

46^a Reunião Anual da SBQ

28 a 31 de Maio de 2023

Águas de Lindóia · SP
Hotel Monte Real

ANAIS

SOCIEDADE BRASILEIRA DE QUÍMICA

Anais da 46^a Reunião Anual da SBQ



Águas de Lindóia-SP
2023

Copyright © 2023 para os autores

Revisão textual e gramatical: Resposanbilidade dos respectivos autores.

Todos os direitos reservados 2023
A reprodução não autorizada desta publicação, no todo ou em parte,
constitui violação de direitos autorais (Lei 9.610/98).

Dados Internacionais de Catalogação na Publicação (CIP)
(Câmara Brasileira do Livro, SP, Brasil)

Reunião Anual da SBQ (46. : 2023 : Águas de
Lindóia, SP)
Anais 46^a reunião anual da SBQ [livro
eletrônico] / organização Sociedade Brasileira de
Química (SBQ). -- 1. ed. -- Águas de Lindóia, SP :
Aptor Software, 2023.

PDF

Vários autores.
Vários colaboradores.
Bibliografia.
ISBN 978-85-63273-51-2

1. Química - Estudo e ensino 2. Sociedade
Brasileira de Química (SBQ) 3. Trabalhos acadêmicos
I. Sociedade Brasileira de Química (SBQ). II. Título.

23-169398

CDD-540

Índices para catálogo sistemático:

1. Química 540

Aline Grazielle Benitez - Bibliotecária - CRB-1/3129

PREFÁCIO

No período de 28 a 31 de maio de 2023, a comunidade Química brasileira esteve reunida em Águas de Lindóia/SP na 46ª Reunião Anual da Sociedade Brasileira de Química (46RASBQ). As Reuniões Anuais da SBQ constituem um dos eventos mais importantes e tradicionais da ciência brasileira e reúnem um grande número de estudantes participantes, entre alunos de graduação e pós-graduação, professores e pesquisadores (jovens e sêniores) de química e áreas afins. Nos últimos dez anos as reuniões atraíram, anualmente, entre 2000 e 4500 participantes, inscritos e convidados, nacionais e internacionais. As características mais importantes das reuniões anuais da SBQ são o forte caráter científico e a interdisciplinaridade da programação, sempre voltada para temas na fronteira do conhecimento. Em Águas de Lindóia não foi diferente, foram mais de 1300 participantes, representantes de 27 estados do Brasil, subdivididos principalmente em 33% de pesquisadores, 35% de estudantes de pós-graduação e 20% de alunos de iniciação científica das mais diversas áreas de Química e afins de todo Brasil e do exterior. Este ano, o tema da reunião foi "Química: Ligando ciências e neutralizando desigualdades". A 46ª Reunião Anual contou com uma programação rica e bastante diversificada, envolvendo os mais diversos e atuais aspectos da química. Nos três dias de evento, tivemos as seguintes atividades: 10 workshops, uma conferência de abertura, 10 minicursos, 16 conferências convidadas, 2 simpósios, 5 sessões temáticas, 20 sessões coordenadas, 2 sessões de *flash poster presentation*, uma inovação na RA, e 2 sessões de painéis. Nestas atividades 110 pesquisadores, 112 alunos de pós-graduação e 38 alunos de iniciação científica fizeram apresentações orais de seus trabalhos, e um total de 946 trabalhos apresentados na forma de painéis. Desta forma, a 46RASBQ contribuiu para um dos seus principais objetivos que é a formação de recursos humanos qualificados na área de Química e afins.

SUMÁRIO

1	AMB - Química Ambiental
58	ANA - Química Analítica
169	BEA - Alimentos e Bebidas
187	BIO - Química Biológica
204	CAT - Catálise
253	EDU - Ensino de Química
309	ELE - Eletroquímica e Eletroanalítica
397	FIS - Físico-Química
422	FOT - Fotoquímica
435	INO - Química Inorgânica
574	MAT - Química de Materiais
713	MED - Química Medicinal
756	ORG - Química Orgânica
864	QPN - Produtos Naturais
962	QVE - Química Verde
970	TEC - Química Tecnológica
979	TEO - Química Teórica

AMB

Química Ambiental

46^a Reunião
Anual da **SBQ**

28 a 31 de Maio de 2023

Águas de Lindóia · SP
Hotel Monte Real

Adsorption of phosphorus from aqueous solution by poly(vinylidene fluoride)/modified bentonite membrane: Performance study.

Gabriela Tuono Martins Xavier (PG),^{1*} Alessandro Lamarca Urzedo (PG),¹ Renan da Silva Nunes (PG),¹ Pierre Le-Clech (PQ),² Dalmo Mandelli (PQ),¹ Pedro Sergio Fadini (PQ),³ Wagner A. Carvalho (PQ).¹

gabriela.xavier@ufabc.edu.br

¹ Center for Natural and Human Sciences (CCNH), Federal University of ABC (UFABC), Santo André – SP, Brazil; ² UNESCO Centre for Membrane Science and Technology, School of Chemical Engineering, The University of New South Wales (UNSW), Sydney – NSW, Australia; ³ Chemistry Department (DQ), Federal University of São Carlos (UFSCar), São Carlos – SP, Brazil.

Keywords: adsorption, membrane process, phosphorus recovery, circular economy.

Highlights

Modified bentonite was incorporated into a PVDF membrane, and showed better performance than the pristine membrane. The membrane was

Abstract

Eutrophication is one of the principal environmental problems worldwide, and it is directly related to the excess of nutrients, mainly phosphorus (P) and nitrogen (N), in water bodies. The two main sources of anthropogenic nutrients in these waters are agriculture runoff and domestic/industrial wastewater disposal. Different materials and technologies to remove and recover P from effluents have been studied globally. In this work, a poly(vinylidene fluoride)/modified bentonite membrane was obtained and used to adsorb P from an aqueous solution during filtration experiments. The produced membrane showed a better permeability and rejection of P compared to the pristine membrane, related to the formation of larger finger-like pores after incorporating clay particles. The dynamic adsorption experiments were conducted in a *dead-end* filtration cell, and it was possible to observe that the increase of pressure in the system had no significant effect on P adsorption by the produced membrane (Figure 1) (ANOVA, $p = 0.055$). Furthermore, the adsorption capacity (Q) of PVDF/modified bentonite membrane was 24.0 mg P/m^2 ($C_0 = 5.8 \text{ mg P/L}$, 3 bar, surface area – 13.85 cm^2), and it rose as the feed solution's P concentration increased (Figure 2), while the flux observed was relatively constant. The mechanism of P removal by the PVDF/modified bentonite membrane proved to be P-species' adsorption onto the adsorbent incorporated into the membrane matrix, as no P rejection was observed in the feed solution. Therefore, the composite membrane might be employed to adsorb P from an aqueous solution, combining the advantages of membrane processes and adsorbents.

Figure 1 - Effect of pressure in P adsorption by PVDF/modified bentonite membrane ($C_0 = 5.8 \text{ mg P/L}$; pH 7.0, 23 °C)

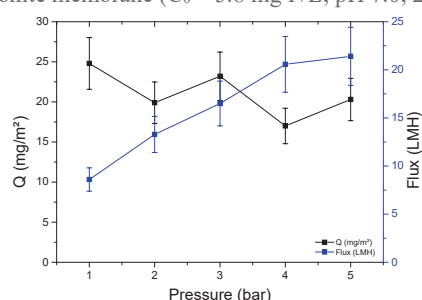
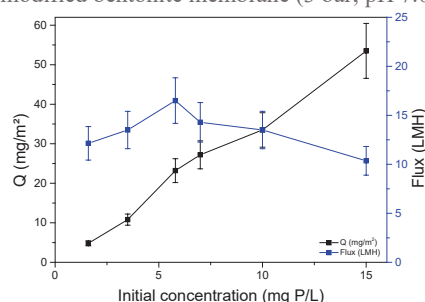


Figure 2 - Effect of P concentration on the adsorption by PVDF/modified bentonite membrane (3 bar; pH 7.0, 23 °C)



Acknowledgments



This study was financed in part by the Coordenação de Aperfeiçoamento de Pessoal de Nível Superior – Brazil (CAPES) – Finance Code 001.

Air quality impact estimation from Capuava Petrochemical Complex in Metropolitan Area of São Paulo, Brazil

Monique Silva Coelho (PG)^{1*}, Daniel Constantino Zacharias (PQ)¹, Tayná Silva de Paulo (IC)¹, Rita Yuri Ynoue (PQ)¹, Adalgiza Fornaro (PO)¹

adalgiza.fornaro@iag.usp.br; monique.coelho@iag.sup.br*

¹Departamento de Ciências Atmosféricas (DCA), Instituto de Astronomia, Geofísica e Ciências Atmosféricas, Universidade de São Paulo (IAG-USP), São Paulo, São Paulo, Brasil.

Key-words: Industrial emissions, Dispersion modeling, Volatile organic compounds, Particulate matter.

Highlights

Uncontrolled emissions from complex showed concentrations of pollutants was two times higher.

Complex emissions could have been responsible for more than 60% of the benzene concentration.

VOC plume had the potential to reach a large part of Mauá and Santo André.

Resumo/Abstract

In the second quarter of 2021, the companies at the Capuava Petrochemical Complex (CPC) carried out a 50-day scheduled shutdown for the maintenance and installation of new industrial equipment. This process resulted in uncontrolled emissions of particulate matter (PM) and volatile organic compounds (VOC) in a densely populated area (CETESB, 2021). Our study evaluated emissions from this acute episode (April-May 2021) by comparing hourly data from the official air quality station (AQS) for PM₁₀, benzene and toluene (CETESB), with data from four previous years (2017-2020). Near-field simulations were also performed to evaluate the dispersion of pollutants from these industries, applying the Gaussian plume model AERMOD (Venkatram et al., 2001), thus estimating the concentrations of VOC and particulate matter (PM₁₀). Compared to the four previous years, an increase in the mean concentrations was observed by a factor of 2 for PM₁₀, benzene, and toluene, reaching maximum values concentrations during the episode: 174.0 µg m⁻³ (PM₁₀), 79.13 µg m⁻³ (benzene) and 58.7 µg m⁻³ (toluene). AERMOD model gives 1-h average for PM and VOC concentrations providing temporal series that were compared with the data from Capuava AQS. The comparison between PM and VOC provided by AERMOD versus PM₁₀, benzene, and toluene, was in agreement with the peaks. Linear correlation indicates that CPC could have been responsible for more than 60% of benzene measured at the Capuava AQS. However, the PM₁₀ behavior was not fully explained by the model, it is hard to estimate the particulate matter inside an uncontrolled soot emission from a refinery flare. AERMOD showed that the VOC plume had the potential to reach a large part of Mauá and Santo André municipalities, with the potential to affect the health of more than 1 million inhabitants.

Referências/References

CETESB (2021) CETESB multa empresas do Polo Petroquímico Capuava [WWW Document]. Blog - Cia. Ambient. do Estado São Paulo. URL <https://cetesb.sp.gov.br/blog/2021/04/14/cetesb-multa-empresas-do-polo-petroquimico-capuava/> (accessed 6.10.21).

Venkatram, A., Brode, R., Cimorelli, A., Lee, R., Paine, R., Perry, S., Peters, W., Weil, J., Wilson, R. (2001). A complex terrain dispersion model for regulatory applications. *Atmospheric Environment*, 35 (24), 2001, 4211-4221, 1352-2310, DOI:10.1016/S1352-2310(01)00186-8

Agradecimentos/Acknowledgments

The authors thank FAPESP (2020/07141-2) and CNRS-France for the founding of the international collaboration project (BIOMASP+) and CETESB for air quality data. The authors thank the financial support and scholarship (Monique Silva Coelho) by CAPES-PROEX (Post-graduation program in Meteorology, IAG-USP).

A multi-instrumental approach to quantify polycyclic aromatic hydrocarbons in seawater from the northeast coast of Brazil after the mysterious oil spill

Thayane C. S. Moreira (PG),^{1*} Ana F. B. Oliveira (PG),¹ Estefani S. Nascimento (PG),² Leonardo M. F. Almeida (PG),² Alex S. Moura (PQ),¹ Cristiane M. V. Araújo-Castro (PQ),² Lino A. V. Rojas (PQ)³, Gilvan T. Yogui (PG),³ Eliete Zanardi-Lamardo (PQ),³ Jandyson M. Santos (PQ)¹

cthayane36@gmail.com; jandyson.machado@ufrpe.br

¹Department of Chemistry, UFRPE; ²Department of Animal Morphology and Physiology, UFRPE; ³Department of Oceanography, UFPE.

Keywords: gas chromatography, fluorescence, oil spill, aromatic hydrocarbons, contamination, seawater

Highlights

- A multi-instrumental approach for analysis of PAHs in seawater samples after the oil spill of 2019
- A high level of contamination for PAHs was found in some samples one year after the oil spill

Resumo/Abstract

In 2019, occurred the biggest environmental disaster in Brazil with an impact on the Northeast coast due to the coming of a large volume of material from oil exploration, which was possibly identified as coming from a Greek ship in transit. The state of Pernambuco – Brazil was one of the most affected by the spill, and three years after the disaster continues to suffer the impacts, which recurrently affect the coast. This disaster caused several impacts on the environment since part of the material's composition is considered toxic. It caused impacts on both public health and the economy, directly affecting tourism and fishing. For the oil composition, the two main classes of organic compounds are aliphatic (HAs) and polycyclic aromatic (PAHs) hydrocarbons, which are considered geochemical biomarkers, and have been studied by several researchers due to their carcinogenic, mutagenic, and teratogenic contents. The objective of this study was to evaluate the level of environmental contamination on the coast of Pernambuco, Brazil through the identification and quantification of PAHs in 50 seawater samples collected in the summer and winter of 2021 (named P01 to P25). The samples were extracted by liquid-liquid extraction with *n*-hexane from method described by Lemos *et al.* (2014) and were analyzed by fluorescence spectroscopy (FS) to quantify the dissolved/dispersed polycyclic aromatic hydrocarbons (DDPAH), and gas chromatography-mass spectrometry (GC/MS) with electron ionization and quadrupole analyzer to quantify 16 PAHs, which is pointed as priority from United States Environmental Protection Agency. Ecotoxicity tests were evaluated to verify the killing effect of a microcrustacean (*Tisbe biminiensis*) during 24 h in the presence of the collected seawaters from the method described by Lavorante *et al.* (2013). The concentration of DDPAH varied from 0.27 to 32.62 $\mu\text{g L}^{-1}$ and from 0.04 to 9.78 $\mu\text{g L}^{-1}$ in the summer and winter seasons, respectively. For GC/MS, the ΣPAHs varied from 0.92 to 233.53 ng L^{-1} , and from 0.74 to 33.28 ng L^{-1} in the summer and winter seasons, respectively, and we have found the P20 sample (collected in summer) as the most affected (collected near a paradisiac beach named of Barra de Sirinhaém, which is located at 87.6 km from Recife). Diagnostic ratios as LMW/HMW, demonstrated contamination from pyrolytic and petrogenic sources. For the P20 sample, significant differences between the concentrations of PAHs were observed during the summer and winter periods, in the way that the ΣPAHs decrease from summer to winter, indicating that there was possibly a recovery of the environmental system overtime. We have found in ecotoxicity tests that three samples (including P20 sample) exhibited a lethal toxic effect on the environment and high mortality rates of the microcrustacean. A multivariate statistical analysis was performed using principal component analysis (PCA) and hierarchical cluster analysis (HCA/Heatmap), and the results pointed to identify the regions most affected by the oil spill. Therefore, it was possible to point out some regions of high contamination by PAHs in seawaters collected on the coast of Pernambuco one year after the oil spill. The results showed the need for continuous monitoring of the regions affected by the spill since they are regions that have areas of environmental protection and with great social and economic importance.

References:

Lavorante, B. R. B. O. *et al.* Ecotoxicology and Environmental Safety, v. 95, 2013, p. 52-59.
Lemos, R.T.O. *et al.* Marine Pollution Bulletin, v. 82, 2014, p. 183–188.

Agradecimentos/Acknowledgments

FACEPE, LaMTESA/UFRPE, PPGQ/UFRPE, PEM/UFRPE, DMFA/UFRPE, DOCEAN/UFPE

Analysis of the Impact of the COVID-19 Pandemic on the Environmental Efficiency of the Largest Wastewater Treatment Plant in Rio de Janeiro

Ricardo Soares(PQ),^{1,2,3*} Rafaela Naegele Alvernaz(PQ),² Márcia Cristina S. Mello(PQ),² Carlos Eduardo S. C. P. Cunha(PQ)^{2,3}

Ricardos@inea.rj.gov.br, Ricardo.soares@uva.br

¹State Environmental Institute, INEA; ²Solid Waste Observatory of the State of Rio de Janeiro, UVA; ³Civil Engineering Department, UVA³

Keywords: COVID-19 Pandemic, Wastewater Treatment Plant; Environmental Efficiency; Pollution Control; Guanabara Bay.

Highlights

- The wastewater flow rate at the *ETE Alegria* increased significantly after the start of the COVID-19 pandemic.
- The *ETE Alegria* is capable of treating the main pollutants present in the sanitary sewage as required by the federal and state laws of Rio de Janeiro.

Resumo/Abstract

The *Alegria* Wastewater Treatment Plant (*ETE Alegria*) has an environmental license to treat up to 2,500 L s⁻¹ daily (216,000 m³ day⁻¹), thus benefiting a population of approximately 1.5 million inhabitants of the city of Rio de Janeiro. However, since the World Health Organization (WHO) decreed the beginning of the COVID-19 pandemic in 2020, there have been changes in the consumption habits and customs of the population in Brazil in general and in the state of Rio de Janeiro in particular. The massive adoption of Non-Pharmacological Intervention Measures has brought significant negative environmental impacts on the management of sanitary sewage and solid waste throughout Brazil. Therefore, the objective of this study is to analyze the impact of the COVID-19 pandemic on the Environmental Efficiency of the *ETE Alegria* in the treatment of all 46 legislated parameters/pollutants. It was observed that after the beginning of the pandemic of COVID-19, the flow of treated sewage from the *ETE Alegria* showed a statistically significant increase of 27.59% (Friedman chi-squared = 784.93, p-value < 2.2e-16) (Figure 1). Although the sewage flow to be treated increased after the pandemic of COVID-19, there were no significant negative impacts on the ability of the *ETE Alegria* to adequately treat the parameters of Biochemical Oxygen Demand (BOD), Chemical Oxygen Demand (COD), Total Suspended Solids (TSS) and total Ammoniacal Nitrogen. The concentrations of As and metals were below the maximum allowable values during the whole period. The organic compounds present in the sanitary wastewater (benzene, toluene, ethylbenzene, xylenes, and others) were below the detection limit practically over the entire evaluated historical series. It seems that the *ETE Alegria* maintained adequate technical efficiency in reducing, neutralizing, or eliminating the pollutants present in the sanitary sewage generated by almost 10% of the Rio de Janeiro state population, thus protecting Guanabara Bay's surface waters.

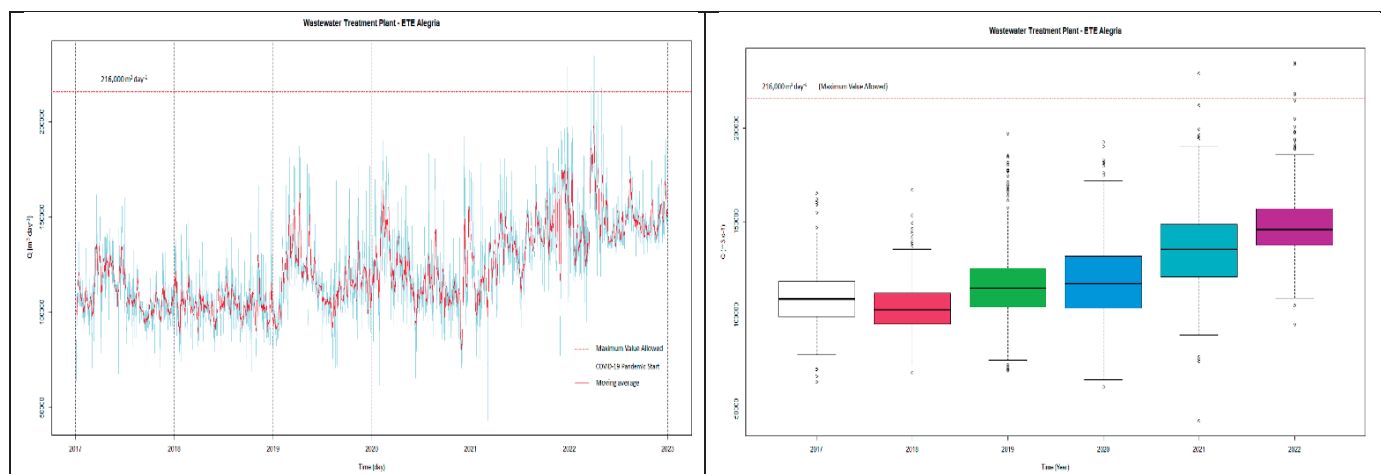


Figure 1. Historical series and box-plot of the sanitary sewage flow treated at the *ETE Alegria* in the evaluated period (2017-2022).

References: Silva, C. M.; Soares, R.; Machado, W.; Arbilla, G. *Rev. Virtual Quím.*, 12, 1001-1016, 2020.

46^o Reunião Anual da Sociedade Brasileira de Química: "Química: Ligando ciências e neutralizando desigualdades"

Analysis of the spatiotemporal distribution of total lead in concentric rings of trees as biomonitoring on geologic failure areas

Kevin Felipe Ramos (PG)¹, Marcos Fernando de Souza Teixeira* (PQ)¹. [*marcos.fs.teixeira@unesp.br](mailto:marcos.fs.teixeira@unesp.br)

¹Department of Chemistry and Biochemistry, School of Science and Technology, São Paulo State University "Júlio de Mesquita Filho" (UNESP), Presidente Prudente, SP, Brazil.

Keys-words: Biomonitoring, arboreal growth rings, lead, geological fault

Highlights

- Environmental variables are recorded in the tree growth rings of biomonitor trees.
- Correlation between spatiotemporal variables and total lead concentration in tree growth rings of tree species *Licania Tomentosa* and *Caesalpinia pluviosa*.
- High variability in total lead concentrations in regions insusceptible to induced geological fracture zones.

Abstract

The analysis of the space-time distribution of potentially toxic metals in the tree rings is a significant contribution to the biomonitoring method, since the environmental variables are recorded in the core of the tree woods¹. The aim of this research was to analyze the spatiotemporal distribution of total lead in arboreal rings of *Moquilea tomentosa* and *Caesalpinia pluviosa* over geological fault zones. The study area was integrated between two geological fault lineaments, in the western region of the state of São Paulo. Cylindrical samples of the concentric rings of the tree species under study were extracted by a metallic probe coupled to a motorized equipment. The sample digestion method was adapted from the USEPA 350 system. To determine the total concentration of lead in the samples, the anode stripping differential pulse voltammetry technique was applied. From a statistical point of view, the Principal Component Analysis (Fig. 1 a and b) was obtained through the values of lead concentration in each sample and data on annual environmental variations.

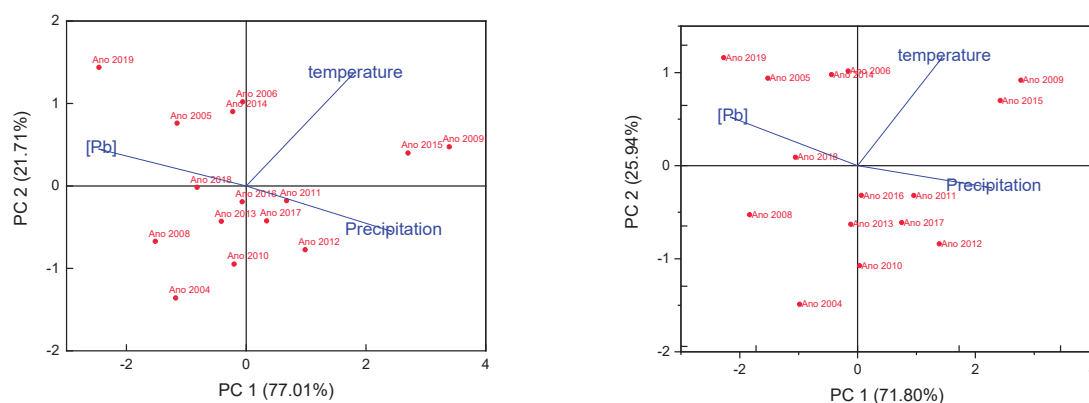


Fig. 1 a) PCA of seasonal variables of the tree species *Licania tomentosa*. b) PCA of seasonal variables of the tree species *Caesalpinia pluviosa*.

From the obtained results, it was verified that the annual variations of the total lead concentrations in the arboreal species, correlate inversely with the environmental variations, and directly with the direction of the probable geological fault in the region, resulting in the emanation of the effective and intense radon gas, coexisting with a high concentration of lead.

Acknowledgments

The authors acknowledge CAPES and CEPID-FAPESP (2013/07296–2) for the financial support.

¹Badamasi, H. **MAYFEB J Environ Sci**, 2, 2017, 27.

An automated, self-powered and integrated IoT analytical platform for on-line and in-situ air quality monitoring.

Danielle S. Sousa (PG)^{1*}, Vanderli G. Leal (PG)¹, Gustavo T. Reis (PG)¹, Sidnei G. da Silva (PQ)¹, Arnaldo A. Cardoso (PQ)², João Flávio S. Petrucci (PQ)¹.

Daniellesousa1006@gmail.com

¹Institute of Chemistry, UFU; ²Institute of Chemistry, UNESP

Key-Word: Air pollution monitoring; Air quality; ozone; nitrogen dioxide; remote gas sensing.

Highlights

An IoT platform was designed for monitoring the levels of two pollutants, O₃ and NO₂, in the outdoor atmosphere of two Brazilian cities.

Abstract

Air quality monitoring networks are challenging to implement due to the bulkiness and high prices of the standard instruments and the low accuracy of most of the described low-cost approaches. This study presents a low-cost, automated, self-powered Internet of Analytical Things (IoAT) platform to determine the hourly levels of O₃ and NO₂ in urban atmospheres. Atmospheric air was sampled at a constant airflow of 100 mL min⁻¹ directly into vials containing 800 µL of indigotrisulfonate and the Griess-Saltzman reagent solutions for ozone and nitrogen dioxide, respectively. The analysis holder containing a light-emitting diode and a digital light sensor enabled the acquisition of the analytical signal on-site and immediately after the sampling time. The data were transmitted to a laptop via Bluetooth, rendering remote hourly monitoring. The platform was automated using two Arduino Uno boards and fed with a portable battery recharged with a solar panel. The method provided a limit of detection of 5 and 1 ppbv for O₃ and NO₂, respectively, which are below the maximum limit established by worldwide regulatory agencies. The IoAT platform was employed to determine the levels of both pollutants in the atmosphere of two Brazilian cities, in which one of them was equipped with an official air quality monitoring station. Comparing the results (Table 1) of both techniques revealed suitable accuracy for the proposed analytical platform. Information technology (IT) allied to reliable chemical methods demonstrated high potential to create air quality monitoring networks providing valuable information on pollutants emissions and ensuring safety to the population.

Table 1: Comparative results obtained by the proposed method and the official air quality station.

Hour	O ₃ IoAT platform (ppbv)	O ₃ Air quality station (ppbv)	NO ₂ IoAT platform (ppbv)	NO ₂ Air quality station (ppbv)	Temp (°C) and RH (%)
2-3 pm	69	54	<LOQ	2	27 / 30
3-4 pm	71	56	4	3	27 / 27
4-5 pm	53	55	6	4	27 / 27
5-6 pm	52	49	12	8	27 / 27
6-7 pm	<LOQ	28	26	20	26 / 30
7-8 pm	<LOQ	26	26	23	24 / 34
8-9 pm	<LOQ	24	28	25	23 / 37

Acknowledgments

CNPq, CAPES and IQ-UFU

Área: AMB

Application of Factorial Design to Optimize Nitrate Removal from Groundwater by Pulsed Current

Antonio R. Alves Jr. (PQ),^{1*} Taís C. Parente (PQ),¹ Eliezer F.A. Neto (PQ),¹ J. T. Oliveira (PQ),¹ Ronaldo F. Nascimento (PQ)¹

ribeirolvs@gmail.com

¹Department of Chemistry, Federal University of Ceará, Av. Humberto Monte, SN-PICI, 60000-000 Fortaleza, CE, Brazil.

Palavras Chave: Electrocoagulation, nitrate, groundwater, factorial design

Highlights

The objective of this work was the optimization of the electrocoagulation (EC) process for the removal of nitrate in groundwater, as an alternative water treatment technology of supply for Ceará.

Resumo/Abstract

The water crisis in Ceará makes it necessary to use groundwater as an alternative source of supply. However, one of the difficulties in using this water is the amount of nitrate, a value higher than the maximum contaminant level (MCL) of 10 mg L⁻¹ of N-NO₃⁻ established in drinking water legislation. The methemoglobinemia is one of the main human health problems due to the high levels of nitrate in drinking water. Other potential health effects associated with high levels of nitrates are cancer and tumor (Gupta et al. 2000). The electrocoagulation (EC) technique is an effective process for nitrate removal (Koparal, et al. 2002). In order to optimize the EC process, a factorial design was applied 2⁴, with the influence of the variables: added NaCl concentration, electrode spacing, stirring and pulse frequency were studied. The experimental work was performed in a batch mode to perform the nitrate removal from groundwater. The circuit was connected to a 12 V Power Supply voltage source which provided the potential difference to the system. In the experiments a home-made circuit was installed to generate pulsed current, 4,00 L of water was added with known concentration of N-NO₃⁻. Four aluminium electrodes connected in parallel, monopolar and time of 20 minutes were run in the test.

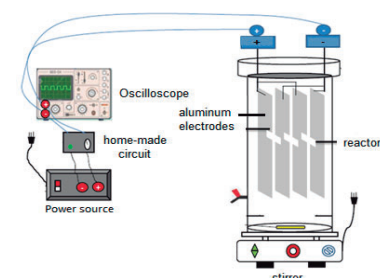
Table 1. Analysis of variance for removal of nitrate into groundwater.^a

Source of variation	Sum of squares	Degrees of freedom	F _o	F _{1,8}	Level of significance
Distance Electrodes in mm (b)	0,02%	1	0,113		
NaCl concentration in mg / l (c)	0,08%	1	0,049		
Frequency in Hz (d)	0,06%	1	0,006		
bc	0,02%	1	0,003		
bd	0,01%	1	0,008	5,318	0,05
cd	0,00%	1	0,000		
bcd	0,00%	1	0,001		
Error	41,06%	8			
Total	41,31%	15			
Model	0,25%	7			

^a Was despised the "A" effect related to the agitation factor of the system for apply ANOVA

The table 1 shows the treatment results. We can observe that the three factors: sodium chloride concentration, electric pulse frequency and electrode spacing in this test did not significantly alter the results of nitrate removal. The F statistic was used to test the effect of the set of independent factors on the experimental response, which this served to verify if at least one of the experimental factors explains the variation of the Y, that is, the experimental response. Thus, it was observed that the null hypothesis (H₀) none of the factors affect the nitrate reduction in the sample was accepted. It can be observed in Table 1 that the factors and interactions were not significant in the trial. Thus, the statistical analysis showed that the best nitrate removal efficiency was observed with the frequency of 125 Hz, electrode distance of 2 mm, agitation of 200 rpm and no addition of NaCl.

Figure 1. Batch mode to perform the nitrate removal from groundwater.



Agradecimentos/Acknowledgments

UFC, Cagece, LAT and Labpoa group.

[1] Gupta SK, Gupta AB, Gupta RC, Seth AK, Bassain JK, Gupta. A Recurrent acute respiratory tract infections in areas with high nitrate concentrations in drinking water. Environ Health Perspect 108:363–365, (2000).

[2] Koparal, A.S., Ogutveren, U.B. Removal of nitrate from water by electroreduction and electrocoagulation, J.Hazard. Mater. Jan 4;89(1):83-94, (2002).

[3] WHO (World Health Organization). Guidelines for drinking water quality, 3rd edn. WHO, Geneva, (2004).

Aquatic ecotoxicological evaluation of organic compounds from burning mixtures of S10 diesel with 1G ethanol, 2G ethanol and HVO using *Daphnia similis*

Clara R. Pereira (PG)¹, Eliete C. Alves (TC)¹, Adriano C. S. Guimarães (IC)¹, Madson Nascimento (PQ)²; Lilian L.N. Guarieiro (PQ),¹

clara.r.pereira@gmail.com; eliete.alves@fieb.org.br; carvalho.adriano21@gmail.com; lilian.guarieiro@fieb.org.br

¹ Centro Universitário SENAI CIMATEC;

² Universidade Federal da Bahia (UFBA).

Keywords: *Daphnia*, *Daphnia Similis*, Ecotoxicity, Fuels.

Highlights

Organic compounds from the burning of different mixtures of S10 diesel with both 1G and 2G ethanol was evaluated.

The addition of 2G Ethanol to Diesel promotes a reduction in toxicity emissions.

Resumo/Abstract

Aquatic ecotoxicology seeks to assess the impact of contaminating substances on the water ecosystem, to detect the effects that can be found in the organisms that inhabit this environment. Daphnias are the main bioindicators used to assess the toxicology of water quality, which have species that can be found both in the sea and in fresh water and are constantly applied in ecotoxicity tests. This study sought to evaluate the aquatic ecotoxicity of the *Daphnia Similis* species (Figure 1) in the presence of organic compounds from the burning of different mixtures of S10 diesel with 1G ethanol, 2G ethanol. A diesel cycle engine (4 cylinders, continuous power 82CV, 66KVA, intermittent power 90CV, 73KVA and turbo aspiration) mounted under a stationary dynamometer (AVL with a capacity to absorb up to 240 kW) was used. The engine worked at a fixed speed (1500 rpm) and a fraction of the gases from the incomplete burning of the selected fuel mixtures passed through a system composed of 2 bubblers in series containing *Daphnia Similis* culture solution. The exposure of *Daphnia Similis* to the collected medium was evaluated through acute tests lasting 48 hours, in which 10 *D. Similis* were exposed to 30 mL of the collected sample, per replicate, considering a triplicate, in addition to a control containing 10 *D. Similis* in pure culture medium, totalizing 30 organisms for each sample. Therefore, the results (Figure 2) showed an increase in mortality with pure S10, considering that with the addition of 1G ethanol to diesel, there was a reduction from 43% to 30% of dead daphnias, in the same way as for the diesel mixture S10 with 2G Ethanol there was an even greater reduction in mortality compared to pure diesel (13% of dead daphnias). This showed that the addition of 2G Ethanol promotes a reduction in toxicity taking into account a scenario of the incidence of these particles in an aquatic environment.

Figure 1. Simplified anatomy of *Daphnia Similis*

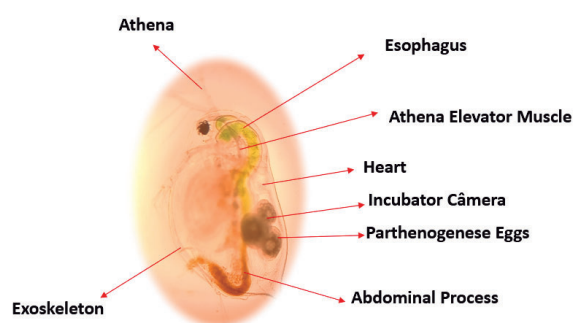
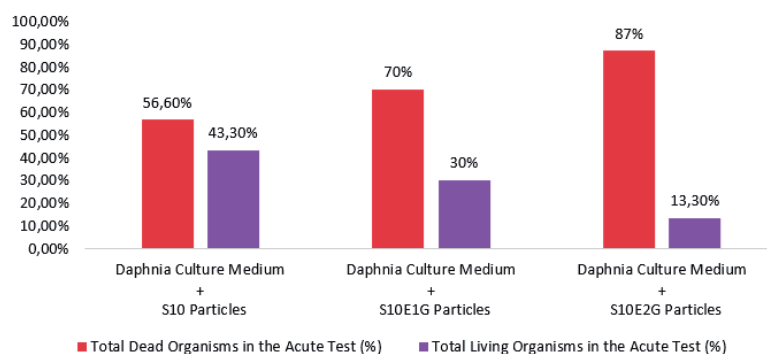


Figure 2. Number in percentage of living and dead organisms after acute test with different fuel mixtures.



Área: AMB

(Inserir a sigla da seção científica para qual o resumo será submetido. Ex: ORG, BEA, CAT)

Assessment of potential biases for microplastics during the digestion of environmental samples

Walter R. Waldman (PQ),^{1*} Ana C.C. Moreira (PG)².

walter@ufscar.br

¹Departamento de Física, Química e Matemática, Federal University of São Carlos; ²Institute of Geography, University of Augsburg,

Palavras Chave: *Microplastics, Digestion, Degradation, Advanced Oxidative Processes.*

Highlights

Advanced Oxidative Processes and mechanical stimuli during the digestion of environmental samples affect microplastic morphology and foster fragmentation and thus affecting the assessment.

Resumo/Abstract

Once discarded in the environment, plastics degrade and fragment into smaller particles. Since photodegradation and weathering can turn microplastics into brittle materials and are also prone to have their surface modified or even eroded by the advanced oxidative processes (AOP) used to disassemble and digest environmental samples. We tested some protocols in the literature to process and digest environmental samples containing microplastics and checked if degradation of the microplastics plays any role in biasing the digestion results by fragmenting the microplastics and then inflating the number of particulates found in the environmental samples. To verify whether AOP affects the fragmentation of degraded polymers in any fashion, we assessed the effect of Fenton reagents and alkaline solution on polymer samples with different levels of photodegradation. Samples with higher carbonyl concentrations showed morphological variations after the AOP protocols, mainly the formation and deepening of crackings on the surface. In contrast, samples with little or no carbonyl concentration showed no variations. These results confirm the interaction of AOP with the photodegraded materials. Therefore, this type of analysis can influence the number of fragments obtained after the chemical digestion of environmental samples containing weathered microplastics. Furthermore, these results put into perspective the monitoring of microplastics.

Agradecimentos/Acknowledgments

The authors acknowledge the Capes fellowship for the master course of ACCM.

Assessment of the ozone-forming potential of hydrocarbons emitted by vehicle exhausts

Bruno Siciliano^{1*} (PG), Cleyton M. da Silva^{1,2} (PQ), Graciela Arbilla¹ (PQ)

sicilianoig@gmail.com

¹Instituto de Química da Universidade Federal do Rio de Janeiro, ²Engenharia Ambiental, Universidade Veiga de Almeida.

Keywords: hydrocarbons, vehicle exhaust, incremental reactivity, ozone-forming potential, multidimensional gas chromatography.

Highlights

Hydrocarbons stand out among volatile organic compounds in urban environments. Incremental reactivity scales were used to estimate ozone-forming potential. Alkenes from exhaust emissions contribute considerably to ozone formation.

Abstract

In this work, the ozone-forming potential (OFP) of hydrocarbons (HC) emitted by the exhaust of two vehicles (PROCONVE L5 and PROCONVE L6) fueled with gasoline (E22) and hydrous ethanol (H100) and using the EPA-75 driving cycle (ABNT/NBR 6601) was studied. The determination of HC was performed by using multidimensional heart-cutting gas chromatography. The separation of the HC in the C₂-C₁₂ range was carried out with two chromatographic columns (DB-624 and PoraPLOT Q-HT), interconnected by a Deans Switch (Figure 1).¹

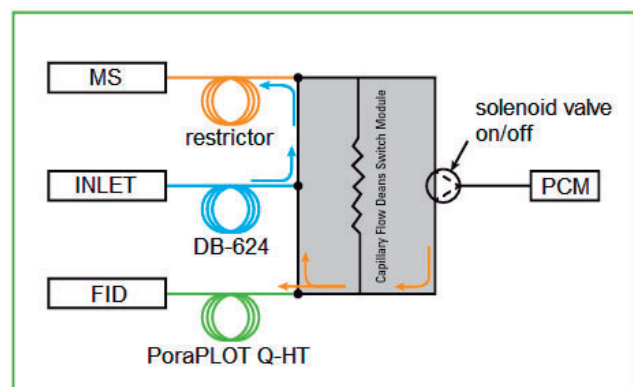


Figure 1. Deans Switch. Source: Adapted from Agilent, 2013.

Table 1. OFP values for MIR, MOIR and EBIR scales.

OFP MIR / g O ₃ km ⁻¹		
	E22	H100
PROCONVE L5	0.0884	0.1110
PROCONVE L6	0.0151	0.0324
OFP MOIR / g O ₃ km ⁻¹		
	E22	H100
PROCONVE L5	0.0370	0.0451
PROCONVE L6	0.0066	0.0132
OFP EBIR / g O ₃ km ⁻¹		
	E22	H100
PROCONVE L5	0.0210	0.0270
PROCONVE L6	0.0039	0.0080

In order to quantify the OFP of the HC emission, three incremental reactivity scales, proposed by Carter (2010),² were used (Table 1). Each scale corresponds to an urban scenario with different volatile organic compounds/nitrogen oxides ratios (VOC/NO_x): Maximum Incremental Reactivity (MIR), Maximum Ozone Incremental Reactivity (MOIR) and Equal Benefit Incremental Reactivity (EBIR). Regardless of the scale, alkenes (mainly ethylene) contributed the most to the OFP (around 60% and 90%, when vehicles were fueled with E22 and H100, respectively). Tests with H100 showed larger OFP values than those with E22, mostly due to the larger amount of ethylene, which is highly reactive and a common product of ethanol combustion. The results showed the relevance of the determination of light-end HC for the ozone formation evaluation.

Acknowledgements

The authors would like to thank CNPq, FAPERJ, FUNADESP and ANP for the financial support and research scholarships.

¹ Agilent. Capillary flow technology: Deans Switch brochure. 2013.

² Carter. Development of the SAPRC-07 chemical mechanism. *Atmos. Environ.* 44, 5324-5335, 2010.

Biossorção-Dessorção de Crômio Hexavalente em Palha da Cana-de-Açúcar *in natura*

Alinec Laura Modesto Lima (IC),^{1*} Luciana Maria Saran (PQ).²

lm.saran@unesp.br; *alince.laura@unesp.br

^{1,2}Departamento de Biotecnologia Agropecuária e Ambiental (DBTAA), Faculdade de Ciências Agrárias e Veterinárias (FCAV), Universidade Estadual Paulista, campus de Jaboticabal, São Paulo, Brasil.

Palavras-Chave: Biorremediação, Material Biológica, Adsorção, Metal Presado, Metal Potencialmente Tóxico, Bioprocesso.

Highlights

Biosorption-Desorption of Hexavalent Chromium in Sugarcane Straw *in natura*.

Sugarcane straw adsorbs hexavalent chromium from solution.

Nitric acid solution as a desorbent can degrade sugarcane straw.

In batch biosorption-desorption cycles there is a loss of biosorbent mass.

Resumo

A palha da cana-de-açúcar (PCA), subproduto abundante gerado por indústrias do setor sucroenergético, têm potencial de biosorver íons metálicos potencialmente tóxicos, como crômio hexavalente, Cr(VI), de soluções.^{1,2} Entretanto, a possibilidade de reutilizar o biosorvente é fator importante para a aplicação, em larga escala, da tecnologia de biossorção na remoção de íons metálicos potencialmente tóxicos de águas residuárias. Considerando o exposto, foram estudados o efeito da concentração de soluções de ácido nítrico (HNO₃) para dessorção de Cr(VI) de palha da cana-de-açúcar *in natura* (PCAN) e a viabilidade de reutilizar a PCAN em mais de um ciclo de biossorção. Para tanto, PCAN “carregada” com Cr(VI) foi tratada com HNO₃(aq) 0,5; 1,0; 2,0; 4,0 e 6,0 mol L⁻¹, visando avaliar qual concentração proporcionaria a maior taxa de dessorção.³ Definidas as melhores condições à dessorção do íon metálico de interesse, a PCAN foi empregada em 6 ciclos de biossorção, sendo que, entre um ciclo e outro, o biosorvente foi submetido a dessorção com solução de HNO₃.⁴ As soluções resultantes dos ensaios de dessorção com HNO₃(aq) 4,0 e 6,0 mol L⁻¹ apresentaram cor amarelo-alaranjado intensa, sendo as respectivas taxas de dessorção cerca de 100 % e superior a 100 %, respectivamente, as quais, possivelmente, ficaram “superestimadas” em razão da presença de solução residual de Cr(VI), que não foi completamente removida após a centrifugação das suspensões e da provável dissolução/extração de compostos presentes na composição da PCAN. O tratamento da PCAN com HNO₃(aq) 4,0 e 6,0 mol L⁻¹, alterou a aparência e “consistência” deste biosorvente, sinalizando sua possível degradação. Houve variação da massa do biosorvente ao longo dos seis ciclos de biossorção-dessorção efetuados. A perda de massa observada ao longo dos ciclos sucessivos de biossorção-dessorção, empregando-se HNO₃(aq) 1,0 e 2,0 mol L⁻¹, para dessorção, pode ter sido decorrente da separação insatisfatória da PCAN durante a etapa de centrifugação, e principalmente, a danos físicos e químicos da matriz estrutural da PCAN durante os ciclos de biossorção-dessorção.⁴ A taxa de remoção (TR) do Cr(VI) pela PCAN diminuiu significativamente nos cinco ciclos de biossorção subsequentes (TR ≅ 20 %) ao primeiro ciclo (TR ≅ 70 %). Esse resultado pode estar relacionado a diminuição da massa do biosorvente, a dessorção incompleta do Cr(VI) e a alterações físicas e químicas da matriz estrutural do biosorvente, durante os ciclos de biossorção-dessorção.^{3,4} Conclui-se que o uso de solução de HNO₃ para a dessorção do Cr(VI) da PCAN, pode acarretar a degradação da matriz estrutural da PCAN, com perda de massa do biosorvente e diminuição significativa da taxa de remoção do Cr(VI) pela PCAN, nos ciclos de biossorção subsequentes aos primeiro ciclo, inviabilizando o seu reuso em processos realizados em batelada.

References

¹Salata, C. R.; Vicentini, T. S.; PEREIRA, G. T.; Saran, L. M. *Livro de Resumos da 42ª Reunião Anual da Sociedade Brasileira de Química: eixos mobilizadores em química*. 2019. http://www.s bq.org.br/42ra/anexos/42RASBQ_programa_e_resumos.pdf

²Saran, L. M.; Salata, C. R.; Vicentini, T. S. *Anais do 17º Congresso Nacional de Meio Ambiente de Poços de Caldas*, 2020. <http://www.meioambientepocos.com.br/anais2020.html>

³Tytlak, A.; Olezczuk, P.; Dobrowolski, R. *Environmental Science and Pollution Research*. 2015, 22(8), 5985. DOI: [10.1007/s11356-014-3752-4](https://doi.org/10.1007/s11356-014-3752-4)

⁴Saeed, A.; Iqbal, M. *Water Research*. 2003, 37(14), 3472. DOI: [10.1016/S0043-1354\(03\)00175-1](https://doi.org/10.1016/S0043-1354(03)00175-1)

Acknowledgments

A pró-reitoria de pesquisa da Unesp (PROPe – Unesp) pela bolsa de iniciação científica concedida (Proposta N. 1639/Edital 1/2020 – PIBIC).

46ª Reunião Anual da Sociedade Brasileira de Química: “Química: Ligando ciências e neutralizando desigualdades”

Black carbon and particulate matter mass concentrations in the metropolitan region of Rio de Janeiro, Brazil

Alex R. Huaman De La Cruz (PQ)¹, Luiz Felipe Menezes Silva (PG)¹, Luis Fernando Mendonça da Silva (PG)¹, Ricardo Henrique Moreton Godoi (PQ)², Vanesa Abelaira dos Anjos (PG)², Adriana Gioda (PQ)^{1*}

¹ Chemistry Department, Pontifical Catholic University of Rio de Janeiro (PUC-Rio), Gávea – RJ

² Environmental Engineering Department, Federal University of Parana, Parana

*agioda@puc-rio.br

Keywords: Black carbon, PM_{2.5}, PM₁₀, Metropolitan region of Rio de Janeiro

Highlights

Black carbon in particulate matter; black carbon emission related to vehicular traffic and industrial activities.

Resumo/Abstract

Particulate matter (PM) is a severe air pollution issue due to its heterogeneous mixture and because pose the greatest health risk [1], [2]. High PM₁₀ and PM_{2.5} mass concentration are characteristics of areas densely populated and with heavy vehicular traffic [3], [4]. A significant portion and one of the more toxic species present in PM_{2.5} is the Black Carbon (BC) [5], [6]. BC pollution has become in a global environmental problem due to that has negative implications on public health, urban air quality, agriculture, reduces the visibility, and cause global climate change. Likewise, it is responsible for producing a positive radiative forcing, due to that absorb solar radiation, leading to the warming of the atmosphere. BC is primary produced and emitted by incomplete combustion of fossil fuels, related to traffic, wood, petrol, agricultural waste, biomass burning, biofuel, and industrial processes. Thus, the present study aims to fill that gap information by measuring PM_{2.5}, PM₁₀ and BC at ten cities from the Metropolitan region of Rio de Janeiro (MRRJ) in the periods of 2018 and 2019. The information obtained will be essential to improve the existing air quality policies. In the Figure 1 is showed the concentration of PM_{2.5} and BC (in PM₁₀ and PM_{2.5}) monitored at 10 monitoring stations of the MRRJ.

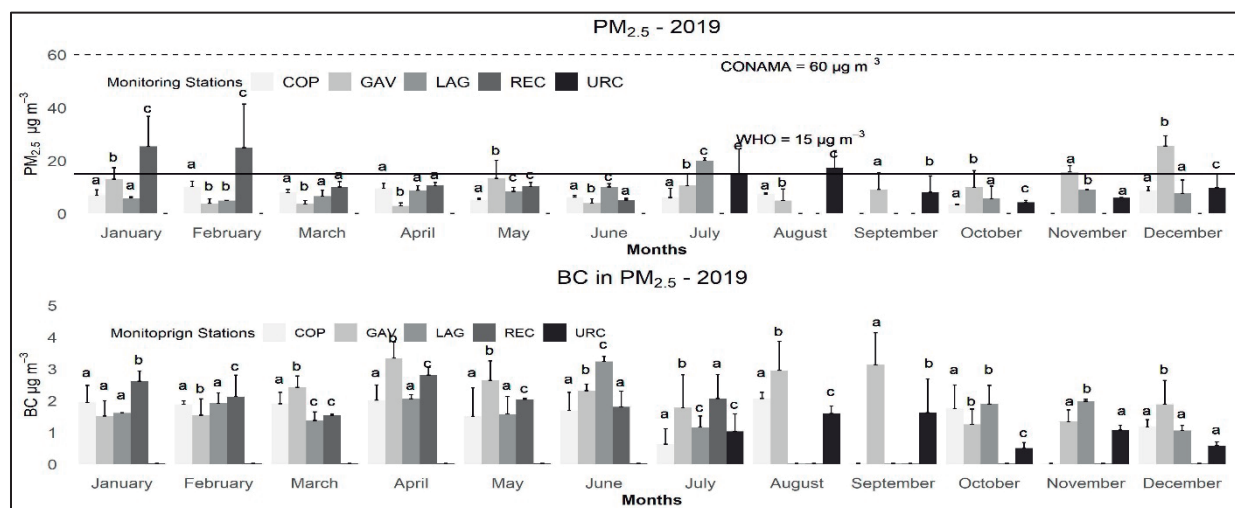


Figure 1. PM_{2.5} concentrations and BC concentrations in PM_{2.5} at five monitoring station from the MRRJ.

Agradecimentos/Acknowledgments

To CAPES, CNPq, FAPERJ by financial support.

- [1] EPA, "Particulate matter (PM) pollution," *Environmental Protection Agency*, 2022. <https://www.epa.gov/pm-pollution/particulate-matter-pm-basics> (accessed Nov. 11, 2022).
- [2] EPA, "How Does PM Affect Human Health?," *Environmental Protection Agency*, 2022. <https://www3.epa.gov/region1/airquality/pm-human-health.html> (accessed Nov. 11, 2022).
- [3] Z. Liu *et al.*, "Characteristics of PM_{2.5} mass concentrations and chemical species in urban and background areas of China: emerging results from the CARE-China network," *Atmos. Chem. Phys.*, vol. 18, no. 12, pp. 8849–8871, Jun. 2018, doi: 10.5194/acp-18-8849-2018.
- [4] A. Mukherjee, M. C. McCarthy, S. G. Brown, S. M. Huang, K. Landsberg, and D. S. Eisinger, "Influence of roadway emissions on near-road PM_{2.5}: Monitoring data analysis and implications," *Transp. Res. Part D Transp. Environ.*, vol. 86, no. July, p. 102442, 2020, doi: 10.1016/j.trd.2020.102442.
- [5] V. Engelhardt, T. Pérez, L. Donoso, T. Müller, and A. Wiedensohler, "Black carbon and particulate matter mass concentrations in the Metropolitan District of Caracas, Venezuela: An assessment of temporal variation and contributing sources," *Elem. Sci. Anthr.*, vol. 10, no. 1, pp. 1–22, Aug. 2022, doi: 10.1525/elementa.2022.00024.
- [6] L. Kirago, M. J. Gatari, Ö. Gustafsson, and A. Andersson, "Black carbon emissions from traffic contribute substantially to air pollution in Nairobi, Kenya," *Commun. Earth Environ.*, vol. 3, no. 1, pp. 1–8, 2022, doi: 10.1038/s43247-022-00400-1.

Catalytic co-pyrolysis of plastics and oil sludge using k10 clay and the effect in diesel oil production

Ana Cristina da Silva Serra (PG),¹ Monica Regina C. M. Calderari (PQ),¹ Jacyra Guimarães Faillace (PQ),²
anacriprofquimica@gmail.com.

¹Programa de Pós-graduação em Química, UERJ; ²Cordenação de Química, IFRJ

Palavras Chave: pyrolysis, plastic, oil sludge, k10, clay, recycling.

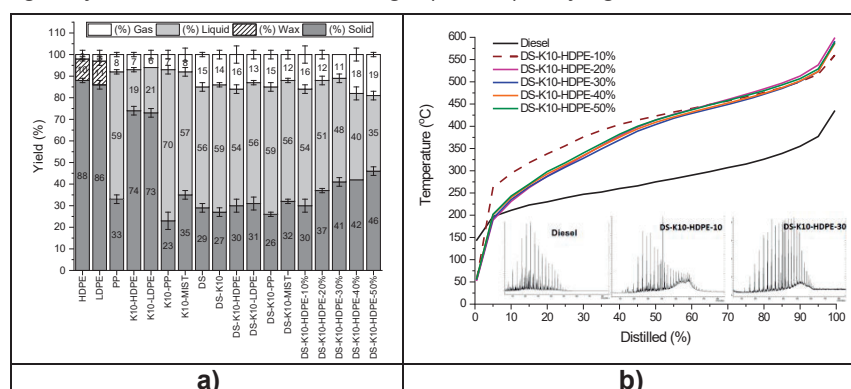
Highlights

Co-pyrolysis of oil sludge and high-density polyethylene (HDPE), low-density polyethylene (LDPE) and Polypropylene (PP) with K10 produced high proportion of pyrolytic liquid with 40% of diesel oil;

Increasing HDPE proportions in catalytic co-pyrolysis with oil sludge raise the diesel production up to 50%.

Abstract

Oily sludge is a toxic residue generated in large volumes by O&G industry. Plastic residues, as polyolefins, can also generate several negative environmental impacts due to higher volumes, inadequate disposal and resistance to decomposition. Pyrolysis is a chemical recycling method which involves a thermal cracking of organic material in a non-oxidizing atmosphere generating a liquid with potential combustible¹. This work is about pyrolysis of polyolefins (HDPE, LDPE and PP), oil sludge (DS) and co-pyrolysis of oily sludge added to polyolefins (10%w/w) both with K10 clay (10% w/w) as catalyst. It was observed an increasing in the proportion of pyrolytic liquid in catalytic pyrolysis of polyolefins if compared to thermal cracking of polyolefins (Figure 1a). Pyrolytic liquid produced had high content of light hydrocarbons in diesel range (C₉-C₂₄) varying from 75% to 90%. These high proportions of paraffinic products



generated are favored by moderate acidity and porous size from clays catalysts in oligomerization bimolecular reactions².

Figure 1 – Proportions of gas, solid liquid and wax in pyrolysis of polyolefins and oil sludge in (a) and distillation curves of diesel and catalytic co-pyrolysis of polyolefins/oil sludge in (b).

Addition of oil sludge in catalytic co-pyrolysis of polyolefins increased proportions of pyrolytic liquid if compared to polyolefins without this sludge. This

positive synergic effect on pyrolysis has been observed in previous studies³ (Figure 1a). Textural properties of K10 clay such as high surface area (229 m²/g), mesopores volume (0,31 cm³/g) and high content of acid sites (617 μmols/g) favored the cracking reaction. Despite increasing of pyrolytic liquid quantities in co-pyrolysis, the proportions of light hydrocarbons in diesel range were around 40 % (Figure 1b). The effect of increasing HDPE concentrations in co-pyrolysis from 20% up to 50% has shown that HDPE proportions above 30% causes a decrease in the generation of pyrolytic liquid (Figure 1a). In distillation curves of the catalytic co-pyrolysis of oil sludge with concentrations of HDPE above 20% was observed an increasing in proportions of light hydrocarbons in diesel range reaching around 50%, while with 10% of HDPE generated only 40% of diesel (Figure 1b).

References

- Wang, Z.; Gong, Z.; Wang, Z.; Li, X.; Chu, Z.; *Environ. Eng. Res.* **2020**, 26, 0.
- Silva, D. C.; Silva, A. A.; Melo, C. F.; Marques, M. R. C.; *J. Anal. Appl. Pyrolysis* **2017**, 124, 290.
- Faillace, J. G.; de Melo, C. F.; de Souza, S. P. L.; da Costa Marques, M. R.; *J. Anal. Appl. Pyr.* **2017**, 126, 70.

Acknowledgments

We thank to FAPERJ, CNPq, CAPES and FINEP by financial support.

Chemistry x Society: Evaluation of the environmental conditions of an urban park in Rio de Janeiro city.

Adriana H. Nudi (PQ),^{1*} Rafael C.C. Rocha (PG),¹ Daniela W. Rosman (IC),² Henrique S. Magalhães (IC),² Juliana H. Gonzaga (IC),² Maria Luisa A.S. Lima (IC),² Maria Paula S. Gaglianone (IC),² Dominic Palatnik (IC),² Michel Matsuda (IC), Hitalla Rafaela (IC),² Valentina Gori (IC),² Matheus Coppo (IC),² Paulo Zuim (IC),² Tatiana D. Saint Pierre (PQ).¹

ahn@puc-rio.br¹ Department of Chemistry, PUC-Rio; ² Department of Biology, PUC-Rio

Keywords: *Urban parks, Environmental Quality, Trace Elements, Atmospheric Emissions, Environmental Legislation*

Highlights

The work aims to bring the science closer to the society. The scientific method was didactically applied. An urban park was monitored and the effects of contaminants on the environment is discussed.

Abstract

Urban parks are geographically delimited public spaces with a predominance of tree-shrub vegetation that have aesthetic, ecological, leisure, and recreation functions. These spaces represent the main outdoor leisure area and the conservation of environmental systems in cities.¹ Monitoring is usually based on environmental indicators,² and little information exists regarding the assessment of contaminants in these areas. Besides, they can be important subjects to bring science closer to the society. Themes about the environment are easy mechanisms to present in a playful way the scientific method for the population. This work proposes the evaluation of the environmental conditions of Parque Alice, an urban park located in Laranjeiras, Rio de Janeiro (RJ), maintained by a collective of residents of Rua Alice. The area was vacated in the 1990s and restored by the Department of the Environment of the municipality of Rio de Janeiro. It is a residential place of moderate vehicular traffic. The hypothesis of the work was to know if the area is free of pollutants, natural or anthropogenic, and to evaluate the effects on the neighborhood.

Sampling occurred in September 2021. Soil, Zebrina plant, and lichens were sampled, in triplicate, in three locations within the park: The lower part (entrance), the middle and upper parts, (approximately 100 m and 200 m distant from the entrance, respectively). The samples were lyophilized to constant weight. The sample preparation followed the EPA 3050B method: Approximately 250 mg were weighed in a polypropylene (falcon) tube and added 2.5 mL of bidistilled HNO₃. The tubes were left overnight (12 h) at room temperature, and then, heated to 100 °C for 4 h in a closed system. After returning to room temperature, 1.0 mL of H₂O₂ (suprapur, Merck) was added and the tubes heated at 100 °C for more 15 min. Then the tubes were filled to 25 mL with ultrapure water. Twenty-one elements included in CONAMA 420 (soil)³ were determined in the samples' solutions by inductively coupled plasma mass spectrometry (ICP-MS). The methodology employed was THE 6020B, by using 6 points for building the analytical curve, with concentrations ranging from 1.0 µg L⁻¹ to 1500 µg L⁻¹, depending on the element of interest. Soil (NRC PACS-2) and plant reference materials (NIST SRM 1515, Apple Leaves and NIST SRM 1573a, Tomato Leaves), which were prepared following the same process as the samples, were used to evaluate the accuracy of the methodology. The coefficient of determination of the calibration curves (R²) were all better than 0.999 and the measured concentrations presented recoveries from 80% to 120% of the certified values. The Statistic 6.0 program was used to treat the results. Most elements determined were below the limits established by CONAMA. Statistically, there were differences (p<0.05) between the sites in the soil samples for Mg, Ni, and Fe. This can be justified by the emission of vehicular atmospheric particulates. The analyses of plants and lichens also presented low values. A second collection will be performed to evaluate the effect of the occupation after two years. In conclusion, the present study showed that Alice Park is free of anthropogenic influences regarding toxic elements. The neighborhood of the park was pleased to know that they live in a healthy environment.

Acknowledgments

FAPERJ, CAPES, CNPq

References

¹Martins, L.f.V.; Venturi, L.A.B; Wingter, G.B. Proposta de um sistema para o monitoramento de parques urbanos em fundos de vale. *Ambiente & Sociedade* n São Paulo. Vol. 22, 2019 n Artigo Original n 2019;22:e00243

²Oliveira, P.T.S.B.; Bitar, O.Y. Indicadores ambientais para monitoramento de parques urbanos. *Revista de Gestão Integrada em Saúde do Trabalho e Meio Ambiente* - v.4, n.2, Artigo 5, maio/ ago. 20

³CONAMA. Resolução No 420, DE 28 DE DEZEMBRO DE 2009 Dispõe sobre critérios e valores orientadores de qualidade do solo quanto à presença de substâncias químicas e estabelece diretrizes para o gerenciamento ambiental de áreas contaminadas por essas substâncias em decorrência de atividades antrópicas. Disponível em [Resolução CONAMA nº 420 de 28/12/2009 \(normasbrasil.com.br\)](https://www.normasbrasil.com.br/Resolucao-CONAMA-n-420-de-28-12-2009) Acessado em 09/01/23.

Área: AMB

CO, O₃ and NO₂ concentrations in Rio de Janeiro, from 2019 to 2021, with emphasis in the lockdown period during the COVID-19 pandemic.

Guilherme de Sousa Dantas^{1*} (PG), Cleyton M. da Silva^{1,2} (PQ), Graciela Arbillá¹ (PQ)

guidantas93@hotmail.com

¹Instituto de Química da Universidade Federal do Rio de Janeiro; ²Engenharia Ambiental, Universidade Veiga de Almeida.

Palavras Chave: *Química atmosférica, Poluentes legislados, Ozônio troposférico, Fontes de emissão.*

Highlights

CO and NO₂ presented lower concentrations during the partial lockdown. O₃ concentrations did not change significantly. Emission sources do have an influence on the air quality of the city.

Resumo/Abstract

Em 11 de março de 2020, a Organização Mundial de Saúde (OMS) classificou o surto de coronavírus (COVID-19) como pandemia. A partir disso, países se organizaram numa iniciativa no combate ao vírus. Entre as medidas adotadas, pode-se destacar a quarentena e o distanciamento social, com o intuito de diminuir a propagação da doença. No Brasil, houve uma restrição no fluxo de veículos automotivos e a circulação de pessoas, que ficou conhecido como *lockdown* parcial (meio de março ao fim de abril), que criou um cenário único no estudo de poluição atmosférica.

O objetivo deste trabalho consiste na análise da variação da concentração de poluentes legislados no período de 23 de março a 30 de abril nos anos de 2019 a 2021, na cidade do Rio de Janeiro. Os dados foram obtidos das estações de monitoramento automático da Secretaria Municipal do Ambiente e Clima (SMAC). As regiões estudadas foram Bangu, Irajá e Tijuca, que possuem perfis distintos de fontes de emissão. Os poluentes legislados analisados foram NO₂, CO e O₃. Apesar de ser importante no estudo de poluição atmosférica, MP_{2,5} (Material particulado com diâmetro inferior a 2,5 de μm) não foi avaliado por quantidade insuficiente de dados. Os dados foram tratados com utilização do *software* RStudio através do pacote OpenAir, onde as distribuições e medianas de cada poluente foram calculadas.

Foi observada a diminuição na concentração de CO e NO₂ no ano de 2020, quando comparada com os outros dois anos estudados. Na estação de Bangu, a mediana da concentração de CO foi de 0,28 ppm, uma diminuição de aproximadamente 30% quando comparada ao ano de 2019 (0,41 ppm) e voltou ao seu nível em 2021 (0,46 ppm). Esse comportamento também foi observado na estação da Tijuca, com uma mediana de 0,19 ppm, uma diminuição de aproximadamente 37% quando o valor é comparado ao do ano de 2019 (0,30 ppm), e que também voltou ao nível de concentração maior no ano de 2021. Para NO₂, a diminuição percentual foi de aproximadamente 31% em Bangu e 21% em Irajá, ambas retomando níveis de concentração mais elevados em 2021. Esses dois poluentes possuem como fonte de emissão principal a veicular, sendo CO proveniente da queima incompleta de combustível nos veículos leves, e NO₂ majoritariamente da queima de diesel, principal combustível em ônibus e caminhões.

Para o caso de ozônio troposférico, não foi observada diminuição significativa nas estações estudadas no ano de quarentena parcial. Isso se deve ao O₃ ser um poluente secundário, que depende das concentrações e reatividade de hidrocarbonetos (proveniente não somente de fontes veiculares como também de fontes industriais, que não tiveram uma redução tão significativa das atividades em período de *lockdown* parcial) e óxidos de nitrogênio presentes na atmosfera, assim como das razões entre as concentrações desses poluentes.

Considerando que o ozônio é considerado pela OMS um dos principais poluentes atmosféricos, quando são considerados os efeitos sobre a saúde das pessoas, pode-se concluir que a diminuição de fluxo veicular numa cidade com fontes mistas de emissão como o Rio de Janeiro não leva a uma melhora significativa na qualidade do ar.

Agradecimentos/Acknowledgments

Os autores agradecem ao CNPq, FAPERJ e FUNADESP pelo financiamento e a SMAC pela disponibilização dos dados.

Área: AMB

Determination of rare earth elements in soil and rocks using microwave assisted digestion and quantification with ICP-MS

Gabriela S. Caldeira (PG),^{1*} Pedro Costa Evangelista (IC),² Nicholas Egger Bernhard (IC),¹ Geraldo Magela Santos Sampaio (PQ),³ Fernando Barbosa Egreja Filho (PQ),¹ Cláudia Carvalhinho Windmoller (PQ).¹

gcaldeira.q@gmail.com; gcaldeira.q@gmail.com

¹Departamento de Química, UFMG; ²Departamento de Química, CEFET-MG; ³Departamento de Geologia, UFOP

Palavras Chave: REE, ICP-MS, fluorides, microwave digestion, soil, mine tailing

Highlights

Determination of rare earth elements in soil and rocks using microwave-assisted digestion and quantification with ICP-MS

Compare sample preparation methods after microwave-assisted digestion with steps to eliminate fluoride ion and determination of rare earth elements with ICP-MS in soil and rocks.

Resumo/Abstract

Rare earth elements (REEs) have been gaining space in the world market due to their applications in modern industry and also in the understanding of geological processes. Brazil is in third place in the world ranking of reserves of rare earth elements. Thus, there is a great need to analyze environmental samples in order to determine concentrations of REEs in samples of soil, rocks and mine tailing to subsidize regulatory norms in Brazil in quality reference values; additionally, they could be possible tracers of the origin of certain contaminants. However, the digestion of samples when using HF is a challenge, since the formation of fluorides from REEs may occur, not achieving good accuracy of the method, requiring subsequent stages of digestion to remove excess fluoride ions. Therefore, the present work aims to compare sample preparation methods after microwave-assisted digestion using inductively coupled plasma mass spectrometry (ICP-MS) in the determination of rare earth elements in soil, rocks and mine tailing samples. Different sample preparation procedures were carried out using microwave-assisted digestion, comparing the method of evaporation to total dryness with the addition of boric acid. Iridium at 5 ug/L was used as an internal standard to evaluate the analysis method in ICP-MS. The correlation coefficients of the calibration curves for all elements were greater than 0.99. For the rare earth elements in digestion of Certificate Reference Material Till-3 of soil, some of these, obtained recoveries greater than 80%, such as Lu, Nd, Sc and Yb and for the other rare earth elements, recoveries close to 50% were achieved. For other elements, in the two procedures, of total dryness of acids and addition of boric acid, Li, V, Cr, Mn, Co, Ni, Zn, As, Mo, Ag, Sb, Pb and U, recoveries greater than 80% were obtained. For digestion of sample of Quality Control Material Iron Formation, for all 28 elements analyzed, was achieved promise values of accuracy and precision, with values greater than 95% of recoveries and values less than 10% for precision. This demonstrates a challenging path in the digestion of soil, rocks and mine tailing samples with microwave-assisted radiation, highlighting the need to optimize methods to ensure better recoveries for the other elements. After optimization and validation of the methods, analysis of numerous samples of soil, rocks and mine tailing scattered in the Brumadinho dam disaster, in Brumadinho, will be conducted, with the aim of setting up a database regarding the occurrence of these elements in these samples.

Agradecimentos/Acknowledgments

The authors gratefully acknowledge Brumadinho project Scientific Technical Committee and Centro de Referência Ambiental (CRA) of UFMG.

Área: BEA

Development of HS-GC-MS method for determining ethanol in Kombucha

Lucas Micqueias Arantes (FM),¹ **Julia Tristão do Carmo** (FM),¹ **Adelmo Carlos Siqueira Silva** (PG),^{1*} **Rúben Santana Ramos da Silva** (IC),¹ **Edgar Nascimento** (PQ),¹ **Tiago Gomes dos Santos** (PQ)¹, **Demétrio de Abreu Sousa** (PQ).¹

lucas.arantes@ifmt.edu.br; admadelmo@gmail.com

¹IFMT campus Cuiabá/Bela-vista

Keywords: *HS-GC-MS Analysis, Fermented Beverages, Volatile Compounds; Low Alcohol Beverages.*

Highlights

In Brazil, the quality standard defines that the ethanol content in kombucha must be less than 0.5% v/v, as it is a non-alcoholic beverage. HS-GC-MS proved to be an alternative for determining it.

Abstract

The age-old beverage kombucha, with a low alcohol content, obtained from the infusion of tea in water, sugars and symbiotic colonies of bacteria and yeasts (SCOBY), ascended in the last decade as a functional drink. Recently, in Brazil, the identity and quality standard of kombucha was regulated, defining the ethanol content of less than 0.5% v/v for it to be considered a non-alcoholic beverage, as it impacts on the beverage's taxation. This work proposed the development of a sampling method by headspace and gas chromatography combined with mass spectrometry detection (HS-GC-MS) for the determination of ethanol content in kombucha. A total of 120 examples of ethanol solutions and 384 examples of commercial kombuchas were collected for this work. The kombucha samples, composed of 4 flavors (beetroot with ginger and grape, hibiscus with rose water and apple, lemon with ginger, passion fruit with lemongrass), produced in Cuiabá/MT were collected during production batches of a company in the first quarter of 2021. They were collected from three manufacturing batches, in two stages of the beverage fermentation process, before bottling and after the final bottling for consumption. HS-GC-MS analysis were carried out in a gas chromatograph coupled to a mass spectrometer with a Triple-Axis detector. Ethanol standards (0.1; 0.3; 0.5; 0.6; 0.7; 1.0% (v/v)) were tested for the construction of the analytical curve. The headspace technique was used before injection into a VF-WAXms column to concentrate the analytes in the volatilized fraction of the vials, 100:1 split-type injection to preserve the column. The chromatographic run had a total time of 6min per sample and was performed starting at 40°C, followed by a temperature ramp of 50°C/min up to 140°C maintained for 1 min. Detection occurred in a mass spectrometer operating in mass scan mode between 10 and 30. After chromatographic analyses, it was possible to verify a detection limit of 0.001% (v/v), quantification limit was 0.003% (v/v), coefficient of linear correlation of 0.99, coefficient of determination was 0.98 and linear regression defined by the equation of the straight line $y=0.4165+4.3334x$. The method was developed from adaptations of the literature and the tests were verified considering the guidelines of the analytical method validation document from the National Institute of Metrology, Quality and Technology (DOQ-CGRE-008). The statistical program R 4.2.1 was used in all mathematical stages of treatment of test results of this analytical method validation. The use of the HS-GC-EM technique proved to be linear, sensitive and accurate for determining the ethanol content in kombucha. Therefore, this studied method should contribute to the general community given the importance of recent regulations related to kombucha and the commercial needs of this beverage.

Acknowledgments

IFMT Campus Cuiabá - Bela Vista e Pró-reitoria de Pesquisa, Pós-Graduação e Inovação do IFMT.

Área: AMB

Estudo da propriedade de superfície de carvão magnético ativado em atmosfera de CO₂ visando aplicação ambiental

Jaqueline Rodrigues Lopes (PM)¹, Maria Eduarda Parussolo (IC)¹, Altair Benedito Moreira (PQ)¹, Odair Pastor Ferreira (PQ)², Márcia Cristina Bisinoti (PQ)¹.

jr.lopes@unesp.br

¹Departamento de Química e Ciências Ambientais, UNESP IBILCE; ²Departamento de Química UEL.

Palavras Chave: *Materiais carbonáceos, carvões magnéticos, carbonização hidrotérmica, ativação.*

Highlights

Study of surface property of activated magnetic carbon in CO₂ atmosphere via environmental application. Thermophysical activation functionalizing the magnetic carbon surface. Production of porous and low-cost material through a raw material with a large volume available, economically and environmentally viable.

Resumo/Abstract

Materiais carbonáceos têm chamado atenção da comunidade científica pela sua eficiência na remoção de contaminantes em meio aquoso. Dentre esses, os carvões magnéticos (CM) se destacam devido sua fácil preparação através do processo de carbonização hidrotérmica (CHT) de biomassa de resíduos agrícolas juntamente com sais de ferro (III) e facilidade de remoção por meio da propriedade magnética. Para aumentar a porosidade e funcionalização de poros na superfície, o material pode ser ativado termoquimicamente, através de processos químicos e físicos, sendo um processo bastante eficiente a ativação com o gás CO₂. Nesse sentido, o objetivo foi sintetizar e ativar carvão magnético avaliando as propriedades de superfície por meio do emprego de sondas catiônica e aniônica. Foi produzido um CM empregando CHT em uma etapa, na presença de solução de nitrato de ferro (III) a 250°C, este denominado CM250. Foi realizada a ativação com CO₂ em duas temperaturas : a 700°C (CMA250-7) e a 900°C (CMA250-9) durante o intervalo de 60 minutos. As propriedades dos CM e CMA foram avaliadas por Espectroscopia no infravermelho por transformada de Fourier (FTIR) empregada para identificar os grupos funcionais presentes, sendo a ligação oxigênio-metal observada em todos os compostos. Foi também caracterizado por Difração de raios X (DRX), para o CM250 foi constatado picos referentes a fase hematita (α -Fe₂O₃) e magnetita (Fe₃O₄) e para ambos CMA250-7 e CMA250-9, foi notado uma melhor definição dos picos sugerindo um aumento no ordenamento estrutural das amostras, provavelmente decorrente do tratamento térmico aplicado. Os difratogramas também indicaram uma transição da fase do α -Fe₂O₃ para Fe₃O₄. E por fim, para determinar a percentagem de componentes inorgânicos presente foi empregada a Análise termogravimétrica (ATG) feita em atmosfera de ar estático, os materiais apresentaram uma porcentagem de óxido de ferro de 21,3% para CM250, 73,7% para CMA250-7 e de 101,1% para CMA250-9. Essas evidências são coerentes com a elevada magnetização destes materiais. Foi utilizado o azul de metileno (AM) e o corante reativo 19 (R19) como sondas catiônicas e aniônicas, respectivamente, para avaliar as características de carga das superfícies dos carvões. O experimento revelou que a ativação funcionalizou a superfície do carvão e que a elevação da temperatura de ativação de 700°C para 900°C teve um impacto negativo significativo, esse efeito pode ser atribuído à ampliação dos microporos para mesoporos. No estudo de adsorção utilizando os corantes o CMA que apresentou melhor adsorção foi o CMA250-7, com saturação dos poros em 168 mg g⁻¹ para R19 e 62 mg g⁻¹ para AM. Conclui-se que o material apresenta possibilidade de remover competitivamente poluentes catiônicos e aniônicos do meio.

Agradecimentos/Acknowledgments

Agradeço a FAPESP : Proc.: 2022/05004-3 e Proc. : 21/09126-3. E a CAPES : Proc. CAPES nº 88887.798904/2022-00 que através dos processos referidos são de total importância para o desenvolvimento da pesquisa.

Evaluation of chrysotile asbestos fibers in particulate matter

Lincoln G. S. de Aquino (IC),¹ Danielle C. Schnitzler (PQ).²

lincoln.1997@alunos.utfpr.edu.br; daniellec@alunos.utfpr.edu.br

^{1,2}Departamento Acadêmico de Química e Biologia, UTFPR.

Palavras Chave: *chrysotile asbestos; particulate matter; scanning electron microscopy.*

Highlights

Asbestos is a common carcinogenic mineral fiber in fiber cement tiles; degradation of roof tiles release fibers to the environment; tiles were supported to verify the presence of fibers in particulate matter; different sample preparations were used to characterize the fibers in SEM-EDS.

Resumo/Abstract

Chrysotile asbestos $[\text{Mg}_3(\text{Si}_2\text{O}_5)(\text{OH})_4]$ is a tubular, curvilinear mineral fiber with a silky appearance that has Mg atoms on its surface, has the following characteristics: resistance (mechanical, electrical, chemical and thermal) and low extraction cost, which favors its use in various materials, mainly used in civil construction, such as fiber cement tiles ¹. Despite the characteristics, the fibers are proven to be carcinogenic ¹. In Brazil, the use of asbestos is not officially banned, despite the vote for its ban having already been held with the Federal Supreme Court ². However, tiles are present in roof coverings throughout Brazil, mainly in regions with lower purchasing power. In this sense, the research group has studied the possibility of releasing asbestos fibers from tiles into water and it was noted that it is possible to expose the fibers. Thus, this work sought to evaluate the presence of fibers in particulate matter (PM). PM is known as a complex mixture of liquid and solid particles, ranging in size from a few nanometers to approximately $100 \mu\text{m}$ ³. In this sense, the analyzes were carried out in the Contestado Settlement, located in the municipality of Lapa - PR, 50 km from Curitiba. The site is free of anthropic influence and fiber cement materials. For the development of the work, tiles from different origins (coastal, plantation) were supported under a protective structure in the shape of a box made of wood and musketeer rifle netting with a canvas bottom for a period of 15 days. After this exposure time, the PM deposited on the canvas surface was collected with the aid of a previously cleaned portable vacuum cleaner. The samples were placed in the storage device of the vacuum cleaner itself. In the laboratory, the samples were submitted to the procedures of (i) preparation without previous digestion of the sample and (ii) preparation with digestion by EPA method 3050B ⁴. The samples were analyzed by Scanning Electron Microscopy coupled to the Dispersive Energy System (SEM-EDS). It was possible to identify the presence of chrysotile fibers. Furthermore, when the digestion method was applied, the removal of Mg atoms present in the surface layer of the chrysotile fiber sheet was observed. It is concluded that roof tiles exposed to the environment, submitted to the weathering process, can suffer degradation and, as a consequence, release the fibers to the environment.

References

1. RADVANEK, Journal Of Hazardous Materials, v. 252-253, p. 390-400, may 2013;
2. MARTINS, M. Carta Capital. 04 dec. 2017;
3. SOUZA, Química Nova, v. 33, n. 6, p. 1247-1253, 2010;
4. USEPA. Method 3050B acid digestion of sediments, sludges, and soils.

Acknowledgments

UTFPR; LEMASSA-UTFPR; LAMAQ-UTFPR; MPT-PR; CME-UFPR; CMCM-UTFPR.

Área: AMB

EVALUATION OF CONTAMINATION BY PETROLEUM HYDROCARBONS IN SEDIMENTS OF IPOJUCA RIVER, PERNAMBUCO, BRAZIL

Bianca M. M. G. Acioli (PG),¹ **Thayane C. S. Moreira** (PG),^{1*} **Rebeca S. França** (PG),² **Alex S. Moraes** (PQ),¹ **Giovana A. Bataglion** (PQ),² **Jandyson M. Santos** (PQ),¹

biancammga@gmail.com; cthayane36@gmail.com*; jandyson.machado@ufrpe.br

¹Departamento de Química, UFRPE. ²Departamento de Química, UFAM.

Keywords: *Ipojuca River; Hydrocarbons; Sediments; Petroleum; Contamination.*

Highlights

- Quantification of petroleum hydrocarbons to evaluate the level of contamination of sediments.
- We have found petrogenic and pyrogenic sources in the formation of sedimentary organic matter.

Resumo/Abstract

The hydrographic basin of the Ipojuca River, state of Pernambuco, Brazil, is about 320 km long and includes 25 counties, one of them being the city of Caruaru, which has regional financial importance. In Caruaru, the river is used for tourism, fishing, human, agricultural, and industrial supply, and may be exposed to several contaminants, including those from the use of petroleum derivatives. Therefore, it is essential to evaluate the level of contamination and the impact caused to aquatic environments, through the identification and quantification of geochemical biomarkers, aiming to identify the compounds of the classes such as aliphatic (AHs) and polycyclic aromatic (PAHs) hydrocarbons, which are considered bioaccumulative and toxic, and can present carcinogenic and mutagenic potential. The present study aimed to carry out the chemical characterization of ten surface sediments samples collected from the Ipojuca River, in the stretch related to the city of Caruaru, aim to identify and quantify AHs and PAHs to obtain the level of contamination of the aquatic system. The sampling was performed along 7 km of the river course, and ten sediments (named from C1 to C10) were collected. The extraction and fractionation of organic compounds followed the methodology developed by Frena *et. al* (2017), and the analysis were performed by GC-FID and GC-MS. The AHs were detected with carbon numbers from *n*-C₁₅ to *n*-C₃₇, and the Carbon Preference Index (CPI) indicated values close to 1, which pointed to contamination by petrogenic sources in eight sediments (C1, C2, C5, C6, C7, C8, C9, and C10). On the other hand, CPI > 2 indicated the occurrence of contamination from a biogenic source, presented in samples C3 and C4. The pristane (Pr) and phytane (Ph) were also identified in all sediments, and the Pr/Ph ratio was found to be close to 1 in three samples (C2, C9 and C10), which may be an indication of the presence of petroleum hydrocarbons in the sedimentary organic matter. For PAHs, we have quantified 21 compounds, and according to the absolute concentration values and diagnostic ratios such as Flr/(Flr+Pyr), Ant/(Ant + Phen) and Σ LMM/ Σ HMM, we can classify the contamination of the sediments at a level of moderate to high, indicating petrogenic and pyrogenic sources as the primary form of sedimentary organic matter. Thus, we were able to infer that there is a relevant contamination level in the studied aquatic system from petroleum biomarkers of AHs and PAHs classes. We expected that the results obtained can guide and help agencies responsible for the preservation and recovery of the Ipojuca River in Pernambuco, Brazil.

References:

FRENA, M. *et al.* *Distribution and Sources of Aliphatic and Polycyclic Aromatic Hydrocarbons in Surface Sediments of Itajaí-Açu Estuarine System in Brazil.* *J. Braz. Chem. Soc.*, 2017 28(4), 2017.

Agradecimentos/Acknowledgments

CAPES, LaMTEsa, UFRPE, PPGQ/UFRPE, FACEPE, GRUPO PEM.

Área: **AMB**

Evaluation of extractive process for demineralization of lignocellulosic biomass

Karen Giacobe (PG),¹ Vanessa R. do Nascimento (PG),¹ Paola de A. Mello (PQ),¹ Fábio A. Duarte (PQ),¹ Cezar A. Bizzi (PQ)^{1*}

karengiacobe@gmail.com; cezar.bizzi@ufsm.br

¹Departamento de Química, UFSM

Keywords: *Biomass, Inorganic constituents, Ultrasound, Extraction.*

Highlights

The inorganic constituents (minerals) present in biomass can corrode/clogging pipelines and reactors, as well as cause problems in the equipment.

The ultrasound-assisted extraction (UAE) is an attractive alternative for the extraction of inorganic constituents from biomass.

Abstract

Lignocellulosic biomasses, such as those considered as agro-industrial wastes, can be used in chemical industry for producing biofuels (second generation ethanol, bio-oil, biochar, among others), and for energy generation through thermal conversion. These lignocellulosic wastes are composed mainly for cellulose, hemicellulose, lignin, extractives, and inorganic constituents.¹ The inorganic constituents² are undesired for several industrial process, since their presence is associated with pipelines clogging, and reactor corrosion while the biomass is converted. The inorganic constituents (minerals) can be extracted by conventional methods (mechanic stirring, leaching, Soxhlet, or conventional extraction).³ These methods tend to require long processes times, excessive volumes of reagents, among others. In this work ultrasound-assisted extraction (UAE) was proposed to increase the efficiency of the mineral extraction when compared with the conventional protocols. The proposed method was investigated for metals (Al, Ba, Ca, Cu, Fe, K, Mg, Mn, Na, P, Sr, and Zn) extraction, which were determined by Inductively Coupled Plasma Optical Emission Spectrometry (ICP-OES, Optima 4300V DV, Perkin Elmer, EUA) in sugar cane bagasse sample. The evaluated parameters for the UAE were the volume and the extractant solution, ultrasound (US) frequency and the delivered energy, and operational conditions such as temperature, and the extraction time. The sample mass was evaluated from 250 mg up to 25 g. The optimal conditions found for UAE were US reactor operating at 45 kHz (70% amplitude, 75 W/dm³ as delivered energy), 30 min extraction at 50 °C, sample mass of 250 mg extracted with 20 mL of 1 mol L⁻¹ H₂SO₄. The elements presents in the *in natura* sugar cane bagasse were in the range of: Al: 200 ± 12; Ba: 4.65 ± 0.63; Ca: 288 ± 45; Cu: 3.84 ± 0.11; Fe: 290 ± 22; K: 1248 ± 70; Mg: 314 ± 24; Mn: 19.2 ± 0.9; Na: 11.7 ± 0.2; P: 103 ± 7; Sr: 3.64 ± 0.08; and Zn: 5.53 ± 1,00 µg g⁻¹, which were totally extracted from biomass using UAE. When 25 g of biomass was extracted with a 2 L of 1 mol L⁻¹ H₂SO₄, an extraction efficiency near to 100% was achieved. In addition, a kinetic study was carried out to evaluate the efficiency of demineralization process, where it was possible to achieve extraction efficiency as high as 93% after just 1 min of sonication. When the proposed UAE protocol was compared with conventional extraction (same operational conditions, but in the absence of US energy), an efficiency lower than 70% was obtained at the same process time. Thus, the proposed UAE method was efficient for the extraction of metals (demineralization process), reducing the solvent concentration and the extraction time, being in accordance with the green chemistry recommendations.

¹Cortez, L. A. B. et al. Biomassa para energia, 773, 2008.

²Negrao, D. R. et al. Inorganics in sugarcane bagasse and straw and their impacts for bioenergy and biorefining: A review. Renewable and Sustainable Energy Reviews, v. 148, p. 111268, Sept. 2021

³Jiang, L. et al. Influence of different demineralization treatments on physicochemical structure and thermal degradation of biomass. Bioresource technology, 146, 2013, 254.

Acknowledgments

CAPES, CNPq, Bio-Value/BEECOL, FAPERGS, and UFSM.

Evaluation of physicochemical Properties associated with trace elements and influence of anthropic and/or natural sources on the water quality of the Ipiranga River, Linhares – ES, Brazil.

Ana K.S. Rocha (PG),¹ Jenifer R. Almeida (PG)¹, Mayra N. Moura (PG)¹, Evelyn S. Pinheiro (TC¹), Paola L. Demuner (TC)², Fadima G. A. Augusto (TC)², Gilberto A. Sipioni (TM)², Geisamanda P. Bandrão (PQ)¹, Vinicius C. Costa (PQ)¹, Maria T. Weitzel (PQ)¹

ana,kellysimoerocha@gmail.com;

¹Departament of Chemistry, UFES; ²State Institute of Environment (Iema-ES)

Key Words: Trace Elements, Surface Water, Ipiranga River, Contamination, quality scores, PCA.

Highlights

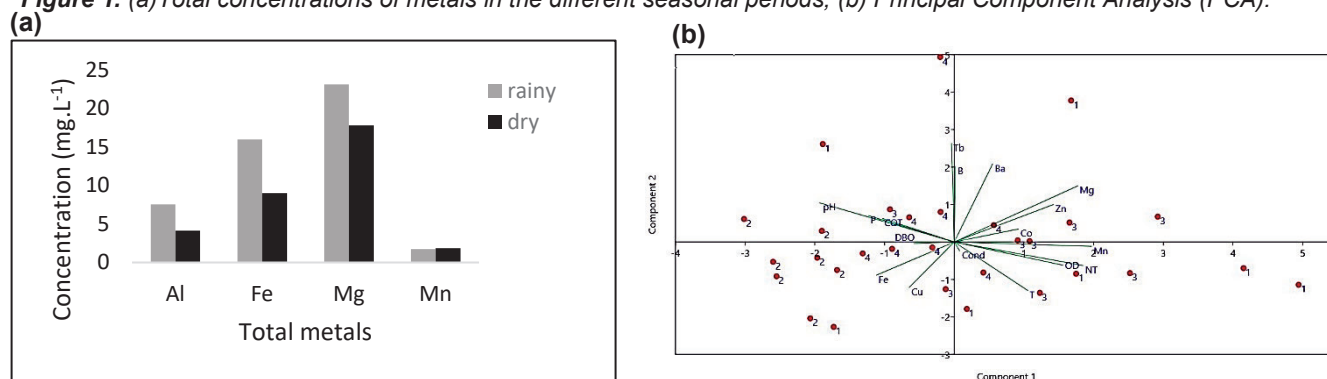
- The occurrences of selected trace elements in the Ipiranga River were different between the sampling points and seasonal periods;
- Anthropogenic activities were the most important contributors to the contamination of the Ipiranga River compared to natural sources;
- Metals were the main contributors in raising the level of contamination at the sampled points;

Resumo/Abstract

Rivers represent 0,49% of the Earth's total freshwater, yet they are the main sources of drinking water for the world's population, in addition to sustaining cultivation, manufacturing, energy, Transportation and natural resources¹. Consequently, there is an increase in surface water pollution in many rivers, mainly by trace elements that impair their quality in many regions, since they become dangerous for humans when above the threshold levels of bioavailability². The objective of this work is to evaluate the water quality of the Ipiranga River, using data provided by an environmental agency (Iema-ES), based on the calculation of environmental quality indices and principal component analysis (PCA) applied to the relationship between metal concentration, physical-chemical and organic parameters, to study possible anthropic and/or natural influences on water quality at the sampled points.

The results obtained by evaluating the environmental quality indices (IQW, IETE, IPTE, CF, m-Cd) showed water contamination by trace elements. Elements Al, Fe, Mn and Mg had the greatest influence on some contamination indices, as they were the elements with the highest concentrations throughout the entire monitoring period (Figure 1a). In ACP (Figure 1b), it was noted in CP1 that a group of samples located in P1, P3 and P4 showed similar behavior indicating high contamination by metal at a very acidic pH and low contamination by organic matter, a result of agricultural activities and weathering. The CP2 indicated that in a group of samples contamination by organic matter was higher in certain sample periods, due to oil activities in the region.

Figure 1. (a) Total concentrations of metals in the different seasonal periods; (b) Principal Component Analysis (PCA).



Bibliographic references: ¹Yakovlev, E. et al. Assessment of physical and chemical properties, health risk of trace metals and quality indices of surface waters of the rivers and lakes of the Kola Peninsula (Murmansk Region, North-West Russia). *Environmental Geochemistry and Health*, v. 44, n. 8, p. 2465–2494, 2022.

²Thai-Hoang, L. et al. Influences of anthropogenic activities on water quality in the Saigon River, Ho Chi Minh City. *Journal of Water and Health*, v. 20, n. 3, p. 491-504, 2022.

Agradecimentos/Acknowledgments

The CAPES, the PPGQUI – UFES, the Iema – ES and the CT-GRSA.

Área: AMB

First report on essential and toxic element binding to metalloproteins in the bile of the endangered Groovebelly Stingray (*Dasyatis hypostigma*)

Regina Fonsêca de Almeida (PG)^{1,2*}, Amanda Pontes Lopes (PG)², Marcelo Vianna (PQ)^{3,4}, Tatiana D. Saint’Pierre (PQ)^{1*}, Rachel Ann Hauser-Davis (PQ)^{2*}

*refonseca25@gmail.com; tatispierre@puc-rio.br; rachel.hauser.davis@gmail.com

¹Departamento de Química, PUC-Rio; ²Instituto Oswaldo Cruz, FIOCRUZ; ³Instituto de Biologia, UFRJ; ⁴IMAM-Aquario.

Keywords: Metalloproteins, Biliary fluid, Ecotoxicology, Environmental contamination, Metals.

Highlights

- Metalloprotein binding to metals and metalloids in elasmobranch bile were assessed by SEC-HPLC-ICP-MS
- Metallothioneins (MT) eluted from 20 to 25 min
- This is the first report of differential metalloprotein binding, including MT, to toxic and essential elements in elasmobranch bile

Abstract

Elasmobranchs, a taxonomic group that includes rays and sharks, play an important role in maintaining aquatic ecosystem equilibrium. However, due to their life history characteristics, these animals are highly exposed to chemical contaminants.¹ One of the biochemical metal-detoxification routes in vertebrates comprises binding to metallothionein (MT), a low-molecular weight metalloprotein. This metalloprotein plays several metabolic roles, including against oxidative stress and in the detoxification of both toxic and essential elements present in excess in the organism.² Studies on the detoxification route of these elements in fish, however, mostly focus on the liver³, although bile, a fluid excreted after each feeding episode by the liver, has also been applied as an indicator of recent exposure to pollutants in bony fish. Biliary evaluations in this regard in elasmobranchs, however, are still non-existent. In this context, this study presents a first-time report on toxic and essential metal and metalloid binding to thermostable proteins present in the bile of the Groovebelly stingray (*Dasyatis hypostigma*), an endangered elasmobranch sampled off the coast of Rio de Janeiro, southeastern Brazil. Following a thermal extraction procedure⁴, 40 µg of total protein determined by the Lowry method modified by Peterson⁵ were injected into a Superdex 75 Size Exclusion column (GE Healthcare®) coupled to a liquid chromatograph hyphenated to an ICP-MS (SEC-HPLC-ICP-MS). Proteins were monitored at 254 and 280 nm and the chromatograms were superimposed on the obtained spectra to assess metalloprotein retention times during 60 min runs using different-sized proteins for column calibration (Bovine Serum Albumin– 67 kDa, Ovalbumin – 45 kDa, Ribonuclease – 13.7 kDa, Reduced Glutathione – 0.3 kDa). Biliary MT eluted between 20 and 25 min, mostly around the same time as As, Cd, Ni and Ti and the essential elements Cu, Mo, Se and Zn, although peaks bound to other metalloproteins eluting between 20 and 30 min were also observed. This indicates that the biochemical MT-detoxification route plays an important role in metal homeostasis and detoxification in this species, although additional studies are required to further elucidate this biochemical route and potential associations to other metalloproteins in elasmobranchs.

1. Hauser-Davis, R. A. **PeerJ**, v. 8: e10293, 2020.
2. Hidalgo, J., et al. **Camp. Biochem. Physiol.**, v. 81C, 1, p. 159-165, 1985.
3. Hauser-Davis, R. A., et al. **Journal of Trace Elements in Medicine and Biology**, v. 68: 126813, 2021.
4. Erk, M., et al. **Talanta**, v. 57, n. 6, p. 1211-1218, 2002.
5. Peterson, G.L.A. **Analytical Biochemistry**, v. 83, p. 346-356, 1977.

Acknowledgments

This study was financed in part by the Coordenação de Aperfeiçoamento de Pessoal de Nível Superior - Brasil (CAPES) - Finance Code 001. TDSP acknowledges FAPERJ and CNPq for research grants. RAHD acknowledges FAPERJ (JCNE 2021-2024 and process number E-26/21.460/2019) and CNPq (productivity grant) for financial support. The implementation of the Projeto Pesquisa Marinha e Pesqueira is a compensatory measure established by the Conduct Adjustment Agreement under the responsibility of the PRIO company, conducted by the Federal Public Ministry – MPF/RJ.

Heterogeneous Photocatalysis: An Efficient Alternative in the Treatment of Laboratory Residues Containing NSAIDs

Jairo F.L. Pires (PG),^{1*} Lanna K. Silva(TC)¹, João L. B. Junior (TC)², Gilmar S. Silva(PG),¹ Maysa Furlan (PG)², Adriana B. Araújo (PQ),¹

adriarau@ifma.edu.br; jairo.pires@acad.ifma.edu.br

¹Department Chemistry, IFMA; ² Department of Biochemistry and Organic Chemistry, UNESP

Keywords: Waste; FilmTiO₂; Drugs.

Highlights

This work proposes a heterogeneous photocatalysis treatment using Ag/TiO₂ films immobilized in glass tubes for the treatment of laboratory chemical residues containing Non Steroidal Anti- Inflammatory Drugs (NSAIDs).

Abstract

Pharmaceuticals are nowadays recognized as a threat for aquatic ecosystems¹. In this work we evaluated a treatment proposal for laboratory chemical residues containing the anti-inflammatory drugs naproxen (NPX), diclofenac (DCF) and Mefenamic acid (MFN) in its composition. The technique used was based on degradation by heterogeneous photocatalysis (FH) with Ag/TiO₂ films immobilized on glass support². The catalysts, obtained via sol-gel, were efficient in removing about 95% of NPX and completely degrading the other drugs in a 24 h treatment interval. The degradation products were identified by the technique of liquid chromatography coupled to mass spectrometry (HPLC-MS/MS), which demonstrated that the FH was also effective for degradation products, since at the end of the process these substances also showed signs of high rate of degradation.

In the study of the degradation products formed during the photocatalytic treatment and the control tests (photolysis), HPLC-MS/MS was used, which indicated the formation of five products of the NPX (m/z: 401, 417, 445, 185 and 177), three from DCF (m/z: 310, 312 and 256) and one from MFN (m/z: 283), and the degradation products showed a reduction significant of its chromatographic peaks in the 24 h treatment by photocatalysis, while in photolysis only the m/z products: 283; 401 and 445 showed signs of degradation.

Acknowledgments

Foundation for the Support of Scientific and Technological Research and Development of Maranhão (FAPEMA)

1. MEZZELANI, M.; GORBI, S.; REGOLI, F.; Mar. Environ. Res., 2018, 140, 41.
2. ARAÚJO, A. B. Tese (Doutorado em Química), Universidade Estadual Paulista, Araraquara, Brasil, 2006.

Increased NO₂ and O₃ concentrations in Rondonópolis - MT as a due of Amazonas, Pantanal, and Cerrado fires

Walter A. Bezerra (PG),^{1*} João Flávio da S. Petrucci (PQ),² Arnaldo A. Cardoso (PQ),¹.

walteraparecidobezerra@gmail.com

^{1*} Institute of Chemistry of Araraquara, Department of Analytical Chemistry (UNESP). Araraquara/SP, Brazil

² Institute of Chemistry, Federal University of Uberlandia (UFU). Minas Gerais, Brazil

Keywords Atmospheric pollution, Burning biomass, nitrogen dioxide and ozone, passive sampler.

Highlights

The study reports NO₂ and O₃ concentrations in Rondonópolis, cerrado region over a year. Significant variations in ozone concentrations were observed during the burning season in the region. Ozone values exceeded maximum air quality limits. Trajectory data of air masses show that they came from fires in the Amazon, Pantanal, and Cerrado biomes.

Abstract

The primary source of NO₂ in the atmosphere is the combustion of fuels, such as coal, oil, natural gas, and renewable sources. The NO₂, which acts as a photocatalyst oxidizes volatile organic compounds (VOC) and forms ozone. Ozone is toxic at a concentration as low as 80 ppb or 160 µg m⁻³ for 1 hour (World Health Organization, WHO). Many studies have linked NO₂ to cardiopulmonary mortality, lung cancer, and asthma exacerbations.

In Rondonópolis, a study of these pollutants was carried out over 12 months. In six locations in the urban perimeter, samplings were carried out approximately every 15 days, in each location 23 samples were taken in triplicate. The samplings were carried out for 8 or 24 hours using passive samplers. For NO₂ collection, a cellulose filter impregnated with triethanolamine was used. The Griess-Saltzman reagent was used for colorimetric determination at 550 nm. For ozone, the filter was impregnated with indigotrisulfonate (ITS), and the ITS's ozonolysis reaction (bleaching) could be determined at 600 nm. For air quality, the Brazilian legislation (CONAMA 491/2018), NO₂ levels must not exceed 200 µg/m³ or 106 ppb for 1 hour. The ozone limit is 100 µg/m³ (51 ppb) for 8 h.

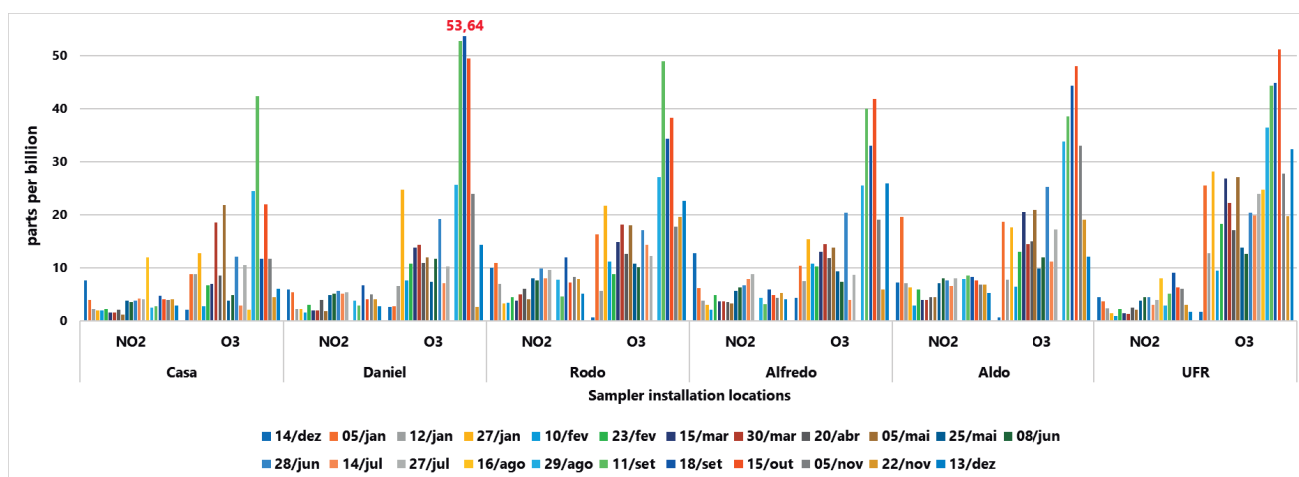


Figure 1: NO₂ and ozone concentrations Rondonópolis 24-hour sampling

The highest ozone peak occurred in September (figure 1), a value higher than the 51 ppb limit established by national legislation. Samples taken over 8 hours (day) showed higher ozone concentrations than those sampled over 24 hours (day and night). A peak of 83 ppb was observed in daytime samples taken over 8 hours. There are records of concentration close to 90 ppb in the capital of Mato Grosso, Cuiabá, in the month of September. The HYSPLIT air mass trajectory model indicated that the air masses that arrived in Rondonópolis, between August and October, passed through regions of the Pantanal, Amazon and Cerrado where intense biomass burning occurred due to forest fires. According to the National Institute for Space Research in Brazil (INPE), at this time of the year there is a peak of fires in regions of the states of Mato Grosso and Goiás, due to forest fires, so it is possible that the increase in ozone is related to the increase in fires, as wind can carry pollutants over long distances.

Acknowledgments

Financial support: CAPES and CNPq Walter Aparecido Bezerra acknowledges financial support from SEDUC-MT
46ª Reunião Anual da Sociedade Brasileira de Química: "Química: Ligando ciências e neutralizando desigualdades"

Investigation of the collaborative effect of adsorption and decolorization of methylene blue with two magnetic biochars from green coconut shell

Evelyn S. Bezerra (IC),¹ João P. C. F. Brunhosa (IC),¹ Isac M. Dias (PQ),¹ Larissa S. Mota (PG)¹, Camila A. Wegermann (PQ)¹, Bruno S. Peixoto (PQ)¹, Marcela C. de Moraes (PQ)¹ *.

mcmoraes@id.uff.br

¹ BioCrom, Instituto de Química, Universidade Federal Fluminense, Niterói, RJ, Brasil

Keywords: adsorption, magnetic biochar, catalytic transmission

Highlights

Magnetic biochar from green coconut shell was applied for dye removal of water; The methylene blue dye was used in the tests of adsorption and catalytic oxidation.

Abstract

Water pollution is a severe global problem and one of the major contaminants comprises organic compounds such as dyes. The presence of those substances in water blocks the entry of light and affects photosynthesis and aquatic life. Consequently, the remediation of these contaminants in the water is an important task. In this work, the collaborative effect of adsorption and catalytic oxidation of methylene blue dye (MB) was investigated using two magnetic biochars (MBC1 and MBC2) previously prepared in our research group through the pyrolysis of the green coconut shell impregnated with ferric chloride. Aiming to understand the catalytic activity of the biochars, the adsorptive features of those materials were determined by adsorption isotherm and kinetic assays. For the kinetic studies, the adsorption equilibrium time increases to 1000 min for MBC1 and 4000 min for MBC2. For both biochars, the pseudo-second order is the equation that best fits the experimental data which means that the limiting step of the process is the adsorption at the active sites¹. By the adsorption isotherms of MBC1 and MBC2, the adsorptive capacity of the materials for the MB removal was determined given a value of 10 mg/g. The experimental data of the MB adsorption were fitted to the classical models of Freundlich, Langmuir, and Sips. For MBC1, the parameter of the Sips equation ($R^2=0,99960$) fitted better with the features of the biochar indicating a relatively heterogeneous surface, which strongly agrees with the material characterization that is composed of a surface mixture with predominantly apolar pores and a polar external surface due to the functional groups of acids and iron oxides. The Langmuir model fitted well with the MB adsorption by MBC2 ($R^2=0,99938$). However, a good fit was also obtained for the Sips model ($R^2=0,99960$), so it is not yet possible to distinguish which model is more representative for MB adsorption by this material. The iron composition for activated carbons MBC1 and MBC2 was subject to catalytic investigation of MB decolorization in presence of H_2O_2 in deionized water without pH control. The catalytic reactions were promoted after keeping the biochars incubated with MB for 48 h and 96 h for MBC1 and MBC2 respectively. In all cases, a large enhancement in the decolorization rates was observed for the catalyzed reactions compared to the control reactions. For all assays, H_2O_2 was chosen as an oxidant. The MBC1 displayed a decolorization percent over 95% using a proportion of 1:2000 (MB: H_2O_2), while the MBC2 only achieved a maximum decolorization rate of 98% using a proportion of 1:4000 (MB: H_2O_2). In order to investigate the role of hydroxyl radicals in the reaction catalysis, the experiment in presence of the radical scavenger² isopropanol, 1MB:1500 H_2O_2 :3000 *iso*, for MBC1 and dye leading to an absorbance reduction and consequently to a reduction of the decolorization rate in comparison to the regular reaction. These results induce us to assume that the active species of the oxidation is the free radicals generated in situ through peroxide cleavage at the Fenton reaction. The easy removal of the magnetic biochars combined with their adsorptive and heterogeneous catalytic activity make these materials promising agents for future applications in water treatment.

Acknowledgments

CNPq, FAPERJ, PPGQ-UFF, PROAP-UFF, CNPq-PIBIC, CAPES

[1] J. Wang and X. Guo, Journal of Hazardous Materials 390 (2020) 122156.

[2] Wang, L.; Li, B.; Dionysiou, D. D.; Chen, B.; Yang, J. e Li, J. Environ. Sci. Technol. 2022, 56, 6, 3386.

Ionic characterization of particulate matter collected in urban, sugar cane, and natural areas.

Luis Fernando Mendonça da Silva (PG),^{1*} Cibele Maria Stivanin de Almeida (PQ),² Maria Cristina Canela (PQ),² Hellen Gonçalves Vieira (PG),² Rodrigo Stellet Ferreira (PG),² Luiz Francisco Pires Guimarães Maia (PQ),³ Adriana Gioda (PQ).¹

Luisfernando2903@gmail.com; agioda@puc-rio.br

¹Pontifícia Universidade Católica do Rio de Janeiro (PUC-Rio), Departamento de Química, Rio de Janeiro, Brasil; ²Universidade Estadual do Norte Fluminense Darcy Ribeiro (UENF), Laboratório de Ciências Químicas, ³Universidade Federal do Rio de Janeiro (UFRJ), Departamento de Meteorologia, Instituto de Geociências, Rio de Janeiro, Brasil.

Keywords: Atmospheric chemistry, Atmospheric pollution, PM_{2.5}, Ionic composition.

Highlights

The daily concentrations of PM were below the values suggested by CONAMA, but 44 % of the samples had values above the stipulated by the OMS and EPA. Most of the ions come from anthropogenic sources.

Resumo/Abstract

Air pollution has become a global environmental and public health problem. Among the pollutants, particulate matter (PM) has been highlighted by its aerodynamic diameters. The lower the diameter, the more dangerous it becomes, due to its ease of entering the human body. In this sense, the present study aims to characterize samples of particulate matter (PM_{2.5}) from the region of Campos dos Goytacazes (CG), Gávea (GA), and Serra dos Órgãos National Park (PARNASO) to identify the sources and level of anthropic influence. All samples were collected according to Brazilian standards (ABNT-NBR 9547/86) and the United States Environmental Protection Agency (US EPA) methods (Method IO – 2.1). The PM concentrations were determined by dividing the PM mass by the sampled air volume. For ion analysis, acute extraction of the filter was performed and taken to ion chromatography. Daily PM_{2.5} concentrations ranged from 8 to 31 µg m⁻³, with an average of 16 ± 7 µg m⁻³ for the GA region and, 13 to 45 µg m⁻³ with an average of 31 ± 15 µg m⁻³ for the PARNASO region and, from 5 to 33 µg m⁻³, with an average of 13 ± 11 µg m⁻³ for CG for the days sampled from February to June 2022. Considering these values, no day sampled exceeded the value suggested by Brazilian legislation (60 µg m⁻³), but 44 % of the samples showed higher daily concentrations than suggested by EPA (35 µg m⁻³) and WHO (15 µg m⁻³). The main ions found in GA and PARNASO were: SO₄²⁻>Na⁺>Cl⁻>NO₃⁻>C₂O₄²⁻>K⁺>Ca²⁺, while in CG, Na⁺>SO₄²⁻>NO₃⁻>Cl⁻>C₂O₄²⁻>K⁺>Ca²⁺. The SO₄²⁻ and NO₃⁻ anions presented a correlation (r = 0.8; p=0.001), suggesting the contribution of anthropogenic sources. Even though the neighborhood of Gávea suffered from marine influences, it was not possible to affirm the common origin between Na⁺ and Cl⁻ using correlation because the ratio of the two ions were lower than the values found in seawater (1.81). This can be justified by the loss of chlorine through volatilization in the form of acids, like HCl, but some anions of carboxylic acids such as oxalate can help in the deficit of Cl⁻, which showed a correlation with Cl⁻ (r = 0.96; p = 0.002)¹. The K⁺ and Ca²⁺ ions showed a strong correlation (r = 0.7; p=0.005), but none showed a correlation with Cl⁻, which suggests that they do not present a significant marine contribution, and through the analysis of air mass trajectories, the continental contribution was observed. In PARNASO, high concentrations of oxalate may be from biogenic emissions. In CG, K⁺ and C₂O₄²⁻ and, NO₃⁻ and Na⁺ presented strong correlation (r = 0.97; p = 0.02), suggesting that these were preferably in the form of sodium and potassium salts.

Agradecimentos/Acknowledgments

CAPES, FAPERJ, CNPq.

¹Zhao, Y., & Gao, Y. (2008). *Science of the total Environment*, 407(1), 541-547.

46ª Reunião Anual da Sociedade Brasileira de Química: "Química: Ligando ciências e neutralizando desigualdades"

Área: _____
(Inserir a sigla da seção científica para qual o resumo será submetido. Ex: ORG, BEA, CAT)

Mapeamento e desenvolvimento de tecnologias socioambientais associadas à incorporação de resíduos vítreos.

Wladimir Teodoro da Silva (PG),^{1*} Janaína P. Silva (PG),¹ Raphaela F. Santos (PG),¹ Bernardo Rossi B. Ladeira (TC),¹ Fernando Lameira (PQ),² Rochel M. Lago (PQ),¹ Rita C. O. Sebastião (PQ),^{1*}

wladmirt@ufmg.br; ritacos@ufmg.br;

¹Departamento de Química, UFMG; ²CDTN

Palavras-Chave: Resíduo Vítreo, Vidro, Sustentabilidade, Desenvolvimento Socioambiental, Desenvolvimento Tecnológico

Highlights

Mapping and development of socio-environmental technologies application associated with incorporation of vitreous waste

Tecnologias associadas a resíduos vítreos

Startups brasileiras que conectam tecnologia, negócios e resíduo vítreo

Desenvolvimento de produtos e serviços associados ao processamento de resíduos vítreos

Resumo/Abstract

O Brasil produz cerca de 1,3 milhões de toneladas de vidro por ano, dos quais apenas 47% são reciclados. Somado ao resíduo proveniente de produtos importados, são aproximadamente 3 milhões de toneladas de resíduo não processado por ano. Esse trabalho tem o objetivo de mapear processos químicos utilizados como iniciativas sustentáveis, que visam reduzir o impacto ambiental gerado pelo descarte desses resíduos e pela extração de matérias primas, associadas ao desenvolvimento de novos produtos. Após o mapeamento dos processos químicos mais utilizados nessas atividades investigamos aprimoramentos químicos ao processo e pretendemos elaborar um plano de negócios, para que esta atividade a ser implementada, promova a redução de impactos socioambientais às comunidades vinculadas ao seu manejo e/ou desenvolvimento tecnológico. O mapeamento foi realizado com vistas a compreender quais são as principais aplicações tecnológicas que utilizam o resíduo vítreo como agregado ou aditivo. Foram analisados 35 artigos com mais de 100 citações, publicados entre 2002 e 2020. Esses trabalhos abordam prioritariamente a incorporação de resíduos de vidro à concreto, cimento e materiais poliméricos de alta compressão. Os resultados demonstram que algumas dessas tecnologias já são consolidadas em processos de P&D, porém, outras são emergentes e carecem de maior investimento em pesquisas e negócios. Foram identificadas 16 *startups* consolidadas no mercado brasileiro, com ações que contemplam desde Tecnologia *Blockchain*, logística reversa, economia circular, dentre outras, todas focadas em negócios de impacto socioambiental. Após este mapeamento, apresentamos agora a 2ª fase do projeto que consiste na utilização do resíduo vítreo para o desenvolvimento de piso ecológico de base cerâmica-resíduo vítreo e cimento-resíduo vítreo. A fase atual das atividades conta com o desenvolvimento um projeto para implantação de uma unidade de processamento de resíduo vítreo a baixo custo, execução de testes de corpo de prova, aprimoramento químico da metodologia de produção e o estudo de viabilidade técnica e econômica para a implementação e consolidação de novos negócios socioambientais.

Referências: BÓ, Souza-Dal et al. Estudo da cadeia de reciclagem de vidro: perspectivas para os municípios da região carbonífera (AMREC) a partir da economia circular. 2019.

Agradecimentos/Acknowledgments

The authors would like to thank INCT Midas, CNPq, FAPEMIG and UFMG/PRPq/Proex for financial support.

Matrix effect challenges to pesticide quantification in different layers of sugarcane

Mariana A. Dias (PG)^{1*}, Éder V. Araújo (PG)¹, Cassiana C. Montagner (PQ)¹

*marimari.dias@gmail.com

¹Environmental Chemistry Laboratory, Institute of Chemistry, University of Campinas, Build I-155, Brazil

Keywords: 2,4-D, Fipronil, Fipronil degradation products, QuEChERS.

Highlights

A simple and fast method to quantify pesticides in sugarcane was satisfactorily validated. Fipronil degradation products and 2,4-D were detected in some layers of sugarcane.

Abstract

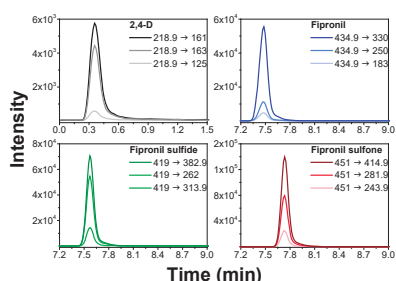


Fig. 1 MRM chromatograms in solvent curve at 50 µg L⁻¹.

Brazil has been the largest producer of sugarcane in the world since 1980 (750 million tons per year). Also, the country has been the major consumer of several pesticides. The herbicide 2,4-D and the insecticide fipronil are the main pesticides used in sugarcane cultivation. Thus, an analytical method was developed and validated using QuEChERS sample preparation and liquid chromatography coupled with mass spectrometry in tandem (LC-MS/MS) to determine 2,4-D, fipronil and its degradation products (fipronil sulfide and sulfone) in different layers of sugarcane (fresh leaf, dry leaf and culm). The parameters affecting the extraction efficiency of the QuEChERS method were optimized by multivariable designs. The analytes were identified and quantified using selected reaction monitoring mode (SRM) (Fig. 1). The 2,4-D ring ¹³C₆ and fipronil-pyrazole-¹³C₃, cyano-¹³C was used as internal standard. Linearity, limit of quantification (LOQ), trueness, precision, and matrix effect were assessed as the merit figures to method validation. The linearity ranged between 0.5-500 µg L⁻¹ and the LOQ was 0.12 µg kg⁻¹ for all analytes. Recoveries showed acceptable values between 63% and 123%, with RSD ≤ 20%. 2,4-D presented a sign suppression in all layers of sugarcane (Fig. 2). On the other hand, a slight enhancement of analytical response was observed for fipronil and its degradation products. Therefore, the matrix-matched calibration method with internal standard was chosen to quantify these analytes in all samples. The validated method was applied to sugarcane samples collected from an experimental farm in São Paulo Agribusiness Technology Agency (Brotas-SP, Brazil). Sugarcane tillers (n = 5) and plants at ripening (n = 5) were collected in triplicate each and divided into three layers. No pesticide was detected in the culm samples. For both sugarcane growth stages, fipronil sulfide and sulfone were detected in fresh leaves at 0.2-0.4 µg kg⁻¹ and 0.2-0.3 µg kg⁻¹, respectively. Fipronil was not applied in the last sugarcane cycle production, as consequence, it was not detected in samples, showing that the residual concentrations are irrelevant. However, the presence of fipronil degradation products could be related to the residual concentrations from previous cycles. 2,4-D was applied on the farm 6 months before the sampling, showing residual concentrations in dry leaves from sugarcane tillers (1-50 µg kg⁻¹) and plants at ripening (0.8 µg kg⁻¹). The developed method was successfully validated and can be easily applied to assess the fate of pesticides in the environment, in combination with studies involving other matrices, like water, soil, and air.

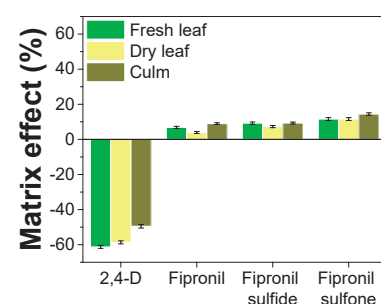


Fig. 2 Matrix effect (%) in different layers of sugarcane.

Acknowledgments

This study was financed in part by the Coordenação de Aperfeiçoamento de Pessoal de Nível Superior – Brasil (CAPES) #2015/18790-3 – Finance Code 001 | FAPESP #2015/18790-3 | INCTAA | UNICAMP

46^a Reunião Anual da Sociedade Brasileira de Química: "Química: Ligando ciências e neutralizando desigualdades"

Mercury determination in biohazard samples by GFAAS using Noviplex card sampling

Emerson C. Almeida (PG),^{1*} Nubya G. Cavallini (PG),¹ José C. S. Vieira (PD),¹ Jiri Adamec (PQ),² Camila P. Braga (PQ),³ Marcelo O. Lima (PQ),⁴ Pedro M. Padilha (PQ),¹

pedro.padilha@unesp.br; emerson.carlos@unesp.br

¹Department of Chemical and Biological Sciences, IBB-UNESP/SP; ²Department of Interdisciplinary Oncology, LSUHSC School of Medicine/USA; ³Department of Redox Biology, UNL/USA; ⁴Evandro Chagas Institute, Belém-PA

Palavras Chave: Noviplex™ card system, Materials biohazard sampling, Mercury determination, Electrothermal atomization

Highlights

- New sampling device for biohazard samples.
- Biohazardous materials sampling without the need for a preservation process freezing.
- Simple and fast sampling strategy of biohazard samples for mercury determination.

Resumo/Abstract

Sample collection and preparation is one of the most important steps in the process for monitoring mercury toxicity in biological samples. In recent decades, several strategies for sample preparation and subsequent mercury determinations have been published (Zhang et al. 2012; Moraes et al. 2013; Queiroz et al. 2018). However, the difficulties related to sampling of biological materials *in situ* and subsequent determination by manipulating the sample as little as possible have not yet been overcome. In this context, the Noviplex™ card system developed by Kim and collaborators (Kim et al. 2013) is an innovative biological fluid collection device that can be used to collect blood aliquots and/or biological extracts. Its viability lies in the sophisticated collection method, which does not require special bottles, equipment, or refrigeration, and in the ability to transport samples without losing the physical and chemical properties of the material. An absorbent disc is saturated with the sampled biological fluid and percolation occurs within three minutes through capillary action, making it possible to transport the cards economically and with minimal biohazard risk to a central laboratory for further analysis, e.g., for mercury. This paper presents a method for sampling biohazardous materials (mercury-contaminated human and fish blood/plasma and muscle and liver tissue homogenates) using percolation on Noviplex cards for total mercury determination by graphite furnace atomic absorption spectrometry (GFAAS). For the sampling process, 50 µL of the biohazardous material was percolated onto the sampling disk of the Noviplex card. Three minutes after percolation of the sample aliquot, the sample adsorbed on the card sampling disk was already dry and showed stability at room temperature for six months. After the sampling process, the card sampling disks with the percolated samples were mineralized in an acidic medium containing 18 mol L⁻¹ H₂SO₄ and 0.02 mol L⁻¹ KMnO₄ in a 1.0:0.50 (v/v) ratio. Mercury determinations of the acid extracts were performed via GFAAS by injecting 15 µL of sample + 5 µL of zirconium nitrate (chemical modifier) into the graphite tube of the spectrometer, in which the inner wall was coated with tungsten carbide (permanent chemical modifier). The reaction conditions provided thermal stabilization of mercury at atomization temperatures up to 1700 °C. The method was validated for total mercury determinations with extracts from DORM-4 and DOLT-4 reference materials. The calculated LODs and LOQs ranged from 12 to 43 µg kg⁻¹, respectively. The sampling method proved to be quite robust for mercury determinations for samples from blood/plasma, muscle and liver tissue homogenates from fish and for human blood/plasma samples.

References

- Kim J. H. et al. *Analytical Chemistry* 85(23):11501-11508, 2013.
Moraes P. M. et al. *Food Chemistry* 141:2614-2617, 2013.
Queiroz et al. *Biological Trace Element Research*, 184:517-522, 2018.
Zhang et al. *Analytica Chimica Acta*, 721, 22-27, 2012.

Agradecimentos/Acknowledgments

São Paulo Research Foundation - FAPESP Processes: 2019/02538-4 and 2016/19404-2; National Council for Scientific and Technological Development – CNPq, Processes: 304768/2018-9 and 404485/2016-2 and Coordination of Superior Level Staff Improvement - CAPES, Project CAPES-Print AUXPE-Process: 88881.3107432018-0.1

Microplastics in the atmosphere of São Carlos (São Paulo): quantification and physical characterization

Gabriel M. Ferraz (PG),*¹ Aline S. de Moraes (IC),¹ Gustavo B. dos Santos (IC),¹ Ingrid T. de Miranda (IC),¹ Roberta C. Urban (PQ)¹

gabriel.ferraz@estudante.ufscar.br

Chemistry Department, Federal University of São Carlos (UFSCar – São Carlos)

Keywords: Microplastics, Atmosphere, Indoor and outdoor environments, School.

Highlights

Quantification and physical characterization of atmospheric microplastics both indoors and outdoors at Alvaro Guião School – São Carlos.

Resumo/Abstract

Microplastics, defined as plastic particles with a size between 1 μm and 5 mm, are ubiquitous contaminants, however, their presence in the atmosphere is still poorly studied.¹ In this study, atmospheric samples were collected indoors and outdoors at Alvaro Guião School in São Carlos (São Paulo – Brazil), from November 2021 to July 2022, using a passive sampler. The atmospheric microplastics (MPs > 25 μm) were quantified and physically characterized by optical microscopy. In the outdoor environment, the mean concentrations of atmospheric MPs were 38.69 ± 20.89 fragments $\text{m}^{-2} \text{day}^{-1}$ and 1.26 ± 0.88 fibers $\text{m}^{-2} \text{day}^{-1}$ in the dry period (April to October), and 25.63 ± 25.51 fragments $\text{m}^{-2} \text{day}^{-1}$ and 0.29 ± 0.51 fibers $\text{m}^{-2} \text{day}^{-1}$ in the rainy period (November to March) (**Figure 1**). In the indoor, the mean concentrations were 39.84 ± 22.43 fragments $\text{m}^{-2} \text{day}^{-1}$ and 18.08 ± 6.09 fibers $\text{m}^{-2} \text{day}^{-1}$ in the dry period, and 10.52 ± 17.95 fragments $\text{m}^{-2} \text{day}^{-1}$ and 7.56 ± 4.55 fibers $\text{m}^{-2} \text{day}^{-1}$ in the rainy period.

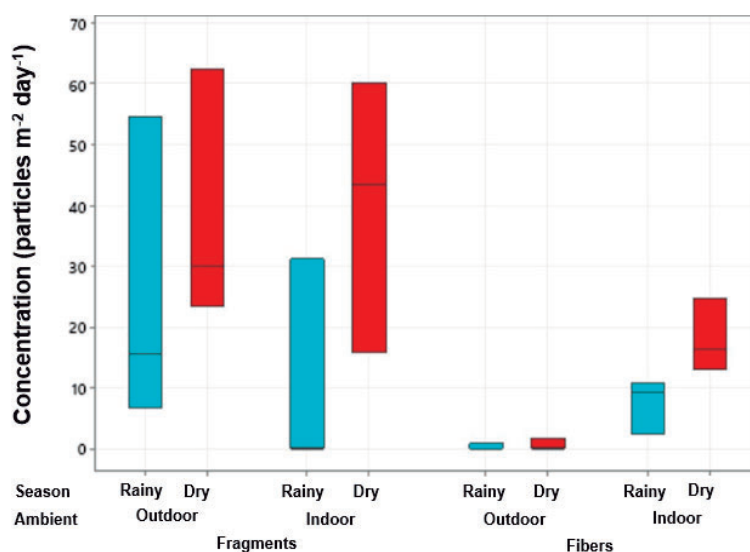


Figure 1. Mean concentrations of atmospheric MPs (fragments and fibers) in samples collected in the dry and rainy seasons in indoor and outdoor environments at Alvaro Guião School – São Carlos (São Paulo).

The mean concentrations of fragments and fibers were higher in the dry season than in the rainy season (Mann-Whitney test). In addition, the fiber concentrations were higher in the indoor environment than in the outdoor, in both seasons (Mann-Whitney test). Fragments are mostly smaller than 60 μm in both periods and environments, while the fibers varied between 100 and 3000 μm in the rainy season and <60 μm to 3000 μm in the dry period. White, black, and red fragments were determined, while black, white, red, green, and blue fiber-like MPs were found. The presence of MPs was demonstrated in both environments and seasons in the city of São Carlos, as well as higher concentrations of smaller particles, which may be more harmful to human health.

- Zhang, Y.; Kang, S.; Allen, S.; Allen, D.; Gao, T.; Sillanpää, M. ; *Earth Sci Rev* **2020**, *203*, 103118.

Agradecimentos/Acknowledgments

Coordenação de Aperfeiçoamento de Pessoal de Nível Superior - Brasil (CAPES, Finance Code 001), São Paulo State Research Foundation (FAPESP, grant #2018/04820-6; #2021/10187-7; #2022/03087-9), INCTAA (CNPq, grant #465768/2018-8; FAPESP, grant #2014/50951-4).

46ª Reunião Anual da Sociedade Brasileira de Química: "Química: Ligando ciências e neutralizando desigualdades"

Modified clays for removing phosphorus from domestic wastewater and potential use of generated sludge as fertilizer

Alessandro Lamarca Urzedo (PG),^{1*} Gabriela Tuono Martins Xavier (PG),¹ Renan da Silva Nunes (PG),¹ Dalmo Mandelli (PQ),¹ Pedro Sérgio Fadini (PQ),² Wagner Alves Carvalho (PQ).¹

a.lamarca@ufabc.edu.br

¹Center for Natural and Human Sciences (CCNH), Federal University of ABC (UFABC), Santo André – SP, Brazil; ²Chemistry Department (DQ), Federal University of São Carlos (UFSCar), São Carlos – SP, Brazil.

Keywords: sewage sludge, phosphorus recovery, phytotoxicity, sustainability

Highlights

TechPhos[®], a modified clay, is used as an alternative and cheap phosphorus adsorbent from sewage. The final sludge containing TechPhos[®] presented potential application as biofertilizer.

Abstract,

Phosphorus (P) is a critical element related to life. This element is an important nutrient because it is present in several key biomolecules. As a result, P mineral sources, like phosphate rocks (PR) are important for fertilizer production. However, food production is threatened by the depletion of PR, which is predicted to be vanished in 50 to 100 years. To overcome this risk, P recovering from wastewater has gained attention recently, since it corresponds to an alternative and sustainable source of P. The purpose of this experimental research was to use a modified clay, identified as TechPhos[®], for removing P from wastewater by adsorption; as well as evaluate potential applications of P recovered on sewage sludge as a fertilizer and investigate mechanisms of adsorption-desorption of P on TechPhos[®] sites. TechPhos[®] is a clay-based material modified for improvement on P adsorption, with maximum adsorption capacity of approximately 20 mg g⁻¹ under pH 3.7 – 4.5, and equilibrium time of 1 h for adsorption. The mechanisms for P removal are combinations of chemical and physical adsorption represented by Langmuir and Freundlich models, both with R² values higher than 0.95. The initial P concentration in the effluent tested from wastewater municipal treatment plant, WTP, in São Carlos, SP, was 3.70 mg P L⁻¹; the adsorption capacity (q) of P by TechPhos[®] was 10.80 mg g⁻¹ which represents a removal of 65.40 %. Each liter of treated wastewater produced 2.29 g of sludge (dry basis). When the tests are performed with a aqueous solution with the same P concentration, pH and temperature as the effluent, the retention decreases from 10.80 mg g⁻¹ to 8.47 mg g⁻¹. This reduction is related to the ability of TechPhos[®] to aggregate fine organic particles containing part of the P present in the effluent. Thus, both P removal and effluent turbidity are favored. The sludge obtained was named ST (sludge with TechPhos[®]), and a control sludge (SC) was collected on WTP for comparison. Both materials were characterized by Scanning Electron Microscopy (SEM); Fourier transforms infrared (FTIR); X-Ray Diffraction (XRD). The morphology; organic functions vibrational stretching and crystalline peaks of ST and SC presented negligible differences on SEM, FTIR and XRD analysis. Phytotoxicity parameters presented lower toxicity for ST using *L. sativa* seeds compared to SC, probably due P burst of nutrients on seeds, which overcome deleterious effects of organics of wastewater sludge. In order to predict the P release potential in real applications of ST or SC in the soil, desorption tests were carried out using NaOH, so that the P reversibly bound to calcium, aluminum and iron can be quantified. The P release profile on NaOH extraction reached 1.74 ± 0.06 mg P g⁻¹ and 2.05 ± 0.08 mg g⁻¹ from SC and ST, respectively. The potential application and advantage of ST over SC is granted by its lower toxicity maintaining fertilization capacity with same P released. Therefore, the TechPhos[®] application has a great potential for P recovery with generation of environmentally friendly material that might be used as biofertilizer.

Acknowledgments

We would like to thank CNPq (Brazilian National Council for Scientific and Technological Development - process 140840/2021-4), CAPES (Brazilian Coordination for the Improvement of Higher Education Personnel). The authors are also grateful to Multiusers Experimental Facilities (UFABC) for the experimental support and to Environmental Biogeochemical Lab (UFSCar).

Monitoramento ambiental da concentração elementar no sistema praial de Aracruz/Fundão, Espírito Santo, Brasil

Lívia Davel Gomes (IC),^{1,2*} Helena Bezerra Ferrari (IC),^{1,2} Antony Luca Luna Vieira de Abreu (IC),³ Lázaro Brandão Zardini (PG),⁴ Luana Santos Moreira (PQ),^{1,2} Maiara Krause (PQ),² Larissa Dias Roriz (TC)², Bruna Silva Correa (TC),² Geisamanda Pedrini Brandão (PQ),^{1,2} Renato Rodrigues Neto (PQ),⁴ Maria Tereza W.D.Carneiro(PQ).^{1,2}

livia.d.gomes@edu.ufes.br

¹Departamento de Química, UFES; ²Núcleo de Competências em Química do Petróleo – NCQP, Laboratório de Espectrometria Atômica – LEA, UFES; ³IFES - Aracruz; ⁴Departamento de Oceanografia, UFES.

Palavras Chave: *Contaminantes químicos, Rio Doce, Sedimento, Avaliação espaço-temporal, Análise exploratória, Índices de referência.*

Highlights

Environmental monitoring of elemental concentration in the beach system of Aracruz/Fundão, Espírito Santo, Brazil

- The PCA indicated a trend in the formation of 2 groups separated by campaign carried out
- The element As presented higher values than PEL
- Praia Grande is the sampling station with the highest concentration of the studied elements

Resumo/Abstract

Após a construção do estaleiro Jurong em Aracruz/ES, no ano de 2014, e a tragédia do rompimento da barragem de Mariana/MG, em 2015, diversos monitoramentos e estudos em praias do litoral do Espírito Santo vem sendo realizados, a fim de avaliar se o ambiente está impactado. Durante o ano de 2022, foi feito um monitoramento de 12 estações amostrais distribuídas ao longo do litoral norte do estado do Espírito Santo, de Barra do Riacho - Aracruz à Praia Grande - Fundão. Sete campanhas mensais (janeiro a julho 2022) foram realizadas na área de pós-praia, no subponto da face inferior, e as amostras de sedimento analisadas quanto à concentração elementar. Para a decomposição parcial das amostras de sedimento foi utilizado o método normalizado US EPA 3051A e o teor dos elementos químicos Al, Fe, Ni, Mn, As, Co, Cr, V, Ba, Cd, Cu, Pb e Zn foi determinado por Espectrometria de Emissão Óptica com Plasma Indutivamente Acoplado (ICP OES) e Espectrometria de Massas com Plasma Indutivamente Acoplado (ICP-MS). A Análise de Componentes Principais (PCA) foi aplicada aos dados para verificar possíveis tendências na distribuição dos elementos entre as amostras investigadas. Aproximadamente 75% da variabilidade dos dados foi explicada por PC1, PC2 e PC3. Os gráficos de escores mostraram uma tendência na formação de 2 grupos. O primeiro composto por amostras das campanhas 1 e 2 agrupadas no quadrante negativo da PC1 e positivo da PC2. O gráfico de pesos indicou alta correlação das amostras do grupo 1 com Ni, Mn, As, Co, Cr e V. O segundo grupo, composto por amostras das campanhas 3 a 7, indicou uma tendência na formação de um subgrupo contendo as amostras da campanha 3, localizado no quadrante positivo da PC2 e negativo da PC3, e de alta correlação com o Mn. As amostras das campanhas 4 a 7, que formam o maior grupo na PCA, estão localizadas nos quadrantes negativos das PCs 2 e 3, evidenciando uma baixa correlação destas com o Ni. De forma geral, não foram observadas variações significativas nas concentrações dos elementos estudados entre as campanhas realizadas, com exceção do Ni, cuja concentração diminuiu um fator de 6 vezes entre as campanhas 1 e 7. O nível de contaminação do sedimento por elementos químicos foi avaliado de forma qualitativa por TEL e PEL, índices de referência para contaminantes inorgânicos em sedimento marinho. Durante o tempo de monitoramento, os elementos Ba, Cd, Cr, Cu, Pb e Zn apresentaram valores abaixo de TEL, enquanto o Ni apresentou valores acima de TEL em todas as estações da campanha 1. Para o As, foram obtidos valores maiores que PEL em todas as campanhas realizadas e em diferentes estações de coleta, indicando alta contaminação por este elemento em toda a região estudada. Para a praia Grande, por exemplo, o valor de PEL obtido na campanha 1 foi 2 vezes maior que o valor de referência. Esta estação amostral também apresentou altas concentrações para a maioria dos elementos estudados. Os elementos Al, Co, Fe, Mn, Se e V não apresentam valores de referência para TEL e PEL. Há um forte indicativo de alta contaminação por elementos químicos na região estudada. No entanto, para uma avaliação mais assertiva sobre o status de contaminação do sistema praial Aracruz/Fundão, outros índices de referência devem ser aplicados.

Agradecimentos/Acknowledgments

FACTO, CNPq, FAPES, UFES/NCQP/LEA

New COVID-19 surveillance strategies using wastewater-based epidemiology (WEB)

Gabriela F Matos (PG)¹, Geovana de M. Mendes (PG)¹, Paulo Felipe N. Estrela (PG)¹, Marcio N. de Souza Junior (PG)¹, Núbia N. de Brito (PQ)¹, Andréa F. Arruda (PQ)¹, Matheus R. Augusto (PG)², Ieda C. M. Claro (PG)², Adriana F. A. Duran (PG)², Aline D. Cabral (PG)², Rodrigo de F. Bueno (PQ)², Gabriela R. M. Duarte (PQ)^{1*}

gabimatoss@discente.ufg.br; gabriela_duarte@ufg.br*

¹Instituto de Química, UFG; ²Centro de Engenharia, Modelagem e Ciências Sociais Aplicada, UFABC.

Keywords: SARS-CoV-2; Early warning; Wastewater-Based Epidemiology.

Highlights

The emergence of new variants of SARS-CoV-2 has provided new waves of the pandemic around the world. WBE can be implemented as part of COVID-19 pandemic surveillance, especially in emerging countries.

Abstract

The COVID-19 pandemic completes its third year, and the world is currently dealing with new waves that arise with new variants of the SARS-CoV-2 virus. Unfortunately, the extent of the COVID-19 infection still needs to be fully explored due to insufficient testing in several countries fighting against economic slowdown¹. Wastewater-Based Epidemiology (WBE) has shown to be a promising tool for the surveillance and tracking of infections. Virus RNA fragments can be found in sewage since all infected people (symptomatic, pre-symptomatic, or asymptomatic) excrete the virus through their biological fluids. Thus, the viral load present in wastewater can be linked to the level of viral circulation in the population and be used to anticipate new waves of infection². From May 2021 to January 2022, the SARS-CoV-2 viral load was monitored in wastewater samples from Goiânia-Brazil. Through pre-concentration, extraction, and purification of viral RNA, followed by reverse transcription-quantitative polymerase chain reaction (RT-qPCR), the presence of fragments of SARS-CoV-2 nucleic acid with varying viral loads (10^5 to 10^8 RNA copies L^{-1}) was detected in 83.78% (31/37) (Figure 1 a). The viral load in the sewage samples was related to the clinical data of the city, thus demonstrating the prospect of the WEB in promoting an Early Warning System (EWS) facing a pandemic. Statistical analysis of prevalence using the Monte-Carlo model made it possible to estimate the weekly viral load spreading in the population (Figure 1 b). So far, our group have issued two early warning notes to public health authorities, which were later confirmed given the increase in clinical cases in the city, demonstrating the method's ability to promote an Early Warning System (EWS) with time to manage the crisis. Therefore, wastewater surveillance has proven to be a fundamental tool to help combat the spread of the pandemic by anticipating new waves and possibly the incidence of new variants.

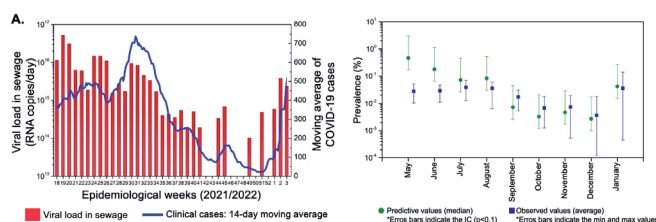


Figure 1. Wastewater-based epidemiology in Goiânia-GO. **A.** Relation between SARS-CoV-2 viral load quantified in sewage samples and the moving average of clinical cases in Goiânia-GO. **B.** Relationship between modeled and observed prevalence.

Agradecimentos/Acknowledgments

[CNPq (402694/2020-1 and 402432/2020-7), FAPEG (202010267000273), MPT and SANEAGO]

1. Kumar M., Jiang G., Thakur, A. K. Chemical Engineering Journal. <https://doi.org/10.1016/j.cej.2022.135936>.
2. Bueno, R.F., Claro, I.C. M. Journal of Environmental Chemical Engineering, <https://doi.org/10.1016/j.jece.2022.108298>.

New design of gas diffusion electrode based on Printex L6 carbon supported on carbon cloth towards the electrogeneration of H₂O₂ for water treatment.

Matheus S. Kronka¹, Beatriz T. Marin¹, Ignasi Sirés², Marcos R. V. Lanza¹

mskronka@usp.br

¹Instituto de Química de São Carlos, Universidade de São Paulo- USP

²Facultat de Química, Universitat de Barcelona, Martí i Franquès 1-11, 08028 Barcelona, Spain

Palavras-Chave:(Eletrodo de difusão gasosa; Eletrogeração de H₂O₂; Processos oxidativos avançados eletroquímicos; Tratamento de efluente; baixa condutividade).

Highlights

The new GDE design based on PL6C offered significant advantages compared to GDE commercial, including a longer time-life and a larger surface area. The new design of GDE more durable and efficient.

Resumo/Abstract

Gas diffusion electrodes (GDEs) have been widely used for the electrochemical production of H₂O₂ in aqueous media due to their highly porous structure, which allows for direct release of O₂ on the electrode surface increasing the reaction efficiency. However, the development of efficient and stable new designs of GDEs for producing H₂O₂ in complex aqueous matrices with low conductivity is a challenge that has been widely studied to enable homogeneous wastewater treatment processes [1,2]. In this work, we present a comparison between a commercial GDE and a new GDE made of Printex L6 Carbon (PL6C), both supported on carbon cloth, to produce H₂O₂. The PL6C-based GDE was produced using a hot press technique, consisting of applying a load of 10 mg cm⁻² of PL6C/20% PTFE on a PX30-PW03 carbon cloth, pressed with 0.5 tons at a temperature of 270°C for 15 minutes. Comparative studies of H₂O₂ electrogeneration and Fe²⁺ regeneration were performed using an electrolyte of 50 mmol L⁻¹ H₂SO₄ at pH 3 (8.2 mS) by applying current densities from 5 to 80 mA cm⁻², using the GDEs as cathode (under air flow of 0.2 L min⁻¹) and DSA® anode, both with 3 cm². It was found that after 300 minutes of electrolysis, the H₂O₂ production obtained by the GDEs showed significant similarities at all studied currents. However, the PL6C GDE achieved double the values obtained for Fe²⁺ regeneration compared to the commercial GDE. The similarity in H₂O₂ production between the GDEs can be explained by the fact that the reaction was not controlled by O₂ mass transport. On the other hand, the superiority of the Fe²⁺ regeneration values by the PL6C-based GDE compared to the commercial GDE can be justified by the higher surface area of the first (47.82 m² g⁻¹), compared to the second (14.85 m² g⁻¹). Another property in which the PL6C-based GDE was superior to the commercial GDE was related to the life-time tests, which were performed by applying a current density of 10 mA cm⁻² in a filter press reactor with pre-pilot scale of a 2.5-liter solution capacity, scaling the electrode area from 3 to 20 cm². The results showed that the life-time of PL6C-based GDE was 6000 minutes while for the commercial GDE it was 4600 minutes, in accordance with the contact angle results that showed higher wettability of the commercial GDE over 30 minutes of a 15 μL water droplet staying. Thus, the PL6C GDE was economically viable for electrochemical production of H₂O₂ in low conductivity solution of 12 mmol L⁻¹ H₂SO₄ at pH 3 (3.1 mS), as found in real wastewater, for current densities of 5 and 10 mA cm⁻². We studied different electrochemical advanced oxidation processes (EAOPs) at 10 mA cm⁻² for the removal of Tebuconazole (TBZ) present in real wastewater, having found the photoelectro-fenton process (PEF) as the most efficient process after completely removing TBZ in 1h, apart from achieving the highest percentage of mineralization (~30%) among the studied EAOPs after 180 min.

Agradecimentos/Acknowledgments

FAPESP (Proc. FAPESP 2014/50945-4, 2017/10118-0, 2017/23464-3, 2021/10973-2, 2021/06129-1), CAPES – Código de financiamento 001) e CNPq (Proc. 465571/2014-0 e 303943/2021-1).

Referências

- [1] Santos, G. O. S. et al. *Current Opinion in Electrochemistry* 36 (2022) 101124
[2] Xie, J., et. al. *Journal of Environmental Chemical Engineering* 10 (2022) 107882

Área: AMB

New portable device for sampling nitrogen dioxide, NO₂, in open and indoor environments

Laís da Silva Guidorizi (IC),¹ Vinícius Sousa Mano (IC)¹ Arnaldo A. Cardoso (PQ),¹.

¹ Instituto de Química de Araraquara, Dep. de Química Analítica, (UNESP). Araraquara/SP, Brasil

Palavras Chave: Dióxido de nitrogênio, Poluição atmosférica, Poluição indoor.

Highlights

This work presents a new low-cost portable sampler for NO₂. Portability is essential for extending monitoring to locations far from the laboratory. The sampler can be used for monitoring both open and indoor atmospheres.

Resumo/Abstract

O dióxido de nitrogênio, NO₂, é o poluente gasoso mais comum presente na atmosfera de cidades. Sua formação é resultado, principalmente, do calor resultante de combustão de materiais que promovem a reação entre N₂ e O₂ presente no ar. O NO₂ também pode ser encontrado também em atmosfera de ambientes fechados como cozinhas e salas com lareiras. O amostrador proposto foi construído utilizando uma bomba de ar (12V) conectado por uma mangueira plástica com uma válvula de agulha para controle da vazão de amostragem (fig 1) e que finalmente é conectada a uma coluna C-18 impregnada com trietanolamina (TEA), reagente conhecido por absorver o gás NO₂ (fig 2). Após a coleta do NO₂ o analito é desorvido da C-18 com solução etanol e água. Na sequência é utilizado o reagente de Griess Saltzman que produz um corante de cor rosa. Após o processo de desorção, analisamos a amostra em um espectrofotômetro em uma faixa de 540nm. O peso do

amostrador é de cerca de 174 gramas. O custo total é de cerca de 50 dólares, não incluindo a coluna de C18 e os reagentes. A coluna de C18 pode ser reutilizada diversas vezes após passar por processo de limpeza com a solução de etanol. O teste prévio obtido em análise de ambientes externos e internos com amostragens de 60 min foi: A amostragem, feita em rua de movimento ao lado do Instituto de Química, resultou em 76,5 ppb. A amostragem em ambiente interno foi feita em três etapas em uma cozinha de 30,6 m³: janelas e portas abertas, sem uso do fogão: 16 ppb. A 2^a amostragem, janelas e portas fechadas e após 10 minutos com um bico de gás do fogão aceso resultou em 138 ppb. E a 3^a com janelas e portas fechadas e após 10 minutos com 4 bicos de gás do fogão aceso resultou em 254 ppb. O amostrador é de fácil construção, de baixo custo e pode ser utilizado em ambientes diversos contendo NO₂ na atmosfera.



Fig 1. Visão Geral do amostrador e seus componentes

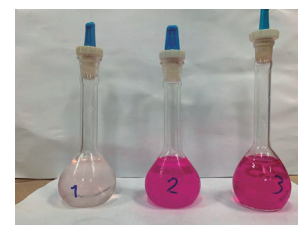


Fig 2: reação do NO₂ e formação do produto

Agradecimentos/Acknowledgments

Agradecemos a CNPq que financiou parte do material do projeto.

Occurrence and contents of trace metals and rare earth elements on plastic pellets

Lais A. Souza (PQ),^{1*} Ana C.S.S. Santos (PG),² Josepha M. Leão (IC),² Otto C. Schaeppi (IC),² Vanessa Hatje (PQ).²

lais.asouza@ufpe.br

¹Departamento de Química Fundamental, UFPE; ²Centro Interdisciplinar de Energia e Ambiente, UFBA

Palavras Chave: Microplastic, REE, Sandy Beaches, Brazil, Contamination, Metals.

Highlights

Fluvial inputs influence the distribution and composition of pellets. Concentrations of \sum REE varied between 359-1739 $\mu\text{g kg}^{-1}$. Pellets are transport vectors and an exposure route for REE and metals.

Resumo/Abstract

Plastic products are suited for a variety of applications. Globally, ~400 million tons of plastic were produced in 2018¹, and it is estimated that this number will exceed 33 billion tons in 2050. Plastics can be found in all environmental compartments in diverse sizes. The microplastics (MPs) are minute (<5 mm in diameter) plastic debris (fibers or fragments) or pellets. Pellets have been encountered in marine waters and sandy beaches all around the world², as well as in the viscera of fish, birds, and marine invertebrates, including species used for human consumption³. The ubiquity of microplastics on beaches around the world is widely known and increasing, becoming a global concern since the durability of this material is associated with high potential risks to aquatic organisms and human health. The objective of this study was to evaluate the occurrence and composition of pellets on oceanic and sheltered sandy beaches and the potential effect of fluvial contribution on the occurrence of these MP on the coast of Bahia, Brazil. We also evaluated the concentrations of trace metals, including REE, in pellets of different colors collected on sand beaches. First, we determined metals in pellets sorted by color, i.e., white/ transparent, yellow, brown, and black. Then we analyzed pellets contamination on beaches that presented a sufficient mass of pellets (>0.7 g) for chemical analysis. Whereas there are numerous reports on the occurrence of pellets in sand beaches worldwide, this is one of the first reports of REE and other trace elements in pellets. It was found that the presence/absence of rivers influences the distribution of pellets. The studied ocean beaches exhibited a very low pollution index (PPI), indicating that the isn't a relevant source of pellets for this region. The concentrations of REE and other trace metals were highly variable among beach types and color of pellets. The highest concentrations of REE and other metals were observed in white pellets, which presented visual signals of erosion and fractures in their surfaces, possibly facilitating the sorption of contaminants. Our study indicates that pellets may be a vector of transport and exposure route for REE and other trace metals. While the concentrations measured here are not particularly high, there is currently no threshold for REE contamination in the environment, and there is a high expectation that REE levels in the environment will increase in the near future due to their extensive use in high technology products (e.g., smartphone, computers, batteries, magnets) and processes.

¹PlasticsEurope, E. P. R. O. "Plastics—the facts 2019. An analysis of European plastics production, demand and waste data." PlasticEurope <https://www.plasticseurope.org/en/resources/publications/1804-plastics-facts-2019> (2019).²Andrady, A.L., 2011. Microplastics in the marine environment. *Mar. Pollut. Bull.* 62, 1596–1605. <https://doi.org/10.1016/j.marpolbul.2011.05.030>.³Pagano, G., Thomas, P.J., Di Nunzio, A., Trifuoggi, M., 2019. Human exposures to rare earth elements: present knowledge and research prospects. *Environ. Res.* 171, 493–500. <https://doi.org/10.1016/j.envres.2019.02.004>.

Agradecimentos/Acknowledgments

This work was supported by CNPq (441264/2017-4; 407297/2018- 9) and GASBRAS/FINEP. The authors were sponsored by CAPES (ACSSS, Finance Code 001), CNPq (VH, 304823/2018-0; LAS, 441264/2017-4). We are grateful to all students that participated in the fieldwork.

Occurrence of antibiotics in aqueous matrices: an outlook about the situation in Brazil

Jany H. F. de Jesus (PQ),¹ Karla V. L. Lima (PG),¹ Raquel F. P. Nogueira (PQ)^{1*}

jesusjanyhf@gmail.com; raquel.pupo@unesp.br

¹ São Paulo State University (UNESP), Institute of Chemistry of Araraquara.

Keywords: Pharmaceuticals, Surface water, Wastewater, Hospital effluent.

Highlights

The occurrence of antibiotics in Brazilian waters was carefully revised. 20 antibiotics were detected in 4 matrices ranging from ng L^{-1} to $\mu\text{g L}^{-1}$. Antibiotic concentrations reached up to 37300 ng L^{-1} .

Abstract

Antibiotics are among the most important tools in medicine, but their misuse and overuse can stimulate bacterial evolution and the spread of resistance, one of the principal threats to public health in the 21st century¹. This study presents data regarding the occurrence of antibiotics in several aqueous matrices in Brazil in the last twelve years (from 2010 to 2022). The search was thoroughly carried out using Science Direct, Web of Science, and Scielo databases. A total of 20 scientific papers were found to develop this work (Fig. 1A). Despite the low number of studies regarding this subject, Brazil is the Latin American country with the highest number of published data on the occurrence of antibiotics in surface water. These studies are still limited to the south and southeast regions. Only two studies were carried out in the Northeast region and there is an absence of data in other regions (North and Central West), leaving Brazil without a general scenario about the occurrence of antibiotics. Data from these papers show the detection of 20 antibiotics in 4 aqueous environments, occurring at concentrations in the range from ng L^{-1} to $\mu\text{g L}^{-1}$. Sulfamethoxazole was the most frequently found and the one with the highest concentration, 37300 ng L^{-1} in a hospital effluent (Fig. 1B and C). As expected, in studies about seasonal variation, the highest levels of the antibiotics commonly prescribed to treat respiratory infections were found in winter, while antibiotics used for other types of infections are generally climate independent.

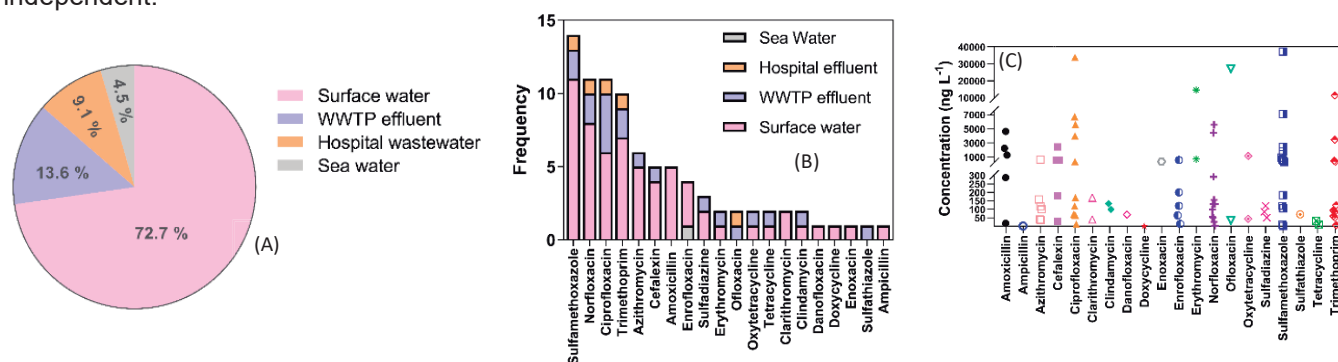


Figure 1: (A) Distribution of studies by matrix (B) Frequency of antibiotic by matrix and (C) Maximum antibiotic concentrations found.

The large variations in climate and social conditions play an important role in the consumption of antibiotics in different regions. For example, according to the Brazilian Diagnostic of Water and Sewage Services², only 54.1% of the population has a sewage treatment service, predominantly the urban population and centered in the most populous region, causing a direct impact on the occurrence of antibiotics in surface water. Since most of the occurrence studies were conducted in south and southern regions, the data available are only representative of these regions and is not an appropriate standard for the rest of the country. Furthermore, considering the environmental and health urgency associated with this topic, and consequently, for future inclusion of antibiotics to the standards related to water quality, it is necessary: (i) further studies to evaluate the capacity of the wastewater treatment plants (WWTPs) for removing antibiotics; (ii) the studies of occurrence in the other regions of the country.

References

¹ WHO, 2018. WHO Report on Surveillance of Antibiotic Consumption 2016 – 2018.

² SNIS, B., 2019. 24^o Diagnóstico dos Serviços de Água e Esgotos - 2018. Brasília: SNS/MDR.

Acknowledgments

FAPESP (grants 2018/12780-4 and 2019/22218-4), CNPq, CAPES (Finance Code 001) and PROPe-PROPG/UNESP. 46^o Reunião Anual da Sociedade Brasileira de Química: "Química: Ligando ciências e neutralizando desigualdades"

Área: AMB Nº de Inscrição: 813

Otimização de metodologia para análise de hidrocarbonetos policíclicos aromáticos (HPAs) em matrizes aquosas por CG-DIC

Vitória A. P. dos Santos (IC)^{1,2}, Gislaíne N. S. Costa (PQ)¹, Natália G. de Figueiredo (PQ)¹

vitoria@int.gov.br; vitoria.perassoli@id.uff.br

¹Divisão de Química e Biotecnologia (DIQIM), Laboratório de Tabaco e Derivados (LATAB), Instituto Nacional de Tecnologia (INT), Av. Venezuela, 82, CEP 20081-312, Rio de Janeiro-RJ, Brasil; ²Instituto de Química (IQ), Universidade Federal Fluminense (UFF), Outeiro de São João Batista s/n, Campus do Valonguinho, CEP 24020-141, Niterói - RJ, Brasil

Palavras Chave: Análise ambiental, Hidrocarbonetos Policíclicos Aromáticos, HPAs, Validação de métodos analíticos, CG-FID.

Highlights

Optimization of methodology for polycyclic aromatic hydrocarbons (PAHs) analysis in aqueous matrices by GC-FID. Development of analytical methods for environmental matrices. Analytical methods validation. Analysis of polycyclic aromatic hydrocarbons.

Resumo

Os HPAs compreendem um grupo de mais de 100 moléculas orgânicas, cujas fontes podem ser naturais ou antropogênicas¹. As propriedades químicas destes compostos variam de acordo com a estrutura da molécula. HPAs de baixa massa molecular têm toxicidade aguda, enquanto HPAs de alta massa molecular apresentam alto potencial mutagênico e carcinogênico¹. Devido aos impactos que estes compostos podem causar a saúde humana e ao meio ambiente, a *United States Environmental Protection Agency* classifica 16 HPAs como prioritários para monitoramento em matrizes aquosas, dentre os quais o naftaleno, antraceno, pireno, criseno e benzo[g,h,i]perileno^{1,2}. A cromatografia gasosa com detector de ionização por chama (CG-DIC) é uma técnica amplamente usada, uma vez que atende a uma ampla variedade de compostos. Neste sentido, o objetivo deste trabalho foi a otimização de um método para a análise de HPAs em matrizes aquosas, utilizando o processo de extração em fase sólida (EFS) e CG-DIC. Foram realizados testes utilizando um mix contendo os 16 HPAs em diferentes solventes (diclorometano (DCM), metanol e metanol/DCM (1:1)), de forma a avaliar a influência dos mesmos na separação dos analitos. Para os testes de EFS, utilizou-se cartuchos C18 de 3 mL e 500 mg, 250 mL de água Milli-Q fortificada, DCM como solvente de co-extração e 2 HPAs (naftaleno e benzo[g,h,i]perileno). Para a análise qualitativa e avaliação dos parâmetros de desempenho do método, preparou-se uma solução estoque a partir de um mix de HPAs (3,6 - 76,9 µg mL⁻¹) em DCM. Utilizou-se cromatógrafo a gás 7890A (Agilent®) com DIC, coluna HP-5 30 m x 0,320 mm x 0,25 µm, hélio (1,3 mL min⁻¹), volume de injeção de 1 µL, injetor e detector com temperaturas de 250 e 300 °C, respectivamente. A programação da temperatura do forno foi de 40 °C (1 min), 25 °C/min até 160 °C, 5 °C/min até 270 °C (11 min) e o tempo de corrida de 35 min. As curvas de calibração (6 pontos) foram preparadas contendo HPAs na faixa entre 0,46 e 26,9 µg mL⁻¹. Os limites de detecção (LD) e de quantificação (LQ) foram determinados pelo cálculo de 3 e 10 vezes o desvio padrão médio obtido pela injeção do mix de HPAs no menor nível de concentração detectado³. O DCM apresentou melhores resultados, devido a um menor ruído na linha de base, menor alargamento dos picos cromatográficos e menor formação de picos residuais. O método proposto apresentou coeficientes de determinação (R²) > 0,99 para o naftaleno, acenaftileno, acenafteno, fluoreno, fenantreno, fluoranteno, pireno, benzo[a]antraceno e criseno, com coeficientes de variação (CV) < 10% (n=3). Os LDs e LQs situaram-se entre 0,01 e 0,18 µg mL⁻¹, e 0,04 e 0,54 µg mL⁻¹, respectivamente. Para os demais HPAs (antraceno, benzo[b]fluoranteno, benzo[k]fluoranteno, benzo[a]pireno, indeno (1,2,3-c,d)pireno, dibenzo[a,h]antraceno e benzo[g,h,i]perileno) o R² variou entre 0,90 e 0,98, com CV < 6,2% (n=3). As curvas de calibração serão novamente preparadas e analisadas. Caso necessário, serão realizados pequenos ajustes nos parâmetros analíticos do método otimizado, considerando-se o volume de injeção, a temperatura do injetor e a temperatura final da rampa de aquecimento. Nos testes de EFS, a concentração do naftaleno se mostrou abaixo do LD do método. Para o benzo[g,h,i]perileno os limites não foram determinados (R² < 0,99). Dentre outras vantagens, a análise simultânea reduz o volume de solventes usados, de resíduos gerados e a exposição aos HPAs. Além disto, os dados obtidos podem embasar futuros estudos relacionados ao monitoramento de sítios contaminados, como rios e lagoas e, à exposição humana.

Referências: ¹Bispo, J. R. L., et al. *J. Anal. Chem.*, v.2, p. 971-978, 2011. ²Onyidinma, U. P., et al. *Groundw. Sustain. Dev.*, v.6, p. 1-13, 2021. ³INMETRO - DOQ-CGCRE-008. Orientação sobre validação de métodos analíticos. 2020.

Agradecimentos

Conselho Nacional de Desenvolvimento Científico e Tecnológico (CNPq) pela bolsa PIBIC-INT concedida.

Photocatalytic antibiotics degradation by semiconductor-based materials.

Bruna R. Serino (IC),¹ Vitor Gabriel Pastana (PG)¹, Ingrid F. Silva (PQ)², Ivo F. Teixeira (PQ)^{1*}, Luís F. G. Noieto (PG)¹, Danielly T. S. Costa (PG)¹.

bruna.serino@estudante.ufscar.br; ivo@ufscar.br.

¹Department of Chemistry, UFSCar; ²Department of Colloid, Max Planck Institute of Colloids and Interfaces, Potsdam, Germany.

Key words: Photocatalysis, Degradation, Carbon Nitride, Antibiotics.

Highlights

Photodegradation of amoxicillin by Poly Heptazine Imide exchanged with different metal single-atoms. Na-PHI, Fe-PHI and Pt-PHI were evaluated. Fe-PHI displays the best activity, 72% removal in 8h under visible light.

Resumo/Abstract

-Contaminants of Emerging Concerns (CECs) are a class of pollutants not removed or eliminated by conventional water treatment. In addition, their environmental impact and health human problems are very little known and their literature is still limited^[1]. In this way, semiconductor-mediated photocatalysis becomes a green and efficient alternative compared to conventional techniques due to their electronic structure and unique physicochemical properties. Highly crystalline carbon nitride structures can be reached by thermally treating melamine in the presence of salts. Sodium cations are stabilized by nitrogen atoms with negative charges in between layers, resulting in the Sodium Poly Heptazine Imide (Na-PHI) (**Fig. 1.a**). Later the sodium cations can be exchanged for other metals single-atoms, by suspending the carbon nitride material in an aqueous solution with a metal salt. In this work, photocatalytic degradation tests of the Amoxicillin antibiotic (AMX) were carried out employing PHI exchanged with different single-atoms (i.e. Fe and Pt). Photocatalytic tests were performed under white LED lamp irradiation with a power of 150 W, adding 30 mg of the photocatalyst in 2 ppm AMX aqueous solution. Some results of the AMX degradation are shown in Fig. 1b. First, the AMX adsorption was evaluated by keeping the reaction in the dark for 90 minutes. For the Fe-PHI, it was observed significant adsorption, of about 27%. After that, the AMX photodegradation was evaluated for 8 hours under light illumination. The three catalysts evaluated showed high activity for AMX photodegradation when compared with the blank reaction (only AMX under visible light). Among all the catalysts, the Fe-PHI was the most efficient for photodegradation, with about 72% degradation after 8 hours of exposure. The catalysts were completely characterized by HR-TEM, STEM-HAADF, XRD, FT-IR and UV-Vis. We intend in the next few months test PHI exchanged by other metals, such as Ni, Cu and Co. Furthermore, zeta potential will be performed in order to evaluate the influence of the charges on the photocatalyst surface into the adsorption/photodegradation of AMX.

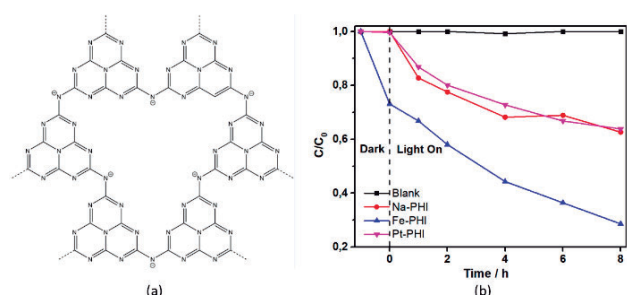


Figure 1. (a) Na-PHI structure; **(b)** AMX degradation for different irradiation times under white LED lamp.

[1] SILVA, Ingrid F. et al. Amoxicillin photodegradation under visible light catalyzed by metal-free carbon nitride: An investigation of the influence of the structural defects. *Journal of Hazardous Materials*, v. 401, p. 123713, 2021.

Agradecimentos/Acknowledgments

The authors are thankful for CNPQ, CAPES, FAPESP and UFSCar.

Photodegradation of acetaminophen as an emerging contaminants model by TiO₂ nanoparticles

Mariana Rodrigues Meirelles(PG)¹, Nirton Cristi Silva Vieira (PQ)¹, Elias de Barros Santos (PQ)¹, Raquel Aparecida Domingues (PQ)¹, Maraísa Gonçalves (PQ)¹

goncalves.maraisa@unifesp.br; radomingues@unifesp.br

¹Federal University of São Paulo, Science and Technology Institute, Talim Street, 330, São José dos Campos, SP, Zip Code: 12231-280, Brazil

Palavras Chave: *Photocatalyst, activated carbon, titanium dioxide, emerging contaminants.*

Highlights

- High photodegradation of acetaminophen by prepared TiO₂

Resumo/Abstract

Predictions of water crises have been highlighted in recent decades due to the high amount of inorganic and organic pollutants that have been released on a large scale in waters. An alternative to minimize the effects of pollutants is the removal of organic contaminants through photocatalytic conversion [1]. TiO₂ has been applied as a photocatalyst for the purpose mentioned above because it can generate radicals when subjected to solar or artificial radiation [2]. This work aimed to prepare semiconductors-based TiO₂ to study its photocatalytic effect in the degradation of paracetamol. The TiO₂ was prepared via the sol-gel method and the study of photocatalysts was divided into two stages: *i.* without the presence of hydrogen peroxide (H₂O₂) and *ii.* with the presence of H₂O₂ during the synthesis. In the first stage, the materials introduced via sol gel were calcined for 2 h at different temperatures. The results showed a phase change from anatase to rutile at high temperatures (650 °C). The correlation between calcination temperature, surface area and crystallite size was also verified. Materials calcined at 350, 400 and 450°C showed greater photocatalytic efficiency, removing 63, 62 and 57%, respectively. In the second stage, to verify the best photocatalytic activity, H₂O₂ was added to the synthesis and later the prepared TiO₂ was calcified at 350 and 450°C. For the temperature of 350 °C, the heat treatment time was varied by 2, 4 and 6 h. All prepared TiO₂ showed photocatalytic efficiency in the degradation of Paracetamol contaminant, with removal between 92% and 98%. TiO₂ calcined at 350 °C for 4 hours, TiO₂-H₂O₂-350_4h, demonstrated the highest photocatalytic efficiency.

References

- [1] Sophocleous M. Global and regional water availability and demand: prospects for the future. *Natural Resources Research*. 2004;13(2):61-75.
- [2] Hanafi MF, Sapawe N. A review on the water problem associate with organic pollutants derived from phenol, methyl orange, and remazol brilliant blue dyes. *Materials Today: Proceedings*. 2020;31:A141-A50.

Agradecimentos/Acknowledgments

The authors acknowledge the financial support received from the Brazilian Funding Institution FAPESP (2019/13471-8 and 21/02354-0).

Photodegradation of Rifampicin by PHI (poly heptazine imide) based catalysts

Vitor G. S. Pastana (PG),^{1*} Marcos A. R. Silva (PG),¹ Luís F. G. Noleto (PG),¹ Bruna R. Serino (IC),¹ Carla da Silva Cunha (IC),¹ Danielly T. S. Costa (PG) 1, Ivo F. Teixeira (PQ).¹

vitorgabrielpastana500@gmail.com; vitorgabrielpastana500@gmail.com

¹Department of Chemistry, UFSCar

Keywords: Emerging contaminants, Photodegradation, Carbon Nitride Based Catalysts

Highlights

Photodegradation of Rifampicin, an emerging contaminant, was investigated through the use of Fe-PHI photocatalyst in eco-friendly conditions. In less than 1h of reaction, 100% of substrate was degraded.

Resumo/Abstract

Emerging Contaminants belongs to a class of chemicals that do not yet have regulation by environmental agencies or have their danger to humans and the environment fully known. Rifampicin is an antibiotic used to treat bacterial infections, in which tuberculosis cases are their greatest application. Remediation of emerging contaminants are not always an easy task, precisely because of the lack of information about our target substance. Photocatalysts materials absorbs light and brings itself to higher levels of energy, allowing the reaction to occur. Carbon nitrides are one kind of newcomer materials, owning promising properties, making them an multifunctional platform for catalytic applications. Sorted structures of C_3N_4 , known as PHI (poly heptazine imides), have emerged as a high ordered and crystalline host option for Single Atoms. In Single-atom catalysts (SACs), the single atoms are isolated and stabilized by the support, in our case, Fe-PHI structures (**Fig. 1**). The preparation method of the support occurs through a thermal treatment of melamine with sodium chloride (NaCl), providing us Na-PHI structures. To obtain the catalyst in question, Fe-PHI, a cationic exchange of Na^+ ions for Fe^{3+} ions is performed, sonicating a quantity of material for 30 minutes with a $FeCl_3$ solution. The catalysts were characterized by HR-TEM, STEM-HAADF, XRD, FT-IR and UV-Vis. An eco-friendly method, using only an aqueous solution of Rifampicin, the heterogeneous catalyst and 410 nm LED irradiation was developed. First, the antibiotic was purchased in a local drugstore, extracted and isolated of the other components of the tablet with chloroform (solvent that it is soluble), filtered (the other unwanted compounds are not soluble in the chosen solvent) and then left to evaporate on heating, resulting in the target compound, and at the end, a 50 ppm red-orange colored aqueous solution was prepared. To the reaction apparatus, 10 mL of substrate and 30 mg of catalyst are used. To monitor adsorption effects, the solution is stirred in the dark for 10 minutes. Then a 50 W 410 nm LED irradiates the solution. Aliquots are taken at predetermined time intervals, filtered in a 0,45 μm filtration unit and analyzed by a UV-Vis Spectrophotometer. **Figure 2** shows the UV-Vis spectrum of rifampicin (black line), the reduction in 40 min of reaction without catalyst (red line) and in the presence of catalyst (blue line) in the same time interval. Under the conditions described, there was a significant reduction in the presence of rifampicin in the medium by the time of 40 min of irradiation (**Fig. 3**). The spectrum band chosen to follow the photodegradation is the visible one (600 nm - 400 nm). Despite the decrease in bands being observed, compounds that absorb in regions of shorter wavelength, which can be by-products, persist in the reaction medium. The role of the Fe-PHI photocatalyst in the removal of Rifampicin proved to be quite effective, although the degradation mechanism and degree of mineralization are still not fully understood, but establishing a potential for the future use of this catalyst in several other applications in emerging contaminants.

Fig. 1

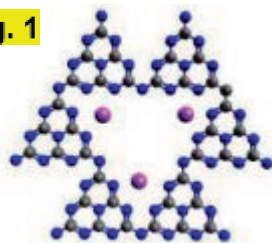


Fig. 2

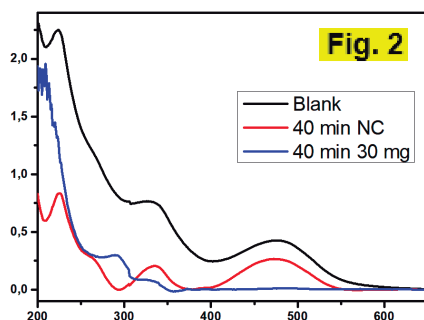
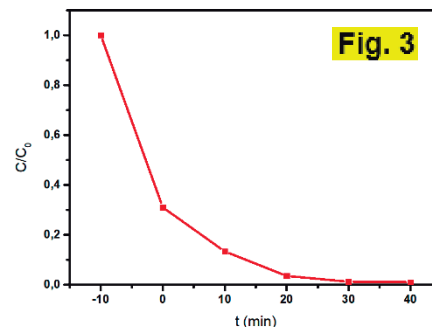


Fig. 3



Fe single-atoms in PHI structure (Fig. 1), adsorption bands of blank and reacted rifampicin (Fig. 2) and C/C_0 degradation curve along the time (Fig. 3).

Agradecimentos/Acknowledgments

Gratitude to the brilliant research group "Lablvo" and CAPES, FAPESP and UFSCar.

PM_{2.5} and metals determination in PM_{2.5} collected in São Paulo during the Covid-19 Pandemic

Camila N. Farias (PG),¹ José V. Martins (TC),² Pérola de C. Vasconcelos (PQ).^{1*}

camila.farias@usp.br

¹Instituto de Química, Universidade de São Paulo (IQ-USP); ²Instituto de Geociências, Universidade de São Paulo (IGc-USP)

Palavras Chave: Particulate Matter; Covid-19; Pandemic; Air Pollution

Highlights

Fifty PM_{2.5} samples were collected during quarantine in São Paulo (March to August 2020). Trace elements determination was performed by ICP-MS and enrichment factors were calculated.

Resumo/Abstract

In 2020, the covid-19 pandemic challenged global health systems. To contain the advance of virus transmission, social isolation with different levels of restriction were adopted in several countries, including Brazil, promoting a reduction in the anthropogenic activity. The vehicular traffic reduction and activities of some industries led to a decrease in atmospheric pollution. To assess the effects of social restriction measures on air quality, fifty PM_{2.5} samples were collected (from March to August, 2020) in São Paulo at a site in the University of São Paulo campus (urban area), using a high volume sampler and quartz fiber filters. Trace elements in PM_{2.5} were determined by ICP-MS after microwave acid extraction.¹

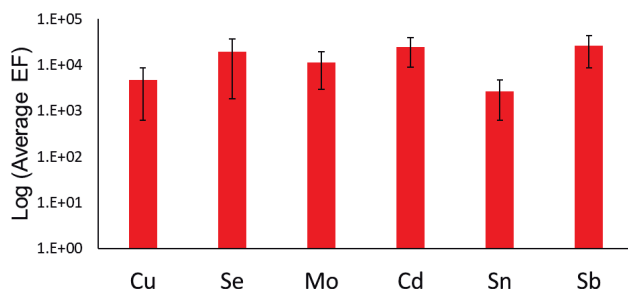


Figure 1. Enrichment factors for trace elements in PM_{2.5}

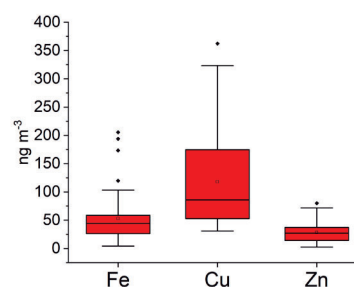


Figure 2. Major elements in PM_{2.5}

Enrichment factors (EFs) were calculated and Fe was considered as a reference element due to its greater abundance in the crust. Fig.1 presents the elements with higher EFs. Cu, Zn, As, Se, Rb, Mo, Cd, Sn, Sb and Pb presented EFs>10, indicating influence of anthropogenic emissions, such as industries, non-exhaust emissions (e.g. brake and tire wear) and fuel combustion.^{1,2} V, Ti, Cr, Mn, Ni, Ba and Sr showed EFs<10, indicated that soil dust resuspension was the main source.² Cu (95 ng m⁻³), Fe (45 ng m⁻³) and Zn (27 ng m⁻³) presented higher concentrations in PM_{2.5} (Fig. 2). Mo, Sn and Sb are mainly related with brake wear emissions.^{2,3,4} Cu is associated with brake wear and, ethanol use and gasohol emissions (engine corrosion)², and Cd and Se are associated with combustion sources.⁴ These results indicate that during the period of social restriction, anthropogenic emissions from industrial activities and vehicular traffic contributed to metal enrichment in PM_{2.5}, despite of the lower concentrations than previous studies.² PM_{2.5} concentrations ranged from 5 to 35 µg m⁻³, median concentration was over 17 ng m⁻³.

REFERENCES

- [1] **Sci. Total Environ.**, 856, 159006, 2023.
- [2] **Atmos. Chem. Phys.**, 17, 11943-11969, 2017.
- [3] **Atmos. Environ.**, 176, 60-70, 2018.
- [4] **Atmos. Environ.**, 99, 257-265, 2014.

Agradecimentos/Acknowledgments

The authors thank CAPES (Project 2017/20826-1), CNPq (Project 301503/2018-4) and METROCLIMA (Project 2016/18438-0).

46ª Reunião Anual da Sociedade Brasileira de Química: "Química: Ligando ciências e neutralizando desigualdades"

Área: AMB

(Inserir a sigla da seção científica para qual o resumo será submetido. Ex: ORG, BEA, CAT)

Polycyclic aromatic hydrocarbons (PAHs) in street dust of Belém, Pará, Brazil: Particle size distribution, sources and cancer risk assessment

Thalita de Moura Negrão (PG), Annibal D. Pereira Netto (PQ)

annibal.netto@id.uff.br

Programa de Pós Graduação em Química, Instituto de Química, UFF
LaQAFa, Instituto de Química, UFF

Palavras Chave: PAHs, Particle-size distribution; Source evaluation, Cancer risk assessment

Highlights

Evaluation of PAHs in street dust samples of Belém, Pará, Brazil
The distribution of PAHs and their total concentrations varied according to the fraction size
Pyrogenic PAHs seem to predominate in the samples and fractions

Resumo/Abstract

Belém, PA is a tropical Brazilian city located in the North Region of Brazil and characterized by tropical humid weather with around 1,5 million people. Samples of street dust (SD) were collected in different urban areas of Belém in two periods: August 2020 and January 2023. Samples were treated and analyzed for eighteen polycyclic aromatic hydrocarbons (PAHs) (the sixteen EPA-PAHs, and benzo[e]pyrene and perylene) as described elsewhere (Franco et al., 2017). Briefly, the samples were dried, sieved and fractioned in different sizes, and extracted in an ultrasonic bath using 3 portions of dichloromethane. Individual extracts were combined, reconcentrated by rotary evaporation, and analyzed by gas chromatography coupled to mass spectrometry, under optimized conditions using a DB-17 column and perdeuterated internal standards. Adequate analytical figures of merit were found for all PAHs. Coefficients of determination were larger than 0,98 and limits of quantification were lower than 1 ng g⁻¹. PAH concentrations varied widely from <LOQ up to several tens of ng g⁻¹. Some PAHs predominated (anthracene, fluoranthene, and pyrene) predominate in most samples but individual PAH concentrations and total PAH concentration seemed to be not related to the sample fraction size. Carcinogenic PAHs (such as benzo[a]pyrene, benzo[a]anthracene, benzo[b]fluoranthene and benzo[k]fluoranthene) were also observed in many samples. Calculations of cancer risk assessment are being carried out.

Agradecimentos/Acknowledgments

CNPq (Projects 312288/2017-4, 315480/2020-3 and 420351/2016-7), CAPES
Lais Ferreira for her kind help in some laboratory activities

Reference:

Caroline F. J. Franco, Michele F. de Resende, Leonardo de A. Furtado, Taila F. Brasil, Marcos N. Eberlin, Annibal D. Pereira Netto. Polycyclic aromatic hydrocarbons (PAHs) in street dust of Rio de Janeiro and Niterói, Brazil: Particle size distribution, sources and cancer risk assessment. *Sci. Total Environ.* 599–600 (2017) 305–313

QUALI-QUANTITATIVE IDENTIFICATION OF MICROPLASTICS IN PUBLIC SUPPLY WATER IN THE REGIÃO METROPOLITANA DE BELÉM – PA

Naiara H. F. Braz (IC),^{1*} Eduardo C. R. Neto (IC),^{1,2} Fabíola R. D. de Souza (IC),¹ Andréia C. Pereira (PQ).¹

andreiaqmc@hotmail.com; naiarahelena2010@gmail.com

¹Faculdade de Geologia, UFPA; ²Bolsista PET-Geologia, UFPA.

Keywords: Microplastics, Public Supply Water, Tap Water.

Highlights

- The consumption of tap water as a means for the ingestion of microplastics.
- Absence of legislation for the control of microplastics in supply water.

Abstract

Microplastics (MP) are polymeric particles smaller than 5 mm that can be observed in different environments (e.g. air, water and soil). These microparticles can be disposed of in the domestic sewage reaching the Sewage Treatment Stations (ETEs). Due to its size, the presence of MP in water from treatment plants and therefore in tap water is possible. Currently, there is not reference in legislation for filtering and/or controlling MP in public supply water, however recent studies have shown that many MP contain chemical substances used to change their properties or colors and many of them have toxic or endocrine disrupting characteristics. MP can also attract other pollutants (e.g. metals and some pesticides). Although it is not habit to drink tap water, it is not uncommon for a portion of the population to drink tap water directly. Furthermore, water is used for cooking, which may contribute to MP ingestion, and heating may release substances adhered to the surface of microparticles. The aim of this work is the identification and characterization of MP in public water supply of the Metropolitan Region of Belém (RMB), regarding their shapes, colors and quantity. The public supply water of the RMB was sampled using glass bottles with capacity for 1 L and filled with tap water from houses of different neighborhoods the RMB, totaling 13 samples, 11 from Belém and 2 from Ananindeua. Samples were passed through a 63 µm sieve to retain MP. Then, they were transported to a becker, in which was added 20 mL of hydrogen peroxide and of iron(II) sulfate solution in acidic medium with concentration of 6 g/L in order to remove organic matter. These solutions were heated up to 60°C and maintained in this temperature for 30 minutes. After cooling, the solutions were filtered under vacuum using Whatman® glass microfiber filters (GF/C) with 1.2 µm pore size and 47 mm diameter. Lastly, the filters were placed in petri dishes and covered with aluminum paper. MP were observed and described using stereomicroscope with magnification up to 6 times. The Figure 01 presents the distribution of microplastics in the samples of cities of RMB based on shapes and colors of MP. As a result, it was observed that all samples presented MP e the amount found ranged from 145 to 613 microparticles per liter. Mostly, the MP found were in the form of fibers and transparent. Also, it is noticeable there is a variety of colors, highlighting yellow and blue shades. The white nodular fragments found might be signs of polystyrene fragmentation, although that cannot be confirmed only by visual characterization, further chemical analysis might be carried out. Considering the potential consequences of MP for human organisms, the data obtained reinforce the need to improve the efficiency of ETEs for a better retention efficiency of microplastics as well as the need to search for alternatives to reduce the generation of these microparticles.

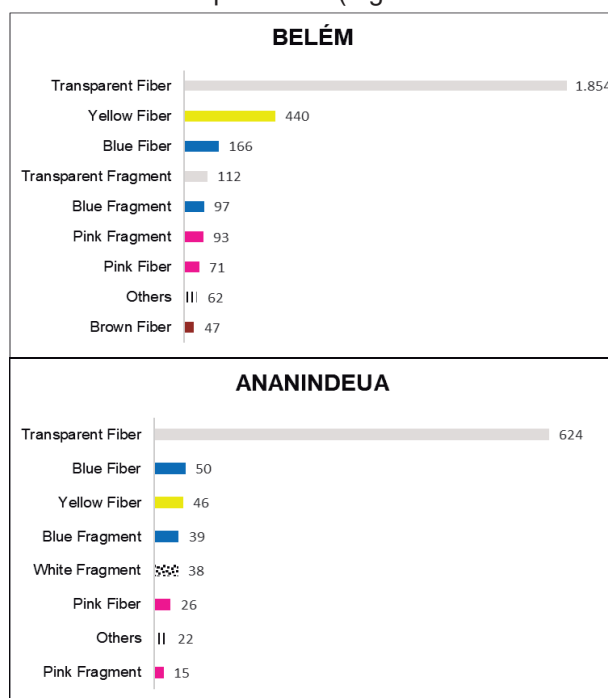


Figure 01 – Distribution of shapes and colors of microplastics in the samples.

Acknowledgments

To the Chemical Analysis Laboratory (IG/UFPA) and the people involved in the samples collection.

QUALI-QUANTITATIVE IDENTIFICATION OF MICROPLASTICS IN SEDIMENTS FROM THE EAST MARGIN OF BAÍA DO GUAJARÁ, BÉLEM – PA

Eduardo C. R. Neto (IC),^{1,2*} Naiara H. F. Braz (IC),¹ Fabíola R. D. de Souza (IC),¹ Andréia C. Pereira (PQ).¹

eduardo2012_net@hotmail.com

¹Faculdade de Geologia, UFPA; ²Bolsista PET-Geologia, UFPA.

Keywords: *Microplastics, Estuarine Sediments, Baía do Guajará.*

Highlights

- Microplastics in estuarine sediments are results of modern pollution and inadequate plastic disposal.

Abstract

Microplastics (MP) are small fragments of synthetic polymers with size under 500 μm and can be found in many environments such as beach sediments, oceans, rivers and potable waters, atmosphere and even human blood, according to various researches. These particles occur in all these environments due mainly to inadequate plastic disposal and inefficient public management of the population waste. Some of these polymers can release toxic substances into the environment. This paper consists in the identification of MP in sediments and their morphology classification in order to collaborate with the acknowledgment of these particles and understand how they present themselves in the geological environment. The sediments were sampled in the east margin of Baía do Guajará, an estuarine channel that bathes the western portion of Belém city. They were collected in two locations: The Icoaraci district and the tourist complex of Ver-o-Rio. In total, six samples were assembled, three in each location. The samples were collected along three portions of the area with two meters spaced apart, in average, from the tide line towards the city coast. The methodology for extracting the MP in laboratory includes the drying of the samples in laboratory oven and their weighing in analytical balance, which were around 100 g. Then, 200 mL of NaCl solution 25% was added to the beakers with the sediments and it was stirred for 3 minutes and then rested for 5 minutes. This process was repeated 5 times with each sample. After, the supernatant solution was passed in a 63 μm sieve to retain the MP particles in suspension. 20 mL of hydrogen peroxide and of iron(II) sulfate solution in acidic environment with concentration of 6 g/L were added in order to remove organic matter. These solutions were heated up to 60 °C and maintained in this temperature for 30 minutes. Afterwards, the solutions were passed through glass filters with 47 mm of diameter in a vacuum pump to contain the MP. Finally, the filters were placed in petri dishes and the MP were observed and described using stereomicroscope with magnification up to 6 times. All of the 6 samples presented MP and they were mainly perceived as fibrous and fragmented shapes in a variety of colors, as displayed in the bar graphs in Figure 01. In both samples, around 80% of the small polymers were recognized as thin curvy fibers and around 70% were transparent or translucent, which might indicate a possible provenance of a type of polymer widely used by the population. Also, when present, yellow and blue seem to be the most common colors in these particles. Comparing the amount of MP in each sample, in both locations it was noticed that their quantity in the sediments increases towards the Baía do Guajará, which relates to the coastal line dynamics and their association with the sediments into the estuarine channel. The identification of a variety of types and colors of MP and a big number of these particles found in these urban environments show that they do not disappear from the space, on the opposite, it tends to fragment into smaller pieces and to spread around into the geological and biological systems, evidencing the increasing need of the population to reduce the pollution of these natural spaces. Further chemical and image analyses might contribute with the characterization and identification of the types of polymers present in these sediments.

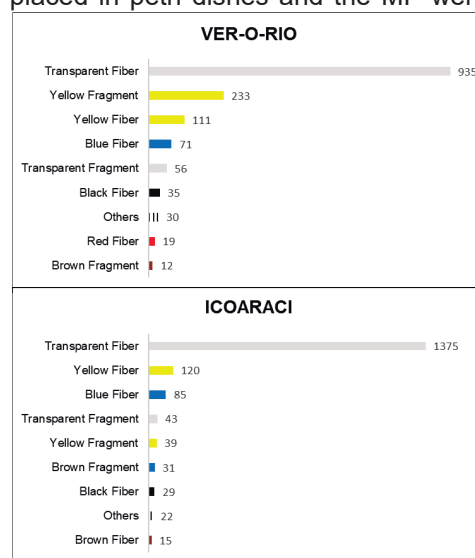


Figure 01 – Distribution of the morphology and quantity of the microplastics from Icoaraci and Ver-O-Rio.

Acknowledgments

To the Chemical Analysis Laboratory and Pará-Iso Laboratory of IG/UFPA.

Removal of malachite green dye in water by adsorption on green coconut husks activated carbon

Natália Pinheiro Pimentel (IC)¹, Larissa Silva de Oliveira Mota (PG)^{1,2}, Bruno Salarini Peixoto (PQ)², Marcela Cristina de Moraes (PQ)^{1,2}

nataliapinheiro1475@gmail.com

¹BioCrom, Departamento de Química Orgânica, UFF; ²Programa de Pós-Graduação em Química, UFF

Palavras Chave: *activated carbon, adsorption, dye, malachite green, green coconut*

Highlights

An abundant Brazilian urban waste is used to produce the activated carbon. Activated carbon demonstrates a great ability to remove malachite green dye.

Abstract

Water contamination by organic pollutants has drawn much attention since they can generate several adverse effects on exposed organisms. Among these substances, dyes are worth mentioning due to their ability to block the passage of light through water, hindering photosynthesis and, consequently, affecting the entire aquatic ecosystem. In addition, dyes can have toxic, carcinogenic, and teratogenic effects (1). A promising strategy for removing these pollutants is through adsorption with activated carbon. These materials can be produced from the pyrolysis of lignocellulosic biomass, such as agro-industrial wastes, which makes its production economically viable and environmentally friendly. Thus, the objective of this work is to evaluate the adsorption of the malachite green model dye on activated carbon obtained from the husk of green coconut.

Activated carbon was previously produced in the research group through the pyrolysis of green coconut shell impregnated with H_3PO_4 at 500 °C for 2 hours (2). The characterizations of the material showed that it has a high surface area ($1242 \text{ m}^2 \cdot \text{g}^{-1}$) and a pH_{pzc} of 2, due to many oxygenated groups on its surface. For the quantification of malachite green dye by spectrophotometry, an analytical curve was constructed. For this, dye solutions in ultrapure water in the range of $1\text{-}10 \text{ mg} \cdot \text{L}^{-1}$ were prepared, in triplicate, and the absorbances were evaluated at 615 nm in a Jasco V-730bio spectrophotometer. The analytical curve was validated on 3 different days, using the precision, accuracy, and linearity criteria recommended by ANVISA (3). As for the adsorption tests of malachite green by activated carbon, they were carried out in batches. To evaluate the adsorption kinetics, 10 mL of dye solution in ultrapure water ($125 \text{ mg} \cdot \text{L}^{-1}$) was added to flasks containing 5 mg of biochar, and the mixture was stirred in a thermostatic bath at 180 rpm and 25°C for times ranging from 1 to 48 hours, in triplicate. Then, the samples were filtered and diluted for further analysis in the spectrophotometer. As can be seen in Figure 1, the adsorption rate increases considerably in the first 6 hours of agitation from that time on, it is observed that the adsorption rate slowly decreases until equilibrium is reached, in 24 hours. In equilibrium, activated carbon showed a great ability to remove the dye, but studies will still be carried out to evaluate the maximum adsorptive capacity of the material through the adsorption isotherm. Plotting the kinetic adsorption models showed that the pseudo-first order model ($R^2=0.97755$) is more representative for this system compared to the pseudo-second order model ($R^2=0.87999$), which means that external or intraparticle diffusion is a limiting step of adsorption kinetics.

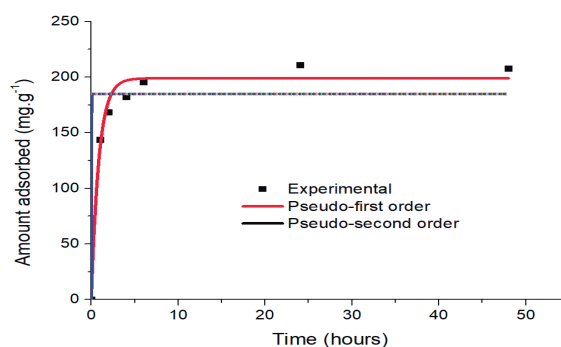


Figura 1. Adsorption kinetics of malachite green dye by activated carbon from green coconut shell

Acknowledgments

CAPES, CNPQ, and FAPERJ

References

- (1) Tkaczyk, A. et al. Synthetic organic dyes as contaminants of the aquatic environment and their implications for ecosystems: A review. In: Science of The Total Environment. 2020.
 - (2) Peixoto, B. S. et al. Adsorbent magnetic materials based on green coconut husks biochar and superparamagnetic iron oxides. In: 43ª Reunião Anual Virtual da SBQ. 2020.
 - (3) ANVISA. RDC Nº 166, de 24 de julho de 2017
- 46ª Reunião Anual da Sociedade Brasileira de Química: "Química: Ligando ciências e neutralizando desigualdades"

Removal of nitrate from aqueous solutions by adsorption processes on clay-carbon composites

Lucas G. dos Santos (PG),¹ Wagner A. Carvalho (PQ),^{1*} Dalmo Mandelli (PQ),¹ Pedro S. Fadini (PQ).^{2*}

lucas.gorito@ufabc.edu.br; wagner.carvalho@ufabc.edu.br.

¹ Center for Natural and Human Sciences (CCNH), Federal University of ABC (UFABC), Santo André – SP, Brazil; ² Chemistry Department (DQ), Federal University of São Carlos (UFSCar), São Carlos – SP, Brazil.

Keywords: adsorption, nitrate, clays, biochar, tertiary treatment.

Highlights

The presence of nitrate in water bodies is an unmistakable sign of contamination. Its removal prevents eutrophication processes. The use of a clay-carbon composite represents a natural alternative.

Abstract

Nitrate is a pollutant present in most surface and groundwater, being used worldwide as a contamination indicator due to its high mobility, which allows it to reach large areas. Excess nitrate in aquatic environments poses a potential threat to ecosystems and human health, contributing to eutrophication and even causing severe methemoglobinemia. The nitrate potability pattern for human consumption, established by the Ministry of Health, is 10 mg/L as nitrogen (N-NO₃⁻).¹ Conventional biological sewage treatment systems are designed to remove solids and dissolved organic matter, respectively identified as primary and secondary treatment, resulting in effluents with nitrogen concentrations close to those of raw sewage. Thus, the present work aimed to evaluate the retention behavior of nitrogen in the nitrate form present in synthetic effluents by adsorbents developed from glycerol's carbon, FeCl₃ and sewage sludge treated with TechPhos® (an adsorbent used in the removal of phosphorus from domestic effluents). Furthermore, the effect of the insertion of nitrogenous functional groups on the retention of nitrate was investigated, through a thermal treatment under NH₃ flow (ammonization) on the surface of the solids.^{2,3} Glycerol's carbon obtained by hydrothermal carbonization in the presence of H₂SO₄ and FeCl₃(s) did not show significant nitrate retention capacity (≈0.6%). However, the ammonization of this material considerably altered its behavior, allowing it to reach 27% of nitrate retention, indicating that there was insertion of N groups on the surface of the solid. In addition, the higher the ammonia content in the solid treatment gas, the better the performance against nitrate (for example, the TechPhos®-Sludge composites pyrolyzed under a 5% NH₃/He flow showed nitrate adsorption values lower than 2%). The literature indicates that the presence of positive charges due to different metallic ions or -NH₃⁺ and -OH₂⁺ groups on the surface of adsorbents promotes the attraction of anions in solution.⁴ Thus, the processes of ammonization of the composite containing sewage sludge are being investigated and optimized, since this can be easily carbonized and subsequently ammonized. The composite will represent an important source of nutrients, as it combines both phosphorus and nitrogen retention processes.

¹ Varnier, C. 1. ed. São Paulo: SIMA/IG, 2019; ² Shafeeyan, M. S. *et al* *Fuel*, v. 94, pp. 465-472, 2012; ³ Kumar, I.A; Viswanathan, N. *Ind Eng Chem Res*, v. 58, no. 47, pp. 21521-21530, 2019; ⁴ H.T. Banu, H.T, *et al*. *Int J Biol Macromol*, v. 130, pp. 573-83, 2019

Acknowledgments



REMOVAL OF RHODAMINE-B FROM WATER USING RICE HUSK BIOCARBON

Sedami T. R. Agassin (PG)*, Mirlene P. Vitorino (PG), Karine P. Naidek (PQ), Alexandre T. Paulino (PQ)

alexandre.paulino@udesc.br; romainagassin@gmail.com

Universidade do Estado de Santa Catarina, Departamento de Química, Rua Paulo Malschitzki, 200, Zona Industrial Norte – Joinville/SC

Keywords: Sorption; Removal, Rice husk biocarbon; Rhodamine B, Water treatment, Textile industry.

Highlights

-Sorption of pollutant in rice husk biocarbon by varying time of contact, mass of adsorbent, pH, initial concentration, temperature, and stirring was performed.

-Thermodynamic study confirmed a spontaneous sorption process ($\Delta G_{ads} < 0$), being favored by increase in temperature.

-Enthalpy variation indicated exothermic sorption process, with removal of Rhodamine B by physisorption.

Introduction

Rice husk biochar to promote the sorption and removal of Rhodamine B (RB) from water. In this case, the sorption phenomena can be evaluated via kinetic and thermodynamic results, involving chemical and physical

interactions. The success of this methodology generates social numerous benefits, such as clear water and friendly environment for populations.

Results and Discussion

The sorption capacity of rice husk biochar for RB observed in Figure 1 can be explained by the point of zero-charge of the sorbent, as well as by the molecular structure of the dye. Higher sorption capacity was determined with the increase of the sorption time, with saturation of the sorbent structure after 200 min. Moreover, when the pH of the dye solution is lower than the zero-charge point of the sorbent, which was lower than 9.75, the sorbent surface is positively charged. Based on the studies performed in the current work, rice husk biochar is an efficient sorbent for RB, with the experimental part organized by factorial design to optimize the study.

It is also possible to observe that the RB sorption capacity has been increased when the pH varied from 3.50 to 4.04, as the surface of carbons present in the biochar is negatively charged due to the deprotonation of functional groups on the surface of the adsorbent material, such as OH ion, improving sorption through electrostatic attraction (AHMAD; SMOKE. 2010). As RB is a cationic dye, its sorption is theoretically favored at pH values above the point of zero-charge, that is, above 9.75. However, there is an opposite effect because RB can be in its zwitterionic form as showed in Figure 2.

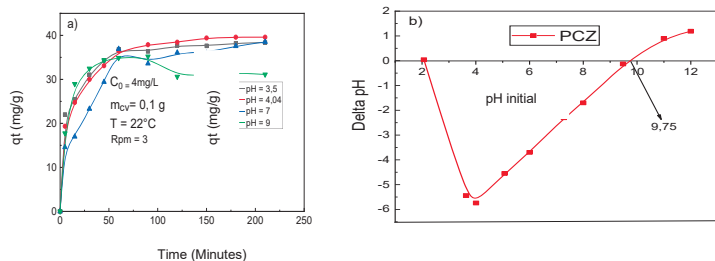


Figure 1 - Effect of pH on the sorption process of RB (a) and point of zero charge for rice husk biochar (b).

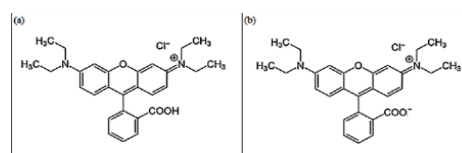


Figure 2 - Molecular structure of Rhodamine B in its cationic (a) and zwitterionic form (b).

The zwitterionic form of the molecule is globally neutral in its load, however, it has a local load due to the presence of its ionizing groups (PETROSYAN; KHOLIN, 2004).

Conclusion

Rice husk biochar is an excellent sorbent for dyes, with percentage of RB removal of 98%. Water could be purified by filters containing rice husk biochar as ecofriendly sorbent.

Acknowledgments

FAPESC, CNP, CAPES

REFERÊNCIAS

AHMAD, R.; FUMAR, R. Journal of Environmental Management, v. 91, n. 4, p. 1032-1038, 2010.

PETROSYAN, N. O. M.; KHOLIN, Y. V. Russian Journal of Applied Chemistry, v. 77, n. 3, p. 414-422, 2004

Sorção de ácido 2,4-diclorofenóxido acético em hidrogel de pectina modificado com dióxido de titânio

André L.D. Santos (IC), Carolina Kuberesky (IC), Carolina Lona (IC), Mirlene P. Vitorino (PG), Karine P. Naidek (PQ), Alexandre T. Paulino (PQ)*

*E-mail: andre.lsantos0202@gmail.com ; alexandre.paulino@udesc.br

Universidade do Estado de Santa Catarina, Centro de Ciências Tecnológicas, Departamento de Química, Rua Paulo Malschitzki, 200, Zona Industrial Norte – Joinville/SC, Brasil

Highlights

- Synthesis of pectin hydrogel modified with TiO₂ for 2,4-D acid sorption at different pH values;
- Possibility of photodegradation of pollutants using pectin hydrogels containing metallic oxides.

Resumo/Abstract

O objetivo desta pesquisa foi desenvolver uma estratégia de limpeza de corpos hídricos contaminados por herbicidas como o ácido 2,4-diclorofenóxido acético (2,4-D). Esse herbicida é um composto de baixo custo e amplamente usado no controle de ervas daninhas em culturas agrícolas. Além disso, seu uso é muito comum em regiões que têm solos pobres em nutrientes e pouca biodiversidade. As culturas mais comuns que recebem esse tipo de herbicida são as culturas de milho, soja e arroz. Porém devido a sua solubilidade, o 2,4-D acaba contaminando o solo, o ar e a água com facilidade, e consequentemente contaminando os seres humanos, causando danos à saúde pública (ECYCLE, 2023). Como alternativa para remover este pesticida das águas, pode ser utilizado hidrogéis de polissacarídeos naturais.

Hidrogéis são compostos macromoleculares formados por uma ou mais redes poliméricas tridimensionais que se ligam através de interações físicas ou ligações químicas (geralmente ligações covalentes) (AOUADA e MATTOSO, 2009). Portanto, os hidrogéis são hidrofílicos e insolúveis, ou seja, são ótimos em absorver e reter água. Sua rede tridimensional hidrofílica proporciona a capacidade de absorver de 20% a até 100% de água em relação a sua massa original seca (ARTIFON, VARNIER E PAULINO, 2017).

Para a síntese do hidrogel estudado neste trabalho foi primeiramente realizada a modificação química da pectina com metacrilato de glicidila com o objetivo de adicionar grupos vinílicos a sua estrutura. O processo de reticulação foi realizado utilizando persulfato de potássio e poliácridamida. A modificação do hidrogel de pectina foi realizada com diferentes proporções de dióxido de titânio (1, 5 e 10% em relação à massa total da solução). Todos os hidrogéis produzidos foram utilizados para a sorção de 2,4-D em solução em diferentes valores de pH, avaliando como essa variável pode afetar a sorção na aplicabilidade do hidrogel no mundo real. Esse tipo de hidrogel é um potencial candidato para a realização de estudos de fotodegradação de poluentes em água devido a presença de dióxido de titânio em sua rede polimérica tridimensional.

Os estudos de sorção do 2,4-D foram realizados de modo a determinar qual composição do hidrogel possui a maior capacidade de reter o poluente, e se o valor de pH afeta a sorção, os estudos foram realizados nos valores de pH 3,0; 4,5; 5,5; 6,5; 7,5 e 9,0. Com a variação do pH foi possível estabelecer uma condição para a remoção do poluente e verificar a interferência de tal parâmetro na sorção em um efluente real. Além disso, outras condições experimentais foram controladas para os estudos de sorção, incluindo a massa de 100 mg de hidrogel seco, percentagens de dióxido de titânio de 0, 1, 5 e 10%, tempo de sorção de 24h e volume de solução de 100 mL com concentração de 2,4-D de 50 mg L⁻¹. A quantificação do herbicida no meio foi realizada por espectrofotometria de absorção molecular (UV-Vis). Com isso foi possível concluir que a concentração de dióxido de titânio na estrutura do hidrogel e o pH da solução não alteram de forma significativa a sorção de 2,4-D no meio, com uma eficiência de remoção em todos os experimentos superior a 90%, um ponto favorável pois amplia o leque de aplicabilidade em condições reais. Isso confirma que todos as composições de hidrogéis testadas são eficientes para a sorção desse poluente, o qual poderia ser fotodegradado durante um processo de purificação de água por fotodegradação.

AOUADA, Fauze Ahmad; MATTOSO, Luiz Henrique Capparelli. Hidrogéis biodegradáveis: uma opção na aplicação como veículos carreadores de sistemas de liberação controlada de pesticidas. 2009.

ECYCLE. Conheça o herbicida 2,4-D e seus impactos.

VARNIER, Karine; ARTIFON, S. E. S; PAULINO, Alexandre Tadeu. Cinética de intumescimento de hidrogéis magnéticos constituídos de polissacarídeos. 2017.

Agradecimentos/Acknowledgments

CNPq, CAPES, FAPESC

Área: AMB*(Inserir a sigla da seção científica para qual o resumo será submetido. Ex: ORG, BEA, CAT)***Sorption differences of pesticides onto sand and polyethylene microplastics****Karen N. Morishita (PG),* Cassiana C. Montagner (PQ)****k171389@dac.unicamp.br***Analytical Chemistry Department, Institute of Chemistry, University of Campinas, Campinas, São Paulo, Brazil*Palavras Chave: *Microplastic, Sand, Sorption, Pesticide.***Highlights**

Sorption of imidacloprid and hexazinone was higher onto polyethylene microplastic than onto sand. It shows microplastics can interfere in aquatic systems' dynamics.

Resumo/Abstract

Introduction: Microplastics, small plastic particles (<5 mm), have been considered ubiquitous in the environment¹. The efforts to understand their potential harm to the environment include numerous studies about their role as sorbents of organic pollutants². However, it must be taken into consideration that sorption of substances also happens onto non-anthropogenic source sorbents, such as soil. This work aimed to understand if sand and polyethylene microplastics have different sorption capacities in aqueous solution. Two pesticides present in Brazilian surface waters were studied: imidacloprid and hexazinone³.

Materials and methods: Sand sample collected in Juquehy beach (SP – Brazil) and pristine polyethylene microplastics were used as sorbents. 3 mL of an ultrapure water contaminated with 50 µg L⁻¹ imidacloprid and hexazinone was kept in contact with 30 mg of sorbent for 96 h. After filtration, the solutions were analyzed in HPLC-DAD in a previous validated method to quantify these analytes. Decrease in concentration was calculated as sorption onto the sorbents.

Results and discussion: Polyethylene microplastics showed higher sorption efficiency (10 and 16% for imidacloprid and hexazinone, respectively) than sand (<1% for both pesticides) as shown in Figure 1. Studies that have also sought to compare sorption of organic pollutants onto microplastics and natural sediments also found that microplastic has higher sorption capacity⁴⁻⁶. On the other hand, when compared to other river sediments such as ash and charcoal, sorption onto microplastics was smaller⁷. Therefore, evaluating the impact of the presence of microplastics in a system must take into account the polymer type, composition of soil and matrix.

Conclusion: Polyethylene microplastics may alter imidacloprid and hexazinone dynamics in a sand environment in ultrapure water due to its higher sorption capacity.

References: 1 - Rochman, C. M. (2018) *Science* 360: 28–29. | 2 - Montagner, C. C. *et al.* (2021) *Quím. Nova* 44: 1328–1352. | 3 - Acayaba, R. D. *et al.* (2021) *Environ Sci Pollut Res* 28: 9824–9835. | 4 - Teuten, E. L. *et al.* (2007) *Environ. Sci. Technol.* 41: 7759–7764. | 5 - Wang, W.; Wang, J. (2018) *Ecotoxicol Environ Saf.* 147: 648–655. | 6 - Chen, X. *et al.* (2021) *Chemosphere* 263: 127947. | 7 - Fatema, M.; Farenhorst, A. (2022) *J. Soil Sediments* 22: 1876–1884.

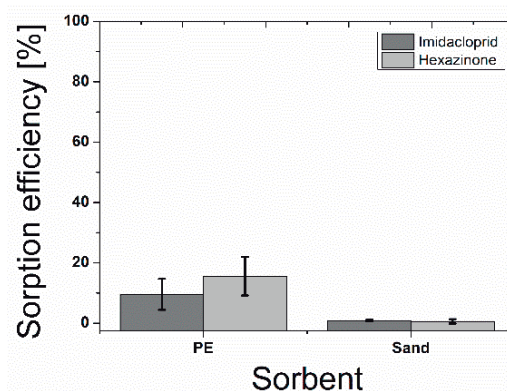


Figure 1. Sorption efficiency of imidacloprid and hexazinone onto sand and polyethylene microplastics (PE)

Agradecimentos/Acknowledgments

We would like to thank CAPES and INCTAA for funding this research.

SORPTION KINETIC OF RHODAMINE B IN BIOCARBON

Mirlene P. Vitorino (PG), Sedami T. R. Agassin (PG)*, Karine P. Naidek (PQ), Alexandre T. Paulino (PQ),
 mirlene.vitorino19@gmail.com; romainagassin@gmail.com

Universidade do Estado de Santa Catarina, Departamento de Química, Rua Paulo Malschitzki, 200, Zona Industrial Norte – Joinville/SC

Keywords: Sorption; Kinetic; Biocarbon; Rhodamine B, Water.

Highlights

- Sorption kinetic was studied after interaction of rhodamine B with rice husk biocarbon at different sorption times.
- Kinetic models were employed to evaluate the resistance to mass transfer of rhodamine B from water to sorbent structure.
- Pseudo-second order and Elovich kinetic models, as well as Langmuir isotherm are efficient to explain the experimental results.

Introduction

Sorption processes involving pollutants in aqueous solutions can be explained by sorption kinetic and isotherm models. These types of studies are important to provide information about sorbent-sorbent, sorbent-sorbate, and sorbent-solution interactions, in addition to possibility of determination of the efficiency of the sorption process (MUKHERJEE *et al.*, 2007). Either the rate constant or sorption rate can also be evaluated in these types of studies as described elsewhere (NOROUZI *et al.*, 2018). Kinetic and isotherm models are affected by various parameters, including diffusion. Different models are normally used for defining the proper mechanism controlling sorption.

Results and Discussion

The sorption kinetic of rhodamine B (RB) in biocarbon was studied for 250 min by considering pseudo-first order, pseudo-second order, intraparticle diffusion, and Elovich kinetic models. Some results of the kinetic studies are presented in Figures 1 and 2.

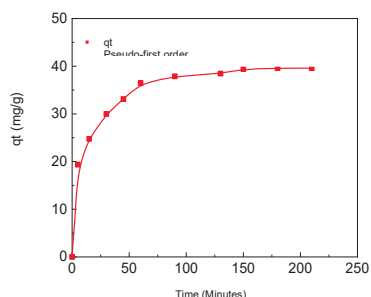


Figure 1 - Pseudo-first order sorption kinetic on optimized experimental conditions: temperature of 22°C; adsorbent mass of 0.1 g, pH = 4.04, $C_0 = 4 \text{ mg L}^{-1}$ and stirring of 3 rpm for 250 min.

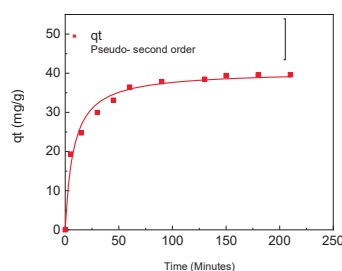


Figure 2 - Pseudo-second order sorption kinetic on optimized experimental conditions: temperature of 22°C; adsorbent mass of 0.1 g, pH = 4.04, $C_0 = 4 \text{ mg L}^{-1}$ and stirring of 3 rpm for 250 min.

The nonlinear pseudo-second order, nonlinear Elovich kinetic models confirmed the best fits for the results, with a q_{max} (experimental) of 39.40 mg g^{-1} and q_{max} (calculated) of 40.56 mg g^{-1} .

Conclusion

The sorption process of RB using rice husk biocarbon is efficiently described by pseudo-second order and Elovich kinetic models, as well as Langmuir isotherm. It implies in a maximum sorption capacity of approximately 56.18 mg g^{-1} .

Acknowledgments

FAPESC, CNPq, CAPES

REFERÊNCIAS

- MUKHERJEE, S. *et al.* **Chemical Engineering Journal**, v.129, p. 133–142, 2007.
 NOROUZI, S. *et al.* **Bioresource Technology**, v. 258, p. 48-56, 2018.

Study of air quality in homes that use rudimentary wood-burning stoves for cooking

Luiz Felipe de M. C. Da Silva(PG)¹, Alex R.H. De La Cruz(PQ)¹, Adriana Gioda(PQ)^{1*}

*agioda@puc-rio.br

¹Chemistry Department, Pontifícia Universidade Católica do Rio de Janeiro, Gávea – RJ

Key words: Household air pollution, Particulate matter, Firewood

Highlights

Use of firewood for cooking; air pollution in indoor and outdoor environments; Emission of particulate material from biomass burning.

Abstract

The process of complete combustion only takes place in ideal situations. The burning of solid fuels, such as firewood, releases several pollutants, including carbon monoxide (CO), formaldehyde (HCHO), nitrogen oxides (NO_x), volatile organic compounds (VOC) and particulate matter (PM_{2.5} and PM₁₀), present in the smoke released¹. The situation is aggravated to the extent that the combustion takes place inside or around homes in rustic stoves with inefficient burning. This is because it exposes residents to high levels of pollutants in the home environment on a daily basis, especially women and children. According to WHO data², 3,2 million people die prematurely each year from diseases related to exposure to household air pollution.

In this perspective, this work aimed to assess the levels of air pollution in homes of the Quilombo Calolé, located in Cachoeira (BA), which use firewood and rudimentary stoves for cooking food. The concentrations of gases (CO₂ and HCOH) and particles (MP_{2.5} and MP₁₀), as well as temperature and relative humidity were measured with the TEMTOPm2000 sensor during the time of stove use (8h-16h).

Temperature and relative humidity ranged from 25 °C to 30 °C and from 75 % to 93 % in the kitchens, respectively. The outside temperature was in the range of 21 °C and the relative humidity around 90 %. CO₂ concentrations ranged from 400 to 650 ppm during wood burning, while the external range was 420 to 520 ppm. Formaldehyde levels were below the WHO recommendations (0,1 mgm⁻³ every 30 min). On the other hand, particulate matter levels (PM₁₀ and PM_{2.5}) were extremely high during most of the period of stove use in all investigated houses. Many of the measurements taken exceeded the detection limit of the sensor (1000 µg m⁻³). Outdoor concentrations were much lower than in the kitchens, between 8 and 10 µg m⁻³, indicating that wood burning is the main source of PM.

Based on the results obtained, it is evident that the practice of cooking using solid fuels, such as firewood, becomes extremely arduous and harmful due to the low efficiency of the traditional stove. In addition to the high biomass demand, the traditional stove favors the spread of smoke by not having a chimney, resulting in exposure to high concentrations of particulate matter (MP_{2.5} and MP₁₀) and other pollutants to the occupants of the enclosure.

The fuels used for cooking also influence outdoor air quality and global warming, as a large part of the emissions are released into the atmosphere. Therefore, improving household stoves can provide an efficient way to mitigate carbon emissions. The impacts caused by particulate matter, both regionally and globally, make the modernization of cooking technologies an important initiative to reduce the effects on the climate in the short term.

Acknowledgments

To CAPES, CNPq, FAPERJ and Petrobras for the financial support. To Instituto Perene for coordinating the project and the quilombola community of Calolé, BA, for their support.

¹ Xu M, Ke P, Wang C, Di H, Meng X, Xia W, Gan Y, He Y, Tian Q, Jiang H, Lu Z (2022) Cooking with biomass fuels and mortality among Chinese elderly people: a prospective cohort study. *Indoor*

²World Health Organization, 2022. <https://www.who.int/data/gho/data/indicators/indicator-details/GHO/household-air-pollution-attributable-deaths>

Synergic photocatalytic effect of TiO₂ dispersed onto activated carbon from coffee husk waste for dye degradation.

Carolina Inácio Portela (PG),¹ Tayra Rodrigues Brazil (PQ),¹ Thais Aline Prado Mendonça (PG)¹, Nirton Cristi Silva Vieira (PQ)¹, Elias de Barros Santos (PQ)¹, Raquel Aparecida Domingues (PQ)¹, Maraisa Gonçalves (PQ)¹
gongalves.maraisa@unifesp.br; ci.portela@unifesp.br

¹Federal University of São Paulo, Science and Technology Institute, Talim Street, 330, São José dos Campos, SP, Zip Code: 12231-280, Brazil

Palavras Chave: Coffee Husk Waste, Activated carbon, Photocatalysis, dyes pollution.

Highlights

- High dispersed TiO₂ onto activated carbon from agriculture waste.
- High photodegradation of Victoria blue B dye by TiO₂/AC.

Resumo/Abstract

Industrial effluents from the textile industry containing several synthetic organic dyes have not been treated conventionally. Then, when released into bodies of water can be risks to the ecosystem into which they were inserted. Several techniques, such as photocatalysis, have emerged promising to degrade many organic dye pollutants from wastewater. The radicals, such as °OH, generated during the photocatalysis reaction do not migrate very far from the active centers of the TiO₂. Then, the adsorption of contaminants onto the high-surface materials is crucial for effective degradation [1]. Therefore, AC has excellent electron transport ability, which can transfer e⁻ from the semiconductor to AC to diminish the e⁻/h⁺ recombination [2]. The recombination occurs when the electron return of conduction band to the valence band, then the photocatalyst loses the activity. Thus, this suggests that TiO₂/AC is an effective and low-cost material for pollution removal. This work aimed to prepare an AC from coffee husk waste to TiO₂ dispersion by sol-gel methods. Two different materials were prepared and characterized.

The surface area for AC is high, about 700 m²/g. The phase anatase was obtained for the TiO₂ and showed very dispersed onto the AC surface. The kinetics of TiO₂/AC photocatalytic activity was swift, removing about 99 % of the Victoria blue dye after 120 minutes of reaction time (Figure 1(a)). The adsorption process also efficiently removes approximately 80% of the Victoria Blue dye (Figure 1(a)). Besides, the photoactivity of two prepared TiO₂/AC is similar to the TiO₂ commercial (TiO₂-P25), as shown in Figure 1(b). The recyclability of the photocatalyst was evaluated in three consecutive reactions, and satisfactory results were obtained, maintaining the photocatalyst's efficiency. Thus, this work proved the feasibility of using coffee husk wastes for AC preparation and your use as a photocatalyst support.

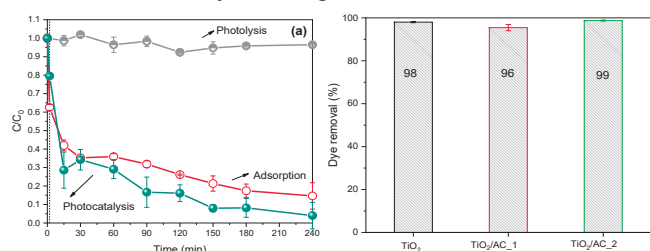


Figure 1. Victoria Blue removal with TiO₂/AC (a); Photocatalysis efficiency of different materials (b). Reactions conditions: the amount of materials = 0.50 mg and 100 mL of dye solution = 15 mg L⁻¹; reaction time: 140 min.

References

- [1] C. Minero, F. Catozzo, E. Pelizzetti, Role of adsorption in photocatalyzed reactions of organic molecules in aqueous titania suspensions, *Langmuir*, 8 (1992) 481-486.
 [2] W. Liu, B. Wang, M. Zhang, Effect of Process Parameters on the Microstructure and Performance of TiO₂-Loaded Activated Carbon, *ACS Omega*, 6 (2021) 35076-35092.

Agradecimentos/Acknowledgments

The authors acknowledge the financial support received from the Brazilian Funding Institution FAPESP (2019/13471-8 and 21/02354-0), IEAMar-UNESP for TEM analysis and the support from NAPCEM (Núcleo de Apoio à Pesquisa em Ciência e Engenharia de Materiais) of Federal University of São Paulo (UNIFESP).

Tijuca Forest: The metropolis and the Atlantic Forest

Graciela Arbilla (PQ),^{1*} Cleyton M. da Silva (PQ).^{1,2}

gracielaiq@gmail.com

¹Instituto de Química, UFRJ; ²Universidade Veiga de Almeida

Key words: *Tijuca Forest, hydrocarbons, air quality, heart-cutting multidimensional chromatography.*

Highlights

C₂-C₁₂ hydrocarbons were determined in the Tijuca Forest. Total concentrations were in the interval 8-50 µg m⁻³. Results showed the forest effect on the reduction of pollutant concentrations.

Abstract

The Metropolitan Region of Rio de Janeiro has 7,535 km². More than 35% is covered by the Atlantic Forest (Mata Atlântica). The Tijuca Forest (29.52 km²) is the largest secondary urban forest in the world and divides the city of Rio de Janeiro in the southern and northern areas. The forest is a significant green belt for the city and was considered by UNESCO as a World Heritage Site. The main goal of this study is to characterize the main hydrocarbons (HCs) in areas of the Tijuca Forest which are currently visited by tourists and population in general and to compare the determined concentrations with values obtained in an urbanized district located at approximately 10 km.

Material and Methods: Samples were collected at six locations: at Sector A of the Tijuca National Park, at Grajaú State Park (both part of Tijuca Forest) and at Saens Pena Square (Tijuca District, with high vehicular flow). Air samples were collected using 6.0 L stainless steel canisters and flux restrictors (1-hour sampling). HCs (C₂-C₁₂) were analyzed by heart-cutting multidimensional gas chromatography with two detectors (MS and a FID) and two columns (primary column - DB 624 and secondary column - Poraplot Q-HT). Compound were trapped at -20°C and thermally desorbed at 300 °C. The limits of detection and quantification were 0.2 and 0.6 µg m⁻³, respectively. The individual HCs were identified and quantified using a standard reference mixture (57 compounds, ozone precursors).

Results and Discussion: Total HCs concentrations in the forest and in the city were in the intervals 8 - 50 and 85 - 108 µg m⁻³, respectively. The main HCs in the forest (in decreasing order of abundance) were: n-butane, propane, ethane, toluene, n-pentane, isopentane, n-hexane and 2-methyl-pentane. Isoprene (mainly of biogenic origin) levels were in the interval 0.4 - 4.0 µg m⁻³. The main difference between the forest and the city were the ratios isoprene/total HCs (0.08 and 0.05, respectively). In spite of the forest being surrounded by the city and the sampling points were relatively near the area with traffic flow (500 - 3000 m), results showed the forest effect on the reduction of HCs

concentrations, probably caused by the absorption of pollutants by vegetation.



Figure 1. Sampling locations and total HCs concentrations (minimum and maximum, in units of µg m⁻³).

Acknowledgments

FAPERJ (APQ1, CNE and JCNE), CNPq, FUNADESP, Agilent Technology Brazil.

ANA

Química Analítica

46^a Reunião
Anual da **SBQ**

28 a 31 de Maio de 2023

Águas de Lindóia · SP
Hotel Monte Real

3D printed electrochemical sensor for tetracycline determination

Rafael R. Silva (IC),¹ Lucas C. Duarte (PQ),¹ Vinícius A. O. P. da Silva (PG),² Bárbara G. S. Guinatti (PG),¹ Bruno C. Janegitz (PQ),² Wendell K.T Coltro (PQ).^{1*}

rafaelrodrisilva@discente.ufg.br;

¹Instituto de Química, Universidade Federal de Goiás; ²Departamento de Ciências Naturais, Matemática e Educação, Universidade Federal de São Carlos;

Palavras Chave: 3D printing, Antibiotics, Compact Sensor, Additive Manufacturing.

Highlights

Minituarized 3D printed electrochemical cell was utilized to analysis tetracycline. Preliminary tests demonstrated that cell is capable to detect tetracycline quickly, requires low sample consumption and low-cost materials.

Abstract

Since the development of 3D printing, electrochemical sensors are becoming more accessible and cheap, due to the fact it's used thermoplastics filaments.¹ Tetracyclines comprise a class of antibiotics with bacteriostatic activity used in veterinary medicine to prevent and treat animal infections. They are the second most produced antibiotics and are a focus of study because it's not biodegradable, being present in milk and river waters.² In this study, we developed a 3D printed electrochemical cell (Figure 1A) in polylactic acid (PLA) which is biodegradable, and PLA-carbon black (PLA-CB) to analyze tetracycline antibiotic based on voltametric measurements. The sensor was firstly characterized by cyclic voltammetry using ferrocenemethanol employing electrode before and after pre-treatment stages. Chemical treatment was done with dimethylformamide (DMF) to remove the PLA in the surface region of electrode and then expose the electroactive sites of carbon black. Pre-treatment increased the current in comparison with the electrode without pre-treatment, as it can be seen in Figure 1B. The electroactive area was made in PLA-CB, the insulating region of PLA. The geometrical area of the working electrode was 28,3 mm² and electroactive area was 36 mm², representing an increase of 28% in the area. The sample volume added on the 3D printed cell was 50 µL. Initial tests were realized based on the adding of 50 µM tetracycline in Britton-Robinson buffer (pH 3), resulting in current response of 0.055 µA for square wave voltammetry (SWV) and 0.041 µA for differential pulse voltammetry (DPV), as it can be seen in Figure 1C. From that, SWV technique was selected for tetracycline analysis. The proposed sensor will be focused on the screening of tetracycline in milk samples.

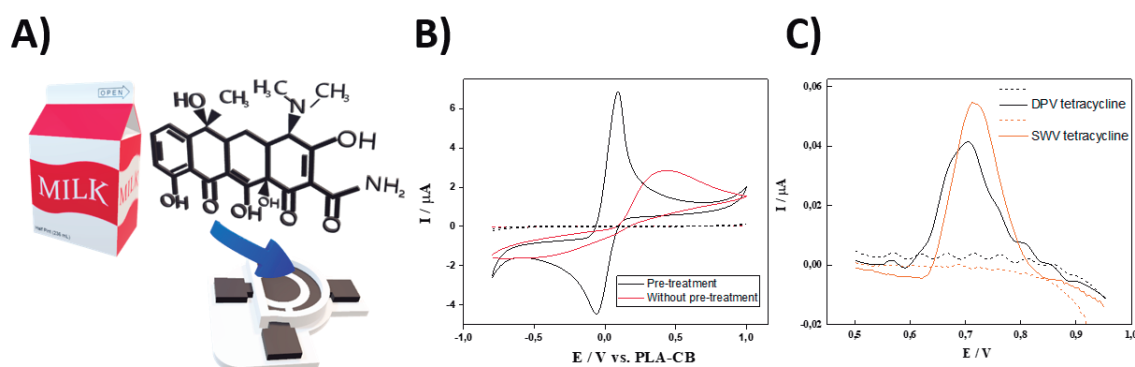


Figure 1. (A) Scheme of tetracyclines analysis on 3D printed sensor. (B) Cyclic voltammograms comparing pre-treated and non-treated electrodes. (C) DPV and SWV comparison analyzing 50 µM tetracycline.

Acknowledgments

[UFG, UFSCar, CNPq, FAPEG, CAPES, FAPESP, INCTBio, Macofren Tecnologias Químicas]

1. Delgado, K. P., Raymundo-Pereira, P. A., Campos, A. M., Oliveira Jr, O. N., & Janegitz, B. C. (2018). *Electroanalysis*, 2018, 30(9), 2153-2159.
2. Duarte, L. C., Baldo, T. A., Silva-Neto, H. A., Figueredo, F., Janegitz, B. C., & Coltro, W. K. *Sens. Actuators B Chem.*, 2022, 364, 131850.

4-Aminoantipyrine: An efficient, cheap and quick color spot test method for the presumptive detection of the street drugs NBOHs

Cláudia M. Rocha (PG),^{1*} Clésia Cristina Nascentes (PQ),¹ Ângelo de Fátima (PQ).¹

mancilha.claudia@gmail.com

¹Departamento de Química, UFMG. Av. Presidente Antônio Carlos, 6627 - Pampulha, Belo Horizonte - MG – Brasil

Keywords: colorimetric test, phenylethylamines, illicit drugs, blotter papers.

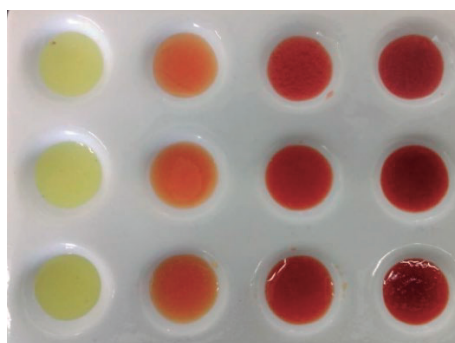
Highlights

The 4-aminoantipyrine is a promising colorimetric reagent for selective NBOH's identification in street drugs, with limit of detection at 0.05 mg mL⁻¹ analyte concentration.

Resumo/Abstract

Recently identified in different countries around the world, including Brazil, as blotter papers, popularly known as “smiles” or “NBomb”, NBOHs are substituted phenethylamine derivatives, part of the new psychoactive substances (NPS) group. Due to frequent structural modifications made on this class of illicit drugs, allied to the difficulty of developing a fast, easy, and specific test that identifies them, it arises as a public health problem¹. This work has developed a colorimetric test for *in situ* applications that explicitly identifies 25H-NBOH and its analogs. To the initial tests, 300 µL of blank solution or a 25H-NBOH methanolic solution (at 0.1-2.0 mg mL⁻¹) was added to a porcelain spot plate, followed by a buffer solution NH₄OH/NH₄Cl pH = 10, K₃Fe(CN)₆ 8% (w/v) and 4-aminoantipyrine 2.0% (w/v) aqueous solution. The spots containing the blank remain bright yellow due to the presence of potassium ferricyanide. Although, those having the analyte turn colored orange-red immediately, indicating the presence of 25H-NBOH. These results show the method's relevance, which gives excellent results using stable and cheap reagents (costing R\$ 0.10/test). For the future, the final step is to apply the test to actual samples seized by police agencies.

Figure 1 – Colors observed for a) blank and analyte concentration at b) 0.1 mg mL⁻¹, c) 0.5 mg mL⁻¹, and d) 0.75 mg mL⁻¹, triplicate.



[1] Coelho Neto, J. *et al. Forensic Toxicology*, 2017, 35, 415

Acknowledgments

This study was funded by the Fundação de Amparo à Pesquisa do Estado de Minas Gerais (FAPEMIG/Brazil; Grant #RED- 00042-16), Conselho Nacional de Desenvolvimento Científico e Tecnológico (CNPq/Brazil; Grant #429121/2018-0) and Coordenação de Aperfeiçoamento de Pessoal de Nível Superior (CAPES/Brazil – Finance Code 001 – Process #88881.516313/2020-01).

A bidimensional porous polymer monolithic platform for enrichment, cleanup and quantification of lysozyme in egg white samples

Fernando H. do Nascimento (PQ)¹, Renan Vitek (PG)¹ and Jorge C. Masini (PQ)¹.

fernandoslifer@gmail.com

¹Departamento de Química Fundamental, Instituto de Química, Universidade de São Paulo, IQ-USP, Av. Prof. Lineu Prestes 748, 05508-000, São Paulo, SP.

Keywords: *polymer monoliths, separation, pre-concentration, clean up, orthogonality, liquid chromatography.*

Highlights

- Weak cation exchange to enrich low abundant lysozyme in the presence of egg albumins
- Orthogonality in sample preparation was easily achieved using polymer monoliths

Abstract

Monolithic polymeric columns work for solid phase extraction (SPE)¹ and chromatographic separations² of large molecules such as proteins. This communication demonstrates the determination of lysozyme in egg-white samples after enrichment and cleanup by weak cation exchange following separation by reversed-phase liquid chromatography. The cation exchange column was prepared from glycidyl methacrylate (GMA, functional monomer) and ethylene glycol dimethacrylate (EDMA, crosslinker), followed by functionalization of the epoxy groups with iminodiacetate (IDA). Reversed-phase columns were prepared using butyl methacrylate (BMA, functional monomer) and EDMA. The reaction mixtures were prepared in the porogenic solvents n-propanol and 1,4-butanediol, and the monoliths were formed by photopolymerization inside vinylized polypropylene ink-pen tubes³ and by thermopolymerization inside functionalized Silcosteel® tubes. The cation exchange and reversed-phase columns were labeled as IDA@poly(GMA-co-EDMA) and poly(BMA-co-EDMA), respectively. The preparation of poly(GMA-co-EDMA) was fast (about one 2 h), including all steps, from preparing the ink-pen tube to washing the formed monolith with acetonitrile (ACN), generating less than 3 mL of waste per column produced, but functionalization demands an overnight period of pumping IDA in the column inside a water bath thermostated at 80 °C. Preparation of the poly(BMA-co-EDMA) also demands an overnight period for heated at 60 °C, with subsequent washing the formed monolith also with ACN. Egg-white samples diluted at a 1:10 (m v⁻¹) in phosphate buffer (pH 7.0) were injected first through IDA@poly(GMA-co-EDMA) to retain and concentrate lysozyme (isoelectric point, pI 10.5 – 11.5), as well as remove the proteins with a pI < 7.0, such as the abundant ovalbumin. Elution of the lysozyme from the cation exchange column was made by elution with 5% (v v⁻¹) acetonitrile in 0.1% (v v⁻¹) trifluoroacetic acid (TFA), which protonates the carboxylates of the cation exchanger, breaking the electrostatic interactions between the column and lysozyme. Reversed-phase LC then analyzes this eluate with a gradient from 5 to 70% ACN in 0.1% TFA, monitoring the absorbance at 220 nm. External calibration curves were prepared with 0.25 to 1.50 mg mL⁻¹ lysozyme reference solutions. Egg-white lysozyme concentrations varied between 2.26 ± 0.06 and 4.41 ± 0.08 mg g⁻¹, and addition/recovery experiments at two concentration levels (0.25 and 0.50 mg mL⁻¹) resulted in recoveries from 94 to 115%, thus demonstrating the columns working with orthogonal selectivity provided enrichment of less abundant lysozyme and accurate chromatography, provided by an efficient cleanup of the sample matrix.

1- Potter, O.G. & Hilder, E.F. *J Sep Sci.* 31 (2008) 1881–1906.

2- F. Svec, F & Lv, Y. *Anal Chem.* 87 (2015) 250–273.

3- Do Nascimento, F.H.; Trazzi, C.R.L.; et al. *J Sep Sci.* 43 (2020) 4123–4130.

Acknowledgments

CAPES (88882.315696/2019-01 and 88887.499941/2020-00) and CNPq (306674/2021-1).

Área:

ANA

(Inserir a sigla da seção científica para qual o resumo será submetido. Ex: ORG, BEA, CAT)

Abordagens quimiométricas para a avaliação dos dados obtidos a partir da análise de quimiotipagem de madeiras por espectrometria de massas: um método alternativo para a identificação de madeiras.

Thays V. C. Monteiro (PG)¹, Antônio Unias (PG)¹, Alexandre Gontijo (PQ)³, Werickson F. Rocha (PQ)¹, João Latorraca (PQ)⁴, Álex Rosini (PG)⁵, Salvador Sánchez (PG)⁵, Andréia Porcari (PQ)⁵, Ana Baddini (PQ)^{2*}, Maíra Fasciotti (PQ)^{1*}

mfasciotti@inmetro.gov.br; ana.baddini@ifrj.edu.br

¹ Instituto Nacional de Metrologia, Qualidade e Tecnologia – INMETRO, Duque de Caxias, RJ, Brazil, 25250-020, ² Instituto Federal do Rio de Janeiro – IFRJ, Rio de Janeiro, RJ, Brazil, 24315-375, ³ Laboratório de produtos florestais – LPF, Brasília, DF, Brazil, 70818-900, ⁴ Universidade Federal Rural do Rio de Janeiro – UFRRJ, Seropédica, RJ, Brazil, 23897-045, ⁵ Universidade de São Francisco – USF, Bragança Paulista, SP, Brazil, 12916-900

Keywords: Quimiotipagem; espectrometria de massas; madeira; quimiometria

Highlights

Wood identification based on metabolites molecular fingerprints by mass spectrometry. Exploratory analysis (PCA) showed well-defined clusters for some genera with a large number of replicates. 100% of accuracy, sensitivity and selectivity with PLS-DA classification for the genera *Caryocar* spp. and *Copaifera* spp.

Resumo/Abstract

A extração ilegal de madeira é um grave problema no Brasil, pois o país concentra grande parte da biodiversidade do mundo, e biomas extremamente ricos como a Amazônia. O desmatamento fez com que o governo criasse leis listando espécies de madeiras ameaçadas de extinção, cujo corte é proibido. Embora protegidas por lei, essas espécies ainda são alvo do comércio ilegal por serem “nobres”. Apesar de esforços para se combater a extração ilegal de madeira com base em leis, na prática a fiscalização e controle de madeira de origem ilegal ainda é muito falho. Sendo assim, esse trabalho teve como objetivo implementar uma linha de pesquisa no INMETRO para o desenvolvimento de um método para identificar espécies de madeira, através da análise de quimiotipagem, que utiliza perfis químicos baseados em metabólitos secundários, que são basicamente impressões digitais moleculares em função de gênero e espécie. Neste estudo, foram utilizadas 61 espécies de madeiras distintas e suas replicatas, totalizando 187 amostras. As madeiras foram extraídas com MeOH/H₂O 3:1 com adição de solução aquosa de bicarbonato de sódio 0,05 mol.L⁻¹ e diretamente infundidas na fonte de íons ESI de um espectrômetro de massas Synapt HDMS QTOF, em modo positivo. O método foi validado qualitativamente, avaliando parâmetros como: repetibilidade, precisão intermediária e seletividade. Comparando os espectros, observaram-se perfis bem característicos para diferentes amostras e grande similaridade entre replicatas de uma mesma espécie. Uma análise exploratória dos dados foi realizada por PCA, em que 28 classes (gêneros distintos) foram consideradas. Somente gêneros com muitas replicatas (>20 indivíduos) apresentaram clusters bem definidos. PCA não é a abordagem mais indicada, pois algumas amostras têm muita influência no modelo. Posteriormente, foi realizada a construção de modelos PLS-DA para classificação de amostras dos gêneros *Caryocar* spp., *Copaifera* spp. e *Eucalyptus* spp. 117 amostras foram colocadas no conjunto de calibração e 59 amostras no conjunto de validação externa. Cada modelo foi construído com duas classes, uma classe contendo amostras do gênero de interesse e a outra contendo as amostras dos gêneros restantes. Para evitar o desbalanceamento de classes na obtenção do modelo PLS-DA foram utilizadas as quintuplicadas das medidas espectrais das amostras na classe do gênero de interesse, enquanto na outra classe foi utilizado um espectro por amostra. Desta forma, o número integrantes em uma classe foi próximo ao número de integrantes da outra. Ao realizar a validação externa, os modelos dos gêneros *Caryocar* spp. e *Copaifera* spp. apresentaram 100% de seletividade, sensibilidade e exatidão. Já o modelo para a identificação de *Eucalyptus* spp. apresentou 98 % de exatidão, 80 % sensibilidade and 100 % de seletividade. Os resultados demonstram que o método desenvolvido é extremamente promissor para ser empregado no controle e fiscalização da exploração ilegal de madeiras.

Agradecimentos/Acknowledgments



Accessing different compounds in a crude oil sample by ultra-high resolution mass spectrometry and different ionization sources

João V. A. Oliveira (IC),^{1*} Deborah V. A. Aguiar (PG),¹ Gesiane S. Lima (PQ),¹ Boniek G. Vaz (PQ).¹

oliveiraataide@discente.ufg.br

¹Instituto de Química, Universidade Federal de Goiás, Campus Samambaia, Goiânia/GO, Brasil

Palavras Chave: *Characterization, Ultra-high resolution mass spectrometry, Crude oil, Ionization sources*

Highlights

Different ionization sources in ultra-high resolution mass spectrometry are complementary and provide a greater amount of molecular information on the composition of the crude oil sample.

Resumo/Abstract

Crude oils are complex mixtures containing mostly hydrocarbons, but it also includes some classes of molecules that contain heteroatoms, such as oxygen (O), nitrogen (N), and sulfur (S) [1]. The presence of heteroatom-containing compounds is problematic for the oil industry, as they contribute to emulsion formation, resistance to catalytic processes, corrosion, and incrustation. Therefore, a comprehensive characterization of the compounds present in crude oil samples is critical in developing solutions to these problems [2,3]. In this work, a crude oil sample provided by Petrobras, with an API grade of 29.9 and a TAN of 0.22, was performed using a Fourier transform ion cyclotron resonance mass spectrometer (FT-ICR MS) 7T SolariX 2xR (Bruker Daltonics, Germany) coupled to electrospray ionization (ESI), atmospheric pressure chemical ionization (APCI), and atmospheric pressure photoionization (APPI) sources.

For the FT-ICR MS analyses, samples were prepared by dissolving 1.0 mg of the crude oil in 1.0 mL of toluene. Afterwards, 0.5 mL of the solution was diluted with 0.5 mL of methanol, to obtain a final concentration of 0.5 mg.mL⁻¹ in toluene:methanol (1:1, v:v). Samples were doped with formic acid (1.0 %) or ammonium hydroxide (2.5 %) for positive and negative ionization mode analysis, respectively. Initially, the data obtained from the FT-ICR MS analyses were calibrated using the DataAnalysis software (Version 5.0, Bruker Daltonik GmbH, Germany), and subsequently, the molecular formulas were assigned to the signals recorded in the mass spectra using the Composer software (Version 1.5.3, Sierra Analytics, USA). The Thanus software was used for graphical constructions.

The ESI analysis in negative ionization mode allowed us to observe mostly species of class N, O, and O₂, which represent carbazoles, phenols, and organic acids, respectively. While in positive ionization mode, we observed mostly class N, representing pyridines. With the use of APCI, in positive ionization mode, the presence of medium polarity compounds such as high molecular weight polyaromatic hydrocarbons, aliphatic hydrocarbons, and sulfurated compounds was observed. Through the APPI analysis in positive ionization mode, the presence of non-polar aromatic compounds was observed. Furthermore, a large number of molecular formulas were detected. Some formulas were common to more than one ionization source, while others were characteristic of a specific ionization source.

These results indicate that the use of different ionization sources is crucial for obtaining the chemical profile of crude oil. The combination of ESI, APCI, and APPI sources accesses a large number of molecules in a complementary manner, providing a comprehensive understanding of the molecular composition of the sample.

Agradecimentos/Acknowledgments

We thank the Petrobras/ CENPES for giving the samples and financial support.

[1] Han, Y.; Zhang, Y.; Xu, C.; Hsu, C. S.; *Fuel* 2018, 221, 144.

[2] Niyonsaba, E.; Manheim, J. M.; Yerabolu, R.; Kenttämää, H. I.; *Anal. Chem.* 2019, 91, 156

[3] Rodgers, R. P.; Schaub, T. M.; Marshall, A. G.; *Anal. Chem.* 2005, 77, 20 A.

A Factorial Design development for Disposable Pipette Extraction (DPX) for LC-MS method for six N-Nitrosamines in Valsartan medicine determination

Almir C. B. Junior (PG)¹, Lucas S. Machado (PG)¹, Boniek G. Vaz (PQ)¹, Andrea R. Chaves (PQ)¹

custodioalmir16@gmail.com

¹ Instituto de Química, Universidade Federal de Goiás, 74690-900, Goiânia, GO, Brazil

Key words: N-Nitrosamines, Disposable Pipette Extraction, Valsartan.

Highlights

- Analysis of six N-Nitrosamines in valsartan by LC-MS;
- The sample preparation is essential to ensure high accuracy and precision;
- Optimization of DPX applying a 2⁵⁻¹ fractional factorial design, evaluating the main variables.

Abstract

N-Nitrosamines have been broadly studied due to their mutagenic and carcinogenic potential¹. The occurrence of this molecules in low amounts is widely known in tobacco smoke, and in cooking or fermentation food. Recently, these molecules were found in medicines containing valsartan, which lead to further studies aiming the investigation in other drugs². In order to evaluate the content of N-nitrosamines in these medicines, efficient and sensitive analytical methods must be developed. However, due to the low levels of these compounds presents in medicines and the higher levels of other constituents that could contribute to generating new N-Nitrosamines residues or degradation products, the development of higher sensitive methodology is urgent. The use of chromatographic techniques coupled to identification by mass spectrometry (LC-MS) has shown appropriate to this purpose^{1,3}. The step of sample preparation is essential to ensure high accuracy and precision to the proposed methodology. An alternative to classical techniques as solid phase extraction (SPE) is the Disposable Pipette Extraction (DPX). This is a miniaturized extraction technique based on SPE that displays advantages as high analyte transfer rate, reduced extraction time, high recovery rate and still maintaining the versatility of sorvent⁴. In order to optimize the main parameters of DPX, a design of experiments approach presents suitable, such as a fractional factorial design of experiments. This method promotes variations of DPX parameters simultaneously, which allows reduction of experiments with gain of information⁵. Therefore, this work aims to optimize the method of extraction of six principal related N-nitrosamines from valsartan medicine by DPX applying a fractional factorial design followed by identification and quantification using LC-MS analysis. The studied nitrosamines were diethylnitrosoamine, 1-nitrosopiperidine, N-nitroso-N-methylethylamine, nitrosomorpholine, N-nitrosodi-n-butylamine and 1-nitrosopyrrolidine. The LC-MS analysis were performed on a Shimadzu LC-20A coupled on a Bruker micrOTOF-Q III equipped with electrospray ion source in positive mode. The chromatography was carried using a Zorbax Eclipse XDB-C18 (4.6x50mm, 1.8 µm) column at 40°C, using a mobile phase A formic acid 0.1% and mobile phase B methanol and flow rate of 0.6 mL/min. The parameters used for the MS analysis were capillary voltage 4kV, nebulizer 4 Bar and dry temperature 200°C. The extraction method by DPX was optimized evaluating commercial sorvents as silica, discovery DSC-SCX, discovery DSC-NH₂ and envi-carb phases. A 2⁵⁻¹ factorial design was performed, evaluating 5 variables, each in 2 different levels. The chosen variables were pH, solvent of elution, equilibrium time and cycles of extraction and desorption. The proposed factorial design led the extraction to its optimal results, which displayed a recuperation over 80% in low pH values and high equilibrium time. The factorial design showed that the pH had a significant contribution for the extraction process as well the equilibrium time. The next step of this study will be to investigate more levels of these parameters, validated and submit the method for commercial valsartan medicine samples.

1. Tuesuwan B.; Vongsutilers. Nitrosamine Contamination in Pharmaceuticals: Threat, Impact, and Control. 2021
2. Johnson, G. E. *et al.* Permitted daily exposure limits for noteworthy N-nitrosamines. 2021
3. Anvisa - Guia sobre o Controle de Nitrosaminas em Insumos Farmacêuticos Ativos e Medicamentos Guia nº 50/2021. 2022
4. Carasek, E.; Morés, L. Huelsmann, R.D. Disposable pipette extraction: A critical review of concepts, applications, and directions. 2022
5. Tibon J.; *et al.* Speciation analysis of organoarsenic species in marine samples: method optimization using fractional factorial design and method validation. 2021

Acknowledgments

LaCEM/IQ-UFG, CAPES and FUNAPE

ANALYSIS OF MONOETHYLENE GLYCOL IN PETROCHEMICAL SAMPLES BY MICELLAR ELECTROKINETIC CHROMATOGRAPHY ON MICROCHIPS

Mauricio M. L. Pereira (IC),^{1*} Kariolanda C. A. Rezende (PG),¹ Wendell K. T. Coltro (PQ).¹

mauricio.matheus@discente.ufg.br

¹Universidade Federal de Goiás, Instituto de Química, Goiânia, GO, 74690-900

Palavras-Chave: Gas condensate, Separation, Microfluidics, Portability, Microsystems, Electrophoresis.

Highlights

We reported the development of analytical methodology using integrated electrophoretic devices with capacitively coupled contactless conductivity detection for the analysis of monoethylene glycol in gas condensate.

Resumo/Abstract

Monoethylene glycol (MEG) is widely used in the petrochemical industry as a thermodynamic inhibitor of hydrate formation, preventing the obstruction of ducts due to the formation of gas hydrates.¹ This process is not only effective but also economically interesting, since MEG can be reused in the extraction process after undergoing a regeneration step. In this regeneration, MEG must be extracted to be reinjected for other extraction of petrochemical samples. On the other hand, gas condensate samples should no longer have traces of this inhibitor. Based on this, the present study describes the development of an analytical methodology using electrophoresis microchips (ME) devices integrated with capacitively coupled contactless conductivity detection (C⁴D) for MEG detection. For this purpose, it was used a commercial instrumentation supplied by eDAQ including glass ME devices containing microchannels (100 μm wide; 10 μm deep) arranged in a double-T format and two pairs of integrated sensing electrodes (200 μm wide \times 500 μm long \times 200 nm thick spaced by 250 μm) made of Pt/Ta. The best sensitivity was obtained by applying a 1200- kHz sinusoidal wave with 100% excitation voltage. The separation of MEG was performed through micellar electrokinetic chromatography due to its ability to promote the separation of neutral analytes. The separation was performed using 50 mM phosphate buffer (pH = 9) containing 30 mmol L⁻¹ sodium dodecyl sulfate (SDS). For sample injection, a potential of 600 V was applied in the injection channel during 10 s. Afterwards, a separation voltage of 700 V was then applied to the separation channel and the resulting signal was monitored in real time. As it can be seen in Fig. 1, MEG was successfully detected within 270 s. Under these conditions it was possible to identify MEG in analyzes of approximately 300 s. The separation through MEKC mode on microchips provided satisfactory repeatability values. For 12 consecutive injections, the RSD values calculated for the peak area was 4.2%. The proposed strategy revealed a linear behavior in the concentration from 150 to 450 $\mu\text{mol L}^{-1}$ (Fig. B) and limit of detection of 25 μmol . The proposed approach has also demonstrated potential to be used for in-field analysis.

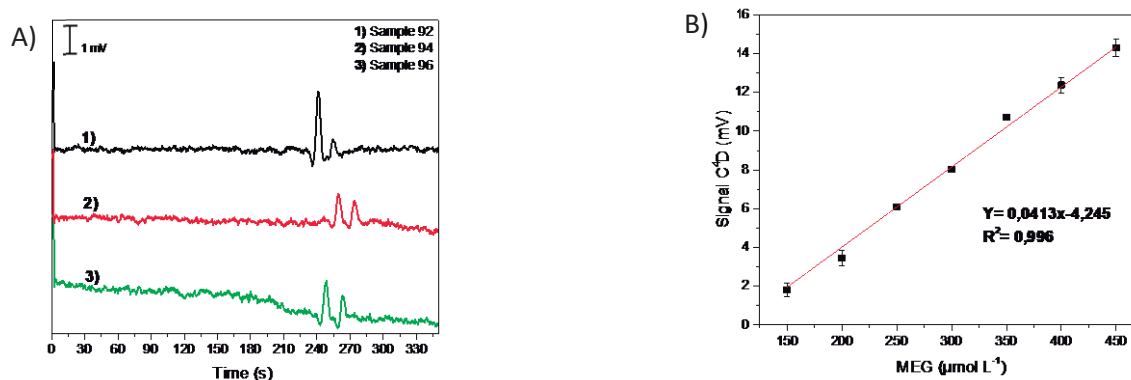


Figure 1. MEG analysis in condensate gas supplied by Petrobras (A). Analytical curve obtained from the electrophoretic detection of MEG in range from 150 $\mu\text{mol L}^{-1}$ to 450 $\mu\text{mol L}^{-1}$ (B).

Agradecimentos/Acknowledgments

[UFG, PETROBRAS, CNPq, CAPES]

¹- ALEF, Khalid et al. The effect of regenerated MEG on hydrate inhibition performance over multiple regeneration cycles. *Fuel*, v. 222, p. 638-647, 2018.

ANCHORING PAPER-BASED DEVICES ON DRONE FOR COLORIMETRIC MONITORING OF TROPOSPHERIC OZONE

Pedro P. E. Campos (IC)^{1*}, Habdias A. Silva-Neto (PG)¹, Vanderli G. Leal (PG)², Lucas C. Duarte (PQ)¹, João F. S. Petrucci (PQ)² and Wendell K. T. Coltro (PQ)¹

ppedro@discente.ufg.br

¹Universidade Federal de Goiás, Instituto de Química, Goiânia, Goiás, Brazil, 74690-900

²Universidade Federal Uberlândia, Instituto de Química, Uberlândia, Minas Gerais, Brazil, 38400-902

Palavras Chave: *Environmental Analysis, Portable Devices, Colorimetric Assays, Atmospheric Air, Ozone Detection.*

Highlights

Use of UAVs, combined with colorimetric devices manufactured in 3D printers for the detection of pollutants in atmospheric air.

Abstract

Unmanned aerial vehicles (UAVs; Drone) have emerged as powerful and versatile analytical approaches for remote monitoring. A current trends in Chemical sciences is the fabrication of “do it yourself” analytical tools, such as paper-based analytical devices (PADs). The combination of PADs and drones is an excellent alternative for sampling and monitoring gas at trace levels in outdoor environments. In this study, we propose for the first time the simple assembling of PADs into a drone to monitor the gaseous ozone in the troposphere. For manufacturing the PAD, chromatographic paper, vinyl stencil ($\varnothing = 5$ mm) and glass varnish were successfully utilized as materials. A commercial generator is utilized as a standard source of O_3 (~ 229 mg h^{-1} , characterized by iodometric titration method). Initially, the colorimetric reaction for ozone quantification was evaluated spotting the reaction zones with 1.5 μ L of 1 mmol L^{-1} potassium indigotrisulfonate (ITS), 1.5 μ L of poly(ethylene glycol) 400 (PEG) and the presence of ozone was verified by changing color from blue to colorless. After the reaction, the PADs were digitalized on a desktop scanner and the analytical signals were extracted using CORELDRAW software. Aiming to improve the analytical performance of the colorimetric analysis, optimization in terms of reaction time, order of addition of reagents and concentration of PEG 400 were performed in the presence of 1 mmol L^{-1} ITS. Under optimized conditions, the analytical curve of O_3 , repeatability and reproducibility experiments were also acquired. The obtained relation between the mass of ozone and the color channel cyan exhibited acceptable values with a linear range between 0.95 to 7.63 mg of O_3 ($R^2 = 0.99$), limit of detection (LOD) of 146 μ g and relative standard deviation (RSD) ranged from 1.6 to 3.4% for the reproducibility and repeatability studies. A plastic holder was manufactured on a 3D printer tool aiming for anchored the PADs upon the drone (Figure 1). The drone anchored with four different PADs was positioned ~ 20 meters from the ground and the sampling and analysis of ozone was realized during ~ 2 min. The obtained colorimetric analysis indicated amount of O_3 ranged from 6.8 ± 0.7 to 7.3 ± 0.2 mg that is similar to found amount of O_3 reported in literature involving trace gas in the atmospheric air. Thus, we believe that the analytical tool introduced herein has the potential for fast, remote and spatial monitoring of trace gases in the troposphere.



Acknowledgments

[UFG, UFU, PETROBRAS, CNPq, FAPEG, CAPES, INCTBio]

A novel spectrophotometric method for determination of bisphenol A in water samples exploring cloud point extraction

Paula V. de Jesus* (IC), Vivian Maringolo (PG), Diogo L. Rocha (R),

Federal University of ABC, Center for Natural Sciences and Humanities, Santo André, São Paulo, Brasil,
CEP 09210-580

*e-mail: villlela.jesus26@gmail.com

Keywords: Bisphenol A, Diazo-coupling Reaction, Cloud Point Extraction, Preconcentration, Spectrophotometry.

Highlights

Determination of bisphenol A in waters using a diazo-coupling reaction and cloud point extraction for pre-concentration.

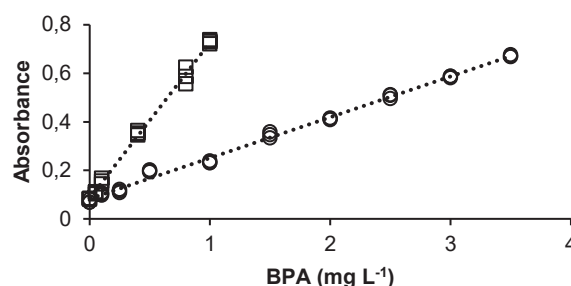
Resumo/Abstract

Bisphenol A (BPA) is an endocrine disrupter that may compose polycarbonate-based plastics. Due to its presence in industrial wastewaters, it is considered as an emerging pollutant. International regulations¹ point out that the concentration of BPA in waters must be $< 100 \mu\text{g L}^{-1}$. A spectrophotometric analytical procedure was previously proposed based on a diazo-coupling reaction with sulfamethoxazole (SMZ) and NaNO_2 for determination of BPA², forming a yellow solution ($\lambda=446 \text{ nm}$). In this case, the detection limit was not suitable for water analysis. In this work, a similar reaction was employed by replacing SMZ for sulfanilamide (SMD), as it shows lower cost and toxicity. The parameters were optimized using a full factorial design (FullFD) ²⁴. The evaluated range and the selected values are presented in Table 1. Linear response was observed up to 3.50 mg L^{-1} , described by the equation $A=0.168 C_{\text{BPA}} + 0.0828$ ($R^2 = 0.995$), where A is absorbance and C_{BPA} is BPA concentration in mg L^{-1} . Detection limit and coefficient of variation ($n = 20$) were estimated at 0.26 mg L^{-1} and 1.3%, respectively. The quantification limit was lowered by using cloud point extraction (CPE). BPA solutions were submitted to heating with Triton X-114 prior to the chemical derivatization in the rich-phase. The main parameters were optimized using FullFD ²³, including surfactant concentration (1 - 5%), heating time (30 - 150 s) and centrifugation time (5 - 15 min), and the selected values were 1%, 150 s and 15 min, respectively. After extraction, linear response was observed between 0.050 and 1.0 mg L^{-1} , described by the equation $A=0.642 C_{\text{BPA}} + 0.0850$ ($R^2 = 0.996$). Detection limit and coefficient of variation ($n = 8$) were estimated at 0.02 mg L^{-1} and 2.6%, respectively.

Table 1. Optimized parameters and optimum conditions for the determination of BPA

Parameter	-1	0	1	Optimum value
SMD, mol L^{-1}	0.01	0.02	0.03	0.03
NaNO_2 , mol L^{-1}	0.15	0.33	0.50	0.50
HCl, mol L^{-1}	1.0	2.0	3.0	1.0
Stirring time, min	0	5	10	zero
Phosphate buffer pH	9	11	13	12

Figure 1. Calibration curves obtained without (-○-) and with CPE (-□-) for BPA determination.



By comparing the analytical curves with and without CPE (Figure 1), it is clear that sensitivity was enhanced by the extraction. The ratio between slopes yielded an enrichment factor of 3.8, which is a common value observed for CPE. The results showed a promising alternative for the determination of BPA in waters without chromatographic separations. In future steps, the accuracy will be deeply evaluated for the application on water analysis.

¹ R. Huelsmann and E. Martendal, J. Braz. Chem. Soc., Vol. 31, No. 8, 2020, p. 1575-1584, 2020, doi: 10.21577/0103-5023.20200043.

² A. Karrat and A. Amine, Microchemical Journal, Vol. 168, May 2021, p. 106496, 2021, doi: 10.1016/j.microc.2021.106496.

³ S. Zhong, S. Tan, L. Ge, W. Wang and J. Chen, Talanta, Vol. 85, p. 488-492, 2011, doi: 10.1016/j.talanta.2011.04.009.

Agradecimentos/Acknowledgments

CAPES (Finance code 001).

APLICAÇÃO DE ENERGIA MICRO-ONDAS NA SÍNTESE DE MIP PARA EXTRAÇÃO EM FASE SÓLIDA DE SERTRALINA EM AMOSTRAS AMBIENTAIS

Ridien G. Alencar (PG)¹, Ailton J. Moreira (PQ)², Roberto Bertholdo (PQ)¹ e Gian P. G. Freschi (PQ)¹,
gianpgfreschi@gmail.com; ridien.alencar@sou.unifal-mg.edu.br.

¹ LAFEQ - Instituto de Ciência e Tecnologia, Universidade Federal de Alfenas (UNIFAL-MG).

² LIEC – Departamento de Química, Universidade Federal de São Carlos (UFSCar)

Palavras Chave: Contaminantes Emergentes, Antidepressivos, Polímeros de Impressão Molecular, Fármacos, Micro-ondas, águas residuais.

Highlights

SYNTHESIS OF MOLECULARLY IMPRINTED POLYMER BY MICROWAVE FOR SOLID PHASE EXTRACTION AND PRE-CONCENTRATION OF SERTRALINE ENVIRONMENTAL SAMPLES

- Sertraline is a contaminant of emerging concern.
- MIPs shows high potential as pre-concentrator for sertraline low traces detection.
- Microwave in an efficient alternative energy to MIP synthesis.

Resumo/Abstract

This paper has two main lines of work: the synthesis of molecularly imprinted polymers (MIP) assisted by microwave energy and the use of this material in solid-phase extraction (SPE) for environmental analysis and sertraline remediation. Eight polymers were synthesized using the precipitation method, including MIPs and their respective NIPs (Non imprinted polymer). Microwave-assisted Polymers occurred at different parameters of power, heating ramp time and power, and amount of solvent employed. After the synthesis, the materials were subjected to analysis its structures (FTIR), thermal stability (DSC and TGA), surface area, pore size (BET) and average particle size (SEM). It was confirmed the incorporation of ethylene glycol dimethacrylate (crosslinker), and methacrylic acid (monomer) in the polymer structure by the Fourier-transform infrared spectroscopy (FTIR). The polymers were used in adsorption and desorption studies for 10 mg. L⁻¹ sertraline aqueous solution (ultrapure water), and the average removal rate was: 95,46%, 60,96%, 93,21%, and 97,78%, for MIPs I, II, III and IV, respectively, and 88,75%, 66,61%, 76,44%, and 93,31% for NIPs I, II, III, and IV. These results demonstrate the increase in the adsorptive capacity of the materials by using sertraline as the template molecule, except by MIP/NIP II. Moreover, it may indicate the successful formation of selective sites for sertraline adsorption in the present MIPs. To measure the polymers selectivity, studies were carried out using solution containing the following drugs in the same concentration: 17 α ethinyl estradiol, diclofenac sodium and sertraline. The studies confirmed the existence of selective sites in the MIP structure, mainly by the comparing the selective adsorption values of MIP and NIP for sertraline compared to the other drugs tested. Moreover, the same studies were also carried out using three different environmental water samples (mineral water source, sewage) in order to determine the influence of physicochemical properties and the presence of other contaminants in the MIP adsorption efficiency. The adsorption efficiency for sertraline obtained in this samples was 1,32%; 3,29 % average higher for MIPs I and III than the ultrapure water (95,46%; 93,21% average) samples using the same analyte concentration, the values for MIP IV was 1,57% lower. Analyzing both the physical properties, adsorption and desorption, and selectivity, MIP III was selected as the best material produced and used in selectivity in environmental samples, pre-concentration, and reuse studies. MIP III showed good high removal rates (85,50% average) of sertraline in the complex samples studied (sewage and treated sewage samples doped with 30 mg. L⁻¹ of sertraline, diclofenac sodium, and 17 α ethinyl estradiol). The MIP III capacity of preconcentration up to 200 times a solution with 5 μ g. L⁻¹ sertraline was confirmed by studies performed in ultrapure water. The possibility of reuse/regeneration of the MIPs were confirmed in at least one adsorption cycle without significant adsorption efficiency loss. The materials produced demonstrated good applicability in environmental samples, emphasizing the use of microwave energy for a faster and more efficient production of these adsorbent materials.

Agradecimentos/Acknowledgments

The authors would like to acknowledge FAPEMIG (APQ-00601-22) for the financial support of his work.

Aplicação de metodologia quantitativa para determinação de imunossupressores via MALDI-MS em matrizes biológicas

Julia Lavorenti (IC),* Diogo de Oliveira Silva (PQ)

julialavorente@gmail.com; dosilva@unifesp.br

Laboratório de Bio-orgânica e Biocatálise (GBB), Universidade Federal de São Paulo (UNIFESP) -Campus Diadema

Palavras Chave: Quantificação; Tacrolimo; Sirolimo; MALDI-TOF; HPLC-PDA

Highlights

Development of a quantitative methodology for determination of immunosuppressants Tacrolimus and Sirolimus by MALDI-MS.

Application of quantitative methodology for determination of tacrolimus and sirolimus in human plasma by MALDI-MS.

Resumo/Abstract

Os imunossupressores foram um dos pilares que tornaram o transplante de órgãos um processo rotineiro nos hospitais pelo mundo. Dentre os milhares de compostos que possuem atividade imunossupressora, podemos destacar o tacrolimo (TAC) e o sirolimo (SIR).¹⁻³ A quantificação destes imunossupressores para o monitoramento terapêutico, durante o processo de obtenção dos mesmos e para o controle de qualidade dos medicamentos são de extrema importância para a segurança dos seus consumidores. Assim, este projeto teve como objetivo o desenvolvimento de uma metodologia quantitativa para a determinação de tacrolimo e sirolimo via MALDI-MS. Para comparação dos resultados obtidos, adaptou-se uma metodologia quantitativa via HPLC-PDA para os compostos.²⁻⁴

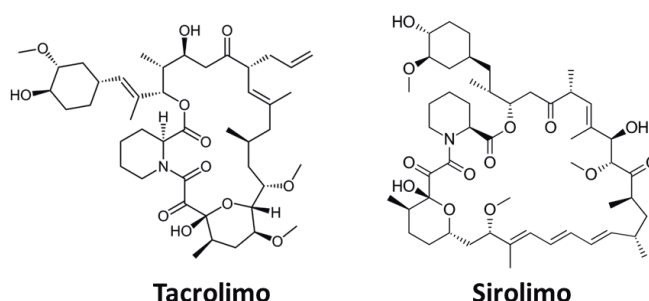


Fig. 1: Estruturas do Tacrolimo e Sirolimo

Trabalhos anteriores realizados pelo grupo, demonstraram que o MALDI-MS apresenta um grande potencial para ser utilizado como ferramenta quantitativa. O método desenvolvido para quantificações dos imunossupressores tacrolimo e sirolimo apresentaram linearidade, obtendo-se $R^2 \geq 0,990$, nas curvas e acurácias dentro da faixa estipulada de 85-115%.

Os primeiros testes realizados contaram com a utilização de amostras de plasma fortificados com soluções de concentrações intermediárias das curvas de calibração de tacrolimo e sirolimo. Figuras de mérito como coeficiente de correlação, reprodutibilidade e efeito matriz foram avaliados para a análise dos imunossupressores em plasma. Os resultados preliminares do protocolo se mostraram com potencial para a sua aplicação em matrizes biológicas visando a determinação de tacrolimo e sirolimo.

[1] *Transplantation*. 2004, 77, S41–43. [2] *Int. J. Pharm. Pharm. Sci.* 2011, 3, 219–222. [3] *Iran. J. Pharm. Res.* 2013, 12, 77–81. [4] *Molecules*. 2020, 25, 1–69.

Agradecimentos/Acknowledgments

CNPq-PIBIC/PIBITI (Bolsa JL)

Assessment of antioxidant activity, total phenolics and oxidative stability in different extracts of *Rosmarinus officinalis*, after additivation in biodiesel using UV-Vis and Rancimat.

Tayná de S. V. Moura (PG),^{1*} Bruno A. S. dos Santos (PG),² Renato de O. Soares (PQ),³ Vânia Mori (PQ),³ Eduardo H. S. Cavalcanti (PQ),³ Kátia R. de Souza (PQ).¹

tayna@ime.eb.br

¹Seção de ensino de engenharia química, IME; ²Departamento de Química, UFF; ³LACOR, INT.

Palavras-chave: *Rosmarinus officinalis*; biodiesel; antioxidant activity; oxidative stability; Rancimat

Highlights

The present work evaluated the antioxidant activity and oxidative stability in different extracts of *Rosmarinus officinalis*. A known methodology for extraction was used, but the extracts differ in terms of particle size, the smallest showed better results. A commercialized extract was also evaluated. From there, it was added to pure biodiesel. The results found were promising.

Resumo/Abstract

Biodiesel é um combustível pouco poluente, proveniente de óleos vegetais ou gordura animal, que possui alta reatividade com o oxigênio, sofrendo oxidação, resultando em seu envelhecimento e prejuízos severos aos sistemas de injeção, filtragem e ao motor dos automóveis. Devido à baixa estabilidade deste, frente a processos oxidativos, torna-se necessária a adição de antioxidantes a fim de preservar o limite mínimo de 12 h para estabilidade oxidativa (EO), conforme exigido pela resolução ANP nº 45 de 2014. Este trabalho tem como objetivo avaliar e analisar diferentes extratos do *Rosmarinus officinalis* (alecrim), que serão aditivados no biodiesel puro (B100) como antioxidante. Foram preparadas duas extrações, segundo metodologia já existente, porém com diferença em duas variáveis: o material de partida foi a parte já seca (otimizando o preparo de amostra) e a variação na granulometria para cada extrato. O extrato 1 passou por trituração, pesagem (240 g), seguido da adição de 1L de etanol, e o extrato 2 foi submetido à trituração, maceração, peneiração (mesh 100) e pesagem (36 g), seguido da adição de 200 mL de etanol. Ambos foram agitados manualmente por 15 dias consecutivos e agitados em mesa agitadora no último dia, por 2h. Após, foram filtrados a vácuo e levados ao rotaevaporador. Também foi utilizado um extrato comercial de alecrim contendo teor etanólico de 40%. Foram adicionados 1000 mg L⁻¹ de cada extrato ao biodiesel em triplicatas, para determinação da EO no equipamento Rancimat. Para a análise de atividade antioxidante (AA), foram utilizados padrões de controle: ácido ascórbico e trolox, que apresentaram respectivamente, atividade antioxidante, iguais à 98,62% e 96,6%. As análises foram realizadas no espectrofotômetro pelo método de Folin-Ciocalteu para fenólicos totais (FT) e o DPPH para (AA). Os resultados obtidos de AA e EO estão apresentados na Tabela 1. Em relação aos FT, os valores obtidos em mg L⁻¹ seguem a ordem crescente de **extrato 2 < extrato 1 < comercial** (48, 68, 82, respectivamente). Observa-se, a partir desse conjunto de dados, que não é possível estabelecer uma relação direta entre FT e AA entre os extratos analisados. Contudo, a AA para ambos os extratos apresentam altas porcentagens, indicando fortemente AA, que podem ser utilizados como antioxidante no biodiesel. Apenas o extrato comercializado apresentou alto teor de FT. Conclui-se que o extrato 2 é o melhor resultado obtido para AA e EO. A partir dos resultados de EO apresentados, percebe-se que o extrato 2 pode ser empregado como antioxidante natural em substituição aos antioxidantes sintéticos (TBHQ, Terc-butilhidroquinona e BHT, Butilhidroxitolueno), por estar em conformidade com as exigências da ANP. Vale destacar que os antioxidantes sintéticos são prejudiciais ao meio ambiente e, conseqüentemente, ao ser humano.

Tabela 1. Teor de fenólicos totais, atividade antioxidante e estabilidade oxidativa para os extratos de *Rosmarinus officinalis*.

Amostras	Atividade antioxidante (%) ± SD	Estabilidade oxidativa (h) ± SD
Extrato 1	89,69 ± 3,6	8,43 ± 0,41
Extrato 2	94,64 ± 5,5	15,17 ± 0,83
Extrato comercial	85,6 ± 4,7	6,19 ± 0,15

Agradecimentos/Acknowledgments

Este estudo foi financiado em parte pela Coordenação de Pessoal de Nível Superior -(CAPES)- Código Financeiro 001, FAPERJ (edital nº05/2020) e IME (Instituto Militar de Engenharia).

Avaliação de marcadores de qualidade de cafés certificados brasileiros

Angelo Pedott Apel (PQ),^{1*} Edmar Martendal Dias de Souza (PQ).¹

angelopedott@gmail.com.

¹Laboratório de Química Analítica e Nanomateriais Inorgânicos – LABQAN, Departamento de Química, CCT-UDESC, Joinville-SC, Brasil.

Palavras Chave: Café, GC-MS, HPLC, PCA, Cafés especiais.

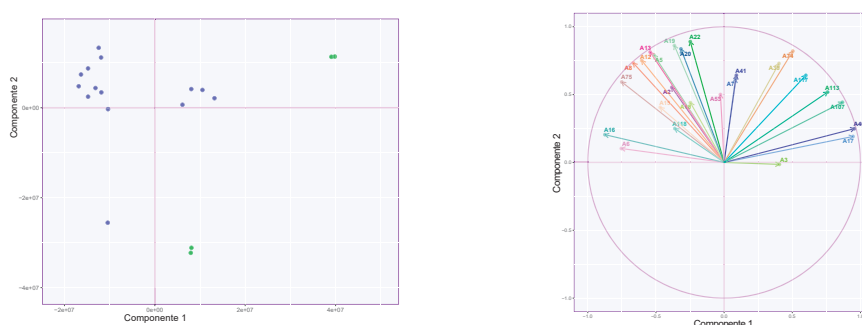
Highlights

Evaluation of quality markers of certified Brazilian coffees. Development of a methodology for compositional analysis of Brazilian certified coffees by chromatographic analysis. PCA was used to identify possible quality markers for coffees.

Resumo/Abstract

O café é um dos produtos mais comercializados internacionalmente no mercado mundial, com valores agregados dos grãos subindo a cada dia. O termo “cafés especiais” identifica cafés com alta qualidade, impactando no sabor. Dessa forma, para além das análises sensoriais se mostra relevante o desenvolvimento de metodologias de análise e caracterização da composição dos cafés especiais, podendo servir como métodos de autenticação e classificação [1]. Este trabalho tem como objetivo o desenvolvimento de uma metodologia de análise para componentes voláteis e não voláteis de cafés brasileiros com finalidade de analisar, através do uso de ferramentas quimiométricas, possíveis marcadores de qualidade de cafés certificados. Para isso, foi estudado a influência da moagem na extração sólido-líquido (Fina, Média e Grossa) e a influência da filtração no extrato (filtro 0,45 µm). As condições cromatográficas para a cromatografia líquida, modificador ácido da fase aquosa (ácido acético e ácido fosfórico), eluições em gradiente e isocrática e solvente da fase orgânica (acetonitrila e metanol). Para cromatografia gasosa foram estudadas a temperatura de injeção (270°C, 260°C) e a programação do forno. A seleção das amostras analisadas utilizou as bases de dados da associação brasileira da indústria do café e da Brazil specialty coffee association, buscando encontrar cafés de classificações distintas (tradicional e especiais) em regiões próximas. A partir dos dados das análises foram selecionadas 137 componentes para serem utilizadas na análise de componentes principais, resultando no plano PC1xPC2 na Figura 1. Podemos observar uma separação entre as amostras de cafés tradicionais (em verde) e as amostras de cafés especiais (azul).

Figura 1 - Plano PC1xPC2 contendo amostras de cafés e o gráfico de loadings das variáveis



Analisando os *loadings* das variáveis analisadas, foram selecionados os analitos de participação significativa para PC1 e PC2, sendo identificado que compostos derivados da pirazina podem ser indicadores de cafés especiais e derivados do fenol sendo indicadores de cafés tradicionais. É proposto aumento no número de amostras para uso nos modelos e avaliação das outras componentes, juntamente com uso de outros modelos quimiométricos.

[1] DOMINGUES, D. S. et al. Food Chemistry Vol. 146, pp. 353–362 (2014)

Agradecimentos/Acknowledgments

CMU/CCT-UDESC, FAPESC, CAPES and CNPq

46ª Reunião Anual da Sociedade Brasileira de Química: “Química: Ligando ciências e neutralizando desigualdades”

Calibration transfer between two FT-NIR spectrometers to PLS prediction of acid value in andiroba seed oils

Gabriela C. Caldas (IC),^{1*} Rayanna F. R. Reis (IC),¹ Neirivaldo C. da Silva (PQ),¹

gabriela.caldas@icen.ufpa.br

¹Faculdade de Química, Instituto de Ciências Exatas e Naturais, UFPA, Belém, Pará, Brasil, 66075110.

Keywords: Andiroba seed oil, Acid value, NIR spectroscopy, PLS regression, Calibration transfer.

Highlights

Direct and reverse standardization between FT-NIR instrument.
RS and DS RMSEP values comparable to primary PLS model.
Recalibration of PLS models to predict acid value in andiroba oil can be avoided.

Resumo/Abstract

The attractive chemical composition of andiroba seed oil (ASO)¹ makes it valuable for the cosmetic and medicinal segments, and economically very important for local communities in Amazon rainforest. NIR spectroscopy (NIRS) can be a potential alternative for assessing acid value (AV) in ASO. It can enable sustainable and environmentally responsible methodologies when compared to reference analytical method to determine AV (time and chemicals consuming). In the context of quality monitoring programs which involves several instruments, especially when they are located far away from each other, the time and cost for transporting samples and PLS recalibrating new spectral responses may be a relevant inconvenient. This can be avoided by means of calibration transfer methods. The present work evaluates the use of reverse (RS) and direct (DS) standardization methods to correct spectral responses from two benchtop FT-NIR spectrometers to enable prediction of AV in ASO. This application has not been found in literature up to now. Reference AV ranged from 5.5 to 81.2 and were expressed as the number of mg of potassium hydroxide needed to neutralize 1 g of the sample². ASO samples (39) were purchased from popular markets or local company. An ABB MB3600 and a Thermo Scientific Antaris II spectrometers were employed (1 mm optical path, 12800 to 4000 cm⁻¹ range, 16 scans and absorbance measured every 4 cm⁻¹). The 1st derivative, 2nd order polynomial and 31 points Savitzky-Golay filter was the most appropriate preprocessing. Cross-validation and prediction sets were selected by SPXY algorithm. Venetian blinds cross-validation method was used. In the DS approach, the PLS model built with Antaris II original spectra (primary) was applied to corrected prediction samples from MB3600 (secondary). In the RS approach, a new PLS model was built using Antaris II corrected spectra and applied to original prediction MB3600 samples. Ten transfer samples were selected using SPXY algorithm. Table 1 presents the figures of merit achieved by the PLS models built.

Table 1. Figures of merit of the PLS models developed in both instruments and after DS and RS approach.

PLS models	Nº of cross-validation samples	Nº of prediction samples	Nº of latent variables	Cross-validation			Prediction		
				RMSE	Bias	R ²	RMSE	Bias	R ²
Antaris II (primary)	21	9	4	3.6	-0.34	0.97	2.5	0.43	0.96
MB3600 (secondary)	27	12	7	4.4	-0.41	0.95	3.1	0.06	0.96
Direct standardization approach	20	12	7	3.2	-0.12	0.98	4.1	-1.77	0.96
Reverse standardization approach	20	12	3	3.9	-0.19	0.97	3.9	-0.16	0.94

PLS loadings are mainly in the region of 1st overtone C-H bands, around 5750 cm⁻¹. Antaris II PLS model achieved the lower RMSEP value, although RMSEP showed no significant different for the four models (F-test, confidence level of 95%). Significant bias was observed for PLS model developed after DS approach only (t-test at, confidence level of 95%). It is worth noting that a biased prediction can be easily corrected by a simple slope and bias correction, if the RMSEP values were similar. The number of samples clearly is a limitation, but preliminary results demonstrate that standardization approaches between FT-NIR instruments for PLS predictions of AV in ASO are potentially feasible. Reverse standardization has achieved more satisfactorily results, considering the lower bias.

¹ Narvaez, LEM; Ferreira, LMMC; Sanches, S; Gyles, DA; Silva-Júnior, JOC; Costa, RMR. *Molecules*, 27, 2733, 2022.

² Odair Zenebon, Neus Sadocco Pascuet and Paulo Tiglia - São Paulo: Instituto Adolfo Lutz, 2008.

Agradecimentos/Acknowledgments

The authors would like to thank to FAPESPA, CNPq, Amazon Oil Company, Group of Advanced Analytical Spectrometry and Center for the Valorization of Amazonian Bioactive Compounds.

Características do estudo de linearidade relacionados à incerteza de medição em química analítica.

Bruna Drielen Ferreira Gonçalves (PG), ^{1*} Vitor Hugo Polisél Paces (PQ),¹ Igor Renato Bertoni Olivares (PQ),¹ Emanuel Carrilho (PQ),¹

bdrielen21@gmail.com; brunadrielen@usp.br

¹Departamento de Química e Física Molecular, IQSC-USP

Palavras-Chave: (linearidade, estatística, incerteza de medição, validação de método).

Highlights

Characteristics of linearity studies related to measurement uncertainty in analytical chemistry.

If linearity is not evaluated in a statistically adequate way, erroneous results can be masked. It is one of the sources that most significantly contributes to measurement uncertainty.

Resumo/Abstract

Esta pesquisa foi desenvolvida para, entre outros aspectos, verificar o baixo entendimento e a aplicação de ferramentas estatísticas na área Química Analítica e afins. Dentre as informações obtidas pela pesquisa, o objetivo deste trabalho foi apresentar discussões de resultados relacionados aos estudos de linearidade durante o processo de validação do método.

Foram realizadas avaliações de conformidade e verificações de cálculos estatísticos de dados analíticos publicados em diferentes periódicos, comparando os resultados publicados com os resultados obtidos por softwares validados para este fim denominados ConfLab Validação e ConfLab Incerteza, mediante aplicação dos respectivos dados brutos dos artigos, verificando os resultados de testes estatísticos que o software de validação realiza para o estudo de linearidade: avaliação da homocedasticidade (homogeneidade das variâncias dos resíduos); exatidão (desvio); coeficiente de variação (precisão) e coeficiente de determinação (r^2). Os resultados e as aplicações da validação, foram submetidos aos critérios de aplicação e aceitação de resultados de validações de métodos contidos em protocolos e legislações vigentes e verificadas suas conformidades. Os softwares são validados para aplicação da gestão de qualidade em laboratórios, e se baseiam no Ciclo de Garantia de Qualidade Analítica (AQAC) bem como nos guias Eurachem/Citac, por isso foram utilizados como valor referência. Os critérios para seleção dos documentos foram: artigos, teses, dissertações ou trabalhos de conclusão de curso que tratavam sobre desenvolvimento de método analítico com objetivo de detectar, quantificar, identificar, caracterizar algum analito em alguma matriz e continham os dados brutos obtidos durante o processo de validação.

Os resultados mostraram que, 64% dos estudos de linearidade não foram realizados dentro das recomendações do protocolo de validação para obtenção de dados. Com relação às características dos cálculos e testes estatísticos relacionados ao estudo de linearidade, obteve-se que, dentre as validações: a precisão dos pontos da curva foi calculada corretamente em apenas 37%; o desvio (erro relativo dos pontos da curva) não foi realizado em 89%; coeficiente de determinação (r^2) foi calculado em todas as validações, mas calculado incorretamente em 74% delas. Além disso, 70% das validações não apresentaram teste estatístico para investigar qual modelo de regressão era o mais adequado (teste de homocedasticidade). Ainda neste contexto, conforme os critérios, a frequência com que os estudos de linearidade foram executados com testes estatísticos suficientes foi de apenas 3% das validações.

Uma vez determinadas as potenciais variações provenientes da validação, as estimativas de incerteza de medição associadas aos métodos foram calculadas. Como consequência dos resultados de linearidade, dentre os parâmetros que mais contribuíram para as estimativas de incerteza, esta foi o parâmetro mais frequente quando avaliada entre os primeiros pontos da curva de calibração do método (usualmente nas menores concentrações do respectivo método), ocorrendo em 81% dos estudos avaliados. Para os pontos finais da curva, a ocorrência é em 41% dos estudos. Em concentrações intermediárias, a linearidade manteve o nível de contribuição (38%). É possível determinar, segundo a literatura, que o coeficiente de determinação (r^2) é inconclusivo quando utilizado isoladamente no estudo da linearidade, uma vez que não está relacionado a outros fenômenos que podem ocorrer durante este estudo. É importante salientar que depende diretamente de um teste de homocedasticidade que, se não realizado ou realizado de forma inadequada, pode mascarar a qualidade dos resultados baseados nesse estudo de linearidade.

Agradecimentos/Acknowledgments

Este estudo reuniu o apoio de: CAPES, CNPq, IQSC/USP e dos Softwares ConfLab.

Área:

ANA

Caracterização molecular de petróleos: óleos crus versus óleos fracionados

Iasmim A. de Souza (IC),¹ Thamara A. Barra (PG),¹ Dayane M. Coutinho (PQ),¹ Débora de A. Azevedo (PQ),¹

iasmimamorim@gradu.iq.ufrj.br;

¹Universidade Federal do Rio de Janeiro, Instituto de Química, LADETEC/LAGOA

Palavras Chave: óleos, espectrometria de massas de alta resolução, compostos polares, caracterização molecular.

Highlights

Petroleum molecular characterization: crude oil versus fractionated oils.

Molecular formula assignments of polar compound by high resolution mass spectrometry;

Evaluation of crude oil and fractionated oil polar compound analysis;

Assessment of discrimination applying different methods for polar compounds characterization.

Resumo/Abstract

O petróleo (óleo cru somado ao gás) é uma mistura complexa de hidrocarbonetos que contém os compostos polares com nitrogênio, oxigênio e enxofre (N, O, S) em menor quantidade. Tais compostos podem ocasionar problemas em equipamentos na cadeia petrolífera, entupimentos e outros inconvenientes. Para que problemas como estes sejam evitados, a caracterização do óleo é essencial. Devido à complexidade da composição do petróleo, existem métodos de fracionamento de óleos crus. Estes são realizados como um pré-tratamento dos óleos para análise por diferentes técnicas analíticas para caracterização molecular. O espectrômetro de massas de alta resolução do tipo Orbitrap (Orbitrap HRMS) proporciona uma análise rápida e é uma importante ferramenta para caracterização molecular de misturas como petróleo. Este instrumento analítico apresenta alta resolução e acurácia em massa e permite a detecção de compostos polares quando acoplado a fonte de ionização por eletrospray. A análise da fração de compostos básicos por Orbitrap HRMS, obtida pelo fracionamento do óleo cru, pode agregar à caracterização em relação a análise do óleo cru já que é obtida uma fração concentrada em compostos nitrogenados básicos importantes na caracterização do petróleo. Esse trabalho visa o estudo da fração básica de óleos utilizando a técnica de Orbitrap HRMS no modo positivo de ionização ESI (+) de duas maneiras: pela análise das frações dos óleos obtida por fracionamento por cromatografia líquida e pela análise dos óleos crus, sem fracionamento. As 3 amostras de óleo cru estudadas foram fornecidas pela Agência Nacional do Petróleo, Gás Natural e Biocombustíveis (ANP). Para obtenção da fração neutra/básica, a massa de 100 mg de cada óleo bruto foi pesada em balança analítica calibrada e separadas as frações neutra/básica e ácida pelo fracionamento em coluna recheada com sílica inicialmente impregnada com KOH. Após a eluição e recolhimento das frações básica/neutra de cada óleo, as quais em média representaram 78 % da massa de óleo inicial, estas foram solubilizadas em tolueno/metanol 1:1 (v/v) e foi utilizado o ácido fórmico como aditivo em modo de ionização positivo. A concentração final para injeção foi de 2,5 mg mL⁻¹ com 0,1 % (v/v) de aditivo. Os espectros de massas foram processados no programa Composer. Como resultado inicial, os três óleos crus apresentaram um número maior de fórmulas moleculares atribuídas às massas assinaladas, mostrando que houve uma perda de resposta na detecção, de aproximadamente 13 % em termos de moléculas assinaladas, e identificação de alguns íons nas frações de compostos básicos. Isso pode indicar que houve discriminação de algumas moléculas durante o método de preparo.

Agradecimentos/Acknowledgments

CNPq, FAPERJ, CAPES.

Characterization of cocaine samples seized by the Federal Police using low-cost NIR spectrophotometers and multivariate data analysis

Jamille C. Souza (PG),¹ Jennifer A. Cavalcante (PG),² Celio Pasquini (PQ),² Jarbas J. R. Rohwedder (PQ),² Adriano O. Maldaner (PG),³ Maria C. Hespanhol (PQ).^{1*}

jamille.c.souza@ufv.br; *mariacarmo@ufv.br

¹Departamento de Química, UFV; ²Instituto de Química, UNICAMP; ³Instituto Nacional de Criminalística, PF.

Keywords: Cocaine hydrochloride, Free base cocaine, Seized samples, NIR spectroscopy, Multivariate analysis, In situ analysis.

Highlights

Seized cocaine samples were characterized using multivariate analysis of their NIR spectra.
Feasibility study of portable and low-cost NIR spectrometers for in-situ analysis of seized drugs.

Abstract

Characterization of suspected substances at the time of seizure is of great importance to avoid failures and to allow law enforcement agents acting correctly and effectively, providing reliable evidence for future judicial decisions. Currently, the rapid tests performed for the *in situ* identification of cocaine (an illicit drug in many countries) are based on colorimetric reactions, which are generally not very trustworthy (since they produce many false-positives results).¹ Thus, the objective of this work was to develop an *in situ*, fast and non-destructive, method to chemically characterize cocaine samples, using low-cost miniaturized near-infrared (NIR) spectrometers and multivariate data analysis. For this, NIR spectra of 907 cocaine samples seized by the Federal Police in different locations of Brazil during 2020 and 2021 were collected (Figures 1A and 1B). These samples, which had already been previously characterized at the Institute National of Criminalistics (DF, Brazil), were analyzed using two spectrometers: the NanoNIR (Texas Instruments Inc. Austin, USA), that monitors the spectral range of 900 – 1700 nm; and the NeoSpectra micro-FT-NIR (Si-ware, Egypt), operating between 1350 to 2550 nm. Subsequently, the data set obtained was pre-processed and treated using the Unscrambler 11.0 software (Aspen Technologies, USA). First, the data were transformed using the 2nd derivative (Savitzky-Golay, 11 points, 2nd-degree polynomial), to minimize scattering and improve samples' spectral features. Then, principal component analysis (PCA) was performed on this data set (Figures 1C and 1D). Both NanoNIR (Figure 1C) and NeoSpectra (Figure 1D) instruments show the difference between the free base cocaine and cocaine hydrochloride already in the first two principal components (PCs). The component that best distinguishes between these two forms is PC1. However, as this feature has a great weight in the distribution of the scores, the next analyses were conducted using, separately, the cocaine hydrochloride and free base cocaine subgroups. PCA was also used to differentiate between pure and adulterated samples and to qualitatively identify the main cocaine adulterants (benzocaine, phenacetin, caffeine, lidocaine, aminopyrine, levamisole, procaine, hydroxyzine and diltiazem). In addition, PLS regression models were constructed, allowing quantify the cocaine content of the samples [RMSEP = 9.93 %]. Therefore, it was possible to develop a green and low-cost analytical method to identify and quantify cocaine and its main adulterants *in situ*.

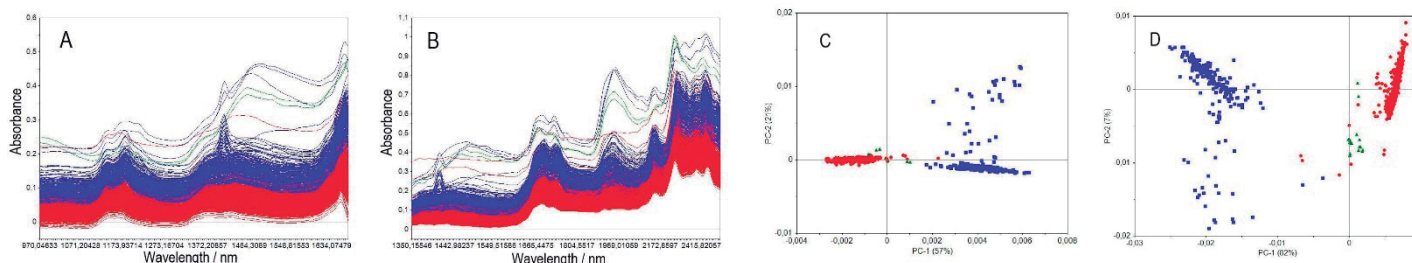


Figure 1. Raw spectra set of the seized cocaine samples: (A) NanoNIR; (B) NeoSpectra. And PCA scores distribution of the whole sample spectra: (C) NanoNIR; (D) NeoSpectra. ! Free base cocaine; , cocaine hydrochloride; 7 non-identified.

¹CONCEIÇÃO, V. N. et al. Estudo do teste de Scott via técnicas espectroscópicas: um método alternativo para diferenciar cloridrato de cocaína e seus adulterantes. *Química Nova*, v. 37, p. 1538–1544, 2014.

Acknowledgments

INCTAA/CNPq-FAPESP, FAPEMIG, CNPq, CAPES/PROCAD – Segurança Pública e Ciências Forenses.

Characterization of pen inks by Raman, FT-IR and Video Spectral Comparator analyses for forensic purposes: document fraud.

Rosane R. Souza (PG),¹ **Lucas M. Duarte** (PQ)^{2*}, **Gláucio B. Ferreira** (PQ)^{3*}.

rosaners@id.uff.br; duartelucas@id.uff.br; glauciobf@gmail.com.

¹Programa de Pós-graduação em Química, UFF; Instituto de Criminalística Carlos Éboli, ICCE; ²Departamento de Química Analítica, UFF; ³Departamento de Química Inorgânica UFF.

Palavras Chave: *Raman scattering, Infrared spectroscopy, Forensic ink analysis, Spectral Comparator.*

Highlights

Spectroscopic methods are useful for the characterization of pen inks. Combination of RS and FT-IR with UV-Vis spectroscopy for document fraud detection and obtaining unequivocal technical evidence.

Resumo/Abstract

A elucidação de fraudes documentais é importante para o esclarecimento de muitos crimes. Devido ao caráter de vestígio criminal das amostras, os métodos não destrutivos são preferíveis. Portanto, a caracterização de tintas de caneta, depositadas em papel, por técnicas analíticas sensíveis, reprodutíveis, confiáveis e que preservem o material questionado é de grande interesse.¹

O presente trabalho propõe a aplicação da espectroscopia vibracional na região do infravermelho (FT-IR) e Raman (RS), bem como a utilização do comparador espectral de vídeo (VSC) na obtenção de espectros de absorvância na região do visível, em amostras de canetas de diferentes marcas e modelos, disponíveis no mercado do Rio de Janeiro, a fim de verificar a viabilidade de utilização dessas técnicas, para a diferenciação das tintas analisadas.

A relação de amostras empregadas neste estudo está descrita na **Tabela 1**. As amostras foram produzidas pelo depósito das tintas na forma de traços verticais e de discos com aproximadamente 2 mm de diâmetro, em suporte de papel de gramatura 75 g.m⁻², de formato A4 e da marca Chamex. As análises foram realizadas nos Espectrômetros FT-Raman *Bruker MultiRAM* (laser 1064 nm) e *Thermo iS-50* com acessório ATR, no Microscópio Raman Confocal *InSpect* (laser 785 nm) e no VSC *Regula 4307*.

As tintas utilizadas em canetas são sistemas coloidais complexos.² Para terem as propriedades ideais são necessários vários componentes adicionais aos colorantes e ao veículo,^{2, 3} isto é, os aditivos proporcionam as características reológicas adequadas à distribuição da tinta no papel, conforme o tipo da ponta da caneta – esfera metálica rotatória (esferográfica, *Rollerball* e gel) ou ponta porosa.³

As análises de RS com o laser de 1064 nm possibilitaram a obtenção apenas do espectro do papel, visto que as amostras foram degradadas. As análises de RS com o laser 785 nm e lente *Leica L 50x/ 0.5*, destacaram a heterogeneidade das tintas sobre as fibras do papel e obteve-se espectros Raman com as seguintes características: boa qualidade - amostras (1) e (2); degradado – amostras (3), (4) e (5); baixa qualidade - amostra (6); com fluorescência - amostra (7). Os espectros de FT-IR permitiram identificar em 4 das 7 amostras analisadas a banda referente ao corante triarilmetano (1584 cm⁻¹).⁴ Os resultados obtidos pelas análises no VSC indicaram a diferenciação de fabricação das tintas, das amostras analisadas, devido à variação das bandas de absorção dos cromóforos, por exemplo as canetas BIC apresentaram 3 bandas características em 427, 547 e 683 nm. A proposta de combinação dessas técnicas é promissora para a caracterização de tintas de caneta.

REFERÊNCIAS: (1)Gomes, J. A.; Sercheli, M. S. *Revista Brasileira de Criminalística* **2011**, 1, 22. (2)Buzzini P. Suzuki E., *J. Raman Spectrosc.* **2016**, 47, 16. (3)Gondra, M. E.; Grávalos, G. R. *Análise Forense de Documentos Instrumentos de Escrita Manual e suas Tintas*, Millennium: Campinas, 2012. (4)Bojko K.; Roux C.; Reedy B. J., *J Forensic Sci.* **2008**, 53, 6, 1458.

Tabela 1- Características das canetas utilizadas no estudo.

	MARCA	MODELO	FABRICAÇÃO	TINTA	Cor da tinta	DIÂMETRO DA PONTA (mm)
1	BIC	Clássica E-H-29	Brasil	pastosa	azul	1,0
2	BIC	Ultra fine L-G-18	México	pastosa	azul	0,7
3	COMPACTOR	07 EEA9	Brasil	pastosa	azul	0,7
4	FABER-CASTELL	TRILUX 032 M	Brasil	pastosa	azul	1,0
5	FABER-CASTELL	TRILUX 035 F	Brasil	pastosa	azul	0,8
6	PILOT	BPS GRIPAZ	Brasil	gel	azul	0,7
7	PILOT	SUPER GRIP NI	Brasil	pastosa	preta	1,0

Agradecimentos/Acknowledgments

PPGQ – UFF e Instituto de Criminalística Carlos Éboli/ DGPTC/ SEPOL.

Chemical characterization by GC/MS of sugarcane bagasse bio-oils produced by hydrothermal liquefaction (HTL)

Rayane Maria do Nascimento (PG),^{1*} Flávio Montenegro (PG),² Raquel Santos (PG),³ Leandro Danielski (PQ)³, Diogo A. Simões (PQ)⁴, Maria Fernanda Pimentel (PQ),³ Jandyson M. Santos (PQ)¹

rayane.mar.nasc@gmail.com; jandyson.machado@ufrpe.br

¹Departamento de Química, UFRPE; ²Departamento de Química, UFPE; ³Departamento de Engenharia Química, UFPE; ⁴Departamento de Engenharia Bioquímica, UFPE.

Keywords: Bio-oil, Sugarcane bagasse, Hydrothermal liquefaction, GC/MS, Experimental design.

Highlights

Chemical characterization by GC/MS of sugarcane bagasse bio-oils produced by hydrothermal liquefaction (HTL)

- The production of sugarcane bagasse bio-oils by HTL was investigated and characterized by GC/MS;
- A factorial design was employed to evaluate the effects of temperature, presence of catalyst, and time.

Resumo/Abstract

The growing energy demand has encouraged studies dedicated to the development of fuels based on renewable sources, such as those that use waste biomass to produce bio-oils through thermal processes. Thus, chemical characterization of bio-oils at the molecular level by chromatographic and mass spectrometric analytical techniques assists in the chemical understanding of the products generated and can be used to evaluate the conditions of the bio-oil production process. The objective of the present study was to investigate the production process of sugarcane bagasse bio-oils by hydrothermal liquefaction (HTL) and to characterize the bio-oils by gas chromatography/mass spectrometry (GC/MS). The bio-oil production process was performed, based on the application of a 2³ complete experimental design, with replicates and including a central point. The variables evaluated were: (T) Temperature between 300-350 °C at high pressures in water, (t) residence time from 0 to 30 minutes, (C) potassium carbonate catalyst between 0 and 0.5 mol L⁻¹. After production, the mixture of bio-oil, the solid phase, and the aqueous phase was separated by vacuum filtration. Then, the bio-oil and the solid phase were extracted with acetone in Soxhlet for 8h. The organic extract was rotary evaporated to obtain the liquid bio-oils, which were analyzed by GC/MS (model QP2010 SE, Shimadzu Co., Japan) after derivatization with BSTFA. From the comparison of the retention times of the chromatographic peaks and their respective mass spectra, with the aid of the NIST Library, the compounds present in the bio-oils were assigned and grouped into classes according to their organic functions. The preliminary results revealed a majority chemical composition of oxygenated compounds such as esters, alcohols, and phenols. When we evaluated the experimental design, the significant effects (at 95% confidence) for alcohol and ester classes, based on the percentage of classes, were the main effects of T, C, and the interaction T x C. For the alcohol response, the effect of changing the temperature from 300 °C to 350 °C, when no catalyst is used (low level), is a decrease in the content of alcohols by 43.3%. No significant effect is observed for T, when the catalyst concentration is 0.5 mol L⁻¹. The effect of the presence of the catalyst is only observed when the temperature is 350 °C, increasing the alcohol content in 43.6%. In the case of ester content, similarly, a significant effect for the temperature is only observed when the catalyst is in the lower level (no catalyst), resulting in an increase for the ester content in 47.5%. The effect of C is also only observed when the temperature is 350 °C, decreasing the ester content in 44.7%. For the hydrocarbon class (HC), the main effect of t and all interactions are statistically significant. The experimental condition that produces the higher amount of HC (~16%) is: T = 300 °C, C = 0 mol L⁻¹; t = 0 min. The phenol class was detected in low percentages, as well as carboxylic acids, aldehydes, ethers, nitrogenous, and thiocompounds. Thus, the application of experimental design for the evaluation of the HTL process allowed obtaining different bio-oils with diversified chemical composition for different organic classes, making it possible to infer the best conditions of temperature, catalyst, and time in order to obtain target classes.

Agradecimentos/Acknowledgments

NUQAAPÉ, INCTAA, FACEPE, CNPQ, CAPES, PETROBRAS, SUZANO, KLABIN, EMBRAER PRPPG/UFRPE.

Colorimetric detection of creatinine on paper-based analytical devices using digital microfluidics for automatic sample manipulation

Larissa G. Velasco (PG)^{1*}, Danielly S. Rocha (PG)¹, Wendell K. T. Coltro (PQ)¹

larissa.garcia.velasco@discente.ufg.br

¹Universidade Federal de Goiás, Instituto de Química, Goiânia, Goiás, Brazil, 74690-900

Digital microfluidics, Colorimetric detection, μ PAD, Creatinine, Automated operations.

Highlights

The use of digital microfluidics coupled to a μ PAD for colorimetric detection of creatinine, a useful biomarker for renal function with automated sample manipulation is reported in this study.

Resumo/Abstract

Digital microfluidics (DMF) is a platform to manipulating droplets in nano- to microliter-scale in an array of insulated electrodes, applicable in different areas due to its reconfigurable arrangement. This technology enables fluidic operations of multiple droplets in parallel, which is one of the main advantages of the operation automation such as: dispensing from reservoirs, merging, mixing, splitting, and directed movement¹. Colorimetric detection is a simple, low-cost and usual method for several biomolecules, however, this technique requires efficient light control². Therefore, this study proposes the automatic manipulation of samples with DMF coupled to microfluidic paper-based analytical device (μ PAD) image capture and analysis through a desktop scanner due to its efficient light control. As a proof-of-concept, the detection of creatinine (CR) was explored as a model. CR is a useful biomarker for the assessment of renal function as it is the metabolite waste product of muscle contraction excreted by the kidneys³. The colorimetric detection of CR was performed using the Jaffé reaction, which consists of the reaction of alkaline picrate with creatinine to form an orange-red product. First, a polyester plate containing 96 square zones and a scanner were used to optimize the concentration of picric acid (PA) and NaOH. The captured images with the scanner were analyzed with the Corel Photo-Paint software in the CMYK color system, exploring the yellow channel. Then, the mix type and mixing time on the DMF chip and the image acquisition time of the PADs after the reaction were optimized. Finally, an automated protocol was developed on the DMF chip for the construction of the CR analytical curve. The range of AP concentration analyzed was from 0.5 to 10 mmol L⁻¹, keeping the NaOH concentration fixed at 250 mmol L⁻¹, and the best result was achieved using 5 mmol L⁻¹ of PA. The NaOH concentration was optimized ranging from 50 to 450 mmol L⁻¹, and the highest color intensity was observed at 300 mmol L⁻¹. These experiments were performed using CR solutions prepared at concentrations of 8 and 32 mg dL⁻¹. For manipulation of the drops on the DMF chip, Tetronic 90R4 surfactant at 0.1% (v/v) was used. Linear and circular mixtures were analyzed on the DMF chip with time varying from 15 to 60 seconds, the highest intensity and lowest standard deviation were obtained with the circular mixture in 45 seconds. Under optimized conditions, the integrated system involving DMF and PAD showed great potential for CR detection. Preliminary results revealed a linear behavior in the concentration range between 2 and 32 mg dL⁻¹. Future efforts will be devoted to complete automation involving the entire analytical procedure, i.e., from sample preparation to detection and application to real samples.

¹Campos RPS, et al. Analytical Chemistry, 91, 2019, 2506

²Fan Y, et al. Measurement, 171, 2021, 108829

³Mathaweesansurn, et al. Talanta, 210, 2020, 120675

Agradecimentos/Acknowledgments

CNPq, FAPEG, CAPES, INCTBio.

Área: ANA

(Inserir a sigla da seção científica para qual o resumo será submetido. Ex: ORG, BEA, CAT)

COLORIMETRIC TEST STUDY FOR THE IDENTIFICATION OF DRUGS USING IN SILICO AND STATISTICAL METHODS

Caio Henrique Pinke Rodrigues (PG),¹ Aline T. Bruni (PQ),¹

caio.pinke.rodrigues@usp.br; caio.pinke.rodrigues@usp.br

¹ Instituto Nacional de Ciência e Tecnologia Forense (INCT Forense) e Departamento de Química, Faculdade de Filosofia, Ciências e Letras de Ribeirão Preto, Universidade de São Paulo. Ribeirão Preto, SP, Brasil, 14040-900.

Keywords: Chemometrics, Amphetamine-type stimulants, Presumptive test, DFT.

Highlights

We observed that an objective distinction between the drug classes was impossible.

We demonstrated that the methodology used was adequate for evaluating presumptive tests.

Resumo/Abstract

Police, customs, prisons, and other public institutions have always demanded rapid drug detection methods. Simple presumptive tests based on color coding are used to identify drugs. One of the most known classes of drugs is Amphetamine-type stimulants (ATS). The main objective of this research was to evaluate, by *in silico* methods, the possibility of using fluorescein isothiocyanate (FITC) as a presumptive test for identifying ATS. Twenty-eight molecules were studied, 14 amphetamines and 14 structurally homologous cathinones. The isolated structures and those forming the bond with the FITC were optimized with B3LYP/6-31G** in the ORCA software. The absorption spectra calculation of these structures used the TDDFT (Time-Dependent Density Functional Theory) with the same methodological level. The CPCM (conductor-like polarizable continuum model) method considered methanol and hexane solvents. The evaluated wavelengths ranged from 600 to 400 nm. Data were organized in a spreadsheet and evaluated according to Pearson's correlation and by exploratory analysis (PCA – Principal Component Analysis) using the Pirouette v.4.5 software (Infometrix). The results indicated that the absorption (λ_{max}) for drug identification ranged from 280 to 480 nm, with two principal peaks. These regions agreed with the absorption regions of the alkyl and benzodioxol groups (with $\pi \rightarrow \pi^*$ transitions). We observed no well-defined pattern between amphetamines and cathinones using Pearson's correlation coefficient. With PCA, we observed that 90.93% of all initial information was within two principal components. The scores indicated no relationship that could differentiate amphetamines from cathinones. Both responses were diffuse, making it impossible to establish an objective standard for interpretation. We concluded that using *in silico* methods can be a faster and less costly alternative for evaluating drug identification tests. This work demonstrated this, as we provided information on the viability or otherwise of reactions and showed that *in silico* methods are a valuable ally in forensic matters.

Agradecimentos/Acknowledgments

The Conselho Nacional de Desenvolvimento Científico e Tecnológico (CNPq, 465450 / 2014-8) and the Coordenação de Aperfeiçoamento de Pessoal de Nível Superior (CAPES, Financial Code 001) for financial support.

Combination of an Efficient Digestion Method and Multi-Collector Inductively Coupled Plasma-Mass Spectrometry for Crude Oil Isotopic Analysis

Alessandra S. Henn (PQ),^{1,2} Stepan M. Chernonozhkin (PQ),³ Frank Vanhaecke (PQ),³ Erico M.M. Flores (PQ)^{1*}

alessandrahenn@gmail.com; ericommf@gmail.com

¹Departamento de Química, UFSM; ² Departamento de Química, UTFPR, ³ Department of Chemistry, UGent

Palavras Chave: Crude oil, Isotopic Analysis, MC-ICP-MS, Magnesium, Lead, Strontium.

Highlights

Isotopic analysis of crude oil was possible combining efficient digestion and MC-ICP-MS
Time-consuming methods and large amounts of reagents were avoided
Promising tool to decipher the formation history of crude oil reservoirs

Resumo/Abstract

Information related to the formation history of crude oil, as well as its origin, type and migration can be obtained from the isotopic composition of some target elements. Elements such as Mg, Sr and Pb have been used as tracers in several applications, including geochemical, environmental and biomedical. The isotopic analysis of Mg, Sr and Pb has been already performed in several matrices, such as environmental, geological and archeological materials, as well as biological fluids and tissues. However, only a few studies were found in the literature on Sr and Pb isotopic composition in crude oil (four related to Pb and only a single study was found for Sr). Moreover, no papers have reported Mg isotopic analysis of crude oil so far. It is well known that a major challenge in crude oil analysis is the sample decomposition step, as an efficient decomposition of the crude oil matrix is not always achieved. As a result, information on the isotopic composition of Mg, Sr and Pb in crude oil is still lacking. Thus, the goal of the present study was to develop methods for Mg, Sr and Pb isotopic analysis of crude oil combining efficient digestion and high-precision multi-collector inductively coupled plasma-mass spectrometry (MC-ICP-MS). In this sense, microwave-assisted wet digestion with a pressurized digestion cavity (MAWD-PDC) was evaluated as sample preparation method. This system allows higher digestion temperatures and pressures (up to 300 °C and 199 bar) than conventional systems, assuring a more efficient digestion of hard-to-digest samples, such as crude oil. Using MAWD-PDC, up to 500 mg of crude oil was efficiently digested using just 6 mL of 14 mol L⁻¹ HNO₃ (75 min, temperature of up to 250 °C). MAWD-PDC was shown to be a suitable sample preparation method for subsequent Mg, Sr and Pb determination and their isotope ratios. Isolation protocols were fine-tuned to the composition of crude oil solutions obtained after MAWD-PDC. For Mg, isolation was successfully carried out using a cation exchange resin (AG 50W-X8). The isolation of Sr and Pb, on the other hand, was performed by applying a sequential isolation protocol using the Sr-spec resin. The Mg-Sr-Pb isotopic composition of the Brazilian crude oils evaluated in this study was within the range observed for seawater and the deposit bedrock. Finally, the methods developed in this study can be considered as promising tools to decipher the formation history of crude oil reservoirs.

Agradecimentos/Acknowledgments

CNPq, CAPES, CAPES-PrInt and FAPERGS

Área: ANA

(Inserir a sigla da seção científica para qual o resumo será submetido. Ex: ORG, BEA, CAT)

Comparação de métodos de preparo de amostra para análise multielementar de extratos medicinais de *Cannabis* por ICP-MS

João Victor Meirelles Leite (PG)^{1,*}, Monica Costa Padilha (PQ)², Tatiana D. Saint’Pierre (PQ)¹.

jvmeirelles18@gmail.com; monicapadilha@iq.ufrj.br; tatispierre@puc-rio.br;

¹Departamento de Química, DQ-PUC-Rio; ²Instituto de Química, IQ-UFRJ;

Keywords: *Cannabis*, ICP-MS, wet digestion; block digester; dilute-and-shoot, multielement analysis

Highlights

Comparison of sample preparation methods for multielement analysis of medicinal *Cannabis* oils by ICP-MS. Method development for a multielement analysis of cannabis oils by ICP-MS. Wet digestion in hot plate, in a digester block and a *dilute-and-shoot* approach were applied to different vegetable oils and statistically evaluated.

Resumo/Abstract

A *Cannabis* é uma espécie de planta altamente diversa e polimórfica, com uma extensa capacidade de biossíntese de metabólitos variados. O potencial psicoativo da *Cannabis* já é conhecido há mais de 5 milênios e a busca por seu aproveitamento, tanto medicinal quanto recreativo, se encontra atualmente em expansão. Mais de 40 tipos diferentes de produtos derivados de *Cannabis* se encontram disponíveis comercialmente e, dentre os itens de caráter medicinal, os extratos oleosos se destacam como um potencial insumo farmacêutico. Conforme avanços judiciais ocorrem quanto à regulamentação da *Cannabis*, urge a necessidade de se desenvolver e padronizar métodos de avaliação de riscos e de controle de qualidade. Dentre os principais alvos de estudo encontrados na literatura, pode-se destacar a identificação e quantificação de espécies inorgânicas. Os metais e metalóides são componentes determinantes da matriz, podendo representar, tanto contaminantes tóxicos passíveis de bioacumulação quanto cofatores essenciais nas vias de biossíntese da *Cannabis*. A análise elementar dos óleos medicinais de *Cannabis* por técnicas espectrométricas se mostra desafiadora, visto a alta carga de matéria orgânica presente na matriz – majoritariamente constituída de óleos vegetais ricos em triglicerídeos de cadeia média – e a conseqüente necessidade de métodos apropriados de preparo de amostra para minimização da mesma. Neste trabalho, 3 diferentes métodos de preparo de amostra foram comparados para a determinação de 29 elementos em diferentes óleos vegetais, por espectrometria de massa com plasma indutivamente acoplado (ICP-MS): (i) decomposição ácida em chapa de aquecimento; (ii) decomposição ácida em bloco digestor; e (iii) uma abordagem *dilute-and-shoot* em solvente orgânico. As duas primeiras abordagens foram otimizadas quanto à massa de amostra, ao volume de solvente empregados e ao tempo de tratamento térmico, de forma multivariada, seguindo um planejamento fatorial fracionário e um planejamento Doehlert, enquanto a metodologia *dilute-and-shoot* foi otimizada de forma univariada quanto ao diluente empregado, ao fator de diluição e ao método de calibração. Óleos comerciais de gergelim e de coco foram adquiridos na cidade do Rio de Janeiro e empregados como matriz da amostra neste trabalho. Recuperações entre 94% e 135% foram obtidas para as digestões ácidas enquanto a diluição em xileno forneceu recuperações entre 79% e 114%. Os parâmetros de massa de amostra e de volume de solvente foram estatisticamente demonstrados como os fatores de maior contribuição no rendimento da digestão ácida das amostras. Após o desenvolvimento dos métodos, avaliados com óleos de gergelim e de coco, os mesmos serão aplicados a amostras de óleo de *Cannabis*.

1. NIE, B.; HENION, J.; RYONA, I. The Role of Mass Spectrometry in the Cannabis Industry. **Journal of Mass Spectrometry**, v. 30, n. 5, p. 719–730, 2019.
2. DAMAK, Fadwa et al. Comparison of sample preparation methods for multielements analysis of olive oil by ICP-MS. **Methods and protocols**, v. 2, n. 3, p. 72, 2019.
3. ALIFERIS, K. A.; BERNARD-PERRON, D. Cannabinomics: Application of Metabolomics in Cannabis (*Cannabis sativa* L.) Research and Development. **Frontiers in Plant Science**, 2020.

Agradecimentos/Acknowledgments

The authors gratefully acknowledge the financial support from Conselho Nacional de Desenvolvimento Científico e Tecnológico (CNPq) and Laboratório Brasileiro de Controle de Dopagem (LBCD).

Comparison of the chemical profile of alcoholic and non-alcoholic brewing products by of multivariate analysis.

Marco Aurelio D. Sasso (TM)^{1*}; Ananda da S. Antonio (PQ)¹; Gabriela V. Costa (PQ)¹.

dalsasso@iq.ufrj.br*; gabrielavanini@iq.ufrj.br

¹Universidade Federal do Rio de Janeiro, Instituto de Química, Núcleo de Análises Forenses (NAF), CEP 21941-598, Brasil

Keywords: Non-alcoholic beer, GC-MS, PCA, HCA, Volatile fingerprinting.

Highlights

33 compounds were identified within brewing products

PCA and HCA grouped samples by yeast, alcohol content, and ethanol removal process

Easy and fast methodology to quality control in brewing industry

Resumo/Abstract

Beer is one of the oldest and most consumed fermented beverage in the world. Its popularity is mainly related to the pleasant sensory features and lower cost compared to other alcoholic beverages¹. However, several factors, such as changes in legislation, religious and health issues, have driven the development of non-alcoholic and low alcoholic beers. Alcohol removal can be achieved by methods, such as reverse osmosis, evaporation, or biological processes. The use of these techniques can cause significant changes in beer sensorial features. Yet, consumers expect the non-alcoholic product to have the same characteristics as the original. The objective of this work was to compare the chemical profile of alcoholic beers (n = 3) and their non-alcoholic counterparts (n = 3) from three brands available in the Brazilian market by multivariate analysis². For this purpose, samples were extracted by liquid-liquid extraction, with 1 mL of tert-butyl methyl ether. The obtained extracts were chemically characterized by gas chromatography tandem mass spectrometry (GC-MS). After the identification of compounds, the chemical fingerprints of each sample were compared through Principal Component Analysis (PCA) and Hierarchical Clustering Analysis (HCA). GC-MS analysis enabled the identification of 33 substances, including acids, aldehydes, esters, higher alcohols, and other compounds. Based on these 33 compounds relative concentration in each sample (n = 6), PCA and HCA clustered them in two distinct groups, which were consistent to samples classification as alcoholic and non-alcoholic beers. Among the 33 compounds used as response-variable in multivariate analysis, six of them had greater influence in the distinction between alcoholic and non-alcoholic samples. These chemical markers included 2-methyl-propan-1-ol (1), 3-methylbutan-1-ol (2) and tyrosol (3). In non-alcoholic beers, the concentration of (1) and (2) was lower than similar alcoholic beers. As (1) and (2) are volatiles compounds, their concentration in non-alcoholic samples may have decreased during the ethanol removal process. PCA also enabled to identify that the ethanol removal process applied by each of the different brands evaluated can significantly impact the final product chemical fingerprint. For instance, the alcoholic and non-alcoholic samples of one specific brand (Brand C) demonstrated less dissimilarity among them, when compared to the pair of samples from the other brands (Brand A and B). The ethanol removal process used by Brand A caused a significant difference on (3) concentration among the alcoholic and non-alcoholic product. Compound (3) is formed during fermentation, and its lower concentration suggests that the process used affected this step. Thus, this component may indicate that different types of yeast were used in the production processes. We can conclude that the ethanol removal process had a significant impact on the profile of the most volatile compounds, except for Brand C. The multivariate analysis was able to group the different brands and products according to alcohol content, the ethanol removal process and the type of yeast used. This type of statistical analysis can be used as a tool for monitoring the process and in the development of new ethanol removal technologies.

¹ Salantă, L. C.; Coldea, T. E.; Ignat, M. V.; Pop, C. R.; Tofană, M.; Mudura, E.; Borsa, A.; Pasqualone, A. e Zhao, H. *Processes* 2020, 8, 1382.

² Zhao, H.; Li, H.; Sun, G.; Yang, B. e Zhao, M. J. *Sci. F. Agric.* 2013; 93: 910–917

Agradecimentos/Acknowledgments

CNPq, Faperj, CAPES

Comparison of variable selection methods for acid value PLS prediction in andiroba seed oil using two FTNIR spectrometers

Rayanna F. R. Reis (IC),^{1*} Gabriela C. Caldas (IC),¹ Neirivaldo C. da Silva (PQ),¹

ncs@ufpa.br; rayanna.reis@icen.ufpa.br

¹Faculdade de Química, Instituto de Ciências Exatas e Naturais, UFPA, Belém, Pará.

Palavras Chave: Andiroba seed oil, NIR spectroscopy, Acid value, Variable selection, PLS regression.

Highlights

NIR based PLS models to predict acid value (AV) in andiroba oil.
VIP and *i*PLS variables selection improved PLS predictions for AV.
Selected variables corresponding to C-H combinations and 1st overtones.

Resumo/Abstract

Andiroba seed oil (ASO) is economically very important for local communities in Amazon rainforest, with attractive chemical composition for cosmetic and medicinal segments¹. Because it is a fast and practical technique, near infrared spectroscopy (NIRS) can be a potential alternative for assessing acid value (AV) in ASO, as it enables sustainable and environmentally responsible methodologies when compared to AOAC and AOCS method (a time and chemicals consuming analytical method). Variable selection approaches enable to investigate the feasibility of predicting AV in ASO using narrower NIR spectral ranges which are attractive for field quality control analysis using miniaturized spectrometers. This work compares full spectra PLS models with two variable selection approaches for prediction of AV in ASO, which is not described in literature so far. Thirty-nine ASO samples were acquired, including local market samples and a 6-year historical bank of a company located in Pará state. Reference AV (5.5 to 81.2) were expressed as the number of mg of potassium hydroxide needed to neutralize 1 g of the sample². Absorbance spectra were acquired in two spectrometers: an ABB MB3600 and a Thermo Scientific Antaris II (1 mm optical path, 12800 to 4000 cm⁻¹, 16 scans and absorbance measured every 4 cm⁻¹). Variable importance in projection (VIP) and interval PLS (*i*PLS) variable selection methods were tested. The 1st derivative, 2nd order polynomial and 31 points Savitzky-Golay filter was the most appropriate preprocessing. Cross-validation and prediction sets selected by SPXY algorithm were: 27 and 12 for MB3600; and 21 and 9 for Antaris II, respectively. Venetian blinds cross-validation method was adopted. Table 1 presents the figures of merit for the full spectra, VIP and *i*PLS approaches.

Table 1. Figures of merit of the PLS models developed.

		N° of spectral variables	N° of latent variables	Cross-validation			Prediction		
				RMSE	Bias	R ²	RMSE	Bias	R ²
MB3600	Full spectra PLS	4669	4	4.8	-0.49	0.94	3.6	-0.43	0.93
	VIP-PLS	478	4	4.8	-0.58	0.95	3.5	-0.32	0.93
	<i>i</i> PLS-PLS	250	2	3.8	0.1	0.96	3.0	0.04	0.95
Antaris II	Full spectra PLS	4279	5	2.9	-0.01	0.98	1.4	-0.1	0.99
	VIP-PLS	410	4	2.7	0.08	0.98	1.3	-0.1	0.99
	<i>i</i> PLS-PLS	250	5	3.9	-0.34	0.96	3.0	-0.39	0.97

All PLS models showed no significant bias (t-test, 95% confidence level). RMSEP values were not significantly different between MB3600 PLS models, while VIP-PLS and *i*PLS-PLS used a substantially lower number of spectral variables. For Antaris II, *i*PLS-PLS model showed a significantly higher RMSEP compared to full spectra PLS. VIP-PLS model performed significantly better for Antaris II than for MB3600. RMSEP comparisons were carried out based on an F-test (95% confidence level). NIR based PLS regression models performed satisfactorily to determine AV in ASO samples. Spectral ranges selected by both VIP and *i*PLS methods are in the region of combination and 1st overtone C-H bands, commonly present in operation ranges of relatively low-cost miniaturized NIR spectrometers.

¹ Narvaez, LEM; Ferreira, LMMC; Sanches, S; Gyles, DA; Silva-Júnior, JOC; Costa, RMR. *Molecules*, 27, 2733, 2022.

² Odair Zenebon, Neus Sadocco Pascuet and Paulo Tiglia - São Paulo: Instituto Adolfo Lutz, 2008.

Agradecimentos/Acknowledgments

The authors would like to thank to FAPESPA, CNPq, Amazon Oil Company, Group of Advanced Analytical Spectrometry and Center for the Valorization of Amazonian Bioactive Compounds.

Compatibility studies between two medications in eyedrops, Brimonidine Tartarate and Timolol Maleate in the presence of some excipients

Lucas Y. Sato (IC)^{1*}, Maria Inês G. Leles (PQ)¹.

yugosato@discente.ufg.br; yugosato@discente.ufg.br

¹Laboratório de Métodos de Extração e Separação, Universidade Federal de Goiás (UFG), Goiânia, Brazil

Palavras Chave: BRIMONIDINE, TIMOLOL, EXCIPIENTS, COMPATIBILITIES, TGA, DSC.

Highlights

In the present work Brimonidine Tartarate, Timolol Maleate and three excipients were analyzed by TGA and DSC. Thermal analysis is a useful tool and important step in pre-formulation studies.

Resumo/Abstract

Glaucoma is one of the leading causes of blindness in the world due to the elevation of intraocular pressure (IOP) caused by insufficient drainage and/or excessive production of aqueous humor (AH). Brimonidine Tartarate (BMT), a highly selective α_2 -adrenergic agonist, and Timolol Maleate (TM), a non-selective β -blocker are both topical medications, commonly used in the form of eyedrops to treat glaucoma. Both of them work similarly by reducing the production of AH and increasing the AH outflow through the uveoscleral pathway and showed additive effects when administered together [1]. Formulations with BMT and TM often contain excipients such as Benzalkonium Chloride (BAC) and different types of phosphates. It's important to run pre-formulation tests with the active pharmaceutical ingredient (API) and the excipients to check if there are any incompatibilities between them. This is normally done through thermal analysis (TGA and DSC). In the present work, BMT, TM, BAC, dibasic sodium phosphate anhydrous (DSPA) and Monobasic sodium phosphate monohydrate (MSPM) were thermally studied, analyzing both API alone and binary mixtures of API + excipients (50:50 w/w). TG curves of the APIs and excipients were obtained using a model TG/SDTA/ 851^e Mettler Toledo by heating approximately 7.000 mg of sample from 25 to 1000 °C in a α -Al₂O₃ pan. The DSC curves of the APIs and the binary mixtures of API + Excipients (BMT + BAC, BMT + DSPA, BMT + MSPM, TM + BAC, TM + DSPA and TM + MSPM) were obtained using a model DSC 822^e Mettler Toledo by heating approximately 5.000 mg of sample in a perforated Aluminum pan from 25 to 300 °C. In both analysis a N₂ atmosphere was used with a flow rate of 50 mL min⁻¹ and a heating rate of 20 °C min⁻¹. The DSC curve of BMT showed a sharp melting endothermic peak at 220 °C and two exothermic peaks at around 270 °C attributed to its decomposition. The DSC curve of TM showed two endothermic events in succession at 210 °C and at 220 °C attributed to its melting and decomposition, respectively. For the DSC curves of the binary mixtures, in all of them, each thermal event that occurred while the components were heated separately, appeared at the same temperature while combined in the mixture. In all cases, for each thermal event attributed above that caused mass losses appeared in their respective TG curves. In conclusion, a formulation of BMT and TM in the presence of BAC, DSPA and MSPM is possible given that there were no interactions between them.

[1] Lee AJ, McCluskey P. Fixed combination of topical brimonidine 0.2% and timolol 0.5% for glaucoma and uncontrolled intraocular pressure. Clin Ophthalmol. 2008 Sep;2(3):545-55. doi: 10.2147/oph.s3840. PMID: 19668752; PMCID: PMC2694019.

Agradecimentos/Acknowledgments

The authors of this work are grateful for the financial support provided by FUNAPE

Development of a passive sampler for the determination of formaldehyde in indoor atmospheres

Alana Melo Magalhães (IC),¹ Arnaldo Alves Cardoso (PQ),^{1*} Marcus Augusto dos Santos Catai (PG).¹

alana.melo@unesp.br; arnaldo.cardoso@unesp.br

¹ Institute of Chemistry, Department of Analytical Chemistry, São Paulo State University (UNESP)

Keywords: Formaldehyde, Indoor pollution, Gas analysis

Highlights

This work is analyzing the best conditions to build a passive sampler that quantifies formaldehyde in indoor atmospheres in order to obtain meaningful data for the health of people in these environments.

Abstract

Formaldehyde is a component present in many household products, so it is common for it to be emitted into the atmosphere. When the concentration of this gas in the indoor atmosphere reaches high values, it can result in deleterious effects to health, therefore, evaluations on the concentration of these aldehydes in indoor environments, such as schools, work environments and shopping areas associated with leisure, are important and the lack of portable analytical methods, easy to use and that do not interfere in the internal activities of these environments is a problem to be overcome, because as a consequence there is a lack of systematic data on this problem in Brazil.

The purpose of this project is to develop a passive sampler for the determination of formaldehyde concentration in air, with low sampling time and easy to use. Among the adsorbent reagents with reaction potential for formaldehyde determination, those that use water as solvent are being evaluated and prioritized, thus avoiding the use of organic solvents that require specific disposal. The compound 3-METHYL-2-BENZOTHAZOLINE HYDRAZONE (MBTH), is recognized as one of the reagents for formaldehyde and is soluble in water. After its reaction with formaldehyde a solution of Fe(III) is added. The oxidation of the solution promotes the formation of an ionic compound with an intense blue color.

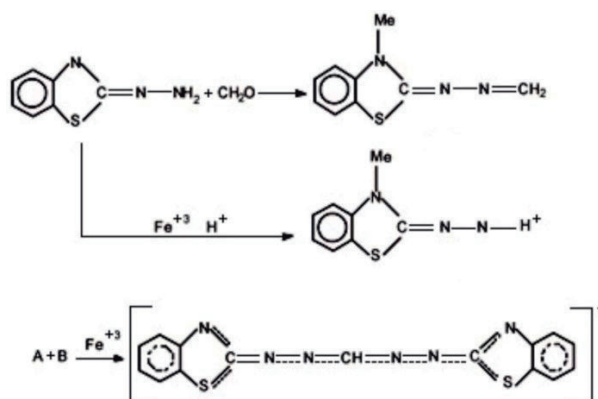


Figure 1: Reaction of formaldehyde with MBTH forming the blue dye.

1.Sawicki, E., Hauser, T. R., Stanley, T. W., & Elbert, W. (1961). The 3-methyl-2-benzothiazolone hydrazone test. Sensitive new methods for the detection, rapid estimation, and determination of aliphatic aldehydes. *Analytical Chemistry*, 33(1), 93–96.

The reaction was initially performed using a cellulose filter, which would work as a support for the sampler, impregnated with different volumes of the MBTH solution. The project continues to seek the best conditions for the reaction, which will take place inside the sampler, with an adequate support that does not interfere in the quantification. The samplers will be exposed to air containing formaldehyde and, at this stage, different diffusion paths will be evaluated. The color will be determined by absorbance measurements, using the principles of the Lambert-Beer law, which relates the concentration of formaldehyde with the color observed from a calibration curve that was performed with standard solutions of the analyte.

Acknowledgments

CNPq for the scholarship granted to develop the research.

Contaminantes inorgânicos em chocolates *Bean-to-bar* do BrasilVitor H. Burgon (PG)¹, Manuela L. N. Silva (IC)¹, Raquel F. Milani (PQ)¹, Marcelo A. Morgano (PQ)^{1*}morgano@ital.sp.gov.br; vitorhburgon@gmail.com¹Centro de Ciência e Qualidade dos Alimentos, ITALPalavras Chave: *Chocolate artesanal, Cádmiio, Chumbo, ICP-MS***Highlights****INORGANIC CONTAMINANTS IN CHOCOLATES BEAN-TO-BAR FROM BRAZIL**

- Cadmium and lead were evaluated in Bean to Bar chocolates from different regions of Brazil.
- The highest levels of inorganic contaminants were found in chocolate samples from Amazonas.

Resumo/Abstract

O chocolate *Bean-to-bar* (da amêndoa a barra) é um tipo de chocolate menos industrializado, geralmente com produção artesanal, controlada e mais sustentável que os tradicionais. Em seu processamento utilizam-se amêndoas de cacau de origem conhecida e açúcar orgânico. Neste trabalho foram estudados os contaminantes inorgânicos cádmio e chumbo em amostras comerciais de chocolates *Bean-to-bar* procedentes de oito regiões do Brasil. Para o preparo das amostras foi utilizado a digestão ácida em sistema fechado assistido por micro-ondas, pesando-se 0,5 g de chocolate e adicionando-se 8 mL de HNO₃ purificado por destilação *sub-boiling* (Berghof, Alemanha) e 2 mL H₂O₂ 30% (m/v) (Merck, Alemanha). A digestão foi realizada em 4 estágios, com temperatura máxima de 170°C e tempo total de 40 min. Os tubos foram avolumados para 25mL com água purificada por osmose reversa (Gehaka, Brasil) e para a quantificação dos contaminantes foi utilizada a técnica de ICP-MS (iCap RQ Thermo Fisher Scientific, Alemanha) em condições otimizadas (m/z ¹¹¹Cd e ²⁰⁸Pb). O método foi validado utilizando materiais de referência certificados de chocolate (ERM BD512) para Cd e folhas de pêssego (NIST SRM 1547) para Pb, com recuperações de 90% e 101% e precisão de 3% e 14% para Cd e Pb, respectivamente. Os resultados obtidos para Cd e Pb nas amostras de chocolates são apresentados na Tabela 1.

Tabela 1. Média e intervalo de concentração para os contaminantes inorgânicos Cd e Pb em amostras de chocolates *Bean-to-bar* (n=64) do Brasil: Amazonas, Amapá, Bahia, Espírito Santo, Floresta Amazônica, Mata Atlântica, Pará e Rondônia.

Região	n	Cd (mg kg ⁻¹)	Pb (mg kg ⁻¹)
Amazonas	7	0,145 (0,03 - 0,74)	0,014 (<LOD - 0,03)
Amapá	2	0,054 (0,007 - 0,1)	0,019 (0,02 - 0,02)
Bahia	35	0,046 (0,01 - 0,18)	0,012 (<LOD - 0,05)
Espírito Santo	8	0,05 (0,01 - 0,09)	0,022 (<LOD - 0,06)
Floresta Amazônica	2	0,08 (0,04 - 0,12)	0,0040 (<LOD - 0,01)
Mata Atlântica	4	0,036 (0,01 - 0,06)	0,0038 (<LOD - 0,008)
Pará	4	0,021 (<LOD - 0,07)	0,010 (<LOD - 0,04)
Roraima	2	0,024 (0,016 - 0,031)	0,015 (0,01 - 0,02)

LOD: Cd = 0,001 mg kg⁻¹ e Pb = 0,005 mg kg⁻¹.

Em geral, níveis seguros foram observados para os contaminantes estudados. A partir da Tabela 1, verifica-se que os teores mais elevados de cádmio foram encontrados em amostras de chocolates *Bean-to-bar* das regiões do Amazonas e da Bahia. Na região do Amazonas, uma amostra apresentou nível superior ao limite máximo estabelecido para Cd (0,3 mg kg⁻¹) pela legislação nacional (IN 160) [1].

[1] Brasil. Instrução Normativa IN 160 - Estabelece os limites máximos tolerados (LMT) de contaminantes em alimentos, 01/07/2022.

Agradecimentos/Acknowledgments

Os autores agradecem à FAPESP (2020/16170-6 e 2022/02658-2), CAPES (código de financiamento 001, bolsa MS) e CNPq (407080/2021-0 e 306054/2020-5).

Copper Mobility in Soils: Investigation through Adsorption Isotherms and Column Percolation Studies with Copper Fungicide.

Leticia M. Rodrigues (PG)^{1*}, Maycon Lucas de Oliveira (PG)¹, Marcia A.M.S. da Veiga (PQ)¹

lmrodrigues@usp.br

¹Chemistry Department, FFCLRP, University of São Paulo, Postal Code 14040-901, Ribeirão Preto, SP, Brazil.

Keywords: (Mobility; Copper; Fungicide; Isotherms; Groundwater; Contamination).

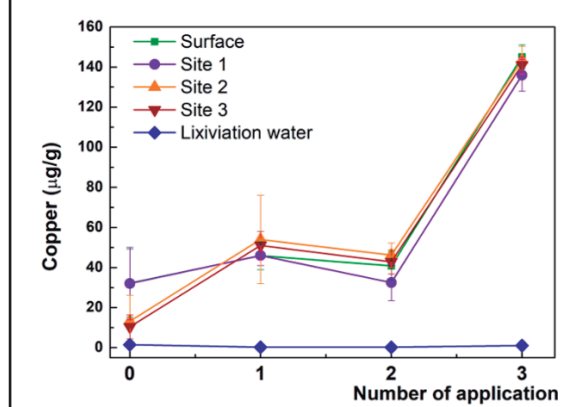
Highlights

Adsorption isotherms revealed distinct Cu mobility in soils
Column study showed different metal concentrations at the lixiviation water site
Fungicide Copper may pose a risk to groundwater contamination

Abstract

Copper fungicides, such as $\text{Cu}_2\text{Cl}(\text{OH})_3$, are widely used in agriculture to combat fungal diseases in legume leaves. However, leaching these fungicides into the soil can contaminate groundwater, posing an environmental risk. This study aimed to evaluate copper's retention and potential mobility from fungicides in soil by conducting physical-chemical soil characterization, isothermal adsorption experiments, and column percolation studies. Three PVC soil columns were prepared: a control column, a column with the addition of $1,52 \cdot 10^{-6}$ g of Cu from standard solution, and a column with the addition of $1,52 \cdot 10^{-6}$ g of Cu from Cuprozeb[®] Fungicide ($170 \text{g} \cdot \text{Kg}^{-1}$ Cu). The soil columns were prepared with collection sites at different distances, including a lixiviation water site. The study was performed by applying three applications of each solution over 30 days. The isothermal adsorption experiments were conducted to evaluate the adsorption capacity of the fungicide copper compared to the standard solution copper. All copper concentration measurements were performed by inductively coupled plasma optical emission spectrometry, axial mode, Model Avio200 (Perkin Elmer), wavelength 324 nm. The soil was classified as having a Blunt texture, with a pH of 5.1 ± 0.2 in water and 4.9 ± 0.2 in CaCl_2 . Its moisture content was $7.710 \cdot 10^{-3} \pm 0.002$ kg water $\cdot \text{kg}^{-1}$ soil, density was 1.18 ± 0.02 g $\cdot \text{mL}^{-1}$, organic matter content was 16.1 ± 3.5 g $\cdot \text{Kg}^{-1}$, cation exchange capacity was 3.29 cmolc $\cdot \text{Kg}^{-1}$ and initial copper concentration in soil was 21.9 $\mu\text{g} \cdot \text{g}^{-1}$. The column percolation study showed that the copper concentration was homogenized throughout the columns, with similar concentrations at the surface and bottom sites for the same application. However, the metal concentration of the lixiviation water site significantly differed from the other sites, as shown in Figure 1. The isothermal adsorption experiments indicated that the fungicide copper had a lower adsorption capacity and higher mobility than the standard solution copper, leading to its leaching and potential groundwater contamination risk, as shown in Frame 1.

Figure 1: Total copper concentration of each application of the Cuprozeb[®] fungicide



Frame 1: Adsorption isotherm parameters for the copper from the fungicide and the copper standard solution

Copper Fungicide		
Model	Q_{\max} (mg $\cdot \text{g}^{-1}$)	R_L
Langmuir	1.42	0.284 to 0.543
Standard Copper Solution		
Model	Q_m (mg $\cdot \text{g}^{-1}$)	ϵ
Freundlich	6.36	-0.3502

Q_{\max} and Q_m refer to the maximum adsorption capacity. R_L predicts the favorability of the adsorption process: unfavorable ($R_L=1$), favorable ($0 < R_L < 1$), and irreversible ($R_L=0$). The ϵ indicates the adsorption favorability: good (2 to 10), moderately hindered (1 to 2), and with few adsorptive characteristics (<1). Due to its lower adsorption capacity, the copper from the fungicide has higher mobility in the soil than that from the standard solution, resulting in more significant leaching.

Acknowledgments

Grant #2021/05635-0, São Paulo Research Foundation (FAPESP).

46^ª Reunião Anual da Sociedade Brasileira de Química: "Química: Ligando ciências e neutralizando desigualdades"

Crickets as a bioindicator of rare earth elements: a microwave-induced combustion sample preparation approach

João L. K. Rocha (PG),¹ Gustavo Gohlke (IC),¹ Thiago C. Pereira (PG),¹ Alessandra S. Henn (PQ),² Jussiane S. Silva (PQ),¹ Érico M. M. Flores (PQ)^{1*}

joaokr12@gmail.com; ericommf@gmail.com

¹ Universidade Federal de Santa Maria, Departamento de Química, Santa Maria, RS, Brazil, 97105-900

² Universidade Tecnológica Federal do Paraná, Campus Medianeira, Medianeira, PR, Brazil, 85884-000

Keywords: *Crickets, REE, bioindicator, MIC, USN-ICP-MS*

Highlights

Sample preparation of cricket was studied for REE determination
MIC allows the digestion of higher sample mass and final solutions with lower carbon content.

Abstract

The exploration of rare earth elements (REE) has increased due to their extensive industrial and technological applications. Discovering REE reserves is challenging and requires extensive geological research. As an alternative, insects can be used as a bioindicator for these elements. Insects can contain different concentrations of REE due to their diet and the presence of the environment. Inductively coupled plasma mass spectrometry with ultrasonic nebulization (USN-ICP-MS) is a powerful analytical technique that allows the determination of REE at low concentration (ppt range). However, it requires the sample in a liquid form, and a sample preparation step is mandatory. Sample preparation of insects can be considered an analytical challenge because they are composed of hard-to-digest lipids, proteins, carbohydrates, and an inorganic fraction. Microwave-induced combustion (MIC) is a sample preparation method that allows lower carbon and acid content in the final solutions compared to conventional acid digestion methods. Therefore, the present study aimed to evaluate the use of MIC for sample preparation of crickets for further determination of Y, La, Ce, Pr, Nd, Eu, Sm, Tb, Gd, Dy, Ho, Er, Tm, Yb, and Lu by USN-ICP-MS. Cricket samples (from China, Thailand, and Brazil) were dried, ground, and pressed as pellets for MIC. The following parameters were evaluated: maximum sample mass, 100 to 600 mg, and absorbing solution, 6 mL of 14.4 mol L⁻¹ HNO₃ or a mixture of 12 mol L⁻¹ HCl and 14.4 mol L⁻¹ HNO₃ 1:3, 2:1, and 3:1 (v/v). Microwave-assisted acid digestion (MAWD) was used as the reference method, and 300 mg of the sample were digested using 6 mL of 14.4 mol L⁻¹ HNO₃. In addition, the carbon content of the solutions obtained by both methods was determined by inductively coupled plasma optical emission spectrometry (ICP-OES). Up to 500 mg of cricket were combusted by MIC without exceeding the maximum pressure of the system. Recoveries higher than 90% were obtained for REE using a mixture of HCl and HNO₃ 3:1 as an absorbing solution. The carbon concentration in solutions obtained after MIC was lower than 13.6 mg L⁻¹, while the concentration in digests obtained after MAWD (reference method) was about 150 mg L⁻¹. For all samples and REE studied, there was no significant difference (t-test, 95% confidence level) between the results obtained by MIC and the reference method. The limits of quantification for MIC ranged from 0.029 (for Lu) to 43.5 µg g⁻¹ (for La), while for MAWD, they ranged from 1.42 (for Lu) to 146 µg g⁻¹ (for La). Therefore, the MIC method proved to be a promising sample preparation method for further determination of Y, La, Ce, Pr, Nd, Eu, Sm, Tb, Gd, Dy, Ho, Er, Tm, Yb, and Lu in cricket samples, presenting solutions with low carbon content and low limits of quantification.

Acknowledgments

The authors would like to thank CNPq, FAPERGS, and CAPES.

Área: ANA

Desempenho analítico de extração simultânea de lipídios totais e mRNA em amostras de tecido biológico conservado em solução TRIzol® por espectrometria de massas

Ricardo Alves Bernardo¹(PQ)*, Gabriela Guimarães Souza¹(IC), Charles Ivo de Oliveira Júnior^{1,2}(PG), Carlos Arterio Sorgi³(PQ), Boniek Gontinjo Vaz¹(PQ), Andréa Rodrigues Chaves¹(PQ).

ricardo.alber@outlook.com; gabrielaguimaraes@discente.ufg.br

¹Instituto de Química, UFG; ²Departamento de Química, UFJ; ³Departamento de Química, Faculdade de filosofia, Ciências e Letras de Ribeirão Preto, USP..

Palavras Chave: *Espectrometria de massas, lipidômica, multiômica.*

Highlights

Analytical performance of simultaneous extraction of total lipids and mRNA in gingival tissue samples conserved in TRIzol® solution by mass spectrometry.

- Optimization of a sample preparation technique based on Bligh & Dyer protocol extraction.
- Simultaneous extraction of total lipids and mRNA using the same biological sample.

Resumo/Abstract

A solução TRIzol® é amplamente utilizada para extração de mRNA em análises transcriptômicas. Contudo, o protocolo descarta a fração orgânica produzida na extração, limitando as informações que podem ser adquiridas de uma única amostra. Sendo assim, o presente estudo propõe a avaliação de parâmetros analíticos para extração simultânea de mRNA e lipídios totais utilizando a mesma amostra biológica. Para tanto, amostras de língua de porco foram conservadas e homogeneizadas em solução TRIzol® na proporção de 10% m/v, e enriquecidas com padrão interno PC(17:0/17:0). Posteriormente, submetidas à extração adaptada baseada no método de Bligh & Dyer, para avaliação de figuras de mérito. Os extratos lipídicos foram analisados por infusão direta no espectrômetro de massas utilizando fonte de ionização por *electrospray*, AB Sciex TripleTOF 5600+ em modo positivo e negativo na faixa de massa de 200 – 1200 Da, em modo de *scan MS/MS*^{All}. Por fim, o método foi aplicado em amostras de tecido gengival.

O método desenvolvido apresentou linearidade na faixa de 50 a 2000 ng mL⁻¹ com $r^2 > 0,99$. Os valores de precisão e exatidão intra e inter-dia variaram de -9,6 a 4,9% e recuperação absoluta entre 90,4 a 103,2%. O efeito matriz foi avaliado e não se apresentou significativo para a metodologia proposta.

Os resultados apresentam um método promissor para avaliação multiômica, uma vez que permitiu a avaliação de lipídios presentes em amostras de tecido gengival conservado em solução de TRIzol®.

Agradecimentos/Acknowledgments



Determination of alkaline and alkaline earth elements in crude oil by MIP OES after microwave-assisted demulsification

Gustavo R. Bitencourt (PG), Alice P. Holkem (PG), Ana Luísa Seeger (IC), Andres C. Souza (IC), Giuliano Agostini (IC), Rochele S. Picoloto (PQ) Paola A. Mello (PQ)*

gustavorbitencourt@hotmail.com; paola.mello@ufsm.br*

Universidade Federal de Santa Maria, Departamento de Química, Santa Maria, RS, Brazil, 97105-900

Keywords: Crude oil, Metal contaminants, MIP OES, Demulsification, Microwave radiation.

Highlights

Feasibility of MIP OES for alkaline and alkaline earth element determination in crude oil after microwave-assisted demulsification was presented;
Effects due to C, Ca, and Na content on the determination by MIP OES are demonstrated.

Abstract

Alkaline and alkaline earth elements can be present at higher concentrations in crude oil emulsions from some reservoirs, being normally associated with chloride as a salt (such as NaCl, MgCl₂, and CaCl₂), dissolved in emulsified water. These elements can cause damages in refineries, including incrustation and corrosion of pipes, valves, and pumps, as well as catalyst poisoning.¹ Thus, the determination of these elements in crude oil emulsions is crucial. For this, the microwave-induced plasma optical emission spectrometry (MIP OES) can be investigated for the determination of alkaline and alkaline earth elements in crude oil emulsions, with simple instrumentation, suitable limits of detection (LODs), and low gas acquisition costs.² In this study, the suitability of MIP OES for the determination of Ba, Ca, K, Li, Mg, Na, and Sr in crude oil emulsion was investigated. A natural crude oil emulsion, classified as a medium crude oil (API 27) was used for all optimizations. Sample preparation was performed by microwave-assisted demulsification which was carried out in a microwave oven (model Multiwave 5000, Anton Paar, Austria). For this procedure, 14 g of sample, 15 mL of ultrapure water (as extraction solution) and five glass spheres, in quartz vessels, are heated using the following microwave program: *i*) 30 min of ramp and *ii*) 20 min of holding, at 1400 W. After cooling, the water is collected and filtered through a PTFE filter (0.22 µm) for further element determination by MIP OES (model 4210 MP-AES, Agilent, USA). Extracts were also analyzed by inductively coupled plasma optical emission spectrometry (ICP OES, model Spectro Ciros CCD, Spectro Analytical Instruments, Germany) for results comparison. Reference values were obtained by ICP OES after microwave-assisted wet digestion (MAWD, model Ultrawave™, Milestone, Italy) according to ASTM 7876. An investigation on interferences on MIP OES was carried out by using the digests from MAWD. Finally, dissolved carbon in digests and extracts was determined by ICP OES. Initially, since MIP OES is prone to matrix effects due to the low plasma temperature (c.a. 5000 K),² the influence of carbon, Ca, and Na content on the measurements was investigated. Digests from MAWD were evaluated after several dilutions (from 1000-fold up to concentrated digest), containing 100 µg L⁻¹ of the analytes. The concentration of dissolved carbon, Ca, and Na in the digest was 1873, 19.4, and 139 mg L⁻¹, respectively. From the results, a signal suppression (until 50%) for Ba, Mg, and Sr was observed, which can be mainly related to the concentration of Na (higher than 35 mg L⁻¹). Thus, for MAWD a minimum dilution (4-fold) was necessary. However, the sample mass used in the demulsification protocol (14 g) is higher than that used in MAWD (0.5 g). Thus, the concentration of dissolved carbon, Ca, and Na in the extract was higher (1582, 766, and 5968 mg L⁻¹, respectively). Then, in this case, a minimum dilution of 200-fold must be performed before the determination by MIP OES. No statistical difference (*t*-test, 95% of confidence level) was observed for the results obtained by MIP OES compared to those by ICP OES using the demulsification method. Agreement ranging from 70 to 108% was observed between the results and the reference values (obtained by ICP OES after MAWD), for all analytes. These results enable to consider the MIP OES as a suitable approach for alkaline and alkaline earth element determination in crude oil emulsions after microwave-assisted demulsification. Additionally, the proposed protocol can be a greener approach, since only water is used (without acid reagents) and due to the lower time required (about 1 h for demulsification, against more than 2 h for MAWD).

¹Speight, J. **Handbook of Petroleum Product Analysis: Second Edition**, 2015, 350 p.

²Müller, A.; Pozebon, D.; Dressler, V. L. **Journal of Analytical Atomic Spectrometry**, 35, 2113-2131, 2020.

Acknowledgments

The authors are grateful to CENPES-PETROBRAS, CNPQ, CAPES, and FAPERGS.

DETERMINATION OF BIOGENIC AMINES BY CAPILLARY ZONE ELECTROPHORESIS WITH DANSYL CHLORIDE AS A DERIVATIZING AGENT

Elisabete A. Pereira (PQ),¹ Luís Moreira Gonçalves (PQ)² Jéssica O. F. Mantoanelli (PG),^{2*}

Ealves@ufscar.br; jofmantoanelli@usp.br

¹Departamento de Física, Química e Matemática, UFSCar-Sorocaba; ²Departamento de Química, Instituto de Química, USP-SP

Palavras Chave: Biogenic amines, capillary electrophoresis, dairy products, food quality

Highlights

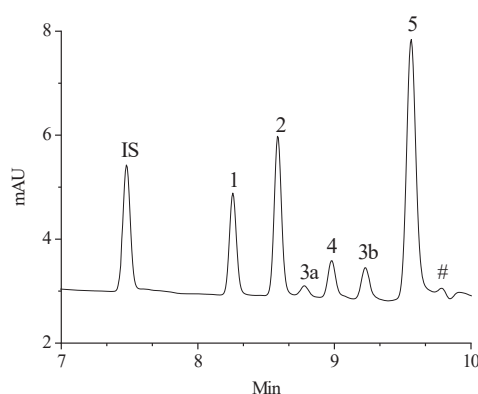
A new method of biogenic amines determination

Dansyl chloride as derivatizing agent

Resumo/Abstract

Biogenic amines (BAs) are naturally found in low concentrations in several varieties of protein-rich foods and beverages [1]. BAs are formed from degradation of amino acids by the action of microorganisms [1]. Consumption of high amounts of BAs may result in different symptoms of intoxication [1]. The development of analytical methods for the determination of BAs in food and beverages is important both for their toxicological effect on consumers and due to quality indicators. The present work describes a new method using dansyl chloride (DNS) as a derivatizing reagent for the separation and analysis of biogenic amines by capillary zone electrophoresis (CZE). The biogenic amines (benzylamine, putrescine, cadaverine, tyramine, histamine, and tryptamine) were reacted with DNS reagent to form adducts with maximum absorbance at 214 nm. Different analytical and instrumental parameters were evaluated. Method development was performed using a CE system (Agilent Technologies, model 7100 A) with a diode array detector set to 214 nm and temperature control maintained at 23°C. Fused silica capillaries (48.5 cm total length) were used. A mixture consisting of 120 mmol L⁻¹ phosphoric acid and acetonitrile 5% (v/v), pH 2.5 was used as a running buffer. The system was operated in normal polarity and a constant voltage of 18 kV. Samples were injected hydrodynamically at 25 mbar during 6 s (Figure 1). The calibration curves were linear ranging from 1.0 to 10.0 mgL⁻¹ with r² higher than 0.99. Intra and inter-day precision were in average 1.1 and 9.9 %, respectively and, recoveries ranged from 87 to 110 %. The limits of detection were in the range of 0.04 to 0.2 mg L⁻¹ (S/N = 3). The developed method was successfully applied to cheese and yogurt analyses.

Figure 1. Optimized separation of BAs-DNS



Legend: Electropherogram of a mixture of amines-DNS (2,5 mL⁻¹ of each amine). Electrolyte: 120 mmol L⁻¹ phosphoric acid and acetonitrile 5% (v/v), pH 2.5; 18 kV, 23°C; 25 mbar x 6 s. Peak identification: IS: Benzylamine; 1. Putrescine; 2 Cadaverine; 3a and 3b. Histamine; 4 Tyramine; 5. Tryptamine; # not identified.

[1] Mantoanelli, J.O.F.; Gonçalves, L. M.; Pereira, E.A; *Chromatographia*, **2020**,83,767-778.

Agradecimentos/Acknowledgments

EAP wishes to acknowledge FAPESP for financial support (2019/03582-7). JOFM wishes to acknowledge CAPES (code 001) for the fellowship granted.

46ª Reunião Anual da Sociedade Brasileira de Química: "Química: Ligando ciências e neutralizando desigualdades"

Determination of Hg in oral medication with high inorganic content by CVG-ICP-MS after microwave-induced combustion

Vinicius P. de Souza (IC),¹ Vitoria H. Cauduro (PG),¹ Emanuele Frozi (IC),¹ Thiago C. Pereira (PG),¹ Cristian R. Andrioli (PG),¹ Rochele S. Picoloto (PQ),¹ Erico M. M. Flores (PQ).^{1*}

souza.vinicius@acad.ufsm.br; ericommf@gmail.com

¹Universidade Federal de Santa Maria, Departamento de Química, Santa Maria, RS, Brazil, 97105-900;

Keywords: Sample preparation, pharmaceuticals, microwave-induced combustion, inductively coupled plasma mass spectrometry, cold vapor generation.

Highlights

Microwave-induced combustion was proposed for decomposition of oral tablet samples containing high inorganic excipient content for further Hg determination by cold vapor generation coupled to inductively coupled plasma mass spectrometry. The proposed method was quick and efficient, using only 6 mL of diluted HNO₃ solution, with reduced reagent use and waste generation.

Resumo/Abstract

Long-time exposure to elemental impurities present in pharmaceuticals can be very harmful to health. In this sense, the ICH guidelines established permitted daily exposure (PDE) values for elemental impurities,¹ which must be monitored from feedstock to final product, especially in the case of toxic elements such as Hg. In this sense, microwave-induced combustion (MIC) is a well-established sample preparation method that could potentially be used for elemental impurities determination in medication. This method provides the complete digestion of the organic matrix in samples followed by a reflux step, improving the recovery of the analytes.² However, samples with high inorganic content (such as tablets containing inorganic excipients) can be a challenge for combustion-based methods, as the necessary heat for analyte volatilization might not be achieved, since the organic matter works as the fuel for combustion.² Therefore, the aim of the present study was to develop a MIC method for pharmaceutical samples with high inorganic excipient content and further determination of Hg. For this purpose, cold vapor generation coupled to inductively coupled plasma spectrometry (CVG-ICP-MS) was used for analyte determination. For method optimization, commercial samples of sitagliptin phosphate (SITA) tablets, used in the treatment of type 2 diabetes, were used. The accuracy of the method was evaluated by standard addition experiments at the PDE level for Hg, and by applying the proposed method to certified reference materials (CRM) of dogfish liver (DOLT-4), lobster hepatopancreas (TORT-2), and aquatic plant (BCR-60). The following parameters were evaluated: sample mass (150 to 400 mg), use of microcrystalline cellulose (300 to 600 mg) or NH₄Cl (300 mg) as combustion aids, and composition and concentration of absorbing solution (H₂O or HNO₃). Samples were grinded and pressed as pellets with combustion aids. The pellets were placed in quartz holders on paper moistened with 50 µL of igniter (NH₄NO₃ 6 mol L⁻¹), and then transferred to quartz vessels. Combustion was performed in closed quartz vessels pressurized at 20 bar with O₂, with 6 mL of absorbing solution. The reflux time was set to 5 min with 20 min of cooling. The optimized condition was set using 400 mg of sample, 300 mg of microcrystalline cellulose, and diluted HNO₃ as absorbing solution. Analyte recovery ranged between 99% and 109%, and no significant differences were observed between experimental and certified values for CRM analysis (Student's *t*-test, 95% of confidence). The proposed method was suitable for decomposition of oral tablet samples with high content of inorganic excipients for further Hg determination by CVG-ICP-MS, and LOQ values were adequate for determination according to ICH Q3D limits for Hg for oral route.

¹ Guideline for Elemental Impurities Q3D(R1). International Council For Harmonisation of technical requirements for pharmaceuticals for human use.

² Flores EMM, Barin JS, Paniz JNG, Medeiros JA, Knapp G, Analytical Chemistry, 76, 2004, 3525.

Agradecimentos/Acknowledgments

The authors would like to thank CNPq, FAPERGS and CAPES.

Determination of naphthenic acids in petroleum samples by two-dimensional gas chromatography coupled to high-resolution mass spectrometry

Millena Couto dos Santos (IC), Naiara M. F. M. Sampaio (PQ), Leandro W. Hantao (PQ).

Instituto de Química, Universidade Estadual de Campinas (IQ-UNICAMP). E-mail: m203837@dac.unicamp.br

Key-words: GCxGC, petroleomics, sample preparation, oil and gas industry.

Highlights

Naphthenic acids with a wide range of molecular weights were efficiently extracted by SPE. In addition, the GCxGC—HRMS technique allowed the identification of several naphthenic acids in petroleum.

Abstract

Naphthenic acids (NAs) are carboxylic acids that naturally occur in oil. This class of compounds is a matter of concern, since they are known to cause operational problems in the oil and gas industry. NAs can act as surfactants, self-organizing at the oil-water interface, thus contributing to the formation and stabilization of emulsions. These acids are also a problem for the environment due to their toxicity and recalcitrant nature. Furthermore, NAs are a complex mixture of compounds with a wide range of molecular weight and structures, making the separation, identification and quantification of these acids a challenge. The molecular formula of the naphthenic acids is given by $C_nH_{2n+z}O_2$, herein Z is the hydrogen deficiency due to cyclic moieties, which is related to the double bond equivalent (DBE) value. Therefore, this work aimed to extract NAs from crude oil samples by solid phase extraction (SPE) and molecular characterization by comprehensive two-dimensional gas chromatography coupled to high-resolution mass spectrometry (GCxGC—HRMS). The acids were extracted using an aminopropyl-based sorbent phase and eluted with an adequate eluotropic series of organic solvents. The extract was dried in a rotary evaporator and reconstituted with isooctane. Analytes were derivatized with N-tert-butyltrimethylsilyl-N-methyltrifluoroacetamide (MTBSTFA) with 1% (v/v) tert-butyltrimethylchlorosilyl (t-BDMCS). The acids were separated on a GCxGC—HRMS assembled on a Q Exactive GC system fitted with a non-polar × mid-polar column set and thermal modulation. Naphthenic acids were found in the studied samples, with carbon numbers ranging from 8 to 20 and DBE-value from 1 to 6. Most abundant acids exhibited mono- (DBE=2) and bicyclic moieties structure (DBE=3).

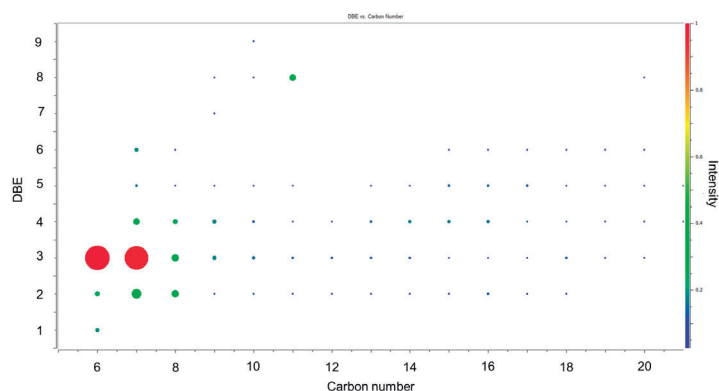


Figure 1. Group-type analysis of *t*-BDMS-derived naphthenic acids illustrating the carbon number and double-bond equivalent values.

Agradecimentos/Acknowledgments

The authors thank PETROBRAS, FAPESP, CNPq, Nova Analítica and ThermoFisher Scientific for supporting our research.

Determination of PAH and derivatives by comprehensive two-dimensional chromatography and passive sampling in surface waters.

Nathan S. Coelho¹ (PG)*, Helvécio C. Menezes¹ (PQ), Zenilda L. Cardeal¹ (PQ)*

¹Universidade Federal de Minas Gerais, Department of Chemistry /ICEx, Belo Horizonte, M.G., Brazil, 31270-901

*e-mail: nathancoelho@ufmg.br

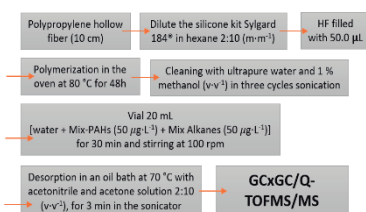
Keywords: GCxGC/Q-TOFMS/MS, LPME, PAHs and derivatives, Passive sampling.

Highlights

A new method for passive sampling of surface water for PAHs and derivatives was developed, and the determinations were performed on a comprehensive two-dimensional chromatography system coupled with mass spectrometry.

Abstract

The assessment of water resources contamination is usually done through conventional sampling, which commonly consumes time, financial resources and does not allow the detection of contamination episodes over a long period [1]. Valenzuela et al¹, proposed a simple device for pesticides passive sampling using the hollow fiber liquid phase microextraction (HF-LPME) technique. Besides, Dos Santos used solid phase microextraction with polydimethylsiloxane, PDMS, for the analysis of PAHs and derivatives [2]. Thus, the objective of this work was to develop new PDMS fibers for HF-LPME passive sampling analysis of PAHs and its oxygenated and nitrated derivatives in surface water with determinations by GCxGC/Q-TOFMS/MS.



The comprehensive two-dimensional gas chromatography system comprises a GCxGC Agilent system model 7890 coupled to an Agilent 7250 Q-TOF-MS/MS, equipped with a split/splitless injector, an GC autosampler 80 and a Zoex ZX2 thermal modulator. Separation was performed using HP-5MS UI column in 1D and DB-17HT column in 2D. All work was based on 16 PAHs, 4 Oxi-PAHs and 4 Nitro- PAHs. Figure 1. Process of production, cleaning and extraction of the analytes with the HF-LPME.

As shown in fig. 2 the column set of DB-5MS (nonpolar) as 1D and, the DB-17HT (medium polarity) as 2D, provided perfect separation and identification of PAHs and derivatives. Additionally, the 8 s modulation period supplied a good distribution of the analytes in the contour plot without a wrap-around effect.

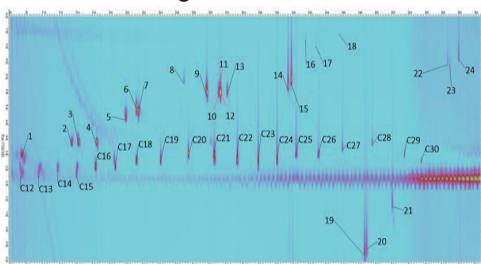


Figure 2. Color diagram of a standard solution of 16 PAHs and 8 derivatives: 1_Naphtalene, 2_Acenaphthleny, 3_Acenaphthene, 4_Fluorene, 5_9-Fluorenone, 6_Phenanthrene, 7_Anthracene, 8_9.10-Anthraquinone, 9_Fluoranthene, 10_2-Methylantra-quinone, 11_2-Nitrofluorene, 12_Pyrene, 13_9-Nitroanthracene, 14_Benzo[a]anthracene, 15_Chrysene, 16_3-Nitrofluoranthene, 17_1-Nitropyrene, 18_5,12-Nafthacenequinone, 19_Benzo[b]-fluoranthene, 20_Benzo[k]fluoranthene, 21_Benzo[a]pyrene, 22_Indeno[123-c,d]pyrene, 23_Dibenzo[a,h]anthracene, 24_Benzo[g,h,i]perylene.

A calibration study for the passive sampling of analytes using the new sampler was also performed and the parameters of method validation were tested following Eurachem Guide. The new HF-LPME fiber showed good results for passive sampling of PAHs and derivatives in surface waters.

The developed GCxGC/Q-TOFMS method showed good performance for environmental determination.

REFERENCES

- [1] Valenzuela, E. F.; Menezes, H. C.; Cardeal, Z. L. Environmental Chemistry Letters. [S.L.]: Springer., 1 Jul. 2020
 [2] Dos Santos, R. R. Et Al. Journal Of Chromatography A, V. 1584, P. 64–71, 11 Jan. 2019

Agradecimentos/Acknowledgments

This work was financed by Companhia Energética de Minas Gerais (CEMIG) and the National Council for Scientific and Technological Development (CNPq).

Área: ANA

Determination of parabens and bisphenol A in sludge samples using hydrophobic deep eutectic solvents by Py-GC/MS

Karen Chibana Ferreira (PG)^{1*}, Thais Rodrigues (PG)¹, Mario Henrique Gonzalez (PQ)², Paulo Clairmont Feitosa de Lima Gomes (PQ)¹

karen.chibana@unesp.br

¹Instituto de Química Unesp – Araraquara; ²Departamento de Química e Ciências Ambientais Unesp - São José do Rio Preto.

Palavras Chave: *Pirolisador; Otimização; Preparo de amostra; HDES*

Highlights

Chemometric tools to optimize injection into the pyrolyzer (Py-GC/MS) and DLLME; Prepare of new hydrophobic deep eutectic solvents

Abstract

Over the years, the search for solvents or materials that have low toxicity to the analyst and to the environment has become relevant. To meet these demands, a new generation of solvents was developed, including hydrophobic deep eutectic solvents (HDES), which represent a subgroup of deep eutectic solvents (DES), which are produced from the mixture of two or three precursors performing intermolecular hydrogen bonds involving a donor species (HBD) with an acceptor species (HBA). The application of HDES in environmental matrices makes it possible to determine emerging contaminants in accordance with the green analytical chemistry requirements. Dispersive liquid-liquid microextraction (DLLME) is an interesting alternative for sample preparation. Therefore, the aim of this research is to prepare HDES and use it in the DLLME as extraction solvent. Moreover, HDES were applied to determine parabens and bisphenol A in sludge samples using a GC/MS with a pyrolyzer during the sample introduction. Chemometric tools were applied to optimize the analysis conditions considering the sample introduction and DLLME parameters. The preparation of HDES were simple and fast, the mixture of HBA and HBD precursors is taken to a heated stirrer (60°C) for 20 minutes and cooled to room temperature. The combinations between precursors such as DL-menthol has been widely used and acts as HBA, and organic (decanoic, dodecanoic, acetic acids) as HBDs. All HDES had a clear appearance, only the mixture containing dodecanoic acid showed a yellowish color, due to the characteristic of the precursor. The density and viscosity were evaluated both have a strong influence on the extraction process, the HDES showed lower densities than water sample, so the organic phase can be collected easily for further analysis. The HDES were characterized by Infrared spectroscopy (FTIR) and Thermogravimetric analysis (TG) which proved the solvent formation. The factorial planning of the injection evaluated the temperature, time and volume of the sample in the pyrolyzer. The water samples were spiked with the standards at a concentration of 6 mg L⁻¹. Based on the obtained the results, the analytical response tends to increase with the augment of injection volume, this variable was the most significant. In this first evaluation the optimal volume indicated was 10 µL. Afterwards, a univariate was performed to evaluate temperature was fixed in 320°C and time of 0.5 min. The injection volume varied from 2 µL to 20 µL. The best condition for this measurement was 20 µL. For the DLLME step, a full factorial design evaluated the salting-out effect, pH, volume of dispersing solvent and extractor. The sludge samples were initially filtered, the liquid phase was analyzed by Py-GC/MS to assess the presence of analytes. The results demonstrated the analytes were not present in the samples, therefore, the samples were fortified with parabens and bisphenol A at a concentration of 3 mg L⁻¹. Thereafter, the DLLME parameters were optimized using the previous described experiment. The most significant variable was the volume of HDES used as extraction solvent. The optimal conditions for DLLME in sludge samples were 300 µL of HDES, 300 µL of ACN, pH = 10 and a value of 5 % m/v of NaCl. After the injection optimization and factorial design of DLLME, it was possible to apply HDES as extraction solvent in sludge samples. Then, more sludge samples, (the liquid and solid phase) will be analyzed using a standard addition in order to quantify the analytes using the developed method.

References:

CALDEIRÃO, L. et al. A novel dispersive liquid-liquid microextraction using a low density deep eutectic solvent-gas chromatography tandem mass spectrometry for the determination of polycyclic aromatic hydrocarbons in soft drinks. *Journal of Chromatography A*, 2020.
FLORINDO, C.; BRANCO, L.; MARRUCHO, I. Development of hydrophobic deep eutectic solvents for extraction of pesticides from aqueous environments. *Fluid Phase Equilibria*, 2017, 448, 135–142.

Acknowledgments



Área: ANA

Determination of polybrominated flame retardants in sludge samples using magnetic ionic liquids and PY-GC/MS

Thais Rodrigues (PG)^{1*}, Karen Chibana Ferreira (PG)¹, Josias de Oliveira Merib (PQ)², Paulo Clairmont Feitosa de Lima Gomes (PQ)¹

*thais.rodrigues1@unesp.br

¹Instituto de Química Unesp - Araraquara; ²Universidade Federal de Ciências da Saúde de Porto Alegre (UFCSPA).

Palavras Chave: *magnetic ionic liquid, emerging contaminants, pyrolyzer, Py-GC/MS, microextraction, sample preparation.*

Highlights

Magnetic ionic liquid (MIL) prepared to extract of brominated flame retardants (PBDES); Optimization of the pyrolyzer and DLLME parameters using chemometrics tools.

Resumo/Abstract

Some classes of substances are classified as chemical emerging compounds, since they are found in different kind of samples including environmental samples such as water and sewage. The CECs are characterized by high environmental persistence and the lack of legislation for their control and monitoring. To determine these contaminants, separation techniques coupled to mass spectrometry are generally employed. Therefore, sample preparation techniques present a keyhole in this analysis. In this context, the importance of dispersive liquid-liquid microextraction (DLLME) stands out, since it reduces the sample volume and solvents. The liquid ionic magnetic (MIL) presents physicochemical properties similar to ionic liquids featuring additional responses to magnetic fields by incorporating a paramagnetic component within the structure. Therefore, the use of MIL in DLLME simplifies the procedure excluding the centrifugation step. Thus, the aim of this study was to prepare a magnetic ionic liquid (MIL) and apply it in the DLLME as an extraction solvent, in order to analyze polybrominated flame retardants (PBDEs) in sludge samples by GC/MS with sample introduction through a pyrolyzer. The DLLME and sample introduction parameters were optimized using a multivariate approach. MIL was prepared based on the work described by Merib et al (2018), MIL ($[P_{66614}^+][MnCl_4^{2-}]$) using trihexyltetradecylphosphonium chloride ($[P_{66614}^+][Cl^-]$) and manganese chloride (II) tetrahydrate ($MnCl_2 \cdot 4H_2O$) under stirring by 24 h and without heating. The MIL was dried in an oven and analyzed by UV-Vis the wavelength in the region between 425 nm and 465 nm referring to the manganese ion were monitored. Also, Infrared and Raman analysis were performed proving the incorporation of the manganese ion in the structure of the ionic liquid. In the chromatographic method, a pyrolyzer was used in the sample introduction stage (Py-GC-MS), the injection conditions were optimized in multivariate approaches by Box-Behnken using three variables. The optimum condition achieved was temperature of 220 °C, pyrolysis time of 0.6 min and injection volume of 9 µL. The DLLME optimized conditions were 5 mg of MIL, 5 µL of acetonitrile (ACN) as disperser solvent, and an extraction time of 120 s with sample volume of 3 mL. The conditions optimized for Py and DLLME allowed suitable PBDEs separation in sludge samples, without the centrifugation step.

References

Sophia, C.; Lima, E. C. Removal of emerging contaminants from the environment by adsorption. *Ecotoxicology and Environment Safety*, v. 150, p. 1-17, 2018.
MERIB, J.; SPUDEIT, D. A.; CORAZZA, G.; CARASEK, E.; ANDERSON, J. L. Magnetic ionic liquids as versatile extraction phases for the rapid determination of estrogens in human urine by dispersive liquid-liquid microextraction coupled with high-performance liquid chromatography-diode array detection. *Analytical and Bioanalytical Chemistry*, 2018.

Agradecimentos/Acknowledgments

Acknowledgements to the National Council for Scientific and Technological Development (CNPq), Fundação de Amparo à Pesquisa do State of São Paulo (FAPESP) and Coordination for the Improvement of Higher Education Personnel (CAPES). Graduate Program in Chemistry at the Institute of Chemistry UNESP Araraquara. National Institute of Alternative Technologies for Detection, Toxicological Assessment and Removal of Emerging and Radioactive Contaminants (DATREM INCT).

Determination of total phenolic content in extra virgin olive oils using colorimetric assays combined with smartphone digital image

Aline D. M. Vieira (PG),¹ Maria Eduarda B. Coutinho (IC),¹ Bruna R. S. Gomes (PG),¹ Jandyson M. Santos (PQ),^{1*}

almelooliveira@hotmail.com; jandyson.machado@ufrpe.br

¹Department of Chemistry, UFRPE

Key-words: Smartphone, total phenols, digital image analysis and, extra virgin olive oil.

Highlights

- We have evaluated the best conditions of the colorimetric method by design of experiments
- Total phenolic content was obtained using UV-Vis analysis and smartphone digital images

Resumo/Abstract

Extra virgin olive oil (EVOO) is an essential product in the diet due to its nutritional and biological properties. Its benefits are related to its high phenolic content and monounsaturated fatty acids. The main antioxidant compounds are carotenes and phenolic compounds, the latter protecting the oil from oxidation and presenting several benefits to human health, such as anti-inflammatory activity and increased plasma antioxidant capacity (Klikarová, 2019). The commonly used method for determining total phenolic content in colored solutions is ultraviolet-visible spectrometry (UV-Vis) (Fuentes, 2012). As an alternative, we proposed the use of smartphones for the acquisition of digital images that are taken of the sample of interest and processed in the application to obtain the concentration of the analyte based on the intensity of the red-green-blue (RGB) channels. In the measurements, the color level of the substance may be proportional to the concentration of the analyte. The objective of this study was to develop a methodology for the determination of total phenolic content present in EVOOs using smartphone digital images in comparison with the reference method by UV-Vis. For the quantification of total phenols in eight commercial EVOOs samples, initially, it was performed the extraction of phenols by the liquid-liquid extraction (LLE) method was based on the procedure proposed by Ricciutelli (2017), in which the phenolic content was extracted in a falcon tube with 4 mL of water and 0.5 mL of methanol. The colorimetric reaction of total phenolic compounds was performed by the Folin-Ciocalteu (FC) method, but we have optimized it through a design of experiments (DoE) using a full factorial design of 2⁴, and we have evaluated four parameters: (I) volume of FC reagent (0.25 mL and 1 mL); (II) volume of sodium carbonate (Na₂CO₃) (2 mL and 4 mL); (III) concentration of Na₂CO₃ (1 % *m/v* and 10 % *m/v*); and (IV) reaction time (30 min and 90 min). The parameters were evaluated through 16 experiments and 5 repetitions in the central point at a total of 21 experiments. The total phenolic content was obtained using a UV-Vis spectrometer model UV1800 dual-beam (Shimadzu Co., Japan) in the absorbance at 760 nm. As preliminary results, we have found the best conditions for the colorimetric method from the DoE processing, and significant effects were negatively obtained for FC reagent volume, positively for the concentration of Na₂CO₃, and the secondary interaction between both. The numerical optimization was performed and the best experimental conditions related to obtaining the highest UV-Vis absorbance of 760 nm were found as: (I) volume of FC reagent at 0.25 mL; (II) volume of Na₂CO₃ at 2 mL; (III) concentration of Na₂CO₃ at 10% *m/v*; and (IV) reaction time at 30 min. The optimized experiments showed a desirability level of 91.4%. Using the best conditions of the colorimetric method, it was applied to an EVOO sample and the phenol content was determined by the UV-Vis reference method, then the sample was also analyzed from the acquisition of digital images with a smartphone, and similar results were obtained. The results of the total phenolic content in the other samples are being performed by UV-Vis and digital images and will be presented at the congress.

References:

- Fuentes, E. *et al.* Food Analytical Methods, v. 5, p. 2012, p 1311-1319.
Klikarová, J. *et al.* Food Analytical Methods, v. 12, 2019, p. 1759-1770.
Ricciutelli, M. *et al.* Journal of Chromatography A, v. 1481, 2017, p. 53-63.

Agradecimentos/Acknowledgments

FACEPE, LaMTESA/UFRPE, PPGQ/UFRPE, LABMAQ

Development of a dynamic method for the production of a gaseous standard: a simple and low-cost alternative

Diandra N. Barreto (PG),¹ João Flávio S. Petrucci (PQ)¹

diandra.nbarreto@gmail.com;

¹ Federal University of Uberlândia, Institute of Chemistry. Av. João N. de Ávila, 2121, 13400-970, Uberlândia, MG, Brazil

Key words: gaseous standard, dynamic methods, low cost, continuous gas extraction.

Highlights

The preparation of gaseous standard solutions is crucial for the development of methods for gaseous samples. Herein, we describe a simple method for the preparation of gaseous standard mixtures of acetone.

Resumo/Abstract

The preparation of gaseous standard solutions or mixtures is a major challenge for method development and analysis of gaseous samples. A standard solution must have constant concentration over time and the values of uncertainties and errors must be known. Static methods use a known volume of the target gas within a closed container (e.g. cylinder). The main disadvantage of these methods is the adsorption or permeation of the components through the container walls, decreasing the shelf life of the standard. On the other hand, dynamic methods are systems that continuously produce gas mixtures with known concentrations, using a gas flow that is continuously and constantly fortified with the target gas. In this work we developed a dynamic method based on continuous gas extraction for the production of a gaseous standard of acetone. Theoretical values of the gaseous standard concentration by the method can be obtained using Equation 1. Experimental values were acquired using a standard gaseous system, controlled flow rate ranging from 50 to 200 mL/min. The air flow was bubbled into a glass flask containing acetone maintained at 25°C. After 10 minutes of equilibrium, the air samples were collected using a Tedlar® bag and injected into a GC-FID. The concentration values obtained for each air flow are shown in Table 1.

Table 1. Concentration of acetone vapor generated using the proposed method

Experimental			Theoretical
Air flow rate (mL/min)	C% (n=3)	RSD (%)	C%
50	34	1,4	36
100	25,5	2,1	29
200	16	1,4	19

$$C_{\%} = \frac{24.5 \times 10^2 q_L \rho}{q_D M} \quad \text{Equation 1}$$

The proposed method showed results similar to the theoretical values, therefore, it is an alternative of easy execution and low cost. In addition, it allows the production of standard solutions of various gaseous substances without the need to purchase permeation tubes or cylinders of the gas of interest.

Agradecimentos/Acknowledgments

IQ-UFU, CAPES CNPQ

Área: ANA

DEVELOPMENT OF A MICRODEVICE FOR THE SAMPLING OF GLYPHOSATE AND ITS DERIVATIVE AMPA IN SURFACE WATER

Maria Fernanda M. Carvalho (IC),¹ Zenilda L. Cardeal (PG),¹ Helvécio C. Menezes (PG)^{1*}

mfmariamf@gmail.com; hmenezes@ufmg.br

¹Universidade Federal de Minas Gerais – UFMG/ICEx - Campus Pampulha, Belo Horizonte/MG, CEP 31270-901

Palavras Chave: *Glyphosate, AMPA, passive sampling, surface water, mesoporous carbon, GC/MS.*

Highlights

When used irresponsibly, Glyphosate (GLY) and its derivative aminomethyl phosphonic acid (AMPA) can induce issues such as contamination of surface water, decreased soil fertility, and adverse effects on soil microbiota. Due to the worldwide intensive use of this herbicide, its necessary developments in the extraction and pre-concentration of these compounds, especially when these are performed in water. This work's objective was to develop a new microdevice for passive sampling based on the use of a mesoporous carbon (MC) [1] fixed on polydimethylsiloxane fiber [2] to extract and pre-concentrate glyphosate and AMPA in surface water samples.

Abstract

The extraction of the analytes in surface water was performed by the passive sampling method. The procedure consisted in submerging the MC fiber with a diameter of 1.0 mm and a length of 2.0 cm in the sample for extraction and preconcentration. After this step, the system was magnetically stirred for 30 minutes. The desorption consisted in adding the fiber to a 2 mL polypropylene (PP) flask with 1.1 mL of acetonitrile for 2 minutes at 45°C in an ultrasonic bath.

Then, towards the derivatization, 25 µl of the lastest step was put on a 2 mL PP flask, then 400.0 µL Trifluoroethanol and 800.0 µL Trifluoroacetic anhydride were added followed by heating to 100° C for 1 h. Subsequently, the aqueous part was evaporated under nitrogen flow, and finally, 1.0 mL of ethyl acetate was added to the polypropylene vial and 1.0 µL was injected.

The analysis of the extraction efficiency was performed by a GC-MS Shimadzu QP-2010, the chromatography separation was performed on an HP5-MS column (30 m x 0.25 mm x 0.25 µm). As shown in Fig. 1 the MC fiber exhibited superior efficiency in the extraction of GLY and AMPA compared to the PDMS fiber.

REFERENCES

- [1] SILVA, R. C. F. Et Al. Chemical Engineering Journal, v. 407, p. 127219, 2021
 [2] COELHO, N. S. Et Al. IV Simpósio da Bacia Hidrográfica do Rio São Francisco, Belo Horizonte, 2022.

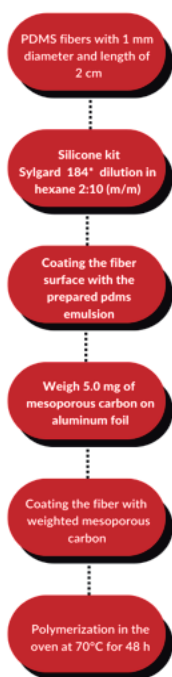


Fig. 1 – Preparation process of MC fiber.

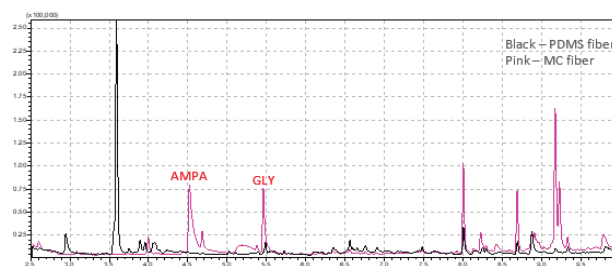


Fig. 2 – Chromatogram comparison of a PDMS fiber with mesoporous carbon fiber for the extraction of GLY and AMPA.

Acknowledgments

This work was financed by Companhia Energética de Minas Gerais (CEMIG), Fundação de Amparo à Pesquisa do Estado de Minas Gerais (FAPEMIG) and the National Council for Scientific and Technological Development (CNPq).

DEVELOPMENT OF AN ANALYTICAL METHOD FOR DETERMINING TRACE ELEMENTS IN URINE SAMPLES BY ICP-MS AND ICP OES

Ketolly N.S. Leal (PG),^{1*} Olívia B.O. Moreira (PG),² Ana B.S. Silva (PQ),¹ Lúcio M. Lemos (PQ),³ Marccone A.L. Oliveira (PQ),² Marco A.Z. Arruda (PQ).¹

ketollynataneg@gmail.com

¹Spectrometry, Sample Preparation and Mechanization Group, Institute of Chemistry, State University of Campinas – Unicamp, Campinas - SP, Brazil, 13083-970.

²Analytical Chemistry and Chemometrics Group (GQAO), Institute of Exact Sciences, Juiz de Fora Federal University – UFJF, Juiz de Fora – MG, Brazil, 36036-90.

³Lemos Laboratory of Clinical Analysis, 36025-290, Juiz de Fora, MG, Brazil.

Keywords: Homeostasis, Biological samples, Analytical methods; Inductively coupled plasma mass spectrometry, ICP OES.

Highlights

Quantification of 10 trace elements in human urine by ICP-MS and ICP OES using a single method. The developed method can be an important tool to assess nutritional imbalances or metabolic disorders.

Abstract

Trace elements are present in the human body in concentrations that can vary from ng/L to mg/L, being responsible for playing important roles in several body functions.¹ Their deregulation can lead to several health problems, such as anemia and immunodeficiency problems, in addition to affecting cellular processes.¹ Thus, the identification and quantification of trace elements can allow for monitoring health conditions, and diagnosing and preventing diseases.² In this context, inductively coupled plasma mass spectrometry (ICP-MS) and inductively coupled plasma optical emission spectrometry (ICP OES) are commonly used to quantify trace elements in biological samples such as blood, urine, and tissues. One of the challenges associated with this technique is the spectral and non-spectral interferences that impact the veracity of the result, especially when the matrix is complex, such as urine which contains a large amount of organic matter and salts. In this sense, the objective was to determine 10 trace elements in urine (Fe, Cu, Zn, Se, Mo, P, K, Ca, Mg, and S) in a single method. Samples were decomposed using a DTG-100 microwave oven (Provecto Analítica), adding 3 mL of sample, 1 mL of HNO₃ (65% v v⁻¹), and 1 mL of H₂O₂ (30% v v⁻¹). After this process, the final volume was adjusted to 50 mL with deionized water (Figure 1). ICP-MS (iCAP TQ, Thermo Scientific) and ICP OES (Thermo Scientific, iCAP 6000) were used to determine the total concentration of trace elements. Indium (In) was used as an internal standard (1 ng/L). Calibration curves were constructed using elemental standards of 1000 mg L⁻¹. The precision of the method was verified using the addition and recovery test (Spike), and calculated according to the FDA guideline.³ The figures of merit LOD, LOQ, linearity, and sensitivity are found in Table 1, as well as the recoveries obtained.

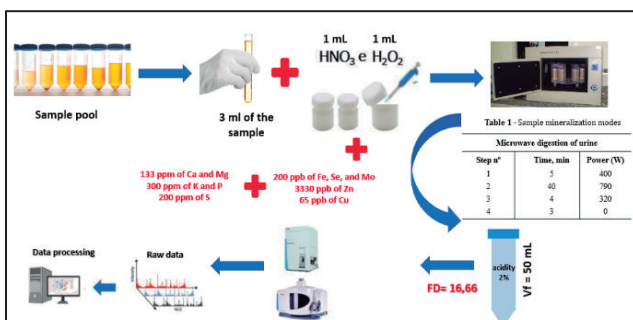


Figure 1 - Workflow

	Fe/In (ng/L)	Cu (ng/L)	Zn (ng/L)	Se (ng/L)	Mo/In (ng/L)	Ca (mg/L)	K (mg/L)	Mg (mg/L)	P (mg/L)	S (mg/L)
Concentration	1.6	0.30	12.89	0.57	3.03	7.00	21.50	6.60	29.50	23.80
Recovery (%)	85 ± 6	122 ± 9	87 ± 3	103 ± 2	87 ± 9	74 ± 3	103 ± 1	77 ± 3	87 ± 7	100 ± 6
%RSD	7	5	3	2	8	2	1	3	7	6
LOD	0.23	0.07	0.16	0.03	0.02	0.01	0.46	0.0014	0.02	0.02
LOQ	0.75	0.23	0.54	0.10	0.06	0.028	1.53	0.004	0.08	0.07
Slope	18465,51	56833,46	17579,37	3478,91	26731,99	38881,17	578,41	179165,68	87,92	110,98
R ²	0.9975	0.9937	0.9988	0.9945	0.9976	0.9970	0.9968	0.9996	0.9998	0.9996

Results Expressed as mean ± standard deviation (n=3) Table 1 - Results obtained

According to the data (Table 1) the 10 trace elements were identified and quantified. The accuracy of the method was in the range of 75% to 122% with a relative standard deviation in the range of 1% to 8%. The limits of detection and quantification were 0.02 µg L⁻¹ and 0.06 µg L⁻¹, respectively. The 10 trace elements were successfully determined, allowing their application in biomonitoring studies of health conditions, and the identification of possible nutritional imbalances or metabolic disorders.

¹De Jesus, J. R. & De Araújo Andrade, T. (2020). *Metallomics*, 12(12), 1912–1930.

²Arruda, M.A.Z., De Jesus, J.R., Blindauer, C.A., Stewart, A.J. (2022). *Journal of Proteomics*, v.263. 104615.

³FDA (2022). *Bioanalytical Method Validation Guidance for Industry*.

Acknowledgments

The authors thank Fapesp (2014/50867-3, 2017/50085-3, 2018/25207-0, 2019/24445-8, 2020/06934-9, and 2020/08543-7) and CNPq (303231/2020-3, and 200475/2022-3/SWE).

Development of a new direct magnetic sorbent sampling device (DMSS-FF-AAS) for highly sensitive cadmium determination

Paula Mantovani dos Santos (PG),^{1*} Ana Carla Ranucci Carneiro (IC),¹ Lucimara Mendonça Costa (PG),² Odair Pastor Ferreira (PQ),^{1,3} Francisco Holanda Soares Junior (PG),^{3,4} João Maria Soares (PG),⁵ Lais Helena Sousa Vieira (PG),³ Eduardo Costa de Figueiredo (PQ),² Marcela Zanetti Corazza,¹ César Ricardo Teixeira Tarley (PQ),^{1,6}

*paulamantovani@live.com

¹Departamento de Química, UEL; ²Laboratório de Análises de Toxicantes e Fármacos, UNIFAL; ³Laboratório de Materiais Funcionais Avançado, UFC; ⁴Departamento de Ensino, IFC; ⁵Centro de Síntese e Análise de Materiais, UERN; ⁶Instituto Nacional de Ciência e Tecnologia de Bioanálítica, UNICAMP.

Keywords: solid sampling; atomic absorption spectrometry; magnetic nanocomposite; highly sensitive determination.

Highlights

- ❖ A new method for the highly sensitive determination of cadmium in environmental and food samples.
- ❖ A method well aligned with the concept of green analytical chemistry.

Abstract

A novel and highly sensitive method for cadmium determination at ultrace levels combining dispersive magnetic solid phase extraction (DMSPE), direct magnetic sorbent sampling (DMSS), and flame furnace atomic absorption spectrometry (FF-AAS) is described in this work. Magnetic carbon-based nanocomposite ($\text{Fe}_3\text{O}_4@\text{C}$) was used as sorbent for cadmium preconcentration using DMSPE. The characterization of $\text{Fe}_3\text{O}_4@\text{C}$ was performed by thermogravimetric analysis (TGA), Fourier transform infrared spectroscopy (FTIR), electron microscopy (SEM), and vibrating sample magnetometry (VSM). Under optimized preconcentration conditions, a 30 mL aliquot of the sample (pH = 8.0) was preconcentrated in 2.0 mg of $\text{Fe}_3\text{O}_4@\text{C}$ for 2.0 min using vortexing. Subsequently, the $\text{Fe}_3\text{O}_4@\text{C}$ particles were easily separated from the aqueous medium by employing a magnetic stainless steel rod and directly inserted inside of a nickel tube heated by flame (Fig. 1). The method (DMSS-FF-AAS) showed substantially higher analytical performance when compared to FAAS, TS-FF-AAS (direct analysis), as well as TS-FF-AAS using preconcentration and elution step, evidenced by a remarkable increase in the sensitivity of 2502, 151 and 41 times, respectively. The limit of detection, linearity, and the precision in terms of repeatability ($n=10$) assessed as relative standard deviation (RSD%) were found to be 5 ng L⁻¹, 15 – 750 ng L⁻¹, and 1 – 4%, respectively. The method was compared to other methods of extraction and pre-concentration of Cd²⁺ ions reported in the literature and proved to be advantageous and promising. The accuracy of the method was attested by analysis of certified reference materials, CRM – 1643e (water) and CRM – 1573a (tomato leaves). The proposed method was successfully applied for cadmium determination in mineral and lake water samples ranging from 16 to 465 ng L⁻¹.

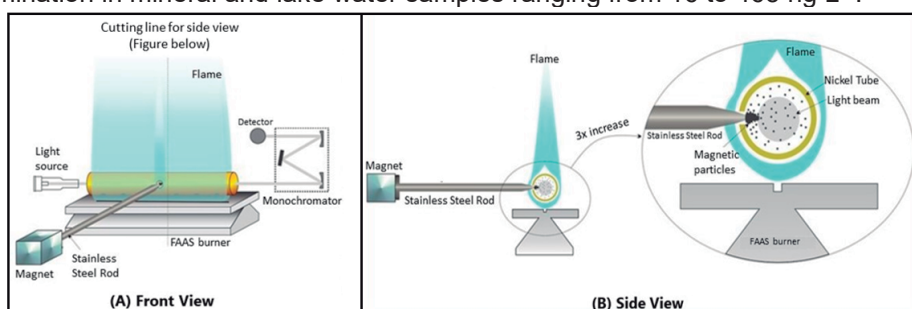


Figure 1. Schematic insertion of magnetic stainless steel rod containing the magnetic nanocomposite attached to the tip inside the nickel tube. (A) front view. (B) side view.

Agradecimentos/Acknowledgments

The authors are grateful for the collaboration of CNPQ (grant no. 427365/2018-0, 420097/2021-0, 307505/2021-9, and 313637/2019-9), FAPEMIG (process APQ-00043-21), CAPES, Araucária Foundation (PBA2022011000002) and INCT (FAPESP Process nº 2014/50867-3 and nº 465389/2014-7). OPF also appreciates the support of FUNCAP (grant number PRONEX PR2-0101-00006.01.00/15 and 'Rational Design of Nanomaterials and Applications in Environmental Remediation, Agriculture and Health').

Development of a non-destructive method for dating pen ink in documents using infrared spectroscopy and ambient ionization mass spectrometry with multiset data modeling

Kauanny B. N. Braga (PG),^{1*} Lanaia I. L. Maciel (PG),² Licarion Pinto (PQ),³ Boniek G. Vaz (PQ),² Jandyson M. Santos (PQ).¹

kauannybeatrizbraga@gmail.com; jandyson.machado@ufrpe.br

¹Chemistry Department, UFRPE; ²Chemistry Institute, UFG; ³Chemistry Department, UERJ

Key-words: Forensic chemistry; Documentoscopy; Pen ink; Dating; Infrared; DESI-MS

Highlights

- Dating of pen ink dyes in real and artificial documents;
- Analysis of pen ink dyes by infrared spectroscopy and ambient ionization mass spectrometry;
- Construction of a predictive ink dating using multiset data modeling.

Resumo/Abstract

Among the different areas that make up forensic chemistry, documentoscopy is of great importance, since it is responsible for providing historical information about a document and evaluating its veracity for judicial purposes. The ink dating of documents is one of the most difficult problems to solve in the field of forensic science, this is because the dyes used in the manufacture of pen inks are more stable over time since their degradation is much slower than that of other components. Exposure of the document to light is the main factor in the long-term degradation of pen ink dyes. This process can last for several years under natural conditions, making it possible to date ancient documents. This study aims to develop a fast and non-destructive method for dating pen ink in documents, through the analysis by Fourier transform mid-infrared spectroscopy in attenuated reflection mode (IR-ATR) and Desorption electrospray ionization mass spectrometry (DESI-MS) using a multiset data modeling. Two sets of paper samples with blue inks were studied, the first was a paper sample that was artificially aged in a simulation chamber arranged with blue, white, and ultraviolet lights, with exposure in different time variations at 0, 24, 48, 72 and 96 hours. The second set of samples were real documents with natural pen inks dated from 1960 to 2022 (a total of 39 samples). All samples were directly analyzed by IR-ATR and DESI-MS, without any type of sample preparation. We have found that it was possible to observe differences among the IR spectra of the artificially aged samples over time, especially a trend of decreases of absorbances in the $\sim 1584\text{ cm}^{-1}$ band, which suggests that there is a chemical modification in the molecular structure of one of the main dyes used in the paint composition, which is the Basic Violet 3 (BV3). The $\sim 1584\text{ cm}^{-1}$ band is related to the stretching frequencies of C=N of BV3 molecule. The same behavior was also found in the IR spectra of the naturally aged samples of documents when we compared the samples over time. Multiple linear regression (MLR) was performed for both sets of samples, using the genetic algorithm (GA) for variable selection (spectrum bands), and we have obtained a model prediction with an error of ± 8.0 hours for the simulated samples, and ± 6.6 years for the real samples. The DESI-MS also showed differences between the real samples in the pen inks with different ages with the identification of 5 different dyes, and the most common was the BV3 and the presence of its molecular and degradation ions (m/z 372, 358, 344, 330, 316) in the MS profiles, which was present in all real samples and simulated samples. The multiset data modeling was applied for combining the DESI-MS and IR-ATR results through GA-MLR, which resulted in a final prediction model. After data fusion, the prediction error for the simulated samples was ± 0.27 hours and ± 4.1 years for naturally aged pen inks. The data fusion technique proved to be more efficient for dating ink than the modeling obtained individually for IR-ATR. Thus, the multiset data modeling from DESI-MS and IR-ATR analysis of pen inks can be used for document dating in routine forensic analysis, as it is fast, practical, non-destructive, and with a low error of prediction.

Agradecimentos/Acknowledgments

FACEPE, LaMTESA/UFRPE, PEM, PPGQ/UFRPE, LABMAQ, UFG, UERJ.

Development of a non-invasive sampling method for metabolomic analysis of exhaled air by TD-GC×GC-MS

Guilherme C. Bernardo (IC),^{1*} Leandro W. Hantao (PQ).¹

g170755@dac.unicamp.br;

¹Institute of Chemistry, University of Campinas (IQ-UNICAMP), 13083-862, Campinas, SP, Brasil.

Keywords: Breath analysis, Breath sampling, GC×GC, Mass spectrometry, Thermal desorption, Volatile organic compounds.

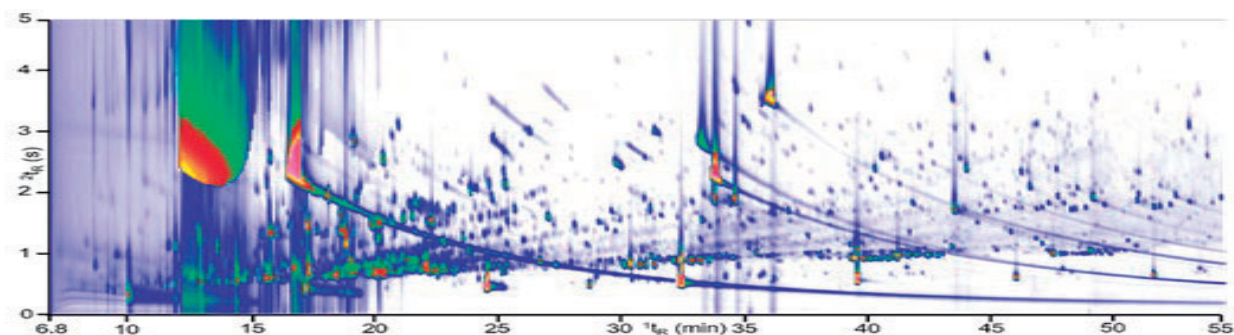
Highlights

Important parameters for breath analysis were optimized such as volume and portion collected, instructions for sampling and minimization of contaminants. Furthermore, a method comparison test was performed.

Abstract

Metabolomics is defined as the comprehensive analysis of set of metabolites present in a biological system, being able to identify metabolic signatures directly related to exogenous and endogenous changes in the individuals under study from a wide range of matrices. Exhaled air is a challenging biological matrix that has attracted interest in both health and exposure studies, mainly due to its non-invasive sampling methods¹. The volatile fraction comprises less than 1% of the total volume of exhaled air, even then it contains hundreds of volatile organic compounds (VOCs) that can be detected, identified, and measured using the appropriate analytical instrumentation. So, the measure of the entire set of VOCs, even those at trace amounts, can be used to provide valuable information about the metabolic state of an organism. However, for breath analysis to be implemented in routine analysis it is essential to overcome the lack of standardization in its analytical methodologies, which have exhibited many variations between different research groups, hampering the progress in this area. To achieve this goal, two of the most important steps are optimizing the parameters of each method and developing comparison tests that allows meta-analyses of data and inter-group discussions². This work aims to develop and evaluate an analytical method for breath analysis using inert polymeric bags (Tedlar® Bags) for sampling and thermal desorption for pre-concentration of the analytes. This workflow is followed by molecular analysis using comprehensive two-dimensional gas chromatography coupled to mass spectrometry (GC×GC-MS) (**Figure 1**). Important parameters were optimized such as volume and portion collected, necessary instructions to volunteers and minimization of contaminants. To evaluate the methodology, a recently proposed test based on the ingestion of peppermint capsules was carried out². Lastly, an untargeted metabolomic analysis of VOCs present in exhaled air from two different study groups was performed using the developed method and chemometric tools.

FIGURE 1: Chromatogram of exhaled breath from a human volunteer using GC×GC-TOFMS with a non-polar × mid-polar column set and a modulation period of 5 s.



¹ Lawal, Oluwasola, et al. Exhaled breath analysis: a review of 'breath-taking' methods for off-line analysis. *Metabolomics* 13 (2017) 1-16.

² Wilkinson, Maxim, et al. "The peppermint breath test: a benchmarking protocol for breath sampling and analysis using GC-MS." *Journal of Breath Research* 15 (2021) 026006.

Acknowledgments

Acknowledgments to São Paulo Research Foundation (FAPESP), grant #2022/07571-2

46ª Reunião Anual da Sociedade Brasileira de Química: "Química: Ligando ciências e neutralizando desigualdades"

Development of colorimetric paper analytical device (PAD) for forensic markers identification and determination in biological samples

Amanda Luise A. Nascimento (PG)^{1,*}, Daniela S. Anuniação (PQ)¹, Wendell K.T. Coltro (PQ)²,
Josué Carinhonha C. Santos (PQ)¹

daniela.anuniao@iqb.ufal.br; amanda.luise@yahoo.com.br

¹Universidade Federal de Alagoas, Campus A. C. Simões, Maceió - AL, Brasil. ²Universidade Federal de Goiás, Goiânia - GO, Brasil.

Keywords: sexual crimes; forensic application; fructose; colorimetric detection.

Highlights

Low-cost, portable, sensitive, and selective device for semen identification in sexual crimes exploring the colorimetric detection of biological markers to assist in the elucidation of crimes against women.

Abstract

A identificação de fluidos corporais é uma etapa crucial na investigação criminal¹ especialmente se tratando de crimes sexuais, devido à alta recorrência de violência desta natureza em que 1 entre 5 mulheres sofreram abuso². A coleta de amostras biológicas, como sêmen, na cena do crime ou na vítima, é importante para confirmar o possível estupro, viabilizando também, identificar o perpetrador. Diferentes metodologias de identificação de marcadores³ presentes no sêmen em altas concentrações, como frutose, têm sido avaliadas, porém, ainda se verifica uma demanda por testes rápidos e de baixo custo para auxiliar na perícia criminal. Assim, o presente trabalho visou o emprego de um dispositivo analítico baseado em papel (PAD) baseado na variação colorimétrica dos sistemas reativos devido à frutose presente na amostra de sêmen, gerando cromóforo de coloração azul (Fig.1a). A mudança colorimétrica nas zonas de teste foi observada visualmente e as imagens capturadas pelo *scanner* permitem obter uma resposta analítica quantitativa. Diferentes parâmetros foram otimizados no desenvolvimento do dispositivo, buscando melhorar a identificação e sensibilidade do método, como: ordem de adição e concentração dos reagentes, sistema tampão e tempo de secagem, permitindo obter resposta linear para frutose na faixa (25 - 200 mg L⁻¹), com limite de detecção de 10 mg L⁻¹.

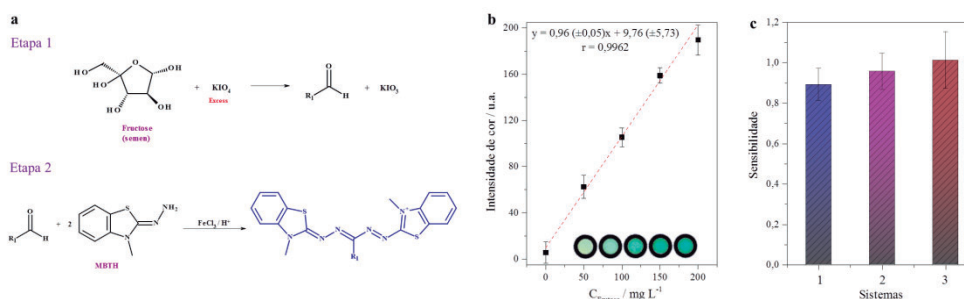


Fig. 1. (a) Reação de oxidação da frutose com conseqüente formação do cromóforo. (b) Curva analítica da intensidade de cor em função da concentração de frutose. (c) Avaliação de possíveis interferentes. Sistemas: (1) frutose; (2) frutose + glicose (proporção 2,5:1); e (3) frutose + Inositol (proporção 2:1).

O intervalo de concentração normalmente reportado em amostras de sêmen varia de 1400 a 6300 mg L⁻¹,^{4,5} indicando que o método atende perfeitamente à finalidade, e, destaca-se que para amostras de sangue, urina e saliva os níveis de frutose são dezenas a centenas de vezes menor. O estudo da seletividade, foi realizado com interferentes como glicose e inositol (Fig. 1b), não apresentando diferença significativa ($\alpha = 0,05$). O dispositivo aplicado em amostra real mostrou-se sensível e confiável cujas análises quali e quantitativas diretamente na cena do crime surge como uma inovação científica e tecnológica que contribuirá na elucidação desses crimes.

References

¹Das et al. *Microchemical Journal*. **2021**, 171, 106810 // ²Brasil, Anuário Brasileiro de Segurança Pública, **2021** // ³Zha et al. *Forensic Sciences Research*. **2020**, 5, 119-125. // ⁴Trang et al. *MOJ Biorg. Org. Che.* **2018**, 2, 185-190 // ⁵Owen; Katz. *Journal of andrology*. **2005**, 26, 459-469.

Acknowledgments

UFAL, IQB – PPQGB, Capes (Procad), CNPq e FAPEAL.

Development of element detection method in vape liquids using ICP-MS

Carlos L.R. Fragoso (PG)¹, Guilherme V. Espinosa (IC)¹, Anna De Falco (PQ)¹, Tatiana D. Saint'Pierre (PQ)¹, Adriana Gioda (PQ)^{1*}

carlostst@gmail.com; agioda@puc-rio.br

¹Departamento de Química, PUC-Rio.

Keywords: electronic cigarette, e-liquid, element determination, ICP-MS

Highlights

Elements such as Ag, As, Ba, Ca, Cd, Co, Cr, Cu, Hg, Li, Mg, Mo, Na, Ni, P, Pb, Pd, S, Sb, Se, Si, Sn, Ti, Tl, V, and Zn were detected over LOQ on e-liquid samples by ICP-MS. The developed method was validated, and the internal and external curves showed a non-significant difference and element recovery between 80 and 110 % (SD = 0.058).

Resumo/Abstract

Electronic Nicotine Delivery Systems (ENDS) or Electronic Smoking Devices (ESD), commonly called electronic cigarettes (vapers or e-cigarettes), are devices used for the consumption of nicotine without the need to burn tobacco leaves. For this purpose, these devices heat a mixture of propylene glycerin and propylene glycol containing different concentrations of nicotine and other additives, called e-liquid (or even juice)^{1,2}. Upon heating, the mixture forms an aerosol, which is inhaled, carrying nicotine into the lung and then into the bloodstream. The composition of these e-liquids varies by origin, brand or consumer's taste (homemade production). Since the e-cigarette trade is prohibited in Brazil by ANVISA Resolution No. 46, of August 28th, 2009, every product that reaches the Brazilian consumer lacks quality control analysis, raising concerns for the health surveillance organs. This concern is due to toxic metals in the aerosol and, possibly, in liquids^{3,4}. While the concentrations determined are smaller than such limits, the elements in the e-liquid must be considered potentially harmful to the user's health since the concentration increases in the aerosol coming from the device leaching and decomposition. The study aimed to detect and assess the accuracy of the results obtained using the sample dilution in ultrapure water, 1 % and 5 % HNO₃, and 1 % HCl for acidification solutions.

After an initial semiquantitative analysis, the analytical method to determine Ag, As, Ba, Ca, Cd, Co, Cr, Cu, Hg, Li, Mg, Mo, Na, Ni, P, Pb, Pd, S, Sb, Se, Si, Sn, Ti, Tl, V, and Zn by inductively coupled plasma mass spectrometry (ICP-MS) was developed, by using e-liquid raw material (glycerin and propylene glycol, in different ratios). Nine samples of e-liquid of brands from the USA, Brazil and Paraguay was used and diluted in a ratio of 1:5 wt/wt. To correct non-spectral interferences, ¹⁰³Rh was used as the internal standard. External curve and standard addition calibration methods were used to evaluate such correction by comparing the slopes using the Student *t*-test, Kolmogorov-Smirnov for the normality test, and ANOVA and Bonferroni tests for correlation and significance. Each analysis was made in triplicate. Recovery studies were performed to evaluate the method's accuracy, and the figures of merit were calculated using the appropriate calibration method. The comparison of the calibration methods showed that the non-spectral interferences for Ni, Ti and Zn were not significant, while standard addition calibration should be used for the other elements. Concentrations above the method's limit of quantification were obtained, except for Pb, for which a smaller dilution was used. The results stayed at 0.01 µg L⁻¹ for Tl to 200 µg L⁻¹ for Zn. The recovery experiments results were between 80 to 110 %, ratifying the accuracy of the analytical method.

- (1) Kaur, G.; Pinkston, R.; McLemore, B.; Dorsey, W. C.; Batra, S. Immunological and Toxicological Risk Assessment of E-Cigarettes. *Eur. Respir. Rev.* **2018**, *27* (147). <https://doi.org/10.1183/16000617.0119-2017>.
- (2) Ghosh, A.; Coakley, R. C.; Mascenik, T.; Rowell, T. R.; Davis, E. S.; Rogers, K.; Webster, M. J.; Dang, H.; Herring, L. E.; Sassano, M. F.; Livraghi-Butrico, A.; Van Buren, S. K.; Graves, L. M.; Herman, M. A.; Randell, S. H.; Alexis, N. E.; Tarran, R. Chronic E-Cigarette Exposure Alters the Human Bronchial Epithelial Proteome. *Am. J. Respir. Crit. Care Med.* **2018**, *198* (1), 67–76. <https://doi.org/10.1164/rccm.201710-2033OC>.
- (3) Gaur, S.; Agnihotri, R. Health Effects of Trace Metals in Electronic Cigarette Aerosols—a Systematic Review. *Biol. Trace Elem. Res.* **2019**, *188* (2), 295–315. <https://doi.org/10.1007/s12011-018-1423-x>.
- (4) Gray, N.; Halstead, M.; Gonzalez-Jimenez, N.; Valentin-Blasini, L.; Watson, C.; Pappas, R. S. Analysis of Toxic Metals in Liquid from Electronic Cigarettes. *Int. J. Environ. Res. Public Health* **2019**, *16* (22), 4450. <https://doi.org/10.3390/ijerph16224450>.

Agradecimentos/Acknowledgments

The authors would like to thank all students, including special graduation student Gabriel Barros and Ph.D. student Luis Fernando da Silva, for their support on experiments and laboratory routine. Also thank to Dr. William Serra and Guilherme for samples donations, and CNPq, CAPES and FAPERJ for financial support.

DEVELOPMENT OF FIELD TEST FOR DETERMINATION OF ADULTERATION OF ETHANOL FUEL BY METHANOL

Débora França de Andrade (PQ),¹ Vanessa G. F. da Cruz (PG),^{1*} Cristiane G. de Souza (PQ),¹ Rafael C. dos Santos (PG),² Renan de O. Muniz (PG),² Luiz Antonio d'Avila (PQ)² o (PQ).^{1*}

debora.franca.andrade@gmail.com; vanessagfcruz@gmail.com

¹Federal University of Rio de Janeiro, Institute of Chemistry, Rio de Janeiro, Rio de Janeiro, Brazil, 21941-909; ²Federal University of Rio de Janeiro, Chemistry and Biochemistry Processes Engineering Program, School of Chemistry, Rio de Janeiro-RJ, Brazil, 21941-909

Passwords: *Adulteration, methanol, ethanol fuel, quality control.*

Highlights

Ethanol fuel has been adulterated with methanol. Quality control is based on gas chromatography. This work aims to develop a simple, fast and low-cost test, which could be carried out in field.

Abstract

Ethanol is the most used biofuel in Brazil. However, this fuel has been adulterated with methanol, of fossil origin, which, in addition to the environmental and tax impacts, may cause damage to the health of consumers, due to its toxicity. The National Agency of Petroleum, Natural Gas and Biofuels (ANP), from Resolution no. 19, of 2015¹, establishes that the maximum content of methanol in ethanol fuel must not exceed 0.5%, by volume. With the issue of ANP Resolution No. 696, of 2017/08/31, rectified on 2017/10/03², it became mandatory to analyze the methanol content in ethanol fuel by suppliers of this fuel and distributors of liquid fuels, in order to curb the use of methanol as an ethanol adulterator. The reference method for determination of methanol in ethanol is based on the gas chromatography technique, NBR 16041/2015 (ANP, 2015). An alternative method, based on high performance liquid chromatography, was developed³ but both require expensive equipment and are only feasible in laboratories. Thus, the main objective of this work was to develop a simple, fast and low-cost test, which could be carried out in field, using Nile blue chloride dye and digital images processing of colorimetric reactions to determine adulteration of ethanol fuel with methanol. An experimental plan was constructed with the aim of identifying the best concentration of this dye and relating it to the colorimetric responses in ethanol and methanol solvents. Concomitantly, the influence of different cameras and smartphones were evaluated, and the results were obtained in the RGB (Red, Green and Blue) system, using the ImageJ software, and compared to select the channel with the highest sensitivity. As a result, the combination of a portable camera and a 64-megapixel smartphone allowed the identification of a greater difference in the response of RGB values between ethanol and methanol at low dye concentrations (0.005 g L⁻¹). The linearity of the method was determined in the ranges of 0 to 100%, 0 to 20% and 0 to 1%, by volume of methanol in ethanol. The results showed good linearity in the concentration ranges from 0 to 100% and 0 to 20%, by volume of methanol in ethanol, which can be demonstrated by coefficients of determination (R^2) greater than 0.90. Red Channel showed a more sensitive response compared to the other ones and partially linear, with coefficients of variation between 4% and 24% in the concentration ranges from 0 to 100% and 0 to 20%, being potentially applicable for quantification. The developed method is promising, requiring optimization of the experimental conditions to be used in the identification of adulteration of fuel ethanol with methanol, in field, making the monitoring of ethanol fuel more accessible and, therefore, improving its quality.

1. Agência Nacional de Petróleo, Biocombustíveis e Gás Natural (ANP). Resolução ANP n° 19 de 15 de abril de 2015. Brasil, 2015.
2. Agência Nacional de Petróleo, Biocombustíveis e Gás Natural (ANP) Resolução ANP n° 696 de 31 de agosto de 2017, Brasil, 2017.
3. Dias GP, Santos RC, Carvalho RC, Souza CG, Santos APF, Andrade DF and d'Avila LA, J. Braz. Chem. Soc., Vol. 31, n° 5, 1055-1063, 2020.

Acknowledgments

Sociedade Brasileira de Química (SBQ)

Thanks to the Institute of Chemistry at UFRJ, the Graduate Program in Chemistry at UFRJ and the financial support from FAPERJ and PRH20.1.

Direct analysis of amino acids by reactive paper spray mass spectrometry for newborn screening

Eduardo L. Rossini (PQ),^{1,2*} Emanuel Carrilho (PQ).^{1,2}

elrossini@usp.br; emanuel@iqsc.usp.br

¹Instituto de Química de São Carlos, Universidade de São Paulo, São Carlos, SP, Brazil, 13566-590; ²Instituto Nacional de Ciência e Tecnologia de Bioanalítica-INCTBio, Campinas, SP, Brazil, 13083-970.

Palavras Chave: Newborn screening, Amino acids, Microfluidic paper device, Ambient ionization, Online derivatization, Diagnostics.

Highlights (up to 200 characters with spaces)

Increase ionization of polar compounds using reactive paper spray;
Microfluidic paper device to collect, store and analyze plasma samples;
Rapid diagnostic of aminoacidopathies for newborn screening.

Abstract

Newborn screening is considered one of the most significant advances in preventive medicine and one of the largest public health campaigns. The early diagnosis of diseases, even for the rare ones, can reduce or eliminate irreversible sequels that could occur if they were not detected prematurely.¹ A group of rare diseases analyzed in newborn screening is the aminoacidopathies, which are metabolic disorders caused by a specific deficiency in determined enzymes or transporters, such as phenylketonuria, leucinosi (maple syrup urine disease), and tyrosinemia type II.² The classic analysis for newborn screening involves the utilization of dried blood spots followed by chromatographic techniques with mass spectrometry detection analysis, however, dried plasma spot (DPS) is a simpler and easier-to-use sampling method that reduces the risk of contamination for the operator, eliminates the hematocrit interference, and facilitates transportation and storage.³ In this way, we proposed to use reactive paper spray (PS) mass spectrometry as a tool to increase the ionization efficiency of high polar molecules as amino acids and integrate the advantages of a paper platform (3D- μ PAD), such as low cost, availability, flexibility, hydrophilicity, light weight, biocompatibility, and power-free fluid transport with the reliability of mass spectrometric.

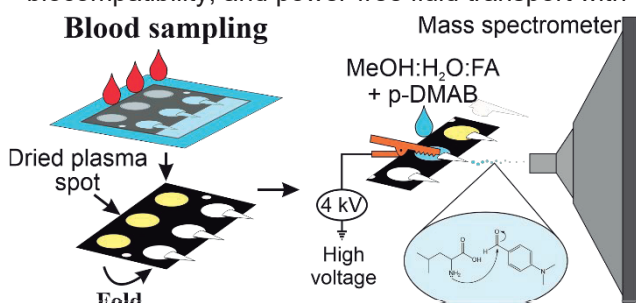


Fig. 1 – Illustration of the 3D- μ PAD device for blood collection and DPS analysis by reactive PS-MS.

The proposed 3D- μ PAD device fabricated using lamination, paper, toner, and plasma separation membrane can be employed to sample blood, separate the red cells to form DPS, and store the plasma sample for analysis and/or shipping. The 3D- μ PAD device reproducibility and homogeneity to separate the red cells to form DPS was tested using fingertip blood ($\sim 20 \mu\text{L}$) and analyzed by an offline spectrophotometric ninhydrin assay. No statistical difference ($p < 0,05$) between the DPS formed in the device's detection layers demonstrates a homogenous distribution by the plasma ($\text{CV} < 10\%$), showing that it can be used for blood microsampling to form DPS.

After sampling, the detection layer of the proposed device was removed, folded, and positioned in front of the mass spectrometer inlet using an alligator clip. An aliquot of *p*-dimethylaminobenzaldehyde (*p*-DMAB) solution in MeOH:H₂O:formic acid 80:19:1 was added to the DPS to extract the analyte and generate the spray to promote the determination via reactive PS-MS. The online derivatization among the *p*-DMAB and the amino acids was possible because the microdroplet spray environment accelerated the derivatization reaction. Analytical curves were constructed from 2.5 to 100 mg L⁻¹ for valine (267 \rightarrow 150), leucine (281 \rightarrow 150), isoleucine (281 \rightarrow 150), phenylalanine (315 \rightarrow 150), and tyrosine (331 \rightarrow 150) via the loss of the specific amino acid using a multiple reaction monitoring in a TSQ Quantum Access mass spectrometer (Thermo Fisher/ triple quadrupole). Limits of detection between 0.57 and 0.95 mg L⁻¹ and limits of quantification between 1.47 and 1.91 mg L⁻¹ for the selected amino acids were obtained. The 3D- μ PAD was successfully integrated with mass spectrometry analysis using reactive paper spray ionization and the proposed methodology can be used to determine amino acids with no sample preparation in plasma samples for aminoacidopathy screening.

¹Howse JL, Katz M, Pediatrics, 106, 2000, 595

²Wasim M, Awan FR, Khan HN, Tawab A, Iqbal M, Ayesha H, Biochemical Genetics, 56, 2018, 7.

³Verplaetse R, Henion J, Analytical Chemistry, 88, 2016, 6789.

Acknowledgments

FAPESP, nº 2020/07195-5, 2017/01189-0 and 2014/50867-3 (INCTBio), and Instituto de Química de São Carlos.

Estudo comparativo entre celas de fluxo de três diferentes geometrias para detecção de quimiluminescência

Rafael A. Alexandre (PG)¹, Boaventura F. Reis (PQ)^{1*}. rafaelalcarde@usp.br; reis@cena.usp.br.

¹ Centro de Energia Nuclear na Agricultura, USP;

Palavras Chave: Quimiluminescência, celas de fluxos, multicomutação em análise em fluxo, instrumentação fotométrica, automação em química analítica.

Highlights

Comparative study involving flow cells of three different geometries for chemiluminescence detection

Flow cell is the core in chemiluminescence detection for analytical purpose. Flow cell geometry affect sensitivity, Flow cells presenting geometries helical, cylindrical and hollow coin were studied.

Resumo/Abstract

A quimiluminescência observada a partir de uma reação química, pode ser entendida como a emissão de incontáveis flashes de luz visível (radiação eletromagnética) emitidos em todas direções. A utilização dessa radiação para fins analíticos, não precisa de fonte de radiação externa e nem de instrumentos ópticos como prisma, lente ou rede de difração, reduzindo o custo do equipamento de detecção. Em geral, a reação é muito rápida, portanto, a mistura entre as espécies químicas envolvidas deve ocorrer o mais próximo possível da janela de observação do fotodetector (fotomultiplicadora ou fotodiodo). Fotomultiplicadora (mais sensível) e fotodiodo (mais barato e robusto) são os dispositivos mais usados para detecção em procedimentos analíticos baseados em quimiluminescência. A mistura rápida e eficiente tem sido obtida empregando o processo de análise por injeção em fluxo, onde a geometria da cela de fluxo é determinante. Dentre as configurações encontradas na literatura, a cela de geometria helicoidal tem destaque, pois pode ser construída enrolando um tubo transparente em uma placa de vidro ou de acrílico e instalada entre dois fotodiodos. Neste trabalho foi comparada a resposta de três celas de fluxo com as seguintes geometrias: helicoidal, constituída por tubo de teflon enrolado no formato de bobina em uma placa de acrílico; cilíndrica, construída em um bloco de acrílico tendo dois cilindros de vidro como coletores de radiação; moeda oca, moldada em vidro. O módulo de análise baseado no processo de multicomutação em análise em fluxo, foi controlado com uma plataforma Arduino Due, usada também para realizar a aquisição de dados. Como reagentes foram usadas soluções de luminol (reagente quimiluminescente) e hipoclorito de sódio (oxidante). O luminol oxidado pelo hipoclorito emite radiação eletromagnética ($\lambda \approx 420$ nm) proporcional à concentração do oxidante. As condições experimentais foram as mesmas para as três celas de fluxo. Considerando-se a sensibilidade como parâmetro a ser avaliado foram obtidos os resultados mostrados abaixo.

Resultados relacionados às três celas de fluxo

Geometria	Volume* (μL)	Faixa (μmolL^{-1})	Intercepte	Coefficiente angular	R ²	LD**
Moeda oca	10	10 - 400	- 2,85	10,082	0,998	0,11
Helicoidal	10	10 - 400	13,48	8,142	0,995	0,21
Cilíndrica	10	10 - 400	33,91	5,446	0,993	0,38

*Volume de hipoclorito injetado em cada replicata. **LD = limite de detecção ($\mu\text{mol/L}$).

Estes resultados indicam vantagem para a cela de fluxo com geometria no formato de uma moeda oca, embora não seja significativa quando comparado com os dados da cela de fluxo de geometria helicoidal. A cela de fluxo com geometria cilíndrica foi usada pela primeira vez neste trabalho. A sensibilidade é 45% menor que a observada para a cela de fluxo no formato de moeda oca, entretanto, esta cela é mais fácil de ser construída. A cela de fluxo no formato helicoidal, requer menos recursos de oficina para sua construção, no entanto, o fotodetector precisa ter área sensível maior. Neste caso, usamos em todos experimentos o mesmo par de fotodiodos com área sensível de 38 mm².

Agradecimentos/Acknowledgments

INCTAA, CAPES, CNPQ.

Ethanol quantification in liquids applying a dispersive NIR spectrometer built using a polymer filament 3D printer

Ítalo P. Caliari (PQ)¹, Kísla S. Furtado (IC)¹, Ana B.M.X. Rufino (IC)¹, Marcio H.P. Barbosa (PQ)², Reinaldo F. Teófilo(PQ)^{1*}

rteofilo@ufv.br

¹Chemistry Department, UFV; ²Agronomy Department, UFV;

Keywords: Beverage, PLS regression, Multivariate calibration, OPS.

Highlights

The 3D-printed instrument provided a predictive performance for ethanol quantification. Ethanol quantification was possible in different types of distilled or fermented alcoholic beverages.

Abstract

This work aims to quantify ethanol in liquids using a dispersive NIR spectrometer built with the fitting of optical components in supports made by 3D printing. The 3D printed instrument near-infrared (NIR) spectrometer¹ was

constructed in the region from 800 to 1600 nm and applied in this work to quantify ethanol in matrices of cachaça, rum, beer, brandy, vodka, mouthwash, alcohol gel, and commercial ethanol solutions. Ethanol reference contents were obtained by a refractometer for a range of 0 to 75% m/m. Partial least squares regression models were built for the 3D printed instrument and two commercial NIR instruments, i.e., the MPA II (Bruker) and the NIR DLP® NIRscan™ (Texas Instruments). The total number of samples used in this study for each instrument was 180, with 75% in the calibration set and 25% in the external validation set. The samples in the calibration and prediction sets were kept the same for each instrument. The ethanol contents ranged between 5 and 70% m/m. As a way of evaluating the overall performance of the instrument and its applicability, calibration models were constructed using PLS regression and the OPS variable selection method, and the results were compared.

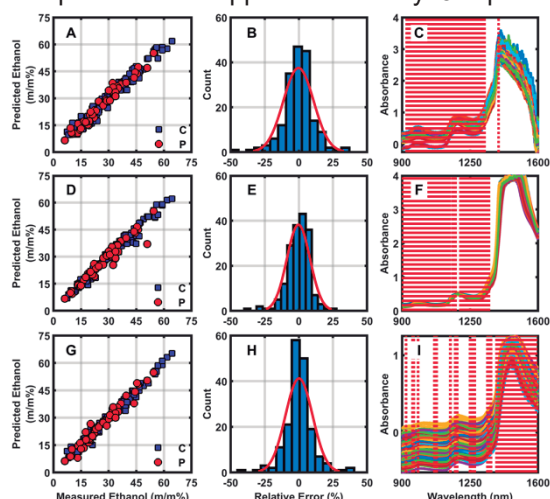


Figure 1. Measured versus predicted values of ethanol m/m% achieved by the model built with the 3D printed instrument (A), MPAII (D), and NIRscan (G) datasets with the “C” calibration and “P” prediction samples set. Histogram of relative errors achieved by the model built with the 3D printed instrument (B), MPAII (E), and NIRscan (H) datasets. 3D printed instrument (C), MPAII (F), and NIRscan (I) spectral datasets with the variables selected by the OPS algorithm marked as red dotted lines.

The spectral datasets for the three instruments are presented in Figures 1C, 1F, and 1I, respectively. Three prominent bands can be observed from 900 to 1600 nm. These main bands can be attributed to alcohols in hydrogen bonding². The region at ~1000 nm can be attributed to the second overtone of OH stretching (1047 nm)²; the combination of the first overtone of OH stretching and twice the methyl CH deformation (1065 nm)²; the combination of the first overtone of OH stretching with three times the CO stretching (1029 nm). The band at ~1200 nm can be attributed to the first overtone region of bonded OH (1280 nm)² and the second overtone of CH stretching of ethanol molecule (1200-1260 nm). The 1400 to 1600 nm region can be attributed to overlapping the first overtone of OH stretching of alcohols and water².

The three instruments achieved excellent predictive capability with similar root mean square error results of cross-validation (2.36 to 2.68) and prediction (2.31 to 2.87). The correlation coefficients of cross-validation and prediction for all models were between 0.97 and 0.98. The 3D printed instrument provided a predictive performance for ethanol quantification comparable to commercial benchtops and portable spectrometers, proving suitable for building calibration models.

1. Caliari, I.P. et al. *Anal. Chem.* **2021**, 93(33), 11388-11397.

2. Workman, Jr., J.; Weyer, L. *Practical Guide to Interpretive Near-Infrared Spectroscopy*; CRC Press, **2007**.

Agradecimentos/Acknowledgments

This study was supported by FAPEMIG, CNPq and CAPES for the financial incentive.

Evaluating features and optimizing parameters for optical sensors application in portable low-cost analytical devices.

Diogo M. de Jesus (PG)^{1*}, Caio C. S. Machado (PG)¹, Yugo S. N. da Mota (IC)², Sidnei G. da Silva (PQ)¹

diogo.morais@ufu.br

¹Institute of Chemistry, Federal University of Uberlândia – UFU; ²Electrical Engineering Department - UFU

Keywords: Photodiodes sensors, Light dependent resistor, Internet of Analytical Things, Analytical instrumentation

Highlights

Results showed a great linear ratio with measures on dye solutions. Data obtained with a spectrophotometer showed similar results. The devices include low-cost sensors and 3D-printed parts.

Abstract

As technology ushers into faster and smaller data transference and acquiring ways, analytical chemistry harnesses these advances by developing easy access devices. This accessibility includes a more diverse approach to detection and quantification problems, low-cost and D.I.Y devices with 3D printed parts, and portable connected devices with Bluetooth and Wi-Fi features. In this work, three light sensors (TSL2591, BH1750, and a light-dependent resistor — LDR) were used in the color measurement of methylene blue (MB) solutions, a very common dye with maximum absorbance at 667 nm. The experimental apparatus includes a 3D printed capsule for cuvette (2), a light emitting diode (LED) with an emission peak at 632 nm (1), and the sensor (3) connected to an Arduino-Uno microcontroller (4) **Fig 1**. Using a benchtop spectrophotometer, as a monochromatic light source, the sensors could be tested on a wide range from 390 to 840 nm. This test showed TSL2591 and BH1750's inability to work at wavelengths under 470 nm as well as the TSL2591's red and near IR strong relative detection. The LDR showed the broadest operation being able to work in wavelengths above 400 nm up to 770 nm. In analytical terms, the spectral response helped to study the sensibility of the sensors along the spectrum and give the parameters that match its sensitivity to the aimed analyte wavelength absorption and complementary emission. The devices assembled using TSL2591 and BH1750 as photometers could successfully measure absorbance between 0.5 $\mu\text{mol/L}$ and 55 $\mu\text{mol/L}$ dye solutions with limits of detection (LOD) of 0.31 $\mu\text{mol/L}$ and 0.34 $\mu\text{mol/L}$ respectively. The good linearity obtained in calibration graphs ($R^2 = 0.9989$ and 0.9994 for TSL and BH respectively) with about $40 \cdot 10^3$ molar absorptivity coefficient for both sensors highly confirms the better sensitivity in the working-range wavelength. The sensors also showed great accuracy capacity with RSDs of 0.68% and 0.57% (TSL2591 and BH1750 respectively) as well as standing as good low-cost competitors against benchtop spectrophotometers. With a relevantly different mechanism, the LDR device reached better results with concentrations below 25 $\mu\text{mol/L}$ ($R^2 = 0.9996$ and $22 \cdot 10^3$ molar absorptivity coefficient) and RSD of 0.27% on blank measurements. Other parameters such as integration time, signal amplifying (gain), and LED amperage were all unchanged after being tested and found optimum. All absorbance measurements used LED supplied with 18 mA and the sensor operation was set at the highest signal amplifying option provided by the sensor's manufacturers without reaching signal saturation.

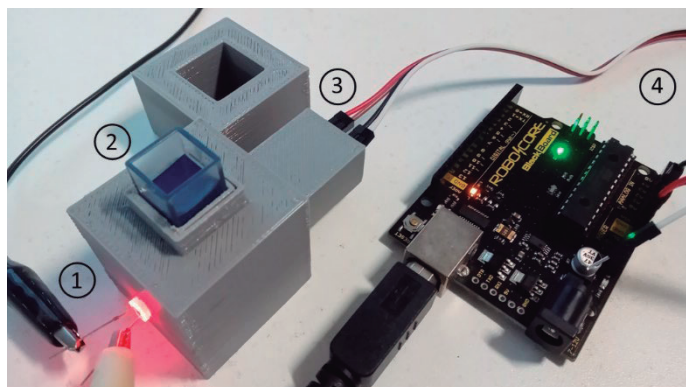


Fig 1: Photo showing device main components.

Acknowledgments

CNPq (process number 403929/2021-0) and FAPEMIG (process number APQ-01395-22)

46^ª Reunião Anual da Sociedade Brasileira de Química: "Química: Ligando ciências e neutralizando desigualdades"

Evaluation of crude oil composition by GC-FID and chemometric tools

Mônica C. Santos (PD),¹ Miguel A. J. S. do Nascimento (IC),¹ Taís de O. Reis (IC),¹ Clarisse L. Torres (PQ),¹ Dayane M. Coutinho (PQ),¹ Raquel V. S. Silva (PQ),¹ Vinicius B. Pereira (PG),¹ Marco A. Dal Sasso (PG),¹ Daniel S. Dubois (PQ),² Francisco R. Aquino Neto (PQ),¹ Débora A. Azevedo (PQ).^{1*}

mcs@iq.ufrj.br; deboraa@iq.ufrj.br

¹Universidade Federal do Rio de Janeiro, Instituto de Química, Ilha do Fundão, Rio de Janeiro, RJ 21941-598, Brazil

²Petrobras, CENPES, Ilha do Fundão, Rio de Janeiro, RJ 21941-915, Brazil

Keywords: Crude oils, Fingerprint, GC-FID, Chemometric analysis

Highlights

Oil fingerprinting is an important tool for characterizing compositional heterogeneities in reservoir geochemistry studies. Chemometrics reduce data complexity and explore the similarity between samples.

Abstract

Reservoir geochemistry is a branch of organic geochemistry that investigates compositional variations in fluid distributions along petroleum reservoirs. Due to its relatively low cost, gas chromatography with flame ionization detection (GC-FID) analysis is widely used to evaluate differences in the chemical composition of petroleum fluids. However, the presence of natural convection currents can make the compositional profile of oils at different depths of reservoirs very similar, making it difficult to evaluate composition differences only by chromatographic analysis. Thus, this work aimed to use chemometric tools to assist in understanding fluid heterogeneities in geological time scales.¹ A set of 47 pre-salt crude oils from the Búzios field were evaluated. This field is currently the second largest oil and gas producer in Brazil, is located in the Santos Basin from the same reservoir. The samples were analyzed by GC-FID using an HP-5ms column from Agilent Technologies. The injection volume was 1 μ L in split ratio mode (1:20). The injector and the detector were maintained at 290 °C and 370 °C, respectively. The GC temperature programming was set from 40 °C (1 min) to 320 °C (10 min) at a rate of 6 °C min⁻¹.² The GC-FID whole oil analyses allow the separation and identification of major components found in oils, such as *n*-alkanes (*n*-C₇ to *n*-C₃₅), branched and cyclic alkanes, besides pristane and phytane (**Figure 1A**). In addition, it was possible to verify the contamination of major crude oils with drilling fluids (**Figure 1B**), principally above *n*-C₁₂. Thus, the C6 to C10 range was selected for evaluation by chemometric. Principal Component Analysis (PCA) was used to reduce the size of the GC-FID datum matrix followed by the application of the supervised method k-Nearest Neighbors (kNN) to explore variations in chemical composition and to identify similar samples. The GC-FID data, which form the **X** matrix, are organized into a two-way matrix with *i* \times *j* dimensions, representing compound retention times and peak height, respectively. The data used is **X** (47 \times 57) for *i* = 47 crude oil samples, characterized by *j* = 57 normalized peak intensities in GC-FID. The chromatograms were evaluated using the Orange software (version 3.33). The results using a PCA analysis showed an explained variance of 83 % of the C6 to C10 range of the GC-FID. The kNN classification was performed based on the similarity measure by the Euclidean distance, being the number of neighbors considered one to five. kNN exhibited 79% accuracy of discrimination. The use of GC-FID associated with multivariate methods such as PCA and kNN constitutes an efficient tool in the identification and practical approach of crude oils.

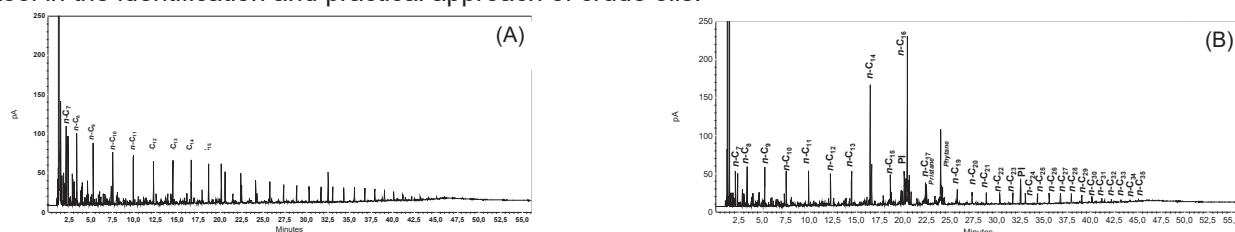


Figure 1. (A) Whole oil chromatogram and (B) Whole oil chromatogram contaminated with drilling fluids.

¹Curiale & Curtis. *Journal of Unconventional Oil and Gas Resources*, (13), 1-31, 2016.

²Barra et al., *Organic Geochemistry* (152) 104146, 2021.

Acknowledgments

The authors thank CENPES-Petrobras for authorizing this study and providing the crude oil samples. We thank the financial support of Petrobras, CNPq, and FAPERJ.

Evaluation of the molecular chemical profile of Brazilian oils applied in the investigation of environmental crimes in forensic studies

Flavia R. Alvares (PG)^{1*}, Vinicius B. Pereira (PG)², Luiz Augusto de O. Costa (PQ)³, Eduardo J. F. Senna (PQ)³, Francisco R. de Aquino Neto (PQ)¹, Gabriela V. Costa (PQ)¹

flavia.rodrigues@hotmail.com; gabrielavanini@iq.ufrj.br

¹Núcleo de Análises Forenses (NAF), Instituto de Química, UFRJ; ²Laboratório de Geoquímica Orgânica, Molecular e Ambiental (LAGOA), Instituto de Química, UFRJ; ³IBAMA

Palavras Chave: Biomarker, Forensic Geochemistry, Petroleum, GC×GC-TOFMS, Orbitrap-HRMS.

Highlights

Orbitrap-HRMS and GC×GC-TOFMS techniques applied in forensic geochemistry. Analysis of Brazilian oils with a wide range of API gravity. Evaluation of biomarkers in forensic studies aimed at environmental crimes.

Resumo/Abstract

The growing increase in offshore oil production in Brazil has resulted in the need for geochemical characterization of these new oils, as distinct aspects of molecular composition are essential for understanding the contribution of organic matter, thermal evolution, and biodegradation [1,2]. The aim of this study was to perform molecular analysis of seven oil samples from different spill sites in Brazil (four in Fernando de Noronha and three in Ceará) using comprehensive two-dimensional gas chromatography with time-of-flight mass spectrometry (GC×GC-TOFMS) and high-resolution mass spectrometry (Orbitrap-HRMS) for geochemistry biomarkers investigation [1]. Oil samples were extracted using Soxhlet extractor and then it was realized asphaltene precipitation analyses. The samples were fractionated in liquid chromatography, separating them into saturated, aromatic, and polar compounds. Cyclic and branched hydrocarbons were isolated in the saturated fraction using urea adduct, analyzed by GC×GC-TOFMS (Figure 1). The biodegradation of the oil samples can be classified according to the presence of 25-nor-hopane (25-NH), 25,28-bis-nor-hopane (25,28-BNH), 25,30-bis-nor-hopane (25,30-BNH) and 25,28,30-tris-nor-hopane (25,28,30-TNH) and their geochemical ratios with 17 α (H),21 β (H)-29-hopane (H29) and 17 α (H),21 β (H)-30-hopane (H30) [3]. In all samples from Fernando de Noronha, the biodegradation parameters had average values: 25NH/H30= 0.09; 25,28BNH/H30= 0.03; 25,30BNH/H29= 0.05; 25,28,30TNH/H29= 0.04; 25,28,30TNH/H30= 0.14. These values indicate low biodegradation

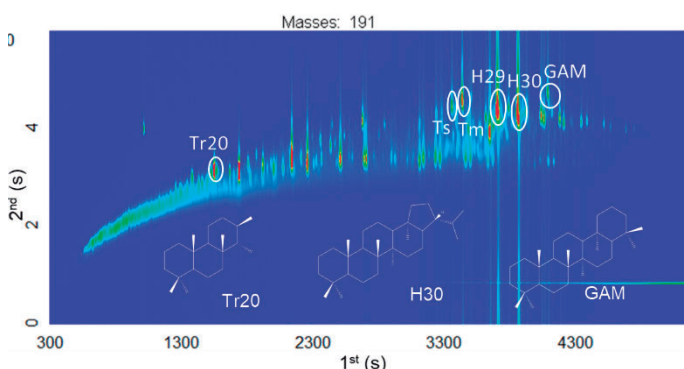


Figure 1. EIC ($m/z = 191$) of oil spill sample.

in all samples. In Ceará's samples, these parameters could not be determined due to the low concentration of 25-norhopanes in the samples. The samples also can be related using origin parameters. Hopanes and steranes gives information to distinguish source rocks in different oil reservoirs. The geochemical reason $H30/Est27 > 7$ is related to the lacustrine origin and can be observed as a characteristic of all oil samples. Thermal maturity evaluates the heat level received by organic matter to enable its transformation into oil. About the ratios of steranes $C27\alpha\alpha\alpha S/(R+S) = 0.50$ and $C27[\alpha\beta\beta]/(\alpha\alpha\alpha+\alpha\beta\beta) = 0.4$ in Fernando de Noronha samples it is possible to infer that they have low thermal evolution. The next steps of this work involves

1. Vanini, G. et al. Fuel **2020**, 282, 118790
2. Wang, Z. et al. Environmental Forensics **2006**, 7, 105-146
3. SOARES, R. F. et al. J. Braz. Chem. Soc. **2013**, 24, 1570-1581

Agradecimentos/Acknowledgments

The authors gratefully acknowledge the financial support from the IBAMA, PRH-ANP, Finep, CNPq and CAPES.

Evaluation of the Quality of Captopril Drug acquired in pharmacies and drugstores in Anápolis-Go

¹Fabrcia Rejane G. Silva (PG)*,¹ Wesley de Almeida Brito (PQ),¹ Eduardo Lopes de Paula(PQ)²
fabriciarejane2@hotmail.com.

¹Universidade unievangélica de Goiás –UNIEVANGÉLICA, Anápolis-Go

² Faculdade Metropolitana de Anápolis, FAMA, Anápolis-Go

Palavras Chave: *Impurezas, captopril, Dissulfeto de captopril, medicamentos.*

Highlights

- Evaluate the formation of captopril disulfide impurity using the High Performance Liquid Chromatography (HPLC) technique. The drug is low cost, integrating the list of essential medicines (RENAME).

Resumo

O presente estudo consiste em caracterizar o fármaco captopril, e avaliar o percentual de impureza em amostras genéricas, na forma sólida oral comprimido produzido na rota sintética farmacêutica. O Captopril DCB 01699, CAS n°62571-86-2 (1-[(2S)-3-Mercapto-2-methylpropionyl]-L-proline) é um fármaco o qual pertence à classe dos inibidores da enzima conversora de angiotensina (IECA) amplamente utilizado no tratamento de hipertensão¹. Sendo um composto orgânico altamente sensíveis agentes externos como oxigênio, causando a degradação por oxidação ligando a grupos *tióis*, formando subprodutos tóxicos caracterizados como impurezas. Em síntese é um desafio controlar a formação do dímero o disulfeto de captopril uma das principais impurezas de degradação do fármaco. Nesse contexto foi avaliado o perfil de degradação de medicamentos comercializados em farmácias e drogarias do município de Anápolis–Go, partindo de excipientes listados na composição de cada amostra, do fármaco nas concentrações de 25mg e 50mg das marcas mais comercializadas do município, e inclusa na lista de medicamentos *Rename*. Assim foram submetidas à ensaios de quantificação de teor do fármaco bem como a formação do principal produto de degradação por meio da técnica de Cromatografia Líquida de Alta Eficiência. Os métodos analíticos utilizados foram de compêndios da Farmacopeia Brasileira 6ª edição e Farmacopeia Americana (36), descritos em especificações de acordo com o RDC 53/2015 presumido pelo ICH Q3A. A impureza dissulfeto encontrada fora do limite de especificação nas amostras (A) e (H) pode ser observada por meios do gráfico 1 bem como em picos cromatográficos sobrepostos representativos abaixo gráfico 2.

Gráfico 1. Percentual de limite de dissulfeto presente em cada amostra

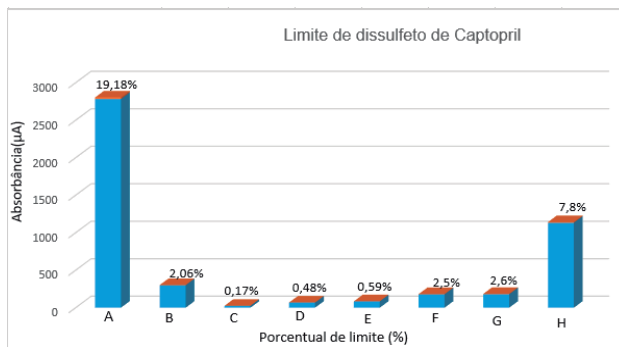
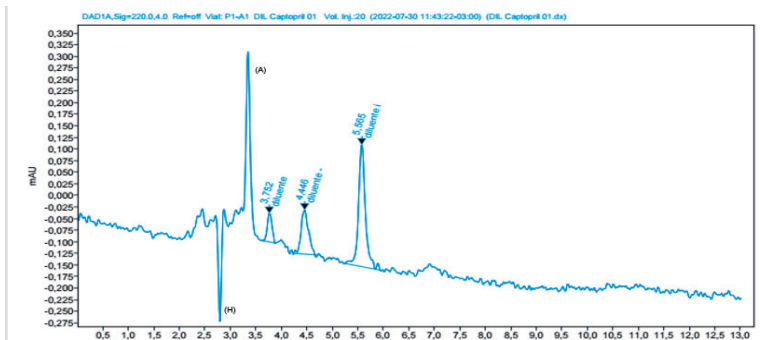


Gráfico 2. Cromatograma das impurezas dissulfeto das amostras A e H



Para comprovação dos resultados foram realizados ensaios com misturas binárias objetivando avaliar a influência dos diferentes excipientes no processo de degradação através de ensaios comparativos de estabilidade acelerada, por um período de 24 horas. Posteriormente as amostras foram submetidas a testes calorimétricos, por meio da técnica termo analíticas (DSC) onde foram detectadas interações entre o fármaco e os excipientes, demonstrado valores significativos de degradação, posteriormente tratados na pela equação de *Van't Hoff*, afim de verificar a degradação do fármaco. Assim foi possível avaliar os agentes degradantes por meios dos excipientes utilizado na rota sintética farmacêutica de medicamentos genéricos.

[1]D. G. Vidt, E. L. Bravo, and F. M. Fouad, "Captopril," *New England Journal of Medicine*, vol. 306, no. 4, pp. 214–219, 1982.

Agradecimentos/Acknowledgments

Programa de Pós-Graduação em Ciências Farmacêuticas (PPGCF)—UNIEVAGÉLICA,
 Indústria Farmacêutica- Anápolis-Go- GEOLAB

Evaluation of tryptoquialanine mycotoxins produced by *Penicillium digitatum* on different orange juice models and different inactivation treatments aiming juice quality control

Éder de Vilhena Araújo (PG)^{1*}, Franciele F. Souza Jesus (IC)¹, Beatriz Lederman Valente (PG)³, Marcelo Cristianini (PQ)³, Cassiana C. Montagner (PQ)², Taicia Pacheco Fill (PQ)¹

*e164664@dac.unicamp.br

¹Microbial Chemistry Laboratory, Institute of Chemistry, University of Campinas, Build 118, Brazil; ²Environmental Chemistry Laboratory, Institute of Chemistry, Build 155, Brazil; ³Department of Food Technology, School of Food Engineering, University of Campinas, Build 80, Brazil

Keywords: Orange juices, *Penicillium digitatum*, Mycotoxins, Tryptoquialanines, Inactivation treatments.

Highlights

Evaluation of the efficiency of thermal and HPP treatment methods for tryptoquialanines A and B inactivation. Tryptoquialanines analysis in fresh and industrial 100% orange juices. Mycotoxins determination through QuEChERS and LC-MS/MS.

Resumo/Abstract

Recently, there has been an increasing trend for fresher and more nutritious food around the world. In this regard, orange juice is one of the most popular fruit juices worldwide especially, due to its high nutritional value, taste, and low caloric content. However, during pre-harvest or post-harvest stages, problems in distribution, storage and processing, can facilitate the infection of several fungal species on citrus fruits.

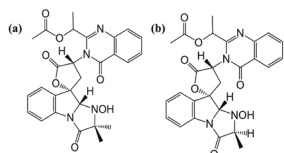


Fig. 1 The chemical structure of the *P. digitatum* mycotoxins (a) tryptoquialanine A $C_{21}H_{24}N_2O_5$, 518.180 g mol⁻¹; (b) tryptoquialanine B $C_{21}H_{24}N_2O_5$, 504.1645 g mol⁻¹.

The fungus *P. digitatum*, is the major citrus post-harvest pathogen and is responsible for up to 70-90% of the total losses. During infection in the citrus host, *P. digitatum* synthesizes the tremorgenic alkaloids tryptoquialanines A (TA) and B (TB) (Fig.1). Therefore, a method was developed and validated for determination of TA and TB, on different orange juice models (Fig.2) based on QuEChERS (Quick, Easy, Cheap, Effective, Rugged and Safe)

extraction and liquid chromatography coupled with mass spectrometry (LC-MS/MS) analysis. The method showed an excellent linearity over a high range of 1–1000 $\mu\text{g kg}^{-1}$ and low range of 1-75 $\mu\text{g kg}^{-1}$ with $r^2 \geq 0.998$. The limits of detection (LOD) and quantification (LOQ) were 1 and 3 $\mu\text{g kg}^{-1}$, respectively. Recoveries showed values between 57 and 83%, with RSD $\leq 13\%$. In this study, we developed and validated an analytical method to determine TA and TB mycotoxins on different orange juice models for the first time (SANCO, 2021). Analysis of orange juice models showed major contamination of the TA alkaloid in fresh and industrial 100% orange juices. Reduction on TA and TB contents after thermal and high-pressure processing (HPP) treatments were $\leq 32\%$. Therefore, the proposed method for this study, proved to be an important tool to quantify mycotoxins on different orange juice models and can be applied in routine analysis. Since, the mycotoxin contents found for the tryptoquialanines on orange juices are within the range of values of tremorgenic mycotoxins that can cause neurological disorders at vertebrates and may be considered relevant.

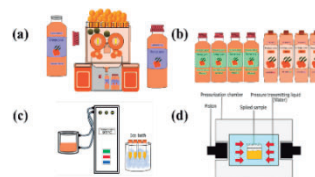


Fig. 2 Simplified representation of evaluated orange juice models. (a) First orange juice model, homemade simulated orange juices (03 *P. digitatum* 50% infected oranges suspended by a package of healthy oranges until 0.75 L); (b) second model, fresh (03 replicates, 04 weeks sampling, 05 different grocery stores) and industrial 100% orange juices (03 replicates, 04 different number lots, 05 orange juice brands) and the inactivation treatments (c) thermal treatment (pasteurization); (d) High-pressure processing (HPP).

Agradecimentos/Acknowledgments

This study was financed in part by the Coordenação de Aperfeiçoamento de Pessoal de Nível Superior – Brasil (CAPES) #2015/18790-3 – Finance Code 001 | FAPESP #2021/00728-0

References

- de Vilhena Araújo É, Vendramini PH, Costa JH, Eberlin MN, Montagner CC, Fill TP. Determination of tryptoquialanines A and C produced by *Penicillium digitatum* in oranges: Are we safe? Food Chem. 2019 Dec 15;301:125285.
- SANCO, EUROPEAN COMMISSION. Document No. SANCO / 12571/2021.

Exploiting digital-images and videos for urea determination in milk based on an enzymatic-colorimetric reaction.

Isabela C. Gonçalves* (PG), Gabriel M. Fernandes (PG), Fábio R.P. Rocha (PQ).

gmartins3510@gmail.com; isabela.camargo.goncalves@usp.br

¹Centro de Energia Nuclear na Agricultura, Universidade de São Paulo, Piracicaba, SP, Brasil, 13416-000

Palavras-Chave: (Urea, Digital-image photometry, Smartphone, Digital videos).

Highlights

Application of smartphone-based digital images for kinetic monitoring; A novel colorimetric-enzymatic method for urea determination; Milk quality control assurance and detection of adulteration.

Resumo/Abstract

Milk is a relatively inexpensive source of proteins and nutrients widely consumed worldwide. On the other hand, milk has been often a target of adulteration^[1], and a common fraud involves dilution to increase the volume aiming for economic gains. Dilution often occurs with the addition of a nitrogen source aiming to mask the decrease of the protein content. Urea is often added with this aim, although it can be found in milk in concentrations lower than 500 mg L⁻¹. Urea intake in concentrations above 700 mg L⁻¹ can cause some health problems, such as indigestion, stomach acid, ulcers, cancer, and kidney dysfunction^[2]. The Brazilian sanitary legislation has established a threshold ranging from 0.14 to 0.5 g L⁻¹ of urea^[1], taking into account its native concentration and aiming to inhibit frauds. The official method for the determination of nitrogen compounds in milk is based on Medium infrared spectroscopy (MIR)^[3,4], which requires a suitable calibration model for quantification. This work proposes a novel method for urea quantification in milk based on colorimetric measurements using a smartphone camera. It is based on the urea hydrolysis catalyzed by the urease, which increases the medium's pH due to ammonia formation. The photometric measurements were then based on the consumption of the acid form of an acid-base indicator (phenol red, $\lambda_{\text{máx}} = 550 \text{ nm}$). To optimize the reaction conditions and ensure quantitative urea hydrolysis, 30 min videos were recorded, and analytical information (RGB color system, channel G) was extracted using ImageJ[®] software from frames taken each 60 s. Under optimized conditions, the digital images were acquired by a smartphone camera under controlled conditions (illumination, distance from the camera to the Eppendorf, and region of interest) and the intensity of the reflected radiation was converted to the RGB color system using a free app (PhotoMetrix[®]) after 20 min of reaction. The optimized procedure showed a linear response within 2.0-15.0 mg L⁻¹ urea ($r = 0.998$), with a coefficient of variation ($n = 10$) and limit of detection (95% confidence level) estimated at 1.6 % and 0.5 mg L⁻¹, respectively. The procedure requires only 30 μg of phenol red indicator, 50 μg urease enzyme, and 500 μL of a 10-fold diluted sample, thus generating 850 μL of waste per determination. Urea quantification was carried out by the standard addition's method aiming to circumvent matrix effects. Recoveries from 95 and 115 % were estimated from samples spiked with urea and results for commercial milk samples agreed with the reference method at the 95% confidence level. These characteristics demonstrate that the proposed method is a simple and cost-effective alternative approach for determining urea in milk.

1. Honorato Santos Neto J, dos Santos LO, dos Santos AMP, Galvão Novaes C, Luis Costa Ferreira S. A new and accessible instrumentation to determine urea in UHT milk using digital image analysis. *Food Chem.* 2022;381(January). doi:10.1016/j.foodchem.2022.132221

2. Xie WQ, Yu KX, Gong YX. Rapid and quantitative determination of urea in milk by reaction headspace gas chromatography. *Microchem J.* 2019;147(March):838-841. doi:10.1016/j.microc.2019.03.063

3. Godden SM, Lissemore KD, Kelton DF, Lumsden JH, Leslie KE, Walton JS. Analytic validation of an infrared milk urea assay and effects of sample acquisition factors on milk urea results. *J Dairy Sci.* 2000;83(3):435-442. doi:10.3168/jds.S0022-0302(00)74900-9

4. BS ISO 9622 : 2013 BSI Standards Publication Milk and liquid milk products — Guidelines for the application of mid-infrared spectrometry. Published online 2013.

Agradecimentos/Acknowledgments

The authors are grateful to the Brazilian agencies: Conselho Nacional de Desenvolvimento Científico e Tecnológico (CNPq), Coordenação de Aperfeiçoamento de Pessoal de Nível Superior (CAPES) and Fundação de Amparo à Pesquisa do Estado de São Paulo (FAPESP). This is a contribution of the National Institute of Advanced Analytical Science and Technology (INCTAA).

Extraction of pesticide residues from frog liver tissues using a Mini-QuEChERS method

Allyson L.R. Santos (PG),¹ Igor M. Lima (IC),¹ Andressa T. Vieira (PG),¹ Giselle O. Carvalho (PG),¹ Patrícia M. Gondim (PG),² Paulo Cascon (PQ),² Anizio M. Faria (PQ),^{1,3*}

allyson@ufu.br; anizio@ufu.br

¹Institute of Chemistry UFU; ²Department of Biology UFC; ³Institute of Exact and Natural Sciences of Pontal UFU

Palavras Chave: Amphibian, method validation, HPLC-DAD, optimization, reduced-scale extraction.

Highlights

Development, optimization, and validation of a new reduced-scale QuEChERS method. Identification of residues of three pesticides in tissues of two frog species collected in Baixo Jaguaribe/CE.

Resumo/Abstract

Anuran species are highly susceptible to pesticides and have a decline in agricultural regions. Pesticide residues in frog liver may be an indicator in confirming the relationship between frog decline and polluted habitat. This work presents a scaled-reduced QuEChERS method for extraction of atrazine, chlorpyrifos, α - and β -endosulfan, α -, β -, θ - and ζ -cypermethrin in the liver tissue of two anuran species: *Leptodactylus macrosternum* and *Scinax x-signatus*. The method was optimized for a scale according to the reality of the samples, using chicken liver tissue as a model tissue. Different extraction solvents and cleanup sorbents were optimized, achieving better recoveries (91-110%) with 2.00 mL of acetonitrile as extracting solvent and 15 mg of PSA, and 15 mg of C₁₈ as cleanup sorbents (Fig. 1A). The analyzes were performed by high-performance liquid chromatography with a diode-array detector, with a total analysis time of 15 min (Fig. 1B). The scaled-reduced QuEChERS method (mini-QuEChERS) was validated following the European Community guidelines, document No. SANTE/2021/11312. The optimized method showed a moderate matrix effect for some pesticides, which was corrected using matrix-matched calibration. The limits of quantification of pesticide residues in liver tissue ranged from 4 to 28 ng g⁻¹. Pesticide recovery rates ranged from 91.8 to 108.0%, while repeatability and intermediate precision showed relative standard deviations < 10.9%. The mini-QuEChERS method was evaluated for robustness by Youden's test, with an RSD < 2%.

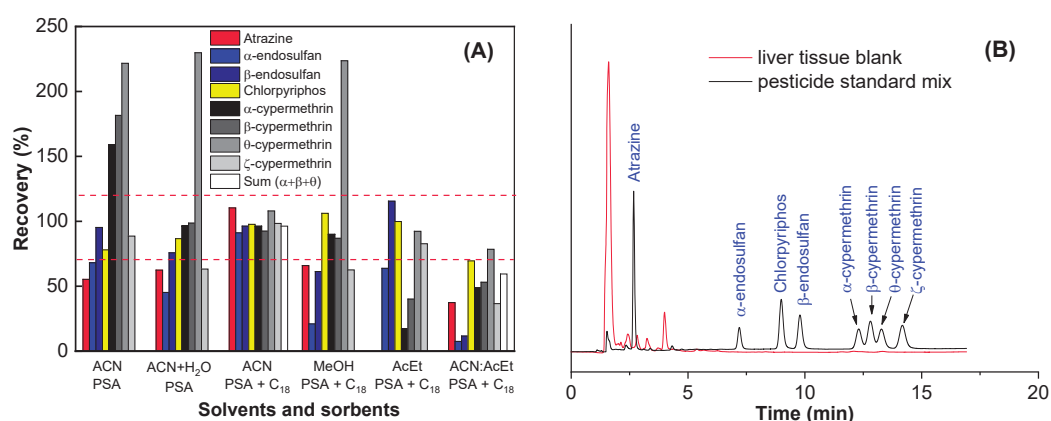


Figure 1. (A) Optimization of mini-QuEChERS method. (B) Chromatogram of the pesticide mixture separation.

The mini-QuEChERS method was applied to sixty samples of liver tissues of anuran collected near agricultural regions in Baixo Jaguaribe/CE. Residues of endosulfan, chlorpyrifos, and cypermethrin were identified in twenty-eight samples. The results confirm the effectiveness of the mini-QuEChERS method and indicate the risk of the anuran species as agricultural production expands in the study area.

Agradecimentos/Acknowledgments

CNPq, CAPES, and FINEP (01.13.0371.00; 01.11.0135.00).

Fabrication of colorimetric paper-based sensors for inexpensive clinical diagnostics

Laura C. Motta (IC),¹ William R. Araujo (PQ)¹.

laura.motta9@gmail.com; wra@unicamp.br

¹ Portable Chemical Sensors Lab, Department of Analytical Chemistry, Institute of Chemistry, State University of Campinas – UNICAMP, P.O. Box 6154, 13083-970, Campinas, SP, Brazil.

Keywords: Paper-based Analytical Devices, Colorimetric sensors, biomarker analysis.

Highlights

We developed colorimetric paper-based sensors for the detection of biomarkers of clinical interest. Methods for glucose, nitrite, and creatinine were developed using digital colorimetry.

Resumo/Abstract

Microfluidic paper-based analytical devices (μ PADs) have potential use in telemedicine^{1,2}. They become applicable to remote areas or with inadequate laboratory infrastructure because of their portability, accessibility, and simplicity. The μ PADs also allow non-specialist persons to perform their analyses periodically for the anticipation of possible health problems and continuous monitoring of treatments⁴. In this work, low-cost and simple colorimetric paper-based sensors were fabricated for the detection of glucose, creatinine, and nitrite aiming to decentralized clinical diagnostics.

The paper devices were fabricated on qualitative filter paper using two approaches: i) physical patterning with a paper punch and ii) patterning by wax printing (Xerox ColorQube 8570) followed by a heating process (100 °C for 1 min). All devices presented a 1 cm diameter and were sealed with *parafilm* or adhesive tape to avoid the leakage of solution through the back side. Glucose was analyzed by an enzymatic method with Glucose Oxidase (GOx); nitrite by Griess reaction³, and creatinine by Jaffé reaction⁴. Selective tests were also performed to evaluate possible interferences of other metabolites (ascorbic acid, urea, uric acid, glucose, creatinine and nitrite) present in saliva and urine biofluids. The colorimetric results were obtained using the camera of a Samsung S20 FE.

The analytical results showed adequate sensitivity for clinical diagnostic purposes of the three analytes studied (glucose, nitrite, and creatinine). The colorimetric assays for creatinine used 10.0 mmol/L picrate in 1.0 mol/L NaOH and presented linear behavior in the concentration range of 25.0 to 175.0 μ mol/L. The colorimetric assays for nitrite detection were performed with N-naphthyl ethylenediamine dihydrochloride (NED; 0.01 mol/L) and 0.05 mol/L sulfanilamide. Under optimal conditions it presented a linear response in the range of 2.0 to 150.0 μ mol/L. The enzymatic assay for glucose used a mixture of 0.3 mmol/L 4-aminoantipyrine, 10 mmol/L phenol, 1.5 kU/L peroxidase and 4 U/ μ LGOx in 100 mmol/L phosphate buffer (pH = 7.5). A calibration curve was built in the concentration range of 0.005 to 2.5 mmol/L, with a sensitive linear range between 0.005 and 0.5 mmol/L. Selective tests using relevant concentrations of major biomarker species demonstrated adequate selectivity, without any false positive results. Collectively, it was possible to achieve adequate sensitivity and selectivity for the detection of glucose, creatinine and nitrite in clinically relevant concentration ranges using colorimetric reactions and a smartphone camera as a portable and affordable detector, with rapid analyses (30 min).

1) T. Ozer, C. McMahon, C. S. Henry. *Annual Review of Analytical Chemistry*, 2020, 13, 85-109.

2) E. J. Maxwell, A. D. Mazzeo and G. M. Whitesides, *MRS Bull.*, 2013, 38, 309–314.

3) T. M. G. Cardoso, P. T. Garcia and W. K. T. Coltro, *Anal. Methods*, 2015, 7, 7311–7317.

4) H. Husdan and A. Rapoport, *Clin. Chem.*, 1968, 14, 222-238.

Agradecimentos/Acknowledgments

We would like to thank the funding agencies CNPq, CAPES, and FAPESP (Grants:2018/08782-1, and 2022/03250-7). Special thanks to SBQ Campinas for the support and registration fee.

Fe(III) determination in water samples using a paper based devices and analysis by smartphone

Ana Alice Silva (IC) *, Eduarda Garcia Santana (IC), Vanessa Nunes Alves (PQ).

anaalicesilva566@gmail.com; eduardagarciasantana212@gmail.com

¹Instituto de Química, Universidade Federal de Catalão, Catalão – GO, Brasil.

Palavras Chave: iron ions, analytical devices, smartphone, paper.

Highlights

Development of a methodology for the analysis of Fe(III) in aqueous samples, using paper devices for image processing analysis

Resumo/Abstract

A demanda analítica contemporânea impulsionou a construção de dispositivos em diversos materiais, dentre eles, o papel. As análises realizadas nestes dispositivos miniaturizados podem estar correlacionadas com o uso de smartphones para determinações analíticas, onde, a partir da intensidade da cor da amostra em canais do tipo RGB e da conversão desta intensidade em absorbância, é possível determinar a concentração do analito. Desta forma, neste trabalho foi desenvolvida uma metodologia para determinação de íons Fe(III), através do processamento de imagens digitais obtidas por um smartphone. A reação entre o íon ferro e o íon tiocianato, foi realizada em um dispositivo de papel do tipo transparência, com barreira hidrofóbica para retenção das soluções (Figura 1). A barreira hidrofóbica foi construída com parafina, pelo método de carimbagem, fazendo uso de uma peça metálica de 2 cm de diâmetro. Uma folha de papel branco foi posicionada abaixo do papel transparência para obtenção de um fundo branco. Para a formação do complexo de coloração vermelho intensa, foram utilizadas apenas gotas de solução, o que faz com que o método gere pouquíssimas quantidades de resíduos. Quatro gotas de solução de íons Fe(III) em concentrações de acordo com o necessário, foram misturadas diretamente no dispositivo em papel com 1 gota de ácido clorídrico $0,1 \text{ mol L}^{-1}$ e 4 gotas de solução de tiocianato de amônio 1 mol L^{-1} . As imagens foram obtidas por Smartphones A30 e A03s, ambos da marca Samsung, e pelo Smartphone Motorola G9 visando avaliar a interferência do detector (smartphone) no método. As imagens obtidas foram analisadas nos canais do Sistema RGB, sendo o canal Green escolhido para análise dos parâmetros das imagens. Inicialmente uma curva de calibração com concentrações entre 2 e 50 mg L^{-1} , obtida pelo processamento das imagens neste canal, forneceu um coeficiente de correlação de 0,99197 e sensibilidade 0,02552. Posteriormente, para avaliar a interferência da luz durante o processo de obtenção das imagens, uma curva de calibração foi construída a partir da obtenção de imagens em ambiente natural (sem controle de iluminação) e em ambiente controlado (caixa de MDF $15,2 \text{ cm} \times 10 \text{ cm} \times 10,5 \text{ cm}$ com iluminação proveniente de fitas de LEDs). Nesse estudo observou-se nos casos das imagens obtidas em ambiente controlado, que a incidência de luz no papel transparência causa reflexos que interferem no processamento das imagens. Assim, a captura das imagens sem controle de iluminação apresentou os melhores resultados ($R^2 = 0,9965$; sensibilidade = 0,0258). A distância para obtenção das imagens também foi avaliada, e melhores resultados ($R^2 = 0,9987$; sensibilidade = 0,0241) foram obtidos quando o smartphone foi posicionado a 3 cm do dispositivo. Devido ao uso de iluminação natural, e sua variação do decorrer do dia, realizou-se captura de imagens em diferentes horários, para análise da interferência de iluminação no método, sendo estes às 09:00 ($R^2 = 0,96733$; sensibilidade = 0,0166), às 12:00 ($R^2 = 0,99525$; sensibilidade = 0,0241), às 15:00 ($R^2 = 0,99845$; sensibilidade = 0,0231) e às 17:00 ($R^2 = 0,99357$; sensibilidade = 0,0221). Diferentes modelos de smartphones utilizados demonstram pouca variação na sensibilidade do método, não influenciando de maneira significativa nas características analíticas. Assim, o método desenvolvido mostrou-se promissor para detecção e quantificação de íons Fe(III) em amostras aquosas, utilizando poucas quantidades de amostra e reagentes, com baixo custo quando comparado às técnicas espectroscópicas, tradicionalmente utilizadas. Nas condições ótimas a menor concentração que pode ser analisada com precisão foi de 2 mg L^{-1} .



Figura 1: Microdispositivo em Papel Transparência de Retroprojetor

Agradecimentos/Acknowledgments

CNPq, CAPES e ao IQ-UFCAT.

Área: ANA*(Inserir a sigla da seção científica para qual o resumo será submetido. Ex: ORG, BEA, CAT)***Flow analysis system for applications in agronomic samples, fully produced in the laboratory****Marcos A.S. Brasil (PQ),¹ Marcos Y. Kamogawa (PQ)¹****kamogawa@usp.br; brasilmas@terra.com.br**¹Departamento de Ciências Exatas, ESALQ/USP;Palavras Chave: *Automatic flow analysis system, analytical instrumentation, multicommutation, additive manufacturing, electronic prototyping.***Highlights**

Flow analysis system for applications in agronomic samples, fully produced in the laboratory. Automatic analysis and recording multicommutation flow system for agronomic samples. Construction based on innovative and low-cost techniques such as additive manufacturing and electronic prototyping.

Abstract

Modern and low-cost techniques, such as electronic prototyping and additive printing, allowed the development of this automatic analyzer, based on the multicommutation in flow analysis for applications in agronomic samples. Flow analysis systems have a strong green appeal, with the use of microvolumes of reagents and samples, producing a reduced volume of waste. The potential of flow systems is undeniable, however, most of the equipment that compose it is imported and of high cost, aiming to overcome this limitation, we propose in this work the construction of an efficient, robust and low cost system and applied to the national demand. The objective of this work was to evaluate the robustness and performance of components such as peristaltic pumps, solenoid valves, diffusion chambers and detectors, built from components purchased locally and/or manufactured using additive printing technology or CNC machining.

In the presented application, determination of total nitrogen in soils and plants, reagents with low environmental impact were used, such as sodium hydroxide ($0,5 \text{ mol L}^{-1}$) and the purple indicator of bromocresol ($2,0 \text{ mg L}^{-1}$). The colorimetric determination is based on the reaction of the ammonium ion in an alkaline medium, which produces the gaseous species ammonia, which permeates through the Teflon membrane (pores of $0.2 \mu\text{m}$), and is received in the purple bromocresol solution, which proportionally changes its color, due to the change in pH. We can highlight the figures of merit, the detection limit of detection of 0.2 mg L^{-1} of NH_4^+ , quantification limit of 2.2 mg L^{-1} , linear range between 2.2 to 25 mg L^{-1} , frequency analysis of 40 determinations per hour, coefficients of variation $< 0.1\%$, variation of the analytical signal less than 1% with variation of up to 5% of the concentration of reagent solutions. All components were obtained from local shops, at a total cost of BRL 500.00. All supports and connections used additive prototyping on a 3d printer and CNC milling to make the gas diffusion chamber and flow cuvette. From the results obtained, we can conclude that it is feasible to build national equipment with performance and quality compared to similar imported ones.

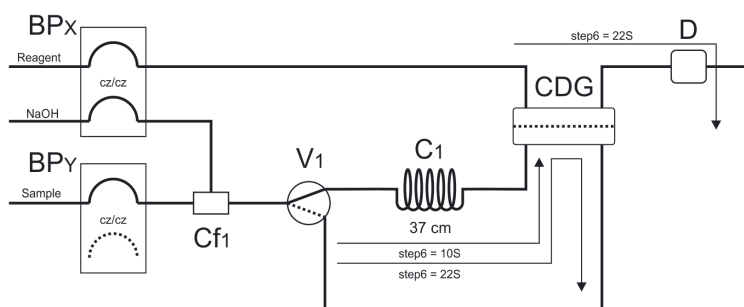


Figure 1. Analytical system for nitrogen determination. BP_{x,y} – peristaltic pumps, Cf₁ – confluence 1, V₁ – three-way valve, C₁ – mixing and reaction coil, CDG – gaseous diffusion chamber, D – detector.

quantification limit of 2.2 mg L^{-1} , linear range between 2.2 to 25 mg L^{-1} , frequency analysis of 40 determinations per hour, coefficients of variation $< 0.1\%$, variation of the analytical signal less than 1% with variation of up to 5% of the concentration of reagent solutions. All components were obtained from local shops, at a total cost of BRL 500.00. All supports and connections used additive prototyping on a 3d printer and CNC milling to make the gas diffusion chamber and flow cuvette. From the results obtained, we can conclude that it is feasible to build national equipment with performance and quality compared to similar imported ones.

Acknowledgments

The authors would like to thank the Luiz de Queiroz College of Agriculture (ESALQ) and the Center for Nuclear Energy in Agriculture (CENA) for all the infrastructure and support.

FLUORESCENT PROBES (OFF-ON) DERIVED FROM BENZOTHAZOLES FOR THE DETECTION OF NUCLEIC ACIDS IN BIOLOGICAL SAMPLES

Karlyly T.O. Pimentel (PG)¹; Alessandra S. Silva (G)¹; Anita J. Marsaioli (PQ)²; Verônica D. da Silva (PQ)¹; Isis M. Figueiredo (PQ)¹; Dimas José da Paz Lima (PQ)¹; Josué Carinhanha C. Santos (PQ)^{1,*}

josue@iqb.ufal.br

¹Instituto de Química e Biotecnologia, Universidade Federal de Alagoas; ²Instituto de Química, UNICAMP.

Palavras Chave: DNA; RNA; fluorescência molecular, ciências forenses.

Highlights

Fluorometric probes exploring the off-on concept containing the benzothiazole nucleus were synthesized ($n = 14$), which proved effective for determining total nucleic acids in biological samples (saliva, urine, and semen).

Abstract

Nucleic acids determination, especially DNA, is a continuous demand in different applications, with an emphasis on forensic sciences, since the DNA can be used for the future identification of a suspect [1]. In this sense, molecular probes that have distinct spectroscopic properties in the presence and absence of the macromolecule can be used to detect DNA in biological samples. In the present work, 14 probes containing a benzothiazole nucleus were synthesized and characterized, of which eight probes (Fig. 1A) showed outstanding sensitivity using ctDNA (*Calf thymus*) and RNA (*Torula yeast*) as models. Probe **5a** showed higher sensitivity in the presence of macromolecules, being more selective for DNA compared to RNA (Fig. 1B). Furthermore, the analytical response between **5a**-macromolecule did not show a significant difference at pH 5, 7, and 9, except for compounds that have -OH in the R₁ position (Fig. 1A), where a drastic reduction in the emission signal was observed at pH 9. Under the conditions optimized at pH 7, HEPES buffer (100 mM) was used, with probe concentration of 3 μM, $\lambda_{ex} = 550$ nm and $\lambda_{em} = 597$ nm (Stokes shift of 47 nm). The increase in ionic strength reduced analytical sensitivity, indicating that the interaction process has electrostatic forces. Six binding mode marker compounds were employed, meaning that **5a** and derivatives preferentially interact in the minor groove of the DNA. Under optimized conditions, the spectrofluorimetric method using **5a** presented LOD of 0.1 and 0.35 mg L⁻¹ for DNA and RNA, respectively, for a linear range of 0.5 to 7 mg L⁻¹ of each nucleic acid. The quantum yield (Φ) was 0.28 (DNA) and 0.15 (RNA), using rhodamine B as a reference. The method's selectivity was compared against 25 possible interferents (proteins, sugars, metabolites, and metal ions, among others). Finally, it was possible to perform quantitative recoveries for samples of saliva (88 - 102%), urine (85 - 97%), and semen (86 - 105%) for DNA in real samples. Besides was possible to visually identify real samples of semen after dilution in buffer (1:10 and 1:20) and exposure to UV light (365 nm), indicating potential for quantitative and qualitative applications regarding DNA detection.

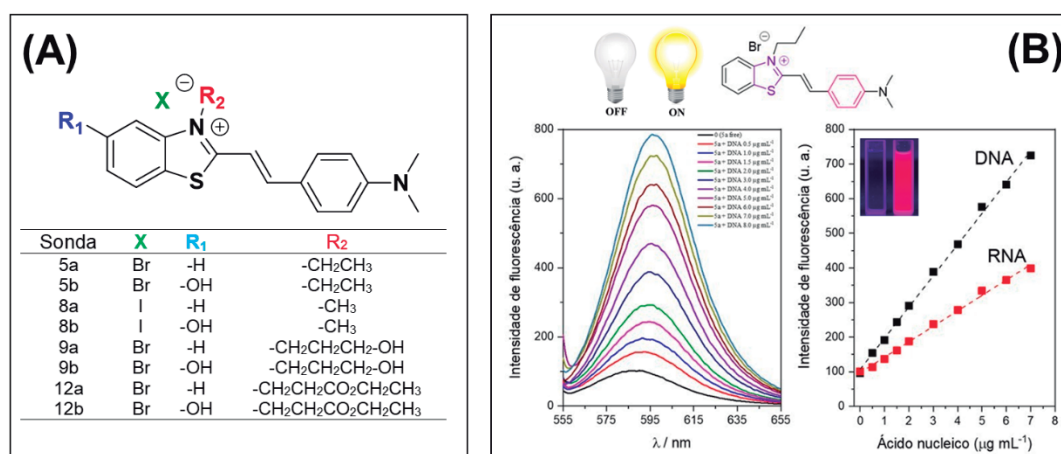


Fig. 1. (A) Chemical structure of the evaluated compounds with outstanding performance; (B) Emission spectrum of the **5a**-ctDNA and **5a**-RNA interaction, and the respective analytical curves under optimized conditions.

[1] Frumkin D. et al., *Forensic Science International: Genetics*, 4, 95-103, 2010.

Acknowledgments

IQB-UFAL, PPGQB, Capes, PROCAD - Segurança Pública e Ciências Forenses, CNPq, Fapeal.

Área: ANA

Inserir a sigla da seção científica para qual o resumo será submetido. Ex: ORG, BEA, CAT)

Fractionation and spatial distribution imaging of trace elements in wild and farmed shrimp from northeast Brazil

Francisco L. F. da Silva (PQ)^{1,2}, Wladiana O. Matos (PQ)², Savarin Sinaviwat (PQ)³, Andrea Raab (PQ)⁴, Eva M. Krupp (PQ)³, Jorg Feldmann (PQ)⁴.

luan.fonseca@uece.br; wladianamatos@ufc.br

¹Faculdade de Educação de Crateús (FAEC)-Universidade Estadual do Ceará; ²LEQA-Departamento de Química Analítica e Físico-Química, Centro de Ciências, Universidade Federal do Ceará; ³TESLA-Department of Chemistry, University of Aberdeen, Scotland; ⁴TESLA – Analytical Chemistry, Institute of Chemistry, University of Graz, Austria.

Palavras-chave: Trace elements, Fractionation, Shrimp, LA-ICP-MS, Spatial distribution, Bioimaging.

Highlights

Trace elements content differ between wild and farmed samples. As is predominant in muscle tissue and in wild samples exceeding 10 times the value recommended by current legislation. There is a spatial relationship between As, Se and S.

Abstract

Trace elements is naturally present in environment and anthropogenic activities have been increasing their concentration levels. Some of them develop important roles in biochemical functions but some elements are toxic or potentially toxic. Trace metals and metalloids bioaccumulate in aquatic organisms, such as shrimps, posing a threat to the marine ecosystem and compromising the food safety of seafood consumers. Shrimp is an important commodity and the whole animal body can be used in culinary preparations. Thus, it is important to evaluate not only trace elements content in shrimp, but also their distribution through different fractions of the body animal. In this work sample of farmed and wild shrimp from northeast of Brazil were fractionated (muscle tissue, carapace and viscera) and the following elements were analyzed in the whole and in each fraction of the animal: As, Co, Cu, Cr, Mn, Mo, Se and V by ICP-MS, and Al, Fe and Zn by MIP-AES. The freeze-dried shrimp samples were decomposed by microwave oven cavity using a mixture of 65% w w⁻¹ HNO₃ and 30% w w⁻¹ H₂O₂ previous ICP-MS and MIP-AES analysis. The CRMs TORT-2 and DORM-4 were analyzed to check the trueness of the analytical method (83-115% of recovery). Farmed and wild shrimp shown different content of almost all inorganic elements, except for Co and Mn. The contents of Cu, Mo, and Zn were higher in farmed shrimp. A remarkable difference in V content is found between the farmed and wild shrimp, the last presenting V level around one order of magnitude higher than the farmed sample. Some toxic elements as Al, Cd and V are present mainly in carapace, while As has higher concentration in muscle tissue. For international legislation, As and Cd in wild sample exceed the allowance limit, around 10 times for As and 4 times for Cd. LA-ICP-MS was used to obtain a mapping of some elements (⁷⁵As, ⁶³Cu, ⁵⁷Fe, ³¹P, ³²S, ⁷⁸Se) in a cross-section of farmed and wild whole shrimp samples. The bioimage results for As corroborate those obtained by ICP-MS since they also shown the predominance of this element in shrimp muscle tissue. Arsenic spatial distribution in shrimp is closely related to that presented by Se and S (Figure 1) represent similar mechanisms of absorption and uptake. Iron, Cu and P was predominant in carapace sample.

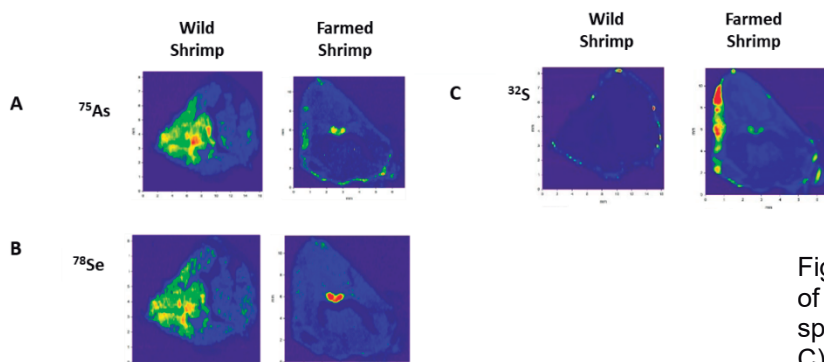


Figure 1: A) Bioimage of a cross-section of farmed and wild whole shrimp with spatial distribution of A) ⁷⁵As, B) ⁷⁸Se and C) ³²S

Acknowledgments

UFC, PGQUIM, University of Aberdeen, CAPES-PRINT - 88887.364637/2019-00, CNPq-421096/2018-7.

Genomagnetic assay for detection of influenza viral RNA in saliva by digital imaging in a 3D-printed 66-well platform

Daniel J. A. dos Santos(PG),^{1*} Matias E. Melendez(PQ),² Ester C. Sabino(PQ),³ Tássia R. de Oliveira(PG),¹ Ronaldo C. Faria(PQ),¹ Oldair D. Leite(PQ),⁴.

oldair.leite@gmail.com; danilequimico10@gmail.com;

¹Department of Chemistry, Federal University of São Carlos, São Carlos, SP, Brazil; ²National Cancer Institute, Rio de Janeiro, Rio de Janeiro, Brazil; ³Institute of Tropical Medicine, Faculty of Medicine, University of São Paulo, São Paulo, SP, Brazil; ⁴Federal Technological University of Paraná, Medianeira, PR, Brazil.

Keywords: Molecular diagnosis, Digital image detection, oligonucleotides-modified magnetic beads, 3D printing

Highlights

- Magnetic manipulation of labeled primers for viral RNA capture in molecular diagnostics;
- Detection by digital image on platforms, with reduced volumes, produced in 3D printing;
- Genomagnetic protocol for diagnosing influenza virus in saliva samples with detection by digital imaging.

Resumo/Abstract

Influenza is a respiratory viral infection that threatens human health and can be responsible for a large number of deaths worldwide each year. A simple and rapid test with adequate sensitivity and specificity at the lowest possible cost is required in the appropriate clinical setting. In this sense, we present a molecular diagnostic strategy for the influenza virus based on the capture and magnetic separation of viral RNA with labeled primers and detection by the digital image on a prototyped 3D platform. The assay, for the determination of viral RNA, occurs in stages, which are carried out in 500 μ L Eppendorf-type microtubes, where capture and detection probes are used to obtain, at the end of the procedure, a sandwich-type bioconjugate labeled with the enzyme peroxidase (HRP). To carry out the assay, the saliva samples are thermally inactivated at 56 °C for 30 min, under constant agitation at 600 rpm. The main stages of the genomagnetic protocol can be summarized as follows: A) the hybridization stage between the viral genetic material exposed by thermal inactivation (opening of the nucleocapsid) and the capture probes, oligonucleotides immobilized on magnetic spheres (MB-cpDNA), detection probes (dpDNA-biotin), primers marked with biotin, B) step of marking the bioconjugate formed with HRP and, C) step of oxidation of the chromogen substrate, use of the chromogenic substrate of HRP (solution containing 3,3',5',5'-tetramethylbenzidine (TMB) and hydrogen peroxide (H₂O₂)). It should be noted that the bioconjugates are conveniently fixed on the walls of the Eppendorf with the aid of a magnetic shelf during the test (steps A-C), in the procedures for removing the solution, washing, and/or conditioning with an appropriate buffer solution, avoiding losses by leaching. Next, the detection of oxidized TMB by digital image is carried out on a prototyped platform in a 3D printer, which contains 66 wells, and has a design similar to the microplate used in the ELISA tests. After optimizing the reaction conditions of the genomagnetic protocol and detection by digital imaging, a linearity of response, or linear relationship (LR), of the signal with the target concentration of influenza RNA, between 1 fmol L⁻¹ to 500 fmol L⁻¹, with limits of detection (LoD) and quantification (LoQ), estimated at 1.0 fmol L⁻¹ and 10.34 fmol L⁻¹ respectively. The proposed molecular protocol was successfully applied in the detection of viral RNA in 36 saliva samples from healthy patients and those with Influenza, and the result obtained demonstrated high specificity and sensitivity (assessed by the ROC curve, a tool that allows the diagnosis of a system binary classifier (sensitivity – true positive rate versus specificity false positive rate)), consistent with the results obtained by the gold standard technique (PCR), but without the use of extraction kits, or carrying out amplification steps, where several reagents are necessary, as well as the use of more sophisticated equipment such as the thermal cycler, inherent to the PCR method.

Agradecimentos/Acknowledgments

Recognition to the support to this work: FINEP, FAPESP, Araucária Foundation, CAPES, CNPQ, UFSCar – DQ, UTFPR - MD, and to the research groups, LaBiE- UFSCar and LAITEC-UTFPR MD.

Gold nanoparticles synthesized on paper substrate by ring-oven for intensification of LIBS emission

Ana Flávia L. M. Nascimento (PG)* and Ivo M. Raimundo Jr. (PQ)

a203754@dac.unicamp.com.br

Instituto de Química, UNICAMP, CP 6154, CEP 13083-970, Campinas, São Paulo

Key words: Laser-induced breakdown spectroscopy (LIBS), Nanoparticle enhanced LIBS, Gold nanoparticles, Ring-oven.

Highlights

Gold nanoparticles (AuNP) prepared directly on filter paper by ring-oven approach.
LIBS signal enhancement due to AuNP interaction with laser pulse
Superposition of analyte ring on the AuNP ring allows higher sensitivity

Abstract

Laser-induced breakdown spectroscopy (LIBS) has several outstanding features, which are important in Analytical Chemistry: simplicity, minimal or no sample preparation, high analytical frequency, multielemental analysis, non-destructive character. However, one of its disadvantages is the direct analysis of liquid samples, which is challenging due to the formation of splash, in addition to the poor limit of detection, usually around mg L^{-1} . As a strategy to overcome these drawbacks, liquid samples are usually transferred to a solid support (filter paper, for example) and submitted to a pre-concentration step. The ring-oven approach employs a device to heat a disk of a filter paper, on which the sample is added drop by drop at its center, being transported to the edge of the paper while the liquid is evaporated. As a consequence, the analyte is concentrated in the form of a ring, which can be analyzed by LIBS.¹ The use of metallic nanoparticles to improve laser ablation techniques in LIBS is known and is named Nanoparticle Enhanced Laser Induced Breakdown Spectroscopy (NELIBS). When deposited on a solid substrate or on the surface of the sample itself, the nanoparticles provide a greater number of electrons so that the ablation and excitation of the plasma are more efficient, since the laser-matter interaction is crucial for the effectiveness of the technique, improving the analytical performance. The present work describes the production of gold nanoparticles (AuNP) direct on the surface of a filter paper (Whatman 40) by means of a ring-oven device, with subsequent concentration of analyte (Cu(II) was chosen to proof of concept) aimed at improving the sensitivity of LIBS technique. The AuNP ring was formed by dropping 100 μL of a $5.1 \times 10^{-6} \text{ mol L}^{-1}$ tetrachloroauric solution, followed of 100 μL of a $7.8 \times 10^{-2} \text{ mol L}^{-1}$ sodium citrate solution, which caused the reduction of Au(III) ions and producing the AuNP ring as shown in Figure 1. Afterwards, 100 μL of a $7.9 \times 10^{-5} \text{ mol L}^{-1}$ Cu(II) solution was dropped on the paper, followed of 150 μL of a 0.01 mol L^{-1} HCl solution. As a means of evaluating the signal enhancement, a Cu(II) ring was also prepared using the same solution, as well as 500 μL of the Cu(II) solution was deposited on the filter paper with and without the AuNP ring, followed of drying. The filter paper disk was placed on a rotating platform, which allowed to fire 120 laser pulses (Q-switched Nd:YAG laser, Brilliant Quantel B, 1064 nm, 20 Hz and 5-ns pulse) to fulfill the ring circumference. The emitted radiation was collected with a 5-mm diameter lens, focused on the tip of 105- μm diameter optical fiber, which guided the radiation to an echelle polychromator (Andor Technology) and an ICCD detector (iStar DH 734, Andor Technology). Compared to the emission intensity of Cu I (324,76 nm) obtained with the filter paper prepared by the deposition of 500 μL of the Cu(II) solution, the signal increased 67 % with the Cu(II) ring, 74 % with the AuNP ring and the deposition of 500 μL of the Cu(II) solution, and 89 % with the AuNP ring to which a Cu(II) ring was superimposed. These results demonstrate the feasibility of preparing AuNP rings directly on the filter paper, which is a powerful tool to increase LIBS signal, in special when the analyte ring is superimposed to which.



Figure 1: AUNP ring.

¹CORTEZ, J.; PASQUINI, C. Ring-Oven Based Preconcentration Technique for Microanalysis: Simultaneous Determination of Na, Fe, and Cu in Fuel Ethanol by Laser Induced Breakdown Spectroscopy. **Analytical Chemistry** 85 (2013) 1547–1554.

Acknowledgments

Authors are grateful to Instituto Nacional de Ciências e Tecnologias Analíticas Avançadas (CNPq 465768/2014-8 and FAPESP 2014/50951-4) as well as to CAPES for the fellowship to AFLMN.

Graphene-based nanomaterials for preconcentration and determination at ultratrace-levels by atomic spectrometry and chromatography

Jefferson S. de Gois (PQ),* Deborah C. Vargas (PQ)

jeffersonsgois@gmail.com; jefferson.gois@uerj.br

Department of Analytical Chemistry, Institute of Chemistry, Rio de Janeiro State University, Rio de Janeiro, RJ, Brazil.

Palavras Chave: Sample preparation, Adsorption, Nanomaterial, FIA-HG-AAS, preconcentration, HPLC-DAD.

Highlights

Ultrasensitive determination of contaminants; Graphene oxide as a sorbent for preconcentration techniques; Atomic spectrometry and chromatography for ultratrace determination.

Resumo/Abstract

Pre-concentration methods are notorious approaches to increase the sensitivity of an analytical method, among the available methods, the dispersive solid-phase microextraction (DSPME) has been drawing attention for separation and pre-concentration of analytes at trace levels.¹ In this case, the analyte extraction occurs by applying a vigorous stirring, thus allowing a quick interaction between the analytes and the adsorbents, like magnetic nanoparticles (MNPs), called magnetic dispersive solid-phase microextraction (MDSPME).^{2,3} Among the materials that can be applied as adsorbents for MDSPME, graphene oxide (GO) has found wide applications due to its mechanical and thermal stability, high surface area, and functional groups that can promote adsorption,²⁵ this material can be incorporated onto iron oxides, such as magnetite (Fe₃O₄) and maghemite (γ -Fe₂O₃), facilitating the separation and improving the adsorption capacity of the material. Therefore, this work presents the synthesis and application of magnetic nanoparticles of graphene oxide (GO/ γ -Fe₂O₃) as a sorbent for solid-phase extraction and pre-concentration of estrogens in tap water samples followed by the determination using high-performance liquid chromatography with a fluorescence detector and the development of an analytical method for the preconcentration of Se in digested fish samples and determination by hydride generation atomic absorption spectrometry and flow injection analysis (FIA-HG-AAS). The GO/ γ -Fe₂O₃ nanoparticles were synthesized via co-precipitation and characterized by X-ray diffraction, Fourier transform infrared spectroscopy, N₂ adsorption-desorption and scanning electron microscopy. The adsorption of estrogens was performed after the optimization of the domain for the factors time, pH, and nanoparticle/analyte ratio using a central composite design consisting of eight factorial points (2³), six axial points, and five replicates of the central point. The optimal adsorption conditions were obtained at 40 min, pH 6, and 9 mg of magnetic nanoparticles. The analytes were eluted using 500 μ L of a solution composed of ethanol/water/acetic acid (80:20:1, v/v/v). The enrichment factor achieved were 91 \pm 6 for 17 β -estradiol and 119 \pm 7 for 17 α -ethinylestradiol, whereas the limits of detection achieved for 17 β -estradiol and 17 α -ethinylestradiol were 2.7 and 0.8 ng L⁻¹, respectively. Recovery tests ranged from 83 to 98%, and the short-term precision was % RSD \leq 7 (n=10). For the determination of Se in digested fish samples, the domain of the factors pH, MNPs mass, and adsorption time was optimized, as well as the flow of carrier gas, the concentration of hydrochloric acid (HCl), and sodium borohydride (NaBH₄) for the hydride generation system. The optimized experimental conditions were obtained at pH 2, 60 mg of MNPs, and 30 min for the adsorption process, and 4.5 (m/v) % HCl, 0.19 (m/v) % NaBH₄, and 273.5 mL min⁻¹ of carrier gas flow for hydride generation. Under optimized conditions, the enrichment factor and the limits of detection were 70 and 30 ng g⁻¹, respectively. The short-term precision of the method, defined by the relative standard deviation (RSD) (n=10), was 7.54%. The accuracy of the method was assessed through recovery tests, as well as the analysis of certified reference materials (CRM). The recovery values ranged from 103.8 to 117.3% and the Se concentration determined in the CRMs agreed with the certified values through a t-test at a 95% confidence level.

Agradecimentos/Acknowledgments

UERJ, IFRJ, CNPq, FAPERJ, CAPES.

1. E. Kazemi, S. Dadfarnia and A. M. Haji Shabani, *Talanta*, 2015, **141**, 273–278.
2. P. Mohammadi, M. Masrounia and Z. Es'haghi, *J. Iran. Chem. Soc.*, 2020, **17**, 3285–3298
3. A. Bazmandegan-Shamili, S. et al., *Food Anal. Methods*, 2016, **9**, 2621–2630.

Hydrophobic deep eutectic solvent based on decanoic acid and tetrabutylammonium bromide: characterization and evaluation towards electrode modification

Karen K. L. Augusto (PG),^{1*} Paulo C. Gomes-Júnior (PG),¹ Renan O. Gonçalves (PG),¹ Júlio C. O. Almeida (IC),¹ Gustavo P. Longatto (IC),¹ Éder T. G. Cavaleiro (PQ),² Orlando Fatibello-Filho (PQ)¹

k.kenlderi@gmail.com

¹Department of Chemistry, Federal University of São Carlos, São Carlos, SP, Brazil; ²São Carlos Institute of Chemistry, University of São Paulo, São Carlos, SP, Brazil

Keywords: Deep eutectic solvent, Hydrophobic eutectic mixtures, Eutectic point, Modified electrode, Sustainable procedure

Highlights

Eutectic point determination of decanoic acid and tetrabutylammonium bromide mixtures, Improved analytical response for hydroquinone detection using an electrode modified with the eutectic mixture.

Abstract

Deep eutectic solvents (DES) emerged as a new category of green solvents able to substitute hazardous organic ones. Since then, these solvents have been broadly studied due to their outstanding features, such as biodegradability, non-volatility, and low toxicity¹. Understanding the characteristics of DES has supported further applications of this new class of solvents contributing to the development of sustainable procedures^{2,3}. In this context, this work aimed to investigate the synthesis of a hydrophobic deep eutectic solvent based on decanoic acid (DecA) and tetrabutylammonium bromide (TBAB) and its application as a modifier of a new electrochemical electrode. Several DecA:TBAB hydrophobic mixtures with different molar ratios were prepared and subsequently characterized by differential scanning calorimetry (DSC), to determine the eutectic point of the system. In short, the DecA:TBAB composition of 1.5:1 (mol/mol) (named HEM – hydrophobic eutectic mixture) presented the lowest melting temperature ($-7.63\text{ }^{\circ}\text{C}$, **Fig. 1(a)**), indicating that this composition resulted in the eutectic mixture. Furthermore, FTIR studies were conducted to evidence the interactions between these precursors. From the FTIR spectra (**Fig. 1 (b) (c) and (d)**), one can highlight the shift in the stretching vibrational band of the decanoic acid carboxyl group from 1693 cm^{-1} to 1724 cm^{-1} due to interactions with tetrabutylammonium bromide. These results agreed with NMR results. To finish, HEM was mixed with multi-walled carbon nanotubes (MWCNT) and NafionTM forming a suspension to modify a glassy carbon electrode (GCE). Hydroquinone (H_2Q , 1.0 mmol L^{-1}) was used as a redox probe to evaluate the electrochemical response of the proposed electrode. According to the cyclic voltammograms (**Fig. 1 (e)**), HEM enhanced the analytical response for H_2Q , with a 1.63 and 1.20-fold increase in the anodic and cathodic currents, respectively, compared to the MWCNT/GCE (without HEM). In addition, **Fig. 1 (e.i)** shows a decrease in the peak-to-peak separation potential (ΔE_p) for HEM-MWCNT/GCE electrode; ΔE_p to the electrode modified with HEM was 1.45 and 1.38-fold lower than those for GCE and MWCNT/GCE electrodes, respectively. The outcomes demonstrated in this work indicate that the proposed hydrophobic eutectic mixture is promising for developing new electrochemical electrodes. Also, the complete characterization achieved can support an understanding of how the eutectic solvents' interactions are formed.

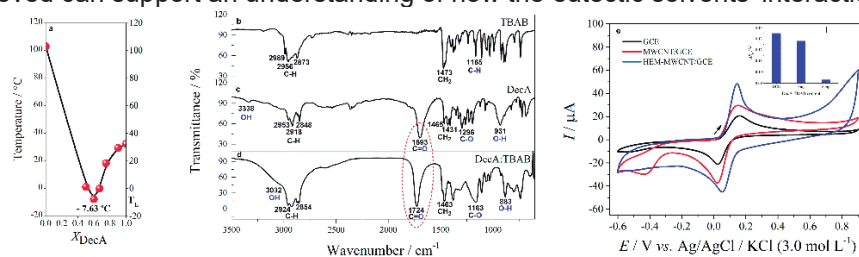


Figure 1 – Eutectic phase diagram of the system DecA:TBAB (a). FTIR analysis for the eutectic mixture and its components: (b) TBAB, (c) DecA, and (d) DecA:TBAB (HEM). And cyclic voltammogram at (—) GCE, (—) MWCNT/GCE, and (—) HEM-MWCNT/GCE electrodes scan rate of 50 mV s^{-1} (e). Inset: Peak-to-peak separation potential of the proposed electrodes.

¹Zhang et al. *Chem Soc Rev* **41**, 2012; ²Augusto et al. *Analytical Methods* **14**, 2022; ³Piton et al. *J Braz Chem Soc* **32**, 2021.

Acknowledgments

The authors thank grant #140406/2021-2 from CNPq, #2022/15513-2 and #2020/01050-5 from FAPESP, and CAPES – Finance code 001 for the financial support during this research.

46^o Reunião Anual da Sociedade Brasileira de Química: "Química: Ligando ciências e neutralizando desigualdades"

Área: ANA

Incorporating ionic liquids on paper surface for enhancing the analytical performance of glucose enzymatic assays based on colorimetric readout

Daniel S. de Paula (IC),¹ Larissa G. Velasco* (PG),¹ Thiago M. G. Cardoso (PQ),¹ Muhammad I. Qadir (PQ),¹ Wendell K. T. Coltro (PQ),¹

daniel.santos@discente.ufg.br; larissa.garcia.velasco@discente.ufg.br

¹Instituto de Química, Universidade Federal de Goiás.

Keywords: Ionic Liquids, PADs, Enzymes, Colorimetric, Glucose.

Highlights

The use of ionic liquids as PAD's surface modifiers to enhance the color homogeneity on the detection zone for glucose colorimetric assay is successfully reported.

Abstract

In this study, we show for the first time the use of ionic liquids (IL) incorporated on microfluidic paper-based analytical devices (μ PADs) as a novel strategy to enhance the color homogeneity on detection zones for glucose colorimetric detection. μ PADs were fabricated by laser cutting in a design containing three microzones (5-mm diameter) interconnected by microfluidic channels (10 mm long, 2 mm wide)¹. This protocol was selected to avoid the use of hydrophobic barriers, which can be damaged when used in association with IL. Four ILs were tested including 1-n-butyl-3-methylimidazolium acetate (AO), 1-n-butyl-3-methylimidazolium tetrafluoroborate (BF), 1-n-butyl-3-methylimidazolium trifluoromethylsulfonylimide (Nt), and 1-methoxyethyl-3-methylimidazolium trifluoromethylsulfonylimide (Ome). Each IL was added on the detection and allowed to dry overnight. After adding the enzymes (glucose oxidase and horseradish peroxidase) and chromogens, the resulting color response was evaluated, especially its intensity and uniformity, in the Corel Photo Paint software. Similarly, we evaluated two colorimetric indicators including potassium iodide (KI) and 4-aminoantipyrine (4-AAP). For all assays, the volume of reagents (enzymes and chromogenic solutions) was 0.5 μ L which was added on detection zone and allowed to dry for 5 min. Among the four IL, the best color intensity and uniformity was observed using BF. A comparison of the recorded images is depicted in Figure 1 using KI and 4-APP as chromogenic solutions. As it can be observed, there is a noticeable improvement on the color distribution inside the detection zone. When KI was used as indicator, the color intensity increased from 204 ± 42 to 234 ± 10 AU in the presence of IL. On the other hand, the addition of IL promoted a decreasing on color intensity from 217 ± 42 to 201 ± 20 AU. This was somehow expected once the use of KI provided a more intense electrostatic interaction with the formed membrane. Regarding the color distribution, both indicators in association with IL provided an enhancement in the colorimetric readout. The color gradient generated by the poor uniformity was noticeably reduced from 20 to 4% and from 19 to 10% when using KI and 4-APP, respectively. Future investigation will be dedicated on quantitative analysis of glucose on biological fluids.

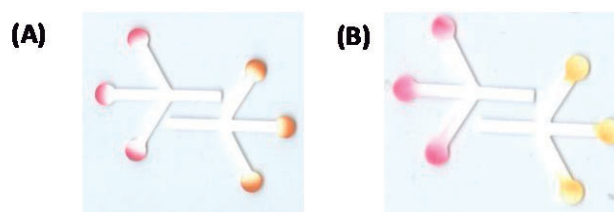


Figure 1. Recorded optical images showing the resulting color distribution for glucose enzymatic reactions performed using 4-APP (magenta color) and KI (yellow color) (A) without and with (B) BF as ionic liquid.

Agradecimentos/Acknowledgments

CNPq, FAPEG, CAPES, INCTBio and UFG.

¹ de Freitas, S.V. et al., *Analytical Chemistry*, 90, 2018, 11949-11954.

In silico infrared spectroscopy applied to the study of 25B-NBOH and 25B-NBOMeLivia Salviano Mariotto (PG),^{1*} Caio Henrique Pinke Rodrigues (PG),¹ Aline Thaís Bruni (PQ)aline.bruni@usp.br; livia.mariotto@usp.br¹ Instituto Nacional de Ciência e Tecnologia Forense (INCT Forense); Departamento de Química, Faculdade de Filosofia, Ciências e Letras de Ribeirão Preto, Universidade de São Paulo.

Key Words: New Psychoactive Substances, NBOHs, NBOMes, Infrared Spectroscopy, In silico methods

Highlights

We use in silico methods to obtain IR spectra for 25B-NBOH and 25B-NBOMe.

Data were validated by comparison to experimental libraries.

We conclude that in silico tools were able to find IR spectra.

Abstract

Identifying New psychoactive substances (NPS) places forensic drug evaluation at a crossroads. The rapid emergence of these drugs caused a lack of spectroscopic standards. Infrared (IR) spectroscopy is an essential technique for identifying NPS because it allows for structural information and high selectivity. Two groups of NPS, NBOHs and NBOMes, have an effect like Lysergic acid diethylamide (LSD), which is responsible for many deaths. This work aimed to study 25B-NBOH and 25B-NBOMe (Figure 1) regarding their spectroscopic properties employing *in silico* methods. These substances are derivatives of 2C-B (4-Bromo-2,5-dimethoxyphenethylamine), a psychedelic drug of the 2C family.

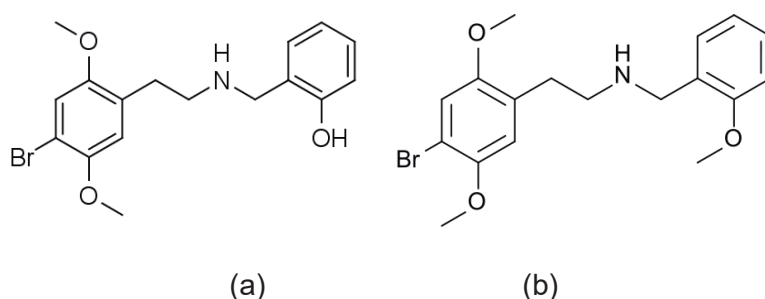


Figure 1: Molecular Structures of (a)25B-NBOH and (b) 25B-NBOMe.

We have performed the systematic conformational analysis for both molecules, and one minimum energy structure was found for each one. The minimum energy structure was optimized in ORCA software, with B3LYP and PBE0 Density Functional Theories with a TZVP basis set. Infrared spectroscopic signals were obtained from optimized structures. We used infrared library data from the Scientific Working Group for the Analysis of Seized Drugs (SWGDRUG) and the European Network of Forensic Science Institutes (ENFSI) as experimental references. All data were set to transmittance, and a gaussian transformation was applied to fit them to the same dimension. The Z-score transformation was used as pre-treatment. We performed a correlation map to assign a Hit Quality Index (HQI). This metric relates the distances between each pair of theoretical and experimental spectra. Results showed that each theoretical spectrum was more like its experimental correspondent's spectrum than the other molecules. We concluded that in silico tools could provide spectroscopic information and could be used to benchmark experimental data by offering standards for unknown NPS.

Acknowledgments

Conselho Nacional de Desenvolvimento Científico e Tecnológico (CNPq, Project 465450/2014-8) and Coordenação para o Aperfeiçoamento de Pessoal de Nível Superior (CAPES, Financial Code 001).

INVESTIGAÇÃO DO PERFIL QUÍMICO DE COMPRIMIDOS DE ECSTASY APREENDIDOS EM JOINVILLE (SC) POR GC-MS E QUIMIOMETRIA

Caroline Nicolodi (PG)¹, William H. Slominski (PG)¹, Gisele Chibinski Parabocz (PQ)², Suellen Pericolo (PQ)², José Augusto Da-Col (PQ)^{1*}, Edmar Martendal (PQ)¹.

jose.col@udesc.br

¹Universidade do Estado de Santa Catarina (UDESC), Departamento de Química (DQMC), Joinville, SC. ²Polícia Científica, Superintendência Regional de Joinville, Joinville, SC

Palavras Chave: Perfil Químico, Caracterização Química, Ecstasy, MDMA, Quimiometria.

Highlights

CHEMICAL PROFILE INVESTIGATION OF ECSTASY TABLETS SEIZED IN JOINVILLE (SC) BY GC-MS AND CHEMOMETRICS. Chemical profiles are important to identify synthetic routes of ecstasy tablets. Probable synthetic routes for MDA and MDMA are reducing routes (reductive amination or Leuckart reaction) and scarecrows route.

Resumo

No Brasil, o ecstasy (MDMA ou MDA) foi a droga mais apreendida dentre as do tipo anfetamina de 2010 a 2017, enquanto Santa Catarina apresentou um índice crescente de apreensões a partir de 2013, seguindo a tendência global e nacional. Para determinar a origem e as rotas sintéticas desses comprimidos, seus perfis químicos são uma importante ferramenta. Nessa linha, empregou-se a cromatografia a gás e a quimiometria na investigação dos perfis químicos de 44 amostras de ecstasy apreendidas em Joinville, SC, em 2019 e 2020. Essas amostras foram cedidas pela Polícia Científica de SC em Joinville. Para a geração dos perfis cromatográficos, utilizou-se a microextração em fase sólida por headspace (HS-SPME) com fibra DVB/CAR/PDMS, seguida de análise por GC-MS. Compostos voláteis e semivoláteis foram extraídos, como solventes, adulterantes, precursores e intermediários de rotas sintéticas de MDA e MDMA. Dentre eles, pode-se citar o safrol, isosafrol, piperonal, 3,4-metilenodioxifenilacetona, α -metil-3,4-metilenodioxifenilpropionitrila e N-formil-MDA/MDMA. Para facilitar a interpretação dos resultados, empregou-se a Análise de Componentes Principais (PCA), auxiliando na identificação de algumas prováveis rotas sintéticas redutoras (aminação redutiva ou reação de Leuckart) e da rota Scarecrows (a partir do helional). O modelo foi feito com valores das áreas de picos autoescalados de 11 compostos no software MATLAB R2009a (Mathworks, Natick, MA, EUA). Assim, cerca de 80% de variância explicada foi obtida com 4 PC. Na **Figura 1**, temos o gráfico de escores PC1 (40,13%) versus PC2 (20,21%), onde é possível observar que as amostras contendo somente MDA estão mais à direita do gráfico, indicando a influência do MDA e do intermediário N-formil-MDA, da reação de Leuckart, em sua produção. Já as amostras 859-10, 3872-5 e 486-5 (conjunto MDA+MDP2P) apresentaram influência dos intermediários da reação de *Scarecrows*, demonstrando o poder do modelo de indicar as rotas sintéticas de produção.

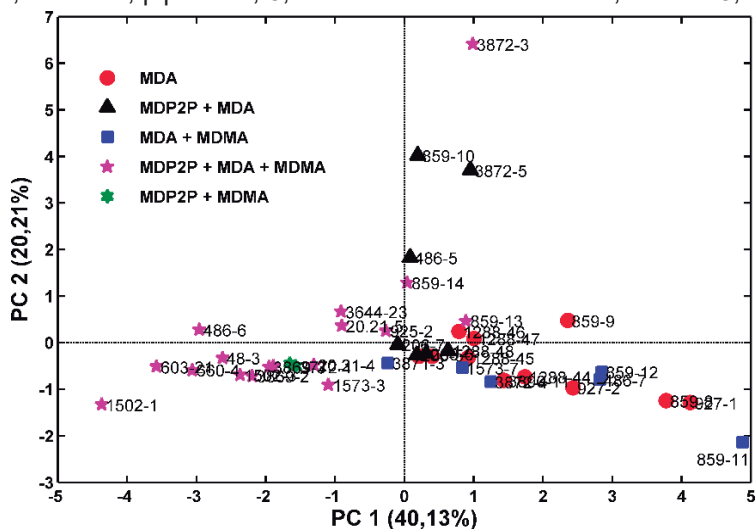


Figura 1. Gráfico de escores da PC1 (40,13%) versus PC2 (20,21%) para o modelo das amostras de ecstasy apreendidas em Joinville, SC. O modelo foi construído com as áreas dos picos cromatográficos autoescaladas.

SOUZA JÚNIOR, J.L. *et al.* *J Forensic Sci*, **65**: 906-912, 2020.

UNODC, Drug Market Trends: Cocaine, Amphetamine-Type Stimulants. World Drug Report, United Nations Publication, n. E.21.XI.8, 2021.

Agradecimentos

Os autores agradecem a Polícia Científica de SC pelas amostras e ao CNPq e à FAPESC, pelo auxílio financeiro.

Investigation of thermal behavior of the antiviral Famciclovir by Thermogravimetry and Differential Thermal Analysis

Luciano C. R. Rais (PG),¹ Éder T. G. Cavalheiro (PQ).¹

lucianorais@usp.br cavalheiro@iqsc.usp.br

¹Instituto de Química de São Carlos, USP.

Keywords: Famciclovir, Thermogravimetry, Derivate Thermogravimetry, Differential Thermal Analysis.

Highlights

Thermal behavior of famciclovir was investigated by thermogravimetric techniques. Thermal events were described.

Abstract

Famciclovir ([2-(acetyloxymethyl)-4-(2-aminopurin-9-yl)butyl], C₁₄H₁₉N₅O₄) is an antiviral prodrug obtained synthetically from the nitrogenous base guanine, with molar mass 321.33 g mol⁻¹.

TG/DTG and DTA curves were obtained in a simultaneous SDT Q600 modulus (TA Instruments) using sample mass of c.a. 7.0 ± 0.1 mg, heating rate of 10 °C min⁻¹, under dynamic N₂ and air atmospheres (flow 50 mL min⁻¹) in open α-alumina sample holders.

Under nitrogen atmosphere, TG/DTG curves of famciclovir present one stage of mass loss, Figure (1.a). The famciclovir was stable up to 204.4 °C. The single mass loss represents 97.2% of the sample. After decomposition of the drug undergone pyrolysis of the carbonized material with a final residue of 0.66% at 1000°C.

Famciclovir TG/DTG curves under air atmosphere (Figure 1.c), revealed that the sample decomposition occurs in two stages. In the first stage of mass loss of 85.9% in the temperature range of 206.6 °C to 393.6 °C. While the second stage occurs from 293.6 °C to 682.9 °C with a loss of 9.44%. In the sequence, another loss between 682.9 °C and 1000.0 °C referring to the burning of the carbonized material, with a final residue of 4.38% at the end of the experiment. In the DTA curve (Figure 1.b), one exothermic event and three endothermic events. The first event is characterized by melting of the drug 103.5 °C (T_{peak}). The exothermic events referred to the thermal decomposition of the drug and that the oxidation of the material is accompanied the by burning of the carbonized, the peaks 354.9 °C, 550.6 °C and 680.1 °C, respectively.

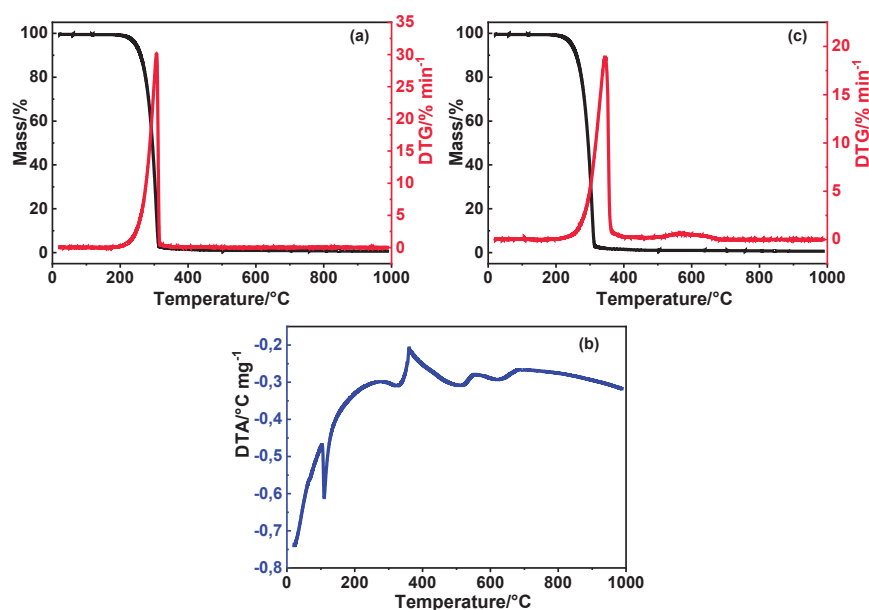


Figure 1: Famciclovir TG/DTG curves under dynamic N₂ atmosphere (a) TG/DTG, (b) DTA and in air atmosphere (c) TG/DTG in air atmosphere (flow rate: 50 mL min⁻¹) and heating rate 10 °C min⁻¹, in open α-alumina sample holder with mass of 6.89 mg and 6.76 mg, respectively.

Acknowledgments

LATEQS, IQSC-USP, CAPES, FAPESP.

LAB-ON-A-DRONE WITH REAL-TIME DATA TRANSMISSION FOR ENVIRONMENTAL APPLICATIONS

Vagner B dos Santos (PQ),¹ Vinícius A Carvalho (IC)¹, João Paulo B. de Almeida (PG)¹

Vagner.bsantos@ufpe.br

¹LIA³ (Laboratório de Automação e Instrumentação Analítica) / Departamento de Química Fundamental, UFPE)

Palavras Chave: (Drone, Lab-on-a-chip, emergent pollution, real-time monitoring, environmental water)

Highlights

An adapted UAV for environmental water sampling in difficult access area.
A fast and low-cost environmental monitoring.
In situ analysis using portable and low-cost instrumentation.
Transmission of data in real-time using an embedded sensor.

Resumo/Abstract

Unmanned aerial vehicles (UAV) have been used as a new environmental tool due to being fast, and the possibility to monitor a wide region of interest and access to difficult areas. The present work is based on the concept of Lab-On-a-Drone, to obtain real-time data from voltammetry referring to studies of contaminants in environmental water. For this, all apparatus were developed and adapted under a UAV remotely controlled via Wifi by a smartphone to trigger a microcontrolled water sampling system using micro pumps (MP), micro valves (MV), to fill an electrochemical cell to perform voltammetric methods using an embedded mini potentiostat and sending data during flight. As a proof of concept of the Lab-On-a-Drone the detection of Pb^{2+} in environmental waters was performed using an electrochemical cell containing a miniaturized BDD electrode as a working electrode, Ag/AgCl as a reference and graphite as a counter electrode. For quantification purposes, analytical curves were constructed for the determination of Pb^{2+} in environmental waters for a concentration ranging from $0.50 \mu\text{g L}^{-1}$ to $50 \mu\text{g L}^{-1}$, with a detection limit of $0.1 \mu\text{g L}^{-1}$. The Lab-On-a-Drone with electrochemical detection was used to measure Pb^{2+} in water reservoirs used to supply the cities of the Metropolitan Region of Recife-Brazil with real-time data transmission, Fig. 1. The Lab-On-a-Drone makes it possible to assess possible environmental impacts, being a monitoring tool for some productive activity, with greater socio-environmental responsibility. The tool can be used by governments and non-profit organizations to monitor water resources and/or water in environmental reserves, using a fast, low-cost, with autonomy, and access to remote areas, without risk to the professionals involved in the collection or detection of pollutants, as well as preservation of the collected sample, and greater speed in obtaining the analysis result, and consequent decision making. This work opens up or creates a new class of fully automated analytical instrumentation with sensors in flying that can map or spatially scan for remote monitoring purposes using sensitive and selective sensors.



Figure 1. UAV adapted (a) for water sampling with 1 (battery), 2 (MP), 3 (SV), and UAV used to collect water and real time data transmission (b). Image of Water reservoir captured using the UAV during the in situ analysis (c).

Agradecimentos/Acknowledgments

CNPq 421147/2018-0, FACEPE (APQ-0413-1.06/21 & APQ-0346-1.06/14).

Lipidomics insights in the treatment of refractory depression disorder with ayahuasca

Emerson Andrade Ferreira dos Santos (PG), Flávia da Silva Zandonadi (PQ), Alessandra Sussulini (PQ)

afs.emerson@gmail.com; sussulini@unicamp.br

Laboratório de Bioanalítica e Ciências Ômicas Integradas (LaBIOmics), Departamento de Química Analítica, UNICAMP

Palavras Chave: *Ayahuasca, Depression, Lipidomics, Mass Spectrometry.*

Highlights

Depression is a health issue worldwide.

Psychedelics such as ayahuasca demonstrated promising effects against depression.

Ayahuasca consists in a mixture of two Amazonian plants.

Resumo/Abstract

Major depression disorder is one of the health issues that most contribute to the burden of diseases worldwide. According to the WHO, around 280 million people suffer under depression.¹ It has a complex matrix, involving many different mechanisms, and is rather conceived as a bio-psycho-social disease.

Ayahuasca is an indigenous Amazonian beverage, made with barks of the vine *Banisteriopsis caapi* and leaves of the bush *Psychotria viridis*. *B caapi* contains beta-carboline compounds that work in a synergic way with *N,N*-dimethyltryptamine (DMT), found in *P. viridis*, allowing the triggering of psychedelic effects. The beverage demonstrated promising effects against depression in clinical researches.²

Lipidomics³ is a branch of metabolomics, an omics science that aims to access information about an organism phenotype by analyzing the intermediate compounds and end products involved in the metabolism. While metabolomics focuses on polar metabolites (hydrophilic), lipidomics investigates the less polar ones (hydrophobic), which is most constituted by lipids.

In this work, serum samples of depression patients and healthy volunteers, to whom ayahuasca or placebo were administrated, were analyzed by an untargeted lipidomics approach, in order to obtain insights into the biochemistry of depression regarding alterations in metabolic pathways and in relative concentrations of its constitutive compounds. After extraction, samples were analyzed by an UHPLC-MS system coupled to an Orbitrap mass spectrometer, data was pre-treated using the software MS-DIAL, and then submitted to biostatistics and in the online software MetaboAnalyst.

Differential lipids in the comparison of healthy and depression patients groups were found to pertain to classes of di-glycerides, triglycerides, sphingomyelin, phosphatidylcholine, and hexosylceramide.

1. <https://www.who.int/news-room/fact-sheets/detail/depression>
2. Palhano-Fontes, F. *et al.* (2019) *Rapid antidepressant effects of the psychedelic ayahuasca in treatment-resistant depression: a randomized placebo-controlled trial.* *Psychol. Med.*, 49(4), 655-663.
3. Wenk, M. R. (2010) *Lipidomics: New Tools and Applications.* *Cell*, 143(6), 888-895.

Agradecimentos/Acknowledgments

FAPESP, CNPq, CAPES, INCTBio, FAEPEX-Unicamp.

Magnetic GO/ γ -Fe₂O₃ nanoparticles for dispersive solid-phase microextraction of pesticides in river water and determination by HPLC-DAD

Luciana R. Marcelo (PG),^{1,2*} Deborah C. Vargas (PQ),¹ Jefferson S. Gois (PQ),¹

luciana.marcelo@ifrj.edu.br

¹Department of Analytical Chemistry, Institute of Chemistry, Rio de Janeiro State University, Rio de Janeiro, RJ, Brazil.

Keywords: Magnetic graphene oxide, Pesticides in surface water, Preconcentration, High performance liquid chromatography.

Highlights

Synthesis and application of an adsorbent with improved properties for pesticides preconcentration. Development miniaturized method of solid phase extraction for pesticides determination in water.

Resumo/Abstract

The occurrence of several pesticide residues in aqueous matrices throughout Brazil have been reported in the literature.^{1,2} Due to the low concentration ($\mu\text{g L}^{-1}$ and ng L^{-1}) of pesticides in environmental samples, a sample pretreatment step prior to instrumental analysis may be necessary. Solid phase extraction (SPE) and its variations are the most commonly used techniques for the preconcentration of pesticides.³ In recent years, magnetic nanoparticles (MNPs) combined with graphene oxide (GO) have been proposed as sorbents for magnetic dispersive solid-phase microextraction (m-d-SPE). therefore, this work reports the development of a new method for preconcentration and determination of trace pesticides from river water samples using GO/ γ -Fe₂O₃ nanocomposite as solid phase extraction sorbent and analysis by high-performance liquid chromatography-diode array detector (HPLC-DAD). Graphene oxide was synthesized from graphite oxidation by a modified Hummers method. GO/ γ -Fe₂O₃ was synthesized by the *in situ* chemical coprecipitation of Fe²⁺ and Fe³⁺ in an alkaline solution in the presence of GO. Six pesticides from different chemical classes, *i.e.*, acetamiprid, atrazine, diuron, imidacloprid, thiacloprid, and thiamethoxam, were selected for this work because they are widely used in Brazil. The affecting parameters on extraction of pesticides were evaluated and optimized using a central composite design (CCD) with of eight points in the kernel part (2³), six points in the star part, and six replicates of the central point. The level of the factors was optimized: extraction time (20 to 120 min), pH of the sample solution (3.0 to 8.0), and mass of adsorbent (20 to 120 mg). All data treatment was carried out using RStudio software version 3.5.3. The effect of desorption solvent type, desorption solvent volume and ionic strength were investigated separately, one at a time. The results of X-ray diffraction, Fourier transform infrared (FT-IR) spectroscopy and scanning electron microscopy analyses of the synthesized material indicated that the GO/ γ -Fe₂O₃ nanocomposite was successfully achieved. The regression model generated was checked using the coefficient of determination (R²). In this study, the adjusted R² value ranged from 0,9601 – 0,9933 demonstrating that only 1 to 4% of the total variations were not explained by the model. The residues of the models were proven to follow a normal distribution according to a Shapiro-Wilk test (p=0.05). The desirability function was used to obtain the optimum values for the extraction and preconcentration method, which were achieved at the extraction time of 84 min, pH of 5.4, and amount of adsorbent of 115 mg. The maximum % adsorption values ranged from 46.5 to 92.0%. To determine the desorption conditions, five organic solvents, namely, acetone, acetonitrile, mixture acetonitrile-water/phosphoric acid (2.5:7.5, v/v), methanol, and methanol-acetic acid (9:1, v/v) were used for desorption of analytes from the GO/ γ -Fe₂O₃. Methanol-acetic acid (9:1, v/v) was the best eluting solvent compared to other studied. In addition, the influence of methanol-acetic acid (9:1, v/v) volume on the desorption efficiency of the analytes was also investigated, and 1.0 mL was the optimum volume of desorption solvent. Finally, the ionic strength in the extraction recoveries was studied. The optimum NaCl concentration in the sample solution was fixed at 1% (w/v). Under optimum conditions, the limits of detection were from 0.13 to 0.84 $\mu\text{g L}^{-1}$. The relative standard deviations (RSDs) were $\leq 7.6\%$ (n = 10). The proposed method was successful applied for extraction and determination of acetamiprid, atrazine, diuron, imidacloprid, thiacloprid and thiamethoxam in river water samples (recoveries > 83%). Remarkably, the adsorbent could be used at least 6 times without affecting the extraction efficiency.

Agradecimentos/Acknowledgments

UERJ, IFRJ, CNPq, FAPERJ, CAPES.

¹Albuquerque, A. F. et al. *Environmental Science: Processes and Impacts*, 18 (7), 779–787, 2016.

²Caldas, S. S. et al. *Journal of the Brazilian Chemical Society*, 30 (1), 71–80, 2019.

³Mahpishanian, S.; Sereshti, H.; Baghdadi, M. *Journal of Chromatography A*, 1406, 48–58, 2015.

46^o Reunião Anual da Sociedade Brasileira de Química: "Química: Ligando ciências e neutralizando desigualdades"

Metabolite profile differentiation study for lettuce in soil-base and hydroponic substrates using PSI-MS methodology.

Yuri A. Rocha (IC),¹ Lucas S. Machado (PG),¹ Lanaia Í. L. Maciel (PG),¹ Almir C. B. Junior (PG),¹ Jussara V. Roque (PG),¹ Boniek G. Vaz (PQ),¹ Andréa R. Chaves (PQ).

yuriarrates@gmail.com; andrearchaves@gmail.com

¹ Laboratório de Cromatografia e Espectrometria de Massas, Instituto de Química, Universidade Federal de Goiás, Goiânia, Brazil, 74690-900.

Key Words: Mass Spectrometry, Metabolomic, Chemometry, Paper spray ionization

Highlights

- Application of analytical approaches to distinguish lettuce according to the growth condition, soil-based agriculture or hydroponic, and also differentiate between the varieties of lettuce.
- Use of PSI-MS for fingerprinting and differentiation according to the ion profile of the main metabolites of the different cultivation methods of lettuce.
- Chemometrics tools applied in order to highlight the most important variables to classify the extracts.

Resumo/Abstract

Over the decades, many efforts have been made to find potential analytical approaches to evaluate the chemical profile of different substrates. The production of lettuce considers two main approaches, which are conventional soil-based agriculture and hydroponic medium. The literature has been showing the difference between the crops of these two approaches. Conventional methods of differentiation bring some important pieces of information, but they still don't consider the chemical profile of the crop with this different growth conditions. The application of analytical approaches capable to generate the chemical ion profile of the sample can be used to create a fingerprint of the plant, allowing the distinguishing of the plant according to the growth condition submitted. Paper spray ionization-mass spectrometry (PSI-MS) is one of the ambient mass spectrometry (AIMS) methods, this technique has been reported in the literature for the fingerprint of food sources to perform the discrimination and differentiation according to the chemical profile of the samples [1]. Although, the application of PSI-MS for fingerprinting and differentiation according to the ion profile of different cultivation methods of lettuce has not been described in the literature. Hence, this study aims to the application of PSI-MS for the fingerprint discrimination of the ion profile of lettuce samples submitted in soil-based agriculture and hydroponic approaches by chemometric data treatment. As PSI-MS method shows itself as simple technique, and faster ionization approach, contributing with the green analytical chemistry principles, due to its low solvent consumption. The grown soil lettuce and hydroponic lettuce samples were obtained in local markets (Goiânia, Goiás – Brazil). The study evaluated three different varieties of lettuce (*Lactuca Sativa* L.) popular known as Iceberg Lettuce, Escarole Lettuce and Oak Leaf Lettuce. For the sample preparation, 300 mg of the lettuce was extract using 10mL of methanol/water (80:20 v/v) mixture followed by infusion and sonication for 30 minutes at room temperature (25°C). The extract was centrifugated at 10000 rpm for 10 minutes. The PSI-MS analysis were performed both in positive and negative ionization mode in a Q Exactive hybrid Quadrupole-Orbitrap mass spectrometer using 20 µL of the extract onto the surface of a triangular paper. Chemometrics tools were applied, and due to the higher number of variables, PCA and PLS-DA was used to reduce the number of dimensions to a small number of principal components. The chemometric models showed specific ions for the characterization of the analyzed species and also the cultivation mode. The ions pointed out by chemometrics tools were submitted to the Global Natural Products Social Molecular Networking (GNPS) database for identification and structural elucidation, and also confirmed by MS/MS analysis. According to this, PSI-MS proof be effective to identify and differentiate metabolites of lettuce in soil-base and hydroponic substrates, being a simple technique who reduces solvent consumption.

[1] Santos, A.M.S.; et al. Paper Spray Ionization Mass Spectrometry Applied for Quantification of Pesticides and Discrimination from Tomato Varieties. *Journal of Food Composition and Analysis* **2022**, *109*, 104467, doi:10.1016/J.JFCA.2022.104467.

Agradecimentos/Acknowledgments

LaCEM IQ/UFG, CAPES, CNPq e FAPEG.

Metabolomics applied in the COVID-19 pandemic

Thales F.D. Pereira (PG)*, Alessandra Sussulini (PQ)

thalespdf@gmail.com; sussulini@unicamp.br

Laboratório de Bioanalítica e Ciências Ômicas Integradas (LaBIOmics), Departamento de Química Analítica, UNICAMP

Keywords: *Metabolomics, Lipidomics, COVID-19, SARS-CoV-2, Pandemic*

Highlights

- ✓ A review of the role of metabolomics-based investigations in combating the COVID-19 pandemics.
- ✓ Main differential metabolites classes: amino acids, carbohydrates, cholesterol, and fatty acids.

Resumo/Abstract

With the first reports of COVID-19 spreading in China at the end of 2019 and with the pandemic officially declared by the World Health Organization on March 11, 2020, the scientific community around the world has mobilized to rapidly improve our knowledge on the pathogenesis of this disease, caused by SARS-CoV-2. In this work, we sought to investigate the role of metabolomics in the context of this new disease. The search carried out on the Scopus platform for articles whose terms “metabolomics” or “lipidomics” must appear together with the terms “SARS-CoV-2” or “COVID-19” showed that between July 2020 and November 2022, a total of 130 articles were published in which the metabolomics approach was used in the COVID-19 pandemic. Just for comparison purposes, when searching on the same platform for articles whose terms “metabolomics” or “lipidomics” appear together with the terms “H1N1”, “SARS-CoV”, “MERS-CoV”, “Zika”, or “Ebola”, and not containing “SARS-CoV-2” or “COVID-19”, revealed less than three dozen works published in the last 10 years. This review reports that metabolomics approaches were mainly employed to suggest biomarker metabolites that would distinguish COVID-19 from other common and low-risk respiratory diseases to classify patients according to risk with great precision. Besides, the main expressive changes due to SARS-CoV-2 infection were found in amino acid metabolism, glucose metabolism, cholesterol metabolism, and fatty acid metabolism. Knowing about the metabolic alterations, some studies proposed treatments that mitigate the effects in severe cases. To a lesser extent, some studies applied metabolomics to understand which metabolic alterations remain after recovery and others evaluated the effects of vaccination. **Figure 1** summarizes the curve of academic production related to the topic in the period, the main analytical techniques employed, the sample matrix studied and the most predominant type of metabolomics approach.

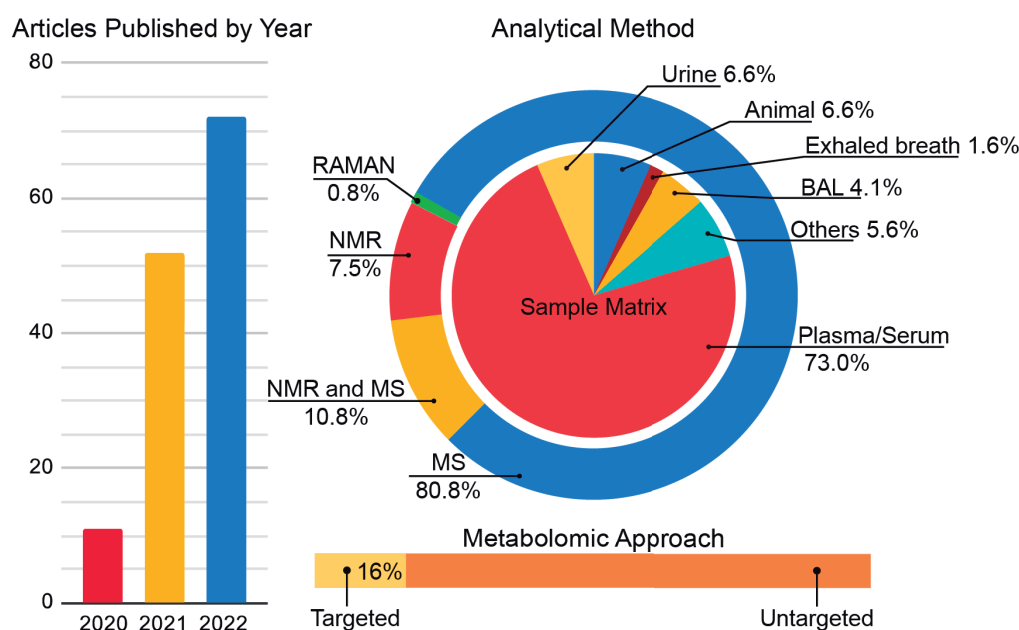


Figure 1. Summary statistics of the production of works applying metabolomics to the study of COVID-19. On the left, the bar graph shows the increase in publications between the first days of 2020 and the end of 2022. The donut graph (outer circle) shows the analytical techniques employed and predominance. The pie chart (inner circle) summarizes the types of matrices studied. Below is the type of metabolomics approach most used (BAL = bronchoalveolar lavage).

Agradecimentos/Acknowledgments

FAPESP, CAPES, CNPq, FAEPEX-UNICAMP, IQ/UNICAMP and the research group LaBIOmics.

Molecular test for COVID-19 diagnosis based on a colorimetric genomagnetic assay

Wyllian Neves Miranda (PG),^{1*} Tássia Regina de Oliveira (PQ),¹ Taíse Helena Oliveira Leite (PG),¹ Erika Regina Manuli (PG),² Fábio Leal (PG),² Ester Sabino (PQ),³ Henrique Pott-Junior (PQ),⁴ Matias Melendez (PQ),^{5,6} Ronaldo Censi Faria (PQ).¹

wyllian.nm@gmail.com;

¹Department of Chemistry, Federal University of São Carlos; ²Municipal University of São Caetano do Sul; ³Institute of Tropical Medicine, University of São Paulo; ⁴Department of Medicine, Federal University of São Carlos; ⁵Cloning Solutions Ltda; ⁶Molecular Carcinogenesis Program, National Cancer Institute;

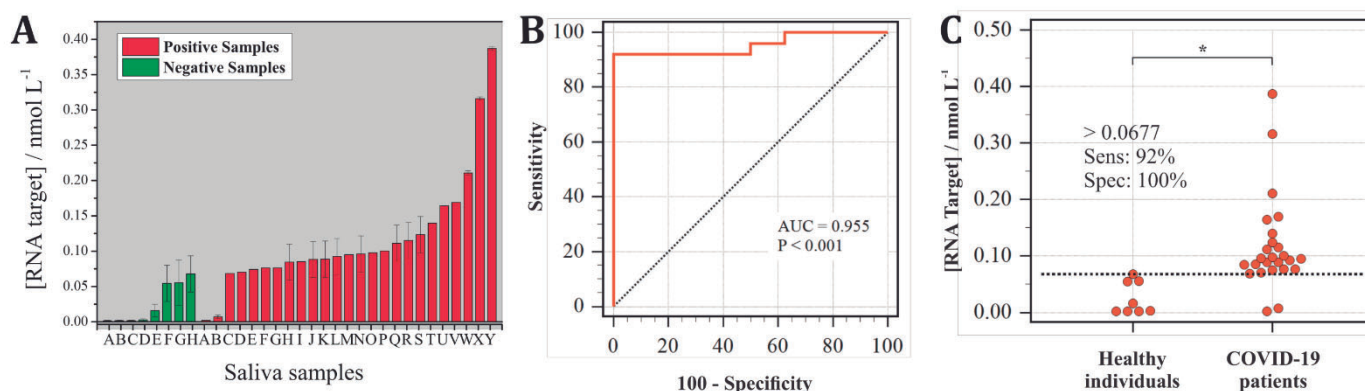
Palavras Chave: Molecular, Diagnosis, SARS-CoV-2, COVID-19, Colorimetric, Genomagnetic.

Highlights

This test can be conducted without amplification or extraction steps, in microtubes or in 96-well microplates for high-throughput COVID-19 diagnostics based on use of low-cost equipment and reagent.

Resumo/Abstract

The world is in prolonged pandemic caused by the SARS-CoV-2 virus, and widespread diagnostic testing is still needed to support efforts to control the disease and spread of new coronavirus variants and prevent. Herein, we present a simple and accurate colorimetric genomagnetic test for the diagnosis of COVID-19 using saliva as sample. To carry out the test, magnetic beads (MBs) modified with a sequence of single-strand DNA (ssDNA) complementary to the *N* gene of the SARS-CoV-2 RNA were designed and used for magnetic capture and separation from a complex saliva sample. A second biotinylated ssDNA sequence was applied, and the colorimetric detection was performed by adding streptavidin-horseradish peroxidase conjugate, H₂O₂, and tetramethylbenzidine (TMB) as chromogenic substrate. The test does not require viral RNA isolation nor transcription or amplification steps and can be performed at room temperature. The molecular assay test can be run in a single microtube or using 96-well microplates, allowing the diagnosis of a large number of samples within 90 min. A simple support for magnets was designed and constructed using a 3D printer that allows the magnetic separations directly in the 96-well microplate. The colorimetric test showed excellent ability to distinguish healthy individuals from patients infected with SARS-CoV-2, with 92% and 100% of clinical sensitivity and specificity, respectively. This performance was similar to that achieved using the gold standard RT-PCR technique. The proposed genomagnetic assay offers an opportunity to greatly increase population testing, contribute to controlling the spread of the virus, and improve health equity in COVID-19 testing.



Agradecimentos/Acknowledgments



Área: ANA

Monitoring the kinetics of the biodiesel oxidation using soft-modeling MCR-ALS and Raman spectroscopy

Maycom Cezar Valeriano (PG)^{1*}, Antônio Carlos Ferreira Batista (PQ)², Mónica Benicia Mamián-López (PQ)¹

*maycom.cezar@ufabc.edu.br

¹Federal University of ABC, Human and Natural Sciences Center. Santo André, São Paulo, Brazil, 09210-580; ²Federal University of Uberlândia. Pontal Institute of Exact and Natural Sciences. Chemistry Department, Ituiutaba, Minas Gerais, Brazil, 38304-402

Palavras Chave: (Biodiesel, Raman, Chemometrics, Machine Learning, Kinetic).

Highlights

Using Raman spectroscopy and soft-modeling MCR-ALS to monitoring biodiesel oxidation kinetic process.

Resumo/Abstract

One of the most critical biodiesel properties is oxidation stability. The biodiesel oxidation process generates contaminants that can compromise the engine's operation. The oxidation process of biodiesel occurs by forming radicals close to unsaturations, where oxygen binds, causing the formation of acids that can lead the generating of species such as aldehydes and even the formation of polymers. In this context, Raman spectroscopy can provide important structural information and, when associated with multivariate analysis, allows monitoring of these degradation processes and enables the study of the kinetic process. In this work, Raman spectroscopy and soft-modeling - alternating least squares (MCR-ALS) were applied to study the kinetics of the biodiesel oxidation reaction. Biodiesel was kept at 40°C, and a continuous airflow (10 kgf/cm²) was injected into the sample. Aliquots were collected each 30 min, and their respective FT-Raman spectra ($\lambda_0 = 1064$ nm) spectra were acquired. Multivariate resolution done by MCR-ALS suggests that the oxidation process follows a one-step mechanism. The calculated spectral profiles show a decrease in the intensity of the C=O bands (1750 – 1700 cm⁻¹) and an increase in the CH₂ and CH₃ bending and stretching vibrational modes (1320 – 1290 cm⁻¹ and 2900 – 3100 cm⁻¹).

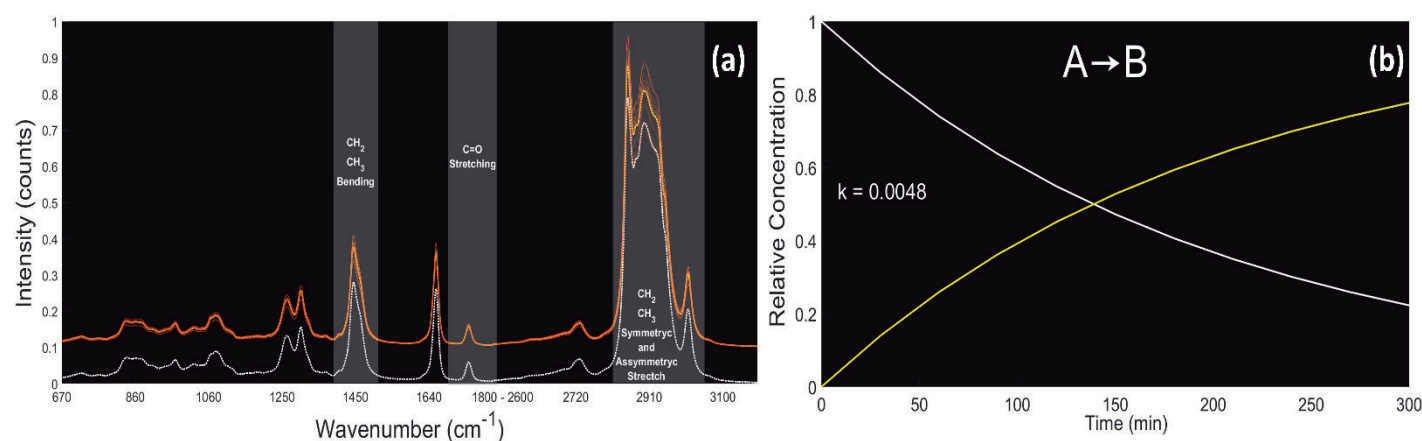


Figure 1: (a) Optimized profiles of biodiesel (white) and product (yellow) of the intermediates from the MCR-ALS soft-modelling, and (b) relative concentrations as a function of time from biodiesel and the oxidation product.

Agradecimentos/Acknowledgments

This work was supported by PRH-ANP (grant No. 045919). The authors thank the Laboratory of Molecular Spectroscopy of the Institute of Chemistry of the University of São Paulo (USP, Brazil) (FAPESP, grant 2016/21070-5).

Nanoecotoxicity assay and the effect of environmental parameters on the stability of nanohematite dispersion

Maycon Lucas de Oliveira (PG)^{1*}, Juliana Cancino-Bernardi (PQ)¹, Márcia A. M. S. Veiga (PQ)¹.

maycon.lucas.oliveira@usp.br;

¹Chemistry Department, FFCLRP, University of São Paulo, Postal Code 14040-901, Ribeirão Preto, SP, Brazil.

Keywords: *Nanohematites*, *Nanoecotoxicity*, *Lactuca sativa* L., *Aquatic environment*.

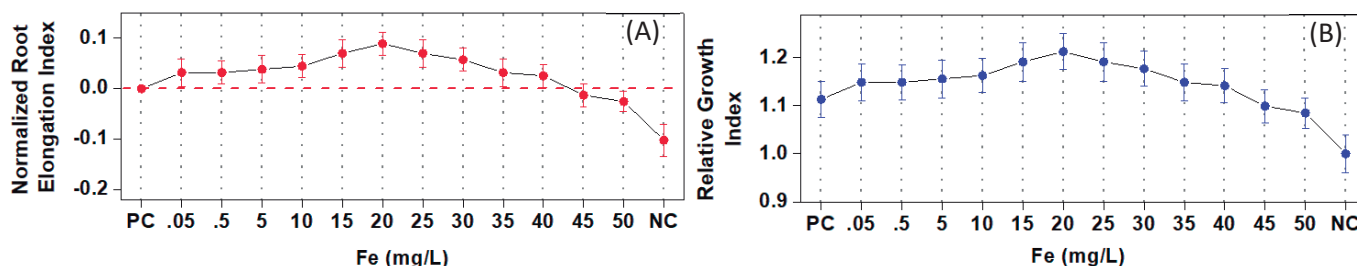
Highlights

HemNPs below 40 mg/L exhibit a hormesis effect in *Lactuca sativa* L.
HemNPs are potentially toxic in aquatic environments at pH 6-7, 25°C, hard water, and 36 h exposure time.

Abstract

Hematite ($\alpha\text{-Fe}_2\text{O}_3$) is the most common iron mineral in the Earth's crust and has been a subject of technological interest due to its high chemical and thermal stability. The nanoscale has attracted attention from a scientific standpoint due to the enhancement of its properties and the emergence of new and unique characteristics. However, the large-scale production of nanomaterials raises concern about potential environmental impacts on aquatic systems, macrofauna, and microfauna. Thus, this work aimed to synthesize and characterize nanohematites (HemNPs) and evaluate nanoecotoxicity through the germination test of *Lactuca sativa* L. (cv. Mimososa). Moreover, since the stabilization of nanoparticle suspensions is directly related to the manifestation of nano-toxic effects, the impact of environmental parameters (pH, hardness, temperature, and exposure time) directly associated with contamination cases was evaluated. The iron contents in the nanoparticles sample were quantified by flame atomic absorption spectrometry (F AAS) at 248.327 nm. The results indicated that the HemNPs were hexagonal, with a crystallinity of 60.9% and size dimension of 68 ± 15 (SEM) and 9 ± 2 (DLS). Experimentally, the iron content was 61,5% m/m compared to the theoretical 69.4% HemNPs, a discrepant value as a function of moisture and washing residues. The nanoecotoxicity assays did not indicate restrictive effects on germination. However, as can be seen in figure 1A, there was a manifestation of hormesis (NREI > 0; better condition at 20 mg/L) and low toxicity to concentrations higher than 40 mg/L (NREI < 0). In addition, the experiment showed a good ability of the plant to obtain nutrients and water with a maximum RGI of 20% (figure 1B). Regarding the stability of dispersions, it was found that the quadratic effect predominates in the four parameters evaluated. Generally, the highest concentration of iron (nanoparticles and ionic iron in suspension) was found when the combined results were in high-hardness waters, with pHs between 6 and 7. In contamination cases, the effects would be prominent in 30 to 36 hours and at 25 °C. Despite the HemNPs showing no nanoecotoxicity according to the germination test results, considering the potential environmental impacts of iron dispersion is concerning since ionic iron can be released from nanoparticle surface generating radicals by homogenous catalysis causing oxidative stress and consequent toxicity for different life forms.

Figure 1 – Nanoecotoxicity assay with *Lactuca sativa* L. (green Mimososa): (A) Normalized Root Elongation Index - NREI and (B) relative growth index - RGI.



Acknowledgments

This study was financed in part by the Coordenação de Aperfeiçoamento de Pessoal de Nível Superior – Brasil (CAPES/PROEX) – Finance Code 001.

Área: ANA

Non-chromatographic arsenic speciation by MSPE-ICP OES in seaweed samples from northeast Brazil

Débora R. de O. Silva (PG)¹, Francisco L. F. da Silva (PQ)^{1,2}, Davino M. Andrade-Neto(PQ)³, Fernando L. de Menezes (PG)³, Pierre B. A. Fachine (PQ)³, Andrea Raab (PQ)⁴, Eva M. Krupp (PQ)⁵, Jorg Feldmann (PQ)⁴, Gisele S. Lopes(PQ)¹, Wladiana O. Matos (PQ)¹.

debora_fos@hotmail.com; luan.fonseca@uece.br.

¹LEQA-Departamento de Química Analítica e Físico-Química, Centro de Ciências, Universidade Federal do Ceará; ²Faculdade de Educação de Crateús (FAEC)-Universidade Estadual do Ceará; ³GQMAT- Departamento de Química Analítica e Físico-Química, Centro de Ciências, Universidade Federal do Ceará; ⁴TESLA – Analytical Chemistry, Institute of Chemistry, University of Graz, Austria. ⁵TESLA-Department of Chemistry, University of Aberdeen, Scotland;

Palavras-chave: Seaweed, Arsenic Speciation, MSPE, HPLC-IPC-MS, ICP-OES.

Highlights

An MSPE method was used to quantify in the northeastern algae with values similar to the chromatographic method. The present work shows itself as a low cost and viable alternative for iAs speciation algae.

Abstract

Seaweed is known as a primary producer in their ecosystems and have capability to bioaccumulate trace elements, particularly arsenic (As). Algae can biotransform As producing several arsenocompounds, as arsenosugars that is precursor of arsenobetaine. Due to the increased of seaweed consumption for food and cosmetic purpose, As analysis is required. There is a lack in the literature about the As content and As speciation analysis in algae from northeast Brazil, the mainly region producer in the country. In this work, As species from algae samples (*Gracilariaria birdiae* and *Solieria filliformis*) were extracted in aqueous media, and then a procedure using iron-based nanoparticles was applied to separate and preconcentrate inorganic arsenic (iAs) which was quantified by ICP-OES. HPLC-ICP-MS was used as a comparative iAs analysis method and to total As speciation analysis. The iron nanoparticles were modified with an iethylenetriamine penta(methylene phosphonic acid) (DTPMP) as solid phase for iAs extraction/preconcentration which was performed employing the following experimental conditions: 4 mL of buffer solution pH 4.0, 20 mg of nanomaterial and 15 min. of extraction. The iAs contents found were 0.383 mg kg⁻¹ and 0.332 mg kg⁻¹ for *Gracilariaria birdiae* and *Solieria filliformis* samples, respectively. The HPLC-ICP-MS results shows that the major species found in the samples studied are arsenosugars (44%). More experiments are required to a complete analysis of algae from this region of Brazil, but preliminary results demonstrated the presence of iAs and arsenosugar in samples that are As compounds that required attention with regard to food security.

Acknowledgments

UFC, PGQUIM, University of Aberdeen, CAPES-PRINT - 88887.364637/2019-00, CNPq-421096/2018-7. FUNCAP, NUTEC.

Obtaining high purity lanthanum and cerium from nickel metal hydride battery waste using hydrophobic eutectic solvent

Kaïque A.M.L. Cruz (PG),¹ Fábio R. P. Rocha (PQ),² Maria C. Hespanhol (PQ)^{1*}

kaique.cruz@ufv.br; *mariacarmo@ufv.br;

¹Grupo de Análises e Educação para a Sustentabilidade (GAES), Departamento de Química, CCE, UFV

²Laboratório de Química Analítica "Henrique Bergamin Filho", CENA, USP

Keywords: Hydrophobic eutectic solvent, Liquid-liquid extraction, Lanthanum and cerium separation, High selectivity, NiMH

Highlights

Separation efficiency of transition metals and lanthanides was achieved using a two-phase system consisting of acid leachate nickel metal hydride battery + hydrophobic eutectic solvent.

Abstract

The development of processes that aim to exploit secondary resources as a way to mitigate the shortage of critical raw materials (CRM) is challenging, despite being increasingly necessary. Nickel metal hydride (NiMH) batteries deserve special attention because they have a high CRM content (15 and 4% by mass of lanthanides, Ln, and cobalt, respectively).¹ The newly developed hydrophobic eutectic solvents (HES)² are shown to be more sustainable methods for recovering metals from NiMH residues, especially in the CRM separation stage, because unlike organic solvents, HES can be non-volatile, non-flammable and non-toxic. In this work, a HES based on trioctylphosphine oxide (TOPO) and decanoic acid (DA) was investigated to perform the separation of Ln present in acidic leachates from NiMH residues. TOPO was chosen due to its easy availability, cost and for being an effective extractant for Ln³. The parameters investigated were: i) nature of the acid used in the leaching (HNO₃, H₂SO₄ and CH₃SO₃H) of NiMH residues and ii) mass proportion of aqueous and eutectic phases, WP1:EP1, (1:1, 1:2, 2:1, 1:4 and 1:8). These parameters indicated that the biphasic system (BS) formed by HES and the leachate obtained in 2.0 mol HNO₃ L⁻¹ presented the best condition for separation between transition metals and Ln, due to the formation of complexes between TOPO, Ln and NO₃⁻ ions. For this BS, a WP1:EP1 ratio equal to 1:8 resulted into 96 and 98% extraction of La and Ce, respectively, for EP1. Separation factors equal to 763 and 1149 for La and Ce, respectively, in relation to Ni were obtained, demonstrating the high selectivity of the BS used, since Ni is the major element (31 g kg⁻¹) in the leachate. The removal of Ln from EP1 was possible by adding a 4.0 mol L⁻¹ HCl solution to this phase due to the formation of complexes between Ln and Cl⁻ ions. The Ln being preferentially extracted into a new HCl-rich WP (WP2). La and Ce in WP2 were separated from each other by adding H₂O₂ and adjusting the pH to 3.3. The Ce (III) species was oxidized to Ce (IV) and precipitated as neutral hydroxide, which has low solubility. While the remaining La in WP2 was precipitated by adding oxalate solution, given the low solubility of lanthanum oxalate in the medium. SEM-EDS analysis of each solid obtained in the precipitation steps indicated the formation of Ce (OH)₄ and La₂(C₂O₄)₃ with purity of 99.9 and 99.8%, respectively. The EP1 was washed with a 2.0 mol L⁻¹ HNO₃ solution, and reused to separate the Ln from new nitric leachate, making it possible to perform at least five complete cycles to obtain the Ln. Thus, a process was developed to obtain CRM (La and Ce) with high purity from a secondary source using a minimum of separation steps, green solvent, low-cost reagents and reuse of the green solvent for a new cycle of obtaining the Ln compounds.

¹ Ebin, B., Petranikova, M., Ekberg, C. J. Mater. Cycles Waste Manag. **2018**, 20, 2018–2027.

² van Osch, D.J.G.P., Zubeir, L.F., van den Bruinhorst, A., Rocha, M.A.A., Kroon, M.C. Green Chem. **2018**, 17, 4518–4521.

³ Schaeffer, N., Conceição, J.H.F., Martins, M.A.R., Neves, M.C., Pérez-Sánchez, G., Gomes, J.R.B., Papaiconomou, N., Coutinho, J.A.P. Green Chem. **2020**, 22, 2810–2820.

Acknowledgments

INCTAA/CNPq-FAPESP, CAPES/FCT, FAPEMIG, CNPq

One-pot synthesis of fluorescent molecularly imprinted nanoparticles for highly selective “turn-off” detection of captopril in urine and wastewater

Weida Rodrigues Silva (PG),^{1*} Maria Del Taboada Sotomayor (PQ)², João Flávio da S. Petrucci (PQ).¹

weidarodrigues@gmail.com

¹Instituto de Química – Universidade Federal de Uberlândia – UFU; ² Departamento de Química Analítica - Universidade Estadual Paulista – UNESP.

Keywords: Molecularly imprinted fluorescent polymers, emerging pollutants, synthesis sol-gel, silica nanoparticles.

Highlights

An one-pot approach was employed to prepare fluorescent molecularly imprinted polymers (FMIPs) using the autocatalytic silica sol-gel polymerization strategy based on the self-catalytic polymerization capability of 3-aminopropyltriethoxysilane (APTES).

Resumo/Abstract

Captopril (CPT) is an antihypertensive drug widely used in Brazil and worldwide. After ingestion, it is metabolized in the liver and excreted mainly through urine. The drug and its metabolites can contaminate various environmental compartments, such as water, and therefore are considered micro-contaminants. The quantification of captopril in urine and in the aquatic environment is fundamental for monitoring the presence of this pollutant¹. Molecularly imprinted polymers (MIPs) are materials with high molecular recognition due to the creation of specific cavities of the target molecule. The synthesis of fluorescent MIPs (FMIPs) combines the selectivity of molecularly imprinted polymers with the sensitivity of fluorescent detection², resulting in sensors with excellent performance. Fluorescent MIPs based on silica nanoparticles (Si-FMIPs) are particularly attractive due to higher stability, better analytical performance, and low cost. Thus, the goal of this study was to synthesize a molecularly imprinted fluorescent silica nanoparticle-based (Si-FMIP) polymer using a one-pot synthesis route for application as a chemical sensor for the selective and sensitive determination of captopril in urine and water. The fluorescent monomer was previously prepared by mixing fluorescein isothiocyanate (FITC) and APTES. Si-FMIPs were synthesized using the sol-gel method according to the following procedure: 0.1 mmol of CPT, 0.3 mmol of APTES (catalyst and functional monomer), and 1 mmol of the fluorescent monomer were added into a reaction flask containing 10 mL of a water/ethanol mixture (8:2). Then, 1 mmol of tetraethoxysilane (TEOS) dissolved in 0.5 mL of ethanol was poured into the flask. The mixture was stirred at room temperature for 48h. After polymerization and template removal, specific recognition cavities complementary to the template would be left behind in the Si-FMIPs. To remove the template molecule, the mixture was subjected to 10 cycles of washes with phosphate buffer (pH 8.5). Non-imprinted fluorescent polymers (Si-FNIPs) were synthesized using the same procedure but without the addition of captopril. After synthesis, the performance of the polymers in selective CPT recognition was evaluated. The optimized conditions were (i) suspension of concentration (ii) contact time (iii) captopril concentration, Figure 1 shows the same results.

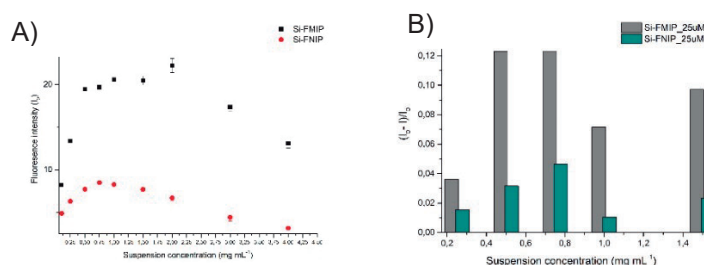


Figure 1. A) Fluorescence quenching as a function of Si-FMIP and Si-FNIP suspension concentration. B) Variation of fluorescence quenching with 25 µM of CPT. I_0 = initial fluorescence intensity; I = fluorescence intensity in the presence of CPT. Fluorescence intensity measurements (λ_{EX} = 490 nm and λ_{EM} = 520 nm).

It is observed that the analytical signal generated by the interaction between captopril and Si-FMIP is higher than Si-FNIP in the evaluated concentration. This fact indicates a great potential for its application as a chemical sensor for captopril determination. The Si-FMIPs were synthesized using the sol-gel method in one step and showed good selectivity in CPT recognition. The next steps consist of optimization and development of an analytical method for the determination of captopril in wastewater and urine samples. ¹ Shi, Y.; Peng, J.; Meng, X.; Huang, T.; Zhang, J.; He, H.; *Anal. Bioanal. Chem.* **2018**, *410*, 7373; ² Wang, F.; Wang, D.; Wang, T.; Jin, Y.; Ling, B.; Li, Q.; Li, J.; *RSC Adv.* **2021**, *11*, 7732.

Agradecimentos/Acknowledgments

IQ-UFU, IQ – UNESP, FAPEMIG, CAPES, CNPq (nº processo 141054/2020-4)

Online spectrophotometric determination of bisphenol A in foods and beverages using a simple calibration strategy

Vivian Maringolo* (PG), **Paula V. de Jesus** (IC), **Diogo L. Rocha** (R),

Federal University of ABC, Center for Natural Sciences and Humanities, Santo André, São Paulo, Brasil,
CEP 09210-580

*e-mail: vivian.maringolo@ufabc.edu.br

Keywords: *diazo-coupling reaction, flow analysis, multi-dispersion calibration, bisphenol A.*

Highlights

Fast online determination of BPA using a simple calibration strategy with transient signals.

Abstract

Bisphenol A (BPA) may be present in plastics and coatings of food and beverage packages. Due to the toxicity of BPA, the World Health Organization recommends the content $< 0.6 \text{ mg kg}^{-1}$ [1]. Analytical procedures for BPA determination have been proposed, including simple spectrophotometric ones [2]. These methods may present low analytical frequency, especially if standard addition calibration (SAC) is used to avoid matrix effects. Recently, multi-energy calibration (MEC) was used to circumvent drawbacks of SAC [3], based on the relation between the absorption spectra of sample with and without the addition of a known concentration of the analyte. Considering that dispersion in a flow system is reproducible, a similar strategy can be exploited using transient signals, herein denominated multi-dispersion calibration (MDC). In this work, a multicommutated flow system was proposed (Figure 1) for the spectrophotometric determination of BPA using a diazotization coupling reaction to yield a colored solution ($\lambda=446 \text{ nm}$). The parameters were optimized using a 2^4 full factorial design, and the selected values for sulfanilamide concentration, NaNO_2 concentration, coil B_2 size and sample volume were 30 mmol L^{-1} , 150 mmol L^{-1} , 150 cm and $2400 \mu\text{L}$, respectively. The concentrations of HCl (for diazotization) and phosphate buffer (pH 12, for the coupling step) were kept, respectively, at 1.0 and 0.5 mol L^{-1} . Linear response was observed between 0.25 and 3.5 mg L^{-1} . Detection limit, coefficient of variation ($n=17$) and determination rate were $20 \mu\text{g L}^{-1}$, 3.6% , and 24 h^{-1} , respectively.

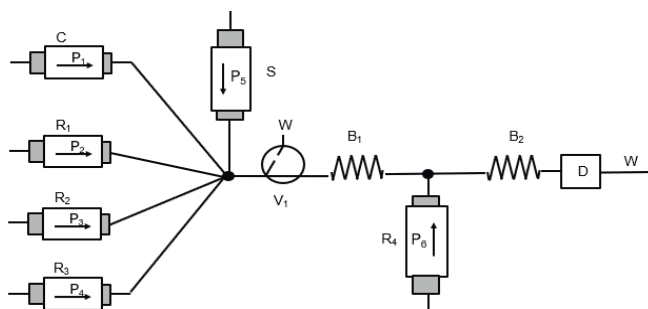


Figure 1: Flow-based system for BPA determination: C: H_2O , S: Sample, R_1 : 30 mmol L^{-1} sulfanilamide, R_2 : 150 mmol L^{-1} NaNO_2 , R_3 : 1 mol L^{-1} HCl, R_4 : 0.5 mol L^{-1} phosphate buffer pH 12. B_1 and B_2 : reaction coils, D: detection system ($\lambda=446 \text{ nm}$), W: waste.

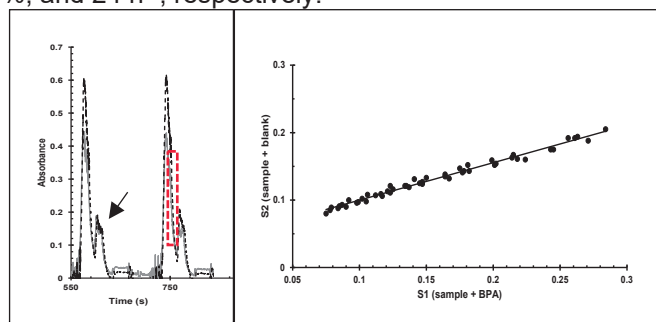


Figure 2: Overlay of the transient signals of a soda sample containing 2.0 (—) and 3.5 mg L^{-1} (---) BPA (A) and calibration curve ($n=2$) obtained with the retrieved data from the region in the dashed rectangle (B). The arrow indicates the Schlieren effect observed for the samples.

MDC was evaluated using a degassed soda sample after the addition of 2.0 and 3.5 mg L^{-1} BPA (Figure 2A). This experiment simulated the addition of 1.5 mg L^{-1} of the analyte to a sample containing 2.0 mg L^{-1} BPA. The retrieved data from a region of the transient signals indicated in Figure 2A were used to obtain the calibration curve (Figure 2B), resulting in the equation $S_2 = 0.555 S_1 + 0.044$ ($R^2 = 0.985$), where S_2 and S_1 are the signals of the sample with 2.0 and 3.5 mg L^{-1} BPA, respectively. Similarly to MEC [3], the slope equals $C_A / (C_A + C_P)$, where C_A is BPA concentration in the sample and C_P is the added BPA. The calculated C_A was 1.90 mg L^{-1} , which compared to the theoretical value (2.0 mg L^{-1}), indicates that MDC is a promising alternative for a fast calibration, requiring two transient signals (obtained in 300 s). Future experiments will be carried out to evaluate the precision and accuracy of the method.

1 WHO, "Toxicological and Health Aspects of Bisphenol A," no. November, 2010, p. 60.

2 A. Karrat and A. Amine, *Microchemical Journal*, vol. 168, no. May, 2021, p. 106496, 2021, doi: 10.1016/j.microc.2021.106496.

3 S. Soares, F.R.P. Rocha, *Talanta*, vol. 209, no. March, 2020, p. 120584, doi: 10.1016/j.talanta.2019.120584

Agradecimentos/Acknowledgments

FAPESP (grant number 2015/12172-6), and CAPES (Finance code 001).

46ª Reunião Anual da Sociedade Brasileira de Química: "Química: Ligando ciências e neutralizando desigualdades"

Optimization and use of AS7341 spectrometer sensor and μ PAD's for colorimetric determinations

Caio C. S. Machado* (PG)¹, Cecilia M. Falaguasta (IC)¹, Yugo S. N. da Mota (IC)², Diogo M. de Jesus (PG)¹, Sidnei G. da Silva (PQ)¹.

*cesarcaio12@gmail.com

¹Institute of Chemistry, Federal University of Uberlândia; ²Electrical Engineering Department, Federal University of Uberlândia.

Keywords: Analytical Instrumentation, Optical sensor, ESP-32, Internet of Things

Highlights

A portable, cost-effective approach for colorimetric determinations. Spectral resolution and sensor response similar to that obtained with a photometer. Ready to Internet of Analytical Things.

Abstract

Imaging analysis based on the use of μ PAD's allows the development of a portable device, with a range of analytical applications, such as clinical, environmental and food analysis. Those devices have the main advantage the improvement of the sample throughput, easy handling, cost-effective and low consumption of samples and reagents. The AS7341 sensor is a spectrometer sensor used for quantitative determinations. The visible spectrum detection is based-on eight channels (415, 445, 480, 515, 555, 590, 630 and 680 nm) which given simultaneously light intensity for each channel. The μ PAD's used in this work are made of filter paper and has 2x1 cm. A 3D Printed gray holder was manufactured in 3.5 x 2.5 x 2 cm to allocate the sensor and to fix a constant distance between the sensor and the μ PAD's (5 mm). An ESP-32 was used as a microcontroller to receive the signals of the sensor. To facilitate, a computer interface based on Visual Basic ® was developed. The sensor allows adjusting gain and LED current, in order to increase the sensitivity. The measurements are based on the reflectance of the light, at specific wavelengths, that passes through an analyte reflected to the detector. For each one of his eight channels (415, 445, 480, 515, 555, 590, 630 and 680 nm) the best condition of gain and LED current was obtained to guarantee better sensitivity for the measurements. Aiming to investigate and relate the desired analytical parameters to the developed system, to obtain quantitative information, the use of Bordeaux Red (BR), Tartrazine Yellow (TY), Sunset Yellow (SY), Bromocresol Green (BG), and Phenolphthalein (PH) were evaluated. and the analytical parameters of linear range, limit of detection (LoD), limit of quantification (LoQ) and RSD were obtained. **Table 1** shows the results obtained by the proposed device.

Table 1: Analytical features and instrumental parameters obtained using AS7341 and μ PAD's for five different dyes. (Considering equation plot: $Y = aX + b$)

Parameter	BR	TY	SY	BG	PH
Channel	515 nm	415 nm	480 nm	480 nm	555 nm
LED current (mA)	90	80	50	50	70
Sensor Gain	8	64	16	16	8
a	0.179	0.0997	0.092	0.130	0.118
b	0.0745	0.0382	0.0734	0.0516	0.114
Linear Range (mmol L ⁻¹)	0.15-1.5	0.25-1	0.35-1.25	0.35-1,5	0.5-2
LoD (mmol L ⁻¹)	0.0460	0.0823	0.0891	0.0630	0.0697
LoQ (mmol L ⁻¹)	0.150	0.274	0.297	0.210	0.232
RSD (%)	1.68	1.49	1.99	1.14	0.94

The proposed device shows potential to detect low concentrations (mmol L⁻¹) of different dyes. Furthermore, this device allows the development of versatile and miniaturized and connected system contributing to achieve the requirements to generate an Internet of Analytical Things dispositive.

Acknowledgments

CNPq (Process number: 403929/2021-0). FAPEMIG (Process number: APQ-01395-22).

Área: **ANA**

Optimization of a Method for the Determination of Ca and Mg in Organic Milk by Flame Atomic Absorption Spectrometry

Bianca C. Moreira (PG),¹ Pedro P. Moura (IC),¹ Fabiano F Costa (PQ),² Rafael A Souza (PQ).^{1*}

bianca_moreira7593@hotmail.com; rafael.arromba@gmail.com.

¹Departamento de Química, UFJF; ²Departamento de Farmácia, UFJF.

Palavras Chave: Acid Digestion, F AAS, Hot plate.

Highlights

Optimization of an acid digestion method using hot plate with high precision and accuracy for the determination of Ca and Mg by Flame Atomic Absorption Spectrometry.

Resumo/Abstract

The minerals calcium and magnesium are essential for human health and may be ingested daily. They are present in cow's milk, in which their concentration can reach and the recommended daily intake requirements. ¹ The Acid digestion is a one of the methods for the of wet preparation of samples, widely used. However, there is no consensus in the literature about the sample preparation procedure prior the quantification of such minerals in milk by Flame Atomic Absorption Spectrometry (F AAS). ^{2,3,4} Based on this fact, this work aimed to optimize a sample preparation method by acid digestion for the determination of Ca and Mg in organic milk by Flame Atomic Absorption Spectrometry (F AAS).

The sample preparation method established was based on other studies, ^{4,5} and the acid digestion was performed on a heating plate at 100 ± 5 °C. Then, in a beaker, Ca. 0.13 g of previously freeze-dried raw milk was mixed with of nitric acid and hydrogen peroxide in a 3:1 ratio, and a watch glass was placed over it to allow reflux. Repeated additions of the oxidizing agents were made, for the complete release of the nitrous vapors. In the digested obtained there was the formation of a mass of residual solid (not reported elsewhere), which was filtered and diluted to 25.00 mL in a with deionized water. The residual solid obtained after filtration was taken to a desiccator and, after drying, was solubilized in absolute ethyl alcohol, diluted to 40% v/v in water, and then submitted to F AAS analysis, in order to evaluate the existence of Ca and Mg minerals in the solid.

The calibration of the atomic absorption spectrometer was done from an external curve constructed in the same acidity medium as the sample solutions. Then, the validation of the method was started through parameters such as limits of detection (LOD), precision and accuracy. The intermediate precision obtained by the method were less than 4%, for both analytes, demonstrating a low dispersion of the data. The LOD obtained for Mg was 0.22 mg/L and for Ca 0.81 mg/L, which are below the concentrations of both analytes in the samples. The accuracy tests were performed for different types of milk (fluid, powdered and freeze-dried), obtaining values between 93% and 107%, which are in agreement with other studies in the literature. ⁵ Besides, The results obtained by analyzing the residual solid were below the method's LOD, and it was not possible to quantify it. This means that the formed solid does not interfere in the determination of such minerals. From this, it is possible to conclude that the established method has proven to be efficient for the determination of Ca and Mg in different types of milk samples (fluid, powdered and freeze-dried).

(1 Zwierchowski, G.; Ametaj, B. N. *Foods*, 2019, 8, 8.; 2 Nicholas, P. K., Padel, S., Cuttle, S. P., Fowler, S. M., Hovi, M., Lampkim, N. H. e Weller, R. F. *Bio. Agric. & horticulture*. 2004, 22, 3.; 3 Rey Crespo, F., Miranda M.; López- Alonso, M. *Food and Chemical Toxicology*. 2013, 55.; 4 Ribeiro, A. S., Arruda, M. A. Z., Cadore, S., Moretto, A. L. *Microchimica Acta*. 2003, 3, 141.; 5 Oreste, E. Q., Souza, A. O. de., Pereira, C. C., Lisboa, M. T., Cidade, M. J. A., Vieira, M. A., Cadore, S., Ribeiro, A. S. *Food analytical methods*. 2016, 9, 3.)

Agradecimentos/Acknowledgments

UFJF, Embrapa Gado de Leite (Dr. Fernanda Samarini Machado) and CAPES.

Otimizações de parâmetros para a análise de espécies de arsênio via microextração/derivatização simultânea líquido-líquido por GC-MS

William Henrique Slominski (PQ),^{1*} Ailton Coelho Junior (PG),¹ Catarinie Diniz Pereira (PQ),² Edmar Martendal (PQ), Tatiane de Andrade Maranhão (PQ)³

Williamhe.slo@gmail.com

¹Laboratório de Química Analítica e Nanomateriais Inorgânicos – LABQAN, Departamento de Química, CCT-UDESC, Joinville-SC, Brasil. ²Departamento de Química, UEM, Maringá-PR, Brasil. ³Laboratório de Espectrometria Atômica e de Massa, Departamento de Química, UFSC, Florianópolis-SC, Brasil.

Palavras Chave: Arsênio, GC-MS, TGM, BCR 627.

Highlights

Parameter optimizations for arsenic species analysis via simultaneous liquid-liquid microextraction/derivatization by GC-MS. Development of an analytical method for the analysis of MMA, DMA and inorganic arsenic. The method validation was made by using the certified reference material, BCR 627 (tuna tissue).

Resumo/Abstract

O arsênio é encontrado em águas naturais em diferentes formas, sendo o arsênio inorgânico mais tóxico do que os orgânicos. Para isso, a determinação de arsênio total e sua especiação é importante para a avaliação da toxicidade^[1]. Neste trabalho, foram estudados os parâmetros que influenciam a reação de derivatização das espécies orgânicas, ácido monometilarsônico (MMA) e ácido dimetilarsínico (DMA), e as espécies inorgânicas (As III e As V), utilizando o éster metílico de ácido tioglicólico (TGM). As variáveis envolvendo as etapas de microextração e derivatização foram otimizadas por meio de abordagens multivariadas (CCD e fatorial 2k) e univariada: volume de TGM (50-500 µL), pH (1-6), efeito salting-out (0-5,5 mol.Kg⁻¹ de NaCl), tempo de extração (1-4 min) e volume de solvente de extração clorofórmio (50-200 µL). As variáveis instrumentais estudadas foram: temperatura de injeção (200-280 °C), vazão inicial do gás de arraste (1-5 mL.min⁻¹), temperatura da fonte de íons (150-250°C), tempo de splitless (45-110 s) e a voltagem do detector (1,1-1,5 Kv). Os resultados das otimizações são apresentados na tabela 1. Nas condições ótimas, os principais parâmetros de mérito foram determinados: limites de detecção na faixa de 0,1-1 µg/L, faixas lineares entre 0,3-3 µg/L e coeficiente de determinação superiores a 0,99. A exatidão da metodologia desenvolvida foi avaliada utilizando um material de referência certificado, BCR 627 (tecido de atum), o método de preparo para a extração das espécies orgânicas ocorreu com a adição de HNO₃ diluído e H₂O₂, a 80 °C em uma chapa de aquecimento. A metodologia para a digestão apresentou resultados satisfatórios para o DMA, com uma concordância de 97 ± 3,80% com o valor certificado, e aos padrões de arsênio das espécies orgânicas não apresentaram interconversões das espécies. com uma concordância de 97% com o valor Certificado. Como perspectiva futura, pretende-se otimizar um método de preparo, visando a digestão e a mineralização total, para esta metodologia que utiliza a derivatização, avaliando possíveis interconversões das espécies.

Tabela 1- Condições obtidos a partir das otimizações multivariadas e univariada (n=3) para as variáveis instrumentais, microextração e derivatização simultânea líquido-líquido.

Microextração/Derivatização		Instrumental	
Volume de TGM	90 µL	Temperatura de injeção	257 °C
pH	3,15	Temperatura da fonte de íons	200 °C
Efeito salting-out	0 mol.Kg ⁻¹	Vazão inicial do gás de arraste	1,60 mL.min ⁻¹
Tempo de extração (vórtex)	4 min	Tempo de splitless	60 s
Volume de clorofórmio	75 µL	Voltagem do detector	1,2*;1,3** Kv

*Para as espécies orgânicas derivatizadas; ** Para a espécie inorgânica derivatizada

[1] Yang, S.J., Lee, Y. & Nam, S.H.. *J Anal Sci Technol* **13**, 45 (2022).

Agradecimentos/Acknowledgments

CCT-UDESC, FAPESC, CAPES and CNPq

Paper microfluidic devices for acetylsalicylic acid titration based on distance measurements

Jordanna E.A. dos Santos (IC-EM),¹ Monise C.R. Casanova (FM),^{1*} Lucas C. Duarte (PQ),² Wendell K.T. Coltro (PQ).²

jordanna.emilly@estudantes.ifg.edu.br; monise.coltro@ifg.edu.br

¹Departamento de áreas acadêmicas, IFG; ²Instituto de Química, UFG

Palavras Chave: *distance-based detection, paper titration, miniaturization.*

Highlights

- Low-cost, disposable and equipment free devices;
- An innovative teaching method for acetylsalicylic acid titration;
- Paper-based analytical devices (μ PAD) distance-based for acid-base titrations.

Resumo/Abstract

Microfluidic paper-based analytical devices (μ PADs) have attractive features for applications in analytical and bioanalytical chemistry due to their low-cost, global affordability and reduced consumption of sample and reagents¹. Colorimetric detection has been one of the most popular approaches used in association with μ PADs because of this instrumental simplicity and inherent portability. Among the different alternatives, distance-based measurements^{2,3} have demonstrated to be one of the simplest methods for applications in laboratories with low-resource settings and they emerge as a huge potential for teaching analytical chemistry including acid-base titrations for high-school and undergraduate classes. This study describes the fabrication of μ PADs for acetylsalicylic acid titration using distance-based measurements. The devices were wax printed on chromatographic paper in a layout containing a circular zone with 5 mm diameter connected to a rectangular channel of 40 mm long x 2mm wide. For performing the titrations, paper channel was first filled with 4.5 μ L of 0.05 mol L⁻¹ NaOH solution (containing phenolphthalein as indicator). After drying at room temperature for 2 min, aliquots of 4.5 μ L of sample solution (acetylsalicylic acid) prepared at different concentrations were added in the circular zone. When the sample travels along the channel, a discoloration of the channel was observed. The length of the discolored zone length was then measured using a digital caliper. The travelled distance by the sample revealed a linear behavior ($R^2 = 0.9949$) ranging from 5.0 to 16.4 mm when the concentration varied from 0.005 to 0.05 mol/L. Considering the recorded data, the limit of detection was estimated to be 0.001 mol/L, which promoted a displacement of ca. 2 mm. Based on the achieved data, the use of μ PADs allied to distance-based measurements have offered satisfactory performance for quality control in commercial analgesics. Future efforts will be dedicated to quantitative analysis of drugs and a comparison with a conventional titration. Furthermore, titrations with distance-based detection have proven to be a low-cost method with lower sample/reagent volume requirements in comparison with conventional titrations (μ L versus mL) and shorter analysis times. Consequently, paper-based titration can be considered a green approach in modern analytical chemistry with potential to replace conventional experimental practices in teaching laboratories.

Agradecimentos/Acknowledgments

UFG, IFG, CNPq, FAPEG and INCTBio.

¹Santos-Neto, H.A. et al., Trends in Analytical Chemistry, 158, 2023, 116893.

²Nguyen, M.P. et al., Analytica Chimica Acta, 1100, 2020, 156-162.

³Tian, T. et al., Lab on a Chip, 16, 2016, 1139-1151.

Parâmetros de qualidade como ferramentas para a diferenciação entre marcas de cigarros comercializadas no Brasil

Lucas Soares Rodrigues (PG)¹ ; José Marcus de Oliveira Godoy (PQ)²

lucassrodrigues31.12.2014@gmail.com; jmgodoy@puc-rio.br

^{1 e 2}Departamento de Química, Pontifícia Universidade Católica do Rio de Janeiro (PUC-Rio)

Cigarros, Contrabando, Diferenciação, Análises Gravimétricas, Métodos Analíticos.

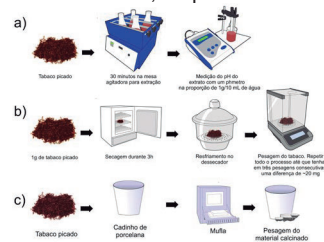
Highlights

Quality parameters as tools for differentiating between brands of cigarettes marketed in Brazil. Development of an analytical method for determining the quality parameters and differentiation between cigarette brands.

Resumo/Abstract

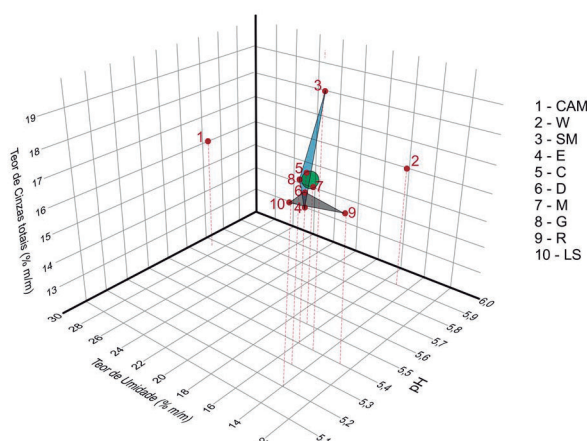
O tabaco (*Nicotiana tabacum* L.) é uma planta cultivada no mundo todo, tendo grande importância econômica e social. Atualmente cerca de 8 milhões de mortes são associadas ao tabagismo. Visando um maior controle, medidas de fiscalização foram adotadas por órgãos regulamentadores, uma vez que o tabaco é conhecido por conter diversas substâncias nocivas ao organismo humano. Alinhado a este fato, ainda se tem a presença de cigarros contrabandeados no mercado nacional. Nos últimos 6 anos ocorreram aumentos sucessivos da participação de cigarros ilegais (contrabandeados ou falsificados) no mercado nacional, ao ponto de, somente na última década o Estado brasileiro ter deixado de arrecadar 70 bilhões de reais devido a presença desses produtos no território nacional. Fatores como acidez, umidade, teor de silicatos e óxidos metálicos constituem parâmetros importantes para a verificação da qualidade deste produto. Este trabalho almejou propor uma diferenciação entre marcas de cigarros comercializadas no Brasil a partir de parâmetros gravimétricos (% cinzas totais e % de umidade) e de acidez (pH). Selecionou-se marcas de cigarros que melhor representam o mercado nacional, sendo marcas de cigarros legalizadas e contrabandeadas. As amostras de cigarros foram compradas em tabacarias locais. Os procedimentos para a medição de cada um dos parâmetros são ilustrados a seguir. (Fig.1).

Fig.1. Esquema das metodologias analíticas adotadas, onde a), b) e c) referem-se os métodos para determinações do pH, % umidade e % cinzas totais, respectivamente.



Os resultados (Fig.2) mostraram que todas as marcas apresentaram valores de pH do extrato abaixo de 6, significando uma menor oferta de nicotina livre para os consumidores. No entanto, todas as marcas apresentaram % cinzas totais acima do recomendado (acima de 12%, recomendado pela ANVISA), significando a presença elevada de óxidos metálicos e silicatos nos produtos. Além disso, cerca de 70% das marcas analisadas apresentaram % de umidade acima do recomendado (acima de 14%, recomendado pela ANVISA), podendo contribuir para o aumento da presença de microrganismos nos produtos e do aumento do diâmetro das partículas emitidas durante a combustão do cigarro.

Fig.2. Resultado do processo de medição dos parâmetros e correlação entre as marcas estudadas



Também foi possível diferenciar as marcas de cigarros contrabandeadas, representadas pelos números 3, 4 e 8 das demais marcas de cigarros. Além disso, as marcas pertencentes as mesmas empresas se agruparam próximas umas das outras (pontos 5 e 7 e pontos 6,9 e 10), com exceção das marcas 1 e 2.

Agradecimentos/Acknowledgments

À CNPq, à CAPES e à PUC-Rio

46ª Reunião Anual da Sociedade Brasileira de Química: "Química: Ligando ciências e neutralizando desigualdades"

Área: ANA

Plataforma de sensoriamento colorimétrica baseada em papel modificada com indol para detecção de nitrito

Bianca Fagundes Teles (IC)¹, Pedro Victor Valadares Romanholo (PG)¹, Suzana M. L. de Oliveira Marcionilio (PQ)², Livia Flório Sgobbi (PQ)^{1*}

bianca@discente.ufg.br; livia_sgobbi@ufg.br

¹Instituto de Química, UFG; ²Departamento de Química, IFGO – Rio Verde

Palavras Chave: Nitrito, Sensor colorimétrico, Sensor de papel, Indol, Smartphone.

Highlights

Paper-based colorimetric sensing platform modified with indole for nitrite detection. The reaction between indole and nitrite in acidic medium forms a pink-red product. The color change is seen by naked eye for qualitative analysis and recorded using a smartphone for quantitative ones.

Resumo/Abstract

A determinação do nitrito é uma questão muito importante do ponto de vista ambiental e de saúde. O nitrito é utilizado como conservante em alimentos, para inibir a proliferação de microorganismos. Tanto o nitrito, como o nitrato, ocorrem em ambientes aquáticos como parte do ciclo biogeoquímico do nitrogênio. A contaminação da água por compostos nitrogenados pode levar a processo de eutrofização. Segundo os padrões estabelecidos pela legislação (CONAMA), o teor máximo tolerado de nitrito é de 1,0 mg/L para manter o padrão de potabilidade. Os métodos mais usados para detecção do nitrito são os espectrofotométricos, como o método de Griess, que utiliza a sulfanilamida e N-(1-naftil)-etilenodiamina, como reagentes. O presente projeto tem o objetivo de desenvolver um método alternativo ainda mais simples para a detecção similar através de um sensor colorimétrico em papel cromatográfico. Utilizou-se o indol como reagente a partir de uma solução em meio ácido. A reação entre uma solução de indol em meio de ácido clorídrico (5 mol/L) na presença de nitrito de sódio (50 mg/L) resulta em um composto rosa. A concentração do indol foi variada entre 0,05% e 25% (m/v) dissolvido em etanol. Encontrou-se um melhor resultado em termos de coloração na concentração de 5%, já a concentração do ácido se manteve fixa durante a fase de testes. A proporção entre os reagentes variou entre 3:1 a 2:6 microlitros, devido ao tamanho da zona de detecção com diâmetro de 5 mm, feito sobre o papel cromatográfico com caneta permanente, a proporção de 2:2 demonstrou resultados mais homogêneos. A ordem de deposição dos reagentes que apresentou melhores resultados, até então, consiste em adicionar primeiro o indol, e posteriormente o ácido. Durante a realização de testes de otimização foram obtidas imagens das zonas reacionais a partir do uso de smartphone. Os resultados obtidos até o presente momento indicam caminhos para a variação de outros parâmetros, como concentração do nitrito e de ácido, a distância entre o smartphone e a zona de detecção para aquisição de imagens, e estudos de interferentes.

Agradecimentos/Acknowledgments



Predictive models for forensic soil identification in georeferenced databases

Luciana Rodrigues Mendes (PG), Márcia Andreia Mesquita Silva da Veiga (PQ). *

luciana.mendes@usp.br; marcia.veiga@usp.br*

¹Chemistry Department, FFCLRP, University of São Paulo.

Keywords: Forensic science, soil provenance, predictive models, trace evidence.

Highlights

Publicly available soil data was used to build predictive maps using QGIS for classifying pixels with attributes matching samples in criminal investigations, reducing the search area at crime scenes.

Abstract

Soil is a common and helpful source of information in criminal investigations. The lack of robust databases in Brazilian soil profiles and composition evidences the need for alternate and transparent methods to identify soil samples in related crime scenes. Hence, this work has the purpose of utilizing rasters with soil attributes and confidence limits, such as silt, clay and sand content, pH, apparent density, and cation exchange capacity, publicly available through government agencies, specifically Embrapa, on their GeoINFO platform in 90 m spatial resolution to build predictive soil sample provenience maps in different locations in the metropolitan region of Ribeirão Preto. This prediction has significantly reduced the extension of the original search area. Each resultant raster was computed from an algorithm that searched and classified pixels in which all the six conditions as compositional attributes were satisfied in the samples in question. This tool can be incorporated into criminal investigations, helping to determine the authorship and materiality of a crime.

Figure 1: % of probable search area reduced after the target values and confidence values were computed into an algorithm.

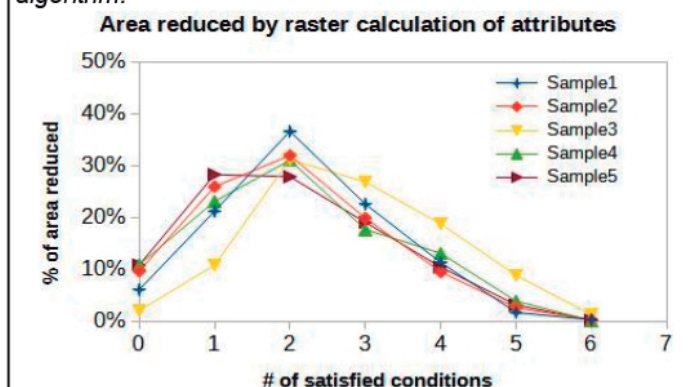


Figure 2: Probability density heatmap resultant from six different soil attribute rasters for Sample1 (QGIS 3.24.3)

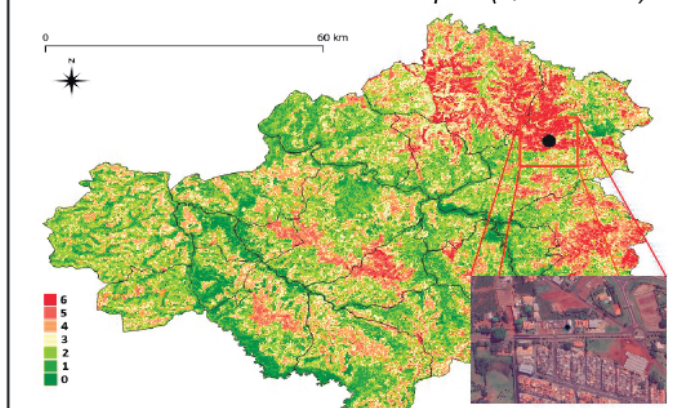


Figure 3: Algorithm used to combine different soil attribute rasters according to target values and confidence limits of questioned samples

```
(lwr_pmtr <= "sand_xdepth" AND "sand_xdepth" <= uppr_pmtr) + ( lwr_pmtr <= "silt_xdepth" AND "silt_xdepth"<= uppr_pmtr) + ( lwr_pmtr <= "clay_xdepth" AND "clay_xdepth" <= uppr_pmtr ) + ( lwr_pmtr <= "apdensity_xdepth" AND "apdensity@1_xdepth" <= uppr_pmtr) + (lwr_pmtr <= "pH_xdepth" AND "pH_xdepth" <= uppr_pmtr) + (lwr_pmtr <= "CEC_xdepth" AND "CEC_xdepth" <= uppr_pmtr)
```

Acknowledgments

This work has been supported by the Brazilian research agency CNPq (Conselho Nacional de Desenvolvimento Científico e Tecnológico) and financed by Coordenação de Aperfeiçoamento de Pessoal de Nível Superior – (CAPES/PROCAD), finance code 001.

Procedimento automático baseado em multicomutação em análise em fluxo para determinação fotométrica de alumínio em águas potáveis

Eliei Brandão^{1,3}, Boaventura F. Reis². ¹Universidade Federal do Amazona (UFAM); ²Centro de Energia Nuclear na Agricultura, Universidade de São Paulo, Piracicaba, SP, Brasil; ³Universidade Federal de São Carlos (UFSCar).

e-mail: reis@usp.br

Palavras Chave: Método automático, Determinação fotométrica de alumínio em águas, fotômetro de LED, cela de fluxo de caminho óptico longo, controle e aquisição de dados com Arduino Due.

Highlights

Automatic procedure based on multicommutation in flow analysis for photometric determination of aluminum in drinking water.

Flow analysis setup controlled by an Arduino Due board, High sensitivity homemade LED based photometer; Flow cell of long optical pathway, Analytical method environmentally sustainable.

Resumo/Abstract

O alumínio é usado em diversas atividades industriais, e sua presença em águas de superfícies e subterrâneas é considerada ocorrência natural. Compostos de alumínio são usados no processo de purificação de água para consumo, podendo aparecer de forma residual. O Ministério da Saúde do Brasil estabeleceu que o limite máximo permissível é $200 \mu\text{gL}^{-1}$ (Portaria GM/MS Nº 888, 04/05/2021), a qual está abaixo dos limites de detecção dos métodos analíticos baseados em espectrofotometria UV-vis. Neste trabalho, empregamos um fotômetro constituído por um LED de alto brilho e um fotodiodo encapsulado na mesmo invólucro com a unidade de amplificação de sinal. O fotômetro foi projetado para trabalhar com cela de detecção (cela de fluxo) com caminho óptico longo¹, visando alcançar sensibilidade para atender o limite legalmente estabelecido, sem recorrer a uma etapa de pré-concentração.

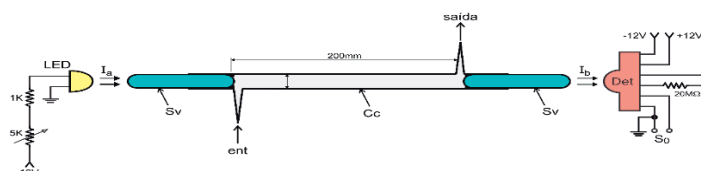


Diagrama do fotômetro de LED. LED = diodo emissor de luz ($\lambda_{\text{max}} = 540 \text{ nm}$); Sv = cilindros de vidro, 20 mm de comprimento e 2,0 mm de diâmetro; Cc = corpo de a cela de fluxo, diâmetro interno de 2,0 mm; Det = fotodetector OPT301(Burr Brawn); I_a e I_b = feixes de radiação eletromagnética emitida pelo LED e recebida pelo fotodetector, respectivamente; ent = entrada de fluido; S_0 = sinal gerado pelo fotômetro (mV).

O cromoazurol S usado como reagente cromogênico, forma composto com os íons Al^{3+} , e em $\text{pH} \approx 6$, absorve radiação em comprimento de onda em torno de 545 nm^2 . O método proposto apresentou as seguintes características: Faixa de resposta linear, $50 - 300 \mu\text{gL}^{-1}$ ($r^2 = 0,999$), limite de detecção, $61 \mu\text{gL}^{-1}$; faixa de recuperação, 94 - 117%; coeficiente de variação 1,26%; consumo de reagente e geração de efluente por determinação, $16 \mu\text{mol}$ e 1,9 mL, respectivamente. Estes dados demonstram que este método pode ser uma alternativa de baixo custo para análise de água. Atende aos requisitos de química limpa; parâmetro considerado na avaliação da sustentabilidade ambiental de métodos analíticos.

1)T. R. Dias, M. A. S. Brasil, M. A. Feres, B. F. Reis, Sens. Actuators B 198 (2014) 448–454.

2) R. B. R. Mesquita, A. O. S. S. Rangel, J. Braz. Chem. Soc., 19 (2008) 1171-1179.

Agradecimentos/Acknowledgments
INCTAA, CAPES, CNPQ.

Área: ANA

Production of a latent fingerprint developer for wet and non-porous surfaces from industrial residue

Ramana R. S. Souza (IC), Rafael M. Dornelas (PQ), Wagner F. Pacheco (PQ)

ramanaramalho@id.uff.br

Departamento de Química Analítica, Universidade Federal Fluminense, Laboratório Peter Sørensen de Química

Keywords: forensic chemistry, developer, fingerprint, small-particle reagent

Highlights

Development of a latent fingerprint developer for wet and non-porous surfaces. Sustainable and economic characteristics. The efficiency of this material is comparable to the imported product.

Abstract

Fingerprints are one of the essential pieces of evidence for human identification. Therefore, identification becomes even more necessary when dealing with a criminal investigation. These fingerprints, composed chiefly of lipids¹, form an image when they are deposited on the surface and may not be visible or latent. Consequently, a developer is required so that the image left by the sebaceous residues can be highlighted and finally revealed. This project aimed to develop a synthetic route for producing a latent fingerprint developer for wet and non-porous surfaces, such as glass, metal, and some plastics², called small particle reagent (SPR). This developer, composed of surfactant, water, iron ore, and choline chloride, started to be produced from the surfactant preparation, in which 2 mL of Triton X-100 was added to 1 g of choline chloride in 250 mL of water. After the first step, 20 mL of the prepared surfactant and 3g of residue (obtained from a Ternium steel mill in Santa Cruz/RJ) were used and mixed with 180 mL of water. The application of the reagent was crucial to avoid damaging the deposited image. To achieve broader coverage without causing disruption and to simplify the process, it was necessary to use a spray applicator. In order to corroborate the efficacy of the product, tests were performed, as shown in Figure 1. The result of the tests could be seen as the characteristic points of the fingerprint (named minutiae), which are unique for each human being. On account of previous elucidation, it was comprehended that the small particle reagent produced in this project presented satisfactory results in the revelation of latent fingerprints. Thus, it is as efficient as the commercial product, which was used as a comparative (Small Particle Reagent Dark, Sirchie), illustrated in Figure 2. In this regard, this study indicated an alternative way to reduce the cost of imported developers by using a waste of iron ore in their composition. Finally, the cost reduction, added to the national manufacturing, constitutes a more economical and sustainable scenario.



Figure 1: Image revealed on the glass with the SPR produced.

Figure 2: Image revealed on the glass with the imported SPR.

Acknowledgments

CNPq, CAPES, FAPERJ, SBQ and UFF.

References: ¹ CARVALHO, João. Estudo do envelhecimento da composição química de resíduos de impressão digital latente por espectroscopia Raman. Universidade De Brasília Instituto De Física, Brasília 2022. ² BUMBRAH, Gurvinder Singh. Small particle reagent (SPR) method for detection of latent fingerprints: A review. Egyptian Journal of Forensic Sciences 2016.

Production of colored magnetic developer powder from industrial steel waste for latent fingerprint development

Louise G. Franco (IC), Ramana R. S. Souza (IC), Rafael M. Dornellas (PQ), Wagner F. Pacheco (PQ)

louisefranco@id.uff.br

Departamento de Química Analítica, Universidade Federal Fluminense, Laboratório Peter Sørensen de Química Analítica.

Keywords: Gentian violet, Latent fingerprint, Iron magnetic nanoparticles.

Highlights

Colored magnetic powder for latent fingerprint development. Economical and sustainable material. Its efficiency was compared with commercial material (imported).

Abstract

Latent fingerprints are invisible to the naked eye and consist substantially of natural secretions from human skin. For this reason, they must go through a development process to be identified ¹. This work aims to produce a violet color revealing magnetic powder made from steel industry waste dust (Ternium - Santa Cruz/RJ), apply it to different surfaces, and compare it to the market-leading commercial black powder (Sirchie, USA). The production consisted of mixing 15 g of industrial dust in 120 mL of water under agitation for 15 min. After that, the mixture was washed five times with the substances in the following sequence: deionized water, HNO₃ 0.1 mol/L, deionized water, NaOH 0.1 mol/L, and deionized water. From the mentioned compounds, 13 mL were used. Afterward, 300 mL of water, 30 mL of NH₄OH 28% - 32%, and 0.75 g of gentian violet were added to the treated material. The mixture was stirred and heated at 90°C for 30 minutes. Subsequently, the content was filtered, and only the solid resulting from the separation was collected, transferred to a Petri dish, and taken to dryness in the oven. Once it was dried, the solid was crushed until it turned into a fine powder, ready to be used as a latent fingerprint developer. The development of fingerprints with this powder was analyzed on five different surfaces (glass, metal, plastic, paper and cardboard). These analyses showed sufficient clarity in the revelation, considering the efficiency in the counting of digital minutiae - which are structures in the printed lines that differentiate the fingerprints of each person ² - and the contrast on the observed surfaces. Figure 1 represents the application of the powder produced on the glass and 35 minutiae in the regions marked in red. Figure 2 represents the application of the commercial black powder also on glass, and 25 minutiae were observed to compare both materials and prove the powder's effectiveness. The efficiency of the material was evaluated from the deposition in duplicate of a fingerprint on the different surfaces tested (one being revealed by the powder produced in this work and the other by Sirchie's commercial powder) and the count of minutiae obtained on an equivalent surface. Although the number of minutiae found and the definition of the image varied with the solid substrate used in the deposition of the fingerprint, greater clarity and more minutiae were always obtained in this work.



Fig. 1: Minutiae count revealed with produced powder



Fig. 2: Minutiae count revealed with commercial powder

¹INTRODUÇÃO às impressões digitais latentes. **Forensics Brasil**, 2020. Disponível em: < https://www.forensicsbrasil.com.br/catalogos/sirchie/impressoes_latentes.pdf >. Acesso em: 09 de fevereiro de 2022.

²CASADO, R.S. **Extração de minúcias em imagens e impressões digitais**. Universidade de São Paulo. Escola de Engenharia de São Carlos. Departamento de Engenharia Elétrica. São Carlos, 2008.

Acknowledgments

CNPq, CAPES, FAPERJ and UFF.

Qualitative Identification of Synthesized Isoniazid Derivatives by Atemporal Technique: UV-Visible Spectrophotometry

Felipe W. V. Paulino (PG)¹, Aldeneide S. de Paiva (IC)², Leilane G. Rodrigues (IC)², Maria N. Nascimento (IC)², Hécio S. dos Santos (PQ)^{1,2}, and Murilo S. S. Julião (PQ)^{1,2*}.

E-mail: felipe.wesley@aluno.uece.br; murilosan@gmail.com*

¹Programa de Pós-graduação em Ciências Naturais, Universidade Estadual do Ceará (UECE); ²Centro de Ciências Exatas e Tecnologia, Universidade Estadual Vale do Acaraú (UVA/CE).

Keywords: Absorption bands, Chalcones, Hydrazone, N-acylhydrazone, Synthesis.

Highlights

Ultramodern analytical techniques must also be hyphenated with cheaper and less complex techniques such as UV-visible spectrophotometry in the elucidation of structures of organic synthesis products.

Abstract

Introduction: Isoniazid (IZD) containing the hydrazone moiety, has been widely used in the synthesis of N-acylhydrazones with possible pharmacological actions. The IZD is a prodrug used as the first choice for the chemotherapy treatment of tuberculosis, an infection caused by the bacillus *Mycobacterium tuberculosis* (ARRUDA; MACEDO; MACEDO et al., 2020). In the structural identification of organic compounds, spectroscopic techniques are generally used, such as: Fourier-transformed infrared, ¹H and ¹³C NMR, and mass spectrometry, which despite their importance and selectivity in this type of identification, are very expensive, require specialized personnel to handle them and most of the time are difficult to access for most Brazilian teaching and research institutions. Thus, objective of this work was to verify the feasibility of UV-visible spectrophotometry in the qualitative identification of hydrazone compounds obtained from the synthesis reaction between aldehydes and chalcones using the drug isoniazid (IZD).

Materials and methods: The synthesis of N-acylhydrazone (isonicotinic acid (2-hydroxy-benzylidene)-hydrazone) was performed from a mixture of 0.50 mM aldehydes or chalcones and 0.50 mM IZD, deionized water and H₃PO₄ concentrated. For spectral measurements, all solutions of reagents and probable products of synthesis were prepared in ethanol, and spectra were recorded in a UV-Vis spectrophotometer Genesys 10S to the 190-500 nm spectral range.

Results and discussion: Scheme 1(a) presents the synthetic route of the compound called HC4ATIOF (C₁₉H₁₆N₄O₅) from the reaction of chalcone called CPATIOF (C₁₃H₁₁NO) with isoniazid (C₆H₇N₃O), however it is observed through the UV-visible spectra of the reagents and the desired product, Figure 1(A), that the absorption bands of the functional groups of HC4ATIOF compound are actually the same as those of chalcone CPATIOF.

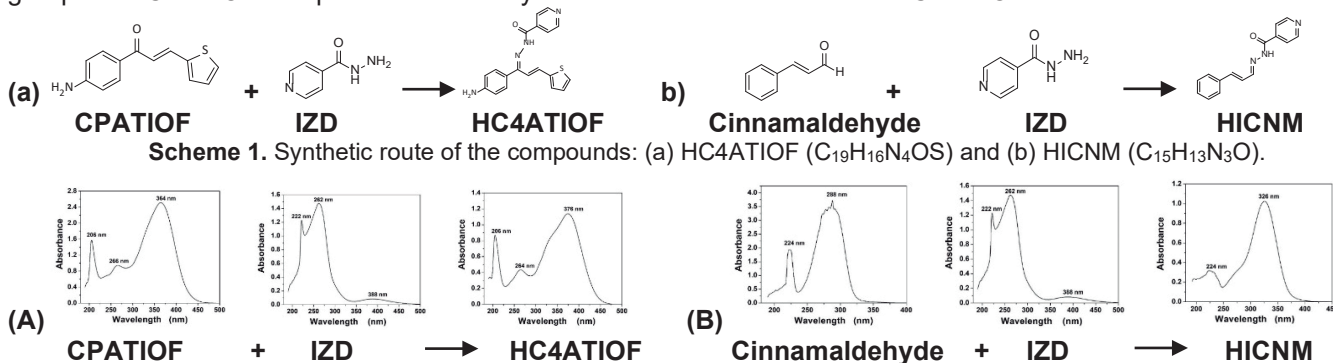


Figure 1. UV-Vis spectra recorded for: (A) 94.3 μM CPATIOF, 559 μM IZD, and 35.0 μM HC4ATIOF; (B) 18,6 μM Cinnamaldehyde; 559 μM IZD, and 29,9 μM HICNM.

Conclusions: The spectra registered in the UV-visible region made it possible to affirm the occurrence of the synthesis of acylhydrazones from aldehydes, since the absorption bands registered in the spectra of the reagents and product obtained are completely different, this indicates that the registered spectrum is of a new substance, HICNM, Figure 1(B). On the contrary, synthesis of acylhydrazones from chalcones were not successful, because when comparing the UV-Vis spectra of the reagents with that of the desired products, it is seen that the spectral profiles of the latter are practically identical to those of the chalcones used and this fact may be related both to the lower reactivity of the conjugated ketone and steric hindrance present in the chalcone structures. Based on these assumptions, it's possible to affirm the viability of using a century-old analytical technique, as UV-visible molecular absorption spectrophotometry in the qualitative identification of organic synthesis products.

References: ARRUDA, I. E.; MACEDO, B. V. S.; MACEDO, J. C. et al. *Química Nova*, v. 43, p. 642-648, 2020.

Acknowledgments

To FUNCAP for the financial support granted. Processes: BP4-00172-00017.01.00/20 and BP4-0172-00075.01.00/20.

Rapid detection of Chikungunya virus (CHIKV) by RT-LAMP for point-of-care applications

Laura Souza Abdallah (IC),^{1*} Kézia Gomes de Oliveira (PG),¹ Ana Maria Bispo de Filippis (PQ),² Gabriela R. Mendes Duarte (PQ).¹

lauraabdallah@discente.ufg.br; lauraabdallah@discente.ufg.br

¹Instituto de Química, UFG; ²Instituto Oswaldo Cruz, Fiocruz.

Key words: *chikungunya, molecular tests, Point-of-Care testing, serum samples*

Highlights

The molecular test developed is capable of diagnosing CHIKV in 20 minutes, directly in serum samples. Due to its easy interpretation and simple execution, the low-cost test can be applied at POCT.

Resumo/Abstract

Chikungunya is a disease caused by the chikungunya virus (CHIKV) and its main symptoms are: fever, headache, nausea, myalgia, rash, arthralgia severe and persistent, which may last for weeks or years in chronic cases of illness. Most of the symptoms can be confused with other arboviruses, like dengue and zika virus. Considering the similarity of the initial symptoms of chikungunya with a series of other infections, especially dengue, it is essential that the public health system has access to rapid, unequivocal, and low-cost diagnostic tests for the differential diagnosis of patients, so that control measures and epidemiological surveillance are fulfilled. In this study, we propose the development of a rapid, sensitive, and low-cost molecular diagnosis capable of detecting the RNA of the CHIKV directly in serum samples, without the extraction step, with high sensitivity and specificity. The test developed here uses the reverse transcription technique followed by loop-mediated isothermal amplification (Reverse transcription loop-mediated isothermal amplification - RT-LAMP) and has great potential for application in places with scarce laboratory infrastructure because it is a simple test, with colorimetric detection of results using pH indicators. After optimization of reaction, RT-LAMP mixture contained 2 μM of external primers, 16 μM of internal primers, 8 μM of loop primers and 1.5 μL of serum sample. The assays were isothermally heated at 68 °C for 20 min and at the end of the incubation time, all tubes were removed from the thermoblock and the results were interpreted based on the color of the reaction, which changed from pink (negative) to yellow (positive) (Figure 1A).

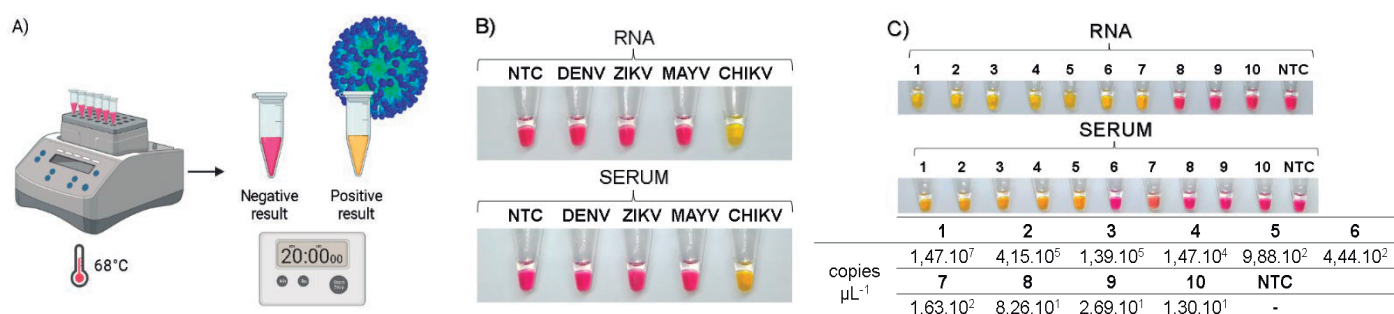


Figure 1. A) Methodology used for colorimetric detection, B) Analytical specificity and C) Analytical sensitivity of CHIKV detection by RT-LAMP from RNA and directly in serum samples.

With optimized reaction conditions, we confirmed the high specificity of the primers, not showing cross-reactions with Dengue, Zika and Mayaro viruses (Figure 1B). The limit of detection was 1,63.10² copies. μL^{-1} for RNA and 9,88.10² copies. μL^{-1} for serum (Figure 1C). A panel of 58 CHIKV RNA samples and 58 serum samples were blind tested. The detection showed 74.36% sensitivity, 100% specificity, and 85.29% accuracy for serum. The success of the results obtained in the panel of real samples demonstrated the great applicability of the test at the point-of-care, since the test does not require sample preparation or use sophisticated equipment and the results are easy to read, taking 20 minutes to perform a molecular test with high reliability.

Agradecimentos/Acknowledgments

Laboratório de Biomicrofluidica, Universidade Federal de Goiás, CNPq and Fiocruz.

RESTRICTED ACCESS MOLECULARLY IMPRINTED MICROEXTRACTION FOR THE DETERMINATION OF ANTI-HELMINTICS IN MILK SAMPLES

Amanda A.M. Lourêdo (PG)¹, Helton Hanchuck Pereira (IC)¹, Gabriel O.A. Costa (IC)¹, Rudy Bonfilio (PQ)² Mariane Gonçalves Santos (PQ)¹.

amanda_marques17@hotmail.com; amanda_marques17@hotmail.com

¹Departamento de Química, UNIFAL-MG; ²Faculdade de Ciências Farmacêuticas, UNIFAL-MG

Palavras Chave: Anti-helmínticos; Polímeros molecularmente impressos de acesso restrito; Extração em ponteiros descartáveis; Micro extração em fase sólida, HPLC-UV

Highlights

- Restricted molecularly imprinted polymer coated with BSA (RAMIP-BSA), was synthesized for selective extraction of albendazole and mebendazole in milk samples for the determination using HPLC-UV.
- The polymer was characterized by FT-IR, thermogravimetry and the capacity of exclude macromolecules, as well as the adsorption kinect and isotherm were evaluated.
- RAMIP-BSA was then used for the direct extraction of mebendazole and albendazole from milk samples.

Introdução

A elevada utilização de anti-helmínticos na medicina veterinária tem despertado preocupação em relação ao consumo de alimentos derivados de animais, devido a possibilidade de resíduos desses fármacos causarem problemas à saúde dos consumidores expostos¹. Para que seja possível monitorar a presença e a concentração desses fármacos em alimentos, são necessários métodos analíticos, eficientes, robustos, rápidos e confiáveis. Neste sentido, a síntese e utilização de sorventes multifuncionais, como os polímeros de acesso restrito molecularmente impresso (RAMIP) apresentam-se como uma alternativa promissora para a extração de anti-helmínticos de amostras complexas como o leite, visto que são capazes de reter seletivamente os analitos de interesse e impedirem a adsorção de macromoléculas como as proteínas na superfície do material extrator². Nesse contexto, foram sintetizados e caracterizados os polímeros RAMIP e RAMIP-BSA que são polímeros de impressão molecular de acesso restrito revestidos com monômeros hidrofílicos e albumina sérica bovina, para a micro extração direta em ponteira de pipeta de albendazol e mebendazol em amostras de leite, seguida da determinação por cromatografia líquida de alta eficiência com detecção ultravioleta (HPLC-UV). formação de uma superfície hidrofílica sobre o RAMIP. Em seguida, realizou-se o revestimento com albumina sérica bovina, gerando o RAMIP-BSA. Os materiais foram caracterizados por

análise termogravimétrica e por Espectroscopia no Infravermelho por Transformada de Fourier para verificar a eficiência da síntese e revestimento com a BSA. Os materiais obtidos RAMIP e RAMIP-BSA foram submetidos a testes de exclusão de proteínas sendo que as taxas de exclusão foram de 82 e 94,7% respectivamente, quando percolada uma solução aquosa de 1 mg mL⁻¹ de caseína. Os teste preliminares foram feitos em soro de leite e leite bovino sendo os melhores resultados de adsorção obtidos com soro de leite. Além disso, estudos de cinética e isothermas de adsorção foram realizados. Para a cinética o equilíbrio foi atingido em 5 minutos e o modelo que mais se adequou foi o de pseudo-primeira ordem. Para a isoterma, o melhor ajuste foi obtido com o modelo de SIPS e o equilíbrio de adsorção ocorreu em torno de 600 ng mg⁻¹ de material. Para a determinação cromatográfica dos analitos, as condições ideais foram otimizadas e os melhores resultados foram obtidos com coluna analítica C18 25 cm X 4,6mm, fase móvel tampão fosfato 0,05M e metanol (40:60) e detector de UV em 295 nm. A extração foi inicialmente otimizada por meio de um planejamento fatorial completo 2⁴ em que foram avaliados volume de amostra e eluente (metanol), pH da amostra e massa de adsorvente (RAMIP-BSA).

Conclusão

As análises realizadas com o material obtido, mostraram-se promissoras, pois em diferentes testes há adsorção seletiva dos analitos e exclusão simultânea de proteínas em uma única etapa, sem necessidade de tratamentos prévios.

Referência

1 YOO, Kyung-Hee. *et al.* *Journal of pharmaceutical analysis*, v. 11, n. 1, p. 68-76, 2021.

2 DE OLIVEIRA, Gabriel. *et al.* *Analytical and bioanalytical chemistry*, v. 405, n. 24, p. 7687-7696, 2013.

Agradecimentos/Acknowledgments

CAPES, FAPEMIG, CNPQ.

Salting-out induced liquid-liquid microextraction for antidepressant drugs determination in hospital effluent by LC-MS

Darlina M. Souza (PQ)*, Renata V. Correa (IC), Luana Formagini (IC), Natalia P. Rocha (IC), Luana D. Silveira (IC), Gabriel V. Larruscahim (IC), Ana Luiza G. Mendes (PG), Jaqueline F. Reichert (PQ), Paola A. Mello (PQ).

darliana.souza@ufsm.br

Departamento de Química, UFSM

Palavras Chave: SILLME, Microextraction, Salting-out, Hospital effluent, Psychodrugs.

Highlights

- ✓ An eco-friendly, robust, and cost-effective salting-out induced liquid-liquid microextraction (SILLME) method coupled with LC-MS was developed for the preparation, extraction, and quantitative determination of antidepressant drugs in hospital effluent samples.
- ✓ Method developed includes antidepressant drugs: sertraline, venlafaxine, and escitalopram.

Abstract

The consumption of antidepressants has increased on a global scale. These medications are frequently prescribed to treat mental health-related disorders and their usage is expected to rise in the future because the COVID-19 pandemic has intensified these problems significantly. These compounds have recently been detected in several environmental compartments, raising concerns about their potential impacts. Despite some progress and excellent studies, remains a need for research, especially in the development of fast, simple, and sensitive methods for the extraction and unambiguous determination of these analytes. In this regard, this study aimed to develop a time and cost-effective multi-residue method to extract and determine three antidepressant drugs in hospital effluent. Target analytes were sertraline, venlafaxine, and escitalopram. The quantification was performed with liquid chromatography quadrupole mass spectrometry (LC-MS, model LCMS-2020, Shimadzu, Kyoto). The instrumental conditions for LC-MS were as follows: Shim-pack CLC-OSD column (5 μm , 150 x 4.6 mm); column oven at 35 ° C; injection volume of 10 μL ; gradient elution mode for mobile phase (0.4 ml min^{-1} constant flow) composed by (i): eluent A - 5 mmol L^{-1} of ammonium formate containing 0.1% formic acid and (ii) eluent B - acetonitrile containing 0.1% formic acid; total running time of 12 min; electrospray ionization in positive mode. The SILLME technique was optimized for analyte extraction. The critical factors that influence the extraction efficiencies of the target analytes, such as the type of extraction solvent and salting-out reagent, volume of extractant, salt amount, sample pH, and sample volume, were investigated. The optimum conditions were attained using 10 ml of sample, at pH 9, and 2 ml of ethyl acetate, with the addition of 2 g sodium sulfate, followed by agitation (2 min) and centrifugation (5 min). Finally, the supernatant was removed, evaporated under nitrogen flow at 40 ° C, and resuspended in methanol for analysis by LC-MS. The method was developed and validated according to the International Conference on Harmonization guidelines M10 and SANTE (2021). The method was linear, accurate, and precise. The results showed that the salting-out induced liquid-liquid microextraction is a suitable method for the quantification of antidepressant drugs in hospital effluent. The proposed SILLME method has some advantages in terms of sensitivity, easiness, solvent consumption, and waste reduction.

Acknowledgments

CAPES, FAPERGS, CNPq, and UFSM.

Sample preparation and electrochemical detection: combining gas diffusion extraction with miniaturized electrochemical devices for nitrite quantification

Diele A.G. Araújo (PQ)^{1*}; Ana C.M. Oliveira (PG)²; Regina M. Takeuchi (PQ,^{2,3}; André L. Santos (PQ)^{2,3}; Rodrigo A.A. Munoz (PQ)²; João Flávio S. Petrucí (PQ)²; Thiago R.L.C. Paixão(PQ)¹.

dielearaujo@usp.br

¹Institute of Chemistry, Department of Fundamental Chemistry, USP, ²Instituto de Química, UFU; ³Instituto de Ciências Exatas Naturais do Pontal, UFU.

Palavras Chave: Separation Method, Miniaturization, Electrochemical Sensors, Electroanalysis.

Highlights

Gas-diffusion extraction and electrochemical detection in a single step. Inexpensive analytical system for nitrite determination.

Resumo/Abstract

Nitrite is used as a food additive and preservative (E249–E252), mainly for meat products, inhibiting the growth of microorganisms. However, exposure to excessive amounts of nitrite can cause serious health problems. Most conventional analytical methods are time-consuming, high-cost, and require several sample preparation steps. This study presents a simple and low-cost 3D-printed analytical device for quantifying nitrite coupling gas-diffusion extraction and electrochemical detection in a single step. The miniaturized electrochemical sensor was fabricated using micropipette tips and metallic wires (Pt and Ag). The device was assembled by inserting a 3D printed and miniaturized electrochemical cell (acceptor reservoir) in the glass sample reservoir, which was filled with 10 mL of the nitrite standard or sample solutions and 1 mL of HCl 12 mol L⁻¹. PTFE (Polytetrafluoroethylene) membranes (pore size of 1 μm; Amanco, Brazil) allowed gas diffusion of the generated NO₂ and separation between the sample reservoir (donor solution) and the electrochemical cell containing the acceptor solution (supporting electrolyte). Figure 1-A showed that good analytical performance (LOD = 58 μmol L⁻¹ and R² = 0.99596) was obtained for the analytical curve constructed using 500 μL of nitrite standard solutions without extraction by gas diffusion, indicating that the sensor has great potential for nitrite determination. Next, we evaluated the proposed system's potential to detect nitrite after gas extraction.

Figure 1: A) Analytical curve constructed in the linear range of 100 to 1100 μmol L⁻¹. **B)** Real-time extraction curve for 100 μmol L⁻¹ of the nitrite in donor solution.

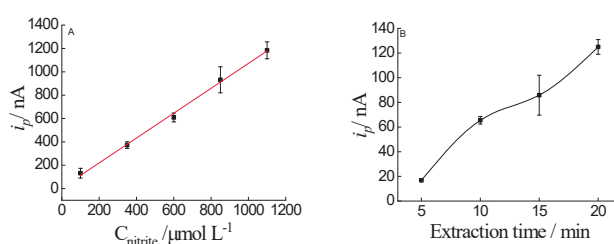


Figure 1-B shows a sharp increase in the nitrite signal during the first 20 min of the extraction, indicating that nitrite can be extracted and collected by the supporting electrode. Further optimization will be performed to improve the analytical performance of the method. The preliminary results demonstrated that the approach described here is a promising way to fabricate a simple, efficient, and cost-accessible analytical device that couples the sample preparation step and electrochemical detection for quantifying nitrite in food samples.

Agradecimentos/Acknowledgments

CNPq, Fapemig, Finep, Capes and FAPESP.

Sample preparation of edible insects for potential toxic elements determination

Gustavo Gohlke (IC),¹ Thiago C. Pereira (PG),¹ Cristian R. Andriolli (PG),¹ Vitoria H. Cauduro (PG),¹ Alessandra S. Henn (PQ),^{1,2} Érico M. M. Flores (PQ)^{1*}

gustavogohlke@gmail.com; ericommf@gmail.com

¹ Universidade Federal de Santa Maria, Departamento de Química, Santa Maria, RS, Brazil, 97105-900

² Universidade Tecnológica Federal do Paraná, Campus Medianeira, Medianeira, PR, Brazil, 85884-000

Keywords: *Edible insects, MIC, Potential toxic metals, ICP-MS*

Highlights

Sample preparation of edible insects was studied for As, Cd and Pb determination;
Combination of high sample mass, diluted acid and lower carbon content was possible;

Abstract

The consumption of edible insects is an alternative to food demand because they have a higher nutritional value than conventional proteins such as meat. However, these insects may contain potentially toxic elements (such as As, Cd, and Pb) due to the substrate and water used in their production. In this sense, analytical methods for the determination of As, Cd, and Pb in edible insects need to be developed to ensure consumer health and safety. Inductively coupled plasma-mass spectrometry (ICP-MS) is an analytical technique that provides multi-element capabilities and low limits of quantification (LOQ). However, the ICP-MS instrument, when working with the conventional sample introduction system, requires samples in a liquid form. In this sense, a previous sample preparation step is required. Microwave-induced combustion (MIC) is a sample preparation method that promises low carbon and acid concentrations in the final solution compared to conventional acid digestion methods. Thus, the present study goal was to evaluate the use of MIC for the sample preparation of edible insects for further determination of As, Cd and Pb by ICP-MS. For this, samples of edible insects (cricket, beetle, grasshopper, and tenebrio molitor larva) were dried, ground and pressed into pallets for combustion. The maximum sample mass (100 to 600 mg), the concentration of HNO₃ used as absorbing solution (3 to 14.4 mol L⁻¹), reflux step time (5 to 15 minutes), and mass of microcrystalline cellulose (100 mg and 200 mg) were evaluated. Microwave-assisted acid digestion in a single reaction chamber (MAWD-SRC) was used as a reference method. For MAWD-SRC a sample mass of 300 mg and 6 mL of 14.4 mol L⁻¹ HNO₃ were used. The accuracy evaluation was performed using two certified reference materials of fish protein (DORM-3 and DORM-5). The residual carbon content of solutions obtained by both methods was determined by inductively coupled plasma optical emission spectrometry (ICP-OES). Masses of 500 mg of cricket were combusted by MIC without exceeding the maximum pressure of the system. Recoveries higher than 90% were obtained for As, Cd and Pb using 7 mol L⁻¹ HNO₃ as absorbing solution and a reflux time of 5 minutes for cricket, beetle, and grasshopper samples. However, due to the high ash content (13%), tenebrio molitor larva sample showed only 75% recovery for As. In this sense, the addition of 100 mg of microcrystalline cellulose was necessary to increase As recovery. The residual carbon content of the solutions obtained after MIC was lower than 13.6 mg L⁻¹, while for MAWD-SCR (reference method) was about 150 mg L⁻¹. For As, Cd, and Pb, there was no significant difference (t-test, 95% confidence level) between the MIC and MAWD-SRC results in all the samples studied. No significant difference (t-test, 95% confidence level) was found between the proposed method and the certified values for DORM-3 and DORM -5. The MIC method provided LOQs of 6.59, 3.38, and 39.7 ng g⁻¹ for As, Cd, and Pb, respectively, and the MAWD-SRC method resulted in LOQs of 46.9, 8.60, and 54.5 ng g⁻¹ for As, Cd, and Pb, respectively. Therefore, the MIC method proved to be a promising sample preparation method for edible insects and further As, Cd, and Pb determination, combining solutions with lower carbon content, diluted acids, and higher sample mass.

Acknowledgments

The authors would like to thank CNPq, FAPERGS and CAPES.

Seminal zinc determination in semen stain using digital image analysis: a comparison between solutions and solid support

Leandro G. Benzi (PG),¹ Maria das Graças A. Korn (PQ),¹ Rodolfo M.M. Santana (PQ),¹

leo-benzi@hotmail.com; rodolfommsantana@gmail.com; korn@ufba.br

¹Departamento de Química, UFBA

Keywords: Colorimetry, Zinc, PAN, Biological Fluid, Visual Detection

Highlights

An analytical method was developed to seminal zinc determination in semen stain.

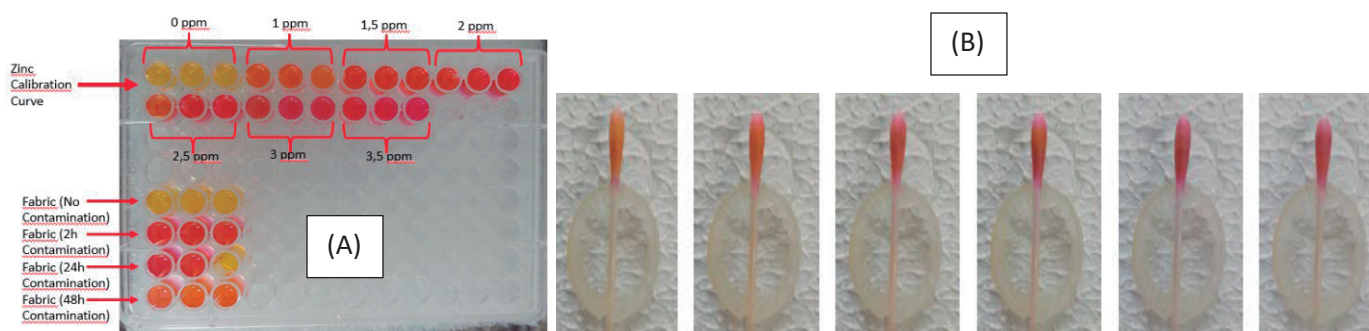
Smartphone camera was used to image acquisition and analysis.

Image analysis performed in solution and solid support.

Resumo/Abstract

The 1-(2-pyridylazo)-2-naphthol (PAN) spectrophotometric method has been extensively evaluated for seminal Zn determination¹. However, digital colorimetric analysis is poorly exploited for Zn(PAN)₂ complex, especially for forensic purposes. The present work proposes an analytical method to seminal zinc determination in semen stain using smartphones for image acquisition. Aqueous media and solid, on cotton swab cellulose fiber, were evaluated for impregnation and measure of the Zn(PAN)₂ complex (Figure 1). Chromogenic solution was prepared containing PAN, BR buffer pH 9,5 and masking agent citrate, fluoride, iodide, tartrate and thiosulfate. To perform real sample analysis, the fabric was contaminated with 200 µL of semen with different drying time: 2, 24 and 48h and then added to a solution containing triton x-100(1%v/v) to stain extraction. A better sensitivity was observed to R and B channels for images in cotton swab cellulose fiber and aqueous solution respectively. However, no significant differences between methods sensitivity were observed ($S_R/S_B = 1,03$). Both methods presented good linearity ($R^2 \geq 0.99$) with LOD 0,20 and 0,12 mg/L for cellulose fiber and solutions respectively. The color changes in the plate are much clearer, but the cotton swab is an interesting alternative to quick and auto tests, analysis kit and other possibilities to develop a simple and portable method. No significant differences were observed ($p=0.05$) between signals generated by the two methods regardless of the contamination time with the semen.

Figure 1. Image analysis for Zn(PAN)₂ complex on (A) 96 well-plate and, (B) cotton swab color change: $C_{Zn}=0$ to 3 mg/L



¹Fuentes, J; Miró, J.; Riera, J.; Simple colorimetric method for seminal plasma zinc assay. *Andrologia*, v 14, p. 322-327 (1982)

Agradecimentos/Acknowledgments



Sound spectrometry: Propose a new analytical technique for determining the majority components in liquid matrices.

Lorryne Moreira Zampier (PG),¹ Sergio Lineu Olivo (PG),² André Fernando de Oliveira (PQ),^{1*} Álvaro Viana Novaes de Carvalho Teixeira (PQ),³ Maria Eliana Lopes Ribeiro de Queiroz (PQ),¹ Antônio Augusto Neves (PQ),¹ Rafael Ferrari (PQ),².

andref.oliveira@gmail.com;

¹Departamento de Química, UFV; ² Faculdade de Engenharia Elétrica e de Computação, UNICAMP; ³ Departamento de Física, UFV

Palavras Chave: Sound frequency, Wine, Alcohol, Acidity, Sugars, Chemometrics

Highlights

Sound Frequency is used for majority components; a low cost and chemometric wine analysis instrumentation is proposed; a new analytical technique emerged.

Resumo/Abstract

Introduction The sound and ultrasound are mechanical waves, and therefore the propagation occurs through a physical medium. The composition of this medium influenced, for example, the wave velocity and attenuation. Several devices based on the use of ultrasound (2-12 MHz) are known, for the determination of fat, protein and other majorities compounds or fundamental studies of solutions, such as the Eigen studies in the 1950 decades. However, this use of sound has never been proposed. The important limitations of using ultrasound are the electronic complexity and cost of the electronic sound system differently. In this context, we propose a new Sound spectrometry allied to chemometric techniques for determining the majority compounds in liquid samples. For example, this work determines alcohol, sugars and acidity in wine. **Experimental Part** A sound spectrometer system was developed and assembled, which used an oscilloscope (Rigol model D1054Z), in which the signal sent to it was obtained through a signal generator (Dual Channel/DDS Signal Generator/Counter). A software called *PUTTY* was developed for control all system and collect data.

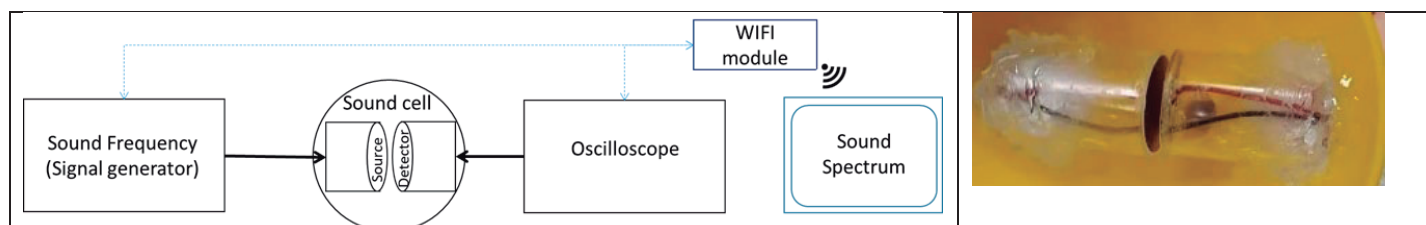


Figure – Scheme of Sound frequency spectrometer and the two piezoelectric transducers in a cell.

Sound cells were made with acrylic tubes and two piezoelectric transducers, in which one was responsible for producing the acoustic waves (source) and the other for receiving them (detector). The distance between the transducers is from 2.5 to 15 mm (Fig.1). A sine wave with a frequency range from 100 Hz to 20 kHz is used. The acrylic tubes cell was rigidly assembled. The spectra of mixtures of alcohol, sugar and acetic acid, besides wine samples, were studied using Principal Components Analysis (PCA) and Partial Least Square (PLS). The smoothing was done with different methods such as Savitzky-Golay, FFT, and Wavelet Transform. The alcohol concentrations had relative errors between 2,5 and 3,9% compared with those obtained by the distiller method. No matricial error was observed. **Conclusion:** In this paper, a new analytical technique was proposed. The sound spectrometer was developed based on the attenuation of sound frequency waves to analyse various liquid matrices. It was found that the instrument was able to recognise standards, grouping different solutions according to their characteristics (qualitative analysis). Furthermore, it was also possible to perform quantitative analysis in authentic matrices, in which a prediction model of the alcohol content in wines was obtained, proving to be fundamental the use of chemometrics and pre-treatments, in this case, through PLS and Wavelet Transform, respectively. The built instrument was of low cost and more straightforward instrumentation. The analysis was carried out more practically and simply than near-infrared or similar to others.

Acknowledgments

FAPEMIG and CNPq

Statistical-based approach to evaluate the influence of synthetic sampling of imbalance datasets on the figure of merits

Alexander de P. Rodrigues (PG),^{1*} Aderval S. Luna (PQ),¹ Licarion Pinto (PQ).¹

alexanderdep.rodrigues@gmail.com;

¹ *Department of Analytical Chemistry, Rio de Janeiro State University, Graduate Program Chemical Engineering, Rua São Francisco Xavier, 524 – Maracanã – Rio de Janeiro, RJ, Brazil, 20550-013*

Keywords: Chemometrics, QSAR, sampling methods, imbalanced datasets, RStudio.

Highlights

Statistical-based approach to evaluate the influence of synthetic sampling of imbalance datasets on the figure of merits

- Synthetic sampling to enhance the figure of merits of imbalance QSAR datasets
- Evaluation of types of sampling and models influence the figure of merits
- Simultaneous enhancement of the figure of merits

Abstract

This work proposed a new approach to study the influence of different types of synthetic sampling and pattern recognition models on three imbalance quantitative structure-activity relationship (QSAR) datasets. This approach evaluates the influence of both the sampling method and pattern recognition algorithm on the figure of merits using an experimental design organization strategy. The factors were analyzed using each figure of merits individually and simultaneously with the Derringer and Suich function. Here the aim was not for optimization but to better understand the influence of synthetic sampling on pattern recognition models' figure of merits and to develop a strategy to choose the sampling and model that may lead to models with robust metrics. For this purpose, three imbalanced QSAR datasets were used. Previously to the classes balancing, it was applied for all datasets, an autoscaling, a near-zero variance filter, and a spatial signal transformation. Three downsamplings (regular downsampling, under-sampling based on Clustering, Tomek-Links), three oversampling (regular upsampling, SMOTE, ADASYN), and two hybrid samplings (SMOTE-TL, SPIDER) methods were used to balance the data sets previously to the evaluation with the proposed strategy. Due to these datasets' non-parametric characteristics, the classification models used were based on support vector machine, radial base function, C5.0, artificial neural network, extreme gradient boosting, and random forest algorithms. All sampling methods and pattern recognition models were performed using R language with the RStudio interface. Over-sampling methods tend to increase the type I error and the accuracy, while downsampling increases and reduces the type I error. Hybrid methods tend to increase all the merits, but it is harder to balance the samples between the classes correctly. Except for the third dataset, over-sampling methods lead to a better overall figure of merits.

Acknowledgments

FAPERJ, CNPq, LEAMS, LTAP, PPGEQ/UERJ, UERJ.

Sulfate determination in waters by Raman Spectroscopy

Elisa M. B. Santos (PG)*, Nilvan A. Silva (PG), Ivo M. Raimundo Jr. (PQ), Wiliam R. Araújo (PQ)

elisamsantos@gmail.com

Instituto de Química, UNICAMP, CP 6154, CEP 13085-563, Campinas, São Paulo

Key-words: Sulfate, Raman Spectroscopy, marine water.

Highlights

Sulfate determination by Raman Spectroscopy

Use of paper-based spot tests in Raman Spectroscopy

Abstract

One of the major problems in offshore oil extraction processes is the incrustation phenomenon, which occurs due to the precipitation of insoluble inorganic salts in pipelines of different processes. Sulfate ions have an important role in the precipitation of earth-alkaline metal ions, causing problems such as decreasing of the productivity and increasing the pressure during oil pumping. Thus, the quantification of sulfate ions in marine waters becomes a relevant factor for the monitoring of incrustation in offshore oil extractions.

The present work describes the use of Raman spectroscopy for the determination of sulfate in waters, based on the scattering by this ion around 980 cm^{-1} , which is free from water interference. Measurements were performed with a spectrophotometer equipped with a diode laser of $784.8 \pm 0.5\text{ nm}$ (bandwidth of 40 pm , power of 500 mW), an Andor/Oxford SR-500i-C-SIL monochromator (Czerny-Turner, focal length of 50 cm and diffraction grating of 600 lines/mm) and an iCCD Andor/Oxford iDUS 416 camera (matrix sensor of $256 \times 2000\text{ pixels}$). All spectra were obtained with a signal integration of 180 s .

The sulfate determination was studied by three different strategies. The direct determination in aqueous solution provided an analytical response range from $500\text{ to }3000\text{ mg L}^{-1}$ and limits of detection and quantification of 90 mg L^{-1} and 300 mg L^{-1} , respectively, which are not adequate for application in marine waters. The pre-concentration strategy based on an ion exchange resin was evaluated employing a column prepared with 500 mg of the Amberlite IRA 910 resin, through which 100 mL of $100\text{ to }400\text{ mg L}^{-1}$ sulfate solutions were pumped at a flow rate of 1 mL min^{-1} . The retained sulfate was eluted with 2 mL of a 1 mol L^{-1} NaCl solution, providing a linear response and a detection limit of 0.30 mg L^{-1} . Despite the low detection limit, the addition of 1.0 and 2.5% sodium chloride to the sulfate solutions caused significant effects in the pre-concentration step, therefore, this method could not be applicable to marine waters. Finally, the current strategy was based on the precipitation of barium sulfate salt in 2-mm diameter spot tests, produced by wax printing on A4 office paper. In order to obtain the BaSO_4 precipitate, $2.0\text{ }\mu\text{L}$ of 0.1 mol L^{-1} barium chloride was transferred to the paper spot, followed of $4 \times 7.0\text{ }\mu\text{L}$ sulfate solutions ($100\text{ to }500\text{ mg L}^{-1}$). The paper was dried at $60\text{ }^\circ\text{C}$ after each solution addition and, then, Raman spectrum was obtained (30 s of exposure and 5 accumulations). A linear response range was obtained ($R^2 = 0.97$), providing a detection limit of 2 mg L^{-1} . These results demonstrate the potentiality of Raman spectroscopy for the determination of sulfate in marine waters, avoiding the interference of sodium chloride.

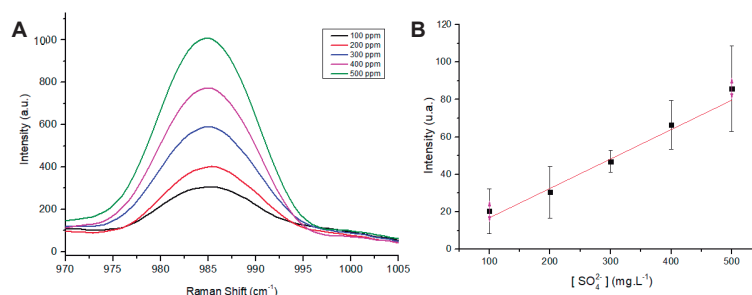


Figure 1: Raman spectra of barium sulfate on paper spot tests (A) and respective analytical curve (B) from 100 mg.L^{-1} to 500 mg.L^{-1} .

Acknowledgments

Authors are grateful to Instituto Nacional de Ciências e Tecnologias Analíticas Avançadas (CNPq 465768/2014-8 and FAPESP 2014/50951-4) as well as to CAPES for the fellowship to EMBS.

Synthesis, characterization, and evaluation of the extracting capacity of ionic liquids supported on graphene oxide for determining pesticides by LC-MS/MS.

Alessandra Timóteo Cardoso (PG),^{1*} Fernando Mauro Lanças (PQ)¹.

alessandracardoso@usp.br.

¹Instituto de Química de São Carlos, IQSC-USP.

Palavras Chave: Graphene oxide (GO), Ionic Liquids (ILs), Sorbents, Sample Preparation, Pesticides, LC-MS/MS.

Highlights

Synthesis of new selective extractor phases for determination of selected pesticides by LC-MS/MS. Good extractability of carbamates and triazines compared to commercial phases.

Abstract

One of the main advantages of using ionic liquids in sorbents for sample preparation is the various combination possibilities between the ions to favor pronounced interactions with the compound of interest, improving the cleaning and pre-concentration of the analytes.¹ Thus, this work aimed to develop and characterize two phases based on ionic liquids supported on graphene oxide, with subsequent evaluation of their extraction capacity for selected pesticides, with determination by LC-MS/MS. Two ionic liquids with imidazole cation were developed: a zwitterionic² – ILz (1-vinyl-3-(butyl-4-sulfonate)imidazolium), and a hydrophilic³ – [VHiM]Br (1-vinyl-3-hexylimidazolium bromide), and anchored in GO according to the methodology of Zhang et al.⁴ Characterization analyzes were carried out to confirm the deposition of ILs on the surface of GO nanosheets. As it is possible to observe in Figure 1A, there are differences between the GO spectra after the anchoring of the ionic liquids (b and c) referring to the appearance of bands of the 1-vinylimidazolium cation bonds (1585 cm⁻¹ and 2927 cm⁻¹) and decrease of some bands concerning pure GO (a) (1053 cm⁻¹ and 3600 cm⁻¹). After this stage, experiments were carried out to evaluate the selectivity and adsorption capacity of the sorbents for the pesticides: 5 mg of each sorbent were weighed in triplicate and placed in Eppendorf (2 mL), and separately 1 mL of the standard solution of triazines and carbamates to 100 ng mL⁻¹ were added and stirred for 1 h. Then, the supernatant was collected and filtered through a 0.22 μm membrane and injected into UPLC-MS/MS (Waters, Milford) under the following conditions: Column C18 (ACQUITY UPLC® HSS T3, 1.8 μm - 300 μm X 150 mm); oven temperature: 35 °C; injection volume 0.5 μL; mobile phase constant flow rate: 10 μL min⁻¹ in gradient elution mode composed of: (A) water / 0.1% formic acid (B): ACN / 0.1% formic acid v:v; total

running time 10 min; ESI+ ionization mode with MRM acquisition mode monitoring the following m/z transitions for carbamates (carbofuran: 165.1>123, carbaryl 145>127, methomyl 88>106) and for triazines (amethrin: 95>90, atrazine: 95>103, simazine: 131>123). It was possible to observe (figure 1B) that, in general, for the extraction of triazines, the best sorbent was ILz@GO. For carbamates, the best sorbent was [VHiM]Br@GO, presenting a greater extraction capacity than the C18 phase in both cases. This occurs because ILs anchored to GO have multiple adsorption mechanisms, such as π-π and electrostatic interactions promoted by GO, in addition to hydrogen bonds between the imino groups and the electronegative atoms of the analytes and ion exchange between the imidazole ring of the cation and ionized analytes. Thus, the extractive phases developed proved to be selective for the extraction of selected pesticides, as they showed high extraction capacity, which makes them suitable for later application in sample preparation techniques involving sorption mechanisms.

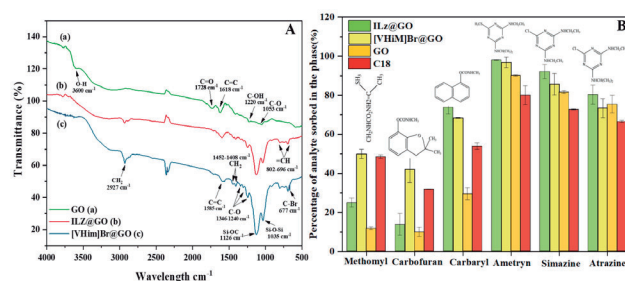


Figure 1. (A) IR spectra (a) GO, (b) ILz@GO, and (c) [VHiM]Br@GO; **(B)** adsorptive capacity of synthesized phases (%).

References: ¹Maciel, EVS et al. *TraC*. 119, 2019. ²Qiao, L. et al. *J Chromatogr. A*. 1286, 2013 137–145. ³Zheng X. et al. *J. Chromatogr. A*. 39-45, 2014. ⁴Zhang, H. et al. *Food Chem*. 290-297, 2018.

Acknowledgments

CNPq (Grant 308843/ 2019-3), FAPESP (Grant 2017/02147-0; 2017/21984-0 – EMU; 2017/21985-6 – EMU), and CAPES (Finance Code 001) for financial support. IQSC and CROMA for the provided framework.

46^o Reunião Anual da Sociedade Brasileira de Química: “Química: Ligando ciências e neutralizando desigualdades”

SYNTHESIS OF A NEW SUPERABSORBENT HYDROGEL FOR THE ADSORPTION OF AMARANTH DYE

Amanda de Souza Nicotte Silva (IC),¹ Igor Coreixas de Sá (PG),¹ Wagner Felipe Pacheco (PQ),¹

amandasns@id.uff.br; igorcoreixas@gmail.com; wfpacheco@id.uff.br

¹Departamento de Química Analítica, Universidade Federal Fluminense (UFF), Niterói/RJ, Brazil;

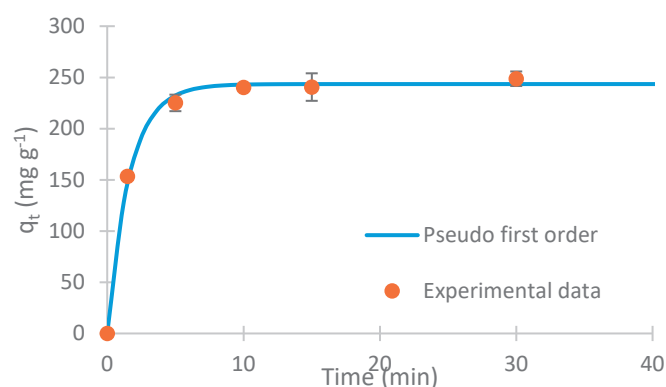
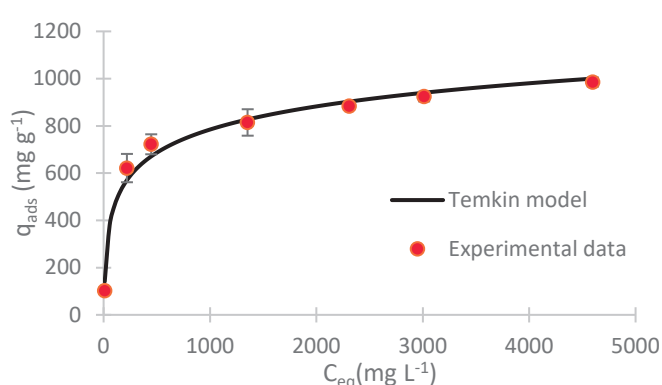
Keywords: Hydrogel, Dye removal, Adsorption, Superabsorbent

Highlights

- The adsorption capacity calculated reached more than 1000 mg/g.
- The synthesized hydrogel removed more than 95% of the dye in less than 10 min.

Abstract

Pollution from excessive disposal of dyes in industrial effluents is one of the main causes of environmental contamination, so that some of these dyes contain components that are toxic to aquatic organisms and humans.¹ Amaranth (FD&C No. 2) is a dark red water-soluble azo dye, mainly used in jams, drinks and cosmetics. In this bias, the removal of dyes can be done by different processes, and one of them is adsorption, an attractive removal method for having low cost, high efficiency and having different types of adsorbent materials.² Hydrogels are adsorbent polymers with high water retention capacity and, therefore, have desirable properties to act as adsorbents. It is proposed, from this perspective, the resourcefulness of a hydrogel to remove amaranth dye from aqueous solutions. The hydrogel, synthesized by radical polymerization, is composed of N,N-methylenebisacrylamide (MBA) and ammonium persulfate (APS) as cross-linking reagent and redox initiator, respectively, and by the monomers 2-trimethylammonioethyl methacrylate chloride (METAC) and acrylamide. The best adsorption was evaluated by pH studies, since the adsorption efficiency of ionic dyes can be influenced by this parameter², as there is dissociation of functional groups present on the surface of the adsorbent, in order to affect the adsorption equilibrium. Thus, the pH was evaluated in a range of 2.0 - 12.0, and what best promoted the removal of the dye was found at 6.0. Regarding thermodynamic tests, the Temkin isotherm best represented the experimental points obtained (graph 1), in which adsorption is discerned by a uniform distribution of binding energies. With regard to adsorption kinetics, an equal mass of hydrogel was placed in 50 mL of dye solutions, buffered at optimal pH, at room temperature and under agitation at 90 rpm. Given the time at defined intervals, the measurement of the remaining concentration of dye was carried out by UV-VIS spectrophotometer, as illustrated in graph 2, where the adsorption kinetics pointed out that the data was best described by the pseudo-first order model.



Graphs 1 and 2: Thermodynamic result of the dye under the Temkin isotherm and result of the adsorption kinetics described under the first pseudo-order model, respectively.

Acknowledgments



¹A.M. Elgarahy, K.Z. Elwakeel, S.H. Mohammad, G.A. Elshoubaky, A critical review of biosorption of dyes, heavy metals and metalloids from wastewater as an efficient and green process. *Cleaner Engineering and Technology* 4, 2021.

²R. Xu, J. Mao, N. Peng, X. Luo, C. Chang, Chitin/clay microspheres with hierarchical architecture for highly efficient removal of organic dyes, *Carbohydr. Polym.* 188, 2018.

Synthesis of magnetic nanoparticles modified with molecularly imprinted polymers for sarcosine determination

Ademar Wong (PQ),¹ Shakeel Zed (PG)¹ and Maria Del Pilar Taboada Sotomayor (PQ)¹

ademar.wong@unesp.br; m.sotomayor@unesp.br

¹Department of Analytical Chemistry, State University of São Paulo (UNESP), Araraquara, SP, Brazil.

Keywords: Core@shell, Mag@MIP, Sarcosine, Prostate cancer, Selectivity and Sensibility

Highlights

- ❖ Molecularly imprinted polymer with magnetic properties obtained by core@shell method.
- ❖ Sarcosine is an amino acid produced by the human body and can be used as a biomarker.
- ❖ Prostate cancer detection based in the detection and quantification of sarcosine.

Resumo/Abstract

Prostate cancer (PCa) has become the second most common malignancy tumors in male genito-urinary system and is an important tumor marker for the early screening and diagnosis of PCa. But the detection of PSA has poor sensitivity and specificity, it may lead to false-positive test result and make many patients have to accept unnecessary biopsy procedures. Therefore, finding a new tumor marker of PCa has become a hot spot of research. Sarcosine is a tumor metabolite which will increase significantly with the depravity and metastase of prostate cancer. In the tissue cells of PCa patients, the concentration of sarcosine is high, but low in the urine of patients with benign prostatic hyperplasia. So, it is possible that sarcosine will become a valuable tumor marker for the diagnosis of prostate cancer [1]. For sarcosine detection an alternative to achieve this goal is through the development of a class of compounds called MIP (Molecularly Imprinted Polymers). The MIPs are obtained from a polymerization, so that they present selective sites, complementary to the template molecule [2]. This recognition takes place through the affinity and interactions between the functional monomer, which constitutes the MIP, and the analyte. The functional monomer was chosen by computational simulation. In order to obtain a sensitive and selective material, a magnetic-MIP (Mag@MIP) of the core@shell type was proposed taking into account the magnetic properties that will be very useful for the process of separating the analyte from other interferences.

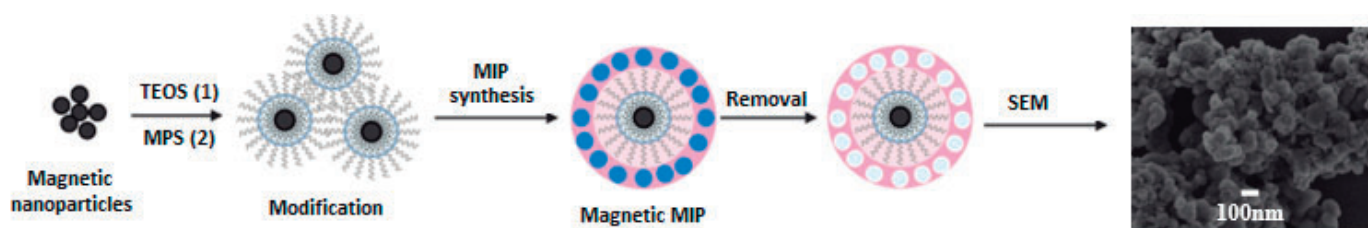


Figure 1: Illustrative image of the magnetic-MIP synthesis and morphological aspect of the Mag@MIP using scanning electron microscopy (SEM).

References:

- [1] M. Wang, L. Valenzuela, G. Murphy, and T. Chu, Purification of a human prostate specific antigen, *Journal of Urology*, v. 197, S148-S152, 2017.
- [2] C. R.T. Tarley, M. D. P. T. Sotomayor, L.T. Kubota, *Polímeros biomiméticos em química analítica. parte 1: preparo e aplicações de MIP*, *Química Nova*, v. 28, 1076–1086, 2005.

Agradecimentos/Acknowledgments

Institute of Chemistry, Unesp, Araraquara and PROPe (edital nº 13/2022)

Área: ANA

(Inserir a sigla da seção científica para qual o resumo será submetido. Ex: ORG, BEA, CAT)

Synthesis of molecularly imprinted polymers for selective casearin extraction**Gilberto Matos (PG),¹ Ademar Wong,¹ Maria Del Pilar Taboada Sotomayor (PQ),¹ Flávio Alexandre Carvalho (PQ)², André Faibicher (PQ)², and André Gonzaga dos Santos (PQ)²**g.matos@unesp.br¹Department of Analytical Chemistry, São Paulo, State University (UNESP), Araraquara, SP, Brazil.²Department of Drugs and Medicines, São Paulo State University (UNESP), Araraquara, SP, Brazil.Keywords: *Casearia sylvestris*; Molecularly imprinted polymer, Phytochemistry**Highlights**

- ❖ New nanostructured material for the pre-concentration, separation and subsequent quantification of casearins (clerodane diterpenes) isolated from *C. sylvestris* leaves through molecularly imprinted polymers.
- ❖ (MIP: Molecularly Imprinted Polymer) have been applied to the recognition of these biomolecules.
- ❖ Casearin D (CAS D) was used as a template for clerodane diterpenes extracted from *C. sylvestris*.

Abstract

Casearia sylvestris Sw. (*Salicacea*) is a plant of Brazilian folk medicine known as guaçatonga. Its leaves have an enormous pharmacological arsenal with great molecular diversity and bioactive potential. Bioactive clerodane diterpenes from its leaves showed different pharmacological activities such as antiulcer, anti-inflammatory and antitumor. However, current phytochemical separation techniques have proven to be expensive, consuming time and resources to detect, isolate, separate and purify active compounds from these plants, mainly complex compounds, with the presence of interferents and with low abundance. Thus, alternative analytical methods using specific recognition adsorbents, such as the use of molecularly imprinted polymers (MIP: Molecularly Imprinted Polymer) were carried out, as well as a sequence of phytochemical separation experiments for isolation and purification of casearin used as a template for extracting clerodane diterpenes from *C. sylvestris*. It was possible to isolate Cas D, with a mass of 289 mg and purity of 97%. The polymer showed satisfactory retention considering adsorption of the analyte as a function of mass increase, with 10mg and pH 8.5 offering the best adsorption results. The analyzes were performed by thin layer chromatography (TLC) and HPLC-UV.

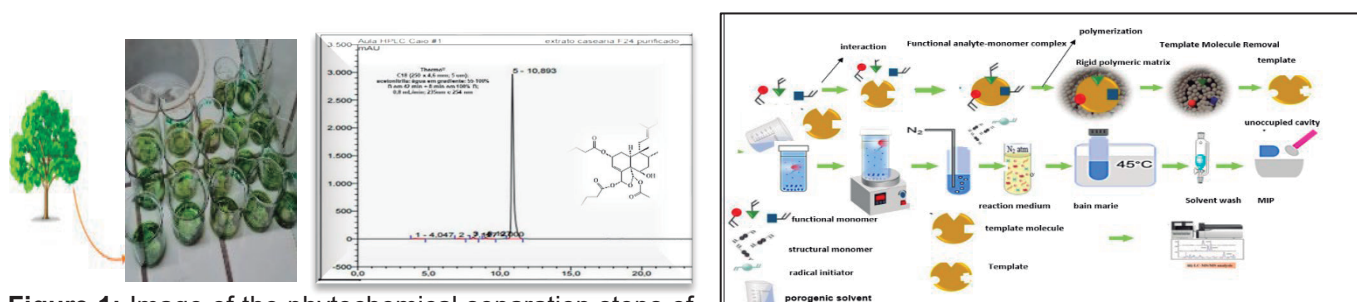


Figure 1: Image of the phytochemical separation steps of the active compounds where it was possible to isolate CasD, and synthesis of the Molecularly Imprinted Polymer for its specific recognition.

References:

- [1] SANTOS AG, et. al. Casearin X, its degradation product and other clerodane diterpenes from leaves of *Casearia sylvestris*: evaluation of cytotoxicity against normal and tumor human cells. **Chem Biodivers**. p. 1-7, 2010.
- [2] C. R.T. Tarley, M. D. P. T. Sotomayor, L.T. Kubota, Biomimetic polymers in analytical chemistry. part 1: preparation and applications of MIP, *New Chemistry*, v. 28, 1076–1086, **2005**.

Acknowledgments

Institute of Chemistry, Unesp, Araraquara and CAPES

Voltammetric determination of cadmium using magnetic graphite-epoxy composite electrode modified with magnetic nanoparticles

Paula Mantovani dos Santos (PG),^{1*} Felipe Augusto Gorla (PG),¹ Ademar Wong (PQ),² Marcela Zanetti Corazza,¹ Maria Del Pilar Taboada Sotomayor (PQ),² Mariana Gava Segatelli¹, César Ricardo Teixeira Tarley (PQ),^{1,3}

*paulamantovani@live.com; tarley@uel.br

¹Departamento de Química, UEL; ²Departamento de Química Analítica, UNESP; ³Instituto Nacional de Ciência e Tecnologia de Bioanalítica, UNICAMP.

Keywords: Graphite-epoxy electrode, Sensitive determination, Cadmium, Voltammetric method and Electroanalysis.

Highlights

- Cadmium can cause serious problems in the environment and to human health.
- An accurate and sensitive electrochemical method for monitoring of cadmium ions in real samples.
- Dispersive Magnetic Solid Phase Extraction combined to voltammetry method.

Abstract

In the present study, dispersive magnetic solid-phase extraction (DMSPE) was combined to the voltammetric method using a magnetic graphite-epoxy composite (m-GEC) electrode to determine of cadmium (Cd^{2+}). For this, a magnetic adsorbent (Fe_3O_4 -poly(atu)-PAN) was prepared and used as adsorbent material during the extraction step. The Fe_3O_4 -poly(atu)-PAN nanocomposite consisted of the synthesis of magnetic poly(allylthiourea) loaded with the ligand 1-(2-pyridylaz)-2-naphthol (PAN). Being the choice of the poly(allylthiourea) was due to its ability to form metal complexes with cationic ions, while azo compounds, such as PAN can form stable and colored complexes with metals. The characterization of the Fe_3O_4 -poly(atu)-PAN was performed by Fourier-transform infrared spectroscopy (FTIR), textural analysis, scanning electron microscopy (SEM), transmission electronic microscopy (TEM), thermogravimetric analysis (TGA), and vibrating sample magnetometry (VSM). The textural analysis of Fe_3O_4 -poly(atu)-PAN using the BET method showed lower porosity, volume and pore diameter when compared to the nanocomposite without PAN, suggesting that the PAN molecule was inserted into the internal pores of the material, decreasing the volume of the interior pores and the specific surface area. The morphological characteristics observed in the SEM and TEM images demonstrated a complex reticular structure due to the clear formation of the polymeric network in the material, favoring the adsorption of Cd^{2+} ions. The developed method involves two steps: (a) the extraction of Cd^{2+} by Fe_3O_4 -poly(atu)-PAN, and (b) the determination of preconcentrated Cd^{2+} ions on the surface of m-GCE using square wave anodic stripping voltammetry (SWASV). In this sense, studies were performed to evaluate the effect of PAN on the magnetic polymer. In the results obtained was found that PAN considerably increased Cd^{2+} adsorption in the nanocomposite due to the multiple binding sites. The effect of the experimental parameters on the preconcentration of Cd^{2+} ions (amount of sorbent, pH value of the sample solution and extraction time) and the voltammetric stripping step (reduction time, potential and supporting electrolyte) were investigated by SWASV technique. Thus, an aliquot of 30 mL of the sample (pH = 6.0) was preconcentrated in 2.0 mg of Fe_3O_4 -poly(atu)-PAN for 2.0 min in vortex. The nanocomposites loaded with Cd^{2+} ions were separated from the sample matrix with the aid of a magnet and subsequently deposited on the surface of the m-GCE for electrochemical analysis that occurred at potential of -0.7 V. The proposed method when compared to other methods of extraction and preconcentration of Cd^{2+} ions reported in the literature proved to be advantageous and promising, showing an anodic peak current of approximately 165 μA for 30 mL of sample using a concentration of 50 $\mu\text{g L}^{-1}$ of Cd^{2+} . Furthermore, good repeatability, and stability were achieved with the built sensor. Finally, the proposed sensor provided promising applications in the electrochemical determination of Cd^{2+} in real samples.

Agradecimentos/Acknowledgments

The authors are grateful for the collaboration of CNPQ (grant no. 142485/2020-9, and 307505/2021-9), CAPES, Araucária Foundation, INCT, UEL, and Institute of Chemistry at UNESP.

BEA

Alimentos e Bebidas

46^a Reunião
Anual da **SBQ**

28 a 31 de Maio de 2023

Águas de Lindóia · SP
Hotel Monte Real

A multicommuted flow system with immobilized enzyme and solid reagent for urea determination in milk

Julyana C. Rodrigues (PG),¹ Karla B. O. Silva (PG),^{2*} Joicy B. S. Costa (PQ),² Caio S. Bezerra (PG),³ Wagner E. Silva (PQ),¹ André F. Lavorante (PQ),¹ Ana Paula S. Paim (PQ).²

ana.paim@ufpe.br; karla.beatriz@ufpe.br

¹Departamento de Química, UFRPE; ²Departamento de Química Fundamental, UFPE; ³Departamento de Ciências da Computação, UFRPE.

Keywords: Metal-organic framework, Spectrophotometry, Urea, Milk, Enzyme immobilized

Highlights

A multicommuted flow system was proposed for urea determination in milk using a column with immobilized enzyme urease and solid reagent (MOF-Cu²⁺)
The urea levels in the analyzed milk are below 40 mg dL⁻¹

Abstract

The presence of urea in milk at concentrations above the permitted levels (40 mg dL⁻¹) is considered as a fraud. The determination of urea in milk cannot be verified by the official method as it detects only total nitrogen. This work describes an automated procedure to determine urea in milk samples using a multicommuted approach (Fig.1) with urease enzyme immobilized in bacterial cellulose and a solid reagent (metal-organic framework, MOF) as a colorimetric reagent. The urea quantification was based on the urea hydrolysis reaction catalyzed by urease, producing NH₄⁺, which reacts with MOF-Cu²⁺ forming tetraamminecopper (II) monitored at 450 nm. FTIR results of MOF showed the presence of the characteristic groups of MOF-Cu²⁺ containing carboxylate ions as ligands. The proposed system consists of two solenoid micro-pumps, a three-way solenoid valve, a column made of polymethyl methacrylate (PMMA) composed of two equal parts (0.36 mL), separated by a silica disk, where the enzymatic reaction occurs. The colorimetric reaction was detected by a multichannel (UV/VIS) spectrophotometer, model USB 4000 (Ocean Optics®). The system control was developed using C language programming through an arduino® UNO board. After the system evaluation, linear responses were obtained between 10.0 and 500.0 mg L⁻¹ urea (R = 0.997, n = 11) with detection and quantification limits of 0.82 mg L⁻¹ and 2.72 mg L⁻¹, respectively, analytical frequency of 7 determinations per hour, 0.8 mL sample solution consumption, with a total 1.4 mL of residue. Potential interfering studies (Cystine, Cysteine, Tryptophan, Thymine, Cyanocobalamin and Lactose) have shown the selectivity of the proposed method. Addition and recovery tests were performed, obtaining variation between 90 and 103%, Table 1, demonstrating the efficiency of the proposed method in detecting urea in milk samples. Comparing the results obtained by the proposed method and the reference method (KIT Urea CE) and applying the F test (precision) and t-test (accuracy), the results showed no significant difference at the 95% confidence level. The proposed system was robust with a structure of easy implementation and operation enabling its application in routine analysis.

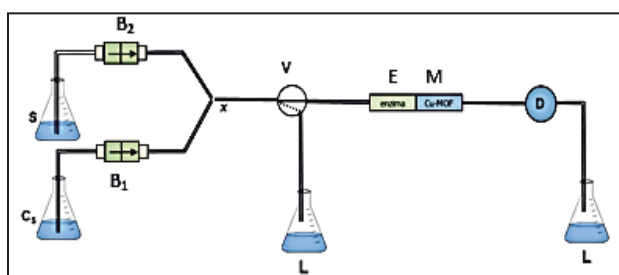


Fig. 1 Flow system diagram. B1 and B2: solenoid minipumps, V: three-way solenoid valve, D: detector, S: sample, Cs: phosphate buffer solution (pH 6.5), L: waste, E and M: column made of the PMMA with immobilized enzyme urease (E) and solid reagent (MOF-Cu²⁺) (M).

Table 1. Results for the recovery study in milk samples, with 10 and 25 mg dL⁻¹ urea added

Milk sample	Proposed method (mg dL ⁻¹)	Found (mg dL ⁻¹)	Recovery (%)
Natural	31.9 ± 0.4	39.1 ± 1.3	91.2
		53.2 ± 0.5	95.0
Powder	24.8 ± 2.7	32.6 ± 0.7	94.0
		46.5 ± 1.2	92.0
Skimmed UHT	19.1 ± 1.2	28.1 ± 2.5	97.1
		40.0 ± 2.3	91.4
Semi-skimmed UHT	31.4 ± 0.3	37.8 ± 0.7	90.7
		51.5 ± 1.4	92.4
Zero lactose	26.9 ± 0.5	38.1 ± 1.3	103.0
		48.3 ± 1.2	93.7

Acknowledgments

The authors are grateful to FACEPE (PRONEX/NUQAAPE) and CAPES for financial support

Área: ANA

ANALYTICAL AND CHEMOMETRIC STRATEGIES FOR ELUCIDATION OF YERBA MATE COMPOSITION

Allan dos Santos Polidoro¹ (PQ), Claissa Nied Peixoto¹ (IC), Vitória Carolina Prestes de Souza¹ (IC), Anai Loreiro dos Santos² (PQ), Adriano de Araújo Gomes¹ (PQ), Rosângela Assis Jacques^{1*} (PQ)

rosangela.j@iq.ufrgs.br;

¹Instituto de Química, UFRGS;

²Instituto de Tecnologia e Pesquisa – ITP, UNIT

Palavras-Chave: *Yerba mate*, Phenolic, PARAFAC, PCA, UHPLC-QTOF-MS.

Highlights

First application of a multivariate optimization methodology to extract non-volatile secondary metabolites from yerba mate by UAE. The extraction efficiency obtained was expressively superior to that obtained with conventional techniques described in the literature. First successful application of commercial yerba mate sample segregation, based on its non-volatile metabolic profile using molecular fluorescence and liquid chromatography, combined with PCA and PARAFAC chemometric tools.

Resumo/Abstract

Yerba mate (*Ilex paraguariensis* A. St. Hil.) is a plant native and cultivated in Brazil, Argentina, and Paraguay, consumed mainly as an infusion of its leaves and branches. Its leaves have several nutritional and medicinal properties attributed to their secondary metabolites, whose composition can vary depending on factors such as the type of cultivation, climate, agronomic conditions, and industrial processing.¹ Therefore, the present study aimed to develop strategies to elucidate the phenolic composition of yerba mate samples from different countries. The non-volatile metabolites were extracted employing ultrasound-assisted extraction, optimized using a 2³ central composite design. The dependent variables evaluated were extraction yield, TPC, TFC, antioxidant activity, and area of the total absorbance chromatogram obtained by HPLC-DAD analysis. The independent variables used were temperature (30 – 80 °C), extraction time (11.6 – 28.4 min), and percentage of ethanol in the hydroethanolic extractor phase (8 – 92%). The extracts were analyzed by molecular fluorescence, and the results were modeled by Parallel Factor Analysis (PARAFAC), which showed that Brazilian samples have a higher pigment content, while those from other countries have a higher phenolic content. Furthermore, the extracts were characterized by UHPLC-QTOF-MS, which allowed the identification of 13 chlorogenic acids, and two methylxanthines, among other compounds, which were quantified by HPLC-DAD. These results were also modeled using a PCA, which showed that yerba mate leaves produced from cultivated yerba mate have a higher amount of chlorogenic acids and that samples from Argentina, Paraguay, and Uruguay have a higher concentration of most chlorogenic acids and flavonoids when compared to the Brazilian samples.

¹Heck, C. I. & de Mejia, E. G. Yerba Mate Tea (*Ilex paraguariensis*): a comprehensive review on chemistry, health implications, and technological considerations. *J. Food Sci.* 72, R138-51 (2007).

Agradecimentos/Acknowledgments

The authors thank Conselho Nacional de Desenvolvimento Científico e Tecnológico (CNPq), and Coordenação de Aperfeiçoamento de Pessoal de Nível Superior (CAPES) for financial support and scholarships.

Determinação de mercúrio em pirarucu fresco e salgado por TDA AAS e avaliação de risco à saúde humana

Charles M. S. Borges (PG),^{1*} Kelly G. F. Dantas (PQ),¹

charles.msb@hotmail.com; kdgfernandes@ufpa.br

¹Programa de Pós-Graduação em Química, UFPA

Palavras-Chave: Mercúrio, Pirarucu, DMA-80, Índice de ingestão estimada, Risco a saúde.

Highlights

Determination of mercury in fresh and salted pirarucu by TDA AAS, and human health risk assessment. The DMA-80 proved to be a very efficient technique for the determination of total mercury in pirarucu samples. The Hg levels found were considerably high in some samples. Assessment of exposure and risk to human health was performed for all samples.

Resumo/Abstract

A contaminação por Hg na região amazônica está diretamente relacionada ao seu uso em atividades ilegais de mineração de ouro, o que causa indiretamente desmatamento, erosão do solo, assoreamento nos rios da região e sendo uma fonte de contaminação para os sistemas aquáticos locais [1][2][3]. O pescado é um dos recursos alimentares mais importantes para a população amazônica, sendo também a principal via de contaminação de Hg para a população [2]. Sendo assim, esse estudo teve como objetivo a quantificação de mercúrio em pirarucu (Arapaima gigas) fresco e salgado provenientes de Manaus-AM, Santarém-PA e Marituba-PA (criação em cativeiro) por espectrometria de absorção atômica com decomposição térmica e amalgamação (TDA AAS). As oito amostras de pirarucu frescas (A3 e A8) e salgadas (A1, A2, A4, A5, A6 e A7) foram adquiridas nas principais feiras e comércios de Belém-PA. Uma massa de aproximadamente 0,05 g de cada amostra in natura e previamente homogeneizada foi pesada em uma barquinha de níquel e transferida para o analisador direto de mercúrio (DMA-80 Tri-Cell, Milestone, Itália). A escolha da célula de leitura utilizada (cell 0, cell 1 e cell 2) foi realizada automaticamente, dependendo da quantidade de mercúrio total na amostra. O comprimento de onda utilizado foi 253,7 nm. Os teores encontrados nas amostras foram quantificados na cell 1 ($0 - 20 \text{ ng}$; $A = 0,04628583 \cdot \text{Hg (ng)} + 0,01044856$; $R^2 = 0,9984$) e na cell 2 ($50 - 200 \text{ ng}$; $A = 0,0007438572 \cdot \text{Hg (ng)} + 0,00010,010448569$; $R^2 = 0,9999$). O desvio padrão relativo variou de 0,6 – 8,0 % ($n=3$). Os valores de LD e LQ encontrados foram 0,01 e 0,04 ng g^{-1} , respectivamente. A exatidão do procedimento proposto foi avaliada usando o material de referência certificado de proteína de peixe (DORM-4), onde uma recuperação de 102,4% foi obtida para o valor de referência certificado (410 $\mu\text{g kg}^{-1}$). As concentrações de mercúrio encontradas nas amostras variaram de 4,0 (A3) a 2050,0 $\mu\text{g kg}^{-1}$ (A1). Dentre as amostras estudadas, duas amostras de pirarucu salgado (A1 e A4) estão acima do valor máximo permitido pela legislação para mercúrio (1000 $\mu\text{g kg}^{-1}$) em pescado (carnívoro). O índice de ingestão semanal estimada (ISE) e a avaliação de risco à saúde humana (RSH) foram calculados de acordo com Felix *et al.* (2022) [4]. Os valores obtidos de ISE e de RSH nas amostras variaram de 0,01 a 5,1 $\mu\text{g kg}^{-1}$ e 0,01 a 3,18, respectivamente. As amostras A1 (5,12 $\mu\text{g kg}^{-1}$), A4 (3,90 $\mu\text{g kg}^{-1}$) e A5 (1,95 $\mu\text{g kg}^{-1}$) ficaram acima do valor de ingestão semanal tolerável (1,6 $\mu\text{g kg}^{-1}$). Os valores de RSH obtidos foram maiores que 1,0 (A1: 3,18; A4: 2,42; A5: 1,21) demonstrando um possível risco à saúde humana. Os resultados obtidos mostraram a importância desse estudo na investigação dos níveis de contaminação que a população pode estar exposta e da necessidade de maiores estudos sobre a contaminação de mercúrio em peixes da região amazônica.

[1] WINDMÖLLER, Cláudia Carvalhinho et al. Use of a direct mercury analyzer® for mercury speciation in different matrices without sample preparation. *Analytical Methods*, v. 9, n. 14, p. 2159-2167, 2017.

[2] NEVADO, JJ Berzas et al. Mercury in the Tapajós River basin, Brazilian Amazon: a review. *Environment international*, v. 36, n. 6, p. 593-608, 2010.

[3] VIEIRA, José Cavalcante Souza et al. The effects of mercury exposure on Amazonian fishes: An investigation of potential biomarkers. *Chemosphere*, p. 137779, 2023.

[4] FELIX, Caio SA et al. Determination and human health risk assessment of mercury in fish samples. *Talanta*, v. 247, p. 123557, 2022.

Agradecimentos/Acknowledgments

A Coordenação de Aperfeiçoamento de Pessoal de Nível Superior (CAPES)

Área: BEA

Determination of ethanol in Kombucha using HS-GC-MS associated with chemometrics techniques

Julia Tristão do Carmo (FM),¹ Lucas Micqueias Arantes (FM),¹ Adelmo Carlos Siqueira Silva (PG),^{1*} Rúben Santana Ramos da Silva (IC),¹ Edgar Nascimento (PQ),¹ Tiago Gomes dos Santos (PQ)¹, Demétrio de Abreu Sousa (PQ).¹

julia.tristao@ifmt.edu.br; admadelmo@gmail.com

¹IFMT campus Cuiabá/Bela-vista

Keywords: *HS-GC-MS Analysis, Fermented Beverages, Volatile Compounds; Low Alcohol Beverages, Partial Least Squares.*

Highlights

Kombucha is a functional drink with low alcohol content. HS-GC-MS associated with Chemometrics techniques proved to be an applicable and adequate alternative to determine alcohol content in kombucha.

Abstract

The age-old beverage kombucha, with a low alcohol content, obtained from the infusion of tea in water, sugars and symbiotic colonies of bacteria and yeasts (SCOBY), ascended in the last decade as a functional drink. Considering that the composition of this drink is influenced by factors such as variations in SCOBY characteristics, ambient temperature, pH, acidity, exposure to oxygen, among others in the production process, the manufacturing control of this drink impacts on the analytical parameters established in the identity standard and quality (PIQ) of kombucha, mainly the alcoholic content. The objective of this work was the development of a chemometric model using partial least squares regression to determine the ethanol content in kombuchas. The kombucha samples, composed of 4 flavors (beetroot with ginger and grape, hibiscus with rose water and apple, lemon with ginger, passion fruit with lemongrass), produced in Cuiabá/MT were collected during production batches of a company in the first quarter of 2021. They were collected from three manufacturing batches, in two stages of the beverage fermentation process, before bottling and after the final bottling for consumption. HS-GC-MS analysis were carried out in a gas chromatograph coupled to a mass spectrometer with a Triple-Axis detector. 256 samples were used for the calibration step in the construction of the chemometric model, while others 128 samples were separated for testing it. Selectivity, repeatability, precision, intermediate precision, sensitivity, limit of detection and limit of quantification were evaluated according to the National Institute of Metrology, Quality and Technology guideline document DOQ-CGCRE-008. The statistical acceptance limit was 5% of significance and for the alcohol content the maximum limit of 0.5 in % v/v was considered. The chemometric model presented RMSEC = 0.6354 and $R^2 = 0.77$, RMSEP = 0.6256 and $R^2 = 0.81$ (for a range of values between 1.5 and 7.5, considering isopropanol/ethanol ratio) and proved to be linear, precise and selective in the studied work range, being, therefore, an applicable and adequate alternative for analyze this drink and assist in decision making in the manufacturing process and product quality assurance. The specificities of the ethanol quantification method are ensured by the unprecedented sample size for kombucha and statistical rigor in the analytical method validation processes. Considering the planning, experimental conditions and obtained results the method can be consistently implemented in other laboratories within its field of application.

Acknowledgments

IFMT Campus Cuiabá - Bela Vista e Pró-reitoria de Pesquisa, Pós-Graduação e Inovação do IFMT.

Área: BEA

Determination of metals in Pork Lard: a fast and low cost sample preparation method by RP-DLLME

Eder L.M. Flores (PQ)¹, Mayara P.O Santos (PG)², Deisy A. Drunker (PQ)³, Cristiane Canan (PQ)³, Oldair D. Leite (PQ).^{1*}

eder@utfpr.edu.br; oldairleite@utfpr.edu.br

¹Departamento de Química, UTFPR – Campus Medianeira; ²Programa de Pós-graduação em Tecnologia de Alimentos – UTFPR/MD; ³Departamento de Alimentos, UTFPR – Campus Medianeira.

Palavras Chave: *sample preparation, fat, flame atomic absorption, microextraction*

Highlights

- Sample preparation procedure using RP-DLLME for metals extraction from solid fat;
- Simultaneous microextraction and preconcentration of analytes, followed by determination by FAAS;
- Low consumption of solvents and use of diluted acid.

Resumo/Abstract

Typically, sample preparation methods for subsequent heavy metal determination in matrices such as oils and fats used closed systems and traditional heating or microwaves, as well as concentrated acids such as HNO₃ and/or HClO₄. These methods have drawbacks such as time consuming and expensive decomposition systems and the use of concentrated acids. As a result, this study proposes an alternative method for sample preparation of pork lard using dispersive liquid-liquid microextraction in reversed-phase (RP-DLLME) for subsequent determination of Cu, Fe, Mg, Mn, and Ni by flame atomic absorption spectrometry (F AAS). The parameters of dispersant (n-propanol and isopropanol) and extractant (diluted HNO₃ and HNO₃ + HCl (1:1 v/v) solvents, stirring time, ultrasound influence, and centrifugation time were evaluated. External calibration using aqueous reference solutions in the range of 0.25 to 2 mg L⁻¹ was performed for all analytes for F AAS determination. The limits of quantification for Cu, Fe, Mg, Mn, and Ni were 0.010, 0.013, 0.042, 0.016, and 0.012 mg kg⁻¹, respectively. For all analytes, the accuracy ranged from 95 to 104%, and the precision (RSD) was less than 6%. The method was tested on various brands of commercial pork lard. Because of the pre-concentration of the analytes, the RP-DLLME procedure was suitable for the preparation of pork lard samples, allowing determination by F AAS. We obtained acceptable recovery values and low LOD values. According to Green Analytical Chemistry principles, the proposed RP-DLLME method present low reagent consumption, use of diluted acids, simplicity of operation, and reduced time consumption are all desirable aspects.

Kalschne, DL; Canan, C; Barin, JS; Picoloto, RS; Leite, OD; Flores, ELM. *Food Analytical Methods*, 13, 2019, 230.

Kalschne, DL; Canan, C; Beato, MO; Leite, OD; Flores, ELM. *et al. Talanta*, 208, 2019, 120409.

Agradecimentos/Acknowledgments

We thank the financial support of UTFPR, CAPES, Fundação Araucária, and CEANMED - Central Analítica Multiusuário/UTFPR.

Determination of total mercury in bovine and buffalo liver raw and after thermal processing by TDA AAS

Kelly G. F. Dantas (PQ),^{1*} Charles M. S. Borges (PG),¹ Heronides A. Dantas Filho (PQ).¹

kdgfernandes@ufpa.br; charlesmsborges@hotmail.com; heronides@ufpa.br

¹Faculdade de Química, UFPA

Palavras Chave: Mercury, Liver, Thermal processing, Bovine, Buffalo, Direct mercury analysis.

Highlights

Low concentrations of mercury was found in bovine and buffalo liver. Low level of mercury was found in bovine (grilled) when compared with bovine liver raw. Buffalo liver grilled and cooked in air fryer showed a higher mercury content when compared with buffalo liver raw.

Resumo/Abstract

Mercury is a toxic metal in the environment and it has the tendency to accumulate and reaches the food chain [1]. A rapid method and simple was used for the determination of total mercury in liver samples (raw and processed) by thermal decomposition amalgamation atomic absorption spectrometry (TDA AAS). Samples of livers (bovine and buffalo) were cut into strips of 1.0 cm. Each type of liver was randomly mixed. The samples were divided in raw (uncooked without any manipulation), grilled in skillet for 3 min on each side in the preheated skillet for 90 s, cooked in air fryer at 180 °C for 10 min, and cooked in air fryer at 200 °C for 10 min. Raw, grilled and cooked samples were ground in a processor. Approximately 0.3 g of each liver was weighed in nickel boats and then analyzed in the direct mercury analyzer (Tri cell, DMA-80, Milestone, Italy). Certified fish protein reference material (DORM 4) was used to assess the accuracy of the analysis procedure. The recovery obtained was 102.1% (certified value: 0.412 mg kg⁻¹; found value: 0.417 mg kg⁻¹). The limits of detection and quantification were 0.01 and 0.03 µg kg⁻¹, respectively. The levels of mercury (µg kg⁻¹) obtained in bovine and buffalo liver varied of 3.22 and 3.49 (raw), 2.9 and 5.62 (grilled), 4.83 and 6.08 (air fryer at 180 °C), and 4.09 and 6.07 (air fryer at 200 °C), respectively. Low level of mercury was observed in bovine (grilled) and higher level of mercury were found bovine and buffalo liver (air fryer at 180 °C and air fryer at 200 °C) when compared to the values obtained in raw samples. Buffalo liver grilled showed a higher mercury content when compared with bovine liver raw. The mercury contents found in raw or processed samples were higher than the values obtained in bovine liver in Spain (0.002 µg kg⁻¹) and Zambia (0.0003 µg kg⁻¹) [2,3]. Goran et al. (2016) [4] observed an increase of Zn concentration in thermally processed beef samples and this was related to the increase of the insoluble Zn fraction from denatured proteins. Higuera et. al. (2021) [5] found the mass fraction of Zn and Cu increased when compared to the raw samples and the other cooking procedures. This study showed the influence of several cooking processes on mercury level in liver studied.

[1] R.F.L. Ribeiro, R. F. L. Germano, A. Microchemical Journal, 2015, 121, 237.

[2] Lopez-Alonso, M., Miranda, M., Benedito, J.L., Pereira, V., Garcia-Vaquero, M. Meat Sci., 2016, 121, 47–52.

[3] Yabe, J., Nakayama, S.M., Ikenaka, Y., Muzandu, K., Ishizuka, M., Umemura, T. J. Vet. Med. Sci., 2012, 74, 1345.

[4] Goran, G. V.; Tudoreanu, L.; Rotaru, E.; Crivineanu, V.; Sci. 2016, 118, 117.

[5] Higuera, J. M. de; Santos, H. M.; Oliveira, A. F. de; Nogueira, A. R. A. J. Braz. Chem. Soc. 2021, 32, 2111.

Agradecimentos/Acknowledgments

CAPES

DEVELOPMENT OF METHOD FOR QUANTIFICATION OF RESIDUES OF ENROFLOXACIN AND CIPROFLOXIN IN BOVINE RAW MILK BY HPLC-DAD

Gabriel Gosling Stollar (IC)¹, Leonardo Ayzawa Queiroz Quadra da Silva (IC)¹, Caroline Pais de Carvalho (PGD), Cintia Sílvia Minafra e Rezende (PQ)², Rosineide Costa Simas (PQ)¹.

biel.gosling@gmail.com

¹Faculdade de Química -EE-Universidade Presbiteriana Mackenzie ; ²Escola de Medicina Veterinária -UFG

Keywords: Antibiotic Residues, Milk quality, Antimicrobials and HPLC

Highlights

The validated method was successfully applied for the determination of Enrofloxacin and Ciprofloxacin in 60 sample raw milk by HPLC DAD.

HPLC-DAD is a sensitive and cost-effective technique that can effectively detect and control quinolones in raw milk.

Abstract

The use of antibiotics in animal production is a fundamental tool for the treatment of diseases, and the first uses of these substances in dairy cattle were directed to the treatment of mastitis, from 1940. To be considered safe and of high quality, milk must be free from residues of veterinary drugs such as antibiotics and pesticides¹⁻². Thus, the presence of antibiotic residues in milk is a factor that negatively affects the safety and quality of dairy products. Before collecting milk from the tank, the dairy industries routinely collect an individual sample from each producer for composition evaluation, water addition, total bacterial count, somatic cell count) and antibiotic residue detection. Brazil has the Milk Waste Control Program (PCRL) that carries out surveillance actions to control the improper use of veterinary drugs. The most common veterinary drugs are antimicrobial with Quinolones (enrofloxacin, ciprofloxacin, danofloxacin, marbofloxacin). The objective of this work was to analyze the presence of antimicrobials residues in the refrigerated raw milk of 60 milk producers from three Brazilian states (MA, MT and GO). The method relies on a simple Quechers step curves were prepared by using a combined working solution to spike matrix blanks (30, 60, 90, 120, and 150 µg.L⁻¹ for quinolones). The limits of detection (LODs) were chosen as the concentration of each compound that gave a S/N ratio greater than 3:1. All LODs for the compounds were below 5 µg.L⁻¹. The recovery and reproducibility results based on matrix spiked standards are acceptable for quinolone residue determination in milk subject to regulation. The results obtained allowed the conclusion that only one producer presented a positive antibiotic result for the Quinolones family, while the other producers analyzed had a negative result. Fat, protein, total somatic cell count and total bacterial count were also analyzed.

Acknowledgments

We thank CPA-UFG by providing the samples for the application of the method and bromatological analyses and flow cytometry.

References:

- 1-Oliveira, R.V.; Pietro, A.C.D.; Cass, Q.B. Quantification of cephalexin as residue levels in bovine milk by high-performance liquid chromatography with on-line sample cleanup. *Talanta* 2007, 71, 1233–1238.
- 2-Christodoulou, E.A.; Samanidou, V.F. Multiresidue HPLC analysis of ten quinolones in milk after solid phase extraction: Validation according to the European Union Decision 2002/657/EC. *J. Sep. Sci.* 2007, 30, 2421–2429.

Evaluation of bioactive compounds in tea made with fermented grape pomace residue

Elisa N. V. Resende (IC)*, Juliana A. Pires (PG), Wanessa R. Melchert (PQ)

***elisanvresende@usp.br;**

College of Agriculture "Luiz de Queiroz", University of São Paulo

Keywords: Anthocyanins; Antioxidant activity; Tannins; Waste management; Winemaking residue.

Highlights

This work sought to evaluate the bioactive compounds that grapes typically have in their pomace, but when it is prepared as a tea. The study may bring new ways to control the disposal of grape pomace.

Abstract

Fermented grape pomace is the main by-product of the winemaking process. It is the residue after the fermentation, consisting of the grape's seeds and skin. It's a valuable antioxidant agent with an extended list of bioactive compounds that can benefit the organism¹. This study aims to evaluate the bioactive compounds (condensed tannins, anthocyanins, and antioxidants) when Bordo grape fermented pomace residue was employed to make tea. Two waste harvests, 2019 and 2020, were employed. The draining process was carried out on the part of the waste samples, and the analyzes were carried out with drained waste and without draining. The samples were weighed at 2 g each and infused in three different temperatures: hot (± 100 °C), cold (± 4 °C), and room temperature (± 26 °C), and then the obtained extracts were analyzed for bioactive compounds. The temperature of the water in which the tea was infused is the parameter that most influenced the concentrations since the draining process did not affect them. For tannins, concentrations were higher in samples infused in hot water (0.60 ± 0.05 g/L) than in cold water (0.23 ± 0.01 g L⁻¹) or room temperature (0.42 ± 0.03 g L⁻¹). While for anthocyanins, higher concentrations were found for room temperature (0.0041 ± 0.0004 mg L⁻¹) than > hot (0.0024 ± 0.0001 mg L⁻¹) or cold temperatures (0.0015 ± 0.0001 mg L⁻¹). As for antioxidants, the concentrations were 0.93 ± 0.01 , 0.56 ± 0.03 , and 0.31 ± 0.01 µg L⁻¹ for the cold, room, and hot temperatures, respectively. This different behavior for each bioactive is expected since the temperature directly influences the extraction due to improving the solvent-analyte contact process. Still, it can also promote the degradation of some bioactive. In the case of the bioactive studied, better yields are expected at temperatures: (i) cold for antioxidants; (ii) environment for anthocyanins; and (iii) hot for tannins. All the values found for tannins, anthocyanins, and antioxidants activity are similar to those in literature². However, since it's a tea, lower concentrations are expected than other types of extractions made with fermented grape pomace, which can be seen in other studies³, which use organic solvents (ethanol, methanol, and others) according to their official methodologies. The following steps of the work are to evaluate the extraction behavior in total phenolic compounds, and the use of a traditional filter or tea bag can affect the extraction.

¹Zhu F, Du B, Zheng L, Li J. Food Chemistry, 186, 2015.

²Silva JK, Batista AG, Cazarin CBB, Dionisio AP, Brito ES, Marques ATB, Junior MRM. LWT-Food Science and Technology, 76, 2017

³Beres C, Costa GN, Cabezudo I, Silva-James NK, Teles AS, Cruz APG, Silva CM, Tonon RV, Cabral LMC, Freitas, SP. Waste management, 68, 2017.

Acknowledgments

The authors acknowledge the financial support from the Coordination for the Improvement of Higher Education Personnel - Brazil (CAPES), and Sao Paulo Research Foundation (FAPESP - Grant 2018/24029-1).

Evaluation of phenolic compounds of roasted coffee obtained from the Circuito das Águas Paulista region

Bruna Luiza Duarte Guedes (PG),* Wanessa R. Melchert (PQ).

brunaluiza@usp.br

College of Agriculture "Luiz de Queiroz", University of São Paulo, Piracicaba, SP, Brazil;

Keywords: Coffee, Phenolic compounds, HPLC, Spectrophotometry

Highlights

Quantification of total phenolics and identification of the compounds from the roasted coffee samples.

Abstract

Coffee is a widely known stimulating drink, being number two in the ranking of beverage consumption worldwide due to its characteristic aroma and flavor. These sensory characteristics result from the chemical composition of the coffee bean as well as from processes involving cultivation, storage, roasting, and also from edaphoclimatic factors. The Brazilian region of *Circuito das Águas Paulista* has specific geographical features such as altitude, latitude, climate, and relief that may facilitate the adaptation of the coffee tree, resulting in high quality beans with the potential of reaching "specialty coffee" status. Therefore, this study aimed to quantify the total phenolic compounds and identify the compounds based on the time of retention of their analytical standards in addition to the caffeine content. The coffee samples provided by the regional producers were roasted, ground, and standardized using a 20-mesh sieve. Regarding the preparation of the beverages, the extraction method followed the Specialty Coffee Association of America protocol for sensory coffee analysis, in which 1.4 g of grounded coffee stayed in contact with 25 mL of water heated to a temperature of 90 °C, during 5 minutes and later filtered with conventional filter paper. The beverage was then diluted in a 1:50 water/coffee ratio, and the resultant extract was analyzed on the spectrophotometer at 770 nm according to the Folin-Ciocalteu method to determine the total phenolic compounds. As for the chromatographic analysis, the extraction method used was infusion, with 1.0 g of grounded coffee filtered with conventional filter paper by pouring 15 mL of 90 °C heated water over it. The extract was also filtered with a syringe filter, and later on 30 µL were injected into the high performance liquid chromatography (HPLC) with a mobile phase of 95% (5% acetic acid in water) and 5% acetonitrile, C18 column (4.6 x 250 mm – 5 µm) and flow rate of 0.8 mL/min for 45 minutes at 280 and 320 nm. **Table 1** represents the total phenolic compounds in roasted coffee samples determined by spectrophotometric analysis, and the results vary from 3370.68 to 3967.57 mg EGA per 100 g of coffee. The phenolic compounds identified with the HPLC were 5-Hydroxymethylfurfural, 3,4-Hydroxybenzoic, Catechin, Chlorogenic Acid, Caffeic Acid, and also Caffeine.

Table 1. Determination of total phenolic compounds in roasted coffee samples by the Folin-Ciocalteu method

Samples	mg EGA / 100 g of coffee
C1	3490.06 ± 129.39
C2	3376.63 ± 25.44
C3	3967.57 ± 28.98
C4	3751.36 ± 28.53
C5	3672.93 ± 86.36
C6	3856.20 ± 67.92
C7	3666.34 ± 78.76
C8	3637.67 ± 95.63
C9	3370.68 ± 34.54
C10	3831.22 ± 48.97
C11	3583.72 ± 108.31
C12	3805.93 ± 39.82

Acknowledgments

The authors acknowledge the financial support from the Coordination for the Improvement of Higher Education Personnel - Brazil (CAPES), National Council for Scientific and Technological Development - Brazil (CNPq), and São Paulo Research Foundation (FAPESP).

Evaluation of the free and bound fractions of carbonyl compounds in craft beers

Marinice Santiago dos Santos Acácio (PG)¹, Eliete Costa Alves (TC)¹, Bruna A. Souza Machado (PQ)¹, Jailson B. de Andrade (PQ)^{1,2,3}, Jeancarlo Pereira dos Anjos (PQ)^{1,2*}.

marinicesantiago@yahoo.com.br; * jeancarlopanjos@gmail.com

¹Centro Universitário SENAI CIMATEC, Salvador, BA, Brasil; ²INCT de Energia e Ambiente, UFBA, Salvador, BA, Brasil; ³Centro Interdisciplinar de Energia e Ambiente – CIEnAm, Salvador-BA, Brasil.

Palavras Chave: Carbonyl compounds, Craft beer, Derivatization, 2,4-DNPH, HPLC-DAD

Highlights

Carbonyl compounds can be present in beer in free and bound forms. All craft beer samples showed bound-carbonyl compounds, which can negatively influence on the quality of the beverage.

Resumo/Abstract

Some compounds with undesirable characteristics can be formed during the craft beer production process, as carbonyl compounds (CC), which influence the sensory properties, in addition to their toxicity. The formation of bound-CC, in craft beers, is favored by the high reactivity of these substances. Bound-CC are considered the most relevant for the formation of unpleasant flavors in beer.^[1,2] This work aimed to identify and quantify 15 carbonyl compounds, in free and bound forms, in craft beers. Free- and bound-carbonyl compounds were analyzed in craft beer samples after derivatization using 2,4-dinitrophenylhydrazine (2,4-DNPH), pre-concentrated by solid phase extraction (SPE) and analysis by HPLC-DAD. The bound-CC were analyzed indirectly, through the quantification of free-CC and total-CC ($CC_{\text{bound}} = CC_{\text{total}} - CC_{\text{free}}$). The proposed method was validated and presented satisfactory figures of merit (selectivity, linearity, LOD, LOQ, precision) to attest to the analytical quality of the results. Acetaldehyde concentrations ranged from 8.83 to 466.1 $\mu\text{g L}^{-1}$ (free fraction) and from 22.47 to 1665 $\mu\text{g L}^{-1}$ (bound fraction). Other compounds found were formaldehyde (free_{max.}: 15.77 $\mu\text{g L}^{-1}$; bound_{max.}: 97.73 $\mu\text{g L}^{-1}$), acrolein (free_{max.}: 2897 $\mu\text{g L}^{-1}$; bound_{max.}: 713.4 $\mu\text{g L}^{-1}$), crotonaldehyde (free_{max.}: 199.5 $\mu\text{g L}^{-1}$; bound_{max.}: 464.0 $\mu\text{g L}^{-1}$); benzaldehyde (free_{max.}: <18.39 $\mu\text{g L}^{-1}$; bound_{max.}: 1326 $\mu\text{g L}^{-1}$). It was possible to identify and quantify free- and bound-CC at low concentrations and with good precision. Craft beers showed a proportion of up to 76% for CC in the bound form (Figure 1), which can be related to undesirable flavors in beverage.

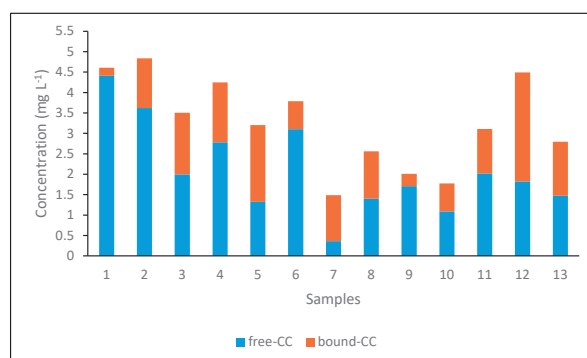


Figure 1. Total carbonyl compounds concentration (free-CC + bound-CC) and distribution of concentrations for free and bound forms in craft beer samples (CC = carbonyl compounds).

^[1]Trueba, P. B., et al.. *J Chromatogr A* **2019**, 1604, 460467; ^[2]Trueba, P. B., et. al.. *J. Food Research International* **2021**, 140, 110049.

Agradecimentos/Acknowledgments

CAPES, CNPq, FAPESB e INCT-E&A

46ª Reunião Anual da Sociedade Brasileira de Química: "Química: Ligando ciências e neutralizando desigualdades"

Área: BEA

Exploratory metabolomic analysis of nattô using mass spectrometry and molecular networking.

Britney S. Toyama (PG),^{1*} Felipe Souza (TM),¹ Carla Porto (PQ)², Eduardo J. Pilau (PQ)¹

pg4040380@uem.br

¹Laboratory of Biomolecules and Mass Spectrometry, Department of Chemistry, State University of Maringá (UEM), Maringá, PR, Brazil; ²Researcher at the startup of technological innovation in chemical analysis (MS Bioscience), State University of Maringá, Maringá, PR, Brazil

Key words: Nattô, Mass Spectrometry, *Bacillus subtilis*, Metabolomic Analysis.

Highlights

Natto is a traditional Japanese food made from fermented soybeans and has a sticky texture and strong flavor. It is high in protein, vitamins, probiotics and others. It is a food with health benefits.

Abstract

Metabolomics is the study of small molecule metabolites in biological systems and their changes in response to genetic or environmental factors. Mass spectrometry is a powerful analytical tool used in metabolomics to identify and quantify metabolites in a sample. The combination of metabolomics and mass spectrometry allows for a comprehensive analysis of the metabolic profile of a biological sample, providing insights into cellular processes and metabolic pathways. In this study, we analyzed Natto to try to understand the process involved during a fermentation process. For this, 100 mg of nattô (previously macerated) was extracted using a chloroform:methanol (9:1; v:v) solution. The system solvent was evaporated using nitrogen and then resuspended in 1000 µL of methanol, filtered using an hydrophilic PTFE membrane filter (Flowsupply; 0,22 µm; 13 mm) and subsequently 2,00 µL of each extract were analyzed using a ultra-high performance liquid chromatography (Shimadzu, Nexxera X2, Tóquio, Japão) coupled to a high resolution mass spectrometry Q-TOF geometry y (Impact II, Bruker Daltonics Corporation, Bremen, Alemanha) equipped with a electrospray ionization source. All the analyses were realized in positive ionization mode. In this study, several compounds of different classes were found and some of them identified. The Molecular Networking tool based in mass spectrometry allows users to visually and structurally evaluate related metabolites with similar fragmentation patterns providing the possibility to interpret large metabolomics data sets and prospect metabolites. Some molecular features were identified using the GNPS (Global Natural Products Social Molecular Networking) library (Figure 1) and others will be analyzed in further studies.

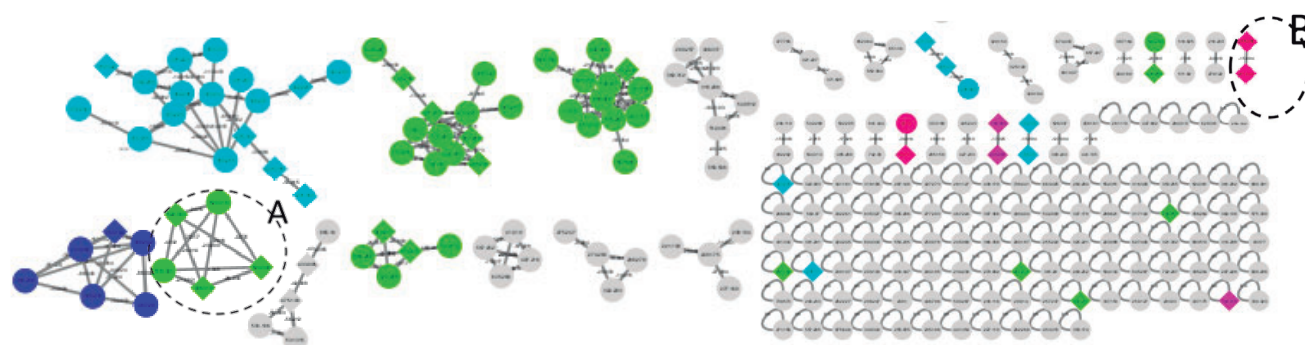


Figure 1: Molecular network - Clusters of molecular families (A) Phosphatidylcholine family, (B) Genistein compounds.

Acknowledgments

The authors would like to thank the State University of Maringá (UEM), the Federal Foundation for Brazilian Research and Development (FINEP), Coordination for Improvement of Higher Education Personnel (CAPES), the National Council for Scientific and Technological Development (CNPq) and Applied Research Program- Araucária Foundation to Support Scientific and Technological Development of the State of Paraná.

Gas chromatography combined with chemometrics to differentiate special from traditional classification in coffees: a preliminary study

Gabriela M.R.N. Alcantara (PG)^{1*}, Winston P. C. Gomes (PG)¹, Gisele G. Bortoleto (PQ)², Renata A. Sermarini (PQ)³, Wanessa R. Melchert (PQ)³

gabriela.nascimento@usp.br;

¹Center for Nuclear Energy in Agriculture, University of São Paulo; ²FATEC of Piracicaba "Dep. Roque Trevisan"; ³College of Agriculture "Luiz de Queiroz", University of São Paulo

Keywords: Coffee, Chemometrics, Chromatography, Decision tree, Food Analytical Chemistry, Food Analysis

Highlights

Chemometric tools using volatile compound data can classify green and roasted coffee beans. The E/M ratio has the potential as a differentiator between special and traditional classes.

Abstract

The quality of coffee, both green (peeled fruit and waiting for the roasting process) and roasted, is influenced by several factors, such as the production method, chemical composition of the beans, and the roasting and preparation processes¹. In this study, it was investigated, in a preliminary way, the special and traditional classification of green and roasted coffees through the concentrations of ethanol and methanol determined by gas chromatography and chemometric tools. Although ethanol and methanol, present in coffee, do not have functions defined in the literature, the ethanol/methanol ratio in coffee gives a flavor known as "Solai" or "up-country", whose characteristic is desirable since a higher ratio confers better quality to coffee². The methodology used was the determination of ethanol and methanol levels, and the evaluation of supervised analyses. For this, 16 and 20 samples of traditional and special coffee were employed, respectively with half the green and the other roasted coffee. All samples were previously ground and standardized to 20 mesh. About 0.55 g was weighed in a 20 mL flask with incubation in the headspace sampler oven (CTC Analytics, Pal System) and subsequent injection of the gaseous phase in a chromatograph gas with flame ionization detection, PerkinElmer®, model Clarus 600 (HS-GC-FID). Special coffee, both green (0.88 ± 0.32 , $n=10$) and roasted (0.13 ± 0.01 , $n=10$), adopted a higher mean factor than traditional ones (0.12 ± 0.01 and 0.06 ± 0.01 , green ($n=8$) and roasted ($n=8$), respectively). Therefore, the ethanol/methanol ratio can be used to differentiate special exhibitions from traditional ones. Decision trees were used to identify the variables that most contribute to the classification of coffee, as well as their levels. Due to the small sample group, resampling techniques were added to each data set (green and roasted), 200 for each classification. A regression tree was constructed for each augmented dataset using the ANOVA method using the statistical software R. The assumed additive model was given by: "Classification = Ethanol + Methanol + Ratio". The model was not validated, considering the sample group was small. For green coffee, methanol was not an important variable carrying out the classification. Thus, the decision tree needed 3 nodes to classify 100% of the special beans, where we were able to establish the following rule: coffee beans that present a ratio ≥ 0.2648 (88.57% of the beans are already classified), ethanol ≥ 0.2256 and finally ethanol < 0.263 (100% of the classification). As for roasted beans, the three variables were important for building the model and thus classifying the samples. For roasted coffee, the model needed many more nodes (7). This could be due to the small number of variables, demonstrating the complexity of roasted coffee beans, or the variability that roasted samples have in their ethanol levels (0.77 ± 0.72 and 0.46 ± 0.05 , special ($n=10$) and traditional ($n=8$), respectively) and methanol (6.76 ± 31.11 and 10.33 ± 22.01 , special ($n=10$) and traditional ($n=8$), respectively). For roasted samples, the ethanol and methanol values may not be the most suitable for the classification model. Even with satisfactory results for green coffee, the authors understand the need to increase the sample group of green and roasted coffees so that the creation of the classification model is possible, and it can be confirmed that the ethanol and methanol compounds and their ratio can be employed as class discriminators for coffees, this being foreseen for the future stages of the work.

¹Alcantara GMRN, Dresch D, Melchert WR, Food Chemistry, 360, 2021.

²Flament, I. Coffee flavor chemistry. Hoboken, NY: John Wiley & Sons, 2001.

Acknowledgments

The authors acknowledge the financial support from the Coordination for the Improvement of Higher Education Personnel - Brazil (CAPES), National Council for Scientific and Technological Development - Brazil (CNPq), and São Paulo Research Foundation (FAPESP - Grant 2018/24029-1).

Microwave-assisted extraction of total phenolic content in coffee samples

Maryane Montagner de Moura* (IC), **Wanessa R. Melchert (PQ)** *maryanemontagner@usp.br

College of Agriculture "Luiz de Queiroz", University of São Paulo, Piracicaba, SP, Brazil

Keywords: Coffees, Microwave, Extraction, TPC, Quantification compounds.

Highlights

The proposed study extracted total phenolic in traditional, special, and green coffee samples using microwave-assisted extraction.

Resumo/Abstract

Phenolic content is organic substances in all vegetables, including coffee, that benefit human health and have a preventive capacity for oxidative damage caused by free radicals. The objective of this study was to evaluate the use of microwave extraction of the total phenolic content from samples of traditional, special, and green coffee. The temperature and extraction time of the microwave and ethanol concentration were optimized using the univariate method. All samples were previously ground and standardized to 20 mesh. About 0.5 g of sample with 30 mL of ethanol was added to the microwave flask. The total phenolic content was determined by the Folin-Ciocalteu method with the spectrophotometric measurement at 770 nm. A 600 μL aliquot of the diluted extract (1:25) was transferred to a 15 mL Falcon® tube with the addition of 3000 μL of Folin-Ciocalteu 10% (v/v) reagent. After 5 minutes of reaction, 2250 μL of 7.5% (w/v) K_2CO_3 was added, and the mixture was kept at room temperature and protected from light for 40 minutes. The calibration curve was built in the range of 10 to 50 mg L^{-1} of gallic acid. Results were expressed in mg of gallic acid per gram of sample (mg GAE g^{-1} of the dry sample). The temperature varied from 30 to 70 °C for 5 min, using 50% (v/v) ethanol. The results obtained for the traditional, special, and green coffee samples were, respectively, in the range of 53.34 – 56.64, 32.29 – 42.86, and 28.70 – 32.34 mg GAE g^{-1} dry sample. The extraction time was varied from 5 to 30 min, at 50 °C, using ethanol 50% (v/v). The results obtained for the traditional, special, and green coffee samples were, respectively, in the range of 48.83 – 57.79, 34.45 – 36.69, and 17.56 – 31.55 mg GAE g^{-1} dry sample. While the ethanol concentration varied from 10 to 99% (v/v), during 10 min, at 50 °C, the results obtained for the traditional, special, and green coffee samples were, respectively, in the range of 3.57 – 54.36, 3.11 – 39.57 and 2.14 – 36.77 mg GAE g^{-1} dry sample. This way, the most satisfactory extraction method for coffee samples was 60 °C for 15 min and an extractor solution of 10% (v/v) ethanol. In the procedure of reference were obtained 30.66, 23.91, and 26.67 mg GAE g^{-1} dry samples, respectively, for traditional, special, and green coffees. The total phenolic content found in the microwave extraction was more satisfactory in a shorter time, demonstrating the viability of the methodology.

Agradecimentos/Acknowledgments

The authors acknowledge the financial support from the Coordination for the Improvement of Higher Education Personnel - Brazil (CAPES), National Council for Scientific and Technological Development - Brazil (CNPq), and São Paulo Research Foundation.

NIR spectral determination of genetic improvement and light accessibility effects and interactions in chemically modified yerba mate leaves

Ieda S. Scarminio (PQ),^{1*} Andressa G. de Almeida (PG),¹ Elis D. Pauli (PQ),² Miroslava Rakocevic (PQ),³ Ivar Wendling (PQ),³ Roy E. Bruns (PQ),² Gustavo G. Marcheafave (PQ).²

ieda@uel.br

¹Laboratory of Chemometrics in Natural Sciences (LQCN), Department of Chemistry, State University of Londrina, P.O.Box 6001, 86051-990 Londrina-PR, Brazil.

²Institute of Chemistry, State University of Campinas, P.O.Box 6154, 13083-970 Campinas-SP, Brazil.

³Embrapa Florestas, P.O.Box 319, Colombo, PR, 83411-000, Brazil.

Palavras Chave: Leaves, Caffeine, Chemometrics, DOE, ASCA, NIRS

Highlights

NIR fingerprints on yerba mate leaves captured the environmental stress response. ASCA determined that genetic improvement and light accessibility effects modifying the chemical composition of yerba mate leaves.

Resumo/Abstract

Genetically improved yerba mate clones are classified into two groups of interest to a selective consumer public, decaffeinated and high caffeine plants. Due to the environmental variation of planting in an agroforestry system, chemically modified yerba mate can change its chemical composition and not meet market criteria. This work aimed to investigate the chemical variation of decaffeinated plants due to five different shading levels (0%, 40%, 51%, 76%, and 82%) through direct NIR fingerprinting. To determine the significance of the chemical modification, the analysis of variance – simultaneous component analysis (ASCA) method was adopted as a chemometric investigation strategy. For the ASCA model, genetic improvement (with and without caffeine) and shading levels (0%, 40%, 51%, 76%, and 82%) dominated factors 1 and 2, respectively. Preprocessing selection of NIR spectra was based on a three-level full factorial design (3³) with the factors: normalization (standard normal variate - SNV, multiplicative signal correction - MSC and without normalization), moving average (3, 7 and 11) and derivation (without, 1st, and 2nd). The best preprocessing condition based on the smallest residual of the ASCA model was the 2nd derivative, 11-point moving average, and SNV normalization. In this case, around 50% of the total variance is due to the residual variation, *i.e.*, the variation not represented by the model and which corresponds to the signal spectral differences among the replicates. Genetic improvement has the most significant effect on the NIR spectral variability, accounting for more than 44% of the total variation, whereas shading is only 3.84% - both with $p < 0.05$. The significance of the genetic improvement confirms the chemical difference between caffeinated and decaffeinated yerba mates observed in the NIR fingerprint regardless of the light condition. Despite being low (1.84%), the effect of the interaction between genetic improvement and shading is significant ($p < 0.05$). The significance of the interaction between genetic improvement \times shading demonstrates that plants have different behaviors due to shading levels. Satisfactorily, the ASCA method associated with NIR fingerprinting indicates that the behavior of the plant with chemical modification is different from the control plant, regardless of the shading level, and can serve the consumer market.

Agradecimentos/Acknowledgments

This research received partial financial support from the Coordenação de Aperfeiçoamento de Pessoal de Nível Superior - Brasil (CAPES) - Finance Code 001 (AGA) that authors gratefully acknowledge. ISS, REB, MR and EDP thank the Conselho Nacional de Desenvolvimento Científico e Tecnológico (CNPq) for granted fellowships (PQ, Process: 302204/2018-0, 302574/2019-0; PV, Process: 350509/2020-4; PDS, Process: 102416/2022-2). GGM thanks to grant 2020/11463-5, São Paulo Research Foundation (FAPESP).

Olives salting study using self-organizing maps (SOM)-type artificial neural networks.

Heloisa H. P. Silva (IC),¹ Julia W. Campos (IC),¹ Nathan F. Silva (IC),¹ Eduardo G. de Sousa (IC),¹ Hágata C. Silva (PQ),¹ Karina B. Angilelli (PQ),¹ Marco A. J. Clemente (PQ),¹ Letícia T. Chendynski (PQ),² Dionisio Borsato (PQ).^{1*}

hhelena.p3@gmail.com; dborsato@uel.br

¹Departamento de Química, UEL; ²Instituto Federal do Paraná, Campus Ivaiporã - PR

Keywords: Multicomponent diffusion, Simulation, Stationary film, Self-organizing maps.

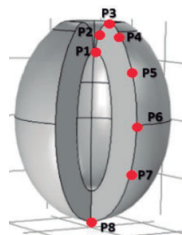
Highlights

The stationary film influence was observed in the diffusion of NaCl and KCl at the solution/olive interface. Artificial neural networks of the SOM type were an adequate tool to evaluate its behavior.

Abstract

Olives are fruits of significant importance in diet and health, since olive oil consumption reduces the risk of heart diseases. However, due to its high water activity, there is an increase in the loss of their sensory qualities. One way to preserve olives consist in immersion in sodium chloride (NaCl) brine. In order to have a healthier diet with reduced sodium content, the salt used is partially replace by potassium chloride (KCl). Inorganic salts penetrate in the biosolid through mass diffusion, which is influenced by parameters such as Biot number, that represents the film resistivity formed on the food interface in contact with a liquid. To determine these parameters during salting, semi-empirical methods are used, which includes experimental data and diffusion process simulation, and they are analyzed by self-organizing maps (SOM)-type artificial neural network. This neural network is an easy-to-view tool to evaluate the stationary film behavior through input data transformation into a discrete two-dimensional weight map. The objective of this research was to estimate the necessary salting time for the olive/brine interface to reach similar concentrations, evaluating the stationary film influence in different olive regions, applying SOM-type artificial neural networks. Olives samples were immersed in static brine containing 1196 mol m^{-3} of NaCl and 402 mol m^{-3} of KCl, and were collected during 60 h. Using finite element method and applying main diffusion coefficients, $D_{11} = 0.43 \times 10^{-12}$ and $D_{22} = 0.54 \times 10^{-12}$, cross coefficients, $D_{12} = 0.29 \times 10^{-13}$ and $D_{21} = 0.32 \times 10^{-13}$, and Biot number, $Bi = 82.05$, the inorganic salts concentrations at 8 points on the olive's surface (Figure 1) were tabulated and processed by SOM network in a 4x4 hexagonal topology and with 10000 training epochs. Olives immersion time was tested until the concentration in the chosen points were similar to the brine's, which was observed in the weight map for NaCl and KCl diffusion generated by the network. The discrete maps showed that, initially, the concentration rate increase was higher in more pronounced concavity regions (P1 and P2), which induce a longer time for film formation. However, once the film thickness had naturally increased, the diffusion rate at these points decreased relative to the others. It is worth noting that NaCl and KCl diffusion through the film, despite having similarities, differed in some ways, especially due to these ion's mobility in aqueous solution, since potassium ions have greater mobility because of its lower hydration shell. Thus, concentration sequence after the first hour was $P1 > P2 > P3 = P6 > P5 > P4 = P8 > P7$ to NaCl and $P1 = P3 > P2 = P6 > P4 > P8 > P5 = P7$ to KCl, and this sequence changed during salting process, individually for each salt. SOM-type artificial neural networks facilitated the visualization of how the stationary film influences on solutes diffusion, varying according to biosolid geometry and immersion time. Furthermore, it was possible to determined that NaCl diffusion takes 6800 h and KCl, 5100 h of salting so that the surface and brine concentrations are equivalent.

Figure 1. Chosen points on the olive surface to analyze the stationary film's behavior.



Acknowledgments

To UEL, CNPq, CAPES and Araucaria Foundation.

46ª Reunião Anual da Sociedade Brasileira de Química: "Química: Ligando ciências e neutralizando desigualdades"

Study of the origin of special green coffee beans through the determination of minerals

Eloá S. Magalhães^{a*}(PG), Winston P. C. Gomes^b (PG), Abílio Paschoalinotte Neto^a (IC), Wanessa R. Melchert^a (PQ)

*esmagalhaes@usp.br

^aCollege of Agriculture "Luiz de Queiroz", University of São Paulo, Piracicaba, SP, Brazil

^bCenter for Nuclear Energy in Agriculture, University of São Paulo, Piracicaba, SP, Brazil

Palavras Chave: Green coffee, Minerals, Microelements, FAAS

Highlights

This work aimed to use mineral determination to classify green coffee beans according to the Brazilian state of origin.

Abstract

Brazil is the largest coffee producer in the world¹. The green coffee bean (peeled fruit and waiting for roasting) has great commercial prominence. It presents varied concentrations of minerals that can change according to edaphoclimatic characteristics, demonstrating that these can be indicators of quality and differentiation². This work aimed to determine the minerals (Na, Co, Cr, Ni, Mg, K, Ca, Mn, Fe, Cu, and Zn) present in green coffee beans according to their origin and use them for characterization. A total of 10 samples were used from 5 different Brazilian states, Bahia, Espírito Santo, Minas Gerais, Paraná, and São Paulo. Dry digestion was carried out, in which 1 g of the sample was weighed in a calcined porcelain crucible and then taken to a muffle (550 °C) until the ashes turned white. The determination was carried out through a photometer and flame atomic absorption spectrometer (FAAS). The results obtained were submitted to ANOVA and Tukey analyses with a confidence level of 95% ($\alpha = 0.05$). After the data autoscaling, principal component analysis (PCA) was used in the differentiation. The most relevant Biplot are presented in Figure 1, in which the PC1xPC2 of Figure 1A and 1B present 60.27% and 60.85% of the total data variation, respectively. Statistically, K, Ca, Mn, Zn, Fe, Mg, Co, Cu, and Cr contents showed significant differences between the states. Higher Ca, Mn, Co, and Cr concentrations were estimated for São Paulo. While, Zn, Fe, Mg and Cu for Espírito Santo and K for Paraná. Figure 1 represents the PCA of the minerals correlated (a) with and (b) without the altitude variable. The altitude factor did not influence the separation of samples from the studied states since all the grains were already of excellent quality, but the concentration of the present minerals (Figure 1b). Probably due to the altitude being much more related to the organic fraction (well established in the literature) than inorganic, the latter being more influenced by the composition of the soil where the cultivation is carried out.

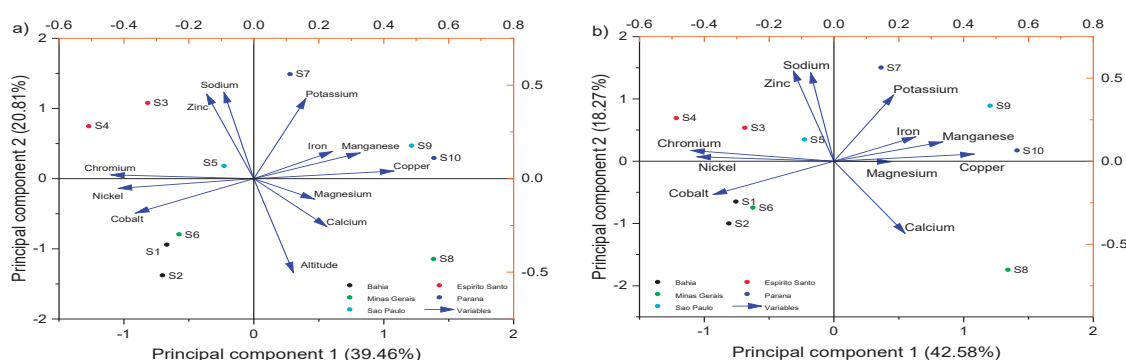


Figure 1 - Biplot of the first two main components for the special green coffee samples (S1 to S10). Mineral concentrations correlated (a) with and (b) without the altitude variable.

¹International Coffee Organization - ICO. World coffee consumption 2022. Acesso em: 20 set. 2022.

²Pohl P, Stelmach E, Welna M, Szymczycha-Madeja A. Food Analytical Methods, 2013.

Acknowledgments

The authors acknowledge the financial support from the Coordination for the Improvement of Higher Education Personnel - Brazil (CAPES), National Council for Scientific and Technological Development - Brazil (CNPq), and São Paulo Research Foundation (FAPESP).

Área: BEA

Variability of the profile of volatile compounds of robusta coffee (*Coffea canephora* var. *robusta*) from the state of Rondônia

Rodrigo Mendonça Vellozo da Silva (PG),¹ Paula Fernandes de Aguiar (PQ),¹ Vinicius Tadeu Kartnaller Montalvão (PQ),¹ Humberto Ribeiro Bizzo (PQ),² Aline Gomes Lopes Pinheiro,³ Claudia Moraes de Rezende (PQ).^{1*}

claudia.rezendeufrij@gmail.com

¹ Instituto de Química, Universidade Federal do Rio de Janeiro; ² Embrapa Agroindústria de Alimentos, Rio de Janeiro; ³ Instituto Federal de Educação Ciência e Tecnologia de Rondônia, campus Cacoal.

Palavras Chave: cromatografia gasosa-espectrometria de massas quadrupolo, microextração em fase sólida, cafés robusta, clones, análise de componentes principais, Rondônia.

Highlights

Coffees from the state of Rondônia were evaluated regarding the volatile profile and showed, among 9 analyzed variables, that the clone type is one of the main factor in differentiating them by PCA.

Resumo/Abstract

Brazil is the world's leading producer of raw coffee beans and the second largest producer of *Coffea canephora*. The main Brazilian regions producing Canephora coffee are in Espírito Santo state, followed by Rondônia, where production is concentrated in the central and northern regions of the state, especially in the municipalities of Cacoal, Alta Floresta d'Oeste, São Miguel do Guaporé, Machadinho d'Oeste, Ministro Andreazza and Nova Brasilândia D'Oeste, which produce more than 60% of the state's total. The transformations in coffee growing in this state have a strong sustainable appeal. In the last 10 years, the planted area has been reduced by 54%, but its productivity has increased by more than 155%. Accompanying these impactful numbers, there is a strong trend in the production of fine Robustas, with exotic and differentiated aromas and flavors. The productive processes of coffee growing in Rondônia involve genetic studies developed by Embrapa and a strong post-harvest follow-up, which gave rise to the movement of clones of "Robustas Amazônicos" coffees and some previous chemical analyses (Vienzk et al, 2023). Due to the peculiar sensorial aspects observed in the Robustas of this region, this work aimed to evaluate the volatile profile of 68 samples of roasted coffees from the 2021 harvest in Rondônia, having as variables: location of production, sensorial notes of the beverages, number of defects, presence of mocha beans, clone types, fermented or natural processing, type and of number of days of the drying process. Roasted (medium roast) and ground coffees were analyzed by gas chromatography coupled to mass spectrometry (GC-MS) with a quadrupole analyzer, using the technique of microextraction in solid phase with triple resin (SPME), using an automatic Combi PAL injector and internal standard. So far, the samples have only been analyzed using the GC-MS and analyzes are being processed using the GC-flame ionization detector (GC-FID), also using an internal standard (imidazole). Principal component analysis of the 68 samples, taking into account the area corrected by the internal standard of all volatile constituents detected in the GC-MS and the 9 variables considered above, preliminarily showed that the type of clone was responsible for the separation of the samples, plus of the impact of the number of days of drying, which was basically carried out by a natural process. No significant influence of other variables was detected in the separation of the analyzed coffees. Among the analyzed clones (03, 08, 10 and 25), the best separation was verified for clone 25. This plant stands out for its high grain yield during processing (ripe fruit/bean processed ratio), an aspect that corroborates the observation of the highest concentration of the sum of volatile compounds for this clone, since the degree of ripening of the coffee bean has an impact relevant in the volatiles produced in the roasting, as well as in the better sensorial classification of the coffee beverages (Velasquez et al, 2019). The main classes of volatile compounds observed were composed by pyrazine and furans, besides ketones and aldehydes, other *N*-heterocyclic compounds and sulfur derivatives. Aspects regarding the drying process of these grains are under evaluation.

References: Velásquez et al. Food Chem. v. 274, p. 137-145, 2019; Vienzk et al. J. Food Comp. Anal. v.117, p.105140, 2023.

Agradecimentos/Acknowledgments

The authors thank Faperj, CNPq, Capes and Embrapa Café for financial support and scholarship.

BIO

Química Biológica

46^a Reunião
Anual da **SBQ**

28 a 31 de Maio de 2023

Águas de Lindóia · SP
Hotel Monte Real

Biotransformation of perillyl alcohol into perillyl butyrate using lipases (*Rhizomucor miehei*) immobilized on lignin from cashew apple bagasse.

Vanessa Moreira Frota (IC),¹ Emanuella Cristina dos Santos Moita (IC),¹ Carlos Alberto Chaves Girão Neto (PG),² Jean Parcelli Costa do Vale (PQ),¹ Hécio Silva dos Santos (PQ),¹ Kirley Marques Canuto (PQ),³ Maria Valdez Pontes Rocha (PQ),² Tigressa Helena Soares Rodrigues (PQ).^{1*}

Categorias: Pesquisador (PQ), Estudante de graduação (IC).

vanessa-frota1@hotmail.com; thelenasr@yahoo.com.br

¹Departamento do Curso de Química, Centro de Ciências Exatas e Tecnologia, Universidade Estadual Vale do Acaraú – UVA;

²Departamento de Engenharia Química, Centro de Tecnologia, Universidade Federal do Ceará – UFC;

³Embrapa Agroindústria Tropical (CNPAT-EMBRAPA);

Palavras Chave: Esterification, Terpenic esters, Immobilization.

Highlights

- Application of magnetic-lignin as support for lipases immobilization and perillyl butyrate production
- Higher yields, productivity were achieved with lipases immobilized
- Recycling kept satisfactory results of perillyl butyrate yields

Resumo/Abstract

Biotransformation is an alternative route for the biomolecules production of industrial interest (Almeida SÁ et al., 2017). Despite the numerous advantages of biocatalysis, the cost of the biocatalyst becomes a major challenge in the consolidation of biotransformation (Bilal and Iqbal, 2019). In this sense, the production of terpene esters using enzymes immobilized on low-cost supports such as cashew apple bagasse becomes a promising alternative for these derivatives obtention. Thus, the objective of this work was to study the enzymatic esterification of perillyl alcohol into perillyl butyrate using free and immobilized lipases (*R. miehei*) in lignin from cashew apple bagasse. The immobilization support (magnetic-lignin) was obtained from a mixture of $\text{FeSO}_4 \cdot 7\text{H}_2\text{O}$ and $\text{FeCl}_3 \cdot 6\text{H}_2\text{O}$ in solution with lignin solubilized in NH_4OH . The enzymatic esterification of perillyl alcohol was carried out in two molar ratios (1:1 and 1:2) of terpenic alcohol and butanoic acid and two temperatures (50 and 55 °C) for 24 hours and 200 rpm. Heptane was used as solvent and the biocatalyst (free and immobilized) was used at the concentration of 10 mg/mL. The acid and alcohol consumption, ester formation were monitored via gas chromatography coupled to a flame ionization detector (GC-FID). Yields were calculated based on the ester and terpene alcohol areas obtained from the chromatogram (Ferraz et al., 2015). The results showed that for both biocatalysts (free and immobilized) it was possible to obtain perillyl butyrate, with the best yield result (90.5%) obtained for RML immobilized in 10 hours of esterification. In the same period, the ester was obtained with a yield of 61.4% when free lipase was used. It should also be noted that for the immobilized enzyme, a high yield of perillyl butyrate (86.1%) was obtained in 2h of esterification, a value higher than the yield (11.3%) using free enzyme. Increasing the acid ratio and temperature did not result in a significant increase in ester yield. Recycling the immobilized enzyme for seven consecutive cycles kept the perillyl butyrate yield in the 91-95% range. Thus, it can be seen that the use of immobilized lipase in magnetized lignin confers operational stability to the biocatalyst, allowing to obtain bioproducts with high yields and productivity. In addition, the satisfactory yields achieved with recycling makes the biotechnological route a promising alternative in obtaining terpene esters.

Agradecimentos/Acknowledgments

BPI/Funcap (n° BP4-0172-00122.01.00/20)

Área:

-BIO-

(Inserir a sigla da seção científica para qual o resumo será submetido. Ex: ORG, BEA, CAT)

Boronic acids with inhibitory action on the P2X7 receptor do not act on the cannabinoid receptor.

Noemi de J. Hiller (PG),¹ Caio F. Souza (PG),² Ana L. M. Ventura (PQ),² Robson X. Faria (PQ),³ Daniela, de L. Martins (PQ)¹

fernandopenteado@seuemail.com; felipesshmelo@seuemail.com (do autor que submete E do autor principal, separados por;) dlmartins@id.uff.br, www.danielamartinsgroup.com.br

¹Universidade Federal Fluminense, Grupo de Pesquisa em Catálise e Síntese (CSI), Laboratório 413, Niterói, RJ, Brasil. www.danielamartinsgroup.com.br; ²Departamento de Neurobiologia- UFF; ³Fiocruz, Laboratório de Avaliação e Promoção de Saúde Ambiental, Rio de Janeiro, RJ, Brasil.

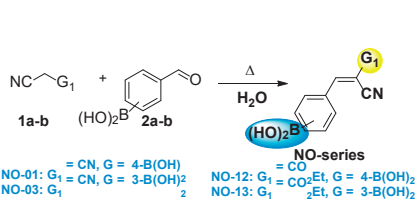
Palavras Chave: (máximo 6, separadas por vírgula, primeiras letras em maiúscula, arial 9, itálico)-Chicken retinal cell, neurons, retinal glial cells, Knoevenagel, boronic acids, organoboron,

Highlights

NO series boronic acid derivatives inhibit P2X7 receptor.
NO series boronic acid derivatives do not inhibit cannabinoid receptors.
NO series has no toxicity in chicken retinal cell cultures.

Resumo/Abstract

In chicken retinal cell cultures, both ATP, through the P2X7 receptor, and cannabinoids can induce cell death. On the other hand, NO series boronic acid derivatives are capable of inhibiting P2X7 receptor activation in macrophages. In this work, the effect of the boronic acid organoboron derivatives NO-01, NO-02, NO-12 and NO-13 on cultured retinal cell death induced by WIN 55212-2, a nonselective synthetic cannabinoid, was investigated. The NO series was prepared through Knoevenagel condensation in an aqueous medium (Scheme 1).



Scheme 1 - Knoevenagel condensation of the NO series

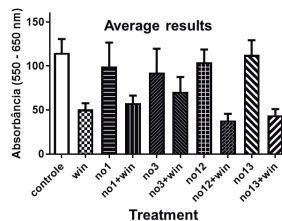


Figure 1 - Viability test with MTT, 24 h treatment with 20 μM of NOs and 1 μM of WIN 55212-2

The chicken embryo cells were incubated for 24 h with 1 μM WIN 55212-2 in the presence or absence of 20 μM derivatives NO-01, NO-03, NO-12 and NO-13. Cell survival was estimated by the MTT assay. Treatment of cultures with WIN induced a significant ~55.8% decrease in cell survival in cultures. No decrease in cell viability was observed when cultures were treated with 20 μM NO compounds, suggesting that these molecules do not show toxicity to neurons or retinal glial cells at this concentration (Figure 1). No attenuation of the WIN-induced decrease in cell viability was observed when cultures were treated with WIN + NOs. Additionally, we analyzed higher concentrations (30 - 50 μM) of NO-01 and NO-03 derivatives (P2X7 IC₅₀ macrofago: 0.630 μM), the main boronic acid compounds that inhibit P2X7 receptor activation, was not able to block the deleterious effect induced by WIN in retinal cultures. Thus, these data suggest that NO-01, NO-02, NO-12 and NO-13 derivatives are neither toxic nor capable of blocking cannabinoid receptors in retinal cells.

Agradecimentos/Acknowledgments

Sociedade Brasileira de Química (SBQ)

Agradecemos ao fomento: CNPq (número de processo: 308755/2018-9, 455739/2014-5, 316568/2021-0), CAPES e FAPERJ (número de processo: E-26/010.001861/2019; E-26/203.246/2017, [E-26/210.242/2019](#), E-26/211.025/2019, E-26/200.982/2021, E-26/211.343/2021. [PROPP/UFF edital FOPESQ-2022](#). O presente trabalho foi realizado, em parte, com apoio da Coordenação de Aperfeiçoamento de Pessoal de Nível Superior - Brasil (CAPES) - Código de Financiamento 001.

Recomendamos fortemente o uso da língua inglesa nos resumos, uma etapa importante na internacionalização do evento.

Formatado: Espaçamento entre linhas: simples

Formatado: TA_Main_Text, À esquerda, À direita: 0 cm

Formatado: Justificado, Espaço Depois de: 0 pt, Espaçamento entre linhas: simples

Área: BIO_

(Inserir a sigla da seção científica para qual o resumo será submetido. Ex: ORG, BEA, CAT)

Capillary bioreactors based on nucleoside hydrolase from *Leishmania donovani*: A direct approach for ligand identification and characterization

Camila A. Wegermann (PQ)¹, Evelyn S. Bezerra (IC)¹, João P. C. F. Brunhosa (IC)¹, Isabella G. M. Sant'Anna (PG)¹, Luzineide W. Tinoco² (PQ), Marcela C. de Moraes¹ (PQ)*

mcmoraes@id.uff.br

¹ BioCrom, Instituto de Química, Universidade Federal Fluminense, Niterói, RJ, Brasil

² IPPN, Universidade Federal do Rio de Janeiro, RJ, Brasil

Palavras Chave: *Inibidores, Leishmaniose, Cromatografia, nucleosídeo hidrolase*

Highlights

A capillary bioreactor based on nucleoside enzyme was prepared. The reactor was inserted in a multidimensional chromatographic system for on-flow activity and inhibition assays.

Resumo/Abstract

Leishmaniosis disease is a current disease in underdeveloped countries and despite the severity of the treatment, the discovery of drugs more efficiently is poorly encouraged. Its severe form is visceral leishmaniasis and its main protozoa causative agent is *Leishmania donovani*. This protozoan life is exclusively dependent on the purine salvation pathway for nucleoside acquisition¹. Therefore, the nucleoside hydrolase *Leishmania donovani* (*LdNH*) enzyme is an important target for new bioactive compounds. This project aims the development, validation, and application of a multidimensional liquid chromatography method to monitor *LdNH* activity, after immobilizing it in fused-silica capillaries, through the quantification of the formed product. Firstly, *LdNH* enzyme was covalently immobilized onto fused-silica capillary tubes (10 cm and 50 cm), creating the *LdNH*-IMERs², which were inserted in the first dimension of the chromatography system. The activity of the obtained IMERs were monitored online in a multidimensional liquid chromatography system, by the quantification of the inosine hydrolysis product, hypoxanthine, formed throughout the enzymatic reaction. For that, an octyl column (Luna-Phenomenex 100, 10 μ m, 10 x 0.46 cm) was inserted in the second dimension to furnish the chromatographic separation of inosine and hypoxanthine. For the *LdNH*-IMER, phosphate buffer saline (KH₂PO₄ 300 mmol/L and NaCl 20 mmol/L, in water, pH 7.4) was used as the mobile phase at a flow rate of 0.05 ml/min, while the mobile phase containing triethylamine (1% in water, v/v, acidified with AcOH pH 6.0):MeOH (95:5), at flow rate 0.8 mL.min⁻¹ was used for the analytical column. The analytical method was validated by studying its linearity through the determination of a calibration curve for hypoxanthine ranging from 0.4 to 1.0 mmol/L ($y = 7919x - 161600$, $R^2 = 0.9989$). The intra- and inter-day precision and accuracy of the method were evaluated by analyzing quality control samples at three different concentrations, namely 450, 650, and 950 μ mol/L. The kinetic analysis indicated a K_M value of 4424.57 ± 143.33 μ mol/L for 50 cm *LdNH*-IMER and 2341.08 ± 112.58 μ mol/L for 10 cm *LdNH*-IMER, which is approximately 12 times or 6 times higher than that of the free enzyme ($K_M = 370$ μ mol/L) respectively. At this point, quinolonic ribonucleoside derivative (compound 17A) was used to validate the 50 cm *LdNH*-IMER as an inhibitor screening method. *LdNH*-IMER exhibited a concentration-dependent response to this inhibitor, and the IC_{50} value was 72.3 μ mol/L. The tests of IC_{50} for 10 cm *LdNH*-IMER and the inhibition constant for both bioreactors are under investigation using the 17A compound and analogs. The results revealed that the *LdNH*-IMERs herein described represent a useful tool for *LdNH* inhibitor automated screening of several compounds, using only a few amounts of the enzyme to prepare the bioreactor. The study also indicates the possibility of screening new substances and complex mixtures.

Agradecimentos/Acknowledgments

CNPq, FAPERJ, PPGQ-UFF, PROAP-UFF, CAPES, BIOCROM.

[1] MORAES, M. et al. Journal of Pharmaceutical and Biomedical Analysis 211 (2022)

[2] MORAES, M. et al. Journal of Chromatography A, (2012) 110-115

Cerulenin-producing *Sarocladium oryzae* BRM 59907 as a promising biocontrol agent against phytopathogenic fungi in postharvest diseases

João Rogério B. A. Rodrigues (PG),^{1*} Otniel F. Silva (PQ),² Marcio Vinicius C. B. Côrtes (PQ),³ Elisa D. Cavalcanti (PQ),⁴ Denise M. G. Freire (PQ).⁴

joao.rogerio.borges.amorim@hotmail.com

¹Biochemistry Graduate Program (PPGBq), Federal University of Rio de Janeiro (UFRJ); ²EMBRAPA Agroindústria de Alimentos; ³EMBRAPA Arroz e Feijão, Brazilian Agricultural Research Corporation; ⁴Department of Biochemistry, Federal University of Rio de Janeiro (UFRJ).

Palavras Chave: *Sarocladium oryzae*, Postharvest diseases, Cerulenin, Biological control, *Penicillium expansum*.

Highlights

For the first time *in vitro* assays suggest that *Sarocladium oryzae* BRM 59907 exhibits good antagonistic activity against *Penicillium expansum*, a psychrophilic fungus that causes blue mold in citrus.

Resumo/Abstract

Food safety and the environmental impacts caused by the application of synthetic pesticides has stimulated the use of biopesticides by Brazilian farmers. After the creation of the National Program for Biobased Agricultural Inputs (2020), so far there has been no product registration against post-harvest pathogens, which cause critical losses for the horticultural sector in the state of Rio de Janeiro. Among them, *Penicillium expansum* can infect citrus fruit in the mature stage and produce carcinogenic mycotoxin patulin. Some strains of *Sarocladium oryzae* has a high capacity to produce cerulenin, a potent low-toxicity and biodegradable fungicide¹.

The present work aimed to evaluate *in vitro* antagonism of *Sarocladium oryzae* BRM 59907 strain against *P. expansum*. The isolates of each fungus were grown in 90 mm x 15 mm Petri dishes containing PDA medium, which were incubated in a BOD chamber at 25 °C for 7 day. The paired method was used, in which 5 mm mycelial discs of the phytopathogen and the biological control agent (BCA) were removed from the edge of actively growing culture and transferred to the center of another Petri dish with sterile PDA, on opposite sides, spaced about 40 mm from each other. The assay was performed in triplicate and mycelial growth was monitored for 15 days. The percentage of *P. expansum* mycelium growth inhibition was calculated according to Bruissson and coworkers² by the formula: Inhibition percentage = 100% × (A_c - A_b - A_t)/(A_c - A_b), where A_c - A_b is the area available for the phytopathogen growth in Petri dish and A_t is the area effectively colonized in Petri dish. The areas were measured in treated pictures with software WebPlotDigitizer³. The results are shown in figure 1, where bars represent average inhibitions with standard deviation. After the fifteenth day, a mean percentual inhibition of (73,8 ± 2,89)% for *P. expansum* was achieved without mycelium contact, showing interaction type B in Badalyan rating (deadlock at distance)⁴, while BCA experienced just a small inhibition of (18,2 ± 2,28)%. It suggests some extracellular metabolites of *S. oryzae* can be responsible for its great antagonistic activity, making it a good biopesticide candidate for *in vivo* tests in citrus.

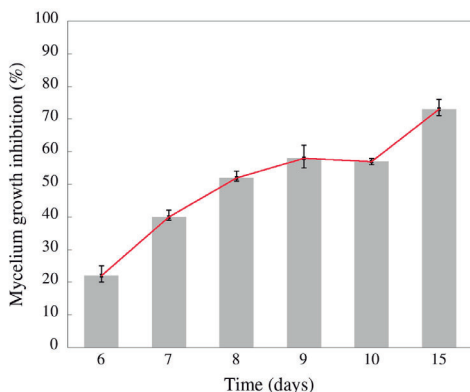


Figure 1. Mycelium growth inhibition of *P. expansum* in 6, 7, 8, 9, 10 and 15 days.



Figure 2. *In vitro* dual culture test of phytopathogen *P. expansum* (T1) paired with *S. oryzae* (T2) after 15 days.

¹Cortês et al. *Fungal Biology Reviews*, 27, 1-7, 2021.

²Bruissson et al. *Frontiers in Microbiology*, 10, 2726, 2019.

³Rohatgi, A. (2015). WebPlotDigitizer (Version 3.9). Retrieved from <http://arohatgi.info/WebPlotDigitizer>

⁴Badalyan et al. *Phytopathol. Mediterr.*, 43, 44–48, 2004.

Agradecimentos/Acknowledgments

The authors are grateful to CAPES, FAPERJ and ANP for financial support.

Cobalt Ferrite Magnetic Nanoparticles as Novel Solid Supports to Enzyme Immobilization for Screening Assays

Miguel F. S. de Abreu¹ (IC),¹ Renato C. S. Lessa (PG)¹, Pamela C. O. de Oliveira (PG)¹, Martin Albino² (PQ) , Claudio Sangregorio² (PQ), Marcela C. DE MORAES¹ (PQ)*

miguelfranco@id.uff.br; mcmoraes@id.uff.br

¹ Biocrom, Departamento de Química Orgânica, UFF ; ²Instituto de Química Ugo Schiff, UNIFI – Florença, Itália

Key Words: *Magnetic, Nanoparticles, enzymes, screening assays, optimization.*

Highlights

SmMTAP was immobilized on cobalt ferrite magnetic nanoparticles. Its activity was monitored by HPLC-DAD. Kinetic, stability, and reusability assays were conducted.

Abstract

Schistosomiasis is a neglected parasitic disease caused by parasitic flatworms of the genus *Schistosoma*, which transmission has been reported in 78 countries. According to WHO (World Health Organization, 2023), at least 236.6 million people required preventive treatment in 2019, which should be repeated over several years. Praziquantel, the most employed anti-schistosomal drug, however, it does not prevent reinfection and the emergence of drug resistance is relevant. Therefore, seeking the discovery of new potential drugs for schistosomiasis treatment, biochemical pathways vital to the parasite have been investigated. ¹ *Schistosoma mansoni*. is exclusively dependent on the salvage pathway for its purine requirement, to which the 5'-deoxy-5'-methylthioadenosine phosphorylase (SmMTAP) enzyme belongs. ² Therefore, the development of new screening assays to rapidly identify new SmMTAP is an important task.³ Screening assays using immobilized enzymes furnish lower cost and interference, reusability, and increase enzyme stability. For that matter, magnetic nanoparticles (MNP) are being used as solid support for enzyme immobilization in the development of in a variety of bioassays.⁴ This work describes SMTAP immobilization on cobalt ferrite MNP and the further activity monitoring through the quantification of the formed product (adenosine) by high-performance liquid chromatography (HPLC). The cobalt ferrite nanoparticle (Co x Fe 3-x O 4) was obtained by the thermal decomposition of iron (III) acetylacetonate and cobalt (II) acetylacetonate in benzyl ether, using oleic acid as a stabilizing agent and oleylamine as reductor agent. This particle was functionalized with amine groups and thereafter reacted with glutaraldehyde as a crosslinking agent. The HPLC-DAD method performed the separation of adenine adenosine using an octadecyl column (150 × 4,6 mm i.d., 3 µm, Sigma Aldrich) and a solution of NH₄OAC 20mmol L⁻¹/ACN (95:5) as mobile phase, at a flow rate of 0,8 mLmin⁻¹. The detection was conducted at 260 nm. The developed method was validated with respect to linearity ($y = 17824x + 1066.6$, $R^2 = 1$), accuracy, intermediate precision, and limits of quantification and detection. The next step involved the enzyme immobilization via the formation of a Schiff base, and the optimization of the enzyme-support incubation time: 4h and 16h. The reactional conditions for the biocatalysis were optimized taking into account different reaction times (5, 10, and 20 minutes) and the amount of SmMTAP-coated MNPs (5, 10, and 25 µg). For the SmMTAP-MNP incubation during the immobilization process, it was concluded that 4 h yielded the highest active IMER. The best enzyme-support incubation time was 4h, while the best catalysis conditions involved 5 µg of SmMTAP-coated MNPs and 20 min of reaction time. Stability assay indicates immobilized SmMTAP retained approximately 100% of its initial activity within 7 days. The reusability revealed a capacity of up to 7 cycles until the activity reached 50% of the initial rate. At last, the Michaelis-Menten constant was estimated as $68 \pm 7,6 \mu\text{M}$. These results, alongside the achieved time/ support amount relationship, demonstrate that the immobilized SmMTAP-MNP is suitable for future activity-based screening assays.

Acknowledgments

Faperj, CAPES e CNPq.

References: ¹World Health Organization. Schistosomiasis. 01/08/2022. Available on : [Schistosomiasis \(who.int\)](https://www.who.int). Accessed 01/27/2023. ²Gryseels, B., Polman, K., Clerinx, J., & Kestens, L. *The Lancet*, 368 (9541), 1106–1118, **2006**. ³Trindade Ximenes, I. A., de Oliveira, P. C. O., Wegermann, C. A.; de Moraes, M. C. *J Pharm and Biomed Anal*, 204, 114-286, **2021**.⁴de Moraes, M.C., Cardoso, C.L. & Cass, Q.B. *Anal Bioanal Chem* 405, 4871–4878, **2013**.

Área: BIO

(Inserir a sigla da seção científica para qual o resumo será submetido. Ex: ORG, BEA, CAT)

Development of a novel screening method for *SmMTAP* enzyme inhibitors

Renato C.S. Lessa (PG),¹ **Miguel F.S. Abreu** (IC),¹ **Vinicius G.C. Madriaga** (PQ),² **Thiago M. Lima** (PQ),² **Vanessa G.P. Severino**,³ **Marcela C. Moraes** (PQ).^{1*}

renatolessa@id.uff.br; mcmoraes@id.uff.br

¹Departamento de Química Orgânica, UFF; ²Departamento de Química Inorgânica, UFF; ³Instituto de Química, UFG

Palavras Chave: HPLC, Natural matrixes, Immobilized enzymes, Screening assay, Selective interaction

Highlights

The enzyme *SmMTAP* was immobilized in a solid support to screen for selective bioactive compounds, in complex natural matrixes, that act as enzyme inhibitor to treat schistosomiasis.

Resumo/Abstract

Enzyme immobilization on solid supports is a process that allows the same enzymes to be employed in successive assays and increases their mechanical, thermic, and pH resistance. Moreover, the catalytic medium becomes heterogeneous, allowing simple separation methods for enzyme recovery, a process that would be unviable in a homogeneous media.¹ This approach is particularly interesting for medicinal chemistry to screen for novel potential selective bioactive compounds, that act as enzyme inhibitors, such as complex natural matrixes, since laborious purification and identification of each component present in the matrix is not necessary. Therefore, the enzyme *SmMTAP* (5'-deoxy-5'-methyladenosine phosphorylase from *Schistosoma mansoni*) was covalently immobilized in dendritic silica, a solid support classified as a mesoporous material.² This enzyme was chosen as the pharmacological target for this project since schistosomiasis is a neglected tropical disease that lacks efficient drugs to adequately control and treat it.³ A HPLC-DAD method for separating the catalytic product adenine from the substrate adenosine was previously optimized⁴ and employed in the direct quantification of the product adenine for *SmMTAP* activity monitoring. The bioreactor containing the immobilized *SmMTAP* consisted of 50 µg of solid support containing the immobilized enzyme for a final volume of 200 µL in K₂HPO₄ 100 mM pH 7.4 medium and 20 minutes of reaction under rotative mixing. For the kinetic study, adenosine concentrations ranging from 2 to 896 µM were used in the activity assays in duplicity. The obtained data yielded a hyperbolic graph that fitted the Michaelis Menten enzymatic behavior with a R² of 0.9944 and Michaelis Menten constant value of 64.7 ± 6.7 µM. The stability assays demonstrated that at 4°C in TRIS HCl 100mM pH 7.4 buffer, bioreactor retained maximum level of its activity over the first three days, differently from K₂HPO₄ 100mM pH 7.4 (optimal enzymatic activity buffer) in which enzymes lost almost 70% of their activity at the same time. Reusability assays pointed out great potential to employ the same enzymes in successive assays, as no significant loss in catalytic efficiency was observed over seven consecutive cycle assays. Lastly, a screening assay with over fifteen natural extracts at concentrations of 200 µg/mL allowed the easy identification of sources of potentially bioactive compounds against schistosomiasis, with three of them showing inhibition between 67.5 and 81.6%. Those extracts will be further investigated in a ligand fishing assay to isolate the bioactive compounds.

References: 1) De Oliveria, P. C. O.; Lessa, R. C.; Ceroulo, M. S.; Wegemann, C. A.; De Moraes, M. C. *Front. Anal. Sci.* **2022**, 2:1004113; 2) Jorge, E. Y. C.; Lima, C. G. S.; Lima, T. M.; Marchini, L.; Gawande, M. B.; Tomanec, O.; Varma, R. S.; Paixão, M. W. *Green Chem.* **2020**, 22, 1754; 3) Wang, J.; Paz, C.; Padalino, G.; Coghlan, A.; Lu, Z.; Gradinaru, I.; Collins, J. N. R.; Berriman, M.; Hoffmann, K. F.; Collins III, J. J. *Science* **2020**, 369, 1649; 4) Kiebling, P.; Scriba, G. K. E.; Sub, F.; Werner, G.; Knoth, H.; Hartmann, H. *J. Pharm. Biomed. Anal.* **2004**, 36, 535.

Agradecimentos/Acknowledgments

Faperj, CAPES and CNPq.

Enzymatic esterification for perillyl valerate production using lipases (*Rhizomucor miehei*) immobilized on cashew apple bagasse lignin.

Amanda Santos da Silva (IC),¹ Vanessa Moreira Frota (IC),¹ Maria Gisele Medeiros Chaves (IC),¹ Carlos Alberto Chaves Girão Neto (PG),² Jean Parcelli Costa do Vale (PQ),¹ Hécio Silva dos Santos (PQ),¹ Lorena Mara Alexandre e Silva (PQ),³ Maria Valderez Ponte Rocha (PQ),² Tigressa Helena Soares Rodrigues (PQ).¹

Categorias: Pesquisador (PQ), Estudante de graduação (IC).

amandasantodasilva1993@outlook.com; thelenasr@yahoo.com.br

¹Departamento do Curso de Química, Centro de Ciências Exatas e Tecnologia, Universidade Estadual Vale do Acaraú – UVA;

²Departamento de Engenharia Química, Centro de Tecnologia, Universidade Federal do Ceará – UFC;

³Embrapa Agroindústria Tropical (CNPAT-EMBRAPA);

Palavras Chave: *Biotransformation; Enzymes; Immobilization.*

Highlights

- Biotransformation of perillyl alcohol in perillyl valerate
- Lipases (*R. miehei*) immobilization in magnetic-lignin from cashew apple bagasse
- Perillyl valerate yields two-times higher for immobilized enzyme

Resumo/Abstract

Terpene esters are compounds consisting of a terpene alcohol and an organic acid, generally short-chained, which are of great interest in the pharmaceutical, cosmetics and food industries. As the biocatalyst is the most expensive component of this process, the application of immobilized enzymes on low-cost supports becomes an alternative for the industrial consolidation of the biotransformation. In this sense, the objective of this work was to study the enzymatic esterification of perillyl alcohol in perillyl valerate using free and immobilized lipases (*R. miehei*) in magnetic-lignin from cashew apple bagasse. The immobilization support was produced from a solution of FeSO₄.7H₂O and FeCl₃.6H₂O and a solution of lignin in NH₄OH. The enzymatic esterification of perillyl alcohol and valeric acid was performed in two stoichiometric ratios (1:1 and 1:2) at two temperatures (50 and 55 °C) during a period of 24h and 200 rpm. Heptane was used as solvent with lipases at 10 mg/mL. An aliquot of 0.1 mL was used for esters yields determination via gas chromatography coupled to a flame ionization detector (GC-FID). Yields were calculated based on the ester and terpene alcohol areas obtained from the chromatogram. The results showed that for lipases free and immobilized it was possible to obtain perillyl valerate, however, a higher yield was obtained with immobilized enzyme (90.3%) when compared to the yield with free enzyme (41.6%), in the ratio of 1:1 at a temperature of 50 °C after 10h of esterification. Furthermore, in 2h of esterification, the yield with immobilized lipases (85.8%) was 11 times greater than that of esterification with free lipase (7.5%). This result can be attributed to the operational stability of the biocatalyst that is achieved by the immobilization process. There was no significant increase in ester yield when the acid ratio and temperature was increased. Furthermore, the reuse of the immobilized enzyme in 7 consecutive cycles kept the ester yield constant in the range of 91-94%. According to the data obtained, it can be seen that the study of immobilized lipases in magnetized lignin allowed obtaining satisfactory yields of perillyl valerate in seven consecutive cycles, adding important advantages to its use such as support low-cost and recycling.

Agradecimentos/Acknowledgments

BPI/Funcap (n° BP4-0172-00122.01.00/20)

Enzyme immobilization on magnetic nanoparticles for in-line activity-based screening assays

Pamella C.O. Oliveira (PG),^{1,*} Pedro R.C. Medeiros (IC),¹ Martin Albino (PQ),² Luzineide W. Tinoco (PQ),³ Gilberto A. Romeiro (PQ),¹ Claudio Sangregorio (PQ),² Marcela C. Moraes (PQ)¹

pamella_ortega@id.uff.br

¹Departamento de Química, UFF-Niterói; ²Departamento de Química, UNIFI-Florença; ³IPP, UFRJ-Rio de Janeiro

Keywords: Magnetite, High throughput assay, On-flow system, Nucleoside hydrolase, Visceral leishmaniasis.

Highlights

Direct on-flow monitoring of nucleoside hydrolase activity. Novel application of superparamagnetic iron oxide nanoparticles. Kinetic study of different LdNH IMERs.

Resumo/Abstract

Automated high-throughput systems enable the evaluation of large libraries and accelerate the identification of new inhibitors in the drug discovery program. In the development of new screening assays, magnetic particles (MP) are considered versatile solid supports with outstanding properties.¹ This work reports the immobilization of the Nucleoside hydrolase (NH) enzyme, an important biological target for the development of antiparasitic drugs, on magnetic nanoparticles (MNP). NH is considered essential for the protozoa survival and replication.² The development of new reliable and automated screening assays for the rapid identification of potential drugs is of paramount importance. MNP with different coatings were synthesized and evaluated in the development of a high-efficiency activity assay. For this, iron oxide MNP of 25 nm was submitted to two coating/functionalization approaches: silica shell (SS) and surface ligand exchange (LE). The proposed immobilization procedure was based on a previous work, that used commercial micrometric magnetic particles for this assay, in which glutaraldehyde was used as a crosslinking agent to covalently immobilize the LdNH enzyme. After immobilization, LdNH-MNPs were trapped inside a TFE Teflon tube (0.3 mm i.d. x 1.6 mm o.d. x 10 cm) using 8 neodymium magnets, resulting in an immobilized-enzyme reactor (IMER). Each IMER was connected in series to an analytical column - Eclipse XBD C18 Agilent column (150 x 4.6 mm) - in a HPLC system (Figure 1). The chromatographic conditions used a Et₃N solution (1% v/v, pH 6.0 acidified with AcOH)/MeOH (95:5), as the mobile phase of the pump B, at a flow rate of 0.8 mL.min⁻¹; and PBS buffer (20 mmol.L⁻¹, pH 7.4, 300 mmol.L⁻¹ NaCl) as the mobile phase of pump A with a flow rate of 0.02 mL.min⁻¹. Kinetic studies provided the Michaelis-Menten constant (K_M) for the substrate for each assembled IMER (Table 1). This study revealed that even smaller amounts (30 ng) of MNP could be used for activity assays without affecting substrate-NH affinity as evidenced by the similar K_M values to the one obtained for the IMER with commercial particles. The NP-LE presented a higher enzyme mass that enables using lower quantities of LdNH-MNPs maintaining the lower K_M values.

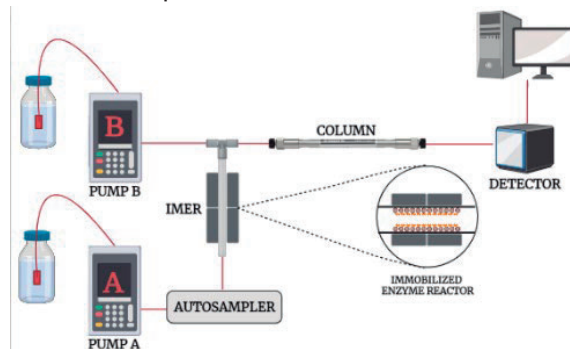


Figure 1: Representation of inline system with LdNH IMER.

Table 1: Kinetic studies for IMERs with different MNPs.

Particles	NH/Support (wt/wt)	K _M (μM)	
		1.0 μg support	0.03 μg support
MP _{Commercial}	0.97	2079 ± 87 ³	-
NP-LE	1.44	3134 ± 135	2180 ± 114
NP-SS	1.04	3722 ± 251	2898 ± 221

[1] Ximenes, I. A. T. et al. J. Pharm. Biomed. Anal. 2021, 204, 114286.

[2] Figueroa-Villar, J.S.; Sales, E.D. Chem. Biol. Interact. 263, 18-27, 2017.

[3] Oliveira, P.C.O. et al. 44^a RAVSBQ 2020.

Agradecimentos/Acknowledgments

This study was financed in part by the Coordenação de Aperfeiçoamento de Pessoal de Nível Superior – Brasil (CAPES) – Finance Code 001; CAPES-PRINT, FAPERJ and CNPq.

Evaluation of the enzyme inhibition activity and *in silico* study of *n*-substituted cinnamic esters against acetylcholinesterase (AChE) present in the larval extract of *Ae. aegypti*

Saraliny B. França (PG),^{1*} Ari S. Guimarães (PG),¹ Marcone G. dos Santos (PG),¹ Jamilly E. S. Rodrigues (IC),¹ Sônia S. Machado (PQ),¹ Edeildo F. Silva – Júnior (PQ),¹ Dimas J. P. Lima (PQ).¹

sara.liny15@hotmail.com

¹Graduate Program in Chemistry and Biotechnology, UFAL;

Key words: Protein quantification, Biological activity, Cinnamic acid derivatives, Covalent docking, Physical-chemical properties and Insects.

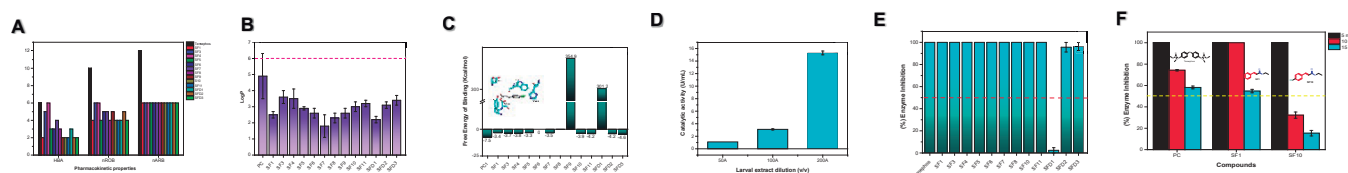
Highlights

The larval extract showed 15.3 U/mL of AChE. Inhibitory and *in silico* studies of the cinnamic esters show that the larvicidal action is due to partial inhibition of AChE.

Resumo/Abstract

AChE has the function of degrading one of the neurotransmitters, responsible for the excitation of insects, acetylcholine.¹ Most insecticides act through this route, as organophosphates, especially temephos, however they are toxic to the ecosystem.¹ Thus, the cinnamic esters have demonstrated larvicidal action against *Ae. aegypti*, however its route of action is still unknown.² Thus, the objective of this work is to evaluate the mechanistic route from *in silico* studies and the AChE present in the larval extract of *Ae. aegypti*. The *in silico* results corroborate the larvicide study,² and the pharmacokinetic properties are consistent with good insecticides (Fig. 1A-B).³ Furthermore, through covalent docking studies it was possible to observe that cinnamic esters with electro-withdrawal groups (-Cl, -Br, -NO₂, -CF₃, -OCF₃, -F and -CN) had effective bond free energies of -3.3 to -4.6 Kcal/mol, while temephos (positive control) had -7.5 Kcal/mol (Fig. 1C).

Fig. 1 In Silico results and analysis of catalytic and inhibitory activity of cinnamic esters.



Legenda: A - Physical-chemical properties; B - Lipophilicity, C - Covalent Docking, D - Catalytic activity of the larval extract; E- enzymatic inhibition; F- Enzyme inhibition kinetics.

From the protein quantification, it can be seen that the crude extract has 2.380 µg/mL of total proteins, presenting 15.3 U/mL of AChE in the dilution of 200 v/v (Fig. 1D). Furthermore, in the inhibitory study, esters with electro-withdrawal groups showed promise at a concentration of 100µM, consistent with temephos (Fig. 1E). Thus, through the kinetic study of the half-life of temephos, ethyl cinnamate (SF1) and ethyl *p*-chlorocinnamate (SF10) at a concentration of 15µM, it is possible to observe a 100% inhibitory action in the initial 5 minutes, right after the AChE's catalytic activity is initiated (Fig. 1F). Therefore, these compounds may act as AChE inhibitors present in *Ae. aegypti* in its larval stage, through the process of enzymatic hydrolysis to express its insecticidal action.

Agradecimentos/Acknowledgments

CAPES, CNPq, FAPEAL, UFAL, LMC e LEAp.

References: [1] BRAGA, I. M & VALLE, D. *Epidemiologia e Serviço de Saúde*, 16, 2007; [2] FRANÇA S. B. et al, *Bioor. Med. Chem*, 44, 2021; [3] HAO, G. et al, *Mol. Inf*, 30, 2011.

Evaluation of the protective effect of piceatannol against glycation of human hemoglobin

Tauane S. Rocha (PG),¹ Rosylene P. C. Lopes (IC),¹ Iara B. Valentim,² Josué C. C. Santos (PQ),¹ Marília O. F. Goulart (PQ),¹ Jadriane A. Xavier (PQ)^{1*}

tauane.rocha@iqb.ufal.br; jadrianexavier@iqb.ufal.br

¹Instituto de Química e Biotecnologia, UFAL. ²Instituto Federal de Alagoas, IFAL

Palavras Chave: Hemoglobina, Antiglicação, Piceatannol, Soret, ThT.

Highlights

Hemoglobin glycation was evaluated by analyzing the production of AGEs, by structural changes in the Soret band, and the formation of amyloid fibrils using ThT. An inhibition of 73% was obtained with 300 μM of piceatannol.

Abstract

Glycation, also known as the Maillard reaction, is a non-enzymatic reaction that occurs in the biological environment or in foods, between sugars (glucose/fructose) and nucleophilic groups of biomolecules¹, generating several addition products, mainly advanced glycation end products (AGEs). AGEs can induce several effects on human health, such as neurodegenerative diseases, including Alzheimer's and Parkinson's, as well as other metabolic disorders like diabetes, heart disease, and even cancer². As such, the objective of this study was to obtain the progression or decrease of Hb's glycation (biomarker for diabetes), through the measurement of fluorescent advanced glycation end-products (AGEs), by analysis of the structural changes in the Soret band of Hb, and by the formation of Hb aggregates, in the presence of natural antioxidants. Fructose was used as the reducing sugar, in the process. Therefore, the therapeutic potential of piceatannol (PIC), one of the major phytochemicals present in yellow passion fruit seeds (*Passiflora edulis*), was evaluated. PIC was chosen due to its previously reported antiglycant and fibrillation inhibitory potential, recently reported by our group in the ethanol extract of passion fruit seeds³. The anti-glycation capacity of PIC was measured at different concentrations (10 – 300 μM), during the initial stage of fructose-induced protein glycation and performed over a period of 5 weeks. PIC (Figure 1) showed a great ability to inhibit glycation (73%), at the concentration of 300 μM (Figure 2). The protective effects of PIC toward changes in the heme group of Hb (Figure 3A) and the formation of amyloid fibrils (Figure 3B) were evident, and the performed assays suggest the potential use of PIC in controlling AGE's production.

Figure 1. PIC structure.

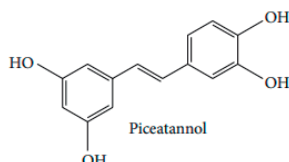


Figure 2. Monitoring of fluorescence intensity at concentrations (10 – 300 μM) of PIC and at different incubation times (A) and spectra of fluorescence intensity at different concentrations of PIC referring to the 5th week of incubation (B).

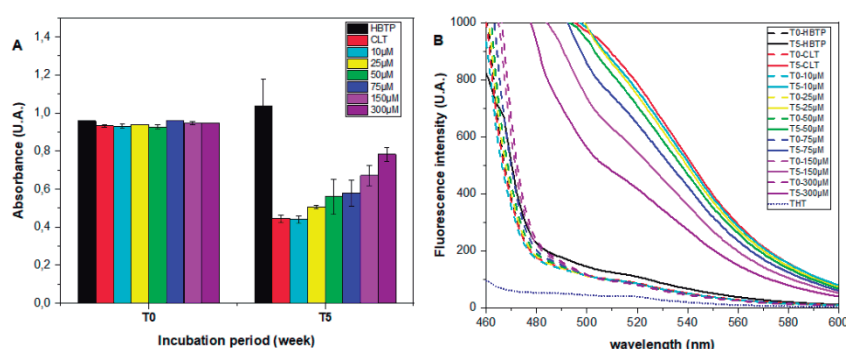
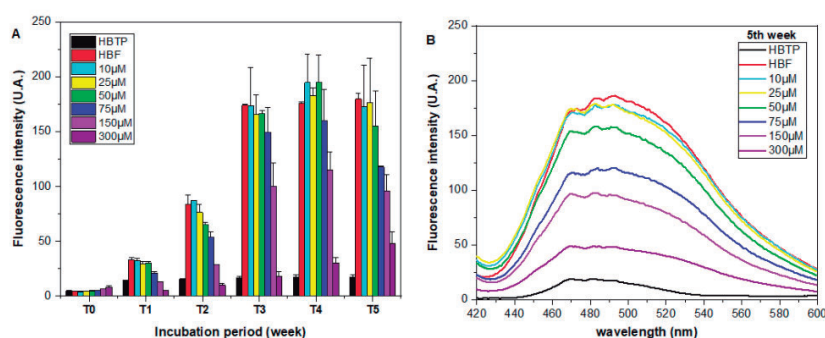


Figure 3. The maximum absorption of the Soret band of glycated hemoglobin with fructose and PIC was measured at the 1st and 5th week of incubation (A), and the monitoring of ThT fluorescence intensity was performed at different concentrations (10 – 300 μM) of PIC at various incubation times (B).



¹ ANIS; SREERAMA. *Food Chemistry*, v.315, p.126-265, 2020. ² FERROZ et al. *Int J Biol Macro*, p.1844-1858, 2020. ³ SANTOS et al. *Molecules*, v.27, n.13, 2022.

Acknowledgments

CAPES, CNPQ and FAPEAL.

46^a Reunião Anual da Sociedade Brasileira de Química: "Química: Ligando ciências e neutralizando desigualdades"

Exploring the application of magnetic nanoparticles in the screening of Nucleoside Hydrolase potential inhibitors on natural products

Pedro R.C. Medeiros (IC)^{1,*}, Pamella C.O. Oliveira (PG)¹, Martin Albino (PQ)², Bruno C. B. Marques (PG)³, Jorge L.S. Simão (PG)⁴, Gabriel F. dos Santos (PG)⁵, Gilberto A. Romeiro (PQ)¹, Claudio Sangregorio (PQ)², Luzineide W. Tinoco (PQ)³, Vanessa G.P. Severino (PQ)⁴, Rosane N. Castro (PQ)⁵, Marcela C. Moraes (PQ)¹.

pedrorcm@id.uff.br; mcmoraes@id.uff.br

¹Departamento de Química Orgânica, UFF; ²Instituto de Química Ugo Schiff, UNIFI – Itália; ³IPPN, UFRJ; ⁴Instituto de Química, UFG; ⁵Instituto de Química, UFRRJ.

Keywords: Iron oxide nanoparticles, Amino-functionalization, *Leishmania donovani*, Propolis extracts, Plant extracts.

Highlights

Nanosized magnetic support to immobilize LdNH. After the characterization of the obtained system, different extracts of natural products were selected as source of potential leishmanicidal agents.

Abstract

Visceral leishmaniasis (VL) is the most severe form of leishmaniasis and is caused by *Leishmania donovani* (Ld) or *L. infantum*. The high cost and toxicity related to the current treatment of VL demonstrate the need to develop new drugs. The enzyme Nucleoside Hydrolase (NH) is essential for RNA and DNA biosynthesis in *Leishmania*, acting in the purine salvage pathway. Therefore, the NH can be considered a promising target for the development of potential new drugs.¹ The use of magnetic particles (MPs) as solid supports for immobilizing macromolecules has been widely used due to their easy functionalization and recovery.² The MP coated with the biological target is an interesting approach to developing screening methodologies.³ Herein, the NH enzyme of *L. donovani* (LdNH) was immobilized on magnetic nanoparticles (MNPs) with two different coatings: silica shell (NP-SS) and ligand exchange (NP-LE). The immobilization of LdNH on the surface of MNPs functionalized with -NH₂ groups was performed using glutaraldehyde by the formation of Schiff bases. Through kinetic studies, the Michaelis-Menten constant was determined as 726.5 ± 69.7 and 486.5 ± 30.0 μmol.L⁻¹ for NP-SS and NP-LE, respectively. Slight differences in the K_M values may be associated with peculiarities in the immobilization process. NP-SS may favor multipoint immobilization and affect the enzyme conformation, and, consequently, the affinity for the substrate. MNP-LdNH was then applied in screening assays on different extracts of *Banisteriopsis laevifolia*, *Croton antisiphiliticus*, and *Annona coriacea*. Additionally, green propolis extracts from *Apis mellifera* and geopropolis extracts from *Melipona rufiventris* and *Melipona quadrifasciata* were evaluated. The catalytic activity of the enzyme was monitored by direct quantification of the product (HYPO) from substrate hydrolysis (INO) through HPLC-DAD. Chromatography separation of INO and HYPO was achieved by using an C-18 Ascentis Express column (50 mm x 4.6 mm, 5 μm) and a Et₃N 1% in H₂O, v/v, acidified with AcOH, pH 6.0:MeOH (95:5) solution as mobile phase, at flow rate 0.8 mL.min⁻¹. The assays were conducted using INO at 500 μmol.L⁻¹, MNP-LdNH at 0.8 μg.mL⁻¹, and extracts at 200 μg.mL⁻¹. Inhibition percentages were calculated by comparing the amount of product formed in the presence of the extract with a blank sample. Results are summarized in tables 1 and 2.

Table 1: Inhibition results of propolis and geopropolis extracts (200 μg.mL⁻¹) in different solvents.

Inhibition	Green propolis			Geopropolis (<i>M. rufiventris</i>)			Geopropolis (<i>M. quadrifasciata</i>)		
	EtOH	Hexane	MeOH	EtOH	Hexane	DCM	EtOH	Hexane	DCM
NP-SS	92%	74%	87%	63%	80%	48%	67%	94%	54%
NP-LE	92%	91%	91%	77%	77%	68%	61%	80%	58%

Table 2: Inhibition results of different extracts at 200 μg.mL⁻¹.

Inhibition	<i>B. laevifolia</i> (EtOH ext.)		<i>C. antisiphiliticus</i>		<i>A. coriacea</i> (EtOH ext.)			
	Leave	Flower	EtOH-Leave	H ₂ O-Root	Leave	Flower	Stem	Seed
NP-SS	99%	97%	> 89%	> 95%	86%	91%	99%	96%
NP-LE	99%	99%	> 96%	> 98%	56%	53%	99%	41%

The results obtained in the screening assays using NP-SS are consistent with those obtained employing NP-LE. This initial screening showed that most extracts and fractions inhibit LdNH by more than 60%, with *B. laevifolia*, *C. antisiphiliticus* and Green propolis being the most promising.

¹Figueroa-Villar, J.D.; Sales, E.M. *Chem.-Biol. Interact* **2017**, 263, 18; ²Ximenes, I. A.T. et al. *Pharm. Biomed. Anal.* **2021**, 204, 114286; ³Lima, J. M. et al. *Anal. Methods*, **2020**, 12, 4116.

Acknowledgments

CNPq, FAPERJ, CAPES – Finance Code 001, and CAPES Print.

46^o Reunião Anual da Sociedade Brasileira de Química: "Química: Ligando ciências e neutralizando desigualdades"

Identification of new inhibitors of the enzyme Nucleoside hydrolase from *Leishmania donovani* by an onflow methodology

Millena S. Ceroullo (IC)¹, Pamella C. O. de Oliveira (PG)¹, Rodrigo C. da Silva (PG)², Maria Cecilia B. V. de Souza (PQ)², Fernanda C. S. Boechat (PQ)², Luzineide W. Tinoco (PQ)³, Marcela C. Moraes (PQ)^{2*}

¹ Departamento de Química Orgânica, UFF – Niterói, RJ; ² IPPN, UFRJ – Rio de Janeiro, RJ;

millenasc@id.uff.br; mcmoraes@id.uff.br

Keywords: Visceral Leishmaniasis, Enzyme Inhibitors, Liquid Chromatography, Kinetic Studies, Flow Method

Highlights

Identification of novel oxiquinoline ribonucleoside as LdNH enzyme inhibitors through an on-flow screening assay by liquid chromatography.

Abstract

The enzyme Nucleoside hydrolase (NH) catalyzes the hydrolysis of the C-N glycosidic bond of ribonucleosides, such as inosine, leading to the formation of free ribose and the corresponding nitrogenous bases, such as hypoxanthine. This enzyme acts in the purine salvage pathway and it is considered a biological target for the development of new antileishmanial agents. *Leishmania donovani* (*Ld*) is one of the etiological agents of visceral leishmaniasis, that can be fatal. The actual treatment presents several disadvantages, such as drug resistance, toxicity, and high cost. Like other neglected diseases, it mostly affects economically vulnerable individuals.¹ In this work, the enzyme LdNH was covalently immobilized on commercial magnetic particles and trapped in a TFE Teflon tube (0.3 mm i.d. x 1.58 mm o.d.; 10 cm) using magnets, providing an immobilized enzyme reactor (IMER). The produced IMER was used to screen a library containing oxiquinoline ribonucleoside derivatives. The performed assay directly quantifies the reaction product, hypoxanthine, by HPLC-DAD. This methodology addresses the versatility of magnetic particles to the automatization of the bioassay, allowing the enzymatic reaction within the system and subsequent separation of inosine and hypoxanthine. The chromatographic separation of inosine and hypoxanthine was performed using a C18 column (150 x 4.6 mm) and an aqueous solution of Triethylamine (1% v/v, pH 6.0 acidified with AcOH)/Methanol (95:5), 0.80 mL·min⁻¹ and $\lambda = 249$ nm. The validated method was used to screen inhibitors in a library of 19 synthetic oxoquinoline ribonucleosides. First, the percentage of inhibition at 200 $\mu\text{mol}\cdot\text{L}^{-1}$ was evaluated. In this step, all compounds with >30% of LdNH-IMER inhibition were selected. Then, the inhibitory capacities (IC₅₀) for the new inhibitors were determined by varying the inhibitor concentration in a fixed substrate concentration. Plotting dose-response curves, IC₅₀ values were obtained in the range of 42.3 ± 3.0 to 243.2 ± 29.9 $\mu\text{mol}\cdot\text{L}^{-1}$. Lastly, the inhibition mechanism of each compound was assessed and the Lineweaver-Burk double reciprocal plot revealed competitive mechanisms for three new inhibitors, with K_i values ranging from 54 to 365.²

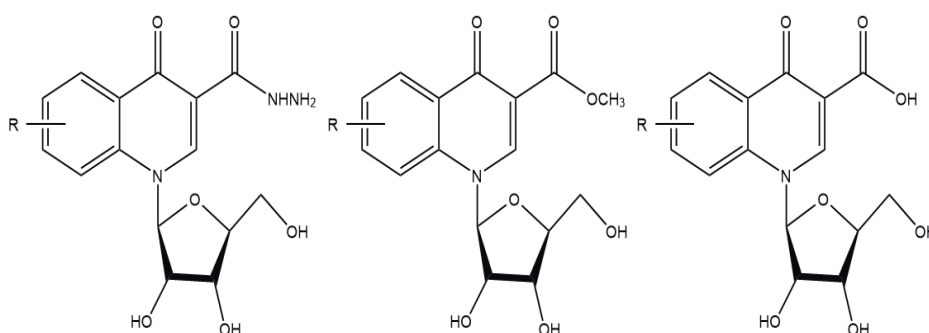


Figure 1: Structure of the ribonucleosides evaluated (R = H, Cl, Br, F₃C).

¹FIGUEROA-VILLAR, José D.; SALES, Edijane M. *Chemico-Biological Interactions*, v. 263, p. 18-27, 2017.

²NIRMA, Charlotte et al. *RSC advances*, v. 9, n. 32, p. 18663-18669, 2019.

Acknowledgments

CNPq, FAPERJ, Coordenação de Aperfeiçoamento de Pessoal de Nível Superior – Brasil (CAPES) – Finance Code 001, and CAPES Print

***In vitro* metabolism and inhibition studies of the main human CYP450 enzymes by the pesticide acephate and its toxic metabolite methamidophos**

Leandro Oka Duarte (PG),¹ Maria Carolina Hebling Grili (IC),¹ Gabriel Balbino Rodrigues (IC),¹ and Anderson Rodrigo Moraes de Oliveira (PQ)¹.

leandro.oka@usp.br

¹Departamento de Química, FFCLRP-USP

Key words: Acephate, Methamidophos, Cytochrome P450, Human liver microsomes, *In vitro* metabolism, *In vitro* inhibition.

Highlights

Acephate was not metabolized into methamidophos by the human liver microsomes. Except for the CYP1A2, there was no evidence of inhibition of the main CYP450 enzymes involved in drug metabolism.

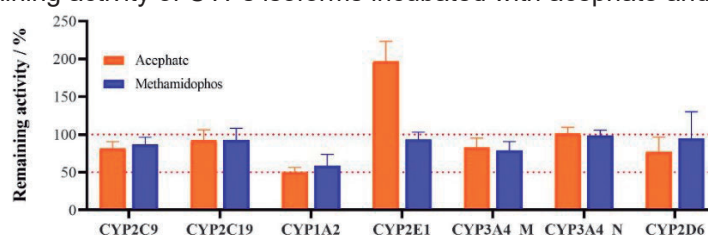
Resumo/Abstract

Acephate is an organophosphate insecticide that is used in countries such as China, Brazil, and India. Some studies showed that methamidophos (a banned pesticide) may be produced after acephate metabolism or degradation. Cytochrome P450 (CYP450) enzymes are involved in the metabolism of several xenobiotics and drugs. In addition, their inhibition may lead to drug-xenobiotics interaction which may cause failure in the treatment or drug toxicity. Considering that pesticides have been found in food, water and in biological human fluids, the purpose of the study is to evaluate, *in vitro*, the effect of acephate and methamidophos over the main CYP450 enzymes present in human liver microsomes (HLM) and assess the pesticide-CYP450 interactions through direct inhibition assay. Data were analyzed by using previously optimized LC-MS methods. The metabolism of acephate was studied at three protein concentrations (0.25 - 1.0 mg mL⁻¹) and three-level concentrations (10 - 100 µmol L⁻¹). To verify the conversion of acephate into methamidophos, the chromatographic area of control groups (0% metabolism) was compared with the test samples. The inhibition screening was performed by adding the pesticides at 100 µmol L⁻¹ to the incubation solution and the remaining enzyme activity (REA%) was monitored by using probes for specific metabolic reactions [acetaminophen (CYP1A2); 1'-hydroxybufuralol (CYP2D6); 4'-hydroxydiclofenac (CYP2C9); 6-hydroxychlorzoxazone (CYP2E1); 4'-hydroxymephenytoin (CYP2C1); and 1'-hydroxymidazolam and dehydronifedipine (CYP3A4)]. The percentage of acephate metabolism was very low which prevents us to infer that the observed results were due to the metabolism or due to the inherent bias of the method (Table 1). In addition, the methamidophos' peak was not observed at any evaluated condition. Regarding the inhibitory capacity (Fig. 1), CYP1A2 was the only enzyme inhibited with a REA% of 58% for methamidophos and 50% for acephate. These findings provide important insights into the behavior of acephate and methamidophos in the human organism and may have implications for the safe use of these compounds in human health and the environment.

Table 1. Percentage of acephate metabolism in human liver microsomes

Protein conc. / mg mL ⁻¹	0.25			0.5			1.0		
Acephate con. / µmol L ⁻¹	10	20	100	10	20	100	10	20	100
Metabolism / %	9.34	4.99	12.7	6.92	14.1	8.27	0.17	0.78	0.72

Figure 2. Remaining activity of CYPs isoforms incubated with acephate and methamidophos.



Agradecimentos/Acknowledgments

CAPES, CNPq, FAPESP and INCT-DATREM.

46ª Reunião Anual da Sociedade Brasileira de Química: "Química: Ligando ciências e neutralizando desigualdades"

Metalloproteomics investigation in rats brain exposed to mercury

José C. S. Vieira (PQ)^{1*}, Maria Gabriela A. Santiago (IC)¹, Renata A. Martins (PG)¹, Andrey Sávio A. Assunção (PG)¹, Grasieli de Oliveira (PG)¹, Izabela C. Bataglioli (PG)¹, Camila P. Braga (PQ)², Jiri Adamec (PQ)² e Pedro M. Padilha (PQ)¹.

cavalcante.vieira@unesp.br; pedro.padilha@unesp.br

¹Laboratory of Bioanalytical and Metalloproteomic (LBM), Department of Chemical and Biological Sciences, Institute of Biosciences - UNESP – Botucatu. ²Department of Interdisciplinary Oncology, LSUHSC School of Medicine/USA

Keywords: Proteins, Two-dimensional electrophoresis, GFAAS, mercury exposure.

Highlights

- ✓ Mercury exposure alters the protein expression in rats brain.
- ✓ The exposure time influences the mercury bioaccumulation in rats body.
- ✓ Mercury exposure can alter protein pathways and affect important biological processes.

Abstract

Mercury is a toxic element, responsible for environmental and human contamination. Prolonged exposure to the element can cause serious damage to the nervous system, such as cerebellar ataxia, visual field changes, and sensory and auditory disturbances. The symptoms and severity of poisoning are related to the amount and frequency of mercury exposure. Thus, this study aimed to analyze the metalloproteomic profile of rats brain exposed to mercury. For this, rats (Wistar, n=5) were exposed to a single dose of 4,6 $\mu\text{g kg}^{-1}$ of mercury and weekly doses of 0,49 $\mu\text{g kg}^{-1}$ to replace losses were administered for 30 and 60 days. Control groups received saline solution at the same doses and frequencies as the mercury-exposed groups. For mercury quantification and proteomic analysis, pools samples from the five animals in each group were made. Mercury concentrations were determined by graphite furnace atomic absorption spectrometry (GFAAS). Proteins were fractionated by two-dimensional polyacrylamide gel electrophoresis (2D-PAGE). Protein spots analyzed using ImageMaster 2D Platinum 7.0 software and proteins identified by mass spectrometry (ESI-MS/MS). The results showed that protein pellets from rats exposed to mercury for 60 days had 43,40% more mercury ($61,50 \pm 1,05 \mu\text{g kg}^{-1}$) when compared to those exposed for 30 days ($42,90 \pm 0,92 \mu\text{g kg}^{-1}$). The number of differentially expressed protein spots in rats exposed to mercury for 60 days (148 spots) was also higher when compared to those exposed for 30 days (67 spots). In these differentially expressed protein spots were identified 18 and 30 mercury-associated protein spots in rats groups exposed to mercury for 30 days and 60 days, respectively. Bioinformatics analysis showed that the proteins identified in mercury-associated protein spots participate in different biological processes in the body, the most common being: cellular processes (14% and 16% of the proteins in the 30 and 60 days group, respectively); metabolic processes (12% and 13% respectively); biological regulation (10% and 12% respectively). Binding processes and catalytic activity assembled 45% and 25% of the proteins identified in the group exposed to mercury for 30 days and 48% and 37% in the group exposed to mercury for 60 days, respectively. Other functions such as detoxification, localization, cell signaling, antioxidant activity, and responses to stimuli were also observed as activities associated with the identified proteins. The preliminary results showed that mercury exposure can alter the expression of a set of proteins in the rats brain exposed to this xenobiotic. The exposure time also showed an influence on the amount of altered proteins, the longer the exposure time the greater the number of altered proteins and possibly the greater risk of damage caused by mercury to the nervous system of living beings.

Acknowledgments

São Paulo Research Foundation - FAPESP Processes: 2019/02538-4 and 2016/19404-2; National Council for Scientific and Technological Development – CNPq, Processes: 304768/2018-9 and 404485/2016-2 and Coordination of Superior Level Staff Improvement - CAPES, Project CAPES-Print AUXPE-Process: 88881.3107432018-0

Urease interaction of Schiff bases derived from hybrid pyrazoles with thiosemicarbazides: inhibition and biophysical studies

Ari Souza Guimarães (PG),^{1,*} Emilly dos Santos Sousa (IC),¹ Jeniffer do Nascimento Ascencio Camargo (PG),² Fernanda Andreia Rosa (PQ),² Josué Carinhanha Caldas Santos (PQ),¹ Isis Martins Figueiredo (PQ)¹

*ari.sguimaraes@gmail.com

¹Instituto de Química e Biotecnologia-Universidade Federal de Alagoas- UFAL. ²Departamento de Química- Universidade Estadual de Maringá, UEM

Keywords: urease; enzimatic inhibitor; biophysical studies; Schiff bases.

Highlights

Compound **312** showed a better IC₅₀ of urease inhibition and function as an uncompetitive inhibitor. In the complex **312**-urease, the allosteric site presented binding affinity when compared with the active enzyme site.

Resumo/Abstract

Urease is a nickel-dependent enzyme that catalyzes the hydrolysis of urea to NH₃ and CO₂. This reaction is associated with several problems, including gastrointestinal infections caused by *Helicobacter pylori* and low urea absorption in the soil [1,2]. Thus, considering the importance of new urease inhibitors, the inhibitory profile of a Schiff base derived from hybrid pyrazoles with thiosemicarbazides (**Fig. 1A**) was evaluated in this work. The compounds **307** - **310** and **312**, with variation in the substitution pattern, led to a higher urease (*Canavalia ensiformis*) inhibition in the assessed concentration (100 μM). The **312** presenting an electron-withdrawing substituent, was the most activity in the series, with an IC₅₀ = 24.7 ± 1.1 μM, smaller than the standard thiourea (TIO) ($p \leq 0.05$, Tukey test) (**Fig. 2B**). Furthermore, **312** was classified as an uncompetitive type of inhibition (**Fig. 1C**) with K_m and V_{max} of 14.03 ± 0.46 mM and 4.08 ± 0.07 μmol NH₄⁺ min⁻¹ mg⁻¹ protein, respectively. The interaction of **312** with urease carried out the formation of a non-fluorescent supramolecular complex (**Fig. 1D**) with a K_{SV} = 8.08(±0.33) × 10³ M⁻¹, and a binding constant (K_b) of 3.88(±0.34) × 10⁸ M⁻¹, where the complex exhibited a stoichiometry 2:1 (ligand:enzyme). Complex formation was confirmed by UV-vis, where at the same concentration [A_{complex} - A₃₁₂] ≠ A_{urease} (**Fig. 1E**). Additionally, based on the biomolecular extinction rate constant (K_q = 8.08 × 10¹¹ M s⁻¹), the dominant quenching in the supramolecular system as static. Finally, in the molecular docking studies with urease (PDB ID: 4H9M), **312** showed the highest correlation energy (fitScore, 61.9) in allosteric site interaction (**Fig. 1F**) compared to the other compounds, corroborating with the experimental data. Besides, **312** interacts with 18 amino acid residues through hydrophobic bonds, halogen, π-anion, π-cation, and an H-bond with a distance of 2 Å with the glutamate residue (GLU 718). Finally, studies with **312** to evaluate its potential as a urease inhibitor in soil samples with different levels of organic matter are under development.

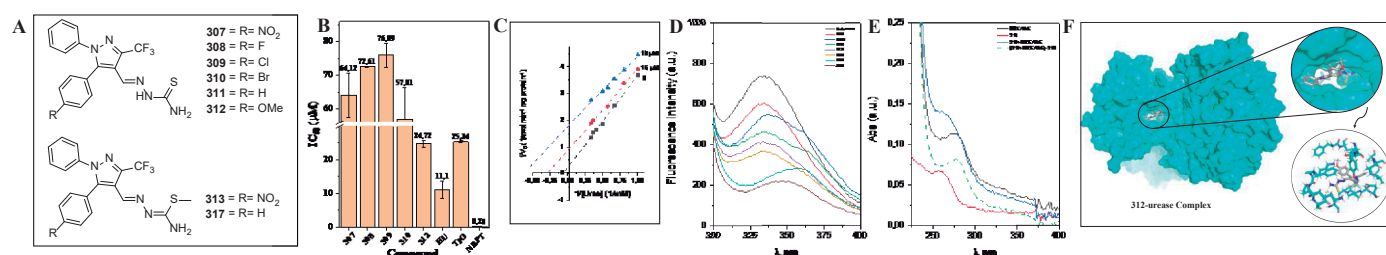


Fig. 1. **A.** Compounds evaluated in the study. **B.** Graph representing the IC₅₀ of the most active compounds of the standards. **C.** Type of inhibition of **312** against urease. **D.** Fluorimetric titration of urease with **312**. **E.** UV-vis study confirming the formation of the complex. **F.** Interaction of **312** with allosteric site amino acid residues.

[1] Tavares M.C. et al., *Talanta*, 230, 122301, 2021. [2] Tavares M.C. et al., *Industrial Crops & Products*, 178, 114580, 2022.

Agradecimentos/Acknowledgments

IQB-PPGQB-UFAL, Fapeal, CAPES, CNPq.

CAT Catálise

46^a Reunião
Anual da **SBQ**

28 a 31 de Maio de 2023

Águas de Lindóia · SP
Hotel Monte Real

5-HMF Oxidation via Photobiocatalysis by Laccase from *Aspergillus* Immobilized on Graphite Carbon Nitride

Bernardo Haber **D. Pires** (IC),¹ Marcelo A. Nascimento (PG),¹ Mauro R. B. P. Gomez (PQ),¹ Raquel A. C. Leão (PQ),¹ Robert Wojcieszak (PQ),² Ivaldo I. Junior (PQ),³ Rodrigo O. M. A. de Souza (PQ).^{1*}

bernardohaber@eq.ufrj.br; souzarod21@gmail.com*

¹ Biocatalysis and Organic Synthesis Group, Instituto de Química da Universidade Federal do Rio de Janeiro–IQ–UFRJ.

² Univ. Lille, CNRS, Centrale Lille, Univ. Artois, UMR 8181 - UCCS - Unité de Catalyse et Chimie du Solide, Lille, France;

³ Department of Biochemical Engineering, School of Chemistry, Federal University of Rio de Janeiro, Brazil.

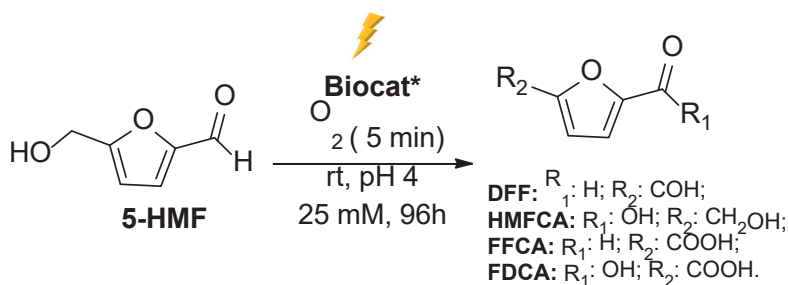
Keywords: Biocatalysis, Photochemical, Oxidation, Immobilized, Laccase.

Highlights

Novel approaches for the 5-HMF oxidation photo-biocatalyzed by laccase from *Aspergillus* immobilized on graphite carbon nitride. Study of the synergistic effect between support and enzyme for the oxidation of 5-hydroxymethylfurfural (5-HMF) in the presence and absence of light.

Abstract

5-HMF is one of the most promising biomass-based chemicals which could be obtained by dehydration of certain sugars, for example, levoglucosan.¹ Its structure consists in a furan ring containing an alcohol and an aldehyde functional group. In a oxidation reaction it can be converted to many important compounds like 2,5-furandicarboxylic acid (FDCA), 5-formyl-2-furancarboxylic acid (FFCA), 2,5-diformylfuran (DFF) and 5-hydroxymethyl-2-furancarboxylic acid (HMFCFA) (Scheme 1).² These derivatives are important building blocks, which potential application in chemical, fuels, medical intermediates, polymers, etc; to achieve this many applications selectivity is an important topic, and different conditions can favoured an of this products.³



Scheme 4: Schematic overview of the possible products that can be formed during the oxidation of 5-HMF.

In this context, our research aims to study the selectivity of free and immobilized Laccase from *Aspergillus* in the 5-HMF oxidation at light. Thereby, the immobilization will be evaluated on graphite carbon nitride such as support by two via chemical adsorption and covalent bonding. Up to now we are able to observe full conversion of the starting material after 96 hours of reaction. Further studies are under way in order to elucidate the contribution of the enzyme and the photo activates support on the starting material conversion.

Acknowledgments

CNPq, CAPES and FAPERJ

¹ Itabaiana Junior, *et al. Green Chem.*, **2020**, 22, 5859-5880.

² C. Zhang *et al. Int. J. Biol. Macromol.*, **2019**, 128, 132-139.

³ Shuai Xu, *et al. J. Am. Chem. Soc.*, **2017**, 139, 14775-14782.

Acetone hydrodeoxygenation over one-dimensional Fe-supported catalysts

Guilherme B. Strapasson (PG),^{1,2*} Ângela A. T. Neto (PQ),² Cristiane B. Rodella (PQ),² Daniela Zanchet(PQ).¹

g216373@dac.unicamp.br

¹Institute of Chemistry, University of Campinas, UNICAMP, Campinas, SP, Brazil; ²Brazilian Synchrotron Light Laboratory, CNPEM, Campinas, SP, Brazil.

Keywords: Heterogeneous catalysis, Nanomaterials, Acidity, Metal oxides, Hydrodeoxygenation

Highlights

Metal-support interactions over one-dimensional metal oxides led to the preferential growth of Fe crystallites

Generation of active interfacial sites on Fe-supported catalysts enhanced C-O bond cleavage

Abstract

Catalyst design and engineering of active sites have helped the development of catalytic systems with unique properties. A class of materials explored in heterogeneous catalysis is nanostructured metal oxides, especially those of one-dimensional morphology (1D). Reducible metal oxide supports that associate redox and acid properties with a metallic phase can result in potential catalytic systems for different reactions. The hydrodeoxygenation (HDO) reaction is one of the main biomass-derivate upgrading processes to obtain biofuels and deals with the selective cleavage of C-O bonds under a hydrogen-rich atmosphere combined with a solid catalyst, reducing the oxygen content to produce hydrocarbons as the main products. Thus, in this work, 1D Fe-supported catalysts were synthesized and evaluated in the acetone HDO reaction. Supports based on TiO₂ nanoribbons (TiO₂NRs) were synthesized using a hydrothermal route, while core@shell-like TiO₂NRs@Nb₂O₅ nanostructures were prepared through wet impregnation of the Nb precursor to obtain 10 at.% Nb (Nb: Ti). Fe-supported catalysts (5 wt.%) were prepared through the incipient wetness impregnation method over the oxide nanostructures. Textural, structural, and electronic characterizations of the catalysts were conducted using various techniques, such as N₂ physisorption, XRD, XPS, SEM, TEM, TPD, TPR, and FTIR of adsorbed model molecules. SEM micrographs demonstrated that well-defined TiO₂NRs with a few micrometers in length were obtained (Fig. 1a), and some cavities were observed on its surface through HR-TEM. SEM and TEM images of TiO₂NRs@Nb₂O₅ were similar to the ones of TiO₂NRs, suggesting that Nb was evenly dispersed over the TiO₂NRs surface. EDS-TEM analysis confirmed the formation of core@shell-like structures, with Nb concentrations in the 5-10 at.% range in the middle of the TiO₂NRs@Nb₂O₅ and above 20 at.% at the edges. XRD patterns demonstrated the formation of TiO₂ (B) crystal structure, whereas crystalline phases related to Nb oxides were not observed for the TiO₂NRs@Nb₂O₅ (Fig.1b). The relative XRD peak intensities agree with a preferential growth along a- and c-axis and the formation of NRs morphology. TEM images of the corresponding Fe-supported catalysts presented FeO_x particles with cuboidal morphology in the 15-30 nm range (Fig. 1c). A preliminary analysis indicated that particles epitaxially grew over the supports, driven by the match of the interplanar distances of the support and the Fe phase. Concerning the catalytic performance over acetone HDO reaction, Fe-supported TiO₂NRs presented similar results with the bare support; on the other hand, Fe-supported TiO₂NRs@Nb₂O₅ enhanced C-O bond cleavage compared to its bare support, suggesting that active interfacial sites were generated in the presence of Nb.

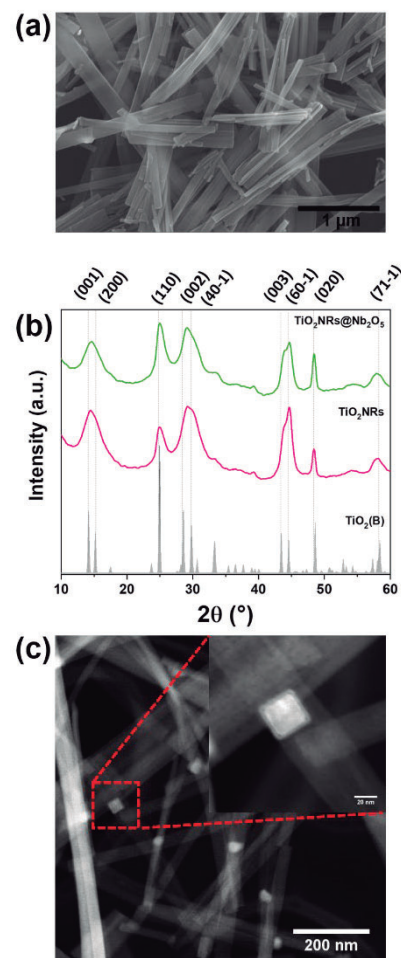


Figure 1: (a) SEM micrograph of TiO₂NRs; (b) XRD patterns of TiO₂NRs and TiO₂NRs@Nb₂O₅; and (c) HAADF-STEM images of Fe-supported TiO₂NRs.

Acknowledgments

We thank FAPESP (2018/01258-5 and 2020/12986-1), CNPq, and CAPES for funding.

A Periodical DFT Study on the Interaction of the $C_4H_7^+$ System with Alkali Metal Ion-exchanged Zeolite Y

Maria E. A. Alves (IC),¹ Nilton Rosenbach Jr (PQ),¹ Claudio J. A. Mota (PQ)²

mariaeduarda@carvalhoz.org; nilton.rosembach.junior@uerj.br

¹Faculdade de Ciências Exatas e Engenharias, UERJ; ²Instituto de Química, UFRJ

Palavras Chave: Zeolite, Bicyclobutonium, Periodical DFT calculations, Solid Solvent.

Highlights

Periodic DFT calculations at the GGA-PPBE were carried out to achieve a better understanding of the influence of the polarity of the zeolite cavity on the stability of carbocation intermediates inside these materials. The results show that local electrostatic interactions play a major role in stabilizing such species on the zeolite surface.

Resumo/Abstract

Zeolites are porous aluminosilicates widely used as catalysts in the petrochemical industry, mainly because of their activity and selectivity. Based on the similarities with superacid media, most of the initial studies suggested that carbocations were the key intermediates in zeolite-catalysed hydrocarbon transformations. We have been studying the nature of carbocations adsorbed on the zeolite surface employing metal-exchanged zeolite and alkyl halides. In these systems, the metal cation acts as a Lewis acid site, coordinating with the alkyl halide to form a metal-halide species and a carbocation inside the zeolite cavity. Based on theoretical and experimental studies, we proposed that zeolites might behave as solid solvents, inducing ionization of the substrate and stabilization of the ionic species formed. It suggests that coulombic interactions can play a major role in the stabilization of ionic intermediates and transition states, rather than confinement effects. Here, we use DFT calculations to investigate the relative stability of the $C_4H_7^+$ species within the pores of zeolite Y-impregnated LiCl, LiBr, NaCl and NaBr. The results (Table 1) show that the presence of all MX units significantly increases the stability of the bicyclobutonium (BCB) cation, reducing the energy difference between the cation and the cyclobutyl (CB), cyclopropylcarbonyl (CPC), and allylcarbonyl (AC) alkoxides. The degree of stabilization increases further when another NaCl unit is introduced in the cavity as shown in Figure 1. These results reinforce the hypothesis that zeolites behave as a solid solvent in which short-range interactions, such as hydrogen bonds and electrostatic forces, play a more significant role in stabilizing ionic species rather than long-range van der Waals interactions.

Table 1. Relative stability of $C_4H_7^+$ species on Y zeolite (kcal mol⁻¹).

Specie	Y	LiClY	LiBrY	NaClY	NaBrY
CB alkoxide	5.7	5.7	6.0	6.9	6.7
CPC alkoxide	3.8	4.1	4.2	4.7	4.8
AC alkoxide	0.0	0.0	0.0	0.0	0.0
BCB cation	22.8	12.6	12.9	13.9	14.5

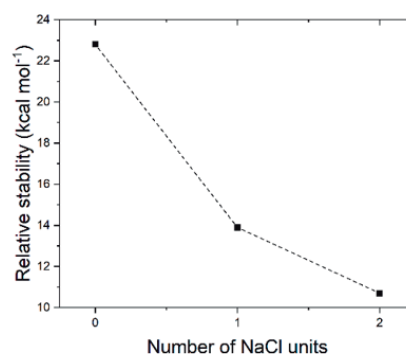


Figure 1. Relative stability of BCB cation and AC alkoxide as a function of NaCl units.

Agradecimentos/Acknowledgments

We thank CNPq, CAPES and FAPERJ for financial support.

46ª Reunião Anual da Sociedade Brasileira de Química: "Química: Ligando ciências e neutralizando desigualdades"

Application of porous silicates impregnated with vanadium in the glycerol acetalization reaction with acetone to obtain Solketal

Adriana M. França (PQ),^{1*} Gabriel L. Catuzo (PQ),² Luiz G. Possato (PQ),² Leandro Martins (PQ),² Celso V. Santilli (PQ),¹

adriana.maneira@unesp.br

¹GFQM /Departamento de Química Analítica, Físico-Química e Inorgânica, Instituto de química, UNESP/Araraquara ; ²GPCAT/ Departamento de Engenharia, Física e Matemática, , Instituto de química, UNESP/Araraquara

Keywords: (Porous Silicates, Vanadium Oxide, Impregnation, Glycerol Acetalization, Solketal, Heterogeneous Catalysis)

Highlights

The texture of the support influences the vanadium species formed its surface.

The mesoporous silicate SBA-15 supported with vanadium has good catalytic performance to the glycerol acetalization.

Resumo/Abstract

Although vanadium-based catalysts are mainly used in oxidation reactions, they can also be used as acid catalysts in reactions such as the acetalization of glycerol for the production of solketal, a molecule that has aroused interest because it can be used as an additive in fossil fuels. [1] Although vanadium has low acidity and surface area, but these characteristics can be improved when the vanadium is well dispersed in high surface area supports, such as porous silicates [2]. In this work, three types of porous silicates, including microporous silicalite-1, mesoporous SBA-15 and macroporous Fumed silica, were applied to demonstrate how the support texture influences the formation of VOx species. These supports were impregnated with 5% (w/w) of vanadium. The chemical and structural properties of the catalysts were characterized by SAXS, XRD, N₂ physisorption, ²⁹Si NMR, FTIR, DR-UV-Vis spectroscopy and TPR-H₂. Different species of vanadium, such as tetrahedral, square pyramidal and octahedral VOx, and degrees of polymerization of these were found according to each support. The catalysts impregnated with vanadium were tested in the acetalization reaction of glycerol with acetone to obtain Solketal. The reaction took place at 60 °C using the following proportions: 20 mg of catalyst, 200 mg of glycerol and 1 mL of acetone. The products were analyzed by gas chromatography at different time intervals between 0 and 120 min. The catalytic test showed that the mesoporous catalyst had the best catalytic performance in 120 min of reaction, showing increasing values for glycerol conversion and selectivity for the product of interest, the solketal, above 80%, throughout the reaction.

[1] T. Ancuta, E. Paul, P. Timea, *Renewable Sustainable Energy Reviews*, 62 (2016) 804–814.

[2] T. Abreu, C. Meyer, C. Padró, L. Martins *Microporous and Mesoporous Materials*, 273 (2019) 219.

Agradecimentos/Acknowledgments

Instituto de Química da UNESP, GFQM, GPCat, CNPq, CAPES e FAPESP.

A Sustainable Approach to Selective Hydrogenation of Unsaturated Esters and Aldehydes with Ruthenium Catalysts

Victor M. Agramunt (PG),^{1,2} Lucas H. R. Passos (PG),¹ Dmitry G. Gusev (PQ),³ Eduardo Peris (PQ),² Eduardo N. dos Santos (PQ)^{1*}

vagramun@uji.es; *nicolau@ufmg.br

¹Departamento de Química, UFMG; ²Universitat Jaume I, Castelló, Espanha; ³Wilfrid Laurier University, Canada.

Key words: Hydrogenation, Homogeneous catalysis, Organometallic, Ruthenium, Selectivity.

Highlights

Ester hydrogenation was carried out under mild conditions. A homogeneous ruthenium catalyst was used. Selective hydrogenation of unsaturated ester was carried out. Anisole was used as solvent.

Abstract

The reduction of esters and aldehydes to alcohols is an important reaction in the chemical industry for the production of a wide range of bulk and fine chemicals.¹ This transformation has been typically accomplished using stoichiometric reactants, or catalysts under harsh reaction conditions.² Herein we report a comparative study of three Ru-catalysts (**Ru-1**, **Ru-2** and **Ru-3**, Figure 1) for the hydrogenation of esters and aldehydes.³⁻⁵

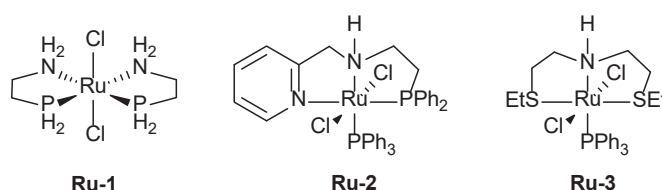


Figure 1 – Ruthenium catalysts used in the work

Our results show that these substrates can be reduced under mild conditions (as low as 40 °C and 5 bar of H₂). For ester and aldehydes containing a C=C bond, it was possible to carry out the selective hydrogenation of the ester or aldehyde functionality while keeping the C=C double-bond unreacted (Figure 2). Furthermore, we demonstrated that anisole, a solvent with a high sustainability rank, is suitable for these catalytic hydrogenations.⁶

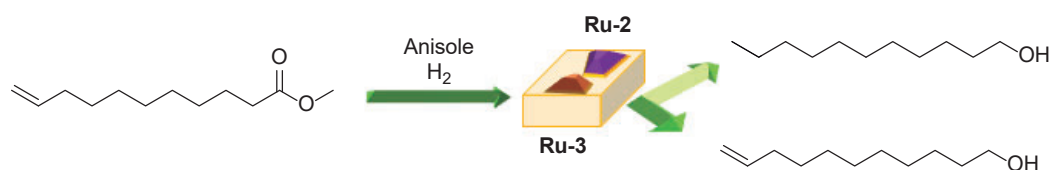


Figure 2 - Selective hydrogenation of the methyl - 10- undecenoate with **Ru-2** and **Ru3**

Reference

- ¹ D. Milstein, D. Srimani, A. Mukherjee, et al. *Angew. Chem.* **54**, (2015), 12357
- ² A Zanotti-Gerosa, L. Wong, D. Grainger, et al. *Catalysis&biocatalysis* **37**, (2019), 4, 8
- ³ L. A. Saudan, C. M. Saudan, C. Debieuxi, P. Wyss. *Angew. Chem. Int.* **46**, (2007), 7473
- ⁴ D. Spasiuk, S. Smith, D. G. Gusev, *Chem. Int. Ed.* **51**, (2012), 2772-2775
- ⁵ D. Spasiuk, S. Smith, D. G. Gusev. *Angew. Chem. Int.* **52**, (2013), 2538-2542
- ⁶ Catherine M. Alder, a John D. Hayler, b Richard K. Henderson, et al. *Green Chem.* **18**, (2016), 3879-3890.

Acknowledgments

We thank CNPQ (140669/2020-5) from Brazil for the scholarship to L. H. R. P. European Union (NextGenerationEU). Universitat Jaume I, Spain is thanked for the fellowship to V. M-A (MGS/2021/07). CNPq (INCT-Catálise). FAPEMIG are thanked for financial support and to the chemistry department (UFMG) for access to its facilities.

Behaviour of iron catalysts supported on MOF UiO-66(Zr) in the selective oxidation of cyclohexane

Wandson Lukas do Nascimento Amorim (PG) ^{1*}, Wagner Alves de Carvalho (PQ) ¹, Dalmo Mandelli (PQ) ¹.

wandson.amorim@ufabc.edu.br; dalmo.mandelli@ufabc.edu.br

¹Center for Natural and Human Sciences, UFABC.

Keywords: Metal-Organic Frameworks (MOFs); Heterogeneous Catalysis; Valorisation of Alkanes; Cyclohexane Oxidation.

Highlights

Ferric chloride (FeCl_3) was used as a catalyst precursor supported on MOF UiO-66(Zr). The catalyst was active with 36% conversion and an average cyclohexanol yield of 7% after 2h of reaction. The leaching tests indicate that the catalyst has a predominantly heterogeneous behaviour.

Abstract

Cyclohexane is an important alkane for the polymer industry such as nylon-6 and nylon-6.6. The oxidation of this compound forms two main products, cyclohexanol and cyclohexanone (KA oil), which are industrially produced using homogeneous catalysts based on cobalt salts and boric acid under pressures between 10 and 20 bar and temperatures between 140 and 180 °C, with conversion rates around 7% and low yields, however, with a selectivity of nearly 80% [1]. Currently, metal-organic frameworks (MOFs) have drawn attention to the construction of heterogeneous catalysts due to their crystallinity, high porosity, large specific surface area and chemical, thermal and structural stability [2]. In this work, the MOF UiO-66(Zr) was used to support Fe species to catalyze the selective oxidation of cyclohexane with hydrogen peroxide (50% m/m) under mild reaction conditions. The materials were analyzed and evaluated by ASAP, PDRX, FTIR, SEM-EDS and TGA. The products were quantified by gas chromatography with a flame ionization detector (GC-FID) and by mass spectrometry (GC-MS).

The DRX and TGA analyzes demonstrate that the support and the catalyst present structural and thermal stability after post-synthesis processes and reaction cycles. The FTIR results show a reduction in the intensity of the band referring to $\text{C}=\text{O}$ (1665 cm^{-1}) in the catalyst after use, indicating possible chemical instability in the solid. The specific surface area of the support was $1621\text{ m}^2/\text{g}$ and of the catalyst $1347\text{ m}^2/\text{g}$. The area reduction in the catalyst was expected due to the mechanical and thermal processes to which it was submitted. The presence of Fe in the catalyst was evidenced by EDS, indicating a content between 1.0 and 1.5% of the metal. The results of the catalytic tests showed that the catalyst was active with 36% of cyclohexane conversion with an average yield of 7% for cyclohexanol, but with limited selectivity (18%). Finally, the leaching tests showed that the catalytic system is mostly heterogeneous, as there was a reduction in cyclohexanol production over time, proving that this process occurs with greater intensity in the presence of the catalyst (**Figure 1**). However, Fe species was also detected, via atomic absorption (% of the initial Fe was leached), but they were almost not active.

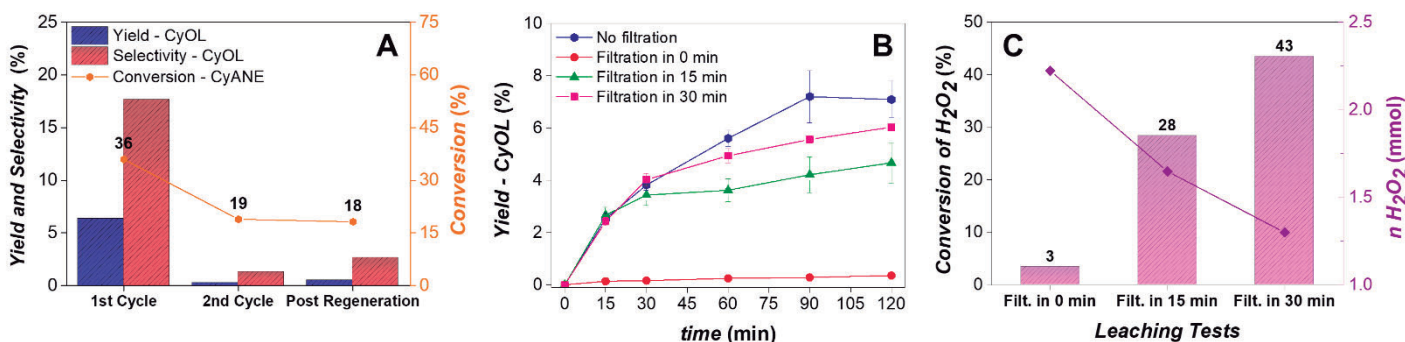


Figure 1. Catalytic tests (A), kinetic behaviour in the presence of Fe(III)-UiO-66(Zr) and leaching tests (B) and quantification of H_2O_2 in the leaching tests (**Conditions:** Catalyst (Fe(III)-UiO-66(Zr) = 50 mg); 0.13 mL H_2O_2 (50% m/m, 2.30 mmol); 0.30 mL (2.75 mmol) of cyclohexane and H_2O (3.61 mmol, provided by H_2O_2) at 40 °C and 1000 RPM (magnetic stirring) for 2 h (120 min) in 2.07 mL of acetonitrile (MeCN) as a solvent).

[1] U. Schuchardt et al. *Applied Catalysis A: General*, v. 211, n. 1, p. 1-17 (2001);

[2] O. Kholdeeva; N. Maksimchuk. *Catalysts*, v. 11, n. 2, p. 283 (2021).

Acknowledgments

This work was supported PRH/ANP N°49, UFABC (PPG-CTQ/CCNH), CEM-UFABC, FAPESP, FINEP, FUNDEP, CAPES, CNPq, LEMUP-UFU and MCTI/SisNANO/INT-CENANO-CNPq.

Bifunctionalization of carboxymethyl cellulose with imidazole and hydroxamic acids: designing biocatalysts to neutralize organophosphates

Mariana Helena Nazareno (IC),¹ Willian H. Takarada (PG),¹ Rilton A. de Freitas (PQ)² and Elisa S. Orth (PQ)¹
mariana.helena@ufpr.br;

¹Department of Chemistry and ²Department of Pharmacy, Universidade Federal do Paraná (UFPR) – Curitiba, PR, Brazil.

Key words: Carboxymethyl cellulose, hydroxamic acid, imidazole, dephosphorylation, biopolymer, pesticide.

Highlights

Chemical modification of carboxymethylcellulose with two anchored nucleophilic groups, hydroxamic acid and imidazole, to develop biocatalysts that efficiently degrade organophosphates, a highly toxic molecule.

Resumo/Abstract

Organophosphate compounds, both natural and artificial are highly stable due to their P-O bonds, making their cleavage possible naturally only in the presence of enzymes. Due to their high toxicity and stability, phosphoric esters were chosen for the development of pesticides and chemical weapons, because they are resistant to water, soil and air, and can reach the target without being chemically altered, accumulating in tissues and causing harm to living beings. Therefore, the study of the reaction mechanisms involving these compounds, the monitoring of their use and the study of neutralization reactions is of paramount importance. A method that is being studied here for the degradation of organophosphates is the development of catalysts with two nucleophilic groups (FIGURE 1A), namely imidazole and hydroxamic acid, molecules already studied in the catalysis reactions of these compounds. The bifunctionalization of carboxymethylcellulose (CMC) was carried on the carboxylic acid sites using hydroxylamine hydrochloride and API (nome completo do API), leading to sustainable biocatalysts (FIGURE 1B), containing imidazole and hydroxamic acid groups. Characterization by several techniques (FTIR, complexation with iron (III), potentiometric titration) confirm the chemical functionalization. Finally, kinetic studies were performed. Samples were tested in reactions with 2,4-dinitrophenyl phosphate (DEDNPP) to analyze the catalytic activity. The bifunctionalized samples showed greater catalytic activity (up to 10⁴-fold) compared to the hydrolysis indicating the success of the work proposal. Also, the bifunctionalized biocatalysts showed higher activity than the monofunctionalized analogues. So far, the results obtained are promising, with success in bifunctionalization and great catalytic activity, which enables the design of sustainable biocatalysts that can be used from chemical detoxification to artificial enzymes and genetic therapy.

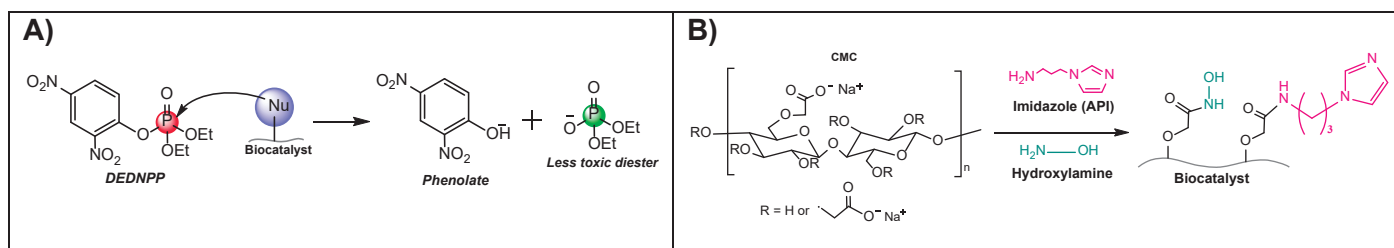


Figure 1. A) Dephosphorylation reaction of DEDNPP; **B)** Functionalization route scheme for CMC-IMZandHDA; **C)** FTIR spectra of the samples; **D)** pH rate profile of the samples reactions with DEDNPP at 21°C

Agradecimentos/Acknowledgments

UFPR, CAPES, CNPq, Fundação Araucária, L'Oréal UNESCO-ABC, PhosAgro/UNESCO/IUPAC, FINEP.

Catalytic conversion of starch over NbOPO₄-based catalysts

Giovanni L. Souza (IC),¹ Simone J. Canhaci (PQ),¹ Kryslaine M. A. Santos (PQ),¹ Marco A. Fraga (PQ),¹
marco.fraga@int.gov.br.

¹Instituto Nacional de Tecnologia, Laboratório de Catálise - Av. Venezuela, 82 - Saúde, Rio de Janeiro - RJ.

Keywords: Starchy biomass, sorbitol, 5-HMF, NbOPO₄.

Highlights

The sequential reaction of starch to form 5-HMF and sorbitol depends on the type of acid site the catalyst presents. NbOPO₄-based catalysts showed promise for this reaction.

Resumo/Abstract

The use of starch, derived from starchy biomass, has become a potential alternative for producing compounds with high industrial demand, such as glucose, 5-hydroxymethylfurfural, and sorbitol. Starch hydrolysis over acidic sites leads to glucose, which, by hydrogenation on metallic sites, leads to the formation of sorbitol. Alternatively, glucose can be dehydrated to 5-HMF on the same acidic sites. This work aims to study the formation of 5-HMF and sorbitol from starch over catalysts based on NbOPO₄, which was used *in natura*, calcined in a muffle furnace at 400°C for 5 h (NbOPO₄-400) and containing 1% Pt on its surface (Pt/NbOPO₄). Catalytic tests were carried out in a Parr reactor at 150°C and pressure of 40 bar (N₂ or H₂) for 6 h, and aliquots were collected in regular periods of 1 h. Product formation was quantified using HPLC on a Waters Alliance 2695 chromatograph with an Aminex HPX-87C column. Initially, preliminary tests were carried out to evaluate the type of acidity required for the first step of the reaction using a catalyst with only Lewis acidity (Al₂O₃) and one with only Brønsted acidity (Amberlyst-36). The results in 3 h of reaction showed yields of glucose of 69% and only traces of 5-HMF when using Amberlyst-36. No reaction products were detected using Al₂O₃, which shows the effectiveness of Brønsted sites. Figure 1 shows that the glucose yield obtained has a similar trend for the three catalysts tested. However, the *in natura* catalyst (Figure 1A) showed higher yields of glucose (70% in 2 h) compared to the other materials. This may be due to the greater number of Brønsted sites in the catalyst since the acidic properties of this material are modified with heat treatment.¹ Glucose is consumed with reaction time in the three tested systems. In 6 h of reaction, the yield of 5-HMF was the same using both NbOPO₄ and NbOPO₄-400 (Figures 1A and 1B) with values of ~17%. This result suggests that the density of acid sites in the catalyst impacts the hydrolysis step but does not cause a significant difference in the dehydration of glucose to 5-HMF. The catalyst containing metallic sites was efficient in hydrogenating glucose, presenting a yield of 20% of sorbitol, evidencing the interplay between acidic and metallic sites on this cascade reaction.

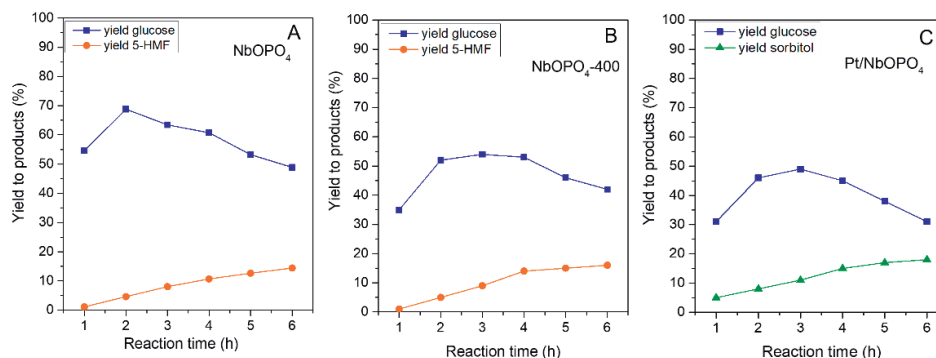


Figure 1. Yield of products formed from starch using catalysts based on NbOPO₄.

1- Amos, T.G., Sleight, A. W. Journal of Solid State Chemistry, 160, 230-238 (2001).

Agradecimentos/Acknowledgments

The authors thank CNPq and FAPERJ for the financial support and CBMM for supplying NbOPO₄.

46ª Reunião Anual da Sociedade Brasileira de Química: "Química: Ligando ciências e neutralizando desigualdades"

Catalytic properties and structural characterization of the Fe-FeOx phases applied to the acetone hydrodeoxygenation reaction

Pedro B. de M. Nunes (IC),^{1*} Guilherme B. Strapasson (PG),^{1,2} Daniela Zanchet (PQ).¹

p236605@dac.unicamp.br

¹Instituto de Química, Unicamp; ² Brazilian Synchrotron Light Laboratory, CNPEM.

Keywords: Nanomaterials, Heterogeneous Catalysis, Iron Oxide, Hydrodeoxygenation.

Highlights

- Evaluation of oxidized and metallic phases of iron in the acetone HDO reaction
- Different thermal pre-treatments induce the coexistence of iron phases and determine the catalytic selectivity

Resumo/Abstract

Due to the imminent shortage of fossil fuels and the growing energy demand, the search for renewable and green energy sources has rapidly become one of the biggest priorities of the century. Lignocellulosic biomass is a natural compound that, after being submitted to processes such as rapid pyrolysis, is transformed into a material known as bio-oil, which is a promising alternative to replace non-renewable fuels and chemical intermediates in the industry. However, due to its high oxygen content, this mixture requires upgrading processes that lead to a decrease in the oxygen content of the targeted compounds, through the selective cleavage of C-O bonds, in the presence of a heterogeneous catalyst under a H₂-rich atmosphere. The use of model molecules of biomass derivatives, such as acetone, is frequently employed due to the complex composition of bio-oils. Thus, in this work, we evaluated the effects of metallic and oxidized phases of iron, an earth-abundant element, in the HDO reaction of acetone, with a correlation of the catalytic sites with the preferred reaction pathways. Commercial γ -Fe₂O₃ nanopowder (particle size <50 nm; specific surface area of 97.8 m²/g) was subjected to reducing and oxidizing thermal pre-treatments, which directly impacted the acetone conversion, the deoxygenation degrees, and the overall products' selectivity. The catalytic results indicated the presence of different catalytic sites, i.e., oxygen vacancies, metallic, and Bronsted/Lewis acid sites. Acetone HDO performance of the as-received γ -Fe₂O₃ catalyst at 300 °C caused an average deoxygenation degree (DD) of 11.4% and acetone conversions of about 27%. Mesityl oxide (C₆H₁₀O), an aldol condensation product formed through acidic sites, was the main product (71.2%). After a reducing pre-treatment at 550 °C (30% H₂/ 70% He) for 3h, however, the catalyst's average DD increased almost 8 times, favoring the formation of propylene and propane as the main products, together representing 85.4% of the total products. The appearance of these products can be associated with the combination of metallic and acid sites, through a bifunctional mechanism or the direct deoxygenation route via oxygen vacancy sites.

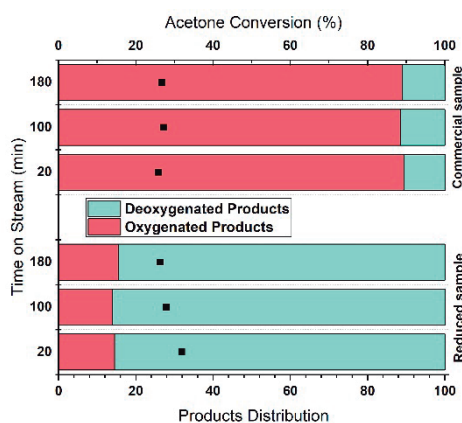


Figure 1 shows the comparison between samples regarding their HDO products distribution and acetone conversion.

Reduction/Calcination pre-treatments have also been carried out, with calcination temperatures varying between 150 °C and 500 °C. Structural characterization conducted using XRD demonstrated that the reducing/oxidizing pre-treatments led to the coexistence of oxidized and metallic Fe phases. Further characterizations and HDO testing are soon to be done. We expect that these structural variations will directly impact the catalytic performance, representing a pathway to fine-tune the selectivity towards the desired products.

Agradecimentos/Acknowledgments

FAPESP (2018/01258-5, 2020/12986-1, 2022/09325-9), CNPq, and CAPES for funding.

Continuous Processes for Enzymatic Hydrolysis of Vegetable Oil

Lucas B. Barbosa (PG), Mauro R. B. P. Gomez (PG), Marcelo A. do Nascimento (PG), Raquel A. C. Leão (PG), Rodrigo O. M. A. de Souza (PQ)*

barrosbluc97@gmail.com; souzarod21@gmail.com*

Biocatalysis and Organic Synthesis Laboratory, Chemistry Institute – Federal University of Rio de Janeiro – IQ – UFRJ.

Keywords: Hydrolysis, vegetable oil, lipase, flow chemistry.

Highlights

This work develops a biotechnological strategy for vegetable oil hydrolysis in high yield and productivity under continuous flow conditions.

Abstract

Hydrolysis of vegetable oils have been carried out traditionally in batch reactors with a lot of success in the last years. For this purpose, Biocatalysis approach towards oil hydrolysis have been studied by several authors over literature but in most cases the need of a surfactant in order to establish a better mixing between oil and water phases¹, can make the downstream process more difficult. One alternative to avoid the use of surfactants and have been applied with much success in food industry is ultrasound² which can enhance the rate of mixing between the two phases and together with the efficiency of continuous flow micro reactors could lead to a very interesting process. The combination of these technologies can allow high space-time yield, that is, product mass per reactor volume and time, and productivity, mass product per time and mass of catalyst.³ First we evaluated quantitative parameters in both immobilized and free enzymes, then we studied the best configuration for promoting the reaction in continuous flow. Figure below presents some of the configurations used for immobilized enzyme, which use a fixed bed reactor. In preliminary studies, we found that the complexity didn't increase the rate of reaction and simple mixture in a "T" joint is the best option in this case (Configuration (B) in Figure).

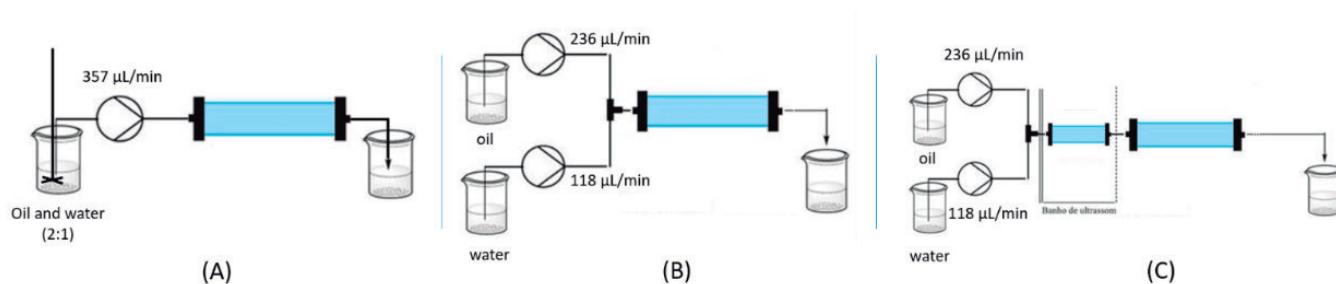


Figure. Configurations (A), (B) and (C) for vegetable oil hydrolysis in continuous flow

By the other hand, when studies were run out with free enzymes in continuous flow, it showed great increase of rate when the ultrasound mixing were added. In a coil PTFE reactor of 12 mL, the conversion and selectivity achieved was 95 %, and the productivity was $36,1 \mu\text{L}\cdot\text{mg}_{\text{enzyme}}^{-1}\cdot\text{min}^{-1}$, proving the efficiency of the process. As perspectives, we would like to explore other immobilization supports for enzymes and stronger sources of ultrasound to achieve >90% conversion.

Acknowledgments

CNPq, CAPES and FAPERJ

- (1) Sande, D.; Colen, G.; dos Santos, G. F.; Ferraz, V. P.; Takahashi, J. A. Production of Omega 3, 6, and 9 Fatty Acids from Hydrolysis of Vegetable Oils and Animal Fat with *Colletotrichum Gloeosporioides* Lipase. *Food Sci. Biotechnol.* **2018**, *27* (2), 537–545. <https://doi.org/10.1007/s10068-017-0249-1>.
- (2) de Castro, T. F.; Cortez, D. V.; Gonçalves, D. B.; Bento, H. B. S.; Gonçalves, R. L. N.; Costa-Silva, T. A.; Gambarato, B. C.; de Castro, H. F.; de Carvalho, A. K. F. Biotechnological Valorization of Mycelium-Bound Lipase of *Penicillium Purpurogenum* in Hydrolysis of High Content Lauric Acid Vegetable Oils. *Process Saf. Environ. Prot.* **2022**, *161*, 498–505. <https://doi.org/10.1016/j.psep.2022.03.013>.
- (3) Plutschack, M. B.; Pieber, B.; Gilmore, K.; Seeberger, P. H. The Hitchhiker's Guide to Flow Chemistry. *Chem. Rev.* **2017**, *117* (18), 11796–11893. <https://doi.org/10.1021/acs.chemrev.7b00183>.

Effect of different acid modulators in the synthesis of MOF UiO-66(Zr)

Paola C. Oliveira (PG) ^{1*}, Wandson L. N. Amorim (PG) ¹, Carla R. Moreira (PQ) ², Marco A. Fraga (PQ) ², Dalmo Mandelli (PQ) ¹.

paola.caroline@ufabc.edu.br

¹Federal University of ABC, UFABC; ²Instituto Nacional de Tecnologia, INT

Keywords: UiO-66; Metal-Organic Frameworks; Synthesis; Modulator.

Highlights

The synthesis of UiO-66(Zr) can be performed with different modulators, that directly impact physical properties such as crystal size and morphology, pore diameter, pore volume, and specific surface area.

Abstract

MOFs are crystalline hybrid materials synthesized from the reaction between organic and inorganic molecules, through molecular self-assembly leading to widely different structures, and distinct properties such as low density, high porosity, and specific surface area. When constructed using zirconium (Zr) as a metallic cluster, they draw attention due to the higher values of thermal, chemical and structural resistance in relation to other metals-containing MOFs. Among them, UiO-66 stands out as a stable material holding 1,4-benzenedicarboxylates as an organic linker. MOF UiO-66(Zr) can be synthesized from terephthalic acid and zirconium chloride (ZrCl₄), however, crystal growth can be controlled using a modulator, a compound or substance that assists in the growth rate and affects various physical properties of the materials. In this work hydrochloric, formic, acetic, and benzoic acids were used as modulators to synthesize UiO-66(Zr), exploring the influence of those acid strength on the MOFs physical properties.

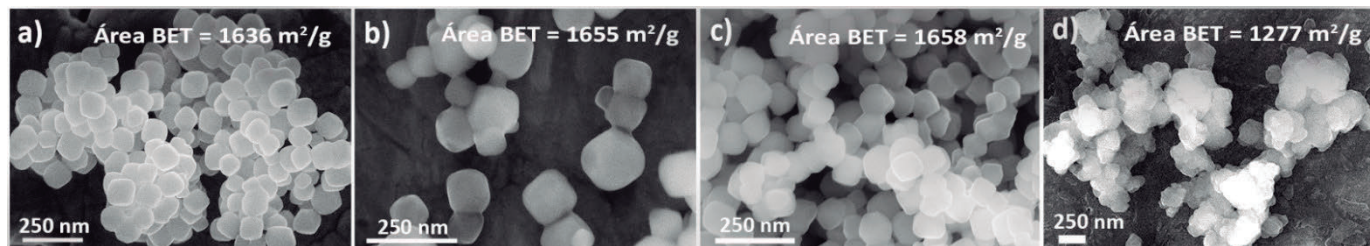


Figure 1. SEM images of UiO-66 synthesized with different modulators and their influence on surface area, morphology and crystal size. Crystals sizes: a) acetic acid (96 nm), b) benzoic acid (106 nm), c) formic acid (84 nm) and d) hydrochloric acid (the lack of uniformity makes the measurement unfeasible).

Evaluating the synthesized MOFs in terms of crystallinity and chemical bonds, it was observed that the proposed synthesis proved to be efficient. However, results showed that the modulator chemical nature has indeed a strong influence on morphology and sizes of the formed crystals as shown in Fig. 1. Acids with lower pKa promoted the formation of totally non-uniform crystals, making it difficult to measure their sizes as in the case of MOF synthesized in HCl (Fig. 1d). On the other hand, when increasing the pKa of the modulating acid, a change in the specific surface area, size and uniformity of crystals was observed. These MOF UiO-66(Zr) presented more uniform square crystal shapes (Fig. 1a-c) with sizes ranging from 84 to 106 nm, obeying the following ascending order: formic < acetic < benzoic acid. In addition, the strength of the acid was also found to be capable of increasing the specific surface area of the material that ranged within 1277 - 1658 m²/g. Total pore and micropore volumes followed the same trend, allowing to choose the most promising acid modulator according to the required MOF application. Even influencing several properties, changing the acid modulator did not affect the thermal resistance of these materials as they still showed stability until around 560 °C.

These results outline that it is feasible to tailor some properties of UiO-66(Zr), which widens their potential applications, such as a catalyst in different types of reactions, such as the conversion of CO₂ into oxygenated products, mostly alcohols and aldehydes.

Acknowledgments

This work was supported by CAPES, FAPERJ, FAPESP, UFABC, CEM, INT and we thank CENANO-INT/SISNANO (CNPq-SisNANO 442604/2019-0) for the SEM-EDS and STEM analyses.

Effects of alkaline promoters on platinum catalysts supported on metal oxides in the reverse water gas shift reaction (RWGS)

Natalia A. Oliveira (IC),^{1*} Natália M. B. Ladeira (PG),¹ Leonardo S. Sousa (PG),¹ Daniela Zanchet (PQ).¹

n217783@dac.unicamp.br

¹Group of Catalysis and Nanomaterials, Institute of Chemistry (IQ), University of Campinas (UNICAMP), Campinas, SP, Brazil;

Keywords: Heterogeneous Catalysis, Alkali Metals, Platinum, CO₂.

Highlights

Performance evaluation of different heterogeneous platinum catalysts in the reverse water gas shift reaction (RWGS) with emphasis on metallic phase dispersion and the use of alkali metals as promoters, aiming at identifying more promising systems for CO₂ conversion.

Abstract

The CO₂ conversion to products is strategic for reducing the carbon footprint in various processes. The Reverse Water Gas Shift (RWGS) reaction leads to the formation of synthesis gas (CO, H₂) from CO₂ according to the equation: CO₂(g) + H₂(g) ⇌ CO(g) + H₂O(g). Using H₂ obtained from renewable sources becomes strategic because the synthesis gas is used directly as raw material in the production of several products, such as higher alcohols (AS) through the Fischer-Tropsch synthesis (FTS, nCO + 2nH₂ ⇌ C_nH_(2n+1)OH + (n-1)H₂O). In this context, the development of catalysts for RWGS becomes viable to produce AS using renewable energy and resources.

The problem with converting CO₂ into CO is the low reactivity of CO₂ and the presence of parallel reactions, such as the formation of CH₄. Thus, the development of active and selective CO catalysts is fundamental. Typically, a metallic phase highly dispersed over porous oxides constitutes the heterogeneous catalysts used in RWGS. This work focuses on the performance of platinum catalysts in the RWGS reaction, with the dispersion of the metallic phase and the use of alkali metals (sodium and potassium) as promoters, with the final objective of understanding the trend of catalytic activity in this type of reaction.

The synthesis of a set of 1% Pt/TiO₂ catalysts prepared by the wet impregnation method and subjected to thermal treatment was carried out. Promoters (K or Na) were added at different levels (0.1-1%) through co-impregnation or sequential impregnation. The catalysts were tested in the reaction of RWGS in a fixed bed, 2% CO₂, 8% H₂, and 90% He and total flow of 100 ml.min⁻¹, in four temperature steps (70 minutes each): 400°C, 500°C, 600°C, and 400°C.

Figure 1 shows the reaction results of four samples obtained by sequential impregnation. It is possible to conclude that materials with 1.0%K and 0.5%K arrive at their saturation concentrations, and even at a lower concentration the presence of the promoter acts as a poison in the obtained catalysts. Other forms of preparation are being evaluated, as well as the use of other supports.

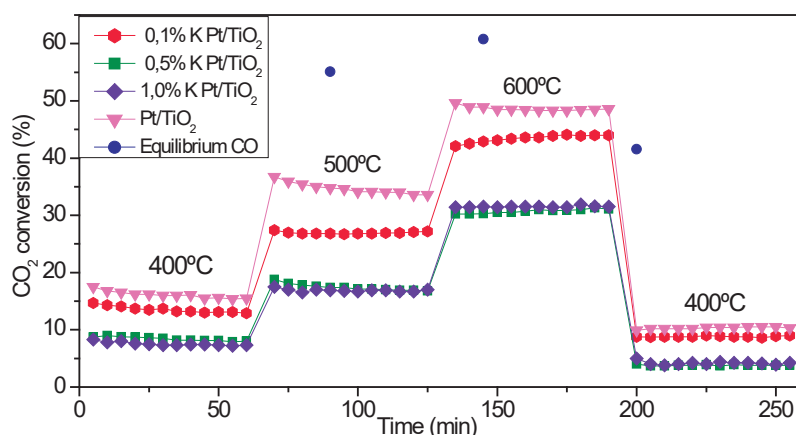


Figure 1. RWGS reaction rate for four catalysts with different promoter/Pt ratio

Acknowledgments



Evaluating the operating conditions of olefins production *via* catalytic CO₂ hydrogenation by Reverse Water-Gas Shift and Fischer–Tropsch reactions.

Guilherme Salvador (PG),² Maria A. Baldanza (PQ),² Fabio Souza Toniolo (PQ),² Carlos A. Ortiz-Bravo (PQ),^{1*}.
toniolo@peq.coppe.ufrj.br; carlosortiz@id.uff.br.

¹Departamento de Físico-Química, UFF; ²Programa de Engenharia química, COPPE/UFRJ.

Palavras Chave: Fe-based catalysts, CO₂ hydrogenation, operating conditions, FTS, and RWGS.

Highlights

Moderately reactor pressure is required to produce olefin via the RWGS-FT route.

Higher H₂/CO₂ molar feed ratios favor the C₂-C₅₊ olefin formation.

Resumo/Abstract

Using CO₂ as a source of carbon atoms to produce light olefins via catalytic hydrogenation is interesting not only because it recycles atmospheric CO₂ associated with the greenhouse effect and climate change, but also because it is a process compatible with the current storage/distribution network of energy. There are two routes for the catalytic hydrogenation of CO₂ to light olefins: the reverse water-gas shift (RWGS) coupled with the Fischer–Tropsch (FT) reaction route, using Fe-based catalysts, and a MeOH-mediated route, combining CO₂ hydrogenation to MeOH and a subsequent methanol-to-olefins reaction. Among hundreds of materials tested for the RWGS-FT route, Na-Fe₂O₃ is pointed out in the literature as a promising catalyst, since it delivers high C₂-C₅₊ olefin yields (> 50 wt.% at 320 °C and 30 bar).¹ However, to progress CO₂ hydrogenation to the industrial level, the effect of the operating conditions should be examined. This work analyzes three critical operating conditions for CO₂ hydrogenation by the RWGS-FT reaction route: catalyst bed temperature (300, 320, and 340 °C), reactor pressure (1, 5, 10, and 20 bar), and H₂/CO₂ molar feed ratio (3 and 6). The 0.5%Na-Fe₂O₃ catalyst was synthesized by a one-pot coprecipitation method as described elsewhere.¹ Powder XRD analysis shows diffraction peaks related to the crystalline Fe₂O₃ rhombohedral phase (#ICSD 201097), FRX analysis only detects Fe presence because of the low Na concentration, and the N₂-physisorption allows to calculate a surface area of 55 m²/g by the B.E.T method, in agreement with the literature.^{1,2} CO₂ conversion at 1 bar increases with temperature (9.6, 22.1, and 24.1% at 300, 320, and 340 °C, respectively), but olefins production is negligible (< 1 wt.%). At 320 °C, increasing pressure from 5 to 10 and 20 bar progressively increases CO₂ conversion (from 25 to 30 and 50 %, respectively), decreases the CO concentration (from 43.4 to 30.4 and 22.4 wt.%), and increases the C₂-C₅₊ olefin concentration (from 41.1 to 53.2 and 57.0 wt.%). Finally, at 320 °C and 20 bar, increasing the H₂/CO₂ molar feed ratio (from 3 to 6) increases the CO₂ conversion (from 50 to 59%), decreases the CO concentration (22.4 to 10.8%) and increases the concentration of methane (from 13.0 to 14.4 wt.%) and the C₂-C₅₊ olefin concentration (from 57.0 to 65.1 wt.%).

Agradecimentos/ Acknowledgments

This study was financed in part by the Coordenação de Aperfeiçoamento de Pessoal de Nível Superior - Brazil (CAPES)- Finance Code 001 and the Fundação Carlos Chagas Filho de Amparo à Pesquisa do Estado do Rio de Janeiro (FAPERJ).

Referências/References

- (1) Liang, B.; Duan, H.; Sun, T.; Ma, J.; Liu, X.; Xu, J.; Su, X.; Huang, Y.; Zhang, T. Effect of Na Promoter on Fe-Based Catalyst for CO₂ Hydrogenation to Alkenes. *ACS Sustain. Chem. Eng.* 2019, 7 (1), 925–932.
- (2) Wang, W. C.; Tao, L. Bio-Jet Fuel Conversion Technologies. *Renew. Sustain. Energy Rev.* 2016, 53, 801–822.

Area: CAT

EVALUATION OF PHOTOCATALYTIC DEGRADATION OF ATRAZINE BY SILVER TUNGSTATE SYNTHESIZED WITH MICROWAVE ENERGY

Otávio A.P. Pereira (PG)¹; Ailton J. Moreira (PQ)²; Gian P. G. Freschi (PQ)¹; Roberto Bertholdo (PQ)¹; roberto.bertholdo@unifal-mg.edu.br; otavio.pereira@sou.unifal-mg.edu.br

¹MACAA - Instituto de Ciência de Tecnologia, Universidade Federal de Alfenas (UNIFAL-MG)

²LIEC - Departamento de Química, Universidade Federal de São Carlos (UFSCar)

Key Words: Atrazine, Photocatalysis, Silver Tungstate, Microwave.

Highlights

- Silver tungstate synthesis by hidrothermal method using microwave energy
- Conventional water and sewage treatments aren't efficient in organic pollutants removal
- Advanced oxidative processes are an alternative to treat organic pollutants

Abstract

The increase of contamination by organic pollutants has boosted researches focused on the treatment of such contaminants using different processes. Organic pollutants can persist in the environment causing problems as the soil, surface water and groundwater contamination, mainly. Among the most organic pollutants, it is possible to list pesticides, pharmaceutical products and some classes of dyes. For treating effluents that contain these pollutants, heterogeneous photocatalysis has been widely studied by the use of different semiconductor materials that act as photocatalysts in the oxidation of these pollutants. Silver tungstate (Ag_2WO_4), is an semiconductor with outstanding photocatalysts properties, because when it is irradiated by ultraviolet (UV) or visible (Vis) light, it is able to produce hydroxyl radicals, peroxides or superoxides that have high potential of oxidation. In this context, this research initial objective involves silver tungstate semiconductor synthesis by the hidrothermal method using microwave energy. After the material characterization, their potential application in the photodegradation of Atrazine in aqueous solution was studied. In the silver tungstate synthesis, 20 mL of a 2 mmol solution of silver nitrate was added to 100 mL of a 1 mmol solution of sodium tungstate under magnetic agitation at room temperature. Then, the suspension was transferred to 4 PTFE vials, hermetically closed and put in a Mars 6 microwave oven. The reaction was managed at 136 °C during 50 minutes. The obtained beige precipitate was separated by centrifugation, washed 3 times with Milli-q water and dried in an oven at 65°C until constant mass. The material was analyzed by powder XRD, that made it possible to verify the $\alpha\text{-Ag}_2\text{WO}_4$ formation, mainly, which is the photactive phases. SEM-FEG images shows the presence of orthorhombic end rods was noticed, confirming the presence of $\alpha\text{-Ag}_2\text{WO}_4$. By DRS spectra, it was verified that the material presented a band gap value of 3,3 eV, and the analysis of surface area showed that the material isn't very porous ($1,7 \text{ m}^2\cdot\text{g}^{-1}$). In the application of Ag_2WO_4 in the degradation of Atrazine, photocatalytic essays were done using an aqueous solution $10 \text{ mg}\cdot\text{L}^{-1}$ containing 5 mg of Ag_2WO_4 , equilibrium time of adsorption of 30 minutes and different times of exposure to visible light in a reactor. Essays adding 2 mL of H_2O_2 to the Atrazine solution containing the photocatalysts were also done. The obtained solutions were filtered and analyzed by HPLC for quantification of remaining Atrazine from photodegradation and its by-products. It was verified that the Atrazine removal was 35 % in 30 minutes in the presence of H_2O_2 and that there wasn't by-products formation.

Acknowledgments

The authors would like to thank the FAPEMIG, CNPq, CAPES, ICT/UNIFAL, EMBRAPA INSTRUMENTAÇÃO and LIEC/UFSCar.

EVALUATION OF REACTION SYSTEMS FOR PHOTODECARBOXYLATION OF FATTY ACIDS MEDIATED BY CvFAP

Ana L. P. da Silva (IC),¹ Alexandre S. França (PQ),¹ Gabriela Y. Breda (PQ),¹ Raquel A. C. Leão (PQ),¹ Rodrigo V. Almeida (PQ),² Rodrigo O. M. A. de Souza (PQ)^{1*}

anapssanha@gmail.com; souzarod21@gmail.com*

¹ Biocatalysis and Organic Synthesis Laboratory, Chemistry Institute – Federal University of Rio de Janeiro – IQ – UFRJ.

² Laboratório de Microbiologia Molecular e Proteínas – Federal University of Rio de Janeiro – IQ – UFRJ.

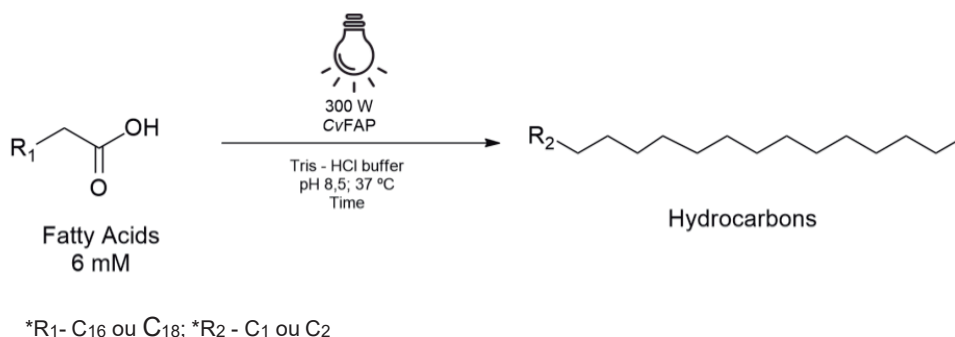
Keywords: CvFAP, Fatty Acid, Photodecarboxylase, Blue Light, Decarboxylation.

Highlights

CvFAP, an enzyme from the unicellular photosynthetic green microalgae *Chlorella variabilis*, has gained importance in the industrial sector since it is used as an alternative strategy for synthesizing long chain alkanes. This flavoenzyme has an affinity for long-chain hydrocarbons, and when photoexcited, it can convert fatty acids into hydrocarbons.

Abstract

Sorigué and collaborators¹ have shown that the CvFAP enzyme, which belongs to the group of photodecarboxylase (FAP), it's capable of converting fatty acids into hydrocarbons in the presence of blue light ($\approx 430\text{-}490\text{ nm}$). Huijbers and collaborators in 2018² described conversions above 99 % in palmitic acid decarboxylation in 3 hours of reaction time and proves a more significant activity of CvFAP for long-chain fatty acids (Scheme).



Scheme: Scope of decarboxylation mediated by CvFAP.

Thus, aiming to broaden the scope, our work shows the optimization of enzymatic photodecarboxylation reactions using different substrates in short reaction times previously optimized by our research group.³ The current project used four substrates (palmitic acid C₁₆H₃₂O₂, linolenic acid C₁₈H₃₆O), linoleic acid C₁₈H₃₂O₂, and oleic acid C₁₈H₃₄O₂) and obtained conversions above 99 % for all of them in 10 minutes of reaction time. These promising results allow development protocols for obtaining hydrocarbon fuels from different resources, using biocatalysis as a strategy.

Acknowledgments

CNPq, FAPERJ and CAPES

¹ Sorigué et al., *Science* **2017**, 357, 903-907.

² Huijbers et al., *Angew. Chem.* **2018**, 57, 13648-13651.

³ Benincá et al., *Mol. Cat.* **2022**, 528, 112469-112475.

Evolving the approaches against organophosphates: from functionalized biocatalysts to neutralizing gels

Willian Hideki Takarada (PG),^{1*} Mariana H. Nazareno (IC),¹ Rilton A. de Freitas (PQ)² and Elisa S. Orth (PQ)¹

*hidetak10@gmail.com;

¹Department of Chemistry and ²Department of Pharmacy, Universidade Federal do Paraná (UFPR) – Curitiba, PR, Brazil.

Keywords: Biopolymers, Carboxymethyl cellulose, Dephosphorylation, Hydroxamic Acid, Imidazole, Paraoxon.

Highlights

Hydroxamate- and imidazole-derived biocatalysts were obtained from colloidal carboxymethyl cellulose. The samples were also developed in the gel form. The materials efficiently neutralize organophosphates.

Resumo/Abstract

Organophosphates encompasses toxic compounds employed as agrochemicals and chemical warfare. Their neutralization reactions (*i.e.*, dephosphorylation reactions) are challenging due to highly-stable P-O bonds but possible using catalysts. Nucleophilic groups, such as hydroxamates and imidazoles, are reactive and promising for neutralizing these compounds, although with some undesirable features (*e.g.*, selectivity and recycling). Thus, the use of templates (*e.g.*, biopolymers) to anchor these groups can improve the catalysis and the neutralization process. Carboxymethyl cellulose (CMC) is a cellulose-derived biopolymer and presents water-solubility and viscous aspects at high polymer concentration. Herein, hydroxamate- and imidazole-derived materials from CMC (colloidal and gel biocatalysts) were developed pursuing the degradation of organophosphates. Carboxylic groups on CMC were functionalized (using 1-ethyl-3-(3-dimethylaminopropyl) carbodiimide (EDC) and N-hydroxysuccinimide (NHS) approach) into hydroxamates (resulting in the colloidal CMC-HDA) and imidazoles (whose different imidazole-side chains resulted in CMC-IMZ(A) and CMC-IMZ(H) samples) (Figure 1A). Functionalization was confirmed and estimated by several techniques (*e.g.*, FTIR, TGA) according to Figure 1C. Then, the colloidal samples were evaluated as catalysts in the dephosphorylation reactions of model-organophosphate diethyl 2,4-dinitrophenyl phosphate (DEDNPP) and real pesticide Paraoxon, unveiling rate enhancements up to 10⁴-fold compared to the spontaneous reactions, results among the best reported (Figures 1B and 1D). The colloidal biocatalysts were also used as additives to develop CMC neutralizing gels. The CMC-IMZ(A)-derived gel were evaluated via *in vitro* permeation assays in a Franz cell with DEDNPP – a intoxication prevention simulation – with prominent results that indicate efficient catalytic detoxification promoted by these materials (Figure 1E). Thus, these materials enable several applications and further development of green, efficient, selective and low-cost (bio)sensors and detoxifying agents for organophosphates, a worldwide concern.

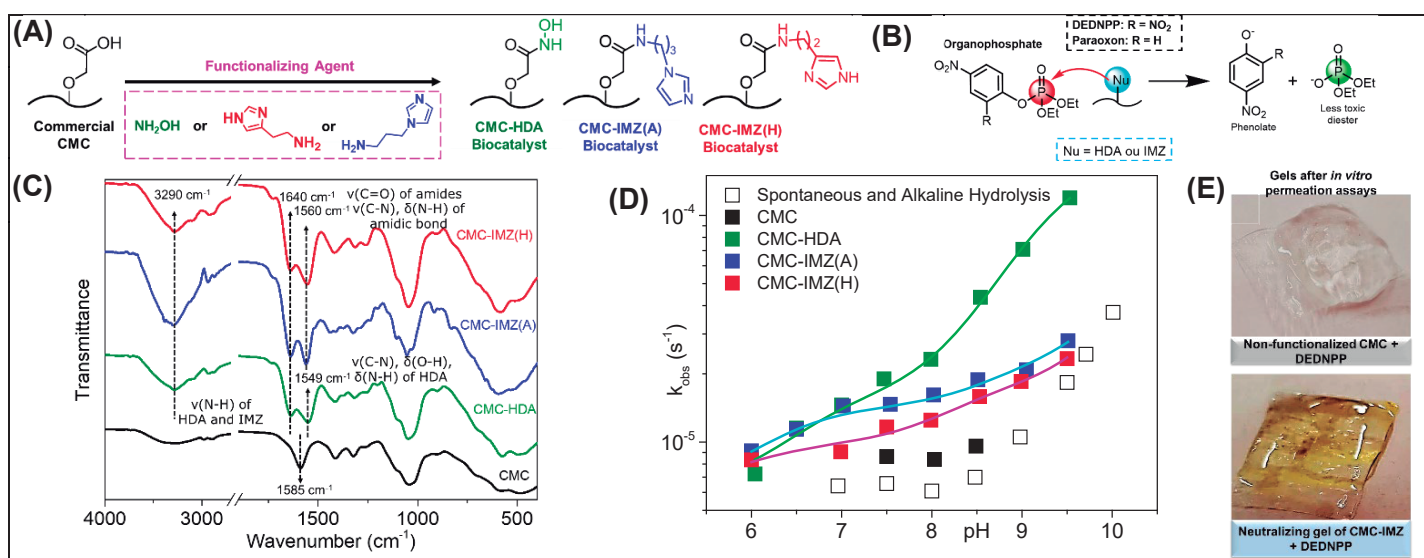


Figure 1. (A) Functionalization route scheme for the biocatalysts; (B) Neutralization reactions of DEDNPP and Paraoxon; (C) FTIR spectra of the samples; (D) pH rate profile of the samples reactions with DEDNPP at 21°C; (E) Gels after *in vitro* permeation assays simulating intoxication prevention.

Acknowledgements: UFPR, CAPES, CNPq, Fundação Araucária, L'Oréal UNESCO-ABC, PhosAgro/UNESCO/IUPAC, FINEP. 46ª Reunião Anual da Sociedade Brasileira de Química: "Química: Ligando ciências e neutralizando desigualdades"

Extraction of pequi oil (*Caryocar brasilienses*) and esterification reaction assisted by ultrasound at room temperature

Daniel Garcez Santos Quattrociochi (PQ),^{1*} Mikael Rocha Bandeira (IC),² Felipe Pereira de Moura (PG),² Maria Clara Oliveira Ribeiro (IC),¹ Manuela Garchet de Souza Magalhaes Matheus (IC),¹ Ruan Stevan de Almeida Ribeiro (PG),¹ Fabio Barboza Passos (PQ),² Thiago de Melo Lima (PQ)¹, Andre Von Held Soares (PQ).²

danielgarcez@id.uff.br

¹Departament of Inorganic Chemistry, UFF; ²Departament of chemical and petroleum engineering, UFF.

Keywords: Pequi; vegetable oil; esterification; catalysis; biodiesel.

Highlights

Obtaining graphitic carbon nitride from urea calcination;
Extraction of pequi oil using ultrasound and soxhlet extractor;
Production of biodiesel from pequi oil by homogeneous and heterogeneous basic catalysis.

Abstract

The growing global energy demand and the depletion of fossil sources is a current problem. The use of petroleum products is essential for the modern world, with means of transport and industry extremely dependent on this non-renewable resource.¹ In this sense, biofuels have been reported as promising to meet part of the demand for fuels. Among them, homogeneous and heterogeneous catalysis can obtain biodiesel from vegetable oils.^{2,3} The present study aimed to find the best condition of the oil extraction process from the pequi pit, using ultrasound equipment, with solvents acetone, ethyl acetate, ethyl alcohol, hexane, and water. The extraction also was performed with Soxhlet extractor and ethanol as solvent. In addition, obtaining biodiesel through the esterification reaction as it is the most used route at the industrial level and lower the cost of reagents. In this sense, the esterification reaction also was studied under heterogeneous conditions employing graphitic carbon nitride (g-C₃N₄) as catalyst. The characterization of the extracted samples and products by GC-MS was also performed. The catalyst (g-C₃N₄) was characterized by X-ray diffraction, thermogravimetric analysis and infrared spectroscopy. The homogeneous reaction procedure consisted of the addition of 0.18 g of KOH and 13 mL of MeOH in 25 mL of pequi oil and the molar ratio of methanol:oil was 9:1.³ The reaction with heterogeneous catalysis was performed 1.4 g of oil, 5 mL of methanol and 25 mg of g-C₃N₄ for 4 hours of reaction on ultrasound in room temperature.⁴ The g-C₃N₄ showed good thermal stability with a degradation temperature above 400 °C. The diffractogram pattern was in accordance with literature data for the same phase found. The crystallographic plans (002) and (100) correspond to the peaks observed in 2θ = 14° and 27°, respectively. These planes are associated with the interplanar distance between the tri-s-triazine units and the distance between the planes of the leaves formed by conjugated aromatic units.⁵ The infrared spectrum presented the bands corresponding to the stretches of the C-N bonds and a broadband 3600 to 2800 cm⁻¹ of the hydrogen bonds of the O-H group from water adsorbed in the polymer and the stretches of the N-H bonds of amino groups in addition to the C=N (1615 cm⁻¹ and 1555 cm⁻¹) and C-N bond stretches (1450, 1400, 1315 and 1230 cm⁻¹). The pequi oil with ultrasound contains palmitic primarily (71%) and oleic (12%) fatty acids. The extraction yield with ultrasound was higher with hexane (57%) as solvent. Ethyl alcohol was used for hot extraction increasing in comparison with cold extraction, the yield of 37.9 % to 50 %. Both the homogeneous and heterogeneous catalysis esterification resulted in the complete conversion of the fatty acids in the respective methyl esters. However, using g-C₃N₄ allows easy separation and reuse of the catalyst and does not require additional steps to obtain the products, thus furnishing a greener feature to the biodiesel production process.

Acknowledgments

This study was financed in part by the Coordenação de Aperfeiçoamento de Pessoal de Nível Superior – Brasil (CAPES), Conselho Nacional de Desenvolvimento Científico e Tecnológico (CNPq) and Fundação Carlos Chagas Filho de Amparo à Pesquisa do Estado do Rio de Janeiro (FAPERJ). The authors also acknowledge to Laboratório de Reatores, Cinética e Catálise (RECAT).

References

1. AMBAT, I.; SRIVASTAVA, V.; SILLANPÄÄ, M. Renewable and Sustainable Energy Reviews, Mikkeli, v. 90, p. 356-369, 2018.
2. DI SERIO, M. et al. Heterogeneous catalysts for biodiesel production. Energy & Fuels, v. 22, n. 1, p. 207-217, 2008.
3. ROCKEMBACH, Caroline T. et al. Revista Virtual de Química, v. 6, n. 4, p. 884-897, 2014.
4. BAIG, RB Nasir et al. Scientific Reports, v. 6, n. 1, p. 39387, 2016.
5. SUN, B. W.; YU, H. Y.; YANG, Y. J.; et al., Physical Chemistry Chemical Physics, v. 19, n. 38, p. 26072–26084, 2017.

From biomass to fuels: a novo carbon-efficient route

Marcelo Maciel Pereira (PQ),^{1*} Leandro Soter de Mariz e Miranda (PQ)^{1*} Yiu Lau Lam(PQ),^{1*} Juliana Carvalho(PQ),¹ Cristiane Cardoso(PG),¹ Débora Nobrega(PG)¹, Matheus Souza(PQ)¹, Thais Corrêa (IC),¹ Alessandra Vieira(PG)¹

maciel@iq.ufrj.br; leandrosoter@iq.ufrj.br; yiulaulam@gmail.com

¹Instituto de Química, UFRJ;

key-words: Carbon-footprint, Refinery, Biomass, Green-fuel, Sugar, Ketal

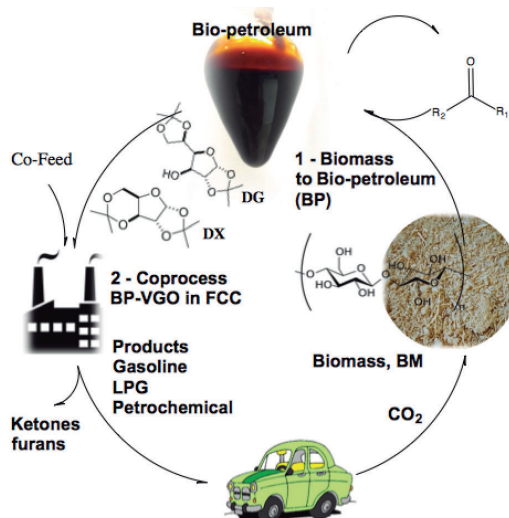
Highlights

Biomass introduction into a refinery. Green products like GLP, gasoline, jet fuel, diesel, light olefin, and BTX. High efficiency (green carbon efficiency >70%) and low-cost route.

Abstract

One of the greatest challenges to Science is to balance energy production with the carbon footprint. Beyond avoiding climate change, only renewable energy sources can provide energy for our and future generations[1]. The amount of second-generation biomass can support the entire production of green-fuel and petrochemical inputs [2] as fuel consumes $\approx 1/4$ of worldwide energy. Our proposed circular technology, figure 1, initiates with a mild ketalization of second-generation biomass to give a liquid product BP which shows feasible physical-chemical properties for subsequent transformation (density $1.2 \text{ g}\cdot\text{cm}^{-3}$, viscosity 200 cp (60°C), specific heat $1.8 \text{ J}\cdot\text{g}^{-1}\cdot\text{C}^{-1}$). As detailed in our publications, it is composed mainly of ketal-sugar derivatives, composition $\approx \text{C}_{2n}\text{H}_{3n}\text{O}_n$ (ranges $\text{C}_{1.4-2}\text{H}_{2.2-2.9}\text{O}_{1\text{N}_{0.007}}$) [3]. BP and representative compounds like DG and DX (fig 1) can be transformed into aromatics [4-6], paraffins, isoparaffins, and cycloalkanes[7-9] with high yields and low coke amount. The flexibility to be converted in typical refinery processes to various products strongly suggests that BP could progressively substitute mineral oil. Hence, the oil refinery can benefit from reducing its carbon footprint. Further research and developments to approach zero net-carbon fuels will have great impacts and demands in advances in chemistry and especially in heterogeneous catalysis. In conclusion, our approach can be a secure transition in the structure of the matrix of energy to reduce carbon footprint and circumvent oil depletion. **Figure 1:** Circular economy of biomass to fuel in two steps.

Step 1- BP production in mild condition (temperature from $90\text{-}140^\circ\text{C}$, mineral acid from $0.1\text{-}0.4 \text{ wt.}\%$, flexible to carbonylate type, like acetone and 2,5-hexadione for example, pressure varies in function of temperature and type of carbonylate, from room to 7 atm). **Step 2 –** BP and example of representative compounds **DG**; 1,2:5,6-di-O-isopropylidene- α -D-glucofuranose and **DX**; 1,2:3,5-di-O-isopropylidene- α -D-xylofuranose are converted to value products. For instance, BP mixture with vacuum gasoil (VGO) in a typical fluid catalytic cracking process conditions gives drop-in fraction in gasoline and liquefied petroleum gas (LPG), petrochemicals, and oxygenates (ketones can be recycled to prepare BP, furans derivatives used as gasoline booster).



catalytic cracking process conditions gives drop-in fraction in gasoline and liquefied petroleum gas (LPG), petrochemicals, and oxygenates (ketones can be recycled to prepare BP, furans derivatives used as gasoline booster).

Acknowledgments

To FAPERJ, CAPES and CNPq

- [1] A. Goldthau, *nature*, 546 (2017) 203./[2] M. H. Langholtz, *et al.*, 2016 Billion-Ton Report, in: A. D. R. f. a. T. Bioeconomy (Ed.), U.S. Department of Energy, 2016, pp. 411./[3] D. Nobrega, *et al.*, *Sustainable Energy & Fuels*, 4 (2020) 4158./[4] J. F. R. Pinto, *et al.*, *Fuel*, 254 (2019) 115684./[5] J. Pinto, *et al.*, *Frontiers in Chemistry*, 7 (2019) 1. [6] N. Batalha, *et al.*, *ChemSusChem*, 7 (2014) 1627./[7] M. O. Souza, *et al.*, *Frontiers in Chemistry*, 9 (2021). [8] S. C. Pereira, *et al.*, *Applied Catalysis a-General*, 609 (2021)./[9] S. Pereira, *et al.*, *Sustainable Energy & Fuels*, 4 (2020) 1312.

Hidrogênio verde a partir do ácido fórmico catalisado por complexos organometálicos de rutênio (II).

Cássio R. A. do Prado (PG)¹, Leonardo T. Ueno (PQ)², Valdemiro Pereira de Carvalho Júnior (PQ)³, Antonio Carlos Ferreira Batista (PQ)⁴, Luís Rogério Dinelli (PQ)⁴, André Luiz Bogado (PQ)^{4*}.

cassiorobertoaprado@gmail.com; bogado@ufu.br

¹Instituto de Química, UFU; ²Departamento de Química, ITA; ³Faculdade de Ciências e Tecnologia, UNESP, ⁴Instituto de Ciências Exatas e Naturais do Pontal, UFU

Palavras-Chave: Hidrogênio verde, organometálico de rutênio, ácido fórmico, catálise homogênea.

Highlights

Green hydrogen from formic acid catalyzed by organometallic ruthenium (II) complexes.

Conversion of formic acid to H₂ and CO₂ were obtained at rate of 95% for the best pre-catalyst.

An attempt to recycle the catalyst produced 99% of conversion and TOF = 953 h⁻¹.

Kinetic and DFT outcomes suggest a dissociative pathway for the dehydrogenation reaction.

Resumo/Abstract

O hidrogênio molecular (H₂) é uma importante fonte de energia limpa e sustentável, que a cada dia vem ganhando mais espaço, podendo ser utilizada para transporte, aquecimento e geração de energia. Porém, existem alguns impeditivos que dificultam o uso em larga escala atualmente, como a estocagem e transporte do gás, que é altamente inflamável. Uma alternativa é a geração *in situ* do H₂, utilizando uma molécula de sacrifício no processo, auxiliada por um agente catalisador para aumentar a velocidade de conversão. Neste trabalho, foi utilizado como fonte de H₂ o ácido fórmico, que possui 4,4 % de hidrogênio em massa, produzindo H₂ via reação de desidrogenação, gerando também CO₂ no processo. A trietilamina foi utilizada como base e complexos de rutênio do tipo [RuCl(*p*-cym)(N-N)]PF₆ (onde N-N corresponde a ligantes diimínicos derivados de anilinas substituídas), foram utilizados como pré-catalisadores, sintetizados e previamente caracterizados por UV/vis, IV, RMN ¹H e ¹³C, análise elementar, condutimetria, voltametria cíclica e cálculos de DFT. A reação de desidrogenação utilizada foi adaptada a partir do método descrito na literatura¹: 2 mL (0,014 mol) de trietilamina, 0,75 mL (0,02 mol) de ácido fórmico e 16,61 μmol de catalisador foram adicionados a um balão de fundo redondo, a temperatura controlada de 60 °C. A produção dos gases foi monitorada por cromatografia gasosa, não sendo observada a presença de CO e de nenhum outro gás. O pré-catalisador que apresentou os melhores resultados continha o ligante N1,N2-*bis*(2,6-dimetilfenil)etano-1,2-diimina (C₁₈H₂₀N₂), com taxa de conversão de cerca de 95% e TOF = 652 h⁻¹. Os valores obtidos de velocidade foram de 1,81 x 10⁻⁴ mol min⁻¹ e *k* = 8,71 x 10⁻³ min⁻¹. Na segunda adição de ácido fórmico, houve um aumento na taxa de conversão para 99 %, ocorrendo em um menor intervalo de tempo, resultando em valores de TOF = 953 h⁻¹, *v* = 2,65 x 10⁻⁴ mol min⁻¹ e *k* = 1,32 x 10⁻² min⁻¹. Os parâmetros físico-químicos foram determinados utilizando as equações de Arrhenius e Eyring, determinando-as pela mudança na temperatura das reações. Para Eyring, o valor de ΔS[‡] calculado foi de 49,6 eu., indicando que o mecanismo da reação é dissociativo. Outros reagentes foram utilizados como base no lugar da trietilamina. Valores semelhantes de conversão foram obtidos utilizando tripropilamina, porém o tempo de reação foi superior a 8 horas, resultando em valores de TOF baixos (140,63 h⁻¹). Com etanol como base, a conversão foi baixa, cerca de 15 %. Valores parecidos de conversão foram obtidos utilizando formiato de sódio (17,86 %) e formiato de potássio (18,97 %). Em *tert*-butóxido de potássio como base, houve um pequeno aumento na taxa de conversão (22,32 %). Na presença de piridina como base (0,02 mol) nenhuma reação foi observada, indicando uma competição da piridina pela porção de coordenação do sítio catalítico. A trietilamina como uma boa base de Brønsted-Lowry, foi mais eficiente que as demais bases utilizadas na desprotonação do ácido fórmico. Uma proposta de mecanismo utilizando cálculos de DFT sugere a troca do ligante Cl por formiato, seguido por uma eliminação β-hidreto para gerar um hidreto complexo liberando CO₂ e H₂ como produtos.

[1] Z. Treigermann, Y. Sasson, Chemistry Select. 2 (2017) 5816.

Agradecimentos/Acknowledgments

CAPES, pela concessão da bolsa de Doutorado e à FAPEMIG, FINEP, FAPESP e ao CNPq.

Hydrogenation Photocatalyzed by Nickel Single-Atoms supported on Crystalline Carbon Nitride

Pietra Flores R. Martins (IC),¹ Guilherme F. S. R. Rocha (PG),¹ Marcos A. R. da Silva (PG),¹ Ivo F. Teixeira (PQ).¹
 pietraflores12@gmail.com

¹Department of Chemistry, UFSCar.

Key words: Carbon Nitride, Poly(heptazine imide), Photocatalyst, Hydrogenation, Single-atoms

Highlights

Perform the hydrogenation of nitrobenzene into aniline, using hydrogen coming from water and nickel single-atoms supported in crystalline carbon nitride as a photocatalyst, developing a sustainable and cheap route for solar to chemical energy conversion.

Resumo/Abstract

A highly crystalline carbon nitride structure can be reached by thermally treating melamine in the presence of NaCl. Sodium cations are stabilized by nitrogen atoms negatively charged in between layers, obtaining Na-PHI (Fig. 1a), PHI standing for poly (heptazine imide). Later, the sodium cations are exchanged for nickel single-atoms, by suspending the material in an aqueous solution of nickel chloride. The obtained Ni-PHI was employed to perform hydrogenations, using hydrogen directly provided from water (instead of the usual fossil fuel H₂ source), enabling a more sustainable and green way to perform this important class of reaction. It is worth highlighting that the Ni active site responsible for reducing water and transferring hydrogen is a non-noble metal catalyst to activate and reduce the water molecule. High conversion and selectivity rates could be observed in the hydrogenation of nitrobenzene to aniline, using TEOA as a hole scavenger, in a very short irradiation time. In only five hours, a yield of 100% was reached (Fig. 1b). Triethanolamine being a toxic and expensive reagent, motivated us to test glycerol as the sacrificial reagent. Even though a decrease in the conversion rate is noticeable, proximally 60% at its highest (Fig. 1c), is still worth investigating, trying to increase the results while keeping the reaction entirely eco-friendly. In order to be certain that the hydrogen source was water, a test without its presence was performed, in which almost no nitrobenzene was converted to aniline (Fig. 1d), indicating that water is, indeed, the main hydrogen source. Tests replacing H₂O with D₂O are planned and might confirm that the hydrogen is sourced by water.

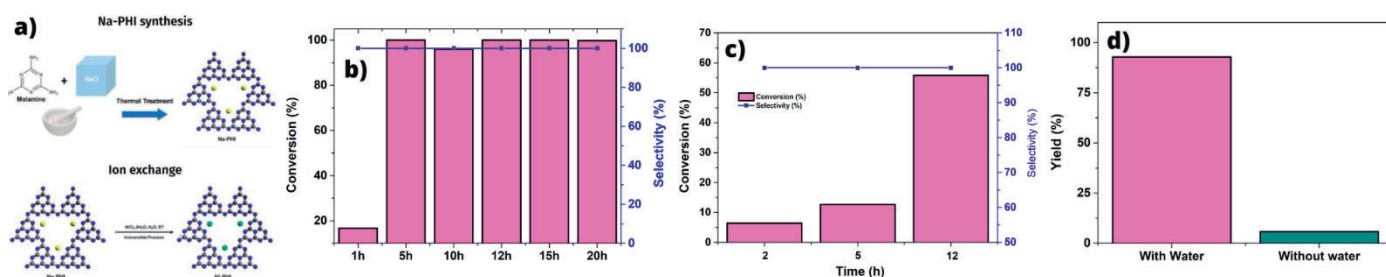


Figure 1: (a) Ni-PHI synthesis; (b) Nitrobenzene conversion rate to aniline for different irradiation times in 410 nm 10 W lighting, using TEOA; (c) Nitrobenzene conversion rate to aniline for different irradiation times in 410 nm 10 W light irradiation, using Glycerol; (d) Nitrobenzene reaction yield with and without the presence of water.

Agradecimentos/Acknowledgments

The authors are thankful for FAPESP, CAPES, CNPQ, Embrapa and UFSCar.

Hydrothermal pretreatment of energy cane using niobium phosphate catalyst

Victória L. da Silva (IC)¹, Raiane P. S. Pinto (IC)¹, Igor M. Gonçalves (PG)¹, Luiz Alexandre Peternelli (PQ)², Márcio H.P. Barbosa (PQ)³, Reinaldo F. Teófilo (PQ)¹.

victoria.lessa@ufv.br; igor.m.goncalves@ufv.br

¹Chemistry Department, UFV; ²Agronomy Department, UFV; ³Statistic Department, UFV

Palavras Chave: Energy cane, Xylose, Furfural, Pretreatment, Niobium phosphate.

Highlights

Niobium phosphate catalyst is effective in hemicellulose solubilization for energy cane pretreatment. Different yields of pentoses and furfural were obtained by varying the temperature.

Abstract

Usually, the main objective of sugarcane cultivation is to increase sugars in the stalks. However, this concept has changed since the production of second-generation fuels became more accessible. These fuels have as a source lignocellulosic biomass. Thus, the term “energy cane” surged as a management concept aiming to produce more sugarcane biomass.¹ However, the natural recalcitrance of lignocellulosic material becomes an obstacle to converting biomass into biofuel or biochemical. One of the stages in the deconstruction of bagasse is pretreatment. The pretreatment can be time and energy-consuming; therefore, using a catalyst becomes desirable.² Among catalysts, niobium phosphate (NbP) has high acidity and is easy to handle.³ This work studied different temperatures in the hydrothermal pretreatment of EC using NbP. Pentoses and furfural were analyzed by Shimadzu Prominence HPLC in a Bio-Rad Aminex HPX-87H column.

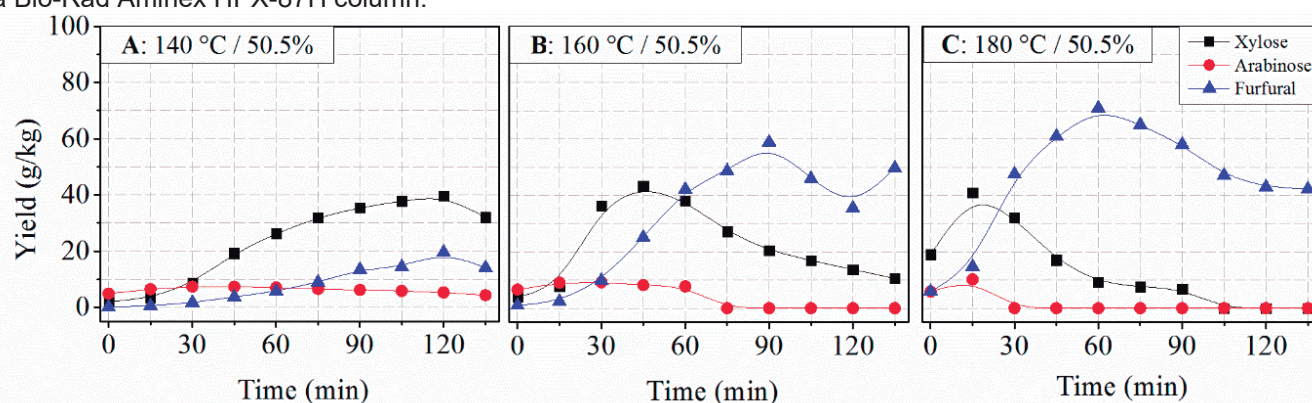


Figure 1. Pretreatment of EC using NbP at the proportion of 50.5% over the time of 135 minutes. The experimental conditions were: 15 g of EC, 7.575 g of NbP, and agitation of 900 rpm.

At lower temperatures (140 °C), it was observed maximum xylose yield was at greater times (Fig. 1A). The opposite was true; at higher temperatures (180°C), the maximum xylose yield was observed at lower times since occur a faster conversion of xylose to furfural (Fig. 1C). Above 60 min in Fig. 1C was seen a decrease in furfural yield, this was probably due to its condensation and formation of hydrochar. At 160°C (Fig 1B), the release of pentoses was faster than at 140°C. On the other hand, furfural conversion was slower than at 180°C condition. Therefore, an increase in the temperature favored the formation of furfural, decreasing xylose yield in the presence of the catalyst.

1. Matsuoka, S. *et al. Adv. Bot.* **2014**, 1–13 (2014).
2. Soltanian, S. *et al. Energy Convers. Manag.* **212**, 112792 (2020).
3. Catrinck, M. N. *et al. Fuel Process. Technol.* **207**, 106482 (2020).

Agradecimentos/Acknowledgments

This study is supported by Biovalue Project (Petrobras, Suzano Papel e Celulose, Klabin, Embraer), FAPEMIG, APESP, FACEPE, and FAPERGS. To CNPq and CAPES for the financial incentive and Brazilian Metallurgy and Mining Company (CBMM) for the niobium phosphate catalyst.

Identification of metal single-atoms on crystalline carbon nitrides using CO-DRIFT-FTIR

Isadora Guedes Farias (PG),¹ Gabriel Ali Atta Diab (PG),¹ Marcos Augusto Ribeiro da Silva (PG),¹ Ivo Freitas Teixeira (PQ)¹.

isadoragfarias@gmail.com

¹Departamento de Química, Universidade Federal de São Carlos (UFSCar).

Palavras Chave: Single-atoms, DRIFT, Characterization, Carbon Nitride, Poly(heptazine imide).

Highlights

SACs characterization by DRIFT with CO as a probe molecule, to investigate the adsorption bands on Ni-PHI and Na-PHI.

Resumo/Abstract

Carbon nitrides (C_3N_4) are a class of semiconductor polymers that provide a two-dimensional support for the stabilization of single atoms, as they exhibit a greater uniformity and controlled structure, which together with the high content of negative nitrogen species offers an abundance of well-defined coordination sites (**Fig. 1b**). In this way, they are very promising for catalytic energy conversion applications acting as photocatalysts. Single-atom catalysis (SACs) despite being a very promising area is at the same time quite limited by the resolution of analytical methods, its characterization requires a series of complementary techniques that are not easily accessible, such as EXAFS and AC STEM-HAADF. Herein, the objective of this work was to use the DRIFT-FTIR with CO as a probe molecule to compare the CO bands on Ni-PHI and Na-PHI, in order to differentiate CO coordinated to Ni single-atoms. It was selected a Ni-PHI sample previously characterized by STEM-HAADF (**Fig. 1c**) and EXAFS, confirming the presence of Ni single-atoms. During the experiment, the samples were placed in the cell, then it was heated at 350 °C with pure He for 10 min. After, it was cooled to room temperature under the He flow (20 mL min⁻¹) and later CO was introduced by 0.5 h at a rate of 10 mL min⁻¹. Finally, helium was passed for 0.5 h to remove not CO molecules. The spectrum was recorded at all stages. In preliminary studies, bridge-type Ni bonding at wavelengths between ~2075 (cm⁻¹) and linear bonds at wavelengths between 2250 and 2300 cm⁻¹ can be assigned in the Ni-PHI spectra after all the sta. More systematic studies will be carried out employing catalysts with different nickel concentrations to confirm their position in the spectra and it is hoped that this work will be a game-changing in single-atom catalysis characterization.

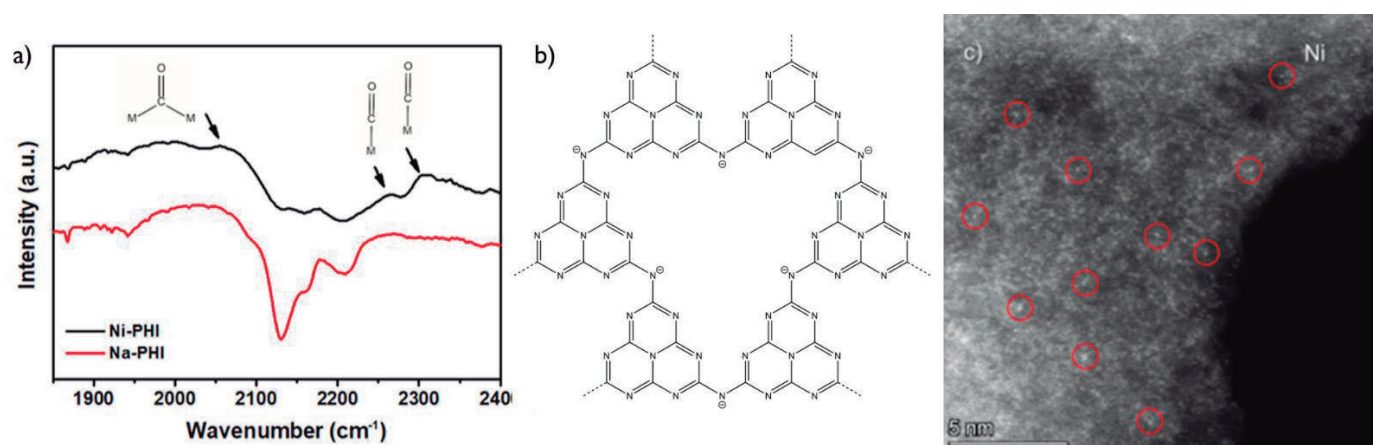


Figure 1: a) DRIFT spectra of Ni-PHI and Na-PHI with chemisorbed CO molecule; b) PHI structure and c) STEM-HAADF image of Ni-PHI showing isolated single-atoms in their structure.

Agradecimentos/Acknowledgment



IRON OXIDE NANOPARTICLES AS CATALYSTS IN ACETONE HYDRODEOXYGENATION REACTION

Breno Artuzi (IC),¹ Gabriel B. Báfero (PG)¹, Guilherme B. Strapasson (PG)^{1,2}, Daniela Zanchet (PQ)¹
b213771@dac.unicamp.br; zanchet@unicamp.br

¹ Instituto de Química, UNICAMP; ² Laboratório Nacional de Luz-Síncrotron, CNPEM.

Keywords: Heterogeneous catalysis, Nanoparticles, Iron oxide, Hydrodeoxygenation

Highlights

Synthesis of iron oxide nanoparticles and application into hydrodeoxygenation of acetone.

Iron oxide NPs led to better catalysts, and the results depended on the NPs loading.

Resumo/Abstract

Iron nanoparticles (NPs) and their oxides have been widely explored in different applications due to their low cost and interesting properties. Among the preparation methods of NPs, colloidal synthesis is a versatile way to tune size, morphologies, and crystalline structure, that directly impact their properties. This project proposes the synthesis of iron oxide NPs, with sizes between 5 nm and 20 nm, and their application as catalysts in the acetone hydrodeoxygenation (HDO reaction). The Fe NPs were synthesized through the thermal decomposition of iron pentacarbonyl dioctyl ether (solvent) in the presence of oleic acid [1]. Trimethylamine N-oxide was added to promote full oxidation forming γ -Fe₂O₃ NPs. SiO₂ was used as support to produce catalysts using the same batch of NPs and different loadings, i.e., 10 wt.% (Fe₂O₃/SiO₂_10%) and 30 wt.% (Fe₂O₃/SiO₂_30%)> The catalysts were prepared by wet impregnation method and calcination at 400° C. XRD of the NPs showed the formation of γ -Fe₂O₃ (or Fe₃O₄) crystal phase with crystallite mean size of 4 nm (due to peak broadening is difficult to distinguish between γ -Fe₂O₃ and Fe₃O₄ phases). TEM confirmed the formation of NPs with an average size of approximately 7 nm. Acetone HDO catalytic evaluation demonstrated that both loadings of NPs led to similar conversions at 400 °C (> 30 %), but the products distribution was impacted. For Fe₂O₃/SiO₂_30%, the deoxygenation products correspond to 41,4 %, whereas for Fe₂O₃/SiO₂_10%, they reach 52,8 %. For comparison, a catalyst made using Fe(NO₃)₃.9H₂O as a precursor, Fe(III)/SiO₂_10%, deactivated in the first hour on stream, showing lower conversion (~20 %) and deoxygenation products (38,2%). Studies are underway to correlate the catalytic performance with the iron oxide exposed surface and size-dependent properties.

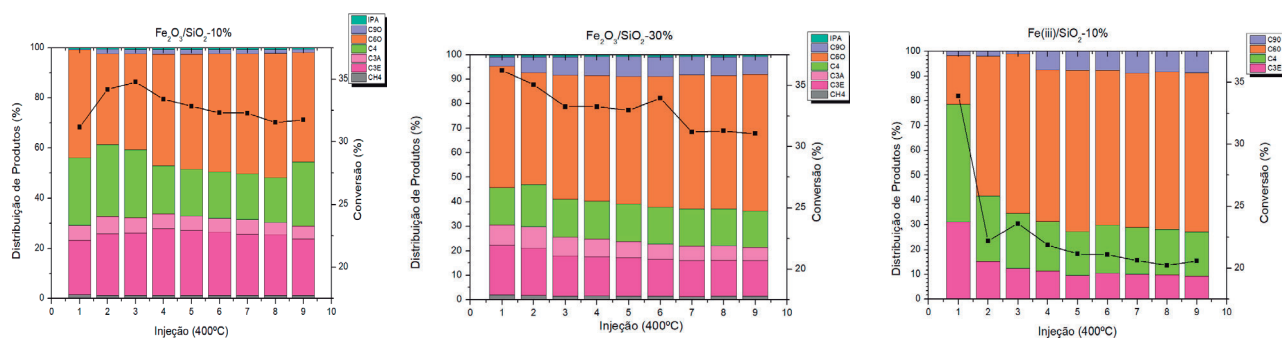


Figure: Conversion (black squares) and products distribution of Fe₂O₃/SiO₂_10%, Fe₂O₃/SiO₂_30%, and Fe(III)/SiO₂_10% applied in acetone HDO reaction. Main products: isopropanol (IPA), condensation products (C6O and C9O), and deoxygenated products (C6, C3A, C3E, CH₄).

[1]J. Park, S.S. Lee; et al. Angew. Chem. Int. Ed. 44 (2005) 2872 – 2877

Agradecimentos/Acknowledgments

FAPESP (2018/01258-5, 2020/12986-1), CNPq, CAPES and PIBIC - PRP UNICAMP for funding.

Iron oxide supported on sand as a catalyst for solar photo-Fenton degradation of antibiotics.

Karla V.L Lima (PG),^{1*} Jany H. Jesus (PQ),¹ Raquel F.P. Nogueira (PQ).¹

k.lima@unesp.br; karlavllima@gmail.com

¹Instituto de Química, UNESP - Araraquara

Key-words: Pharmaceuticals; Trimethoprim, Sulfamethoxazole, Photodegradation, Solar irradiation

Highlights

A stable iron oxide catalyst supported on sand was obtained.
The catalyst was effective to degrade antibiotics under solar irradiation.
The catalyst maintains its activity even after 5 cycles of use.

Abstract

This study aims to produce an iron oxide supported on sand (IOSS) as catalyst for use in a photo-Fenton process and to evaluate its effectiveness for degrading two antibiotics, sulfamethoxazole (SMX) and trimethoprim (TMP), in ultrapure water and Wastewater Treatment Plant (WWTP) effluent. The IOSS catalyst was synthesized based on the methodology described by Benjamin *et al.*, and characterized by X-ray fluorescence (XFR), X-ray diffraction (XDR), and Scanning Electron Microscopy (SEM). The XRF results confirmed the presence of iron in the IOSS and XRD patterns revealing the presence of quartz, and hematite identified by comparison with the database. The SEM image (Fig.1A) showed that the iron oxide particles were supported on the sand surface. The catalytic activity of IOSS was evaluated based on the degradation of TMP and SMX, in 250 mL of ultrapure water and WWTP effluent, both spiked with 200 $\mu\text{g L}^{-1}$ of each antibiotic, at pH 3, using 0.5 g L^{-1} of IOSS and 10 mmol L^{-1} of H_2O_2 . The experiments were performed in a homemade glass photoreactor (5.5 cm height and 9.5 cm diameter) under magnetic stirring and solar or UV lamp irradiation and the antibiotics concentrations were determined using high-performance liquid chromatography. The IOSS catalyst demonstrated effectiveness in degrading antibiotics under both solar and UV lamp radiation (Fig.1B and 1C), with better performance under solar radiation (100% degradation of SMX and TMP after 120 min) compared to blacklight UV lamp (63% degradation of SMX and 77% of TMP after 120 min). Additionally, after an initial decrease of about 20% in antibiotic degradation between the first and second cycle, the catalytic activity of IOSS was maintained after four cycles, demonstrating the stability of the catalyst (Fig.1D). Overall, the IOSS catalyst has potential for use in removing antibiotics from complex matrices such as urban wastewater, and is a candidate to be applied in fluidized bed reactor, avoiding their release into the aquatic environment.

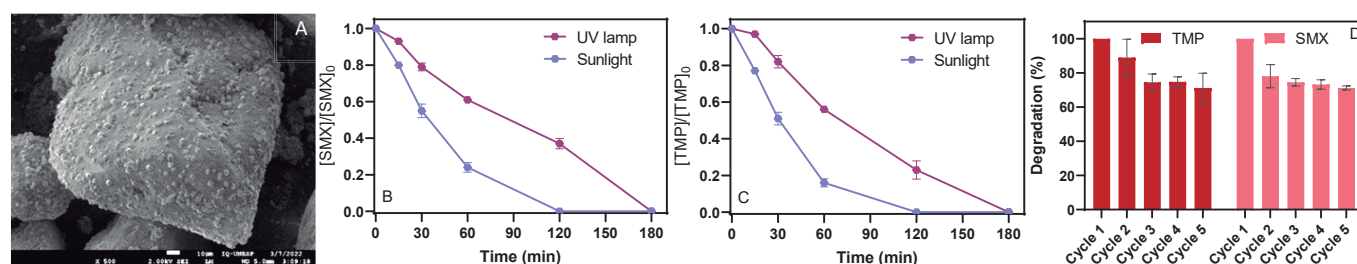


Fig 1: SEM image of the IOSS catalyst (A), degradation results of SMX and TMP in WWTP effluent under natural solar irradiation and UV lamps (B and C), and percentage degradation of SMX and TMP antibiotics using IOSS after 5 cycles in water (D). Conditions: 200 $\mu\text{g L}^{-1}$ of TMP and SMX, 0,5 g L^{-1} of IOSS, 10 mmol L^{-1} of H_2O_2 , at pH 3,0.

[1]. Benjamin, M.M. *et al.* (1996) 'Sorption and filtration of metals using iron-oxide-coated sand', *Water Research*, 30(11), pp. 2609–2620. doi:10.1016/S0043-1354(96)00161-3.

Acknowledgments

The authors are grateful to the Coordination for the Improvement of Higher Education Personnel (CAPES, Finance Code 001) and to the São Paulo Research Foundation, Brazil, (FAPESP, grants 2018/12780-4 and 2019/22218-4).

Levulinic acid esterification to ethyl levulinate over Nb-based catalysts

Camila C. Lopes (PG),^{*1,2} Alanna S. Moraes (PQ),² Vinícius W. Faria (PQ),² Marco A. Fraga (PQ),^{1,2}

camila.lopes@int.gov.br; camila.lopes@int.gov.br

¹Instituto Militar de Engenharia, IME; ²Instituto Nacional de Tecnologia, INT

Palavras Chave: biomass, Green chemistry, niobium, esters.

Highlights

NbOPO₄ is an efficient catalyst for levulinic acid esterification. Catalyst reached high ethyl levulinate selectivity (93%) with 30% yield.

Resumo/Abstract

Levulinic acid (LA) is a lignocellulosic biomass chemical that presents a series of advantages both from environmental and economic point of view. One of the possibilities for using LA is in the form of alkyl esters (levulinates) that can be used as biofuel, fuel additive or biolubricant.^[1] In this contribution, the use of niobium-based solids as acid catalysts for esterification of LA is assessed. For this study, commercially available samples of niobium oxide (Nb₂O₅.nH₂O) and niobium phosphate (NbOPO₄.nH₂O) were tested as received (called Nb₂O₅-in and NbP-in, respectively) and calcinated at 400 °C (Nb₂O₅-400 and NbP-400). Three additional samples were prepared by treating niobium oxide with different phosphoric acid concentrations, named Nb₂O₅-PO₄(X), where X is the acid solution concentration of 0,5, 1, or 2 mol.L⁻¹. The catalysts were characterized by XRD, N₂ physisorption, total (TPD-NH₃) and Brönsted (TPD-n-propylamine) acidity. Catalytic tests were performed in a semi-batch reactor, using an ethanol:LA molar ratio of 1:5, 10%wt catalyst, ethanol reflux temperature (78 °C), 400 rpm for 6 h. The LA consumption and products formations were accompanied by GC/MS. Control experiments were performed without using a catalyst. All catalysts were active for LA esterification but distinct performances were observed as regarding the selectivity to ethyl levulinate (EL). Figure 1 displays products selectivity over all catalysts at isoconversion (~25%).

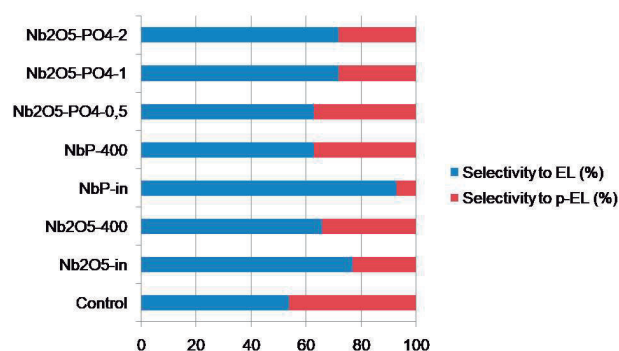


Figure 1: Products selectivity over all catalysts at isoconversion.

NbP-in was the most efficient catalyst leading to ester selectivity of 93%. Bare and phosphate oxides, on the other hand, achieved only around 66-77%. Thermal treated catalysts exhibit quite low activity. These results could be well correlated to the catalyst acidity, which decreases upon calcination. Grafting phosphate groups on Nb₂O₅, however, enabled to keep catalytic performance despite their lower selectivity. Besides ethyl levulinate, a pseudo-levulinate (p-EL) was also identified. This side product is proposed to be formed from an intermediate lactone.^[2]

Agradecimentos/Acknowledgments

Authors acknowledge financial support from CNPq and FAPERJ. ASM thanks PCI/CNPq/INT for her scholarship (Proc. 300426/2022-4).

[1] Appaturi, J. N.; Andas, J.; Ma, Y.; Phoon, B. L.; Batagarawa, S. M.; Khoerunnisa, F.; Hussin, M. H.; Ng, E. Recent advances in heterogeneous catalysts for the synthesis of alkyl levulinate biofuel additives from renewable levulinic acid: A comprehensive review. *Fuel*, v. 323, 124362, 2022.

[2] Chaffey, D. R.; Bere, T.; Davies, T. E.; Apperley, D. C.; Taylos, S. H.; Graham, A. E. Conversion of levulinic acid to levulinate Ester biofuels by heterogeneous catalysts in the presence of acetals and ketals. *Applied Catalysis B: Environmental*, v. 293, 120219, 2021.

Mechanosynthesis of cyanohydrin derivatives catalyzed by MOF.

Cristiane Kelly de Oliveira (FM),^{1,3*} Thiago Muniz de Souza (PQ)², Severino Alves Júnior (PQ),³ Ricardo Luiz Longo (PQ),³ Ivani Malvestiti (PQ).³

ckoliveira@gmail.com

¹Escola de Referência em Ensino Médio Professor Ernesto Silva, ²Universidade Federal Rural de Pernambuco, UFRPE;

³Departamento de Química Fundamental, UFPE.

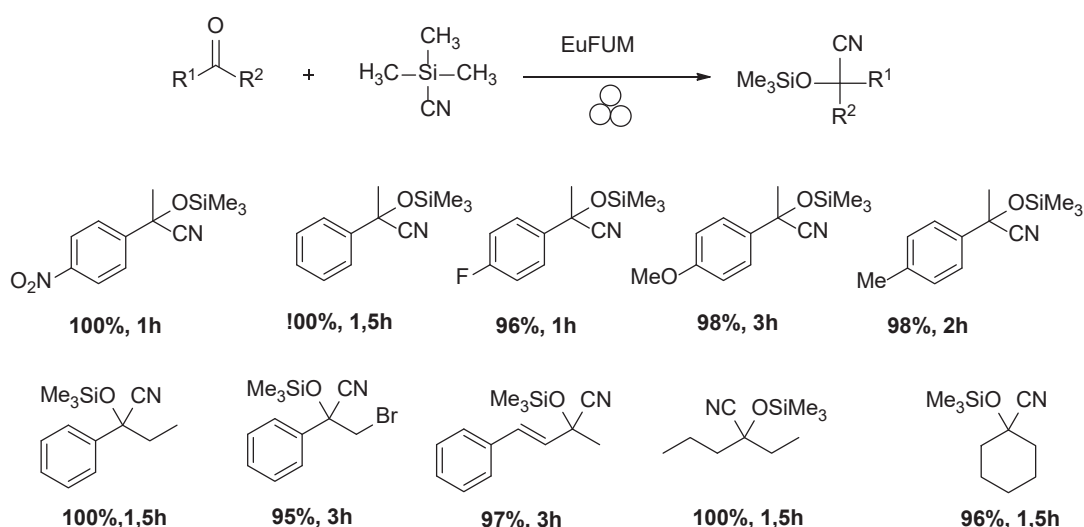
Palavras Chave: Mechanochemistry, Metal-Organic Frameworks, cyanosilylation, catalysis, ketones.

Highlights

This work presents an efficient, solvent-free and green synthesis of cyanohydrin derivatives by ball milling method, with good to quantitative yields, through catalysis with a metal-organic framework of europium (Eu-MOF).

Resumo/Abstract

Cyanohydrins, in addition of being biologically active, are used in the preparation of β -aminoalcohols, α -hydroxy-ketones and α -hydroxy-acids which are important intermediates in the synthesis of fine chemicals, pharmaceuticals, and agrochemicals. In this work, three Eu-MOF, EuFum, EuFumOX and EuBTC, were tested in the cyanosilylation reaction of ketones. The mechanochemical reactions were performed without solvent and the best results were obtained with $\text{Eu}_2(\text{fum})_3 \cdot 7\text{H}_2\text{O}$ (EuFum), scheme 1. The scope of the method was evaluated with aliphatic and aromatic ketones substituted with electron donating and withdrawing groups, obtaining yields in the range of 82-100%. The presence of electron donating and withdrawing substituents did not significantly affect the reaction yields. The yields obtained are similar to those of conventional methods, however, the mechanochemical method is solvent-free and requires shorter reaction times between 1-3 hours while in the literature it requires 24 hours¹.



Scheme 1: Scope of Cyanosilylation reaction.

Therefore, this work presents a green, robust and efficient method to obtain cyanohydrin derivatives with good to quantitative yields in 1-3 hours via mechanochemistry.

¹DOI:10.3390/catal12030299.

Agradecimentos/Acknowledgments

UFPE, FACEPE, CNPq, CAPES.

Molecularly Defined Precursors for Pt Nanoparticle Controlled Growth and Speciation Targeting CO₂ Conversion

Leonardo S. Sousa (PG),^{1*} Guilherme B. Strapasson (PG),¹ Renan B. Guerra (PQ),¹ Caio C. Oliveira (PQ),¹ Daniela Zanchet (PQ)¹

l178387@dac.unicamp.br

¹Institute of Chemistry, UNICAMP, CAMPINAS-SP

Palavras Chave: Molecularly Defined Precursors, Coordination Compounds, Platinum, Heterogeneous Catalysis, CO₂ reduction

Highlights

We synthesized Pt/TiO₂ catalysts using Pt coordination compounds. We demonstrate how the metal precursor and pre-treatments impact the catalyst activity toward CO₂ reduction to CO.

Resumo/Abstract

It has been reported that Pt and TiO₂ present a dynamic interaction that can be understood by the strong metal support interaction mechanisms, which encompass (i) charge transfer at the interface between the metal and oxide; (ii) encapsulation, when a non-stoichiometric TiO_x coat cover the metallic nanoparticle; and (iii) alloy formation, when the system is over-reduced and Ti atoms are incorporated into Pt lattice. Our goal is to employ organic complexes in the heterogenization of platinum on titanium dioxide and evaluate how these precursors impact the dynamics of Pt/TiO₂. Figure 1 (a) shows selected complexes' synthesis and respective yields. These compounds differ in their carbon content, and electronic structure, in which C2 and C3 have more carbon atoms than C1, and C3 is an example of π extended system.

Figure 1(b) depicts the XANES spectra of the materials heterogenized on TiO₂ and pyrolyzed at 500 °C. All materials show an intermediate electronic state between Pt²⁺ and Pt⁰ standards, indicating that pyrolysis reduced the samples but kept a certain degree of electronic deficiency, with C2/TiO₂_P500 being the most deficient and C1/TiO₂_P500 the least. The difference in the electronic state among the samples had a clear impact on the catalytic activity for CO₂ conversion to syngas through the reverse water gas shift reaction (RWGS: CO₂ (g) + H₂ (g) → CO (g) + H₂O (g)). The same trend observed in XANES was reflected in the catalytic activity, with C2/TiO₂_P500 having the highest conversion rate and C1/TiO₂_P500 having the smallest one. These examples demonstrate how modifications to the precursor can be a promising strategy for modulating Pt NPs' properties, such as metal speciation, particle size, and metal-support interaction. A broad library of complexes is under study to further explore this methodology.

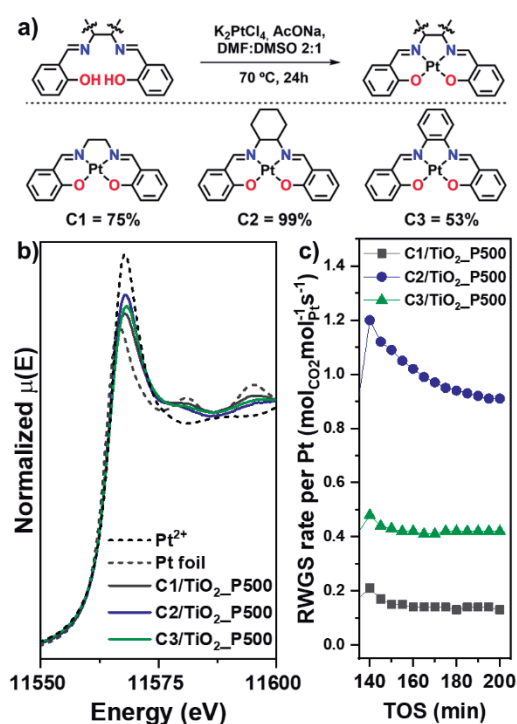


Figure 1. (a) Complexes' synthesis and yield; (b) XAFS spectra for three complexes heterogenized on TiO₂ and pyrolyzed at 500 °C; (c) RWGS rate for three catalysts (Reaction conditions: 500 °C, 2% CO₂, 8% H₂, 90% He, 100 ml.min⁻¹).

Agradecimentos/Acknowledgment



CNPq



(20/08575-6; 18/01258-5)



(309412/2018-8)

Multifunctional heterobimetallic Ru^{II}/Ni^{II} complex linked by an N,N,O ligand and synergic effect in catalysis

Gustavo H. C. Masson (PG),^{1*}, Bruna Pes Nicola (PG),² Douglas Henrique Nunes Santos (PG)¹, Beatriz E. Goi (PQ),¹ Katia Bernardo Gusmão (PQ),² Valdemiro P. Carvalho-Jr. (PQ),¹

*massonghc@gmail.com.

¹Departamento de Química e Bioquímica, FCT-UNESP.

²Instituto de Química, Universidade Federal do Rio Grande do Sul (UFGRS).

Keywords: polymerization; multifunctional catalyst, synergistic effect.

Highlights

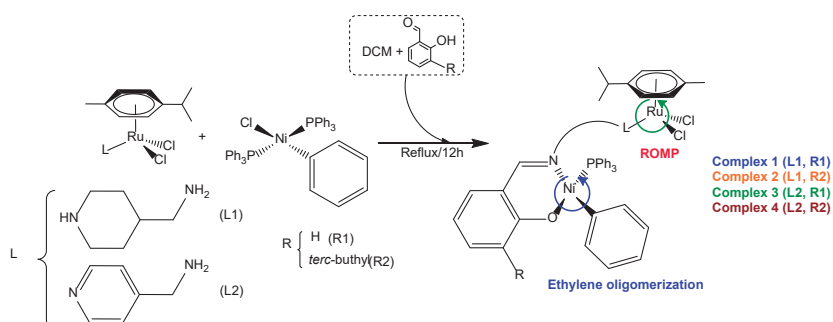
Bimetallic complexes based on Ru-Ni.

Multifunctional catalyst for ethene oligomerization and ROMP of Bicyclo[2.2.1]hept-2-ene.

Abstract

Late transition metal complexes have been used to catalyze many reactions. Among them, complexes based on Ni^{II} or Ru^{II} have attracted much attention. Ni in the oxidation state 2+ shows high activity in catalysis, mainly in ethylene polymerization and oligomerization due the easily activation of olefins, besides to act as a Lewis acid in the presence of olefins. On the other hand, Ru^{II} can be coordinated to a great number of ligands, what must change its behavior in catalysis. Due its good π -donnor effect, this metal is a good alternative for Ring Opening Methathesis Polymerization (ROMP). The use of heterobimetallic complexes as homogeneous catalysts aims to expand the catalytic scope, besides increases their reactivity via an electronic or mechanistical synergism [1].

In this work, we reported the synthesis, characterization, and catalytic activity of Ru^{II}-Ni^{II} heterobimetallic complexes to act in two mechanism: ethylene oligomerization and ROMP. Thus, new heterobimetallic complexes [Ph(PPh₃)Ni(N,O)-Ru(*p*-cymene)pip] (**1**), [Ph(PPh₃)Ni(N,O-*tert*-butyl)-Ru(*p*-cymene)pip-Cl₂] (**2**), [Ph(PPh₃)Ni(N,O)-Ru(*p*-cymene)-pyridineCl₂] (**3**), and [Ph(PPh₃)Ni(N,O-*tert*-butyl)-Ru(*p*-cymene)pyridineCl₂] (**4**) were obtained by the reaction of the appropriated ruthenium precursor, [(Ph)Ni(PPh₃)₂Cl], and the desired aldehyde in an 1:1:1 ratio (**Scheme 1**). The complexes were fully characterized by spectroscopy techniques as FTIR, UV-Vis, and ¹H and ³¹P{¹H}, besides cyclic voltammetry (CV). The CV of heterobimetallic complexes were performed using CH₂Cl₂ as solvent, tetrabutylammonium hexafluorophosphate as supporting electrolyte, a platinum disco (2 mm) as working electrode, a platinum wire as auxiliary electrode, and Ag/AgCl as reference electrode. All bimetallic species showed an irreversible process assigned to the Ni^{II/III} redox pair, and reversible processes related to the Ru^{II/III} pair around 1.20 V. Previously work showed that the monometallic Ru fragment has an irreversible behavior of the Ru^{II/III} redox pair on CV, around 1.36 V, using the same conditions [2]. The shift on oxidation potential (Ru fragment) could be attributed to a synergic effect between Ru-Ni. In contrast, Ru fragment was able to polymerize norbornene reaching 80% in 60 minutes of conversion using **2** with [NBE]/[Ru] = 5000 and [EDA]/[Ru] = 10 in chloroform at 50° C, while monometallic Ru polymerized NBE with 40% conversion using the same conditions [2]. The Ni fragment oligomerized ethylene using ethylaluminium sesquichloride (EASC) in a molar ratio Al/[Ni] of 2100, toluene as solvent, 220 psi of ethylene, and 25° C, reaching a turnover frequency about 150 s⁻¹. The major part of products was C₄ chains, with lower amount of C₆ (around 25% related to the C₄).



Scheme 1. Overview of the reaction to obtain **1-4**.

The complexes were fully characterized by spectroscopy techniques as FTIR, UV-Vis, and ¹H and ³¹P{¹H}, besides cyclic voltammetry (CV). The CV of heterobimetallic complexes were performed using CH₂Cl₂ as solvent, tetrabutylammonium hexafluorophosphate as supporting electrolyte, a platinum disco (2 mm) as working electrode, a platinum wire as auxiliary electrode, and Ag/AgCl as reference electrode. All bimetallic species showed an irreversible process assigned to the Ni^{II/III} redox pair, and reversible processes related to the Ru^{II/III} pair around 1.20 V. Previously work showed that the monometallic Ru fragment has an irreversible behavior of the Ru^{II/III} redox pair on CV, around 1.36 V, using the same conditions [2]. The shift on oxidation potential (Ru fragment) could be attributed to a synergic effect between Ru-Ni. In contrast, Ru fragment was able to polymerize norbornene reaching 80% in 60 minutes of conversion using **2** with [NBE]/[Ru] = 5000 and [EDA]/[Ru] = 10 in chloroform at 50° C, while monometallic Ru polymerized NBE with 40% conversion using the same conditions [2]. The Ni fragment oligomerized ethylene using ethylaluminium sesquichloride (EASC) in a molar ratio Al/[Ni] of 2100, toluene as solvent, 220 psi of ethylene, and 25° C, reaching a turnover frequency about 150 s⁻¹. The major part of products was C₄ chains, with lower amount of C₆ (around 25% related to the C₄).

Acknowledgments

This work was supported by the Coordenação de Aperfeiçoamento de Pessoal de Nível Superior – Brasil (CAPES) – Finance Code 001. FAPESP, Proc. 2021/11873-1 and 2021/13128-1.

[1] MATA, José A.; HAHN, F. Ekkehardt; PERIS, Eduardo. Heterometallic complexes, tandem catalysis and catalytic cooperativity. *Chemical Science*, v. 5, n. 5, p. 1723-1732, 2014.

[2] MASSON, Gustavo HC et al. Ruthenium–nickel heterobimetallic complex as a bifunctional catalyst for ROMP of norbornene and ethylene polymerization. *New Journal of Chemistry*, v. 45, n. 26, p. 11466-11473, 2021.

Nd_{0.90}Yb_{0.10}AlO₃ perovskite nanocrystals as photocatalysts for hydrogen generation under focused infrared laser excitation

João M. Gonçalves* (PQ),¹ Włodzimierz Mista (PQ),² Przemysław Wiewiorski (PQ),¹ Mariusz Stefanski (PQ),¹ Robert Tomala (PQ),¹ Wiesław Strek (PQ).¹

j.goncalves@intibs.pl

¹Department of Optical Spectroscopy, Institute of Low Temperature and Structure Research Polish Academy of Science;
²Department of Nanomaterial Chemistry and Catalysis, Institute of Low Temperature and Structure Research Polish Academy of Science.

Palavras Chave: Photocatalysis, Hydrogen, Infrared excitation, Nanocrystals, Lanthanides

Highlights

Nd_{0.90}Yb_{0.10}AlO₃ perovskite nanocrystals as photocatalysts for hydrogen generation under focused infrared laser excitation

- Nd_{0.90}Yb_{0.10}AlO₃ were obtained by sol-gel Pechini and under focused infrared laser excitation produced a broadband white emission
- Bubbles were produced at the surface of the material as a result of focused excitation
- Major component of bubbles was determined to be hydrogen

Resumo/Abstract

Several materials present a broadband white emission when submitted to focused infrared excitation in a phenomenon generally called Laser Induced White Emission (LIWE). This process is not only comprised of a broadband emission comprising the whole visible, but electron emission has also been observed in graphene¹. However, LIWE has been widely described only in vacuum or air. Recently, using graphene as a target, LIWE was also observed in liquid media, such as methanol, ethanol and water and due to ejection of hot electrons from the surface of the material, the light emission was accompanied by production of H₂ in liquid media²⁻⁴. However, due to the organic nature of the photocatalyst, relatively high generation of undesirable gaseous byproducts, such as CH₄, and a possible degradation of the material to carbon dots was observed. In this context, inorganic materials might overcome this drawbacks: since they lack carbon in their composition, their production of carbon-containing byproducts is expected to be significantly lower and their supposed degradation will not produce carbon dots. Herein, we propose the use of Nd_{0.90}Yb_{0.10}AlO₃ perovskite nanocrystals as a photocatalyst for H₂ production with focused infrared laser excitation. Due to the presence of Nd³⁺ and Yb³⁺, this material presents a particular electronic structure with absorption of both lanthanides, which makes it attracting for focused laser induced photocatalysis.

References

- 1 W. Strek, R. Tomala, M. Lukaszewicz, B. Cichy, Y. Gerasymchuk, P. Gluchowski, L. Marciniak, A. Bednarkiewicz and D. Hreniak, *Scientific Reports*, 2017, **7**, 41281–41281.
- 2 W. Strek, W. Mista, P. Wiewiorski and R. Tomala, *Chemical Physics Letters*, 2021, **775**, 138649–138649.
- 3 W. Strek, P. Wiewiorski, W. Mista, T. Hanulia and R. Tomala, *ACS Omega*, 2021, **6**, 3711–3716.
- 4 W. Strek, P. Wiewiorski, W. Mišta, R. Tomala and M. Stefanski, *Molecules*, **27**, 718.

Agradecimentos/Acknowledgments

The authors would like to acknowledge NCN project for financial support (Grant No. NCN-2020/37/B/ST5/02399).

Palladium pincer organometallic complexes as a source of homogeneous and heterogenized metal catalysts

Davi dos S. Leite (PG),¹ Júlio Cezar Pastre (PQ),¹ Daniela Zanchet (PQ).¹

d264584@dac.unicamp.br.

¹Instituto de Química, UNICAMP

Palavras Chave: *organometallic complexes, heterogeneous catalysis, heterogenization*

Highlights

Triflate palladium(II) PCP pincer complexes are used as either homogeneous or heterogeneous catalysts in cross-coupling reactions. Different immobilization techniques are employed to access the heterogeneous versions.

Resumo/Abstract

The use of easily synthesized and tunable catalysts is of great interest in both homogeneous and heterogeneous catalysis. The combination of a tridentate pincer ligand and a transition metal center in a complex allows for the suitable balance between thermal stability and reactivity in an often-rigid *meridional* coordination mode^[1]. While these complexes can be directly used as homogeneous catalysts for organic reactions^[2], they have been only superficially explored in heterogeneous catalysis. This work focuses on the use of triflate palladium(II) PCP pincer complexes as either direct homogeneous catalysts or as precursors for heterogeneous catalysts through the attachment of the complex (by the ligand or by the metal center) to the free surface hydroxyl groups of oxide support^[3]. The ligands and homogeneous complexes are characterized by routine ¹H, ³¹P{¹H} NMR and FTIR spectroscopies. For the heterogeneous versions, the mesoporous SBA-15 was selected as initial support due to its high surface area and pore size, allowing for more effective complex immobilization. The support, synthesized following Zhu's method^[4] and calcined at 400°C, presents an 896 m²/g surface area, a 3.38 OH/nm² hydroxyl group density, and a 99 Å average pore size while retaining no considerable amount of organic residues as shown by TGA analysis. Besides, solid-state ²⁹Si NMR shows that 50% of the hydroxyl groups are non-condensed and could be used as anchoring points. Further studies in the immobilization and application to cross-coupling reactions are envisioned to better understand the immobilization technique's effectiveness and impact on the catalyst performance.

[1] E. Peris, R. H. Crabtree, *Chem. Soc. Rev.* **2018**, *47*, 1959–1968.

[2] N. Selander, K. J. Szabó, *Chem. Rev.* **2011**, *111*, 2048–2076.

[3] S. Liu, J. M. *et al*, *ACS Catal.* **2016**, *6*, 8380–8388.

[4] Y. Zhu *et al*, *CrystEngComm.* 2011, *13*(2), 402–405.

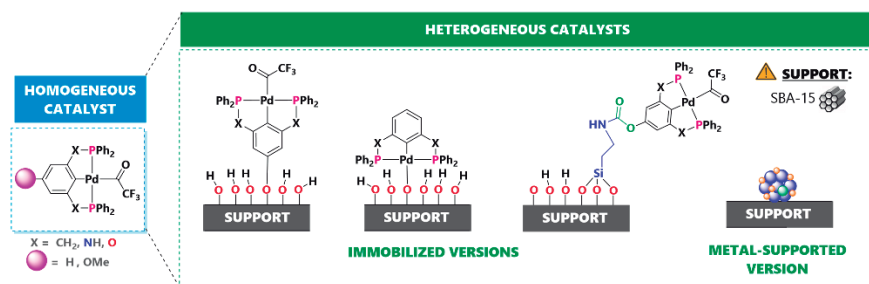


Figure 1. Catalyst formulations with triflate palladium(II) PCP pincer complexes.

Agradecimentos/Acknowledgments



(RCGI-CCU-P63-PSR-001-00)

(2022/11173-2,

(88887.667685/2022-00)

2020/15230-5)

Performance evaluation of multiple Prussian Blue Analogues' nanostructures for Water Oxidation Reaction

Gabriel R. Alvarenga (PG),¹ **Juliano A. Bonacin** (PQ),¹

g172422@dac.unicamp.br; jbonacin@unicamp.br

¹Instituto de Química, UNICAMP;

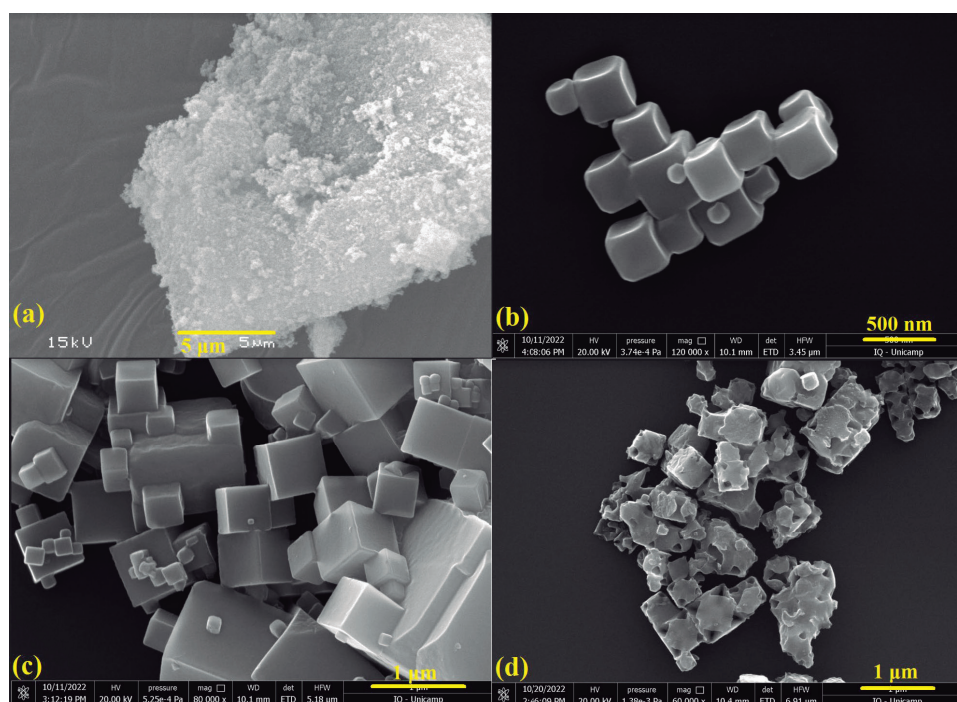
Palavras Chave: Prussian Blue, Morphology, Water Splitting

Highlights

We have synthesized Cobalt Prussian Blue Analogues (CoPBA) with multiple nanostructures and we shall evaluate their effectiveness as catalysts for water splitting.

Abstract

Humankind's energy generation was established thanks to fossil fuels due to their inexpensiveness in comparison with other sources of energy, but the alarming effects of greenhouse effect gases that are byproducts of the combustion of said compounds in global warming became one of the major incentives to replace them for more environmental-friendly alternatives and, at the same time, efficient in terms of cost and yield. In the face of the current situation, hydrogen gas (H₂) takes the spotlight due to being a renewable, carbon-free, energy source. The main goal of the project is to develop Prussian Blue Analogue (PBA) catalysts with controlled morphological structures for Water Oxidation Reaction (WOR) and evaluate their respective electrocatalytic behavior.



Acknowledgments



Phosphine-functionalized chitosan microparticles as support material for palladium nanoparticles in Heck reactions

André F.P. Biajoli (PQ),¹ André R. Fajardo (PQ),¹ Jaqueline F. de Souza (PG),¹ Thalia S.A. Lemos (IC)¹

andre.biajoli@ufpel.edu.br; andre.fajardo@pq.cnpq.br

¹*Centro de Ciências Químicas, Farmacêuticas e de Alimentos, UFPel*

Keywords: *Heterogeneous catalysis, Polysaccharides, Palladium*

Highlights

Functionalized chitosan microparticles. Full characterization. Nanoparticle stabilization. Heck olefination of aryl iodides. Reuse experiments.

Abstract

In this work we investigated the activation and stabilization of Pd nanoparticles using phosphine-functionalized chitosan microparticles. The catalytic activity of the prepared material was assessed in a series of Heck reactions, demonstrating its potential regarding yields and reaction scope. Comparative experiments confirmed the superior performance of the phosphine-modified material with respect to a similar catalyst derived from non-functionalized chitosan. Finally, the prepared catalyst also exhibited appreciable activity even after four consecutive reaction runs, with minimal loss of Pd by leaching.

Acknowledgments

The authors are thankful to CNPq (Process 404744/2018-4). A.R.F. also thanks CNPq for his PQ fellowship (Process 303872/2019-5). This study was financed in part by the Coordenação de Aperfeiçoamento de Pessoal de Nível Superior, Brazil (CAPES/Proap), Finance Code 001.

Photocatalytic CO₂ reduction to CH₄ in continuous flow reactor using Fe₂TiO₅ enhanced by magnetron sputtering-deposited Cu nanoparticles

Gustavo H.C. Santos (PG),^{1*} Renato V. Gonçalves (PQ),² Liane M. Rossi (PQ)^{1*}

ghcsantos@usp.br; lrossi@iq.usp.br

¹Departamento de Química Fundamental, Instituto de Química, Universidade de São Paulo; ²São Carlos Institute of Physics, University of São Paulo.

Palavras Chave: Photocatalysis, CO₂, sputtering, nanoparticles, methane, Copper

Highlights

Fe₂TiO₅ converted CO₂ into CH₄ (0.11 μmol g_{cat}⁻¹h⁻¹) using water, under simulated solar light irradiation. After deposition of high-disperse ~3 nm Cu nanoparticles on Fe₂TiO₅ by magnetron sputtering, the CH₄ yield increased in 23%.

Resumo/Abstract

The CO₂ emissions from fossil fuel and industry activities reached 37.9±3 GtCO₂ in 2021, getting closer to pre-pandemic values and threatening global environmental security.¹ Strategies to reduce atmospheric CO₂ concentration have been studied to mitigate the environmental consequences. In contrast with the conventional thermal catalytic CO₂ reduction, where most efforts have been applied, photochemical approaches use milder conditions and light absorption to overcome the high energy input required to break CO₂ stability. In this context, Artificial Photosynthesis (AP) consists of using the water oxidation reaction to drive CO₂ reduction into most valuable products under solar light, as in biological systems. Due to its properties, such as feasible band position and narrow bandgap that enable suitable overlap with solar emission, Fe₂TiO₅ emerges as a candidate semiconductor to carry out CO₂ reduction under AP conditions.² In this work, Fe₂TiO₅ was synthesized through solvothermal method, treated under different temperatures and characterized using XRD, DRS, Raman, XPS, MEV and TEM. Catalytic tests conducted under 800 mW cm⁻² simulated sunlight irradiance, showed that Fe₂TiO₅ dispersed in NaHCO₃ solution reduces CO₂ to CH₄ on a 0.11 μmol g_{cat}⁻¹ h⁻¹ rate, in absent of sacrificial reagent and without H₂ production. Sputtering deposition of highly disperse ~3 nm nanoparticles of Cu on Fe₂TiO₅ for different deposition times indicates an increase of CH₄ production to 0.51 μmol g_{cat}⁻¹ h⁻¹, under same conditions. To our knowledge, this is the first report of Fe₂TiO₅ directly applied as CO₂ photocatalyst.

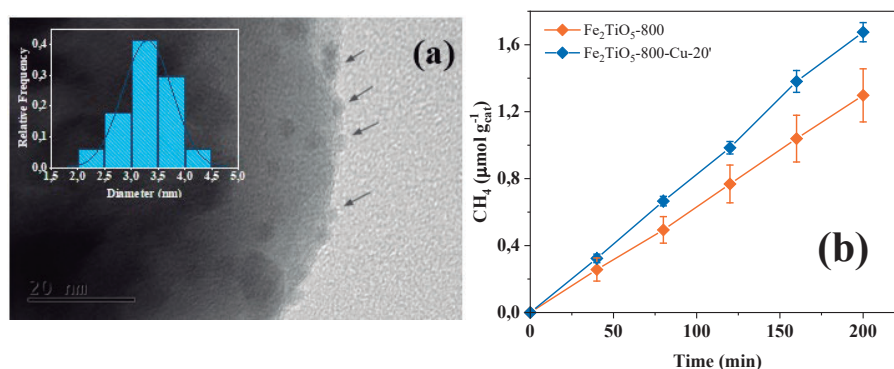


Fig. 1. (a) TEM images of Fe₂TiO₅-800-Cu(20'); (b) Accumulated CH₄ yield comparison for Fe₂TiO₅ calcined.

1 C. Barzak, *The Closing Window.*, 2011, vol. 20.

2 H. A. Centurion, M. A. Melo, L. G. Rabelo, G. A. S. Alves, W. S. Rosa, I. Rodríguez-Gutiérrez, F. L. Souza and R. V. Gonçalves, *J. Alloys Compd.*, 2023, **933**, 167710.

Agradecimentos/Acknowledgments

We gratefully acknowledge support of the RCGI – Research Centre for Greenhouse Gas Innovation, hosted by the University of São Paulo (USP) and sponsored by FAPESP – São Paulo Research Foundation (2014/50279-4 and 2020/15230-5) and Shell Brasil, and the strategic importance of the support given by ANP (Brazil's National Oil, Natural Gas and Biofuels Agency) through the R&D levy regulation.

Photocatalytic water splitting by highly crystalline carbon nitride-based catalyst: A route without noble metals

Gabriel Ali Atta Diab (PG),^{1*} Bruna Rocha Serino (IC),¹ Marcos Augusto Ribeiro da Silva (PG),¹ Guilherme Freitas Silva Rodrigues Rocha (PG),¹ Ivo Freitas Teixeira (PQ).¹

gabrieldiab2000@gmail.com

¹Departamento de Química, Universidade Federal de São Carlos (UFSCar)

Palavras Chave: Hydrogen Evolution, Water Splitting, Photocatalysis, Crystalline Carbon Nitride, Poly(Heptazine imide).

Highlights

New strategies toward overall water splitting without noble metal cocatalyst using highly crystalline carbon nitride-based photocatalyst.

Resumo/Abstract

With the decline of fossil fuels and continuous global energy demand, it is necessary to seek new strategies to produce green energy from renewable sources. As a clean, reliable and potentially sustainable energy vector, hydrogen is one of the most important fuels to supply this demand and minimize global warming effects. Nowadays, most of the H₂ is produced by steam reforming of methane, which needs high pressures and temperatures, apart from lead to CO₂ emissions. Photolysis of water can play a pivotal role in hydrogen production using solar light as driven force. Carbon nitride, a robust semiconductor composed solely by carbon and nitrogen with absorption in visible light range, has been demonstrating high efficiency for water splitting reaction, although with relevant quantities when scavenger reagents and noble metals are employed.¹ Nevertheless, the use of scavenger and noble metal makes the process unfeasible due to its high cost. To overcome this, new strategies involving the use of abundant metals and alternative electrons donators or even avoiding their use could open new perspectives in the application of carbon nitrides in energy generation. This work is focused on investigate new strategies using highly crystalline carbon nitride formed by polycondensation of heptazines units, obtaining poly(heptazine imide) – PHI. Na-PHI was synthesized by melamine polymerization in the presence of NaCl. Then several cocatalyst metal-based were introduced in the scaffold by a simple cation exchange in aqueous solution, obtaining a generic M-PHI.² The water splitting tests were carried out in a sealed reactor with an inert atmosphere (Ar) using triethanolamine as electrons donator and H₂PtCl₄ solution to compare the hydrogen production in the system without their presence. The best result show Ni as a potential substitute of Pt, producing 580 μmol/L in 24 h and using a blue LED light (410 nm). Studies involving replacement of the scavenger are being performed.

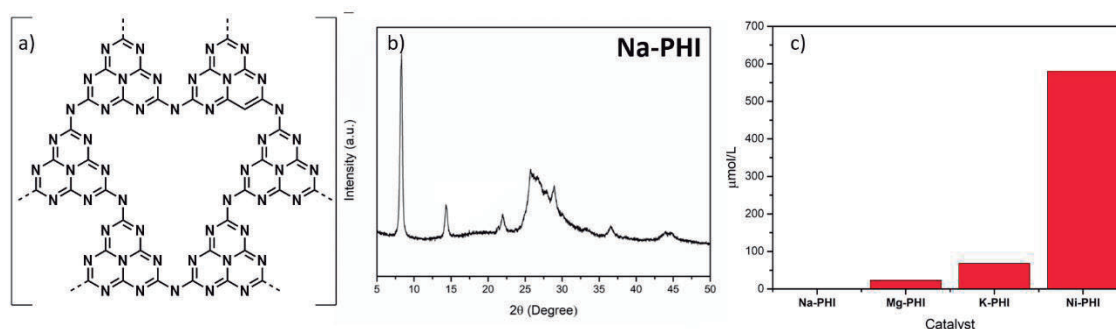


Figure 1: a) Structure of Na-PHI; b) diffraction pattern; c) hydrogen evolution of each photocatalyst w/o Pt.

¹ da Silva, M. Appl. Catal, 304, 2022, 120965.; ² Teixeira. I. J. Mater. Chem. A, 2022, 10, 18156-18161

Agradecimentos/Acknowledgments

This research is being supported financially by FAPESP, CNPQ and CAPES.

Reduction-carburization of MoO₃ throughout acetone hydrodeoxygenation reaction drives new surface properties

Gabriel B. Báfero (PG),¹ Guilherme B. Strapasson (PG),^{1,2} Davi S. Leite (PG),¹ Daniela Zanchet (PQ).^{1,*}

g155426@dac.unicamp.br; zanchet@unicamp.br

¹Group of Catalysis and Nanomaterials, Institute of Chemistry (IQ), University of Campinas (UNICAMP), Campinas, SP, Brazil;

²Brazilian Synchrotron Light Laboratory (CNPEM), Campinas, SP, Brazil

Keywords: Catalysis, Hydrodeoxygenation, Molybdenum oxide, Molybdenum oxycarbide.

Highlights

MoO₃ surface can be reduced-carburized under acetone HDO atmosphere into a MoO₂/MoO_xC_y mixture

As the reaction progresses, MoO_xC_y shows acidic/electronic properties that impact the catalyst performance

Abstract

Metal oxides have attracted attention as heterogeneous catalysts due to their abundance and inexpensiveness and the possibility of combining different surface properties in a single material (acid-base, redox, and oxygen vacancy sites). In this way, they have even been tested in the hydrodeoxygenation reaction (HDO), one of the processes that aim the bio-oil upgrading by reducing its oxygen content. MoO₃ can be reduced-carburized under the HDO atmosphere, generating an oxycarbide phase (MoO_xC_y). The stabilization of the unusual Mo⁵⁺ species through MoO_xC_y has been explored in some studies; however, a more in-depth characterization connecting its properties and catalytic performance is still lacking.

By subjecting a commercial MoO₃ nanopowder to acetone HDO reaction at 350 °C, an interesting catalytic profile was obtained (Figure 1). The initial products were propylene (C₃E), isopropanol (IPA), and larger molecules related to acetone condensation (C₆O), obtained, in principle, through oxygen vacancies, hydrogenating sites, and acidic sites, respectively. XRD analysis showed that the catalyst structure changed along TOS from MoO₃ to a mixture of MoO₂ and MoO_xC_y phases after 6 h due to a reduction-carburization process. The conversion increase after 3 h on stream was associated with the crystalline transition between structures. IPA generation decreased along TOS, favoring propane (C₃A) formation and other hydrogenolysis products (C₁, C₂, C₄, C₆). The ³¹P-MAS-NMR of adsorbed TMPO showed that MoO_xC_y presents stronger acid sites, which may be related to more extensive IPA dehydration. At the same time, the more reduced molybdenum species presented in the phase mixture, verified through XPS, may be associated with C₃A favoring through more hydrogenating sites.

It was possible to observe that the formation of a MoO₂/MoO_xC_y mixture throughout the reaction considerably altered the products distribution and the catalytic profile. The nature of the sites that commonly mediate the reaction mechanisms, together with these results and surface characterizations, have already allowed us to address some still unexplored characteristics of MoO_xC_y, such as its acidity and the cooperation with MoO₂.

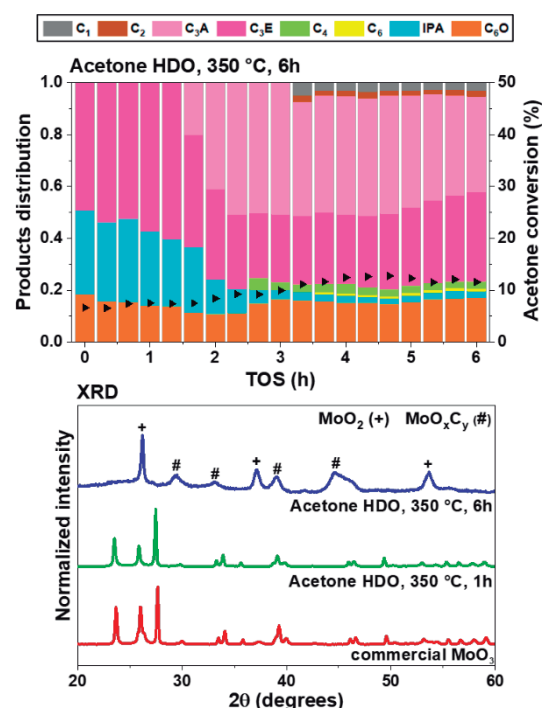


Figure 1: Products distribution (colored bars) and conversion (arrows) of acetone HDO reaction for commercial MoO₃; and XRD patterns of initial and spent catalyst (1 and 6 h).

Acknowledgments

The authors thank the financial support of the Fundação de Amparo à Pesquisa do Estado de São Paulo (2018/01258-5), the Conselho Nacional de Desenvolvimento Científico e Tecnológico and the Coordenação de Aperfeiçoamento de Pessoal de Nível Superior (CAPES finance code 001).

Ru^{II}/Pd^{II} heterobimetallic complexes as bifunctional catalysts to obtain copolymers via ROMP coupling and Ethylene Polymerization.

Douglas. P. Oliveira (PG),^{1*} Valdemiro P. C. Júnior (PQ),² Beatriz E. Goi (PQ),²

douglas.poletto@unesp.br; valdemiro.carvalho@unesp.br; beatriz.goi@unesp.br;

¹Departamento de Química e Bioquímica, UNESP; ²Departamento de Química e Bioquímica, UNESP; ²Departamento de Química e Bioquímica, UNESP.

Keywords: Bifunctional catalysts; Polymerization; ROM; Ethylene.

Highlights

Synthesize an unprecedented bimetallic complex, based on palladium and ruthenium to act in the synthesis of copolymers via ROMP coupling and Ethylene Polymerization.

Resumo/Abstract

The functionalized monomer NBE-Aryl-Br was synthesized through an adaptation of the Steglich esterification parameters, using 5-norbornene-2-carboxylic acid and 4-Bromophenol, characterized by FTIR, UV-vis and ¹H NMR. The [(NBE-Aryl)Ni(PPh₃)₂Br] (**complex 1**) was synthesized by the oxidative addition reaction between the precursor complex [Pd(PPh₃)₄] and NBE-Aryl-Br. The complex [RuCl₂(η⁶-*p*-cymene)((4-methylamino)-piperidine)] was obtained (**complex 2**) from the insertion of the ligand 4-(aminomethyl)piperidine to the dimer [Ru(*p*-cymene)Cl₂], which was used as a precursor, along with complex 1 for the synthesis of the heterobimetallic complex [RuCl₂(η⁶-*p*-cymene)(μ-pipNH₂)Pd(Ph)(PPh₃)Br] (**complex 3**). All complexes were analyzed by spectroscopic techniques: FTIR and UV-vis. Additionally, **complex 1** was characterized by ¹H NMR. In addition, complexes 1-3 were characterized by cyclic voltammetry, identifying processes referring to the interconversion of Pd^{IV/III} and Ru^{III/II} on **complex 3**. The catalytic activity of **complex 3** was evaluated in norbornene ROMP reactions, in which the temperature (25 and 50 °C) and the reaction time (10-60 min) were varied.

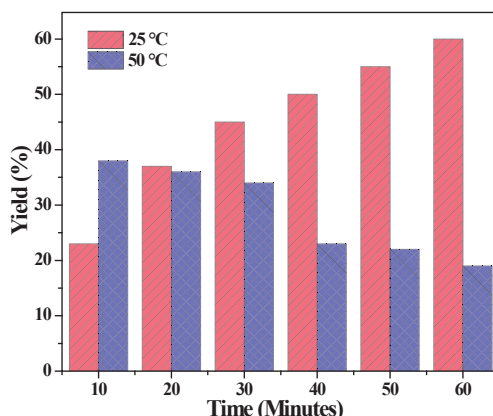


Figure 1. Yield dependence as a function of temperature, at 25 and 50 °C, for NBE ROMP with complex 4 in CHCl₃ and 60 min; [NBE]/[EDA]/[Ru] = 5000/28/1. The numbers correspond to the IPD values for each polymer obtained.

Agradecimentos/Acknowledgments



Síntese de óxidos mistos via decomposição de MOFs pós modificados e aplicação em hidrogenação catalítica de CO₂.

Thiago Rui Casagrande (IC),¹ Ayla Borges Serra (PG)*,² Osvaldo Antonio Serra (PQ).¹

thiagocasagrande@usp.br; aylarbserra@gmail.com

¹Departamento de Química, FFCLRP-USP; ²Departamento de Engenharia Química, UFSCar.

Palavras Chave: MOFs, Catálise, Hidrogenação de CO₂

Highlights

Synthesis of mixed oxides via decomposition of post-modified MOFs and application in catalytic CO₂ hydrogenation.

Zirconium and copper nanostructured materials are extensively studied due their catalytic properties and for their high chemistry and thermal stability.

The catalyst oxide nanoparticles was obtained by porous inorganic polymer synthesis (3D), post synthetic modification and pyrolysis.

The catalysts showed excellent yields in methanol production of 580 gMeOH/Kgcat.h⁻¹ at 265 °C and 3 Mpa, and 77% selectivity.

Resumo/Abstract

Devido ao efeito estufa, que está relacionado ao aumento do nível de CO₂ na atmosfera, tecnologias de captura, armazenamento e utilização deste poluente têm sido de extrema importância e recebido atenção global nos últimos anos. Com isso, há uma crescente pressão para redução das emissões de CO₂, assim como desenvolvimento de sistemas eficientes de captura e utilização do mesmo. Nessa perspectiva, o desenvolvimento de sistemas catalíticos capazes de converter CO₂ em materiais com valor agregado, como metanol, é de grande interesse para o desenvolvimento tecnológico e manutenção da vida. Materiais a base de zircônio e cobre nanoestruturados vêm sendo extensivamente estudados devido a suas propriedades catalíticas e por apresentarem alta estabilidade química e térmica. Nos catalisadores metálicos, a diminuição do tamanho de partícula leva ao aumento do número de átomos superficiais, modificando a interação de interfaces, estado de oxidação e interações entre óxidos, responsáveis pela formação dos sítios ativos. Variações estruturais e morfológicas podem ser obtidas modificando os métodos e condições sintéticas na obtenção dos óxidos. Neste trabalho sistemas bimetálicos do tipo ZrO₂:CuO foram obtidos a partir da decomposição da MOF UiO-66, com potencial aumento de eficiência na hidrogenação catalítica de CO₂ para produção de metanol. Para isso, foram realizadas sínteses desses polímeros inorgânicos porosos (3D) modificados pós sinteticamente, com posterior pirólise para obtenção das nanopartículas desejadas. Os materiais apresentaram ótimos rendimentos na produção de metanol de 0,58 g_{MeOH}/g_{cat}.h a 265 °C a 3 Mpa, 18,5 % de conversão do CO₂ e seletividade de 77%. Esse rendimento é superior ao catalisador industrial de Cu-ZnO-Al₂O₃ de 0,15 g_{MeOH}/g_{cat}.h (250 °C, 5 MPa), acima mesmo dos catalisadores de In₂O₃/ZrO₂ com rendimento de 0,35 g_{MeOH}/g_{cat}.h (300°C, 5MPa).

Agradecimentos/Acknowledgments

USP, UFSCar, FAPESP, CNPq, CAPES.

Síntese de nanocatalisadores Cu-SiO₂ com diferentes arquiteturas

Wellington Luiz Saraiva Soares (PG),^{1,2*} Andréa M. Duarte de Farias (PQ),² Leon F. Feitosa (PQ),² Carla R. Moreira (PQ),² Marco A. Fraga (PQ)^{1,2*}

wellington.saraiva@int.gov.br; marco.fraga@int.gov.br.

¹Instituto Militar de Engenharia – IME, Rio de Janeiro; ²Instituto Nacional de Tecnologia – INT, Rio de Janeiro

Palavras-chave: Catalisadores de cobre, core-shell, nanopartículas de Cu, esferas de SiO₂, estabilidade.

Highlights

Synthesis of Cu-SiO₂ nanocatalysts with different architectures. Cu-SiO₂ catalysts with different architectures were prepared providing systems containing different Cuⁿ⁺ species.

Resumo/Abstract

Catalisadores à base de metais não-nobres são uma alternativa economicamente mais viável para aplicações em larga escala do que catalisadores à base de metais nobres. No entanto, metais não-nobres são mais propensos a sofrer fenômenos de desativação (lixiviação e/ou sinterização), principalmente em meio aquoso. Para minimizar e/ou eliminar estes problemas, catalisadores com diferentes arquiteturas empregando métodos não convencionais de síntese vêm sendo desenvolvidos com o objetivo de obter estruturas mais resistentes à desativação. Neste cenário, foram preparados catalisadores contendo Cu e SiO₂ com arquiteturas diferentes para este trabalho. O método convencional de impregnação ao ponto úmido foi usado para preparar um catalisador de cobre suportado em sílica (**Cu/SiO₂**). Nanopartículas de cobre (NPCu) foram sintetizadas para serem usadas em dois catalisadores diferentes. Em um deles as NPCu foram suportadas em sílica (**NPCu/SiO₂**). Em um outro procedimento, foram usadas para a obtenção de um catalisador com morfologia núcleo-casca (*core-shell*), onde nanopartículas de cobre foram recobertas por sílica (**NPCu@SiO₂**), usando uma síntese solvotérmica. Por fim, um último catalisador foi preparado a partir de esferas de sílica e o cobre foi incorporado em sua superfície (**SiO₂@Cu**) por método hidrotérmico. Os materiais sintetizados foram caracterizados por técnicas diferentes. Por microscopia eletrônica de varredura (MEV) e de transmissão (MET), foram identificados detalhes intrínsecos da estrutura/morfologia de cada um. No caso do **NPCu@SiO₂** obtivemos estrutura encapsulada multi nuclear. A estrutura predominante da **SiO₂@Cu** foi um núcleo único possivelmente de Cu-Si, com um espaçamento entre o núcleo e a casca de sílica. Ambas as estruturas também apresentaram NPCu com morfologia de “agulhas” na superfície externa das esferas de sílica. Na difração de raios X (DRX), a amostra **Cu/SiO₂** apresentou picos de difração da fase CuO, nas outras não foram observados picos característicos de cobre, indicando a presença de nanopartículas de cobre. Os perfis de temperatura a redução programada (TPR) indicaram a redução de Cu⁺² a Cu⁰ na faixa de 230 °C a 260 °C nos catalisadores. Além disso o **SiO₂@Cu** apresentou um pico adicional de redução em 298 °C, indicando uma espécie de cobre que se reduz em uma temperatura mais alta. Este resultado indica a presença de duas espécies de CuO, uma mais resistente a redução que a outra. O perfil do catalisador **Cu/SiO₂** foi mais largo, sugerindo que as partículas do CuO têm uma maior variação de tamanho. Resultados da análise termogravimétrica (TGA) do **NPCu@SiO₂** confirmou que a amostra sintetizada contém ainda matéria orgânica proveniente da preparação. A amostra foi submetida a calcinação a 500 °C, para garantir a efetiva remoção destes materiais, o que foi confirmado por TGA após esse tratamento. A espectroscopia fotoeletrônica de raios X (XPS) mostrou que, de fato, a amostra **NPCu@SiO₂** continha resíduos orgânicos da síntese, permitindo identificar a presença de polivinilpirrolidona (PVP) usado como estabilizante. Da mesma forma, confirmou sua remoção após a calcinação. Em relação ao estado de oxidação do cobre, a técnica mostrou que os catalisadores **Cu/SiO₂** e **SiO₂@Cu** apresentam apenas espécies Cu²⁺. Já a amostra **NPCu@SiO₂**, tanto antes quanto depois da calcinação, apresentou uma mistura de Cu²⁺ e Cu reduzido (Cu⁺ e/ou Cu⁰). O conjunto de resultados mostrou que diferentes espécies Cuⁿ⁺ podem ser obtidas e são dependentes da arquitetura do catalisador. Sistemas com arquiteturas avançadas como do tipo *core-shell* permitem a obtenção de NPCu menores e uma mais ampla distribuição de espécies Cu.

Agradecimentos/ Acknowledgments

CAPES pela bolsa de estudos, CENANO-INT/SISNANO (CNPq-SisNANO 442604/2019–0) pelas análises de STEM e LABNANO-CBPF pelas análises de TEM-EDX.

Área: ORG

(Inserir a sigla da seção científica para qual o resumo será submetido. Ex: ORG, BEA, CAT)

Selenoxide-pillar[5]arene catalyst for efficient nucleophilic reactions under water**Pâmella Cordeiro (PG),¹ Victor Menezes (IC),¹ Clara Barroso (IC),¹ Ingrid Chipoline (PG),³ Alix Ángel (PG),² Eduardo Alberto (PQ),² Vanessa Nascimento (PQ)¹****pamellacordeiro@id.uff.br**¹Supraselen laboratory, Federal Fluminense University, Niteroi, Brazil; ²Department of Chemistry, Federal University of Minas Gerais University, Belo Horizonte, Brazil; ³Department of Chemistry, Federal University of Rio de Janeiro, RJ, Brazil.

Key words: Selenium, pillararene, catalyst.

Highlights

In this work, we promote the synthesis of nitriles compounds in a greener reactional media through the use of pillar[5]arenes combined with organochalcogens as catalysts.

Resumo/Abstract

Because of the singular electron-rich cavity and easy functionalization, pillar[n]arenes have been extensively studied for several applications.^[1] Besides, selenium compounds are highlighted in different fields, including catalytic potential in promoted organic reactions.^[2] Therefore, the objective this work is the synthesis and application of selenoxidepillar[5]arene as organocatalyst. For the development of this project, it was first established the obtation of the selenocatalysts. Thus, a selenoxide-pillar[5]arene **P[5]** were obtained previously for our group. This structure is derived from selenoxides, which provide better solubility in the aqueous medium. Thus, the synthesized compounds were tested as catalyst in the obtation of nitriles in water – which are excellent synthetic precursors. Noticeably, the best reactional condition formed the product with 75% yield, using **P[5]** 1 mol%, NaCN (2eq.) during 16 hours. From these promising results, we proceed to the variation of the reaction leaving group and nucleophile, using other halogens and sodium azide, respectively. And, once again, the catalyst proved to be efficient and tolerable to such variations. In addition, the scalability and catalyst recovery also were evaluated and proved to be very satisfactory. Furthermore, studies was carried out to explore the reaction mechanism that can be seen figure 1. To finalize, the reaction scope continues to be explored with the use of other substituted bromides.

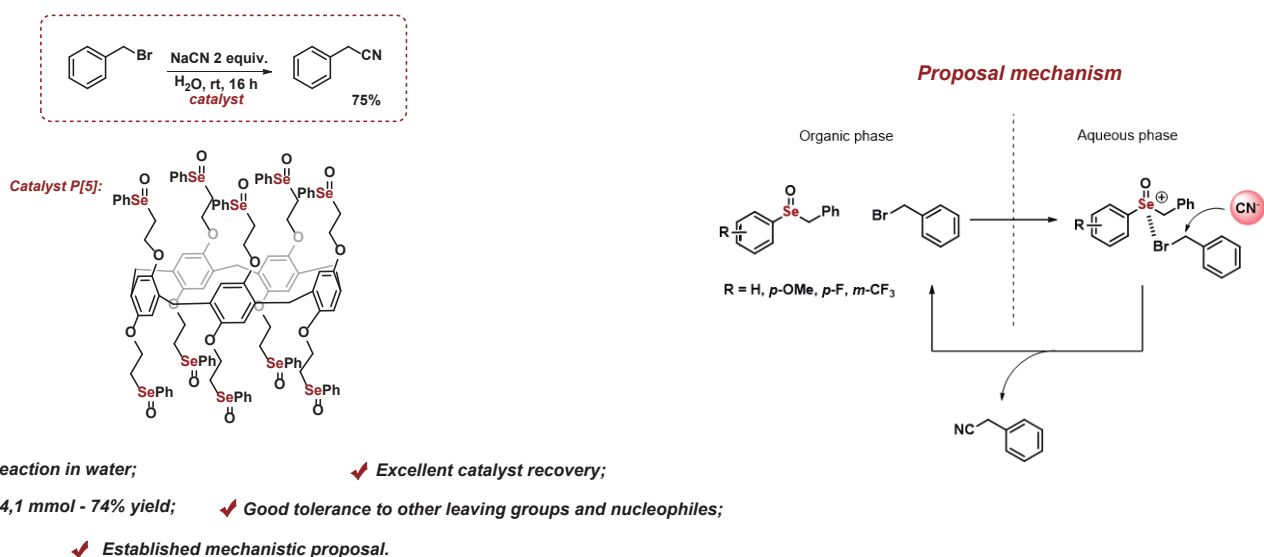


Figure 1: Graphical abstract

Agradecimentos/Acknowledgments

FAPERJ, UFF, UFMG

¹Yang et al.; Pillararene-based molecular-scale porous materials, *Chem. Commun.*, **2021**,57, 13429-13447. ²Alberto, E. et al.; From Stoichiometric Reagents to Catalytic Partners., *Adv. Synth. Catal.* **2021**, 364,87-93.

46ª Reunião Anual da Sociedade Brasileira de Química: "Química: Ligando ciências e neutralizando desigualdades"

Single-Atoms on Crystalline Carbon Nitrides for Selective C-H Photooxidation: A Bridge to Achieve Homogenous Pathways in Heterogenous Materials

Marcos A. R. da Silva (PG),^{1*} Carla S. Cunha (IC),¹ Vitor G. S. Pastana (PG),¹ Bruna R. Serino (IC),¹ Guilherme F. S. R. Rocha (PG),¹ Gabriel A. A. Diab (PG),¹ Ivo F. Teixeira (PQ).¹

marcosgusto96@gmail.com

¹Department of Chemistry, UFSCar.

Key words: Carbon Nitride, Poly(heptazine imide), Single-Atom, Photocatalysis, Selective Oxidation.

Highlights

In this work, we synthesize metal single-atoms coordinated on crystalline carbon nitrides and apply these catalysts in toluene photooxidation reactions with high yields through a homogeneous-like mechanism of high-valent species.

Abstract

Single-atom catalysts (SACs) are promising materials to achieve maximum atomic utilization and higher turnover numbers for metal-catalyzed reactions. More important, the production of single-atoms could mimic the environment of metal complexes, with discrete molecular orbitals and enhanced metal-ligand electronic transfer. To date, most of the works evidence the improvement of metal utilization with SACs, but few reported the resemblance of these materials with homogenous catalysts. For example, iron and manganese high-valent species have been proposed as key intermediates in catalytic biological reactions. These species have already been predicted in SACs with N-doped carbons and graphene supports. However, these materials possess poorly reproducibility and laborious synthetic methods. Crystalline carbon nitrides, especially poly(heptazine imide) structures (PHI), are suitable supports for single-atom coordination. The synthesis of such compounds is made with a thermal condensation of melamine with NaCl. The ionic character of this material, called Na-PHI, enables the ionic exchange of Na⁺ by transition metals, like Fe³⁺ or Mn²⁺. The atomically dispersion of iron sites is revealed with HAADF-STEM images (Fig. 1a) and proved with EXAFS analysis (Fig. 1b), showing that Fe-Fe bonds are not present in Fe-PHI catalyst. In this work, Fe and Mn-PHI were applied for selective photooxidation of hydrocarbons, such as toluene. Photocatalytic tests under LED irradiation (410 nm) and O₂ as oxidant have shown excellent yields towards benzaldehyde. Fe-PHI exhibits a conversion of 94% with 85% of selectivity to benzaldehyde in 20 hours, while Mn-PHI possess 90% of conversion and 88% of selectivity in 12 hours (Fig. 1c). These high yields can only be achieved with iron and manganese since other metals such as Ni, Cu and Pt does not present the same conversions, as well as the pristine Na-PHI. Although these compounds are photocatalysts, they do not generate reactive radicals in solution, as depicted by EPR (Fig. 1d). This feature occurs due to the production of high-valent metal species, formed by the photogenerated holes of PHI (Fig. 1e). These high-valent species are confirmed by XANES assays, showing a shift to higher energies when the light is turned on (Fig. 1f-h). More important, the trend is observed for iron and manganese, indicating the ability of these catalysts to mimic homogeneous complexes.

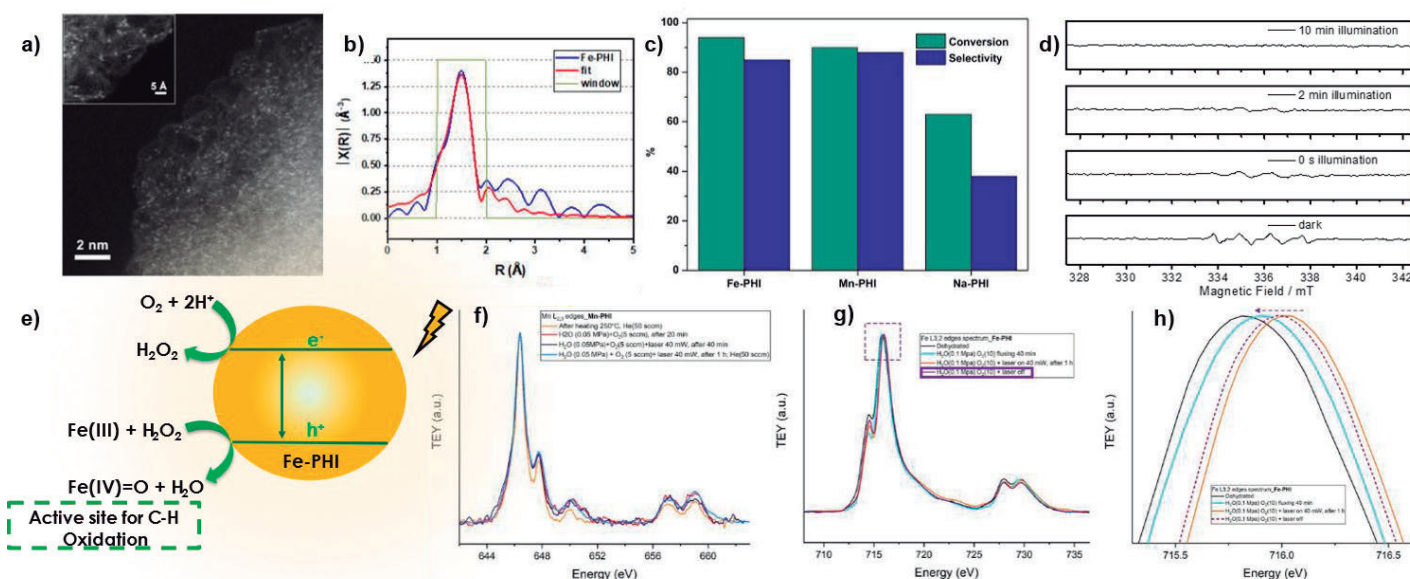


Figure 1: a) HAADF image of Fe-PHI; b) EXAFS of Fe-PHI; c) Photocatalytic toluene oxidation to benzaldehyde results; d) Spin-trapping EPR assays in reaction system; e) Mechanism of Fe high valent species; XANES analysis of Mn-PHI (f), Fe-PHI (g) and amplification of XANES shift (h) under reaction conditions (O₂ and light).

Sunlight Palmitic Acid Decarboxylation Mediated by CvFAP

Matheus C. Silva (IC),¹ Alexandre S. França (PQ),¹ Gabriela Y. Breda (PQ),¹ Raquel A. C. Leão (PQ),¹ Rodrigo V. Almeida (PQ),² Rodrigo O. M. A. de Souza (PQ).^{1*}

matheuscandidoo732@gmail.com; souzarod21@gmail.com*

¹ Biocatalysis and Organic Synthesis Laboratory, Chemistry Institute – Federal University of Rio de Janeiro – IQ – UFRJ.

² Laboratório de Microbiologia Molecular e Proteínas – Federal University of Rio de Janeiro – IQ – UFRJ.

Keywords: CvFAP, Fatty Acid, Photodecarboxylase, Solar Light, Decarboxylation.

Highlights

The long-distance fuel sector is one of the fastest-growing carbon emission sources. In this way, new sustainable technologies are necessary as an alternative to traditional long-distance fuel. Fatty acids photodecarboxylase from *Chlorella variabilis* (CvFAP) provides promising approaches to produce various hydrocarbon biofuels. However, this reactional system requires some improvement in its parameters to be an environmental process as preconized by the green chemistry concepts.

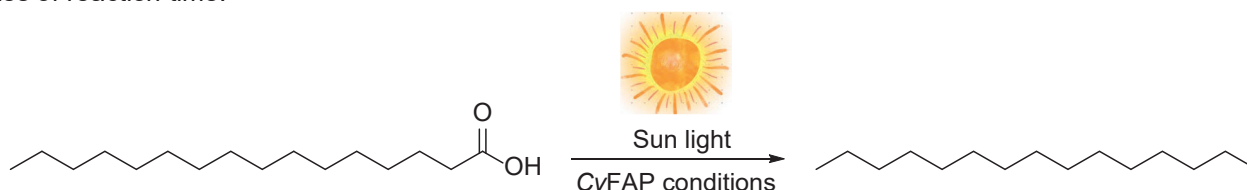
Abstract

The photodecarboxylase from *Chlorella variabilis* (CvFAP) promotes the elimination of CO₂ of fatty acids converting it into alkanes or alkenes in a light-driven and irreversible reaction¹ as shown in Scheme 1:



Scheme 1: Palmitic acid decarboxylation via CvFAP.

The first protocol published by Huijbers and co-workers 2018² for palmitic acid decarboxylation is the most used until now, in this way alternative conditions using or not, different co-solvent were tested aiming a new method for total product conversion (without co-solvent gave us >99 % of product). Therefore, other investigation conducted was finding new light sources ($\approx 430\text{-}490\text{ nm}$ [a]) to carry the photodecarboxylation via CvFAP under natural conditions. In this way, was evaluated the efficiency of solar light as shown in Scheme 2, and It gave us a complete conversion in twenty minutes of reaction time.



Scheme 2: Palmitic acid decarboxylation via CvFAP using Solar light.

Acknowledgments

CNPq, CAPES and FAPERJ

1. Sorigué et al., *Science* **2017**, 357, 903-907.

2. Huijbers et al., *Angew. Chem.* **2018**, 57, 13648-13651.

Synthesis and characterization of biodiesel using Licuri (*Syagrus coronata*) as raw material

David Thomas Duarte Arruda (PG),^{1*} Denise Ramos Moreira (PG),¹ Gabriel Érik Patrício de Almeida (IC),¹ Felipe Soares Correira (IC),¹ Nágila Maria Pontes Silva Ricardo (PQ),¹

davidthomasduar@gmail.com

1. Universidade Federal do Ceará - UFC, Departamento de Química Orgânica e Inorgânica, Campus do Pici, BI – 935, Fortaleza, CE, CEP 60455-760.

Keywords: *Syagrus coronata*, Biodiesel, Monoalcohol Basic Catalysis .

Highlights

Synthesis and characterization of biodiesel using Licuri (*Syagrus coronata*) as raw material, via basic homogeneous catalysis using monoalcohols.

Resumo/Abstract

With environmental problems impacting in greater proportions and also gaining more space in international discussions about how to obtain new solutions. Energy reserves always remain the focus of these discussions, especially when considering fuels, and how to reduce their consumption, or make them less harmful to the environment. Taking this into account, biofuels gained a lot of space, as they can be produced from different biodegradable raw materials of vegetable or animal origin. Biodiesels are a mixture of esters that have undergone a transesterification reaction from vegetable oils or animal fat, in a synthetic route that can be both acidic and basic in the presence of alcohols, mainly methyl, and ethyl alcohol. Native to the caatinga biome, the Licuri (*Syagrus coronata*) is a kind of palm tree whose fruit is rich in fatty acids, consisting mainly of lauric acid, a saturated acid. Licuri oil is a raw material still little explored in the bioenergy segment and, therefore, it is an important species to be used in the synthesis of biodiesel. For biodiesel to reach the consumer, it must meet technical standards, established by regulatory bodies, which guarantee the quality of the biofuel. Thus, the aim of this work was to synthesize biodiesel using monoalcohols, methanol, and ethanol from the Licuri oil (LO). Licuri oil was purchased already purified and had an acidity of 1,6 mg/g KOH. As a biodiesel production route, the transesterification reaction of LO with methanol (MBL) and ethanol (EBL) was carried out through basic homogeneous catalysis. It was possible to determine the structure of the licuri biodiesel by FTIR and ¹H and ¹³C NMR. The composition of the oil was established by gas chromatography coupled to mass spectrometer (GC-MS). The thermogravimetric behavior under synthetic air flow was evaluated and a characteristic thermal event of ester degradation was presented, both for methyl and pro ethyl biodiesel. The degradation initiation temperatures of the first thermal event, at a rate of 10 °C.min⁻¹, were close to 120 °C (MBL) and to (EBL). The thermal stability of biodiesel was considered satisfactory, with high DTG and DSC onset temperatures. which indicates promising substances to be used as an ecological lubricant. The results indicate that Licuri oil is a promising raw material for the production of quality and environmentally friendly fuels.

Agradecimentos/Acknowledgments

UFC, CAPES e CNPq.

Área: CAT

(Inserir a sigla da seção científica para qual o resumo será submetido. Ex: ORG, BEA, CAT)

Synthesis of biofuel additive and green solvent from lignocellulosic biomass-derived compounds using hierarchical ZSM-5 zeolite as catalyst

Sancler C. Vasconcelos (PG),¹ **Vinicius Rossa** (PQ),¹ **Domingos S. A. Silva**² (PG), **Monize Picinini**² (PG), **Ernesto A. Urquieta-González**² (PQ), **André V. H. Soares**³ (PQ), **Fabio B. Passos**³, **Thiago M. Lima** (PQ).^{1*}

sanclervasconcelos@id.uff.br; tmlima@id.uff.br.*

¹ Instituto de Química, Universidade Federal Fluminense; ² Departamento de Engenharia Química, Universidade Federal de São Carlos; ³ Departamento de Engenharia Química e Petróleo, Universidade Federal Fluminense.

Palavras Chave: Hierarchical zeolites, Furfural hydrogenation, Biomass upgrading, Domino reactions, Statistical planning

Highlights

ZSM-5 hierarchical zeolites were studied as catalysts in producing biofuels additives in a green route, departing from furfural and other platform molecules with high conversion and selectivity.

Resumo/Abstract

Increasing energy consumption and CO₂ emissions have several consequences for the planet's ecosystem. It is pivotal to search for sustainable alternatives to diminish the dependence on fossil fuels. In that matter, lignocellulosic -derived molecules, such as Furfural (FUR), presents great potential, since it is a platform molecule that can be used as a precursor to several value added products, such as alkyl levulinates. Zeolites are bifunctional catalysts widely used in industry and suitable for acid-catalyzed reactions. However, their employment in biomass valorization reactions is limited, since the small micropores lead to humins formation, and thus blocking the acid active sites. Hence, alkaline treatments were performed in different Si/Al ratios ZSM-5 zeolites (Si/Al ratio = 23, 38 and 48) to form hierarchical zeolites, containing both micro and mesopores. The effectiveness of the treatment was accessed by XRD, XRF, N₂ physisorption, FTIR-pyridine, TPD-NH₃, and SEM. The hierarchical catalysts formed was tested in the FUR domino reaction to obtain isopropyl levulinate (PL) using isopropanol as solvent and H donor. Preliminary tests indicated that the enhancement in mesopore volume and high acidity in the catalysts led to increased conversion and selectivity to PL. Aiming to maximize PL production, a factorial statistical design was performed in 2 levels and 3 factors (2³), where the influence of reaction temperature, catalyst mass and isopropanol volume were evaluated. As result, a 99% FUR conversion and a 95% PL selectivity was obtained. Different substrates such as furfuryl alcohol, levulinic acid, and α-angelica-lactone were tested, leading to high PL selectivity. Furthermore, the use of HMF as substrate led to several products, including (E)-4-(5-(hydroxymethyl)furan-2-yl)but-3-en-2-one (HMB, 82% of selectivity), an aldol condensation product that has been studied as a hypoxia medicine.

[1] Jorge, E. Y. C. et al. Metal-exchanged magnetic β-zeolites: Valorization of lignocellulosic biomass-derived compounds to platform chemicals. *Green Chem.* 19, 3856–3868 (2017)

[2] Serrano, D. P., Melero, J. A., Morales, G., Iglesias, J. & Pizarro, P. Progress in the design of zeolite catalysts for biomass conversion into biofuels and bio-based chemicals. *Catal. Rev. - Sci. Eng.* 60, 1–70 (2018)

[3] Vasconcelos, S. C. et al. Selective Synthesis of Levulinic Ester from Furfural Catalyzed by Hierarchical Zeolites. *Catalysts* 12, 783-801 (2022)

Agradecimentos/Acknowledgments

CAPES, CNPq, FAPERJ, RECAT-UFF, CPqMAE-UFSCar.

Synthesis of mannitol (di)esters envisaging potential environmental application.

Gabriel Francisco Souza da Silva (IC),¹ **Mayllon S. de Oliveira** (IC),¹ **Alan José C. Manso** (PG), **Gizele C. F. Sant'Ana** (PQ),² **Jaqueline D. Senra** (PQ).^{1*}
gabriel.2409francisco.ss@gmail.com; jaqueline.senra@uerj.br

¹Departamento de Química Geral e Inorgânica, IQ-UERJ; ²Departamento de Tecnologia de Processos Bioquímicos, IQ-UERJ.

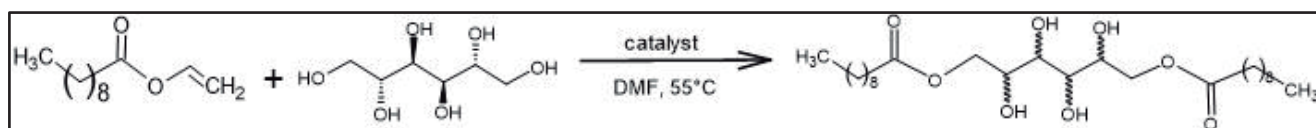
Palavras Chave: Organogels, Biocatalysis, Transesterification, Lipases, Carbohydrates.

Highlights

Transesterification products between vinyl decanoate and D-mannitol were prepared in moderate yields. Results indicated that the selectivity for the diester product is better at low temperatures (55°C) with K₂CO₃ as base in DMF, when compared to the same reaction at 110°C. Model esterification tests with lipases were then carried out for the evaluation of activity envisaging its use as biocatalysts for the transesterification reaction.

Resumo/Abstract

The great technological advance has been responsible for the increase in consumption and industrial production. However, the current environmental issues have led to efforts to promote methods that can reduce impacts, aiming at increasing the quality of life and the recovery of ecosystems. In case of oil spill cleanup, supramolecular organogels are interesting materials and represent a low cost alternatives, especially by virtue of the ease in obtaining rapid modulation of physicochemical properties due to changes in temperature and pH. In this context, low molecular weight gelators (LMWGs) containing carbohydrates are biocompatible and furnish hierarchically defined structures as a result of the multiple stereogenic sites. Following this idea, this work aims to combine a simple and low-cost route for the preparation of new mannitol (di)esters as potential organogels for future use in environmental remediation. The model reaction consisted in the study of vinyl decanoate and D-mannitol in DMF at 55°C and 110°C (Scheme 1). The preliminary HPLC-MS results showed that inorganic bases (K₂CO₃ and Cs₂CO₃) led to low to moderate product yields for the D-mannitol mono and diesters (1:1.3, up to 60%), indicating low product selectivities for the diester product. In order to improve reaction yield and selectivity, we started the study with lipases as remarkable biocatalysts. To first evaluate the enzymatic activity of *Candida antarctica* type B – CALB (Novozym 435) and *Rhizopus* sp. L04 LipB we chose the model reaction between lauric acid and 1-propanol towards These lipases have been tested to prove their potential for application in esterification/transesterification reactions.



Scheme 1: Model transesterification reaction between vinyl decanoate and D-mannitol.

The lipase activity in esterification reactions was determined by titration of aliquots of the reaction between lauric acid and 1-propanol - with acid-alcohol molar ratio of 1:1 -, with sodium hydroxide (NaOH) at 0.01 molar, to determine the amount of lauric acid that reacted with alcohol and the activity of each lipase. The reaction took place in a jacketed reactor at 60°C. Aliquots of 150 µL were withdrawn at the beginning and at the end of the reaction. The tested lipases showed esterification activity with high potential in the reaction of interest. The application of the studied lipases in the transesterification reaction is underway.

Agradecimentos/Acknowledgments

We acknowledge CNPq, FAPERJ and CAPES for funding and Central Analítica Fernanda Coutinho at Institute of Chemistry of the Rio de Janeiro State University for the HPLC-MS analyses.

The utilization of acid heterogeneous catalysts in lignocellulosic biomass pretreatment as a more sustainable alternative to depolymerization

Vinicius G. C. Madriaga¹ (PG), Daniel G. S. Quattrociochi¹(PQ), Saulo Bom Pinheiro¹ (IC), Maria Clara O. Ribeiro¹ (IC), Fábio Barboza Passos² (PQ), Thiago de Melo Lima¹ *(PQ).

tmlima@id.uff.br

¹Departamento de Química Inorgânica, UFF; ²Departamento de Engenharia Química, UFF.

Palavras Chave: biochar, biomass, sugar, heterogeneous catalyst, zeolite

Highlights

Here, we propose the utilization of two acid catalysts (a zeolite and a sulfonated biochar) to promote the depolymerization of cellulose and hemicellulose from raw lignocellulosic biomass to obtain a mixture of sugars

Resumo/Abstract

Recent research in the lignocellulosic biomass field have already shown how powerful this source is in obtaining several value-added products and energy. However, the process of transforming biomass in these products might be very complex since it is necessary to perform multiple reactions to obtain different compounds, such as furfural, levulinic acid, furfuryl alcohol, and many others. One of the most critical steps is biomass pretreatment, which separates biomass fractions (cellulose, hemicellulose, and lignin) and promotes hemicellulose and cellulose depolymerization, to obtain sugar units. For this reaction, an acid reaction medium is essential, which can be provided by a Brønsted - acid catalyst.¹

To achieve a greener perspective, this work proposes the utilization of two heterogeneous acid catalysts: a commercial beta zeolite (H-BEA-25) and a sulfonated coffee-derived biochar for the aforementioned reaction. The biochar was obtained from coffee grounds by heating this biomass at 350 °C for 2h, in an oxidative atmosphere and followed by sulfonic acid groups functionalization.² In Figure 1, the IR spectra confirm the functionalization since the band in 1030 cm⁻¹ appears, indicating the presence of S-O stretch. The acidity of both materials was also obtained by titration methods, (0,53 mmol/g for H-BEA-25 and 0,96 mmol/g for sulfonated biochar) indicating that these materials have the requirements to be applied as catalysts.³ As a perspective, further characterizations are still needed, and also, the catalytic performance of these materials is under evaluation. However, both materials show a potential application as catalysts, which might represent a new perspective in this field since there are only a few heterogeneous catalysts for this reaction.¹

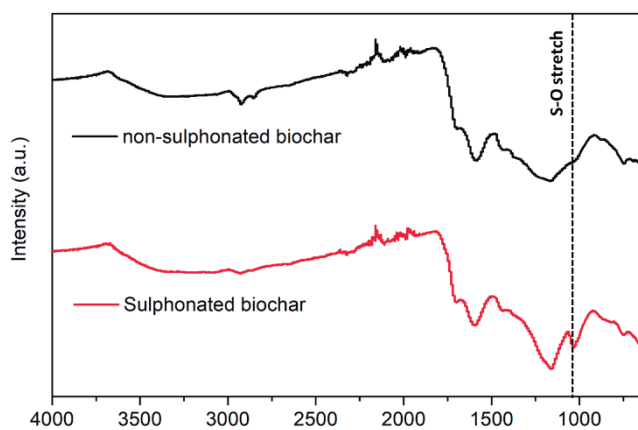


Figure 1 – IR spectra of biochars

References

- (1) Ganguly, A.; Chatterjee, P. K.; Dey, A. *Renew. Sustain. Energy Rev.* **2012**, *16* (1), 966–972.
- (2) Verma, S.; Baig, R. B. N.; Nadagouda, M. N.; Len, C.; Varma, R. S.. *Green Chem.* **2017**, *19* (1), 164–168.
- (3) Jorge, E. Y. C.; Lima, C. G. S.; Lima, T. M.; Marchini, L.; Gawande, M. B.; Tomanec, O.; Varma, R. S.; Paixão, M. W. *Green Chem.* **2012**, *22* (5), 1754–1762.
- (4) Qadoos, K., Nawaz, A., Mukhtar, H. *Advances in Lignocellulosic Biomass Pretreatment Strategies*. In: Zaporozhets, A. (eds) *Advanced Energy Technologies and Systems I. Studies in Systems, Decision and Control*, vol 395. Springer, Cham.

Agradecimentos/Acknowledgments

CAPES, CNPq, FAPERJ, Laboratório de Reatores, Cinética e Catálise (Recat), UFF.

Área: CAT

(Inserir a sigla da seção científica para qual o resumo será submetido. Ex: ORG, BEA, CAT)

Understanding CO₂ hydrogenation selectivity on nickel catalysts by *in situ* and *operando* techniques

Liane M. Rossi (PQ),*¹ Thalita S. Galhardo (PQ),¹ Adriano H. Braga (PQ),¹ Bruno H. Arpini (PG),¹ János Szanyi (PQ),² Renato V. Gonçalves (PQ)³

lrossi@iq.usp.br

¹Institute of Chemistry, University of São Paulo, 05508-000 São Paulo, SP, Brazil; ²Institute for Integrated Catalysis, Pacific Northwest National Laboratory, Richland, Washington 99352, United States; ³Instituto de Física de São Carlos, Universidade de São Paulo, CP 369, 13560-970 São Carlos, SP, Brazil

Palavras Chave: *catalysis, nickel, carbon dioxide, selectivity, in situ, operando, XPS, EXAFS.*

Highlights

The extensive spectroscopic (XAS, XPS, DRIFTS) and morphologic (XRD, TEM) evaluation of the Ni catalyst at different life stages present a clear evidence of the role of surface Ni₃C species formed in-situ at high temperatures in suppressing CH₄ formation during CO₂ hydrogenation.

Resumo/Abstract

Carbon dioxide (CO₂) is one of the most abundant wastes and its emission has harmful and unequivocal impact on global warming. Carbon capture storage and utilization (CCSU) technologies should be implemented for an immediate and sustained reduction in greenhouse gas emissions. Once captured, CO₂ could be stored or even converted into liquids via catalytic hydrogenation. In this context, the hydrogenation of CO₂ can lead to various C1 products, such as CO via the reverse water–gas shift (RWGS) reaction, CH₄ via Sabatier or methanation reaction, CH₃OH via selective hydrogenation and, ultimately, C₂+ hydrocarbons, olefins, or even oxygenates. Selectivity remains an issue. The first step, which is the hydrogenation of CO₂ through RWGS to form CO and water, is an equilibrium-limited endothermic reaction favored at high temperatures and methane is concomitantly formed over most catalysts as an undesired side product at low temperatures (< 600 °C). Here, we describe a multi-technique *in situ* and *operando* approach to characterize and understand how carbon accumulation on Nickel catalysts under CO₂ hydrogenation conditions affects selectivity. The Ni catalyst was tested under CO₂ hydrogenation conditions (10 °C min⁻¹ from 100 to 800 °C) under 1/4 CO₂/H₂. The freshly reduced catalyst produced CO (RWGS) and CH₄ (methanation reaction) concomitantly at temperatures between 300 and 600 °C. The production of CH₄ was suppressed on the spent catalyst, and CO was the main product at all temperature. Spectroscopic studies by CO-DRIFTS, XPS, and EXAFS under *operando* conditions suggest that a Ni₃C-like phase accumulates on the catalyst, which may be responsible for preventing the formation of CH₄. Overall, the adsorption strength of CO is greatly diminished with the deposition of C on the surface of metallic Ni particles, which ultimately results in the almost complete elimination of the CO methanation pathway.

Agradecimentos/Acknowledgments

We gratefully acknowledge support of the RCGI – Research Centre for Greenhouse Gas Innovation, hosted by the University of São Paulo (USP) and sponsored by FAPESP (2014/50279-4 and 2020/15230-5) and Shell Brasil, and the strategic importance of the support given by ANP (Brazil's National Oil, Natural Gas and Biofuels Agency) through the R&D levy regulation. Acknowledgments are given to LNNano (proposal #TEM-24456) and LNLS for access to DXAS and XAFS2 beamlines (proposals #20170290 and #20170171). Acknowledgements are given to the Environmental Molecular Sciences Laboratory (EMSL), a DOE Office of Science User Facility located at the Pacific Northwest National Laboratory, for access to Transient Kinetics Analysis (proposal #50697).

Uso da Céria na degradação fotocatalítica da tetraciclina sob radiação no UV/Visível

Gabriel Castro de Sousa (PG)^{1*}, Ayla Roberta Borges Serra (PQ)², Osvaldo Antonio Serra (PQ)¹

gabrielsousa@usp.br

¹Departamento de Química, FFCLRP; ² Departamento de Engenharia Química, UFSCAR.

Palavras-Chave: Fotocatálise, MOFs, Céria, Tetraciclina, Terras raras.

Highlights

Use of Ceria for the photocatalytic degradation of tetracycline under UV/Visible radiation. Ceria nanoparticles derived from Ce-MOF were obtained. Removal of up to 100% of the pollutant was achieved.

Resumo/Abstract

Antibióticos são extremamente importantes para o combate de diversas infecções. Entretanto, muitas substâncias não são metabolizadas por completo pelos organismos vivos e acabam contaminando corpos d'água e sistemas de saneamento com metabólitos e até mesmo com o próprio medicamento em seu estado primário. A presença destes tipos de poluentes, no meio ambiente, traz vários riscos à saúde humana e aos ecossistemas. Dessa forma, se faz necessário o desenvolvimento de tecnologias que sejam eficientes para a remoção destes resíduos. O óxido de cério está entre os Lantanídeos mais utilizados para catálise devido a sua estrutura e propriedades redox. O cério existe em dois estados, o trivalente (+3) e tetravalente (+4), e a transição entre esses dois estados pode gerar vacâncias de oxigênio resultando numa melhor remoção dos poluentes. Dessa forma, céria (CeO₂) é comumente utilizada como fotocatalisadora e adsorvente para remoção de metais pesados e corantes. O método de obtenção da céria gera mudanças nas propriedades de adsorção do composto. Ao calcinar MOFs (estruturas metal-orgânicas) de cério, o óxido obtido possui uma estrutura porosa e com grande área superficial, similar ao de seu precursor, que aumenta sua capacidade fotocatalítica. A céria obtida a partir do MOF Ce-BTC foi submetida a testes fotocatalíticos para determinar sua eficácia. Os testes consistiam em um recipiente com solução de tetraciclina em água ao qual foi adicionado o catalisador. A solução foi mantida sob agitação em temperatura ambiente. Na primeira parte dos experimentos foi avaliada a adsorção do material. Com a lâmpada desligada, foram coletadas alíquotas por 1 hora, com intervalos de 10 minutos, que após centrifugação, foram analisadas espectrofotometricamente no UV-Visível. Em seguida, a lâmpada xênon de 300W, que simula a luz solar, com comprimento de onda 280-420 nm foi ligada. Alíquotas foram coletadas de 20 em 20 minutos por 2 horas. As amostras também foram analisadas por espectrofotometria. Os testes foram repetidos para outros materiais, como a céria comercial. Os resultados comparando a eficácia do material obtido neste projeto com a céria comercial estão representados abaixo, na figura 1.

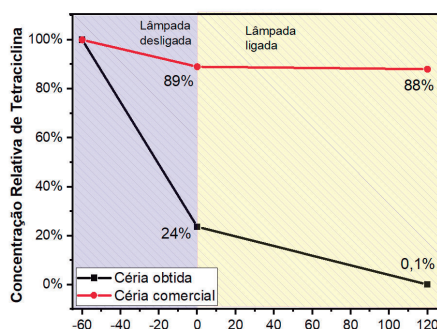


Figura 1 - Remoção da tetraciclina: céria obtida versus céria comercial

Agradecimentos/Acknowledgments

Grupo de pesquisa do Laboratório de Terras Raras, Universidade de São Paulo, Pró-Reitoria de Pesquisa, CAPES, CNPQ, FAPESP.

Utilização de complexo dioxo-halogenosselenito de níquel como sensibilizador de diferentes sólidos suportes para a produção de H₂(g)

Cândida Brandl (PG),^{1*} Tanize Bortolotto (PQ),¹ Camila Cechin (PQ),¹ Robert Burrow (PQ),¹ Arthuro Barbosa (IC),¹ Bernardo Iglesias (PQ),² Ernesto Schulz Lang (PQ)¹ e Bárbara Tirloni (PQ)¹.

Cândida.brandl@acad.ufsm.br;

¹Departamento de Química, LMI – Laboratório de Materias Inorgânicos - UFSM.

²Departamento de Química, LBMP – Laboratório de Bioinorgânica e Materias Porfirínicos - UFSM.

Palavras Chave: Dioxo-halogenosselenito, Fotocatálise, Hidrogênio.

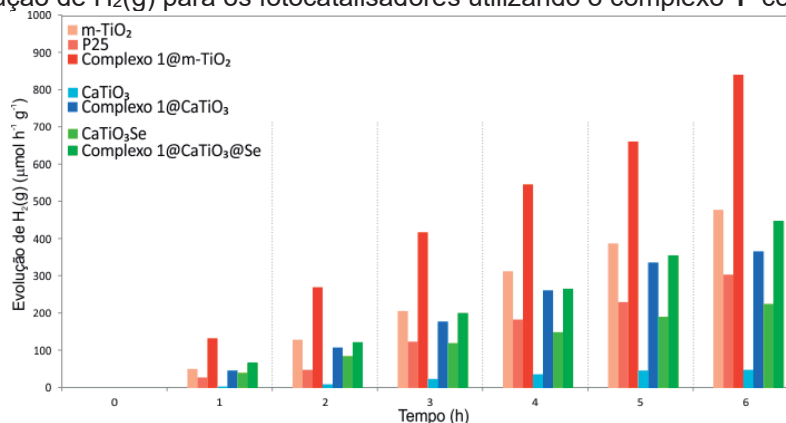
Highlights

Use of nickel dioxihaloselenite complex as a sensitizer of different solid supports to produce H₂(g). The complex has good H₂(g) production performance against heterogeneous processes for three different solid supports.

Resumo/Abstract

A produção de H₂(g), combustível limpo, barato e que não gera gases poluentes à atmosfera, através da divisão da água, substrato renovável e limpo, tem sido amplamente investigada através do uso da fotocatálise utilizando luz solar.^{1–3} O presente trabalho busca investigar a produção de H₂(g) através da fotólise da água, sintetizando diferentes fotocatalisadores, a serem utilizados no processo fotocatalítico heterogêneo. Para isso, é empregado um complexo de níquel(II) contendo o ligante dioxo-halogenosselenito, [NiBr(SeO₂Br)(phen)₂] (**1**), já que esse apresenta *band gap* adequado para o processo, absorção de luz visível e boa atividade fotocatalítica. O complexo **1** foi utilizado como sensibilizador de materiais semicondutores (m-TiO₂, CaTiO₃ e CaTiO₃@Se). Os fotocatalisadores preparados foram utilizados para a divisão fotocatalítica da água, com o objetivo de melhorar a produção de H₂(g). Foram comparados os resultados entre os diferentes sólidos suportes, e os resultados para a evolução de H₂(g) (Fig. 1) utilizando o complexo **1** como sensibilizador foi cerca de 900 μmol g⁻¹ para o sólido suporte m-TiO₂, 400 μmol g⁻¹ para o sólido suporte CaTiO₃ e 500 μmol g⁻¹ para o sólido suporte CaTiO₃@Se, após 6 horas de reação fotoinduzida. Ainda, os resultados obtidos foram comparados aos sistemas sem o uso do complexo **1**, confirmando a boa performance do complexo de níquel(II) contendo o ligante dioxo-halogenosselenito frente aos processos heterogêneos para os sólidos suportes m-TiO₂, CaTiO₃ e CaTiO₃@Se. Sendo assim, demonstra-se a eficiência do complexo **1** como sensibilizador ao ser impregnado nesses sólidos suportes, melhorando consideravelmente a produção de H₂(g).

Figura 1 – Produção de H₂(g) para os fotocatalisadores utilizando o complexo **1** como sensibilizador.



Fonte: autoria própria.

Agradecimentos/Acknowledgments

Universidade Federal de Santa Maria, CAPES, CNPq, RITEs- Fapergs e Fapergs (Processo: 21/2551-0002123-3).

Referências

- (1) Song, H.; Luo, S.; Huang, H.; Deng, B.; Ye, J. Solar-Driven Hydrogen Production: Recent Advances, Challenges, and Future Perspectives. *ACS Energy Lett.* **2022**, 7 (3), 1043–1065. <https://doi.org/10.1021/acseenergylett.1c02591>.
- (2) Younas, M.; Shafique, S.; Hafeez, A.; Javed, F.; Rehman, F. An Overview of Hydrogen Production: Current Status, Potential, and Challenges. *Fuel* **2022**, 316 (December 2021), 123317. <https://doi.org/10.1016/j.fuel.2022.123317>.
- (3) Ishaq, H.; Dincer, I.; Crawford, C. A Review on Hydrogen Production and Utilization: Challenges and Opportunities. *Int. J. Hydrogen Energy* **2022**, 47 (62), 26238–26264. <https://doi.org/10.1016/j.ijhydene.2021.11.149>.

EDU

Ensino de Química

46^a Reunião
Anual da **SBQ**

28 a 31 de Maio de 2023

Águas de Lindóia · SP
Hotel Monte Real

A cooperative learning approach using the Jigsaw method with other teaching strategies in public schools of Ceará

Gisele S. Lopes (PQ),¹ Magno Ferreira de Melo Junior (PG/FM),^{2,3} Athus Torres Florambel (FM),^{2,4} Isaías Batista de Lima (PQ),²

gslopes@ufc.br; magno.melo@educacao.fortaleza.ce.gov.br

¹Departamento de Química Analítica e Físico-Química, UFC; ²Mestrado Profissional em Ensino de Ciências e Matemática, Centro de Ciências, UFC; ³Escola Municipal Conego Francisco Pereira da Silva, Fortaleza, CE; ⁴Centro Educacional Evandro Ayres de Moura, Fortaleza, CE.

Palavras Chave: cooperative learning, jigsaw method, teaching strategies.

Highlights

The jigsaw method was used with other teaching strategies. Sensory experiments were applied for teaching acids and bases to high school students. Students were actively involved in sharing ideas and work cooperatively to complete the tasks.

Resumo/Abstract

In this work we present some strategies for didactic activities based on the precepts of cooperative learning (Jigsaw format) associated with other didactic teaching tools. The pedagogical potential of using the Jigsaw cooperative learning method (FATARELI et al, 2010) can reinforce a more active participation of students in classes, as well as promote the collective socialization of students. This technique associated with experiments involving the sense organs (taste, smell and vision) aimed to stimulate and reinforce the reading of texts on the subject of acids and bases, as well as increase curiosity and instigate the students to the investigative process. The preparation for the application of the jigsaw class associated with sensory experiments was divided into 3 stages organized as follows, 1st stage: fragmentation of the content to be worked on (acids and bases) to generate the specific contents of the groups of specialists with the proper elaboration or selection (if the teacher has access to didactic material that fits the requirements of the jigsaw method) of supporting texts; 2nd stage: formation and distribution of functions of the base group; 3rd stage: preparation of the experiments. Two semi-structured questionnaires were used to evaluate the strategy, one to analyze the contributions of the class in the proposed model to the learning of the subject acids and bases and another one to analyze acceptance of the method, in which the students expose their perceptions about the influence of the cooperative work in their learning, organization and relevance of the stages, didactic resources used and the topic addressed. The observed results show that the proposed strategy caused significant advances in the acquisition of knowledge by the students, about the theme addressed, and it was very well accepted, including reducing the resistance of students to perform reading activities. The second strategy is in progress and guides the use of the jigsaw method in classes on current issues in environmental education for elementary school students in a municipal school. In this second study, reports on environmental disasters and their consequences are being used. Students are being instructed to set up "podcasts" in the groups to present the proposed topics in environmental education. Through interaction the students learn to interrogate issues, share ideas, clarify differences, and construct new understandings. Therefore, it is concluded that combining different didactic methods with the teaching and learning process can result in an important instrument for stimulating students' learning, with potential to accommodate the various forms of student learning.

Ref.: FATARELI, E. F.; FERREIRA, L. N. A.; FERREIRA, J. Q.; QUEIROZ, S. L. **Método cooperativo de aprendizagem jigsaw no ensino de cinética química**. Química Nova na Escola, v. 32, n. 3, p. 161–168, 2010.

Agradecimentos/Acknowledgments

Secretaria Municipal de Educação de Fortaleza (SME) and Universidade Federal do Ceará (UFC).

Área: EDU

Acrilamida em Alimentos como Temática de Estudos de Caso Interrompidos na Promoção do Ensino Superior de Química dos Alimentos

^{1*}Ricardo Matos (PG), ¹Guilherme B. Silva (PG), ¹Mikeas S. Lima (PG), ¹Salete L. Queiroz (PQ).

ricardo2.matos@usp.br

¹Instituto de Química de São Carlos, Universidade de São Paulo

Palavras-Chave: estudo de caso interrompido, acrilamida, ensino superior.

Highlights

Acrylamide in Food Products as Theme of Interrupted Case Studies in Promoting the Teaching of Food Chemistry in Higher Education.

Three interrupted case studies on the topic acrylamide in food products were solved by first-year undergraduate chemistry students.

The pre-test and post-test results provide evidence of the case studies' effectiveness in promoting students' understanding of several chemical concepts.

Resumo/Abstract

O método de estudo de caso interrompido tem potencial na promoção de avanços conceituais e desenvolvimento de variadas habilidades. Os casos podem ser histórias reais ou fictícias sobre dilemas que são resolvidos com respaldo em conceitos científicos. Este trabalho tem como objetivo reportar as contribuições da aplicação de 3 estudos de caso de caráter interrompido sobre a mitigação de acrilamida em alimentos para o entendimento de conceitos relacionados à temática. Os estudos de caso, que tratavam da acrilamida em café, pão e batata, foram aplicados em 2 turmas de 31 e 32 estudantes de um Curso de Bacharelado em Química. A aplicação ocorreu de maneira remota, devido às restrições físicas impostas pela pandemia de COVID-19, sendo utilizados os ambientes virtuais Google Meet e Tidia-Ae para realização das atividades. Os estudantes foram divididos em 6 grupos de 5 integrantes, com cada caso sendo solucionado por 2 grupos simultaneamente. Atendendo ao caráter interrompido dos estudos de caso, a sua aplicação na disciplina compreendeu quatro etapas, nas quais os grupos que trabalharam com o mesmo caso realizaram sessões virtuais conjuntas com a professora, com duração de aproximadamente 30 min, nos quais eram apresentados fragmentos da narrativa pertinentes a cada etapa e atividades a serem desenvolvidas. Repostas escritas para as atividades deveriam ser entregues no Tidia-Ae. Para análise das contribuições dos estudos de caso para o entendimento de conceitos relacionados à temática, foram aplicados um pré e um pós-teste com 15 afirmativas sobre conceitos envolvendo a Química dos Alimentos, mais especificamente sobre a Reação de Maillard (8 questões sobre a formação de acrilamida e mecanismos da reação) e Conceitos Fundamentais (7 questões sobre mitigação da acrilamida, técnicas analíticas para sua determinação e curiosidades a seu respeito). O pré-teste foi aplicado antes e o pós-teste foi aplicado após as sessões de aplicação dos estudos de caso. As respostas de cada um dos estudantes foram classificadas em 3 categorias: resposta satisfatória (RS), resposta insatisfatória (RI) e não respondeu (NR). A categoria RS corresponde as respostas corretas, já na categoria RI os participantes responderam incorretamente à afirmativa e, por fim, a categoria NR contempla os estudantes que não responderam as questões. Valores obtidos por meio de teste t para amostra de pares revelam diferença estatística significativa entre os resultados dos testes ($p < 0,05$). Dessa forma, se aceita a hipótese alternativa: o emprego da metodologia contribui para avanços conceituais de química. Isso é corroborado pelas médias de acerto às respostas obtidas em ambos os testes, sendo observado o incremento de 43,6 para 52,2 do pré para o pós-teste. O emprego da metodologia também contribuiu para o entendimento da Reação de Maillard, o que é corroborado pelas médias de acerto às respostas obtidas em ambos os testes, em que houve um aumento de 42 para 47,42 do pré para o pós-teste. O avanço no entendimento conceitual dos estudantes pode estar atrelado as atividades didáticas desenvolvidas, já que a literatura aponta que um dos entraves para o entendimento da Reação de Maillard e da formação da acrilamida é a falta de conexão desse conteúdo com o cotidiano.

Agradecimentos/Acknowledgments

Ao CNPq (Processo 304974/2020-0) e a FAPESP (Processo 2018/23809-3).

46ª Reunião Anual da Sociedade Brasileira de Química: "Química: Ligando ciências e neutralizando desigualdades"

Adaptações de experimentos para o ensino de química em diferentes contextos: abordagem sobre fluorescência e cromatografia

Mateus Feitosa Santos (IC),^{1*} Sulcimilena Mady Flores (TC),¹ Nívea Cristina G. Munin (PQ).¹

niveaqueudes@ufam.edu.br; mateusfeitosa035@gmail.com

¹Instituto de Ciências Exatas e Tecnologia, UFAM

Palavras Chave: análise química qualitativa, separação de misturas, ensino médio, ensino superior.

Highlights

Adaptations of experiments for teaching chemistry in different contexts: topics of fluorescence and chromatography. The experiment enabled the separation of flavonoids and terpenoids. The students were able to glimpse through the experiment the use of hyphenated techniques chromatography and molecular fluorescence. The experiment can be used for high school education in the different chemistry concepts.

Resumo/Abstract

A pandemia ocasionada pelo novo coronavírus exigiu do docente mudanças no ensino de química, sobretudo no ensino remoto, trazendo desafios para o ensino de técnicas fundamentais da química analítica em um contexto em que aulas experimentais não podem ser realizadas na íntegra, seja em cursos sem equipamentos e laboratórios sofisticados ou no caso da pandemia, em aulas remotas. O objetivo deste trabalho foi propor uma aula experimental para disciplina de química analítica instrumental que envolve conceitos de cromatografia e fluorescência molecular para o público universitário. Em complemento a esta proposta, agregou-se o fator cotidiano dos alunos ao escolher extratos de plantas de uso popular, bem como propor adaptação às aulas práticas para o ensino de química no nível básico ou demonstração por vídeo aula. Independentemente do nível de ensino que será abordado o experimento, o professor deve organizar o seguinte planejamento da aula: título, público-alvo, disciplinas relacionadas, objetivos educacionais, justificativa, conteúdos trabalhados, materiais utilizados e tempo disponível¹. O protocolo experimental inicia-se com coleta e separação do material para confecção dos extratos. Neste trabalho escolheu-se as folhas de *Arrabidaea chica* (crajiuru), *Melissa officinalis* (erva cidreira), *Baccharis trimera* (carqueja), *Mangifera indica* (mangueira) todas coletadas no entorno do campus universitário (Instituto de Ciências Exatas e Tecnologia da UFAM) e conhecidas pela população local. As folhas foram lavadas com água e secas ao ar livre para o preparo do extrato aquoso e etanólico (pode ser comercial), sob leve aquecimento. Filtrou-se o extrato (com algodão, filtro de café ou papel de filtro de laboratório). Este extrato foi usado para realizar a) experimento de cromatografia em papel com diferentes eluentes + fluorescência, b) análise qualitativa pela reação de Taubouk adaptada² com análise em câmara escura UV-Vis (ou lâmpadas ou Leds UV comerciais). Tanto a cromatografia em papel quanto o resultado pela reação de Taubouk revelaram a presença de várias classes de flavanóides: auronas (cor vermelha), antocianinas (lilás-roxo), flavonóides (verde neon a verde escuro), além de terpenoides (azul claro). Como resultado, após aplicação de questionário, os alunos da disciplina de química analítica instrumental puderam avaliar a aplicação do experimento e grande maioria foi capaz de realizar a análise qualitativa dos constituintes, assim como entender o uso de técnicas acopladas (cromatografia e fluorescência) em laboratórios que não tem este tipo de equipamentos. Para o ensino médio, após a adaptação usando matéria acessíveis e de baixo custo, pode-se trabalhar diferentes temas, tais como: separação de misturas, polaridade dos compostos, entre outros considerando as funções orgânicas e grupos funcionais presentes nos constituintes encontrados nos extratos: carbonila (auronas e flavonóides), hidroxila (antocianinas, flavonóides, terpenoides), dupla ligação, anéis aromáticos e outros.

1. Vadim R. Viviani. Aula prática de Fotossíntese. Journal of biochemistry Education. V14, n1, 2016.

2. COSTA, S. et al.. South American Journal of Basic Education, Technical and Technological, v. 8, n. 2, p. 664–676, 2021.

Agradecimentos/Acknowledgments

PROGESP e PROEG da Universidade Federal do Amazonas (UFAM) pelas bolsas de iniciação científica e monitoria.

“Nobel Reaction in Orgexp2”: demonstration of a Click Chemistry reaction in the undergraduate laboratory of Experimental Organic Chemistry 2

Ana Carolina de O. Pereira (IC),¹ Gabriel L. S. dos Santos (IC),¹ Thamires J. J. Silva (PG),¹ Vinicius de O. C. Felisberto (IC),¹ Tiago L. da Silva (PQ),² Camilo H. S. Lima (PQ),¹ José C. Barros (PQ).^{1*}

jbarros@iq.ufrj.br

¹ Universidade Federal do Rio de Janeiro, Instituto de Química, Avenida Athos da Silveira Ramos, nº 149, Bloco A, 7º andar, Centro de Tecnologia, Cidade Universitária, Rio de Janeiro, RJ, CEP: 21941-909, Brasil

² Universidade Federal do Rio de Janeiro, Campus Macaé, Avenida Aluizio da Silva Gomes, nº 50, Granja dos Cavaleiros, Macaé, RJ, CEP: 27930-560, Brasil

Keywords: Nobel Prize, Click Chemistry, STS.

Highlights

Nobel Prize is an interesting subject in class. Click Chemistry is quite simple to perform in the laboratory. A student kit was prepared. It allowed for students to easily perform the reaction in the lab and discussions.

Abstract

The Nobel Prize is one of the most recognized events in Science. The Nobel prize in Chemistry 2022 was awarded to Bertozzi, Meldal and Sharpless for the development of Click Chemistry and Bioorthogonal Chemistry [1]. Notably in the last year, the subject of this Prize due to its simplicity allowed not only for theoretical discussions with the students, but for perform the experiment in the undergraduate laboratory of Experimental Organic Chemistry 2 without a change in the course syllabus.

Initially, slides, blackboard and molecular models (a,b) were used to introduce the subject of the Nobel Prize, and the concept of the Click Chemistry. Next, students employed an in-house built kit (c) previously prepared by professor and tutors to perform the Click Chemistry reaction in class (d) (Figure 1). The kit was prepared based on a literature procedure [2]. Reaction was quite simple to perform, motivated students and inspired questions and discussions about the Prize, mechanisms, medicinal and industrial applications, dialoguing with the concepts of Science, Technology and Society (STS).

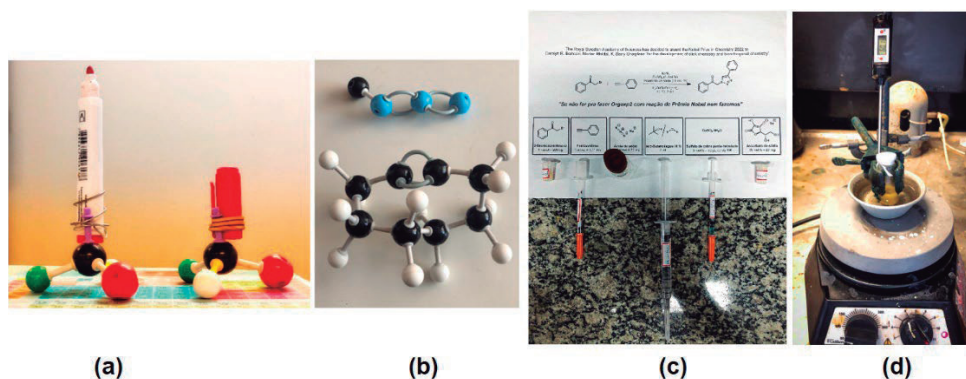


Figure 1 – Molecular models (a,b), student kit (b) and reaction setup (c)

References:

[1] The Nobel Prize in Chemistry 2022. Available at: <https://www.nobelprize.org/prizes/chemistry/2022/summary/>. Accessed in 05 Dec. 2022.

[2] Hansen, T. V.; Wu, P.; Sharpless, W. D.; Lindberg, J. G. *Journal of Chemical Education*, v. 82, n. 12, p. 1833-1836, 2005.

Acknowledgments

Authors acknowledge CAPES, CNPq, FAPERJ and PIBIC-UFRJ.

46ª Reunião Anual da Sociedade Brasileira de Química: “Química: Ligando ciências e neutralizando desigualdades”

'Mini museum of Glass: Marrying chemistry and glass' as a case of study for science, outreach, and awareness about glass material.

Victor Murilo Poltronieri da Silva (PG),¹ Naiza Vilas Bôas (PG),¹ Liane Miranda Carvalho (PG),¹ Guilherme Felipe Lenz (PG),¹ Ricardo Santos Baltieri (PG),¹ Francis Dayan Rivas Garcia (PG),¹ Renato Grigolon Capelo (PG),¹ José Hermes da Silva Soares (PG),¹ Thiago Augusto Lodi (PG),² Gustavo Galleani (PG),² Leonnam Gotardo Merizio (PG),² Andrea S. S. de Camargo (PQ),² Danilo Manzani (PQ).^{1*}

victor.murilo.silva@usp.br; dmanzani@usp.br

¹São Carlos Institute of Chemistry, University of São Paulo (USP), São Carlos, SP, Brazil

²São Carlos Institute of Physics, University of São Paulo (USP), São Carlos, SP, Brazil

Keywords: Museum, Glass, IYoG, Science Literacy, Science Communication.

Highlights

Glass teaching can be challenging in undergraduate chemistry courses and even more applied in scientific outreach projects. The Mini Museum of Glass set a stone for the first official academic museum of glass.

Abstract

As a centuries-old material, glass plays many important roles in current society, from containers to optical fibers that run the world's internet. Humanity is living in The Age of Glass. Indeed, the year 2022 was celebrated as the International Year of Glass (IYoG), hence, the Laboratory of Inorganic and Vitreous Materials (LaMIV) from the University of São Paulo (USP) inaugurated the Mini Museum of Glass ('Minimuseu do Vidro'). The core value of this project is to disseminate glass knowledge throughout society. To accomplish it, graduate students and research fellows from the São Carlos Institute of Chemistry (IQSC-USP), supported by LeMaF (IFSC-USP), joined forces to put in practice and build 6 scientific modules addressing different topics about the glass' nature and properties: (i) Crystalline vs. non-crystalline materials, (ii) Mini Collection of Glass, (iii) Colors in Glass, (iv) Candy Glass, (v) Transparency and Optical Fibers, and (vi) Luminescent glass. Each module was composed of an interactive part (exhibition) and an explanatory banner written at the undergraduate level. Still, the glass topic is not only difficult to implement in an outreach project but rather labored to even teach undergraduate students, thus evidenced by education activity applied in 3rd year's discipline in a chemistry undergraduate course. In summary, the museum materials were designed to consider the science literacy indicators, balancing scientific background information with the social interface between scientific knowledge and society. The first step was taken, to adapt the texts to a more accessible language, considering the Scientific indicator and the social interface superficially. Further improvements need to be done to gain interactivity with the exhibition and develop a connection with the non-science community.



Figure 1. Mini Museum of Glass current exhibition at "Prof. Johannes Rüdiger Lechat" library - IQSC.

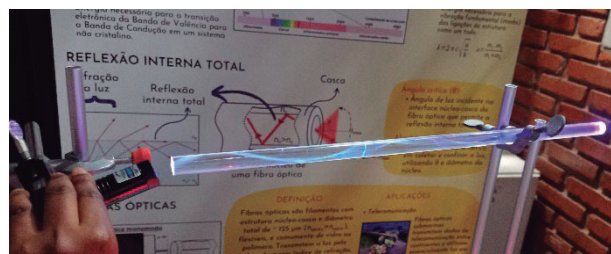


Figure 2. Illustration of total internal reflection phenomenon – module V.

Acknowledgments

The Brazilian agency CAPES and PROCEU-USP are acknowledged for financial support and the members of LaMIV-IQSC and LeMaF-IFSC for intellectual and personal support.

And now, teacher? Artificial intelligence and Chemistry teaching: reflections on ChatGPT in the description of chemical concepts

Bruno S. Leite (PQ).^{1*}

brunoleite@ufrpe.br

¹Departamento de Educação, UFRPE

Keywords: Artificial intelligence, Chemistry teaching, ChatGPT, Chemical concepts.

Highlights

An investigation was carried out on the ability of ChatGPT to answer questions about the definitions of chemical concepts, identifying its potential and limitations.

Abstract

In recent years, digital technologies have stood out with numerous possibilities for application in Education. Teachers and students can use apps, software, videos, games, the internet, etc. The insertion of technologies in education was/is often questioned by those involved (teachers, directors, parents, students). When the calculator (calculating machine) appeared, schools had to adapt the way they taught math calculations. Similarly, with videos, smartphones, and the Internet. Recently, a new challenge has emerged through the use of artificial-intelligence (AI), the chatbot called ChatGPT, that has taken the world. The ChatGPT, which was released as a free-to-use tool in November 2022 is a large language model (LLM), which generates convincing sentences by mimicking the statistical patterns of language in a huge database of text collated from the Internet. In this context, this research aimed to investigate the potentialities and limitations of the ChatGPT tool in which we evaluate the performance of ChatGPT on its ability to answer questions about Chemical concepts. For this, we analyzed ChatGPT's responses regarding five chemical concepts (Covalent Bond, Substance, Isomerism, Stoichiometry, and Atom) and compared them with definitions present in literature (scientific articles and books) and on the internet. The results show that the answers presented by ChatGPT are compiled from definitions that are already available in the literature and on the internet, that is, from websites, digital repositories, scientific articles published in virtual journals, and from books. ChatGPT has ability to generate fluent language, churning out sentences that are increasingly hard to distinguish from texts written by people. Unlike other platforms, such as Wikipedia (which requires some caution depending on the concept addressed), ChatGPT presented, in relation to the chemical concepts investigated, coherent definitions that can be used for the process of building chemical knowledge. On the other hand, one of the limitations observed initially is that ChatGPT's answers may present plagiarism, which raises concerns about whether the student/teacher will be able to recognize a copied text or if the AI will recognize the ethical nuances of scientific research. ChatGPT does not understand what it responds to. It responds based on what probability indicates, using as a base the data it had access to when it was trained. Thus, it is necessary that in the teaching of chemical concepts, we can go beyond the question and answer ("What is this?"; "The answer is this!"), but discuss, debate ideas, and argue (at a deeper level than provided by AI). The ChatGPT has excellent linguistic capabilities, but is limited in logic, abstraction, high-level reasoning, and is not capable of maintaining a coherent discussion that can be achieved through teacher-student and student-student interaction. ChatGPT should be understood as another opportunity for the teacher to overcome the teaching paradigm content-centered, teacher-centered and memorization-focused. These are challenges that come with the advent of technologies in education. So, and now teacher, what to do? Stimulating critical writing skills among students and reflecting on what is written can be an initial path.

Acknowledgments

To CNPq (proc. 422587/2021-4), FACEPE (proc. APQ-0916-7.08/22), LEUTEQ, UFRPE.

Argumentação de graduandos em química sobre a temática polímeros

Pablyana L.R. Cunha (PQ),^{1,2*} Raíla R. de S. Almondes (PG)², Salete L. Queiroz (PQ)²

***pablyana@ufc.br**

¹Departamento de Química Orgânica e Inorgânica, UFC; ² Instituto de Química de São Carlos, USP

Palavras-Chave: Casos investigativos, Química, Argumentação, Ensino Superior.

Highlights

Argumentation of undergraduate chemistry students on the thematic polymers

This work aims to analyze the argumentation of undergraduate chemistry students based on the resolution presented to an interrupted case study on biofilm applications in fruits.

Resumo

No Brasil, o leque de pesquisas sobre argumentação relacionadas ao ensino de química tem se ampliado, indicando a sua potencialidade na promoção do entendimento dos alunos sobre conceitos científicos, além do desenvolvimento de habilidades como a comunicação em linguagem científica, raciocínio e pensamento crítico¹. Este trabalho visa à análise da capacidade argumentativa de graduandos de um Curso de Bacharelado em Química, tendo como base a resolução textual apresentada por eles a um caso investigativo de caráter interrompido sobre a temática biofilmes poliméricos usados na proteção de uvas. Para determinação da qualidade da argumentação, foram selecionados textos produzidos por cinco alunos (doravante denominados de A, B, C, D e E), que foram posteriormente analisados, com base no *Quadro Analítico* de Souza e Queiroz². Para a análise do **nível de produção argumentativa**, considerou-se o total de unidades de análise (UA) presentes nos textos, sendo possível perceber uma diferença entre a quantidade de UA (Fig. 1A), variando de 20 a 35. A análise do **nível de complexidade argumentativa** foi feita pela classificação das UA em categorias que expressam, ou não, algum conteúdo argumentativo e os coeficientes de complexidade argumentativa (CCA) atribuídos a elas (Fig. 1B).

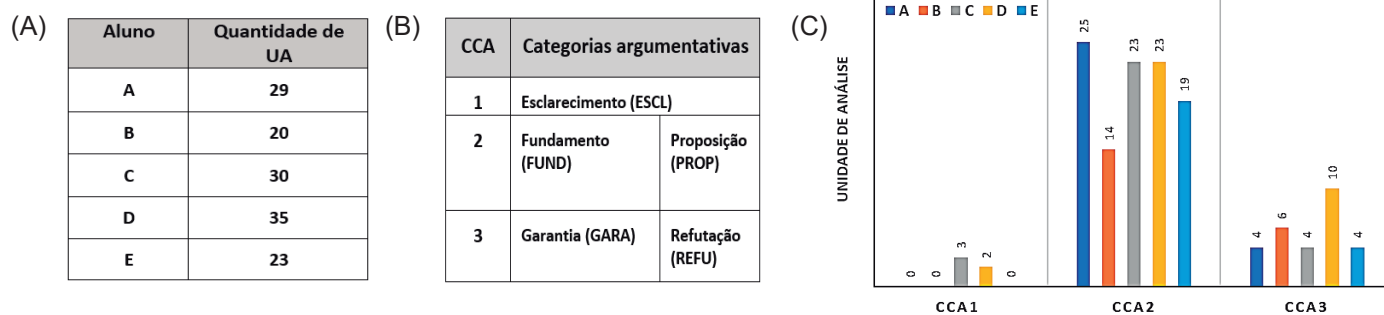


Figura 01 – (A) Total de UA dos textos; (B) Categorias e seus respectivos CCA; (C) Distribuição da UA pelos CCA.

O gráfico da Fig. 1C indica que os picos com a maior concentração de UA se localizaram no CCA 2, no qual constam as categorias de **PROP e FUND**, mostrando que os textos apresentam componentes da premissa básica de um argumento. O segundo CCA mais presente nos textos foi o CCA 3, estando presentes **GARA e REFU**, mostrando que, além da premissa básica de um argumento, os alunos se preocuparam em produzir componentes que validassem as premissas e que apontassem suas condições de exceção. O CCA 1 só apareceu para os textos dos alunos C e D, na categoria de **Esclarecimento**. Considera-se que, de uma forma geral, a premissa básica de um argumento foi atingida nos textos (fundamento, proposição e garantia) e que a aplicação de estudos de caso favoreceu a promoção da argumentação.

¹PORTO, P. A.; QUEIROZ, S. L., *Química Nova na Escola*, 43, 1, 3, 2021. ²SOUZA, N.; QUEIROZ, S. *Investigações em Ensino de Ciências*, 23, 3, 145-170, 2018.

Agradecimentos

À UFC pelo afastamento da Professora Pablyana Cunha, para realização de estágio de pós-doutoramento na USP.

KIT DIDÁTICO AUTOMATIZADO DE TITULAÇÃO PARA LABORATÓRIOS DE CIÊNCIAS

Gustavo L. Silvestre (IC),¹ Edson A. Duarte (FM),¹ Daltamir J. Maia (FM)¹.

glaurentino@outlook.com; daltamir.maia@gmail.com;

¹Instituto Federal de São Paulo – IFSP – Câmpus Campinas

Palavras Chave: *Titulação ácido-base, automatização, kit didático, Arduino uno.*

Highlights

AUTOMATED DIDACTIC TITRATION KIT FOR SCIENCE LABS

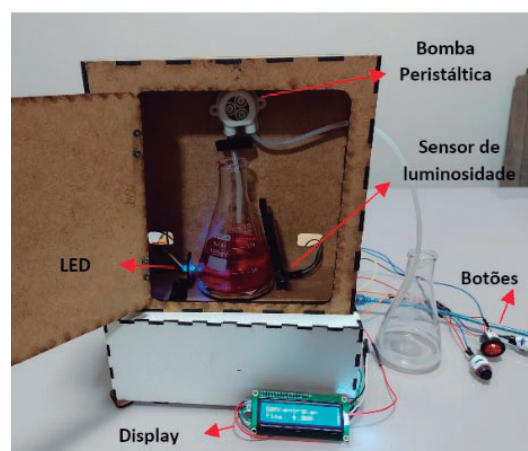
Automated kit for performing acid-base titrations using: Arduino uno, luminosity sensor, magnetic stirrer, peristaltic pump to control the volume of titrant to be added.

Resumo

Esse trabalho teve o objetivo de projetar um equipamento de automatização do processo de titulação ácido-base para laboratórios de ciências e que, ao mesmo tempo, seja portátil, compacto e de baixo custo. Além da importância analítica na determinação das concentrações de um ácido ou de uma base, a titulação ácido-base pode ser um ótimo momento para discutir os conceitos de reações químicas, equilíbrio químico, acidez e basicidade, balanceamento, concentração das soluções, diluição além de outros tópicos associados à Química.

O controle automático é feito através de uma placa microcontroladora Arduino Uno que controla o passo a passo da titulação; a adição da solução titulante é feita através de uma bomba peristáltica; o ponto de viragem é detectado por um sensor de luminosidade TSL2561 que interrompe a titulação quando ocorre a mudança de cor (indicador fenolftaleína), seja de incolor para rosa (o titulado é um ácido) ou de rosa para incolor (o titulado é uma base); uma fonte de alimentação 12 V; um display LCD de sinal de saída do microcontrolador para mostrar todas as informações ao usuário. Após o fim da titulação, um programa determina a concentração do titulado automaticamente. A Figura ao lado ilustra o kit completo; o titulado é confinado em um ambiente escuro para impedir que a luminosidade externa atrapalhe a leitura do sensor na mudança de cor, garantindo assim a reprodutibilidade dos resultados.

Depois de alguns ajustes tais como a velocidade de gotejamento da solução titulante, leitura de luminosidade para definir o ponto de viragem da titulação, os resultados se mostraram satisfatórios para um experimento que tem por objetivo principal o ensino, mais que a precisão dos valores de concentração da solução do titulado. Este protótipo foi manufaturado em um ambiente maker com componentes comerciais que possibilitam a sua reprodução a baixo custo e mais do que isso “a popularização da Ciência”.



Agradecimentos

IFSP – Instituto Federal de São Paulo;

CEPIN – Centro de Pesquisa e Inovação de Tecnologias Educacionais;

46ª Reunião Anual da Sociedade Brasileira de Química: “Química: Ligando ciências e neutralizando desigualdades”

Beyond chemistry triplet: infusion of nature of chemistry in experimental chemistry teaching

Saulo Quintana Gomes (PQ)^{1*}

saulo.quintana@ufca.edu.br

¹Instituto de Formação de Educadores – Universidade Federal do Cariri

Palavras Chave: *Chemistry teaching, Nature of science, Nature of chemistry, Experimentation.*

Highlights

There is a lack of including the nature of chemistry in chemistry teaching. It is possible to think of the infusion of the current nature of chemistry in chemistry teaching through experimental practices.

Abstract

The literature does not pay enough attention to include the nature of chemistry in chemistry teaching¹. This can be observed in an absolute or comparative way since “among the school science subjects [...] chemistry continues to be a relatively uninterrogated domain in terms of its epistemic aspects”². This lack of attention can be due to the pragmatic vocation of chemistry³, which is also reflected in its teaching. However, from the decade of 1990⁴ onwards, a research field around the philosophy of chemistry was mobilized. Even so, “unfortunately, the same dynamism of scholarship cannot be attributed to the infusion of philosophy of chemistry in chemical education research and practice.”². Most of the research in this interface is theoretical and deals with problems such as model building or key chemical concepts. On the other hand, chemistry teaching has a long tradition of applying experimental activities^{5,6}. Even so, none of the recent and stimulating discussions about the philosophy (or nature) of chemistry is related to experimentation in the field’s publications.

In the present work, I argue that it is possible to establish this relationship, which is to think about the infusion of the current nature of chemistry notions – informed by research on the philosophy of chemistry – in chemistry teaching through experimental practices. The structuring idea is that epistemological aspects of chemistry and experimentation have already been brought together in chemistry teaching through classic Johnstone's triangle, or chemical triplet⁷. Therefore, it remains to mediate an update in philosophical arguments in relation to experimental possibilities (or impossibilities), a task to which I contribute through the discussion of some of the main characters of chemistry, namely: relational, producer of its study object, pragmatic, dual (technoscientific) and visual. This discussion highlights experimental strategies for teaching about the nature of chemistry. Some limitations of the proposed approach are also considered, particularly on the visual character of chemistry taken as realistic.

References

1. Teo, T. W., Goh, M. T. & Yeo, L. W. Chemistry Education Research Trends: 2004-2013. *Chem. Educ. Res. Pract.* 15, 470–487 (2014).
2. Erduran, S. & Kaya, E. *Transforming Teacher Education Through the Epistemic Core of Chemistry: Empirical Evidence and Practical Strategies.* (Springer, 2019).
3. Ribeiro, M. A. P. A emergência da Filosofia da Química como campo disciplinar. *Rev. Bras. Pesqui. em Educ. em Ciências* 16, 215–236 (2016).
4. Scerri, E. R. Are chemistry and philosophy miscible? *Chem. Intell.* 3, 44 (1997).
5. Hodson, D. Laboratory work as scientific method: three decades of confusion and distortion. 37–41 (2006).
6. Hofstein, A. The laboratory in chemistry education: thirty years of experience with developments, implementation, and research. *Chem. Educ. Res. Pract.* 5, 247–264 (2004).
7. Taber, K. S. Revisiting the chemistry triplet: Drawing upon the nature of chemical knowledge and the psychology of learning to inform chemistry education. *Chem. Educ. Res. Pract.* 14, 156–168 (2013).

Agradecimentos/Acknowledgments

Universidade Federal do Cariri - Instituto de Formação de Educadores

Categorization of images presente in the development of “electrochemical cells”, in textbooks of Natural Sciences approved by PNLD 2021.

***Carlos A. P. Domingues** (PG)¹, Elaine P. Cintra (PQ)²

¹carlos6hm@yahoo.com.br; ²elainecintra@ifsp.edu.br

^{1,2}Mestrado Profissional em Ensino de Ciências e Matemática (Encima) do IFSP-SP

Palavras Chave: PNLD, Pilhas, Taxonomia, Livro Didático.

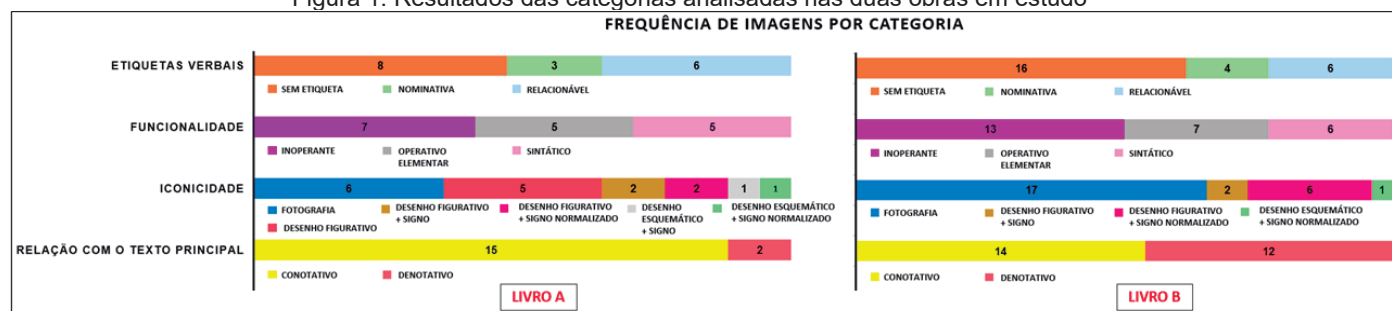
Highlights

Analysis of images related to electrochemical cells in PNLD 2021 works. The results point to a high occurrence of photographs and low synoptic relationship, compromising understanding.

Resumo/Abstract

As imagens estão presentes na esfera educacional como um recurso importante para auxiliar na explicação de conceitos e, portanto, atuando como facilitador dos processos de ensino-aprendizagem. Segundo PERALES e JIMENEZ (2002), as imagens também podem assumir funções como: despertar o interesse, tornar a obra mais atraente, descrever fenômenos, entre outros. Neste sentido, o uso de imagens é incentivado, sobretudo nos conceitos que demandam maior carga de abstração. Na química, um exemplo clássico são as dificuldades enfrentadas na compreensão envolvendo conceitos de eletroquímica. O presente trabalho busca responder à questão: Como se caracterizam as imagens sobre a temática “pilhas”, presentes em livros didáticos aprovados no PNLD 2021? Foi realizada uma pesquisa de análise documental, de metodologia mista, onde foram analisadas 43 imagens presentes em duas obras de ciências da natureza, sendo 17 imagens da coleção “Multiverso”, editora FTD - LIVRO A - e 26 da coleção “Matéria”, editora Scipione - LIVRO B. A categorização foi realizada utilizando a taxonomia de Perales e Jimenez (2002) e as classificações propostas foram discutidas pelos autores do trabalho. Os resultados são apresentados na Figura 1.

Figura 1: Resultados das categorias analisadas nas duas obras em estudo



Após categorizações, foram comparados os resultados das obras, levando em consideração os percentuais de ocorrência. Na categoria Iconicidade, as duas obras apresentaram maior incidência de imagens do tipo Fotografia sendo 35% das ocorrências no LIVRO A e 65,4 % no LIVRO B. Este tipo de imagem possui função motivacional, cabendo apenas o papel de observação (baixa iconicidade). De acordo com o critério de Funcionalidade, observou-se a predominância de imagens com função Inoperante – tipo de figura que não apresenta elementos utilizáveis para a compreensão do conceito – sendo 41,2% das ocorrências no livro A e 50% no livro B. Na categoria Relação com o Texto Principal, notou-se maior ocorrência da unidade “Conotativo” (sem estabelecimento de relação com texto principal) chegando a 88,2% no LIVRO A. Para a maioria das imagens dos dois livros não foram constatadas referências às imagens nos textos (sem etiqueta verbal) que poderiam auxiliar na compreensão do conceito investigado. Considerando as dificuldades relacionadas à temática das pilhas, seria oportuno um maior sincronismo entre o texto e a imagem, proporcionando uma sinergia no processo de compreensão da temática (relação sinóptica), redução de imagens meramente ilustrativas (maior grau de iconicidade).

Referências/References

PERALES, F. J.; JIMÉNEZ, J. de D. Las ilustraciones en la enseñanza-aprendizaje de las ciencias: análisis de libros de texto. *Enseñanza de las ciencias: revista de investigación y experiencias didácticas*, v. 20, n. 3, p. 369-386, 2002.

Área: EDU

CO₂ REDUCER: Knowing your environmental footprint from the STEAM approach in Basic Education

Gisele S. Miranda (PQ-FM),^{1*} Victoria S. Alves (IC),² Paula Helena M. dos Santos (IM),¹ Camile Vitória A. Cagide (IM),¹ Ana Clara S. Lourenço (IM),¹ Ana Carolina P. Brito (IM),¹ Matheus M. Lanci (IM).¹

giselemiranda@id.uff.br; vialves@id.uff.br

¹Colégio Universitário Geraldo Reis – COLUNIUFF; ²Instituto de Química da Universidade Federal Fluminense - IQUFF

Keywords: STEAM Education, Carbon Credits in Basic Education, Application Development, Teaching Chemistry through Experimentation.

Highlights

To think about the future is to act in the present. It was with this idea that a group of students from the basic education proposed a technological solution to reduce carbon emissions into the atmosphere.

Resumo/Abstract

Thinking about the future is acting now. It was with this idea that a group of students from segments F2 and High School proposed a technological solution to reduce carbon emissions in the atmosphere. These students are part of the research group called Gender, Science and Basic Education at COLUNIUFF, which, besides researching on the subject, develop a series of actions aiming to encourage and promote the participation of students, especially girls, in science. This work was developed from the STEAM teaching strategy, which proposes the investigation of real situations, integrating Natural Sciences with Technologies, Engineering and Mathematics. This approach to teaching and learning is based on the integration between two or more areas of knowledge and is materialized through questioning, observation, investigation, and search for problem solving. Thus, for the development of this proposal, we rely on the works of ¹Sanders, 2009, ²Riley, 2014, and ³Bacich and Holland, 2020, aiming at the development of competencies and skills anchored in knowledge and technologies permeated by innovation and creativity; and on the works of ⁴Frison, 2016, to promote the proactive, autonomous, self-regulated, and supportive cognitive development of individuals. Seeking to understand the guidelines of "SDG 13: action against global climate change" and how each individual action could contribute to reduce the negative impacts on the environment, the GT CO₂Reducer created a prototype application in order to favor the monitoring of the environmental footprint of ordinary citizens, due to their consumption pattern, and thus allow everyone to make better choices, in terms of environmental impacts, of products and services. Knowing the CO₂ emissions of each process, it is the common citizen himself who will drive industries and companies to seek new production processes, which are in accordance with the maintenance of life on the planet. Some companies already make available the amount of CO₂ emitted in the production or provision of services, such as airlines, which facilitated the collection of this data. However, the vast majority is unaware of the process of calculating CO₂ emissions and the GT CO₂Reducer has been developing a partnership with other institutes to develop this calculation for different production processes. Developing a methodology to promote the demystification of science made it perceived as an important tool for social transformation committed to sustainability at different levels across the planet.

References: ¹SANDERS, M. STEM, STEM Education, STEMmania. In: The Technology Teacher, v. 68, n. 4, p. 20–26, 2009. ²RILEY, S. Arts integration and STEAM: quick resource pack. The Institute for Arts Integration and STEAM: Westminster, MD, 2020. ³BACICH, L. HOLANDA, L. (Orgs). STEAM em sala de aula: a aprendizagem baseada em projetos integrando conhecimentos na educação básica. Porto Alegre: Penso, 2020. ⁴FRISON, L.M.B.. Monitoria: uma modalidade de ensino que potencializa a aprendizagem colaborativa e autorregulada. Pro-Posições, v.27, n. Pro-Posições, 2016 27(1), jan. 2016.

Agradecimentos/Acknowledgments

We would like to thank to Faperj, ProgradUFF, and COLUNIUFF for the financial support.

Combining a Memory Game with Experimentation: A Proposal for the Teaching of Periodic Table.

Isadora Cavalcante Josino (IC),¹ Maria Aparecida Bezerra de Oliveira (IC),¹ Maria Leidiana Nogueira Amaro(IC),¹ Thiago Muniz de Souza (PQ)¹

isadorajosino5@gmail.com

¹Unidade Acadêmica de Serra Talhada- Universidade Federal Rural de Pernambuco - UAST/ UFRPE

Keywords: Chemistry Teaching, Experimentation, Games, Playful activity, Periodic Table, Vygotsky.

Highlights

This abstract presents a proposition of a playful activity associated with an experimental practice to teach the periodic table and its properties in basic education from the social-interactionist theory of Vygotsky.

Resumo/Abstract

The use of games in the teaching of chemistry is an efficient didactic tool in the process of teaching and learning in which new methodologies with the use of this playfulness have been used in basic education. In this context, the present work is a proposal of a ludic activity in the intention of developing a game together with an experimental activity in order to study the social-interactionist behavior during the application of this game, and in particular, to try to answer the following question: *What attracts the attention of the learner who initially is not interested in participating in the ludic activity and in the course of the game such a learner becomes completely included in the ludicity?* In this perspective, the didactic game aims to enable access to chemical knowledge to reinforce the concepts previously seen in the classroom. In other words, the game is applied after the conceptual discussion, and it is called a didactic game (Soares & Rezende, 2019). The game will be developed with 42 cards, which are complementary pairs, a model like the games of memory cards, each card contains an image, and the other complementary card contains information about the image, the application of the game will be done in groups, each team should have a maximum of 5 people and, thus, the winning group will be the one that forms the largest number of pairs. The existing content on the cards will be related to the theme of the periodic table, electronic distribution, and its properties. Fiurini & Carvalho (2014) also developed a type of memory game with the same theme; However, they were based on the theory of meaningful learning and not on the social-interactionist theory. Despite this, some researchers claim that the memory game is not a pedagogically efficient game. To make it interesting, the experiment known as the flame test will be used concomitantly with the game, where each hit on the pair of cards will have an experimental verification by means of a practice present on the pair of cards. Such association (game/experimentation) is in fact the great differential of the proposal, because few reports of didactic games have been associated with experimentation in the classroom. The game proposal has as theoretical reference based on conception of the Lev Vygotsky to understand that the game is a mediation channel for the developing of the students through the intervention of the sign system. Furthermore, it can be suggested that the use of the game with an emphasis on the memory game, linked to experimentation, can be a viable alternative to improve the pedagogical part of this type of game.

References

Fiurini, G. F & Carvalho, M. O lúdico como ação motivadora no ensino da tabela periódica. Cadernos PDE, Curitiba, v. 1, p. 3-21, 2014.

Soares, M. H. F. B & Rezende, F. A. M. (2019). Análise teórica e epistemológica de jogos para o ensino de química publicados em periódicos científicos. Revista Brasileira de Pesquisa em Educação em Ciências, 747-774.

Agradecimentos/Acknowledgments

We thank the extension program SONUS/UFRPE- 2020 and the School of Reference in High School Cornelio Soares of the State of Pernambuco-Brazil.

Creation of a Popular Science Text on Metal-Organic Frameworks (MOFs) to teach Chemistry

Leonardo L. Silva (PG), Carolina M. Primo (PG), Amadeu M. Bego (PQ), Regina C. G. Frem. (PQ).

leonardo.l.silva@unesp.br

São Paulo State University (UNESP), Institute of Chemistry, Araraquara, Brazil.

Keywords: Public communication of science, Popular science text, Metal-organic frameworks.

Highlights

Once there is a gap between society and the academic realm, in this research it is proposed the creation of a popular science text inspired by a scientific research on Metal-Organic Frameworks (MOFs).

Resumo/Abstract

Nowadays, it can be observed a gap between society and research developed by scholars within the academic realm. That distancing might cause a devaluation of science by the society, which worsens even more, for example, an increasing phenomenon: the science denialism. Thus, it is mandatory to foster measures that aim at strengthening the relationship between the academic realm and society. The public communication of science has been mentioned as a feasible solution for that, given that this kind of effort aims at making science popular and contributing to science literacy of laypersons. One of the several formats of scientific divulgation is by means of the Popular Science Text (PST), which is described by specialized literature in that field as a specific speech genre, according to Mikhail Bakhtin's heritage, and it presents the following characteristics: i) content focused on science; ii) accessible communication style for laypersons; and iii) compositional structure, which is integrated. Therefore, this research aimed at writing a Popular Science Text based on a research carried out within the academic realm regarding the synthesis and characterization of a Metal-Organic Framework (MOF) and its use in Forensic Chemistry, more specifically in Document Examination by Experts. The Popular Science Text created is entitled "Fake or Authentic? MOFs potential in preventing sophisticated document fraud". To that end, based on specialized literature in that field, an instrument that guided the writing process of the Popular Science Text has been created to make its formulation easier, as well as to adjust it to the main features in a well-structured PST. Thus, one can say the result met all requirements properly and reasonably in terms of content, format and language, which are core characteristics for making laypersons aware of scientific content. Furthermore, the PST written may pose a great educational potential, since it has been properly created for teachers so they can specifically use it aiming at coherent and well-established goals when thinking of putting it into practice in the classroom, being possible to foster students' learning and development in terms of building a reading habit of scholarly papers, making them get in touch with such content and acknowledging its importance, not to mention to acquire knowledge on steps within science and making students get more engaged in the classroom, boosting their scientific literacy.

Agradecimentos/Acknowledgments

I would like to thank CNPq, the Research and Innovation Network in teaching of Chemistry (RIPEQ, abbreviation in Brazilian Portuguese for "Rede de Inovação e Pesquisa do Ensino de Química"), the Tutorial Education Programme (PET, abbreviation in Brazilian Portuguese for "Programa de Educação Tutorial"); the Applied Metal-Organic Frameworks Research Group and the Institute of Chemistry, located in Araraquara, at the State University of São Paulo.

Desenvolvimento de competências e habilidades em tecnologias verdes e sustentabilidade de jovens estudantes do ensino médio da rede pública através da produção de biopigmentos com microalgas da espécie *Dunaliella salina*

Valéria Belli Riatto¹ (PQ), **Fabiane Lima Santos**^{2,3} (PG), **Yasmin Santos Anunciação**^{2,4} (IC), **Fernando Leal Barreiros Moutinho**^{1,2*} (PG)

vriatto@ufba.br; fernando.vian@fieb.org.br

¹Instituto de Química, Departamento de Química Orgânica, UFBA; ²Serviço Social da Indústria, SESI-BA; ³Instituto de Educação, UFBA-UEFS; ⁴Instituto de Biologia, UFBA;

Palavras Chave: *Green skills*, *Desenvolvimento sustentável*, *Mulheres na Ciência*, *Microalgas*.

Highlights

Design of a green skills for public schools' young students. Principles for an education in green technologies and sustainable development. Women in science. Microalgae biomass as pigments in paints.

Resumo/Abstract

Abordagens educacionais baseadas no desenvolvimento de competências e habilidades verdes (*green skills*), são fundamentais para a formação e inserção de jovens dentro dos Objetivos de Desenvolvimento Sustentável (ODS), estabelecidos pela Assembleia das Nações Unidas em 2015.^{1,2} Contudo, ainda vivemos a presença-ausência de mulheres nas ciências, devido às inúmeras dificuldades que estas enfrentam em relação ao seu acesso e permanência em espaços de produção de conhecimento científico.³ Este contexto nos incentivou a participar, pela primeira vez, da 7ª edição do Programa Futuras Cientistas MCTI, do Centro de Tecnologias Estratégicas do Nordeste (CETENE),⁴ cujo escopo propõe aumentar o interesse e a participação de estudantes mulheres nas diversas áreas de ciência e tecnologia, promovendo a cooperação e o intercâmbio de informações com vistas a eliminar a discriminação contra a mulher e alcançar a igualdade de gênero em vários campos, sendo que um destes diz respeito ao tema mulher e ciência. Para tanto, foi desenvolvido um plano de trabalho para imersão de algumas jovens mulheres em ciência/ inovação e desenvolvimento sustentável, destinado a estudantes da rede pública. De acordo com o programa, foram selecionadas 05 jovens mulheres, estudantes do ensino médio de escolas estaduais da região metropolitana de Salvador/BA. O trabalho experimental foi realizado entre os dias 03 e 30 de janeiro de 2023, quando as estudantes tiveram a oportunidade de frequentar um laboratório de pesquisa e desenvolver um biopigmento para tinta látex, a partir de biomassa de microalgas da espécie *Dunaliella salina*. Neste período, as estudantes realizaram o cultivo das microalgas, extração de sua biomassa para obtenção do biopigmento e posterior aplicação em tinta látex. Ao final das atividades práticas, e de posse dos conceitos adquiridos, as estudantes consolidaram seus conhecimentos e descobertas em um relatório descritivo, que foi utilizado como base para a construção de uma apresentação oral que ocorreu durante a finalização do Programa, através de um evento virtual, que reuniu e envolveu todas as participantes inscritas. Nesta apresentação, foram discutidas as habilidades adquiridas e competências verdes desenvolvidas ao longo de todo processo experimental, destacando como as alunas aprenderam a utilizar recursos renováveis (biomassa) para o desenvolvimento de um produto sustentável (biopigmento), dentro de uma perspectiva aplicada e inserida nos 12 princípios da Química Verde. Esta oportunidade foi o primeiro contato destas jovens estudantes com um ambiente de pesquisa, resultando na construção de uma perspectiva de carreira na química, que até então era desconhecida por elas.

Referências:

1. NAKAMURA, M. *et al.*; **Navigating the Structure of Research on Sustainable Development Goals**. Institute for Scientific Information, Web of Science Group, 2019.
2. RAVINDRANATH, M. J. *et al.*; *International Journal of Education & Management*, **10(2)**, 175-178, 2020;
3. PATROCINO, L. B. *et al.*; *Caderno Espaço Feminino*, 33(1), 418-441, 2020.
4. <https://linktr.ee/futurascientistas>, acesso em 05/01/2023

Agradecimentos/Acknowledgments

CNPq, Capes, INCT E&A, SESI-BA, CETENE, MCTI.

Desenvolvimento de disciplina eletiva para o Ensino Médio com a temática relacionada aos Objetivos do Desenvolvimento Sustentável

Bruna de Araújo Costa (FM)^{1*}, Larissa Garcia Velasco (IC)², Denilsan Monteiro dos Santos (FM)¹, Felipe A. M. Rezende (PG)², Ana Paula C. Teixeira (PQ)^{3,4}, Rochel Montero Lago (PQ)^{3,4}, Nyuara A. S. Mesquita (PQ)^{2,4}, Márlon Herbert F. Barbosa Soares (PQ)^{2,4}

bruna.costa@ifgoiano.edu.br

¹ Colégio Estadual Jardim Europa. ² Laboratório de Educação Química e Atividades Lúdicas – Instituto de Química – Universidade Federal de Goiás. ³ Departamento de Química – Universidade Federal de Minas Gerais. ⁴ INCT-Midas.

Palavras-Chave: *disciplina eletiva; objetivos da química para o desenvolvimento sustentável; reciclagem; lixo.*

Highlights

Development of an elective course for High School with the theme related to the Sustainable Development Goals. This work presents the development of an elective discipline at the secondary level of education to discuss waste recycling and its relationship with the sustainable development goals (SDGs)

Resumo/Abstract

A Sociedade Brasileira de Química liderou o Movimento Química Pós 2022 - Sustentabilidade e Soberania, nos anos de 2021 e 2022. O objetivo principal deste movimento é desenvolver ações que reflitam sobre a contribuição da Química para a construção de uma sociedade mais sustentável e para a soberania do Brasil. Como resultado, foram criados dois Objetivos da Química para o Desenvolvimento Sustentável (OQDS)¹. O primeiro deles, OQDS 1, é "Promover a sustentabilidade através da Química na Educação Básica". Para alcançar esse objetivo, foram desenvolvidos cursos online para professores, produção de podcasts, experimentos e jogos educativos relacionados à temática da sustentabilidade, além de disciplinas eletivas sobre o assunto que serão oferecidas em escolas públicas. Este trabalho descreve a implementação de uma disciplina eletiva intitulada "Meio Ambiente" em um colégio público em Goiânia, Goiás, durante o período de janeiro a novembro de 2022, com a participação de 81 alunos. A abordagem adotada na disciplina utilizou a metodologia de pesquisa-ação educacional, que consiste em quatro etapas: identificação do problema, planejamento de soluções, implementação e monitoramento de ações e avaliação dos resultados. Em relação à identificação do problema, foi constatado que o descarte inadequado do lixo na escola era uma questão importante a ser resolvida. Um questionário prévio foi aplicado aos estudantes para avaliar o seu conhecimento sobre o assunto. Para o planejamento da solução do problema identificado, a professora e os estudantes criaram e identificaram lixeiras recicláveis na escola e sensibilizaram a comunidade escolar sobre a importância da temática Objetivos de Desenvolvimento Sustentável. Na implementação da ação, foi constatado um baixo nível de conhecimento sobre o correto descarte de resíduos, levando à elaboração de material de identificação das lixeiras, produção de textos, pesquisas científicas na internet e na biblioteca e efetiva resolução de exercícios sobre o tema. A comunidade escolar foi informada através de apresentações orais e divulgação nas redes sociais da escola. No monitoramento e avaliação, houve um aumento gradual na conscientização dos estudantes sobre a importância do correto descarte dos resíduos. Isso se mostrou positivo, especialmente em uma escola com uma grande quantidade de pessoas presentes por boa parte do dia. A partir do aumento na percepção da quantidade de lixo e tipo de descarte, os estudantes passaram a se sentir indignados e a mudar efetivamente suas atitudes em relação ao descarte de resíduos na escola. Para difundir as ações e resultados alcançados, eles produziram vídeos que foram compartilhados com a comunidade escolar, nas redes sociais da escola e nas redes sociais dos próprios estudantes. O impacto foi notável tanto na escola quanto na comunidade ao redor, já que os estudantes levaram o conhecimento adquirido na disciplina para suas casas e outras convivências, transformando-se em multiplicadores dessas informações.

¹Silva, I. F.; Nascimento, P.H. P.; Lago, R. M.; Ramos, M. N.; Galembeck, F.; Rocha Filho, R. C.; Teixeira, A. P. C. **Química Nova**, 45(4), 497-505, 2022.

Área: _____
(Inserir a sigla da seção científica para qual o resumo será submetido. Ex: ORG, BEA, CAT)

Desenvolvimento de metodologia de avaliação de impacto de atividades de extensão que visam a popularização da ciência para educação básica

Janaina de Paula e Silva (PG),¹ Wladimir T. Silva (PG),¹ Mikaelly V. S. Magalhães (IC),¹ Bárbara R. Vicensoni (IC),¹ Janice Henriques da Silva Amaral (PQ),² Rita C. O. Sebastião (PQ),¹

janainapaulasilva@ufmg.br; janainadepaulaesilva@gmail.com

¹⁻⁵Departamento de Química, ICEX, UFMG; ²Instituto de Ciências Biológicas, UFMG

Palavras-Chave: *Avaliação de impactos, Extensão, Divulgação científica, Popularização da ciência, Metodologia Delphi, Educação básica*

Highlights

Development of a methodology for evaluating the impact of extension activities for popularizing science at basic education. Mapping of indicators used to evaluate the impact of extension in universities. Development of a methodology for evaluating the impact of activities aimed at basic education.

Resumo/Abstract

A extensão universitária é um dos pilares que juntamente com o ensino e a pesquisa, definem o papel social que as universidades devem desempenhar. Discutir a extensão universitária é discutir a própria universidade como instituição e o papel social que ela desempenha.

Neste estudo, investigamos a concepção e o uso de indicadores de avaliação da extensão universitária. O objetivo principal é verificar a existência de indicadores que avaliem, de forma eficiente, o impacto de atividades específicas e propor uma metodologia simples e clara para esta avaliação. O foco do estudo são atividades de extensão que visam a divulgação científica e popularização da ciência dentro da Universidade Federal de Minas Gerais no período compreendido entre o ano de 2000 e 2022. Esse recorte foi dado à pesquisa após avaliação, junto às escolas de educação básica, da necessidade de tornar mais acessível a este público as atividades desenvolvidas pela academia, principalmente aquelas relacionadas às ciências químicas e físicas, porque são mais difíceis de serem compreendidas. Tais atividades de extensão, por vezes, acabam por tornar o ensino dessas disciplinas mais atrativo e interessante. Por se tratar de um conjunto grande de atividades, justifica-se então a necessidade de ter indicadores que meçam a qualidade e o impacto dessas ações junto à educação básica.

Para a evolução da pesquisa, foi necessário desenvolvermos um breve histórico do surgimento da extensão universitária, revisando o contexto e diversas fases, modelos e políticas adotados na universidade brasileira bem como o contexto histórico do desenvolvimento da avaliação no âmbito da extensão universitária. Como procedimentos metodológicos usamos a pesquisa exploratória, análise de documentos e a metodologia Delphi, utilizada como instrumento de coleta de dados de 20 especialistas em extensão universitária (Gupta e Clarke 1996). Os resultados da coleta serão transcritos e analisados, seguindo estratégias elaboradas por Laurence Bardin (2011), numa Análise de Conteúdo.

Como resultado, espera-se trazer um panorama atual sobre a avaliação da extensão universitária e uma proposta metodológica inovadora com indicadores chaves para avaliar, de forma clara, os resultados e impactos de relevância para atividades de extensão que são realizadas para o público da educação básica.

Referências:

- Bardin, Laurence. Análise de Conteúdo. Tradução Luís Antero Reto, Augusto Pinheiro. São Paulo; Edições 70, 2011.
- Gupta, U. G., Clarke, R. E. (1996). Theory and application of the Delphi technique: a bibliography (1975-1994). *Technological Forecasting and Social Change*, 53, 185-211.

Agradecimentos/Acknowledgments

The authors would like to thank INCT Midas, CNPq, FAPEMIG and UFMG/PRPq/Proex for financial support.

Desmistificando o uso de produtos domissanitários: uma lição de higiene que pode salvar vidas

Maria Júlia N. Pegorelli (IC)^{1*}, Ana C. Simões (IC)¹, Julia R. Rettodin (IC)¹, Erika Watanabe (TC)², Janksyn Bertozzi (PQ)², Alessandra Stevanato (PQ)².

mpegorelli@alunos.utfpr.edu.br

¹Departamento Acadêmico de Engenharia de Materiais, UTFPR – Campus Londrina; ²Departamento Acadêmico de Química, UTFPR – Campus Londrina.

Palavras-Chave: Coronavírus. Higienização. Pandemia.

Highlights

Demystifying the use of household products: a hygiene lesson that can save lives. With the arrival of the COVID-19 pandemic, the world found itself again in a changing situation. New habits were revealed, such as the use of a protective mask, and old habits perpetuated, such as the use of household products for hand hygiene. In this context, the project's main objective is to promote in the community reflections on hygiene habits resulting from the post-pandemic world in a practical way, so that it transforms the quality of life of those who were sensitized during the process.

Resumo/Abstract

Muito se têm discutido, recentemente, acerca do uso de produtos domissanitários para a erradicação da propagação do vírus SARS – CoV-2, responsável pelo início do colapso global em 2019. Em 2020, as vendas de álcool subiram mais de 85%, de sabão líquido mais de 33% e de antisséptico para as mãos mais de 623%. Com a flexibilização das medidas protetivas, é fundamental o trabalho de conscientização sobre a importância da higienização, em especial, locais com agrupamento de pessoas, como no caso de escolas. Diante dessa situação, foi pensado em um projeto de extensão que busca, desenvolver estratégias de educação sobre hábitos de higiene junto à comunidade escolar. O estudo baseou-se na proposta didática dos três momentos pedagógicos, atualmente incorporada em diversas propostas de ensino e, em especial, no ensino de química. Esta metodologia dialógico-problematizadora é organizada em três momentos com funções específicas: 1) *Problematização inicial*: momento em que o professor age como mediador, fomentando uma discussão de modo a explorar explicações, levantando as limitações do conhecimento; 2) *Organização do conhecimento*: momento em que são apresentados e organizados os conhecimentos para responder aos possíveis questionamentos que surgiram no momento anterior; 3) *Aplicação do conhecimento*: momento em que a situação inicial é analisada e interpretada com base nos conhecimentos expostos no segundo momento para que os estudantes possam responder a situação-problema. Sendo assim, este trabalho teve por objetivo analisar as contribuições da oficina denominada “Desmistificando o uso de produtos domissanitários: uma lição de higiene que pode salvar vidas”, apresentada na Escola Municipal Roberto Alves Lima Júnior, localizada na cidade de Londrina – PR, com 115 alunos, sendo turmas do 9º no do ensino fundamental, 1º, 2º e 3º anos do ensino médio, do período matutino. Em termos metodológicos, a pesquisa de abordagem qualitativa, foi desenvolvida a partir da análise de questionários, baseada na análise de conteúdo, no que se refere a três categorias: problematização inicial, organização do conhecimento e aplicação do conhecimento. Os alunos foram incentivados a pensar sobre as causas e consequências do uso de produtos domissanitários e sua implicação para reduzir a propagação do vírus Sars-Cov-2 (etapa que deve instigar os estudantes a levantarem hipóteses). Na organização do conhecimento, esclareceu-se o que foi a pandemia e a composição do coronavírus, a função de produtos domissanitários, importância da higienização. Essas atividades foram pensadas para promover a interação entre o aluno-aluno e professor-aluno, estimulando a autonomia na construção do conhecimento. Na etapa da aplicação do conhecimento, a situação problema foi retomada utilizando os conhecimentos científicos desenvolvidos na fase anterior. Antes da realização da oficina foram aplicados 115 questionários contendo 04 questões cada, havendo um índice de acerto de 62%, após a realização da oficina esse índice subiu para 79%. Os resultados evidenciaram as lacunas conceituais existentes no aprendizado dos alunos, principalmente o que se refere à dificuldade dos estudantes em conceituarem e relacionarem situações reais com os conhecimentos químicos apresentados e mostra a ainda a necessidade de ações em espaços de ensino que promovam uma aprendizagem significativa dos conceitos abordados.

Agradecimentos/Acknowledgments

Sociedade Brasileira de Química (SBQ)

À Universidade Tecnológica Federal do Paraná – campus Londrina e ao Departamento Acadêmico de Química, à PROREC/PROGRAD pela concessão da bolsa e a Escola Municipal Roberto Alves Lima Júnior.

Development of an augmented reality app for teaching isomers: the use of mobile devices as facilitators in the learning process of organic chemistry

Cibele Zanatta da Silva Pereira (FM),¹ Márcia Andreia Mesquita Silva da Veiga (PQ).¹

cibelezanatta@usp.br; marcia.veiga@usp.br

¹Chemistry Department, FFCLRP, University of São Paulo, Postal Code 14040-901, Ribeirão Preto, SP, Brazil.

Keywords: Augmented reality, QRCode, Isomerism, Organic Chemistry, Educational Technologies.

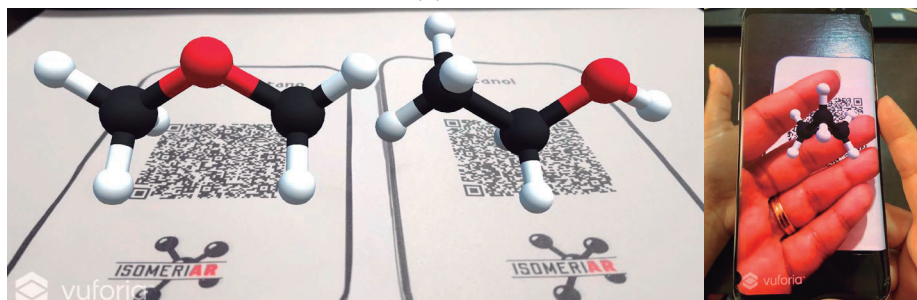
Highlights

An application was developed to teach isomerism through augmented reality and QRCode as markers. Three-dimensional images of organic compounds display on the screen of a mobile device, and the user can interact with these virtual molecules.

Abstract

Contemporary society has had its daily life modified and leveraged by the rise of the digital age, which has transported us to the information era. The use of smartphones in education is already a reality; nonetheless, high school students know a lot about the use of technology but need to be made aware of how to relate it to science and their daily lives. In this context, this research project aimed to use technologies such as augmented reality (AR), Quick Response Codes (QR Code), and online platforms in teaching isomerism in organic chemistry to high school students. For this purpose, we used programs such as Unity, Blender, Vuforia, and Jmol to develop an application called IsomeriAR. The application developed projected, successfully, on the screen of a mobile device, three-dimensional images of organic compounds allowing, besides the spatial visualization, the manual interaction of the user with the virtual molecules. It is, therefore, an immersive media because the student can manipulate, rotate, and zoom in and out the size of the virtual object and compare two structures simultaneously. To use this pedagogical resource, we present suggestions based on the strategy of active methodologies for learning organic chemistry, which provides the student with the development of autonomy, and protagonism, acting as a facilitator of the teaching-learning process. Molecular visualizers in AR are known to have been in use for a few years. In 2014, Colin Berry and Jason Board* presented the structure of a protein in AR. However, more than a 3D molecule viewer, this pedagogical resource, combined with a didactic sequence based on the strategy of active methodologies for learning organic chemistry, provides the student with the development of autonomy, and protagonism, acting as a facilitator of the teaching-learning process. The visualization and manipulation of molecules through the smartphone screen minimize the students' difficulty understanding spatial isomerism, arousing greater interest and engagement in the subject. The actual manipulation of these molecules is not feasible, so AR is an excellent pedagogical resource for teaching isomerism. The product developed is viable, and improvements are being made for its application in the classroom. (*) DOI 10.1002/bmb.20805

Methoxymethane and Ethanol - Function Isomers (a) and user interaction with the virtual molecule (b).



Source: Screenshot from author's smartphone

Acknowledgments

Coordenação de Aperfeiçoamento de Pessoal de Nível Superior (CAPES), PROFQUI, PRPG-USP

Development of pedagogical material in Computational Chemistry to Assist Organic Chemistry and Biochemistry learning

Edith C.M. Ordoñez (PG),^{1*} Adriano M. Gonçalves (PQ),² Nailton M. do Nascimento Junior (PQ)³

ecm.ordonez@unesp.br; adrianogoncalvesbio@gmail.com; nailtonjr@gmail.com

^{1,3}Departamento de Química, UNESP; ²Departamento de Química UNESP; UNIARA

Keywords: *Chemistry education; Computational Chemistry; Teaching material; 3D visualization*

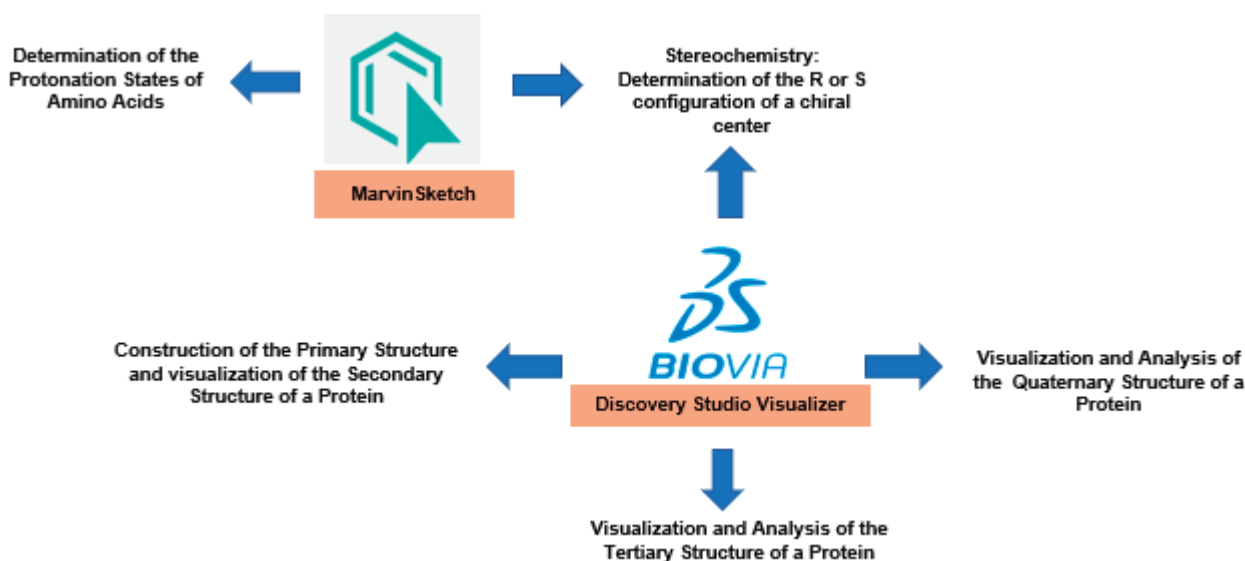
Highlights

Development of pedagogical material in Computational Chemistry to assist Organic Chemistry and Biochemistry.

Computational Chemistry can be used in university courses. Herein the development of video and written tutorials to assist in Organic chemistry and Biochemistry learning is presented.

Resumo/Abstract

Taking into account the importance of education in all sociocultural sectors and the modifications that have been carried out by world events in recent years such as the COVID-19 pandemic, the use of Computational Chemistry resources for teaching has been sought. In this sense two free softwar, MarvinSketch and Discovery Studio Visualizer, were used to develop pedagogical material through videos and written support tutorials to assist in Chemistry and Biochemistry learning. This kind of tools may contribute significantly to student learning, through a better visualization of the atomic world from a three-dimensional point of view and, in turn, train students to acquire a better technological performance throughout their research life, generating confidence in themselves to propose new solutions to the problems of science. The designed material approaches 5 important topics of Chemistry, being protein structure, states of protonation of molecules and stereochemistry for the determination of the absolute R, S configuration of a compound. A total of 9 videos and Y written materials were developed, and will be freely available on YouTube and Google Drive in mid of 2023. Presenting the following scheme for its application and later analyzing the respective results with the persecution of the students with this type of material.



Acknowledgments



Development of the SD Diagram for electronic distribution of all block D elements

Thalyta Raquel do Nascimento Alves (FM),^{1*} Francisco Adilson Matos Sales (PQ),²

thalyta.alves@prof.ce.gov.br; adilson.sales@ifce.edu.br

¹Secretaria de Educação do Estado do Ceará – EEM Beni Carvalho; ²Departamento de Ensino IFCE – campus Aracati

Keywords: *Electronic distribution, Transition elements, Rich-Suter diagram, Periodic table.*

Highlights

This research resulted in the development of the SD Diagram for the electronic distribution of elements of d block of the Periodic Table.

Resumo/Abstract

The electron configuration of an atom in its ground state is a topic covered at all levels of chemistry education - from 9th grade in Primary School until Higher Education. Students are usually taught to perform the electron distribution using Pauling's Diagram, which is based on Schrödinger's proposed model, filling the sublayers in increasing order of energy. The method is efficient for most chemical elements, especially the representative elements. However, it fails to describe the distribution of some transition elements in the d and f blocks in their ground state. Some chemistry teachers try to explain these anomalies by the fact that the semi-filled or fully filled orbitals are more stable. This claim could explain the electron distribution for some elements - such as Copper and Chromium - but it is not correct for anomalies in general - such as Niobium and Ruthenium, for example. Rich-Suter Diagrams^{1,2} are a useful tool for explaining the electron configurations of transition elements. These diagrams have as their main characteristic the energy of electrons with spin α (-1/2) and spin β (+1/2) not being the same, meaning that the two electrons in the 5s orbital, for example, have different energy due to their different spin angular momentum. Knowing this, this work proposes a new diagram based on Rich-Suter diagrams to facilitate the electron distribution of chemical elements in the d block. This diagram directs the electron distribution in a simple and coherent way optimizing the graphs proposed by Rich-Suter, contemplating the anomalous distributions that Pauling's diagram does not contemplate. In the SD Diagram, presented in Frame 1, the distinction of alpha and beta orbitals was not made, as this would make the diagram inconsistent, but it was assumed that the first filled s orbital will always be an s(α) orbital and the second will always be an s(β) orbital. A similar reasoning was performed for the d orbitals. In the diagram, a limit of electrons to be distributed was established depending on the transition period of the chemical element and only the valence electrons were considered for distribution.

Frame 1: SD Diagram for electronic distribution of block d elements.

		1st transition period					
		Limit of electrons	1 a 5	6 a 10	11 a 12	-	Limit of electrons
2st transition period	1 a 4 →	s	s	d	d	-	
	5 a 6 →	s	d	s	d	← 10 a 12	3st transition period
	7 a 9 →	d	s	d	s	← 7 a 9	
	10 a 12 →	d	d	s	s	← 1 a 6	

Source: Created by the author himself

Reference

¹ RICH, R. L.; SUTER, R. W.; Periodicity and Some Graphical Insights on the Tendency toward Empty, Half-full, and Full Subshells. *J. Chem. Educ.*, Vol. 65 (8), 702-704, 1988.

² OROFINO H.; MACHADO, S. P.; FARIA, R. B. The use of Rich and Suter Diagrams to Explain the electron configurations of transition elements. *Quim. Nova*, Vol. 36 (6), 894-896, 2013.

Agradecimentos/Acknowledgments



ELABORAÇÃO E VALIDAÇÃO DE UM INSTRUMENTO DE ANÁLISE PARA LIVROS DIDÁTICOS DE QUÍMICA NA TEMÁTICA NANOTECNOLOGIA

Diogo Ramos Pereira (IC),¹ Carla Juliana Silva Soares (PG),¹ Monique Gabriella Angelo da Silva (PQ).¹

Diogo.pereira@iqb.ufal.br

¹Instituto de Química e Biotecnologia, UFAL.

Palavras Chave: Instrumento de análise, Livro didático, Nanotecnologia.

Highlights

ELABORATION AND VALIDATION OF AN ANALYSIS INSTRUMENT FOR CHEMISTRY TEXTBOOKS ON THE THEME OF NANOTECHNOLOGY. The present work proposes an analysis instrument that serves to evaluate the theme Nanotechnology in a standardized way a textbook.

Resumo/Abstract

A Nanociência e Nanotecnologia são ramos da ciência moderna que englobam um conjunto de atividades e mecanismos em escala reduzida em prol do desenvolvimento científico, proporcionando a inovação de diversos setores. Desse modo, por ter ampla importância reconhecida na sociedade, este trabalho apresenta um instrumento de validação que serve para averiguar de forma **padronizada** como a temática vem sendo abordada nos livros didáticos de Química do PNLD. Para este trabalho, o instrumento foi i) elaborado e ii) validado com base na coleção Química Ser Protagonista dos PNLD (2012 – 2020) que é a coleção majoritariamente distribuída no Brasil.

Para a **criação do instrumento** se fez necessário uma revisão na literatura sobre os principais temas abordados na nanotecnologia para uma análise coerente da presença da temática no livro didático. Após a revisão foram definidos eixos temáticos para enquadrar os conteúdos a medida que aparecem no livro, são eles: *História e Conceitos em Nanotecnologia, Saúde, Fontes Energéticas, Meio Ambiente, Tecnologia e Pontos Negativos*. Tendo selecionado os eixos, as questões do livro foram integralmente analisadas e neles enquadradas pelos autores deste trabalho. Para validar essa análise se fez necessário que esse instrumento fosse aplicado por estudantes, professores, especialistas e pesquisadores com afinidade na temática Nanociência e Nanotecnologia.

A **validação do instrumento** foi realizada com 10 usuários seguindo as orientações de (SOUZA et al, 2017) que considera este quantitativo uma amostra significativa. A partir das respostas coletadas no formulário, utilizou-se o coeficiente de Kuder-Richarson ou KR20, como parâmetro estatístico, para avaliar a consistência interna dos resultados. Ver Figura 1. Na fórmula da figura 1, o “p” está relacionado ao número de pessoas na amostra que responderam as questões de forma correta; O “q”, relaciona o número de pessoas na amostra que responderam as questões de forma incorreta; Por fim, o “pq” são o produto de p e q.

Figura 1: Fórmula do coeficiente de Kuder-Richardson:

$$P_{KR20} = \frac{K}{K-1} \left(1 - \frac{\sum_{j=1}^k p_j q_j}{\sigma^2} \right)$$

Os resultados foram tratados via *excel*. Ver tabela 1.

Tabela 1 - Resultados de PKR20 da validação dos instrumentos de análise de Nanotecnologia:

K	12
$\sum pq$	2,07
varp	6,61
P_{KR20}	0,749277

O resultado obtido foi satisfatório. Visto que quanto mais próximo de 0,7 ou próximo a 1 for o resultado, mais próximo do ideal estará, por outro lado os valores abaixo de 0,6 são considerados insatisfatório (BISPO, CAZARINI, 2007).

Referência: BISPO, Carlos Alberto Ferreira; CAZARINI, Edson Walimir. **Teste do coeficiente de fidedignidade escolhido para ser utilizado na avaliação qualitativa paraconsistente**. Anais, 2007.

SOUZA, A. C. de; ALEXANDRE, N. M. C.; GUIRARDELLO, E. de B. **Propriedades psicométricas na avaliação de instrumentos. Avaliação da confiabilidade e da validade**. Epidemiologia e Serviços de Saúde, V. 2017.

Área: EDU

Elementos representacionais e conceituais das teorias de ligação química em livros-textos de Química para o Ensino Superior

Lucas César da Silva (FM),^{1,2*} Juliana Fedoce Lopes (PQ),² Evandro Fortes Rozentalski (PQ)³

lucasesardasilva1@gmail.com

¹Escola Estadual Professor Antônio Rodrigues d'Oliveira, EEPARO; ²Laboratório de Química Computacional LaQC, Universidade Federal de Itajubá, UNIFEI. ³Grupo de Pesquisa em Práticas Formativas e Educativas em Ciências e Matemática (PFECiM), Universidade Federal de Itajubá, UNIFEI.

Palavras Chave: Teorias de ligação, Ligação química, Livros didáticos, Orbitais.

Highlights

Representational and conceptual elements of chemical bonding theories in Chemistry textbooks for superior education could be misleading regarding to quantum chemical concepts.

Resumo/Abstract

Na literatura, diferentes trabalhos são encontrados sobre as representações utilizadas em livros textos de química para abordagem dos conceitos sobre a ligação química e a influência destas no ensino de seus conceitos. Nesses estudos, destaca-se o pouco singularismo admitido para cada teoria no que diz respeito às suas representações, dificultando a aprendizagem significativa¹. Desta forma, o seguinte trabalho teve como objetivo analisar os livros-textos de Química para o Ensino Superior quanto à abordagem dos modelos teóricos para ligação química, em particular, a Teoria de Ligação de Valência e a Teoria do Orbital Molecular. O referencial de análise destes livros se deu a partir dos construtos teóricos de Johnstone² que compreende os três níveis de representação do conhecimento químico: nível macro e tangível que envolve parâmetros fenomenológicos; o nível molecular e invisível que envolve a construção conceitual; e o nível simbólico e matemático que constitui as ferramentas representacionais.

Os livros selecionados para a análise foram definidos por meio de um questionário disponibilizado a professores do Ensino Superior de diferentes universidades, obtendo-se, porém, apenas respostas dos docentes da instituição de origem desta pesquisa. Foram analisados três livros de Química Geral e três livros de Química Inorgânica por meio da Análise Textual Discursiva. Este estudo identificou que as imagens utilizadas pelos livros para representar os orbitais atômicos e moleculares podem contribuir para interpretações incorretas dos conceitos que sustentam as teorias de ligação, como por exemplo, o entendimento de que é por meio de uma sobreposição física de orbitais atômicos que se obtêm os orbitais moleculares quando se representa a combinação linear dos orbitais por figuras com sombreados. Além disso, a não explicitação coesa das formas de obtenção e construção das imagens foi também considerado como elemento que pode acarretar dificuldades na aprendizagem de conceitos pelos estudantes. Observou-se uma similaridade entre os livros quanto às representações dos diagramas de orbitais moleculares para diferentes compostos e que em alguns deles não foi exposto de forma significativa a explicação para a inversão desses diagramas o que possibilita a construção incompleta de conceitos pelos estudantes.

Por fim, este trabalho destaca a importância do nível representacional para a construção de conceitos sobre ligação química nos livros-textos de Química e sua relação com o nível teórico e salienta ainda a necessidade de se procurar estratégias de complementação desses materiais para o cunho educacional, alçando a proposta da utilização das ferramentas da química computacional que podem vir a favorecer a elaboração de amostras visuais de representação molecular que abarque, por sua vez, a interpretação quântica dos modelos de ligação.

¹GÓMEZ, P. J.S.; MARTÍN, F. "QUANTUM vs. Classical" Chemistry in University Chemistry Education: A Case Study of The Role of History in Thinking the Curriculum. *Chemistry Education: Research and Practice*, v. 4, n. 2, p. 131-148, 2003.

²JOHNSTONE, A. H. Macro and Microchemistry. *The School Science Review*, v. 64, n. 227, p. 377-379, 1982.

Agradecimentos/Acknowledgments

UNIFEI, PPGMQ-MG, CNPq, FAPEMIG, CAPES.

Ensino do conteúdo de termoquímica no contexto da sustentabilidade usando a leitura de texto

Roberto A. Ribeiro (PQ).

roberto.ribeiro@ifnmg.edu.br

Instituto Federal do Norte de Minas Gerais- campus Salinas

Palavras Chave: Educação, Química, Leitura, Texto.

Highlights

Teaching thermochemistry content in the context of sustainability using text reading
Biodegestion and the Brazilian energy matrix were discussed. Discursive questions were answered and debated by the students. The method was efficient in promoting debate and satisfactory responses.

Resumo

Introdução

É muito comum o uso de leitura de texto em sala de aula para explorar um determinado conteúdo de Química. A leitura é uma habilidade essencial para a aprendizagem e a formação de leitores críticos¹. Dessa forma, foi elaborado um texto envolvendo a sustentabilidade e o conteúdo de termoquímica. A estrutura do texto é apresentada na Figura 1. O tema sustentabilidade foi conduzido a partir da definição de Boff² e aspectos de termo-

química como tipos de energia, unidades de medida e poder calorífico foram estudados. O trabalho foi desenvolvido em duas turmas do 2º ano do curso técnico integrado ao ensino médio de Agropecuária. Após a leitura, uma questão discursiva sobre o texto foi sorteada e respondida pela equipe de alunos. Em seguida, cada equipe expôs sua resposta para a turma e assim iniciar um debate. Será apresentado aqui um recorte do trabalho realizado, considerando apenas uma das turmas e duas questões respondidas pelos alunos. As questões foram: 1- “Descreva como o ser humano pode contribuir para a sustentabilidade do meio em que vive do ponto de vista social” e 2- “Calcule a porcentagem de aumento previsto na produção de energia na matriz de 2024 em relação à de 2026. Este aumento é necessário? Por quê?” As respostas foram analisadas através da análise textual discursiva³.

Resultados e Discussão

Na resposta da questão 1, foram identificadas as categorias: descarte adequado do esgoto doméstico, consumo consciente de água, energia e produtos industrializados, chamar a atenção das indústrias sobre o descarte de resíduos nos rios. Na questão 2, a categoria identificada na resposta dos alunos foi o aumento da população, sendo realizado corretamente o cálculo solicitado. As categorias da questão 1 estão relacionadas com o tema resíduo, o que está em consonância com a dica de sustentabilidade ecológica dada por Boff². Na questão 2, a categoria identificada mostra que os alunos associaram corretamente o aumento da produção de energia com o aumento da população. A realização do cálculo dentro do contexto descrito pode ter contribuído para os alunos compreenderem a necessidade e a importância da matemática na Química⁴. Sendo assim, os resultados obtidos foram considerados satisfatórios devido à coerência das respostas dadas e o cálculo correto.

Referências

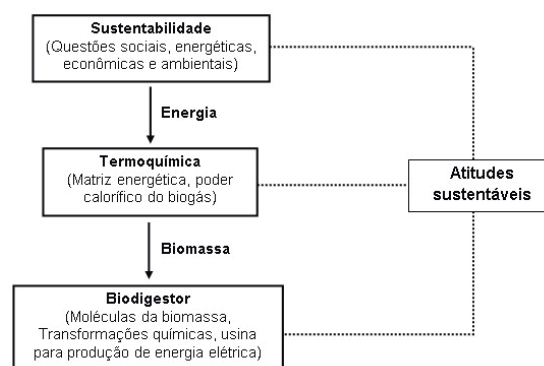
¹SOLE, I. Estratégias de leitura. Porto Alegre:Penso, 1998.

²BOFF, L. Sustentabilidade: o que é - o que não é. Petrópolis: Vozes, 2018.

³MORAES, R.; GALLIAZI, M. do C. Análise textual discursiva. Ijuí:Unijuí, 2016.

⁴SÁ, M.B.Z.; SANTIM FILHO, O. Revista Ibero-Americana de Estudos em Educação, v.12, 2017.

Fig. 1. Estrutura dos conteúdos do texto elaborado para a abordagem dos temas propostos.



Agradecimentos

Alunos(as) do 2º Ano de Agropecuária e profa. Daiane.

Excel software as a teaching tool in the teaching of Chemistry: Periodic properties and physics of elements.

Breno Kelison da Silva Braga (IC),^{1*} Francisco Adilson Matos Sales (PQ).¹

breno.kelison@gmail.com; adilson.sales@ifce.edu.br

¹Departamento de Ensino, IFCE – campus Aracati.

Palavras Chave: Excel, Periodic table, Properties of elements.

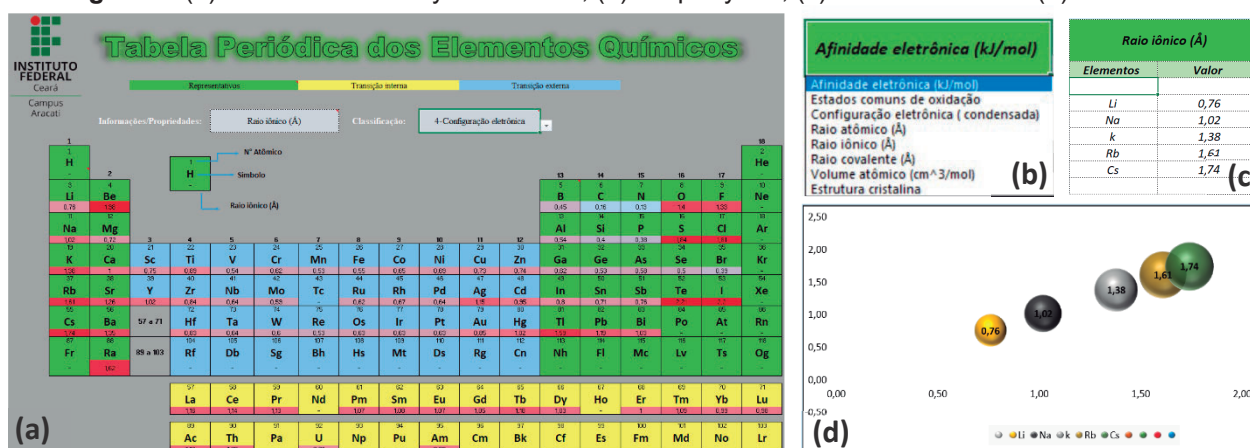
Highlights

This research resulted in the development of one Periodic table, which provides the creation of graphs with comparative effect of the properties of elements, which enables its use as a data source.

Resumo/Abstract

The present work was developed covering the study of information and communication technologies (ICT)¹ in Chemistry teaching, particularly on the periodic properties of elements, with the purpose of creating a teaching tool to aid students and teachers. All data presented in the worksheet were taken from the CRC Handbook of Chemistry and Physics 95th². Graphs are presented in the worksheet according to the property to be analyzed comparing data of certain elements and their properties in order to facilitate the presentation of the difference and similarity of these properties. The visual effect is presented through various types of graphs that aid in teaching. In this perspective, the Excel® software proved to be a great tool for creating teaching materials, despite some difficulties in use and limitations that the software has. Consequently, it was not possible to develop everything that was planned, given that, as a rule, we have little knowledge of a tool that has numerous resources. However, it was possible to develop a dynamic Periodic table in which the generated graphs can be used by teachers, for preparation of lessons, presentation of work, and development of theories, as well as serving a good source of knowledge, as it contains various data about the elements of the periodic table. The worksheet contains a total of 14 chemical and physical properties, 5 units of measurement, 16 graphs including some in 3D scale, 7 choice tabs, information on 118 elements, and 15 macros. Figure 1 presents the periodic table and the various resources available for its use.

Figure 1: (a) Overview of the dynamic table; (b) Property tab; (c) Element tab and (d) Bubble chart.



Reference

- 1 GUIARDI, M. M. M. A inserção das TICs no ensino fundamental: limites e possibilidades. Revista científica de educação à distância. vol. 2 (25), 2022.
- 2 HAYNES, W. M.; LIDE, D. R.; BRUNO, T. J. CRC Handbook of Chemistry and Physics: A Ready-Reference Book of Chemical and Physical Data, 95th, CRC Press, 2014.

Agradecimentos/Acknowledgments



Experimentação investigativa utilizando a palma de forrageira como ferramenta didática no ensino médio

Lorena C. N. Félix (PG),^{1*} Gabriel B. de L. Vitorino (IC),² Andréa M. S. S. Brito (PQ),² Maria J. F. Gomes (PQ),¹
jose.filqueiras@ufrpe.br; lorenaurpe@gmail.com

¹Departamento de Química, UFRPE; ²Unidade Acadêmica de Serra Talhada, UFRPE.

Palavras Chave: Experimentação Investigativa; Três momentos pedagógicos; Palma Forrageira, Kit experimental.

Highlights

Investigative experimentation using the forage palm as didactic tools in high school.
Experimental kits with forage palm as didactic material to aid in the teaching of chemistry.
Production of soap from forage palm.
Cochineal as a pH indicator natural.
Production of cake from palm flour.

Resumo/Abstract

A experimentação investigativa associada à contextualização, através da abordagem de questões sociais que fazem parte da realidade da comunidade na qual a escola está inserida, tem sido apontada como uma estratégia eficaz no ensino e aprendizagem de conceitos científicos e processos científico-tecnológicos. Entre as práticas pedagógicas de ensino, os Três Momentos Pedagógicos (3MP), que consiste em três etapas, a problematização inicial, organização do conhecimento e aplicação do conhecimento, é atualmente incorporada em diversas propostas de ensino, pois possibilita o aluno compreender a realidade de forma crítica e coletiva, se envolvendo ativamente em seu processo de formação. Com relação aos recursos didáticos, o uso de kits experimentais utilizando materiais alternativos de fácil acesso e/ou de baixo custo, é uma ferramenta bastante disseminada nas escolas que não possuem laboratórios equipados, pois permite o contato dos alunos com os fenômenos químicos, possibilitando a criação dos modelos que tenham sentido para eles, a partir de suas próprias observações, transformando-os em protagonistas do seu processo de aprendizagem. Nesse sentido, a presente pesquisa teve como principal objetivo analisar as contribuições de atividades didáticas pautada na abordagem experimental investigativa e na dinâmica 3MP, através do uso de três kits com experimentos (figura a), empregando a palma de forrageira (1b), na produção de bolo (figura 1c), sabão (figura 1d) e cochonilha como indicador de pH (figura 1e), de modo a promover a compreensão dos conteúdos separação de misturas, transformação da matéria, estequiometria, reações de ácido – base e reação de saponificação. As atividades foram desenvolvidas em uma turma do 3º ano do ensino médio, em uma escola localizada no município de Calumbi/PE, com o total de 14 aulas e duração de 50 min/aula. Para análises dos dados, 8 questionários mistos foram adotados e categorizados. Do total de 28 alunos que participaram, 61% eram residentes da zona rural e 93% responderam que relacionar os conceitos de química com os experimentos empregando a palma de forrageira, que está presente no cotidiano, facilitou o aprendizado. Com relação ao aprendizado dos temas propostos, 70,7% responderam de forma satisfatória, demonstrando assim que essa pesquisa promoveu diálogos entre os saberes populares, científicos e escolares, ampliando o conhecimento dos estudantes sobre a utilização da palma forrageira. Os resultados desta pesquisa culminaram na construção de uma cartilha, contendo a metodologia e as atividades realizadas com os kits experimentais.



Figura 1: (a) kit



(b) palma de forrageira



(c) bolo de palma



(d) sabão de palma



(e) indicador de pH

Agradecimentos/Acknowledgments

Feminismos e Academia: mulheres cientistas e o impacto da violência simbólica de gênero na carreira científica

Ana Luiza do Prado Lima (PG), Nyuara Araújo da Silva Mesquita (PQ), Márlon Herbert F. B. Soares (PQ),
analuzapradolima@gmail.com; marlon@ufg.br

Laboratório de Educação Química e Atividades Lúdicas – Instituto de Química – Universidade Federal de Goiás.

Palavras Chaves: Mulheres Cientistas; Feminismos; Violência Simbólica; Carreira Científica.

Highlights

Feminism and Academia: Women Scientists and the Impact of Gender Symbolic Violence on Scientific Career. This work presents the "dribble of pain" and the "scissor effect" as gender symbolic violence from the conversation with 12 researchers from a chemistry course at a federal university.

Resumo/Abstract

O gênero pode ser caracterizado como uma construção social, histórica e cultural, mantida por meio das relações de poder de um sujeito (masculino) operado contra outro sujeito (feminino)¹. Além do marcador gênero, aspectos interseccionais como raça, classe e sexualidade, também operam nesse sistema hierárquico de poder. Nesse sentido, enquanto produto cultural e social e moldada na noção binária de gênero, o campo científico é marcado pela exclusão feminina e a violência simbólica de gênero. Para Bourdieu (1997)² a violência simbólica está na consideração de que a hierarquia e a desigualdade social não são mantidas puramente pelo exercício da força física, mas através de simbolismos e significados que buscam subordinar determinados grupos. Um aspecto das violências simbólicas é que tendem a acontecer no campo do psicológico, da violência moral, somatizado por fatores culturais das hierarquizações de poder e desigualdades sociais, podendo evoluir para violências físicas. No sentido de procurar entender algumas violências simbólicas que pesquisadoras/professoras sofrem em seu ambiente acadêmico, conversamos com doze professoras de um instituto de química de uma universidade federal brasileira, a fim de compreender como estas relações são construídas. Dessa forma, apropriamo-nos da conversa como metodologia de pesquisa, que, conforme explicita Sampaio, Ribeiro e Souza (2018)³ “[...] *Assumir a conversa como metodologia de pesquisa significa, portanto, assumir que a investigação não tem objetivos fechados, mas interesses.*” Justifica-se ainda uma vez que, os conhecimentos expostos nas conversas, além de não hierarquizados são plurais e singulares. Após transcritas as conversas, gravadas via aplicativo de conversas em vídeo, foi possível perceber marcadores da violência simbólica de gênero a partir do “*drible da dor*” em que há a necessidade de uma descorporificação de características consideradas femininas para alcançarem novos espaços. Um dos relatos de uma pesquisadora, é representativo dessa violência: “*a gente tem que vestir uma carapuça de uma pessoa ruim, porque senão as pessoas passam por cima. [...] e eu começo a entender que é porque as mulheres não possuem espaço na área da ciência*” (P3). Outra violência simbólica de gênero se deu a partir do “*efeito tesoura*”, conforme relata outra professora, no que se refere ao fato de que não se conseguiu eleger uma mulher para um cargo de poder na própria instituição: “*ah... é essa situação do machismo... Não tem nenhuma outra explicação. Porque se a gente tem 50% de mulheres, inclusive muitas técnicas, eu penso que a gente já deveria ter tido uma oportunidade de eleger mulheres [...]*” (P6). À guisa de considerações finais, é perceptível a existência de fatores que contrapõem a ideia da neutralidade e meritocracia científica. À vista disso, é salutar destacar a urgência das discussões sobre a violência simbólica de gênero e seu impacto na carreira científica.

¹SCOTT, J. *Educação & Realidade*, v.15, n.2, p. 71-99, 1990.

²BOURDIEU, Pierre. *Meditações Pascalianas*. Paris: Seuil, 1997.

³SAMPAIO, C. S.; RIBEIRO, T.; SOUZA, R. *Conversa como metodologia de pesquisa: por que não?*. Rio de Janeiro: Ayvu, 2018.

Agradecimentos/Acknowledgments

À CAPES, pela bolsa concedida e ao Laboratório de Educação Química e Atividades Lúdicas, pelo espaço de acolhida e apoio.

Área: EC

Ferramenta Colaborativa para análise de livros didáticos com ênfase na temática sistema terrestre

Yuri J. S. de Lima (PG),¹ Maria J. R. Amaro (PG)², Monique G. A. Da Silva (PQ)³

Maria.amaro@iqb.ufal.br; yuri.lima@iqb.ufal.br; maria.amaro@iqb.ufal.br; monique.silva@iqb.ufal.br

¹Instituto de Química e Biotecnologia, UFAL; ²Instituto de Química e Biotecnologia UFAL

Palavras Chave: (Indicadores, alfabetização científica).

Highlights

COLLABORATIVE TOOL FOR ANALYSIS OF TEXTBOOKS WITH EMPHASIS ON THE THEME "EARTH SYSTEMS": This work proposes a textbook evaluation tool on the Earth system theme as a way of unifying the analysis of questions. Allowing the teacher to select what the student will develop. We selected high school chemistry books to be protagonists of the last three years. In analyzing the questions by thematic axes and considering the indicators, we used the Kuder-Richardson equation (KR 20) which stipulates reliability and for criterion validity we used the gold standard

Resumo/Abstract

Para qualificarmos se um livro didático de química possui potencial de alfabetização científica em uma determinada temática, é necessário uma ferramenta que proporcione essa análise de maneira padronizada para que possa ser reproduzida por qualquer outro investigador. Este trabalho apresenta uma ferramenta de análise para a investigação da temática Sistemas Terrestres em livros didáticos de química. A coleção analisada pelos autores foi a Química Ser protagonista do último triênio do PNLN sob a luz dos indicadores de alfabetização científica propostos por Pizarro. Para a construção da ferramenta foram selecionadas 20 questões aleatórias do livro enquadradas como parte do conteúdo Sistemas Terrestres e enviadas para um grupo seletivo de pesquisadores, especialistas na área, professores e estudantes para analisarem as questões e classificarem segundo os indicadores. Foi utilizada a equação de Kuder-Richardson (KR 20) que estipula a confiabilidade. E para a validade de critério utilizamos a do padrão ouro. O método de confiabilidade, Kuder-Richardson estabelece valores que podem ter resultado confiável ou não, conforme a imagem a seguir: Neste trabalho os resultados possuem valores confiáveis, tanto para os indicadores (0,82237), como para os eixos temáticos (0,80717). O intervalo de confiança dado pela KR 20 está entre 0,70 e 0,90

Condição	Kuder-Richardson (KR)
Não-recomendado	< 0,70
Aceitável	$0,70 \leq KR \leq 0,79$
Recomendado	$0,80 \leq KR \leq 0,90$
Não-recomendado	> 0,90

Parâmetro Ideal:
 $0,70 \leq KR \leq 0,90$

Referência

Pizarro, Mariana Vaitkunas. **Alfabetização científica nos anos iniciais: necessidades formativas e aprendizagens profissionais da docência no contexto dos sistemas de avaliação em larga escala.** / Mariana Vaitkunas

Pizarro, 2014 355f.: il.

RICHARDSON, R. J. **Pesquisa Social: métodos e técnicas.** 3. ed. São Paulo, Atlas, 1999. 334 p. ISBN: 85-224-2111-0.

Flash Cards of the Periodic Table

Rodrigo Alves de Souza (FM) ¹rodralves@gmail.com¹ Secretaria da Educação do Estado de São Paulo, Diretoria Regional de Ensino de Araraquara, Araraquara/SP, Brasil.

Palavras Chave: Flash cards, Ferramenta pedagógica, Tabela periódica, Ensino Médio, Sequência didática.

Highlights

A pedagogical tool named flash card (FC), integrating analogic and digital concepts applied to periodic table.

Resumo/Abstract

Apesar de ser um instrumento versátil e capaz de compilar variadas informações, a tabela periódica carrega consigo um “título” de algo difícil na Educação Básica. Segundo Trassi e colaboradores [1] se pratica, em muitas escolas, um ensino da tabela que privilegia a teoria pautada em componentes complexos, vinculada a memorização de elementos e de suas propriedades, apenas, sem considerar as necessidades do alunado. Além disto, as dificuldades enfrentadas pelos docentes para tratar de tabela periódica e temas correlatos são relatadas [2].

Para conturbar a questão, os aspectos históricos, observados na década anterior, apresentavam-se dissociados do conteúdo específico, tanto nas obras do Plano Nacional do Livro Didático, da Educação Básica [3], como em muitos livros de Química Geral, adotados para o nível Superior [4]. Neste último caso, trazendo pouca importância à abordagem histórica ou, quando tratada, reforçando concepções impróprias.

Todavia, encontram-se alternativas interessantes para se trabalhar a temática, ora envolvendo o viés lúdico [5] e recursos em espaços não formais [6], ou mesmo as plataformas de vídeos, como o caso do canal *Periodic Videos* [7]. Contudo, as duas últimas são limitadas, seja pela localidade inacessível ou pela barreira do idioma.

Portanto, suprir a escassez de recursos com as possibilidades analógicas (“o fazer” com materiais acessíveis), integrando-se o universo da internet, comum ao cotidiano estudantil, parece estratégico para driblar as dificuldades estruturais/materiais e se compatibilizar aos modos contemporâneos dos jovens.

Assim, o objetivo deste trabalho foi desenvolver uma ferramenta pedagógica nomeada *Flash card*, junto com os discentes, de maneira a promover uma maior apropriação e aproximação deles aos conteúdos da tabela periódica.

As atividades ocorreram em uma escola pública estadual do Programa Ensino Integral, em Araraquara/SP, com três turmas da primeira série do Ensino Médio. As turmas personalizaram os elementos a partir de uma escolha prévia, de cada estudante, orientada pelo docente. Assim, tiveram entre 24 e 26 elementos produzidos nos FC por turma. O conteúdo envolvia “Símbolos dos elementos e equações químicas” e “Organização dos elementos de acordo com suas massas atômicas na tabela periódica”, conforme previsto no Currículo do Estado [8].

Cada FC foi concebido a partir da metade de uma folha A4 (148,5 mm × 105 mm). Na frente continha o símbolo do elemento, em destaque, e o nome. No verso, um resumo de informações oriundas das pesquisas de cada discente, para o seu respectivo elemento. Tais informações faziam alusão ao WWW da internet e ao ‘atalho’ de indagações da Língua Inglesa, sendo W1 = *where* (onde estaria inserido ou localizo o elemento), W2 = *what* (o que compõe ou qual fonte natural ele faz parte) e W3 = *with* (com quem ou como reage quimicamente o elemento).

Desde as orientações iniciais até a produção final da ferramenta foram transcorridos 500 min de uma sequência didática, incluindo-se exposições (do docente) sobre a organização dos elementos na tabela, tira dúvidas, momentos de pesquisa estudantil, revisões dos FC produzidos e a socialização deles. Ocorreram também debates, curiosidades levantadas e a possibilidade de se observar a criatividade exposta nas personalizações dos FC, com cores ou ilustrações, que remetiam ao uso do elemento ou alguma característica marcante dele.

Notaram-se uma variedade ampla de elementos apresentados nos FC, incluindo-se representantes de todas as “famílias” comumente tratadas no Ensino Médio, bem como metais de transição e até elementos transurânicos.

A personificação indivíduo–produção nos FC gerou uma extensão de pensamentos daquilo que os estudantes assimilaram, fosse na confecção do trabalho ou sobre o elemento químico. A transposição individual–coletivo se deu de modo proveitoso, já que na dialogicidade da sequência das aulas se teve maior participação estudantil nos debates que em aulas outrora ocorridas, antes dos FC produzidos. Segundo os relatos deles, em sua maioria, a atividade foi estimulante, rompendo-se a ideia prévia de que a tabela seria algo tão dificultosa para a aprendizagem.

[1] TRASSI, R. C. M.; et al. *Acta Scientiarum*, v. 23, n. 6, p. 1335–1339, 2001.[2] FERREIRA, L. H.; CORREA, K. C. S.; DUTRA, J. L. *Química Nova na Escola*, v. 38, n. 4, p. 349–359, 2016.[3] MEHLECKE, C. M.; et al. *Revista Electrónica de Enseñanza de las Ciencias*, v. 11, n. 3, p. 521–545, 2012.[4] LEITE, H. S. A.; PORTO, P. A. *Química Nova*, v. 38, n. 4, p. 580–587, 2015.[5] PINHEIRO, I. A. M.; et al. *Holos*, v. 8, p. 80–86, 2015.[6] CÉSAR, E. T.; REIS, R. C.; ALIANE, C. S. M. *Química Nova na Escola*, v. 37, n. 3, p. 180–186, 2015.[7] YouTube. *Periodic Videos*. Disponível em: <<https://www.youtube.com/user/periodicvideos>>. Acesso: 12 fev. 2023.[8] GOVERNO DO ESTADO DE SÃO PAULO. *Currículo do Estado de São Paulo*: Ciências da Natureza e suas tecnologias. São Paulo: SE, 2011.

Identificação de Conceitos de Limiar na Disciplina de Química Orgânica

Kerlyn K.M. Hiraga (PQ)¹, Antonio Aprigio da Silva Curvelo (PQ)¹

kerlynk@usp.br

¹Instituto de Química de São Carlos, IQSC-USP;

Química Orgânica; Ensino Superior; Conceitos Limiares; Conceitos Portais; Estudo de Caso.

Highlights

Identification of Threshold Concepts in Organic Chemistry Class. In a class of Organic Chemistry with the aid of a conceptual diagnostic tool developed we identified topics of difficulties, the propagation of such difficulties and Threshold Concepts.

Resumo/Abstract

A partir de um estudo de caso com embasamento teórico na teoria da Aprendizagem Significativa foi realizado um mapeamento curricular conceitual da disciplina de Química Orgânica I do curso de Bacharelado em Química do IQSC-USP. Este mapeamento foi a base para o desenvolvimento de uma ferramenta diagnóstica conceitual capaz de investigar tanto os tópicos nos quais os estudantes apresentaram dificuldades, como a propagação destas dificuldades ao longo do desenvolvimento da disciplina. Através das análises realizadas e dos resultados obtidos, um aspecto relevante para o processo de Aprendizagem Significativa, a Estase Conceitual, pôde ser verificada. A Estase conceitual considera a natureza não pontuada da aprendizagem, ou seja, que aprender é um processo não linear que inclui longos momentos de estagnação seguidos de momentos de rápida aprendizagem (Land & Meyer, 2006). De acordo com esse processo, existem conceitos, denominados Conceitos Limiares ou Conceitos Portais (**Figura 1**), que segundo Kinchin (2010, p. 54) "... são alguns conceitos - chave de uma disciplina que devem ser ultrapassados, antes que um aluno necessite desenvolver sua compreensão além de um nível de iniciante". Através da investigação do aproveitamento dos estudantes, observou-se que aqueles que apresentaram desempenhos superiores obtiveram representativa diferença de aproveitamento em comparação aos demais estudantes no conceito de *Orbitais Atômicos e Orbitais Moleculares*. Também, em análises onde foram utilizados grafos, observou-se expressiva diferença de aproveitamento neste conceito. Desta forma, a partir dos pressupostos acima descritos é que se propõe que o conceito de *Orbitais Atômicos e Orbitais Moleculares* se caracterize como um conceito Portal para a disciplina de Química Orgânica.

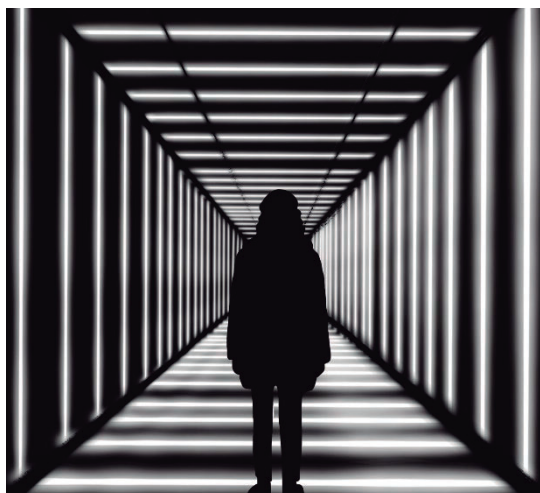


Figura 1: De acordo com Meyer e Land (2006) os conceitos limiares são portais que dão acesso a formas características de pensar e praticar que uma comunidade possui. Atravessar esses portais equivale a pertencer, participar e por consequência contribuir com uma determinada comunidade. Segundo os mesmos autores, um conceito portal, deve ser um conceito:

- Transformativo,
- Irreversível,
- Integrativo
- Limitado e
- Potencialmente Problemático

Agradecimentos/Acknowledgments

Instituto de Química de São Carlos (IQSC-USP), Conselho Nacional de Desenvolvimento Científico e Tecnológico (CNPq).

Kinchin, I. M. (2010). Solving cordelia's dilemma: threshold concepts within a punctuated model of learning. *Journal of Biological Education*, 44(2), 53–57. <https://doi.org/10.1080/00219266.2010.9656194>

Land, R., & Meyer, J. H. F. (2006). Overcoming barriers to student understanding: Threshold concepts and troublesome knowledge. In *Overcoming Barriers to Student Understanding: Threshold Concepts and Troublesome Knowledge*. <https://doi.org/10.4324/9780203966273>

Área: EDU

Nº de Inscrição: _____

Impactos da implementação de um Caso Investigativo para o ensino de Química Inorgânica na motivação de estudantes de um curso de bacharelado em Química

Vitor H. V. Rodrigues (IC)^{1*}, Carolina M. Primo (PG)¹, Regina Frem (PQ)¹, Amadeu M. Bego (PQ)¹.

vitor.vieira@unesp.br; amadeu.bego@unesp.br.

¹ São Paulo State University (UNESP), Institute of Chemistry, Araraquara, Brazil.

Palavras-chave: Case Studies, Motivation, Metal Organic Framework.

Destaques

Quais os impactos da implementação de um Caso Investigativo sobre MOFs (Metal-Organic Frameworks) na motivação de estudantes de um curso de bacharelado em química?

Resumo

O ensino de química na graduação, em geral, apresenta características do modelo tradicional de ensino, em que o professor é considerado a figura central e o detentor do conhecimento em sala de aula, tendo como finalidade a transmissão dos conteúdos para os alunos em aulas puramente expositivas. Os alunos se reduzem a meros expectadores da aula e recorrem a técnicas de memorização e reprodução mecânica dos conteúdos. A literatura tem apontado que essa metodologia pode acarretar em diversos impactos, como falta de interatividade no processo de ensino e aprendizagem, baixa autonomia dos estudantes, além da reprodução do conteúdo de forma acrítica e mecânica. Esses impactos podem influenciar a motivação dos estudantes em sala de aula. Nesse sentido, há algum tempo a literatura vem discutindo sobre as potencialidades do uso de Casos Investigativos (CI) como estratégia didática inovadora em aulas de ciências, inclusive no ensino superior, possibilitando o desenvolvimento do protagonismo do aluno e incentivando sua aprendizagem ativa e auto-dirigida. O objetivo deste trabalho foi investigar os impactos da implementação de um CI na motivação de estudantes de um curso de bacharelado em química de uma universidade pública do interior do estado de São Paulo. O CI utilizado na intervenção pedagógica visa o ensino de Química Inorgânica, especificamente para o conteúdo de Metal-Organic Frameworks (MOF), abordando a síntese, caracterização e aplicação forense de uma MOF luminescente. O CI em questão foi elaborado no contexto do Programa de Educação Tutorial (PET-Química) e foi baseado em Textos de Divulgação Científica sobre as produções científicas de um grupo de pesquisa da universidade. Para a coleta de dados foram utilizados instrumentos propostos e validados pela literatura especializada e a gravação audiovisual das aulas. O CI implementado apresentou o formato interrompido, ocorrendo em 3 aulas distribuídas ao longo de 3 semanas. Para avaliar a motivação dos alunos, a pesquisa foi fundamentada na Teoria da Autodeterminação (TAD) e foram utilizados três questionários já validados internacionalmente: Science Motivation Questionnaire; Basic Psychological Needs in General e Perceived Competence for Learning. Esses questionários foram aplicados ao longo das semanas de intervenções a fim de medir e possibilitar análises estatísticas acerca da variação de motivação dos alunos. A análise dos dados possibilitou a investigação do perfil motivacional dos estudantes da turma e sua relação com a tendência e a variação das escalas ao longo do processo durante 3 semanas. Os resultados mostram a potencialidade do uso dos CI nas aulas de Química da graduação no que diz respeito a um impacto positivo na motivação dos graduandos quanto à autonomia, ao vínculo e à competência.

Agradecimentos

Ao CNPq, à Rede de Inovação e Pesquisa no Ensino de Química (RIPEQ), ao Programa de Educação Tutorial (PET), ao grupo de pesquisa Applied MOFs e ao Instituto de Química da Unesp de Araraquara.

Inductive effect as a Didactic Resource for General Chemistry Content in High School

Eduardo L. Silva (PG),¹ **Marcelo V. Migliorini** (PQ),^{*1,2}

eduardo-silva04@uergs.edu.br; marcelo-migliorini@uergs.edu.br

¹PPGSTEM - UERGS Guaíba; ²Engenharia de Bioprocessos e Biotecnologia UERGS – Santa Cruz do Sul.

Palavras Chave: *Inductive effect; Eletronegativity; meaningful learning.*

Highlights

Inductive Effect is an important tool for understanding molecular structure and reactivity; The relationship with electronegativity is possible for a better understanding of contents about General Chemistry contents.

Resumo/Abstract

The inductive effect is characterized by being an important tool within the concepts of structure and reactivity involving the discipline of Organic Chemistry at advanced levels when compared to high school. In the traditional approach to Teaching Chemistry at secondary level,¹ students are presented with a series of contents, approached, in general, in a fragmented way, making it difficult for them to understand and perceive their interrelationships.²

Thinking about favoring a Meaningful Learning, the present work investigates the applicability of the concept of Inductive Effect, based on electronegativity, as a link between the different chemical concepts (such as: bond polarity, acid-base theory, among others), aiming to collaborate in understanding the correlation of structures and properties of molecules through conceptual reframing.

According to Ausubel, the essence of the Meaningful Learning process is that the ideas expressed symbolically are related to information previously acquired by the student through a non-arbitrary and substantive relationship. As such, concepts serve as meaningful and strategic anchor points. Accordingly, Moreira points out that the conceptual reframing, based on a base concept that serves as a conducting wire for correlations, can lead to the formation of a more consistent meaningful learning about the concepts considered relevant, since they will be expanded among the other conceptual structures.

Having as a reference the Significant Learning proposed by Ausubel and Moreira,³ an applied, participatory and open action research is in the execution phase, with a target audience of 150 high school students from the Escola Estadual de Ensino Médio Bento Gonçalves, located in Canoas-RS. The expected results turn to the consistent conceptual chemical alignment, without fragmentations, providing a better cognitive development.

References:

- [1] MORTIMER, E.F.; MACHADO, A.H.; ROMANELLI, R.I. A proposta curricular de Química do estado de minas gerais: fundamentos e pressuposto. *Química Nova*, 23(2), 2000. p.274
- [2] OLIVEIRA, M.A.M, Ressignificação da maior parte dos conceitos de Química no Ensino Médio, através do assunto eletronegatividade, Dissertação de Mestrado, 2022. PPGSTEM-UERGS.
- [3] MOREIRA, M.A.; MASINI, E.F.S. *Aprendizagem Significativa. Condições para sua ocorrência e lacunas que levam a comprometimentos.* São Paulo: Vetor, 2008.

Agradecimentos/Acknowledgments

PPGSTEM-UERGS

Interdisciplinarity in Teaching Radioactivity

Thalita F. M. de Souza (FM)*,¹ **Gilze B. C. Borges (FM)**,¹ **Andresa F. B. Guimarães (FM)**,¹ **Siméa P. C. Ceballos (FM)**,¹ **João U. V. Filho (FM)**,¹ **Paula R. F. Arruda (FM)**,¹ **Isabel C. V. B. Bastos (FM)**,² **Luis G. M. Santos (FM)**,¹ **Lilian V. Silva (FM)**.¹

thalita.menegassi@ifsuldeminas.edu.br

¹Instituto Federal de Educação, Ciência e Tecnologia do Sul de Minas Gerais (IFSULDEMINAS) Campus Avançado Carmo de Minas; ²Instituto Federal de Educação, Ciência e Tecnologia do Ceará (IFCE) Campus Cedro

Palavras Chave: *Filme, Ciências da Natureza, Ciências Humanas, Linguagens e Ensino Remoto.*

Highlights

Teaching sequence integrating scientific knowledge with historical-cultural aspects about Radioactivity for contribution of technical and humanistic development of the students.

Resumo/Abstract

Este resumo tem como objetivo apresentar a atividade interdisciplinar realizada a partir do tema central Radioatividade envolvendo as áreas do conhecimento de Ciências da Natureza e suas Tecnologias, de Ciências Humanas e Sociais Aplicadas, de Língua Portuguesa, de Arte e da área técnica de Alimentos. A proposta de trabalho buscou uma abordagem para o ensino de radioatividade que integrou os conhecimentos científicos aos aspectos histórico-culturais, contribuindo para a construção de uma visão de ciência não dogmática, dinâmica e social. A atividade foi realizada nos meses de junho e julho de 2020 com as duas turmas do 3º ano dos Cursos Técnicos Integrados oferecidos pelo campus. Cabe ressaltar que todas as atividades foram realizadas por meio do ensino remoto devido a pandemia da COVID-19. Os estudantes foram divididos em 5 grupos contendo de 4 a 6 integrantes, e a atividade foi realizada em 4 etapas. Na Etapa 1, os estudantes assistiram ao filme "Radioactive" (Radioativo) que é uma cinebiografia da cientista Marie Curie mostrando a sua trajetória na Ciência e as suas descobertas que mudaram o mundo. Após um momento de discussão, cada grupo preencheu um formulário eletrônico com questões sobre o filme e o seu impacto na sociedade. As respostas das questões foram o ponto de partida para as próximas discussões sobre o tema. Em seguida, na Etapa 2, cada grupo elaborou uma manifestação artística e, orientado pelos professores das disciplinas, aprofundou os estudos em 5 subtemas, que foram: I - A influência dos contextos histórico-social e filosófico na produção dos conhecimentos acerca da radioatividade e a mulher na comunidade científica; II - As aplicações da radioatividade na química e na física; III - As aplicações da radioatividade na medicina, na saúde e nos processos de datação; IV - Irradiação de alimentos e aplicação industrial; V - Fissão e fusão nuclear: acidentes radioativos e aspectos ambientais. Com o objetivo de promover um espaço para os alunos desenvolverem a expressão verbal, foi realizado, na Etapa 3, um seminário em que cada grupo apresentou o seu respectivo subtema e a sua manifestação artística aos demais estudantes e professores. Por fim, na Etapa 4, os estudantes elaboraram individualmente uma produção textual dissertativa-argumentativa para o desenvolvimento da sua escrita. Após a realização da atividade interdisciplinar, os professores concluíram que a proposta de trabalho cumpriu com os objetivos definidos. Os estudantes foram engajados e apresentaram resultados finais demonstrando excelente compreensão dos conteúdos técnico e científico. Além disso, as discussões realizadas durante a atividade interdisciplinar contribuíram para a formação humanística dos estudantes prevista pelo IFSULDEMINAS.

Agradecimentos/Acknowledgments

Instituto Federal de Educação, Ciência e Tecnologia do Sul de Minas Gerais (IFSULDEMINAS).

Intervenção didática baseada na experimentação investigativa para o estudo de ácido-base no Ensino Médio

Maria C.N. Nogueira_(FM)*,¹ Ivoneide L. C. Barros (PQ)², Verônica T. S. Batinga (PQ)².

ivoneide.lopes@ufrpe.br; cibellynovaes@gmail.com

¹EREM Antônio Gomes de Lima; ²Programa de Mestrado Profissional em Rede Nacional – PROFQUI/UFRPE

Palavras Chave: Ácidos, Bases, Solo, Experimentação Investigativa, Ensino Médio

Highlights

Didactic intervention based on investigative experimentation for the study of acid-base in high school.

Investigative experimentation for acid-base approach.

Contextualized teaching based on the reality of rural school students.

Easy-to-reproduce didactic intervention for chemistry teachers.

Resumo/Abstract

A experimentação investigativa parte de problemas que possam interessar os alunos a participarem da investigação, na qual eles irão buscar informações, propor e/ou testar hipóteses, elaborar explicações sobre o fenômeno em estudo, discutir os resultados da resolução dos problemas em grupos, e elaborar as conclusões acerca do problema. No Ensino Médio, o conhecimento sobre ácidos e bases é fundamental para a formação de conceitos em química, uma vez que possuem grande aplicação no dia a dia. Contudo, é pouco relacionado com as outras áreas do conhecimento e com a própria vivência do estudante. Por isso, eles têm dificuldades de estabelecer relação deste conteúdo com fenômenos que ocorrem no cotidiano. Nessa perspectiva, foi desenvolvida uma pesquisa com 46 estudantes de escola pública do sertão pernambucano, a fim de analisar as possibilidades de uma intervenção didática, com base na experimentação investigativa, para o estudo de ácidos e bases, no 3º ano do Ensino Médio. A metodologia usada apresentou elementos da experimentação investigativa, com nível um de abertura de investigação, constando de cinco etapas: (i) avaliação diagnóstica, (ii) proposição, (iii) resolução de problemas, (iv) sistematização dos conhecimentos de forma coletiva e (v) avaliação, sendo esta correspondente à sistematização individual do conhecimento aprendido. O conteúdo - ácidos e bases - foi abordado partindo de dois problemas articulados à experimentação investigativa, nos quais foram levados em consideração para sua elaboração o cotidiano do aluno e o contexto em que escola está inserida. O primeiro consistiu na identificação da acidez e basicidade de alguns materiais de limpeza. O segundo considerou a análise da acidez e basicidade de solos, já que a pesquisa foi realizada numa escola de área rural. A análise dos conhecimentos prévios (etapa i) mostrou que poucos estudantes sabiam definir ácidos e bases e relacioná-los aos temas solos e materiais de limpeza. Dentre as poucas tentativas de respostas foi observada a existência de diferentes concepções alternativas para o conceito de ácidos e bases; sendo mais abordado o conceito de ácidos, e sempre associando-o a algo perigoso e corrosivo e, também a alimentos. Houve participação efetiva dos estudantes na experimentação proposta para a resolução dos problemas, resultando em maior engajamento e apropriação dos conteúdos estudados à medida que analisavam, formulavam e testavam suas hipóteses de respostas, contribuindo para a construção do conhecimento. A validação das respostas dos estudantes à avaliação (etapa v) consistiu na proposição de um novo questionário sobre o conhecimento químico envolvido nos problemas propostos. A análise dos resultados do processo de resolução de problemas e do questionário mostrou que a experimentação investigativa foi bem aceita pelos alunos e contribuiu para aprendizagem dos conceitos de ácidos e bases no contexto do tema solos e materiais de limpeza, sendo de fácil reprodutibilidade, podendo ser adaptada de acordo com a realidade da escola, e adotada por professores de química que buscam uma participação ativa dos estudantes no processo de ensino.

Referências:

[1] SOUZA, F.L. et al. Atividades experimentais investigativas no ensino de química. São Paulo: Edusp, 2013.

[2] BRUNING, V.; ZORZI DE SÁ, M. B. Uma Abordagem sobre Ácidos e Bases no Cotidiano: Trabalhando com Atividades Experimentais Investigativas na Educação Básica. Os Desafios da Escola Pública Paranaense na Perspectiva do Professor PDE. V. 1, 2013.

[3] LEÃO, A.F.C.; GOI, M. E. J. Revisão de literatura sobre a experimentação investigativa no ensino de ciências. Comunicações Piracicaba | v. 28 | n. 1 | p. 315-345 | jan.-abr. 2021 DOI: <http://dx.doi.org/10.15600/2238-121X/comunicacoes.v28n1p315-345>.

Agradecimentos/Acknowledgments

Ao Programa de Mestrado Profissional em Química em Rede Nacional – PROFQUI/UFRPE e à Escola de Referência em Ensino Fundamental e Médio Dário Gomes de Lima.

Área: **EDU**

Kit impresso por 3D para uma nova aplicação dos indicadores naturais de pH nas aulas experimentais de ácido-base em colégios sem laboratório

João P. de O. Loureiro¹ (IC); Luana M. Villafuerte¹ (IC); Carla V. B. dos Santos² (FM); Wagner F. Pacheco¹ (PQ); Felipe S. Semaan¹ (PQ); Rafael M. Dornellas^{1,*}(PQ). *rafaeldornellas@id.uff.br

¹ Universidade Federal Fluminense, Laboratório Peter Sørensen de Química Analítica, Outeiro São João Batista, s/n – Niterói - RJ – Brasil.

² Colégio Estadual Pandia Calógeras, Rua João Cesariano s/n - São Gonçalo - RJ - Brasil.

Palavras Chave: Impressão 3D; indicadores naturais de pH; baixo custo; reutilizável.

Highlights

3D printed kit for a new application of natural pH indicators in experimental acid-base classes in schools without a laboratory. 3D-printed plates, with natural indicators, make it possible to carry out practical acid-base classes with the greatest interest from students without the need for a laboratory in schools.

Resumo/Abstract

A área de tecnologia é o setor que mais atrai atenção do público jovem, despertando nos adolescentes um maior interesse no aprendizado, é perceptível que a necessidade de se reinventar é essencial para manter a atenção dos alunos em sala de aula. As grandes inovações e sistemas como o uso da impressão 3D tem mostrado bons resultados para a proposta de ministrar uma aula dinâmica, prática e lúdica atraindo a atenção dos alunos. O objetivo deste trabalho foi desenvolver um kit de placas impresso por 3D e posteriormente impregnados com extratos de indicadores de pH naturais¹ (repolho roxo, cebola roxa, feijão e beterraba) através da metodologia de *drop-casting* (Para formar o filme de indicador natural sobre as placas, 65 µL de extrato foi adicionado as cavidades (n=3) e em seguida, levou-se à estufa para evaporação do solvente e impregnação na superfície (10min)), como uma metodologia alternativa para ser aplicada em aulas práticas de acidez e basicidade no ensino de química (ensino médio), sem a necessidade da estrutura de laboratórios. A funcionalidade do kit 3D foi avaliada em aulas de química das redes públicas estadual (100 alunos) e federal (30 alunos) no estado do Rio de Janeiro, inseridas na grade curricular do ensino médio. Foram testadas substâncias comuns do dia a dia como suco de limão, refrigerante, vinagre, bicarbonato de sódio, desengordurante, alvejante e soda cáustica onde aplicou-se uma alíquota (20 µL) de cada produto nas cavidades da placa 3D do kit impregnada com o respectivo indicador natural. Foi possível observar as mudanças de cor e os alunos foram orientados a construir uma escala correlacionando a coloração do indicador e a faixa de pH. A implementação dessa nova abordagem de ensino com o uso de peças impressas em 3D apresentou a possibilidade de uma nova abordagem para aulas práticas de pH, em locais sem a estrutura de um laboratório, com vantagens destacam-se a sustentabilidade, visto que gera o mínimo de resíduos e as placas são reutilizáveis (laváveis), o baixo custo de produção da placa e extrato (R\$010 a confecção da placa e R\$0,05 a reaplicação do extrato), uma maior durabilidade do indicador natural seco sobre a placa (9 meses armazenados à temperatura ambiente), facilidade de transporte, maior praticidade e segurança o que permite o manuseio pelos alunos dando assim uma maior autonomia no aprendizado quando comparado a utilização do extrato bruto ou papel de filtro impregnada com extrato de feijão preto². Desta forma a metodologia torna os processos de aprendizagem mais práticos e modernos.

¹ B. DA CUNHA, M.; O. LIMA, F. A Saga do Repolho Roxo no Ensino De Química. Química Nova na Escola, v. 44, n. 3, 2022. ²NUNES, C.; JANSEN, A.; QUINÁIA, S. otimização da extração de antocianinas presentes no feijão-preto e impregnação do extrato em matriz polimérica natural para uso como indicador de pH. Química Nova, v. 45, n. 1, 2022.

Agradecimentos/Acknowledgments

FAPERJ, CNPq, CAPES, PIBIC UFF e PROPI UFF.

Labvivo: discutindo desinformação, química e valores por meio de uma estratégia experimental investigativa

Guilherme Andrade Marson (PQ)¹ *, Paula S. R. Ferreira (PG)¹, Dante M. B. Del Manto (IC)¹, Pedro N. Lima (IC)¹, Cristian U. C. Florido (IC)¹, Giuliana A. C. Durynek (IC)¹, Leonardo B. Septon (IC)¹, Giovanni V. N. dos Santos (IC)¹, Henrique T. O. Okigami (IC)¹, Stefhanie C. Merino (IC)¹, Gabriel S. Bingres (IC)¹

gamarson@iq.usp.br*

¹Departamento de Química Fundamental, Instituto de Química – Universidade de São Paulo

Palavras Chave: licenciatura, intersetorialidade, curso de extensão

Highlights

Labvivo: discussing disinformation, chemistry and values by means of an investigative experimental strategy. Our results indicate that Labvivo subsidized the analysis of disinformation with scientific concepts and, in connection, fostered questioning values that undermine the advance of our society.

Resumo/Abstract

Labvivo surgiu em 2020 numa disciplina de licenciatura em química, no contexto do ensino remoto. Contemplada com o prêmio Prof. Rubens Murillo Marques em 2021¹, propõem que licenciandos atuem como professores num curso de extensão, partindo do desafio de tomar uma peça de desinformação, submetê-la ao exame científico em atividade experimental investigativa², e situá-la numa trama relacional de valores. Ressalta-se que o papel da desinformação em redes sociais nos projetos retrógrados autocráticos aprofunda este desafio para além das questões conceituais^{2,3}. Este trabalho baseia-se na análise da produção dos licenciandos que atuaram como professores em cursos de extensão presenciais realizados em junho e outubro de 2022, em suas notas de observação e na produção de estudantes do ensino médio da rede pública que participaram dos cursos. A peça de desinformação usada é um vídeo propagado via *Whatsapp*: um homem branco de meia idade (P1), em linguagem coloquial, de sua cozinha, afirma que a inalação de vapores de solução de NaHCO₃ previne COVID-19, apoiando-se em peculiar explanação sobre pH, e estimulando repassar a mensagem. O percurso investigativo Labvivo consiste em traduzir as informações do vídeo em hipóteses que possam ser testadas empregando-se escala de pH tendo extrato de repolho roxo como indicador. O estudo realizado na edição de junho de 2022, (66 estudantes de 3 escolas) indicou que, para muitos estudantes, a origem sócio cultural aparente de P1 é mais relevante para desqualificar a informação do que as inconsistências científicas de seu discurso, explicitadas no percurso experimental investigativo. Isto levou a inserção de novos elementos na edição de outubro de 2022. Foram incluídos depoimentos fictícios em vídeo, de personagens representando marcadores sociais de raça e sexo⁴: um homem branco de meia idade concordando com a desinformação (P2) e uma jovem negra discordando da desinformação (P3). Antes do experimento, os estudantes deveriam indicar sua concordância com as pessoas nos vídeos e, depois do percurso, manter ou mudar de opinião, justificando-se. A proposta foi testada com dois grupos de estudantes da região metropolitana de São Paulo: GA (*n*=28), do ensino médio regular, que já haviam estudado a desinformação como conteúdo escolar; GB (*n*= 23) do ensino técnico em química, que não haviam estudado a desinformação. Da análise dos resultados categorizados destaca-se que: antes do experimento, a vasta maioria dos estudantes de GA e GB identificam a desinformação, discorda de P1 e P2 e concorda com P3; após o experimento, as opiniões se mantêm; nos dois grupos, de modo geral, os argumentos mais indicados fazem menção aos conceitos e às pessoas no vídeo; em GB, predominam menções aos conceitos associados ao experimento; em GA prevalecem menções às pessoas, em conexão com o termo “fake news”. Os resultados reportados sugerem que a proposta Labvivo é apropriada para subsidiar a análise crítica da desinformação com conceitos científicos, e, em conexão, questionar valores que emperram o avanço da sociedade.

Referências

- 1: Marson et al.; *Textos FCC*, 2021, 59, 34 [https://doi.org/10.18222/fcc-pprmm2021_21]
- 2: Souza et al.; *Atividades experimentais investigativas no ensino de química*. 1ª ed., CETEC, São Paulo 2014.
- 3: Tuleikytė, J.; *O Mundo contemporâneo desumanização e humanização*, palestra proferida em 24/05/2022. [<https://www.youtube.com/watch?v=B6BbB4TCvk8>]. Acesso em 11/2/2023.
- 4: Crenshaw, K.; *Univ. of Chicago Legal Forum*, 1989 1(8). [<http://chicagounbound.uchicago.edu/uclf/vol1989/iss1>] Acesso em 11/2/2023.

Agradecimentos/Acknowledgments

À CAPES e à USP pelas bolsas de P. R. S. Ferreira e D. Del Manto, respectivamente. Aos Profs Emiliano B. Alvarez, Rafael H. Trindade e Daniela Rubio pela colaboração com o programa Labvivo.

LIVRO DE NANOTECNOLOGIA E MEIO AMBIENTE COM POTENCIAL DE ALFABETIZAÇÃO CIENTÍFICA PARA EDUCAÇÃO BÁSICA

Carla Juliana Silva Soares* (PG)¹, **Diogo Ramos Pereira** (IC)¹, **Monique Gabriella Angelo da Silva** (PQ)¹

soarescarlajuliana@gmail.com

¹Instituto de Química e Biotecnologia, UFAL;

Palavras Chave: Alfabetização científica, Material didático, Nanotecnologia, Meio ambiente.

Highlights

NANOTECHNOLOGY AND ENVIRONMENT BOOK WITH SCIENTIFIC LITERACY POTENTIAL FOR BASIC EDUCATION. The present work intends to present a proposal for a textbook on the themes of Nanotechnology and Environment with a focus on the discipline of Chemistry for students of basic education based on the potential for scientific literacy.

Resumo/Abstract

A Alfabetização Científica (AC), segundo Lorenzetti e Delizoicov (2001), é o desenvolvimento da capacidade de ler, compreender e expressar opinião sobre os assuntos que envolvam a Ciência na educação básica e posterior a ela. É sabido que os livros didáticos são excelentes suportes no processo da Alfabetização Científica e com base nisso, este trabalho apresenta um livro didático sobre Nanotecnologia e Meio ambiente. Para poder iniciar a construção do livro, buscou-se conhecer a frequência e a forma como as temáticas Nanotecnologia e Meio Ambiente estão sendo abordadas nos livros didáticos de Química Ser Protagonista (QSP) PNLD 2012 a 2023 e se estão possibilitando a construção do processo de Alfabetização Científica dos alunos. Para isto, foi realizada uma análise técnica do conteúdo de 4.305 páginas, 9.771 questões, 204 capítulos e 78 unidades da coleção QSP. No total, a temática de Nanotecnologia apresentou 96 ocorrências e Meio Ambiente 1377 vezes. Identificadas as ocorrências das temáticas, as mesmas foram analisadas sob a luz dos indicadores de alfabetização científica propostos por Pizarro (2014): articular ideias, problematizar, argumentar, ler em ciências, escrever em ciências, investigar, criar e atuar (Ver tabela 1)

Tabela 1. Panorama geral dos indicadores analisados no QSP

Indicador	Meio Ambiente	Nanotecnologia
Articular Ideia	53,45%	41,66%
Ler em Ciências	14,60%	31,25%
Problematizar	14,16%	21,87%
Argumentar	05,40%	03,14%
Investigar	05,01%	02,08%
Escrever em Ciências	03,41%	00,00%
Atuar	02,25%	00,00%
Criar	01,74%	00,00%

Observando os dados supracitados, nota-se que a temática de Meio ambiente aparece com maior frequência se comparada com Nanotecnologia e aparece contemplando todos os indicadores de AC. No caso de Nanotecnologia, o tema é raramente abordado e em nenhum momento, por exemplo, estimula a participação ativa do aluno, pois não contempla os indicadores, *escrever em ciências*, *atuar* e *criar*. Com o respaldo destes dados, o livro didático "*Nanotecnologia e Meio Ambiente*" visa preencher as lacunas identificadas durante a análise da coleção Química Ser Protagonista.

Referência:

LORENZETTI, Leonir; DELIZOICOV, Demétrio. **Alfabetização científica no contexto das séries iniciais.** Ensaio Pesquisa em Educação em Ciências (Belo Horizonte), v. 3, n. 1, p.45-61, jun. 2001.

PIZARRO, M. V. **Alfabetização científica nos anos iniciais:** necessidades formativas e aprendizagens profissionais da docência no contexto dos sistemas de avaliação em larga escala, 355f. Tese (Doutorado em Educação para a Ciência). Faculdade de Ciências, UNESP, Bauru, 2014.

Movimento Química Pós-2022 SBQ – Elaboração e disponibilização de experimentos em plataforma digital para conscientização de estudantes

Rita C. O. Sebastião (PQ),¹ Natália R.S. Araujo (PG),¹ Janáina P. Silva (PG),¹ Wladimir T. Silva (PG),¹ Márton H. F. B. Soares (PQ),^{2*} Nyuara Mesquita (PQ),² Alfredo Matheus (PQ).^{3*}

ritacos@ufmg.br; marlon@ufg.br, almateus@gmail.com

¹Departamento de Química, UFMG; ²Departamento de Química, UFG; Colégio Técnico de Minas Gerais, Coltec.

Palavras Chave:(Sustentabilidade, Ensino básico, Plataforma digital, Capacitação de professores, Experimentos químicos).

Highlights

Post-2022 Chemical Movement – Development and Availability of Experiments on a digital platform to raise awareness elementary school students

Network interaction to promote sustainable development

Accessible communication between academic research and society

Students' awareness of the chemistry role for sustainable development

Resumo/Abstract

Em 2021, a SBQ lançou o **Movimento Química Pós 2022 – Sustentabilidade e Soberania**, com o objetivo de promover reflexões sobre como a Química pode contribuir para a sustentabilidade e a soberania do Brasil (Silva, I., 2022). O primeiro Objetivo da Química para o Desenvolvimento Sustentável (OQDS) é “Promover a sustentabilidade através da Química na Educação Básica”. Dentro desta temática, este trabalho visa divulgar o projeto desenvolvido em parceria pelo programa 1000 Futuros Cientistas (1000FC) da UFMG, o Pátio da Ciência – UFG e o Instituto Nacional de Ciências e Tecnologia Midas (INCT Midas). Este projeto visa promover a interação entre a universidade e estudantes e professores do ensino básico, por meio da divulgação e popularização da ciência, levando discussões sobre os OQDS em uma plataforma digital. Tecnologias desenvolvidas pelos pesquisadores INCT Midas foram adequadas às práticas de laboratórios, atividades lúdicas e oficinas de experimentos (Silva, J., 2021). O desenvolvimento e adequação das práticas ocorre através da utilização de linguagem apropriada e contextualização da tecnologia, demonstrando sua aplicação em problemas sociais cotidianos, com foco em sustentabilidade e impacto social. Destacam-se duas propostas de ações/experimentos já mapeados e adaptados para a sala de aula de nível básico: (i) “Meu xixi é adubo!” fundamentado na tecnologia de produção de fertilizante a partir de urina e (ii) “Produzindo Madeira com plásticos” fundamentado na tecnologia de produção da Madeira Plástica. O Programa 1000FC já recebeu mais de 1000 estudantes de 21 escolas (de 11 diferentes cidades) no Departamento de Química para visita e execução de experimentos em laboratórios de ensino. No evento I Dia com Ciência e II Congresso Nacional de Inovação e Popularização da Ciência, promovido pelo Programa 1000FC em outubro de 2022 na UFMG, foram doados cerca de 100 kits com densímetros para professores do ensino básico, que receberam treinamento sobre um experimento de adulteração de combustível a ser realizado com o kit. Este evento contou com cerca de 1800 participantes, entre alunos de graduação e pós-graduação e professores e alunos do ensino fundamental. O projeto também busca incentivar o protagonismo do professor de química, com desenvolvimento de material de capacitação para abordagem do tema nas escolas. Em implementação constante e com perspectiva de desenvolvimento de mais experimentos, o projeto tem potencial para atingir um público nacional, fomentando a discussão sobre sustentabilidade e química, com entrega de produtos que podem ser utilizados pelos professores e permitindo uma aproximação entre universidade e sociedade.

SILVA, Ingrid F. et al. Movimento Química pós 2022: construção de um plano de ação para que a Química e Seus Atores impactem a Sustentabilidade e Soberania no Brasil. *Química Nova*, 2022, 45, 497.

Silva, Janáina P. et al. Methodological Process to Select, Develop, and Execute a Chemical Experiment for an Innovative Extension Project: Connecting Technological Research to Basic Education, *J. Chem. Educ.*, 2021, 98, 1562.

Agradecimentos/Acknowledgments

Os autores gostariam de agradecer ao INCT Midas, Proex e CNPq pelo apoio financeiro.

O pioneirismo da Professora Doutora Maria Falce de Macedo em exposição no Museu da História da Medicina do Paraná

Camila Silveira (PQ)^{1*}, Patricia Gomes Vidal Corrêa (PG)¹

camilasilveira@ufpr.br*

¹Departamento de Química/PROFQUI, UFPR

Palavras-Chave: *Mulheres pioneiras, Mulheres cientistas, Educação em museus, Divulgação Científica.*

Highlights

The pioneering spirit of Professor Doctor Maria Falce de Macedo on display at the Museum of the History of Medicine of Paraná: reports the main data of a historical research on the first female doctor trained in Paraná and the first full professor in Brazil, which culminated in a museographic exhibition.

Resumo/Abstract

O pioneirismo das cientistas precisa ser amplamente divulgado para que a sociedade possa (re)conhecer e valorizar os importantes feitos protagonizados pelas mulheres. Neste sentido, a partir de visitas mediadas ao Museu da História da Medicina do Paraná (MHMP) e de estudos realizados no acervo deste museu, identificamos que a primeira médica formada no Paraná e primeira professora catedrática do Brasil, a Professora Doutora Maria Falce de Macedo (1897-1972), atuou por muitas décadas como docente de Química/Bioquímica na Faculdade de Medicina da Universidade (Federal) do Paraná, sendo responsável pela formação de centenas de profissionais no campo da Medicina e da Farmácia. Com isto, evidenciamos o seu papel de destaque no ensino superior, lecionando conteúdos químicos e contribuindo com o desenvolvimento curricular da disciplina de Química Orgânica e Biológica, impulsionando-nos à realização de uma investigação científica sobre a sua formação e atuação acadêmica. Assim, a partir dos fundamentos da pesquisa histórica, tomamos como fontes de informação documentos institucionais e pessoais compreendendo todo o período de vida da cientista. Tais dados foram levantados em arquivos das instituições nas quais Maria Falce atuou, bem como por meio de entrevistas com familiares, que colaboraram com a composição do percurso historiográfico. Como exemplos de resultados, sublinhamos o tema de sua tese para o concurso de catedrática (*Função Cyanica*, 1928) e o estágio realizado no Laboratório de Química Orgânica do professor Otto Rothe, em 1926. Em sua biblioteca particular, localizamos diversos livros clássicos de Química e um apreço pelas produções de Marie Curie. Ensinava um vasto conteúdo programático, que incluía funções químicas, reações orgânicas, isomeria etc. Para além das questões acadêmicas, os achados da pesquisa revelaram dimensões de sua liderança feminina em outras instâncias da sociedade. Ainda, documentos comprovaram seu cargo como Médica Chefe da Seção de Bacteriologia, Parasitologia e Química Médica do Laboratório de Pesquisas e Análises do Estado do Paraná (1928). Ademais, fundou o primeiro laboratório particular de Análises Clínicas do Paraná. Por muitos anos, ela foi a única mulher do corpo médico do hospital da Santa Casa e do corpo docente da Faculdade de Medicina da Universidade. Após sete meses de trabalho de campo, a equipe de pesquisadoras envolvidas no estudo, dedicou-se à produção de uma exposição sobre o pioneirismo e protagonismo da cientista em questão, para além de sua formação e atuação acadêmica dada a relevância do acervo organizado. Em cartaz no MHMP desde o dia 18 de outubro de 2022, a exposição reúne objetos pessoais e profissionais, fotografias, vídeos, documentos, dentre outros, e tem despertado grande interesse do público visitante, apontando caminhos possíveis e potentes para uma prática de divulgação e educação científica sobre mulheres cientistas em espaços museais.

Agradecimentos/Acknowledgments

Museu da História da Medicina do Paraná, Associação Médica do Paraná, Santa Casa de Misericórdia de Curitiba, Biblioteca Central da UFPR, Centro Paranaense Feminino de Cultura, familiares da Dra. Maria Falce, Meninas e Mulheres nas Ciências, equipe de pesquisadoras, CNPq, CAPES.

Podcast as a guiding tool for experimental practices within an investigative and potentially significant didactic sequence on Chemical Kinetics.

José R. Gregório (PQ),² Águeda C. Aguiar (FM),^{1*} Daniele T. Raupp (PQ),²

irg@ufrgs.br; quimicaagueda@gmail.com

¹E.T.E. José Feijó SEDUCRS; ²Instituto de Química UFRGS

Palavras-Chave: *Ensino de Química; Novas Tecnologias; Aprendizagem Significativa; Experimentos Investigativos.*

Highlights

The need to use new technologies in Chemistry Teaching is necessary for better integration and contextualization in the reality of the students. The activity developed herein, in addition to relating the contents of Chemical Kinetics with low-cost experiments, guides them through narratives recorded in easily available audio (podcasts). The structure of the didactic sequence used the Predict, Observe and Explain (POE) technique, relating it to meaningful learning using prior knowledge.

Abstract

The practices of the Didactic Sequence developed were organized in an investigative way, using the Predict, Observe and Explain technique, guided by the Theory of Meaningful Learning, with the objective of building a potentially meaningful and accessible educational product. During the execution of the didactic sequence, the student is in the role of a researcher, with great autonomy when guided via podcast for the execution of experiments. The teacher acts as a mediator. The results show that the teaching of Chemical Kinetics was facilitated by the investigative experimental approach and by the use of the Predict, Observe and Explain technique. This technique allows students to discuss and reflect on many kinetic phenomena, which often leads to cognitive conflict, which makes possible for the students to rethink their subsumers and rearrange them. The podcast, as a mean of guiding the experimental classes, provided an environment where the student is more active, participative and independent of the teacher who, in fact, works as a mediator in the process. Justi and Gilbert (1999)¹ point out that the integrated understanding of many fundamental concepts is necessary, such as the particular nature of matter and the interactive and dynamic character of chemical reactions for the understanding of kinetic phenomena.

The podcast was chosen as a mean of guiding the experimental classes, so that the student had access to all the steps of the procedure and could listen the instructions again as many times as necessary (and even before performing the experiment), creating greater autonomy during the experimental and observation processes. For each experimental class, quantitative data was made pre-available in a very summarized way, leaving the greatest support and guidance to the podcast created by the teacher. As most students have a cell phone or a smartphone that supports mp3 audio, it becomes an easily accessible resource. Freire (2013)² reflects on the positive aspects of the podcast in the educational field, such as the possibility of taking a less usual position, in addition to the malleability of listening in different times and places, resources that enhance communicative practice.

The results of the application of the Predict, Observe and Explain technique showed that, in general, the students presented a construction of knowledge in a more concrete way when comparing their previous knowledge with their observations and the theoretical knowledge acquired in the sequence, building greater connections with the reality. Many students reported, after the activity, that they enjoyed it a lot and that they had effectively learned in class with the POE technique. In this way, and using prior knowledge, the construction of new knowledge became more participatory, making this method potentially significant.

The Didactic Sequence addressed concepts such as: essential factors for the occurrence of a reaction, evidence for the occurrence of a reaction, collision theory, activation energy, dependence of the slow step in determining the rate of the reaction, effects on the reaction rate and influence of catalysts in chemical reactions. The practices carried out (all guided via podcast) were iodine clock (Landolt reaction), effervescent tablets in different water temperatures, reaction of bicarbonate solution in different concentrations with acetic acid from vinegar and reaction of hydrogen peroxide with potato catalase under different conditions.

¹JUSTI, R.; GILBERT, J. K. History and Philosophy of Science Through Models: The Case of Chemical Kinetics. *Science and Education*, v.8, p. 287-30, 1999.

²FREIRE, E. P. A. Conceito educativo de *podcast*: um olhar para além do foco técnico. *Educação, Formação & Tecnologias*, América do Norte, v. 6, n. 1, p. 35-51, 2013.

Acknowledgements

This study was financed in part by the Coordenação de Aperfeiçoamento Pessoal de Nível Superior - Brasil (CAPES) - Finance Code 001. We also acknowledge PROFQUI/UFRGS for support.

Programa Química na Prática: uma parceria entre o Instituto Sua Ciência, indústrias químicas, universidades e escolas de educação básica.

Juliana M. Sampaio Furlani (PQ),^{1*} Natália de Paiva Diniz (PG),² Jane Raquel S. de Oliveira (PQ)¹

jufurlani@unifei.edu.br;

¹Instituto de Física e Química, Unifei; ²Faculdade de Ciências, Campus de Bauru, Unesp.

Palavras Chave: Química na Prática, Indústrias, Terceiro setor, Universidades públicas, Educação em ciências.

Highlights

Chemistry in Practice Program: a partnership between Instituto Sua Ciência, chemical industries, universities and basic education schools. Emancipatory scientific education. Interdisciplinary and contextualized activities. Role of science and the importance of scientific information, especially with regard to chemical sciences and their numerous everyday, industrial and technological applications.

Resumo/Abstract

O programa Química na Prática se propôs a unir indústria, academia e terceiro setor para evoluir o ensino de ciências na educação básica no Brasil, com foco em química. Foi conduzido seguindo a missão e os valores do Instituto Sua Ciência (ISC), com foco em ação emancipatória de crianças e jovens por meio da educação científica. A parceria com a indústria se estabeleceu a partir de uma ideia inicial de um grupo de voluntários da Basf, base de Guaratinguetá/SP. Essa ideia foi desenvolvida pelo ISC, culminando em um projeto que obteve aporte financeiro da Basf e doação de equipamentos, reagentes e vidrarias pela Oxiteno, atual Indorama. As ações do programa ocorreram de julho/2021 a dezembro/2022. Para iniciá-lo, um edital nacional foi lançado e selecionou quatro propostas de projetos para o desenvolvimento de atividades interdisciplinares e contextualizadas que contribuíssem para a melhor compreensão sobre o papel da ciência e a importância da informação científica, especialmente no que se refere às ciências químicas e suas inúmeras aplicações cotidianas, industriais e tecnológicas. Cada equipe era formada por um docente universitário, um licenciando em química, um professor de química e dois estudantes da educação básica, sendo um total de 20 pessoas nos quatro projetos. O financiamento obtido, no valor de R\$200.000,00, propiciou o pagamento mensal de bolsas para os estudantes das equipes e bolsas de gestão e coordenação para os colaboradores que estruturam e tornaram possível a articulação entre a escola e as empresas, assim como deram suporte às atividades realizadas. Foram oferecidos dois cursos de formação na modalidade a distância para os professores das escolas parceiras (Abordando a Natureza da ciência em sala de aula e Tecnologias digitais na sala de aula). Durante o desenvolvimento do programa, a equipe de gestão produziu peças de divulgação científica em diferentes formatos, abordando temas como tratamento de água, solubilidade, modelos atômicos, origem dos elementos químicos, corpo humano, entre outros, publicadas principalmente no *Instagram* e no *Facebook*. As interações nas redes sociais são essenciais para o estabelecimento do contato com o público e a garantia do acesso à informação segura e de qualidade, assim como para a disseminação e incentivo à replicabilidade das ações desenvolvidas. As ações desenvolvidas pelas escolas e universidades parceiras atingiram mais de 5700 pessoas de forma presencial. Os projetos também utilizaram as mesmas redes sociais que, somadas, tinham mais de 5300 seguidores. Ocorreu grande mobilização das escolas em torno dos projetos, culminando com alunas e alunos da educação participando e sendo premiados em eventos científicos.

Agradecimentos/Acknowledgments

O ISC agradece às empresas parceiras, Basf e Indorama (Oxiteno), pela confiança que tornou esta ação possível. Agradece aos executores, em todos os níveis do programa, pelo tempo, energia e conhecimento dedicados à educação em ciências no Brasil.

REALIDADE AUMENTADA E VIRTUAL NO ENSINO DE QUÍMICA: REVISÃO SISTEMÁTICA DA LITERATURA

Maria J. R. Amaro (IC),^{1*} Monique G. A. Silva (PQ)²

Maria.amaro@iqb.ufal.br; monique.silva@iqb.ufal.br.

¹Instituto de Química e Biotecnologia, UFAL; ²Instituto de Química e Biotecnologia, UFAL.

Palavras Chave: Realidade Virtual, Realidade Aumentada e Metaverso.

Highlights

AUGMENTED AND VIRTUAL REALITY IN THE TEACHING OF CHEMISTRY: A SYSTEMATIC REVIEW OF THE LITERATURE VIRTUAL. The advances in technology are surprising and offer numerous advantages to consumers in various fields. Two technologies that have been very promising are Augmented Reality (AR) and Virtual Reality (VR), especially in the educational field. Such realities, when applied in a school environment, are able to allow a more immersive experience, where learning becomes easier, stimulating the student's memory and guaranteed better results.

Resumo/Abstract

Os avanços da tecnologia são surpreendentes e oferecem inúmeras vantagens aos consumidores em diversos campos. Duas tecnologias que têm sido muito promissoras são a Realidade Aumentada (RA) e a Realidade Virtual (RV), em especial no campo educacional. A RA cria camadas dentro de uma realidade existente como observamos uma molécula tridimensional sobre a mesa de estudo com o auxílio da camera de um celular, por exemplo. E a RV cria uma nova realidade, simulando, por exemplo, um ambiente real. Tais realidades, quando aplicadas em um ambiente escolar, são capazes de permitir uma experiência mais imersiva, onde o aprendizado se torna mais facilitado, estimulando a memória do aluno e garantido melhores resultados.

Com o uso dessas tecnologias é possível desenvolver livros, jogos didático, ambientes virtuais e interatividade no ambiente escolar. O metaverso, por exemplo, é um recurso que tenta replicar a realidade, somando (RV, RA e a internet), viabilizando a criação de espaços coletivos e virtuais compartilhados, semelhante às salas de aulas. Esse tipo de ferramenta engloba os processos de exploração, descoberta, observação e construção do conhecimento como é proposto pelo desenvolvimento de algumas habilidades da Base Nacional Comum Curricular (BNCC), como a EF05CI01 e EF05CI05.

Deste modo, o objetivo deste trabalho foi realizar uma revisão sistemática da literatura pautada nas palavras chaves: *Realidade Virtual, Realidade Aumentada, Química e Ensino de Química, com foco nas áreas de Ciências e ensino de Química*, visando delinear os modos como essas realidades vêm sendo aplicadas na educação, especificamente no ensino de Ciências/Química. Tal levantamento de dados respalda a elaboração e o desenvolvimento de novas ferramentas tecnológicas que tenham potencial real de utilidade e aplicação. Podemos observar na tabela abaixo, os principais resultados encontrados durante os últimos onze anos (ver Tabela 1).

Tabela 1. RV e RA na Química e no ensino de Química (2011 a 2022)

Categorias	Quantidades		
	RV E RA – Química	RV – Ensino de Química	RA – Ensino de Química
Congresso Brasileiro de Informática na Educação	2	1	1
Sociedade Brasileira de Ensino de Química (SBEnQ)	0	0	0
Sociedade Brasileira de Química - Divisão de Ensino de Química (SBQ)	0	0	0
Revista Virtual de Química	70	35	20
Revista Química Nova na Escola- QNEsc	158	139	19

Fonte: autores, 2022

Na Tabela é possível observar quantas publicações foram encontradas nos últimos anos, sobre *RV no ensino de Química*, e sobre *RA no ensino de Química*, esses resultados podem ser explicados devido as uma novas abordagens, para o ensino de química e ciências. Somado a isso nos últimos três anos com a propagação da pandemia, onde o online passou a ser normalizado nas instituições de ensino se dá o aumento de publicações em revistas virtuais, como podem ser observado.

REFERÊNCIAS BIBLIOGRÁFICAS

CARDOSO, Alexandre. *Uma arquitetura para elaboração de experimentos virtuais interativos suportados por Realidade Virtual Não-Imersiva*. 2002. Tese de Doutorado. Tese de Doutorado, Universidade de São Paulo, USP. CARVALHO, Fábio Câmara Araújo de; IVANOFF, Gregorio Bittar. *Tecnologias que educam: ensinar e aprender com as tecnologias de informação e comunicação*. Pearson Prentice Hall, 2010.

RELATO DE EXPERIÊNCIA DA UTILIZAÇÃO DA QUÍMICA FORENSE PARA O ENSINO DE COMPOSTOS DE COORDENAÇÃO

Joice Lima Carvalho (PG), Renata C. Nunes (FM)*

joicelimacis@gmail.com; renatacn@iff.edu.br

Instituto Federal de Educação Ciência e Tecnologia Fluminense – campus Cabo Frio, IFFluminense

Palavras Chave: *Compostos de coordenação, Química forense, Metodologias ativas, Teste de Scott, Detecção de chumbo.*

Highlights

An experience report employing forensic chemistry to teach coordination compounds

Forensic chemistry was employed to contextualize coordination compounds to graduated students.

The students showed motivation to perform the activity besides the difficulties to answer the questions.

Resumo/Abstract

A disciplina de Química Inorgânica II que trabalha compostos de coordenação na Licenciatura em Química vem apresentando ao longo dos anos altos índices de reprovação¹. A utilização de metodologias ativas e temas que despertem o interesse dos estudantes pode contribuir para a melhora desse quadro. O objetivo desse trabalho é relatar a experiência da utilização da química forense aplicada aos compostos de coordenação, especificamente os testes para cocaína e detecção de chumbo. A fim de executar a atividade elaborada, a proposta foi aplicada na disciplina de Química Inorgânica 2 no campus Cabo Frio no segundo semestre de 2022, onde participaram da atividade dez estudantes, sendo que apenas dois estavam cursando pela primeira vez. Para resolver os problemas propostos, os alunos deverão possuir conhecimentos sobre geometria de compostos de coordenação, efeitos que afetam cores em complexos, Teoria do Campo Cristalino e Teoria do Campo Ligante. A atividade foi dividida em três etapas, realizada em quatro grupos: na primeira delas, realizada em sala de aula, com duração de 30 minutos, foi distribuído um conto de mistério e atividades para os estudantes² que deveriam levantar hipóteses para resolver o mistério e definir quais seriam as estratégias de pesquisa. Na segunda etapa, eles deveriam pesquisar e embasar cientificamente respostas para questões propostas na atividade testes e entregar duas semanas após o início da atividade. Nessa mesma data, houve o fechamento da atividade com as discussões das respostas apresentadas por eles. Na primeira etapa, os grupos apontaram corretamente quem havia disparado a arma de fogo, mas não houve unanimidade com relação ao teste do papelote, se de fato era cocaína. Todos os grupos sinalizaram a necessidade de pesquisa sobre os testes para conseguirem explicar como funcionavam. A análise das respostas revelou maiores dificuldades em conceitos básicos como número de coordenação, geometria e isomeria do que nas teorias de ligações em compostos de coordenação. Dois grupos consideraram que a mudança de cor já seria indício para resíduos de disparo por arma de fogo, bem como, para detecção positiva de cocaína sem buscar embasamento para esse posicionamento. Essa é uma concepção preocupante, pois algumas mudanças de cores em testes colorimétricos indicam a ausência do analito, além da possibilidade de resultados falso-positivos. A atividade foi avaliada de forma bastante positiva pela turma que pode retomar conceitos que tinham dúvidas. Como a atividade ocorreu antes das provas finais da disciplina, pode ter colaborado para o aumento do índice de aprovação dos estudantes, que foi de 70%.

¹NUNES, Renata. A aprendizagem baseada em problemas (ABP) aplicada ao ensino de Química Inorgânica: as cores dos minerais. # Tear: **Revista de Educação, Ciência e Tecnologia**, v. 11, n. 2, 2022.

²Disponível em https://drive.google.com/file/d/15fDP2zyzxxva8avJltolubOR_8cHHP97m/view?usp=sharing.

Área: EDU

REVISÃO DA LITERATURA SOBRE INTERDISCIPLINARIDADE ENTRE A QUÍMICA E A CONFEITARIA

Vitória Cristina P. de Oliveira Silva (PG), Monique G. Ângelo da Silva² (PQ)

vitoria.silva.ufal@gmail.com

¹Instituto de química e biotecnologia, UFAL;

Palavras Chave: revisão da literatura, química, confeitaria.

Highlights

This work aims to carry out a systematic review of the literature on confectionery and chemistry teaching for a better understanding of what has already been developed and how these publications were made, their methodologies and approaches.

Resumo/Abstract

A confeitaria é a arte de fazer doces e é considerada uma das áreas mais difíceis da culinária mundial. Sendo comparável como a área de ciências exatas do mundo da gastronomia, baseada em números precisos de quantidades de cada elemento. Podemos encontrar pratos à base de diferentes tipos de massas como pudins, biscoitos, panquecas, bolos e tortas, sorvetes e doces gelados. É dentro desse contexto que é possível encontrar uma gama de possibilidades de se trabalhar a química de forma contextualizada, desmistificada, agradável e “apetitosa”, realizando um percurso interdisciplinar entre a Química e a Confeitaria, enquadrando-se desta forma nas exigências da Base Nacional Comum Curricular – BNCC para ser vista não como algo isolado, mas como parte de um todo na sociedade. Trabalhar a química dos alimentos possibilita estudar a composição, propriedades e as transformações químicas que os alimentos sofrem durante a manipulação, processamento e armazenamento (DAMODARAN;FENNEMA;PARKIN,2010).

Objetivando a tomada de decisões para a construção de um produto técnico tecnológico no ramo educacional, este trabalho propõe como etapa inicial uma revisão sistemática da literatura para quantificar as publicações acerca da temática confeitaria e ensino de química nos últimos dez anos (2013 a 2022). A revisão da literatura foi realizada em duas etapas: i) nas seguintes plataformas de busca: Scielo, BDTD – Biblioteca Digital de Teses e Dissertações, e na seleção de 15 revistas de ensino da lista da CAPES de 2023 com Qualis A e B, com as palavras chaves: *Química, Ensino e Confeitaria* (ver tabela 1) apenas com o filtro do tempo; ii) categorização das publicações encontradas (tabela 2).

Tabela 1. Quantitativo de publicações de 2012-2023

Periódico Capes	0
Scielo	0
BDTD	7
Revistas de ensino de química ou ciências;	25

FONTES : AUTOR,2023

Tabela 2. Categorias das publicações

Categoria 1. História e referencial teórico	11
Categoria 2. Metodologias Ativas	16
Categoria 3. Análise de livros didáticos	1
Categoria 4 . Consciência ou educação alimentar	4

FONTES : AUTOR,2023.

No total foram encontrados 32 artigos que abordaram a temática, dentre eles 50% apresentavam metodologias ativas com aplicação em sala de aula e 30% trabalham de maneira teórica os conceitos, essas categorias foram criadas pelas autoras para melhor compreensão do que está sendo produzido na área de acordo com as propostas dos trabalhos analisados e com a perspectiva do desenvolvimento de um produto técnico tecnológico que auxilie os professores da educação básica a utilizarem essa temática como recurso de ensino-aprendizagem. Fennema, O. R.; Damodaran, S.; Parkin, K. L. *Química de Alimentos de Fennema*. Editora. Artmed, 4ª Edição, 2010

Ciência e literatura nos anos iniciais do ensino fundamental: as propriedades dos materiais em uma abordagem investigativa

Aline Patrícia Pasqui Bonini (FM; PG)^{1*}, Gabrielle Anália Cristiano (TC)², Tathiane Milaré (PQ)³.

tmlare@ufscar.br; alinepasqui@gmail.com

¹CI José Reinaldo Ribeiro Brugnaro; Programa de Pós-graduação em Educação em Ciências e Matemática - UFSCar; ²Egressa do curso de Licenciatura em Química - UFSCar; ³Departamento de Ciências da Natureza, Matemática e Educação, UFSCar.

Palavras Chave: Alfabetização Científica, Literatura infantil, Experimentação.

Highlights

Science and literature in the early years of elementary school: the properties of materials in an investigative approach

This paper approaches Inquiry-based Sequence Teaching through the use of retelling of “Three Little Pigs” to teach material properties and Scientific Literacy development.

Resumo/Abstract

Dentre os desafios para a abordagem da Química os anos iniciais do Ensino Fundamental destacam-se: professores sem formação suficiente em ciências da natureza, a ênfase no processo de alfabetização e no ensino de matemática e a concepção de que os conhecimentos químicos se restringem a conceitos abstratos e complexos que pouco se articulam com a realidade das crianças. Com o intuito de contribuir para a superação desses desafios, buscou-se utilizar estratégias já utilizadas em sala de aula com as crianças, como é o caso da literatura infantil, estabelecendo as questões de pesquisa: como articular histórias infantis e o ensino investigativo de química? Quais são as contribuições dessa articulação para a promoção da Alfabetização Científica (AC) das crianças? A história “Os três porquinhos” foi escolhida por abordar a construção de casas com diferentes materiais. Verificou-se a necessidade de adaptá-la para explorar outros materiais e propriedades por meio de atividades práticas. Foram elaborados testes experimentais com casinhas feitas de metal, PVC, palha, parafina, madeira, cimento, papel, acrílico, buscando avaliar alterações que fossem perceptíveis pelas crianças quando submetidas à variação de temperatura, à umidade e à combustão. Com base nos resultados, foi elaborado um reconto no qual a continuação da história estava condicionada à realização dos experimentos. Elaborou-se desta forma uma sequência de ensino investigativa (SEI)ⁱ, que foi realizada em uma turma de 3º ano de uma escola pública do interior de São Paulo. As atividades foram gravadas e transcritas. Os dados foram analisados com base na Análise de Conteúdoⁱⁱ, buscando evidências dos indicadores de ACⁱⁱⁱ. Os resultados evidenciaram as contribuições das atividades realizadas e da articulação entre ciência e literatura, uma vez que foi possível discutir com as crianças as propriedades dos materiais; identificar os indicadores de Alfabetização Científica; sensibilizar, contextualizar e proporcionar diversas reflexões e debates em sala de aula, que relacionaram a história, as vivências das crianças e o conhecimento químico.

Agradecimentos/Acknowledgments

CAPES, CNPQ, FAI/UFSCar e Diretoria do CCA/UFSCar.

ⁱ CARVALHO, A. M. P. (org.). *Ensino de ciências por investigação: condições para implementação em sala de aula*. São Paulo: Cengage learning, 2013. 152p.

ⁱⁱ BARDIN, L. *Análise do Conteúdo*. Lisboa: Edições 70, 2005.

ⁱⁱⁱ SASSERON, L. H.; CARVALHO, A. M. P. Almejando a alfabetização científica no ensino fundamental: a proposição e a procura de indicadores do processo. *Investigações em Ensino de Ciências*, v. 13, n. 3, p. 333-352, 2008.

Science and Social Media: Communicating Science through Instagram® at @iq.ufrgs

Juliana Christina Thomas (PQ)*, Marina Thoma Rockenbach (IC), Bruna de Brito de Souza Canali (IC), Francielle Pereira Pedrosa (IC), Vinícius Pospichil Gil (IC), João Paulo Bizarro Lopes (PQ), Marcelo Priebe Gil (PQ), Nathália Marcolin Simon (PQ)

institutoquimica.ufrgs@gmail.com

Instituto de Química, Universidade Federal do Rio Grande do Sul - UFRGS

Palavras Chave: Social Media, Science Communication, Thematic Posts, Instagram

Highlights

Science communication via social media at @iq.ufrgs through thematic posts was a valuable way to strengthen the relationship between Instituto de Química, UFRGS and their community.

Abstract

Social media are valuable resources to communicate science in a quickly way. On the other hand, any information can be published on social media, regardless its scientific value. To minimize spreading wrong information, academics are more and more engaged to science communication through social media. In this context, herein we report the use of an Instagram® profile (@iq.ufrgs) to strengthen the communication and popularization of science between Instituto de Química, UFRGS and their community.

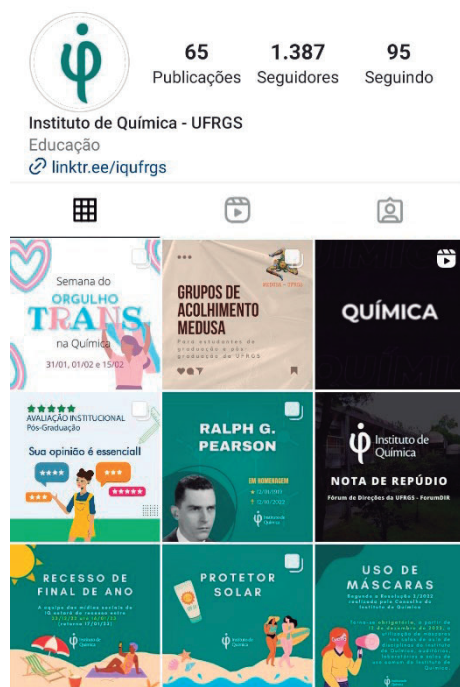


Figure 1. @iq.ufrgs Instagram® profile

@iq.ufrgs (Figure 1) was created on July, 2021 and focused mainly on showing research projects in an accessible way.

Later on, a series of posts about the relationship between chemistry and festive dates was published, which became the most successful posts. Regarding Instagram® statistics, these posts had the largest numbers in comments, shares and saves, as well as greater reach, therefore, the most effective way to communicate science to the community.

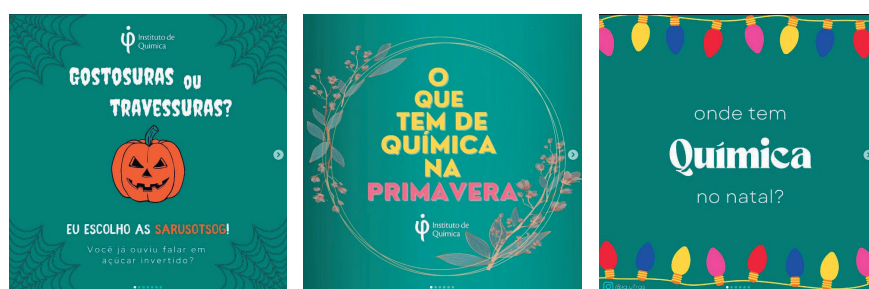


Figure 2. Chemistry of festive dates: representative posts from @iq.ufrgs

These thematic posts were highly shared by the community and helped to emphasize the presence of science in everyone's lives.

Thorp, H. H. *Science*, **2022**, 375, 593; Teruya, L. C. *et. al. Quim Nova*, **2013**, 36, 1561.

Acknowledgments

Pró-reitoria de Extensão (PROEXT), Pró-reitoria de Pesquisa (PROPESQ), Universidade Federal do Rio Grande do Sul – UFRGS.

Sustentabilidade e química verde: um olhar em uma coleção de ciências da natureza e suas tecnologias

Renata C. Nunes (FM),* Richard F. Andrade (IC), Joice L. Carvalho (FM), Maria Eduarda Q. S. Tavares (TM)

renatacn@iff.edu.br

Instituto Federal de Educação Ciência e Tecnologia Fluminense – campus Cabo Frio, IFFluminense

Palavras Chave: *Química verde, Sustentabilidade, Ensino de química, Programa Nacional do Livro Didático.*

Highlights

Sustainability and green chemistry: an analysis of natural sciences and their technologies`collection
Concepts related to sustainability and green chemistry are presented on the analyzed books, however there are some gaps.
It is possible to discuss them more interdisciplinarity.

Resumo/Abstract

O objetivo desse trabalho foi realizar a análise da inclusão da sustentabilidade e química verde (QV) nos capítulos de química da coleção “Moderna Plus - Ciências da Natureza e suas Tecnologias”. Essa coleção foi selecionada por ter sido aprovada pelo PNLD 2020 e foi a mais adotada pelas escolas brasileiras¹. Essa é a primeira vez na qual não há mais divisão dos livros por disciplinas: química, física e biologia foram agrupadas em um conjunto de seis livros. A sustentabilidade é um conceito amplo que envolve a relação entre ambiente, sociedade e economia. É baixa a inclusão de conceitos da QV nas Licenciaturas em Química² e há uma tendência desses futuros professores não abordarem esses conceitos em sala de aula³. A presença da QV e sustentabilidade nos livros didáticos pode contribuir sua abordagem, visto que são muitas vezes o principal, ou único, recurso didático que os professores dispõem⁴. A promoção de atitudes sustentáveis está explícita na BNCC, mas também em documentos anteriores como Diretrizes Curriculares Nacionais e PCN⁺. Em uma análise geral, a questão ambiental mostra-se presente em quase todos os capítulos analisados. No entanto, observa-se que os problemas vivenciados pelo planeta predominam com relação às discussões de propostas sustentáveis. O capítulo que trata de estequiometria poderia introduzir os conceitos de economia atômica e fator-E como exemplos de sucesso da indústria para melhorar esses indicadores. O capítulo que aborda os gases não menciona a poluição atmosférica que é tratada em outro volume, mas há vantagem para o aprendizado dos estudantes quando os temas são trabalhados de forma interdisciplinar. Pesquisas anteriores já apontavam para essa abordagem descontextualizada e fragmentada da questão ambiental⁵. Nesse mesmo volume, há um capítulo denominado “Sustentabilidade ambiental”, que traz um pequeno tópico sobre alternativas para o futuro, não obstante se restringe àquelas relacionadas à energia. O capítulo que trata da poluição ambiental e sustentabilidade é um destaque positivo pois trabalha temas relacionados à sustentabilidade e QV. Em trabalhos anteriores, os professores relatavam que eram insuficientes a inserção desses temas nos livros didáticos⁶. O livro representa um avanço no tratamento das questões de interesse comparado aos livros de edições passadas, mas ainda há espaço para trabalhar outros temas sem sobrecarregar o conteúdo do ensino médio.

¹<https://www.fnde.gov.br/index.php/programas/programas-do-livro/pnld/dados-estatisticos>

²GOMES, L. S. et al. Panorama da Inclusão dos conceitos de Química Verde nas Licenciaturas em Química dos Institutos Federais. **Ambiente & Educação**, v. 27, n. 1, p. 1-24, 2022.

³SANTOS, D. M.; ROYER, M. R. Análise da percepção dos alunos sobre a química verde e a educação ambiental no ensino de química. **Revista Debates em Ensino de Química**, v. 4, n. 2, p. 142-164, 2018.

⁴ZAMBON, L. B.; TERRAZZAN, E. A. Livros didáticos de Física e sua (sub) utilização no Ensino Médio. **Ensaio Pesquisa em Educação em Ciências**, v. 19, 2017.

⁵CASSIANO, K. F. D.; ECHEVERRÍA, A. R. Abordagem ambiental em livros didáticos de Química: Princípios da Carta de Belgrado. **Química Nova na Escola**, 2014.

⁶PRSYBYCIEM, M. M. et al. Educação Ambiental e a Sustentabilidade: concepções e práticas de professores de Química do ensino médio. **Revista ESPACIOS**, v. 35, n. 10, 2014.

Agradecimentos/Acknowledgments

CNPq, FAPERJ, IFFluminense

Sustentabilidade no Brasil a partir da Química: projetos em desenvolvimento envolvendo o OQDS 1 no ano de 2023

Larissa L. Maia (PG),¹ Maryna M. Barros (PG),² Ingrid F. Silva (PQ),³ Izadora R. S. Menezes (PG),² Márlon Herbert. F. B. Soares (PQ),⁴ Shirley Nakagaki (PQ),⁵ Rochel M. Lago (PQ),² Ana Paula de C. Teixeira (PQ).^{2*}

larissalisboamaia8@gmail.com; anapct@ufmg.br

¹Instituto de Ciências Exatas e Tecnológicas, UFV; ²Departamento de Química, UFMG; ³Department of Colloid Chemistry, MPIKG; ⁴Instituto de Química, UFG; ⁵Departamento de Química, UFPR.

Palavras-chave: OQDS 1, Sustentabilidade, Ensino de Química, Educação Básica.

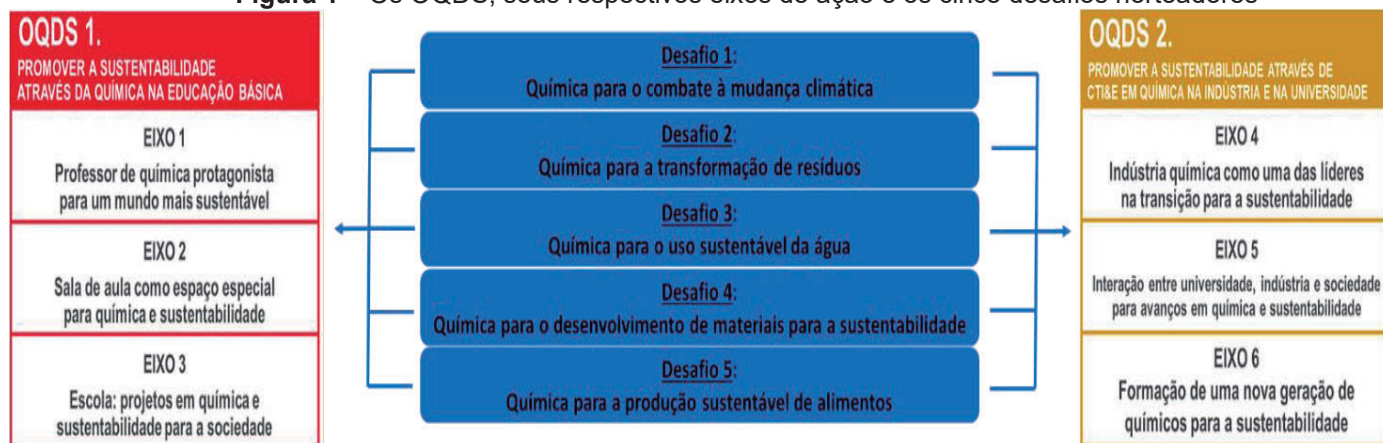
Highlights

Sustainability in Brazil from Chemistry: projects under development involving OQDS 1 in 2023.
Project for implementation of sustainability and sovereignty in Brazil from Chemistry.
OQDS 1: Promoting sustainability through the subject of Chemistry in Middle and High School.

Resumo/Abstract

O “Movimento Química Pós 2022 – Sustentabilidade e Soberania”, criado pela Sociedade Brasileira de Química (SBQ) está sendo implementado por diversas frentes. Dentre essas frentes, temos o plano de ação “Química e Seus Atores para um Brasil Sustentável e Soberano”, que visa implantar a sustentabilidade e soberania no país por meio da Química. A partir de entrevistas com profissionais de diferentes setores, os envolvidos nesse plano de ação propuseram dois Objetivos da Química para o Desenvolvimento Sustentável (OQDS), cada um com três eixos de ação. A estrutura desses OQDS foi inspirada na Agenda 2030 e nos Objetivos para o Desenvolvimento Sustentável (ODS), conforme Figura 1. Depois de propostos os OQDS, um grupo de inteligência com especialistas de diferentes setores selecionou cinco desafios que irão direcionar a implementação de ações e projetos em cada um dos OQDS em 2023, conforme apresentamos na Figura 1:

Figura 1 – Os OQDS, seus respectivos eixos de ação e os cinco desafios norteadores



Para que os desafios comecem a ser executados, temos como resultado a implementação de algumas ações relacionadas ao OQDS1, de responsabilidade de diversos grupos de pesquisa envolvidos no Movimento. Essas ações foram divididas em: a) elaboração e aplicação de experimentos e jogos educativos com viés de sustentabilidade na sala de aula e na formação de professores; b) produção de vídeos educativos para plataformas online; c) produção de podcasts na temática e d) implementação de um curso formativo para professores de Química para a Educação Básica, inicialmente voltado para o desafio 3 (Figura 1) de maneira remota, na perspectiva de produzir materiais que sirvam como subsídios para os professores introduzirem a sustentabilidade em sua prática pedagógica. Outro resultado a partir das decisões dos grupos envolvidos foi o entendimento que a ação de um curso formativo em uma plataforma, pode congrega todas as ações anteriores, de forma coletiva, sem que se cesse as ações independentes. Em 2023, o desafio 3 vem sendo objeto de estudo, elaboração e aplicação em sala de aula a partir das ações descritas. As propostas piloto, tanto presencialmente, quando remotamente podem direcionar as ações descritas para que contemplem os outros desafios nos próximos anos, a partir de uma análise qualitativa das ações para o desafio 3.

Agradecimentos/Acknowledgments

A Capes, CNPq, Fapemig, INCT Midas, SBQ, Abiquim, CFQ, Escalab e aos participantes do Grupo de Inteligência.

46ª Reunião Anual da Sociedade Brasileira de Química: “Química: Ligando ciências e neutralizando desigualdades”

Teacher education: a scientometric study on the development and validation of research instruments.

Douglas Cezars A. R. Almeida (PG)^{1*}, Amadeu Moura Bego (PQ)¹

douglas.cezars@unesp.br; amadeu.bego@unesp.br

¹São Paulo State University (UNESP), Institute of Chemistry, Araraquara, Brazil.

Palavras-Chave: teacher education; scientometrics; research instruments; development; validation.

Highlights

Based on a scientometric study, this paper aims to describe the scenarios of publications on the development and validation of research instruments, with a focus on teacher education

Resumo/Abstract

Research instruments are of utmost importance in the field of education and, therefore, it is necessary to have theoretically and methodologically grounded instruments in the literature that allow for the extraction of the answers sought for the objectives set. However, national research indicates a lack of studies that focus on the processes adopted in the development and validation of research instruments in the field of Education. In view of this scenario, this research aims to: I) describe the international scenario of publications on teacher education focused on the development and validation of research instruments; II) analyze their theoretical perspectives and relations with the teacher education process and III) point out the trends, theoretical and methodological propensities, gaps and future challenges on the subject. To reach the proposed objectives, we opted for a scientometric study of the literature. To observe the trends of publications, seven searches were conducted using the Web of Science (WoS) database, using the descriptors instrument develop*; instrument design*; instrument validation; tools develop*; tools design*; assessment instrument; assessment tools; combined with the descriptors: teacher education; teacher training; teacher preparation. As a result of the search, 105 articles were found that addressed the theme. The initial data analysis relied on examining the following elements: I) number of citations; II) authors; III) journals; IV) countries; V) institutions; VI) year of publication; VII) keywords used by the authors. Furthermore, through the 20 most relevant articles, the theoretical perspectives and the methodological aspects adopted in the development and validation of research instruments were identified. The initial results indicate that in the last 10 years the number of publications and citations of articles about the development and validation of research instruments had a significant leap. Through the keywords it was possible to identify the trends of specific themes published on the studied topic, these being: professional development; competencies for teaching; beliefs about self-efficacy; Pedagogical Content Knowledge (PCK); Technological Pedagogical Content Knowledge (TPACK). Moreover, the keywords indicate that the research instruments are related to the process of initial teacher education. Finally, the term questionnaire was identified as a recurring keyword. Through the analysis of the 20 most cited articles, it was identified: I) Likert scales (varying points) are widely used in the development of the instruments; II) in the development of the constructs, the articles present a theoretical foundation on the theme studied and a literature review on instruments that research the same theme; III) on the component items of the instruments, two tendencies were observed, namely, a) the items are developed in discussion groups that involve the researcher and theme specialists and b) there is a preference for adapting items that already exist in instruments validated in the literature; III) the procedures adopted for the validation of the instruments involve three main processes: validation by subject matter experts (content validation); validation by confirmatory or exploratory factor analyses (construct validation); calculation of reliability and internal consistency performed through Cronbach's α . Finally, although we did not observe specific procedures that are repeated in the processes of analyzing the results, all articles use grounded statistical techniques that are appropriate to the research objectives. Therefore, with this research, we expected to contribute to discussions, at the national level, on the development and validation of instruments, as well as to indicate the trends adopted in the development and validation of instruments already consolidated in the literature.

Agradecimentos/Acknowledgments

The authors would like to thank the Chemistry Institute of UNESP Araraquara for the support and the CNPQ for funding this research.

Área: EDU

Teaching Chemistry Inclusively: an educational tool using 3D printing

João Victor Firmino Felício (IC)*, Ingrid GS Machado (IC), Denise BA Barbosa (PQ).

joaovtf2016@gmail.com

Departamento de Educação e Ciências - Laboratório de Pesquisas e Experimentos em Nanociência - IF SUDESTE MG

Palavras Chave: *pedagogical methods; 3D printing; Inclusion*

Highlights

The work presents the concept, design and manufacturing of an educational tool using 3D printing. This method provides valuable aid in offering the students a tactile and practical experience in their study, especially if they are visually impaired or if they have Attention deficit hyperactivity disorder (ADHD and Down's syndrome).

Resumo/Abstract

With regards to inclusive chemistry education there are three types of barriers to need to be achieved for the success of the students: (i) pedagogical (lack of preparation of the teachers), (ii) accessibility (limited access to laboratories and equipment), and the most significant barrier that is (iii) acceptance (negative attitudes of educators who believe that students with disabilities cannot succeed in learn Chemistry). Traditional teaching still has a strong influence on high school especially for preparing ENEM. Priority is usually given to the accumulation of conceptual contents, and students are expected to assimilate these previously organized conceptual structures in a passive, receptive manner. Overcoming these barriers to learning became a significant challenge in our Institute, and especially in a classroom with students carries cognitive impairments (one with Down's syndrome and six with ADHD).

Trying to provide students with opportunities to engage in activities which stimulate their visual and tactile senses to improving spacio-visual ability, and to lead a deeper understanding of the content, and their performance in assessments, were produced several models that represent molecular structures and/or crystal structures by offering students a suitable for to improve their concepts about, Periodic Table, Molecular Geometry and Intermolecular Forces. Making possible the "visualization" of these structures for all students, without exception (with or not impairments), can feel the objects and to better assimilate the knowledge. Even if this method has not provided a perfect replica of the structures in their minds, it has made it possible that for the first time in their lives, these students could have some visualization of any structure within the classroom of chemistry. Remembering that Chemistry is a discipline with an important visual component. In addition to this progress, which would be enough for us to consider the work satisfactory. Our results showed that, for those students diagnosed with ADHD, the learning was more significant. We verified that students with ADHD also benefited from the production of these models because, according to them, it was easier to be interested in the lessons and thus maintain focus on it for much longer, which made them "understand" the lessons they had much better 3d models in the hands, in relation to the subjects in which they did not have.

After the positive feedback from the work, we take the time to extend this accessibility to another student in a special situation in the classroom, whose has Down's syndrome, as he has his own way of interpreting the information that comes to him, sometimes it results in some very distorted concept of the discipline, but with the models, he had a solid reference, which even resulted in increase, not only in his grades, but also in his interest in the classes.

References

Abels, S.. Scaffolding inquiry-based science and chemistry education in inclusive classrooms. In N.L. Yates (Ed.), *New Developments in Science Education Research*. Hauppauge: Nova science publisher. 2015;pp. 77-95

K.Waseem, and O. H.Qureshi, *Innovation in Education - Inclusion of 3D-Printing Technology in Modern Education System of Pakistan :Case from Pakistani Educational Institutes*, 8(1), 2017; 22–28

Miner, D. L.; Nieman, R.; Swanson, A. B.; Woods, M. *Teaching Chemistry to Students with Disabilities: A Manual for High Schools, Colleges, and Graduate Programs*, 4th ed.; American Chemical Society: Washington, DC, 2001; pp 70–73; ISBN 0-8412-3817-0.

Agradecimentos/Acknowledgments

Instituto Federal de Educação, Ciência e Tecnologia do Sudeste de Minas Gerais

Área: EDU

Teaching, research and extension: the implementation of a design for the elaboration of Popular Science Texts and Case Studies inspired by a scientific research on luminescent Metal-Organic Framework

Carolina M. Primo (PG)¹, Amadeu Moura Bego (PQ)¹, Regina Frem (PQ)¹.

carolina.martins@unesp.br

¹São Paulo State University (UNESP), Institute of Chemistry, Araraquara, Brazil.

Palavras Chave: *Science Communication, Case Studies, Metal-Organic Framework.*

Highlights

What are the processes involved in the elaboration of Popular Science Texts and Cases Studies inspired by scientific research?

Resumo/Abstract

Brazilian public universities are based on the principle of indissolubility between teaching, research, and extension. This principle means that, in addition to producing knowledge from scientific research, universities play a fundamental role in transmitting this knowledge through teaching and also by their dialogical interaction with the society. Currently, what is observed is that scientific knowledge generated by scientific research does not go beyond academic boundaries and consequently does not reach a large portion of society. Another aggravating factor is that undergraduate chemistry teaching is often disconnected from these new scientific researches and has been historically traditional, in which students find themselves in the position of mere passive spectators of the process. Therefore, the aim of this work was to develop and implement a design, based on the principle of indissolubility between teaching, research and extension, for the elaboration of Popular Science Texts (PST) and Cases Studies (CS) inspired by scientific productions developed by a research group of an university. The inspiring research chosen deals with the synthesis and characterization of luminescent Metal-Organic Frameworks (MOF), as well as their application in the context of forensic chemistry. The design was planned by a multidisciplinary team and based on the Design-Based Research principles. The implementation took place in the context of the Tutorial Education Program (PET-Química). In general, the project presented three main progressive cycles, which involved: I) deepening studies of the chemical contents of MOF; II) studies and production of PST based on this scientific research; III) studies and production of CS inspired by the PST. Each cycle involved a series of relevant activities to the formative process of learning the fundamentals of these materials and, subsequently, of their production. In all, four PST and four CS were elaborated. The PST, for example, presents accessible language to the non-specialist public and compositional construction specific to this textual genre. The CS, in turn, presents the necessary characteristics to be considered good cases, according to the literature. In addition to the PST and CS as final products, the implementation of the design generated knowledge about optimized processes that involve the production of materials inspired by a certain scientific research and that comply with different roles, interrelating the three pillars of the university: teaching, research and extension.

Agradecimentos/Acknowledgments

We would like to thank CNPq, the Research and Innovation Network in Chemistry Education (RIPEQ, abbreviation in Brazilian Portuguese for “Rede de Inovação e Pesquisa do Ensino de Química”), the Tutorial Education Program (PET, abbreviation in Brazilian Portuguese for “Programa de Educação Tutorial”); the Applied Metal-Organic Frameworks Research Group and the Institute of Chemistry of the São Paulo State University.

The aspects of Environmental Education in Integrating Projects of Natural Sciences: in focus the PNLD 2021

Wárica Santos Souza (PG),¹ Márlon Herbert Flora Barbosa Soares (PQ),¹ Nyuara Mesquita (PQ)^{1*}

nyuara@ufg.br; waricasouza@gmail.com

¹ Laboratório de Educação Química e Atividades Lúdicas – Instituto de Química/Universidade Federal de Goiás - UFG

Palavras-Chave: *Macrotendências, Projetos Integradores, Educação Ambiental.*

Highlights

It discusses the inclusion of Environmental Education in public school books that focus on the development of projects that integrate the different knowledge of Chemistry, Physics and Biology.

Resumo

No Programa Nacional do Livro Didático (PNLD) de 2021, os livros didáticos não são mais separados por disciplinas, mas por área do conhecimento. Dessa forma as disciplinas de Química, Biologia e Física estão contidas na área de Ciências da Natureza e suas Tecnologias (CNT). No referido PNLD, o Objeto 1 refere-se aos Projetos Integradores (PI) que trazem projetos da área de CNT para serem desenvolvidos nas escolas na etapa do Ensino Médio. Nesses materiais, os projetos são pensados a partir de temas que integram os conhecimentos de Química, Física e Biologia, além de outras temáticas das demais áreas (Matemática e Ciências Humanas). O presente trabalho visou analisar as vertentes de Educação Ambiental (EA) presentes nesses Projetos Integradores. Para isso, foi realizada uma análise documental das treze obras didáticas aprovadas na área de CNT utilizando como aporte teórico o trabalho de Layrargues e Lima (2014)¹ e buscando identificar a inserção da EA nesses novos materiais didáticos. Salientamos que estes materiais visam integrar os conhecimentos de Ciências às demais áreas de conhecimento e que a EA perpassa as diferentes áreas de conhecimento, inclusive a Química. Adotamos como categorias de análise as macrotendências conservacionista, pragmática e crítica, sobretudo por serem categorias que apresentam objetivos distintos em relação ao meio ambiente e à sociedade, o que caracteriza a multiplicidade de caminhos para realização da EA e seus diferentes objetivos formativos. Cada uma das treze obras aprovadas apresenta seis projetos tendo-se um total de 78 projetos contidos nos materiais didáticos. Ao identificarmos os projetos que apresentavam a EA como elemento estruturador das discussões e propostas elaboradas obtivemos o total de 31 projetos com relação direta com o tema. No que tange às macrotendências e vertentes, observamos a presença das três tendências nos diferentes projetos, de maneira que a tendência pragmática predomina em algumas propostas, difundindo visões reducionistas das problemáticas ambientais, permeados pela ideia das responsabilidades individuais de “cada um faz sua parte”. A EA crítica se sobressai mais que a vertente conservacionista tendo em vista a ênfase na necessidade do posicionamento e do papel político do sujeito, visto que são essas ações que têm o potencial transformador da sociedade, que é um dos principais objetivos dessa tendência. Os resultados quantitativos de inserção das macrotendências nos materiais analisados são apresentados na Figura 1.

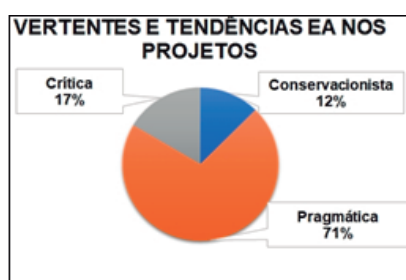


Figura 1. Projetos com foco na EA nos PI.

Referências

1. LAYRARGUES, P. P. LIMA, G. F. C. **As macrotendências político pedagógicas da educação ambiental brasileira.** Ambiente & Sociedade, v. XVII, p. 23-40, 2014

46ª Reunião Anual da Sociedade Brasileira de Química: "Química: Ligando ciências e neutralizando desigualdades"

The concepts of citizenship and competence: a comparison between BNCC and the Amazonian educational documents.

^{2,3,4*} **Carlos E.P. Aguiar** (PG/FM), ¹ **Maria E.R. Marcondes** (PQ)

cerodafe@usp.br; mermarco@iq.usp.br

¹Instituto de Química, USP; ²Secretaria de Estado de Educação e Desporto do Amazonas-SEDUC-AM; ³Secretaria Municipal de Educação de Manaus-SEMED-Manaus; ⁴Programa de Pós-Graduação Interunidades em Ensino de Ciências USP.

Palavras Chave: *Cidadania, Competências, Referenciais Curriculares.*

Highlights

Analysis of concepts of competence and citizenship presented in the Base Nacional Comum Curricular-BNCC. Establishing similarities and differences with the Amazon curriculum documents. we analyzed both: the general principles and those established for science teaching.

Resumo/Abstract

O termo “Competências” bem como a expressão “Exercício da Cidadania”, vêm sendo relevantes em discussões no campo educacional por envolverem processos de ensino e aprendizagem que têm como objetivo promover o desenvolvimento integral do estudante. Os referenciais curriculares atuais como a BNCC e os referenciais amazonenses – o Referencial Curricular Amazonense-RCA (estadual) e Currículo Escolar Municipal-CEM (manauense), apresentam discursos em favor de uma formação que desenvolva competências e prepare o sujeito para uma plena participação cidadã em sua comunidade¹. Diante disso, como parte de nossa pesquisa, investigamos as concepções de competências e de cidadania manifestadas nesses documentos. Com base em trabalhos sobre esses conceitos^{2,3,4}, foram elaborados dois instrumentos para análise das oito competências específicas de Ciências da Natureza-CN dos três referenciais. “Atender demanda da sociedade”; “Enfrentar situações”; “Transformar as realidades sociais”, foram as categorias utilizadas como identificação da visão de competências; enquanto “Reconhecimento dos direitos e deveres sociais”; Participação ativa na transformação da sociedade”; “Atuação em prol da promoção do bem-estar social”, as categorias para identificação da visão de cidadania. As análises foram validadas por pesquisadores de nosso grupo. Como resultados parciais, já que se trata de uma parte da pesquisa, foi possível perceber um alinhamento entre os discursos dos três referenciais quanto às visões de competências, prevalecendo a ideia de enfrentar situações com a aplicação dos saberes adquiridos pelos estudantes em situações que lhes exijam uma intervenção imediata. Quanto à cidadania, a ideia de cidadania como direitos e deveres não aparece, sendo que na BNCC o discurso que prevalece é o da promoção do bem-estar social quando comparado ao de participação ativa na transformação da sociedade, enquanto que nos referenciais amazonenses essas duas concepções estão igualmente presentes. Consideramos que nosso estudo pode subsidiar o aprofundamento e orientar outras pesquisas relativas aos temas competências e cidadania.

Referências

- ¹BRASIL. Ministério da Educação. **Base Nacional Comum Curricular-BNCC**. Brasília: MEC, 2017.
- ²CARVALHO, J.M. Cidadania no Brasil: O longo caminho. 30ª ed. Rio de Janeiro, 2012.
- ³DIAS, L.S. Competências em educação: conceito e significado pedagógico. **Revista Semestral da Associação Brasileira de Psicologia Escolar e Educacional**, SP, v. 14, n. 1, 2010, p. 73-78.
- ⁴MOTOKANE, M.T. Sequências didáticas investigativas e argumentação no ensino de ecologia. **Revista Ensaio, Belo Horizonte**, v. 17, n. especial, p. 115-137, 2015.

Agradecimentos/Acknowledgments

Aos pesquisadores do nosso grupo.

The playfulness in The Teaching of Organic Chemistry: A Report of Experience

Maria Leidiana Nogueira Amaro (IC)¹, Chaianne Kaialle da Silva Nascimento (IC)¹, Isadora Cavalcanti Josino (IC)¹, Thiago Muniz de Souza (PQ)¹.

leidianeamaro0@gmail.com

¹Universidade Federal Rural de Pernambuco, UFRPE;

Keywords: Chemistry Teaching, Organic Chemistry, Playful Activities, Teaching Material.

Highlights

Here, it is a report of experiences from a board game aimed at developing a meaningful teaching and learning process from a social-historical theoretical framework.

Resumo/Abstract

The use of playful activities has been a relevant topic in teaching chemistry because it promotes, besides playfulness, a two-way communication between students and teachers. Such playful approaches become a versatile strategy in relation to when they will be applied in the classroom, ranging from before the presentation of the content (educational games) and after the delivery of the lesson (didactic games) (Rezende & Soares, 2019). The present report aims to present the observations made during the application of an analogical and didactic game with the theme functions and properties of the organic compounds, in the School Cornelio Soares High School in Serra Talhada-PE. This was organized based on Vygotsky's epistemological references, in which the playful activity acts as a mediation channel (Chaiklin, 2011) between pairs: The teacher (or game enforcer) and student (player) through the zone of proximal development (imminent).

The board game (figure 1), similar to traditional ludo (with modifications), it was organized in a dynamic question and answer format, using cards with multiple choice questions, numbered according to the number of cards on the board (with 52 pack of cards), selected according to the colour of each trajectory of time, game pawns in the shape of test tubes, through which the players moved and dice that indicated how many squares they should advance. Throughout the application of the game, it was noticeable that the students felt at ease to express their opinions, correcting, or complementing them, according to the knowledge of the group and what they had learned in class and/or experienced in daily life. This game proved to be a complementary resource and facilitator in the acquisition (accommodation/assimilation) of content and socialization (via behavioral analysis) and of the chemical

knowledge, because it allowed students, teachers, and extension agents to interact in an egalitarian and horizontal way, causing reconstruction of knowledge in a playful way. As in the work of Zanon, Guerreiro & Oliveira (2008), which also proposes the use of ludo in teaching chemistry, however aimed at the nomenclature of organic compounds, in which the players had to match the name of the compound with the structural formula or vice-versa. Through the observations made during the application of the game, it is possible to notice that the insertion of activities that "escape" from the traditional method of teaching, allows a better teacher-student interaction, making possible the inclusion of the students as subjects in the teaching-learning process.

References

- CHAIKLIN, S. A zona de desenvolvimento próximo na análise de Vigotski sobre aprendizagem e ensino. *Psicologia em Estudo*, Maringá, v. 16, n. 4, p. 659-675, out./dez. 2011. Disponível em: <<https://www.scielo.br/j/pe/a/jCGfKbkrHPCr8KyZD4xjB3C/?lang=pt>> Acesso em: 16 jan. 2023.
- REZENDE, F. A. M.; SOARES, M. H. F. B. Análise teórica e epistemológica de jogos para o ensino de química publicados em periódicos científicos. *RBPEC*, 747-774, 2019. Disponível em: <<https://periodicos.ufmg.br/index.php/rbpec/article/view/12296/12994>> Acesso em: 12 out. 2021.
- ZANON, D. A. V.; GUERREIRO, M. A. S.; OLIVEIRA, R. C. Jogo didático Ludo Químico para o ensino de nomenclatura dos compostos orgânicos: projeto, produção, aplicação e avaliação. *Ciênc. cogn.*, Rio de Janeiro, v. 13, n. 1, p. 72-81, mar. 2008. Disponível em <http://pepsic.bvsalud.org/scielo.php?script=sci_arttext&pid=S1806-58212008000100008&lng=pt&nrm=iso>. Acesso em: 02 jan. 2023

Agradecimentos/Acknowledgments

We thank the extension program SONUS/UFRPE- 2020 and the School of Reference in High School Cornelio Soares of the State of Pernambuco-Brazil.

The use of social media in the teaching of Chemical kinetics

Paulo Victor Alves de Souza (PG), Ana Cristina F. de Brito Pontes (PQ)*, Daniel de Lima Pontes (PQ)

[*ana.cristina.pontes@ufrn.br](mailto:ana.cristina.pontes@ufrn.br) ¹Instituto de Química, UFRN

Palavras Chave: *chemistry teaching, TICs, social media, Chemical kinetics.*

Highlights

The use of information technologies social media is considered by many as a means of distraction. The twitter, Facebook, Instagram and TikTok are new ways of communicative yet not explored by the school.

Resumo/Abstract

The twitter, Facebook, Instagram and TikTok are new ways of communicative yet not explored by the school and that have great potential for scientific dissemination and communication with young students. In this way, the objective of this work is to propose to identify the students' learning after the use of social media in the teaching of chemical kinetics. The research was carried out with public school students in the city of Aroeiras, in Paraíba, in three classes of the second year of high school, with 65 students. The survey was carried out completely online due to the COVID-19 pandemic and the reform of the school's physical structure. Classes took place on the Google Meet videoconferencing platform and the communication with the students took place through the WhatsApp application. A didactic sequence was applied divided into 4 different moments (each class of 100 minutes) in which the content was worked on accompanied by the exposition of videos with discussion about the experiments presented. Next, activities were proposed to the students, the elaboration of a) video on the topic of the class applied in everyday life and b) a scientific dissemination leaflet, in the format for the Instagram feed. These produced materials were later discussed in the classroom. The data collection methods, two questionnaires using the Likert¹ scale model (1932), one before the application of the didactic sequence, to collect information regarding internet access, use of social networks and knowledge of chemistry, the other was applied at the end, to collect information from in order to identify the students' learning about the didactic sequence. Figure 1 (a) shows the data obtained in the quiz.

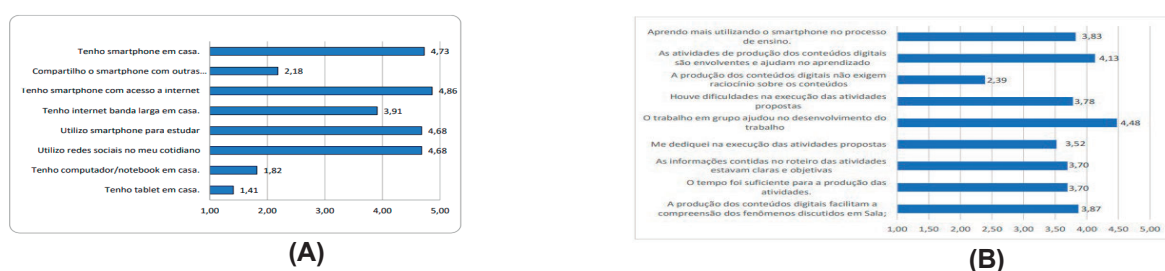


Figure 1: (A) data obtained from the questionnaire regarding access to social media and (B) students' perception after applying the didactic sequence.

Figure 1 (B) shows the students' perception after applying the didactic sequence using social media. Most students had positive responses regarding the use of this methodology, however they also demonstrated some difficulties in preparing the material because they did not have access to computers, which made typing the texts difficult at some point. Some students also deviated from the theme proposed by the activity and were instructed to redo it.

¹LIKERT, R. A technique for the measurement of attitudes. Archives of Psychology. v. 22, n. 140, p. 44-53, 1932.

Agradecimentos/Acknowledgments

PROFQUI – UFRN E PROFQUI-UFRJ.

46ª Reunião Anual da Sociedade Brasileira de Química: "Química: Ligando ciências e neutralizando desigualdades"

ELE

Eletrquímica e Eletranalítica

46^a Reunião
Anual da **SBQ**

28 a 31 de Maio de 2023

Águas de Lindóia · SP
Hotel Monte Real

3D-printed amperometric sensor for the detection of ethanol in saliva

Theodora Wrobel von Zuben (PG)*,¹ Cristiane Kalinke (PQ),¹ Bruno Campos Janegitz,² Airton Gonçalves Salles Jr. (PQ),¹ Juliano A. Bonacin (PQ).¹

*t177584@dac.unicamp.br

¹Instituto de Química, Universidade Estadual de Campinas, 13083-970 Campinas – SP, Brasil

²Departamento de Ciências da Natureza, Matemática e Educação, Universidade Federal de São Carlos, 13600-970 Araras – SP, Brasil

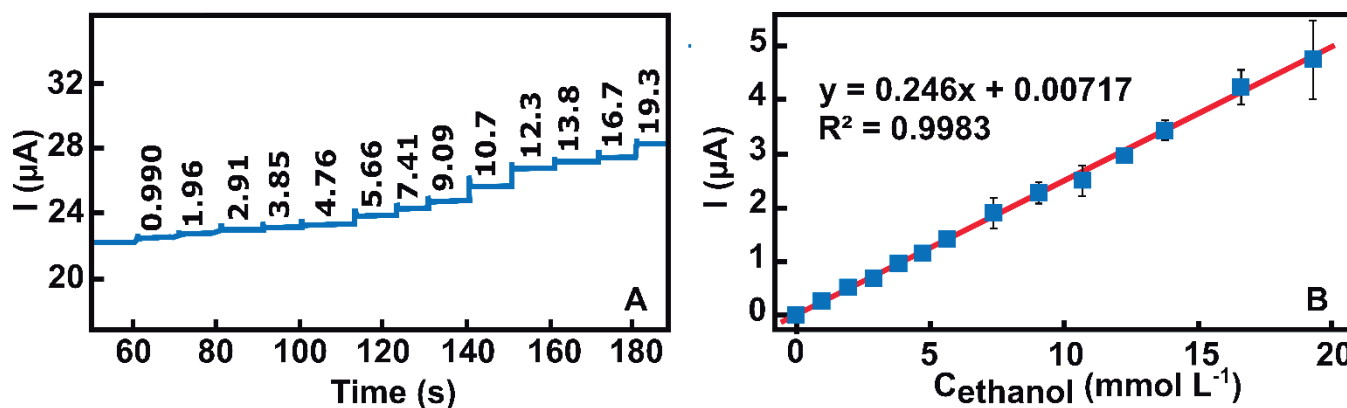
Palavras Chave: 3D-printed electrode, Surface activation, Ethanol sensing, Alcohol limits.

Highlights

Herein, we report the use of a 3D-printed electrode as a sensor for electrochemical detection of ethanol in saliva.

Abstract

In this work, we report a non-enzymatic and metal-free ethanol sensor based on 3D PLA-graphene electrodes. We evaluated the best activation treatment of PLA-graphene to achieve a sensor to monitor ethanol levels in saliva sample following the driver's laws of several countries. The analytical performance was obtained by amperometry, presenting linear range for the detection in supporting electrolyte (0.99–19.3 mmol L⁻¹) and in saliva sample (0.99–17.4 mmol L⁻¹), with limits of detection of 0.135 and 0.239 mmol L⁻¹, respectively. The 3D-printed sensor showed good repeatability and reproducibility. The method was successfully applied for the detection of ethanol in saliva samples, demonstrating an interesting alternative method for the detection of ethanol in drivers, considering the alcohol limits in different countries.



Acknowledgments



3D printing pen: an alternative tool to fabricate electrochemical sensors applied to Pb²⁺ quantification in remote localization by SWASV.

Renato S.O. Lins (PG)¹, William B. Veloso (PG)¹, Débora N. Medeiros (PG)¹, Lauro A. Pradela-Filho (PQ)¹, Thiago R. L. C Paixão (PQ)¹, Mauro Bertotti (PQ)^{1*}

renatolins@usp.br; rsolins@ufam.edu.br

keywords: 3D printed pen; Remote localization; Square-Wave Anodic Stripping Voltammetry; Lead detection.

Highlights

3D printing pen affords the fabrication of low-cost 3D-printed sensors. A promising approach is reported for Pb²⁺ determination in remote localization. The studies were performed in the presence and absence of Bi²⁺, a chemical modifier.

Resumo/Abstract

Disposable electrochemical systems for heavy metals detection are important for attending remote localizations affected by anthropogenic factors involving mining activities [1]. Herein, electrochemical sensors were developed with a 3D printing pen and poly(methyl methacrylate) mold. The electrodes were printed with Carbon Black/Poly(lactic acid) (CB/PLA) filaments. The resulting devices, tested as working electrodes (Figure 1A), were applied to Pb²⁺ detection. For electrochemical measurements, a Pt wire was used as an auxiliary electrode (AE) and Ag/AgCl (KCl sat.) as a reference electrode. The square-wave anodic stripping voltammetry (SWASV) was performed in the absence and presence of 1 μmol L⁻¹ Bi²⁺. The results (Figure 1B) showed a lower background current in the presence of Bi²⁺. Additionally, a remarkable increase (3.7-fold) in the analytical signal was observed in the presence of Bi²⁺, demonstrating the possibility of using the proposed sensor for Pb²⁺ detection at low concentrations. Therefore, a 3D printing pen affords the fabrication of miniaturized sensors for point-of-need applications. The proposed device will be used to quantify Pb²⁺ in remote locations of the Amazon state. As a result, this project involves the collaboration of the Federal University of Amazon and the University of São Paulo, in agreement with the main purpose of the annual conference of the Brazilian Chemical Society.

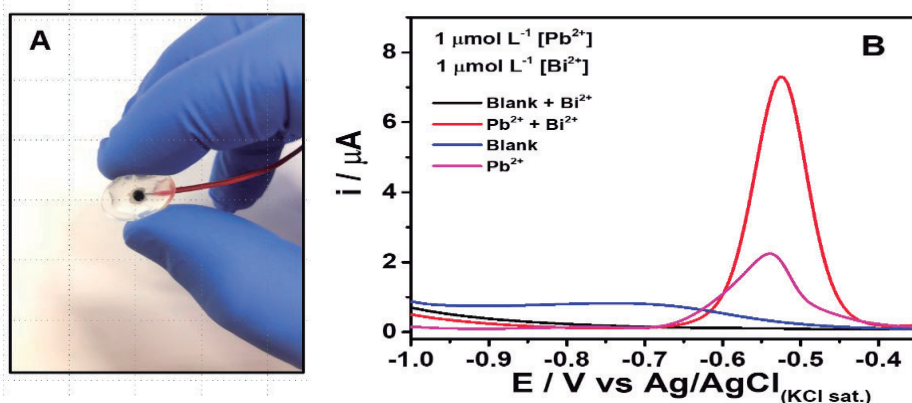


Figure 1. (A) Image of the electrodes. (B) SWASVs recorded in 1 μmol L⁻¹ Pb²⁺ solution in the absence and presence of 1 μmol L⁻¹ Bi²⁺. Supporting electrolyte: 0.1 mol L⁻¹ acetate buffer (pH 4.5). E_{deposition} -1.2 V; t_{deposition}: 80 s; E_{cleaning} 0.7 V; t_{cleaning} 15 s; Amplitude: 60 mV; Frequency: 60 Hz; Increment of potential: 5 mV.

[1] Bernalte E, Arévalo S, Pérez-Taborda J, Wenk J, Estrela P, Avila A, Di Lorenzo M, Sensors and Actuators B: Chemical, 307, 2020,127620.

Agradecimentos/Acknowledgments

São Paulo Research Foundation - FAPESP (2021/00205-8, 2019/15065-7, 2018/08782-1), Coordenação de Aperfeiçoamento de Pessoal de Nível Superior - CAPES (PROEX: 88887.673431/2022-00, 8882.328249/2019-01), and Conselho Nacional de Desenvolvimento Científico e Tecnológico - CNPq (140462/2021-0).

A 3D carbon black disposable electroanalytical sensor modified with reduced graphene oxide used to the sensitive determination of levofloxacin

Thalles P. Lisboa (PQ), Raylla S. Oliveira (PG), Wallace B. V. de Oliveira (PG), Cassiano C. de Souza (PG), Guilherme F. Alves (PG), Maria Auxiliadora C. Matos (PQ) and Renato C. Matos (PQ).*

thallespl_jf@hotmail.com; renato.matos@ufjf.edu.br

Departamento de Química, Universidade Federal de Juiz de Fora, 36026-900, Juiz de Fora-MG, Brasil

Palavras Chave: Carbon black/polylactic acid filament, Reduced graphene oxide, Levofloxacin, Modified 3D electrochemical sensor, Antibiotic.

Highlights

A 3D-printed sensor for levofloxacin electrochemical monitoring. Simple and effective 3D-printing systems for the construction of electrochemical sensors. Analysis with minimal sample preparation.

Abstract

Levofloxacin (LEV) is a third-generation fluoroquinolone mostly used for prophylactic treatment in aquatic cultures and in bacterial infestation in humans to treat pneumonia, urinary tract infection, and acute kidney infection. Antibiotics and their metabolites generally exhibit high stability, which has increased concern in the scientific community due to the emergence of resistant bacteria. In addition, the indiscriminate use of antibiotics for the treatment of infections in humans and animals can worsen the situation due to the contamination of aquatic environments and animal products. Thus, since LEV is considered an emerging pollutant, the development of selective and sensitive methods is highly required [1].

Therefore, in this work we present a simple method for the fabrication of a carbon black/polylactic acid composite (3D-CB/PLA) using a 3D-pen, the sensor was latter modified with reduced graphene oxide (rGO), and for the first time used for monitoring levofloxacin (LEV) in pharmaceutical formulations, synthetic urine, and tap water samples by differential pulse voltammetry (DPV). The characterization by scanning electron microscopy (SEM), electrochemical impedance spectroscopy (EIS), and cyclic voltammetry (CV) demonstrated that the electroanalytical performance of the modified sensor compared to the unmodified electrode was increased 3.7-fold and it was observed anticipation of 120 mV in the peak potential, which characterizes the electrocatalytic effect promoted by the rGO nanosheets attached on 3D-printed carbon black surface. Additionally, the proposed method presented a linear working range from 10 to 50 $\mu\text{mol L}^{-1}$ (Figure 1) and a detection limit of 2.17 $\mu\text{mol L}^{-1}$. Moreover, excellent precision ($\text{RSD} < 6.5\%$) and accuracy with recovery for spiked samples ranging from 95.4 to 104.8% were obtained. The sensor was also selective against the main antibiotics reported in the literature. Therefore, it can be concluded that 3D printed electrochemical devices are currently promising analytical tools that can be implemented in routine methods.

[1] Lisboa, T.P. *et al.* *New Journal of Chemistry*, 2023 [DOI: [10.1039/D2NJ05338A](https://doi.org/10.1039/D2NJ05338A)]

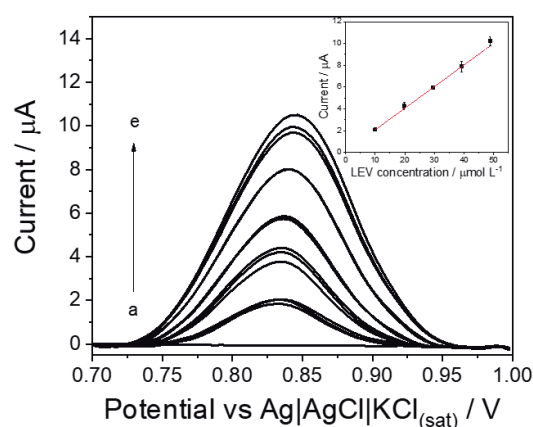


Figure 1. Analytical curve of LEV by DPV using rGO/3D-CB/PLA electrode.

Acknowledgments

This research was supported by FAPEMIG (Research Support Foundation of the State of Minas Gerais) (process: APQ-00042-21), CNPq (National Council for Scientific and Technological Development, process: 303815/2022-1), CAPES (Coordination for the Improvement of Higher Education Personnel) and PROPESQ/UFJF.

A IMPEDIMETRIC SENSOR BASED ON π -CONJUGATED POLYMER-NANOGOLD FOR THE DETECTION OF μ -PATHOGENS

Miqueias de Lima Portugal (IC),¹ Marcelo J. M. Bartholomei (TC),¹ André Olean-Oliveira (PQ),² Marcos F. S. Teixeira (PQ).^{1*}

miqueias.portugal@unesp.br; marcos.fs.teixeira@unesp.br

¹São Paulo State University School of Science and Technology Presidente Prudente FCT-UNESP; ²UNIVERSITY of Duisburg-Essen, Germany

Keywords: Nanocomposite, Impedimetric, Gold Nanoparticle, Resistive Sensor.

Highlights

- Development of an impedimetric sensor to detection of *Listeria monocytogenes*.
- Investigation of interfacial phenomena between the bacterium and redox impedance transduction.

Abstract

The π -conjugated polymers have been widely explored as transducers in the development of chemical sensors due to the presence of active redox sites in their structure that allows detection at low concentrations. In addition, the presence of electrochemically synthesized nanoparticles in situ from the polymer monomer allows to increase the sensitivity of the sensor due to a significant increase in the surface of the active area.

The objective of this work was the development of a chemocapacitor sensor based on the electrochemical response of poly(o-phenylenediamine) (poly(o-PD)) with gold nanoparticles (AuNP) for detection and quantification of the pathogenic microorganism *Listeria monocytogenes*. The study proposes an alternative methodology using dissolved oxygen as a redox probe. This approach is possible due to the selective and sensitive response to the dissolved oxygen reduction reaction with conducting polymer.

The device was prepared by a single-step technique [1] by potential cycling between -0.70 and $+1.60$ V (vs. SCE) for 20-cycle scans at a scan rate of 15 mV s⁻¹ in a deaerated solution containing 2.00 mmol L⁻¹ 1,2-phenylenediamine monomer and 1.00 mmol L⁻¹ HAuCl₄ in 0.10 mol L⁻¹ H₂SO₄ medium.

The impedimetric response of the poly(o-PD)-Au film to different concentration of *Listeria monocytogenes* colony was carried out in a universal buffer (pH 6.6) solution containing dissolved O₂ saturated in atmospheric equilibrium. By charge resistance measurements, an increase in the system impedance was observed with the increase in the concentration of the bacteria in solution. This behavior is due to the increase in the number of species occupying and blocking the electrode surface, resulting in an increase in R_{redox} as a function of the "gate effect" generated for dissolved oxygen molecules to access the redox sites of the polymer. In evaluating the redox capacitance, a direct linear relationship was observed with the concentration of the *Listeria monocytogenes* colony. The complex capacitance values were analyzed by the graph C'' vs. Hz, using the following relationship:

$$C'' = \frac{Z'}{\omega|Z|^2}$$

The sensor response was linear in the range of 0.00 to 177 CFU mL⁻¹ for *Listeria monocytogenes*.

References

¹OLEAN-OLIVEIRA, André; SERAPHIM, Patricia Monteiro; TEIXEIRA, Marcos FS. Methylated DNA impedimetric immunosensor based on azo-polymer-AuNPs dots and 5-methylcytosine antibody using dissolved oxygen as a redox probe. **Electrochemistry Communications**, v. 136, p. 107242, 2022.

Acknowledgments

The authors acknowledge CEPID-FAPESP (2013/07296-2) and CNPq (145584/2021-6) for the financial support.

Amperometric detection of indapamide on glassy carbon electrode

Thawan G. Oliveira (PG)¹, Berlane G. Santos (PG)¹, Josué M. Gonçalves (PQ)¹, Lúcio Angnes (PQ)^{1*}

Thawan.oliveira@usp.br; thawan.oliveira@usp.br

¹ Departamento de Química Fundamental, Instituto de Química, Universidade de São Paulo (IQUSP)

Keywords: Indapamide, Flow injection analysis (FIA), Amperometric measurements, Glassy carbon electrode (GCE).

Highlights

Fast method for quantification of indapamide; Advantageously to the classical chromatographic methods.

Abstract

In this work was developed a fast, precise and reliable voltammetric method for the quantification of indapamide, an orally active diuretic sulfonamide used for hypertensive treatment. This compound acts inhibiting sodium reabsorption and increasing the elimination of water. This characteristic was responsible for his banishment by the International Olympic Committee since 1999. The study begins by finding an adequate potential range to avoid poisoning the working glassy carbon electrode (GCE) in phosphate buffer (pH = 12.0). Utilizing flow injection analysis, linear responses between $2.0 \times 10^{-6} \text{ mol L}^{-1}$ to $2.5 \times 10^{-5} \text{ mol L}^{-1}$ of indapamide ($R^2 = 0.995$), and detection limit (LOD) $3.0 \times 10^{-7} \text{ mol L}^{-1}$ were obtained. This method was applied for the quantification of indapamide in tablets and in synthetic urine. The same flow system was used for the analysis of commercial drugs and the response obtained corresponded to 98% of the concentration indicated on the drug label. The velocity of analysis using flow methods compares advantageously to the classical chromatographic methods. For synthetic urine, linear responses were obtained in samples spiked in the region from $5.0 \times 10^{-6} \text{ mol L}^{-1}$ to $30 \times 10^{-6} \text{ mol L}^{-1}$ ($R^2 = 0.991$) and LOD $3.0 \times 10^{-7} \text{ mol L}^{-1}$.

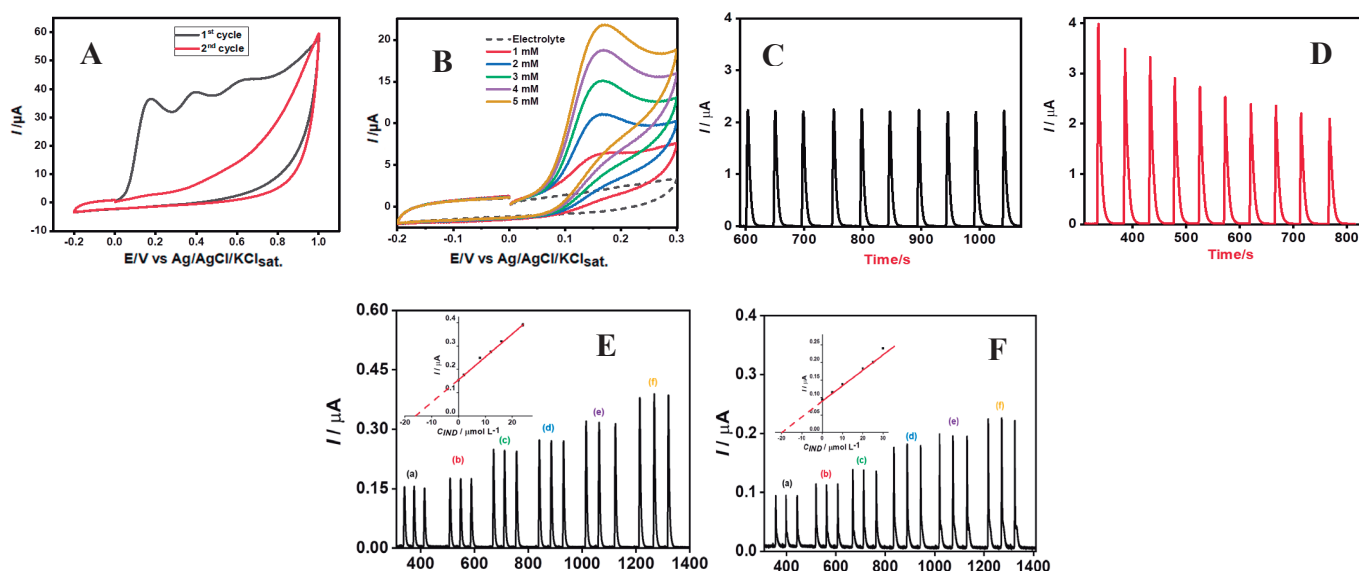


Figure 1. Voltammetric study of indapamide in aqueous medium (A) Sequence of two cyclic voltammograms in the potential window from -0.2 V to +1.0 V; (B) Series of voltammograms performed in the electrolyte (dashed line) and in presence of 1.0 to 5.0 mM of indapamide in the potential window situated between -0.2 V and +0.3 V. (C) Flow injection analysis experiments at 0.2 V and 0.5 V (D) for injections of indapamide 200 μM using the single line FIA system at a flow rate of 4.0 mL min^{-1} , volume injected of 125 μL . (E) Records of a series of injections of Pharmaceutical samples of indapamide (F) Analysis of indapamide in synthetic urine sample.

Acknowledgments



An electrochemical biosensor to diagnose COVID-19 based on gold nanoparticles conjugated with antibody specific to RBD domain.

Fabiola L. Castro (PG),¹ Ana C. H. Castro-Kochi (PQ)¹, Vivian L. de Oliveira (PQ)², Silvia B. Boscardin (PQ)³, Lídia M. Andrade (PQ)⁴, Wendel A. Alves Melo (PQ)¹.

Fabiola.c@ufabc.edu.br

¹Centro de Ciências Naturais e Humanas, Universidade Federal do ABC, Santo André, São Paulo; ²Laboratório de Imunologia, LIM19, Instituto do Coração (InCor), Hospital das Clínicas da Faculdade de Medicina da Universidade de São Paulo (HCFMUSP), São Paulo; ³Departamento de Parasitologia, Instituto de Ciências Biomédicas, Universidade de São Paulo, São Paulo; ⁴Departamento de Física, ICEx, Universidade Federal de Minas Gerais, Belo Horizonte, MG.

Keywords: Biosensors, SARS-CoV-2, Anti-RBD-antibodies, Zinc Oxide.

Highlights

In this study, we have created an electrochemical biosensor for diagnosing COVID-19 by utilizing gold nanoparticles conjugated with antibodies specific to the RBD (Receptor-Binding Domain) of the Spike protein of SARS-CoV-2.

Abstract

The COVID-19 pandemic has been a major concern for the global community for the past two years. To tackle the spread of this disease, it is crucial to invest in diagnostic methods that are simple, fast, and cost-effective. With this in mind, we have developed an impedimetric biosensor for detecting SARS-CoV-2 based on FTO (Fluorine-doped Tin Oxide) electrodes modified with zinc oxide nanorods (ZnONRs) and anti-RBD (Receptor-Binding Domain) monoclonal antibodies conjugated with gold nanoparticles (AuNPs). This solution provides a real-time monitoring tool for COVID-19 and a cost-effective alternative to traditional diagnostic methods. The ZnONRs electrodes were characterized using Scanning Electron Microscopy (SEM), as shown in Figure 1A. Our group has previously described the methodology for producing these electrodes.^[1] The AuNPs-anti-RBD conjugates onto the surface electrode were performed using electrochemical impedance spectroscopy (EIS) and cyclic voltammetry (CV). The target antigen was successfully detected, as demonstrated by decreased oxidation peak potential in the cyclic voltammetry analysis (Figure 1C, purple curve). This enabled us to construct a calibration curve consistent with previous literature data, which in turn allowed a more accurate and precise evaluation of the antigen levels in the sample.

An Atomic Force Microscopy (AFM) study was conducted on the AuNPs-anti-RBD conjugates samples to understand better the interaction between the antibody and the gold nanoparticles. The AFM images (Figures 1D and 1E) revealed that the conjugated antibodies were clustered around the gold nanoparticles, which suggests a higher degree of organization in the system. To evaluate the detection-response performance of the antibody, an ELISA (Enzyme-linked immunosorbent assay) was performed using the RBD recombinant protein of 5 SARS-CoV-2 Variants of Concern (VoC) (Alpha, Beta, Gamma, Delta, and Omicron). The results, shown in Figure 1F, demonstrate that the antibody exhibited good detection-response performance against all variants, including the Omicron variant (blue bullets). This improved biosensor performance can significantly contribute to the early detection and monitoring of COVID-19, ultimately helping control and manage the disease.

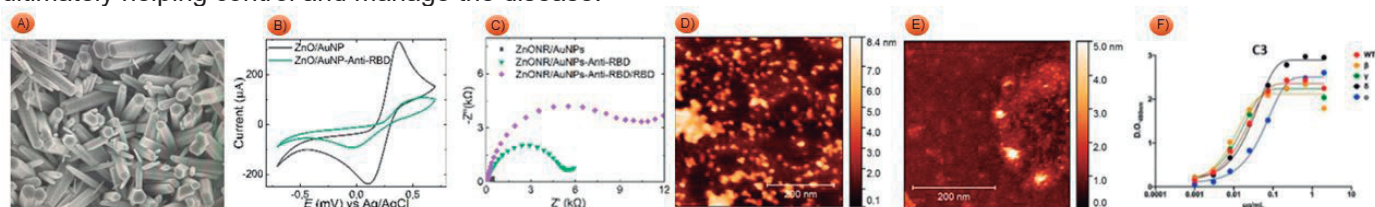


Figure 1. (A) Scanning Electron Microscopy image of ZnONRs. (B) Cyclic voltammogram of the FTO electrode modified with ZnONRs and the AuNP-conjugated anti-RBD antibody. (C) Nyquist diagram of the electrochemical impedance spectroscopy measurement demonstrating the performance of the FTO/ZnONRs electrode in the presence of the AuNP-conjugated antibody. (D) Atomic Force Microscopy image of 8 µg/mL of AuNP-conjugated antibodies. (E) Atomic Force Microscopy image of antibodies. (F) Results of the Enzyme-Linked Immunosorbent Assay test using the anti-RBD antibody against SARS-CoV-2 variants Alpha (red), Beta (yellow), Gamma (green), Delta (black), and Omicron (blue).

[1] Nunez, F.A.; Castro, A.C.H.; de Oliveira, V.L.; Lima, A.C.; Oliveira, J.R.; de Medeiros, G.X.; Sasahara, G.L.; Santos, K.S.; Lanfredi, A.J.C.; Alves, W.A. *ACS Biomater. Sci. Eng.* **2023**, *9*, 458-473.

Acknowledgments

FAPESP, CNPq, CAPES, InCor / HC-FMUSP, INCT de Bioanalítica.

Anodic processes in washing machine effluents for production of value added chemicals

Suelya S.M. Paiva (PG)¹, Herbet L. Oliveira (PG)^{1*}, Thalita M. Barros (PG)¹,

Carlos A. Martínez-Huítile (PQ)², Elisama V. Santos (PQ)¹, José E. L. Santos (PG)²

suelyapaiva@live.com; herbet.lima.097@ufrn.edu.br

¹Programa de Pós-Graduação em Engenharia Química, UFRN

²Instituto de Química, UFRN

Palavras Chave: *Electrooxidation, Hydrogen production, washing machine effluent*

Highlights

The actual washing machine effluent is one of the primary sources of microplastics and other significant compounds that frequently come into contact with the environment without being pre-treated.

Hydrogen, considered a clean fuel, environmentally friendly, and with high energy power, becomes an attractive alternative, mainly being produced from the electrolysis process.

Resumo/Abstract

Because they are domestic effluents, washing machine effluents receive little attention in the study of effluent treatments. However, there are a variety of micropollutants in this type of effluent, such as microplastics, surfactants, fibers, and others, which cause an increase in the organic load that is frequently not eliminated by conventional effluent treatments [1]. In addition, in the field of renewable energies, the production of hydrogen is a process that has been extensively studied since hydrogen is a fuel with a high energy content and can be produced through a simple electrolysis of water. Searching for routes in which hydrogen can be produced in a clean way and at the lowest possible cost becomes essential. The electrochemical treatment of real washing machine effluent coupled with the simultaneous production of green hydrogen was evaluated. The electrochemical reactor consisted of two electrodes of dimensions (15.0 cm² BDD and 18.2 cm² SS), protected inside a (10.0×7.5×1.7 cm) acrylic case, with pre-drilled holes for solution inlet, outlet, and for electrical connections. Electrolysis of 1 L of mixture of effluents collected from a washing machine, in 0.1 M H₂SO₄ or 0.1 M Na₂SO₄ as the supporting electrolyte was performed by applying 7.5, 15, 30 and 60 mA cm⁻² for 150 min in a thermoregulated glass tank at 25°C. The H₂ produced at cathodic reservoir, in concomitance with the electrolysis of effluents collected from a washing machine at anodic compartment, was collected over distilled water, as reported in previous works. The results showed that increasing the current density resulted in greater degradation of the contaminants present in the effluent, with a reduction of 24% of COD in Na₂SO₄ and 33% in H₂SO₄ for a current density of 60 mA cm⁻². This behavior is also visible in the absorbance spectrum, where increasing current density causes a greater decrease in absorbance peaks. For both electrolytes, hydrogen production increased with increasing current density, with a volume of hydrogen produced of 7.4 L in Na₂SO₄ and 7.6 L in H₂SO₄ for a current of 60 mA cm⁻². As a result, the electrochemical oxidation used in effluent treatment can serve as a low-cost hydrogen production route.

References

1. Duran, F. E., de Araujo, D. M., do Nascimento Brito, C., Santos, E. V., Ganiyu, S. O., & Martinez-Huítile, C. A. (2018). Electrochemical technology for the treatment of real washing machine effluent at pre-pilot plant scale by using active and non-active anodes. *Journal of Electroanalytical Chemistry*, 818, 216-222.

Agradecimentos/Acknowledgments

Financial supports from Conselho Nacional de Desenvolvimento Científico e Tecnológico (CNPq, Brazil) (306323/2018-4, 312595/2019-0, 439344/2018-2, 315879/2021-1, 409196/2022-3, 408110/2022-8), and from Fundação de Amparo à Pesquisa do Estado de São Paulo (Brazil), FAPESP 2014/50945-4 and 2019/13113-4, are gratefully acknowledged.

A novel electrochemical sensor based on hydrophobic deep eutectic solvent for 17 β -estradiol detection.

Júlio C. O. Almeida (IC),^{1*} Karen K. L. Augusto (PG),¹ Paulo C. Gomes-Júnior (PG),¹ Renan O. Gonçalves (PG),¹ Gustavo P. Longatto (IC),¹ Éder T. G. Cavalheiro (PQ),² Orlando Fatibello-Filho (PQ).¹

almeidajulio@estudante.ufscar.br;

¹Department of Chemistry, Federal University of São Carlos, São Carlos, SP, Brazil; ²São Carlos Institute of Chemistry, University of São Paulo, São Carlos, SP, Brazil.

Keywords: Hydrophobic deep eutectic solvent, Electrochemical sensors, Green chemistry, Endocrine disrupting.

Highlights

Characterization of hydrophobic deep eutectic solvent based on octanoic acid and tetrabutylammonium bromide, Determination of 17 β -estradiol using an electrode modified with the eutectic solvent.

Resumo

Os solventes eutéticos profundos (*Deep eutectic solvent*, DES) surgiram como opções sustentáveis aos solventes orgânicos de altas toxicidade e volatilidade¹. Desde então, eles vêm sendo aplicados em diversos procedimentos devido às suas propriedades únicas como biodegradabilidade, termoestabilidade e baixa ou ausência de toxicidade². O presente trabalho teve como objetivo caracterizar um solvente eutético profundo hidrofóbico (HDES) formado pelo ácido octanóico (OctA) e brometo de tetrabutilamônio (TBAB). A melhor razão molar encontrada foi 1,85:1 (OctA:TBAB). A caracterização do eutético e dos precursores por FTIR é mostrada nas **Fig. 1 (a) (b) e (c)**, sendo destacada a mudança na vibração de estiramento da carbonila do OctA na presença do TBAB, a qual foi deslocada de 1705 cm⁻¹ para 1728 cm⁻¹. Em seguida, o OctA:TBAB foi utilizado para modificar um eletrodo de carbono vítreo (GCE) juntamente com nanotubos de carbono de paredes múltiplas (MWCNT) ou *carbon black* (CB) e Nafion[®]. Diferentes massas de MWCNT ou CB foram estudadas na otimização do sensor proposto. Os resultados da **Fig. 1 (d)** mostram que o sensor com MWCNT apresentou um aumento de 83,29 % na corrente de pico anódica e de 97,50 % na corrente catódica, apesar de ter apresentado um aumento de 32,8 % na separação de potencial de pico (ΔE_p) comparado ao sensor com *carbon black*. Sendo assim, selecionou-se o MWCNT para modificar o eletrodo juntamente com a mistura eutética. Por fim, o sensor proposto foi utilizado para determinação do 17 β -estradiol (**Fig. 1 (e)**), sendo obtidos resultados promissores para a determinação deste analito com aumentos das correntes anódica e catódica iguais a 57% e 56%, respectivamente, em relação ao eletrodo sem a presença de OctA:TBAB (MWCNT/GCE).

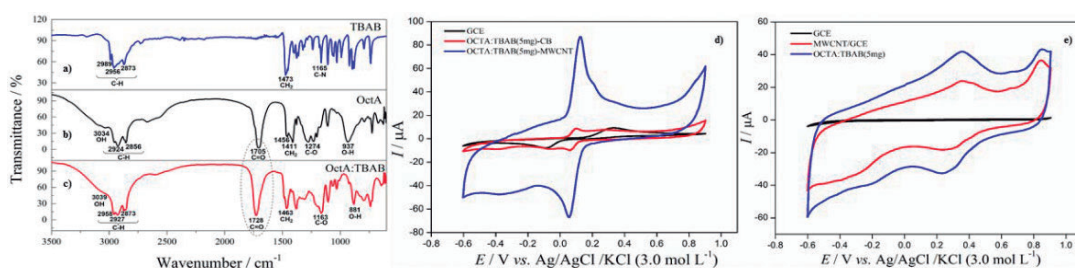


Figure 1: FTIR analysis for the eutectic mixture and its components a) TBAB, b) OctA, and c) OctA:TBAB; d) Cyclic voltammogram with Hydroquinone (H_2Q 1,0 mM); e) Cyclic voltammogram with 17 β -estradiol (1,0 mMol).

¹Joshua R. et. al Chem. Rev. 121, 2021. ²Piton et al. J Braz Chem Soc 32, 2021.

Agradecimentos

O autor agradece o apoio de todas as instituições que financiaram o desenvolvimento do presente trabalho: CNPq (#2022/15513-2), FAPESP (#140406/2021-2 e 2020/01050-5) e CAPES – Finance code 001.

Aptasensing of Alzheimer's disease by a CO₂ laser-ablated 3D-printed platform integrated with leaf-shaped gold nanodendrites

Masoud Negahdary ^{1,*}, William Barros Veloso ¹, Raphael Prata Bacil ¹, Rafael Martos Buoro ², Thiago RLC Paixão ¹, Wilson Akira Ameku ¹, Mesaque Carvalho França ¹, Thawan Gomes de Oliveira ¹, Claudimir Lucio Do Lago ¹, Solange Kazumi Sakata ³, Michelangelo Durazzo ³, Lúcio Angnes ^{1,†}

¹ Department of Fundamental Chemistry, Institute of Chemistry, University of São Paulo
Av. Prof. Lineu Prestes, 748, 05508-000, São Paulo, Brazil

² Institute of Chemistry of São Carlos, University of São Paulo, Av. Trabalhador São-Carlense, 400, 13556-590, São Carlos, Brazil

³ Nuclear and Energy Research Institute, National Commission of Nuclear Energy (IPEN/CNEN - SP), São Paulo, SP, 05508-000, Brazil

*Corresponding author, E-mail: mnegahdary@iq.usp.br;

†Corresponding author, E-mail: luangnes@iq.usp.br.

Highlights

In this research, we designed and produced a CO₂ laser-ablated 3D-printed platform electrode. Then the electrode surface was modified with LSG NDs using an electrodeposition method, which created a suitable space for interaction with the aptamer strands intended for A β ₍₁₋₄₂₎ detection. The primary goal of this research, which was not trailed in other previous research, included the use of innovative materials and interfaces in the design of aptasensor for AD diagnosis, which, by integrating with the efficient role of LSG NDs, the aptasensor was able to achieve excellent diagnostic performance for A β ₍₁₋₄₂₎ as the preferred diagnostic biomarker of AD.

Resumo/Abstract

An aptasensing platform has been designed to detect beta-Amyloid (A β), a vital biomarker of Alzheimer's disease (AD). Here, a CO₂ laser-ablated 3D-printed electrode, as an innovative signal transducer, was developed via modification with leaf-shaped gold nanodendrites (LSG NDs, mean diameter: ~ 92 nm), which could provide an ultra-efficient interface for immobilizing aptamer strands. The modified electrode with LSG NDs had approximately 7 times enhanced electrochemically active surface area compared to the bare electrode. This modification confirms the special size, morphology, and distribution of LSGNDs in amplifying electrochemical signals to provide a highly sensitive infrastructure for analyte detection. The strands of a thiol-functionalized aptamer sequence interacted with the gold surface and could provide an optimized biointerface to detect A β in a linear range from 0.1 pg mL⁻¹ - 10 ng mL⁻¹ (limit of detection (LOD): 83.7 fg mL⁻¹, (S/N = 3)). The developed aptasensor confirmed logical stability, desired reproducibility and regeneration, and even minimal impact of interfering agents. In addition, the application of this aptasensor was monitored via assay of spiked analyte concentrations in 20 samples, including CSF and serum.

Agradecimentos/Acknowledgments

The authors would like to thank the Sao Paulo Research Foundation-FAPESP (projects 2019/27021-4, 2017/13137-5, and 2014/50867-3) and the National Council for Research-CNPq (processes 311847-2018-8 and 465389/2014-7). The authors are also appreciative to Central Analítica (IQ-USP), and Laboratório de Microscopia e Microanálise do Centro de Ciência e Tecnologia de Materiais do IPEN/CNEN-SP for material characterization facilities.

A rotating disk voltammetric study of the anodic oxidation of nitrite at a Pt-TRP (Tetraruthenated Cobalt (II) Porphyrzine) modified electrode

Leonardo M. A. Ribeiro (PG)*¹, Hiago N. Silva (PG)¹, Marcos M. Toyama(PQ)², Henrique E. Toma(PQ)¹, Mauro Bertotti (PQ)¹

leonardo.ma.ribeiro@usp.com.br

¹Departamento de Química Fundamental, Instituto de Química, Universidade de São Paulo (IQ – USP); ²Departamento de Química, Instituto Mauá de Tecnologia (IMT)

Keywords: Porphyrzine, Rotating disk electrode, Nitrite electrocatalysis, Modified electrodes

Highlights

Rotating disk voltammetric experiments were performed to understand the kinetics of the nitrite anodic oxidation at a Pt electrode modified with a film of Cobalt (II)–tetra(3,4-pyridyl)-porphyrzine (TRP).

Abstract

The nitrite ion (NO_2^-) is a common chemical in our routine, recurrently found on cured meat, human saliva, and urine. In 2015, the International Agency for Research on Cancer (IARC) classified NO_2^- as “probably carcinogenic to humans”. Hence, strategies to easily, quickly, and inexpensively monitor such compound are welcome. This can be achieved by using electrochemical sensors and providing mediators capable of facilitating the electron transfer step is an issue of continuous research. This work shows our efforts to modify platinum surfaces with a film of Cobalt (II)–tetra(3,4-pyridyl)-porphyrzine (TRP), which has already been reported as a good electrocatalyst¹. In a previous study, we demonstrated that the anodic oxidation of nitrite on a modified Pt-TRP microelectrode takes place at less positive potentials than the bare Pt microelectrode². In the present study, the kinetics of the reaction involving nitrite and immobilized TRP was investigated using rotating disk electrode (RDE) voltammetry. Hence, sensors with better performance can be rationally designed. The influence of the rotation rate and nitrite concentration indicated that the rate of the cross-chemical reaction between cobalt porphyrzine centers immobilized into the film and nitrite controls the overall process.

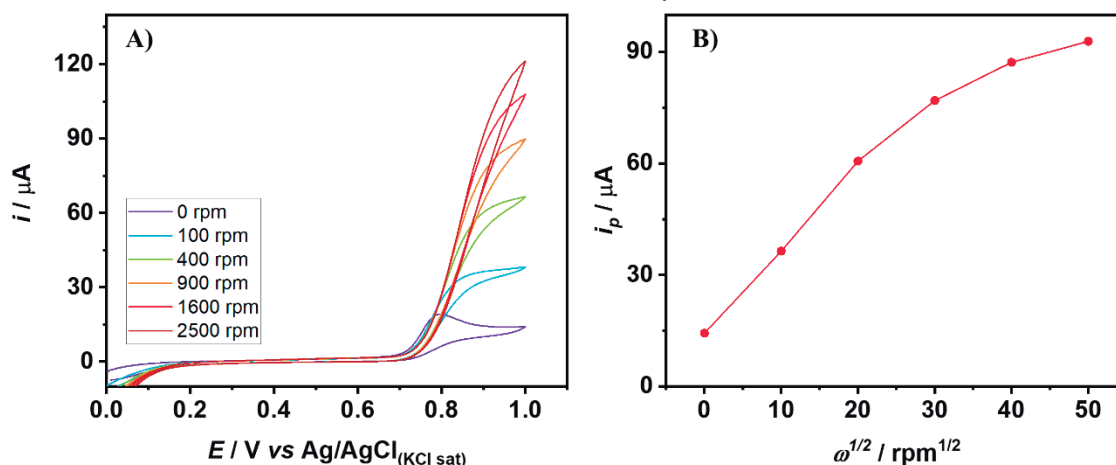


Figure 1 – A) Cyclic voltammograms recorded in PBS (pH = 7) containing 1mM NO_2^- using a Pt-TRP rotating disk electrode at varying rotation rates (scan rate = 10 mV s^{-1}). B) Peak current (i_p) values (at 0.9 V) as a function of the square root of the rotation rate.

Acknowledgments



¹ SILVA, Hiago N. et al. A New Supramolecular Tetraruthenated Cobalt (II) Porphyrzine Displaying Outstanding Electrocatalytical Performance in Oxygen Evolution Reaction. *Molecules*, v. 27, n. 14, p. 4598, 2022.

² RIBEIRO, L. M. A.; et. al. Pt sensor based on a new porphyrzine to nitrite determination. *In: Encontro Brasileiro De Química Analítica*, 20., 2022, Bento Gonçalves. **Resumo** [...]. São Paulo: BrJAC, 2022. p. 30

A spray-processable and all-solid-state electrochromic device

Marivone Gusatti (PG),^{1*} Daniel A. R. Souza (PG),¹ Marcelo Nalin (PQ).¹

m.gusatti@unesp.br

¹Instituto de Química, Departamento de Química Analítica, Físico-Química e Inorgânica, UNESP, Campus Araraquara, SP

keywords: *Spray Coating, ECD, Al Counter Electrode, PEDOT:PSS.*

Highlights

An electrochromic device with glass/Al/Alq₃/PEDOT:PSS structure was designed.
Low-cost deposition technique of thin films.
The device showed low operational voltage, good contrast, and fast response time.

Abstract

The electrochromic (EC) phenomenon refers to a reversible change in the optical properties of electrochromic materials under an applied external voltage. Recently, EC materials have attracted much attention due to their wide range of applications, including energy-efficient information displays, electronic labels, smart windows, and switchable mirrors [1]. In this study, we describe the assembly of an all-solid-state electrochromic device (ECD) completely free of indium-doped tin oxide, lithium, and tungsten trioxide, without liquid or gel electrolyte in its structure. The ECD is based on a new structure formed by an Al counter electrode covered with an Alq₃ film, as the anode species, and a working electrode of PEDOT:PSS, as the electrochromic material, on a glass substrate. This solid-state ECD contains internal layers that are fully solution-processable at low temperatures by a cost-effective spray coating technique.

The ECD achieved a transmittance variation of about 7.02 % at 580 nm (Fig. 1) under an applied voltage of +3V, with good color homogeneity. With a positive voltage applied to the working electrode, electrons are injected into the PEDOT:PSS film, and the ECD changes color from light blue to dark blue. On the other hand, with a negative voltage applied to the working electrode, the ECD restores its optical property, returning to its original color. In addition, the switching speed between colored and bleached states is fast under an applied voltage of +2 V and -3.5 V, with a coloration time of 13.78 s and a bleaching time of 4.28 s.

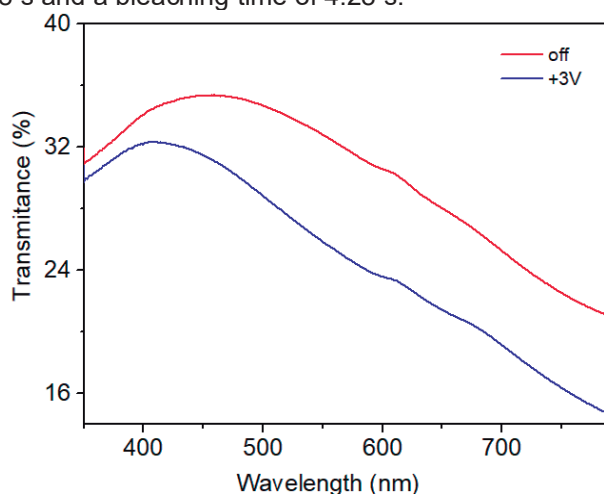


Fig. 1. The optical transmittance spectra of the ECD in the initial and colored state.

Thus, these results indicate that the ECD has good performance and promising applications in the industrial field. Furthermore, this study presents an opportunity to take advantage of low-cost solution-processing methods for producing high-quality EC devices.

[1] M. A. Khalifa, K. Sheng, Z. Wang, J. Zheng, C. Xu, *Adv. Mater. Interfaces* 2022, 9, 2100945.

Acknowledgments

The authors thank the UNESP (PROPG-PROPe 05/2022) and FAPESP Grant n° 2013/07793-6 for providing financial support to carry out this research.

Assembly and ion transfer properties of MoS₂/graphene nanocomposites at liquid-liquid interfaces.

Ariane Schmidt (PG)^{1,2*}, Hussain A. Al Nasser (PG)², Aldo J. G. Zarbin (PQ)¹, Robert A. W. Dryfe (PQ)²

arianeschmidt@ufpr.br

¹Chemistry Department, Federal University of Paraná (UFPR), 81531-980 Curitiba, Paraná, Brazil; ²Department of Chemistry, Henry Royce Institute for Advanced Materials, University of Manchester, Oxford Road, Manchester M13 9PL, United Kingdom.

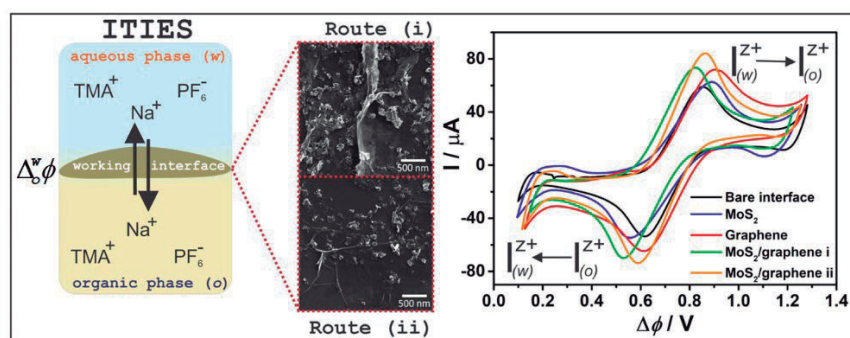
Keywords: Ion Transfer, ITIES, 2D Materials, Liquid-Liquid Interfaces, Thin Films.

Highlights

MoS₂/graphene nanocomposites were assembled at the liquid-liquid interface, and the ion transfer properties were studied at the interface between two-immiscible electrolyte solutions.

Abstract

The ion transfer through the interface between two-immiscible electrolyte solutions (ITIES) has been extensively explored and presents applications in electroanalysis, ion separation, and more.¹ The modification of the ITIES interface can influence the ion transfer properties by blocking the path of the ion or by enhancing the membrane selectivity. Herein, we investigate the ion transfer properties of MoS₂/graphene thin films assembled at L/L interfaces.² For this, two routes were used for the preparation of the nanocomposites: i) MoS₂ and graphene dispersions were combined in a one-pot biphasic system, or ii) previously prepared neat MoS₂ and graphene films were combined in a new L/L interface. All samples were fully characterized, showing that the materials' organization depends on the route used. Using (i), interconnected and wrinkled sheets of MoS₂/graphene were obtained, while using (ii), the sheets were more spread out. For the ion transfer studies, a four-electrode cell with water|1,2-DCB was used to polarize the interface, Scheme 1. The presence of the interfacial layer of MoS₂/graphene enhances the facilitated Na⁺ ion transfer compared to the isolated MoS₂ or graphene and even more compared to the bare interface. This could be associated with the increase in the interfacial area due to the roughness of the film or by the accumulation of the ion at the interface. This trend was followed for the ion transfer of tetramethylammonium cation (TMA⁺) and hexafluorophosphate anion (PF₆⁻), but the current for ion transfer decreases by repeated cycling, which could indicate the entrapment of the ions through the film, acting as a nanofiltration membrane. This study can shed a light on the transport properties of those films, as well as the selectivity, which can be further improved by modifying the proportion of each material or the thickness of the film, besides the study in scalable membranes through the liquid-liquid assembly of those films.



Scheme 1. Ion transfer at ITIES, scanning electron microscopy images of MoS₂/graphene composites and cyclic voltammogram with and without the interfacial film for the facilitated Na⁺ transfer.

1. Molina, A., Torralba, E., Serna, C., *et al.* Phys. Chem. Chem. Phys., **14**, 15340-15354, 2012.
2. Zarbin, A. J. G. Mater. Horiz., **8**, 1409-1432, 2021.

Acknowledgments

Authors acknowledge CAPES, CAPES-PRInt, CNPq, INCT-Nanocarbono, INCT-NanoVida, EPSRC-UK for financial support.

Co₃O₄ nanostructures as catalysts in the electrosynthesis of ammonia

Marina D. Saraiva (PG),^{1,2} Thiago M. Mariano (PQ),^{1,2} Manuel E. G. Winkler (PQ),^{1,2} João A. V. Meirelles (IC),¹ Evelin Medeiros (IC),¹ Rafael L. Germscheidt (PG),¹ Larissa E. R. Ferreira (PG),¹ Juliano A. Bonacin (PQ),^{1,2} Italo O. Mazali (PQ),¹ Raphael Nagao (PQ)^{1,2*}

marinadsaraiva@gmail.com; nagao@unicamp.br

¹Institute of Chemistry, University of Campinas; ²Center for Innovation on New Energies

Keywords: Co₃O₄ nanoplates, Co₃O₄ nanowires, Nitrate reduction, Ammonia electrosynthesis, Electrocatalysis.

Highlights

Using two different Co₃O₄ morphologies for NO₃⁻ reduction as a method for generating NH₃. Co₃O₄ electrocatalysts, analysed in the same condition, produces more NH₃ when it has larger active surface area.

Resumo/Abstract

Ammonia (NH₃) has become one of the main focuses of study in the energy sector, as a precursor of clean energy based on hydrogen. An alternative to the production of NH₃ by the Haber-Bosch process, economical and environmentally friendly, is the electrocatalytic reduction of nitrate (NO₃⁻)¹. For this, it is still necessary to work on challenges such as increasing the electrocatalytic efficiency, stability and selectivity of the materials used as catalysts. Therefore, the present study proposes to adopt cobalt oxides as a catalyst in the electrosynthesis of NH₃ from the NO₃⁻ reduction reaction (NO₃RR). Cobalt and its compounds have been highlighted in the literature as promising catalysts in NO₃RR, it happens because, even at lower potentials, there is a significant rate of selectivity for NH₃ as a product in the reaction². This study has been working with two Co₃O₄ morphologies, i.e., nanoplates (NP) and nanowires (NW) (Figure 1), as catalysts to obtain NH₃. The NP was supported in glassy carbon with 0.196 cm² of geometric area and the NW were electrodeposited in FTO with 1.0 cm² of geometric area. The materials were characterized by cyclic voltammetry (CV) at 20 mV s⁻¹ with NaOH 1.0 mol L⁻¹ as electrolyte and with the electrolyte with NaNO₃ 14.0 mmol L⁻¹. As shown in the Figure 1, both materials have reducing activity to reduce in the presence of NO₃⁻. The NP showed reducing activity from -0.2 V vs RHE while the NW showed activity closer to 0 V vs RHE of potential. In this way, to study the catalysts, a chronoamperometry (CA) was carried out at -0.2 to -0.8 V vs RHE for the NP, and at -0.1 to -0.5 V vs RHE for the NW. The electrolysis was taken for 1 hour and the currents obtained (i) were normalized for the geometric area of the electrodes. In this work, it was selected the values of -0.2 and -0.4 V vs RHE of applied potential for the comparative studies. At these potentials, the use of NP resulted in the production of 0,04 and 0.19 mmol L⁻¹ h⁻¹ of NH₃, respectively. Concomitantly, the NW generate, at the same potentials, 0.23 and 2.17 mmol L⁻¹ h⁻¹ of NH₃, respectively, these values are the mean values of the triplicates. With these results, it is already possible to indicate that the difference in the morphology of the oxide makes it possible to increase the production of NH₃ in the electroreduction of NO₃⁻. We point out that, for a better discussion of the results, the faradaic efficiency (FE), selectivity and yield are still in progress as well as other electrochemical measurements and material characterizations.

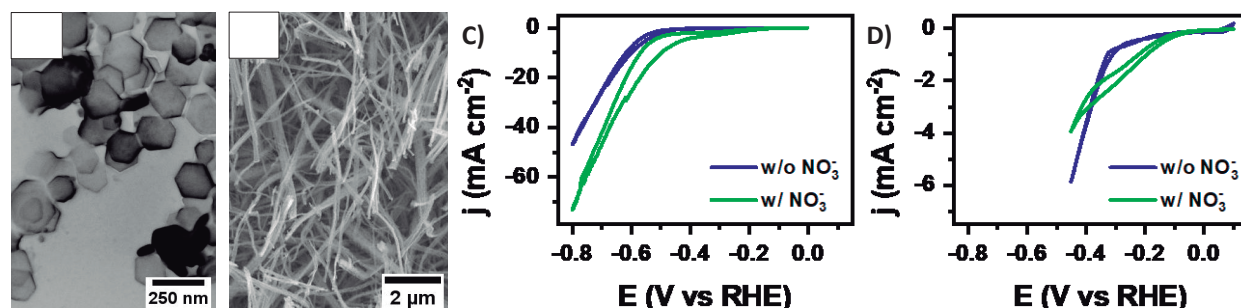


Figure 1. SEM micrographs Co₃O₄ of A) NP and B) NW. Voltammograms at 20 mV s⁻¹ in NaOH 1.0 mol L⁻¹ with NaNO₃ 14.0 mmol L⁻¹ and Co₃O₄ electrodes as C) NP and D) NW.

- Zhiheng Gong et al. Applied Catalysis B: Environmental 305, (2021).
- Liu, J.-X., Richards, D., Singh, N. & Goldsmith, B. R. ACS Catal. 9, 7052–7064 (2019).

Agradecimentos/Acknowledgments

This work was supported by CNPq, FAPESP, CAPES and Shell.

CO₂ conversion promoted by a bias-free electrolyzer with a Cu₂WO₄ gas diffusion photocathode and a BiVO₄ photoanode

Jéssica Costa Alvim (PG),¹ Leonardo Carvalho Soares (PG)¹, Nadia Guerra Macedo (PQ)¹, Márcio Sangali (PG)², Rubens Caram Jr (PQ)², Claudia Longo (PG)¹

costaalvimjessica@gmail.com; l264622@dac.unicamp.br; clalongo@unicamp.br

¹Departamento de Físico-Química, Instituto de Química - UNICAMP; ²Faculdade de Engenharia Mecânica - UNICAMP

Palavras Chave: CO₂ reduction, Photoelectrochemical cell, Bias-free system

Highlights

Bias-free photoelectrochemical cell for CO₂ reduction reaction
Photocathode: p-type Cu₂WO₄ semiconductor on gas diffusion electrode for CO₂RR
Photoanode: n-type BiVO₄ semiconductor for O₂ Evolution Reaction
Ethanol produced from CO₂ conversion, achieved without external bias, with 14 % of Faradaic Efficiency.

Resumo/Abstract

The search for sustainable pathways for CO₂ reduction reaction (CO₂RR) to value-added chemicals is a remarkable challenge due to the high stability of CO₂ molecule and low selectivity for C₂₊ products from carbon dioxide conversion. Photoelectrochemical (PEC) devices that spontaneously promote CO₂RR, without any external applied potential, would be a sustainable and low-cost alternative for producing molecules from emitted CO₂. Here we demonstrated a PEC reactor to promote solar-driven CO₂RR using photo-responsive semiconductor electrodes. The cathodic compartment for CO₂RR includes a gas diffusion electrode (GDE) prepared by deposition of Cu₂WO₄ (a p-type semiconductor) particles by hand-painting method on carbon paper (Sigracet 39BC), placed between two titanium mesh to improve the electrode mechanical stability (GDE|Cu₂WO₄|Ti-mesh). At the anodic compartment, oxygen evolution reaction (OER) takes place on BiVO₄ photoanode prepared with a Ti foil covered with a film of BiVO₄ prepared by successive ionic layer adsorption and reaction (SILAR) method and modified with Ni-Fe hydroxides by electrodeposition. Thus, the Ti|BiVO₄|FeOOH|NiOOH (9.0 cm²) photoanode was connected with the GDE|Cu₂WO₄|Ti-mesh (7.5 cm²) photocathode under CO₂ flow in a H-type PEC cell, using 0.5 M NaHCO₃ aqueous solution in both compartments (ca. 150 mL). Irradiated by a metallic vapor light source (irradiance of ~ 65 mW/cm²), without any external bias, this PEC reactor showed an open circuit potential of 0.4 V; also, a short-circuit photocurrent of ca. 0.7 mA flowed in the cell, continuously sustaining OER and CO₂RR in each compartment. After 2 hours, the main liquid product generated from CO₂RR in this system was ethanol, with (14 ± 3) % of Faradaic Efficiency. Considering the studies performed with each electrode, we conclude that the spontaneous current in the PEC-Cell results from the low onset potentials required by Cu₂WO₄ for CO₂RR, as well as, for OER on BiVO₄|FeOOH|NiOOH. Therefore, association of adequate semiconductor electrodes can promote bias-free CO₂ conversion in a photoelectrochemical reactor.

Agradecimentos/Acknowledgments

The authors gratefully acknowledge support from CINE, FAPESP, Faepex-UNICAMP, CNPEM, CNPq and CAPES.

Composite Material Immobilized in 3D-printed Support, an Economical Approach for Electrochemical Sensing of Nimesulide

Wallace B. V. de Oliveira (PG),* Thalles P. Lisboa (PQ), Raylla S. Oliveira (PG), Cassiano C. de Souza (PG), Maria Auxiliadora C. Matos (PQ), Renato C. Matos (PQ).

wallacemnj@gmail.com; renato.matos@ufjf.edu.br

Departamento de Química, Universidade Federal de Juiz de Fora, 36026-900, Juiz de Fora-MG, Brazil

Palavras Chave: 3D-Printed support, Graphite composite material, Nimesulide, Anti-inflammatory.

Highlights

A 3D printed support with graphite and nail polish composite material for electrochemical monitoring of Nimesulide using a low-cost and easy mass production sensor for anti-inflammatory detection.

Abstract

Nimesulide is a non-steroidal anti-inflammatory drug from the sulfonanilide group that has analgesic and antipyretic action, it is used to control acute pain in the treatment of diseases, such as osteoarthritis, by inhibiting cyclooxygenase enzymes^{1,2}. This work aimed to build a disposable electrode, cheap, and robust, with a maximum manufacturing value of US\$ 0.02 per sensor, whose basic structure is a composite material (CM) immobilized on 3D support of acrylonitrile butadiene styrene (ABS), to the determination of Nimesulide (NIM) in different samples. The surface characterization of the electrodes was made by scanning electron microscopy (SEM), electrochemical impedance spectroscopy (EIS), and cyclic voltammetry (CV). The electrochemical response for NIM obtained was compared with a commercial Glassy Carbon Electrode (GCE), where a 70% increase in the analytical response was observed. The sensor was applied for the quantification of NIM by the square wave voltammetry (SWV) method in pharmaceutical formulations, tap water, synthetic urine, and breast milk, the mechanism of the reaction was also investigated (Figure 1). The optimized method presented a satisfactory linear range of 10 to 50 $\mu\text{mol L}^{-1}$ (Figure 2), with a simple sample treatment, good precision (RSD < 3.38%), and an excellent detectability (limit of detection of 0.018 $\mu\text{mol L}^{-1}$). Samples were spiked at three concentration levels to evaluate the accuracy of the method, obtaining recovery values from 96.2 to 112.8%. Thus, the disposable proposed device proves to be a promising analytical tool for routine analysis of NIM in different samples with a minimum sample preparation step (simple dilution).

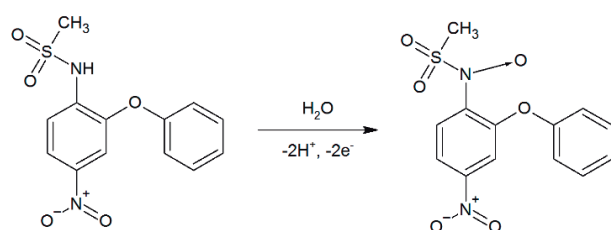


Figure 1: Electrochemical mechanism for the NIM oxidation process on 3Ds-NPGE surface.

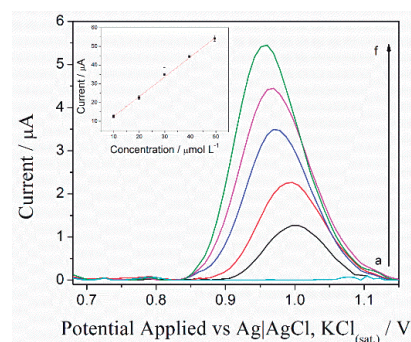


Figure 2: SWV voltammograms for analytical curve of NIM using 3Ds-NPGE with concentrations ranging from blank (a) to 50 (f)

¹de Sousa JM, de Araújo Neto MF, Partata AK (2016) Ação antiinflamatória da nimesulida e seu grau de hepatotoxicidade. Rev Científica do ITPAC v9:1–11

²Davis R, Brogden RN (1994) Nimesulide: An Update of its Pharmacodynamic and Pharmacokinetic Properties, and Therapeutic Efficacy. Drugs 48:431–454

Agradecimentos/Acknowledgments

This research was supported by FAPEMIG (Research Support Foundation of the State of Minas Gerais) (process: APQ-00042-21), CNPq (National Council for Scientific and Technological Development, process: 303815/2022-1), CAPES (Coordination for the Improvement of Higher Education Personnel) and PROPESQ/UFJF.

Coupling between TiO₂ nanotubes and Cu-MOF for CO₂ photoelectrochemical reduction into value-add products

Juliana de Almeida (PQ),^{1,2} Gabriela Maria Previde (IC),^{1,2} Isabela Disigant (PG),^{1,2} Christiane de Arruda Rodrigues (PQ).^{1,2}

juliana.almeida17@unifesp.br

¹Departamento de Engenharia Química, UNIFESP; ²INCT-DATREM Instituto de Química, UNESP.

Palavras Chave: Absorption, CO₂ conversion, Metal-Organic Framework, Methanation, Photoelectrocatalysis, TiO₂ nanotubes.

Highlights

Cu-MOF increased methanol production efficiency due to improvements in CO₂ capture.

A synergistic combination between TiO₂ nanotubes and Cu-MOF improves CO₂ conversion.

Resumo/Abstract

The growing dependence on fossil fuels in recent decades and the pollution resulting from their use has driven the development of technologies that reduce carbon dioxide emissions. In this perspective, the CO₂ conversion is a promising alternative that consists of applying semiconductors able to reduction of CO₂ in value-added compounds. Among these materials, copper oxides are the only material that promote the production of alcohols and C₂ products. While TiO₂ is an excellent oxidant, providing methyl radicals and facilitating the formation of alcohols^{1,2}. In addition, the metal-organic frameworks (MOF) are porous three-dimensional structures, with a high surface area and affinity for CO₂ adsorption¹. In order to increase the efficiency of this process, this study synthesized TiO₂ nanotubes modified with Cu-MOF by drop casting technique. Thus, the preparation of TiO₂ nanotubes (NT/TiO₂) was produced via an anodizing process in an electrochemical cell containing an aqueous solution of HF, followed by heat treatment. After, the NT/TiO₂ was modified with Cu-MOF using the drop casting technique. Previously, Cu-MOF was synthesized by the solvothermal method, in which a solution of CuNO₃, DMF, and terephthalic acid was placed in a closed reactor at 130°C for 48 hours, followed by washing, filtering, and drying. The MOF was characterized using the Brunauer–Emmett–Teller (BET) method based on adsorption isotherms of nonreactive nitrogen, this material showed able to load CO₂ molecule in the cavities. The morphology and structure of the NT/TiO₂@Cu-MOF electrode were characterized by scanning electron microscopy and X-ray diffraction, such analyzes showed the presence of octahedral nanoparticles deposited on the surface of NT/TiO₂. Meanwhile, the photoelectrochemical characterization was conducted by linear voltammetry (0.1 M Na₂SO₄) and stability in phosphate buffer solution. These analyzes showed cathodic behavior of the electrodes and high stability in front light, respectively. The CO₂ conversion was conducted in a two-compartment reactor using a 1.0 M NaHCO₃, pH 7.0, solution with CO₂ bubbled. After 120 min of continuous irradiation and application of ~0.4 V, the electrode produced methanol in a remarkable concentration detected using a GC-FID. The electrode showed a synergic activity between the semiconductor and MOF. While the Cu-MOF increase the capacity of CO₂ adsorption and favored its reduction, the TiO₂ was essential to provide methyl radical to the reaction of methanol formation, improving the efficiency of the process.

References:

- Cardoso, J. C. *et al. Appl Catal B* **225**, 563–573 (2018).

Agradecimentos/Acknowledgments

INCT-DATREM (Proc. CNPq 465571/2014-0), São Paulo Research Foundation (Proc. FAPESP 2014/50945-4), Coordination for the Improvement of Higher Education Personnel (Proc. CAPES 88887136426/2017/00), Project PITE-FAPESP 2020/12263-0.

Cu₂O nanocubes as catalysts for the electro-reduction of nitrate to ammonia

Igor Messias (PG)^{1,2}; Manuel E. G. Winkler (PQ)³; Gabriel F. Costa (PG)^{1,4}, Thiago M. Mariano (PQ)³, Maria R. Pinto (PG)^{1,5}, Marina D. Saraiva (PG)^{1,3}, João B. S. Junior (PQ)⁶, Raphael Nagao (PQ)^{*1,3}

manuelgw@unicamp.br; nagao@unicamp.br

¹Institute of Chemistry, UNICAMP, ²Argonne National Laboratory, ³Center for Innovation on New Energies, ⁴University of Michigan, ⁵Leiden University, ⁶Brazilian Nanotechnology National Laboratory, LNNano.

Palavras Chave: Cu₂O nanocubes, nitrate reduction, ammonia production.

Highlights

- Cu₂O nanocubes as catalysts for the electro-reduction of nitrate to ammonia;
- Cu₂O nanocubes with sizes of 47.98 ± 13.15 nm showed high catalytic activity for electroreduction of NO₃⁻ to NH₃;
- 94.4 ± 4.3 % Faradaic Efficiency was observed at -0.30 V vs RHE.

Resumo/Abstract

Ammonia (NH₃) is a multifunctional compound employed in several applications. Conventionally, it is produced by the Haber-Bosch, which produces twice the amount of greenhouse gases and consumes 1 to 2 % of all the energy produced worldwide annually¹. Therefore, electrochemical reduction of nitrate (NO₃RR) to NH₃ is an ideal technology, as it can use renewable electricity as the energy source¹. Cu₂O nanoparticles were synthesized through a one-step water-based reduction method². HAADF-STEM and EDX revealed cubic particles containing Cu and O elements uniformly distributed (Figure 1 A-C). The average cube size was 47.98 ± 13.15 nm, calculated from the count of 100 particles (Figure 1D). To further confirm the chemical composition of the prepared samples, high-resolution XPS analysis was performed and the fitted peaks at 934.3 eV and 954.2 eV refer to CuO, while the peaks at 933.2 eV and 952.4 eV correspond to Cu₂O (Figure 1 E). The performance as a catalyst for NO₃RR was evaluated in an H-type electrochemical cell in 14 mM NaNO₃ and 1 M NaOH with argon flow. Linear Sweep Voltammetry (LSV) results showed a high catalytic activity, with an onset potential at -0.10 V vs RHE, and a much higher current in the presence of NO₃⁻ (Figure 1F). Quantification of ammonia produced in the potential range of -0.1 to -0.6 V vs RHE showed that NH₃ is produced in the entire potential range, with a maximum Faradaic Efficiency at -0.30 V (94.4 ± 4.3 %). Thus, Cu₂O nanocubes stand as a promising low-cost catalyst for ammonia production via NO₃RR.

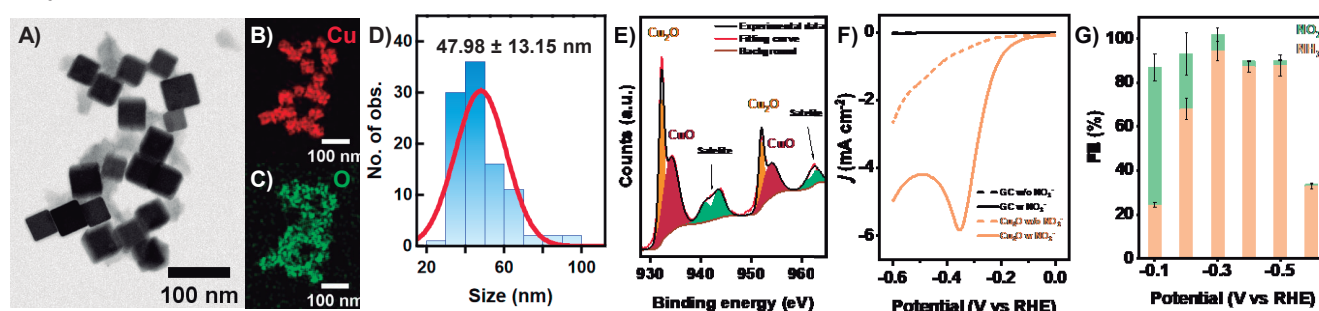


Figure 1. A) HAADF-STEM, B) and C) EDX mapping of Cu and O, respectively, D) size distribution, and E) high-resolution XPS of Cu₂O nanocubes. F) LSV curves (20 mV s⁻¹) of the Cu₂O catalyst and the substrate (glassy carbon) in 1 M NaOH with and without 12 mM NaNO₃, and G) FE for NH₃ and NO₂⁻ at different potentials.

¹ Wu, L. *et al.*, Pure Appl. Chem. **2021**; 93(7): 777–797.

² Herzog, A. *et al.*, Angew. Chem. Int. Ed. **2021**, 60, 7426–7435

Agradecimentos/Acknowledgments

This work was supported by Shell, FAPESP, CNPq, CAPES, and LNNano.

Degradation of the antibiotic ciprofloxacin by the photo-electrochemical method using a photoanode of the type FTO/Fe₂O₃/BiOI@BiOBr as catalytic material

Maria H.A. Feitosa (PG),¹ Anderson M. Santos (PQ),¹ Esther M. Angelini (IC),¹ Fernando C. Moraes (PQ).¹

helenaifpi@gmail.com

¹Departamento de Química, UFSCar

Keywords: Ciprofloxacin, Photo-electrocatalysis, Degradation, Emerging contaminants, Environment pollution.

Highlights

- The photoanode FTO/Fe₂O₃/BiOI@BiOBr showed higher degradation efficiency than FTO/Fe₂O₃;
- Photo-electrocatalysis performed better than electrocatalysis and photocatalysis.

Abstract

In recent years, several materials with semiconductor properties have been widely investigated in photo-electrocatalysis for environmental applications. In this work, hematite (α -Fe₂O₃) was chosen as a semiconductor material for the fabrication of a type II heterojunction with BiOI@BiOBr as catalytic material. This catalytic material was used as photoanode at the removal of ciprofloxacin in water. Thus, the manufactured photoanode was used for ciprofloxacin (CIP) degradation under several conditions: pH, electrolyte concentration, drug concentration and work potential under radiation of a 9.0 watt UVC lamp.

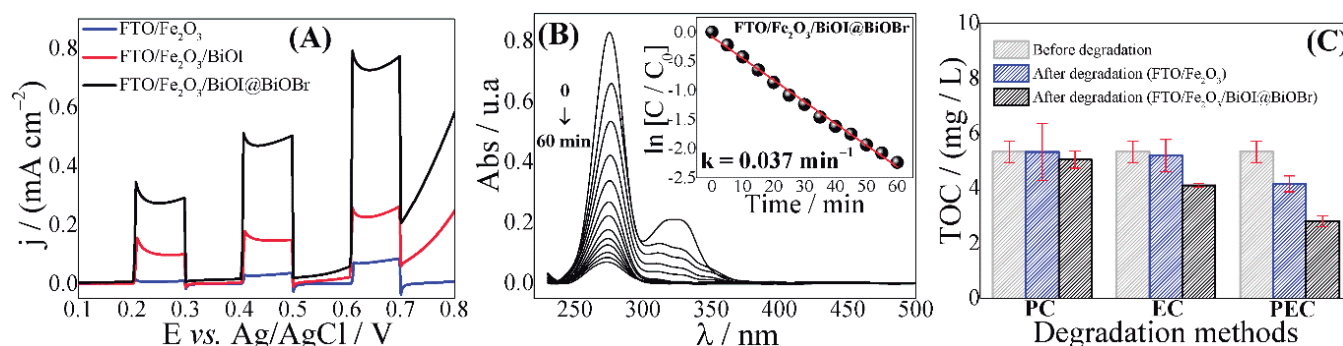


Figure 1: (A) Photocurrent response of semiconductor materials; (B) Ciprofloxacin degradation by photo-electrocatalysis using the optimized photoanode; (C) TOC data from the initial sample and after 1h of degradation.

It was possible to observe in Fig 1(A) that when introducing the BiOI material under the surface of the FTO/Fe₂O₃, there was an increase in the photocurrent of approximately 61.9 %. The addition of the BiOBr semiconductor on the FTO/BiOI surface increased the analytical response by 75.5 %. Thus, when comparing the electrode (FTO/Fe₂O₃) with the modified electrode of ternary composition, there was an increase of 184.1 %. With this catalytic material, different degradation tests were carried out, as displayed in Fig 1(B). It can be noted that the maximization of the concentration decay occurred at pH 6.0; [Na₂SO₄] = 0.1 mol L⁻¹; [CIP] = 30 μ mol L⁻¹ and $E = +2.0$ V. In this scenario, it is observed that in 1 hour the CIP concentration decreased approximately 91.9 % with a pseudo first order at K_c of 3.7×10^{-2} min. Tests that were also performed with FTO modified only with hematite proved to be 2.14 times less efficient than the modified electrode. Finally, the determination of the total organic carbon proposes that for the two photoanodes in different methods (electrocatalysis (EC), photocatalysis (PC) and photo-electrocatalysis (PEC)) there is a higher mineralization rate for the FTO/Fe₂O₃/BiOI@BiOBr by the PEC method in 47.4 %, while the others showed a lower possibility of mineralization organic matter into inorganic, as presented in Fig. 1 (C).

Acknowledgments

The authors thank the Department of Chemistry - UFSCar. Financial support and scholarships granted by FAPESP processes (n^os 2017/10118-0 and 2022/05454-9) and by CAPES - Financial Code 001.

Desenvolvimento de sensor eletroquímico biomimético baseado em polímero funcionalizado para detecção de pesticidas organofosforados

Julia Garcia de Oliveira (IC)¹, João Vitor Souza de Oliveira (IC)¹, Bruno Silveira de Souza (PQ)², Jamal Rafique (PQ)¹, Sumbal Saba (PQ)¹, Lívia Flório Sgobbi (PQ)^{1*}

juliagarcia@discente.ufg.br; livia_sgobbi@ufg.br

¹Instituto de Química, UFG; ²Departamento de Química, UFSC

Palavras Chave: Enzimas artificiais, Polímeros, Pesticidas organofosforados, Desfosforilação, Sensor eletroquímico.

Highlights

Development of a biomimetic electrochemical sensor based on a functionalized polymer for the detection of organophosphorus pesticides. A polymer functionalized with imidazole moieties works as an efficient artificial enzyme for dephosphorylation of methyl-paraoxon. The product released in the dephosphorylation reaction was electrochemically detected. The biomimetic system exhibited high potential to be used in electrochemical sensing platforms.

Resumo/Abstract

A Química Biomimética lida com sistemas químicos que podem simular fenômenos biológicos. Neste cenário, a produção de enzimas artificiais por meios sintéticos tem despertado grande interesse, uma vez que as naturais, apesar da eficiência catalítica e seletividade notáveis; têm atividade afetada dependendo das condições experimentais (pH, temperatura, etc), além do custo elevado, o que inviabiliza a sua aplicação em biossensores. O desenvolvimento de sistemas biomiméticos que imitem as reações enzimáticas e que possam ser produzidos em grande escala é de grande interesse para a Ciência. Diante disso, o presente trabalho tem como objetivo a investigação do comportamento do polímero funcionalizado com grupos imidazóis (PECIM) (Figura 1A) na reação de desfosforilação do pesticida metil-paraoxon (Figura 1B) para aplicação em plataformas de sensoriamento eletroquímico [1]. A atividade catalítica do polímero foi avaliada na presença do pesticida por monitoramento espectrofotométrico da reação de desfosforilação, utilizando 3 g/L de polímero misturados na presença de 0,1 mmol/L de pesticida em tampão BR pH 9. Em tais condições, observou-se o aparecimento de um pico em 400 nm, referente à liberação de *p*-nitrofenolato, resultante da desfosforilação do pesticida. A hidrólise espontânea do pesticida também foi avaliada em pH 9, sendo esta negligenciável nas condições experimentais avaliadas. Posteriormente, a detecção do *p*-nitrofenolato liberado na reação foi realizada por voltametria de onda quadrada de +1,2 V a -1,2 V, utilizando-se um eletrodo impresso de carbono, onde observou-se um pico em torno de -0,90 V relacionado à redução do *p*-nitrofenolato. O efeito de hidrólise espontânea também foi avaliado em tampão BR pH 9, a partir de uma concentração fixa de pesticida, monitorada em diferentes tempos. Como a produção de *p*-nitrofenolato foi menor que àquela produzida pela reação com o polímero, o sinal obtido também foi inferior. Deste modo, o polímero funcionalizado demonstrou potencial para ser aplicado com uma enzima artificial no desenvolvimento de um sensor eletroquímico.

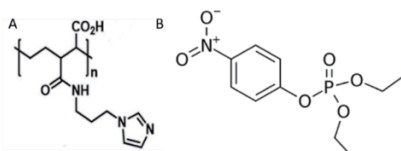


Figura 1. A) Polímero PECIM. B) Metil-paraoxon.

Referências

[1] LEOPOLDINNO, E. C.; PINHEIRO, G.; ALVES, R. J.; GEROLA, A.; SOUZA, B. S. Post-modified polymer with imidazole groups as an efficient and reusable heterogeneous catalyst for organophosphate degradation. **Materials Today Communication**, v. 26, P; 1011904 2021.

Agradecimentos/Acknowledgments

UFG-IQ, UFSC (Departamento de Química), CNPq.

Detection of the anti-A β 42 autoantibody biomarker from Alzheimer's diseases using electrochemical and electrical measurements associated with PCA

Anna Laura Yuri Yokomichi (PG)¹, Ana Livia de Carvalho Bovolato (PQ)², Arthur Oscar Schelp (PQ)², Sidney J. L. Ribeiro (PQ)³, Elenice Deffune (PQ)², Marli Leite de Moraes (PQ)^{1*}

marli.moraes@unifesp.br

¹Federal University of São Paulo, Instituto de Ciência e Tecnologia, São José dos Campos, SP, Brazil; ²São Paulo State University, Hemocentro de Botucatu, Botucatu, SP, Brazil; ³São Paulo State University, Instituto de Química, Araraquara, SP, Brazil

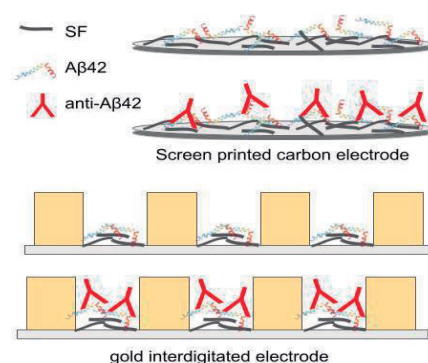
Palavras Chave: Autoantibodies, Alzheimer's disease, Amyloid-beta, Immunosensor, Impedance Spectroscopy, Principal Component Analysis

Highlights

Autoantibodies detection against A β 42 peptide is described to support Alzheimer's disease diagnosis using immunosensor technology. A β 42 immobilized on silk fibroin recognized its antibodies as seen by electrochemical and impedance spectroscopy response in real samples. The developed immunosensor seems be a promising complementary exam to Alzheimer's disease diagnosis, through the anti-A β 42 autoantibody detection.

Resumo/Abstract

Increased levels of autoantibodies against A β 42 peptide have been detected in the serum of Alzheimer's patients, suggesting as potential biomarker to Alzheimer's disease (AD) diagnostic. In this work was investigated the anti-A β 42 autoantibody detection for AD diagnosis using a simple and efficient system. The A β 42 was immobilized into thin films with the silk fibroin (SF). Two systems were investigated, one A β 42 on the SF (SF/A β 42) and the other a mix of these materials (SF+A β 42), on screen-printed carbon electrode and gold interdigitated electrode, for electrochemical and electrical measurement, respectively. Films containing only SF and a nonspecific peptide on the SF were studied as control systems. Films formation and morphology were analyzed by increasing the voltammogram area and changes in the atomic force microscopy images. When A β 42 was added on SF and the mix (SF/A β 42) on electrode the voltammogram area increase of 3.3 (SF) to 144.1 μ A.V and 2.2 (bare electrode) to 152.9 μ A.V, respectively. Comparing the response of cyclic voltammetry and impedance spectroscopy (IS), both detection methods showed more resistance to current flow when interaction antigen-antibody occurred and there was more variation for each anti-A β 42 concentration for the specific system SF/A β 42 using IS. Non-specific antibody was tested with SF/A β 42 film and the same electrical behavior of control systems was observed confirming the immunosensor specificity. Patient samples were used to check the immunosensor viability, it can distinguish the positive of negative samples and data were analyzed using the principal component analysis (PCA) statistical tool that showed the immunosensor selectivity and specificity.



Agradecimentos/Acknowledgments

This work was financially supported by Fundação de Amparo à Pesquisa do Estado de São Paulo, FAPESP (proc. 2018/04648-9) and Coordenação de Aperfeiçoamento Pessoal de Nível Superior, CAPES (proc. 88882.430905/2019-01).

Determination of the metanil yellow dye as an adulterant in turmeric powder samples by its electropolymerization on a BDD surface

Júlia T. Ichikura* (IC),¹ Jhonys M. Freitas (PQ),¹ Romeu C. Rocha Filho (PQ).¹

julia.tiemy@estudante.ufscar.br

¹LaPE – Laboratório de Pesquisas em Eletroquímica, Departamento de Química, UFSCar.

Key words: Metanil Yellow, Turmeric Powder, Boron-Doped Diamond, Electropolymerization, Square-Wave Voltammetry, Food Flavoring Adulteration.

Highlights

A stable film is obtained by the electropolymerization of the MY dye on a BDDE. The electroactivity of the film is used to determine the possible adulteration with MY in turmeric powder samples.

Abstract

According to a Brazilian Ministry of Health report released in 2020,¹ 44% of the turmeric (*Curcuma longa* L.) samples marketed in India had a content of 4 to 6 mg/g of the metanil yellow dye (MY) in their composition. This dye is a potentially toxic chemical, very harmful to health, and potentially carcinogenic in humans. This work presents the initial studies to develop an electroanalytical method for identifying MY in turmeric samples by using a cathodically pretreated boron-doped diamond electrode (BDDE) and 0.1 mol L⁻¹ H₂SO₄ as the supporting electrolyte. For the determinations, cyclic voltammetry (CV) was used to perform the MY electropolymerization² and square-wave voltammetry (SWV) to detect the reversible electrochemical process of MY around 0.45 V vs. (Ag/AgCl/KCl 3.0 mol L⁻¹). Figure 1A presents the electrochemical behavior of 50.0 μmol L⁻¹ MY at an anodically (APT) or cathodically pretreated (CPT) BDDE.

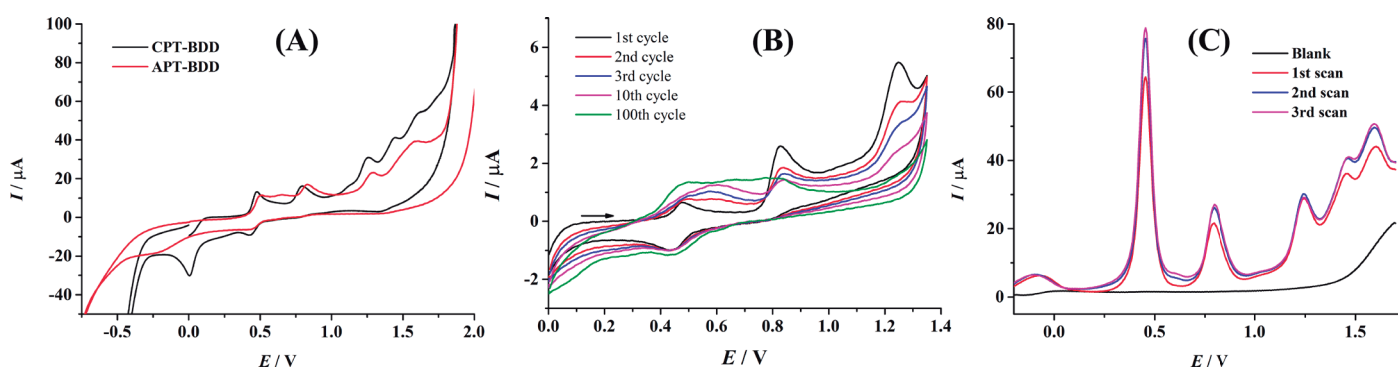


Fig. 1. (A) CV voltammograms at the anodically or cathodically pretreated BDD electrode for 50.0 μmol L⁻¹ MY; (B) Subsequent CV voltammograms for 5.0 μmol L⁻¹ MY. (C) Subsequent SWV voltammograms for 50.0 μmol L⁻¹ MY. Supporting electrolyte: 0.1 mol L⁻¹ H₂SO₄. For CV: $v = 0.1 \text{ V s}^{-1}$; For SWV: $E_{\text{sw}} = 20 \text{ mV}$; $\Delta E = 5 \text{ mV}$; $f = 25 \text{ s}^{-1}$.

After choosing the CPT-BDDE for further studies, evidence of the polymeric film formation could be seen even for a low concentration of MY (5.0 μmol L⁻¹) as the current increases for the reversible electrochemical process around 0.45 V in subsequent CV cycles, as shown in Fig. 1B. From SWV voltammograms (Fig. 1C), it can be noted that there is a significant increase in the sensibility for the peak around 0.45 V. However, the peak growth could affect the repeatability of the method. Therefore, CV scans were run before the SWV scans to stabilize the film formed. After optimizations, six CV scans were set to obtain excellent intra-day repeatability (RSD = 0.9%, $n = 20$) for 5.0 μmol L⁻¹ MY. Studies for different concentrations of MY, comprising a submicromolar level, are being performed, along with the application to determine the presence of MY directly in turmeric powder samples.

¹ Ministry of Health. Department of Pharmaceutical Assistance and Strategic Inputs. **Informações Sistematizadas da Relação Nacional de Plantas Mediciniais de Interesse ao SUS: *Curcuma longa* L., Zingiberaceae – Açafraão-da-terra** – Brazil, 2020.

² KISS, László; KISS, András; KUNSÁGI-MÁTÉ, Sándor. Anion effect on the electropolymerization reaction of metanil yellow in aqueous media and characterization of polymer films. **Periodica Polytechnica Chemical Engineering**, v. 65, n. 2, p. 192-199, 2021.

Acknowledgments

CAPES, CNPq, and FAPESP are gratefully acknowledged for financial support and scholarships.

46ª Reunião Anual da Sociedade Brasileira de Química: "Química: Ligando ciências e neutralizando desigualdades"

Development of a porphyrazine – decorated nanoporous gold microsensor for ascorbate detection.

Pedro H. A. Damasceno (PG)^{1*}, Douglas P. M. Saraiva (PG)¹, Gilberto J. Silva Junior (PG)¹, Leonardo M. A. Ribeiro (PG)¹, Hiago N. Silva (PG)¹, Marcos M. Toyama (PQ)², Henrique E. Toma (PQ)¹, Mauro Bertotti (PQ)¹.

pedrodamasceno@usp.br

¹Department of Fundamental Chemistry, Institute of Chemistry, University of São Paulo, São Paulo, SP, Brazil, 05508-900;

²Mauá Institute of Technology, Department of Chemistry/IMT, São Paulo, SP, Brazil, 09580-900.

Palavras Chave: *Microelectrode, Nanoporous gold, Porphyrazine, Ascorbate, Catalytic effect.*

Highlights

Gold microsensors were modified with nanoporous gold and cobalt (II) porphyrazine to detect ascorbate in natural orange samples by differential pulse voltammetry.

Resumo/Abstract

Ascorbate is a water-soluble vitamin with many functions. Among them, antioxidant is one of the most important and known. In the immunologic system, ascorbate is a potent agent against free radicals produced endogenously and exogenously, and humans can get it by alimentation¹. In this work, we show our efforts towards fabricating a cobalt (II) – porphyrazine/nanoporous gold sensor for ascorbate electrochemical detection. The microelectrode was lab-made using a 25 μm diameter gold fiber. The surface of the bare gold microelectrode sensor (μAu) was first activated through a dynamic hydrogen bubble template (DHBT)² method, and then modified with a cobalt-porphyrazine³ compound. Briefly, a -3.0 V potential was applied for 150 s in a 5 mmol L⁻¹ HAuCl₄ + 0.5 mol L⁻¹ H₂SO₄ solution. During this step, the chloroauric anion was reduced at the electrode surface simultaneously with the hydrogen bubble evolution, creating the nanoporous structure (NPG). Then, the NPG surface was modified by dip coating in a 100 $\mu\text{mol L}^{-1}$ cobalt (II)-tetra(3,4-pyridyl)- porphyrazine (TRP) solution prepared in methanol. Compared to the μAu surface, the anodic oxidation of ascorbate exhibited a peak potential shift of about 850 mV to a less positive value using the NPG/TRP modified electrode, and a 100-fold current increase. Such a remarkable performance can be attributed to the synergic effect caused by the presence of numerous active sites in the NPG structure and the catalytic activity of the immobilized porphyrazine. Morphological and electrochemical characterizations were performed by Scanning Electron Microscopy (SEM) and Energy Dispersive Spectroscopy (EDS) techniques to evaluate the distribution of the catalyst particles in both sensors and to understand the mechanism involving the electron transfer step. An interference study was carried out, and a calibration curve was obtained along an extended ascorbate concentration range. The sensor will be applied as a miniaturized tool to get information on the role of ascorbate against cellular disorders caused by oxidative stress induced by UV irradiation in HaCaT cells (intra and extracellular).

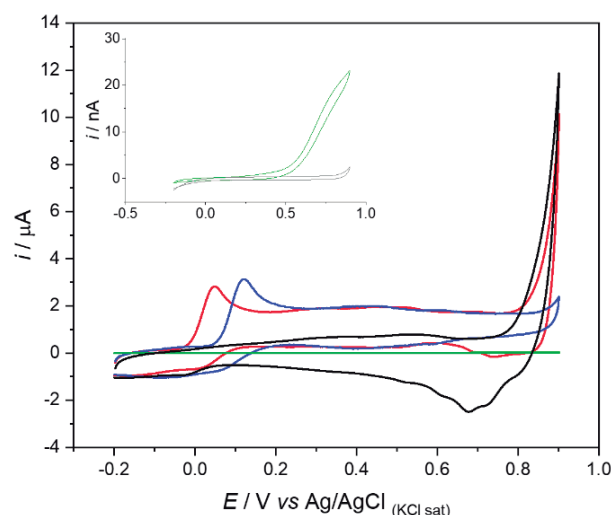


Figure 1 – Cyclic voltammograms (second cycle) recorded in phosphate buffer solution (pH \approx 7) using a bare microelectrode (green curve) and the NPG-TRP modified microelectrode (black curve), and in phosphate buffer solution (pH \approx 7) + 4 mmol L⁻¹ AA with the NPG modified microelectrode (blue curve) and the NPG-TRP modified microelectrode (red curve). The inset shows a magnified CV recorded with the bare microelectrode in phosphate buffer solution (pH \approx 7) + 4 mmol L⁻¹ AA. Scan rate: 100 mV s⁻¹.

[1] Pisoschi, A. M.; Pop, A.; Serban, A. I.; Fafaneata, C.; *Electrochim. Acta* **2014**, 121, 443.

[2] Regiart, M. et al. ; *ChemElectroChem* **2020**, 7, 1558.

[3] Silva, H.N. et al. *Molecules* **2022**, 27, 4598.

Acknowledgments



Development of electrochemical sensors with metallic nanoparticles synthesized in deep eutectic solvents

Gustavo P. Longatto (IC), ^{1*} **Karen K. L. Augusto** (PG), ¹ **Paulo C. Gomes-Júnior** (PG), ¹ **Renan O. Gonçalves** (PG), ¹ **Júlio C. O. Almeida** (IC), ¹ **Éder T. G. Cavalheiro** (PQ), ² **Orlando Fatibello-Filho** (PQ). ¹

gustavo.longatto@estudante.ufscar.br

¹Department of Chemistry, Federal University of São Carlos, São Carlos, SP, Brazil; ²São Carlos Institute of Chemistry, University of São Paulo, São Carlos, SP, Brazil

Keywords: Electrochemical Sensor, Metallic Nanoparticles, Deep Eutectic Solvent.

Highlights

Synthesis of metallic nanoparticles in deep eutectic solvent (ethaline) and their role as electrochemical sensor modifiers.

Abstract

Deep Eutectic Solvents (DES) are analogous to ionic liquids and have become relevant in recent decades as alternatives to toxic and volatile conventional solvents¹. DES have been widely investigated for various applications due to their advantageous physical and chemical properties. Due to their characteristics, DES are considered a good option for the synthesis of nanometric materials without the need for extreme temperature and pressure conditions (60–80 °C at 1 atm)², which provides a gentler route for the formation of reduced size and uniform morphology metal nanoparticles (MNPs). In this study, the ethaline, DES formed by choline chloride (ChCl) and ethylene glycol (EG) in a molar ratio of 1:2, was employed as the medium for the synthesis of MNPs from cerium chloride using hydrazine sulfate as the reducing agent. The cerium nanoparticles (CeNPs) were analyzed using two characterization techniques: energy-dispersive X-ray spectroscopy (Fig 1 (a)) and transmission electron microscopy (Fig 1 (b)). The analysis also showed that the CeNPs were arranged in clusters, had an average size of 4 nm, and were predominantly composed of oxides. The CeNPs were incorporated into a suspension containing carbonaceous materials (multi-walled carbon nanotubes (MWCNTs) or carbon black (CB)) and a polymeric film-forming agent (Nafion™)³. The sensors were modified by drop-casting the suspension onto a glassy carbon electrode (GCE). Cyclic voltammetry analysis with hydroquinone (H₂Q) revealed that CB promotes higher anodic and cathodic peak currents (17% and 36%, respectively, compared to MWCNTs), as illustrated in Fig. 1(c). Based on these analyses, it can be concluded that the proposed method was effective in synthesizing the CeNPs, which showed promising results.

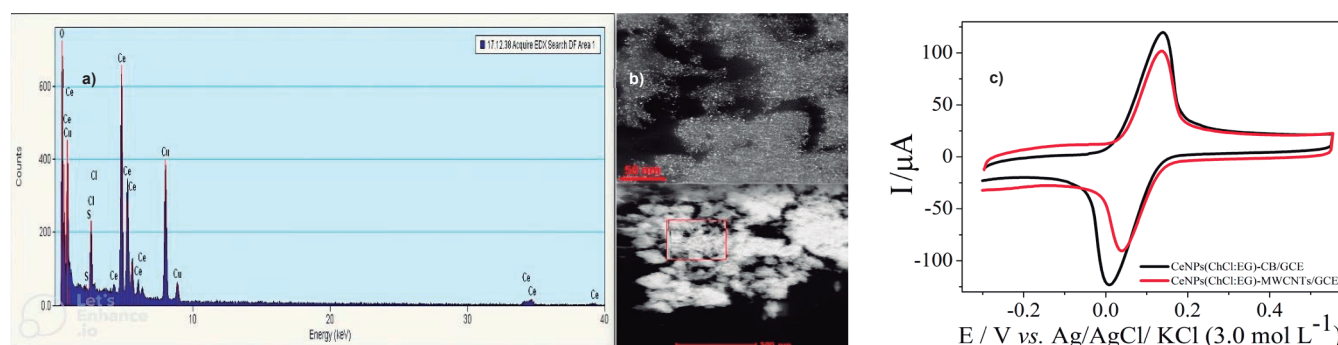


Figure 1 - (a) Cyclic voltammogram for 1.0 mmol L⁻¹ H₂Q at (—) CeNPs-CB/GCE and (—) CeNPs-MWCNTs/GCE sensors. **(b)** EDX spectrum of CeNPs-CB film and **(c)** TEM image of CeNPs

¹Abbott. *et al. Chem. Commun.* **19**; ²Lee, J. S. *Nanotechnology Reviews* **6**; ³Wong, A., *et al. Microchemical Journal* **147**, 2019.

Acknowledgments

The authors thank grant #140406/2021-2 from CNPq, #2022/15513-2 and #2020/01050-5 from FAPESP, and CAPES – Finance code 001 for the financial support during this research.

Development of electrochemical sensor using 3D printing pen and commercial conductive filament

Débora N. Medeiros (PG),^{1*} **William B. Veloso** (PG),¹ **Lauro A. Pradela-Filho** (PQ),¹ **Thiago R. L. C da Paixão** (PQ).¹

d.nascimento.medeiros@usp.br

¹Departamento de Química Fundamental, USP

Keywords: 3D printing pen, electrochemical sensor, surface renewable.

Highlights

3D printing pen simplifies sensor fabrication. The electrodes dispense surface treatment for application. The proposed electrochemical devices are promising platforms for wearable and microfluidic systems.

Resumo/Abstract

3D printing has been extensively used to develop cost-effective electrochemical sensors [1]. Herein, disc electrodes were fabricated with a 3D printing pen, poly(methyl methacrylate) templates, and commercial conductive filament. The filament is based on polylactic acid and carbon black. The resulting materials were tested as working electrodes without any surface treatments. They were characterized using hexaammineruthenium (III) as an electrochemical probe. The printing processing parameters were submitted to optimization studies. They include the thickness and diameters of the electrodes. The diameter was evaluated from 1 to 4 mm. The electrode diameter was restricted by the 3D printing pen's nozzle dimension. Additionally, larger diameters generate small cracks on the electrode surface, affecting their analytical signal. Consequently, 2 mm was the best condition. Even though no signal difference was observed by varying the printing layer between 2 and 3 mm, higher thickness might increase the electrical resistance of the electrodes, compromising their electrochemical response. Considering that 2 mm of thickness allowed the renewal of the electrode surface multiple times, this condition was selected for printing. Under optimized conditions, Figures 1A and B show images of the electrochemical chips. Sharp voltammetric profiles (Figure 1C) are observed for $[\text{Ru}(\text{NH}_6)]^{2+}/[\text{Ru}(\text{NH}_6)]^{3+}$. Additionally, the fabrication process is reproducible (RSD = 4%), demonstrating the proposed electrodes are promising materials for sensing applications. Therefore, the analytical applicability of the sensors will be evaluated for caffeine and caffeic acid, thinking in food applications.

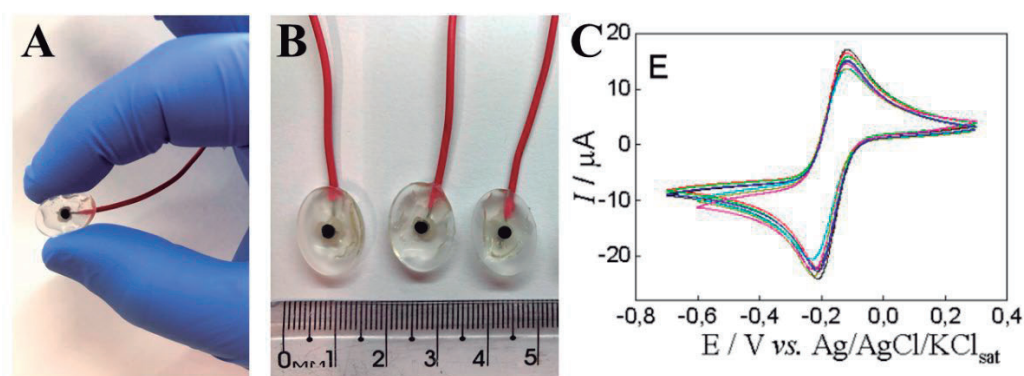


Figure 1. A and B) Electrodes' images. C) Cyclic voltammograms were recorded in $5 \text{ mmol L}^{-1} [\text{Ru}(\text{NH}_6)]^{3+} + 1 \text{ mol L}^{-1} \text{ KCl}$ at 50 mV s^{-1} .

[1] A. Ambrosi, M. Pumera, Chem. Soc. Rev. 2016, 45, 2740.

Agradecimentos/Acknowledgments

São Paulo Research Foundation - FAPESP (2021/00205-8, 2019/15065-7, 2018/08782-1), Coordenação de Aperfeiçoamento de Pessoal de Nível Superior - CAPES (PROEX: 88887.673431/2022-00) and Conselho Nacional de Desenvolvimento Científico e Tecnológico - CNPq (140462/2021-0).

46ª Reunião Anual da Sociedade Brasileira de Química: "Química: Ligando ciências e neutralizando desigualdades"

Área: ELE

Disposable Gold-modified Electrochemical Sensors for Quantification of Nitrite and Nitrate in Drinking Water

João Vitor Fernandes Paiva (PG)^{1*}, Daniel A. de Azevedo (PG)², Pedro V. V. Romanholo (PG)¹, Sergio A. S. Machado (PQ)³, Livia Florio Sgobbi (PQ)¹.

joaoouvitor97@discente.ufg.br; livia_sgobbi@ufg.br

¹ Instituto de Química, UFG; ² Instituto de Física, UFG; ³ Instituto de Química de São Carlos, USP.

Palavras Chave: Electrochemical sensors, screen printed electrodes, modified electrodes, nitrite, nitrate.

Highlights

Disposable electrochemical sensors made of conductive carbon ink and modified with gold and cadmium nanoparticles to detect nitrite and nitrate, sequentially. Fast analysis, cost-effective and low volume sampling technology.

Resumo/Abstract

Nitrite and nitrate ions are inorganic compounds available in nature from the nitrogen cycle and are also part of metabolic processes in various organisms. However, at high concentrations, these ions originated from the increasing use of agricultural fertilizers and food additives for bacterial control have generated a large increase in contamination of surface and underground water systems, causing eutrophication of rivers and lakes, as well as endocrine changes in living aquatic organisms. In humans, nitrate reduces to nitrite forms nitrosamines that are carcinogenic, causing esophageal and gastric cancer. The conversion of hemoglobin to methemoglobin also occurs, which can lead to death from respiratory failure due to low oxygen transport. Due to their toxicities, the Ministry of Health and the National Council for the Environment (CONAMA) defined that the maximum limit of nitrite and nitrate in drinking water should be 1.0 mgL⁻¹ and 10.0 mgL⁻¹, respectively. The conventional analytical techniques, such as chromatography, spectrophotometry and chemiluminescence present precise results and high selectivity. However, they are expensive, time-consuming and require highly qualified professionals. Based on this, electrochemical sensors have emerged as a viable alternative, since they are easy-to-construct, portable, low cost and they are highly sensitive and enable on-site fast analyses. Electrochemical sensors can be modified with metallic nanoparticles in order to obtain improved sensitivity and selectivity by increasing the electroactive area, greater electron transfer, greater electrode conductivity and electrocatalytic effect. This work presents the electrodeposition of gold and cadmium nanoparticles on the surface of a conductive carbon ink electrode fabricated by screen printing on polyethylene terephthalate (PET) substrate for detection and quantification of nitrite and nitrate in drinking water. Gold electrodeposition was performed by chronoamperometry, applying -0.3 V for 600 s in a 1.5 mmolL⁻¹ tetrachloroauric acid solution. The characterization of the modified electrodes was performed by Cyclic Voltammetry, Scanning Electron Microscopy and Energy Dispersive Spectroscopy. The detection was performed by square wave voltammetry, monitoring the oxidation of nitrite (5.0 mmolL⁻¹) in NaClO₄ (0.1 molL⁻¹) + H₂SO₄ (pH 3) and the reduction of nitrate (5.0 mmolL⁻¹) catalyzed by the electrodeposition of cadmium (1.0 mmolL⁻¹) in NaClO₄ (0.1 molL⁻¹) + H₂SO₄ (pH 3). Nitrate generated a detection signal in the square wave voltammogram at -1.5 V, while nitrite was detected at 0.6 V. The next steps include the optimization of the quantitative detection of nitrite and nitrate by square wave voltammetry, for the further application in drinking water.

Agradecimentos/Acknowledgments



Área: ELE

Effect of different experimental conditions in the voltage oscillation during Nb anodization in spark regime.Jonata R. D. Batista (PG)*¹, Franciso Trivinho-Strixino (PQ)¹, Patricia S. Araujo (PG)¹.

jonata@estudante.ufscar.br;

¹Departamento de Física, Química e Matemática (DFQM-So), UFSCar.

Key-Words: Voltage oscillation, PEO, Niobium anodization.

Highlights

- Presence of voltage oscillation during Nb anodization in spark regime.
- Electrolyte temperature and composition effect on the oscillatory voltage behavior during NB anodization in spark regime.

Resumo/Abstract

Plasma Electrolytic Oxidation (PEO) is a process that allows obtaining oxide films with several interesting properties, such as antibacterial coatings [1] and biocompatibility [2]. Under specific conditions and with different substrates, electrolyte temperatures, and composition, unusual behavior is observed in voltage during anodization. Low-frequency oscillations are detected during the spark regime and modify the anodic oxide film, similar to what was observed in silicon anodization [3]. In this study, metallic niobium substrates were anodized in three different electrolytes: C₂H₂O₄, H₃PO₄, and KOH, each with a 0.1 mol/L concentration, to track the presence of this voltage oscillatory behavior. The substrate anodization was carried out in a constant current mode, and a voltage and digital temperature recorder were used to register these parameters during the process, according to Table 1. The oscillatory behavior is present at certain electrolyte conditions, as shown in Table 1.

Table 1 – Qualitative comparison for different experimental conditions at which voltage oscillations are present. The symbol “✓” confirms the voltage oscillations, whereas “✗” denotes the absence of the voltage oscillation.

Temperature (°C)	Electrolyte		
	C ₂ H ₂ O ₄	H ₃ PO ₄	KOH
15	✓	✗	✗
25	✓	✓	✓
30	✓	✓	✓

According to Table 1, the voltage oscillations are influenced by the electrolyte temperature, indicating a minimum temperature condition for each electrolyte for the voltage oscillation to be present. The samples were characterized by scanning electron microscopy (SEM), dispersive energy spectrometry (EDS), and X-ray diffraction (XRD) to check if the variation of the experimental conditions modified the anodic oxide properties obtained.

References

- [1] Santos, J. S. ; Rodrigues, A. ; Simon, A. P. ; Ferreira, C. H. ; Santos, V. A. ; Sikora M. S. ; Cruz, N. C. ; Mambrini, G. P. ; Trivinho-Strixino, Francisco . One-step synthesis of antibacterial coatings by Plasma Electrolytic Oxidation of aluminum. *Advanced Engineering Materials*, v. 21, p. 1438-1656, 2019.
- [2] SIMON, A. P. ; LIMA, A. S. ; SANTOS, V. A. ; Santos, Janaína S. ; Trivinho-Strixino, F. ; Sikora M. S. . Optimization of TiO₂ coatings properties and photochemical Ag-functionalization: Implications on bioactivity and antibacterial activity. *JOURNAL OF MATERIALS RESEARCH*, p. 4243, 2022.
- [3] Parkhutik, V. Silicon anodic oxides grown in the oscillatory anodization regime – kinetics of growth, composition and electrical properties. *Solid-State Electronics*, 45, 1451–1463, 2001.

Agradecimentos/Acknowledgments

This work was supported by the Brazilian funding agencies CAPES (financial code 01), FINEP Martha, and FAPESP (2022/05191-3) projects. The authors also thank CBMM for the ammonium oxaloniobate (ANO) salt donation.

Electrocatalytic reaction of hydrogen evolution from *Eichhornia crassipes* and bovine manure biochar

Michael Douglas Santos Monteiro (PG),^{1*} Marcos Vinicius Quirino dos Santos (IC),¹ Wandson Almeida dos Santos (PG),¹ José Felipe dos Santos (IC),¹ Alberto Wisniewski Junior (PQ),¹ Eliana Midori Sussuchi (PQ)¹

michaelquimica96@gmail.com

¹Universidade Federal de Sergipe, Departamento de Química, São Cristóvão, Sergipe, Brazil, 49.100-000

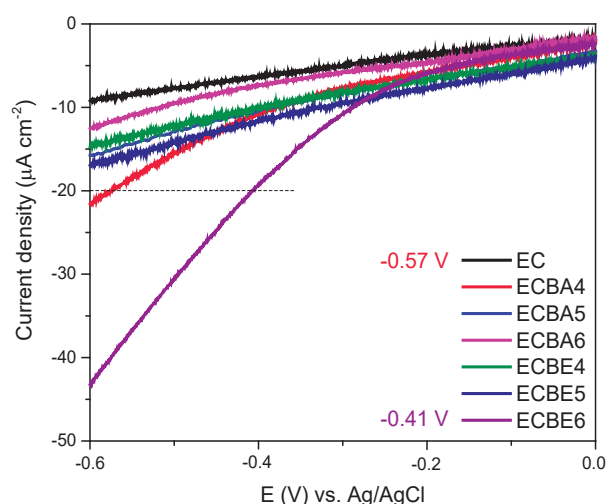
Keywords: Green hydrogen, Biochar, Renewable Energy.

Highlights

Electrodes with *Eichhornia crassipes* and bovine manure biochar.
H₂ is the most promising solution to environmental problems and energy crisis.
This work contributes with green energy technology.

Abstract

Energy is one of the main sources for the stability of the population's way of life and quality of life^{1,2}. Hydrogen gas (H₂) is the most promising solution for environmental problems and energy crisis, as it can replace finite fossil fuels, in addition to promoting sustainability and greater safety³. The objective is the development of the modified electrodes based on biochar, produced from *Eichhornia crassipes* and cattle manure, biomass very abundant in the state of Sergipe. These electrodes were applied as catalysts in electrochemical reactions to hydrogen evolution reaction (HER). The production of biochar samples were obtained by pyrolysis at temperatures of 400, 500 and 600 °C, designed BA4, BA5 and BA6, to *Eichhornia crassipes* and BE4, BE5, and BE6 to manure biochar, respectively. The electrodes were prepared from 5 mg of biochar, 30 µL of perfluorinated nafion[®] resin, 250 µL of ethanol and 720 µL of deionized water were mixed and ultrasonicated for 40 min to achieve a homogeneous catalyst-ink mixture. To prepare the electrodes, 5 µL of the was collected and deposited on the 3 mm polished surface of the electrode and dried. The linear sweep voltammetry (LSV) technique was used to assess the electrocatalytic capacity of the electrodes. The analyzes were performed from potential 0.0 V to -0.6 V (versus Ag/AgCl) at scan rate of 5 mV s⁻¹. Figure 1 shows that among the catalysts used, biochar from bovine manure pyrolyzed at 600 °C (ECBE6) presented the highest current density (*j*) and the lowest overpotential (η) (-0.41 V). This factor is essential for the choice of biochar, because for the process to occur, it is necessary to overcome the η in the HER. The result obtained can be explained, as the pyrolysis temperature is essential to obtain good conductivity and is beneficial to form a porous structure that indicates high specific surface area, in addition to offering fast ion channels and large active surface areas.



1. Chen, J. *et al.* International Journal of Hydrogen Energy 2021.
2. Liu, H. *et al.* Journal of Cleaner Production 2021, 310, 127293.
3. Sun, J. *et al.* International Journal of Hydrogen Energy 2022.

Fig. 1. Linear sweep voltammetry analysis in 1 mol L⁻¹ H₂SO₄, using a glassy carbon electrode (EC), ECBA4, ECBA5, ECBA6, ECBE4, ECBE5 and ECBE6 electrodes, under N₂, scan rate of 5 mV s⁻¹.

Acknowledgments

This project is funded by the Green Hydrogen Innovation Program (iH₂Brasil) carried out by the Brazil-Germany Alliance for Sustainable Development and is implemented by GIZ (Deutsche Gesellschaft für Internationale Zusammenarbeit GmbH) and the Ministry of Mines and Energy (MME) with support from Federal Ministry for Economic Cooperation and Development (BMZ) of Germany. The authors thanks to CLQM (Center of Multi-users Chemistry Laboratories), Corrosion and Nanotechnology Laboratory (LCNT), Sergipe Oil and Gas Competence Center (NUPEG/PETROBRAS/UFS) from the Federal University of Sergipe for providing support to carry out the experiments.

Electrocatalytic reaction of hydrogen evolution from electrodes modified with Carbon dots Of *Moringa Oleifera*

Marcos Vinicius Quirino dos Santos (IC),^{1*} Michael Douglas Santos Monteiro (PG),¹ Wandson Almeida dos Santos (PG),¹ José Felipe dos Santos (IC),¹ Alberto Wisniewski Junior (PQ),¹ Eliana Midori Sussuchi (PQ)¹

quirino98@academico.ufs.br

¹Universidade Federal de Sergipe, Programa de Pós-Graduação em Química, Departamento de Química, São Cristóvão, Sergipe, Brazil, 49.100-000.

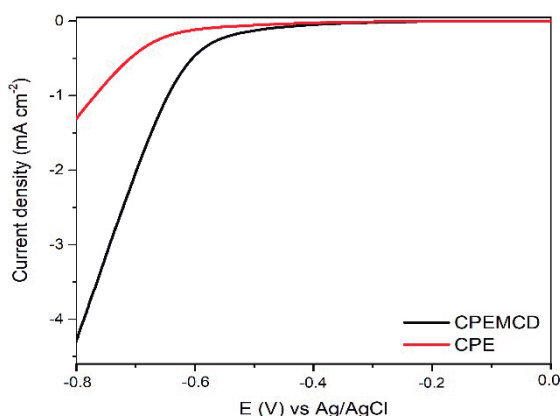
Keywords: *Moringa Oleifera*, Carbon dots, Biomass, hydrogen evolution reaction, Energy.

Highlights

Electrodes with Carbon dots of *Moringa Oleifera*.
 H₂ is the most promising solution to environmental problems and energy crises.
 This work contributes with green energy technology.

Abstract

Carbon Dots (CDs) have attracted attention due to their excellent properties, in addition to having several sources of raw materials and low-cost preparation methods. Recently, there have been some attempts to use biomass residues as a raw material in the production of CDs¹. In this work, the hydrothermal route was used to obtain CDs, and as a carbon precursor, 5.0 g of *Moringa Oleifera* leaves were applied, which were left for 4 hours at 240°C in an autoclave reactor. The characterizations of the material properties were made by the techniques of visible ultraviolet spectroscopy, Fourier transform infrared spectroscopy and fluorescence spectroscopy. The electrode without modification (CPE) was constituted by graphite and binder (6.5:3.5%) (w:w) and electrodes modified with *Moringa Oleifera* (CPEMCD) were composed of graphite, mineral oil and CDs of *Moringa Oleifera* in different proportions (5.0 %, 10.0% and 15.0%). The components to obtain the electrodes were macerated for 5 min with a mortar and pestle, until a homogeneous paste was obtained and inserted into a polypropylene tube ($\Phi_{int}=4.8$ mm), and the electrical contact was established through the insertion of a copper wire ($\Phi_{int}=3.0$ mm). FTIR analysis it was possible to observe bands of functional groups of interest, such as the NH₂/NH of amine/amide and C=O of acetyl and carboxylic groups. The absorption spectrum shows two bands at 192 nm, attributed to $\pi-\pi^*$ transitions, characteristic for *sp*² carbon of aromatic groups. At 272 nm, the absorbance band referring to $n-\pi^*$ transitions are found, attributed to carbonyl or nitrogen groups that may be present on the surface of the CDs of *Moringa Oleifera*². The linear sweep voltammetry (LSV) technique was used to assess the electrocatalytic capacity of the electrodes. Analyses were performed from potential 0.0 V to -0.8 V (versus Ag/AgCl) at scan rate of 5 mV s⁻¹. Fig. 1 it is possible to observe the results referring to hydrogen evolution reaction, where we have that the electrode modified with CDs of *Moringa Oleifera* presented better overpotential and current density for the production of H₂ in comparison with the non-modified electrode, this result can be intensified with the increase in the number of cycles.



1. W. Li *et al. Mater. Chem. Front.*, vol. 4, no. 1, p. 277–284, 2020, doi: 10.1039/c9qm00618d.
2. W. Meng, X. *et al Energy Environ. Mater.*, vol. 2, no. 3, p. 172–192, 2019, doi: 10.1002/eem2.12038.

Fig. 1. Linear sweep voltammetry analysis in 1 mol L⁻¹ H₂SO₄, using a CPE(--); and CPEMCD(--), scan rate of 5 mV s⁻¹.

Acknowledgments

This project is funded by the Green Hydrogen Innovation Program (iH₂Brasil) carried out by the Brazil-Germany Alliance for Sustainable Development and is implemented by GIZ (Deutsche Gesellschaft für Internationale Zusammenarbeit GmbH) and the Ministry of Mines and Energy (MME) with support from Federal Ministry for Economic Cooperation and Development (BMZ) of Germany. The authors thanks to CLQM (Center of Multi-users Chemistry Laboratories), Corrosion and Nanotechnology Laboratory (LCNT), Sergipe Oil and Gas Competence Center (NUPEG/PETROBRAS/UFES) from the Federal University of Sergipe for providing support to carry out the experiments.

Área: ELE

ELECTROCATALYTIC REFORM OF LIGNIN IN ALKALINE SOLUTION: THE EFFECT OF NANOSTRUCTURATION OF COBALT ELECTRODES

Lívia C. S. Epifanio (IC), Hamilton Varela (PQ), André H.B. Dourado (PQ).

ciciliniivia@usp.br; andre.dourado@usp.br

Instituto de Química de São Carlos, USP - Av. Trabalhador São Carlense, 400 – 13566-590 – São Carlos, Brasil

Key-words: *Lignin valorization, biomass electrochemical reforming, cobalt electrocatalyst*

Highlights

Electrochemical activity as a function of the morphology.

Surface area control by electrochemical deposition.

Optimal electrode area

Resumo/Abstract

Kraft lignin is a known pulp and cellulose by-product. This macromolecule can be oxidized, generating monoaromatic chemical products and, if the oxidation process is electrochemical, also producing H₂, a high energy density fuel. For the electrochemical lignin oxidation, alkaline electrolytes are needed, so the macromolecule can be soluble in aqueous media. In this work, Cobalt (Co) was selected as electrocatalyst, since it has a low cost and is stable in alkaline media. Another advantage of Co is that this catalyst has a high selectivity not only for aldehyde products, but also specifically for vanillin, which is unexpected and not understood by the literature. For this reason, it is proposed to systematically investigate Coelectrochemical behavior for kraft lignin oxidation. To carry out the study, Co electrodeposition was selected to synthesize the catalyst, since this is a low cost process and easy to control. After that, the obtained electrodes were tested for lignin oxidation and mass transport influence was found, due to the peak current linearization against sweep rate. Changing the deposition conditions, the electrode roughness also changed. Checking the activity of these different electrodes, it was found that there is an optimal surface area for this reaction.

Agradecimentos/Acknowledgments

FAPESP (2022/09720-5) FAPESP (2019/22183-6 e 2020/15230-5), Shell Brasil e CNPq (306060/2017-5).

Electrochemical behavior of carbon paste electrode modified with ternary natural deep eutectic solvent for determination of carbendazim in tap water.

Suysia R. D'Almeida (PG),¹ Rafael M. Buoro (PQ)^{1*}.

suysiadalmeida@usp.br; rafbuoro@iqsc.usp.br

¹Departamento de Química e Física Molecular, Instituto de Química de São Carlos, Universidade de São Paulo

Keywords: Natural deep eutectic solvent, ternary NADESs (t_NADES), Carbon paste electrode, Electroanalysis.

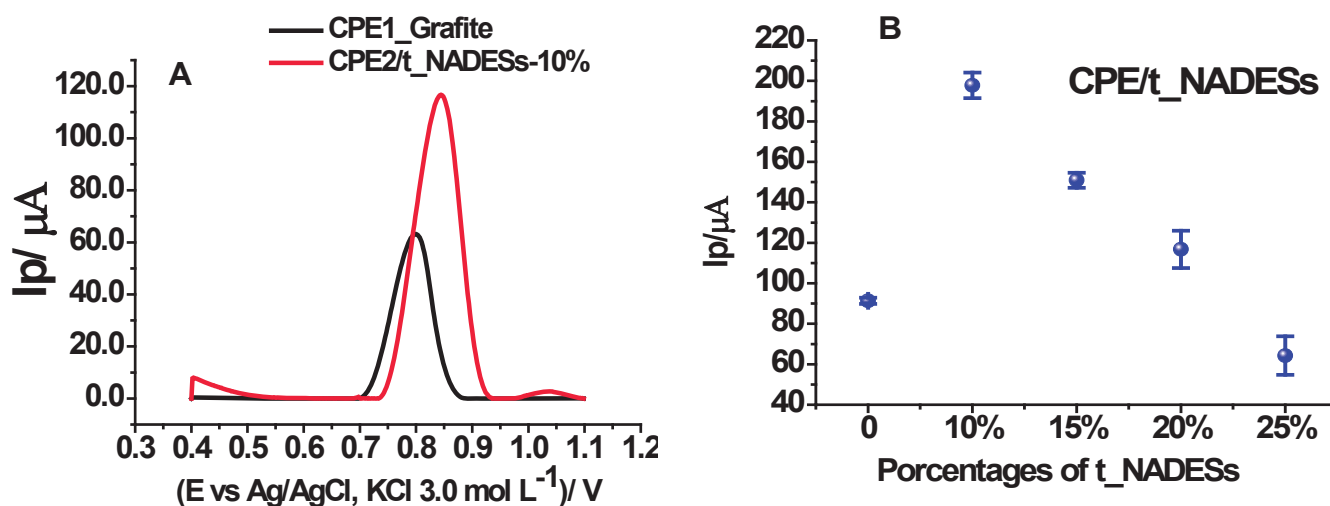
Highlights

The t_NADES modified CPE presented superior performance when compared to CPE. CPE2/t_NADES-10% compared as binder modifying agents. The CPE/t_NADES presented superior performance for oxidation of CRZ.

Resumo/Abstract

Carbon paste electrodes (CPE) have been used for the electrochemical determination of toxic contaminants due of many advantages such as easiness surface renewal, low manufacturing cost, and possibility of direct modification of the composite [1]. Natural Deep Eutectic Solvent (NADESs) can be defined as a mixture of two or more natural organic compounds when at a particular molar ratio, having a melting point significantly lower than that of either individual component [2]. In this work, a new ternary NADESs based on sugars was proposed for the modification of carbon paste electrodes. The t_NADES was synthesized adapting the method proposed by Abbott [3]. D (+) glucose (HBA), L (+) tartaric acid and glycerol (HBD) were mixed simultaneously in a 1:1:5 (mHBA/mHBD) ratio under vigorous stirring and controlled temperature (80 °C). A homogeneous liquid was obtained and then allowed to be cooled to room temperature. The carbon paste composite was prepared by substituting a fraction (10-25%) of the binder (mineral oil) by the eutectic mixture. The electroanalytical performance of the electrodes was evaluated and characterized using cyclic and square wave voltammetry. The modified carbon paste electrodes (CPE/t_NADES-10%) were evaluated towards their efficiency for determination carbendazim (CRZ) by electrochemical techniques. The CPE/t_NADES-10% showed the best peak current performance compared to CPE (Fig. 1A and B). For percentages higher than 10%, the decrease in the peak current is associated to the loss of cohesion of the carbon paste due the increase of the water affinity by the composite.

Fig. 1: (A) square wave voltammograms for 500 $\mu\text{mol L}^{-1}$ carbendazim in phosphate buffer (pH 7.0) for CPE and CPE_NADESs.



Acknowledgments

This study was financed in part by the Coordenação de Aperfeiçoamento de Pessoal de Nível Superior – Brasil (CAPES) – Finance Code 001, CNPq and São Paulo Research Foundation - FAPESP (2017/13307-8).

References:

- [1] Svancara, *et al.* Central European Journal of Chemistry 7 (2009) 598 – 656.
- [2] Choi, *et al.* Plant Physiol 156 (2011) 1701 – 1705.
- [3] Abbott, *et al.* Chem. Comum. (2003) 70 – 71.

Electrochemical degradation of paracetamol using electrochemical advanced oxidation process with DSA anode in sodium chloride medium

Ludmila Lorrane Martins Silva* (IC),¹ Guilhermina Ferreira Teixeira (PQ),² Flávio Colmati (PQ)²

colmati@ufg.br; ludmilalorrane@discente.ufg.br

¹Faculty of Pharmacy, Federal University of Goiás- UFG; ²Institute of Chemistry, Federal University of Goiás-UFG

Keywords: drug degradation; environment decontamination; wastewater treatment; dimensionally stable anode.

Highlights

The paracetamol solution was degraded in an electrochemical reactor.
The dimensional stable anode (DSA) was composed of Ti/Ru_{0.3}Ti_{0.7}O₂.
After 5 minutes, 95% of the paracetamol was degraded.

Abstract

Paracetamol is one of the most consumed analgesics and antipyretics worldwide. However, its occurrence along with its metabolites in aquatic effluents can pose a significant threat to organisms that come into contact with polluted water. In this work, we explored the use of electrolysis as a potential solution for treating contaminated water. We conducted experiments on two different concentrations of paracetamol (10 and 20 mg.L⁻¹) in a sodium chloride medium with a concentration of 0.05 mol.L⁻¹. The efficiency of degradation was analyzed through UV-visible spectroscopy, especially by measuring the absorbance at 246 nm. At a current density of 7.6 mA.cm⁻², approximately 95 % of the 10.0 mg.L⁻¹ paracetamol solution was degraded after 5 minutes (Figure 1a), and the same degradation efficiency was achieved after 15 minutes for the more concentrated paracetamol solution (Figure 1b). Decreasing the current density, only 2.4% of the 20.0 mg.L⁻¹ paracetamol solution was degraded after 60 minutes (Figure 1 c). Additionally, a band around 290 nm was observed, indicating the formation of a degradation byproduct (Figure 1 a-b). Our initial results showed that paracetamol is rapidly degraded using eletrolysis; however, it is necessary to identify the resulting products.

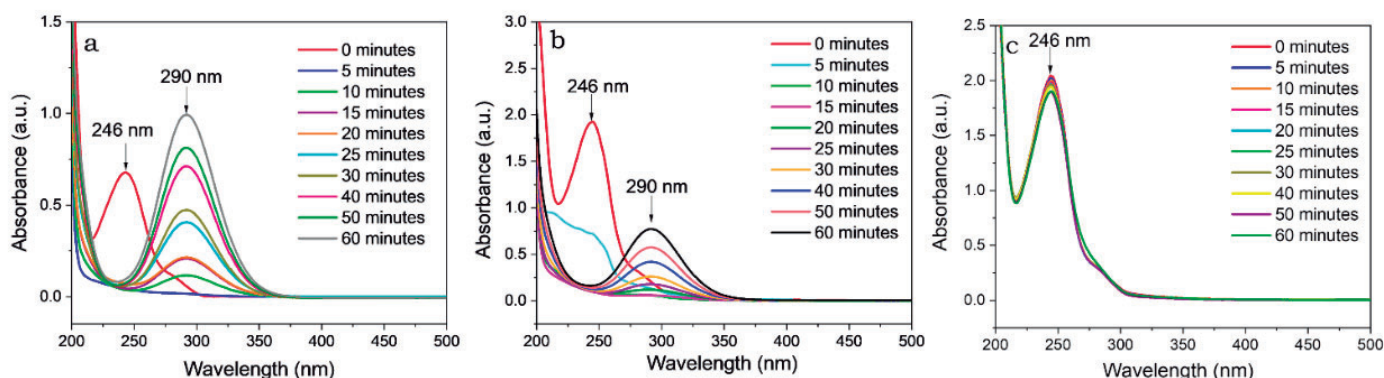


Figure 1: Uv-visible spectra of paracetamol a) 10 mg.L⁻¹, 7.6 mA.cm⁻² (V= 4V) ; b) 20 mg.L⁻¹, 7.6 mA.cm⁻² (V= 4V) and c) paracetamol 20 mg.L⁻¹ 0.16 mA.cm⁻² (V= 2V)

References:

- Brune, K.; Renner, B.; Tiegs, G. *European Journal of Pain*, v. 19, p. 953–965, 2015
 Farto, C.; Júnior, G.; Sena, R.; Rosenhaim, R. *Revista de Gestão de Água da América Latina*, v. 18, e6, 2021.
 Jallouli, N.; Elghniji, K.; Trabelsi, H.; KSIBI, M. *Arabian Journal of Chemistry*, v. 10, p. S3640–S3645, 2017.
 Smolinka, T. *Encyclopedia of Electrochemical Power Sources*, p. 394–413, 2009.
 Rathi, B. S.; Kumar, P. S. *Environmental Pollution*, v. 280, p. 116995, 2021.

Acknowledgments

The authors thank the Brazilian research agencies CAPES (Processes number: 88882.306480/2018-1), CNPq and Federal University of Goiás Research Initiation Program.

Electrochemical method for detection of mRNA-208b using disposable devices and magnetic beads decorated with DNA hairpin probe

Vagner da Silva Santos (PG),^{1*} Pablo R. L. da Silva (PG),¹ Evair D. Nascimento (PG),¹ Ronaldo C. Faria (PQ).¹

vhagnersantos@outlook.com;

¹ Department of Chemistry, Federal University of São Carlos-UFSCar, Rod. Washington Luís km 235, São Carlos, SP, 13565-905, Brazil

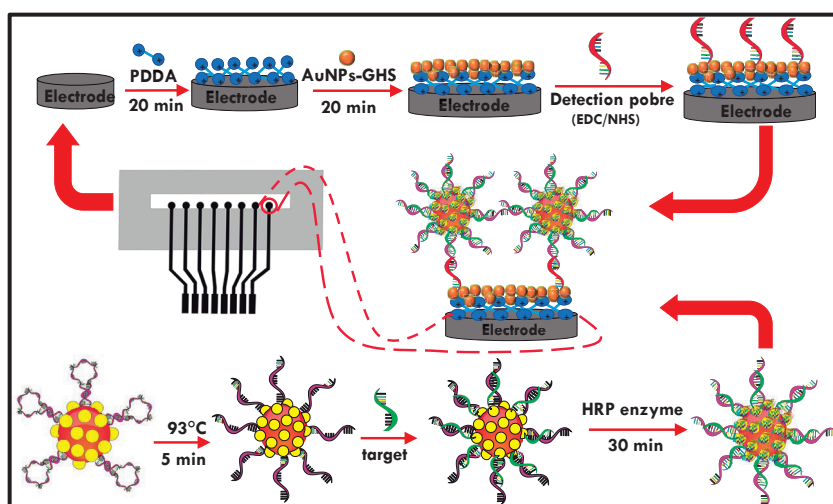
Keywords: Electrochemical method, Disposable device, mRNA-208b, DNA hairpin probe, coronary heart disease.

Highlights

An electrochemical method for ultrasensitive detection of circulating mRNA using hairpin DNA probe, magnetic beads, and disposable electrodes for the diagnosis of cardiac problems was developed.

Resumo/Abstract

Coronary diseases (CDs) are the most common type of cardiovascular disease, affecting the heart and blood vessels and are one of the leading causes of death not only in Brazil, but worldwide. The diagnosis of CDs is accomplished using an electrocardiogram or the monitoring of serological markers. Regardless of whether these are the most used methods for assessing these diseases, they require specialized personnel and use nonspecific markers that take hours to detect in the bloodstream. As a result of these limitations, we propose an electrochemical method that uses DNA sonda (hairpin) in magnetic spheres to detect mRNA-208b, which is specific for myocardial infarction and is released at the start of cardiac necrose. The presented method consists of magnetic spheres coated with hairpin and biotin which, when heated, favors the opening and girdling of the hairpin with mRNA-208b. After that, the bioconjugate is incubated with streptavidin-HRP. Thus, the temperature and time of denaturation were evaluated, as well as the concentration of hairpin, detection probe and biotin as described in the table on the side. In addition, the method makes use of a disposable device with eight independent electrochemical cells based on carbon paste, which allows the simultaneous detection of eight different samples or targets. With the chosen conditions, the method produced an analytical range of 0.01 to 5000 fM with a detection limit of 0.01 fM, demonstrating the method's sensitivity in detecting mRNA-208b. The system showed good specificity when evaluated against other to the hairpin non-specific target sequences. In addition, the system's stability was monitored for 24 days, with a significant drop in current signal only on the final day. The method was applied to real samples of blood serum from people with diseases that trigger heart problems. The results demonstrate the method's ability to monitor specific genetic markers for coronary artery disease before the clinical condition worsens.



	Variation	Chosen Condition
Biotin	1 μM e 1mM	1 mM
Hairpin	0,5 μM a 8 μM	8 μM
denaturation temperature	43°C a 93°C	93°C
denaturation time	5 min a 30 min	5 min
Detection probe	0,5 μM a 8 μM	4 μM
Dilution sample	1:100 a 1:300	1:100

In addition, the method makes use of a disposable device with eight independent electrochemical cells based on carbon paste, which allows the simultaneous detection of eight different samples or targets. With the chosen conditions, the method produced an analytical range of 0.01 to 5000 fM with a detection limit of 0.01 fM, demonstrating the method's sensitivity in detecting mRNA-208b. The system showed good specificity when evaluated against other to the hairpin non-specific target sequences. In addition, the system's stability was monitored for 24 days, with a significant drop in current signal only on the final day. The method was applied to real samples of blood serum from people with diseases that trigger heart problems. The results demonstrate the method's ability to monitor specific genetic markers for coronary artery disease before the clinical condition worsens.

Agradecimentos/Acknowledgments



Electrochemical sensor based on Ir/C nanoparticles to determine Bisphenol A in instant noodles cups

Amanda Morais (IC),^{1*} Maria Lurdes Felsner (PQ),^{1,2} Giancarlo Richard Salazar Banda (PQ),³ Katlin Ivon Barrios Eguiluz (PQ),³ Jamylle Yanka Cruz Ribeiro (PG),³ Andressa Galli (PQ)¹

agalli@unicentro.com; am.morais534@gmail.com

¹Departamento de Química, UNICENTRO; ²Departamento de Química, UEL; ³Programa de Pós-graduação em Engenharia de Processos, Universidade Tiradentes

Keywords: *chemically modified electrodes, bisphenol A, validation of electroanalytical methods.*

Highlights

Iridium nanoparticles supported on carbon have high catalytic performance.

A validated analytical method to determine BPA in instant noodles cups was developed.

The limit of detection (LOD) was 9.36 ppb, and a suitable linear range of concentration was achieved.

Abstract

Bisphenol A (BPA, 2,2-bis(4-hydroxyphenyl) propane) is widely used in industry, and its presence is related to water bottles, food packages, baby bottles, and so on [1]. Some residual BPA can migrate to the contents of these objects, which is the primary route of human exposure and contamination with this endocrine disruptor with estrogenic activity [2]. Therefore, the quantification of this compound is essential. Hence, iridium nanoparticles supported on carbon black (Ir/C) were used to modify a glassy carbon electrode (GCE), thereby forming a new electrochemical sensor for BPA. The suitability of the method for the intended purpose was ensured by a validation study considering the parameters selectivity, matrix effect, calibration curve, range, accuracy, precision, and intermediate precision. The sensor exhibits sensitivity, with LOD $0.041 \mu\text{mol L}^{-1}$ ($9.36 \mu\text{g kg}^{-1}$) and LOQ $0.124 \mu\text{mol L}^{-1}$ ($28.35 \mu\text{g kg}^{-1}$), both lower than $0,6 \text{ mg kg}^{-1}$, which is the maximum limit of migration allowed by the ANVISA [3]. Besides, the recovery values found in instant noodles cups were in the range of 90%–110%, which is within the values suggested in the literature for the validation of the method. Moreover, the developed method presented good precision, and suitable linearity in the concentration range analyzed.

- [1] Y. Ma, H. Liu, J. Wu, L. Yuan, Y. Wang, X. Du, R. Wang, P.W. Marwa, P. Petlulu, X. Chen, H. Zhang, The adverse health effects of bisphenol A and related toxicity mechanisms, *Environ. Res.* 176 (2019) 108575. <https://doi.org/10.1016/J.ENVRES.2019.108575>.
- [2] A. Ballesteros-Gómez, S. Rubio, D. Pérez-Bendito, Analytical methods for the determination of bisphenol A in food, *J. Chromatogr. A.* 1216 (2009) 449–469. <https://doi.org/10.1016/J.CHROMA.2008.06.037>.
- [3] Agência Nacional de Vigilância Sanitária (ANVISA). Resolução da Diretoria Colegiada – RDC n° 88, de 29 de abril de 2016, dispõe sobre regulamento técnico sobre materiais, embalagens e equipamentos celulósicos destinados a entrar em contato com alimentos. Diário Oficial da União, Poder Executivo, Brasília, DF, 29 de jun. 2016.

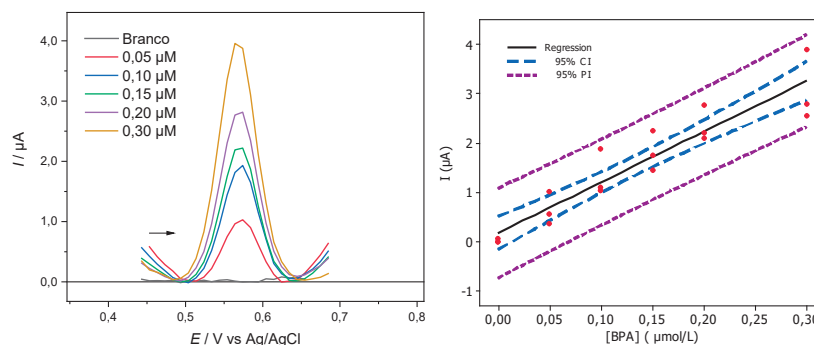


Fig. 1: Square wave voltammograms of BPA made in the linear range of concentration of $0,05\text{--}0,30 \mu\text{mol L}^{-1}$ in $0,1 \text{ mol L}^{-1}$ phosphate buffer, $\text{pH} = 7$, $a = 30 \text{ mV}$, $f = 60 \text{ s}^{-1}$, $\Delta E = 30 \text{ mV}$ (left), and calibration curve (right).

Acknowledgments

The authors thank CAPES, CNPq, Fundação Araucária, UNICENTRO, Grupo de Eletroanalítica e Materiais Nanoestruturados (GEMN), and Laboratório de Eletroquímica e Nanotecnologia (LEN).

Electrochemical Sensor Based On Molecularly Imprinted Polymer For Highly Sensitive Detection Of Albumin Serum Human Biomarker In Oxidative Stress

Heitor F. Trevizan (PG),¹ André Olean-Oliveira(PQ),² Patrícia Monteiro Seraphim (PQ),³ Marcos Fernando de Souza Teixeira (PQ),^{4*}

^aFaculty of Science and Technology, São Paulo State University (UNESP), Pres. Prudente, SP, BR.
marcos.fs.teixeira@unesp.br

Keywords: (Albumin Serum Human; Polymer Molecularly Imprinted; Resistive/capacitive sensor; Molecular recognition; Without redox probe).

Highlights

- Development of a sensor with EIS / ECS transduction without soluble redox probe;
- The MIP impedimetric sensor for selective monitoring of albumin serum human was effective;
- Electrochemical impedimetric sensing responses on molecularly imprinted polymers;
- High sensitivity and selectivity in determining of albumin serum human.

Resumo/Abstract

Albumin is an important protein in the body and plays a critical role in the maintenance of nutrition balance, plasma pressure, and transportation of different substances. Moreover, the change of albumin concentration in the blood or tissue fluids can be used as a biomarker in human health and disease¹. For example, the low concentrations of albumin in blood may suggest changes in the immune system, caused by viral infections such as human immunodeficiency (HIV) and Coronavirus (COVID-19)^{2,3}. In this study, a novel molecularly imprinted polymer (MIP) sensor based on poly(azo-BBY) for the electrochemical detection of albumin is reported. The poly(azo-BBY) MIP film on electrode fluorine tin oxide (FTO) was prepared by electropolymerization of Bismarck Brown Y in the presence of albumin as target molecule.

The MIP and NIP electrodes were characterized by Raman spectroscopy, where the vibrational bands were identical, however with slightly weaker intensities for the MIP electrode, indicating the specific interaction of albumin with the -NH₂ and azo groups of the poly(Bismarck Y). The electrochemical detection properties were investigated via electrochemical impedance/capacitance spectroscopy to confirm the imprinting effect on the MIP films. Analyzing the imaginary capacitance as a function of the applied frequency, the MIP film capacitance system decreased to the low frequency region with increasing albumin concentration. Due to the specific cavities for albumin on the large surface of the MIP sensor, the target molecule can easily be rebinding on these cavities. The device has a linear range of response in the concentration range of 0.25–1.0 ng mL⁻¹ with good correlation between the imaginary capacitance and the albumin concentration ($r = 0.9979$). The prepared sensor shows a sensitivity of 0.156 $\mu\text{F cm}^2 \text{ mL ng}^{-1}$ and a limit of detection (LOD) of 0.215 ng mL⁻¹ (S/N = 3). Other electrochemical studies which determine a sensors performance, such as reproducibility, stability and interference, have also been performed.

Reproducibility was studied using seven independently prepared poly(azo-BBY)-MIP sensors for the detection of albumin (0.5 ng mL⁻¹). As a result, the RSD relative standard deviation of the impedance/capacitance response was less than 9%. Therefore, poly(azo-BBY)-MIP sensors exhibit good reproducibility. After 14 days, the RSD of the poly(azo-BBY)-MIP sensor was 9.8%, indicating excellent stability. The selective recognition performance of the sensor was investigated with concomitant species that possibly act as interferents in biological fluid. The MIP sensor showed high selectivity for ASH adsorption compared to other proteins and aminoacids.

Reference

- 1 Wang L, Zhao L, Colloids and Surfaces A: Physicochemical and Engineering Aspects, v. 632, 2022, p. 127843.
- 2 Gandhi M, Indiramma J, Jayaprakash, NS, Kumar AS, Journal of Electroanalytical Chemistry, 2022, p. 116018.
- 3 Meng XM, Li ZR, Zheng XY, Liu YX, Niu WJ, Qiu XY, Lu HZ, *European Journal of Pharmaceutical Sciences*, v. 167, 2021, p. 105986.

Agradecimentos/Acknowledgments



Electrochemical study of kaempferitrin on the BDD electrode and the proposal of an oxidation mechanism supported by quantum chemical calculations

Carolina G. Simião (PG)¹, Fernanda Bettanin (PQ)², Kathia Maria Honório (PQ)^{2,3}, Thiago Veiga (PQ)¹, Eliana Maira Agostini Valle (PQ)¹, Hueder Paulo Moises de Oliveira (PQ)³, Lucia Codognoto (PQ)¹

lucia.codognoto@unifesp.br; simiao.carolina@gmail.com

¹Departamento de Química - Unifesp; ²EACH-USP; ³CCNH - UFABC

Palavras Chave *Bauhinia forficata*, BDD electrode, kaempferitrin, electrochemistry, mechanism.

Highlights

Study of the electrochemical behavior of kaempferitrin on boron-doped diamond electrodes and proposal of the oxidation mechanism with the aid of quantum chemical calculations.

Resumo/Abstract

A canferitrina (CFT), Fig. 1, é um flavonoide glicosilado com atividade hipoglicemiante, principal marcador analítico e farmacológico nas folhas da *Bauhinia forficata*. Neste trabalho o objetivo foi fazer o estudo eletroquímico da CFT utilizando o eletrodo de diamante dopado com boro (BDD) e propor o seu mecanismo de oxidação com a auxílio de cálculos químico-quânticos. Inicialmente, foi realizado um estudo eletroquímico da CFT, utilizando a voltametria cíclica (tampão BR 0,1 mol L⁻¹ e pH = 7) e observou-se que a CFT tem um pico de oxidação em +0,75 V vs Ag/AgCl (pico 1) e um segundo pico em +0,95 V vs Ag/AgCl (pico 2), Fig 2, com características de processo irreversível e dependente do pH do meio. Para o estudo do mecanismo de oxidação da CFT, foram conduzidos experimentos por comparação com os resultados voltamétricos encontrados para outros dois flavonoides, as flavonas apigenina e crisina, que apresentam estruturas químicas semelhantes¹⁻³. A partir dos resultados obtidos via estudos voltamétricos e dados da literatura¹⁻⁴, foi possível levantar a hipótese de que a CFT possui um mecanismo de oxidação sobre o eletrodo de BDD similar ao da apigenina, onde os pontos de oxidação acontecem nas posições 4' (anel B) e 7 (anel A). Desta forma, um mecanismo de oxidação para a CFT sobre o eletrodo de BDD foi proposto (Fig. 3). Para confirmar as posições de oxidação 4 e 7, foram realizados cálculos químico-quânticos usando a Teoria do Funcional da Densidade (DFT), com o funcional B3LYP e a base 6-31g(d), incluindo efeito do solvente (água) utilizando o modelo de solvatação IEFPCM. A partir das propriedades calculadas (energia total, energia livre de Gibbs, cargas atômicas, energia do orbital de fronteira HOMO, mapa de contribuições atômicas para os orbitais HOMO e mapa de potencial eletrostático) para as espécies sob análise, foi possível corroborar o mecanismo proposto (Fig. 3) via experimentos eletroquímicos.

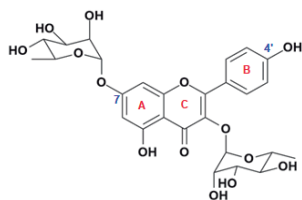


Fig. 1: Estrutura química da CFT.

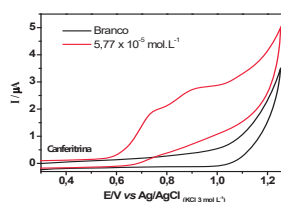


Fig. 2: Voltametria cíclica para a canferitrina ($1,57 \times 10^{-5}$ mol L⁻¹), em tampão BR 0,1 mol L⁻¹, pH = 7,0 e $v = 100$ mV s⁻¹.

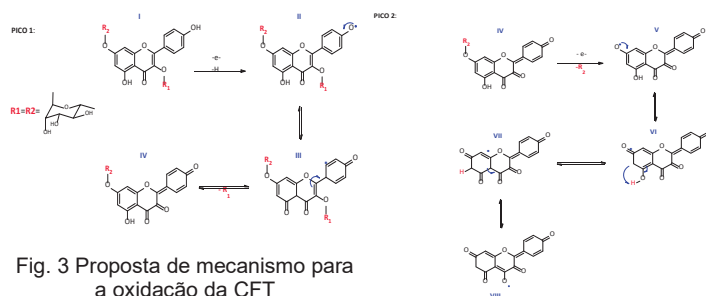


Fig. 3 Proposta de mecanismo para a oxidação da CFT

[1] - XING, T.L.; WANG, F.; MAO, Y.Y.; WANG, L.P.; YE, B.X.; J Chin Chem Soc, 56, pp. 303-309. 2009.

[2] - XIE, Z.; LI, G.; FU, Y.; SUN, M.; YE, B. Talanta, Volume 165, Pages 553-562, 2017. ISSN 0039-9140.

[3] - JANEIRO, P.; CORDUNEANU, O.; BRETT, A.O.. Electroanalysis, 17: 1059-1064. 2005.

[4] - JØRGENSEN, L.V.; CORNETT, C.; JUSTESEN, U.; SKIBSTED, L.H.; DRAGSTED, L.O. Free Radical Research, 29:4, 339 350, 1998.

Agradecimentos/Acknowledgments

FAPESP, CNPq, CAPES.

Electrochemical study of the removal of toxic metals (cadmium, lead, mercury and nickel) from the aqueous medium using *Opuntia ficus indica*

¹Karla Beatriz O. Silva* (PG), ²Rogério T. Ribeiro (PQ), ¹Ana Paula S. Paim, ¹Madalena C. C. Areias (PQ).

karla.beatriz@ufpe.br; rogerio.ribeiro@mintconsultoria.com.br

¹Departamento de Química Fundamental, Centro de Ciências Exatas e da Natureza, Universidade Federal de Pernambuco (UFPE); ² Diretoria de Pesquisa & Inovação, Consultoria em Materiais e Inovação Tecnológica Ltda (MInT consultoria) - PE.

Palavras Chave: *Metals; Opuntia; Voltammetry.*

Highlights

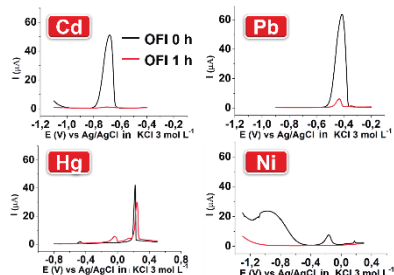
Natural coagulant used to remove toxic metals.

Redissolution voltammetry used in the study of removal of Cd, Hg, Ni and Pb using *Opuntia ficus indica*.

Resumo/Abstract

Opuntia ficus indica (OFI) is a cactus commonly found in semi-arid or water-scarce regions. It can be classified as a natural coagulant because it has a high capacity to adsorb various types of pollutants from the aqueous environment, such as toxic metals, which have bioaccumulative capacity and can cause short, medium and long-term damage to the environment in which it is inserted ¹. Due to the existing affinity between metals and natural coagulants, interest arose in evaluating the interaction between OFI and some metals, such as Cd, Hg, Ni and Pb, which in concentrations above 0.001; 0.0002; 0.025 and 0.01 mg L⁻¹, respectively, are considered toxic ². In this context, we used the technique of anodic stripping voltammetry (VRA) as the main investigation tool. Differential

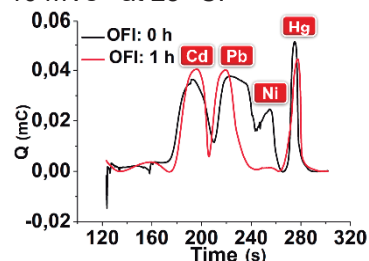
Figure 1. Voltamograms of anodic stripping in solution of Cd²⁺, Pb²⁺ and Hg²⁺ (10⁻⁵ mol L⁻¹) and Ni²⁺ (10⁻⁴ mol L⁻¹) in 0.1 mol L⁻¹ HCl medium with $\nu = 10$ mVs⁻¹



pulse voltammetry was used in a potential window of -1.3 to 0.5 V, deposition potential (E_{dep}) equal to -1.3 V and a deposition time (T_{dep}) of 600 s, when the metals were separated, and 60 s, when the metals were together in 0.1 mol L⁻¹ HCl solution. When analyzing the metals in isolation (Figure 1), it was observed that after 1 hour of contact with OFI, the intensity of the anode peak current (I_{pa}) presents a reduction of 99%, 91% and 33% for Cd²⁺, Pb²⁺, Hg²⁺, respectively. For Ni²⁺ this percentage was not determined due to the absence of peaks characteristic of this metal after the addition of OFI. The small percentage of extracted Hg indicates that a longer contact time (TC) between this metal and OFI would be required. Previous studies have shown that a 2 hour TC results in a removal percentage of 54% for this metal. Figure 2 shows the results

obtained with the simultaneous presence of all investigated metals in the medium. In this case, the charge was used as a parameter to determine the amount of metals. A tendency similar to the previous case was observed, since after 1 hour of contact between the metals and the OFI, there was a reduction of 22%, 26%, 6% and 52% for Cd²⁺, Pb²⁺, Hg²⁺ and Ni²⁺, respectively. The amount of metal extracted was lower than the system where the ions are isolated in the middle, this indicates that there is probably a dispute between these metal ions for the available active sites of OFI. In addition, it was also observed that Hg²⁺ was the least extracted metal in both systems, strengthening the hypothesis that a TC longer than 1 hour or a more rigorous treatment is necessary to remove this metal. Finally, it is believed that OFI has affinity for the metals Cd²⁺, Pb²⁺, Hg²⁺ and Ni²⁺ and in just 1 hour it was possible to notice the partial removal of these ions.

Figure 2. Voltamogram of anodic stripping in 0.1 mol L⁻¹ HCl solution of Cd²⁺, Pb²⁺, Hg²⁺ and Ni²⁺ (10⁻³ mol L⁻¹), with $\nu = 10$ mVs⁻¹ at 25 °C.



Agradecimentos/Acknowledgments

CNPq, CAPES e UFPE.

¹BABY, J. et al. International Journal of Biological and Chemical Sciences, 2011. ² Resolução CONAMA 357, 2005.

46ª Reunião Anual da Sociedade Brasileira de Química: "Química: Ligando ciências e neutralizando desigualdades"

Electroreduction reaction of carbon dioxide in materials containing Sn and Bi for the production of formate

Maria R. Pinto (PG),¹ James C. Pessoa (IC),¹ Igor Messias (PG),¹ Gabriel F. Costa (PG),¹ João B. S. Junior (PQ),² Raphael Nagao* (PQ)^{1,3}

j237271@dac.unicamp.br; nagao@unicamp.br

¹Institute of Chemistry, UNICAMP; ²National Nanotechnology Laboratory, CNPEM, ³Center for Innovation in New Energies, UNICAMP

Keywords: *Metallic Catalysts, Nanomaterials, CO₂ Electroreduction reaction, Formate, Tin, Bismuth*

Highlights

Formate production by carbon dioxide electroreduction reaction. A synthesis and study of catalyst materials with Sn and Bi. Physicochemical characterization of catalysts.

Abstract

The study of the electroreduction reaction of CO₂ (ERCO₂) is one of the alternatives studied to mitigate the effects of the increasing CO₂ concentration in the atmosphere. ERCO₂ supplies different products that can be used as fuels, as they are good energy carriers¹, and in the chemical industry. Formate is known to be selectively produced in materials with Sn and Bi in its composition. In this study, Sn, Bi and a SnBi bimetallic material supported on carbon Vulcan catalyst materials were synthesized through solvothermal² method. These materials were characterized by XRD, XPS, SEM and also cyclic voltammetry (figure 1A). The Faradaic Efficiency (FE) for formate (figure 1B) was evaluated at different potentials in 1-hour long electrolysis in the range from -0.2 to -1.2 V. In this range, the highest FE were obtained at the potential of -0.9 V being: 97% for Bi, 65% for Sn and 71% for SnBi. The formate partial current gives us information about the activity of these materials, which considers the FE and absolute currents in electrolysis experiments. To improve the activity and selectivity of these materials, a gas diffusion electrode (Figure 1C) setup is being used for long-term electrolysis studies that will allow us to analyze the stability of the materials in ERCO₂.

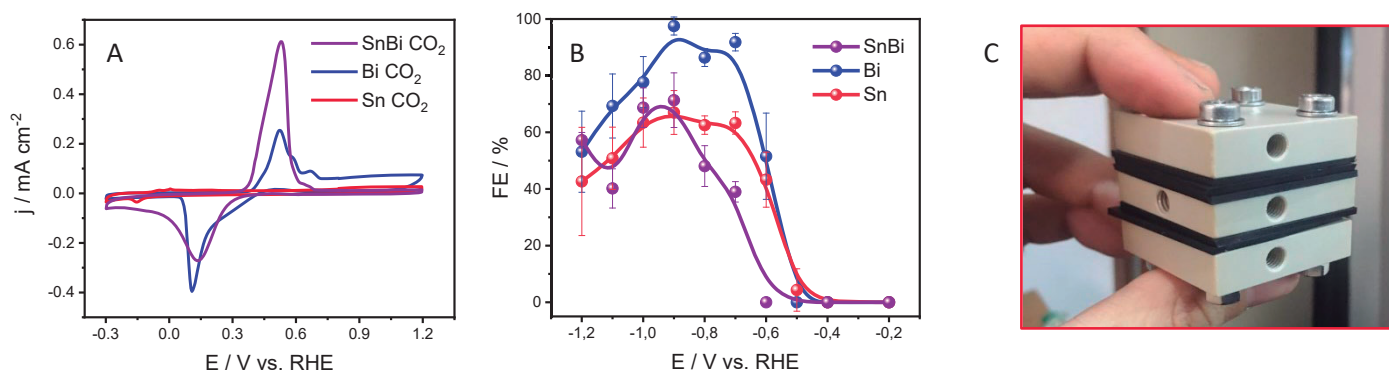


Figure 1: (A) cyclic voltammetry of Sn, Bi and SnBi at 0.5 M KHCO₃ at 20 mV s⁻¹. (B) Faradaic efficiency for formate production Sn, Bi and SnBi at 0.5 M KHCO₃ during ERCO₂. (C) Gas diffusion electrode to study the stability of the materials.

[1] Mardinil, Nour, et al. International Journal of Hydrogen Energy vol. 46, p. 13050–60, **2021**.

[2] Philips, Matthew F., et al. ACS Applied Energy Materials, vol. 5, no 2, p. 1720–30, **2022**.

Acknowledgments

J.C.P acknowledge SAE/UNICAMP, CNPq, M.R.P (22/03750-0), G.F.C. (22/01799-1); R.N. (21/08868-6) acknowledge FAPESP and Shell (DEC 17/11986-5); I.M. acknowledge CAPES (001).

Enhancing stability and efficiency of self-doped TiO₂ nanotubes electrodes for electrochemical generation of reactive sulfate species

Bruna L. Finkler (IC),*¹ Cleber A. Lindino (PQ),¹ Guilherme G. Bessegato (PQ).^{1,2}

bruna.finkler@unioeste.br

¹Engineering and Exact Sciences Center, UNIOESTE/Campus Toledo; ²UTFPR/Campus Dois Vizinhos

Keywords: Electrocatalysis, Self-doping, TiO₂ nanotubes, Degradation.

Highlights

Self-doping process induced excellent electrochemical properties on TiO₂ electrodes. Until 100% degradation without irradiation. SDTNTs are alternative candidates to the use of more expensive electrodes.

Abstract

Emerging contaminants are target of concern all around the world and, because of its complexity and difficulty of degradation, efficient removal methods are required, such as advanced oxidation processes (AOPs)¹. Radicals generation, that are the base of AOPs, can be performed through many ways, including transition metals, such as TiO₂ nanotube (TNT) electrodes, which have gained notoriety in different photoelectrochemical applications due to their nanometric morphology. More recently, the electrochemical self-doping of TNTs has been highlighted due to the possibility of 'activating' the electrode for oxidation reactions in the absence of light^{2, 3, 4}. Then, several opportunities for the application of self-doped TNT (SDTNT) emerged, such as the electrochemical oxidation of organic contaminants. However, the service time of these electrodes is limited, their efficiency can be improved and there is a lack of studies elucidating the influence of the electrocatalysis conditions³. In this work, TNT electrodes were produced by electrochemical anodizing of metallic Ti plates in different electrolytes based on aqueous, glycerol and ethylene glycol solutions. The TNTs underwent thermal treatment at 350, 400, 450 and 500 °C for 2 h and self-doped applying -2.5 V vs Ag/AgCl for 5 min in 0.1 M Na₂SO₄. The efficiency and stability of the electrodes in the degradation of a 7.5 mg L⁻¹ methylene blue solution in 0.1 M Na₂SO₄ under 7.5 mA cm⁻² were compared. The anodizing conditions significantly influence the degradation efficiency and especially the time of use of SDTNTs. Glycerol-based electrolyte showed longer service time, which could be related to the stronger adhesion of the oxide film on the Ti substrate. Treatment temperature (for crystallization of TiO₂) was evaluated, as well as the parameters of electrocatalysis, such as current density, pH of the electrolyte, temperature, and sulfate concentration to apply the optimized electrode and conditions in the degradation of an emerging contaminant (ibuprofen).

Table 1 – Optimized electrolysis parameters

Parameter	Optimum
Electrode	Glycerol-based
Treatment temperature	400 °C
Current density	15 mA cm ⁻²
pH	7.5
Electrolysis temperature	25 °C
Sulfate concentration	0.1 mol L ⁻¹

Source: Author, 2022

Optimized parameters are shown in Table 1. Electrodes treated at 400 °C also showed a better

service time, which can be explained through the anatase phase, that is more stable than rutile and amorphous phases. The electrode and the optimum parameters were used to perform the oxidation of the drug ibuprofen (30 mg L⁻¹), which resulted in almost 100% of degradation in 60 min of treatment. Thus, SDTNT can be considered alternative candidates to boron-doped diamond electrodes, for example, and further investigation of the conditions that increase their efficiency and stability is needed.

References

- ¹OH, W., *et al.* **Applied Catalysis B: Environmental**. v. 194, p. 169-201, 2016.
- ²Kim, C., *et al.* **ACS Applied Materials & Interfaces**. v. 7, p. 7486–7491, 2015.
- ³Bessegato, G. G., *et al.* **Electrocatalysis**. v. 10, p. 272–276, 2019.
- ⁴Cai, J., *et al.* **Applied Catalysis B: Environmental**. v. 257, p. 117902, 2019.

Acknowledgments

Acknowledgments to UNIOESTE and to GIPeFEA lab, for providing the physical space to conduct the research. To CNPq (process 428014/2018-6), for financial support to the project. To PETq and to FNDE, for the scholarship granted.

Estudo da Eletro-oxidação de Etanol Comercial sobre Eletrodos de Platina

Caio A.C. Bertolini (IC),¹ André H.B. Dourado (PG),^{1*} Hamilton Varela (PQ).¹

caio.augusto28@usp.br; andre.dourado@usp.br

¹Instituto de Química de São Carlos, Universidade de São Paulo

Palavras Chave: Oxidação eletroquímica do etanol, Instabilidades cinéticas, Eletrodos de platina

Highlights

A Study of Commercial Ethanol Oxidation on Platinum Electrode

Different oscillatory behavior and enhanced electrochemical properties, depending on the ethanol sample.

Resumo/Abstract

Devido ao interesse crescente em utilizar etanol como combustível para células a combustível e/ou sua reforma eletrocatalítica para a geração de H₂ verde, propõe-se a utilização de etanol combustível comercial, disponível em postos de combustíveis na cidade de São Carlos – SP para a verificação da influência dos contaminantes no comportamento eletroquímico do etanol. Para tanto, o presente estudo utiliza-se de três diferentes amostras de etanol, sendo uma o álcool etílico para análise (PA), com título de 96,5% (m/m), considerado “puro”, e amostras provenientes de dois postos de combustíveis, 1 e 2.

O estudo foi realizado em uma célula eletroquímica de três eletrodos convencional, sendo o de trabalho e o auxiliar placas e platina e o referência uma bolha encapsulada de H₂. O eletrólito foi H₂SO₄ 0,5 mol L⁻¹.

Para cada amostra, realizaram-se varreduras lineares de corrente (5 μA s⁻¹), como mostrado na figura.

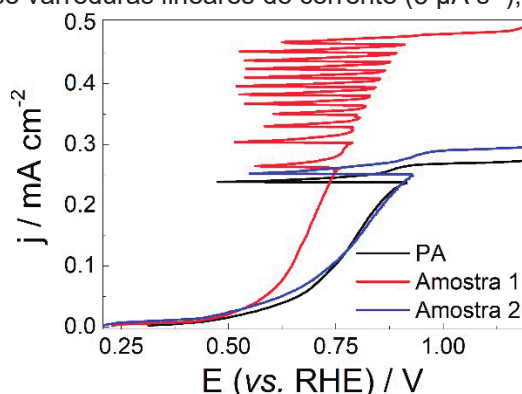


Figura 1. Perfil galvanodinâmico obtido para as amostras de etanol testadas em H₂SO₄ 0.5 mol L⁻¹ a 5 μA s⁻¹.

Assim, tendo apresentado maiores correntes a menores sobrepotenciais durante as medidas galvanodinâmicas, a amostra otimizada foi a 1, superando inclusive, a atividade da amostra controle, PA. Por tratar-se de uma reação que apresenta instabilidades cinéticas, durante as varreduras galvanodinâmicas também foram observados intervalos de corrente nas quais oscilações de potenciais ocorreram. A amostra que apresentou a maior janela de correntes também foi a 1, sugerindo que para esse sistema, o envenenamento do eletrodo devido ao acúmulo de venenos catalíticos é mais dificultado, aumentando a vida útil de um potencial dispositivo.

Agradecimentos/Acknowledgments

CNPq (#306060/2017-5 e #2022/3407), FAPESP (#2019/22183-6 e #2020/15230-5) e Shell Brasil.

Área: ELE

Estudo Nanogravimétrico da Eletro-oxidação de Moléculas Orgânicas Pequenas sobre Platina dispersa em Polianilina

Tifany L. R. Guercia (IC), André H.B. Dourado (PQ), Hamilton Varela (PQ).

tifanylaila@usp.br; hamiltonvarela@usp.br

Instituto de Química de São Carlos, USP - Av. Trabalhador São Carlense, 400 – 13566-590 – São Carlos, Brasil

Palavras Chave: *Eletrocatalise, Nanogravimetria, Polianilina.*

Highlights

Nanogravimetric study of the electro-oxidation of small organic molecules on platinum dispersed in a polyaniline matrix

Methanol oxidation reaction (MOR) is kinetic and diffusional limited on Au and Pt.

MOR follows a Frumkin isotherm on both metals.

There are mass variations during PANI's redox behavior due to charge compensation.

Resumo

A polianilina (PANI) é um polímero condutor que pode ser utilizado como matriz de dispersão para catalisadores em células eletroquímicas, devido à alta estabilidade e capacidade de reduzir a forte adsorção de CO em catalisadores como a Pt, aumentando a vida útil do dispositivo. Ela também apresenta um perfil redox reversível na janela de potencial do seu estado de oxidação mais condutor e estável (esmeraldina), o que dá a ela um conjunto de características de grande interesse para aplicações em conversão de energia utilizando a oxidação de pequenas moléculas orgânicas, como o metanol. Como a PANI apresenta um perfil característico de compensação de cargas e processos de adsorção são facilmente investigáveis pela nanobalança eletroquímica de cristal de quartzo (EQCN, em inglês), essa técnica foi selecionada para a investigação da influência da PANI na reação de oxidação do metanol (MOR, em inglês) sobre eletrodos de Au e Pt. O estudo da MOR permitiu identificar processos eletroquímicos limitados cineticamente e por transporte de massa, através do estudo voltamétrico a diferentes velocidades de varredura. A dependência da corrente de oxidação com a concentração de metanol permitiu o ajuste de uma isoterma de Frumkin para o metanol sobre Au. O ajuste também sugere que os mesmos intermediários estão presentes em diferentes etapas reacionais. A mesma metodologia foi aplicada para o eletrodo de Pt. Partindo para os efeitos gravimétricos da PANI, foram investigados inicialmente através de um processo de compensação de cargas utilizando diferentes eletrólitos, identificando assim a interferência deles na reversibilidade do processo de oxidação-redução do polímero. Em seguida, foi realizado o estudo da interferência do metanol na matriz polimérica e seus efeitos gravimétricos consequentes.

Agradecimentos

Universidade de São Paulo (PUB #83.1), FAPESP (#2013/16930-7 e #2019/22183-6) e CNPq (#306060/2017-5).

Evaluation of palladium decorated nanoporous gold sensor for hydrogen peroxide detection.

Paula C. Falcoswki (PG),¹ Douglas P.M. Saraiva (PG),¹ Mauro Bertotti (PQ)¹
 paula.calli@usp.br ; mbertott@iq.usp.br;

¹Department of Fundamental Chemistry, Institute of Chemistry, University of São Paulo - USP; São Paulo – SP, Brazil.

Keywords: Hydrogen peroxide, Nanoporous gold, Palladium-Gold, Modified electrode.

Highlights

The synergistic effect of palladium and gold nanostructures were exploited for development of a new hydrogen peroxide sensor.

Abstract

Hydrogen peroxide (H_2O_2) is a metabolite involved in numerous biological processes, acting as a signaling agent in stress response. It is considered the major reactive oxygen species (ROS) in redox regulation. The molecule can reversibly oxidize specific proteins, altering their activity and contributing to different processes in the organism, such as differentiation and the control of growth factors. Moreover, hydrogen peroxide is formed as a defense mechanism of the cell against more harmful ROS, being an indicator of oxidative stress¹. Therefore, this substance detection is very important in biological systems. Although gold electrodes have poor efficiency for H_2O_2 detection, nanoporous gold (NPG) has been demonstrated to be a good platform for both reduction and oxidation. Palladium electrodes, on the other hand, are a well-known substrate for hydrogen peroxide reduction. Nonetheless, only a few works reported the use of both components together. In this work, we have evaluated the performance of a nanoporous gold electrode decorated with palladium for hydrogen peroxide detection. The nanoporous gold layer was prepared onto a conventional bare Au electrode by the dynamic hydrogen bubble template (DHBT) method (-4 V for 60 s in a 2 mmol L⁻¹ gold (III) chloride solution in an acid solution). In this method, hydrogen is formed in the electrode surface concurrently with the gold deposition, which helps the porous formation. The addition of palladium in the electrode surface was carried out by a similar process applying -4 V for 120 s in a 4 mmol L⁻¹ palladium (II) bis(acetylacetonate) solution. The comparative response of different electrodes in a 5 mmol L⁻¹ hydrogen peroxide solution is shown in Fig. 1. The Au bare electrode presents a small response at about -0.3 V, and a significant potential shift (0.2 V) and a corresponding current enhancement are noticed using the NPG electrode. Performance even better is observed with the nanoporous gold palladium decorated electrode, and its response to hydrogen peroxide excels that obtained with a platinum electrode. The synergic effect between gold and palladium onto the nanoporous surface is a likely explanation for such an outstanding feature. Preliminary voltammetric studies indicated a good correlation between signal and hydrogen peroxide concentration in the 0.5 to 8.0 mmol L⁻¹ concentration range. Further studies will be directed to optimize the experimental conditions toward fabricating a sensitive microsensor for hydrogen peroxide detection. The influence of dissolved oxygen on the sensor response will also be the subject of the following studies.

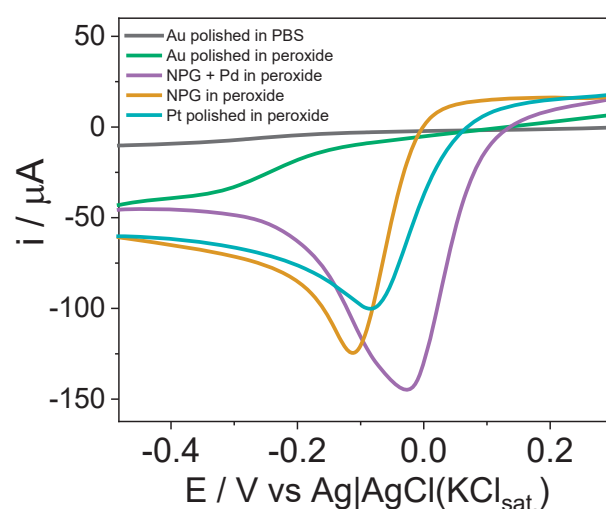


Fig.1: Voltammetry of modified and unmodified Au electrodes and platinum electrode in a 5 mmol L⁻¹ peroxide solution

¹ Sies, H., & Jones, D. P. (2020). Reactive oxygen species (ROS) as pleiotropic physiological signalling agents. *Nature Reviews Molecular Cell Biology*, 21(7), 363–383.

² Plowman, B. J., Jones, L. A., & Bhargava, S. K. (2015). Building with bubbles: the formation of high surface area honeycomb-like films via hydrogen bubble templated electrodeposition. *Chemical Communications*, 51(21)

Acknowledgments

The authors would like to thank São Paulo State Research Foundation, grant number FAPESP 2018/08782-1. DPMS was funded by the National Council for Scientific and Technological Development, grant number 141394/2019-6. PCF was funded by the São Paulo State Research Foundation, grant number 2022/03665-2

Electrochemical behavior of DNA in carbon paste electrodes modified with hydrophilic and hydrophobic natural deep eutectic solvents (NADES)

Beatriz A. Fernandes (PG)^{1*}, Rafael M. Buoro (PQ)¹.

beatrizall1@usp.br;

¹ Departamento de Química e Física Molecular, Instituto de Química de São Carlos- Universidade de São Paulo

Palavras-Chave: Carbon paste electrode, Natural Deep eutectic solvent, DNA.

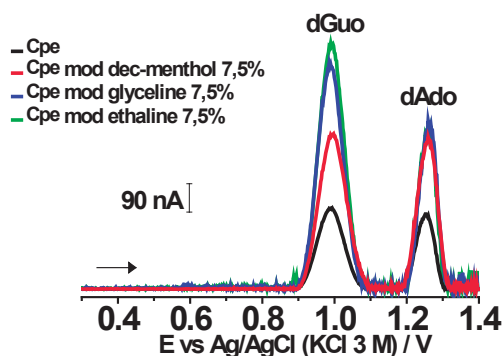
Highlights

Carbon paste electrodes were modified with hydrophilic and hydrophobic natural deep eutectic solvents. The hydrophilic NADES modified electrodes presented higher current nucleoside oxidation peaks.

Abstract

Carbon paste electrodes with different modifier binders have been studied to develop DNA-based sensors that allow the quantitative determination and study of the interaction mechanism of DNA with small molecules. Natural deep eutectic solvent (NADES) is an alternative class of electrode carbon paste modifiers, considered a class of green solvents generally composed of a hydrogen-bond acceptor (HBA) and a hydrogen bond donor (HBD) [1]. Understanding the redox behavior of the DNA in novel binders is critical for the design and successful application of the sensor. In this work, it was investigated the electrochemical behavior of DNA at paste carbon electrodes modified with hydrophilic (ethaline and glyceline) and hydrophobic (dec-menthol) NADES (CPE NADES) using cyclic (CV) and differential pulse voltammetry (DPV). The used NADES were prepared by mixing HBA and HBD in a specific molar ratio under stirring and controlled temperature (60 °C) until the formation of a homogeneous liquid [2]. The CPEs NADES modified-DNA were prepared by successively covering the electrode surface with three drops each of 10 μL from a 50 $\mu\text{g mL}^{-1}$ dsDNA [3]. The DPV voltammograms showed two well-defined peaks corresponding to deoxyguanosine (dGuo) oxidation, at $E_{pa} = + 1,05 \text{ V}$, and deoxyadenosine (dAdo), respectively at $E_{pa} = + 1,3 \text{ V}$ as previously stated in literature, but with increased currents for the NADES modified binders. Adding NADES to the binders reduces the intrinsic hydrophobicity of the mineral oil, as choline chloride is a positively charged ammonium quaternary salt. Therefore, the dsDNA negatively charged phosphate backbone interacts with the electrode surface through electrostatic interactions extending the dsDNA and leaving the nitrogenous bases more available to be oxidized. Thus, this study showed that the NADES can be used with binders in CPES for developing DNA-based sensors with increased sensitivity and evinced that the electrochemical behavior of dsDNA and current intensity of dGuo and dAdo depends on the binder hydrophilicity. The ethaline modified carbon paste electrode with 7,5% presented as the best substitution percentage with superior electroanalytical performance and was selected for the preparation of carbon paste DNA- modified for future studies of the interaction mechanism of DNA with small molecules.

Figure 1. DP voltammogram baseline-corrected in 0.1 M acetate buffer solution pH 4.5 of 50 $\mu\text{g mL}^{-1}$ dsDNA.



Acknowledgments

This study was financed in part by the Coordenação de Aperfeiçoamento de Pessoal de Nível Superior- Brasil (CAPES) -Finance Code 001 and FAPESP.

References:

- [1]. Brett, Christopher M.A. **Current Opinion In Electrochemistry**, Coimbra, v. 10, p. 143-148, ago. 2018.
- [2]. Cariati, Larissa ;Buoro,Rafael M .**Electrochemistry Communications**, Brasil, v. 109, p.106605, dez.2019.
- [3]. Buoro, R. M et al. **Bioelectrochemistry**, v. 99, p 40–45.2014.

Exploring the impact of laser scan gap on the electrochemical response of electrodes manufactured by laser-induced carbon pyrolysis.

Davi M. de Farias (PG),¹ Bruno Ferreira (PG), Gabriel N. Meloni (PQ), Thiago R.L.C. Paixão (PQ)

daviimarques@usp.br*

Institute of Chemistry, Department of Chemistry, University of São Paulo, 05508-900, São Paulo-SP, Brazil.

Palavras Chave: CO₂ laser, Laser pyrolysis, Electrochemical devices.

Highlights

The impact of different CO₂ laser scan gaps on the electrochemical performance of resulting electrodes is investigated. Changing the scan gap impacts the analytical response of electroanalytical methods.

Resumo/Abstract

Laser-induced pyrolysis to fabricate electrochemical devices from carbon-based polymers is very attractive. It involves a single fabrication step and can be used on several inexpensive substrates, including flexible ones. The electrode geometry is formed by selective pyrolyzing substrate regions using a CO₂ laser, moving in a raster pattern. The impact of fabrication parameters, besides laser power, on the electrochemical response of these electrodes has yet to be investigated in depth. We investigate the impact of the scan gap (the separation between each line in the raster pattern - Fig. 1A) on the electrochemical response of electrodes using the outer-sphere redox probe [Ru(NH)₆]³⁺. Scan gap values between 0.1 and 0.025 mm were investigated, and the cathodic and anodic peak potential difference (ΔE_p - Fig. 1B gray) and current ratios (I_{pa}/I_{pc} - Fig. 1B red) of voltammograms recorded with [Ru(NH)₆]³⁺ were used to quantify the electrochemical response. A trend of decreased I_{pa}/I_{pc} with decreased scan gap is seen, while ΔE_p decreased to a certain point, followed by a decrease, pointing to an optimal gap value.

Similarly, the absolute value of the cathodic and anodic currents approaches the expected value for the electrode geometric area and then decreases. These analyses suggest that at large scan gaps, only a partial area of the electrode surface is electroactive, while these parts interconnected and separated by non-pyrolyzed phenolic islands. Most of the surface is pyrolyzed at the optimal scan gap, and the separation between the electroactive areas allows for diffusional overlap. At the smaller scan gap, the electrode surface might be degraded by the continuous laser incidence. Electrodes fabricated with the optimal scan gap (smaller ΔE_p and closer to unit I_{pa}/I_{pc}) were used, as a proof of concept, to detect fluoroquinolones (Levofloxacin) and then compared with GCE electrodes at the same conditions. When the obtained result is contrasted with what is obtained for the largest gap electrode, it is clear that optimizing the fabrication parameters can have a huge impact on the development of electrochemical sensors.

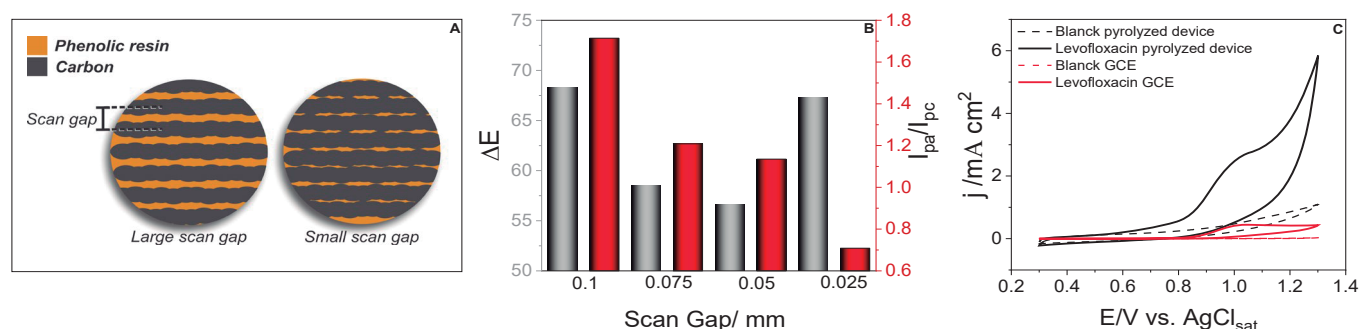


Figure 1 – A) Schematic representation of substrate pyrolysis varying scan gaps distance B) Effect of the scan gaps distance on ΔE (gray bars) and I_{pa}/I_{pc} (red bars). C) CVs recorded in the absence (dashed lines) and presence (solid lines) of 1.0 mmol L⁻¹ Levofloxacin using GCE electrodes (red lines) and pyrolyzed electrodes (black lines). Supporting electrolyte PBS buffer pH 7 and scan rate 50 mv s⁻¹.

Agradecimentos/Acknowledgments

São Paulo Research Foundation - FAPESP (2022/03382-0), Coordenação de Aperfeiçoamento de Pessoal de Nível Superior - CAPES (88887.601733/2021-00) and Conselho Nacional de Desenvolvimento Científico e Tecnológico - CNPq (140463/2021-6).

Fabrication of carbon fiber microelectrodes insulated with polymers.

Daniel V. Braga (IC),¹ Douglas P.M. Saraiva (PG),^{1*} Mauro Bertotti (PQ)¹

dpm.saraiva@gmail.com;

¹Department of Fundamental Chemistry, Institute of Chemistry, University of São Paulo - USP; São Paulo – SP, Brazil.

Keywords: Microelectrode, Fabrication, Carbon Fiber, Polymer Insulation.

Highlights

A simple and easily scalable method for the fabrication of microelectrodes is presented.

Abstract

We herein report a new method for the construction of small outline microelectrodes. The proposed method was based on the insulation of a carbon microfiber with a polymer by dip coating, and polydimethylsiloxane (PDMS), polycyanoacrylate (PCA), and epoxy resin (ER) were examined as insulating materials. After the dip coating step, the electrode was spun perpendicular to its axis to remove any polymer excess from the electrode body and to guarantee a homogeneous coating. The coating was cured with an infrared lamp, and a scalpel was used to release a cross-section of the carbon disc microfiber. Attempts to remove the coating were also based on immersing the coated electrode in concentrated sulfuric acid or other solvents, hence cylindrical microelectrodes were obtained. Many parameters require optimization, including the number of polymer layers and their composition, the G-force applied during the rotating step, the duration of the rotation step, and the power of the infrared lamp. Nonetheless, preliminary results were auspicious with microelectrodes prepared with two-layer PCA/PDMS and two-layer PCA/ER coatings. The two-layer coatings granted a high level of insulation, and an excellent electrochemical response to ferricyanide was noticed after exposing the cross-section, as seen in Fig.1. For instance, a well-defined sigmoidal voltammogram with very low hysteresis was obtained as a consequence of the radial diffusion associated to mass-transport at microelectrodes. The microelectrode radius was determined with the equation $i = 4nFDcr$, where i is the steady state current, n is the number of electrons involved in the reaction, F is the Faraday constant, D is the diffusion coefficient of the electroactive species in the medium, C is the concentration, and r is the radius of the disc microelectrode. Using this equation, the radius was determined a 6.4 μm , which represents a slight variation from the nominal fiber diameter (7 μm). One of the more significant strengths of the proposed method is its easy scalability for the simultaneous fabrication of microelectrodes, its simplicity, and the use of inexpensive equipment. Such micrometric electrodes will be further applied for neurotransmitter detection as implanted devices. Thus, biocompatibility, penetration capacity without causing damage to brain tissues, and further surface modification for enhancing the sensitivity and selectivity for neurotransmitter detection will be further studied.

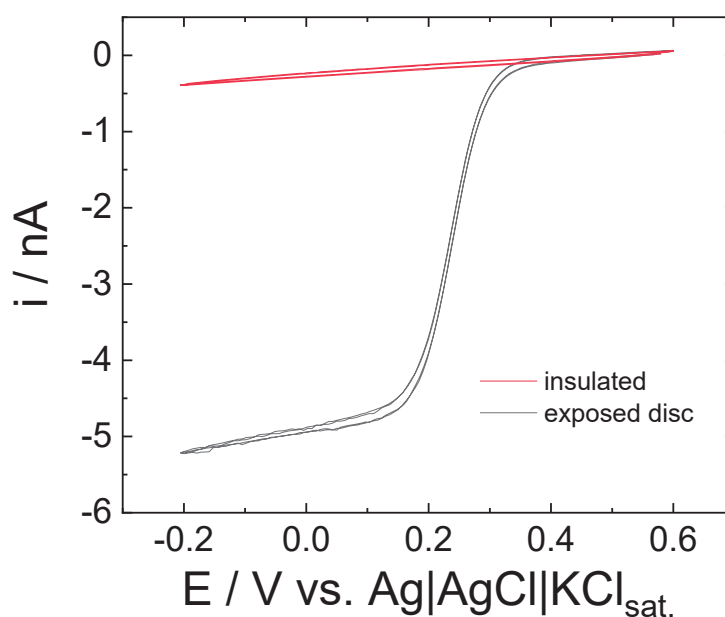


Fig.1 – Voltammograms recorded with insulated and exposed disc microelectrodes in a 5 mM $[\text{Fe}(\text{CN})_6]^{3+}$ and 500 mM KCl solution. Scan rate: 0.1 V s^{-1} . Microfiber nominal diameter: 7 μm .

Acknowledgments

The authors thank São Paulo State Research Foundation, grant number FAPESP 2018/08782-1. DPMS was funded by the National Council for Scientific and Technological Development, grant number 141394/2019-6. DVB was funded by the Coordination for the Improvement of Higher Education Personnel.

HEMIN/MWCNT FILM ON GLASSY CARBON ELECTRODE TO IDENTIFY FREE RADICAL FORMATION FROM NITROFURAZONE IN AQUEOUS MEDIA

Charles de L. Brito (PQ)^{1*}, Elizabeth I. Ferreira (PQ)¹, Mauro A. La-Scalea (PQ)².

mauro.scalea@unifesp.br; charles.brito@usp.br

¹Departamento de Farmácia, FCF-USP; ²Departamento de Química, UNIFESP-Diadema

Palavras Chave: Nitrofurazone, Hemin, Carbon nanotube, Electrochemical sensors, Cyclic voltammetry, Nitro-anion radical.

Highlights

The effect of electrocatalysis was proved in the GCE-CNT-F-HEM sensor due to reduction of overpotential and increasing of current values.

The radical was better stabilized on GCE-CNT-F-HEM system.

Resumo/Abstract

Nitrofurazone (NF), a nitroheterocyclic compound that is regularly used in burns as an antimicrobial and also has antichagasic activity, presents itself as a promising prototype in the search for new antichagasic drugs, with the objective of improving its biological activity^{1,2}. The proposed mechanism of action predicts the formation and stabilization of nitro-anion radical ($R-NO_2^{\bullet-}$). Hemin (HEM) when linked to functionalized carbon nanotubes (CNT-F) can allow an increase in electrocatalytic performance and a reduction in charge transfer resistance which makes it more suitable for mechanistic and analytical applications³. Cyclic voltammograms (CV) were recorded by using an electrochemical cell with three electrodes: Ag/AgCl_(sat.), Pt and modified glassy carbon electrode with functionalized CNT combined with HEM (GCE-CNT-F-HEM), being 1,3 dioxolane as dispersing agent, in aqueous medium (alkaline pH). Figure 1A shows a comparison among the voltammograms GCE-CNT-F-HEM, GCE-CNT-F and glassy carbon bare (GCE-SM) which corresponds to the electron-transfer process involving the $R-NO_2/R-NO_2^{\bullet-}$ couple at pH 10.04. The experiments presented a clear register, in which the redox pair $R-NO_2/R-NO_2^{\bullet-}$ occurred at less negative reduction potential for GCE-CNT-F-HEM compared to the GCE-SM and GCE-CNT-F, reaching to a variation of 250 and 50 mV, respectively. The peak currents, $I_{pc,2}$ was 13 times higher than GCE-SM and 2 times higher than GCE-CNT-F. Figure 1B presents, molecular oxygen as the best radical scavenging agent, when compared to the thiol groups, cysteine and glutathione, because the nitro radical was completely consumed. The current ratio ($I_{pa,2}/I_{pc,2}$) was used to evaluate the radical kinetic stability, as the electrogenerated nitro-anion radical underwent a second-order disproportionation chemical reaction. The rate constant of this reaction, k_2 , was determined in 0.1 mM NF solutions, and the values found to GCE-CNT-F-HEM, GCE-CNT-F and GCE-SM were 10700, 12860 and 22600 L/mol s, respectively, being the half-life times, $t_{1/2}$, 0.93, 0.78 and 0.44 seconds, respectively.

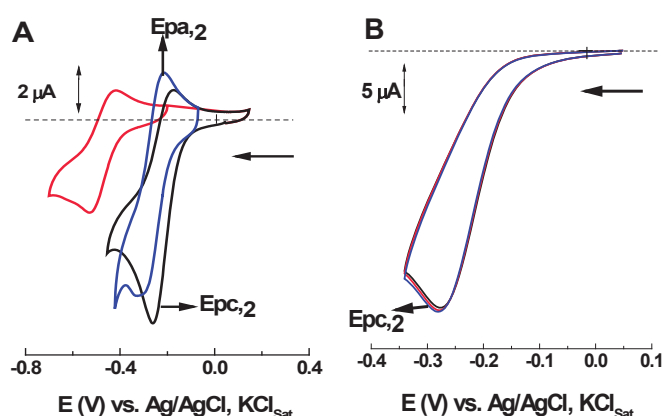


Figure 1. CV (1st cycle) recorded in NF 0.1 mM solution, pH = 10.04. **(A)** GCE-SM (red), GCE-CNT-F (blue) and GCE-CNT-F-HEM (black), in range of $v = 0.2 \text{ V s}^{-1}$; **(B)** presence of molecular oxygen after gas bubbling (1 mL/min) for 5 min (black), 10 min (red) and 15 min (blue), $v = 0.1 \text{ V s}^{-1}$.

¹Patterson, S., Fairlamb, A.H.; *Curr. Med. Chem.*, 26 (2019); ² Scarim, C;B, Chin, C.M.; *Med. Chem. Res.* 28 (2019) 2099-2108; ³ Santos, R.M. et al., *Biosens. Bioelectron.* 44 (2013), 152-159.

Hierarchical architectures of graphene as sensitive membranes for electrochemical sensors

Volodymyr Zaitsev (PQ),^{1*} Albina Mikhralieva (PQ),¹ Olena Artiushenko (PQ),¹ Mykhailo Nazarkovskyi (PQ),¹ vnzaitsev@puc-rio.br

¹Departamento de Química, PUC-Rio

Palavras Chave: *graphene quantum dots, mesoporous graphene, graphene nanosponge, sensors*

Highlights

Graphene derivatives such as graphene quantum dots, mesoporous graphene, and graphene nanosponge can essentially increase the sensors' sensitivity and selectivity due to their hierarchical architectures.

Resumo/Abstract

Carbon-based nanoparticles have gained enormous research interest in the last decade due to their excellent electrochemical and photochemical properties. Among them are 2D nanoparticles, such as graphene (G) and graphene oxide (GO); 1D nanostructures, such as carbon nanotubes; and 0D nanoparticles, such as nanodiamonds and carbon nanodots (CNDs). Recently we obtained a new type of carbon-based 2D nanoparticles: mesoporous Graphene (GMP) and Graphene nanosponge (GNS), which, contrary to G and GO, have porous morphology, Fig. 1b-c. In the search for materials that can increase the sensitivity of electrochemical sensors, GMP and GNS were immobilized on the surface of a glassy carbon electrode, and analytical properties of the sensors were tested in the determination of endocrine disruptors, clinically essential chemicals such as glucose, and neurotransmitters. The results were compared with sensors having electrocatalytically active membranes with GO, graphene quantum dots (GQDs) and graphene with tremella-like structure (TGO), Fig.1a,d. Due to the porous and hierarchical electroactive structure, the nanomaterials have increased sensitivity and improved sensor selectivity.

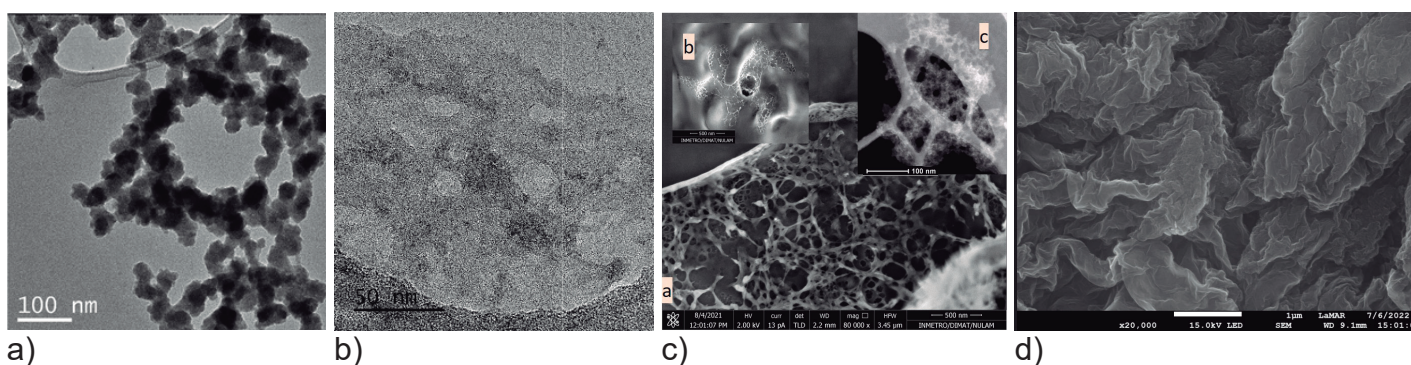


Figure 1. Electron microscopy images of (a) graphene quantum dots (GQDs), (b) mesoporous graphene (GMP), (c) graphene nanosponge (GNS), (d) graphene with tremella-like structure (TGO).

Agradecimentos/Acknowledgments

The authors are grateful for financial support of this research from the National Council for Scientific and Technological Development (CNPq), Grants 438450/2018-3 and 315125/2021-7, and Fundação de Amparo à Pesquisa do Estado do Rio de Janeiro – FAPERJ, Grants E-26/010.1556/2019, E-26/200.018/2020, E-26/204.448/2021, E-26/210.449/2021 and E-26/200.939/2021.

Investigation of RhFe/C and Rh/C nanoparticles for nitrogen reduction reaction

Rodrigo Gomes de Araujo (PG),¹ Joelma Perez (PQ),¹

rodrigogomesaraujo@usp.br

¹ São Carlos Institute of Chemistry (USP)

Keywords: electrocatalyst, nitrogen reduction reaction, ammonium synthesis

Highlights

The main product of N₂ electroreduction is ammonia;

The potential control allows producing other subproducts like N₂H₄;

Bimetallic material modifies the activity for NRR.

Abstract

The electroreduction of nitrogen to ammonia under temperature and ambient pressure has gained prominence since it provides an alternative to the reform process, drastically reducing CO₂ emissions via NH₃ synthesis. The nitrogen reduction reaction (NRR) was investigated using nanoparticles of Rh and RhFe catalysts dispersed in carbon. The polyol technique was utilized to synthesize Rh/C and RhFe/C catalysts with the same mean crystallite size. The reaction products were examined by UV-VIS using indophenol blue for ammonia detection and the *Watt and Chrisp* for hydrazine detection methods. Figure 1 shows the cyclic voltammetry results for the RhFe/C and Rh/C catalysts together with the x-ray diffraction (XRD) data. The XRD results confirmed the size of approximately 3 nm for both catalysts, showing that the polyol synthesis was adequate to obtain nanoparticles of the same size. The metallic alloy exhibits a more significant NRR catalytic activity.

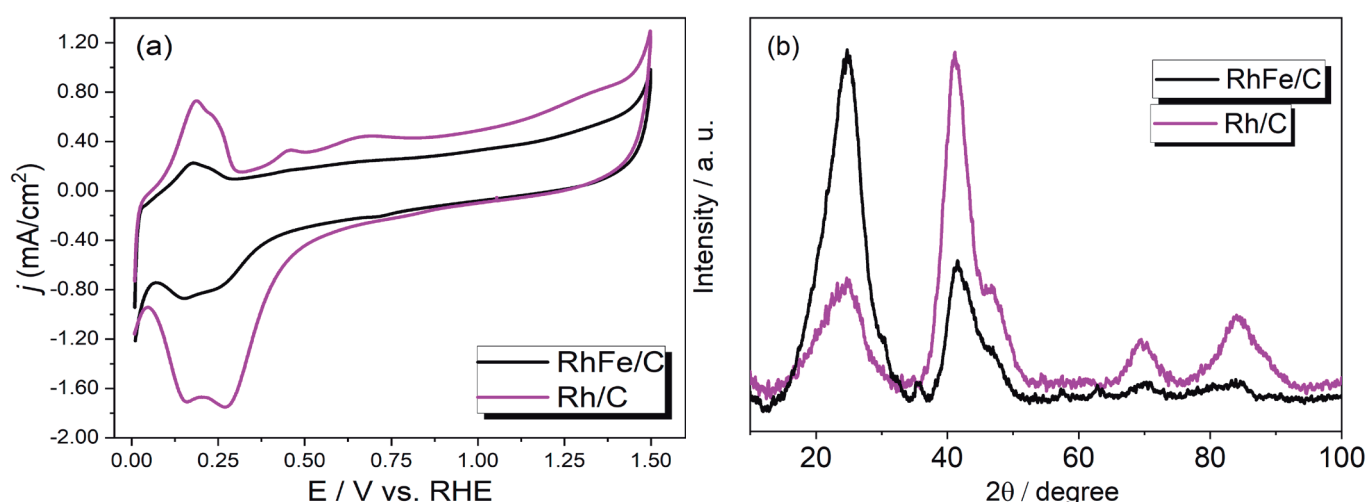


Figure 1. (a) Cyclic voltammetry of the material, (b) DRX analysis.

Acknowledgments

Thanks to CNPq and FAPESP for the financial support.

Investigations of the voltage oscillations during Nb anodization under spark regime

Francisco Trivinho-Strixino (PQ)*¹, Jonata R. D. Batista (PG)¹, Patricia S. Araujo (PG)¹.

fstrixino@ufscar.br;

¹Departamento de Química, Física e Matemática (DFQM-So), UFSCar.

Key-Words: Voltage oscillations, Niobium anodization.

Highlights

- Peculiar voltage oscillations with high amplitude and low frequency are observed during Nb anodization in the spark regime.
- Deposition of Nb₂O₅ inside the pores during Nb anodization might trigger the voltage oscillation behavior.

Resumo/Abstract

Electrolytic plasma oxidation is a technique that has been widely studied to obtain oxide films, such as Niobium oxides, that are interesting due to their properties as a semiconductor material, biocompatibility, and high corrosion resistance [1]. The electrochemical behavior during this process can change according to the anodization parameters and can influence characteristics such as thickness, morphology, and crystal structure of the obtained anodic film. When produced under specific conditions, anodic silicon oxides exhibit oscillatory voltage behavior [2]. The authors addressed this behavior with a different mechanism of active oxide dissolution during the process. For our study, the voltage oscillations were investigated using different approaches. Although obtained using different anodization procedures, some similarities between silicon and niobium anodization might bring some clues to these unusual voltage oscillations. Niobium substrates were anodized in a C₂H₂O₄ solution in galvanostatic mode. A voltage and temperature digital recorder was used for curve registration during the process. The samples were characterized by scanning electron microscopy (SEM), dispersive energy spectrometry (EDS), and X-ray diffraction (XRD). The anodic oxide morphology transient was registered inside a voltage oscillation period. At the end of the study, a possible mechanism was suggested that caused the voltage oscillations.

References

- [1] Babaei, K., Fattah-alhosseini, A., Chaharmahali, R. A review on plasma electrolytic oxidation (PEO) of Niobium: Mechanism, properties and applications. *Surfaces and Interfaces*, 21, 100719, 2020.
- [2] Parkhutik, V. Silicon anodic oxides grown in the oscillatory anodization regime – kinetics of growth, composition and electrical properties. *Solid-State Electronics*, 45, 1451–1463, 2001.

Agradecimentos/Acknowledgments

This work was supported by the Brazilian funding agencies CAPES (financial code 01), FINEP Martha, and FAPESP (2022/05191-3) projects. The authors also thank CBMM for the niobium foil donation.

Isolated Pd sites on functionalized carbon supports towards hydrogen peroxide electrosynthesis: A study of activity and stability

Guilherme V. Fortunato^{1,2}, **Marc Ledendecker**², **Marcos R. V. Lanza**¹

g.fortunato@usp.br

¹Instituto de Química de São Carlos, Universidade de São Paulo- USP

²Department of Technical Chemistry, Technical University Darmstadt, Alarich-Weiss-Straße 8, 64287 Darmstadt, Germany

Palavras-Chave: (Hydrogen peroxide, Selective 2-electron oxygen-reduction, Electrocatalysts, Single-atom catalysts, Electrochemical stability).

Highlights

The stability of single-atom catalysts (SACs) under harsh conditions in real-world applications is still a concern for the implementation of electrochemical H₂O₂ production. Here, we synthesized and applied Pd-based SACs to address this challenge. The performance, selectivity, and durability of these catalysts were thoroughly evaluated under realistic conditions.

Resumo/Abstract

The *in-situ* electroproduction of hydrogen peroxide (H₂O₂) via selective 2-electron oxygen-reduction (ORR-2e⁻) has gained a lot of attention in recent years because of its wide applicability ranging from industrial processes to water treatment technologies.[1] However, making the implementation of electrochemical H₂O₂ production a reality is still a challenge, as it requires the development of electrocatalysts that are more active, selective, and stable, while also using less noble metal content.[1,2] Single-atom catalysts (SACs) have emerged as a promising solution to this problem as they provide unprecedented levels of metal dispersion and unparalleled activity and selectivity towards ORR-2e⁻. [2] But the (electro)chemical stability of SACs under harsh conditions in real-world electrochemical devices is still a concern.[3,4] To address this challenge, we synthesized and applied SACs based on palladium (Pd) dispersed in carbon support with functional groups that stabilize the isolated metallic center, resulting in highly efficient electrocatalysts for selective H₂O₂ production. We thoroughly evaluated the performance, selectivity, and durability of the newly synthesized Pd SAC-based electrocatalysts under realistic conditions using testing protocols that simulate actual H₂O₂-producing devices. Based on the experimental results, we highlight important structural factors for enhancing stability, including customizing the coordination environment around the active center and the importance of the carbon material.

Agradecimentos/Acknowledgments

FAPESP (#2014/50945-4, #2017/10118-0, #2019/04421-7, and #2021/14194-8).

Referências

- [1] G. V. Fortunato, E. Pizzutilo, I. Katsounaros, D. Göhl, R.J. Lewis, K.J.J. Mayrhofer, G.J. Hutchings, S.J. Freakley, M. Ledendecker, Analysing the relationship between the fields of thermo- and electrocatalysis taking hydrogen peroxide as a case study, *Nat. Commun.* 13 (2022) 1973. doi:10.1038/s41467-022-29536-6.
- [2] J. Gao, B. Liu, Progress of Electrochemical Hydrogen Peroxide Synthesis over Single Atom Catalysts, *ACS Mater. Lett.* 2 (2020) 1008–1024. doi:10.1021/acsmaterialslett.0c00189.
- [3] E. Kollé-Görge, G. Fortunato, M. Ledendecker, Catalyst Stability in Aqueous Electrochemistry, *Chem. Mater.* 34 (2022) 10223–10236. doi:10.1021/acs.chemmater.2c02443.
- [4] F.D. Speck, J.H. Kim, G. Bae, S.H. Joo, K.J.J. Mayrhofer, C.H. Choi, S. Cherevko, Single-Atom Catalysts: A Perspective toward Application in Electrochemical Energy Conversion, *JACS Au.* 1 (2021) 1086–1100. doi:10.1021/jacsau.1c00121.

Laser-scribed pencil lead electrode fabrication and their application in flow injection analysis (FIA)

Thawan G. Oliveira (PG)¹, Irlan S. Lima (PG)¹, Wilson A. Ameku (PQ)¹, Josué M. Gonçalves (PQ)¹, Lúcio Angnes (PQ).^{1*}

Thawan.oliveira@usp.br; thawan.oliveira@usp.br

¹ Departamento de Química Fundamental, Instituto de Química, Universidade de São Paulo (IQUSP)

Keywords: Laser, Graphite, Graphene, Indapamide, Cyclic Voltammetry (VC), Flow Injection Analysis (FIA)

Highlights

Modification of pencil lead surface by laser heat treatment; Production of moldable, Sensitive and low-cost electrode; Determination of indapamide by FIA.

Abstract

Laser heat treatment produces conductive graphene-on-graphite surfaces, improving their electrochemical performance, producing low-cost, and sensitive, sensors quickly and environmentally friendly. Improvement was assessed by electrochemical tools such as cyclic voltammograms and electrochemical impedance spectroscopy using $[\text{Fe}(\text{CN}_6)]^{3-/4-}$ and dopamine as redox probes. The electrochemical results demonstrated that a treated surface resulted in improvement in electron transfer and less resistance to charge transfer. The resulting material was adequately characterized by Raman spectroscopy and scanning electron microscopy, where an irregular surface composed of crystalline graphite particles was observed. Furthermore, as a proof of concept, the detection of indapamide in a sample of synthetic urine by flow injection analysis was applied-Indapamide is a diuretic drug often used by athletes to change the urine composition to hide the consumption of prohibited substances in performance tests doping.

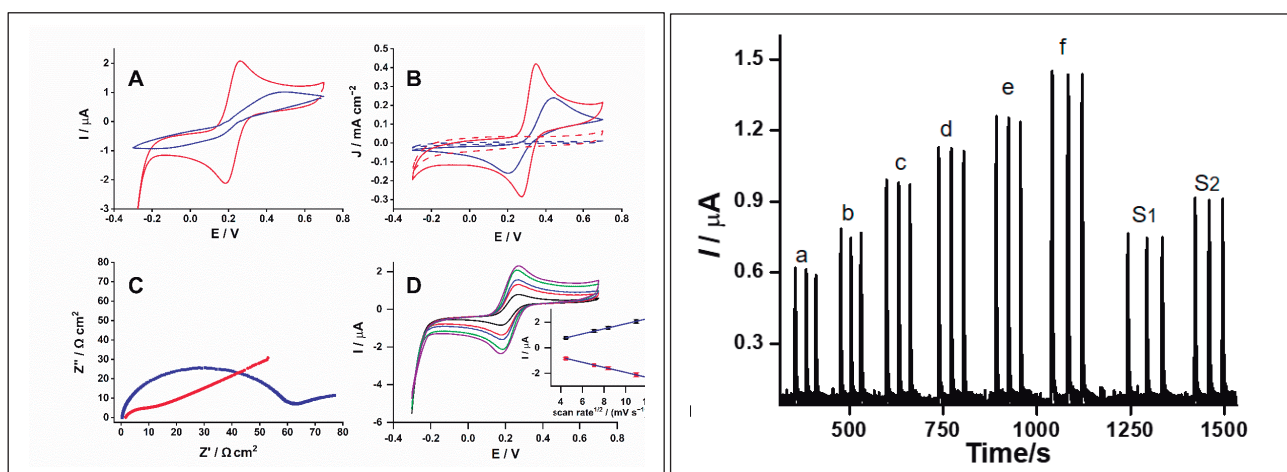


Figure 1 – Left: Cyclic voltammograms (CVs) and electrochemical impedance spectroscopy (EIS) recorded using non-treated (LNGr) (blue) and treated (LTGr) (red) H-type graphite; Right: Records of a series of injections of a solution containing indapamide.

Acknowledgments



Lignin Oxidation on CuO: (Electro)chemical Approaches

André H. B. Dourado (PQ), Matheus Santos (PG), Antonio A. S. Curvelo (PQ), Hamilton Varela (PQ)

andre.dourado@usp.br; hamiltonvarela@usp.br

São Carlos Institute of Chemistry, Universidade de São Paulo – Av. Trabalhador São-carlense, 400 – 13566-590 – São Carlos, Brazil

Key-words: *Lignin valorization, CuO Catalyst, Multi-frequency Mott-Schottky, Biomass, Hydrogen Generation.*

Highlights

Lignin was (electro)chemically oxidized by CuO catalyst
Preference to aldehydes generation on both pathways
Electrochemical mechanistic investigation took place
Oxygen vacancies tested by multi-frequency Mott-Schottky

Abstract

Lignin is a macromolecule present in biomass and with practically no industrial application nowadays. In general, it is obtained as a side-product of pulp and paper industry, or bioethanol production, and normally used as fuel for thermoelectricity production. However, this molecule is a natural source of aromatic compounds, which are normally obtained from fossil sources in actual techniques. Because of this, it is of high interest to investigate catalytic processes that can depolymerize lignin to obtain these products. By heterogeneous catalysis, CuO is a potentially good candidate. At temperatures as high as 180 °C, along with high O₂ pressures, CuO can provide good yield to monoaromatic phenol molecules with ketonic or aldehydic carbonyl, or carboxylic acids in para position. In *ortho*, these products can have zero, one or two methoxy groups, depending on the monomeric distribution of the starting macromolecule. Cu oxides are already known in electrochemical literature to be good oxidative catalysts in alkaline media. This approach cannot just find a new way to oxidate the lignin, but also can provide insights into the understanding of general lignin oxidation paths for this catalyst. The electrochemical approach generates the same monoaromatic products observed in heterogeneous catalysis, identified, and quantified by gas chromatography, suggesting a faradic efficiency of 20 % for aldehydes and 4 % for ketones and carboxylic acids each, a similar distribution observed for the heterogeneous catalysis. The catalyst was electrochemically characterized by electrochemical impedance spectroscopy, and capacitive cyclic voltammetry for surface area changes investigation and for the oxide characteristics investigation by multi-frequency Mott-Schottky analysis (mf M-S), which showed a slope of $-6.17 \cdot 10^{13} \text{ F}^{-2}$. The negative slope is a characteristic of intrinsic n-type semi-conductors, and the absolute slope decreased after the potential polarization. This decrease was observed to be dependent on the oxidation potential applied, suggesting that the charge carriers (oxygen-vacancies) are involved in the electrochemical mechanism and probably in the heterogeneous one as well.

Agradecimentos/Acknowledgments



2019/22183-6
2021/09630-3



2020/15230-5



306060/2017-5

Magneto-assay for detection of SARS-CoV-2 Spike protein for the diagnosis of COVID-19 using a disposable electrochemical device

Evair D Nascimento (PG),¹ Wilson T.Fonseca (PG),¹ Tássia R.de Oliveira (PG),¹ Pablo R. L. da Silva (PG),¹ Vagner S. Santos (PG),¹ Ronaldo C.Faria (PQ)¹

Evair190@gmail.com

¹ Department of Chemistry, Federal University of São Carlos-UFSCar, Rod. Washington Luís km 235, São Carlos, SP, 13565-905, Brazil

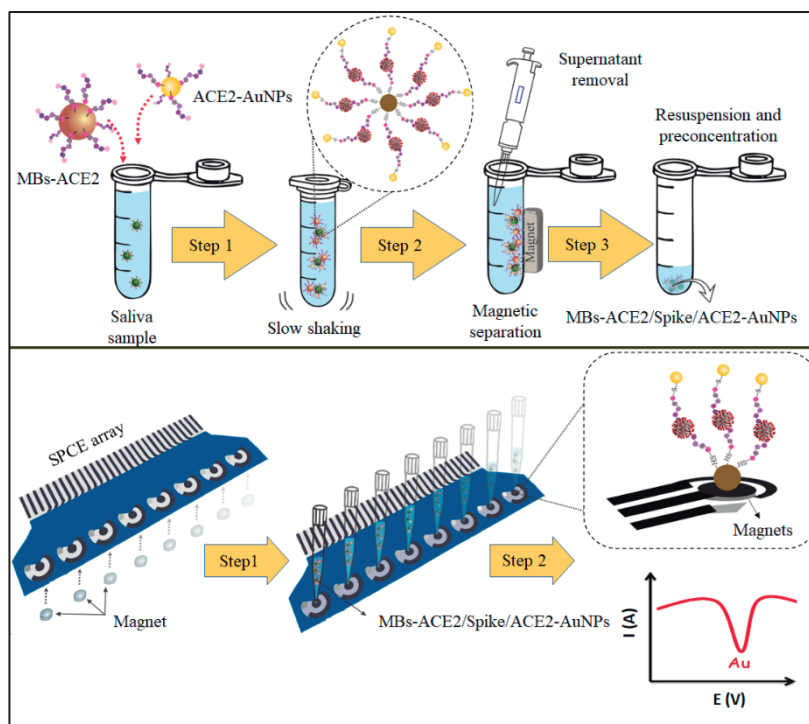
Palavras Chave: *Electrochemical Device, SARS-CoV-2, COVID-19, Diagnosis, Spike Protein, Saliva*

Highlights

We used an ultrasensitive magneto-assay for the diagnosis of COVID-19 application of magnetic beads and AuNPs conjugated with ACE2 for the capture and detection of Spike protein SARS-CoV-2 in saliva

Resumo/Abstract

Since the emergence of the COVID-19 pandemic, caused by the Severe Acute Respiratory Syndrome of the Coronavirus 2 (SARS-CoV-2), it has fueled the search for tests that help in the diagnosis of the disease in order to control and reduce viral transmission. The primary technique used to diagnose individuals infected with Coronavirus disease (COVID-19) is the Reverse Transcription Polymerase Chain Reaction (RT-PCR) technique. However, considering the high number of cases and the underlying limitations of the RT-PCR technique, particularly with regard to the accessibility and cost of the test, it is necessary to develop new, less expensive testing techniques that can aid in the early diagnosis of the disease. With that in mind, we developed an ultrasensitive magnetoassay using Magnetic Beads (MBs) and gold nanoparticles (AuNPs) conjugated with human Angiotensin-Converting Enzyme 2 (ACE2) peptide (Gln²⁴-Gln⁴²) for the capture and detection of SARS-CoV-2, respectively, in human saliva samples. The method proposed involved the use of a disposable electrochemical device containing eight screen-printed carbon electrodes that allow the simultaneous analysis of eight samples. The magneto-assay exhibited an ultra-low detection limit of 0.35 mg mL⁻¹ for the detection of Spike SARS-CoV-2 protein in human saliva. The magneto-assay was tested on saliva samples from both healthy and SARS-CoV-2 infected individuals. In terms of efficiency, the proposed technique showed a sensitivity of 100.0% and a specificity of 93.7% for the Spike protein of SARS-CoV-2. It showed great similarity with the RT-PCR technique. The results obtained point to the potential application of this simple and low-cost magnetoassay for saliva-based point-of-care diagnosis of COVID-19.



Agradecimentos/Acknowledgments



Área: ELE

(Inserir a sigla da seção científica para qual o resumo será submetido. Ex: ORG, BEA, CAT)

Magneto-immunoassay for serological diagnosis of COVID-19 by detection of anti-Spike antibodies using disposable microfluidic device.

Pablo R. L. da Silva (PG),^{1*} Sthéfane V. Almeida (PG),¹ Vagner S. Santos (PG),¹ Evair D. Nascimento (PG),¹ Ronaldo C. Faria (PQ).¹

Pablo.silva@estudante.ufscar.br

¹ Department of Chemistry, Federal University of São Carlos-UFSCar, Rod. Washington Luís km 235, São Carlos, SP, 13565-905, Brazil

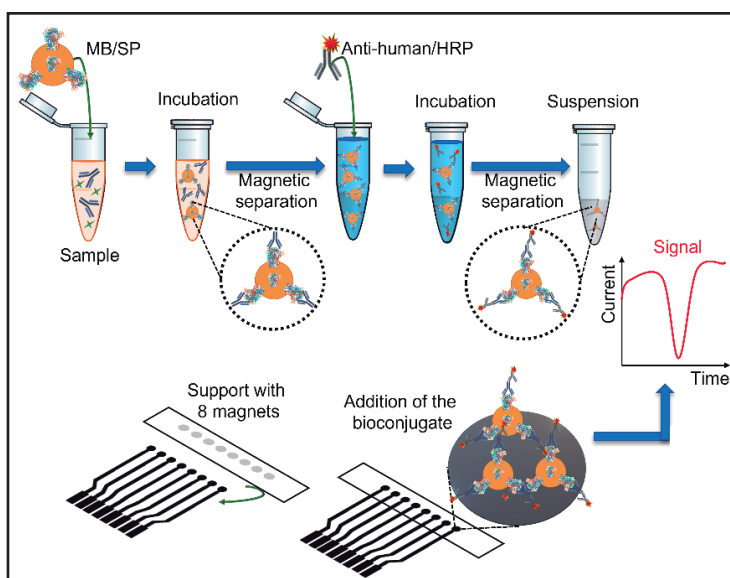
key words: Microfluidic Device, Magnetic Beads, Antibody, Diagnosis, Spike Protein, Magneto-immunoassay.

Highlights

Development of an ultrasensitive immunosensor for the detection of anti-Spike antibodies for the diagnosis of COVID-19 using magnetic beads conjugated with the Spike protein to capture and quantify anti-Spike IgG and IgM antibodies.

Resumo/Abstract

Since the onset of the pandemic caused by the severe acute respiratory syndrome coronavirus 2 (SARS-CoV-2), efforts have been made to find means that can assist in the diagnosis of the disease, with the aim of controlling and reducing viral transmission. Among the available diagnostic tests in the market are RT-PCR, which detect the virus's genetic material, and serological tests which detect antibodies. Among these tests, immunological tests have presented difficulties not only in diagnosing COVID-19, but also in evaluating the type of antibodies, both in individuals with the disease and in vaccinated individuals, thus presenting a high rate of false negative or positive results. However, the detection of anti-SARS-CoV-2 antibodies is a useful tool for diagnosing COVID-19, as IgG antibodies (persist for a long time) are an indicator of a past infection and provide immunity to the virus. While IgM antibodies are produced by the immune system at the beginning of a viral infection and are an indicator of a current or recent infection. Electrochemical immunosensing is an interesting method for detecting antibodies and can provide information about current and past infections by the virus and even evaluate the type of antibodies in vaccinated individuals. In this sense, an ultra-sensitive immunosensor using magnetic beads (MBs) with the SARS-CoV-2 virus Spike (SP) protein has been developed for the capture and separation of antibodies from the serum sample and for the detection and quantification. The developed method used a disposable microfluidic electrochemical device containing eight screen-printed electrodes that allow the analysis of eight samples simultaneously. The developed method showed an ultra-low detection limit of 0.01 and 0.1 fg mL^{-1} for the detection of anti-Spike protein IgG and IgM antibodies, respectively. In conclusion, the electrochemical immunoassay is a highly sensitive and specific method for detecting IgG and IgM antibodies. Its simplicity, speed and ability to detect small amounts of target antibodies make it a useful tool for the diagnosis of COVID-19 and antibody monitoring at the point of care.



The developed method used a disposable microfluidic electrochemical device containing eight screen-printed electrodes that allow the analysis of eight samples simultaneously. The developed method showed an ultra-low detection limit of 0.01 and 0.1 fg mL^{-1} for the detection of anti-Spike protein IgG and IgM antibodies, respectively. In conclusion, the electrochemical immunoassay is a highly sensitive and specific method for detecting IgG and IgM antibodies. Its simplicity, speed and ability to detect small amounts of target antibodies make it a useful tool for the diagnosis of COVID-19 and antibody monitoring at the point of care.

Agradecimentos/Acknowledgments



Manufactured 3D- Printed electrodes for electroanalytical applications using polyacrylate hydrogels as a medium.

Amanda G. Batista (IC)¹, Igor C. de Sá (PG)¹, Suellen F.L. do Nascimento (PQ)¹; Lucas V. de Faria (PQ)¹, Felipe S. Semaan (PQ)¹, Wagner F. Pacheco (PQ)¹, Rafael M. Dornellas (PQ)¹

amanda_batista@id.uff.br;

¹ Departamento de Química Analítica, Universidade Federal Fluminense (UFF), Niterói/RJ, Brazil

Keywords: 3D-Printed electrode, Hydrogel, Electrolytic cell, Polyacrylate composite

Highlights

- Cyclic voltammograms showed that the redox reaction is reversible, and diffusion governs the mass transfer in the hydrogel medium.
- The p(MA-co-AC-co-AA) hydrogel behaves like an electrolytic solution itself, there is no need for an electrolyte addition.
- Each electrode costs less than a US dollar (\$1) to manufacture.

Abstract

Composite electrodes are composed of an insulating and a conducting phase, which can give semiconductive properties to the material¹. Polylactic acid is a thermoplastic and insulating polymer but with the addition of Carbon Black (CB) it becomes conductive². These material characteristics allows the use of 3D printing techniques for the manufacture of a portable and low cost electrochemical electrode for in locus analysis. The proposed electrode consists of a case printed by a 3D resin, in which it has holes that connect the PLA-CB composite material, extruded by a 3D printing pen, to the potentiostat. This printed device consists of combining the working, reference and counter electrodes without the need to use of any commercial electrode. Furthermore, a hydrogel was made by polymerizing three different monomers (Acrylamide/Methacrylic acid/ Acrylic acid) and applied as both the solution medium as well as the support electrolyte as it contains in its structure ionic sites that not only is capable of swelling water but also is responsible for the charge transfer process. Besides, as the studied hydrogel is anionic, it can adsorb cations efficiently. Therefore, it's also possible to preconcentrate an analyte and improve it's detection limits for several cationic species, such as metals. An analytical curve was performed using cyclic voltammetry technique with the 3D-printed electrode and the hydrogel placed over the surface of the electrode without using any additional electrolyte, in different concentrations of $K_3[Fe(CN)_6]$ (Image 1). In order to characterize the mass transport that governs the proposed system, cyclic voltammetry was performed using $K_3[Fe(CN)_6]$ (5mM), alternating the scan rate of from 10 to 1000 $mV.s^{-1}$ (image 2) observing a reversible and diffusional process. Finally, the constant K0 and the electroactive area of the electrode were also calculated, obtaining 0.0084 and 0.030 cm^2 , respectively.

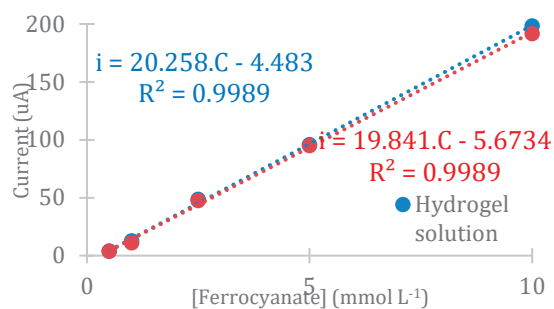


Image 1: Calibration curve using the hydrogel and in aqueous:

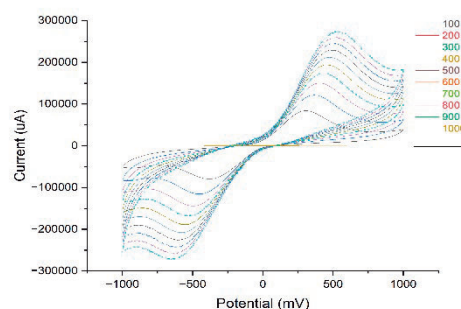


Imagem 2: Cyclic voltammogram in various scan rates in hydrogel

Acknowledgments

The authors would like to thank CAPES, FAPERJ, UFF and Peter Sorensen Laboratory

[1] GIBSON, R.F., Principles of composite material mechanics, McGraw-Hill, Inc, 1994.

[2] MCCREERY, R. L. Advanced carbon electrode materials for molecular electrochemistry, Chem. Ver., v.108 (7), p.2646, 2008.

Manufacture of composite electrodes based on graphite and aluminum oxide dispersed in the polylactic acid matrix for electrochemical sensing

Natália Marinho Caldas (IC)¹, Anderson de Oliveira Alves (IC)¹, Suellen F. L. do Nascimento (PQ)¹, Lucas V. de Faria (PQ)¹, Felipe Semaan (PQ)¹, Wagner F. Pacheco (PQ),¹ Rafael M. Dornellas (PQ)¹

Nataliamarinho@id.uff.br

¹Departamento de Química, UFF.

Keywords: composite electrodes, polymers, aluminum oxide, electrochemistry.

Highlights

Lab-made composite electrodes; Cost-effective strategy for large-scale electrode production; Potential usefulness in 3D printing.

Abstract

Composite electrodes consist of mixtures between at least two phases, an insulator, and a conductor, generating material with enhanced physical and chemical properties. Graphite-based materials are low-cost and have attractive electrical properties, making them great candidates for this purpose. Polymers are widely used as insulating phase, where polylactic acid (PLA) stands out, biodegradable and thermostable with good mechanical resistance, characteristics that allow its use in additive manufacturing [1]. Previous studies have shown that alumina oxide (AO) provides improved sensitivity and selectivity and electrocatalytic effects in electrochemical sensing [2]. Thus, in this work, composite electrodes were produced based on graphite, PLA, and AO, where graphite mass was fixed at 65 %w/w while the remaining 35% w/w corresponded to different proportions between PLA and OA (varying the percentage of OA from 0% (EP0) to 12.25% (EP5)). Preliminary studies by cyclic voltammetry using $[\text{Fe}(\text{CN})_6]^{3-/4-}$ as a redox probe showed that increased amounts of alumina increased the electroactive sites. While for the electrode containing only graphite and PLA, an active area of 0.1190 cm² was estimated, for the electrode containing 12.25% AO, a value of 0.1755 cm² was found, suggesting an increase of 1.5-fold in the electroactive area. Studies were also performed using dopamine (1.0 mmol L⁻¹) as a model molecule. As shown in Figure 1, the increased proportion of AO allowed a more enhanced electrochemical response, considering that higher anodic and cathodic current intensities and less peak-to-peak separation (better reversibility) were achieved. Such material shows promise for large-scale sensor production in laboratories with minimal structure, aiming at organic and inorganic species sensing in routine analysis.

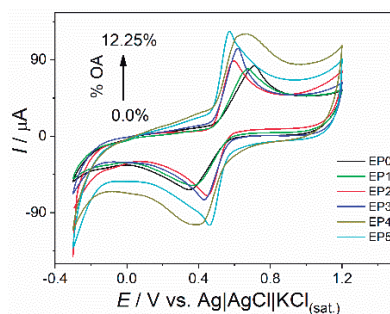


Figure 1: Cyclic voltammograms recorded for 1.0 mmol dopamine using electrodes prepared with different amounts of OA (0% for EP0 and 12.25 % for EP5).

- [1] A.L. Silva, M.M. *et al.* New J. Chem. 42 (2018) 19537–19547.
 [2] A.P. Lima, *et al.* Sensors Actuators B Chem. 262 (2018) 646–654.

Acknowledgments

We thank the CNPq, CAPES, FAPERJ, UFF and SBQ.

46^o Reunião Anual da Sociedade Brasileira de Química: "Química: Ligando ciências e neutralizando desigualdades"

Área: ELE

New Insights on the Formation of Gold Nanoparticles and Polydopamine Nanocomposites by Single Electrodeposition Step

Natalia Marçal Silva (IC), Heitor Furlan Trevizan (PG), Celso X. Cardoso (PQ), Marcos F. S. Teixeira (PQ)*
natalia.marcal@unesp.br; marcos.fs.teixeira@unesp.br

School of Science and Technology, São Paulo State University (UNESP), Presidente Prudente, SP, BR.

Key words: *Conductive polymers, Polydopamine films, Nanocomposites, Electrochemical study.*

Highlights

- Formation of polydopamine with gold nanoparticle.
- One-step electrodeposition.
- Investigation of interfacial phenomena.

Abstract

Recently, conductive metal-polymer nanocomposites have attracted much attention for investigations of new electrocatalytic materials, sensorial platforms and microelectronic devices. Polydopamine, a π -conjugated conducting polymer is of particular interest due to its high conductivity, high visible light transmissivity, excellent stability, and very good film-forming properties. Alternatively, electrochemically induced polymerization is an attractive strategy to deposit polydopamine films. The cyclic voltammetry in oxygen-free basic dopamine solution is employed to deposit polydopamine.

The aim of this work was to develop a single-step synthesis of AuNPs/polydopamine nanocomposite by cyclic voltammetry. Gold nanoparticle and polydopamine nanocomposites were prepared employing in-situ electropolymerization of dopamine and tetrachloroauric acid. The oxidation of dopamine and the reduction of gold(III) ions occurred simultaneously in a single step, which resulted in formation of nanocomposites based on gold nanoparticles entrapped within the polydopamine.

During the first positive scan, an oxidation peak at +0.63 V vs SCE was observed, which is attributed to the oxidation of dopamine leading to dopamine-quinone and consequently 5,6-indolequinone as a polymerizable species. The current related to the polymer redox response progressively increased in the range of 0.0 - 0.5 V. The SEM image shows the formation of gold nanoparticles in the form of nanoclusters encapsulated by a thin layer of polydopamine evenly distributed over the entire surface of the electrode. The voltammetric response of the electrode increased gradually cycle-by-cycle up to 20 scans. Subsequent scans did not show any increase in voltammetric response of the electrode. Detailed study of the nanocomposite was carried out by electrochemical impedance to understand the interfacial phenomena.

Acknowledgments

(2013/07296-2)



(303282/2020-7)



Nickel-magnetite nanoparticles as electrocatalysts for urea electro-oxidation reaction via MagnetoElectroCatalysis

Eduardo M. Rodrigues (PG),¹ Caio M. Fernandes (PG),¹ Evelyn C. S. Santos (PQ),² Flávio Garcia (PQ),² Odivaldo C. Alves (PQ),¹ Júlio César M. da Silva (PQ).^{1*}

ed_rodrigues@id.uff.br; julioocms@id.uff.br

¹Departamento de Físico-Química, UFF; ²Centro Brasileiro de Pesquisas Físicas

Palavras Chave: *Nanoparticles, Nickel-magnetite, Hyperthermia, Electrocatalysis, Urea electro-oxidation.*

Highlights

Use of an alternating magnetic field to generate localized heat in nickel-magnetite nanoparticles during the urea electrooxidation reaction. A new approach to the field of electrocatalysis.

Abstract

Urea is a compound that is commonly found in water bodies and can naturally be decomposed into ammonia which is toxic to humans and animals.^[1] Nickel-based electrocatalysts shows high catalytic activity for the urea electro-oxidation reaction (UER), a process that degrade urea into H₂, N₂ and CO₂.^[2] A parameter that can enhance the UER process is the increase in the temperature of the reaction.^[3] Magnetite has attracted attention of the scientific community due to its exceptional magnetic property, having good prospects in biomedical applications due to its ability to generate heat when subjected to an alternating magnetic field.^[4] The objective of this work consists in synthesize nickel-magnetite nanoparticles aiming at its application as catalysts for UER under an alternating magnetic field in order to generate localized heat at the anode electrode, enhancing the UER process. It is important to point out that is a new approach was named as MagnetoElectroCatalysis by the author of the present work. The magnetite nanoparticles were synthesized via co-precipitation method, and the nickel nanoparticles via sodium borohydride reduction.^[1,4] The nickel-magnetite nanoparticles were synthesized (mass ratio 3:2) via sodium borohydride reduction, using the magnetite previously synthesized. All materials were supported on carbon cloth (CC) and used as anode electrode. The diffractograms from X-ray diffraction showed the presence of Fe₃O₄, Ni and NiO. The images obtained by transition electron microscope showed nickel nanoparticles with diameters from 2 to 4 nm and magnetite nanoparticles with an average diameter of 20 nm. The hyperthermia measurements showed that the Fe₃O₄ and NiFe₃O₄ nanoparticles generated heat, and Ni nanoparticles did not. The magnetization curves demonstrates that the magnetic saturation decrease in the following order: Fe₃O₄ > NiFe₃O₄ > Ni, which is expected since the magnetic moment of nickel is smaller than that of magnetite. The cyclic voltammograms performed in 1 mol L⁻¹ NaOH from 0 to 0.7 V vs Hg|HgO showed the characteristics peaks of the transition Ni²⁺/Ni³⁺ for the nickel and nickel-magnetite nanoparticles.^[1] There was not observed any peaks related to the magnetite in this experiment. Chronoamperometric experiments 0.55 V vs Hg|HgO in 1 mol L⁻¹ NaOH and 0,33 mol L⁻¹ urea were carried out to investigate the effect of the alternating magnetic field (565.7 Oe and 224.7 kHz), at the anode during the UER. The results related to NiFe₃O₄ catalysts showed that right after the magnetic field was turned on the current density from UER rose sharply (28%), demonstrating that the electrocatalytic activity of the material was enhanced due to the heat of the NiFe₃O₄. For Ni and Fe₃O₄ any affect was observed, as expected. The influence of the amplitude of alternating magnetic field in the related process using NiFe₃O₄ was also investigated, and the results shows that the current from UER increases linearly with the field amplitude varying from 149.2 to 888.9 Oe.

References

- [1] J. R.Barbosa et al. *Electrochimica Acta*. 355, (2020), 136752.
- [2] LIU, D. et al. *Journal of Colloid and Interface Science*. 529, (2018), 337.
- [3] N.A.M. Barakat, et al. *Journal of Advanced Research*. 16, (2019), 43.
- [4] KOWALIK, P. et al. *The Journal of Physical Chemistry C*.124, (2020), 6871.

Acknowledgments

CBPF, CNPq, CAPES, Capes-PrInt (88887.310269/2018-00), FAPERJ (E-26/211.371/2019, E-26/201.435/2021, E-26/211.389/2021, E-26/210.793/2021, E-26/210.770/2021).

Nitrogen-doped Carbon Spherical Shells: a sustainable alternative to designing miniaturized electrochemical sensor

Nathalia O. Gomes (PG)^{1*}, Marcelo L. Calegari (PQ)¹, Sergio A. S. Machado (PQ)¹, Paulo A. Raymundo-Pereira (PQ)² sasmach@iqsc.usp.br; nathalia@usp.br

¹ São Carlos Institute of Chemistry, University of São Paulo, ² São Carlos Institute of Physics, University of São Paulo

Keywords: Sensors, sodium diclofenac, tap water samples, eco-friendly route, carbon spherical shells, nitrogen

Highlights

Simple, easy and inexpensive electrochemical sensor functionalized with greener Nitrogen-doped Carbon Spherical Shells for ultrasensitive detection of diclofenac at a low detection limit (358 nM) toward quality control of tap water

Resumo/Abstract

Introduction: Monitoring of drugs in water and the environment is crucial for human health due to the deleterious effect on the human health. The human can be exposed to the hazardous substances through the consumption of contaminated supply water since the processes in treatment plants cannot totally eliminate the contaminants. Electrochemical sensors are an emergent technologies able to detect hazardous compounds in water samples [1]. Thus, we have synthesized and used Nitrogen-doped Carbon Spherical Shells (N-CSS) as sensing layer in electrochemical sensors to detect anti-inflammatory diclofenac, an emerging pollutant, in water samples.

Results: First, we proposed a hydrothermal route to prepare Nitrogen-doped Carbon Spherical Shells (N-CSS) which offer a simple, non-toxic, low cost and green procedure to insert nitrogen heteroatom in pristine CSS to provide new sustainable material. Under optimized conditions, the N-CSS was prepared using a 1:100 ratio of (CSS:urea) followed by hydrothermal treatment at 160 °C for 3h. The XPS survey spectrum reveals a peak close to 399 eV related to N1s with an atomic percentage of 2.6%. The deconvoluted high-resolution N1s spectra of N-CSS (2.6%) showed three components with the binding energy at 399.6, 400.5, and 405.9 eV related to amide, O=C-N-C=O, and N-oxides, respectively. These results indicate the well-succeeded nitrogen doping of the CSS material using a green route. The N-CSS was incorporated into labmade screen-printed carbon electrode (SPCE) surfaces. Sodium diclofenac was chosen as a proof-of-concept molecule to show the feasibility of the proposed sensor. Differential pulse voltammetry (DPV) was used to perform the electrochemical detection of sodium diclofenac using the bare SPCE, SPCE/CSS, and SPCE/N-CSS devices. The relation between current and concentration is provided by the equations: $I \text{ (A)} = 1.35 \times 10^{-8} + 0.042C_{\text{diclofenac}} \text{ (mol L}^{-1}\text{)}$ ($R^2 = 0.99$), $I \text{ (A)} = 6.9 \times 10^{-9} + 0.07C_{\text{diclofenac}} \text{ (mol L}^{-1}\text{)}$ ($R^2 = 0.982$), $I \text{ (A)} = 7.99 \times 10^{-9} + 0.12C_{\text{diclofenac}} \text{ (mol L}^{-1}\text{)}$ for bare SPCE, SPCE/CSS and SPCE/N-CSS devices, respectively. The nitrogen-doped material indicated an increase in sensitivity values and linear range when compared to the other surfaces. The detection limit estimated was of 0.358 μM for SPCE/N-CSS. Thus, the nitrogen groups can facilitate sodium diclofenac oxidation and improve the analytical performance of the sensor. The SPE/N-CSS sensor was used to detect sodium diclofenac in multiple samples including tablets, urine, saliva and tap water samples giving good recoveries values (94 -104%). All those outcomes indicate the potential of the N-CSS material as a sensing layer in the electrochemical sensors for environmental and clinical applications.

Agradecimentos/Acknowledgments

São Paulo Research Foundation (FAPESP) [grant numbers [2020/09587-8](#), [2016/01919-6](#) and [2022/02164-0](#). Brazilian National Council for Scientific and Technological Development (CNPq) (grant numbers [151200/2022-0](#), [307070/2022-0](#), [423952/2018-8](#), and [164569/2020-0](#)).

References:

[1] GOMES, N.O. Flexible and integrated dual carbon sensor for multiplexed detection of nonylphenol and paroxetine in tap water samples. *Microchimica Acta*, p. 1–10, 2021.

Área: **ELE**

Nova célula eletroquímica impressa em 3D inspirada em um design de favo de mel para a detecção de metil-paration em amostras de mel

Bruno C. Janegitz^a (PQ), Robert D. Crapnell^b (PQ), Paulo Roberto de Oliveira^a (PQ), Cristiane Kalinke^c (PQ), Criag E. Banks^c (PQ)

brunocj@ufscar.br; R.Crapnell@mmu.ac.uk; paulo.oliveira@ufscar.br; cristiane.kalinke@gmail.com; C.Banks@mmu.ac.uk

^aDepartment of Nature Sciences, Mathematics, and Education, Federal University of São Carlos, 13600-970, Araras, São Paulo, Brazil

^bFaculty of Science and Engineering, Manchester Metropolitan University, Manchester M1 5GD, United Kingdom

^cInstitute of Chemistry, University of Campinas (Unicamp), 13083-859 Campinas, São Paulo, Brazil

Palavras Chave: impressão 3D, agrotóxicos, sensores eletroquímicos, manufatura aditiva

Highlights

A new electrochemical cell is proposed

The methyl parathion was detected in the system with 6 electrodes

The new system does not need any chemical/electrochemical treatments

Abstract

O desenvolvimento e o aumento do número de culturas na agricultura levaram recentemente a uma maior eficiência na produção mundial de alimentos e a um maior consumo de agrotóxicos. Nesse contexto, o uso desordenado de agrotóxicos tem afetado a diminuição da população de insetos polinizadores, além de causar contaminação de alimentos. Portanto, métodos simples, de baixo custo e rápidos podem ser alternativas interessantes para verificar a qualidade de alimentos como o mel. Neste trabalho, propusemos um novo dispositivo impresso em 3D inspirado em um favo de mel, com 6 eletrodos de trabalho (Fig. 1) para a análise eletroquímica de metil-paration em amostras de alimentos e ambientais. Sob os parâmetros otimizados, o sensor proposto apresentou faixa linear entre 0,85 e 19,6 $\mu\text{mol L}^{-1}$, com limite de detecção de 0,20 $\mu\text{mol L}^{-1}$. Os sensores foram aplicados com sucesso em amostras de mel e água da torneira usando o método de adição padrão. A célula proposta feita de ácido poliláctico e o filamento condutor (negro de fumo) é de fácil construção, não havendo necessidade de tratamentos químicos a serem utilizados. Esses dispositivos são plataformas versáteis para análises de alimentos e ambientais baseadas em eletroanálise, capazes de realizar detecção em baixas concentrações.

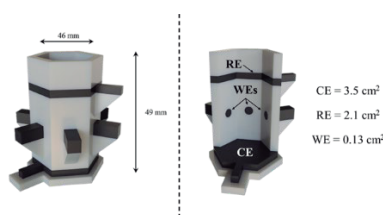


Fig. 1. Célula eletroquímica proposta com multieletródos

Acknowledgments

Os autores agradecem às agências brasileiras FAPESP (2017/21097-3, 2019/00473-2, 2021/07989-4 e 22/01601-7), CAPES (88887.636021/2021-00, e 001, 88887.712315/2022- 00) e CNPq (303338/2019-9) pelo apoio financeiro.

Numerical study of electrochemical potential variations on the surface of particles and intercalation waves in Li-ion Batteries.

Robson Pinheiro (IC),¹ Eduardo Parma (PG),² Raphael Nagao (PQ).^{2,3*}

r.258828@dac.unicamp.br, *nagao@unicamp.br

¹Institute of Physics Gleb Watagin, UNICAMP; ²Institute of Chemistry, UNICAMP; ³Center for Innovation in New Energies, UNICAMP.

Keywords: Li-ion batteries, Computational numerical modeling, Phase-separating porous electrodes, Surface energy.

Highlights

Modeling of voltage oscillations in lithium-ion batteries to understand the impact of surface energy on the propagation direction of lithium phases during intercalation.

Abstract

In 2018, the first potential oscillations during charging and discharging of lithium-ion batteries were reported¹, obtained in a battery with LTO anode ($\text{Li}_4\text{Ti}_5\text{O}_{12}$). This recent result was the starting point for the investigation of the lithiation mechanism in these systems, emphasizing that there is still no detailed description of the chemical dynamics associated with these oscillations. In this context, computational modeling² presents itself as a powerful tool for investigating the intercalation mechanism, considering that it allows the monitoring of Li^+ concentrations and electrical potentials at each point of the system. Thus, this work describes the search for a numerical description of the potential oscillations faithful to the experimental data, followed by the investigation of the mechanism behind the intercalation process. In fact, to understand this mechanism, we base ourselves on the Li^+ concentration data and on the electric potential, varying the parameter $\frac{dy}{dc}$ in such numerical tests. It was studied how the potential evolves in time through plots of *cathode filling vs. time*, and *cell potential per cathode filling*. It is noteworthy that being able to predict this type of behavior is also very important from a technological point of view, as the device being powered by the battery may not be compatible with non-stationary potentials, which may lead to damage or loss of efficiency.

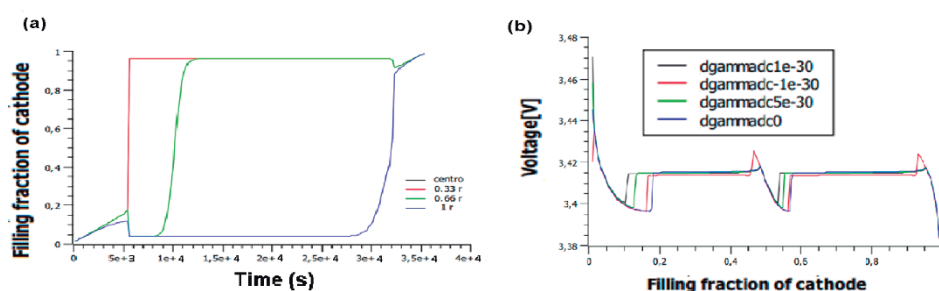


Figure 1. Effect of $\frac{dy}{dc}$ on oscillations; (a) Fraction of Li^+ in the cathode (one particle, $\frac{dy}{dc} = -10^{-3} D$); (b) Surface electrochemical potential (two particles, $\frac{dy}{dc} : dgamadc$).

References:

- (1) Li, D.; Sun, Y.; Yang, Z.; Gu, L.; Chen, Y.; Zhou, H. *Joule* **2018**, 2 (7), 1265–1277.
- (2) Smith, R. B.; Bazant, M. Z., *J. Electrochem. Soc.*, **2017**, 164 (11), E3291-E3310.

Acknowledgments

SAE-Unicamp, FAPESP, CNPq, Shell and ANP.

Numerical Study on the Mass Transport and Surface Energy Effects on Voltage Oscillations in Li-ion Batteries

Eduardo Parma (PG),¹ Raphael Nagao* (PQ),^{1,2*}

e170193@dac.unicamp.br; nagao@unicamp.br

¹Institute of Chemistry, UNICAMP; ²Center for Innovation in New Energies, UNICAMP

Keywords: Oscillations, Li-ion batteries, Phase-separating porous electrodes, Phase-field modeling.

Highlights

Computer simulations are used to investigate how cell parameters and electrode surface properties impact the voltage oscillations in Li-ion batteries, providing recommendations for experimentalists.

Abstract

For the first time in 2018, voltage oscillations were reported for Li-ion batteries during galvanostatic operation. This phenomenon results from $\sim 10^{11}$ electrode nanoparticles phase-separating in synchrony.¹ Yet, little is known about this synchronization process, and how it relates to cell and component properties. Computational techniques are being used to study such oscillations, as they provide extensive parameter control and a wealth of time and space resolved data.² In this work, we use simulations to show how improved mass transport and surface energy contributions promote synchronization among particles, increasing oscillation amplitude. Mass transport effects were investigated by changing the electrolyte diffusion constant and porous electrode thickness, resulting in larger oscillations at the start of the time series for lower characteristic diffusion times. Li^+ concentration plots along the electrode show that this comes from the increased interaction between particles on opposite ends of the electrode. Regarding surface energy, we swept values for $\frac{d\gamma}{dc_s}$, expressing how surface energy varies with surface Li^+ concentration. Both positive and negative values for the parameter lead to oscillations with considerably larger amplitude, with the sign dictating oscillation morphology and frequency. These results may inform experimentalists on how to design experiments, and also provide them insight on what techniques to use for electrode material characterization, aiming for a better understanding of the oscillation mechanism.

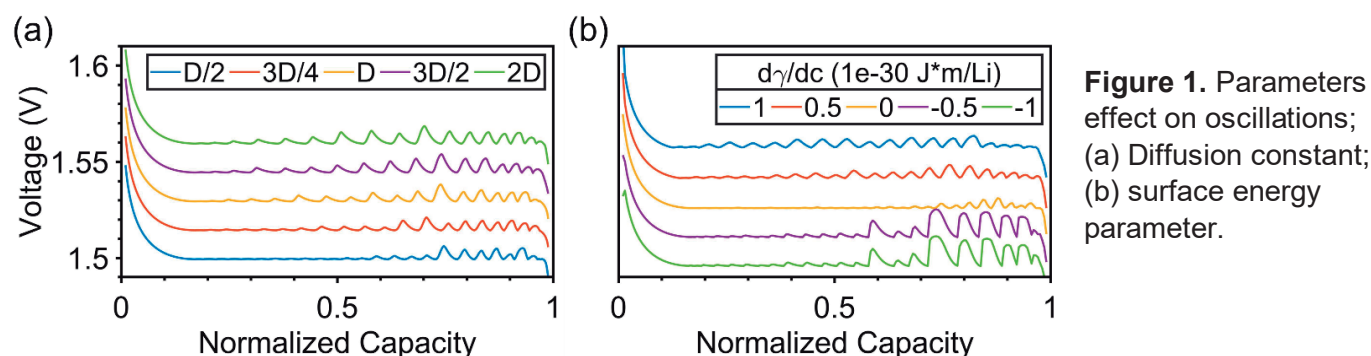


Figure 1. Parameters effect on oscillations; (a) Diffusion constant; (b) surface energy parameter.

References:

- (1) Li, D.; Sun, Y.; Yang, Z.; Gu, L.; Chen, Y.; Zhou, H. *Joule* **2018**, 2 (7), 1265–1277.
- (2) Parma, E.; Costa, G. F.; Nagao, R. *J. Phys. Chem. C* **2022**, 126 (29), 11900–11906.

Acknowledgments

E.P. (20/12632-5) and R.N. (16/01817-9, 21/08868-6) acknowledge FAPESP, R. N. acknowledge CNPq (405235/2018-6, 402481/2021-6), Shell (Division 1 – Dense Energy Carriers – 17/11986-5) and ANP.

On the detection of the RBD domain of the spike protein of SARS-CoV-2 using electrochemical impedance spectroscopy

Augusto Etchegaray (PQ),^{1,2*} Julius J.T.J. Paul (PG)¹, Isabela M.U. Magri (IC),² Wyllerson E. Gomes (PQ),³ Renata K. Mendes (PQ),^{2,3}

¹Programa de Pós-Graduação em Ciências da Saúde, Escola de Ciências da Vida; ²Faculdade de Química; ³Programa de Pós-Graduação em Sistemas de Infraestrutura Urbana, Escola Politécnica, PUC-Campinas.

Keywords: (SARS-CoV-2, COVID-19, Spike protein, RBD domain, Electrochemical impedance spectroscopy, biosensor)

Highlights

Antibodies against the RBD domain of the S protein of SARS-CoV-2 were desorbed from iron-magnetic nanoparticles in linear response to antigen concentration as determined by electrochemical analysis.

Abstract

The SARS-CoV-2 pandemic has changed the world in many aspects due to a sanitary and economic crisis. Research in clinical and biotech labs has focused on ways to immunize the population and perform tests to confirm infection, aiming to prevent the spread of the virus. Three years have passed, and COVID-19 is still a matter of concern, given its slow global resurgence. Following this rationale, this work has focused on the development of an analytical device that could be used to detect SARS-CoV-2 that is easy to prepare, and it is not expensive. Biosensors were prepared using iron magnetic nanoparticles containing monoclonal antibodies against the receptor binding domain (RBD) of the spike protein of SARS CoV-2. Antibodies were directly adsorbed to nanoparticles (NPs) without functionalization. Surface-modified NPs were added to a glassy carbon electrode, dried, and connected to an electrochemical cell. Electrochemical impedance spectroscopy (EIS) and ELISA experiments indicated that antibodies were desorbed from the NPs upon the addition of the RBD domain of the spike protein. The obtained biosensors produced linear curves with decreasing charge transfer resistance due to removal of antibodies, suggesting that a detection method can be designed based on antibody desorption. Figure 1 shows a representative analytical curve produced using the non-orthodox designed biosensor, based on antibody desorption. In Figure 2, a scheme showing antibody (Ab) desorption was drawn based on the results.

Figure 1. Resistance X antigen concentration.

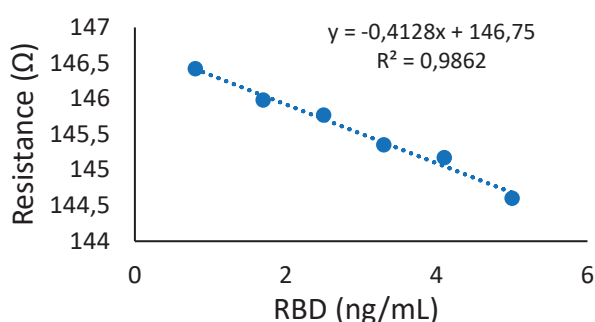
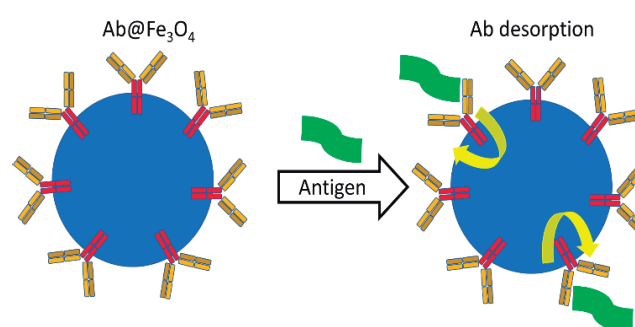


Figure 2. Antibody desorption from the Nps.



Acknowledgments

This study was financed in part by the Coordenação de Aperfeiçoamento de Pessoal de Nível Superior – Brasil (CAPES) - Finance code - 001. - Scholarship PNPd to WEG.

Área:

ELE

(Inserir a sigla da seção científica para qual o resumo será submetido. Ex: ORG, BEA, CAT)

Optimization of an Electrochemical Test for Quantification of Deleterious Phases in UNS S32750 Super Duplex Stainless Steel

Marcelo T. G. de Sampaio (PG)^{1*}, Anderson B. Furtado (PG)¹, Marcelo D. C. Ignácio (IC)¹, Sergio S. M. Tavares (PQ)², Juan M. Pardal (PQ)², André R. Pimenta (PQ)²⁻³ e Eduardo A. Ponzio (PQ)¹

eduardoariel@id.uff.br; Marcelo_sampaio@id.uff.br

¹ Laboratório de Materiais da UFF (G₂E/LaMUFF), Instituto de Química, Universidade Federal Fluminense, Niterói, Rio de Janeiro, Brasil; ² Programa de Pós-Graduação em Engenharia Mecânica e Montagem Industrial, Universidade Federal Fluminense, Niterói, Rio de Janeiro, Brasil; ³ Laboratório de Instrumentação e Simulação Computacional LISCOMP, Instituto Federal do Rio de Janeiro, Paracambi, Rio de Janeiro, Brasil

Keywords: Super Duplex Stainless Steel, Sigma Phase, Linear Sweep Voltammetry, Morphology

Highlights

Optimized electrochemical test for Sigma Phase quantification. Great correlation between the electrochemical response and microstructure. An electrochemical analysis of sigma phase morphology.

Resumo/Abstract

The objective of this work was to optimize the linear voltammetry in KOH (LSV-KOH test) in order to obtain an alternative electrochemical test, more precise and with a better detection limit, for quantification deleterious phase know as sigma phase in UNS S32750 superduplex stainless steels. KOH solutions are widely reported as sigma phase etching for metallographic analysis (1). The reason for this is due to the Cr and Mo transpassive dissolution that occurs preferably in alkaline media, once sigma phase is Cr and Mo richer than steel matrix this one is attacked primarily (2). For optimization of this new procedure for sigma phase quantification, a multivariate experimental design (Doehlert Matrix) was employed. Four specimens were subjected to different heat treatments in order to generate different sigma phase volume fractions. The initial quantification was measured by optical microscopy. The optimization aimed to achieve the best linearity between sigma phase volume fractions and the electrochemical response (Charge Density), thus creating a calibration curve. Three electrochemical factors were optimized: initial potential, scan rate and KOH concentration. After optimization process, the ideal factors values were obtained: 0.818 V for initial potential, 3,42 mV⁻¹, and 3,55 mol L⁻¹ for KOH concentration. In addition to the 4 original specimens, eleven more UNS 32750 super duplex stainless steel specimens, in two different grain sizes, were added to the calibration curve. After this step, a linear regression coefficient of 0.95 was obtained indicating good correlation between sigma phase and charge density in voltammograms. Another feature observed in LSV-KOH, is the qualitative analysis of the sigma phase morphology present in the Specimens. Depending on the sigma precipitation stage, changes were observed in the behavior of the voltammograms. In specimens where, lamellar morphology is present the voltammograms show two peaks curve. Meanwhile, in specimens where occurred also divorced precipitation of sigma the voltammograms changes to a 3 peaks curve. This feature is due to the dissolution of sigma phase boundaries which has different compositions according the form of sigma precipitation. In this study, we can conclude that LSV-KOH technique was more accurate in deleterious phase quantifying than the classical DL-EPR (3) technique, the LSV-KOH was able to detect and quantify the amount of deleterious phase present, which was the principal objective of this work. These additional peaks have a great concordance with observed morphology in optical microscopy and are correlated to composition mainly Ni behavior in Cr and Mo depleted zones in sigma boundaries.

(1) Michalska, J.; Sozańska, M. *Materials Characterization*, 56, n. 4-5, p. 355-362, 2006.

(2) Domínguez-Aguilar, M. A.; Newman, R. C. *Corrosion Science*, 48, n. 9, p. 2560-2576, 2006.

(3) De Sampaio, M. T. G., et al. *Corrosion Engineering, Science and Technology*, p. 1-11, 2022.

Agradecimentos/Acknowledgments



Palladium-Ceria Electrocatalysts for Application in Alkaline Direct Urea Fuel Cells

Carolina R. da Silva (IC), ¹ Tuani C. Gentil (PG), ¹ Victor S. Pinheiro (PG), ¹ João P. C. Moura (PG), ¹ Mauro C. Santos (PQ). ^{1*}

carolina.rufino@aluno.ufabc.edu.br; mauro.santos@ufabc.edu.br

¹Centro de Ciências Naturais e Humanas (CCNH), Universidade Federal do ABC (UFABC)

Key Words: fuel cells, urea, palladium, ceria.

Highlights

Development of palladium hybrid electrocatalysts with ceria nanorods for application in direct urea alkaline fuel cell.

Resumo/Abstract

Among the emerging technologies that seek to replace dependence on fossil fuels, fuel cells stand out. The use of urea as a direct fuel can be considered a promising alternative, as it is an abundant, low-cost organic compound and has an energy density in the liquid state 10 times higher than the energy density of H₂ [1]. For the development of electrocatalysts with high catalytic activity, Pd was used together CeO₂. Pd has already been widely studied and in alkaline solutions has shown promising results, and CeO₂, used to reduce the poisoning of active sites and the cost of the electrocatalyst [2]. CeO₂ NR was synthesized by the hydrothermal method and Pd nanoparticles by the sodium borohydride reduction method. [2]. For the incorporation of the CeO₂ nanorods to the mixture of Pd Vulcan XC-72, the impregnation method was used [3]. The expected percentages of Pd, CeO₂ NR and C for the hybrid electrocatalysts Pd₁₀(CeO₂)₂₀(Vn)₇₀ and Pd₁₅(CeO₂)₁₀(Vn)₇₅, estimated by EDS, were 10%, 20% and 70% and 15%, 10% and 75%, respectively. TEM images indicated Pd nanoparticles and CeO₂ NR well distributed on the carbon support of the hybrid electrocatalysts. The EDS mappings also confirmed the homogeneity in the distribution of nanostructures and the XRD patterns indicated that there was no alloy formation between them [3]. The results of Raman Spectroscopy showed a greater number of oxygenated species on the surfaces of the hybrid electrocatalysts when compared to the surface of the simple electrocatalyst Pd/C Alfa Aesar [3]. The curves obtained in cyclic voltammetry and chronoamperometry, using the hybrid electrocatalysts and the simple electrocatalyst in a solution of 1 mol L⁻¹ urea in 1 mol L⁻¹ KOH with potential from 0.00 to +0.80V (vs. SCE) and sweep rate of 10mV s⁻¹, for cyclic voltammetry and study potential +0.65V for chronoamperometry, are shown in Figure 1 and Figure 2, respectively. It is verified that the electrocatalyst Pd₁₀(CeO₂)₂₀(Vn)₇₀ obtained the highest mass activity among the electrocatalysts evaluated for the urea oxidation, being approximately 4 times higher than the mass activity of Pd/C. It is also verified, in both electrochemical measurements, that the presence of CeO₂ improves the catalytic activity, which can be attributed to the supply of oxygenated species that favor the oxidation reaction [4]. The preliminary fuel cell results showed the increasing of power densities using urea as fuel and Pd₁₀(CeO₂)₂₀(Vn)₇₀ as electrocatalyst.

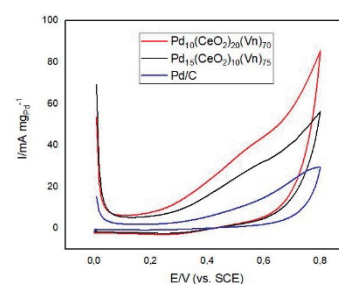


Figure 1.

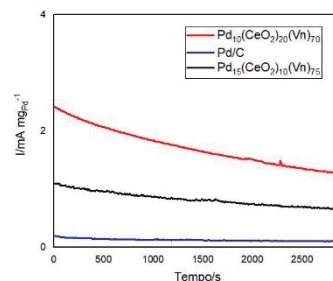


Figure 2.

[1] Journal of Power Sources, 417 (2019), 159-175; [2] Energy & Environmental Science, v. 2, n. 9, p. 915, 2009; [3] International Journal of Hydrogen Energy, 46 (2021), 15896-15911; [4] Science, 309(5735) (2005), 713-714.

Agradecimentos/Acknowledgments

PRH-ANP UFABC, ANP, UFABC, LEMN, CEM, FAPESP (2017/21846-6, 2017/10118-0 2017/26288-1, 2018/18675-8, 2021/10033-0)

Photovoltaic electrochemically-driven degradation of organic pollutants with simultaneous green hydrogen production

Suelya da S. Mendonça de Paiva (PG),² Mayra Kerolly Sales Monteiro (PQ),⁴ José Eudes Lima Santos (PQ),¹ Jussara Câmara Cardozo (PQ),¹ Edney Rafael V. P. Galvão (PQ),⁴ Marco A. Quiroz (PQ),¹ Djalma Ribeiro da Silva (PQ),¹ Carlos A. Martínez-Huitle (PQ),^{1,3} Elisama Vieira dos Santos (PQ),^{2,3}

mayra.kerolly@gmail.com; suelyapaiva@live.com

¹ Institute of Chemistry, Federal University of Rio Grande do Norte, P59078-970 Natal, RN, Brazil; ² School of Science and Technology, Federal University of Rio Grande do Norte, Campus Universitário, P59078-970 Natal, RN, Brazil; ³ National Institute for Alternative Technologies of Detection, Toxicological Evaluation and Removal of Micropollutants and Radioactives (INCT-DATREM), Institute of Chemistry, UNESP, P.O. Box 355, Araraquara 14800 900, SP, Brazil; ⁴ Human Resources Program of the National Agency for Petroleum, Natural Gas and Biofuels – PRH-26-ANP, Graduate Program in Chemical Engineering - PPGEQ, Lagoa Nova, Natal/RN, 59078

Palavras Chave: (Green Hydrogen Production; Electrochemical Oxidation; photovoltaic energy; BDD; stainless-steel ⁽³¹⁶⁾)

Highlights

Green hydrogen was produced by electrochemical oxidation (EO) of an aqueous solution including benzene, toluene, and xylene (BTX) in a PEM-type electrochemical cell powered by a photovoltaic (PV) energy source in this work.

Resumo/Abstract

For green hydrogen production, EO was performed on a Nb/BDD anode at three current densities (15, 45, and 60 mA cm⁻²), while a stainless steel (SS) cathode was utilized. For 180 min, the tests were carried out in a flow reactor with a mass transfer coefficient of 5.11×10⁻⁵ (m s⁻¹). The degradation of aromatic compounds via electrochemical oxidation was monitored by means of absorbance analysis and gas chromatography. The results of the analysis clearly shown that the oxidation of the BTX after 180 min of electrolysis time by applying 60 mA cm⁻² reached up to 100% of degradation. Therefore, the objective of this work is to demonstrate that hydrogen is efficiently produced simultaneously with the EO of BTX, using as a sacrificial analyte with a split electrochemical flow cell, featuring a BDD electrode as anode and a 316-type stainless-steel as cathode. The technology proposed here uses a photovoltaic array as an energy source to drive the operation of the designed PEM-type cell, establishing a promising, efficient, and sustainable alternative to produce green hydrogen. The amount of hydrogen produced in the cathodic compartment was determined simultaneously with the occurrence of the EO of BTX in the anodic compartment during a new set of experiments. For these experiments, the chosen anolyte was a 20 mg L⁻¹ of BTX solution in 0.25 M H₂SO₄ solution. The hydrogen production volumes obtained when concentrations of 20 mg L⁻¹ of BTX as organic model pollutants were about ±0.431 L, after 180 min of electrolysis.

References

Santos, J.E.L., Silva, D.R., Martínez-Huitle, C.A., dos Santos, E.V., Quiroz, M.A. (2020). Cathodic hydrogen production by simultaneous oxidation of methyl red and 2,4-dichlorophenoxyacetate in aqueous solutions using PbO₂, Sb-doped SnO₂ and Si/BDD anodes. Part 2: hydrogen production. RSC Advances, 10, 37947-37955.

Câmara Cardozo, J.; da Silva, D.R.; Martínez-Huitle, C.A.; Quiroz, M.A.; Dos Santos, E.V. (2022) Photovoltaic Electrochemically Driven Degradation of Calcon Dye with Simultaneous Green Hydrogen Production. Materials, 15, 7445.

Agradecimentos/Acknowledgments

Financial supports from Conselho Nacional de Desenvolvimento Científico e Tecnológico (CNPq, Brazil) (306323/2018-4, 312595/2019-0, 439344/2018-2, 315879/2021-1, 409196/2022-3, 408110/2022-8), and from Fundação de Amparo à Pesquisa do Estado de São Paulo (Brazil), FAPESP 2014/50945-4 and 2019/13113-4 and financial support to the Human Resources Program of the National Agency of Petroleum, Natural Gas and Biofuels – PRH-26-ANP through the Post-Doctoral Scholarship granted to Mayra, are gratefully acknowledged.

Portable Analysis Kit for Quality Control of Narrow Therapeutic Index Drugs using Boron-Doped Diamond Electrode in a 3D-printed Electrochemical Cell

Débora A.R. Moreira (PG),¹ Dilton, M. Pimentel (PG),¹ Wallans T.P. dos Santos (PQ)²

debora.ufvjm2009@yahoo.com.br; wallanst@yahoo.com.br

¹Departamento de Química, FVJM; ²Departamento de Farmácia, UFVJM, *Universidade Federal dos Vales do Jequitinhonha e Mucuri, Diamantina, Minas Gerais, Brasil.*

Keywords: *Analysis Kit, 3D Electrochemical Cells, Boron-Doped Diamond, Drug Quality Control, Manipulation Pharmacies, Electrochemical Sensors.*

Highlights

- Simple and fast voltammetric analysis Kit for drugs determination in pharmaceutical samples;
- Selective electrochemical screening of drugs for application in the quality control in manipulation pharmacies;
- Low cost and waste generation method for drugs quality control in formulation pharmaceutical.

Abstract

The narrow therapeutic index (NTI) drugs are active principles that require an efficient quality control, since their therapeutic dosages are very close to their toxic dosages [1]. In Brazil, 22 active principles are considered as to be NTI drugs, which many cases of intoxication with these compounds have been reported. The official methods for NIT drugs determination are mainly based on high performance liquid chromatography with ultraviolet detection. Electrochemical methods have been widely reported for drugs determination in pharmaceutical samples due to their advantages, such as simplicity, portability and low-cost. In this context, we present, an analysis Kit for NIT drugs determination using boron-doped diamond electrode (BDDE) in a 3D-printed electrochemical cell with detection by differential pulse voltammetry (DPV). Electrochemical measurements were performed on an Autolab PGSTAT 128N potentiostat/galvanostat. Electrochemical cell was composed of three electrodes: a BDDE (0.13 cm²) with a doping level of 8000 ppm as working electrode; Ag/AgCl (saturated KCl) and platinum wire, as reference and auxiliary electrodes, respectively. The electrochemical platform fabricated by 3D printing allowed analysis of small volumes (1000 µL) and easy coupling of BDDE with reproducible geometric area ("rubber ring"). Slicer software, Simplify 3D (Cincinnati, USA) was used in 3D-printed electrochemical cell. The BDDE was pre-treated cathodically in 0.5 mol L⁻¹ H₂SO₄, applying a current of +1.0 mA for 120 s and then applying -30 mA for 360 s. The electrochemical behavior of the NIT drugs was evaluated by cyclic voltammetry in different pHs and supporting electrolytes. The optimized condition for NIT drugs electrochemical detection was obtained using a 0.15 mol L⁻¹ phosphate buffer solution in pH 2. Although, twenty (20) NTI drugs were investigated by proposed method, only fourteen (14) showed to be electroactive on BDDE for electrochemical detection. These electroactive NTI drugs were: aminophylline, carbamazepine, clindamycin, clonidine, clozapine, colchicine, minoxidil, oxcarbazepine, prazosin, procainamide, quinidine, theophylline, warfarin and verapamil. The developed analysis Kit presented wide working linear ranges ($r^2 > 0.999$) and limits of detection sufficiently low for determination of all NTI drugs in pharmaceutical samples ($< 0.44 \mu\text{mol L}^{-1}$). An adequate stability of the electrochemical responses was also obtained for successive analyzes using the same (N = 10) or different (N = 6) working electrodes, with relative standard deviations smaller than 5.0 % and 4.7%, respectively. Addition-recovery studies of NIT drugs in pharmaceutical samples were close to 100%, which the obtained results were validated by official methods. The use of the BDDE in 3D-printed electrochemical cell with detection by DPV demonstrated to be a simpler, faster, lower cost and waste generation method for drugs determination than official methods. Therefore, the proposed method presents a promising analysis kit for NIT drugs quality control in pharmaceutical samples, providing an efficient and feasible application in manipulation pharmacies.

Acknowledgments

FAPEMIG, CNPq, UFVJM, RQ-MG e CAPES

References:

[1] Brasil. RDC 67 de outubro de 2007. ANVISA, Ed.:BRASIL, 2007.

46ª Reunião Anual da Sociedade Brasileira de Química: "Química: Ligando ciências e neutralizando desigualdades"

Preconcentration followed by electrochemical degradation in methanol medium as a strategy to increase the efficiency of the clindamycin removal

¹Júlia Faria Silva (IC), ¹William Santacruz (PG), ¹Rodrigo de Mello (PG), ¹Artur de Jesus Motheo (PQ)*

juliafsilva@usp.br; artur@iqsc.usp.br

¹ São Carlos Institute of Chemistry, University of São Paulo, P.O Box 780, CEP 13560-970, São Carlos, SP, Brazil

Palavras Chave: *Clindamycin, Electrochemical Degradation, Adsorption, Methanol Medium.*

Highlights

- Clindamycin removals up to 98% after 1 hour of electro-oxidation in methanol medium
- The adsorption of clindamycin was accomplished using activated carbon

Resumo/Abstract

Numerous studies have demonstrated the presence of various types of pollutants in the environment. Some of them are called emerging pollutants because they are harmful to the environment and human health and occur in low concentrations. Many municipal wastewater and runoff contain antibiotics such as clindamycin, which are challenging to remove using conventional water treatment processes. Therefore, it is necessary to develop useful strategies for water treatment^{1,2}. Preconcentration by adsorption is very promising due to its high efficiency, low energy consumption and feasibility, in which the adsorbent can be reused³. The subsequent desorption step with methanol leads to a highly concentrated clindamycin solution that can be treated by electrochemical degradation. In this work, a preconcentration step of adsorption/desorption was performed before the electrochemical degradation of clindamycin. Adsorption tests onto granular activated carbon (GAC) were carried out for 100 mg L⁻¹ clindamycin solution until the thermodynamical equilibrium be reached, and adsorption isotherms were calculated. Clindamycin concentration was monitored by high performance liquid chromatography (HPLC). Electrooxidation of clindamycin was performed in water and methanol medium containing 0.03 mol L⁻¹ NaCl and 100 mg L⁻¹ clindamycin, using a Dimensionally Stable Anode (DSA). The degradation of clindamycin showed a removal of 93.3% in water and 98.0% in methanol after 1 hour. Degradation in water showed a faster kinetic constant, but after 1 hour of electrooxidation, the removal of clindamycin in methanol medium was greater. Variation of different current densities was evaluated and showed that electrooxidation in water was more efficient at 3.5 mA/cm² and 88.3% of clindamycin was removed in the first 15 minutes. In the chromatograms, the formation of some by-products can be seen in both water and methanol media and the intensity of which increases with decreasing clindamycin concentration. After the complete removal of the impurity, the by-products formed are also degraded, and at the end of the electrochemical treatment no further by-product was detected. Electrochemical degradation of clindamycin showed great removal of the contaminant in water and methanol media. These results highlight the possibility of using methanol as an electrolytic medium as efficiently as water. Therefore, a prior process of enrichment of the pollutant may be a viable proposal to improve the efficiency of this type of technology, and it proves to be a promising alternative for the treatment of wastewater.

[1] PULIZZI, F.; SUN, W. Treating water with nano. **Nature Nanotech**, v. 13, p. 633, 2018.

[2] GEISSEN, V.; MOL, H.; KLUMPP, E.; UMLAUF G.; NADAL, M.; VAN DER PLOEG M.; ZEE, S.; RITSEMA, C. Emerging pollutants in the environment: A challenge for water resource management, v. 3, n. 1, p. 57-65, 2015.

[3] DE MELLO, Rodrigo et al. Combination of granular activated carbon adsorption and electrochemical oxidation processes in methanol medium for benzene removal. **Electrochimica Acta**, v. 425, p. 140681, 2022..

Agradecimentos/Acknowledgments

The authors gratefully acknowledge the financial assistance granted by the São Paulo Research Foundation (FAPESP, Brazil) [2017/10118-0; 2018/16308-8; 2022/11761-1] and the Coordination for the Improvement of Higher Education Personnel (CAPES, Brazil) [88887.713883/2022-00] in support of this research.

Simultaneous determination of amoxicillin and clavulanate in pharmaceutical samples using BIA with amperometric detection.

Anastácio A. Boane (PG)^{1,2*}, Lucas V. de Faria (PQ)¹, David R. Ramos (PG)¹, Mariana C. Marra (PQ)¹ Rodrigo A.

A. Muñoz (PQ)¹, Eduardo M. Richter (PQ)¹.

emrichter@ufu.br; anasboas@yahoo.com.br

¹Institute of Chemistry, UFU, Av. João Naves de Ávila, 2121 - Santa Mônica, Uberlândia - MG, 38408-100, ² Faculty of Natural and Exact Sciences, Av. FPLM, 111 – Cimento Neighborhood, Massinga –Mozambique

Highlights

First electrochemical method for simultaneous determination of amoxicillin (AMX) and clavulanate (CLA). Unique advantages of pulsed amperometric detection have been explored.

Abstract

Introduction: AMX is a β -lactam antibiotic that is usually formulated with CLA, forming a synergistic antibiotic pair for antibacterial applications [1, 2]. AMX and CLA can be determined simultaneously by high performance liquid chromatography (HPLC), infrared spectroscopy, chemiluminescence, and capillary electrophoresis (CE) [2-4]. However, to our knowledge, electrochemical methods for the simultaneous quantification of AMX and CLA have not yet been reported. Therefore, a simple and rapid method for the simultaneous quantification of AMX and CLA using batch injection analysis with amperometric detection (BIA-AD) is proposed.

Results/discussion: The electrochemical profiles of AMX and CLA were evaluated by cyclic voltammetry using boron-doped diamond as working electrode and Britton-Robinson (BR) buffer solution as supporting electrolyte. Better results (peak separation and response stability) were obtained using 0.3 mol L⁻¹ of BR buffer solution, pH 10.0. A strategy using amperometry with application of three sequential pulses was used: (i) +1.3 V for detection of AMX only, (ii) +1.8 V for detection of both AMX and CLA, where the CLA signal was obtained taking into account the correction factor (FC) and the following expression ($I_{CLA} = I_{+1.8V} - (FC \cdot I_{+1.3V})$, where FC is the ratio of the AMX oxidation current at +1.8V and +1.3V, and (iii) +2.0V/20s for cleaning the electrode surface. Potential pulses (+1,3 V and +1,8 V) were applied as a function of time to allow for replicate injections (n = 5). Linear ranges between 10 and 60 $\mu\text{mol L}^{-1}$, and 5 and 30 $\mu\text{mol L}^{-1}$ were obtained for AMX and CLA, respectively. Successive measurements (n=10) using concentrations of 10 and 50 $\mu\text{mol L}^{-1}$ AMX and 5 and 25 $\mu\text{mol L}^{-1}$ CLA were performed and RSD values below 8% for AMX and 3% for CLA attested to the good repeatability of the method. The method was applied for the simultaneous determination of both active principles in two pharmaceutical samples (**Fig. 1**) and the results obtained are shown in **Table 1**. At a 95% confidence level, no significant differences were observed between results obtained by proposed BIA and CE methods [4].

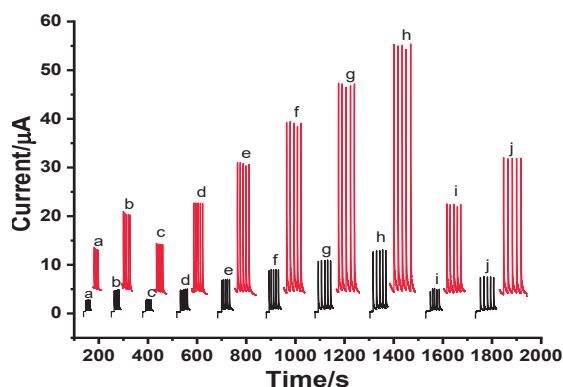


Fig.1 Amperograms obtained for the simultaneous determination of AMX and CLA in pharmaceutical samples. Concentrations ($\mu\text{mol L}^{-1}$) of AMX or CLA and AMX, respectively: (a) 10, (b) 20, (c) 5 and 10; (d) 10 and 20, (e) 15 and 30, (f) 20 and 40, (g) 25 and 50, (h) 30 and 60, (i) Sample 1; (j) Sample 2. Black line: +1.3V; red line: +1.8V.

Table 1. Results obtained by BIA-AD and CE for the determination of AMX and CLA in pharmaceutical samples.

Sample	Analyte	Concentrations found	
		BIA-AD	CE
A	AMX	506±19 mg	506±7 mg
	CLA	145±12 mg	144±2 mg
B	AMX	6.3±0,15 g	5.6±1 g
	CLA	0.81±0.03g	0.91±0.02g

A – Amstar de 500 mg AMX + 125 mg CLA; B – amostra de 5,6 g AMX + 0,798 g CLA

Conclusions: In this study, for the first time, the possibility of simultaneous determination of AMX and CLA using an electrochemical method was demonstrated. The proposed method is simple, fast, reliable and low-cost viable alternative to chromatographic methods for routine analysis of pharmaceutical formulations.

Acknowledgments

CAPES, CNPQ, FAPEMIG, UFU, PPQUI, NuPE.

References: [1] Atici E.B. *et al.*, Journal of Pharmaceutical and Biomedical Analysis 136 (2017) 1–9; [2] Bejjani A. *et al.*, Nuclear Instruments and Methods in Physics Research B 371 (2016) 392–395; [3] Hasanpour F. *et al.*, Analytica Chimica Acta 670 (2010) 45-50; [4] Marra M.C. *et al.*, Journal of Separation Science 40 (2017) 3557-3562.

Stainless Steel as Catalytic Support for Glycerol Oxidation

Paula Barione Perroni (PG),¹ Teko W. Napporn (PQ),² Hamilton Varela (PQ),¹

paula.perroni@usp.br; hamiltonvarela@gmail.com

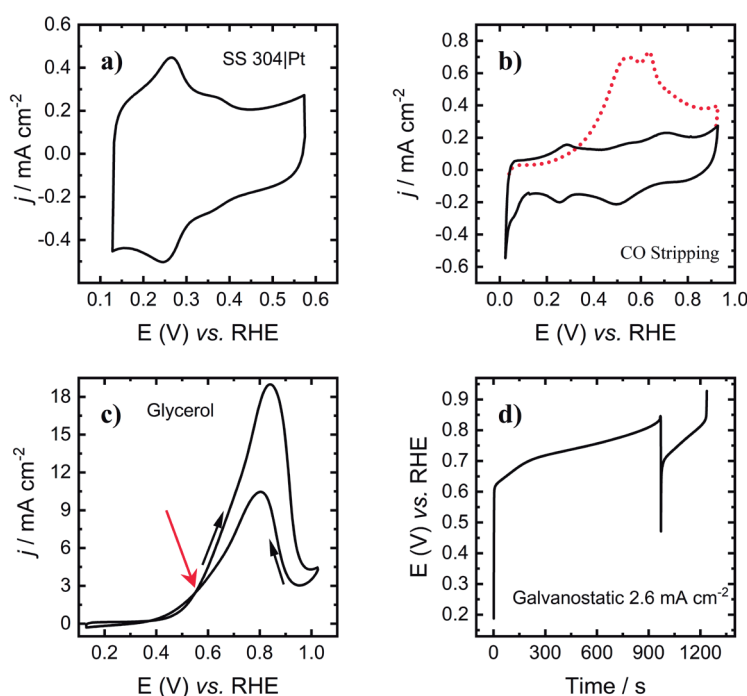
¹ Instituto de Química de São Carlos, USP; ² Université de Poitiers, IC2MP

Palavras Chave: stainless steel, glycerol oxidation, platinum, alkaline medium, oscillation

Highlights

Platinum is easily deposited at stainless steel surface. The catalyst obtained is good for glycerol oxidation.

Resumo/Abstract



The Pt is deposited at stainless steel surface by chemical reaction between the Pt and the alloy surface. Firstly, the SS304 was etched in H_2SO_4 30 w.t.% at 60°C for 5 min, then it is washed and right after the electrode was submitted in a slightly acid solution of $3.9 \times 10^{-5} \text{ mol L}^{-1}$ of H_2PtCl_6 and HCl 0.06%, under controlled temperature of 70°C during 20 minutes.[1] The electrode was tested for 0.1 M glycerol oxidation at solution KOH 1M, and the results are summarized in Fig. 1. Both cyclic voltammetry of the material without the organic and CO stripping confirm the Pt deposition at the steel. In Fig 1a) is possible to identify the typical Pt hydrogen region below 0.4 V and the respective double-layer above it. The window potential was set until 0.6V so the surface would not go under oxide modifications. Two peaks appear in CO stripping between 0.5 and 0.8V, as can be seen in Fig 1b), ascribed to CO oxidation at different size Pt particles.[2] The Fig 1c) shows a typical glycerol oxidation voltammetry profile where the main peak corresponds to its partial oxidation to glyceraldehyde and subsequently to glyceric acid.[3] A systematic study was made under galvanostatic study and only at 2.6 mA cm^{-2} (the current density is highlighted in the CV image by the

Figure 1: a) cyclic voltammetry of Pt deposited at SS304 in KOH 1M and scan rate of 20 mV s^{-1} b) CO stripping at scan rate of 10 mV s^{-1} ; c) glycerol 0.2 M electrooxidation at SS304|Pt and scan rate of 20 mV s^{-1} ; d) chronopotentiometry at $j=2.6 \text{ mA cm}^{-2}$.

red arrow) was possible to access oscillatory profile, as demonstrated in Fig 1d). After 800 seconds just one cycle with 0.37 V of amplitude appeared. In a summary we showed that the stainless steel is a good substrate for Pt deposition and further organic molecule oxidation. Both H_2 adsorption/desorption region in CV and CO stripping confirm the Pt presence and the material appears to be good catalyst for glycerol oxidation. However, under galvanostatic conditions more study is necessary.

References

- [1] C.M. Chen, C.H. Chen, T.C. Wei, *Electrochim. Acta.* 55 (2010) 1687–1695.
- [2] F. Maillard, S. Schreier, M. Hanzlik et al. *Phys. Chem. Chem. Phys.* (2005) 375–383.
- [3] Y. Kwon, K.J.P. Schouten, M.T.M. Koper, *ChemCatChem.* 3 (2011) 1176–1185.

Agradecimentos/Acknowledgments

P.B.P acknowledges Coordenação de Aperfeiçoamento de Pessoal de Nível Superior (CAPES) for financial support (88887.372103/2019-00 and 88887.463441/2019-00), FAPESP (#2019/22183-6 and #2020/15230-5), Shell Brasil and CNPq (#306060/2017-5)

Studies on the voltammetric behavior and determination of salicylic acid in alkaline solutions

Giulia C.P. Freitas (IC),^{1*} Regina M. Takeuchi (PQ),¹ André L. Santos (PQ),¹

giulia.freitas@ufu.br

¹Instituto de Ciências Exatas e Naturais do Pontal, UFU.

Keywords: Cu electrode, Cyclic voltammetry, Pharmaceutical analyses.

Highlights

Cu electrode and NaOH solutions are promising for the voltammetric determination of salicylic acid. Electrode fouling was overcome by simply stirring the solution between the voltammetric scans.

Resumo/Abstract

Salicylic acid (SA) is a physiologically important molecule for plants that has analgesic effects and is widely used in the cosmetic industry, mainly due to its exfoliating action. Thus, high-performance and cost-effective analytical methods for the quantification of SA are necessary since they could contribute to detecting pathologies in plants and ensuring the quality control of pharmaceutical and cosmetic products. Voltammetric techniques are promising for SA quantification since they combine high sensitivity, operational simplicity, and a relatively low cost of instrumentation. In this context, the objective of this study was to evaluate the voltammetric behavior of SA in alkaline solutions, aiming at the development of a voltammetric method to quantify SA in different matrices. The electrochemical behavior of SA was studied by cyclic voltammetry on glassy carbon (GCE), Pt, and Cu working electrodes in 0.3 mol L⁻¹ NaOH aqueous solution (Fig. 1A).

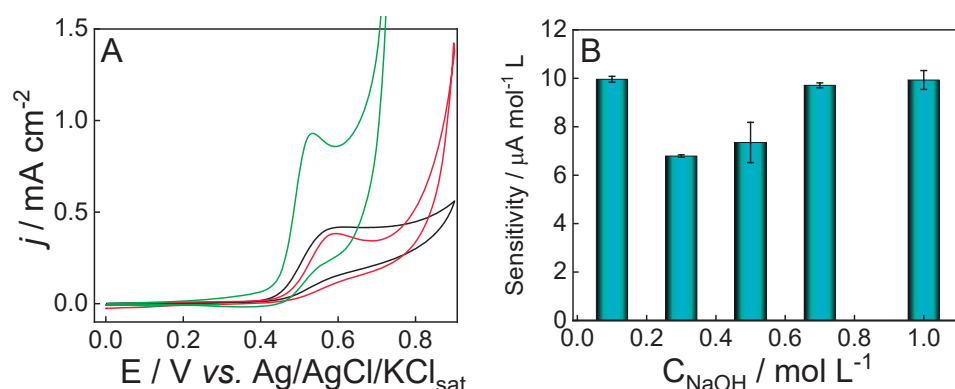


Fig. 1 – **A)** Cyclic voltammograms recorded with different working electrodes in 0.3 mol L⁻¹ NaOH in the presence of 1.0 mmol L⁻¹ of SA, $v = 100$ mV s⁻¹. (—) GCE ($\Phi = 3$ mm); (—) Pt ($\Phi = 3$ mm) and (—) Cu ($\Phi = 1.3$ mm). **B)** Sensitivity towards SA with Cu working electrode as a function of the NaOH concentration.

Fig. 1A shows that SA electrooxidation gave rise to an anodic peak that could be observed on the three working electrodes studied. Cu electrode provided the highest peak current, the lowest peak potential (+0.53 V), and the best peak definition. Analytical curves were constructed for SA ranging its concentration from 1.0 to 4.0 mmol L⁻¹ and the sensitivity observed with the Cu electrode was 1.9 and 2.6 times higher than that observed for Pt and GCE, respectively. Therefore, Cu is the most promising working electrode to be used for the voltammetric determination of SA in alkaline solutions. The sensitivity towards SA with the Cu working electrode was determined in different concentrations of NaOH (Fig. 1B). It was observed that the best sensitivities were observed at 0.1; 0.75 and 1.0 mol L⁻¹ NaOH. Thus, 0.1 mol L⁻¹ was selected for the subsequent experiments since this concentration minimizes the consumption and waste of chemicals without compromising sensitivity. Even though some decrease in peak current was observed as successive cyclic voltammograms were recorded, the initial signal was completely restored by simply stirring the solution for approximately 30 s between the voltammetric scans. Therefore, this study suggests that the combination between Cu working electrodes and alkaline solutions is a promising approach to developing voltammetric methods for SA determination. Satisfactory sensitivity was obtained even in 1.0 mol L⁻¹ NaOH as the supporting electrolyte which could be advantageous since strongly alkaline solutions could be required in the sample pretreatment procedure.

Agradecimentos/Acknowledgments

FAPEMIG (APQ-01316-22)

Studying the synthesis of a new catalyst based on gold nanoparticles supported on ZrO₂/carbon black for efficient H₂O₂ production applied on wastewater treatment process

Matheus S. Kronka¹ (PG), Guilherme V. Fortunato¹ (PQ), Leticia Mira¹ (PG), Alexsandro J. dos Santos¹ (PQ), Marcos R. V. Lanza¹ (PQ)*

* marcoslanza@usp.br

¹Instituto de Química de São Carlos, Universidade de São Paulo- USP

Palavras-Chave: Eletrocatalisadores, Suporte híbrido à base de carbono, Processos eletroquímicos oxidativos avançados, Tratamento avançados de efluentes.

Highlights

Two-step synthesis of Au-ZrO₂/PL6C catalyst showed higher selectivity (97%) for H₂O₂ production compared to the one-step route (89%). Efficient removal of Carbaryl by using electro Fenton and photo-electro Fenton process.

Resumo/Abstract

Materiais carbonáceos têm sido considerados catalisadores eficazes para a produção eletroquímica de H₂O₂ a partir da reação de redução de oxigênio, no entanto sua baixa atividade catalítica pode demandar elevado consumo de energia [1-3]. Para diminuir o consumo energético desses sistemas, uma abordagem amplamente investigada na literatura é a modificação de materiais de base carbono com metais nobres e não nobres. Neste trabalho, os autores avaliaram duas rotas de síntese para produzir um novo material baseado em nanopartículas de ouro ancoradas em ZrO₂/carbono Printex L6, como catalisador estável e eficiente para produção de H₂O₂ em meio ácido [3]. Foram testadas duas rotas de síntese: uma em etapa única pelo método hidrotermal assistida por microondas e outra em duas etapas, com a síntese inicial do substrato ZrO₂/PL6C pelo método assistido por microondas e o crescimento das NPs de Au em uma segunda etapa hidrotermal, sem o auxílio de microondas. A partir dos resultados de caracterização física, constatou-se uma melhor dispersão das partículas de ouro suportadas em ZrO₂/PL6C, produzidas através da rota de duas etapas, resultando em um catalisador com maior seletividade na obtenção de H₂O₂ (97%) em comparação com o Au-ZrO₂/PL6C produzido por meio de uma única etapa (89%). A eficiência catalítica elevada do Au-ZrO₂/PL6C produzido em duas etapas foi comprovada em testes quantitativos de produção de H₂O₂, utilizando eletrodos de difusão gasosa (GDE), atingindo uma produção máxima de 710 mg L⁻¹, enquanto, com um GDE não modificado, foi alcançada uma produção de apenas 140 mg L⁻¹ após 120 minutos de eletrólise a 50 mA cm⁻², em ambos os casos. O GDE modificado foi aplicado na degradação de 10 mg L⁻¹ de Carbaryl (CBR) em escala de laboratório avaliando diferentes processos eletroquímicos oxidativos avançados (PEOA). Os processos electro Fenton (EF) e foto-electro Fenton (FEF) apresentaram semelhantes valores de cinética de pseudo primeira ordem, removendo totalmente o CBR em 10 e 6 minutos, respectivamente. Porém, o FEF apresentou maior porcentagem de mineralização (89%) graças aos processos fotocatalíticos da radiação UVC, comparado ao processo EF (59%) após 120 min. Com base nos resultados obtidos, foi concluído que o catalisador de Au-ZrO₂/PL6C produzido por meio de síntese em duas etapas foi altamente eficiente na produção de H₂O₂ em um sistema eletroquímico e aplicado com sucesso para remoção rápida de Carbaryl utilizando o processo FEF.

Agradecimentos/Acknowledgments

FAPESP (2014/50945-4, 2017/23464-3, 2017/10118-0, 2019/20634-0 e 2019/04421-7), CAPES (Código de financiamento 001) e CNPq (465571/2014-0 e 303943/2021-1).

Referências

- [1] Santos, G. O. S. et al. *Current Opinion in Electrochemistry*, (2022), 36:101124.
- [2] Kronka, M.S. et al. *Materials Chemistry and Physics*, 267 (2021), 124575.
- [3] Kronka, M. S. et al. *Chemical Engineering Journal*, 452 (2023), 139598.

Study of carbon matrix gas diffusion electrode for electrogeneration of oxidants species in an electrochemical reactor using membrane

Taynara O. Silva* (PG),^{1,2} Marcos R. V. Lanza (PG),¹ Manuel A. R. Rodrigo (PG),²

taynaraos1994@usp.br; taynaraos1994@usp.br

¹ Chemistry Institute of São Carlos – University of São Paulo, Av. Trab. São Carlense, n°400, São Carlos, Brazil.; ² Chemical Engineering Department, University of Castilla-La Mancha, C. Altagracia, n° 50, Ciudad Real, Spain

Palavras Chave: Hydrogen peroxide, Electrosynthesis, Nanomaterial, Carbon black, Electrochemical degradation

Highlights

New reactor for eletrogenation on H₂O₂ and oxidants espécies

The use of membrane increases the values of H₂O₂ electrogenerated

New material based on carbon gas diffusion electrode

Resumo/Abstract

One of the main challenges of environmental studies is the removal of pollutants, among them, are: pesticides, plasticizers, antibiotics, etc., [1,2] In this context, studies addressing alternative forms of degradation have been studied, Advanced Oxidative Processes (AOPs) are one of the highlights, having the hydroxyl radical (OH•) as the principal oxidant species [2,3]. Hydrogen peroxide (H₂O₂) is one of the most used reagents in the advanced oxidated process (AOPs) for being the main precursor of OH•.

This oxidant is formed by the oxygen reduction reaction (ORR), where one of the limitations of this reaction is the solubilization of oxygen in the reaction medium [1]. Thus, gas diffusion electrode (GDE) of carbon matrix appears to overcome this problem due to its triple interface. For this reason, Studies seeking to scale up the electroproduction of hydrogen peroxide in reactors have been growing.

In this work, the gold was to study current density conditions for the electrogeneration of hydrogen peroxide in a flow reactor, using different counter electrodes and evaluate their influence on the reaction. The current density studies were: 25 mA cm⁻², 50 mA cm⁻², 100 mA cm⁻², 150 mA cm⁻², and 200 mA cm⁻². In an acid medium Na₂SO₄ 0,5 M; pH 2.5 adjusted with H₂SO₄ 1M using a volume of 1 L, and flow of O₂ 50 mL h⁻¹.

Used approach, the first without membrane in a single compartment of solution and the second one with a double compartment dived with a membrane, the studies show that with the membrane it is possible to achieve higher values of H₂O₂ and presents different kinetic and behavior of generation. One of the advanced of use membranes is the possibility of avoiding the consumption of H₂O₂ at the anode.

Calculations of current efficiency and energy consumption were also performed to evaluate the performance of the material and the reactor.

References

- [1] Assumpção, M.H.M.T. et al, *Carbon*, 49 (2011) 1842.
- [2] Moreira, J. et al. *Applied Catalysis B: Environmental*. 248 (2019) 95-107.
- [3] V. B. Lima. *Chemosphere*, 247 (2020) 125807.

Agradecimentos/Acknowledgments

University of São Paulo, Chemistry Institute of São Carlos University of Castilla - La Mancha, Chemical Engineering Department, FAPESP Process: 2019/08701-4; 2017/10118-0; 2022/07227-0.



Study of single atom catalysts for nitrate reduction reaction to produce green NH₃.

Thiago de Morais Mariano (PQ),^{1,2} Valnei Monteiro de Amorim(IC)¹, Marina Dias Saraiva (PG),^{1,2} Manuel E. G. Winkler(PQ),^{1,2} Luis Fernando G. Noleto (PG),³ Ivo Teixeira (PQ),³ Raphael Nagao (PQ).^{1,2}

marianot@unicamp.br nagao@unicamp.br

¹Physical Chemistry Department, UNICAMP; ²Center of Innovation on New Energies CINE; ³Chemistry Department UFSCar

Keywords: Single atom, Electrocatalysis, Nitrate reduction, Ammonia, Energy.

Highlights

Co, Fe, Ru and Cu single atom catalysts employed to convert nitrate ions into ammonia. Catalysts show high HER overpotentials, avoiding competition with NO₃RR, tend to increase Faradaic Efficiency.

Abstract

NH₃ is considered a safer energy carrier for hydrogen than hydrogen itself, once ammonia can be transported and stored safely and less expensively compared to hydrogen. NO₃RR (Nitrate Reduction Reaction) requires 8 electrons to form NH₃, with a potential of -0.12 V vs SHE (Standard Hydrogen Electrode) in alkaline medium, relying on direct and indirect NH₃ formation mechanisms. Given this scenario, the catalysts used for the NO₃RR play a key role in the efficient conversion to NH₃, as well as mitigate the influence of competition from HER (hydrogen evolution reaction). Single atom catalysts (SAC) have attracted attention in recent years for their very high performance in electrocatalysis, due to their activity, stability and selectivity¹.

In this work, four SAC catalysts were prepared: Fe-SAC, Co-SAC, Ru-SAC and Cu-SAC; All catalysts were synthesized by cation exchange method starting from Na-PHI and characterized by HR-TEM (High Resolution-Transmission Electronic Microscopy), AC-HAADF-STEM (High Angle Annular Dark Field-Scanning Transmission Electronic Microscopy) and Cyclic Voltammetry. HR-TEM (Fig. 1a)² shows no particle formation, whilst HAADF-STEM images display single atoms (Fig. 1b-c). Electrochemical characterization was performed in an alkaline medium in the absence and in the presence of the NO₃⁻ and presented similar profiles to those observed in Hydrogen Evolution Reactions (HER), showing HER onset potential at more negative potentials, indicating that they are good catalysts for the NO₃RR. Co-SAC catalyst the onset potentials for HER were similar, i.e., it is not possible to identify whether there is the reduction of NO₃⁻; In Cu-SAC, it is observed that after the addition of NO₃⁻ the onset potential for HER is -0.2 V vs RHE (Reversible Hydrogen Electrode), while with the electrolyte alone the HER showed onset potential of -0.5 V vs RHE; Fe-SAC catalyst showed onset potential for HER at -0.4 V vs RHE, lower than when adding NO₃⁻, suggesting that NO₃RR is initiating at approximately -0.4 V vs RHE; Ru-SAC showed onset potential after NO₃⁻ addition at approximately -0.6 V vs RHE. This shows that this catalyst has good potential for NO₃RR, by mitigating the competition from RHE, and consequently raising the faradaic efficiency for NH₃ formation. Overall, the isolated atom catalysts presented good results, even though preliminary, and show that they have potential to be applied in the NO₃RR, with the exception of Co-SAC, which did not present any significant alteration in the voltammograms with the addition of NO₃⁻.

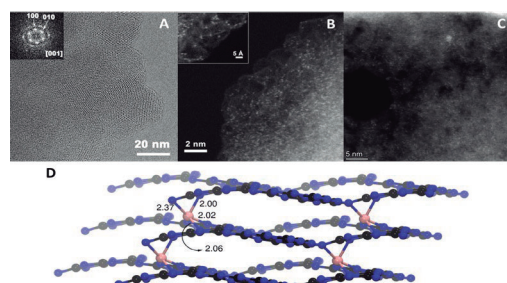


Fig. 1. (A) HR-TEM image of Fe-PHI (0.1%) and the corresponding FFT (left) indexed in a hexagonal lattice; (B) Annular dark-field scanning transmission electron microscopy image of Fe-PHI showing metal single-atoms; (C) STEM-HAADF microscopy image of Cu-PHI (0.1%) showing metal single-atoms; (D) The atomic structure of Fe-PHI obtained from spin-polarized DFT simulation. The distances between Fe and nearest N atoms are marked in Å units. Atoms color: C-black, N-blue and Fe-pink.

1. Cardoso JS, Silva V, Rocha RC, Hall MJ, Costa M, Eusébio D.. *J Clean Prod.* 2021;296. doi:10.1016/j.jclepro.2021.126562
2. da Silva MAR, Silva IF, Xue Q, et al.. *Appl Catal B.* 2022;304:120965. doi:10.1016/j.apcatb.2021.120965

Acknowledgments

FAPESP, SHELL, CAPES, LNNano and CNPq.

STUDY OF THE PREPARATION OF AN IMPEDIMETRIC DEVICE TO DETECT METHYLATED DNA

Pedro Costa Monteiro Pizzol (PG),^{1*} Miquéias de Lima Portugal (IC),¹ Patrícia Monteiro Seraphim (PQ),² Marcos F. S. Teixeira (PQ).^{1*}

pedro.pizzol@unesp.br; marcos.fs.teixeira@unesp.br

¹São Paulo State University (UNESP) - Department of Chemistry and Biochemistry - School of Science and Technology, Presidente Prudente. ²São Paulo State University (UNESP) - Department of Physiotherapy - School of Science and Technology, Presidente Prudente.

Keywords: Methylated DNA sensor; Gold nanoparticle-polymer; Oxygen probe.

Highlights

- Development of a sensor with redox impedance transduction based on the dissolved oxygen probe.
- Impedimetric sensor for selective monitoring of methylated DNA.

Resumo/Abstract

Immunosensors based on electrochemical impedance spectroscopy (EIS) stand out as a transduction model, mainly due to the high sensitivity achieved by the technique, which can reach detection limits on the picomole scale. Most of these works use ferrocene as a redox species in solution to increase the signal-to-noise (S/N) response to antigen-antibody interactions at the electrode surface. However, the presence of excess redox probes can be accompanied by problems associated with false-positive sensor responses. This study proposes an alternative methodology using dissolved oxygen, already naturally present in the reaction system, as a redox probe for the immunoassay of detection of 5-methylcytosine for the determination of global levels of methylated DNA. The present work describes the development of an electrochemical immunosensor for the direct determination of methylated DNA using dissolved oxygen as the redox probe. The oxygen-sensitive response is possible due to the presence of the redox conducting polymer based on the poly(o-phenylenediamine) (poly(o-PD)). In addition to conducting polymer, gold nanoparticles (AuNPs) were formed in the polymer film by encapsulation to increase the active surface area and enhance sensor performance. The platform was easily synthesized using a single-step electropolymerization technique in a solution containing the 1,2-phenylenediamine monomer and H₂AuCl₄ salt. The immunosensor was developed by simply immobilizing the 5-methylcytosine antibody (Ab-5-mC) with high affinity to 5-mC on the surface of the device coated with poly(o-PD)-AuNPs. No secondary antibody and enzyme were used in constructing this device. The immunosensor performance was evaluated by EIS in different concentrations of 5-methylcytosine (5-mC) in 0.10 mol L⁻¹ phosphate buffer solution (PBS) solution containing atmospheric oxygen. The pyrazine rings of the polymer are more available for reaction with dissolved oxygen (Eq. 1), resulting in an increased sensitivity of the device.



The analysis of the element impedimetric parameters revealed that the presence of dissolved oxygen decreased the R_{ct} value. This wide sensitivity of the poly(o-PD)-AuNP-coated electrode to the variation of oxygen in solution will be used as a redox probe to accompany the analysis of methylated DNA. The system impedance increased with increasing concentration of 5-mC in solution as a function of increasing surface blocking after binding between 5-mC and Ab-5-mC. The interaction of 5-mC and Ab-5-mC hinders the permeation of molecular oxygen to the redox sites of the polymer and consequently increases the electrical resistance of the polymer.

Agradecimentos/Acknowledgments

The authors acknowledge CEPID-FAPESP (2013/07296-2) and CNPq (145584/2021-6) for the financial support.

Study of the voltammetric behavior of ammonia in alkaline solutions on Pt electrodes aiming its electrochemical sensing

Vitoria B. Messias (IC),^{1*} Regina M. Takeuchi (PQ),¹ André L. Santos (PQ),¹

vitoriabrambilla10@gmail.com

¹Instituto de Ciências Exatas e Naturais do Pontal, UFU.

Keywords: Environmental analysis, Differential pulse voltammetry, Cyclic voltammetry.

Highlights

NH₃ electrooxidation yielded a well-defined voltammetric peak in alkaline solutions. Differential pulse voltammetry showed attractive analytical performance. Promising approach for NH₃ quantification.

Resumo/Abstract

Determination of free and total ammonia in wastewater and natural water has become a major concern in environmental chemistry since NH₃ is highly toxic to several aquatic organisms and human beings. Voltammetry is a promising technique to quantify NH₃ regarding its high sensitivity, operational simplicity, and low cost of instrumentation. Therefore, the objective of this study was to evaluate the voltammetric behavior of NH₃ on Pt electrodes in alkaline solutions aiming to find the experimental conditions capable to provide better analytical performance. All the voltammetric experiments were conducted with a 2.0 mm Pt disc working electrode using KOH aqueous solutions as the supporting electrolyte. The analytical performances of cyclic (CV), differential pulse (DPV), and square wave voltammetry (SWV) were evaluated. CV has shown that NH₃ electrooxidation yielded an anodic peak at -0.28 V (Fig. 1, green curve) which is in close agreement with previous reports [1].

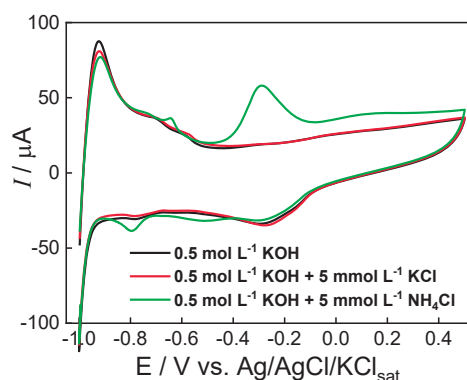


Fig. 1: Cyclic voltammograms recorded with a Pt working electrode ($\Phi = 2.0$ mm), $\nu = 100$ mV s⁻¹.

Table 1: Analytical parameters for NH₃ with different voltammetric techniques.

Technique	Linear range*	Linear equation*	R ²	LOD*	LOQ*
CV	100 - 750	$A = 1.70 + 0.04 C_{\text{NH}_3}$	0.9929	68	226
DPV	2.5 - 20	$A = 0.34 + 0.53 C_{\text{NH}_3}$	0.99841	0.79	2.64
SWV	5.0 - 75	$A = -0.95 + 0.24 C_{\text{NH}_3}$	0.98784	3.9	13

*Concentration of NH₃ in $\mu\text{mol L}^{-1}$. A – area under the voltammetric peak.

A linear relationship between peak current (i_p) from CV and the square root of scan rate ($\nu^{1/2}$) was observed according to the equation: i_p (μA) = $136 \nu^{1/2}$ ($\text{V}^{1/2} \text{s}^{-1/2}$), $R^2 = 0.99846$, indicating that NH₃ electrooxidation is a diffusion-controlled electrode process. Analytical curves were constructed by using CV ranging the concentration of NH₃ from 0.1 to 1.0 mmol L⁻¹ at different concentrations of KOH as the supporting electrolyte. It was observed that the concentration of KOH did not affect the sensitivity towards NH₃, thus 0.1 mol L⁻¹ KOH was selected as the supporting electrolyte for the analytical studies. After optimizing the voltammetric parameters, it was observed that DPV provided the best analytical performance (Table 1). For all the voltammetric techniques evaluated, the use of the area under the voltammetric peak as the analytical signal instead of i_p provided the best linearity. The results obtained in this study allow us to conclude that DPV combined with Pt electrodes in alkaline solutions is a promising approach to quantifying NH₃ in wastewater and natural water samples.

Agradecimentos/Acknowledgments

FAPEMIG (APQ-01316-22)

[1] Wang et al., *J. Electroanal. Chem.* 922, **2022**, 116721. DOI: <https://doi.org/10.1016/j.jelechem.2022.116721>

Synthesis of platinum nanoparticles in deep eutectic solvent for application in electrochemical sensors

Paulo C. Gomes-Junior (PG),^{1*} Karen K. L. Augusto (PG),¹ Renan O. Gonçalves (PG),¹ Gustavo P. Longatto (IC),¹ Júlio C. O. Almeida (IC),¹ Éder T. G. Cavalheiro (PQ),² Orlando Fatibello-Filho (PQ).¹

paulojunior@estudante.ufscar.br

¹ Department of Chemistry, Federal University of São Carlos, São Carlos 13565-905, SP, Brazil

² São Carlos Institute of Chemistry, University of São Paulo, São Carlos, SP, Brazil

Keywords: Platinum nanoparticles, Deep eutectic solvent, Electrochemical sensors.

Highlights

Eutectic synthesis of PtNPs in reflux using reline as a stabilizing medium.

PtNPs and MWCNTs were incorporated into a Nafion film, increasing electrocatalytic activities for riboflavin detection.

Abstract

Deep eutectic solvents (DES) were introduced by Abbot et al.¹ in 2001 and proved to be alternatives to non-aqueous solvents and ionic liquids with various applications, mainly because the characteristics they present, such as low toxicity, biodegradability, and high thermal stability². In this work, we synthesize platinum nanoparticles (PtNPs) by a reflux method using a DES based on choline chloride and urea (reline) in a 1:2 molar ratio. Then, the PtNPs were incorporated into a composite sensor based on multi-walled carbon nanotubes (MWCNTs) for electrochemical detection of riboflavin (RB). The synthesized PtNPs were characterized by transmission electron microscopy (TEM). The PtNPs were small-sized nanoparticles with an average diameter of (0.200 ± 0.001) nm. The cyclic voltammetry results showed that PtNPs-ChCl:U/MWCNTs/GCE sensor presented an increase of electrocatalytic activity in comparison to those of glassy carbon (GCE, inset (i)) and MWCNTs/GCE (inset (ii)) sensors (Figure 1a) for the RB determination. Then, the effect of potential scan rate, pH, supporting electrolyte, and square wave voltammetry (SWV) operational parameters were evaluated using the PtNPs-ChCl:U/MWCNTs/GCE sensor to establish the electrochemical behavior and optimal conditions to determine RB. The potential scan rate effect revealed that RB electro-reduction is an adsorptive-diffusion-controlled process. The pH effect (2.0 - 9.0 in BR 0.2 mol L^{-1} buffer) showed that peak potential (E_p) vs. pH was linear for RB (1.0 mmol L^{-1}) with a slope of -0.059 V pH^{-1} , suggesting an equal number of protons and electrons in the reduction process. In addition, pH 7.0 was chosen, and the supporting electrolyte effect showed that peak currents were higher in the phosphate buffer solution (PBS) than in the BR buffer solution at the same ionic strength and pH. The RB response in PBS was optimized by varying the SWV parameters with the selected conditions: frequency (f) = 8 Hz, amplitude (a) = 100 mV, and increment (ΔE_s) = 5 mV. Under these conditions, the analytical curve was constructed (Figure 1b) with the following equation: $-I_{cp} (\mu\text{A}) = -3.2 + 247.1 [C_{RB}, \mu\text{mol L}^{-1}]$ ($R^2 = 0.99$). The detection (LOD) and quantification (LOQ) limits obtained were 1.8 nmol L^{-1} and $0.01 \mu\text{mol L}^{-1}$, respectively. Intra ($n = 15$) and inter-day ($n = 3$) repeatability studies were performed for RB at 0.20, 0.50, and $0.98 \mu\text{mol L}^{-1}$. The relative standard deviation (RSD) results were lower than 7 and 5%, respectively, suggesting good precision of the method by applying of the sensor in RB detection. The sensor efficiency was tested in samples of biological fluids fortified with RB at the following concentrations: 0.05, 0.25, and $0.73 \mu\text{mol L}^{-1}$ for synthetic urine and 0.12, 0.37, and $0.84 \mu\text{mol L}^{-1}$ for serum. The recoveries obtained ranged from 92.1 to 104.7% in the samples, which denotes a low matrix effect on the response with the PtNPs-ChCl:U/MWCNTs/GCE sensor, which suggests potentiality in the determination of RB in real biological samples.

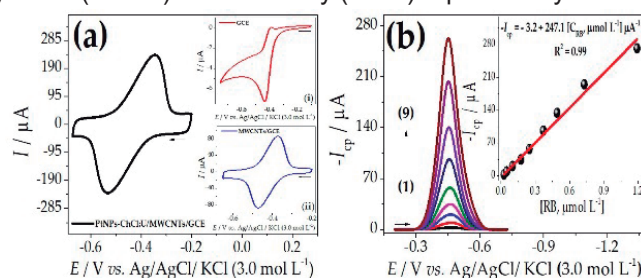


Figure 1: (a) Cyclic voltammograms obtained for RB at 1.0 mmol L^{-1} with PtNPs-ChCl:U/MWCNTs/GCE sensor in PBS 0.2 mol L^{-1} (pH 7.0), $v = 50 \text{ mV s}^{-1}$ and Insets: (i) GCE and (ii) MWCNTs/GCE. (b) Analytical curve obtained for RB at concentrations (1) $0.02 \mu\text{mol L}^{-1}$ to (9) $1.0 \mu\text{mol L}^{-1}$, with the sensor PtNPs-ChCl:U/MWCNTs/GCE in PBS 0.2 mol L^{-1} (pH 7.0), using SWV with $a = 100 \text{ mV}$, $f = 8 \text{ Hz}$ and $\Delta E_s = 5 \text{ mV}$.

1. Abbott, A. P., Capper, G., Davies, D. L., Munro, H. L. & Rasheed, R. K. Preparation of novel, moisture-stable, Lewis-acidic ionic liquids containing quaternary ammonium salts with functional side chains†. *Chem. Commun.* 2010–2011 (2001).

2. Shishov, A., Bulatov, A., Locatelli, M., Carradori, S. & Andrich, V. Application of deep eutectic solvents in analytical chemistry. A review. *Microchem. J.* **135**, 33–38 (2017)

Acknowledgments

The authors gratefully acknowledge the financial support and scholarships granted by CAPES (Proc. 88887.597443/2021-00 and 88887.607018/2021-00), CNPq (#140406/2021-2) and FAPESP (2022/15513-3 and 2020/01050-5).

46ª Reunião Anual da Sociedade Brasileira de Química: "Química: Ligando ciências e neutralizando desigualdades"

The effect of an electrochemical pretreatment on the performance of lab-made screen-printed carbon electrodes.

Dayane Vasconcelos Petine (IC),^{1*} Vinícius C. Oliveira (IC),¹ Regina M. Takeuchi (PQ),¹ André Luiz dos Santos (PQ),¹

dayane.petine@ufu.br

¹ Instituto de Ciências Exatas e Naturais do Pontal, Universidade Federal de Uberlândia.

Keywords: Screen-printed electrodes, Conductive inks, Cellulose acetate.

Highlights

The main goal of this study is to evaluate cellulose derivatives such as cellulose acetate as alternative binders for the fabrication of carbon conductive inks.

Resumo/Abstract

The attractive characteristics of electrochemical sensors are the high sensitivity, simplicity and relatively low cost of the instrumentation required by these sensors stand out. A recent and promising approach to make electrochemical sensors even more attractive is the use of screen-printed electrodes (SPEs), which are cheap, disposable, and miniaturized. In this context, the objective of this study is mainly focused to evaluate the reproducibility of lab-made carbon screen-printed electrodes prepared in different batches, the effect of aging of the conductive ink and electrodes, and the effect of electrochemical activation on the voltammetric performance of these SPEs. The binder agent used in this work was prepared by dissolving 1.25 g of cellulose acetate in 20.0 mL of acetone at constant stirring for 1 hour followed by 24 hours in the refrigerator. The conductive ink is prepared with 4.0 g of carbon powder and 10.0 g of the polymer solution. The as-prepared ink was transferred onto the substrate, which was an overhead projector sheet in the mold made on a cutting printer. These electrodes were characterized by cyclic voltammetry in 1.0 mol/L KCl in the presence of 2.0 mmol/L of $[\text{Fe}(\text{CN})_6]^{4-}$ at a scan rate of 50 mV/s in the range of -0.5 to +0.8 V. Fresh-prepared electrodes provided $\Delta E_p = 150$ mV and I_{pa}/I_{pc} ratio close to 1, indicating a reversible process. Three different batches were produced and with the aging of the conductive ink, kept in the refrigerator for approximately two months, the voltammetric peaks of $[\text{Fe}(\text{CN})_6]^{4-}$ almost disappeared (Fig. 1, red curve). Thereby, it was introduced an electrochemical procedure as an attempt to restore the activity of the electrode surface. This procedure consisted in performing 10 potential cycling in the range of -0.5 to +1.8 V in the presence of H_2SO_4 , HNO_3 , and KOH 0.1 mol/L. The best results were achieved by using H_2SO_4 , for which $\Delta E_p = 108$ mV for $[\text{Fe}(\text{CN})_6]^{4-}$ was observed (Fig. 1, black curve). In conclusion, over time the stored conductive ink ages, and its capacity to conduct electric current decreases so it is necessary to use electrochemical activation procedures to restore the electrode performance.

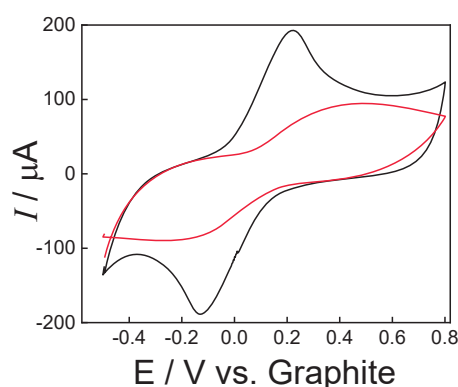


Figure 1. Cyclic voltammograms recorded with SPE in KCl 0.1 mol/L, 50 mV/s in the presence of 2.0 mmol/L of ferrocyanide. (—) Activated by potential cycling in H_2SO_4 0.1 mol/L from -0.5 a +1.8 V (—) Two months-aged electrode without activation.

Agradecimentos/Acknowledgments

Prof^ª. Dr^ª. Rosana M. N. de Assunção for kindly supplying us with the cellulose acetate, CNPq, FAPEMIG (APQ 01316-22), and CAPES.

Ultrasensitive Electrochemical Detection of the Alzheimer Disease Biomarker miR-206 in Human Plasma

Amanda Carrico (PG),^{1*} Loanda Cumba (PQ),¹ Miguel Medina (PQ),² Tobias Engel (PQ),³ Robert J. Forster (PQ)¹

amanda.carrico2@mail.dcu.ie

¹National Centre for Sensor Research, School of Chemical Sciences, Dublin City University, Dublin 9, Ireland. FutureNeuro, The SFI Research Centre for Chronic and Rare Neurological Diseases ; ²Network Center for Biomedical Research in Neurodegenerative Diseases (CIBERNED), Madrid, Spain. CIEN Foundation, Queen Sofia Foundation Alzheimer Center, Madrid, Spain ; ³FutureNeuro, The SFI Research Centre for Chronic and Rare Neurological Diseases, Royal College of Surgeons in Ireland.

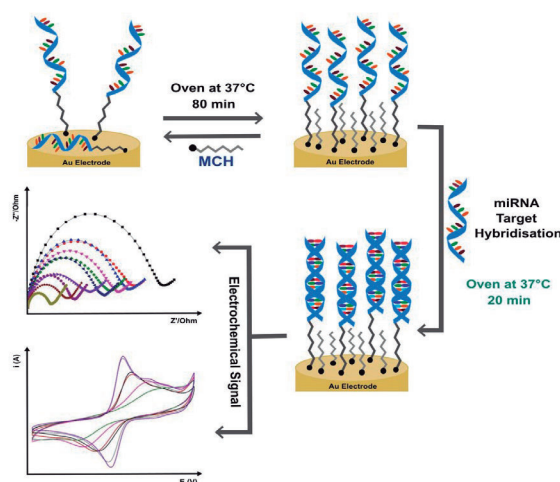
Keywords: Label-free, Biosensor, miR-206, Alzheimer disease, Electrochemical impedance spectroscopy

Highlights

A stable, label-free biosensor for the ultralow, selective detection of a blood circulating miRNA related to Alzheimer disease, miR-206, was developed. The platform was tested in real plasma samples.

Resumo/Abstract

An ultrasensitive, amplification free, biosensor for the selective detection of miR-206, a biomarker for Alzheimer disease, has been developed. The principle was grounded in the changes in the charge transfer resistance (RCT) as an effect of intramolecular forces between miRNAs and ferro/ferricyanide in a well-structured transducer platform. A compact well-ordered mixed monolayer made of co-immobilized 6-mercapto-1-hexanol (MCH) to miRNA probe in a 1:4 ratio (at 37°C), uplifted the performance of the sensor through effectively assisting the orientation of the oligonucleotides. In this work, the remarkable response of the sensor was generated through new insights over the use of different miRNA and MCH moieties to control interfacial constants, surface densities and hybridization efficiency. A very low limit of detection, 0.15 aM, is achieved and the sensor has a wide linear dynamic range (from aM to μ M), high selectivity, low non-specific binding and good stability (less than 10% change in response after 14 days storage). Significantly, the sensor can measure the concentration of miR-206 in real plasma samples and the results correlate directly with those obtained using qPCR. Nanomolar concentrations of miR-206 are found in the plasma of confirmed AD patients, but in healthy controls, it is pM and lower. The ability of the biosensor to quantitatively detect miR-206 in plasma without the need for amplification is significant and opens the possibility of developing a point of care diagnostic device for AD screening which is critical for early detection.



Agradecimentos/Acknowledgments

This work has emanated from research supported in part by a research grant from Science Foundation Ireland (SFI) under Grant Number 16/RC/3948 and co-funded under the European Regional Development Fund and by FutureNeuro industry partners.

Urea electro-oxidation reaction on nickel-magnetite nanorings catalyst via MagnetoElectroCatalysis

Caio Machado Fernandes (PG),^a Eduardo M. Rodrigues (PG),^a Odivaldo C. Alves (PQ),^a Evelyn C.S. Campos (PQ),^b Flávio Garcia (PQ),^b Júlio César M. Silva (PQ).^{a*}

caiomf@id.uff.br; julio.cms@id.uff.br

^aDepartamento de Físico-Química, UFF; ^bCentro Brasileiro de Pesquisas Físicas

Palavras Chave: *Nanoparticles, Nickel-Magnetite Electrocatalyst, MagnetoElectroCatalysis, Urea Electro-oxidation Reaction*

Highlights

A new approach to the field of electrocatalysis. External alternating magnetic field applied to urea electro-oxidation reaction. Nickel-magnetite nanoparticles supported on carbon cloth electrode.

Resumo/Abstract

Nowadays, there are two major problems directly related to global development: the environmental pollution and the energy crisis. Urea is a substance present in the human and animal urine and can also be part of industrial wastewaters, if used or produced in their processes. The crucial concern is that if urea-rich effluents flow into the environment, it can decompose into ammonia a toxic substance. Therefore, it is of paramount importance to explore methods to mitigate this problem. The urea electro-oxidation reaction (UER) is an excellent process to decompose urea into H_2 , N_2 , and CO_2 .¹ Nickel and nickel-based electrocatalysts shows high catalyst activity toward UER.^{1,2} Besides the catalyst composition, the temperature of the UER is key parameter to the process and suitable results are obtained increasing the temperature of the process from 25 °C to 45 °C.² However, most of the time, the energy required to heat the catalytic bed is enormous, which makes this process unfeasible. It is well known from the biomedical area that magnetite nanoparticles are very susceptible to heat dissipation under an alternating magnetic field, a technique called localized hyperthermia.³ Therefore, synthesizing nickel-magnetite nanoparticles and using this material as electrocatalyst towards UER under an alternating magnetic field applied to the anode electrode can be an excellent new strategy, since nickel is an active catalyst for UER and magnetite dissipate heat, increasing local temperature at the anode and consequently accelerating the process. This recent field of research was named as MagnetoElectroCatalysis by the authors of the present work. It is important to point out that the energy involved to generate localized heat at the catalyst is significantly lower than to that involved to heat the catalytic bed. Thus, this work aims to report the effect of an alternating magnetic field applied to $NiFe_3O_4$ nanorings supported on carbon cloth in the process UER in alkaline media (1 mol L⁻¹ NaOH + 0.33 mol L⁻¹ urea). Magnetite nanoparticles were synthesized via hydrothermal method and reduction at a continuous flow, while nickel nanoparticles were prepared via sodium borohydride method. They were characterized by XRD, showing peaks related to Fe_3O_4 , Ni, and NiO, by TEM and SEM, where the micrographs showed interaction between nickel nanoparticles (sizes from 2 to 4 nm) and magnetite nanorings (125 nm), and by magnetization curves showing that $NiFe_3O_4$ has relevant magnetization saturation, but lower than pure magnetite, which is expected after nickel insertion, since Ni has a lower magnetic moment. Hyperthermia experiments showed that both Fe_3O_4 and $NiFe_3O_4$ nanoparticles deposited on carbon cloth heat up due to the effect of the alternating magnetic field (565.7 Oe and 224.7 kHz), which was not observed for nickel nanoparticles. Chronoamperometric curves displayed unequivocally that the current originated from the UER on $NiFe_3O_4$ sharply increased (16%) in the presence of an alternating magnetic field (565.7 Oe) and that the increase of the obtained current had higher value as the applied magnetic field increased (149.2, 298.4, 447.6, 565.7, 739.7, and 888.9 Oe).

References: [1] *Electrochimica Acta* 355 (2020) 136752; [2] *Journal of Advanced Research* 16 (2019) 43; [3] *ACS Applied Nano Materials* 4 (2021) 3148.

Agradecimentos/Acknowledgments

UFF, CBPF, CNPq, CAPES, Capes-PrInt (88887.310269/2018-00), FAPERJ (E-26/211.371/2019, E-26/201.435/2021, E-26/211.389/2021, E-26/210.793/2021., E-26/210.770/2021).

Urea electro-oxidation reaction on nickel nanoparticles supported on carbon cloth via pulsed laser deposition

Júlio César M. Silva (PQ),¹ Mengying Ma (PG),² Caio Machado Fernandes (PG),¹ Mengfei Li (PG),² Angela Caroliny A. Pinto (IC),² Camilla M. Alves (PQ),² Dante F. Franceschini (PQ),² Eduardo M. Rodrigues (PG),¹ Eduardo A. Ponzio (PQ),¹ Yutao Xing (PQ).^{2c}

juliocms@id.uff.br, xy@id.uff.br

¹Departamento de Físico-Química, UFF; ²Instituto de Física, UFF.

Palavras Chave: Nickel nanoparticles, PLD, Carbon Cloth, Urea electro-oxidation

Highlights

Nickel nanoparticles supported on carbon cloth via Pulsed Laser Deposition. Different deposition times by PLD resulted in different agglomeration of Ni nanoparticles and distinct catalytic for UER.

Resumo/Abstract

Urea-containing wastewater has become an ecological problem, and the treatment of urea-rich wastewaters turns as an important topic for researchers around the globe [1]. The urea electro-oxidation reaction (UER) is considered a valuable approach to decompose urea into H₂, N₂, and CO₂. It is important to highlight that H₂ is considered the most promising fuel for the 21st century, and urea electrolysis has become very appealing for this process due to lesser energy consumption involved to produce H₂ when compared to H₂O electrolysis (E° = 0.37 V vs E° = -1.23 V, respectively) [2]. Regarding the catalyst for UER, nickel and nickel-based materials stand out because of the suitable electrocatalytic activity. Taking into account the different methods used to synthesize nickel catalyst nanoparticles, Pulsed Laser Deposition (PLD), which is a physical method, shows some advantages, since no chemical reactions involved during preparation of nanoparticles, the size of the nanoparticles can be easily tuned by changing the inert gas pressure in the chamber, and the amount of nanoparticle loading on electrode substrate can be easily controlled by changing the deposition time [3]. Thus, in this work, nickel nanoparticles supported on carbon cloth (NiNP/CC) were prepared via PLD with three different deposition time (20s, 40s and 60s). The materials were evaluated as electrocatalysts for urea UER in alkaline media. From the micrographs obtained by Scanning Electron Microscopy (SEM) and Energy Dispersive X-ray Spectroscopy, it was observed that the agglomeration of nickel nanoparticles on carbon cloth (CC) increased as the PLD deposition time increased. The electrochemical characterization by cyclic voltammetry (CV) in 1 mol L⁻¹ KOH (from 0.0 to 0.8 V vs Hg|HgO) showed the characteristics peaks of Ni²⁺ [Ni(OH)₂] oxidation to Ni³⁺ (NiOOH) and the reduction of tNi³⁺ (NiOOH) to Ni²⁺ [Ni(OH)₂] for all the three synthesized samples. Regarding UER in 1 mol L⁻¹ KOH + 0.33 mol L⁻¹ urea, the maximum current density from CV normalized by electroactive surface area (ESA) obtained with NiNP/CC 20s catalysts was approximately 35.5% and 67.9% higher than the ones obtained with NiNP/CC 40s and NiNP/CC 60s catalysts, respectively. The current density from UER in Chronoamperometry measurements at 0.55 V vs Hg|HgO for 60 minutes followed the same trend. From the SEM images it was seen that the nickel particles of NiNP/CC 20s are less agglomerated and better dispersed than the other samples, which led to better results in the UER, what agrees with a previous work [3]. Thus, in the present work, it was shown that PDL is as effective method to synthesize nickel nanoparticles directly supported on carbon cloth, which is a resistant and flexible material that could be used in real applications.

References

- [1] J. R. Barbosa et al. *Electrochimica Acta*. 355, (2020), 136752.
- [2] Singh, R. K et al. *Electrochimica Acta*. 278, (2018), 405.
- [3] Coelho, I. F et al. *Materials for Renewable and Sustainable Energy*. 9, (2020), 20.

Agradecimentos/Acknowledgments

CBPF, CNPq, CAPES, Capes-PrInt (88887.310269/2018-00), FAPERJ (E-26/211.371/2019, E-26/201.435/2021, E-26/211.389/2021, E-26/210.793/2021, E-26/210.770/2021).

Uric acid quantification with pencil-drawn graphite electrodes modified with niobium oxide and electrochemically reduced graphene oxide

Douglas P.M. Saraiva (PG),^{1*} Bruno Ferreira (PG),¹ Leonardo M.A. Ribeiro (PG),¹ Lauro A. Pradela Filho (PQ),¹ Thiago R.L.C. Paixão (PQ),¹ Mauro Bertotti (PQ)¹

dpm.saraiva@gmail.com;

¹Department of Fundamental Chemistry, Institute of Chemistry, University of São Paulo - USP; São Paulo – SP, Brazil.

Keywords: Uric acid, Pencil drawn electrode, Niobium oxide, Graphene oxide.

Highlights

Low-cost sensors were produced with a pencil-drawn technique. Niobium oxide and reduced graphene oxide were used as modifiers. The sensors were explored for uric acid quantification.

Abstract

Uric acid is the primary product of purine metabolism, being generated by enzymatic reaction with xanthine oxidase. Abnormal uric acid concentrations in humans are indicators of chronic renal, cardiovascular, hyperuricemia, gout, Lesch-Nyhan syndrome, and so forth. Uric acid is usually found in blood serum in concentrations ranging from 240 to 520 $\mu\text{mol L}^{-1}$, and in urine, from 1.44 to 4.43 mmol L^{-1} .^[1] Pencil-drawn graphite electrodes are valuable tools for routine analysis as disposable devices. Although first described in 1960, only recently have they been used in various applications. Some studies, however, have reported that they provide poor analytical performance for some species, which can be overcome by electrode surface modification. Although largely studied, a few works have used niobium oxide for uric acid detection. Graphene oxide has been extensively used to detect uric acid, but the modification of pencil-drawn electrodes with both oxides has never been reported. In this work, a pencil-drawn electrode modified with niobium oxide and electrochemically reduced graphene oxide was evaluated to determine uric acid. The results showed a synergistic effect of both materials, with the pencil-drawn modified electrode leading to a peak potential shift of ~ 400 mV compared to the non-modified one. In addition, the peak current significantly enhanced (118%) after modification with both oxides. A good correlation between signal and concentration was found between 50 to 1000 $\mu\text{mol L}^{-1}$, with a limit of detection (LOD) of 29 $\mu\text{mol L}^{-1}$. Considering the LOD values, the sensors might be used for uric acid determination in urine and blood serum samples. Additionally, the reproducibility was good, with an RSD of 4.6%. The device cost was estimated, and the value is ~ 1 dollar cent per unit. This is considerably low, making the proposed sensors attractive analytical platforms for various applications.

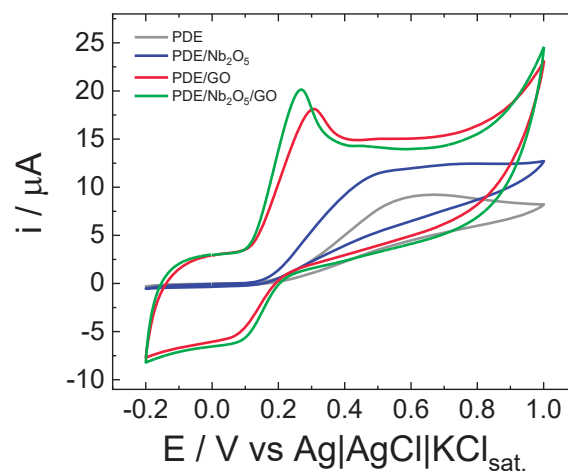


Figure 1 – Cyclic voltammograms recorded in PBS with pencil-drawn electrodes (PDE) at 0.1 V s^{-1} in a 2.0 mmol L^{-1} uric acid solution.

Acknowledgments

The authors thank São Paulo State Research Foundation, grant number FAPESP 2018/08782-1. DPMS and LMAR were funded by the National Council for Scientific and Technological Development, grant numbers 141394/2019-6 and 140259/2021-0. BF was funded by the Coordination for the Improvement of Higher Education Personnel, grant number 88887.601733/2021-0. LAPF was funded by the São Paulo State Research Foundation, grant number FAPESP 2021/00205-8.

¹ Shang, K.; Wang, S.; Chen, S.; Wang, X. *Biosensors* 2022, 12, 588. <https://doi.org/10.3390/bios12080588>

Utilization of mass spectrometry to evaluate Pt catalysts for ammonia electrooxidation in alkaline medium

Seiti I. Venturini (PG),¹ Denis Ricardo Martins de Godoi (PQ),² Joelma Perez (PQ),¹

Seiti.venturini@usp.br

¹São Carlos Institute of Chemistry(USP); ²Araraquara Institute of Chemistry (Unesp)

Keywords: Mass spectrometry, electrocatalyst, ammonia oxidation reaction.

Highlights

- The main product of ammonia electrooxidation is N₂;
- The potential control allows producing other subproducts like NO_x;
- The crystallite size affects the activity for oxidation of ammonia.

Abstract

One of the alternatives for electricity production is converting the chemical energy of ammonia molecules via a fuel cell, and the ammonia oxidation reaction (AOR), which has the advantage of not having CO₂ as a product. The AOR was studied in an alkaline medium utilizing Pt commercial catalyst dispersed on carbon via OEMS (Operando Electrochemistry Mass Spectrometry). These catalysts have different size particles, confirmed by X-ray diffraction and transmission electron microscopy analysis. The particle size follows the sequence: Pt2<Pt3<Pt4<Pt6. The main activity for AOR observed is in the Pt2 catalyst; it has 3 nm of crystallite size. In figure 1, we observed the m/z 28 mass signal (Nitrogen) for voltametric analysis; nitrogen is the major product. These results showed that we have less activity for larger particle sizes and slight changes in the curve profile of mass spectrometric results.

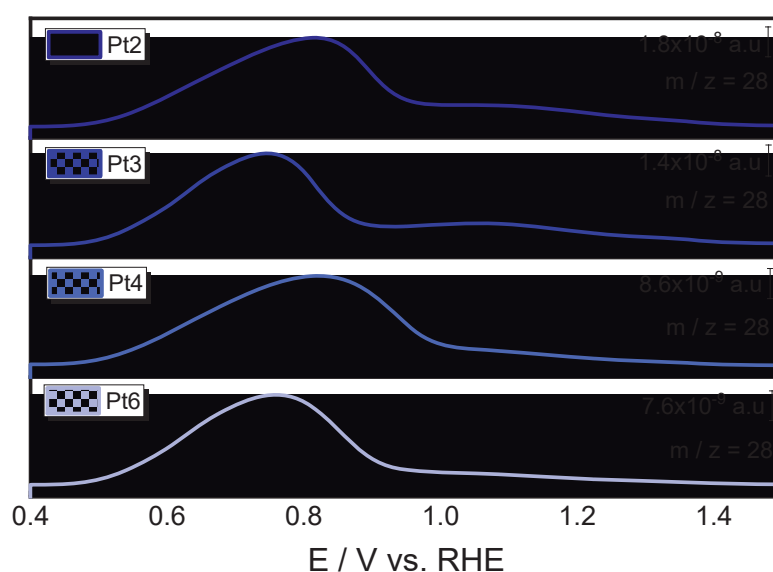


Figure 1. OEMS analysis for cyclic voltammetry, analyzing m/z 28 signal.

Acknowledgments

Thanks to CNPq and FAPESP for the financial support.

Voltammetric determination of bisphenol A using a screen-printed electrode modified with graphene and quantum dots

Anderson M. Santos (PQ),^{1*} Maria H.A. Feitosa (PG),¹ Ademar Wong (PQ),¹ Orlando Fatibello-Filho (PQ),¹ Fernando C. Moraes (PQ).¹

andersonmartinsts@gmail.com

¹ Department of Chemistry, UFSCar

Keywords: Nanostructured material, Quantum dots, Electrochemical electrode, Screen-printed electrode, Endocrine interfering.

Highlights

- Determination of the endocrine interfering bisphenol A;
- Voltammetric determination of bisphenol A;
- Screen-printed electrode modified with graphene and quantum dots;
- Bisphenol A detection in environmental samples.

Abstract

Bisphenol A (BPA) is an endocrine disruptor with high demand since it is used in several industrial processes. Nowadays, there are several reports that mention the presence of BPA in rivers, lakes, oceans, and soils. This fact is due to the inappropriate disposal of this substance in the environment. Therefore, the monitoring of BPA is very important due to its high toxicity in the environment. In this work, we use graphene and quantum dots as modifiers of a screen-printed electrode to determine bisphenol A in river waters. The characteristics of the materials were evaluated by fluorescence spectra, X-ray diffraction, transmission electron microscopy and scanning electron microscopy. The electrochemical behavior of the proposed modified electrode was performed using cyclic voltammetry and the BPA quantification by square-wave voltammetry. As can be seen in Fig. 1A, cyclic voltammograms obtained showed well-defined oxidation peaks at a potential of +0.30 V vs. Ag/AgCl/KCl (3.0 mol L⁻¹). Additionally, it was observed an increase in the analytical signal with the modification of electrode with graphene (blue) and QDs-graphene (black). After the selection of the experimental conditions, such as pH, supporting electrolyte and the square-wave voltametric parameters, the analytical curve for BPA was linear in BPA concentration range from 0.020 to 9.0 μmol L⁻¹ (Fig. 1B) with a limit of detection of 3.4 nmol L⁻¹. Finally, the method was successfully applied in the determination of BPA in river water samples with recoveries close to 100 %.

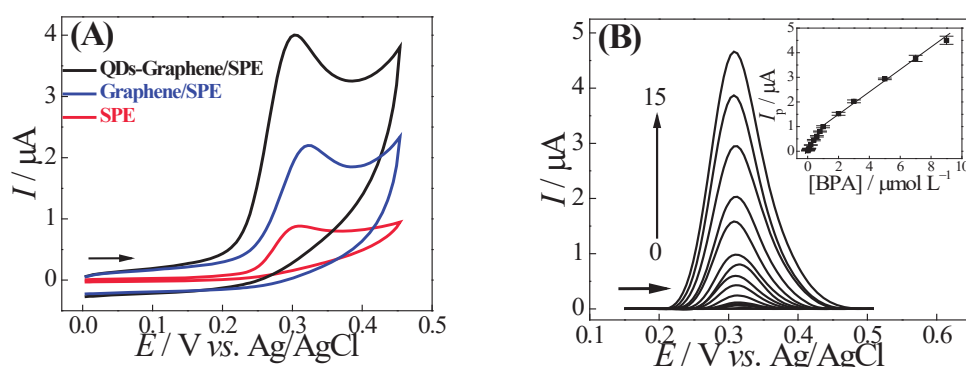


Fig. 1 – (A) Cyclic voltammograms ($v = 50 \text{ mV s}^{-1}$) obtained for $10.0 \text{ } \mu\text{mol L}^{-1}$ bisphenol A in 0.10 mol L^{-1} phosphate buffer solution (pH 7.0) using SPE (—), Graphene/SPE (—), QDs-Graphene/SPE (—). **(B)** SW voltammograms obtained using the QDs-Graphene/SPE electrode in 0.10 mol L^{-1} phosphate buffer solution (pH 7.0) containing different concentrations for BPA: $0.020 - 9.0 \text{ } \mu\text{mol L}^{-1}$ and analytical curve (inserted).

Acknowledgments

This study was financed in part by the Coordenação de Aperfeiçoamento de Pessoal de Nível Superior - Brazil (CAPES) - Finance Code 001. The authors gratefully acknowledge the financial support granted by FAPESP (grant numbers 2017/10118-0 and 2022/05454-9).

Voltammetric sensor for ciprofloxacin antibiotic based on green-synthesized silver nanoparticles and carbon black

Laís Muniz Meireles (PG),¹ Rafael Matias Silva (PG),² Renata Pereira Lopes Moreira (PQ),² Tiago Almeida Silva (PQ)²

laismuniz_meireles@hotmail.com; tiago.a.silva@ufv.br

¹Departamento de Metalurgia e Química, Centro Federal de Educação Tecnológica de Minas Gerais, Timóteo-MG, Brasil;

²Departamento de Química, Universidade Federal de Viçosa, Viçosa-MG, Brasil.

Keywords: green chemistry, metallic nanoparticles, electrochemical sensors, antibiotics.

Highlights

Silver nanoparticles (AgNPs) synthesized by black tea extract. Glassy carbon electrode modified with chitosan film containing AgNPs and carbon black. Voltammetric determination of ciprofloxacin.

Abstract

The synergistic effect that can be obtained by combining nanomaterials has been widely studied to improve the analytical performance of electrochemical sensors. Due to its low-cost and high surface area, carbon black (CB) becomes an interesting material to develop electrochemical devices, as well as silver nanoparticles (AgNPs) because of its high conductivity and chemical stability. In this work, a novel voltammetric sensor for ciprofloxacin (CIP) antibiotic is designed based on AgNPs synthesized by a green route and CB nanoparticles. AgNPs were synthesized using black tea extract to reduce Ag^+ ions and also stabilizing the nanoparticles, called $\text{AgNPs}_{\text{green}}$. From UV-Vis spectroscopy analyzes was verified the success of the $\text{AgNPs}_{\text{green}}$ synthesis. Glassy carbon electrode (GCE) surface was modified with an aqueous dispersion based on $\text{AgNPs}_{\text{green}}$, CB and crosslinked chitosan (Ch). The electrochemical response of CIP was tested on the bare GCE, CB-Ch/GCE and $\text{AgNPs}_{\text{green}}$ -CB-Ch/GCE for comparative purposes. The analyte displayed an irreversible oxidation, and it is clear from the cyclic voltammograms (CVs) of Fig. 1 (a) that the anodic peak current obtained using the modified electrode was significantly superior to that one recorded using the bare GCE. After that, the effect of pH and scan rate on the CIP response was evaluated in different CV measurements. For analytical purposes, the square-wave voltammetry (SWV) was explored for the determination of CIP. Thus, in addition to pH, optimal experimental conditions were determined for the technical parameters of of frequency (f), amplitude (a) and potential increment (ΔE_s). The analytical curve for CIP using the proposed $\text{AgNPs}_{\text{green}}$ -CB-Ch/GCE sensor and SWV was constructed, and it can be observed in Fig. 1 (b), as well as the SW voltammograms obtained towards different concentrations of CIP. Two linear ranges were obtained: (1) of 0.1 to 24.8 $\mu\text{mol L}^{-1}$ and (2) of 36.9 to 130.3 $\mu\text{mol L}^{-1}$, with a limit of detection (LOD) of 0.48 $\mu\text{mol L}^{-1}$.

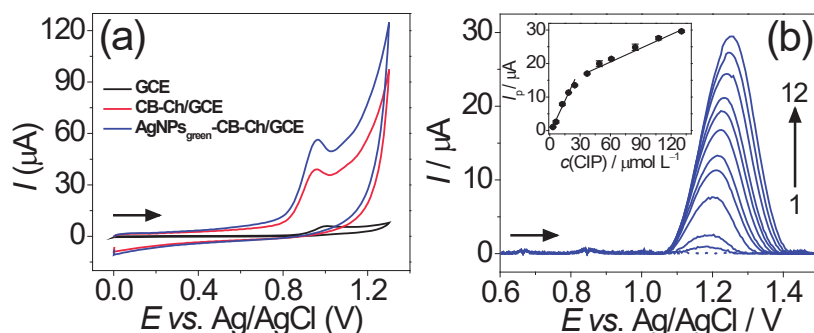


Figure 1. (a) CVs recorded using different working electrodes in 0.1 mol L⁻¹ phosphate buffer solution (pH = 7.0) containing 0.49 mmol L⁻¹ CIP. $v = 50 \text{ mV s}^{-1}$. (b) SWVs obtained using $\text{AgNPs}_{\text{green}}$ -CB-Ch/GCE in 0.1 mol L⁻¹ phosphate buffer solution (pH = 2.0) containing different CIP concentrations: (1) 0.0 (blank); (2) 3.1; (3) 6.2; (4) 12.4; (5) 18.6; (6) 24.8; (7) 36.9; (8) 49.02; (9) 61.0; (10) 84.5; (11) 107.7 and (12) 130.3 $\mu\text{mol L}^{-1}$. SWV parameters: $f = 70 \text{ Hz}$; $a = 90 \text{ mV}$; $\Delta E_s = 5 \text{ mV}$. Inset: Analytical curve for CIP (I_p vs. $c(\text{CIP})$).

Acknowledgments

The authors are grateful for the financial assistance of FAPEMIG (APQ-00083-21 and APQ-03113-22).

46^o Reunião Anual da Sociedade Brasileira de Química: "Química: Ligando ciências e neutralizando desigualdades"

Área: ELE

Wearable glove-based electrochemical sensor for forensic applications

Paula Cristine Rocha Corsato (IC),¹ Lucas Felipe de Lima (PG),¹ Mayra Venturini Paschoarelli (IC),¹ William Reis de Araujo (PQ)¹

pcorsato15@gmail.com; pcorsato15@gmail.com

¹ Portable Chemical Sensors Lab, Department of Analytical Chemistry, Institute of Chemistry, State University of Campinas – UNICAMP, P.O. Box 6154, 13083-970, Campinas, SP, Brazil.

Keywords: Electrochemical, Picric Acid, Diazepam, Wearable sensor, Portable sensor, Forensic.

Highlights

Glove-based sensor enables in-situ analysis of forensic compounds. The flexible stencil-printed electrodes were applied for analyses of picric acid explosive and diazepam, a crime-facilitating drug.

Resumo/Abstract

Portable sensors are valuable tools for on-the-spot examination of latent evidence, prohibited substances, drug testing, and hazards substances to support law enforcement and facilitate rapid and effective crime investigation.¹ Therefore, in this work, we fabricated an accessible and disposable wearable electrochemical sensor manufactured by a stencil-printing method on nitrile gloves using flexible and conductive carbon and Ag/AgCl inks. The working electrode was modified with multiwalled carbon nanotubes (MWCNTs) and poly(3,4-ethylenedioxythiophene): poly(styrene sulfonate) (PEDOT:PSS) for rapid and sensitive detection of nitroexplosive picric acid (PA) and the crime-facilitating drug Diazepam (DZ). Morphological characterizations performed by scanning electron microscopy (SEM) revealed that the MWCNTs appear entangled in bundles with a uniform diameter and micrometric length dispersed in the PEDOT:PSS polymeric structure, which contributes to the increased active area and high electron transfer properties. The redox characterization of PA and DZ was performed by cyclic voltammetry and demonstrates that both species present irreversible and pH-dependent reduction processes involving a 1:1 electron:proton ratio. The electrochemical quantification of PA and DZ was performed by the square wave voltammetry (SWV) technique under optimized experimental conditions using 0.1 mol L⁻¹ Britton-Robinson buffer (pH=7.0 for DZ and 2.0 for PA). An analytical curve was built for PA using the peak current values of the reduction process close to -0.6 V and exhibited a linear behavior in a concentration ranging from 5.0 µmol L⁻¹ to 100.0 µmol L⁻¹, with a limit of detection (LOD) of 0.24 µmol L⁻¹ and limit of quantification (LOQ) of 0.79 µmol L⁻¹. The analytical curve for DZ was built using the peak current values from the reduction process close to -1.3 V and exhibited 2 linear interval responses in the concentration ranging from 0.5 µmol L⁻¹ to 100.0 µmol L⁻¹, resulting in a LOD and LOQ of 0.06 µmol L⁻¹ and 0.21 µmol L⁻¹, respectively. The robustness and accuracy of the developed wearable electrochemical sensor were evaluated through addition and recovery protocol, by spiking different concentrations (5 µmol L⁻¹ to 50 µmol L⁻¹) of PA in tap and lake water and DZ in orange juice and whiskey samples. The recoveries ranged from 94.4% to 116.1% for PA and 95.8% to 112.2% for DZ, highlighting the adequate accuracy of our method. To provide adequate portability for onsite analysis using our glove-based wearable device, we coupled the sensor with a miniaturized and portable potentiostat controlled by a smartphone for real-time on-finger touching analyses. As proof of applicability, the fingertip sensor was swiped across the investigated surface containing the analytes in both aqueous/sprayed and solid powder conditions for sampling. Following, the fingertip sensor was joined with the thumb finger containing an ionic gel prepared with agarose (2.5%; m/v) and appropriate BR buffer solution, which completed the electrochemical cell and enabled a voltammetric measurement. The glove-based sensor was also explored for rapid identification of powder samples of PA and DZ (ranging from 0.5 mg to 2.0 mg) to simulate analyses of potential evidence at a crime scene. Based on the attractive analytical parameters and feasibility tests, we can indicate this lab-on-a-glove sensor as an excellent alternative approach for rapid, simple, and in-field analyses of nitro explosives and drug testing.

1- Portable analytical platforms for forensic chemistry: A review, *Analytica Chimica Acta*, 1034, 2018, 1-21.

Agradecimentos/Acknowledgments

We thank the funding agencies CNPQ, CAPES, and FAPESP (Grants: 2018/08782-1, and 2022/03250-7). Special thanks to SAE/PRP/UNICAMP (Serviço de Apoio ao Estudante) for the scholarship and SBQ Campinas for the support and registration free.

ZnO-based electrochemical immunosensor to assess vaccine-induced antibody-mediated immunity against wild-type and Gamma SARS-CoV-2 strains^[2]

Freddy A. Nunez (PG)¹, Ana C. H. Castro-Kochi (PQ)¹, Isabela P. Daher (PG)^{2,4}, Edecio Cunha-Neto (PQ)², Jorge Kalil (PQ)², Silvia B. Boscardin (PQ)⁴, Alexandre J. C. Lanfredi (PQ)³, Vivian L. de Oliveira (PQ)^{1,2}, Wendel A. Alves (PQ)¹

freddynz18@gmail.com; castro.achonorato@gmail.com

¹Centro de Ciências Naturais e Humanas, Universidade Federal do ABC, Santo André, São Paulo; ²Laboratório de Imunologia, LIM19, Instituto do Coração (InCor), Hospital das Clínicas da Faculdade de Medicina da Universidade de São Paulo (HCFMUSP), São Paulo; ³Centro de Engenharia, Modelagem e Ciências Sociais Aplicadas, Universidade Federal do ABC, Santo André, São Paulo; ⁴Departamento de Parasitologia, Instituto de Ciências Biomédicas, Universidade de São Paulo, São Paulo.

Keywords: SARS-CoV-2; electrochemical immunosensor; zinc oxide nanorods; COVID-19 vaccines; ChAdOx1-S, BNT162b2

Highlights

We modified the surface with Gamma variant S protein (P1). We have proven the versatility of the sensor. The update allows evaluating the response of the variants. Platform has relevance in public policies

Resumo/Abstract

The evaluation of serological responses to COVID-19 is crucial for population-level surveillance, developing new vaccines, and evaluating the efficacy of different immunization programs. Research and development of cutting-edge point-of-care test technologies remain essential to improve immunity assessment, especially for SARS-CoV-2 variants that partially evade vaccine-induced immune responses. This work uses an impedimetric biosensor based on the immobilization of the recombinant trimeric wild-type Spike Protein (S-protein) on zinc oxide nanorods (ZnONRs) was employed for serological evaluation.^[1] We successfully assessed its applicability using serum samples from Spike-based COVID-19 vaccines: ChAdOx1-S (Oxford-AstraZeneca) and BNT162b2 (Pfizer-BioNTech). Overall, the ZnONRs/ Spike-modified electrode displayed sensitive results for both vaccines, showing excellent potential as a tool for the assessment and monitoring of seroprevalence in the population (see Figure 1). A refined outcome of this technology was achieved when the ZnO immunosensor was functionalized with the S-protein from the Gamma variant (P.1 lineage).^[2] Serological responses against samples from vaccinated individuals were acquired with excellent performance. The ZnONRs/Spike immunosensor data reveal that Oxford-AstraZeneca vaccinated individuals present significantly less antibody-mediated immunity against the Gamma variant than the Pfizer-BioNTech vaccine, highlighting the great potential of this point-of-care technology for evaluating vaccine-induced humoral immunity against new SARS-CoV-2 strains.

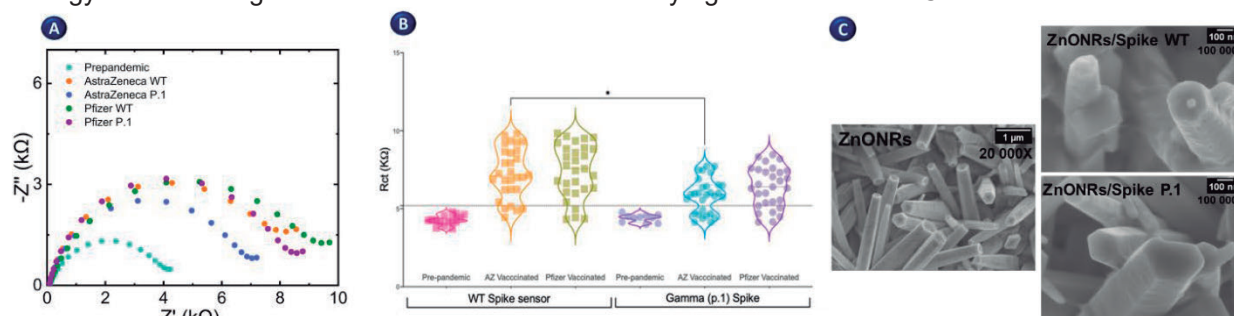


Figure 1. Electrochemical biosensor performance. (A) Assessment of polyclonal antibody response in the sera of ChAdOx1-S and BNT162b2 vaccinated individuals using the FTO-ZnONRs/spike WT and FTO-ZnONRs/spike P.1 variant (B) Comparison of ZnONRs/Spike WT and ZnONRs/Spike P.1 immunosensor response between a representative set of clinical samples from Spike-based vaccinated individuals. Violin plots where symbols represent individual participants. * $p < 0.05$ using Kruskal–Wallis test with Dunn’s post-hoc test for multiple comparisons. (C) SEM images.

[1] Nunez, F.A.; Castro, A.C.H.; de Oliveira, V.L.; Lima, A.C.; Oliveira, J.R.; de Medeiros, G.X.; Sasahara, G.L.; Santos, K.S.; Lanfredi, A.J.C.; Alves, W.A. *ACS Biomater. Sci. Eng.* **2023**, *9*, 458–473.

[2] Nunez, F.A.; Castro, A.C.H.; Daher, I.P.; Cunha-Neto, E.; Kalil, J.; Boscardin, S.B.; Lanfredi, A.J.C.; de Oliveira, V.L.; Alves, W.A. *Biosensors* **2023**, submitted to publication.

Agradecimentos/Acknowledgments

FAPESP, CNPq, CAPES, InCor / HC-FMUSP, LECC/COPPE/UFRJ, INCT de Bioanalítica.

FIS

Físico-Química

46^a Reunião
Anual da **SBQ**

28 a 31 de Maio de 2023

Águas de Lindóia · SP
Hotel Monte Real

Assessment of a Nylon filtering fabric for the phosphorus release from granulated organomineral fertilizer in water.

Henrique de Araujo Sobreira (PG),^{1*} Anizio Marcio de Faria (PQ),^{1,2} Rosana Maria Nascimento de Assunção (PQ).^{1,2}

*henriquedeasobreira@gmail.com

¹Institute of Chemistry, UFU; ²Institute of Exact and Natural Sciences of Pontal, UFU.

Keyword: Release, Phosphate, Organomineral Fertilizer.

Highlights

The investigation of the phosphate release rate in fertilizers is one of the solutions to reduce environmental pollution. A Nylon filtering fabric with reduced mesh avoids the dispersion of granulated organomineral fertilizer in the water.

Resumo/Abstract

Currently, the study of slow or controlled release in phosphate fertilizers is necessary to solve environmental problems caused by the excessive use of these products. In this technique, it is possible to propose mathematical models by investigating the phosphate release rate to minimize losses such as leaching and avoiding high doses of fertilizer in the soil, reducing environmental pollution. The objective of the present study was to evaluate the conditions for obtaining better efficiency of phosphate release in samples of granulated organomineral fertilizers (GOF) dispersed in water or retained in a Nylon filtering fabric with a 400 mesh (Nff400). The Nff400 was used to simulate the GOF disposition in the soil and to avoid an accelerated release of phosphorus due to the dissolution of fertilizer granules in water excess. For the study of phosphate release in GOF samples, the MAPA¹ protocol was used. All measurements were performed in triplicates. Figure 1 shows the kinetic curve profiles of phosphate releases from GOF samples, with and without Nff400. Table 1 summarizes the kinetic models of controlled release under the studied conditions.

Figure 1: Organomineral phosphate release behavior in water

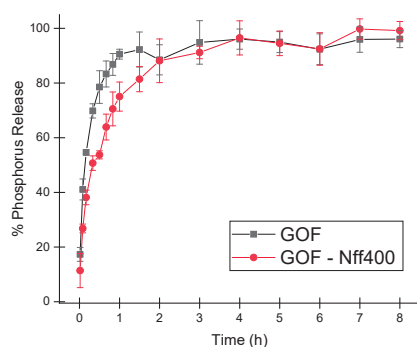


Table 1: Kinetic Parameters of Granular Organomineral Fertilizer Release

Samples	Higuchi model		Korsmeyer-Peppas model		
	R ²	K _H (min ^{-0,5})	R ²	K (min ⁻ⁿ)	n
GOF-Nff400	0,899	5,92	0,973	25,4	0,234
GOF	0,765	6,21	0,939	41,6	0,151

Initially no significant change in the phosphate release process from GOF samples, with and without Nff400 (Figure 1). However, after a half hour, there was a delay in the release process using the Nff400. To characterize the phosphate release mechanism, the Korsmeyer-Peppas and Higuchi models were used, for which the values of the constants and the release exponent (n) were obtained, as shown in Table 1. Phosphate release using the Nff400 presented a better fit to the models used in this work, indicated by the coefficient of determination (R²). GOF samples without Nff400 show an increase in the released phosphate dosage in the first hour. Probably this occurs due to the dissolution of the sample granules, increasing the access to released phosphorus. According to these results, the use of a control container, compacting the GOF as occurs in soil, can affect the proposition of the GOF release mechanism/model. Therefore, the Korsmeyer-Peppas model is the best one to describe the system using the Nff400.

[1] BRASIL. Ministério da Agricultura, Pecuária e Abastecimento. **Manual de métodos analíticos oficiais para fertilizantes e corretivos / Ministério da Agricultura, Pecuária e Abastecimento. Secretaria de Defesa Agropecuária.** Brasília: MAPA, 2017.

Agradecimentos/Acknowledgments

CNPQ; FINEP (01.11.0135.00/01.13.0371.00); UFU; PROAP; AGROCP.

Área: FIS

ASSOCIATING OPPOSITELY CHARGED NANOCELLULOSE: A STRATEGY FOR THE DESIGN OF SUPER-RESISTANT FOAMS

Maria C. S. Oliveira* (IC),^{1,2} **Diego M. Nascimento (PQ)**,² **Elisa S. Ferreira (PQ)**,² **Juliana S. Bernardes (PQ)**.^{2,3}

maria.oliveira@lnnano.cnpem.br.

¹Universidade Estadual de Campinas (Unicamp); ²Laboratório Nacional de Nanotecnologia (LNNano); ³Universidade Federal do ABC (UFABC).

Keywords: Electrostatic complexation, Cationic cellulose nanofibrils, Anionic cellulose nanofibrils, foams.

Highlights

- A pathway for production of all-nanocellulose foams in water was developed.
- Resistant and wet-resilient nanocellulose foams by electrostatic complexation.

Resumo/Abstract

The demand for more environment-friendly products and processes according to the green chemistry principles has highlighted the use of renewable feedstock instead of petroleum derivatives. In this context, cellulose nanofibrils (CNFs) foams have been investigated due to their unique combination of cellulose features such as abundance, renewability, and non-toxicity with properties as low density, large surface area, and high porosity. However, the applications of CNF foams are limited to their low mechanical and water resistances, in comparison to foams derived from synthetic polymers. In this work, CNFs were functionalized with cationic and anionic groups and these nanomaterials were combined to obtain super-resistant and water-resilient foams. Charged CNFs were produced from microfibrillated cellulose by oxidation with sodium hypochlorite mediated by the radical 2,2,6,6-tetramethylpiperidine-N-oxyl (TEMPO) and cationization with glycidyltrimethylammonium chloride (GTMAC), obtaining anionic and cationic cellulose materials, respectively. After functionalization, CNFs were produced by mechanical disintegration (3 and 15 cycles) using a microfluidizer. For preparing the foams, anionic and cationic CNFs were mixed in different proportions (65:35, 50:50, and 35:65), the excess of water was removed by centrifugation and lightweight materials were obtained by freeze-drying. Porous and open cellular structures were assembled for all tested conditions (porosity >90%), as revealed by scanning electron microscopy. Compressive testing revealed that the most resistant foams were obtained with equivalent amounts of negatively and positively charged CNFs produced at an intermediate degree of disintegration (compressive modulus ~2MPa). Besides mechanical strength, CNF foams with electrostatic complexation were less sensitivity to water compared to foams without the association of charged CNFs. This route to produce cellulose foams using electrostatic complexation is a simple and versatile strategy to create lightweight and mechanically resistant materials.

Agradecimentos/Acknowledgments



Colorimetric detection of acephate and glyphosate: simple, fast and selective

Patricia M. Soares (PG),¹ Alex R. Teixeira (PG),¹ Renan B. Campos (PQ),² Elisa S. Orth (PQ).^{1*}

patriciasoares@ufpr.br; elisaorth@gmail.com

¹Departamento de Química, UFPR; ²Departamento Acadêmico de Química e Biologia, UTFPR

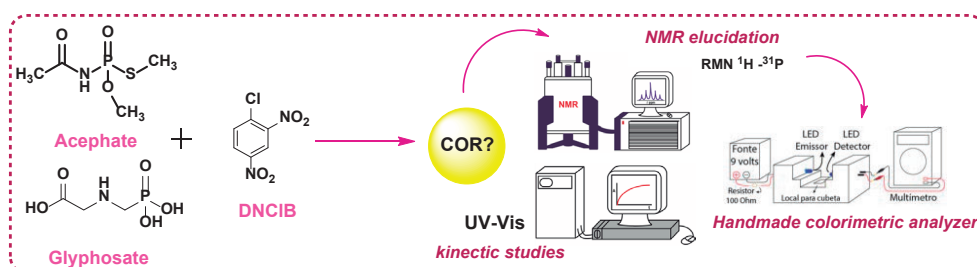
Palavras Chave: (pesticide, derivatization, colorimetric detection, organophosphate)

Highlights

- Promote reaction that leads to a colored product
- Promote the monitoring of pesticides in a fast, efficient and cost-effective way

Resumo/Abstract

The use of pesticides is an important tool with regard to guaranteeing the demand for food. They are widely used and it is essential that their presence be monitored, both in food and in the environment.¹ Organophosphates such as acephate and glyphosate are widely used worldwide but are difficult to monitor, especially due to their simple and small structure. Thus, it is the focus of this study to search for simple organic molecules that allow the detection of these pesticides in a fast, reproducible and efficient way. We are proposing here the use of derivatizing agents such as 1-chloro-2,4-dinitrobenzene (DNCIB). The reactions carried out so far are very promising and show the formation of a product that absorbs in the UV-Vis region (~400 nm), enabling the colorimetric detection. Studies are underway to optimize reaction conditions and adjust kinetic data, as well as mechanistic elucidation through NMR spectroscopy. In addition, studies to evaluate the selectivity is being carried out, indicating that the process is highly selective for organophosphates. Finally, real life samples of the agrochemicals were also evaluated regarding the effect of interferents in their formulation, which don't seem to affect the detection pursued. Overall, the present studies sheds light towards the colorimetric detection, which is usually desired due to its simple and straightforward response. The kinetic studies showed to be very important in order to distinguish the competing reactions: derivatization and hydrolysis.



Agradecimentos/Acknowledgments

UFPR, CAPES, Finep, CNPq, PhosAgro/Unesco/IUPAC, Fundação Araucária and L'Oréal-UNESCO-ABC.

References:

1. Valle, A.L. et al. Environ. Chem. Lett (2019) 17:291–317

Área: FIS

Development of cationic cellulose nanofibrils-based adhesive reinforced with natural rubber latex with enhanced water resistance

Daiane B. Silva (IC)¹, Diego M. Nascimento (PQ)¹, Pedro I. C. Claro (PQ)¹, Rubia F. Gouveia (PQ)^{1,2}, Juliana S. Bernardes^{1,2}

juliana.bernardes@Innano.cnpem.br

¹ Brazilian Nanotechnology National Laboratory, Brazilian Center for Research in Energy and Materials, Campinas, SP, Brazil.

² Nanoscience and Advanced Materials, Federal University of ABC, Santo André, SP, Brazil

Keywords: cationic cellulose nanofibers, natural latex rubber, electrostatic interaction, adhesion

Highlights

Cationic cellulose nanofibers (CCNFs) have excellent bonding capacity for multiple solid surfaces

Natural rubber latex (NRL) improves CCNFs cohesion in water by electrostatic assembly

Resumo/Abstract

The potential to replace petroleum-based materials has recently drawn attention to materials extracted from natural and renewable sources. One industry where this substitution has been taken into consideration is the adhesives sector. In this area, environmentally friendly products can be created by employing renewable feedstocks or by using water in place of organic solvents. Since they are biodegradable, biocompatible, and have the capacity for chemical alteration, substances derived from lignocellulosic biomass, such as nanocelluloses, stand out as excellent possibilities in this situation.

Herein, the adhesion property of cationic cellulose nanofibers (CCNFs) to different substrates (aluminum foil, polypropylene, and paper) was evaluated, as well as the improvement of wet adhesion through electrostatic complexation between CCNFs and natural rubber latex (NRL) particles. Uniaxial tensile tests of dried single lap joints demonstrate that CCNF dispersion (0.8 wt. %) is an effective adhesive for all analyzed systems since bonded areas resist mechanical tension close to the rupturing force of substrates. Force distance curves obtained by colloidal probe microscopy revealed that the adhesion of CCNFs to aluminum foil and polypropylene is mainly governed by electrostatic attraction, while for paper, it is primarily due to mechanical interlocking between the cellulosic fibers. Additionally, wet adhesion of polypropylene and aluminum foil was substantially improved (about 70% and 200%, respectively) by adding NRL to CCNF dispersion due to the reduction of nanofibers swelling.

This work provides a novel approach for preparing efficient renewable water-based adhesives for aluminum foil, polypropylene, and paper through a single mixture of biopolymers.

Agradecimentos/Acknowledgments

FAPESP and CNPq

Estudo da degradação do corante reativo amarelo Color Supra AC 2R pelo uso de peroxidase da raiz forte e Fenton: Uma comparação da eficiência dos métodos.

¹João Vitor dos Santos Goll (IC), ¹Nicholas Johann Berner (IC), ¹Paulo Cesar de Jesus (PQ)*, ¹Endler Marcel Borges de Souza (PQ); ¹Jurgen Andreas (PQ).

pcj@furb.br; jvsgoll@furb.br

¹Departamento de Química, Universidade Regional de Blumenau, FURB, Blumenau, SC; 89030-903.

Palavras-Chave: Corante, Amarelo Color Supra AC 2R, Descoloração, Degradação, Peroxidase, Fenton.

Highlights

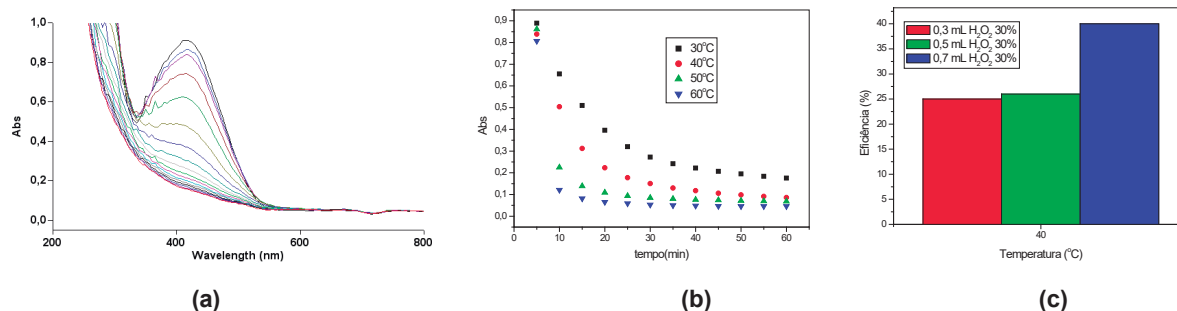
Study of the degradation of the reactive yellow Color Supra AC 2R dye using horseradish peroxidase and Fenton: A comparison of the efficiency of the methods.

The efficiency of decolorization and degradation of the yellow reactive Color Supra AC 2R dye using horseradish peroxidase (PeO) and Fenton was evaluated. The Fenton system containing H₂O₂ 3% was the most efficient, with 90% in 15 minutes. Using PeO the efficiency was 40%, with H₂O₂ 30% in 60 minutes.

Resumo/Abstract

O estudo da degradação de corantes vem sendo investigado, na busca de métodos que diminuam o impacto ambiental causado pelos mesmos.^{1,2} Neste trabalho foi estudado a degradação do corante reativo amarelo Color Supra AC 2R, aplicando a reação de Fenton e enzima peroxidase da raiz forte (PeO 906) com atividade 2009,2 KU/g, com diferentes concentrações de H₂O₂ (30%, 3%, 0,3%). Foi preparada solução de corante na concentração de 0,06 gL⁻¹ e solução de Fenton (H₂O₂/FeSO₄) com 0,225g de FeSO₄ em 100mL de diferentes concentrações de H₂O₂, ajustando o pH para 2 com H₂SO₄. Foram transferidas para uma cubeta de quartzo termostatizada, 3 mL da solução de corante e 0,2 mL da solução de Fenton. Para as reações enzimática foram utilizadas 2,5 mL de solução de corante, quantidade diferentes de PeO (0,5mg, 0,7 mg e 1 mg) e H₂O₂ (0,3mL, 0,5mL, 0,7mL). Leituras da absorbância no comprimento de onda máximo do corante (λ_{\max} = 425 nm) foram realizadas de 5 em 5 minutos, nas temperaturas de 30°C, 40°C, 50°C e 60°C. A eficiência de descoloração e degradação da solução do corante foi determinada. Experimentos foram realizados em duplicatas e os brancos também foram realizados destacando a observação da eficiência de descoloração para somente H₂O₂ em 20% nas condições experimentais. A **Figura 1a e 1b** mostra o decaimento da absorbância vs tempo com H₂O₂ 3% a 40°C para o Fenton. A **Figura 1c** mostra a eficiência na degradação obtida com a PeO e diferentes quantidades de H₂O₂ 30%. Com a peroxidase o processo de descoloração e degradação foi mais lento, levando 60 minutos para se observar bons resultados. Apesar do método com Fenton ser mais promissor, não devemos descartar a possibilidade de melhorar a aplicação do uso da peroxidase, cujo impacto ambiental é praticamente desprezível.

Figura 1 (a) decaimento da absorbância vs tempo para Fenton 3% H₂O₂ a 40°C, (b) gráfico da eficiência da descoloração do Fenton com H₂O₂ 3% em diferentes temperaturas. (c) gráfico da eficiência da descoloração da peroxidase da raiz forte com diferentes quantidades de H₂O₂ 30% a 40°C.



Referências e notas

(1) Santana, C. S.; Velloso, C.C.V.; Aguiar, A., *Rev. Virtual Quím.* **2019**, 104. (2) Mittersteiner, M.; Farias, N. R.; Barbieri, M.R.; Scharf, D. R.; Borges, E. M.; João, J. J.; De Jesus, P. C.; *J. Mol. Liq.* **2021**, 325.

Agradecimentos/Acknowledgments

Ao PIBIC/CNPq, FURB/UNIEDU, INCT Catálise e FAPESC.

46ª Reunião Anual da Sociedade Brasileira de Química: "Química: Ligando ciências e neutralizando desigualdades"

Exploring biopolymers for catalytic neutralization of organophosphates: target functionalization of (nano)bio-based and waste-derived materials

Willian Hideki Takarada (PG),^{1*} José G. L. Ferreira (PG),¹ Mariana H. Nazareno (IC),¹ Bernardo M. Régner (PG),¹ Cassiano Pires (PG),² Izabel C. Riegel-Vidotti (PQ),¹ Rilton A. de Freitas (PQ)² and Elisa S. Orth (PQ)¹

hidetak10@gmail.com; elisaorth@gmail.com

¹Department of Chemistry and ²Department of Pharmacy, Universidade Federal do Paraná (UFPR) – Curitiba, PR, Brazil.

Keywords: Gum arabic, shrimp husk, cellulose, dephosphorylation, pesticides

Highlights

Efficient biocatalysts for neutralization of toxic organophosphates were obtained by functionalization of polysaccharides (commercial and waste sources) with amidoximates, hydroxamates and imidazoles.

Resumo/Abstract

Organophosphates comprise toxic compounds employed as pesticides and nerve agents. Dephosphorylation reactions that neutralize these compounds are very slow and challenging due to highly-stable P-O bounds. Target functionalization of nucleophilic groups on biopolymeric templates (under mild synthesis conditions) allows the development of efficient and sustainable catalysts for organophosphates degradation. Our approach (Figure 1) aims to green up the process through the rational mono- and bi-functionalization of the carboxylic acids groups with imidazoles, hydroxamates and/or amidoximates in: (i) gum arabic (commercial and tannin industry byproduct), (ii) cellulosic-materials (carboxymethyl cellulose and nanocellulose-derivatives) and (iii) cellulosic-waste (rice and shrimp husk). The use of nucleophiles anchored in templates improve neutralization by catalysis and promote selective and recycle paths for detoxification. Furthermore, samples were obtained in different forms, such as solid, colloidal and gel. Covalent-functionalization was confirmed and estimated by several techniques (e.g., FTIR, TGA, potentiometric titrations). Then, all the samples were evaluated as catalysts in the dephosphorylation reactions of model-substrate diethyl 2,4-dinitrophenyl phosphate (DEDNPP) and real pesticide Paraoxon, unveiling rate enhancements up to 10⁴-fold compared to the spontaneous reactions, results among the best in the literature. Bi-functionalized samples also reveals some insights about groups neighboring effects on catalysis. Cellulose-derived nanocatalyst unveil insights about the coverage effect in catalysis. We also developed carboxymethyl cellulose-derived neutralizing gels and results so far using DEDNPP indicate potential in intoxication prevention. Overall, efficient and promising neutralizing agents were synthesized in solid, colloidal and gel form, enabling several applications and further development of green, efficient, selective, low-cost, waste-derived detoxifying agents for organophosphates, a worldwide concern.

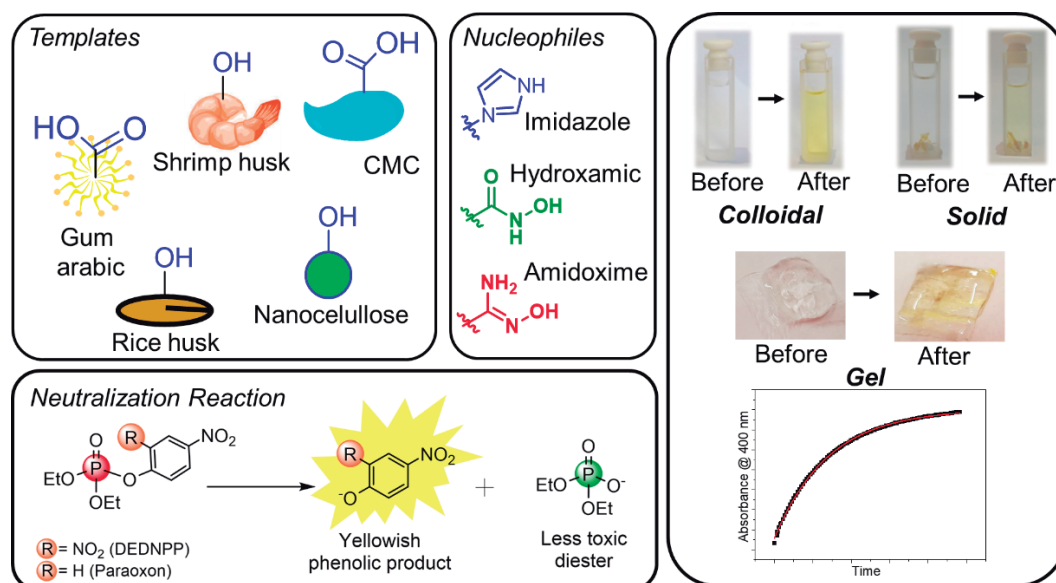


Figure 1. Main features of this work: templates and nucleophiles selection and neutralization process

Acknowledgements: UFPR, CAPES, CNPq, Fundação Araucária, L'Oréal UNESCO-ABC, PhosAgro/UNESCO/IUPAC, FINEP. 46^a Reunião Anual da Sociedade Brasileira de Química: "Química: Ligando ciências e neutralizando desigualdades"

Exploring the kinetic instabilities in the electro-oxidation of isopropanol

Gianluca Ragassi*, André H. B. Dourado, Hamilton Varela

São Carlos Institute of Chemistry, University of São Paulo, Av. Trabalhador São-carlense, 400, 13566-590, São Carlos – Brazil

*ragassigianluca@gmail.com

The electro-oxidation of isopropanol (isopropyl alcohol, 2-propanol) on platinum proceeds with very high selectivity to acetone through a two-electrons process. The reversibility of the isopropanol ($\text{H}_3\text{C-HCOH-CH}_3$)/acetone ($\text{H}_3\text{C-CO-CH}_3$) pair is particularly appropriate for hydrogen transfer, and fuel cells operating with isopropanol present low crossover rates, and open circuit potential of 810 mV, which is considerably higher than 580 mV observed for methanol, under identical conditions.[1] Furthermore, isopropanol is non-toxic and often used for disinfection and cleaning. Mechanistically speaking,[2] acetone is also the main poisoning species, as no adsorbed CO, CO_{ad} , is detected and only very small amounts of CO_2 is observed at high potentials. Kinetic instabilities, namely self-organized potential oscillations, in the electro-oxidation of isopropanol on platinum and platinum-based catalysts, are often referred to as the cause of performance decrease and even a limiting factor to the wider use of this system. This is in contrast with our recent findings in several liquid fuels employed in fuel cell and also in electrochemical reformer to produce clean hydrogen. (see [3] and references therein). The main goal of this work is to understand the electrochemical oscillations observed in the electro-oxidation of isopropanol on platinum and then tune the reaction parameters in order engineer the oscillations towards the optimization of practical devices. A set of data exploring the effect of reaction temperature is given in Fig. 1. The voltametric signatures illustrate the effect of T on reaction rates along the sweep. In the range between 25 and 60 °C, and the oscillation frequency varied from c.a. 5×10^{-3} to 10^{-2} Hz, with the oscillatory activation energy (at constant current) around $25 \text{ kJ} \cdot \text{mol}^{-1}$. Interestingly, previous unreported mixed-mode oscillations depicted in Fig. 1(b) were found at 60 °C. From the fundamental perspective, the isopropanol/acetone system is very interesting as all electrochemical oscillators in this class involves CO_{ad} .

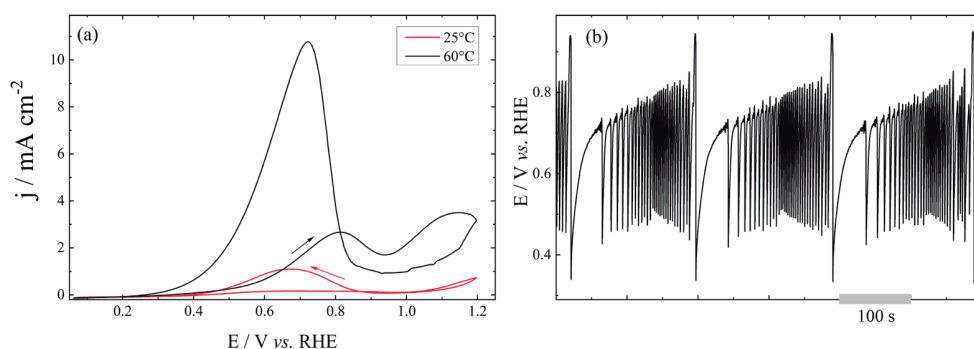


Figure 1: (a) voltametric profiles of the electro-oxidation of isopropanol on Pt at 25 and 60 °C, and (b) potential oscillations recorded at $j = 0,4 \text{ mA cm}^{-2}$ and 60 °C. Electrolyte: aqueous solution containing $[\text{H}_2\text{SO}_4] = 0.1$ and $[\text{H}_3\text{C-HCOH-CH}_3] = 1 \text{ mol} \cdot \text{L}^{-1}$.

Acknowledgements: FAPESP (#2019/22183-6, #2020/15230-5, #2021/09630-3, and #2021/13564-6), and CNPq (#306060/2017-5).

- [1] A. Santasalo, T. Kallio, K. Kontturi, *Platinum Metals Rev.* **53** (2009) 58.
- [2] F. Waidhas, S. Haschke, P. Khanipour, L. Fromm, A. Görling, J. Bachmann, I. Katsounaros, K. J. J. Mayrhofer, O. Brummel, J. Libuda, *ACS Catal.* **10** (2020) 6831.
- [3] G. Melle, T. Altair, R. Romano, H. Varela, *Energy Fuels* **35** (2021) 6202.

Influence of cellulose nanofibrils on bile salt aggregates

Davi Siqueira da Silva de Souza (PG),¹ **Vinícius Augusto Peixoto Tartare** (IC),² **Giovana Cristina Zambuzi** (PG),¹ **Brenda da Silva Bega** (IC),² **Kelly Roberta Francisco** (PQ).^{1,2*}

davissouza@hotmail.com; kfrancisco@ufscar.br*

¹Programa de Pós-Graduação em Ciência dos Materiais, UFSCar; ²Departamento de Ciências da Natureza, Matemática e Educação, UFSCar

Keywords: *Self-aggregation, Bile salt, Sodium taurodeoxycholate, Cellulose nanofibril, Rheology.*

Highlights

Bile salts with nanofibrils form different aggregates depending on the proportion between them. An increase in the amount of bile salts and nanofibrils leads to a more viscoelastic system, suggesting longer self-assembling aggregates.

Abstract

Bile salts are surfactants that at concentrations above the critical micellar concentration (cmc) form aggregates spontaneously in ordered and/or disordered phases, driven by hydrophobic interactions in the aqueous phase [1] and hydrogen bonds in the organic phase [2]. The structure of self-aggregates can be altered in the presence of certain molecules [3], such as cellulose nanofibrils (CNF), affecting the size, shape and distribution of the aggregates, and, consequently, leading to changes in the rheological behavior of the systems. In this work, the self-assembly of CNF with sodium taurodeoxycholate (NaTDC) in the proportions of CNF:NaTDC 1:27, 1:11 and 1:5 was investigated using Dynamic Light Scattering (DLS), Zeta Potential and rheology. DLS results showed that CNF/NaTDC aggregates were larger than pure surfactant or nanocellulose, with size particles ranging from 1.48 to 3.36 μm and small populations on the nanometer scale for 1:11-CNF:NaTDC and 1:5-CNF:NaTDC, with values of 67 and 98 nm, respectively. All systems showed negative electrical potential less than -35 mV, indicating good colloidal stability of the aggregates in aqueous medium. Moreover, the increment of CNF particles promoted greater colloidal stability in the systems. Flow curves of all systems showed that the apparent viscosity of the systems increased with the increment of the nanocellulose particles. Additionally, the systems presented the phenomena of shear thinning followed by shear thickening, indicating the non-Newtonian behavior of fluids [4, 5]. Rheological curves obtained in the oscillatory mode confirm that systems are viscoelastic and an increment in CNF amount increases the viscoelasticity of the systems, suggesting CNF/NaTDC aggregates were more structured and longer than pure surfactant and nanocellulose, since the elasticity modulus G' increased. Summing up, cellulose nanofibrils associated with bile salt formed different structures depending on the proportion of the nanoparticles and surfactant, modulating the rheological behavior of the systems and also, they can be a promising system for the controlled release of substances.

[1] CHEN, Y. *et al.* **Journal of Colloid and Interface Science**, v. 608, p. 405-415, 2022.;

[2] KANAZAWA, S. *et al.* **Langmuir**, v. 36, n. 26, p. 7627-7633, 2020.;

[3] MUKHERJEE, B. *et al.* **RSC Advances**, v. 6, n. 3, p. 1769-1781, 2016.;

[4] GOODWIN J. W., HUGHES R. W. **Rheology for chemists: An introduction**. The Royal Society of Chemistry, London, 2000.;

[5] MACOSKO C. W. **Rheology: Principles, Measurements and Applications**, Wiley-VCH, New York, 1994.

Acknowledgments



(Fellowships: 88887.713911/2022-00;
88887.713913/2022-00)



(Fellowships: 22/02092-9;
22/02089-8)



Influence of the size of the gold core to obtain Au@Pt bimetallic nanoparticles

Francesca Fornasier (PG),^{1*} Ana Maria Percebom (PQ).¹

francesca@hotmail.com

¹Laboratory of Macromolecules & Nanoparticles (M&N Lab), Department of Chemistry, Pontifical Catholic University of Rio de Janeiro, PUC-Rio, Brazil

Keywords: Bimetallic Nanoparticles, Au@Pt NPs, Successive Route, Plasmon Resonance

Highlights

Bimetallic Au@Pt nanoparticles were synthesized. A successive Route, two different sizes of gold core and, H₂PtCl₆ was used as a platinum precursor. The samples showed different plasmonic properties.

Resumo/Abstract

Gold and platinum bimetallic nanoparticles have shown great potential for applications in several scientific fields. The deposition of a second metal on the surface of spherical gold nanoparticles allows tuning the nanoparticles' optical properties, making them multifunctional nanoplatforms.¹ A successive route can be used for this purpose allowing control over the final physicochemical properties of the nanoparticles. In the present study, we used two different sizes of spherical gold core (approximately 20 and 40 nm) and chloroplatinic acid (H₂PtCl₆) as precursor, to obtain bimetallic nanoparticles with a molar ratio of 1 Pt/Au. Elemental mapping of images obtained by transmission electronic microscopy (TEM) revealed that the samples are formed by gold decorated with 2 - 3 nm platinum nanoparticles, which we called Au@Pt NPs. Figure 1 shows, by spectroscopy, the broadening of the LSPR band (Figure 1A, green line) and the red shift for the sample with gold core of approximately 20 nm (Figure 1A, black line). The sample with gold core of approximately 40 nm (Figure 1B, black line) did not show significant broadening of the LSPR band and red shift (Figure 1B, yellow line), the variation in the size of the gold core can influence the plasmonic properties of Au@Pt bimetallic nanoparticles. These results indicate the parameters that can be controlled to tune the final properties of Au@Pt NPs, facilitating their potential applications.

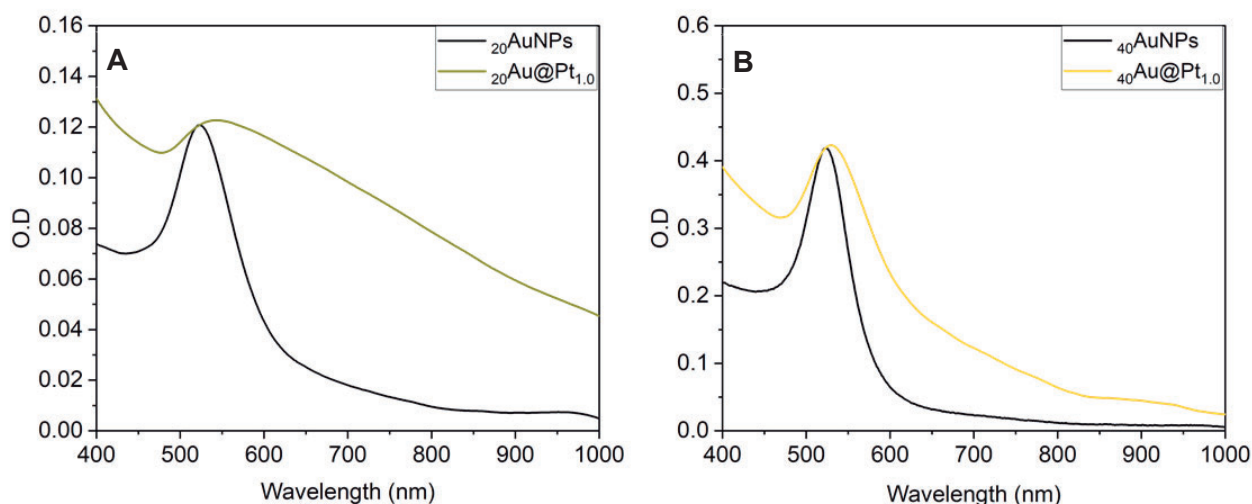


Figure 1. (a) Spectra of $_{20}\text{AuNPs}$ and $_{20}\text{Au@Pt}_{1.0}$ NPs and, (b) Spectra of $_{40}\text{AuNPs}$ and $_{40}\text{Au@Pt}_{1.0}$ NPs

1. Gao, Z. *et al.* Platinum-Decorated Gold Nanoparticles with Dual Functionalities for Ultrasensitive Colorimetric in Vitro Diagnostics. *Nano Lett* **2017**, 17, 5572–5579.

Agradecimentos/Acknowledgments

CNPq, LNNano, CAPES

Inorganic Ligands for Quantum Dots Through Ligand Exchange Method

Isabela Jeane O. Vieira (PG),^{1,2*} Olavo F. Verruma (PG), João B. Sousa Junior (PQ),^{1,2}

isabela.vieira@innano.cnpem.br;

¹Brazilian Center Research in Energy and Materials, CNPEM - Brazilian Nanotechnology National Laboratory, LNNano; ²Chemistry Institute, UNICAMP.

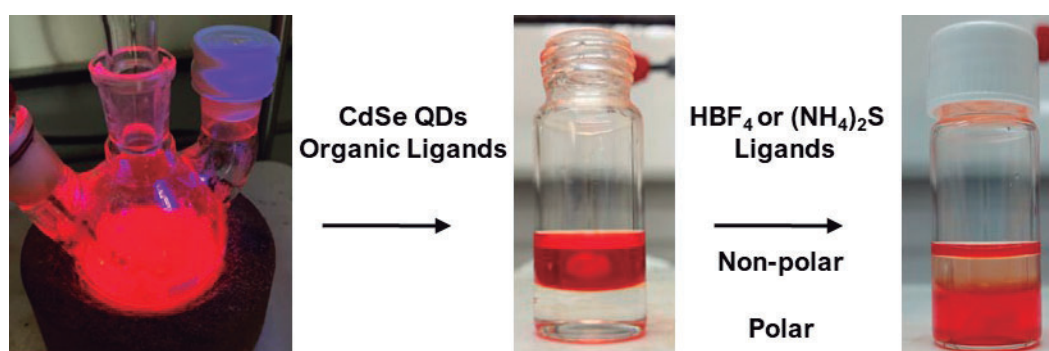
Keywords: Cadmium selenide, Quantum dots, Ligands exchange, Inorganic ligands, Semiconductor devices.

Highlights

A stable colloidal solution of inorganic ligand (S^{2-}) capped CdSe Quantum Dots was obtained using a two-phase ligand exchange process. Colloidal stability and photoluminescence (PL) efficiency were kept after the ligand exchange process.

Abstract

Spherical colloidal nanocrystals of semiconductor materials, known as quantum dots (QD), can be synthesized by wet routes in high boiling point organic solvents. After synthesis and purification, the QD presents organic ligands on the surface that promote colloidal stability by steric stabilization. Organic ligands are necessary during the synthesis protocol to control nanocrystal size and morphology, which is the key point of using QDs on optoelectronics devices, the quantum confinement effect that leads to extremely narrow PL emission (color purity). However, applying QD on optoelectronic devices requires the absence of those organic molecules on the surface of nanocrystals to enhance electronic transport. Aiming to achieve higher charge transport efficiency on QDs optoelectronics devices, the ligand exchange method was studied to obtain inorganic ligand-capped QD. Spherical CdSe QD (~ 3.0 nm) with surface organic ligands (oleylamine and oleic acid) was synthesized with narrow PL emission. To exchange or remove the organic ligands, QD dispersed in non-polar solvents are mixed and stirred with polar solvent solutions with $(NH_4)_2S$ (Ammonium Sulfide) or HBF_4 (fluoboric acid) until the complete transfer of the NPs to the polar phase¹. We characterized the QD before and after ligand exchanges by UV-Vis spectroscopy, photoluminescence (PL), and X-ray photoelectron spectroscopy (XPS). The results demonstrate that the ligand exchange processes preserved the colloidal stability of QD in polar solvents. In the presence of the $(NH_4)_2S$ ligand, CdSe QDs demonstrate greater luminescent efficiency. Those S^{2-} -capped CdSe QD has great potential to be applied in optoelectronics devices such as FET (Field Effect Transistor) and light-emitting diodes (LED)².



1. Nag, A. *et al.* **J. Am. Chem. Soc.** 133, 10612–10620 (2011).
2. Talapin, D. V. *et al.* **Chem. Rev.** 110, 389–458 (2010).

Acknowledgments

The authors thank the Brazilian Center for Research in Energy and Materials (CNPEM) and Brazilian National Nanotechnology Laboratory (LNNano). This work was supported by the State of São Paulo Research Foundation (FAPESP) grants 2021/03321-9 and 2022/02435-3.

Investigação de Parâmetros na Obtenção de Quitosana a partir de Casca de Camarão

Renata Coutinho de Oliveira (IC)¹, **Maria Eduarda S. E. de Abreu (IC-Jr)¹**, **Tatyane Claudio Araujo (TM)¹**, **Angela Sanches Rocha (PQ)^{1,2,3,4}**, **Célia Sousa (PQ)^{2,3,4}**, **Priscila Tamiasso-Martinhon (PQ)^{2,3,4}**

¹Programa de Pós-Graduação em Química, PPGQ/UERJ, ²Programa de Mestrado Profissional em Química em Rede Nacional, PROFQUI/UFRJ. ³Grupo Interdisciplinar de Educação, Eletroquímica, Saúde, Ambiente e Arte, GIEESAA/UFRJ. ⁴Grupo Interinstitucional e Multidisciplinar de Ensino, Pesquisa e Extensão em Ciências, GIMEnPEC/UFRJ
angela.sanches.rocha@gmail.com

Palavras-Chave: Biopolímero, Quitina, Sustentabilidade

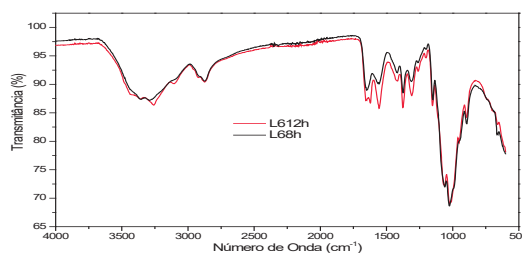
Highlights

Investigation of Parameters for chitosan obtain from Shrimp Shell. Reuse of polluting materials. Chitosan is a biopolymer, biodegradable, non-toxic. Deacetylation of chitin in the exoskeleton of crustaceans and insects. Applied in effluent treatment as photocatalysis and adsorbents.

Resumo/Abstract

A comunidade pesqueira tem grande importância para economia, sendo que em algumas regiões litorâneas, é a principal fonte de renda. Porém há a preocupação com o descarte indevido dos resíduos gerados por esta prática. Visando a um destino para esse resíduo, é possível reutilizá-los, como na obtenção de quitosana. A Quitosana é um biopolímero, biodegradável, atóxico e obtido através da desacetilação da quitina, abundante em exoesqueletos de crustáceos e insetos, além de fungos. A casca de camarão é uma matéria prima rica em quitina e, a partir dela, foi feita uma investigação para obtenção da quitosana, além de melhorias do processo estabelecido. Este polímero é conhecido por ter potencial para uso no tratamento de efluentes como componente de fotocatalisadores e adsorventes.

O presente trabalho tem como objetivo a investigação de parâmetros para obtenção da quitosana usando como fonte a casca de camarão marinho. Com isso, foram feitos testes para que se obtivesse o biopolímero em tempo mais reduzido e com maior rendimento. As cascas limpas, secas e moídas são desmineralizadas com HCl e desproteinizadas com solução de NaOH, mas na última etapa do processo, a desacetilação, foi feita a separação do material e foram feitos dois testes, um com o aquecimento de 12 horas com temperatura a 65 °C (L612H) e outro com o aquecimento de 8 horas com temperatura a 90°C (L68H) usando autoclave, ambas o sexto lote. Através da caracterização com o teste de solubilidade em ácido acético 1%, entre as duas amostras foi possível observar que a segunda amostra se solubilizou melhor, e que a primeira amostra formou precipitado. Já na análise dos espectros de FTIR (Figura) foi possível observar que as duas amostras são semelhantes, mas a banda em torno de 1400 cm⁻¹, indicativa da desacetilação, é maior na amostra desacetilada por 12h, indicando que nesta condição, a conversão de quitosana em quitina é mais efetiva.



Agradecimentos/Acknowledgments

O presente trabalho foi realizado com apoio da Coordenação de Aperfeiçoamento de Pessoal de Nível Superior – Brasil (CAPES) – Código de Financiamento 001.

Área: FIS

Kinetic of combustion in spark ignition engines – applying chemistry methodology in mechanical engineering

Natália R. S. Araujo (PG),¹ Felipe S. Carvalho (PG),¹ João Pedro Braga (PQ),¹ Fabrício J.P. Pujatti (PQ),² Rita C. O. Sebastião (PQ),^{2*}

nataliarsaraujo@ufmg.com; ritacos@ufmg.br

¹Departamento de Química, UFMG; ²Departamento de Engenharia Mecânica, UFMG.

Keywords: *Internal combustion engines, Kinetic of combustion, Energetic efficiency, Mass Burned Fraction.*

Highlights

A new methodology to determine the kinetics of fuel combustion in internal combustion engines.

Simplified kinetics to compare fuels and additives combustion processes.

Combustion efficiency mapping to fuel or operation conditions in internal combustion engines.

Abstract

An internal combustion engine works with the energy from the heat released during the combustion of the oxidizer-fuel mixture. The process of fossil fuels and biofuels combustion can be described by its kinetic properties. The knowledge of these properties allows the characterizing of chemical reactions, their velocities, and the mechanism of the process. From this information, one can inform decisions such as the addition or substitution of components that are significant to a specific reaction, allowing one to speed up or slow down a process. It can be a determinant step to improve the energetic efficiency of engines. In this sense, this research proposes the use of a new methodology, based on a neural network, applied in two fronts of work to compare fuel combustion processes: using thermogravimetric analysis (TG and DSC data) and using the Mass Burned Fraction (MBF), measured in internal combustion engines. Thermogravimetry stands out in the fuel combustion kinetic study since it represents a validated and internationally accepted chemistry methodology.

The proposed methodology allows the determination of the kinetic triplet: activation energy (E_a), frequency factor (A) and mechanism of reaction throughout the combustion process. The results from thermogravimetric data represent the baseline of fuel combustion kinetic once they are obtained at atmospheric pressure and controlled temperature program. The results obtained from MBF data show how the in-cylinder combustion progresses as a function of the crank angle, varying in pressure and engine speed. This work proposes to adapt the methodology that uses thermogravimetric data to determine the fuel combustion kinetic in spark ignition engines using MBF data. The determined triplet kinetic according to both methods will be compared, which allows the study of the influence of engines operation condition (i.e., geometry, pressure) in the combustion process. From the comparison, it is expected to obtain simpler and representative kinetic models of real engines.

ARAÚJO, Natália R. S. et al. Kinetic models and distribution of activation energy in complex systems using Hopfield Neural Network. *Thermochimica Acta*, v. 697, p. 178847, 2021.

QUIROGA, Luis Carlos Rios; BALESTIERI, José Antonio Perrella; ÁVILA, Ivonete. Thermal behavior and kinetics assessment of ethanol/gasoline blends during combustion by thermogravimetric analysis. *Applied Thermal Engineering*, v. 115, p. 99-110, 2017.

Acknowledgments

The authors would like to thank CNPq, FAPEMIG and UFMG/PRPq for the financial support.

Lightweight wood materials templated by wet foams

Elisa S. Ferreira¹⁻³ (PQ), Elizabeth Dobrzanski (PG)^{2,3}, Prashant Agrawal (PQ),⁴ Praphulla Tiwary (PQ),⁴ Richard Chen (PQ),⁴ Emily D. Cranston (PQ)^{2,3,5*}

elisa.ferreira@lnnano.cnpem.br; emily.cranston@ubc.ca

¹Brazilian Nanotechnology National Laboratory (LNNano), Brazilian Center for Research in Energy and Materials (CNPem), Campinas, Brazil; ²UBC BioProducts Institute, Vancouver, Canada; ³Department of Wood Science, The University of British Columbia (UBC), Vancouver, Canada; ⁴Department of Chemical and Biological Engineering, UBC, Vancouver, Canada; ⁵Plantee Bioplastics Inc., Vancouver, Canada

Palavras Chave: *lightweight material, foam, wood, aqueous foam.*

Highlights

In this work, lightweight solid foams (0.13 g cm^{-3}) with low thermal conductivity ($0.042 \text{ W m}^{-1} \text{ K}^{-1}$) were produced from forest residue by a green and easily scalable route.

Resumo/Abstract

Colloids assembled as lightweight materials, such as solid foams and aerogels, can absorb mechanical, sound, and heat energies very efficiently, with distinct performance over their respective condensed materials [1]. Polymer foams are typically produced by incorporating a gas phase in polymer fluids during synthesis (e.g. polyurethane (PU) foams) or in molten plastics (e.g. polyolefin foams). As wood cannot be processed as a fluid, we propose a route to prepare wood foams by oven-drying aqueous foams. The characteristic instability of wet foams was overcome by combining wood particles with poly(vinyl alcohol) (PVA) and sodium dodecyl sulphate (SDS), which reinforced the wet structure and enabled the foam to be dried without collapse. To assemble wood particles without chemical refining, PVA was added as a binder, holding the components together in a composite structure with dimensional stability. The wet foams were oven-dried, creating a lightweight material (0.13 g/cm^3 , Fig 1.) with thermal conductivity (0.042 W/mK) close to PU foams. The wood foams could be fully recycled by re-dispersing and re-foaming the components in water, producing foams with the original density and performance. This route to produce solid bio-based foams opens new opportunities for the creation of cellular bio-based materials by assembling particles and colloids at the air/water interface [5]. Moreover, the application of water-soluble colloids allows for recovering pristine components and reassembling them into new structures, overcoming plastic disposal issues.

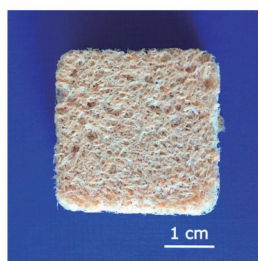


Figure 1. Wood foam prepared from aqueous wet foams.

[1] L.J. Gibson, M. F. Ashby, *Cellular Solids: Structure and Properties*, 1999, 1, 6, University Press, Cambridge, UK.

[2] E.S. Ferreira, C. A. Rezende, E. D. Cranston, *Green Chemistry*, 2021, 23, 10, 3542.

[3] E.S. Ferreira, E. Dobrzanski, P. Tiwary, P. Agrawal, R. Chen, E.D. Cranston. *Materials Advances*, 2023, 4, 641-650.

Agradecimentos/Acknowledgments

NRCan (2019-F0041-C00001), NSERCC (RGPIN-2018-06818), Mitacs Accelerate (IT22973 and IT30768), UBC BioProducts Institute, Plantee Bioplastics, and LNNano-CNPem.

Natural siliceous spherulites filled by organic matter, a preliminary assessment by Raman spectroscopy

Antonio Carlos Sant'Ana (PQ),¹ Lenize F. Maia (PQ),^{1*} Rafael de Oliveira (PG)¹, Dalva A. L. Almeida (PQ),¹ Gabriel A. Barberes (PQ),¹ André Luiz S. Pestilho (PQ),² Delano M. Ibanez (PQ),² Luiz Fernando C. de Oliveira (PQ)¹

antonio.sant@ufjf.br; lenmaia@uol.com.br

¹Núcleo de Espectroscopia e Estrutura Molecular, Departamento de Química, UFJF, Juiz de Fora, MG.; ²Centro de Pesquisas da Petrobras, Rio de Janeiro, RJ.

Palavras Chave: Silicon oxide, Spherulites, Geochemistry, Minerals, Carbon species

Highlights

- Chemical composition of spherulites revealed by Raman spectroscopy
- Identification of silicon oxide as a major inorganic component in the spherulitic matrix
- Diverse spectral pattern of the organic matter was identified in the core of the spherulites

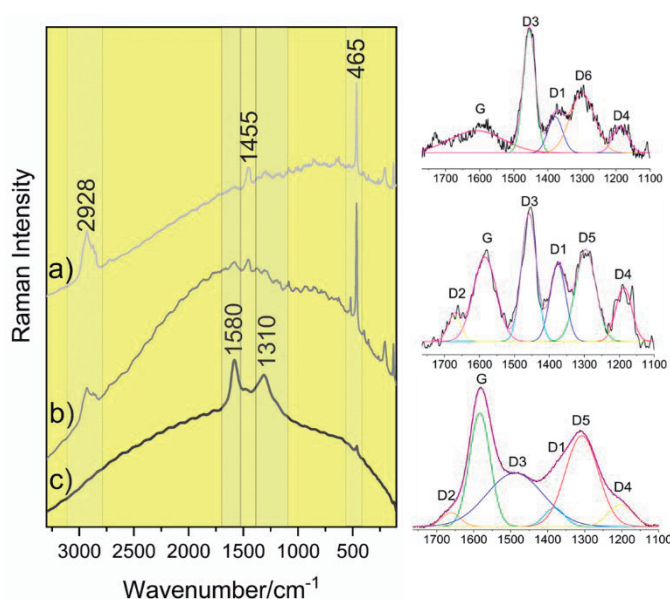
Resumo/Abstract

The natural occurrence of spherulites is a well-known phenomenon resulting from a series of geochemical and sedimentological processes. In this particular case, the analyzed spherulites are derived from the Barra-Velha Formation (BVF) in the Santos sedimentary basin (Brazilian Atlantic margin). Literature data have reported the presence of “calcite spherulites” as part of lacustrine carbonates (CaCO_3) from BVF¹, however, Raman spectral analyses (Fig.1) revealed the occurrence of silicon oxide (SiO_2) instead, due to Raman bands at 465, 358, 398, and 207 cm^{-1} . In addition, the samples presented Raman bands attributed to carbonaceous materials in the range of 3000 to 2800, and 1700 to 1100 cm^{-1} (Fig.1) distributed in the

central core of spherulite. The spectral deconvolution of the first-order region showed a complex mixture of carbon-based compounds (Fig.1 a-c).

Both the inorganic and organic content identified from the BVF spherulites are a matter of debate. The replacement of the CaCO_3 to SiO_2 may result from hydrothermal flow or as an interaction with the matrix (broadly referred to as mud), composed of clay minerals, calcite, dolomite, and silica. The organic matter identified in the central core surrounded by SiO_2 has generated a series of questions about the sequence of diagenetic processes.

Fig.1- Raman spectra from a spherulite (Barra Velha Formation), obtained with laser line at 632.8 nm.



Agradecimentos/Acknowledgments

The authors would like to thank CNPq, CAPES, CENPES/PETROBRAS

¹Gomes, J.P; Bunevich, R.B., Tedeschib, L.R. et al. *Mar. Pet. Geol.* **2020**, *113*, 104176.

Novel green surfactants display foaming properties similar to sodium dodecyl sulfate

Carolina R.A. Lopes (PG),^{1*} Guilherme A. Ferreira (PQ),¹

carolina.ravazzano@ufba.br

¹Departamento de Físico-Química, Instituto de Química, Universidade Federal da Bahia, Salvador, BA, Brasil

Keywords: Aqueous foams, Green surfactants, Cardanol

Highlights

Foam formation and stability in aqueous solutions containing novel cardanol-based surfactants and their mixtures with sodium dodecyl sulfate.

The green surfactants do not improve the properties of foams made from sodium dodecyl sulfate solutions.

Some of the green surfactants display interesting foaming properties and are considered promising substituents to currently available nonionic surfactants.

Resumo/Abstract

Aqueous foams have a wide range of practical applications, playing an important role in cleaning, personal hygiene, pharmaceutical and food products, among others. Nonetheless, such systems are thermodynamically unstable in virtue of their high interfacial free energy, often displaying short half-life times. The simplest way of controlling foam stability is based on the use of surfactants. Owing to their amphiphilic properties, these species are able to rearrange at the interface, reducing the energy required to expand it and contributing to foam kinetic stability. However, since most of the available surfactants are obtained via petrochemical routes, their use may incur in (eco)toxicological hazards [1]. In the light of green chemistry principles, sustainable and bio-based alternatives to petroleum-derived surfactants have been widely studied. In this work, aqueous solutions containing three (3) ethoxylated nonionic surfactants derived from cardanol, a phenolic compound extracted from cashew nutshell liquid, had their foaming properties assessed. Both pure and mixed (with sodium dodecyl sulfate, SDS) surfactant solutions were tested. The cardanol-derived surfactants shared identical hydrophobic moieties, differing from one another solely on the number ($n = 7, 9$ or 12) of ethoxy units (EO) attached to their hydrophilic moiety. Foam stability was evaluated through the Tessari (double-syringe) technique [2] at different concentrations for both the individual nEO solutions and their mixtures with SDS. Foamability tests were conducted with the use of an electric stirrer and the obtained foam height for each system was compared to the height of the starting solution. Dynamic surface tension and surface rheology data for nEO solutions at a concentration of 2% v/v were also determined by the pendant drop method. Foamability and stability results suggest that there is no synergy between SDS and cardanol-derived surfactants: mixed systems showed no improvement in the aforementioned solution properties. On the other hand, for most of the concentrations tested, 9EO solutions achieved a significant improvement in foam life-time, demonstrating a superior stabilization effect when compared with reference SDS solutions. Both 9EO and 12EO surfactant solutions also produced a considerable amount of foam for all tested concentrations, with the exception of the 9EO solution at 0.1% v/v. It's worth mentioning that, for all tested concentrations, 12EO solutions displayed a similar foamability to that of SDS solutions. These results are now being correlated with the determined surface properties in an effort to elucidate the underlying mechanisms involving foam formation and stabilization by nEO aqueous solutions. Nevertheless, cardanol-derived surfactants are promising foaming agent alternatives, balancing desirable foaming properties while complying with green chemistry principles.

[1] R. Jahan, A. M. Brodatti, M. Tsianou, P. Alexandridis, *Adv. Colloid Interface Sci.* **275**, 102061 (2020).

[2] L. Zhang, L. Tian, H. Du, S. Rouzière, N. Wang, A. Salonen, *Langmuir* **33(29)**, 7305-7311 (2017).

Agradecimentos/Acknowledgments

CNPq, CEPETRO/UNICAMP and Cardolite.

Periodic chaos. A new nonlinear dynamic behavior.

Romulo O. Pires (PQ), Roberto B. Faria (PQ)^{1*}

faria@iq.ufrj.br

¹Instituto de Química, UFRJ

Palavras Chave: *chaos, oscillating reactions, bursts, nonlinear behavior, periodic chaos.*

Highlights

A period of chaos appears, regularly, before a cluster of bursts.

Resumo/Abstract

In a small range of chlorate concentration and flow rate (k_0) values, a period doubling sequence of oscillations (period-1, period-2, period-4) followed by a chaotic behavior was observed between clusters of bursts (Fig. 1a) in the simulation of the chlorate-nitrous acid-iodine-iodide oscillating reaction [1] by a mechanism containing 33 chemical reactions and 27 independent chemical species. The burst pattern is regular and repetitive (Fig. 1b), but it is chaotic immediately before the onset of the cluster of bursts. The clusters of bursts may contain different numbers of bursts, depending on the chlorate concentration and k_0 . This behavior disturbs the paradigms of chaos science because the chaotic behavior appears regularly inside a regular pattern, without any change in the parameters. This behavior, which we call periodic chaos, expands the possibilities when chaotic behavior can be observed.

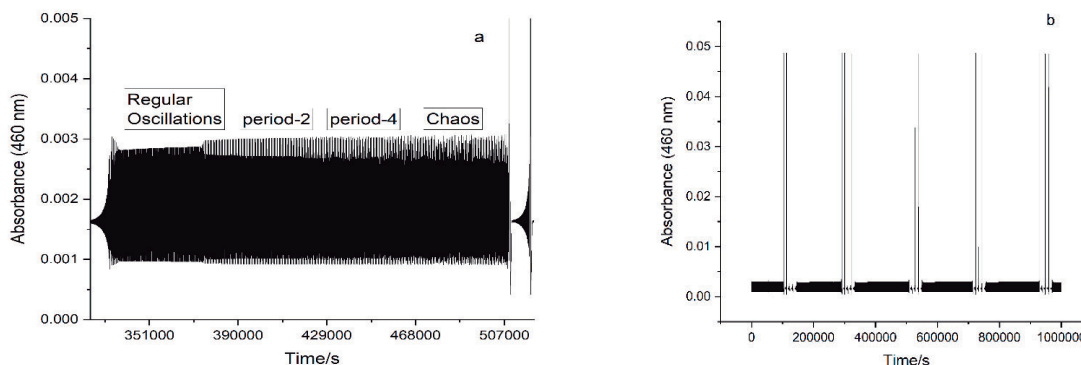


Figure 1. Periodic chaos. $[\text{ClO}_3^-] = 0.0130 \text{ M}$, $[\text{HNO}_2] = 0.0016 \text{ M}$, $[\text{I}_2] = 0.000274 \text{ M}$, $[\text{I}^-] = 0.0084 \text{ M}$, $[\text{O}_2] = 0.000258 \text{ M}$, $[\text{H}^+] = 0.02 \text{ M}$, $k_0 = 3.9842 \times 10^{-5} \text{ s}^{-1}$.

[1] E. V. Monteiro, J. P. R. Queiroz, R. B. Faria, The chlorate-nitrous acid-iodine-iodide oscillating reaction, *ACS Omega* **2021**, *6*, 7959-7965. DOI: 10.1021/acsomega.1c00933.

Agradecimentos/Acknowledgments

CNPq (303.260/2019-0). This study was financed in part by the Coordenação de Aperfeiçoamento de Pessoal de Nível Superior - Brasil (CAPES) - Finance Code 001

Preparação de compósito de óxidos de ferro em quitosana para estudo de adsorção de corantes sintéticos

Bruna Cristina Badalotti (IC),¹ Reinaldo Aparecido Bariccatti (PQ).

bruna1234badalotti@gmail.com; reinaldo.bariccatti@unioeste.br.

¹Departamento de Química, UNIOESTE

Palavras Chave: nanopartículas, adsorção, magnéticas.

Highlights

Composite preparation of iron oxides/chitosan with the purpose of studying the adsorption of dyes. The synthesized iron oxide is a magnetic material, which incorporates this property in chitosan and preserves its adsorptive properties.

Resumo

A síntese de compósitos tem grande interesse tecnológicos e dada a sua ampla aplicação em meio ambiente, alimentos e fármacos.¹ As associações entre diferentes substâncias apresentam propriedades interessantes como alta capacidade adsorptiva e ferromagnetismo, favorecendo a aplicação em processos de adsorção. Para isto sintetizou o Fe_3O_4 na presença de quitosana com objetivo de manter as propriedades de adsorção e incorporar propriedades magnéticas ao compósito. Os estudos na caracterização do compósito foram acompanhados por microscopia eletrônica de varredura MEV e espectroscopia no infravermelho FT-IR. No MEV, verificou um aumento da rugosidade da superfície, indicando a incorporação do Fe_3O_4 (magnetita) na superfície da quitosana. O aumento da rugosidade foi acompanhado de um aumento no número de partículas agregadas, isto é associado a propriedade magnética do compósito. Os espectros de FT-IR mostraram que a magnetita mascara/reduz as bandas da quitosana. Para os estudos

cinéticos e de equilíbrio os frascos das misturas heterogêneas foram posicionados sobre um ímã de neodímio por cerca de 10 segundos, garantindo a precipitação do compósito e obtenção do espectro da solução com uma linha base próxima de zero, comprovando a facilidade de separação do sólido pelo campo magnético. Com objetivo de estudar a adsorção de corante geradores de oxigênio singlete obteve a cinética de adsorção com o corante eritrosina. Observou-se uma adsorção significativa do corante, reduzindo sua absorbância em solução na presença do compósito. Realizou-se estudos cinéticos de adsorção e aplicou os modelos cinéticos de ordem 0, 1 e 2, tendo como melhor ajuste de ordem 0, fornecendo R^2 de 0,9986 e uma constante de $2,93 \pm 0,05 \cdot 10^{-7} \text{ mol.L}^{-1}.\text{min}^{-1}$. Para estudo de equilíbrio se fez necessário determinar coeficiente de absorção molar em 308nm onde está banda possui uma absorção considerável, mas não é tão intensa quando a obtida no visível ($\epsilon = 10.650 \text{ L cm}^{-1} \text{ mol}^{-1}$), em

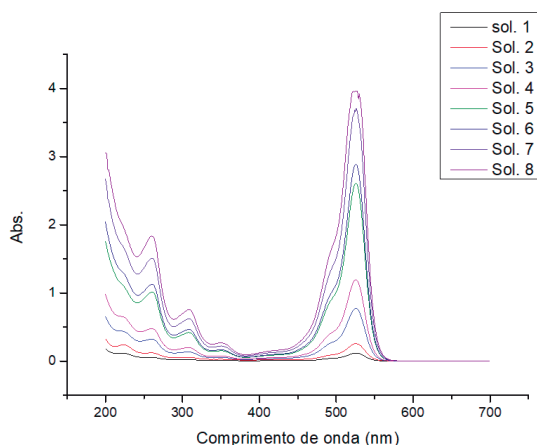


Figura 01: Espectro de adsorção das soluções eritrosina após 24 horas com contato com adsorvente.

seguida foram obtidos os espectros de absorção das soluções do corante após alcançar o equilíbrio na presença do adsorvente (Figura 01). Observou-se a redução na intensidade de absorção em relação as soluções originais e aplicou-se os modelos de adsorção de Langmuir e de Freundlich. Segundo os valores obtidos o melhor ajuste é o modelo de Freundlich ($Y=A.X^b$, com R^2 de 0,864) com $A=1,50 \pm 0,88$ e $b=0,29 \pm 0,06$, adsorvendo cerca de 0,090 g de corante por grama de adsorvente.

¹ Ferreira H. S. e Rangel M. C. (2009). Nanotecnologia: Aspectos Gerais e Potencial da Aplicação em Catálise. *Química. Nova*, **32**, 1860-1870.

Agradecimentos/Acknowledgments

Fundação Araucária, UNIOESTE, GIPeFEA e CNPq.

Área: FIS

Síntese e aplicação de nanocompósito $\text{Eu}^{3+}:\text{SiO}_2\text{-PMMA}$ para detecção de impressões digitais latentes em investigações forenses

Luiz F.S. Andrade (PG),^{1*} Victor H.V. Sarmiento (PQ),² Filipe A. Jesus (PQ),³

Luiz21045@outlook.com; Luiz21045@outlook.com

¹Programa de Pós-Graduação em Química, UFS; ²Departamento de Química, UFS; ³Instituto Federal de Alagoas, IFAL.
Palavras Chave: Impressões digitais, Európio, Sol gel, Luminescência.

Highlights

- ❖ As amostras contendo nanocompósito $\text{Eu}^{3+}:\text{SiO}_2\text{-PMMA}$ exibem fortes emissão de luminescência devido ao processo de transferência de energia intramolecular lantanídeos-ligantes;
- ❖ Os lantanídeos dopados em uma matriz de sílica possuem um poder de emissão de luz que pode ser utilizado em vários setores, como lasers, nanosensores.

Resumo

A onda de violência no Brasil vem ganhando força e, junto dela, os crimes. Atrelado a esses delitos, está a Química Forense (QF), área que consiste na aplicação dos conhecimentos da ciência química aos problemas de natureza forense. A atuação dos peritos criminais na investigação de um caso é um exemplo de aplicação da QF, aonde ele utiliza de métodos e técnicas que auxiliam na análise de evidências. A técnica de identificação de impressões digitais é uma delas. O reconhecimento de indivíduos por impressões digitais é uma das técnicas mais eficientes em relação a todos os outros métodos de reconhecimento biométrico para identificação de pessoas. Entretanto, os métodos de identificação por impressões digitais necessitam cada vez mais de melhorias em tornar visíveis de forma seletiva as impressões digitais otimizando a identificação inequívoca de indivíduos. Com objetivo de tornar essas técnicas de identificação de impressões digitais ainda mais eficazes, alguns nanomateriais semicondutores podem ser utilizados para melhorar a capacidade de detecção, atuando como um tratamento químico. Neste sentido, foi realizado a síntese do nanocompósito $\text{Eu}^{3+}:\text{SiO}_2\text{-PMMA}$ preparados pelo processo sol-gel. Os efeitos foram avaliados através de caracterizações por Espalhamento de Raios X a baixo ângulo (SAXS), Espectrofotômetro de Infravermelho por Transformada de Fourier (FTIR), Difração de Raio (DRX), Termogravimetria (TG), Microscopia Eletrônica de Varredura (MEV) e Espectroscopia de Fotoluminescência (EF), que possibilitaram a caracterização dos grupos funcionais, da estabilidade térmica das estruturas e elucidar os efeitos promovidos pela adição do Tetraetilortossilicato (TEOS) sobre a formação das estruturas de sílica e analisar possíveis modificações na luminescência dos íons Eu^{3+} incorporados. Os resultados obtidos mostraram que as curvas de SAXS estão de acordo com a análise dos resultados de TG, que demonstrou maior proteção do polímero nos híbridos com quantidades de TEOS mais elevadas em suas composições. Há também boa concordância entre as curvas de SAXS e os espectros de FTIR, uma vez que estes evidenciaram a presença de estruturas mais condensadas nas amostras com maiores conteúdos inorgânico. Além disso, os resultados denotaram a formação de estruturas de sílica maiores e mais condensadas à medida que esse precursor foi incorporado em quantidades mais elevadas, bem como notou-se o aumento da estabilidade térmica dos híbridos em virtude das mudanças na fase inorgânica. Quanto à luminescência, os espectros demonstraram que não houve alterações significativas nas propriedades de emissão dos híbridos. No entanto, a adição de maiores quantidades desse alcóxido reduziu a eficiência e a intensidade de emissão dos íons Eu^{3+} , que, provavelmente, coordenam-se às estruturas de sílica nesses híbridos confirmando que os fatores experimentais associados à composição de híbridos $\text{Eu}^{3+}:\text{SiO}_2\text{-PMMA}$, de fato, exercem forte influência sobre as características estruturais e as propriedades luminescentes dos materiais mencionados. Os valores de Eficiência quântica do estado emissor das amostras realizadas foram superiores a híbridos similares e a matrizes dopadas com complexos altamente luminescentes, o que as caracteriza como materiais muito promissores para desenvolvimento de um novo pó seletivo, eficiente e confiável para revelação de impressões digitais latentes em superfícies porosas e não porosas. Além, de um produto de melhor relação custo x benefício em comparação com os produtos utilizados atualmente, baseado nos aspectos da confiabilidade dos resultados produzidos.

Agradecimentos

A CNPq pela bolsa de pós-graduação, a Universidade Federal de Sergipe e ao CLQM (Centro de Laboratórios de Química Multiusuários) da Universidade Federal de Sergipe pelo suporte às análises.

Área: FIS

Self-aggregated systems formed by bile salt, lecithin and propylene glycol

Giovana C. Zambuzi (PG)¹; Brenda da Silva Bega (IC)²; Davi Siqueira da Silva de Souza (PG)¹; Vinícius Augusto Peixoto Tartare (IC)²; Kelly Roberta Francisco (PQ)²

giozambuzi@gmail.com

¹CCTS – UFSCar; ²DCNME - UFSCar

Keywords: Lecithin, Sodium taurodeoxycholate, Propylene glycol, Self-aggregation, Rheology

Highlights

Systems formed by bile salt and lecithin in different proportions with the addition of propylene glycol were prepared. It was obtained aggregates with different sizes and, therefore, systems with different viscoelastic behaviors.

Resumo/Abstract

Lecithin (LEC) is a natural surfactant, predominantly composed of polar and neutral phospholipids, it is mainly found in soybeans and egg yolks. It is used as a dietary supplement and as an emulsifier.^[1] Bile salt (sodium taurodeoxycholate) is an amphoteric physiological surfactant, is excreted in the small intestine and has fat- digestion function.^[2] The combination of these components can allow the formation of different structures, such as reverse micelles, liposomes and wormlike micelles.^[1;2] The addition of small molecules can significantly change the size, shape and rheological properties of those self-assembling systems^[3]. In this work, we evaluated the addition of propylene glycol on the structure of NaTDC/LEC aggregates and viscoelasticity of the systems. The systems were prepared by mixing a stock solution of 200 mol/L lecithin with 100 mol/L sodium taurodeoxycholate (NaTDC) solubilized in methanol in the proportions of NaTDC/lecithin 0.2; 0.4 and 0.8 (w/w). After removal of methanol, 0.001g of propylene glycol (PG) and 10 ml of cyclohexane were added to the systems and stirred for 24 h at 100 rpm. After resting, the formation of at least two phases was observed in the systems, which the lower phase was more viscoelastic. The size of the formed aggregates was determined by Dynamic Light Scattering (DLS), and the addition of propylene glycol molecules led to an increase in the size of the aggregates for the proportions of 0.2 and 0.4 NaTDC/LEC, and a decrease in the aggregate size for the 0.8 NaTDC/Lecithin system. The flow curves showed that the addition of propylene glycol increased the apparent viscosity for the 0.4 NaTDC/LEC system, decreased its value for the 0.8 NaTDC/LEC solution, and showed no significant difference for the 0.2 NaTDC/LEC system, when their values were compared with the systems without the addition of the solute. The oscillatory curves showed that 0.4 NaTDC/LEC system with propylene glycol had a higher modulus of elasticity, G' , compared to the solution without the solute. However, for the 0.8 NaTDC/LEC solution, the addition of the solute decreased its viscoelastic properties. This result indicated that propylene glycol promoted the formation of longer wormlike micelles and with a longer relaxation time for the solution containing bile salt and lecithin in the proportion of 0.4.

References:

[1] TUNG, S. H. et al. JACS. 128 (2006) 5751.

[2] CAUTELA, J. et al. Colloids and Surfaces A. 532 (2017) 411.

[3] HANIO, S. et al. Langmuir. 37 (2021) 2543.

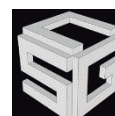
Agradecimentos/Acknowledgments



Fellowships: 88887.713913/2022;
0088887.713911/2022-00



Fellowships: 22/02092-9;
22/02089-8



Área: FIS

Spectroscopic, electronic and vibrational studies of different compounds of **Bis-Chalcones**

Vitória B. Costa (IC)¹, Alexandre M. R. Teixeira (PQ)², Hécio S. Santos (PQ)³ and Antonio C. Sant'Ana (PQ)^{1*}.

vitoria.basilio@estudante.ufjf.br; antonio.sant@ufjf.br.

¹Laboratory of Plasmonic Nanostructures – LabNano, Univ. Fed. Juiz de Fora; ²Department of Biological Chemistry, Regional University of Cariri; ³Science and Technology Centre - Course of Chemistry, State University Vale do Acaraú.

Keywords: Chalcones, Dibenzalchalcones, UV-VIS Spectroscopic, Raman Spectroscopic.

Highlights

The interest in the characterization of *bis*-chalcones by UV-VIS, Raman, SERS and ATR-FTIR spectroscopies is from their antioxidant activity that make them potential good drugs.

Resumo/Abstract

Bis-chalcones (BC) are organic compounds formed by the double condensation reaction of a ketone that has two active sites with two equivalents of aromatic aldehyde.¹ They are known for their wide range of biological activities, including anti-inflammatory, antioxidant and antitumor properties.¹ BC has been extensively studied as potential drugs for the treatment of various diseases, such as cancer and cardiovascular disease.¹ They can be of natural or synthesized origin.¹ (Figure 1).

The aim of this work was the characterization of different BC through ATR-FTIR, UV-VIS, Raman and Surface-Enhanced Raman Scattering (SERS) spectroscopies. Solid BC samples were solubilized in suitable solvents at concentrations close to 1.0×10^{-3} mol L⁻¹ for UV-VIS spectroscopic analysis. Absorption bands were observed at 220 –

500 nm range, giving them yellowish colors. Vibrational analyses showed bands at 1600 cm⁻¹, assigned to C=C stretching modes, at 2800-3100 cm⁻¹ range, assigned to C-H stretching modes, and at 1000 cm⁻¹, assigned to C-C stretching of aromatic rings. SERS spectra are being carried out using silver nanoparticles in aqueous suspensions.

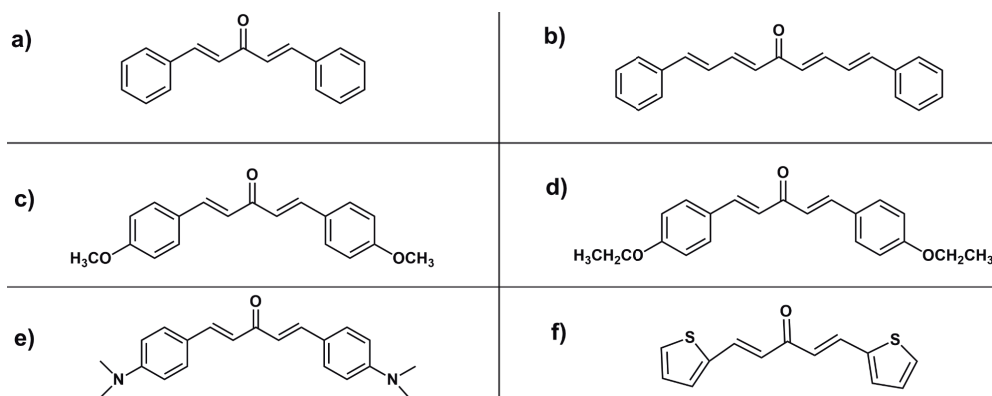


Figure 1: Structures of synthesized BC: (a) (1E,4E)-1,5-diphenylpenta-1,4-dien-3-one; (b) (1E,3E,6E,8E)-1,9-diphenylnona-1,3,6,8-tetraen-5-one; (c) (1E,4E)-1,5-bis(4-methoxyphenyl)penta-1,4-dien-3-one; (d) (1E,4E)-1,5-bis(4-ethoxyphenyl)penta-1,4-dien-3-one; (e) (1E,4E)-1,5-bis(4-(dimethylamino)phenyl)penta-1,4-dien-3-one; (f) (1E,4E)-1,5-di(thiophen-2-yl)penta-1,4-dien-3-one.

References:

¹ DE OLIVEIRA, M. M., *et al.*, Full Spectroscopic Characterization and Cytotoxicity Activity of Synthetic Dibenzalacetone Derivatives, **J. Molecular Structure**, v. 1231, 2021, 129670.

Agradecimentos/Acknowledgments

The authors would like to thank LabNano research group, Federal University of Juiz de Fora for the Scientific Initiation scholarship and the funding agencies CNPq, CAPES and FAPEMIG.

Study of self-association of sodium taurodeoxycholate in the presence of cellulose nanocrystals

Vinicius Augusto Peixoto Tartare (IC),¹ Davi Siqueira da Silva de Souza (PG),² Brenda da Silva Bega (IC),¹ Giovana Cristina Zambuzi (PG),² Kelly Roberta Francisco (PQ).^{1,2*}

viniciustartare.ufscar@gmail.com; kfrancisco@ufscar.br*

¹Departamento de Ciências da Natureza, Matemática e Educação, UFSCar; ²Programa de Pós-Graduação em Ciência dos Materiais, UFSCar.

Keywords: Self-aggregation, Bile salt, Sodium taurodeoxycholate, Cellulose nanocrystal, Rheology.

Highlights

Taurodeoxycholate and nanocrystals aggregates were obtained at different proportions. The nanocellulose promoted the formation of longer structures when associated with the bile salt.

Abstract

Bile salts can form mixed structures with each other, with non-ionic surfactants, ionic surfactants and polymers [1, 2, 3]. However, there are few works that studied the aggregation of bile salts in the presence of cellulose nanocrystals [4]. In this way, it is fundamental to understand the intermolecular interactions between bile salts and nanocellulose, creating procedures for obtaining rheological modifiers for the various industrial sectors. In this work, cellulose nanocrystals (CNC) were mixed with sodium taurodeoxycholate (NaTDC) in CNC:NaTDC proportions of 1:5, 1:2 and 1:1 in order to evaluate the size of the aggregates, colloidal stability and viscoelasticity of the systems by using Dynamic Light Scattering (DLS), Zeta Potential and rheological measures, respectively. DLS results showed that mixed aggregates formed are larger than pure surfactant or nanocrystal. Increasing CNC concentration led to the formation of larger-sized nanometer and micrometer CNC/NaTDC aggregates. Zeta potential values for all systems became more negative with the increment of nanocellulose particles, indicating that the addition of CNC increases the stability of the systems. The flow curves confirmed that all systems presented the phenomena of shear thinning followed by shear thickening at high shear rate, indicating the non-Newtonian behavior of fluids [4, 5]. Also, the highest value of apparent viscosity was observed for the system with higher amount of surfactant and nanocrystal. Curves obtained in oscillatory mode confirm that fluids are viscoelastic and presented a rheological behavior similar to wormlike systems, where the viscous modulus G'' is greater than elastic modulus G' at low frequency and at high frequency G' is higher than G'' . The relaxation time, determined at the frequency of cross-over, is dependent of the nanocellulose and surfactant proportions, where longer relaxation time was observed for the systems formed by 1:1 CNC:NaTDC. Finally, nanocrystals can be used as rheological modifier in the presence of bile salts due to the formation of long self-aggregating particles.

[1] MUKHERJEE, B. *et al.* **RSC Advances**, v. 6, n. 3, p. 1769-1781, 2016.;

[2] CAMARGOS, C. H., REZENDE, C. A. **ACS Applied Nano Materials**, v. 4, n. 10, p. 10505-10518, 2021

[3] CHEN, S.; DONG, H.; YANG, J. **Sensors**, v. 20, n. 6, p. 1690, 2020;

[4] GOODWIN J. W., HUGHES R. W. **Rheology for chemists**-An introduction. The Royal Society of Chemistry, London, 2000.;

[5] MACOSKO C. W. **Rheology**: Principles, Measurements and Applications, Wiley-VCH, New York, 1994.

Acknowledgments



(Fellowships: 22/02092-9;
22/02089-8)



(Fellowships: 88887.713911/2022-00;
88887.713913/2022-00)



The influence of poly(ethylene glycol) on the rheology of bile salt/ lecithin reverse wormlike micelles

Brenda da Silva Bega (IC),¹ **Giovana Cristina Zambuzi** (PG),² **Vinícius Augusto Peixoto Tartare** (IC),² **Davi Siqueira da Silva de Souza** (PG), ¹**Kelly Roberta Francisco** (PQ),^{1,2*}

brendabega3@gmail.com; kfrancisco@ufscar.br*

¹Departamento de Ciências da Natureza, Matemática e Educação, UFSCar; ²Programa de Pós-Graduação em Ciência dos Materiais, UFSCar

Keywords: *Sodium taurodeoxycholate, Lecithin, Polyethylene glycol, Self-aggregation, Rheology.*

Highlights

The addition of propylene glycol (PEG) to sodium taurodeoxycholate (NaTDC) and lecithin (LEC) systems promoted aggregates with different sizes depending on the NaTDC/LEC ratio and changes in the viscoelasticity of the systems.

Abstract

Bile salts are natural surfactants important in the digestion and absorption of lipids and cholesterol.^[1] Lecithin is a natural zwitterionic surfactant that contains two tails in its molecular structure, and is found primarily in egg yolks and soybeans.^[2] The mixture of these two surfactants leads to the formation of mixed structures that self-organize forming aggregates such as spherical micelles, wormlike micelles, liposomes and lamellae.^[1;2,3] In this work, we have studied the effects that polyethylene glycol (PEG) has produced on the size, shape and structure of wormlike micelles formed by taurodeoxycholate (NaTDC) and lecithin (LEC), as well as evaluating changes in the rheological properties of the systems. The systems were prepared in methanol ^[3] from stock solutions of 100 mol/L NaTDC and 200 mol/L LEC in NaTDC/LEC ratios 0.2, 0.4 and 0.8 (w/w). After removing the solvent, 0.004 g of polyethylene glycol (PEG) 400 g/mol and 10 mL of cyclohexane were added to the systems, which were left under stirring for 48 h. Dynamic light scattering (DLS) results showed that the presence of PEG leads to a decrease in the size of aggregates in 0.2 and 0.8 NaTDC/LEC and to an increase in 0.4 NaTDC/LEC. Flow curves showed that the addition of PEG leads to a decrease in apparent viscosity for 0.2 and 0.4 NaTDC/LEC systems and an increase for NaTDC/LEC proportion of 0.8. The Shear thinning was observed at low shear rates and the shear thickening appeared at higher shear rates. The oscillatory tests showed that the addition of PEG promoted an increase in the elastic modulus G' for 0.8 NaTDC/LEC system compared to the system without the addition of the solute. However, the addition of PEG to 0.4 NaTDC/LEC leads to a loss in the viscoelastic properties of the system. We suggest that wormlike micelles in the 0.4NaTDC/LEC became less elongated by the addition of PEG, as the solute acts to disrupt the aggregates. However, the addition of PEG to the 0.8 NaTDC/LEC systems leads to a greater structuring of the wormlike micelles, increasing the viscoelasticity of the solution. Furthermore, wormlike micelles formed in this work presented very long relaxation times, indicating that these structures are very long and that their breakage and recombination takes place at their edges.

[1] Cautela J. *et al.* **Colloids and Surfaces A**, v. 532, p. 411-419, 2017. [2] Tung, S. H. *et al.* **Journal of the American Chemical Society**, v. 128, n. 17, p. 5751-5756, 2006. [3] HANIO, S. *et al.* **Langmuir**, v. 37, n. 8, p. 2543- 2551, 2021.

Acknowledgments



(Fellowships: 22/02092-9; 22/02089-8)



(Fellowships: 88887.713911/2022-00;
88887.713913/2022-00)



Understanding the chemical kinetics of H₂O ices irradiated by different ionizing agents in space environments.

Carolina Hahn da Silveira (PD),^{1*} Sergio Pilling (PQ),¹

cahdsilveira@gmail.com

¹Laboratório de Astroquímica e Astrobiologia, Instituto de Pesquisa e Desenvolvimento, Universidade do Vale do Paraíba, UNIVAP/São José dos Campos-SP.

Palavras Chave: Astrochemistry, Astrophysical Ices, H₂O, Computational Methodology.

Highlights

We employ the PROCODA code to calculate the chemical reaction rates and molecular abundances in astrophysical ice analogs processed by radiation, such as cosmic rays, electrons and ionizing photons.

Resumo/Abstract

Water is one of the most abundant molecules found in space, especially in cold environments, such as molecular clouds and protostellar objects, in the form of the named astrophysical ices. The study of the behavior of such ices rich in water is of great importance since they are a nursery of several chemical species and also a source for molecules that will desorb to gas-phase. The ionizing radiation (fast ions, electrons and energetic photons) in space induce chemical changes in such ices increasing the chemical complexity of the interstellar medium. We report the use of the PROgram for solving COupled Differential equations in Astrochemistry (PROCODA)^{1,2,3} in pure water ices at very low temperature under the presence of chemical processing by ionizing radiation. The program uses experimental data in the infrared and solves a set of chemical coupled reactions. The program characterizes the chemical equilibrium that appears in the ice at large radiation fluences and de radiation-induced molecular. In this work, the experimental data were taken from the literature and covers ices bombarded by cosmic rays, X-rays, UV and electrons. The code described the evolution of 9 species (H₂O, H₂O₂, and O₃ observed in the experiments; H, O, H₂, OH, O₂, HO₂ non-observed in the experiments but predicted) by employing 50 chemical reaction plus 9 desorption-induced reaction. Some reactions are illustrated in Figure 1. Figure 2 presents a typical output of the code with the evolution of molecular concentration (in terms of column density) as a function of time, for the data employing cosmic ray in 12 K H₂O ice.

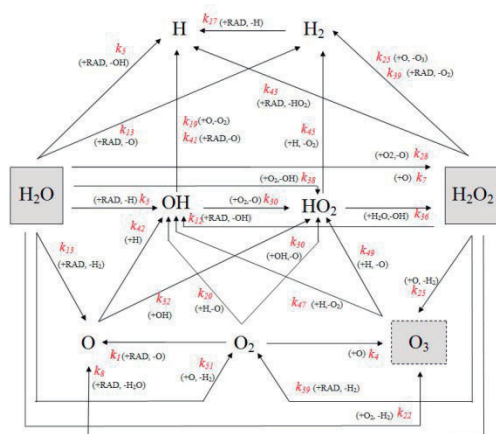


Figure 1. Scheme of chemical reactions in pure water ice.

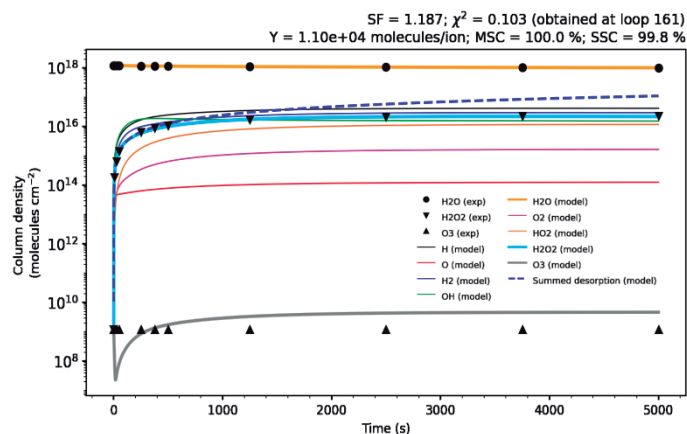


Figure 2. Molecular abundance evolution employing the PROCODA in the H₂O ice at 12 K irradiated by cosmic rays.

The program calculates the effective rate constants of radiation-induced destruction reactions, bimolecular reactions and desorption reactions and also characterizes the molecular abundances at chemical equilibrium phase (constant chemical scenario that appeared in the ice at large radiation fluences). We expect the numerical values obtained in this work, when employing in astrochemical models, provides better understanding of the chemistry of cold space environments.

¹ Pilling et al. *The Astrophysical Journal*, v. 925, n. 2, p. 147, 2022.

² Carvalho et al. *MNRAS*, v. 515, p. 3760, 2022.

³ Pilling et al. *Adv. Space Research*, accepted, 2023.

Agradecimentos/Acknowledgments

We thank the research funding agencies CAPES and CNPq.

FOT

Fotoquímica

46^a Reunião
Anual da **SBQ**

28 a 31 de Maio de 2023

Águas de Lindóia · SP
Hotel Monte Real

Chalcones functionalized with methoxy groups (-OCH₃): Preparation, characterization and spectroscopic studies

Elizabeth Aparecida Alves (PG),¹ Carla Cristina Schmitt Cavalheiro (PQ),¹

alvesselizabeth@usp.br; carla@iqsc.usp.br

¹Institute of Chemistry of São Carlos, USP, São Carlos, SP – Brasil.

Key words: Chalcone, methoxy, α,β -unsaturated, Claisen-Schmidt condensation.

Highlights

Chalcones are directly affected by the insertion of substituent groups on their aromatic rings. Spectroscopy allows investigating how this highly conjugated system of π bonds is affected in the presence of methoxy substituents.

Abstract

Natural and synthetic chalcones are molecules known to have pharmacological and biological activity, widely exploited due to their antioxidant, anti-inflammatory, anticonvulsant, antitumor and bactericidal properties, among others. Its basic structure, Figure 1, consists of two aromatic rings that are connected by a carbonyl system α,β -unsaturated. The most used synthesis method for the preparation of these compounds is the Claisen-Schmidt condensation, which occurs between an acetophenone and a benzaldehyde by acid or base catalysis. Chalcones are directly affected by the insertion of different substituent groups on their aromatic rings, in which the carbonyl moiety of chalcones has its charge density altered due to the effect of substituents. In this work, it is reported how the methoxy group (-OCH₃), a strongly electron-donating substituent, affected the electronic properties of the α,β -unsaturated carbonyl system of chalcones. Disubstitution in ring B by methoxy groups was also investigated, evaluating its effect on the α,β -unsaturated carbonyl set. FTIR spectra showed characteristic bands, as the HC=CH (α - β) bond of the α,β -unsaturated system in the region close to 977 cm⁻¹ for all compounds, indicating that they were obtained. By ¹H NMR, confirmation of obtaining α,β -unsaturated products could be observed in the region of 7.65 ppm for α hydrogen and in the region of 7.95 ppm for β hydrogen. The absorption spectra in the UV-Vis region showed that all compounds present an intense band in the region between 298 and 344 nm, characteristic of a $\pi \rightarrow \pi^*$ transition, with mixed character $\pi_{\text{cinnamoyl}} \rightarrow \pi^*$ and $n_{\text{C=O}} \rightarrow \pi^*$. Spectroscopic studies with solvents EtOAc; CH₃CN; EtOH; MeOH and PBS 7.4; showed a bathochromic shift, characteristic of positive solvatochromism for all compounds. The UV-Vis absorption spectrum of the -OCH₃ substituent at the para position showed great influence, shifting the absorption bands to the region of longer wavelength, confirming that electronic transitions $\pi_{\text{cinnamoyl}} \rightarrow \pi^*$ and $n_{\text{C=O}} \rightarrow \pi^*$ feel the effect of a donor group. These results are part of the photophysical study of the interaction of methoxylated chalcones with albumin proteins (BSA, HSA) in phosphate buffered saline (PBS).

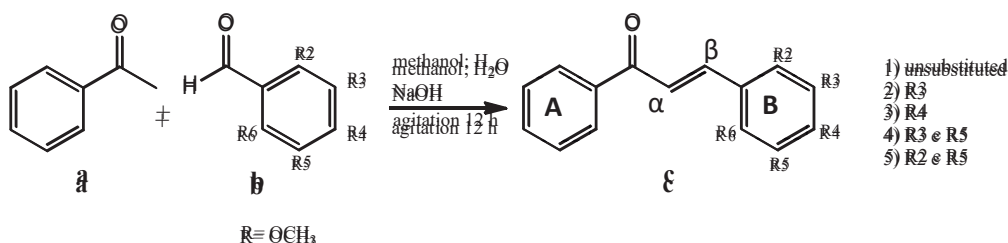


Figure 1. a) acetophenone; b) benzaldehyde; c) basic structure of chalcones [1,3-diphenyl-2-propen-1-one].

Acknowledgments

CNPQ, FAPESP, CAPES.

Fe(III) complex with NHC ligands for methyl methacrylate photo-ATRP

Botter, Maria Luisa (PG),¹ Bignardi, Camila (PG),¹ Pesqueira, Naralyne M.(PG),¹ Carvalho Júnior, Valdemiro P. de (PQ),¹ Goi, Beatriz E. (PQ).^{1*}

maria.botter@unesp.br; beatriz.goi@unesp.br

¹Departamento de Química e Bioquímica, FTC-UNESP

Palavras Chave: Photo-ATRP; Iron(III) complex; Methyl methacrylate.

Highlights

This work presents a new Fe(III) complex bearing NHC ligand as a photo-redox mediator in photo-ATRP. The system presented a polydispersity index of 1.15, and significant temporal control and selectivity.

Resumo/Abstract

There has been a great increase in the interest of development of new controlled radical polymerization (CRP) systems in recent years. Based on this, this work presents the synthesis of a new Fe(III) complex with carbene N-heterocyclic ligands (NHC) (Figure 1). The precursors, ligand and complex were synthesized and further characterized by absorption spectroscopy in the UV-Vis region, vibrational spectroscopy in the infrared region (FTIR), cyclic voltammetry and nuclear magnetic resonance (NMR ¹H). The [Fe(Pmb)₂Br] complex was used as a photo-redox mediator in photo-ATRP (Atom Transfer Radical Polymerization) reaction of methyl methacrylate (MMA) in different molar ratios [MMA]/[EBPA]/[Fe^{III}]. The kinetic study of the polymerization system presented a pseudo-first order profile to all the conditions. In the proportion with an intermediate concentration of iron(III) complex, (200/1/0.04), the highest conversion (50%) and good polymerization control were observed, with a polydispersity index of 1.15 (Figure 2). As it was found that the system has temporal control, in which in the absence of light there is no continuity of polymerization. Therefore, the developed system uses an unprecedented Fe(III) complex for MMA polymerization, with a significant temporal control and selectivity (photo-induced).

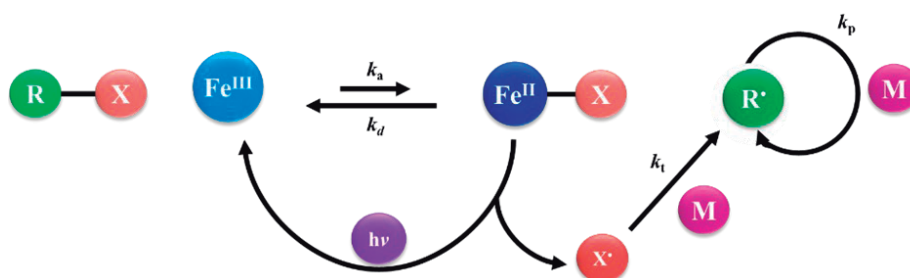


Figure 1. Photo-ATRP system.

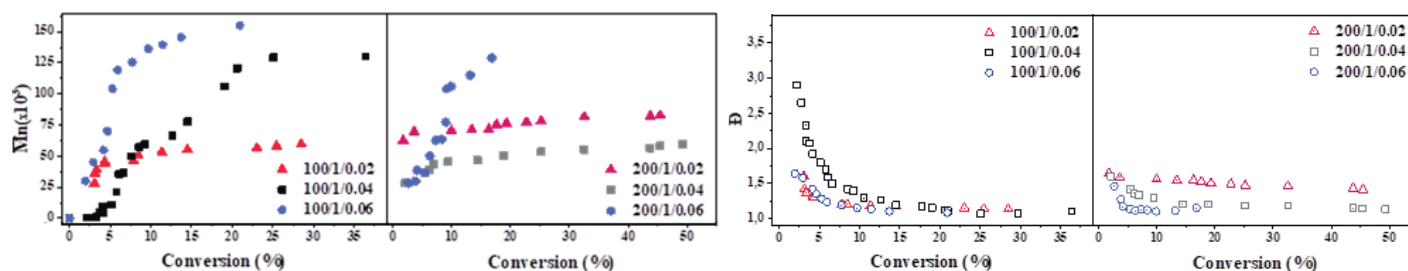


Figure 2. Dependence of Mn and Đ on MMA conversion with iron(III) complex, in all six conditions tested, at 25°C.

Agradecimentos/Acknowledgments



Design of a polymer optical fiber luminescent solar concentrator

Daniel A. R. Souza (PG),^{1*} Marivone Gusatti (PG),¹ Fabio J. Caixeta (PG),¹ Marcelo Nalin (PQ),¹ Sidney J. L. Ribeiro (PQ).¹

daniel.arg@gmail.com

¹Instituto de Química, Departamento de Química Analítica, Físico-Química e Inorgânica, UNESP, Campus Araraquara, SP

keywords: Polymer Optical Fiber, LSC, Photovoltaic Cell, Rhodamine 6G.

Highlights

Luminescent solar concentrator (LSC) based on cylindrical optical fiber.
 Manufacture of hollow-core PMMA fibers.
 Preparation of composite based on resin and photoluminescent dye.

Abstract

Current photovoltaic (PV) cells exhibit efficiencies of 10% to 40% [1]. The mismatch between the absorption of photovoltaic cells and the solar irradiance on earth is one of the major limitations towards more efficient PV energy conversion. Currently, to increase the PV system power, large-area panels are required. In urban centers, the maximum power achieved is often limited by the rooftop area [2]. Significant attention is directed towards luminescent solar concentrators (LSCs) which have emerged as an interesting solution for concentrating a large area of sunlight into a small beam of high field intensity. This action strategy provides greater use of solar energy by photovoltaic cells and allows better integration in urban environments. Luminescent polymer optical fibers provide a flexible platform for LSCs applications, where, the luminophores can convert some part of the solar spectral emission into a range belonging to the maximum conversion range of a given PV cell [3]. In this operation, the spectral conversion can resort to modes called downconversion (DC), upconversion (UC), or down-shifting (DS), that spectral converters exploit the photoluminescence processes to capture low- or high-energy photons that cannot be used by the PV cell and thus, convert them to photons with a useful energy.

In this work, an LSC based on polymeric fiber optics was fabricated. The LSC is composed of two main parts, the first one is the PMMA optical fiber that acts as a waveguide and the second one is the luminescent material that performs the spectral conversion. In the manufacturing process, the hollow-core PMMA fibers were obtained from pulling technique. To transform the optical fiber into a bi-component LSC, the photoluminescent dye known as rhodamine 6G was dispersed in acrylic resin and injected into the fiber core. Figure 1 shows an image of the LSCs illuminated by a solar simulator.

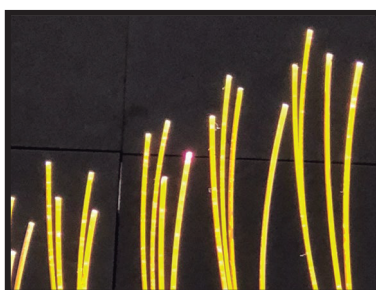


Fig. 1: LSCs illuminated by a solar simulator.

[1] The National Renewable Energy Laboratory: <https://www.nrel.gov/pv/cell-efficiency.html> (2020), Accessed 1st Feb 2023.

[2] F. Meinardi, A. Colombo, K.A. Velizhanin, R. Simonutti, M. Lorenzon, L. Beverina, R. Viswanatha, V.I. Klimov, S. Brovelli, Nat. Photonics, 8 (2014), pp. 392 - 399.

[3] A.R. Frias, E. Pecoraro, S.F.H. Correia, L.M.G. Minas, A.R. Bastos, S. Garcia-Revilla, R. Balda, J. Mat. Chem. A; 6: 8712-8723, 2018.

Acknowledgments

The authors thank the CNPq (Grant n° 382428/2022-6), SISFÓTON-MCTI project, FAPESP (Grant n° 2020/13309-3), and UNESP (PROPG-PROPe 05/2022) for providing financial support to carry out this research.

Development of a new Mn(II) complex bearing NHCs as a potential photoredox catalyst for CRP2 reaction.

Camila Bignardi (PG)¹, Naralyne M. Pesqueira (PG)¹, Valdemiro P. de Carvalho Jr. (PQ)¹, Beatriz E. Goi (PQ)^{1*}

c.bignardi@unesp.br; beatriz.goi@unesp.br *

¹Departamento de Química e Bioquímica, FCT-UNESP, Presidente Prudente.

Keywords: N-heterocyclic carbenes, Manganese (II), photocatalyst, CPR2

Highlights

A new Mn(II) complex was synthesized from the py-mesethylimidazole and further applied as a photoredox catalyst to the *Controlled Radical Photopolymerization (CRP2)* of the MA using TEA and EBPA as the additives in a reductive pathway

Abstract

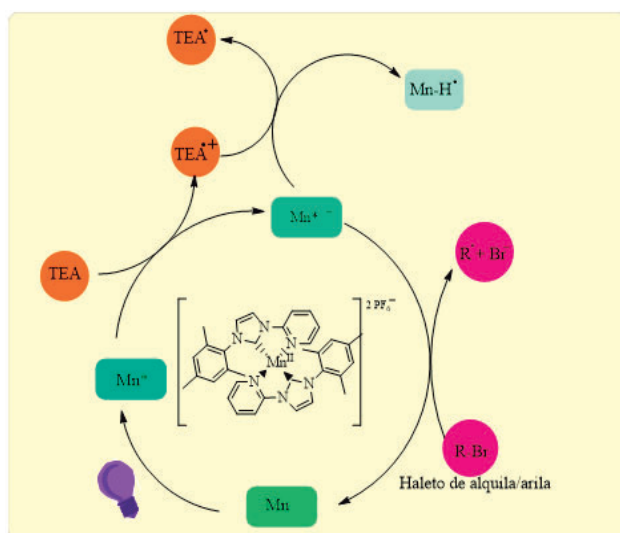


Figure 1. Reductive pathway for the CRP2 of MA catalyzed by the Mn^{II} complex in the presence of TEA and EBPA.

The photoredox polymerization has been used as a green method to obtain well-defined polymers. One of the most studied methods is the *Controlled Radical Photopolymerization (CRP2)*.^{1,2} The [Mn^{II}(py-mesethylimidazole)₂](PF₆)₂ complex was synthesized from the NHC, pymesethylimidazole, and further characterized. The py-mesethyl imidazole ligand was characterized by FTIR, UV-Vis, fluorescence spectroscopy and ¹H NMR. The complex [Mn^{II}(py-mesethylimidazole)₂](PF₆)₂ by FTIR and UV-Vis, cyclic voltammetry, MALDI-TOF and fluorescence spectroscopy. The synthesized complex was additionally studied photophysically in the presence of polymerization additives at 365 nm, and where the Stern-Volmer constant ($K_{SV} = 0.387 \text{ mol}^{-1}\cdot\text{L}$) was estimated. The behavior of the complex obtained was also monitored against irradiation at 365 nm, and its

sensitivity to air. The synthesized complex was active as a photocatalyst in methyl acrylate (MA) CRP2, using α -ethyl-bromophenylacetate as initiator and triethylamine (TEA) as electron donor. The obtained polymers exhibited uniform masses with $\bar{D} < 2$. The best condition for the photocatalysis was in the molar ratio of [MA/EBPA/Mn^{II}/TEA] = 200/1/0.12/1 with $M_n = 160000 \text{ g}\cdot\text{mol}^{-1}$ and $\bar{D} = 1.4$ with 73% conversion. The same ratio was used in the kinetic monitoring of the polymerization of methyl acrylate, showing that the complex, in addition to catalyzing a pseudo-first order reaction ($k_{obs} = 2.1 \times 10^{-3} \text{ min}^{-1}$), keeps the system slightly controlled.

1- Federico Bella, Roberta Bongiovanni. Photoinduced polymerization: An innovative, powerful and environmentally friendly technique for the preparation of polymer electrolytes for dye-sensitized solar cells. *Journal of Photochemistry and Photobiology C: Photochemistry Reviews*, 16, 1-21.(2013)

2- Mao Chen, Mingjiang Zhong, and Jeremiah A. Johnson. Light-Controlled Radical Polymerization: Mechanisms, Methods, and Applications. *Chem. Rev.* 116, 17, 10167–10211 (2016).

Acknowledgments



Proc. 2021/11873-1 and 2021/13128-1



Methyl methacrylate photo-ATRP mediated by the Fe(III) complexes coordinates to symmetric Schiff bases

Yasmin de M. Shimizo (IC),^{1*} Camila Bignardi (PG),² Naralyne M. Pesqueira (PG),² Valdemiro P. de Carvalho Jr. (PG),² Beatriz E. Goi (PG).²

*yasmin.shimizo@unesp.br; beatriz.goi@unesp.br

¹Departamento de Química e Bioquímica, FCT-UNESP, Presidente Prudente.

Keywords: Fe(III) complexes, photo-ATRP, control radical polymerization, symmetrical Schiff bases.

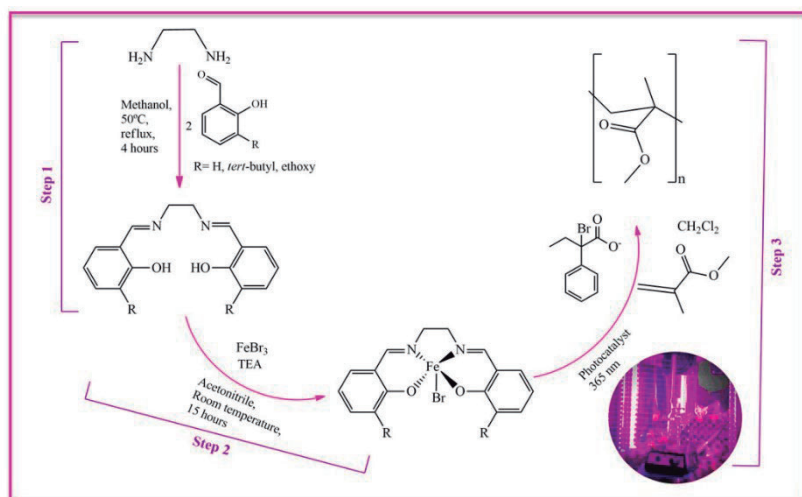
Highlights

Schiff base ligands and their respective Fe (III) complexes were synthesized and characterized. The mediating ability of the complexes in the photopolymerization of methyl methacrylate under 365 nm LED irradiation was evaluated.

Abstract

Atom Transfer Radical Polymerization (ATRP) is a technique that uses metal-based catalysts to control the growth of polymer chains through a reversible redox process that involves the transfer of halogen atoms to activate dormant species generating initiator radicals and to disable propagation chains. Iron complexes are less toxic, inexpensive, and biocompatible catalytic systems and interesting due to the abundance of iron¹.

In this research, Schiff base ligands were synthesized and characterized by H¹ NMR, FTIR and UV-Vis. Then, Fe(III) complexes were also synthesized and characterized by FTIR, UV-Vis, MALDI-TOF and cyclic voltammetry. Thus, the mediating ability of the complexes in the polymerization of methyl methacrylate under 365 nm LED irradiation was evaluated. The general reaction for the synthesis of ligands, complexes and the photopolymerization are shown in Scheme 1.



Scheme 1. General reaction for the synthesis and photopolymerization.

The controlling capability of complexes **1-3** on the radical photopolymerization by transfer of atom (photo-ATRP) of methyl methacrylate (MMA), was evaluated in the molar ratio of 500/1/0.02 [MMA/EBPA/Fe³⁺] at 25°C for 24 hours. The initiator used was ethyl bromophenylacetate (EBPA). Furthermore, the complexes **1-3** showed a good control ability in the photoATRP, following a pseud-first order kinetic profile, as reported in the literature. It was also possible to observe the increasing of molecular mass with conversion and the Đ values indicated a slightly controlled polymerization. The complexes also showed a photo regulated polymerization.

1. Dadashi-Silab, S.; Matyjaszewski, K. Iron Catalysts in Atom Transfer Radical Polymerization. *Molecules*. 2020, apr 3; 25(7), 1648.

Acknowledgments

Proc. 2021/11873-1 and 2021/13128-1



Nickel Complexes as Potential Photocatalysts for Controlled Radical Photopolymerization (CRP2) of methyl acrylate

Naralyne Martins Pesqueira (PG),^{1*} Camila Bignardi (PG),¹ Valdemiro P. de Carvalho Jr (PQ),¹ Beatriz Eleutério Goi (PQ).¹

*naralyne.pesqueira@unesp.br; beatriz.goi@unesp.br

¹Departamento de Química e Bioquímica, FCT-UNESP, Presidente Prudente.

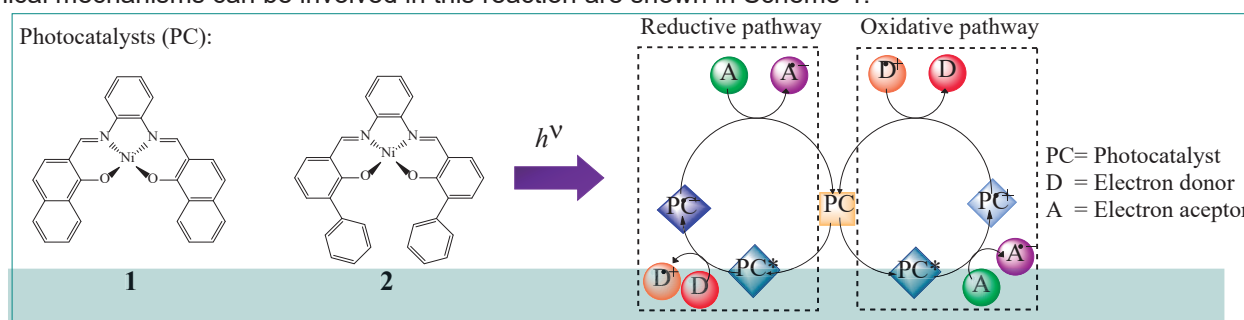
Keywords: Schiff bases, Ni(II) complexes, fluorescence experiments, LED irradiation, photopolymerization, CRP2.

Highlights

Ni(II) complexes with Schiff-base ligands were prepared and characterized by FTIR, UV-Vis, RMN and fluorescence spectroscopy. The polymerization of methyl acrylate was evaluated under LED irradiation.

Abstract

The science of photopolymerization has gained attention because excellent spatial and temporal quality is easily achieved with intrinsic advantages and superiorities compared with the conventional thermal polymerization method for the synthesis of polymers. Hence, a photocatalyst (PC) must have at least one photosensitive function (chromophore) to absorb the light (photons) and therefore to produce active species (radical, cations, etc.) able to initiate the photopolymerization reaction. Three properties of PCs are important for the efficiency of the photopolymerization: light absorption, redox potentials, and long lifetime of the excited states.¹ The tetradentate symmetric Schiff bases ligands were synthesized and characterized by FTIR, UV-Vis e ¹H and ¹³C RMN. The Ni(II) complexes were synthesized and characterized by FTIR, UV-Vis, ¹H and ¹³C RMN, Cyclic Voltammetry and Fluorescence spectroscopy. Thus, Ni(II) complexes were investigated as PCs. Their chemical structure and different chemical mechanisms can be involved in this reaction are shown in Scheme 1.



Scheme 1. General scheme of CRP2 and structures of Ni(II) complexes.

In addition, the spectrofluorometer was used to study the fluorescence properties of the nickel complexes. Moreover, solvent effect experiments were carried out to gain deeper insights onto the nature of the absorption processes and emitting excited state in toluene, THF, CH₂Cl₂ and DMF. These complexes have strong visible-light absorption at 350-400 nm, emission at 400 nm and excitation at 365 nm. They were combined with an alkyl bromide 2-bromoacetophenone (EBr) and an aromatic amine Ethyl 4-(dimethylamino)benzoate (EDB) under LED irradiation. The molar ratios were of 200/1/0.02/1 and 200/1/0.12/1, ([MA]/[EBr]/[Ni^{II}]/[EDB]). The conversion degree and the respective polymerization rate were investigated by FTIR spectroscopy in conjunction with Attenuated Total Reflection (ATR), monitoring the band of the olefin in the MA (methyl acrylate) monomer at 1635 cm⁻¹. Interestingly, the results of photopolymerization showed polymers with Mn ($\cong 110 \times 10^3$ g.mol⁻¹) and narrow Đ = 1.3 -1.6 using those molar ratios between complexes 1–2 and MA, respectively. The conversions were between 20-60% in total time of approximately 10 min and 3 hours for Complexes 1 and 2, respectively. Therefore, the Ni(II) complexes can initiate the photopolymerization (CRP2) of methyl acrylate as photocatalysts under irradiation at 365 nm, using a very low quantity of complex and additives.

- Lalève J, Telitel S, Xiao P, Lepeltier M, Dumur F, Morlet-Savary F, et al. Metal and metal-free photocatalysts: Mechanistic approach and application as photoinitiators of photopolymerization. *Beilstein Journal of Organic Chemistry*. 2014 Apr 15;10:863–76.

Acknowledgments



Proc. 2021/11741-8, 2021/11873-1 and 2021/13128-1



Photoinduced organometallic mediated radical polymerization of VAc mediated by Mn^{II} complexes of bearing tetradentate Schiff-base ligands

Beatriz E. Goi (PQ)^{1*}, Camila Bignardi (PG)¹, Naralyne M. Pesqueira (PG)¹, Valdemiro P. de Carvalho Jr. (PQ)¹.

beatriz.goi@unesp.br*

¹Departamento de Química e Bioquímica, FCT-UNESP, Presidente Prudente.

Keywords: photocontrolled-OMRP, manganese complexes (II), Schiff bases.

Highlights

Four Mn^{II} Schiff base complexes were synthesized and further characterized. The complexes **1-4** were applied as mediators in the photo-OMRP reactions in order to evaluate their mediating ability.

Abstract

The organometallic-mediated radical polymerization (OMRP) has been widely used as a powerful polymerization technique to synthesize structurally precise functional polymers, with controlled molecular weight and narrow dispersity (\mathcal{D}) under mild conditions (light stimuli is included). It is based in the activation/deactivation mechanism which may occur either by reversible termination (RT) or degenerative transfer (DT) mechanisms, depending on the experimental conditions.¹ In this work, four new Mn^{II} Schiff base complexes were synthesized and further characterized by Maldi-TOF, cyclic voltammetry, EPR measurements, FTIR and UV-Vis. The four Schiff bases were obtained by the condensation reaction of 3-tert-butyl-salicylaldehyde, 3-ethoxy salicylaldehyde and propanediamine. They were coordinated to the manganese chloride (MnCl₂), obtaining the complexes **1-4** ([Mn^{II}(Salen-*tert*-butyl)], [Mn^{II}(Salen-di-*tert*-butyl)], [Mn^{II}(Salen-ethoxy)] and [Mn^{II}(Salen-di-ethoxy)]). These complexes **1-4** were applied as mediators in Organometallic Mediated Radical Polymerization reactions (photo-OMRP) using vinyl acetate (VAc) as monomer and diphenyl(2,4,6-trimethylbenzoyl)phosphine oxide (TPO) as initiator and DMSO as solvent. The tests were carried out in a photoreactor with 390 and 400-800 nm LEDs at 25°C (Figure 1), varying the concentrations of monomer and initiator. The condition that presented the best results of conversion and polydispersity index for each complex was applied in a kinetic study in order to evaluate the controlling capability of the complexes **1-4**.

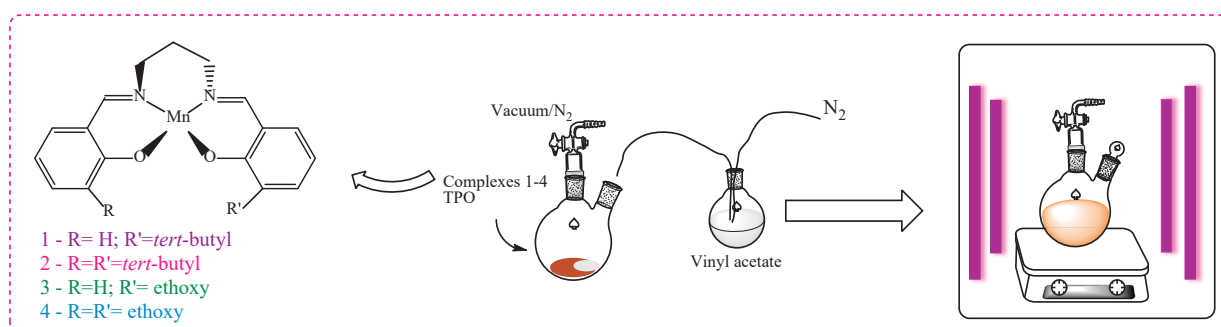


Figure 1. General procedure for photo-OMRP of VAc at 25°C.

1. L. F. Oliveira, C. Bignardi, N. M. Pesqueira, B. A. Riga-Rocha, A. E. H. Machado, V. P. Carvalho-Jr, B. E. Goi, Eur. Polym. J., 2021, 110757.

Acknowledgments

Quenching of horseradish peroxidase-generated triplet acetone by sorbate and ethyl sorbate

Thiago M. V. Gomes (PG),¹ Luiz D. Ramos (PG),² Cassius V. Stevani (PQ),² Etelvino J. H. Bechara (PQ)^{1,2*}

thiagodamata20@usp.br; ejhbechara@gmail.com

¹Departamento de Bioquímica, Instituto de Química, Universidade de São Paulo, Brazil; ²Departamento de Química Fundamental, Instituto de Química, Universidade de São Paulo, Brazil

Palavras Chave: Photochemistry in the dark, Triplet acetone, Sorbate, HRP, Chemiluminescence, Quenching.

Highlights

1. Triplet carbonyls are produced by dioxetane and peroxy radical intermediates of biological processes.
2. Quenching of carbonyl triplets by conjugated dienes like sorbates is diffusion-controlled.

Abstract

Triplet excited carbonyls can initiate typical photochemical reactions even in the absence of light. This "photochemistry in the dark" paradoxical hypothesis was chemically anchored by synthesis and studies of 1,2-dioxetanes and 1,2-dioxetanones, which thermolysis yield triplet carbonyls, that exhibit ultraweak chemiluminescence. Due to their long lifetime and alcoxyl radical-like reactivity, it may start and propagate deleterious reactions on biological systems.¹ In this work, the quenching properties, with the classical Stern-Volmer treatment, of sorbate (2,4-hexadienoate) and ethyl sorbate (ethyl 2,4-hexadienoate) against horseradish peroxidase (HRP)/isobutanal (IBAL)-generated triplet acetone (Fig. 1) was investigated. The kinetic quenching constants (k_q) for sorbate, $3.0 \times 10^9 \text{ M}^{-1}\text{s}^{-1}$, and ethyl sorbate, $8.6 \times 10^9 \text{ M}^{-1}\text{s}^{-1}$, were obtained, when triplet acetone lifetime is $1.2 \mu\text{s}$.² These values are in agreement with a collisional suppression process, in which k_q expected is close to the reported diffusional coefficient in water ($\sim 5 \times 10^9 \text{ M}^{-1}\text{s}^{-1}$).³ SDS-PAGE and CD show that enzymatic-generated triplet acetone may cause secondary and tertiary structural damages to the HRP. The use of sorbate and its alkyl ester during the reaction revealed the protection properties of the conjugated 1,2-dienes against IBAL-induced HRP structural damages.

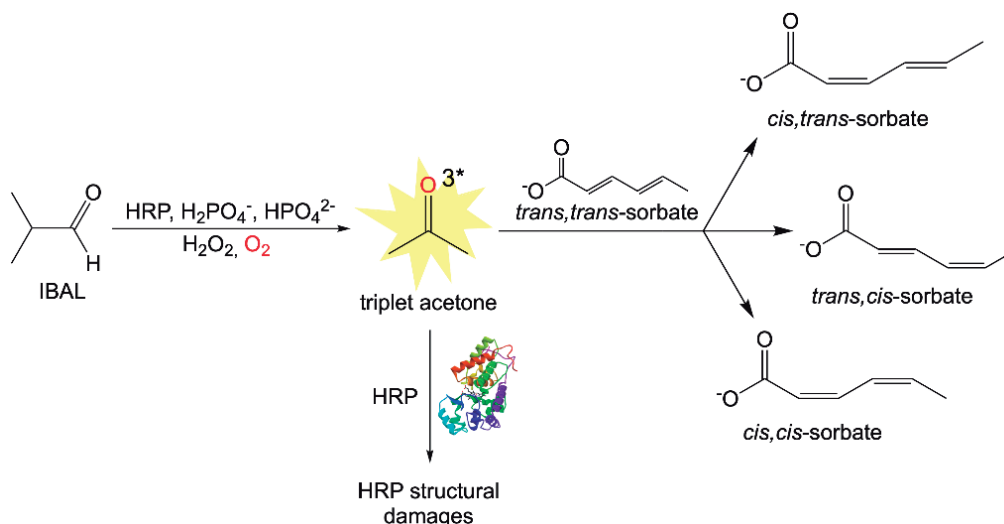


Fig. 1. Horseradish peroxidase (HRP)/isobutanal (IBAL)-generated triplet acetone mechanism, HRP structural damages and quenching of triplet acetone by sorbate, possibly generating *cis,trans* isomers.³

[1] BAADER, W. J. et al., Braz. Chem. Soc. 2015, 12, 2430-2447. [2] CATALANI, L. H. et al., Photochem. Photobiol. 1987, 45, 273-281. [3] VELOSA, A. C. et al., Chem. Res. Toxicol. 2007, 20 (8), 1162-1169.

Acknowledgments

The authors are grateful to FAPESP and CNPq for founding the research.

Structural and Spectroscopy Studies of the Organophosphate Pesticides Fenthion, Fenamiphos and Azamethiphos

Stefanny G. Costa (IC),^{1*} Thays de S. Lima (PQ),² Fernanda Bettanin (PQ)³, Lucia Codognoto (PQ),⁴ Hueder P. M. de Oliveira (PQ)¹.

hueder.paulo@ufabc.edu.br; stefanny.g@aluno.ufabc.edu.br

¹Universidade Federal do ABC, UFABC; ²Universidade de São Paulo, IQSC-USP; ³EACH-USP; ⁴Universidade Federal de São Paulo – Campus Diadema, UNIFESP.

Keywords: Organophosphate pesticides, DFT, Molecular orbitals, Electrochemistry

Highlights

- Study the properties of the organophosphate compounds using computational modeling;
- Chemistry computational being a source support of experimental results;

Resumo/Abstract

By the evolution of chemistry several new compounds are developed every day, it becomes even more necessary to study their impact on the environment. Thus, this study aims to support future work under the organophosphate pesticides Fenthion, Fenamiphos and Azamethiphos providing information about the molecules through the molecular modeling technique based on the density functional theory (DFT), in figure 1 is possible to see the molecular structure of these compounds. The pesticide structures were geometrically optimized starting from the three-parameter hybrid functional combined with a gradient-corrected functional correlation-B3LYP and the 6-31G(d) base set. The chemical-quantum calculations were performed using the Gaussian 09 software by ChelpG method for semi-empirical calculations. Therefore, using the output generated the charges and energies of the molecules were analyzed, the electrostatic potential surfaces and the molecular orbitals were modeled, the UV-VIS absorption spectra were simulated. With all these results obtained it is possible to infer some proprieties of these compounds and to make some comparison with electrochemical analyses. The generated data show a similarity between the results obtained through the Gaussian calculations and the electrochemical experimental. There by, from an electrochemical perspective it can be concluded that the compounds oxidation through the analysis of HOMO orbital energy determined computationally is favored starting from Fenamiphos (-0.2196 eV), Fenthion (-0.2257 eV) and Azamethiphos (-0.2455 eV). In addition, the theoretical result obtained is in line with the analysis of experimental Cyclic voltammetry data where the oxidation order is favored according to the order Fenamiphos (1.2 V), Fenthion (1.3 V) and Azamethiphos (1.7 V), thus indicates that the computational study corroborates the use of electrochemical techniques for pesticide oxidation.

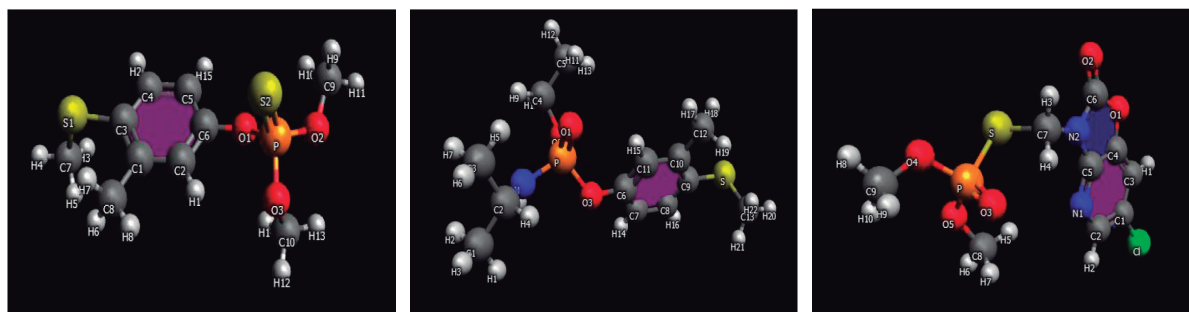


Figure 01- (left to right) Molecular Structure of Fenthion, Fenamiphos and Azamethiphos.

Agradecimentos/Acknowledgments

CNPq, CAPES, UFABC, UNIFESP

Área: FOTO

(Inserir a sigla da seção científica para qual o resumo será submetido. Ex: ORG, BEA, CAT)

Synthesis and characterization of Fe(II) complexes coordinated to ligands Schiff bases for application as photocatalysts in CRP2

Sergio M. M. Yamada (PG),^{1*} Beatriz E. Goi (PQ),¹ Valdemiro P. C. Júnior (PQ).¹

Sergio.yamada@unesp.br; beatriz.goi@unesp.br; valdemiro.carvalho@unesp.br.

¹Departamento de Química e Bioquímica, UNESP; ¹Departamento de Química e Bioquímica, UNESP; ¹Departamento de Química e Bioquímica, UNESP.

Palavras Chave: Fe(II) complexes, photopolymerization, Schiff bases.

Highlights

To investigate the reactivity of Fe(II) complexes coordinated to Schiff base ligands against CRP2-type reactions.

Ascertain the influence of the complexes on the final characteristics of the polymers.

Resumo/Abstract

This work presents the syntheses of new Fe(II) complexes coordinated to non-symmetrical Schiff base ligands for application in the CRP2 Controlled Radical Photopolymerization reaction. Initially, non-symmetrical Schiff base ligands were synthesized and characterized by FTIR, UV-Vis and ¹H NMR. Subsequently, the complexes were also synthesized and characterized by FTIR, UV-Vis and MALDI-TOF. In total, three ligands were synthesized, varying the amine in its structure, namely: ethylenediamine (ethoxy-salen), 1,2-diaminocyclohexane (ethoxy-saloex) and ortho-phenylenediamine (ethoxy-salophen). From these Schiff Bases, three complexes were synthesized, all of which showed to be active as photocatalysts in CRP2 using a system of Methyl Acrylate (MA) as monomer, α -ethyl-bromophenylacetate as initiator and TEA as donor of electrons. The results of photopolymerization showed high conversions, but little control over the characteristics of the polymeric chains when using smaller amounts of complex and low conversion and greater control over the characteristics of the chains when using larger amounts of complex. As shown in Table 1.

Table 1. Polymerization assays for the complex [Fe(II)(ethoxy-salophen)]

Ensaio	M/I/[Fe ^{II} (etoxy-salophen)]/TEA	Conv. (%)	M. Molar	\bar{M}_n
1	200:1:0,00:1	---	---	---
2	200:1:0,02:0	---	---	---
3	200:1:0,02:1	87	180000	2,8
4	200:1:0,05:1	76	125000	2,2
5	200:1:0,12:1	30	73000	2,0

Agradecimentos/Acknowledgments



Área: FOT

Synthesis, characterization and photophysical studies of a new azo dye and its application as an optical sensor of chemical microenvironments

Lucas H. Pereira (IC)^{1*} Willy G. Santos (PG)¹ and Sidney J. L. Ribeiro (PQ)¹

lh.pereira@unesp.br

¹ Instituto de Química, Departamento de Química analítica, Físico-química e Química inorgânica, Universidade Estadual Paulista (UNESP)

Palavras Chave: Azo dyes, Fluorescent probes, Pyrylium, Molecular sensors

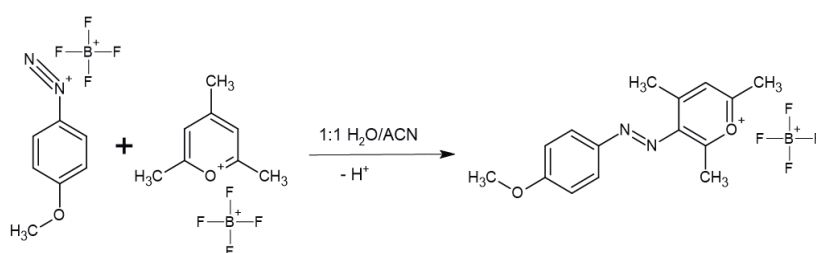
Highlights

A new synthetic route was proposed for a new azo-dye structure. Fluorescence intensity and the maximum absorption is modulated by the chemical nature of microenvironments such as micelle media.

Resumo/Abstract

The photophysical and photochemical properties of azo dyes have been extensively studied, presenting a vast number of studies in the literature. Applications foreseen include optical probes for sensing, since such properties have a clear dependence on the chemical microenvironment in which it is found. In this work, a new synthesis route was used for the formation of a new azo dye (Pyrylazo), containing trimethylpyrylium as part of the structure of the luminescent dye, as shown in Fig. 1. Pyrylazo was characterized by different spectroscopic techniques: (a) IR, UV-vis, ¹³C-NMR, ¹H-NMR. The photophysical properties were investigated in the presence of solvents of different polarities. A linear dependence of λ_{\max} with the polarity of the medium was verified. Studies in organized media (cell and micelle) demonstrated that the dye has a higher intensity of fluorescence, due to the restriction of thermal relaxation processes of the dye, such as rotation modes and vibrations of the molecule. Knowing this, the luminescent dye Pyrylazo has considerable potential in the investigation of sensing cellular structures and/or macromolecular media.

Figure 1: Synthesis of a new class of azo-dyes: **Pyrylazo**



Agradecimentos/Acknowledgments

This research is part of SISFóton program supported by MCTI. Willy G. Santos thanks CNPq/MCTI/Sisfóton for the personal financial research (382715/2022-5). Sidney J. L. Ribeiro also thanks FAPESP, CNPq and Capes for the financial support.



Synthesis of Salen-type Co(II) complexes to mediate *photo-OMRP*

Larissa F. de Oliveira (PG),¹ Valdemiro P. Carvalho Jr. (PQ),¹ Beatriz. E. Goi (PQ)¹

larissa.fazoni@unesp.br

¹Departamento de Química e Bioquímica, FCT-UNESP, Presidente Prudente.

Palavras Chave: *photo-CMRP*, Cobalt(II) complexes, Salen-type non-symmetrical ligands.

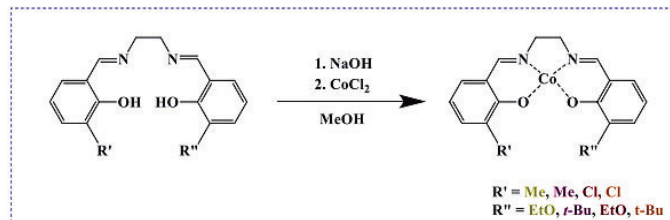
Highlights

Four Cobalt(II) complexes coordinated to Salen-type non-symmetrical ligands were synthesized as potential mediators in Cobalt-Mediated Radical Photopolymerization (*photo-CMRP*).

Abstract

The Cobalt-Mediated Radical Photopolymerization (*photo-CMRP*) technique allows the production of polymers with complex architecture and well-defined properties. This occurs due to the instantaneous concentrations of radicals generated in the polymeric medium, that are reduced by coordinating these radicals at the Cobalt(II) center. Therefore, four Cobalt(II) complexes coordinated to Salen-type non-symmetrical Schiff base ligands were synthesized to mediate *photo-CMRP* reactions. The proposal is to evaluate different combinations of coordinated ancillary ligands, verifying the electronic and steric effect in the metal center of Cobalt(II) and, consequently, in the *photo-CMRP* reaction. [1,2]

Figure 1. General scheme of the synthesis of Cobalt(II) complexes.



Both Cobalt(II) complexes and ligands were characterized by FTIR, UV-Vis and cyclic voltammetry. In the FTIR spectra obtained for the ligands, it can be observed the main characteristic stretching of the molecules, which includes the stretch $\nu(\text{C}=\text{N})$ in the $1629 - 1633 \text{ cm}^{-1}$ region. In the FTIR spectra obtained for Cobalt(II) complexes, a displacement of these stretch was noticed for greater energy, indicating the formation of the complexes. The formation of the complex can also be evidenced in the UV-Vis spectra, through the formation of transition bands of the MLCT type as well as a displacement in the $\pi-\pi^*$ transitions of the iminic group ($\text{C}=\text{N}$) of the complexes in relation to the respective ligands. In the cyclic voltammograms, oxidation and reduction of the redox pair Co(II)/Co(III) were observed.

[1] Silva, T. T.; Silva, Y. F.; Machado, A. E. H.; Maia, P. I. S.; Tasso, C. R. B.; Lima-Neto, B. S.; Sá, J. L. S.; Carvalho-Jr, V. P.; Batista, N. C.; Goi, B. E. *Journal of Macromolecular Science, Part A Pure and Applied Chemistry*. v. 56, n. 12, p. 1132–1140. 2019.

[2] Debuigne, A.; Jêrome, C.; Detrembleur, C. *Polymer*. 2017, 115, 285–307.

Acknowledgments



INO

Química Inorgânica

46^a Reunião
Anual da **SBQ**

28 a 31 de Maio de 2023

Águas de Lindóia · SP
Hotel Monte Real

A busca por propriedades sinérgicas de transição de spin e magnetos de uma molécula.

Luisa Fernanda Roldan Florez (IC), Giordano Poneti (PQ), Rafael A. Allão Cassaro (PQ)

Luisa1624@gmail.com;

Instituto de Química – Universidade Federal do Rio de Janeiro, UFRJ;

Química de Coordenação, Magnetismo Molecular, transição de spin, magnetos de uma molécula.

Highlights

Looking for synergy between spin crossover (SCO) and Single Molecule Magnets (SMM). We synthesized and characterized cationic complex with potential to exhibit SCO and anionic SMM.

Resumo/Abstract

Um composto pode atuar como um Interruptor Molecular (IM) quando este pode ter a interconversão reversível da sua distribuição eletrônica a partir de estímulos externos como temperatura, alteração de pressão ou incidência de luz. Em complexos de metais da primeira série de transição com configurações d^4 - d^7 , a transição entre o estado de alto spin e de baixo spin é conhecida como transição de spin - spin crossover (SCO).¹ Complexos com essas características são considerados IMs e possuem potencial aplicação na construção de dispositivos eletrônicos e sensores. Complexos catiônicos do tipo $[\text{Co}(\text{pyterpy})_2]^{2+}$ são conhecidos por apresentar o comportamento de SCO.² Outro comportamento magnético em compostos de coordenação de bastante interesse é conhecido como magneto de uma molécula (Single Molecule Magnet – SMM). Estes complexos possuem alta anisotropia magnética, normalmente observada em complexos de Dy^{3+} , Tb^{3+} ou Co^{2+} . Os SMMs apresentam relaxação lenta da magnetização e podem exibir ciclos de histerese (efeito de memória magnética). Eles são considerados como um ponto final da miniaturização dos dispositivos de armazenamento de alta densidade de informação. Compostos que exibem a coexistência ou sinergia dos fenômenos SCO e SMM são escassos na literatura.³ Neste trabalho será reportado a síntese de complexos catiônicos e aniônicos que podem apresentar, respectivamente comportamento de SCO ou SMM. O complexo catiônico foi sintetizado pela reação entre o ligante pyterpy (4'-(piridin-4-il)-2,2':6',2''-terpiridina) e sulfato de cobalto(II) hidratado na proporção 2:1. O novo complexo obtido teve a sua estrutura resolvida por meio da difração de raios por monocristal e caracteriza-se por um complexo mononuclear de cobalto(II) coordenado de forma tridentada por duas moléculas de pyterpy de forma meridional. Medidas de magnetometria estão em andamento para verificar a existência de transição de spin. Foram também sintetizados os complexos aniônicos $\text{Na}[\text{Co}(\text{acac})_3]$ e $\text{N}(\text{Et})_4[\text{Co}(\text{hfac})_3]$, onde acac é o pentano-2,4-diona, hfac é o 1,1,1,5,5,5-hexafluoropentano-2,4-diona e $\text{N}(\text{Et})_4$ é o cátion tetraetilamônio, sendo que o último complexo apresenta comportamento de SMM.⁴ Os complexos aniônicos foram caracterizados por espectroscopia de absorção na região do infravermelho (IV) e difração de raios X em policristal. Esforços para sintetizar complexos que podem apresentar coexistência ou sinergia dos fenômenos de SCO e SMM estão em andamento por meio de reações de metátese entre o complexo catiônico, que podem exibir comportamento de SCO e os aniônicos que podem apresentar comportamento de SMM.

1- J. A. Real, A. B. Gaspar, M. Carmen Muñoz, *Dalton Trans.* **2005**, 2062-2063

2- S. Hayami, Y. Komatsu, T. Shimizu, H. Kamihata, Y Hoon Lee, *Coord. Chem. Rev.* **2011**, 255, 1981.

3- I. A. Gass, S. Tewary, A. Nafady, N. F. Chilton, C. J. Gartshore, M. Asadi, D. W. Lupton, B. Moubaraki, A. M. Bond, J. F. Boas, S-X Guo, G. Rajaraman, K. S. Murray, *Inorg. Chem.* **2013**, 52, 7557.

4- A. V. Pali, D. V. Korchagin, E. A. Yureva, A. V. Akimov, E. Y. Misochko, G. V. Shilov, A. D. Talantsev, R. B. Morgunov, S. M. Aldoshin, B. S. Tsukerblat, *Inorg. Chem.* **2016**, 55, 19, 9696

Agradecimentos/Acknowledgments

Aos laboratórios de difração de raios X do IQ-UFRJ, LDRX-UFF e CENABIO. Ao CNPq pela bolsa de iniciação científica e a FAPERJ pelo apoio financeiro.

A case of abnormally high intensity parameters in Eu(III)-indandionate complexes

Israel F. Costa (PQ),^{1*} Lucca Blois (PG),¹ Vitor H. Paschoal (PQ),¹ Albano N. Carneiro Neto (PQ),³ Renaldo T. Moura Jr. (PQ),⁴ Victor M. Deflon (PQ),⁵ Luís D. Carlos (PQ),³ Wagner M. Faustino (PQ),² Maria Claudia F. C. Felinto (PQ),⁶ Ricardo L. Longo (PQ),⁷ Romulo A. Ando (PQ),¹ Ercules E.S. Teotonio (PQ),² Hermi F. Brito (PQ),¹ Oscar L. Malta (PQ).⁷

*israelc@iq.usp.br;

¹Department of Fundamental Chemistry, Institute of Chemistry, University of Sao Paulo (USP), São Paulo–SP, Brazil; ²Department of Chemistry, Federal University of Paraíba, João Pessoa–PB, Brazil; ³Physics Department and CICECO, University of Aveiro, Aveiro, Portugal; ⁴Department of Chemistry and Physics, Federal University of Paraíba, Areia–PB, Brazil; ⁵São Carlos Institute of Chemistry- University of Sao Paulo (USP), São Carlos–SP, Brazil; ⁶Nuclear and Energy Research Institute–IPEN/CNEN, São Paulo–SP, Brazil; ⁷Department of Fundamental Chemistry, Federal University of Pernambuco, Recife–PE, Brazil

Keywords: trivalent europium, indandionate, luminescence, Judd-Ofelt parameters, molecular thermometers

Highlights

The highest value of Judd–Ofelt intensity parameter (Ω_2) for the europium (III) compound reported in the literature. The Eu(III)-indandionate complexes exhibit high PLQYs (Q_{Eu}^L) in solid state.

Resumo/Abstract

Luminescent coordination compounds based on trivalent europium ions (Eu^{3+}) materials have attracted much attention in the last decades due to their potential applications, such as optoelectronics, molecular thermometers, and biomedical devices. The most important features of these materials may be associated with narrow emission bands, which arise from intra-configurational Laporte forbidden $4f - 4f$ transitions (${}^5\text{D}_0 \rightarrow {}^7\text{F}_J$). On the other hand, the energy structures of the organic ligands in the complexes play the most important role in the Eu^{3+} luminescence sensitization process¹. In this context, this work reports about theoretical, syntheses, structural (Figure 1a), vibrational (FTIR/Raman) and photoluminescence studies of a series of tetrakis complexes containing tetraethylammonium, $\text{Et}_4\text{N}^+[\text{Ln}(\text{acind})_4]^-$ (Et_4N^+ : tetraethylammonium cation, Ln: Gd and Eu, and acind: 2-acyl-1,3-indandionate). The experimental intensity parameter (Ω_λ), lifetime (τ), radiative (A_{rad}) and non-radiative (A_{nrad}) coefficients, intrinsic quantum yield (Q_{Eu}^{Eu}) and experimental absolute luminescence quantum yield values (Q_{Eu}^L) were calculated (Table 1). Furthermore, the intrinsic quantum yield (Q_{Eu}^{Eu}) are in excellent agreement with the experimental absolute luminescence quantum yield values (PLQYs). Studies of luminescent properties have shown that tetrakis Eu^{3+} complexes with acind ligands presents high intensity emission (Figure 1b). These results suggesting that these complexes constitute a new class of coordination compounds with great potential for application as red emitting layer in OLEDs.

Table 1. Experimental intensity parameters (Ω_λ in 10^{-20} cm^2), lifetime (τ/ms), radiative (A_{rad} in s^{-1}) and non-radiative (A_{nrad} in s^{-1}) coefficients, intrinsic quantum yield (Q_{Eu}^{Eu}), and experimental absolute luminescence quantum yield ($Q_{Eu}^L/\%$) for the $\text{Et}_4\text{N}^+[\text{Eu}(\text{acind})_4]^-$ complex at 300 K.

Complexes	Ω_2	Ω_4	τ	A_{rad}	A_{nrad}	Q_{Eu}^{Eu}	Q_{Eu}^L
$\text{Et}_4\text{N}^+[\text{Eu}(\text{isovind})_4]^-$	73.5	8.9	0.337	2468	562.3	81.4	80
$\text{Et}_4\text{N}^+[\text{Eu}(\text{bind})_4]^-$	59.1	13.0	0.299	2109	1235	63	61
$\text{Et}_4\text{N}^+[\text{Eu}(\text{mbind})_4]^-$	46.3	11.5	0.201	1673	2286	42.3	40
$\text{Et}_4\text{N}^+[\text{Eu}(\text{Brbind})_4]^-$	49.0	12.7	0.306	1782	1487	54.5	54
$\text{Et}_4\text{N}^+[\text{Eu}(\text{nind})_4]^-$	29.1	9.5	0.513	1131	817.5	58.0	60

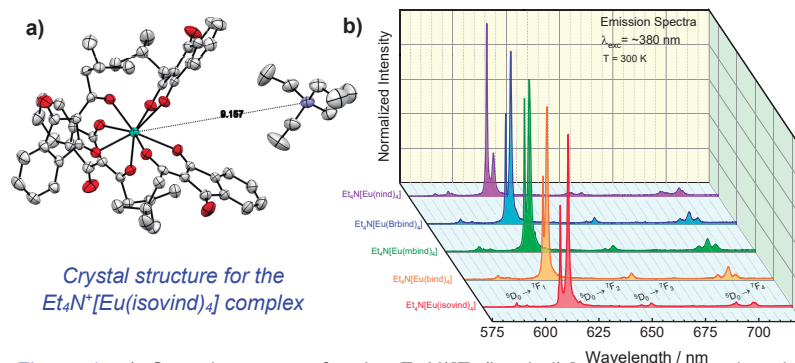


Figure 1. a) Crystal structure for the $\text{Et}_4\text{N}^+[\text{Eu}(\text{isovind})_4]^-$ complex showing the intermolecular interactions between Et_4N^+ cation and indandione groups in the structure of the $\text{N}(\text{Et})_4[\text{Eu}(\text{acind})_4]^-$ compound. b) Emission spectra of $\text{Et}_4\text{N}^+[\text{Eu}(\text{acid})_4]^-$ complex from 300 K.

Reference

¹ A.N. Carneiro Neto. *et al.*, in: J.-C.G. Bünzli, V.K. Pecharsky (Eds.), *Handb. Phys. Chem. Rare Earths*, Vol. 56, Elsevier, **2019**: pp. 55–162.

Agradecimentos/Acknowledgments

This work was supported by FAPESP, CNPq and CAPES.

Acetamide ligand for application as ionic sensor

Iane Alves (IC),¹ Izilda A. Bagatin (PQ),¹

iane.alves@unifesp.br

¹Instituto De Ciências Ambientais, Químicas e Farmacêuticas – ICAQF – UNIFESP – Diadema - SP
Laboratório de Química de Calixarenos, Espectroscopia Molecular e Catálise LQCEMC

Palavras Chave: (ionic sensor, thiazole, pyridine).

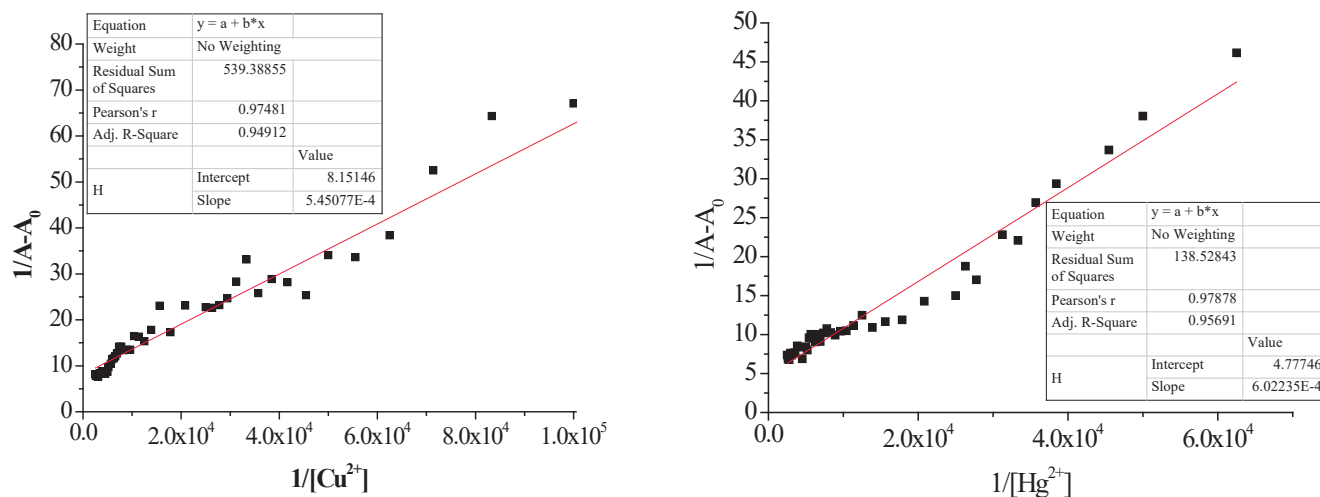
Highlights

Development of ionic sensor,

Toxic metals in the environment

Resumo/Abstract

The development of ionic sensors has attracted attention due to their range of applications. It is largely motivated by the increase in diseases and environmental contamination caused by toxic ions, whose altered concentrations induce different harmful responses to human health and the environment. However, the detection techniques normally used to determine these species are complex and expensive [1][2][3]. For this reason, the synthesis of a new molecule, 3-((2-oxo-2-(thiazol-2-ylamino)ethyl)amino)pyridin-1-ium bromide, was carried out so that it would present selectivity and sensitivity properties. This molecule was characterized by: 1) ¹H-NMR: (D₂O, 300 MHz), 8.07 ppm (m, H_{ar}), 8.01 ppm (m, H_{ar}), 7.76 ppm (m, H_{ar}), 7.72 ppm (m, H_{ar}), 7.46 ppm (d, H_{ar}), 7.19 ppm (d, H_{ar}) and 5.50 ppm (s, 2H, CH₂); 2) FTIR (KBr, cm⁻¹): 1693 (νC=O), 2926 (ν_{ass}CH₂), 2861 (ν_sCH₂), 1585 (νC=C), and 3350 (νNH), 3) Elemental analysis 38,07 (C%), 3,47 (H%), 17,79 (N%) and 10,31 (S%). The selectivity studies depicted interactions with Hg²⁺ (K_{ass} = 7.93.10³, R² = 0,95) and Cu²⁺ (K_{ass} = 1.5.10⁴, R² = 0,95) with stoichiometry of 1:1 through the Job Plot method.

Figure 1: Binding constants for Cu²⁺ and Hg²⁺ by Benesi-Hildebrand method.

References: [1] Aruna, A., Rani, B., Swami, S., Agarwala, A., Behera, D., & Shrivastava, R. (2019). Recent progress in development of 2,3-diaminomaleonitrile (DAMN) based chemosensors for sensing of ionic and reactive oxygen species. *RSC Advances*, 9(52), 30599–30614. doi:10.1039/c9ra05298d, [2] Hafiz Muhammad Junaid, Madeeha Batool, Farah Wahida Harun, Muhammad Saleem Akhter & Nabila Shabbir (2022) Naked Eye Chemosensing of Anions by Schiff Bases, *Critical Reviews in Analytical Chemistry*, 52:3, 463-480, doi: 10.1080/10408347.2020.1806703, [3] Liu, W., Wang, Y., Bai, Z., Li, Y., Wang, Y., Chen, L., ... Wang, S. (2017). Hydrolytically Stable Luminescent Cationic Metal Organic Framework for Highly Sensitive and Selective Sensing of Chromate Anions in Natural Water Systems. *ACS Applied Materials & Interfaces*, 9(19), 16448–16457. doi:10.1021/acsami.7b03914 .

Agradecimentos/Acknowledgments

CNPq

A Mononuclear Nickel(II) Catalyst in a Model Oxidative Process

Henrique C. L. Soares*¹ (IC), Marília R. Mello¹ (PG), Roberto B. Faria¹ (PQ), Marciela Scarpellini¹ (PQ)*

marciela@iq.ufrj.br*; henriquecastro@ufrj.br*

¹Departamento de Química Inorgânica, Instituto de Química, UFRJ.

Palavras Chave: Nickel complexes, Catalysis, Oxidative process, Bioinorganic Chemistry.

Highlights

Investigation of a mononuclear nickel(II) complex as catalyst in oxidation of 3,5-DTBC. Catalytic parameters V_{MAX} and K_M are $2.421 \times 10^{-8} \text{ mol L}^{-1} \text{ s}^{-1}$ and 17.61 mol L^{-1} , respectively.

Abstract

Oxidative processes are widely spread in many biological systems and play an important role in the survival of the living beings. These types of reactions often need the presence of enzymes to catalyze typical process. Nickel is one of the most common metals found in the active site of metalloenzymes. Usually, it participates in electron transfer reactions. The bioinorganic chemists search for biomimetic complexes that can catalyze a wide variety of oxidative processes.¹ The use of polynitrogenated ligands allows the complex display labile sites in *cis* position, suitable to the substrate coordination.² The model substrate typically used to investigate the oxidation ability of new metal complexes is the 3,5-di-*tert*-butylcatechol (3,5-DTBC). The *tert*-butyl groups assist the electron transfer reaction, while they prevent other side oxidative processes. The product of the 3,5-DTBC oxidation is the 3,5-di-*tert*-butyl-*o*-quinone (3,5-DTBQ), which can be spectroscopically monitored at 400 nm.³ Therefore, the main goal of this work is evaluate the promiscuity of the nickel(II) complex, [Ni(bis(1-methylimidazol-2-yl)methyl)(2-(pyridil-2-yl)ethyl)amine](H₂O)Cl]ClO₄, as a catalyst in the oxidation of 3,5-DTBC, since it was previously investigated as an electrochemical catalyst for the pH dependence in the H₂ and O₂ generation in water. The complex was synthesized and characterized as previously described.² The complex reactivity was observed by reaction with 3,5-DTBC in methanol saturated O₂. Initially, the electronic spectra were recorded sweeping wavelengths between 300 and 1100 nm, every 30 s, in a methanolic solution ([Complex] = $1 \times 10^{-5} \text{ mol L}^{-1}$ and [3,5-DTBC] = $1 \times 10^{-3} \text{ mol L}^{-1}$) for 30 min. The formation of a band in 400 nm, was observed. After that, the reaction was carried in the same conditions, however, different buffer solutions were used to monitor how the product formation rate varies with the pH. The reaction was followed at 400 nm, and the pH of the solutions were in the range 7.0 – 11.5. Thereby, it was observed that the complex has a higher activity in basic pH. Lastly, the reaction was set in pH 9.0, varying the substrate concentration ($0.5 \times 10^{-1} - 5.0 \times 10^{-1} \text{ mol L}^{-1}$) and keeping complex concentration in $1 \times 10^{-3} \text{ mol L}^{-1}$. Using the initial rates, the Michaelis-Menten curve and the Lineweaver-Burk plot, the V_{MAX} and the K_M value obtained were $2.421 \times 10^{-8} \text{ mol L}^{-1} \text{ s}^{-1}$ and 17.61 mol L^{-1} , respectively. At the moment, it is possible to conclude that this complex presents the promiscuity ability to catalyze different substrates with environmental interest.

Acknowledgments

CNPq, CAPES, FAPERJ, PIBIC-UFRJ

1 TREVIÑO, R. E.; SHAFAT, H. S. Protein-based models offer mechanistic insight into complex nickel metalloenzymes. *Current Opinion in Chemical Biology*, 2022, v. 67, p. 102110.

2 PADILHA, D. S.; BORTOLUZZI, A. J.; SCARPELLINI, M. An unusual partial occupancy of labile chloride and aqua ligands in cocrystallized isomers of a nickel(II) complex bearing a tripodal N₄-donor ligand. *Acta Crystallographica Section C*, 2022, v. 76, n. 1, p. 17-22.

3 POSADA, N. B. M. *et al.* Influence of the secondary coordination sphere on the physical properties of mononuclear copper(II) complexes and their catalytic activity on the oxidation of 3,5-di-*tert*-butylcatechol. *Polyhedron*, 2018, v. 141, p. 30–36.

Antioxidant Effects of Complexes Containing Modified Phenanthroline

Victoria Cristina Oliveira (PG)¹, Izilda A. Bagatin (PQ)¹

oliveira,cristina@unifesp.br

¹Instituto De Ciências Ambientais, Químicas E Farmacêuticas – ICAQF – UNIFESP – Diadema - SP
Laboratório de Química de Calixarenos, Espectroscopia Molecular e Catálise LQCEMC

Palavras Chave: 1,10-Phenanthroline-5,6-Dione; Ruthenium; Palladium; Zinc; Cyclic Voltammetry.

Highlights

Oxide-reduction potentials of metal complexes, antioxidant, and antineoplastic activities studies transition complexes, characterization of the complexes by spectroscopic techniques

Resumo/Abstract

Transition complexes have been used as chemotherapeutic agents and antioxidants since 1860 when the FDA approved Rosenberg's study on cisplatin to combat testicle, breast, ovary, head, and neck tumor cells. Since then, interests have arisen in producing antineoplastic and antioxidant agents based on metallic ions that could interact with the cells, reducing their nephrotoxicity and hepatotoxicity. In general, metal complexes have a positively charged metal center that binds to negatively charged biomolecules, targeting proteins and nucleic acids and increasing their interaction with DNA, which may occur by the nitrogenous bases or the phosphate group through intercalation. As intercalating agents, we can cite the modified phenanthrolines, which will be the focus of our work linking them to metallic ions such as Ru²⁺, Zn²⁺, and Pd²⁺, to evaluate their antioxidant potential, besides the evaluation as antineoplastic agents *in Vitro* and *in Vivo* studies.^[1,2,3] After synthesizing the ligand and complexes, the characterization was made using spectroscopic techniques such as ¹H NMR and FTIR. FTIR signals of 1,10-Phenanthroline-5,6-Dione depicted vibrational frequencies as C=N and C=C in 1580 cm⁻¹ and 1555 cm⁻¹, that shifted to 1575 cm⁻¹ and 1565 cm⁻¹ in [RuNOCl(1,10-Phenanthroline-5,6-Dione)₂]²⁺, to 1589 cm⁻¹ and 1565 cm⁻¹ in [Zn(CF₃SO₃)₂(1,10-Phenanthroline-5,6-Dione)] and 1575 cm⁻¹ and 1565 cm⁻¹ in [PdCl₂(1,10-Phenanthroline-5,6-Dione)] complexes, respectively. ¹H NMR in DMSO_{d6} showed us displacement of the (1,10-Phenanthroline-5,6-Dione) ligand bands at 7.6 ppm (c-H, dd, ³J = 8.0 Hz), 8.6 ppm (b-H, dd, ³J = 7.5 Hz) and 9.2 ppm (a-H, dd, ³J = 4.2 Hz a-H) to 9.63 ppm (a-H, dd, ³J = 4.5 Hz); 8.81 ppm (b-H, dd, ³J = 7.7 Hz); 8.12 ppm (c-H, dd, ³J = 8.0 Hz) for [RuNOCl(1,10-Phenanthroline-5,6-Dione)₂]²⁺ complex; to 8.53 ppm (a-H, dd, ³J = 4.5 Hz a-H); 7.8 ppm (*), for complex [Zn(CF₃SO₃)₂(1,10-Phenanthroline-5,6-Dione)] and to 9.23 ppm (a-H, dd, ³J = 4.8 Hz); 8.77 ppm (b-H, dd, ³J = 7.7 Hz); 8.03 ppm (c-H, dd, ³J = 8.0 Hz) for [PdCl₂(1,10-Phenanthroline-5,6-Dione)] complex.

References:

- [1] M. J. Hannon, *Pure appl Chem*, pp. 2243-2261, 2007.
- [2] D. V. A. Luís, Lisboa: Universidade Nova de Lisboa, 2011.
- [3] R. Franklin e L. Costello, pp. 211-217, 2007.

Agradecimentos/Acknowledgments

O presente trabalho foi realizado com apoio da Coordenação de Aperfeiçoamento de Pessoal de Nível Superior – Brasil (CAPES) – Código de Financiamento 001

Antiproliferative effects and topoisomerase II inhibitory activity of a novel silver compound containing thiosemicarbazone

Ana B. Lazzarini (PG),¹ Andresa A. de Lima (PG),¹ Angelica E. Graminha (PQ),¹ José Clayston Melo Pereira (PQ),¹ Mauro A. Lima (PG),² Fillipe V. Rocha (PQ),² Adelino V. G. Netto (PQ),¹

ana.lazzarini@unesp.br (ABL)

¹São Paulo State University (UNESP), Institute of Chemistry, Department of Analytical, Physical Chemistry, and Inorganic Chemistry, Araraquara, SP, Brazil; ²Federal University of São Carlos (UFSCar), Department of Chemistry, São Carlos, SP, Brazil.

Keywords: Cancer, Metal complex, Silver(I), Thiosemicarbazone, Topoisomerase, Biological evaluation

Highlights

A new silver(I)-based complex was active against a cisplatin-resistant cell line (A2780cis) and induced the inhibition of topoisomerase II α activity.

Abstract

The platinum(II)-based chemotherapeutics used in cancer treatment are limited by cell resistance and side effects¹. Owing to silver(I) multi-target mode of action and low cytotoxicity in healthy cells, this metal centre has been receiving great attention². Aiming at better understanding the structure-activity relationship in Ag(I) compounds containing both 1,10-phenanthroline (phen) and thiosemicarbazone (TSC) moieties, in this work we report a new metal complex (**C1**) with formula [Ag(cTSC)(phen)]NO₃.H₂O {cTSC = trans-cinnamaldehyde-*N*(4)-ethyl-thiosemicarbazone}. **C1** was synthesized according to Silva *et al.*³ with some modifications. The new compound was characterized by spectroscopic (¹H NMR, IR) and spectrometric techniques (ESI-MS), molar conductivity, and elemental analysis. The cell viability studies were performed by MTT assay towards A2780cis (cisplatin-resistant ovarian cancer) and MRC-5 (lung fibroblast) cell lines. **C1** exhibited IC₅₀ values of 3.76 ± 0.25 μM (A2780cis) and 5.18 ± 0,1 μM (MRC-5) whereas cisplatin displayed cytotoxic indexes of 16.76 ± 0.57 μM and 21.62 ± 0,80 μM, respectively. Clonogenic assays with ovarian cancer cells (A2780cis) demonstrated cytotoxic and cytostatic activity of **C1** at 1.1 μM in comparison

to control. However, at a concentration of 4.4 μM, **C1** induced changes in the cell morphology within 48h, which may indicate apoptosis. With the purpose of studying which are the possible biological targets, it was evaluated the ability of **C1** to induce the topoisomerase II α activity (TOP2A). The Ag(I)-based complex inhibited the activity of TOP2A at a concentration > 10 μM.

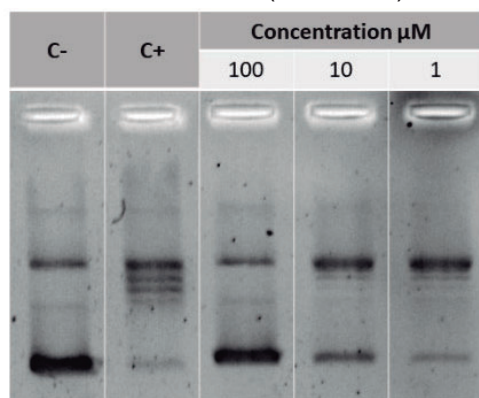


Figure 1. Agarose gel electrophoresis of DNA in the presence of TOP2A and increasing amounts of **C1** (1, 10 and 100 μM); C- = Supercoiled DNA, C+ = DNA and TOP2A

¹ OUN, R.; MOUSSA, Y. E.; WHEATE, N. J. Dalton Trans. **2018**, v. 47, n. 19, p. 6645-6653.

² MEDICI, S. *et al.* Coord. Chem. Rev. **2016**, v. 327-328, p. 349-359.

³ SILVA, D. E. S. *et al.* Dalton Trans. **2020**, v. 49, n. 16, p. 5264-5275.

Acknowledgments

Financial support of CNPq (132024/2020-9; 422105/2016-3), FAPESP (2022/14041-0; 2016/17711-5; 2019/11242-1; 2022/02876-0; 19/17762-7), and CAPES (Finance Code 001) are acknowledged.

Antitumor trials revealed a palladium-based complex for regression of MCF-7 breast tumour cell growth in BALB/c nude mice

Renan L. Farias (PQ),^{1*} Cauê B. Scarim (PQ),² Mauro A. Lima (PG),³ Fillipe V. Rocha (PQ),³ Javier Ellena (PQ),⁴ Nailton M. Nascimento-Júnior (PQ),⁵ Saulo S. Garrido (PQ),⁵ Adriano B. Oliveira (PQ),⁶ Adelino V.G. Netto (PQ)⁷

renan.farias@puc-rio.br

¹Departamento de Química, PUC-Rio; ²Departamento de Fármacos e Medicamentos, FCFAR-UNESP; ³Departamento de Química, UFSCar; ⁴Instituto de Física de São Carlos, USP; ⁵Departamento de Bioquímica e Química Orgânica, IQAR-UNESP; ⁶Departamento de Química, UFS; ⁷Departamento de Química Analítica, Físico-Química e Inorgânica, IQAR-UNESP

Keywords: Metallo drug, Palladium-complexes, Topoisomerase IIa, Preclinical screening, In vivo evaluation

Highlights

Design and synthesis of potential antitumor Pd-complexes.
In silico and *in vitro* studies endorse TOP2A inhibitory activity.
In vivo assays reveal the anti-MCF-7 breast cancer cell proliferation.

Abstract

In this work, four Pd(II)-complexes were obtained with general formulae [PdCl₂(L)PPh₃]Cl (**1-4**), where PPh₃= triphenylphosphine and L= *trans*-cinnamaldehyde-*N4*-R-thiosemicarbazone; R= H (**1**), Methyl (**2**), Ethyl (**3**), and Phenyl (**4**). As follows, **1-4** were characterized by IR, NMR, microanalysis, and molar conductivity. Complexes **2** and **3** formed suitable single crystals for X-ray diffraction. Both crystalized in a monoclinic crystal system, *P2₁/n* for **2** and *P2₁/c* for **3**. The asymmetric unit comprises a Pd(II)-ion 4-fold coordinated by a κ^2N,S -donor ligand. One chloride and PPh₃ complete the slightly distorted square-planar environment, **Fig. 1**. The compounds were screened against the human breast MCF-7 tumour cell line and non-tumour lung fibroblasts MRC5. Compounds **3** and **L3** exhibited promising IC₅₀ values against MCF-7 (4.42 – 6.48 μ M) and demonstrated to be more cytotoxic than cisplatin. However, at concentrations close to the IC₅₀, only **3** showed non-toxic profile in the RBC assay (haemolysis < 9 %). Based on biomolecular fluorescence trials, **3** promotes a quenching in the HSA emission band (λ_{max} = 333 nm) by dynamics mechanism.¹ Also, the low K_b value of 6.63×10³ M⁻¹ from the spectrophotometric titration and the competition assay with Hoechst 33258 suggested a weak affinity of **3** for the ctDNA structure.² The anti-MCF-7 cell growth activity of **3** was investigated *via* xenograft implantation of MCF-7 cells in BALB/c nude mice. These specimens were separated into three groups (*n* = 5): placebo (**POS**), treatment (**RL-3**) and cisplatin (**CIS**) groups. A single dose (i.p) of cisplatin and **3** (5 mg kg⁻¹ day⁻¹) induced a similar tumour weight regression from the 2nd to 16th day of treatment, **RL3** = 46.77 % and **CIS** = 54,63 %, **Fig. 2**. Finally, molecular docking predicted **3** and **4** as TOP2A allosteric modulators,³ which is validated via partial inhibition of kDNA decatenation, mediated by the TOP2A, in agarose gel electrophoresis assay.

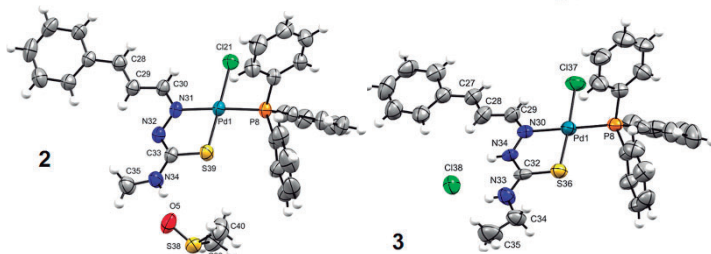


Fig. 1 ORTEP for **2** and **3**, showing the atom labelling and displacement ellipsoids drawn at 50 % probability level.

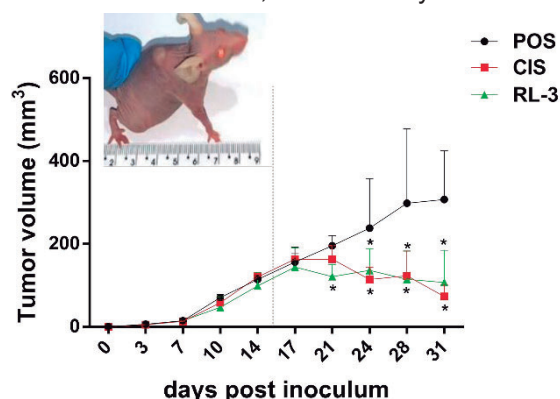


Fig. 2 Effect of **3** and cisplatin on MCF-7 cell growth in BALB/c nude mice. **Note:** This *in vivo* study is approved by CEUA/FCF/Car 02/2019.

¹Reis, F.C.C. *et al.*, *Inorg. Chem. Comm.* 63, (2016), 96-100.

²Kellet, A. *et al.*, *Chem. Soc. Rev.* 48, (2019), 971-988.

³Rocha, F.V. *et al.*, *J. Inorg. Biochem.* 199, (2019), 110725.

Acknowledgements

The authors are grateful for the regular financial support provided by FAPERJ, FAPESP, CNPq, and CAPES foundations.

Área: INO

Antiviral activity of Co(II) and Ni(II) trinuclear complexes with an oxamate-type ligand derived from bis-thiazol

Mariany dos Santos Silva (PG),¹ Natasha M. Cassani (PG),² Uriel Enrique A. Ruiz (PG),² Shiraz F. Leite (PG),² Lucas H. G. Kalinke (PQ),³ Douglas H. Nakhata (PQ),¹ Ana Carolina G. Jardim (PQ),² e Danielle Cangussu (PQ).^{1*}

santos234@discente.ufg.br, danielle_cangussu@ufg.br

¹Instituto de Química, Universidade Federal de Goiás, UFG; ²Instituto de Ciências Biomédicas – ICBIM, Universidade Federal de Uberlândia – UFU; ³Instituto Federal Goiás - Câmpus Anápolis.

Palavras Chave: ZIKV, CHIKV, Inibição, Viabilidade celular, Estabilidade.

Highlights

Co(II) and Ni(II) oxamate complexes as inhibitors of Zika and Chikungunya virus replication; UV–visible spectral study on the stability of Co(II) and Ni(II) oxamate complexes.

Resumo

O estudo sobre a contribuição dos íons metálicos para a manutenção da homeostase em organismos vivos é um importante tópico investigado pela ciência em diferentes áreas. A química de coordenação é uma das áreas que tem contribuído de forma significativa nos estudos dos complexos metálicos com aplicações medicinais.^{1,2} Nessa perspectiva, o presente trabalho teve por objetivo preparar complexos contendo um ligante do tipo oxamato³, avaliar a estabilidade em soluções tampão de pH fisiológico e estudar atividades biológicas. Foram sintetizados os compostos $K_6Co_3(dabtoz)_3 \cdot 8H_2O \cdot MeOH^3$ ($K_6Co_3L_3$) e $Na_6Ni_3(dabtoz)_3 \cdot 10H_2O$ ($Na_6Ni_3L_3$) [onde dabtoz (L) = *N,N'*-(4,4'-bitiazol-2,2'-diil)-bis(oxamato)] sob a forma de monocristais obtidos por difusão lenta em metanol e caracterizados por espectroscopia no infravermelho e difração de raios X de monocristal. A atividade antiviral foi investigada em linhagens celulares infectadas pelos vírus Chikungunya (CHIKV) e Zika (ZIKV), na presença ou ausência dos compostos. Foi avaliada a porcentagem de viabilidade celular de células incubadas com os compostos, a porcentagem de replicação viral em células infectadas, e a inibição de replicação viral em células incubadas com determinadas concentrações dos complexos. Os resultados demonstraram que as células toleram diferentes concentrações de cada composto. O composto $K_6Co_3L_3$ inibiu a replicação (94.8 %) do CHIKV de forma mais eficiente que o $Na_6Ni_3L_3$, ainda que os dois compostos apresentem a íon trinuclear $[M_3L_3]^{6-}$ com estrutura semelhante. Para ZIKV, novamente o composto de Co(II) foi o mais ativo, apresentando relevante inibição (52.5 %) de replicação viral quando as células foram tratadas previamente com o composto na concentração de 2 μM . Em paralelo, foram realizados experimentos utilizando a espectroscopia na região do ultravioleta e visível para avaliar a estabilidade destes complexos em solução tampão fosfato com pH= 7,4 e a 37° C, condições adequadas para o meio fisiológico. A cada 24 horas as amostras foram analisadas três vezes durante três dias e os espectros das amostras apresentaram bandas de absorções no UV-Vis constantes em todos os testes indicando que os complexos possuem estabilidade em pH biológico. Assim, o trabalho mostra que o composto $K_6Co_3L_3$ apresenta promissora atividade antiviral, cujos mecanismos de ação estão sendo investigados.

Referências:

1. RONCONI, Luca; SADLER, Peter J. Using coordination chemistry to design new medicines. **Coordination Chemistry Reviews**, v. 251, n. 13-14, p. 1633-1648, 2007.
2. STORR, Tim. **Ligand design in medicinal inorganic chemistry**. John Wiley & Sons, 2014.
3. KALINKE, Lucas H. G. et al. Trinuclear Cobalt (II) Triple Helicate with a Multidentate Bithiazolebis (oxamate) Ligand as a Supramolecular Nanomagnet. **Inorganic Chemistry**, v. 61, n. 15, p. 5696-5700, 2022

Agradecimentos

UFG, UFU, FAPEMIG, CAPES e CNPq.

Association of antibiotics with metal ions as a drug repositioning strategy: Norfloxacin combined with Co²⁺ and Zn²⁺ ions.

Jeane P. C. dos Santos (PG),¹ Ricardo Schneider (PQ),² Ronan F. F. de Souza (PQ),¹ Sílvia D. de Campos (PQ),¹ Pedro H. O. Santiago (PQ),³ Javier A. Ellena (PQ),³ Élvio A. de Campos (PQ).^{1*}

patriciajeane125@gmail.com; elvio.campos@unioeste.br

¹Centro de Engenharias e Ciências Exatas, Unioeste; ²UTFPR – Campus Toledo; ³Instituto de Física de São Carlos, USP.

Palavras Chave: Metal complexes, Coordination polymers, Quinolones, Antimicrobial agent.

Highlights

The hydrothermal reaction of M(NO₃)₂ (M = Co²⁺ or Zn²⁺) with norfloxacin produces the complexes [M(HNorfloxacin)₂(H₂O)₂](NO₃)₂.

The same reaction condition using the MOFs [M(glutamate)(H₂O)₂]_n (M = Co²⁺ or Zn²⁺) as metal ions source produces the unprecedented coordination polymers [M(Norfloxacin)₂]_n.

Different from [Co(Norfloxacin)₂]_n, the unit cell of the coordination polymer [Zn(Norfloxacin)₂]_n contains six H₂O molecules as a host.

Resumo/Abstract

Antibiotic complexes bearing metal ions attract the attention of scientists searching new drugs, as well as those striving to increase the activity of antibiotics. The bioactivity of antibiotics can be increased through the coordination of metal ions¹. Furthermore, such complexes allow the reduction of the dose of drugs introduced into the body and improve their bioavailability² and may also be employed for the treatment of other diseases, in a kind of drug repositioning³. In this context, we present the combination of norfloxacin, a quinolone used mainly to treat infections associated with the gastrointestinal or genitourinary systems by inhibiting DNA replication⁴, with Co²⁺ and Zn²⁺ metal ions using two distinct metal precursors: the metal nitrate and the BioMOF [M(glutamate)(H₂O)₂]_n. The reactions were carried out in a 100 mL teflon lined stainless steel autoclave, where 0.5 mmol of the metal ion precursors, 1 mmol of norfloxacin and 12 mL of pure water were treated at 105 °C by 48 h. The reactor was kept in the oven until room temperature and the crystals were collected after cooling or ageing of the resulting filtered solution. The products were characterized by XRD, IR and TGA. The reaction of Co(NO₃)₂ or Zn(NO₃)₂ with norfloxacin produces a metal complex of general formula [M(HNorfloxacin)₂(H₂O)₂](NO₃)₂, and crystallises in a triclinic unit cell belonging to the *P*-1 space group. The zinc complex is registered as CCDC n. 140820, while the structure of the cobalt complex was solved by single crystal X-ray diffraction. However, the reactions using the BioMOF of general formula [M(glutamate)(H₂O)₂]_n as a source of metal ions, led to the formation of inedited one-dimensional coordination polymers with 1:2 metal ligand ratio, whose structures were solved by single crystal X-ray diffraction. They belong to the monoclinic crystalline system, space group P2/n (cobalt compound) and P2₁/c (zinc compound) and both are thermal stable until 300 °C. The cobalt compound presented high activity against *Pseudomonas aeruginosa*.

1 - *Chem. Sci.* **2020**, 11, 2627. <https://doi.org/10.1039/c9sc06460e>

2 - *Trends in Analytical Chemistry* **2020**, 123, 115771. <https://doi.org/10.1016/j.trac.2019.115771>

3 - *Pharmaceuticals* **2022**, 15, 1010. <https://doi.org/10.3390/ph15081010>

4 - *The Comprehensive Pharmacology Reference* **2007**, Elsevier Inc., Amsterdam, pp. 1-5. <https://doi.org/10.1016/b978-008055232-3.62306-2>

Agradecimentos/Acknowledgments

This study was financed in part by the Coordenação de Aperfeiçoamento de Pessoal de Nível Superior – Brasil (CAPES) – Finance code 001.

A theoretical approach to primaquine and amodiaquine copper(II) complexes

Frederico Henrique do C. Ferreira (IC),¹ Maribel Navarro (PQ),² Luiz Antônio S. Costa (PQ),¹

frederico.h@outlook.com; luiz.costa@ufjf.br

¹NEQC – Núcleo de Estudos em Química Computacional, UFJF, Juiz de Fora - MG; ²LAQBIC – UFJF Juiz de Fora - MG

Palavras Chave: quinolines, molecular dynamics, copper, malaria

Highlights

The search for a drug against malaria lead to the simulations of copper(II)-primaquine/amodiaquine complexes which demonstrated good interactions energies with key Plasmodium biomolecules.

Abstract

One of the most successful antimalarial drugs was chloroquine, which incorrect administration as prophylactic led to the development of resistance in some *Plasmodium* strains. Nowadays, it is necessary to use some drug cocktails to achieve the very same result. The idea of this project is to study copper(II) complexes containing primaquine and amodiaquine as ligands. It was evaluated the interaction between those copper complexes and some key molecules to *Plasmodium* metabolism, such as the heme group, haematin and DNA, which were carried out by molecular dynamic simulations.

The interaction energies demonstrated the intermolecular interactions as a thermodynamic favouring process, i.e., $\text{CuPQCl}_2 \cdots \text{HEME}$ presents an interaction energy of $-15.6 \pm 2.5 \text{ kcal mol}^{-1}$ and $\text{CuPQ}(\text{NO}_3)_2 \cdots \text{Haematin}$ $-10.5 \pm 1.8 \text{ kcal mol}^{-1}$. Those associations are mainly $\pi \cdots \pi$ ring related, as shown in figure 1, since van Der Waals is the greatest contribution in energy.

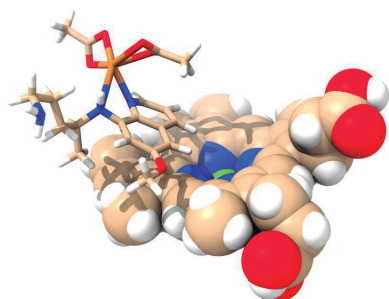


Figure 1. Interaction Haematin \cdots $\text{CuPQ}(\text{Ac})_2$ demonstrating the $\pi \cdots \pi$ ring interaction.

Another analysis that showed the dynamics of the interaction along the simulated time was the solvent accessible surface area (SASA), thus exhibiting the blockage to solvent caused by all studied compounds that may lead to the reduction in the biological activity. Copper amodiaquine calculations are in progress, their results will be presented in the final presentation.

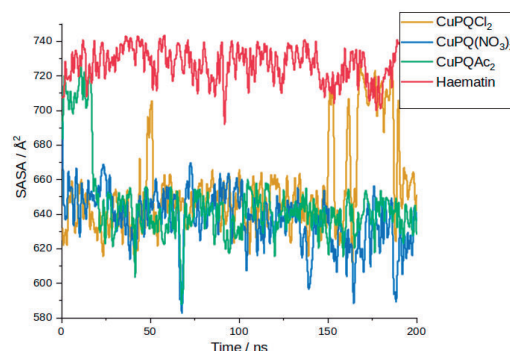


Figure 2. SASA analysis of the simulated complexes along with Haematin.

So far, the results demonstrated a favouring interaction between the species that may be fruitful for the further investigation of those complexes as antimalarial agents.

References:

- Pereira, C. de S. *et al. Pharmaceuticals*. **2022**, 14, 1251.
Villarreal W. *et al. Pharmaceuticals*. **2022**, 15, 921.

Acknowledgments

CNPq, Santos Dumont/LNCC

Diaquabis(1,3,5-tris(4-carboxyphenyl)benzoate)phenanthrolinecobalt(II): Synthesis, Characterization and Polymeric Crystal Structure

Henrique V. P. Hollauer (PG)¹, Gabriel Salomão (IC)¹, Guilherme P. Guedes (PQ)², Livia B. L. Escobar (PQ)^{1*}

¹Departamento de Química, Pontifícia Universidade Católica do Rio de Janeiro, Rua Marquês de São Vicente, 225 Gávea, 22451-900, Rio de Janeiro-RJ, Brasil.

²Instituto de Química, Universidade Federal Fluminense, Campus Valonguinho, Outeiro de São João Batista s/n, 24020-007, Niterói-RJ, Brasil.

henriquehollauer@gmail.com; liviablescobar@puc-rio.br

Keywords: coordination polymers, crystal structure

Highlights

In this resume, we present a new 1D coordination polymer using Co(II) ion, the polycarboxylate anion 1,3,5-tris(4-carboxyphenyl)benzene (BTB), and the auxiliary ligand, phenanthroline.

Abstract

Coordination polymers (CPs) are complexes that form one-dimensional (1D) extended chains, two-dimensional (2D) sheets, or three-dimensional (3D) frameworks. Crystalline materials, such as some CPs, have attracted a great deal of attention for the past two decades for their application in areas such as gas storage/separation, small molecule adsorption, luminescence and magnetism [1]. Several kinds of ligands can be used to produce CPs and the most famous class is the aromatic polycarboxylate ligands. This class of ligands is interesting for the development of this type of material because they have high structural stability, the ability to propagate magnetic interaction and several coordination sites [2]. In this work, we prepared the new coordination polymer, $\{[Co(H_2O)_2(BTB)_2phen]\}_n$, according to the scheme described in Figure 1a:

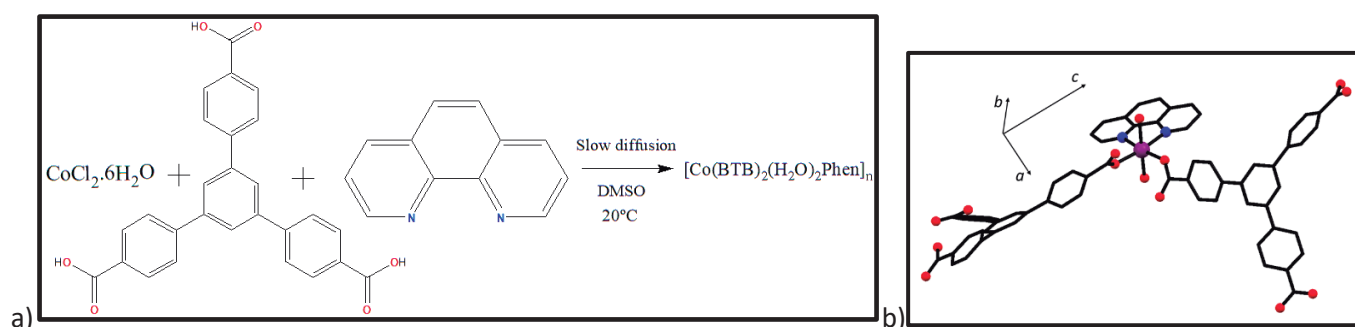


Figure 1: a) Synthetic route for the preparation of $\{[Co(H_2O)_2(BTB)_2phen]\}_n$. b) Fragment of the crystal structure of $\{[Co(H_2O)_2(BTB)_2phen]\}_n$.

After a few days, pink single crystals were obtained. The single-crystal x-ray analysis revealed that the Co(II) ion presents a distorted octahedral geometry, with the nitrogen atoms from the phenanthroline ligand occupying two of the equatorial positions forming a chelate ring of five members. The other two equatorial positions of the Co(II) are coordinated with the oxygen atoms from two different BTB ligands in a bridge mode. Water molecules occupy the axial positions. Magnetic properties are currently being investigated.

Acknowledgments

CNPq e PUC-Rio

[1] Davarci, D.; Duyar, C.; Zorlu, Y. 3D Ag(I) coordination polymer constructed from a flexible pyridyloxycyclotetraphosphazene linker: Synthesis, crystal structure and dye adsorption properties. *Polyhedron*. V. 231, 2023.

[2] Wu, F.; Wu, Y.; Wang, Z.; He, X.; Li, M. Structural variation of hydroxide-metal clusters and three Co(II)/Zn(II) coordination polymers assembled by tripodal 3,5-bis(4-carboxybenzyloxy)benzoic acid. *Inorganic Chemistry Communications*, v. 146, 2022.

Calcium phosphate containing silica as structural reinforcement

Lauany M. Pontes^{1*} (PG), João Vitor G. de Faria¹ (IC), Lucas A. Rocha¹ (PQ), Eduardo J. Nassar¹ (PQ).

lauanymazzon@gmail; eduardo.nassar@unifran.edu.br

¹ Departamento de Química, UNIFRAN

Keywords: Biomaterials, Biocompatibility, Sol-Gel, Bioactive Biomaterials, Bone Tissue.

Highlights

Calcium phosphate, present in the bone matrix, is used as biomaterial. Structural modification may increase its mechanical resistance, biocompatibility, bioactivity, and osteoconduction, broadening the scope of its applications.

Resumo/Abstract

Population ageing has led materials researchers to seek innovative solutions for medical procedures in an attempt to improve patients' well-being. In this context, research interest in biomaterials has grown. The demand for biomaterials, used to treat various tissue or organ deficiencies of natural or accidental origin, has increased. Biocompatibility is the main feature of a biomaterial: it prevents the material from being rejected by the body and ensures that it will elicit the desired effect. Other important biomaterial features include biodegradability, biactivity, and bioabsorptivity. Calcium phosphate (CP), an inorganic component of bones, is a bioceramic that is employed as biomaterial. However, CP presents low mechanical resistance. This study aims to boost CP resistance by adding SiO₂ to the CP structure. Infrared vibrational spectroscopy of pure CP and CP reinforced with SiO₂ revealed peaks at 634 and 571 cm⁻¹, attributed to PO₄³⁻ stretching. The typical Ca-O vibrations appeared at 1451 cm⁻¹. Both pure CP and reinforced CP displayed a broad peak between 1000 and 1100 cm⁻¹, due to PO₄³⁻ vibrations, but this is an overlap region. The peaks at 941 and 498 cm⁻¹, related to Si-OH and Si-O-Si, were only detected for reinforced CP. The X-ray diffractogram of reinforced CP presented the standard peaks of CP and calcium silicate (see Figure 1). Europium III addition during the synthesis helped to monitor the structural variation: the europium III emission spectrum allows the number of calcium sites in the materials to be determined. The band at 580 nm was due to the ⁵D₀ → ⁷F₀ transition, which does not split under the crystalline field effect.

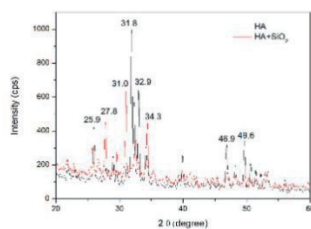


Figure 1: XRD for pure CP and CP+SiO₂

The emission spectrum of europium III in pure CP displayed three bands, indicating three sites. CP reinforced with SiO₂ presented two bands, indicating that one site disappeared upon SiO₂ addition, as confirmed by the reduction in the number of bands of the other transitions.

Agradecimentos/Acknowledgments

CAPES, CNPq and FAPESP

Catalytic Oxidation of Hidroquinone by an Illuminated Dicopper(II) Metallacyclophane Complex

Jackson J. Santos (IC),¹ Maria Clara Oriol Edimio Souza (PG),¹ Pedro Victor Valadares(PG),¹ Renato Rabelo (PQ),¹ Lucas Hoffmann Gregghi Kalinke (PQ),² Joan Cano (PQ),⁴ Livia Flório Sgobbi(PQ),¹ Danielle Cangussu (PQ).¹

Jackson.souza@discente.ufg.br; danielle_cangussu@ufg.br

¹Departamento de Química, UFG; ²Instituto Federal de Goiás, Campus Anápolis IFG; ⁴Instituto de Ciência Molecular, Universitat de València.

Palavras Chave: Química de coordenação, Fotoquímica, Catálise, Biosensores.

Highlights

Photoactive dicopper(II) metallacyclophane complex with an oxamate ligand and a comparative study of the catalytic activity of this complex and its illuminated species towards the hydroquinone oxidation is presented herein.

Resumo/Abstract

Enzimas a base de cobre são amplamente estudadas por desempenhar importantes funções biológicas. As enzimas oxidase possuem diversas aplicações biotecnológicas, em especial biosensores. Apesar da importância dessas enzimas, seu uso é limitado devido à baixa estabilidade térmica e a meios não fisiológicos. Visando minimizar esses problemas, pesquisas na área de síntese de complexos podem levar a compostos que mimetizam as funções enzimáticas como de catalisadores de reações-modelo para biosensores. Neste trabalho estudou-se o dímero de cobre (II) de fórmula $[\text{Cu}_2(\text{acriba})_2(\text{H}_2\text{O})_2]^{4-}$ (**1**) utilizando o ligante $\text{Et}_2\text{H}_2\text{acriba}$ [onde *acriba* = *N,N'*-2,7-diaminoacridina-bis (oxamato)], que apresentou funções catalíticas para oxidação da hidroquinona (HQ). O composto **1** irradiado ($\lambda_{\text{máx}}=250\text{nm}$) apresentou uma mudança na sua função catalítica aumentando a velocidade da reação de oxidação da hidroquinona (HQ) para benzoquinona (BQ) (Figura 1).

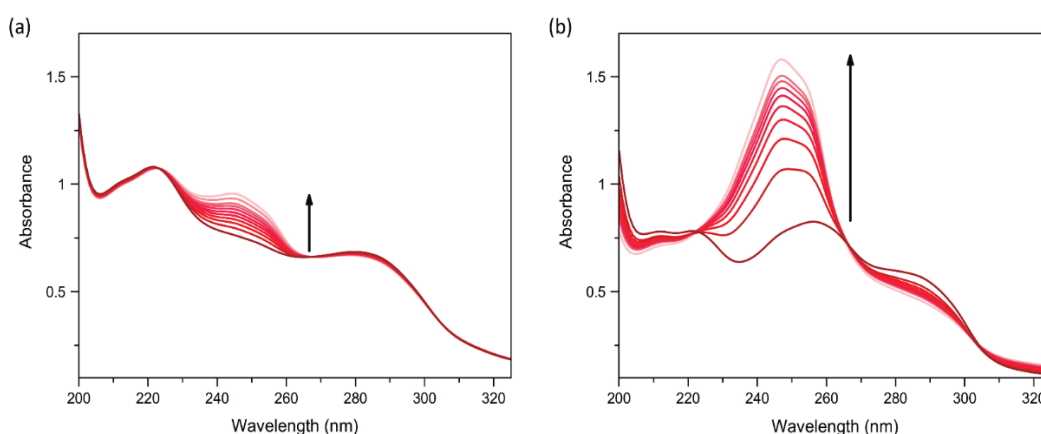


Figura 1. Evolução do espectro de absorção de uma solução aquosa de HQ 75 μM e composto **1** (15 μM) antes (a) e depois (b) da irradiação com luz UV por 5 minutos. As setas indicam o curso da reação de oxidação.

Agradecimentos/Acknowledgments

CNPq, Capes, FAPEG, UFG

Área: INO*(Inserir a sigla da seção científica para qual o resumo será submetido. Ex: ORG, BEA, CAT)***Cellulose-based up converting composites with translucent proprieties and high efficiency****Elaine A de Mattos (PG),¹ Rodrigo Piassentin (IC),¹ Douglas Lourenço Fritzen¹, Veronica Texeira² and Lucas C. V. Rodrigues (PG),^{1*}****elaine.mattos@usp.br; lucascvr@iq.usp.br**¹Departamento de Química Fundamental, IQ-USP;²Brazilian Center for Research in Energy and Materials (CNPEM), Brazil*up conversion, nanoparticules, Surface plasmon resonance, plasmon enhanced up conversion.***Highlights**

Up converting rare earth based fluorides obtained by solvothermal synthesis. HPMC based up converting transparent films. Increase in intensity of emission via Plasmon enhanced up conversion.

Resumo/Abstract

The up conversion phenomenon converts two or more lower-energy photons into one higher-energy photon. One of its main limitations is the phenomenon's inherent low yield, and in order to mitigate this problem, we studied the enhancing effect of metallic nanoparticles on cellulose-based polymeric transparent composites with up converting properties. For this purpose, $\text{YF}_3: \text{Yb}^{3+}, \text{Er}^{3+}$ nanoparticles were prepared via a solvothermal method and incorporated, alongside AuNps, into hydroxypropylmethylcellulose (HPMC) films using a drop-casting process. X-ray fluorescence nanomapping registered at the Carnúba beamline from Sirius Synchrotron facility was used to understand the dispersion of the nanoparticles in the film after the casting process, and, showed, serendipitously, that the gold nanoparticles interact preferentially with the fluoride nanoparticles over the carbonyl ends of the HPMC. That proximity is responsible for the plasmon enhanced up conversion phenomena. The photoluminescence study showed an intensification of the up conversion phenomenon by 1000x in the presence of gold nanoparticles and a 100x increase in quantum yield.

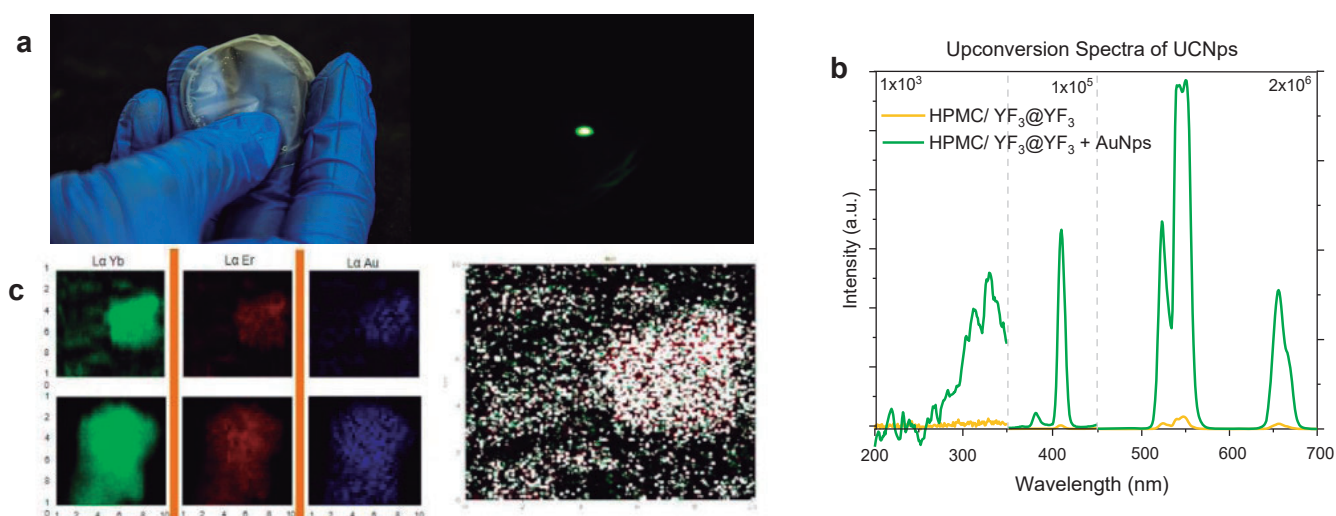


Figure 1: (a) Photograph of the UCNPs in the dark under 980 nm laser excitation and picture of the thin HPMC/UCNps film in white light and with 980 nm laser excitation, (b) up conversion spectra of the HPMC/UCNps with and without AuNps, (c) Images obtained from x-ray fluoresce Nano mapping of regions of the HPMC/UCNps + AuNps.

Agradecimentos/Acknowledgments

Acknowledgments: CNPq.

46ª Reunião Anual da Sociedade Brasileira de Química: "Química: Ligando ciências e neutralizando desigualdades"

Cerium vanadate (CeVO_4) nanoparticles for combined luminescence and catalysis

Alicya C.S. Abdala (PG),¹ Rafael V. Perrella (PQ),² Paulo Cesar de Sousa Filho (PQ)^{1*}

alicya.abdala@gmail.com, pcsfilho@unicamp.br

¹Institute of Chemistry, University of Campinas (UNICAMP). ²Laboratoire de Physique de la Matière Condensée, Ecole Polytechnique (Palaiseau, France).

Keywords: Rare earth, Luminescence, Catalysis, Nanoparticle.

Highlights

Direct aqueous coprecipitation synthesis afforded homogeneous CeVO_4 elongated nanoparticles with enhanced defect density and showing Eu^{3+} emissions under UV excitation, thus opening interesting perspectives for combining luminescent and catalytical properties in colloidal oxide nanocrystals.

Abstract

Rare earth oxide nanoparticles are extensively explored as luminescent materials because of the unique spectroscopic properties of lanthanide (Ln^{3+}) emissions, also affording interesting catalytic properties due to oxygen mobility and redox activity. For instance, cerium(IV) oxide is a classic non-stoichiometric material with multiple applications in catalysis.[1] Although cerium vanadate (CeVO_4) is a less explored example of catalytically active oxide, this composition is highly promising due to a more complex redox chemistry ($\text{Ce}^{3+}/\text{Ce}^{4+}$, $\text{V}^{4+}/\text{V}^{5+}$), which in turn allows applications in hydrocarbon/phenol degradation and as cytochrome c-oxidase and superoxide-dismutase-like catalysts.[2] Despite these advantages, luminescence of Ln^{3+} ions in CeVO_4 are scarcely studied due to multiple quenching channels in this host, but responsive luminescence can be achieved by controlling the defect chemistry and microstructure.[3] We therefore investigate strategies for combining luminescent and catalytic properties in CeVO_4 nanoparticles aiming at multifunctional nanomaterials. $\text{CeVO}_4:\text{Ln}^{3+}$ ($\text{Ln}=\text{Eu}, \text{Yb}/\text{Er}$) and $\text{CeVO}_4:\text{Zr}^{4+}$ nanoparticles were prepared by direct precipitation with metal nitrates and NH_4VO_3 in water at 25 °C for 48 h.[4] The initial pH of the mixture (5.2, 7.3, or 8.3) caused only minor alterations in the general morphology of the final solids (Figure 1), which are nearly monocrystalline elongated particles (5-10 nm width, 30-40 nm length). However, Zr^{4+} -doping resulted in a higher degree of nanovoiding in the particles, as a consequence of a higher density of structural defects. The solids crystallized in the tetragonal $I4_1/amd$ structure regardless the nature of the dopants as shown by X-ray diffractograms and Raman spectra. Eu^{3+} emissions in CeVO_4 were observed at under 280 nm excitation at different europium concentrations, showing that the nanostructural character of the particles overcomes at least partially the possible $\text{Ce}^{4+}/\text{Eu}^{2+}$ quenching channels even at high Eu^{3+} concentrations (20%). Although upconversion luminescence under 980 nm excitation was not detected for pristine $\text{CeVO}_4:\text{Yb}/\text{Er}$ particles, we currently investigate if controlled annealing of the solids enable detection of Er^{3+} emissions and further study of potential thermometric applications. Our results confirm the formation of homogeneous CeVO_4 particles with enhanced defect density (Zr -doping) and showing UV-excited luminescence (Eu -doping), which opens further perspective to investigate the catalytic behavior towards different oxidation reactions.

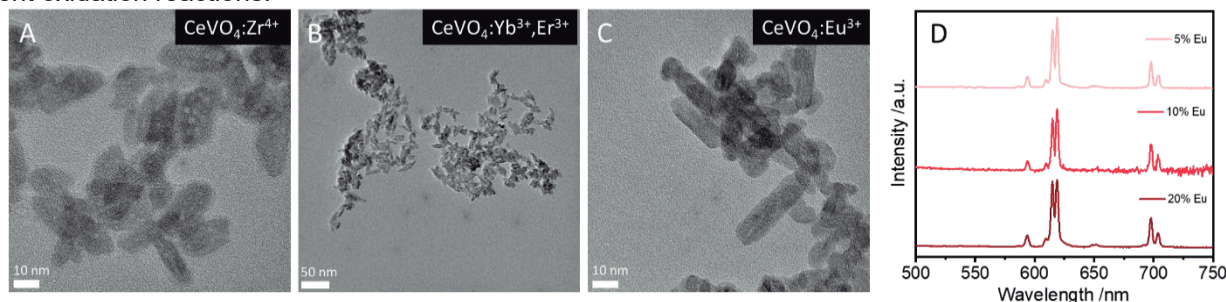


Figure 1. TEM micrographs of (A) $\text{CeVO}_4:\text{Zr}^{4+}$, (B) $\text{CeVO}_4:\text{Yb}^{3+}, \text{Er}^{3+}$ and (C) $\text{CeVO}_4:\text{Eu}^{3+}$ nanoparticles. (D) Emission spectra of powder $\text{CeVO}_4:\text{Eu}^{3+}$ with different Eu^{3+} concentrations (5, 10 and 20%) under UV excitation ($\lambda_{\text{exc}}=280$ nm).

References:

[1] J. Catal. 2021, 397, 116-127. [2] Angew. Chem. Int. Ed. 2019, 58, 7797-7801. [3] Nano Lett. 2022, 22, 9, 3569–3575. [4] Langmuir, 2020, 36, 9124-9131.

Acknowledgments

The authors thank CAPES, CNPq (136329//2022-5), and FAPESP (2022/03442-3) for financial support.

$\{[\text{Co}(\text{Dca})_2(4\text{-hydroxypyridine})]\}_n$: Synthesis, Characterization and Crystal Structure

Brendo M Gonçalves (IC),¹ Guilherme P. Guedes (PQ),² Lívia B. Escobar (PQ).^{1*}

¹Departamento de Química, Pontifícia Universidade Católica do Rio de Janeiro, Rua Marquês de São Vicente, 225 Gávea, 22451-900, Rio de Janeiro-RJ, Brasil.

²Instituto de Química, Universidade Federal Fluminense, Campus Valonguinho, Outeiro de São João Batista s/n, 24020-007, Niterói-RJ, Brasil.

liviabescobar@puc-rio.br brendo@aluno.puc-rio.br @guilherme_guedes

Keywords: Polynitrile Anions, Crystal Structure

Highlights

Coordination compounds have the potential for a multitude of applications, from gas adsorption properties, ion exchange, and magnetism to luminescence [1]. Here, a new Co-based polymer is reported.

Resumo/Abstract

To produce such complexes, N-donor and polynitrile anions such as the dicyandiamide anion (dca^{-1}) are often chosen, as they can facilitate the transmission of magnetic properties, as well as favor the polymerization [2]. To design structures with intriguing topologies and interesting properties, chemists can play with several kinds of ligands. In this work, our main was to produce a multifunctional complex and to do that, we have used as an auxiliary ligand, 4-hydroxypyridine, which also acts as a bridging ligand. Thus, a new coordination polymer containing the high anisotropic ion Co (II), dca^{-} and 4-pyridinol, $\{[\text{Co}(\text{dca})_2(4\text{-hydroxypyridine})]\}_n \cdot 2\text{H}_2\text{O}$, was synthesized, characterized and the study of its magnetic and gas adsorption properties is in progress.

The 1D coordination polymer, $\{[\text{Co}(\text{dca})_2(4\text{-hydroxypyridine})]\}_n \cdot 2\text{H}_2\text{O}$, was synthesized by slow diffusion, according to the scheme represented by figure 1a):

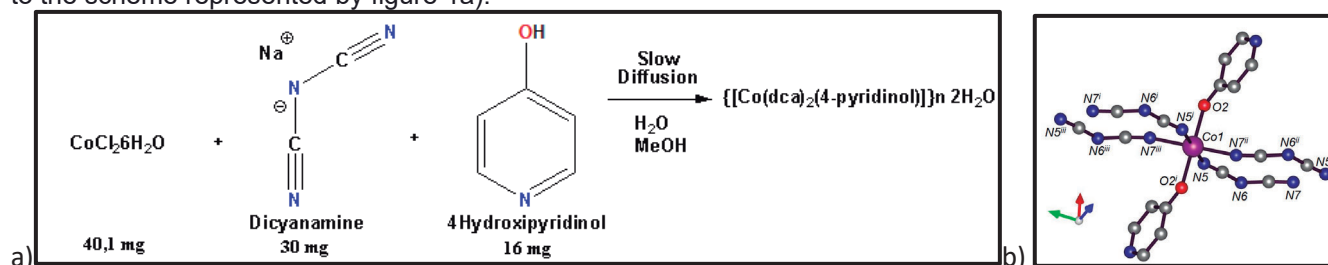


Figure 1: a) Synthetic route for the preparation of $\{[\text{Co}(\text{dca})_2(4\text{-hydroxypyridine})]\}_n \cdot 2\text{H}_2\text{O}$. b) Fragment of the crystal structure of $\{[\text{Co}(\text{dca})_2(4\text{-hydroxypyridine})]\}_n \cdot 2\text{H}_2\text{O}$.

In the infrared spectrum the main bands referring to the dca^{-} ligand were shifted to higher wavenumbers when compared to the free ligand [$\nu_{\text{as}} + \nu_{\text{s}}(\text{C}\equiv\text{N})$: 2286 cm^{-1} , $\nu_{\text{as}}(\text{C}\equiv\text{N})$: 2232 cm^{-1} and $\nu_{\text{s}}(\text{C}\equiv\text{N})$: 2179 cm^{-1}] indicating that the dca^{-} ligand is coordinated in a $\mu_{1.5}$ bridge mode to the Co(II) site. Bands corresponding to the 4-hydroxypyridine ligand appear at 3590 cm^{-1} ($\nu_{\text{O-H}}$) and $1580\text{-}1490\text{ cm}^{-1}$ ($\nu_{\text{CC/CN}}$).

Figure 1b) shows the coordination environment of the Co(II) ion, its coordination geometry is a distorted octahedron being coordinated to four nitrogen atoms from the dca^{-} anion in the equatorial positions, and to two oxygen atoms from the 4-hydroxypyridine ligand in the axial sites.

Agradecimentos/Acknowledgments

CNPq, FAPERJ e PUC-Rio.

[1] Mehdi Boutebdja *et al.*; *J. Mol. Struct.*; 1271, **2023**, 134041.

[2] Xin Zhang *et al.*; *J. Funct. Biomater.*; 13(4), **2022**, 215.

Área: INO

Comparative study of the catalytic reaction of the complex of ruthenium and bisimidazole with other analogous complexes

Mariana Rodrigues Oliveira (IC)¹, Marcelo Carpes Nunes (PG)¹, André Luiz Barboza Formiga (PQ)¹

m236006@dac.unicamp.br; m262826@dac.unicamp.br; formiga@unicamp.br

¹Institute of Chemistry (IQ) – University State of Campinas;

Keywords: Ruthenium complexes, Ligand Bisimidazole, water oxidation, homogeneous catalysts.

Highlights

Synthesis and purification of ruthenium complexes; N-heterocyclic ligands; water oxidation reaction, catalysts; water splitting; Proton-coupled electron transfer.

Abstract

The fossil fuel crisis has spurred increased research on sustainable energy sources and new technologies. Significant increases in oil prices and demand, driven by increased consumption and growth in the world's rapidly developing economies, have made its development and application more urgent (Meyer, 2012). A very promising alternative is the use of hydrogen as fuel, which can be obtained using complexes such as catalysts in the electrochemical or photocatalytic oxidation of water, which has received great attention since the energy of this gas is clean. In this process, the semi-reaction of water oxidation ends up being the limiting factor of the process, since it occurs with a large overpotential. In our group, we observed that the association of coordinated imidazole groups reduces the oxidation potentials through the transfer process of electrons coupled to protons, causing this reaction to occur at lower potentials. In this work, the bisimidazole ligand and its ruthenium complex (shown in the figure 1 below) were synthesized and characterized to investigate their catalytic activity. A ruthenium(II) complex containing dissociable protons, $[\text{Ru}(\text{tpy})(\text{H}_2\text{bim})\text{OH}_2]\text{PF}_6$, was synthesized and characterized, where the H_2bim and M-OH_2 ligands are expected to serve as proton dissociation sites. The structure of the synthesized complex is shown in the scheme below, where it was carried out using the methodology described by Okamura, M. et al. (2012).

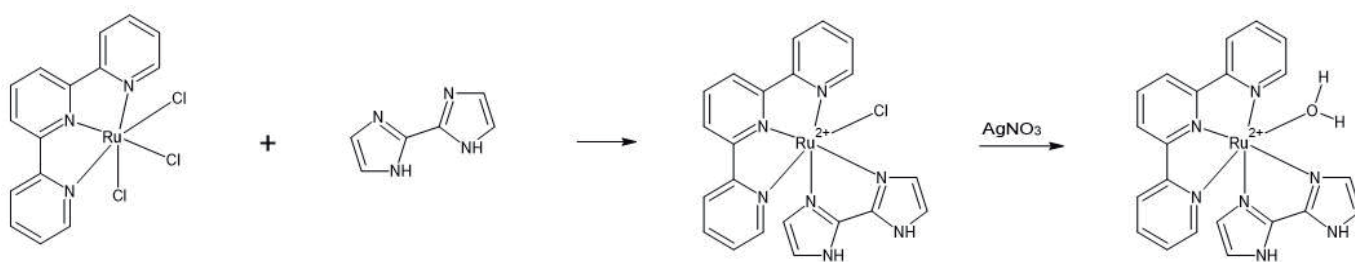


Figure 1. Synthetic route for obtaining the complex $[\text{Ru}(\text{tpy})(\text{H}_2\text{bim})\text{OH}_2](\text{PF}_6)_2$ Source: Author (2023).

The complex was synthesized by the reaction between $[\text{Ru}(\text{tpy})\text{Cl}_3]$ with the ligand BimH_2 , obtaining the complex $[\text{Ru}(\text{tpy})(\text{H}_2\text{bim})\text{Cl}](\text{PF}_6)$ which was purified by column chromatography, where 4 fractions were obtained and found to be pure by CCD. The 3rd fraction obtained was identified as the intermediate of interest, its FR was found to be 0.33. NMR was also performed, showing that the complex obtained was similar to the compound described in the literature. From this complex the chloride ligand was removed with AgNO_3 in the presence of water, obtaining the complex of interest - $[\text{Ru}(\text{tpy})(\text{H}_2\text{bim})\text{OH}_2](\text{PF}_6)_2$, which had its structure confirmed by NMR. Further characterization measurements for both complexes are currently underway. In the future, we will describe the electrochemical properties and catalytic behavior of the complex of interest.

Concepcion, J. J.; House, R. L.; Papanikolas, J. M.; Meyer, T. J. **Chemical approaches to artificial photosynthesis**, Proceedings of the National Academy of Sciences, vol. 109, n. 39, p. 15560–15564, 2012.

Okamura, M. et al. **A mononuclear ruthenium complex showing multiple proton-coupled electron transfer toward multi-electron transfer reactions**. Dalton Transactions, v. 41, n. 42, p. 13081–13089, 10 out. 2012.

Acknowledgments

The authors would like to thank CNPq, CAPES, FAPESP, Unicamp, and CINE. (FAPESP 2017/11986-5).

Comparison between two acetylhydrazone-derived *N*-acylhydrazones and their interactions with aluminum in the context of neurodegenerative diseases

Roberta Lamosa (IC),^{1*} Dayanne M. Silva (PG),¹ Nicolás A. Rey (PQ).¹

*lamosaroberta@gmail.com

¹ Laboratory of Organic Synthesis and Coordination Chemistry Applied to Biological Systems (LABSO-Bio), Department of Chemistry, Pontifical Catholic University of Rio de Janeiro (PUC-Rio)

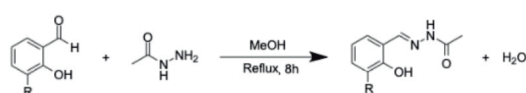
Keywords: Neurodegeneration, *N*-acylhydrazones, Aluminum, UV-Vis spectroscopy.

Highlights

Aiming at the promising effects of *N*-acylhydrazones for the treatment of neurodegenerative diseases and knowing their affinity towards metal ions, new hydrazone ligands were developed and evaluated regarding their aluminum(III) chelating properties.

Abstract

Chelation therapy for the treatment of neuropathologies such as Alzheimer's (AD) and Parkinson's diseases (PD) has attracted considerable interest in recent years due to the controversial role of toxic metals, such as aluminum, in neurotoxicity associated with these conditions. Schiff bases with proper placement of additional donor atoms can form stable complexes with metal ions, behaving as highly biocompatible chelators. Thus, in this work we focused on the stability and coordination ability of two new acetylhydrazone-derived *N*-acylhydrazones towards aluminum(III). The ligands were synthesized according to Mozghan Tahriri *et al.* (2017) (Figure 1) and characterized using solid-state and solution spectroscopic techniques.



R = H for **SALACTIN** and CH₃ for **MALOCTIN**

Figure 1. General scheme for the synthesis of both ligands.

SALACTIN: white precipitate with a yield of 64%. MP: 204 ± 1 °C. IR(KBr) ν_{max} : 3428, 3074, 1684, 1621, 1575, 1315 cm⁻¹. ¹H NMR (DMSO-*d*₆) δ 2.16 (s, 3H); 6.87 (t, 1H); 7.24 (t, 1H); 7.48 (dd, 1H); 7.61 (dd, 1H); 8.32 (s, 1H); 11.18 (s, 1H); 11.60 (s, 1H).

MALOCTIN: white precipitate with a yield of 79%. MP: 223 ± 2 °C. IR(KBr) ν_{max} : 3432, 1679, 1620, 1608, 1498, 1535, 1498, 1315 cm⁻¹. ¹H NMR (DMSO-*d*₆) δ 1.98 (s, 3H); 2.18 (s, 3H); 6.82 (dd, 1H); 7.18 (dd, 1H); 7.24 (dd, 1H); 8.26 (s, 1H); 10.52 (s, 1H); 11.79 (s, 1H).

The study in a 1% DMSO/water solution demonstrated the stability of the ligands within 48 hours at 25 °C (Figure 2A). In the metal interaction studies, the formation of a 2:1 (M:L) complex between Al³⁺ and the compounds was observed (Figure 2B), indicating the efficiency of these hydrazones in chelating Al³⁺, and supporting their use as possible agents for the treatment of neuropathologies aggravated by heavy metal intoxication.

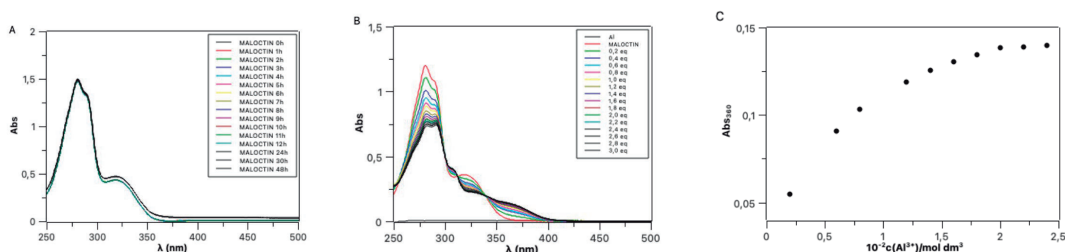


Figure 2. (A) Absorbance profile curves of **MALOCTIN** ($c = 5 \times 10^{-5}$ mol L⁻¹) (B) Spectrophotometric titration with AlCl₃ in DMSO/water 1/99 mixture. $l = 1$ cm. $\theta = (25.0 \pm 0.1)^\circ\text{C}$; between 250 and 500 nm (C) Dependence of absorbance at 384 nm on Al³⁺ concentration.

Tahriri, M., Yousefi, M., Mehrani, K. et al. Synthesis, Characterization and Antimicrobial Activity of Two Novel Sulfonamide Schiff Base Compounds. Pharm Chem J 2017, 51, 425–428.

Acknowledgments

This work was supported by FAPERJ, CAPES and CNPq.

Complexos de rutênio contendo diferentes bifosfinas utilizados como modificadores de eletrodo na determinação eletroquímica de íon nitrito.

Leonardo Corsi Custódio (IC)¹, André Luiz Bogado (PQ)¹, Luís Rogério Dinelli (PQ)^{1*}

leonardo.corsi2@hotmail.com; dinelli@ufu.br

¹Instituto de Ciências Exatas e Naturais do Pontal, UFU

Palavras-Chave: Eletrodo modificado, Pasta de carbono, Rutênio, Nitrito

Highlights

Ruthenium complexes with different bisphosphines used as electrode modifiers in the electrochemical determination of nitrite ion. The electrode modified with *cis*-[RuCl₂(bipy)(dppb)] complex showed the best result for the voltammetric determination of nitrile ion; All modified electrodes showed a wide linear range of nitrite ion determination; The modified electrode was used for the determination of nitrite in a real sample (bacon)

Resumo/Abstract

A síntese dos complexos de rutênio de fórmula geral *cis*-[RuCl₂(bipy)(P-P)] onde ; P-P = dppe, dppp e dppb foram realizadas conforme descritos na literatura¹. Os eletrodos de pasta de carbono modificados foram confeccionados utilizando o seguinte procedimento geral: uma mistura de 65% de grafite em pó, 32% de parafina e 3% de modificador foi aquecida em banho maria a uma temperatura de 80°C até a fusão da parafina e em seguida homogeneizados e transferidos para uma seringa e o contato elétrico foi feito utilizando uma haste de cobre. Os complexos sintetizados foram caracterizados por voltametria cíclica e todos apresentaram somente um processo eletroquímico quase reversível referente ao par redox Ru(II)/(III). Os eletrodos modificados com os complexos sintetizados foram utilizados para a determinação voltamétrica de íon nitrito. A figura 1A mostra os resultados dos eletrodos modificados para a determinação de nítrico comparando com o eletrodo de pasta de carbono sem modificador (PC). Pode-se observar por esta figura que o eletrodo modificado contendo o complexo *cis*-[RuCl₂(bipy)(dppb)] mostrou-se mais sensível (maior corrente de pico) ao nitrito. Na figura 1B mostra o voltamograma, utilizando o eletrodo contendo o *cis*-[RuCl₂(bipy)(dppb)], do nitrito em diferentes concentrações. Pode-se observar um aumento de corrente em função do aumento de concentração do nitrito com faixa linear de $1,1 \times 10^{-4}$ e $1,3 \times 10^{-3}$ mol L⁻¹. Esse eletrodo modificado foi utilizado para a determinação de nitrito em uma amostra de bacon, e o valor encontrado de nitrito foi de 6,23 mg/kg, que é um valor abaixo do recomendado para esse íon pelo Ministério da Saúde.

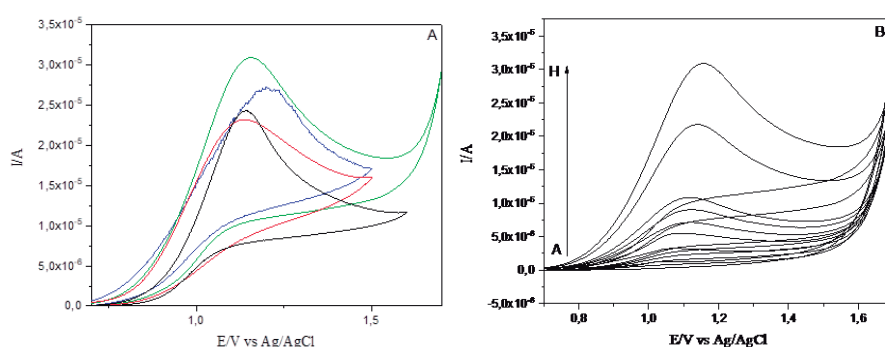


Figura 1 A: Voltamogramas cíclicos do nitrito ($1,3 \times 10^{-3}$ mol.L⁻¹) em tampão acetado 0,1 mol L⁻¹ utilizando os eletrodos: PC (—), dppe (—), dppp (—) e dppb (—); **Figura 1B:** Voltamogramas cíclicos registrados com o eletrodo *cis*-[RuCl₂(bipy)(dppb)], em uma solução de tampão acetato 0,1 mol L⁻¹ em diferentes concentrações de nitrito; A: 0; B: $1,10 \times 10^{-4}$; C: $1,96 \times 10^{-4}$; D: $2,91 \times 10^{-4}$; E: $3,85 \times 10^{-4}$; F: $4,76 \times 10^{-4}$; G: $9,1 \times 10^{-4}$ e H: $1,3 \times 10^{-3}$ mol L⁻¹.

¹SOUZA, C. M. L.; SANTOS, T. A.; PRADO, C. A.; LIMA, B. A. V.; CORRÊA, R. S.; BATISTA, A. A.; OTUBO, L.; ELLENA, J.; UENO, L. T.; DINELLI, L. R.; BOGADO, A. L. *Royal Society of Chemistry*, v. 6, p. 53130-53139, 2016.

Agradecimentos/Acknowledgments

FAPEMIG, CAPES e o CNPq.

Computational study of physicochemical and electronic properties of palladium complexes with antitumor potential

Catherine R. S. de Souza (PG),^{1*} Willian T. G. Novato (PQ),¹ Diego F. S. Paschoal (PQ)^{1*}

catherinesiqueira1@hotmail.com; diegofspaschoal@macae.ufrj.br

¹Núcleo de Química Teórica e Computacional de Macaé, Polo Ajuda, Instituto Multidisciplinar de Química, Centro Multidisciplinar UFRJ-Macaé, Universidade Federal do Rio de Janeiro, 27.971-525, Macaé, RJ, Brazil;

Keywords: Cancer, Pd complexes, DFT, Electronic properties.

Highlights

Assessment of the relationship between the electronic properties and the cytotoxic activity of palladium complexes against the K562 cell line.

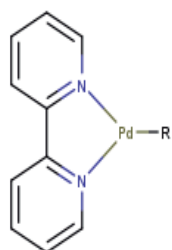
Strong correlation between $\Delta\epsilon$ (eV) and CC_{50} (μM) was found, with a $R^2 = 0.9852$.

Abstract

Pd complexes are promising compounds for the treatment of cancer, as they have fewer adverse effects and have significant antitumor activity. *In silico* methods allow obtaining electronic properties and, consequently, information about

their activity, optimizing the process of searching for new drugs.¹ The present work aims to search for correlations between the antitumor activity described by a set of Pd(II) complexes and their electronic and physicochemical properties. Initially, a set of seven Pd(II) complexes (Figure 1) that show antitumor activity for the K562 cell line were selected¹. The geometries of complexes were optimized and characterized as a minimum point on the potential energy surface (PES) through harmonic frequency calculations at B3LYP/Paschoal-DZP/def2-SVP/IEF-PCM(UFF) in GAUSSIAN 16 Rev. C.01 program. The computational protocol was defined for having the best computational cost/quality in previous kinetic

studies.² The electronic properties such as frontier orbital energies (ϵ_{HOMO} , ϵ_{LUMO} , and $\Delta\epsilon$), hardness (η), chemical potential (μ), electronegativity (χ), and electrophilicity (ω) were calculated³, and correlations with the biological activity (CC_{50} , μM) described in the literature for the Pd(II) complexes were attempted. In addition, octanol/water partition coefficient ($\log p_{o/w}$) will also be calculated. We can highlight that the results indicate a strong correlation between $\Delta\epsilon$ (eV) x CC_{50} (μM) (Figure 2), indicating that the frontier orbitals are excellent descriptors of the activity of Pd(II) compounds. Then, theoretical CC_{50} values were calculated and compared with experimental values (Figure 3), showing excellent results. Concluding, the results showed important correlations between the electronic properties and the antitumor activity of the studied Pd complexes, which may help to explain differences between the activity of molecules, in addition to helping predict CC_{50} values. Subsequently, the number of Pd complexes is being increased to 22 and other properties are also being evaluated.



R₁= ethyldithiocarbamate;
R₂= butyldithiocarbamate;
R₃= n-hexyldithiocarbamate;
R₄=morpholinedithiocarbamate;
R₅= piperidinedithiocarbamate;
R₆= glycinato;
R₇= octylglycinato;

Figure 1. General structure of the Pd(II) complexes

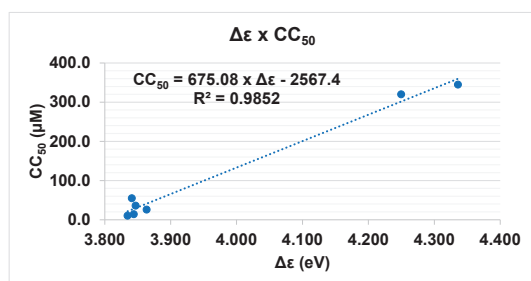


Figure 2. Linear regression between $\Delta\epsilon$ x CC_{50}

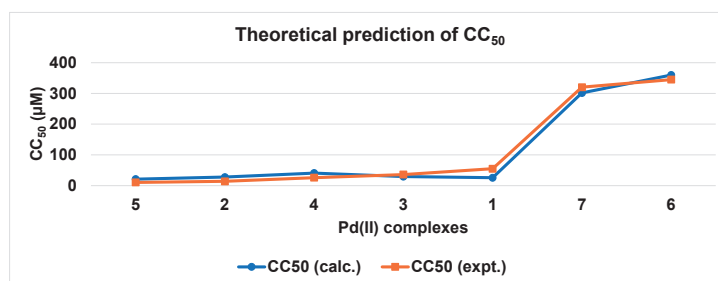


Figure 3. Correlation between calculated and theoretical CC_{50} values

¹Jahromi, E. Z. et al. J Iran Chem Soc, v. 13, p. 967-989, 2016;

²De Souza, C. R. S. et al. Assessment of a computational protocol for studying the aquation reaction of Pd(II) complexes (in preparation).

³Feizi-Dehneyebi, M. et al. Spectrochim Acta, Part A, v. 249, p. 119215, 2021.

Acknowledgments

The authors would like to thank the Brazilian agency FAPERJ (E-26/201.336/2022 – BOLSA) and CAPES (Finance Code 001) for the financial support.

46^o Reunião Anual da Sociedade Brasileira de Química: "Química: Ligando ciências e neutralizando desigualdades"

Área: INO

Cyclometalated iridium(III) complex with N^O chelating pyrazine ligandGustavo M. Martinez (IC)¹, Renan C. Silva (PG)^{1,2}, Ana M. Pires (PQ)^{1,2}, Sergio A. M. Lima (PQ)^{1,2}

g.martines@unesp.br

¹Department of Chemistry and Biochemistry, FCT-UNESP; ²Department of Chemistry and Environmental Sciences, IBILCE-UNESP.

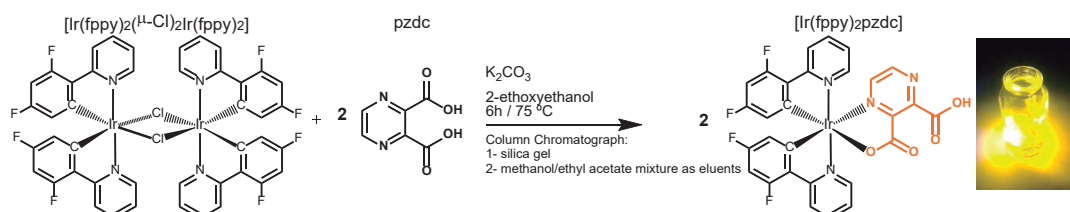
Keywords: Luminescence, Ir(III), Spin–Orbit Coupling (SOC), Solvatochromism.

Highlights

New phosphorescent iridium(III) complex.

Abstract

The phosphorescent heteroleptic iridium(III) complexes are extraordinary d-block luminophore because of their high quantum yields (Φ) and easy photophysical tuning of the ³LC -^{1,3}MLCT hybrid excited state [1]. The highly efficient emission originates from the strong spin–orbit coupling of the Ir(III) ion, which leads to the formation of a hybrid state mixing the triplet ligand-centered (³LC) and both singlet/triplet metal-to-ligand charge transfer (^{1,3}MLCT) states. Heteroleptic iridium(III) complexes have been widely explored in devices like dye-sensitized solar cells (DSC) and organic light-emitting diodes (OLEDs), and in the biological area as bioimaging agents and photodynamic therapy. Thus, here we report the synthesis of the complex [Ir(fppy)₂pzdc] where, fppy = 2-(2,4-difluorophenyl) and pzdc = 2,3-pyrazinedicarboxylic acid (Scheme 1).



Scheme 1: Synthesis of the heteroleptic Ir(III) complexes with N^O chelating pyrazine ligand [2]. Photograph of the complex in powder form under laser ($\lambda_{exc} = 410$ nm). Yield (46%), of a yellow powder. FTIR–ATR (ν_{max}/cm^{-1}): 1632 ($\nu_{C=O}$)_{pzdc}, 1600, 1570, 1557 ($\nu_{C=N}$, $\nu_{C=C}$)_{fppy}, 1333 (ν_{COO})_s, 1108 ($\nu_{C=N}$, $\nu_{C=C}$)_{pzdc}. CHN Analysis Calcd for IrC₂₈H₂₃N₄O₈F₄: C, 41.43%; H, 2.86%; N, 6.90%. Found: C, 41.50%; H, 3.02%; N, 6.20%.

Coordination by the pyrazine N^O site is indicated by IR spectra, where the pyrazine stretching bands disappear in the complex. The photophysical properties were studied by UV-Vis and Photoluminescence Spectroscopy by varying the solvent: DMSO, DCM, ACN, and MeOH. High molar absorptivity was observed. LC and MLCT singlet/triplet transitions are verified, Fig 1(a). In Figure 1(b) the normalized excitation spectra exhibited a broad band with a similar profile for all solvents. The emission spectra obtained for each solvent are seen in Fig. 1(c) in normalized form and in Fig.(d) as a function of intensity, where broad yellow-orange-red emissions with shift of the maxima are observed. The Φ was determined: DMSO (7.7%), DCM (9.2%), ACN (6.9%), and MeOH (1.2%). The observed solvatochromism effect indicates a great MLCT character, exhibiting higher Φ in aprotic solvents, while, in the protic MeOH it exhibits a lower Φ . The presence of hydrogen bonds in the complex can affect its phosphorescence.

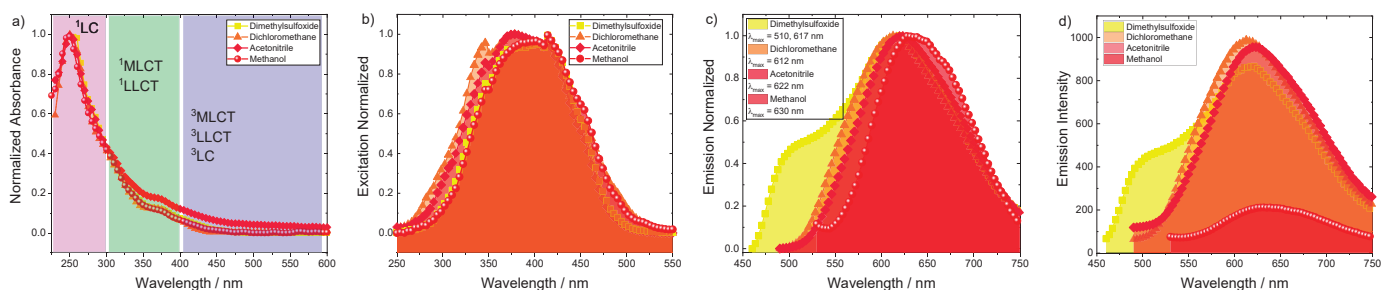


Figure 1: (a) UV-Vis absorption spectra in 1.0×10^{-5} mol.L⁻¹ solutions. (b) excitation spectra ($\lambda_{em} = 613$ nm), (c) normalized emission ($\lambda_{ex} = 400$ nm) and (d) as a function of intensity in different solvents at concentrations 2.0×10^{-4} mol.L⁻¹.

References: [1] Deaton JC, Castellano FN. Archetypal Iridium(III) Compounds for Optoelectronic and Photonic Applications: Photophysical Properties and Synthetic Methods. John Wiley & Sons Ltd. (2017). [2] Govindaswamy, P. et al. Mono and dinuclear iridium, rhodium and ruthenium complexes containing chelating carboxylato pyrazine ligands: Synthesis, molecular structure and electrochemistry. J. Organomet. Chemi. (2007).

Acknowledgments

This work was supported by CNPQ (PIBIC: n°6179) and FAPESP (2019/26103-7).

Decavanadates containing nickel(II) and copper(II) complexes

Heloísa de Souza Camilo (PG),^{1*} Juliana Morais Missina (PQ),¹ Gabriel Barros Baptistella (PG),¹ Patrizia Rossi (PQ),² Paola Paoli (PQ),² Jaisa Fernandes Soares (PQ)¹, Giovana Gioppo Nunes (PQ).¹

sc.heloisa@gmail.com

¹Departamento de Química, UFPR, Brazil; ²Dipartimento di Ingegneria, Università degli Studi di Firenze, Firenze, Italy.

Key words: (Decavanadate, POVs, Cyclen, Nickel(II) complexes, Copper(II) complexes)

Highlights

Two new decavanadate (V_{10}) salts containing nickel(II)- and copper(II)-cyclen complexes were synthesized and characterized by SC-XRD, FT-IR, P-XRD, TG and EPR. Distinct structural modes of interaction with V_{10} were found. Both products are being evaluated as adsorbents of organic dyes from aqueous solution.

Resumo/Abstract

Recently it has been demonstrated by our research group that decavanadate salts are able to bleach aqueous solutions of organic cationic dyes.¹ Herein, two novel bimetallic decavanadates $[\text{Ni}(\text{cyclen})(\text{H}_2\text{O})_2]_2[\text{H}_2\text{V}_{10}\text{O}_{28}]\cdot 2\text{H}_2\text{O}$ (**1**) and $[\{\text{Cu}_2(\text{cyclen})_2\}(\text{H}_2\text{V}_{10}\text{O}_{28})]\cdot 6\text{H}_2\text{O}$ (**2**), where cyclen = 1,4,7,10-tetraazacyclododecane, are described. Single-crystal X-ray diffraction analysis revealed that, in **1**, two hexacoordinated $[\text{Ni}(\text{cyclen})(\text{H}_2\text{O})_2]^{2+}$ complexes counterbalance the charge of a discrete diprotonated V_{10} anion, while in **2**, the $[\{\text{Cu}_2(\text{cyclen})_2\}]^{2+}$ moiety is bound to V_{10} through a $\mu_3\text{-O}$ atom (Figure 1). To the best of our knowledge, it is a new coordination mode of copper(II) complexes to V_{10} . Both complexes were also characterized by P-XRD, spectroscopic techniques (FTIR, Raman, EPR and UV/vis), and thermogravimetric analysis (TGA). The IR spectra of the products presented bands characteristic of the V_{10} anion and the organic parts ($\nu(\text{N-H})$ at 3323 and 3233 cm^{-1} , $\nu(\text{C-H})$ at 2943 and 2883 cm^{-1} , $\nu(\text{V=O})$ at 960 cm^{-1} , and $\nu(\text{V-O})$ at 831, 748 and 613 cm^{-1}). The copper(II) center in **2** adopts a square pyramidal geometry. The solid-state EPR spectrum of **2** showed only one signal at 3200 G, characteristic of an isotropic Cu^{II} species ($g = 2.098$), which could be related to a dynamic Jahn-Teller effect. Both complexes were employed in dye adsorption studies for wastewater treatment purposes using methylene blue as model. Bleaching assays were performed by the direct addition of each compound to aqueous solutions of methylene blue (MB), monitoring the absorption at 664 nm. Both complexes were effective in bleaching the dye solution. The efficacy of **2** to bleach MB solutions in the presence of hydrogen peroxide was remarkable, achieving nearly 81% of color removal in only 30 min.

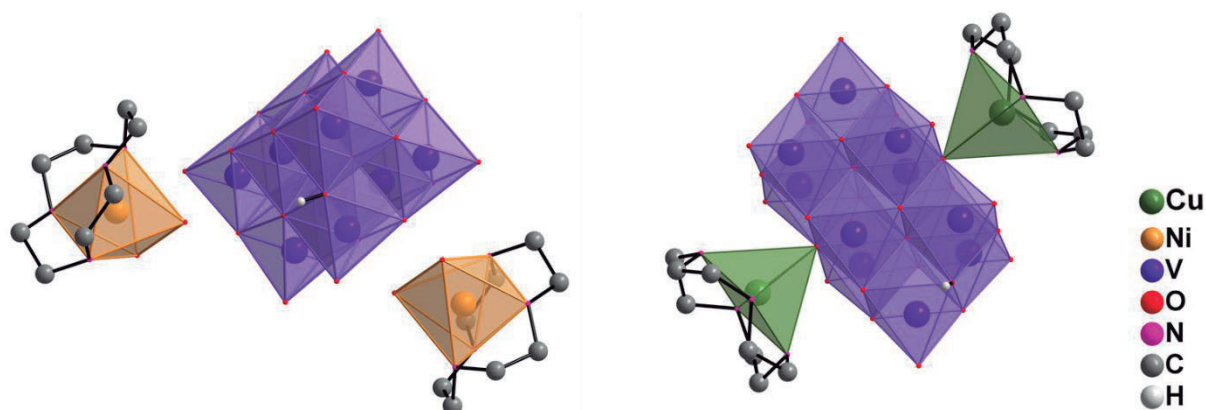


Figure 1. Representations of $[\text{Ni}(\text{cyclen})(\text{H}_2\text{O})_2]_2[\text{H}_2\text{V}_{10}\text{O}_{28}]\cdot 2\text{H}_2\text{O}$ (**1**) $[\{\text{Cu}_2(\text{cyclen})_2\}(\text{H}_2\text{V}_{10}\text{O}_{28})]\cdot 6\text{H}_2\text{O}$ (**2**).

1 MISSINA, *et. al.*, Polyhedron, 114414, 2020.

Agradecimentos/Acknowledgments

UFPR, CNPq, CAPES-PrInt, Fundação Araucária

Degradação de corantes utilizando nanopartículas core-shell $\text{Fe}_3\text{O}_4@\text{Nb}_2\text{O}_5$ como fotocatalisadores.

Aaron M. dos Santos (IC),¹ **Adriana Seidel** (PG),² **Karine P. Naidek** (PQ)^{1*}

mewsaaron@gmail.com; karine.naidek@udesc.br

¹Departamento de Química, Centro de Ciências Tecnológicas, Universidade do Estado de Santa Catarina (UDESC) – Joinville/SC

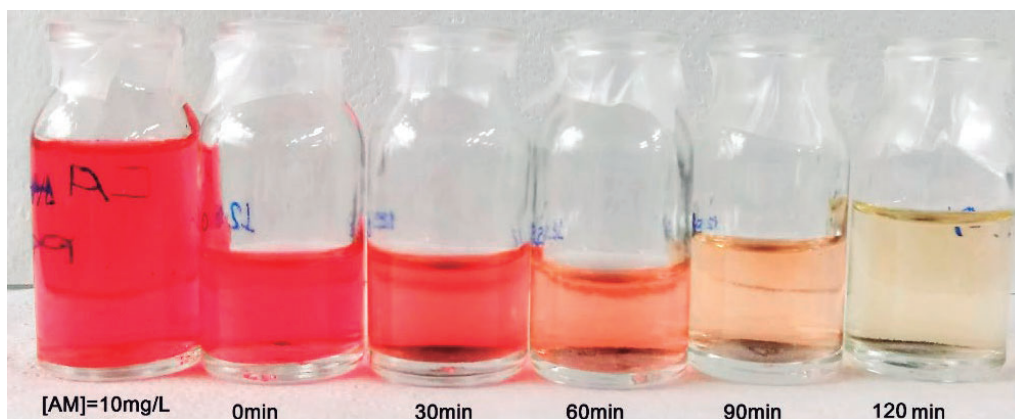
Palavras Chave: Fotocatálise, Nanopartículas, Core-Shell, Nióbio, Magnético.

Highlights

Dye degradation using $\text{Fe}_3\text{O}_4@\text{Nb}_2\text{O}_5$ core-shell nanoparticles as photocatalysts. $\text{Fe}_3\text{O}_4@\text{Nb}_2\text{O}_5$ core-shell was synthesized, with photocatalytic discoloration efficiency 90% or better. Cycling experiments indicate that the discoloration efficiency remained 86% or better after five cycles.

Resumo/Abstract

Corantes provenientes das mais diversas atividades industriais dão origem a um grande volume de efluentes que, se tratados incorretamente, podem destinar corantes orgânicos para o meio aquático. Uma alternativa que vem ganhando destaque como possibilidade de tratamento para esses efluentes é a fotocatálise, destacando-se o emprego de nanopartículas. Uma forma de potencializar esse processo é revestir nanopartículas magnéticas (NPMs) com óxido de nióbio(V) a fim de promover uma maior fotodegradação no meio. Sendo assim, o objetivo desse trabalho é sintetizar, caracterizar e identificar a atividade de NPMs do tipo *core-shell* em fotocatálise dos corantes alaranjado de metila (AM), vermelho de metila (RM) e violeta de metila (VM), pois esses são comumente utilizados em processos industriais. A metodologia envolvida possui três etapas: 1) a síntese das NPMs a partir de sais de ferro; 2) o recobrimento da NPMs com óxido de nióbio(V) para gerar $\text{Fe}_3\text{O}_4@\text{Nb}_2\text{O}_5$ e caracterização via FTIR, DLS e TEM; e 3) teste da eficiência na degradação e descoloração dos corantes orgânico AM, RM e VM via fotocatálise. Os resultados apontam que foi possível sintetizar $\text{Fe}_3\text{O}_4@\text{Nb}_2\text{O}_5$ e caracterizar via FTIR, DLS e TEM, utilizar o nanocatalisador em fotocatálise e degradar os corantes AM (90%), RM (80%) e VM (81%) em 120 min. A influência de parâmetros na eficiência da descoloração, foi estudada por meio de cinética de primeira ordem e o melhor resultado obtido foi na condição em pH = 2, 0,5 g L⁻¹ de nanocatalisador, concentração de AM igual a 5 mg L⁻¹ e tempo no ultrassom de 20 min. Por fim, foi possível avaliar a reutilização do nanocatalisador, que em 5 ciclos sua eficiência se manteve acima de 86% de degradação em 120 min de fotocatálise.



Agradecimentos/Acknowledgments

UDESC, FAPESC, Centro Multiusuários CCT/UDESC.

Development and characterization of europium(III)-doped gadolinium(III) hydroxychloride to obtain oxychloride with potential applicability in ionizing radiation detectors

Gabriel L. Colombo, (IC)¹ Marco A. Cebim, (PQ)^{1*}

gabriel.colombo@unesp.br, marco.cebim@unesp.br

¹Institute of Chemistry, Department of Analytical Chemistry, Physico Chemical, and Inorganic, São Paulo State University (UNESP)

Keywords: Scintillators, Lanthanides, Luminescence.

Highlights

Development of materials with scintillation property; Layered double hydroxides of lanthanides.

Abstract

Currently, with the advances in technology, different forms of ionizing radiation are present in the daily life of human beings, such as in medical examinations (X-ray, UV), power generation, detection devices in airports, etc. Thus, the quantification of radiation present in certain environments, so that it does not exceed the safe exposure limit for humans, is extremely important. Through materials called scintillators, materials responsible for absorbing high energy radiation and converting it to lower energy radiation, it is possible to quantify this radiation through the emission of light. Thus, the importance of studying new materials that have the property of scintillation is increasing. In this work, lamellar precursors of lanthanides were developed through the synthesis by the hydrothermal method, with the purpose of synthesizing oxychlorides from the thermal decomposition of these precursors. Lanthanide oxychlorides have scintillation properties, so they can be applied in ionizing radiation detectors. The materials obtained, with the general formula $Gd_{4-x}Eu_xO(OH)_9Cl.yH_2O$ (Figure 1A), ([Eu(III)] in relation to [Gd(III)] = 0.5%, 1%, 2%, 4%, and 8%), were characterized via FTIR (Figure 1B), where one can notice binding bands with OH and bonds of metals with oxygen and metals with chloride. They were also characterized via XRD (Figure 1C), where one can notice the formation of lanthanide hydroxides, with the general formula $Gd_{1-x}Eu_x(OH)_3$.

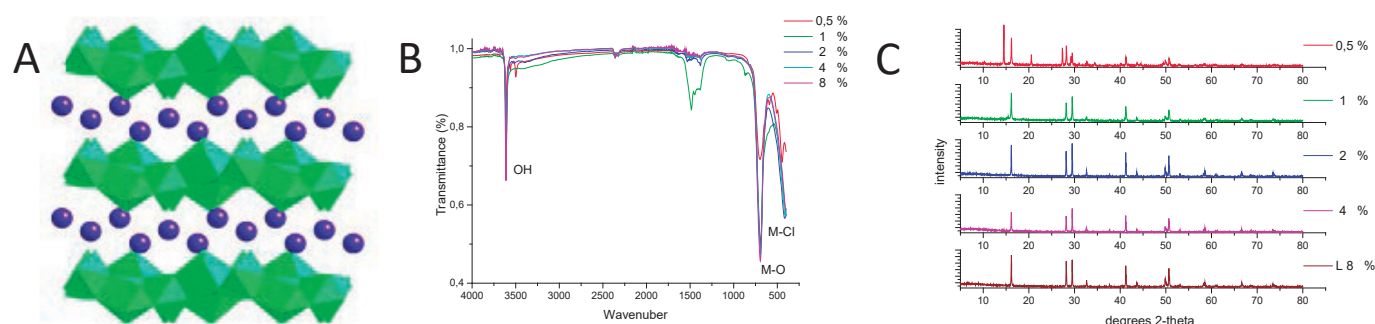


Figure 1: (A) Spatial representation of synthesized materials, (B) Infrared spectrum, (C) X-ray diffraction of the obtained compounds.

Agradecimentos/Acknowledgments

CAPES and CNPq (procs: 141081/2020-1 e 317610/2021-0)

Development of pH Sensors Based on Eu(dbm)₃ Complexes and 1,10-Phenanthroline Derivatives: Synthesis and Spectroscopic Analysis.

Jean D. C. Menezes (IC),¹ Rodolpho A. N. Silva (PG),¹ Ana M. Pires (PQ)^{1,2}, Marco A. Cebim (PQ)¹ and Marian R. Davolos (PQ)¹.

jean.dominique@unesp.br; marco.cebim@unesp.br

¹São Paulo State University (Unesp), Institute of Chemistry, Araraquara, Brazil

²São Paulo State University (Unesp), School of Technology and Sciences, Presidente Prudente, Brazil

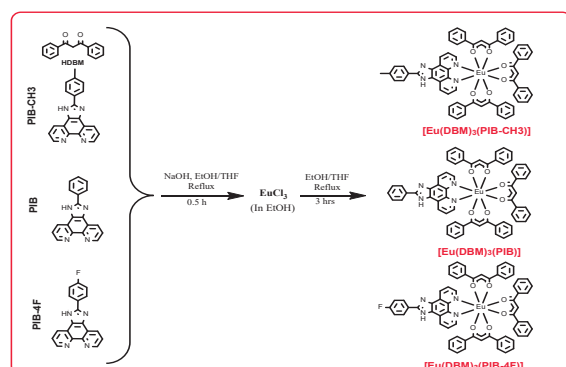
Keywords: Lanthanide, Luminescence, coordination, sensor

Highlights

Three complexes with the general formula [Eu(DBM)₃(Phen-derivative)] were synthesized, characterized and had their optical properties evaluated, showing higher luminescence than the precursor complex.

Abstract

Lanthanide ions are widely used due to their established optical properties, such as bioluminescent markers and sensors, which arise from intraconfigurational 4f-4f transitions. However, these electronic transitions are forbidden by Laporte's rule, resulting in low molar absorption. To overcome this limitation, organic molecules can be inserted to absorb and transfer energy to the emitting ion in a phenomenon known as the antenna effect. In this work, three new complexes were synthesized, with a structure based on a derivative of 1,10-phenanthroline (PIB, PIB_4CH₃, or PIB_4F) and three units of β-diketone (DBM). The complexes were characterized via FTIR and Raman, where the displacement of the C=N and C=O stretches indicated the coordination of the ligands to the ion. The presence of molecular ions was verified by mass spectrometry, suggesting success in the synthesis of the complexes. Finally, photoluminescence spectroscopy revealed a significant increase in the emission quantum efficiency (Table 1) for the synthesized complexes compared to the precursor complex, indicating that the replacement of water molecules the precursor complex 1,10-phenanthroline derivatives played an important role in improving the emission quantum efficiency.



Complex	Emission quantum efficiency (%)	Increase (%)
Eu-DBM-H ₂ O	10	-
Eu-DBM-PIB	51	510
Eu-DBM-PIB_4F	38	380
Eu-DBM-PIB_4CH ₃	23	280

Figure 1: Scheme of synthesis of the produced complexes. **Table 1:** Emission quantum efficiency values and relative increase.

Acknowledgments

CAPES and CNPq (procs: 141081/2020-1 e 317610/2021-0)

Dinuclear Gold(I) diphosphine metallacycles with pyridyldicarboxamide-bis(thiosemicarbazides)

Ana J. Z. Londero (PG),¹ Vânia Schwade (PQ),¹ Ernesto S. Lang (PQ),¹ Ulrich Abram (PQ),² Pedro I. S. Maia (PQ)^{3*}

anajulialondero@gmail.com; pedro.maia@uftm.edu.br

¹Departamento de Química, UFSM, Santa Maria, Brazil; ²Institute of Chemistry and Biochemistry, Freie Universität Berlin, FUB, Berlin, Germany; ³Department of Chemistry, UFTM, Uberaba, Brazil

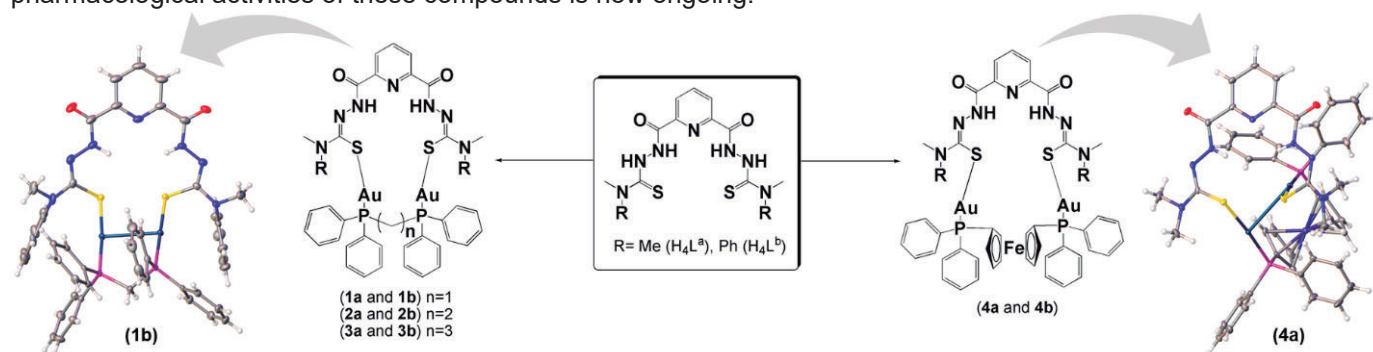
Keywords: Gold(I) complexes, Thiosemicarbazides, X-ray diffraction.

Highlights

A novel thiosemicarbazide-type ligand class with a potential N₃S₂-donor set, H₄L^R, was prepared. Dinuclear Gold(I) metallacycles were obtained from reactions of H₄L^R and [(AuCl)₂(dppx)].

Resumo/Abstract

Thiosemicarbazones and thiosemicarbazides are classes of compounds with wide pharmacological versatility, such as antiviral, antitumor and antimicrobial activities.¹ Besides that, the coordination chemistry is interesting due to their variable donor ability and structural diversity. Considerable efforts have been made to development non-platinum anticancer agents, for example, gold complexes have attracted significant attention since gold(I) and gold(III) compounds have been found to inhibit tumor cell growth.¹ In this work, we report the synthesis and spectroscopic characterization of H₄L^{a,b} and their gold(I) metallacycles [Au₂(dppm)H₂L] (**1a,b**), [Au₂(dppe)H₂L] (**2a,b**), [Au₂(dppp)H₂L] (**3a,b**) and [Au₂(dppf)H₂L] (**4a,b**) [H₄L^a = 2,6-Bis(4,4-dimethylthiosemicarbazide-1-yl-carbonyl)pyridine; H₄L^b = 2,6-Bis(4,4-diphenylthiosemicarbazide-1-yl-carbonyl)pyridine; dppm = 1,1'-bis(diphenylphosphino)methane; dppe = 1,1'-bis(diphenylphosphino)ethane; dppp = 1,1'-bis(diphenylphosphino)propane; dppf = 1,1'-Bis(diphenylphosphino)ferrocene]. The preparation of H₄L was performed using 2,6-pyridinedicarbonyl dichloride and the thiosemicarbazide derivative in THF in the presence of a base. H₄L^{a,b} were characterized by FT-IR spectroscopy, ¹H NMR, ESI-MS and elemental analysis. The structure of H₄L^b was also confirmed by single-crystal X-ray diffraction. The complexes were synthesized by reaction of H₄L with [(AuCl)₂(dppx)] in CH₂Cl₂ at room temperature and were precipitated by addition of diethyl ether (Scheme 1). The gold(I) complexes were fully characterized by FT-IR spectroscopy, ¹H and ³¹P{¹H}-NMR, ESI-MS and elemental analysis. The complexes **1b**, **2b** and **4a** were further characterized by single-crystal X-ray diffraction, revealing the formation of gold(I) metallacycles upon coordination of the bis(thiosemicarbazide) ligands via the sulfur atoms. The linear (173-178°) coordination around the gold atoms is completed by the phosphine ligand. Strong Au...Au interactions are observed in the structures which are responsible for the stability of the metallacycles. The evaluation of the pharmacological activities of these compounds is now ongoing.



Scheme 1. Synthesis of complexes 1–4.

Agradecimentos/Acknowledgments

CNPq and CAPES

¹ P.I.S. Maia, V.M. Deflon, U. Abram, *Future Med. Chem.* 6(13), 2014, 1515–1536.

46ª Reunião Anual da Sociedade Brasileira de Química: "Química: Ligando ciências e neutralizando desigualdades"

Distinctive single-molecule magnet behavior of two related dysprosium(III) complexes with different geometries

Francielli S. Santana (PG),^{1*} Fabio Santanni (PQ),² Matteo Briganti (PQ),² Mauro Perfetti (PQ),² Giovana G. Nunes (PQ),¹ Roberta Sessoli (PQ),² Jaísa F. Soares (PQ).¹

francielli.s.santana@ufpr.br

¹Departamento de Química, Universidade Federal do Paraná, Curitiba-PR, Brazil; ²Dipartimento di Chimica "Ugo Schiff", Università degli Studi di Firenze, Florence, Italy

Palavras Chave: Single-Molecule Magnets, Dysprosium, PCS Agent, Computational Calculations.

Highlights

A new, well-performant single-molecule magnet as a potential PCS agent candidate. Detailed computational and experimental studies on the different magnetic behavior of two structurally-related dysprosium(III) compounds.

Abstract

Complexes based on lanthanoid ions (Ln^{3+}) with the ligand **bbpen**²⁻ (H_2bbpen = *N,N'*-bis(2-oxidobenzyl)-*N,N'*-bis(pyridin-2-ylmethyl)ethylenediamine), and their derivatives, give rise to well-performant magnetic and optical materials.¹ These compounds belong to the Single-Molecule Magnet (SMM) class, which shows slow magnetic relaxation in the absence of an external magnetic field. SMM candidates are those that present, among other features, a large magnetic anisotropy determining a high effective energy barrier for magnetization reversal (U_{eff}). Moreover, as a consequence of such significant anisotropy, Ln-SMM constitute good candidates for pseudocontact shift agents (PCS) in structural studies of macromolecules by Nuclear Magnetic Resonance (NMR), as shown in a previous work by some of us on the pentagonal-bipyramidal (PBP) compound **[Dy(bbppn)Cl]** (**1-Cl**, Figure 1, H_2bbppn = *N,N'*-bis(2-oxidobenzyl)-*N,N'*-bis(pyridin-2-ylmethyl)-1,2-propanediamine).² Notwithstanding the excellent performance of the air-stable SMM **1-Cl**, its practical application as PCS tag is limited by low solubility in polar solvents, with dimethylsulfoxide (dmsO) as an exception. From the slow evaporation of a dmsO solution of **1-Cl**, colorless crystals of **1-dmsO** were isolated. Single-crystal X-ray diffraction analysis of **1-dmsO** revealed a distorted square antiprismatic geometry (Figure 1), in which Cl⁻ acts as a counter ion after being displaced from the Dy³⁺ inner coordination sphere by two dmsO molecules. Surprisingly, powder X-ray diffraction (PXRD) analysis revealed reversal to the structure of **1-Cl** after the crystals of **1-dmsO** were stored in air for a few weeks and finally grounded for analysis. Magnetic measurements confirmed the SMM nature of freshly prepared **1-dmsO**, which is strongly axial at low temperatures. Detailed computational calculations by CASSCF

method allowed us to explain the significant change in the magnetic relaxation dynamics of **1-dmsO** as compared to **1-Cl**, which arises from the structural differences between them. Due to its considerable magnetic anisotropy and better solubility in polar solvents as compared to **1-Cl**, **1-dmsO** qualifies for investigation as a potential NMR tag in protein structural studies.

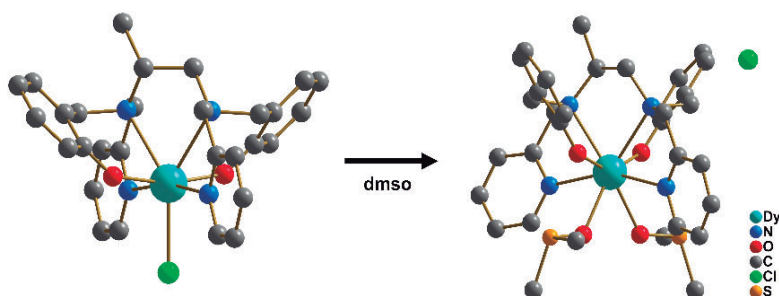


Figure 1. Structural representation of the compounds **1-Cl** (left) and **1-dmsO** (right).

References:

- [1] Qu, Y-X. *et al.* *Coord. Chem. Rev.* **2023**, 475, 214880.
 [2] Santana, F. S. *et al.* *Chem. Sci.* **2022**, 13, 5860.

Acknowledgments

UFPR; CAPES; CNPq; UNIFI.

DNA interaction and *in silico* studies of bioinspired copper(II) complexes containing *n*-alkyl chains

Fernando R. Xavier (PQ),¹ Maiara Ignês N. dos Santos (PG),¹

fernando.xavier@udesc.br

¹Laboratório de Síntese e Catálise – SINCA, Departamento de Química, CCT/UEDESC, Joinville-SC, Brazil.

Keywords: Bioinspired ligands; copper(II) complexes; DNA interaction; molecular docking.

Highlights

Metal complexes containing bioinspired ligands are growing in a variety of medicinal applications. Three copper complexes were prepared and had their physicochemical properties determined. Their ability to interact with salmon DNA was assessed spectrophotometrically and binding constants are being calculated and corroborated by *in silico* studies (molecular docking).

Resumo/Abstract

Cancer is a chronic disease characterized by the uncontrollable cell growth that invade tissues and organs. One of the means of combating this dysfunction is to block the cellular DNA replication. Metal complexes have been extensively studied as potential chemotherapeutic agents with antitumor activity [1]. Copper-based complexes can be considered good candidates as antineoplastic agents once Cu(II) ions have less systemic toxicity for non-tumor cells than platinum for example [1,2]. Parallel to this, a good example of bioinspired ligand that can interact with DNA is the bis(2-picolyl)amine (bpma), which consists in a quite versatile molecule which can be easily functionalized with pendant R-groups.[3] Thus, the ligands bpma, L^{C6OH}, and L^{C10OH} were synthesized and characterized accordingly. All [CuL₂](ClO₄)₂ complexes were prepared by adding a solution of the respective ligand (1,0 mmol) in methanol (10 mL) in a solution of Cu(ClO₄)₂·6H₂O (0,5 mmol) also in methanol (10 mL) at room temperature where color became deep blue. [Cu(bpma)₂](ClO₄)₂ (**1**) was isolated as dark blue crystals whereas [Cu(L^{C6OH})₂](ClO₄)₂ (**2**) and [Cu(L^{C10OH})₂](ClO₄)₂ (**3**) consisted in greenish-blue thick oils (Fig. 1, left). These compounds were analyzed by elemental analysis, infrared spectroscopy, molar conductivity, ultraviolet and visible spectroscopy, electrochemistry, and mass spectrometry. The electronic structure and molecular arrangement were calculated via DFT and TD-DFT studies for the three complexes, which helped with their IR and UV-Vis assignments. The ability of interaction between all complexes with nucleic acids was evaluated through spectrophotometric studies, and intrinsic binding constants (*K_b*) with the probable complex/DNA binding modes being determined and corroborated by molecular docking (*in silico* analysis).

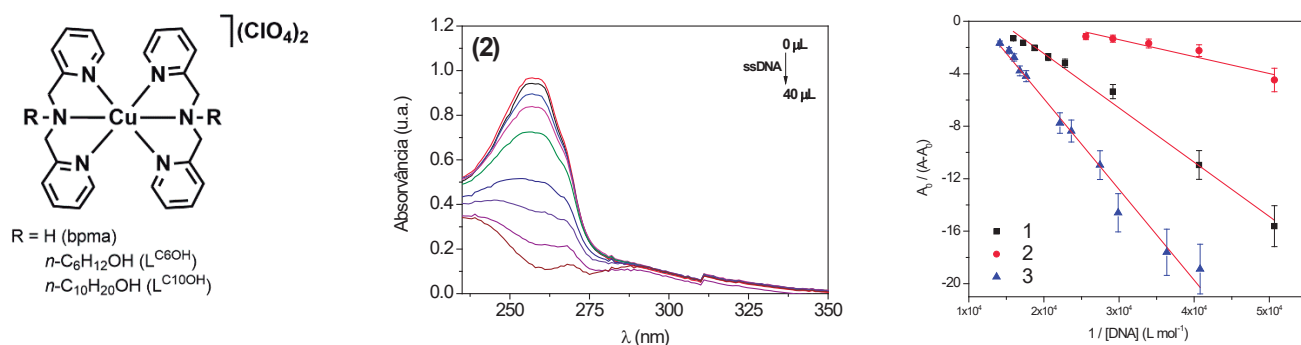


Fig. 1 – Complexes herein studied (left), spectral variation of **2** during DNA titration (middle) and Benesi-Hildebrand plot for complexes **1-3** (right). *K_b* values obtained: 4.24, 1.92, and 1.15×10⁴ L mol⁻¹. For **1-3**, respectively.

[1] LIU, Ya-xian et al. *Trans. Met. Chem.* 43(3) (2018) 259-271. [2] T.J.P. McGivern et al. *Inorg. Chim. Acta.* 472 (2018) 12-39. [3] C. Wende, et. al. *Eur. J. Inorg. Chem.* 16, (2014) 2585.

Agradecimentos/Acknowledgments

CMU/CCT-UEDESC, IQ-USP, UFSC, FAPESC, CAPES and CNPq.

Effects of substituent in *meso*-tri-pyridyl porphyrin derivatives: synthesis and photophysical analysis

Rafaela Copello (IC)¹, Bernardo Almeida Iglesias (PQ)¹

rafacop09@gmail.com

¹ Laboratório De Bioinorgânica e Materiais Porfirínicos, Departamento De Química, Universidade Federal De Santa Maria, UFSM, Av. Roraima 1000, 97105-900 Santa Maria, RS, Brazil;

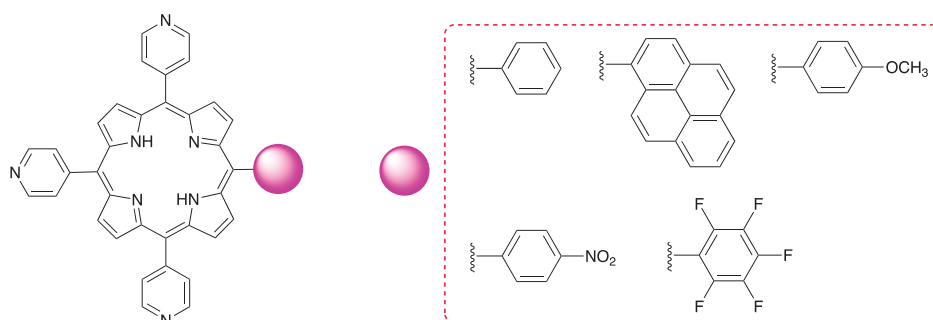
Palavras Chave: *Porphyrins, Photophysical, Steady-state fluorescence, Fluorescence lifetimes.*

Highlights

Photophysical investigation of asymmetric porphyrin derivatives; Solution behavior in several solvents; Use of steady-state and time-resolved fluorescence emission techniques;

Resumo/Abstract

Porphyrins, in general, are tetrapyrrolic macrocycles that present attractive photophysical properties, mainly according to the change in solvent polarity. Depending on the nature of the solvent, they may show different behavior in the ground state and in the excited state^{1,2}. Porphyrin derivatives containing peripheral coordinating groups (for example, pyridyl units) may be interesting for the formation of cationic derivatives, which may have different photophysical properties. In this work, we report, the photophysical analysis of tri-substituted porphyrin derivatives with pyridyl and diverse aromatic substituents at *meso*-5-position. Porphyrins in several solutions (DCM, ACN, 1,4-Diox, EtOH, DMF, DMSO) are studied and photophysical behavior by absorption UV-Vis and emission analysis (steady-state and time-resolved fluorescence) were used. Preliminary results show that these derivatives are influenced by the nature of the solvent (mainly by variations in the Soret bands), emitting fluorescence in the region between 600-800 nm and presents shorter fluorescence lifetimes (between 2.0 to 10 ns). Photostability, ROS generation assays (singlet oxygen and superoxide) and electrochemical behavior are evaluated. Moreover, this class of compounds can be used as platform for coordination chemistry at peripheral pyridyl positions, forming tri-cationic derivatives with some polypyridyl complexes, such as Pt(II) or Pd(II) derivatives.



Agradecimentos/Acknowledgments

The authors thanks to CNPq, FAPERGS and CAPES/PROEX – Finance code 001 for financial supporting.

¹Lopes, J.M.S.; *et al.* Spectrochimica Acta Part A: Molecular and Biomolecular Spectroscopy 238 (2020) 118389.

²de Souza, V.B.; *et al.* Molecules 28 (2023) 1385.

Electronic investigation of the effect of substituents on the SOD mimic activity of copper (II) complexes with 8-hydroxyquinoline-derived ligands

Talis U. Silva (PQ),^{1,2*} Everton T. Silva (PQ),³ Karina C. Pougy (PG),¹ Camilo H. S. Lima (PQ),¹ Sérgio P. Machado (PQ).¹

talisus2506@gmail.com; sergiopm@iq.ufri.br

¹Instituto de Química, UFRJ; ²Instituto de Química, UFRRJ, ³IFRJ

Palavras Chave: SOD mimic activity, 8-hydroxyquinoline derivatives, Copper complexes, Molecular orbital, DFT, Electronic affinity.

Highlights

The theoretical electron affinity of the Cu-complexes has correlated with their superoxide dismutase mimic activity. Electron-withdrawing substituents increased the reduction ability of the compounds.

Resumo/Abstract

Introduction: Superoxide dismutase (SOD) is an important antioxidant defense in live organisms, responsible for the dismutation of the $O_2^{\cdot-}$. Cu-complexes are possible SOD mimetic systems.¹ The main objective of this work was to use DFT calculations to provide details on the structural and electronic properties of the oxidized and reduced forms of the ligands and Cu^{2+} -complexes (SOD mimics) obtained by Ceolin and coworkers (**Figure 1**),² and to study the influence of substituents of different electronic natures on the reactivity of these compounds.

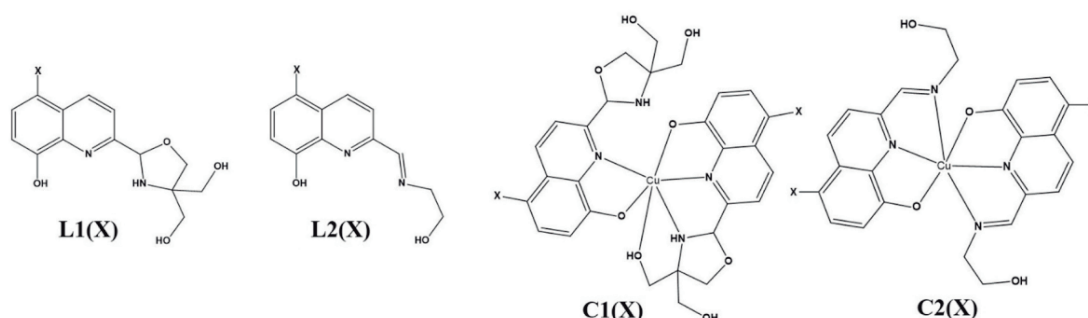


Figure 1. Scheme of the ligands and Cu-complexes studied. X = -NH₂, -OCH₃, -CH₃, -H, -Cl, -CN, -NO₂.

Computational methods: All calculations were done in Gaussian 09 package with B3LYP/LanL2DZ(Cu-atom)/D95V(other atoms) level theory using solvent effect (PCM = water). Electron affinity (EA) was obtained with EA = E_{red} - E_{oxi} (E_{red} and E_{oxi}, energies of reduced and oxidized structures).

Results and discussion: The theoretical parameters obtained were compared and validated with the experimental data available. The results showed that the reduction and oxidation steps occur with greater participation of the 8-HQ ligand and copper atom, respectively, indicating that the electron received during the reduction step is used to reduce Cu(II) → Cu(I). The EA showed a good correlation with the experimental SOD activity, and the analysis of EA, total charge, and molecular orbitals (MO) indicated an increase in the SOD activity with the insertion of electron-withdrawing substituent groups in the structures.

References:

- DAIER, V. A et al. *J. Inorg. Biochem.* 163, 162–175, 2016. Doi: <https://doi.org/10.1016/j>
- CEOLIN, J. et al. *Appl. Organomet. Chem.* 32(4), e4218, 2018. Doi: <https://doi.org/10.1002/aoc.4218>.

Agradecimentos/Acknowledgments

To CAPES (Financial code 001; PhD Scholarship for TU da Silva); FAPERJ (E-26/010.001003/2016 and E-26/010.210.513/2019); CNPq (304402/2017).

Erbium (III) Oxamato-Based Coordination Polymer: Magnetic properties

Jhonny Willians Maciel (PG),¹ Renato Rabelo (PQ),¹ Meiry Alvarenga (PG),¹ Lucas Hoffmann Gregghi Kalinke (PQ),² Felipe Terra Martins (PQ),¹ Danielle Cangussu de Castro Gomes (PQ),¹

jhonnywmaciel@gmail.com;

¹Instituto de Química, UFG; ²Departamento das Áreas Acadêmicas, Instituto Federal de Goiás - Campus Anápolis

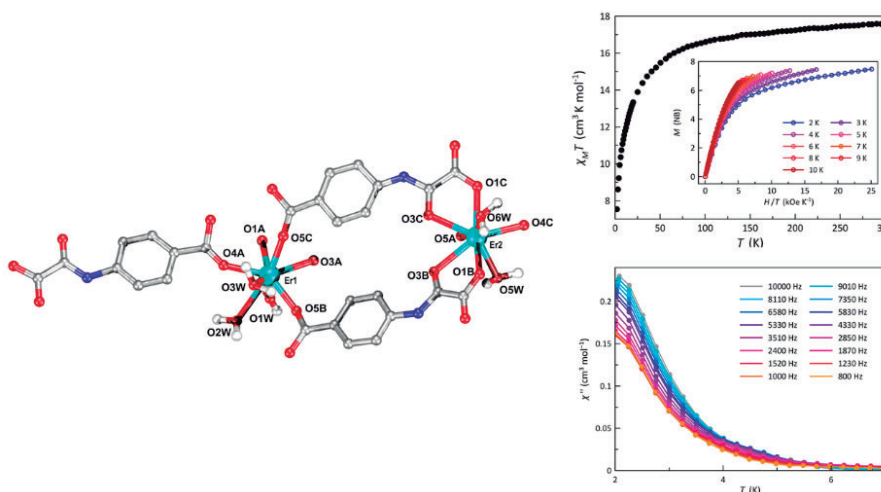
Palavras Chave: Oxamato, EtH₂pcpa, Er(III).

Highlights

In this work, we present the preparation, magnetic properties and structural results concerning the formation of the complex between the Erbium(III) ion with the *N*-(4-carboxyphenyl)oxamic acid (EtH₂pcpa).

Resumo/Abstract

The preparation of coordination compounds based oxamate ligand has been widely explored with numerous examples where the synthesis strategy leads to different structural topologies and physical properties.[1],[2] In this work, we present the structural results and magnetic properties of coordination polymer containing the Er^{III} ions with Na₂Hpcpa [H₃pcpa = *N*-(4-carboxyphenyl)oxamic acid]. The complex was obtained in the form of single crystals by slow diffusion of aqueous solutions of the ligand and metal at 1:1 stoichiometry in an H-shaped tube (yield of 72%). The structure of the complex of formula [Er₂(Hpcpa)₃(H₂O)₅]_n was determined by X-ray single crystal diffraction. The crystallographic results reveal that it crystallizes in the monoclinic *Cc* space group. The asymmetric unit comprises two crystallographically independent Er^{III} metal ions (Er1 and Er2), three anionic Hpcpa²⁻ ligands, and six water molecules. The polymer obtained is isostructural to those previously reported [3]. The plot of $\chi_M T$ versus T of the Er complex shows a value of $\chi_M T$ at room temperature of 17.5 cm³mol⁻¹K, which continuously decreases with cooling because of the thermal depopulation of the M_J states and reaches 7.5 cm³mol⁻¹K at 1.9 K. No χ_M'' signals were found in the absence of an applied d_c magnetic field (H_{dc}) due to QTM effects. However, when a non-zero H_{dc} is applied, χ_M'' signals appear below 6.0 K, indicating the occurrence of the phenomenon of slow relaxation of the magnetization induced by H_{dc} .



Agradecimentos/Acknowledgments

CNPQ, CAPES, FAPEG e UFG.

Referências:

- [1] Maciel J, Kalinke L, Valdo A, et al., J Braz Chem Soc.,30(11):2413-2429 (2019).
- [2] T. L. Oliveira et al., Polyhedron, 81, 105–114 (2014).
- [3] Maciel, J. W. et al., Inorg. Chem. 60, 6176–6190 (2021).

Área: ELE

(Inserir a sigla da seção científica para qual o resumo será submetido. Ex: ORG, BEA, CAT)

Estudo da degradação do pesticida Carbendazim em presença dos íons metálicos Chumbo e Cobre

Aymara da Silva Santos (IC),¹ Lucia Codognoto (PQ), Eliana Maíra Agostini Valle (PQ),¹
aymarasnts@gmail.com; emavalle@gmail.com

¹Universidade Federal de São Paulo – Instituto de Ciências Ambientais, Químicas e Farmacêuticas, UNIFESP – campus Diadema

Palavras Chave: Carbendazim, Chumbo, Cobre, complexo, degradação.

Highlights

Study of the degradation of the pesticide Carbendazim in the presence of the metal ions Lead and Copper

Carbendazim (MBC) is an example of a harmful pesticide, which has atoms of nitrogen and oxygen in its structure that can form complexes with metal ions. Thus, in this work was studied the influence of the complexes on the degradation of Carbendazim by an advanced oxidative process.

Resumo/Abstract

O Carbendazim é fungicida que possui em sua molécula um grupo benzimidazol e um grupo carbamato, atua de forma sistêmica nas raízes e folhas, inibindo a formação de microtúbulos [1]. A estrutura molecular do carbendazim apresenta átomos de nitrogênio e oxigênio que podem interagir com íons metálicos [2]. Estudos prévios mostram uma interação entre os íons metálicos cobre e chumbo e o pesticida carbendazim, em água ultrapura. Neste trabalho avaliou-se a influência dos complexos na degradação do Carbendazim por processo oxidativo avançado.

As medidas foram realizadas a partir de soluções estoque de carbendazim $1,0 \times 10^{-3} \text{ mol L}^{-1}$, em etanol, $\text{Cu}(\text{NO}_3)_2$ $1,0 \times 10^{-3} \text{ mol L}^{-1}$ e $\text{Pb}(\text{NO}_3)_2$ $1,0 \times 10^{-3} \text{ mol L}^{-1}$, em água ultrapura. O estudo da degradação foi realizado em um Potenciostato/Galvanostato AUTOLAB PGSTAT 128N, com três compartimentos. Eletrodo de trabalho: diamante dopado com boro; Eletrodo de Referência: Ag/AgCl (KCl sat.); Eletrodo auxiliar: placa de platina; Eletrólito de suporte: tampão de Na_2HPO_4 ($0,1 \text{ mol L}^{-1}$). A degradação do pesticida foi acompanhada por espectroscopia na região do UV-Visível.

Para o estudo da degradação do CBZ, CBZ-Cu e CBZ-Pb foram realizadas eletrolises com potencial fixo em 3 V. Ao final das eletrolises, o sinal espectroscópico das espécies foi monitorada. Para o CBZ sozinho, observou-se a diminuição da resposta espectroscópica, reduzindo sua concentração inicial de $1,00 \times 10^{-4} \text{ mol L}^{-1}$ para $5,58 \times 10^{-5} \text{ mol L}^{-1}$, ou seja, um percentual de 44,2%. Quando avaliado a influência do metal na degradação do fungicida, observou-se que a presença de chumbo, dificultou a degradação do CBZ, observando uma redução de 26% da concentração inicial. Já em presença de cobre, observou-se a redução de 62% de CBZ em relação a concentração inicial, concluindo que a complexação com cobre facilitou a degradação do mesmo.

Referências

- [1] ARYA, R., SHARMAL, R., MALHOTRA, M., KUMAR, V., SHARMA, A. K. Biodegradation Aspects of Carbendazim and Sulfosulfuron: Trends, Scope and Relevance. Current Medicinal Chemistry, v. 22, n. 9, p. 1147–1155, 2015.
[2] Costa, I.M., Codognoto, L., Valle, E.M.A. J Solid State Electrochem (2017). <https://doi.org/10.1007/s10008-017-3746-5>.

Agradecimentos/Acknowledgments

Ao Instituto de Ciências Ambientais, Química e Farmacêuticas da Universidade Federal de São Paulo – campus Diadema.

Laboratório de Eletroquímica e Eletroanalítica e Bioinorgânica Ambiental (LABEE-BIA) CNPq, CAPES e FAPESP (2017/24235-8) pelo suporte financeiro.

Estudo da oxidação catalítica do ciclohexeno mediada por um complexo bioinspirado de cobre via análise multivariada

Larissa Chimilouski (PG)¹, William Henrique Slominski (PG)¹, Edmar Martendal (PQ)¹ e Fernando Xavier (PQ)¹

larissa.c17@edu.udesc.br

¹Laboratório de Síntese e Catálise – SINCA, Departamento de Química, CCT/UEDESC, Joinville-SC, Brasil.

Palavras-chave: Oxidação catalítica, Ciclohexeno, Análise multivariada.

Highlights

A reação de oxidação catalítica do ciclohexeno gera produtos importantes que são intermediários sintéticos envolvidos na indústria química. Através de uma análise multivariada, foi avaliado a influência da quantidade de catalisador, oxidante (H₂O₂) e o tempo na formação dos produtos de reação. Nas condições ótimas encontradas há formação majoritária da 2-ciclohexen-1-ona (à 20 °C). Estudos de variação de temperatura estão em curso para avaliar a seletividade entre os demais produtos formados.

Resumo/Abstract

A reação de oxidação do ciclohexeno vem sendo objeto de intensos estudos, uma vez que os produtos obtidos, como o 1,2-ciclohexanodiol e ciclohexanona, são intermediários sintéticos envolvidos na produção de produtos químicos finos e na síntese do poliéster^[1]. Neste trabalho, foi aplicado um planejamento multivariado para avaliar simultaneamente as variáveis (quantidade de catalisador, oxidante e tempo) na reação de oxidação catalítica homogênea do ciclohexeno promovido pelo complexo [Cu(bpy)₂](ClO₄)₂. O complexo foi sintetizado e caracterizado de acordo com métodos já descritos^[2]. A oxidação catalítica foi realizada em CH₃CN, onde os intervalos das variáveis foram: Catalisador (0,1-3,0 mol%), peróxido de hidrogênio (1-20 vezes de excesso) e tempo (8-24h). Para tal, foi utilizado um desenho Box-Behnken como metodologia de superfície de resposta, totalizando 15 experimentos. A temperatura foi mantida a 20°C e os principais produtos da reação foram separados e quantificados por GC-MS. Dentre os 15 experimentos, foram identificadas as condições reacionais em que foi quantificado a maior quantidade de produtos gerados (tabela 1). Como não foi detectado todos os produtos nos experimentos, foi feita uma avaliação da influência da temperatura na oxidação do ciclohexeno nas condições ótimas e observou-se que com o aumento da temperatura (35°C e 50°C) foram observados mais produtos, sendo o 2-ciclohexen-1-ona com maior conversão em relação aos demais. Em estudo futuro será avaliado a inclusão da variável temperatura no planejamento multivariado e o impacto na conversão dos produtos desta reação.

Tabela 1. Pontos ótimos na oxidação catalítica do ciclohexeno à 20°C. Onde: 1 (Ciclohexanol); 2 (2-ciclohexen-1-ona); 3 (2-Ciclohexen-1-ol); 4 (1,2-Ciclohexanodiol); 5 (1,2-epoxiciclohexano).

Entrada	Cat. (mol%)	H ₂ O ₂ (n/n _{CyH})	Tempo	Conversão %				
				1	2	3	4	5
2	3,00	10,5	8	-	2,3	0,5	3,0	-
8	1,55	20,0	24	-	60,1	5,3	5,3	-

^[1] Boudjema; Rabah; Choukchou-Braham. *Acta Physica Polonica A*, v. 132, 3, p. 469-472, 2017.

^[2] A. I. Tillmann. *Dissertação de mestrado*. UDESC (2022).

Agradecimentos/Acknowledgments

CMU/CCT-UEDESC, FAPESC, CAPES and CNPq.

Eu³⁺, Tb³⁺, Al³⁺ and Zn²⁺ complexes derived from 2-(4-hydroxiazobenzene)benzoic acid.

Vinicius Flores da Silva¹ (IC), Izilda A. Bagatin (PQ).¹

vinicius.flores@unifesp.br¹;

¹Instituto De Ciências Ambientais, Químicas E Farmacêuticas – ICAQF – UNIFESP – Diadema - SP
Laboratório de Química de Calixarenos, Espectroscopia Molecular e Catálise LQCEMC

Palavras Chave: Europium, Terbium, Zinc, Aluminium, Luminescence, HABA.

Highlights

Coordination compounds with Eu³⁺, Tb³⁺, Al³⁺, and Zn²⁺ can be used to develop Organic Light Emitting Diodes (OLEDs).

Resumo/Abstract

The luminescence phenomenon has a large application in science, from Organic Light Emitting Diodes (OLEDs) to biosensors. The coordination between an organic ligand and Rare Earth metals or transition metals is a classic example of how to achieve luminescent compounds¹. The fluorescence emission of Eu³⁺ and Tb³⁺ complexes is achieved by the energy transfer from the organic ligand excited triplet state to the ⁵D₀ state from Eu³⁺ and ⁵D₄ state from Tb³⁺, a process known as Antenna Effect². Since the transitions from Eu³⁺ (⁵D₀ → ⁷F₂) and Tb³⁺ (⁵D₄ → ⁷F₅) are permitted by an electric dipole, the radiative emission of these lanthanide ions is placed in the visible region. Moreover, due to the coordination, the fluorescence of Zn²⁺ and Al³⁺ complexes results from the shift of ligand π → π* transition. This work aims to synthesize coordination compounds using mild reactions between Eu³⁺, Tb³⁺, Al³⁺, Zn²⁺, and 2-(4-hydroxiazobenzene) benzoic acid and investigate the luminescence properties of the complexes. The reactions were performed in acetonitrile using NaOH or Et₃N as bases and the corresponding metal triflate under an inert atmosphere. The ¹H NMR characterization showed the broadening of the H signals, especially due to the paramagnetic character of Eu³⁺ and Tb³⁺. The signals for HABA and complexes are ¹H NMR (300 MHz, DMSO-*d*₆) 8,79 ppm (dd, 2H), 8,50 ppm (dd, 1H), 8,40 ppm (dd, 1H), 8,29 ppm (t, 1H) e 8,21 ppm (t, 1H) e 7,60 ppm (dd, 2H), Eu³⁺: ¹H NMR (300 MHz, DMSO-*d*₆) 7,75 ppm (6H), 7,44 ppm, 7,27 ppm (12 H), 7,03 ppm (6H), Tb³⁺: ¹H NMR (300 MHz, DMSO-*d*₆) 7,66 ppm (18 H), 6,94 ppm (6 H), Al³⁺: ¹H NMR (300 MHz, DMSO-*d*₆/CDCl₃) 7,74 ppm (6 H), 7,55 ppm, 7,48 ppm (12 H), 6,90 ppm (6H), Zn²⁺: ¹H NMR (300 MHz, DMSO-*d*₆) 7,73, 7,63 ppm (6 H), 7,42 ppm (6H), 6,83 ppm (4H). The FTIR analyses showed a shifting in the stretching frequency of the C=O bonding, showing the coordination as bidentate. FTIR (KBr, cm⁻¹) νC=O for HABA and complexes: 1710 cm⁻¹ for HABA, 1657 cm⁻¹ for Eu³⁺, 1693 cm⁻¹ for Tb³⁺, 1626 cm⁻¹ for Al³⁺ and 1631 cm⁻¹ for Zn²⁺. The luminescence assay was performed in the solid state, and the results are placed in the table below:

Compound	λ _{em} (nm)	λ _{exc} (nm)
HABA	482	350
Eu(HABA) ₃	613	225
Tb(HABA) ₃	542	270
Al(HABA) ₃	605	484
Zn(HABA) ₂	623	500

Referências

¹Valeur, B. Molecular Fluorescence: Principles and Applications, 2 ed, WEINHEIM Wiley – VCH, 2012.

²Ungur, Liviu; Szabo, Bernat. Mechanisms of Luminescence in Lanthanide Complexes: A Crucial Role of Metal–Ligand Covalency, *Inorg. Chem*, 61,16, 2022.

Agradecimentos/Acknowledgments

FAPESP, CNPq and UNIFESP.

Europium(III) circularly polarized luminescence of core@shell nanoparticles

Nagyla A. Oliveira (PG),¹ Isabela M. S. Diogenis (PG),¹ Bruna F. F. Silva,¹ Fernando A. Sigoli (PQ).^{1*}

n234905@dac.unicamp.com; fsigoli@unicamp.br

¹Instituto de Química, UNICAMP

Palavras-Chave: CPL, Lanthanides, Nanoparticles

Highlights

Chiral ligand functionalized-core@shell nanoparticles showing downshifting circularly polarized luminescence (CPL) and dissymmetry factor (g_{lum}) values are around 0.3.

Resumo/Abstract

Circularly polarized luminescence (CPL) is often associated with molecules due to the many possibilities to understand and even control the chirality in these structures. However, currently the development of chiral nanomaterials has become increasingly attractive for researchers. Insert chiral ligands on the surface of nanoparticles is one way of inducing chirality in nanomaterials. This surface modification has proven to be efficient, with high values of the dissymmetry factor, allowing the application in chiroptical devices.^{1,2} In this work, we presented the core@shell nanoparticles $\text{NaGd}_{0,5}\text{Tm}_{0,01}\text{Yb}_{0,49}\text{F}_4@/\text{NaGd}_{0,85}\text{Eu}_{0,15}\text{F}_4$, functionalized with (+)-3-heptafluorobutyryl camphorate-(hfbc), and an investigation about their CPL properties. The nanoparticles were synthesized by thermal decomposition method in the hexagonal (β) and cubic (α) crystalline structures were confirmed by DRX analysis. The bands of the β -diketonate of hfbc, seen in FTIR spectra confirms the functionalization. All the spectroscopic analysis were obtained from using an acetonitrile suspension 3 mg mL^{-1} . UV-VIS and Circular dichroism (CD) spectra show a band with maximum about 310 nm assigned to camphorate ligand. Furthermore, CD spectra confirm the positive orientation of ligand. The $^5\text{D}_0 \rightarrow ^7\text{F}_2$ electronic transition of the Eu(III) was monitored in downshifting PL spectra indicating the ligand \rightarrow metal ion energy transfer. Therefore, downshifting CPL analysis were obtained analyzing the emitted photons at about 595 nm and 612 nm, corresponding to Eu(III) transitions, $^5\text{D}_0 \rightarrow ^7\text{F}_1$ and $^5\text{D}_0 \rightarrow ^7\text{F}_2$, respectively. For both nanoparticles, the CPL analysis indicate the preferential left-circularly polarized emission confirmed by positive dissymmetry factor (g_{lum}) values of 0.12 and 0.07 to β -NPs and 0,32 e 0,38 to α -NPs, relating to electronic transitions $^5\text{D}_0 \rightarrow ^7\text{F}_1$ and $^5\text{D}_0 \rightarrow ^7\text{F}_2$, respectively. The obtained g_{lum} values are relatively high when compared to those already registered, suggesting high efficiency of CPL emission, which makes the investigation of these materials promising for possible optical applications.

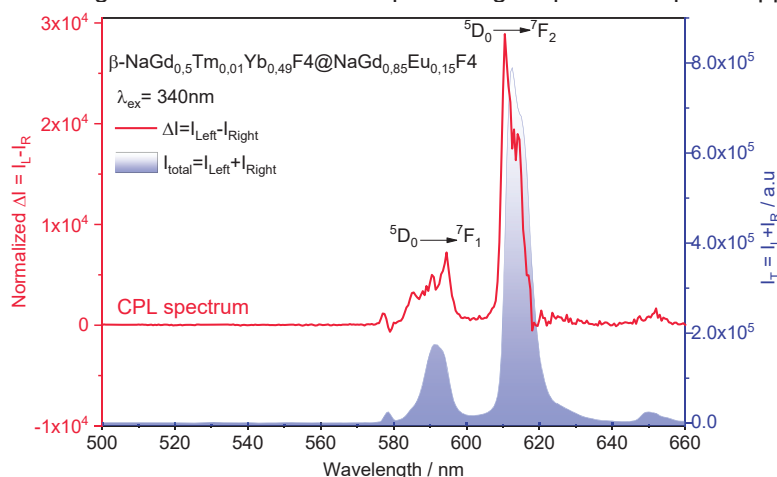


Figure 1: Intensity variation (ΔI) and total Intensity (I_T) to emission intensities to the left and right NPs $\beta\text{-NaGd}_{0,5}\text{Tm}_{0,01}\text{Yb}_{0,49}\text{F}_4@/\text{NaGd}_{0,85}\text{Eu}_{0,15}\text{F}_4$, (I_L and I_R are the left and right polarized emission intensities).

Agradecimentos/Acknowledgments

The authors are grateful to CNPq, FAPESP, CAPES, CNPEM, LNNANO and INOMAT.

¹ [1] D. P. Sebastiano and D.B. Lorenzo, *Inorg. Chem.* **51**, 12007-12014 (2012).

² Han, D., Li, C., Jiang, C., Jin, X., Wang, X., Chen, R., Cheng, J., Duan, P., *Aggregate* 2022, 3, e148.

46ª Reunião Anual da Sociedade Brasileira de Química: "Química: Ligando ciências e neutralizando desigualdades"

[Eu(TTA)₃(Phen-derivative)] type complexes: influence of 1,10 - phenanthroline substituents on their optical properties

Rodolpho A. N. Silva (PG),¹ Jean D. C. Menezes (IC),¹ Marco A. Cebim (PQ),¹ Marian R. Davolos (PQ),¹ Sergio A. M. Lima (PQ),^{1,2} Ana Maria Pires (PQ).^{1,2*}

alessandro.nesta@unesp.br; ana.maria@unesp.br

¹Department of Physical Chemistry, Inorganic, and Analytical Chemistry, São Paulo State University – Chemistry Institute, Araraquara, Brazil

²Department of Chemistry and Biochemistry, São Paulo State University – Presidente Prudente, Brazil

Keywords: Lanthanides, Europium, Luminescence, Coordination compounds.

Highlights

Three luminescent complexes, general formulae [Eu(TTA)₃(Phen-derivative)], were synthesized, characterized, and their optical properties evaluated in comparison to the precursor complex.

Abstract

The success in the development of highly efficient luminescent complexes containing Eu(III) as emitting ion strongly depends on the adequate choice of ligands. Furthermore, it is necessary to avoid water molecules coordinated to the emitting ion, as they contribute to luminescence quenching processes. In tris β-diketonate complexes, a way to achieve this goal is the insertion of molecules such as 1,10 – phenanthroline, which, in addition to displacing water molecules via the chelate effect, also prevents the coordination of new molecules via steric hindrance. Moreover, alterations in the structure of 1,10 – phenanthroline is relatively ease and may further favors the luminescence of the respective complexes. Therefore, in this study, three complexes were synthesized (C2, C3, and C4, Figure 1) and evaluated regarding the influence of the substituent inserted in the on the luminescence of the produced systems. Modifications in the spectral profiles in FTIR measurements assigned to the C=N and C=O bonds of the ligands compared to the complexes corroborate their formation. Mass spectrometry data, in turn, revealed signals related to the molecular ions of the idealized complexes, in the proportion Eu/β-diketone/Phen of 1/3/1, respectively (Figure 1). Finally, photoluminescence spectroscopy data associated with the application of the LUMPAC software indicated that the presence of the substituent in the structure of 1,10 – phenanthroline can result in a significant decrease or increase in the quantum emission efficiency of the complexes (Table 1). The results discussed above show that the substituents present in the 1,10 – phenanthroline derivatives acted importantly for the modulation of the luminescence of the complexes, and complexes C2 and C3 are very promising materials as luminophors.

Complex	τ (ms)	Ω ₂ (10 ⁻²⁰ cm ²)	Ω ₄ (10 ⁻²⁰ cm ²)	A _{rad} (s ⁻¹)	A _{nrad} (s ⁻¹)	η (%)
Eu-TTA-H ₂ O (C1)	0.23	29.53	6.64	1050.34	3299.38	24.15
Eu-TTA-PIB (C2)	0.41	26.11	6.61	956.45	1468.38	39.44
Eu-TTA-PIB_4CH ₃ (C3)	0.43	25.71	6.51	941.11	1384.47	40.47
Eu-TTA-PIN_2OH (C4)	0.15	24.35	5.72	890.81	5740.49	13.43

Table 1: Photophysical parameters of the synthesized complexes.

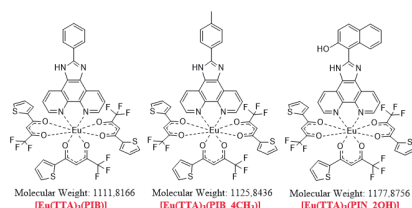


Figure 1: Representation of the synthesized complexes.

Acknowledgments

CAPES and CNPq (procs: 141081/2020-1 e 317610/2021-0)

46ª Reunião Anual da Sociedade Brasileira de Química: "Química: Ligando ciências e neutralizando desigualdades"

Evaluation for synergistic effects of reactive oxygen and nitrogen species originated from ruthenium porphyrin derivative compounds in cancer cells

Matheus Torelli Martin (PG)^{1*}, Amanda Blaque Becceneri (PG)¹, Roberto Santana da Silva (PQ),¹

m.torelli@usp.br

¹Departament of Biomolecular Sciences, School of Pharmaceutical Sciences of Ribeirão Preto, University of Sao Paulo, Ribeirão Preto, SP-Brazil.

Keywords: Cancer, Photodynamic Therapy, Ruthenium complexes

Highlights

Ruthenium-porphyrin photosensitisers based on generation of Reactive Nitrogen-Oxygen Species (RNOS) show cytotoxic effect only in the presence of irradiation in cancer cell lines.

Photosensitizers generators of RNOS combined with PDT have potential for cancer treatment.

Abstract

Photosensitizers are molecules capable of interacting with light to generate reactive oxygen species (ROS) and other radicals. In this way, these molecules are used in photodynamic therapy (PDT) to selectively treat diseased areas of human tissue, like some types of carcinoma and resistant infections. Furthermore, reactive nitrogen species (RNS), such as nitric oxide (NO) has been reported as an important agent in tumorigenesis depending on its concentration. Mechanisms of DNA damage, DNA damage repair response, modulation of cell cycle arrest and apoptosis induction are being studied concerning this radical.^{1,2} Thus, the aim of this work was to synthesize and study the photochemical and photophysical properties of a new candidate photosensitizer based on a *meso*-substituted porphyrin with nitro-ruthenium complexes able to photo-release NO while generating ROS and evaluate its cytotoxicity on cancer cell lines. The [H₂TPyP{Ru(NO₂)(bpy)₂}]₄ complex was synthesized from the precursor 5,10,15,20-tetra(4-pyridyl)porphyrin (H₂TPyP) and characterized by UV-visible, FT-IR, ESI-TOF spectrometry, among others. The fluorescence quantum yield (Φ_f) by excitation at 420 nm was $\Phi_f = 4.8 \times 10^{-3}$ for the complex, while the H₂TPyP $\Phi_f = 5.1 \times 10^{-2}$. We have hypothesized that this effect took place due to the electronic withdrawal by substituted nitro-ruthenium complexes. We have also determined the singlet oxygen quantum yield (Φ_Δ) by direct measurement of phosphorescence at 1270 nm, the H₂TPyP presented $\Phi_\Delta = 0.47$ and the complex $\Phi_\Delta = 0.29$ in oxygen-saturated DMSO, excitation by 400 nm LED module. NO photo-release efficiency (Φ_{NO}) assays were performed in PBS (pH = 7.4) using a 415 nm LED array and a selective amperometric sensor. The results show $\Phi_{NO} = 2.85 \times 10^{-5}$. Triplet decay times (τ_T) were measured with flash photolysis ns-Nd³⁺-YAG pumped OPO, the H₂TPyP presented $\tau_T = 985 \mu s$ and the [H₂TPyP{Ru(NO₂)(bpy)₂}]₄ $\tau_T = 463 \mu s$ in deaerated DMSO, which explains the Φ_Δ decrease comparing the precursor and the synthesized complex. Cytotoxicity studies were carried out with A375 and B16F10 cell lines. The results showed that the complex, after 4 h of treatment in the absence of light, does not present toxicity with any concentrations tested (0-50 μM). However, when the cells are treated with PDT (415 nm, 4 J cm⁻²) high cytotoxicity is observed, with IC₅₀ values less than 1 μM . Comparing these results with several other porphyrin species suggest a novel role of cell death in the enhanced cytotoxicity by production of NO and ¹O₂ in cancer cells. This has originated a great deal of work on the potential PDT applications of compounds capable to produce synergistic cytotoxic radical molecules.

1. Khan, F. H. *et al. Int J Mol Sci* **21**, 9393 (2020).

2. Sampaio, R. N. *et al. Journal of Physical Chemistry A* **116**, 18–26 (2012).

Acknowledgments

FAPESP (2020/03367-6; 2019/19448-8), CAPES (88887.714781/2022-00), CNPq and FCFRP-USP. We would like to thank Dr. Mauricio da Silva Baptista and Dr. Helena C. Junqueira from IQ-USP for singlet oxygen and lifetime measurements.

Evaluation of the electrocatalytic water oxidation reaction promoted by Copper-Prussian blue after thermal decomposition

Fiorella Z.F. Herrera (PG),^{1*} Juliano A. Bonacin (PQ).¹

f227961@dac.unicamp.com

¹Institute of Chemistry, UNICAMP

Keywords: Water oxidation reaction, Thermal treatment, Heterogeneous catalyst, Prussian blue analogue, Copper Hexacyanoferrate (II).

Highlights

Detailed study of the preparation, thermal analysis and electrochemical characterization of Copper hexacyanoferrate (II).

The catalysts prepared at 420 °C and 550 °C shown better performance in the water oxidation reaction.

Abstract

The following work aims to evaluate the efficiency of different types of Prussian Blue catalysts ($[\text{Cu}[\text{Fe}(\text{CN})_6]_{0.5} \cdot n\text{H}_2\text{O}]$) towards the water oxidation reaction. The catalysts evaluated were prepared via thermal decomposition under different temperatures.

To evaluate the performance of the catalysts, their electroactive area (A_e), the onset value, and the Tafel curve were calculated, and an Electrochemical Impedance Spectroscopy (EIS) study was performed.

Tabla N°1. Electrochemical characterization of CuFe(II) PB catalysts

Heat Treatment	CuFe(II) PB				
	60°C	135°C	200°C	420°C	550°C
Onset potential (RHE)	1.72	1.45	1.55	1.42	1.03
Tafel Slope ($\text{mV} \cdot \text{dec}^{-1}$)	314	617	680	262	223
RS (Ω)	24.09	19.94	23.08	19.09	28.66
RCT (Ω)	300.15	200.91	243.19	56.56	88.61
ECSA cm^2	0.476	0.93	0.84	1.12	1.01

The results show that the catalysts with the highest water content (CuFe(II) PB 60°C, CuFe(II) PB 135°C and, CuFe(II) PB 200°C) present a lower performance towards the water oxidation reaction. Although CuFe(II) PB 60°C has shown a higher overpotential compared to the catalyst prepared at 135°C and 200°C, its water oxidation process was found to be kinetically faster. This could indicate that the water of hydration molecules in the CuFe(II) PB 60°C might accelerate the reaction. In addition, it is observed that the catalysts prepared at 420°C and 550°C show the best performance and the highest number of active sites. These results indicate that it is essential to carry out more chemical characterization studies, and analyze the effect of water, and the surface on these catalysts under mild conditions to better understand the oxidation mechanism of water and further advance in the development of new catalysts.

References:

[1]Rafael L. Germscheidt et.al. ACS Applied Energy Materials 5(8), 9447-9454, 2022.

[2]Priscilla J. Zambiasi et. al. Dalton Transactions 49,16488, 2020.

Acknowledgments

This study was financed in part by the Coordenação de Aperfeiçoamento de Pessoal de Nível Superior – Brasil (CAPES) – Finance Code 001. The authors are grateful to the CAPES, CNPq (308203/2021-6), FAPESP 2017/11986-5, 2018/25092-9, 2021/05976-2.

Evaluation of the metallophoric potential of an *N*-acylhydrazone in the context of Alzheimer's disease: Interaction with Cu^{2+} , $\text{O}_2^{\cdot-}$ radicals and $\text{A}\beta_{1-16}$

Barbara Marinho Barbosa (IC),^{1*} Leonã S. Flores (PQ),² Charlane C. Correa (PQ),² Daphne S. Cukierman (PQ),¹ Nicolás A. Rey (PQ).¹

barbaramarinoharbosa@gmail.com;

¹ Laboratory of Organic Synthesis and Coordination Chemistry Applied to Biological Systems (LABSO-Bio), Department of Chemistry, Pontifical Catholic University of Rio de Janeiro (PUC-Rio)

² Department of Chemistry, Federal University of Juiz de Fora, Brazil

Keywords: Metallophores, Hydrazones, Copper, Benzodioxole, Alzheimer's disease.

Highlights

Based on the pathophysiological role of copper(II) ion in Alzheimer's disease, a benzodioxole-containing *N*-acylhydrazone, namely **X1Diox**, was studied regarding its metallophoric potential, showing promising results.

Abstract

Physiological metal ions, such as Cu^{2+} , have been associated with Alzheimer's disease, increasing the oligomerization of $\text{A}\beta$ peptide as well as the aggregates' toxicity.¹ In this context, metallophores have been developed to compete with the peptide for the abnormal interaction with those metals, in order to restore the metal homeostasis.² In this work, a benzodioxole-containing *N*-acylhydrazone, **X1Diox**, was synthesized and characterized in solution and in the solid state, including by single-crystal XRD, being isolated in the form of a hydrated hydrochloride. The hydrazone showed high resistance towards hydrolysis, remaining in 95% aqueous solution for 48h, at physiological pH 7.4. The Method of Continuous Variation was used to estimate the stability of the ML copper(II) complex of **X1Diox** and indicated a moderate affinity ($\log K = 5.97 \pm 0.01$), as expected for a metallophoric compound. The interaction of **X1Diox** with the fragment $\text{A}\beta_{1-16}$ in the presence of Cu^{2+} was evaluated by UV-Vis spectroscopy, and the formation of the ternary complex $\text{A}\beta_{1-16}\text{-Cu}^{2+}\text{-X1Diox}$ could be observed. Furthermore, the *N*-acylhydrazone was able to reduce the amount of electrochemically generated $\text{O}_2^{\cdot-}$ in solution, in a concentration-dependent process (Figure 1). Preliminary tests on yeast showed that, even at high concentrations ($750 \mu\text{mol.L}^{-1}$), **X1Diox** has no toxic effect on more than 80% of cells. In addition, some pharmacological parameters were calculated and all values were in accordance with what was expected by the Lipinski's Rule of Five. Finally, the neutral ML_2 complex $[\text{Cu}(\text{X1Diox})_2]$ was synthesized and characterized by IR, ICP-OES, conductometry and cyclic voltammetry.

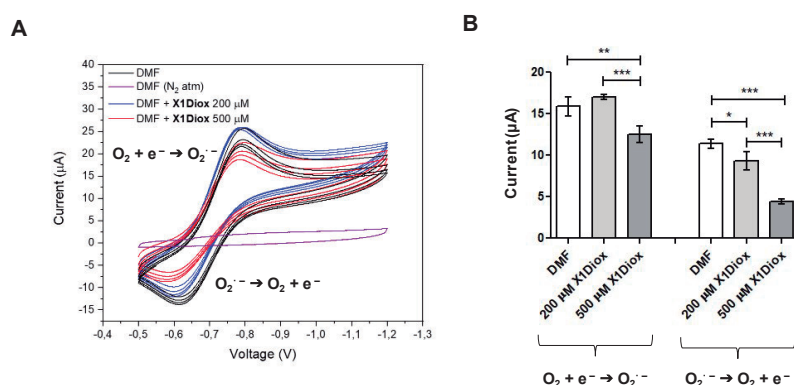


Figure 1. Study of the interaction between **X1Diox** and electrochemically generated superoxide radicals in a TBAPF₆ 0.1 mol.L⁻¹ solution. **(A)** Voltammogram of O_2 dissolved in DMF with different ligand concentrations. **(B)** Influence of **X1Diox** concentration on the current produced for the O_2 reduction and oxidation processes. The symbols (*), (**) and (***) represent a statistically significant difference, in ascending order.

¹ Acevedo, K. *et al.*; J. Biol. Inorg. Chem. **2019**, 24, 1141.

² Sales, T. *et al.*; Int. J. Mol. Sci. **2019**, 20, 1829.

Acknowledgments

This work was supported by CNPq and FAPERJ.

Explorando o uso de meio aquoso para obtenção da 2-*N*-piridilporfirina de Mn(III) (MnT-2-PyPCI) e otimização quimiométrica da nova rota

Jacqueline C. Bueno-Janice (PQ),^{1,2} Victor H.A. Pinto (PQ),¹ José F. Sarmiento-Neto (PQ),^{1,3} Wallace D. Fragoso (PQ),¹ Júlio S. Rebouças (PQ).^{1*}

jsreboucas@quimica.ufpb.br

¹Departamento de Química, UFPB. ²Departamento de Biofísica, UFPE, ³Departamento de Ciências Farmacêuticas, UFPE.

Palavras Chave: Mn-porfirinas, agentes terapêuticos redox-ativos, porfirinas hidrossolúveis.

Highlights

Exploring the use of aqueous media to prepare Mn(III) 2-*N*-pyridylporphyrin (MnT-2-PyPCI) and chemometric optimization of the new route.

- Exploring N-pyrrole and N-pyridyl rich acid-base equilibrium of 2-*N*-pyridylporphyrin for synthesis.
- New Mn-metallation route using aqueous acid as solvent.
- Chemometric optimization of metallation yields via Doehlert design.

Resumo/Abstract

As Mn-porfirinas derivadas das 2-*N*-alquilpiridínioporfirinas compreendem uma classe versátil de porfirinas estudadas tanto como modelos biomiméticos de enzimas oxidorreduzidas (superóxido dismutases, citocromos P450, peroxidases, catalase) como agentes terapêuticos redox-ativos em doenças e estados patológicos associados ao estresse oxidativo;¹ dois complexos de Mn(III) dessa classe avançaram para fase II de estudos clínicos em humanos no Canadá e EUA.² A metodologia clássica de obtenção das *N*-alquilpiridínioporfirinas de Mn(III) (MnTalquil-2-PyPCI₅) é realizada em duas etapas: a primeira etapa é caracterizada pela alquilação da *N*-piridilporfirina neutra (H₂T-2-PyP) gerando a *N*-alquilpiridilporfirina catiônica correspondente (H₂Talquil-2-PyP⁴⁺), enquanto, na segunda etapa, realiza-se a complexação metálica (MnTalquil-2-PyP⁵⁺).³ A purificação desses compostos catiônicos (base-livre ou complexo) é realizada por sucessivas precipitações via metátese OTs⁻/PF₆⁻/Cl⁻ ou Cl⁻/PF₆⁻/Cl⁻ usando água e acetona como solventes.³ Uma rota alternativa para obtenção das Mn-porfirinas derivadas das 2-*N*-alquilpiridínioporfirinas é via formação de um intermediário de síntese, a MnT-2-PyPCI (Fig. 1), obtida pela metalação da H₂T-2-PyP em solventes orgânicos,⁴ para posterior alquilação para obtenção de diversas MnTalquil-2-PyPCI₅. Neste trabalho apresentamos uma nova metodologia para a síntese da MnT-2-PyPCI (Fig. 1) por meio de uma rota sintética ambientalmente mais amigável, utilizando meio aquoso ácido e um método de purificação sem uso de solventes orgânicos. Para tanto, investigou-se a influência de diferentes fatores (concentrações de ácido, excesso de Mn e temperatura) na obtenção da MnT-2-PyP⁺, em pequena escala, através de um estudo quimiométrico usando planejamento de Doehlert.⁵ Posteriormente, foram selecionadas duas condições do estudo quimiométrico para preparação em maior escala da MnT-2-PyPCI e foi desenvolvido um método de purificação sem uso de solventes orgânicos, obtendo-se rendimentos isolados superiores a 79%. A partir da derivatização da MnT-2-PyPCI podem ser obtidas as MnTalquil-2-PyPCI₅ de interesse para o desenvolvimento de modelos biomiméticos e agentes terapêuticos redox-ativos.

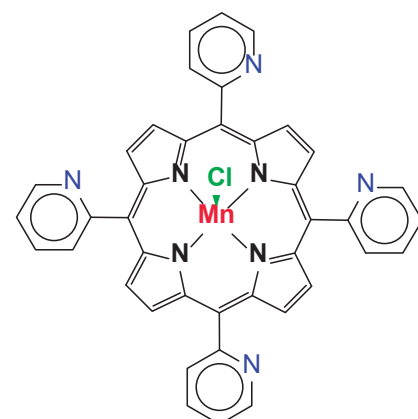


Figura 1. MnT-2-PyPCI

¹ I. Batinic-Haberle, J.S. Rebouças, I. Spasojevic. Redox-Active Therapeutics. Zurique: Springer International Publishing, **2016**. ² I. Batinic-Haberle *et al.*, *Oxid. Med. Cell. Longev.* 2021:653790, **2021**. ³ I. Batinic-Haberle, J.S. Rebouças, L. Benov, I. Spasojevic. Chemistry, Biology and Medical Effects of Water-Soluble Metalloporphyrins. In: K.M. Kadish; K.M. Smith; R. Guilard. (Org.). Handbook of Porphyrin Science. New York: World Scientific Publishing, 11:291-393, **2011**. ⁴ J.S. Rebouças, M.E.M.D de Carvalho, Y.M. Idemori, *J. Porphyr. Phthalocyanines*, 6:50-57, **2002**. ⁵ S.L.C Ferreira *et al.*, *Talanta*, 63:1061-1067, **2004**.

Agradecimentos/Acknowledgments

CNPq, CAPES, FINEP, UFPB, INCT-INFo, INCT-CiMol.

Área: INO

Gold complex with dithiocarbamate ligands as a potential anticarcinogenic agent

Arthur H. Rodrigues Neto (IC)¹, Thaiz Cristina Soares dos Santos (PG)¹, Ana Luiza de Andrade Querino (PG)¹, Heveline Silva* (PQ)¹

arthurneto123@ufmg.br, hevelinesilva@ufmg.br

¹Universidade Federal de Minas Gerais Av. Pres. Antônio Carlos, 6627 - Pampulha, Belo Horizonte - MG, 31270-901

Palavras Chave: Chemotherapy, Gold, Complex, Dithiocarbamate, Inorganic

Highlights

Gold complexes have shown great potential as antitumor agents. DTC (dithiocarbamate) compounds can have their selectivity and cytotoxicity increases considerably after metal coordination.

Resumo/Abstract

Gold complexes has gained great attention in antitumoral treatment since cisplatin was discovered as an active drug against most of cancer types. The gold has some similar chemical proprieties comparing with platinum, what gave visibility to the metal. In the synthesis of the complex introduced in this work, the gold precursor [Cl-Au-PPh₃] was added in the 30DTC ligand in a 1:1 ratio, and thus a substitution reaction occurs with the displacement of Cl⁻ ligand and DTC ligand binds the metal giving the desired complex (figure 1).

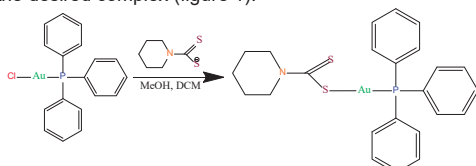


Figure 1. Scheme of synthesis

After the synthesis, that lasted 3 days, the solution was removed under low pressure. A solid yellow (55,63 % yelt) were investigated by IR^v, and NMR as described in the table below:

	NMR (ppm)				IV (cm ⁻¹)
30 DTC	δ 212,46 (C-S)	δ 1,54 (C-H) Piperidine	δ 4,27 (N-C-H) Piperidine	-	1621 cm ⁻¹ (C=S)
Au30DTC	δ 202,36 (C-S)	δ 1,68 (C-H) Piperidine	δ 4,13 (N-C-H) Piperidine	δ 156,14 (C aromatic)	3043 cm ⁻¹ (C-H _{ar})

Cytotoxicity assays were performed *in vitro* against human breast cells (tumor- MDA, MCF-7 and non tumor MCF-10). In all of them, the complex was extremely cytotoxic, but not very selective. The IC₅₀ were found as 0,68 μM, 0,82 μM and 0,29 μM for MCF-7, MDA and MCF-10, respectively. The compound is very active, specially compared with the activity of his own ligand, that has shown cytotoxicity, but in higher concentrations. The IC₅₀ of the ligand were found as 2,40 μM, 2,87 μM and 0,95 μM for MCF-7, MDA and MCF-10, respectively. The coordination of the gold potentiated the cytotoxicity of the ligand in all cell lineages.

Agradecimentos/Acknowledgments

FAPEMIG, CNPQ, UFMG

Delgado, Giset; Condé, Camila; Santos, Hélio; Navarro, Maribel. Compostos quimioterápicos de ouro: uma nova visão geral dos complexos anticâncer de Au(I/III) em relação à estrutura do ligante. *Química Nova* **2020**, *43*, 1104-1124. <http://dx.doi.org/10.21577/0100-4042.20170566> Alavizadeh, S.; F. Gheybi, F.; Nikpoor, A.; Badiie, A.; Golmohammadzadeh, S.; Jaafari, M. Therapeutic Efficacy of Cisplatin Thermosensitive Liposomes upon Mild Hyperthermia in C26 Tumor Bearing BALB/c Mice. *Mol. Pharmaceutics* **2017**, *14*, 712-721. [doi.org/10.1021/acs.molpharmaceut.6b01006](http://dx.doi.org/10.1021/acs.molpharmaceut.6b01006)

46ª Reunião Anual da Sociedade Brasileira de Química: "Química: Ligando ciências e neutralizando desigualdades"

Comentado [HS1]: Você não comparou com os valores do ligante. Tem que colocar e mostrar que o ouro melhorou a atividade.

Formatado: Contorno do Texto, Preenchimento de Texto

Formatado: Fonte: 10 pt

Formatado: Fonte: (Padrão) Arial, 10 pt

Formatado: Fonte: (Padrão) Arial, 10 pt, Negrito

Formatado: Fonte: (Padrão) Arial, 10 pt

Sociedade Brasileira de Química (SBQ)

² Garcia, A., Machado, R.C., Grazul, R.M. et al. Novel antitumor adamantane–azole gold(I) complexes as potential inhibitors of thioredoxin reductase. *J Biol Inorg Chem* **2016**, 21, 275–292 . doi.org/10.1007/s00775-016-1338-y

Formatado: Fonte: (Padrão) Arial, 10 pt

Green-emitting Tb³⁺ complex dispersed in PMMA and PVDF films and their application as phosphor-converted UV LED

Ariane C. F. Beltrame (PG)^{*1,2}, Felipe S. M. Canisares (PG)^{1,3}, Leonardo F. Saraiva^{1,2}, Airtón G. Bispo-Jr (PQ)⁴; Ricardo V. Fernandes (PG)⁵, Sergio A. M. Lima (PQ)^{1,2,3}, Ana M. Pires (PQ)^{1,2,3}.

¹Department of Chemistry and Biochemistry, São Paulo State University (UNESP), Presidente Prudente, Brazil; São Paulo State University (Unesp), ²Institute of Biosciences, Humanities and Exact Sciences, São José do Rio Preto-SP, Brazil; São Paulo State University (Unesp), ³Institute of Chemistry, Araraquara-SP, Brazil; ⁴University of Campinas (Unicamp), Campinas-SP, Brazil; ⁵State University of Londrina (UEL), Londrina-PR, Brazil.

Keywords: Terbium(III); Luminescence; Lanthanides; Rare-earth; Solid State Lighting; LEDs.

Highlights

Tb³⁺ tetrakis complexes dispersed in polymeric films were applied as efficient green emitting coatings of LED prototypes.

Abstract

Luminescent materials are of high interest due to several applications, such as for light-emitting diodes (LEDs) and organic light-emitting diodes (OLED) devices, cell markers, sensors, and lasers^{1,2,3}. Focusing on lighting, this study deals with the preparation and characterization of films produced by the drop-casting method containing the green emitter complex Na[Tb(acac)₄] tetrakis (acac = acetylacetonate), and using poly(methyl) methacrylate (PMMA) or poly(vinylidene) fluoride (PVDF) as the polymer matrix, while computational tools based on theoretical methods were used to obtain further insights into the luminescent aspects. FTIR, TGA, elemental analysis (C, H, N), diffuse reflectance, and photoluminescence data ensured the synthesis success of the water-free Na[Tb(acac)₄] complex. The luminescent films were characterized by FTIR, diffuse reflectance, scanning electron microscopy (SEM), X-ray diffraction and photoluminescence. The ratio between the Na[Tb(acac)₄] complex and polymer was varied to produce films at 0.5, 0.75, 1.0, 2.0 or 5.0% by weight. The geometry was optimized through Orca 5.0.3 with the r²SCAN-3c functional and Def2-TZVP basis set. The optimized structure was submitted to excited-state calculations with the ωB97x-D4 functional, where C, O, H was described with the new valence polarized double-ζ basis set (Def2-vZDP), and the 53MWB *Stuttgart-Cologne* effective-core potential (ECP) for Tb³⁺. Although the PMMA or PVDF films were opaque due to the low solubility of the Tb³⁺ complex, all samples exhibited the characteristic green emission assigned to the usual set of ⁵D₄→⁷F_J (J = 6-2) Tb³⁺ transitions. The excited-state calculations for the isolated complex showed that the first triplet state (T1) lies above in energy (22,276.2 cm⁻¹) compared to the ⁵D₄ of Tb³⁺ (20,284.1 cm⁻¹), leading to an efficient sensibilization through energy transfer. However, the increment of the polymer amount led to a lowering in energy of the T1, enhancing the backward energy transfer, from the ⁵D₄→T1, diminishing the quantum yield (QY). This assumption was also confirmed from the localized vibrational modes, as described by Moura Jr, et al [4], higher vibrational mode values promote higher energy transfer rates. From an experimental sight, the ⁵D₄ lifetime, intrinsic (Φ_{Tb}^{Tb}) and absolute emission quantum yield parameters exhibited a non-linear dependence with the amount of complex, due to the tendency to form clusters as the concentration increase. From all produced films, regardless of the polymer, those containing 5.0% of complex exhibited the higher global emission quantum yields, 48.20% (PMMA) and 16.70% (PVDF), and consequently, they were selected for construction the LED prototypes. The one coated with the PMMA film exhibited the characteristic Tb³⁺ green emission, while the device produced with the PVDF film generated yellowish green emission, due to the LED blue emission scattered in the opaque film. Therefore, a detailed study on the electronic structure of the complex was performed, concluding that the polymer matrix can interfere in the device emission color, and with the PMMA-prototype, the green emission of the Tb³⁺ complex was preserved.

Acknowledgments

This work was supported by FAPESP (2019/26103-7), CNPq (Grants number 304003/2018-2 and 309448/2021-2), CAPES (Grant number 88887.672234/2022-00), FAPESP (2022/08409-4)

References

- [1] YANG, Daqing et al, *Synthetic Metals*, **221**, 236-241 (2016).
- [2] QUIRINO, W. G. et al. *Thin Solid Films*, **494**, 23-27 (2006).
- [3] MONTEIRO, J. H.S.K. *Molecules*, **25**, 1-34 (2020).
- [4] MOURA Jr, R. T., et al, *Optical Materials: X*, 16 100216 (2022).

Área: INO

Highly emissive green and orange PMMA films blended with heteroleptic Ir(III) complexes

Vytor C. Oliveira¹, Felipe S. M. Canisares², Ana M. Pires^{1,2} and Sergio A. M. Lima^{1,2}

E-mail: vytor.campos@unesp.br

¹Department of Chemistry and Biochemistry, University of São Paulo State, Presidente Prudente, Brazil

²Department of Analytical, Physical-Chemistry and Inorganic Chemistry, University of São Paulo State, Araraquara, Brazil

Palavras Chave: heteroleptic complexes, iridium(III), coated UV-LED

Highlights

Green- orange-emitting heteroleptic Ir(III) complexes dispersed in PMMA films.

Abstract

The production of iridium complexes has been extensively studied, as result of their high quantum yields, high emission lifetimes, chemical stability, and easy tunable color emission, which may vary from blue to red, and beyond, according to the energy of ligands coordinated to the iridium ion [1-2]. In this way, the syntheses of two heteroleptic complexes were performed, $[\text{Ir}(\text{fppy})_2(\text{pdc})]$ (1a) and $[\text{Ir}(\text{fppy})_2(\text{pqc})]$ (1b), where Fppy = 2-(2,4-difluorophenyl)pyridine, pdc = 2,2'-bipyridine-4-carboxylate, and pqc = 2-Pyridin-2-yl-quinoline-4-carboxylate. For this, the $[(\text{fppy})_2\text{Ir}(\mu\text{-Cl})_2\text{Ir}(\text{fppy})_2]$ dimer was dissolved in chloroform and added to an aqueous solution of Hpdc or Hpqc, which resulted in a biphasic system; thus, methanol was added to turn homogeneous, allowing the reaction to take place. The solution was kept under stirring at room temperature for ~ 2 h, and then the organic solvent was evaporated by heating, leading to the precipitation of the complexes in aqueous solution. Both complexes were characterized by FTIR, MALDI-TOF analysis, UV-Vis and ^1H NMR, which results confirm the formation of the proposed structures. Under UV excitation at 266 nm, the complex (1a) exhibited green emission with a broad band centered at ~555 nm; on the other side, the complex (1b) showed also a broad emission in the orange/red region of the visible spectrum with a maximum at 640 nm. PMMA (Poly(methyl methacrylate)) films containing each complex were produced by drop-casting method, using dichloromethane as solvent. The weight percentage of complexes was varied in the polymer (0.1%, 0.25%, 0.5%, 0.75%, and 1.0%) in order to determine the most suitable proportion for UV-LED coating. All films exhibited transparency, regardless of the complex concentration, and maintained their green and red characteristic emissions. These emission colors are essential for the creation of lighting devices based on RGB system (red, green and blue), as it enables the generation of any color within the visible range in the electromagnetic spectrum.

Acknowledgments

CNPq (304003/2018-2, 309448/2021-2), FAPESP (19/26103-7) and PROPE-Unesp.

References

- [1] Yi-Lu Chang and Zheng-Hong Lu, *Journal of display technology*, **9**, 459-468, 2013
[2] CHEN, F. et al. *Inorg. Chem.*, **47**, 2507-2513, 2008.

High quantum yield of a red-emitting Ir(III) complex in aqueous solution

Augusto F. B. Almeida (IC),¹ Felipe S. M. Canisares (PG),^{1,2} Ana M. Pires (PQ),^{1,2} Sergio A. M. Lima (PQ)^{1,2}

af.almeida@unesp.br

¹São Paulo State University (Unesp), School of Technology and Sciences, Presidente Prudente-SP, Brazil; ²São Paulo State University (Unesp), Institute of Chemistry, Araraquara, Brazil.

Keywords: iridium, red emission, spin-orbital coupling.

Highlights

Red-emitting Ir(III) complex. High emission quantum yield in aqueous solution.

Abstract

Several research groups are focusing their efforts on the creation of new materials aiming applications in different fields, especially in biology, and medicine¹. Ir(III) luminescent complexes are known in the literature for their high quantum emission yields and long lifetimes, attributed to their high spin-orbital coupling, around 4,430 cm⁻¹. This coupling acts on the mixture of the ligand singlet and triplet excited states creating an overpopulated emissive state that intensifies the radiative decay rate and generates complexes with high emission efficiency. The emission wavelength in iridium(III) complexes can be easily modulated by changing the ligands structure- used to synthesize the complexes, varying the color emission from blue to red, And beyond. One of the recent highlights of the application of luminescent iridium(III) complexes in the biological field is their use as markers allowing the visualization of both cell shape and its internal organization in *in vivo* or *in vitro* studies². However, the cell medium itself is self-luminescent in the blue and green region, which may interfere with the probe emission. Therefore, a red emitting probe is highly desirable as the observer can easily distinguish between these two signals. Thus, inspired to create new luminescent red probes to be applied in the biological field, a new-emitting Ir(III) complex is introduced here. For the Ir(III) complex synthesis, the precursor Ir(III) dimer, [(Fppy)₂Ir(μ-Cl)₂(Fppy)₂], (Fppy = 2-(2,4-difluorophenyl)pyridine) was dissolved in dichloromethane followed by the addition of an aqueous solution of the bqdc ligand, potassium [2,2'-biquinoline]-4,4'-dicarboxylate, and methanol, to form a homogeneous system. The mixture was left under stirring at room temperature for 4 h, then the organic solvents were evaporated by heating and the complex precipitated in aqueous medium. The complex formation was confirmed by FTIR, ¹H NMR, UV-Vis, and MALDI TOF analyzes. By photophysical characterization of the Ir(III) complex in aqueous solution, it was possible to verify that it exhibits a broad emission band centered at 607 nm under 272 nm excitation with a emission quantum yield of 62%, one of the highest found in the literature so far. Therefore, the desired red-emitting complex was successfully produced exhibiting optical features that qualify it as a promising candidate for biological application as a luminescent probe.

Acknowledgments

Capes (88887.341772/2019-00), CNPq (304003/2018-1 and 309448/2021-2) and Fapesp (2019/26103-7).

[1] N. Ahmed, et al., Theranostic application of nanoparticles in cancer, Drug Discov. Today 17 (2012) 928-934

[2] P. M. A. de Farias, B. S. Santos, R. L. Longo, R. Ferreira, C. L. Cesar, Mat. Chem. Phys., 89 (2005)1, 21-27.

Influence of terpyridine ruthenium(II) complexes in the HSA self-aggregation

Mauricio de Oliveira (IC),¹ and Renata Galvão de Lima (PQ)^{1,2}

mauricio.oliveira1@ufu.br

¹Instituto de Ciências Exatas e Naturais do Pontal-ICENP, Universidade Federal de Uberlândia, Ituiutaba, MG, Brasil; ²Instituto de Química (IQ), Universidade Federal de Uberlândia (UFU), Uberlândia/MG, Brasil

Palavras Chave: Terpyridine ruthenium (II) complexes, Human serum albumin, Fluorescence spectroscopy, Protein aggregation.

Highlights

[Ru^{II}(tpy)(NH.NHq-COOH)(L)]ⁿ⁺ complexes modified the microenvironment of protein close to Trp-214.

The HSA aggregation process were induced: more pronounced by RuNO⁺ and RuNO₂ than RuH₂O.

Resumo/Abstract

Human serum albumin (HSA) aggregation in aqueous solution can be governed by several factors as pH, temperature, and protein concentration^[1]. The understanding of the HSA aggregation mechanism and potentially the design of suitable inhibitor molecules for stabilizing its native conformation, are of utmost importance^[2]. In this work we proposed evaluate the influence of different co-ligand in the terpyridine ruthenium (II) complex in the HSA self-aggregation process. The [Ru^{II}(tpy)(NH.NHq-COOH)(L)]ⁿ⁺ (**Ru-L**) complexes, where L = NO⁺, NO₂⁻ and H₂O were obtained similar described in literature^[3]. The fluorescence spectra under $\lambda_{exc}=320$ nm at different temperatures (308 and 318K), were observed two populations of heat-induced protein aggregation^[1] with the increase in temperature. The aggregated species were characterized by fluorescence emission at 360 nm (tryptophan) and 400-450 nm (β -sheet rich oligomeric interfaces of albumin)^[4] (Figure 1a). The aggregates processes at 318K in presence of **Ru-L** complexes, where L = NO⁺ and NO₂⁻ were more pronounced than L=H₂O (Figure 1b). Bessas and co-workers^[3] suggest that these complexes modified the microenvironment of protein close to Trp-214, becoming with hydrophilic character. Probably, these different ions complexes affect the electrostatic force in protein, which affect the protein-protein interaction and promote the aggregates formation.

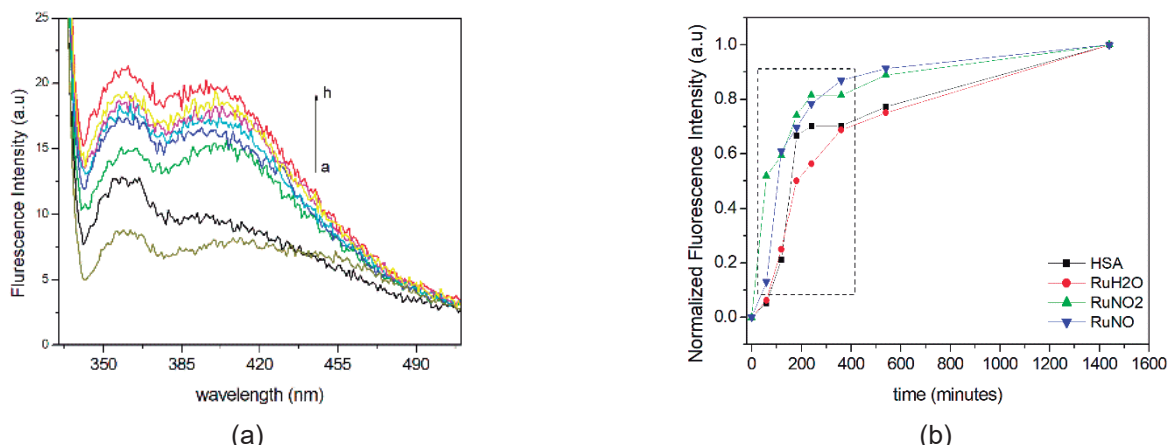


Figure.1. Fluorescence emission spectra of RuNO⁺-HSA in PBS solution at 318K during different time (a: 0:1440 minutes), under $\lambda_{exc}=320$ nm (a) and normalized fluorescence intensity at 400 nm vs time (b).

[1] Radomska, K.; Wolszczak, M., *International Journal of Molecular Sciences*, (2022), 23, 15, 8090.

[2] Maciążek-Jurczyk, M., et al., *Molecules*, (2020), 25, 618.

[3] Bessas, N.C., et al., *Luminescence*, (2021), 36, 391.

[4] Hedberg, Y., et al., *Colloids and Surfaces B: Biointerfaces*, (2019), 173, 751.

Agradecimentos/Acknowledgments

RELAM (UFU Multiuser Laboratory). CNPQ-PIBIC for Mauricio's scholarship.

Inhibition of Cis_2His_2 and Cis_3His zinc-fingers domains by palladium-phosphine complexes

Carolina Galuppo (PG),¹ Camilla Abbehausen (PQ).^{1*}

cgaluppo@unicamp.br; camilla@unicamp.br

¹Institute of Chemistry, UNICAMP

Palavras Chave: Zinc finger; Metal interaction; Mass spectrometry; Phosphines; Coordination chemistry; Bioinorganic chemistry.

Highlights

Pd^{II} -phosphine complexes inhibit zinc-finger domains demonstrated by mass spectrometry. The reactivity depends on complex structure, and coordination chemistry can modulate the protein interaction.

Abstract

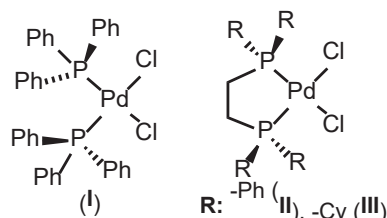


Figure 1: Molecular structures of Pd^{II} -phosphine complexes. (I) $\text{PdCl}_2(\text{tpp})_2$; (II) $\text{PdCl}_2(\text{dppe})$; (III) $\text{PdCl}_2(\text{dcpe})$.

Zinc fingers (ZF) are protein's structural motifs in which Zn^{II} ion stabilizes their conformation by coordinating cysteine and histidine residues. Due to the important roles

involved in genic regulation, ZFs are also related to the biochemical pathways of various pathologies, which and make them attractive pharmacological targets. The mechanism of ZF inhibition includes the removal or replacement of Zn^{II} from the domain. Our research group studied the design of metal-phosphine complexes to inhibit retroviral ZF selectively.[1-3]

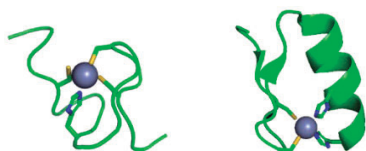


Figure 2: PyMOL constructed structures from PDB for the second ZF domain of NCp7 protein from HIV-1 (PDB# 1ESK, left) and the third ZF domain of Sp1 (PDB# 1MEY, right). Residues coordinated to Zn^{II} appear highlighted.

Herein, the behavior of Zn^{II} replacement by Pd^{II} -phosphine complexes (Fig. 1), and $\text{K}_2[\text{PdCl}_4]$, was

analyzed in two ZF domains (Fig. 2): a Cys_2His_2 motif, the third ZF domain of the human transcription factor Sp1, which appears to be overexpressed in several types of human cancers; and a Cys_3His motif, the second ZF domain of NCp7 protein from HIV-1, a protein which plays a decisive role in the infectious capacity of the virus.

The $\text{K}_2[\text{PdCl}_4]$ interaction with the Cys_2His_2 ZF domain promotes highly specific hydrolysis, forming mainly the c18 fragment of Sp1 as the product. The complex (I) mitigates the hydrolysis effect, reacting to form a variety of Pd finger species, varying the number of Pd^{II} and ligand (tpp) present. Differently, complexes (II) and (III) interacted with the Cys_2His_2 ZF domain forming the Pd-phosphine finger. While phosphine ligands favored the interaction of Pd^{II} center with Cys_3His ZF, the $\text{K}_2[\text{PdCl}_4]$ leads to the formation of only small amounts of Pd finger after incubation. Although the presence of unreacted ZF is observed in the products, Zn^{II} ejection products with one and two Pd-phosphine units are observed for the three complexes.

References

- [1] C. Abbehausen *et al.*, *Inorg. Chem.*, **52**, 11280 (2013)
- [2] C. Abbehausen *et al.*, *Inorg. Chem.*, **57**, 218 (2018)
- [3] C. Galuppo *et al.*, *J. Inorg. Biochem. In Press*, 112117 (2022)

Acknowledgments

This project was supported by FAPESP (2019/16904-2) and CNPq (142280/2017-8, 404668/2021-6).

Área: INO

In Silico Studies of Biologically Relevant Ligand Exchange Reactions of the Drug Candidates [AuCl(NHC)] and [CuCl(NHC)]

Gustavo C. Rodrigues (IC)^{1*}, Manoel V. F. Barrionuevo (PG)¹, Miguel A. San Miguel (PQ)¹, Camilla Abbehausen (PQ)¹.
gustavoclaussr@gmail.com

¹Institute of Chemistry, UNICAMP

Palavras Chave: Organometallic complexes, DFT, Ligand exchange, Relaxed Surface Scan.

Highlights

Linear Au(I) and Cu(I) organometallics have been investigated as chemotypes. They can exchange their ligands in solution, affecting the biological outcome. This work investigates in silico these reactions.

Resumo/Abstract

Au(I) and Cu(I) are thiophilic; therefore, they undergo ligand exchange reactions in biological systems. N-heterocyclic carbenes (NHC)^[1] are excellent σ -donating, resulting in linear, stable, and inert complexes with these metal centers. An example of an NHC ligand is the symmetric mesitylated (IMes), present in the complexes studied in this work, [AuCl(IMes)], and [CuCl(IMes)] (Fig 1). Among different NHC structures, these organometallics presented significant anti-Leishmania and anti-Chikungunya replication activities



Figure 1. IMes, [AuCl(IMes)] and [CuCl(IMes)] structures.

In silico methods are growing in the pharmaceutical drug research area due to their numerous advantages^[2]. In this study, we used DFT (PBE0, DEF2-TZVP/BJ, RIJCOSX, CPCM for DMSO implicit solvation, and ZORA for gold) to study ligand exchange reactions of [Au(IMes)Cl] and [Cu(IMes)Cl], more specifically, the Cl⁻ substitution for DMSO and cysteine (Cys), as also as the ligand scrambling reaction (where two molecules of [MCl(IMes)] react forming [M(IMes)₂]⁺ and MCl₂⁻, M = Au(I) and Cu(I)), observed in several linear Au(I) and Cu(I) complexes^[3].

Firstly, the geometry of reactants and products was optimized using DFT in ORCA. Vibrational frequencies and Fukui function surfaces were also

calculated. The relaxed surface scan was used to search transition state (TS) candidates of each reaction, using the semiempirical GFN-xTB, with 120 steps. Then, the structures were analyzed and selected as TS guesses, which were used as input for TS optimization (OPTTS) using DFT. At least one optimized TS was obtained for each of the six reactions studied, and it was possible to calculate the activation energy (E_a) and Gibbs free energy variation (ΔG) of each reaction in kJ/mol (Table 1)

Table 1. E_a and ΔG for [AuCl(IMes)] and [CuCl(IMes)] reactions.

Reaction	[Au(IMes)Cl]		[Cu(IMes)Cl]	
	E_a (kJ/mol)	ΔG (kJ/mol)	E_a (kJ/mol)	ΔG (kJ/mol)
L = DMSO	101,42	77,59	103,50	84,17
L = Cys	58,66	-32,28	275,40	-13,67
Scrambling	196,15	58,70	135,05	54,75

The TS structures suggested that DMSO reacted with [Au(IMes)Cl] via an associative mechanism, while Cys via dissociative. The opposite was observed for [Cu(IMes)Cl] reactions. In summary, Cl replacement by Cys was exergonic, in contrast to Cl replacement by DMSO. However, the kinetic barrier for the reaction with Cys is considerably different compared to Cu(I) and Au(I).

REFERENCES

- BENHAMMER, Jan; FRISON, Gilles; HUYNH, Han. Chemistry Europe, v. 19, ed. 38, p. 12892-12905, 2013.
- SHAKER, Bilal; AHMAD, Sajjad; LEE, Jingyu. Computers in Biology and Medicine, v. 137, p. 104851, 2021.
- AIRES, Rochanna; SANTOS, Igor; FONTES, Josielle; BERGAMINI, Fernando; JARDIM, Carolina; ABBEHAUSEN, Camilla. Metallomics, v. 14, ed. 8, 2022.

Agradecimentos/Acknowledgments

We gratefully acknowledge financial support from CNPq 406444/2018-8, FAPESP 2020/11727-2 and 2019/16904-2, and CENAPAD-SP project#638 for computer time

Investigation of CO redox release by oxo-centered carbonyl-triruthenium clusters

Amanda Batista Silva (IC),¹ Sofia Nikolaou (PG)²

amandaq56@usp.br; sofia@ffclrp.usp.br

^{1,2}Departamento de Química, Faculdade de Filosofia Ciências e Letras de Ribeirão Preto, Universidade de São Paulo

Palavras Chave: CORM, redox release, triruthenium clusters

Highlights

In this work, it is presented the CO redox release dependence on the axial pyridine ligands L in the $[\text{Ru}_3\text{O}(\text{CH}_3\text{COO})_6(\text{L})_2\text{CO}]$ compounds, where L = 2,6-dimethylpyrazine, piridine and aminopyridine. By the analysis of the rate constants, it was concluded that the compound bearing the ligand with the highest pKa delivery CO more efficiently.

Resumo/Abstract

The increasing development of CO releasing molecules (CORMs)^{1,2} is due to the role of carbon monoxide in physiological process^{3,4} and potential applications in disease treatments.^{1,2} In face of that, the LABiQSC² research group has been studying the physical-chemical and biological proprieties of the centered carbonyl-triruthenium clusters with general formula $[\text{Ru}_3\text{O}(\text{CH}_3\text{COO})_6(\text{L})_2\text{CO}]$, where L = N-heterocyclic ligand.⁵ In a previous work it was demonstrated that the complex $[\text{Ru}_3\text{O}(\text{CH}_3\text{COO})_6(\text{py})_2\text{CO}]$, py = piridine, release CO by oxidative stimulus in aqueous environment.⁶ By a kinect approach, it was proven that the CO release was dependent on the concentration of complex, oxidant and pH. In order to advance these studies, this work analyzed the CO redox release dependence on the ancillary ligands, L = 2,6-dimethylpyrazine(dmpz), piridine(py) and aminopyridine(ampy), described in figure 1. For the experiments, 1,06 mmol/L solutions of each complex were prepared in methanol. After that, 500 μL of each solution were mixed with 2,00 mL of methanol and 500 μL of 37% dihydrogen peroxide. The initial concentrations were 177 $\mu\text{mol/L}$ of complex and 2.0 mol/L of H_2O_2 . The methanol was chosen considering the solubility of the complexes. The procedure was repeated three times and the reactions were monitored by UV-vis spectroscopy at 23°C. The analysis was made by calculating the reactions rate constants (k) from the mono-exponential plot of absorbance changes at 675 nm (λ_{max} of the $[\text{Ru}_3\text{O}(\text{CH}_3\text{COO})_6(\text{L})_2\text{S}]^+$ products) versus time. The k values obtained were 4.86 min^{-1} for the complex with L = dmpz, 14.56 min^{-1} for the complex with L = py and 62.60 min^{-1} for the complex with L = ampy. These results indicate that the complex with L = ampy is a better CORM than the others, once the CO delivery rate is higher. This conclusion agrees with previous works where it was found that ligands with higher pKa values facilitate the oxidation of $[\text{Ru}_3\text{O}(\text{CH}_3\text{COO})_6(\text{L})_2\text{CO}]$ by stabilization of higher oxidation states of the unit $[\text{Ru}_3\text{O}]$ and it will help to design new CORMs.⁵

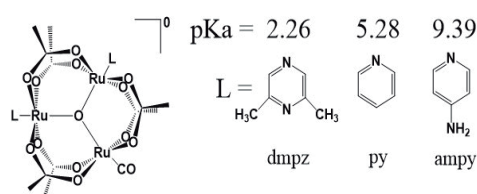


Figure 1. Complexes studied with their respective ligands

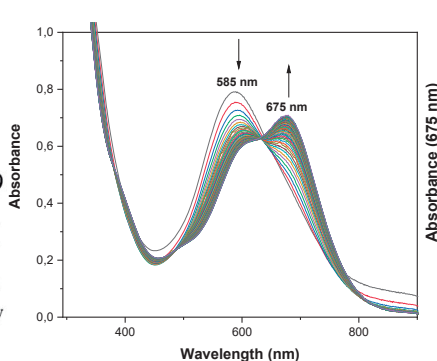


Figure 2. Spectral changes during CO release

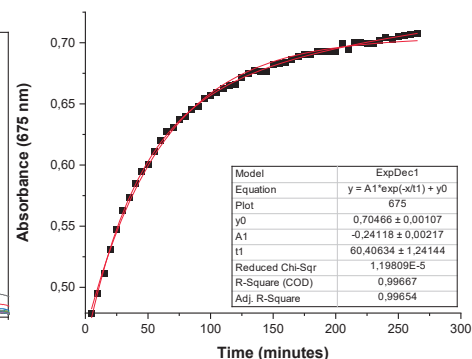


Figure 3. Kinect data for CO release

[1] K. LING, *Journal of Medicinal Chemistry*, 61, 2611 (2018). [2] W. ADACH, *Chemical-Biological Interactions*, 318, 108973 (2020). [3] S.W. RYTER, *The Korean Journal of Internal Medicine*, 28, 123 (2013). [4] C.S.F. QUEIROGA, *British Journal of Pharmacology*, 171, 1533 (2015). [5] M.B. MOREIRA, *Danton Transactions*, 45, 16799 (2016). [6] SILVA, A.B. 2022. "Carbonyl redox release by the complex $[\text{Ru}_3\text{O}(\text{CH}_3\text{COO})_6(\text{py})_2\text{CO}]$ in Aqueous Environment". Comunicação apresentada no XX BMIC - Brazilian Meeting on Inorganic Chemistry, Bento Gonçalves, Brazil, setembro de 2022.

Agradecimentos/Acknowledgments

Fundação de Amparo à pesquisa (FAPESP) and Conselho Nacional de Pesquisa e Desenvolvimento Tecnológico (CNPq)

46ª Reunião Anual da Sociedade Brasileira de Química: "Química: Ligando ciências e neutralizando desigualdades"

Investigation of noncovalent interactions in the crystal structure of new nickel(II) complex with a thiosemicarbazide ligand

Gustavo Jones Lima (IC),^{1*} Claudia Cristina Gatto (PQ)¹

*gustavo.joneslima@gmail.com; ccgatto@gmail.com

¹Laboratory of Inorganic Synthesis and Crystallography, University of Brasília (IQ-UnB), Brasília-DF, Brazil

Keywords: nickel(II) complex, thiosemicarbazide ligand, crystal structure, noncovalent interactions.

Highlights

A new nickel(II) complex with thiosemicarbazide was studied by X-ray crystallography. A 3D Hirshfeld surface was analyzed to verify noncovalent interactions upon the molecular packing.

Resumo/Abstract

Thiosemicarbazides are important ligands in bioinorganic and coordination chemistry.¹ A few drugs are derived from this ligand, showing promissory results in microbial, fungicide, and cancer therapy.^{2,3} A considerable number of nickel(II) complexes have been intensively studied for their pharmacological properties and biological applications. Additionally, thiosemicarbazides ligands are able to form stable metal complexes with an extensive variety of metal ions, which evince an abundant diversity of applications for this ligand and their metal complexes.

The present work reports the structural elucidation and investigation of noncovalent interactions of new nickel(II) complex, $[\text{Ni}(\text{ptsc})_3]\text{Cl}_2 \cdot 2\text{H}_2\text{O}(\text{DMF})$ with 4-phenyl-thiosemicarbazide ligand (ptsc). The metal center is coordinated by three ligand molecules with an NS-donor system and the coordination geometry to the nickel(II) atom is observed as a distorted octahedral, Figure 1(a). The asymmetric unit of the compound also shows two chloride ions, DMF and water solvent molecules. The analysis of the packing architecture with the Hirshfeld surface shows many noncovalent interactions, Figure 1(b).

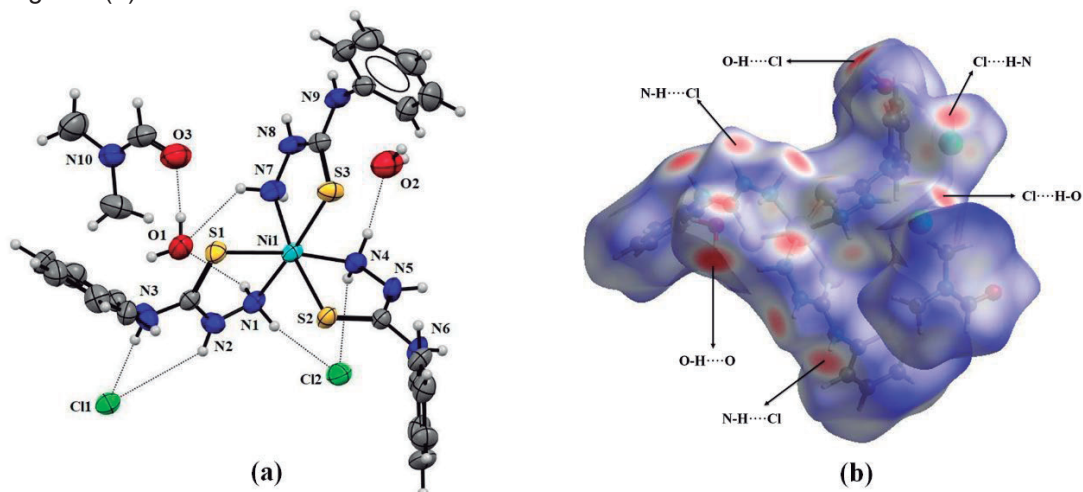


Figure 1. (a) Molecular structure of $[\text{Ni}(\text{tsc})_3]\text{Cl}_2 \cdot 2\text{H}_2\text{O}(\text{DMF})$ showing intermolecular hydrogen interactions (dotted lines). (b) Hirshfeld surface mapped with d_{norm} of the complex $[\text{Ni}(\text{tsc})_3]\text{Cl}_2 \cdot 2\text{H}_2\text{O}(\text{DMF})$.

¹A.S. Antsyshkina, G.G. Sadikov, T.V. Kokisharova, V.S. Sergienko, *Russian Journal of Inorganic Chemistry*, **2014**, 59, 50.

²C. Popovici, C.M. Pavel, V. Sunel, C. Cheptea, D.G. Dimitriu, D.O. Dorohoi, D.D.V. Closca, M. Popa, *Int. J. Mol. Sci.* **2021**, 22, 12139.

³X. Zhang, P. Lei, T. Sun, S. Jin, X. Yang, Y. Ling, *Molecules*. **2017**, 22, 2085.

Agradecimentos/Acknowledgments



Lanthanide coordination polymers containing *N*-phthaloylglicinate and terephthalate ligands: Synthesis, structure and optical properties.

Joaldo G. Arruda (PG)¹, Israel F. Costa (PQ)², Victor M. Miranda (PG)³, Rafaela B.P. Pesci (PG)¹, Victor M. Deflon (PQ)³, Wagner M. Faustino (PQ)¹, Hermi F. Brito (PQ)², Huayna Terrasche (PQ)⁴, Ercules E.S. Teotonio (PQ)^{1,4*}.

teotonioees@quimica.ufpb.br;

¹Departamento de Química, UFPB; ²Instituto de Química, USP; ³Instituto de Química de São Carlos, USP; ⁴Institute of Inorganic Chemistry, CAU.

Keywords: *N*-phthaloylglycine, Terephthalic acid, Mixed carboxylate, Coordination polymers, Lanthanide, Photoluminescent.

Highlights

- The lanthanide mixed carboxylate coordination polymers were prepared.
- Structural and photoluminescent properties were investigated.

Abstract

Novel lanthanide coordination polymers of general formula $\{[Ln_2(\text{phthgly})_4(1,4\text{-dbc})(\text{H}_2\text{O})_6](\text{H}_2\text{O})_4\}_n$, Eu-(**1**) and Gd-(**2**) for Ln: Eu and Gd, respectively; where phthgly: *N*-phthaloylglycinate and 1,4-dbc: terephthalate, were synthesized by the reaction between an aqueous solution of $Ln(\text{NO}_3)_2 \cdot 5\text{H}_2\text{O}$ and a mixed of phthgly and 1,4-dbc carboxylate ligands. These compounds were characterized by elemental analysis, infrared spectroscopy, and thermogravimetric analysis (TGA). The results of single-crystal X-ray diffraction reveal that these coordination polymers are isostructural, crystallizing in the triclinic space group $P\bar{1}$. The molecular structures of Eu-(**1**) and Gd-(**2**) (Fig. 1a) are formed by polymeric chains of symmetric binuclear units bridged by 1,4-dbc ligand. Surprisingly, all ligands participate in hydrogen bonding interactions, creating a highly rigid crystalline structures (Fig. 1b). Furthermore, the carboxylate groups adopt different coordination modes (bidentate chelate, bidentate bridging)^[1,2]. TGA/DrTGA analyses show two consecutive weight loss events from 55 to 123 °C attributed to the releasing of lattice and coordination water molecules, respectively. In addition, several consecutive thermal events above 350 °C may be assigned to the thermal decomposition of the anhydrous materials. The luminescence data indicated that the Eu^{3+} ion exhibits high luminescence intensity with high color purity under direct excitation or via intramolecular energy transfer from ligands (Fig. 1b). The color coordinates (Fig.1c) of the Eu(**1**) compound depict reddish emission. These novel coordination polymers offer a more attractive platform for developing functional materials for different applications.

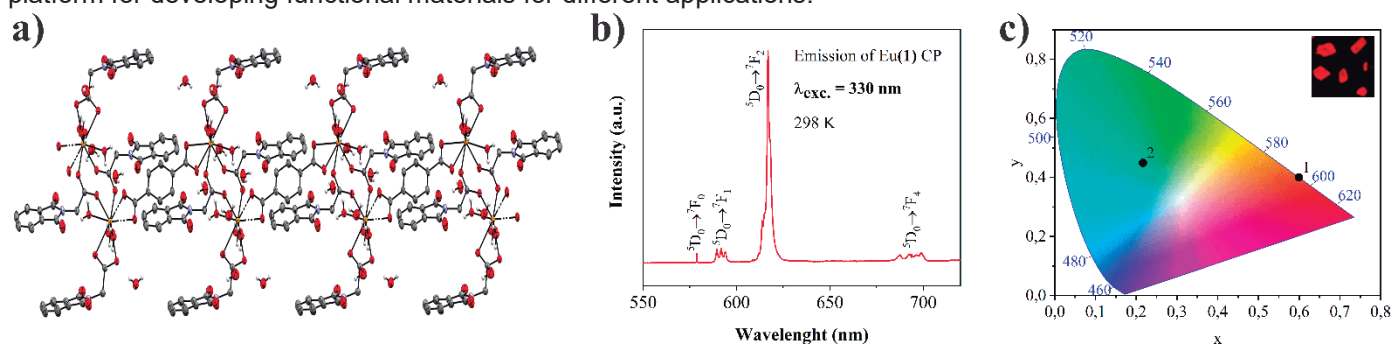


Figure 1. (a) Packing along *a* axis of coordination polymer **1**; (b) Emission spectrum of complex **1** under excitation at 330 nm and (c) CIE color coordinates of complex **1** and **2**. Inserted a photo of complex **1** upon excitation at 330 nm.

[1] E.E.S. Teotonio, G.M. Fett, H.F. Brito, A.C. Trindade, M.C.F.C. Felinto, Novel unexpected Tb^{3+} coordination polymer containing two carboxylate ligands: Syntheses, structure and photoluminescent Properties, *Inorg. Chem. Commun.* 10 (2007) 867–872.

[2] F.G. Chávez, H. Najera, M.A. Leyva, O.S. Feria, F. González, I. Beltrán, New 2D Lanthanide MOFs Constructed from Bis(imide) Pyromellitic Alanine Ligands with Enhanced Fluorescence toward Activation and Modulation of Microstructure, *Cryst. Growth Des.* 20 (2020) 4273–4292.

Acknowledgments

The authors acknowledge CNPq, CAPES, FINEP and FAPESP for financial support.

Layer-by-Layer Assembly Of NaYF₄:Yb³⁺/Er³⁺ UCNPs@Cystein And Antibody: A Sensor For *Escherichia Coli* Bacteria

Beatriz B. S. Ramin (PG),¹ Willy G. Santos (PQ),¹ Marli L. de Moraes (PQ),² Sidney J. Ribeiro (PQ)^{1*}

beatriz.schulz@unesp.br; sidney.jl.ribeiro@unesp.br

¹São Paulo State University, Chemical Institute, Araraquara, SP, 14800-060, Brazil; ²Universidade Federal de São Paulo, Instituto de Ciência e Tecnologia, São José dos Campos, SP, 12247-014, Brazil.

Palavras Chave: biosensor, bacteria, nanoparticle, Up-conversion, fluorescence emission.

Highlights

A sensor to detect *E. Coli* bacteria based on LbL films of UCNPs modified with cysteine and *E. Coli* antibody was developed to improve the biocompatibility of the biosensor and recognition of *E. Coli*.

Resumo/Abstract

Every year, millions of people die from a pathogenic bacterial infection, which requires the development of efficient detection methods. Films from nanoparticles for up-converting energy NaYF₄:Yb³⁺/Er³⁺ UCNPs were developed for detection of *E. coli*. The surface of the UCNPs was modified with cysteine (Cys) and then bioconjugation with an *E. coli*-specific antibody (Ab) was performed. However, UCNPs exhibit water-induced UC emission quenching, thus decreasing the sensitivity of the sensor in aqueous media. Therefore, we propose a Layer-by-layer (LbL) film sensor in PVS for biosensor assembly. The biosensor response, the specific antigen-antibody interaction, was investigated using fluorescence. A reformulated Stern-Volmer equation was used to investigate the quenching rate constant values and statistical results, respectively. The limit of detection was $\sim 5 \times 10^{-6}$ g L⁻¹ *E. coli*. Furthermore, the proposed method achieved great advantages such as easy operation and high sensitivity.

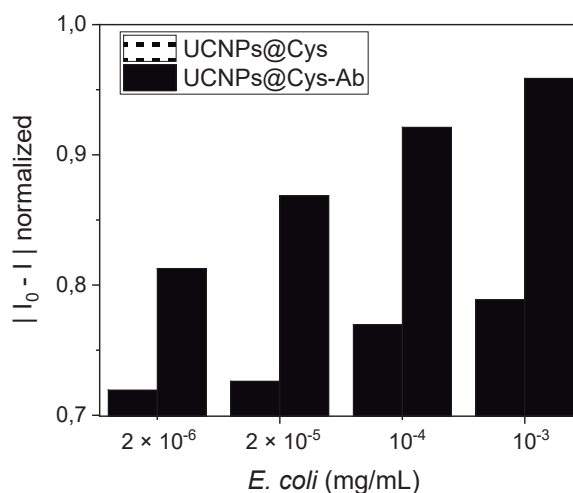


Figure 1. Optical sensor response $|I_0 - I|$ at 656 nm as a function of the concentration of the *E. coli* extract.

Acknowledgments



Process FAPESP: 2020/14009-3; 2019/15227-7.

Luminescent Eu³⁺-doped gadolinium niobate: effect of doping concentration and annealing temperature on the stabilization of crystalline phases

Daniela Caroline Silva (IC),¹ Guilherme Primac Costa (IC),¹ Hayra do Prado Labaki (PG),¹ Rogéria Rocha Gonçalves^{1*}.

danielacarolineml@usp.br; rrgoncalves@ffclrp.usp.br

¹ Laboratório de Materiais Luminescentes Micro e Nanoestruturados – Mater Lumen, Departamento de Química, FFCLRP, Universidade de São Paulo, 14040-900, SP, Brazil.

Palavras Chave: Nanoparticles, Gadolinium Niobate, Europium, Luminescence, Morphology, Spectroscopy.

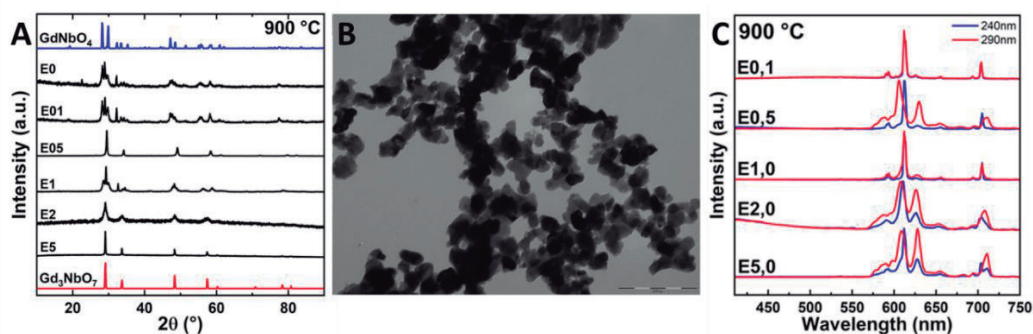
Highlights

Gd₃NbO₇ (orthorhombic) and GdNbO₄ (monoclinic) were preferentially crystallized depending on the annealing temperatures and the Eu³⁺ content, with consequent impact on the morphology and luminescence of the particles.

Resumo/Abstract

Eu³⁺ doped gadolinium niobate nanoparticles were synthesized by the sol gel process, using 2-ethoxyethanol, niobium ethoxide, Gd(NO₃)₃, EuCl₃, and ethanol as precursor and adding ethanolic solution of NH₄OH for basic catalysis. The colloidal suspension was maintained under stirring for 1 hour. The resulting solid was isolated by centrifugation, washed with ethanol, and dried for 24 hours at 60 °C, and then was annealed at 900, 1000, or 1100 °C for 10h. The Eu³⁺ content varied from 0.1 (E0,1) to 5.0 (E5,0) % in mol. The structural, morphological, vibrational, and photoluminescent properties were evaluated. Upon annealing at 900 °C, the Eu³⁺ content favors the Gd₃NbO₇ stabilization (Figure 1A), which is also crystallized at higher annealing temperatures. Transmission electron microscopy showed the formation of nanoparticles after annealing at 900 °C, with an average diameter below 100 nm (Figure 1B); and even for higher annealing temperatures, small nanoparticles were still observed. The Raman spectra for the undoped sample confirmed the presence of Gd₃NbO₇ and/or GdNbO₄ phases upon distinct annealing temperatures, and attesting a relatively low phonon energy of the gadolinium niobate of about 800 cm⁻¹. The excitation spectra showed the characteristic intraconfigurational *f-f* transitions of Eu³⁺, and a broadband, below 300 nm, which is ascribed to the charge transfer band and its position and intensity were directly correlated with the crystalline phases stabilized in the samples. Figure 1C displays the emission spectra of the Eu³⁺-doped gadolinium niobate under selective excitation at 245 and 299 nm. The excitation at 245 nm, preferentially excites the Eu³⁺ substituting the single symmetry site of Gd³⁺ in GdNbO₄ structure, which results in more define Stark components. However, under excitation at 299 nm, an inhomogeneous broadening is observed due to the presence of Eu³⁺ in the Gd₃NbO₇ phase. In the case of samples doped with 1.0 mol% of Eu³⁺, a distinct profile was observed, characteristic of a single symmetry site occupation.

Figure 1. (A) X-ray diffractograms, (B) TEM Images (0.5 mol% Eu³⁺), and (C) emission spectra upon excitation at 240 (GdNbO₄) and 290 nm (Gd₃NbO₇) for the Eu³⁺-doped gadolinium niobate annealed at 900 °C for 10 h.



Agradecimentos/Acknowledgments

This work was supported by Conselho Nacional de Desenvolvimento Científico e Tecnológico (CNPq), Coordenação de Aperfeiçoamento de Pessoal de Nível Superior (CAPES) and Fundação de Amparo à Pesquisa do Estado de São Paulo (FAPESP) and Photonics National Institute for Science and Technology (INFO).

Área: INO

Luminescent high-entropy rare earth vanadate nanoparticlesDayane V. N. dos Santos (PG),^{1,2} Júlio C. Cezar (PQ),² and Paulo C. de Sousa Filho (PQ)^{1*}

d169791@dac.unicamp.br; *pcsfilho@unicamp.br

¹Institute of Chemistry, University of Campinas (UNICAMP); ²Brazilian Synchrotron Light Laboratory (LNLS), CNPEM.

Palavras Chave: High-entropy materials, Luminescence, Nanoparticles.

Highlights

We synthesized rare earth vanadate nanocrystals containing a mixture of five cations as major lattice components to describe potential high-entropy effects on the microstructure and luminescence of oxide nanoparticles.

Abstract

High-entropy materials (HEM) are increasingly explored in solid-state chemistry towards understanding how disordered multicomponents change structural stability, ion mobility, thermal or ionic conductivity, among other properties. Although high-entropy oxides (HEO) afford several advantages in comparison to the conventional counterparts in catalysis and energy conversion, few works have explored luminescent properties and microstructural effects of rare earth based HEO [1,2]. Herein we propose to study the luminescence and structure of high-entropy rare earth vanadate nanoparticles (NPs) using Eu^{3+} as a spectroscopic probe, also discussing how the thermometric response of Er^{3+} -doped HEO nanoparticles compare with conventional particles. UV-excitable $(\text{Y}_{0.19}\text{La}_{0.19}\text{Gd}_{0.19}\text{Yb}_{0.19}\text{Lu}_{0.19}\text{Eu}_{0.05})\text{VO}_4$ and $(\text{Y}_{0.95}\text{Eu}_{0.05})\text{VO}_4$, and NIR-excitable $(\text{Y}_{0.19}\text{La}_{0.19}\text{Gd}_{0.19}\text{Yb}_{0.19}\text{Lu}_{0.19}\text{Er}_{0.05})\text{VO}_4$ and $(\text{Y}_{0.75}\text{Yb}_{0.20}\text{Er}_{0.05})\text{VO}_4$ nanoparticles were prepared by aqueous coprecipitation of mixtures of metal nitrates and sodium metavanadate at 25 °C [3]. The obtained particles showed polycrystalline nature and elongated morphology (Figure 1a) with hydrodynamic diameters around 65 ± 15 nm. Interestingly, annealing of the HEO particles resulted in significant nanovoiding and faceting (Figure 1b), which will be further investigated by *in situ* techniques. Although the general elemental distribution is homogeneous (Figure 1c), the HEO particles possibly underwent preferential concentration of larger ionic radius La^{3+} at the surface in comparison to the inner volume of the particles, as suggested by XPS analysis. Both HEO and reference materials showed the characteristic *I41/amd* tetragonal structure, confirming the incorporation of all ions in the crystal lattice. The Eu^{3+} emission spectra of the HEO (Figure 1d) showed an increased intensity ratio between the B2 (614.8 nm) and E (618.8 nm) components of the ${}^5\text{D}_0 \rightarrow {}^7\text{F}_2$ transition when compared to the conventional nanoparticles and other $\text{YVO}_4:\text{Eu}^{3+}$ particles reported in the literature. This suggests a high degree angular distortion around the *D2d* Eu^{3+} coordination polyhedron in agreement with expected effects introduced by the high-entropy conditions [4]. This indicates that we can possibly probe and quantify systematically the degree of high entropy in REVO4 nanoparticles via Eu^{3+} spectra. The Er^{3+} -doped solids showed low relative thermal sensitivities ($<0.26\% \text{ K}^{-1}$ at ~ 300 K) between 77 and 580 K, but the sensitivity profile of the HEO material deviated from the reference particles. Further investigation will enable us to correlate the thermal response to effects introduced by the high entropy in the thermal conductivity of the vanadate nanoparticles.

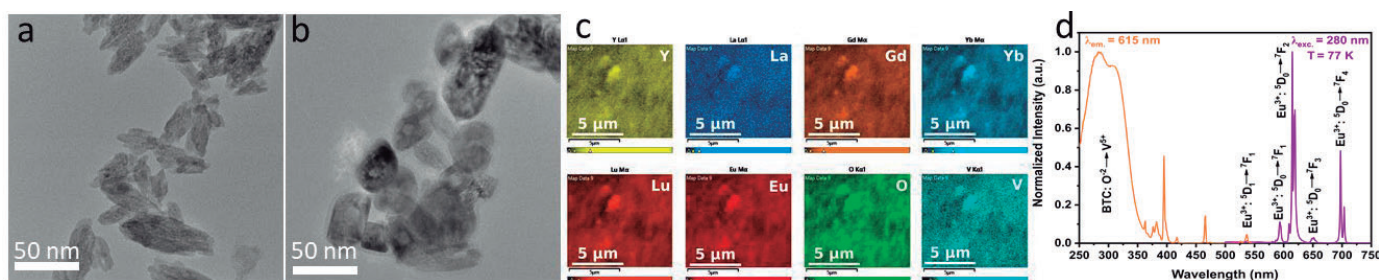


Figure 1. TEM images of (a) as prepared and (b) 900 °C-annealed $(\text{Y}_{0.19}\text{La}_{0.19}\text{Gd}_{0.19}\text{Yb}_{0.19}\text{Lu}_{0.19}\text{Eu}_{0.05})\text{VO}_4$ particles. (c) SEM-EDS elemental mappings and (d) excitation (orange, $\lambda_{\text{exc}}=615$ nm) and emission (purple, $\lambda_{\text{exc}}=280$ nm) spectra of the Eu^{3+} -doped HEO.

References:

[1] J. Mater. Chem. A, 2021, 9, 782-823.; [2] Adv. Sustainable Syst., 2022, 6, 2200067.; [3] Langmuir, 2020, 36, 9124-9131.; [4] Nanoscale, 2021, 13, 4931-4945.

Acknowledgments

The authors thank CAPES, CNPq, and FAPESP (2022/03442-3) for financial support.

Luminescent nanothermometers decorated with metal nanoparticles to assess thermal contributions in plasmonic catalysis

Tamires M. Oliveira (PG),¹ Gabriel Moronari (IC),¹ Rafael V. Perrella (PG),¹ Pedro H. C. Camargo (PQ),² Paulo Cesar de Sousa Filho* (PQ)¹

tamires.maira.oliveira@gmail.com; *pcsfilho@unicamp.br

¹Department of Inorganic Chemistry, Institute of Chemistry, University of Campinas (UNICAMP); ²Department of Chemistry, University of Helsinki.

Key-words: Nanothermometry, Spectroscopy, Plasmonic, Catalysis.

Highlights

Combining luminescent rare earth vanadates and gold nanorods (AuNRs) resulted in enhanced activity towards reduction of 4-nitrophenol, providing an interesting system to study the underlying mechanisms in plasmonic catalysis via optical determination of the local temperature.

Abstract

Plasmonic metal nanoparticles (NPs) show notable properties for emerging applications photocatalysis, which motivates fundamental research in this field¹. However, accurate description of mechanisms of reaction mediated by metal NPs is still limited by the difficult determination of local temperatures to attribute thermal contributions². Marrying optical nanothermometers based on lanthanide emissions and plasmonic NPs is therefore an interesting approach to afford insights into the underlying mechanisms in plasmonic photocatalysis. We proposed a rare-earth vanadate-based platform combined with gold nanoparticles or nanorods (REVO₄-AuNPs/AuNRs), in which the REVO₄ phase shows a luminescent thermometric response to measure the temperature around the metal NPs during photocatalytic assays. Comparing (Y,Yb,Tm,Er)VO₄ particles and AuNRs-functionalized systems revealed changes in the profile of Er³⁺ ²H_{11/2}→⁴I_{15/2}, ⁴S_{3/2}→⁴I_{15/2} upconversion emissions under λ_{exc}=808 nm excitation, where the high energy band showed increased intensities due to the increase of the local temperature caused the metal NPs. This effect is suppressed if this sample is dispersed in water, thus indicating a higher degree of energy dissipation. Intensity vs. power profiles also showed the effects of AuNRs on upconversion mechanisms, with a decrease in the number of photons required for Er³⁺ emissions when AuNRs interact with the vanadate particles. This was also confirmed by *in situ* luminescence measurements monitoring progressive deposition of AuNRs over (Y,Yb,Tm,Er)VO₄ particles. Catalysis assays of 4-nitrophenol reduction by NaBH₄ under λ_{exc}=740 nm demonstrated a positive interaction between the (Y,Yb,Tm,Er)VO₄ support and AuNRs, where an improved catalytic activity was observed in the combined system. Our results points toward multimodal systems to potentially provide detailed information on temperature fluctuations around the AuNRs and on the effects of REVO₄ as catalytic supports in plasmonic catalysis reactions.

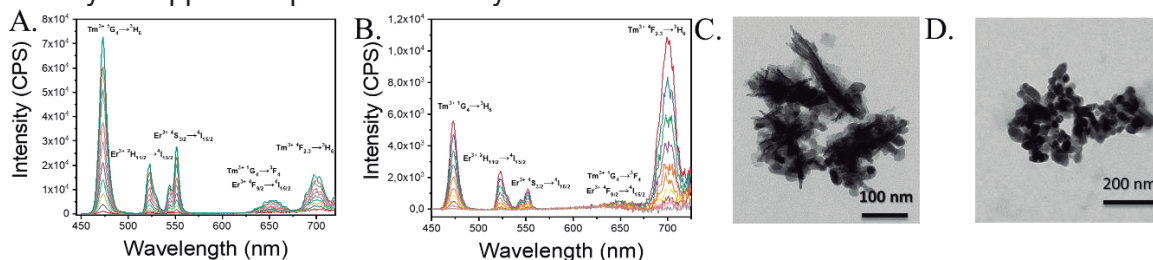


Figure 1. Power-dependent spectrum to A. (Y,Yb,Tm,Er)VO₄ and B. (Y,Yb,Tm,Er)VO₄-AuNRs show the influence of the presence of Au in the spectroscopy results and the TEM images to C. (Y,Yb,Tm,Er)VO₄ and D. (Y,Yb,Tm,Er)VO₄-AuNRs depict the deposition of gold over REVO₄.
¹ *Nature Materials*, 2015, 14, 567.

Acknowledgments

The authors thank CAPES, CNPq, and FAPESP (2019/21896-9, 2021/08107-5, 2022/05118-9, and 2022/03442-3) for financial support.

Luminescent Perovskite like structure of RE³⁺-doped NaTaO₃: from cubes to spheres for Biophotonics

Ana C. da Costa (IC)¹, Hayra do P. Labaki (PG)¹, Rogéria R. Gonçalves (PQ)¹

ana_cda@usp.br; rrogoncalves@ffclrp.usp.br

¹Laboratório de Materiais Luminescentes Micro e Nanoestruturados – Mater Lumen, Departamento de Química, FFCLRP, Universidade de São Paulo, 14040-900, SP, Brazil.

Keywords: luminescence, perovskite, biophotonics, lanthanide, nanoparticles, tantalate

Highlights

In this work, we report the synthesis, structural, morphological and spectroscopic features of Red emitting redispersible nanocubes and nanospheres RE³⁺ doped sodium tantalate.

Resumo/Abstract

Sodium tantalates have been remarkably explored as a new photocatalyst system for water splitting since they have unique photocatalytic properties. However, only a few papers focus on the use of NaTaO₃ as host materials for rare earth ions. Furthermore, this perovskite can be a promising host for RE³⁺ ions owing to its high density (7.09 g/cm³) which can be interesting for scintillation studies, low phonon energy (cutoff 693 cm⁻¹) hindering a luminescence quenching, chemical stability, and nontoxicity [1,2]. The NaTaO₃ also exhibits a rich polymorphism over wide temperature ranges, which are the result of the flexibility of the framework that can tolerate the tilting of MO₆ octahedra and explain their difficulty to crystallize a pure phase. In this work, we report the synthesis, structural, morphological and spectroscopic studies of Eu³⁺ doped sodium tantalate. Nanoparticles were observed by transmission electron microscopy (TEM) images, as can be seen in Figure 1(A), which shows the formation of fully dispersed nanoparticles with an average size of 60 nm. Furthermore, it is observed that modifying the base volumes added during the synthesis, there is a change in the morphology of the particles, changing from cubic to spherical. In addition to the homogeneous distribution and control of particle size and morphology, the synthesis adopted in this work stabilizes the pure orthorhombic structure of NaTaO₃, with Pbnm space group (JCPDS No. 88375) and cell parameter defined as a=5.48109(9) b=5.52351(9) c=7.79483(12). Furthermore, a selective occupation of Eu³⁺ ions from sites on the crystalline structure and on the surface of nanoparticles were identified using lanthanide ions as structural probe. In conclusion, the luminescent nanoparticles of NaTaO₃ have properties which may be promising for application in biological media and in photocatalysis studies.

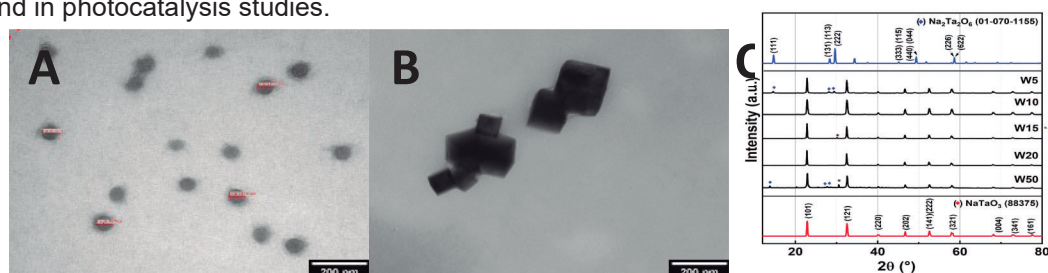


Fig. 1. TEM of NaTaO₃ (A) 50 mL NaOH, (B) 20 mL NaOH and (C) XRD diffractogram of NaTaO₃ samples

REFERENCES

- [1] Vishnu Shanker, Saroj L. Samal, Gopal K Pradhan, Chandrabhas Narayana and Ashok K. Ganguli "Nanocrystalline NaNbO₃ and NaTaO₃: Rietveld studies, Raman spectroscopy and dielectric properties." *Solid State Sciences*, 11, 2, 562-569, 2009.
- [2] Hanggara Sudrajat, Sandhya Babel, Indika Thushari and Kritapas Laohasurayotin "Stability of La dopants in NaTaO₃ photocatalysts." *Journal of Alloys and Compounds*, 775, 1277-1285, 2019.

Agradecimentos/Acknowledgments

This work was supported by Conselho Nacional de Desenvolvimento Científico e Tecnológico (CNPq), Coordenação de Aperfeiçoamento de Pessoal de Nível Superior (CAPES) and Fundação de Amparo à Pesquisa do Estado de São Paulo (FAPESP) and Photonics Nacional Institute for Science and Technology (INFO)

Mechanism of interaction of yttrium and lanthanum in cationic resin from the loading of acidic mine water (AMW) in sulfate-rich.

Alexandre C. Bertoli (PQ),^{1*} Gabriela C. Silva (PQ),² Ana Cláudia Q. Ladeira (PQ),² Luciano T. Costa (PQ),¹ Hélio A. Duarte (PQ),³ Wagner B. Almeida (PQ).¹

bertolialexandre@yahoo.com.br

¹Instituto de Química, UFF; ²Centro de Desenvolvimento da Tecnologia Nuclear, CDTN; ³Departamento de Química, UFMG.

Keywords: Ionic Exchange, DFT, Acid Mine Water.

Highlights

Elution using CaCl₂ removes the Ln from the resin loaded with AMW. DFT indicate the chemical speciation of [LnSO₄(H₂O)₇]⁺ and [Ln(SO₄)₂(H₂O)₅]⁻. Functional group in the resin acts as a complexing agent.

Resumo/Abstract

Lanthanum and yttrium can be found in ores as well as in secondary sources such as acid mine water (AMW). Due to their crescent use in green technology the secondary sources have become attractive and promising. The ion exchange process to recover rare earth elements (REE) from acid waters is investigated using combined experimental and theoretical approaches. Experiments of loading and elution of acidic cation resin were carried out in batch and continuous (in the column) using laboratory solutions as well as crude AMW samples. The loading of the resin, which assessed the competition of different species during the ion exchange process, showed that the resin presents higher loading for La³⁺ in detriment to Y³⁺. Elution in columns with 2.0 M CaCl₂ showed that as the flow rate decreased there was an increase in the elution from ~80% to 100% for La³⁺ and ~50% to 90% Y³⁺. The theoretical studies, using DFT calculations indicated that [LnSO₄(H₂O)₇]⁺ and [Ln(SO₄)₂(H₂O)₅]⁻ (Ln=La, Y) species are adequate models to describe the chemical speciation. The free reaction energies of displacing the Ln³⁺ species from the resin by [Ca(H₂O)₆]²⁺ to release the species [LnSO₄(H₂O)₇]⁺ and [Ln(SO₄)₂(H₂O)₅]⁻ are 7.7 and 5.2 kcal mol⁻¹, respectively, for La³⁺, and 4.8 and 3.8 for Y³⁺. These values must be compared to the same process in the absence of SO₄²⁻, which yields the values of 3.1 and 3.4 kcal mol⁻¹ for La³⁺ and Y³⁺, respectively. According to our calculations, the presence of sulfate slightly disfavors the elution process for the La³⁺ and it is marginally the same for Y³⁺. The estimated free energies are less favorable by at least 5 kcal mol⁻¹. Unexpectedly, the presence of sulfate does not affect the thermodynamics of the REE loading and elution processes. In other words, the formation of less charged species of Ln³⁺/SO₄²⁻ does not affect their interaction with the resin. This is an unexpected result since it is expected that the positively charged species are crucial for the effectiveness of the ion exchange process using cationic resins. We have shown that the resin acts as a complexing agent anchored in a solid matrix.

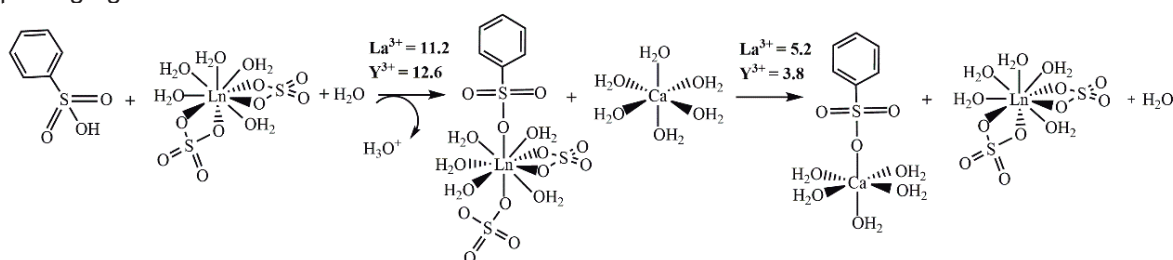


Figure 1 – Reaction mechanism of the loading and elution processes. Values are in kcal mol⁻¹.

Agradecimentos/Acknowledgments

FAPERJ and FAPEMIG. Based Mineral High-Performance Materials and Processes Network–RENOVAMin (Proc. RED-00102-16).

Metal biomolecule framework from metal carbonates and glutamic acid.

Rodrigo V. Rodrigues (IC),¹ Natália C. Zanotelli (PG),¹ Sílvia D. de Campos (PQ),¹ Ronan F. F. de Souza (PQ),¹ Elvio A. de Campos (PQ).^{1*}

rodrigovieira3007@gmail.com; elvio.campos@unioeste.br

¹Centro de Engenharias e Ciências Exatas, Unioeste – Campus Toledo PR.

Palavras Chave: *Metal organic framework, Coordination polymer, Self-assembly, Crystal structure, Supramolecular structure.*

Highlights

The metal biomolecule frameworks (MBioFs) with general formula $[M(\text{glutamate})(\text{H}_2\text{O})_2]_n$ where $M = \text{Co}^{2+}$, Cu^{2+} , or Zn^{2+} are prepared by an eco-friendly method.

A procedure for recrystallization of the obtained MBioFs is presented.

Resumo/Abstract

The combination of metal ions with glutamate can result in several compounds that are classified as BioMOFs (metal-organic frameworks for biological and medical applications) or MBioFs (metal biomolecule frameworks), such as copper¹, zinc² and cobalt³. These can be prepared by different methods, such as slow evaporation of aqueous solutions in stoichiometric mixtures of salts⁴ or metallic oxides⁵ with glutamic acid without any pH control, or with pH adjusted with K_2CO_3 ¹ or NaOH ², in a water/methanol mixture in the presence of triethylamine⁶ and also by the hydrothermal method in a closed reactor at 100 °C in the presence of triethylamine as a proton trap³. In both methods the same structure is obtained, which macroscopically appears as orthomorphous crystals belonging to the space group $P2_12_12_1$ in variable yields. Herein are the results of simple reactions, carried out in aqueous media, between basic carbonates of cobalt, copper, and zinc with glutamic acid according to the conditions described in Table 1. In both reactions crystalline compounds were obtained and characterised by XRD, Infrared and UV-Vis spectroscopy (solids by photoacoustic), and TGA. These techniques confirmed that the structures obtained were identical to those described in the literature for the compound with general formula $[M(\text{glutamate})(\text{H}_2\text{O})_2]_n$ (**I**) where $M = \text{Co}^{2+}$, Cu^{2+} , or Zn^{2+} .

Table 1: Experimental conditions for reactions between metal carbonates and glutamic acid.

Metal ion source	H ₂ O vol. (mL)	Mass (g)	Mols	Temp. °C	Yield (%) [*]	Unreacted solid	Final pH
$\text{CoCO}_3 \cdot x \text{H}_2\text{O}$	60 mL	4.0202	0.026	50	43	**	7
$\text{CuCO}_3 \cdot \text{Cu}(\text{OH})_2$	250 mL	4.4224	0.020	95	47	$\text{Cu}(\text{OH})_2$	4
$2\text{ZnCO}_3 \cdot 3\text{Zn}(\text{OH})_2$	250 mL	2.1960	0.004	95	85	-	5

^{*} Based on glutamic acid. ^{**} Mixture of cobalt oxides and hydroxides and part of the excess CoCO_3 .

Due to the fast precipitation of the $[M(\text{glutamate})(\text{H}_2\text{O})_2]_n$, part of them is retained when filtering the solution resulting from the reaction between metal carbonates and glutamic acid. This product was recovered by treatment with a 1.5% (v/v) acetic acid aqueous solution at temperature between 50 and 70 °C, and the solid formed showed X-ray diffraction pattern identical to that observed for (**I**), which configures a possible recrystallisation method of the obtained MOFs. Both compounds are thermally stable up to 100 °C, temperature at which the loss of the two water molecules from the structure (one coordinated and one hosted) begins. Organic matter decomposes above 200 °C, resulting in the respective metal oxide in the case of copper and cobalt compounds and carbonate in the case of zinc compound.

1 - *Inorg. Chim. Acta* 1998, 283, 105-110. **2** - *Chem. Commun.* 2016, 52, 280-283. **3** - *J. Coord. Chem.* 2009, 62, 1959-1963. **4** - *Acta Cryst.* 1966, 21, 594-600. **5** - *Acta Cryst.* 1966, 21, 600-605. **6** - *New J. Chem.* 2020, 44, 3961-3969.

Agradecimentos/Acknowledgments

This study was financed in part by the Coordenação de Aperfeiçoamento de Pessoal de Nível Superior – Brasil (CAPES) – Finance code 001. R. V. Rodrigues thanks to Fundação Araucária for the scholarship.

Metallo-Octa-Carboxy-Phthalocyanine Coordination Polymers as Efficient Oxygen Evolution Reaction (OER) Electrocatalysts.

Ítalo Reis Machado (PG),¹ Raphael Bacil Prata (PQ),¹ Helton Pereira Nogueira (PQ),¹ Koiti Araki (PQ),^{1*}
 italo.machado@usp.br; koiaraki@iq.usp.br

¹ Departamento de Química Fundamental, Instituto de Química, Universidade de São Paulo.

Key Words: oxygen evolution reaction; electrocatalysis; coordination polymers; phthalocyanine

Highlights

Carboxy-phthalocyanine based amorphous coordination polymers; Building-blocks united by first row transition metal ion; Efficient and stable OER electrocatalysts.

Resumo/Abstract

Oxygen evolution reaction (OER) stands as a key challenge for the realization of sustainable energy conversion and storage technologies such as fuel cells and water-splitting. Based on the attractive properties of metalated phthalocyanines (Pc) and coordination polymers (CP), especially of first row transition metal elements in electrocatalysis, noble-metal-free CPs based on iron and cobalt octa-carboxy-phthalocyanines (FeOcPc and CoOcPc) were prepared by bridging them with first row transition metal ions (Fe²⁺, Co²⁺ and Ni²⁺). The materials were characterized through FT-IR, WAXS and EDX. The enhanced electrocatalytic activity of these amorphous materials was demonstrated by voltammetric techniques, in 1.0 mol L⁻¹ KOH electrolyte solution. FeOcPc-Ni was the one with the lowest overpotential at 10 mA cm⁻² (299 mV) and Tafel slope (46.4 mV dec⁻¹) among them, whist also exhibiting stability throughout 15 h of experiment at current density of 10 mA cm⁻². Therefore, showing a promising capability as OER electrocatalyst.

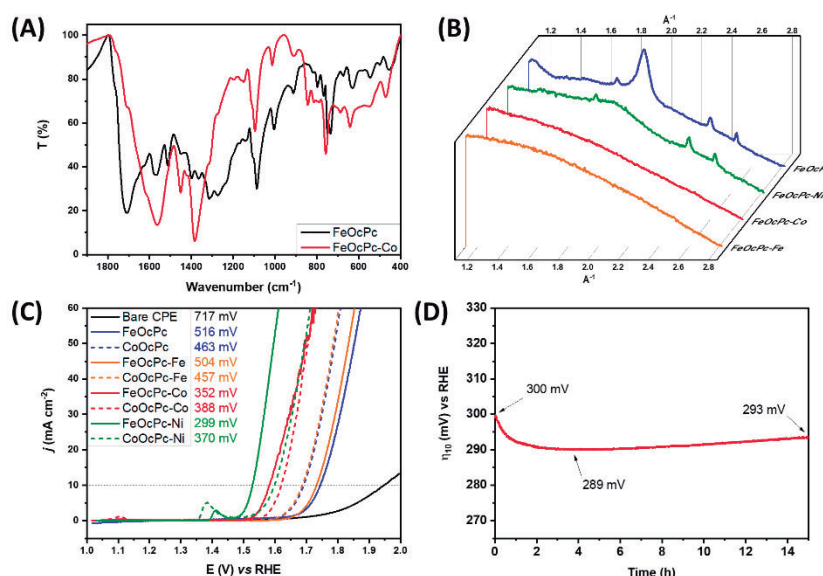


Fig 1: (A) Comparative FT-IR of FeOcPc and FeOcPc-Co CP; (B) Comparative WAXS of FeOcPc and this respective FeOcPc-M_b CPs; (C) LSV of M_aOcPc and M_aOcPc-M_b loaded on carbon past electrode (CPE); (D) 15 h chronopotentiometry at $j = 10 \text{ mA cm}^{-2}$ with FeOcPc-Ni CP.

Agradecimentos/Acknowledgments

CNPq, CAPES, FAPESP and SisNANO-USP

Área: INO

Modification of natural São Simão's kaolinite with β -alanine and L-phenylalanine amino acids as interesting strategy to enhance functional properties.

Eduardo Henrique Donzelli,¹ Denis Talarico de Araújo¹, Eduardo José Nassar¹, Katia J. Ciuffi¹, Emerson Henrique de Faria¹

donzelliengquimica@gmail.com, denistalarico@gmail.com, eduardo.nassar@unifran.edu.br,
katia.ciuffi@unifran.edu.br and emerson.faria@unifran.edu.br

¹Grupo de Pesquisas em Materiais Lamelares Híbridos (GPMatLam) - Universidade de Franca (UNIFRAN). Av. Dr. Armando Salles Oliveira, 201. Pq. Universitário, CEP 14404-600.

Keywords: biohybrid material, clay minerals, amino acids, release systems.

Highlights

Kaolinite was modified by displacement method using kaolinite intercalated with DMSO as precursor. Functionalized kaolinite presents higher basal spacing depending of molecular size of aminoacid employed. FTIR and thermal analysis confirm the grafting of kaolinite.

Resumo/Abstract

Organic-inorganic hybrid materials stand out for combining the thermal stability and rigidity of inorganic materials with the malleability and versatility of organic compounds. The unique properties not present in isolated materials can also arise, in addition to significantly increasing the functional properties of inorganic solids allowing applications such as controlled release systems, adsorbents, catalysts and among others. Thus, the addition of amino acids to kaolinite can be done through intercalation (weak bonds hydrogen bonds) and also by chemical reactions (grafting via covalente bonds). The reactions between organic units and inorganic solids results in many cases in covalent bonds between the amino acids and the kaolinite surface, resulting in the incorporation of the amino acids into the kaolinite structure. Modification with amino acids can improve kaolinite properties in various aspects, as example, the solubility, stability, biocompatibility and controlled release capacity of compounds could be improved. Furthermore, the addition of amino acids can make kaolinite more compatible with diferente biological matrices and can be used to increase the retention of proteins and other compounds on the surface of kaolinite. Thus, in this work, brazilian's são simão kaolinite was functionalized with the amino acids β -alanine and L-phenylalanine through the displacement method widely discussed in the literature and used by our research group¹. 10 g of Kao-DMSO was added to 50 g of L-proline in a reflux system (ratio of 5:1) with temperature slowly rising from 60°C to 105°C, close to the melting/decomposition temperature of the amino acid. After 24h, the material was washed with ethanol by a soxhlet system for 24h and then vacuum filtered. The resulting material was designated as Kao-Ala. The same process was carried out with the amino acid L-phenylalanine, however with the reaction temperature slowly rising between 60°C to 275°C, the resulting material being designated as Kao-Phe. The functionalization of kaolinite with β -alanine and phenelalanine were confirmed by various techniques, XRD confirm the expansion of the interlayer space, from 7.14 Å to 11,23 Å in the kaolinite-alanine solid, and from 7.14 Å to 12.0 and 7.8 Å in the kaolinite-phenylalanine solid. This result suggests that occurs the intercalation of both amino acids in the kaolinite interlayer space. FTIR and thermal analysis confirms that covalent bonds occurs between carboxylate from amino acids and aluminol groups from kaolinite. Interlayer Al-OH vibration at 938 cm⁻¹ it is not observed in both biohybrids, and also the interlayer OH at 3654, 3667 cm⁻¹ confirming the functionalization. Briefly, the modification of the structure of kaolinite through amino acids is a promising technique to improve the properties of this material and make it more functional in applications such as controlled release of drugs, biocatalysts and other biotechnological applications. Kaolinite was successfully functionalized by both amino acids containing different groups. the amino acid b-Ala and L-Phen proved to be efficient for increasing kaolinite organophilicity, being a reaction route suitable for Green Chemistry, with low cost, and easily reproducible. This materials could be applied as efficient catalysts support for metallocomplexes, adsorbents, drug delivery systems and among others.(da Silva et al., 2020)

da Silva, A. F., de Pádua, G. S., de Araújo, D. T., Vieira, C. A., de Faria, E. H. (2020). Immobilization of L-alanine into natural kaolinite via amidation catalyzed by boric acid for the development of biohybrid materials. Journal of Solid State Chemistry, 287, 121332. <https://doi.org/10.1016/j.jssc.2020.121332>

Agradecimentos/Acknowledgments

CAPES (código de financiamento 001), FAPESP, CNPq (310151/2021-0).

46ª Reunião Anual da Sociedade Brasileira de Química: "Química: Ligando ciências e neutralizando desigualdades"

N-(3-hydroxypropyl)-1,8-naphthalimide as a fluorescent sensor.

Keryn H. V. Souza (PQ)¹, Izilda A. Bagatin (PQ)¹

Keryn.hapuk@unifesp.br

¹Instituto De Ciências Ambientais, Químicas E Farmacêuticas – ICAQF – UNIFESP – Diadema – SP
Laboratório de Química de Calixarenos, Espectroscopia Molecular e Catálise LQCEMC

Palavras Chave: *Calixarenos, Naphthalimides, Luminescence.*

Highlights

Development of fluorescent chemosensor ligand. Functionalization of naphthalimides in calixarenes.

Resumo/Abstract

The naphthylimides are chemical species widely used either as luminophores or as dyes, having their photophysical properties changed according to the replacement of its radical, and may offer promising results in the development of light-emitting materials [1,2]. Calixarenes, in turn, are organic synthon molecules able to transport and host ions and molecules selectively in their cavities when functionalized with appropriate organic groups [3]. In this work, we use n-(3-hydroxypropyl)-1,8-naphthylimide (**1**) as a chromophore ligand. Initially, ligand **1** was synthesized from the 1,8-naphthalic anhydride and 3-amino-1-propanol reagents, which formed a crystalline product with high purity, observed by the ¹H NMR signals of the hydrogens of the conjugated rings at 8.65 ppm (dd, CH), 8.27 ppm (dd, CH) e 7.79 ppm (t, CH), and at 3.16 ppm (s, OH) and 2.01 ppm (m, N-CH), 4.4 ppm (t, O-CH₂) and 3.6 ppm (t, CH₂) from the propanol signals. FTIR depicted the bands at 1525cm⁻¹ (ν-C=C), 1693cm⁻¹ (ν-C=O), and 3479 cm⁻¹ (ν-O-H). The band at 1442cm⁻¹ can be assigned to CH₂-N; the intensity of the bands near 780cm⁻¹ characterizes the vibration of the aromatic rings of the molecule. The calix[4]arene matrix was then functionalized with 1,3-dibromopropane, which formed ligand **2** (5,11,17,23-tetra(tert-butyl)-25,27-bis(3-bromopropoxy)-26,28-(dihydroxy)calix[4]arene), already described previously by the group [4], which will be linked to ligand **1**. Analyses will be performed to check for ions that are potentially harmful to the environment.

References: [1] O. V. Prezhdo, B. V. Uspenskii, V. V. Prezhdo, w. Boszczyk, V. B. Distanov. *Dyes and Pigments* 72, 2007, 42 – 46. [2] S. Kagatkar, D. Sunil. *J Mater Sci* 57, 2022, 105 – 139. [3] P. M. Marcos, S. Félix. *Química* 107, 2007, 31-37. [4] I. A. Bagatin, H. E. Toma, *New J. Chem.*, 2000, 24, 841-844.

Agradecimentos/Acknowledgments

O presente trabalho foi realizado com o apoio da Coordenação de Aperfeiçoamento de Pessoal de Nível Superior – Brasil (CAPES) - Código de Financiamento 001.

Nanozyme peroxidase-like activity of luminescent LaVO₄ colloidal particles

Magna S. Santos (PG),¹ Paulo Cesar de Sousa Filho (PQ)^{1*}

m265974@dac.unicamp.br, *pcsfilho@unicamp.br

¹Department of Inorganic Chemistry, Institute of Chemistry, UNICAMP.

Keywords: Rare earths, nanoparticles, luminescence, nanozyme, nanothermometry.

Highlights

A sacrificial template method enables low temperature formation of monazite-type LaVO₄ colloidal nanoparticles. Ln³⁺-doping of LaVO₄ provided multifunctional particles combining upconversion thermometric response and nanozyme behavior, showing efficient peroxidase-like oxidation of 3,3',5,5'-tetramethylbenzidine.

Abstract

Lanthanum vanadate (LaVO₄) crystallizes in a kinetically stable tetragonal phase (*I4₁/amd*) and in a thermodynamically stable monoclinic phase (*P2₁/n*). Because of the high oxygen mobility and non-stoichiometry of this composition, these polymorphs have been extensively explored as photo- or electrocatalysts towards pollutant degradation, CO oxidation, selective transformations of methane, among other reactions.[1] Because LaVO₄ is also an attractive host for luminescent lanthanide ions (Ln³⁺), this oxide provides interesting perspective for multifunctional materials combining enzyme-like catalysis and luminescence. Specifically, LaVO₄ colloids are highly promising as potential nanozymes (*i.e.* inorganic particles showing enzyme-like catalytic activity) combining thermometric luminescent properties. We herein report the synthesis, luminescence, and catalytic ability of colloidal LaVO₄ particles doped with different Ln³⁺. The solids were prepared by one-pot colloidal conversion of hydroxycarbonate sacrificial templates (La_xLn_{1-x}CO₃OH.nH₂O) with NH₄VO₃ in water/ethylene glycol via a previously developed protocol.[2] The synthesis yielded 50-100 nm particles (ζ potential \sim -20 mV) formed by aggregated 5-8 nm crystallites, resulting in increased porosity (Figure 1a). The colloidal conversion of hydroxycarbonates enabled the unusual formation of monoclinic (La_{0.99}Eu_{0.01})VO₄ at low temperatures (*i.e.* 95 °C), since aqueous synthesis of LaVO₄ particles generally yields the kinetically stable tetragonal phase. Replacing La³⁺ by large amounts of smaller lanthanides (*i.e.* Yb³⁺/Er³⁺) afforded tetragonal (La_{0.65}Yb_{0.15}Er_{0.20})VO₄ particles, which remained structurally stable after calcination at 900 °C as shown by X-ray thermodiffraction. The Eu³⁺-doped solids showed the characteristic lines under λ_{exc} =280 nm, whereas as-prepared Yb³⁺/Er³⁺-doped particles showed thermally responsive upconversion (λ_{exc} =980 nm) emissions (Figure 1b). The particles also showed peroxidase-like activity in the oxidation of 3,3',5,5'-tetramethylbenzidine (TMB) by hydrogen peroxide [3] forming 3,3',5,5'-tetramethylbenzidine-diimine (ox-TMB, Figure 1c). Therefore, our results confirm that the prepared particles effectively behave as nanozymes, opening interesting perspectives towards combination of thermometry and enzyme-like catalysis at the nanoscale.

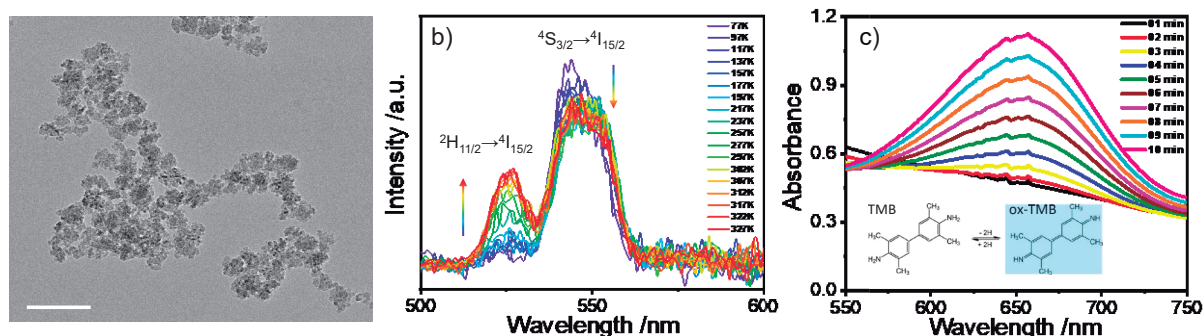


Figure 1. a) TEM images, b) upconversion spectra (λ_{exc} =980 nm) at different temperatures (77-327 K), and UV-vis absorption spectra showing the peroxidase-like activity of the (La_{0.65}Yb_{0.15}Er_{0.20})VO₄ particles.

References

- [1] Chem. Eng. J, 2021, **420**, 130529
- [2] Nanoscale, 2021, **13**, 4931-4945
- [3] Colloids Surf. A Physicochem, Eng. Asp., 2021, **618**, 126427

Acknowledgments

The authors thank CNPq, CAPES and FAPESP (2022/03442-3).

46ª Reunião Anual da Sociedade Brasileira de Química: "Química: Ligando ciências e neutralizando desigualdades"

New 2p-4f heterospin systems: synthesis, crystal structure and magnetic properties

**Livia B. L. Escobar (PQ)^{1,2,3*}, Vinicius R. Campos (PQ)¹, Stéfane Soriano (PQ)⁴, Mateo Briganti (PQ)^{1,5},
Stephen Hill (PQ)², Guilherme P. Guedes (PQ)¹, Maria G. F. Vaz (PQ)¹**

¹Instituto de Química, Universidade Federal Fluminense, Campus Valonguinho, Outeiro de São João Batista s/n, 24020-007, Niterói-RJ, Brasil.

²National High Magnetic Field Laboratory, Florida State University, Tallahassee, Florida 32310, United States.

³Departamento de Química, Pontifícia Universidade Católica do Rio de Janeiro, Rua Marquês de São Vicente, 225 Gávea, 22451-900, Rio de Janeiro-RJ, Brasil.

⁴Instituto de Física, Universidade Federal Fluminense, Campus Praia Vermelha, Av. Gal. Milton Tavares de Souza, s/n, 24210-036, Niterói-RJ, Brasil.

⁵Laboratory of Molecular Magnetism (LaMM), Department of Chemistry "Ugo Schiff", University of Florence, Italy.

liviabescobar@puc-rio.br

Keywords: Heterospin Complexes, Lanthanides, Magnetic Properties.

Highlights

Heterospin systems can present interesting magnetic properties such as high-density data storage and data processing devices [1]. We present the synthesis and EPR studies of the new LnN₃tempo family.

Resumo/Abstract

In this work, we have synthesized and studied the magnetic properties of a new family of compounds obtained through a one-pot reaction by using [Ln(hfac)₃] (hfac = hexafluoroacetylacetonate, Ln = Dy(III), Tb(III) or Gd(III)) and the nitroxide radical 4-azido-2,2,6,6-tetramethylpiperidine-1-oxyl radical (N₃tempo) [2]. Figure 1 presents the asymmetric unit of the complexes in which it is possible to note that each {Ln(hfac)₃(N₃tempo)} moiety results from the coordination of the organic radical, through the nitroxide oxygen atom, to the lanthanide ion. The two crystallographically nonequivalent lanthanide ions are coordinated by three hfac⁻ chelating ligands, one nitroxide oxygen atom, and one aqua ligand. The coordination geometry of lanthanide ions Ln1 and Ln2 in these compounds is distorted bicapped trigonal prismatic.

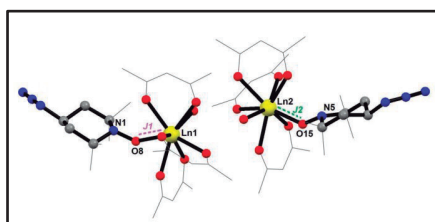


Figure 1- Asymmetric unit of the LnN₃tempo derivatives evidencing the magnetic exchange between the radical and the lanthanides ions.

The magnetic susceptibility analysis indicated the presence of weak antiferromagnetic interactions between the Gd(III) ion and the N₃tempo radical. The hyperfine structure is defined in the High-frequency EPR spectrum of the Gd(III) derivative and simulations are in progress.

Agradecimentos/Acknowledgments

CNPq, CAPES, FAPERJ, NSF, NHMFL

[1] Mateus S. Souza *et al.*; *Inorg. Chem.*; 61; 31; **2022**; 12118.

[2] Livia B. L. Escobar *et al.*; *Inorg. Chem.*; 53; 14; **2014**; 7508.

New Copper (II) Complexes Based on 1,4-Disubstituted-1,2,3-Triazole Ligands with Promising Antileishmanial Activity

João P.C. Nascimento (PG),^{1*} Natali L. Faganello (PG),¹ Adriano C.M. Baroni (PQ),¹ Gleison A. Casagrande (PQ),¹

Cruz.nascimento@ufms.br

¹Institute of Chemistry, Federal University of Mato Grosso do Sul - UFMS.

Keywords: Copper (II) Complexes; Crystal Structure; Biological Activity.

Highlights

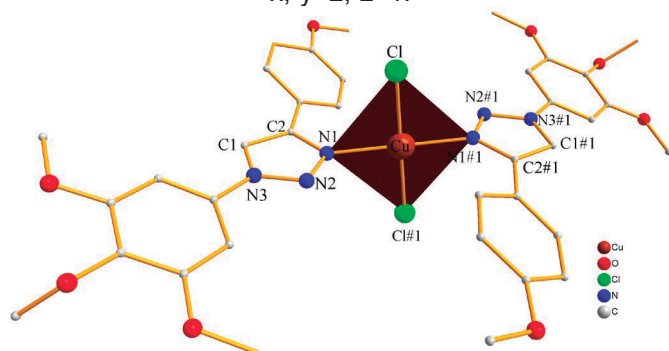
New Cu^{II} complexes were fully characterized and tested for antileishmanial activity. Biological activity for complex 1 was IC₅₀ of 0.37 μM on the amastigote form of Leishmania.

Abstract

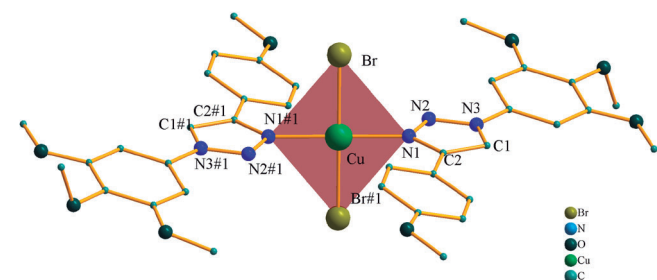
Leishmaniasis is one of the most lethal parasitic diseases in the world, affecting the health of individuals living in intertropical and temperate regions of the planet, where treatment is irregular and ineffective with first and second-line drugs, which bring side effects greater than the benefits attributed to them. Thus, the study of new bioactive compounds brings benefits, once the development of new drug candidates containing 1,4-disubstituted-1,2,3-Triazole centers coordinated to Cu^{II} metal centers is a good strategy to face Leishmaniasis. The X-ray diffractometry data show a triclinic crystalline system, belonging to group $P\bar{1}$ for both complexes, figure 1.

Figura 1. DIAMOND projection of the molecular structure of complex 1(a) and complex 2(b). Hydrogen atoms have been omitted for clarity.

a) Symmetry operation to generate equivalent atoms #1 $-x, -y+2, -z+1$.



b) Symmetry operation to generate equivalent atoms #1 $-x+1, -y, -z+1$.



The asymmetry unit found for both complexes is formed by 1 ligand and a halogen atom bonded to the metal

atom. A characteristic of the group $P\bar{1}$ is low symmetry, with the presence of an inversion center that assembles the molecular structure and makes two asymmetric units are present within each cell. The calculated coordination index 4 for both complexes is $\tau_4=0$, where this value is assigned to a square planar coordination environment. UV-Vis spectroscopy demonstrated the hyperchromic effect for the complexes in solution, in addition to the presence of a single band in the 200-350 nm region attributed to intraligand $\pi \rightarrow \pi^*$ or $n \rightarrow \pi^*$ transitions. The solid-state study showed the same band as in solution, but with the presence of a second band assigned to transition in the d orbitals of the metal, $v1\ 2t_2 \rightarrow 2E_2$ (D). The nature of the electronic transitions elucidated by TD-DFT calculations demonstrated LMCT, IL, and XLCT electronic transitions for complex 1 in dichloromethane solution. The infrared spectroscopy showed the unfolding of the band referring to C-H trz in the ligand, for a band referring to C-H sp^2/trz in both complexes. It was also possible to observe an increase in the frequency of vibration of the stretching $\nu(C=N)$, from 1598 cm^{-1} in the ligand to 1614 and 1612 cm^{-1} in complexes 1 and 2, respectively. This increase may be related to the LMCT transition observed in the TD-DFT calculations. The biological activity tested against promastigotes and amastigotes forms of Leishmania (*L.*) amazonenses, showed that both complexes had better activity than their respective ligand in both forms, with complex 1 showing a IC₅₀ value of 0.37 μM for the amastigote form, a value better than the regulated drug, besides showing a selectivity value of 9.7, i.e., the complex has a preference for the parasite instead of the mammalian cell.

Agradecimentos/Acknowledgments

We thank the instituto de química da UFMS, CAPES and CNPQ.

We thank the FUNDECT MS - GRANT AGREEMENT: 330/2022, SIAFEM: 32268, Process: 71/033.044/2022

New Gold(I) Complex Based on Thiocarbamoyl-naphthylpyrazoline-1,3,5-Trisubstituted Ligand.

Natali L. Faganello (PG),¹ **João P. C. Nascimento** (PG),¹ **Yasmin L. Santos** (IC),² **Clara A. Da Silva** (IC),² **Lucas Pizzuti** (PQ),² **Davi F. Back** (PQ),³ **Gleison A. Casagrande** (PQ).¹

natali_faganello@hotmail.com

¹Department of Chemistry, UFMS; ²Department of Chemistry, UFGD, ³ Department of Chemistry, UFSM.

Keywords: Pyrazoline, spectroscopy, crystal structure.

Highlights

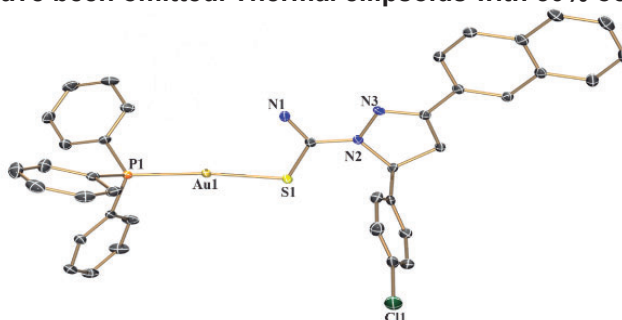
A new Au^I complex was synthesized and characterized. The X-ray studies revealed a linear geometry around Au^I atom. Complete characterization also involved IR, UV-Vis, and NMR spectroscopic analyses.

Abstract

Pyrazoline compounds have been presented with broad pharmacological potential as anticancer, antitumor, and antioxidant activities. The metalation of biologically active ligands is a strategy to enhance their biological activities and broaden their applications in other areas such as materials chemistry and medicinal chemistry. Thus, the synthesis and characterization of new gold(I) complex with pyrazoline ligand is the focus of this work.

X-ray diffractometry studies revealed (Figure 1) a molecular structure of gold(I) as a cationic complex with general formulae [Au(PPh₃)(L)]PF₆.MeOH.

Figure 1. Projection of the asymmetric unit of the complex. For clarity, the hydrogen atoms, MeOH solvate, and the PF₆ - anion have been omitted. Thermal ellipsoids with 50% occupational probability.



The cationic unit contains the pyrazoline ligand coordinated in a monodentate manner via the sulfur atom to the gold(I) metal center which completes its coordination sphere with a phosphorus atom coming from the auxiliary ligand triphenylphosphine. The P(1)-Au(1)-S(1) bond angle of 172.744 shows an approximately linear coordination geometry for the Au^I atom.

The data from the infrared vibrational spectroscopy obtained for the complex show the main bands as found in the free ligand. The stretch attributed to the thiocarbonyl grouping ($\nu(\text{C}=\text{S})$) that appears in the region of 1388 cm^{-1} in the free ligand was shifted to lower wavenumber (1369 cm^{-1}) in the complex, which may be related to the coordination via sulfur atom to the gold(I) metal center.

The molecular absorption study in the UV-Vis region shows a similarity in the spectra of the ligand and complex. After coordination, a hyperchromic effect is observed in the spectrum of the complex. The main absorption band observed in the complex spectrum is attributed to the LMCT-type electronic transitions of the ((N-C=S) $\pi^* \rightarrow \text{Au-P}$) type.

The ¹³C NMR data for the complex when compared to the ligand shows a smaller chemical shift of the signal corresponding to the thiocarbonyl carbon atom (C=S), indicating greater shielding of this atom. It is suggested that this behavior may be related to the coordination of the ligand to the gold(I) metal center. The gold(I) complex synthesized in this work will be submitted to biological anticancer assays and also tested as a new candidate molecule for bioimaging application.

Acknowledgments

We thank the Chemistry Institute at UFMS, CAPES, and CNPQ.

We also thank FUNDECT/MS - Grant: 30/2022, SIAFEM: 32268, Process: 71/033.044/2022.

New organometallic tin(IV) complex with hydrazone ligand: crystal structure and noncovalent interactions study

Rafaela Caixeta de Souza (IC),^{1*} Claudia Cristina Gatto (PQ)¹

*rafaelacaixetasouza@gmail.com; cggatto@gmail.com

¹Laboratory of Inorganic Synthesis and Crystallography, University of Brasilia (IQ-UnB), Brasília-DF, Brazil.

Keywords: organotin(IV) complex, hydrazone, crystal structure, noncovalent interactions.

Highlights

A new Organotin(IV) complex with a hydrazone ligand was studied by X-ray crystallography. The 3D Hirshfeld surface was analyzed to verify noncovalent interactions upon the molecular packing.

Resumo/Abstract

Hydrazones are Schiff bases and an important class of ligands in bioinorganic and coordination chemistry with growing interest due to their versatility and applications.¹ These ligands are derived from a class of biologically active drugs important for medicinal chemistry, highlighting their extensive pharmacological property, including antitumor, antiviral, and antituberculosis activities.^{1,2,3} Polydentate hydrazone ligands can form stable complexes with different transition metals.¹ A considerable number of organotin(IV) complexes with hydrazone ligands have been intensively studied for their bactericidal and antitumor activities.⁴

The present work reports the structural elucidation and investigation of noncovalent interactions of new organotin(IV) complex [Sn(apbh)Me₂Cl] with 2-acetylpyridine-benzoylhydrazone ligand (Hapbh). The Schiff base was found bidentate with NO-donor atoms to the metal atom and deprotonated. The metal center shows distorted square-based pyramidal coordination geometry, coordinated by a ligand molecule, two methyl groups, and a chloride ion. Hirshfeld surface was used to investigate the relevant and important stacking interactions and hydrogen bonds, shown in Figure 1.

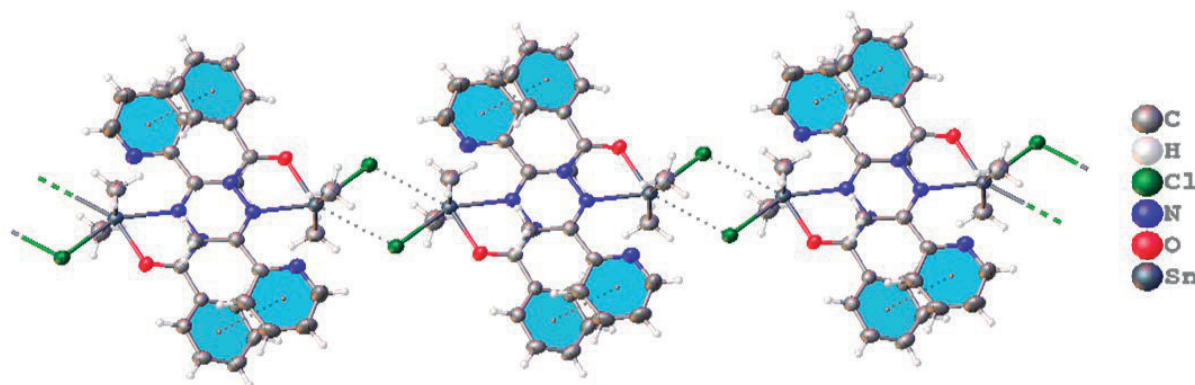


Figure 1. View of the complex [Sn(apbh)Me₂Cl] showing the $\pi\cdots\pi$ stacking interactions and hydrogen bonds.

¹P. Santiago, F.S. Tiago, M.S. Castro, P. Souza, J. Martins, C.C. Gatto, *J. Inorg. Biochem.*, **2020**, 204, 110949.

²A.A.R. Despaigne, L.F. Vieira, I.C. Mendes, F.B. da Costa, N.L. Speziali, H. Beraldo, *J. Braz. Chem. Soc.*, **2010**, 21, 1247.

³J. Patole, U. Sandbhor, S. Padhye, D.N. Deobagkar, C.E. Anson, A. Powell, *Biorg. Med. Chem.*, **2003**, 13, 51.

⁴M. Hong, H.-D. Yin, S.-W. Chen, D.-.-Q. Wang, *J. Organomet. Chem.*, **2010**, 605, 653.

Agradecimentos/Acknowledgments



Área: INO
(Inserir a sigla da seção científica para qual o resumo será submetido. Ex: ORG, BEA, CAT)

Novel ascorbic acid based Ce-Doped Titanium Oxo Clusters for enhancing visible light driven water splitting

Marcelo Victor Cunha do Amaral (PG),¹ Juliana Fonseca de Lima (PQ)¹.

Marcelinho7x@hotmail.com; Juliana.lima@uerj.br

¹Departamento de Química Geral e Inorgânica, UERJ

Keywords: Fuels, Hydrogen, *Water Splitting*, Titanium, Solar Energy

Highlights

- Novel Titanium oxo clusters (TOCs) are proposed with different ligands.
- Ce doping for enhancing charge transfer and lowering band gap range.
- Construction of photoactive electrodes with synthesized TOCs.
- Electrodes will be applied for photo assisted water splitting.

Resumo/Abstract

Hydrogen as a clean fuel that has been receiving a lot of attention lately since it can be produced in ways in which no greenhouse gasses are emitted, usually in a process called water splitting. This process consists of the electrolytic decomposition of water into hydrogen and oxygen by means of an electrolytic cell in which hydrogen (HER) and oxygen (OER) evolution happens on the cathode and anode respectively. However, the process is expensive due to mechanistical and thermodynamical hindrance during reaction, especially concerning OER, which is not able to happen without the use of metallic catalysts that are usually noble metal based like Ru and Ir, and expenses regarding used electricity are also significant.¹ For that reason, new, cheaper and efficient catalysts must be researched, in such ways both hindrances and electricity costs can be lowered.¹ Ce doped Titanium oxo clusters (TOCs) are candidates as catalysts for that process, since they can obtain adequate Band Gap values and expressive photocurrent generation following the work reported by Wang (2021) in which his benzoate based Ce doped TOC with band gap 1,65 eV obtained clear photocurrent generation under visible light with a photocurrent density of 0,58 $\mu\text{A}\cdot\text{cm}^{-2}$.² In this research, we proposed the synthesis and characterization by XRD, FTIR and SEM of novel Ce doped TOCs for the construction and evaluation of photo electrodes designed for light assisted water splitting, aiming the further development of TOC chemistry.

Figure 1: TOC A IR spectra

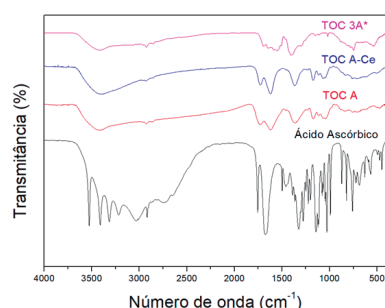


Figure 2: TOC 3A* XRD pattern

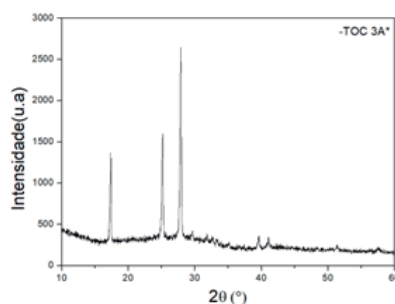
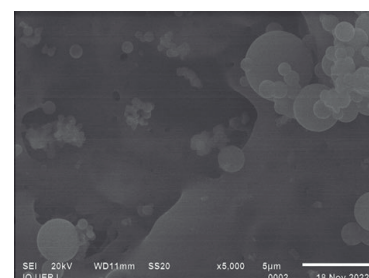


Figure 3: TOC 3A* SEM image



1 - Moreira, D.E.B. **Design of new cobalt-based Prussian Blue Catalysts for water oxidation: how the synthetic route affects the material performance?** 2022. (62 p.) Dissertação (mestrado) - Universidade Estadual de Campinas, Instituto de Química, Campinas, SP.
2 - Wang, C. et al. **Synthesis of lanthanide-doped titanium-oxo clusters for efficient photocurrent responses.** Journal of Solid State Chemistry 304 (2021) 122586

Agradecimentos/Acknowledgments

CAPES, CNPq, SBQ, UERJ

Novel copper(II) complexes of a furan-containing *N*-acylhydrazonic ligand: Synthesis, characterization and potential antitumor activity

Fagner S. Moura (PG),¹ Ygor S. Sobrinho (IC),¹ Carolina S. Stellet (IC),¹ Carolina B. P. Ligiero (PQ)², Renata Diniz (PQ),³ Nicolás A. Rey (PQ)¹

*92mourafagner@gmail.com;

¹ Laboratory of Organic Synthesis and Coordination Chemistry Applied to Biological Systems (LABSO-Bio), Department of Chemistry, Pontifical Catholic University of Rio de Janeiro (PUC-Rio)

² Laboratory of Supramolecular Chemistry and Nanotechnology, Department of Inorganic Chemistry, Federal Fluminense University (UFF)

³ Laboratory of Crystallography (LabCri), Department of Chemistry, Federal University of Minas Gerais (UFMG)

Keywords: complexes, antitumor, copper(II), *N*-acylhydrazones, coordination chemistry

Highlights

Copper(II) coordination compounds with a wide range of ligands, have been shown to induce cell death by apoptosis.¹ Given this scope, a furan-containing *N*-acylhydrazonic ligand was synthesized and characterized, along with two of its new copper(II) complexes that might show promising antitumor activity.

Abstract

The literature has reported mononuclear and binuclear copper(II) complexes with encouraging results regarding their cytotoxic activity, in some cases even more potent than cisplatin.^{2, 3} In this context, the present work reports the synthesis and characterization of two new copper(II) complexes containing an *N*-acylhydrazonic ligand (H₂B2). The organic synthesis, *via* condensation reaction, between 5-methylsalicylaldehyde and furan-2-carbohydrazide, had a yield of 89.0% with the formation of a light yellow crystals. MP: 150±2 °C; IR(KBr) ν_{max} : 3134; 1660; 1623; 1596; 1271 cm⁻¹. The copper(II) binuclear complex [Cu₂(B2)₂(IsoOH)₂] was obtained from the reaction of the ligand with copper(II) perchlorate hexahydrate, in a basic medium with isopropanol. Copper(II) mononuclear complex [Cu(HB2)Cl], on the other hand, was obtained from copper(II) chloride dihydrate, in methanol. Dark green single crystals were obtained from the syntheses, and their structures were elucidated (Figure 1A and B). Cyclic voltammetry of the complexes was performed in DMF with TBAPF₆ 0.1 mol. L⁻¹. The binuclear complex showed a cathodic peak at -0.8 V and two anodic peaks at -0.86 V and -1.07 V, while the mononuclear showed a cathodic peak at -0.6 V and an anodic peak at -0.85 V (Figure 1C). The molar conductivity of the complexes was performed in a 1.10⁻³ mol. L⁻¹ solution in DMF. The value of 2.68 cm²Ω⁻¹mol⁻¹ for the binuclear complex suggests a non-electrolyte complex. For the mononuclear complex, molar conductivity of 25.9 cm²Ω⁻¹mol⁻¹ between a non-electrolyte and a 1:1 electrolyte complex. This might be due to the equilibrium between ionized and non-ionized species, in cancer cells involving H₂B2 and both complexes are underway.

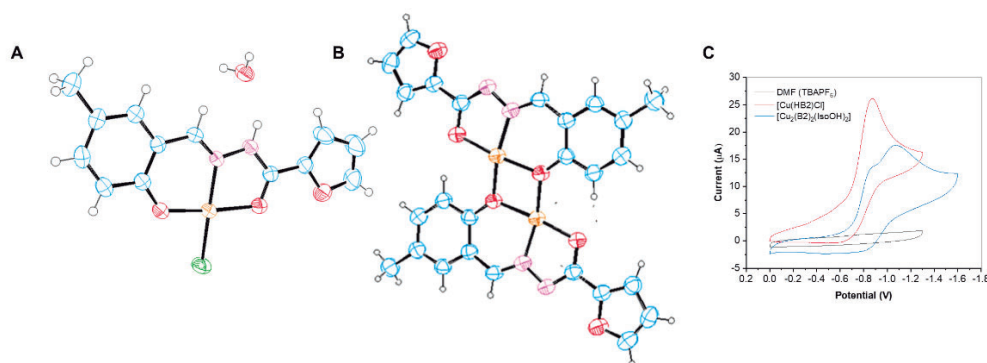


Figure 1. (A) ORTEP representation of [Cu(HB2)Cl]. (B) ORTEP representation of [Cu₂(B2)₂(IsoOH)₂] – solvent molecules were hidden for the sake of simplicity. (C) Comparative cyclic voltammograms between mononuclear and binuclear complexes at 100mV.s⁻¹ in DMF (TBAPF₆ 0.1mol.L⁻¹), under inert atmosphere at 25 °C.

¹ SANTINI, C.; *et al.* *Chem. Rev.* **2014**, 114, 815.

² TAN, C.P. *et al.* *Metallomics* **2014**, 6, 978.

³ FEKRI, R. *et al.* *Inorganica Chimica Acta* **2019**, 484, 245.

Acknowledgments

This work was supported by FAPERJ, FAPEMIG, Finep, CAPES and CNPq.
46ª Reunião Anual da Sociedade Brasileira de Química: "Química: Ligando ciências e neutralizando desigualdades"

Novel quinolone functionalized Schiff base silver(I) complexes: synthesis and characterization

Lorena de Souza Teixeira (IC),¹ Gustavo Bezerra da Silva (PQ).^{1*}

gusbezerra@ufrrj.br

¹Instituto de Química, Universidade Federal Rural do Rio de Janeiro (UFRRJ), Seropédica, RJ, CEP 24000-000.

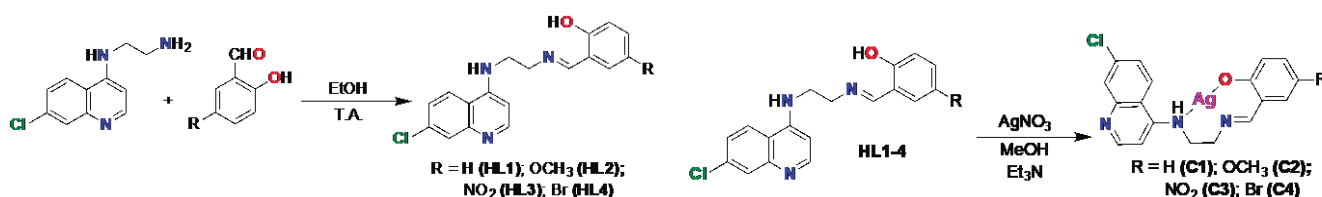
Keywords: Quinoline, Silver(I) complexes, Schiff bases.

Highlights

Synthesis and characterization of silver(I) complexes designed with potential quinoline derivatives.

Abstract

To the best of our knowledge, silver(I) complexes are widely known by their bactericide activity.¹ However, recently studies have also shed some light on their cytotoxic behavior.² A judicious strategy to obtain compounds with improved pharmacological activity is molecular hybridization. In this scope, the complexation of quinoline derivatives, such as Schiff bases, to silver(I) is promising due to their wide range of pharmacological potential.³ Therefore, this work aimed the synthesis and characterization of novel silver(I) complexes (**C1-C4**) with Schiff bases of quinolone derivatives (**HL1-4**, Scheme 1).



Scheme 1. Quinoline functionalized Schiff bases **HL1-4** and their silver(I) complexes **C1-C4**.

Firstly, a series of Schiff bases quinoline-based of the type (*E*)-2-(((2-(((7-chloro-4a,8a-dihydroquinolin-4-yl)amine)-ethyl)imine)methyl)-4-*R*-phenol, *R* = H (**HL1**), OCH₃ (**HL2**), NO₂ (**HL3**) e Br (**HL4**) was synthesized upon addition reaction of *N*¹-(7-chloroquinolin-4-yl)ethane-1,2-diamine and their respective 5-*R*-2-hydroxybenzaldehyde, at room temperature. Products were obtained as yellow solids, without further purification (yields: 40-84%). Finally, the complexation reactions were investigated in a proportion 1:1 of ligands **HL1-4** and silver(I) nitrate in the presence of trimethylamine in order to deprotonate the phenolic ring. The complexes **C1-C4** were obtained as brownish-green solids (yields: 65-90%).

All compounds were fully characterized by analytical (m.p. and elemental analysis) and spectroscopic (IR, ¹H NMR and ¹H X ¹H COSY) methods. IR data have shown that νC=N(imine) of ligands was almost unaffected upon coordination which indicates that imine nitrogen remains uncoordinated. However, bands attributed to the phenolic ring were absent in spectra of complexes, in accordance of deprotonation upon coordination of phenolate ring. ¹H NMR spectra data have also corroborated that imine does not coordinate while hydrogen of amine has shown higher chemical shift upon coordination, indicating the coordination of amine to silver(I).

In summary, four novel quinoline functionalized Schiff base silver(I) complexes were obtained. The proposed structures are [Ag(**L1-4**)], in which ligands coordinate through phenolate ring and amine moieties to silver(I). Fully characterization and bactericide activity and *in vitro* cytotoxicity are underway.

[1] Zanon, V. S.; Vargas, M. D. et al *J. Inorg. Biochem.* **2019**, 191, 183. [2] Adeleke, A. A.; Zamisa, S. J. et al *Molecules* **2021**, 26, 1205. [3] Altay, A.; Sahin, O. et al *Polyhedron* **2018**, 151, 170.

Acknowledgments

Central Analítica at PPGQ-UFRRJ and Profs. Maria D. Vargas (PPGQ-UFF) and Maurício Lanznaster (GQI-UFF) for donations of reagents/solvents.

Obtaining BioMOF from glutamic acid and basic nickel carbonate.

Luana T. C. Silva (PG),¹ Rodrigo V. Rodrigues (IC),¹ Sílvia D. de Campos (PQ),¹ Ronan F. F. de Souza (PQ),¹ Elvio Antônio de Campos (PQ)^{1*}

luanacasagrande18@gmail.com; elvio.campos@unioeste.com.br

¹*Cento de Engenharias e Ciências Exatas, Unioeste – Campus Toledo – PR.;*

Palavras Chave: *Metal Organic Framework, Self-assembly, Metal-Biomolecule Framework, Crystal Structure*

Highlights

A metal-biomolecule framework (BioMOF) was obtained from a metal complex.

The structure of the BioMOF is similar to the structure of cobalt, copper and zinc coordination compounds with the same ligand.

The synthesis method used is more ecological than those described for similar compounds.

Resumo/Abstract

BioMOFs are crystalline and porous structures belonging to the class of metallic organic structures that have been attracting attention in studies of new materials and synthetic routes, due to their simple and low-cost synthesis. These compounds have several potential applications, from gas storage, catalysis and even pharmaceutical purposes such as drug delivery. Glutamic acid (H₂Glu) is a non-essential amino acid present in many living organisms and has a carboxylic acid group in the main chain as well as the side chain, allowing for strategic uses as a polydentate ligand to synthesize MOF-like structures. Several structures bearing this ligand are known and can be classified as BioMOFs or MBioFs, for instance, cobalt¹, copper² and zinc³ compounds. However, the combination of glutamic acid with Ni²⁺ ions, at least to our knowledge, is not described in the literature. The synthesis process started with the reaction in aqueous medium of 5 mmol of basic nickel carbonate, NiCO₃·2Ni(OH)₂·4H₂O, with 10 mmol of glutamic acid at 90 °C. As Ni(OH)₂ does not react with glutamic acid, after CO₂ release ceased, the mixture was filtered, the solvent volume was reduced to 10% of the initial value and the material was dried in an oven at 100 °C for 2 h and then in a desiccator over sulfuric acid for 2 weeks, obtaining the vitreous complex [Ni(Hglutamate)₂(H₂O)₂] with 82% yield based on glutamic acid. This complex was characterized by elementary analysis, infrared and UV-vis spectroscopy and thermogravimetric analysis, since it is difficult to crystallize similarly to palladium compounds with the same ligand⁴ or the nickel compound with aspartate⁵. To obtain the BioMOF, 1 mmol of the nickel complex was dissolved in 12 mL of pure water and kept in a teflon lined stainless steel autoclave at 100 °C by 24 h, resulting after cooling to room temperature in 0.12 g (45% yield) of [Ni(glutamate)(H₂O)₂]_n. This compound was characterized by XRD, IR and TGA. It presents the X-ray diffraction pattern identical to those observed to similar compounds of cobalt, copper and zinc and its crystalline structure was solved by single crystal X-ray diffraction that confirms the orthorhombic unit cell belonging to the P2₁2₁2₁ space group.

1 - *CrystEngComm*. **2003**, 5, 34-37. <https://doi.org/10.1039/B210753H>

2 - *Acta Cryst.* **1966**, 21, 594-600. <https://doi.org/10.1107/S0365110X66003517>

3 - *Chem. Commun.* **2016**, 52, 280-283. <https://doi.org/10.1039/C5CC07781H>

4 - *Z. Anorg. Allg. Chem.* **1962**, 319, 101-106. <https://doi.org/10.1002/zaac.19623190113>

5 - *J. Chem.* **2016**, Article ID 7317015. <http://dx.doi.org/10.1155/2016/7317015>

Agradecimentos/Acknowledgments

This study was financed in part by the Coordenação de Aperfeiçoamento de Pessoal de Nível Superior – Brasil (CAPES) – Finance code 001.

On the use of a microspectrometer for analyzing Rare Earth marked gunshot residues

Rodrigo Galvão dos Santos (PQ)¹, Jorge Fernando Silva de Menezes (PQ)^{2,3}, Vinícius Santos de Santana (IC)²
rodrigo.galvao@pefoce.ce.gov.br; jorge_fernando@ufrb.edu.br

¹Crime Scene Investigator - Perícia Forense do Estado do Ceará, Fortaleza/CE, Brazil; ²Universidade Federal do Recôncavo da Bahia, Amargosa/BA, Brazil; ³National Institute of Science and Technology in Energy and Environment, Universidade Federal da Bahia, Salvador/BA, Brazil

Keywords: gunshot residues, spectroscopy, rare earth ions.

Highlights

A microspectrometer was used to analyze rare earth marked gunshot residues. The equipment allowed for fast, contactless and non destructive assessment of the fluorescence emission at low mass concentrations (0.17% wt.).

Abstract

According to the latest official reports, there are about 4.4 million firearms in private hands in Brazil [1], which translates to approximately 2 guns for every 100 people. On the other hand, Brazil still registers over 20 homicides for every 100 thousand people, thus being the 8th most violent country in the world. Taking into account that firearms are used in 76% of the homicides in the country, the development of new methods for forensic ballistics is of great interest, particularly for the identification of gunshot residues (GSR) produced from firearms. In Brazil, the colorimetric test for Pb is still commonly used. However, one of its major drawbacks is the possibility of contamination with other lead sources, thus leading to false positive results [2,3]. In order to overcome these limitations, some techniques have been proposed involving Rare Earth (RE) marked GSR, such as Electrospray Ionization Fourier Transform Ion Cyclotron Resonance Mass Spectrometry (ESIFT-ICR MS) [4] and fluorescence spectroscopy with mixed $\text{Eu}^{3+}/\text{Tb}^{3+}$ frameworks]. Two RE based luminescent compounds were chosen in this study: $[\text{Tb}(\text{ACAC})_3(\text{H}_2\text{O})_3]$ and $[\text{Eu}(\text{TTA})_3(\text{H}_2\text{O})_2]$ (ACAC=acetylacetone, TTA=thenoyltrifluoroacetone), which give a green and red emission respectively. These hydrated β -diketone based compounds are well known in the literature and thus can be used as benchmarks for the technique. The materials were prepared following tried-and-true methods and a high resolution spectrometer (microspectrophotometer) was used to investigate the luminescence emission of RE marked GSR. The microspectrophotometer in question is a dual-video spectral comparator (Regula 4308), which is originally intended for authenticity verification of documents. In order to assess the effectiveness of the Regula 4308 to identify RE marked GSR, a test was conducted using ten rounds of .380 ACP ammunition (CBC company Non-Toxic Ammunition). Each of the rounds was disassembled using an inertia bullet puller and 10 mg (0.17% wt.) of the Tb^{3+} compound was added to the gunpowder of five rounds, while the same amount of Eu^{3+} compound was added to the remaining five. The 10 rounds were fired using two similar pistols and the ten cartridge cases were recovered for analysis. Using the microspectrophotometer module of the Regula 4308, the ten cases can be analyzed in a single run. Under magnification, fragments of the luminescent compounds were visible under a 365 nm excitation. A 2 s integration time was used for the spectral acquisition and the color coordinates in the CIE 1931 color space were calculated. The coordinates are close to the spectral locus of the CIE diagrams, as a result of the high color purity of the RE emission spectra, particularly for the Eu^{3+} compound, which is still preserved after the gunpowder ignition. The results indicate the effectiveness of a microspectrometer for rapid, contactless and non destructive analysis of RE marked GSR. The luminescence emission was also detectable inside the gun barrels and visible to the naked eye using a portable 365 nm light source (Convoy S2+ UV flashlight), thus allowing for on-site crime scene photography. This technique can also be used to assess new RE based markers or nanoparticles, besides being able to identify different batches of ammunition with different color emission signatures.

Acknowledgments

The authors are grateful to the Fundação de Amparo à Pesquisa do Estado da Bahia (FAPESB) and the Conselho Nacional de Desenvolvimento Científico e Tecnológico (INCT-Energia e Meio Ambiente) for financial support.

References

- [1] Anuário Brasileiro de Segurança Pública. Year 16 (Brazil, 2022).
- [2] M. R. Bartsch, H. J. Kobus, and K. P. Wainwright, *J. Forensic Sci.* 41, 14047J (1996).
- [3] S. Charles and N. Geusens, *Forensic Sci. Int.* 216, 78–81 (2012).
- [4] C. A. Destefani et al., *Microchem. J.* 116, 216–224 (2014).

Área: INO

Optical and structural effects of Ce³⁺/Ce⁴⁺ doping variation in SrY₂O₄ matrix

Caique M. Tavares (IC),^{1*} Leonardo F. Saraiva (PG),² Ana M. Pires (PQ),^{1,2} Sérgio A.M. Lima (PQ).^{1,2}

caique.tavares@unesp.br

¹Department of Chemistry and Biochemistry, FCT-UNESP; ²Department of Chemistry and Environmental Sciences, IBILCE-UNESP.

Keywords: Solid State Lighting; Luminescence; Cerium(III/IV); Modified Pechini Method.

Highlights

Ce³⁺/Ce⁴⁺ doped matrix from the modified Pechini method. Monitoring of the SrY₂O₄ host lattice in the presence or absence of the dopant. Feasibility of application in solid state lighting.

Abstract

The single-phase red-emitting SrY₂O₄:Ce^{4+/3+},Eu³⁺ phosphor produced by an adapted Pechini route under softer synthesis conditions (1100 °C in CO reducing atmosphere) than the traditional solid-state synthesis [1] has been investigated envisaging its application as red component for solid-state lighting [2]. It has been prior determined that cerium is present in a mixed oxidation state, where the proportion of Ce⁴⁺/Ce³⁺ was 70/30% by X-ray photoelectron spectroscopy (XPS), and this influences the SrY₂O₄ phase stabilization by increasing the point defect concentration. Thus, a more in-depth study of the influence of varying cerium concentration in the SrY₂O₄ matrix on its structural and optical properties becomes necessary. Therefore, this matrix doped with 0, 2, 4 and 6 at% of Ce³⁺ was synthesized by the modified Pechini method from the mixture of precursor aqueous solutions of Sr(NO₃)₂, Y(NO₃)₃ and Ce(CH₃COO)₃ under stirring and heating. Then, the complexing and polymerizing agents citric acid and D-sorbitol were added, respectively, to form the polymeric resin, that was pre-calcined at 350°C for 3h to generate the precursor charcoal which, after deagglomeration, was calcined at 1100°C for 5h under CO atmosphere. In the FTIR spectra, except for the non-doped sample, the presence of a band at 1740 cm⁻¹ assigned to the carbonate anion stretching mode was verified, and that may be related to the formation of both Sr₂CO₃ and Ce₂(CO₃)₃, probably on the surface of the particles, due to the basic character of these cations. The band at 1460 cm⁻¹, characteristic of Sr-O bonding deformation, in turn, undergoes a slight displacement as a function of the cerium concentration, evidencing changes in the bond angle caused by the difference in radius between Sr²⁺ and the dopant. The vibrational mode at 857 cm⁻¹ related to (YO-) bond deformation also shifts to higher wavenumber according to dopant insertion. Finally, the band within the 400 – 610 cm⁻¹ range assigned to Y-O vibration practically does not change with increasing dopant concentration, which may be an indication that cerium is in fact preferentially occupying Sr²⁺ sites or interstices. From the diffuse reflectance spectra, and by applying the Kubelka-Munk's approximation, the optical bandgap values were estimated as being 3.89, 3.82, 3.41 and 3.37 eV for the samples doped with 0, 2, 4 and 6 at% of Ce, respectively, indicating that the increase in dopant concentration tends to decrease of the bandgap. Finally, concerning luminescence measurements, all samples exhibited similar behaviour, regardless of the dopant presence or absence. In the excitation spectra, broad and intense bands were found centered at 250 nm that can be associated with M-O²⁻ charge transfer transitions, and by exciting the samples in this region, a band centered at 485 nm, characteristic of defects is viewed [1]. Therefore, it can be concluded that the synthesis of Ce-doped matrices using the modified Pechini method produced the matrix as expected, but the system was not adequate for Ce³⁺ stabilization in sufficient quantity for emission observation. This reinforces its functionality only as a co-dopant in this host lattice, and not as a main activator.

Acknowledgments

CNPq (120394/2022-7, 304003/2018-2 309448/2021-2), FAPESP (2022/08409-4) and LaCOM FCT-UNESP.

[1] SARAIVA, Leonardo F. et al. Eu³⁺-activated SrY₂O₄:Ce^{4+/3+} red-phosphor for WLEDs: Structural and luminescent insights from experimental and theoretical approaches. *Journal of Alloys and Compounds*, v. 938, p. 168595, 2023.
[2] BISPO-JR, Airton G. et al. Recent prospects on phosphor-converted LEDs for lighting, displays, phototherapy, and indoor farming. *Journal of Luminescence*, v. 237, p. 118167, 2021.

Optimization of Eu^{3+} -doped $\text{Li}_2\text{ZnSn}_3\text{O}_8$ stannate materials prepared *via* Solid-state methods for sensitive thermometry applications

Matheus S.N. Saula (PG)^{1*}, Israel F. Costa (PQ)¹, Maria C.F.C Felinto (PQ)², Luiz A.O. Nunes (PQ)³; Oscar L. Malta (PQ)⁴, Hermi F. Brito (PQ)¹.

msalgado@iq.usp.br;

¹Chemistry Institute – Department of Fundamental Chemistry, USP; ²Chemistry and Environment Center, IPEN; ³Physics Institute of São Carlos, USP; ⁴Chemistry Institute – Department of Fundamental Chemistry - UFPE.

Keyword : Luminescent materials, europium, stannates, solid-state synthesis, thermometry.

Highlights

Here, we report the synthesis, structural and spectroscopic studies of the $\text{Li}_2\text{ZnSn}_3\text{O}_8$:%mol Eu^{3+} luminescent materials synthesized by the microwave-assisted solid-state and ceramic methods.

Resumo/Abstract

Europium-doped inorganic luminescent materials have been widely applied in the fields of solid-state lasers, biological and forensic markers, anti-counterfeiting products, thermal sensors and in other several photonic technologies areas. Further, the relatively easy production, inexpensiveness and thermal stability of stannate-based host matrices, as well as their favorable band gap to allow persistence luminescence phenomenon, have attracted significant attention in the research field. In this work, $\text{Li}_2\text{ZnSn}_3\text{O}_8$: Eu^{3+} materials were synthesized varying the activating dopant ion's concentration by the ceramic and microwave assisted solid-state (using a domestic equipment^[1] – Fig.1a) methods after gridding Li_2CO_3 , ZnO , SnO_2 , Eu_2O_3 precursor oxides. The materials were characterized by thermal analysis, powder X-ray diffraction, scan electron microscopy (SEM), FTIR, Raman and diffused reflectance spectroscopy. The PXRD patterns indicate the formation of the desired $\text{Li}_2\text{ZnSn}_3\text{O}_8$ matrix phase when doped with different concentrations of the Eu^{3+} ion, showing a high crystallinity. The photoluminescence properties were determined based on the excitation and emission spectra of the $\text{Li}_2\text{ZnSn}_3\text{O}_8$:0.5%mol Eu^{3+} materials (Fig.1b) showing intense emission colors that varies from white to red depending on the sum of host matrix's and dopant activator ion's contribution to luminescence of the material at a given temperature (Fig.1c). The emission spectra in Fig.1b shows narrow emission bands (characteristic of $^5\text{D}_0 \rightarrow ^7\text{F}_{0-4}$ Eu^{3+} transitions) and a host matrix broad emission band (covering the 500 to 720 nm range). Upon lowering the temperature from 298 to 77 K, the emission intensity of the $^5\text{D}_0 \rightarrow ^7\text{F}_2$ transition from the Eu^{3+} ion decreases significantly while the host matrix broad emission band increases in function of the temperature (Fig.1b), which explains the change in the color emission of the material at different temperatures and allow its application studies as luminescent thermal sensors.

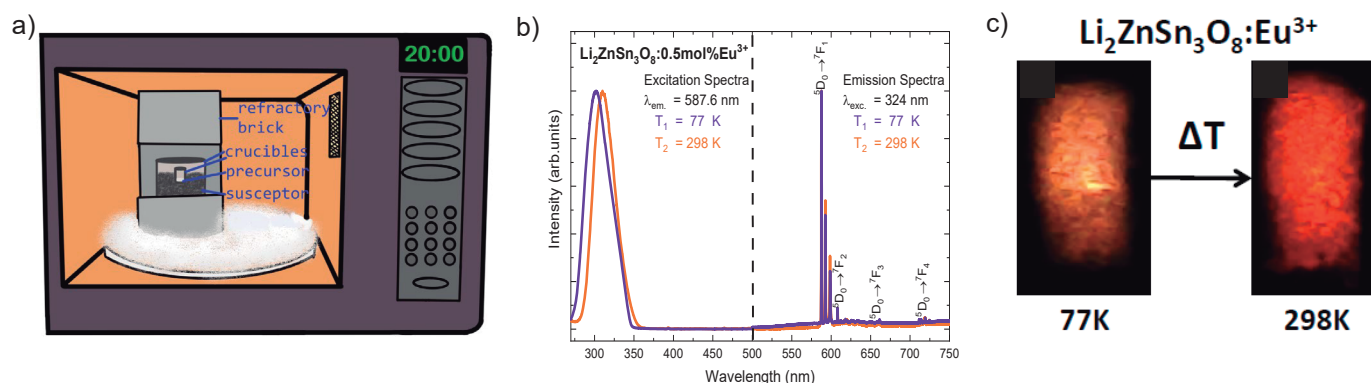


Fig. 1 – a) Domestic microwave heating system b) $\text{Li}_2\text{ZnSn}_3\text{O}_8$:0.5mol% Eu^{3+} luminescent material's excitation and emission spectra and c) luminescence emission color of $\text{Li}_2\text{ZnSn}_3\text{O}_8$:0.5mol% Eu^{3+} according to temperature.

Reference: [1] J. Miranda de Carvalho, C. C. S. Pedroso, M. S. de N. Saula, M. C. F. C. Felinto, H. F. Brito, *Molecules* 2021, 26.

Agradecimentos/Acknowledgments

The authors are thankful to FAPESP (2020/10228-2) and to CNPq for the research grants (306951/2018-5).

Orthopalladated oximes compounds containing 2,6-lutidine: Synthesis, structure, DNA binding studies and cytotoxic assays

Ana M. R. Polez (PG),^{1*} Renan L. de Farias (PQ),² Andresa Alves (PG),¹ Ana B. Lazzarini (PG),¹ Victor M. Miranda (PG),³ Victor M. Deflon (PQ),³ Mauro A. Lima (PG),⁴ Fillipe V. Rocha (PQ),⁴ Adelino V. G. Netto (PQ)¹.

ana.polez@unesp.br

¹Departamento de Química Analítica, Físico-Química e Inorgânica, UNESP; ²Departamento de Química, PUC RIO; ³Instituto de Química, USP; ⁴Departamento de Química, UFSCar.

Keywords: Cyclopalladated complexes, Antitumor activity, DNA binding studies.

Highlights

New orthopalladated oximes active against tumor cells and low affinity toward DNA.

Resumo/Abstract

This work deals with the synthesis, structural characterization and antiproliferative effects of three novel Pd^{II} complexes (**1-3**) of the type [PdCl(C²,N-L1)(luti)], [PdCl(C²,N-L2)(luti)] and [PdCl(C²,N-L3)(luti)], where L1 = acetophenone oxime, L2 = benzaldehyde oxime, L = tetralone oxime and luti = 2,6-lutidine, as potential antitumor agents. Compounds **1-3** have been fully characterized by elemental analysis and spectroscopic techniques (FTIR and NMR). The crystal and molecular structures of **1-2** have been determined by X-ray diffraction analysis. In all the cases, it has been observed a nearly square planar environment around Pd atom composed by the C,N-donor atoms from cyclopalladated oxime, one N atom from lutidine and one chloro ligand. The N atoms are oriented in a *trans* configuration (Fig 1). All compounds have been screened against tumor cell lines (MCF-7, A549 and MDA-MB-231) and fibroblasts (MRC5) via MTT assays. In particular, complex **3** has exhibited cytotoxic effects against MDA-MB-231 (7.54 ± 0.33 μM) and MCF7 (IC₅₀ = 14.78 ± 0.06 μM). Preliminary DNA binding studies on **3** have been carried out through spectrophotometric titrations and circular dichroism experiments. The increase of the concentration of **3** has not resulted in meaningful changes in the spectral CD profile of ct-DNA (Fig 2), indicating that the cyclopalladated establishes a weak interaction with DNA. Upon successive addition of aliquots of **3** to the DNA-Hoescht 33258 solution, a decrease of fluorescence intensity (ca. 10 %) has been detected (Fig 3), suggesting that **3** binds weakly to DNA.

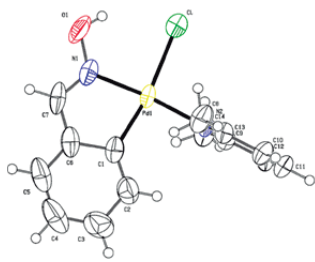


Fig 1. The molecular structure of **2**, showing the atom-labelling and displacement ellipsoids.

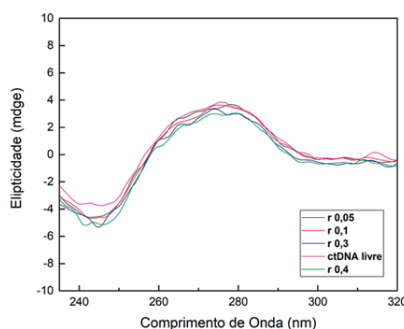


Fig 2. CD spectra of ct-DNA (85 μM) in Tris-HCl in the absence and presence of the palladium complex **3**.

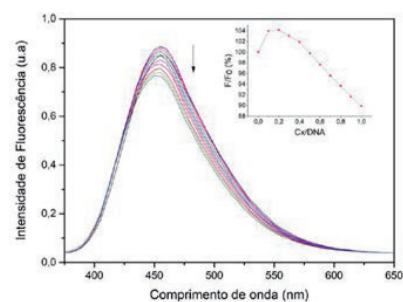


Fig 3. Fluorescence emission spectra for the Hoechst 33258 solution (λexcitation = 350 nm) with increasing amounts of the complex **3**.

Agradecimentos/Acknowledgments

This work was sponsored by grants from CNPq-PIBITI, FAPESP (proc. 2016/17711-5 and 2022/14041-0) and CAPES (finance code 001).

[Pd(P-P)(lap)]PF₆ complexes: Synthesis, characterization, cytotoxicity and mechanism of action. (P-P) = diphosphine; lap = lapachol

Jocely L. Dutra (PG),^{1*} João Honorato (PQ),¹ Marcos V. Palmeira-Mello (PQ),¹ Carlos A. Moraes (PQ),¹ Javier Ellena (PQ),² Alzir A. Batista (PQ).¹

jocely.dut@hotmail.com

¹Chemistry Department, UFSCar; ²São Carlos Institute of Physics, USP.

Keywords: Cancer, Lapachol, Palladium, DNA, Phosphines.

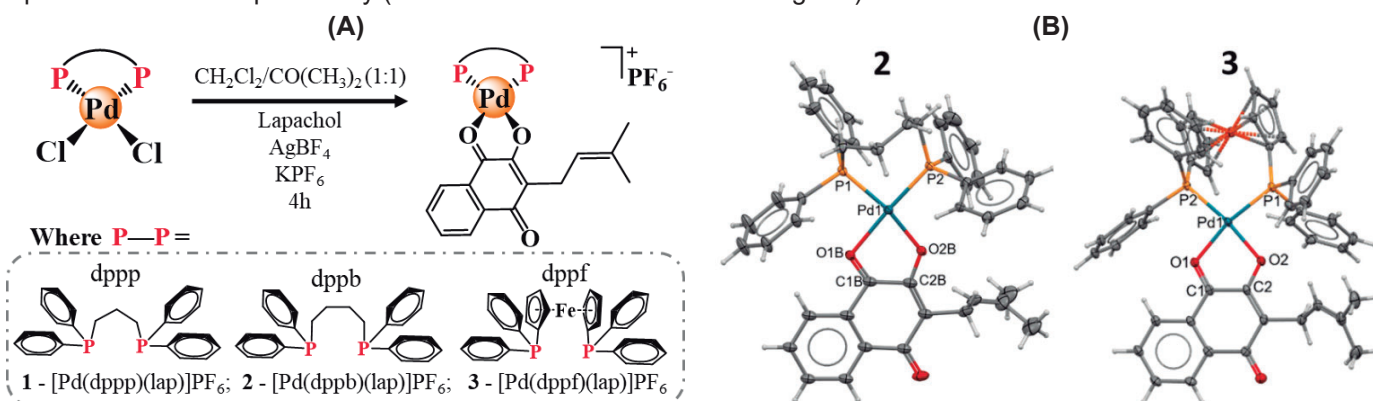
Highlights

Three new palladium/phosphine/lapachol complexes were synthesized, characterized, and their cytotoxicity was evaluated against several cancer cell lines. The complex [Pd(dppf)(lap)]PF₆ (**3**) presents a good selectivity index.

Resumo/Abstract

In this work Pd^{II} complexes, employing lapachol (lap) and diphosphines as ligands, were synthesized [Fig. 1(A)] and characterized, resulting in compounds of general formula [Pd(PP)(lap)]PF₆ [PP = **1** - dppp (1,3-bis(diphenylphosphino)propane); **2** - dppb (1,4-bis(diphenylphosphino)butane) and **3** - dppf (1,1'-bis(diphenylphosphino)ferrocene)]. The values of molar conductivity, in DMSO, show cationic complexes (1:1). The ³¹P{¹H} NMR spectra of the complexes show a double doublet signals, indicating the no magnetic equivalence of the phosphorus atoms *trans* to oxygens of lap. The NMR experiments (¹H, ¹³C{¹H}, COSY, HSQC, HMBC) suggest a planar square structure for the complexes. The mass experiments were performed adopting the Agilent 6545 qTOF MS, equipped with an electrospray interface. The theoretical values of the molecular ion mass are in agreement with the correspondent founded peak mass for the complexes, without contra ion: M-PF₆ = [Pd(PP)(lap)]⁺. In FTIR experiment the displacement of the bands ν(C=O) to a region of lower energy in the complexes, when compared with the free lap, indicates the coordination of ligand to the metal, by the O–O atoms. The slow evaporation of **2** and **3**, in CH₃OH/CH₂Cl₂ (1:1) solution resulted in single crystals suitable for X-ray diffraction, the structures are shown in Fig. 1(B). The cytotoxic activities of the complexes were evaluated in several cell lines. The activities for **3** were observed in the A2780cis (cisplatin-resistant ovarian cancer cell line) with the IC₅₀ = 4.4 ± 0.8 μmol/L, and the high activity in the non-cancer lung cells (MRC-5), IC₅₀ ≥ 40 μmol/L, gives this complex a remarkable selectivity index of 9.1 (IC₅₀ MRC-5/ IC₅₀ A2780cis). In order to investigate the mechanisms of death of **3**, we carried out experiments on cell morphology, colony formation, and wound healing. DNA is one of the main targets for metal-based anticancer drugs. Therefore, we investigated the interaction between **1-3** and DNA by viscosity measurements, gel electrophoresis, circular dichroism, and displacement assay using Hoechst 33258.

Fig. 1. (A) Synthetic Route used to obtain complexes **1-3** **(B)** Crystal structure of **2** and **3** showing the atom labels and ellipsoids with 30% of probability (the counterions were omitted in Fig. 1B).



Agradecimentos/Acknowledgments

The authors thank CNPq, CAPES and FAPESP for the financial support.

Photoactivated ruthenium complex induces cytotoxicity and apoptosis of lung cancer cells in three-dimensional culture

Amanda Blanque Becceneri (PQ)¹, Matheus Torelli Martin (PG)¹; Roberto Santana da Silva (PQ)^{1*}

amandabecc@usp.br; silva@usp.br

¹Departament of Biomolecular Sciences, School of Pharmaceutical Sciences of Ribeirão Preto (FCFRP), University of Sao Paulo, Ribeirão Preto, SP-Brazil.

Keywords: Cancer, Photodynamic Therapy, Ruthenium.

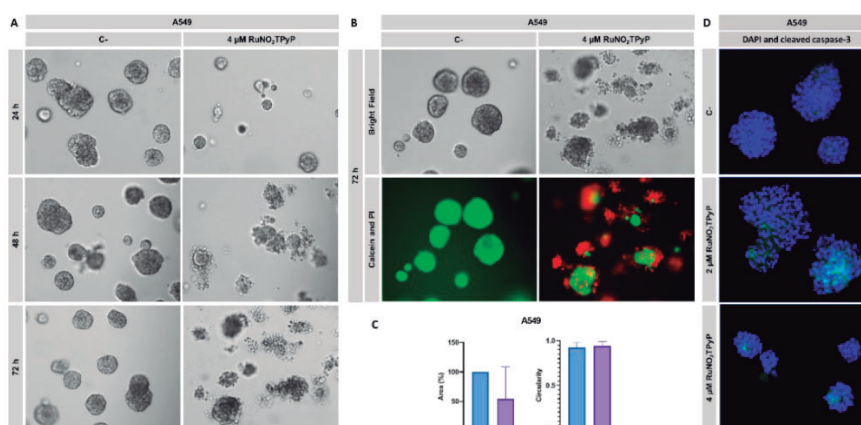
Highlights

The ruthenium meso-substituted porphyrin complex alters the morphology, induces cytotoxicity, and induces apoptosis of A549 cells in 3D culture after a 24 h treatment followed by light irradiation.

Resumo/Abstract

Cancer is a general term for a variety of illnesses that can affect almost any organ or tissue in the body¹. According to recent estimates, cancer remains a significant global public health issue². Cancer treatment is determined by the type and stage of the disease, but traditional cancer treatments, such as surgery, radiotherapy, and chemotherapy, have many limitations and side effects³. Photodynamic therapy emerges as a type of non-invasive therapy that may be used in place of traditional cancer treatments or in addition to them for increased efficacy⁴. The goal of this work was to analyze the effects of a photoactivated ruthenium complex, the TPyP-meso- $\{[Ru(bpy)_2(NO_2)](PF_6)_4\}_4$, on lung cancer multicellular structures (A549) grown in three-dimensional culture after 24 h treatment followed by light irradiation (415 nm, 4 J.cm⁻²). The 3D culture represents an important step towards testing new compounds with antitumor potential⁵. Using the on top cultivation method, cell morphology, cytotoxicity, and immunofluorescence assays were performed. The morphology assay (Fig. 1A) revealed that the complex altered the shape of the 3D A549 structures, and the cytotoxicity assay (Fig. 1B), which involved double staining with calcein-AM and propidium iodide, revealed that, in contrast to the control, the treated multicellular structures began to fragment, and the red color intensified, indicating cell death. The area of the structures was also reduced (Fig. 1C). It was possible to see the positive labeling for cleaved caspase-3 (in green) in the immunofluorescence assay using the anti-cleaved caspase-3 antibody, especially in the center of the multicellular structures at all the concentrations examined (Fig. 1D). Additional investigations are going to be carried out given the interesting results obtained with this model, which can better mimic the tumor microenvironment.

Figure 1 – Effects of photoactivated ruthenium complex after 24 h treatment on A549 multicellular structures in three-dimensional culture.



References: ¹WHO. Cancer. (2022); ²Siegel, R. L., Miller, K. D., Fuchs, H. E. & Jemal. CA. Cancer J. Clin. 72, 7–33 (2022); ³Nurgali, K., Jagoe, R. T. & Abalo, R. Front. Pharmacol. 9, 1–3 (2018); ⁴Da Silva, E., Pereira, E., Santos, D. & Ricci-Júnior, E. 211 Rev. Bras. Farm 90, 211–217 (2009); ⁵Fontoura, J. C. et al. Mater. Sci. Eng. C (2020).

Agradecimentos/Acknowledgment

This work was supported by FAPESP (grant 2020/03367-6; 2019/19448-8), CAPES, CNPq and FCFRP-USP.

Photobiological assays of mono-substituted corroles containing phenothiazine and carbazole moieties

Bruna M. Rodrigues (IC)¹, Otávio A. Chaves (PG)², Diego F. de Oliveira (IC)³, Rafael de Q. Garcia (Ms)³, Leonardo De Boni (PQ)³, Bernardo Almeida Iglesias (PQ)¹

matuzzirodrigues@gmail.com

¹ Laboratório De Bioinorgânica e Materiais Porfirínicos, Departamento De Química, Universidade Federal De Santa Maria, UFSM, Av. Roraima 1000, 97105-900 Santa Maria, RS, Brazil; ² Departamento de Química, Universidade de Coimbra, Portugal; ³ Instituto de Física de São Carlos, Universidade de São Paulo, Caixa Postal 369, 13560-970 São Carlos, SP, Brazil.

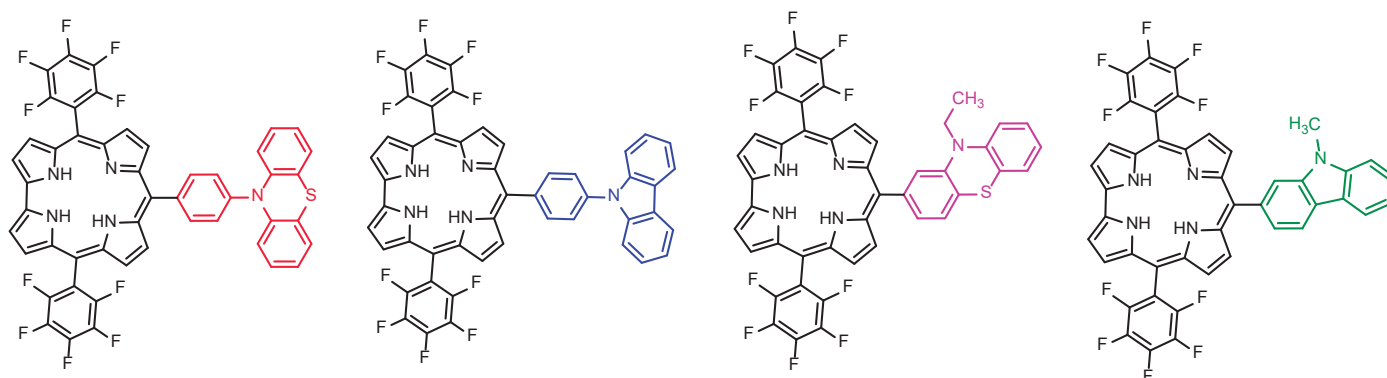
Palavras Chave: Corroles, Photophysical, Photobiology, DNA, HSA.

Highlights

Four mono-substituted corroles were used to photobiological assays; Interactive analysis between DNA and corroles evaluated by spectroscopic methods; HSA-binding properties by spectroscopic multi-techniques;

Resumo/Abstract

Corroles are macrocycles of the porphyrin class but they contain a direct C-C bond between the pyrrole units. Like porphyrins, they are compounds that have photophysical and photobiological properties of interest^{1,2}. In this work, we report, the photophysical and photobiological study of mono-substituted corrole derivatives with phenothiazine and carbazole units. The results show that studied compounds presents low fluorescence emission, good triplet excited states population, higher oxygen singlet (¹O₂) production and can be strong interact with DNA and HSA biomacromolecules (binding constants about 10⁵ M⁻¹). All biomolecule-interactive study were evaluated by spectroscopic techniques (absorption, emission and CD analysis) and also by theoretical molecular docking analysis, being able to distinguish the specific sites of interaction.



Agradecimentos/Acknowledgments

The authors thanks to CNPq, FAPERGS, CAPES/PROEX – Finance code 001 and FAPESP for financial supporting.

¹Acunha, T.V.; *et al.* Journal of Molecular Liquids 340 (2021) 117223.

²Rodrigues, B.M.; *et al.* Journal of Inorganic Biochemistry 242 (2023) 112149.

Photocatalytic Generation of Green H₂O₂ by Modified Poly (Heptazine Imides)

Luis F.G. Noletto (PG),¹ Andrea Rogolino (PG),² Vitor G.S. Pastana (PG),¹ Danielly T.S. Costa (PG),¹ Bruna R. Serino (IC),¹ Ivo F. Teixeira (PQ).¹

Fernandoguimaraes621@gmail.com; andrea.rogolino@studenti.unipd.it

¹Department of Chemistry, Federal University of São Carlos, Washington Luis Highway s/n Km 235, São Carlos, 13565-905, São Paulo, Brazil; ²Galilean School of Higher Education, University of Padova, Via Venezia 20, Padova, 35131, Italy.

Keywords: Photocatalysis, Carbon nitrides, Hydrogen peroxide, Poly (heptazine imides), Oxygen reduction.

Highlights

- Catalytic tests showed better performances for the precursor H-PHI and Na-PHI.
- H-PHI produced up to 1556 mmol L⁻¹ h⁻¹ g⁻¹ H₂O₂ under 410 nm irradiation using glycerin as a sacrificial electron donor.

Abstract

Photocatalysis provides a sustainable route for large-scale production of hydrogen peroxide (H₂O₂) from atmospheric O₂ via oxygen reduction reaction (ORR), an attractive alternative to the traditional anthraquinone method. Carbon nitrides are interesting heterogeneous photocatalysts that can be applied in ORR, especially the poly (heptazine imides) (PHIs), a subgroup whose structure provides high crystallinity and a scaffold to host transition metal single atoms.^[1] In this work, PHI was synthesized, functionalized with single atoms (M = Na, Fe, Ni, Co, Ru, and H-PHI), and fully characterized, including photoluminescence (PL) spectroscopy (Fig. 1b).^[2] Fig. 1a presents the photocatalytic results of the tests carried out with all modified PHIs. H-PHI exhibits high two-electron activity under visible light, with up to 1556 mmol L⁻¹ h⁻¹ g⁻¹ H₂O₂ production from O₂. Similar to this result, Na-PHI displayed conversion rates of 1077 mmol L⁻¹ h⁻¹ g⁻¹. It was noted that functionalization with transition metals is not beneficial for H₂O₂ synthesis, as the metal also catalyzes its decomposition, as evidenced by the kinetic data. The PL spectra (Fig. 1b) suggests that H-PHI shows better activity due to its long lifetime in an excited state.^[2] Overall, this work reports the high photocatalytic activity of H-PHI and highlights the efficiency of photocatalytic synthesis of H₂O₂ using inexpensive covalent materials.

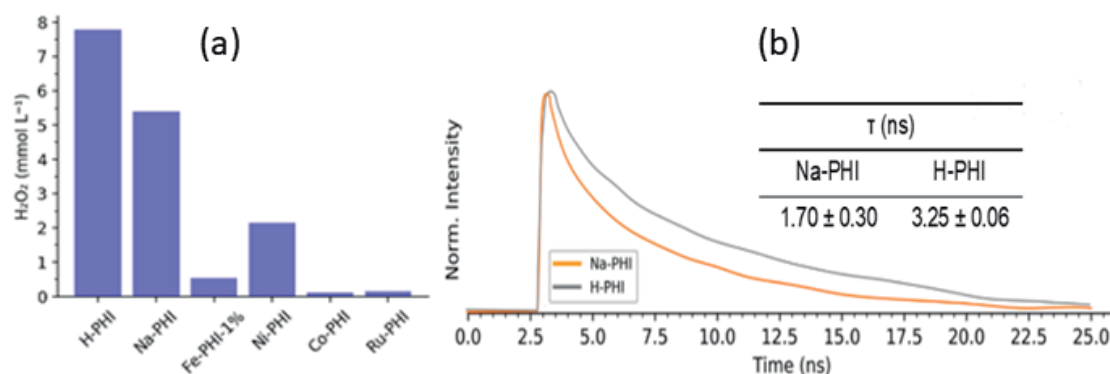


Figure 1. (a) Comparison of different M-PHIs in photocatalytic H₂O₂ production; (b) Time-resolved photoluminescence decay curves of Na-PHI and H-PHI aqueous suspensions. Reaction conditions: 5 mg catalyst, 2 mL 3.5% w/w glycerin, bubbled O₂ 1 min before reaction, 410 nm (100 W), r.t, 1h.

1. Shiraishi, Y. *et al.* Highly Selective Production of Hydrogen Peroxide on Graphitic Carbon Nitride (g-C₃N₄) Photocatalyst Activated by Visible Light, *ACS Catal.* 2014, 4, 3, 774–780.

2. Rogolino, A. *et al.* Modified Poly (Heptazine Imides): Minimizing H₂O₂ Decomposition to Maximize Oxygen Reduction. *ACS Applied Materials & Interfaces.* 2022, 14, 44, 49820-49829.

Acknowledgments

CAPES, CNPq, FAPESP and Max Planck Society

Photophysical properties of bis-cyclometalated Iridium(III) complexes

Leonardo H. de Macedo (PG)¹, Karina P. Morelli Frin (PQ)*¹.

karina.frin@ufabc.edu.br

¹ Federal University of ABC - UFABC, Av. Dos Estados, 5001, Santo Andre - SP – Brazil - 09210-170.

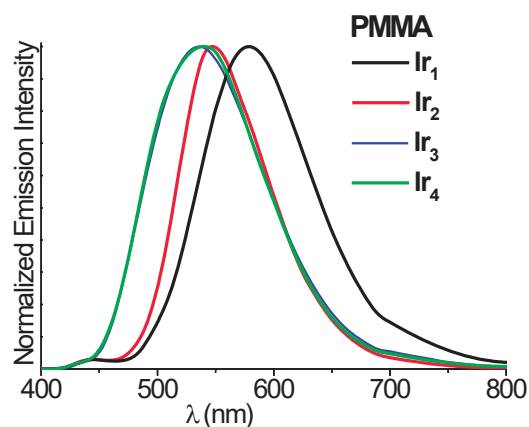
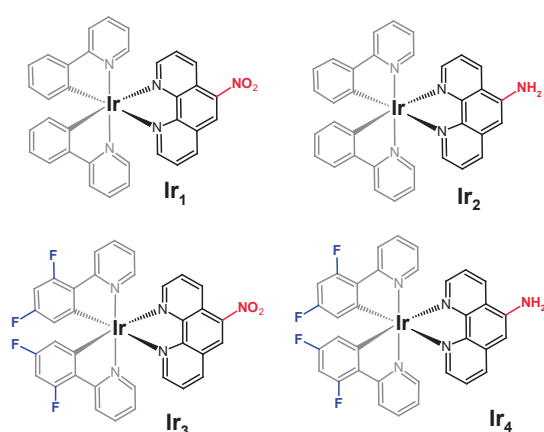
Palavras Chave: Iridium(III), Phosphorescence, MLCT, OLED, LEEC.

Highlights

Electrochemical and photophysical investigation of bis-cyclometalated iridium(III), $[\text{Ir}(\text{CN})_2(\text{NN})]^+$ aiming their evaluation as an emissive layer in OLED and/or LEEC devices.

Resumo/Abstract

Significant research efforts have been devoted to the development of photoinduced molecular devices based on metal complexes for sensing, energy conversion, and other applications. In this work, the electrochemical and photophysical behaviors of bis-cyclometalated iridium(III) complexes of general structure $[\text{Ir}(\text{CN})_2(\text{NN})]^+$, Ir_1 - Ir_4 , have been investigated aiming their evaluation as an emissive layer in OLED (Organic Light-Emitting Diode) and/or LEEC (Light-Emitting Electrochemical Cell) devices.



The electrochemical results allowed us to understand that the F substituents in the CN ligand stabilize the energy level of HOMO, while the substituents in the NN ligand (NO_2 and NH_2), stabilized and destabilized the energy level of LUMO, respectively. The complexes Ir_2 ($\lambda_{\text{max}} = 570 \text{ nm}$; $\tau = 0.840 \mu\text{s} \pm 0.010$; $\phi_{\text{em}} = 1.30\% \pm 0.07$) and Ir_4 ($\lambda_{\text{max}} = 575 \text{ nm}$; $\tau = 0.660 \mu\text{s} \pm 0.010$; $\phi_{\text{em}} = 0.75\% \pm 0.04$) are emissive in CH_3CN solution, while Ir_1 and Ir_3 complexes no detectable emission in solution were obtained. On the other hand, the emission can be observed for the four complexes in rigid media (PMMA) as a function of the rigidochromic effect and ascribed to $^3\text{MLCT}$ excited state. It is important to emphasize that the use of the $-\text{NH}_2$ and $-\text{NO}_2$ groups, which have extreme and opposite donor/acceptor electronic properties, generated complexes with very different photophysical properties in solution, which can be softened in a more rigid medium and, therefore, can still be evaluated as emissive layers in devices.

References:

- Márcia R. Gonçalves, Karina P.M. Frin, Journal of Molecular Structure 1224 (2021) 129312.
- Márcia R. Gonçalves, Adriano R.V. Benvenho, Karina P.M. Frin, Optical Materials 94 (2019) 206–212.

Agradecimentos/Acknowledgments

UFABC, FAPESP, and CAPES.

pH-Switching of the Luminescent, Redox and Magnetic Properties in a Spin Crossover Cobalt(II) Molecular Nanomagnet

Renato Rabelo (PQ),^{1*} Mario Inclán (PQ),² Enrique García-España (PQ),² Jorge Pasán (PQ),³ Rafael Ruiz-García (PQ),² Francisco Lloret (PQ),² Joan Cano (PQ),² Danielle Cangussu (PQ).¹

renato_rabelo@ufg.br

¹Instituto de Química, UFG; ²Instituto de Ciencia Molecular, Universitat de València; Laboratorio de Materiales para Análisis Químico, Universidad de La Laguna.

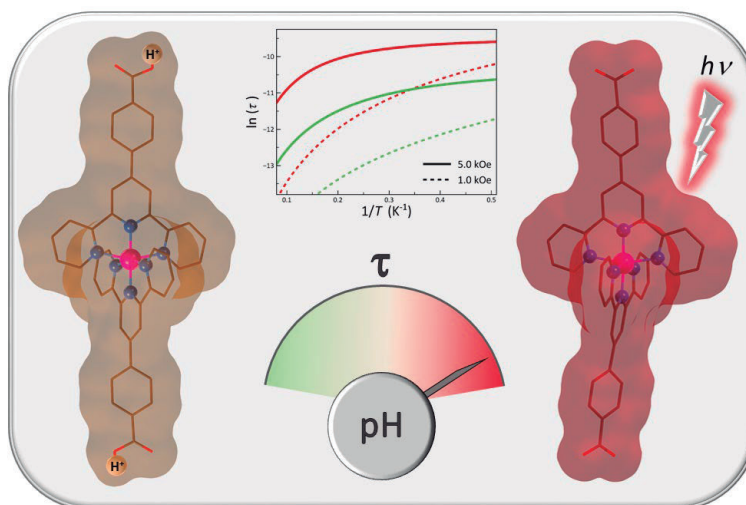
Palavras Chave: Coordination chemistry, Spin crossover, Slow magnetic relaxation, Dynamic molecular system.

Highlights

Reversible changes in the luminescent, redox and magnetic properties through pH-control in a spin crossover cobalt(II) molecular nanomagnet with a carboxylic acid group-containing terpyridine-type ligand are presented herein.

Resumo/Abstract

Using mononuclear first-row transition metal complexes as dynamic molecular systems to perform specific and selective functions under the control of an external stimulus that appropriately tunes their geometric (shape, size, or conformation) and electronic (optical, redox, or magnetic) properties may have a great impact in several domains of molecular nanoscience and nanotechnology. Here we present two mononuclear cobalt(II) complexes of formulas $\{[\text{Co}^{\text{II}}(\text{HL})_2][\text{Co}^{\text{II}}(\text{HL})]\}(\text{ClO}_4)_3 \cdot 9\text{H}_2\text{O}$ (**1**) and $[\text{Co}^{\text{II}}\text{L}_2] \cdot 5\text{H}_2\text{O}$ (**2**) [HL = 4'-(4-carboxyphenyl)-2,2':6',2"-terpyridine] which were isolated as a mixed protonated/hemiprotonated cationic salt or a deprotonated neutral species. They constitute a unique example of bistable bis(benzoic acid-substituted terpyridine)cobalt(II) complex exhibiting reversible changes in luminescence, redox, and magnetic (spin crossover and spin dynamics) properties as a result of the ligand deprotonation, either in solution or in the solid state. The fine-tuning of the optical, redox, and magnetic properties in this new class of pH-responsive spin crossover molecular nanomagnets offers fascinating possibilities envisaging multifunctional and multiresponsive magnetic devices for molecular spintronics.



Agradecimentos/Acknowledgments

CNPq, CAPES, FAPEG, Generalitat Valenciana.

Platinum (II) complexes with a diacetylmonooxime ethylthiosemicarbazonate ligand: from mononuclear to polynuclear complexes

Viviane Ap. da Silveira (PG),¹ Ana C. R. Gonçalves (PG),¹ Antônio E. H. Machado (PQ),² Victor M. Deflon (PQ),³ Pedro I. S. Maia (PQ).^{1*}

vivianesacra@gmail.com; pedro.maia@uftm.edu.br

¹Programa Pós-graduação Multicêntrico em Química de Minas Gerais-PPGMQ-MG, UFTM, Uberaba, Brasil; ²Instituto de Química, UFU, Uberlândia – MG, Brazil; ³Instituto de Química, USP, São Carlos – SP, Brazil.

Palavras Chave: Thiosemicarbazones, Platinum (II) complexes, Spectroscopy, X-Ray crystallography.

Highlights

The chemistry of thiosemicarbazones with platinum (II) is explored. Different synthetic routes have been used in order to enable the formation of different oligomers.

Abstract

Thiosemicarbazones are bioactive ligands with a versatile coordination chemistry.¹ The additional pair of electrons from the sulfur atom is frequently explored in order to form bridges with more than one metal center.² This work presents the synthesis and characterization of three new di, tri and tetranuclear Pt^{II} complexes derived from the monomeric complex [PtCl(L1)] (1), where L1²⁻ = diacetylmonooxime-ethyl-thiosemicarbazonate. The dinuclear (2), trinuclear (3) and tetranuclear (4) complexes were obtained from reactions of the precursor [PtCl(L1)] (1) with NaN₃, K₂[PtCl₄] and Et₃N, respectively (Figure 1a). It is important to highlight that the formation of the dinuclear complex occurs after decomposition of the azide in solution, which should probably occur after the formation of the complex with N₃⁻. The formation of the trinuclear complex is explained by the order of addition of the reagents, while the tetranuclear complex is formed upon deprotonation of the OH group consequent formation of Pt-S bonds.

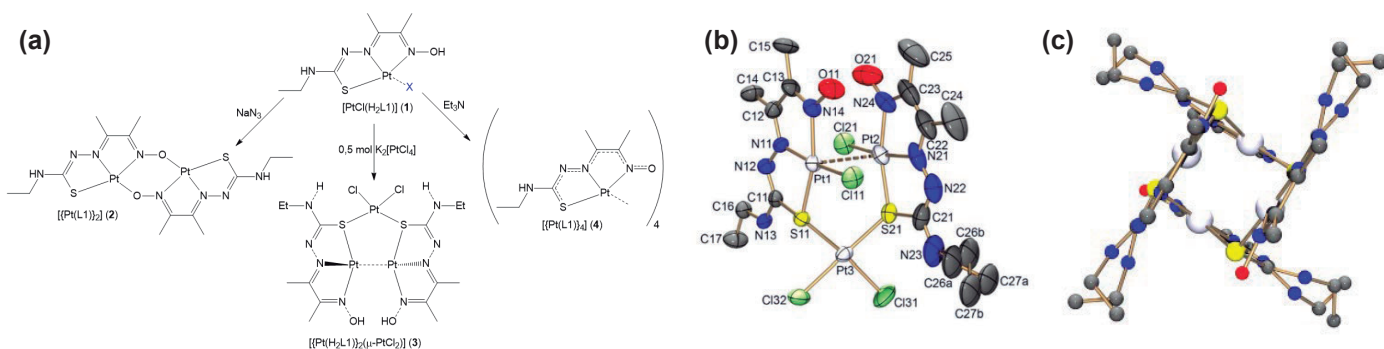


Figure 1: (a) Synthesis reactions of the dinuclear (2), trinuclear (3) and tetranuclear complexes (4). (b) Crystalline and molecular structure of the complex 3. (c) View of tetramer [Pt(L1)₄] along the c axis.

The compounds were analyzed by IR, ¹H-NMR, CHNS and molar conductivity. These analyses indicated the formation of neutral complexes according to the proposed compositions. The confirmation of the formation of the dinuclear complex [Pt(L1)₂] (2) was based on the high resolution ESI(+) mass spectrum, which showed a peak related to the [M+H]⁺ ion at *m/z* 791,0806 (calculated = 791.0837). Suitable crystals for X-ray diffraction analysis were obtained for the complexes 3 and 4. The complex 3 crystallizes in the monoclinic space group *P2₁/c*, while 4 presents the tetragonal space group *P4₂/n*. DFT studies are now underway in order to explain the formation of these oligomers and also de Pt...Pt interactions.

Acknowledgments

CNPq, CAPES and FAPEMIG

1. H. Yan, et al. *Tetrahedron Lett.* 54, 2013, 154-157.
2. L. Adrio, et al. *J. Organomet. Chem.* 694, 2009, 747-751.

Predicting Pt-195 NMR chemical shift in Pt(II) complexes using the new NMR-ZORA basis sets

Joyce H. C. e Silva (PG),¹ **Diego F. S. Paschoal (PQ)^{1*}**

diegofspaschoal@macae.ufrj.br or diegopaschoal01@gmail.com

¹Núcleo de Química Teórica e Computacional de Macaé, Polo Ajuda, Instituto Multidisciplinar de Química, Centro Multidisciplinar UFRJ-Macaé, Universidade Federal do Rio de Janeiro, 27.971-525, Macaé, RJ, Brazil;

Keywords: Cancer, Pt(II) complexes, Pt-195 nucleus, NMR, NMR-ZORA, Computational protocol.

Highlights

New NMR-ZORA basis sets were proposed for H-He, Li-Ne, Na-Ar, and Pt atoms.

Calculated Pt-195 NMR chemical shift at GIAO-BP86-SC-ZORA/NMR-ZORA/C-CPM for a set of 30 Pt(II) complexes with a MAD of 114 ppm and R² of 0.9853.

Abstract

Nuclear magnetic resonance (NMR) spectroscopy has played an important role in studying Pt(II) complexes with antitumor potential, since the Pt-195 nucleus is very sensitive to the nature of the ligands in the coordination sphere and the oxidation state of the metal.¹ The theoretical prediction of the Pt-195 NMR chemical shift ($\delta^{195}\text{Pt}$) is a difficult task, several factors must be taken into accounts, such as basis sets, electronic correlation, solvent, and relativistic effects.¹ Previously, Paschoal et al.¹ developed the NMR-DKH basis sets and a nonrelativistic protocol for predicting the Pt-195 NMR chemical shift. The authors studied a set of 258 Pt(II) complexes and obtained a mean absolute deviation (MAD) of 168 ppm. However, DKH calculations are not implemented in most computational packages. Thus, in the present study, NMR-ZORA basis sets were proposed and a computational protocol for predicting the $\delta^{195}\text{Pt}$ was proposed.

Initially, the NMR-DKH basis sets were recontracted as NMR-ZORA for H-He, Li-Ne, Na-Ar, and Pt atoms, with the contraction coefficients through the coefficients of atomic orbitals calculated at Hartree–Fock level with ZORA scalar relativistic correction. The structures of Pt(II) complexes studied were optimized and characterized as a minimum point on the potential energy surface (PES) at B3LYP/LANL2TZ(f)/def2-SVP/C-PCM level. Then, the chemical shift was calculated according to equation: $\delta^{195}\text{Pt}_{\text{calc}} = \sigma_{\text{ref}} - \sigma_{\text{calc}}$, where σ_{ref} is the calculated shielding constant for internal reference $[\text{PtCl}_6]^{2-}$ in D₂O.¹ The shielding constants (σ) were calculated at GIAO-DFT-Functional-SC-ZORA/NMR-ZORA/C-PCM level. All calculations were carried out in ORCA 5.0.3 program.

Initially, cisplatin and carboplatin, that present experimental data for $\delta^{195}\text{Pt}$ available in the literature were selected as models. The NMR calculations were obtained for a set of 36 DFT functionals, with the smallest mean relative deviations (MRD) being found when GGA functionals are considered, with the BP86 and OPBE functionals showing MRD of only 0.3%. Then, the protocols BP86/NMR-ZORA/CPCM and OPBE/NMR-ZORA/CPCM were applied in the study of a set of 30 Pt(II) complexes, which present experimental data for $\delta^{195}\text{Pt}$. The calculated results (Figure 1) with BP86 showed excellent agreement with the experimental values, with a MAD of only 114 ppm and a coefficient of determination (R²) of 0.9853 (Figure 2), showing the quality of the proposed NMR-ZORA and computational protocol for studying Pt-195 NMR.

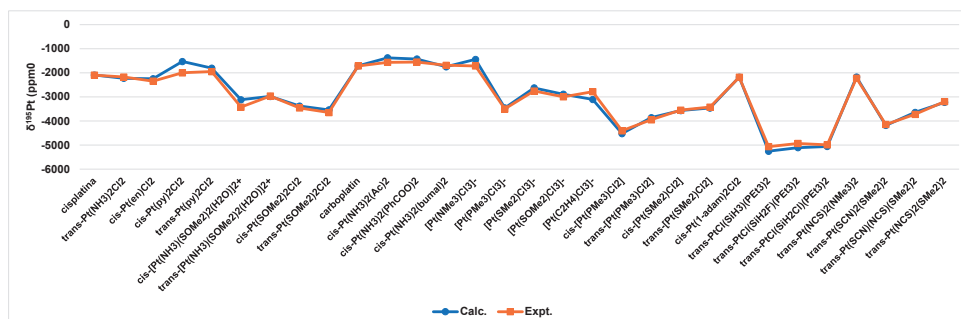


Figure 1. Calculated $\delta^{195}\text{Pt}$ at GIAO-BP86-SC-ZORA/NMR-ZORA/C-PCM level for a set of 30 Pt(II) complexes.

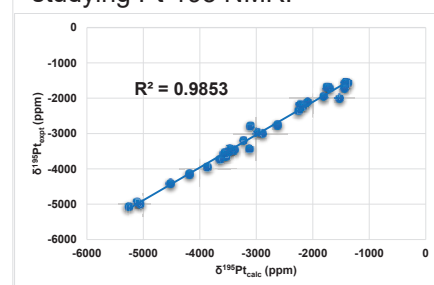


Figure 2. Correlation between calculated and experimental $\delta^{195}\text{Pt}$.

¹Paschoal et al., J. Comput. Chem., v. 37, p. 2360-2373, 2016.

Acknowledgments

The authors would like to thank the Brazilian agency FAPERJ (E-26/201.336/2022 – BOLSA) and CAPES (Finance Code 001) for the financial support.

46^o Reunião Anual da Sociedade Brasileira de Química: "Química: Ligando ciências e neutralizando desigualdades"

Preparação de um complexo trinuclear de paládio(II) a partir de uma tiossemicarbazona derivada de uma β -dicetona

Andressa R. Rettondin (PG),¹ Bruna Possato (PQ),² Adelheid Hagenbach (PQ),³ Sérgio de Albuquerque (PQ)², Ulrich Abram (PQ),³ Pedro Ivo da Silva Maia (PQ).^{1*}

prof.andressarettondin@gmail.com; pedro.maia@uftm.edu.br

¹Departamento de Química, Universidade Federal do Triângulo Mineiro, Uberaba - MG; ²Faculdade de Ciências Farmacêuticas de Ribeirão Preto, USP; ³Freie Universität Berlin, Berlin, Alemanha

Palavras-Chave: Complexo trinuclear de paládio, Tiossemicarbazonas, Infravermelho, Difração de raios X, UV-vis

Highlights

Preparation of a trinuclear palladium(II) complex from a thiosemicarbazone derived from a β -diketone.

Thiosemicarbazones are versatile ligands. A new trinuclear palladium(II) complex was synthesized and characterized. Using the same ligand, platinum(II) and palladium(II) yield different types of complexes.

Resumo/Abstract

As tiossemicarbazonas são utilizadas como ligantes há muito tempo, principalmente por oferecerem múltiplos modos de coordenação, levando a estabilização dos centros metálicos em diversos estados de oxidação em diferentes geometrias e muitas vezes ainda são capazes de surpreender. Um exemplo é o complexo [Pt(phen)L^{Ph}],¹ onde L^{Ph} = 5-hidroxi-3-metil-N,5-difenil-4,5-diidro-1H-pirazol-1-carbotiamida,² onde se observou um acoplamento C-C entre a fenantrolina e o carbono α em relação ao fragmento cetona do ligante tiossemicarbazonato para formação de um quelato *N,N,N,S*-tetradentado na formação do complexo. No presente trabalho, buscou-se avaliar a influência do centro metálico na reação de acoplamento C-C trocando-se a platina(II) por paládio(II). Para tanto, foram usadas as mesmas condições anteriores,¹ alterando-se o precursor metálico para [Pd(phen)Cl₂]. Imediatamente após a adição de Et₃N na mistura reacional, observou-se a mudança de cor do meio, de bege para vermelho escuro. Após remoção do solvente, o produto bruto da reação foi cromatografado utilizando-se sílica como fase estacionária e um gradiente de ACN:DCM como fase móvel. A partir da alíquota com maior concentração do complexo foram obtidos monocristais que foram devidamente caracterizados. No espectro de infravermelho (ATR) observou-se a ausência da banda alargada característica de $\nu(\text{O-H})$, indicando a mudança na estrutura do ligante. A ausência da banda intensa característica dos compostos carbonilados ($\nu(\text{C=O}) \sim 1600 \text{ cm}^{-1}$) é um indício de uma acentuada deslocalização eletrônica causada pela coordenação ao paládio. A reação de formação de $[\{\text{PdL}^{\text{Ph}}\}_3]$ foi acompanhada por UV-vis durante 540 s, registrando-se 1 espectro a cada 10 s. Foi possível se observar o aparecimento de uma banda alargada na região de 400 nm compatível com uma transição eletrônica do tipo intracluster, apontando a formação do composto trinuclear. Finalmente, a estrutura molecular do complexo foi determinada por difração de raios X, revelando a formação de um complexo trinuclear (Figura abaixo), onde ocorre a coordenação do ligante em modo *O,N,S*-tridentado e a labilização da fenantrolina durante a reação.

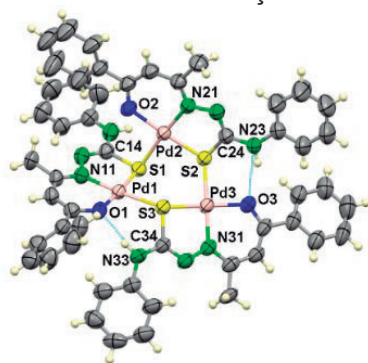
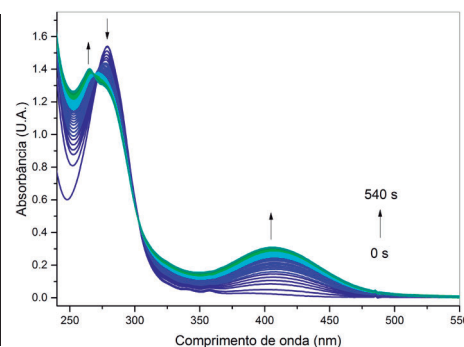


Tabela. Estrutura elucidada por DRX e comprimento e ângulos de ligações selecionadas

Ligação	Comprimento de ligação (Å)	Ligação	Ângulo (°)
Pd1-S1	2.2393	Pd2-S2-Pd3	120.29
Pd1-S3	2.3572	Pd1-S1-Pd2	99.09
Pd1-O1	2.005	Pd3-S3-Pd1	127.47
Pd1-N11	2.009		
Pd2-S2	2.2267	O1-Pd1-S1	177.03
Pd2-S1	2.3293	O1-Pd1-S3	87.21
Pd2-O2	1.993		
Pd2-N21	1.984	O2-Pd2-S2	175.12
Pd3-S2	2.3183	O2-Pd2-S1	91.57
Pd3-S3	2.2494		
Pd3-O3	2.015	O3-Pd3-S3	172.29
Pd3-N31	1.993	O3-Pd3-S2	85.48



¹ Gonçalves, A. C. R. et al., *Dalton Transactions*, v. 49, n. 28, p. 9564-9567, 2020.

² Rettondin, A. R. et al., *Eur. J. Med. Chem.*, 120, 217-226. 2016.

Agradecimentos/Acknowledgments

CNPq, FAPEMIG, FAPESP (2017/17579-2).

Preparation of multifunctional catalyst based on manganese porphyrin immobilized in inorganic composites towards a sequential reaction

Renaldo Marcos da Silva Junior¹ (PG), **Everton Henrique dos Santos**¹ (PG), **Shirley Nakagaki**^{1*} (PQ).

renaldo.junior@ufpr.br; shirleyn@ufpr.br

¹Laboratório de Bioinorgânica e Catálise - Departamento de Química – Universidade Federal do Paraná (UFPR) – CEP 81531980, Curitiba-PR, Brazil.

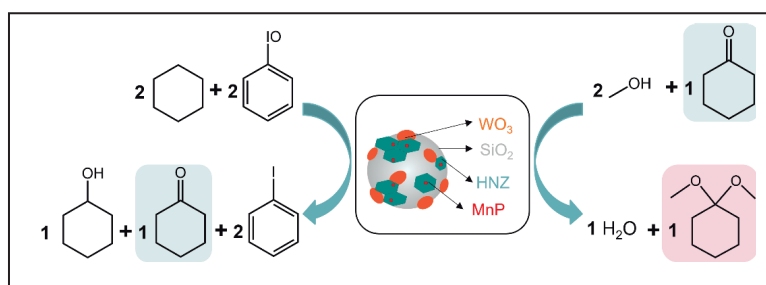
Keywords: *Porphyrin, Composites, Support, Catalyst, Multifunctional, Sequential reactions.*

Highlights

- Immobilization of manganese(III)porphyrin to produce reusable and multifunctional solid catalysts.
- Silica/WO₃/layered material solids as supports for immobilization of catalyst species.
- One-pot assisted Tandem reaction of cyclohexane oxidation and cyclohexanone acetalization.

Resumo/Abstract

Inspired by natural systems like cytochrome P-450, researchers have investigated synthetic metalloporphyrins (MPs) as catalysts in various single organic reactions [1]. Immobilization of this family of complexes on solid supports has been explored to stabilize MPs and to allow them to be reused [1, 3]. Considering the stability and the diverse mechanisms through which MP-based solids can act and depending on the catalytic reaction and the chemical characteristics of the support, immobilized MPs can be investigated in one-pot sequential reactions involving one or more mechanisms (domino or cascade and Tandem, respectively) [2]. This approach allows the potential of MPs to be explored even further and generates less waste.



Here, we have developed multicomponent and multifunctional solid catalysts based on the tetra-anionic manganese(III)porphyrin Na₄[Mn(TDFSP)(Oac)] (MnP) immobilized on inorganic supports composed of silica/WO₃/layered material and investigated their catalytic activity in one-pot cyclohexane oxidation to cyclohexanol and cyclohexanone with PhIO followed by ketalization of the cyclohexanone carbonyl group to dimethyl cyclohexanone ketal with methanol. We expected that the MnP would catalyze cyclohexane oxidation, and that the acid sites of the silica/WO₃/layered material would assist cyclohexanone/methanol ketalization. After establishing the optimal conditions for the single organic reactions separately, we proposed the proof-of-concept one-pot Tandem reaction of cyclohexane oxidation to cyclohexanol and cyclohexanone with PhIO catalyzed by silica/WO₃/layered material/MnP and ketalization of the cyclohexanone carbonyl groups with methanol to obtain dimethyl cyclohexanone ketal as final product. Albeit modest, ketal production catalyzed by the solids confirmed that the one-pot Tandem reaction occurred successfully, proving the multifunctionality of the catalysts. The results could be attributed to the adequate preparation of the catalysts in terms of composition, morphology, and textural properties. The MnP on the support was available for catalyzing cyclohexane oxidation, whereas the support assisted cyclohexanone ketalization under the conditions employed in this work. The latter reaction was possible thanks to the catalytic acid sites attributed mainly to the presence of zinc(II) in the layered component of the support.

References:

- [1] D. Dolphin, T.G. Traylor, L.Y. Xie, *Acc. Chem. Res.* 30 (1997) 251.
 [2] E. H. Santos, C. Carvalho, C. M. Terzi, S. Nakagaki, *Molecules*, 23 (2018) 2796.
 [3] K.C.M. Westrup, R.M. da Silva, K.M. Mantovani, L. Bach, J.F. Stival, P.G.P. Zamora, F. Wypych, G.S. Machado, S. Nakagaki, *Appl. Catal. A Gen.* 602 (2020) 117708.

Agradecimentos/Acknowledgments



Preparation of silver vanadate (β -AgVO₃) and collagen dispersions

Bianca R. Brito (PG),^{1*} Rúbia Camila Bottini (PQ),² Bruna C. Becker (IC),³ Luiz F. Pereira (PQ),³ Eduardo L. Sá,¹ Giovana G. Nunes (PQ).¹

biancarigonatto@gmail.com

¹Departamento de Química, UFPR; ²Departamento de Química, UTFPR; ³Escola de Ciências da Vida, PUCPR

Palavras Chave: (Silvervanadate, β -AgVO₃, Collagen, Microscopy, Morphology, Angiogenic).

Highlights

β -AgVO₃ was synthesized by a simple methodology. The product was characterized by employing spectroscopic and diffractometric technics. β -AgVO₃ collagen dispersions were prepared using sonication. The homogeneity and morphology of films were analyzed by scanning electron microscopy and atomic force microscopy, respectively.

Resumo/Abstract

Silvervanadate (AgVO₃) exhibits a variety of crystalline structures and applications. β -AgVO₃ is one of the most stable phases of this oxide, being explored in biosensors, photocatalysis, tribology, lithium-ion battery, biomedicine, and medical applications.¹ The reaction between NH₄VO₃ and AgNO₃ produced a yellow solid that was treated at 200°C for one day, given an orange solid. The powder X-ray diffractogram presented peaks that can be indexed to the pure β -AgVO₃ phase (JCPDS 29-1154 card). The solid was also characterized by vibrational spectroscopies (IR and Raman) and electronic spectroscopy. Scanning electron microscopy (SEM) showed a homogeneous morphology formed by silver vanadate rods with micrometric length (Figure 1a). EDS spectrum confirms the presence of silver, vanadium and oxygen atoms. Different amounts of the orange solid (0.25 mg and 0.10 mg) were dispersed in a collagen suspension under sonication. Atomic force microscopy (AFM) analysis confirms the incorporation of the silver vanadate into collagen films (Figure 1b). Preliminary studies using the chicken chorioallantoic membrane model point to an angiogenic effect in concentrations below 35.0 μ g mL⁻¹. (Animal assays were pre-approved by the institutional ethical committee of PUC/PR, Project n° 850/2013 and license n° 01657/2019).

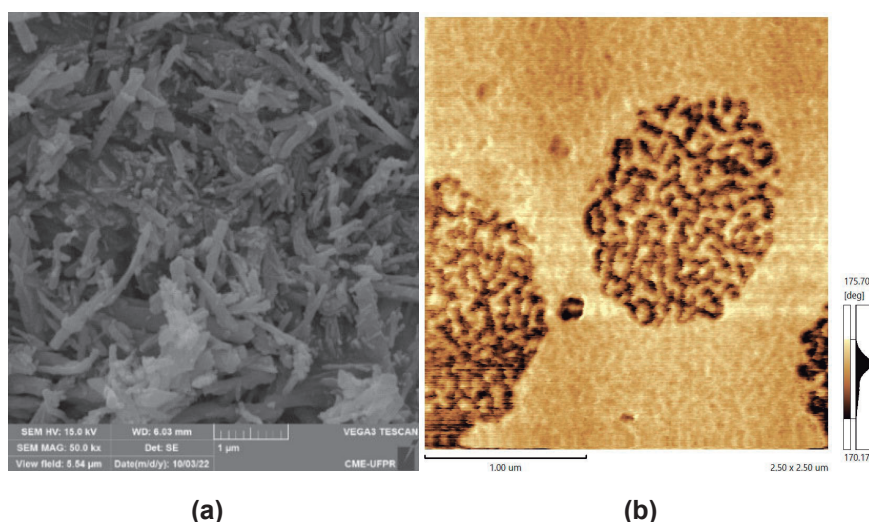


Figure 1: (a) Scanning electron microscopy (SEM) image of β -AgVO₃ at 1 μ m. (b) AFM analysis of the suspension of 0,10mg of β -AgVO₃ in collagen.

Agradecimentos/Acknowledgments

UFPR / CAPES / CNPq / FUNDAÇÃO ARAUCÁRIA / PROEX

[1] W. Klöckner, **Materials Letters**, **278**, 128403, (2020).

Questioning the solubility evaluation methods for coordination compounds

João Madureira (PQ),¹ Maria Luiza de Assis Marcolan (IC),¹ Thalita Lopes da Silva Pereira (IC), Geovanna Batista Florentino (IC), Ana Caroline Moreno Alves Netto (IC).¹

jmadureira@id.uff.br

¹Departamento de Química Inorgânica do Instituto de Química, UFF.

Palavras Chave: (Solubility, Coordination compounds).

Highlights

Organic compounds solubility methods are inadequate to study coordination compounds.

Solubility is a classic property but no systematic studies for coordination compounds exist.

The best counter-ions for synthesis are inadequate to study solubility in closed systems mimicking in vivo conditions.

Counter-ion exchange is explored to improve solubility and better represent extracellular conditions.

There is no reason to keep large anions when performing solubility studies for in vivo prediction.

Resumo/Abstract

Solubility is a classic physicochemical property, but it's not considered a "true" research field by itself. No systematic studies about the solubility of coordination compounds or organometallics can be found. Even old handbooks and encyclopedia data are restricted to inorganic salts or neutral compounds studies, while coordination compounds are typically cationic. Due to the scarcity of solubility studies for such compounds, we started a systematic bibliography search to build a database that can help us to understand their solubility and to predict the solubility of new or yet to be synthesized compounds. The results found so far are summarized in this work.

Since the solubility is one of the critical properties to be assured during the development of a drug and our research group is interested in the development of coordination compounds for chemotherapy and parasitic diseases treatment, it is critical to follow an adequate method approach to evaluate their solubility in complex media (extracellular fluids), since the usual approach is intravenous fluid application. Since metallodrugs solubility evaluation is seldom determined in water we questioned the adequacy of such an approach.

Coordination compounds are typically big metal cations stabilized with large counter ions like PF₆⁻, BF₄⁻ or similar ones. While such an approach results in higher yields and purity improvement, it also significantly decreases the solubility in aqueous media. Furthermore, cation-anion interactions are expected to be strong in closed systems, where such studies are performed; while in vivo can be classified as open systems that eliminate the original counter-ion, replacing it with chloride.

To improve the solubility methodology for coordination compounds, developed as potential metallodrugs, we evaluated the solubility of [Ru(bpy)₂(phen)](PF₆)₂ in water, 0.1 mol/L NaCl and simulated extracellular body fluid (EBF). The values are less than 1 mmol/L and show only small differences among them. Recrystallization of the compound in the three media gives the same anhydrous crystal as PF₆⁻ confirming that strong counter-ion interactions avoid the determination of the true solubility of the drug when present in plasma. The complex counter-ion exchange to its chloride form shows a very strong solubility increase (> 200 mmol/L) on all three media, indicating that the first approach does not represent the true behavior of the drug in vivo. Similarly, many of the cationic drugs are to be much more soluble than what is expected from the values determined in closed systems with the original counter-ions present.

Agradecimentos/Acknowledgments

M. L. A. Marcolan thanks FAPERJ for an IC grant.

Ruthenium(II) metronidazole complexes: cell cycle arrest at G1/S transition and apoptosis induction in MCF-7 cells

Caio Cesar Candido (PG)^{1*}, Henrique V. R. Silva (PG)¹, Bruno Zavan (PQ)², Marisa Ionta (PQ)², Marília I. F. Barbosa (PQ)^{1*}, Antônio C. Doriguetto (PQ)^{1*}

caiocandido95@hotmail.com; mariliaifrazaob@gmail.com; doriguetto@unifal-mg.edu.br

¹Instituto de Química, UNIFAL-MG; ²Departamento de Ciências Biomédicas, UNIFAL-MG

Palavras Chave: Ruthenium complexes, Metronidazole, Anticancer activity, Breast cancer.

Highlights

Synthesis and characterization of ruthenium(II) metronidazole complexes. Cytotoxicity profiles and DNA interaction study. Inhibition of the proliferative behavior of estrogen-positive breast carcinoma cells. Cell death by apoptosis.

Resumo/Abstract

Ruthenium compounds are known to be potential drug candidates since they offer the potential for reduced toxicity over platinum-based complexes, making them suitable for use in biological applications [1]. Metronidazole (MTNZ), a nitroimidazole derivative, is widely used to treat a variety of infections due to its antibacterial and antiprotozoal activity [2]. Additionally, was considered to be anti-tumor active due to its affinity for penetration and accumulation in hypoxic tumors [3]. So, ruthenium(II) complexes with metronidazole as a ligand were obtained of the type [RuCl(MTNZ)(dppb)(N-N)]PF₆ (Figure 1) where: dppb = 1,4-bis(diphenylphosphino)butane, MTNZ = metronidazole, N-N = 4,4'-Mebipy = 4,4'-dimethyl-2,2'-bipyridine (**1**), 4,4'-Methoxybipy = 4,4'-dimethoxy-2,2'-bipyridine (**2**), bipy = 2,2'-bipyridine (**3**) and, phen = 1,10-phenanthroline (**4**). The complexes were characterized by elemental analysis, molar conductivity, infrared and UV-Vis spectroscopy, cyclic voltammetry, ³¹P{¹H}, ¹H, ¹³C{¹H}, and Dept 135 NMR, and mass spectrometry. The interaction of complexes with DNA was evaluated and the demonstrated behavior has characteristics of the intercalation, and their cytotoxicity profiles were determined for tumor cell lines derived from human estrogen-positive breast cancer, MCF-7, (Table 1). We demonstrated that complexes (**1**) and (**3**) are promising antitumor agents once they inhibited the proliferative behavior of MCF-7 cells and induced apoptosis.

Figure 1. Synthetic route and general structure of the Ru(II)-MTNZ

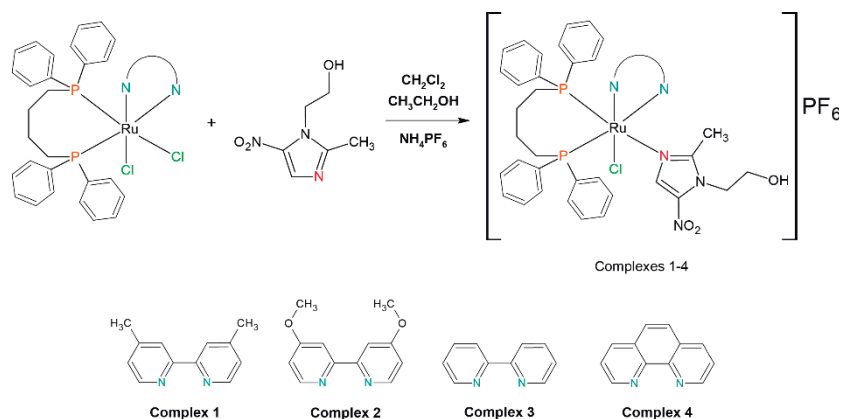


Table 1. IC₅₀ values (μM) and selectivity index (SI) determined after 48h of treatment with complexes (1-4) and free metronidazole. Data show means + SD of three independent experiments.

Compound	IC ₅₀ ± SD (μM) MCF-7	SI
1	17.47 ± 1.14	2.7
2	31.99 ± 1.72	1.2
3	16.88 ± 0.97	2.9
4	25.69 ± 1.65	1.1
Metronidazole	> 250	-
cisplatin	8.58 ± 1.77	0.3

[1] S. Thota, *et al.*, J. Med. Chem., 61 (2018) 5805-5821.

[2] A.H. LAU, *et al.*, Clin. Pharmacokinet., 23 (1992) 328-364.

[3] D. Zyro, *et al.*, Cancers, 14 (2022) 900-924.

Agradecimentos/Acknowledgments

The authors are grateful for the financial support from CAPES (Finance code 001 and research fellowships), CNPq (428475/2018-3 and 308893/2019-0), FINEP (CT-INFRA), and FAPEMIG (APQ-02036-21 and APQ-01835-18).

Ruthenium organometallic complexes containing α -diimine ligand: Synthesis characterization, halide effect, reactivity and antioxidant activity

Janaína S. da Silva (PG)¹, Otávio Fuganti (PG)¹, Davi F. Back (PQ)², André L. Bogado(PQ)³, Juliana P. da Silva (QP)⁴, Márcio P. de Araujo (PQ)^{1*}.

mparaujo@ufpr.br

¹Departamento de Química, UFPR; ²Departamento de Química, UFSM; ³Departamento de Química, FACIP-UFU; ⁴Departamento de Química, UFSC

Palavras Chave: Ruthenium-cymene, α -Diimine, Electrochemistry, Halide effect, Gas-phase behavior, Antioxidant

Highlights

Ru-X bond strength analyzed by DFT and ESI-MS;

The ligand α -diimine facilitate the reduction process under cyclic voltammetry conditions;

The halide coordinated to the ruthenium affects the antioxidant activity.

Resumo/Abstract

Over the years, halides have been widely used as leaving groups in Ru-arene complexes, and their ability to influence the mechanism of action and cytotoxicity associated with the hydrolysis stability of such complexes.

This work describes the studies of ruthenium(II) complexes with general formula $[\text{RuX}(\eta^6\text{-}p\text{-cymene})(\text{Me-DAB})]\text{PF}_6$ (X = Cl; Br; I).

The complexes were synthesized from the reaction of the precursors $[\text{RuX}_2(\eta^6\text{-}p\text{-cymene})]_2$ followed by addition of KPF_6 , and fully characterized by NMR (^1H , ^{13}C), vibrational and electronic spectroscopy, elemental analysis, cyclic voltammetry, X-ray diffraction (**Figure 1**) and ESI-MS. The ^1H NMR experiments allowed the evaluation of the complexes stability related to the Ru-X bonds solvolysis process (X = Cl, Br, I), in which the compounds were stable in DMSO-d_6 / D_2O for a period up to 72 h. The Ru-X bond strength determined by DFT and collision-induced dissociation (CID) follows the sequence $\text{Ru-Cl} < \text{Ru-Br} < \text{Ru-I}$. The cyclic voltammetry experiments (**Figure 2**) revealed that the complexes present two independent processes, one irreversible oxidation process attributed to the $\text{Ru}^{3+}/\text{Ru}^{2+}$ pair and one irreversible reduction process leading to the formation of Ru^0 complex. Finally, these complexes were applied as antioxidant agents using the DPPH radical removal method. All complexes demonstrated the ability to remove the DPPH radical (**Table 1**). The results showed that complexes with the chlorido ligand have more significant antioxidant activity than the complexes with the bromido ligand, followed by iodido one.

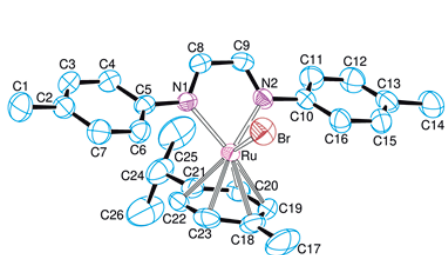


Figure 1. Molecular structure of $[\text{RuBr}(\eta^6\text{-}p\text{-cymene})(\text{Me-DAB})]\text{PF}_6$ solved by X-ray diffraction (hydrogen atoms and PF_6^- are omitted).

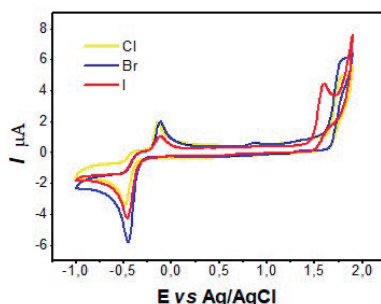
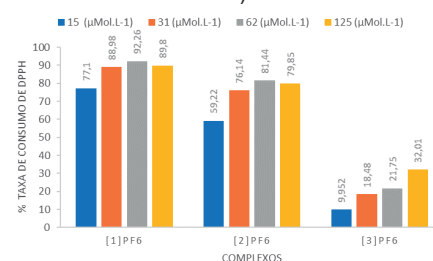


Figure 1. Cyclic voltammograms of $[\text{RuX}(\eta^6\text{-}p\text{-cymene})(\text{Me-DAB})]\text{PF}_6$ complexes (X = Cl, Br, I).

Table 1. Radical scavenging of DPPH (%) (180 min)



Agradecimentos/Acknowledgments

The authors thank CNPq and CAPES for financial support.

Synthesis, characterization and photoluminescence study of the complex [Eu(TTA)₃(PIB_4CH₃)]

Bianca V. Alves (IC),¹ Rodolpho A. N. Silva (PG),¹ Sergio A. M Lima (PQ),^{1,2} Ana M. Pires (PQ),^{1,2} Marian R. Davolos (PQ)^{1*}

bianca.veleda@unesp.br; marian.davolos@unesp.br

¹Institute of Chemistry, São Paulo State University (Unesp), Araraquara; ²School of Technology and Sciences, São Paulo State University (Unesp), Presidente Prudente

Keywords: Lanthanide, Photoluminescence, Coordination Compounds

Highlights

The complex [Eu(TTA)₃(PIB_4CH₃)] was synthesized and characterized, showing high luminescence, explained by the presence of PIB_4CH₃ and β-diketone TTA in the coordination sphere of the lanthanide ion.

Abstract

Lanthanide(III) ions present 4f-4f transitions that are prohibited by Laporte's and spin rules, resulting in low molar absorptivities. The use of molecules coordinated with lanthanide ions is a valid strategy to increase the energy absorbed that can be transferred to the lanthanide ion, in a phenomenon called the antenna effect. This phenomenon results in compounds that present high luminescence, which can be modulated according to their respective applications. Such systems can be used in different ways, such as the development of biomarkers, luminescent sensors, and electronic devices. In this work, a new complex containing one unit of the phenanthroline derivative (PIB_4CH₃) and three units of the β-diketone ligand (TTA) was synthesized. (Figure 1A).

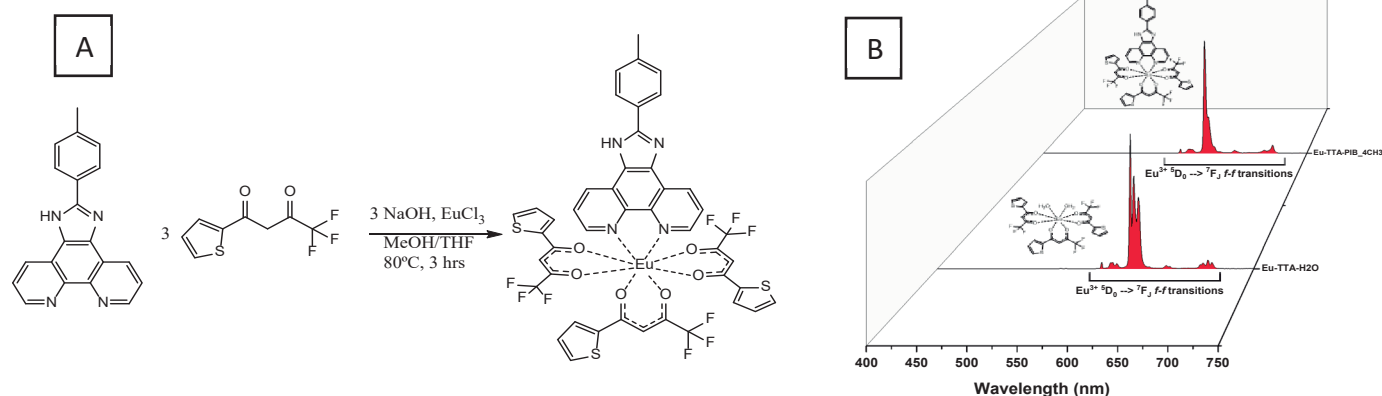


Figure 1: (A) Equation of the synthesis reaction. (B) Emission spectra of the synthesized complex (back) and the precursor complex (front).

The complex was characterized by FTIR and Raman techniques, where the displacements of the C=N and C=O vibrations, present in the ligands, suggest the coordination in the europium (III) ion. Via mass spectrometry, the signal referring to the idealized complex was observed ($[M - 1H]^+$ = 1111 Da). Via the photoluminescence spectroscopy technique and using the LUMPAC software, it was possible to observe that only the Eu(III) transitions are in the spectra. This is a strong suggestion that energy transfer from ligands to lanthanide ions is taking place efficiently. It is also verified that the synthesized complex has a higher quantum efficiency value when compared to the precursor complex, due to the replacement of water molecules by organic ligands. It is concluded, therefore, that the proposed complex was successfully synthesized and that it is potentially applied in areas such as bioimaging and sensing, for example.

Acknowledgments

CNPq (procs: 141081/2020-1 and 317610/2021-0).

46^o Reunião Anual da Sociedade Brasileira de Química: "Química: Ligando ciências e neutralizando desigualdades"

Sensitization of lanthanide complexes through direct spin-forbidden singlet - triplet excitation

Airton G. Bispo-Jr (PQ),¹ Italo O. Mazali (PQ),¹ Fernando A. Sigoli (PQ)^{1*}

agbj@unicamp.br; fsigoli@unicamp.br

¹Department of Inorganic Chemistry, Institute of Chemistry, University of Campinas, Unicamp, Brazil.

Keywords: Luminescence, Rare-earths, Lanthanides, Coordination chemistry, Energy conversion.

Highlights

Which would be the photophysical parameters if lanthanide (Ln^{III}) complexes could be directly excited through spin-forbidden singlet (S₀) - triplet (T_n) transitions?

Herein, homobimetallic Eu^{III}, Tb^{III}, Er^{III}, and Yb^{III} complexes with halogen-substituted benzoate ligands are presented.

As halogens and Ln^{III} atomic numbers increase, intense singlet - triplet absorption/excitation bands and relative quantum yields up to 18% were achieved due to an increased spin-orbit coupling effect.

The near-UV-shifted excitation may enable application in luminescent solar concentrators, where Yb^{III} near-infrared luminescence matches the maximum efficiency of the crystalline Si photovoltaic cell.

Abstract

The bright photoluminescence coming from 4*f*-4*f* electronic transitions of lanthanide (Ln) complexes has attracted constant interest for application in cell imaging, solid-state lighting, sensors, and luminescent solar concentrators, for instance.^[1,2] Among these fields, luminescent solar concentrators based on Ln^{III} complexes have been investigated to improve the power conversion efficiency of crystalline Si photovoltaic (PV) solar cells taking advantage of their strong absorption within the near-UV or blue spectral regions, where the PV absorption is negligible, and efficient emission within 600 – 1100 nm, while Yb^{III} emission at 980 nm matches the maximum external quantum efficiency of such PVs.^[3] Despite the well-known antenna effect based on S₀ → S_n excitation transitions, which are responsible for the classical Ln^{III} photoluminescence in complexes, new strategies toward improving their luminescent features have still been envisaged.^[1,2] In this context, herein, a new photo-induced excitation pathway for Ln^{III} complexes is presented, based on spin-forbidden S₀ → T_n electronic transitions in a series of homobimetallic Eu^{III}, Tb^{III}, Er^{III}, and Yb^{III} complexes with halogen (X = Cl or Br)-substituted benzoate (bza) ligands.^[1] As the Ln^{III} and ligand weight increase in the [Ln₂(X-bza)₆(H₂O)₂] complexes, intense S₀ → T_n absorption/excitation bands (340 – 450 nm) are favored due to spin-orbital coupling in the organic moieties that relaxes the S₀ → T_n transition selection rule, which also decreases the pseudo-Stokes shift.^[1] Moreover, emission quantum yields up to 18% were achieved due to the characteristic Ln^{III} emissions within the visible (Eu^{III} and Tb^{III}) or near-infrared (Er^{III} and Yb^{III}) spectral regions.^[1] The near-UV-shifted absorption enables application in luminescent solar concentrators where Yb^{III} near-infrared luminescence lacking photobleaching and thermal quenching matches the maximum efficiency of crystalline Si photovoltaic cells.^[1] Therefore, this study opens up new research opportunities to boost the luminescent properties of Ln^{III} complexes through S₀ → T_n absorption transition by designing new ligands with superior spin-orbital coupling.^[1]

Acknowledgments

INCT/INOMAT - (CNPq: 465452/2014-0 and FAPESP: 50906-9/2014), FAPESP: 2021/06326-1 and 2020/02614-0 and CAPES.

[1] A. G. Bispo-Jr, F.A. Sigoli and co-workers, *Phys. Chem. Chem. Phys.*, **2022**, *24*, 13565–13570.

[2] A. G. Bispo-Jr; F.A. Sigoli and co-workers, *J. Lumin.*, **2022**, *252*, 119406.

[3] M. J. Crane and co-workers, *ACS Appl. Energy Mater.*, **2019**, *2*, 4560–4565.

Silver(I) complex of isatin-thiosemicarbazone: synthesis, cytotoxicity and DNA binding studies

Andresa A. de Lima (PG),^{1*} Ana B. Lazzarini (PG),¹ Renan D. Zanetti (PQ),¹ Mauro A. Lima (PG),² Fillipe V. Rocha (PQ),² Adelino V. G. Netto (PQ).¹

andresa.lima@unesp.br;

¹Department of Analytical, Physical Chemistry and Inorganic Chemistry, UNESP; ²Department of Chemistry, UFSCar.

Keywords: Cancer; Metal complex; Silver; Isatin-thiosemicarbazone; 1,10-phenanthroline; DNA;

Highlights

A new silver(I)-based complex is active against a panel of tumor cells with low binding affinity to ct-DNA.

Resumo/Abstract

Platinum-based tumor agents have been playing a key role in the treatment of cancer. However, these drugs have some limitations such as toxicity and resistance to some cell lines, reducing the effectiveness of the treatment.¹ Silver complexes have attracted attention due to their anti-proliferative action against microorganisms and tumor cells as well as their low toxicity in humans.² In this study, a new silver complex of formula [Ag(ITSC-Et)(phen)]NO₃.H₂O (ITSC-Et = isatin-thiosemicarbazone and phen = 1,10-phenanthroline) was synthesized based on adaptations of the procedure described by Silva et al.³ The ¹H and ¹³C NMR spectra suggests that ITSC-Et and phen coordinate to Ag(I) as bidentate ligands. Mass spectrometry (ESI-MS), conductivity measurements and elemental analysis are in accordance with the proposed structure. The complex was stable in DMSO solution and in the presence of Cl⁻ ions for 48h. Thereby, the cell viability was evaluated by MTT assay against a panel of tumor cell lines: A2780 cis (cisplatin-resistant ovarian), A549 (lung), MCF-7 (breast) and fibroblast MRC-5 (lung). The silver complex exhibited IC₅₀ values ranging of 5.76 - 8.58 μM. It is noteworthy that the complex was more active in the A2780 cis cell than the reference drug cisplatin. DNA binding assays were performed by spectroscopic titration and circular dichroism techniques. These results suggested that it interacts weakly with DNA (K_b = 7.52 × 10⁴ M⁻¹). Competitive binding assays with Hoechst 33258 and thiazole orange (TO) showed that, upon successive additions of the silver compound, a quenching of 80% and 39%, was observed respectively. Therefore, the interaction with DNA occurs probably via minor groove or by electrostatic forces.

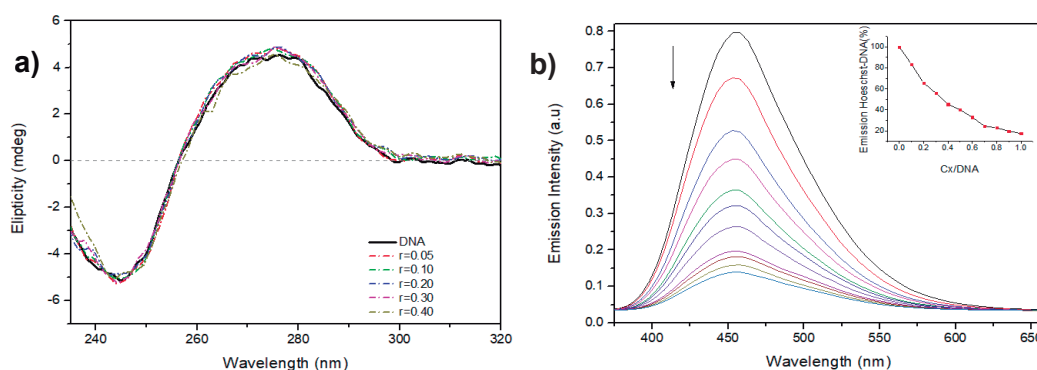


Figure 1: a) CD spectrum in the absence and presence of ct-DNA. b) Emission spectrum of DNA-Hoechst 33258 adducts in the presence of increasing amounts of silver complex.

¹ DILRUBA, S. et al. *Cancer Chemother. Pharmacol.* **2016**, v. 77, n. 6, p. 1103-1124.

² MEDICI, S. et al. *J. Med. Chem.* **2019**, v. 62, n. 13, p. 5923-5943.

³ SILVA, D. E. S. *Dalton Trans.* **2020**, v. 49, n. 16, p. 5264-5275.

Agradecimentos/Acknowledgments

The authors are grateful for the financial support of CAPES (Finance Code 001), CNPQ (132024/2020-9; 422105/2016-3) and FAPESP (2016/17711-5 and 2022/14041-0).

SOD-like activity of copper complexes with amino acids, promising application in agriculture.

Jennyfer C. Silva (PG),¹ Camilla Abbehausen (PQ),¹ Hudson W. P. Carvalho (PQ),² Tiago Tezotto (PQ),² Laura G. Nuevo (IC).^{2*}

jennyfer005@hotmail.com; camilla@unicamp.br

¹Institute of Chemistry, UNICAMP; ²Nuclear Energy Center for Agriculture, USP

Palavras Chave: Copper, Complexes, Amino acids, Superoxide Dismutase, SOD-like, Oxidative stress.

Highlights

Superoxide dismutase (SOD) is an enzyme present in aerobic organisms to protect them from the deleterious action of superoxide ions. Compounds that mimic the action of SOD can present pharmacological benefits and offer protection against stress in plants. The use of metal amino acid chelates as fertilizer has demonstrated several benefits for different cultures. In this project, we evaluated the *in vitro* SOD-like activity of three [Cu(aa)] and we found significant activity. Further studies will be performed to demonstrate the benefits for the cultures of soybean.

Resumo/Abstract

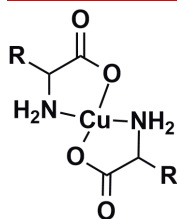


Figure 1. Structure of [Cu(aa)]. aa = Gly, His and Tyr

Aerobic beings such as plants can suffer oxidative stress, caused by reactive oxygen species (ROS), which leads to cellular damage¹. In agriculture, abiotic stress factors such as dry periods, pollutants, salinity, and light intensity, can increase ROS production, resulting in loss of growth and productivity, damage to biomolecules such as lipids, protein

synthesis and, mainly, reducing the photosynthetic rate^{2,3}. The organisms produce a series so defending biomolecules to make ROS less harmful to tissues. Among them, the SOD is a class of metalloenzymes capable of promoting superoxide dismutation into molecular oxygen and hydrogen peroxide⁴. In several conditions, such as disease and stress, the organisms have a significant increase of ROS production or defense mechanisms impaired. In these cases, small molecules could help, and metallic compounds are considered the best candidates to mimic SOD.

Thus, the present work sought to synthesize complexes with antioxidant capacity mimetic the Cu/Zn metalloenzyme SOD1. As the use of metal amino acid chelates have been demonstrating benefits for the supplementation of cultures of foodstock, in this work we preconized whether they could act as SOD mimetics under stress conditions. Firstly, we evaluated the SOD-like activity *in vitro*, finding the best candidates.

The Cu(II) complexes (Figure 1) were obtained from the reaction of amino acids such as Glycine (Gly), Histidine (His) and Tyrosine (Tyr), along with Cu(II) salt. The obtained complexes were characterized by infrared and Uv-Vis spectroscopy (ATR-FTIR). Subsequently, the **CuGly**, **CuHis** and **CuTyr** complexes were tested in the NBT photoreduction competition assay, for superoxide ion generation assay by means of methionine and riboflavin. This assay can quantify the inhibition of formazan formation by scavenging radical superoxide, in different ranges of the complex concentrations, allowing it to correlate with the catalytic activity of SOD. As a result, we calculated the inhibitory concentration at 50% (IC₅₀). The IC₅₀ results correlate with the McCord Fridovich constant (k_{MCCF}) which quantifies the rate of dismutation of the superoxide ion. k_{MCCF} of the native enzyme SOD1 is 5.10¹¹ M⁻¹.s⁻¹. The k_{MCCF} values for the complexes obtained, are discrepant among themselves varying the amino acids (**CuGly** 2,09.10⁷ M⁻¹.s⁻¹, **CuHis** 10,80.10⁷ M⁻¹.s⁻¹ e **CuTyr** 172.10⁷ M⁻¹.s⁻¹). These complexes will be further submitted for *in vivo* tests in soybean plants, to evaluate the antioxidant capacity after suffering saline stress.

- [1]. Liu, J. et al. *Jour. of Agri. and Food Chem.* **2020** 68 (47), 13608-13619;
- [2]. Rene, J. et al. *Front. in Plant Sci.* **2022** 12 778270;
- [3]. Oikawa, K. et al. *Nat Commun.* **2022** 13 7493;
- [4]. Demidchik, V. *Envir. and Exp. Botany.* **2015** 109 212-228

Agradecimentos/Acknowledgments

This project was supported by Capes, FAPESP 2019/16904-2 and CNPq 404668/2021-6.

46^o Reunião Anual da Sociedade Brasileira de Química: "Química: Ligando ciências e neutralizando desigualdades"

Soot reduction catalysts CeO₂ obtained by thermal decomposition of cerium-based Metal-Organic Frameworks MOF-76

Viviane de Carvalho Gomes (PG),¹ **Oswaldo Antonio Serra** (PQ),^{1*} **Ayla Roberta Borges Serra** (PG).²

vivianegomes@usp.br; osaserra@usp.com.br

¹Departamento de Química, FFCLRP-USP; ²Departamento de Engenharia Química, UFSCar.

Keywords: Rare Earths, Catalysis, Ceria, Soot, MOFs.

Highlights

Here we synthesized ceria (CeO₂) catalysts by thermal decomposition of MOF-76 at different temperatures from 300°C to 900°C. Usually the soot (Printex®) decomposes at 610°C but in the presence of catalysts it is possible decrease. For example, in the presence of ceria obtained by Pecchini's method the soot decomposition occurs at 458°C. Using CeO₂ obtained from MOFs this temperature dropped to 370°C, the best result found in literature until now. CeO₂ calcined at lower temperatures (<500°C) showed larger surface area (S_{BET}) than ceria synthesized by usual methods, and superior volume of adsorbed gas at lower programmed reduction temperature (TPR).

Resumo/Abstract

Particulate matter (PM) has become an issue causing diseases and decreasing life expectancy around the world, turning eminent the necessity for efficient catalyzer for the soot reduction process. Cerium-based oxide catalysts were synthesized from thermal decomposition of MOF-76 (Metal-Organic Frameworks). The synthesis of the MOF Ce-BTC was made through a simple process of direct precipitation at low temperature (50°C) using water and ethanol as solvent. Thermal decomposition was carried out at different temperatures: 300°C, 400°C, 500°C, 700°C and 900°C, obtaining ceria (CeO₂) with fluorite structure. The TGA/DSC and XRD analyzes showed that oxides obtained at temperatures under 500°C has amorphous characteristics, which crystallinity grows with increase of calcination temperature until 900°C. SEM analysis indicates the major presence of nanorod morphology with dimensions varying from 100 to 120 nm for samples calcined by lower temperatures, while the presence of nanospheres increases with high calcination temperatures. The adsorption/desorption of N₂ isotherms, combined with BET and BJH analysis indicated that oxides calcined under 500°C has good interaction with gas (Type IV), large surface area S_{BET} (69,01 to 95,05 m².g⁻¹), beyond materials with high porosity (0,108 to 0,128 cm³.g⁻¹) and mesoporous well distributed by the structure (54,8 to 69,5 Å). On the other hand, ceria obtained by decomposition above 500°C demonstrated weaker interaction with gas phase (Type V), inferior surface area S_{BET} (5,43 to 17,20 m².g⁻¹) and lower porosity (0,009 to 0,039 cm³.g⁻¹) with porous shortly distributed (97.3 to 126 Å). Catalytic tests were performed by homogeneous mixture between the catalyst and soot of Printex® model, which the blends were submitted to TGA/DSC analysis, identifying the highest point of the soot's decomposition T_m. Soot without catalyst decomposes around 610°C, soot in contact with ceria obtained by the usual Pecchini's method decomposes at 458°C, while soot at presence of the produced ceria from MOF-76 lowered this temperature to the range of 425 to 370°C. Among the produced ceria from MOF-76 through direct precipitation, the CeO₂ calcinated at 400°C demonstrated greater catalyst properties (BET and TPR) and higher catalyst efficiency reaching the lowest registered soot's reduction temperature with ceria catalyst (TGA/DSC).

[1] Liu K., You H., Zheng Y., Jia G., Huang Y., Yang M., et al. Room-temperature synthesis of multi-morphological coordination polymer and tunable white-light emission. *Cryst Growth Des.* 2010;10(1):16–9.

[2] Nascimento L.F., Serra O.A. Washcoating of cordierite honeycomb with ceria-copper mixed oxides for catalytic diesel soot combustion. *Process Safety and Environmental Protection.* 2016;101:134–43.

[3] Chen Z., Chen L., Jiang M., Gao X., Huang M., Li Y., et al. Controlled synthesis of CeO₂ nanorods and their promotional effect on catalytic activity and aging resistibility for diesel soot oxidation. *Appl Surf Sci.* 2020;510.

Agradecimentos/Acknowledgments

CNPq, CAPES e FAPESP.

46ª Reunião Anual da Sociedade Brasileira de Química: "Química: Ligando ciências e neutralizando desigualdades"

Spectroscopic and theoretical study of a red-emitting Eu^{3+} -phosphor/PMMA film: An adapted approach to extract the photophysical parameters

Leonardo F. Saraiva (PG)^{1,2}, Airtton G. Bispo-Jr (PQ)^{3,4}, Sergio A. M. Lima (PQ)^{1,2}, Ana M. Pires (PQ)^{1,2}.

leonardo.f.saraiva@unesp.br

¹Department of Chemistry and Biochemistry, FCT-UNESP; ²Department of Chemistry, IBILCE-UNESP; ³Institute of Chemistry, IQ-UNICAMP; ⁴ Department of Chemistry and Biomolecular Sciences, University of Ottawa.

Keywords: Lanthanides, Photoluminescent spectroscopy, Theoretical methods, Red-emitting film, New procedure, LEDs.

Highlights

The photophysical properties of the new red-emitting $\text{SrY}_2\text{O}_4:\text{Ce}^{3+}, \text{Eu}^{3+}/\text{PMMA}$ film were thoroughly studied from PL spectroscopy and an adapted theoretical approach, revealing its potential for LED application.

Abstract

Luminescent materials based on trivalent lanthanide ions, Ln^{3+} , have often been employed in light-emitting diodes (LEDs), which is currently the main solid-state lighting (SSL) technology [1]. Tailoring the phosphor photophysical aspects is essential to map strategies to boost their performance, which can also be done by employing theoretical approaches to obtain further opto-structural correlations. The theoretical approaches reported so far for Ln^{3+} systems mainly encompass complexes, inorganic phosphors, or glasses [2], while no description has been found for Ln^{3+} -based polymeric films whose luminescent and structural features enable their use in SSL. Therefore, an adapted theoretical approach is introduced here, based on modeling the surface interaction between the supercell containing Eu^{3+} and the poly(methyl) methacrylate (PMMA) polymer in the novel $\text{SrY}_2\text{O}_4:\text{Ce}^{3+}(2\%), \text{Eu}^{3+}(3\%)/\text{PMMA}$ film. All the calculations were performed using the extended tight-binding GFNn-xTB code by adding over 50 monomer groups around a $2 \times 2 \times 2$ supercell considering the Y^{3+} sites replacement by Eu^{3+} [1]. The polymer effect in the $\text{Eu}-\text{O}$ bonds was extracted from the Hellmann-Feynman theorem to calculate the theoretical Judd-Ofelt (JO) intensity parameters (Ω_λ , $\lambda = 2, 4, 6$). Photoluminescence emission spectra of all films obtained by changing the phosphor weight amount exhibited the usual set of $^5\text{D}_0 \rightarrow ^7\text{F}_{0-4}$ transitions in the orange-red spectral region characteristic of Eu^{3+} occupying low-symmetry sites. The theoretical description unraveled the presence of non-covalent interactions in the phosphor-PMMA surface, whose forces were decomposed from the Hellmann-Feynman theorem, allowing the estimation of the effective force constants, which were inversely proportional to the $\text{Eu}-\text{L}$ distance. Also, the strengthening of the phosphor-PMMA interactions promoted angular distortions of the axial oxygens in the EuO_6 polyhedra, leading to variations in the experimental Ω_2 values since they are sensible to bond angle deformations. Additionally, the proximity of different groups with Eu^{3+} in the supercell favors the deactivation of the $\text{Eu}^{3+} \ ^5\text{D}_0$ excited-state, due to oscillations of the polymer chain. Lastly, the theoretical $\Omega_{2,4,6}$ were determined by decomposing the parameters into the forced-electric dipole (FED) and dynamic coupling (DC) mechanism contribution, where the latter was dominant in all cases. Hence, a computational methodology was developed to derive the $\Omega_{2,4}$ parameters of the $\text{SrY}_2\text{O}_4:\text{Ce}^{3+}, \text{Eu}^{3+}/\text{PMMA}$ film with a suitable concordance with the experimental data. Furthermore, the obtained data on the photo-structural features enable designing and tailoring new materials for solid-state lighting.

Acknowledgments

FAPESP (2022/08409-4), CNPq (304003/2018-2 and 309448/2021-2) Laboratory of Luminescent Materials from IQ-UNESP.

[1] L. F. Saraiva, A. G. Bispo-Jr, S. A. M. Lima, A. M. Pires, *J. Alloys and Compounds* 938 (2023) 168595

[2] A. N. C. Neto, et al. *Handbook on the Physics and Chemistry of Rare Earths* – Chapter 310, 56 (2019) 55 – 162

Spectroscopic investigation of the recombinant human cofilin-1: a bioinorganic study

Ana Claudia Silva Gondim* (PQ)¹, Leonardo Alves Linhares (IC)¹, Luiz Henrique da Costa Souza (PG)¹, Eduardo Henrique Silva de Sousa (PQ)¹, Izaura Cirino Nogueira Diógenes (PQ)¹.

acgondim@dqoi.ufc.br

¹Laboratório de Bioinorgânica, Universidade Federal do Ceará, Fortaleza, Brazil

Palavras Chave: Parkinson's disease, Cofilin-1, Spectroscopy, Bioinorganic.

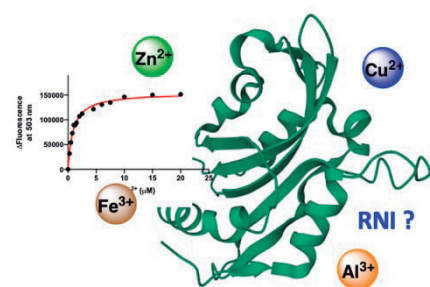
Highlights

Cofilin-1 is implicated in Parkinson's disease

Recombinant production of cofilin-1 and spectroscopic investigations

Interaction and structural modifications promoted by metal ions and RNI

Resumo/Abstract



Complex and incurable neurodegenerative diseases such as Alzheimer's and Parkinson's disease affect millions of people around the world and have raised great interest and concern of the scientific community.¹ The formation of protein aggregates has been a hallmark of neurodegenerative diseases including Parkinson's Disease (PD). Some proteins expressed in the brain are susceptible to misfolding and aggregation processes such as α -synuclein, which has been implicated along with others in Parkinson's disease². The role of transition metals or other agents in the protein aggregation process, particularly α -synuclein, has been explored by bioinorganic chemistry community. In this context, human cofilin-1, a protein with several biological roles, including

potentially involved in PD, has likely an important role in the early stages of neurodegenerative process³. Aiming to shed light on species that could interact with cofilin-1 and eventually lead to misfolding and or aggregation, recombinant production and structural investigation of this protein was carried out. By employing fluorescence, circular dichroism and thiol reactive reagent, metal ions were investigated as well as RNI (reactive nitrogen species, e.g., NO and HNO). Initially, optimization of the routine of fluorescence assay involving the human Cofilin-1 in the reduced and oxidized forms (free thiols or disulfide bridges) was carried out along with the investigation of its possible interaction with ions (Fe^{3+} , Zn^{2+} , Cu^{2+} and Al^{3+}). Intrinsic and extrinsic fluorescence were explored either using excitation of the tryptophan residue or bis-ANS. The results suggested an apparent interaction of the ions at least with native cofilin-1. There are changes in the maximum of the protein emission indicating conformational changes along with an increase in the light scattering using Zn^{2+} even at below $15 \mu\text{mol L}^{-1}$, which was also noticed for Al^{3+} . This observation is encouraging and may, eventually, assist on further investigation of the possible mechanisms of cofilin-1 in the neurodegenerative diseases, especially in PD. Extrinsic fluorescence using bis-ANS showed a K_d for this probe at $3.9 \mu\text{mol L}^{-1}$, whose studies indicated disturbance of profile upon use of metal ions. These measurements provided an apparent K_d for some of the metal ions. Zinc ions showed binding without much change in the bis-ANS emission profile, while iron(III) and copper(II) ions caused major changes. Circular dichroism has been done to evaluate conformational changes as well oxidation of the thiols of cofilin-1, which has also been explored upon treatment with NO and HNO donors. These studies opened exciting opportunities to shed some light on the possible biological role of these metal ions and reactive nitrogen species with human cofilin-1, considering these species might be detected in the brain.

Agradecimentos/Acknowledgments

All the authors are thankful to CAPES (Finance Code 001, PROEX 23038.000509/2020-82) and FINEP (CV. 01.22.0174.00) for the financial support and Dr Fábio Klamt (UFRS) for biological discussions.

¹DORSEY, E. R. et al. *The Lancet Neurology*, v. 17, n. 11, p. 939–953, 2018

²SOTO, C.; PRITZKOW, S. *Nature Neuroscience*, v. 21, n. 10, p. 1332–1340, 2018.

³LOPES, F. M. PhD Thesis, Universidade Federal do Rio Grande do Sul, Porto Alegre, 2017.

Spectroscopic Observation and Characterization of a Ruthenium-Enoic Carbene Complex Relevant to Olefin Metathesis

Leonildo A. Ferreira (PQ)¹ and Henri S. Schrekker (PQ)²

leonildoferreira@ufg.br

¹Instituto de Química, Universidade Federal de Goiás - UFG, Campus Samambaia, Goiânia, GO; ²Instituto de Química, Universidade Federal do Rio Grande do Sul - UFRGS, Campus do Vale, Agronomia, Porto Alegre, RS.

Palavras-Chave: Metátese de olefinas, Alquilideno, Carbeno, Rutênio, Ressonância magnética nuclear.

Highlights

Reaction between Grubbs second generation complex with maleic acid.

First time a ruthenium-enoic carbene was detected during a reaction.

Novel complex observed and characterized NMR spectroscopy.

Abstract

The olefin cross-metathesis with acrylic or maleic acid derivatives offers a remarkably efficient protocol to prepare market-relevant chemicals. Nevertheless, drawbacks associated with the low reactivity of such electron deficient olefins and the presumably high instability of the organometallic intermediates generated during the olefin metathesis catalytic cycle typically demand the use of unpracticable amounts of the catalyst, hindering the development of low-cost processes. Understanding the nature of such intermediates could potentiate the efforts in designing more robust catalysts and surpass such obstacles, as has been demonstrated for other intermediates formed during the catalytic cycle in olefin metathesis. In this sense, the reaction of second-generation Grubbs metathesis complex (**GII**) with maleic acid (**MA-H**) was monitored by ¹H and ³¹P{¹H} NMR spectroscopy (Chart 1). The reaction was chosen as an attempt to observe the formation of a ruthenium-enoic carbene complex since this is, *a priori*, the only possible alkylidene intermediate for this reaction. The intermediate could be observable as a trapped 16-electrons complex. Gratifyingly, the reaction resulted in the formation of only a novel ruthenium-alkylidene complex and occurred at mild conditions (°C, in thf-*d*₆) over the course of several hours. The formation of this novel alkylidene was identified to be a ruthenium-enoic carbene complex (**Ru-CHCO₂H**) by ¹H-¹³C HSQC and ¹H-¹³C HMBC NMR. Unfortunately, formation of unidentified alkylidene-free species rivels with the enoic complex, turning the purification and isolation of **Ru-CHCO₂H** highly difficult.

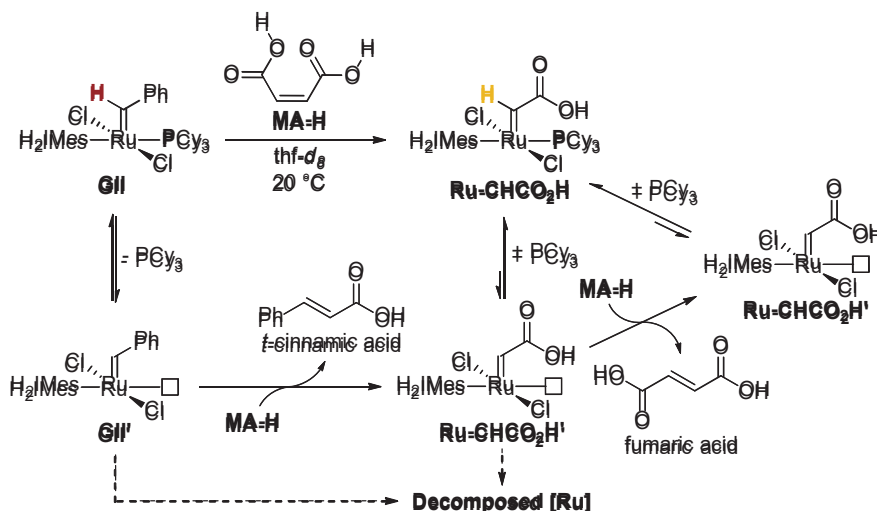


Chart 1. Schematic representation of the reaction between **GII** and maleic acid resulting in the formation of the Ru-enoic carbene complex.

Acknowledgments

Coordenação de Aperfeiçoamento de Pessoal de Nível Superior (Capes) is thanked for the financial support.

Structural and luminescent investigation of Eu^{3+} -activated MgAl_2O_4 co-doped with alkaline metals for WLEDs

Maria Eduarda Marra Mesti¹, Leonardo Figueiredo Saraiva¹, Ana M. Pires^{1,2} and Sergio A. M. Lima^{1,2}

E-mail: marra.mesti@unesp.br

¹Department of Chemistry and Biochemistry, University of São Paulo State, FCT-UNESP, Presidente Prudente – SP, Brazil;

²University of São Paulo State, Institute of Biosciences, Humanities and Exact Sciences, IBILCE-UNESP, São José do Rio Preto - SP, Brazil.

Palavras Chave: solid-state lighting, europium(III), aluminates

Highlights

Red-emitting Eu^{3+} -activated $\text{MgAl}_2\text{O}_4:\text{M}^+$ ($\text{M} = \text{Na}, \text{K}$) phosphors synthesized from an adapted Pechini route exhibiting the ${}^5\text{D}_0 \rightarrow {}^7\text{F}_{0-4}$ set of transitions with high color purity in the red spectral region.

Abstract

Nowadays, LEDs are considered as the state-of-the-art technology in solid-state lighting, due to their lower energy consumption and higher efficiency compared to other sources [1]. They are widely used in different fields, and further improvement of their properties is the focus of several researchers. Among the methods for producing white LEDs (WLEDs), the current used commercially is the phosphor-converted hybrid-LED, although it suffers from a low color rendering index (CRI) and high color correlated temperature (CCT) due to the lack of red-emitting component [1]. This study reports the photoluminescence properties of Eu^{3+} -based MgAl_2O_4 co-doped with Na^+ or K^+ , at 2 and 3%, red-emitting phosphor synthesized by an adapted Pechini route [2] at 1000 °C, and air atmosphere. XRD data confirmed that all samples formed by the MgAl_2O_4 spinel single-phase. From Rietveld refinement, the M-O experimental bond length ($\text{M} = \text{Mg}^{2+}, \text{Al}^{3+}$) was determined, and the arrangement of one Mg^{2+} tetrahedra-site was elucidated. XPS analysis for Eu^{3+} -doped sample indicated the absence of surface contamination. Excitation spectra of samples monitoring the ${}^5\text{D}_0 \rightarrow {}^7\text{F}_2$ transition at 619.5 nm displayed the charge transfer band (CTB) $\text{O}^{2-} \rightarrow \text{Eu}^{3+}$ as the most intense, while the narrow band assigned to ${}^7\text{F}_0 \rightarrow {}^5\text{L}_6$ at 394 nm exhibited the highest relative intensity among the $f-f$ transitions. Emission spectra recorded under excitation in the CTB revealed the splitting of the ${}^5\text{D}_0 \rightarrow {}^7\text{F}_0$ transition into two components, implying the insertion of Eu^{3+} in at least two non-equivalent low-symmetric sites lacking an inversion center [3], since the band assigned to the ${}^5\text{D}_0 \rightarrow {}^7\text{F}_2$ hypersensitive transition was the one with the highest relative intensity. In this sense, ten components were expected for this transition, following the splitting of $2J+1$ for non-Krammer ions; however, only four components were observed at room temperature. Among all samples, the 3%- $\text{Eu}^{3+}, \text{K}^+$ -doped exhibited the highest relative intensity, suggesting the decrease of defect concentration in the lattice with the insertion of the co-dopant, leading to higher radiative decay rates. Lastly, the 1931 Chromaticity Diagram (CIE) of the samples reveal high color purity in the red spectral region, with a value of approximately 99%. Thus, all results ensure that the red-emitting phosphor was successfully synthesized as suggested and the spectroscopic data confirmed that it is a promising candidate for developing a WLED prototype.

Acknowledgments

CAPES 88887.686150/2022-00, FAPESP (22/09504-0), CNPq (304003/2018-2 and 309448/2021-2).

References

- [1] A. G. Bispo-Jr; L. F. Saraiva; S. A. M. Lima; A. M. Pires; M. R. Davolos. *Journal of Luminescence*, 237, 2021, 118167. [<https://doi.org/10.1016/j.jlumin.2021.118167>]
- [2] Oliveira, N. A.; Bispo-Jr, A. G.; Shinohara, G. M. M.; Lima, S. A. M.; Pires, A. M. *Mat. Chem. And Phys.* 2021, 257, 123840. [<https://doi.org/10.1016/j.matchemphys.2020.123840>]
- [3] Binnemans, K. *Coord. Chem. Rev.* 2015, 295, 1. [<https://doi.org/10.1016/j.ccr.2015.02.015>]

Structural and photoluminescent properties of novel lanthanide dipivaloymethanate complexes: A platform for investigation of LMCT transitions

Paulo R. S. Santos (PG)^{1*}, Ashely A. S. S. de Jesus (IC)¹, William B. de Lima (IC)¹, Wagner M. Faustino (PQ)¹, Israel F. Costa (PQ)², Lucca B. Guimarães (PG)², Maria Claudia F. C. Felinto (PQ)³, Hermi F. Brito (PQ)², Renata Diniz (PQ)⁴ and Ercules E.S. Teotonio (PQ)¹

roberto.santos.p.s@outlook.com

¹Department of Chemistry, Federal University of Paraíba, João Pessoa–PB, Brazil; ²Institute of Chemistry, University of São Paulo (USP), São Paulo–SP, Brazil; ³Nuclear and Energy Research Institute–IPEN/CNEN, São Paulo–SP, Brazil ⁴Department of Chemistry ICE, Federal University of Minas Gerais

Keywords: Lanthanide complexes, dipivaloymethanate, LMCT transitions, bis(diphenylphosphine)

Highlights

Novel Ln-dipivaloymethanate complexes with bis-phosphine oxide ligands were successfully synthesized. The role of LMCT states in the luminescent properties have been investigated.

Resumo/Abstract

Luminescent lanthanide compounds are widely studied due to their unique photophysical properties for applications in optical materials, LED's, sensors and biological markers, luminescent thermometers. However, most of these systems have been obtained in the form of simple molecular entities. Recently, new di- or polynuclear systems containing diketonate ligands have been investigated in focusing on a deeper understanding of energy processes. In particular, Eu-dipivaloymethanate complexes are characterized by low energy charge transfer (LMCT) states.[1] In this context, the present work reports the synthesis, characterization and photophysical properties of compounds with the general formula $[Ln_2(dpm)_6(dppeO_2)]$, where dpm: dipivaloymethane dppeO₂: 1,2-bis(diphenylphosphino)ethane oxide, Ln: Eu³⁺, Tb³⁺, Sm³⁺, Dy³⁺ and Gd³⁺. These complexes were prepared by direct reaction between ethanolic solutions of the respective LnCl₃·6H₂O salts with dppeO₂ and dpm ligands in the molar ratio 1:1:3.[2] The FT-IR spectra of the complexes show a redshift of the band attributed to the vibrational mode $\nu(C=O)$, suggesting that dpm is coordinated to the Ln³⁺ ion in chelating mode. All complexes had their structures elucidated by the single crystal X-ray technique, indicating that they are isomorphs and crystallize in a triclinic crystal group, P-1 space group. In addition, The structures are constituted by a symmetric dinuclear unit, in which the lanthanide ion is found in a chemical environment belong to C_{3v} point group (**Fig. 2b**). The diffuse reflectance spectra of the Eu³⁺, Tb³⁺ and Gd³⁺ complexes (**Fig. 1a**) exhibit strong absorption bands in the 200-450 nm range attributed to dpm ligand S₀→S₁ transition. For [Eu₂(dpm)₆(dppeO₂)] complex, it is also observed a shoulder in the longer wavelength region that can be assigned to a low energy LMCT transition. The high relative intensities between the ligand excitation band and the 4f-4f transitions in the Tb³⁺, Sm³⁺ and Dy³⁺ complexes indicate an efficient ligand-to-lanthanide energy transfer process. On the other hand, the ligand band exhibit very low intensity for the Eu³⁺ complex (**Fig. 1b**), indicating the presence of an efficient suppression channel from ligand states via LMCT. Overall, the emission spectra display characteristic narrow bands attributed to the intraconfiguration Ln³⁺ ion transitions. The absence of a broad band in these spectra efficient suggest an efficient intramolecular energy transfer (**Fig. 1c**) for the complexes of Tb³⁺, Sm³⁺ and Dy³⁺ ions.

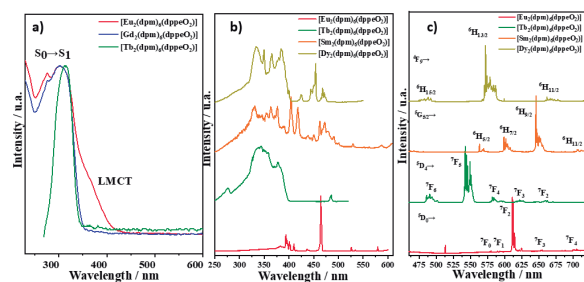


Figure 1. (a) Reflectance spectra in the UV-VIS region. (b) Complex excitation spectra 77 K and (c) Complex emission spectra 77 K

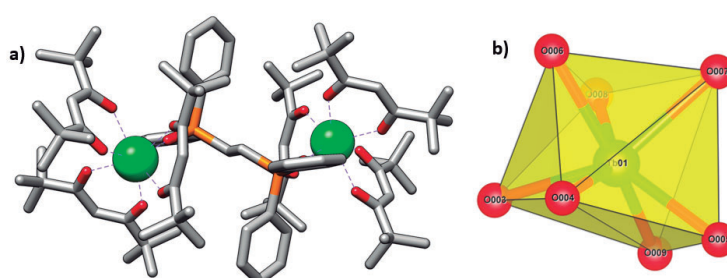


Figure 2. Structure of complex $[Ln_2(dpm)_6(dppeO_2)]$ Ln = Eu³⁺, Tb³⁺ e Gd³⁺

Acknowledgments

This work was supported by CNPq, FAPESP, FINEP, CAPES and UFPB.

[1] Kitagawa, Y. *et al.* (2017) *Chemistry - A European Journal*, 27(1), pp. 264–269.

[2] Teotonio, E. E. S. *et al.* (2009) *Optical Materials*, 32, pp. 345-349.

Structural and spectroscopic characterization of a diorganotin(IV) complex with an isoniazid derivative

Pedro H. de O. Santiago (PQ),¹ Claudia C. Gatto (PQ),² Javier Ellena (PQ)¹

pedrophs.santiago@gmail.com

¹Instituto de Física de São Carlos, Universidade de São Paulo - USP; ² Instituto de Química, Universidade de Brasília - UnB

Palavras Chave: Hydrazone, Diorganotin(IV) complex, Crystallography.

Highlights

A pentacoordinated dimethyltin(IV) with hydrazone ligand was obtained and characterized by single crystal X-ray diffraction and spectroscopic techniques.

Abstract

The use of isoniazid and its derivatives for the development of new metal complexes attracted interest in the last years due to the possibility of obtaining bioactive compounds, which can show antitumor, antitubercular and antibacterial properties.¹⁻³ In this work, we report the synthesis and characterization of a dimethyltin(IV) complex with isoniazid derivative as a ligand, aiming to obtain a complex with antitumor properties.

The reaction of 2-hydroxyacetophenoneisonicotinichydrazone (H_2L) with the diorganotin(IV) complex resulted in the complex $[SnMe_2(L)]$. The NMR (1H and ^{13}C), FTIR and UV-Vis experiments indicate the formation of a mononuclear complex, with the metal center in a pentacoordinated environment attached to two methyl ligands and to one hydrazone ligand. The single crystal X-ray diffraction analysis confirms the proposed structure (Figure 1a), with the hydrazone acting as a tridentate ligand, coordinated to the Sn(IV) cation through the *ONO* chelating system, and the Sn1 ion in a distorted square pyramid geometry. The Hirshfeld surface analysis (Figure 1b) showed the presence of non-classical hydrogen bonds, and $Sn\cdots N$ and $\pi\cdots\pi$ stacking interactions in the crystal lattice of the complex.

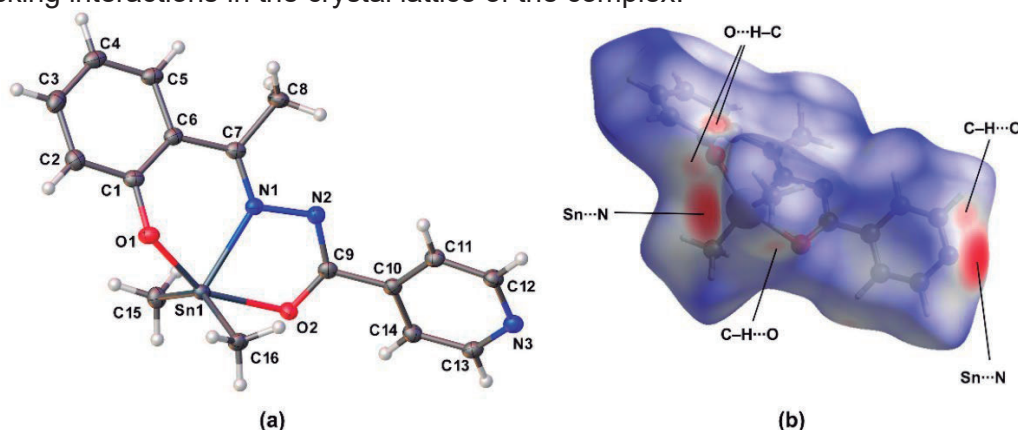


Figure 1. (a) Crystal structure of $[SnMe_2(L)]$ and (b) Hirshfeld surface mapped with d_{norm} .

[1] Fregonezi, N. F. et al.; *Regulatory Toxicology and Pharmacology*, **2020**, 113, 104653.

[2] Firmino, G. S. S. et al.; *Biometals*, **2016**, 29, 953.

[3] Mezey, R. et al.; *Polyhedron*, **2015**, 102, 684.

Acknowledgments

The authors are grateful for the support from IFSC-USP, IQ-UnB and FAPESP (2017/15850-0 and 2021/10066-5).

Study of a new chemosensor based on 1.8 naphthalic anhydride.

Janail R. Silva¹ (PG), Izilda A. Bagatin (PQ).¹

janail.rodrigues@unifesp.br¹;

*Instituto De Ciências Ambientais, Químicas e Farmacêuticas – ICAQF – UNIFESP – Diadema - SP
Laboratório de Química de Calixarenos, Espectroscopia Molecular e Catálise LQCEMC*

Palavras Chave: *Chemosensor, hydrogen bond, fluorescence*

Highlights

Potential probe for ions such as F⁻, Br⁻, Ni²⁺, and Hg²⁺. Utilization of amide-bonded working groups and associated luminescent groups. Ligand with solid potential to recycle high-value materials.

Resumo/Abstract

New chemosensors have been constantly developed to identify potentially toxic environmental species¹. In this sense, a luminescent molecule was developed to identify species through hydrogen bonding. In the first step, 4-bromobenzohydrazine-1.8-naphthylimide was synthesized, obtaining the following ¹H NMR signals (δ CDCl₃, 300 MHz), ppm: 7.68, (d, Ar-CH) and 7.78 (d, Ar-CH), 7.82 ppm (t, CH) 8.31 ppm (dd, CH), 8.42 ppm (s, NH), 8.69 ppm (dd, CH). In preliminary analyses using UV-Vis spectroscopy, it was possible to determine the pKa of this new molecule obtaining a value of 9,3, demonstrating its operating range. To verify the synthesized compounds' interaction with the proposed ions, titrations of the ligand were performed, and good interaction with fluoride ions was observed. An isosteric point was found at approximately 240 nm and 256 nm. Also, the band's decrease at 231 nm and its respective bathochromic shift to 233 nm, adding two new bands at 248 nm and 275 nm, depicted the ligand equilibrium with F⁻-occurring. This typical interaction must be linked to the hydrogen bonding of the N-H group with F⁻, i.e., N-H...F⁻ without intermediates. Further analyses will be performed to confirm such interactions using luminescence techniques. The results are preliminary but demonstrate a potential probe.

¹ ZIMMERMANN-DIMER, Lizandra Maria; MACHADO, Vanderlei Gageiro. Quimiossensores cromogênicos e fluorogênicos para a detecção de analitos aniônicos. Química Nova, v. 31, p. 2134-2146, 2008.

Agradecimentos/Acknowledgments

O presente trabalho foi realizado com apoio da Coordenação de Aperfeiçoamento de Pessoal de Nível Superior – Brasil (CAPES) – Código de Financiamento 001

Study of the behavior of complexes $[\text{Ru}_3\text{O}(\text{CH}_3\text{CO}_2)_6(\text{py})_2\text{NO}]\text{PF}_6$ and $[\text{Ru}_3\text{O}(\text{CH}_3\text{COO})_6(\text{py})_2(\text{NO}_2)]$ in aqueous medium.

Hugo E. Barbosa (PG),¹ Amanda B. Silva (IC),¹ Ana P. de L. Batista (PQ)², Sofia Nikolaou (PQ)¹

hugoelias@usp.br

¹Departamento de Química, Faculdade de Filosofia, Ciências e Letras de Ribeirão Preto (FFCLRP-USP)

²Departamento de Química, Universidade Federal de São Carlos (UFSCAR)

Keywords: (Triruthenium cluster, metallodrug, reactivity, NORMs).

Highlights

In this work it was verified that the complex $[\text{Ru}_3\text{O}(\text{CH}_3\text{COO})_6(\text{L})_2\text{NO}]\text{PF}_6$ (**1**) has reactivity in aqueous medium dependent on the pH. The spectral changes are significant at high pH values (above pH 9) and literature suggests that the product of this reactivity is $[\text{Ru}_3\text{O}(\text{CH}_3\text{COO})_6(\text{py})_2(\text{NO}_2)]$ (**2**). However, in acid environment, the nitrite compound does not convert to **1**. From **2** electronic spectrum profile, it was suggested a high lability of NO_2^- ligand in aqueous environment.

Resumo/Abstract

In recent years our research group has been studying the coordination compounds of general formula $[\text{Ru}_3\text{O}(\text{CH}_3\text{COO})_6(\text{L})_2\text{NO}]\text{PF}_6$ (L = 4-acetylpyridine; 4-tertbutylpyridine; isoquinoline; 3-methylpyridine and 4-methylpyridine).¹ The complexes of this class constitute multiconfigurational systems better described by the Enemark-Feltham notation $\text{Ru}(\text{III})\text{Ru}(\text{III})[\text{RuNO}]^6$, where $[\text{RuNO}]^6$ stands for different contributions of the main configurations $\text{Ru}(\text{III})\text{-NO}^0$ and $\text{Ru}(\text{II})\text{-NO}^+$.¹ These compounds perform NO controlled release and interesting chemical properties,¹ therefore it is necessary to investigate their behavior in aqueous medium aiming their biological applications. The synthesis of the complex $[\text{Ru}_3\text{O}(\text{CH}_3\text{COO})_6(\text{py})_2\text{NO}]\text{PF}_6$ was made according to the literature¹ and the reactivity experiments were performed by adding 650 μL of a 60 mM complex solution in acetonitrile to 2.35 mL of water solutions at different pH values (produced by adding NaOH or HCl). The solutions were left to stand for 30 min and the spectral changes were recorded with an Agilent Carry 60 UV-vis spectrometer at 35 °C. From pH 1 to pH 9, compound **1** is inert, since there are no spectral changes (Figure 1). At pH 10, it was observed the formation of an intermediate with $\lambda_{\text{max}} = 551 \text{ nm}$ and, above this pH value, it is converted to a final species with $\lambda_{\text{max}} = 355 \text{ nm}$ and 882 nm . The species produced at pH 10 was monitored during 12 hours. After this time interval, it was noticed its conversion to the same spectral profile observed at pH 13, confirming the intermediate character of the species displaying $\lambda_{\text{max}} = 551 \text{ nm}$. With this in mind, and knowing that in basic medium there may be a nucleophilic attack by OH^- ions that converts coordinated NO^+ to NO_2^- ,² the final species ($\lambda_{\text{max}} = 355 \text{ nm}$ and 882 nm) observed between pHs 10 and 14 was assigned as $[\text{Ru}_3\text{O}(\text{CH}_3\text{COO})_6(\text{py})_2(\text{NO}_2)]$. The fact that the nucleophilic attack is observed at relatively high pH values agrees with molecular modeling results³ which described the ground-state electronic structure of **1**, confirming its multiconfigurational character and revealing a major contribution of the $\text{Ru}(\text{III})\text{-NO}^0$ configuration, that would be less susceptible to nucleophilic attack. We have then compared the acid-base behavior of the complex $[\text{Ru}_3\text{O}(\text{CH}_3\text{COO})_6(\text{py})_2(\text{NO}_2)]$ (**2**), obtained according to literature.⁴ Surprisingly, in a pH 1 water solution of **2** the expected conversion of **2** to **1** was not observed. The spectra of aqueous solutions of **2** at different pH values were invariant, indicating that the NO_2^- ligand might be dissociated before its conversion to coordinate NO^+ .

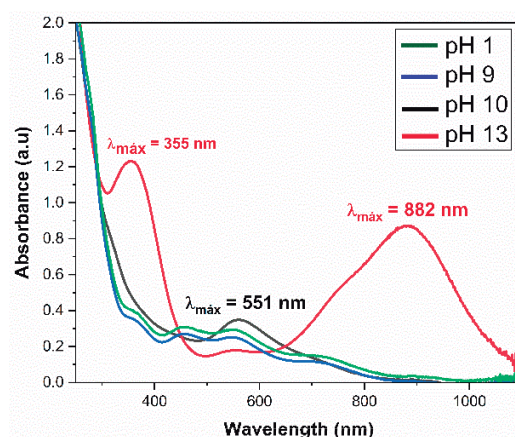


Figure 1. Electronic absorption spectra of the $[\text{Ru}_3\text{O}(\text{CH}_3\text{CO}_2)_6(\text{py})_2\text{NO}]\text{PF}_6$ complex in aqueous solution at various pHs after 30 minutes.

1. N. A. P. dos Santos, A. B. Silva, C. F. N. da Silva, A. D. P. Alexiou, S. Nikolaou, *New Journal of Chemistry* 2022, 46, 4819. 2. E. Tfouni, M. Krieger, B. R. McGarvey, D. W. Franco, *Coord Chem Rev* 2003, 236, 57.3. A. P. L. Batista, J. Pavan, M. A. Ribeiro, S. Nikolaou, *Inorg Chem* 2023 (submitted). 4. H. Ohtsu, N. Oka, T. Yamaguchi, *Inorganica Chim Acta* 2012, 383, 1.

Agradecimentos/Acknowledgments

Conselho Nacional de Pesquisa e Desenvolvimento Tecnológico (CNPq), Fundação de Amparo à Pesquisa (Fapesp) and Coordenação de Aperfeiçoamento de Pessoal de Nível Superior (CAPES).

Submicrometric rare earth-based luminescent thermometers for combination with plasmonic nanoparticles

Gabriel Moronari (IC),¹ Tamires M. Oliveira (PG),¹ Paulo Cesar de Sousa Filho (PQ),*¹

g178420@dac.unicamp.br; *pcsfilho@unicamp.br

¹Institute of Chemistry, University of Campinas (UNICAMP)

Keywords: Sacrificial templates, Luminescence, Upconversion, Plasmonic nanoparticles.

Highlights

Single phase and heterostructured rare earth-based particles were successfully synthesized and showed thermally responsive upconversion luminescence, enabling further combination with AuNRs for heating/thermometry.

Abstract

Real-time temperature monitoring via optical, contactless nanothermometers is a powerful tool for medical diagnosis and treatment of various diseases.^[1] Furthermore, combination of luminescent thermometers and plasmonic metal nanoparticles (AuNRs) can be helpful for theranostic applications, such as all-in-one local submicron- or nanoheaters with intrinsic thermometric response. We hereby report the preparation of different rare earth (RE³⁺-based) particles with upconversion luminescence for further deposition of Au nanorods. We used sacrificial hydroxycarbonate templates (RECO₃OH.*n*H₂O, RE=Y_{0.77}Yb_{0.18}Er_{0.02}Tm_{0.03})^[2] (Figure 1a) to afford vanadate-phosphate (REVO₄-REPO₄, Figure 1b) and vanadate-fluoride (REVO₄-NaREF₄, Figure 1c) heterostructures as well as pure REVO₄ (Figure 1d) via hydrothermal synthesis at 200 °C for 18 h. The particles showed homogeneous size distribution and submicrometric sizes (~200-300 nm), thus conserving the general properties of the templates. AuNRs were prepared by seed-mediated reduction of HAuCl₄ by NaBH₄,^[3] showing homogeneous sizes and aspect ratios (Figure 1e), and plasmon absorption maxima at 515 and 800 nm. The thermometric assays performed with (Y_{0.77}Yb_{0.18}Er_{0.02}Tm_{0.03})VO₄ particles under λ_{exc}=980 nm (Figure 1f) resulted in relative thermal sensitivities between 0.3-0.9 % K⁻¹ at 77-473 K.

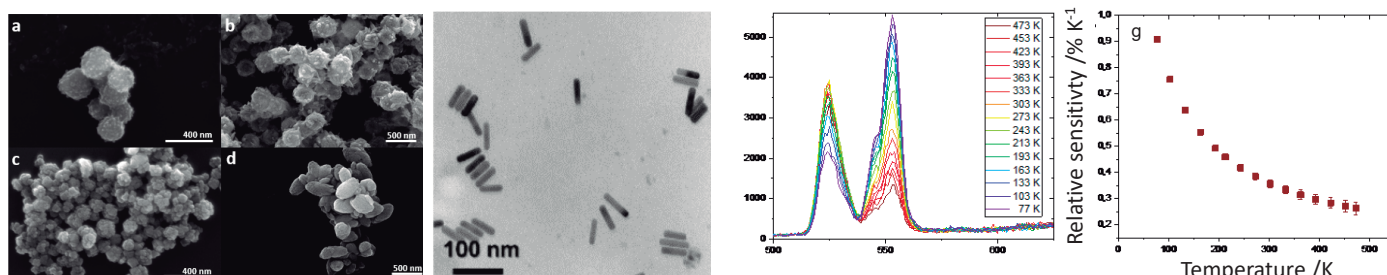


Figure 1. (a-d) Scanning and (e) transmission electron micrographs of (a) hydroxycarbonate templates (RECO₃OH.*n*H₂O), (b) REVO₄-REPO₄, (c) REVO₄-NaREF₄, (d) REVO₄, and (e) gold nanorods (AuNRs). (f) Temperature dependent upconversion spectra (λ_{exc}=980 nm) and (g) relative thermal sensitivity of REVO₄ particles (RE=Y_{0.77}Yb_{0.18}Er_{0.02}Tm_{0.03}).

Both the vanadate-based luminescent thermometers and the AuNRs were successfully obtained. We therefore envisage to optimize methodologies for controlled combination of the luminescent and plasmonic particles using reverse emulsion and surface ligands for direct anchoring, thus enabling to tune the loading of AuNRs over RE³⁺-based particles. This will allow to evaluate the effects of plasmonic nanoparticles in the luminescence of RE³⁺ ions for further applications as combined optical heaters-thermometers.

References: [1] Li, Y. et al. *ACS Nano*, 2016, 10, 2766-2773. [2] de Sousa Filho, P. C. et al, *ACS Appl. Mater. Inter.*, 2017, 9, 1635-1644. [3] Nikoobakht, B.; El-Sayed, M. A., *Chem. Mater.*, 2003, 15, 1957-1962.

Acknowledgments

The authors thank CNPq/PIBIC, CAPES, and FAPESP (2022/03442-3) for financial support.

Substitution of the *trans* ligands in the metallo-drug candidate $[\text{Ru}_2\text{O}(\text{CH}_3\text{COO})_2(\text{py})_4(\text{THIQ})_2](\text{PF}_6)_2$: the importance of the aquation reaction

Pedro H.O. Nazar (IC),¹ Sofia Nikolaou (PQ)¹ pholiveiranazar@usp.br

¹Departament of Chemistry, FFCLRP-USP.

Keywords: Ruthenium complex; Aquation reaction; Metallo-drug, Lability.

Highlights

The basicity of the incoming ligands impacts the $[\text{Ru}_2\text{O}(\text{CH}_3\text{COO})_2(\text{py})_4(\text{THIQ})_2(\text{PF}_6)_2$ substitution reactions. The $[\text{Ru}_2\text{O}]$ core has affinity for Pearson's hard bases. The aquation reaction is important for biological applications.

Resumo/Abstract

The ruthenium binuclear complex $[\text{Ru}_2\text{O}(\text{CH}_3\text{COO})_2(\text{py})_4(\text{THIQ})_2(\text{PF}_6)_2$ (**1**) is a metallo-drug candidate due to its activity against melanoma B16F10 cells, being less cytotoxic to human adenocarcinoma (MCF7 cells).¹ An interesting feature of μ -oxo bridged ruthenium binuclear complexes is the lability of the *trans* bonds to the μ -oxo bridge, due to the "trans effect".² Considering that the most successful metallo-drug in use, cisplatin (cis-[Pt(NH₃)₂Cl₂]), is a labile compound, the importance of studying the reactivity of such ruthenium complexes is evident. We have verified that the lability of **1** can be potentiated by two factors: 1. Due to the acidic nature of the $[\text{Ru}_2\text{O}]$ core, the relative basicity of the ligands in *cis* and *trans* position affects the substitution reactions in such a way that more basic ligands tend to substitute faster less basic ligands at the *trans*-position. Therefore, in the presence of 4-acetylpyridine (pKa 3.60),³ the THIQ (pKa 7.0)¹ ligand is less labile than in the presence of 4-aminopyridine (pKa 9.39).³ 2. Pearson's hard bases, such as water, promotes the solvolysis of the *trans* position to the μ -oxo bridge in the $[\text{Ru}_2\text{O}]$ unit.⁴ Performing a series of experiments with different proportions of dry acetone and water (90:10; 75:25; 50:50; 25:75 and 10:90 v/v) during 470 min (T = 293 K), it was verified that larger proportions of water generated more pronounced spectral changes over time ($\lambda_{\text{max}} = 582.0$ nm and A = 0.59 a.u. to $\lambda_{\text{max}} = 576.0$ nm and A = 0.45 a.u. for the 10:90 v/v). In the absence of water, we have observed very discrete spectra changes when **1** was monitored in a non-coordinating organic solvent (dry acetone, 24 h, T = 293 K), although the presence of excess of 4-aminopyridine resulted in a more pronounced effect than excess of 4-acetylpyridine. Once we have demonstrated that the aquation reaction is an important step for the lability of the complex and given our interest in a potential biological application, the kinetics of the reaction between histidine and complex **1** were investigated (Table 1). The experiments were carried out 310 K, in phosphate buffer (0.01 M; 0.027 M KCl; 0.137 M NaCl; pH 7.6), tris buffer (50 mM; 5 mM NaCl; pH 7.6) and deionized water in the presence and absence of histidine, monitoring the reactions in a UV-Vis spectrophotometer. The data indicate that the reactive unit interacting with histidine is actually the $[\text{Ru}_2\text{O}(\text{CH}_3\text{COO})_2(\text{py})_4(\text{H}_2\text{O})_2](\text{PF}_6)_2$ species, demonstrating the importance of the aquation reaction in the process. The aminoacid concentration directly influences the kinetic constant obtained, suggesting that the substitution mechanism is probably associative.

Table 1. Kinetic data of the complexes in different solvents and histidine concentrations. K_{obs} value obtained from the exponential curve of absorbance data at 580 nm (λ_{max}) as a function of time.

Complex	Solvent	[complex] (μM)	[histidine] (mM)	k_{obs} ($\times 10^{-4} \text{ s}^{-1}$)
$[\text{Ru}_2\text{O}(\text{CH}_3\text{COO})_2(\text{py})_6](\text{PF}_6)_2$	Phosphate buffer	50.0	10.0	1.97 \pm 0.13
		100.0	10.0	1.90 \pm 0.07
		50.0	20.0	2.7 \pm 0.2
		25.0	10.0	2.02 \pm 0.08
		50.0	5.0	1.53 \pm 0.06
$[\text{Ru}_2\text{O}(\text{CH}_3\text{COO})_2(\text{py})_4(\text{THIQ})_2](\text{PF}_6)_2$	Phosphate buffer	50.0	-	0.89 \pm 0.03
		50.0	-	0.699 \pm 0.003
		50.0	10.0	1.627 \pm 0.013
		50.0	0.1	0.817 \pm 0.005
		50.0	-	0.748 \pm 0.008
	Deionized water	50.0	-	0.690 \pm 0.019

¹ REIS, F. C. C. "[$\text{Ru}_2\text{O}(\text{CH}_3\text{COO})_2(\text{py})_4(\text{THIQ})_2](\text{PF}_6)_2$: síntese, caracterização, cinética de troca de ligantes, comparação com complexo análogo e estudos biológicos". Tese de Doutorado, Universidade de São Paulo. **2018**. ²IDO, Y. et al. Eur. J. Inorg. Chem., pp. 3641–3650, **2013**. ³ MOREIRA, M. B. et al. Dalton Trans., v. 17, p. 3342–3350. **2016**. ⁴HUSSAIN, A. et al. Inorg. Chimica Acta, v. 362, pp. 1101-1108. **2009**.

Agradecimentos/Acknowledgments

The authors would like to thank the Laboratory of Biological Activity and Supramolecular Chemistry of Coordination Compounds (LABiQSC²), the Unified Scholarship Program (PUB) of University of São Paulo (USP), the CNPq and FAPESP Brazilian agencies for funding this project.

Área: INO

(Inserir a sigla da seção científica para qual o resumo será submetido. Ex: ORG, BEA, CAT)

Synthesis and Characterization of a heterogeneous photocatalyst using Nontronite clay as support for titanium dioxide.

Yan P. Vedovato (IC)*, Lorrana V. Barbosa (PG), Liziane Marçal (PQ), Emerson H. de Faria (PQ)

¹Grupo de Pesquisa em Materiais Lamelares Híbridos (GPMatLam) – UNIVERSIDADE DE FRANCA (UNIFRAN). Av. Dr. Armando Salles Oliveira, 201. Pq. Universitário. Franca/SP, Brasil. 14404-600

e-mail: yan.pita185@gmail.com and emerson.faria@unifran.edu.br

Keywords: *Heterogeneous photocatalysis, sol-gel, nontronite, terephthalic acid, titanium dioxide*

Highlights

Nontronite was purified by the dispersion and decantation method and applied as a support for the immobilization of the titanium dioxide semiconductor. The heterogeneous photocatalyst was synthesized by the sol-gel process. The resulting solid was calcined to evaluate the influence of temperature on photocatalytic activity. The photocatalytic activity was evaluated as a function of the terephthalic acid hydroxylation reaction.

Resumo/Abstract

Advanced oxidative processes, mainly heterogeneous photocatalysis is a widely used technique for effluent treatment and contaminant degradation. Currently, one of the main challenges of this process is the use of semiconductors to take advantage of the greater absorption of light, preferably from natural sources such as the sun light. In this sense, the optimization of this process, either for the improvement of the efficiency of degradation and generation of hydroxyl radicals, or in the reaction time, cost and use of the technique become fundamental. Thus, clay minerals have attracted great prominence to support semiconductors, such as kaolinite, montmorillonite, halloysite, and among others clay minerals. Nontronite is a clay mineral from the smectite group, which is a species rich in iron (III). Nontronite or Fe-smectites are authigenic species of clays, they are usually found above basalt on the sea floor, and can also be formed by hydrothermal weathering processes of basalt and rocks. In this study, the heterogeneous photocatalyst based on Nontronite was prepared via sol-gel methodology. For this, the titanium (IV) isopropoxide precursor was used as ethanol solvent, and acetic acid as a stabilizing agent, the clay mineral nontronite, from the municipality of Bambuí-MG, was used as a support for the immobilization of the semiconductor. This clay mineral was selected considering its potential for generating hydroxyl radicals, using a greater range of absorption of solar, visible and ultraviolet radiation to promote the improvement in photocatalytic efficiency, due to its specific surface area and its structure. The solids were characterized using X-ray diffraction techniques, thermal analysis and scanning electron microscopy. Thermal analysis was used as a reference technique for defining the heat treatment temperatures, and the initially dry sample was divided into 4 fractions, one of which was stored and the others calcined at 400, 700 or 1000°C. X-ray diffraction of the sample at room temperature reveals a reduction in nontronite crystallinity after semiconductor immobilization. The solid calcined at a temperature of 400°C showed the characteristic peaks of nontronite clay mineral with lower crystallinity. However, for the solids calcined at 700 and 1000°C the nontronite structure is completely collapsed resulting in the formation of mixtures of aluminum, silicon and iron oxides. It should be noted, however, that from 400°C onwards, the characteristic peaks of the anatase phase of titanium dioxide can already be observed. Kinetic assays of photolysis of terephthalic acid were carried out to verify if there would be degradation of this compound when exposed to UV light ($\lambda=254$ nm and $P=96W$), and also heterogeneous photocatalysis assays with the solids obtained. These results were analyzed via photoluminescence spectroscopy, as 2-hydroxyterephthalic acid, resulting from the reaction with hydroxyl radicals, presents a characteristic emission band at 425 nm. It was possible to observe in the photolysis test that the terephthalic acid underwent any change in its structure, the absence of the band at 425 nm (typical for hydroxylated specie) and that the best profile of this hydroxylation reaction was obtained with the solid NON-TiO₂-400, which confirms that the structure of the lamellar clay mineral provided increased exposure of the TiO₂ semiconductor to UV radiation, and induced greater formation of hydroxyl radicals. These results are compatible with those obtained in the characterization of the materials that demonstrated that nontronite structure was preserved until 400°C.

Agradecimentos/Acknowledgments

CAPES (código de financiamento 001), CNPq (310151/2021-0), FAPESP (2013/19523-3 and 2017/15482-1)

Synthesis and characterization of a novel palladium(II) complex with memantine

Laura Barros Silva* (IC),¹ Anna Karla dos Santos Pereira (PQ),² Igor Andrade Santos (PG),³ Ana Carolina G. Jardim (PQ),³ Pedro Paulo Corbi (PQ).¹

ppcorbi@unicamp.br; l176631@dac.unicamp.br

¹Institute of Chemistry, University of Campinas-UNICAMP. ²Federal University of Tocantins-UFT. ³Institute of Biomedical Sciences, Federal University of Uberlândia-UFU.

Keywords: Aminoadamantanes, Palladium(II), Spectroscopy

Highlights

◆ A palladium(II) complex with memantine is presented. ◆ Elemental and thermal analyses permitted proposing its composition. ◆ Spectroscopic analyses suggest a square-planar geometry for the complex.

Abstract

Adamantanes are a class of organic compounds that consist of a single diamond-like carbon cage [1]. Memantine is a representative drug of this class that is used to treat Alzheimer's Disease. In our group, this drug has been studied as an antiviral agent, with promising results against Chikungunya virus (CHIKV) [2]. Palladium complexes have been reported as potential antineoplastic and antimicrobial agents [3]. In this work, we report the synthesis and spectroscopic characterization of a novel Pd(II) complex with memantine (Pd-mtn).

The complex was prepared by the reaction of Li_2PdCl_4 and memantine hydrochloride in methanol under stirring for 2 hours and at room temperature. The pH was adjusted with a solution of KOH. The yellowish solid obtained was collected by filtration, washed with methanol and dried. Yield 67.3%. The 1:2 palladium:memantine molar composition was confirmed by elemental analysis. Anal. Calcd. for $\text{PdC}_{24}\text{H}_{42}\text{N}_2\text{Cl}_2$ (%): C 53.8, H 7.90, N 5.23. Found (%) C 53.7, H 7.60, N 5.21. The complex is soluble in dimethylsulfoxide. Thermal analysis confirmed the proposed composition of the complex. Decomposition starts at 200°C and seems to occur in two steps. Infrared (Figure 1) and ^1H , ^{13}C and $\{^{15}\text{N}, ^1\text{H}\}$ nuclear magnetic resonance data confirmed coordination of memantine to Pd(II) by the nitrogen atom of NH_2 group. The ^1H NMR spectrum is shown in Figure 2. The square-planar coordination sphere was completed by two chloride ions. No ligand exchange was observed in a study based on ^1H NMR spectroscopy in dimethylsulfoxide for 24 hours.

References

- [1] A. K. dos S. Pereira et al., *New J. Chem.*, vol. 44, no 27, p. 11546–11556, jul. 2020, doi: 10.1039/D0NJ02009E.
- [2] A. K. dos S. Pereira et al., *Pharmacol. Rep.*, vol. 73, no 3, p. 954–961, jun. 2021, doi: 10.1007/s43440-021-00216-4.
- [3] A. T. Fiori-Duarte, et al., *J. Mol. Struct.*, vol. 1186, p. 144–154, jun. 2019, doi: 10.1016/j.molstruc.2019.03.020.

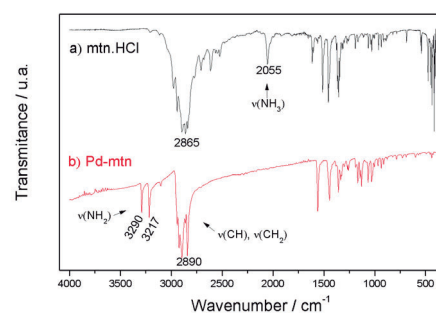


Figure 1: Infrared absorption spectra for a) memantine hydrochloride and b) Pd-mtn complex

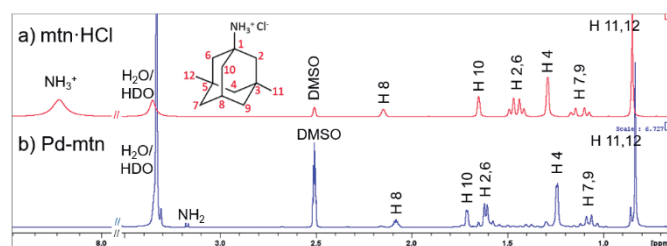


Figure 2: ^1H nuclear magnetic resonance spectra for a) memantine hydrochloride and b) Pd-mtn complex

Acknowledgments

The authors would like to thank to FAPESP (Grant # 2021/08717-8), FAEPEX and CNPq for financial support.

Área: INO

Synthesis and Characterization of $\text{NaYF}_4:\text{Yb}^{3+}/\text{Er}^{3+}$ UCPs for Polymer Composites and Applications Based on Upconversion Luminescence

Matheus V. B. Silva (PG),^{1*} Harumi Otaguro (PQ),² Rosana M. N. Assunção (PQ),¹ Sidney J. L. Ribeiro (PQ).³
mvicente.quim@gmail.com

¹Instituto de Química, UFU; ²Centro de Estudos do Mar, UFPR; ³Instituto de Química, Unesp.

Palavras-Chave: *Upconversion, UCPs, Rare earths.*

Highlights

$\text{NaYF}_4:\text{Yb}^{3+},\text{Er}^{3+}$ UCPs were efficiently synthesized by hydrothermal route.

Hexagonal phase UCPs had better upconversion luminescence.

PEG-6000 induced the production of cubic phase UCPs.

Resumo/Abstract

Luminescent materials produced from rare earths (RE), especially those with upconversion property, have aroused great interest due to their diversified application potential. In this work, particles of $\text{NaYF}_4:\text{Yb}^{3+},\text{Er}^{3+}$ system with upconversion property (UCPs) were synthesized and characterized aiming to incorporate them into polymer matrices in order to obtain new materials. Three luminophores of this system were synthesized by the hydrothermal route, each based on different additives: 1) EDTA, 2) EDTA, and PEG-6000 and, 3) oleic acid (OA). The upconversion emission spectra of UCPs were acquired by photoluminescence spectroscopy (PL), the size and morphology were characterized by scanning electron microscopy (SEM), the crystalline structure were characterized by X-ray diffraction (DRX). The UCPs produced from EDTA and OA (named RE/EDTA and RE/OA, respectively) resulted in hexagonal crystalline phase materials with good luminescence intensity. The UCP produced from EDTA and PEG-6000 (named RE/EDTA-PEG) resulted in a cubic crystalline phase material with low luminescence. The morphologies of three luminophores were quite different from each other: RE/EDTA UCPs had a hexagonal prism shape with length ranging between 2.5 and 6 μm ; RE/OA ones had an acicular shape with length ranging between 0.6 and 2 μm ; and RE/EDTA-PEG had a shape like small spheres with diameters varying between 145 and 180 nm. PEG-6000 acted not only reducing the size of UCPs, but by altering their crystalline phase. The hexagonal phase UCPs exhibited better luminescence than cubic phase one. Subsequently, the UCPs produced will be incorporated into polymeric matrices of PVP and CAB, two polymers with promising characteristics for several applications.

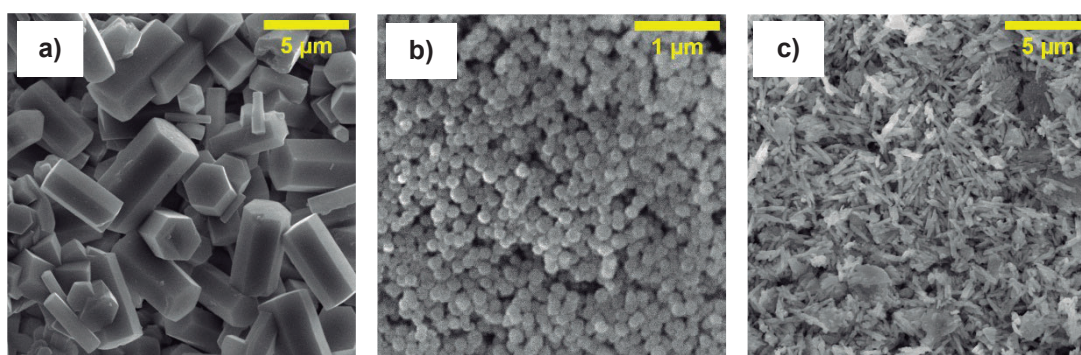


Figure 1: SEM microscopies of (a) RE/EDTA, (b) RE/EDTA-PEG and (c) RE/OA UCPs.

Agradecimentos/Acknowledgments



Synthesis and characterization of ruthenium(II) organometallic complexes containing aroylthiourea ligands

Marcielli Indira de Oliveira (PG),¹ Sailer Santos dos Santos (PQ),² Adailton João Bortoluzzi (PQ),¹ Márcio Peres de Araujo (PQ),³ Juliana Paula da Silva (PQ).^{1*}

j.p.silva@ufsc.br; marcielli.oliveira@posgrad.ufsc.br

¹ Department of Chemistry, UFSC; ² Department of Chemistry, UFSM; ³ Department of Chemistry, UFPR

Keywords: Ru(II) organometallics, aroylthiourea

Highlights

Solid and solution characterization of two new series of ruthenium (II) organometallic complexes containing aroylthiourea ligands. Strong N-H...Cl interaction in solid and solution.

Abstract

Thiourea-based compounds have several pharmacological applications. If we consider their Ru(II) organometallic complexes with this type of ligands, just a few examples are known, and the development of new ruthenium compounds can be interesting based on the fact that ruthenium-based drugs have been used as promising substitutes for platinum complexes in the biological field due to their lower toxicity. Among the most interesting thiourea-based ligands, aroylthioureas exhibit a rich and very well documented coordination chemistry. The present work reports the synthesis and characterization of aroylthioureas ligands coordinated to Ru(II) leading two new serie of complexes with the general formula: [Ru(HL-κS)(Cl)₂] (**1**) and [Ru(HL-κS)₂(Cl)]BF₄ (**2**), where L= *N*-benzoyl (*N,N'*-diethylthiourea) (**a**), *N*-benzoyl(*N,N'*-diisobutylthiourea) (**b**), *N*-benzoyl(*N,N'*-morpholythiourea) (**c**) and *N*-benzoyl(*N,N'*-dibenzylthiourea) (**d**). In complex **1a**, the ligand acts as a monodentate (κ-S) donor, while in complex **2a** two ligands act as a monodentate (κ-S) donor forming cationic species after addition of the BF₄ counterion. Both series consist of hexacoordinated ruthenium organometallic structures. Coordination of two ligands in this type of complex is unusual and provides interesting structures. Figure 1 depicts the molecular structure of **1a** and **2a**.

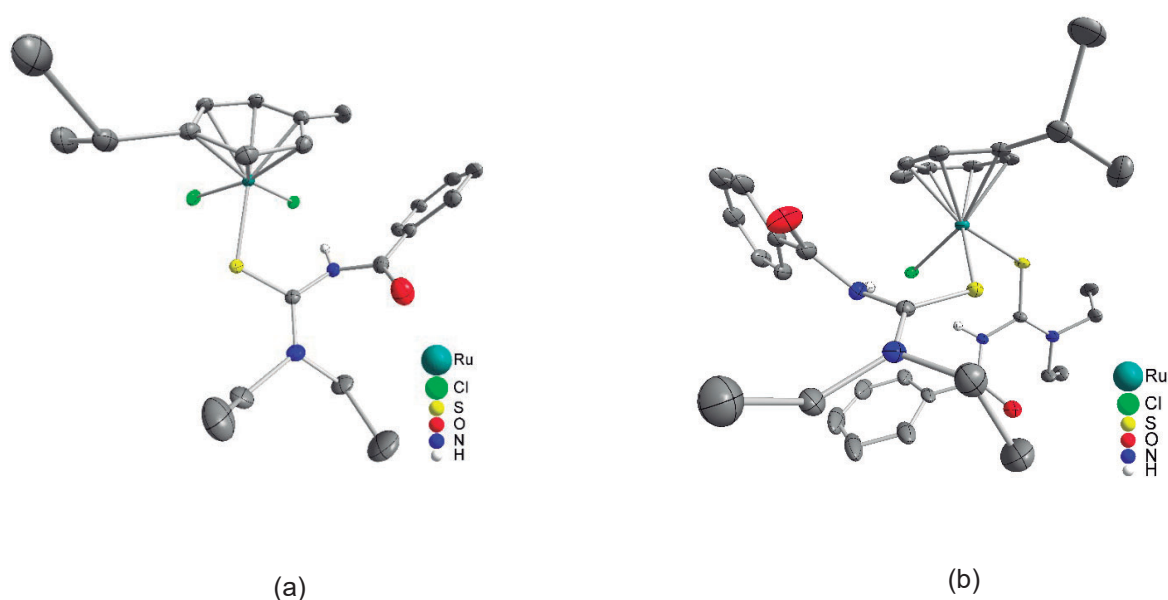


Figure 1. Molecular structures of complexes **1a** (a) and **2a** (b). Hydrogen atoms are omitted in both projections except for *N-H* hydrogen atom connections. In (b) counterion is omitted.

Acknowledgments

Brazilian agencies CAPES and CNPq supported this work.

Synthesis and characterization of two new oxazoline complexes containing rare terminal titanium-chalcogen (Ti-X, X = S or Se) bonds

José S. C. Neto (PG),^{1*} Francielli S. S. Seckler (PG),² Giovana G. Nunes (PQ),² Matteo B. (PQ),² Jaísa F. Soares (PQ)¹

joseseveriano1992@gmail.com

¹Departamento de Química, UFPR; ²Universidade de Florença, UniFi.

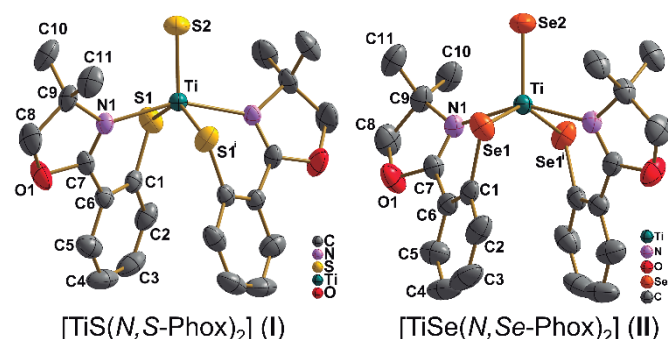
Palavras-Chave: Oxazoline, Titanium(IV), Chalcogenides, Structural Parameters, Redox Reaction

Highlights

Two new oxazoline complexes of titanium(IV) exhibit terminal titanium-chalcogen multiple bonds, which are highly uncommon in coordination chemistry.

Abstract

Oxazoline complexes with 6-membered chelate rings, such as those formed from (4,4-dimethyloxazolin-2-yl)thiophenolate (*N,S*-Phox⁻), have shown promising results as enantioselective catalysts due to their high structural rigidity.¹ Additionally, their catalytic properties can be finely tuned due to the relatively easy oxazoline ring functionalization. In this context, efforts have been made to synthesize more efficient catalytic species. In the present work, the 1:2 reaction between [TiCl₃(thf)₃] and the proligands Li(*N,S*-Phox) and Li(*N,Se*-Phox) in thf originated the two isostructural, five-coordinated titanium(IV) complexes [TiS(*N,S*-Phox)₂] (I) and [TiSe(*N,Se*-Phox)₂] (II), with two units of the bidentate oxazoline ligand and a terminal titanium-chalcogen (S or Se) bond. The formation of these complexes was attributed to redox reactions involving the starting materials and excess of elemental sulfur or selenium present in the reaction media. Both products



crystallized in the C2/c space group, with small variations in the lattice parameters. The structural parameter tau (τ_5) was calculated from the largest values of bonding angles involving the metal center, with τ_5 equaling 0.18 and 0.12 in I and II respectively. These values are compatible with a slightly distorted square pyramidal geometry² whose distortion increases with decreasing chalcogen radius. Reports on multiple titanium-chalcogen (S or Se) terminal bonds are rare, with only three occurrences in each

case according to a CCDC (Cambridge Crystallographic Data Center) search. In our work, the measured Ti–S and Ti–Se bond lengths were 2.092(11) Å and 2.224(9) Å respectively, close to the few available literature values.³ Bond valence sum calculations using crystallographic parameters – bond lengths – gave BVS values for titanium of 3.86 and 3.95 in I and II respectively, supporting the +IV oxidation state. The other species formed in this reaction, which were isolated and characterized by spectroscopic techniques, were identified as the bis-oxazolines Phox-N,S-S,N-Phox and Phox-N,Se-Se,N-Phox, compatible with the oxidation of both the thio(seleno)phenolate and titanium(III) to produce the terminal sulfide and selenide ligands in products I and II. We are now investigating the possibility of synthesizing the related [TiX(*N,S*-Phox)₂] and [TiX(*N,Se*-Phox)₂] with titanium(III) (X = halide) for comparative catalytic and magnetic studies.

References:

- [1] Ibrahim. K. T. *et al.* Monatsh. Chem. Rev 2022, 153, 837-871.
- [2] Addison. A. W. *et al.* Dalton Trans. 1984, 7, 1349-1356.
- [3] Kisko. J. L. *et al.* J. Am. Chem. Soc. 1997, 32, 7609-7610.

Acknowledgments

UFPR, CNPq, Capes, Fundação Araucária, PPGQ-UFPR

Synthesis and Crystal Structure of a Coordination Polymer based on Copper(II) and Mixed Ligands

Marye A.R. Silva (IC)^{1*}; Rafaela M.R. da Silva¹ (PG); Javier Ellena² (PQ); João H. de Araujo-Neto² (PQ); Maria Vanda Marinho¹ (PQ).

marye.silva@sou.unifal-mg.edu.br

¹Instituto de Química, Campus Santa Clara, Universidade Federal de Alfenas, Alfenas, MG, 37133-840, Brasil.

²Instituto de Física de São Carlos, Universidade de São Paulo, São Carlos, SP 13566-590, Brasil.

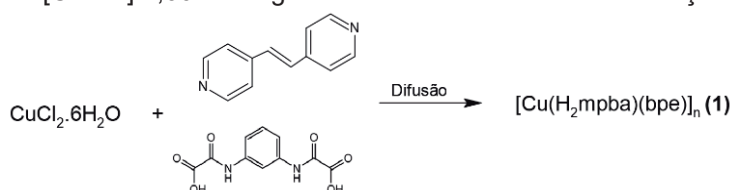
Palavras Chave: Polímeros de coordenação, Oxamatos, ligante nitrogenado, Estrutura cristalina

Highlights

- Synthesis, spectroscopic characterization, and crystal structure;
- New coordination polymer derived from copper(II) and H₄mpba = 1,3-phenylenebis(oxamic) acid;
- 2D network based on 1,2-Bis(4-pyridyl)ethylene (bpe) and H₂mpba²⁻ as bridge ligands.

Resumo

Complexos/polímeros/ redes de coordenação envolvem basicamente a coordenação por ligação covalente entre cátions de metais de transição (íons e/ou blocos construtores) como ácido de Lewis e ligantes orgânicos como base de Lewis, e dentro da Química Supramolecular através das interações intermoleculares, podem dar origem a diferentes arranjos supramoleculares.^[1-2] O presente trabalho pautou na síntese e caracterização no estado sólido do íon cobre(II) com dois ligantes orgânicos, sendo um responsável pela carga do composto, o ligante 1,3-fenilenobis(oxamato) (H₂mpba²⁻), e outro, um ligante auxiliar 1,2-di(4-piridil)etileno (bpe) levando a formação do polímero de coordenação bidimensional de fórmula: [Cu(H₂mpba)(bpe)]_n (**1**). Até o momento, uma busca baseada no software Conquest (CSD)^[3] há somente três polímeros de coordenação contendo o H₂mpba²⁻,^[1] tornando bastante interessante sua obtenção e caracterização. A síntese de **1** pode ser visualizada no Esquema 1. Os dados de IV exibem intensos picos de absorção ν(CO) em 1660/1610 cm⁻¹ provavelmente devido a coordenação do H₂mpba²⁻ parcialmente desprotonado ao centro metálico através dos grupos carbonil-amida e carboxilatos.^[1-2] Bandas em 1650 cm⁻¹ indicam a coordenação do ligante bpe ao centro de cobre(II), com estiramento ν(CC/CN) em 1620 cm⁻¹ (ν(CC/CN) = 1597 cm⁻¹ para ligante bpe livre). Dados de difração de raios X por monocristal revelam a formação de um polímero de coordenação zigue-zague contendo o ligante H₂mpba²⁻ coordenado de modo bidentado *syn-syn* μ₂-κ²O,O':κ²O'',O'''. O ligante bpe coordena ao centro metálico através do átomos de nitrogênio no modo em ponte μ₂-κN:κN' levando a formação da rede bidimensional. Cada centro de cobre(II) exibe uma geometria octaédrica coordenado por quatro átomos de oxigênio e dois átomos de nitrogênio, cujas as distâncias do plano basal [Cu-O1; Cu-O3; Cu-O6; Cu-N3] são: 1,974, 2,319, 2,346 e 2,002 Å, respectivamente. As distâncias apicais são: [Cu-O4] 1,979 e [Cu-N4] 2,002 Å. Figura 1 ilustra a esfera de coordenação bem como a rede polimérica bidimensional (2-D) em **1**.



Esquema 1. Representação da metodologia reacional.

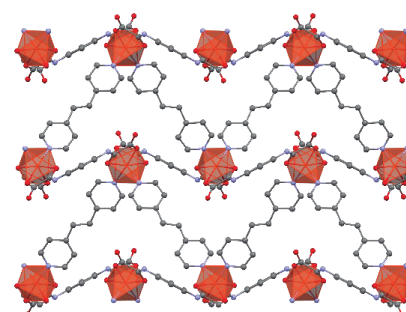


Figura 1. Visão da rede bidimensional ao longo do plano *bc* em **1**.

Agradecimentos

Funding: PIBITI-UNIFAL-MG (CNPq); FAPEMIG-Project CEX-APQ-01597-17.

Referências:

- [1] Campos, N.R. De; *et al*, Building-up Host–Guest Helicate Motifs and Chains: A Magneto-Structural Study of New Field-Induced Cobalt-Based Single-Ion Magnets. *Dalton Trans.* **2021**, *50*, 10707–10728.
- [2] Mariano, L.D.S.; *et al*, Polymorphic Derivatives of Ni^{II} and Co^{II} Mesocates with 3D Networks and “Brick and Mortar” Structures: Preparation, Structural Characterization, and Cryomagnetic Investigation of New Single-Molecule Magnets. *Cryst. Growth Des.* **2020**, *20*, 2462–2476. [3] Macrae, C. F.; Edington, P. R.; McCabe, P.; Pidcock, E.; Shields, G. P.; Taylor, R.; Towler, M.; Streek, J. v. *J. Appl. Cryst.*, **2006**, *39*, 453.

Synthesis and structural analysis of a 1,3,4-thiadiazole-based molecule and its coordination copper(II) complexes

Ana Júlia Zimmermann Londero (PG),¹ Vânia Denise Schwade (PQ)¹, Ernesto Schulz Lang (PQ)¹.

[anajulialondero@gmail](mailto:anajulialondero@gmail.com)

¹Universidade Federal de Santa Maria, Departamento de Química, Av. Roraima, 1000, Camobi, Santa Maria-RS-Brasil.

Keywords: Thiadiazoles, Copper(II) complexes, Spectroscopic characterization.

Highlights

A new ligand was prepared from 4-fluorobenzoyl chloride and 5-(methylthio)-1,3,4-thiadiazole (HL). Two copper(II) complexes were obtained: [Cu(HL)₂Cl₂] (**1**) and [Cu(L)₂] (**2**).

Abstract

The chemistry of 1,3,4-thiadiazoles and their derivatives are remarkable because they have a wide range of applications, and can be used in the pharmaceutical and agricultural industries and in the chemistry of new materials. Due to the presence of the -C=N- bonds, 1,3,4-thiadiazoles exhibit a broad spectrum of biological activities¹. However, reports of crystal structures of metal complexes with ligands derived from 1,3,4-thiadiazole are still scarce. In order to clarify the molecular structures and properties of these complexes, in this work we report the synthesis and spectroscopy characterization of HL and its complexes [Cu(HL)₂Cl₂] (**1**) and [Cu(L)₂] (**2**) [HL = *N*-(1,3,4-thiadiazole-2-methylthio)-4-fluorobenzamide]. The preparation of HL was performed using 5-amino-1,3,4-thiadiazole-2-thiomethyl and 4-fluorobenzoyl chloride in THF in the presence of triethylamine as base. The structure of HL was confirmed by single-crystal X-ray diffraction (SC-XRD), being also characterized by FT-IR, ¹H NMR and ¹⁹F NMR spectroscopies, ESI-MS and elemental analysis. The complexes were synthesized by reaction of HL with copper(II) chloride (**1**) and copper(II) acetate (**2**), in a MeOH/CH₂Cl₂ (2:1 v/v) solvent mixture. Complex **1** has been structurally analyzed by SC-XRD. The metal center adopts a square planar arrangement, which is composed by two nitrogen atoms from the thiadiazole rings of the HL molecules, and by two chloride ions. The ¹H NMR spectrum in DMSO evidenced antiferromagnetic exchanges of a new copper(II) specie. Electron paramagnetic resonance (EPR) experiments were proceeded in DMSO (77 K) and CH₂Cl₂ (77 K and room temperature) and demonstrate the typical paramagnetic behavior of the Cu^{II} unpaired electron. The FT-IR spectrum of complex **1** (Fig. 1) presents the ν(CO) and ν(CN) vibration bands at 1669 and 1522/1511 cm⁻¹, respectively. The FT-IR spectrum of complex **2** suggests the coordination of the ligand in a monoanionic manner through the enolized (C=O) oxygen atom, and probably one of the nitrogen atoms from the thiadiazole ring in a chelation mode. The shift of the ν(CO) vibration band from 1662 (in free HL) to 1451 cm⁻¹ and the ν(CN) vibration band at 1491 cm⁻¹ support the proposed structure (Fig. 1).

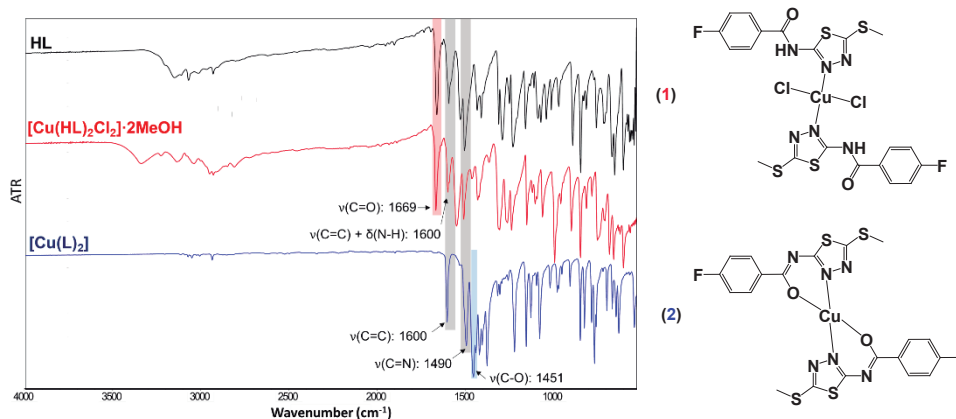


Figure 1: FT-IR spectra of ligand and complexes (left); Molecular structure of the copper(II) complexes (right).

Acknowledgments

UFSM, Cnpq, CAPES, FAPERGS.

¹ A) X.-H. Yang et al. *Bioorg. Med. Chem.* (2012) 1181–1187. B) H. Rajak et al. *Bioorg. Med. Chem. Lett.* 21 (2011) 5735. C) W. M. Xu et al. *Pestic. Biochem. Physiol.* 101(2011) 6. D) Zoumpoulakis, P. et al. *Bioorg. Med. Chem.* 20 (2012) 1569.

46^o Reunião Anual da Sociedade Brasileira de Química: "Química: Ligando ciências e neutralizando desigualdades"

Synthesis and structural characterization of a tetranuclear Co(II) complex containing an oxazolidine-based ligand

Francielle X. dos Santos (IC),¹ Brunno P. Freitas (PG),¹ Guilherme P Guedes (PQ),^{1*}

franciellexavier@id.uff.br; guilherme_guedes@id.uff.br

¹Universidade Federal Fluminense, Instituto de Química, Departamento de Química Inorgânica

Keywords: tetranuclear compound, X-ray diffraction, coordination chemistry, crystal structure.

Highlights

A tetranuclear Co(II) complex containing an oxazolidine-based ligand was synthesized following an one-pot methodology. The crystal structure was solved by single-crystal X-ray diffraction.

Resumo/Abstract

A combinação de ligantes orgânicos e íons de metais de transição pode levar à obtenção de materiais multifuncionais, visto que os cátions metálicos podem agregar outras propriedades ao sistema, tais como ópticas e/ou magnéticas.¹ As oxazolidinas pertencem a uma classe de compostos orgânicos heterocíclicos de cinco membros que contém um átomo de oxigênio e um de nitrogênio nas posições 1 e 3, cujos derivados podem ser explorados na química de coordenação devido à presença de dois heteroátomos doadores de densidade eletrônica.² Além disso, diversos complexos tetranucleares de cobalto já foram reportados na literatura devido suas interessantes propriedades magnéticas, especialmente como magnetos moleculares de uma única molécula (*Single-Molecule Magnets* - SMMs).³ A obtenção de um novo composto tetranuclear foi feita através da metodologia one-pot a partir de uma solução etanólica contendo um equivalente de 2-amino-2-(hidroximetil)-1,3-propanodiol (tris) e de 2-piridino-carboxialdeído.⁴ Essa mistura foi aquecida à 50 °C durante uma hora e, então, foi adicionado o nitrato de cobalto(II) na mesma proporção. Após 45 dias, monocristais de coloração marrom-avermelhada foram obtidos e caracterizados por espectroscopia de absorção na região do infravermelho e difração de raios X. Foram observadas bandas na região de 3440 cm⁻¹ (νOH), 3225 cm⁻¹ (νNH_{oxazolidina}), 1068 cm⁻¹ (νCO) e 1018 cm⁻¹ (νCN). A estrutura cristalina do complexo está apresentada na **Figura 1a**. Os dados obtidos pela difração de raios X de monocristal mostram que o complexo possui fórmula molecular [Co₄(L)₂(Tris)₂(H₂O)₂](NO₃)₂, na qual os íons metálicos ocupam vértices alternados de um cubo defletido, (Figura 1b). Dois íons Co(II) são coordenados a dois átomos de nitrogênio dos anéis das porções piridina e oxazolidina do ligante formado *in situ* durante a reação, por dois átomos de oxigênio da porção álcool do mesmo ligante, e também pelos átomos de oxigênio e o de nitrogênio do ligante tris. Já os outros dois íons Co(II) são coordenados por uma molécula de água cada, pelos átomos de oxigênio da porção álcool de cada ligante derivado de oxazolidina e por um átomo de oxigênio de cada ligante tris. Posteriormente, serão estudadas as propriedades espectroscópicas na região UV-visível do composto obtido em estado sólido e em solução.

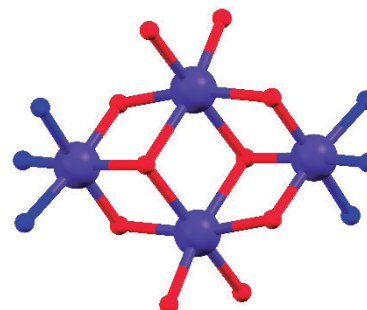
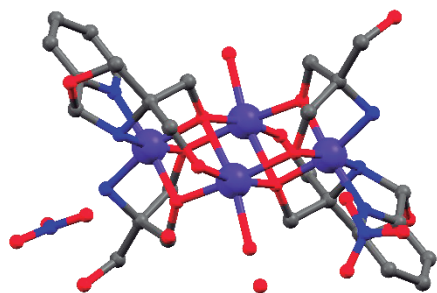


Fig. 1. Estrutura resolvida por difração de raios-X de monocristal do complexo obtido. Os átomos de hidrogênio foram omitidos por questões de clareza da visualização.

Fig. 2. Representação do núcleo [Co₄O₁₀N₆] do complexo obtido.

¹ SALEEM, A. et al., *Dalton Trans.*, **2018**, 47, 6156.

² SHAGHAFI, M. B., GROTE, R. E., JARVO, E. R., *Organic Letters*, **2011**, 12, 2884-2887.

³ GUEDES, G. P. et al. *Eur. J. Inorg. Chem.* **2012**, 5642-5648.

⁴ AREAS, E. et al., *Inorganica Chimica Acta*, **2022**, 529, 120664.

Agradecimentos/Acknowledgments

CNPq, FAPERJ, CAPES and LDRX-UFF.

Área: INO

Synthesis and structural characterization of Cu(II) and Ni(II) complexes containing a chiral oxazolidine-based ligand

Brunno P. Freitas (PG),¹ Guilherme P. Guedes (PQ),^{1*}

brunnopf@id.uff.br; guilherme_guedes@id.uff.br

¹Universidade Federal Fluminense, Instituto de Química, Departamento de Química Inorgânica

Keywords: oxazolidine, mononuclear compounds, X-ray diffraction, crystal structure.

Highlights

Two Cu(II) and Ni(II) complexes containing a chiral oxazolidine derivative ligand were synthesized following an one-pot methodology. The structures were solved by single-crystal X-ray diffraction.

Abstract

Oxazolidines are a class of saturated five-membered heterocyclic organic compounds containing an oxygen and nitrogen atoms at 1 and 3 positions, respectively (Figure 1). The saturated form of the oxazolidine ring is of great interest from a structural point of view, since the insertion of different substituent groups in the ring at the positions 2, 4 and 5 or the amine nitrogen atom allows the design of a series of derivatives. Besides, such derivatives can even be exploited in coordination chemistry due to the presence of electron donating groups.¹

The two complexes (1 and 2) were synthesized by the one-pot methodology.² To an ethanolic solution containing 2-amino-2-(hydroxymethyl)-1,3-propanediol (Tris) was added one equivalent of pyridine 2-aldehyde. This mixture was left under heating at 50°C for one hour and then copper(II) (1) or nickel(II) (2) perchlorate salts were added. Both complexes were characterized by infrared spectroscopy and X-ray diffraction. The IR spectra showed two typical bands which indicated the formation of the oxazolidine-based ligand (Figure 2); 3207 cm⁻¹ (νNH_{oxazolidine}) and 1023 cm⁻¹ (νCN) (1); 3255 cm⁻¹ (νNH_{oxazolidine}) and 1016 cm⁻¹ (νCN) (2); 1610 cm⁻¹ (νC_{aromatic}) and 1106 cm⁻¹ (νClO_{perchlorate}) (1); 1611 cm⁻¹ (νC_{aromatic}) and 1108 cm⁻¹ (νClO_{perchlorate}) (2).

The crystal structures of complexes 1 and 2 are shown in Figures 3(a) and 3(b), respectively. Both complexes are mononuclear systems with molecular formula [M(L)₂](ClO₄)₂, M = Cu(II) (1) and Ni(II) (2). The metal ion is coordinated to four pyridine and oxazolidine nitrogen atoms and two oxygen atoms from alcohol groups. As indicated by IR spectra, the formation of a chiral oxazolidine derivative was also confirmed by SC-XRD. The crystal lattice of both complexes is stabilized by intermolecular hydrogen bonds between alcohol and perchlorate moieties (1 and 2) and between the lattice water molecule and alcohol groups (only in 2).

Comentado [GPG1]: Seria bom colocar outras bandas além dessas. A banda Cl-O, por exemplo, do perclorato e alguma coisa aromática.

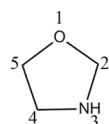


Fig. 1. Molecular structure of the oxazolidine ring.

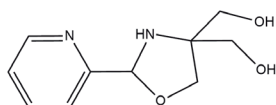


Fig. 2. Molecular structure of the oxazolidine-based ligand.

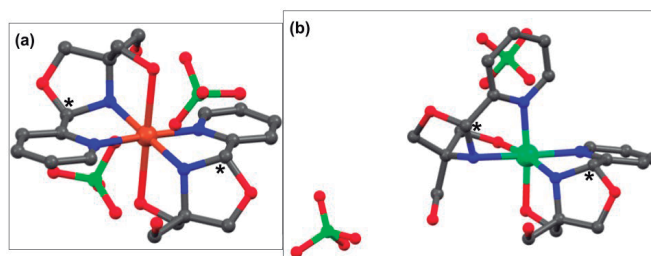


Fig. 3. Crystal structure of 1(a) and 2(b). * Representation of asymmetric carbon atoms. Hydrogen atoms were omitted for sake of clarity.

¹ CORDERO, F. M. et al., *Progress in Heterocyclic Chemistry*, 2021, 32, 365-395.

² AREAS, E. et al., *Inorg. Chim. Acta*, 2022, 529, 120664.

Acknowledgments

CNPq, FAPERJ, CAPES and LDRX-UFF.

Synthesis and study of the photoluminescent properties of new β -diketonate components of the Eu^{3+} ion with the ligand fg2ap

Anna Paula R. Queiroga (PG),^{1*} Iran F. Silva (PG),² Bruno F. Lira (TC),² Wagner M. Faustino (PQ).²

annapaula_rocha@hotmail.com

¹Instituto de Química, UNICAMP; ²Departamento de Química, UFPB.

Keywords: Luminescence, β -diketones, amides as ligands, energy transfer.

Highlights

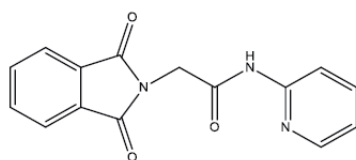
The replacement of water molecules by the 2-(1,3-dioxoisindolin-2-il)-n-(piridin-2-il)acetamid (fg2ap) in Eu^{3+} ion complexes increases the intrinsic quantum yields of luminescence.

Resumo/Abstract

The coordination compounds of trivalent lanthanide ions are widely studied due to their peculiar photophysical properties that allow their use in several applications. For this, it is extremely important to study and determine organic ligands that are efficient for the luminescence sensitization process of these ions. With this in mind, the synthesis of a new class of tris β -diketonates of the Eu^{3+} ion and its Gd^{3+} analogues with the compound 2-(1,3-dioxoisindolin-2-yl)-N-(pyridin-2-yl)acetamide (fg2ap) (**Fig. 1**) as an auxiliary ligand, aiming to investigate its photoluminescent properties. The amide auxiliary linker was obtained from the reaction between 2-aminopyridine and N-phthaloylglycine chloride with a yield of 56.18%. The ligand synthesis was confirmed by melting point data, infrared absorption spectroscopy and ^1H and ^{13}C nuclear magnetic resonance. The complexes, on the other hand, were synthesized from the substitution of the water molecules of the tris β -diketonates hydrated complexes by the amide ligand fg2ap, presenting yields from 26 to 83%. These were characterized by complexometric titration, infrared spectroscopy, thermogravimetric analysis and had their spectroscopic properties experimentally analyzed. The data obtained by complexometric titration and thermogravimetric analysis suggest that the complexes have a general formula $[\text{Ln}(\beta\text{-dic})_3(\text{fg2ap})]$, and the coordination of the β -diketonates ligands occurs through the oxygen atoms of the carbonyl groups and the auxiliary ligand fg2ap through one of the carbonyls and heterocyclic nitrogen, according to the absorption spectra in the infrared region. The replacement of water molecules by this amide in Eu^{3+} ion complexes increases the intrinsic quantum yields of luminescence (**Table 1**). The triplet states determined experimentally through the emission spectra of the Gd^{3+} complexes indicate favorable resonance conditions between the lowest energy triplet states of the ligands with the $^5\text{D}_0$ emitter level of the Eu^{3+} ion.

Table 1 - Parameters of experimental intensity (Ω_λ), radiative rate (A_{rad}), non-radiative rate (A_{nrad}), emission level lifetime (τ) and intrinsic emission quantum yield (Φ_{LnLn}) of Eu^{3+} hydrated and substituted complexes at 300 K and 77 K. ($\lambda_{\text{exc}} = 394 \text{ nm}$).

Complexos	$\Omega_2 (10^{-20} \text{ cm}^2)$		$\Omega_4 (10^{-20} \text{ cm}^2)$		$A_{\text{rad}} (\text{s}^{-1})$		$A_{\text{nrad}} (\text{s}^{-1})$		$\tau_{394 \text{ nm}} (\text{ms})$		$\Phi_{\text{LnLn}} (\%)$	
	300K	77K	300K	77K	300K	77K	300K	77K	300K	77K	300K	77K
$[\text{Eu}(\text{btfa})_3(\text{H}_2\text{O})_2]^{2+}$	14,8	13,9	7,8	1,6	642	507	1840	1551	0,39	0,37	24,7	18,9
$[\text{Eu}(\text{tta})_3(\text{H}_2\text{O})_2]^{2+}$	26,9	27,6	6,3	7,1	980	1018	3525	2873	0,24	0,29	23,3	29,3
$[\text{Eu}(\text{dbm})_3(\text{H}_2\text{O})]^{2+}$	31,6	41,3	4,2	3,1	1124	1415	7804	3280	0,07	0,26	8,2	37,1
$[\text{Eu}(\text{btfa})_3(\text{fg2ap})]$	21,3	20,5	6,5	6,4	838	807	1385	1234	0,45	0,49	37,7	39,5
$[\text{Eu}(\text{tta})_3(\text{fg2ap})]$	25,9	25,0	6,2	6,3	975	950	1525	1091	0,40	0,49	39,0	46,5
$[\text{Eu}(\text{dbm})_3(\text{fg2ap})]$	24,4	25,2	5,5	9,5	929	1021	4953	1757	0,17	0,36	15,8	36,8



2-(1,3-dioxoisindolin-2-il)-N-(piridin-2-il)acetamida

Fig 1. Estrutura molecular do ligante auxiliar fg2ap. ^a Data obtained from the reference [1].

Agradecimentos/Acknowledgments

This work was supported by CNPq, FINEP, CAPES and UFPB.

[1] G.B.V. Lima, J.C. Bueno, A.F. da Silva, A.N. Carneiro Neto, R.T. Moura, E.E.S. Teotônio, O.L. Malta, W.M. Faustino, Novel trivalent europium β -diketonate complexes with N-(pyridine-2-yl)amides and N-(pyrimidine-2-yl)amides as ancillary ligands: Photophysical properties and theoretical structural modeling, *J. Lumin.* 219 (2020). <https://doi.org/10.1016/j.jlumin.2019.116884>.

Synthesis, characterization and biological activity of a new melatonin derivative and its silver complex

Bruna Possato (PQ)^{1*}, João Stempkoski (IC)¹, Murilo Helder de Paula (TM)¹, Flavio da Silva Emery (PQ)¹, Sérgio de Albuquerque (PQ)^{1*}

brunapossato@usp.br; sdalbuq@fcrfp.usp.br

¹ Faculdade de Ciências Farmacêuticas de Ribeirão Preto, Universidade de São Paulo.

Keywords: Melatonin derivatives, Silver complexes, Trypanosoma cruzi, in vitro cytotoxicity

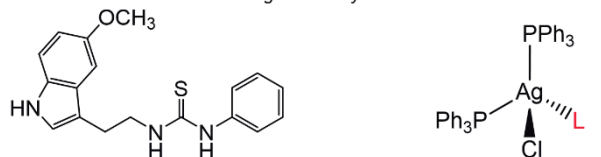
Highlights

New melatonin-derived thiourea and its silver complex were successfully synthesized. The silver complex was more active against *Trypanosoma cruzi* and PC3 (human prostate cancer) than both free ligand and precursor complex.

Abstract

Melatonin, the sleep hormone, is secreted by the pineal gland and has aroused the interest of researchers because it has antioxidant, anti-inflammatory and anti-aging properties. Because it is linked to immune function, it has been shown to be a potential antiparasitic agent,¹ so the synthesis of new derivatives is promising, especially those with a structure that favors coordination to metal centers, which can increase their biological activity.² Silver complexes, for example, are known antimicrobial agents and are widely used in the treatment of wounds and burns.³ In this work, we will present the synthesis of a new thiourea derived from melatonin and its silver complex, as well as the study of their trypanocidal activity and cytotoxicity *in vitro* against both healthy and cancer strains. To achieve that, the thiourea (L) was obtained by refluxing 5-methoxytryptamine and phenyl isothiocyanate in the presence of triethylamine in tetrahydrofuran for 3 h, followed by washing with brine, evaporation of the solvent and precipitation in ethanol. The formation of the silver complex, [AgCl(PPh₃)₂L], was performed by the reflux between the aforementioned thiourea and the precursor [AgCl(PPh₃)₂] during two hours in chloroform, and precipitation in ethanol after reducing the volume of the reaction medium. Both free ligand and complex were characterized by ¹H-NMR, UV-Vis and IR. The ¹H-NMR spectrum of the complex displays more hydrogens signs in the aromatic rings region (~7.5 - 7.0 ppm), caused by the presence of two triphenylphosphine groups as co-ligands in its coordination sphere. The vibrational spectrum of the free thiourea showed $\nu(\text{N-H}) \sim 3250\text{-}3650 \text{ cm}^{-1}$, $\nu(\text{C-H}) \sim 3200 \text{ to } 2750 \text{ cm}^{-1}$, aromatic $\nu(\text{C=C}) \sim 1700 \text{ to } 1300 \text{ cm}^{-1}$ and $\nu(\text{C=S}) \sim 1250 \text{ cm}^{-1}$. The complex presents $\nu(\text{P-C}) \sim 750 \text{ and } 650 \text{ cm}^{-1}$. The absorption spectra of thiourea and [AgCl(PPh₃)₂L] show bands with λ_{max} at 268 and 256 nm, respectively. The *in vitro* trypanocidal activity of the compounds was determined through the CPRG assay, using intracellular amastigotes (in LLC-MK2) of the Tulahuen strain (LacZ) incubated with the compounds for 72 h. Along with the trypanocidal activity, the *in vitro* cytotoxicity against LLC-MK2 strain (monkey kidney) was also evaluated using the MTT method. Similarly, *in vitro* cytotoxicity against PC3 (human prostate cancer) and PNT2 (human prostate) was determined. In both experiments, [AgCl(PPh₃)₂L] was more active than the free ligand and the precursor (see Table), corroborating the proposition that coordination to the metallic center would increase the activity of the melatonin derivative.

Table. Structure from the melatonin-derivative thiourea, its silver complex and biological activity data.



	IC ₅₀ <i>T. cruzi</i> (μM)	CC ₅₀ LLC-MK2 (μM)	CC ₅₀ PC3 (μM)	CC ₅₀ PNT2 (μM)
Thiourea	39,2	48,7	>50	>50
[AgCl(PPh ₃) ₂ L]	3,20	3,03	0,69	4,48
[AgCl(PPh ₃) ₂]	9,38	6,57	1,79	5,22

¹Providello, M. V. et al. *Can. J. Physiol. Pharmacol.* **2021**, 99 (8), 795–802

²Possato, B. et al. *J. Inorg. Biochem.* **2017**, 176, 156–158.

³Sadler, P. J. *Adv. Inorg. Chem.* **1991**, 36, 1–48; Siqueira, F. dos S. et al. *Microb. Pathog.* **2023**, 175, 105960

Acknowledgments

FAPESP (2017/17579-2, 2018/24544-3, 2019/19835-1) CAPES and CNPq

Area: INO

Synthesis, characterization and biological applications of a novel Ru^{II}-NO₂ compound as a metallopharmaceutical candidate

Renan R. Bertoloni (PG)¹, Alexia M. Silva (PG)², Sofia Nikolaou (PQ)³, Claudia Turro (PQ)⁴

renanrbert@usp.br

^{1,3} Departamento de Química, Faculdade de Filosofia Ciências e Letras de Ribeirão Preto (FFCLRP – USP)

^{2,4} Department of Chemistry and Biochemistry, The Ohio State University (OSU)

Keywords: Coordination Chemistry, Ruthenium, Metallopharmaceutical, NORMs

Highlights

A novel compound with formula [Ru(tpy)(dppz)(NO₂)](PF₆) was synthesized and characterized by UV-Vis, ¹H-NMR, CV and XRD techniques. Initial studies of its biological applications show that the complex interacts with DNA, as it was able to increase the melting temperature (T_m) of CT-DNA in phosphate buffer by 5°C.

Resumo/Abstract

Since the discovery of the antitumor activity of cisplatin by Barnet Rosenberg in the 1960s, coordination complexes have been increasingly studied as drug candidates, especially ruthenium compounds, which, when combined mainly with polypyridine ligands, can have biological properties of interest through interaction with DNA¹ and/or photochemical and photophysical properties that enable its application in photodynamic therapy through the generation of ¹O₂.² Another factor influenced by the presence of polypyridine ligands is a modification in the electronic levels of the coordination complex, which makes a monodentate ligand more photolabile and may generate other interesting applications for the complex.³ Bearing these possible applications in mind, the aim of this work was the synthesis and characterization of a novel complex with the formula [Ru(tpy)(dppz)(NO₂)](PF₆) (tpy = 2,2':6',2''-terpyridine; dppz = dipyrido[3,2-a:2',3'-c]phenazine) and the verification of some of its biological properties. The monodentate ligand NO₂⁻ was chosen as a source of nitric oxide (NO), since there is information in the literature showing that this release followed by the conversion of NO₂⁻ to NO occurs through an enzymatic catalysis.⁴ The synthesis was performed starting from the precursor [Ru(tpy)(dppz)(Cl)](PF₆) with NaNO₂ in a 1:1 acetone/H₂O solution maintained at reflux for 3h (yield: 47%) and the purification was carried out in an alumina column using acetonitrile as mobile phase to remove the precursor and a 20% ACN/80% MeOH solution to remove the complex of interest. The characterization was performed by UV-Vis, ¹H-NMR, CV and DRX, whose crystal structure is illustrated in Figure 1. It was verified that the presence of dppz in the structure causes the complex to interact with the DNA, increasing by 5°C the melting temperature (T_m) of CT-DNA in phosphate buffer (1mM PO₄³⁻, 1mM NaCl, pH = 7.0). The next steps for the work are the determination of the quantum yield of ¹O₂ generation and the verification of the release of NO in biological medium.

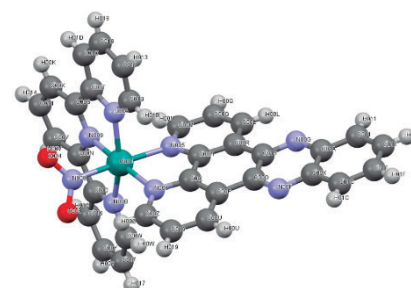


Figure 1: X-Ray Crystal Structure of [Ru(tpy)(dppz)(NO₂)](PF₆).

1. di Pietro, M. L., la Ganga, G., Nastasi, F. & Puntoriero, F. Ru(II)-dppz derivatives and their interactions with DNA: Thirty years and counting. *Applied Sciences (Switzerland)* **11**, (2021).
2. Aksakal, N. E., Kazan, H. H., Eçik, E. T. & Yuksel, F. A novel photosensitizer based on a ruthenium(ii) phenanthroline bis(perylene-diimide) dyad: synthesis, generation of singlet oxygen and in vitro photodynamic therapy. *New Journal of Chemistry* **42**, 17538–17545 (2018).
3. Dixon, I. M., Bonnet, S., Alary, F. & Cuny, J. Photoinduced Ligand Exchange Dynamics of a Polypyridyl Ruthenium Complex in Aqueous Solution. *Journal of Physical Chemistry Letters* **12**, 7278–7284 (2021).
4. Pereira, A. D. C., Ford, P. C., da Silva, R. S. & Bendhack, L. M. Ruthenium-nitrite complex as pro-drug releases NO in a tissue and enzyme-dependent way. *Nitric Oxide* **24**, 192–198 (2011).

Agradecimentos/Acknowledgments

The authors would like to thank the Brazilian agencies Conselho Nacional de Pesquisa e Desenvolvimento Tecnológico (CNPq), Fundação de Amparo à Pesquisa (Fapesp) and Coordenação de Aperfeiçoamento de Pessoal de Nível Superior (CAPES) for the financial support for this work.

Synthesis, characterization and crystal structure of a new 2D coordination polymer containing Cu(II) and 2-aminoterephthalic acid

Gabriel Salomão (IC)¹, Rachel C. V. Novas (PG)¹, Carolina Ligiero (PQ)¹, Camilla D. Buarque (PQ)¹,
Livia B. L. Escobar (PQ)^{1*}

¹Departamento de Química, Pontifícia Universidade Católica do Rio de Janeiro, Rua Marquês de São Vicente, 225 Gávea, 22451-900, Rio de Janeiro-RJ, Brasil.

gsdearaujo@hotmail.com, liviablescobar@puc-rio.br, cligiero@yahoo.com.br, chemistrykel@gmail.com

Keywords: Coordination Polymers, Crystal Structure

Highlights

Coordination polymers (CPs) have received a lot of attention due to their potential in interesting applications such as magnetism [1] and biologicals properties [2]. Here, a new CP, $\{[Cu_2(ATA)_2(DMF)_2]\}_n$, is presented.

Abstract

To produce a multifunctional CP, we have chosen two different classes of ligands, the aromatic carboxylates that can provide stability to the structure and the coumarins, which present important fluorescence and biologicals properties [2]. Coumarins are a class of compounds that exhibit a broad spectrum of biological properties including anticoagulant, anti-inflammatory, antioxidant, antiviral, antimicrobial, and anticancer agents as well as enzyme inhibitors. On the other hand, it has been reported that the incorporation of a metal ion into coumarin derivatives can increase the activity of such complexes compared to coumarin-based ligands [2]. Considering this, we tried to combine a coumarin derivative and the 2-aminoterephthalic acid to produce a coordination polymer that could show both magnetic and biological properties. The copper polymer was obtained according to the procedure shown in figure 1a):

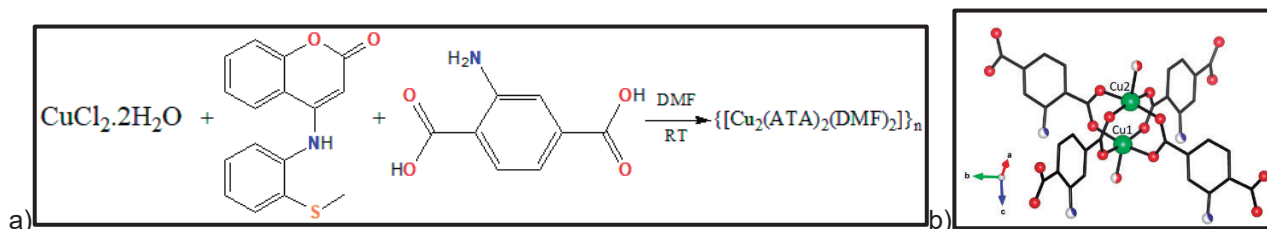


Figure 1: a) Synthetic route for the preparation of $\{[Cu_2(ATA)_2(DMF)_2]\}_n$. b) Fragment of the crystal structure of $\{[Cu_2(ATA)_2(DMF)_2]\}_n$.

After a few days, it could be seen some green crystals. Unfortunately, the infrared spectrum suggested that only the ATA ligand was coordinated to metal ion, and this was confirmed by the x-ray single crystal analysis. Figure 1b) shows the fragment of the crystal structure of the dimeric unit of repetition of the 2D polymer. Both Cu (II) ions are coordinated to four oxygen atoms from ATA ligand and one oxygen atom from a DMF molecule. The coordination geometry is square pyramidal. Given the short distance between Cu(1) and Cu(2), 2.64Å, interesting magnetic properties might be involved and this study is in progress.

Acknowledgments

CNPq and PUC-Rio

[1] Zhong-Yi Li *et. al.*; *Inorg. Chem. Com.*; **2023**; 148; 110348.

[2] Balewski Ł, Szulta S. *et. al.*; *Front. Chem.*; **2021**; 9; 781779.

Synthesis, characterization, and electronic structure of cobalt complexes with aryl imidazol ligand

Débora A. Steffler^{*1} (IC), Thiago L. P. Magalhães¹ (PG), Marcelo C. Nunes¹ (PG), Dr. Maurício P. Franco¹ (PD), Prof. Dr. André L. B. Formiga^{**1} (PQ)

*d233471@dac.unicamp.br; **formiga@unicamp.br

¹Chemistry Institute, UNICAMP

Keywords: Cobalt Complex, Aryl imidazol ligand, Electrosynthesis, DFT.

Highlights

Cobalt complex synthesized by electrosynthesis. Use of DFT and characterization of the coordination compound by NMR, HRMS, HPLC, CHN, Conductivity, UV-Vis, and FTIR.

Resumo/Abstract

The main goal of artificial photosynthesis is to mimic plants using sunlight to form high-energy compounds.[1] Coordination compounds can be used as efficient catalysts for fundamental reactions of artificial photosynthesis. The main complexes used in this process are ruthenium and iridium derivatives, which have a low abundance and high cost. However, a first-row transition metal known to catalyze water oxidation since the 1960s is cobalt,[2] which has a greater abundance and lower cost. Our group has an interest in pyridyl and imidazole ligands, the latter can be deprotonated, thus helping to control the oxidation potential of this possible catalyst. In this sense, we will present two cobalt complexes $[\text{Co}^{\text{II}}(\text{Impy})_3]^{2+}$ and $[\text{Co}^{\text{III}}(\text{Impy})_3]^{3+}$ and their synthesis and characterization (described in Figure 1).

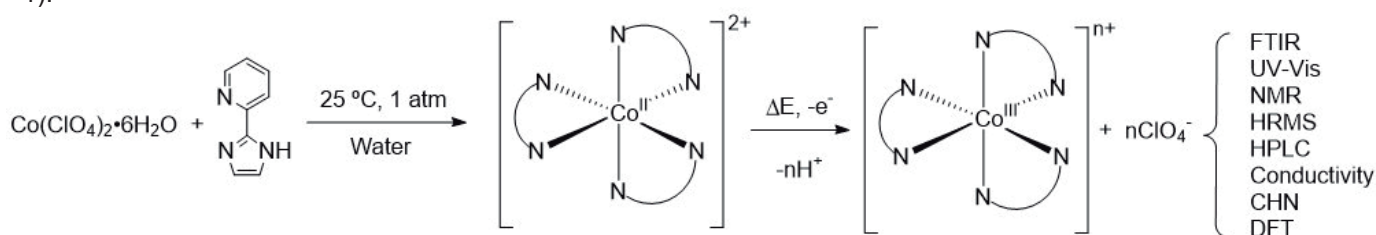


Figure 1. Synthesis e characterization of the complexes $[\text{Co}^{\text{II}}(\text{Impy})_3]^{2+}$ and $[\text{Co}^{\text{III}}(\text{Impy})_3]^{3+}$

Spectroscopy techniques and elemental analysis confirmed the proposed structure. In the conductivity measurement in acetonitrile, it was obtained that the molar conductivity for cobalt(II) and cobalt(III) complexes are 276.93 Scm^2/mol and 28.86 Scm^2/mol , respectively. Both values are higher than the pure solvent conductivity (0.45 $\mu\text{S}/\text{cm}$). In the case of the cobalt(II) complex, the value suggests the presence of one fully protonated complex $[\text{Co}^{\text{II}}(\text{Impy})_3]^{2+}$ and two perchlorates. Moreover, cobalt(III) complex conductivity values are between a ratio of 1:1 and no electrolytes, suggesting that there is a balance between monoprotonated and fully deprotonated species. By DFT, only fully deprotonated complexes were calculated. The spin density of both the facial and meridional isomers of the $[\text{Co}^{\text{II}}(\text{Impy})_3]$ complex is on cobalt, which confirms that oxidation occurs at this site, forming Co^{III} . Moreover, the facial and meridional isomers are isoenergetic, but there is a significant difference between the isomers during the reduction of Co^{III} to Co^{II} . There is no significant difference between the isomers in the binding distance of cobalt to the ligand.

The proposed compounds were synthesized and characterized experimentally and theoretically. According to the conductivity results, the cobalt(II) complex is fully protonated and there is a mixture of the cobalt(III) complexes in different degrees of protonation. Future voltammetric measurements will reveal the potential of the complex to be a catalyst for the water oxidation reaction. In addition, attempts will be made to crystallize the complexes for further X-ray diffraction (XRD) analysis.

[1] Concepcion, J. J., House, R. L., Papanikolas, J. M., & Meyer, T. J. (2012). Chemical approaches to artificial photosynthesis. *Proceedings of the National Academy of Sciences of the United States of America*, 109(39), 15560–15564.

[2] Anbar, M., Pecht, I., King, E., Mason, H. S., Morrison, M., & Wiley, J. (1937). The Oxidation States of the Elements and Their Potentials in Aqueous Solutions. In *Advances in Chemical Series* (Vol. 59, Issue 2). American Chemical Society.

[3] Ali, I., Wani, W. A., & Saleem, K. (2013). Empirical formulae to molecular structures of metal complexes by molar conductance. *Synthesis and Reactivity in Inorganic, Metal-Organic and Nano-Metal Chemistry*, 43(9), 1162–1170.

Acknowledgments

The authors would like to thank CNPq, CAPES, FAPESP, Unicamp, and CINE. (FAPESP 2017/11986-5).

Synthesis, characterization and interaction studies with HSA of a novel trinuclear ruthenium complex $[\text{Ru}_3\text{O}(\text{CH}_3\text{COO})_6(2\text{-OHIm})_3]\text{CH}_3\text{COO}$

Nathan C. Fernandes (IC),^{1*} Bruno F. A. Pinheiro (PG),¹ Sofia Nikolaou (PQ).¹

nathancamposfer@usp.br

¹Departamento de Química da Faculdade de Filosofia, Ciências e Letras de Ribeirão Preto – Universidade de São Paulo

Palavras-Chave: (Metallopharmaceutical, Ruthenium, HSA).

Highlights

A novel and water-soluble trinuclear ruthenium acetate containing 1(2-hydroxyethyl)imidazole ligands was synthesized. Fluorescence measurements indicates the formation of an adduct with HSA.

Resumo/Abstract

Trinuclear ruthenium acetates of general formula $[\text{Ru}_3(\mu_3\text{-O})(\mu\text{-OOCCH}_3)_6\text{L}_3]^+$, where L = N-heterocyclic ligand, represent an important class of metal complexes due to their reversible oxiredution chemistry and intramolecular charge transfer. In 2014, research groups revealed the cytotoxicity of trinuclear complexes $[\text{Ru}_3(\mu_3\text{-O})(\mu\text{-OOCCH}_3)_6\text{L}_3]^+$ and $[\text{Ru}_3(\mu_3\text{-O})(\mu\text{-OOCCH}_3)_6(\text{L})_2(\text{NO})]^+$ against lung (A549 strain) and murine melanoma (B16F10 strain) tumor cells, respectively.^{1,2} Aiming to expand the biological applications of this class of complexes, this study involves the synthesis of a novel and water-soluble trinuclear ruthenium acetate of formula $[\text{Ru}_3\text{O}(\text{CH}_3\text{COO})_6(2\text{-OHIm})_3]\text{CH}_3\text{COO}$, where 2-OHIm = 1(2-hydroxyethyl)imidazole. The characterization of the compound was performed using spectroscopic techniques such as UV-vis, H-NMR and FTIR.

UV-vis (H_2O): $\epsilon_{673} = 5016 \text{ M}^{-1} \text{ cm}^{-1}$ at 673 nm and $\epsilon_{498} = 1943 \text{ M}^{-1} \text{ cm}^{-1}$ at 498 nm. ¹H-NMR ($(\text{CD}_3)_2\text{SO}$): δ 6.9 (s, 2.88 H, NCHC), 5.69 (t, 6.15 H, OCH₂), 4.24 (t, 6.27 H, NCH₂), 4.07 (s, 2.82 H, NCHC), 1.97 (s, 2.84 H, NCHN), 1.66 (s, 18.00 H, C₂H₃O₂). IR (KBr): $\pi(\text{Ru}_3\text{O})$ 683, $\nu(\text{NCH}_2)$ 1105, $\delta_s(\text{CH}_3 \text{ (Ac)})$ 1350, $\nu_s(\text{CO}_2)$ 1430, $\nu_{\text{as}}(\text{CO}_2)$ 1530, $\nu(\text{OH})$ 3382 cm^{-1} .

Furthermore, the interaction of $[\text{Ru}_3\text{O}(\text{CH}_3\text{COO})_6(2\text{-OHIm})_3]\text{CH}_3\text{COO}$ with Human Serum Albumin (HSA) was evaluated from the quenching of albumin's fluorescence by the addition of a complex solution at 27 °C ($\lambda_{\text{exc}} = 295 \text{ nm}$ and $\lambda_{\text{em}} = 335 \text{ nm}$). Lifetime measurements were also performed at 27 °C for HSA solutions containing different concentrations of complex. No significant changes in the albumin's excited state lifetime were observed, indicating a purely static quenching mechanism.³ From the data treatment, the equilibrium constant ($K_{\text{SV}} = 17310 \text{ M}^{-1}$) for the adduct complex-HSA formation was obtained from Stern-Volmer plots. Thermodynamic parameters are going to be evaluated from van't Hoff equation by repeating the fluorescence titrations at different temperatures.

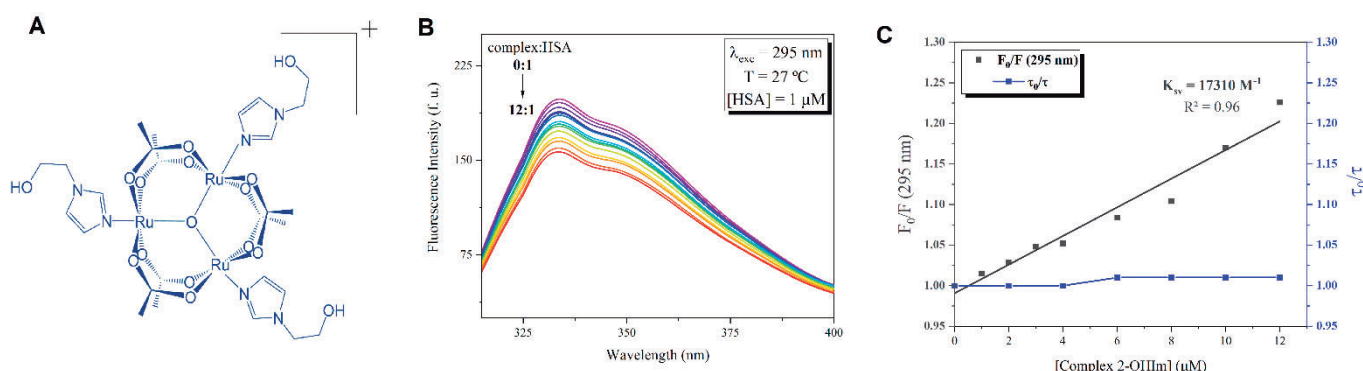


Figure 1. (A) Structural representation of $[\text{Ru}_3\text{O}(\text{CH}_3\text{COO})_6(2\text{-OHIm})_3]\text{CH}_3\text{COO}$ (B) Fluorescence quenching of HSA by the addition of $[\text{Ru}_3\text{O}(\text{CH}_3\text{COO})_6(2\text{-OHIm})_3]\text{CH}_3\text{COO}$ complex; (C) Stern-Volmer plot and lifetime measurements of HSA solutions with different complex concentrations.

[1] Tauchman J., Paul L. E. H., Furrer J., Therrien B., Süß-Fink G. *Inorg. Chem.*, 423 (2014), p. (16-20). [2] Carneiro Z. A., Biazoto, J. C., Alexiou, A. D. P., Nikolaou S. J. *Inorg. Biochem.*, 134 (2014), p. (36-38). [3] Balzani, V., Ceroni, P., & Juris, A. (2014). *Photochemistry and Photophysics*. Wiley-VCH.

Agradecimentos/Acknowledgments



Synthesis, characterization and *in vitro* antibacterial activity of a silver(I) complex with 5-(trifluoromethyl)uracil

Gabriele de M. Pereira (PG)¹, Fernando R. G. Bergamini (PQ)², Silmara Cristina L. Frajácómo (PQ)³, Wilton R. Lustrí (PQ)³ and Pedro P. Corbi (PQ)¹

gabriele_menezes@hotmail.com; ppcorbi@unicamp.br

¹Institute of Chemistry, University of Campinas-UNICAMP; ²Institute of Chemistry, Federal University of Uberlândia-UFU; ³Biological and Health Sciences Department, University of Araraquara-UNIARA.

Keywords: 5-(Trifluoromethyl)uracil, Silver(I), Antibacterial activity.

Highlights

- ◆ A novel silver(I) complex of with 5-(trifluoromethyl)uracil is presented.
- ◆ Spectroscopic data suggest ligand coordination to Ag(I) by nitrogen and oxygen atoms.
- ◆ The complex was inactive over Gram-positive and Gram-negative strains.

Resumo/Abstract

Metal complexes are used in medical practice for different purposes [1]. Silver complexes, as silver sulfadiazine for example, have been used to treat bacterial skin infections for a long time [2]. One strategy for overcoming bacterial resistance is the combination of well-known bioactive metals with ligands that already possess medicinal applications [3]. Nucleotide analogs are a class of bioactive molecules that have been used in medicine as antiproliferative agents. One representative nucleotide analog widely used in the treatment of various types of cancer is 5-fluorouracil (5-FU) [4]. Due to the established use of nucleotide analogues in cancer treatment, new molecules of this class have also been studied as potential antibacterial agents. Considering this context, the present work describes the synthesis and biological study of the silver complex with the nucleotide 5-(trifluoromethyl)uracil.

The silver(I) complex with 5-(trifluoromethyl) uracil (Ag-5TFMU) was prepared by the reaction of 1.0 mmol of an alkaline aqueous solution 5-(trifluoromethyl)uracil with 1.0 mmol of silver nitrate. The reaction was carried out under magnetic stirring for 2 hours without heating. The complex was collected by filtration, washed, and dried. The composition found for this complex was $\text{AgC}_5\text{H}_2\text{F}_3\text{N}_2\text{O}_2$. Anal. Calcd. for $\text{AgC}_5\text{H}_2\text{F}_3\text{N}_2\text{O}_2$: C 20.93%; H 0.70%; N 9.76%. Found: C 20.83%; H 0.59%; N 9.73%. Mass spectrometric data permitted the identification of $[\text{Ag}_3(5\text{TFMU})_2]^+$ and $[\text{Ag}_4(5\text{TFMU})_3]^+$ ions at m/z 680.7256 and 968.6370, respectively. The presence of the species with four silver atoms may be due to a recombination during the fragmentation process of the sample under analysis, or even by the presence of a polymeric arrangement for the silver(I) complex with 5-(trifluoromethyl)uracil. Infrared (IR) and solid-state ^{13}C nuclear magnetic resonance (NMR) spectroscopies suggest coordination of the ligand to silver by oxygen and nitrogen atoms in a bidentate mode.

The antibacterial activity of the Ag-5TFMU complex was preliminarily evaluated by minimal inhibitory concentration (MIC) assays. The complex was inactive over Gram-positive (*S. aureus* and *B. cereus*) and Gram-negative (*P. aeruginosa* and *E. coli*) bacteria at concentrations of 3.80 to 7.61 $\text{mmol}\cdot\text{L}^{-1}$. Further studies over other bacterial strains are envisaged.

References

- [1] TESAURO, D. Metal complexes in diagnosis and therapy. *International Journal of Molecular Sciences*, v. 23, n. 8, p. 4377, 2022.
- [2] CANDIDO, T. Z. et al. Silver Nimesulide Complex in Bacterial Cellulose Membranes as an Innovative Therapeutic Method for Topical Treatment of Skin Squamous Cell Carcinoma. *Pharmaceutics*, v. 14, n. 2, p. 462, 2022.
- [3] CIOL, M. R. et al. A silver complex with cycloserine: synthesis, spectroscopic characterization, crystal structure and *in vitro* biological studies. *ChemistrySelect*, v. 3, n. 6, p. 1719-1726, 2018.
- [4] NUNES, J. H. B. et al. Synthesis, characterization and *in vitro* biological assays of a silver(I) complex with 5-fluorouracil: A strategy to overcome multidrug resistant tumor cells. *Journal Fluorine Chemistry*, v. 195, p. 93-101, 2017.

Agradecimentos/Acknowledgments

The authors would like to thank to CAPES, FAPESP (grant # 2021/08717-8), FAEPEX and CNPq (Brazilian agencies)

Synthesis, characterization and solution studies of the interaction of a new *N*-acylhydrazone containing the 3,4,5-trimethoxybenzene group with aluminum

Dayanne Martins (PG),^{1*} Roberta Lamosa (IC),¹ Daphne S. Cukierman (PQ),¹ Nicolás A. Rey (PQ),¹

*dayanne.martinspppp@gmail.com

¹ Laboratory of Organic Synthesis and Coordination Chemistry Applied to Biological Systems (LABSO-Bio), Department of Chemistry, Pontifical Catholic University of Rio de Janeiro (PUC-Rio)

Keywords: Parkinson's disease, Synucleinopathies, Aluminum, *N*-acylhydrazones.

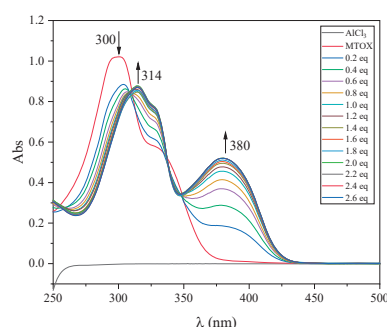
Highlights

Due to the involvement of metal ions in the process of neural degeneration, a new *N*-acylhydrazone was synthesized and evaluated for aluminum(III) chelation properties. The study of *N*-acylhydrazone-derived chelating agents has held promise with potential bioactivity in the treatment of diseases such as Parkinson's disease (PD).

Resumo/Abstract

Metal dyshomeostasis and the presence of exogenous metals in humans have been linked to neuropathologies such as Parkinson's disease (PD), by their action on protein aggregation processes and oxidative stress, causing neuronal death. Aluminum(III), in particular, constitutes a neurotoxic agent of known effect on the nervous system¹. In addition to elevating the production of reactive oxygen and nitrogen species², exposure to Al³⁺ also causes iron dyshomeostasis through increased Fe³⁺/Fe²⁺ oxireduction activity³. Developing new drugs that preclude the accumulation of metal ions that induce protein aggregation and, in the case of Al³⁺, contribute to oxidative stress, is crucial to slowing the progression of PD. In this work, the ligand 2-hydroxy-3-methyl-benzaldehyde 3,4,5-trimethoxybenzoyl hydrazone (MTOX) was synthesized, characterized using solid-state and solution spectroscopic techniques, and its toxicity was evaluated by exposure of increasing concentrations to the yeast *Saccharomyces cerevisiae*. We also investigated the binding properties of this ligand against Al³⁺ ions in solution. The synthesis, via Schiff's base condensation reaction, had a yield of 78.1% with the formation of a pale yellow precipitate; MP: 180±1°C; IR(KBr)_{vmax}: 3177; 1652; 1605; 1586; 1240 cm⁻¹. Preliminary results show stability of the binder against hydrolysis within 12 hours at 25 °C. The ligand showed low toxicity at concentrations up to 900 μM, indicating the feasibility of its use in *in vitro* cell-based and *in vivo* systems. Spectrophotometric studies evaluating the interaction with Al³⁺ ions showed a bathochromic shift of hydrazonic absorption from 300 to 314 nm after complexation (Figure 1), and the appearance of a new band attributed to a charge transfer process from the ligand to the metal (TCLM). The absorbance constant value at the absorbance maximum of the complex was reached approximately 6 hours after mixing in solution of the ligand with metal. The dependence of the absorbance at the spectral maximum at 380 nm (TCLM band) indicates complexation with the addition of two metal equivalents on the ligand, which suggests the formation of a complex with stoichiometry M₂L. Further studies are in progress in order to characterize the complex in the solid state and the effectiveness of the ligand in experimental models of aluminum-related PD.

(a)



(b)

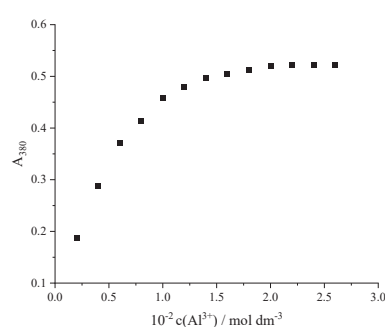


Figure 1. (a) Complexation study of MTOX ($c = 5 \times 10^{-5} \text{ mol L}^{-1}$) with AlCl₃ in DMSO/buffer mixture 10/90. pH = 4.5; $l = 1 \text{ cm}$. $\theta = (25.0 \pm 0.1) \text{ }^\circ\text{C}$. (b) Dependence of absorption at 380 nm on Al³⁺ concentration. (●) experimental.

¹ Exley, C. e Mold, M. J.; *Journal of Biological Inorganic Chemistry* **2019**, *24*, 1279.

² Pasha, A. e Oglu, A.; *MedBioTech Journal* **2017**, *1*, 91.

³ Wael M. et al; *Journal of Hazardous Materials* **2011**, *192*, 881.

Agradecimentos/Acknowledgments

This work was supported by FAPERJ, CAPES and CNPq.

Área: INO*(Inserir a sigla da seção científica para qual o resumo será submetido. Ex: ORG, BEA, CAT)***Synthesis of catalytic rare-earth materials for CO₂ conversion with microwave assisted heating****Marcelo C. Portes (PG),¹ Caique S. Fernandes (IC),¹ Lucas Duriguetto (IC),¹ Pedro M. Vidinha (PG),¹ Lucas C. V. Rodrigues (PG),^{1*}****marcelo.portes@usp.br; lucascvr@iq.usp.br**¹Departamento de Química Fundamental, IQ-USP;Palavras Chave: *rare earth, catalysis, cerium nanoparticles, CO₂ conversion.***Highlights**Microwave-assisted synthesis of cerium oxide nanoparticles. Synthesis of cerium oxide nanoparticles doped with rare earth ions. Catalytic materials for CO₂ conversion.**Resumo/Abstract**

Synthesis and characterization catalysts for CO₂ conversion from the mixture of rare earth cerium doped with lanthanum in order to obtain doped nanoparticles capable of carrying out the catalytic conversion of CO₂ into useful molecules such methanol, ethanol and others, using a supercritical CO₂ reactor. The cerium oxide nanoparticles were synthesized, via microwave assisted solvothermal route having its synthesis optimized for a domestic microwave oven and characterized by X-ray diffraction and SEM (Figure 1 A and B respectively). The nanoparticles presented a promising rate for CO₂ conversion, especially to methanol using a gas mixture of 50/50 of H₂ and CO₂. The nanoparticles presented a 1% conversion rate, from witch almost 30% were converted to methanol (Figure 1C). Finally, other gas mixtures compositions as well as Lanthanum-doped materials were studied for optimization of the catalytic process.

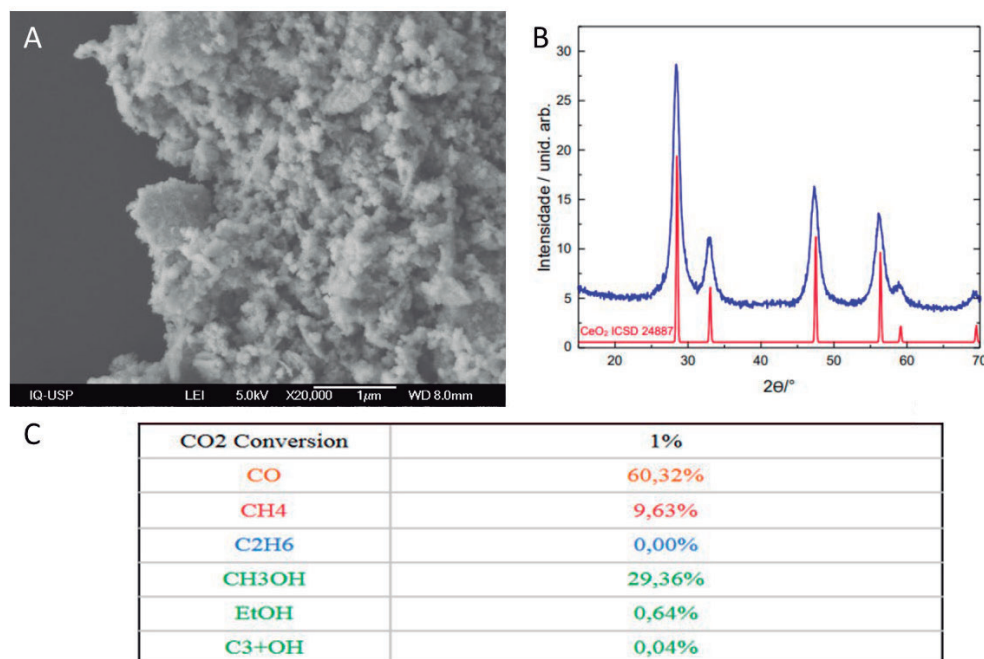


Figure 1. A) SEM image of the non-doped Cerium nanoparticles. B) XRD pattern of the non-doped nanoparticle and C) Table of CO₂ conversion for the non-doped nanoparticle.

Agradecimentos/Acknowledgments

To Universidade de São Paulo (PIPAE 2021.1..10424.1.9)

46ª Reunião Anual da Sociedade Brasileira de Química: "Química: Ligando ciências e neutralizando desigualdades"

Synthesis of fluorescent labelled mesoporous silica nanorod reservoir (MCM-41) for an anticancer nanovalve fabrication

Aline F. M. da Silva (PQ)^{1*}, Daniel P. Levita (IC)¹, Thiago C. dos Santos (PQ)² and Célia M. Ronconi (PQ)^{1*}.

alines@id.uff.br, cmromconi@id.uff.br

¹Departamento de Química Inorgânica, Universidade Federal Fluminense, Campus do Valonguinho, Outeiro de São João Batista, s/n, 24020-141, Niterói, RJ, Brasil; ²Departamento de Química Inorgânica, Universidade Federal do Rio de Janeiro, Cidade Universitária, Outeiro de São João Batista, s/n, 21941-909, Rio de Janeiro, RJ, Brasil.

Keywords: Silica nanoparticles, MCM-41, Nanorods, Drug delivery, Fluorescence labelling, Lanthanide.

Highlights

Silica nanoparticles can form traceable nanovalves through fluorescent labelling. Preparation of labelled nanorods with lanthanides to be used as reservoirs for anticancer drugs is being investigated to be applied as nanovalves for cancer treatment.

Abstract

Mesoporous silica nanoparticles (MSNs) possess properties like biocompatibility, tunable pores and chemically modifiable surface, that make them promising material for drug delivery systems, such as nanovalves.^{1,2} It is known that MSNs morphology plays an important role in drug cell internalization, with better results for rod-shaped systems, demonstrated in our previous work.¹ However, MSNs behavior during and after drug delivery has been not addressed, which is crucial for biomedical applications, thus MSNs labelled can provide more detailed information on the interaction of the material with the cells. Here, we describe the characterization of two types of lanthanide-doped MCM-41 nanorods, prepared by low (r-MS-LLn) and high (r-MS-HLn) additions of Gd³⁺ and Eu³⁺ nitrates during the synthesis, using hexadecyltrimethylammonium bromide (CTAB), tetraethyl orthosilicate and ammonium hydroxide. ATR-FTIR spectra exhibits characteristic Si-O-Si (~1000 and 800 cm⁻¹) and Si-OH (~950 cm⁻¹) vibrational modes, as well as C-H bonds (~2900 cm⁻¹) from CTAB in the mesopores. XRD analysis shows peaks related to MSNs hexagonal symmetry and structure (Figure 1). A *d*₁₀₀-spacing shift and peak decrease in r-MS-HLn may be due to incorporation of more lanthanide heteroatoms or formation of Gd₂O₃ or Eu₂O₃ clusters.³ X-ray fluorescence allows the observation of Si and Gd peaks and reveals a mass composition of 98.17% Si and 1.15% Gd for r-MS-LLn and 97.27% Si and 2.46% Gd for r-MS-HLn, in accordance with the low and high additions of lanthanide nitrates. This result suggests that both materials have been successfully labelled. Our perspectives are to proceed with silica functionalization, drug loading and enclosing of MCM-41, for drug release and biological tests.

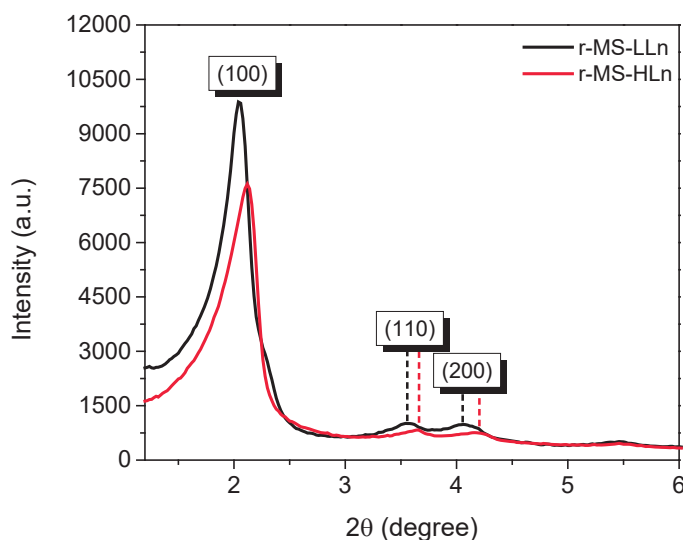


Figure 1. PXRD of r-MS-LLn and r-MS-HLn.

- [1] Da Silva, A. F. M. et al. *ACS Appl. Nano Mater.* **2022**, 13805.
 [2] Chircov, C. et al. *Molecules* **2020**, 25 (17), 3814.
 [3] Liu, J. et al. *RSC Adv.* **2019**, 9 (70), 40835–40844.

Acknowledgments

CAPES, CNPq, FAPERJ (Programa Redes de Pesquisa em Nanotecnologia no Estado do RJ grant number E-26/010.000981/2019), PPGQ-UFF, LAME-UFF, LAMATE-UFF, CMULT-PPGQu-UFRJ.

Área: INO

Synthesis of nano copper ferrite (CuFe_2O_4) prepared from electronic waste printed circuit boards

Ingrid G. S. Machado (IC), João Victor F. Felício (IC), Debora S. Netto (TM), Gabrielly C. B. L. Cavalcante (TM), Maria Karoline C. Souza (TM), Aryanne L. Bonifácio (TM), Marcel L. Machado (TM), Thiago de F. Fortes (TM), Wagner D. Rocha (PQ), Denise B. A. Barbosa (PQ)*.

denise.barbosa@ifsudestemg.edu.br

Laboratório de Pesquisas e Experimentos em Nanociência do IF SUDESTE MG – Campus Juiz de Fora

Key words: Ferrite, Nanomaterials, Electronic waste, Nanoparticles.

Highlights

Nanomaterial synthesis from electronic waste is an effective way for recycle. This work presents a tetragonal copper ferrite CuFe_2O_4 have been synthesized using electronic waste printed circuit boards.

Resumo/Abstract

Firstly, the separation of the different components of the PCBs was carried out. Leaving the plate with only the copper trails, we proceeded to acid leaching with H_2SO_4 and H_2O_2 (Yang and Yang, 2011). Then, the synthesis of copper ferrite nanoparticles was performed by coprecipitation. For each 100 ml of waste, a solution of 2.0 mol/L of NaOH was added drop by drop, under constant stirring, until pH=12. Next, the suspended precipitate was heated to 80°C and kept under stirring for 1 hour. The product obtained was cooled to room temperature, filtered and washed with distilled water. Soon after, the obtained nanoparticles were calcined at 900°C for 4 h. The nanoparticles were characterized by X-ray diffraction in a diffractometer (Bruker D8) using $\text{Cu K}\alpha$ radiation ($\lambda = 1.5406 \text{ \AA}$), in the range (2θ) = 10° - 80° in steps of 5°/s. Peaks were identified in 2θ of 18.3°, 29.9°, 30.5°, 34.7°, 35.8°, 37.1°, 41.8°, 43.7°, 55.4°, 57.8°, 62.1°, 63.6° and 74.6°, which according to the literature (JCPDS Card No. 34-0425) correspond to planes (101), (112), (200), (103), (211), (202), (004), (220), (105), (321), (224), (400) and (413) respectively and close to what is expected for the CuFe_2O_4 ferrite. Also was identified a phase of CuO in 2θ of 48.7°, 65.7° e 68,01°. The average crystal size of CuFe_2O_4 was reached around 24 nm according to the Scherrer equation, which evidently approves the nanometric crystallinity of the prepared copper ferrite. The study of spectroscopy in the infrared region (FT-IR) was carried out in the Frontier FTIR spectrophotometer (Perkin Elmer) in the wave number range (400-3500 cm^{-1}). The presence of a band at 586 cm^{-1} characteristic of the Fe-O of the tetrahedral and at 418 cm^{-1} characteristic of the Metal-Oxygen bond of the octahedral site (site B) was observed. In addition, the structural characteristics of ferrite were studied through metallography. The metallographic tests were performed using optical microscopy, the images were captured using the Olympus GX51 image analyzer. For this analysis, powder samples were made by embedding them in resin, in order to be able to visualize the structure under an optical microscope. Then, the samples were sanded, polished before the metallographic test, to obtain a surface free of irregularities and imperfections. Areas can be observed grain boundary, with intragranular and intergranular pores. The presence of CuO provides an increase in porosity due to the increase in the thickness of the layer of the liquid phase rich in CuO located between the grains, decreasing the apparent density of the samples. The electrical properties was studied as a function of frequency at room temperature in a frequency 20Hz -3MHz range. It was observed, real and imaginary part of the dielectric constant decreases with increasing frequency while AC conductivity increasing. This polarization occurs in all heterogeneous crystalline materials (which are more than one phase). Similar results have been observed in other research of ferrite systems. The Magnetic and Photocatalytic degradation studies are being carried out.

United Nations University (UNU). The Global E-waste Monitor 2020 quantities, flows and the circular economy potential. Germany. 2020. Disponível em: https://wedocs.unep.org/bitstream/handle/20.500.11822/9648/Waste_crime_RRA.pdf?sequence=1&isAllo wed=y. Acesso em: 30 out 2022.

XRD pattern of CuFe_2O_4 nanoparticles with JCPDS. Research Gate, 2021. Disponível em: <https://www.researchgate.net/figure/XRD-pattern-of-CuFe2O4-nanoparticles-with-JCPDS-File-No-340425-and-050667-in-inset-for_fig1_320645913>. Acesso em: 4 nov 2022.

Yang, H., J. Liu and J. Yang, Leaching copper from shredded particles of waste printed circuit boards. Journal of Hazardous Materials, 2011. 187 (1-3)

Agradecimentos/Acknowledgments

IF Sudeste MG – Campus Juiz de Fora

Área: INO

Synthesis of the [Eu(BTFA)₃(PIB_4CH₃)] complex with potential application in red light emitting LEDs

Giovanna C. Marineli (IC),¹ Rodolpho A. N. Silva (PG),¹ Ana M. Pires (PQ),^{1,2} Marian R. Davolos (PQ)^{1*}
 g.marineli@unesp.br; marian.davolos@unesp.br

¹Institute of Chemistry, São Paulo State University (Unesp), Araraquara; ²School of Technology and Sciences, São Paulo State University (Unesp), Presidente Prudente

Keywords: Luminescence, Europium, Coordination compounds, Spectroscopy.

Highlights

In this work, a new complex [Eu(BTFA)₃(PIB_4CH₃)] was synthesized, characterized, and its optical profile was studied via photoluminescence. The complex shows a potential application in LEDs.

Abstract

Complexes containing lanthanide ions have been widely used in luminescent materials, such as in sensors, in LEDs, and other displays, due to the possibility of materials development with high emission intensity, and good thermal and optical stability, among others. In these compounds, the applications are based on the optical properties that come from 4f-4f transitions, prohibited by the Laporte and the spin rules. Thus, lanthanide ions have low molar absorptivity. In coordination compounds containing these ions, the luminescence is improved through the already widely used “antenna effect”, where coordinated organic molecules, absorb the incident energy and transfer this energy to the lanthanide ion, resulting in the high luminescence observed.¹ In this work, a complex was synthesized (Figure 1), with a phenanthroline derivative (PIB_4CH₃) and β-diketone (BTFA) as ligands. The complex was characterized via FTIR, where the variations in the C=O and C=N stretches, as well as the appearance of new stretches attributed to the Eu-O and Eu-N bonds, suggested the formation of the complex. Also, via mass spectrometry, it was possible to observe the molecular ion signal of the complex, at 1106 Da [M - 1H⁺], referring to the target ligands/Eu(III) ratio. Via PLS, it was possible to observe a significant increase in the values of quantum efficiency, when compared with the complex containing BTFA and H₂O as ligands (Table 1), which shows the importance of the ligand PIB_4CH₃ in replacing the water molecules of the system. So, it can be concluded that the compound was successfully synthesized and characterized and its photoluminescence profile indicated a significant improvement in light emission when compared to the “precursor” complex.

Complex	Quantum efficiency (%)
[Eu(BTFA) ₃ (H ₂ O) ₂]	28
[Eu(BTFA) ₃ (PIB_4CH ₃)]	61

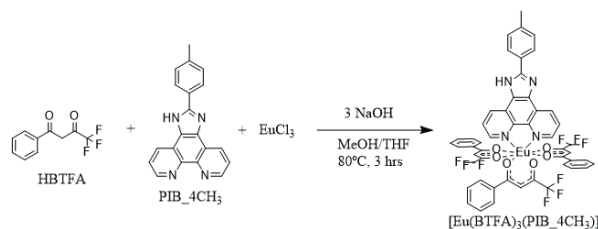


Table 1: Quantum efficiency of the complexes.

Figure 1: Equation of the synthesis reaction.

1. Nathalia B. D. Lima et al. A Comprehensive Strategy to Boost the Quantum Yield of Luminescence of Europium Complexes. Sci. Rep. 3, 2395, 2013.

Agradecimentos/Acknowledgments

CAPES and CNPq (procs: 141081/2020-1 e 317610/2021-0)

46ª Reunião Anual da Sociedade Brasileira de Química: “Química: Ligando ciências e neutralizando desigualdades”

Systematic preparation of metalloporphyrin-based magnetic core@shell catalysts for CO₂ fixation reactions

Everton Henrique dos Santos¹, Vanessa Prevot², Claude Forano², Shirley Nakagaki¹

everhs1@gmail.com; shirleyn@ufpr.br

¹Laboratório de Bioinorgânica e Catálise, - Departamento de Química - Universidade Federal do Paraná, - CP 19032, fax: +55-41-33613186, CEP 81531-980, Curitiba, PR, Brazil; ²Institut de Chimie de Clermont-Ferrand (ICCF) - UMR CNRS 6296, Université Clermont Auvergne, Campus Universitaire des Cézeaux, TSA 60026 CS 6006, 63178 AUBIERE Cedex – France.

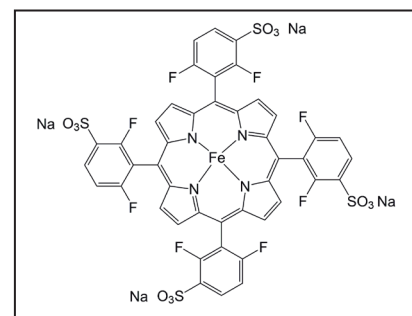
Palavras Chave: Metalloporphyrin, Heterogeneous Catalysis, Sequential Reaction, Core@shell, Magnetite, Layered Solids.

Highlights

Systematic preparation of core@shell-like multifunctional catalysts, based on different metalloporphyrins, layered double hydroxides and magnetite, for CO₂ cyclic addition reactions to epoxide.

Resumo/Abstract

Knowing the metalloporphyrin (**MP**) high efficiency as catalyst towards a range of reactions [1], improving their reusability by producing **MP**-based heterogeneous catalysts is of interest, which also can provide better protection for **MP**, avoiding, for instance, biomolecular interactions that may lead to **MP** deactivation and low solubility in the reaction medium. Additionally, it may consequently bring up new properties as support's intrinsic catalytic sites, magnetic susceptibility and others [2]. Such properties may generate interesting catalysts for wide range of reactions due to synergic effects from catalyst-support [3]. Taking these points in consideration, our goal is to develop core@shell-like supports based on magnetite (Fe₃O₄) as core, using a proposed route, and investigating and understanding the growth of a shell composed of layered double hydroxides (Mg₃Al- or Ni₃Al-LDH), followed by immobilization of different **MP**, e.g. **[M(TDFSPP)]** (Figure), where M = Fe³⁺ (Figure), Mn³⁺, Zn²⁺ or Mg²⁺. The solid supports were analyzed by powder XRD, TEM, FTIR, SEM, ICP-OES and TGA techniques. After that, the catalytic ability of these solids was investigated in different reactions: oxidation of cyclohexane and cyclooctene, photo-assisted H₂ generation and cross-coupling reactions, such as esterification reaction of cyclohexanol and acetic acid, besides the CO₂ cycloaddition to epoxides. Considering the best conditions for each reaction, assisted-Tandem sequential reactions are under study, for example, the cyclooctene oxidation followed by CO₂ addition to cyclic carbonate obtention.



REFERENCES

- [1] D. Dolphin, T.G. Traylor, L.Y. Xie, Acc. Chem. Res. 30 (1997) 251.
- [2] G.S. Machado, G.G.C. Arízaga, F. Wypych, S. Nakagaki, J. Catal. 274 (2010) 130-141.
- [3] E. H. Santos, C. Carvalho, C. M. Terzi, S. Nakagaki, Molecules, 23 (2018) 2796.

Agradecimentos/Acknowledgments



INSTITUT DE CHIMIE
DE CLERMONT-FERRAND

The cytostatic and apoptotic effects of nitrosyl ruthenium complex such as *cis*-[RuNO(bpy)₂(pyridine-x)]³⁺ complex in cancer cell line

Eduardo Rodrigues da Silva^{1*} (IC), Rafaella Rebecchi Rios¹ (PQ), Amanda Blanque Becceneri¹ (PQ), Marcela Tavares Luiz² (PQ), Marlus Chorilli² (PQ) and Roberto Santana da Silva¹ (PQ).

eduardoguedasilva@gmail.com; silva@usp.br

¹School of Pharmaceutical Sciences of Ribeirão Preto - USP, FCFRP; ²School of Pharmaceutical Sciences of São Paulo State University - UNESP, FCFAR.

Keywords: Metallopharmaceutical, Ruthenium complexes, Nitric oxide, Cytotoxicity, Cytostatic.

Highlights

Nitrosyl ruthenium complexes as cytostatic agents.

Abstract

Thenitric oxide delivery agents based on ruthenium complex demonstrate prosperous as new metallopharmaceutical drugs with anticancer activity specially in synergistic effect with reactive oxygen species (ROS)¹. Based on that, it is important to understand the effect of each radical molecule in the biological process. We have synthesized *cis*-[Ru(bpy)₂NO(L)]³⁺ complex (bpy= 2,2'-bipyridine; L= chloride, pyridine, 4-picoline, 4-acetylpyridine) as compounds that release NO exclusively. Details of chemical characterization such as UV-vis, Infrared and cyclic voltammetry are provided on Table 1. The UV-visible spectra show typical shape of nitrosyl ruthenium species with bands centred on UV region attributed to Metal-ligand and intra ligand transitions as judged by molecular orbital calculations. The electrochemical studies are a fascination. In acetonitrile it is observed reversibility process for {Ru^{II}-NO⁺}^{3+/2+} follow by irreversible one attributed to {Ru^{II}-NO⁰}^{2+/+} (Table 1). Different behaviour was observed in aqueous solution, which is better described as in Scheme 1. Studies concerning the cytotoxicity of the *cis*-[Ru(bpy)₂NO(4-pic)]³⁺ complex against the triple negative breast cancer MDA-MB-231 cell line among 7.8 – 250 μM (Figure 1) and CHO-K1 cell line among 50 – 500 μM (Table 2) were performed. No significant cytotoxic effect was observed in CHO-K1 and in the concentrations 125 and 250 μM in MDA-MB-231 the cytotoxic were significant; however the nitrosyl ruthenium complex present incredible cytostatic effect in CHO-K1, based on the Wound Healing experiments (Figure 2). Studies related to the use of nanoparticle to increase cellular uptake are in development and will provide relationship between concentration and activity. In conclusion NO seems to stop the spread of tumor cells through blocking specific molecules, even in very low concentrations, that is involved in tumor progression, which make more effective the use of other chemotherapeutic agents such as singlet oxygen.

Table 1. Spectrophotometric and electrochemical characterizations of the species *cis*-[Ru(bpy)₂(NO)(L)]³⁺.

<i>cis</i> -[Ru(bpy) ₂ (NO)(L)] ³⁺	UV-Vis λ, (log ε)	E (V vs Ag/AgCl) NO ^{+/0} ; NO ^{0/-}	ν(NO) (cm ⁻¹)
4-pic	301, (4,30)	+0,57;-0,34	1954
py	301, (4,22)	+0,58;-0,33	1947
4-acpy	301, (4,27)	+0,58;-0,31	1952
Cl	296, (4,25)	+0,25;-0,55	1932

Table 2. Cytotoxicity of the *cis*-[Ru(bpy)₂NO(4-pic)]³⁺ in CHO-K1 cell line.

Concentrations	
500μM	84,3% ± 0,04
400μM	92,4% ± 0,05
300μM	99,5% ± 0,07
200μM	101,8% ± 0,04
100μM	107,4% ± 0,05
50μM	109,4% ± 0,03

Figure 2. *cis*-[RuNO(bpy)₂(4-pic)]³⁺ cytostatic effect.

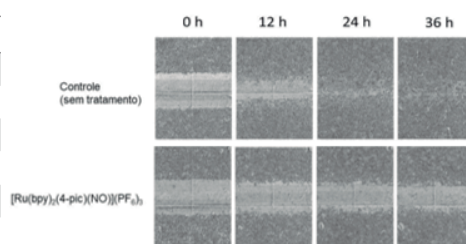
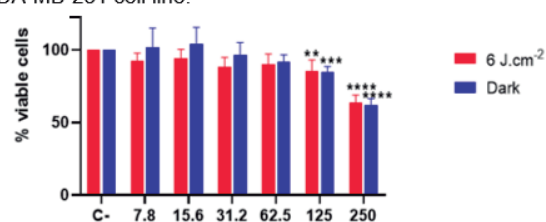
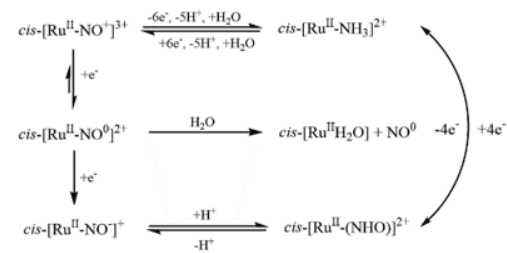


Figure 1. Cytotoxicity of the *cis*-[Ru(bpy)₂NO(4-pic)]³⁺ in MDA-MB-231 cell line.



Scheme 1. Mechanism of conversion of the nitrosyl group in aqueous medium.



[1] R.G. de Lima, R. Rios, A.E. da Hora and R.S. da Silva in: Advances in Inorganic Chemistry, 80, 355, 2023.

Acknowledgments

Acknowledgments: FAPESP (2022/10343-1), CNPq and FCFRP.

The effect of fluorine alkali-earth metals on the thermal, structural and luminescent properties of Eu³⁺-doped niobium oxyfluoride glass

Leandro O. E. da Silva (PG),¹ Marcos de Oliveira Júnior (PQ),² Rodrigo Falci (PQ),³ Victor A. Rivera (PQ),³ Danilo Manzani (PQ),^{1*}

le.olivetti@usp.br; dmanzani@usp.br

¹São Carlos Institute of Chemistry, University of São Paulo (USP), São Carlos, SP, Brazil; ²São Carlos Institute of Physics, University of São Paulo (USP), São Carlos, SP, Brazil; ³Centre d'Optique, Photonique et Laser (COPL), Université Laval, Quebec, Canada.

Keywords: fluorine alkali-earth, Eu³⁺-luminescence, structural properties, niobium oxyfluoride glass

Highlights

Different alkali-earth periodically affects the T_g, Eu³⁺ luminescence and UV-vis absorption; it is supposed that Sr²⁺ occupy the same Pb²⁺ site, presenting exceptional results; Eu³⁺ was used as a structural probe.

Resumo/Abstract

In this work, niobium oxyfluoride glass samples were synthesized with molar compositions 60Pb₂P₂O₇-20Nb₂O₅-20XF₂ and 98.5[60Pb₂P₂O₇-20Nb₂O₅-20XF₂]:1.5Eu₂O₃ (X = Mg, Ca, Sr, and Ba). The effect caused by the presence of different earth-alkali metals were studied from the thermal, structural, optical, and luminescence points of views by using DSC, Raman, ¹⁹F, ³¹P, and ²⁰⁷Pb NMR, UV-vis absorption and Eu³⁺ photoluminescence. Eu³⁺ was used as a structural optical probe to study the effect of different earth-alkali metals on their spectroscopic properties by evaluating the Judd-Ofelt parameters Ω_2 and Ω_4 and lifetimes. Preliminary results demonstrated the presence of other earth-alkali metals directly affects the luminescent properties which was evaluated by the intensity ratio of Eu³⁺ ⁵D₀ → ⁷F₁ / ⁵D₀ → ⁷F₂ transitions. The increase of the earth-alkali ionic radii induces an increase of the local symmetry around Eu³⁺, excepting for Sr²⁺ which demonstrated a higher asymmetry around the ion attested by the intensity ratio, Ω_2 parameter and lower lifetimes when compared with the other samples (1.56 ms, while 1.66, 1.67 and 1.68 ms for Mg²⁺, Ca²⁺, and Ba²⁺, respectively). ¹⁹F NMR indicates the formation of F—Nb and F—X bonds (X = earth-alkali metals), while ³¹P NMR indicates the formation of isolated phosphorus and P—O—P bonds in Q¹ units. Moreover, the increase of the earth-alkali ionic radii induces a decrease in their thermal stability against crystallization, except for Sr²⁺, which showed the lower thermal stability of the series. At the same time, the indirect band gap energy calculated for each glass sample demonstrated similar values of approximately 3.48 eV and 3.45 eV for undoped and Eu³⁺ doped glass samples respectively, with a slight decrease for both Sr²⁺-containing glass samples. Based on the results, these glasses showed potential for rare-earth incorporation to produce efficient materials for light-emitting purposes. Their optical properties can be controlled by adding different earth-alkali metals according to their periodic chemical trend.

Agradecimentos/Acknowledgments

FAPESP for funding (2019/16115-8, 2022/01762-0), IFSC – USP and IQSC – USP for providing the facilities for glass characterization.

Theoretical and spectroscopic study of lanthanide(III)-based complexes containing 4-picolinic acid as antenna ligand

Ana Carolina C. do Nascimento (PG),¹ Esther S. Areas (PQ),¹ Guilherme P. Guedes (PQ),^{1*}

anacellis@id.uff.br; guilherme_guedes@id.uff.br

¹Universidade Federal Fluminense, Instituto de Química, Departamento de Química Inorgânica

Keywords: lanthanides, 4-picolinic acid, TD-DFT, spectroscopy, UV-visible.

Highlights

The spectroscopic properties of a series of lanthanide(III) complexes were studied through a TD-DFT method, in order to understand the role of 4-picolinic acid as antenna ligand.

Abstract

Lanthanide(III) complexes are widely studied due to their possible optical applications.¹ Although the emission of lanthanide ions is usually of low intensity, it can be intensified when coordinated to antenna ligands, which transfer energy to the lanthanide excited levels.² In this work, the spectroscopic properties on the UV-visible region of six mononuclear lanthanide(III)-based complexes with 4-picolinic acid as antenna ligand (Dy(4pic), Eu(4pic), Sm(4pic), Tb(4pic), Er(4pic), and Gd(4pic)) were studied through theoretical methods and compared to experimental data in order to evaluate 4-picolinate's capacity to sensitize the lanthanide ions.

The crystal structures solved by single-crystal X-ray diffraction afforded the initial coordinates to the calculations, and the hydrogen atoms' positions were optimized in the PBE/def2-TZVP level. The theoretical (TD-DFT) UV-visible absorption spectra, considering only vertical electronic transitions, were generated using the B2PLYP double-hybrid functional and the SARC2-DKH-QZVP basis set for the lanthanide ions and def2-TZVP for all ligand atoms.

Figure 1 shows the experimental and calculated spectra along with the calculated oscillator strengths for Eu(4pic) compound. The results reveal a considerable displacement between the theoretical and experimental spectra; however, since they both present similar shapes, the theoretical model can be applied to investigate the orbitals involved in the observed electronic transitions. The electronic transition resulting in the most intense band is showed in **Figure 2**; as expected, it is ligand-centered. Hence, the lanthanide luminescence process can be understood as arising from the antenna effect. The calculations for compounds Dy(4pic), Sm(4pic) and Tb(4pic) were already carried out, displaying similar results.

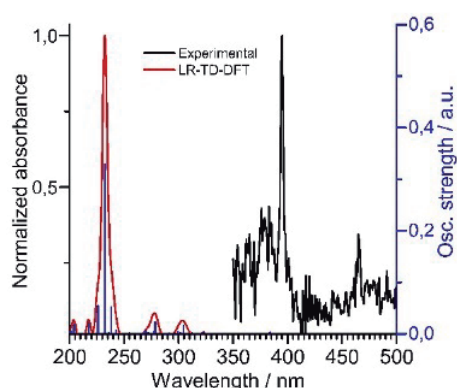


Fig. 1. Theoretical and experimental solid-state UV-visible absorption spectra of compound Eu(4pic).

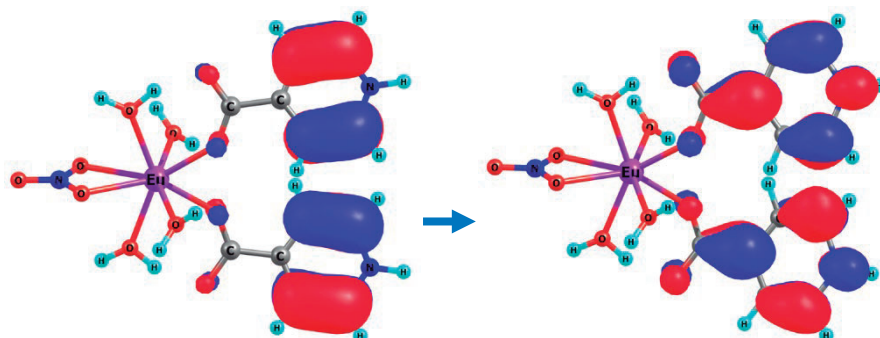


Fig. 2. Selected transition of the most intense absorption band of compound Eu(4pic). $\lambda(\text{calc.})$ 232 nm; $\lambda(\text{exp.})$ 395 nm.

¹ MONTEIRO, J. H. S. K. *Journal of Luminescence*, **2022**, 245, 118768.

² SINGH, A. K. *Coordination Chemistry Reviews*, **2022**, 455, 214365.

Acknowledgments

CNPq, FAPERJ, CAPES, LDRX-UFF, LQC-UFF and LAME-UFF.

The reaction between pyridoxal and L-Histidine in the absence and presence of zinc(II): the role of the metal in impeding Pictet-Spengler cyclization

Bruna V. Paes (PG),^{1*} Bernardo L. Rodrigues (PQ),¹ João P. A. Martins (PQ),¹ Isolda M. C. Mendes (PQ),¹ Rafael P. Vieira (PQ),¹ Heloisa Beraldo (PQ).¹

brunavidal.p@gmail.com

¹Departamento de Química, Universidade Federal de Minas Gerais (UFMG), Belo Horizonte/MG, Brasil.

Palavras Chave: Schiff base, L-Histidine, Pyridoxal, Cyclization, Zinc(II).

Highlights

- The Schiff base with pyridoxal and L-Histidine not was formed as a final product in the absence of zinc(II);
- A new binuclear zinc(II) complex with pyridoxal-L-Histidine Schiff base is described;

Resumo/Abstract

Schiff bases and their metal complexes present antimicrobial, antitumor, antioxidant, and anti-inflammatory activities, among others.¹ Amino acids and their derivatives are excellent building blocks to form ligands due to their coordination properties and biological importance.² Therefore, obtaining Schiff bases derivatives from amino acids and their metal complexes can be an interesting strategy for the synthesis of compounds with potential pharmacological applications. In the present work, the reaction between pyridoxal (Pdx) and L-Histidine (L-His) was studied in the absence and presence of zinc(II). It has been observed that the Schiff base derived from pyridoxal hydrochloride and L-His is not formed as a final product in the absence of zinc(II) but instead Pictet-Spengler cyclization occurs with formation of 4-[3-hydroxy-5-(hydroxymethyl)-2-methylpyridin-4-yl]-4,5,6,7-tetrahydropyridine[3,4-c]imidazole-6-carboxylate of potassium (cyclic compound) (Figure 1).

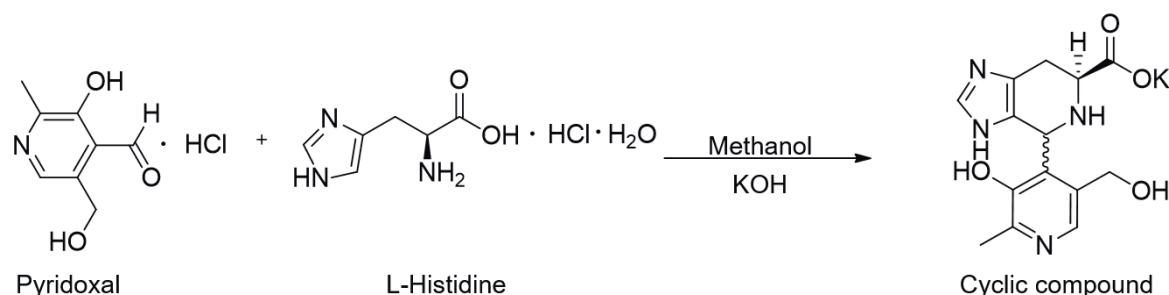


Figure 1. Syntheses scheme of the reaction between pyridoxal and L-Histidine.

It was also observed that this reaction is highly diastereoselective, producing mostly the *cis* diastereoisomer, which was identified by two-dimensional NOESY NMR. Computational calculations using the Density Functional Theory (DFT) with the hybrid exchange-correlation functional (B3LYP) and 6-311++G** basis set were used to determine the Gibbs free energy (ΔG°) of this cyclization reaction taking into account the solvent used. The species (Schiff base and cyclic compound) present at reaction pH 6 were determined using the Chemicalize software. A value of $\Delta G^\circ_{\text{cic}} < 0$ was determined for the [Pdx-His] Schiff base cyclization step, with the formation of the *cis* isomer, which was found experimentally. The one-pot reaction of Pdx with L-His in the presence of zinc acetate gave rise to the complex [Zn(Pdx-L-His)].3H₂O (**C1**). From the synthesis of compound (**C1**) crystals were obtained whose structure was determined by X-ray diffraction as being the binuclear compound [Zn₂(Pdx-L-His)₂Cl(H₂O)]·6.25H₂O (**C1A**). The results suggest that the [Pdx-L-His] Schiff base can only be obtained in the form of its zinc(II) complex and that the metal would have the role of preventing cyclization by complexing the Schiff base. ¹ Hameed, A.; Al-Rashida, M.; Uroos, M.; Ali, S. A.; Khan, K. M. *Expert. Opin. Ther. Pat.* 27 (2017) 63. ² Han, J.; Konno, H.; Sato, T.; Soloshonok, V. A.; Izawa, K. *Eur. J. Med. Chem.* 220 (2021) 113448.

Agradecimentos/Acknowledgments

UFMG, CNPq, CAPES, FAPEMIG, FINEP.

TITANIA DOPED WITH IRON (III) AS PHOTOCATALYST FOR HYDROGEN PEROXIDE PRODUCTION

Marcus V. do Prado (PG)¹, Vinicius Lima (IC)¹, Lorrana Vietro Barbosa (PG)¹, Suelen D. de Souza (PG)¹, Eduardo Nassar (PQ)¹, Liziane Marçal (PQ)¹, Emerson H. de Faria (PQ)¹, Katia J. Ciuffi (PQ)¹, Miguel A. Vicente (PQ)², Raquel Trujillano (PQ)², Vicente Rives (PQ)², Antonio Gil (PQ)³, Sophia A. Korili (PQ)³

¹Universidade de Franca, Franca- Brazil; ²Universidad de Salamanca, Salamanca- Spain; ³Universidad Publica de Navarra, Pamplona- Spain

Palavras Chave: Advanced oxidation process, Hydrogen Peroxide, Iron(III), composites, Clay mineral, Titanium Dioxide.

Highlights

Iron/titanium dioxide photocatalysts were prepared by the Sol-Gel method. The photocatalysts produced several amounts of H₂O₂. Hydroxylation of terephthalic acid was used to measure their photocatalytic performance. All the reactions were carried out under ambient conditions and irradiation with 95-W UV light.

Resumo/Abstract

The demand for H₂O₂ is increasing worldwide. Although it is considered a "green" chemical, its synthesis is environmentally unfriendly. Direct H₂O₂ synthesis is the best way to overcome this issue, but factors as risk of explosion and poor H₂O₂ stability prevent its application at the industrial level. Here, sol-gel processes were used to prepare iron/titania-based photocatalysts that can produce H₂O₂ directly, thus avoiding hydrogen peroxide deactivation and optimizing TiO₂ properties and advantages. More specifically, a natural purified Brazilian kaolinite (São Simão), FeCl₃, and Ti(IV) isopropoxide were used to synthesize a new nanocomposite via a sol-gel route. The resulting solid was dried at 100 °C for 24 h and split into four fractions: one used as dried, and the other three were heated in air at 400, 700, or 1000 °C for 24 h. Drying did not modify the kaolinite basal spacing (7.14 Å). Anatase was formed at 400 °C. At higher temperatures, anatase and rutile were found, and kaolinite was amorphized and transformed into metakaolinite. The characterization of the solids by infrared spectroscopy gave no evidence that titanium alkoxide interacted with lateral hydroxyls of aluminol and silanol in the clay interlamellar layer. Calcination at higher temperatures caused the bands in the region between 3200 and 3700 cm⁻¹ to disappear, evidencing that kaolinite was converted to metakaolinite, which displayed a broad band at 1050 cm⁻¹, characteristic of SiO₂. Calcination at 700 °C led to the emergence of two bands, at 463 and 660 cm⁻¹, attributed to the formation of Fe-O and Fe-O-Ti bonds, respectively, indicating that iron ions were present in the clay matrix. SEM micrographs showed morphological alterations due to kaolinite functionalization with titanium isopropoxide. Increasing heat treatment temperature increased particle fragmentation. EDX analyses confirmed that titanium and iron were present in the clay. The band around 500 nm in UV-Vis spectra, corresponding to the anatase phase, widened; the band at 482 nm was assigned to Fe-Fe interactions or to iron substitution in the anatase structure. The band gap was calculated as 2.55 eV, very close to the band gap of iron, corroborating that iron ions were inserted in the titanium kaolinite matrix. The specific surface area of the solids varied with heating from 21 to 12 m²/g. H₂O₂ production was studied by the proton-coupled electron transfer process. Benzyl alcohol was used as proton and electron donor in a mixture with water (10/1), in the presence of O₂ (which was bubbled for controlled times), under magnetic stirring and irradiation with a Hg lamp (95 W; λ = 310 nm) at room temperature. H₂O₂ concentration was analyzed by photoluminescence (terephthalic acid method). The best result among the tested materials, 70 μmol/L hydrogen peroxide, was achieved with the solids calcined at 400 °C, which had the highest surface area (21 m²/g) and the kaolinite structure preserved. The prepared photocatalysts can be potentially employed for selective H₂O₂ production. Kaolinite promoted dispersion of the active phase on the clay surface, which promoted selective H₂O₂ production.

Agradecimentos/Acknowledgments

CAPES (Finance Code 001), CNPq (305180/2019) and FAPESP (2020/06712-6).

Unusual long 5D_0 excited state lifetime from highly luminescent Eu^{3+} doped $\text{Y}_2\text{Sn}_2\text{O}_7$ ceramics

Maria Vitória Guidorzi* (PG)¹, Fernanda H. Borges (PG)¹, Rogéria R. Gonçalves (PQ)¹

guidorzim@usp.br

¹Laboratório de Materiais Luminescentes Micro e Nanoestruturados-Mater Lumen, Department of Chemistry, FFCLRP, University of São Paulo, Ribeirão Preto, SP, Brazil.

Palavras Chave: luminescence, stannate, lanthanide, spectroscopy, tin oxide, europium

Highlights

Eu^{3+} -doped yttrium stannates ($\text{Y}_2\text{Sn}_2\text{O}_7$) were synthesized via co-precipitation method. Eu^{3+} ions entered into the host replacing Y^{3+} ions in a high symmetry (D_{3d}) site with a long lifetime ($\sim 12\text{ms}$).

Resumo/Abstract

Rare earth (RE)-doped inorganic materials have been widely explored for several Photonics applications, such as waveguides, LEDs, solar cells and biomarkers. The choice of the host for doping with lanthanide ions is important since the crystalline structure influences on their luminescent properties. Eu^{3+} ions are used as structural probes allowing the investigation of the local structure where they are located due to their specific well known and assigned electronic transitions. In this study, we investigated the changes in the structural and luminescence properties of $\text{Y}_2\text{Sn}_2\text{O}_7$ nanoparticles doped with 0.5% in mol of Eu^{3+} ions as a function of annealing temperature. The materials were synthesized by co-precipitation method using as precursors the Tin (IV) chloride pentahydrate, yttrium chloride and ammonium hydroxide. The solution was stirred for 2 hours in a water bath at 80°C . The solids were annealed at 700 , 900 , 1100 and 1300°C for 2 hours. X-ray diffractograms (Fig. 1A) of the Eu^{3+} doped $\text{Y}_2\text{Sn}_2\text{O}_7$ shows the crystallization of $\text{Y}_2\text{Sn}_2\text{O}_7$ pyrochlore phase with space group $Fd-3m$, and cassiterite SnO_2 , space group $P4/nmm$ as a secondary phase (*). The crystallization degree augments with the increasing of the annealing temperature. The Eu^{3+} emission spectra (Fig. 2B) were also used to follow the structural changes, where it is observed the $^5D_0 \rightarrow ^7F_J$ ($J = 0, 1, 2, 3$ and 4) transitions could be observed under different excitation wavelengths. For the sample annealed at 700°C , the observed inhomogeneous broadening is a result of the distribution of the Eu^{3+} ions in a significantly disordered environment and of low symmetry. With the annealing temperature increasing, the profile spectra changes to sharper and the $^5D_0 \rightarrow ^7F_1$ transition stands out, revealing the occupation of the Eu^{3+} ion in a site of higher symmetry (D_{3d}). These samples exhibited a very long 5D_0 excited state lifetime ($\sim 12\text{ms}$). These lattice stand out as a host material for doping with optically active lanthanides ions for a wide range of Photonic applications, such as photocatalytic activity, piezoelectricity, superconductivity, resistance to radiation damage and others.

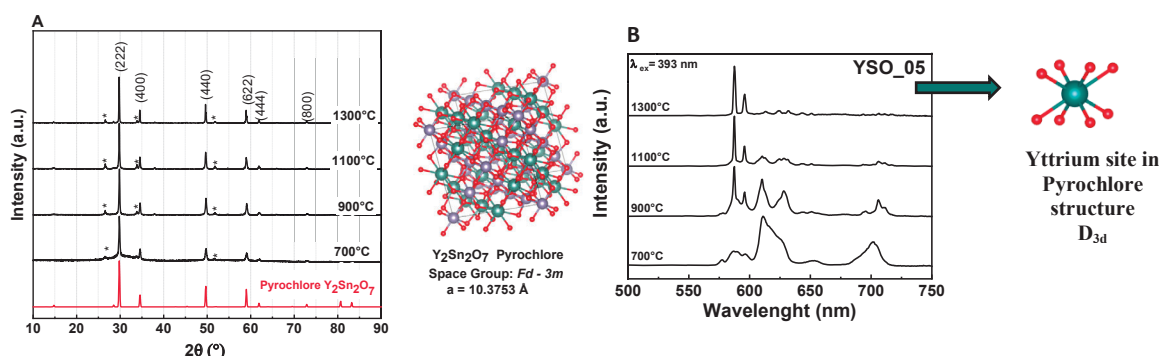


Fig. 1: (A) X-ray diffractograms and (B) Emission spectra of 0.5% Eu^{3+} -doped yttrium stannate samples.

Agradecimentos/Acknowledgments

This work was supported by Conselho Nacional de Desenvolvimento Científico e Tecnológico (CNPq), Coordenação de Aperfeiçoamento de Pessoal de Nível Superior (CAPES) and Fundação de Amparo à Pesquisa do Estado de São Paulo (FAPESP) and Photonics National Institute for Science and Technology (INFO).

Upconversion interparticle energy transfer in NaREF₄ assisted by 3,5-dibromobenzoate, acetylacetonate and tenoyltrifluoroacetate

Sergio F. N. Coelho (PG)¹, Italo O. Mazali (PQ)¹, Fernando A. Sigoli (PQ)¹.

Sergio.fern@hotmail.com;

¹ *Institute of Chemistry, University of Campinas, Campinas, Brazil*

Keywords: *Upconversion, Nanoparticle, Interparticle Energy Transfer.*

Highlights

Upconversion energy transfer from NaGd_{0.50}F₄:Yb_{0.49}Tm_{0.01} to functionalized 3,5-dibromobenzoate or acetylacetonate or tenoyltrifluoroacetate Eu^{III} and/or Tb^{III} doped-NaREF₄ NPs

Resumo/Abstract

Lanthanide-doped UCNPs in particular NaREF₄ are characterized by having narrow absorption or emission bands, low phonon energy, long emission lifetimes, and excellent photostability. These fluoride nanocrystals can provide a large flexibility in hierarchically structure design (core@shell), which facilitates the tuning of the luminescence of lanthanide ions in a given application. However, ligands such as aromatic carboxylic acids and β-diketones may be used to functionalize the surface of these nanoparticles improving light absorption and, therefore, the emission by the well-known antenna effect. In this work, we report on the upconversion emissions of the Eu^{III} and Tb^{III} ions originating from non-radiative interparticle energy transfer from oleate-capped NaGd_{0.50}F₄:Yb_{0.49}Tm_{0.01} nanoparticles to 3,5-dibromobenzoate (bbza⁻), or tenoyltrifluoroacetate (tta⁻)-functionalized NaGd_{0.85}F₄:Eu_{0.15} nanoparticles or acetylacetonate (acac⁻)-functionalized NaGd_{0.85}F₄:Tb_{0.15} and NaGd_{0.635}F₄:Eu_{0.15}Tb_{0.215} nanoparticles, when the former is excited by a 980 nm laser. The nanoparticles have been synthesized by the thermal decomposition methodology. The oleate-uncapped nanoparticles were prepared by acid washing and then their surfaces were functionalized by adding the bbza⁻ or acac⁻ or tta⁻ ligands. The NaREF₄ NPs were characterized by XRD, FTIR, DRS, and PL measurements. The PL results show the upconversion emission in powder mixtures of Eu^{III} and Tb^{III} ions-doped ligand-functionalized NPs, indicating the energy transfer from NaGd_{0.50}F₄:Yb_{0.49}Tm_{0.01} assisted by the ligands-functionalized Eu^{III} and/or Tb^{III} doped-NaREF₄ NPs. Probably, the Eu^{III} and Tb^{III} upconversion emission arise from the energy transfer mainly from Tm^{III} ¹G₄ excited state (power-law indicates n=3) of neighborhood NaGd_{0.50}F₄:Yb_{0.49}Tm_{0.01} nanoparticles to triplet states of the ligands-functionalized nanoparticles. Subsequently, the excited states of the Eu^{III} and Tb^{III} ions are populated leading to their narrow emissions. In this work, we also demonstrate that remote self-referencing luminescent temperature probes can be performed via interparticle energy transfer. The luminescent nanothermometer composed by the powder mixture of NaGd_{0.50}F₄:Yb_{0.49}Tm_{0.01} plus acac-NaGd_{0.635}F₄:Eu_{0.15}Tb_{0.215} exhibits relative thermal sensitivities of 1.33 % K⁻¹ at 367 K.

Agradecimentos/Acknowledgments

INOMAT, FAPESP, CNPq and Capes.

Using aryl-triazenes as fluorescent sensors: photophysical approaches

Jenifer Rosa (IC)¹, Bernardo Almeida Iglesias (PQ)¹

jenifer.rosa@acad.ufsm.br

¹ Laboratório de Bioinorgânica e Materiais Porfirínicos, Departamento De Química, Universidade Federal De Santa Maria, UFSM, Av. Roraima 1000, 97105-900 Santa Maria, RS, Brazil;

Palavras Chave: *Triazenes, Photophysical, Sensors.*

Highlights

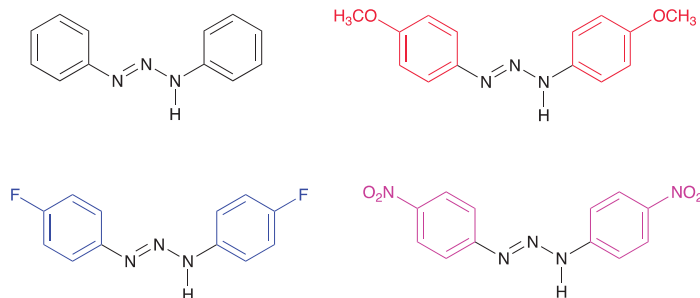
Aryl-triazene molecules were used to possible sensor applications;

Photophysical study in several solvents;

Detection of cationic, anionic and biomolecule targets;

Resumo/Abstract

Triazene derivatives are a class of organic compounds containing -N(H)-N=N- functional group, mainly used in coordination chemistry. In this work, we report, aryl-triazene derivatives with different substituents (Ph, 4-OMePh, 4-FPh and 4-NO₂Ph). The photophysical analysis were conducted in several solvents (DCM, MeOH, ACN, THF, 1,4-Diox, Ethyl Acetate, DMF and DMSO). Also, fluorescent sensor properties in the presence of different analytes (cations, anions and biomolecules) were evaluated by spectroscopic techniques.



Agradecimentos/Acknowledgments

The authors thanks to CNPq, FAPERGS and CAPES/PROEX – Finance code 001 for financial supporting.

Using Electrochemical Impedance Spectroscopy to Understand Charge Carrier Recombination in Perovskite Solar Cells

Lucas P. Souto (PG),*¹ Thayná M. G. dos Santos (PG),¹ Daniel Z. de Flório¹, André S. Polo (PQ)¹

andre.polo@ufabc.edu.br; lucas.polimante@ufabc.edu.br;

¹Universidade Federal do ABC, UFABC. Av. dos Estados, 5001 – Santo André

Palavras Chave: Perovskite Solar Cells, Electrochemical Impedance Spectroscopy, Solar Energy Conversion, Renewable Energy.

Highlights

The composition of the perovskite layer has a direct impact on the electronic & electrochemical processes of the solar cells, as is demonstrated by using Electrochemical Impedance Spectroscopy.

Abstract

Perovskite Solar Cells (PSCs) have some charge carriers processes, such as recombination, ionic migration, and accumulation at the device interfaces, that have a direct impact on their efficiency and long-term stability. Electrochemical Impedance Spectroscopy (EIS) is a powerful tool for identifying and understanding these processes [1]. In this study, we use EIS to investigate the electronic and electrochemical processes in PSCs having different perovskite layers composition, MAPbI₃ or MAFAPI₃, aiming to understand how these modifications change such processes.

The MAPbI₃ and MAFAPI₃ solar cells exhibit high uniformity of the layer and we did not observe defects or holes. The perovskite average grain size is $(1.7 \pm 0.5) \times 10^2$ nm for both compositions. The average solar efficiency for solar cells having MAPbI₃ and MAFAPI₃ is $(14.2 \pm 1.9)\%$, for both materials. The JV curves of the best-performance devices are shown in Fig. 1.

The Nyquist plots determined by EIS measurements show semicircles in high (HF) and low (LF) frequency regions (Fig. 2). To interpret the EIS

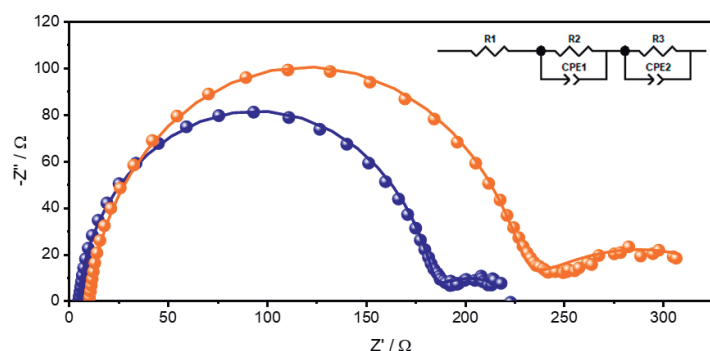


Figure 2 – Nyquist plots of MAPbI₃ and MAFAPI₃ solar cells made by dynamic deposition. (Pirr = 10 mWcm⁻²; frequency = 1 MHz - 10 mHz at V_{OC}; V_{amp} = 10 mV).

the perovskite composition, since the presence of FA⁺ cations leads to more stable materials.

Reference

[1] von Hauff, E. and Klotz, D., *J. Mater. Chem. C*, **2022**,10, 742-761

Acknowledgments

We would like to thank to PRH - ANP, CEM – UFABC; CNPq (406470/2022-7) and FAPESP (2017/11986-5; 2022/07268-8) for their support and contribution to this project.

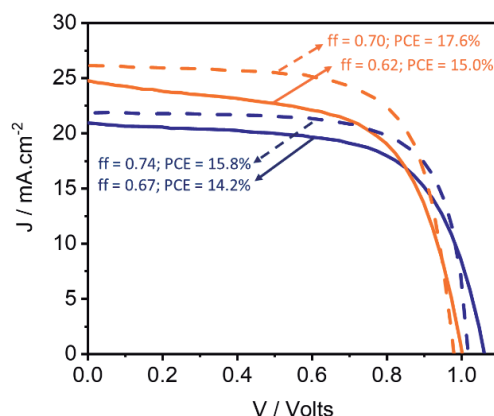


Figure 1 - Current density-voltage curves for the best MAPbI₃ and MAFAPI₃ solar cells made by dynamic deposition. Curves in forward (—) and reverse (---) scan.

results, a Voigt linear equivalent circuit is proposed to fit the experimental data and determine the values for the equivalent electrical R/C components. The high-frequency time constants determined are, 17.7 and 12.8 μs, respectively for MAPbI₃ and MAFAPI₃, which are ascribed to the transport and recombination of charges at the interfaces of the PSCs layers [1]. The low-frequency time constants determined are 107.5 and 301.5 ms, respectively for MAPbI₃ and MAFAPI₃, and are assigned to slow processes such as ionic motion and accumulation in the perovskite layer, leading to recombination sites and due to an electronic-ionic coupling, resulting in processes with higher time constants [1]. The higher constant time value observed for PSCs prepared with the MAFAPI₃ layer is related to a higher recombination resistance, probably due to

Water-induced reversible structural changes in magnetic and optical properties of a Co(II)-based complex

Dayenny L. D. Leite (PG)¹, Carolina B. P. Ligiero (PQ)¹, Isabela A. A. Bessa (PG)¹, Sérgio Pinheiro (PQ)², Henrique C. Silva Jr (PQ)¹, Gláucio B. Ferreira (PQ)¹, Wallace C. Nunes (PQ)³, Catiúcia R. M. O. Matos (PQ)^{1,4} and Célia M. Ronconi (PQ)^{1,*}.

dayennylooise@id.uff.br; cmronconi@id.uff.br

¹Departamento de Química Inorgânica, ²Departamento de Química Orgânica, ³Departamento de Físico-Química, ⁴Departamento de Física, Universidade Federal Fluminense, Niterói, RJ, Brasil; ⁴ University of Limerick, Limerick, Irlanda.

Keywords: Co(II) complex, Water-induced structural change, Magnetic properties

Highlights

A Co(II) complex synthesized from an aminoacid ligand presents water-induced switchable structural changes which influences its magnetic and optical properties.

Abstract

Coordination compounds are constructed by combining metallic cores with a variety of organic ligands, which provides interesting physicochemical properties to the final material. Changing the subunits can modulate the final properties depending on the obtained structure and their nature, e.g., complexes containing metal centers with unpaired d-electrons often exhibits interesting magnetic and electronic interactions [1-2]. Herein, a Co(II) coordination complex was obtained and showed a reversible water-induced structural change upon heating. The pink single crystals of the complex were obtained by adding a MeOH solution of $\text{Co}(\text{CH}_3\text{COO})_2 \cdot 4\text{H}_2\text{O}$ into a 1:1 MeOH:H₂O solution of an aminoacid ligand [3]. Structural analysis from single crystal X ray diffraction revealed that the complex crystallized in a monoclinic space group $P2_1/n$, with a Co(II) center coordinated with two ligand molecules and two water molecules. Completing the asymmetric unit there is one uncoordinated water molecule interacting by hydrogen bonding (Fig. 1a). Thermogravimetric analysis showed the complete dehydration around 100 °C with 18 % of weight loss, where this water removal process results in a crystal color change from pink to purple (Fig. 1b). Powder X-ray diffraction revealed a structure reversibility upon a water absorption/desorption cycle (Fig. 1c). This structural change was accompanied by a change in their magnetic properties, where the complex and its dehydrated form presented $\chi_M T$ values at 300 K of 2.86 and 3.03 $\text{cm}^3\text{Kmol}^{-1}$, respectively, that are significantly higher than the expected value of 1.87 $\text{cm}^3\text{Kmol}^{-1}$ for a magnetically isolated Co(II) ion (Fig. 1d). Also, the dehydrated form did not show a magnetic saturation at 70 kOe, reaching a 1.59 N_{μ_B} at 2 K, suggesting significant crystal-field interactions (Fig. 1e). Theoretical calculations were performed in order to understand and evaluate the electronic and magnetic properties of the complex.

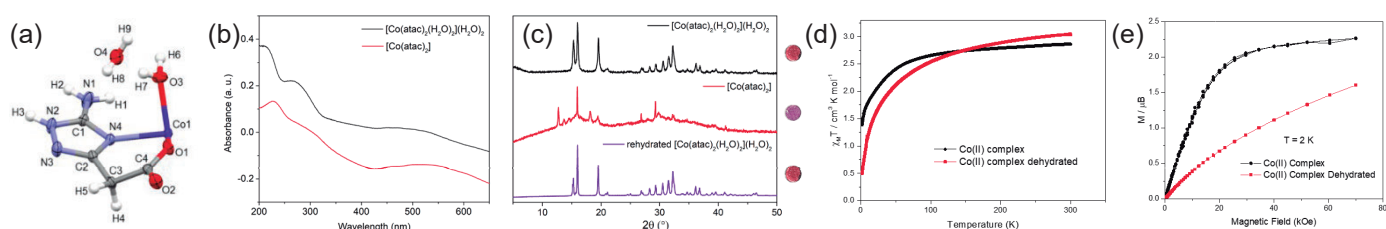


Figure 1: (a) Asymmetric unit of the Co(II) complex; (b) Solid-state UV-Vis spectra; (c) PDRX of the complex dehydrated and after water capture; (d) Temperature dependence of $\chi_M T$ product and (e) Magnetization versus magnetic field curves at 2 K for the polycrystalline sample of Co(II) complex as synthesized and its dehydrated form.

Acknowledgments

UFF, CNPq, CAPES, FAPERJ, LAMATE-UFF, LAME-UFF

[1] K. I. Pashanova, A. I. Poddel'sky, A. V. Piskunov, *Coordination Chemistry Reviews*, **2022**, 459, 214399.

[2] C. R. M. O. Matos, C. V. Sarmiento, H. C. S Junior, G. B. Ferreira, G. P. Guedes, W. C. Nunes, C. M. Ronconi, *Dalton Transactions*, **2021**, 50, 15003.

[3] C. R. M. O. Matos, H. Junior, D. L. D'Amato, A. S. Souza, S. Pinheiro, G. P. Guedes, G. B. Ferreira, O. C. Alves, F. B. de Almeida, F. Garcia, C. M. Ronconi, *Dalton Transactions*, **2020**, 49, 16359.

What are the Tower's method products: Metal-hydroxides or metal-glycerolates?

Josué M. Gonçalves^{1,2*}, Irlan S. Lima^{1*}, Abhijit H. Phakatkar³, Rafael S. Pereira⁴, Paulo R. Martins⁵, Koiti Araki¹, Lúcio Angnes¹, Reza Shahbazian-Yassar².

irlan.santos@usp.br; luangnes@iq.usp.br

¹ Instituto de Química, Universidade de São Paulo, Av. Prof. Lineu Prestes 748, 05508-000 São Paulo, SP, Brazil;

² Department of Mechanical and Industrial Engineering, University of Illinois at Chicago, Chicago, IL 60607, USA;

³ Department of Biomedical Engineering, University of Illinois at Chicago, Chicago, IL 60607, USA;

⁴ Centro de Engenharia, Modelagem e Ciências Sociais Aplicadas, Universidade Federal do ABC, 09210-580 Santo André, SP, Brazil;

⁵ Instituto de Química, Universidade Federal de Goiás, Av. Esperança s/n, 74690-900 Goiania, GO, Brazil;

Key words: Synthesis, Tower's method, Nickel hydroxide, Nickel-glycerolate.

Highlights

It has been long believed that colloidal nickel hydroxide nanoparticles are produced by the reaction of nickel salts, glycerol and potassium hydroxide known as the Tower method. In the present work, we challenge this belief and reveal the reasons for error in identification of nickel products produced by the Tower method.

Abstract

Tower's method has been extensively used in the development of electroactive materials for several electrochemical applications. However, based on XRD data, the materials resulting from the Tower's method show strikingly similar structures to metal-glycerolates prepared by solvothermal methods using similar reagents. In this sense, Ni based materials were carefully prepared and analyzed by structural, morphological, spectroscopic, and electrochemical characterization techniques. Initially, the images obtained by *in-situ* HRTEM (**Figure 1**) showed no evidence of nanoparticles.

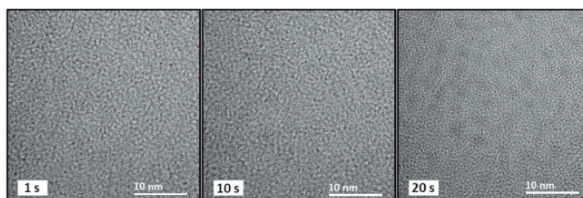


Figure 1. A series of TEM images of a Ni-Gly-KOH film taken at different e-beam exposure times, monitoring the *in-situ* nucleation and growth of nanoparticles induced by the electron beam.

The nickel hydroxide nanoparticles are only formed upon further reaction of Ni-glycerolate precursors with an aqueous alkaline solution. Those new findings shed light on the nature of the metal derivatives obtained by the reaction of Ni²⁺ and glycerol in the Tower method and provide more solid foundation to design electrode materials for batteries, supercapacitors, electrocatalysts and electrochemical sensors.

References and Acknowledgments

O.F. Tower, Note on colloidal nickel hydroxide, J. Phys. Chem. 28 (1924) 176–178;

M.A. Rocha, H. Winnischofer, K. Araki, F.J. Anaissi, H.E. Toma, A new insight on the preparation of stabilized alpha-nickel hydroxide nanoparticles, J. Nanosci. Nanotechnol. 11 (2011) 3985–3996.



Área: INO

(Inserir a sigla da seção científica para qual o resumo será submetido. Ex: ORG, BEA, CAT)

X-ray Photoelectron Fingerprints of High-Valent Ruthenium–oxo Complexes Along the Oxidation Reaction Pathway in Aqueous Environment

Kalil C. F. Toledo¹, Jose Luis Silva², Isaak Unger³, Tiago Araujo Matias¹, Leandro Rezende Franco⁴, Giane Damas², Luciano T. Costa⁵, Tulio C. R. Rocha⁶, Arnaldo Naves de Brito⁷, Clara-Magdalena Saak³, Kaline Coutinho⁴, Koiti Araki³, Olle Björneholm³, Barbara Brena², C. Moyses Araujo² kalilcft@gmail.com

¹ Department of Fundamental Chemistry, Institute of Chemistry, University of São Paulo, Av. Lineu Prestes 748, Cidade Universitária, Butanta, Sao Paulo, SP 05508-000, Brazil.

² Materials Theory Division, Department of Physics and Astronomy, Uppsala University, Box 516, 75120 Uppsala, Sweden

³ Molecular and Condensed Matter Physics Division, Department of Physics and Astronomy, Uppsala University, Box 516, 75120 Uppsala, Sweden

⁴ Instituto de Física, Universidade de São Paulo, 05508-090 Cidade Universitária, São Paulo/SP, Brazil

⁵ Instituto de Química–Departamento de Físico-química, Universidade Federal Fluminense, Outeiro de São João Batista s/n, CEP 24020-150 Niterói, RJ, Brazil

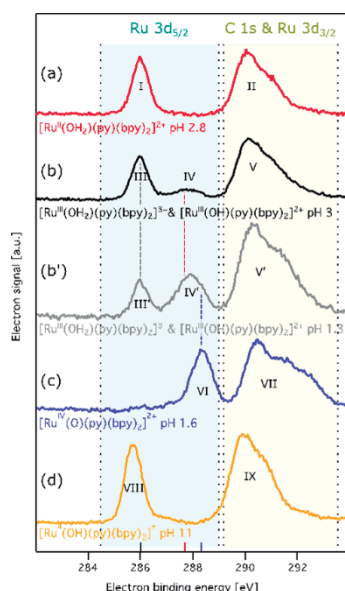
⁶ Brazilian Synchrotron Light Laboratory (LNLS), Brazilian Center for Research on Energy and Materials (CNPEM), PO Box 6192, 13083-970, Campinas, SP, Brazil

⁷ Institute of Physics “Gleb Wataghin”, University of Campinas, 13083-859 Campinas, SP, Brazil

Palavras Chave: Ruthenium Complexes, XPS, *in-operando*, liquid-jet.

Highlights

- In-operando spectroscopy to investigate proton-coupled electron transfer reactions
- Combined theory-experimental approach and synchrotron-based XPS measurements
- The study $[\text{Ru}^{\text{IV}}=\text{O}]^{2+}$ formation

Resumo/Abstract

Recent advances in operando-synchrotron-based X-ray techniques are making it possible to address fundamental questions related to complex proton-coupled electron transfer reactions, such as for instance the electrocatalytic water splitting process. However, it is still a grand challenge to assess the ability of the different techniques to characterize the relevant intermediates, with minimal interference at the reaction mechanism. To this end, we have developed a novel methodology employing X-ray photoelectron spectroscopy (XPS) in connection with the liquid-jet approach to probe the electrochemical properties of a model electrocatalyst, $[\text{Ru}^{\text{IV}}(\text{bpy})_2(\text{py})(\text{OH}_2)]^{2+}$, in an aqueous environment. There is a unique fingerprint of the extremely important higher valence ruthenium oxo species in the XPS spectra along the oxidation reaction pathway. Furthermore, a sequential method combining quantum mechanics and molecular mechanics (S-QM/MM) is used to unveil the underlying physical chemistry of such systems. This study provides the basis for the future development of *in-operando* XPS techniques for water oxidation reactions.

Agradecimentos/Acknowledgments

STandUP for Energy and the Swedish Research Council, FAPESP Process numbers 2017/11986-5, 2017/11631-2, 2013/24725-4, 2018/04523-1, Shell and ANP (Brazil's National Oil, Natural Gas and Biofuels Agency) STINT-CAPES (9805/2014-01), CNPq (401581/2016-0 and 303137/2016-9),

MAT

Química de Materiais

46^a Reunião
Anual da **SBQ**

28 a 31 de Maio de 2023

Águas de Lindóia · SP
Hotel Monte Real

A heterogeneous Fenton-like metal-free catalyst based on cyamelurate-functionalized g-C₃N₄

Wanessa L. Oliveira (PG)¹, Eduarda F. de Oliveira (PG)¹, Taís S. da Cruz¹, Walker V. F. C. Batista (PG)¹, Gabriel A. A. Diab (PG)², Ivo F. Teixeira (PQ)², Dalva E. C. Ferreira (PQ)^{1,3}, João P. de Mesquita (PQ)^{1,2}.

wanessalimaoliveira@gmail.com; joaopm2000@yahoo.com.br

¹Departamento de Química, UFVJM; ²Departamento de Química UFSCAR; ³Departamento de Química UFMG.

Palavras Chave: Metal-free, Polymeric g-C₃N₄, funcionalization, cyamelurate, Fenton-like.

Highlights

Polymeric g-C₃N₄ sheets functionalized with cyamelurate-like functional groups. Evaluation of the degradation of a model molecule *via* dark Fenton-like reactions. High activity in a wide pH range and efficient H₂O₂ utilization.

Resumo/Abstract

The traditional Fenton reaction based on the use of aqueous iron(II), as well as Fenton-like reactions using other metals often result in some problems, including the pH-dependence, high consumption of H₂O₂ and the production of sludge. Metal-free catalysts have been considered an interesting and viable alternative for Fenton-like reactions. Recently were reported the first works on the use of graphitic carbon nitride (g-C₃N₄) as a metal-free catalyst in heterogeneous Fenton-like reactions in the absence of light. g-C₃N₄ is a polymeric carbon-based 2D layered material composed, mainly, of s-heptazine units with the C/N ratio=3/4. We showed that oxygenated g-C₃N₄ obtained at different temperatures (500-600 °C) can degrade indigo carmine in presence of hydrogen peroxide and absence of light and we conclude that Fenton-like activity is directly related to the oxygenated functional groups present on g-C₃N₄ surface.¹ In order to control the nature of the oxygenated functional groups, in this work we propose the use of alkaline hydrolysis reaction as a alternative for the controlled introduction modification of polymeric g-C₃N₄ with the

introduction of cyamelurate-like functional groups. During the reaction, under controlled conditions of temperature and concentration, the degree of fragmentation/functionalization of the sheets formed by s-heptazines can be easily controlled with the formation of cyamelurate-like functional groups. The materials were characterized by a variety of techniques including SEM, TEM and potentiometric titration. The catalytic performance of the materials were evaluated for the degradation of indigo carmine (IC) (Fig. 1). On one hand, the polymeric g-C₃N₄ and H₂O₂ show very low degradation kinetics, the cyamelurate-functionalized g-C₃N₄ exhibits a high performance on the degradation of the dye. Under the experimental conditions tested, all materials showed similar catalytic activity with a 70% degradation of the dye after 30 minutes of reaction. Preliminary results suggest that H₂O₂ reacts with the functional groups forming hydroxyl radicals with the direct participation of the dye molecule.

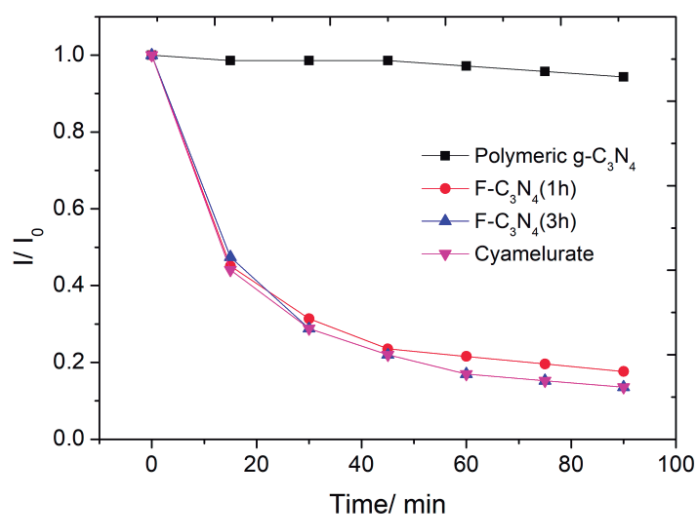


Figure 1. Degradation kinetics of indigo carmine dye in the presence of the samples polymeric g-C₃N₄, fragments and potassium cyamelurate. Conditions: Initial pH 7, 15 mg of catalyst, [IC]= 20 mgL⁻¹ and [H₂O₂] = 9.3 × 10⁻³ M.

Agradecimentos/Acknowledgments

JPM acknowledge grants from CNPq, 102190/2022-4 and APQ-02629-17, the support from UFVJM, CAPES and CNPq. The authors acknowledge MULTIFAR, LMMA and associated projects.

1. Oliveira, W. L. et al. *Journal of Colloid and Interface Science* 2021, 587, 479-488

Artificial Intelligence (AI) Based on Active Learning (AL) for Experimental Design – the MLChem4D Software Results and Outlook

Maicon P. Lourenço^{1*}(PQ), Alain Tchagang²(PQ), Karthik Shankar³(PQ), Venkataraman Thangadurai⁴(PQ) and Dennis R. Salahub⁴(PQ)

maiconpl01@gmail.com

¹Departamento de Química e Física, UFES; ²NRC Canada; Department of Electrical Engineering, ³University of Alberta; Department of Chemistry, University of Calgary⁴.

Keywords: Perovskites, Machine Learning, Active Learning, Design of Experiments, Transition Metal Oxides.

Highlights

An AI method for experimental design was implemented in the MLChem4D software. This technology has the potential to find optimum experimental conditions in organic, inorganic chemistry and materials science.

Abstract

The developed artificial intelligence (AI) method based on active learning¹ (AL) was applied in the experimental design of two important materials: non-stoichiometric perovskites ($\text{Ba}_{(1-x)}\text{A}_x\text{Ti}_{(1-y)}\text{B}_y\text{O}_3$) due to substituting ionic sites with different concentrations and elements ($\text{A} = \text{Ca}, \text{Sr}, \text{Cd}$; $\text{B} = \text{Zr}, \text{Sn}, \text{Hf}$), aiming at the maximization of the energy storage density (in laboratory); stoichiometric ABO_3 perovskites where different elements are changed in the A and B sites for the minimization of the formation energy (*in silico*). The MLChem4D² (Fig. 1) has the potential to be applied in inorganic and organic synthesis (e.g.: search for the optimum concentrations or catalysts, pH to improve the yield) and materials science. The latter marks the first MLChem4D application for the design of perovskite oxides, Fig. 1.

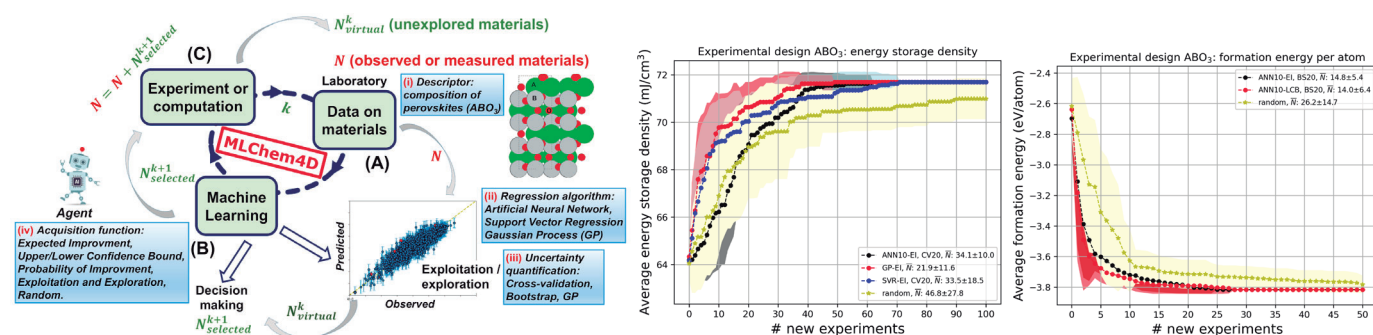


Figure 1. The MLChem4D workflow (left) and the average ABO_3 properties optimized obtained by 30 AL independent runs as a function of the number of new experiments. Center: $\text{Ba}_{(1-x)}\text{A}_x\text{Ti}_{(1-y)}\text{B}_y\text{O}_3$; right: ABO_3 . ANN10: Artificial Neural Network with one hidden layer and ten hidden neurons. SVR: Support Vector Regressor. GP: Gaussian process. El: Expected Improvement. LCB: Lower Confidence Bound with $C=3$. CV-20: K-fold cross-validation with 20 splits. BS20: non-parametric bootstrap with 20 resampling. RS: random search.

The results of the AL applied for perovskites proved to be efficient, allowing us to walk in regions of chemical space for new discoveries, even with small data scenarios. The MLChem4D can be applied in other branches of chemistry.

¹Lookman et al.; *Active learning in materials science with emphasis on adaptive sampling using uncertainties for targeted design*; *npj Comput Mater* 5, 21 (2019). ²Lourenço et al.; *Active Learning for Optimum Experimental Design – Insight into Perovskite Oxides*; *Can. J. of Chemistry*, under review.

Acknowledgments

Fundação de Amparo à Pesquisa do Espírito Santo (FAPES); Conselho Nacional para o Desenvolvimento Científico e Tecnológico (CNPq); Coordenação de Aperfeiçoamento de Pessoal de Ensino Superior (CAPES). National Research Council of Canada, Artificial Intelligence for Design program and by the Natural Sciences and Engineering Research Council of Canada, Discovery Grant (RGPIN-2019-03976).

Área: MAT

(Inserir a sigla da seção científica para qual o resumo será submetido. Ex: ORG, BEA, CAT)

Bentonite modified with n-hexadecyltrimethylammonium bromide (CTAB) and bis- (triethoxysilylpropyl) tetrasulfide (TESPT) by sol-gel methodology

Maria Isabel O. Damas (IC)^{1*}, Fernanda R. Diamantino (PG)¹, Lorrana V. Barbosa (PG)¹, Eduardo Donzelli (PG)¹, Eduardo J. Nassar (PQ)¹, Katia J. Ciuffi (PQ)¹, Emerson H. de Faria (PQ)¹, Liziane Marçal (PQ)¹.

mariaisabel.oliveiradamas@gmail.com; liziane.silva@unifran.edu.br

¹ Universidade de Franca (UNIFRAN). Av. Dr. Armando Salles Oliveira, 201. Pq. Universitário. Franca/SP, Brasil. 14404-600

Keywords: hybrid materials, functionalization, intercalation, hydrophobic properties.

Highlights

Hybrid materials were obtained by intercalation of CTAB and functionalization of TESPT on bentonite. FTIR and XRD confirm the CTAB and TESP intercalation on bentonite. The change on surface properties of bentonite was confirmed by change on hydrophilicity from hydrophilic to hydrophobic in both materials.

Resumo/Abstract

It is already known that industries face great problems in the removal of contaminants in their effluents, due to some factors such as high cost, lack of appropriate resources, and among others. In this context, many alternative adsorbents have been studied to removal these contaminants from aqueous solutions. Clays are increasingly used in this process and can be chemically modified, becoming organofunctionalized. The goal of this study was to synthesize and characterize materials using natural bentonite and functionalized, aiming its application in the application in removal of hydrophobic and/or hydrophilic pollutants. The bentonite clay was modified with bis- (triethoxysilylpropyl) tetrasulfide (TESPT) and/or n-hexadecyltrimethylammonium bromide (CTAB) by sol-gel methodology where 20 grams of purified bentonite clay was added to a beaker with 333mL of distilled water, maintained under vigorous magnetic stirring for 40 minutes. After this period, 1.67 mL of hydrochloric acid, 1.66 mL of ethanol and 20 mL of alkoxide TESPT or 21 g of CTAB were added. The reaction was maintained under mechanical agitation for 24 hours at room temperature. After functionalization, each material was centrifuged to separate the solid at 3000 rpm and washed with distilled water in the Soxhlet system, the synthesis took place at a temperature of 60°C and dried for 96 hours, and the Ben-TESPT and Ben-CTAB samples were obtained. The samples were characterized by X-ray diffractometry (XRD), infrared molecular absorption spectroscopy (FTIR), cation exchange capacity (CEC) determination, specific area (SE) by methylene blue method (SE) and scanning electron microscopy (SEM). The characterization techniques revealed that the bentonite was organofunctionalized with TESPT and CTAB. X-ray diffraction (XRD) analysis, showed an expansion of the interlayer space from 14.23 to 15.22 Å and 16.68 Å, respectively. The FTIR spectra confirm the presence of CTAB and TESPT in the each material due to bands in region of 1290 cm⁻¹ of sulphide groups of alkoxide and typical bands of the quaternary ammonium salt at 2921 cm⁻¹ and 2852 cm⁻¹. The analyzed materials have a CEC values corresponding to 1.98 mmol. 100g⁻¹ of Ben-TESPT and 50 m².g⁻¹ of Ben-CTAB and SE values of 15.50 m².g⁻¹ of Ben-TESPT and 390 m².g⁻¹ of Ben-CTAB. The insertion of organic molecules of the modifier promotes the expansion of interlayer space of bentonite, resulting in change on the hydrophilicity from hydrophilic to hydrophobic. The organic units functionalized (highly nonpolar) promotes the change on surface properties of clay. The samples were characterized by scanning electron microscopy, that shown the presence of small particles into bentonite, and more agglomerated than natural bentonite, this result confirms the modification with TESPT and CTAB and suggest that sol-gel methodology are viable technique to provide new adsorption sites that may be able to adsorb compounds with hydrophobic characteristics such as oil, dyes, pharmacies, pesticides and among others.

Agradecimentos/Acknowledgments

CAPES (Finance Code 001), CNPq and FAPESP.

Bioactive material with microorganisms can enhance the micronutrients solubilization from low reactive sources: insight for application as coating fertilizer granules

Ricardo Bortoletto-Santos* (PQ),^{1,2} Vinícius F. Majaron (IC),³ Marisa G. da Silva (IC),³ Rodrigo Klaic (PQ),⁴ Wagner L. Polito (PQ),⁵ Denise Bevilaqua (PQ),² Cristiane S. Farinas (PQ),⁴ Caue Ribeiro (PQ),⁴ Sidney J.L. Ribeiro (PQ).²

ricbortolettosantos@hotmail.com

¹Universidade de Ribeirão Preto (UNAERP), ²Instituto de Química (UNESP); ³Departamento de Química (UFSCar); ⁴Laboratório Nacional de Nanotecnologia para o Agronegócio (Embrapa Instrumentação); ⁵Instituto de Química de São Carlos (USP).

Keywords: *Acidithiobacillus thiooxidans*; *Aspergillus niger*; Fertilizer; Micronutrients; Starch.

Highlights

The innovative system can ensure the supply of multiple nutrients to plants by using low reactivity sources through a more environmentally-friendly management; The synergy between the nutrients and microorganisms incorporated in the coating resulted in system acidification and increased availability of micronutrients.

Abstract

Fertilization is essential to provide suitable conditions for plant development and crop productivity, but the environmental cost of fertilizers is a drawback for achieving a sustainable agriculture. A potential alternative is the use of unprocessed (raw) nutrient sources such as mineral oxides (ZnO, MnO, CuO) as fertilizers. However, these low reactive sources are not readily available to plants. Here, we developed a bioactive coating material containing microorganisms that allowed different nutrients to be made available from unprocessed nutrient sources. For that, the coating material composed of maize starch, mineral oxides (ZnO, MnO, CuO), and a microbial source (*Aspergillus niger* or *Acidithiobacillus thiooxidans*) was applied on monoammonium phosphate (MAP) granules, as a model fertilizer. Our results revealed that the bioactive coating did not affect the phosphorus (P) release, since it did not impose a physical barrier. However, the acidifying capacity of both microorganisms significantly enhanced the oxide solubilization. The presence of *Aspergillus niger* or *Acidithiobacillus thiooxidans* promoted local acidification, as well as the bioactive coating material with *Aspergillus niger* reached Cu, Zn and Mn solubilization up to 10.9, 14.6 and 34.3% in 42 days of soil incubation. This phenomenon suggested that the organic acids produced by *Aspergillus niger* chelate the cations, reducing precipitation and, therefore, increasing their solubilization. This innovative system can effectively supply nutrients to plants using cheap and low reactivity nutrient sources with the advantage that it can be co-applied on currently used fertilizer granules in a single delivery, making easier the adoption by producers.

Acknowledgments

The authors are thankful for the financial support given by FAPESP (São Paulo State Research Foundation, grant#2016/10636-8, #2017/18673-2, #2018/10448-2, and #2020/03259-9), CAPES (Coordination for the Improvement of Higher Education Personnel, CAPES-Embrapa Program), CNPq (Brazilian National Council for Scientific and Technological Development), SISNANO/MCTI, FINEP, and Embrapa AgroNano research network.

Área: MAT

(Inserir a sigla da seção científica para qual o resumo será submetido. Ex: ORG, BEA, CAT)

Biopolymeric Materials Containing Upconversion Luminescent Nanoparticles for Thermal sensing in smart packaging and labels

Ana Beatriz Acosta (PG)¹, Luís Fernando dos Santos (PG)¹, Francisco Recco Torres (PG)², José Maurício Caiut (PQ)², Rogéria Rocha Gonçalves (PQ)¹.

beatriz.acosta@usp.br

¹Laboratório de Materiais Luminescentes Micro e Nanoestruturados-Mater Lumen, Department of Chemistry, FFCLRP, University of São Paulo, Ribeirão Preto, SP, Brazil.

²NanoLum., Department of Chemistry, FFCLRP, University of São Paulo, Ribeirão Preto, SP, Brazil.

Palavras Chave: NaGdF₄: Er³⁺/Yb³⁺; Rare Earth; Photoluminescence; Smart packaging; Intelligent packaging.

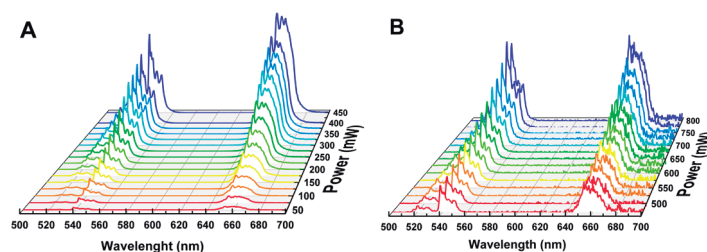
Highlights

Dispersion of NaGdF₄: Er³⁺/Yb³⁺ nanoparticles in gellan gum with the possibility of application in photonics, specially for luminescent thermal sensing.

Resumo/Abstract

One of the great motivations and technological impacts of the chemistry of materials has been the focus on the development of materials with the objective of obtaining properties designed for specific applications. When doping systems with lanthanide ions, we can attribute luminescent properties to a material and, it is of great interest, that it has characteristics such as transparency at the excitation wavelength, high solubility of lanthanide ions in the solid lattice, low phonon energy and chemical and thermal stability [1]. This work aims to carry out the hydrothermal synthesis of NaGdF₄ nanoparticles doped with 5% Er³⁺ and 20% Yb³⁺ followed by their dispersion into biopolymers, i.e. gellan gum, to obtain membranes. Studies were carried out on the structural, morphological, and spectroscopic properties of the nanoparticles and after dispersion into the biopolymer. The formation of the β-NaGdF₄ structure (hexagonal) is observed in the diffractograms, which appear in the form of rods when observed in the TEM images. Spectroscopic properties were studied and upconversion luminescence was detected under excitation at 980 nm (Figure 1). In the emission spectra, bands are observed in the green (525 nm) and red (660 nm) regions referring to the ²H_{11/2}, ⁴S_{3/2} → ⁴I_{15/2}, and ⁴F_{9/2} → ⁴I_{15/2} transitions of the Er³⁺ ions [2], respectively, indicating that the materials have emission in the yellowish green region and that the dispersion in the biopolymer did not generate luminescence quenching. Subsequently, dispersion will be carried out in other polymers, organic-inorganic hybrids and biopolymers, aiming at the production of smart labels.

Fig 1. Emission spectra of NaGdF₄:Er³⁺/Yb³⁺ under excitation at 980 nm a) particle only and b) after incorporation into the biopolymer



[1] Dong H, Sun LD, Yan CH. Energy transfer in lanthanide upconversion studies for extended optical applications. *Chem Soc Rev.* 2015;44:1608–34

[2] TIAN, Linlin *et al.* Hexagonal phase β-NaGdF₄: Yb³⁺/Er³⁺ thin films with upconversion emission grown by electrodeposition. *RSC Advances*, v. 4, n. 38, p. 19896-19899, 2014.

Agradecimentos/Acknowledgments

This work was supported by Conselho Nacional de Desenvolvimento Científico e Tecnológico (CNPq), Coordenação de Aperfeiçoamento de Pessoal de Nível Superior (CAPES), and Fundação de Amparo à Pesquisa do Estado de São Paulo (FAPESP) and Photonics National Institute for Science and Technology (INFO).

Biossensores baseados em nanobastões de ouro para detecção de SARS-CoV-2 através da técnica de espalhamento dinâmico de luz (DLS)

Ana Beatriz C. Souza (IC)¹, Carolina B. P. Ligiero (PQ)^{1*}, Aline F. M. Silva (PQ)¹, Dayenny L. D. Leite (PG)¹, Marcelo A. Strauch (PQ)², Célia M. Ronconi (PQ)^{1*}

ab_costa@id.uff.br; cmronconi@id.uff.br

¹Departamento de Química Inorgânica, Universidade Federal Fluminense, Campus do Valonguinho, Outeiro de São João Batista, s/n, 24020-141, Niterói, RJ, Brasil. ²Instituto Vital Brasil, Niterói, RJ, 24230-410, Brasil

Palavras Chave: Nanobastões de ouro, Espalhamento dinâmico de luz, SARS-CoV-2

Highlights

Biosensors based on gold nanorods (AuNRs) for detection of SARS-CoV-2 through dynamic light scattering technique. Anisotropic AuNRs have interesting optical properties, such as high sensitivity of the translational band measured by DLS. The detection of the presence of an antigen in the environment of AuNRs makes it a promisor sensor.

Resumo

Em razão dos enfrentamentos pandêmicos causado pelo vírus SARS-CoV-2, nosso grupo de pesquisa deu início, em 2020, ao desenvolvimento de biossensores para detecção da proteína S presente na superfície desse patógeno através do DLS^{1,2}. Partículas anisotrópicas constituídas por nanobastões de Au apresentam elevada sensibilidade óptica, podendo ser um sistema interessante mas pouco explorado na literatura para a detecção de moléculas biológicas por meio de DLS. Para comprovar essa hipótese, nanobastões de Au foram sintetizados por crescimento semeado envolvendo duas etapas: a primeira que trata da síntese de uma solução prévia, chamada de solução semente, enquanto a segunda refere-se à produção de uma solução de crescimento³. O DLS normalmente modela a função de auto-correlação para nanopartículas esféricas. Entretanto, partículas em forma de bastões são anisotrópicas, possuindo duas dimensões, que geram dois decaimentos no correlograma convertidos para dois picos de diâmetro hidrodinâmico (D_H), associados aos movimentos rotacional e translacional (Figura 1). O material também foi caracterizado por espectroscopia na região do ultravioleta visível, indicando sua morfologia devido ao surgimento de duas bandas em 518 e 651 nm referentes aos tamanhos transversal e longitudinal dos bastões, respectivamente (Figura 2). O surfactante cetiltrimetilamônio (CTAB) utilizado na síntese, recobre e estabiliza o material, mas é deletério à bioconjugação. Dessa forma, a troca do CTAB pelo citrato é necessária antes de acoplar o ligante⁴. A bioconjugação dos anticorpos anti-proteína S é feita pelo método covalente que garante boa estabilidade aos biossensores, com intermédio do agente de ligação cruzada 3,3'-ditiobis(sulfosuccinimidil propionato), DTSSP. Essa etapa de adição do ligante encontra-se em fase de desenvolvimento e permitirá a determinação da presença ou não da proteína S do vírus estudado através da técnica de DLS.

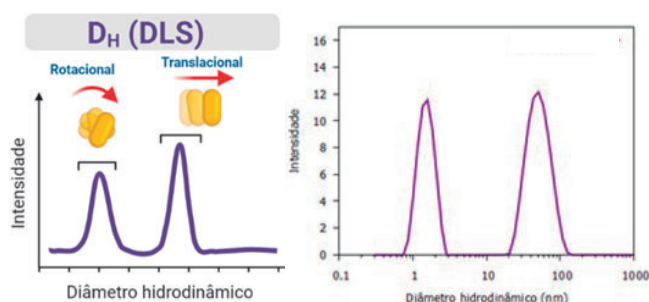


Figura 1: Resultado de DLS a) esperado; b) obtido.

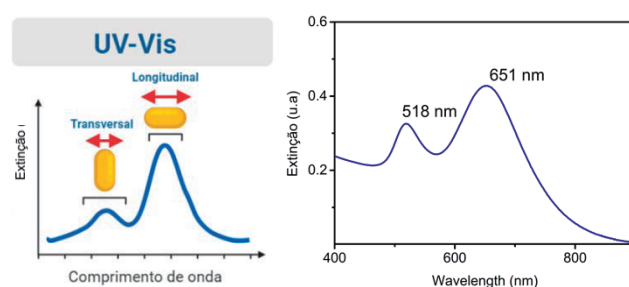


Figura 2: Extinção óptica dos nanobastões a) esperado; b) obtido.

Agradecimentos

UFF, CNPq, CAPES, FAPERJ, LQSN, LAME, LAMATE

[1] LIGIERO, C. S., et al., Influence of particle size on the SARS-CoV-2 spike protein detection using IgG-capped gold nanoparticles and dynamic light scattering. *Mater. Today Chem.* **2022**, 25, 100924.

[2] SILVA, P. B., et al., Detection of SARS-CoV-2 virus via dynamic light scattering using antibody-gold nanoparticle bioconjugates against viral spike protein. *Talanta*. **2022**, 243, 123355.

[3] NIKOOBAKHT, B., et al., Preparation and growth mechanism of gold nanorods (NRs) using seed-mediated growth method. *Chem. Mater.* **2003**, 15, 1957.

[4] MEHTALA, J. G., et al., Citrate-stabilized gold nanorods. *Langmuir*. **2014**, 30(46), 13727.

Bismuth vanadate supported in bacterial cellulose for photodegradation of contaminants of emerging concern

Vinícius A. Silva* (PG),¹ Leonardo Marchiori (PG),¹ Sajjad Ullah (PQ),² Elias P. Ferreira-Neto (PQ),³ Sidney J. L. Ribeiro (PQ).¹

vinicius.a.silva@unesp.br

¹Inorganic Chemistry Department, Institute of Chemistry, UNESP; ²Institute of Chemical Sciences, University of Peshawar; ³Chemistry Department, UFSC

Keywords: BiVO₄, bacterial cellulose, photocatalytic membrane, decontamination, aerogel.

Highlights

An improved synthesis of bacterial cellulose aerogel integrated with BiVO₄, increasing sorption and photocatalytic properties for application in an efficient environmental remediation under sunlight.

Resumo/Abstract

The increasing anthropogenic contamination of water resources and the rising demand for potable water worldwide has increased the urgency of solutions for wastewater treatment. Photocatalysis stands out in the field of the available technologies for this application, mainly due to the use of light, where the absorption of UV to IR radiation by a semiconductor material generates radicals that can interact and degrade contaminants to their mineralization. Bismuth vanadate (BiVO₄) has promising photocatalytic activity, with visible light and part of UV absorption, to apply in the degradation of emerging concern contaminants. The application of photocatalysis materials, commonly synthesized as powders, however, can create problems for their application, such as the separation of the material from the aquatic residue, leading to further contamination. The integration of BiVO₄ with bacterial cellulose (BC) can solve these problems and enhance material utilization, as it has sorption properties and the ability to make surface modifications, as well as being a non-toxic, low cost, and biocompatible material. In the search for solving the availability of water free of emerging concern contaminants, we will investigate the association of BiVO₄ and BC for effective water purification through photocatalysis.

Agradecimentos/Acknowledgments

Financial support from Brazilian agencies FAPESP, CNPq and CAPES is acknowledged.

Cadmium sorption by organic-inorganic nanocomposites based on anionic clays

Juliana C. A. Paiva (IC)^{1*}, Luiz Fernando B. Malta (PQ)¹

¹Instituto de Química, UFRJ – julianaalvesdepaiva3000@gmail.com

PalavrasChave: layered double hydroxide, tartrate, trace metal.

Highlights

- Mg/Al LDH was used as a platform for trace metal sorption
- The functionalization of layered structure with tartrate anion allowed absorbing Cd without decomposing
- The increase of Cd concentration led to a decrease of ionic absorption capacity of LDH-tartrate

Resumo/Abstract

Layered Double Hydroxides are anionic clays that can act for environmental remediation even for trace metal absorption [1]. To do so, intercalation of chelate agents, such as tartrate ion, [2] must be carried out previously. In the present study, the follow-up of previous studies [3] evidenced the improved property of LDH-tartrate in face of LDH alone for cadmium absorption. Mg/Al LDH 2:1 was synthesized using the rising pH approach until precipitation of nitrate precursors at pH10 using NaOH 1mol L⁻¹. The isolated material was exposed to Cd²⁺ solutions at RT for 24h with concentrations ranging from 0.0025 to 0.05 mol L⁻¹. IAC% was calculated according to literature [4]. Materials were characterized by X rays diffraction (XRD) and FT-infrared spectroscopy (FTIR) while Cd²⁺ content was determined by X rays fluorescence(XRF). Indexing XRD data gave hexagonal "c" cell parameter decrease upon tartrate inclusion ("a" = 3,10(9)Å and "c" = 23,4(1)Å to "a" = 3,11(0)Å and "c" = 23,3(7)Å) due to increase of H-bonding in the interlayer space. FTIR spectra evidenced vanishing of 1380 cm⁻¹ band (nNO₃⁻) upon tartrate association, corroborating ion exchange process. XRD patterns (Fig 1a) also revealed LDH structure was partially collapsed upon the presence of Cd²⁺; in contrast LDH-Tartrate nanocomposite successfully absorbed Cd²⁺ maintaining its structure. From XRF results the IAC% versus [Cd²⁺] plot (Fig 1b) revealed decrease of sorption as Cd²⁺ concentration increased. Therefore, the synthesized nanocomposite showed improved capacity to remove Cd²⁺ and maintain its structure allowing possible reutilization.

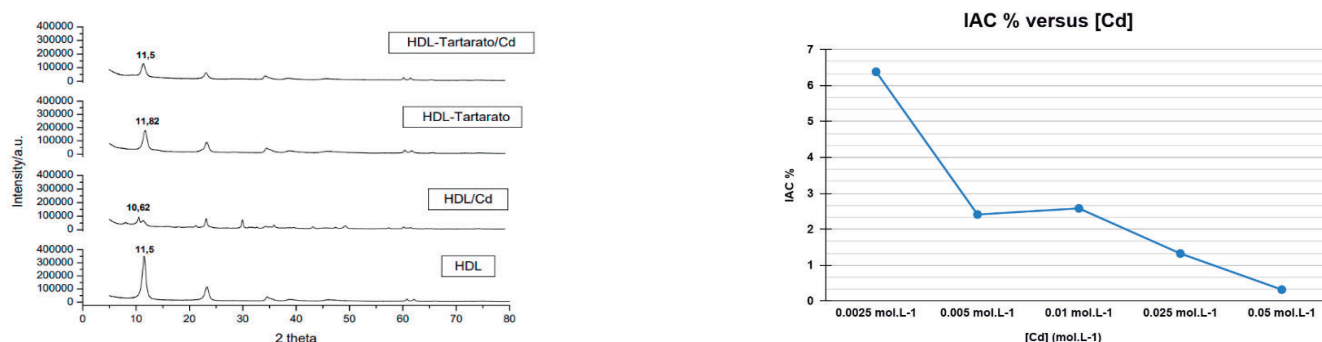


Fig 1: XRD patterns obtained for the LDH, LDH/Cd, LDH-Tartrate and LDH-Tartrate/Cd (a); and IAC % versus [Cd] (mol.L-1) graph (b).

Agradecimentos/Acknowledgments

CAPES, CNPq e FAPERJ.

[1] Zhu, K., Gao, Y., Tan, X., Chen, C. Polyaniline-Modified Mg/Al Layered Double Hydroxide Composites and Their Application in Efficient Removal of Cr(VI). ACS Sustainable Chemistry & Engineering 4, 4361–4369, 2016.

[2] Kameda, T., Takeuchi, H., Yoshioka, T. Ni–Al Layered Double Hydroxides Modified with Citrate, Malate, and Tartrate: Preparation by Co-precipitation and Uptake of Cu²⁺ from Aqueous Solution. Journal of Physics and Chemistry of Solids. 72, 846–851, 2011.

[3] SILVA, C. G. N.; NEVES, V. A.; BOMFIM, J. F.; SENRA, Jaqueline Dias; MALTA, L. F. B. . OTIMIZAÇÃO MULTIVARIADA DA SÍNTESE DO HIDRÓXIDO DUPLO LAMELAR Mg/Al COMO MATERIAIS AD(AB)SORTIVOS PARA APLICAÇÕES AMBIENTAIS, BIOLÓGICAS E CATALÍTICAS. In: Desenvolvimento científico e tecnológico no Brasil: interdisciplinaridade. 1ed.Rio Branco: Stricto Sensu, v. 1, p. 44-60 (2021).

[4] Rocha, L.D.S., Duarte, J.P.P., Medeiros, M.E., Souza, R.M., Malta, L.F.B. Screening of sorption conditions of Cd²⁺ ions by cerium (IV) hydrogenphosphate from aqueous solutions. J Therm Anal Calorim 147, 1177–1186 (2022).

Área: **MAT**

Characterization of bio-oil produced through slow and fast pyrolysis of lignocellulosic biomass

Ana Luiza G. Mendes (PG),¹ Lisiane O. Diehl (PG),² Darliana M. Souza (PQ),¹ Fernanda de Castilhos (PQ),² Paola de A. Mello (PQ).^{1*}

ana.mendes@acad.ufsm.br; paola.mello@ufsm.br

Universidade Federal de Santa Maria, Brazil, ¹Chemistry Department; ²Chemistry Engineering Department

Keywords: *Lignocellulosic biomass, Pyrolysis, Bio-oil, Acidity, Organic Characterization*

Highlights

- ❖ Composition of bio-oil is dependent on the biomass used as raw material for pyrolysis.
- ❖ By increasing the temperature and the heating rate, the acid number and water content can change significantly.
- ❖ The MDGC-MS proved to be a suitable tool for the identification and separation of compounds in bio-oil.

Abstract

Lignocellulosic biomass is a renewable resource with the potential to supply the world's high energy demand. The use of this resource as a raw material to produce biofuels requires transformations through biological, mechanical, or thermal processes, such as pyrolysis.¹⁻² Pyrolysis is a thermochemical conversion process that transforms biomass, under the absence of oxygen, into biochar (solid fraction), bio-oil (liquid fraction), and biogas (gaseous fraction).² Bio-oil is a complex hydrocarbon mixture, containing mainly oxygenated polar organic compounds in a wide range of chemical functions: carbonyl-compounds (ketones, aldehydes, and furanoics), sugars, carboxylic acids, and aromatics (hydrocarbons, PAHs, and phenolics).³ These compounds, such as carboxylic acids, confer the bio-oil high acidity. In the present study, pine wood (PW) and sugarcane straw (SS) agricultural residues were investigated and submitted to slow and fast pyrolysis at 400 to 600 °C for the characterization of the liquid product. Some physical properties of the bio-oils, such as water content and acid number (AN), were determined by standard methods using an automatic titrator (model Titrand 836, Metrohm, Switzerland). The organic characterization was performed by multidimensional gas chromatography mass spectrometry (model MDGC/GCMS-2010, Shimadzu, Japan) for the identification of oxygenated compounds in bio-oil from lignocellulosic biomass. The results obtained showed some differences depending on pyrolysis process parameters. As the temperature increased from 400 °C to 600 °C, it was possible to obtain the highest yield in the bio-oil production (54.7% from PW biomass and 52.8% from SS biomass). By increasing the heating rate and pyrolysis temperature, a reduction of water content was observed. For bio-oil from PW, increasing the heating rate significantly reduced the acidity number for the bio-oil pyrolyzed at 400 °C. The bio-oil from fast pyrolysis of SS at 600 °C presented the lowest acid number. Regarding to the characterization of organic compounds, acetic acid, eugenol, syringol, guaiacol, o-cresol, vanillin, 2-cyclopenten-1-one, 2-(5H)-furanone, furfuryl alcohol, 5-methylfurfural, phenol and levoglucosan were identified. Thus, it was possible to realize that different types of biomasses and experimental conditions of pyrolysis significantly changed the composition of bio-oil and characterization proved to be a crucial point for understanding the influence on the composition, as well as to develop studies regarding the suitability of bio-oils for different applications.

¹ Ghodake SG, Shinde SK, Kadam AA, *et al.*, Journal of Cleaner Production, 297, 2021, 126645.

² Sonil N, Mohanty P, Pant K, *et al.*, Bioenergy Research 6, 2012, 663.

³ McKendry P, Bioresource Technology, 83, 2002, 37.

Acknowledgments

CAPES, FAPERGS, CNPq, PRH 52.1 - ANP (UFSM), Bio-Value/BEECOL, and UFSM.

Chemical synthesis of α -MoO₃ from MoS₂ by reflux in oxidative environment

Arthur L. Santa Maria (PG)¹, Rafaella Ribeiro (PG)^{1*}, Eryza G. de Castro (PQ).¹

arthurleonhardt@gmail.com

¹Chemistry Department, UNICENTRO

Key Words: Molybdenum, Metal Oxide, Nanomaterials, Chemical Synthesis.

Highlights

Molybdenum oxide can be obtained through reflux in an oxidative environment, a simple, and low-cost process. This process uses low temperatures and generates α -MoO₃ with high purity.

Resumo/Abstract

α -MoO₃ is a cheap material with promising properties. It was synthesized from MoS₂ by reflux in HNO₃ 1 mol/L for 300 minutes. After this time, 1 ml of H₂SO₄ is added and left at reflux for another 30 minutes. The resulting solid is washed in distilled water until pH 4 is reached. It was then characterized by FTIR, XRD, and SEM. The FTIR spectrum displays bands at 993, 877, 820, 607, 487 cm⁻¹ characteristics of molybdenum oxide^{1,2}. The peaks obtained by XRD are characteristic of α -MoO₃ with orthorhombic structure^{1,3}. From the SEM image, it is possible to observe reduced size of the particles, showing belt-like morphology. These characterizations shows that α -MoO₃ was formed through reflux of MoS₂ in oxidative environment, allowing different alternatives of synthesis of the material. This study is advantageous compared to other synthetic routes due to its simplicity, since it does not use autoclave, reduced synthesis time and for producing small particles.^{3,4} MoO₃ will be used to obtain composites with conductive polymers, with subsequent application in electrochemical devices.

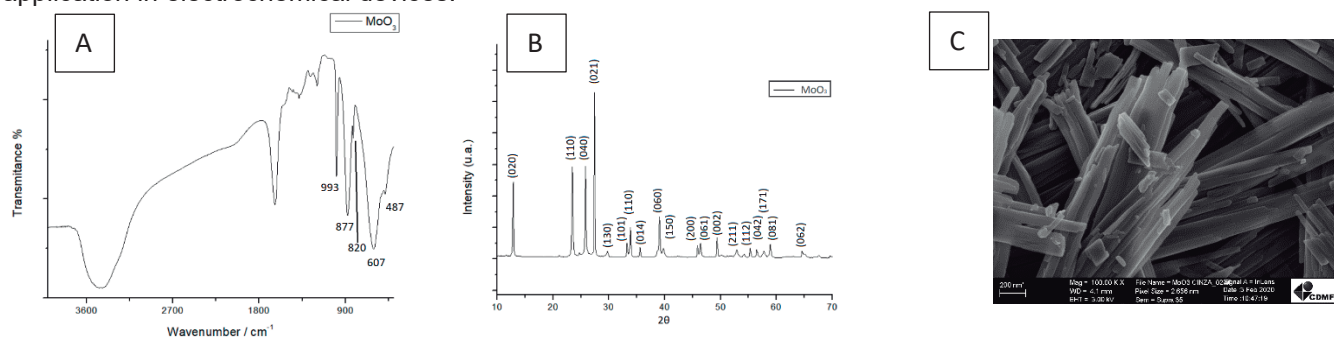
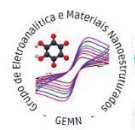


Figure 1: FTIR Spectra (A) XRD diffractogram and (B) SEM image (C). Source: The authors

References

- 1- Fernandes, C.I., s; Capelli, S. C.; Vaz, P. D.; Nunes, C. D. 2015. Highly selective and recyclable MoO₃ nanoparticles in epoxidation catalysis. *Appl. Catal. A Gen.* 504, 344–350.
- 2- Sharma, R. K.; Reddy, G. B. Effect of substrate temperature on the characteristics of α -MoO₃ hierarchical 3D microspheres prepared by facile PVD process, *J. Alloys Compd.*, 598, 177–183.
- 3- Nagabhushana, G. P.; Samrat, D.; Chandrappa, G. P. α -MoO₃ nanoparticles: solution combustion synthesis, photocatalytic and electrochemical properties, *RSC Adv.*, vol. 4, no. 100, 56784–56790.
- 4- Sinaim, H.; Ham, D.J.; Lee, S.J. A. Phuruangrat, S. Thongtem, and T. Thongtem, “Free-polymer controlling morphology of α -MoO₃ nanobelts by a facile hydrothermal synthesis, their electrochemistry for hydrogen evolution reactions and optical properties. *J. Alloys Compd.*, 516, 172–178, 2012.

Agradecimentos/Acknowledgments



Cold and warm white light emission in $\text{GeO}_2\text{-Nb}_2\text{O}_5\text{:Ho}^{3+}/\text{Yb}^{3+}/\text{Tm}^{3+}$ materials under excitation at 980 nm and ultraviolet for solid-state lighting

Vitor dos S. de Souza (PQ),^{1*} Fábio J. Caixeta (PQ),² Rogéria R. Gonçalves.¹

vitor.santos.souza@usp.br

¹Departamento de Química, FFCLRP, USP; ²Instituto de Química, UNESP

Palavras Chave: $\text{GeO}_2\text{-Nb}_2\text{O}_5$; $\text{GeO}_2.9\text{Nb}_2\text{O}_5$; Rare earth; Photoluminescence; White emission; Correlated color temperature.

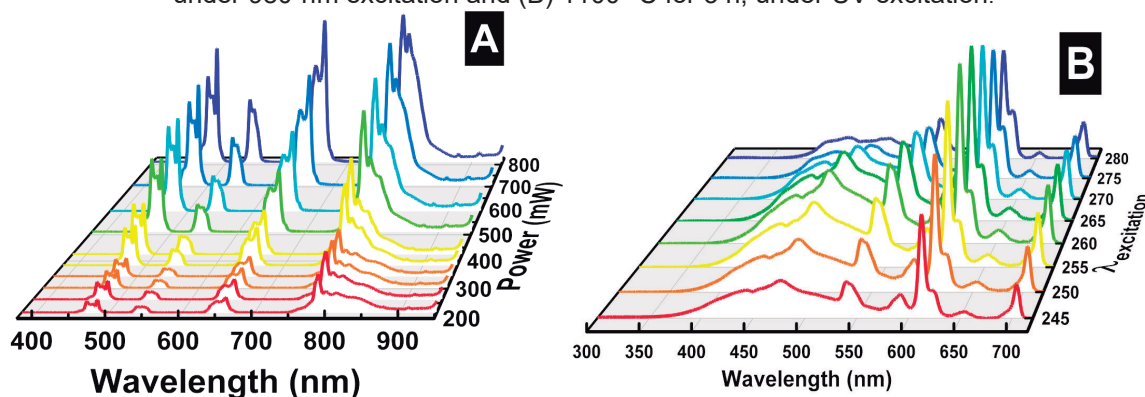
Highlights

White light emission on $\text{Ho}^{3+}/\text{Yb}^{3+}/\text{Tm}^{3+}$ triply doped with $\text{GeO}_2\text{-Nb}_2\text{O}_5$ based material with cold and warm white emitted under excitation at UV and Cold white emitted under excitation at 980 nm.

Abstract

0.3% Ho^{3+} , 1.2% Yb^{3+} , 0.5% Tm^{3+} triply doped $\text{GeO}_2\text{-Nb}_2\text{O}_5$ nanocomposites were synthesized using the sol-gel method. The main objective of this work is the preparation and structural and spectroscopic characterizations of these luminescent materials for white light emission. X-ray diffraction measurements were performed on nanocomposites annealed at 900 and 1100 °C, trigonal phase of germanium oxide GeO_2 was confirmed in both heat treatments. For the sample calcined at 1100 °C, the coexistence of the tetragonal mixed oxide $\text{GeO}_2.9\text{Nb}_2\text{O}_5$ was observed. Under infrared excitation, at 980 nm, the sample calcined at 900 °C showed luminescence upconversion processes, with red, green, and blue emissions, which are the three colors responsible for white light emission. The band at approximately 470 nm (blue) refers to transitions of Tm^{3+} ions, respectively. The green emission around 546 nm is attributed only to the Ho^{3+} ion transitions. In the red region at 658 nm, the transitions attributed to the Ho^{3+} and Tm^{3+} ions occur in all spectra (Fig. 1A). For the sample treated at 1100 °C under ultraviolet excitation (245 to 280 nm), were observed in addition to the host lattice emission band, the emissions of Ho^{3+} ions in 540, 590, 613, 623, and 653 nm, and Tm^{3+} ions emissions in 653, and 704 nm (Fig. 1B). Thus, the sample calcined at 900 °C under excitation at 980 nm and the calcined at 1100 °C under excitation at UV showed emission in the white light region. Such preliminary results demonstrate the relevant potential of these rare earth-doped materials in several photonic applications, in solid-state lighting.^[1]

Fig. 1. Emission spectra of $\text{Ho}^{3+}/\text{Yb}^{3+}/\text{Tm}^{3+}$ triply doped $\text{GeO}_2\text{-Nb}_2\text{O}_5$ nanocomposite annealed at (A) 900 °C for 3 h, under 980-nm excitation and (B) 1100 °C for 3 h, under UV excitation.



[1] SOUZA, V. S. et al. Modulating white light emission temperature in $\text{Ho}^{3+}/\text{Yb}^{3+}/\text{Tm}^{3+}$ triply doped nanostructured $\text{GeO}_2\text{-Nb}_2\text{O}_5$ materials for WLEDs applications. *Journal of Luminescence*, v. 248, p. 118978, 2022.

Acknowledgments

This work was supported by Conselho Nacional de Desenvolvimento Científico e Tecnológico (CNPq), Coordenação de Aperfeiçoamento de Pessoal de Nível Superior (CAPES), and Fundação de Amparo à Pesquisa do Estado de São Paulo (FAPESP). We also thank Companhia Brasileira de Metalurgia e Mineração (CBMM) for supplying Nb_2O_5 and Photonics Nacional Institute for Science and Technology (INFO).

Combining upconversion and persistent luminescence nanomaterials to produce rechargeable bio-emitters

Luidgi Giordano (PQ),^{1,2} Guanyu Cai (PG),² Johanne Seguin (PG),³ Jianhua Liu (PG),³ Cyrille Richard (PQ),³ Bruno Viana (PQ),² Lucas C. V. Rodrigues (PQ),^{1,*}

lucascvr@iq.usp.br

¹Department of Fundamental Chemistry, Institute of Chemistry, University of São Paulo; ²Institut de Recherche de Chimie Paris, CNRS; ³Unité de Technologies Chimiques et Biologiques pour la Santé, Univ. de Paris

Palavras Chave: Persistent Luminescence, Upconversion, Bioimaging, Nanomaterial, Energy storage, In vivo.

Highlights

NIR to green upconversion followed by radiative energy transfer allows charging-recharging of NIR persistent luminescence. In-vivo imaging after nanocomposites sub-cutaneous or oral administration.

Resumo/Abstract

Persistent luminescence in the infrared region is highly desirable due to potential applications in bioimaging [1]. However, it is important to be able to recharge the nanoparticles inside the body to increase the timescale of the imaging. Recently, there is a rush to find ways to charge persistent luminescence using an infrared laser as a power source and an upconversion process. This would allow the expansion of the potential applications for these materials, since both excitation and emission are fully inside the biological window. In this work, by using two materials associated via dry impregnation: β -NaGd_{0.8}Yb_{0.17}Er_{0.03}F₄ nanoparticles, known for their efficient upconversion, and Zn_{1.33}Ga_{1.335}Sn_{0.33}Cr_{0.005}O₄ nanoparticles, known for their persistent luminescence properties we effectively observed radiative energy transfer. This hybrid material exhibited persistent luminescence at 700 nm after charging with a 980 nm laser. Due to this property, in vivo tests with the composite (Figure) confirmed its potential application in bioimaging. Finally, a mechanism was proposed to explain this energy transfer process and the positive results of these tests demonstrate the effectiveness of our novel approach in recharging persistent luminescence and its potential for wider use in the future.

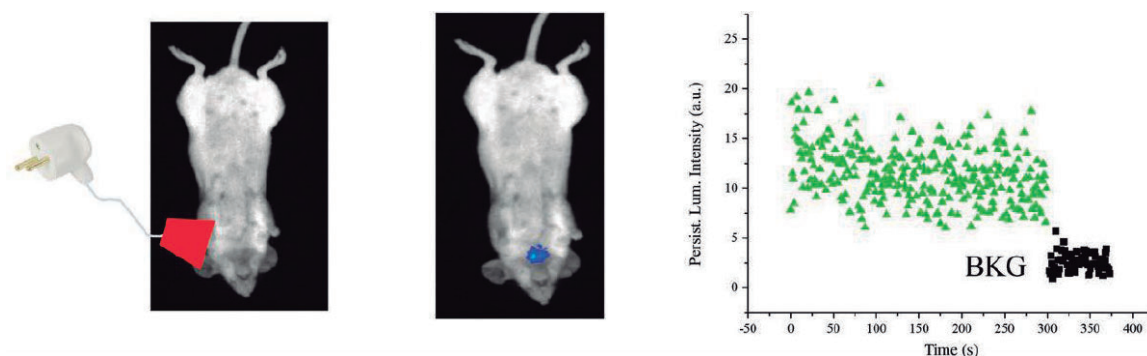


Figure. (left) Excitation of a capsule orally administered in a mouse using a 980 nm laser. (center) Counts after in situ excitation. (right) Decay of in situ persistent luminescence.

Agradecimentos/Acknowledgments

CAPES, CNPq, FAPESP and ANR PERSIST #18-CE0-8-0012 France

Reference

[1] Frtizen, D.L.; Giordano, L.; Rodrigues, L.C.V.; and Monteiro, J.H.S.K; *Nanomaterials* 10 (2020) 2015.

Área: MAT

Controlled release of urea by nanocomposites based on castor oil and laponite

Alexandre Antonio Fidelis Martins Junior* (IC),¹ Ricardo Bortoletto-Santos* (PQ),^{2,3} Vinícius F. Majaron (IC),¹ Wagner L. Polito (PQ),⁴ Sidney J.L. Ribeiro (PQ),³ Caue Ribeiro (PQ).⁵

alexandrejunior@estudante.ufscar.br

¹Departamento de Química (UFSCar); ²Universidade de Ribeirão Preto (UNAERP); ³Instituto de Química (UNESP); ⁴Instituto de Química de São Carlos (USP); ⁵Laboratório Nacional de Nanotecnologia para o Agronegócio (Embrapa Instrumentação).

Keywords: Laponite; Polyurethane; Urea; Fertilizer; Castor oil.

Highlights

Lamellar material is effective to control the N diffusion; PU-coatings modified with laponite can delay the N release from urea.

Abstract

Urea is the main nitrogen source applied in agriculture and directly impacts agricultural productivity. However, it presents significant losses that reduce the nitrogen use efficiency (NUE) by plants, such as ammonia (NH₃) volatilization, leaching, and greenhouse gases emission (N₂O). One strategy to minimize these problems is to protect the fertilizer with nutrient-release barrier materials. Moreover, the coating technology allows to increase the NUE, making the nutrient available gradually and uniformly. Laponite is a synthetic clay formed by tetrahedral silicate layers compressing an octahedral layer of magnesium oxide, which has negative charges on its surface. Thus, the permeation through the polymer can be significantly reduced by the presence of internal diffusional barriers, such as finely dispersed nanoclays (in the nanocomposites form). In this study, we proposed a nanocomposite system based on castor oil-derived polyurethane (PU) and Laponite for controlling the urea release by an ion-exchange mechanism. The nanocomposites were prepared following three proportions (2, 3.5 and 5% by mass). Our results showed that nanocomposites containing laponite were successfully synthesized, as well as the TGA residue results were similar to the nanocomposite formulation. Moreover, the water release results also demonstrated that the nanocomposites successfully retarded the nitrogen release from urea granules, as well as the release times were proportional to the contents of the cation-exchange materials. The combination of small proportions of laponite in the polymeric matrix significantly reduced the urea release, reaching 40% in 250 hours (nanocomposite containing 2% of laponite). The use of PU nanocomposites can significantly improve nitrogen release control, opening a new field for the investigation of controlled-release fertilizers.

Acknowledgments

The authors are thankful for the financial support given by FAPESP (São Paulo State Research Foundation, grant#2020/03259-9), CAPES (Coordination for the Improvement of Higher Education Personnel, CAPES-Embrapa Program), CNPq (Brazilian National Council for Scientific and Technological Development), SISNANO/MCTI, FINEP, and Embrapa AgroNano research network.

Crumpled graphene/Ni(OH)₂ nanocomposites applied as electrochemical sensors for glucose and persistent contaminants

Anna E. Silva¹, Victor H. R. de Souza² e Eduardo G.C. Neiva^{1*}

eneiva@furb.br

¹ Departamento de Química, Universidade Regional de Blumenau (FURB), CEP 89012900, Blumenau, SC, Brasil; ² Departamento de Química, Universidade Federal da Grande Dourados (UFGD), CEP 79825070, Dourados, MS, Brasil.

Palavras Chave: Óxido de grafeno reduzido; Hidróxido de níquel; Glicose; N-acetilcisteína; Famotidina; Hidroclorotiazida.

Highlights

Electrosynthesis of CG/Ni(OH)₂ nanocomposites;

Evaluation of adsorptive and electrochemical methods to Ni²⁺ incorporation on CG;

Developing of electrochemical sensor for glucose and persistent contaminants.

Resumo/Abstract

Diferentes deposições de nanopartículas de Ni foram realizadas utilizando métodos de adsorção e deposição eletroquímica, partindo de uma solução de acetato de níquel. A otimização da deposição de Ni foi realizada levando em consideração o melhor comportamento eletrocatalítico para a oxidação da glicose em meio alcalino empregando cronoamperometria. O melhor comportamento eletroquímico foi obtido pela deposição eletroquímica através da aplicação de 0,7 V por 30 s em solução aquosa de Ni²⁺, seguida da ciclagem em solução aquosa de KOH, de forma a originar filmes finos de grafeno amassado (GA) homogeneamente decorados com nanopartículas de Ni(OH)₂ com tamanho de 3,79±0,04 nm. A detecção de glicose foi otimizada para os filmes finos de GA/Ni(OH)₂ atingindo um baixo limite de detecção (LD) de 0,34±0,04 μmol L⁻¹ para uma ampla faixa linear de detecção (FLD) de 1 a 1000 μmol L⁻¹ com boa reprodutibilidade, repetibilidade e baixo efeito de interferentes. Os filmes finos de GA/Ni(OH)₂ também exibiram LD muito baixo para n-acetilcisteína, hidroclorotiazida e famotidina (0,54±0,07, 2,38±0,45 e 0,91±0,48 μmol L⁻¹, respectivamente) e um FLD amplo.

Agradecimentos/Acknowledgments

Os autores agradecem à FAPESC e ao Instituto Nacional de Ciência e Tecnologia em Nanomateriais de Carbono (INCT-Nanocarbono) pelo suporte financeiro, à CLAIMS pelos equipamentos, à FURB pela infraestrutura e ao Grupo de Química de Materiais (GQM-UFPR) pelas caracterizações de MEV e EDS. Os autores também agradecem ao Centro de Microscopia da UFPR pelas imagens de MET.

Desenvolvimento de soluções sustentáveis para mitigar a colisão de pássaros em vidros.

Victor Chad Paiva (IC)¹, Marcelo Nalin (PQ)¹

victor.chad@unesp.br; marcelo.nalin@unesp.br

¹Departamento de Química Geral e Inorgânica, UNESP IQAr

Soluções Sustentáveis/Sustainable solution, Glasses, Colisão, Pássaros Em Vidros/Bird collisions,

Highlights

Development of Sustainable-sustainable Solutions-solutions to Mitigate-mitigate Bird-bird Strikes-collisions in Glass.

Glass benefit aesthetics and energy savings in buildings.

Bird strikes-collisions impact local fauna and flora.

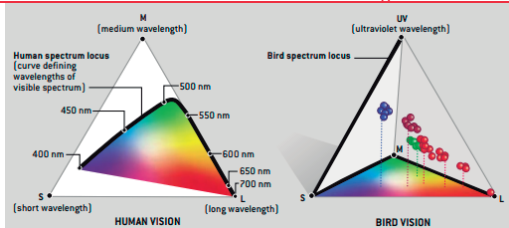
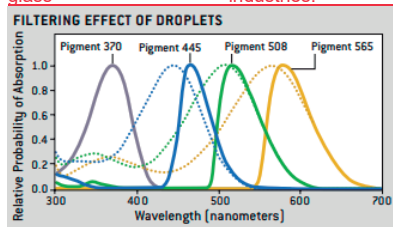
Laws are being created to lessen the impacts just by reducing the use of glass.

Resumo/Abstract

This project aims at the fundamental study of sustainable solutions, through the development of thin films that can be applied to commercial glass surfaces that do not cause problems from an architectural point of view, nor too much increase in production cost. Among the materials listed as candidates, we can highlight the semiconductor oxides with an absorption range in the region between 300 and 400 nm. This prerequisite is necessary since the maximum sensitivity of bird vision is in this spectral range and not in the visible region, as in the case of humans. In this work, two oxides were deposited with different compositions by using two techniques commonly used in the glass industry

, i.e. thermal evaporation and sputtering. Titanium oxide is generally used to infer self-cleaningself-cleaning properties to glass windows and present absorption properties in the desired optical window, however, the results show that even if the absorption band is in the correct energy, the film also absorbs into the visible range, whichat is not desirable. Onn the other hand, zinc oxide has presented very good absorption in the UV range and not present absorption in the visible range. Thus, this oxide is a very promising material in order to mitigate the problem of collisions of birds in glass windows. This is the first study in this sense realized in Brazil and must be intensified in order to bring alternatives to

glass industries.



Formatado: Inglês (Estados Unidos)

Formatado: Inglês (Estados Unidos)

Formatado: Inglês (Estados Unidos)

Formatado: Inglês (Estados Unidos)

Formatado: Inglês (Estados Unidos)

Formatado: Inglês (Estados Unidos)

Formatado: Inglês (Estados Unidos)

Formatado: Inglês (Estados Unidos)

Formatado: Inglês (Estados Unidos)

Formatado: Inglês (Estados Unidos)

Formatado: Inglês (Estados Unidos)

Formatado: Inglês (Estados Unidos)

Formatado: Inglês (Estados Unidos)

Formatado: Inglês (Estados Unidos)

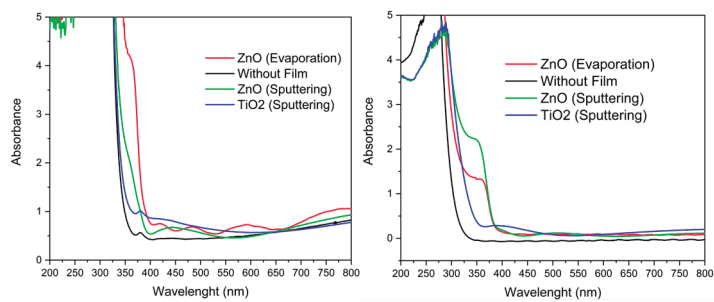
Formatado: Inglês (Estados Unidos)

Formatado: Inglês (Estados Unidos)

Formatado: Justificado, Espaço Depois de: 8 pt

Formatado: Inglês (Estados Unidos)

Source: Timothy H. Goldsmith, What birds see, Scientific American, July (2006) 69-75



Agradecimentos/Acknowledgments

We thank Fundação de Amparo à Pesquisa do Estado de São Paulo (FAPESP) for the scholarship granted, process nº 2021/14878-4.

Formatado: Fonte: (Padrão) Arial, 10 pt

Designing Eco-friendly Cellulose Nanofibrils/Natural Rubber Latex-based Aerogel Nanocomposites for Water Remediation

Marcos V. Lorevice* (PQ),¹ Pedro I. C. Claro (PQ),¹ Nadia A. Aleixo (PG),^{1,2} Livia S. Martins (IC),¹ Ana P. Stelzer (IC),¹ Rubia F. Gouveia (PQ).^{1,2}

marcos.lorevice@Innano.cnpem.br; rubia.gouveia@Innano.cnpem.br

¹Brazilian Nanotechnology National Laboratory (LNNano), Brazilian Center for Research in Energy and Materials (CNPem), SP, Brazil; ²Center for Natural and Human Sciences, Federal University of ABC, 09210-580 Santo André, São Paulo, Brazil.

Keywords: biomass-based porous structure, microfluidizer, TEMPO-oxidation, cellulose nanofibrils, natural rubber latex, pollutants adsorption.

Highlights

A solvent-free route produced fractal 3D structured CNF aerogels with nanopores. The incorporation of NR into CNF aerogels added hydrophobicity and wet resistance. CNF/NR aerogel removed heavy metal or dye even at low concentrations.

Abstract

Cellulose nanofibrils (CNF)-based aerogels have emerged as a sustainable absorbent alternative to remove heavy metal ions and organic compounds from aqueous environments. Although CNF has been proven to be one of the most promising green raw materials of at last few years due to its intrinsic and renewable properties, CNF-based porous materials are unstable in aqueous media due to their high hydrophilicity, presenting poor structural resilience, consequently disassembling their 3D network in water, especially if reusability is demanded. Natural rubber latex (NR) can be blended into CNF porous structures as a physical crosslinker to improve wet resilience and enhance structural resistance in aqueous media [1], besides adding hydrophobicity. This work investigated CNF isolation from oxidation/fibrillation combined approaches to produce CNF-based aerogels. These porous materials were obtained through the ice-templating/freeze-drying method. Oxidated/high-pressure fibrillated CNF aerogels exhibited interesting homogeneous interconnected 3D structure containing micro to nanoporous, achieving robust compressive mechanical properties (Young's modulus ~ 400 kPa). NR was combined with oxidated/high-pressure fibrillated CNF yielding a water-resilient and hydrophobic composite aerogel (Oxi-CNF/NR) and adjusting the flexibility and rigidity of aerogels. The adsorption kinetics indicated pseudo-second-order adsorption, elucidating the chemisorption mechanism of Oxi-CNF/NR. Adsorption capacity ranged from 100-400 mg g⁻¹ for Cu (II) and 150-330 mg g⁻¹ for methylene blue dye, with reuse performance ranging from 60 to 98% over the reuse cycles, respectively. X-ray micro CT analysis and adsorption test were combined and allowed to track metal ion adsorption, indicating ion adsorbed throughout the 3D structure. These findings indicate Oxi-CNF/NR composite aerogels as promising and efficient green adsorbents of pollutants from contaminated water.

Acknowledgments

This work was supported by FAPESP (grants 2020/08651-4 and 2021/03097-1) and CNPq (grants 380312/2020-4, 301362/2020-3, 301356/2020-3 and 380173/2022-0).

References

[1] M.V. Lorevice, E.O. Mendonça, N.M. Orra, A.C. Borges, and R.F. Gouveia, Porous Cellulose Nanofibril–Natural Rubber Latex Composite Foams for Oil and Organic Solvent Absorption, ACS Appl. Nano Mater. 3 (2020) 10954.

Área: MAT

(Inserir a sigla da seção científica para qual o resumo será submetido. Ex: ORG, BEA, CAT)

Determination of Degree of Sensitization using a minicell on HAZ of a supermartensitic stainless steel weld joint, before and after PWHT.

Anderson B. Furtado (PG)^{1*}, Marcelo T. G. de Sampaio (PG)¹, Marcelo D. C. Ignácio (IC)¹, André R. Pimenta (PQ)^{2,3}, Sérgio S. M. Tavares (PQ)³, Eduardo A. Ponzio (PQ)¹.

andersonbarbosa@id.uff.br

¹ Laboratório de Materiais da UFF (G2E/LaMUFF), Instituto de Química, Universidade Federal Fluminense, Niterói, Rio de Janeiro, Brasil; ² Laboratório de Instrumentação e Simulação Computacional LISCOMP, Instituto Federal do Rio de Janeiro, Paracambi, Rio de Janeiro, Brasil; ³ Programa de Pós-Graduação em Engenharia Mecânica e Montagem Industrial, Universidade Federal Fluminense, Niterói, Rio de Janeiro, Brasil.

Palavras Chave: SENSITIZATION, MINICELL, WELDING, PWHT

Highlights

Development of electrochemical minicell. A sensitization gradient in HAZ from top to root was noticed. Delta Ferrite was observed in Top-HAZ. PWHT promotes sensitization.

Resumo/Abstract

Supermartensitic Stainless Steels (SMSS) have both high weldability and higher corrosion resistance than conventional martensitic stainless steel. However, during the weldment process appears Heat Affected Zones (HAZ) become harder than the Base Metal (BM) and consequentially may be harder than required in NACE MR0175/ISO 15156 standard. Post-weld heat treatments (PWHT) were studied as a way to promote the reduction of this hardness peak in the HAZ [1]. However, it is important to analyze the susceptibility to intergranular corrosion of the welded SMSS joint after PWHT, because, during this heat treatment, Cr-rich carbides may precipitate leading to the sensitization process. In this work, a contact minicell with an opening diameter of 0.75mm was used to perform DL-EPR tests in different regions of an SMSS multipass welded joint. This test gives the percentual value of the sensitized area and this value is called the Degree of Sensitization (DOS). The minicell was required as the HAZ in the narrowest region has only 0.7mm wide. The welded joint was subjected to PWHT at 650°C for 5 and 15 minutes. In all specimens the base metal was the most sensitized region (Higher DOS), however, the root-HAZ sensitization was higher than the top-HAZ. This can be attributed to a tempering process on the HAZ as the subsequent welding passes still affect these zones by the thermal conductivity. So, as the Top-HAZ is subjected to fewer welding passes this effect is less markable. The DOS value increased with PWHT time. After 15 minutes at 650°C, the DOS of root-HAZ was 74.5%, very close to the value of 71.9% of the BM in the as-welded (AW) condition. Similarly, the top-HAZ after PWHT had DOS of 45%, close to 49% of root-HAZ-AW. The top also featured delta ferrite which was verified in atomic force microscopy (AFM) images, also noticed that the corrosion occurred mainly around this phase According to Zappa et al [2] tempering process of PWHT cannot eliminate delta ferrite, and in this work, this was also noted in AFM images after PWHT. Therefore, during the weld passes, the root-HAZ region was tempered, in addition to the elimination of delta ferrite. Despite the PWHT acts reducing the hardness, attention must be paid to the fact that there is an increase in sensitization together which was determined thanks to the use of a minicell capable off analyze only the HAZ due to its size. Also, it was verified that the finishes pass performed in this weld joint are deleterious as delta ferrite was noticed in AFM images even after PWHT.

[1] S.S.M. Tavares, et al. *Mater. Res.* 17 (2014) 1336–1343.

[2] S. Zappa, et al. *Forces Mech.* 6 (2022) 100067.

Agradecimentos/Acknowledgments



Development of agro-waste and cellulose-based composite filters and their application for fast removal of lead(II) in water purification

Gabriel B. Carvalho (PG),¹ Pedro E. Costa (IC),² Altamiro X. Souza (PG),³ Marcelo F. Oliveira (PQ),⁴ Daniel Pasquini (PQ),⁵ Luis C. Morais (PQ).^{2*}

gabriel_badagnani@hotmail.com; luis.morais@uftm.edu.br

¹PPGMQ-MG, UFTM; ²Chemistry Department, UFTM; ³PPGBIOCOM, UFU; ⁴Chemistry Department, USP; ⁵Chemistry Institute, UFU.

key words: Cellulosic composites filters, High flow, Fast Lead (II) removal, Low cost, Water purification.

Highlights

Cellulosic-based filters were prepared to remove Lead(II).

Surprisingly, filtration takes place in less than 120 sec having both high flow and removal.

The system can be installed in poor communities.

Resumo/Abstract

There are a great number of environmental issues that some can be mentioned i.e. oil pollution, chemical pollution, ground water pollution, thermal pollution, and agricultural pollution. In this work, the major worried is about chemical pollution from lead(II) and applying one simple strategy to overcome this. The World Health Organization (WHO) recommends a maximum amount of lead(II) in drinking water of 5 $\mu\text{g L}^{-1}$. In humans, the accumulative effect of lead (II) can severely affect brain, blood, kidneys and other organs. These are facts that motivated this work to look for a way to minimize water pollution by lead(II), in an efficient, fast and low cost way when compared to many others that have been employed. For this, cellulosic-composite filters were developed and tested in laboratory. The composites are formed by mixing cellulose nanofibers (CNF), bleached cellulose fibers (BCF) and soy hulls (SH). In the filters preparation the components were mixed in water under mechanical stirring during 15 minutes. After this, the slurry is put on Büchner funnel with a fabric filter. Then, the cellulosic filter is removed and put to dry in temperature under 70 °C. The filters are cut to obtain an area of 18 cm² and put in a manifold system connected to a vacuum pump. One commercial filter (CMF) was used as reference and it consisted of pure cellulose having 8 μm in average of size porous. The tested Lead (II) solution was 11 ppm and 30 mL was eluted on the solvent recipient and thus, filtrated. The eluted solution was analyzed by atomic absorption spectrophotometry. The parameters analyzed were filtration time (s), Flow (L h⁻¹ m⁻²) and removal (%). The CMF took **6 s** to filtrate. It removed 8% of Lead (II) and has a flow of 10.000 L h⁻¹ m⁻², which is an indicative of very fast filtration. However, the BCF filter showed a twice-flow, removed 14% of Lead (II) just in **3 s**. The CNF filter removed 24% of Lead (II) in **10 s** with a flow of 6.000 L h⁻¹ m⁻². After addition of 30% w/w of soy husk in the CNF-BCF cellulosic matrix, the filtration time increase to **90 s** decreasing the flow to 667 L h⁻¹ m⁻², allowing 12.5% of Lead (II) removal. The next tests will involve measurements of mechanical resistance and quantification of use cycling and their respective Lead(II) removal.

Agradecimentos/Acknowledgments

The authors are grateful to the FAPEMIG (Research Support CEX-APQ-01651-17), CNPq (National Council for Scientific and Technological Development), CAPES (Coordination for the Improvement of Higher Education Personnel), Foundation of the State of Minas Gerais), Rede Mineira de Química (RQ-MG). And also to the Federal University of Uberlândia (UFU) by support to the micrographs performed in multi-user in Chemical Engineer Institute.

Área: MAT

Development of ASIC biomimetic systems for antinociceptive drug screening

Willian Silveira (IC),¹ Patrícia Bulegon Brondani (PQ),^{1*} Ismael Casagrande Bellettini (PQ).¹

p.b.brondani@ufsc.br, patyqmc@gmail.com, williansilveira63@gmail.com

¹Centro Tecnológico, de Ciências Exatas e Educação (CTE), Programa de Pós-graduação em Nanociência, Processos e Materiais Avançados (NPMat), UFSC Blumenau.

Palavras Chave: Nociception, Bioinspired Systems, Polymeric Micelles, Acid-Sensing Ion Channels.

Highlights

Stable, simple, and low-cost micellar screening test for antinociceptive drugs;
Directly application in the development of new drugs to treat pain;
Bioinspiration on acid-sensing ion channels;

Resumo/Abstract

Harmful stimuli to the body are associated with pain via the nociceptive system, through specialized sensory receptors called nociceptors. Nociceptors detect pain by the activation of receptors and ion channels present on their surface. For example, so-called ASICs, or acid-sensitive ion channels, are activated by small changes in pH that are related to various disorders. Drugs that stop the stimulus (and pain) antagonize this process. Pain treatment is a serious public health problem and, therefore, there is a great effort for the development of new antinociceptive drugs. Research in this area usually takes place through experiments that cause pain and are carried out predominantly in mammals, such as rats and mice. The purpose of this work is to develop new biomimetic systems based on the functioning of ASICs. These systems will allow the construction of new and simple screening tests (*in vitro*) for the development of potential antinociceptive drugs. This strategy can replace animals in some of the testing steps for investigating new drugs. In addition, it can accelerate the development of new drugs and a better understanding of the nociception system. In our previous work, promising results were achieved using a micellar dispersion of polystyrene-*b*-poly (acrylic acid) (PS-*b*-PAA) encapsulating *p*-nitrophenyl butyrate (*p*-NFB) in the presence of a lipase. When *p*-NFB was released, in the presence of lipase, it was converted to the corresponding phenol, shifting the maximum absorbance wavelength. In this way, the analytical response generated was clear and it was possible to evaluate the effect of the pH of the medium on the release of the encapsulated molecule and the influence of an ASIC antagonist drug, ibuprofen, over the developed system. The results obtained were consistent with the published *in vivo* results, leading to a higher signal in pH 7 when compared to pH 7,4 and a diminishment of the signal when in the presence of ibuprofen. However, the system must be improved so that testing of more antinociceptive drugs is possible. Most of the drugs to be tested present absorbance in the detected region generating interference. For this reason, new highly conjugated molecules (dyes, anthraquinones, anthocyanins,...) are being tested for encapsulation, thus enabling the displacement of the detected wavelength into the visible region. These molecules should be accepted substrates for lipases and have a suitable size and hydrophobicity to be able to be encapsulated. The best results so far were obtained by the use of the ester derived from 1,8-dihydroxyanthraquinone. Among various immobilized lipases tested, lipase Cal-B efficiently converted the ester in the corresponding dihydroxyanthraquinone that generates a signal from 400 nm to 550 nm. The molecule was encapsulated in the PS-*b*-PAA micellar dispersion and the system will be investigated in different pHs and in the presence of several ASICs antagonists to probe the correct functioning.

Agradecimentos/Acknowledgments

CNPq, CAPES, UFSC

Development of biocompatible conductive substrates based on biocellulose, KTCNQ and AgTCNQ for retinal implants applications.

Giulia Santos Machado (IC)¹, Dr. Thales Reggiani de Moura (PQ)¹, Prof. Dr. Renan Lira de Farias (PQ)¹, Prof. Dr. Hernane da Silva Barud (PQ)² and Prof. Dr. Sidney José Lima Ribeiro (PQ)¹.

giulia.machado@unesp.br

¹Instituto de Química, Departamento de Química Analítica, Físico-química e Inorgânica, Universidade Estadual Paulista (UNESP);

²Grupo de biopolímeros e biomateriais, Universidade de Araraquara (UNIARA).

Key Words: Retina, Semiconductor, KTCNQ, AgTCNQ, Biocompatibility.

Highlights

Implants based on metal-organic semiconductors are able to replace retinal photoreceptors and excite neurons. Four methods of film synthesis were used via mild temperature conditions.

Resumo/Abstract

In 2021, around 49.1 million people were diagnosed with blindness around the world ^[1] and Retinitis Pigmentosa is the most common cause of hereditary blindness ^[2]. Due to this worldwide problem, the development of devices able to replace the photoreceptors of the retina and excite the output neurons are being studied for restoring visual perception. An alternative is the development of implants based on metal-organic semiconductors, which have electronic properties similar to those of purely inorganic and also act as biocompatible materials for biological applications ^[3]. In addition, the device must have a conductive, flexible and biocompatible substrate.

Based on that, this study aims to develop biocompatible conductive substrates using bacterial cellulose (*Acetobacter xylinum*) and KTCNQ (K-tetracyano-quinodimethane) as a semiconductor for the elaboration of subretinal devices implantable in the photoreceptor layer of people with degenerative diseases. To that end, four methods of synthesis of conductive films were used, all via mild temperature conditions. The first method consisted in the deposition via spin-coating (SC), in which the SPINCOATER P6700 (SCS) equipment was used; the second method was thermal deposition (DT, 150 °C, 2.10⁻³ mbar); the third method was a deposition from a solid-liquid system (chloroform); and the fourth method was carried out using a Schlenk flask in a chemical oven at 110 °C.

Moreover, it was also synthesized films containing AgTCNQ (Ag-tetracyano-quinodimethane), a semiconductor that has high conductivity, properly used in electronic applications in biocompatible devices. They were prepared from a method of silver deposition on bacterial cellulose followed by immersion in acetonitrile solution with TCNQ.

All obtained films were characterized via vibrational spectroscopy in the IR and RAMAN region and they have undergone mechanical tests and resistance and electrical conductivity tests.

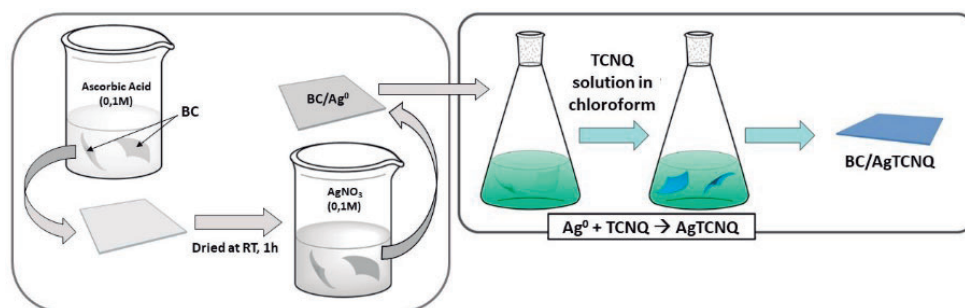


Figure 1 - Synthesis of films containing AgTCNQ

[1] Bourne, R. R. A.; Adelson, J.; Flaxman, S. et al. Investigative Ophthalmology & Visual Science, 2020 61, 2317.

[2] Rare Disease Database (NORD). Retinitis Pigmentosa. Accessed in January, 2023: (<https://rarediseases.org/rare-diseases/retinitis-pigmentosa/>)

[3] Benfenati, F.; Lanzani, G. Lab Anim. 2018, 47, 71.

Agradecimentos/Acknowledgments

To the CNPq-PIBIC, FAPESP and SisFOTON.

Development of lead-free low melting borosilicate glass frits for the production of commercial automotive enamels

Caio C. de Lima (PG),¹ Érico Teixeira-Neto (PQ),² Italo O. Mazali (PQ).¹

caiocarvalho796@gmail.com; erico@metaura.com.br; mazali@unicamp.br

¹Departamento de Química Inorgânica, Instituto de Química, UNICAMP; ²Metaura Pesquisa e Desenvolvimento Ltda.

Keywords: Glass frits, Automotive enamels, Bismuth oxide.

Highlights

The use of bismuth in borosilicate glasses made it possible to obtain a material capable of generating enamels with good fixation on an automotive glass substrate, in addition to excellent opacity.

Abstract

Glass frits are powdered materials obtained from the rapid cooling process of a mixture of molten oxides. The automobile industry uses this type of material in the production of black band enamels, which are used on windshields and car windows, where it plays the role of protecting the adhesive located between the windshield and the bodywork of the vehicle, in addition to playing an aesthetic role. Frits based on $\text{SiO}_2\text{-B}_2\text{O}_3\text{-PbO}$ have become very common in automotive applications due to the interesting properties acquired with their use, such as low melting point, structural stability, and excellent thermal characteristics. For environmental reasons, PbO needs to be replaced by other oxides, where Bi_2O_3 stands out¹. The present work aimed to produce lead-free low melting glass frits for applications in the automotive sector. For this purpose, a sample of vitreous frits based on the composition $\text{SiO}_2\text{-B}_2\text{O}_3\text{-Bi}_2\text{O}_3\text{-ZnO-Na}_2\text{O}$, prepared in an alumina crucible at 1100 °C, was synthesized.

DTA analyses were carried out, where the glass transition was detected around 430°C, which allows a working temperature range between 500-600°C for industrial applications. Spectroscopic techniques revealed the presence of tetrahedral units of Si Q¹ and Q², which indicates low polymerization of the glass structure due to the presence of sodium ions acting as network modifiers.

The application tests consisted of the preparation of enamels for automotive glass mixing the vitreous frits with pigments and organic vehicles. It was observed that similarly to reference products on the market, there was good adherence of the enamel to the glass substrate, in addition to excellent opacity, which is expected from the use of Bi^{3+} , which, due to its high polarizability, offers good absorption of incident radiation. The chemical resistance tests were conducted by submerging the specimens in a H_2SO_4 solution at 80 °C for 4 hours, where it was possible to notice the leaching of the enamel after 1 hour submerged. The increase in zinc contents and the decrease in sodium should improve the chemical durability of the material, which will be investigated in future works.

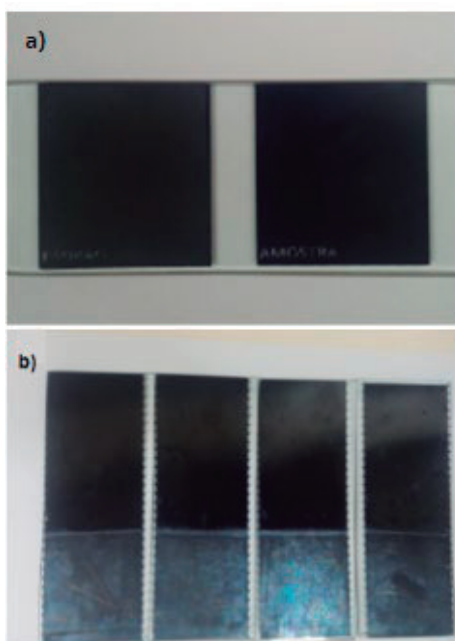


Figure 1: Commercial black band enamel (left) and the developed enamel sample (right) sintered in glass substrate (a); chemical resistance test of the developed enamel in acid medium for 1, 2, 3 and 4 hours, from left to right (b).

References

- [1] S. Gu, Z. Wang, S. Jiang, H. Lin, *Ceramics International* vol. 40, 7643-7645, 2014.

Acknowledgments



Development of sustainable luminescent solar concentrators: from castor oil to photovoltaic cell

Fábio J. Caixeta (PQ)^{1*}, Beatriz D. de Freitas (IC)¹, Bruno S.D. Onishi (PG)¹, Ricardo Bortoletto-Santos (PQ)¹, Francis S.R. Garcia (PG)², Younès Messaddeq (PQ)^{1,3}, Sidney J. L. Ribeiro (PQ)¹.

fcaixeta@alumni.usp.br

¹Institute of Chemistry, UNESP; ²São Carlos Institute of Chemistry, USP; ³Département de physique, de génie physique et d'optique, Université Laval

Keywords: Urethanesil, [Eu(tta)₃(H₂O)₂], Photoluminescence, Sunlight, Photostability, Green energy.

Highlights

Hybrid material based on Castor Oil and 3-(triethoxysilyl)propyl isocyanate. Incorporation of [Eu(tta)₃(H₂O)₂] complex. Cylindrical luminescent solar concentrator for PV energy production enhancement.

Abstract

It is consensus that the tremendous growing in global energy consumption since the beginning of the twentieth century, mainly coming from fossil sources, has led to the recent climate changes. Under this scenery, there is no doubt that the energy of the future is going to be based on natural and renewable sources. Over the last years, much attention has been dedicated to obtaining new materials to be used in photovoltaic (PV) energy production. Several strategies have been adopted in order to improve the PV energy conversion. Notwithstanding, some challenges concerning PV need to be overcome, mainly related to the efficiency of the process. In this sense, luminescent solar concentrators (LSCs) has been successfully used during the last decades for such purpose. Efficient UV absorption, efficient emission quantum yield, photostability, and sustainability are characteristics extremely important concerning LSCs. In the present study we present and discuss outstanding results concerning a sustainable organic-inorganic hybrid (OIH) material based on Castor oil (CO) and containing a Eu³⁺ complex, namely SiCO-[Eu(tta)₃]. Such material was obtained by using the sol-gel process, following the casting method. The results have shown that the SiCO-[Eu(tta)₃] material presents satisfactory thermal stability, broad transparency window (90% of transmittance in the visible and infrared) and efficient UV-to-visible conversion. Furthermore, the photoluminescence results have revealed an expressive increase in the emission quantum efficiency when the [Eu(tta)₃] complex is incorporated into OIH material. Moreover, experiments in progress have shown that SiCO-[Eu(tta)₃] can be used to produce cylindrical LSCs. Which, are more efficient than planar ones. All the results indicate that the obtained material have a huge potential to be used as efficient luminescent solar concentrators and consequently improving PV cells energy conversion.

References

- [1] M. A. Hernández-Rodríguez *et al.*, *J. Appl. Phys.*, **131**, 140901 (2022).
[2] M. A. Cardoso *et al.*, *J. Sol-Gel Sci. Technol.*, **101**, 58 (2022).

Acknowledgments

The authors are grateful to FAPESP (Grant No. 2015/22828-6, 2018/07727-7, 2020/03259-9, and 2022/03652-8) and CNPq (Grant No. 380556/2023-5) for financial support and LAMF-UNESP for providing institutional support and facilities to obtain results, and A. Azevedo Óleos (Brazil) for supplying Castor oil.

Área: **MAT**

(Inserir a sigla da seção científica para qual o resumo será submetido. Ex: ORG, BEA, CAT)

Development of toecap for safety shoes industry using Polymer/Clay composites.

Felipe C. Clementino (PG),^{1,2} Jorge L. D. dos Santos,¹ Emerson H. de Faria (PQ).^{2*}

e-mail: felipec@ipt.br; emerson.faria@unifran.br

¹Laboratório de Química e Manufaturados, LQM do IPT; ²Grupo de Pesquisas em Materiais Lamelares Híbridos, GPMatLam da UNIFRAN

Palavras Chave: EPI, Calçado Profissional, Biqueira, Nanocompósito, Policarbonato, Argilominerais

Highlights

Development of toecap for footwear containing polymeric nanocomposite. Mixtures containing different mass ratio of clay minerals in polycarbonate increases the thermal and mechanical properties of the toecaps.

Resumo/Abstract

The city of Franca is nationally recognized as the footwear capital. A sector that has gained a lot of space recently is professional footwear. Among the various safety components, the toecap for safety shoes is extremely important component to prevent injuries from falling objects on the feet. Thus, in this work, the mechanical and thermal properties of polycarbonate (PC) composites with clay minerals (kaolinite (Kao) and bentonite (Bent)) to evaluate the possible improvement of physical chemical properties of the toecaps. Initially, physical mixtures of the polymer and clay minerals were carried out, varying the mass/mass proportions between 1% and 5%. These materials were then homogenized in a disk milling, extruded and pelletized in the form of granules in a twin screw extruder, co-rotating, brand AX Plasticos, model AX16-DR with a temperature of processing: 220-250°C. They were injected with a mold suitable for tensile testing according to the ASTM D638-01 (standard for tensile testing of plastics). The materials were characterized from the physical-chemical point of view and also their mechanical properties were initially explored. The thermal analysis (TG/DTG/DSC) of the polycarbonate (PC), demonstrate that the thermal decomposition of the polymer occurs at a temperature of 515°C for the first stage and 626°C for the second, with only 0.8% of the residue present, which must be attributed to tough or vitreous carbon. The composites obtained with clay minerals demonstrate that there was an increase in the temperature of thermal decomposition, which suggests the interaction between the polymer and the clay mineral. It is noteworthy that the thermogravimetric curve of the composites PC/Bent 5% and PC/Kao 5% have a profile very similar to the thermogram of the PC due to the high dilution of the inorganic loads in the matrix, however the peaks of thermal degradation of the composite with bentonite happen at temperatures higher than those of pure polycarbonate, being 527 °C for the first stage and 638 °C for the second, increasing approximately 12 °C in each stage, respectively. At the end, a residue of approximately 2.5 is obtained, which must be attributed to the aluminosilicate resulting from the dehydroxylation of the incorporated clay minerals and to a residue of vitreous or resistant carbon from the degradation of the PC. In the X-ray diffraction (XRD) of the PC/Kao and PC/Bent composites, the presence of reflections characteristic of clay minerals and also characteristic halos of polycarbonate could be observed proportionally to the clay minerals concentration in the polymer. The mechanical properties of the materials were investigated, where the parameters were verified; yield stress, elongation and modulus of elasticity. All results were compared to pure polycarbonate (reference material), it should be noted that the use of composite materials based on kaolinite, there was no significant change in the results of elongation and yield stress in this range of mass proportions tested, however the modulus of elasticity was an increase of approximately 11.2% in the result, as for the use of bentonite, there was a reduction of more than 50% in the result of elongation and yield stress, and an increase of 12.1% in the value of the modulus of elasticity. The increase in modulus of elasticity is a very important characteristic for the toecap, as it must withstand a compression of 15 kN, but the loss of intensity in yield stress and elongation is detrimental to the toecap, which must withstand an impact of 200 J, according to the EN ISO 22568 standard, which determines and specifies this safety item. As a next step, there is interest in the use of kaolinite in polycarbonate for application as a toecap for professional shoes, as well as the modification of clay mineral for the same application.

Agradecimentos/Acknowledgments

O presente trabalho foi realizado com apoio da Coordenação de Aperfeiçoamento de Pessoal de Nível Superior - Brasil (CAPES) - Código de Financiamento 001, no qual agradeço a concessão da bolsa de estudos.

E.H. De Faria thanks to CNPq project number: 310151/2021-0 and FAPESP

Dextran-graft-poly(N-isopropylacrylamide) nanoparticles via Schiff base formation for co-delivery of doxorubicin and curcumin

Maria J.M. Carneiro (PG)^{1*}, Cláudio B.A. Paula (PG)¹, Irisvan S. Ribeiro (PG)¹, Laís R.M. de Lima (PG)¹, Raelle F. Gomes (PG)¹, Jéssica M. T. Souza (PG)³, Gisele S. Araújo (PG)³, José D.B. Marinho Filho (PQ)³, Ana J. Araújo (PQ)³, Judith P.A. Feitosa (PQ)¹, Regina C.M. de Paula (PQ)¹

rpaula@dgoi.ufc.br; mariajose_quimica@hotmail.com

¹Departamento de Química Orgânica e Inorgânica, UFC; ²Núcleo de Pesquisa em Biodiversidade e Biotecnologia, ³UFDPAr; Laboratório de Cultura de Células do Delta, UFDPAr

Keywords: *pH-sensitive*, *Cancer*, *Graft copolymer*

Highlights

Graft copolymers exhibited thermal and pH dual-responsive properties.
The copolymers were able to self-assembled on nanoparticles with thermal stimulus.
The drug-loaded nanoparticles exhibited pH-sensitive release profile;
The nanoparticle showed cytotoxicity in HCT-116 cells and reduced cytotoxicity in non-tumor cells.

Resumo/Abstract

Chemotherapy is one of the most used forms of cancer treatment at present, but the effectiveness of monotherapy is generally limited. Studies report that combination chemotherapy can provided a better and sometimes synergistic therapeutic efficacy against cancers.¹ Curcumin, extracted from the rhizomes of *Curcuma longa*, has several pharmacological properties, with emphasis on anticancer activity.² The combination of curcumin (CUR) with chemotherapeutic agents showed an increase in the antitumor effect.³ Stimulus-responsive nanoparticles can promote a selective release of the drug in tissues and tumor cells efficient therapeutic efficacy.⁴ In this work, dextran-g-poly (N-isopropylacrylamide) copolymers were synthesized via Schiff base formation, obtaining self-assembled nanoparticles for pH-sensitive release of doxorubicin and curcumin. The analyzes of dynamic light scattering (DLS) showed that the copolymers were thermal and pH dual-responsive. Doxorubicin (DOX) was conjugated to the copolymers via Schiff base formation and curcumin was encapsulated by hydrophobic interaction, obtaining nanoparticles by self-assembly with size of 61 nm. The drug loading efficiency (DLE) values of DOX and CUR were 78.4% and 66,1%, and the drug loading content (DLC) values of DOX and CUR were 12.6% and 11.0%, respectively. A higher percentage of doxorubicin and curcumin was released at pH 5.0 compared to physiological pH, confirming a pH-sensitive release profile. The *in vitro* cytotoxicity assay demonstrated that DOX/CUR-loaded nanoparticles can inhibit HCT-116 cell proliferation and promote reduced cytotoxicity in non-tumor cells. The DOX/CUR-loading nanoparticles may be a promising drug co-delivery system for anticancer therapy, given the possibility of selective drug delivery in cancer cells.

Agradecimentos/Acknowledgments

CAPES, CNPq, INCT/ Polysaccharide, FUNCAP, FINEP and LCCDelta.

¹SENAPATI, S.; MAHANTA, A. K.; KUMAR, S.; MAITI, P. **Signal Transduction and Targeted Therapy**, v. 3, p. 1–19, 2018.

²ZHENG, B.; MCCLEMENTS, D. J. **Molecules**, v. 25, n. 12, p. 1–25, 2020.

³YOUNES, M.; MARDIROSSIAN, R.; RIZK, L.; et al.. **Plants**, v. 11, p. 2137, 2022.

⁴CHANG, D.; MA, Y.; XU, X.; XIE, J.; JU S. **Frontiers in Bioengineering and Biotechnology**, v. 9, p. 707319, 2021.

Dispersion Analysis of Poly(heptazine imide)/Polyurethane Nanocomposites for Fertilizers

Júlia Antoneli Ibanhes (IC),^{1,2} Guilherme F. S. R. Rocha (PG),¹ Marcos A. R. da Silva (PG),^{1,2} Ivo F. Teixeira (PQ),¹ Ricardo Bortoletto-Santos (PQ),^{2,3} Caue Ribeiro (PQ).²

juliaantoneli@estudante.ufscar.br

¹Department of Chemistry, UFSCar; ²Embrapa Instrumentação, ³Universidade de Ribeirão Preto (UNAERP)

Keywords: Carbon Nitride, Poly(heptazine imide), Fertilizer, Controlled Release, Polyurethane.

Highlights

Prepared carbon nitrides showed negative residual charge; CTAB showed better dispersion of carbon nitrides in polyurethane matrix; This work aimed to study the dispersion processes of nanocomposites composed of crystalline carbon nitrides with castor oil-based polyurethane matrix for controlled nutrient release.

Abstract

Crystalline carbon nitrides with poly(heptazine imide), or PHI, structures emerge as promising materials for many applications, such as sensing, catalysts and ions adsorption. The latter feature is due to the ionic character of these compounds, which is attributed to the deprotonation of carbon nitrides polymers and stabilization with alkali cations. Thus, this ionic material can be employed for nutrient adsorption and controlled release for fertilizers. The PHI structures were synthesized by a thermal condensation of melamine with NaCl, generating an ordered material with sodium cations between the carbon nitride layers, which was named Na-PHI (**Fig. 1a**). Potential zeta analysis indicated, as expected, that Na-PHI possesses negative charges in acid and basic pHs (**Fig. 1b**), indicating that it will react strongly with ammonium (NH_4^+), which has a positive charge, thus urea is a suitable fertilizer to polymeric coating in Na-PHI. However, to prepare Na-PHI/polyurethane nanocomposites, it is necessary to determine the ratio mixture between these components since affects its viscosity. Viscosity analysis of the nanocomposites were made with 1%, 2.5%, 3.5% and 5% of Na-PHI in polyurethane matrix, and was confirmed 5% was the best composition due to the higher viscosity. High viscosities are better for deposition onto irregular interfaces, such as urea granules. Also, a suitable dispersant is required for nanocomposites preparation, whereby CTAB shows the highest viscosity (**Fig. 1c**) among others surfactants, such as PMAA, Tween 20 and Tween 80. The determination of mixture parameters is extremely important for an efficient nanocomposite for controlled nitrogen release on soils.

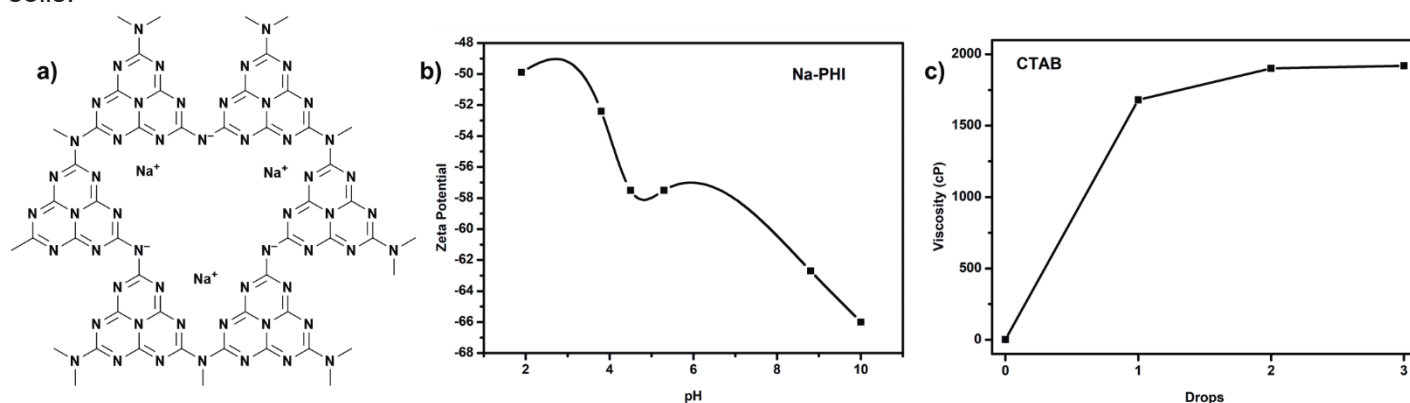


Figure 1: a) Structure of Na-PHI; b) Zeta Potential of Na-PHI; c) Viscosity of the mixture Na-PHI/Polyurethane with CTAB as dispersant.

Acknowledgments

The authors are thankful for FAPESP, CAPES, CNPQ, Embrapa and UFSCar.

Dithiocarbamate intercalated in zinc hydroxynitrate matrix and its behavior in water medium

Eline Barbosa Ferreira (PG)^{1*}, Eder do Couto Tavares (PQ)¹, Fábio da Silva Lisboa (PQ)¹
 eline.bf.ferreira@gmail.com

¹ Institute of physics and chemistry, Federal University of Itajubá – UNIFEI

keywords: Zinc hydroxynitrate, Intercalation, Dithiocarbamate.

Highlights

- Intercalation of dithiocarbamate in the interlayer space of zinc hydroxynitrate compound.
- Behaviour of dithiocarbamate in water with and without the matrix presence.

Abstract

The zinc hydroxynitrate intercalated with dithiocarbamate, $K_2[C_7H_7SO_2N=CS_2] \cdot 2H_2O$, (ZHN+DCBI) was obtained through a coprecipitation reaction, in which a sodium hydroxide solution containing the dithiocarbamate (DCBI) anion was deposited in a beaker with constant and vigorous magnetic stirring, while a zinc nitrate solution was dropped slowly and constantly on the alkali mixture. Figure 1 shows the comparison between the diffractograms of the lamellar matrix of zinc hydroxynitrate (ZHN) and the intercalated material (ZHN+DCBI). It is possible to observe the change in the basal distance from 9.69 Å (200 plane in blue line) to 13.81 Å (red line), that supports the intercalation of the anion in the structure. Figure 2 shows the results obtained through the FTIR technique in which typical vibrational modes of the lamellar matrix and the anion could be observed, such as ν_{CN} (1329 cm^{-1}), $\nu_{SO_{2s}}$ (1130 cm^{-1}), $\nu_{SO_{2as}}$ (1230 cm^{-1}), $\nu_{CS_{2as}}$ (940 cm^{-1}) and ν_{sNO} (1366 and 1353 cm^{-1}). It is possible to verify the presence of dithiocarbamate in the structure by observing the ZHN+DCBI curve (red line). Figures 3 and 4, respectively, show the results obtained for the study of anion's behavior in water, and the influence of the layered structure. When comparing the intercalated compound with the degradation of the anion, it can be stated that the anion's degradation occurs within 960 minutes, while intercalated compound's degradation starts after 270 minutes, which indicates the preservation of the dithiocarbamate in the interlayer space.

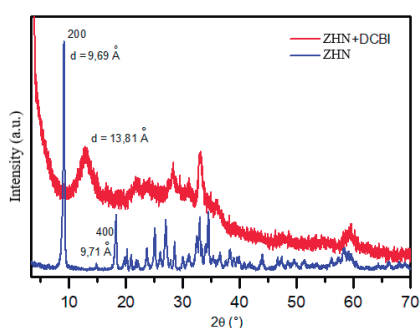


Figure 1: Powder X-ray diffraction of ZHN (blue) and ZHN+DCBI (red).

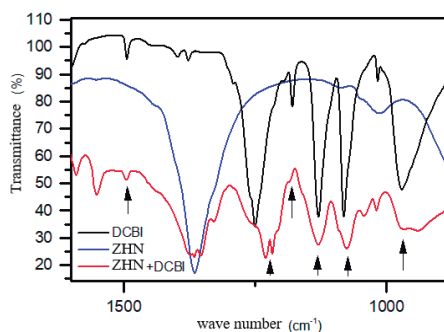


Figure 2: Infrared amplified spectrum of DCBI (black), ZHN (blue), and ZHN+DCBI (red).

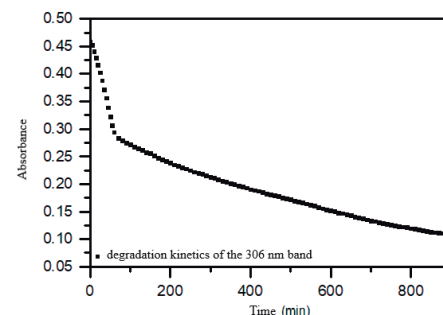


Figure 3: Degradation kinetics of the DCBI's 306 nm band.

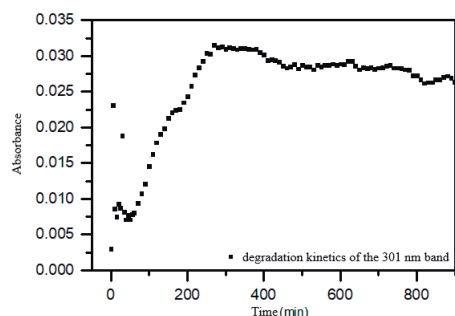


Figure 4: Degradation kinetics of the ZHN+DCBI's 301 nm band.

Acknowledgments



Double doping of Lanthanum-Strontium Titanate: synthesis, characterization, and nanoparticles production by exsolution for solid oxide fuel cell anodes.

Antonio T. B. De Oliveira (PG),¹ Daniel Z. De Florio (PQ).

Oliveira.antonio@ufabc.edu.br; daniel.florio@ufabc.edu.br

¹ Centro de Engenharia, Modelagem e Ciências Sociais Aplicadas, UFABC

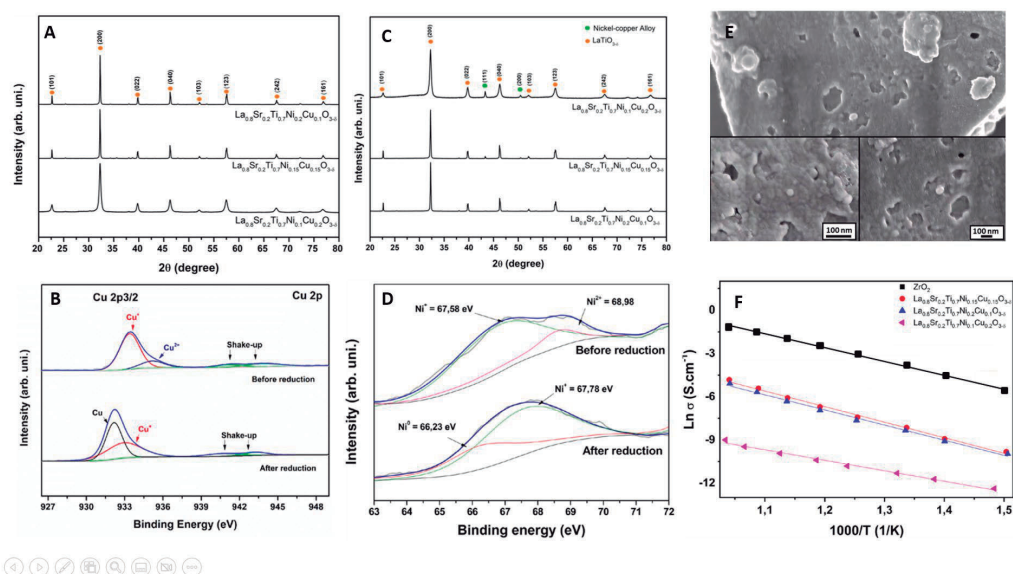
Palavras Chave: Perovskites, exsolution, Solid Oxide Fuel Cell (SOFC), XRD

Highlights

Exsolution for methane conversion

Resumo/Abstract

Solid oxide fuel cells (SOFCs) stand out among several energy conversion devices owing to their high efficiency, fuel flexibility, and low to zero CO₂ emissions. The present work seeks to obtain perovskite materials for use as anodes in SOFC with exsolved metal alloy nanoparticles attached to the structure, with the aim of addressing a more promising material, challenging, and less contemplated in the literature. The nanoparticle catalysts solubilized in a perovskite host were exposed to a reducing H₂ atmosphere. La_{0.8}Sr_{0.2}Ti_{0.7}Ni_{0.3-x}Cu_xO₃ (x = 0.1, 0.15, 0.2) were obtained via the Pechini synthesis route and calcinated at 900 °C for 5 h. To obtain decorated NiCu nanoparticle alloys, the powders were heat treated under 3 vol % H₂/N₂ gas at 900 °C for 10 h. The samples were characterized using X-Ray Diffraction (XRD). Fig. A shows a single-phase perovskite can be observed before the reduction treatment. X-Ray Photoelectron spectroscopy (XPS) revealed the predominance of oxidate states in the prepared samples (Fig. B). After the reduction treatment, XRD analysis showed the presence of new peaks, which could be associated with the nickel-copper alloy (Fig. C). By XPS measurements, metallic nickel and copper were found, confirming the presence of nanoparticles anchored on the surface, (Fig. B and D). Scanning electron microscopy was applied, and spherical nanoparticles were observed after the reduction treatment (Fig. E). Finally, electrochemical impedance spectroscopy was used to compare the electrical properties of the samples (Fig. F) to zirconia-yttria ceramics.



Agradecimentos/Acknowledgments

The author acknowledges CEM-UFABC, PRH49-ANP/UFABC, M2PCINE- FAPES/Shell

Ecofriendly preparation of nanogels based on polyetheramine-bisepoxide as potential multifunctional carriers.

Heber E. Andrada (PG),^{1*} Bruno Andrade Fico (PG),¹ Felipe Breda Alves (PG),¹ Julia Mirian Paulino (PG),¹ Natalia Nascimento Silveira (PG),¹ Raquel Alves Dos Santos (PQ),¹ Eduardo Ferreira Molina (PQ).¹

heberandrada@hotmail.es

¹Laboratório Sol-gel, Universidade de Franca, Av. Dr. Armando Salles Oliveira 201, 14404-600 Franca, SP, Brazil.

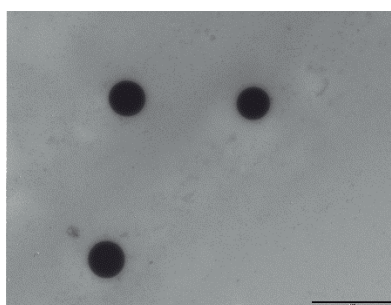
Palavras Chave: nanogels, jeffamine, nanocarriers, drug delivery.

Highlights

Nanogels are three-dimensional cross-linked polymeric networks of submicron size, which have the ability to absorb large amounts of water or biological fluids while maintaining their structure. They have very interesting properties, such as good biocompatibility, high porosity, high stability and high drug or micronutrient loading capacity. For this reason, these nanogels are beginning to be used in various areas of science, such as the pharmaceutical industry and agriculture.

Resumo/Abstract

The development of nanotechnologies has made it possible to achieve important advances in the transport of bioactive molecules in the field of nanomedicine and micronutrients in the field of agriculture. Nanogels are three-dimensional cross-linked polymeric networks of submicron size. These can be prepared from polymeric precursors or by heterogeneous polymerization of monomers^{1,2}. These nanogels have been shown to exhibit reduced premature release of bioactive molecules, increasing the efficacy of targeted drugs, which is why they have been widely used as drug delivery agents^{3,4}. In this work, we evaluated the formation of nanogels based on polyetheramine (PPO) and bisepoxide (BisE), varying the molar ratio of PPO:BisE. The formation of the nanogels was physicochemically characterized using techniques such as DLS, zeta potential, TEM and biological assays were performed to evaluate their biocompatibility and cytotoxicity. It was observed by TEM and DLS techniques that these nanogels have a size between 200 to 500 nm depending on their composition, and that the size increases with increasing temperature. The surface charge was measured by zeta potential. At basic pH the nanogels have a negative surface charge (-33mV), and for pH below 7, their surface charge becomes neutral or slightly positive. Moreover, by TGA measurements, it was observed that the nanogels have the capacity to retain water in their interior up to about 300°C. Finally, cytotoxicity tests were performed and it was observed that the nanogels are biocompatible and therefore viable for use in pharmaceutical formulations.



References

1. Dalir Abdolahinia, E. *et al.* Application of nanogels as drug delivery systems in multicellular spheroid tumor model. *J. Drug Deliv. Sci. Technol.* **68**, 103109 (2022).
2. Topuz, F. & Uyar, T. Advances in the development of cyclodextrin-based nanogels/microgels for biomedical applications: Drug delivery and beyond. *Carbohydr. Polym.* **297**, 120033 (2022).
3. Vashist, A. *et al.* Nanogels as potential drug nanocarriers for CNS drug delivery. *Drug Discov. Today* **23**, 1436–1443 (2018).
4. Fu, X., Hosta-Rigau, L., Chandrawati, R. & Cui, J. Multi-Stimuli-Responsive Polymer Particles, Films, and Hydrogels for Drug Delivery. *Chem* **4**, 2084–2107 (2018).

Agradecimentos/Acknowledgments

Funding: FAPESP (n° 2021/06552-1, 2022/06507-9), CAPES (Finance Code 001), and CNPq (307696/2021-9).

Effect of pluronic® F-127 surfactant amount on textural properties of mesoporous carbon from tannin biomass

Aline C. Marciano^{1*} (PG), Igor B. Gomes¹ (IC), Rayane C. F. Silva¹ (PQ), Victor S. Vaz¹ (IC), Keiliane S. dos Santos¹ (PG), Rubens L. F. Filho¹ (PG), Glaura G. Silva¹ (PQ), Paula Sevenini² (PQ), Ana Paula C. Teixeira^{1**} (PQ).

aline.capelao@gmail.com*; anapct@ufmg.br**

¹ Universidade Federal de Minas Gerais. ² Universidade do Estado de Minas Gerais unidade Divinópolis.

Keywords: Tannin Biomass, solvent-free, porous carbon.

Highlights

Biomass as carbon source are being used for more sustainable and economically friendly synthesis of mesoporous carbon. An increase in amount of surfactant leads to microporous characteristics materials.

Abstract

Mesoporous carbons (MC) are materials consisting of carbon with pore diameters between 2 and 50 nm^{1,2}. By varying the synthesis parameters, it is possible to control size, volume, geometry, and organization of pores. The versatility combined with the intrinsic properties of MCs (physical-chemical stability, surface area and high pore volume) allows the use of these materials in different areas such as catalysis, adsorption, and energy storage. The use of renewable sources such as biomass has gained prominence for enabling the obtainment of carbon materials with different morphologies, low cost, and easy accessibility. Thus, the use of biomass and new synthesis methodologies may be the solution for the use of MC on a large scale, considering economic and environmental aspects^{1,3}. The solvent-free methodology was used for the synthesis of MC⁴. Tannic Acid (TA, Synth) or Tannin Extract (TE, ~70% w/w, Tannac) as carbon source (P), pluronic® F-127 (S, surfactant) and terephthalaldehyde (R, crosslinking agent) were mixed and ground in a planetary mill for 30 minutes. The P:S:R ratio (w/w) used were 2:2:1 (TA1 and TE1) or 2:4:1 (TA2 and TE2). The solid obtained was added to alumina navicles in a quartz tube and inside a tubular furnace for the formation of pores and carbonization of the biomass, in a commercial argon atmosphere with temperature, gas flow and time optimized in the process. The produced MCs were characterized by gas physisorption. The difference in the materials produced refers to the amount of surfactant and the origin of the biomass precursor used. The physisorption isotherms (Figure 1) indicated that TA1 and TE1 presented isotherms with a profile like type IV, characteristic of mesoporous materials. However, TE1 isotherm has a more heterogeneous material profile, as expected due to the purity of the biomass. The MCs produced with double of surfactant (TA2 and TE2) showed isotherms like type I, indicating more microporous characteristics. Furthermore, these two materials did not show clear hysteresis, indicating that the mesoporous, if present, must be very small (2 to 3 nm) and aggregated⁵. By analyzing the textural parameters (Table 1), it is possible to see that the increase in surfactant amount caused a significant decrease in surface area and pore volume in TA2. Despite the difference in these textural parameters not being so significant, TE2 also showed microporous characteristics, as its micropore area was greater than the external area. This indicates the need for new synthetic optimizations to produce a material with higher mesoporous quality for conditions with high amounts of surfactant. Therefore, it is possible to produce mesoporous carbon materials using sustainable precursors as biomass. Nevertheless, the synthesis method is strongly impacted by the amount of surfactant and this study is still in the preliminary stage. The next steps are related to the variation of synthetic parameters such as decreasing the amount and type of surfactant (less costs) and grinding conditions (time and rotation speed). In this way, it will be possible to evaluate the impact of the surfactant on the textural properties of the materials.

Figure 1. Nitrogen Physisorption Isotherm for the materials

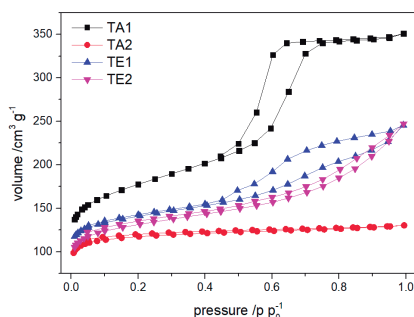


Table 1. Texture parameters of materials from Nitrogen Physisorption analysis

Material	$A_{\text{BET}} / \text{m}^2\text{g}^{-1}$	Pore diameter (BJH) / nm	$V_{\text{total}} / \text{cm}^3\text{g}^{-1}$	$V_{\text{meso}} (\text{BJH}) / \text{cm}^3\text{g}^{-1}$	$V_{\text{micro}} / \text{cm}^3\text{g}^{-1}$	$S_{\text{micro}} / \text{m}^2\text{g}^{-1}$	$S_{\text{ext}} / \text{m}^2\text{g}^{-1}$
TA1	636	5.6	0.343	0.352	0.101	272	364
TA2	391	-	0.198	-	0.148	359	32
TE1	542	5.6	0.392	0.203	0.132	345	196
TE2	488	-	0.351	-	0.152	366	121

¹ Li, W.; Liu, J.; Zhao D. *Nat Rev Mater.* **2016**, *1*, 16023. ² Szcześniak, B.; Choma, J.; Jaroniec, M. *Chem Commun.* **2020**, *56*, 7836.

³ Libbrecht, W et al. *Carbon.* **2017**, *116*, 528. ⁴ Zhao, J. et al. *Chem Eng J.* **2020**, *381*, 122579. ⁵M. Thommes et al. *Pure and Applied Chemistry.* **2015**, *87*, 1051.

Acknowledgments

UFMG, CTNano, Rota 2030, FUNDEP, MIDAS, Capes, CNPq, FAPEMIG, XBM and Bravo Motors Company.

46ª Reunião Anual da Sociedade Brasileira de Química: "Química: Ligando ciências e neutralizando desigualdades"

Effect of surface groups in carbon dots on the cell viability

Mayara Martins Caetano (PG)¹, Amanda Blaque Becceneri (PQ)², Roberto Santana da Silva (PQ)² e Renata Galvão de Lima (PQ)^{1,3}

renatagalvao@ufu.br

¹Instituto de Química (IQ), Universidade Federal de Uberlândia (UFU), Uberlândia/MG, Brasil; ²Faculdade de Ciências Farmacêuticas de Ribeirão Preto, Universidade de São Paulo, Ribeirão Preto, SP, Brasil; ³Instituto de Ciências Exatas e Naturais do Pontal-ICENP, Universidade Federal de Uberlândia, Ituiutaba, MG, Brasil;

Palavras Chave: Carbon dots, Cell viability, Cell morphology alteration, Fluorescence bio-imagem

Highlights

Chemical nature and charge of surface functional groups in carbon dots on cell viability and abnormalities in cell morphology

Resumo/Abstract

Carbon dots (CDs) have been demonstrated as a new class of fluorescent nanomaterials widely used as fluorescent nanoprobe for optical bioimaging^[1]. In this work we reported two CDs obtained from *o*-phenylenediamine (OPDA) and 3,4-hidroxybenzoic acid (DABA) in ethanol/H₂O solution under domestic microwave irradiation. FTIR spectra for both CDs are possible to observe peak at 3.423 cm⁻¹ and 3.319 cm⁻¹ attributed to the stretching vibrations of the O–H and N–H bonds, indicating the presence of a hydroxyl group, and primary amine. Furthermore, stretching in the region of 1.630 to 1.650 cm⁻¹, which can be attributed to the presence of carbonyl group from carboxylate. The zeta potential in pH=7.4 for CDs-DABA and CDs-OPDA equals –5.85 mV, and –0.146 mV, respectively. AFM images showed a particle size distribution for CDs-OPDA equals 5.2 nm while CDs-DABA 14 nm. Both CDs emit yellow fluorescence at 570 nm under $\lambda_{ex}=430$ nm. The cytotoxicity and cellular morphology involve chemical nature and charge of surface functional groups for both CDs were studied on human (A375) and murine (B16F10) melanoma as well as lung fibroblast (MRC-5) cells. In the same concentration interval, the CDs-OPDA showed to be more cytotoxic than CDs-DABA (Fig.1a) in all concentrations tested. The CDs-OPDA showed cell viability lower than 50% starting concentrations of 1.25 mg mL⁻¹ for B16F10 and 0.31 mg mL⁻¹ for MRC-5. Microscope images of A375 cells treated with CDs-DABA did not indicate any morphological changes until a concentration of 1.25 mg mL⁻¹ (Fig.1b). In contrast, cells treated with CDs-OPDA showed the first signs of cytotoxicity already at a concentration of 0.15 mg mL⁻¹ accompanied by possible aggregation of CDs-OPDA. It is possible to conclude that the cytotoxic effect is concentration dependent. Only CDs-OPDA entered in the MRC-5 cell (0.07 mg mL⁻¹) as showed by the yellow emission (Fig.1c).

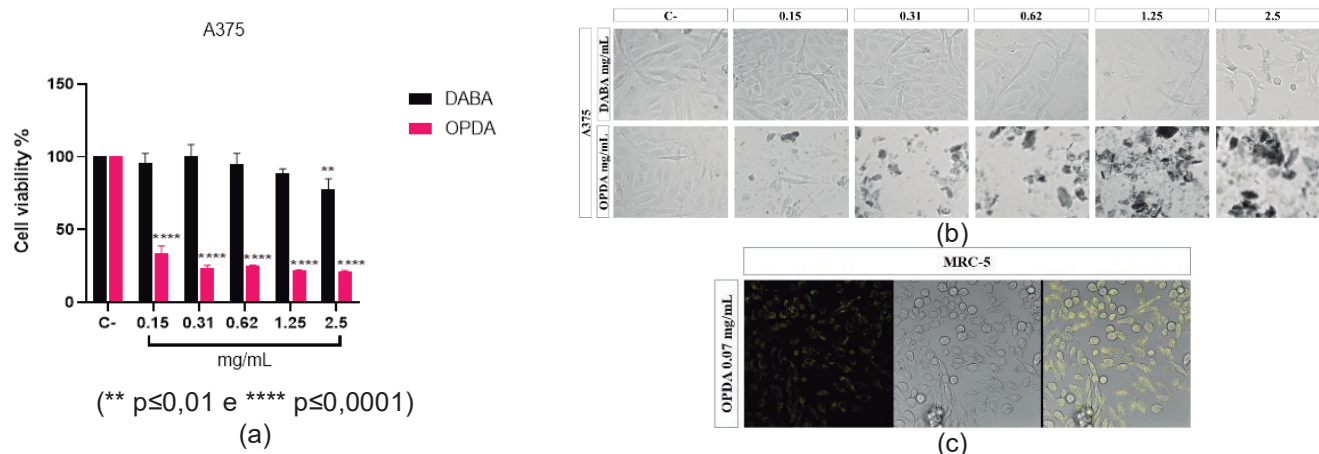


Fig. 1: A375 viability cell (a) and morphology of cells in comparison to control cells (b) in function of CDs concentration after 24 h of incubation. Microscopic confocal laser for MRC-5 labeled with CDs-OPDA.

[1] Havrdova, M. et al., *Carbon* 99 (2016) 238-248.

Agradecimentos/Acknowledgments

RELAM (UFU Multiuser Laboratory); Capes, CNPq and Fapesp

46ª Reunião Anual da Sociedade Brasileira de Química: "Química: Ligando ciências e neutralizando desigualdades"

Área: **MAT**

(Inserir a sigla da seção científica para qual o resumo será submetido. Ex: ORG, BEA, CAT)

Effect of ultrasound treatment on Cellulose and CNF films**André Neubern (AN), Roselena Faez (RF).****andrefelipeneubern@hotmail.com**Laboratório de Materiais Poliméricos e Biossorventes (Lab-MPB), Universidade Federal de São Carlos (UFSCar)- Araras, SP.
Palavras Chave: (ultrassound, cellulose, fertilizer, CNF, blend, slow-release).**Highlights**

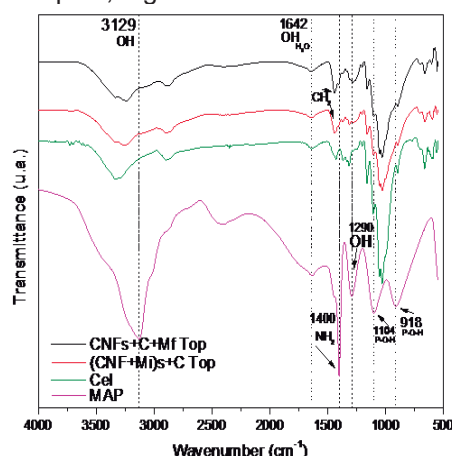
Using ultrasound treatment intensifies the interaction of the fertilizer with the polymeric matrices, resulting in better dispersion of the nutrient into the matrices along the film.

Abstract

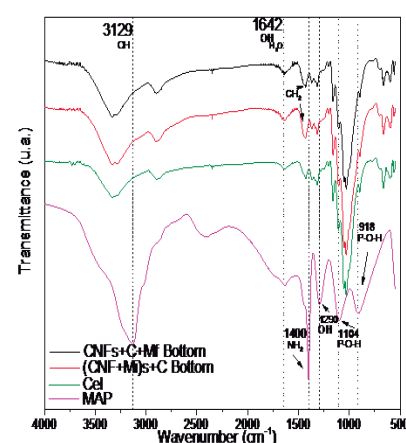
The need to produce more food in the same space is a fact of everyday life and constantly seeking to enhance field management to improve productivity. Enhanced Efficiency Fertilizers (EEF) are one of the alternatives to increase production, making nutrient availability more effective. Employing films as carriers for these nutrients is an option to implement the release of these fertilizers. Thus, we developed a composite of cellulose (Cel, 0.5 wt.%), cellulose nanofibrillated (CNF, 0.2 wt.%), and 40 wt.% of fertilizer (monoammonium phosphate-MAP 40 wt.%) according to the amount of polymer, to obtain plantable pots, Figure 1a.



(a)



(b)



(c)

Figure 1: (a) Image of plantable pot from Cel and CNF; (b) FTIR comparison of the top side of the films (c) FTIR comparison of the bottom side of the films

We prepared films from the sonication of one component (CNF) by adding the nutrient at the end (Mf), and two components (CNF and MAP), considering the nutrient at the beginning (Mi). The casting films from each approach were characterized on both sides (top and bottom) by FTIR analysis. According to the results, the films from the one component sonicated showed intense peaks relative to the fertilizer, indicating a lower interaction between the polymer and the matrix, Figure 1b. However, after CNF-MAP sonication, the dispersion coagulated, indicating interactions between CNF and MAP. Also, from FTIR, we observed lower intensities, especially on the top side. This behavior may indicate the interaction of phosphate and ammonium with cellulose, reducing the intensity of 1370 cm^{-1} and 1313 cm^{-1} peaks referring to the C-H bond bending and CH_2 group vibration of cellulose, respectively. The nutrient concentration on the film's top side is due to the casting method since, after the evaporation of the solvent, the nutrient concentrate is at the top. This behavior is observed in both procedures. The bottom side has similar curves in both films; however, the top side differs. Therefore, we considered the ultrasound treatment of CNF-fertilizer solutions provides better dispersion and a more significant interaction of the nutrient with the matrix.

Acknowledgments

The authors are also grateful for grants 2019/02535-5 from FAPESP and for Suzano Papel & Celulose to provide cellulose and CNF.

Effects of the synthetic method, particle size, and anatase/rutile phases on photocatalytic degradation of sulfathiazole by TiO₂ nanoparticles

Elias B. Santos (PQ),^{1*} Maraisa Gonçalves (PQ),¹ Raquel Domingues (PQ),¹ Nirton C. S. Vieira (PQ),¹ Sara P. Sabino (TC),¹

santos.barros@unifesp.br

¹Instituto de Ciência e Tecnologia, Universidade Federal de São Paulo – UNIFESP.

Palavras Chave: Nanoparticles, TiO₂, Sulfathiazole, Photocatalysis, Effects.

Highlights

- Samples of TiO₂ nanoparticles were prepared with different sizes and mixtures of anatase/rutile phases.
- The particle size and polymorphic phases of TiO₂ have a significant impact on the photocatalytic activity.
- It was also observed that the employed synthesis methods produce nanoparticles with different activities.

Resumo/Abstract

Nanoparticle size has a significant impact on their properties due to the increase of the relative surface area and quantum size effects, which differ significantly from their bulk counterpart. In the case of metal oxides such as titanium dioxide (TiO₂), in addition to the size effect, the polymorphic phase can also impact the properties, since they have different crystalline structures.¹ In the present work, the effect of TiO₂ particle size and the presence of anatase/rutile phases on the photocatalytic activity of sulfathiazole was investigated. For this purpose, different TiO₂ samples were prepared from commercial reagents, such as P25. Another sample was also synthesized from the thermal decomposition of titanium isopropoxide at 700 °C for 4h. The samples were named TiO₂-23, TiO₂-25, TiO₂-35, TiO₂-117, and TiO₂-135 referring to the average particle size, in nanometers, obtained by transmission electron microscopy. All samples presented the anatase and rutile phases identified by X-ray diffraction. The samples were tested, setting the experimental conditions, on photocatalytic degradation of sulfathiazole. The commercial sample P25 showed better catalytic performance, degrading sulfathiazole in 75 min of reaction. The other samples showed lower catalytic efficiency dependent on the particle size, with degradation times ranging from 125 to 350 min. The main difference was the sample TiO₂-23, which is similar in particle size to P25, but with lower catalytic efficiency with a time of 300 min. This sample has small particles but a high degree of aggregation in an aqueous medium. This result indicates that the synthesis method also influences the type of particle with a consequent effect on catalysis.

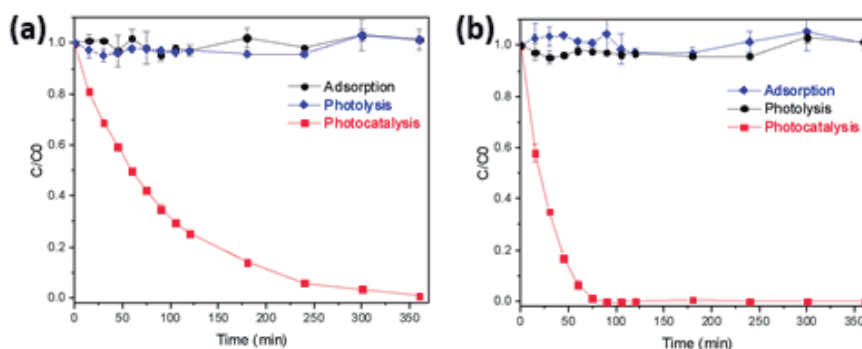


Figure. Photocatalytic degradation of sulfathiazole by TiO₂-23 and TiO₂-25.

Agradecimentos/Acknowledgments

The authors acknowledge the financial support received from FAPESP/M-ERA-NET Project Acronym 3D-Photocat 2019, IEAMar-UNESP for TEM analysis, and the support from NAPCEM of the Universidade Federal de São Paulo.

Reference: Ko K.C. et al. J. Phys. Chem. Lett. 2017, 8, 8893-8898.

Electrically conductive foams based on functionalized cellulose nanofibers and carbon black

Gabriele Polezi (PG),^{1,2} Diego Magalhães do Nascimento (TC),² Juliana da Silva Bernardes (PQ).^{1,2*}

gpolezi@gmail.com; juliana.bernardes@lnnano.cnpem.br

¹Federal University of ABC (UFABC); ²Brazilian Nanotechnology National Laboratory (LNNano) - CNPEM

Palavras Chave: *Sugarcane bagasse, Cellulose nanofiber, Carbon black, Electrical conductivity, Foams.*

Highlights

Colloidal stability of CNF/carbon black dispersions is improved for positively charged CNF. Hybrid foams presents good mechanical properties and high conductivity, suitable for electrical applications.

Resumo/Abstract

Cellulose nanofiber (CNF) is an abundant and biodegradable material that have attracted widespread attention due to their potential to replace petroleum-derived non-biodegradable polymers. CNF-based foams have promising applicability in various fields as renewable functional porous materials. However, compared to petroleum-based polymer foams, CNF foams still need to be improved for their practical applications. In this study, to enhance their mechanical performance and confer electrical properties to CNFs, carbon black (CB) was combined with sugarcane bagasse-derived cellulose nanofibrils to produce hybrid conductive foams.

The cellulose fraction was obtained from sugarcane bagasse fibers by organosolv and bleaching pulping, followed by mechanical fibrillation to separate neighboring nanofibrils. Cellulosic fibers were chemically modified using TEMPO/NaClO/NaBr system or glycidyl trimethylammonium chloride (GTMAC) to synthesize oxidized (OCNF) and cationic (CCNF) nanofibers, respectively. By adding the carbon nanoparticles to the aqueous suspension of the modified CNFs (0.3 wt%) and centrifuging the mixture, it was possible to examine the dispersive capability of CB on these modified CNFs. Foams with a vertically hierarchically porous structure were prepared by unidirectional ice-templating followed by lyophilization. Four different mass ratios of CNF/CB (1:0.1, 1:0.5, 1:1, and 1:2) were used to investigate the effect of particle filler on foams' electrical conductivity. Morphological properties were investigated by scanning electron microscopy (SEM), and electrical conductivity was analyzed by two-probe measurements.

Particle aggregation and sedimentation were only observed for dispersions prepared with OCNF. The better dispersibility of CCNF may be related to the presence of positive charges on the surface of nanofibrils, which induces a delocalization of π -electrons of aromatic rings from CB, resulting in an attractive electrostatic interaction between the CB particles and CNF. Therefore, conductive foams were prepared with positively charged nanofibers. According to SEM images, foams showed a three-dimensional microporous structure, as expected. Control foam (without CB particles) exhibited smooth pore wall surfaces, while the hybrid foams had a rough surface due to carbon particles deposited on the nanofibers. This adsorption promotes the formation of an interconnected conductive network that increases the material's conductivity. The ratio of CB and CNF in these hybrid foams had a noticeable effect on their mechanical properties: higher CB concentrations turned the foam brittle. In the non-compressed state, CCNF/CB 1:0.1 foam did not conduct electrical current, while CCNF/CB 1:0.5, 1:1, and 1:2 presented average conductivity of 0.54, 5.48, and 15.10 mS/cm, respectively. When the foams are compressed (90% of compression), the electrical conductivity increases for all samples, reaching average conductivities of 58.26, 479.14, and 3616.66 mS/cm for CCNF/CB 1:0.5, 1:1, and 1:2, respectively. With compression, the CB particles are closer to each other, decreasing the current flow resistance and improving the electrical conductivity through the material.

A better understanding of interactions between CB and charged CNF could be helpful in the dispersion and stabilization of carbon nanomaterials in an aqueous medium of nanocellulose. The hybrid foams of CCNF/CB produced in this study present structural anisotropy, good mechanical properties, and high electrical conductivity, being a promising material suitable for practical electrical applications and thus enabling the development of high-value-added materials from sugarcane bagasse.

Agradecimentos/Acknowledgments

The authors acknowledge the Brazilian funding agencies FAPESP (Fundação de Amparo à Pesquisa do Estado de São Paulo) and CAPES (Coordenação de Aperfeiçoamento de Pessoal de Nível Superior – Brasil) for financial support.

Environment-friendly free-standing cellulose membranes decorated with high content of silver nanoparticles for catalytic reduction of 4-nitrophenol

Rodolfo P. P. Nunes (PG)*, Larissa V. F. Oliveira (PQ), Fernanda F. Camilo (PQ)

ffcamilo@unifesp.br; rodolfo.nunes20@unifesp.br

Laboratório de Materiais Híbridos (LMH), Departamento de Química, Universidade Federal de São Paulo – Campus Diadema

Keywords: (Cellulose, Ionic liquid, Silver nanoparticles, Catalysis).

Highlights

This work aimed to fabricate free-standing membranes based on the most abundant biopolymer, cellulose, decorated with high content of silver nanoparticles for catalytic reduction of 4-nitrophenol.

Abstract

The aqueous dispersions with a high concentration of silver (from 5 mmol L⁻¹ to 100 mmol L⁻¹) were prepared from the chemical reduction of a silver salt with tetrabutylammonium borohydride in the presence of polyvinylpyrrolidone (PVP). The presence of the surface plasmon surface at 400 nm in the UV-Vis spectra of all samples proved the presence of silver nanoparticles. The TEM images showed that they are spherical and with diameters ranging from 10-80 nm, depending on the sample (Figure 1). The membranes were fabricated in 3 steps: (a) First, microcrystalline cellulose (MCC) was solubilized in the ionic liquid 1-butyl-3-methylimidazolium chloride (BMImCl) (b) Second, water was added in the dispersed cellulose solution and then a wet membrane was obtained (c) Third, the silver nanoparticles were maintained in contact with the wet cellulose membrane for 24 hours. Free-standing membranes were obtained, they do not dissolve in water and have high thermal stability. The nanoparticles are distributed evenly throughout the biopolymer without degrading the primary cellulose structure. These membranes were successfully used in the degradation of 4-nitrophenol. For instance, in less than 45 min, one of the samples (sample CEL_25 mmol L⁻¹_AgNP) caused the complete degradation of the organic pollutant and it was used 5 times in new processes with the same efficiency (Figure 2). The use of membranes in catalytic processes instead of powders avoids the need for more complex separation methods, such as centrifugation and filtration, and increases recyclability[1].

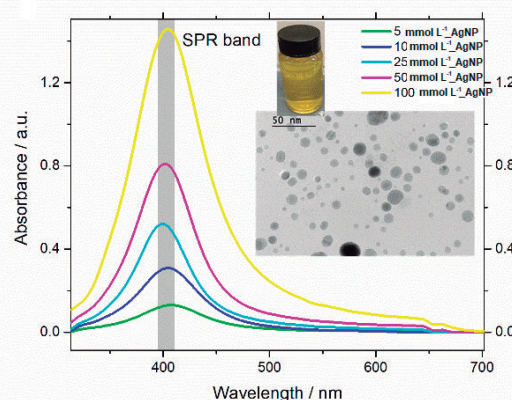


Figure 1: UV-Vis spectra of the silver nanoparticle dispersions
Inset: Photo and TEM image of the 25 mmol L⁻¹_AgNP

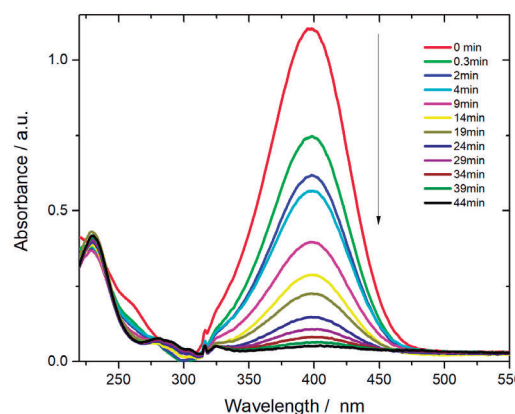


Figure 2: UV-Vis spectra obtained during the 4-nitrophenol reduction using the cellulose membrane prepared with the dispersion 25 mM_AgNP

[1] Camila Rodrigues Cabreira and Fernanda Ferraz Camilo, Cellulose, 2020, 27, pp. 3919–3929.

Acknowledgments

Fundação de Amparo à Pesquisa do Estado de São Paulo (FAPESP) (21/08987-5)

Estudo do efeito do método de funcionalização das AuNPs em biossensores para a detecção da Ptn S do SARS-CoV-2

Camille C. De Mello (PG),¹ Carolina B. P. Ligiéro (PQ),¹ Célia M. Ronconi (PQ).^{1*}

camillemello@id.uff.br; cmronconi@id.uff.br

¹Departamento de Química Inorgânica, Universidade Federal Fluminense, Campus do Valonguinho

Palavras Chave: Biossensores, Nanopartículas de ouro, Funcionalização, Espalhamento dinâmico de luz

Highlights

- Study of the functionalization method effect on AuNPs biosensors for the detection of the SARS-CoV-2 S Ptn.
- Synthesis of biosensors from the surface functionalization of gold nanoparticles, followed by polyclonal antibody coupling. Detection by dynamic light Scattering (DLS).

Resumo

Diante da situação emergencial mundial devido a pandemia de COVID-19 surgiu a necessidade do desenvolvimento de testes de detecção do vírus SARS-CoV-2.^{1,2} A abordagem utilizada consiste na funcionalização de nanopartículas de ouro (AuNPs) com anticorpos policlonais (pAb), resultando em biossensores (pAb-AuNPs). Para a funcionalização foram testados agentes de ligação cruzada com espaçadores de diferentes tamanhos: o 3,3'-ditiobis(sulfosuccinimidila) (DTSSP) com espaçador de 2 carbonos e o ácido 11-mercaptop undecanóico (MUA) com espaçador de 11 carbonos (Figura 1a). Como transdutor escolheu-se a técnica de espalhamento de luz dinâmico (DLS) devido ao grande poder de espalhamento das AuNPs. Aqui trazemos alguns resultados preliminares usando AuNPs com 80 nm. Os resultados mostram as mudanças no diâmetro hidrodinâmico (D_H) durante a síntese do pAb-AuNPs (Figura 1b) e os resultados dos imunoenaios com a Ptn S (Figura 1c). Os nanobiossensores com espaçador mais longo deram respostas muito promissoras (maior ΔD_H) no ensaio preliminar e estudos mais completos estão sendo conduzidos.

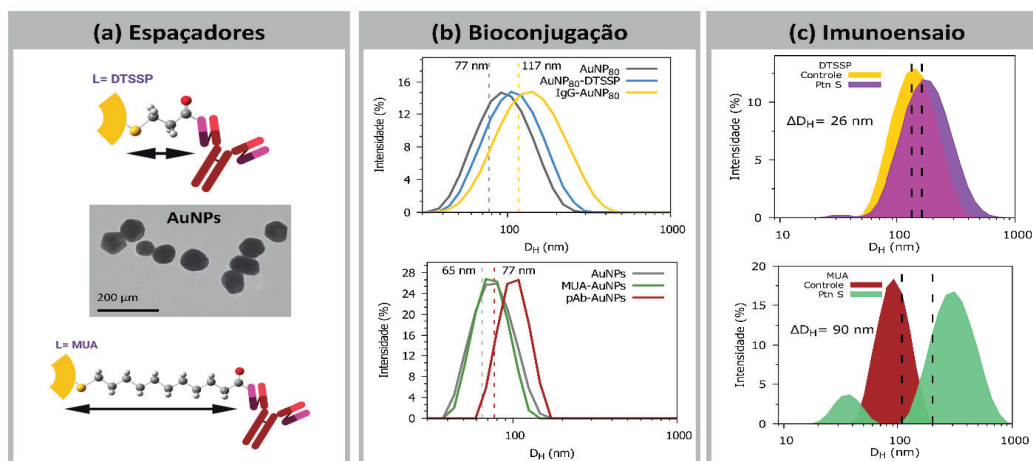


Figura 1: (a) Espaçadores usados e imagem por MET das AuNPs; (b) Mudanças no D_H (DLS) durante as etapas de bioconjugação; (c) Respostas obtidas nos imunoenaios por DLS.

Agradecimentos



¹ Silva, P. B. *et al.*, Talanta, v. 243, p. 123355, 2022.

² Ligiéro, C. B. P. *et al.*, Materials Today Chemistry, v. 25, p. 100924, 2022.

Fabricação e Caracterização de Filmes Amido/Carboximetilcelulose–Argila

Alessandra Stevanato (PQ)¹, Felipe Ferreira Lopes* (PQ)², Delia do Carmo Vieira (PQ)²

stevanato@utfpr.edu.br; felipeflopesengmat@gmail.com

¹Departamento Acadêmico de Química, UTFPR – Campus Londrina; ²Departamento Acadêmico de Engenharia de Materiais, UTFPR – Campus Londrina.

Palavras Chave: Amido, Argila, Carboximetilcelulose, Filmes Biodegradáveis, Caracterização Microestrutural.

Highlights

Manufacture and Characterization of Clay–Starch/Carboxymethylcellulose Films. Polymer–clay nanocomposites have several technological applications, such as biodegradable films, sensor and others. Manufacturing, rheological and microstructural characterizations will be presented at this congresso.

Resumo/Abstract

A fabricação de nanocompósitos polímeros–argila e suas aplicações estão em grande crescimento devido às diversas aplicações tecnológicas relevantes, tais como filmes biodegradáveis, sensores, engenharia de tecido, dentre outras. Neste trabalho investigou-se a formação de filmes a partir de amido solúvel, como carboximetilcelulose sódica (CMC), glicerol e uma argila *in natura* proveniente do sudoeste paulista (pós que passaram na peneira 400 mesh); todas as dispersões foram preparadas em meio aquoso. Diferentes formulações de filmes argila/amido/CMC e uma formulação contendo apenas amido para efeitos de comparação foram obtidas e caracterizadas quanto a sua estabilidade térmica via DSC e TGA, resistência à tração, permeabilidade ao vapor de água, absorção de umidade e solubilidade em água. O comportamento reológico das dispersões em meio aquoso foi estudado por reometria e as imagens destas dispersões também foram investigadas por microscopia ótica. As Figuras 1 e 2, apresentam os resultados das caracterizações reológicas das formulações utilizadas para obtenção dos filmes e as imagens de microscopia ótica de uma das dispersões de Amido/CMC-Argila.

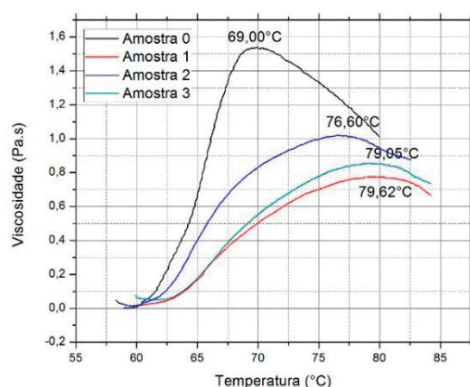


Figura 1. Comportamento reológico das dispersões: amostra 0 contém apenas amido, amostra 1 (12% m/m_{amido} CMC), amostra 2 (12% m/m_{amido} de CMC e 8% m/m_{amido} de argila) e amostra 3 (12% m/m_{amido} de CMC e 15% m/m_{amido} de argila).

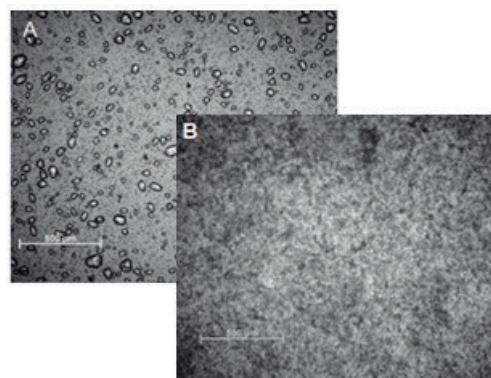


Figura 2. Microscopia ótica de luz polarizada da amostra 3 (12% m/m_{amido} de CMC e 15% m/m_{amido} de argila) com ampliação de 50x em duas temperaturas: (a) temperatura ambiente e (b) 86 °C.

A incorporação de 15% m/m_{amido} de argila resultou em filmes biodegradáveis com melhor atuação de barreira ao vapor de água e com uma maior interação entre a argila e a matriz polimérica. Constatou-se ainda que a incorporação da argila não modificou a estabilidade térmica dos materiais. Os filmes transparentes obtidos poderiam ser utilizados na indústria alimentícia, já que se mostraram mais resistentes quando expostos à água conforme indicado pelos ensaios de permeabilidade e de absorção/solubilidade.

Agradecimentos/Acknowledgments

Aos Departamentos Acadêmicos de Engenharia de Materiais (DAEMA) e de Química (DAQUI) da UTFPR – Campus Londrina.

Factor Analysis of Polymeric Blends Obtained from Starch Modified with Polyvinyl Alcohol and Sorbitol.

Leandro A. Pereira (IC)¹; Josiane Caetano (PQ)¹; Douglas C. Dragunski (PQ)¹

leaoaugusto44@gmail.com

¹Centro de Engenharias e Ciências Exatas, Unioeste, Rua da Faculdade, 645 CEP - 85903-000 - Toledo -PR.

Keywords: Green polymer, cationic starch, biofilms.

Highlights

Factor Analysis of Polymeric Blends Obtained from Starch Modified with Polyvinyl Alcohol and Sorbitol.

Films were produced using the casting technique containing starch, polyvinyl alcohol (PVA) and sorbitol.

The film containing the highest amount of starch and PVA showed the lowest solubility.

When the amount of plasticizer is increased, elasticity is increased, but it can cause exudation.

Resumo/Abstract

In this work, biodegradable polymeric blends of cationic starch (DS 30%) and polyvinyl alcohol (PVA -87% degree of hydrolysis; MM = 87000 g/mol) were produced with sorbitol as plasticizer. For this, a 2³ factorial design was used in order to produce films with properties (solubility, mechanics and swelling) for application in fruit coating. Table 01 contains the proportions used in each film.

Table 01: Amount of components (Starch, PVA and sorbitol) in % by mass present in each film.

Film	Starch (%)	PVA (%)	Sorbitol (%)
1	3	8	30
2	1	4	15
3	2	6	22,5
4	3	4	15
5	1	8	15
6	1	4	30
7	1	8	30
8	3	4	30

The films obtained showed better mechanical properties (lower Young's modulus) when the amount of plasticizer was higher. However, better solubility when the amount of polymers (starch and PVA) was in higher proportions. Thus, films 6 and 7, which have very low proportions of starch in relation to the proportions of sorbitol, presented respectively 400% and 300% of deformation. While the smaller deformations were obtained by films 1 and 3, 20% and 40% respectively, both have more balanced proportions in relation to films 6 and 7. Due to the hydrophilic capacity of the plasticizer during the solubility test, film 7 completely solubilized, while film 8 showed the lowest solubility. Therefore, for use in fruit coating, the film with lower solubility and good elasticity should be used. In this way, film 8 was chosen.

Agradecimentos/Acknowledgments



Fibroin/Bacterial Cellulose Nanocrystals/Gellan Gum hydrogel, aiming application in 3D bioprinting and drug release.

Luygui Gaspardo Silva (IC),^{1*} Sidney José Lima Ribeiro (PQ),^{1**} Hernane da Silva Barud (PQ),^{2***}

sidney.jl.ribeiro@unesp.br; *luygui.gaspardo@unesp.br; *hernane.barud@gmail.com

¹Instituto de Química, Departamento de Química Analítica, Físico-Química e inorgânica, UNESP;

²Biotecnologia, programa de pós graduação em biotecnologia, UNIARA

Key Words: hidrogel nanocompósito, Fibroína, nanocristal de celulose bacteriana, bioimpressão 3D

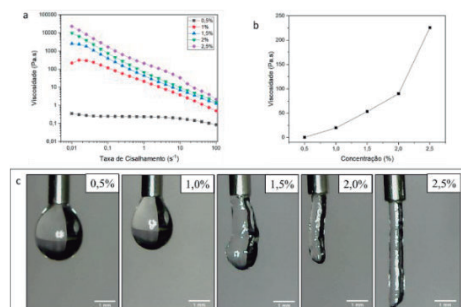
Highlights

For the first time was prepared Fibroin /Bacterial cellulose Nanocrystals /Gellan Gum hydrogel, applicable for the controlled release of drugs, aiming its application in 3D bioprinting.

Abstract

3D Bioprinting is a category of 3D printing that enabled the printing of three-dimensional structures that can be made of viable cells, biological materials, or biomaterials, based on a hydrogel (VENTOLA, 2014). The essence of 3D Bioprinting is hydrogels. Hydrogels are materials that are capable of being printed, allow crosslinking, that is, the connection between linear molecules producing three-dimensional polymers; and are similar to the extracellular matrix, as they have a highly hydratable microenvironment (TAMAY *et al*, 2019). Therefore, to achieve a nanocomposite hydrogel, in this work, bacterial cellulose nanocrystals and fibroin were extracted, which are biopolymers that can be used in wide areas, such as drug delivery and 3D bioprinting. The objective of this work was to evaluate and characterize hydrogels of different concentrations of fibroin/bacterial cellulose nanocrystals/gellan gum, aiming the 3D bioprinting. To evaluate this goal, different mass contents of the BCN/fibroin/gellan gum hydrogels were obtained. BCN/fibroin was used in intervals of 0.5% for the proportion of solids. the concentrations of gellan gum were added following the nomenclature of A: GG 2% (m/m) and B: GG: 2.5% (m/m). The characterization were performed by Fourier Transform Infrared (FTIR-ATR), Scanning Electron Microscopy (SEM), Thermogravimetric Analysis (TGA), and Rheometry methods. The spectrum observed in hydrogels 1A and 1B, by FTIR-ATR, in which there is a mixture of Fibroin and GG, in the region of 1400 cm^{-1} , it is possible to notice a peak in the Gellan Gum that disappears in the hydrogels, thus, the disappearance of this band suggests that the material is a polymeric association. In addition, to assess the morphology of the material, It was possible to conclude from the SEM that the surface of the film is quite smooth and with little roughness, and the absence of particulate elements indicated the homogeneity of the material. Using the TGA, it was possible to conclude that when comparing the thermal analysis of the hydrogels with the pure materials, we can observe that the addition of GG and fibroin did not modify the thermal resistance of the BCN, since all materials have a degradation event at about 250°C . Finally, using Rheometry, it was concluded that all hydrogels presented a pseudoplastic profile. When observing the viscosity data of hydrogel, A, a small variation in its average viscosity is noted as the proportions of NCCB/Fibroin are altered. In addition, it is noted that at concentrations of solids greater than gellan gum, Figure 1, (hydrogel A), fibroin helps in structuring the gel, increasing the average viscosity of the hydrogel. Furthermore, it is observed that fibroin helps to increase viscosity when added to hydrogels containing NCCB and GG.

Figure 1. Data obtained by Rheometry analysis of different concentrations of Gellan Gum (GG), being: **a.** viscosity curves of GG hydrogels versus shear rate; **b.** Average viscosity data of hydrogels with different GG contents. **c.** Optical microscopy images of hydrogels with different GG contents.



TAMAY, D. G.; USAL, T. D.; ALAGOZ, A. S.; YUCEL, DENIZ; HASIRCI, N.; HASIRCI, V. 3D and 4D Printing of Polymers for Tissue Engineering Applications. **Frontiers in Bioengineering and Biotechnology**, v. 7, 2019. VENTOLA, C. Lee. **Medical Applications for 3D Printing: Current and Projected Uses**. P&T, v. 39, p. 704-711, 2014.

Acknowledgments

We thank FAPESP for financial support: Process FAPESP: 2021/09352-3

Fluorophosphate glasses containing CdS quantum dots: Synthesis, characterization, and photoluminescence properties

Vinicius Leonardo Souza (IC),¹ Renato Grigolon Capelo (PG),¹ Danilo Manzani (PQ),^{1*}

vini.chemical019@usp.br; dmanzani@usp.br

¹São Carlos Institute of Chemistry, University of São Paulo (USP), São Carlos, SP, Brazil.

Keywords: fluorophosphate glass, CdS quantum dots, photoluminescence

Highlights

Synthesis and characterization of fluorophosphate glass containing luminescent CdS quantum dots. The CdS containing glasses are promising for photonic applications.

Resumo/Abstract

Quantum dots are an important class of semiconductor nanomaterials with interesting properties in photonics due to their size-controlled light emissions. Quantum dots emissions mainly occur by electronic transitions from the valence to conduction bands and the energy separation (E_{gap}) between these bands defines the emitted light wavelengths. Generally, quantum dots (QDs) are mainly obtained as colloidal materials, which limits their optoelectronic applications. In order to overtake this limitation, which can hamper their applications, different glass families are exploited as a solid matrix for hosting luminescent QDs. Fluorophosphate glasses (FPs) are an interesting matrix that arises from the combination of fluoride and phosphate precursors. Their properties, such as low characteristics temperatures, large thermal stability against crystallization, and wide transparency range from UV (300 nm) to near-infrared (4 μm) make them promising materials for optical and photonic applications.[1] However, even with such great characteristics, fluorophosphate glasses are still poorer explored as QDs hosts. In this sense, this work shows the study, synthesis, and characterization of fluorophosphate glasses containing CdS QDs. A new set of CdS-FP glasses were synthesized by the conventional melt-quenching method with the molar composition $\text{NaPO}_3\text{-ZnO-BaF}_2\text{-AlF}_3\text{-MgF}_2\text{:CdS}$. Then, the CdS QDs growth was carried out by controlled heat treatment above T_g , and the thermal properties were studied by DSC analysis. The structure of the oxyfluoride glasses as well as the network connectivity were studied by Raman, revealing the influence of the fluorine atoms in the glassy network due to the increase of Q^2 and Q^1 units. The optical properties were studied by UV-Vis which showed an increase in the absorbance of the sample with changes in heat treatment. Finally, the photoluminescence changed in function of heat treatment, suggesting the growth of CdS quantum dots, as observed by Transmission Electronic Microscopy (TEM) varying from 0.8 to 4.5 nm size. The obtained CdS containing fluorophosphate glasses showed promising properties for photonic and optoelectronic applications in the visible region.

References

[1] Doris Möncke and Hellmut Eckert. Review on the structural analysis of fluoride-phosphate and fluorophosphate glasses. In *Journal of Non-Crystalline Solids*: X. 2019.

Agradecimentos/Acknowledgments

This work is financially supported by FAPESP. The authors thank the Sao Carlos Institute of Chemistry (IQSC-USP), the Chemistry Institute of Araraquara (IQ-UNESP), and all the collaborators for the infrastructure and resources provided.

Glasses and glass-ceramics containing magnetic crystals and nanocrystals.

Bruna Borges Nascimento (IC),¹ Juliane R. Orives (PQ),¹ Marcelo Nalin (PQ).¹

bruna.borges@unesp.br; juliane_resges@hotmail.com; marcelo.nalin@unesp.br

¹Departamento de Química Analítica, Físico Química e Inorgânica – Instituto de Química, UNESP Araraquara

Key-words: Magnetic nanoparticles, Cobalt-platinum, Phosphate glasses.

Highlights

Synthesis of CoPt magnetic nanoparticles.

Phosphate-glasses containing CoPt nanoparticles covered with a silica layer.

Hybrid glasses prepared by melt-quenching process.

Resumo/Abstract

Glasses are highly functional materials that allow the incorporation of other chemical substances in their structure, for example magnetic nanoparticles. This process has shown to be very interesting for the development of new hybrid materials such as magnetic field sensors, due to its magneto-optical applications.^[1]

Phosphate glasses have good optical properties and present moderate melting point depending on the composition, while CoPt nanoparticles are known for their good magnetic properties and chemical stability.^[2,3] The synthesis of the glasses involves high temperatures, therefore the structure of the nanoparticles, during the process for incorporation into the glasses, needs to be protected, which can be done by covering the nanoparticles with a silica layer (here named CoPt@SiO₂ NP). Silica is known to present very good optical transparency in the visible and infrared regions as well as for its resistance to temperature and corrosion.

This work includes the synthesis of CoPt nanoparticles followed by ~~their~~ incorporation into a phosphate glass. The glass was obtained by mixing ~~the~~ nanoparticles in a polyphosphate coacervate gel and in sequency the mixture was melted at 1025 °C by 15 min. The ~~samples obtained hybrid glasses~~ were characterized by ~~thermal analysis~~, X-ray diffraction, ~~Raman~~, infrared and UV-Vis spectroscopies and transmission electron microscopy. Several contents of CoPt@SiO₂ NP were incorporated, proving the possibility to use this methodology to obtain high optical quality materials ~~besides to~~ and also allow the incorporation of magnetic metallic phases into glasses.

Agradecimentos/Acknowledgments

The authors acknowledge São Paulo Research Foundation, FAPESP (2013/07793-6, 2019/19609-1), CNPq (National Council for Scientific and Technological Development) (2021/3207) and SISFOTON-MCTi for financial support.

References:

[1] Wei, Y.; et al., J. Adv. Opt. Mat., 7, 1900702, 2019.

[2] Shaaban, K.S.; et al., J. of Inorg. Organomet. Polym. and Mat., 30, 4655–4663, 2020.

[3] Orives, J.R.; et al., J. of Alloys and Comp., 848, 2020.

Gold particles embedded in upconverter nanoparticles via modified Pechini method.

Alessandro Bruno Silva Garcia¹ (PG), **Marian Rosaly Davolos**¹ (PQ), **Sergio Antonio Marques Lima**² (PQ), **Ana Maria Pires**^{1,2} (PQ).

alessandro.garcia@unesp.br; ana.maria@unesp.br

¹ Department of Analytical, Physical-Chemistry and Inorganic Chemistry, São Paulo State University, Araraquara, Brazil

² Department of Chemistry and Biochemistry, São Paulo State University, Presidente Prudente, Brazil.

Keywords: upconversion, perovskite, lanthanum aluminum, thulium and ytterbium, gold

Highlights

Synthesis of Tm^{3+} and Yb^{3+} codoped LaAlO_3 nanoparticles via modified Pechini method as blue and red emitters under 980 nm laser excitation; Absorption of gold particles and shift of the dominant emission color from blue to red.

Abstract

Gold nanoparticles have been applied in the field of bio-nanotechnology because of their unique properties and numerous surface functionalization possibilities, such as with thiol or amine groups, and high chemical stability against oxidation under biological conditions. The main difference between gold and other nanoparticles (quantum dots, magnetic and polymeric nanoparticles) is due to the surface plasmon resonance (SPR) [1]. Furthermore, gold nanoparticles can be easily synthesized with citric acid, one of the precursors used in the Pechini method. Phosphors containing Tm^{3+} (emitter) and Yb^{3+} (sensitizer) can absorb in the infrared region and emit in the visible (blue - due to the $^1\text{G}_4 \rightarrow ^3\text{H}_6$ - and red due to the $^3\text{F}_3, ^3\text{F}_2 \rightarrow ^3\text{H}_6$ electronic transitions) via absorption of three and two photons, respectively (upconversion mechanism) [2], and this emission can be modulated by the concentration of gold particles. In this way, gold particles were inserted into Tm^{3+} and Yb^{3+} codoped lanthanum aluminate nanoparticles ($\text{LAO}:\text{Tm}_{0.002}, \text{Yb}_{0.15}$) obtained from a modified Pechini method. The precursors, citric acid and sorbitol in addition to nitrate metals solutions (Al^{3+} , La^{3+} , Tm^{3+} and Yb^{3+}), were heated yielding a polymeric resin that was pre-calcined, macerated and then suspended in water; to this suspension different concentrations of HAuCl_4 were added and kept under stirring, with subsequent drying and calcination. All samples were characterized by X-ray diffraction, FTIR, Raman scattering, diffuse reflectance and photoluminescence (upconversion and downshifting). The gold particles on the upconverter surface leads to a reduction of both blue and red transition, which is due to the absorption band of the metal (absorbing practically all of the visible however, the blue is more absorbed than the red, Fig. 1 (a,c), and as a result a color shift is observed in the sample from blue to red, Fig. 1 (b). Although the luminescent properties have been suppressed, the method proved to be efficient for incorporating gold into luminescent systems using the modified Pechini method enabling color emission tuning.

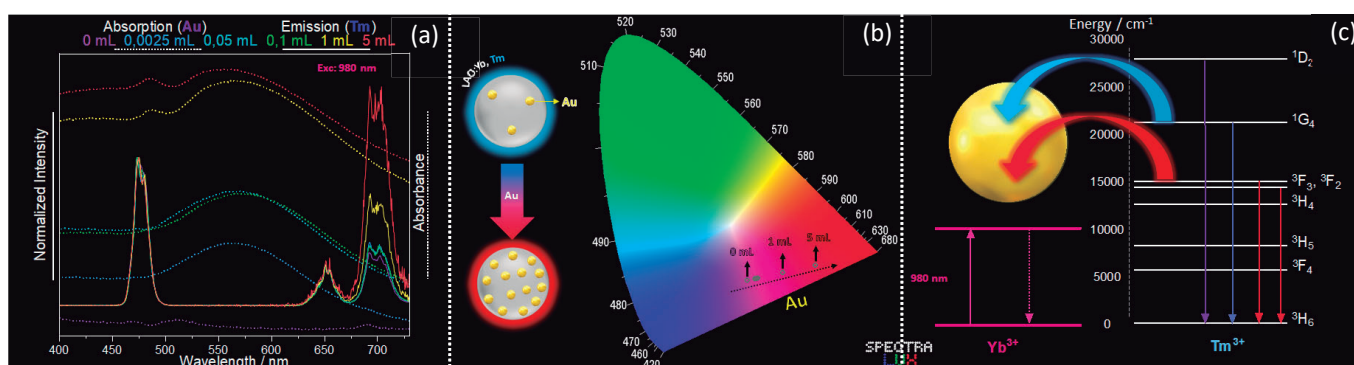


Fig 1. Tm^{3+} emission and absorption spectra of samples before and after Au particles decoration (a), chromaticity diagram varying Au concentration (b), upconversion energy transfer mechanism with energy absorption by Au particles (c).

References

[1] *J. Mater. Chem. B*, 2019, **7**, 3480-3496. [2] *Nanoscale Adv.*, 2019, **1**, 4492-4500.

Acknowledgments

CNPq (Grant N° 141761/2019-9), FAPESP

46ª Reunião Anual da Sociedade Brasileira de Química: "Química: Ligando ciências e neutralizando desigualdades"

Growth and Control of Bi₂S₃ Shell Formation in Bi₂O₃ Nanoparticles

Iara A.T. Gaia (PG),¹ Eder V. Guimarães (PG),² Anielle C.A. Silva (PQ),³ Hanna D. Mikhail (PQ),⁴ Pedro I.S. Maia (PQ),¹ Ricardo S. Silva (PQ).^{2*}

iara_gaia@hotmail.com; ricardo.silva@uftm.edu.br

¹Núcleo de Desenvolvimento de Compostos Bioativos (NDCBio) UFTM; ²Departamento de Física UFTM; ³Instituto de Física UFAL; ⁴Departamento de Engenharia Mecânica UFTM

Key Words: Bi₂O₃/Bi₂S₃ Core/Shell, Aqueous Colloidal Solution, 1-thioglycerol Concentration

Highlights

Bi₂O₃/Bi₂S₃ nanoparticles are semiconductors that have interesting physical and chemical properties, such as high luminescence and excellent photoconductivity, which allows couple them to biological molecules, aiming their use as fluorescent probes.¹ In this way this is possible with the passivation and functionalization of their surface, allowing the bioconjugation of the nanoparticles.²

Resumo/Abstract

In this context, we successfully report the synthesis via aqueous solution of Bi₂O₃/Bi₂S₃ core/shell nanoparticles (CSNPs) using 1-thioglycerol (TG) for surface coating at a temperature of 80 °C. The 1-thioglycerol stabilizer monitors shell formation with the semiconductor Bi₂S₃ (Fig.1a).

The TEM images showed the formation of nanoparticles with an average size of 5.0 nm, which corresponds to the semiconductor Bi₂O₃. The EDS analysis confirms the presence of the chemical elements Bi, O and S. Selected area of electron diffraction (SAED) patterns show the expected peaks associated to the Bi₂O₃ semiconductor. The FTIR spectra show the formation of the S-Bi bond (Fig. 1b). As well, the Raman spectroscopy shows the characteristic vibrational modes of Bi₂O₃ and Bi₂S₃ semiconductors (Fig.1c). With the shift to longer wavelengths in the UV and PL we have evidence of the formation of the Bi₂S₃ shell as the concentration of 1-Thioglycerol (3T and 4T) increases. Overall, the growth of Bi₂O₃ nanoparticles and the control of Bi₂S₃ shell formation is evidenced by the results obtained, which recommends them as promising materials for biotechnological applications involving the manufacture of drugs, fluorescent biomarkers for diagnosis and biosensors.

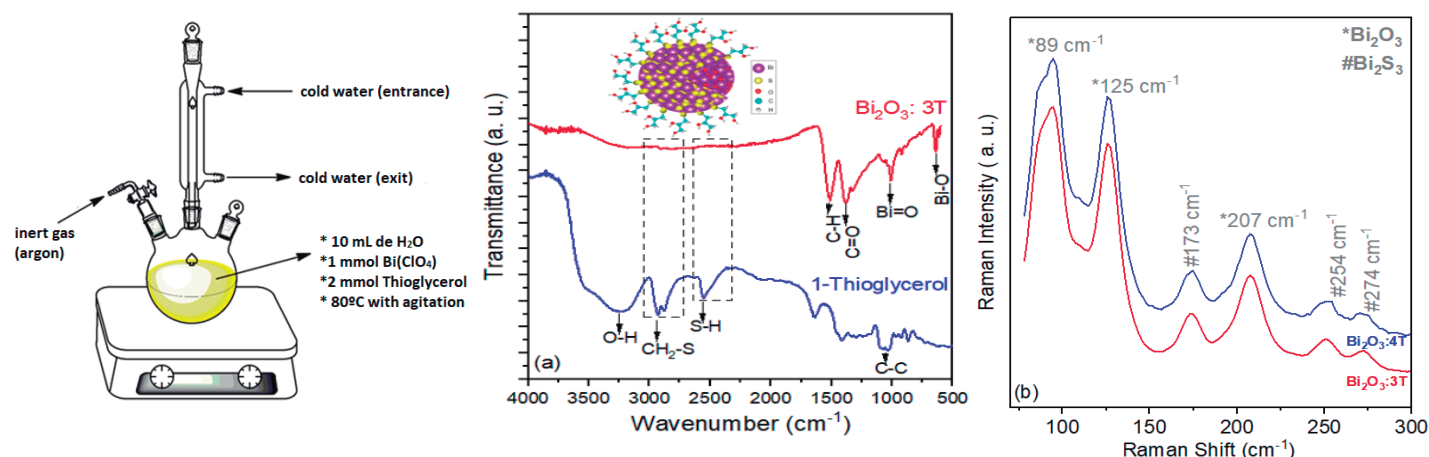


Figure 1. (a) Synthesis via aqueous solution of nanoparticles (b) FTIR spectra of Bi₂O₃ nanoparticles with the stabilizing agent 1-thioglycerol for the Bi₂O₃:3T sample; (c) Raman spectra for Bi₂O₃:3T and Bi₂O₃:4T samples.

1. UDDIN, I. et al. *Current topics in medicinal chemistry*, p. 2019-2025 (2016).
2. TANSIL, N. C. et al. *Nano Today*, 1(1), 28-37 (2006).

Agradecimentos/Acknowledgments

FAPEMIG, CNPq, CAPES and FAPESP

High-entropy metal-glycerolate as a precursor template of spherical porous high-entropy oxide microparticles

Josué M. Gonçalves (PG),^{1,2*} Alireza Ghorbani (PG),¹ Timothy G. Ritter (PG),³ Irlan S. Lima (PG),² Mahmoud Tamadoni Saray (PG),¹ Abhijit H. Phakatkar (PG),⁴ Vinicius D. Silva (PG),¹ Rafael S. Pereira (PG),⁵ Alexander L. Yarin (PQ),¹ Lúcio Angnes (PQ)² and Reza Shahbazian-Yassar (PQ)^{1*}

josuemartins@usp.br; rsyassar@uic.edu

¹Department of Mechanical & Industrial Engineering, University of Illinois at Chicago, Chicago, Illinois, United States

²Instituto de Química, Universidade de São Paulo, São Paulo-SP, Brazil

³Department of Civil & Materials Engineering, University of Illinois at Chicago, Chicago, IL, USA

⁴Department of Biomedical Engineering, University of Illinois at Chicago, Chicago, IL, USA

⁵Centro de Engenharia, Modelagem e Ciências Sociais Aplicadas, Universidade Federal do ABC, Santo André, SP, Brazil

Palavras Chave: High-Entropy Coordination Compound, High-Entropy Metal-Glycerolate, High-Entropy Oxides, Spinel Phase.

Highlights

High-entropy metal glycerolate was synthesized via one-step solvothermal method. The High-entropy metal-glycerolate were used as a precursor in design of porous high-entropy oxide microparticles.

Resumo/Abstract

High-entropy materials have received notable attention concern on account of their unique structure, tunable properties, and unprecedented potential applications in many fields. In this work, for the first time a NiCoMnZnMg-containing high-entropy glycerolate (HE-Gly) particles has been synthesized using a scalable solvothermal method. The HE-Gly particles were used as a precursor in design of porous high-entropy oxide (HEO) microparticles. The morphological and structural characterizations demonstrate that the temperature of the annealing process, and the composition of the metal ions in the HE-Gly precursors play important roles in determining porosity, crystallinity, and phase separation in HEOs. In fact, HE-Gly exhibited a porous structure of spinel HEOs with secreted MgO phase after annealing process at 800 °C (HEO800), while the annealing process at 400 °C (HEO400) led to a low-crystallinity spinel phase without phase segregation (Figure 1). Overall, this work describes a new precursor HE-Gly for a HEOs designer, whose composition, crystallinity, and porosity can be easily controlled. This strategy can lead to future industrial applications, paving a new path toward synthesizing high-entropy materials.

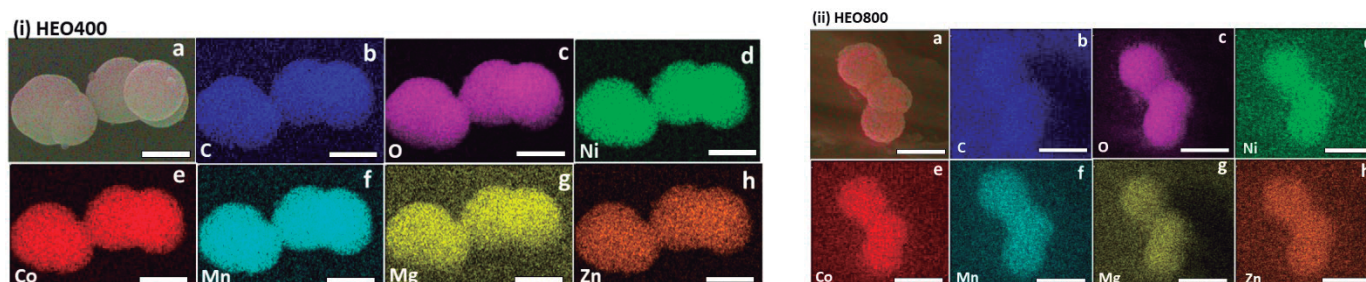


Figure 1. SEM-EDS analysis of (i) HEO400 (scale bar corresponds to 1 μm), and (ii) HEO800 particles (scale bar corresponds to 1 μm). (a) EDS overlap mapping of HEO particles. EDS elemental mapping of individual elements constituting HEO particles indicating the high mixing entropy. (b) carbon (blue), (c) oxygen (magenta), (d) nickel (green), (e) cobalt (red), (f) manganese (light blue), (g) magnesium (yellow), and (h) zinc (orange).

Agradecimentos/Acknowledgments

National Science Foundation DMR-1809439, FAPESP (2018/16896-7 and 2020/06176-7) and CNPq (311847-2018-8, 465389/2014-7, 202290/2020-4). Soft and Hybrid Nanotechnology Experimental (SHyNE) Resource (NSF ECCS-1542205), the MRSEC program (NSF DMR-1720139) at the Materials Research Center.

46ª Reunião Anual da Sociedade Brasileira de Química: "Química: Ligando ciências e neutralizando desigualdades"

Synthesis of highly concentrated dispersions of gold nanoparticles in a non-aqueous solvent

Flávia Tavares da Silva (PG) e Fernanda Ferraz Camilo (PQ)

flavia.tavares@unifesp.br;

Laboratório de Materiais Híbridos (LMH), Departamento de Química, Universidade Federal de São Paulo – Campus Diadema

Key words: (Gold nanoparticles, non-aqueous, nanomaterials, hydrophobic).

Highlights

Dispersions of high concentrations of gold nanoparticles in non-aqueous solvents have wider applications than the ones produced in water in low concentrations. In this sense, in this study, we develop a simple method to produce highly concentrated dispersions of gold nanoparticles in 1-butanol.

Abstract

Metallic materials (Au, Ag, Pt, Pd, etc.) in the nanometric scale have been widely studied due to their distinctive properties in this dimension. Among these nanomaterials, gold nanoparticles (AuNPs) are one of the most studied due to their potential applications as sensors, therapeutic agents, tumor markers, and catalysts [1]. Although there are several preparations for gold nanoparticles, the search for the methods to prepare these dispersions in non-aqueous, hydrophobic solvents and highly concentrated are necessary. Highly concentrated gold nanoparticle dispersions can meet requirements of a large-scale application, and hydrophobic dispersions can be used where the ones produced in water are not possible, for instance, as coating for hydrophobic surfaces. Therefore, in this study we develop a new method to prepare dispersions of gold nanoparticles (AuNPs) in 1-butanol (non-aqueous and hydrophobic solvent) with metal concentration varying from 1 mM to 50 mM. This sample are denoted as AgNP_xmM, where x is the used gold salt concentration. HAuCl₄ solubilized in 1-butanol was reduced with TBH₄ (TBA = tetrabutylammonium) in the presence of polyvinylpyrrolidone (PVP) as stabilizer. In the UV-vis spectra of all dispersions were observed the peak at 536 nm and with the increase as the concentration increases. The samples remaining stable during at least 6 months. The images registered in a transmission electron microscopy (TEM) proved the presence of spherical AuNPs with a diameter between 10-30 nm.

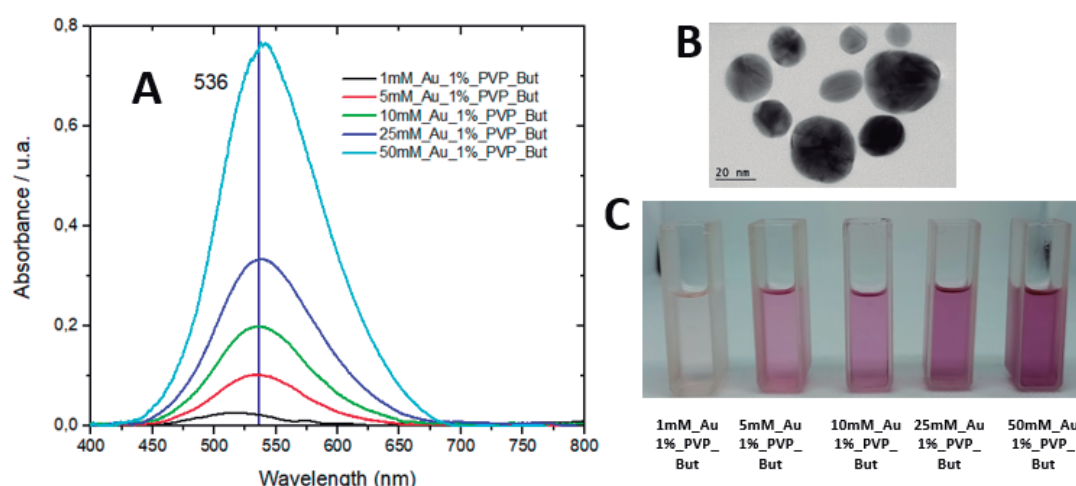


Figure 1: (A) UV-Vis spectra of dispersions; (B) Transmission electron microscopy of sample 5mM_Au_1%_PVP_But; (C) Images of dispersions.

[1] S. Eustis and M. A. El-Sayed, *Chem. Soc. Rev.*, 2006, **35**, 209–21

Agradecimentos/Acknowledgments

Coordenação de Aperfeiçoamento de Pessoal de Nível Superior – Brasil (CAPES) – Finance Code 001

Fundação de Amparo à Pesquisa do Estado de São Paulo (FAPESP) (21/08987-5)

46ª Reunião Anual da Sociedade Brasileira de Química: "Química: Ligando ciências e neutralizando desigualdades"

Área: MAT

Hybrid materials based on chitosan/magnetite/silver nanoparticles for environmental applications

Andressa Luíza Ratajk (IC),¹ Ana Livia de Andrade (IC),¹ Lucas Eduardo Reinke (IC),¹ Marion Isari Buse (PG),¹ Larissa Nardini Carli (PQ).^{1*}

andressa.ratajk@grad.ufsc.br; larissa.carli@ufsc.br

¹Centro Tecnológico, de Ciências Exatas e Educação, UFSC Blumenau

Keywords: Chitosan, Hybrid materials, Adsorption, Photocatalysis, Wastewater treatment

Highlights

Hybrid materials were synthesized using different methods;

The hybrids were characterized by their physical-chemical characteristics;

The hybrids showed adsorption capacity and catalytic activity.

Resumo/Abstract

The preservation of water sources and the search for efficient processes to remove pollutants and microorganisms are great environmental challenges. Hybrid materials based on chitosan associated with silver and magnetite nanoparticles can result in an easily-obtained and versatile device. This hybrid material might exhibit a high capacity for adsorption/degradation of pollutants and inhibit the growth of microorganisms. The application of magnetite nanoparticles is a promising approach, as it allows recovering the materials after use through the application of an external magnetic field. In this context, the aim of this work was to obtain hybrid materials of chitosan, magnetite and silver nanoparticles for application in the adsorption and/or degradation of pollutants. The hybrid materials were produced through two different methodologies and characterized by their morphology, chemical characteristics, and ability to adsorb and degrade methyl violet 2B dye from aqueous solution. The hybrids materials with magnetic response were successfully obtained by both methods and showed characteristic bands of their components (confirmed by Fourier transform infrared spectroscopy (FTIR)). Furthermore, the formation of silver nanoparticles was verified by ultraviolet-visible (UV-Vis) spectrophotometry. Preliminary tests of adsorption/degradation of the methyl violet 2B dye indicated that the materials have adsorption capacity and, mainly, (photo)catalytic activity when applied under ultraviolet radiation in the presence or absence of hydrogen peroxide. Additionally, it is expected that these materials present antimicrobial activity, expanding their potential of application in the treatment of water and effluents from different sources.

Agradecimentos/Acknowledgments

CNPq, UFSC

Immobilization of Au and Ag nanoparticles through 3D microfluidic printing for development of ultrasensitive SERS sensors

Cleber S. Torres (PG),^{1*} Henrique K. K. Ramos (IC),² Edison H. Montoya (PG),¹ Anerise de Barros (PQ),¹ Varlei Rodrigues (PQ),² Fernando A. Sigoli (PQ),¹ Italo O. Mazali (PQ).¹

*cstorres20@gmail.com

¹Laboratory of Functional Materials, Institute of Chemistry, UNICAMP, Campinas, Brazil.

²Institute of Physics "Gleb Wataghin" (IFGW), UNICAMP, Campinas, Brazil.

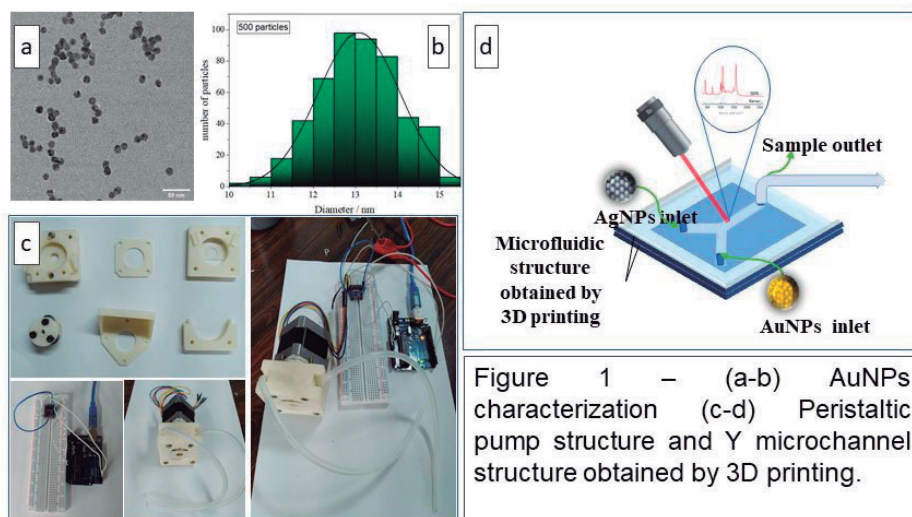
KEYWORDS: Nanoparticle, Gold, Silver, SERS, microfluidic.

Highlights

- Design of "Y" microfluidic channels through 3D printing technology
- Development of SERS sensors based on Au and Ag nanoparticles junctions
- SERS evaluation of 4-ABT molecule

Abstract

Surface-enhanced Raman spectroscopy (SERS) provides a fingerprint of the analyte as well as increased sensitivity compared to conventional Raman spectroscopy. Considering this, studying and developing new substrate manufacturing strategies that allow lower detection limits, reduced analysis time, portability, reproducibility, high sensitivity, and specificity against certain groups of analytes is essential to increasingly expanding the applicability of the SERS tool. Hence, microfluidic devices have been increasingly used, mainly for in situ biological analysis, due to the high homogeneity control provided by a controlled flow and the lower consumption of reagents. Therefore, this work aims to develop SERS substrates employing gold and silver nanoparticles (AuNPs and AgNPs) using microfluidic structures obtained from 3D printing. To verify the quality of the NPs synthesis, UV-VIS spectroscopy and transmission electron microscopy characterizations were performed. The extinction spectra of the colloidal suspension of AuNPs and AgNPs were characterized by the presence of the plasmonic excitation band centered at 520 nm and 407 nm, respectively. The micrographs of the NPs present homogeneous spherical particles with an average size of 12.9 nm, indicating the effectiveness of the methodology used in the synthesis (as illustrated in figures 1a and 1b, referring to the AuNPs). For the deposition of AuNPs, AgNPs, and molecule detection in the 3D printed microchannel (Figure 1d) on the silicon surface, peristaltic pumps (Figure 1c) were chosen because they are based on the alternation of compressions and relaxations of a hose.



The pump was also obtained by 3D printing and characterized by flow and pressure measurements that served to verify the best pump and microchannel coupling region. Flow measurement shows that the pump performs better when coupled to the microchannel outlet compared to the inlet. Regarding the pressure measurement, the outlet hose was stretched vertically, and the height of the water column was measured to verify that the pump can easily pump up to a height of 10 m. This predicts that it can generate 1 bar of water pressure. Thus, this microfluidic system allows the

handling of microscopic amounts of fluids that facilitate the elaboration of sensitive, fast, and versatile devices.

Acknowledgments



Indirect SERS chemosensing for atmospheric Hg detection

Deysiane A. L. dos Santos (PG)¹, Anerise de Barros (PQ)¹, Fernando A. Sigoli (PQ)¹, Italo O. Mazali (PQ)¹
deyseals@gmail.com; mazali@unicamp.br

¹Functional Materials Laboratory - Institute of Chemistry, University of Campinas – UNICAMP, Campinas, Brazil

keywords: Gold, nanorods, SERS sensor, mercury, amalgamation.

Highlights

Indirect SERS sensor for Hg^{0(g)} detection, exploiting the suppression of the plasmonic effect of gold nanoparticles caused by Hg^{0(g)} amalgamation.

Abstract

Mercury is considered a 'global pollutant' and can be emitted into the environment both by natural sources and anthropic sources, with the atmosphere being its main means of transport in nature. Due to its properties, mercury has a residence time in the atmosphere in the order of one year, facilitating its transport over long distances and deposition on a global scale. Hg^{0(g)} is extremely toxic and can cause devastating effects on brain tissues, leading to sensorineural and neuromotor damage. This work presents the development of an indirect surface-enhanced Raman scattering (SERS) sensor for the detection of Hg^{0(g)} based on gold nanorods (AuNRs). The detection is based on the degradation effect of the plasmonic characteristics of the AuNRs during the Au-Hg amalgam formation process. The sensor consists of AuNRs deposited on the surface of a 4 mm² Si substrate functionalized with a 3-mercaptopropyltrimethoxysilane (MPTMS) solution, followed by the deposition of the probe-molecule Rhodamine 6G. The UV-Vis spectrum of the AuNRs suspension verifies for the efficiency of the AuNRs growth method through the appearance of transverse and longitudinal plasmon bands at 515 and 673 nm respectively and the TEM micrographs confirm a good distribution of size and morphologies homogeneity. The quantification of the gold content performed by ICP MS agrees with the expected theoretical result for this synthesis. A better visualization of the Raman spectra was obtained through statistical analysis using multidimensional data projection techniques. The effect of different levels of amalgamation as a function of Hg^{0(g)} content on the plasmonic effect of gold nanoparticles was also investigated by classical electrodynamics simulations based on the boundary element method (BEM). Figure 1(a) presents a schematic illustration of the SERS detection principle for Hg^{0(g)}. Figure 1 (b) presents the averages of all Raman mappings performed for the detection of Hg^{0(g)} in the range from 180 to 38104.1 ng. Figure 1(c) corresponding to the analytical curve based on ΔI as in function of [Hg^{0(g)}] by monitoring the reduction in SERS intensity of the 1509.74 cm⁻¹ band of Rhodamine 6G. These results demonstrate the development of a detection system for Hg^{0(g)} with good reproducibility and sensitivity. This strategy is still little explored in SERS sensors and there is no report in the literature for the detection of Hg^{0(g)}.

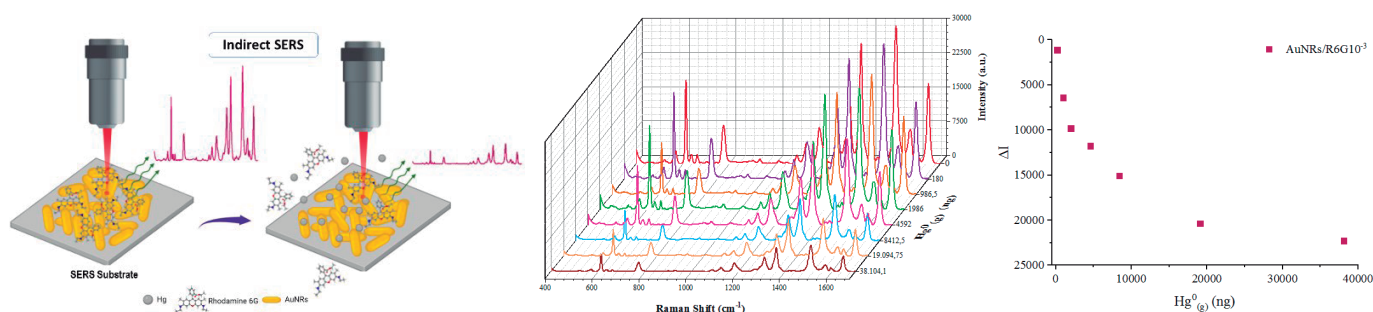


Figure 1. a) Schematic illustration of the SERS detection principle for Hg^{0(g)}; b) SERS intensity reduction of Rhodamine 6G as a function of the increase in Hg^{0(g)} mass from 180 to 38104 ng; (c) Analytical curve for the variation of the SERS intensity of the band 1509.74 cm⁻¹ of Rhodamine 6G as a function of the increase in the mass of Hg^{0(g)}.

Acknowledgments



Influence of magnetic stirring to synthesize titania nanotubes over microwave-assisted synthesis.

Lorrana Vietro Barbosa (PG)¹ and Emerson H. de Faria (PQ)^{1,*}.

e-mail: *emerson.faria@unifran.edu.br

¹Grupo de Pesquisa em Materiais Lamelares Híbridos (GPMatLam) – Universidade de Franca (UNIFRAN). Av. Dr. Armando Salles Oliveira, 201. Pq. Universitário. Franca/SP. 14404-600

Palavras Chave: *nanomaterial, titania nanotubes, microwave assisted synthesis*

Highlights

Titania nanotubes was synthesized under microwave assisted synthesis. Physical-chemical analysis confirmed the synthesis without magnetic stirring. Magnetic stirring under similar conditions promotes the fragmentation of titania nanotubes. Titania nanotubes with higher purity was obtained without magnetic stirring.

Resumo/Abstract

Titanium dioxide is one of the most popular semiconductors employed for different applications such as pigments, thin films, sunscreen, and as photocatalyst in various environmental applications. In this context, titania with nanotubular morphology has attracted prominence as a versatile material under environmental applications, specially photocatalytical, and also to medical purposes as implantation material, due to its unique properties such as higher specific surface area, lower grain size, change of surface charge, and principally to increase drastically the photocatalytical activity of titania. However, as previously discussed by Kasuga *et al.*, 1999 the mechanism of titania nanotubes has not been clarified yet. Are remarkably that various parameters could influences directly the chemical hydrothermal synthesis. In the present work, we investigated the influence of magnetic stirring over microwave assisted synthesis of TiO₂ nanotubes using anatase powder as the raw material. The resulting materials were characterized by X-ray diffraction, infrared absorption spectroscopy, thermal analysis, and scanning electron microscopy. Anatase powder acquired from MERCK, powder (12.5 g), and 100 mL of a 10 M NaOH aqueous solution were placed in a 200 mL Teflon flask, which, in turn, was placed for 2 h in a microwave furnace, using 1200 W, and heating velocity of 10°C/min reaching the 110 °C during 2h with magnetic stirring (350 r.p.m.) and without magnetic stirring. The final solids were several washed with distilled water (200 mL) and then centrifuged at 2500 r.p.m. for 15 minutes to separate the powder from the solution. This procedure was repeated until the conductivity of the supernatant reached 70 µS/cm. The resulting solids were washed also with 150 mL of 0.1 mol L⁻¹ HCl solution and the materials were labeled as NT-TiO₂-MS and NT-TiO₂-NMS for magnetically stirred and static synthesis respectively. XRD of NT-TiO₂-MS reveals the presence of the phase mixture resulting in synthesis under constant magnetic stirring, and confirmed the presence of anatase phase (as in precursor), due to the reflections at 25°, 37°, 48°, 54°, 55° and 62° and also the halo between 5 and 20 °C was observed resulting from an amorphous phase in magnetically stirred synthesis. However, NT-TiO₂-NMS shows the typical reflections of titania nanotubes with broadened reflections at a low angle of 10°, and other reflections at 24°, 28°, and 48°. FTIR shown the typical bands of water at 3600 cm⁻¹ and Ti-O-Ti and Ti-O at 1069 and 930 cm⁻¹ for both samples. SEM analysis confirm the suggested results observed by XRD. The nanotube synthesized without magnetical stirring results in more elongated fibers and typical nanotubular morphology. However, the parent solid NT-TiO₂-MS presents very small spherical particles and some agglomerated nanotube fibers mixed with this smaller particle probably resulting from the fragmentation of titania nanotube fibers. Terephthalic acid hydroxylation over UV light (95W λ=254 nm) reveals that both solids present good photocatalytic activity. It is important to remark that microwave synthesized titania nanotube reduces the reaction time from 20h to 2h, and the gain in energy consume it is very higher and could be highlighted within requirements from sustainable development goals, obviously, other critical points were observed such as the procedure for washing the samples, and also the use of concentrated alkaline medium needs be optimized.

¹Kasuga, T., Hiramatsu, M., Hoson, A., Sekino, T., Niihara, K. *Advanced Materials*. 1999, 11, 1307-1311.

Agradecimentos/Acknowledgments

FAPESP (2017/15482-1), CAPES (finance code 001), CNPq (310151/2021-0),

46ª Reunião Anual da Sociedade Brasileira de Química: "Química: Ligando ciências e neutralizando desigualdades"

Influence of zeolite acidity on heat release rate of an intumescent formulation in fire spread: a theoretical study

Ana L. S. Ventapane,^{1*} Simone P. S. Ribeiro (PQ).¹

analuciaventapane@pos.ig.ufrj.br

¹Instituto de Química, Universidade Federal do Rio de Janeiro, Cidade Universitária, Bloco A, Rio de Janeiro, RJ 21941-909 Brazil

Palavras-Chave: Computational Fluid Dynamics (CFD), Fire Dynamics Simulator (FDS), Zeolite Acidity, Synergistic Agent, Intumescent Formulation, Flame Retardant.

Highlights

The effect of acidic sites of faujasite Y zeolites in an intumescent formulation was investigated by theoretical study using the heat release rate of these composites by computational fluid dynamics.

Abstract

The flammability of polymers can cause several damages. To reduce the effects of fire development, the heat release rate (HRR) in fire must be reduced too. The intumescent formulation is a flame retardant additive that have become a preventive protection in polymers against fire. A strategy to increase the flame retardant properties in intumescent formulation is the use of synergistic agent such as zeolites. In previous work the influence of acidic sites of faujasite Y zeolites on their synergistic action with an intumescent formulation (IF) composed of ammonium polyphosphate (APP) and pentaerythritol (PER) in a polypropylene (PP) matrix was investigated. The zeolites with acid sites demonstrated a positive effect on char formation.¹ To evaluate this results in a real environment fire scenario, a simulation was developed in Fire Dynamics Simulator computational software to analyze the fire behavior on peak heat release rate (pHRR) of sodic zeolite (NaY) and acidic zeolite (HY) on intumescent formulation. Table 1 shows the time of simulation, the room temperature and the heat release on pHRR of these composites.

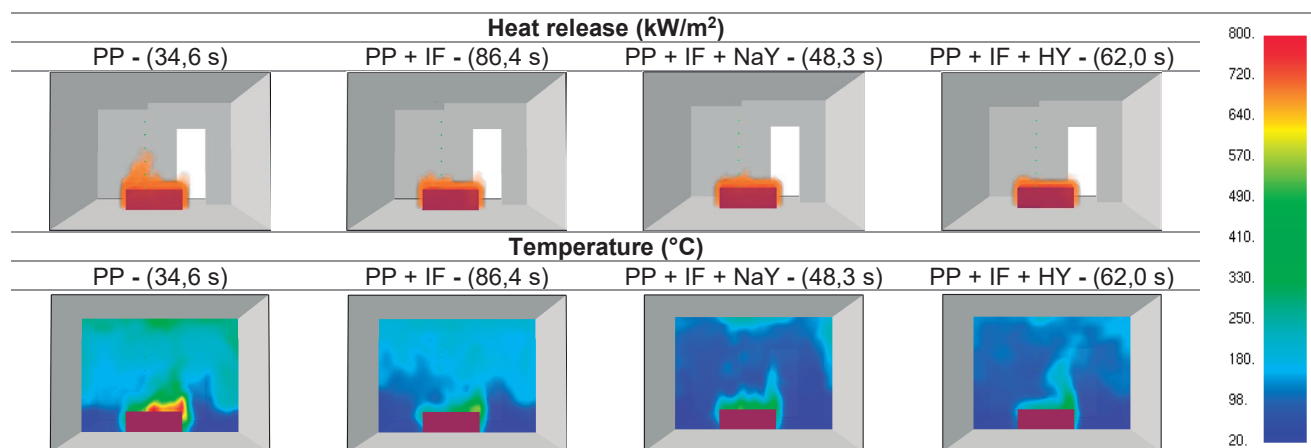


Table 1 – Heat release, temperature and time of simulation on pHRR of composites.

The table shows that the composite with HY lead a considerable reduction on pHRR, room temperature besides the reduction of time simulation witch can improve safety scape on a fire scenario. The zeolite acid sites can catalyze more efficiently the reaction between APP and PER, which produces phosphate esters, precursors of char, improving the thermal stability and enhancing the flame-retardant properties.

¹ RIBEIRO, S. P. S.; *et al.* Influence of the zeolite acidity on its synergistic action with a flame-retarding polymeric intumescent formulation. **Journal of Materials Science**, v. 55, n. 2, p. 619–630, 2019.

Acknowledgments

The author wishes to thank CAPES program for the support.

INVESTIGATION OF THE INTERACTION BETWEEN GLYPHOSATE PESTICIDE AND LIPID AND AMPHIPHILIC PEPTIDE MONOLAYER STRUCTURES USING THE LANGMUIR-BLODGETT TECHNIQUE

Priscila S. Ferreira (PG)*, Barbara B. Gerbelli (PQ), Bruna Cortez (PG), Ana. C. H. Castro-Kochi (PQ), Fabiola L. Castro (PG), Wendel A. Alves (PQ).

priscila.sabbag@ufabc.edu.br

Centro de Ciências Naturais e Humanas, Universidade Federal do ABC, Santo André, São Paulo.

Keywords: Lipopeptides, Glyphosate, Langmuir-Blodgett films, Biosensors.

Highlights

This study presents the design and development of an impedimetric biosensor that utilizes a combination of phosphatidylcholine and lipopeptide assemblies on a solid substrate. The biosensor is fabricated using the Langmuir-Blodgett (LB) method, which allows for the creation of high-quality monolayer films. With this innovative approach, the biosensor offers a highly reliable and efficient means of detecting glyphosate herbicide in environmental waters.

Resumo/Abstract

In recent years, the utilization of pesticides in agriculture has become more prevalent in managing agricultural pests. Given this scenario, developing new analytical tools capable of detecting these substances in food and water is crucial. In this study, we use lipopeptides as functional mimics of the enzyme acetylcholinesterase (AChE) in monolayers of phosphatidylcholine (PC) to detect the presence of glyphosate and N-(phosphonomethyl)glycine (PNG) in the environment. The lipopeptides contain hydrophilic amino acids, L-serine (S), L-proline (P), L-arginine (R), L-tryptophan (W), and L-glycine (G), covalently linked to a long aliphatic chain.^[1] We used different molar ratios between the lipopeptides (LP) and PC ([LP/PC]). For each monolayer composition, we varied the concentration of PNG from 1 to 15 μM . We used the Langmuir-Blodgett technique to investigate the influence of the LP on the lipid monolayer and observed changes in the adsorption isotherm with increasing amounts of LP, such as a decrease in the mean molecular area and a decrease in the maximum pressure (Figure 1A). For [LP/PC]=0.5, increasing the concentration of PNG did not modify the collapse pressure (Figure 1B), but for [LP/PC]=1.0, the maximum pressure decreased until it reached a value of around 23 mN/m (Figure 1C). The Nyquist diagram shows an increase in resistance to charge transfer due to the modification of ITO in the presence of the monolayer and then adding the pesticide (Figure 1D), indicating that the monolayer adheres to the ITO surface and the pesticide interacts with the monolayer. A calibration curve was established by adjusting the concentration of PNG (as depicted in Figure 1E), resulting in a detection limit of 48 nmol L⁻¹.

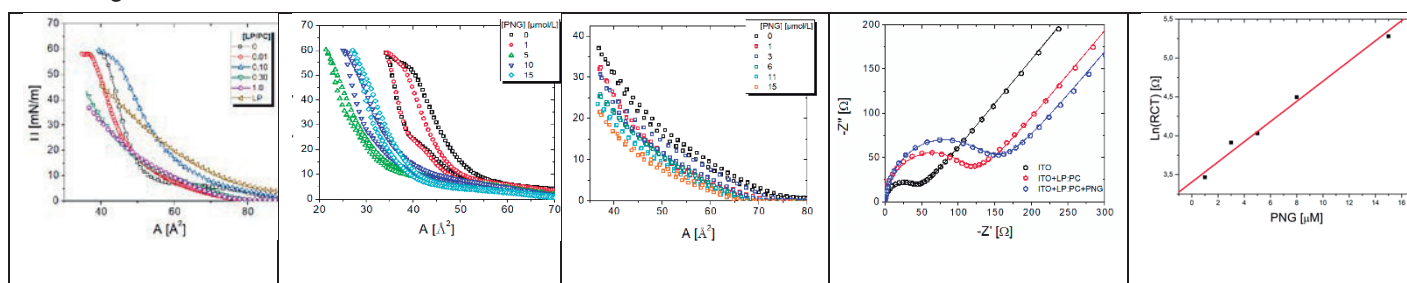


Figure 1. Adsorption isotherm: (A) Different molar ratios between LP and PC ($0.05 \leq [LP/PC] \leq 1$), (B) Different of the molar concentration of PNG on [LP/PC]=0.3 and (C) [LP/PC]=1; (D) Representing the Nyquist diagram of the EIS measurement in the presence and absence of pesticides; (E) Depicting the calibration curve obtained by varying the concentration of PNG.

[1] Gerbelli, B.B.; Oliveira-Filho, P.L.; Cortez, B.; Sodre, P.T.; Coutinho-Neto, M.D.; Hamley, I.W.; Seitsonen, J.; Alves, W.A. *Nanoscale Adv.* **2022**, *4*, 3592-3599.

Agradecimentos/Acknowledgments

FAPESP, CNPq, CAPES, INCT de Bioanalítica.

46ª Reunião Anual da Sociedade Brasileira de Química: "Química: Ligando ciências e neutralizando desigualdades"

Luminescence of Eu^{III} and Tb^{III} Complexes Coordinated to Thermoresponsive Phosphine Oxide-Functionalized Poly(N-Vinylcaprolactam) Nanogels

William M. Oliva (PG)¹, Italo O. Mazali (PQ)¹, Fernando A. Sigoli (PQ)^{1*}.

willmoliva@gmail.com; fsigoli@unicamp.br

¹Institute of Chemistry, University of Campinas (UNICAMP).

Keywords: Europium, Luminescence, Poly(N-Vinylcaprolactam), Nanogel, Terbium, Thermometry.

Highlights

NVCL, a cross-linker and phosphine oxide ligands were copolymerized in aqueous dispersion.

The thermoresponsive nanogels can incorporate Ln^{III} complexes and act as luminescent temperature probes.

Abstract

Poly(N-vinylcaprolactam) (pNVCL) is a thermoresponsive material that undergoes a coil-globule phase transition near human body physiological temperature. It is dispersible in water and shows better biocompatibility than other polymers of similar properties, such as poly(N-isopropylacrylamide) (pNIPAM)^[1]. By interacting with sensitive optical probes, particularly lanthanide ion compounds, the luminescent nanogels based on these polymers can provide nanothermometers for aqueous environments due to their reversible temperature-driven structural changes^[2]. In the present work, allyldiphenylphosphine oxide (adppo) and diphenyl(4-vinylphenyl)phosphine oxide (dppso) – molecules that have both a coordinating P=O group and a polymerizable end – were each copolymerized with N-vinylcaprolactam (NVCL) in water alongside the cross-linker N,N'-methylenebisacrylamide (MBAM) and in presence of the surfactant sodium dodecyl sulfate (SDS). The reaction, carried out using degassed and deionized water at 70 °C for 5 hours, leads to dispersed ligand functionalized-pNVCL nanoparticles. Each phosphine oxide was added at different molar percentages, related to the main monomer, to prepare a comprehensive series of adppo- and dppso-functionalized nanogels. The obtained systems were characterized by nuclear magnetic resonance (NMR), indicating the polymer identity and the phosphine oxide functionalization. Studies by dynamic light scattering (DLS) indicated optimal functionalization concentrations for the nanogels to reproduce the original polymer structural transition as a function of temperature. Separately, trivalent lanthanide ion complexes of Eu^{III} and Tb^{III} with chelating antenna ligands such as 2-thenoyltrifluoroacetate (tta⁻), hexafluoroacetylacetonate (hfa⁻) and acetylacetonate (acac⁻) were also prepared and structurally and spectroscopically characterized as a powder and in ethanolic solutions. Stoichiometric amounts of the complexes, individually and combined, were added to selected dispersions of the phosphine oxide-functionalized pNVCL nanogels and used to verify their potential temperature-dependent energy transfer. The phosphine oxide groups replace the coordinated water molecules of lanthanide complexes, therefore incorporating the complexes into the nanogel network *via* chemical bonding. The resulting luminescent and thermoresponsive nanogels were studied by DLS and photoluminescence spectroscopy, under heating and cooling cycles between 20 °C and 50 °C. The nanogels retain the polymer phase transition and the typical Eu^{III} and Tb^{III} luminescence can be detected in aqueous dispersions, with their intensities and emission lifetimes responding to the temperature variation. However, successive cycles of structural changes can lead to reduction of the optical signal and reproducibility issues in some cases.

References

- [1] N. A. Cortez-Lemuz, A. Licea-Claverie, *Progress in Polymer Science*, **53**, 1 (2016).
[2] J. A. Sobrinho, G. A. Brito Jr., I. O. Mazali, F. A. Sigoli, *New Journal of Chemistry*, **44**, 8068 (2020).

Acknowledgments

The authors are thankful to CAPES, CNPq, FAPESP and INOMAT for funding this research.

Luminescent Glass and Glassceramics for middle infrared applications

Marcelo Nalin (PQ),^{1*} Gabirelli Fernandez Vazques (IC),¹ Juliane Resges Orives (PQ),¹

marcelo.nalin@unesp.br

¹Departamento de Química Analítica, Físico Química e Inorgânica – Instituto de Química, UNESP Araraquara

Palavras Chave: *glass, glassceramics, luminescence, sensors, middle infrared, rare earths*

Highlights

Glass and glassceramics containing rare earths

Luminescence in the middle infrared

Sensing applications for greenhouse gases

Resumo/Abstract

Greenhouse gases, such as CH₄, CO₂, CO, N₂O, etc, are the biggest villains of our times concerning the global warming and related climate changes. For this reason, controlling the levels of such gases is primordial to avoid catastrophic events in the future.

The main problem arising from the presence of such gases is the fact that they absorb energy in the range of the middle infrared region, by the vibrations of their molecules.

It is important to highlight that the glass composition is primordial, once it must be transparent to the optical window in the desired range. For this, we use heavy metal oxide glasses.

Detecting remotely such gases, in any level, is determinant for the success of new technologies. An emerging possibility is the uses of special optical fibers containing crystalline materials in the core of the fiber. The novelty of this project is to obtain dysprosium gallium garnets inside the glasses by a single step methodology. Glasses in the system PbO-Bi₂O₃-Ga₂O₃-GeO₂ containing 1, 2 or 3 mol % of Dy₂O₃ were prepared by classic melt-quenching methodology. This unique system, during the cooling process induces the crystallization of pure Dy₃Ga₅O₁₂ garnet crystalline phase. Depending on the cooling conditions it is possible to control the range of size of the crystals, passing from some microns to dozens of microns. The crystals were characterized by means of X-Ray diffraction and micro-Raman spectroscopy while the optical properties were studied using UV-Vis, FT-IR and luminescence spectroscopies. Luminescence measurements have shown the Stark emissions of dysprosium ions, characteristic of rare earths present into crystalline phases. The crystals have sharper emissions (compared to glasses) in the infrared region and can be used for selective monitoring of greenhouse gases. In this specific case, Dy³⁺ can be used to sensing CO₂ molecules at 4.3 μm. Interesting enough, when the rare earth is changed, it is possible to obtain the respective garnets, such as Er₃Ga₅O₁₂, Tm₃Ga₅O₁₂, Ho₃Ga₅O₁₂, Gd₃Ga₅O₁₂, etc. Such results allow to tune the emissions in the middle infrared to be specific to certain molecules, such as CH₄, CO, NO, etc.

Agradecimentos/Acknowledgments

The authors acknowledge FAPESP (grants 2013/07793-6 and 2021/13981-6) and SISFOTON-MCTI (CNPq grants 440217/2021-0) for financial support.

Magneto-optical borogermanate glasses and fibers containing Tb³⁺

Douglas Faza Franco¹ (PQ), Thiago A. Lodi¹ (PQ), Eduardo O. Ghezzi¹ (IC), Sandra Helena Messaddeq (PQ)², Younes Messaddeq (PQ)², Marcelo Nalin (PQ)¹

douglas.franco@unesp.com

¹Departamento de Físico-Química, Analítica e Inorgânica (IQCAR/UNESP); ²Laval University (Centre d'Optique, Photonique et Laser, COPL, 2375 rue la Terrasse, Quebec, Quebec G1V 0A6, Canada)

Keywords: Magneto-optical glasses, Optical fibers, Faraday rotator, Terbium.

Highlights

- Magneto-optical (MO) glasses and fibers containing Tb³⁺ ions;
- High Verdet constant (V_B) values and good MO performance;
- MO materials for developing sensors of the current and magnetic field.

Resumo/Abstract

Magneto-optical (MO) materials based on the Faraday effect have been increasingly studied for use in new technologies [1,2]. MO materials have been applied as modulators, as optical isolators, and as magneto-optical fiber sensors. A wide variety of transparent MO glasses, crystals, and transparent glass–ceramics containing rare earth (RE) ions such as Tb³⁺, Dy³⁺, Pr³⁺, and Gd³⁺ have been investigated in the last few years. In this work, glass compositions based on borogermanate (BGB-xTb) glasses containing high concentrations of Tb³⁺ ions were developed to produce magneto-optical (MO) fibers. All glasses were synthesized from the melt-quenching process for 2 hours between 1350-1500 °C using platinum crucibles. All samples are completely transparent, and they are attracted for a commercial Neodymium magnet indicating the paramagnetic behavior (Figure 1). Morphological analysis (HR-TEM) of the sample with the highest concentration of Tb³⁺ ions (18 mol%) confirmed the homogeneous distribution of Tb³⁺ ions and the absence of nanoclusters. All the samples presented excellent thermal stability against crystallization ($\Delta T > 100$ °C). An optical fiber was manufactured by a fiber drawing process from the BGB glasses containing 6, 8, 9 and 10 mol% of Tb₄O₇. UV–Vis spectra of the glasses showed Tb³⁺ electronic transitions and optical windows varying from 0.4 to 1.6 μm . The magneto-optical properties and the paramagnetic behaviors of the glasses were investigated using Faraday rotation experiments. The Verdet constant (V_B) values were calculated at 500, 650, 880, 1050, 1330, and 1550 nm. The maximum V_B values obtained at 650 and 1550 nm for the glass with $x = 18$ mol% were -128 and -17.6 rad T⁻¹m⁻¹, respectively. In fact, this result indicates that the V_B values calculated for the BGB-18Tb glass are higher than the commercial TGG crystal at 650 nm ($V_B = -125$ rad T⁻¹.m⁻¹). The V_B values at 500 and 1550 nm for the optical fiber containing 8 mol% of Tb₄O₇ were -110.2 and -9.5 rad T⁻¹m⁻¹, respectively, while the optical loss at around 880 nm was 6.4 dB m⁻¹. In addition, the glass precursors have presented a great potential to be applied as Faraday rotators in the development of miniaturized sensors to detect the magnetic field and electric current of transformers and electrical current.

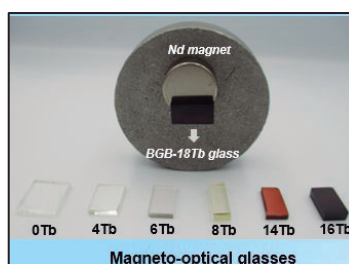


Figure 1: Photographs of the BGB-xTb glasses and the magnetic attraction of the BGB-18Tb glass using a commercial neodymium magnet.

References

- [1] Chen, Q. et al. Bol. Soc. Esp. Ceram. Vidr., 56(1), 1–12 (2017).
 [2] Franco, D.F. et al., Sci. Rep. 11, 9906 (2021).

Agradecimentos/Acknowledgments

The authors are grateful to the São Paulo State Research Foundation (FAPESP, grants 2016/16900-9, 2018/19272-4, and 2013/07793-6) for financial support and to the Centre d'optique, Photonique et laser (COPL) at Laval University – Canada.

Mesoporous carbons: a sustainable alternative for CO₂ capture and storage

Tiago H.S. Madalena (PG),¹ Ana Paula .T. de Carvalho (PQ),² Luciano A. Montoro (PQ),² Alaine C. Herédia (IC),
tiagohsm@outlook.com

¹Departamento de Química, Icox, UFMG.

Key words: CO₂ Capture, Mesoporous Carbons, adsorption, physisorption

Highlights

Mesoporous nitrogen-doped carbons proved to be a sustainable alternative for CO₂ capture and storage.

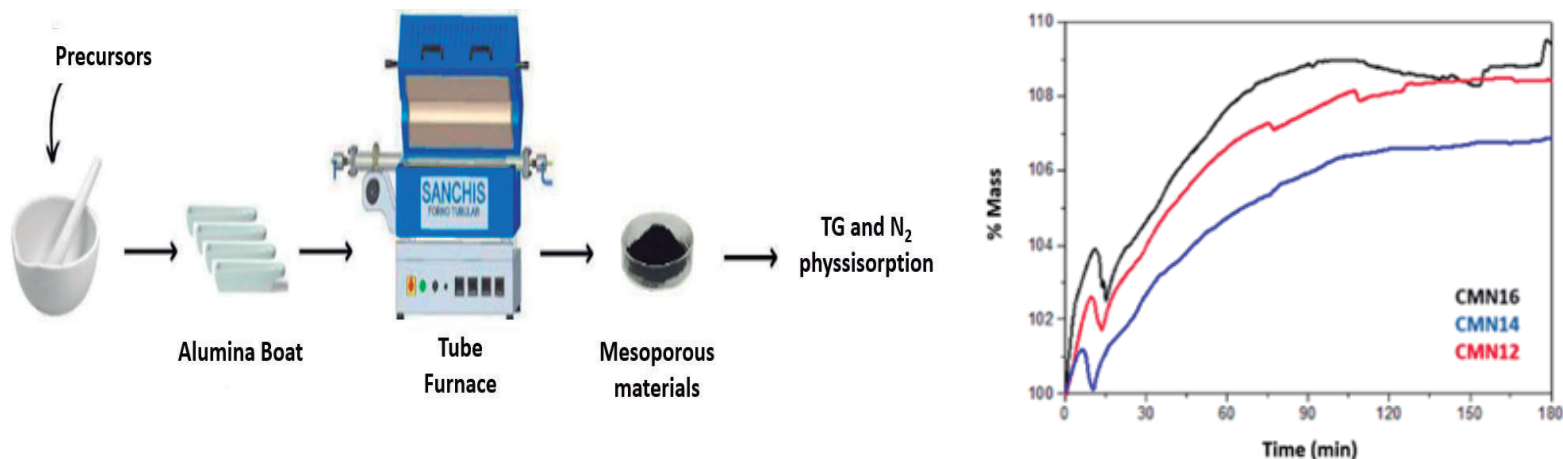
Resumo/Abstract

This work describes the results and conclusions obtained in the preparation and characterization of modified samples of mesoporous carbons (CM) from impregnation with nitrogen considering as a parameter the mass ratio in the proportions between carbon precursor and nitrogen precursor (C:N) for the capture and storage of CO₂. The samples were obtained by the sustainable solvent-free method using Resorcinol and Melamine as carbon and nitrogen precursor sources, respectively. The textural characteristics were determined using nitrogen adsorption and desorption isotherms by the BET method and the BJH method. And they showed that the use of melamine causes a decrease in the textural properties of the materials, however, it is possible to notice that this decrease does not occur in a linear way, since the CMN14 compound presents the highest parameters among the three impregnated materials. The CO₂ capture tests were conducted in a thermogravimetric analysis equipment using an isothermal method at 25 °C in CO₂ saturated environment and revealed that the adsorption capacities are correlated with the changes in the textural properties of the materials as nitrogen is introduced in the structure and again it can be noticed that this property does not present a linearity having the compound CMN16 as material with greater absorptive character for CO₂.

Table 1: N₂ physisorption analysis results and CO₂ capture results

Material	Surface area (m ² g ⁻¹)	Diameter (nm)	Volume(cm.g ⁻¹)	CO ₂ capture (mmol.g ⁻¹)
CM	648.22	4.31	0.42	2.24
CMN12	399.34	3.81	0.12	2.00
CM14	528.90	7.75	0.30	1.76
CMN16	441.80	3.05	0.13	2.08

Figure 1: Production scheme of mesoporous materials and capture CO₂ results



Acknowledgments

UFMG, DQ-UFMG, Capes, CNPq, GRUTAM, ESCALAB, RHI Magnesita.

46ª Reunião Anual da Sociedade Brasileira de Química: "Química: Ligando ciências e neutralizando desigualdades"

Mesoporous carbons produced with biomass using the *solvent-free* method: porous supports for sulfur incorporation

Rayane C. F Silva (PQ)^{1,2}, Rubens L. F. Filho (PG)^{1,2}, Aline C. Marciano (PG)^{1,2}, Keiliane S. dos Santos (PG)^{1,2}, Igor B. Gomes (IC)^{1,2}, Victor S. Vaz (IC)^{1,2}, Danielle D. Justino (PG)^{2,3}, Fernanda G. Gandra (IC)^{1,2}, Mozair C. V. Junior (TC)², Glaura G. Silva (PQ)^{1,2}, Paula S. Pinto (PQ)^{2,4}, Paulo F. R. Ortega (PQ)^{2,3}, João P. C. Trigueiro (PQ)^{2,3}, Rodrigo L. Lavall (PQ)^{1,2}, Ana Paula C. Teixeira (PQ)^{1,2*}.

rayane.silva@ctnano.org; anapaula.cta1@gmail.com

¹Departamento de Química, UFMG; ² Centro de Tecnologia em Nanomateriais– CTNano/UFMG; ³Departamento de Química, CEFET-MG; ⁴Universidade do Estado de Minas Gerais – UEMG-Divinópolis.

Keywords: mesoporous carbons, biomass, lithium sulfur batteries.

Highlights

Mesoporous carbon from biomass and incorporated with sulfur. Higher proportions of sulfur and activation of the material allowed a more effective incorporation.

Abstract

This study reports the synthesis of mesoporous carbon (MC) from tannin biomass and incorporated with sulfur (S). The objective was to evaluate how different synthetic parameters can influence the stability and the S content. Firstly, a MC material was produced by the *solvent-free* method and named as M. Part of M was activated with carbon dioxide (CO₂) and named as: MA.¹ From M and MA, 5 sulfur-embedded materials (SMC) were produced by the autoclave melt diffusion method² (Tab. 1). M and MA presented type IV isotherms (Fig. 1a), typical of mesoporous materials¹. MA showed higher total pore volume (1037 cm³g⁻¹) and BET specific surface area (1485 m²g⁻¹) compared to M (0.452 cm³g⁻¹ and 533 m²g⁻¹). To obtain the incorporated sulfur content, thermogravimetric analysis (TG)² was performed on N₂ for the MCS (Tab. 1 and Fig. 1b, 1c). The main results indicated that the 2:1 ratio (S:MC) tends to increase the S content. The incorporation without opening the autoclave (MS4), shifted part of the incorporated S to a higher temperature range (3° event). For incorporation with the activated material (MS5), the S decomposition temperatures were shifted to the two events with the highest temperature range (2° and 3° event). It is concluded that prior activation of MC and higher proportions of S generated more effective incorporation. The study of these materials is part of *Rota 2030* public notice and it is being developed at UFMG and CTNANO. In fact, electrochemical tests have indicated an improvement in the reversibility of processes with increasing S content and carbon activation. In the future, the SCM will be used to build sustainable lithium-sulfur batteries in the *Rota 2030* project.

Table 1: Sulfur incorporation parameters and thermogravimetric analysis results: T: temperature; t: time; C_T: total content; C: content; T_R: temperature range.

Precursor	Sulfur:MC ratio	Incorporation with sulfur					Thermogravimetric analysis results						
		Step 1		Step 2		Step 1 and 2 performed	C _T / %	1° Event		2° Event		3° Event	
		T/°C	t/h	T/°C	t/h				C ₁ /%	T _{R1} /°C	C ₂ /%	T _{R2} /°C	C ₃ /%
MS1	M	155	24	-	-	-	36	11	149-286	25	211-288		
MS2	M	155	24	-	-	-	43	32	150-246	11	246-286		
MS3	M	155	24	300	2	Separate	47	27	165-232	20	232-278		
MS4	M	155	24	300	2	Together	59	29	169-259	22	259-310	8	329-446
MS5	MA	155	24	300	2	Together	58			48	176-332	10	332-451

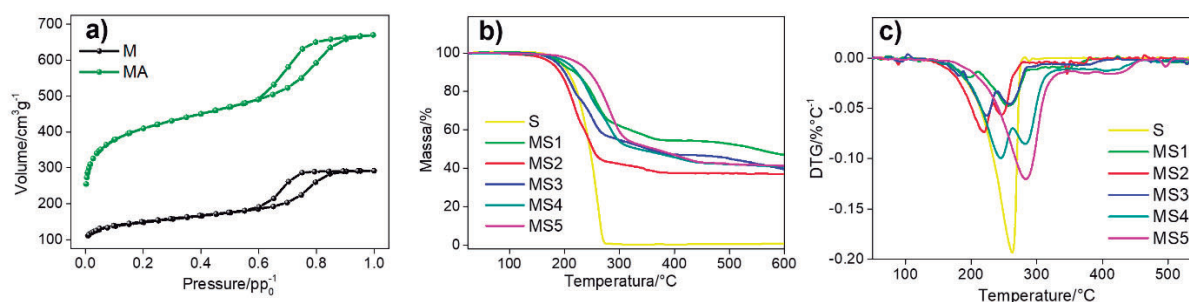


Figure 1: (a) N₂ physisorption isotherms; TG (b) and DTG (c) curves.

References: [1] Jimena Castro-Gutiérrez et al.; *Green Chemist*, Issue 22, 2018; [2] Xiulei Ji, *Nature Materials*, V.8, 2009.

Acknowledgments

UFMG, Rota 2030, FUNDEP, Bravo Motors, XBM, CTNANO, INCT MIDAS, Fapemig, Capes, CNPq, Grutam, CEFET-MG; UEMG-Divinópolis 46° Reunião Anual da Sociedade Brasileira de Química: "Química: Ligando ciências e neutralizando desigualdades"

Microwave-assisted synthesis of polyacrylamide preformed particle gels reinforced with carbon nanomaterials for conformance control

Sthéfany Z. S. do Amparo^{1,3} (PG), Cláudia K. B. de Vasconcelos^{2,3} (PQ), Aline I. A. dos R. Almeida¹ (PG), Laryssa E. B. Sena^{1,3} (IC), Glaura G. Silva^{1,3} (PQ) and Marcelo M. Viana^{1,3} (PQ).

marcelomachado@ufmg.br; marcelo.viana@ctnano.org

¹Departamento de Química-ICEx, Universidade Federal de Minas Gerais, ZIP 30.270-901, Belo Horizonte, MG, Brazil;

²Departamento de Física e Química, Pontifícia Universidade Católica de Minas Gerais, ZIP 30.535-901, Belo Horizonte, MG, Brazil;

³CTNano, Universidade Federal de Minas Gerais, ZIP 31.310-260, Belo Horizonte, MG, Brazil.

Palavras Chave: Polyacrilamide, Nanomaterial, Hydrogel, Graphene oxide, Microwave synthesis, Conformance control.

Highlights

Nano-reinforced PAM hydrogels were prepared using microwave-assisted synthesis. PAM-CNT-ox increased the swelling capacity up to 57%. PPGs prepared are strongly suitable for injection with $\eta < 30$ mPa.s.

Abstract

Enhanced oil recovery (EOR) aims to increase the sweeping efficiency of a reservoir through the injection of displacing fluids or gels. The preformed particle gels (PPGs) acts blocking the high permeability channels and elevate the cost/benefit for oil production. Herein, polyacrylamide (PAM) hydrogels reinforced with graphene oxide (GO) and oxidized carbon nanotubes (CNT-ox) and their PPGs were prepared using microwave-assisted synthesis.

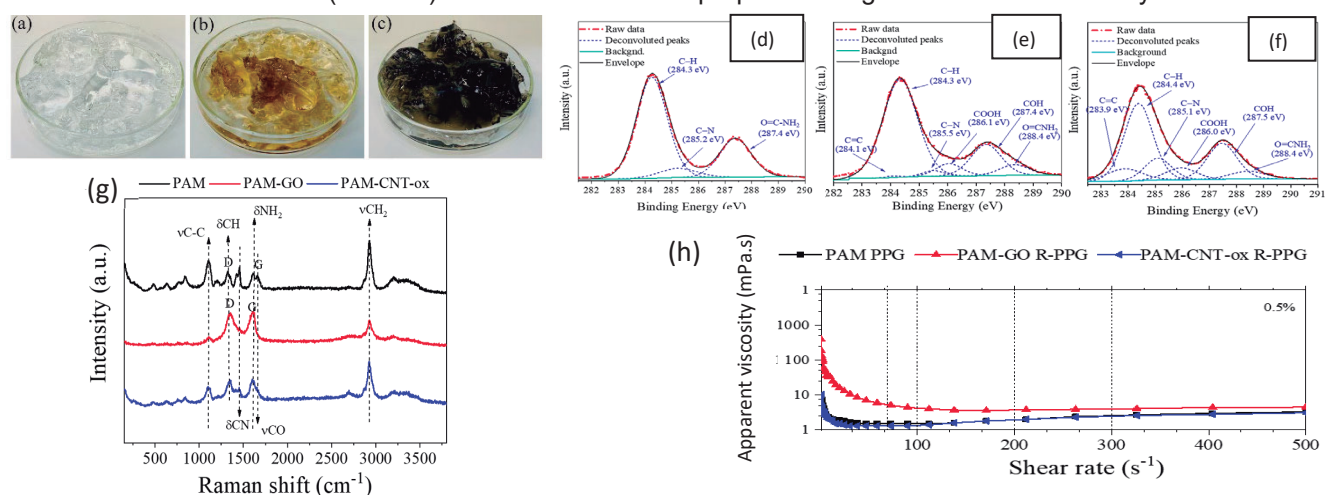


Figure 1. Photographs and XPS core-level spectra of C1 s for (a, d) PAM, (b, e) PAM-GO and (c, f) PAM-CNT-ox hydrogels; (g) Raman spectra of hydrogels; (h) Curves of apparent viscosity as a function of shear rate for saline solution containing 0.5% in mass of PAM PPG, PAM-GO R-PPG and PAM-CNT-ox R-PPG.

Raman spectroscopy and XPS analysis were performed to confirm GO and CNT-ox incorporation on the PAM hydrogel and to identify an *in-situ* acrylamide polymerization with an unusual chemical cross-linkers. The PPG apparent viscosity results showed that all systems containing 0.5 wt.%, 1.0 wt.% and 2.0 wt.% are suitable for injection with $\eta < 30$ mPa.s.

References:

[1] DO AMPARO, Sthéfany ZS et al. Microwave-assisted synthesis of PAM preformed particle gels reinforced with carbon nanomaterials for conformance control in oil recovery. *Fuel*, v. 330, p. 125650, 2022.

[2] AMARAL, Camila NR et al. Preformed particle gels with potential applicability for conformance control of oil reservoirs. *Journal of Applied Polymer Science*, v. 137, n. 15, p. 48554, 2020.

Acknowledgments

This work was financially supported by CNPq, Fapemig, Coordenação de Aperfeiçoamento de Pessoal de Nível Superior Capes - CAPES (Finance code 001) and Petrobras.

Modification of HKUST-1 MOF with gold nanoparticles and SERS characterization of the hybrid material.

Hudson Batista da Silva (PG)^{1*}, Charlane Cimini Corrêa (PQ)¹ and Gustavo Fernandes Souza Andrade (PQ)¹.

HUDSONSILVA@ICE.UFJF.BR.

¹Departamento de Química da Universidade Federal de Juiz de Fora (UFJF).

Palavras Chave: MOF, Nanopartículas de ouro, SERS, Polimorfismo.

Highlights

- Metal-organic frameworks (MOFs);
- Third Generation MOF HKUST-1;
- Gold nanoparticles (AuNPs);
- Modification of HKUST-1 with AuNPs;
- Surface-enhanced Raman spectroscopy (SERS).

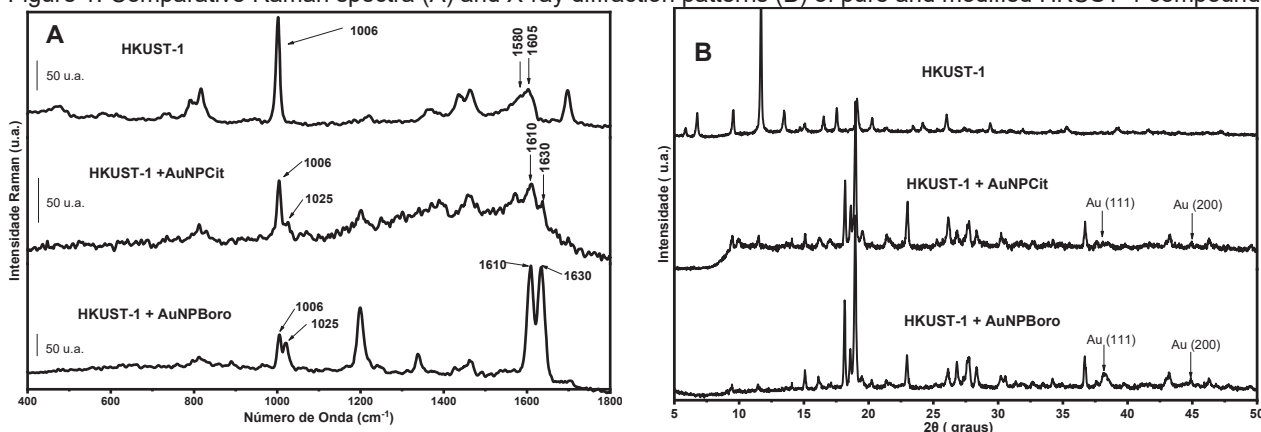
Resumo/Abstract

In the present work, MOF HKUST-1 was modified with AuNPs. Citrate-coated gold nanoparticles (AuNPCit) and borohydride-coated gold nanoparticles (AuNPBoro) were used. The HKUST-1 modified with AuNP coated with sodium citrate (HKUST+AuNPCit) and AuNP coated with sodium borohydride (HKUST-1+AuNPBoro) were characterized using different techniques. Coating was performed by two methods: Modification during MOF synthesis and modification after MOF preparation.

Fig. 1 A shows the Raman spectrum obtained for the pure MOF HKUST-1 and HKUST-1 with post-synthesis modification with the different gold nanoparticles. The appearance of some bands indicating the presence of nanoparticles in the MOF was observed, such as the ring breathing mode appearing at 1006 cm⁻¹ in the band of HKUST-1 already shifting to 1025 cm⁻¹ in the spectra of the modified MOF, or the two bands related to C-C stretching appearing at 1580 and 1605 cm⁻¹ in the spectrum of pure HKUST-1, while these bands shift to 1610 and 1630 cm⁻¹, respectively, in the modified MOF.

Fig. 1 B shows the X-ray diffractogram of the samples modified by post-synthesis with the different nanoparticles. The peaks attributed to the AuNPs can be seen in the diffractograms of the modified samples. An important aspect is the difference between the diffractograms of the pure and the modified HKUST-1. The diffractograms of the modified samples show the same profile but they are clearly different from those of the pure sample. In infrared analysis, the spectra of the samples are identical, indicating that polymorphism has occurred after post-synthesis modification.

Figure 1: Comparative Raman spectra (A) and X-ray diffraction patterns (B) of pure and modified HKUST-1 compounds.



Agradecimentos/Acknowledgments

UFJF, CAPES, FAPEMIG, CNPq.

Molecularly imprinted optical sensor for the determination of glyphosate

Cristiane Dos Reis Feliciano (PG)¹, Taylor Marques (IC)¹, Luciano Sindra Virtuoso (PQ)¹, Mariane Gonçalves Santos (PQ)¹.

crisfeliciano2018@gmail.com; crisfeliciano2018@gmail.com

¹Departamento de Química, UNIFAL;

Palavras Chave: Glifosato; Polímeros Molecularmente Impressos; Pontos Quânticos; Nanopartículas Magnéticas.

Highlights

- Glyphosate is the most widely used herbicide to control weeds in various crops.
- A composite material, capable of selectively extracting and concomitantly detecting glyphosate residues was synthesized based on the molecularly imprinted polymers (MIPs) technology and using CdTe quantum dots (PQs) and magnetite nanoparticles (NPMs) to generate fluorescent and magnetic properties, respectively.
- The obtained composite presented great potential for use as an optical sensor.

Introdução

O glifosato é o herbicida mais utilizado mundialmente. Dentre os seus efeitos adversos, destaca-se a carcinogênese provocada pela exposição crônica. Assim, surgiram preocupações relativas à saúde humana decorrentes da exposição alimentar. O monitoramento e determinação de sua concentração nas mais diferentes matrizes alimentares, são realizados por técnicas analíticas de alto custo, que demandam tempo e mão de obra qualificada. Além disso, por se tratar de uma molécula altamente polar, muitas vezes é necessária uma etapa de prévia de derivatização antes da determinação cromatográfica¹.

Dessa forma, a produção de um material compósito capaz de extrair e concomitantemente detectar seletivamente os resíduos de glifosato em matrizes complexas, como alimentos, de forma prática, com alta sensibilidade, por meio de técnicas analíticas simples é desejável². Neste sentido, o objetivo deste estudo foi produzir um compósito com propriedades fluorescentes e magnéticas baseado na tecnologia de impressão molecular para ser usado como sensor para a determinação de glifosato por fluorimetria.

Resultados e Discussão

Os PQs de CdTe revestidos com ácido tioglicólico, foram sintetizados pela metodologia one-pot em meio aquoso. A síntese das NPMs foi realizada pelo método de co-precipitação. O preparo do compósito foi realizado pelo método sol-gel, in situ utilizando o processo Stöber para a impressão molecular na superfície das nanopartículas, utilizando como molécula molde o padrão de glifosato, obtido da Sigma Aldrich®. O material obtido foi denominado PQs-NPMs-MIP. Após, o compósito foi revestido com quitosana, obtendo-se os PQs-NPMs-MIP-QS. Em seguida, os materiais foram caracterizados por espectroscopia na região do infravermelho e potencial zeta, possibilitando a confirmação da presença da camada de quitosana e o incorporamento dos PQs de CdTe e das NPMs.

Posteriormente, foram realizados os testes iniciais de sensibilidade do compósito à presença do glifosato. Observou-se que os PQs-NPMs-MIP provocavam um aumento da fluorescência quando ligados ao analito, enquanto os PQs-NPMs-MIP-QS, geravam a supressão da fluorescência quando adsorviam o glifosato. Isso ocorreu, provavelmente, devido a uma grande densidade de grupamentos amina nos PQs-NPMs-MIP, provenientes do (3-aminopropil)trióxido de silano usado como monômero funcional, gerando um efeito de "FRET"³ na presença de glifosato. O revestimento com quitosana, por sua vez, resultou num efeito de "quenching" devido ao recobrimento de parte dos grupamentos amina. Além disso, um estudo sobre o tempo necessário para a interação analito-compósito foi realizado em tempos de 0 – 10 minutos. Os resultados demonstraram que a adsorção é imediata, aumentado até atingir a saturação do compósito. Ademais, estudos preliminares de linearidade demonstraram bons resultados.

Conclusão

Conclui-se com as análises realizadas até o momento que os compósitos obtidos se mostraram promissores para a detecção de glifosato em diferentes amostras de forma prática, rápida e com alta sensibilidade, podendo ser empregados como sensores ópticos.

Referência

1 RIGOBELLO-MASINI, M. *et al* *Chromatographia*, v. 82, n. 8, p. 1121–1138, 2019.

2 ZHANG, X. *et al*. *Polymers*, v. 11, n. 7, 2019.

3 GUO, J. *et al*. *Talanta*, v. 125, p. 385-392, 2014.

Agradecimentos/Acknowledgments

CAPES, FAPEMIG, CNPQ

MoS₂ and AuNPs: *in situ* nanocomposites through liquid-liquid interfacial route

Carla R. Klimpovuz (PG),¹ Marcela M. Oliveira (PQ),² Aldo J.G. Zarbin (PQ)^{1*}

carlaklimpovuz@ufpr.br; aldozarbin@ufpr.br

¹Department of Chemistry, UFPR; ²Academic Department of Chemistry and Biology, UTFPR.

Key Words: *Thin Films, Plasmon Band, Metal Nanoparticles, 2D Materials, Plasmonic Nanocomposites*

Highlights

Synthesis of nanocomposites between MoS₂ and AuNPs in a single step. Using the liquid-liquid interfacial route, we obtained thin films of nanocomposites in a simple way and under ambient conditions.

Abstract

Combining the optical properties of plasmonic nanoparticles with the electronic and mechanical properties of two-dimensional materials is the aim of this work. We describe the *in situ* production of nanocomposites between molybdenum disulfide (MoS₂) and gold nanoparticles (AuNPs). The synthesis of nanocomposites occurred spontaneously, in a single step and under ambient conditions. Nanocomposites were obtained and processed in a two-phase system consisting of water, toluene and precursors, resulting in interfacial films. These thin films could be deposited on the most diverse substrates, depending on the purpose of the analysis or application.¹ We obtained different nanocomposites only by varying the synthesis parameters and the proportion between the precursors. Samples were characterized by UV-Vis and Raman spectroscopy, FTIR, XRD, SEM and TEM. The characterizations indicated the spontaneous formation of AuNPs in different shapes and sizes depending on the nanocomposites. Systems consisting of a 3:1 ratio of metallic precursor to exfoliated MoS₂ result in films of different colors – coming from AuNPs of different sizes – depending on the reaction time (24h, 48h or 70h). In addition, a change in the morphology and structure of MoS₂ was observed after its reaction with the metallic precursor. When the synthesis was conducted in smaller proportions of metallic precursor to MoS₂, there was also the formation of AuNPs, but the structural properties of MoS₂ were better preserved. Additional spectroscopic characterizations, such as XPS, are being conducted to elucidate the mechanism of nanocomposite formation in the interfacial system.

[1] Zarbin, A. J. G. Mater. Horiz. 2021, v. 8, p. 1409.

Acknowledgments

CNPq, CAPES, INCT Nanocarbono, INCT-NanoVida and CME-UFPR.

Mudança de fases de PVDF pela presença de HAp incorporada na matriz polimérica

Júnio A.R. Pasqual (PG),^{1*} Carla C. Schmitt (PQ),^{1,2.}

junio.pasqual@usp.br; carla@iqsc.usp.br (do autor que submete E do autor principal, separados por;)

¹Departamento de Engenharia de Materiais, USP-São Carlos; ²Departamento de Físico-Química USP-São Carlos.

Palavras-Chave: Biomateriais, Hidroxiapatita, Poli(fluoreto de vinilideno), Formação de fases.

Highlights

Phase change of PVDF due to the presence of HAp incorporated into the polymeric matrix.

Research using HAp and three types of PVDF for a composite biomaterial verified HAp as a possible β -phase former for PVDF1015 and PVDF5140, thus facilitating its use as a biomaterial.

Resumo/Abstract

Estudos voltados para o bem-estar da população se mostram cada vez mais necessários tendo em vista o aumento recorrente da expectativa de vida. Esse fenômeno é um indicador da tendência de aumento da casos de doenças comuns a população idosa como, por exemplo, osteoporose[1]. Para aumentar a qualidade de vida desse grupo são feitos estudos buscando desenvolvimento de materiais biocompatíveis passíveis de promoção de regeneração óssea [2]. As pesquisas nessa área investigam a obtenção de materiais semelhantes aos encontrados no corpo humano e que apresentem comportamento osteogênico interessante para que o organismo vivo se recupere de maneira satisfatória, numa abordagem minimamente evasiva. A hidroxiapatita (HAp) e o poli(fluoreto de vinilideno) (PVDF) são materiais comumente utilizados para aplicações biomédicas por possuírem propriedades atraentes quando em contato com o tecido vivo [2], [3]. No trabalho proposto foram obtidas membranas compostas de HAp e diferentes tipos de PVDF a fim de verificar a influência da variação da presença do material cerâmico na formação das fases desse polímero que é utilizado como matriz para o compósito proposto. Os polímeros PVDF1015, PVDF5140 e PVDF6008 possuíam viscosidade e densidade diferentes e foram utilizados na forma de pellets ou pó. As análises realizadas foram por FTIR e DRX para verificação da formação da fase β por ser a mais interessante para aplicações de PVDF como biomaterial. Ao final, observou-se que a presença da HAp facilita a formação da fase β para o PVDF1015 e PVDF5140, onde se observou aumento de aprox. 1% na formação dessa fase para uma proporção 90/10 PVDF/HAp. Para o PVDF6008 observou-se uma redução de aproximadamente 9,54% na porcentagem e fase β , mostrando-se um material de menor interessa para aplicações médicas coincidindo com uma menor formação de cadeias na posição CIS. A presença de HAp mostrou uma possível maior influência com relação ao grau de cristalinidade para o PVDF6008, resultando em um aumento de cristalinidade de aproximadamente 22,3%. Observou-se que dos três tipos, o PVDF5140 se apresentou como o mais indicado para obtenção de matriz polimérica de fase β , ou seja, mais indicada para utilização como biomaterial. Mais comparações de concentrações diferentes estão em curso.

[1] J. Zhou et al., "Biomaterials and nanomedicine for bone regeneration: Progress and future prospects," *Exploration*, vol. 1, no. 2, p. 20210011, Oct. 2021, doi: 10.1002/EXP.20210011.

[2] A. Carter, K. Popowski, K. Cheng, A. Greenbaum, F. S. Ligler, and A. Moatti, "Enhancement of Bone Regeneration Through the Converse Piezoelectric Effect, A Novel Approach for Applying Mechanical Stimulation," *Bioelectricity*, vol. 3, no. 4, p. 255, Dec. 2021, doi: 10.1089/BIOE.2021.0019.

[3] L. Wu et al., "Recent advances in the preparation of PVDF-based piezoelectric materials," *Nanotechnology Reviews*, vol. 11, no. 1. De Gruyter Open Ltd, pp. 1386–1407, Jan. 01, 2022. doi: 10.1515/ntrev-2022-0082.

Agradecimentos/Acknowledgments

Os autores agradecem à CAPES pelo apoio financeiro e à Solvay pela doação dos polímeros necessários ao desenvolvimento da pesquisa. Também a todos pela participação e ajuda durante os experimentos e caracterizações.

Multifunctional hydrogels based on guar gum and chitosan as antibacterial and anti-inflammatory skin wound dressing

Matheus X. Oliveira (PG),¹ Francisca Vanessa C. Canafístula (PG),¹ Fábio Oliveira S. Ribeiro (PG),² Alyne R. de Araújo (PQ),² Iásly C. Lima (PG),³ Ana Maria S. Assrey (PQ),³ Judith Pessoa A. Feitosa (PQ).¹

judith@dqoi.ufc.br; matheuxaviero@alu.ufc.br

¹Departamento de Química Orgânica e Inorgânica, UFC; ²Centro de pesquisa em Biodiversidade e Biotecnologia, UFDPAr; ³Instituto Superior de Ciências Biomédicas, UECE.

Keywords: Wound dressings, Chitosan, Galactomannan, Antibacterial, anti-inflammatory action

Highlights

Hydrogel is injectable, self-healing, adhesive, cytocompatible, anti-inflammatory and antibacterial against *S.aureus* resistant. Raw materials are available and inexpensive. Excellent wound dressing

Resumo/Abstract

The skin represents the first mechanical barrier for body protection against harmful agents. According to WHO, millions of people suffer from pathologic wounds, and the required medical care costs will be \$35 billion in 2023. Effective dressings need to be developed primarily based on natural polymers. The depolymerized guar gum after oxidation in three degrees (20, 35, 50%) form hydrogels when mixed with *N*-succinyl chitosan aqueous solution by Schiff base reaction. The hydrogels were characterized by FT-IR, rheological properties, swelling, degradation in PBS at 37°C, and also morphology. Gelation time assure the classification of injectable for all hydrogels. The swelling degree in PBS is in the range of 26-35 g of fluid/g gel. The pore size distribution is heterogeneous with pore varying from 67 to 93 μm. All hydrogels degrade in PBS solution, but still remain around 40% of initial mass after 28 days. In addition, the material is flexible, self-repairing, adhesive and cytocompatible. The innate antibacterial action was confirmed against gram-positive (*Staphylococcus aureus*, *Staphylococcus epidermidis*, *Staphylococcus aureus* - MRSA) and gram-negative (*Escherichia coli*) bacteria. AFM images illustrated morphological changes in *S. aureus* - MRSA (methicillin-resistant) strain in contact with Gel. The *in vivo* assays performed with gel with DGG with degree of oxidation 50% showed that the hydrogel has anti-inflammatory action being able to accelerate the healing process, restoring around 99% of tissue with capillary deposition at 14 days. are excellent candidates to be used as wound healing dressing.

Hydrogel characteristics



Agradecimentos/Acknowledgments

CAPES, CNPq, FUNCAP, UFC, UECE, UFDPAr, INCT-Polysaccharide INCT-Inomat

Yang, Y., Liang, Y., Chen, J., Duan, X., & Guo, B. (2022). *Bioactive Materials*, 8, 341–354.
Gushiken, L. F. S., Beserra, F. P., Bastos, J. K., Jackson, C. J., & Pellizzon, C. H. (2021). *Life*, 11(7), 1–15.
Weng, H., Jia, W., Li, M., & Chen, Z. (2022). *Carbohydrate Polymers*, 294, Artigo 119767.
Ansari, M., Meftahizadeh, H., & Eslami, H. (2022). *Chemical Papers*, 76(3), 1513–1524.

Nanobiointeractions of quantum dots with Zebrafish liver cells: Synthesis, biomolecular corona formation and toxicity assessment

Milena L. Brito (PG)^{1,2}, Matheus P. Baptista (IC)¹, Juliana D. Oliveira (PD)¹, João B. S. Júnior (PQ)¹, Diego S. T. Martinez (PQ)^{1,2*}

milenalb@usp.br; diego.martinez@innano.cnpem.br

¹Laboratório Nacional de Nanotecnologia (LNNano), Centro Nacional de Pesquisa em Energia e Materiais (CNPEM), Campinas/SP.

²Centro de Energia Nuclear na Agricultura (CENA), Universidade de São Paulo (USP), Piracicaba/SP.

Keywords: Nanotoxicology; Protein Corona; Luminescent Nanomaterials, Nanosafety.

Highlights

CdSe@CdS@SiO₂ quantum dots were synthesized and well-characterized for toxicity studies.

The biomolecular corona modulates the nanoparticles' biological identity and its nanobiointeractions and toxicity.

The QDs showed low toxicity to Zebrafish liver cells in the presence of fetal bovine serum (FBS)-corona.

Abstract

Quantum dots (QDs) of CdSe and CdS are semiconductor nanoparticles that show deeply interesting optical and electrical properties for several technological applications¹. Although some toxicological parameters of QDs have already been determined by *in vitro* and *in vivo* assays¹, the complete characterization of the biological identity that these nanoparticles assume in contact with biomolecules present in complex biological media is still lacking^{2,3}. The Zebrafish is frequently used as a biological model in environmental and human health research. Here, we proposed a three-step synthesis of a QD/silica core@shell system – CdSe@CdS@SiO₂ QDs, and their complete solid state and colloidal characterization for toxicological studies. We performed the *in vitro* toxicological assessment of QDs in Zebrafish liver cell line (ZFL) linked to the biomolecular corona formed on the particle' surface in cell culture medium in presence and absence of fetal bovine serum (FBS). To that, we performed the incubation of the QDs in the RPMI/L-15 culture medium, supplemented with 10% FBS. This step allows the protein coronas formation on the particle surface, like the biological functionalization that happens in the regular *in vitro* assays' conditions. This whole characterization enables the description of affinity relationships between colloidal and biological entities. Also provides essential information to establish the QDs biological identity, their toxicological responses, and cellular effects in the Zebrafish *in vitro* assays; an important step towards establishing the Safe-by-Design concept. The synthesized quantum dots showed colloidal stability in deionized water, with 36 nm diameter (by transmission electron microscopy) and 86 nm hydrodynamic diameter (by dynamic light scattering), the surface electrophoretic potential of -33 mV, and emit electromagnetic radiation at 602 nm (visible light – red region). Cell viability assays (MTT, Alamar Blue, and Neutral Red) demonstrated that QDs did not show a toxicity effect greater than 30% to ZFL cells, at concentrations between 0.5 to 250 µg.mL⁻¹ in the presence of FBS in the medium. The characterization of FBS-coronas by polyacrylamide gel electrophoresis demonstrated that the more than 20 proteins (from 10 to 245 kDa) are present and have a strong affinity for the particle surface. Finally, experiments to monitor the FBS-coronas' evolution and their respective cellular effects, internalization and toxicity mechanisms³ are being designed to compose a knowledge database involving a complete characterization of QDs during *in vitro* toxicity assessments towards understanding and controlling the nanobiointeractions for safer applications of this promising luminescent nanoparticles in materials science and biotechnology¹.

References

- (1) Oh, E.; Liu, R.; Nel, A.; Gemill, K. B.; Bilal, M.; Cohen, Y.; Medintz, I. L. Meta-Analysis of Cellular Toxicity for Cadmium-Containing Quantum Dots. *Nat Nanotechnol* **2016**, *11* (5), 479–486. <https://doi.org/10.1038/nnano.2015.338>.
- (2) Dawson, K. A.; Yan, Y. Current Understanding of Biological Identity at the Nanoscale and Future Prospects. *Nat Nanotechnol* **2021**, *16* (3), 229–242. <https://doi.org/10.1038/s41565-021-00860-0>.
- (3) Paula, A. J.; Silveira, C. P.; Martinez, D. S. T.; Souza Filho, A. G.; Romero, F. v.; Fonseca, L. C.; Tasic, L.; Alves, O. L.; Durán, N. Topography-Driven Bionano-Interactions on Colloidal Silica Nanoparticles. *ACS Appl Mater Interfaces* **2014**, *6* (5), 3437–3447. <https://doi.org/10.1021/am405594q>.

Acknowledgments

CNPq, FAPESP, INCT-Inomat and SisNANO/MCTI

Nanocomposites of graphene, graphene oxide and molybdenum disulfide studied by Scanning Probe Microscopy

Amanda F. Pereira (PG),¹ Ariane Schmidt (PG),¹ Camilla K. B. Q. M. Oliveira (PQ),² Aldo J. G. Zarbin (PQ).^{1*}

amanda.figueiredo@ufpr.br; aldozarbin@ufpr.br

¹Chemistry Department, UFPR; ²Physics Department, UFPR

Keywords: Nanomaterials, Graphene, Molybdenum Disulfide, Microscopy, SPM, AFM

Highlights

The properties of nanomaterials can be investigated through the scanning probe microscopy technique that identifies the possible interactions between materials in nanocomposites.

Abstract

The properties of nanomaterials could be investigated using several techniques, and scanning probe microscopy (SPM) has been relevant in the characterization of these materials. The SPM is able to meticulously investigate the different characteristics between the materials of a nanocomposite in addition to verifying the topography (morphology, thickness and roughness) of the samples' surface, thus identifying the origin of the most diverse properties of these materials.¹ In this work, the SPM was used to characterize nanocomposites containing graphene oxide (GO), reduced graphene oxide (rGO), chemical grapheme (GR) and molybdenum disulfide (MoS₂) to study the different properties and the nature of the interaction between the individual components of these nanocomposites. Samples were prepared using the liquid-liquid interfacial route (LLIR)² and they were deposited by film transfer or drop-casting onto Si/SiO₂ and mica substrates. In addition to topographic techniques (contact and dynamic mode), phase contrast microscopy and lateral force microscopy (LFM) were also used to verify the viscoelastic and adhesion properties of the materials, respectively. Furthermore, other characterization techniques were used, such as: UV-Vis spectroscopy, Raman spectroscopy, X-ray diffraction, scanning electron microscopy (SEM), among others, to identify the materials. As a result, rGO, GR and MoS₂ showed more adhesive flakes with the tip than the substrate, while GO presented more adhesive and non-adhesive flakes depending on the sheet size as observed by LFM, and this could be due to the Puckering effect that depends on compression and shear. While in terms of viscoelastic properties, both GO and rGO flakes are harder than the substrate, while MoS₂ is softer. Due to the formation of by-products such as iron oxides, GR showed softer regions (graphene) when compared with these oxides. As nanocomposites, MoS₂ presents smaller flakes that decorate the larger sheets of GO, rGO and GR (SEM and SPM). These have harder and less adhesive characteristics than MoS₂ and this one that is found around the graphene sheets presents a slight modification in the adhesion and viscoelastic properties than the flakes that are only found on the substrate, an indication of the difference in properties between the MoS₂-graphene and MoS₂-substrate interaction. Finally, the spectroscopy techniques prove the formation of the nanocomposite, with characteristic bands of MoS₂ and graphene (UV-vis and Raman) and their characteristic peaks (XRD). Through this study we can elucidate the possible interactions between graphene and MoS₂ and which of these interactions can interfere in the properties of the material obtained.

1. VAZIRISERESHK, Mohammad R. et al. Nano letters, **19**, 5496-5505, 2019.
2. ZARBIN, Aldo J. G. Materials Horizons, **8**, 1409-1432, 2021.

Acknowledgments

UFPR, CNPq, CAPES, INCT Nanocarbono, INCT NanoVida, CME-UFPR.

Área: MAT

Nanocomposites of polyaniline and molybdenum disulfide prepared by liquid-liquid interfacial route (LLIR) for application in photovoltaics

João Victor Gonçalves (IC)¹, Amanda F. Pereira (PG)¹, Aldo J. G. Zarbin (PQ).^{1*}

joao.victorzg06@gmail.com; aldozarbin@ufpr.br

¹Departamento de Química, UFPR

Palavras Chave: Nanomaterials, Molybdenum Disulfide, Conducting Polymers, Photovoltaics.

Highlights

Study of the preparation and properties of MoS₂/PAni nanocomposite thin films by LLIR, and their suitability for application as components in more eco-friendly and sustainable photovoltaic devices.

Resumo/Abstract

Over the past few years, molybdenum disulfide (MoS₂) has been researched as a potential new material for photovoltaic devices; It's relatively easy processability, natural abundance, and lower toxicity, makes it an interesting substitute for the largely utilized photovoltaic materials, such as Indium-Thallium Oxide (ITO), and Platinum (Pt) ¹. Furthermore, conjugated conducting polymers, such as Polyaniline (PAni), have been heavily reported to enhance electric properties of materials when synthesized as composites ².

With that, in this work, thin films of MoS₂/PAni nanocomposites were successfully synthesized by liquid-liquid interfacial route (LLIR)³, utilizing the interface between toluene and two different aqueous phases (HCl and H₂SO₄ solutions), and Ammonium Persulfate (APS) as the oxidizing agent for the interfacial polymerization of aniline. Both films were characterized by UV-Vis Spectroscopy, X-ray Diffractometry and Scanning Electron Microscopy (SEM).

Initial comparisons of both films reveal that the two acids contribute to the formation of films with different morphology and thickness, as well as polymer stability regarding pH changes. Further dissimilarities were found comparing the UV-Vis spectra, pointing to a small divergence in the final structure of the composites. Future studies regarding the difference in electrical properties of the two films are to be conducted, aiming to determine whether they are suitable as photovoltaic components, and if so, which acid solution produces the more interesting material for such.

¹ SINGH, Eric et al. ACS Appl. Mater. Interfaces, **9**, 3223–3245 (2017).

² SALVATIERRA, Rodrigo V., ZARBIN, Aldo J. G. Chem. Mater., **22**, 5222-5234 (2010).

³ ZARBIN, Aldo J. G. Materials Horizons, **8**, 1409-1432 (2021).

Agradecimentos/Acknowledgments

UFPR, CNPq, CAPES, INCT Nanocarbono, GQM-UFPR.

Área:

MAT

(Inserir a sigla da seção científica para qual o resumo será submetido. Ex: ORG, BEA, CAT)

Non-Destructive Test for Sigma Phase Quantification in UNS S32760 Super Duplex Stainless Steel: LSV-KOH as a New Methodology

Marcelo T. G. de Sampaio (PG)^{1*}, Anderson B. Furtado (PG)¹, Marcelo D. C. Ignácio (IC)¹, Sergio S. M. Tavares (PQ)², Juan M. Pardal (PQ)², André R. Pimenta (PQ)²⁻³ e Eduardo A. Ponzio (PQ)¹

Marcelo_sampaio@id.uff.br

¹ Laboratório de Materiais da UFF (G₂E/LaMUFF), Instituto de Química, Universidade Federal Fluminense, Niterói, Rio de Janeiro, Brasil; ² Programa de Pós-Graduação em Engenharia Mecânica e Montagem Industrial, Universidade Federal Fluminense, Niterói, Rio de Janeiro, Brasil; ³ Laboratório de Instrumentação e Simulação Computacional LISCOMP, Instituto Federal do Rio de Janeiro, Paracambi, Rio de Janeiro, Brasil

Keywords: Super Duplex Stainless steel, Sigma Phase, LSV-KOH, Non-Destructive Test

Highlights

Non-Destructive test for Sigma Phase quantification. Linear correlation between electrochemical and optical microscopy analysis. Deepening in microstructure analysis and morphology.

Resumo/Abstract

One of the main problems that these high alloyed stainless steels like super duplex stainless steel (SDSS) can undergo are deleterious phases (DP) precipitation. Sigma, chi, nitrides and carbides are some of DP that can be present in a SDSS. DP can precipitate in a range of 700-1000°C, that usually occurs during fabrication process, welding or operation. The appearance of these DP impairs the properties of the alloy once these phases are Cr-rich and generate nanometric Cr-depleted regions around them. In context of UNS S32760 super duplex stainless steel, the effect of W addition in DP phases precipitation is a study subject. what can be observed is that no agreement of W addition effect on DP precipitation. Some studies show a faster precipitation Kinect than a W free specimen. Meanwhile, other researchers found that W would stabilize chi phase which retards sigma phase precipitation. Torres et al. (1) demonstrated that a 2.1% of W retard its precipitation. Specifically, for 0.7% of W would have an effect that promote sigma phase precipitation. The main objective of this present work was expanding the application of a previous optimized LSV-KOH test for quantification of deleterious phases, especially sigma phase, in super duplex stainless steels. In this case, deleterious phases present in 7 heat-treated specimens of UNS S32760 SDSS were quantified by quantitative metallography using optical microscopy and then the sigma phase volume fractions were plotted versus the current density obtained in LSV-KOH. A calibration curve with a linear regression coefficient of 0.97 was obtained. For comparison the electrochemical quantification was performed in three different solutions widely used in the classical DL-EPR and the best linearity was 0.52. Besides, other investigations were carried out in the surface of the specimens after both electrochemical tests (LSV-KOH and DL-EPR). Atomic force microscopy shown that after DL-EPR test sigma boundaries was deeply attacked as expected, but how this region not necessarily has the same volume fraction of sigma phase DL-EPR normally present inconsistencies with sigma phase amount. In other way, after LSV-KOH we can see an intense growth of the passive film over the phase sigma region. This phenomenon is correlated to Cr and Mo dissolution and a Ni film enrichment (2) that was observed in SEM/EDS analysis. In this way, we can conclude that the LSV-KOH test is more accurate than the DL-EPR test, since the electrochemical response is directly linked to the dissolution of chromium in it, unlike what occurs in the DL-EPR.

(1) Torres, C. et al *Journal of Electrochemical. Society*, 167, 081510, 2020

(2) De Sampaio, M. T. G., et al. *Corrosion Engineering, Science and Technology*, p. 1-11, 2022

Agradecimentos/Acknowledgments



Novel process for production of niobium carbide nanoparticles

Tiago Serodre (PG),¹ Jordan J. Silva (IC),² Clascídia A. Furtado (PQ),¹ Luiz G. O. L. Cançado (PQ),² tms@cdtn.br;

¹Centro de Desenvolvimento da Tecnologia Nuclear; ²Departamento de Física UFMG

Palavras Chave: *Niobium, Graphene, Carbides, High energy milling*

Highlights

Niobium carbide nanoparticles were produced by mechanochemical means using graphene and graphite nanoparticles as carbon sources, and ferroniobium as the niobium source.

Resumo/Abstract

Niobium carbide is a refractory metallic carbide with a very high hardness, melting point exceeding 3800 °C and great chemical stability, not to mention its relatively high electrical conductivity for a ceramic material[1-3]. We describe herein the production of niobium carbide nanoparticles (NbCNP) by mechanochemical means using graphene and graphite nanoparticles as carbon sources, and ferroniobium as the niobium source. The resulting nanoparticles were analysed by X-ray diffraction, transmission electron microscopy, Raman spectroscopy and dynamic light scattering. The nanoparticles were shown to be highly crystalline, with crystal structures consistent with NbC and Nb₆C₅ structures and stoichiometries. The size of the particles was measured to be distributed around 20 to 200 nm. The nanoparticles can be dispersed in aqueous solutions with the aid of surfactants. This property, coupled with their high surface area inherent from their nanoscale, and the aforementioned electrical, chemical and mechanical properties of niobium carbide make NbCNP promising candidates in applications such as batteries, composites and catalysts.

[1] T. Amriou, et al., Phys. B Condens. Matter, vol. 325, pp. 46–56, Jan. 2003

[2] B. Sustarsic, et al., Vacuum, vol. 71, no. 1–2, pp. 77–82, May 2003

[3] L. Wu, et al., J. Alloys Compd., vol. 561, no. April 2018, pp. 220–227, Jun. 2013.

Agradecimentos/Acknowledgments

CAPES, CNPQ, INCT Nanomateriais de Carbono, CNEN, UFMG

Novel rare earth fluorides TiO₂ based composites for photocatalytic applications via upconversion process

Daniel E. B. Moreira (PG)*, Paulo C. de Sousa Filho (PQ)² and Juliana F. Lima (PQ)¹

daniel.estevesbm@gmail.com;

¹ Universidade do Estado do Rio de Janeiro, Instituto de Química, FotoNano

² Universidade Estadual de Campinas, Instituto de Química

Key words: titanium dioxide, rare earths, photocatalysis, upconversion

Highlights

- Organic pollutants are increasing, and alternative treatments are needed
- Photocatalysis is a AOP that uses light to degrade organic molecules, such as dyes
- Semiconductors are usually activated by ultraviolet (UV) radiation (5% of overall solar energy)
- Solar spectrum is majorly composed of Near Infrared Radiation (NIR)
- Upconversion converts low energy photons into higher ones
- Coupling photocatalysts with upconversion materials might be the perfect solution

Resumo/Abstract

Heterogeneous photocatalysis has recently been studied as a promising alternative method used to break organic pollutant molecules into harmless H₂O and CO₂. However, typical photocatalysts, such as TiO₂, are only active at ultraviolet region, while only 5% of solar energy is composed of UV light. Therefore, scientist have been proposing alternatives such as doping with metal ions or non-metal elements aiming to shift the bandgap energy (E_g) to visible radiation. Nevertheless, even if doping effectively transfer E_g to visible wavelengths, solar energy is majorly composed of near infrared radiations (NIR), which corresponds to ~50%. In this scenario, materials with upconversion (UC) emissions might be the perfect solution. Being a hot topic in materials science since 2000s, upconversion nanoparticles are responsible for converting low energy photons, such NIR ones, into energetic UV/visible photons. Therefore, coupling photocatalysts with Ln-based UC nanoparticles can generate a novel composite which will be responsible for a great enhancement of nearly the entire solar radiation. Thus, this work is divided into two approaches, that are the sol-gel based synthesis and characterization of X-TiO₂ (X = Ce(III) or N), and the synthesis and characterization of NaYF₄:TR³⁺ (TR³⁺ = Yb³⁺, Nd³⁺, Tm³⁺, Er³⁺), the UC materials. Here we reported the first part, materials containing different amount of Ce or N were characterized by DRX and SEM; the results are shown in figures 1 and 2, respectively.

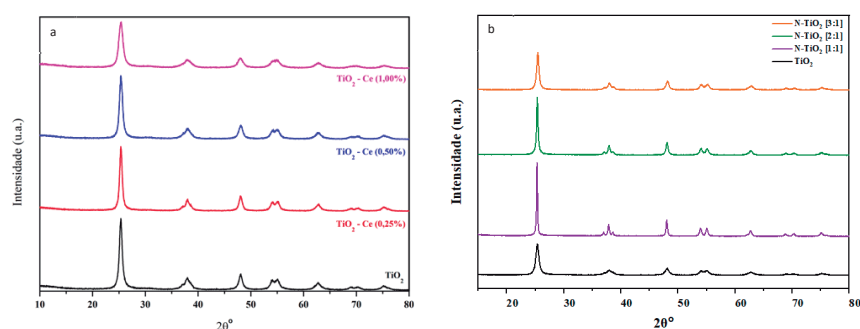


Figure 1: X-Ray results obtained for TiO₂ modified with cerium (a) and nitrogen (b)

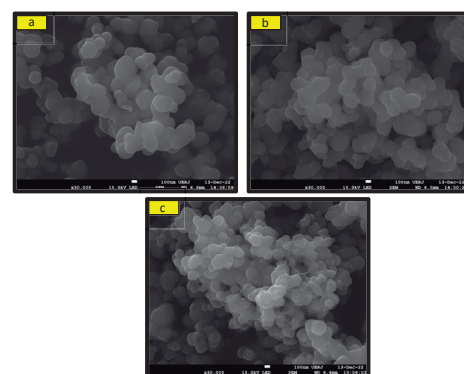


Figure 2: SEM analysis for N-TiO₂ doped with the N:Ti ratio of 1:1 (a), 2:1 (b) and 3:1 (c).

1. Asif, M.; Zafar, M.; Akhter, P.; Hussain, M.; Umer, A.; Razzaq, A.; Kim, W.-Y.; *Applied Sciences* **2021**, *11*, 8264.
2. Wu, Y.; Chan, S. Y.; Xu, J.; Liu, X.; *Chem. Asian J.* **2021**, *16*, 2596.

Agradecimentos/Acknowledgments

FAPERJ, FAPESP, CAPES, CNPq e UERJ.

One-pot three-step synthesis of core cross-linked star polymers featuring palladium nanoparticles

Tanize Bortolotto (PQ),¹ Gabrielly E. Neumann (PG),¹ Suelen G. Trindade (PQ),¹ Vanessa Schmidt (PQ),¹ e Cristiano Giacomelli (PQ),¹

cgiacomelli@ufsm.br

¹Departamento de Química, UFSM.

Palavras-Chave: *Star polymers, Radical polymerization, Capping agents, Palladium nanoparticles.*

Highlights

Particles behaving as highly hydrated unimolecular single objects (so-called nanogels), featuring a water-soluble polymer at the outer shell and an either compact or swollen core, can be synthesized using a cost-effective and environmentally friendly one-pot polymerization approach.

Resumo/Abstract

This study shows that polymer nanogels (well-defined core cross-linked star – CCS – polymers behaving as highly hydrated unimolecular objects) can be synthesized by activators regenerated by electron transfer atom transfer radical polymerization (ARGET ATRP) method with sequential addition of monomers in a one-pot process.

The CCS polymers are formed by cross-linking of preformed macroinitiators via polymerization in a convergent fashion (arm-first star polymer synthesis method). Although the CCS macromolecule is structurally complex, the synthetic method is really simple. We here demonstrate that core functionalization is easy and straightforward, thus leading to particles in which specific intermolecular interactions define their use as cargo vectors or reactors through which reactants and products of organic reactions can diffuse without big constraints.

The main issue encountered in this process was the macromolecular characterization. The reaction mixture at the end of the third step is rather complex, and separation was quite difficult because polymer chains have similar solubility properties. Therefore, we relied on the combination of data obtained from different techniques, mainly ¹H NMR, GPC and DLS, to attest the identity of CCS samples.

The possibility of using these complex structures as nanoreactors was confirmed in a second step. Palladium acetate was reduced with sodium borohydride to obtain the ready-to-use catalyst (~ 25-nm nanogel structures containing ~ 7-nm palladium nanoparticles), which catalytic activity was particularly remarkable in both p-nitrophenol reduction and Suzuki cross-coupling reactions. The results were dependent on macromolecular composition and architecture, metal nanoparticle size and distribution.

One of the most important features of materials investigated here is the cost-effective, environmentally friendly polymerization approach because it uses very low copper concentrations, it does not require stringent experimental conditions (it is, in fact, tolerant to reactants impurities and can even be performed in air), and it is suited for industrial scale up.

Agradecimentos/Acknowledgments

The authors acknowledge financial support from CNPq, CAPES and FAPERGS.

Optimization, characterization and molecular modeling of electrospun membranes of poly(vinyl alcohol) with different degrees of hydrolysis

Ariane Regina de Souza Rossin* (PG),^{1,2} Gabriel Nardi Fraga (PG),^{1,2} Vinicius Martinelli (PG),¹ Josiane Caetano (PQ),² Wilker Caetano (PQ),¹ Douglas Cardoso Dragunski,^{1,2} (PQ)

ariane.rossin@gmail.com; dcdragunski@gmail.com

¹Department of Chemistry, UEM; ²Center of Engineering and Exact Sciences, UNIOESTE

²Centro de Engenharias e Ciências Exatas, Unioeste, Rua da Faculdade, 645 CEP - 85903-000 - Toledo -PR.

Palavras Chave: Polymer molecular modeling, Crosslinking, Rheology

Highlights

Optimization, characterization and molecular modeling of electrospun membranes of poly(vinyl alcohol) with different degrees of hydrolysis

- The different degrees of poly hydrolysis (vinyl alcohol) are studied for application in electrospinning;
- Molecular modeling was used to predict more stable conformation and structural differences in different hydrolysis degrees of PVA;
- citric acid insertion and F127 were also evaluated for the
- Rheology was used to evaluate solution parameters;
- The results show that PVA₈₇ has a more stable conformation, lower viscosity and consequently a more facilitated fiber formation.

Resumo/Abstract

Poly (vinyl alcohol) (PVA) is a polymer widely studied for its vast applicability and can be obtained in different degrees of hydrolysis and molecular weight. For electrospinning, the use of PVA is widely explored in several segments, including medical and filtering. In many cases, PVA fibers must undergo a process of chemical or physical crosslinking for stability in aqueous medium. Therefore, the study seeks to obtain and characterize PVA fibers with hydrolysis grade of 87 and 99% (PVA₈₇ and PVA₉₉) using citric acid (CA) as a reticulante and Pluronic® - F127 as a drug carrier for possible medical applications. Also, obtain molecular modeling of the PVA/CA/F127 mixture for both degrees of hydrolysis. Initially, rheology and scanning electron microscopy (SEM) were used as a characterization method. For computational modeling, the Hartree-Fock (HF) method with long-range interpretations (HF-3c) was used. Molecular modeling presented data not yet reported in the literature, such as the orientation and disposition of THE among pva chains. The more stable geometry of the molecular structure of PVA₉₉ demonstrates more intra- and inter-chain hydrogen bonds and greater stiffness when compared to PVA₈₇. The interaction of F127 with the polymer is dependent on the degree of hydrolysis. Rheology has shown that the degree of hydrolysis is an important factor for the solution to be electrospun, since characteristics such as viscosity and shear are different. For PVA₈₇ there is the formation of fibers in nanoscale and a reduction in diameter with the insertion of the crosslinking agent. For PVA₉₉, new approaches should be used for fiber formation. The results show that the degree of hydrolysis of PVA is a predominant factor for the formation of fibers in the electrospinning process.

Agradecimentos/Acknowledgments

The authors acknowledge UNIOESTE, UEM and CAPES (Coordination for the Improvement of Higher Education Personnel), for the laboratory structure and financial support.

Ordered mesoporous silicas for potential applications in solid vaccine formulations

Matheus C. R. Miranda (PD),^{1*} Vinicius R. De Jesus, (PG)¹ Carmen M. Nunes (IC),¹ Luana F. Santos (IC),¹ Jessica Soares Cardoso (PG),³ Jéssica A. F. Pedro (PG),² Orlando G. Ribeiro (PQ),³ José L. de Souza Lopes (PQ),² Osvaldo A. Sant'Anna (PQ),³ Marcia C. A. Fantini (PQ),² Aryene G. Trezena (PQ),³ Milene Tino-De-Franco (PQ),³ Tereza S. Martins (PQ).^{1*}

* tsmartins@unifesp.br; mcrmiranda@unifesp.br

¹Departamento de Química, Unifesp; ²Instituto de Física/USP, SP, ³Instituto Butantan
Palavras Chaves/Keywords: SBA-15, Bovine serum albumin, Solid Vaccine,

Highlights

Ordered mesoporous silicas for potential application in the production of solid vaccines.

The study about different incorporation methods is important to lead to the successful development of vaccines that are more efficient and easier to produce and handle.

Resumo/Abstract

The vaccines are widely produced and distributed in liquid form and are administered parenterally through injection either via intramuscular or subcutaneous routes, using needles. This form of vaccine delivery faces some limitations, like needle-stick injuries, poor patient compliance and cold chain storage. Therefore, our research project aims to study vaccines for oral administration. This form will minimize the chance of disease transmission from needle-stick injury and increase patient compliance, as it would be pain-free. However, before using solid vaccines for oral administration, tests with the subcutaneous application were performed. Ordered mesoporous silicas (OMS) have been proposed as vaccine adjuvants due to their properties such as high surface area (above 600 m² g⁻¹), pore volume (from 1 to 5 cm³ g⁻¹), adjustable pores (2-50 nm) and narrow pore size distribution¹. In the present study, the OMS (SBA-15) was added to the phosphate-buffered saline (pH ~ 7.4) solution containing bovine serum albumin (BSA), a protein with antigenic characteristics, that was chosen as the model antigen, in two proportions of BSA:SBA (1:10 and 1:25). The resulting mixture was stirred at room temperature for 24 h, then divided into two parts (A and B). Part 'A' was frozen in a freezer at (- 25 ± 5) °C for 24 h and after lyophilized at - 52 °C, under vacuum (35 µmHg), for 48 h and the Part 'B' the solvent was evaporated in a Drying Oven at 35 °C for two days. The immunogenic materials (SBA-15:BSA_A, and SBA-15:BSA_B) were characterized by several physical-chemical techniques and used in the Immunological assays. Small-angle X-ray scattering measurements showed that all materials present the characteristic reflections [(100), (110), (200), (210), and (300) from pure SBA-15 indicating that the silica mesostructure has been preserved after the incorporation of BSA. Nitrogen adsorption-desorption isotherms measurements showed, for all samples, a decrease in surface area and pore volume, indicating that BSA was incorporated into the SBA-15 mesopores. By thermogravimetric analysis and differential scanning calorimetry curves, all samples exhibited higher thermal degradation temperature than pure BSA. The fluorescence spectrum of tryptophan residues in BSA incorporated into SBA-15 was quite similar to that of the pure BSA, showing the preservation of the aromatic residues, corroborating with the CD data. Circular dichroism (CD) spectra of both samples suggest the preservation of protein secondary structure in the process of incorporation into the SBA-15 mesopores. All immunogenic materials (SBA-15:BSA_A and SBA-15:BSA_B) and pure BSA were injected subcutaneously into BALB/c mice (n=6) groups on days 0 and 40. SBA-15:BSA mixtures (1:10 and 1:25) without undergoing any treatment were also injected. Serum samples were obtained from all mice 30 days after each immunization, and IgG anti-BSA antibodies were detected by Enzyme-Linked Immunosorbent Assay. No significant difference was observed between the untreated and the freeze-dried or evaporated groups. However, all groups containing SBA-15 showed almost 3 times higher in antibody titres than the groups with pure BSA. These facts indicate that none of the BSA incorporation methods interfered with the immunogenicity of the SBA-15:BSA complex. Furthermore, the results showed that SBA-15 increased the immunogenic activity of BSA.

References:

1. A.G.Trezena, P.L.O. Filho, L.C.C. da Silva, C.L.P. Oliveira, J.L.S. Lopes, N.S. Antonio, V.F.B. Dettmann, M.A. Akamatsu, T.S. Martins, O.G.Ribeiro, M.C.A. Fantini, O.A. Sant'Anna, M. Tino-De-Franco. *Biologicals* 80 (2022) 18-26.

Agradecimentos/Acknowledgments

This work was supported by the Sao Paulo Research Foundation (FAPESP) (processes numbers 17/17844-8, 19/08582-5, 22/08360-5, 19/19567-7). C.M.N. and L.F.S also thank CNPq (PIBIC and PIBITI) for grants.

Otimização da síntese de biossensores com nanopartículas de ouro com até 200 nm para detecção de proteínas virais.

Mariana C. Oliveira¹ (IC), Carolina B.P. Ligiero¹ (PQ), Dayenny L. D' Amato¹ (PG), Célia M. Ronconi^{1*} (PQ).

marianacarvalhooliveira@id.uff.br; cmronconi@id.uff.br

¹Departamento de Química Inorgânica, Universidade Federal Fluminense (UFF)

Palavras Chave: nanopartículas de ouro, SARS-CoV-2, imunoenensaio, biossensores, espalhamento de luz dinâmico.

Highlights

Optimization of biosensor synthesis with gold nanoparticles up to 200 nm for detection of viral proteins. The present work aims to study the synthetic conditions for bioconjugated gold nanoparticles synthesis in the range of 100-200 nm for use as light scattering sensors for viruses.

Resumo/Abstract

Doenças virais causam grandes prejuízos para a saúde pública gerando enorme perda de vidas. O controle delas depende em grande parte de estratégias de rastreamento e isolamento dos doentes, como ocorreu durante a pandemia de COVID-19. O desenvolvimento de testes rápidos, baratos e eficientes é de grande relevância, especialmente os testes rápidos de antígeno. Nosso grupo de pesquisa mostrou recentemente^{1,2} que nanopartículas de ouro (AuNPs) com até 130 nm bioconjugadas com anticorpos, detectaram com sucesso a proteína S do vírus SARS-CoV-2, através do aumento do diâmetro hidrodinâmico (ΔD_H) utilizando a técnica de espalhamento dinâmico de luz (DLS) (Figura 1a). Esse método, além de rápido, de boa sensibilidade e reprodutibilidade, também demonstrou que maiores AuNPs resultaram em uma melhor resposta nos ensaios. No presente trabalho estão sendo estudadas as condições para síntese de bioconjugados com AuNPs ainda maiores para verificar o tamanho limite que irá gerar um maior espalhamento sem perdas por espalhamento múltiplo. Na primeira etapa, AuNPs com até 200 nm foram sintetizadas e caracterizadas por espectroscopia na região do UV-Visível, Microscopia Eletrônica de Varredura (MEV) e espalhamento de luz dinâmico (Figura 1b, c, d). A bioconjugação foi realizada com anticorpo policlonal equino anti-S, e foi feito o estudo de algumas condições reacionais como o tipo e a concentração do reagente de ligação cruzada e a concentração do anticorpo. Alguns resultados preliminares dos imunoenensaios são mostrados na Figura 1e.

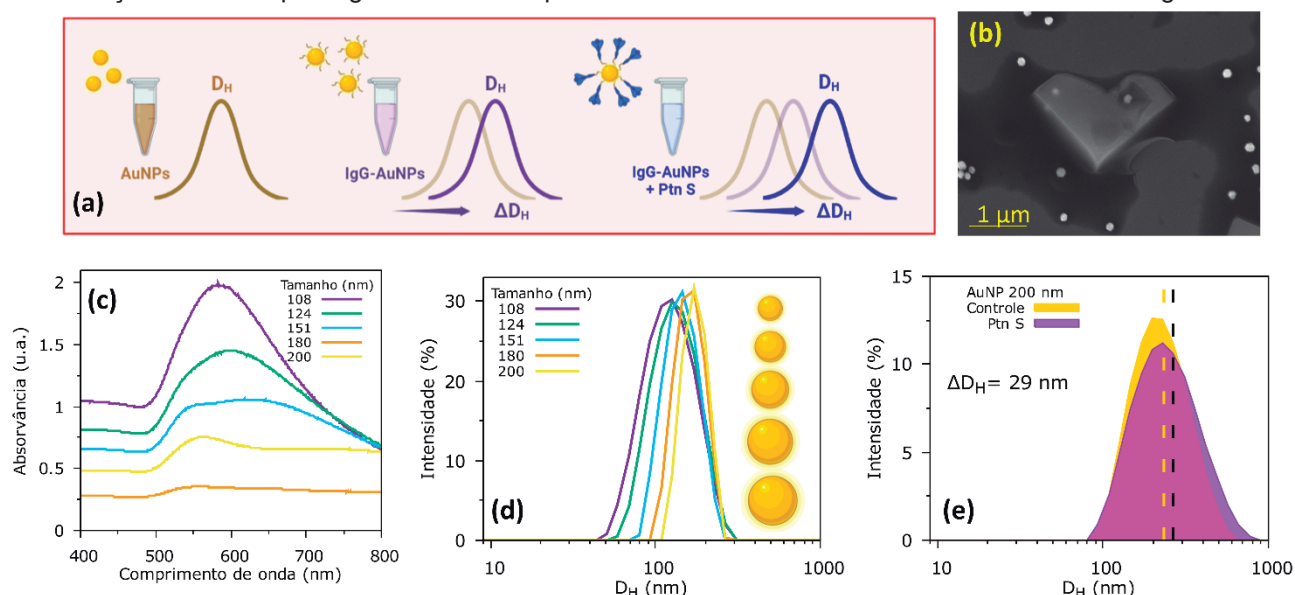


Figura 1: (a) Método de detecção da Ptn S, (b,c,d) caracterização das AuNPs e (e) Imunoenensaio para a detecção de Ptn S.

¹ LIGIERO, C. B. P. et al., *Materials Today Chemistry*, **2022**, 25, 100924.

² SILVA, P.B.S. et al., *Talanta*, **2022**, 243, 123355.

Agradecimentos/Acknowledgments

FAPERJ, CNPq, PPGQ-UFF, LAMATE (UFF), INMETRO, LECC-UFRJ.

Paramagnetic borotungstate glasses – a new magnetic-optical material

Leonardo V. Albino (PG)^{1,2,3}, Thierry Cardinal (PQ)², Marc Dussauze (PQ)³, Frédéric Adamietz (PQ)³, Olivier Toulemonde (PQ)², Véronique Jubera (PQ)², Douglas F. Franco (PQ)¹, Marcelo Nalin (PQ)¹

leonardoalbino63@gmail.com; marcelo.nalin@unesp.br*

¹Laboratório de Vidros Especiais (LaViE), Institute of Chemistry, São Paulo State University (UNESP), Araraquara – SP – Brazil

²Institut de Chimie de la Matière Condensée de Bordeaux (ICMCB), CNRS, UMR 5026, Université de Bordeaux, 33608 Pessac – France

³Institut des Sciences Moléculaires (ISM), CNRS, UMR 5255, Université de Bordeaux, 33405 Talence – France

Palavras Chave: Borotungstate glasses, magnetic-optical materials, lanthanides, Faraday effect

Highlights

- Glasses with high concentrations of lanthanides (> 20 mol%) were synthesized;
- Thermal, structural, optical and luminescent characterizations were carried out;
- Studies and measurements of magnetic and magneto-optical susceptibility were carried out;
- Studies show promising application as magneto-optical materials.

Abstract

Transparent glasses with magneto-optical properties are attracting attention and great technological interest for their broad application prospects, including modulators, magneto-optical isolators, information storage devices, spintronics, magnetic sensors, and magneto-optic (MO) fibers. Borotungstate glasses have the advantage of high lanthanide solubility and high refractive index, which facilitates the optimization of the Faraday effect in the glass due to the high concentration of paramagnetic species [1].

This work involves the synthesis of glassy materials in the $x\text{Ln}_2\text{O}_3\text{-WO}_3\text{-B}_2\text{O}_3$ system (where Ln = lanthanides ions, $x = 20; 22.5; 25; 27.5; 30$ mol%) by a melt-quenching process. Samples were characterized using thermal analysis, FTIR, RAMAN, fluorescence spectroscopy, and magnetic analysis.

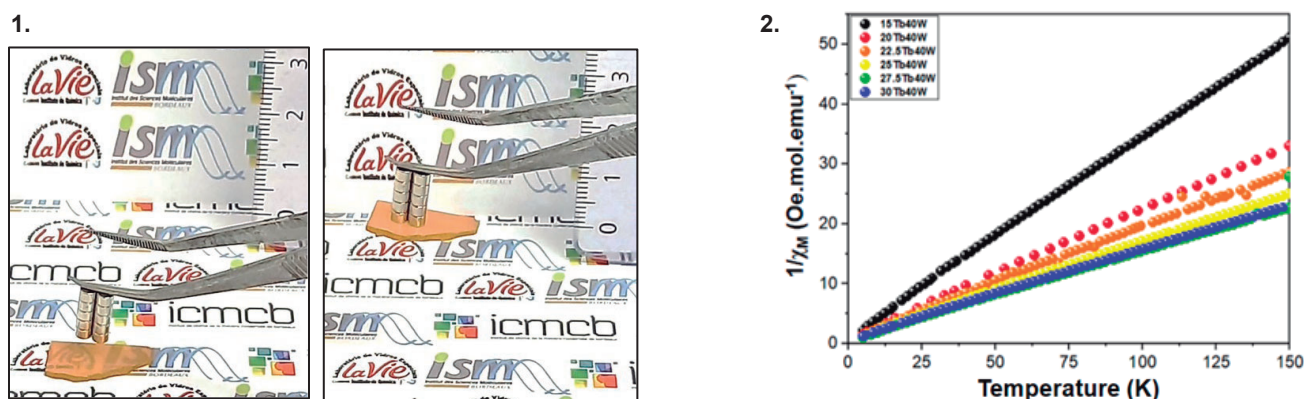


Figure 1. Photograph of the sample 25Ho40W after cutting and polishing being attracted by magnet.

Figure 2. Reciprocal magnetic molar susceptibility (χ_M) vs temperature measurements for a series of glasses with different Tb³⁺ concentrations.

Figure 1 shows the sample 25Ho40W, after cutting and polishing, being attracted by magnet, showing that the samples present magnetic behavior at room temperature. Figure 2 shows the reciprocal susceptibility ($1/\chi_M$) for different concentrations of Tb³⁺ ion as a function of temperature. All data follow the Curie-Weiss law, which estimates the Curie constant (C) from the slope and the Weiss temperature (θ) from the intercept.

Acknowledgments

The authors are grateful to the Coordination for the Improvement of Higher Education Personnel (CAPES, grants 88887.571031/2020-00 and 88882.330082/2019-01), São Paulo State Research Foundation (FAPESP, grant 2013/07793-6) and FUNGlass (funding from the European Union's Horizon 2020 research and innovation programme under the Marie Skłodowska-Curie grant agreement No 823941), for financial support.

Patterned biofilms of gellan gum with silk sericin and studies of their interaction with lanthanides for photonic applications

Francisco R. Torres (PG) ^{1*}, Roberta S. Pugina (PQ) ¹, Molíria V. dos Santos (PQ) ², Hernane S. Barud (PQ) ³, José Maurício A. Caiu (PQ) ¹.

francisco.torres@usp.br

¹Departamento de Química, FFCLRP, Universidade de São Paulo; ²Departamento de Morfologia, Odontopediatria e Ortodontia, Faculdade de Odontologia, Universidade de São Paulo; ³Grupo BioPolMat - Universidade de Araraquara

Keywords: Biomaterials; Luminescence; Iridescence.

Highlights

Iridescent gellan gum and sericin film obtained from a pattern
 Properties of both materials collaborate for a free-standing patterned film
 The luminescence of GG-Eu³⁺ was improved with sericin insertion

Abstract

Gellan Gum (GG) is a natural and biocompatible polysaccharide that can be modified to suit different applications [1]. Seeking a material with better mechanical functionalities and optical properties, GG was combined with sericin (SS), a protein extracted from the cocoon of the silkworm. An interesting property that this material showed when dried in a patterned matrix under ambient conditions was to reproduce the patterns on the surface of its film through the process of soft lithography. Scanning electron microscopy confirmed the formation of periodic micropatterns on the film, shown in Figure 1 - a. The result of these patterns on the surface are angle-dependent iridescent colors (Figure 1 - b), structurally induced in the film by the mold [2]. A GG-only film prepared in the same way did not show the same behavior, just as an SS solution does not form a free-standing film. Therefore, only the combination of the properties of these two biopolymers collaborate for the formation of a patterned film, which can be chemically functionalized, in order to expand its scope of applications, as sensors, random Lasers or structural colors systems. In parallel, preliminary studies have already indicated that the GG matrix has a reduced efficiency to energy transfer in the interaction with lanthanide ions, important in the development of photonic devices due to their distinguished luminescent properties. However, the composite material of GG and SS, doped with Eu³⁺ showed interesting results regarding the sensitization effect from the matrix to the ion (Figure 1 - c), increased by the presence of SS, as well as a longer lifetime of the excited state [3]. These findings make this new material even more promising in photonic applications, due to its structural color with the lanthanides luminescence properties.

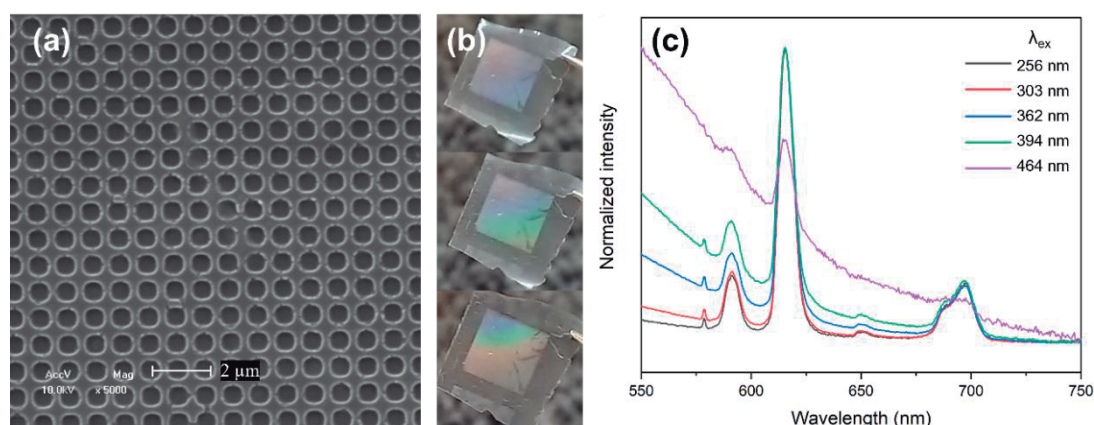


Figure 1. (a) Scanning electron microscopy showing the printed pattern on GG + SS film, (b) their iridescence visible at naked eye; (c) emission spectra from sample 1% Eu³⁺-doped GG + SS film (50/50, w/w).

References: [1] Bacelar, A. H. et al. *Journal of Materials Chemistry B*, v. 4, n. 37, p. 6164–6174, 2016. [2] Perry, H. et al. *Advanced Materials*, v. 20, p. 3070–3072, 2008. [3] Binnemans, K. *Coordination Chemistry Reviews*, v. 295, p. 1–45, 2015.

Acknowledgments

The authors acknowledge the Brazilian agencies FAPESP (2019/18828-1) and CNPq (154100/2022-6) as well as the Universidade de São Paulo (USP) for financial support.

46ª Reunião Anual da Sociedade Brasileira de Química: "Química: Ligando ciências e neutralizando desigualdades"

Phosphorylated Biopolymers: Chitosan and Cellulose modified with phosphate groups. Properties and Applications.

Celso A. Bertran* (PQ),¹ **Thalita M. Missano** (PG),¹ **Tais S. Almeida** (PG),¹ **Carolina R. Grizotto** (IC).¹

bertran@unicamp.br

¹Institute of Chemistry UNICAMP

Keywords: *Biopolymers, Biomaterials, Phosphorylated Chitosan, Phosphorylated Cellulose, Porous Network.*

Highlights

- Phosphorylation of Chitosan and Cellulose.
- Combination of the biofunctionality of biopolymers and calcium phosphate.
- 3D porous network formed by ionic crosslink.

Abstract

Chitosan and cellulose are natural biopolymers widely exploited for various biomedical applications due to their recognized biocompatibility, bioactivity, and osteoconductivity. The modification of these biopolymers through phosphorylation reactions modifies their characteristics, such as solubility and the aggregates and networks formation, opening up new possibilities for use. Phosphorylation allows calcium ions fixation in the polymer structure, forming a 3D network, and also the ionic crosslinking. The functionalization of chitosan and cellulose allows the combining benefits, of the known biofunctionality associated with these biomaterials, with the biofunctionality of calcium phosphates. For chitosan, phosphorylation of the hydroxyl groups with phosphate transforms it into a pH-responsive polymer with pKa 6.70 and 10.08 corresponding to the amino and phosphate groups, respectively, making it soluble at pH above 7 and partially soluble at pH below 2. In addition, its solubility is increased, making it possible to solubilize around 18% (m/m) of the material. The free amino group present in chitosan allows the crosslinking of the polymeric chains, which combined with the reaction of the phosphate groups with calcium ions, results in a consistent gel that, after lyophilization, transforms into a foam-like material with interconnected pores and thin walls (Figure 1a). Tests with fibroblast cells (NIH/3T3) indicate that the material is not cytotoxic and is suitable for biological use, as demonstrated by the cell viability results. For cellulose, in particular, for phosphorylated microfibrils (C μ F) and nanocrystals (CNC), dispersions can organize when subjected to centrifugation followed by lyophilization, forming a 3D network. In addition, phosphorylated CNC/C μ F react with calcium ions and adsorb the cationic surfactant CTAB, changing the surface charge from negative to positive. The 3D network formed by CNC/C μ F and with a positively charged surface works as a template and can adsorb silica nanoparticles. Burning the cellulose template causes the silica to react with phosphate and calcium ions to form the 58S bioglass scaffold (Figures 1b and 1c).

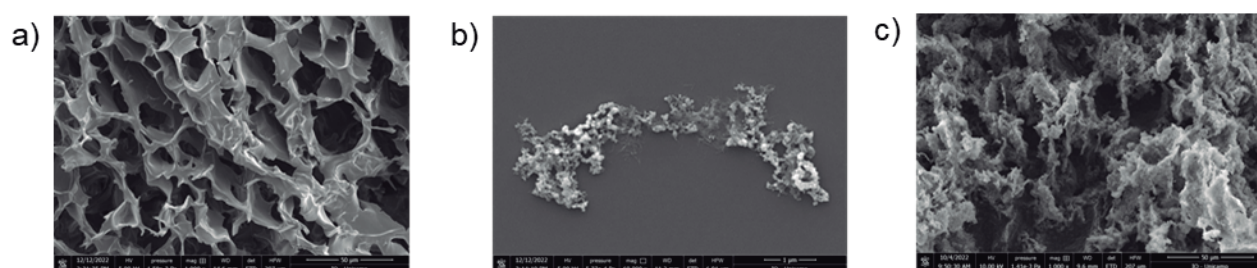


Figure 1: SEM micrographs of: (a) lyophilized chitosan foam; (b) phosphorylated CNC after calcium reaction; (c) 58S bioglass scaffolds.

Acknowledgments

CAPES, CNPQ, FAPESP 2021/11019-0; Institute of Biology – UNICAMP (Biomembranes Laboratory); Institute of Chemistry – UNICAMP; FMI Lab – Functional Materials and Interfaces Laboratory.

Photocatalytic synthesis of PANI.TiO₂ nanocomposites

Vanessa M.M. Vargas (TC),^{1*} Carla Dalmolin (PQ),² Sérgio H. Pezzin (PQ).²

sergio.pezzin@udesc.br; vanessa.vargas@ufsc.br

¹UFSC - Campus Joinville, Rua Dona Francisca, 8300 – Bloco U, Zona Industrial Norte, 89.219-600 Joinville – SC – Brasil;

²Departamento de Química, CCT, UDESC, Rua Paulo Malshitzki 200, Zona Industrial Norte, 89.219-710 Joinville – SC – Brasil.

Palavras Chave: *polyaniline, titanium dioxide, heterogeneous photocatalysis, nanocomposites.*

Highlights

Synthesis of PANI.TiO₂ nanocomposites from oxidation of aniline over TiO₂ by heterogeneous photocatalysis. Formation of PANI by photocatalysis may lead to photosensitive composite catalysts.

Resumo/Abstract

In recent decades, several studies have demonstrated the high efficiency of degradation of organic pollutants by heterogeneous photocatalysis (HP) by TiO₂ photosensitized with a colored conductor polymer, such as polyaniline (PANI), under a variety of light sources. However, PANI.TiO₂-based nanocomposites face the challenge of having an adequate interface to promote synergistic effects, which result in gains in degradation of pollutants by HP, mainly under visible and sunlight. To cover this demand, many synthetic pathways have been developed, but the use of HP itself could become an interesting pathway to synthesize PANI.TiO₂.

This work aimed to synthesize nanocomposites formed by titanium(IV) oxide (TiO₂-P25), and polyaniline (PANI), PANI.TiO₂, by a photocatalytic route at different concentrations of acid and aniline. Our contribution concerns a new proposal to obtain PANI.TiO₂ catalysts without the use of a chemical oxidant or external electrical potential and investigate the ability of TiO₂ nanoparticles to oxidize aniline, under UV light, in a one-pot system. The syntheses were carried out by the irradiation of a dispersion containing TiO₂ (ca. 2 wt%) and aniline in ultrapure water with pH adjusted with H₂SO₄. Prior to the irradiation period, the system was stirred for 30 min in the dark to the achievement of the adsorption/desorption equilibrium between aniline and TiO₂. Irradiation was promoted by a 125 W HP-Hg vapor lamp positioned 10 cm from the top of a 40 mL reactor with water circulation at RT and magnetic stirring. Under these conditions, brown colored oligomer mixtures were obtained, which, in general, presented a microsphere morphology. PANI oligomers were easily solubilized in ethanol and FTIR analyses showed that the insoluble fraction refers to phenazine and cross-linked oligomers. A prominent band at 1627 cm⁻¹ in the FTIR spectra is associated with the presence of phenazine, which is typical of the initial step of PANI synthesis and considered nuclei for the PANI chain propagation step at pH < 2.5. At pH > 3.5 a large part of the aniline is neutral, and the tendency is for ortho-directed reactions, leading to the formation of the brown product (non-protonated oligomers) with no π-π conjugation. The syntheses carried out at pH values close to the pKa of aniline (4.6), achieved higher reaction rates than those performed at lower pH. This effect is associated with the lower oxidation potential required by non-protonated aniline. Another peculiar effect of this synthetic route refers to pH changes throughout the synthesis. For the systems starting at pH 4 and 5, after 30 min of reaction the pH increased to about 6, remaining unchanged until the end of the experiment. For samples prepared at pH 0.7, the pH remained unchanged over the 5 h of irradiation.

The observations of pH change and formation of oligomers demonstrate how the mechanisms of aniline oxidation via photocatalysis with TiO₂ are quite different from the conventional chemical synthesis with ammonium persulfate. It is suggested that in the initial stage the aniline is oxidized via electron transfer from •OH radicals generated in the solution to the organic molecule: •OH + RH to RH• + –OH. In this pathway there is generation of hydroxyl ions responsible for the pH increase in the syntheses at pH 4 and 5. As in the test at pH 0.7 it remains unchanged, it is proposed that, in this case, due to the lower presence of neutral aniline, there was no relevant formation of –OH. Therefore, this preliminary study has given directions to be explored in the photocatalytic synthesis of polyaniline.

Agradecimentos/Acknowledgments

FAPESC, UFSC.

PMMA luminescent films based in inorganic-organic hybrids for application in PC-WLED devices

André Lucas Costa (PG)^{*1,2}, Ariane C. F. Beltrame (PG)^{*1,2}, Sergio A. M. Lima (PQ)^{1,2}, Ana Maria Pires (PQ)^{1,2}.

andre.lucas-costa@unesp.br

¹Department of Chemistry and Biochemistry, FCT-UNESP; ²Department of Chemistry and Environmental Sciences, IBILCE-UNESP.

Keywords: Multicolor-emitting; Europium(III); Terbium(III); Tunable color.

Highlights

Core@shell type luminescent inorganic-organic hybrid dispersed in PMMA polymeric films for application in phosphor-converted white-light-emitting diodes (PC-WLEDs).

Abstract

White-light-emitting diodes (WLEDs) are the main white light source for indoor and outdoor lighting as well as backlighting of displays. Research in solid state lighting (SSL) is now focused not only on increasing luminous efficacy (LE) but also on improving color quality, particularly CCT (Correlated Color Temperature) and CRI (Color Rendering Index).¹ High CCT values disrupt human circadian rhythm, alertness, and neuroendocrine and neurobehavioral physiology, motivating the search for new devices with superior color qualities than the commercially available WLEDs. Thus, luminescent inorganic-organic hybrids have shown to be very promising alternatives both in therapeutic and lighting applications, in addition to multifunctional devices or in bioimaging. In this regard, through a step-by-step process, two inorganic-organic core@shell-like hybrids based on spheroidal-shaped $Y_2O_3:Eu^{3+}@SiO_2-$

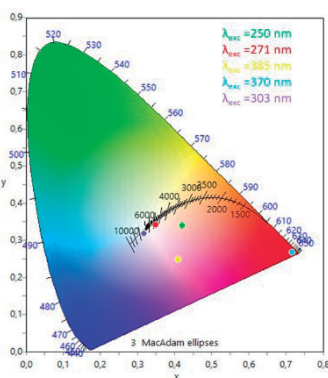


Fig. 1 – The 1931 CIE color diagram for the luminescent film monitoring different excitation wavelengths.

$[Tb(acac)_3(Salen)]$ or $Y_2O_3:Tb^{3+}@SiO_2-[Eu(dbm)_3(Salen)]$ particles with diameter of 170 nm were fabricated from $Y_2O_3:RE^{3+}$ ($RE^{3+} = Eu^{3+}$ or Tb^{3+}) coated with a layer of SiO_2 (2.7 nm), that was imino-functionalized to get Salen ligands to which were finally bonded to $[RE(\beta\text{-diketonate})_3]$ complexes ($\beta\text{-diketonate} = \text{acetylacetonate, acac, or dibenzoylmethanate, dbm}$)². Both hybrids were fully characterized, which data can be found in reference 2. To evaluate the behaviour of both hybrids in a polymeric matrix aiming application in PC-WLEDs, luminescent PMMA films based on a 1:1 mass mixture of these two hybrids using chloroform as solvent, in the proportion of 50% m/m of hybrids/polymer was prepared. From luminescence spectroscopy measurements of the film, the main transitions of Eu^{3+} and Tb^{3+} ions were detected, according to the selected excitation wavelength, indicating that both hybrids keep their emission in the produced material. Therefore, by varying the excitation wavelength, it was possible to tune the global emitted color of the film from the red spectral region, with major emission of Eu^{3+} , to the white emission region due to the combination of Eu^{3+} , Tb^{3+} and of the Salen ligand emissions. This behaviour is illustrated in the color diagram, Fig. 1. It should be emphasized that there is no energy transfer from the RE^{3+} in the core to the

other RE^{3+} on the surface of the particles, avoiding the luminescent quenching of both emitting ions. As a consequence, these results qualify this tunable luminescent film as a promising candidate to be applied in the PC-WLEDs architecture.

Acknowledgments

FAPESP (2019/26103-7), CNPq (304003/2018-2; 309448/2021-2), CAPES (Grant number 88887.686388/2022-00).

References

- [1] BISPO-JR, Airton G. et al. Recent prospects on phosphor-converted LEDs for lighting, displays, phototherapy, and indoor farming. *Journal of Luminescence*, v. 237, p. 118167, 2021.
- [2] A. L. Costa, et al. Multicolor-emitting luminescent $Y_2O_3:RE^{3+}@SiO_2-[RE^{3+}(\beta\text{-diketonate})_3]$ core@shell hybrids featuring dual RE^{3+} activator centers. *Journal of Alloys Compounds*, 843, 2020.

Área: MAT

POLIGLICEROL LINEAR A PARTIR DE CLOROPROPANÓIS E GLICEROL: NOVAS ROTAS DE SÍNTESE

Ticiane Vieira de Paula Souza (PG),^{1*} Michel Neves de Miranda (IC),¹ Aline Silva Muniz (PQ),¹ Valéria Gonçalves Costa (PQ),² Angelo R.S. Oliveira (PQ),¹ Maria Aparecida F. César-Oliveira (PQ).^{1*}

mafco@ufpr.br; ticiane.vieira@ufpr.br

¹LEQUIPE, Departamento de Química, UFPR; ²LAMAP, Divisão de Materiais, INT.

Palavras-Chave: Poliglicerol linear, Cloropropanóis, Glicerol, Poliéter hidroxilado, Controle de massa molar.

Highlights

Linear polyglycerol from chloropropanols and glycerol: new synthetic routes.

New synthetic routes to produce linear polyglycerol of varying molar mass; Step polymerization of mono- and dichloropropanols, with and without glycerol.

Resumo/Abstract

Neste trabalho, novas rotas sintéticas para a obtenção de poliglicerol linear de massa molar variada foram desenvolvidas a partir da polimerização em etapas do 3-cloropropan-1,2-diol (3-MCPD) e da reação do 1,3-dicloropropan-2-ol (1,3-DCP) com glicerol, ambas na presença de um sal de caráter básico, sob temperaturas menores que as tipicamente utilizadas para a polimerização do glicerol. Foi abordada também a utilização de materiais de partida halogenados que são obtidos por modificação química do glicerol, uma matéria-prima abundante e de baixo custo, obtido de fonte renovável. O glicerol é coproduto da produção de biodiesel, que desempenha um importante papel na matriz energética brasileira. As modificações químicas do glicerol permitem a obtenção de diversos produtos com uso nas indústrias farmacêuticas, de cosméticos, polímeros, energia, química fina e muitas outras áreas. Dentre esses produtos se encontra o poliglicerol (PG), que pode ser visto como uma mistura de oligômeros de diferentes tamanhos de cadeia e diferentes geometrias (lineares, ramificados e cíclicos), sendo que os oligômeros de cadeias curtas e lineares, como o di- e triglicerol (166 e 240 g.mol⁻¹), são amplamente utilizados pela indústria alimentícia e obtidos por eterificação catalítica do glicerol. A literatura mostra que, independentemente do método de obtenção, uma dificuldade intrínseca ao processo é a obtenção de PG de massas molares superiores às de oligômeros pequenos, principalmente usando glicerol como reagente. Este trabalho visa, além da utilização do glicerol, a obtenção de um maior controle da massa molar na formação de poligliceróis lineares, assim como o uso de condições reacionais mais brandas, envolvendo temperaturas mais baixas, evitando a formação de subprodutos tóxicos, como a acroleína, por exemplo. Para atingir esses objetivos, foi desenvolvida uma metodologia baseada na reação de eterificação, inspirada nas condições reacionais da Síntese de Williamson, porém aplicadas à polimerização do 3-MCPD, e do 1,3-DCP com o glicerol. As condições de reação variaram, dependendo dos citados materiais de partida, mas ambas realizadas em três etapas utilizando K₂CO₃ como catalisador. O processo foi submetido a um pedido de patente, motivo pelo qual o procedimento experimental não pode ser apresentado com riqueza de detalhes. A primeira etapa foi feita em atmosfera inerte (N₂) na faixa de 140-160°C, durante 2-4 h. Em seguida, a segunda etapa foi realizada em 180-200°C (2-4 h). Na terceira etapa, os produtos residuais foram destilados, à pressão reduzida. O PG obtido por ambas as rotas (3-MCPD ou 1,3-DCP + glicerol) foi separado por solubilização em etanol e filtrado. A purificação foi realizada por resfriamento da solução abaixo de 10 °C, por 12 h, seguida de filtração e rotaevaporação do solvente. Dessa forma, poliglicerol linear foi obtido como produto puro, em rendimentos de 92%, caracterizado por RMN de ¹H e de ¹³C, IVTF e por MALDI TOF que apresentou valores de massa molar em torno de 3100 g.mol⁻¹ para o PG de 1,3-DCP + glicerol e em torno de 1600 g.mol⁻¹ para o PG de 3-MCPD. As rotas sintéticas desenvolvidas produziram PG's lineares que apresentaram massas molares bem superiores, obtidos sob condições reacionais mais brandas, a partir de glicerol e cloropropanóis, que podem ser obtidos a partir de glicerol por meio de métodos já patenteados, consistindo, assim, em uma opção para a valorização da glicerina, coproduto da produção de biodiesel.

Referências: CHONG, C.C. *et al.* Environ. Technol. Innov. 19: 100859. 2020; MARTIN, A. *et al.* Eur J Lipid Sci Technol. 113: 100. 2011; SUTTER, M. *et al.* Chemical Reviews 115: 8609. 2015.

Agradecimentos/Acknowledgments



Polymers of β -Ciclodextrina modified with L-Cysteine: Synthesis, characterization and incorporation of TiO_2 and silver nanoparticles.

Arthur F. Lemos (PG), Yasmin M. Nascimento (IC), Mariane Silva da Cruz (IC), Zaine Teixeira Camargo (PQ)*
marianesilv@hotmail.com; zaine@academico.ufs.br

Department of Chemistry, Federal University of Sergipe (UFS).

Palavras Chave: *nanosponges, TiO_2 nanoparticles, Photocatalysis*

Highlights

- Development of a photocatalyst for environmental decontamination.
- β -cyclodextrin polymer functionalized with L-cysteine and cross-linked with citric acid.
- Nanocomposite with TiO_2 and TiO_2/Ag .

Abstract

β -cyclodextrin Polymers (β CDP) have been used for environmental decontamination, as they are insoluble in water, form inclusion complexes, and have adsorption capacity. Their association with TiO_2 nanoparticles (TiO_2 NP) makes them attractive for photodegradation [1].

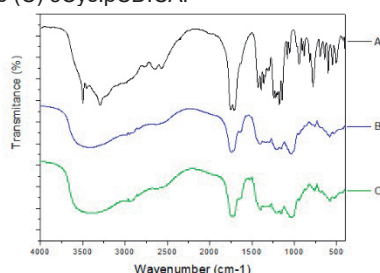
This work aimed to develop a photocatalyst for environmental decontamination using β CDP functionalized with L-cysteine (Cys) and cross-linked with citric acid (CA) to obtain a nanocomposite with TiO_2 NP and TiO_2/AgNP .

The β CD was functionalized with Cys by esterification and TiO_2 NP were obtained by the sol-gel method, from Ti(IV) isopropoxide. The nanocomposites were obtained *in situ* by adding modified β -CD (Cys. β CD) and CA to the TiO_2 NP suspension. AgNO_3 solution was added to the samples and the redox reaction was performed under UV light. FTIR, XRD, DRS, and TEM performed the structural, optical, and morphological investigations. In molar ratios of Cys: β CD 1:1, 3:1 and 5:1 discrete bands were attributed in the FTIR, referring to the ester carbonyl and bands referring to amine and S-H deformation. There were broad peaks by XRD, indicating that

functionalization had occurred (data not shown).

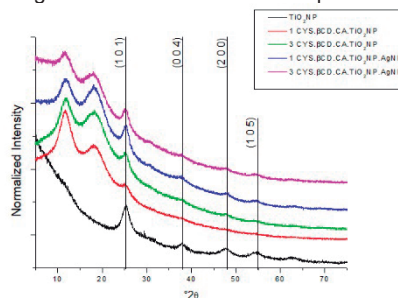
The polymers were obtained with the molar ratios 1:1 and 3:1, being named 1Cys. β CD.CA and 3Cys. β CD.CA. The main feature by FTIR (Figure 1), distinct from Cys. β CD and CA, was the band at 1730 cm^{-1} , attributed to the crosslinked ester carbonyl.

Figure 1 – FTIR: (A) CA, (B) 1Cys. β CD.CA e (C) 3Cys. β CD.CA.



As seen in Figure 2, two broad peaks are observed by XRD referring to polymers in the region of 2θ smaller than 20° , plus the peaks of anatase TiO_2 [2].

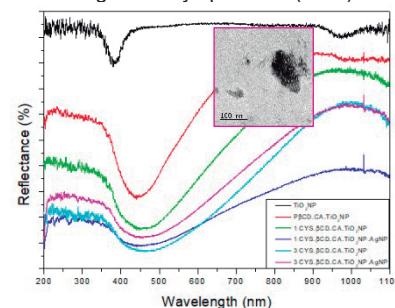
Figure 2 – XRD of the nanocomposites.



The peak of the highest intensity of Ag coincides with the peak of the plane (2 0 0) of TiO_2 , but there was no increase in intensity in the samples with Ag, which may be due to its low proportion.

As seen in Figure 3, the optical reflectance bands of TiO_2 showed a cut-off at 400 nm, in addition to the SPR band of Ag ($\sim 430\text{ nm}$). The morphology was sponge-like with nanoparticles between 3 nm and 10 nm and 30-50 nm nanorods (inset in Figure 3).

Figure 3 - DRS of the nanocomposites and TEM image of 3 Cys. β CD.CA (inset).



As the nanocomposites obtained in this work are promising for photocatalysis, methylene blue photodegradation tests are in progress.

REFERENCES: [1] SHERJE, A. P et al. *Carbohydr. Polym.*, v. 173, p. 37–49, Oct. 2017. [2] MAHMOUD, M. et al. *Program nucl. Energy*, v. 106, p. 51–63, Jul. 2018. ACKNOWLEDGMENTS: CMNano (053/2022); PPGQ-UFS

Polypyrrole/stearic acid-coated *Luffa cylindrica* for enhanced removal of sodium diclofenac from water: Batch and continuous adsorption studies

André Ricardo Fajardo (PQ)^{1*} and Juliê Silveira da Costa (PG)¹

drefajardo@hotmail.com; ju_scosta@yahoo.com

¹Laboratório de Tecnologia e Desenvolvimento de Compósitos e Materiais Poliméricos (LaCoPol), Universidade Federal de Pelotas (UFPEl), Campus Capão do Leão s/n, 96010-900, Pelotas-RS, Brazil.

Keywords: Adsorption, sponge gourd, emerging contaminants, pharmaceuticals, water treatment.

Highlights

- > *Luffa cylindrica* was coated with polypyrrole and polypyrrole/stearic acid.
- > The coated *Luffa* showed different chemistry, morphology, and wettability than raw *Luffa*.
- > The coated *Luffa* was used to adsorb sodium diclofenac in batch and continuous experiments.
- > The coated *Luffa* is a more efficient adsorbent than the raw *Luffa*.
- > This original adsorbent based on biomass can be reused without losing adsorption performance.

Abstract

The hydrophilicity of some vegetal biomasses limits their use as adsorbents for the removal of emerging contaminants from water. As an approach to overcome this limitation, in this study, *Luffa cylindrica* (LF), a 3D natural fiber array biomass, was coated with polypyrrole (PPy) and polypyrrole/stearic acid (PPy/SAc) to increase their adsorption capacity towards sodium diclofenac (DCF). Characterization analyses demonstrated that the PPy and PPy/SAc coatings altered the physicochemical, morphological, and wettability properties of LF. As a result, LF-PPySAc becomes hydrophobic (water contact angle > 124°) benefiting the interaction with DCF (**Fig 1**). Overall, these changes resulted in different adsorption performances for the coated-LF samples regarding raw LF. By using batch and continuous adsorption processes, it was verified that the adsorption capacity was noticeably higher for the LF-PPy and LF-PPySAc, which is explained by the higher interactions between DCF and these adsorbents. Experimentally, it was verified that the PPy/SAc coating enhances the adsorption of DCF by 234% (batch process, **Fig 2a**) and 80% (continuous process **Fig 2b**) compared to raw LF. Kinetic, isothermal, and thermodynamics analyses indicated that the DCF adsorption is mediated mainly by physical forces (H-bonding, π - π interaction, and hydrophobic forces), and intraparticle diffusional processes are involved. The high stability of LF-PPySAc allowed its reuse at least five times without losing adsorption performance in both batch and continuous processes. Thus, the coating of LF with PPy/SAc is ranked as a promising approach to obtaining an adsorbent material with an enhanced capacity to remove hydrophobic contaminants from the aqueous medium.

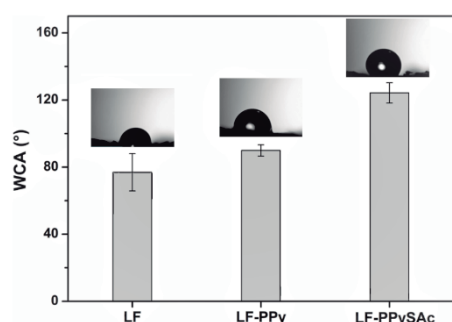


Fig. 1 WCA measurements for LF samples. Inset: Water droplet photographs on each sample.

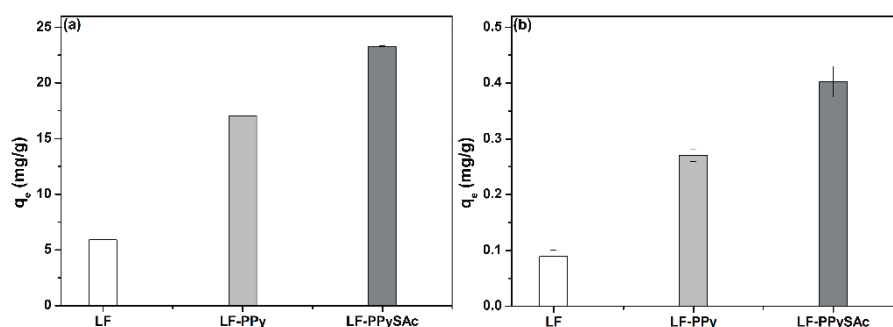


Fig. 2 Adsorption capacity of LF samples for DCF using (a) batch and (b) continuous processes.

Acknowledgments

The authors are thankful to CNPq (Processes 404744/2018-4 and 303125/2022-5). This study was financed in part by the Coordenação de Aperfeiçoamento de Pessoal de Nível Superior, Brazil. (CAPES/Proap), Finance Code 001. Thanks also to the organizing committee of the 46th RASBQ.

Polystyrene films coated with antimicrobial hyaluronic acid/poly (diallyldimethylammonium chloride) polyelectrolyte multilayers

Guilherme L. B. Neto (PG),^{1*} Bruno R. Machado (PG),¹ Paulo R. Souza (PQ),¹ Alessandro F. Martins (PQ).^{1,2}

g.luizbatista15@gmail.com

¹Departamento de Química, UEM; ²Departamento de Química, UTFPR-Apucarana

Keywords: *Layer-by-Layer, Surface coatings, Surface properties.*

Highlights

A novel surface coating based on hyaluronic acid/poly diallyldimethylammonium chloride was deposited on oxidized polystyrene films through the Layer-by-Layer (LbL) approach aiming the obtention of an antiadhesive and antibacterial surface.

Abstract

Diseases caused by the most common pathogen agents, such as bacteria, are public health issues. Surface contamination occurs due to these pathogenic agents' fast spread and propagation. A promissory alternative that comes to researchers' attention is the Layer-by-Layer (LbL) approach. The LbL promotes thin film assemblies, *i.e.*, (nanocoatings) on solid substrates to control microbial growth and attachment. In this facet, the surface coating presence does not compromise the optical and mechanical substrate properties. Also, different surface coatings can be obtained from the LbL method due to its relatively easy and quick achievement. The final modified surface presents the chemical and biological properties of the adsorbed polyelectrolytes. Generally, one polycation and one polyanion are deposited individually onto a solid substrate. Electrostatic interactions between an oxidized substrate with a polycation promote the first layer deposition. Then, the substrate containing one deposited layer is added to a polyanionic polyelectrolyte solution. After the adsorption/deposition of a polycationic-polyanionic polymer bilayer, multilayers (PEMs) are performed upon the solid substrate by repeating the process. The surface properties, including thickness, roughness, wettability, and polarity, are modulated by controlling the number of bilayers deposited on the solid substrate. Hyaluronic acid (HA) (polyanionic electrolyte) and poly (diallyldimethylammonium chloride) (PDADMAC) (polycationic polymer) were deposited on oxidized polystyrene to yield surface coatings (PEMs). HA is a glycosaminoglycan naturally found in the extracellular membrane of all mammalian cells and it is known as one of the most hydrophilic biopolymers in nature.¹ Due to its hydrophilicity, HA can prevent bacterial adhesion on solid surfaces, preventing biofilm formation of *Staphylococcus epidermidis*, *Escherichia coli* (*E. coli*) and *Staphylococcus aureus* (*S. aureus*).² PDADMAC presents quaternary ammonium moieties in its structure. Therefore, its cationic behavior is independent of the pH condition. Bactericidal PDADMAC effects are related to its cationic feature. Studies showed that the PDADMAC supports antimicrobial activity towards *S. aureus*, methicillin-resistant *S. aureus*, *E. coli*, *Pseudomonas aeruginosa* (*P. aeruginosa*), and *Acinetobacter baumannii*.^{3,4} However, the antimicrobial activity is imparted by aqueous PDADMAC solutions. This study shows novel antimicrobial HA/PDADMAC PEMs (5, 6, 14, and 15 layers) obtained on oxidized polystyrene for the first time. The antimicrobial activity depends on the PEM surface features. The PEMs are characterized by water contact angle measurements, Energy Dispersive Spectroscopy and Atomic Force Microscopy. The HA/PDADMAC PEMs present promissory characteristics to inhibit the adhesion and proliferation of *P. aeruginosa* and *S. aureus* on solid surfaces.

Acknowledgments

The authors thank CNPq and CAPES for the research funding and Symbios for providing the hyaluronic acid.

1. DEL HOYO-GALLEGO, S. et al. Construction of antibacterial poly(ethylene terephthalate) films via layer by layer assembly of chitosan and hyaluronic acid. *Carbohydrate Polymers*, v. 143, p. 35–43, 5 jun. 2016.

2. JUNTER, G. A.; THÉBAULT, P.; LEBRUN, L. Polysaccharide-based antibiofilm surfaces. *Acta Biomaterialia*, v. 30, p. 13–25, 15 jan. 2016.

3. TRAN, P. L. et al. The ability of quaternary ammonium groups attached to a urethane bandage to inhibit bacterial attachment and biofilm formation in a mouse wound model. *International Wound Journal*, v. 14, n. 1, p. 79–84, 1 fev. 2017.

4. SANTOS, R. et al. Preparation, Antimicrobial Properties, and Cytotoxicity of Acrylic Resins Containing Poly(diallyldimethylammonium chloride). *The International Journal of Prosthodontics*, 34(5), 635–641. 2021.

Polyurethane membranes modified by hollow aluminum oxide particles

Marla Almeida Siqueira (PG).¹ João Pedro Massaria de Arcanto (PG), Cleocir José Dalmaschio (PQ).

Cleocir.dalmaschio@ufes.br

¹Departamento de Química, Universidade Federal do Espírito Santo

Palavras Chave: *Processo separação, nanoestruturas, polímero.*

Highlights

Polyurethane membranes with incorporated aluminum oxide particles;

Hollow aluminum oxide particles;

Separation process with semipermeable membranes;

Oxide surface functionalization.

Resumo/Abstract

Com os avanços na tecnologia em membranas se ampliam a gama de aplicações desse tipo de estrutura em processos de separação, desde dessalinização, remoção de germes até separação de emulsões, por exemplo¹. A introdução de novas tecnologia na produção de membranas, torna promissora a aplicação deste tipo processos de separação em emulsões óleo em água, pois reduz a contaminação de óleo a níveis aceitáveis nos limites das normas ambientais vigentes. Além disso, as novas tecnológicas permitem produzir membranas com elevado fluxo de permeado, possibilitando assim aplicação em processos industriais que, em geral, possuem alto volume de fluídos a serem tratados. Neste contexto, o desenvolvimento de membranas resistentes e com elevada eficiência em processos de separação são temas relevantes de pesquisa científica e tecnológica. Assim, o objetivo do trabalho foi desenvolver membranas semipermeáveis de poliuretana aditivada com partículas de Al₂O₃.

Para atingir maior relação área/massa, partículas ocas de Al₂O₃ foram sintetizadas empregando moldes de microesferas de carbono, preparadas por processo hidrotérmico. Os íons de alumínio foram depositados, na forma de hidróxido, sobre as microesferas de carbono e após a calcinação foi obtida estruturas do tipo casca oca de Al₂O₃. O padrão de difração de raios-X do material calcinado indica a formação de estruturas na fase gama-Al₂O₃. Imagens de microscopia comprovam a formação do tipo de estrutura oca. As estruturas de óxido foram incorporadas em poliuretana (PU), solubilizada em DMF, e então foi preparado membranas por processo de inversão de fase². Teste de permeabilidade à água indicaram que a modificação da membrana com o óxido reduz a permeabilidade, se comparado a membranas de PU pura. De fato, se observa por microscopia que ao adicionar frações da ordem de 1% em massa já se tem uma alteração da superfície da membrana em função da segregação das partículas de óxido da matriz polimérica. Também se constata que partículas de óxido alteram a hidrofiliicidade, reduzindo efeitos deletérios de inscrutamento, o que evita redução de fluxo ao longo do tempo em emulsões oleosas. Conclui-se que a aditivação com óxido altera a estrutura de superfície em membranas de PU.

1. Yang Y, Ali N, Bilal M, et al. Robust membranes with tunable functionalities for sustainable oil/water separation. *J Mol Liq* 2021;321:114701.

2. Cheng B-X, Gao W-C, Ren X-M, et al. A review of microphase separation of polyurethane: Characterization and applications. *Polym Test* 2022;107:107489.

Agradecimentos/Acknowledgments

UFES, NCQP-UFES, LMC/LPT-UFES, CNPq, CAPES, FAPES.

Potential markers for gunshot residues: LnOFs (Ln= Tb^{III} and Eu^{III}) and Forensic Science

Marye A.R. Silva (IC)^{1*}; Rafaela M.R. da Silva (PG)¹; Javier Ellena (PQ)²; João Honorato de Araujo-Neto (PQ)²; Maria Vanda Marinho (PQ)^{1*}.

marye.silva@sou.unifal-mg.edu.br; maria.marinho@unifal-mg.edu.br

¹Instituto de Química, Campus Santa Clara, LaPI, Universidade Federal de Alfenas, Alfenas, MG, 37133-840, Brasil.

²Instituto de Física de São Carlos, Universidade de São Paulo, São Carlos, SP 13566-590, Brasil.

Palavras Chave: LnOFs, ligante benzenotetracarboxílico, Estrutura cristalina, GSR.

Highlights

- Europium(III) and Terbium(III) coordination networks from 1,2,4,5 benzenetetracarboxylic acid;
- Thermal Stability and Luminescence properties under UV radiation;
- Crystal Structures determined by Single-Crystal X-Ray Diffraction;
- LnOFs as potential application in forensic analysis in crime scenes.

Resumo

LnOFs (lanthanide organic frameworks) são materiais híbridos sintetizados a partir de terras raras “íons lantanídeos” e ligantes orgânicos^[1] e dentre suas inúmeras aplicações, podem atuar como marcadores luminescentes de resíduos de pólvora em locais de crime causado por disparo de arma de fogo usando apenas uma lâmpada ultravioleta, sendo Tb^{III} (marcador -verde) e Eu^{III} (marcador-vermelho)^[2]. Resíduos de disparo de arma de fogo (GSR), sigla do inglês *Gunshot residues*, consiste em partículas sólidas produzidas quando uma arma de fogo é descarregada, e sua detecção fornece evidências importantes em investigações criminais.^[3] Desde o início dos anos 2000, tem-se usado munições livres de metais pesados “*non-toxic ammunition*” tornando necessário novas tecnologias para o trabalho da perícia criminal, destacando assim os marcadores luminescentes a base de íons de terras raras.^[2] A exemplo da LnOF [TbHbtec]_n^[2] sintetizada pelo grupo de pesquisa, estes marcadores têm sido obtidos ora por síntese hidro/solvotermal ora por agitação com uso de algum solvente orgânico. A [TbHbtec]_n^[2] foi testada como funcional marcador verde “Tb^{III}” e primeira LnOF testada como marcador luminescente de resíduos de pólvora com estabilidade térmica acima de 400 °C (Figura 1). Assim, neste trabalho revelamos a obtenção das LnOFs (Tb^{III} and Eu^{III}) com o ligante H₄btec, a caracterização por infravermelho e análise térmica, e difração de raios X por monocristal revelando a estrutura cristalina da rede de coordenação [EuHbtec]_n (Figura 2). Os cálculos pelo software SHAPE^[4] mostram que a geometria em torno do Eu^{III} pode ser descrita como Muffin, Poliedro MFF-9 (grupo pontual Cs). A dimensionalidade da rede bidimensional pode ser observado pela Figura 2.

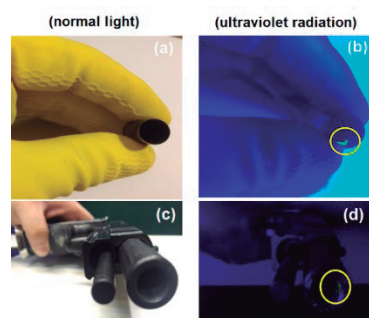


Figura 1- Imagens do marcador “verde” de resíduo de pólvora (GSR) sob luz normal: (a) estojo de cartucho (c) dentro da arma de fogo; e sob luz ultravioleta: (b) estojo de cartucho e (d) dentro da arma de fogo com os LGSR.^[2]

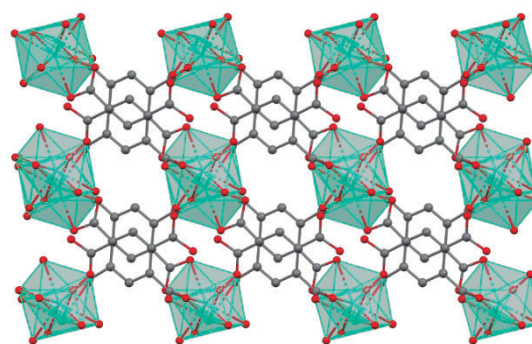


Figura 2- Visão da rede polimérica bidimensional de [EuHbtec]_n.

Agradecimentos

Agradecimento: Aos colaboradores do artigo da caracterização da LnOF sintetizada pelo nosso grupo de pesquisa (LaPI-UNIFAL-MG) de fórmula [TbHbtec]_n^[2].

Funding: PIBITI-UNIFAL-MG (CNPq); FAPEMIG-Project CEX-APQ-01597-17.

Referências: [1] Marinho, M. V.; *et al.*, Photoluminescent and Slow Magnetic Relaxation Studies on Lanthanide(III)-2,5-Pyrazinedicarboxylate Frameworks. *Inorg. Chem.*, **2017**, *56* (4), 2108–2123. [2] Silva, M. A.; *et al.*, A New Photoluminescent Terbium(III) Coordination Network Constructed from 1,2,4,5-Benzenetetracarboxylic Acid: Synthesis, Structural Characterization, and Application as a Potential Marker for Gunshot Residues. *Inorganica Chim Acta* **2019**, *495*, 118967. [3] Lucena, M. A. M., *et al.*, Application of the Metal-Organic Framework [Eu(BTC)] as a Luminescent Marker for Gunshot Residues: A Synthesis, Characterization, and Toxicity Study, *ACS Appl. Mater. Interfaces* **2017**, *9*, 4684-4691. [4] Llunell, M.; *et al.*, Shape: Program for the Stereochemical Analysis of Molecular Fragments by Means of Continuous Shape Measures and Associated Tools. *Electronic Structure Group*, Universitat de Barcelona, **2013**.

Área: MAT

(Inserir a sigla da seção científica para qual o resumo será submetido. Ex: ORG, BEA, CAT)

Preparation and Characterization of a composite from chitosan and a castor oil-Polyurethane

Ricardo S. Medeiros (PG), Ana Paula G. Ferreira (PQ), Éder T.G. Cavalheiro* (PQ)

medeirossricardo@usp.br; cavalheiro@iqsc.usp.br

Instituto de Química de São Carlos - IQSC, Universidade de São Paulo - USP

Key words: Castor oil, Chitosan, Polyurethane, Composites, Infrared Spectroscopy, Thermalanalysis,

Highlights

This work demonstrates the results from preparation and characterization of composites from polyurethane derived from castor oil, methylene diphenyl diisocyanate (MDI) and chitosan (CTS). The obtained composite polymers (PUCTS) were characterized by FTIR, MEV and thermal analytical techniques (TG and DMA).

Abstract

Polyurethane is a class of polymers synthesized from the polyaddition reaction of a polyol (soft segments) with a diisocyanate (hard segments)^[1]. Urethane polymers are widely used in industry due to the versatility of their physicochemical, mechanical and thermal properties. Most polyols used in synthesis are from fossil and non-renewable sources^[2]. In recent years, vegetable oils and polysaccharides derived from plants and animals have emerged as low-cost sources and renewable materials in the preparation of polyurethanes^[3]. Castor oil (CO) became attractive since it is made up of 90% ricinoleic acid, with three hydroxyl groups (OH) attached to carbon 12 of its fatty acids^[4]. Chitosan (CTS) is a copolymer formed by monomeric units of 2-amino-2-deoxy-D-glucopyranose and 2-acetamido-2-deoxy-D-glucopyranose randomly, united by glycosidic β (1 \rightarrow 4) bond. It is obtained from deacetylation reaction of chitin, alkaline hydrolysis^[5]. CTS presents biocompatibility, biodegradability, mucoadhesiveness, antimicrobial activity, nontoxicity, ability of acting as transport matrix, among interesting properties^[5]. Composites of polyurethanes and chitosan were prepared under different conditions by direct 'one-shot' method, in which chitosan was scattered into polyol, derived from CO. After that, it was mixed with methylene diphenyl diisocyanate (MDI) in a reaction flask at room temperature, under stirring. The mixture was degassed and poured into a silicone mold to cure at room temperature. Composites PUCTS were characterized by FTIR, SEM and thermoanalytical techniques (TG, DMA). Regarding to characterization all composites presented similar properties. Changes were observed on FTIR spectral of initial and final products: OH bands of polyol in the region of 3500-3200 cm^{-1} and N=C=O band from MDI at 2189 cm^{-1} were not observed, while it was observed the bands related to C=O and NH in the region of 1750 -1500 cm^{-1} due to the formation of the urethane bond. Moreover, the bands features CTS were also observed with the increase of percentage in composites. According to SEM images, the morphology of PU, in the different magnifications, showed roughness on the surface with circular spots inside, with diameters smaller than 200 μm , characteristic of the outflow of gases during polymerization. The presence of CTS in composites was observed due to the presence of smooth plaques randomly distributed in the PU. TG curves of PUCTS showed five steps of mass loss attributed to loss of water and/or volatile molecules; of urethane, ester of polyol and chitosan decompositions and burning of carbonized material, leaving a residue of about 0,5% at 1000°C. PUCTS samples were thermally stable up to approximately 200°C. DMA curves present the respective glass transition temperature for composites PUCTS in the range of 16-20°C. The results are relevant for the study of polyurethane obtained from renewable sources, considering possible applications in the compatible biological materials area.

[1] Tan, ACW, Polo-Cambrenell, BJ, Provaggi, E, Ardila-Suárez C, Ramirez-Caballero, GE, Baldovino-Medrano, VG, Kalaskar, DM. Design and development of low cost polyurethane biopolymer based on castor oil and glycerol for biomedical applications. *Biopolymers*. 2018 Feb;109(2):e23078.

[2] Cassales A, Ramos LA, Frollini E. Synthesis of bio-based polyurethanes from Kraft lignin and castor oil with simultaneous film formation. *Int J Biol Macromol*. 2020 Feb 15;145:28-4.

[3] Trovati, G., Suman, M. V. N., Sanches, E. A., Campelo, P. H., Bessan Neto, R., Claro Neto, S., Trovati, L. R. Production and characterization of polyurethane castor oil (*Ricinus communis*) foam for nautical fender. *Polymer Testing* 73 (2019) 87-93

[4] Wang, C., Zheng, Y., Xie, Y., Qiao, K., Sun, Yi., Yue, L. Synthesis of bio-castor oil polyurethane flexible foams and the influence of biotic component on their performance. *J Polym Res* (2015) 22: 145

[5] Medeiros, R.S.; Ferreira, A.P.G.; Venâncio, T.; Cavalheiro, É.T.G. Preparation, Characterization and Study of the Dissociation of Naproxen from Its Chitosan Salt. *Molecules* **2022**, *27*, 5801.

Acknowledgments

The authors thank the FAPESP and CNPq for grants.

Protonated Poly(Heptazine Imides): A potential metal-free sunblock

Danielly T. S. Costa (PG)¹, Gabriel A. A. Diab (PG)¹, Luís F. G. Noletto (PG)¹, Vitor G. S. Pastana (PG)¹, Guilherme de F. S. R. Rocha (PG)¹, Dario Batista Fortaleza (PG)¹, Bruna R. Serino (IC)¹, Fillipe V. Rocha (PQ)¹, Ivo F. Teixeira (PQ)¹.

danielly9@estudante.ufscar.br

¹Departamento de Química, UFSCAR.

Key words: Carbon nitride, Catalysis, Sunscreen, Skin cancer.

Highlights

Carbon nitrides are new materials that have great applicability and potential for replacing titanium dioxide (TiO₂), especially as an active ingredient in sunscreens. H-PHI, a protonated variant of Na-PHI, has superior properties and does not require purification steps to remove heavy metals, being especially interesting for application in cosmetics.

Resumo/Abstract

According to data obtained by the Brazilian Society of Dermatology, between 2018 and September 2022, regarding the total number of diagnoses for skin cancer, approximately 250,000 new cases were registered, and compared to previous years, there was an increase of 52 thousand cases. In this sense, carbon nitrides, which are a class of polymeric semiconductors, in their form of protonated poly(heptazine) imide (H-PHI), a protonated variant of Na-PHI (**Fig. 1a**), exhibit superior properties compared to TiO₂, been a potential substitute to TiO₂ as an active ingredient in sunscreens.

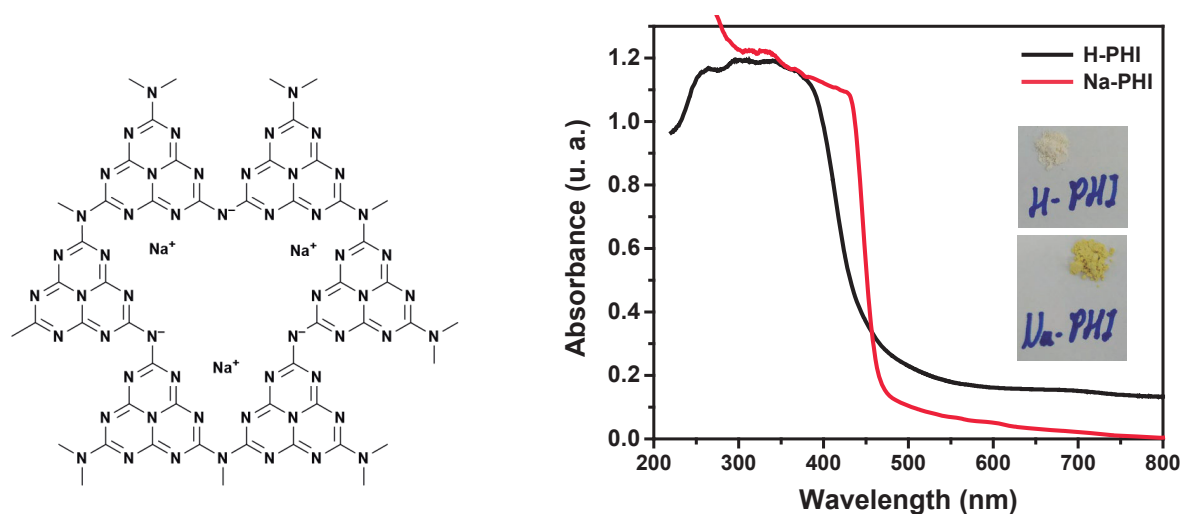


Fig. 1: a) Sodium Poly(heptazine) imide structure; b) UV-Vis Spectra for H-PHI and Na-PHI.

Based on **Fig. 1b**, it is possible to observe that H-PHI completely absorbs the ultraviolet region, being a potential active principle for sunscreens. Compared with Na-PHI, which has a yellow color, H-PHI has a white color due to the protonation of negative nitrogens, leading to resonance breakage between the heptazine rings. In addition to assessing absorption in the UV region, we also performed preliminary biosafety tests on fibroblast cells, developed from lung tissue (MRC-5), which demonstrated that the material is safe and does not affect cell viability, indicating that the material is promising to pass the stage of dermatological tests. Furthermore, formulations substituting TiO₂ for H-PHI are being prepared by our group and tests are being carried out to compare their sun protection factor (SPF).

Agradecimentos/Acknowledgments

CNPq, FAPESP e UFSCar.

Raman Spectroelectrochemical study of CoFe Prussian Blue analogues films on screen-printed electrodes

Rafael L. Gernscheidt (PG)*,¹ Juliano A. Bonacin (PQ),¹

*r226597@dac.unicamp.br

¹Instituto de Química, Universidade Estadual de Campinas, 13083-970 Campinas – SP, Brasil

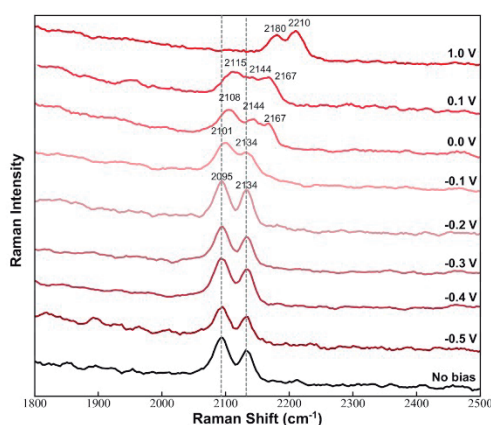
Palavras Chave: cobalt-Prussian blue, water oxidation, water splitting, screen-printed electrodes, spectroelectrochemistry, Raman spectroscopy.

Highlights

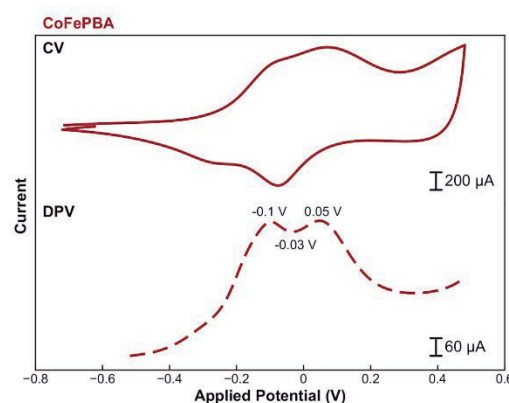
Herein, we report the use of a screen-printed electrode, modified with CoFePBA catalyst for a spectroelectrochemical Raman study, aiming to understand the redox processes on the thin film.

Abstract

Spectroelectrochemistry (SEC) is the combination of spectroscopic apparatus with electrochemical cells, providing a great way for in situ monitoring of reactions and changes in the material structure, being a powerful tool for the identification of reaction intermediates, facilitating mechanistic and kinetic studies. Furthermore, the search for clean, renewable, and environmentally friendly hydrogen sources has made water an excellent feedstock candidate to produce hydrogen. The production of green H₂ from water occurs by a system known as Water Splitting (WS), which is limited by the anodic process, called Oxygen Evolution Reaction (OER), where the Water Oxidation Reaction (WOR) takes place, requiring a catalyst to be effective. Prussian blue analogues (PBA) are one of the most promising examples of WOR Earth-abundant catalysts presenting great performance, activity, and stability under mild condition, and among them, analogues made from Co and Fe are great examples. However, one of the greatest challenges when studying them is to understand reaction mechanisms, since the reaction intermediates usually react very quickly and are hard to be identified. Herein, we report the use of a screen-printed electrode, modified with CoFePBA for a spectroelectrochemical Raman study, aiming to understand the redox processes on the thin film, aiming to assign the redox waves in the cyclic voltammogram. The study shows changes in the spectra $\nu(\text{CN})$ stretching vibration modes with different applied potentials. These changes can be related to redox waves identified in the cyclic voltammogram, allowing a better understanding about the processes and the atoms that are being oxidized during this process. Moreover, the study also helps to understand and propose the oxidation state of the catalyst during the WOR.



Raman spectroelectrochemistry of CoFePBA film.



Cyclic and differential pulse voltammetry from the CoFePBA film.

Acknowledgments



Rapid Synthesis of WO₃ for Oxygen Evolution Reaction: Influence of Microwave and Thermal Treatment

Barbara S. Rodrigues (PG) e Juliana S. Souza (PQ).

barbara.scola@ufabc.edu.br; juliana.souza@ufabc.edu.br

¹Centro de Ciências Naturais e Humanas, UFABC.

Keywords: Microwave-assisted synthesis, Tungsten oxide, Water splitting.

Highlights

Microwave-assisted Synthesis of WO₃; Controlling crystalline structure and morphology; Investigation of annealing temperature; Enhancement of activity towards oxygen evolution after thermal treatment.

Abstract

WO₃ is a widely reported semiconductor for water splitting [1]. Therefore, optimizing its synthesis process by controlling morphology and crystalline structure is advantageous [2]. The monoclinic phase of WO₃ is often reported as the most active phase for photo(electro)catalysis purposes. However, the annealing step is required in several routes to obtain a crystalline material [1]. Here, WO₃ samples were rapidly obtained using WCl₆ and ethylene glycol via microwave approach. The mixture was irradiated in two steps: (i) at 100 °C for 1 min using power of 30 W and (ii) at 240 °C for 10 min, 80 W. The products were washed twice with isopropanol and once with acetone and dried at 60 °C for 2h. The annealing step was investigated at various temperatures for 1 h to track whether the changes are attributed to a microwave effect or a solid-state synthesis during the thermal treatment. Thus, the annealing step was repeated for WCl₄ (the precursor). After that, the microwave-treated materials were tested for oxygen evolution reaction (OER).

The as-prepared material was identified via XRD as WO_{2.79}, exhibiting the most intense peak at 23° that is related to a preferential growth along the plane [010] (Figure 1a) [3]. This proposition is supported by the SEM image of this sample (Figure 1b), where it is possible to observe the needle-like morphology – associated with growth in one dimension. XRD of the annealed samples has shown that at 400 °C WCl₄ does not exhibit a well-defined crystalline structure. The peaks are mostly broad which is commonly associated with low crystallinity. On the other hand, up to 400 °C, the microwave synthesized samples show crystalline phase of WO_{2.79}, and the morphology remains needle-like. Only at 600 °C both samples show a clear phase transition to the monoclinic phase of WO₃. However, only the microwave-treated material exhibits a well-defined morphology of wrinkled rods, probably due to the coalescence of needles. Linear voltammetry (LV) of microwave synthesized samples (Figure 1c) shows that up to 0.4 V, WO_{2.79}, and WO₃ annealed at 400 °C had activity towards OER; however, the current enhanced more than eight times after the thermal treatment at 600 °C.

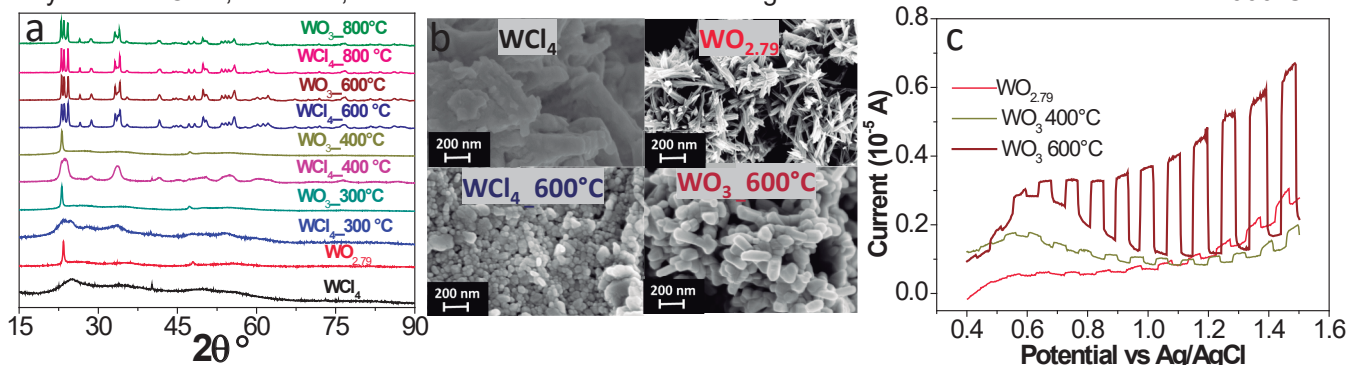


Figure 1. (a) XRD and (b) SEM images of the samples. (c) OER of the microwave synthesized samples before and after annealing LV was performed at 0.5 mol L⁻¹ H₂SO₄, using Pt as counter electrode.

[1] Zheng, G, et.al. *Nanoscale*, **11**, 18968-18994 (2019).

[2] Deshmukh, R. & Niederberger, M. *Chem. – A Eur. J.* **23**, 8542–8570 (2017).

[3] Cheng, W. *Angew. Chem. Int. Ed.* **54**, 340–344 (2015).

Agradecimentos/Acknowledgments

FAPESP (2019/00904-3, 2019/26010-9, 2021/12018-8), CAPES, CEM-UFABC and ETH – Zürich.

Síntese de carbonatos cíclicos a partir de CO₂ em catálise heterogênea utilizando o COF ZnCl₂@RIO-12 como catalisador

Letícia R. C. Corrêa (PG),^{1*} Inês Paninho (PQ),² Ana Nunes (IC),² Luís Branco (PQ),² Pierre M. Esteves (PQ)¹.

leticia.ccorrea@gmail.com

¹Instituto de Química, UFRJ, Rio de Janeiro; ²Departamento de Química FCT-NOVA, Lisboa, Portugal

Palavras Chave: COF, CO₂, carbonatos cíclicos, catálise heterogênea

Highlights

Synthesis of cyclic carbonates from CO₂ and epoxides using ZnCl₂@RIO-12 as the heterogeneous catalyst

This work aimed to produce cyclic carbonates from epoxides and CO₂ catalyzed by a COF. The material used was ZnCl₂@RIO-12. Yields greater than 80% were obtained.

Resumo/Abstract

O dióxido de carbono (CO₂) tem sido amplamente explorado como matéria-prima na produção de carbonatos cíclicos. Nos últimos anos, a importância deste tema aumentou significativamente devido a esta ser uma molécula versátil, os carbonatos cíclicos podem se tornar uma plataforma para introduzir o CO₂ como uma matéria-prima renovável em diferentes áreas do setor químico^[1]. Atualmente, já são utilizados como solventes polares apróticos, aditivos de combustível, eletrólitos para baterias de lítio, intermediários em química fina, bem como monômeros na produção de polímeros^[2].

Uma das rotas mais atraentes para produzir carbonatos cíclicos a partir de epóxidos é a reação de acoplamento econômico atômico entre CO₂ (Figura 1a). Sistemas catalíticos homogêneos binários compostos de complexos metálicos juntamente com líquidos iônicos têm sido usados com sucesso. Neste trabalho o objetivo foi a o desenvolvimento de um catalisador heterogêneo para esta reação. O catalisador consiste em um material nano estruturado de alta área específica do tipo *Covalent Organic Framework* - COF, neste caso foi utilizado o RIO-12^[3], onde o ZnCl₂ foi introduzido em sua estrutura (Figura 1b). As reações foram realizadas em um reator sob pressão de CO₂ (40 bar) e na ausência de solvente e a 60 °C. Foram realizados testes em diferentes condições e a melhor condição foi replicada para diferentes epóxidos (R=epóxido de estireno, propileno de ciclohexano). Os rendimentos obtidos foram, em geral superiores a 80%, sendo bem competitivo com os catalisadores homogêneos.

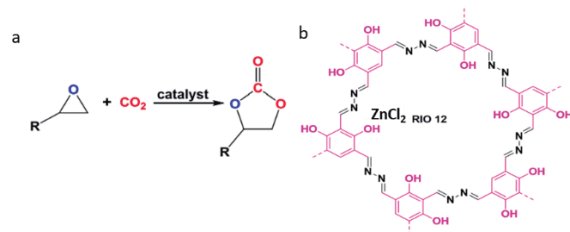


Figura 1: a- esquema da reação; b- catalisador.

Referências Bibliográficas:

[1] PANINHO, A. B. et al. Catalytic effect of different hydroxyl-functionalised ionic liquids together with Zn(II) complex in the synthesis of cyclic carbonates from CO₂. *Molecular Catalysis*, v. 499, p. 111292, jan. 2021. [2] SCHÄFFNER, B. et al. Organic Carbonates as Solvents in Synthesis and Catalysis. *Chemical Reviews*, v. 110, n. 8, p. 4554–4581, 29 mar. 2010. [3] MAIA, R. A. et al. CO₂ Capture by Hydroxylated Azine-Based Covalent Organic Frameworks. *Chemistry – A European Journal*, v. 27, n. 30, p. 8048–8055, 27 abr. 2021.

Agradecimentos/Acknowledgments

FCT-CAPES, CNPq, FAPERJ e FCT-NOVA de Lisboa pelo trabalho desenvolvido em parceria com a UFRJ.

Síntese de dissilicato de magnésio e cálcio dopado com manganês e estudo das propriedades espectroscópicas.

Juliana M. Tavares (IC),¹ Alessandro B. S. Garcia (PG),¹ Ana M. Pires (PQ),^{1,2} Airton G. Bispo Junior (PQ),³ Marian R. Davolos (PQ)^{1*}

juliana.m.tavares@unesp.br; marian.davolos@unesp.br

¹Universidade Estadual Paulista (Unesp), Instituto de Química, Araraquara; ²Universidade Estadual Paulista (Unesp), Faculdade de Ciências e Tecnologia, Presidente Prudente; ³Universidade Estadual de Campinas (UNICAMP), Instituto de Química.

Palavras Chave: Luminescência, Manganês, Silicato de cálcio e magnésio, Síntese no estado sólido.

Highlights

Manganese doped dicalcium magnesium disilicate synthesis and its spectroscopic properties study. Ca₂MgSi₂O₇:Mn²⁺ synthesis through solid-state reaction aiming for its application in lighting. Effect of site symmetry on the luminescence color.

Resumo

O Ca₂MgSi₂O₇ pertence ao sistema cristalino tetragonal, grupo espacial P4₂m e exibe em sua estrutura ao menos três sítios, sendo dos íons Si⁴⁺ e do Mg²⁺ tetracoordenados e do Ca²⁺ octacoordenado ou também hexacoordenado (estrutura incomensurável). Ao ser dopado com Mn²⁺, por conta de seu raio e carga, espera-se que esse ocupe os sítios do Ca²⁺ e/ou Mg²⁺, Figura 1 (a)^[1]. Embora a matriz possa ser obtida por diferentes rotas sintéticas, como pelo método sol-gel, visando sua aplicação em dispositivos de iluminação a síntese via estado sólido é mais vantajosa por resultar em menor número de defeitos na estrutura que reduzam a eficiência luminosa do material. A escolha do íon Mn²⁺ como dopante nesse sistema deve-se à potencial aplicação em PC-LEDs como luminóforo **vermelho**. A transição eletrônica desse íon proibida por spin ⁴T₁→⁶A₁ responsável pela emissão é sensível ao sítio de ocupação, já que a energia do estado excitado ⁴T₁ diminui com o aumento da força do campo cristalino [2]. Geralmente, Mn²⁺ em sítios octaédricos a emissão de luz ocorre na região do espectro eletromagnético de cor **vermelha**, e em sítios tetraédricos resulta em uma emissão de cor **verde**. Para investigar as propriedades espectroscópicas do Mn²⁺ na matriz hospedeira, assim como identificar o sítio ocupado pelo dopante, amostras de Ca₂MgSi₂O₇:Mn²⁺ com 10 e 25 at%, foram sintetizadas via síntese no estado sólido sendo os precursores CaCO₃, MgO, SiO₂ e MnCO₃, os quais foram cominuídos durante 1h na presença de álcool isopropílico e secos em estufa, com posterior calcinação a 1325°C durante 8h. Os materiais obtidos foram caracterizados por difração de raios X, FTIR, reflectância difusa e fotoluminescência. As medidas de fotoluminescência de ambas as amostras indicam a presença do manganês ocupando os sítios com número de coordenação e/ou campos cristalinos maiores, o que pode ser observado pela emissão com máximo em aproximadamente 700 nm, Figura 1 (b), quando a excitação foi fixada em 414,5 nm. Dessa forma pode-se concluir que Mn²⁺ ocupa preferencialmente sítios do Ca²⁺, resultado esse que confronta conclusões encontradas na literatura [3], sugerindo que o luminóforo produzido é um emissor no vermelho potencialmente aplicável em iluminação no estado sólido.

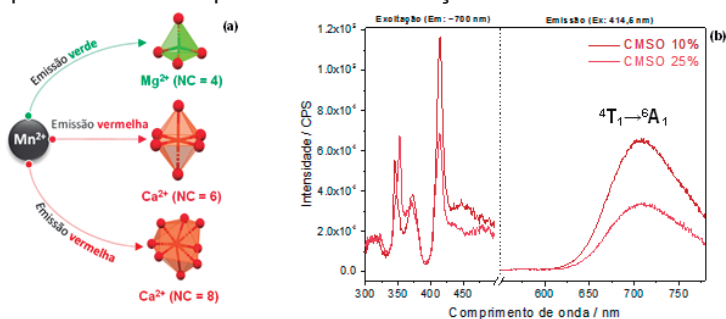


Figura 1. (a) Sítios dos íons Mg²⁺ e Ca²⁺; (b) Espectros de excitação com a emissão fixada em 700 nm, e espectro de emissão com a excitação fixada em 414,5 nm.

Agradecimentos

FAPESP (proc. n° 2020/02614-0) e CNPq (proc. n° 317610/2021-0)

Referências:

[1] *Acta Crystallographica Section B Structural Science*, v. 57, p. 443-448, 2001. [2] *Journal Of Luminescence*, v. 237, p. 118167, 2021. [3] *Applied Physics Letters*, v. 90, p. 161901, 2007.

Síntese e caracterização de $\text{Sr}_3\text{SiO}_5:\text{Eu}^{3+}$ via estado sólido para potencial aplicação em W-LEDs

Vinicius Miquelin (IC),¹ Alessandro B. S. Garcia (PG),¹ Ana M. Pires (PQ),^{1,2} Airton G. Bispo Junior (PQ),³ Marian R. Davolos (PQ)^{1*}

vinicius.miquelin@unesp.br; marian.davolos@unesp.br.

¹Universidade Estadual Paulista (Unesp), Instituto de Química, Araraquara; ²Universidade Estadual Paulista (Unesp), Faculdade de Ciências e Tecnologia, Presidente Prudente; ³Universidade Estadual de Campinas (UNICAMP), Instituto de Química, Campinas.

Palavras Chave: silicato de estrôncio, európio, fotoluminescência, W-LEDs

Highlights

Synthesis and Characterization of $\text{Sr}_3\text{SiO}_5:\text{Eu}^{3+}$ via solid state for potential application in W-LEDs. Parameters synthesis optimization of a red luminescent material based on the $\text{Sr}_3\text{SiO}_5:\text{Eu}^{3+}$.

Resumo

A síntese no estado sólido pode ser utilizada para obtenção de luminóforos contendo lantanídeos, já que esse método apresenta como vantagens o controle estequiométrico, alta pureza, além de garantir o menor número de defeitos, tornando o método ideal para a obtenção de materiais luminescentes eficientes. Para a geração de luz branca o LED disponível comercialmente (YAG:Ce³⁺) apresenta baixos índices de renderização de cor, pela deficiência espectral na região do vermelho. A dopagem de matrizes inorgânicas com lantanídeos tem como característica principal emissão de luz em diferentes comprimentos de onda, em função do dopante. O Eu³⁺ apresenta emissão característica na região do vermelho, com alta pureza de cor devido a bandas finas de emissão, e quando utilizado como dopante em silicatos, que têm altas estabilidades química e térmica, sinergicamente ambos formam materiais com potencial aplicação em dispositivos de iluminação. Esse trabalho tem como objetivo a otimização dos parâmetros da síntese no estado sólido para a obtenção de Sr_3SiO_5 , com posterior dopagem com 1% de Eu³⁺. Os precursores, SrCO₃, SiO₂ e Eu₂O₃, foram cominuídos com álcool isopropílico durante 1 h, secos, sendo por fim tratados termicamente (entre 1300 e 1500°C) durante 5 h. A formação da fase com grupo espacial P4/ncc foi confirmada por difração de raios X (Figura 1 (a, b)) e FTIR, sendo a temperatura de 1450°C a que apresenta menores concentrações de fases secundárias. A temperatura otimizada foi utilizada para obtenção de $\text{Sr}_3\text{SiO}_5:\text{Eu}^{3+}$ (1%), o qual foi analisado por fotoluminescência onde foram observadas transições (⁵D₀ → ⁷F_J, sendo J = 1,2,3,4) características do íon emissor na região do vermelho (Figura 1 (c, d)), indicando a potencialidade desse material para ser aplicado em iluminação.

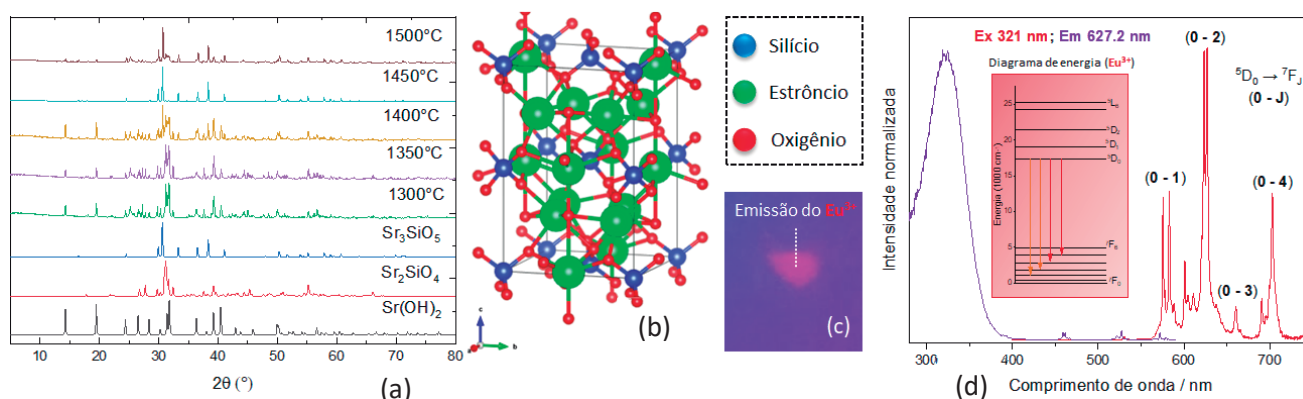


Figura 1: (a) Difratogramas de raios X das amostras em função da temperatura de síntese, (b) Estrutura cristalina do Sr_3SiO_5 , (c) Imagem da amostra $\text{Sr}_3\text{SiO}_5:\text{Eu}^{3+}$ (1%) excitada com lâmpada (285 nm). (d) Espectros de excitação (em.: 627,2 nm) e de emissão (exc.: 321 nm)

Referências: Cogent Physics (2016), 3: 1262573; J. Mater. Chem., 2012, 22, 15887.

Agradecimentos

FAPESP (proc. nº 2020/02614-0) e CNPq (proc. nº 317610/2021-0)

Scalable methods to isolate cellulose nanofibers from sugarcane bagasse.

Pedro S.T. Alonso (IC),¹ Juliana S. Bernardes (PQ)^{2*}

pedro.alonso@Innano.cnpem.br; juliana.bernardes@Innano.cnpem.br

¹Faculdade de Engenharia Química, Unicamp; ²UFABC

Palavras-Chave: Nanocelulose, Escalonamento, Bagaço de cana-de-açúcar

Highlights

Low-cost and low-energy green processes for CNF production

Pilot plant scaling production of Cellulose Nanofibers

Resumo/Abstract



Figure 1. Photograph of cellulose nanofibers suspension.

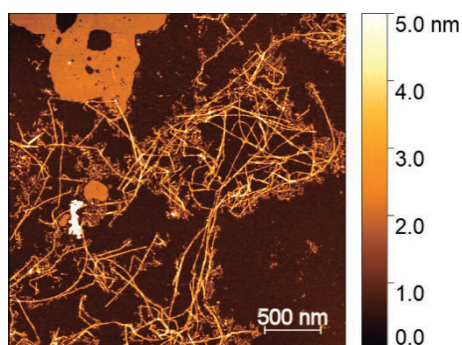


Figure 2. Picture of the nanofiber obtained by Atomic Force Microscopy

Due to their potential uses in many fields, cellulose nanofibers are a distinctive and innovative natural nanomaterial that has attracted considerable attention. Researchers are constantly looking for more effective, commercially viable, and environmentally friendly production processes to meet the expanding demand. Conventional production technologies, which include a variety of physical, chemical, and physicochemical approaches, currently need to be improved for this purpose and have several drawbacks, such as lengthy processing times and high costs. In the present work, we evaluated a simplified TEMPO (2,2,6,6-tetramethylpiperidine 1-oxyl radical)-catalyzed oxidation methodology to extract cellulose nanofibers from sugarcane bagasse on a laboratory scale.

By increasing the oxidant agent concentration (up to 50 mmol of NaClO per gram of cellulose) and the reaction time (from 2h to 6h), we observed that fibers bleaching, and oxidation could simultaneously occur, reducing two processes (pulping and bleaching) and two washing steps. In addition, low-energy mechanical treatment (7 min in Ultraturrax, 20,000 rpm) transformed the fibers suspension into a highly viscous and transparent gel, with high yield (ca 30%). An AFM (Atomic Force Microscopy) characterization (Figure 2) showed that the diameters of the fibers were in fact in the nanoscale, with most of them being under 5nm. These preliminary results reveal that cellulose nanofibers can be successfully isolated from sugarcane bagasse using a simplified methodology and may be a potential route for upscaling at the Pilot Plant from the Brazilian Biorenewables National Laboratory.

Agradecimentos/Acknowledgments

Sensing of pesticide thiamethoxam using gelatin carbon dot

Ana Julia G. Baviera (IC),¹ Maria Vitória P. Vaz (IC),¹ Mayara Martins Caetano (PG)² e Renata Galvão de Lima (PQ)^{1,2*}.

ana.baviera@ufu.br; renatagalvao@ufu.br.

¹Instituto de Ciências Exatas e Naturais do Pontal-ICENP, Universidade Federal de Uberlândia, Ituiutaba, MG, Brasil; ²Instituto de Química (IQ), Universidade Federal de Uberlândia (UFU), Uberlândia/MG, Brasil

Palavras Chave: Carbon dot, Gelatin, Pesticide, Quenching fluorescence emission, and Inner filter effects.

Highlights

The blue fluorescence emission from gelatin carbon dot used by sensing studies for the determination of the pesticide thiamethoxam (THI).

Resumo/Abstract

The fluorescence method using carbon dots (CDs) nanomaterials has been used in determination of pesticides and medicines present in food and wastewater^[1]. The present work presents the preparation of carbon dot from gelatin, as well as sensing studies for the determination of the pesticide thiamethoxam (THI). The carbonaceous precursor used in CDs synthesis were gelatin and the hydrothermal technique via domestic microwave irradiation. The hydrothermal process was done in the presence of NaOH 1mol/L/ethanol. After purification by dialysis bag, the CD_g exhibit fluorescent emission at 395 nm under λ_{ex} = 240 nm and 320 nm and fluorescence stability in aqueous solution (pH=7) during 30 days under 5 °C. At pH ~7 (Britton–Robison buffer solutions) was shown the fluorescence emission maximum. The fluorescence emission of the CD_g, in addition to that of THI, were affected gradually by quenching of the 395 nm band, with increasing concentrations of THI under λ_{ex} = 240 nm (Fig. 1a). The fluorescence quenching was not observed when the studies were done using λ_{ex} = 320 nm. Considering that the THI show electronic absorption at 256 nm (Fig. 1b), it's possible to suppose that the fluorescence quenching mechanism is based in inner filter (IFEs)^[2]. The quenching efficiency (F_0-F/F_0) presented a good linear relationship ($R^2 = 0.9807$) versus the concentration of THI in the range 0.08–1.03 mg/mL (Fig. 1a).

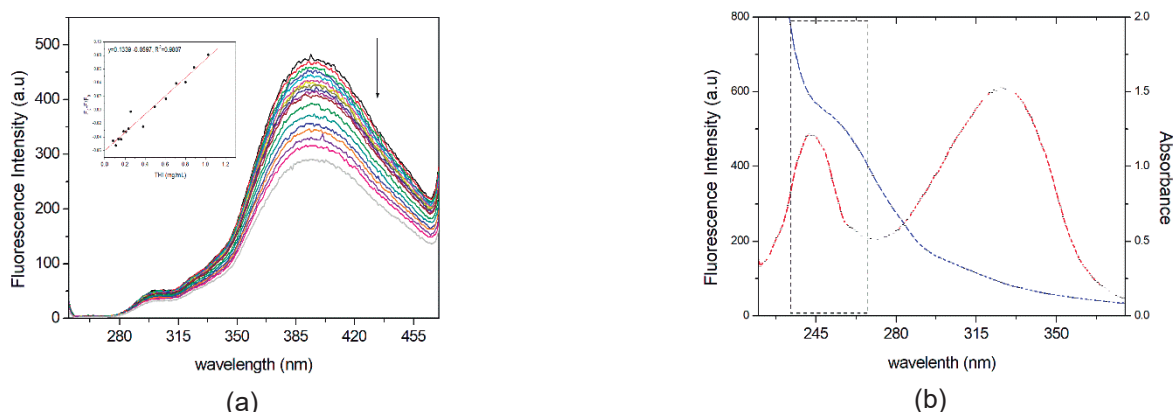


Figure 1. Quenching fluorescence emission of CD_g in presence of THI (0.08–1.03 mg/mL) under λ_{ex} = 240 nm (slit ex:5; em:10) in BR buffer solution at pH=7 (a) and UV visible of THI (blue line) and excitation fluorescence spectra of CD_g (λ_{em} =395 nm) (red line) (b).

[1] MANDAL, P. et al. *New Journal of Chemistry*, 43, 12137-12151, 2019.

[2] SILVA, L.F. et al. *Luminescence*, 2022. <https://doi.org/10.1002/bio.4410>

Agradecimentos/Acknowledgments

RELAM (UFU Multiuser Laboratory).

SERS spectroscopy of chitosan and nanocellulose in films containing silver nanoparticles

Amanda Cota Marques (PG),¹ Daphne Fonseca de Coppoli Lanferini (PG),¹ Antonio Carlos Sant'Ana (PQ),¹ Michele Munk (PQ)².

amandacmarq@gmail.com; daphnecoppoli@gmail.com

¹Departamento de Química, UFJF; ²Departamento de Biologia UFJF

Palavras-Chave: Drug delivery; biodevice; cellulose nanofiber; nanocomposite; surface chemistry; Raman spectroscopy.

Highlights

Chemical interactions of chitosan, nanocellulose and silver nanoparticles were investigated by SERS spectroscopy. Such materials in combination can be used in biological applications as artificial skin.

Resumo/Abstract

Cellulose nanofibers (NFC) can be used as carriers for topical and transdermal drug delivery of antibiotics for possessing novel properties that represents potential for an effective device for controlled drug delivery system (DDS). Therefore, to explore these properties of cellulose nanofibers, we can use those as a DDS for antifungal and antibacterial drugs. NFC also serves as an efficient physical barrier against any external infection. NFC-based

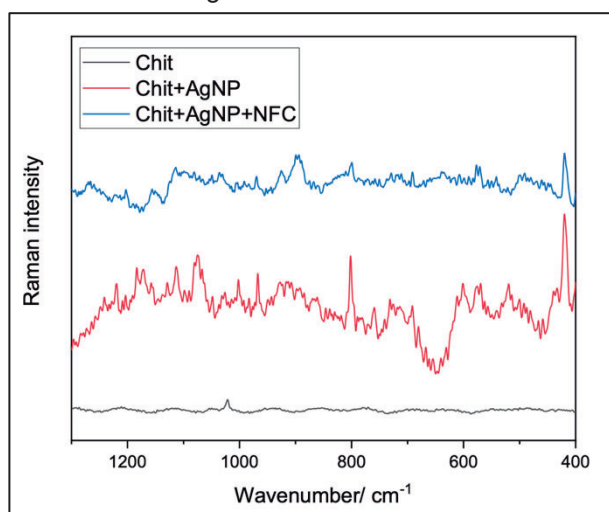


Figure 1: Raman and SERS spectra of analyzed films.

antimicrobial biomaterials are fabricated by the combination of cellulose nanofibers and antimicrobial agents by utilizing physical or chemical strategies. Chitosan (Chit) also exhibits several interesting biological activities, including antimicrobial activity. Silver nanoparticles (AgNP) have attracted intensive research interest because of their important applications in a wide range of applications, including antimicrobial effect, rich surface chemistry and high efficiency as substrate for surface-enhanced Raman scattering (SERS) spectroscopy. In this work, the SERS activity of the combination of NFC, Chit and AgNP in film structures was investigated, aiming for future applications such a material in combination with antifungal and antibacterial drugs for treatments of induced infections. AgNP aqueous suspension was prepared as proposed by Creighton¹ and characterized by UV-VIS-NIR and Zeta potential, showing a maximum extinction at 380 nm, and the average size of 30 nm. Such results are compatible with the requested AgNP characteristics for antimicrobial applications.

References:

- 1) CREIGHTON, J. Alan; BLATCHFORD, Christopher G.; ALBRECHT, M. Grant. Plasma resonance enhancement of Raman scattering by pyridine adsorbed on silver or gold sol particles of size comparable to the excitation wavelength. **Journal of the Chemical Society, Faraday Transactions 2: Molecular and Chemical Physics**, v. 75, p. 790-798, 1979.

Agradecimentos/Acknowledgment

Authors would like to thank the financial agencies CNPq, CAPES and FAPEMIG for financial support and fellowships.

Silica particles decorated with Ir(III)-Eu(III) heterobimetallic complex aiming for oxygen sensing: a luminescent, cytotoxic, and cell imaging study

Felipe S. M. Canisares (PG),¹ João A. O. Santos (PG),¹ Alessandra M. G. Mutti,² Ana M. Pires (PQ),^{1,2} Marian R. Davolos (PQ),² Sergio A. M. Lima (PQ)^{1,2}

manrique.canisares@unesp.br;

¹Departamento de Química Analítica, Físico-química e Inorgânica, IQ-UNESP; ²Departamento de Química e Bioquímica, FCT-UNESP

Keywords: silica particles, bimetallic complex, ratiometric sensing, bioprobe, low cytotoxicity, cell imaging.

Highlights

Homogenous spherical particles, Low cytotoxicity in Huh-7.5 cell line, Luminescence response within the cells, Dual-emission in the visible spectral region.

Abstract

The low concentration of tissue oxygen, hypoxia, is a common characteristic of many diseases such as cardiac ischemia, inflammatory diseases, brain abnormalities, and solid tumors¹. Because of this, oxygen measuring and imaging have drawn attention in the field of diagnosis and therapy due to their important role in understanding different physiological and pathological processes. Among the techniques used to identify and quantify oxygen in biological medium, luminescence imaging methods display several advantages, such as minimal invasiveness, fast response, high sensitivity, etc... For years, these luminescent probes were mainly composed of one emission signal, which have low reliability since their degradation may modify the measuring calibration. Ratiometric probes have the potential to overcome these issues due to their dual-emission, which works as a self-calibration to measure more sensitive and accurate detection². In this work we have synthesized luminescent silica particles (SiO₂) decorated with a bimetallic Ir(III)-Eu(III) complex for future applications as oxygen sensing in biological medium. In a heterobimetallic Ir(III)-Eu(III), the Ir(III) complex acts as a ligand to the Eu(III) ion, and because its excited state is typically a triplet, it may be sensitive to the presence of triplet oxygen. SiO₂ were synthesized by the classical sol-gel method to support the complexes and act as a carrier in biological media, since the complex is not soluble in water. Ir(III)-Eu(III) complex was grafted using a step-by-step procedure resulting in 200 nm-spherical silica particles (SiO₂-Eulr), size estimated by TEM images. The surface charge of -14.20 mV of the nanoparticles, measured by zeta potential in PBS buffer, formed a stable colloidal suspension. The final product exhibited a yellow emission by combining the green and red emissions from the Ir(III) component and the Eu(III) ion, respectively. It was observed that the emission from the Ir(III) complex is quenched by the oxygen concentration, while the Eu(III) emission is not affected. Toxicity assays were carried out using Huh-7.5 cell line, and the SiO₂-Eulr nanoparticles were not toxic in concentrations between 1.56 and 400 µg·mL⁻¹. For acquisition of confocal microscopy images, these cells were incubated in a suspension of 50 µg·mL⁻¹ of SiO₂-Eulr for 4 h. The images revealed the internalization of the nanoparticles by the cells, keeping their luminescent properties, since the green and red emissions were detected individually by different emission channels. These results suggest that the material is a promising ratiometric luminescent probe for labeling cells and detecting oxygen in biological media.

Acknowledgments

Capes (88887.341772/2019-00), CNPq (304003/2018-1), Fapesp (2019/26103-7), and Fulbright.

¹ Wen, Y., Zhang, S., Yuan, W., et al. Afterglow/Fluorescence Dual-Emissive Ratiometric Oxygen Probe for Tumor Hypoxia Imaging. *Analytical Chemistry* (2023).; ² Guo, L., Tian, X., Zhu, C., Hussain, et al. A dual-emission fluorescent ratiometric probe based on bimetallic lanthanide complex interacted in nanoclay for monitoring of food spoilage. *Sensors and Actuators B: Chemical*, 366 (2022) 131992.; ³Chen, F. F., Bian, Z. Q., Liu, Z. et al. Highly efficient sensitized red emission from europium (III) in Ir– Eu bimetallic complexes by 3MLCT energy transfer. *Inorganic chemistry*, 47(7) (2008) 2507-2513.

SILICON QUANTUM DOTS: SYNTHESIS, OPTIMIZATION, CHARACTERIZATION, AND VALIDATION AS ELECTROBIOSENSOR

Heshiley C. Correia da Silva* (PG),¹ **Helen C. Ferraz** (PQ),² **Ana Maria Rocco** (PQ),¹

heshiley95@eq.ufrj.br; amrocco@eq.ufrj.br

¹ Universidade Federal do Rio de Janeiro, Grupo de Materiais Condutores e Energia, Programa de Engenharia de Processos Químicos e Bioquímicos /EPQB; ² Universidade Federal do Rio de Janeiro, Programa de Engenharia Química/COPPE

Palavras-Chave: *Quantum dots, silicon, electrobiosensor*

Highlights

Study of a one-step "green synthesis" of silicon quantum dots.
Carbon paste electrodes modified with silicon quantum dots.
SiQD characterization.

Abstract

Quantum dots (QDs) are synthetic semiconductor nanocrystals with unique optical and electronic properties whose particular characteristics have drawn attention in biotechnology. These particularities have stimulated the intensive use of QDs in bioanalytical, biophysical, and biomedical research [1]. This interest results from characteristics such as having a similar size to proteins and nucleic acids, which allows their functionalization for different analytical systems of interest. In addition, it becomes possible to obtain them in different sizes within the nanometer scale. The modification of electrodes is the most common strategy to improve the performance of electrochemical biosensors, besides being an approach that allows improving the analytical signal (current) of the device and/or introducing functional groups to favor the immobilization of biomolecules [2]. In this sense, this work presents the development and characterization of a carbon electrode produced by incorporating silicon quantum dots (SiQDs) into carbon paste. SiQDs were synthesized by the coprecipitation method [3], modifying the precursors to study the best synthesis conditions. The one-step green synthesis used 3-Aminopropyltriethoxysilane (APTES) and 3-Aminopropyltrimethoxysilane (APTMS) as Si sources and sodium L-ascorbate (AS) as a reducing reagent. TEM, DLS, zeta potential, and spectrophotometry performed characterization. Cyclic voltammetry (CV) monitored all electrode modification steps using a potassium ferrocyanide solution. The SiQDs obtained in an aqueous medium showed a maximum emission at 450 nm (in blue) and a hydrodynamic diameter of (3.04 ± 0.02) nm. In preliminary electrochemical analyses, the SiQD-modified carbon electrode showed variations in signal amplitude with higher current density and shifting of peak current density to lower potentials concerning the CV carbon electrode, thus demonstrating to be an appropriate material for use in studies of electrochemical biosensors. Experiments with dopamine and mercury solutions evaluated the selectivity of SiQD-based electrodes. Trials for immobilization of horseradish peroxidase (HRP) enzyme for peroxide determination are in progress.

Acknowledgments

Coordenação de Aperfeiçoamento de Pessoal de Nível Superior (CAPES)

Reference

- [1] Kargozar, S; Hoseini, S.J; Milan, P.B, Hooshmand, S; Kim, HW, Mozafari, M. Quantum Dots: A Review from Concept to Clinic. *Biotechnology Journal*, v. 15, n. 12, pp. 2000117. <https://doi.org/10.1002/biot.202000117>
- [2] ARYA, S. K. et al. Capacitive aptasensor based on interdigitated electrode for breast cancer detection in undiluted human serum. *Biosensors and Bioelectronics*, v. 102, n. 2017, p. 106–112, 2018. DOI: 10.1016/j.bios.2017.11.013.
- [3] ZHOU, Yanxia et al. Development of silicon quantum dots based nano-fluid for enhanced oil recovery in tight Bakken cores. *Fuel*, v. 277, p. 118203, 2020. <https://doi.org/10.1016/j.fuel.2020.118203>

Simple synthesis of hierarchically porous carbon from spent coffee grounds to remove emerging contaminants.

Rubens Lucas de Freitas Filho* (PG)¹, **Lucas Coelho de Oliveira** (IC)¹, **Ana Paula de Carvalho Teixeira** (PQ)¹
rubensfreitas@ufmg.br; anapct@ufmg.br

¹Departamento de Química, Instituto de Ciências Exatas (DQ-ICEX) - UFMG

Keywords: Hierarchical porous carbon, biomass, spent coffee grounds, adsorption, emerging contaminants.

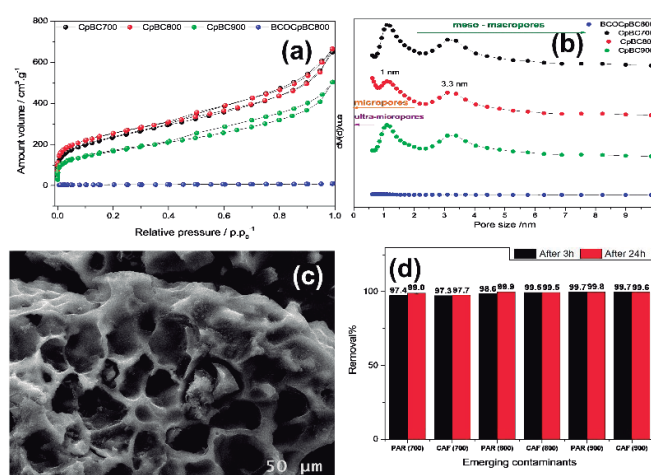
Highlights

Synthesis of hierarchical porous carbon from spent coffee grounds (biomass waste) for removal emerging contaminants (caffeine, paracetamol) from water.

Resumo/Abstract

In this work hierarchical porous carbon (HPC)¹ were prepared using spent coffee grounds as carbon source and zinc chloride as an activated agent.² The HPC were obtained by template-free route from biomass pyrolysis. The materials were characterized by the techniques of elemental analysis (CHNSO), XRD, TG, SEM, Raman spectroscopy, EDS, Physisorption analysis (BET) and zero charge point. The HPCs showed macro/meso/microporosity and specific surface areas between 783 – 919 m².g⁻¹, and total pore volume between 0.920 – 1.029 cm³.g⁻¹. The materials presented high carbon contents (>81%) and a multimodal distribution with maximum 1nm and 3.3 nm, and average diameter of 0.614 and 1.096 nm respectively. The hierarchical porous carbon were applied in the removal of emerging contaminants (caffeine, paracetamol) from water. The materials showed removals capacity above 98% for caffeine and paracetamol in just 3 hours of contact. Kinetic and adsorption isotherms studies for caffeine and paracetamol demonstrated that most materials follow pseudo-second order kinetics. On the other hand, the adsorption isotherms adjusted better to the Sips model obtaining q_{max} values of 376 mg.g⁻¹ and 255 mg.g⁻¹ for caffeine and paracetamol respectively.

Figure 1: Isotherms of nitrogen sorption of HPC(a), Pore size distribution of HPC (b), SEM images of HPC (c) and (d), Adsorption tests for removal emerging contaminants from water.



References:

- 1 R. W. Fu, Z. H. Li, Y. R. Liang, F. Li, F. Xu and D. C. Wu, *New Carbon Mater.*, 2011, **26**, 171–179.
- 2 J. Xu, B. Xue, C. Liu, C. Xia, M. Li and R. Xiao, *Sustain. Energy Fuels*, 2021, **5**, 3884–3894.

Agradecimentos/Acknowledgments

CNPQ, CAPES, UFMG Microscopy Center, ESCALAB, FUNDEP, INCT Midas and Chemistry Department UFMG.

46ª Reunião Anual da Sociedade Brasileira de Química: "Química: Ligando ciências e neutralizando desigualdades"

Singlet Molecular Oxygen Generation via Unexpected Emission Color-Tunable CdSe/ZnS Nanocrystals for Applications in Photodynamic Therapy

¹Zahid U. Khan (PQ), ²Latif U. Khan (PQ), ³Hermi F. Brito (FM), ⁴Magnus Gidlund, ¹Paulo D. Macio (FM).^{1*}

zahid@iq.usp.br; pdmascio@iq.usp.br

¹Department of Biochemistry Chemistry, Institute of Chemistry, University of São Paulo (USP), Zip Code 05508-000, São Paulo, SP, Brazil

²Synchrotron-light for Experimental Science and Applications in the Middle East (SESAME), P.O. Box 7, Allan 19252, Jordan

³Department of Fundamental Chemistry, Institute of Chemistry, University of São Paulo (USP), 05508-000, São Paulo-SP, Brazil.

⁴Department of Immunology, Institute of Biomedical Sciences-IV, University of São Paulo (USP), 05508-000, São Paulo-SP, Brazil.

Palavras Chave: Quantum dots, Ion exchange, Singlet molecular oxygen generation, Cellular labeling, Cellular uptake mechanism.

Highlights

This work presents the synthesis and characterization of series of color-tunable CdSe/ZnS core-shell QDs and their evaluation for photodynamic therapy. The color-tuning was achieved unexpectedly as *result of* interfacial alloying via an anion exchange (AE) of Se²⁻ by S²⁻ during overcoating of CdSe core by ZnS. Solvent system of 1-dodecanthaiol (DDT) and oleylamine (OLA) was used as a sensitive parameter to induce the AE. The QDs demonstrated efficient singlet molecular oxygen generation, induced no cell activation and presented good biocompatibility in RAW macrophages. The cells endocytosed the QDs *via* energy-dependent pathways and displayed enhanced fluorescence in the intracellular regions.

Resumo/Abstract

It is highly desirable in biomedical sciences to utilize the multifunctional nanoparticles of similar size with tunable emission. Since the optoelectronic properties of quantum dots (QDs) originate from size-dependent quantum confinement effects; therefore, we developed an alternate approach to synthesize color-tunable CdSe/ZnS QDs based on interfacial ion exchange (predominantly exchange of Se²⁻ by S²⁻ anion), using 1-dodecanthaiol (DDT) and oleylamine (OLA) solvents system as a sensitive parameter. The wide-range color-tunability (490-570 nm) was achieved unexpectedly as result of interfacial alloying without a significant change in the size (from 4.45 to 4.81 nm) of QDs, as confirmed by XAFS data analysis. Owing to the molecular-like sensitization behavior, the QDs were evaluated for singlet molecular oxygen (¹O₂) efficiency. They were further studied in macrophages cells for biocompatibility, bioimaging and delivering pathways to use for future photodynamic therapy (PDT). The QDs demonstrated efficient singlet molecular oxygen (¹O₂) quantum yields (Φ_{QDs}) of 14, 12, and 18% for QDs (I), QDs (II), and QDs (III), respectively. The QDs treated cells presented high cell viability above 85% and induced no cell activation. Fluorescence and TEM images of cells manifested considerable amount of QDs in the intracellular regions. The pathway-specific inhibition measurements revealed that the QDs were internalized by cells *via* energy-dependent endocytosis predominantly macropinocytosis and other lipid raft-mediated endocytic pathways and accumulated presumably in endosome/lysosomes. This study will open new possibilities of band edge engineering and pathway-specific delivery of QDs-based theranostics into a site of interest for simultaneous bioimaging and photodynamic therapy.

Agradecimentos/Acknowledgments

The authors acknowledge the financial support by Conselho Nacional de Desenvolvimento Científico e Tecnológico (CNPq), The World Academy of Sciences for the advancement of science in developing countries (TWAS) (No. 190932/2015-5), and Fundação de Amparo à Pesquisa do Estado de São Paulo (FAPESP) (No. 2021/00356-6).

Smart packaging for meat-based products from bacterial cellulose, silk fibroin and curcumin

Daniela V. Pereira (PG),^{1*} Beatriz Damasio de Freitas (IC),¹ Hernane da S. Barud (PQ),² Maurício Cavicchioli (PQ),² Ricardo Bortoletto-Santos (PQ),^{1,3} Juliana Farinassi Mendes (PQ),⁴ Sidney J. L. Ribeiro (PG).¹

d.vassalopereira@gmail.com

¹ Institute of Chemistry, UNESP; ² University Center of Araraquara (UNIARA), ³ Universidade de Ribeirão Preto (UNAERP), Empresa Brasileira de Pesquisa EMBRAPA ⁴

Keywords: Smart Packaging, Bioplastics, Silk Fibroin, Bacterial Cellulose, Curcumin, Environmentally Friendly.

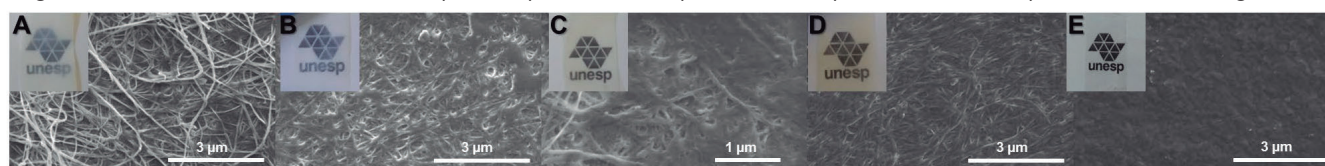
Highlights

Production of environmentally sustainable smart packaging; Silk fibroin and bacterial cellulose as bioplastics; Curcumin as a freshness indicator; Contribution to the 9th objective of the 2030 Agenda.

Abstract

Currently, society has become concerned and aware of environmental sustainability, as well as it is a growing concern among scientists, producers and consumers of the agri-food sector [1,2]. Associated with this sector, food packaging generates plastic waste and food loss, creating the need for new sustainable materials that help extend the shelf life of food. During the shelf life, food can degrade and, in the case of meat foods, release biogenic amines that are harmful to human health [1,2]. The use of intelligent packaging, such as the freshness indicator label, can overcome this problem, as they change color according to the quality of the food. The biogenic amines release can change the pH of the atmosphere inside the package, so the use of halochromic dyes on the label can be a potential option. Furthermore, the base of the sensor can be produced from biopolymers, which are biodegradable and friendly to the environment [2,3,4]. In this scenario, the purpose of this work is the development of an environmentally friendly freshness indicator label, using curcumin as a dye and biopolymers such as silk fibroin (SF) and bacterial cellulose (BC) as its base. The SF was extracted according to Rockwood et al. (2011) and Haider, Arai and Hirabayash (1993) [5,6]. BC production was done as De Salvi et al. (2014) [7]. Films of BC, SF and their mixtures were produced in mass ratio still in a wet state of SF/BC 3:1, 1:1 and 1:3, respectively, and named SF/BC-1, SF/BC-2 and SF/BC-3 – Figure 1.

Figure 1. Photos and SEM of films A) BC, B) SF/BC-1, C) SF/BC-2, D) SF/BC-3 and E) SF from left to right.



Preliminary tests have shown that the curcumin in the SF/BC-2 film has adequate potential as a freshness label. More physical-chemical and mechanical characterizations of the new material are also underway. In addition, such technology is in accordance with the 9th objective on Industry, Innovation and Infrastructure of the 2030 Agenda. Thus, investment in the materials production such as the one presented here can encourage innovation in the use of new technologies in a sustainable way.

[1] SORO, A. B. et al. **Food Packaging and Shelf Life**, v. 29, p. 100722, 2021.

[2] AHARI, H.; SOUFIANI, S. P. **Frontiers in Microbiology**, v. 12, 2021.

[3] POGGI, G.; CHELAZZI, D.; LAURATI, M. **Colloids and Surfaces A: Physicochemical and Engineering Aspects**, p. 128121, 2021. [4] GREGORY, D. A. et al. **Materials Science and Engineering: R: Reports**, v. 145, p. 100623, 2021.

[5] ROCKWOOD, D. N. et al. **Nature protocols**, v. 6, n. 10, p. 1612-1631, 2011.

[6] HAIDER, Z. A.; ARAI, Mitsuo; HIRABAYASHI, Kiyoshi. **Bioscience, biotechnology, and biochemistry**, v. 57, n. 11, p. 1910-1912, 1993.

[7] DE SALVI, D. T. B. et al. **Journal of Thermal Analysis and Calorimetry**, v. 118, n. 1, p. 205-215, 2014.

Acknowledgments

CNPq, FAPESP, CAPES, UNESP, UNIARA, EMBRAPA Instrumentation.

Spectroscopic study of a new composite from Eu^{3+} -doped cellulose nanocrystals/fibroin to obtain luminescent cholesteric film

Pedro H. L. Sanches (PG)^{1*}, Francisco R. Torres (PG)¹, Molíria V. do Santos (PQ)², José M. A. Caiut (PQ)¹.
pedro_sanches@usp.br

¹Departamento de Química, FFCLRP, Universidade de São Paulo, ²Departamento de Morfologia, Odontopediatria e Ortodontia, Faculdade de Odontologia, Universidade de São Paulo.

Keywords: Luminescence; Cellulose nanocrystals; Europium; Fibroin; Liquid Crystal.

Highlights

Obtaining Eu^{3+} -doped whiskers from bacterial cellulose.
 Spectroscopic study of the material using the lanthanide ion as a probe.
 Development of luminescent and cholesteric nanocomposites with fibroin.

Abstract

Nanomaterials have been awakened great worldwide interest as reinforcement materials in polymeric matrices. The cellulose nanocrystals (CNC), nanocrystalline domains that promote strong intermolecular interactions [1], and fibroin, a protein originated from silk that promotes excellent mechanical properties [2], have been used on the development of new functional materials. Thus, the combination of the physicochemical properties of fibroin and CNC, with the luminescent characteristics of lanthanide ions (Ln^{3+}) and optical properties of liquid crystals, may play an important role in exploring photonic development, enabling innovative sensors with great biocompatibility and applicability. In this work, different routes of obtaining CNC were studied, followed by the introduction of fibroin and the interaction of Eu^{3+} due to its characteristics that allow us to study the coordination environment, aiming the production of different structural materials, such as cholesteric films, in order to generate photonic devices with color tunable in response to external action [3]. Initially, the work focused on the preparation and study of the Eu^{3+} -doped CNC, resulting in a film with iridescent characteristics (Fig 1a and 1b), as well as carrying out some tests for the production of films of CNC-fibroin (Fig 1c). The photoluminescence studies confirmed the characteristic Eu^{3+} ion narrow bands from f-f transitions in the excitation and emission spectra. For the latter, it was possible to observe a greater intensity of the Eu^{3+} bands when excited at 318 nm (Fig 1d), the region of the cellulose matrix, when compared with direct excitation at the lanthanide ion. Finally, further studies are been carried out and will be presented, aiming a better knowledge about the coordination of Eu^{3+} ion at CNC structure to keep the cholesteric structure even after fibroin interaction.

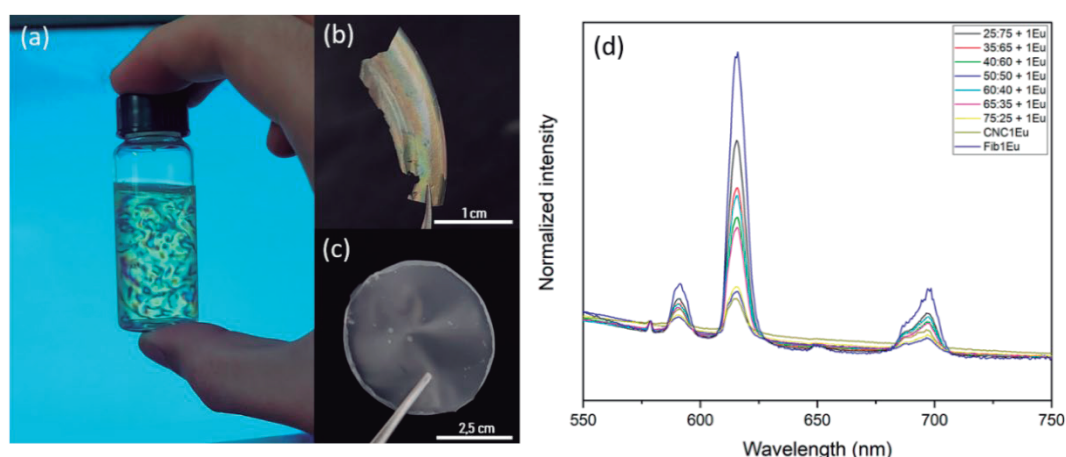


Figure 1 – (a) Suspension of CNC between polarizing filters; (b) Iridescent fragment of a CNC-only film; (c) Film obtained from 50CNC:50Fibroin (%wt) (d) Emission spectra of CNC-Fibroin films with different proportions (%wt) and doped with 1% Eu^{3+} ($\lambda_{\text{ex}} = 318 \text{ nm}$).

References: [1] Vasconcelos, N. F., et al. (2017). *Carbohydrate Polymers*, 155, 425–431. [2] Rockwood, D. N., et al. (2011) *Nature Protocols*, 6(10), 1612–1631. [3] Binnemans, K. (2015). *Coordination Chemistry Reviews*, 295, 1–45.

Acknowledgments

The authors acknowledge the Brazilian agency FAPESP (2019/18828-1) and the Universidade de São Paulo (USP) for financial support. In addition to Professor Dr. Hernane S. Barud, from the BioPolMat Group of UNIARA, for providing the bacterial cellulose membrane samples used.

Sticking with a multifunctional material through Co₃O₄/GO cross-linked heterostructures

Jéssica E. S. Fonsaca (PQ),^{1,2*} Carlos Eduardo L. dos Santos (PG),^{1,2} Sergio H. Domingues (PQ),^{1,2} Christiano J. S. de Matos (PQ).^{1,2}

je.fonsaca@gmail.com; cjsdematos@mackenzie.br

¹Mackenzie Institute for Advanced Research in Graphene and Nanotechnologies – MackGraphe, Mackenzie Presbyterian Institute, São Paulo, Brazil; ²Engineering School, Mackenzie Presbyterian University, São Paulo, Brazil.

Key words: 2D materials, heterostructures, covalent bond, multifunctionality.

Highlights

Covalent bonds were employed to guide graphene oxide (GO) and 2D-Co₃O₄ materials to a cross-linked heterostructure platform that exhibited boosted catalytic and electrochemical features.

Abstract

The vertical stacking of 2D materials has led to the now well-known van der Waals heterostructures (vdW-Hs), which have been highly explored in the nanomaterials field since they show fascinating synergetic properties. Some factors, however, have limited their applications, such as the control of interlayer distance and the chemical nature of interfaces, as they are kept together through vdW interactions. A whole new approach for obtaining these structures is through the covalent bond of the stacked layers, leading to cross-linked heterostructures (CL-Hs).¹ This is a ground-breaking strategy for the design of 3D structures with controlled connections among 2D homo/hetero structures. In this work, we are interested in producing self-standing CL-Hs composed of graphene oxide (GO) and 2D-Co₃O₄. In this sense, 2D-Co₃O₄ was functionalized with APTES (3-aminopropyltriethoxysilane), leaving -NH₂ groups available to connect to GO through amide bonds, leading to the Co₃O₄/GO CL-Hs (Figure 1A). For this to be possible, the carboxylic groups of GO surface were previously activated through the well-known cross-linkers EDC (1-ethyl-3-(3-dimethylaminopropyl) and NHS (N-hydroxysuccinimide). After the synthesis, the materials that were highly hydrophilic, turned into a self-standing hydrophobic platform (Figure 1B), suggesting the functionalization of the hydrophilic groups present in the untreated materials. It is important to highlight that Co₃O₄/GO structures without covalent linkages (*i.e.*, based on van der Waals interactions) were also obtained, and presented high hydrophilicity. Contact angle measurements attested these behaviors. Infrared spectroscopy certified the presence of all functional groups, especially the amide bonds, referred to C=O stretching at around 1640 cm⁻¹ in the spectrum. Finally, scanning electron microscopy (SEM) revealed the layered structure of the produced platform (Figure 1C).

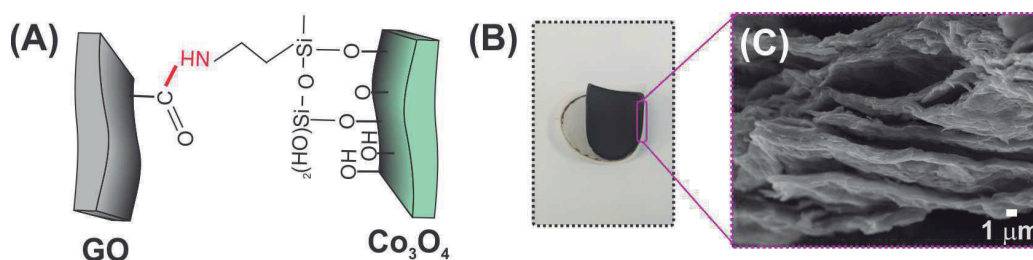


Figure 1. Co₃O₄/GO CL-Hs (A) bonding illustration, (B) photographic and (C) SEM images.

CL-Hs materials are mainly recognized by their enhanced porosity and surface area.¹ Based on that, we have investigated the catalytic and electrochemical properties of both CL and vdW Co₃O₄/GO-Hs. Results attested better catalytic performance and higher specific capacity when compared to its non-covalent analogue. The intriguing confined and controlled spaces between neighboring 2D layers in CL-Hs possibly favor chemical processes.² These new concepts enlighten to new possibilities towards the architecture of 3D platforms based on well-controlled 2D layers.

Acknowledgments

Authors acknowledge FAPESP (#2020/13288-6 and #2018/25339-4), INCT of Carbon Nanomaterials, Mackenzie Presbyterian University, CNPq (306808/2020-0).

References: 1. *Chem. Commun.*, **2017**, 53, 10093-10107. 2. *Chem. Soc. Rev.*, **2017**, 46, 1842-1874.

Study of defects in Platinum Diselenide (PtSe₂) by Raman Spectroscopy

Carolina Pirogini Torres* (TC), **Victor Secco Lemos** (PG), **João Batista Souza Junior** (PQ)

carolina.torres@lnnano.cnpem.br

¹Laboratório Nacional de Nanotecnologia, LNNano Centro Nacional de Pesquisa em Energia e Materiais, CNPEM.

²Instituto de Química, Universidade de Campinas, UNICAMP.

Keywords: Raman spectroscopy, 2D materials, Metal Dichalcogenides, Crystallographic Defects

Highlights

The Transition Metal Dichalcogenides has been studied on several areas. In this work, Raman Spectroscopy was used to study punctual defect formation on 2D materials of Platinum diselenide (PtSe₂).

Abstract

Platinum diselenide (PtSe₂) is a material from the Transition Metal Dichalcogenides (TMD) class and has been studied for applications on hydrogen evolution, optoelectronic devices, and photocatalytic applications. Due to its weak van der Waals interlayer bond, this material can be exfoliated and separated into two-dimensional (2D) sheets. Also, defects on the edges and surface can be formed during this process. The Raman spectroscopy technique is essential for several studies in 2D materials, mainly defects characterization due to the sensitivity of Raman technique with the breaking of the conservation of momentum rule, *i.e.* Raman peaks can shift, broaden, change their relative intensity, or additional peaks occurrence with the presence of defects. The principal defects studied for Raman are vacancies, isolated functional groups, substitutional atoms, dislocation, and grain boundaries. In this work, metallic platinum thin film and nanoparticles were obtained, then, PtSe₂ was synthesized by a new selenization process. The nanomaterial was characterized by Raman spectroscopy, Transmission Electron Microscopy (TEM) and High-Resolution Transmission Electron Microscopy (HRTEM), Scanning Transmission Electron Microscopy (STEM), and X-ray mapping spectroscopy (EDS) before and after the in-situ Raman temperature tests (Figure 1). Afterward, the materials were treated with butyllithium solution and characterized again. It was possible to observe the effects of exfoliation and the generation of defects on the material with the Raman peaks shift to lower energy possibly due to the local atomic change in the structure. TEM also showed that after butyllithium treatment the structure was broken preserving the short-range ordering (SRO), but losing the long-range ordering (LRO).

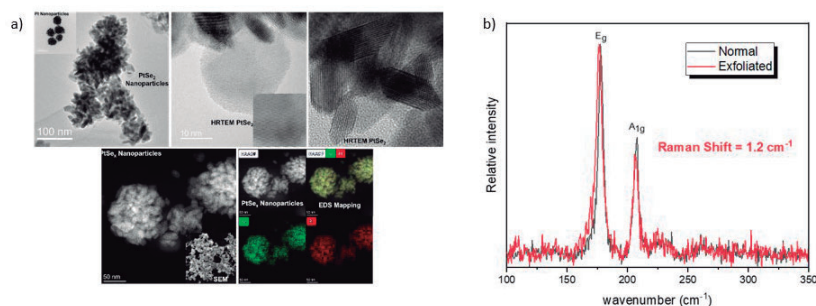


Figure 1. a) Images of TEM/HRTEM of nanoparticles PtSe₂ before and after exfoliation b) Raman spectra of nanoparticles PtSe₂ before and after exfoliation.

Acknowledgments

I would like to thank the funding agency (FAPESP), the National Center for Research in Energy and Materials (CNPEM) for the entire work structure.

Study of ternary Mg-Ca-Al LDH synthesis aiming CO₂ capture.

Rayane de S. Soares (IC),^{1*} Luiza C. de Moura (PQ),¹ Jussara L. de Miranda (PQ).¹

rayanesouzasoares55@gmail.com; lcmoura@acd.ufrj.br

¹Instituto de Química, UFRJ.

Palavras Chave: Carbon dioxide, LDH, Adsorption, Synthesis, Coprecipitation.

Highlights

Carbon dioxide intensifies global warming. LDH are good adsorbents of CO₂. They were synthesized by coprecipitation method. Characterization was performed by X-ray powder diffraction and FTIR.

Resumo/Abstract

The greenhouse effect is a natural and necessary phenomenon for life, but the intensification of the emission of greenhouse gases leads to an increase in temperature, generating global warming. In this sense, the recent technology for capturing, using and storing CO₂ (CCUS) is an alternative to mitigate the greenhouse effect¹. As a result, MMO (mixed metallic oxides) derived from the calcination of layered double hydroxides (LDH) and LDH have been considered in the capture of carbon dioxide, as they have a high surface area, porosity and basicity. LDH, also known as anionic clays, have the following formula: $[M^{2+}_{1-x} M^{3+}_x (OH)_2]^{x+} A^{m-}_{x/m} nH_2O$, which M^{2+} e M^{3+} represent divalent and trivalent metal cations, respectively,, A^{m-} represents intercalated anions and x represents the molar ratio between the cations (M^{2+} e M^{3+})². Herald et al. studied the ternary LDH of calcium, magnesium and aluminum (LDH Ca-Mg-Al) and verified how the reaction time, the molar ratio and the pH influence their formation³. The objective of this work is to obtain LDH-(Mg-x%Ca)₂Al and LDH-(Mg-x%Ca)₃Al intercalated with carbonate ion by the coprecipitation method, evaluating the effect of the concentration of Ca²⁺ and pH, aiming CO₂ capture. The synthesis of LDH-(Mg-10%Ca)₂Al and LDH-(Mg-20%Ca)₂Al were carried out by the coprecipitation method. The materials obtained were left at room temperature for 24h and heated at 120°C for 4h. They were characterized by X-ray diffraction (XRD) and Fourier Transform Infrared Spectroscopy (FTIR). The diffractogram of LDH-(Mg-10%Ca)₂Al presented the following characteristic peaks of LDH: 11,8° (003), 23,4° (006), 34,8° (009), 38,6° (015), 45,9° (018), 60,6° (110) and 62,3° (113). However, it showed peaks 26.3°, 27.5° and 29.7° indicating that a by-product was formed. The FTIR spectrum showed the following bands: O-H stretching in the region 3500-2000 cm⁻¹, water angular deformation at 1640 cm⁻¹ and carbonate ion stretching at 1372 cm⁻¹. In the region from 1200 to 400 cm⁻¹, the vibrational modes of MgO₆ and AlO₆⁴ are observed. The diffractogram of LDH-(Mg-20%Ca)₂Al indicated the formation of CaCO₃. Thus, LDHs are being synthesized with different percentages of calcium and pH, for the formation of ternary HDLs of pure Mg, Ca and Al.

¹XU, Yuen et al. **Resources, Conservation and Recycling**, v. 167, p. 105433, 2021.; ²Moura, L. C. 2001, 119f, Tese de Doutorado- UFRJ; ³HERALDY, E. et al. In: **IOP Conference Series: Materials Science and Engineering**. IOP Publishing, 2016. p. 012025; ⁴KAGUNYA, Winnie et al. **Chemical Physics**, v. 236, n. 1-3, p. 225-234, 1998.

Agradecimentos/Acknowledgments

PRH 20.1, ANP e LABTECH.

Study of the activity of ceria nanorods over the catalytic hydrogenation of α,β -unsaturated compounds using *in situ* Raman spectroscopy

Gustavo D L de Andrade (IC)*,¹ Fernando A. Sigoli¹ (PQ), Italo Odone Mazali (PQ),¹

g171282@dac.unicamp.br*

¹Functional Materials Laboratory - Institute of Chemistry, University of Campinas – UNICAMP, Campinas, Brazil.

Palavras Chave: Nanomaterials, Heterogenous Catalysis, Cerium Oxide, Raman Spectroscopy, Oxygen Vacancies.

Highlights

CeO₂ nanorods were used as catalysts in hydrogenation of α,β -unsaturated compounds, and studied using Raman spectroscopy. The results suggest oxygen vacancies are involved in the reaction mechanism.

Resumo/Abstract

The hydrogenation of α,β -unsaturated compounds for the formation of unsaturated alcohols is an important process for drugs, flavoring and fragrances industries.¹ The development of a new method using heterogenous catalysis would represent a valuable step towards the sustainability of the process. Cerium (IV) oxide nanorods have been recently reported as a selective heterogenous catalyst for the hydrogenation of crotonaldehyde (a 4-carbon α,β -unsaturated compound).² The adsorption of different α,β -unsaturated on the ceria surface has also been recently reported. CeO₂ is known for its high concentration of oxygen vacancies defects, which formation is enhanced by the nanorod morphology.² Furthermore, these vacancies are pointed as essential for the ceria catalytic activity. Raman spectroscopy can be used for the study of the oxygen vacancies abundance in cerium oxide, through the monitoring of the t_{2g} band position.³ In this project, cerium oxide nanorods have been synthesized, characterized, and treated to promote a higher oxygen vacancies concentration. Such nanorods were then tested for the catalytic hydrogenation of different α,β -unsaturated compounds, with the oxygen vacancies behavior being studied using Raman spectroscopy. Figure 1 illustrates the setup used for these experiments.

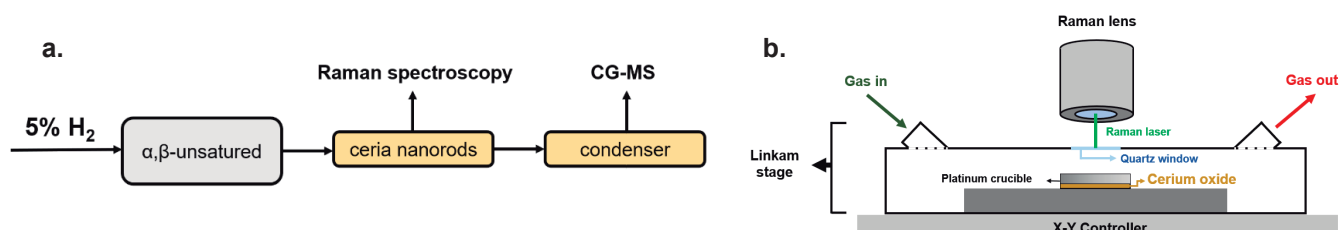


Fig. 1: a) Setup used for the catalytic tests. b) Setup for *in situ* Raman spectroscopy

The catalytic results with crotonaldehyde not only shows that the selectivity towards the carbonyl hydrogenation has been successfully reproduced using the treated nanorods, but it also reveals that the oxygen vacancies are in fact involved in the catalytic process, as shown in Fig. 2.

References:

1. M. Zielinski, W. Juszczyk and Z. Kaszukur, RSC Adv., 2022, 12, 5312–5323.
2. Z. Zhang, et. al. ACS Catal., 2020, 10, 14560–14566.
3. I. C. Silva, F. A. Sigoli, I. O. Mazali, J. Phys. Chem. C, 2017, 121, 12928–12935.

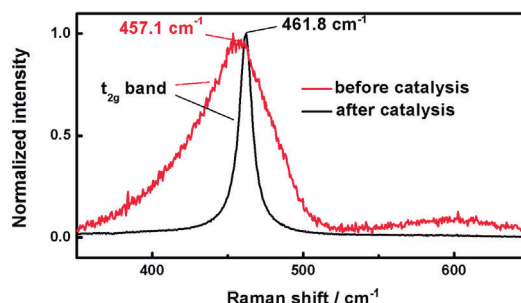


Fig. 2: Raman spectra of ceria nanorods before and after the catalytic tests

Agradecimentos/Acknowledgments



Study of the influence of different electrodes on electrochemical properties in water oxidation reactions catalyzed by Prussian blue cobalt analogue

Gabriel de O. Aparecido (PG),¹ Rafael L. Germscheidt (PG),¹ Juliano A. Bonacin (PQ)*,¹

*jbonacin@unicamp.br

¹Instituto de Química, Universidade Estadual de Campinas, 13083-970 Campinas – SP, Brasil

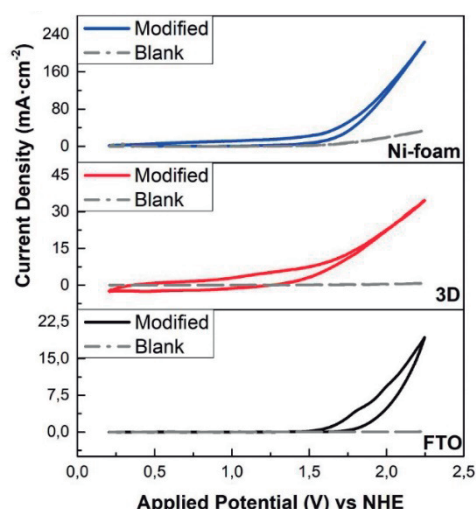
Palavras Chave: cobalt-Prussian blue, water oxidation, water splitting, 3D printed electrodes.

Highlights

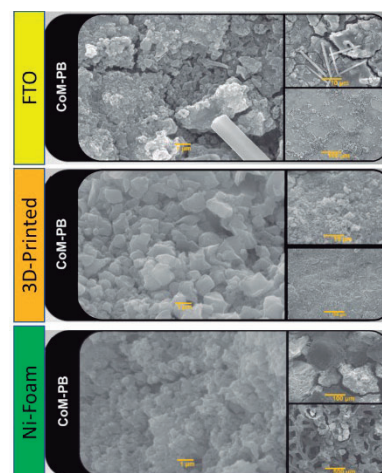
Herein, we study the influence of different electrodes (FTO, 3D printed electrode, and Ni-foam) on electrochemical properties in water oxidation reactions catalyzed by the Prussian blue cobalt analogue under mild conditions.

Abstract

A green fuel alternative to replace fossil fuels is the generation of hydrogen gas through electrolysis. However, the oxygen evolution reaction (OER) is the bottleneck of the process making the process expensive and unfeasible today. Prussian blue analogs (PBA's) are a class of three-dimensional materials that have good performance under mild conditions (pH~7) towards the OER. In this work, we evaluate the performance of the oxygen evolution for cobalt-Prussian blue analogue ($\text{Co}_3[\text{Co}(\text{CN})_6]_2$) in three different electrodes: FTO, 3D Printed electrode and Ni-foam. The differences among the electrode are evaluated using studies of cyclic voltammetry, linear voltammetry, and electrochemical impedance with and without temperature variation in order to understand the interfacial phenomena present in this system. The influence of the electrode in the electronic transfer process is also evaluated, demonstrating how the conductive characteristic of each of the electrodes decreases the resistance to charge transfer, changes the capacitance and stability of the catalyst in the face of water oxidation under mild conditions.



CV in KNO_3 (0.5 molL^{-1}) at 5 mVs^{-1} . The curves were normalized using ECSA.



SEM images of the modified electrodes.

Acknowledgments



Study of the intercalation of clusters in LDH aiming the capture and conversion of CO₂

Giovana P.S. Gonzales (IC),¹ Luiza C. Moura (PQ),¹ Jussara L. Miranda (PQ).¹

giovanagonzales@gradu.iq.ufrj.br; lcmoura@acd.ufrj.br

¹Instituto de Química, UFRJ.

Palavras Chave: LDH, cluster, CO₂ capture, ion-exchange

Highlights

The increase in CO₂ concentration is related to global warming. LDH are good options for CO₂ capture. Clusters are synthesized and intercalated in LDH. Characterization was performed by X-Ray powder diffraction and FTIR.

Resumo/Abstract

Discussions about carbon dioxide (CO₂) have been gaining more and more space due to the increase in its concentration in the atmosphere, related to the advent of global climate changes. In this context, layered double hydroxide (LDH) appears as an alternative to mitigate the effects of global warming, promoting the capture and/or conversion of CO₂¹. LDH, also known as hydrotalcite or anionic clays, are materials that have organized structures and flexible pores like clay minerals, capable of incorporating different anions in their interlayered area. In addition, they have a great ability to adsorb other species due to their large surface area, thermal stability and can be obtained at a relatively low cost. LDHs have been drawing the attention in several applications, such as in the field of antitumor therapies², catalysts² and the capture of greenhouse gases¹. The present work aims to obtain LDH-Mg_xAl-NO₃ (x=2 and 3) by the coprecipitation method and intercalated with molybdenum³ clusters from ion-exchange reactions. Clusters are representatives of a particular class of coordination compounds with metal cations being the central units. Due to the different structures and properties of the clusters, these compounds can be intercalated with LDH, allowing greater versatility in applications. To obtain LDH, Al(NO₃)₃·9H₂O, Mg(NO₃)₂·6H₂O e NaOH were used. Cluster synthesis followed the procedure described by Dorman⁴ starting from MoCl₅, AlCl₃, NaCl and metallic aluminum. The diffractograms of LDH intercalated with nitrate anions, showed 00 ℓ peaks, characteristic of LDH-NO₃, in 2 θ equal to 11.8° (003); 23.7° (006) and 35.7° (009). The infrared spectrum shows a broad band in the region of 3500 cm⁻¹ referring to the O-H stretches. There is also a band at 1640 cm⁻¹, related to the angular deformation of the water. The characteristic bands of the LDH matrix, MgO₆/AlO₆, are observed in the region between 1200 and 400 cm⁻¹. XRD results from preliminary tests indicate cluster intercalation in LDH-NO₃ due to the shift of 00 ℓ peaks to lower 2 θ values.

¹MIRANDA, J. et al. Revista Virtual de Química, v. 10, n. 6, 2018. ²CUNHA, V. R. R. et al. Química Nova, v. 33, n. 1, p. 159-171, 2010; ³MOURA, L. C. 1990. Tese de Mestrado - Pontifícia Universidade Católica do Rio de Janeiro. ⁴Dorman, W. C.; McCarley, R. E.; Inorganic Chemistry, 1974, 13(2), 491-493.

Agradecimentos/Acknowledgments

PRH 20.1, ANP e LABTECH.

Study of the thermal behavior of functionalized Fe₃O₄ nanoparticles.

Daniel B. Fumis (PG),¹ Maria L. Della-Costa (PG),¹ Caroline Gaglieri (PG),¹ Laura T. Ferreira (PG),² Rodrigo F.C. Marques (PQ),² Aroldo G. Magdalena (PQ).¹

aroldo.magdalena@unesp.br

¹Departamento de Química, FC-UNESP - Bauru-SP; ²Departamento de Química Analítica, Físico-Química e Inorgânica, IQ-UNESP – Araraquara-SP

keywords: Fe₃O₄ nanoparticles, α-Fe₂O₃, Thermal behavior, non-isothermal kinetics.

Highlights

The functionalization of the Fe₃O₄ does not change the sequence of reactions but modifies the interval of reactions.

The functionalization of the Fe₃O₄ modifies the mechanism of formation of α-Fe₂O₃.

Abstract

Temperature changes can promote several chemical and physical processes in nanoparticles. Under heating the Fe₃O₄ (magnetite) is converted to γ-Fe₂O₃ (maghemite) and α-Fe₂O₃ (hematite) structures^{1,2}. The surface functionalization of the nanoparticles can change the thermal stability of these transitions. Thus, the objective of this work was to study the thermal behavior of Fe₃O₄ nanoparticles functionalized with chitosan and EDTA (ethylenediaminetetraacetic acid). The synthesis of Fe₃O₄ nanoparticles was carried out by the co-precipitation method³ and later functionalization with chitosan¹ and EDTA². Characterizations were performed using infrared spectroscopy (IR), thermogravimetry and differential thermal analysis (TG-DTA), transmission electron microscopy (TEM) and X-ray diffraction (XRD). DTA results showed an exothermic transition (533°C for Fe₃O₄, 573°C for Fe₃O₄-EDTA and 577°C for Fe₃O₄-chitosan) associated with the formation of hematite (α-Fe₂O₃). This result showed that the chitosan coating was more effective in preventing the magnetite oxidation process². To investigate this transition (α-Fe₂O₃ formation) in more detail, DTA curves were performed at different heating rates (5, 10, 15 and 20°C min⁻¹) and the non-isothermal kinetics were studied for the Fe₃O₄ and Fe₃O₄-EDTA nanoparticles. With the increase in the heating rate, the oxidation and decomposition reaction of chitosan is shifted to the interval of the hematite formation reaction, which made the kinetic study by thermal analysis impossible. During the heating of the para Fe₃O₄ nanoparticles, a discrete exothermic event was observed between 160 and 290° C, which was associated with the formation of the γ-Fe₂O₃ intermediate. Therefore, the formation the sequence of observed reactions was (2 Fe₃O₄ + ½ O₂ → 3 γ-Fe₂O₃ → 3 α-Fe₂O₃). The non-isothermal kinetics results showed that the reaction mechanism of the formation of α-Fe₂O₃ for the Fe₃O₄ nanoparticle resembles the autocatalytic reaction (Cn) with activation energy of 205.6 kJ mol⁻¹; while the Fe₃O₄@EDTA nanoparticle was an autocatalytic reaction (Cn) for the diffusional control associated with nucleation/nuclear growth (according to Avrami/Erofeev -An). The activation energies obtained were 193.4 and 172.5 kJ mol⁻¹, respectively. Its alteration is due to the consumption of vacancies, provided from the functionalization with EDTA. In addition, the kinetic study was considered well done, due to the consistency between the theoretical and experimental curves obtained for each sample with its respective kinetic model, and the statistical results obtained.

References

1. Silva, I. M. B.; Della-Costa, M. L.; Tessarolli, B. O.; Alarcon, R. T.; Gaglieri, C.; Bannach, G.; Magdalena, A. G.; Braz. J. Therm. Anal. **2019**, 8, 79.
2. Fumis, D. B.; Silveira, M. L. D. C.; Gaglieri, C.; Ferreira, L. T.; Marques, R. F. C.; Magdalena, A. G. Mater. Res. **2022**, 25, e20220312.

Acknowledgments

The authors would like to thank Capes (Finance code 001, proc. 024/2012 and 011/2009 Pro-equipament), POSMAT/UNESP, Fapesp (Processes: 2013/09022-7, 2015/00615-0, 2016/015991 and 2021/13835-0) and CNPq (Processes: 302267/2015-8 and 302753/2015-0) for the financial support.

Superwetable anti-fouling nanolayers to improve oil-water separation

Caroline B. Aquino (PG)^{1,2}, Matheus S. Dias (PG)^{1,2}, Camila M. Maroneze (PQ),^{1,2}

carolinebrambilla.aquino@gmail.com; camila.maroneze@mackenzie.br

¹MackGraphe – Mackenzie Institute of Research in Graphene and Nanotechnologies, São Paulo, Brazil;

²Engineering School, Mackenzie Presbyterian University, 01302-907 São Paulo, SP, Brazil

Palavras Chave: Clay minerals, Oil-water separation, Nanochannels membranes.

Highlights

Clay-based nanostructured membrane with antifouling technology tuned by hydrophilic surface properties for oil-water separation.

Abstract

Due to fast industrialization, industrial chemists have increasingly invested in the separation of chemical mixtures and water/effluent system treatments.¹ Also, the complexity and energy costs of the separation methods expanded the search for alternative, efficient and economic processes. Membrane based separation methods can be an order of magnitude more efficient in terms of energy consumption than other technologies (distillation, evaporation, drying, etc.). Therefore, it is needed to find materials that are capable of separating molecules according to their chemical properties or size, resulting in effective membranes, resistant to fouling.² Bidimensional nanomaterials have been used to modify the surface of commercial membranes, modulating their properties through nanolayer architectures. Additionally, exfoliation methods to obtain ultrathin layered materials has enabled the control of the membrane thickness and form selective nanochannels. These features enhance the membrane's performance, successfully improving mass transport and the retention of small species (molecules and ions).³ However, one of the great challenges is inhibiting the fouling effect caused by different organic, inorganic and biological species. In this context, this work studied the exfoliation and application of a clay mineral (vermiculite) for the fabrication of nanostructured membranes for water treatment. Clays are abundant and have shown significant potential to be exploited, because of their special layered structure, high thermal stability, remarkable absorption and adsorption capacity and antifouling attributes for oil-water separation.⁴ Furthermore, the VMT exfoliation were carried out using ion-exchange method, obtaining lithium-VMT nanolayers (Li-VMT) (Figure 1a-b). This material was applied to modify the surface of polyamide (PA) membrane by vacuum filtration (Figure 1c). In addition, water treatment analysis showed that after 8 hours of testing, the Li-VMT nanolayers improved the wettability and fouling resistance of the PA membrane (Figure 1d). In summary, we show how the use of mineral clays can be suitable for the development of efficient membranes for oil-water separations.

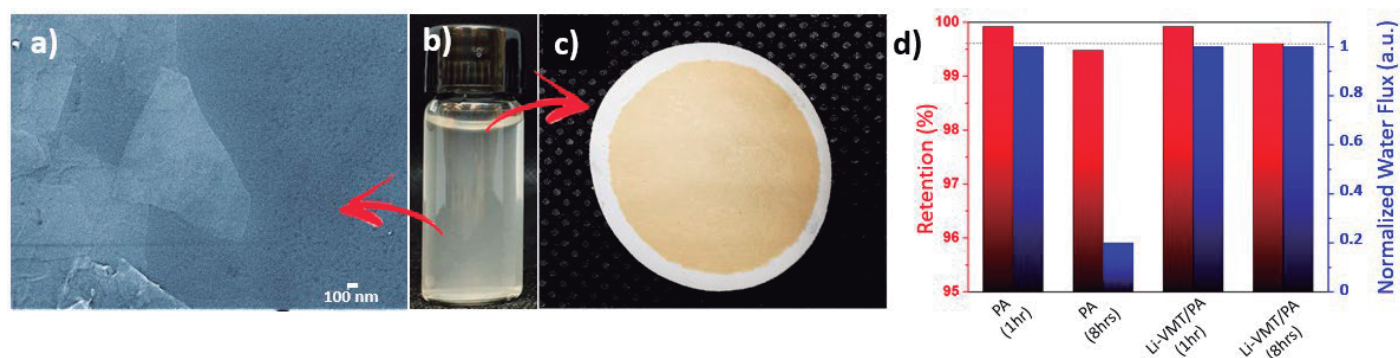


Figure 1. Li-VMT: a) SEM image of nanolayers, b) Aqueous suspension photography and c) PA membrane modified. PA and Li-VMT/PA membrane: d) Retention and Permeability result after 1 and 8 hours of filtration test to analyze efficiency and fouling properties.

Acknowledgments

Petrobras (2018/00459-7), MackGraphe and Mackenzie Presbyterian University (UPM).

References: [1] Shannon, M. A. *et al. Nature* (2008). [2] Elimelech, M. *Journal of Water Supply: Research and Technology - AQUA* (2006). [3] Anna Lee, J. W. E. and S. B. D. *Environ Sci (Camb)* (2015). [4] Zhou, Y. *et al. Adv Funct Mater* (2019).

Supramolecular assembly composed by reduced graphene oxide and cationic pillar[5]arene as a potential chemo-photothermal agent for Leishmaniasis treatment

Isabela A. A. Bessa (PG)*¹, Danilo R. H. Miranda (IC)¹, Carolina B. P. Ligiero (PQ)¹, Brunno R. F. Verçosa (PQ)², Juliany C. F. Rodrigues (PQ)², Thiago C. dos Santos (PQ)³, Célia M. Ronconi (PQ)

isabelabessa@id.uff.br; cmronconi@id.uff.br

¹Departamento de Química Inorgânica, UFF; ²Núcleo Multidisciplinar de Pesquisa em Biologia, UFRJ; ³Departamento de Química Inorgânica, UFRJ

Key-words: drug delivery systems, reduced graphene oxide, pillar[5]arene, amphotericin B, leishmaniasis

Highlights

In the present work, we developed a chemo-photothermal agent based on reduced graphene oxide and cationic ammonium pillar[5]arene, loaded with amphotericin B, for Leishmaniasis treatment.

Abstract

Carbon based materials have gained attention in nano biomedicine as nanocarriers for drug delivery systems. As a result of its similarity with graphene sheets and intrinsic property of absorbed NIR light, reduced graphene oxide is the main choice among these materials. Recently, our research group proved the effect of a photothermal agent against leishmania promastigotes cells [1]. In this work, we developed a new photothermal therapy agent based on reduced graphene oxide and a cationic quaternary ammonium pillar[5]arene, AP[5]A. GO was synthesized by modified Hummers method [2] and rGO-AP[5]A_30 was produced by attaching AP[5]A onto GO surface, by supramolecular interactions, followed by its reduction [3]. The colloidal behavior of this material was studied by zeta potential measurements. The results evidenced the successful functionalization of rGO surface with AP[5]A, since the surface charge changed to -26.4 mV (GO), to +22.4 mV (rGO-AP[5]A_30). The XPS spectra not only corroborated with this fact, but also showed the lower oxygen percentage as a result of GO's reduction by hydrazine. The amphotericin B (AmB) loaded into the system rGO-AP[5]A_30 + AmB presented a higher kinetic release rate under the NIR stimulation (Figure 1a), suggesting that the photothermal property was successfully achieved. The antiproliferative effect against *Leishmania* promastigotes was proved by an inhibition of 86 % of parasites growth, treated with rGO-AP[5]A_30 + AmB (Figure 1b). The evaluation of NIR light irradiation on the antiproliferative effect is still being performed.

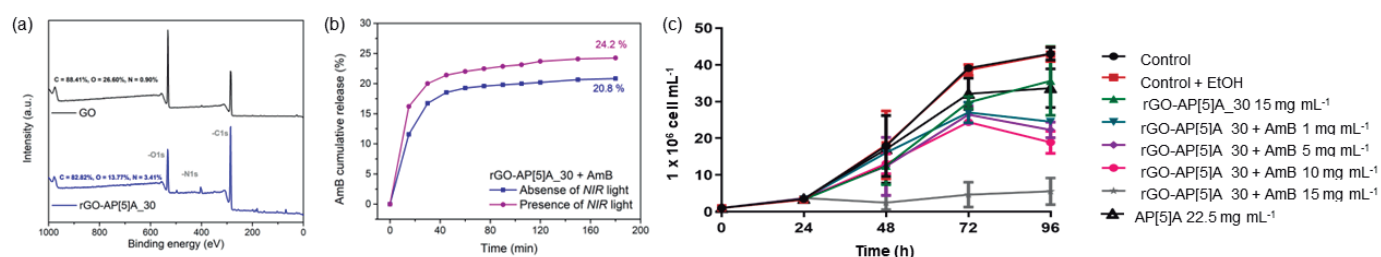


Figure 1: (a) XPS spectra of GO and rGO-AP[5]A_30; (b) AmB cumulative kinetic release curve in the absence and presence of NIR light; (c) antiproliferative effect of rGO-AP[5]A_30 + AmB, and precursors, at different concentrations, in the absence of NIR light.

Acknowledgments

UFF, CNPq, CAPES, FAPERJ, PPGQ-UFF, LQSN, LAME, LAMATE

[1] VITORINO, L. S., et al., *Colloids and Surfaces B: Biointerfaces*, **2022**, 209, 112169.

[2] DOS SANTOS, T. C., et al., *Journal of CO₂ Utilization*, **2021**, 48, 101517.

[3] ZHAO, G. et al., *Biosensors and Bioelectronics*, **2017**, 91, 863.

Supramolecular interaction of arginine with oxidized cellulose

Rafael Giovanini de Lima (PG)^{1,2}, Diego Magalhães do Nascimento (PQ)¹, Juliana da Silva Bernardes (PQ)^{1,2}.

rafaelgiovanini96@gmail.com

¹ Brazilian Nanotechnology National Laboratory, Brazilian Center for Research in Energy and Materials, Campinas, SP, Brazil;

² Nanoscience and Advanced Materials, Federal University of ABC, Santo André, SP, Brazil

Keywords: Cellulose nanofibers, TEMPO oxidation, SARS-CoV-2, Electrostatic interaction, Atomic Force Microscope (AFM), Amino acids.

Highlights

Arginine can be found in the coronavirus spike protein.

Arginine interacts with negatively charged cellulose nanofibers by electrostatic interaction.

The availability of carboxylate groups for interaction plays an important role.

Resumo/Abstract

Surfaces play an essential role in the spread of viruses. The strategy of developing materials that can inactivate them without the need for a cleaning step is very promising for preventing their spread. Recent studies have shown that the electrostatic interaction between the coronavirus and negatively charged molecules reduces its power of infection. The S protein (Spike) of SARS-CoV-2 has a polybasic cleavage site with positively charged arginine, which is exposed and unstable. To better understand this binding behavior, we evaluated, in this work, the interaction of the amino acid arginine with oxidized cellulose nanofibers presenting three charge densities (0.1, 0.62, and 1.16 mmol of COO⁻ per g of cellulose). When arginine is added, the zeta potential of negatively charged CNFs decreases; however, charge inversion was not observed because ARG molecules are zwitterionic at physiological pH, and probably not all carboxylate groups are at the surface of the fibers, available for electrostatic interaction. Furthermore, arginine molecules remain adsorbed to the surfaces of CNFs even after three days of dialysis against water, suggesting that a strong supramolecular interaction occurs. By elemental analyses, we verified that the adsorption capacity of arginine depends on the charge density of CNF, indicating that the electrostatic interaction between the guanidine moiety of arginine molecules and the carboxylate groups of CNFs plays an important role in the binding mechanism. Our results shed some light on the possible interaction between oxidized CNFs and more complex systems.

Agradecimentos/Acknowledgments

Coordenação de Aperfeiçoamento de Pessoal de Nível Superior (CAPES)

Fundação de Amparo à Pesquisa do Estado de São Paulo (FAPESP)

Conselho Nacional de Desenvolvimento Científico e Tecnológico (CNPQ)

Universidade Federal do ABC (UFABC)

Laboratório Nacional de Nanotecnologia (LNNano)

Centro Nacional de Pesquisa em Energia e Materiais (CNPEM)

Sustainable urethanesil based on castor oil doped with europium complex

Beatriz D. de Freitas (IC)^{1*}, Bruno S. D. Onishi (PG)¹, Fábio J. Caixeta (PQ)¹, Ricardo Bortoletto-Santos (PQ)^{1,2}, Francis S. R. Garcia (PG)³, Younès Messaddeq (PQ)^{1,4}, Sidney J. L. Ribeiro (PQ)¹.

bd.freitas@unesp.br

¹Institute of Chemistry, São Paulo State University (UNESP), Araraquara, Brazil; ²University of Ribeirão Preto (UNAERP); ³São Carlos Institute of Chemistry, University of São Paulo (USP), São Carlos, Brazil; ⁴Département de Physique, de génie physique et d'optique, Université Laval, Quebec City, Canada

Keywords: Sol-gel, Organic-Inorganic Hybrid, Luminescent material, Sustainability.

Highlights

Development of Hybrid urethanesil based on CO and ICPTS without metal catalyst and solvent; Incorporation of red-emitting lanthanide complex in the hybrid and the investigation of its optical properties.

Abstract

Polymers based on vegetable oils can be excellent suitable candidates for replacing fossil polymers, for example, polyurethanes (PU) based on castor oil (CO). However, the synthesis of PU materials is normally carried out using organic solvents, metals and high temperatures. To overcome these problems, the sol-gel route is an alternative approach based on mild conditions to produce environmentally friendly organic-inorganic hybrid urethanesil (Ur). Therefore, in this study, we proposed the synthesis of a sustainable organic-inorganic hybrid (OIH) based on Ur derived from CO, as well as the incorporation and interaction of europium β -diketone [Eu(tta)₃(H₂O)₂] in the organic-inorganic hybrid matrix, as shown in the Figure 1. The self-sustaining hybrid of Ur was synthesized from the reaction of 3-(triethoxysilyl)propyl isocyanate (ICPTES) and CO in a 3:1 molar ratio. The films were obtained by the sol-gel process, following the casting method. The CO-based OIH-Ur films showed high transmittance in the visible and infrared spectrum (90%) and the urethanesil showed photoluminescence (PL) with emission at 416.0 nm when excited at 319.0 nm, as shown in Figure 1. The results also revealed an increase in the intrinsic quantum yield of PL (Q_L^{Eu}) for [Eu(tta)₃(H₂O)₂]. It has been verified a Q_L^{Eu} value of 27% for the isolated complex, while a value of 49% was observed when it is incorporated into OIH PU.

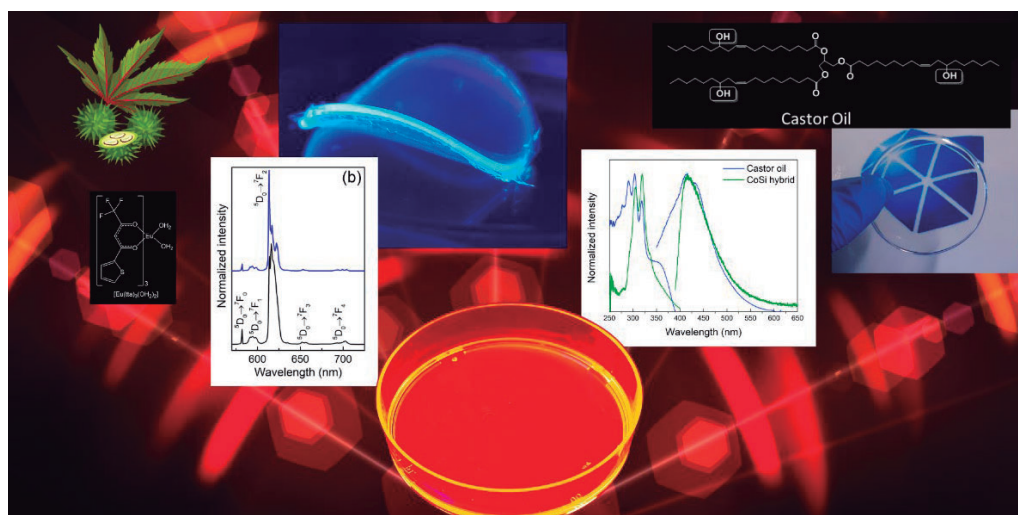


Figure 1 - Main characteristics, namely, the luminescence of the hybrid and the same doped, as well as its precursors.

Acknowledgments

The authors are grateful for financial support given by FAPESP (#2015/22828-6, #2018/07727-7, #2020/03259-9, #2022/03652-8) and CAPES (88887.499004/2020-00) for the scholarship. The authors also thank LAMF UNESP for providing institutional support and facilities to obtain results.

Synthesis and Characterization of Composite Membranes Based on ZIF-8 and Bacterial Cellulose

Augusto Henrique Piva (PG),¹ Hernane da Silva Barud (PQ),² Regina Célia Galvão Frem (PQ).^{1*}

augusto.h.piva@unesp.br; rcgfrem@gmail.com*

¹Department of Analytical, Physical and Inorganic Chemistry, Institute of Chemistry, São Paulo State University, UNESP;

²Department of Medicinal Chemistry, Araraquara University, UNIARA.

Keywords: Composite membranes, ZIF-8, Bacterial cellulose, In situ growth.

Highlights

Composite membranes were obtained by *in-situ* growth of ZIF-8 on bacterial cellulose. The effect of pre-synthesis procedure and functionalization of cellulose in the MOF ratio was investigated.

Resumo/Abstract

Metal-Organic Frameworks (MOFs) are a subfamily of coordination polymers. Due to their wide range of structures and functionalities, these materials have enormous potential for many applications¹. Nevertheless, they are typically obtained as a fine powder, which make their practical applications difficult. Therefore, the integration of MOF powders onto a supporting material creates a more processable MOF-based composite better suited for practical applications². In this work, composites were obtained by *in situ* growth of ZIF-8 on bacterial cellulose (BC) and functionalized cellulose (CMBC), which had carboxylate groups grafted on its surface. The synthesis of ZIF-8 was performed by the methodology adapted from Lai *et al*³. A pre-synthesis procedure was performed, where BC was immersed in the solution of each precursor for 20 min, then the solutions were combined and heated in a microwave oven. The resulting material was named BC/ZIF-8 mw 1. In order to increase the MOF ratio and the coverage of fiber surface, the above procedure was repeated 5 and 10 times, resulting in the materials BC/ZIF-8 mw 5 and BC/ZIF-8 mw 10, respectively. With CMBC, only 1 cycle of pre-treatment was used, and the resulted hybrid was named CMBC/ZIF-8 mw. The functionalization was confirmed by FTIR spectroscopy, while PXRD confirmed the achievement of ZIF-8 as pure phase in all materials. TG analysis allowed to quantify the MOF ratio in each membrane. It was observed an increase of the ratio with the number of cycle, from 24.58%, to BC/ZIF-8 mw 1, to 74.72%, to BC/ZIF-8 mw 5, but only a slightly increase to BC/ZIF-8 mw 10 (82.22%) and with the functionalization (32.64%). FEG-SEM images revealed the formation of nanometer-size particles, with rhombic dodecahedron morphology, but the total fiber coverage was only observed in the composite using CMBC, showing the importance of polar groups for this approach.

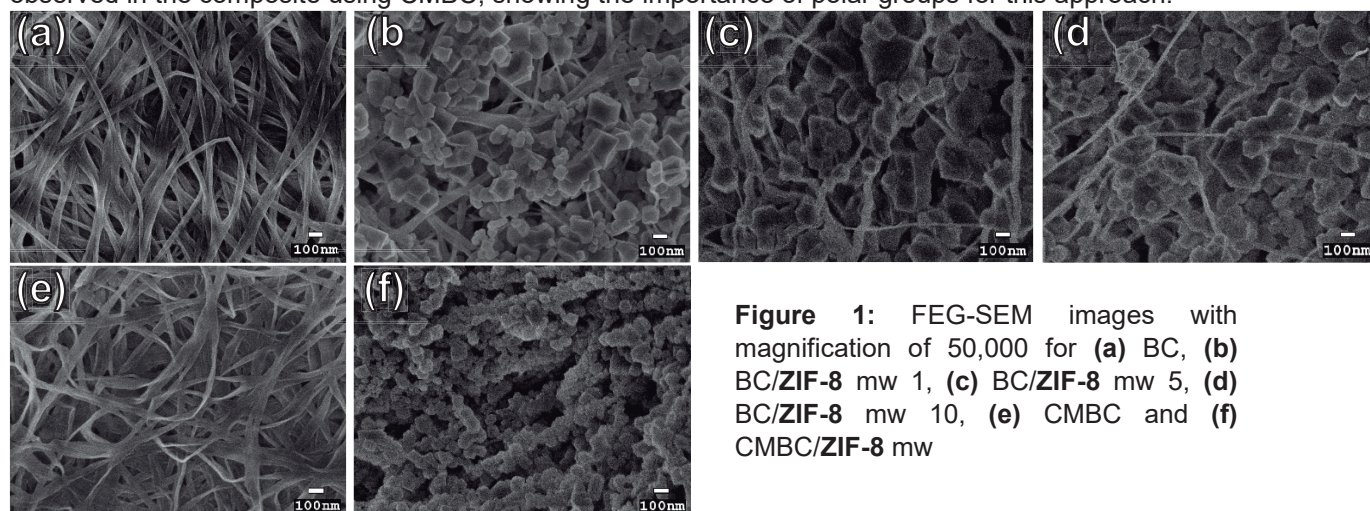


Figure 1: FEG-SEM images with magnification of 50,000 for (a) BC, (b) BC/ZIF-8 mw 1, (c) BC/ZIF-8 mw 5, (d) BC/ZIF-8 mw 10, (e) CMBC and (f) CMBC/ZIF-8 mw

[1] Kirchon, A. *et. al.* Chem. Soc. Rev., 2018, 47, 8611-8638.

[2] Ma, K. *et. al.* Chem. Mater. 2020, 32, 7120-7140.

[3] Lai, L. S. *et al.* Procedia Engineering, 2016, 148, 35-42.

Agradecimentos/Acknowledgments

The authors are grateful for the financial support of CNPq (132508/2020-6) and FAPESP (2019/19453-1).

Área: MAT

Synthesis and characterization of glasses for ultra-sensitive magneto-optical sensors.

Eduardo O. Ghezzi (IC),¹Leonardo V. Albino (PG),¹Thiago A. Lodi (PQ),¹Douglas F. Franco (PQ),¹Marcelo Nalin (PQ).

eduardo.ghezzi@unesp.br

¹Departamento de Físico-Química, Analítica e Inorgânica (IQCAr/UNESP)

Palavras-Chave: *Magneto-optical glass, Optical fibres, Magneto-optical sensors.*

Highlights

- Oxide glasses with magneto-optical (MO) properties;
- Borogalate glasses containing Tb³⁺ ions;
- Magneto-optical glass applied for development of magnetic field and electric current sensors.

Resumo/Abstract

Os vidros óxidos com propriedades magneto-ópticas (MO) vêm exibindo notoriedade em diversas áreas da ciência, além de aplicações industriais de sensores de campo magnético e de corrente elétrica^[1]. Nos últimos anos, o grupo LAVIE (IQAr-Unesp) vem estudando novas composições vítreas contendo altas concentrações de íons paramagnéticos, em especial os íons terras raras, principalmente o Tb³⁺^[1]. No presente trabalho são discutidos os resultados da síntese e caracterização de vidros borogalatos contendo entre 8 e 13 mol% de Tb₄O₇. Os vidros borogalatos foram fundidos pelo método de fusão seguido de choque térmico e caracterizados pelas técnicas de Calorimetria Exploratória Diferencial (DSC), espectroscopia Raman, espectroscopia de absorção na região UV-Vis-NIR e Rotação de Faraday para os cálculos dos valores das constantes de Verdet (V_B) em 632 nm. As curvas DSC dos vidros borogalatos mostram os valores de temperatura de transição vítrea (T_g) e do início do processo de cristalização (T_x) entre 693-704°C e 850-942°C, respectivamente. Os valores calculados para os parâmetros de estabilidade térmica ($\Delta T = T_x - T_g$) são superiores a 150°C. Estes resultados indicam que os vidros são termicamente estáveis frente ao processo de devitrificação, ademais são fortes candidatos para a preparação de fibras com propriedades magneto-ópticas. Os espectros Raman apresentam bandas atribuídas aos principais modos vibracionais de grupos boratos. Em termos de atribuições, observam-se bandas em 484, 703 e 1404 cm⁻¹, atribuídas ao surgimento de espécies B-O⁻ que indica a quebra das ligações B-O-B pela ação modificadora dos íons Tb³⁺ na rede vítrea. Os espectros de transmissão mostram uma ampla faixa de transmissão entre 0,5 µm até 1,54 µm. Em termos da caracterização magneto-óptica, o valor da constante de Verdet (V_B) é um parâmetro extremamente importante para a determinação da performance MO dos materiais. Neste trabalho, o valor de V_B (em 632 nm) obtido para o borogalato contendo a maior concentração de Tb³⁺ (13 mol% de Tb₄O₇) foi igual a $V_B = -125 \text{ rad T}^{-1} \text{ m}^{-1}$. Os resultados obtidos mostram que os vidros possuem grande potencial para a fabricação de fibras MO e para o desenvolvimento de sensores MO de corrente elétrica e campo magnético, visto que os referidos vidros borogalatos apresentam todos os pré-requisitos, tais como, alto valor de Constante de Verdet, boa estabilidade térmica e uma ampla janela de transmissão na região do Vis-NIR.

Referência: ¹ Franco, D. F.; Ledemi, Y.; Correr, W.; Morency, S.; Afonso, C. R. M.; Messaddeq, S. H.; Messaddeq, Y.; Nalin, M.; Sci. Rep, 11(1), 1–16 (2021).

Agradecimentos/Acknowledgments

Ao Professor Dr. Douglas Faza Franco pela co-orientação, ao CNPQ (PIBIT) pela bolsa concedida, à FAPESP (processo no 2013/07793-6) e ao SISFOTON-MCTI pelo auxílio financeiro.

Área: MAT

Synthesis and characterization of hybrid microspheres kaolinite/chitosan/Polyvinyl alcohol and applications in removal of emerging contaminants.

Hugo Fernando Meira dos Santos (IC), Emerson Henrique de Faria (PQ).

e-mail: hugofernando3768@gmail.com and emerson.faria@unifran.edu.br

¹Grupo de Pesquisa em Materiais Lamelares Híbridos (GPMatLam) – UNIVERSIDADE DE FRANCA (UNIFRAN). Av. Dr. Armando Salles Oliveira, 201. Pq. Universitário. Franca/SP, Brasil. 14404-600

Palavras Chave: Clay minerals; adsorption; emerging contaminants; microspheres; composites.

Highlights

Hybrid microspheres containing kaolinite, chitosan and polyvinyl alcohol were prepared and characterized; Stability in aqueous acidic and basic solutions were tested confirming the synthesis of composites stable and candidate to act as adsorbents; Preliminary adsorption studies with methylene blue reveal the higher adsorption capacity of microspheres using the combined biodegradable polymers; Reuse tests reveal the capability to regenerate the microspheres under mild conditions (NaCl saturated solution);

Resumo/Abstract

Brazil is the third major country that mines kaolinite (Kaol) with a great potential for production with higher purity and unique physical-chemical properties. The great pollution of water emerge the demand for the development of materials that could remove dangerous contaminants. In this context, the incorporation of biopolymers in Kaol opens a wide field of applications in this area as adsorbents, catalysts support, filters, barriers, and among others. This work aims to produce a competitive adsorbent with microspheres shape using Kaol, chitosan, to acts as an adsorbent and allows the synthesis of solids with microsphere shape, and also polyvinyl alcohol, commonly used in clay mineral/polymer films to improve physical chemical resistance. Briefly, the synthesis was based on a suspension of 7g of kaol in a 5%(v/v) acetic acid mixture with 2%(m/v) chitosan and 1.5%(m/v) PVAL solution, which was mechanically stirred for 24h. The resulting gel was dried, ground and suspended in a 200ml mixture containing 1%(m/v) chitosan and 1.25%(m/v) PVAL that after vigorous stirring during 2h the suspension was dripped into an 8%(m/v) NaOH solution, the microspheres were dried and washed until pH = 7. Three other microsphere syntheses were prepared for comparison, without PVAL and with single bipolymer layer. Characterization techniques was performed by X-ray diffraction, infrared absorption spectroscopy, UV-Visible Absorption Spectroscopy, thermal analysis, specific surface area using the methylene blue method, cation exchange capacity, scanning electron microscopy, equilibrium, and adsorption kinetics studies, evaluating the parameters: stirring, contact time and initial concentration of contaminant to find optimal adsorption conditions for the microspheres, which will be used in further studies in column tests for further practical applications of this research. The partial results shown that Kaol particles are homogeneously distributed into biopolymer, XRD shown typical Kaol peaks with reduction of the intensity due the mixing with amorphous polymers. FTIR shown that Kaol hydroxyl groups (3600 cm^{-1}) from edges interact with chitosan amine groups and PVAL hydroxyl groups via hydrogen bonds. The adsorption tests with methylene blue shown that a cationic interaction with microspheres is possible, the results shown a monolayer adsorption mechanism (Langmuir model), the microspheres containing chitosan and PVAL presentes the increasing of 10 times in the adsorption capacity than natural clay (with maximum adsorption capacity of 35.6 mg/g).

Agradecimentos/Acknowledgments

CAPES (finance code 001); CNPq(310151/2021-0) and FAPESP (process 2022/07773-4).
46ª Reunião Anual da Sociedade Brasileira de Química: "Química: Ligando ciências e neutralizando desigualdades"

Synthesis and characterization of nanostructured Cobalt - Gadolinium ferrite for use as biopolymeric films with antineoplastic activity

Tatiana Alves Toledo (PG),¹ Lígia Nunes de Moraes Ribeiro (PQ),¹ Denise Barros de Almeida (PQ)²

tatianatoledo04@gmail.com

¹Instituto de Biotecnologia - UFU; ²Departamento de Educação e Ciências - Núcleo de Química IF Sudeste MG

Keywords: ferrite, gadolinium, polymeric films, drug delivery, biocomposite.

Highlights

Synthesis and characterization of magnetic compounds of cobalt and gadolinium ferrite to be incorporated into biopolymeric films for evaluation of cytotoxic activity against tumor cell lines.

Abstract

Cancer is a public health concern and the development of new treatments based on nanostructured systems are promising for antineoplastic therapy. This work aims at the synthesis and characterization of nanostructured magnetic compounds based on cobalt and gadolinium ferrite to be incorporated into biopolymeric films for studies of cytotoxic activity against tumor cell lines.

CoFe_{2-x}Gd_xO₄ nanoparticles were synthesized by the coprecipitation method, with a molar ratio between salts in a proportion of 1:2 (Co:Fe) for the control and 1: (2 - x) : x (Co:Fe:Gd) for the samples, with x equal to 1, 3, 5, 7, 9 and 11. After precipitation, the suspension was heated to 98 °C and calcined at 900 °C for 1.5 h.

XRD and Raman analyzes for the control sample show cobalt ferrite (CoFe₂O₄) patterns, with a mean crystallite size of 44 nm. As for the samples with incorporated gadolinium, which present similar diffractograms, the diffraction and scattering patterns correspond to gadolinium orthoferrite (GdFeO₃), with an average size ranging from 28 to 64 nm – Fig. 1.

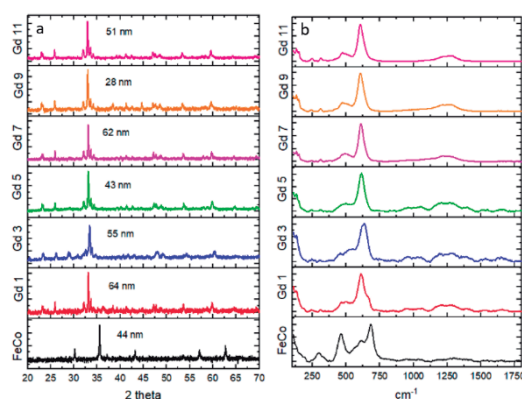


Fig. 1: a) XRD b) Raman

SEM analyzes coupled to a microanalysis detector – EDS indicate the presence of cobalt in all samples and an irregular morphology for samples with gadolinium (Fig. 2).

Amostra	Proporção Co:Fe _(2-x) :Gd _x
FeCo	1 : 1,85 : 0
Gd 1	1 : 0,85 : 1,98
Gd 3	1 : 0,88 : 5,91
Gd 5	1 : 2,61 : 10,10
Gd 7	1 : 4,21 : 14,93
Gd 9	1 : 6,09 : 17,29
Gd 11	1 : 6,79 : 18,75

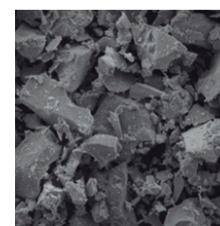


Fig.2 – EDS e MEV

The characterizations indicate that for syntheses by the coprecipitation method there is a solubility limit for the replacement of ions in the cobalt ferrite network. An excess of Fe³⁺ and Gd³⁺ ions was observed in the reaction medium (Fig. 2) that tend to aggregate around the grains in the form of GdFeO₃. This outer envelope can mask and overwhelm signals from XRD and Raman techniques by the disordered surface layer, as observed by SEM.

As future perspectives, magnetic analysis, preparation of nanostructured films and cytotoxicity assays will be carried out.

References:

- [1] R.S. Yadav, et al. *Ultrasonics Sonochemistry* (2017). [2] Hashemi, et al. *Journal of Magnetism and Magnetic Materials*, 492, (2019). [3] Ruffo, et al. *J Mater Sci: Mater Electron* 31, (2020). [4] Pinho, et al. *European Journal of Inorganic Chemistry*, (2018). [5] Joshi, et al. *Magnetism and Magnetic Materials*, 426, (2017).

Acknowledgments

Synthesis, characterization and application of activated carbon produced from polyacrylic acid and KOH

Ana L. A. Simões (PG),¹ Sara S. Vieira (PQ),^{2*} Amanda S. X. dos Santos (IC),¹ Leonardo C. Freitas (IC),¹ Maria H. Araujo (PQ).¹

*sarasilveira@id.uff.br

¹Departamento de Química, UFMG – Belo Horizonte, MG; ²Departamento de Química Inorgânica, UFF – Niterói, RJ.

Keywords: Graphene oxide, Adsorption, Amoxicillin, Carbpol.

Highlights

Activated carbon was synthesized from polyacrylic acid and KOH. Materials presented good superficial area, presence of graphene oxide sheets and excellent results in amoxicillin adsorption.

Abstract

This work describes the synthesis and application of activated carbon produced from polyacrylic acid as precursor and KOH as activating agent (Fig. 1). Raman spectroscopy analysis showed the presence of two typical carbonaceous bands (D and G), indicating that the increase of activating agent produces more defective carbon structures. N₂ adsorption and desorption analysis (Fig. 2) exhibited type I curve and high BET areas for the KOH activated materials, which suggests these materials are highly microporous and may have adsorption applications. Analyzing MET micrographs (Fig. 3), it's possible to identify structures like thin layers, indicating formation of graphene oxide. The carbonization process transforms the original structure into an open and highly complex three-dimensional lattice structure. In this case, it can be suggested that the internal porosity may be caused by the random stacking of crushed graphene-like nanoparticles, mounted along the fiber axis. Isotherm adsorption studies with amoxicillin were conducted and values obtained for maximum adsorption (Table 1) showed these activated carbons have a very promisor future as emerging contaminants adsorption agents.

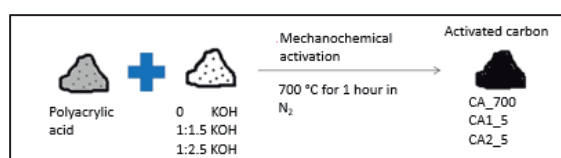


Fig. 1: Activated carbon synthesis scheme.

Table 1: Amoxicillin adsorption values.

Material	CA_700	CA1_5	CA2_5
Q _{máx} (mg g ⁻¹)	82	199	113

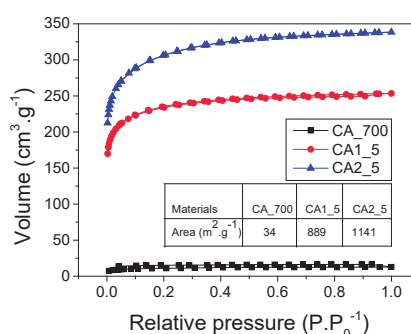


Fig. 2: N₂ adsorption and desorption analysis and BET calculated areas.

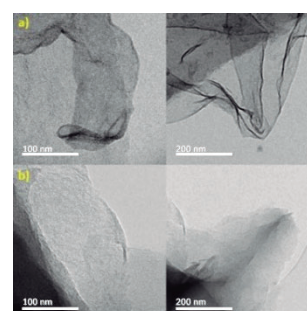


Fig. 3: TEM micrographs for materials a) CA1_5 and b) CA2_5.

Acknowledgments



Synthesis, characterization and application of thin films of graphene nanocomposites and Ni and Co hexacyanoferrates in energy storage

Rou-Yi Pan (IC)* e Eduardo Guilherme Cividini Neiva (PQ)

rpan@furb.br; eneiva@furb.br

Departamento de Química, Universidade de Blumenau (FURB)

Palavras-Chave: Nanocompósitos, Óxido de Grafeno Reduzido, Hexacianoferratos, Níquel, Cobalto, Armazenamento de Energia

Highlights

- ✓ Electrosynthesis of rGO/NiHCFe, rGO/NiCoHCFe_1:1 and rGO/NiCoHCFe_1:2 nanocomposites;
- ✓ Electrochemical and morphological characterization;
- ✓ Study of cyclic voltammetry and charge/discharge measurements;
- ✓ Specific capacity and capacity retention of thin films.

Resumo/Abstract

Os dispositivos pequenos de energia são a maioria a base de Li, porém funcionam somente em eletrólitos orgânicos e apresentam insegurança ambiental. Dessa forma, um dos materiais de interesse é a família dos hexacianometalatos (HCMs), que permite ligação com vários metais e apresenta boa interação com cátions metálicos. Além disso, a síntese de nanocompósitos com grafeno aumenta a estabilidade e a condutividade do material. Foram utilizados na eletrossíntese dos hexacianoferratos (HCFe), três precursores a base de grafeno, Ni e Co (rGO/Ni, rGO/NiCo_1:1 e rGO/NiCo_1:2), os quais foram sintetizados através da modificação do método poliol.^[1] Esses nanomateriais foram processados na forma de filmes finos pelo método de *drop casting* e depositados sobre substratos de vidro recoberto com óxido de estanho dopado com índio (ITO). A eletrossíntese dos HCFe foi realizada em meio de 0,1 mol L⁻¹ KCl (ou NaCl) e 1 mmol L⁻¹ K₃[Fe(CN)₆] e as caracterizações eletroquímicas nos meios de 0,1 mol L⁻¹ KCl, NaCl ou LiCl. Todas as medidas eletroquímicas foram realizadas em sistema de três eletrodos, usando os filmes depositados como eletrodo de trabalho, Ag/AgCl como eletrodo de referência e fio de platina como contra eletrodo.^[2] Em meio de K₃[Fe(CN)₆] com K⁺ houve maior corrente de formação do que em Na⁺, logo foi o eletrólito de suporte de crescimento escolhido para a eletrossíntese do material. As voltametrias de crescimento mostraram que o rGO/Ni produz o HCFe ao longo das ciclagens e em maior quantidade (70 µA de corrente de pico anódico), ao passo que os filmes de rGO/NiCo_1:1 e rGO/NiCo_1:2 obtiveram 38 µA e 30 µA, respectivamente. Na avaliação da estabilidade voltamétrica dos filmes nos meios de KCl, NaCl e LiCl, obteve-se as menores estabilidade para o cátion Li⁺, como esperado, uma vez que ele apresenta maior raio hidrodinâmico e danifica as cavidades receptoras ao entrar e sair da estrutura. A presença de Co favoreceu a capacidade nos ensaios de carga e descarga (CD) empregando baixas correntes, bem como a sua estabilidade frente a 2000 ciclos de CD. A presença do Na⁺ incrementou maiores retenções de capacidade para todos os precursores e o nanocompósito sem Co foi o mais afetado em meio de Li⁺. A morfologia e a distribuição dos HCFe foram analisadas via microscopia eletrônica de varredura (MEV) e demonstraram formação de nanopartículas de HCFe sobre as macropartículas precursoras e as folhas de rGO. A presença do HCFe também foi confirmada pela técnica de EDS. A caracterização da estrutura cristalina pela técnica de difração de raios X (DRX) e a otimização da capacidade estão sendo estudadas no momento.

[1] HOSTERT, L., NEIVA, E. G. C., ZARBIN, A. J. G., ORTH, E. S., Nanocatalysts for hydrogen production from borohydride hydrolysis: graphene-derived thin films with Ag-and Ni-based nanoparticles. *J. Mater. Chem. A*, v. 6, p. 22226-22233, 2018.

[2] NEIVA, E. G. C., ZARBIN, A. J. G., Nickel hexacyanoferrate/graphene thin film: a candidate for the cathode in aqueous metal-ion batteries. *New J. Chem.*, v. 46, p. 11118-11127, 2022.

Agradecimentos/Acknowledgments

Os autores agradecem à FAPESC e ao Instituto Nacional de Ciência e Tecnologia em Nanomateriais de Carbono (INCT-Nanocarbono) pelo suporte financeiro, à CLAIMS pelos equipamentos, à FURB pela infraestrutura e ao Grupo de Química de Materiais (GQM-UFPR) pelas caracterizações de MEV, EDS e DRX.

Synthesis of $\text{CdSiO}_3:\text{Pr}^{3+}$ and co-doped $\text{CdSiO}_3:\text{Mn}^{2+}\text{Pr}^{3+}$ by a hydrothermal method

Elena Iraê A.H.P.Santos (PG), Flavio Maron Vichi(PQ)*

elena.santos@usp.br; fmvichi@iq.usp.br Instituto de Química, Universidade de São Paulo, Av. Prof. Lineu Prestes, 748, Bloco 3T, Sala 325,05508-900 São Paulo-SP, Brazil

Palavras Chave: Cadmiun silicate, Hydrothermal, Synthesis

Highlights

A Hydrothermal method was successfully applied to obtain phosphors with persistent luminescence of $\text{CdSiO}_3:\text{Pr}$, $\text{CdSiO}_3:\text{Mn}$ and co-doped $\text{CdSiO}_3:\text{Pr},\text{Mn}$

Resumo/Abstract

Materials with Persistent luminescence are materials of great interest, with a vast application range due to their property of light emission for long periods. Cadmium silicates are usually synthesized via solid state, using high temperatures above 1050°C , but there are disadvantages, such as high-energy cost and particle agglomeration^[1]. The hydrothermal method is a good alternative because it allows for mild reaction conditions and interesting morphologies^[2]. Cadmium metasilicate was obtained as a single phase and also doped with Mn^{2+} and Pr^{3+} using the hydrothermal method: 50ml of a solution of CdCl_2 were added to a 50ml solution of Na_3SiO_4 in water with a stoichiometric proportion of 1:1. The doping materials MnCl_2 and PrCl_3 where added together with the cadmium precursor in a molar proportion of 1% Mn and 0,5% Pr . pH was adjusted to 6 using HCl. The mixture was stirred during 20 minutes and afterwards added in a Teflon-lined autoclave filled to 70% of its total volume and heated at 180°C for 24 h. Two temperatures of calcination were used: 600°C and 800°C at 4h. The samples were characterized using x-ray diffraction (XRD) and emission and excitation spectra were obtained.

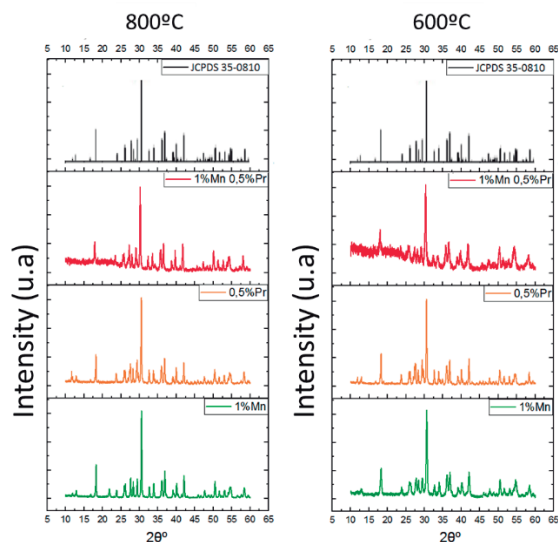


Figure 1. XRD diffractograms of samples

The excitation spectra (fig.2) show excitation wavelengths at 254 nm and 280 nm for samples calcined at 800°C and 600°C , respectively. The emission spectra follow the same order of intensity between the temperatures but with a higher intensity for samples at 800°C . The samples calcined at 600°C also show an emission at 450 nm, associated with the matrix CdSiO_3 .

[1] A. Jain et al; *Renewable and Sustainable Energy Reviews* **65** (2016) 135-153

[2] C. Manjunatha et al./ *J. Mater. Chem.*, **22** (2012), 22392-22397

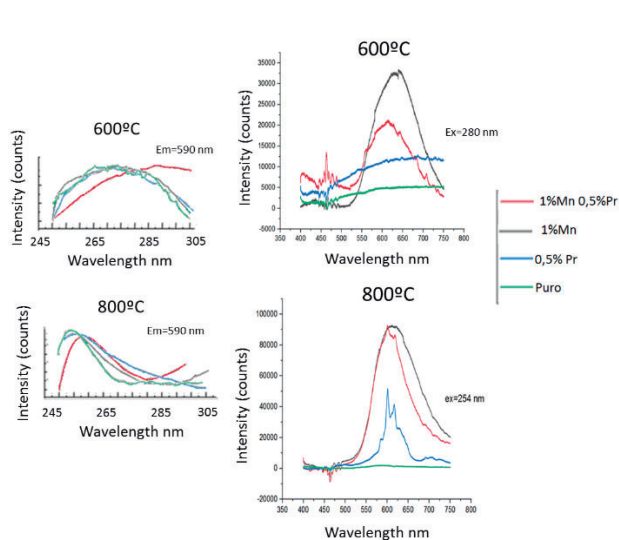


Figure 2. Emission and Excitation spectra

Agradecimentos/Acknowledgments

We thank CAPES, CNPq and FAPESP for the financial support.

Synthesis of hollow ZnO polyhedral derived from zeolitic-imidazole framework-8 for microbial volatile organic compounds detection.

Gustavo S. M. dos Santos (PG),^{1*} Bruna S. de Sá (PG),¹ Tarcísio M. Perfecto (PQ),² Diogo P. Volanti (PQ).¹

diogo.volanti@unesp.br; gustavo.sanghikian@unesp.br

¹Laboratório de Materiais para Sustentabilidade (LabMatSus); ²Laboratório Nacional de Nanotecnologia (LNNano)

Keywords: Microbial Compounds, Nanostructures, MOF, gas sensor, semiconductor

Highlights

MOF-derived hollow ZnO polyhedral synthesis for gas sensor. Morphologies and phase characterizations of nanostructures. Detection of Microbial Volatile Organic Compounds in different temperatures.

Resumo/Abstract

The metabolism of fungi and bacteria produces Microbial Volatile Organic Compounds (MVOCs).¹ That is, some microorganisms release specific MVOCs². Detecting these compounds can help in the non-invasive diagnosis of diseases, then developing MVOC sensors is crucial.³ The ZnO derived from zeolitic-imidazole framework-8 (ZIF-8) is widely used as a gas sensor due to its good performance in gas detection.⁴ Thus, in this work, the ZIF-8 was produced by a mixture of 2-methylimidazole solution and zinc acetate dihydrate $Zn(CH_3COO)_2 \cdot 2H_2O$ solution. This mixture was left at room temperature for 2 h, washed with deionized water, dried at 80 °C for 20 h and then centrifuged to obtain the white particles of ZIF-8. After that, the ZnO was obtained by calcinating the precursor ZIF-8 at 550 °C for 1 h with a heating rate of 5 °C/min. The samples of ZIF-8 and ZnO were characterized by X-ray diffraction, scanning electron microscopy, transmission electron microscopy and energy-dispersive X-ray. As for the structure of ZIF-8, the XRD analysis illustrates diffraction peaks that agree with the literature.⁴ The ZnO has characteristic peaks of wurtzite hexagonal structure (JCPDS 65-3411). The microscope analysis revealed the formation of polyhedral ZIF-8 particles and hollow ZnO polyhedral structures. EDX results of synthesized ZnO showed the presence of zinc and oxygen in the sample. Finally, the sensor test was performed for seven MVOCs. Fig. 1 shows the responses for the sensing measurements using ZnO as a sensor. It is possible to observe a higher response and selectivity for the 3-methyl-1-butanol.

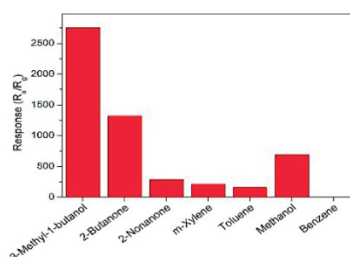


Fig. 1. Sensing measurements of 100 ppm MVOCs at 450 °C.

Agradecimentos/Acknowledgments

This work was supported by Laboratório de Sucroquímica e Química Analítica (LSQA), Laboratório Nacional de Nanotecnologia (LNNano), Embrapa, CAPES under Project Number 88887.694732/2022-00, CNPq (311453/2021-0) and FAPESP (grants 2020/05233-7 and 2020/06421-1).

- Berry, D. R. Products of primary metabolic pathways. Physiology of industrial fungi. **Blackwell Scientific Publications**, Oxford, 1988.
- Bos, L. D. J., Sterk, P. J. & Schultz, M. J. Volatile Metabolites of Pathogens: A Systematic Review. **PLoS Pathogens**, v. 9, n. 5, p. e1003311, 2013.
- Tripathi, K. M. et al. Recent advances in engineered graphene and composites for detection of volatile organic compounds (VOCs) and non-invasive diseases diagnosis. **Carbon**, v. 110, p. 97–129, 2016.
- Zhang, X. et al. ZIF-8 derived hierarchical hollow ZnO nanocages with quantum dots for sensitive ethanol gas detection. **Sensors and Actuators, B: Chemical**, v. 289, p. 144–152, 2019.

Synthesis of stable and lead-free all-inorganic metal halide perovskites

Stéphany de O. Romera (IC)*, Daniel Angeli de Moraes (PQ), Laudemir Carlos Varanda (PQ).

stephany.romera@usp.br; lvaranda@iqsc.usp.br.

¹Chemistry Institute of São Carlos, University of São Paulo, Brazil.

Palavras Chave: *Perovskites, Lead-free structure, Chemical stability, Photovoltaic*

Highlights

The conversion of solar energy into electrical energy has been highlighted in the last decade, and the photovoltaic processes have significantly increased using systems and devices involving perovskites. Hybrid (organic-inorganic) perovskites containing lead proved to be promising materials, with the highest efficiencies but low stability and sustainability, due to lead in their composition. Here, we describe a new route to synthesize lead-free all-inorganic perovskite nanocrystals based on the $\text{Cs}_8\text{Au}_4\text{M}^{\text{III}}\text{X}_{23}$ ($\text{M} = \text{In}^{3+}$, Sb^{3+} , Bi^{3+} ; and $\text{X} = \text{Cl}^-$, Br^- , I^-) structure. Two approaches were employed and compared (i) non-aqueous (hot-injection) and (ii) acidified aqueous systems, corresponding to the desired metal halide type.

Abstract

The syntheses in non-aqueous and aqueous media were based on the methodologies of IMRAN et al., 2018 and LINDQUIST et al., 2021, respectively, adapting some conditions and reagents, such as the use of metal acetates, which have high solubility and low cost. The results showed an improvement for the systems in non-aqueous media, with the $\text{Cs}_8\text{Au}_4\text{BiCl}_{23}$ perovskite phase formation. However, a secondary phase in a small proportion was observed, indicating the need for new adjustments. On the other hand, the results in the aqueous medium system were quite promising since perovskite structures were obtained without secondary phases for the compositions $\text{Cs}_8\text{Au}_4\text{BiCl}_{23}$, $\text{Cs}_8\text{Au}_4\text{InCl}_{23}$, $\text{Cs}_8\text{Au}_4\text{BiBr}_{23}$, $\text{Cs}_8\text{Au}_4\text{InBr}_{23}$, and $\text{Cs}_8\text{Au}_4\text{SbBr}_{23}$. The addition of the surfactant 11-mercaptoundecanoic acid (MUA) optimized the octahedral particle shape. However, this negatively affected the perovskite composition with bromide ions due to the competition between the thiol group with gold ions, avoiding its structuring in perovskite. In contrast, a significant improvement was observed in particle size and shape control for the Cl-containing composition ions, leading to their expected octahedral shape. Because it is a new composition, there is little data in the literature to compare results. The fact that success was achieved in synthesizing them with the adaptations carried out quickly should be highlighted.

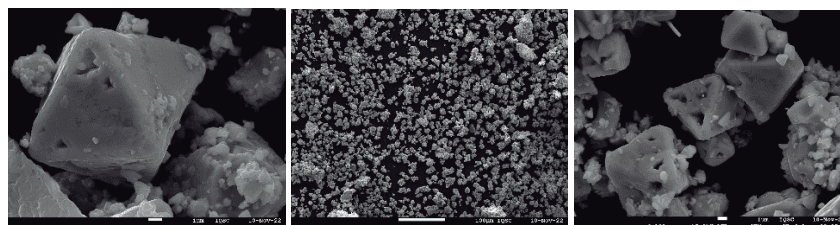
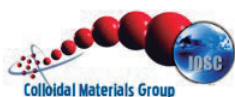


Figure 1. Scanning Electron Microscopy (SEM) images of the perovskites ($\text{Cs}_8\text{Au}_4\text{BiCl}_{23}$) synthesized in the presence of surfactant MUA.

Acknowledgments



Synthesis, structural, and spectroscopic characterization of Eu³⁺-doped yttrium or gadolinium hafnates nanoparticles for Biophotonics application

Caio Faim Lima (IC)¹, Gabriel Silva Canhoto (IC)¹, Fernanda Hediger Borges (PG)¹, Hayra do Prado Labaki (PG)¹, and Rogéria Rocha Gonçalves (PQ)^{1,*}

caiofaim@usp.br; rrgoncalves@ffclrp.usp.br

¹Laboratório de Materiais Luminescentes Micro e Nanoestruturados – Mater Lumen, Departamento de Química, FFCLRP, Universidade de São Paulo, 14040-900, SP, Brazil.

Keywords: Yttrium or Gadolinium Hafnate, Hafnium oxide, Rare earth, Spectroscopy, Photoluminescence, Radioluminescence.

Highlights

Synthesis, structural, morphological, and spectroscopic features of Eu³⁺-doped yttrium or gadolinium hafnates nanoparticles were obtained by different methodologies for biophotonics as photo or radioluminescent materials.

Resumo/Abstract

The HfO₂ system has been studied over the last decades, mainly in the form of thin films, due to its higher dielectric constant ($\epsilon = 25$) with respect to silica. As a result of its very high melting point (over 2700 °C) and its mechanical resistance, hafnia has also found application in refractory protective coatings of thermocouples in harsh conditions as in nuclear applications. Recently in 2019, HfO₂ nanoparticles were approved for radiotherapy treatment in different types of cancer and carcinoma, such as liver, head, and prostate. Nevertheless, yttrium or gadolinium hafnates are less explored in the literature. Ceramics based on rare earth hafnates are known for their low volatility and thermal conductivity, as well as high chemical stability and melting temperatures. It has been also shown that rare earth hafnates are promising for the development of a wide range of new high-temperature materials, such as thermal barrier coatings and casting molds for gas turbine engine blades. Furthermore, these systems are a new series of materials as scintillator hosts due to their high transparency, high density (8.92 g/cm³), and effective atomic number. In this work, we report the synthesis, structural and spectroscopic characterization of yttrium or gadolinium hafnates obtained by distinct methodologies, such as homogeneous precipitation and sol-gel process using NH₄OH or lysine as a basic catalyst agent. The crystalline structure of the materials was attested by X-ray diffraction, FTIR, and Raman spectroscopies. Depending on the rare earth content, methodology, as well as, annealing temperature monoclinic hafnium oxide, tetragonal rare earth stabilized hafnia or rare earth hafnates crystallized. Fig. 1 A shows the stabilization of cubic defect fluorite Ln₂Hf₂O₇, belonging to the *Fm* $\bar{3}$ *m*, for the sol-gel synthesis. Transmission electron microscopy shows the presence of spherical nanoparticles of different sizes, about 30-65 nm for the sol-gel synthesis using NH₄OH, Figure 1B, about 20-40 nm for the sol-gel synthesis using Lysine, Figure 1C, and between 134 to 166 nm for the homogeneous precipitation route,

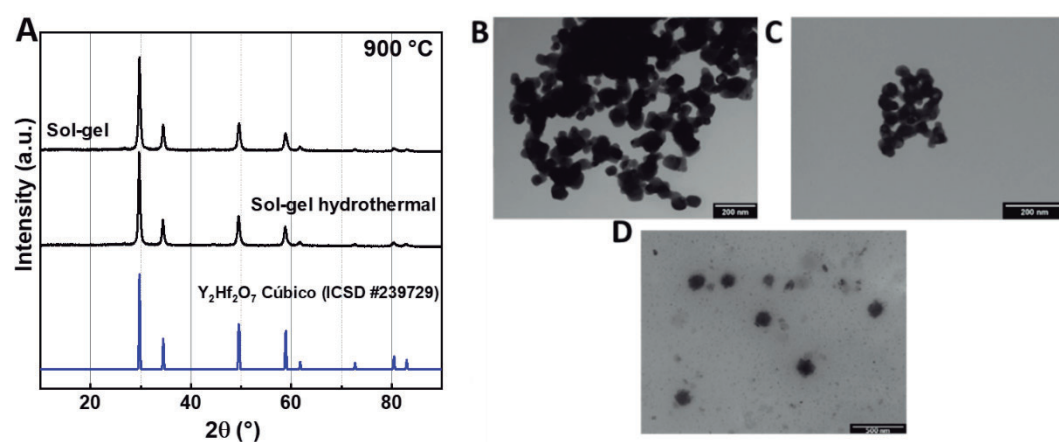


Figure 1D. The excitation spectra depict the Eu³⁺ characteristic *f-f* transitions, as well as, broadband in the UV range ascribed to the O²⁻→Eu³⁺ charge transfer band. Emission bands in the red region (⁵D₀→⁷F_{0,1,2,3} and 4) were observed upon CT band excitation. Intense radioluminescence was also observed suggesting potential application for theranostics.

Fig. 1. (A) XRD diffractogram for the Y₂Hf₂O₇ samples and TEM images for the Ln₂Hf₂O₇ synthesized through a (B) sol-gel, (C) sol-gel using Lysine (followed by a hydrothermal process), and (D) homogeneous precipitation.

Agradecimentos/Acknowledgments

We would like to acknowledge FAPESP, CAPES, CNPQ, and Photonics National Institute for Science and Technology (INFO) for financial support.

Temperature-related ultralong lifetime, thermometry, and radioluminescence of Pr³⁺ and Na⁺ doped yttrium tantalates nanoparticles for nanomedicine advances

Hayra do Prado Labaki (PG)¹, Fábio José Caixeta (PG)^{1,2}, Natasha Policei Marques (PG)³, Éder José Guidelli (PQ)³, Lucas Carvalho Velozo Rodrigues (PQ)⁴, and Rogéria Rocha Gonçalves (PQ)^{1,*}

hayra.labaki@usp.br; rrgoncalves@ffclrp.usp.br

¹Laboratório de Materiais Luminescentes Micro e Nanoestruturados – Mater Lumen, Departamento de Química, FFCLRP, Universidade de São Paulo, 14040-900, SP, Brazil.

²Department of Analytical, Physical, and Inorganic Chemistry, Institute of Chemistry, São Paulo State University (UNESP), 14800-060 Araraquara, SP, Brazil

³Laboratório de Nanotecnologia e Dosimetria de Radiações - NanoDose, Departamento de Física, FFCLRP, Universidade de São Paulo, SP, Brazil.

⁴Departamento de Química Fundamental, Instituto de Química, Universidade de São Paulo, São Paulo-SP, Brazil.

Keywords: Nanomedicine, Yttrium Tantalate, Rare earths, Nanoparticles, Persistent luminescence, Scintillation

Highlights

An ultra-long lifetime, persistent luminescence, nanothermometry, and scintillation features were attested for Pr³⁺ and Na⁺ doped yttrium tantalate nanoparticles making these materials potential candidates for nanomedicine applications.

Resumo/Abstract

Nanomedicine refers to the application of nanotechnology in disease diagnosis, treatment, and/or monitoring. Luminescent materials exhibiting long lifetime of excited state are interesting for this field given that the lifetime of most biological molecules is below the nanosecond level, and a long-lived emission that could remain detectable after removing the excitation for several seconds is very important. In the present work, we report the synthesis, structural, morphological, and spectroscopic characterization of a multifunctional material: the Pr³⁺, Na⁺-doped yttrium tantalate designed by a sol-gel methodology. The X-ray diffraction analysis illustrated the Y₃TaO₇, and M'-YTaO₄ phases crystallization. Transmission Electron Microscopy shows nanoparticles with an average size of 49 nm. Photoluminescence measurements revealed an intense reddish emission, as well as, in the NIR II and IIb regions of the biological windows. The time-resolved emission spectra revealed a relatively intense emission even after 1s of delay. The ¹D₂ lifetime values show an extremely long lifetime of 432 ms upon excitation at the charge transfer band, after annealing at 1100 °C. The lifetime was also temperature-dependent indicating that a sensible nanothermometer arises.

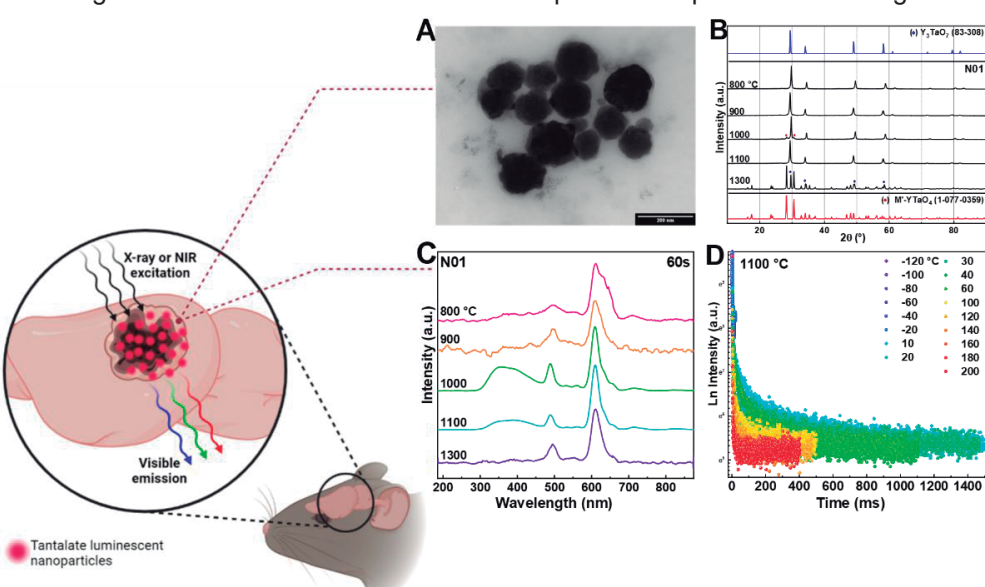


Fig. 1. (A) Transmission Electron Microscopy, (B) XRD diffractogram, (C) radioluminescence, and (D) lifetime decay as a function of the temperature for the Pr³⁺ and Na⁺ yttrium tantalate nanoparticles.

Agradecimentos/Acknowledgments

We would like to acknowledge FAPESP, CAPES, CNPQ, and Photonics National Institute for Science and Technology (INFO) for financial support.

46^o Reunião Anual da Sociedade Brasileira de Química: "Química: Ligando ciências e neutralizando desigualdades"

The effect of copper salt counter ions on green syntheses of copper nanoparticles.

Paulo C. Rodrigues (PG),¹ Italo O. Mazali (PQ),¹ Marco A. Z. Arruda (PQ)²

p231478@dac.unicamp.br

¹ Laboratory of Functional Materials, Institute of Chemistry, UNICAMP, Campinas, Brazil.

² Spectrometry, Sample Preparation and Mechanization Group, Institute of Chemistry, UNICAMP, Campinas, Brazil.

Keywords: Copper Nanoparticles, Green Synthesis

Highlights

Evaluation of the effect of the counter ions, sulphate and hydroxide, on the green synthesis of copper nanoparticles. Hydroxide ions lead to the formation of smaller nanoparticles. Sulphate ions in the solution are capable of guiding, together with the stabilizer, the formation of CuO or CuNPs.

Abstract

The research in nanotechnology is a large potential field for modern technological development due to its size-dependent physical-chemical properties that guarantee unique characteristics to meet the most diverse application purposes. The preparation and application processes of CuNPs in this scenario have gained special attention in recent years, but due to its easy oxidation, a characteristic potentiated at the nanoscale, it has proven to be a challenge in the development of CuNPs with naked surface [1]. As a research group, we have a strong interest in the sustainable and non-toxic synthesis routes of these structures for application in agriculture and SERS materials. The objective of this study is to evaluate the effect of the counterion of the precursor salt on the syntheses of CuNPs, seeking to establish less laborious pathways and the substitution of reagents typically used, such as sodium borohydride, for environmentally friendly alternatives that are better aligned with the principles of green chemistry. To do so, the effect

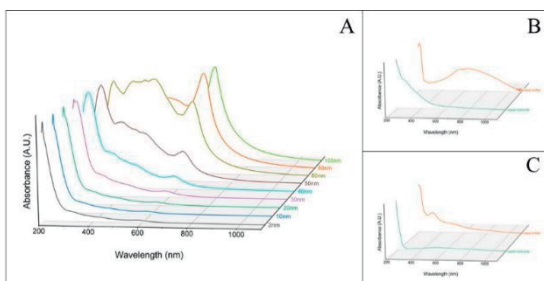


Figure 1: In (A), there are the absorption spectra in the UV-Vis region for copper nanoparticles that range from 2 nm to 100 nm according to the Mie scattering model. In (B), the UV-Vis spectra using ascorbic acid as the stabilizer for synthesis. In (C), the UV and Vis region spectrum for syntheses using gallic acid as stabilizers.

on the surface plasmon resonance bands was evaluated, and to understand the modifications, the results obtained were compared with simulations adopting the Mie dispersion model [2]. The syntheses were carried out using copper hydroxide and pentahydrate sulfate as precursor salts, hydrazine as a reducing agent and ascorbic or gallic acid as stabilizers, occurring at room temperature for two hours, and the products were centrifuged and washed with ultrapure water, and UV-Vis spectra were taken. The choice of these two molecules as stabilizers is based on their great similarity. Both have 4 hydroxyl groups and 1 ketone group, but the partial charges on each of these groups are different for each molecule. This offers the possibility to explore how different interactions of van der Waals forces between the NPs and functional groups result in different synthesis and stability outcomes. It was observed that the impact of the counter-ion of the salt

present in the solution is not only capable of assisting in the self-assembly of the NP's, but its interaction with the stabilizer can lead the synthesis to the formation of CuONPs or CuNPs. In the study, syntheses conducted in the presence of the sulfate ion and gallic acid favored the formation of CuONPs, however, when the stabilizer was changed to ascorbic acid, the preference changed to CuNPs, and it also caused a higher polydispersion of sizes. When the counter-ion in the medium is hydroxide, it was observed that the preference for CuO and CuNP formation is reversed compared to sulfate, and it also leads to the formation of smaller nanoparticles. Additional characterizations are being performed on these materials, as well as studies regarding their repeatability, to eliminate stochastic errors.

[1] S. Yimeng et al., *Eur. J. Inorg. Chem.*, 2022. doi: 10.1002/ejic.202200614.

[2] J.S. Duque et al 2017 *J. Phys.: Conf. Ser.* 850. doi: 10.1088/1742-6596/850/1/012017

Agradecimentos/Acknowledgments



(Proc. 2022/01418-8)



Área: MAT

The effect of the molecular structure of HPMC on the interaction with water for cryogels prepared with and without calcium peroxide

Camila G. Chiaregato (PG),^{1*} Oigres D. Bernardinelli (PQ),² Amin Shavandi (PQ),³ Edvaldo Sabadini (PQ),⁴ Denise F. S. Petri (PQ).¹

camichiaregato@usp.br

¹Department of Fundamental Chemistry, Institute of Chemistry, USP, São Paulo, Brazil; ² Department of Physics, UFSCar, São Carlos, Brazil; ³ BioMatter Unit, École Polytechnique de Bruxelles, ULB, Brussels, Belgium; ⁴ Department of Physical Chemistry, Institute of Chemistry, UNICAMP, Campinas, Brazil

Keywords: hydroxypropyl methylcellulose, transverse relaxation time, swelling rate, contact angle, CaO₂

Highlights

The incorporation of CaO₂ particles into HPMC cryogel reduced the O₂ release.

The molecular characteristics of HPMC drive the swelling rate and wettability.

Abstract

The interaction between polymers and water is critical for determining the final characteristics of a material. Hydroxypropyl methylcellulose (HPMC) belongs to the cellulose ether family that has both hydrophobic methyl groups (DS) and hydrophilic hydroxypropyl groups (MS) on its chain. The interactions between water molecules and cryogels prepared with different types of HPMC, in the presence and absence of a linear nonionic surfactant (containing a dodecyl chain and a PEG chain) and CaO₂ microparticles, were systematically investigated using sorption experiments and Time-Domain Nuclear Magnetic Resonance (TDNMR). Solutions of HPMC at 3.0 wt% containing 0.3 wt% of citric acid (crosslinker) and 0.15 wt% of sodium hypophosphite (catalyst) were prepared. The surfactant concentration was 0.168 g L⁻¹, and 50 mg of CaO₂ was added to 1.6 g of HPMC solution. Then, the precursor gels were frozen for 24 h and freeze-dried during 10-12 h. The resulting cryogels were oven heated at 165 °C for 5 min to promote the esterification reaction between citric acid and HPMC hydroxyl groups. Regardless of the DS and MS of the HPMC, most water molecules showed transverse relaxation time t_2 typical of intermediate water and a small population of more tightly bound water. HPMC cryogels with the highest DS of 1.9 had the slowest swelling rate ($0.519 \pm 0.053 \text{ g}_{\text{water}}/(\text{g.s})$) and the highest contact angle values ($85.250^\circ \pm 0.004^\circ$), providing the best conditions for a slow reaction between CaO₂ and water. The presence of the surfactant increased swelling rate and decreased contact angle values, likely due to hydrophobic interactions possibly favored the exposition of the surfactant's polar head to the medium. The HPMC with the highest MS had the fastest swelling rate and the lowest contact angle. The initial rate (V_0), calculated from the kinetics of O₂ release, was slower for all cryogels compared with pure CaO₂, avoiding burst release. These findings are relevant for the formulations and reactions, where tuning the swelling kinetics is crucial for the final application, such as biomedical applications and wastewater treatment.

Acknowledgments

The authors thank the São Paulo Research Foundation (FAPESP) (2018/13492-2 and 2022/06284-0) and CNPq (304017/2021-3) for the financial support.

The influence of chemical aging on carbonaceous materials for soil application: how can this affect the stability of their water-dispersible colloids?

Laís G. Fregolente (PQ)^{1*}, Maria T. Rodrigues (IC)¹, Naiara C. Oliveira (PQ)¹, Bruno Souza Araújo (PQ)¹, Antônio G. S. Filho (PQ)², Odair P. Ferreira (PQ)^{1,2}

opferreira@uel.br; laisfregolente@fisica.ufc.br

¹Departamento de Física, UFC; ²Departamento de Química, UEL

Palavras Chave: Biochar, Hydrochar, Oxidation, soil conditioner, Hydrothermal Carbonization, Pyrolysis

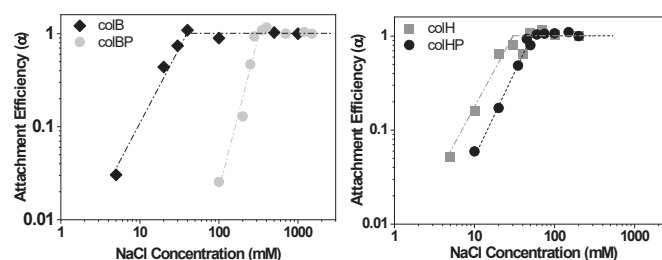
Highlights

- The thermochemical process from biomass provides carbonaceous materials for soil conditioning;
- The aging process could be generating “carbon” colloids affecting the soil stability;
- Biochar colloids stability strongly increased with oxidation, while hydrochar colloids stability slightly change.

Resumo/Abstract

Hydrochar and biochar have been used as soil conditioners, and to understand their role on soil system in a long-term it is necessary to study the changes on their characteristics due aging ¹. Chemical aging is used to simulate the alterations on their physicochemical properties ². Small particles of chars might interact with soil colloids affecting the aggregates formation, stability, and mobility. So, this study explored the effects of aging on hydrochar and biochar, as well as the stability of chars' colloids. Different oxidation methods were assessed using hydrogen peroxide; mixture of nitric and sulfuric acids; and leaching ³. After oxidation processes, samples were mixed with ultrapure water, and sonicated; the dispersed solution was allowed to settle undisturbed during 24 h, filtered, and the solids dried. The distinct characteristics of composition and structure between hydrochar and biochar samples determined their behavior in front of chemical aging. Our results demonstrated that biochar is much more resistant to chemical oxidation, even at extreme conditions, than hydrochar. However, the input of O-containing functional affected material thermal stability due changes on chemical composition ². Further, while biochar exhibited a hydrophilic profile, hydrochar hydrophobicity showed to be a difficult property to overcome with chemical oxidation. The effectiveness of chemical aging treatments for biochar increased in the order of leaching<acid<hydrogen peroxide, while for hydrochar the order was leaching<hydrogen peroxide<acid. The oxidation of biochar (colBP) strongly increased colloidal stability, reflecting on its critical coagulation concentration (CCC), while the improvement of O-containing functional groups on hydrochar surface (colHP) slightly changed its CCC. Therefore, it can be expected changes on carbonaceous materials over time, modifying the small particle dynamics, which requires much more attention to the environmental risks due their application over time.

Figure 1. Aggregation attachment efficiencies of colH, colB, colHP, and colBP to different NaCl concentration (mM).



1 FENG, Z. et al. Science of the Total Environment, 783, 147091, 2021.

2 WANG, Y. et al. Environmental Science and Technology, 53, 8136–8146, 2019.

3 CHANG, R. et al. Environmental Pollution, 254, 113123, 2019.

Agradecimentos/Acknowledgments

Scientific and Technology Development Foundation of the State of Ceará (FUNCAP); National Council for Scientific and Technological Development (CNPq).

46ª Reunião Anual da Sociedade Brasileira de Química: "Química: Ligando ciências e neutralizando desigualdades"

The influence of the thermal behavior of ureasil-polyether (UP) hybrid matrices on the magnetic hyperthermia of UP-CoFe₂O₄ nanocomposites

Willian Max Oliveira de Souza de Santana (PG)*¹, Sandra Helena Pulcinelli (PQ)¹, e Celso Valentim Santilli (PQ)¹

willian.santana@unesp.br

¹Instituto de Química (Câmpus Araraquara), Universidade Estadual Paulista "Júlio de Mesquita Filho" (UNESP)

Palavras Chave: Ureasil-poliéter, Nanocompósito, Hipertermia magnética.

Highlights

- The presence of superparamagnetic nanoparticles did not affect the nanostructure and thermal behavior of the hybrid matrices.
- The thermal behavior of the hybrid matrix influenced the hyperthermia capacity of the UP-CoFe₂O₄ nanocomposites.
- The presence of superparamagnetic nanoparticles in the hybrid matrix did not affect drug diffusion.

Resumo/Abstract

Superparamagnetic nanoparticles (SNP), such as cobalt ferrite (CoFe₂O₄), when exposed to an alternating magnetic field (AMF), convert the energy of this field into heat. Local temperature elevation (~42-46 °C) is known as magnetic hyperthermia (MH).[1] SNP have been associated with polymeric or organic-inorganic hybrid (OIH) materials for applications in tissue engineering, drug delivery and cancer treatments.[1] OIH from the ureasil-polyether family, such as ureasil-poly(ethylene oxide) (UPEO) and ureasil-poly(propylene oxide) (UPPO) have siloxane groups covalently connected to polyether chains in their structure.[2] Unlike UPEO, UPPO hybrids have a low swelling capacity due to the hydrophobicity of the PPO macromer, thus UPPO hybrids have a slower drug release rate.[2] Most studies related to SNP-containing nanocomposites have investigated the influence of SNP characteristics (e.g, size and concentration), paying little or no attention to the host matrix. In this work, we evaluated the influence of UPPO and UPEO hybrid matrices on the MH of UP-CoFe₂O₄ nanocomposites. The results of small angle X-ray scattering (SAXS) and differential scanning calorimetry (DSC) analyzes showed that the nanoscopic structure and thermal properties remained essentially unchanged after the incorporation of CoFe₂O₄ into the hybrid material. The lower heat capacity of the UPPO-CoFe₂O₄ nanocomposite promoted greater MH efficiency when compared to UPEO-CoFe₂O₄. The temperature variations reached by UPPO-CoFe₂O₄ and UPEO-CoFe₂O₄ were 34 and 20 °C, respectively, when subjected to AMF for 240 s. The release profile of diclofenac sodium (chosen model drug) from UPPO or UPEO was not affected by incorporation of SNP or MH.

[1] DAS, P.; COLOMBO, M.; PROSPERI, D. Recent Advances in Magnetic Fluid Hyperthermia for Cancer Therapy, *Colloids Surfaces B Biointerfaces*, v. 174, p. 42-55, 2019.

[2] OSHIRO, A. J., et al. Drug Delivery Systems Obtained from Silica Based Organic-Inorganic Hybrids, *Polymers (Basel)*, v. 8, 2016.

Agradecimentos/Acknowledgments

CNPq, Capes e FAPESP;

Time-dependent shell thickness: controlling the recovering in silica-coated silver nanoparticles Ag@SiO₂

João Antonio Oliveira Santos* (PG),¹ Ana Maria Pires (PQ),^{1,2} Sergio Antonio Marques Lima (PQ),^{1,2**}

*joao.antonio@unesp.br; **sergio.lima@unesp.br

¹ São Paulo State University (UNESP), Institute of Chemistry, Araraquara, SP, Brazil; ² São Paulo State University (UNESP), School of Science and Technology, Presidente Prudente, SP, Brazil

Keywords: plasmonic, nanoparticles, silica coating, Stöber, single-core structures

Highlights

Silver nanoparticles coated with silica using Stöber methodology; Varying shell-thickness by changing the reaction time; Reproducibility and stability of single-core nanostructures.

Abstract

Homogeneous and spherical silver nanoparticles (Ag) have drawn attention for their exceptional plasmonic properties attributed to the localized surface plasmon resonance (LSPR) that occurs in the ultraviolet and visible (350–480 nm) spectral regions [1]. Such property has been explored in plasmonic enhancement studies based on surface-enhanced Raman scattering (SERS), surface-enhanced fluorescence (SEF), and metal-enhanced luminescence (MEL) [2]. However, optical-enhanced effects are strongly dependent on the distance between the Ag surface and the molecules that exhibit such properties [3]. Thus, the simplest way to control this distance is by coating the Ag with layers of optically transparent inorganic compounds, such as silica. Besides acting as a spacer, silica shell promotes a decrease of Ag toxicity, an increase in colloidal stability due to its surface charge in aqueous media, and easy surface functionalization, making core@shell (Ag@SiO₂) structures excellent candidates for applications in biomedical applications. The challenge here is to overcome the instability of Ag in the presence of ammonia during their coating with silica by Stöber methodology [4]. In this work, we report the synthesis and characterization of silver nanoparticles in water and their coating with different thicknesses of silica modulated by reaction time. Water-suspended 30 nm-silver nanoparticles were obtained by reducing silver ions (Ag⁺) in the presence of ascorbic acid and sodium citrate. Next, to obtain the Ag@SiO₂ structures, the Ag suspension was stirred in the presence of tetraethylorthosilicate (TEOS) and injected into a previously prepared mixture of ethanol and ammonium hydroxide. After injection, the growth of the silica layer through reaction time was evaluated by transmission electronic microscopy (TEM) and UV-vis spectroscopy. TEM images of the Ag@SiO₂, Figure 1, showed a gradual growth of the silica layer in different time reactions. It is noticed that the silica shell is not observed up to 30 min of reaction, but at 45 min a well-defined shell of silica around the Ag can be observed. The methodology promoted the formation of predominantly single-core systems. Analysis of the extinction spectra (λ_{LSPR}) showed that the shifts (bathochromic and hypsochromic) observed in the plasmonic bands corroborate the information observed by the TEM images, concluding (i) the rapid growth of the silica layer after the induction time of 30 min (ii) the formation of a plateau in the shell growth after 2h of reaction, and (iii) solubilization of the silver particles after 3h of reaction. Times of 45 min, 1h, 2h, and 3h were selected to evaluate the reproducibility of the synthesis and similar growth patterns were observed. Such results indicate this methodology has potential for coating metallic particles with good-thickness control.

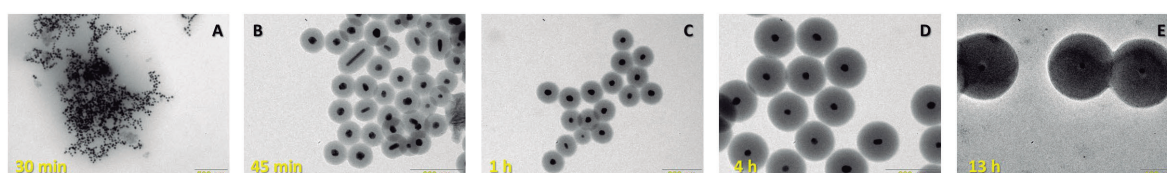


Figure 1. TEM images of 30 nm-Ag coated with different thicknesses of silica (SiO₂) by varying the coating time (a) 30 min, (b) 45 min, (c) 1 h, (d) 4 h, and (e) 13 h.

[1] Lismont, M. et al. J Colloid Interface Sci 2015,447, 40–49 [2] Camacho, S.A. et al. J. Phys. Chem. C 2016, 120, 20530–20535 [3] Wang X-J. et al. Nanomaterials 2018, 8, 98 [4] Y. Kobayashi et al. J Colloid Interface Sci 2005, 283 392–396.

Acknowledgments

Capes-PrInt (88887.695875/2022-00), CNPq (141229/2019-5), and Fapesp (2019/26103-7).

46^o Reunião Anual da Sociedade Brasileira de Química: "Química: Ligando ciências e neutralizando desigualdades"

Treatment crude glycerin from biodiesel industries to carbon dots synthesis

Amanda T. V. Santos (IC),¹ Hevelyn V. E. Machado (IC),¹ Ailton J. Terezo (PQ),¹ Adriano B. de Siqueira (PQ),¹ Mario R. S. Soares (PQ).^{1*}

mario.r5@hotmail.com

¹Grupo de Eletroquímica e Novos Materiais (GENMAT), Departamento de Química-UFMT, Cuiabá/MT, Brasil.

Palavras Chave: Glycerol, Phosphoric Acid; BioC-Dots;

Highlights

Glycerol is interesting precursor to BioC-Dots synthesis. Almost 10% glycerin is obtained in the biodiesel production. Acidification of the crude glycerin is a feasible method to obtain glycerol.

Resumo/Abstract

Glycerol has great relevance due to its high applicability. Among the ways of obtaining it, the one with the highest proportion is derived from biodiesel production through the transesterification reaction, responsible for generating approximately 10% of crude glycerin as a byproduct. In 2021, the year of biggest biodiesel production, 6.765 million m³ of this biofuel were produced in Brazil, leading to approximately 676 thousand m³ of crude glycerin (in 2022, biodiesel production was 5.743 million m³).^[1] However, the crude glycerin resulting from the transesterification reaction has low purity, making it a co-product of little commercial value.^[2]

In this work, the acid treatment of crude glycerin obtained from a local biodiesel industry in Mato Grosso was performed using phosphoric acid (H₃PO₄) 83%. Due to the complexity of the crude sample, a matrix was previously prepared by solubilizing the crude glycerin in water to proceed to the acidification step. The matrix sample presented a pH 10.0. It was acidified to pH 1.0 (GP1), pH 3.0 (GP3), pH 6.0 (GP6) and pH 8.0 (GP8). After the acidification step, each sample was transferred to a separatory funnel and kept at rest for 24h sufficient time to allow the formation of separate layers. Three layers were expected: free fatty acids in the top layer; an intermediate layer rich in glycerol; and precipitated salts in the bottom layer.^[3]

For the GP8 sample, no layer separation was observed, and therefore no further analysis followed. For samples GP1, GP3 and GP6 the separation into two layers only was observed, which means precipitation of the salts was not achieved. Thus, for samples GP1, GP3 and GP6, the top phase rich in organic compounds and the bottom, aqueous phase rich in glycerol and dissolved inorganic salts. The aqueous phase of each sample was submitted to a concentration process using a rotary evaporator system, i.e., the glycerin-rich phase was concentrated by removing water from the solubilization of crude glycerin

and residual alcohol from the transesterification process at the biodiesel production.

The samples GP1, GP3, GP6, as well as GPA (glycerin P.A., commercial), were characterized by simultaneous Thermogravimetric Analysis (TG) and Differential Thermal Analysis (DTA), performed in a Shimadzu apparatus, model DTG-60H. All analyses used 40-30 mg of sample, in an alumina crucible, under synthetic air atmosphere and 100 mL min⁻¹ flow, in the heating range from room temperature to 1000 °C and 10 °C min⁻¹ rate. The results of these analyses are shown in the table.

Table 1 – Results of simultaneous TG/DTA analysis

Sample	TG Weight loss (%)			DTA		
	1st	2nd	3th	1st	2nd	3th
GPA	1.1	98.9	-	endo	endo	-
GP6	8.1	80.8	2.5	endo	endo+exo	endo+exo
GP3	7.5	72.5	5.3	endo	exo	exo
GP1	11.2	41.8	33.2	endo	exo	exo

The results of the TG analyses show the thermal decomposition of the glycerol up to 300°C (GPA) and for the acidified ones second exothermic thermal event immediately after degradation of the glycerol. In addition, for these samples, there is a third thermal event with mass loss, more pronounced for GP1, indicating the decomposition of phosphate salts, which they find dissolved in the concentrated sample.

In this context, we expected BioC-Dots with distinct properties between them due to different composition of precursors, which indicated by TG-DTA results.

References:

- [1] ANP, Agência Nacional do Petróleo, Gás Natural e Biocombustíveis, 2022.
- [2] Nanda, M. R. et al. *Austin J. Chem. Eng.*, 2014, 1.
- [3] Kumar L. R. et al. *Bioresource technology*, 2019, 293.

Acknowledgments

FAPEMAT, CNPq, UFMT and BIO OLEO LTDA.

Upconversion luminescent Y_2SiO_5 : Er^{3+}/Yb^{3+} hollow spheres as Nanoplatforms for Theranostics

Dos Santos, L.F.¹ (PG); **Gomes, L. F. T.**¹ (IC); **Dalossio, V. P.**¹(IC); **Lima, K.O.**¹ (PQ); **Borges, H. S.**² (PQ); **Gusmão, L. A.**²(PG); **Tedesco, A. C.**²(PQ) and **Gonçalves, R.R.**² (PQ)

luiz2.santos@usp.br; rrgoncalves@ffclrp.usp.br

¹Laboratório de Materiais Luminescentes Micro e Nanoestruturados – Mater Lumen, Departamento de Química, FFCLRP, Universidade de São Paulo, 14040-900, SP, Brazil; ² Centro de Nanotecnologia e Engenharia Tecidual – Fotobiologia e Fotomedicina – CNET, Departamento de Química, FFCLRP, Universidade de São Paulo, 14040-900, SP, Brazil.

Keywords: upconversion, hollow spheres, biophotonics, lanthanide, nanoparticles, silicate.

Highlights

Upconversion luminescent hollow spheres of rare earth (RE) doped yttrium silicate is reported, exhibiting high thermal sensitivity and large repeatability to be used as nanothermometer and high cell viability opening the potentiality for theranostics.

Abstract

Upconverting nanoparticles have been used in some research fields, such as nanomedicine [1], energy conversion, sensors, catalysis, for instance. In this work, a synthetic route was developed for the preparation of spherical luminescent nanoparticles based on Er^{3+} , Yb^{3+} co-doped Y_2SiO_5 , starting from yttrium hydroxycarbonate and silica as core and shell precursors respectively. The particles' internal structure was tuned according to the silica thickness over the core and the heat treatment. Dispersed hollow spheres highly crystalline nanoparticles were observed after annealing treatments, corresponding to cubic phase of Y_2O_3 (core) and monoclinic $X1$ - Y_2SiO_5 crystallized on the surface. Intense green emission around 525, 545 nm assigned to the ${}^2H_{11/2} \rightarrow {}^4I_{15/2}$ and ${}^4S_{3/2} \rightarrow {}^4I_{15/2}$, and red emission centered at 650 nm derivated from ${}^4F_{9/2} \rightarrow {}^4I_{15/2}$ from Er^{3+} ion were observed under excitation using a CW laser at 980 nm. The upconversion dynamics was evaluated by the number of photons, which indicated that energy transfer by the upconversion mechanism is the dominant process. On the basis of luminescence nanothermometry measurements, the hollow spheres displayed high thermal sensitivity and large repeatability, and attesting that they can be used as primary thermometer. Besides, in vitro assays were performed attesting a high cell viability, when glioblastoma cells are exposed to the nanoparticles, indicating the possibility of their use as a nanoplatform for cancer therapy, accomplished to be used as temperature sensor, optical bioimaging and as energy converters (NIR to visible) coupled to photosensitizers for reactive oxygen species production for PDT.

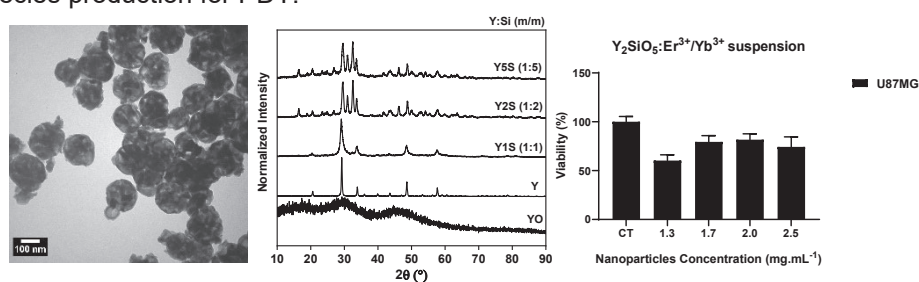


Figure 1. TEM image of $X1$ - Y_2SiO_5 hollow sphere related to Y_2S sample. X-ray diffractograms of nanoparticles prepared in this work, and viability cell on KNS-42 cell line obtained by colorimetric assays performed in duplicate experiments ($n=2$).

References

[1] Linlin Zhao, Jongseon Choi, Yan Lu, So Yeon Kim, NIR Photoregulated Theranostic System Based on Hexagonal-Phase Upconverting Nanoparticles for Tumor-Targeted Photodynamic Therapy and Fluorescence Imaging, *Nanomaterials* 2020, 10, 2332.

Acknowledgments

This work was supported by Conselho Nacional de Desenvolvimento Científico e Tecnológico (CNPq), Coordenação de Aperfeiçoamento de Pessoal de Nível Superior (CAPES) and Fundação de Amparo à Pesquisa do Estado de São Paulo (FAPESP), Photonics National Institute for Science and Technology (INFO) and USP-Cofecub

Área: MAT

Use of lipases in the surface (bio)modification of polyester for the incorporation of chitosan nanoparticles

Wendhy C. Vicente (PG),^{1*} Patrícia B. Brondani (PQ),¹ Larissa N. Carli (PQ).¹
wendhycarolinavicente@gmail.com

¹Centro Tecnológico, de Ciências Exatas e Educação - UFSC Blumenau. Programa de Pós-graduação em Nanociência, Processos e Materiais Avançados, UFSC.

Palavras Chave: Poliéster, Hidrólise enzimática, Biocatálise, Nanotecnologia, Materiais têxteis.

Highlights

- Twenty commercial lipases, immobilized or not, were tested;
- Chitosan nanoparticles were prepared by using different methodologies;
- Chitosan-functionalized polyester fabrics were characterized by their physical-chemical properties;

Abstract

Poly(ethylene terephthalate) (PET) is a considerably interesting polyester synthetic fiber to be functionalized, as it has excellent physical properties, such as high resistance to wear or stretching, low shrinkage and roughness, making it a practical, low-cost material with less need for maintenance. However, polyester fabric has undesirable characteristics that need to be improved, such as low dyeability associated with its hydrophobic nature, accumulation of electrostatic charge, and flammability. One way of functionalizing textile materials is the superficial chemical modification of the fiber, followed by combining different structures, such as nanoparticles. Concerning the surface chemical modification of polyester fiber, biocatalysis (use of enzymes in reactions and processes) has shown to be a methodology with enormous potential to be explored. The use of lipases can result in the hydrolysis of ester groups present on the fabric surface, which improves its hydrophilicity. In the incorporation stage, it is common to use biopolymer bases and their nanosystems as active encapsulants, since the biopolymer itself can add different properties to the fabric. For this reason, chitosan is an interesting candidate to be combined with polyester fiber due to its biocompatibility, biodegradability, and interesting biological properties. In this sense, this research project proposes a study of the action of lipases to perform the superficial hydrolysis of polyester with subsequent impregnation of chitosan nanoparticles to the fiber. To create a process that is in line with the environmental issues of the textile industry, it is also expected to increase the hydrophilicity and dyeability of the fiber by disperse dyes, as well as to incorporate multiple functionalities conferred by chitosan itself, such as antimicrobial action, ultraviolet protection, and flame retardant properties.

Acknowledgments

Uso de Espiropirano para Identificação de Metal Pesado em Solução AquosaLucas G.B. Felício (IC),¹ Flávio B. Miguez (PG),¹ Frederico B. De Sousa (PQ)^{1*}

lucasgbfelicio@gmail.com; fredbsousa@unifei.edu.br

¹Laboratório de Sistemas Poliméricos e Supramoleculares, Instituto de Física e Química, UNIFEI.Palavras Chave: *Espiropirano, Mercúrio, Detecção, Merocianina, Metal Pesado.***Highlights**

Use of Spiropyran for Heavy Metal Identification in Aqueous Solution. Water soluble spiropyran. Selective interaction between spiropyran and Hg²⁺. –OCH₃ group play a role in the Hg²⁺ interaction. Spiropyran was able to sense Hg²⁺ (at 0.75mg.mL⁻¹) in aqueous solution.

Resumo

Os espiropiranos são moléculas que apresentam propriedades crômicas associadas a diversos estímulos externos, isomerizando-se reversivelmente entre as formas denominadas de espiro (**SP** forma fechada) e merocianina (**MC** forma aberta), como representado na **Figura 1a**. Os espiropiranos têm sido utilizados em diversas aplicações, destacando aquelas relacionadas à interação com metais e sensoriamento destes. Logo, a obtenção de derivados de espiropirano solúveis em água é importante para o sensoriamento de íons metálicos em solução aquosa, evitando solventes orgânicos. Neste trabalho, o derivado representado na **Figura 1a** foi obtido e caracterizado por técnicas de espectroscopia de infravermelho e ressonância magnética nuclear. Além disso, o equilíbrio entre as formas protonada (pH 2) e desprotonada (pH 11) pode ser verificado nos espectros de absorção apresentados na **Figura 1b** e confirmado pela titulação ácido-base realizada no com este derivado em solução aquosa. Como a estrutura da MC, em pH 11, favorece a interação com íons metálicos, titulações utilizando soluções aquosas dos nitratos de Cr³⁺, Mn²⁺, Fe²⁺, Co²⁺, Ni²⁺, Cu²⁺, Zn²⁺, Cd²⁺ e Hg²⁺ foram realizadas com o derivado da **Figura 1a**. Com base nas titulações realizadas, ficou evidente para o íon de Hg²⁺ a redução na intensidade da banda em 532 nm em função do aumento da concentração deste íon, **Figura 1c**, sugerindo uma seletividade deste derivado de espiropirano para o metal pesado Hg²⁺. Com o intuito de verificar a maior afinidade do Hg²⁺ pela forma MC, a titulação deste íon foi realizada em pH 7,5, na qual o equilíbrio entre as formas protonada e desprotonada está presente. Nesta titulação, a variação no espectro eletrônico foi menos evidente do que aquela em pH 11. Além disso, para os testes de interação entre os nitratos dos íons metálicos e o derivado de espiropirano, sem o grupo –OCH₃ no anel benzopirano, não foram verificadas mudanças de cor nas soluções, indicando que o derivado MC e a presença do grupo –OCH₃ é fundamental para a interação com o íon Hg²⁺.

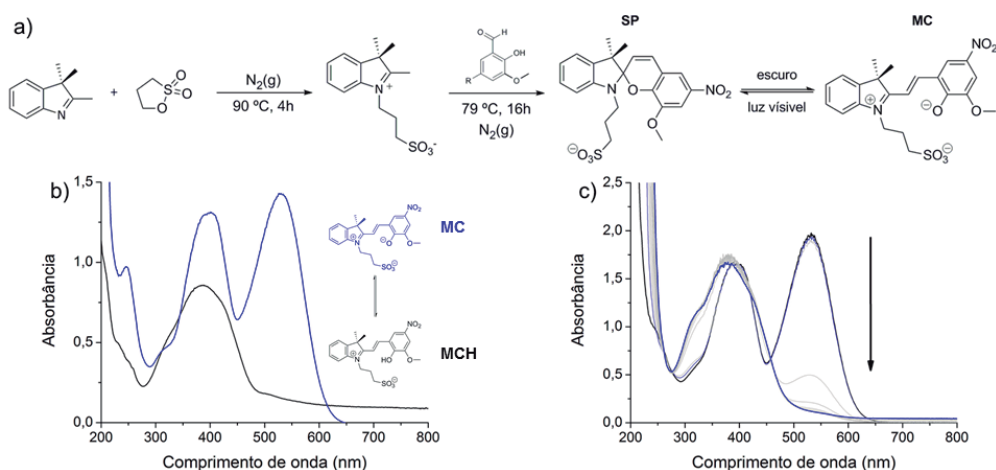


Figura 1: a) Esquema da síntese e equilíbrio entre os isômeros SP e MC, b) Espectros eletrônicos dos isômeros MC e MCH e c) Espectros eletrônicos da MC em função do aumento da concentração de Hg²⁺.

Agradecimentos

À UNIFEI, ao CNPq, à FAPEMIG e à CAPES.

Uso de resíduo de Lama Vermelha na produção de filmes anódicos de Nb₂O₅ e sua aplicação em Fotocatálise Heterogênea.

Patrícia dos Santos Araujo (PG),¹ Jonata Rodrigues Dias Batista (PG),¹ Yasmin Bastos Pissolito (PG),¹ Vagner Romito de Mendonça (PQ),² Francisco Trivinho-Strixino* (PQ),¹

patricsa1501@gmail.com; fstrixino@ufscar.br

¹Departamento de Físico e Química da Universidade Federal de São Carlos-Sorocaba, UFSCar; ²Instituto Federal-Itapetininga IFSP

Palavras Chave: *Oxidação eletrolítica a Plasma; Dopagem Anódica; Fotocatálise Heterogenea; Nb₂O₅; Lama Vermelha;*

Highlights

Use of Red Mud residue in the production of Nb₂O₅ anodic films and its application in Heterogeneous Photocatalysis.

Anodic films of Nb₂O₅ doped with red mud, were produced by plasma electrolytic oxidation.

The sample produced with 0.50% red mud resulted in 64% methylene blue degradation after 2h.

Resumo/Abstract

A indústria, por meio de seus resíduos, gera matérias primas abundantes e baratas que costumam ter amplo potencial de aplicação na produção de produtos nanotecnológicos [1]. Um exemplo é um resíduo gerado durante a fabricação do alumínio, conhecido por lama vermelha, armazenado em bacias de contenção, com riscos ao meio ambiente [2]. A lama possui composição química compatível com o uso no eletrólito durante o processamento de filmes anódicos por oxidação eletrolítica a plasma (PEO) [3]. Neste trabalho foram produzidos filmes de Nb₂O₅ por PEO, utilizando o resíduo da lama vermelha inserido diretamente na solução eletrolítica como elemento dopante. Foram investigadas as condições de preparação do eletrólito e do substrato metálico, as propriedades fotocatalíticas dos filmes obtidos e influência da lama vermelha. Os substratos de Nióbio foram anodizados soluções aquosas de C₂H₂O₄ contendo diferentes % de Lama Vermelha. Foi utilizado um sistema composto por uma fonte de corrente contínua em regime galvanostático, registrador de sinal para coleta das curvas de anodização e controle de temperatura do eletrólito por banho de recirculação externo. As amostras foram caracterizadas por meio de técnicas como microscopia eletrônica de varredura (MEV), espectrometria de energia dispersiva (EDS) e difração de raios x (DRX). As propriedades fotocatalíticas foram investigadas por testes de fotodegradação do Azul de Metileno (MB), em solução aquosa. Com a adição de Lama Vermelha ao eletrólito, houve uma mudança na resposta eletroquímica durante a síntese, ocorreu a redução de tamanho médio de cristalito estimado e aumento da espessura dos filmes. Foram encontrados no filme elementos como Alumínio e Silício, indicando a inclusão desses elementos de origem da lama. Nos teste de fotocatálise com Lama os melhores resultados foram para as amostras contendo 0,50% de lama vermelha com degradação de 64% do azul de metileno após 2h de exposição à luz UVC.

[1] F. Galembeck, C.A.S. Barbosa, R.A. Sousa. Aproveitamento sustentável de biomassa e de recursos naturais na inovação química. **Química Nova**, v. 32, n.3, p. 571–581, 2009.

[2] A. Gelencsér, et al. The Red Mud Accident in Ajka (Hungary): Characterization and Potential Health Effects of Fugitive Dust. **Environmental Science & Technology**, v. 45, p. 1608–1615, 2011

[3] M.P.L. Antunes, . et al. Red Mud from Brazil: Thermal Behavior and Physical Properties. **Industrial & Engineering Chemistry Research**, v. 51, p. 775–779, 2011.

Agradecimentos/Acknowledgments

Este trabalho foi financiado pelas agências de fomento brasileiras CAPES (código financeiro 01) e pelos projetos FINEP Martha e FAPESP (2022/05191-3). Os autores também agradecem à CBMM pela doação da placa metálica de Nb.

Uso de resíduos siderúrgicos como matéria-prima para a síntese de zeólitas

Diego Lopes da Silva (PG),^{1*} José Marcos Sasaki (PQ),² Adonay Rodrigues Loiola (PQ),¹.

diegolopes@alu.ufc.br

¹Departamento de Química Orgânica e Inorgânica, UFC;

²Departamento de Física, UFC.

Palavras Chave: Zeólitas, Resíduo siderúrgico, Síntese.

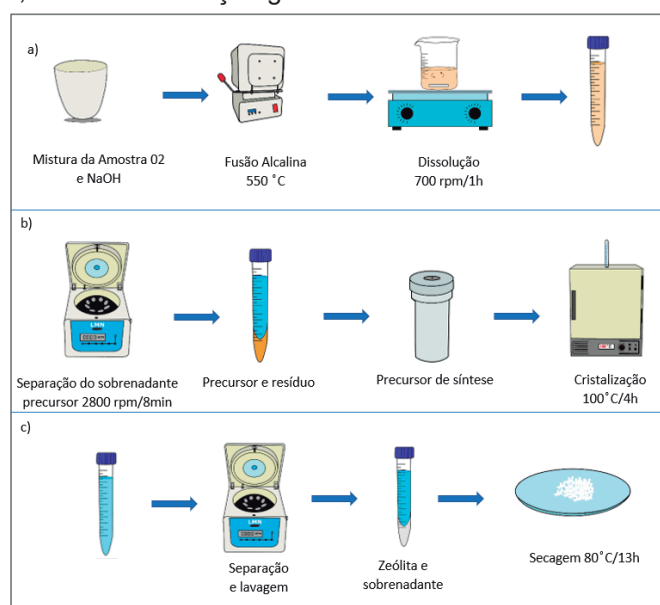
Highlights

Use of steel waste for the synthesis of zeolites

- Use of steel waste for synthesis
- Type A zeolite synthesis
- Zeolites with potential for adsorptive processes.

Resumo/Abstract

A indústria siderúrgica é um dos setores estratégicos que contribuem para o progresso econômico do país, pois fornece matéria-prima para várias partes da cadeia produtiva. Apesar de sua relevância, e mesmo diante de um conjunto de ações direcionadas para a redução de resíduos, os processos siderúrgicos ainda contribuem de forma significativa para a geração de passivos ambientais. Entre esses, destaca-se os materiais refratários, os quais são constituídos por óxidos de silício e alumínio, compostos que podem ser explorados como matéria-prima na produção de zeólitas, aluminossilicatos cristalinos com estruturas porosas bem definidas e que encontram aplicações em catálise, processos de separação de gases, troca iônica etc. Nesta pesquisa, os resíduos refratários foram usados para a síntese de zeólitas, onde foi aplicado o método de síntese hidrotérmica. Assim, foram obtidas zeólitas do tipo A, analcima e faujasita em misturas de fases. Estas foram identificadas por meio das medidas de difração de raios-x, bem como nas imagens de microscopia eletrônica de varredura (MEV) que mostraram as morfologias presentes, evidenciando o formato cúbico da zeólita A. Além das bandas de absorção na região do infravermelho, que estão relacionadas às ligações de Si—Al existentes nas estruturas. Logo, o material obtido tem o potencial de serem utilizados em aplicações futuras, como em adsorção gasosa e troca iônica.



Agradecimentos/Acknowledgments

DotLib, LRX and Federal University of Ceará.

Versatility of ultras-small amorphous TiO₂ nanoparticles for preparation of ZnO@nTiO₂ core@shell nanostructures

Artur Luís Hennemann (PG),¹ Geovanne Lemos de Assis (PG),¹ Robson Raphael Guimarães (PQ),¹ Helton Pereira Nogueira (PQ),¹ Koiti Araki (PQ),^{1*}

koiaraki@iq.usp.br

¹Departamento de Química, Universidade de São Paulo.

Key Words: Core@Shell nanomaterials, TiO₂ nanoparticles, TEM

Highlights

Amorphous ultras-small TiO₂ nanoparticle is shown to be a quite versatile starting material for preparation of ZnO@nTiO₂ core@shell nanostructures.

Resumo/Abstract

Anatase and rutile are the two most common crystalline phases of TiO₂ and have been widely explored, while the amorphous phase has been overlooked due to high disorder and consequent low photoactivity. However, amorphous TiO₂ is more widely available in nature, has larger surface areas and specific adsorption capacities than the crystalline materials, and can be prepared at lower temperatures. A highly water dispersible ultras-small 3 nm amorphous TiO₂ nanoparticles (nTiO₂, Fig. 1C) exhibiting very high affinity for metal ions was developed, as well as its large-scale production method. The amorphous nature, small size and the high affinity of nTiO₂ for Zn(II) ions are currently being explored to prepare core@shell nanostructured system. For example, ZnO nanorods is readily covered up by nTiO₂ demonstrating to be especially interesting in the preparation of ZnO@nTiO₂ core@shell nanostructures. In addition, the thickness of nTiO₂ shell and ZnO nanorods size can be controlled simply by adjusting the reaction stoichiometry, generating new nanostructured materials. The process was monitored by XRD (Fig. 1A) and UV-Vis spectroscopy (Fig. 1B) clearly demonstrating the decrease of the ZnO band-gap transition and XRD diffraction peaks as the proportion of nTiO₂ was increased, as expected for the decrease of the ZnO core size, which was confirmed by TEM (Fig. 1D).

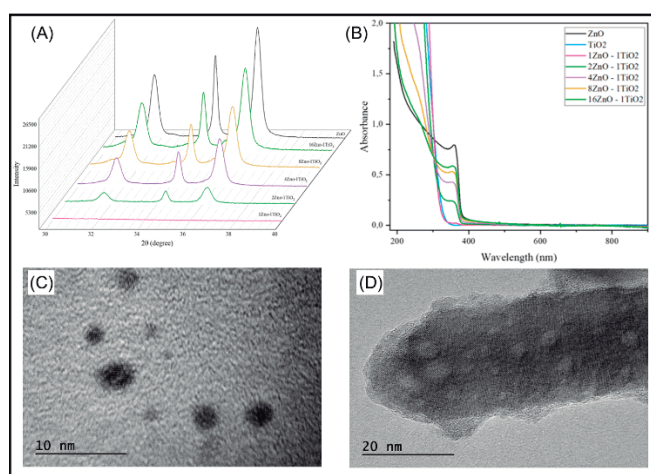


Fig. 1: (A) XRD of the ZnO@nTiO₂ in the 001, 002 and 101 plane region of ZnO showing the effect of the proportion of ZnO:nTiO₂ on the resulting nanostructured material. (B) UV-Vis spectrum of the products of reaction of ananoTiO₂ with ZnO nanorods in different proportions generating ZnO@nTiO₂ nanostructures. TEM image of (C) nTiO₂ and (D) a ZnO@nTiO₂ core@shell nanostructure.

Agradecimentos/Acknowledgments

CAPES, CNPq, FAPESP and SisNANO-USP

Área: MAT

(Inserir a sigla da seção científica para qual o resumo será submetido. Ex: ORG, BEA, CAT)

WO₃.H₂O application as an electrochemical sensor in the detection of Bisphenol-A

Eryza G. de Castro (PQ)¹, Jhonatan Matheus P. da Rocha (PG)¹, Andressa Galli (PQ)¹, Camila Alves de Lima Larissa (PQ)¹, Larissa Panatto Trento (IC).

eryza.castro@gmail.com

¹Chemistry Department, UNICENTRO

Key Words: Tungsten Oxide, Chemical Synthesis, bisphenol A, Sensor.

Highlights

WO₃ can be obtained by recycling material the W from filaments of automotive lamps. WO₃ applied as a modifying agent in the carbon paste electrode (CPE) for the electroanalytical detection of Bisphenol-A (BPA).

Abstract

This study describes the synthesis and characterization of WO₃ from recycled material from automotive lamps and its application as a modifying agent in the carbon paste electrode (CPE) for the electroanalytical detection of Bisphenol-A, a molecule known for its activity as a disruptor of endocrine system. According to the morphological and structural analyzes, it was possible to determine that the synthesis results in a WO₃ sample of high purity and crystallinity, represented by the monohydrated orthorhombic phase of tungsten oxide, tungsite (WO₃.H₂O), with high purity and crystallinity. The tungsite crystals are organized in the form of small needles agglomerated into spheres, as shown by the SEM images. This structure provides a high contact surface, ideal for electron transfer processes. The electrode modified with WO₃, presented a good synergy with the CPE, increasing its catalytic capacity for oxidation of BPA on its surface, when in a proportion of 2.5% of the modifying material for the carbon paste. The oxidation of BPA on the surface of CPE/WO₃ occurs mainly by diffusion of the species to the surface, it was also possible to indicate the involvement of two protons and two electrons in the transfer process electronics, moreover, the process was characterized as totally irreversible. The development of the electroanalytical methodology was carried out using the differential pulse voltammetry technique, under optimized conditions of a_m=75mV t_m=10ms and 6mV increment, using Britton-Robinson buffer (0.1 mol.L⁻¹) at pH=10. The method showed adequate linearity in the BPA concentration range of 1 to 18µmol.L⁻¹, with a correlation coefficient of 98.9%. The linear regression model was evaluated by ANOVA, which demonstrated that the model is statistically significant in generalizing the system, with a non-significant lack of model adjustment for a significance level of 5% (α=0.5). t-test indicated low significance of the linear coefficient in the equation of the line. The residuals showed normality, verified by the Shapiro-Wilk test, and homoscedasticity, by the Cochram test. The analytical calibration curve showed an LD and LQ of 0.345 µmol.L⁻¹ and 1.046 µmol.L⁻¹, respectively. Thus, it was determined that BPA is detectable within the studied concentration range. Accuracy for the developed method was performed by recovery tests using real samples of bottled water, with recovery values around 114-122%.

References

- 1- ZHOU, Y.; YANG, L.; LI, S.; DANG, Y. A novel electrochemical sensor for highly sensitive detection of bisphenol A based on the hydrothermal synthesized Na-doped WO₃ nanorods. *Sensors & Actuators: B. Chemical*, v.245, p. 283, 2017.
- 2- LI, H., Et al. Disposable paper-based electrochemical sensor based on stacked gold nanoparticles supported carbon nanotubes for the determination of bisphenol A. *Electrochemistry Communications*. P. 104, 2016.

Acknowledgments



WS₂-WO₃/rGO: Tackling two different energy problems with one unique and novel nanocomposite

Sergio H. Domingues (PQ),^{1,2*} Carlos Eduardo L. dos Santos (PG),^{1,2} Jéssica E. S. Fonsaca (PQ),^{1,2}

shdomingues@mackenzie.br

¹Mackenzie Institute for Advanced Research in Graphene and Nanotechnologies – MackGraphe, Mackenzie Presbyterian University, São Paulo, Brazil; ² Engineering School, Mackenzie Presbyterian University, São Paulo, Brazil.

Key words: nanocomposites, TMD, TMO, graphene, supercapacitor, HER.

Highlights

A WS₂-WO₃/rGO nanocomposite was synthesized through a hydrothermal route that led to a material with unique properties capable of acting both as a supercapacitor and as electrocatalyst in hydrogen evolution reactions (HER).

Abstract

Dichalcogenides and transition metal oxides, TMDs and TMOs, respectively, as well as graphene derivatives (GO and rGO) are promising materials for energy storage and conversion systems. However, individually, they face limitations such as instability of charge/discharge mechanisms (TMDs and TMOs) and surface area dependence (rGO). The combination of these materials, in a rational way, producing nanocomposites, can eliminate their deficiencies, generating a novel and unique material with superior properties when compared to neat nanomaterials. Based on this, our main goal was to synthesize nanocomposites based on a TMD (WS₂), a TMO (WO₃) and finally a graphene derivative (rGO) in the form of a single electrode and investigate their capacitive and catalytic properties in hydrogen evolution reaction (HER). Therefore, WS₂-WO₃ was obtained by a hydrothermal route, adding tungsten and sulfur precursors in an autoclave (200°C for 24 h). To obtain the WS₂-WO₃/rGO, the rGO was previously synthesized by a modified Hummers method and reduced using hydrazine, being later added to the autoclave containing the WS₂-WO₃ precursors. The products were properly characterized by different techniques. Figure 01A illustrates the comparative Raman spectra of rGO, WS₂-WO₃ and WS₂-WO₃/rGO, where it is clearly noted the presence of dichalcogenide, oxide and graphene derivative bands in the nanocomposite spectrum, proving the success of the synthesis.

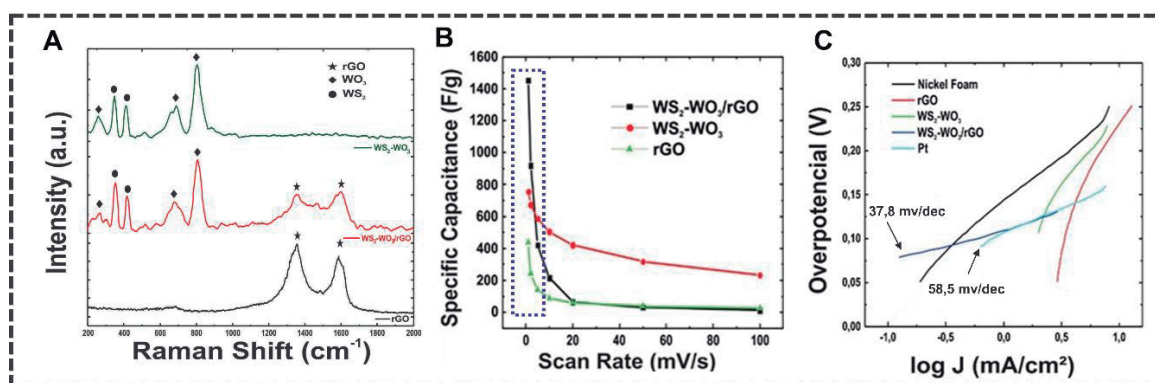


Figure 1. (A) Raman spectra, (B) Specific capacitance and (C) LSV curves at 2mV/s for all studied nanomaterials.

Figure 1B illustrates that in several ranges of scan rates, the nanocomposite presented a much higher capacitance than its individual components, up to four times higher in some cases. Regarding to HER (Figure 1C), the superiority of the nanocomposite is not only evidenced when it is compared to the pure species, but also to platinum, since it presents considerably lower overpotential values in HER reactions in basic medium. In this sense, we attested the possibility of achieving the production of smart materials based on outside-the-box concepts that may be promising for filling in the gaps of energy field.

Acknowledgments

Authors acknowledge CNPq (#306808/2020-0), INCT of Carbon Nanomaterials, Mackenzie Presbyterian University, MackPesquisa, MackGraphe, Brazilian Army and FAPESP (#2020/13288-6).

ZnO/g-C₃N₄ heterostructures decorated with silver nanoparticles for methylene blue photodegradation in real textile wastewater.

Renan Tostes Couto* (PG),¹ **Juliana Fonseca de Lima** (PQ).¹

renantostesc@gmail.com

¹ Grupo de Materiais Fotoativos Nanoestruturados (FotoNANO), Instituto de Química, Universidade do Estado do Rio de Janeiro, Rio de Janeiro, RJ 20550-900, Brasil.

Keywords: Silver nanoparticles, Zinc oxide, g-C₃N₄, Heterojunctions, Photocatalysis.

Highlights

Synthesis of ZnO/g-C₃N₄ heterostructures decorated with silver nanoparticles.

Characterization of the heterostructures by FTIR, XRD, SEM and DRS.

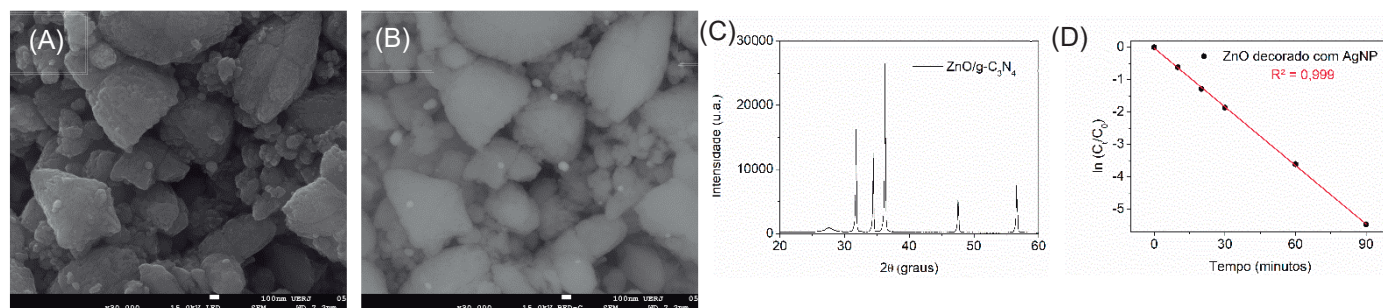
Photocatalysis of methylene blue in real textile wastewater.

Resumo/Abstract

An average textile industry can consume 1.6 million liters of water. The dyeing not only consume high volumes of water but also produces very complex substances. Besides, their high stability and high resistance creates a challenge in conventional wastewater treatments processes. Traditional methods have been used such as adsorption, biological degradation and others but all of them presents some drawbacks. That way, photocatalysis arises as a promising method for dyes removal [1].

Among nanomaterials utilized for photocatalysis of dyes, zinc oxide (ZnO) is vastly employed by presenting great degradation results and excellent absorption in ultraviolet region. However, UV region represents only a small part of solar spectrum. Heterojunction nanocomposites like ZnO and graphitic carbon nitride (g-C₃N₄) stands out as photocatalyst materials due to minimized recombination ratio and improved capability of utilizing solar radiation by band gap alterations. The decoration of silver nanoparticles (AgNP) turns out as a good alternative for visible light absorption due to plasmonic effects [2,3].

In this work, the synthesis of ZnO/g-C₃N₄ heterostructure decorated with AgNP was developed and characterized by FTIR, XRD, SEM and DRS. The photocatalysis of Methylene Blue (MB) was done using an real textile wastewater provided by De Millus S.A.. SEM images ((A) and (B)) reveals presence of AgNP in all of zinc oxide. XRD (C) of ZnO/g-C₃N₄ points out the presence of both materials. Lastly, preliminary results indicate an enhancement of photocatalytic activity (D) with the presence of silver nanoparticles in zinc oxide.



- [1] A. Saravanan, P.S. Kumar, S. Jeevanantham, M. Anubha, S. Jayashree, Environ. Pollut. 298 (2022) 118844.
- [2] V.E. Podasca, T. Buruiana, E.C. Buruiana, J. Photochem. Photobiol. A Chem. 371 (2019) 188–195.
- [3] J.H. Shen, T.H. Chiang, C.K. Tsai, Z.W. Jiang, J.J. Horng, J. Environ. Chem. Eng. 10 (2022) 107352.

Agradecimentos/Acknowledgments

CAPES, CNPq and FAPERJ.

MED

Química Medicinal

46^a Reunião
Anual da **SBQ**

28 a 31 de Maio de 2023

Águas de Lindóia · SP
Hotel Monte Real

4-Hydroxyderricin (4HD) as an antibacterial agent: total synthesis, comprehensive structure-activity investigations and mechanism of action

Alvaro L. Helena (PG),¹ Reinaldo S. Theodoro (PG),¹ Patrick R. Ozanique (PG),¹ Leticia R. Assis (PG),¹ Julyanna A. S. Nascentes (PG),¹ Carlos H. G. Martins (PQ),² Henrique Ferreira (PQ),³ Luis O. Regasini* (PQ).¹

alvaro.helena@unesp.br; luis.regasini@unesp.br

¹Department of Chemistry and Environmental Sciences, Institute of Biosciences, Humanities and Exact Sciences, São Paulo State University (Unesp), São José do Rio Preto, SP, Brazil. ²Departament of Microbiology, Institute of Biomedical Sciences, Federal University of Uberlândia (UFU), Umarama, MG, Brazil; ³Departament of Biochemistry and Microbiology, Institute of Biosciences, São Paulo State University (Unesp), Rio Claro, SP, Brazil.

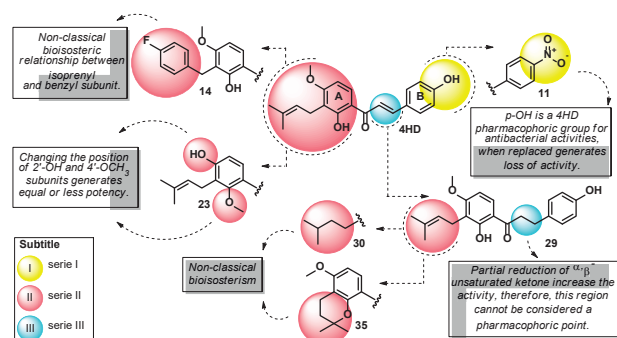
Keywords: Total synthesis, 4-Hydroxyderricin, Regioselective, Prenylated chalcones, Antibacterial, Membrane.

Highlights

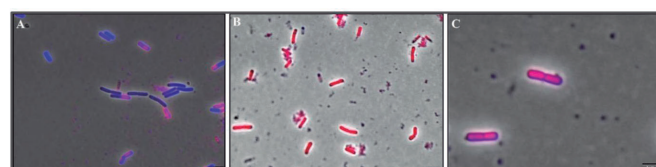
A total synthesis of **4HD** and 45 analogs were carried out. Structure-activity relationships were clarified. Their mode of action was elucidated, indicating membrane disruption of MSSA and MRSA cells.

Abstract

Antibacterial resistance (ABR) has been turned a great concern to global health. The overuse and misuse of antibacterial agents, mainly during COVID-19 pandemic, is strongly associated with the increasing development of ABR. Thus, efforts to discover new antibacterial agents are essential to overcome this worldwide challenge [1]. 4-hydroxyderricin (**4HD**) is a chalcone from *Angelica keiskei* and exhibits potent antibacterial activity [2]. **4HD** was selected as a hit for the design and syntheses of three series of analogs, which were evaluated against human pathogens, including drug-resistant strains. The target compounds, 45 in total, were synthesized using regioselective iodination, Suzuki coupling, sigmatropic rearrangements and reductions. Among them, 26 are new compounds and 8 naturally occurring compounds. Antibacterial and antimycobacterial assays of **4HD** analogs indicated MIC₉₀ values ranging from 1.56 to 25 µg mL⁻¹. **4HD** exhibited a potent inhibitory activity against *Staphylococcus aureus* (MSSA and MRSA) biofilms with a MBIC₅₀ values of 1.56 and 0.78 µg mL⁻¹, respectively. The mode of action of **4HD** and two analogs were elucidated and *B. subtilis* membrane disruption was confirmed by PI-SYTO-9 fluorescence microscopy. The assays with human keratinocytes indicated low toxicity of **4HD** analogs. In addition, three regions of **4HD** structure (α, β-unsaturated ketone bridge and rings A and B) were exploited in SAR conclusions. In brief, this is the first study on total and regioselective synthesis of **4HD** and its analogs as well as their antibacterial mode of action.



Scheme A. SAR of 4HD and its selected analogs.



(A) Negative control (cells treated with 1% DMSO);
(B) Positive control (cells treated with nisin);
(C) Cells treated with 4HD solution in DMSO for 15 minutes. Magnification 100×; Scale bar 5µm.

Scheme B. Fluorescence microscopy of *B. subtilis*.

Acknowledgments

The authors gratefully acknowledge financial support from the Coordination for the Improvement of Higher Education Personnel (CAPES, finance code 001), Brazilian Council for Scientific and Technological Development (CNPq) (Grants 471129/2013-5, 306251/2016-7 and 429322/2018-6), the São Paulo Research Foundation (FAPESP) (Grants 2014/18330-0 and 2018/15083-2). ALH thanks CAPES for his scholarship.

[1] Rossolini, G. M. et al. Epidemiology and clinical relevance, economic burden, mechanisms of resistance determinants versus anti-Gram-positive agents. COMICR. v. 13, p. 582-588, 2010.

[2] Kim, D. W. et al. *Angelica keiskei*, an emerging medicinal herb with various bioactive constituents and biological activities. Arch. Pharm. Res. v. 40, p. 655-675, 2017.

Alkyl/arylaminomethylenecyclohexan-1,3-diones as possible Alternative Oxidase Enzyme (AOX) inhibitors in *Moniliophthora perniciosa*

Leonardo Claudio (IC),^{1*} Paulo C. S. Costa (PG),¹ Victor M. Brandão (IC),¹ Gonçalo A. G. Pereira (PQ),² Antônio Vargas de Oliveira Figueira (PQ),³ Paulo C. M. L. Miranda (PQ),^{1*}

leonardo-claudio@outlook.com.

¹Institute of Chemistry, Unicamp – Campinas, Brazil; ²Institute of Biology, Unicamp – Campinas, Brazil; ³Center for Nuclear Energy in Agriculture, USP – Piracicaba, Brazil.

Palavras Chave: AMCD, AOX, Enzyme Inhibitors, GMO, WBD.

Highlights

Alkyl/arylaminomethylenecyclohexan-1,3-diones (AMCDs) enclose a new class of synthetic compounds designed by QSAR to inhibit the Alternative Oxidase Enzyme (AOX). Biological activities were evaluated using GMO *Pichia pastoris*.

Resumo/Abstract

The enzyme Alternative Oxidase acts as an escape route to the cytochrome c respiratory chain by catalyzing the oxidation of ubiquinol.¹ This mechanism plays a major role in the infection of cocoa by *M. perniciosa*, the witches' broom disease agent. AMCD ligands were proposed after virtual screening and docking studies. A multicomponent reaction (MCR, Panel A in Figure 1) can easily access these compounds, allowing a rapid and highly structurally diversified synthesis. AMCDs (the faded red compound in Panel B in Figure 1) were also selected by their ability to mimic the structure of the AOX natural inhibitor colletochlorin B (the blue compound in Panel B in Figure 1).

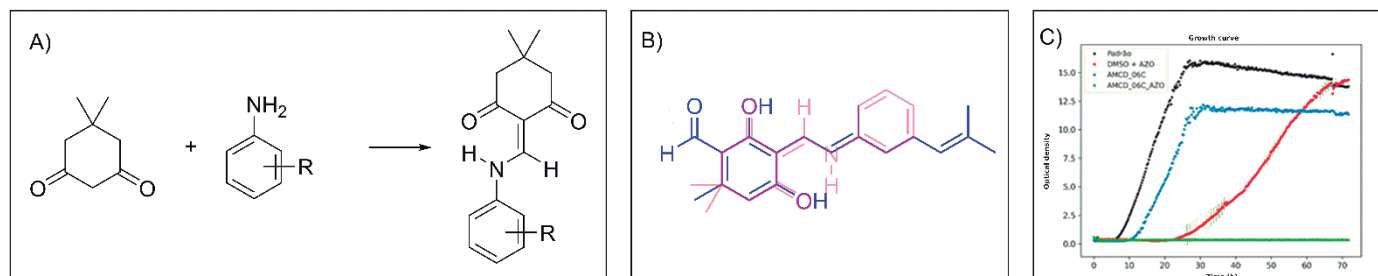


Figure 1. A) Synthetic approach for AMCDs derivatives, B) AMCD (faded red) and colletochlorin B (blue) structural alignment, and C) AMCD biological assay against GMO *Pichia pastoris*.

The OpenEye platform was used for the virtual screening and molecular docking. First, the colletochlorin B structure was used as a pharmacophore to filter the substructures with a similar spatial distribution of chemical properties. After that, the zinc and eMolecules datasets were filtered by the substructures found in the first step. The filtered compounds were docked after an *M. perniciosa* AOX model. The interaction founded by the docking was visualized, and the structure of AMCDs was selected. A total of 40 compounds were synthesized and characterized by ¹H and ¹³C-NMR spectroscopy. The biological assay was performed using a GMO *Pichia pastoris* model. The AMCDs showed low toxicity, and some structures were able to reduce the growth rate of the yeast completely (Panel C in Figure 1).

REFERENCES

1. Purdy LH, Schmidt RA. 1996. Status of cacao witches' broom: biology, epidemiology, and management. Annual Review of Phytopathology 34: 573–594.
2. Lieby-Muller, F., Simon, C., Constantieux, T., & Rodriguez, J. (2006). Current developments in Michael addition based multicomponent domino reactions involving 1,3-dicarbonyls and derivatives. QSAR & Combinatorial Science, 25(5-6), 432-438.

Agradecimentos/Acknowledgments

We kindly thank FAPESP, CAPES and the Institute of Chemistry of UNICAMP for all the support required in this study.

Antileishmanial activity of β -carboline-(piperazinyl)-1,3,5-triazine hybrids

Caroline Fortuna (PG),¹ Rodolfo Bento Balbinot (PG),² Débora Laís Gonçalves (IC),¹ Paula Baréa (PG),¹ Debora C. Baldoqui (PQ),³ Willian F. da Costa (PQ),³ Celso Vataru Nakamura (PQ),² Maria Helena Sarragiotto (PQ).^{1*}

carolinefortunacf@gmail.com; mhsarragiotto@uem.br

¹Programa de Pós-Graduação em Química, UEM; ²Laboratório de Inovação Tecnológica no Desenvolvimento de Fármacos e Cosméticos, UEM; ³Departamento de Química, UEM.

Keywords: β -Carboline, Triazine, Antileishmanial, *Leishmania amazonensis*.

Highlights

The synthesized β -carboline-(piperazinyl)-1,3,5-triazine hybrids (**2a-g**) and their precursors **1a-g** were evaluated against promastigote and amastigote forms of *Leishmania amazonensis*.

Resumo/Abstract

Leishmaniasis is a neglected disease caused by parasites of the *Leishmania* genus, affecting approximately 12 million people in the world, being estimated that a 700 000 to 1 million new cases occur annually.¹ Current drugs for leishmaniasis exhibit high toxicity and several side effects. To discover novel more effective and less toxic antileishmanial agents, several classes of compounds have been investigated, including β -carbolines. In continuing our work with aiming to explore the potential antileishmanial activity of β -carbolines,² we designed a series of hybrids **2a-g**, which were synthesized from the corresponding carboxylic acids **1a-g**, as described earlier (Figure 1).³ In this work the synthesized β -carboline-(piperazinyl)-1,3,5-triazine hybrids (**2a-g**) and their precursors **1a-g** were evaluated against *Leishmania amazonensis*. The 50% inhibitory concentration (IC₅₀) of promastigote and amastigote forms of *L. amazonensis*, cytotoxicity (CC₅₀) for the macrophage J774-A1 cell lines, and the selectivity index (SI) were determined. The assay results for 1-(substituted)- β -carboline-3-carboxylic acids showed that **1a-e** were weakly active for the promastigote form of *L. amazonensis*, with IC₅₀ values in the range of 55.9 to 159.7 μ M. For amastigotes, the compounds exhibited moderate activity, with IC₅₀ values in the range of 18.2-62.6 μ M. Compounds **1f-g** were inactive (IC₅₀ >200 μ M). The results for the *in vitro* activity of **2a-g** are presented in Table 1.

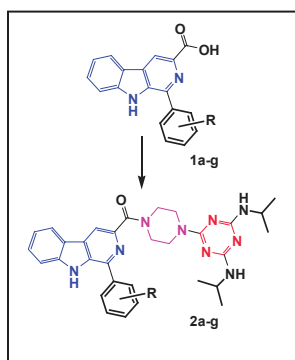


Fig. 1. Structures of **1** and **2**

Table 1. Antileishmanial activity data for **2a-g** against *L. amazonensis*.

Comp.	R	Promastigote IC ₅₀ (μ M)	Amastigote IC ₅₀ (μ M)	J774A1 CC ₅₀ (μ M)	SI	
					Pro	Ama
2a	H	8.3 \pm 1.1	34.9 \pm 2.4	45.1 \pm 5.6	5.40	1.3
2b	4-OCH ₃	>200	nt	346.3 \pm 17.0	-	-
2c	4-F	9.5 \pm 0.7	26.3 \pm 1.9	165.3 \pm 6.8	17.3	6.30
2d	2-Cl	8.7 \pm 0.1	15.1 \pm 0.6	62.57 \pm 4.80	7.21	4.13
2e	4-Cl	156.6 \pm 24.1	>100	335.3 \pm 20.5	2.14	-
2f	3-NO ₂	>200	nt	361.4 \pm 45.	-	-
2g	4-NO ₂	>200	nt	301.3 \pm 15.9	-	-
Miltefosine		22.71 \pm 1.24	1.75 \pm 0.1	54.2 \pm 5.20	2.4	30.9

nt = not tested.

Compounds **2a**, **2c** and **2d** exhibited significant activity for promastigotes, with IC₅₀ ranging of 8.3 to 9.5 μ M, while a moderated activity was observed for amastigotes (IC₅₀ ranging of 15.1 to 34.9 μ M). It is worth mentioning that a better inhibition profile against the amastigote form would be desirable. Compound **2c** (IC₅₀ = 9.5 \pm 0.7 μ M) was 17 times more toxic to the promastigote form of parasite than to J774A cells. The introduction of (piperazinyl)-1,3,5-triazine moiety in the hybrids **2a-g** led to an increase of antileishmanial activity, compared to **1a-g**.

¹ World Health Organization. Leishmaniasis. Acesso em: 27 de janeiro de 2023.

² Baréa, P.; Barbosa, V. A.; Bidóia, D. L.; Paula, J. C.; Stefanello, T. F.; Costa, W. F.; Nakamura, C. V.; Sarragiotto, M. H. *European Journal of Medicinal Chemistry*, **2018**, 150, 579–590.

³ Livro de Resumos 45RASBQ, pag. 667, **2022**, Maceió.

Agradecimentos/Acknowledgments

CAPES, CNPq, FUNDAÇÃO ARAUCÁRIA, DEPARTAMENTO DE QUÍMICA-UEM

Antiureolytic properties of cinnamyl hydroxamic acids

Luciana Pereira Silva Viana (PG),^{1*} Giovanna Marques Naves (IC),¹ Bruno da Costa Tomaz (IC),¹ Ângelo de Fátima (PQ),¹ Cleiton Moreira da Silva (PQ).¹

lucianapereira0410@gmail.com

¹Departamento de Química, Universidade Federal de Minas Gerais, UFMG, 31270-901.

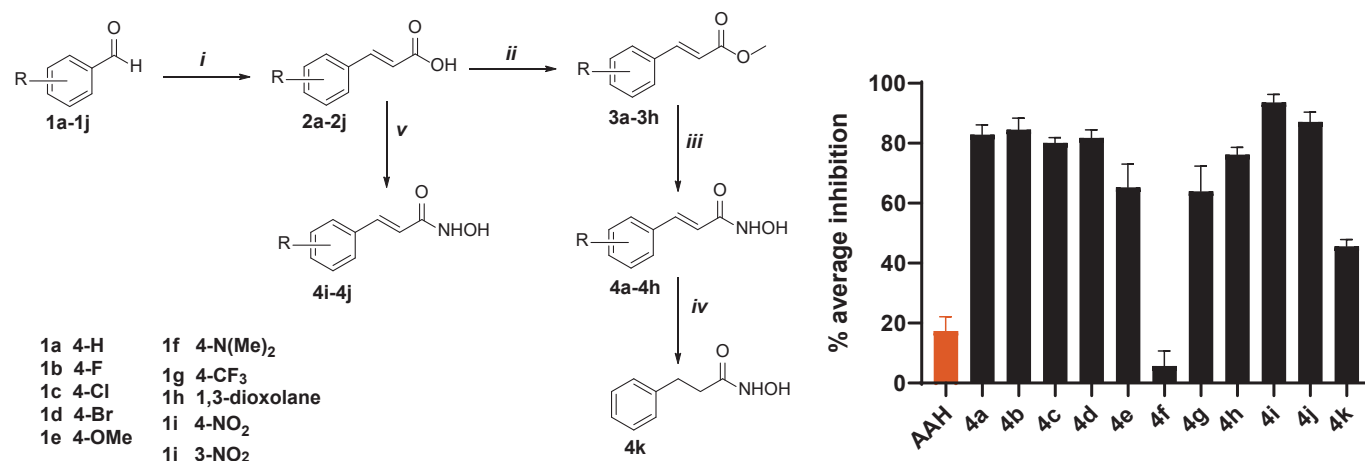
Keywords: Urease inhibitor, Hydroxamic acids, *Helicobacter pylori*.

Highlights

Cinnamyl hydroxamic acids are promising urease inhibitors, with IC₅₀ values between 3.8 – 24.2 μM.

Abstract

Urease is a nickel metalloenzyme responsible for the hydrolysis of urea to ammonia and carbamic acid. This enzyme is mainly present in plants, bacteria and fungi.¹ In human health, the activity of ureases is an important virulence factor in infections caused by ureolytic pathogens, for example *H. pylori*, since urea is the major nitrogenous metabolic product in humans.² The ureolytic activity also impacts agricultural productivity, considering that urea is the main nitrogen fertilizer used in the world.¹ The negative effects of urease activity and the absence of safe and effective inhibitors in the market motivate the development of new urease inhibitors. In this context, hydroxamic acids are an important class of compounds to be investigated, given that acetohydroxamic acid (AAH) has well-established inhibitory properties.³ In this work, 11 hydroxamic acids derived from cinnamic acids (compounds **4a-4k**) were synthesized (Scheme 1) and their urease inhibitory activities evaluated *in vitro* by indophenol method. Initially, the compounds were tested at a concentration of 20 μM and IC₅₀ was determined only for those that were more active than AAH (Fig.1). Compounds with electron donating groups are less active than those with electron withdrawing groups, with compound **4i** being the most active (IC₅₀= 3.8 μM). Compound **4k** (IC₅₀= 24.2 μM) exhibited lower inhibitory capacity than its analogue, compound **4a** (IC₅₀= 7.6 μM). This result indicates the importance of the double bond for the antiureolytic activity.



Scheme 1. Synthetic route of cinnamyl hydroxamic acids. *i*) Malonic acid, piperidine, EtOH, 70°C, microwave irradiation, 45 min. *ii*) TMSCl, MeOH, reflux, 24 h. *iii*) KOH, NH₂OH.HCl, MeOH, r.t. *iv*) Pd/C, H₂, MeOH, r.t., 48 h. *v*) CDI, NH₂OH.HCl, anhydrous THF, inert atmosphere, r.t., 48 h.

Figure 1. % average inhibition at 20 μM. Compound 4f was less active than AAH.

[1] Kappaun, K.; Piovesan, A. R.; Carlini, C. R.; Ligabue-Braun, R. J. *Adv. Res.* **2018**, 13, 3–17. DOI:10.1016/j.jare.2018.05.010

[2] Montecucco, C.; Rappuoli, R. *Nat. Rev. Mol. Cell Biol.* **2001**, 2, 457–466. DOI:10.1038/35073084

[3] Marmion, C. J.; Griffith, D.; Nolan, K. B. *Eur. J. Inorg. Chem.* **2004**, 3003–3016. DOI: 10.1002/ejic.200400221

Acknowledgments

CNPq, FAPEMIG, CAPES - Finance Code 001

Busca por inibidores de Ornitina Descarboxilase de *Leishmania donovani* por modelagem molecular

Joyce R. Melo (PG),¹ Nelilma C. Romeiro (PQ),¹ Paulo de Sousa Maia (PQ)²

joycemeloufrj@gmail.com

¹Laboratório Integrado de Computação Científica-LICC- IMQ CM/UFRJ

²Grupo de Eletrocatalise e Química Bioinorgânica- GEQBio-IMQ CM/UFRJ

ODC, Ornitina descarboxilase, Leishmaniose, Leishmania, Modelagem molecular, Química medicinal

Highlights

Search for inhibitors of Ornithine Decarboxylase from *Leishmania donovani* by molecular modeling

The main objective of this work is to carry out integrated molecular modeling studies aiming at the selection, obtention and pharmacological evaluation of ODC inhibitors, as potential candidates for anti-leishmanial drugs.

Resumo/Abstract

A leishmaniose é uma das sete doenças tropicais e subtropicais mais importantes e representa um grave problema de saúde mundial, com um amplo espectro de manifestações clínicas, sendo potencialmente fatal. Essa doença é causada por *Leishmania sp.*, protozoários parasitas intracelulares da família *Trypanosomatidae*, que são transmitidos aos hospedeiros mamíferos através da picada de fêmeas infectadas de insetos da subfamília flebotomíneos. A Ornitina descarboxilase (ODC), é uma importante enzima do metabolismo redox, sendo limitante da via biossintética das poliaminas. Poliaminas de protozoários parasitas podem ser alvos potenciais para o desenvolvimento de novos fármacos com atividade contra *Leishmania donovani*. Nesse cenário, a realização de estudos *in silico* é uma estratégia para auxiliar no planejamento de novos candidatos a fármacos, reduzindo o custo total inerente ao processo. Assim, foi realizada a busca por inibidores de ODC, já descritos na literatura, no banco de dados de moléculas, alvos e atividades farmacológicas ChEMBL. No processo foram consideradas moléculas testadas nas proteínas de *Leishmania donovani*, *Bos taurus*, *Ratus norvegicus* *Mus musculus* e *Homo sapiens*, que resultou em 235 moléculas. Foi feita a análise dos inibidores encontrados e 8 moléculas de referência foram selecionadas, utilizando como critérios a potência inibitória e esqueletos moleculares inovadores. Em seguida, foi feita a busca por similaridade molecular no ChEMBL e no Pubchem, através da plataforma de bioinformática ChemMine, utilizando como critério um coeficiente de Tanimoto maior ou igual a 80%. No processo, foram utilizadas três ferramentas: 1)- Algoritmo de *Fingerprint* do Pubchem; 2)- Algoritmo de *Fingerprint* do ChEMBL e 3)- Algoritmo EI, que usa uma medida de similaridade baseada em pares atômicos, também no ChEMBL. Os compostos selecionados foram salvos em formato csv e analisados individualmente utilizando critérios de exclusão, tais como inibição já descrita, toxicidade, entre outros. O modelo 3D de ODC construído a partir de sequências de aminoácidos foi feita através do servidor Swiss model, que no total identificou 50 possíveis moldes. O molde escolhido para o servidor construir a ODC de *L. donovani* foi a estrutura cristalográfica da ODC humana, com resolução de 2,1Å, com código PDB 1d7k.1.A. Essa proteína apresenta 43,08% de identidade com a ODC de *Leishmania donovani*, e foi validada e refinada através do Saves, ProsaWeb e Modrifer. Posteriormente, serão realizados estudos de *Docking Molecular*, *Dinâmica Molecular*, e filtros ADMET.

Agradecimentos/Acknowledgments

CAPES, CNPQ, FAPERJ e UFRJ

Design and synthesis of 4,6-stieryl-pyrimidines as curcumin analogues with potential activity against *Trypanosoma cruzi* amastigotes.

Jorge Lucas F. Lacerda (PG),¹ Afonso Santine M. M. Velez (PG),¹ Paulo Pitasse-Santos (PQ),¹ Gabriela A. de Souza (PQ),¹ Debora Decoté-Ricardo (PQ),² Marco Edilson F. de Lima (PQ).^{1*} jorge.lacerda@ufrj.br; marcoedilson@gmail.com*

¹Instituto de Química - Universidade Federal Rural do Rio de Janeiro, Seropédica, RJ; ²Instituto de Veterinária - Universidade Federal Rural do Rio de Janeiro, Seropédica, RJ.

Keywords: Chagas Disease, bioisosterism, diarylheptanoids, cytotoxicity.

Highlights

This work shows the molecular design and the synthesis of 4,6-stieryl-pyrimidines as curcumin bioisosters aiming to potentiate the biological profile of the natural diarylheptanoid against *Trypanosoma cruzi* amastigotes.

Abstract

Chagas Disease (CD) is a parasitic illness caused by the hemoflagellate protozoan *Trypanosoma cruzi*. CD was first described by Carlos Chagas at 1909, and still nowadays is estimated that it affects about 6 to 7 million people around the World. At least 200 thousand people are infected by *T. cruzi* among which at least 13 thousand die per year, since according to PAHO/WHO data. Another alarming fact is that among infected people less than 10% receive a diagnosis and the correct treatment. These values are related to very low investments in new drug development for CD, since only benznidazole and nifurtimox are used today in CD therapy, despite its high toxicity and the need of long-term treatments.¹ All these factors are associated by the fact that CD is a tropical neglected disease and highlight the need of efforts in the research of new drugs suitable for treatment of the chagasic patients with more effectiveness and less harmful side effects.² Natural curcumin (**1**), the major diarylheptanoid isolated by *Curcuma longa* rhizomes, is assigned with various bioactivity in the literature like antibiotics, antioxidant, anti-inflammatory, antiviral and antiproliferative. Recently, Sueth-Santiago³ *et al.* investigated in our research group the activities of curcumin (**1**) and its minor natural analogues (desmethoxycurcumin (**2**), Fig. 1 and bisdesmethoxycurcumin) against *T. cruzi* epimastigotes (Dm28c strain), getting relevant results when compared to benznidazole.³ The authors assigned the anti-*T. cruzi* properties shown by curcumin to its antiproliferative activity which is related to the interactions with parasite's tubulin. In our work the natural curcumin (**1**) and desmethoxycurcumin (**2**) were separated by chromatographic column and assessed against *T. cruzi* amastigotes (Tulahuen C2C4-LacZ strains) showing IC₅₀ values of 17,75 μM and 30,55 μM for curcumin (**1**) and desmethoxycurcumin (**2**), respectively. Additionally, the two natural diarylheptanoids showed also high toxicity to LLC-MK2 cells, what is expected due to its antiproliferative profile.⁴

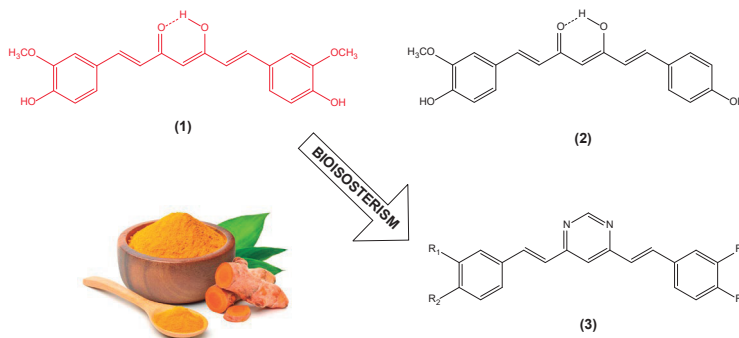


Figure 1. Structures of curcumin (**1**), natural analogue (**2**) and bioisosters (**3**).

Our results obtained with the natural derivatives motivated us to the synthesis of a series of 4,6-stieryl-pyrimidines (**3**, Fig. 1), planned as curcumin bioisosters, to be evaluated against the *T. cruzi* amastigotes. The new analogues obtained (**3a-j**) are shown in Fig. 2 and their structures were confirmed by ¹H and ¹³C NMR and MS. The molecular docking of both natural and synthetic compounds is being performed in β-α-tubulin complex obtained by homology. The set of results obtained herein will provide subsidies for a SAR study of this family of compounds.

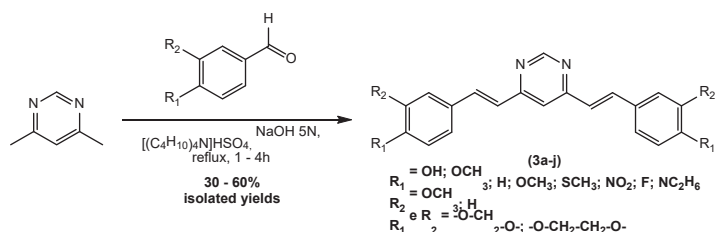


Figure 2. Synthesis of curcumin bioisosters (**3a-j**).

¹ PAN-AMERICAN HEALTH ORGANIZATION/ WORLD HEALTH ORGANIZATION - <https://www.paho.org/pt/brasil>; ² OLIVEIRA, O. V. DE. [s.l.] EdUFSCar, 2018. p. 227–244. ³ SUETH-SANTIAGO, V. *et al.* PLoS ONE 11(9): e0162926; ⁴ CHAKRABORTI, S. *et al.* Journal of Medicinal Chemistry, v. 54, n. 18, p. 6183–6196, 2011.

Acknowledgments

CNPq, CAPES, FAPERJ

Design and synthesis of benzodioxol-hydroxamate hybrids as potential anticancer agents

Lara G. Borges (PG),¹ Thais N.O. Alves (IC),¹ Mônica F.Z.J. Toledo (TC),¹ Roberto Parise-Filho (PQ).^{1*}

lara.gimenez@usp.br; roberto.parise@usp.br

¹Departamento de Ciências Farmacêuticas, USP.

Palavras Chave: HDAC6, Hematological cancer, Capsaicin, Nexturastat A, Molecular Hybridization.

Highlights

Capsaicin and nexturastat A hybrids were designed to be potential antitumoral compounds. Molecular docking studies were performed in HDAC6. Six benzodioxol-hydroxamate hybrids were synthesized and characterized.

Resumo/Abstract

Nexturastat A (HDAC6-selective inhibitor) have shown potential activity in hematological cancer therapy. At the same time, previous studies related to pepper-derived capsaicin and synthetic analogues have contributed to obtaining compounds with high antitumor activity, including hematological malignances [*Molecules*, 26 (2021), 1521-1542]. Thus, this project aims to obtain compounds, designed by the molecular hybridization of nexturastat A and capsaicin (**Figure 1A**), which could generate potential antitumoral candidates, and also new and selective HDAC6 inhibitors. The general scaffold of the hybrid compound started from using capsaicin as the *cap* group of the HDAC inhibitor (variation in this region can modulate selectivity, since the surface of the catalytic cavity of HDACs tolerates a wide molecular diversity) and the benzyl-hydroxamate moiety from nexturastat A as a linker and *Zinc Binding Group* (ZBG). Furthermore, the acyl-amidic carbon chain of capsaicin was replaced by different R groups in order to modulate affinity/selectivity of the *cap* group. Benzodioxol-benzyl-hydroxamate analogues **26a-k** were designed by replacing the vanilloid group with a benzodioxol ring. Our previous studies have demonstrated the strong influence of this bioisosteric substitution into capsaicin-derived compounds, improving selective cytotoxicity [*Bioorg. Med. Chem.*, 28 (2020), 115600-115610; *RSC Med. Chem.*, 11 (2020), 1032-1040; *Bioorg. Med. Chem.*, 27 (2019), 1-21].

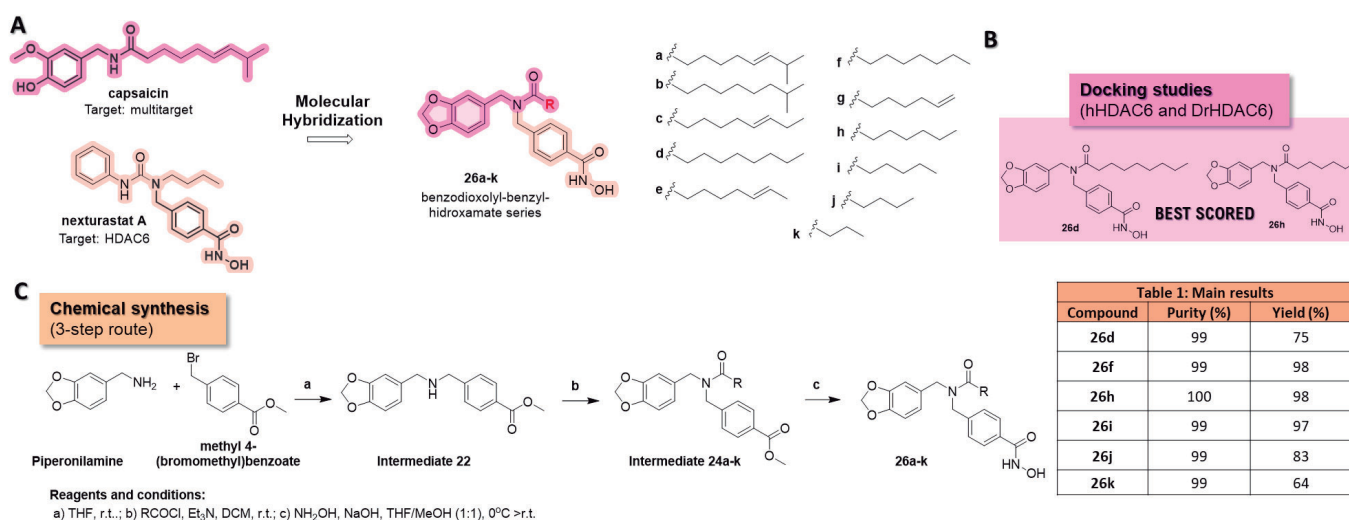


Figure 1: A) Design of compounds; B) Best scored compounds in docking studies; C) Synthetic strategy and main results.

The designed hybrids were submitted to molecular docking studies over human and zebrafish HDAC6 isozymes, and compounds **26d** and **26h** demonstrated the best scores in both enzymes (**Figure 1B**). The best scored compounds (**26d** and **26h**) and further four analogues (**26f**, **26i**, **26j** and **26k**) were synthesized in a facile 3-step synthetic route and they were obtained in good-to-high yields (64%-98%) and, moreover, HPLC purity greater than 99% (**Figure 1C**, **table 1**). All the compounds were characterized by ¹H/¹³C NMR and HRMS. Phenotypic screening against different cancer cell cultures, such as Jurkat, Namalwa and K562, and enzymatic inhibition assay against HDACs are underway.

Agradecimentos/Acknowledgments

The authors are grateful to Faculty of Pharmacy of University of São Paulo, which allowed the development of this work, CAPES and FAPESP for financial support and grants (#2022/02805-5, #2021/08260-8).

Design and synthesis of bis-chalcones as curcumin analogues and evaluation of their toxic activities against *Trypanosoma cruzi* amastigotes

Afonso Santine M. M. Velez (PG)¹, Gabriel A. da Rocha-Silva (IC),¹ Douglas C. Alcântara-Pinto (PG),¹ Gabriela A. de Souza (PQ),¹ Geovana Andrade da Silva (IC),¹ Lorrane de Souza Chaves (IC),² Leonardo Freire-de-Lima (PQ),² Debora Decoté-Ricardo (PQ),³ Marco Edilson F. de Lima (PQ).^{1*}

afonsosv30@gmail.com; marcoedilson@gmail.com*

¹Departamento de Química Orgânica, Instituto de Química - Universidade Federal Rural do Rio de Janeiro, Seropédica, RJ; ²Instituto de Biofísica Carlos Chagas Filho - Universidade Federal do Rio de Janeiro, Ilha do Fundão, Rio de Janeiro, RJ; ³Depart. de Microbiologia e Imunologia Veterinária, Instituto de Veterinária - Universidade Federal Rural do Rio de Janeiro, Seropédica, RJ.

Keywords: molecular simplification approach, tropical neglected diseases, Chagas disease.

Highlights

This work presents the design and synthesis of a series of bis-chalcones as curcumin simplified analogues active against *T. cruzi* amastigotes. The most active derivative assessed had IC₅₀ value of 5.87 μM.

Abstract

Chagas disease (CD) is caused by the hemoflagellate protozoan *Trypanosoma cruzi* being endemic in areas where people live in great economic vulnerability, mainly in South and Central Americas WHO data shows that CD is part of a group of diseases called neglected tropical diseases (NTDs), with CD being considered the most neglected among them due to the very low efforts of pharmaceutical companies to develop new drugs.¹ The treatment available for chagasic patients is limited to only two drugs, nifurtimox and benznidazole. Both options have limited therapeutic potential and low efficacy in the chronic phase of the disease, long treatment times, in addition to presenting serious adverse effects. Natural curcumin (**1**) is assigned with various bioactivities in the literature as antibiotic, antioxidant, anti-inflammatory, antiviral and antiproliferative. Recently, Sueth-Santiago² *et al.* investigated in our research group the activity of curcumin (**1**) against *T. cruzi* epimastigotes (Dm28c strain), getting relevant results. The optimization and simplification of synthetic approaches for the preparation of new chemical entities applicable to the treatment of NTDs is desirable since the accessibility and low costs of possible new drugs is a requirement. In this sense the molecular simplification³ strategy meets the challenges that are imposed on medicinal chemists working in this research field. Derivatives **2-6** (**Fig. 1**) were planned as simplified analogues of curcumin, being synthesized through the acid-catalyzed aldol condensation reactions between suitable ketones and appropriately substituted benzoic aldehydes. The final products were obtained in yields ranging from 60 to 75% and had their purity grades evaluated by HPLC. All the structures were confirmed by ¹³C and ¹H NMR spectral data. The antiparasitic evaluation of the bis-chalcones were carried out against intracellular amastigotes of *T. cruzi* (Tulahuen strain C2C4-LacZ)⁴ and the results are shown below.

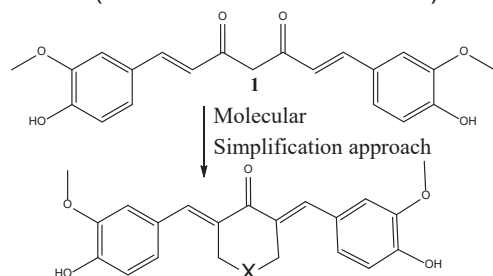


Figure 1. Molecular design of curcumin analogues.

Compound	Activity on <i>T. cruzi</i> amastigotes (Tulahuen C2C4 LacZ)	Cytotoxicity on LLC-MK2 (Host cells)	Cytotoxicity on human total lymphocytes
1	17.75 ± 6.88	25.69 ± 6.05	134.13
2 X = O	12.78 ± 5.17	20.57 ± 4.65	146.31
3 X = N(-CH ₃)	9.60 ± 1.61	25.00	-
4 X = S	5.87 ± 2.89	12.97 ± 2.36	189.74
5 X = S(=O)	16.70 ± 4.67	28.46 ± 5.17	138.36
6 X = S(=O) ₂	7.33 ± 0.43	11.49 ± 3.71	104.95
Benznidazole*	1.50 ± 0.33	>200	-

The results obtained herein highlight the approach of preparing new simplified chemical structures in relation to their natural prototypes may be the way to develop a suitable new drug for the treatment of chagasic patients.

¹WHO- https://www.who.int/health-topics/chagas-disease#tab=tab_1. ²Sueth-Santiago, V. *et al.* PLOS ONE, v. 11, n. 9, 22 set. 2016. ³Crisóstomo P. *et al.* J. Org. Chem. 71, 6, 2339, 2006. ⁴Buckner, F. S. *et al.*, Antimicrob. Agents Chemoth. 40, 2592, 1996.

Acknowledgments

CNPq, CAPES, FAPERJ

Design and synthesis of boronic *N*-acyl hydrazones derivatives as potential inhibitors of SARS-CoV-2 main protease (3CL_{pro}).

Diogo Boreski (IC),^{1*} Juliana Romano Lopes (PG),¹ Jean Leandro dos Santos (PQ)¹ Chung Man Chin (PQ),¹

diogo.boreski@unesp.br;

¹ Drugs and Medicines Department, School of Pharmaceutical Sciences, UNESP, Araraquara, São Paulo

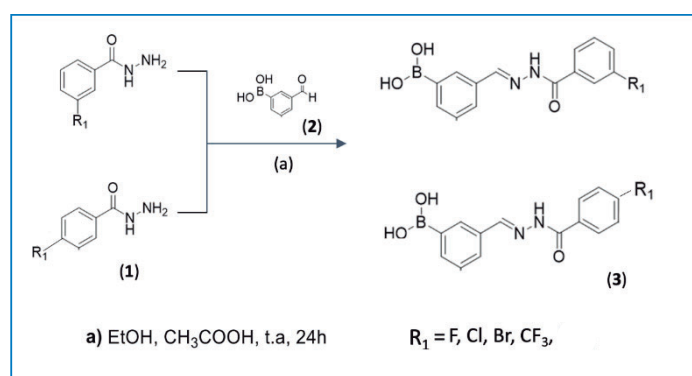
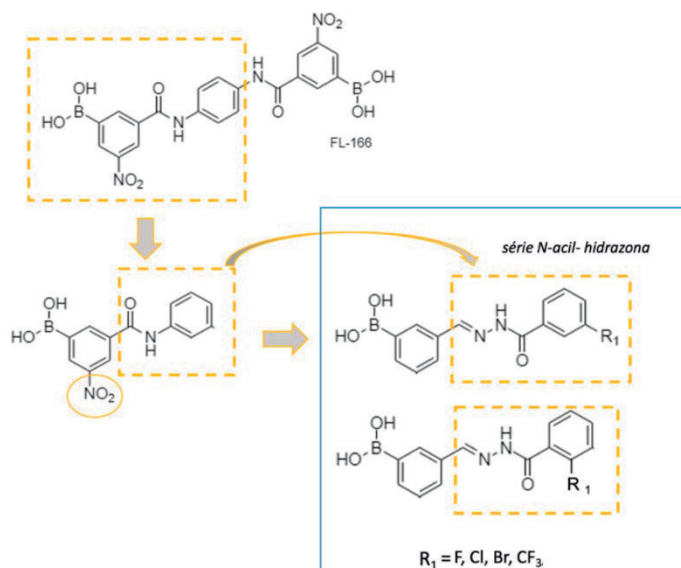
Palavras-Chave: Protease inhibitors, *N*-Acyl-Hydrazones, Boronic acids, SARS-CoV-2

Highlights

The recent COVID-19 pandemic brought along challenges for drug discovery. The main proteases is one of the most tapped targets for antiviral molecules. In this way, this work proposes the synthesis and biological evaluation of eight new compounds exploring some promising groups for modern medicinal chemistry such as boronic acid and *N*-acyl hydrazones due its pharmacological properties and the possibility to target linking.

Resumo/Abstract

As the protease Mpro of SARS-CoV-2 shows a high structural similarity with SARS-CoV, this work aimed to obtain novel compounds and investigate their potential effect to inhibit Mpro of SARS-CoV-2¹. The *N*-acylhydrazones derivatives have been tested for several inflammatory diseases² and the boron is a promise atom to be used in viral diseases drugs³. Based on the structure of FL-166⁴, a SARS-CoV active compound and by the previous computational study of the structure to understand the binding behavior to the target, performed in our laboratory, we used the strategy of molecular modification to design and synthesize eight boronic acylhydrazone derivatives (figures above). They were obtained with 50-85% yield, purified and characterized through IR and NMR spectroscopy and are in stage of evaluation of inhibitory activity of Mpro of SARS-CoV-2.



¹ Jin, Z., Du, X., Xu, Y. *et al.* Structure of M^{pro} from SARS-CoV-2 and discovery of its inhibitors. *Nature* **582**, 289–293 (2020).

²Verma, G *et al.* A review exploring biological activities of hydrazones. *Journal of pharmacy & bioallied sciences*, *6*(2), 69–80. 2014

³ Diaz D.B., Yudin A.K. The versatility of boron in biological target engagement. *Nat Chem.* 2017; *9*:731–742.

⁴Bacha, U. *et al.* Identification of novel inhibitors of the SARS coronavirus main protease 3CL_{pro}. *Biochemistry*, *43*(17), 4906–4912. 2004

Agradecimentos/Acknowledgments

We thank National Council for Scientific and Technological Development for productivity fellowship level 2 [CNPq process numbers: 305174/2020-7 (JS) and 313435/2019 (CM) respectively]. We also thank Fundação de Amparo à Pesquisa do Estado de São Paulo (FAPESP) IC process number (2022/04709-3).



Área: MED

(Inserir a sigla da seção científica para qual o resumo será submetido. Ex: ORG, BEA, CAT)

Design and synthesis of new potential PI3K and HDAC6 hybrid inhibitors for cancer treatment

Karoline B. Waitman (PG),^{1*} **Maurício T. Tavares** (PQ),¹ **Larissa C. de Almeida** (PG)², **Jorge Antonio Elias Godoy Carlos** (PG),² **Thales Kronenberger** (PQ),³ **Mônica F.Z.J. Toledo** (TC),¹ **Leticia V. Costa-Lotuf** (PQ),² **João A. Machado-Neto** (PQ),² **Roberto Parise-Filho** (PQ).¹

karolinewaitman@usp.br; karolinewaitman@usp.br

¹Laboratory of Design and Synthesis of Bioactive Substances (LAPCESSB), Department of Pharmacy, Faculty of Pharmaceutical Sciences, University of São Paulo (USP)

²Department of Pharmacology, Biomedical Science Institute, University of São Paulo (USP)

³Department of Pharmacy, University of Tübingen, EKUT

Palavras Chave: molecular hybridization, histone deacetylase 6, phosphoinositide 3-kinase, anilino-purines, benzyl-hydroxamates, cancer.

Highlights

Pharmacophores of PI3K and HDAC6 inhibitors have been hybridized into a single entity. They were synthesized and its anticancer and enzymatic activities were evaluated.

Resumo/Abstract

Hybrid inhibitors have the potential to overcome cancer resistance, by blocking multiple signaling pathways at once. Both PI3K (phosphoinositide 3-kinase) and HDAC6 (histone deacetylase 6) are commonly mutated on tumors and their inhibition has been shown beneficial for treatment. To construct hybrid PI3K/HDAC6 inhibitors, pharmacophores of known selective inhibitors bearing anilino-purines, benzyl-hydroxamates, and benzyl-benzamides (idelalisib, nexturastat A, and chidamide) have been connected through a linker and hybridized into a single entity (Figure 1).

Eight final compounds and five intermediates have been synthesized with yields from 6–48% and characterized by ¹H, ¹³C NMR, and cancer cell cytotoxicity. The most promising ones were subjected to DMPK tests and personalized enzymatic assays to evaluate their activity on target and selectivity. The results obtained for the most successful compounds are summarized in Table 1.

Table 1: Synthesis, yields and biological evaluation of most promising hybrid compounds.

Compound	Yield (%)	Purity (%)	IC ₅₀ HCT116 (µM)	IC ₅₀ MCF-7 (µM)	IC ₅₀ Jurkat (µM)	IC ₅₀ Namalwa (µM)	IC ₅₀ HDAC1 (µM)	IC ₅₀ HDAC6 (µM)	T _{1/2} human / mouse (min)	Cl _{int} human / mouse (µL/min/mg)	Inhibition CYP450 (%)
6a	31	99.9	9.3	9.3	0.02	0.04	118.4	232.4	>120 / 50	< 6 / 14	50 / 34 / -23 / -16 (1A2 / 2C9 / 2D6 / 3A4)
6c	22	98.7	8.3	19.5	0.05	0.01	83.5	184.3	>120 / 35	< 6 / 20	47 / 42 / -55 / -14 (1A2 / 2C9 / 2D6 / 3A4)
6d	48	97.8	21.7	31.7	0.03	0.04	188.5	341.0	>120 / 35	< 6 / 20	46 / 52 / -39 / -62 (1A2 / 2C9 / 2D6 / 3A4)

1. Waitman, K. & Parise-Filho, R. New kinase and HDAC hybrid inhibitors: recent advances and perspectives. *Future Med. Chem.* **14**, 745–766 (2022).

Agradecimentos/Acknowledgments

The authors are grateful to Faculty of Pharmacy of University of São Paulo, which allowed the development of this work, CAPES, for financial support and grants #2022/07275-4, and #2021/08260-8 from São Paulo Research Foundation (FAPESP).

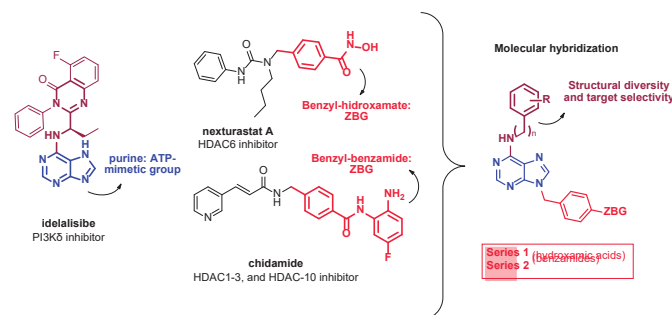


Figure 1: Design of PI3K/HDAC6 hybrid inhibitors.

Área: MED

Design, Synthesis and Anti-*Candida* Activity of Diarylideneacetones Inspired by Curcumin

Davi S. Oliveira (IC),¹ Veridianna C. Pattini (PG),¹ Patrick R. Ozanique (PG),¹ Álvaro L. Helena (PQ),¹ Janaina C. Orlandi (PQ),² Margarete T. G. Almeida (PQ),³ Luis O. Regasini (PQ).^{1*}

davi.santos@unesp.br; luis.regasini@unesp.br

¹Laboratório de Antibióticos e Quimioterápicos, IBILCE, Unesp São José do Rio Preto – SP, Brasil; ²Departamento de Ciências Fisiológicas, UNICAMP Piracicaba -SP, Brasil; ³ Departamento de Ciências Dermatológicas, Infecções e Parasitárias, FAMERP São José do Rio Preto – SP.

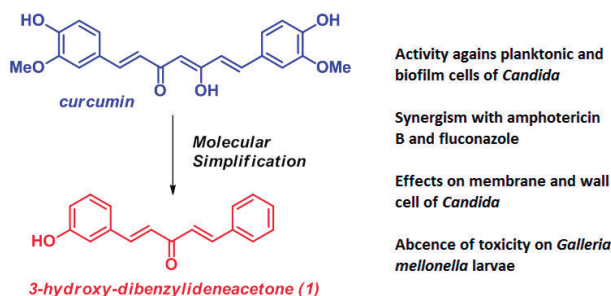
Palavras Chave: Antifungal, Curcumin, *Candida*, Biofilm, *Galleria mellonella*

Highlights

Curcumin was used to design a series of 25 diarylideneacetone analogs, Compound **1** was more active and chemically stable than curcumin. Compound **1** demonstrated antibiofilm and anti-adhesion activities and no toxicity against *Galleria mellonella* larvae.

Abstract

Infections caused by *Candida* species have considerably increased in recent decades. However, the antifungal agents for the treatment of candidiasis are restricted to a few groups of drugs that present some limitations, including high toxicity, reduced efficacy and limited spectrum of action. This perspective encouraged us to synthesize and evaluate a series of 25 diarylideneacetones inspired by curcumin, a natural product recognized as promising antifungal agent. Structure-activity relationship data demonstrated that hydroxyl groups and electronic density on rings A and B, respectively were crucial for anti-*Candida* effect. 3-Hydroxy-dibenzylideneacetone (**1**) was the most active compound against *Candida* species, with Minimum Inhibitory Concentration (MIC) values ranging from 7.8 to 31.2 μM . *Candida albicans* and *Candida krusei* were more susceptible to **1** than fluconazole, which was used as reference anti-*Candida* drug. Compound **1** at sub-MIC was able to reduce *C. albicans* adhesion onto human gingival fibroblasts (HGF-1 cell line) and human epidermal keratinocytes (HaCaT cell lines). Our investigations demonstrated the ability of **1** to inhibit *C. albicans* biofilm formation and preformed biofilm, when tested at respective MIC and 10 \times MIC values. Combinations of **1** and amphotericin B or fluconazole showed synergistic effects against *C. albicans*, with Fractional Inhibitory Concentration Index (FICI) values of 0.5 and 0.2, respectively. Preliminary studies on the fungitoxicity of **1** indicated a dual action, targeting membrane and cell wall of *C. albicans*. Finally, **1** was more stable than curcumin in phosphate buffer and demonstrated low acute toxicity against *Galleria mellonella* larvae. These findings open new avenues for the study of diarylideneacetones as anti-*Candida* prototypes inspired by structure and bioactivity of curcumin.



Acknowledgments

The authors gratefully acknowledge financial support from the Coordination for the Improvement of Higher Education Personnel (CAPES, finance code 001), Brazilian Council for Scientific and Technological Development (CNPq) (Grants 471129/2013-5, 306251/2016-7 and 429322/2018-6), the São Paulo Research Foundation (FAPESP) (Grants 2014/18330-0 and 2018/15083-2) and Multiuser Centre for Biomolecular Innovation (FAPESP 2009/53989-4). DSO thanks CNPq - PIBIC for his scholarship.

Design, synthesis, and biological evaluation of new selective dimeric 2-nitroimidazoles against *Trypanosoma cruzi* amastigotes

Afonso Santine M. M. Velez (PG)¹, Gabriel A. da Rocha-Silva (IC),¹ Douglas C. Alcântara-Pinto (PG),¹ Paulo Pitasse-Santos (PQ),¹ Gabriela A. de Souza (PQ),¹ Debora Decoté-Ricardo (PQ),² Marco Edilson F. de Lima (PQ).^{1*}

afonsosv30@gmail.com; marcoedilson@gmail.com*

¹Departamento de Química Orgânica, Instituto de Química - Universidade Federal Rural do Rio de Janeiro, Seropédica, RJ;

²Departamento de Microbiologia e Imunologia Veterinária, Instituto de Veterinária - Universidade Federal Rural do Rio de Janeiro, Seropédica, RJ.

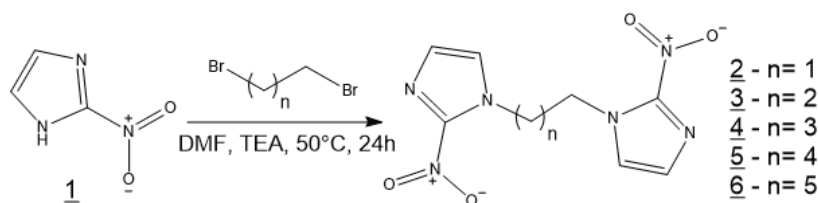
Keywords: nitroheterocycles, N-alkylation, Chagas disease, pharmacophore dimerization.

Highlights

This work presents a molecular design through the dimerization of a pharmacophoric group, the 2-nitroimidazole present in benznidazole, active against *T. cruzi* amastigotes, obtaining IC₅₀ < 1 μM.

Abstract

Chagas disease (CD) is a parasitosis caused by the hemoflagellate protozoan *Trypanosoma cruzi*, which is usually endemic in areas where there are people living in great economic vulnerability, especially in South America. The main route of transmission of the infection is vector, which occurs through the bite of the insect popularly known as "kissing bug" (*Triatoma infestans*). WHO data shows that CD is part of a group of diseases called neglected tropical diseases (NTDs), with CD being considered the most neglected among them due to the very low effort of pharmaceutical companies to develop new treatments.¹ The treatment available for chagasic patients is limited to only two drugs, both nitroheterocycle derivatives, nifurtimox and benznidazole (in Brazil, only benznidazole is available). Both options have limited therapeutic potential and low efficacy in the main phase of the disease, long treatment periods, in addition to presenting serious adverse effects. Considering the presented problem, and with the intention of meeting the humanitarian demand for new antichagasic drugs, a series of simple molecules of N-alkylated 2-nitroimidazole derivatives was synthesized. The nitroimidazole center is the main pharmacophore present in the structure of the drug benznidazole, being one of the main structural characteristics that guarantee its antiparasitic activity. The 2-nitro-1H-imidazole (**1**) (known as: azomycin – a natural antibiotic) has antichagasic activity against *T. cruzi* amastigotes comparable to that of benznidazole.² Dimerization of an active compound is a molecular design strategy that generally results in an enhanced interaction of improved pharmacological properties. This improvement in potency is attributed to a higher concentration of pharmacophores near molecular interaction sites in the biological environment.³ The alkylation reactions were carried out by reacting 2-nitroimidazole with dibromoalkanes, with different chain sizes. The obtained derivatives were analyzed by HPLC-MS, and their structures were confirmed by ¹³C and ¹H NMR spectral data. And the biological evaluation of its cytotoxic and antiparasitic profile against the intracellular replicative form of *T. cruzi* (Tulahuen strain C2C4-LacZ) was carried out.⁴



	Activity on <i>T. cruzi</i> amastigotes (Tulahuen C2C4 lacZ)	Cytotoxicity on LLC-MK2 (Host cells)
	IC ₅₀ (μM)	
1	5.74 ± 1.89	>500
2	10.69 ± 1.04	>200
3	3.57 ± 1.07	>200
4	2.66 ± 0.42	>200
5	1.23 ± 0.01	>200
6	0.59 ± 0.01	>200
Benznidazole*	1,50 (±0,33)	>200

The results obtained show that the strategy of preparing molecules with a simple structure containing two 2-nitroimidazole pharmacophores as a promising approach against *T. cruzi* amastigotes, mainly with the increase of the methylene chain. The new derivatives obtained in this work, in addition to being toxic against *T. cruzi*, also showed reduced cytotoxicity against host cells, evidencing their high selectivities.

¹WHO- https://www.who.int/health-topics/chagas-disease#tab=tab_1. ²Velez, A. S. M. M. et al. 2-Nitro-1-vinyl-1H-imidazole. *Molbank*, **2022**, M1326. ³Paquin, A. et al. *Molecules*, **2021**, 17;26(8):2340. ⁴Buckner, F. S. et al., *Antimicrob. Agents Chemoth.* **40**, 2592, 1996.

Acknowledgments

CNPq, CAPES, FAPERJ

Development of multi-target enzymatic inhibitors for the treatment of victims of snakebites: exploring serine proteases

Sarah H. Louzada (IC)^{1*}, Arthur E. Kümmerle (PQ)², Carlos Mauricio R. Sant'Anna (PQ)¹

sarahhessing@ufrj.br

¹Departamento de Química Fundamental, Instituto de Química, UFRRJ; ²Departamento de Química Orgânica, Instituto de Química, UFRRJ.

Keywords: Snakebite, Semiempirical Method, Serine Proteases, Molecular Docking, Bothrops Jararaca.

Highlights

Theoretical methods were used to evaluate thiosemicarbazones as candidate dual inhibitors of botropic venom serine proteases (SP) and metalloproteases (MP); one new compound containing a boronic acid group was designed which presented favorable interactions with SP as a covalent inhibitor and also with MP.

Abstract/Abstract

Snakebites received the Neglected Tropical Disease status from WHO since 2017. Up to 5.4 million people are bitten by snakes annually, of which 2.7 million develop severe conditions and up to 138,000 die from complications. The action of snake venom is due to the presence of different enzymes, whose main components are phospholipases, serine proteases (SP) and metalloproteases (MP). Our proposal is to design compounds with dual action, capable of inhibiting two classes of such enzymes, so that they can be used complementarily in the future to the use of snake antivenom. Previously, we verified the inhibitory activity *in vitro* and *in vivo* on a bothropic MP of thiosemicarbazones designed by theoretical methods by our group.¹

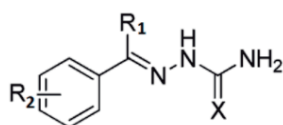


Figure 1: General structure of semicarbazones (X=O) and thiosemicarbazones (X=S).

For this study, a 3D model of bothrombin, an SP of *B. jararaca*, was built with the Swiss-Model server from the UniProtKB-collected sequence P81661. The structures of 13 pairs of (E) and (Z) isomers (figure 1) were built with Spartan'14 (Wavefunction, Inc) and energy-minimized with the semi-empirical method PM6. They were docked in the bothrombin model with ChemPLP function of GOLD 5.7 (CCDC). In general, results indicated that the (E) isomers presented more favorable interactions with the model.

Since we were interested in the design of dual inhibitors, compounds (E)-5a and (E)-5b, which were previously demonstrated *in vitro* as MP inhibitors,¹ were selected for further improvement. They were used to propose candidates for covalent inhibitors of SP. A carboxylic acid group located at the R₁ position was replaced by a boronic acid group, since this group is able to covalently bind to serine residues.² The docking results of these modified compounds, (E)-5ab and (E)-5bb, showed that only for (E)-5ab the boronic acid group was near to the catalytic serine residue. To investigate the formation of the covalent bond, we studied the steps of a possible mechanism for bond formation at the semiempirical quantum-mechanical level. A cutout of the best evaluated enzyme-ligand complex, containing the ligand and the nearest amino acid residues was selected with Deep View 4.1. The enthalpy of the ligand, empty binding site, noncovalent and covalent complexes were calculated after optimization with the PM7 method of MOPAC 2016, with a continuum approach to represent the surrounding medium. With these data, it was possible to calculate the enthalpy change of each step and of the global reaction of the proposed mechanism (Table 1). It can be seen that the global reaction is enthalpically quite favorable (-211 kJ/mol). As we are seeking dual inhibitors, a similar study was also applied with a previous MP model previously prepared by us¹ to determine the interaction enthalpy of (E)-5ab with this enzyme and found an interaction enthalpy of -230 kJ/mol. Combining these results, we suggest (E)-5ab as a dual inhibitor candidate for MP and SP enzymes present in snake venoms.

Table 1: Interaction enthalpies for compound (E)-5ab in SP model.

Step*	ΔH (kJ/mol)
1	-148
2	+246
3	-309
Global reaction	-211

*1: non-covalent complex formation;
2: proton transfer between His and Ser catalytic residues;
3: covalent complex formation.

Acknowledgements/Acknowledgments

FAPERJ, CNPq.

¹ACS Med. Chem. Lett. 2017, 8, 11, 1136–1141

²Chem. Rev. 2012, 112, 4156–4220

46^o Reunião Anual da Sociedade Brasileira de Química: "Química: Ligando ciências e neutralizando desigualdades"

Discovery of new piperine-based antischistosomal efflux pump inhibitors

Jordano F. Reis (PG),^{1*} Quelli Larissa O de Santana (PG),² Rafael F. Dantas (PQ),¹ Walter César G. Valente (TC),¹ Giuliana V. Schirato (TC),¹ Sabrina Baptista Ferreira (PQ)² and Floriano P. Silva-Jr (PQ)¹.

*jordanoreis@outlook.com

¹LABECFAR, Instituto Oswaldo Cruz, FIOCRUZ; ²LabSOPB Instituto de Química UFRJ

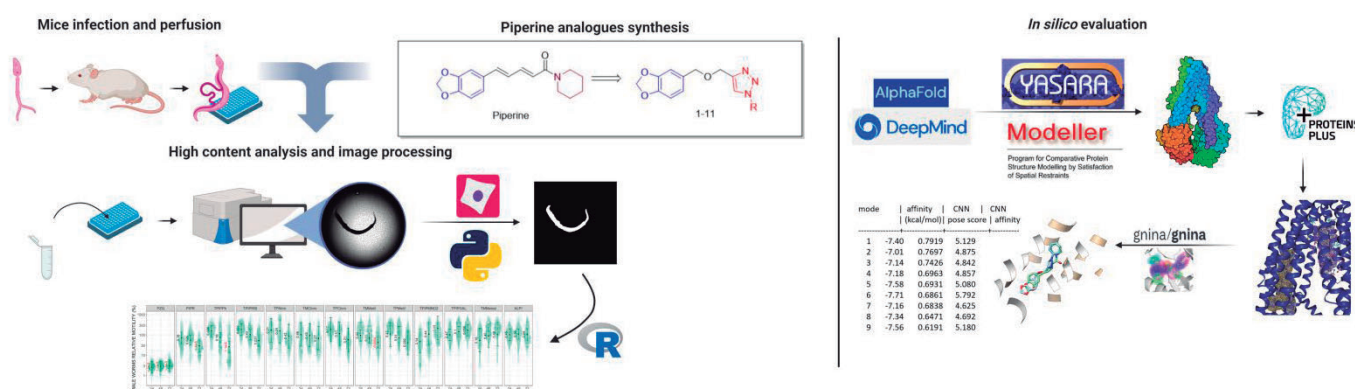
Keywords: Schistosomiasis, Efflux pumps, Drug resistance, Piperine, Drug discovery.

Highlights

Piperine, a human efflux pump inhibitor, and a new analog decreased adult schistosomes motility. Molecular docking revealed their putative interactions with two sites of schistosome efflux pump SMDR2

Abstract

Schistosomiasis, a parasitic disease caused by *Schistosoma* flukes (e.g. *S. mansoni*), affects 250 million people worldwide. Praziquantel is the only available treatment but overuse may result in resistant forms¹. Studies have found a correlation between resistance to Praziquantel and P-Glycoprotein-type ABC transporters (Pgp/ABCB1) in *S. mansoni*². To address this, therapeutic alternatives are needed, and natural products such as piperine, which inhibits human Pgp activity, may offer a solution³. This work aimed to evaluate the anti-schistosomal activity of piperine and 11 new analogous compounds synthesized by our group (Fig 1). To do so, we measured their effects on adult parasite motility using an ex vivo automated microscopy assay. Image analysis was performed in three steps: segmentation of the parasite (convolutional neural network), features extraction (Cellprofiler), and motility measurements (multilevel generalized linear statistical model). Of all molecules, piperine and compound 1 showed activity against adult worms at 50 μ M. In parallel, we used *in silico* approaches to investigate the putative molecular mechanism involved. A model of *S. mansoni* Pgp (SMDR2) was obtained from AlphaFold (Q26599) and energy minimization was performed using YASARA. We validated the structure in the Saves 6.0 portal. For the *in silico* studies, we used DoGSiteScorer to find the putative interaction sites and GNINA 1.0 for docking. We identified two possible interaction sites inside SMDR2 transmembrane region. Piperine seems to bind to both sites but more strongly to site 1, similar to what has been reported in the literature for the human Pgp. As for compound 1, it seems to only interact with site 1. Associating the ex-vivo activity data with *in silico* analyses might be the key to developing more active compounds against SMDR2 and providing better anti-schistosomal compounds. A graphical abstract can found bellow:



1- World Health Organization, A road map for neglected tropical diseases 2021–2030; 2- Messerli et al., Mol Biochem Parasitol 2009, 167(1); 3- Syed et al., Scientific Reports, 2017, 1-18, 7(1).

Acknowledgments

The authors gratefully acknowledge Fábio Jorge V. Júnior for statistical assistance, and the financial support from CAPES, Fiocruz and UFRJ.

Docking-based virtual screening of LaSMMed Chemical Library on arginase of *Leishmania amazonensis*.

Mariana L. Silva (PG),¹ Kaio M. Santiago-Silva (PG),¹ João Gabriel A. Cavalcanti (PG),² Marcelle L. F. Bispo (PQ)^{1*}.

mfbispo@uel.br

¹Departamento de Química, UEL; ²Departamento de Patologia, Análises Clínicas e Tóxicológicas, UEL.

Palavras Chave: *Molecular docking, Arginase, Inhibitors, Leishmaniasis.*

Highlights

Arginase is a crucial enzyme for *Leishmania* spp. A docking-based virtual screening of 66 compounds from our chemical library identified potential hits that exhibited good physicochemical properties related to oral bioavailability.

Resumo/Abstract

Leishmaniasis is a neglected and parasitic disease caused by more than 20 species of *Leishmania* spp, transmitted to humans through the bite of infected female sandflies. Each year, 700000 to 1 million new cases worldwide are estimated. Most occur in the poorest countries and affect vulnerable populations with difficult access to health services. Treatment options for this disease include injectable drugs, only one oral option, and many adverse effects. Given this scenario, the research and development of new drugs are necessary. In this context, an essential aspect in the search for new antileishmanial agents is the identification of molecular targets of specific metabolic pathways that are unique and essential for parasite survival. For example, Arginase (ARG) is crucial for parasite survival and cell replication. It is a manganese-dependent enzyme that participates in the polyamines biosynthesis pathway, catalyzing the hydrolysis of *L*-arginine to *L*-ornithine and urea. Therefore, in this work, we performed a docking-based virtual screening of sixty-six compounds from our in-house chemical library (LaSMMed Chemical Library) on ARG from *L. amazonensis* (LaARG), a species of widespread in the Brazilian territory. The tridimensional structure of LaARG was built by homology in Modeller 10.1, using as a template ARG from *L. mexicana* (PDB: 4ITY, resolution: 1.80 Å)¹, being validated by ProSA and PROCHECK servers. The docking calculations were performed with the program GOLD (v. 2020.1) using the four available scoring functions: ASP, ChemPLP, GoldScore, and ChemScore. We applied a consensual validation by scale² from the obtained fitness score values to rank the best structures. The best four ranked (S-LMed47, R-LMed47, LMed36, and LMed27) were selected to analyze molecular interactions with ARG using PyMOL (v. 2.5). Compound S-LMed47 showed the highest number of hydrogen bonds (four in total) with Thr148, Ser150, Gly151, and Asn152, in addition to the coordination with the Mn²⁺ ion, a critical interaction since ARG is a metalloenzyme Mn-dependent. Conversely, its enantiomer (R-LMed47) showed only one hydrogen bond with residue His139, an essential residue that coordinates the binuclear cluster of Mn²⁺ at the active site. Compounds LMed36 and LMed27 interacted similarly, coordinating with one of the Mn²⁺ ions. Besides, we predicted *in silico* physicochemical properties related to drug-likeness and the pharmacokinetic profile using the SwissADME server. Despite moderate water solubility and interaction with some CYP enzymes, all selected compounds showed good oral bioavailability predictions. The results suggest that LMed47, LMed36, and LMed27 are potential hits as ARG inhibitors and possible antileishmanial agents. *In vitro* assays are in progress to prove this potential. **References:** 1- D'ANTONIO, Edward L. et al. Archives of biochemistry and biophysics, v. 535, n. 2, p. 163-176, 2013; 2- WIGGERS, Helton J. et al. Molecular Informatics, v. 30, n. 6-7, p. 565-578, 2011.

Agradecimentos/Acknowledgments

This study was supported by Coordenadoria de Aperfeiçoamento Pessoal de Nível Superior (CAPES, Brazil) by scholarship financing (Code 001).

Docking of *N*-acyl/sulfonyl-hydrazones designed as potential inhibitors of *Mycobacterium tuberculosis* NADH-dependent enoyl-ACP reductase

Laudicéa do Nascimento Oliveira (PG), Camilo Henrique da Silva Lima (PQ),
Raoni Schroeder Borges Gonçalves (PQ), Magaly Girão Albuquerque (PQ) *

laudiceaoliveira6@gmail.com; camilolima@iq.ufrj.br; raoni.schroeder@iq.ufrj.br; magaly@iq.ufrj.br *

Programa de Pós-Graduação em Química (PGQu), Instituto de Química, Universidade Federal do Rio de Janeiro (UFRJ)

Keywords: Molecular Modeling, Molecular Docking, Structure-Based Drug Design, Tuberculosis, InhA, Substrate Binding Site

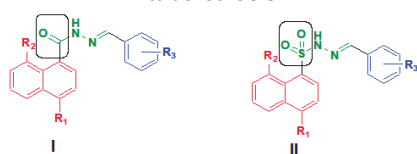
Highlights

Two series of *N*-acyl/sulfonyl-hydrazones (I and II), designed as potential inhibitors of the NADH-dependent enoyl-ACP reductase (InhA) enzyme from *M. tuberculosis* (MTB), were docked into the substrate binding site in order to evaluate their potential binding mode.

Abstract

Tuberculosis (TB) is an infectious disease caused by *M. tuberculosis* (MTB).¹ In 2019, TB was the 13th cause of death in the world and the 1st cause from a single infectious agent.¹ In 2020 and 2021, TB was the 2nd cause of death from a single infectious agent, after CoViD-19.¹ The NADH-dependent enoyl-ACP reductase enzyme, encoded by the MTB inhA gene, is a validated target against TB, since it plays a crucial role in regulating the catalysis of fatty acids and the synthesis of the MTB cell wall.² Isoniazid, for example, one of the first-choice drugs against TB, targets InhA, but in fact, it is a pro-drug, which is activated by MTB catalase/peroxidase KatG, forming a adduct with NADH (cofactor) that binds to InhA, inactivating it, thus being an InhA indirect inhibitor.² The development of InhA direct inhibitors is an attractive approach, since KatG is frequently responsible for resistance.² Based on literature studies,³⁻⁵ we designed two series of *N*-acyl/sulfonyl-hydrazone (I and II) (Figure 1) compounds as potential direct inhibitors of InhA. Therefore, the goal of this work is to investigate the potential binding mode of these designed compounds into the substrate binding site of InhA, by docking simulations, using the AutoDock 4.0 program.⁶

Figure 1. Chemical structures of the two series of *N*-acyl/sulfonyl-hydrazones (I and II) designed as potential direct inhibitors of InhA from *M. tuberculosis*.



Chain E of the crystal structure of InhA (MTB, H37Rv) inhibited by TCU was isolated from the complex (PDB ID: 2X23), excluding the structures of the inhibitor (TCU) and solvent (DMSO and water) molecules, but maintaining the cofactor structure (NAD). All hydrogen atoms were added, Gasteiger partial charges were assigned, non-polar hydrogens were deleted, and their charges were merged with the carbon atoms. Atom types were assigned, defining hydrogen bond (H-bond) acceptors/donors, aromatic, and aliphatic carbon atoms. Rotatable bonds were defined only for ligands.

A grid box of 46 x 46 x 46 (x, y, z) Å³ with a grid spacing of 0.375 Å was defined, considering the ligands size. The grid box was centered on the oxygen atom of the Tyr158 hydroxyl group. The Lamarckian Genetic Algorithm (LGA) / Local search (LS) method was defined as search algorithm and 20 runs were carried out. The ligand structures were constructed and optimized in the Spartan program, using the MMFF94 force field.⁷ The Discovery Studio Visualizer (DSV) program was used to analyze the results.⁸ Redocking of TCU inhibitor showed RMSD = 0.41 (RMSD ≤ 2.0 Å) and estimated free energy of binding (Table 1, E = ΔG_{bind}) of -10.83 kcal/mol. TCU forms H-bond with a hydroxyl (OH) group of NAD and hydrophobic interactions (alkyl, π-alkyl) with Ala191.

Table 1. Estimated free energy of binding (AutoDock 4.0, E = ΔG_{bind}, kcal/mol) of compounds from series I and II docked into the substrate binding site of InhA from *M. tuberculosis*.

#	R ₁	R ₂	R ₃	E
Ia	OCH ₃	H	4-NO ₂	-3.31
Ib	OCH ₃	H	3-OH, 4-OCH ₃	-6.24
Ic	OCH ₃	H	3,4-O ₂ CH ₂	-7.57
Id	OH	OH	3-OH, 4-OCH ₃	-6.34
Ie	OCH ₃	OH	3,4-O ₂ CH ₂	-1.14
IIa	OCH ₃	OCH ₃	4-NO ₂	73.55
IIb	OCH ₃	OCH ₃	3-OH, 4-OCH ₃	-3.92
IIc	OCH ₃	OCH ₃	3,4-O ₂ CH ₂	4.29

Ia (E=-3.31) forms hydrophobic interactions (alkyl, π-alkyl) with NAD. **Ib** (E=-6.24) forms hydrophobic interactions with Ala191; but shows an unfavorable H-bond (donor-donor) with OH group (NAD). **Ic** (E=-7.57) forms van der Waals with NAD oxygen atom, and hydrophobic interactions with NAD and Ala191. **Ie** (E=-1.14) forms H-bond with OH (NAD) and Lys165, and hydrophobic interactions with Ala191. **IIa** (E=73.55) forms hydrophobic interactions with Ala191; but shows two unfavorable H-bond (donor-donor) with OH (NAD). **IIb** (E=-3.92) forms van der Waals interactions with Ser20. **IIc** (E=4.29) forms hydrophobic interactions with Ala191. In conclusion, the top ranked compounds were **Ic**, **Id**, and **Ib**. As a perspective, we intend to synthesize the proposed compounds.

Acknowledgments

CAPES – CNPq – FAPERJ

¹ WHO (2022) Global Tuberculosis Report 2022.; ² Cade, C.E. et al. (2010) Protein Science, 19:458; ³ Lima, C.H.S. et al. (2015) Int. J. Mol. Sci., 16:23695.; ⁴ Joshi, S.D. et al. (2016) Eur. J. Med. Chem., 121:21.; ⁵ Gazzi, T.P. et al. (2017) J. Braz. Chem. Soc., 28:2028.; ⁶ autodock.scripps.edu(1.5.7/Dec_19_18/1999-2011); ⁷ www.wavefun.com(1991-2000); ⁸ discover.3ds.com(2021).

Área: _____
(Inserir a sigla da seção científica para qual o resumo será submetido. Ex: ORG, BEA, CAT)

Docking studies of the Cannabinoids derivatives in O- GlcNAc Transferase (OGT) as anti-cancer candidates

Marissa El Hajje (PG),¹ Haifa Hassanie (PG),¹ Gustavo Goulart Henrique Trossini,¹

marissa.elhajje@usp.br

¹Departamento de Ciências Farmacêuticas, USP

Highlights

Molecular docking is a method that analyzes the conformation and orientation of molecules into the binding site of a macromolecular target. Poses that could be taken are generated by search algorithms and ranked by scoring functions. Some well-known examples of software developed over the past few decades are AutoDock, AutoDock Vina, DockThor, GOLD, FlexX, and Molegro Virtual Docker. In this study we aim to use GOLD software in order to generate distance restraints, which greatly increase protein-small molecule docking accuracy. The visualization is very important to assess cannabinoids binding site, specificity and affinity on OGT protein.

Resumo/Abstract

O-GlcNAc Transferase (OGT) is an enzyme that transfers N-acetylglucosamine from UDP to serines and threonines in cytoplasmic, nuclear, and mitochondrial proteins. Most human malignancies exhibit increased OGT expression, and OGT inhibition reduces cancer cell proliferation. Several chemical classes were tested as OGT inhibitors. Around of that, cannabinoid derivative THC demonstrated a potent inhibitory activity against this target.

Cannabinoids have been shown to be beneficial in the treatment of several diseases. High-thickness tetrahydrocannabinol (THC) may be useful for reducing chemotherapeutic drug resistance. Treatment with CBD has been demonstrated to promote apoptosis and autophagy in various cancer cells. One of the most prevalent diseases in the world and a leading cause of mortality globally is cancer. Over the past 50 years, more innovative treatments and targets have been created, yet the incidence of cancer fatalities has continued to climb.

For a better understanding the cannabinoids derivatives interactions with OGT structure, were performed docking studies between with crystal structure (4GZ3) and cannabinoids derivatives THC and CBD.

The docking results showed that CBD and THC exhibit the same interactions as the co-crystallized ligand where the same residues are involved: Histidine at 498, Leucine at 653 and Histidine at 920. CBD has RMSD of 0.17 and a score of 8.44. THC has an RMSD of 0.24 and a score of 8.18. The interactions are mostly H-bonds and Van der Waals forces. The pharmacophoric features were determined including HB donors, HB acceptors and hydrophobic features. Future work will be focused to select new cannabinoids derivatives with OGT inhibitory activity.

Acknowledgments

We would like to thank CAPES, FAPESP, CNPq, USP and FCFUSP

Efficacy of a larvicide candidate against *Aedes aegypti* Linn (Diptera: Culicidae) in laboratory

Luana M.S. Oliveira (PG),^{1*} **Nathália A. Macêdo** (PG),¹ **Letícia J. Dias** (IC),¹ **Ualace N. Santos** (IC),¹ **Rafaela K. V. Nunes** (PG)¹, **Adriana J. Santos** (PQ),¹ **Rogéria S. Nunes** (PQ),¹ **Roseli La Corte** (PQ),¹ **Sócrates C.H. Cavalcanti** (PQ)¹.

luanamarilia7@gmail.com; socratescavalcanti@yahoo.com.br.

¹Pharmacy Department, UFS;

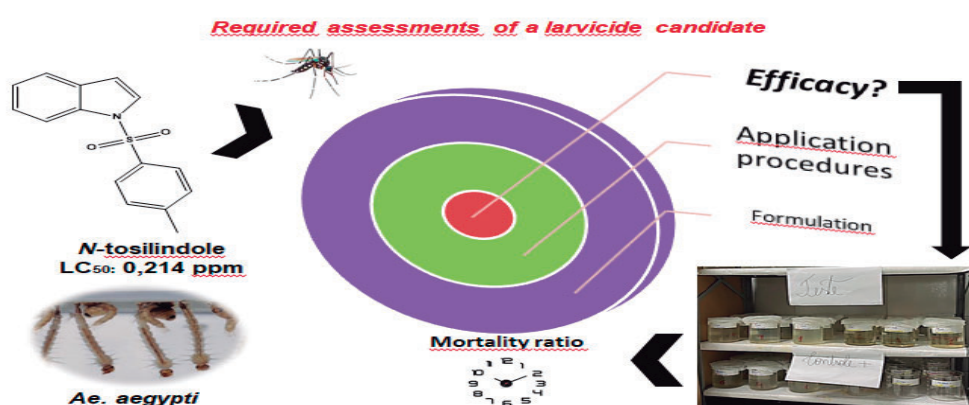
Keywords: Larvicides, *Aedes aegypti*, Efficacy, *N*-tosilindole.

Highlights

Aedes aegypti is a vector of four diseases. *N*-tosilindole is a Larvicide Candidate (LC) against the vector. It is important to know the efficacy of a LC. A control accounted for by larval mortality.

Resumo/Abstract

Aedes aegypti is a vector with ability to cause infections of high Public Health impact, especially in tropical countries. To develop a New Larvicidal Formulation (NLF), a series of testing is necessary to guarantee the effectiveness, safety and selectivity of the formulation to the target arthropod. Among these evaluations, the immediate and residual effect are primarily evaluated in one liter containers of water comparing the NLF to a larvicide currently used and has the function of verifying the length of time the larvicidal formulation exerts its of action, eliminating 100% of the larvae in the reservoirs, as well as the posterior residual effect. *N*-tosilindole is an example of a larvicidal candidate, as it exhibits high larvicidal potency ($LC_{50} = 0.214$ ppm). Therefore, the main goal of this research is to evaluate the efficacy of two formulations containing *N*-tosilindole against *Ae. aegypti* in a laboratory setup. One formulation comprises a granulated solid and the second is based on a surfactant stabilized system. In order to simulate the average household water usage, two different regimes of water volume manipulation were accessed. Controlled release formulations of the active principle must establish a level of control. As well as to predict the necessary frequency of application, maintaining lethal dosages for a period of time accounted for by larval mortality. Therefore, the preliminary results are supported by findings in the literature that confirm the importance of evaluating the two water handling regimes. Furthermore the two formulations indicate a residual effect superior or equivalent to the spinosad larvicide currently used.



PONTES, J. R. S. et al. **Mem Inst Oswaldo Cruz**, v. 105, n. 2, p. 220–224, 2010;

MACÊDO, N. A. et al. **SEMAC**. São Cristóvão, 2015.

Agradecimentos/Acknowledgments



Investigating the lack of cruzain to *Trypanosoma cruzi* activity with chemical space analyses and machine learning

Rafael F. Lameiro (PG),¹ Carlos A. Montanari (PQ).^{1*}

rafael.lameiro@usp.br; carlos.montanari@usp.br

¹Medicinal Chemistry Group (NEQUIMED), São Carlos Institute of Chemistry – University of São Paulo, São Carlos, Brazil.

Keywords: chemical space, cruzain, machine learning, *Trypanosoma cruzi*.

Highlights

Cruzain is an essential enzyme to the parasite *T. cruzi*, but many of its inhibitors are not bioactive. We try to rationalize this using chemical space analyses on calculated molecular descriptors.

Resumo/Abstract

Chagas disease is a neglected tropical disease caused by the protozoa *Trypanosoma cruzi*. Cruzain, its main cysteine protease, is commonly targeted in drug discovery efforts to find new treatments for this disease. Even though the essentiality of this enzyme for the parasite has been established, many cruzain inhibitors fail as trypanocidal agents. This lack of translation from biochemical to biological assays can involve several factors, including suboptimal physicochemical properties. In this work, we aim to rationalize this phenomenon through chemical space analyses of calculated molecular descriptors. These include statistical tests, visualization of projections, scaffold analysis, and creation of machine learning models coupled with interpretability methods. Our results demonstrate a significant difference between the chemical spaces of cruzain and *T. cruzi* inhibitors, with compounds with more hydrogen bond donors and rotatable bonds being more likely to be good cruzain inhibitors, but less likely to be active on *T. cruzi*. In addition, cruzain inhibitors seem to occupy specific regions of the chemical space that cannot be easily correlated with *T. cruzi* activity, which means that using predictive modeling to determine whether cruzain inhibitors will be trypanocidal is not a straightforward task. We believe that the conclusions from this work might be of interest for future projects that aim to develop novel trypanocidal compounds.

Agradecimentos/Acknowledgments

The results of this work have been published: Lameiro, R.F. and Montanari, C.A. (2023), Investigating the lack of translation from cruzain inhibition to *Trypanosoma cruzi* activity with machine learning and chemical space analyses. **ChemMedChem**. Accepted Author Manuscript. <https://doi.org/10.1002/cmdc.202200434>.

R.F.L. receives a PhD Scholarship from the São Paulo Research Foundation (FAPESP) - grant #2021/01633-3. This study was financed in part by the Coordenação de Aperfeiçoamento de Pessoal de Nível Superior – Brasil (CAPES) – Finance Code 001. FAPESP grant #2013/18009-4 is also acknowledged.

Investigation of biological activities of LASSBio Chemical Library to construct a “targetome”

Lucas Silva Franco (PG),^{1,2} Rodolfo do Couto Maia (PQ),^{2,3} Eliezer J. Barreiro (PQ),^{1,2,3}

silvafrancolucas@gmail.com; ejbarreiro@ccsdecania.ufrj.br

¹ Programa de Pós-Graduação em Farmacologia e Química Medicinal, Instituto de Ciências Biomédicas, Universidade Federal do Rio de Janeiro, Avenida Carlos Chagas Filho, 373, Ilha do Fundão, Rio de Janeiro, RJ, Brasil

² Laboratório de Avaliação e Síntese de Substâncias Bioativas (LASSBio®, <http://www.lassbio.icb.ufrj.br>), Instituto de Ciências Biomédicas, CCS, Universidade Federal do Rio de Janeiro, Cidade Universitária, Rio de Janeiro, RJ, Brasil

³ Instituto Nacional de Ciência e Tecnologia de Fármacos e Medicamentos (INCT-INOVAR; <http://www.inctinofar.ccs.ufrj.br/>), CCS, Universidade Federal do Rio de Janeiro, Cidade Universitária, Rio de Janeiro, RJ, Brasil

Keywords: Medicinal Chemistry, Chemical Library

Highlights

Studies of the LASSBio Chemical Library (LCL) exploring medicinal chemistry databases highlighted modulation of targets related to recent drug discovery and development trends.

Resumo/Abstract

BACKGROUND: The LCL contains ca. 2300 compounds, and medicinal chemistry concepts have driven the library content selection.^{1,2} In this work, content characterization of the LCL is presented, focused on identifying of additional biological activities beyond those discovered by LASSBio, and biological activities of compounds structurally similar to LCL's molecules.

METHODS: Drugs & biologics knowledge area of Cortellis Drug Discovery Intelligence (CDDI) - Clarivate Analytics database was used to search compounds labelled with the “LASSBio” tag. The associated biological activity and targets were extracted and processed in KNIME platform. LCL compounds and ChEMBL31 compounds were converted to ECFP_4 chemical fingerprints. Tanimoto coefficient similarity search was employed to extract compounds of LCL from ChEMBL31 (similarity coefficient = 1) in order to identify additional biological activities beyond those discovered by LASSBio. Data related to nearest neighbors – with a similarity coefficient between 0.7 and 1.0 – were obtained for the identification of the potential biological activity of LCL compounds. SQL format of ChEMBL31 was used to extract biological activity and target annotation of LCL compounds and their nearest neighbors.

RESULTS: The CDDI database contains 106 compounds of the LCL, which represent the most active compounds of each publication. Data related to targets modulated by these compounds indicated GPCRs and kinases as the main target families. The collection of targets was depicted and named “targetome” (Figure 1). The ChEMBL31 database contains 412 compounds of the LCL, which are related to more than 12 thousand data points. Data curation indicated a similar profile to that shown by CDDI database analysis.

CONCLUSIONS: Studies of the LCL highlighted its adherence to the recent trends of the drug development process. Activities observed for LCL compounds nearest neighbors may be helpful to guide future molecular repositioning studies.

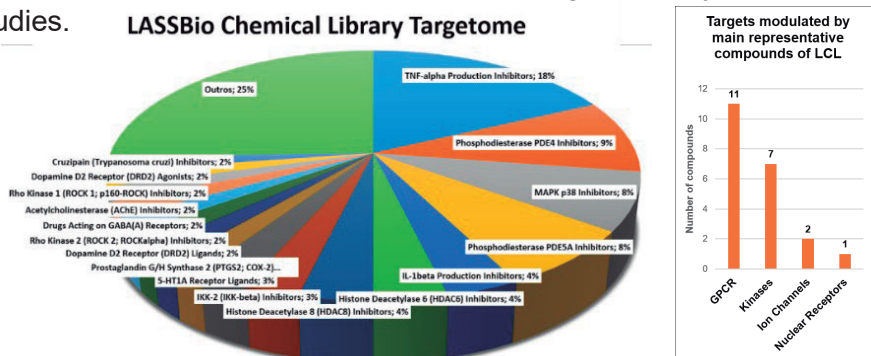


Figure 1: Targetome of the LASSBio Chemical Library representing main targets modulated by this collection.

References

¹COLODETTE, N. M. et al. J. Comput. Aided. Mol. Des., 2020, 34, 1091–1103.

²FRANCO, L. S.; MAIA, R. C.; BARREIRO, E. J. RSC Medicinal Chemistry, 2021, 12, 110-119.

Agradecimentos/Acknowledgments

INCT-INOVAR (CNPq N° 465.249/2014-0) and CNPq.

46ª Reunião Anual da Sociedade Brasileira de Química: “Química: Ligando ciências e neutralizando desigualdades”

Machine learning classification model and molecular dynamics simulation for O-GlcNac transferase (OGT) potential inhibitors discovery

Pedro Henrique R. A. Azevedo (PG),^{1*} Tatiana F. Alves (IC),¹ Bruna R. B. Peçanha (PG),¹ Luiz A. P. Flores-Junior (PG),¹ Luiza R. S. Dias (PG),¹ Estela M. F. Muri (PG),¹ Camilo H. S. Lima (PQ).²

camilolima@iq.uffrj.br; pedrohraa@id.uff.br

¹ Laboratório de Química Medicinal, Faculdade de Farmácia, Universidade Federal Fluminense, Niterói, RJ, Brazil; ² Universidade Federal do Rio de Janeiro, Instituto de Química, Rio de Janeiro, RJ, Brazil;

Keywords: Virtual screening, Machine learning, OGT, Molecular docking, Molecular dynamics simulation, drug repurposing.

Highlights

OGT imbalance may contribute to diabetes and cancer. Consensus machine learning (ML) and molecular dynamics simulation (MDS) were used to identify new OGT inhibitors.

Resumo/Abstract

Introduction: OGT enzyme participates in post-translational glycosylation on the hydroxyl group of serine or threonine residues in nuclear, cytoplasmic, and mitochondrial proteins (1). Overexpression of OGT is relevant in metabolic diseases such as cancer and diabetes (2). Thus, the objective of this work is to carry out a virtual screening of FDA-approved drugs using consensus machine learning (ML) and evaluate this finding using molecular dynamics simulation (Figure 1).

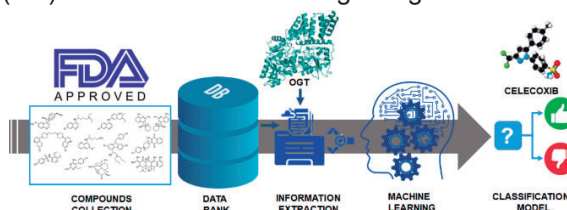


Figure 1 - Illustrated abstract demonstrating the main steps for celecoxib identification as OGT inhibitor

Computational methods: The Knime software was used to prepare the ML procedure. Seven ML algorithms were selected to evaluate an imbalanced data set (28 active: 830 inactive) considering the physicochemical and molecular docking descriptors. Next, the SMOTE approach was applied to resample the data set. After that, the data set was divided into training and test sets (70:30), and a ten-fold cross-validate was applied to each ML algorithm. The statistical parameters as sensitivity, specificity, accuracy, and Matthew's correlation coefficient (MCC) were calculated from the test set. The compound selected by consensus was submitted to MDS using the Charmm36 force field implemented in GROMACS software by 100ns. The RMSD, RMSF, and MM-PBSA were calculated using available modules in GROMACS software.

Results and discussion:

The ML consensus using five algorithms after the SMOTE approach showed excellent statistical values with sensitivity, specificity, and accuracy over 90% and Matthew's correlation coefficient (MCC) values greater than 0.8 to the test set. The FDA-approved drug repurposing identified the non-steroidal anti-inflammatory celecoxib as the best potential inhibitor. The pose analysis obtained by docking revealed hydrogen bond interactions only with the OGT C-Cat domain. The molecular dynamics simulation confirmed that the lack of interactions by hydrogen bonding with the C- and N-Catalytic domains allowed the drug to leave the binding site. The binding energy results showed that celecoxib would be a potentially weak OGT inhibitor.

Reference:

1. Ma, J., Wu, C., & Hart, G. W. (2021). *Chemical Reviews*, 121(3), 1513–1581
<https://doi.org/10.1021/acs.chemrev.0c00884>
2. Albuquerque, S. O. et al. (2020). *European Journal of Pharmaceutical Sciences*, 154, 105510.
<https://doi.org/10.1016/j.ejps.2020.105510>.

Acknowledgments

This study was financed in part by the Coordenação de Aperfeiçoamento de Pessoal de Nível Superior - Brasil (CAPES) - Finance Code 001, National Council for Scientific and Technological Development (CNPq), and FAPERJ - Carlos Chagas Filho Foundation—Grant N° 22/2016 (Project: E-26/200.930/2017), SEI-260003/009792/2021, SEI-260003/007043/2022, and SEI-260003/003788/2022.

Machine learning methods applied for the prediction of biological activities of triple reuptake inhibitors

Gustavo H. M. Sousa (PG),¹ Renan A. Gomes, (PQ)¹ Eliseu O. de Oliveira (PQ),² Gustavo H. G. Trossini (PQ)¹

gustavo.henrique.sousa@usp.br; trossini@usp.br

¹ Departamento de Farmácia, Faculdade de Ciências Farmacêuticas, Universidade de São Paulo, São Paulo, SP, Brazil; ²LifeScius, Inc, Richmond, Virginia, USA

Palavras Chave: Triple reuptake inhibitors; computer aided-drug design; machine-learning; QSAR; Random Forest; Support Vector Machine

Highlights

Making use of the quantitative structure-activity relationship (QSAR) tools and methods, based on state-of-the-art statistical and computational techniques, is possible to predict a compound's physicochemical property or even its biological activity, driving the drug design process towards a more rational approach. From compounds showing *in vitro* activity against three major depression targets: dopamine, norepinephrine and serotonin transporters, we developed a typical quantitative structure-activity relationship workflow, in order to predict the ligands' biological activity. After proper treatment of the data, linear and non-linear algorithms were used to predict the response variable, measured in pKi, achieving best results with algorithms such as Random Forest and Support Vector Machines for the dopamine and norepinephrine transporters and the models were able to predict accurately the test groups.

Resumo/Abstract

Major depressive disorder (MDD) is characterized by a series of disabling symptoms like anhedonia, depressed mood, lack of motivation for daily tasks and self-extermination thoughts. The monoamine deficiency hypothesis states that depression is mainly caused by a deficiency of monoamine at the synaptic cleft and major efforts have been made to develop drugs that inhibit serotonin (SERT), norepinephrine (NET) and dopamine (DAT) transporters in order to increase the availability of these monoamines. Triple reuptake inhibitors (TRIs) can target SERT, NET and DAT simultaneously, and are believed to have the potential to be early onset antidepressants. Quantitative structure-activity relationship models were developed using machine learning (ML) to predict biological activities of a series of triple reuptake inhibitor compounds that showed *in vitro* inhibitory activity against multiple targets. The results, using mostly interpretable descriptors showed that the internal and external predictive ability of the models are adequate, particularly of the DAT and NET by Random Forest (RF) and Support Vector Machine (SVM) models. The non-linear models obtained by RF and SVM presented higher performance when compared to the linear models. The best models were achieved for the dopamine receptor, with the performance metrics depicted below:

Model	Receptor	R ² (training)	RMSE (training)	R ² (test)	RMSE (test)
RF	Dopamine	0,863	0,362	0,817	0,398
SVM	Dopamine	0,811	0,395	0,799	0,418

The current work shows that models developed from relatively simple, chemically interpretable descriptors such as nitrogen electronic state, number of longest aliphatic chain, for example, can predict the activity of TRIs with similar structure in the applicability domain using ML methods.

Agradecimentos/Acknowledgments

We would like to thank CAPES; CNPQ and São Paulo Research Foundation (FAPESP) for supporting this research.

Molecular docking-based virtual screening of an in-house chemical library to identify candidate SARS-CoV-2 M-pro inhibitors

Bruno S. Oliveira (IC)^{1*}, Carlos Mauricio R. Sant'Anna (PQ)²

brunosnadeoliveira@ufrj.br, santanna@ufrj.br

¹Departamento de Ciências Farmacêuticas, UFRRJ; ²Departamento de Química Fundamental, UFRRJ

Keywords: virtual screening, molecular docking, SARS-CoV-2, M-pro, Michael acceptors

Highlights

A docking study applied to an in-house chemical library was able to identify candidate SARS-CoV-2 M-pro inhibitors including two natural products from green propolis that can act as Michael acceptors of the catalytic Cys145.

Resumo/Abstract

Since its creation in 1966, the Graduate Program in Chemistry at UFRRJ (PPGQ-UFRRJ) has produced a number of theses, dissertations and publications, which mostly describe natural products, semi-synthetic and synthetic molecules. This chemical heritage has been gathered by our group to construct a virtual chemical library (QV-PPGQ-UFRRJ). This virtual library can be useful for several studies, including to perform virtual screenings on several biological targets. In view of the serious pandemic caused by the SARS-Cov-2 betacoronavirus and the need to find pharmaco-biological methods of prophylaxis or therapeutic treatment of severe acute respiratory syndrome (the most serious symptom of Covid-19), the objective of the present study was the identification of candidate inhibitors for SARS-Cov-2 M-pro main protease, an essential enzyme for the virus to generate functional polypeptides. For this, theoretical methods were used to predict the ligand-protein interactions between molecules present in the QV-PPGQ-UFRRJ and the M-pro of SARS-Cov-2, with the purpose of identifying candidate inhibitors. 250 molecules of QV-PPGQ-UFRRJ, with protonation states defined with the pKa plugin of the Marvin program (Chemaxon) were energy minimized with PM6 and RM1 methods of the Spartan'14 program (Wavefunction). The 250 optimized structures were used in a molecular docking study with the GOLD 2022 program (CCDC) on the crystallographic structure of M-pro obtained from the Protein Data Bank with the code 7EN8 (1.83 Å resolution); the S atom of residue Cys145, essential for the catalytic activity of the enzyme, was chosen as the center of the binding site, and a site radius of 12 Å was chosen. Initially, a redocking study of the co-crystallized ligand in the A chain of the 7EN8 structure was performed, obtaining RMSD values of 0.228 Å and 0.484 Å for the ChemPLP and Goldscore scoring functions, respectively, indicating good accuracy of these methods in predicting the mode of interaction at this enzyme. With the ChemPLP function and having as reference the score value of 83.78 for the co-crystallized ligand, 40 compounds were identified that presented score values greater than 60. Two of these compounds (Table 1), which contain α,β -unsaturated carbonyls, had the C- β close to the S atom of Cys145. These two structures (rosmarinic acid¹ and cinnamyl caffeate¹) are natural products derived from green propolis and showed good potential for covalent inhibition of SARS-Cov-2 M-pro since they could act as Michael acceptors with the Cys145 residue.

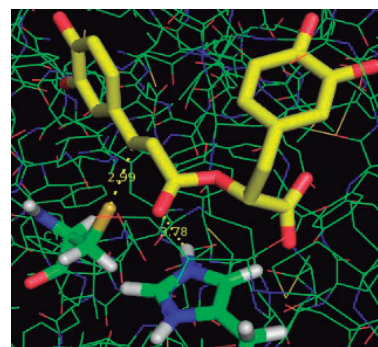


Figure 1: ChemPLP molecular docking pose of rosmarinic acid (C in yellow) at the SARS-CoV-2 M-pro binding site (C in green).

Table 1: Compound	ChemPLP Score	Distance between ligand C- β and Cys145 S
Rosmarinic acid	72,04	2,986 Å
Cynnamyl caffeate	64,1	2,975 Å

¹ Pires, L. O. Orientadora: Castro, R. N. 2019. 124 f. Dissertação (Mestrado), PPGQ, UFRRJ.

Agradecimentos/Acknowledgments

CNPq; Faperj

Molecular Modeling studies of *Leishmania infantum* Methionyl-tRNA synthetase

Marilia Valli (PQ),¹ Henrique R. Teles (PG),¹ Leonardo L.G. Ferreira (PQ),¹ Adriano D. Andricopulo (PQ)¹

marilia.valli@ifsc.com.br; henrique.rodriguesteles@gmail.com

¹Laboratory of Medicinal and Computational Chemistry (LQMC), Center for Research and Innovation in Biodiversity and Drug Discovery (CIBFar), Institute of Physics of São Carlos, University of São Paulo (USP), Av. João Dagnone, n° 1100, São Carlos, SP, Brazil

Palavras Chave: visceral leishmaniasis, homology model, virtual screening, molecular dynamics.

Highlights

Visceral leishmaniasis is a neglected tropical disease, lethal if not treated. We aimed to identify inhibitors of *Leishmania infantum* methionyl-tRNA synthetase, a molecular target for this parasite.

Abstract

Visceral leishmaniasis is a neglected tropical disease (NTD) caused by *Leishmania infantum* and *L. donovani* that is lethal in cases of nontreatment. The treatments are limited by serious drawbacks involving safety, resistance, stability, and high costs. In this work, we aimed to identify inhibitors of *Leishmania infantum* methionyl-tRNA synthetase (*LiMetRS*), a validated molecular target for leishmaniasis drug discovery, using a combination of strategies (Figure 1). Homology modeling was used to obtain the structure of *LiMetRS* based on the crystal coordinates of the enzyme from *Trypanosoma brucei* (*TbMetRS*). A virtual screening using molecular docking identified 10 candidate compounds from among more than 5 million that were included in the initial dataset filtered from the ZINC15. The selected hits were further evaluated using a script created in this work to select only the ligands that interacted with specific amino acids in the catalytic site of the enzyme.

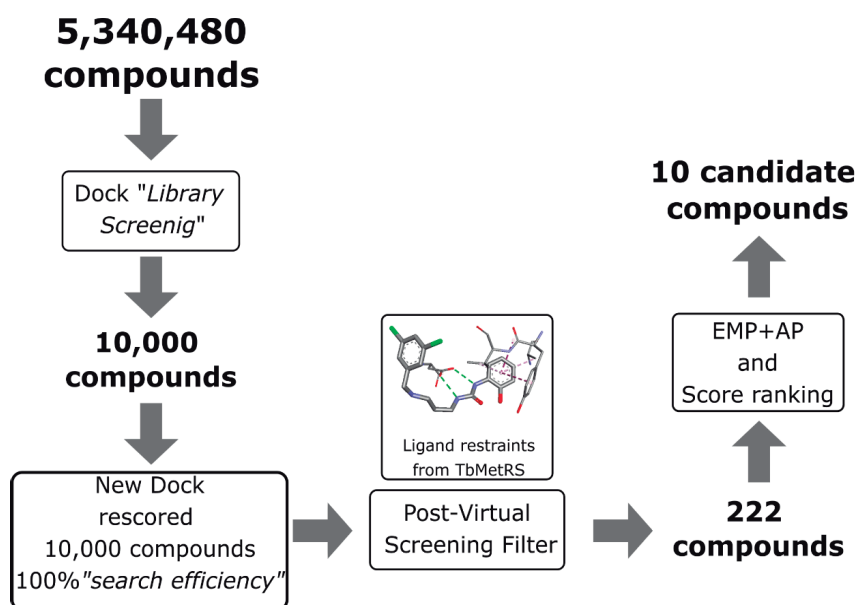


Figure 1. Schematic representation of the virtual screening strategy

Acknowledgments

CIBFar-CEPID FAPESP #2013/07600-3, INCT BioNat FAPESP/ CNPq #2014/50926-0, FAPESP/DFG #2020/11967-3, FAPESP/DAAD PROPASP #2022/08333-8, and Scholarship FAPESP #2019/05967-3.

Área: MED

Multi-approach characterization of *Leishmania braziliensis* dihydroorotate dehydrogenase and screening of potential inhibitors

Thamires Quadros Froes (PQ)^{1,2}, Jyoti Chauhan (PQ)³, Charles, J. Eyermann (PQ)³, Lori Ferrins (PQ)³, Flávio da Silva Emery (PQ)², Maria Cristina Nonato(PQ)^{1,2}

tqfroes@usp.br; j.chauhan@northeastern.edu; c.eyermann@northeastern.edu; l.ferrins@northeastern.edu; flavioemery@usp.br; cristy@fcrfp.usp.br

1) School of Pharmaceutical Sciences of Ribeirão Preto, USP, São Paulo, Brazil; 2) Center for the Research and Advancement of Fragments and molecular Targets (CRAFT); 3)³Dept. of Chemistry & Chemical Biology, Northeastern University, Boston, MA, USA

Palavras Chave: *Leishmania braziliensis*, Dihydroorotate dehydrogenase, Kinetic assay, competitive inhibitors.

Highlights

The complete kinetic characterization of *Lb*DHODH was crucial for developing a reproducible ligand screening assay that allowed us to identify ligands in the μM range. Structural X-ray diffraction studies provided the molecular basis for optimizing the inhibitors.

Resumo/Abstract

Cutaneous leishmaniasis (CL) is a neglected tropical disease spread over 85 countries and responsible for up to 119,600 deaths/year, only in Brazil (PORTELLA; KRAENKEL, 2021). The available drugs display high toxicity and low efficacy, highlighting the need for novel therapeutic alternatives to fight CL. One way to achieve this goal is by identifying essential targets of the parasite that allow selective inhibition. The dihydroorotate dehydrogenase (DHODH) is the rate-limiting step in the *de novo* pyrimidine biosynthetic pathway of *Leishmania braziliensis*. We carried out extensive kinetic characterization to develop inhibitors for this promising target: *Lb*DHODH follows a ping-pong catalysis mechanism with optimal pH (8.0). At this pH, the first-substrate (dihydroorotate - DHO) has $Km^{DHO} = 11.7 \pm 0.3 \mu\text{M}$, the second-substrate (fumarate - FUM) has $Km^{FUM} = 74 \pm 3 \mu\text{M}$, and the global $K_{cat}^{(s-1)} = 5.4 \pm 0.1$, with a Hill coefficient: 1.8 ± 0.1 . Using these parameters, we developed a reproducible screening protocol that validated the product of the first reaction step (orotate) as a natural *Lb*DHODH inhibitor (Fig 1A). The assay was exploited to identify orotate-based *Lb*DHODH inhibitors (Fig 1A) with up to 16-fold improved potency but reduced ligand efficiency (LE) (0.63 (orotate) to 0.25 (NEU83)- Fig 1A). Efforts to overcome this limitation resulted in NEU56 (LE: 0.35). Aiming to provide a structural perspective to this dilemma, we also solved the structure of *Lb*DHODH in complex with orotate (Resolution: 1.7Å), NEU83 (Resolution: 1.9 Å), and NEU56 (Resolution: 1.8 Å) using X-ray crystallography (Fig 1B). Whereas orotate moiety shows a similar binding profile to other DHODH-orotate complexes, the carboxy-naphthalene ring from NEU83 is solvent exposed and provides one additional hydrogen bond to ASN54. On the other hand, the aromatic ring in NEU56 is buried at *Lb*DHODH active site, and no other interaction is found.

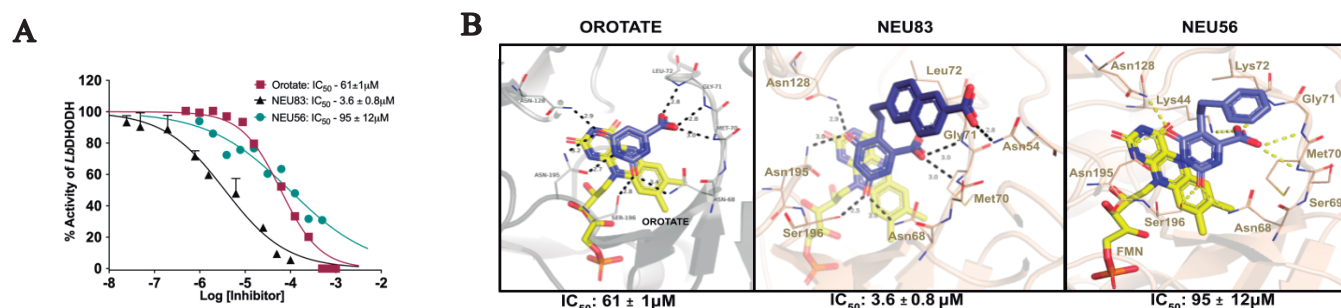


Figure 1: Screening and X-ray studies of *Lb*DHODH inhibitors (A) Inhibitors' IC₅₀ determination. (B) Inhibitors' binding profile at *Lb*DHODH active site.

As our previous hot spot analysis predicted (FROES, T.Q. *et al*, 2021), crystallographic structures also highlighted a loop movement that enhanced *Lb*DHODH's druggability. This information shall be exploited to develop a second round of *Lb*DHODH inhibitors with improved potency. A cryptic site observed in *Lb*DHODH-NEU56 complex is also being investigated for allosteric inhibitors design.

PORTELLA, T. P.; KRAENKEL, R. A. Spatial-temporal pattern of cutaneous leishmaniasis in Brazil. *Infectious Diseases of Poverty*, v. 10, n. 1, 2021.

FROES, T. Q. *et al*. DHODH Hot Spots: An Underexplored Source to Guide Drug Development Efforts. *Current Topics in Medicinal Chemistry*, v. 21, n. 23, p. 2134–2154, 2021.

Agradecimentos/Acknowledgments

FAPESP, CNPq and NIH

46ª Reunião Anual da Sociedade Brasileira de Química: "Química: Ligando ciências e neutralizando desigualdades"

NHC-functionalized compound with Selenium: Synthesis, characterization and anticarcinogenic properties

Thaiz Cristina Soares dos Santos (PG),^{1*} Alix Y. Bastidas Angel (PG),¹ Eduardo Eliezer Alberto (PQ)¹, Heveline Silva (PQ).¹

thaizcristina@ufmg.br

¹ Department of Chemistry, Universidade Federal de Minas Gerais;

Keywords: N-heterocyclic carbene, Imidazole, Cell, Cancer.

Highlights

The combination of Selenium and NHC's groups were the strategy in the search for new antitumor drugs in this work. The synthesis and previous cytotoxicity studies were the first steps to this project.

Abstract

N-heterocyclic carbenes (NHC's) constitute an important class of carbenes. Compounds containing NHC's groups have attracted increasing attention for their use as ligands in reactions catalyzed by transition metals, in the synthesis of drugs and have good antitumor and antimicrobial activity¹. Compounds containing Selenium, due to their antioxidant activity², can help in the redox homeostasis of reactive oxygen species (ROS) in tumor cells³. The aim of this work was to synthesize a compound that contains NHC group functionalized with Selenium (B), then characterize and perform the biological test in tumor cell and compare with the intermediate compound (A). The scheme of synthesis (Figure 1) involved the following reaction mechanisms: diazotization, nucleophilic aromatic substitution, reduction with LiAlH₄, reduction with NaBH₄ and bromination of alcohols.

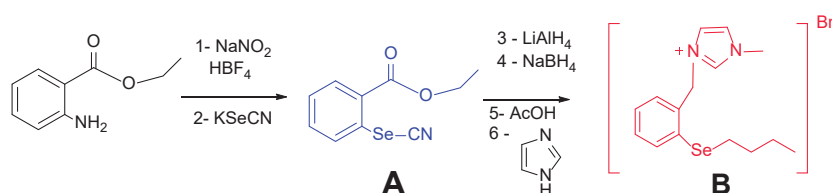


Figure 1: Synthesis route of compounds A and B

The ¹³C NMR spectrum for **A** shows the signal at δ 106,09, corresponding to Se-CN, signal at δ 168,06 corresponding to the C=O of the ester. In comparison, the ¹³C NMR for **B**, shows the Se-C was shifted to δ 32,09, suggesting that the nitrile was replaced by the butyl radical. It was also possible to identify signals at δ 121,83; 123,59 corresponding to the CH₂ of imidazole and C-N at δ 137,69 instead of ester carbons. The ¹H NMR spectrum for **B** shows the signal at δ 10,15 further indicating the presence of H on the N=CH-N in the imidazole ring confirming the formation of NHC group. About the IR spectra it is possible to see the band corresponding the C-O bond of the ester at 1286 cm⁻¹ of compound **A** as also signals referred to nitrile C≡N at 2145 cm⁻¹ which were not observed in compound **B** which instead has a band at 3391 cm⁻¹ referring to the imidazole amine. Cytotoxicity assays were performed *in vitro* against human breast cells (tumor- MDA, MCF-7 and non tumor MCF-10). With respect to MDA cell, **B** was five times more active than **A** (IC₅₀ 6,1 μ M and 29,4 μ M respectively) and no significant difference was observed for MCF-7 cells (IC₅₀ 42,4 μ M and 49,4 μ M respectively). However, neither compound was selective when compared to a normal cell MCF-10. Even though the results are promising, since they present some selectivity to breast carcinoma-MDA (a non-responsive cell to hormone therapy) promoted by structure modification. The future perspective is to use this molecule as a ligand to obtain an organometallic complex expecting a biological activity improvement.

Acknowledgments

CAPES, FAPEMIG, CNPq, UFMG

¹CORREIA, J; *Quim Nova* Vol. 31, 872 - 884, **2008.**, ²GALADARI, S; *Biol. Med.* 104, 144 - 164, **2017.**, ³SOSA, V; *Ageing Res. Rev.* 12, 376 - 390 **2013.**

Novel Bis-naphthoquinone-1,2,3-triazole derivatives as potential pharmacological agents

Gustavo Senra (PQ),¹ Adriane Amaral (PQ),¹ Vítor Ferreira (PQ),¹ Fernando de Carvalho (PQ),¹

senradcarvalho@gmail.com

¹Departamento de Química Orgânica, Instituto de Química, Universidade Federal Fluminense, Niterói-RJ, 24210-141, Brazil

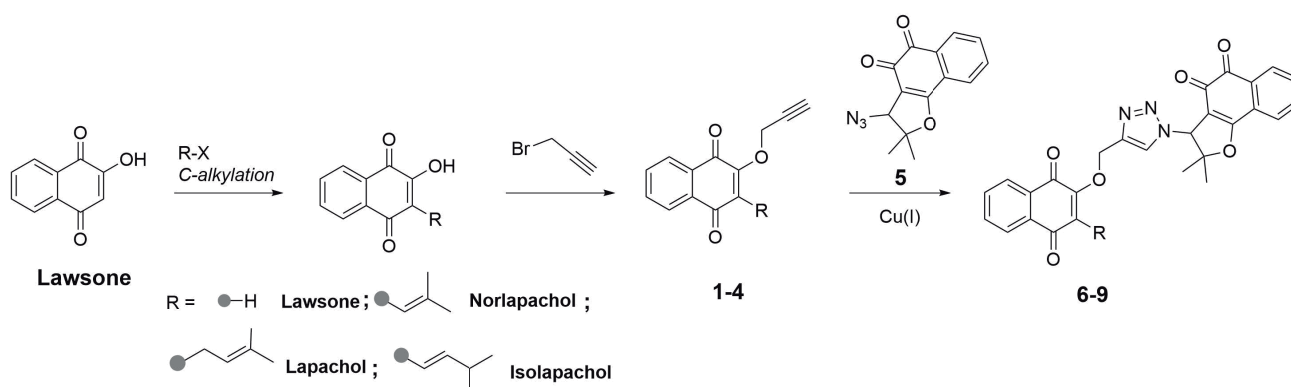
Palavras Chave: Naphthoquinone, 1,2,3-triazole, Click Chemistry, heterocycle.

Highlights

A new set of quinone-1,2,3-triazoles hybrids was obtained via click chemistry. Lapachol, norlapachol, isolapachol and lapachone were used as substrates. Structural modifications in the naphthoquinone unit can considerably alter its action in the redox cycle and promote the elevation of intracellular levels of reactive oxygen species, which play an important role in triggering the apoptosis process.

Resumo/Abstract

Several synthetic and natural low molecular weight naphthoquinones find applications in diverse scientific and technological fields. These naphthoquinones also have potential clinical utility in the treatment of various diseases.¹ Naphthoquinones bearing the pyranic ring, specifically, have been reported to have bioactivity against various microorganisms and cancer cell lines due to their ability to accept one or two electrons in the redox cycle, generating reactive oxygen species (ROS).² Through this mechanism, quinones are cytotoxic and lead cells to their programmed death (apoptosis).³ β -Lapachone, in special, has received great attention due to its pronounced anticancer activity.⁴ On the other hand, heterocyclic rings such as 1,2,3-triazoles are highly important in medicinal chemistry as they are present in the structure of several bioactive compounds.⁵ Considering all these facts, it is reasonable to envision that the combination of the 1,4-naphthoquinone and 1,2,3-triazole moieties has the potential of generating highly bioactive molecules. In this sense, in this work we aimed to synthesize novel quinone-triazole hybrids through the Cu(I)-catalyzed Huisgen cycloaddition between the O-propargylated 1,4-naphthoquinones **1-4** and azido-lapachone **5**, as shown in Scheme 1. Compounds **1-5** were synthesized, in good yield, and characterized. The triazole derivatives of lawsone (60% yield) and nor-lapachol (70% yield) have already been obtained and partially characterized. Once the other triazoles are synthesized and after the complete characterization of all newly synthesized Bis-naphthoquinone-1,2,3-triazoles, their *in vitro* evaluation as pharmacological agents will be performed.



Scheme 1. Synthetic route toward bis-naphthoquinone-1,2,3-triazole hybrids.

References

- ¹ *Current Organic Synthesis* **2016**, 13, 334-371.
- ² *Journal of the American Chemical Society* **2011**, 133, 11557-11571.
- ³ *Current Pharmaceutical Design* **2016**, 22, 5899-5914.
- ⁴ *Bioorganic & Medicinal Chemistry* **2008**, 16, 5635-5643.

Agradecimentos/Acknowledgments



Preparation and characterization of acyclovir-loaded PVA/CA/Zein bioadhesive nanofibers for treatment of herpes simplex virus type 1

Bruna Schoenberger Teixeira (PG),¹ Bárbara Sthéfani Caldas (PQ),¹ Valéria Aquilino Barbosa (PQ),¹ Tânia Ueda Nakamura (PQ),² Eduardo Radovanovic (PQ),¹ Fernanda Andreia Rosa (PQ).^{1*}

bru_schoenberger@hotmail.com; farosa@uem.br

¹Department of Chemistry, State University of Maringá; ²Department of Pharmacy, State University of Maringá

Keywords: poli(vynil alcohol), zein, herpesvirus, bioadhesive.

Highlights

This work was dedicated to preparation of PVA/CA/Zein nanofibers loaded with the antiviral drug acyclovir to produce a bioadhesive for the treatment of Herpes Labialis.

Abstract

Worldwide, 99% of people are infected with the herpes virus during their lifetime. Herpes is a disease that causes blisters and redness on the skin and can lead to more serious illnesses such as encephalitis¹. Acyclovir (ACY) is a purine analogue of the nucleoside guanosine that acts as the most powerful antiviral against herpes simplex virus type 1 (HSV-1)². However, oral administration of the drug is limited, mainly due to its short time of biological half-life. Several drug delivery systems have been investigated in the last decades, such as responsive polymeric delivery systems. Thus, due to the lack of therapies for herpes labialis using bioadhesives, a new formulation for acyclovir was proposed. PVA is a hydrophilic polymer widely used in the preparation of polymeric fibers and biomaterials³. Zein is a corn protein that has several advantages, including hydrophobicity⁴. The bioadhesive nanofibers of PVA (10%) and zein (5%) cross-linked with citric acid (15% wt to PVA) and loaded with the antiviral acyclovir (7% wt to PVA) were prepared using a homemade coaxial electrospinning apparatus, with a rotating collector, covered with waxed paper. Parameters such as flow rate, distance from tip-to-collector, humidity, voltage, and temperature were maintained at 0.65 mL h⁻¹, 15 cm, 40-60%, 20 kV, and 22-25 °C, respectively. The electrospun fibers were treated at 120 °C for 24 hours for the crosslinking reaction. The morphology was characterized by SEM, ATR-FT-IR, and NMR analyses. Mechanical tests of tensile strength, solubility, and swelling were also investigated. The in vitro release profile of acyclovir was determined at 100 rpm and 37 °C, for 15-300 minutes. The straight-line equation was used ($y = 0.05498x - 0.00689$), validated by linear regression for a range of 2.5-15 µg mL⁻¹ of ACY in HCl 0.1 N. SEM images indicated the formation of homogeneous fibers, with a mean diameter of 380±40 nm. The presence of acyclovir was confirmed by ATR-FT-IR and ¹H NMR analysis. The bioadhesive has great mechanical resistance, with Young's modulus of 55.3 MPa, a good degree of swelling of 190%, and solubility in 24 hours of 40%. The drug release profile was determined and indicated a maximum acyclovir release of 87% in 60 min. The results indicated that the methodology, as well as the chosen components of the polymeric blend, were efficient for the new acyclovir formulation.

Acknowledgments



Financial Support: Public Notice CAPES 11/2020 Epidemics.

¹ Esposito, S., Autore, G., Argentiero, A., Ramundo, G., Principi, N. *Autoimmunity Reviews*, **2022**, 21, 12, 103187.

² Schalkwijk, H. H., Snoeck, R., Andrei, G. *Biochemical Pharmacology*, **2022**, 206, 115322.

³ Ghalei, S., Asadi, H., Ghalei, B. *Journal of Applied Polymer Science*, **2018**, 46643.

⁴ Chen, H., Su, J., Brennan, C. S., Van der Meeren, P., Zhang, N., Tong, Y., Wang, P. *Materials Today Advances*, **2022**, 16, 100307.

Purine-derived phenylhydroxamate compounds reduce cell viability and modulate HDAC activity in hematological neoplasm models

Jorge Antonio Elias Godoy Carlos (PG),¹ Larissa Costa de Almeida (PG),¹ Keli Lima (PG),¹ Mauricio Temotheo Tavares (PG),² Karoline de Barros Waitman (PG),² Leticia Veras Costa-Lotufo (PQ),¹ Roberto Parise-Filho (PQ),² João Agostinho Machado-Neto (PQ).¹

jorgegdy@icb.usp.br, jamachadoneto@usp.br

¹Department of Pharmacology, Biomedical Science Institute, University of São Paulo, Brazil. ²Department of Pharmacy, Faculty of Pharmaceutical Science, University of São Paulo, Brazil.

Palavras Chave: Histone deacetylases, purine-derived phenylhydroxamate, antineoplastic activity, Blood cancer, Acute leukemia.

Highlights

High levels of histone deacetylases (HDAC) are reported in patients with hematological and it have been associated with poor prognosis. Three novel purine-derived phenylhydroxamates with potential HDAC inhibitor activity were tested. The novel purine-derived phenylhydroxamates tested presented selective antineoplastic effects in blood cancer cells.

Abstract

Introduction: The histone acetylation process is the best-studied type of post-translational modification, playing a key role in chromatin remodeling regulated by the activity of two enzymes: histone acetyltransferases and histone deacetylases (HDAC). High levels of HDAC have been associated with poor prognosis and are observed in patients with hematological higher levels of its enzymes. The present study aimed to evaluate the cellular effects of three novel potential HDAC inhibitors in hematological neoplasm models. **Material and methods:** A panel containing myeloid (OCI-AML3, Kasumi-1, HL-60, THP-1, MOLM-13, MV4-11, U-937, NB4, NB4-R2, K-562, KU812, SET2, and HEL) and lymphoid (Jurkat, CEM, Namalwa, NALM6, Daudi, Raji, SUP-B15, REH, U266, MM1.S, MM1.R, Karpas 422, and MEC-1) neoplasm cells were used. Peripheral blood mononuclear cells (normal leukocytes) from healthy donors were used for toxicity evaluation (n=4). Three novel purine-derived phenylhydroxamates with potential HDAC inhibitor activity (named here as 82, 83, and 84) were used. Vorinostat was used as a reference drug. Cell viability was assessed by MTT assay, apoptosis by annexin V/propidium iodide labeling and flow cytometry (FC), clonogenicity by autonomous colony formation, cell cycle by propidium iodide and FC, protein expression by Western Blot, and cell differentiation by morphology. IC₅₀ values were obtained by non-linear regression. Statistical analysis was performed by ANOVA and Bonferroni post-test. A $p < 0.05$ was considered significant. **Results:** All compounds tested reduced cell viability at submicromolar concentrations being compound 82 more potent than the others (IC₅₀ ranged from 0.09 to 2.04 μ M). THP1, MOLM13, NB4-R2, and HEL leukemia cells were more sensitive to these compounds and were selected for the next experiments. In normal leukocytes, vorinostat and compound 82 did not reduce cell viability at the same extension as observed for leukemia cells, indicating a selective antineoplastic activity. All compounds induced time- and dose-dependent manner apoptosis in THP-1, MOLM-13, NB4-R2, and HEL cells (all $p < 0.05$). Vorinostat and compound 82 strongly reduced colony formation, being compound 82 more efficient, especially in MOLM-13 and NB4-R2 cells (all $p < 0.05$). Low concentrations of vorinostat and compound 82 lead to reduced cell cycle progression (all $p < 0.05$). THP-1, MOLM13, NB4-R2, and HEL cells were exposed to vorinostat or compound 82 and the expression of proteins involved in apoptosis and HDAC activity was modulated. Low concentration of vorinostat or compound 82 induced differentiation and vacuoles in THP-1 and NB4-R2 cells. **Conclusion:** Our results indicate that the three purine-derived phenylhydroxamates tested presented antineoplastic effects being a future candidate to compose the list of HDAC inhibitors in the antineoplastic arsenal.

Acknowledgments

Supported by FAPESP, CAPES, and CNPq.

Síntese de quinazolinonas e fenil hidrazidas: avaliação leishmanicida e busca de potenciais alvos enzimáticos por quimiogenômica

Patrick P. Pimentel (IC),¹ Tiago R. Navarro (IC),¹ André B. Farias (PQ),^{2,3} Claudia do C. Maquiaveli (PQ),⁴ Edson R. da Silva (PQ),⁴ Nelilma C. Romeiro (PQ),² Evanoel Crizanto de Lima (PQ).^{1*}

pppatrickpedro@gmail.com; *evanoel.crizanto@gmail.com

¹Laboratório de Catálise e Síntese de Substâncias Bioativas, Pólo Ajuda, Centro Multidisciplinar UFRJ-Macaé; ²Laboratório Integrado de Computação Científica (LICC), Centro Multidisciplinar UFRJ-Macaé; ³ Instituto de Matemáticas Aplicadas y Sistemas, Universidad Nacional Autónoma de México, Mérida, Yucatán, México; ⁴Laboratório de Farmacologia e Bioquímica, Faculdade de Zootecnia e Engenharia de Alimentos, USP.

Palavras-Chave: Quinazolinonas, Hidrazidas, Leishmania, Quimiogenômica

Highlights

Synthesis of quinazolinones and phenyl hydrazides: leishmanicidal evaluation and search for a possible enzymatic target through chemogenomics. We have prepared hydrazides and quinazolinones based in previous results. New compounds showed antileishmanial activity however did not inhibit the enzyme arginase. Chemogenomics calculations were used to find possible molecular targets.

Resumo/Abstract

Em 2019, publicamos a síntese de hidrazidas α,α -difluoradas que apresentaram atividade leishmanicida sobre as formas promastigota e amastigota de *Leishmania amazonensis*. Adicionalmente, as moléculas preparadas também apresentaram atividade inibitória da enzima arginase do parasito. Baseando-nos nestes resultados prévios, foram sintetizadas 10 fenil hidrazidas e 3 quinazolinonas, empregando-se simplificação molecular, reduzindo a quantidade de etapas da síntese e os custos envolvidos no preparo dos produtos. As hidrazidas foram obtidas reagindo anidrido isatoico e fenil hidrazinas comerciais, sob refluxo com etanol, por 2h. As quinazolinonas foram obtidas a partir das hidrazidas, com cloreto de acetila e MecN, agitando-se à temperatura ambiente, por 3 a 5h. Algumas hidrazidas apresentaram atividade leishmanicida em culturas de promastigotas superior às dos protótipos fluorados, dentre as quais a mais potente teve $CI_{50} = 1,3\mu M$. As quinazolinonas foram inativas, porém, forneceram informações relevantes sobre a relação estrutura-atividade. Ensaios preliminares de inibição enzimática foram realizados e o resultado mostrou que, apesar de serem mais ativas que os protótipos, as fenil hidrazidas não apresentaram inibição da enzima arginase. Desta forma, foram empregados cálculos de quimiogenômica com o objetivo de encontrar possíveis alvos moleculares para ação dessas substâncias. As moléculas foram preparadas usando o software ChemDraw e submetidas aos cálculos de quimiogenômica utilizando os protocolos do Pidgin (v.3). Os resultados revelaram um conjunto de proteínas com inibidores similares aos do presente trabalho, com destaque para as enzimas pteridina redutase e piruvato quinase, uma vez que são considerados alvos para o desenvolvimento de inibidores contra leishmania. Estudos complementares de *docking* molecular estão sendo realizados para compreender a relação estrutura-atividade das moléculas sintetizadas neste trabalho com os alvos propostos. Os cálculos de *docking* estão sendo realizados no programa Gold e a análise das interações e inspeção visual no programa Discovery Studio e Pymol. Espera-se que esses resultados possam racionalizar a síntese de novas fenil hidrazidas para novos alvos moleculares.

Agradecimentos/Acknowledgments

Authors thank Faperj, Fapesp, CAPES and CNPq for financial support and Farmanguinhos for analytical data.

Structure-based design of new gamma-carboline chloromethyl amides as Inhibitors of SARS-CoV-2 M^{pro} enzyme

Pedro H. O. Borges (PG)¹, Anna Paula P.M. da Silva (PG)¹, Luiz C. Saramago (PQ)², Floriano P. Silva Júnior (PQ),^{2*} Sabrina B. Ferreira (PQ)^{1*}

borges.pho@pos.iq.ufrj.br; floriano@ioc.fiocruz.br; sabrinab@iq.ufrj.br

¹Universidade Federal do Rio de Janeiro, Instituto de Química Laboratório de Síntese e Prospecção Biológica, Rio de Janeiro, RJ, Brasil; ²Fundação Oswaldo Cruz, Instituto Oswaldo Cruz, Laboratório de Bioquímica Experimental e Computacional de Fármacos, Rio de Janeiro, RJ, Brasil

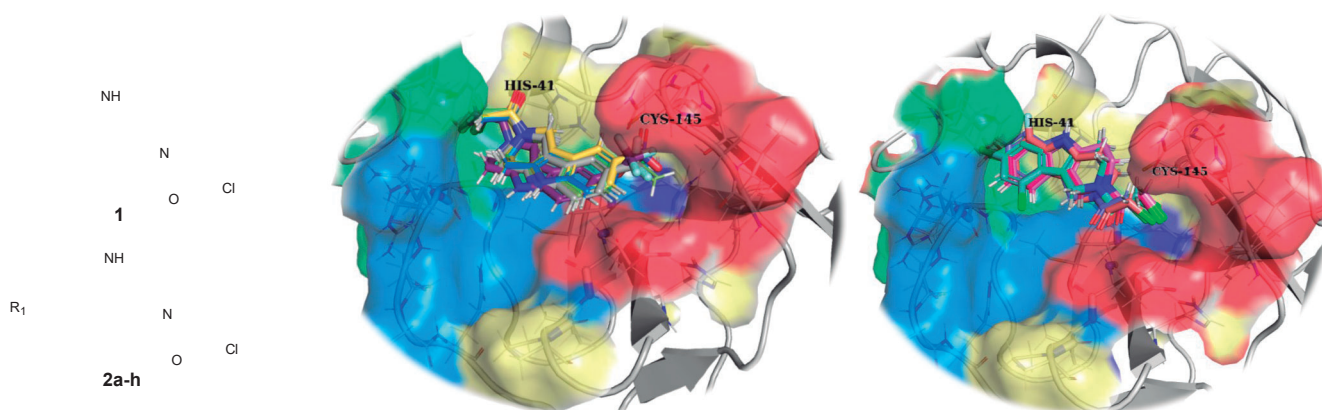
Palavras Chave: Artificial Intelligence, SARS-CoV-2, Mpro, Molecular Docking, Molecular Dynamics

Highlights

Artificial intelligence (AI) models can suggest new molecules based on known inhibitors. Our group's AI model suggested new and potentially active molecules against SARS-CoV-2 M^{pro} and evaluated *in silico*.

Resumo/Abstract

The COVID-19's pandemic caused by the SARS-CoV-2 virus has taken nearly 7 million lives since its outbreak in December 2019, alongside social and economic impact across the world¹. Despite the success of recently developed vaccines and antivirals², the development of new drugs is still necessary. Computational approaches derived from the artificial intelligence (AI) field allow us to quickly propose new and potentially effective molecules. Previously, our group's AI model³ based on generative deep learning methods identified a fragment-like compound (**1**) with inhibitory activity against SARS-CoV-2 main protease (M^{pro}). Optimized compound **1** analogues (**2a-h**) were designed by using molecular docking and molecular dynamics simulations and the best predicted ligands are being synthesized. Molecular docking protocols were carried out by GOLD and AutoDock Vina for consensus docking scores. Docking results have shown interactions of the chloromethylamide moiety with both S1 and S2 subsites, depending on the position and nature of the R₁ substituent. MM-PBSA calculations will be done to estimate ligand affinities against the target enzyme. Our results will aid us in developing inhibitors with stronger molecular binding affinities.



Acknowledgments

The authors gratefully acknowledge the financial support from CAPES, Fiocruz and UFRJ

1. Nalbandian, A.; et al. *Nat. Med.* **2021**, 27 (4), 601–615; 2. Yang, H.; et al. *PLoS Biol.* **2005**, 3 (10); 3. Santana, M. V. S.; Silva-Jr, F. P. De Novo Design and Bioactivity *BMC Chem.* **2021**, 15 (1), 8.

Structure Based Drug Design Driven LASSBio-1632 Optimization

Marcos S. Oliveira (PG),¹ João A. Lima (PG),¹ Vinicius de Frias Carvalho (PQ),³ Eliezer J. Barreiro (PQ),^{1,2} Lídia M. Lima (PQ).^{2*}

marcos.oliver1822@gmail.com; lidalima@ufrj.br

¹LASSBio. Laboratório de Avaliação e Síntese de Substâncias Bioativas. Instituto de Ciências Biomédicas (ICB), UFRJ.

²Programa de Pós-graduação em Farmacologia e Química Medicinal, ICB, UFRJ.

³Laboratório de Inflamação do Instituto Oswaldo Cruz (IOC/Fiocruz)

Keywords: Lead-optimization, SBDD, Phosphodiesterase, Docking

Highlights

We described the optimization of antiasthmatic prototype LASSBio-1632 from structure-based drug design strategy (SBDD), the synthesis of the designed analogues and their inhibitory effects on target.

Abstract

LASSBio-1632 was identified as a new antiasthmatic lead candidate. Structure activity relationship (SAR) studies have revealed the role of the bioactive conformation in its ability to inhibit phosphodiesterase 4 (PDE-4). To start a lead optimization program, we decide to investigate by crystallography studies the comparative conformation of LASSBio-1632 and its non-alkylated analogue LASSBio-1624. These studies showed significant differences in the conformations of LASSBio-1624 and LASSBio-1632. While, the former assumes a linear conformation, the latter presents a folded conformation induced by the presence of the methyl group attached to the nitrogen of the *N*-sulfonylhydrazone subunit. With this information in mind and in order to improve LASSBio-1632 activity, we described here the attempt to optimize LASSBio-1632 structure guided by SBDD (structure-based drug design) strategy. The binding mode of LASSBio-1632 in the docked in the PDE4A10 (PBD ID:2QYK) was established, using the same ligand conformation identified in the previous crystallographic study. We demonstrated that the 3,4-dimethoxy-phenyl scaffold oriented to the Q pocket (cavity with the Gln residue responsible by selectivity that interacts with PDE4 inhibitors) and the group linked to the nitrogen atom of sulfonylhydrazone subunit (N-H to LASSBio-1624 and N-CH₃ to LASSBio-1632) oriented to the metallic site (Zn⁺² and Mg⁺²). However, any interaction of these ligands with the metal ions has been observed. This finding revealed the possibility of maintaining the alkylation of the *N*-sulfonylhydrazone (essential for the bioactive conformation), but exploring groups capable of possessing the ideal distance and characteristics for coordination with the metal site of PDE-4. Therefore, we designed four new LASSBio-1632 analogues that were study by molecular docking, in a comparative manner with LASSBio-1632, using GOLD and PDE4A10 (PBD ID:2QYK). The results confirmed that polar groups introduced to the *N*-sulfonylhydrazone framework can promote mono and bidentate interactions with the divalent ions present in the catalytic site of PDE4, improving the theoretical affinity to PDE4. The new analogues also promoted the same interactions already described for PDE inhibitors with selectivity for the isoform PDE4 (van der Waals interactions between Met485, Ile548, Phe552, and Phe584 residues with benzodioxole scaffold and hydrogen interaction of 3,4-dimethoxy-phenyl scaffold with Gln581 residue). Encouraged by the results the compounds were synthesized, employing classical synthetic methodology, already applied to obtain LASSBio-1632, being obtained in good yields. At this point the compounds were sent to enzymatic assays on PDE-4 and the results will either confirm the hypothesis adopted in the attempt to optimize LASSBio-1632 or refute it.

Acknowledgments

Authors would like to thank FAPERJ, INCT-INOVAR, CAPES and CNPq for financial support.

Área: MED

(Inserir a sigla da seção científica para qual o resumo será submetido. Ex: ORG, BEA, CAT)

Synthesis and antiplasmodial profile of novel triazole-7-chloroquinoline hybrids

Alcione Silva de Carvalho (PQ),¹ Victória Toledo Diniz de Camargo (IC),¹ Beatriz Cunha Tolla de Oliveira (IC),¹ Isabela Alencar Graciano (PG),² Fernando de Carvalho da Silva (PQ),² Carolina Bioni Garcia (PQ),³ Vitor Francisco Ferreira (PQ).¹

AlcioneCarvalho1570@gmail.com; vitorferreira@id.uff.br

¹Departamento de Tecnologia Farmacêutica, FF-UFF; ²Departamento de Química, IQ-UFF; ³Plataforma de Bioensaios de Malária e Leishmaniose, PBML-FIOCRUZ

Palavras Chave: Triazole-quinoline, Hybrids, Chloroquinoline moiety, Antiplasmodium, Synthesis, Medicinal chemistry.

Highlights

Triazole-7-chloroquinoline hybrids have been synthesized through a well-established synthetic methodology. The preliminary results showed good activity against W2 strain of *P. falciparum*.

Introduction

Malaria is one of the most devastating and common infectious disease throughout the world. *P. falciparum* is responsible for nearly one million deaths every year.¹ Quinoline compounds have long been used in clinical treatment of malaria and remained the mainstays of chemotherapy against malaria. The emergence of *P. falciparum* strains resistant to almost all antimalarials prompted urgency of alternative drugs to chemotherapy of malaria.¹ Our research group has achieved promising results through building a single molecular framework containing quinoline and triazole rings by molecular hybridization strategy of medicinal chemistry.^{2,3} Continuing our study, we present this work the synthesis of novel triazole-7-chloroquinoline derivatives (**4-11**) and their antiplasmodial evaluation (Figure 1).

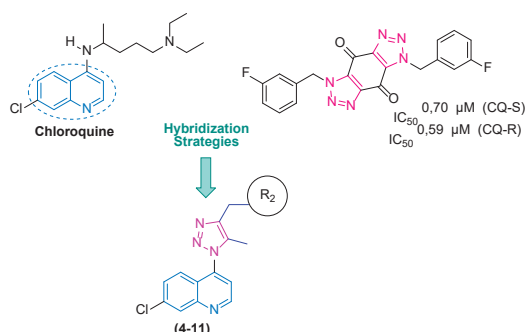
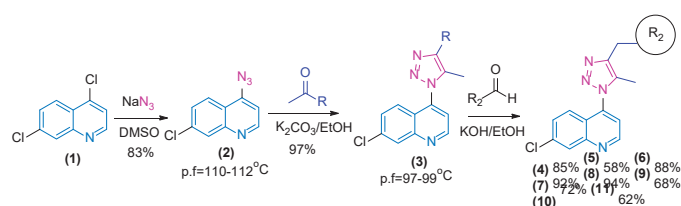


Figure 1. Rational approach to the design of novel triazole-7-chloroquinoline derivatives (**4-11**).

Results and Discussion

The total synthesis of the novel triazole-7-chloroquinoline derivatives (**4-11**), is describing in the Scheme 1.



Scheme 1. Synthetic route of new derivatives (**4-11**).

New triazole-7-chloroquinoline hybrids are being assayed against the W2 - chloroquine-resistant of *P. falciparum* clone. Four of the five compounds already evaluated exhibited IC₅₀ values ranging from 6.3 to 69 μm. Also, cytotoxicity in human blood cells assay is in progress.

Conclusions

A novel series of triazole-quinoline were obtained in excellent yield. Preliminary antiplasmodial activity of these compounds showed good activity against W2 strain of *P. falciparum*. This study can aid in the planning of new hits compounds for malaria disease.

Acknowledgements

PIBIC-CNPQ; CAPES; FAPERJ

1-WHO Global technical strategy for malaria 2016–2030; 2-Chuck, D.C *et al* 2013 *Malaria Journal*, **12**, 234; 3-Graciano, I.A *et al* 2022 *Medicinal Chemistry*, **18**, 521.

Synthesis and biological evaluation of hybrid inhibitors for the treatment of hematologic malignancies

Vinicius A. M. de Souza (IC)¹, Karoline B. Waitman (PG)¹, Mônica F.Z.J. Toledo (TC)¹, Maurício T. Tavares (PQ)¹, Roberto Parise-Filho (PQ)¹.

vini.albu@usp.br; roberto.parise@usp.br

¹Laboratory of Design and Synthesis of Bioactive Substances (LAPCESSB), Department of Pharmacy, Faculty of Pharmaceutical Sciences, University of São Paulo (USP)

Palavras Chave: molecular hybridization, histone deacetylase, phosphoinositide 3-kinase, dual inhibitors, hybrids, cancer.

Highlights

A hybrid PI3K/HDAC6 inhibitor has been designed from two selective molecules for treating hematologic cancer. One final molecule was synthesized.

Abstract

Cancer is a disease characterized by the disordered and accelerated replication of abnormal and dedifferentiated cells within which a vast number of genes are mutated. PI3K δ (phosphoinositide 3-kinase delta) mutations are widespread in leukocytic lineages and so its inhibition is being increasingly explored although the apparent resistance to monotherapy.¹ To overcome this situation, hybrid molecules, especially between PI3K and HDAC6 (histone deacetylase 6) inhibitors, have been shown to be an effective alternative.¹ Therefore, this work aims to synthesize hybrid PI3K/HDAC6 molecules based on the pharmacophores of selective inhibitors of each chosen target, idelalisib (PI3K δ inhibitor) and nexturastat A (HDAC6 inhibitor), as shown in figure 1.

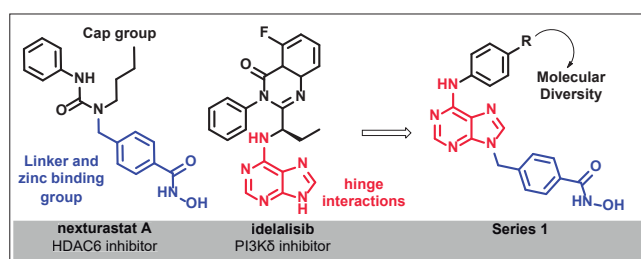
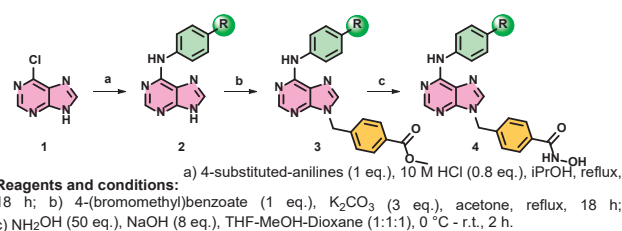


Figure 1: Design of the hybrid inhibitor.

As shown in **Scheme 1**, the hybrid compounds of series 1 were prepared from the reaction of 6-chloropurine (**1**) with 4-substituted-anilines, through nucleophilic aromatic substitution (S_NAr), thus forming the aniline-purine intermediates (**2**). Compounds **2** were reacted with methyl 4-(bromomethyl)benzoate via bimolecular nucleophilic substitution reaction (S_N2), to form benzoate methyl ester intermediates (**3**).

Finally, intermediates (**3**) were reacted with hydroxylamine (NH₂OH) to yield the corresponding hydroxamates (**4**).



Scheme 1. Synthetic route for hybrid compounds.

Final compound **4d**, prepared by the reaction with a 4-bromoaniline, was obtained as a white solid with 51% global yield, as well as its intermediates **2d** (greenish white solid, 81% yield) and **3d** (slightly greene solid, 81% yield) with the route showing good viability. All the compounds were further characterized by ¹H and ¹³C NMR and their high purity will be verified by HPLC soon. In the end, we expect to have ten different final products. After their complete characterization and purity evaluation, the compounds will have their biological activity assessed by cytotoxicity and mechanistic assays in hematological cancer cell lineages and solid tumors, such as Jurkat cell line (T-cell acute lymphoblastic leukemia), Namalwa cell line (B-cell acute lymphoblastic leukemia), MCF-7 (breast cancer cell line) and HCT 116 (colon cancer cell line).

1. Waitman, K.; Parise-Filho, R. *Future Medicinal Chemistry*, **2022**, 14(10), 745–766.

Acknowledgments

The authors are grateful to the Faculty of Pharmaceutical Sciences of University of São Paulo, which allowed the development of this work, and fellowship #2022/12468-6, grant #2021/08260-8, from São Paulo Research Foundation (FAPESP).

Synthesis and Biological Evaluation of New Nitroimidazole-Chalcone Derivatives, Designed as Trypanocide Drug Candidates

Mayara S.S. do Nascimento (PG),^{1,2} Talita C.D. Bernardes (IC),³ Luan C. Martins (PQ),³ Rafaela S. Ferreira (PQ),³ Iara A. Cardoso (PQ),⁴ Maria C. Nonato (PQ),⁴ Samir A. Carvalho (PQ),⁵ Edson F. da Silva* (PQ),⁵ Carlos A.M. Fraga* (PQ)^{1,2}.

mayarasalles6@gmail.com; cmfraga@ccsdecania.ufrj.br; edson.ferreira@fiocruz.br

¹ Programa de Pós-Graduação em Farmacologia e Química Medicinal, Instituto de Ciências Biomédicas, Universidade Federal do Rio de Janeiro, Rio de Janeiro, RJ, Brazil; ² Laboratório de Avaliação e Síntese de Substâncias Bioativas (LASSBio), Instituto de Ciências Biomédicas, Universidade Federal do Rio de Janeiro, Rio de Janeiro, RJ, Brazil; ³ Departamento de Bioquímica e Imunologia, Instituto de Ciências Biológicas, Universidade Federal de Minas Gerais, MG, Brazil; ⁴ Laboratório de Cristalografia de Proteínas, Faculdade de Ciências Farmacêuticas de Ribeirão Preto – USP; ⁵ Instituto de Tecnologia em Fármacos e Farmanguinhos, Fundação Oswaldo Cruz, 21041-250 Rio de Janeiro, RJ, Brazil.

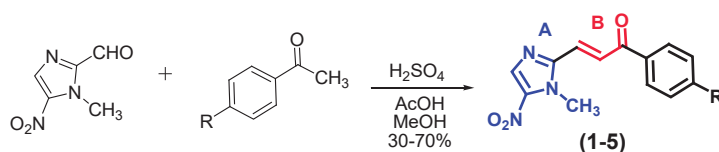
Keywords: *Trypanosoma Cruzi*; Chagas Disease; Nitroimidazole chalcones; Nitroreductase Inhibitors.

Highlights

Five new nitroimidazole-chalcone derivatives were synthesized and evaluated. Nitroimidazole-chalcone derivatives showed to be more efficient substrates of *Tc*-nitro-reductase I than benzimidazole used as standard. Nitroimidazole-chalcone derivatives showed to present moderate activity as cruzain inhibitors.

Abstract

Chagas disease (CD) is a parasitic disease of great relevance caused by the hemoflagellate protozoan *Trypanosoma cruzi*.¹ CD therapy was developed in 1970, and is restricted to two drugs: nifurtimox (Nfx) and benzimidazole (Bzn), which presented limited safety and efficacy in the chronic phase of disease. Therefore, this work describes the synthesis and biological evaluation of five new nitroimidazole-chalcone hybrids (1-5) designed to combine the capability to be bioactivated by type 1 nitro-reductase (TcNTR), due to the presence of nitroimidazole subunit A, furnishing reactive toxic species, and also as cruzain inhibitors, due to the presence of electrophilic α,β -unsaturated ketone subunit B. Target compounds were synthesized in good yields through acid catalyzed condensation substituted acetophenones with 1-methyl-2-nitroimidazolyl-5-carbaldehyde. The obtained results indicated that bromo- and methoxy-substituted derivatives (4) and (5) presented the best profile as TcNTR substrates with a relative metabolism 3.62 and 2.46 times higher than Bzn, which is important to produce nitro-reduced species that could bind to *T. cruzi* macromolecules. Moreover, derivatives (3) and (2) were able to inhibit cruzain activity in 65 and 50%, respectively.



Composto	R	Relative potential as substrate of <i>Tc</i> -nitroreductase I (50 μ M)	% inhibition of cruzain at 100 μ M with pre-incubation	% inhibition of cruzain at 100 μ M without pre-incubation
1	H	1.46	47 \pm 8	ND
2	NO ₂	1.77	50 \pm 10	ND
3	F	ND	65 \pm 7	14 \pm 4
4	Br	3.62	34 \pm 7	ND
5	OCH ₃	2.46	40 \pm 9	ND
Bzn	----	1	----	----
E-64	----	----	93 \pm 1	----

¹Ferreira, W. S; *et al. Bioorg. Med. Chem.*, 2008, **16**, 2984.

²Bock, M. *et al. Bol. Chil. Parasitol.*, 1969, **24**, p. 13.

Acknowledgments

Farmanguinhos, FIOCRUZ, FAPERJ, CNPq and CAPES.

Área: MED

(Inserir a sigla da seção científica para qual o resumo será submetido. Ex: ORG, BEA, CAT)

Synthesis and Evaluation of New CBD Analogues with Antimicrobial Activity

Graziella dos Reis Rosa Franco (PG)^{1*}, Isabela Marie Fernandes (IC)², Vanessa Silva Gontijo (PQ)¹, Luke Wooley (PG)³, Scott Smid (PQ)³, Claudio V. Junior (PQ)¹.**grazireisfranco@yahoo.com.br; grazireisfranco@yahoo.com.br**¹Laboratory of Research in Medicinal Chemistry – PeQuiM, Institute of Chemistry, Federal University of Alfenas (UNIFAL, Brazil); ²Faculty of Pharmacy, UNIFAL; Faculty of Health & Medical Sciences, University of Adelaide (Australia).

Palavras Chave: Cannabidiol, Antimicrobial activity, antibacterial activity, cannabidiol analogues.

Highlights

The increased bacterial resistance to antimicrobials is a global concern

Resistant Gram-positive bacteria still cause substantial mortality worldwide

The structure of CBD represents a prototypical scaffold for the development of new drugs

Resumo/Abstract

Cannabidiol (CBD) is the main non-psychoactive compound in *Cannabis sativa* and its natural isomer is the R(-)-CBD ¹. The first antimicrobial activity of CBD was published in 1973, but only in 2008 new results were published. The new studies of CBD revealed its activity against both Gram-positive bacteria, including resistant strains (MRSA) and Gram-negative strains (*N. gonorrhoeae*) ¹, in addition to safety and low induced resistance^{1,2}. The major importance of these studies was related to the identification of a new class of highly potent antimicrobial compounds, with high natural abundance or easy synthetic access. In this work, we report the antimicrobial results of 42 new synthetic CBD-like compounds. An initial screening was carried out against the ESKAPE pathogens, leading to the identification of compounds **PQM-247**, **PQM-290**, **PQM-291**, **PQM-302**, and **PQM-303** as the most active against Gram-positive bacteria, but not towards Gram-negative ones. The evaluation of Minimal Inhibitory Concentration (MIC) and Minimal Bactericidal Concentration (MBC) against nine Gram-positive bacteria strains - MRSA (USA300, CI-Rudinik, and CI-Seffie), *E. faecium* (19434, CI1, and CI2), and *S. epidermidis* (12228, 14990, and 35984) – confirmed the bioactivity of the five initially identified promising CBD analogues, and highlighted **PQM-291** (MIC/MBC= 32 µg/mL for *E. faecium* – CI1), **PQM-302** (MIC/MBC= 32 µg/mL for both MRSA-USA300 and *E. faecium* – CI1), and **PQM-303** (MIC/MBC= 32 µg/mL for both MRSA-USA300 and *S. epidermidis*) as the most potent and promising analogues, in comparison to CBD and daptomycin used as positive controls.

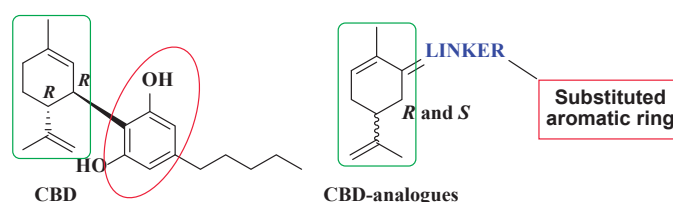


Figure 1- Structural design for the CBD-based analogues

- [1] Blaskovich, M. A. T.; et al. The Antimicrobial Potential of Cannabidiol. *Commun. Biol.* 2021 41 **2021**, 4 (1), 1–18.
 [2] Wu, Q.; Guo, M.; Zou, L.; Wang, Q.; Xia, Y. 8,9-Dihydrocannabidiol, an Alternative of Cannabidiol, Its Preparation, Antibacterial and Antioxidant Ability. *Molecules* **2023**, 28 (1).

Agradecimentos/Acknowledgments



Synthesis and *in-silico* studies of a new hydroxypyridinone derivative designed as HDAC inhibitor presenting a new zinc binding group

Alef D.S. Lima (PG),^{1,2*} Pedro S.M. Pinheiro (PQ),^{2,3} Carlos A.M. Fraga (PQ)^{1,2,3}

aleflimaeq@gmail.com; aleflimaeq@gmail.com

¹Programa de Pós-graduação em Química, Instituto de Química, UFRJ; ²Laboratório de Avaliação e Síntese de Substâncias Bioativas (LASSBio®), Instituto de Ciências Biomédicas, UFRJ; ³Instituto Nacional de Ciência e Tecnologia de Fármacos e Medicamentos (INCT-INOVAR), UFRJ.

Keywords: Medicinal Chemistry, Epigenetic, HDAC, HDAC Inhibition, Hydroxypyridinone.

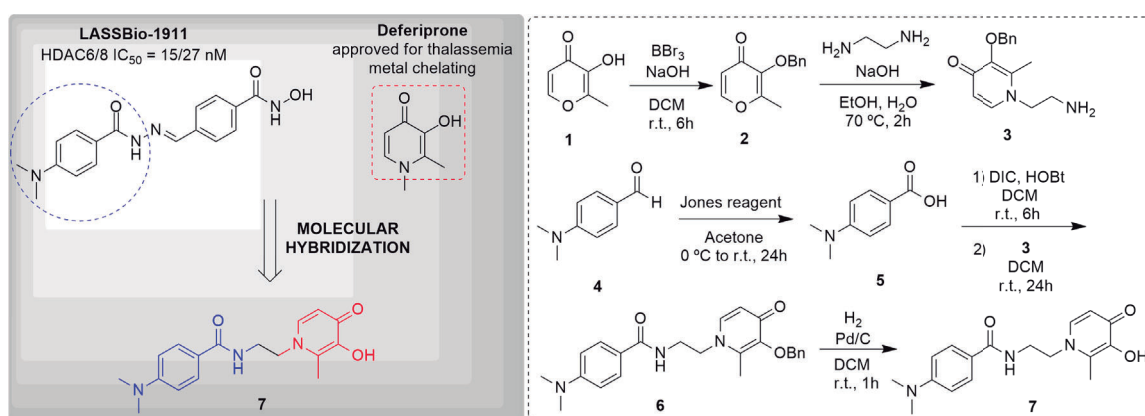
Highlights

HDACs overexpression can develop various diseases including cancer. New zinc binding groups are desired once hydroxamic acids can cause severe side effects due to its potential mutagenicity.

Resumo/Abstract

Histone deacetylases (HDACs) have become a well-explored validated target in recent years. HDAC catalyzes deacetylation of histones and several non-histonic proteins. Deregulation of deacetylation levels of these proteins can lead to the development of various diseases, such as cancer and neurodegenerative diseases. Hydroxamic acid is the most common zinc binding group (ZBG) introduced in HDAC inhibitors, however it can cause mutagenicity and toxicity. LASSBio-1911 is a potent HDAC6/8 inhibitor ($IC_{50} = 15/27$ nM) previously identified by our group, which presents antiproliferative effects against different cancer cell lines (Rodrigues *et al.*, 2016). In this context, this work presents a new compound (**7**) designed as HDAC inhibitor based on molecular hybridization of LASSBio-1911 and Deferiprone, a well-known metal ion chelator with hydroxypyridinone scaffold, introducing a possible new ZBG (Figure 1). Compound **7** was obtained following the steps shown in Figure 1 with moderate yields and characterized by NMR ¹H and ¹³C, while its purity was determined by HPLC. Molecular docking studies show that compound **7** can perform the key interactions with HDAC6 active site, specially chelating the zinc atom bidentally. PhysChem and ADME properties were predicted by Percepta software and compound **7** exhibits a good drug-like profile without Lipinski's rule violations. *In-vitro* studies will be performed to evaluate HDAC inhibition activity of compound **7**.

Figure 1 – Rational design and synthetic route to obtain compound 7.



RODRIGUES, Daniel A. et al. Design, synthesis, and pharmacological evaluation of novel N-acylhydrazone derivatives as potent histone deacetylase 6/8 dual inhibitors. *Journal of Medicinal Chemistry*, v. 59, n. 2, p. 655-670, 2016.

Agradecimentos/Acknowledgments



Synthesis of 1,4-naphthoquinone ester derivatives as potential anti oral cancer agents

Raquel Nery (IC),¹ Robson Corrêa (IC),¹ Ryann S. Nascimento (IC),¹ Gustavo Senra G. de Carvalho (PQ),¹ Daniel Tadeu Gonzaga (PQ),² Vítor Francisco Ferreira (PQ),¹ Fernando de Carvalho da Silva (PQ),¹

raquelnery@id.uff.br

¹Departamento de Química Orgânica, Instituto de Química, Universidade Federal Fluminense, Niterói-RJ, 24210-141, Brazil

²Faculdade de Ciências Biológicas e Saúde, Universidade do Estado do Rio de Janeiro, Rio de Janeiro-RJ, 23070-200, Brazil

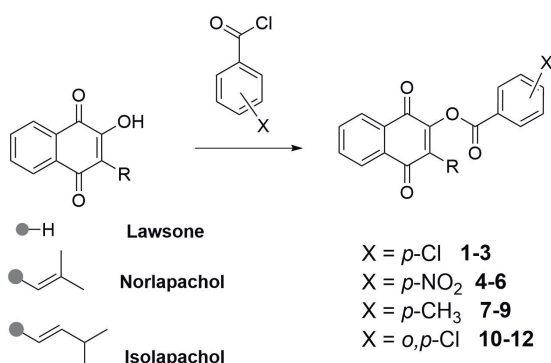
Palavras-Chave: Naphthoquinone, cancer, heterocycle.

Highlights

1,4-Naphthoquinones are a class of compounds with a wide spectrum of pharmacological applications, including activity against certain types of cancer. However, targeted structural modifications have the potential of increasing the effectivity and selectivity associated with such compounds, while also leading to lower toxicity profiles. This work describes our efforts into the development of a straightforward approach toward lawsone-derived 1,4-naphthoquinone aryl esters.

Resumo/Abstract

Several synthetic and natural low molecular weight naphthoquinones find applications in diverse scientific and technological fields. These naphthoquinones also have potential clinical utility in the treatment of various diseases.¹ Naphthoquinones bearing extra aromatic portions have been reported to display bioactivity against various microorganisms and cancer cell lines due to their ability to accept one or two electrons in their redox cycle, generating reactive oxygen species (ROS) *in situ*.² The participation of quinones in the phenomenon of apoptosis is currently regarded as an interdisciplinary frontier research area in medicinal chemistry, and the delineation of rational strategies for the synthesis of new substances to combat neoplasms, mainly those related to cancer, is among the most prominent themes in the literature, especially as anti-oral cancer.⁴ Several research groups are trying to improve the antitumor effects of naphthoquinones by performing chemical modifications. In this context the objective of this work was to synthesize lawsone-derive benzoyl esters employing a simple synthetic methodology, as showed in Scheme 1.⁵ This modification, widely used in medicinal chemistry as prodrug is the synthesis of ester analogues, since they favor the bioavailability providing a classic strategy for masking polar alcohol and carboxylic acid functionalities through first pass effect, improving cell permeability, and due to their simplicity and scalability.⁶ Thus, Ensuing the complete characterization of all the newly synthesized compounds, their *in vitro* evaluation against oral cancer cells is ongoing.



References

- 1 Current Organic Synthesis 2016, 13, 334-371.
- 2 Journal of the American Chemical Society 2011, 133, 11557-11571.
- 3 Current Pharmaceutical Design 2016, 22, 5899-5914.
- 4 Molecules, 2022, 28, 309.
- 5 Tetrahedron 2014, 70, 3266-3270.
- 6 Current Drug Metabolism, 2003, 4, 461-485.

Scheme 1. Synthetic strategy toward novel 1,4-naphthoquinone esters.

Agradecimentos/Acknowledgments



Synthesis of New Hybrid 1,2,3-Triazole Compounds in Combating COVID-19.

Rafael O. Costa (IC),¹ Pedro H. O. Borges (PG),¹ Gabriel A. S. Aquino (PG),¹ Floriano P. S. Junior (PQ),² Sabrina B. Ferreira (PQ).^{1*}

rafaeloc94@ufrj.br; sabrinab@iq.ufrj.br

¹Universidade Federal do Rio de Janeiro, Instituto de Química, Laboratório de Síntese Orgânica e Prospecção Biológica, Rio de Janeiro, Brasil; ²Instituto Oswaldo Cruz, Laboratório de Bioquímica Experimental e Computacional de Fármacos, FIOCRUZ, Rio de Janeiro, Brasil.

Palavras-chave: COVID-19, SARS-CoV-2, Heterocycle, Triazol, Ribofuranose, RNA polymerase.

Highlights

Synthesis of new molecules based on the antiviral drug Favipiravir that will contain nitrogenated heterocycles and 1,2,3-triazoles, with possible applicability in the treatment of COVID-19.

Abstract

SARS-CoV-2 is the biological agent responsible for COVID-19, which has had a catastrophic impact on world demography, causing almost 700,000 deaths in Brazil.^{1,2} The search for drugs presents itself as a way to, not only to help, but also to offer alternatives to the treatment of the disease.³ The purpose of the work is to develop the synthesis of the new molecules with structures based on the antiviral drug Favipiravir that, by means of bioisosterism and molecular hybridization, will contain, in their molecular skeleton, such as nitrogenated heterocycles, nucleoside analogues, and 1,2,3-triazoles, with possible applicability in the treatment of Covid-19. Once the family of compounds is obtained, it will be sent to biological testing. **Figure 1** shows the structure of the final compound we aim to obtain. The synthesis started with 2-aminopyrazine (**1**), which was protected with an acetyl group, followed by a sequence of electrophilic substitution and deprotection obtaining the aryl azide intermediate (**2**). The next steps consist in a Huisgen 1,3-dipolar cycloaddition with different commercial aryl alkynes to give the 1,2,3-triazole intermediate (**3**). This intermediate will be reacted with the protected ribose, which is going to be deprotected to obtain the final products (**4**). Currently, the aryl azide intermediate and the protected ribose are synthesized and the triazole is in progress. In addition, the results obtained so far are satisfactory, with the intermediates being analyzed with ¹H NMR, ¹³C NMR, and infrared.

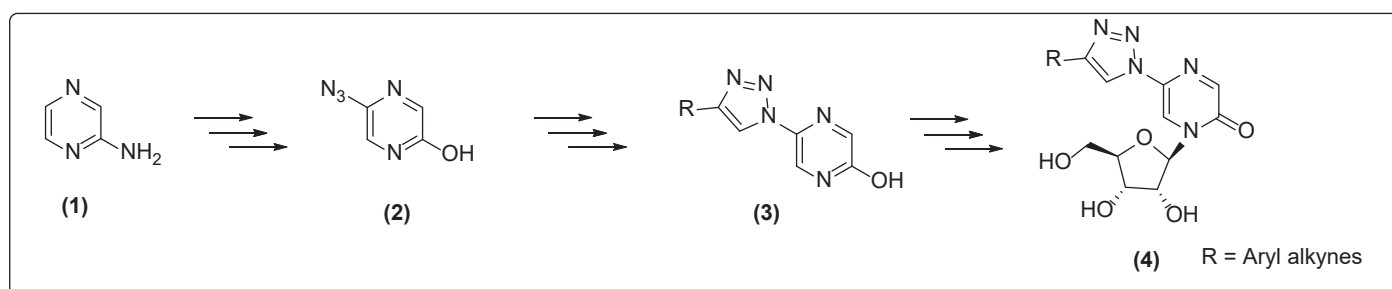


Figure 1: Synthetic pathway to obtain the final products.

1. Chen. Y; Liu. Q; Guo. D. J. *J. Med. Virol.* 2020, 92, 418-423.
2. World Health Organization. WHO Coronavirus (COVID-19) Dashboard, 2023. Disponível em: <https://covid19.who.int>. Acesso em 13/03/2023.
3. GARCIA-BELTRAN, Wilfredo F. et al. v. 184, n. 9, p. 2372-2383, 2021.; SHAMAN, Jeffrey; GALANTI, Marta. *Science*, v. 370, n. 6516, p. 527-529, 2020.

Acknowledgments

I would like to thank CNPq, FAPERJ, LABRMN, and FIOCRUZ for making this research possible.

Synthesis, Photodegradation, and Biological Evaluation of New Photodegradable Antimicrobial Agents

Gabriel A. S. Aquino (PG)¹, Sabrina B. Ferreira (PQ)¹, Magne O. Sydnes (PQ)^{2*}

gabrielalves.aq@gmail.com; magne.o.sydnes@uis.no

¹Universidade Federal do Rio de Janeiro, Instituto de Química, Laboratório de Síntese Orgânica e Prospecção Biológica, Rio de Janeiro, Brasil; ²Department of Chemistry, Bioscience and Environmental Engineering, Faculty of Science and Technology, University of Stavanger, UiS.

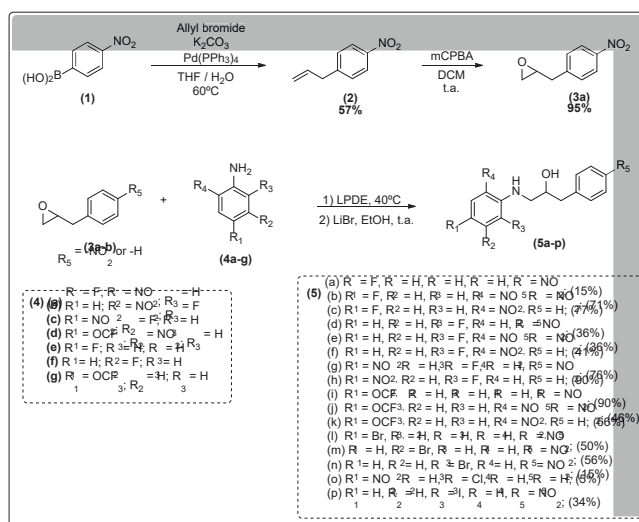
Keywords: Antibiotics, Photodegradation, synthesis

Highlights

This work describes the synthesis of new molecules with applicability as antimicrobial agents and easy degradation properties to prevent accumulation in the environment and multi-drug resistance.

Abstract

Multi-drug resistant (MDR) bacteria are currently a severe public-health problem due to the extensive and indiscriminate overuse of antimicrobial agents. MDR bacteria lead to a problematic situation, where the treatments for infectious diseases are becoming less effective and increasing medical costs and mortality.¹ One of the reasons for the growth of MDR bacteria cases is the high levels of antibiotic residues in bodies of water, leading to a demand to develop new antimicrobial agents, which scaffolds could degrade under ambient light, preventing accumulation in the environment.^{2,3} The present work describes the synthesis, characterization, photodegradation, and biological evaluation of 16 new compounds with potential biological application as photodegradable antimicrobial agents based on our previously reported scaffold.^{4,5}



1. WHO, World Health Organization; Antibiotic resistance; <https://www.who.int/news-room/fact-sheets/detail/antibiotic-resistance> (accessed August 8, 2022).
2. E. D. Brown and G. D. Wright, *Nature* **2016**, *529*, 336-343.
3. M. C. Danner, A. Robertson, V. Behrends and J. Reiss, *Sci. Total Environ.* **2019**, *664*, 793-804.
4. Eikemo, V.; Sydnes, L. K.; Sydnes, M. O. *RSC Adv.* **2021**, *11*, 32339-32345.
5. Eikemo, V.; Holmelid, B.; Sydnes, L. K.; Sydnes, M. O. *J. Org. Chem.* **2022**, *87*, 8034-8047.

Acknowledgments

G.A.S.A. would like to thank CNPq for a PhD fellowship and the Diku funded NorBra project for a six-month scholarship enabling a research stay at the University of Stavanger, Norway. Fridtjof Nansens Fond til Videnskabens Fremme is acknowledged for funding chemicals.

Targeting pancreatic cancer cells by antineoplastic activity of the multikinase inhibitor AD80

Keli Lima (PG),^{1,2} Lívia Bassani Lins de Miranda (PG),² Anali Del Milagro Bernabe Garnique (PQ),³ Bruna Oliveira de Almeida (PG),² Mariane Cristina do Nascimento (PG),^{1,2} Guilherme Augusto Sousa Alcântara (PQ),² Glauca Maria Machado-Santelli (PQ),³ Eduardo Magalhães Rego (PQ),¹ João Agostinho Machado-Neto (PQ).²

jamachadoneto@usp.br

¹Laboratory of Medical Investigation in Pathogenesis and Targeted Therapy in Onco-Immuno-Hematology (LIM-31), Department of Internal Medicine, Hematology Division, Faculdade de Medicina, University of São Paulo, São Paulo, Brazil; ²Department of Pharmacology, Institute of Biomedical Sciences, University of São Paulo, São Paulo, Brazil; ³Department of Cell and Developmental Biology, Institute of Biomedical Sciences, University of São Paulo, São Paulo, Brazil

Palavras Chave: Pancreatic cancer, AD80, Multikinase inhibitor, Autophagy, Aurora kinases.

Highlights

Pancreatic cancer is one of the most lethal human cancers and needs new therapeutic options. AD80 has antineoplastic effects by induction of mitotic aberrations, autophagy, and apoptosis in pancreatic cancer cells.

Abstract

Introduction: Pancreatic cancer is one of the most lethal human neoplasms and its therapeutic repertoire remains limited. AD80 is a multikinase inhibitor that inhibits S6K as well as RET, RAF, and SRC and displays antineoplastic effects in hematological and solid tumors. **Aims:** To uncover cellular and molecular effects of AD80 in pancreatic cancer cells. **Methods:** MIA PaCa-2, PANC-1, and AsPC-1 pancreatic cancer cell lines were used. Cell viability was evaluated by MTT assay, clonogenicity by colony formation assay, DNA content analysis by propidium iodide and flow cytometry, morphology by immunofluorescence (IF), formation of acidic vesicular organelles (AVO) by acridine orange and fluorescence microscopy, and cell signaling by PCR array and Western blot. Spheroid was also used to access the effects of the drug in 3D models. ANOVA and Bonferroni post-test were used. A p -value < 0.05 was considered significant. **Results:** In pancreatic cancer cells, AD80 reduced cell viability in a concentration- and time-dependent manner (all $p < 0.05$). AD80 also strongly decreased clonogenicity (all $p < 0.05$). DNA content analysis indicated an increase in polyploidy cells (all $p < 0.05$), which was confirmed by IF. In the molecular scenario, AD80 reduced S6RP and histone H3 phosphorylation and induced γ H2AX and PARP1 cleavage. AURKA phosphorylation and expression were markedly decreased by the drug. In PANC-1 cells, AD80 strongly induced autophagic flux. A total of 32 out of 84 autophagy-related genes were modulated by AD80 and it was associated with vacuole organization, macroautophagy, response to starvation, cellular response to nitrogen levels, and cellular response to extracellular stimulus (all FDR $q < 0.05$). In 3D pancreatic cancer models, AD80 also effectively reduced cell viability (all $p < 0.05$). **Conclusion:** Our exploratory study establishes novel targets underlying the antineoplastic activity of the drug and provides insights into the development of therapeutic strategies for this disease.

Agradecimentos/Acknowledgments

K.L., L.B.L.M., and B.O.A. received a fellowship from FAPESP (grants #2020/12842-0, #2022/03316-8, and #2019/25421-5). This study was supported by grants #2019/23864-7 and #2021/11606-3 from the São Paulo Research Foundation (FAPESP). This study was financed in part by the Coordenação de Aperfeiçoamento de Pessoal de Nível Superior, Brasil (CAPES), Finance Code 001.

Ugi four-component reactions (UGI-4CR) in synthesis of novel potential inhibitors of SARS-CoV-2 main protease (M^{pro})

Gustavo Barbosa (PG)*¹, Guilherme Nuñez (PG)¹, Luciano Caseli (PQ)¹, Martin Würtele (PQ)², Diogo Oliveira-Silva (PQ)¹.

gustavo.barbosa@unifesp.br, guilherme.nunez@unifesp.br, lcaseli@unifesp.br, martin.wurtele@unifesp.br, dosilva@unifesp.br

¹Intituto de Ciências Ambientais, Químicas e Farmacêuticas, UNIFESP, ²Intituto de Ciência e Tecnologia, UNIFESP.

Keywords: UGI-4CR, multicomponent reaction, SARS-CoV-2, biological activity.

Highlights

The revisited UGI-4CR as synthetic methodology to afford new potential inhibitors of SARS-CoV-2 M^{pro}. The isocyanide *in situ* preparation was the key-event and an 18 peptoid library was produced.

Resumo/Abstract

UGI-4CR has been explored in many fields by its synthetic versatility. This protocol is well known to lead to pseudopeptides, a class of substances with important biological activities and reported as inhibitors of SARS-CoV-2 M^{pro} as well [1]. Therefore, the design of new compounds using UGI multicomponent reaction has been explored last decades aiming increase biological activity opportunities [2]. Figure 1 shows the synthetic approach of this work, where the *in situ* preparation of isocyanide is the key step due to the structural range limitation of commercially available substances, its stability and cost as well. Furthermore, by employing this procedure a variety of substituents in the isonitrile moiety can be provided with no purification requirements.

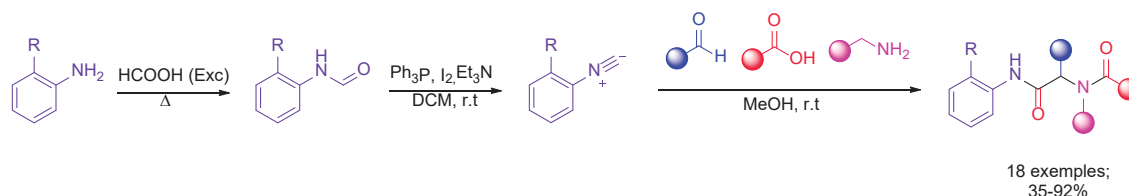


Figure 1. Synthetic approach to provide potential inhibitors of SARS-CoV-2 M^{pro}

The compounds library was prepared in two stages: 1 - by using an aleatory range of starting materials to afford the preliminary set of inhibition assay results; and 2 - by applying precursors able to increase the inhibition rates compared to the first ones. Two criteria were observed to guide the molecular modifications: i- to increase hydrogen bond donors (HBD), acceptors (HBA) and intermolecular interactions as well; and ii- to better fit in Lipinsky rules [3]. All these modifications above mentioned were guided by inhibition factors observed on previous assays, associated to the study of Langmuir's monolayers interference, which was used as a model platform to provide insights about the permeation mechanism of developed compounds through the membrane of a virus infected cell (Figure 2).

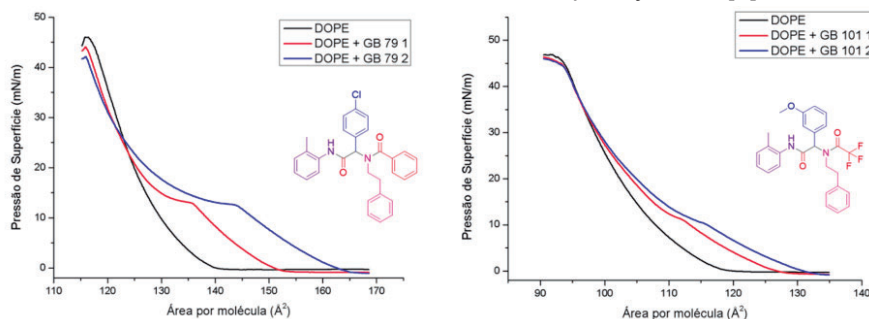


Figure 2. Isotherm profile of two yielded compounds.

[1] *J Med Chem.* 65, 4, 2848-65, 2022. [2] *Chem. Rev.* 112, 6, 3083-35, 2012. [3] *Adv Drug Deliv Rev.* 46, 3-26, 2001.

Agradecimentos/Acknowledgments

FAPESP, CAPES, CNPq and UNIFESP.

ORG

Química Orgânica

46^a Reunião
Anual da **SBQ**

28 a 31 de Maio de 2023

Águas de Lindóia · SP
Hotel Monte Real

4-acyl-1,2,3-triazole Direct Synthesis: A new way to easily obtain antileishmanial hydroxy-1,2,3-triazoles

David C. Zeitune (IC)¹, Marcelo Folhadella M. F. Azevedo (PG)¹, Camilla D. Buarque (PQ)^{1*}.

davidchafi@gmail.com; camilla-buarque@puc-rio.br

¹Departamento de Química, PUC-Rio

Palavras Chave: 1,2,3-triazoles, 1,3-dipolar cycloaddition, solvent-free, one-pot, *Leishmania amazonensis*

Highlights

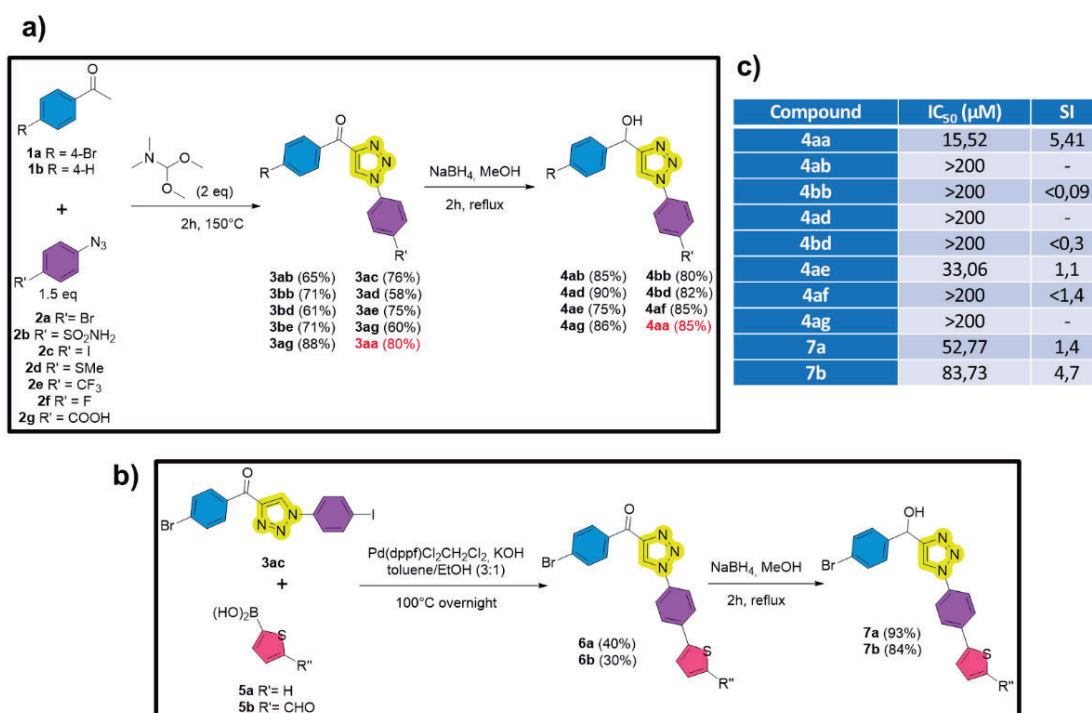
New 4-acyl-1,2,3-triazole were obtained directly from acetophenones in a green-click synthesis

New bioactive 4-hydroxy-1,2,3-triazoles were obtained from 4-acyl-1,2,3-triazole

Selected compounds were tested against *Leishmania amazonensis*.

Resumo/Abstract

4-acyl-1,2,3-triazoles are an important molecular structure with broad applicability, mainly as a platform for bioactive 4-hydroxy-1,2,3-triazoles. Our research group has a remarkable track record in developing new compounds for the treatment of *Leishmania amazonensis*, and compound **4aa** has proven to be our best candidate, effective against both forms of the parasite.^{1,2} In this study, new hydroxy-1,2,3-triazoles (**4**) were obtained in 92-80% yield from 4-acyl-1,2,3-triazoles **3** (obtained directly from acetophenones **1** and aryl azides **2** in a metal and solvent-free *one-pot* method). Type **7** compounds were obtained after triazole **3ac** and **thiophene-based** boronic acids (**5a,b**) Suzuki cross-coupling followed by carbonyl reduction. These selected compounds were tested against promastigote *Leishmania amazonensis* and three promising compounds were identified to be tested in amastigote form.



Scheme 1: (a) hidroxi-1,2,3-triazole synthesis; (b) thiophane-triazole hybrids achievement; (c) antileishmanial activities.

- (1) da Silva, V.; Silva, R.; et. al. *J. Braz. Chem. Soc.* **2020**.
 (2) Almeida-Souza, et. al. *J. Med. Chem.* **2021**, *64* (17), 12691–12704.

Agradecimentos/Acknowledgments

The authors would like to thank CAPES, CNPq and FAPERJ for the financial support. Also, we link to thank PUC-Rio and CALPH for the structure that made the work possible.

A pilot study to produce a certified reference material for Forensic Chemistry

Thais G. Silva (PG),^{1*} Rodrigo O. M. A. de Souza (PQ),² Bruno C. Garrido (PQ),³ Fernanda G. Finelli (PQ)^{1*}

*thaisgoulart@ufrj.br; finelli@ippn.ufrj.br

¹Universidade Federal do Rio de Janeiro, Instituto de Pesquisa de Produtos Naturais, Centro de Ciências da Saúde, Cidade Universitária, RJ; ²Universidade Federal do Rio de Janeiro, Instituto de Química, Centro de Tecnologia, Cidade Universitária; ³Divisão de Metrologia Química e Térmica, Instituto Nacional de Metrologia, Qualidade e Tecnologia

Keywords: CRM, Amphetamines, Flow Chemistry, Wacker-Tsuji oxidation, Reductive amination.

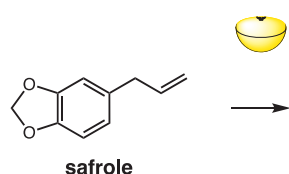
Highlights

We report an efficient synthesis of MDA under batch and continuous-flow conditions and the certification process to produce a CRM and supply an urgent demand from the Instituto Nacional de Criminalística/PF-BR.

Abstract

The use of Certified Reference Materials (CRMs) provides precision and traceability to analytical procedures, making measurements and identification more reliable. Metrological traceability is the only path to achieve comparability between results in different laboratories, which is an essential characteristic of reliable measurements, especially in forensic analyses. Among the investigation targets of the Federal Police, amphetamines are one of the main substances sold on the illegal market as drugs of abuse. However, this class of CRMs is extremely expensive, not produced by the Brazilian industry, and not readily available for importation into Brazil.^{1,2}

In this pilot study, we were able to efficiently synthesize MDA from safrole in two steps after a Wacker-Tsuji oxidation and reductive amination under batch and continuous-flow conditions.^{3,4} After optimization, the desired amphetamine hydrochloride was obtained in 38% overall yield in a process of 40 hours for the two reaction steps under batch conditions. Under continuous-flow conditions, MDA was obtained in 60% overall yield after 65 minutes in a higher selectivity process.



Scheme 1. Synthesis and certification of MDA for Forensic Chemistry

To supply an urgent demand from Instituto Nacional de Criminalística (INC/PF-BR), the MDA produced in a small batch was submitted to a CRM certification process. The material was split into 62 vials containing 10 mg of MDA and analyzed to accomplish the qualitative and quantitative characterization, and the homogeneity, short-term stability, and long-term stability tests. These studies were carried out by HPLC-DAD, HPLC-MS/MS, HRMS, and qNMR analyses. As a result of the CRM certification process for MDA, 25 vials are available for distribution. The certified value of the mass fraction was (991 ± 14) mg/g ($k = 2$) or (99.1 ± 1.4) g/100 g ($k = 2$). The estimated uncertainty for the material includes the uncertainty of characterization, the stability of transport, and the uncertainty of homogeneity.

The results of this study will allow our Federal Police to use a CRM synthesized and certified in our country and this was made possible due to a successful partnership among UFRJ, INMETRO, and PF-BR.

¹Ellison, S. L. R.; Williams, A. *Eurachem/CITAC*, **2019**, 2; ²Kielbasa, A.; Gadzala-Kopciuch, R.; Buszewski, B. *Anal. Chem.*, **2016**, 3, 224-235; ³Heather, E.; Shimmon, R.; McDonagh, A. *Forensic Sci. Int.*, **2020**, 309,110176; ⁴González-Martínez, D.; Gotor, V.; Gotor-Fernández, V. *Adv. Synth. Catal.*, **2019**, 11, 2582-2593.

Acknowledgments

The authors would like to thank Capes, Faperj and CNPq.

Aplicação da red mud em reações de adição de 1,4 na síntese do 3,7-dimetil-3-(feniltio)oct-6-enal, um potencial antibactericida

Sandro Luiz Barbosa (PQ),¹ **David Lee Nelson** (PQ),¹ **Savio E. O. Miranda** (PG),¹ **Milton de S. Freitas** (PQ),¹ **Maria Luiza P. Oliveira** (IC),² **Jeniffer L. S. Soares** (IC),¹ **Lucas Paconio da Silva** (PG),¹ **Franco J. Caires** (PG),².

sandro.barbosa@ufvjm.edu.br

¹Departamento de Farmácia, UFVJM. ² Faculdade de Ciências Farmacêuticas de Ribeirão Preto/SP, USP.

Palavras Chave: Lama vermelha, Adição de Michael, Microwave irradiation, Citral, benzenotiól (PhSH), compostos α,β -insaturados.

Highlights

Application of red mud in 1,4 addition reactions in the synthesis of 3,7-dimethyl-3-(phenylthio)oct-6-enal, a potential antibacterial agent

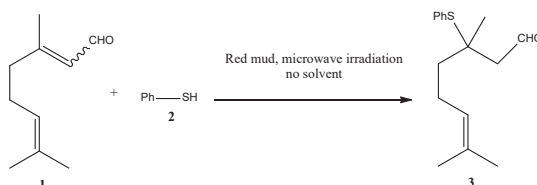
Red mud (RM) is an industrial waste generated during the processing of bauxite into alumina using the Bayer process.

Application of RM as catalyst in Michael addition reaction.

Microwave irradiation process and no solvent.

Resumo/Abstract

RM is a solid residue produced during the production of alumina from the caustic digestion of bauxite ores, a process called the Bayer Process [1]. Approximately 1.5 tons of RM is produced for each ton of alumina. The annual global production of RM is approximately 0.15 billion tons. It is composed of fine particles of various mineral oxides, including aluminum, iron, silicon, titanium and traces of other metals, with a highly alkaline pH of 10-12.5. Due to the alkaline nature and high metal content in the RM, its disposal in landfills causes a significant impact on soils and groundwater [25,30]. Attempts have been made to utilize RM for other industrial and environmental purposes as a component in building bricks, filler in asphalt roads, for the production of coagulants, adsorbent for inorganic and organic compounds and as a catalyst. In this work, the authors describe a simple and efficient method for the synthesis of 3,7-dimethyl-3-(phenylthio)oct-6-enal. This compound was produced by the conjugated addition of PhSH **2** to citral **3** (main component of lemongrass essential oil, *Cymbopogon citratus*), in a Michael addition reaction, in the presence of RM in solvent-free medium and under microwave irradiation (Equation 1).



Red mud was initially dried at 100 °C for 24 h in a hot air oven. The dried RM sample was ground and sieved through a 150-micron sieve to furnish a uniform particle size. The sample was calcined in a muffle furnace at temperatures that varied from 100 °C for 4 h. To a 10 mL microwave reactor vial, 2.00 mmol of citral 1.00 mmol benzenethiol (PhSH) and 0.0360 g of RM (20% w/w in relation to citral) was added. The vial was heated in the microwave reactor at 120 °C for 40 min. The mixture was cooled to room temperature, and 10.0 mL of CH₂Cl₂ was added. The organic solution obtained after filtration of the solid catalyst was transferred to an extraction funnel and partitioned between 10 mL of CH₂Cl₂ and 20 mL of saturated NaHCO₃, dried with magnesium sulfate, filtered, and evaporated under reduced pressure. The residue was subjected to GC-MS analysis, which demonstrated the absence of unreacted PhSH. The residue was then purified by flash column chromatography on silica using hexane-ethyl acetate (9:1) as the mobile phase to yield 3,7-dimethyl-3-(phenylthio)oct-6-enal (90% yield) as a colorless oil. Five more runs could be performed with the same catalyst. Each run was performed in triplicate.

1. Wang X, Zhang Y, Liu J, Hu P, Meng K, Lv F, Tong W, Chu PK. (2017) Dealkalinization of red mud by carbide slag and flue gas. *Clean Soil Air Water*. 46: 1700634.

Agradecimentos/Acknowledgments

The authors acknowledge the support by the PRPPG/UFVJM in response to Resolution 15/2019 and Fapemig (Chamada Universal), 0004022 code.

Application of Cu(II)-N-Ts-(bis)imidazoline in diastereo and enantioselective Henry reaction of aldehydes and nitroethane

Ariadne de Jesus Vicente (PG)*, Alessandro Rodrigues (PQ), Elisângela Vinhato (PQ).

ariadne.vicente@unifesp.br

Departamento de Química, Universidade Federal de São Paulo, Diadema, SP, Brazil.

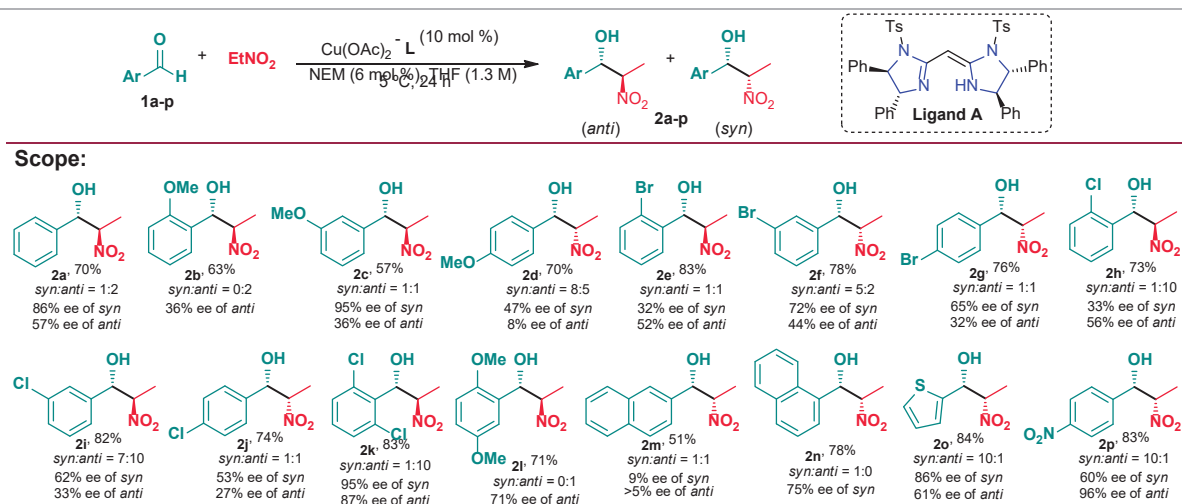
Keywords: Henry Reaction, Enantioselective Catalysis, Imidazoline Ligands.

Highlights

Development of imidazoline ligands for the stereoselective Henry reaction. 16 Examples of nitroaldol products were obtained in yields from 51 to 84%, *dr* up to 10:1 and *ee* up to 95%.

Abstract

The enantioselective catalyzed Henry (nitroaldol) reaction plays a key role in the formation of C–C bonds in a stereoselective manner.^[1] In view of the wide range of synthetic versatility of 1,2-nitroalcohols, the Henry reaction has attracted considerable attention, which has prompted the development of new catalytic systems continuously.^[2] Herein, we report the results on the development of chiral complexes generated *in situ* between copper(II) salts and imidazoline-core ligands in Henry-type reactions. As a starting point, we used benzaldehyde (0.4 mmol reaction scale) as a model compound to optimize the conditions for the Henry reaction with nitroethane. We investigated the influence of different combinations of reaction variables such as Cu(II) source, six chiral imidazoline-type ligands, the equivalents of reaction components, and the nature of the solvent. Based on the screening of reaction parameters, the optimized catalytic methodology uses 10 equiv of nitroethane, ligand *N*-Ts-(bis)imidazoline **A** (10 mol %), Cu(OAc)₂ (10 mol %), NEM (4-Ethylmorpholine, 6 mol %), and THF (1.3 M) at 5 °C for 24 h. The consolidated methodology provided the 1,2-nitroalcohol **2a** in 70% yield, with a *dr* of 1:2, and *ee*'s of 57% for the *anti*-product and 86% for the *syn*-product. Once the methodology was optimized, the scope of the reaction was explored with 15 additional aldehydes (Scheme 1). The *dr* values were determined by ¹H NMR and *ee* values were determined by chiral HPLC analysis. The absolute configurations of the products were assigned by comparison with literature data.



Scheme 1. Diastereo- and enantioselective Henry reaction of various aldehydes with nitroethane.

Our study demonstrates that Cu(II)-imidazoline complexes can catalyze enantio- and diastereoselectively the nitroaldol reaction between 16 aldehydes and nitroethane. Explorations toward the elaboration of a mechanistic model of this transformation are currently underway in our laboratory.

[1] *Mini Rev. Org. Chem.* **2019**, *16*, 1-12. [2] *Aust. J. Chem.* **2022**, *75*, 806-819.

Acknowledgments



Asymmetric dearomatization of indolizines via organocatalytic high-order cycloaddition

Thiago Sabino da Silva (PG),^{1,2} José Tiago Menezes Correia (PQ),¹ Benjamin List (PQ),² Fernando Coelho (PQ).^{1*}

thiagosabinodasilva@gmail.com; facoelho@unicamp.br

¹Institute of Chemistry, UNICAMP, SP, Brasil; ²Max-Planck-Institut für Kohlenforschung, Mülheim an der Ruhr, Germany

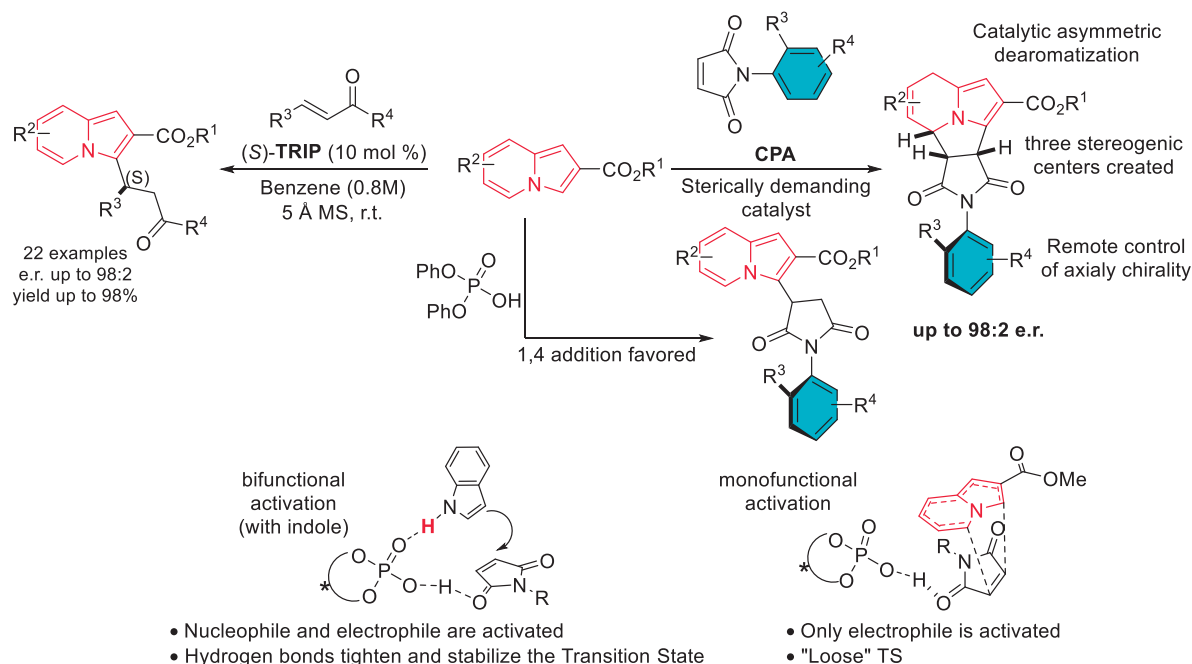
Palavras Chave: High-order cycloaddition; Organocatalysis; Chiral Phosphoric Acids; Asymmetric dearomatization; Indolizines; Atropoisomerism

Highlights

A high-order [8+2] cycloaddition between indolizines and pro-chiral maleimides led to dearomatized adducts with simultaneous remote control of axial chirality. This is the first report of an asymmetric dearomatization of the indolizine core.

Resumo/Abstract

Indolizines are electron-rich indole bioisosteres considered as privileged scaffolds for drug development. The asymmetric organocatalytic functionalization of this core represents a challenge due the lack of an acidic site that can interact with catalysts so that enantioinduction only relies on monofunctional activation of the electrophile. In 2017, List and Coelho described the first asymmetric organocatalytic functionalization of indolizines with enones to afford conjugate adducts using Chiral Phosphoric Acid (CPA). Attempts to expand the electrophile scope to maleimides using sterically demanding CPAs produced dearomatized [8+2] cycloadducts instead of 1,4-conjugate adducts. Here, we disclose the first asymmetric dearomatization of indolizines using prochiral maleimides, during which three adjacent stereogenic centers are generated with concomitant remote control of axial chirality.



Agradecimentos/Acknowledgments



A visible-light-induced multicomponent synthesis of 1,4-Dicarboxyl compounds: A reaction cocktail of CO₂, carbamoyl-DHP and styrene

Kimberly Benedetti Vega (PG)*, ^[1,2] André Luiz Carvalho de Oliveira (IC), ^[1] Prof. Burkhard König (PQ)^[2] and Prof. Dr. Márcio Weber Paixão (PQ) ^[1]

andrelco@estudante.ufscar.br; kbenedetti@utp.edu.co

¹Laboratory for Sustainable Organic Synthesis and Catalysis, Department of Chemistry, Federal University of São Carlos – UFSCar, São Carlos, São Paulo, Brazil; ² Institut für Organische Chemie, Universität Regensburg, Universitätsstrasse 31, 93053, Regensburg, Germany.

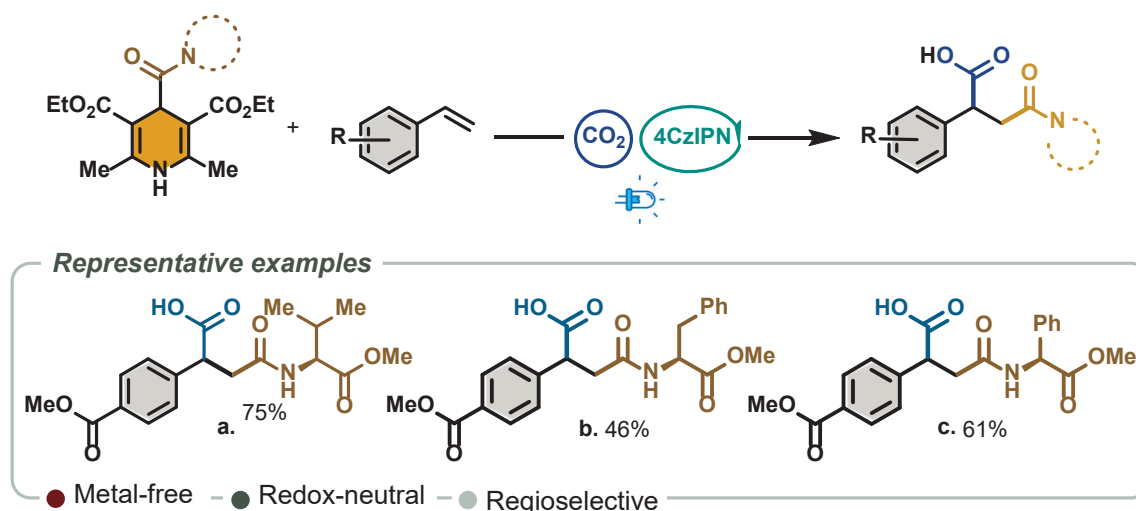
Keywords: Photocatalysis, Carbon Dioxide, 1,4-dihydropyridines, Carboxylic acids, Dicarboxylic compounds.

Highlights

A convenient, efficient and direct approach towards photoinduced 1,2-dicarboxylation of styrenes using carbamoyl radicals and CO₂ has been developed.

Abstract

1,4-Dicarboxyl compounds are interesting structural motifs and versatile precursors to numerous pharmaceutical molecules and natural bioactive compounds.^[1] A challenging alternative for the synthesis of these compounds consists in the concomitant installation of two carboxylic structures onto the olefin's π system.^[2,3] Thus, we developed a metal-free, redox-neutral and regioselective method for the simple and straightforward synthesis of such important chemical architecture using styrenes, carbamoyl radicals and carbon dioxide as carboxylation agents. This strategy allowed the difunctionalization of a variety of styrenes using CO₂ and amino acid-derived 1,4 DHPs, providing 1,4-dicarboxylic compounds in moderate to excellent yields. Due to the high versatility of the C1-synthons used in this protocol, we have the prospect of extending the robustness of our scope by carrying out isotopic labelling experiments with ¹³CO₂, as well as using isotopically labelled 1,4 DHPs.



[1] Young, W. B.; Rai, R.; Shrader, W. D.; Burgess-Henry, J.; Hu, H.; Elrod, K. C.; Sprengeler, P. A.; Katz, B. A.; Sukbunthong, J.; Mordenti, J. *Bioorg. Med. Chem. Lett.* **2006**, 16 (7), 2034–2036. [2] Ju, T.; Zhou, Y.-Q.; Cao, K.-G.; Fu, Q.; Ye, J.-H.; Sun, G.-Q.; Liu, X.-F.; Chen, L.; Liao, L.-L.; Yu, D.-G. *Nat. Catal.* **2021**, 4 (4), 304–311. [3] Xu, P.; Wang, S.; Xu, H.; Liu, Y.-Q.; Li, R.-B.; Liu, W.-W.; Wang, X.-Y.; Zou, M.-L.; Zhou, Y.; Guo, D.; Zhu, X. *ACS Catal.* **2023**, 2149–2155.

Acknowledgments

We are grateful to Brazilian funding agencies CNPq (INCT Catálise, Grants No 444061/ 2018-5 and Universal Project 405052/2021-9) and FAPESP (21/06099-5). KBV thanks to FAPESP (PhD fellowship 21/01354-7). This study was also financed in part by the Coordenação de Aperfeiçoamento de Pessoal de Nível Superior - Brasil (CAPES) - Financial code 001.

Área: ORG

(Inserir a sigla da seção científica para qual o resumo será submetido. Ex: ORG, BEA, CAT)

BIOACTIVITY OF PHENOLIC COMPOUNDS PROFILED BY ESI-QTOF-MS IN *Plathymenia reticulata* BENTH HIDROETHANOLIC EXTRACTS.

Catarina dos Santos (PQ)¹, Vania V. A. Nunes (PQ)¹, Ana Lucia T. G. Ruiz (PQ)², Celio F. F. Angolini (PQ)³, Marcos N. Eberlin⁴ catarina.santos@unesp.br

¹Laboratory of Chemistry of UNESP-Assis (LAQUA), Assis, SP, Brazil. ²Faculty of Pharmaceutical Sciences, University of Campinas (UNICAMP), Campinas, São Paulo, Brazil; ³Mass Spectrometry and Chemical Ecology Laboratory (MS-Cell), Federal University of ABC (UFABC), Santo André, São Paulo, SP, Brazil. ⁴Mackenzie Presbyterian University, São Paulo, SP, Brazil

Keywords: *P. reticulata*, ESI-QTOF-MS, phenolics, biological activities.

Highlights

Plathymenia reticulata Benth. (Fabaceae) is a Brazilian Cerrado tree used to recover degraded areas. From its extracts, it was described inflammatory activities, infections, and snake poisoning. Their polyphenols showed a very good antioxidant scavenging activity and no cytotoxicity for normal cells.

Abstract

Plathymenia reticulata Benth. (Fabaceae) is a Brazilian Cerrado tree used in the recovery of degraded areas and urban reforestation, as well as in the timber sector^[1]. It's described for treating inflammatory diseases, infections, and snake poisoning^[2]. In this study, we profiled the main phenolic constituents of *P. reticulata* hydroethanolic leaf extracts by ESI-QTOF-MS. We also established a correlation between these metabolites and antioxidant and *in vitro* antiproliferative activities. 10g dry and crushed leaves/100mL of EtOH: H₂O 70:30 (v/v) were macerated and re-extracted twice. After filtration, the extract was concentrated under reduced pressure. For ESI-MS, 2 µL of the extract was dissolved in a MeOH/H₂O (1:1 v/v) containing NH₄OH 0,1% solution and injected in a QTOF Agilent 6500 series mass spectrometer (Agilent, USA), operating in the negative ion mode. DPPH assay was performed as described by Costa et al.^[3] Human tumor cell lines: UACC-62 (melanoma), MCF-7 (breast), NCI-ADR/RES (ovarian expressing phenotype with multiple drug resistance), 786-0 (renal), and a non-tumoral cell line VERO (epithelial cells of monkey kidney) were tested^[3]. The total growth inhibition (TGI) values were determined by ORIGIN 8.6® (OriginLab Corporation, USA).

Polyphenols found by ESI-MS in *P. reticulata* leaves extract were mostly flavonoids and catechins: quercetin ([C₁₅H₁₀O₇-H]⁻ m/z 301,0365), rutin ([C₂₇H₃₀O₁₆-H]⁻ m/z, 609,1457): eriodictyol ([C₁₅H₁₂O₆-H]⁻ m/z 287,0561), epicatechin ([C₁₅H₁₄O₆-H]⁻ m/z 289,0765), taxiflorin ([C₁₅H₁₂O₇-H]⁻ m/z 303,0534) and galocatechin ([C₁₅H₁₄O₇-H]⁻ m/z 305,0678). The extract displayed a very good antioxidant scavenging activity (EC₅₀ 7,5 mg/mL) when compared to Trolox (1,13±0,7 mg/mL); and weak antiproliferative activities for NCI-ADR/RES (TGI 16,91 mg/mL) and MCF-7 (TGI 25,23 mg/mL) lineages. For Vero (normal cell), it was detected low cytotoxicity (27,36 mg/mL). For the other lineages tested, the extract was inactive. There was no correlation between the antioxidant and antiproliferative activities. Still, these results suggest that hydroethanolic *P. reticulata* extracts could be a source of antioxidants or drugs against breast and ovarian cancers.

Acknowledgments

Fapesp for funding (grant number 2017/15610-0).

[1] P.E.R. Carvalho, *Espécies arbóreas brasileiras*; Embrapa Informação Tecnológica: Colombo; Brasília, 2009; Vol. 3 [2] V.M.de Moura, et al, *J. Ethnopharmacol.* **2016**, 183, 136 [3] M. F. da Costa, et. al, *Anal. Methods* **2016**, 8, 6056.

(Bio)Electroreduction of acetophenone applying lipases

Patricia Bulegon Brondani (PQ),^{1*} Morgana Aline Voigt (PG),¹ Lidiane Meier (PQ),¹ Eduardo Zapp (PQ).¹

p.b.brondani@ufsc.br, patyqmc@gmail.com

¹Centro Tecnológico, de Ciências Exatas e Educação (CTE), Programa de Pós-graduação em Nanociência, Processos e Materiais Avançados (NPMat), UFSC Blumenau.

Palavras Chave: *Organic electrosynthesis, Biocatalysis, Lipases, reduction of ketones*

Highlights

Electrochemistry and biocatalysis for the selective reduction of acetophenone to 1-phenylethanol;
Hydrolases performing reduction reactions;
Thermomyces lanuginosus leading to 87-94% of 1-phenylethanol.

Resumo/Abstract

Electrosynthesis has its broad application limited by the need for parameter optimizations and relatively low selectivity for some reactions, such as the reduction of acetophenone, in which the pinacol dimer is obtained in addition to 1-phenylethanol.[1,2] Proposals for selectivity control in this reaction exist, but few works present effective or viable alternatives.[3,4] In this study, it is proposed to use electrochemistry allied with biocatalysis to reduce ketones avoiding dimerization and leading to the preferential formation of the alcohol. The chosen enzymes for this function were lipases, commercially available under accessible prices, and exceptionally versatile in organic synthesis. Diverse combinations of electrodes, solvents, supporting electrolytes, and lipases were tested. The optimized reaction conditions led to the formation of 87.8% of racemic 1-phenylethanol and are composed of a tin/lead (63:37) combined working electrode coated with Nafion film modified with lipase from *Thermomyces lanuginosus*, a platinum counter electrode, an applied potential of -2.0 V vs. Ag/AgCl (KCl 3.0 mol L⁻¹), acetate buffer (0.1 mol L⁻¹) pH 5.0 in 4 hours of reaction at room temperature. The same working electrode was used five times over five days, and the conversion to alcohol remained constant. The addition of lipase from *Thermomyces lanuginosus* immobilized in a clay mineral and, commercially, in silica gel (Lipolase 100T) to the electroreduction medium resulted in even higher conversions to 1-phenylethanol (93.2–93.9%). Using the modified electrode made the methodology more advantageous regarding enzyme stability, process reproducibility, and material reusability. The observed results were promising, considering that this work explores a novelty in reduction reactions: the active and joint application of electrosynthesis and lipases to perform organic transformations.

[1] SCHÄFER, H. J. Contributions of organic electrosynthesis to green chemistry. **Comptes Rendus Chimie**, v. 14, n. 7–8, p. 745–765, 2011.

[2] MITSUDO, K. et al. Combinatorial electrochemistry for organic synthesis. **Current Opinion in Electrochemistry**, v. 8, p. 8–13, 2018.

[3] ZHAO, S. F. et al. Electrocarboxylation of acetophenone in ionic liquids: The influence of proton availability on product distribution. **Green Chemistry**, v. 16, n. 4, p. 2242–2251, 2014.

[4] XUE, Y. F. et al. Supramolecular chiral electrochemical reduction of acetophenone with hybridization of a chiral multifarene and Au nanoparticles. **Journal of Catalysis**, v. 404, p. 529–536, 2021.

Agradecimentos/Acknowledgments

CNPq, CAPES, FAPESC, UFSC

Carbocation stabilities from epoxide ring opening: An NMR and DFT investigation

Leonardo F. F. Lopes (IC)^{1*}, Kennedy D. C. Santos (PG)¹, Renan F. Gimenez (IC)¹, Renan V. Viesser (PQ)^{1,2}, Marco A. B. Ferreira (PQ)³ and Cláudio F. Tormena (PQ)¹

leofuzatoferreira@gmail.com.

¹Institute of chemistry, UNICAMP – Campinas – Brazil; ²Department of Chemistry – University of Houston – Houston – USA; ³Department of chemistry – UFSCar – São Carlos - Brazil

Keywords: Stability, Carbocation, Mechanism, NMR.

Highlights

Epoxides are important intermediates in organic chemistry and their opening reactions can lead to non-classical carbocations, providing stereoisomers at different ratio.

Abstract

The epoxide opening reaction^{1,2,3} can occur under a S_N1 mechanism in acidic conditions in which an intermediate carbocation is formed in the solution. In this study we evaluate the structures and stabilities of carbocation^{1,2,3} by unequivocally assigning the structure of products obtained from reaction between α -pinene oxide and hydrogen chloride, combining NMR and Density Functional Theory (DFT)⁴ calculation.

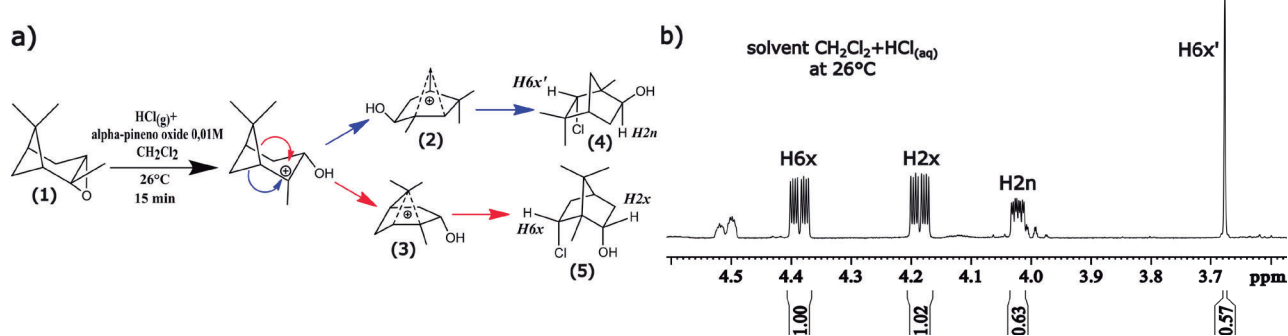


Figure 1. A) Reaction condition⁵ used in this study with intermediaries (2) and (3) and products (4) and (5). B) ¹H NMR spectrum in CDCl₃ at 600 MHz for products (4) and (5), highlighting hydrogen assignment for each isomer.

The structures for α -pinene oxide (1) and products (4) and (5) were assigned through NMR spectra (¹H, ¹³C, COSY, HSQC, HMBC and NOESY). The reactions were carried out using 37% v/v aqueous HCl_(aq) with α -pinene oxide using solvents with different polarities (hexane, CHCl₃ and CH₂Cl₂) and at 26°C stirred for 15 min. At these conditions compound 4 is present in 35% in comparison with compound 5 (65%) in all solvents. The reaction was performed at 3°C in CHCl₃ and the same proportion is observed (35:65), when the reaction was performed at 43°C the proportion of compound 4 increased to 52%. The carbocations (2 and 3) and transition state structures involved in the reaction mechanism are being characterized using DFT applying B3LYP-D3, M062X and ω B97XD functionals and cc-pVTZ basis set.

REFERENCES

1. M. Magre, E. Paffenholz, B. Maity, L. Cavallo, M. Rueping, *J. Am. Chem. Soc.* 2020, 142, 14286–14294
2. K. B. Wiberg, P. R. Rablen, *J. Org. Chem.* 2020 85, 11741-11749.
3. L.C. King, H. Faber, *J. Org. Chem.* 26, 326 (1961).
4. A. Castro-Alvarez, H. Carneros, D. Sánchez, J. Vilarrasa, *J. Org. Chem.* 2015 80, 11977-11985.
5. M. Chini, P. Crotti, C. Gardelli, F. Macchia, *Tetrahedron* 48, 3805 (1992).

Acknowledgments

We thank FAPESP for financial support (grants #2020/10246-0 and #2022/11314-5) and scholarship to LFFL (#2022/16223-8), CAPES for scholarship to KDCS. We also thank Institute of Chemistry of UNICAMP for the multiuser NMR facility.

Chalcogen-naphthoquinones-1,2,3-triazoles hybrids: synthesis and evaluation of photophysical, photobiological and electrochemical properties

Luana S. Gomes (PG),^{*1} Érica O. Costa (IC),¹ Thuany G. Duarte,¹ Fernando C. da Silva (PQ),¹ Vitor F. Ferreira (PQ),² Bernardo A. Iglesias (PQ),³ Vanessa Nascimento (PQ).¹

luanagomes@id.uff.br

¹Departamento de Química Orgânica, Universidade Federal Fluminense, Instituto de Química, Campus do Valonguinho, 24020-141, Niterói-RJ, Brasil; ²Laboratório de Materiais Bioinorgânicos e Porfirínicos, ³ Departamento de Química, Universidade Federal de Santa Maria, 97105-900, Santa Maria-RS, Brasil.

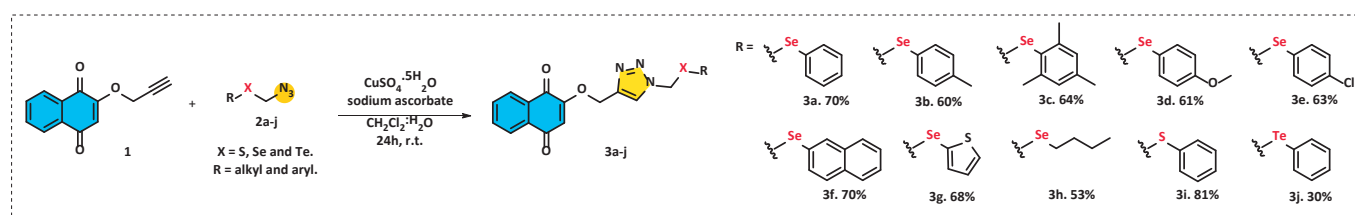
Palavras Chave: lawsone, organochalcogens, molecular hybridization.

Highlights

In this work, a series of new chalcogen-functionalized-1,2,3-triazole naphthoquinones was synthesized and its photophysical and electrochemical properties were evaluated.

Resumo/Abstract

Organochalcogens have been widely studied due to the large number of synthetic and biological applications. Among these activities, the antioxidant or pro-oxidant potential of selenium-containing compounds is often explored.¹ In the other hand, quinones comprise a large and diverse family of naturally occurring metabolites. The interest in these substances has grown in recent years due to their biooxidation-reduction properties and ability to catalyze biological electron transfer processes, mainly in pharmaceutical research studies.^{2,3} Another prominent scaffold is the 1,2,3-triazole nucleus, which are only produced synthetically, that have a wide range of applications and widely used as a link between different groups of interest.⁴ Therefore, in this work, the objective is the preparation of a series of new hybrid substances containing naphthoquinone from lawsone, and organochalcogens connected through a triazole group, for the study of its photophysical, photobiological and electrochemical properties. The target molecules were synthesized using propargylated lawsone **1** and a series of azides containing chalcogens **2a-j** by a 1,3-dipolar cycloaddition reaction catalyzed by Cu(I) salts. By this protocol it was possible to obtain 10 different structures with yields ranging from 30 to 81% (**Scheme 1**).



Scheme 1. Synthesis of chalcogen-naphthoquinones-1,2,3-triazoles **3a-j**.

Agradecimentos/Acknowledgments

UFF, CAPES, FAPERJ, FAPERGS and CNPq.

¹Sak, M.; Al-Faiyz, Y. S.; Elsayy, H.; Shaaban, S. *Antioxidants*, **2022**, 11, 1231.

²Barreiro, E. J.; da Silva, J. E. M.; Fraga, C. A. M. *Quim. Nova*, **1996**, 19, 641.

³Cordeiro, P. S. *et al. J. Braz. Chem. Soc.*, **2022**, 33, 111.

⁴Praveena, K. S. S.; Murthy, N. Y. S.; PAL, S. *J. Chem. Pharm. Res.*, **2015**, 7, 506.

Chemoenzymatic Dynamic kinetic resolution of chiral benzylamines mediated by heterogeneous palladium catalyst supported on dolomite.

José C. Q. Arêas (PG), Larissa M. da Silva (IC), Livia Y. Sawada (IC), Pedro Allan Sousa Veras (IC), Rafael Lamoglie Borges (IC) Fernanda A. de Siqueira (PQ)*

icqareas@unifesp.br; larissa.moises20@unifesp.br; livia.sawada@unifesp.br; pveras04@unifesp.br; rafael.borges@unifesp.br; fasilqueira@unifesp.br*

Laboratory of Organic Synthesis and Catalysis, Federal University of São Paulo (UNIFESP), Campus Diadema, Rua Prof. Arthur Riedel, 275, Bairro Jardim Eldorado, 09972-270 Diadema-SP, Brazil

Keywords: Dynamic Kinetic Resolution; Biocatalysis; Palladium; Chiral Amines; Dolomite.

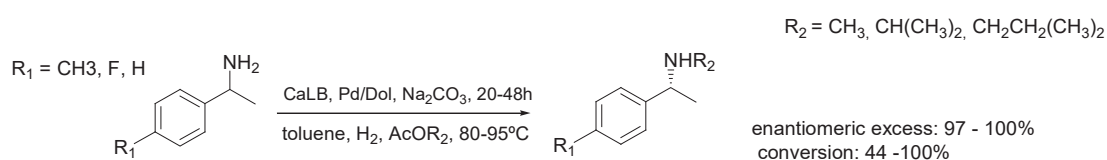
Highlights

Study carried out to understand and optimize DKR reactions of benzylamines in a one-pot reaction system using different reaction conditions.

Resumo/Abstract

Chiral amines constitute one of the most important classes of organic compounds, mainly due to their biological activity. They are widely used in the chemical, agrochemical and pharmaceutical industries due to their versatility.

Obtaining these enantiomerically pure amines can be performed through some processes, such as synthesis, enzymatic kinetic resolution (KR) and dynamic kinetic resolution (DKR), the latter of which has shown to be an excellent option because it presents great cost-effectiveness and several features of green synthesis, such as the use of enzyme, relatively cheap and recyclable catalyst. Furthermore, it can lead to a theoretical 100% conversion.^{1 2} However, amines require drastic conditions for racemization to occur, a crucial step in the kinetic resolution process, which can affect enzymatic activity. This work presents the DKR of 5 benzylamines using different reaction conditions to optimize and obtain the corresponding enantiomerically pure amides. The catalyst used was designed by our research group and has 2.5% m/m load of palladium in dolomite.²



In addition to the compounds mentioned above, (±)1,2,3,4-tetrahydro-1-naphthylamine and (±)1-indanamine were used. Among all variations of acyl donor, in general, ethyl acetate furnished the best results. This can be explained by its smaller size, that can facilitate the lipase approach.³ Among the studied molecules, (±)1,2,3,4-tetrahydro-1-naphthylamine and (±)1-(4-fluorophenyl)ethylamine obtained less than desired results. The reasons can be attributed by steric and electronic effects, that can affect the enzyme approach in the acylation step.

In optimized conditions, the reactions of DKR furnished the corresponding acetamides in excellent conversions and enantiomeric excesses.

1 GUSTAFSON, K. P. J.; Lihammar, R.; Verho, O.; Engström, K.; Bäckvall, J-E. *J. Org. Chem.* 2014, 3747.

2 MENDONÇA, R.C.Z., Esteves, L.M., Oliveira, H.A. *et al.* Recyclable Palladium Catalyst Supported on Dolomite for Dynamic Kinetic Resolution of (±)-1-Phenylethylamine. *Catal Lett* 152, 1205–1214.

3 KAZLAUSKAS, Romas J *et al.* *The Journal of Organic Chemistry*, v. 56, n. 8, p. 2656-2665, 1991

Agradecimentos/Acknowledgments

FAPESP, CAPES, UNIFESP- Diadema

Chemoselective Electrochemical Reduction of 5-arylidene-thiazolidine-2,4-diones and its Potential Application in the Synthesis of Pioglitazone

Pedro P. de Castro (PQ),¹ Ronewalber B. Gomes (IC),¹ Guilherme B. Simoso (IC),¹ Guilherme M. Martins (PQ),¹ Giovanni W. Amarante (PQ),² Timothy J. Brocksom (PQ),¹ Kleber T. de Oliveira (PQ)^{1*}

pedro.possa@ufscar.br; kleber.oliveira@ufscar.br

¹Departamento de Química, UFSCar; ²Departamento de Química UFJF

Keywords: electrosynthesis, thiazolidine-2,4-dione, 1,4-reduction, pioglitazone.

Highlights

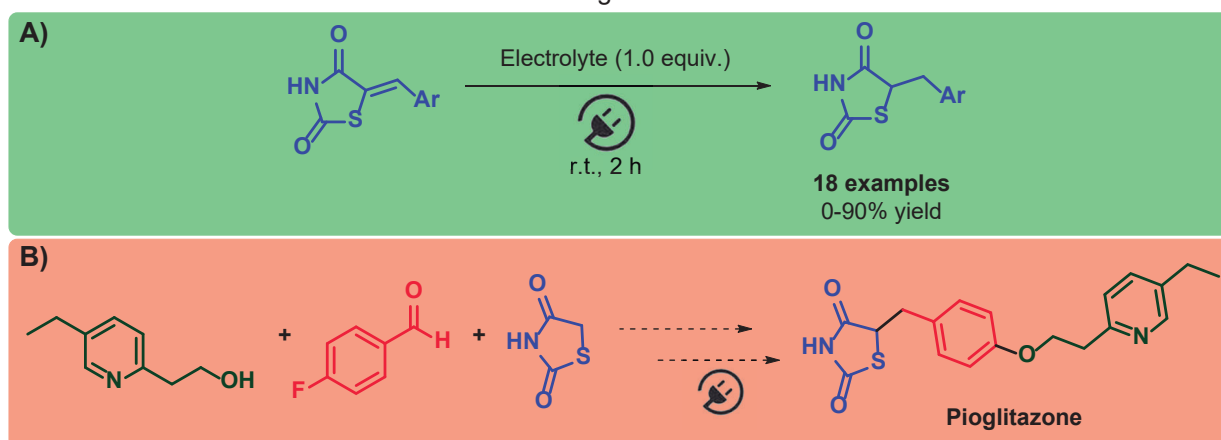
The use of electroynthesis in the chemoselective reduction of 5-arylidene-thiazolidine-2,4-diones is described. Its application in the preparation of pioglitazone highlights the synthetic interest of this protocol.

Resumo/Abstract

The chemical reduction of enones is generally achieved by using transition metal catalysis or potentially hazardous reagents, such as hydrides.¹ The reduction of 5-arylidene-thiazolidine-2,4-diones is of particular interest in this field, since it is involved in the last step of the synthesis of several hypoglycemic drugs, such as pioglitazone, rosiglitazone and ciglitazone.² In this context, electrochemical synthetic approaches are relevant alternatives to these transformations, allowing the use of milder and safer reaction conditions.

The optimization of the electrochemical reduction of thiazolidine-2,4-diones was carried out varying parameters such as the electrodes, electrolytes, solvents, additives, reaction time and temperature. By using the optimized reactions conditions, a representative scope of 18 examples was successfully prepared in up to 90% yield (Scheme 1A). The scale-up of one of these derivatives (Ar = 4-F-Ph) to a gram scale was demonstrated in 78% yield. Several control experiments were performed in order to propose a plausible reaction mechanism, including isotopic labelling, the use of radical scavengers and divided-cell experiments. It was possible to determine the hydrogen atoms origin, as well as to detect the formation of a key side-product. As an application of this methodology, the preparation of pioglitazone is under development and will be reported in due course.

Scheme 1. A) Electrochemical reduction of thiazolidine-2,4-diones; B) Electrochemical reduction in the preparation of Pioglitazone.



References: ¹ *Adv Synth Catal.* **2021**, 363, 2104-2109; ² *Synth. Commun.* **2021**, 51, 57-80.

Agradecimentos/Acknowledgments

FAPESP (grants 2021/13924-2 (P.P.C.), 2022/00074-3 (G.M.M.), 2020/06874-6 (K.T.O)), FAPEMIG, CAPES, and CNPq.

Conformational Concomitant Polymorphism with color change in bis(1-*N,N*-dimethylsulfamoyl-4-imidazolyl)gloxal

Carolina B. P. Ligiero (PQ),^{1*} Lygia S. de Moraes (PQ),² P. C. M. L. Miranda (PQ),³ Rodrigo Bitzer (PQ),⁴ Célia M. Ronconi (PQ)¹

cligiero@yahoo.com.br

¹Departamento de Química Inorgânica, UFF; ²Division of Chemistry and Chemical Engineering, California Institute of Technology; ³Departamento de Química Orgânica, UNICAMP; ⁴Instituto de Química, UFRJ

Palavras Chave: (conformational polymorphism, color change, single crystal X-ray diffraction).

Highlights

Bis(1-*N,N*-dimethylsulfamoyl-4-imidazolyl)gloxal was synthesized with 89 % global yield via benzoin condensation and two crystalline forms (conformational polymorphism) can be obtained concomitantly.

Resumo/Abstract

The ability of a chemical compound to crystallize into different crystalline forms is known as polymorphism. The compound bis(1-*N,N*-dimethylsulfamoyl-4-imidazolyl)gloxal (4-BIG-DMAS (**1**)) was synthesized in four steps with 89 % global yield via benzoin condensation of the protected imidazole-4-carbaldehyde (Figure 1a). (**1**) crystallizes as colorless and yellow crystals from the solutions. Single crystal X-ray diffraction analyses revealed that they are polymorphs of (**1**), which crystallizes concomitantly as different conformers by the rotation of the imidazole groups around the single bond (Figure 1b), adopting *antiperiplanar* or *synclinal* arranges. Other characterization methods of the polymorphs have been conducted such as solid-state NMR (CPMAS-Figure 1c), UV-Vis (Figure 1d), TGA, DSC and hot stage microscopy. Variable temperature XRPD (Figure 1e) shows a phase transition occurring after thermal degradation for both forms at temperatures higher than 150 °C. Moreover, theoretical studies are being carried out to provide a more comprehensive view of the phenomenon.

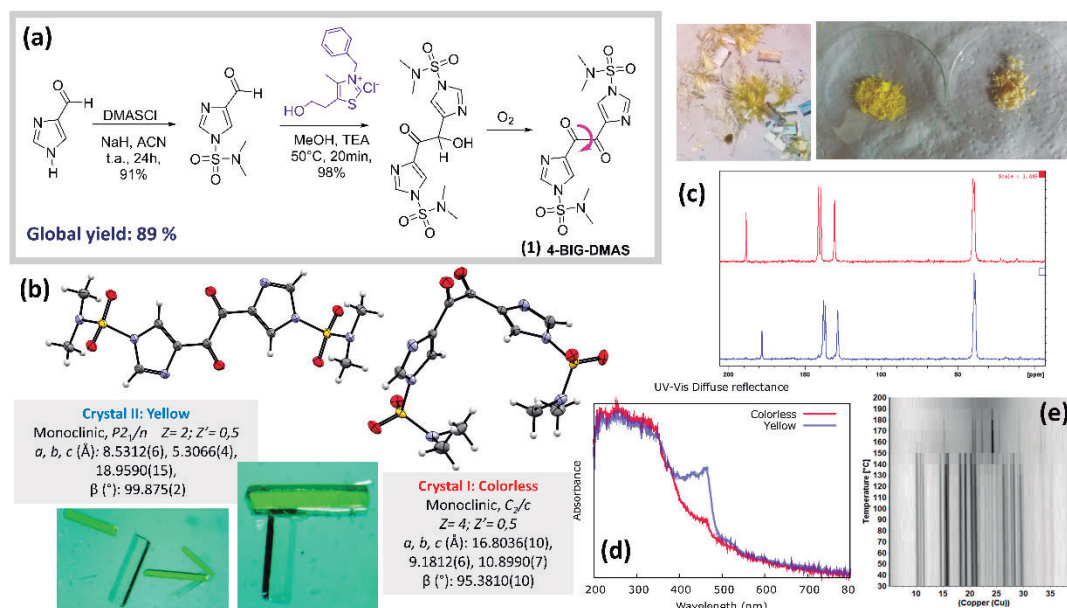


Figura 1. (a) Scheme for the synthesis of 4-BIG-DMAS; (b) structure of yellow and colorless crystals; some photos (c) SSNMR (CPMAS); (d) UV-Vis; (e) XRPD with variable temperature.

Agradecimentos/Acknowledgments

Continuous-Flow Ozonolysis as Efficient Process for Producing Certified Reference Materials

Letícia S. Chaves (IC),¹ Thaís G. Silva (PG),² Caio M. Pacheco (PG),¹ Raquel A. C. Leão (PQ),¹ Bruno C. Garrido (PQ),³ Fernanda G. Finelli (PQ),² Rodrigo O. M. A. Souza (PQ).^{1*}

seiraleticia@gmail.com; souzarod21@gmail.com*

¹ Biocatalysis and Organic Synthesis Laboratory, Chemistry Institute – Federal University of Rio de Janeiro – IQ – UFRJ.

² Instituto de Pesquisas de Produtos Naturais – Federal University of Rio de Janeiro – IPPN – UFRJ.

³ Instituto Nacional de Metrologia, Qualidade e Tecnologia, INMETRO.

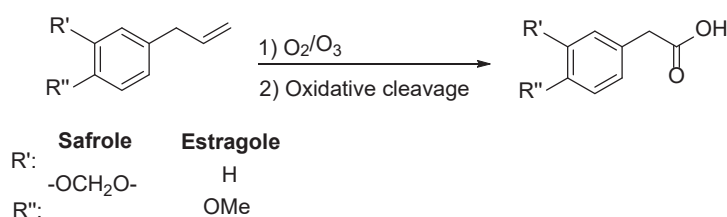
Keywords: ozonolysis, safrole, estragole.

Highlights

This project aims to analyze and optimize different synthetic routes to obtain intermediary predecessors to amphetamine compounds, which are then certified as reference materials.

Abstract

The correct and complete characterization of seized materials by the police is crucial to understand the number of synthetic routes that can develop these illicit compounds. In this sense, the best way to confidently assure the identification of these compounds is through certified reference materials (CRM).¹ Since this type of product is scarce in both national and international markets, the purpose of our work is the synthesis of carboxylic acids as intermediary predecessors to amphetamine compounds. As to the methodology being used to obtain carboxylic acids, we applied ozonolysis reactions. The safrole and the estragole compounds are being treated with an ozone flow.² After the ozonide intermediate formation, we moved on to an oxidative cleavage ("workup") in order to acquire the carboxylic acid. Different reaction conditions are being tested, both in the ozonolysis and in the workup section. Different flows of ozone were also analyzed, since our starting material was being completely degraded due to highly oxidative conditions. We tested different types of ozone introduction, such as atmosphere saturation and even -78 °C reaction temperatures.



Scheme: Ozonolysis of Safrole and Estragole.

Initial results have shown that the amount of ozone introduced into the safrole reaction media is a crucial variable in order to minimize side reactions. As for estragole, we achieved an amount of 99% of conversion and managed to obtain 15% of selectivity for the carboxylic acid synthesis with a flow method using a tube-in-tube reactor, with O₂ gas. Therefore, to maximize product formation, the next step involves optimizing the continuous flow ozonolysis reaction and testing different oxidative cleavages of alkenes, such as photocatalysis for both estragole and safrole.³ Thus, it is expected to produce intermediate predecessors to obtain certified reference materials (CRM).

Acknowledgments

CNPq, CAPES and FAPERJ

¹ ABNT. NBR ISO 17034: 2017

46^o Reunião Anual da Sociedade Brasileira de Química: "Química: Ligando ciências e neutralizando desigualdades"

² Atapalkar, R. S. et al. *Green Chem.*, **2021**,23, 2391-2396.

³ Wise, D. E. et al. *J. Am. Chem. Soc.* **2022**. 144, 15437-15442.

Continuous Flow Synthesis of 4-(4-Aminophenyl)-morpholin-3-one: An Important Rivaroxaban Intermediate

Mayara Carvalho (IC), Felipe L. N. da Silva (PG), Mauro R. B. P. Gomez (PQ), Raquel A. C. Leão (PQ), Rodrigo O. M. A de Souza (PQ). *

mayaracarvalhodc@gmail.com; souzarod21@gmail.com*

Biocatalysis and Organic Synthesis Laboratory, Chemistry Institute – Federal University of Rio de Janeiro – IQ – UFRJ.

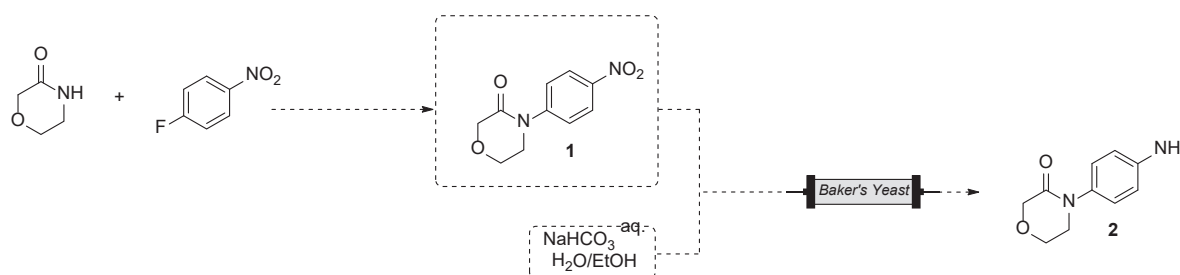
Keywords: *Rivaroxaban, Flow Chemistry, Reduction, Saccharomyces cerevisiae.*

Highlights

Continuous-flow synthesis of 4-(4-aminophenyl)-morpholin-3-one, an important intermediate in the synthesis of the drug Rivaroxaban via cascade nucleophilic aromatic substitution and low-cost NO₂ bioreduction using Baker's Yeast as catalyst.

Abstract

Rivaroxaban is a drug from the oxalizinone class that acts as a factor Xa inhibitor and is recommended for the treatment of deep vein thrombosis¹. It was invented and produced by Bayer, being marketed under the name Xarelto. The synthesis of this drug passes through the intermediate 4-(4-aminophenyl)-morpholin-3-one (**2**), which is obtained through the reduction of 4-(4-nitrophenyl)-morpholin-3-one (**1**) through hydrogenation catalyst with a yield of 37%.¹ Intermediate **1** can be obtained by a nucleophilic aromatic substitution and would be also evaluated by us during the next months. We have decided first to find a suitable alternative to the nitro group reduction. *Saccharomyces cerevisiae* is one of the most widely used yeasts in the world, also known as Baker's Yeast. It is found in the literature several articles that point to its ability to reduce nitro aromatic compounds in aniline with high yields.^{2,3} Continuous flow chemistry, with its system in miniaturized reactors compared to the batch system, enables better efficiency in: mass transfer, heat, energy, better reproducibility, easy scaling, greater purity and yield, and greater productivity.⁴ Since the reaction of interest presents a yield of only 37% for the desired product, this work aims at the synthesis of intermediate **2** through the bioreduction of **1** using baker's yeast in continuous flow (Scheme).



Scheme: composition of the reaction medium to obtain (**2**).

In our first study about the reduction reaction with *Saccharomyces cerevisiae* in basic conditions, we notice some difficult: the time of reaction be very long, but the ease of hydrolyzing the amide under basic condition was the main one. A careful study is being carried out that involves the choice of the base, concentration and temperature of the reaction. We expect that in this way the reduction product will be formed more than the hydrolysis impurity.

Acknowledgments

CNPq, CAPES and FAPERJ.

1. Saeed, A; Fattah, T. A. *Tetrahedron: Asymmetry* **2017**, *28*, 485–504.
2. Selvam, P; Mohapatra, S. K. *Letters in Organic Chemistry*, **2006**, *3*, 901-904.
3. Hanh, et al. *Terrahedron Lett.*, **1994**, *35*, 23, 3965-3966.
4. Seeberg, et al. *Chem. Rev.* **2017**, *117*, 11796–11893.

CYP716C58 and its role in celastrol biosynthetic pathway of *Maytenus ilicifolia*

Otávio Aguiar de Souza (PG),¹ Tatiana Maria de Souza-Moreira (PQ),² Wesley Bruno Botero (PG),¹ Keylla Utherdyany Bicalho (PQ),³ Mariana Marchi Santoni (TC)², Sandro Roberto Valentini (PQ)², Maysa Furlan (PQ).^{1*}

oa.souza@unesp.br; maysa.furlan@unesp.br

¹ NuBBE, Instituto de Química de Araraquara, Unesp; ² Faculdade de Ciências Farmacêuticas, Unesp Araraquara, ³ VIB Center for Plant Systems Biology, Ghent, Belgium

Palavras Chave: *Biosynthesis, Synthetic Biology, Organic Chemistry, Triterpenoid.*

Highlights

CYP716C58 and its role in the reconstitution of celastrol biosynthetic pathway in yeast;

CYP716C58 catalyzes the C-2 oxidation of maytenoic acid to populnic acid in yeast;

This oxidation step is vital to the complete elucidation of the antitumoral celastrol biosynthetic pathway.

Abstract

Celastrol is a quinone methide triterpenoid (QMT) accumulated in plants that belong to the Celastraceae family (such as the Brazilian species *Maytenus ilicifolia*). This QMT is one of the most promising compounds regarding to develop antitumor drugs. However, this compound is produced in very small amounts in the roots of plants, which unviable the direct extraction regardless of the employed technology or approach, and the majority of the enzymes that have a role in the downstream cascade oxidation steps towards the biosynthesis of celastrol remain unknown^{1,2}. Once these factors hinder the large-scale production of celastrol, one more efficient, viable, sustainable and inexpensive alternative is to try to reconstitute this oxidation steps in an heterologous organism (e.g. yeast) aiming to produce this valuable plant-derived compound¹. Previously, the *M. ilicifolia* root transcriptome via RNA-seq was created of and the full-length sequences of one oxidosqualene cyclases (OSCs, friedelin synthase *MiFRS4*) cytochrome P450 (CYPs, CYP712K4, CYP716C58, CYP716A280, CYP716E61, CYP716E62, CYP716E63, MiCYP81AM1) enzymes that shown to be potential candidates in the biosynthetic pathway were Gateway cloned in vectors pESC-URA-tHMG1-DEST, pAG423GAL-ccdB and pAG424GAL-ccdB, and MTR1, a P450 reductase was cloned in the vector pAG415GAL-ccdB³. Following this steps, combinatorial experiments were performed by combining *MiFRS4* and CYP712K4 (experimentally proven to produce friedelin⁴ and maytenoic acid³, respectively, important intermediates in the celastrol biosynthetic pathway) followed by the other cloned P450 enzymes separately and the suitable reductases *tHMG1* and *MTR1*. The vectors with the cloned enzymes were transformed in the yeast *Saccharomyces cerevisiae* (KB13; *MATa*, *MAL2-8c*, *SUC2*, *ura3-52*, *P_{ERG7::PKEX2-ERG7}*, with the auxotrophic markers *trp1Δ0*, *his3Δ0*, *leu2Δ0* and *pah1Δ0* obtained by CRISPR/Cas9³). Yeast transformations were performed using the lithium acetate/single stranded carrier DNA/ polyethyleneglycol method⁵ and the transformed cells were selected on SD medium with suitable dropout supplements. The positive colonies were detected by PCR colony and the yeast cells were cultivated in the presence of methyl-β-cyclodextrin (MβCD) as reported⁶. From the all the combinatorial experiments, the one with combination of *MiFRS4*, *tHMG1*, CYP712K4 and CYP716C58 led to C-2 oxidation of the maytenoic acid to populnic acid (3-hydroxy-2-oxo-D:A-friedelan-3-en-29-oic acid) which was detected by high resolution liquid chromatography-mass spectrometry and molecular networking. This is particularly important and represents an advance since previous biogenetic pathways³ have speculated that an oxidation step leading to populnic acid is vital for further elucidation of the complete metabolic pathway of QMTs such as celastrol, and our findings prove experimentally those assumptions.

References: 1 LU et al. *Med. Res. Rev.* 41(2) 1022-1060, 2021; 2 COURDAVAULT et al. *Trend. Can.* 6 (6) 444-448, 2020; 3 BICALHO et al. *Plant Cell Phys.* 60 (11) 2510-2522, 2019; 4 ALVES et al. *Molecules* 23(3) 700 ; 5 GIETZ and WOODS. *Methods Enzymol.* 87-96, 2002; 6 Moses et al. *PNAS*, 111:1634-1639, 2014.

Acknowledgments

FAPESP (grants 21/05646-2, 13/07600-3 and 14/50926-0), CNPq (grant 2014/465637-0) and Capes (Finance Code 001)

Desenho e caracterização de novas estruturas líquido cristalinas fotoativas derivadas da madeira roxinho

Bruna Thatise Batistel (IC),^{1*} **Caroline S. B. Weber** (PG),¹ **Aloir A. Merlo** (PQ).¹

brunathatise.batistel@gmail.com

¹Instituto de Química, Universidade Federal do Rio Grande do Sul.

Palavras Chave: Cristais líquidos; Estrutura fotoativa; Madeira roxinho; Extração Soxhlet.

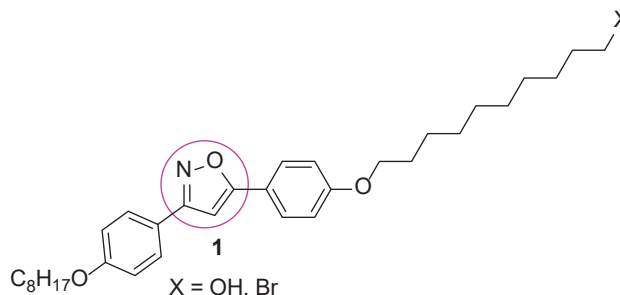
Highlights

Design and characterization of new photoactive liquid crystalline structures derived from roxinho tree wood.

This work is investigating photoactive molecular structures present in roxinho tree wood, connect this material with the isoxazole ring derivatives (an important precursor of mesophases) and combine both properties.

Resumo/Abstract

A investigação de novas estruturas líquido cristalinas com propriedades fotossensíveis tem crescido nas últimas décadas, em função da grande aplicabilidade desses compostos, tais como em células fotovoltaicas [1], armazenamento holográfico de dados [2], fotoalinhamento [3], entre outros. A arquitetura dessas moléculas é a etapa-chave para a obtenção das propriedades fotoativas. Desse modo, procurou-se utilizar um material fotossensível natural, extraído da madeira roxinho, árvore do gênero *Peltogyne*, originária da região Amazônica e da Mata Atlântica. A utilização de tal material é justificada pela importância da preservação da biodiversidade dos ecossistemas. Nesse sentido, pretende-se funcionalizar o substituinte alquila do isoxazol (**1**), importante núcleo indutor de mesofases [4], com o material fotoativo extraído da madeira. A extração do tipo Soxhlet foi empregada para isolar o material de interesse, através da utilização de diclorometano, etanol e acetato de etila como fase móvel. O emprego dos dois últimos solventes foi mais eficiente. O material isolado é fotoativo apenas em solução. São perspectivas futuras desse trabalho, a purificação e a caracterização da estrutura isolada da madeira roxinho, assim como a inserção do anel isoxazol (**1**) em tal material, objetivando a obtenção de um cristal líquido com propriedades fotossensíveis.



[1] *RSC Adv.*, 2016, **6**, 11577-11590.

[2] *Liq. Cryst. Rev.*, 2016, **4**, 83-100.

[3] Vladimir G. Chigrinov, Vladimir M. Kozenkov, Hoi-Sing Kwok. *Photoalignment of liquid crystalline materials: Physics and applications*. John Wiley & Sons, Ltd., 2008. ISBN: 978-0-470-06539-6.

[4] *J. Mater. Chem. C*, 2017, **5**, 12308-12337.

Agradecimentos/Acknowledgments

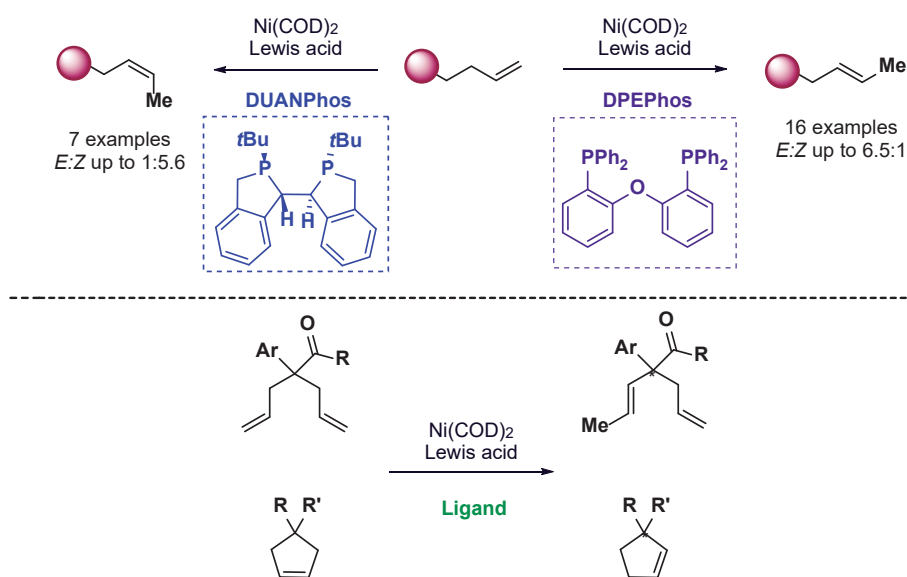
Agradecemos ao CNPq (MCTI/CNPq N° 309661/2020-0) e Fapergs/Edital PqG 002/2014 pelo apoio financeiro.

Desymmetrization of olefins catalyzed by Ni(0).**Eduardo J.C. Junior** (PG),¹ **Henrique S. Almeida** (IC),¹ **Caio C. Oliveira** (PQ).¹

e230035@dac.unicamp.br; h172265@dac.unicamp.br; caio.oliveira@unicamp.br

¹Institute of Chemistry, University of Campinas (UNICAMP)Keywords: *Catalysis, Olefin Isomerization, Nickel, Lewis Acid.***Highlights**The combination of Ni(0) and a Lewis acid allowed the stereoselective isomerization of terminal alkenes under kinetic control.¹**Abstract**

The combination of Ni(0) and Lewis Acid (LA) successfully allowed the transposition of terminal double bonds to yield 1,2-alkenes. Interestingly, only one migration was observed, even when further migrations would lead to a more stable, conjugated isomer.¹ Careful ligand choice allowed the stereocontrol for these reactions. While DPEPhos produce *E*-products, DUANPhos produce *Z* isomers. The success of this method inspired the development of a desymmetrization protocol in route to more complex olefins. Bisallylic and cyclic substrates were successfully isomerized and its enantioselective version is ongoing.

**Scheme 1.** Stereoselective monotransposition of double bonds.

References:

- (1) Carvalho-Junior, E. J.; Oliveira, C. Nickel-Catalyzed Double Bond Transposition under Kinetic Control. ChemRxiv November 25, 2022. <https://doi.org/10.26434/chemrxiv-2022-w9n02>.

Acknowledgments

Determinação de Pureza de Sais de Bunte por RMN Quantitativo de Hidrogênio

Vanessa B. dos Santos (PG),^{1*} Rogério A. Gariani (PQ),¹ Alcindo A. dos Santos (PQ),²

vanessa.boz@outlook.com;

¹Departamento de Química - Laboratório Análise Instrumental – LAI, Universidade do Estado de Santa Catarina, SC, Joinville, CEP 89219-710, Brazil; ² Instituto de Química, Universidade de São Paulo, Av. Prof. Lineu Prestes, 748, 05508-900 São Paulo, SP, Brazil;

Palavras Chave: Determinação de pureza, Calibração interna, Sais de Bunte, Quantificação, RMNq-¹H.

Highlights

Determination of purity of bunte salts by quantitative hydrogen NMR

The pharmaceutical industry associated with the development of new drugs seeks, together with the regulatory agencies, to maintain a high standard of quality for these inputs and, for this, it is necessary, in addition to structural clarification, to determine the purity of the composition, especially those with important biological activities, particularly those derived from Bunte salts. Concerning this problem, a need to study the purity of these substances arises, using a non-destructive, fast and relatively simple technique such as quantitative hydrogen Nuclear Magnetic Resonance (¹H qNMR), able to analyze several compounds in a single measurement and without requiring a standard identical to the substance under quantification. The quantification methodology used in this work was ¹H qNMR with internal calibration, initially used as the internal standard certified calcium formate reference material, which was named as the primary standard to later quantify the purity of the secondary standard dimethylsulfone (DMSO₂) and then use it as reference material. This work was developed aiming to find solutions with better cost-benefit for quality control, specifically of Bunte salts via RMNq-¹H.

Resumo/Abstract

A indústria farmacêutica associada ao desenvolvimento de novos medicamentos busca, juntamente com os órgãos de regulamentação, manter um alto padrão de qualidade destes insumos e, para isso, é necessário além da elucidação estrutural, a quantificação da pureza da composição, especialmente os que apresentam importantes atividades biológicas, como particularmente os derivados de sais de Bunte. Mediante a essa problemática, viu-se a necessidade de estudar a pureza destas substâncias por meio de uma técnica não destrutiva, rápida e relativamente simples como Ressonância Magnética Nuclear quantitativa de hidrogênio (RMNq-¹H), capaz de analisar diversos compostos. A metodologia de quantificação utilizada neste trabalho foi a RMNq-¹H com calibração interna, empregado inicialmente como padrão interno o material de referência certificado formiato de cálcio que foi denominado como padrão primário para posteriormente quantificar a pureza do padrão secundário DMSO₂ e assim, utilizá-lo como material de referência. Sendo assim, para a etapa inicial foram executadas algumas otimizações dos métodos de preparo e aquisição, com o objetivo de obter sinais bem resolvidos e núcleos completamente relaxados, além de uma pesagem mais assertiva. Para garantir a qualidade do método, a validação do método analítico foi baseada nas diretrizes atuais, em que foram verificados: a seletividade, linearidade, precisão, robustez, limites de detecção e quantificação, incerteza combinada e incerteza expandida. Todos os testes foram comparados estatisticamente em termos de porcentagem de coeficiente de variação, não sendo observado diferença significativa ao confrontar os resultados adquiridos. O valor de pureza determinado para o padrão secundário, por meio do ensaio de linearidade foi de 99,72% com $\pm 1,31\%$ de incerteza com 95% de confiança em uma sonda TBI, onde todo o estudo foi realizado. Após a investigação do padrão secundário, este foi aplicado como material de referência nos derivados de sais de Bunte e então obtida a determinação de pureza destes, podendo chegar a uma pureza de 52,44% de S-(2-etoxi-2-oxoetil) tiosulfato de sódio (composto A), com uma incerteza de $\pm 1,44\%$ (95% de confiança). Este trabalho foi desenvolvido visando encontrar soluções com melhor custo-benefício para controle de qualidade, especificamente de sais de Bunte via RMNq-¹H, técnica que se mostra rápida e razoavelmente simples.

Agradecimentos/Acknowledgments

Aos órgãos de fomento CAPES, CNPq e FAPESC, pelo apoio financeiro durante o trabalho.

46ª Reunião Anual da Sociedade Brasileira de Química: "Química: Ligando ciências e neutralizando desigualdades"

Development of new selenotetrazole derivatives and evaluation as corrosion inhibitors

Victor H. M. Costa (IC)¹, Clara Castro Barroso (IC)¹, Pâmella S. Cordeiro (PG)¹, Vinicius M. dos Santos (IC)², Caio M. Fernandes (PG)², Joel S. Reis (PQ)¹, Eduardo A. Ponzio (PQ)² and Vanessa Nascimento (PQ)¹

vhmenezescosta@id.uff.br;

¹Supraselen Laboratory, Chemistry Department, Fluminense Federal University; ²LAMUFF, Department of Chemistry, Fluminense Federal University

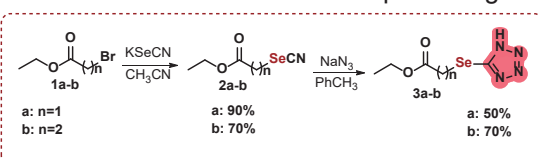
Keywords: Selenium, Tetrazole, Heterocycle, Anticorrosive, Organic synthesis

Highlights

This work aimed to explore the anticorrosive capacity of new molecules containing selenium and the tetrazole core.

Resumo/Abstract

Corrosion consists in the spontaneous degradation of metallic materials due to their interaction with the environment¹. One of the main methods of protecting metal alloys is the application of organic corrosion inhibitors, substances added in small concentrations directly to the aggressive medium in order to hinder, delay or reduce corrosion¹. Compounds containing heteroatoms such as N, O and S and also π -electrons have been described by their ability to increase adsorbent properties on the metal surface because of the donation of electron pairs for empty d orbitals of the atoms of metal surface, forming protective layers¹. Tetrazole is a heterocyclic structure containing four nitrogen atoms and has a great range of applications. In addition, organoselenium compounds are found in the literature linked to a large number of pharmacological activities, however, despite their great potential, much less is reported about their applications in material sciences². Thus, the aim of this project is to evaluate the anticorrosive potential of organoselenium derivatives containing the tetrazole nucleus. Therefore, a series of selenium aliphatic derivatives **2a-b** was synthesized by inserting the SeCN group in commercial bromides **1a-b**. Then, the target molecules **3a-b** were obtained by forming the tetrazole core with a reaction using sodium azide³ (Scheme 1). To evaluate the anticorrosive activity of the synthesized compounds, weight loss study was carried out, where it can be observed that the four organic molecules act as excellent corrosion inhibitors at room temperature (Table 1). Significantly decreasing the corrosion rate and achieving anticorrosive efficiencies in the range of 81 to 93%, approximately, at 2,00 mmol L⁻¹. Additionally, electrochemical tests have shown that these molecules act by decreasing both cathode and anode currents, increasing the polarization resistance of the mild steel and protecting it against corrosion.



Scheme 1. Synthetic pathway of Selenotetrazoles derivatives

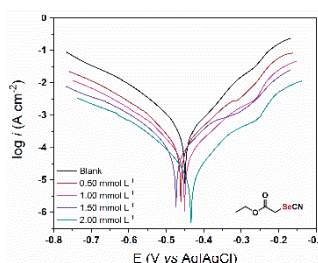


Figure 1. Polarization curves for one of the organoselenium compounds

Table 1. Anticorrosive evaluation

Compound	Concentration (mmol L ⁻¹)	Corrosion Rate (mm year ⁻¹)	η (%)
-	-	1,811 ± 0,050	-
	0,50	0,662 ± 0,022	63,4
	1,00	0,546 ± 0,028	70,0
	1,50	0,400 ± 0,025	77,9
	2,00	0,286 ± 0,036	84,2
	0,50	0,721 ± 0,012	60,2
	1,00	0,624 ± 0,024	65,5
	1,50	0,483 ± 0,057	73,4
	2,00	0,342 ± 0,012	81,1
	0,50	0,406 ± 0,019	77,6
	1,00	0,314 ± 0,020	82,6
	1,50	0,211 ± 0,017	88,3
	2,00	0,130 ± 0,014	92,8
	0,50	0,531 ± 0,021	70,6
	1,00	0,426 ± 0,025	76,5
	1,50	0,323 ± 0,028	82,2
	2,00	0,217 ± 0,020	88,0

Agradecimentos/Acknowledgments

UFF, FAPERJ, SBQ-RJ, CAPES

References

- [1] Fernandes, C. M. et al; *Journal of Molecular Liquids*, **2023**, 375, 12199.
 [2] Abd El-Lateef H. M. et al; *Journal of the Taiwan Institute of Chemical Engineers*. **2022**, 133, 9360.
 [3] Leal, J. G. et al; *New Journal of Chemistry*. **2017**, 41, 5875.

Development of Synthetic Methodology Towards Boronic Acids Derivatives as Potential Therapeutic Agents

Wallace C. de Souza (PG),¹ Bruno C. Ribeiro (IC),¹ Raquel A. C. Leão (PQ),¹ Vagner D. Pinho (PQ),² Leandro S. M. Miranda (PQ),¹ Rodrigo O. M. A. de Souza (PQ).^{1*}

wallacecostadesouza@gmail.com; souzarod21@gmail.com*

¹Laboratório de Biocatálise e Síntese Orgânica, Instituto de Química – Universidade Federal do Rio de Janeiro –RJ

²Microbiológica Química e Farmacêutica - Rua Dr. Nicanor, 238 Inhaúma, Rio de Janeiro, RJ – Brasil CEP 20765-120

Keywords: boronic acids, nucleosides, borylation.

Highlights

Development of a synthetic methodology towards boronic acids derivatives and borylated nucleosides with potential antimicrobial activity.

Abstract

Boronic acids and their derivatives have been studied as potential therapeutic agents due to their physicochemical characteristics, which allow them to act as powerful enzyme inhibitors, among other applications.¹ Thus, the objective of this work is the development of new methodologies for the synthesis of new generation of borylated nucleosides with potential action as antimicrobial agents. In view of the objectives, synthetic strategies were outlined based on the non-selective protease inhibitor synefungin for the development of boronic analogues. Recently, methodologies for borylation reactions have been the subject of intense study. However, the synthesis of nucleoside derived amino-boronic acids are non-existent. Therefore, the analogues **1** and **5**, Figure 1, were projected as model nucleoside derivatives to develop the necessary methodology to introduce the amino-boronic acids functionality into a nucleoside scaffold.

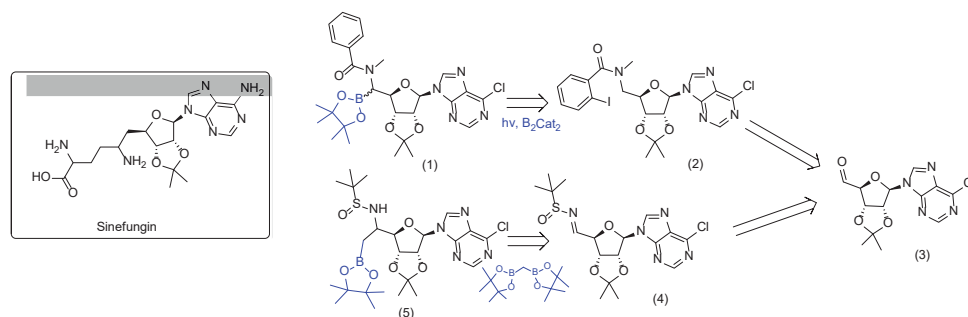
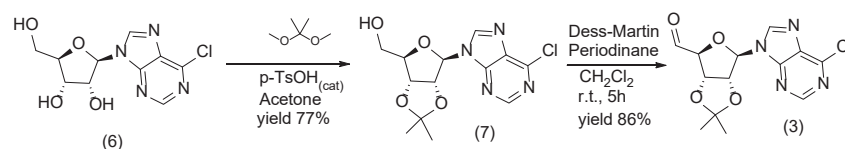


Figure 1: Transformations in the alcoholic portion of the nucleoside

Two different strategies were considered to introduce the amino-boronic acids functions, as depicted in Figure 1. For both, the aldehyde **3** is a common intermediate. Thus, **3** was obtained in 66% global yield from commercial nucleoside **6**, through the reaction sequence comprised of 2,3-*O,O*-isopropylidene introduction for the protection of the C2', C3' position of **6** followed by the Dess-Martin mediated oxidation of the primary position of 7, Scheme 1.



Scheme 1: nucleoside synthesis and oxidation

Reductive amination as well as sulfonamide formation for the synthesis of **2** and **4**, respectively, are under investigation.

Acknowledgments

CNPq, CAPES, FAPERJ

46ª Reunião Anual da Sociedade Brasileira de Química: "Química: Ligando ciências e neutralizando desigualdades"

1. Fernandes, G. F.S; Denny, W.A, et al, *Eur. J. Med. Chem*, **2019**, *179*, 791-804.
2. BTrippier, P. C., & McGuigan, C. *Med. Chem. Comm.*, **2010**, 183-198.

Diels-Alder reaction of chitin-derived furans

Julia Soares Baptista (IC),¹ Camila Souza Santos (PQ),¹ Renan Rodini Mattioli (PG),¹ Vitor H. Menezes da Silva (PQ), Julio Cezar Pastre (PQ)^{1,*}.

j236489@dac.unicamp.br; jpastre@unicamp.br

¹ Institute of Chemistry, University of Campinas - UNICAMP, 13083-970, Campinas, SP, Brazil.

Keywords: N-Acetylglucosamine, 3-acetamido-5-ethylfuran, maleimide. Diels-Alder reaction, chitin derivatives.

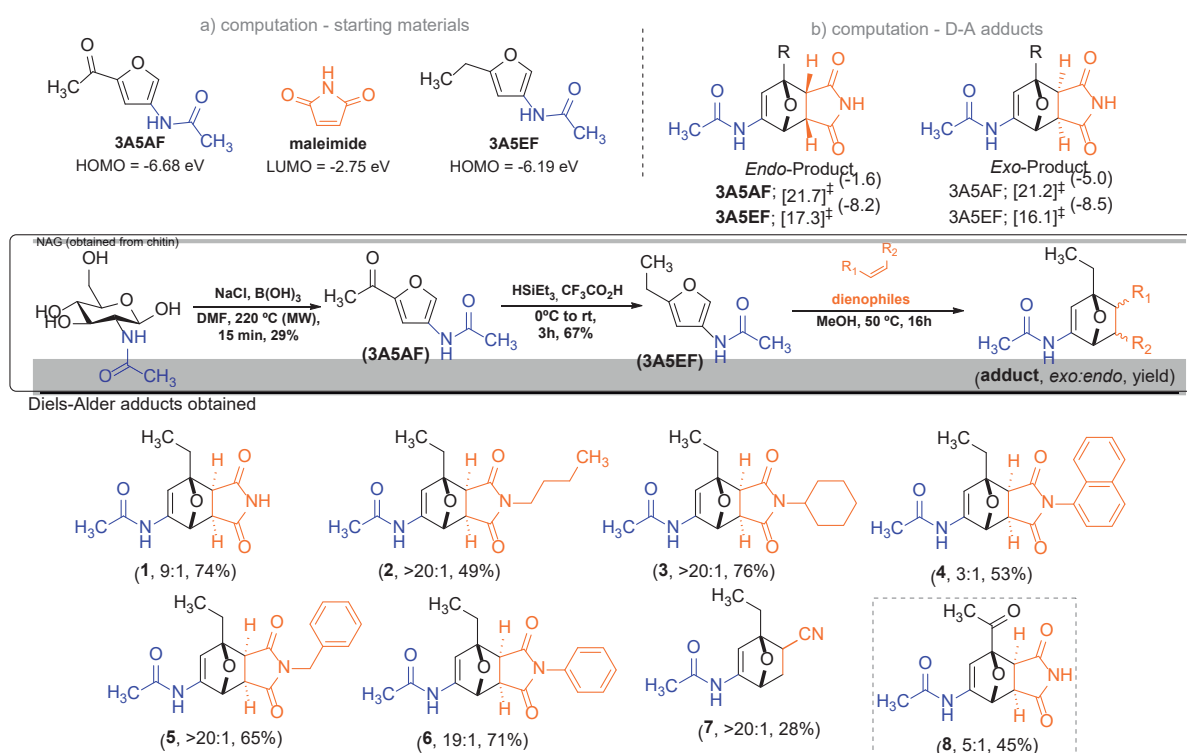
Highlights

Aromatic products that contain nitrogen in their structures are important for the sustainable production of building blocks.

Eight Diels-Alder adducts were obtained by the reaction between chitin-derived furans and several maleimides.

Abstract

The biorefinery concept is very important to the sustainable production of biofuels, functional materials, and fine chemicals, such as, for example, those containing nitrogen in their structures. Chitin is a biopolymer that has great potential for obtaining nitrogen-containing derivatives, such as 3-acetamido-5-acetylfuran (**3A5AF**) which is obtained from the dehydration of *N*-acetyl-*D*-glucosamine (NAG).¹⁻³ We started our study by computationally analyzing the reactivity of two chitin-derived furans, **3A5AF** and **3A5EF**, against the dienophile maleimide by means of Density Functional Theory. Based on the HOMO energies depicted the **3A5EF** is more reactive than **3A5AF**. Indeed, the higher reactivity of **3A5EF** is reflected by considerably reduction of ΔG^\ddagger comparing **3A5AF** with **3A5EF** (4.4 and 5.1 kcal/mol for *endo* and *exo*, respectively). Moreover, the DA reaction for **3A5EF** has higher exothermicity than its counterpart DA reaction with **3A5AF**. Thus, **3A5EF** was chosen to be the diene in the experimental tests of the DA reaction. The reaction between **3A5EF** and maleimides as dienophiles in methanol, at 50 °C in 16 hours gave the best yields and selectivities. The adducts were synthesized with yields between 28–76% (sum of *exo/endo* isomers; *exo* being the major isomer).



References: [1] *Green Energy Environ.*, **2018**, 3, 318–327; [2] *Green Chem.*, **2014**, 16, 2204–2212; [3] *ACS Sustain. Chem. Eng.*, **2018**, 6, 12411–12418.

Acknowledgments

The authors gratefully acknowledge financial support from the São Paulo Research Foundation - FAPESP (Award N.: JCP, 2021/06661-5) and the Brazilian National Council for Scientific and Technological Development – CNPq (Award N.: JSB, 120853/2022-1).

Divergent Functionalization of Styrenes via Radical/Polar Crossover with CO₂ and Sodium Sulfinates

Kimberly B. Vega (PG)*,^[1,2] José A. C Delgado (PG),^[1,2] Lucas V. B. L. Pugal (PG),^[1] Dr. José T. M. Correia (PQ)
^[1] Prof. Burkhard König ^[2] and Prof. Dr. Márcio W. Paixão (PQ)^[1]

kbenedetti@utp.edu.co

¹Laboratory for Sustainable Organic Synthesis and Catalysis - Department of Chemistry, Federal University of São Carlos – UFSCar, São Carlos, São Paulo, Brazil; ² Institut für Organische Chemie, Universität Regensburg, Universitätsstrasse 31, 93053, Regensburg, Germany.

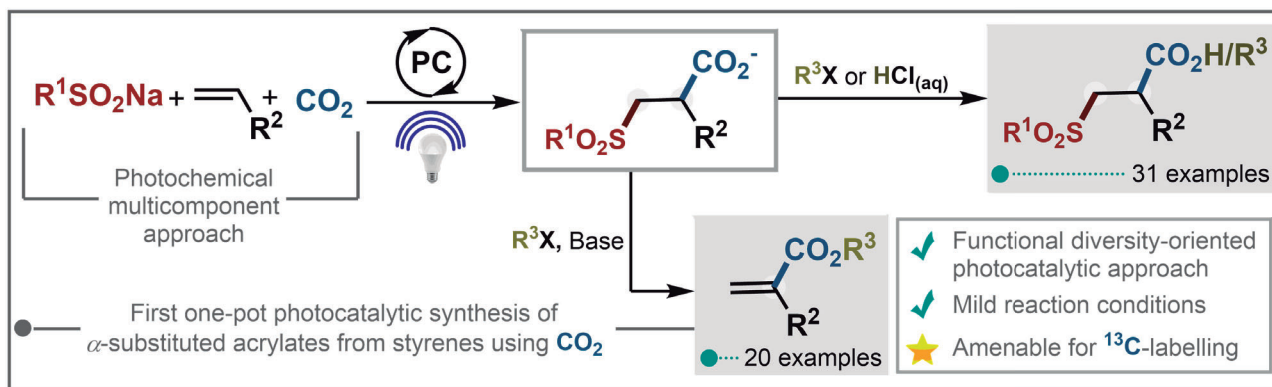
Keywords: Photocatalysis, Sustainability, Carbon Dioxide, Carboxylic acids, α -substituted acrylates

Highlights

The merger of radicalar with polar chemistry has been designed to implement a tunable multicomponent reaction which encompasses CO₂, sodium sulfinates and styrenes to access both β -sulfonylated carboxylic acids and to α -substituted acrylates.

Abstract

Sulfones and carboxylic acids are prominent chemical motifs widely present in the chemical structure of agrochemicals, pharmaceuticals and many other highly valuable compounds.^[1,2] Herein, we describe a conjunctive strategy for the precise installation of these functionalities onto styrenes using sodium sulfinates and CO₂ as coupling partners. The protocol allowed the preparation of carboxy-sulfonylated compounds in good yields and broad functional group tolerance. Additionally, taking advantage of the leaving group ability of the sulfone moiety, a one-pot photocatalytic carboxy-sulfonylation-elimination strategy was developed for the synthesis of α -aryl-acrylates.



[1] *Angew. Chemie* **2020**, *132*, 11717–11723. [2] *ACS Catal.* **2020**, 14984–15007.

Acknowledgments

We are grateful to Brazilian funding agencies CNPq (INCT Catálise, Grants No 444061/ 2018-5 and Universal Project 405052/2021-9) and FAPESP (21/06099-5). KBV thanks to FAPESP (PhD fellowship 21/01354-7). JTMC thanks to FAPESP (postdoc fellowship 17/10015-6 and 19/01560-6). This study was financed in part by the Coordenação de Aperfeiçoamento de Pessoal de Nível Superior - Brasil (CAPES) - Financial code 001. This work was supported by the German Science Foundation (DFG, KO 1537/18-1).

Área: ORG

(Inserir a sigla da seção científica para qual o resumo será submetido. Ex: ORG, BEA, CAT)

Diverse Continuous Photooxygenation Reactions of (+) and (-)- α -Pinenes to the Corresponding Pinocarvones or *trans*-PinocarveolsGabriel H. S. Rosa (IC)¹, Thiago I. S. Santos (PG)¹, Timothy J. Brocksom (PQ)¹, Kleber T. de Oliveira* (PQ)^{1*}

*kleber.oliveira@ufscar.br

¹Departamento de Química, Universidade Federal de São Carlos, São Carlos, 13565-905, Brazil.

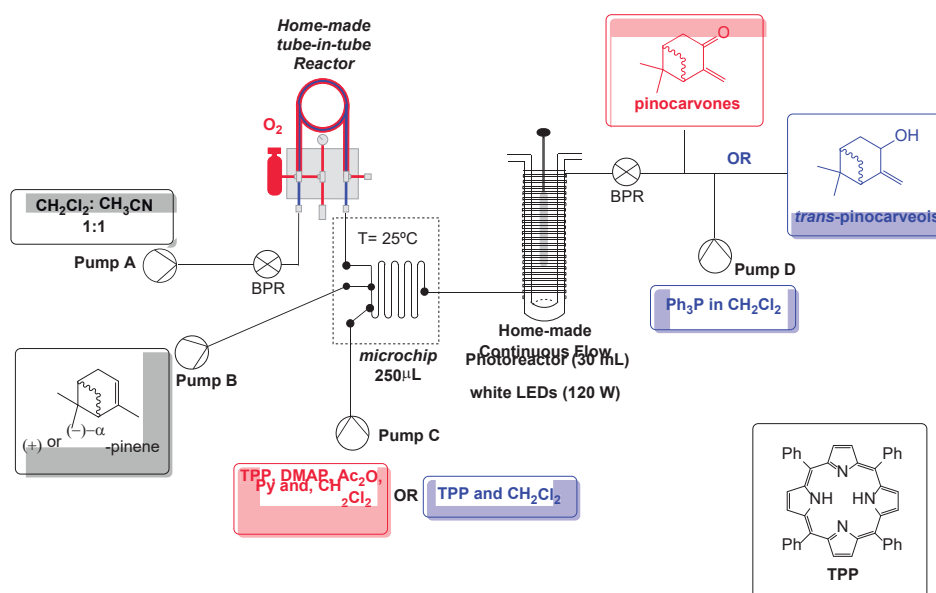
Palavras Chave: Flow chemistry, Photooxygenation, Terpenes, Hydroperoxides, Scale-up

Highlights

Pinocarvones and *trans*-pinocarveols were obtained from the photooxygenation of both (+) and (-) α -pinenes under continuous flow conditions. Multigram experiments were efficiently performed using a tube-in-tube reactor for oxygen diffusion, and a photoreactor for the photooxygenation step. The continuous flow reactors were developed by our research group.

Resumo/Abstract

In this study, the continuous flow photooxygenation reactions of (+) and (-)- α -pinenes are described. The corresponding hydroperoxides (intermediates from the photooxygenation step) were continuously processed under mild conditions using Ac_2O and a base to yield (-) or (+) pinocarvones in up to 79–83% yield (12–13 gram-scale). Alternatively, the hydroperoxides were continuously reduced with a $\text{Ph}_3\text{P}/\text{CH}_2\text{Cl}_2$ solution giving the corresponding pinocarveols up to 61% yield (10.8 g-scale). Our protocols proved to be efficient, easily scaled up, and safe while processing unstable hydroperoxides at the g-scale and during long-term experiments (up to 24 h). We also describe a variable we have named efficiency (E) which is useful to rationalize the best reaction conditions for the best yield and includes the productivity ($\text{g}\cdot\text{day}^{-1}$) and unreacted starting materials.



Agradecimentos/Acknowledgments

The authors would like to thank the São Paulo Research Foundation FAPESP for financial support (grants 2013/07276-1, 2019/27176-8, 2020/06874-6 and G. H. S. R.'s fellowship 2020/04114-4). We also thank CNPq and CAPES.



Dynamic kinetic resolution of chiral benzylamines mediated by palladium catalyst supported on dolomite.

Larissa M. da Silva (IC), José C. Q. Arêas (PG), Livia Y. Sawada (IC), Fernanda A. de Siqueira (PQ)*

larissa.moises20@unifesp.br; [jqcareas@unifesp.br](mailto:jcqareas@unifesp.br); livia.sawada@unifesp.br; fasiqueira@unifesp.br*

Chemistry Department, UNIFESP – Diadema.

Keywords: Dynamic Kinetic Resolution; Palladium; Chiral Amines; Dolomite; Biocatalysts.

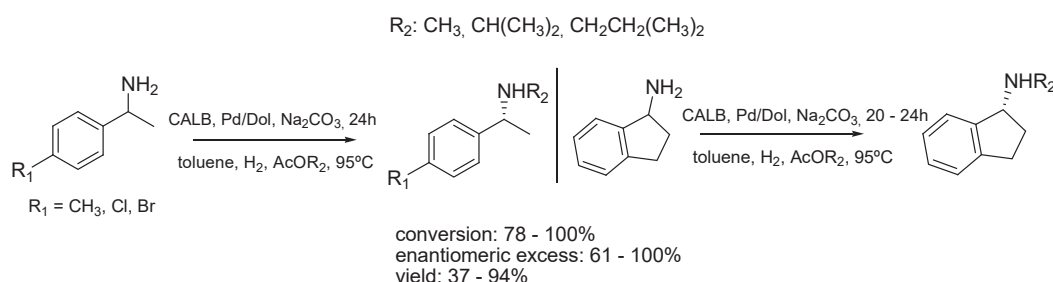
Highlights

Study carried out to understand and optimize DKR reactions of benzylamines using different reaction conditions.

Resumo/Abstract

Enantiomerically pure amines are essential for the chemical, agrochemical and pharmaceutical industries, as they are present in the structures of a series of biologically active compounds. Dynamic kinetic resolution (DKR) has been shown to be a great option for obtaining enantiomerically pure amines, as it is cost-effective and has several features of green synthesis, such as the use of an enzyme, a relatively inexpensive and recyclable catalyst, in addition to being able to lead to a theoretical yield of 100%.¹⁻² However, amines require drastic conditions for racemization to occur, a crucial step in the kinetic resolution process, which can affect enzymatic activity. This work presents the DKR of 4 benzylamines using different reaction conditions in order to optimize and obtain the most enantiomerically pure amines.

The catalyst used was designed by our research group and has 2.5% m/m of palladium in dolomite.²



The substrates used are represented in the scheme and to perform the DKR reactions three different donors of the acyl group were used: isoamyl acetate, isocyl acetate and ethyl acetate. Among all the variations with the acyl donor, in general, ethyl acetate generated the best results in most substrates. This is due to its smaller size, which does not impair the action of the enzymatic catalyst. The use of the three different acyl donors allowed evaluating the best results, with the objective of improving the conditions of DKR.

Among the molecules studied, 4-chlorine- α -methylbenzylamine and 4-bromine- α -methylbenzylamine were converted to the chiral acetamides, but with loss of halogen atom, observed by the analysis of NMR spectrum. For the 4-methyl- α -methylbenzylamine and 1-indanamine the corresponding acetamides were obtained in excellent conversions and enantiomeric excesses.

1 Gustafson, K. P. J.; Lihammar, R.; Verho, O.; Engström, K.; Bäckvall, J.-E. *J. Org. Chem.* 2014, 3747.

2 Mendonça, R.C.Z., Esteves, L.M., Oliveira, H.A. *et al.* Recyclable Palladium Catalyst Supported on Dolomite for Dynamic Kinetic Resolution of (\pm)-1-Phenylethylamine. *Catal Lett* 152, 1205–1214.

Agradecimentos/Acknowledgments

FAPESP, CNPq, UNIFESP - Diadema

Dynamic kinetic resolution of chiral benzylamines using ionic liquids and palladium catalyst supported on dolomite.

Livia Y. Sawada (IC),¹ José C. Q. Arêas (PG),¹ Larissa M. da Silva (IC),¹ Luiz Sidney Longo Júnior (PQ),² Fernanda A. de Siqueira (PQ)^{1*}

livia.sawada@unifesp.br; [jqcareas@unifesp.br](mailto:jcqareas@unifesp.br); larissa.moises20@unifesp.br; luiz.longo@unifesp.br
fasiqueira@unifesp.br

¹Chemistry Department, UNIFESP - Diadema; ²Department of Pharmaceutical Sciences, UNIFESP – Diadema.

Keywords: Dynamic Kinetic Resolution; Ionic Liquids; Palladium; Chiral Amines; Dolomite; Biocatalysts

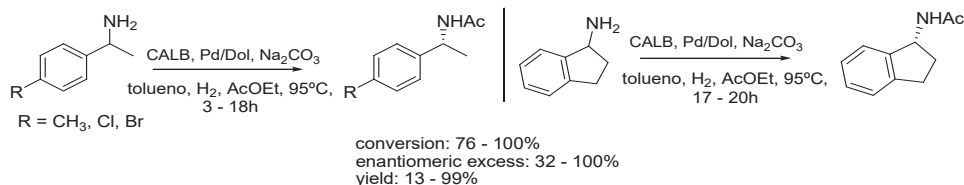
Highlights

Study carried out to understand and optimize DKR reactions of benzylamines using ionic liquids and different reaction conditions.

Resumo/Abstract

Enantiomerically pure amines are essential for the chemical, agrochemical and pharmaceutical industries, as they are present in the structures of a series of biologically active compounds. Dynamic kinetic resolution (DKR) has been shown to be a great option for obtaining enantiomerically pure amines, as it is cost-effective and has several features of green synthesis, such as the use of an enzyme, a relatively inexpensive and recyclable catalyst, in addition to being able to lead to a theoretical yield of 100%.¹⁻² However, amines require drastic conditions for racemization to occur, a crucial step in the kinetic resolution process, which can affect enzymatic activity. This work presents the DKR of 4 benzylamines using different reaction conditions in order to optimize and obtain the most enantiomerically pure amines.

The catalyst used was designed by our research group and has 2.5% m/m of palladium in dolomite.²



In an attempt to improve the metal catalyst efficiency, ionic liquids (N₄₄₄₄.NTf₂, N₈₈₈₈.NTf₂, P₄₄₄₄.NTf₂, P₈₈₈₈.NTf₂) were used as solvents. The use of these solvents is a green alternative, as these are low toxicity and low steam pressure substances. In addition, it is known that the use of polar solvents as ionic liquids contribute to the stabilization of palladium nanoparticles³.

The use of ionic liquids allowed a significant reduction in the reaction time for the substrates 4-methyl- α -methylbenzylamine and 1-indanamine in relation to reactions without these solvents, which generally took about 20 to 24 hours to obtain good results. These reactions without the use of ionic liquids were performed in previous studies by our research group.

However, 4-chlorine- α -methylbenzylamine and 4-bromine- α -methylbenzylamine substrates did not form the expected products. Through analysis of nuclear magnetic resonance (NMR), it was seen that they were converted to the chiral acetamides, but with loss of the halogen atom.

1 Gustafson, K. P. J.; Lihammar, R.; Verho, O.; Engström, K.; Bäckvall, J-E. J. Org. Chem. 2014, 3747.

2 Mendonça, R.C.Z., Esteves, L.M., Oliveira, H.A. *et al.* Recyclable Palladium Catalyst Supported on Dolomite for Dynamic Kinetic Resolution of (\pm)-1-Phenylethylamine. *Catal Lett* 152, 1205–1214.

3 Mukherjee, D. J. Nanopart. Res. 2008, 10, 429

Agradecimentos/Acknowledgments

FAPESP, CNPq, UNIFESP - Diadema

46^o Reunião Anual da Sociedade Brasileira de Química: "Química: Ligando ciências e neutralizando desigualdades"

Efficient two step, one-pot sequential synthesis of functionalized pyrrolo[5,4-*b*][1,5]benzodiazepines

Julia Poletto (PG),^{1*} Michael Jackson Vieira da Silva (PQ),¹ Fernanda Andreia Rosa (PQ).¹

juliapoletto0@gmail.com

¹Departamento de Química, UEM

Palavras Chave: β -enamino diketone, 4-acyl pyrrole-2,3-dione, pyrrolo[5,4-*b*][1,5]benzodiazepine

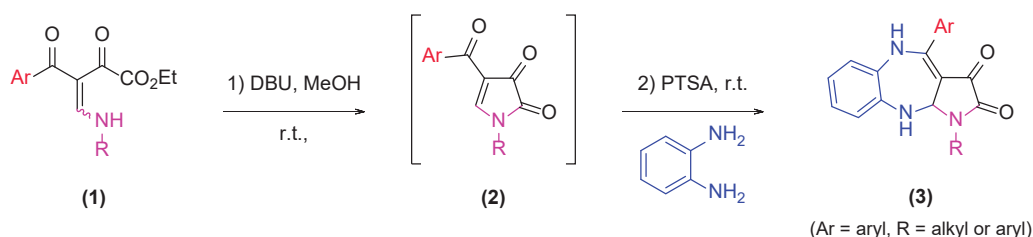
Highlights

A simple and efficient synthetic methodology was developed for the preparation of the pyrrolo[5,4-*b*][1,5]benzodiazepine nucleus from 4-acyl pyrrole-2,3-diones and *o*-phenylenediamine.

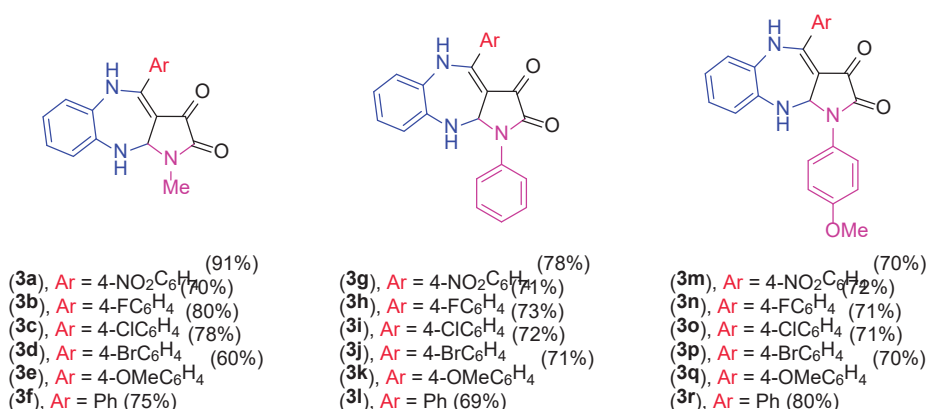
Resumo/Abstract

Benzodiazepine scaffold has great potential as a pharmacophoric subunit in biologically active molecules and drug design.¹ Therefore, we have developed a sequential one-pot method from the *in situ* intermediate 4-acyl pyrrole-2,3-diones (**2**) with *o*-phenylenediamine. Using this protocol, a series of 18 novel pyrrolo[5,4-*b*][1,5]benzodiazepine derivatives **3a-r** were obtained in good to excellent yields (60-91%).

Scheme 1. Synthesis of pyrrolo[5,4-*b*][1,5]benzodiazepines from the reaction of 4-acyl pyrrole-2,3-diones and *o*-phenylenediamine^a



^aReaction conditions: (1) (0.5 mmol), DBU (0.6 mmol), in 10 mL of MeOH, at r.t. for 40 min to 2 h and PTSA (1.1 mmol) and *o*-phenylenediamine (1.0 mmol) for 1 to 12 h. Yield of isolated product.



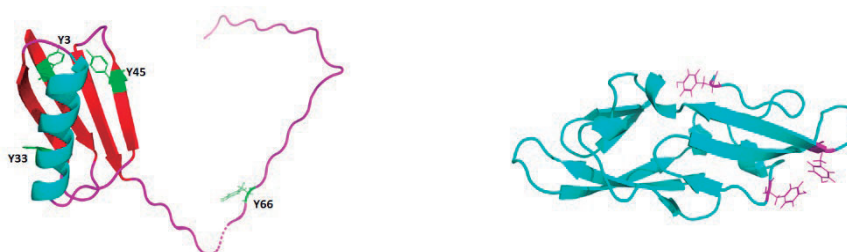
(1) (a) Jeganathan, M.; Pitchumani, K. *ACS Sustainable Chem. Eng.* **2014**, *2*, 1169-1176. (b) Wang, L.; Li, X.; An, Y. *Org. Biomol. Chem.* **2015**, *13*, 5497-5509. (c) Cacchi, S.; Fabrizi, G.; Goggiamani, A.; Iazzetti, A. *Org. Lett.* **2016**, *18*, 3511-3513.

Agradecimentos/Acknowledgments

We thank the CNPq and CAPES for the financial support in the form of fellowships.

Área: ORG*(Inserir a sigla da seção científica para qual o resumo será submetido. Ex: ORG, BEA, CAT)***Electrophilic fluorination of aromatic amino acids and proteins****Lívia C. R. M. da Frota (PQ),¹ Ariana A. Vasconcelos (PQ),² Ícaro P. Causo (PQ),³ Fábio C. L. Almeida (PQ),² Fernanda G. Finelli (PQ).¹****lcrmfrota@gmail.com; finelli@ippn.ufrj.br**¹Instituto de Pesquisa de Produtos Naturais Walter Mors, IPPN-UFRJ; ²Instituto de Bioquímica Médica Leopoldo de Meis and Centro Nacional de Biologia Estrutural e Bioimagem, IBqM-UFRJ; ³Departament of Physics, IBILCE-UNESP.Palavras-Chave: *Fluorination, Amino acids, Proteins.***Highlights**¹⁹F is interesting for biorthogonal labeling since it is not naturally present in biomolecules and is NMR active. Direct fluorination of proteins was selective at tyrosine and tryptophan residues.**Resumo/Abstract**

Biorthogonal chemistry explores non-native functional groups in biomolecules aiming to understand biological processes in living organisms.¹ ¹⁹F NMR of proteins is a great tool for studying protein interactions with small molecule ligands, protein folding and dynamics and it can be considered a biorthogonal technique since fluorine is not naturally present in biomolecules.² One way to incorporate fluorine in proteins is adding the fluorinated amino acids in growth media.³ However, synthetic fluorine-containing amino acids preparation involves multi-step routes and low-yield reactions.⁴ Despite the operational simplicity, direct fluorination of wild-type proteins has never been reported. This work presents studies on the fluorination of aromatic amino acids under biocompatible conditions and its application in the direct fluorination of these residues in proteins. Preliminary results showed that L-tyrosine and L-tryptophan are fluorinated under electrophilic fluorination conditions in buffered medium (pH = 7), while L-phenylalanine remains unreacted. Reaction of GB1, a 7KDa protein with four tyrosine and one tryptophan residues, under the same conditions showed fluorination of tryptophan 43 and tyrosine 3 residues while reaction of Cyanovirin-N, a 11kDa protein containing three tyrosine residues, was fluorinated only in tyrosine 11. Heteronuclear NMR correlation experiments confirmed fluorination at C2 and C4 of the indole ring of tryptophan and at *ortho* position related to hydroxyl group of tyrosine. Mass spectrometry experiment and DFT calculation are ongoing to confirm fluorine incorporation and to explain selectivity.

**Scheme 1.** 3D structure of GB1 (left) and Cyanovirin (right)¹Bird, R. E. *et al*, *Bioconjugate Chem.* **2021**, 32, 2457; ²Arntson, K. E., Pomerantz, W. C. K., *J. Med. Chem.* **2016**, 59, 5158; ³Lang, K. *et al*, *Chem. Rev.* **2014**, 114, 4764; ⁴Moschner, J. *et al*, *Chem. Rev.* **2019**, 119, 10718.**Agradecimentos/Acknowledgments**

CAPES, CNPq and FAPERJ for financial support.

Enantioselective transesterification of propargyl tertiary alcohols: reaction medium engineering and substrate scope evaluation

Laerte G. Neto (PG), Cintia D.F. Milagre (PQ), Humberto M.S. Milagre (PQ).*

laerte.ganeo@unesp.br; humberto.milagre@unesp.br

Institute of Chemistry, São Paulo State University (UNESP)

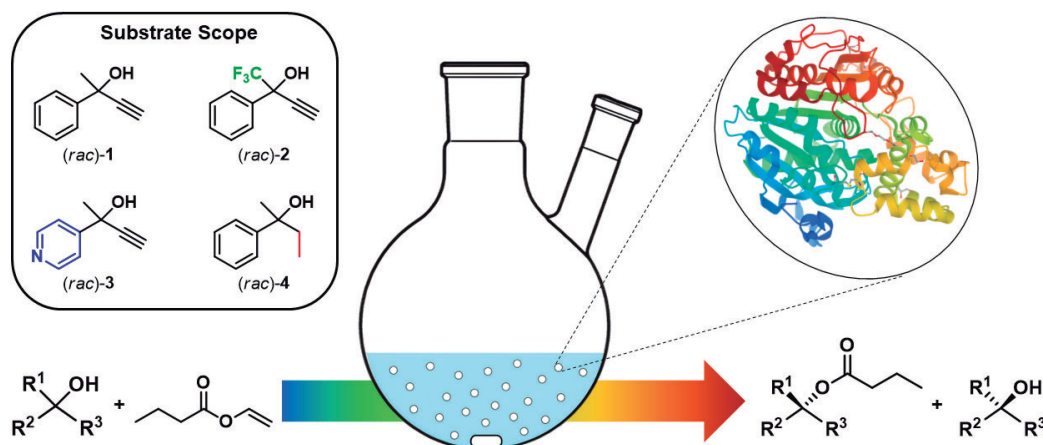
Keywords: Biocatalysis, Kinetic resolution, Propargyl tertiary alcohols, Lipase, Reaction medium engineering.

Highlights

- Kinetic resolution of propargyl tertiary alcohols catalyzed by *Candida antarctica* lipase A;
- Medium engineering study using 2-phenyl-3-butyn-2-ol as model substrate, followed by scope evaluation.

Resumo/Abstract

Propargyl tertiary alcohols and their esters are essential building blocks for the pharmaceutical industry. An example of a drug derived from these alcohols is efavirenz, which is used to treat HIV.¹ Despite their importance, the enantioselective synthesis of these compounds is still a significant challenge to organic chemists, essentially due to sterical hindrance. *Candida antarctica* lipase A (CAL-A) is known to catalyze the kinetic resolution via an enantioselective transesterification reaction of bulky substrates, such as the propargyl tertiary alcohol 2-phenyl-3-butyn-2-ol ((*rac*)-1).^{2,3} The present work reports a reaction medium engineering approach using (*rac*)-1 as the model substrate and CAL-A as the chiral catalyst, evaluating the following parameters: temperature, organic solvent, acyl donor identity, acyl donor concentration and enzyme loading. In the optimized condition, a 33% conversion and 95% *ee* were obtained, similar to the literature, but with the advantages of using a commercially available wild type and immobilized CAL-A, and a lower enzyme/substrate ratio. After the optimization step, a scope of substrates was evaluated, so the sterical and electronic effects could be analyzed.



References:

- [1] Noda, H.; Kumagai, N.; Shibasaki, M. *Asian J. Org. Chem.* **2018**, *7*, 599–612.
- [2] Krishna, S. R.; Persson, M.; Bornscheuer, U. T. *Tetrahedron: Asymmetry* **2002**, *13*, 2693-2696.
- [3] Löfgren, J.; Görbe, T.; Oschmann, M.; Humble, M. S. Backvall, J. *ChemBioChem* **2019**, *20*, 1438-1443.

Agradecimentos/Acknowledgments

This study was financed in part by the Coordenação de Aperfeiçoamento de Pessoal de Nível Superior - Brasil (CAPES) - Finance Code 001; Financial support of the Sao Paulo Research Foundation – FAPESP [grants number 2019/15230-8].

Área: ORG

(Inserir a sigla da seção científica para qual o resumo será submetido. Ex: ORG, BEA, CAT)

ENHANCED NUCLEOPHILIC FLUORINATION OF ALKYL BROMIDES UNDER CATALYSIS OF CROWN ETHER AND HEXAFLUORINATED *TERC*-BUTANOL

Annelise Souza Melo¹ (PG), Josefredo R. Pliego Jr¹ (PQ), Marcelo S. Valle^{1*} (PQ), annelisesouzamelo@gmail.com; marcelovalle@gmail.com

¹ Departamento de Ciências Naturais, Universidade Federal de São João Del Rei.

keywords: organic chemistry, supramolecular catalysis, fluorination.

Highlights

- Formation of 35% of the fluorinated product using HFTB cocatalyst, while the use of BDMb and *tert*-butanol resulted in 22% and 13.5%, respectively, using the same reaction conditions.
- Minimal formation of elimination product at 3% only.

Resumo/Abstract

The development of new fluorinated drugs depends on the advancement of synthetic methodologies of fluorination reactions. In case of aliphatic fluorinated compounds, the great challenge is to use cheap and widely available source of fluorine, such as potassium fluoride. For the fact of being sparingly soluble in polar aprotic solvents, showing low reactivity in polar protic solvents, and the possibility of E2 reactions occurring in parallel, aliphatic fluorination with KF requires a special catalysis via control of intermolecular forces.¹ Recently, it was shown by theoretical calculations, followed by experimental confirmation,^{2,3} that the use crown ether combined with bulky alcohols leads to a nanostructured environment capable of solubilizing and activating the S_N2 reaction involving KF. That study was a proof of concept,² and using 1 mmol of BDMb diol, 1 mmol of substrate (RBr) and 1 mmol of crown ether (18C6) led to a yield of 22% in 24h of reaction in reflux of acetonitrile as solvent. The use of *tert*-butanol rather BDMb resulted in 13.5% yield. Minimum amounts of elimination reaction by-product were obtained. In this work we repeated the experiments with BDMb and explored the use of another alcohol, a hexafluorinated *tert*-butanol (HFTB).

In the experiments, the reactions were carried out at 24 hours under reflux of acetonitrile. We have used 1 mmol of 3-bromopropoxybenzene as substrate, 1 mmol of crown ether associated with 1 mmol of HFTB, and 2 mmol of potassium fluoride, dissolved in 4 mL of acetonitrile as indicated in the Figure 1.

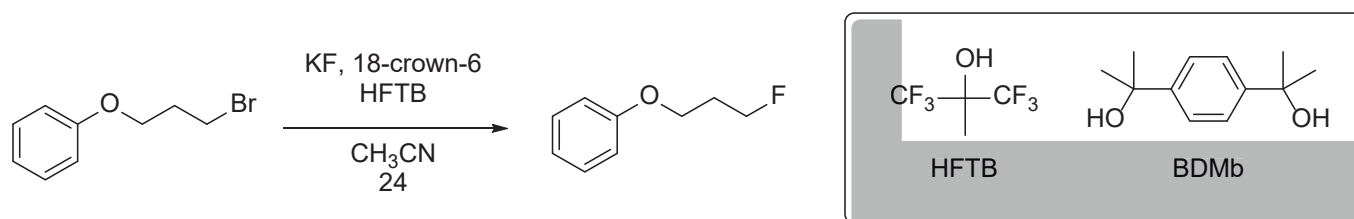


Figure 1. Fluorination of alkyl fluoride using KF, crown ether and bulk alcohol in acetonitrile.

The conversion to the fluorinated product using HFTB was around 35%, proving to be superior to another experiment carried out by our research group using *tert*-butanol with conversion of 13.5%.³ This result demonstrates that with the increase of the hydrogen bond force between the fluorinated bulk alcohol and fluoride ion leads to enhancement of the reaction rate. Preliminary theoretical calculations have indicated that there is a substantial charge distribution inside the F⁻(HFTB) complex, suggesting an increase of the solubility of KF as the main factor for the rate acceleration effect. Another important factor in this experiment was the minimal formation of elimination product, only 3%. The fluoropropoxybenzene compound has been proven by nuclear magnetic resonance analysis.

Agradecimentos/Acknowledgments

¹ Pliego, J. R.; *Org. Biomol. Chem.* **2021**, *19*, 1900.

² Silva, S. L.; Valle, M. S.; Pliego, J. R.; *J. Org. Chem.* **2020**, *85*, 15457

³ Silva, S. L.; Valle, M. S.; Pliego, J. R.; *J. Mol. Liq.* **2020**, *319*, 114211

UFJSJ, CAPES, CNPq, FAPEMIG.

Environmentally friendly and greener method of extraction of hesperidin from peel orange waste (*Citrus x sinensis*).

Caroline A. Santos (IC)^{1,2} and Maurício M. Victor (PQ)^{1,2}

carol.ames@hotmail.com; mmvictor@ufba.br

¹ Organic Chemistry Department, Chemistry Institute, Federal University of Bahia, UFBA, CEP 40170-290, ² National Institute of Science and Technology of Energy and Environmental, UFBA.

Keywords: hesperidin, natural flavonoid, sustainable extraction method, green chemistry.

Highlights

The focus of this research was to make the cost-effectiveness of substances with pharmacological properties, such as hesperidin, more accessible due an attractive and sustainable procedure.

Resumo/Abstract

Our research focused on the investigation to become the extraction of hesperidin **1** from orange (*Citrus x sinensis*) waste more sustainable. The residues were collected in restaurants in the UFBA campus. Our approach was based in the modification of procedure described by our group in the literature¹ to avoid the toxic CH₂Cl₂ and to replace of MeOH by EtOH. Also, number and time of extractions, preparing of waste substrate (albedo), and use of microwave² were explored. Recovering of solvent was estimated. Several methods were explored, and a resume is shown in Table 1:

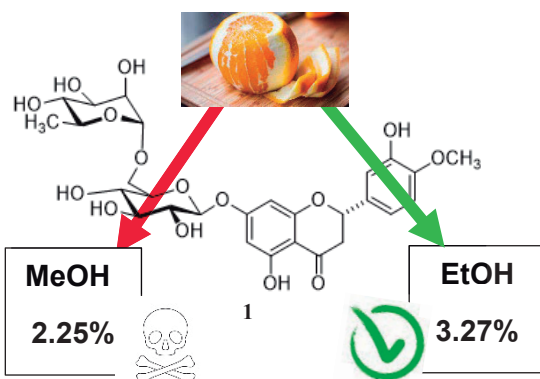


Table 1: different methods of extraction of hesperidin from albedo of citrus waste

Solvent	Solvent Recovery (%)	Yield (%) ^a	Substrate	Time (h)	Method	Cycles
MeOH	91	2.25	Pieces ^b	1.5 + 0.5	Reflux	2
EtOH	48	2.17	Pieces	1.0	Reflux	1
EtOH	32	3.27	Pieces	1.5 + 0.5	Reflux	2
EtOH	41	1.65	Crushed ^c	1.0	Reflux	1
EtOH	37	1.46	Crushed	0.5 + 0.5	US + reflux	1
EtOH	55	1.89	Pieces	0.5 + 0.5	US + reflux	1

a) (w/w) on dry albedo; b) handly cutted; c) using home blender.

As a post-extraction step, treatment of wash of extracted hesperidin was performed with warm water (40°C). In order to make the experiment even more environmentally friendly, in addition to choosing the extractor solvent ethanol, solvent was recovered by distillation to be reused in consecutive extractions.

The research data demonstrate that the best method in view of the variations to which the albedo was subjected was the one where the albedo was cut manually, placed at reflux with absolute ethanol in 2 extraction cycles, one lasting 1 hour followed by another lasting 30 minutes. This mode showed the highest yield of hesperidin obtained (3.27%).

References

- ¹ Victor, M. M.; David, J. M.; Cortez, M. V. M.; Leite, J. L.; Silva, G. S. B.; *Waste Biomass Valori.* **2021**, *12*, 313-320.
² Kantar, S. E.; Rajha, H. N.; Maroun, R. G.; Louka, N.; *J. Food Sci.* **2020**, *85*, 414-420.

Acknowledgments



Enzymatic oxidation of secondary alcohols by non-selective alcohol dehydrogenase

Letícia D. Dantas (PG),¹ Thais G. Silva (PG),² Fernanda G. Finelli (PQ),² Humberto M. S. Milagre (PQ),¹ Rodrigo O. M. A. de Souza (PQ),³ Cíntia D. F. Milagre (PQ).^{1*}

leticia.dantas@unesp.br; cintia.milagre@unesp.br

¹Instituto de Química, UNESP; ²Instituto de Pesquisas de Produtos Naturais, UFRJ; ³Instituto de Química, UFRJ

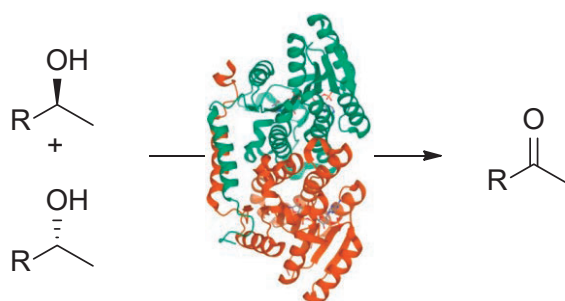
Palavras Chave: Biocatalysis, Alcohol Dehydrogenases, Oxidation.

Highlights

- Enzymatic oxidation of secondary alcohols catalyzed by non-selective alcohol dehydrogenase.

Resumo/Abstract

Alcohol Dehydrogenases (ADH) are enzymes that catalyze the oxidation of alcohols and reduction of carbonyl compounds, utilizing a nicotinamide (NADP(H)) cofactor.^{1,2} Typically, these enzymes are highly enantioselective, which is not interesting in oxidation of racemic alcohols since, in these cases, a maximum of 50% yield would be achieved.¹ Herein, we studied the oxidation of two secondary alcohols catalyzed by an ADH from *Sphingobium yanoikuyae*, reported in the literature as a non-selective enzyme, in order to produce important compounds, such as the intermediates for the synthesis of amphetamines. The preliminary results shown that obtaining conversion with low selectivity, slightly favoring the (*R*)-enantiomer, was possible. In addition, the different substituent groups interfere on the enzyme selectivity. Reaction conditions are currently under optimization to improve the oxidation conversion rates; however, we could already conclude that enzymatic catalysis is advantageous for the oxidation of alcohols, providing a greener and more sustainable alternative.



References:

- [1] De Miranda, A. S.; Milagre, C. D. F.; Hollmann, F. *Front. Catal.* **2022**, *2*. doi: 10.3389/fctls.2022.900554.
 [2] Milagre, C. D. F.; Milagre, H. M. S. *Curr. Opin. Green Sustain. Chem.* **2022**, *38*. doi: 10.1016/j.cogsc.2022.100694.

Agradecimentos/Acknowledgments

Financial support of the Sao Paulo Research Foundation – FAPESP [grants number 2014/50249-8; 2019/15230-8]; This study was financed in part by the Coordenação de Aperfeiçoamento de Pessoal de Nível Superior - Brasil (CAPES) - Finance Code 001. The authors acknowledge CAPES for maintaining the Portal de Periódicos (CAPES publication portal).

Fluorine-Induced *Pseudo*-Anomeric Effect in Fluorinated Cyclohexanes

Bruno A. Piscelli (PG),^{1*} Rodrigo A Cormanich (PQ)¹

b195034@dac.unicamp.br; cormanich@unicamp.br

¹Instituto de Química, Universidade Estadual de Campinas (UNICAMP).

Palavras Chave: Anomeric Effect; Physical Organic Chemistry; Theoretical Chemistry; DFT; NBO.

Highlights

- CF₂ groups can induce substantial *pseudo*-anomeric preferences in differently substituted cyclohexanes through 1,3-diaxial CH_{ax}...OMe electrostatic Non-Conventional Hydrogen Bonds (NCHBs).
- The F atoms can induce NCHB formation even with poor hydrogen bond acceptors (F and OAc).

Resumo/Abstract

The anomeric effect is a well-known stereoelectronic phenomenon in organic chemistry and, in the case of 2-methoxypropan, is often attributed to hyperconjugation between the lone pair of the (*endo*) ring oxygen and the antibonding orbital of the exocyclic C-O bond (*n*_O → σ^* _{CO} overlap), as well as stronger steric hindrance in the equatorial conformation and efficient dipole-dipole relaxation in the axial conformation (see Fig. 1A).

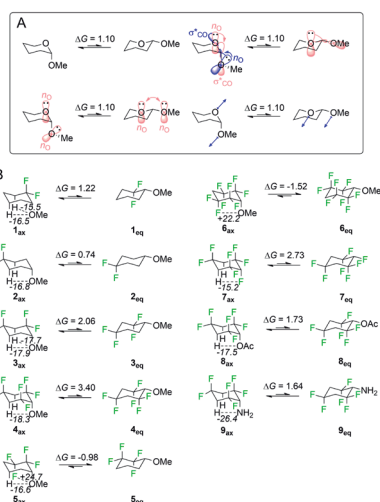


Figure 1. (A) Common explanations for 2-methoxypropan anomeric effect; (B) Calculated ring interconversion and NCHB energies (in kcal mol⁻¹) for 1-9.

In this study, we present a comprehensive analysis of the *pseudo*-anomeric effect in fluorinated cyclohexanes, which suggests that non-classical 1,3-diaxial CH_{ax}...OX hydrogen bonds (NCHBs) are the main driving force behind the effect. The introduction of CF₂ groups into the cyclohexane ring efficiently polarizes the 3,5-diaxial hydrogens in methoxycyclohexanes, which strengthens the CH_{ax}...OMe interactions and stabilizes the axial conformers (Fig. 1 B). This observation is supported by NMR experiments (see Fig. 2 A and B).

Furthermore, we found that the efficiency of the introduction of CF₂ groups into the ring is reinforced by the *pseudo*-anomeric preference observed in compounds 7-9. Even with less electronegative (NH₂) and poor hydrogen bond acceptors (F and OAc) substituents, the CF₂ groups can still induce NCHBs and promote expressive axial stabilization.

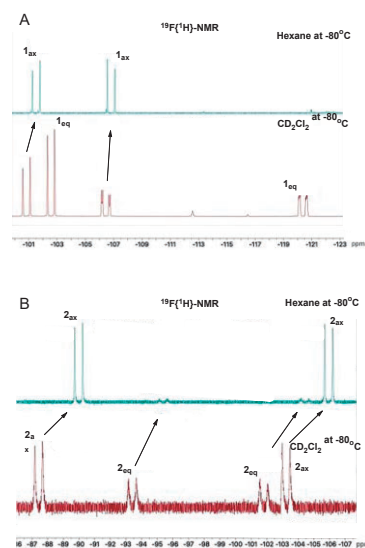


Figure 2. (A) VT-NMR for compound 1; (B) VT-NMR for compound 2.

References

- [1] (a) Piscelli, B. A.; Sanders, W.; Yu, C.; Al Maharik, N.; Lebl, T.; Cormanich, R. A.; O'Hagan, D. *Eur. J. Chem.* **2020**, 26, 11989-11994. (b) Piscelli, B. A.; Cormanich, R. A.; O'Hagan, D. *Phys. Chem. Chem. Phys.* **2021**, 23, 5845-5851.

Agradecimentos/Acknowledgment



Green approach for the design and synthesis of seleno-1,4-naphthoquinones with pharmacological potential

Amanda R. Azevedo (PG),¹ Caroline S. Moreira (PG),¹ Patrick C. Nobre (PQ),¹ Kaila V. S. Santos (IC),¹ Vitor F. Ferreira (PQ),² Fernando de C. da Silva (PQ)¹ and Vanessa Nascimento (PQ)^{1*}

arebelo@id.uff.br; nascimentovanessa@id.uff.br

¹Department of Organic Chemistry, Federal Fluminense University - UFF - Niterói-RJ; ²Department of Pharmaceutical Technology, Federal Fluminense University - UFF - Niterói-RJ

Keywords: Selenium, Biological potential, 1,4-Naphthoquinone derivatives

Highlights

Planning and obtaining, based on the principles of green chemistry, of biologically promising new molecules through the combination of selenoanilines and naphthoquinones.

Resumo/Abstract

Organochalcogens and quinones have been the object of great synthetic interest due to their pharmacological potential.^{1,2} Therefore, we aim to pursue an efficient method for the construction of 1,4-naphthoquinones derivatives containing selenium moieties, for this, we hypothesized that selanylanilines can be employed as a selenium source (Figure 1a). Initially, the preparation of anilines containing selenium was carried out, through the use of two different methodologies^{3,4} it was possible to obtain 4 anilines (**2** or **3**), with different electronic effects, with yields ranging from 40 to 78% (Figure 1b). Then, we started the study, based on previous work,² with selanylaniline **2** and 1,4-naphthoquinone **4** as model substrate. Unfortunately, even evaluating various conditions, under different solvents (H₂O, EtOH and DMSO) no product was obtained (Figure 1c). Thus, we decided modify the selenium source and selanylaniline **3** was chosen. Initially, the naphthoquinone **4** was reacted with selanylaniline **3** in ethanol at room temperature, the reaction was monitored by TLC and after 24h, any product was observed. When the reaction was carried out at reflux temperature under conventional heating, it was possible isolated the desired product with 30% of yield (Table 1, entry 1). These results led us to explore an alternative procedure and the reaction was carried out using microwave irradiation (MW) at 60 °C or 80 °C. By this way, after 1 hour, the yields were 28 and 31%, respectively (Table 1, entries 3 and 4). When the methodology was performed in an ultrasonic bath (US) the product was obtained in 29% yield after 2 h at room temperature. To improve the efficacy, some additives were screened and in basic medium, the formation of the desired product was not observed. However, an acid medium afforded **6** in 42% yield upon isolation (Table 1, entry 7). So far we have synthesized the unpublished and promising desired product in satisfactory yield and in environmentally friendly conditions. New tests are being carried out to improve this yield and, subsequently, expand the scope of the reaction.

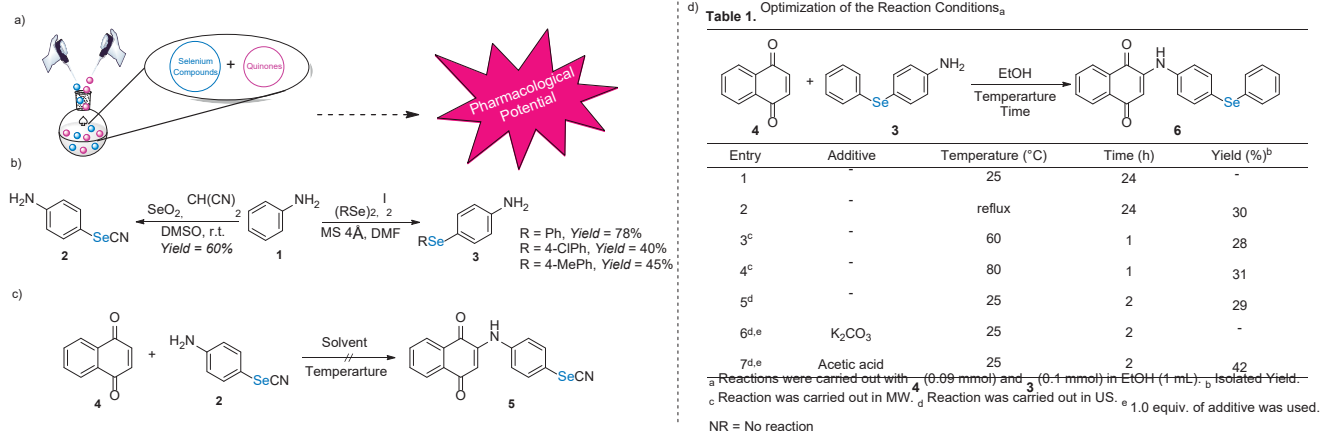


Figure 1

Agradecimentos/Acknowledgments

CNPq, CAPES, FAPERJ, UFF, PPGQ-UFF and LaReMN. **References:** [1] Shelar, D. S.; Dhavan, P. P.; Singh, P. R.; Jadhav, B. L.; Vaidya, S. P.; Manjare, S. T. *J. Mol. Struct.* **2021**, *1244*, 130914. [2] Martinez, S. T.; Silva, B. V.; Pinto, A. C.; Ferreira, V. F.; da Silva, F. C. *Química Nova* **2012**, *35*, 858-860. [3] Shaaban, S.; Shabana, S. M.; Al-Faiyz, Y. S.; Manolikakes, G.; El-Senduny, F. F. *Bioorg. Chem.* **2021**, *109*, 104713. [4] Bai, R.; Dabaria, K. K.; Badsara, S. S. *Synthesis* **2022**, *54*, 2487-2493.

Greener synthesis of coumarin-pyrrole hybrids using heterogeneous catalysis

Alice Karoline de Almeida Martinez (IC)^{1*}, Jhonathan R. N. dos Santos (PG)¹ and Arlene G. Corrêa (PQ)¹¹Centre of Excellence for Research in Sustainable Chemistry, Department of Chemistry, Federal University of São Carlos, São Carlos, SP, Brazil. *alicemartinez@estudante.ufscar.br

Key-words: Coumarins, Pyrroles, Hybrids, Microwave.

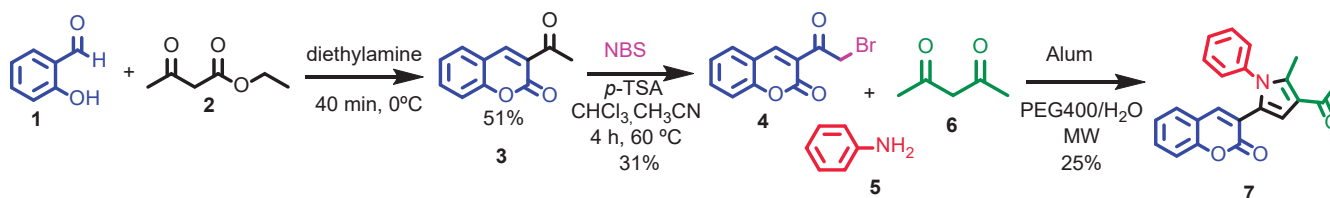
Highlights

Coumarin-pyrrole hybrids were synthesized through multicomponent reactions under microwave radiation and using heterogeneous catalysis, obtaining so far 25% yield using alum as catalyst.

Abstract

Coumarins show a wide spectrum of biological activities and are present in commercially available drugs due to their ability to do non-covalent interactions with protein.¹ Pyrrole derivatives can also be highlighted due to their pharmacological applicability, such as anti-tumor, anti-microbial, anti-inflammatory, etc.² There are several reports concerning the synthesis of pyrroles, including Knorr, Paal-Knorr and Hantzsch reactions,³ however such methodologies usually require metal catalysis, chlorinated solvents and severe reaction conditions. Moreover, the synthesis of coumarin-pyrrole hybrids **7** has been described using alum, in PEG 400-H₂O (3:2) under conventional heating (70 °C for 5 h).⁴

In this work, it is intended to optimize the reaction for obtaining coumarin-pyrrole hybrids **7** using bromocoumarin **4**, aniline (**5**) and acetyl ketone (**6**), under microwave irradiation and heterogeneous catalysis, aiming to greener conditions, such as the reduce in the energy spent, but keeping good yields. Several heterogeneous catalysts have been screened, such as Beta and USY zeolites and clay montmorillonite K-10 with no success. Nevertheless, the desired product **7** was obtained in 25% yield using alum under MW irradiation for 60 min at 70°C.



The perspective is optimizing the reaction conditions, evaluating the temperature, solvent and proportion of the reagents, since in the original publication they are in the same stoichiometry. Furthermore, other heterogeneous catalysts will be tested as well as their recovery and recycle.

References:

- (1) Franco, D. P.; Pereira, T. M.; Vitorio, F.; Nadur, N. F.; Lacerda, R. B.; Kümmerle, A. E. The Importance of Coumarins for Medicinal Chemistry and the Development of Bioactive Compounds in the Last Years. *Quim. Nova* **2021**, *44* (2), 180–197.
- (2) Fatahala, S. S.; Mohamed, M. S.; Sabry, J. Y.; El-Deen Mansour, Y. E. Synthesis Strategies and Medicinal Value of Pyrrole and its Fused Heterocyclic Compounds, *Med. Chem.* **2022**, *18*(10), 1013-1043.
- (3) Shi, T.; Yin, G.; Wang, X.; Xiong, Y.; Peng, Y.; Li, S.; Zeng, Y.; Wang, Z. Recent Advances in the Syntheses of Pyrroles. *Green Synth. Catal.* **2022**, in press.
- (4) Pal, G.; Paul, S.; Das, A. R. Alum-Catalyzed Synthesis of 3-(1H-Pyrrol-2-yl)-2H-Chromen-2-Ones: A Water-Peg 400 Binary Solvent Mediated, One-Pot, Three-Component Protocol. *Synthesis* **2013**, *45* (9), 1191–1200.

Acknowledgments

We thank FAPESP (2013/07600-3, 2014/50249-8 and 2021/050012-3), GlaxoSmithKline, CAPES (Financial Code 001) and CNPq (grants 429748/2018-3 and 302140/2019-0) for funding and grants.

Indetification of the metabolites product by *Waitea circinata* through untarget mass spectrometry experiments

Cecília F. Maciel (IC),¹ Matheus S. Souza (PG),¹ Lucilia Kato (PQ),¹ Leila G. de Araújo (PQ),²

ceciliafrmaci@gmail.com; ceciliafrmaci@gmail.com

¹Instituto de Química, UFG; ²Instituto de Ciências Biológicas, UFG.

Palavras Chave: *Fungus*, *Dereplication*, *Mass Spectrometry*, *GNPS*.

Highlights

Dereplication study of *W. circinata* extracts, a mycorrhizal fungus that assist the control of rice blast, being able to inhibit up to 97% of the in vitro growth of *M. oryzae*, that causes rice blast.

Resumo/Abstract

Waitea circinata, orchidoid mycorrhizal fungus isolated from the root of the orchid *Epidendrum nocturnum*, produces secondary metabolites that help controlling the rice blast, a disease caused by the fungus *Magnaporthe oryzae* that affects the rice plant. Previous studies carried out with *W. circinata* demonstrated the inhibitory action of up to 97% of the in vitro growth of *M. oryzae*, and rice cultures associated with *W. circinata* showed resistance to the disease, suppressing its development in up to 83.3%. (CARVALHO et al., 2015). Knowing the difficulty in isolating extracts from natural products, the molecular networks approach can be used for dereplication by mass spectrometry, since this analysis correlates the spectra and groups them by similarity, in order to help in understanding the composition of this extract. (WANG et al., 2016). The present study aimed to dereplicate the extracts using mass spectrometry data from the mycorrhiza of the fungus *Waitea Circinata*. The methodology used was based on the cultivation of the fungus *W. circinata* (En07-BRM 32644), After the cultivation of the fungus, the mycelial mass was obtained and from it, an extraction was made with the mycelium during the period of 9 days in ethyl acetate/methanol and chloroform/methanol. Afterwards, analyzes of high performance liquid chromatography coupled with high resolution mass spectrometry were made, and with de data obtained with UPLC-MS/MS analysis of the extracts using GNPS were performed. Through the study of chemical dereplication of *W. circinata* extracts using mass spectrometry data and the GNPS platform, it was observed that two of the noted compounds showed considerable similarity with the fragments present on the platform, such compounds are described in figures 1 and 2, and both had their presence confirmed in the EMM1 and EMM2 extracts. In addition, the observed data can be corroborated with data in the literature, since the annotated compounds were described as present in microorganisms of fungal origin, which further reinforces the possibility that, in fact, dehydrocurvularin and 1-palmitoil-2-oleoil-glycerol make up the hall of compounds that originate from *W. circinata*.

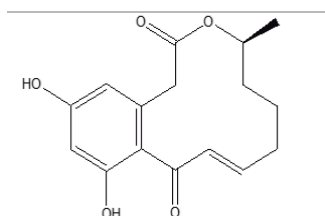


Figure 1. desidrocurvularina

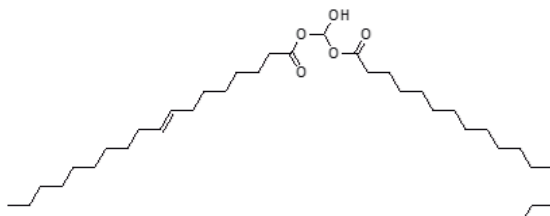


Figure 2. 1-palmitoil-2-oleoil-glicerol

CARVALHO, et al. Trop. Plant. Pathol. , v. 40, p. 151-159, 2015.; WANG, M. et al. Nat. Biotechnol. 34, n. 8, p. 828–837, 2016.

Agradecimentos/Acknowledgments

Laboratório de Produtos Naturais, Laboratório de Genética e Microrganismo, Universidade Federal de Goiás, CRTI.

Identification of compounds in complex mixtures using low-cost, low-resolution, and cryo-free NMR

Leice M. R. de Novais (PQ)^{1*}, Ana C. Q. Marques (TC),¹ Ricardo de O. Mascarenhas (TC),² Caroline R. M. D'Oca (PQ),¹ Andersson Barison (PQ),¹ Kahlil S. Salome (PQ).¹

kahlil.salome@gmail.com; leicenovais@gmail.com*

¹Multiuser NMR Lab, Chemistry Department, UFPR, Curitiba, Paraná, Brazil, 81531-980; ² Technical-Scientific Division, Federal Police, Curitiba, Paraná, Brazil.

Keywords: cryo-free NMR, Forensic Chemistry, Drugs, Counterfeit.

Highlights

Drug adulteration and the adulterants were easily identified using cryo-free benchtop NMR in a fast, easy, and inexpensive way, without deuterated solvent, and little to no sample preparation.

Abstract

Medicines are frequently counterfeit and illegally sold in the parallel market causing various health problems.¹ Anabolic steroids are common targets for adulteration even though these drugs are strictly controlled by ANVISA.² With this control, seized products need to be identified, generating an excessively high demand for enforcement authorities. For the identification and quantification of organic compounds, Nuclear Magnetic Resonance spectroscopy (NMR) has already proved to be quite efficient, since it is possible to analyze these compounds without the need of purification processes, sample preparation, or even the use of chemical standards.³ Therefore, the aim of this work was to evaluate the use of low-resolution and cryo-free NMR on the identification of the chemical composition of seized anabolic steroids.

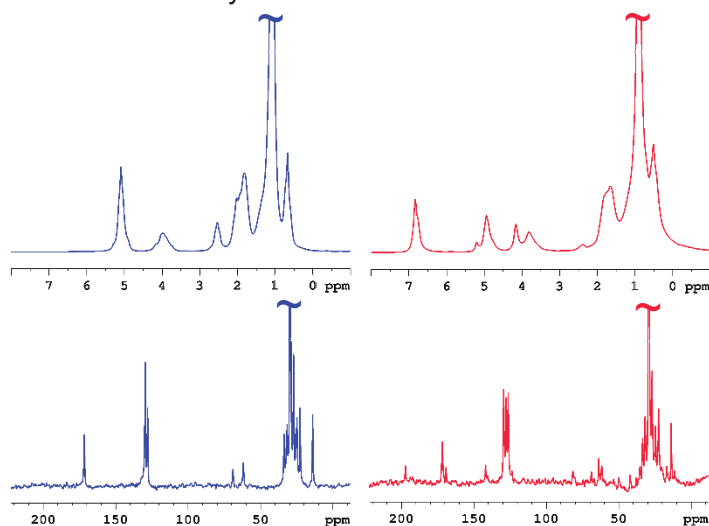


Figure 1: ¹H (top) and ¹³C{¹H} (bottom) NMR spectra of a seized sample (blue) and Durateston® standard (red).

The analyses were carried out in a 1.9T cryo-free benchtop NMR **without deuterated solvents**. About 60 crude seized samples were analyzed and it was possible to identify the anabolic hormones and their active ingredients quickly, unequivocally, and with minimal sample preparation using 1D and 2D NMR. Among the results obtained, the detection of counterfeit products stands out, as shown in Figure 1, where ¹H (top) and ¹³C{¹H} (bottom) NMR spectra of a seized sample (SS, blue) and the Durateston® standard (DS, red) are compared. SS only shows signals of the oil used as excipient, while DS shows signals of testosterone forms: isocaproate, phenylpropionate, propionate, and decanoate.

Thus, cryo-free NMR has proven to be a cheap, fast, robust, and efficient tool to the analysis of complex mixtures such as counterfeit drugs, food, drinks, among many others.

¹ Souza DS e col. Research, Society, and Development, v. 10, p. 1-12, 2021.

² BRASIL. Agência Nacional de Vigilância Sanitária. Portaria nº 344, de 12 de maio de 1998.

³Holzgrabe U e col. J. of Pharmaceutical and Biomedical Analysis. v. 55, p. 679-687, 2011.

Acknowledgments

UFPR, CAPES, CNPq, and Fundação Araucária.

Intercomponent interactions in a [2]rotaxane containing the tetralactam macrocycle: looking beyond the trifurcated hydrogen bond

Suzan K. Kunz (IC),¹ Fellipe F. S. Farias (PG),¹ Gustavo H. Weimer (PG),¹ Marcos A. P. Martins (PQ)^{1*}

suzan.kunz@acad.ufsm.br; marcos.nuquimhe@gmail.com

¹Núcleo de Química de Heterociclos (NUQUIMHE), Departamento de Química, Universidade Federal de Santa Maria (UFSM) 97105-900, Santa Maria, RS, Brasil.

Key words: Rotaxane, Intercomponent Interactions, VT-NMR, QTAIM, Stabilization Energy, Molecular Machines.

Highlights

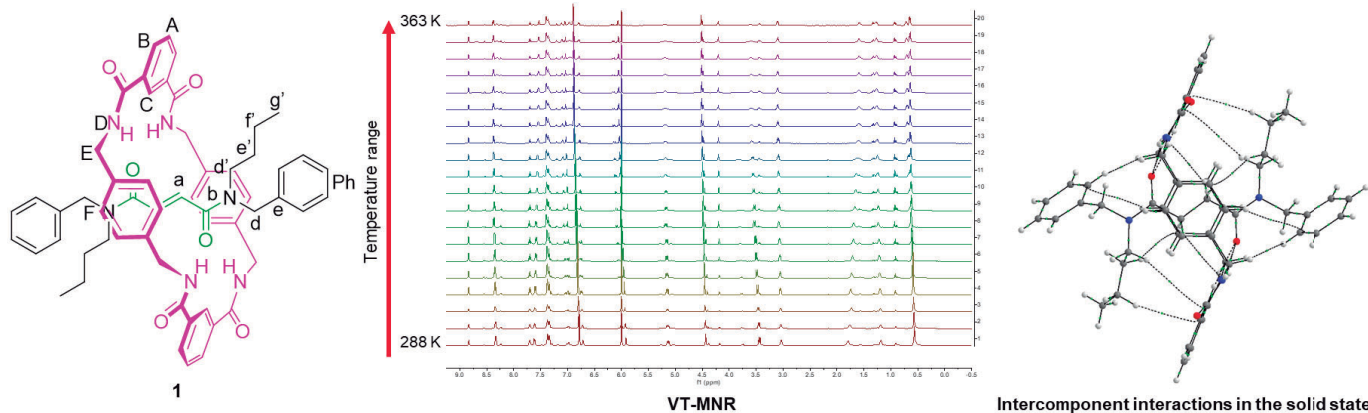
Intercomponent interactions was observed in solution and solid state.

$\pi \cdots \pi$ and $\text{CH} \cdots \pi$ interaction were modified by increasing temperature.

The intercomponent interactions was quantified and measured.

Abstract

A [2]rotaxane molecule maintain its components interconnected by mechanical bonding, an intrinsic result of its molecular topology. The interactions that occur between the macrocycle and the thread, called intercomponent interactions, define the magnitude of the movements and are directly related to the energetic demand to execute them. Previously reported in the Literature, the main interaction that occurs between components in tetralactam-based rotaxanes is the trifurcated H-bond, however, this is not the only influential interaction. Therefore, the objective of this work is to investigate the intercomponent interactions in a [2]rotaxane (compound **1**) in solution and in crystalline solid state. The respective methodologies were employed, in solution, experiments of Variable Temperature of ¹H Nuclear Magnetic Resonance (VT-NMR), and in crystalline solid state, from SC-XRD data, the Quantum Theory of Atoms in Molecules (QTAIM) and the G_{AI} analysis were applied. The analyzed model contains a fumaric diamide station, bulky groups bearing *N*-benzylbutan-1-amine stoppers and the tetralactam macrocycle. The VT-NMR experiment were carried out in the range of 288 to 363 K, observing the chemical shift change of certain hydrogen peaks. The hydrogens that had the greatest chemical shift differences were *d'* and *d* with a difference of 0.1824 and 0.0687 ppm, respectively, and *a* with 0.1523 ppm, these interactions can be characterized as $\pi \cdots \pi$ for *a* and $\text{CH} \cdots \pi$ for *d'* and *d*. In the crystalline solid state, the nature and magnitude of intercomponent interactions in the crystal was determined. The trifurcated hydrogen bond represented 61% of the total stabilization energy (-31.33 kcal·mol⁻¹). The other interactions that occur mainly between bulky groups and the station (but the trifurcated H-bond) along with the macrocycle, represent 39% (-20.38 kcal·mol⁻¹), having significant importance in the molecular stability in the performance of the movements. The main nature of intercomponent interactions observed are $\text{CH} \cdots \pi$ and $\text{H} \cdots \text{H}$. Therefore, it is possible to recognize and measure the intercomponent interactions, both in solution and in the solid state, these data are valuable for the synthesis and application of molecular machines.



Quim Nova, 2021, **44**, 76–85; Chem. –A Eur. J., 2011, **17**, 6076–6087; Eur. J. Org. Chem., 2019, **2019**, 3464–3471.

Acknowledgments

The authors acknowledge the Fundação de Amparo à Pesquisa do Estado do Rio Grande do Sul (FAPERGS), Conselho Nacional de Desenvolvimento Científico e Tecnológico (CNPq) and Coordenação de Aperfeiçoamento de Pessoal de Nível Superior (CAPES) for the financial support.

Investigation of the Solvent Role in the Groebke-Blackburn-Bienaymé ReactionMarcelo H.R. Carvalho (PG),¹ Pedro P. de Castro (PQ),² Brenno A.D. Neto (PQ),³ Giovanni W. Amarante (PQ).^{1*}

carvalho.mhr@gmail.com; giovanni.amarante@ufff.edu.br

¹Departamento de Química, UFJF; ²Departamento de Química, UFSCar; ³Instituto de Química, UnB

Palavras Chave: Multicomponent Reaction, Solvent Effect, GBB, Heterocycles.

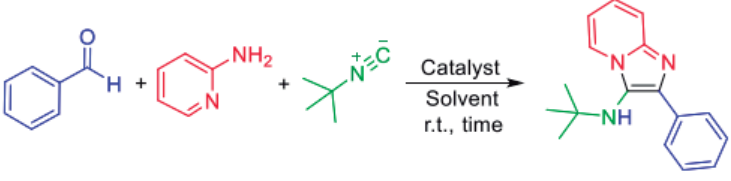
Highlights

Investigations of the Groebke-Blackburn-Bienaymé reaction were carried out. The best effect of methanol among several solvents tested provided insights about the reactivity and the entire mechanism.

Resumo/Abstract

Multicomponent reactions (MCRs) are transformations in which three or more substances are placed in the same reactor and, without variation in the conditions, they react in sequential steps, leading to the formation of product.¹ Multicomponent reactions that have gained a lot of attention are those based on the use of isocyanide, such as Ugi, Passerini, and Groebke-Blackburn-Bienaymé (GBB) reactions.² The GBB reaction involves an aldehyde, an isocyanide and a cyclic amidine as reagents, affording imidazo[1,2-a]-heterocycles as products.

Several works based on GBB reaction have already been published and the most recurrent solvent in these syntheses is methanol, probably due to the high yields and also the low probability of forming side-products.³ A recent work published by our group identified that methanol, besides being a solvent, can act directly on the MCR Ugi mechanism.⁴ Thus, because the GBB reaction passes through some intermediates similar to those of Ugi, we envision methanol acts not only as solvent. Therefore, an optimization of the reaction conditions was carried out (Table 1). Using a Brønsted acid as a catalyst, it was observed that methanol afforded the best results compared to the other alcohols (entries 3-8), water (entry 9), or other polar aprotic and non-polar solvents (entries 10-12). Moreover, methanol has different behavior in the reaction environment being able to lead to the product even in the absence of a catalyst (entries 13-18). Still, a representative scope will be carried out, and also new control experiments, in order to obtain more evidences about the key role of methanol in this reaction.



Entry	Time (h)	Catalyst	Solvent	Conversion (%) ^a
1	2	PTSA (10 mol %)	Methanol	79
2	4	PTSA (10 mol %)	Methanol	85
3	6	PTSA (10 mol %)	Methanol	94
4	6	PTSA (10 mol %)	Ethanol	85
5	6	PTSA (10 mol %)	Isopropanol	45
6	6	PTSA (10 mol %)	n-Butanol	76
7	6	PTSA (10 mol %)	t-Butanol	17
8	6	PTSA (10 mol %)	n-Octanol	23
9	6	PTSA (10 mol %)	Water	Traces
10	6	PTSA (10 mol %)	Acetonitrile	8
11	6	PTSA (10 mol %)	Dichloromethane	15
12	6	PTSA (10 mol %)	Toluene	Traces
13	6	-	Methanol	40
14	6	-	Ethanol	8
15	6	-	Isopropanol	0
16	6	-	n-Butanol	0
17	6	-	Dichloromethane	0
18	6	-	Toluene	0

^a Conversion calculated of the crude mixture through ¹H NMR analysis.

Table 1. Optimization of reaction conditions.

(1) Ugi, I.; Dömling, A.; Hörl, W. Multicomponent Reactions in Organic Chemistry. *Endeavour*. **1994**, 18 (3), 115-122.(2) Sadjadi, S.; Heravi, M. M.; Nazari, N. Isocyanide-Based Multicomponent Reactions in the Synthesis of Heterocycles. *RSC Adv*. **2016**, 6, 53203–53272.(3) Boltjes, A.; Dömling, A. The Groebke-Blackburn-Bienaymé Reaction. *Eur. J. Org. Chem*. **2019**, 42, 7007–7049.(4) Carvalho, M. H. R.; Ribeiro, J. P. R. S.; De Castro, P. P.; Passos, S. T. A.; Neto, B. A. D.; Dos Santos, H. F.; Amarante, G. W. Solvent Dependent Competitive Mechanisms for the Ugi Multicomponent Reaction: A Joint Theoretical and Experimental Study in the α-Acyl Aminocarboxamides vs α-Amino Amidines Formation. *J. Org. Chem*. **2022**, 87 (16), 11007-11020.**Agradecimentos/Acknowledgments**

The authors are grateful for the generous financial support from CAPES (Finance Code 001), UFJF, FAPEMIG, FAPESP, FAPDF and Rede Mineira de Química.

Área: ORG

Knoevenagel hydroxychloroquine analogs and in vitro evaluation against the protozoan disease Leishmaniasis (*L. amazonensis*)

Priscila P. Dario (PG)^{1*}, Gabriel L. Kosinski (IC)¹, Kahlil S. Salome (PQ)¹, Daniel S. Rampon (PQ)¹, Marcelo G. M. D'Oca (PQ)^{1*} priscila.dario@ufpr.br

¹Chemistry Department, Graduate Program in Chemistry, Federal University of Paraná, UFPR, 815321980, Curitiba, PR, Brazil.

Luis H. D. Yamashita (PG)², Danielle Lazarin-Bidoia (PQ)², Celso V. Nakamura (PQ)², Fernanda A. Rosa (PQ)²

²Graduate Program in Pharmaceutical Sciences, State University of Maringá, UEM, 87020-900, Maringá, PR, Brazil.

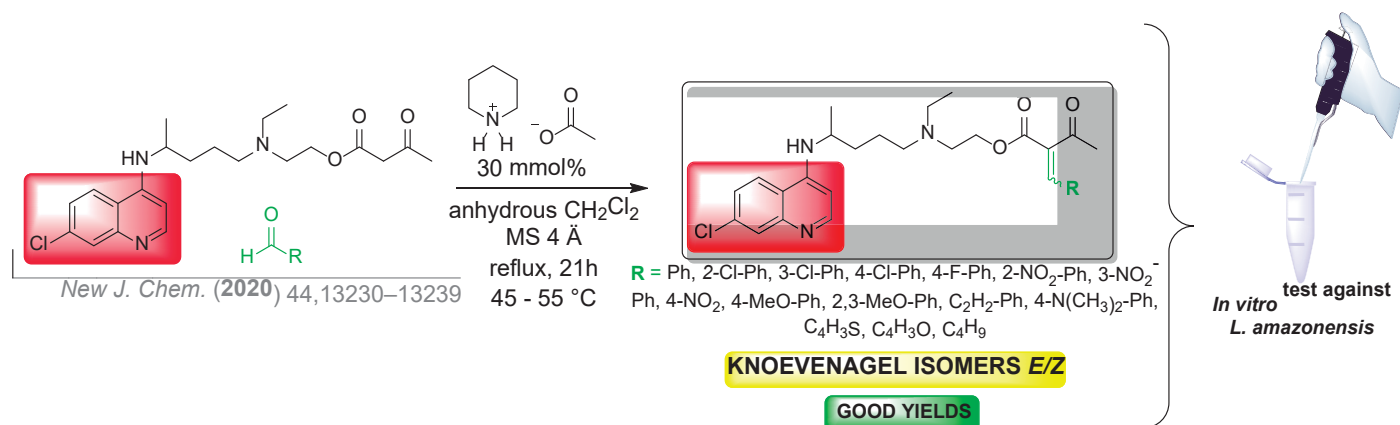
Keywords: Neglected tropical disease, Hydroxychloroquine derivatives, Antileishmanial.

Highlights

15 New alkylidenes derived from hydroxychloroquine were synthesized with satisfactory yields in *E/Z* isomers mixtures. *In vitro* biological tests were performed against the protozoan *L. amazonensis*, which causes Leishmaniasis.

Abstract

Leishmaniasis is a neglected disease^{1,2} that presents high mortality rates. It is caused by the protozoan *Leishmania* mosquito-borne.³ Challenges such as drug resistance in different strains and the high toxicity of existing drugs^{2,3,4,5} pave the way for developing new compounds⁴. Considering the potential of quinoline derivatives for treating diseases caused by protozoa³, the analog 7-chloro-N,N-dimethylquinolin-4-amine shows remarkable efficiency in the strains *L. amazonensis* and *L. infantum* in tests *in vitro* and *in vivo*⁵. Recently, quinoline-isatin hybrid structures demonstrated *in vitro* activity concerning the *Leishmania major*¹. Also, drugs used in malaria treatment, such as chloroquine (CQ), hydroxychloroquine (HCQ), and mefloquine (MFQ), showed exciting results concerning *L. amazonensis*². In this way, the Knoevenagel condensation⁶ have been studied based upon the green chemistry perspective and is one of the most widely exploited reactions in the production of synthetic intermediates and products pharmaceuticals. Thus, in the present work, the Knoevenagel condensation between aldehydes and HCQ acetoacetate afforded fifteen new alkylidenes in good yields (62 to 86%), using HCQ as a precursor. Following, the 15 new hydroxychloroquine alkylidenes are being evaluated *in vitro* against the promastigote form of one of the species (*L. amazonensis*) of the protozoan that causes Leishmaniasis.



Acknowledgments

The authors thank CAPES and CNPq for the fellowship and financial support from PPGQ-UFPR.

References

- Sabt, A.; et al. *Eur. J. Med. Chem.*. 246, 114959, 2023.
- Rocha, V. P. C.; et al. *J. Med. Microbiol.*. 62, 1001-1010, 2013.
- Dorababu A. *ChemistrySelect*. 6(9), 2164-2177, 2021.
- Herrera, L.; et al. *Int J Parasitol Drugs Drug.* 14, 56-61, 2020.
- Soyer, T. G.; et al. *Exp Parasitol.*. 199, 30-37, 2019.
- Alves Sobrinho, R. C. M.; et al. *RSC Adv.*. 7, 3214-3221, 2017.
- 46ª Reunião Anual da Sociedade Brasileira de Química: "Química: Ligando ciências e neutralizando desigualdades"

Laboratory Automation:

Low-Cost Microcontrollers in Real-Time Analysis of Ozonolysis Reaction

Lucas Luís C. de Andrade (IC), Caio M. Pacheco (PG), Raquel A. C. Leão (PQ), Rodrigo O.M.A. de Souza (PQ).*

lucaslca@eq.ufri.br, souzarod21@gmail.com*

Biocatalysis and Organic Synthesis Group, Instituto de Química, Universidade Federal do Rio de Janeiro.

Keywords: *flow chemistry, arduino, code, industry 4.0, ozonolysis.*

Highlights

The present work brings useful automation through microcontrollers such as an ESP32 and Arduino modules simplifying chemical analysis and real-time data acquirement.

Abstract

Continuous-flow process can be readily customized to meet the specific demands of the reaction. The construction of the reactor is often modular being assembled from several specialized yet easily integrated components such as heating and cooling zones, micro-mixers, residence tubing coils, separators, and diagnostic/analysis units. This workflow not only allows for facile automation and continuous operation of such processes, but also enables the chemist to perform more potentially hazardous and otherwise forbidden transformations in a safer and more reliable fashion.¹ The main advantages cited for improved operational safety are principally the reduced inventories of reactive chemicals, the small-contained reactor units and the ability to install real time monitoring of the system leading to rapid identification of problems and the instigation of automated safe shutdown protocols. Control and visualization of processes response are key to keep quality and safety. That is, following in a real-time reaction, for example, can certify that everything is going according to plan. Many types of sensors can be used for different situations. Here in, we will show the integration of pressure, temperature, and ozone sensors, into a 3D printed microreactor, so the data 'pressure/temperature/ozone' versus 'time' can be stored, and a graph plotted. To exemplify our concept study we have optimized a Baeyer-Villiger type reaction of Cyrene, with low residence times and conversion and selectivity above > 99% and we're currently optimizing an ozonolysis β -pinene. Furthermore, creating client and server modules to get data transfer via wi-fi, we could improve the feedback, enabling real-time analysis across the lab to another room, with a weightless portable device (Figure).

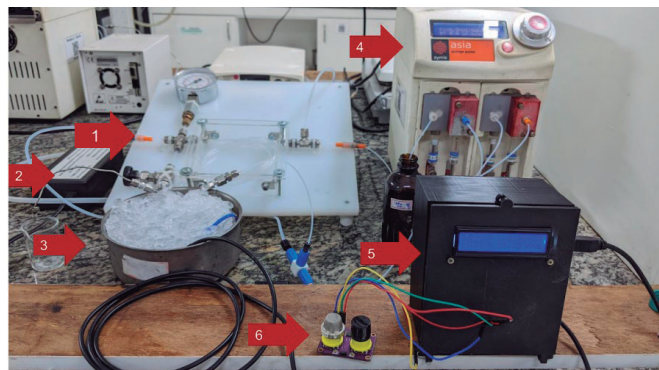


Figure. 1- Tube-in-tube reactor. 2 - Ozone generator 3 - Immersed coil reactor and temperature sensor (DS18B20). 4 - Syringe Pump. 5 - Arduino Mega with LCD display. 6 - Ozone Sensor.

The main goal is to get lab equipment more close to the concept of Industry 4.0 with less expensive do-it-yourself apparatus that can be done at a small fraction of the cost. Some researchers define those features as an important hands-on experience for students in prototyping and computing, and can also be applied to bring engagement in chemical classes.^{2,3} Also, wireless communication for data transfer was explored and the conclusion is that the sensors could precisely form a platform for obtaining data in laboratories and industrial manufacturing.⁴

Acknowledgments

FAPERJ, CNPq and CAPES

1. BAUMANN, M. **2020**, 24, 1802-1813.
2. Kubinová, S.; J. Šlegl, S. *J. Chem. Educ.*, **2015**, 92, 1751-1753.
3. Lopez-Gazpio, J.; Lopez-Gazpio, I. *J. Chem. Educ.* **2020**, 97, 4355-4360.
4. Cherkasov, N.; Baldwin S.; Gibbons, G. J.; Isakov, D. *ACS Sens.* **2020**, 5, 2497-2502.

Mechanistic Investigations on Baeyer-Villiger Reaction of Cyrene

Caio M. Pacheco (PG)^{1*}, Isabela G. Da Silva (IC),¹ Wesley Lima (PG),¹ Pierre M. Esteves (PQ)², Leandro S. M. Miranda (PQ)¹, Rodrigo O. M. A. de Souza (PQ)^{1*}

caioimp@id.uff.br+; souzarod21@gmail.com*

¹Biocatalysis and Organic Synthesis Group, Chemistry Institute, UFRJ, Rio de Janeiro;

²Chemistry Institute, UFRJ, Rio de Janeiro;

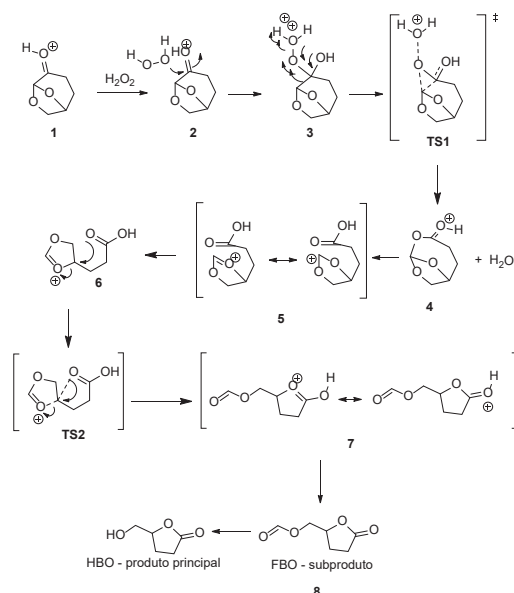
Keywords: Baeyer-Villiger reaction, oxidation, reactive intermediates, carbocations

Highlights

Baeyer-Villiger rearrangements affording stable carbocations

Abstract

The Baeyer-Villiger rearrangement is a chemical reaction in which a ketone or an ester is transformed into an ester or a lactone by the action of a peroxyacid catalyst. This reaction is useful for the synthesis of functionalized lactones, which have a wide range of applications in the pharmaceutical and fine chemical industries. The mechanism involves the formation of a peroxyacid intermediate, which then undergoes carbonyl group migration to give the desired product. When cyrene is used as starting material, an unexpected lactone is obtained as a rearrangement product.¹ In this work, we theoretically investigated the rearrangement involving lactone 1 that leads to HBO and FBO products (Scheme). We verified, through DFT calculations at IEFCM(H₂O)/M06-2X/6-311++G(d,p) level, that the rearrangement barrier must be catalyzed by acid (barrier < 3 kcal mol⁻¹), leading to the formation of a resonance-stabilized carbocation (6), which can subsequently undergo subsequent substitution, with ring opening. The reaction must be acid-catalyzed, as the neutral or basic route of rearrangement leads to much higher reaction barriers. Analysis of IBO orbitals² confirm the proposed electron flow and formation of the carbocation. This discovery opens the possibility of new transformations based on Baeyer-Villiger rearrangements, which will be explored.



Scheme: Proposed Mechanism.

Acknowledgments

CNPq, CAPES, FAPERJ.

[1] Allais, F.; Flourat, A. L.; Bonneau, G. et al. *Green Chemistry*. **2018**, *20*, 2455 – 2458.

[2] (a) Klein, J. E. M. N., Knizia, G. *Angew. Chem. Int. Ed.* **2015**, *54*, 5518. (b) Knizia, G. *J. Chem. Theory Comput.* **2013**, *9*, 4834.

Mechanosynthesis of 4-aryl-itaconic half-esters and telescopic synthesis of benzoazepinone and naphthalenes

Igor Sande (PG),¹ Silvio Cunha (PQ).^{1,2*}

igorsande@gmail.com; silviodd@gmail.com

¹Instituto de Química, Universidade Federal da Bahia, UFBA, 40170-115; ²INCT-Instituto Nacional de Ciência e Tecnologia em Energia e Ambiente, Universidade Federal da Bahia, UFBA, 40170-230

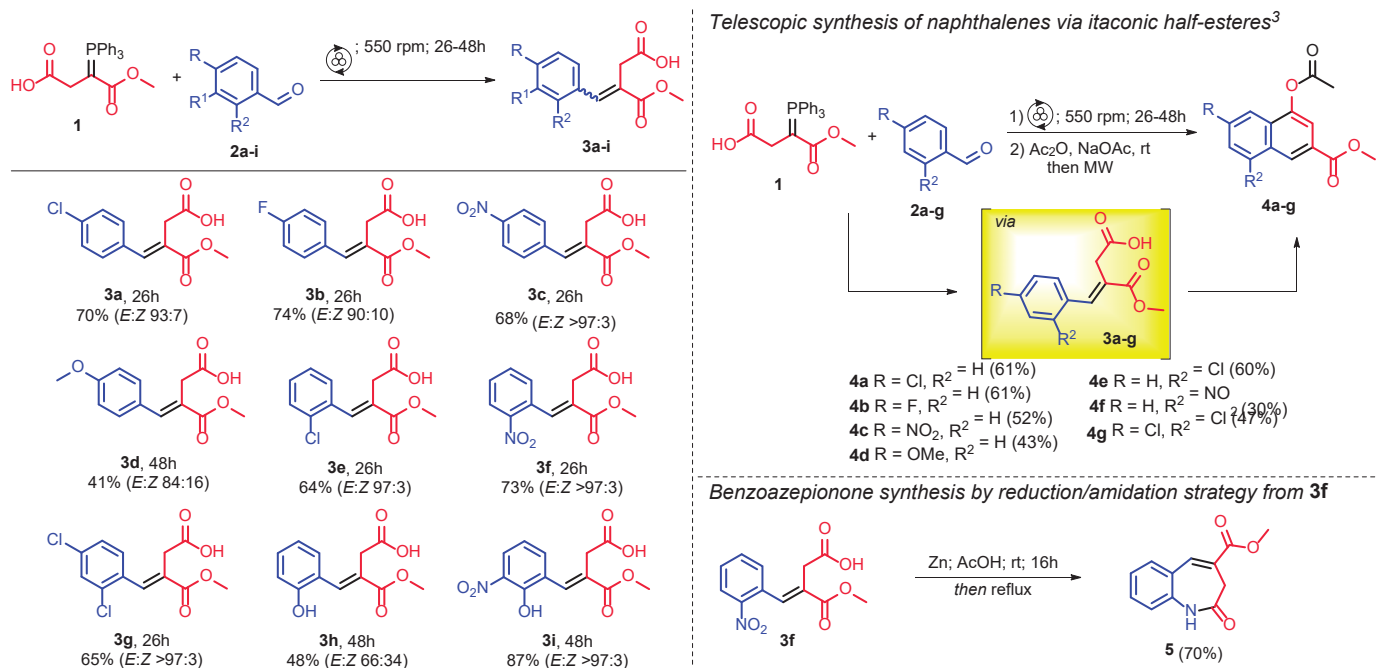
Palavras Chave: Mechanochemistry, Solvent-free, Wittig olefination, Friedel-Crafts reaction.

Highlights

Itaconic half-esters were synthesized under solvent-free mechanochemical conditions by Wittig olefination and synthetic applications were investigated to obtain naphthalenes and benzoazepinone.

Resumo/Abstract

Itaconic half-esters (**3a-i**) can be obtained by Stobbe condensation, however the use of stronger bases under heating are required, or by Wittig olefination. The classical condition to this olefination employing carboxyphosphorane **1** requires dry/toxic solvent, inert atmosphere and, due to the thermal instability of **1**, the Wittig olefination is carried out at room temperature resulting in long reaction time.^{1,2} In this work, we developed a mechanochemical Wittig olefination under solvent-free condition to obtain 4-aryl-itaconic half-esters. Synthetic applications of **3** was investigated in a telescopic synthesis of naphthalenes (**4a-g**) by Wittig/Friedel-Crafts reactions³ and benzoazepinone **5** by reduction/amidation of **3f**.



Agradecimentos/Acknowledgments



fapesb



inct
institutos nacionais
de ciência e tecnologia



(1) Rizzacasa, M. A.; Sargent, M. V. Australian Journal of Chemistry 1987, 40 (10), 1737-1743.

(2) Manna, T.; Rajput, A.; Saha, N.; Mondal, A.; Debnath, S. C.; Husain, S. M. Organic & Biomolecular Chemistry 2022, 20 (18), 3737-3741.

(3) Poster n° 7 presented in 18th Brazilian Meeting on Organic Synthesis (BMOS).

46^a Reunião Anual da Sociedade Brasileira de Química: "Química: Ligando ciências e neutralizando desigualdades"

Área: ORG

Metabolomics-driven exploration of bioactive molecules prior to their purification in *Picramnia sellowii* Planch. by UHPLC-QTOF-MS/MS

Alicia L.C. de Souza (PG),^{1*} Carlos André F. Moraes (PG),¹ Danielle F. da Silva (PQ),¹ Luciano S. Pinto (PQ),² Maria Fátima G.F. da Silva (PQ)¹.

alicia.ludymilla@gmail.com; dmfs@ufscar.br

¹Departamento de Química, UFSCar; ²Departamento de Química, USP

Palavras Chave: *molecular network, mass spectrometry, xanthomonas citri, chlorogenic acid, cluster.*

Highlights

The directed metabolomic study by UHPLC-QTOF-MS/MS to obtain active chemical compounds from a species of the genus *Picramnia*.

Resumo/Abstract

The discovery of new bioactive natural products for agriculture can be inspired by popular information or achieved by screening a collection of extracts for bioactivity using *in vitro* and *in vivo* assays. When a natural extract is deemed bioactive, bioassay-guided fractionation is usually performed. Failure to isolate bioactive compounds during bioassay-guided fractionation is very common and costly. Therefore, it is important to detect candidate bioactive molecules prior to their purification in order to streamline the isolation procedure applied to these substances. Through tandem mass spectrometry (MS), it is possible to accelerate the dereplication of molecules using molecular networks, prior to the subsequent isolation of compounds, and then to identify the potentially bioactive molecules. Therefore, extraction of *P. sellowii* leaves was performed with dichloromethane, methanol, ethanol and EtOH:H₂O (1:1 v/v). The crude extracts of *P. sellowii* in dichloromethane and methanol, and the fractions obtained after SPE column purification (ethanolic fractions F1-F4) were bioassayed against *Xanthomonas citri subsp. citri*, responsible for citrus canker. This bacterium affects all commercially important citrus varieties and species. Citrus canker is an important disease for citrus cultivation in several countries, such as Brazil and the United States, the two largest orange producers in the world. Chemical control of citrus canker in endemic areas is based exclusively on cupric bactericides that have no curative or systemic activity and are therefore applied in preventive management of citrus canker. Thus, in order to search for new bactericides with low environmental toxicity, we first performed microbiological tests on *P. sellowii* extracts and fractions, evaluating their minimum inhibitory concentration (MIC) and minimum bactericidal concentration (MBC). The *Xanthomonas* strains used throughout this study were resistant, tolerant, and susceptible to copper. The results were promising with the fractions F3 and F2, the first one at the concentration of 125 µg mL⁻¹ (MIC and MBC) against all strains (resistant, tolerant, and susceptible), the second one at the concentrations of 250 µg mL⁻¹, 125 µg mL⁻¹, and 250 µg mL⁻¹ (MIC and MBC) against resistant, tolerant, and susceptible strains, respectively. Previous to this study, we considered that *Picramnia* should be given a status of high interest regarding further investigations into its antibacterial activity, since it accumulates anthraquinones, anthrones and glycosylated anthrones, which are bactericidal agents (Diaz-Muñoz *et al.*, 2018). However, LC-MS-based metabolomics data showed that the fractions F3 and F2 are very rich in chlorogenic acids, whereas anthraquinone derivatives were found only in limited amounts (Cluster of chlorogenic acids produced by *P. sellowii* will be discussed). We have already streamlined the isolation procedure applied to these substances; experimental isolation work has been initiated to confirm their respective antibacterial activity.

Diaz-Muñoz, G.; Miranda, I. L.; Sartori, S. K.; de Rezende, D. C.; Diaz, M. A., Anthraquinones: an overview. In *Studies in natural products chemistry*, Elsevier: 2018; Vol. 58, pp 313-338.

Agradecimentos/Acknowledgments



Metal-Free Synthesis and Molecular Rearrangements as a Versatile Tool for the Construction of New Functionalized 1,2,3-Triazoles

Fernanda P. Pauli (PQ),¹ Mariana M. Nunes (IC),² Vinícius R. Campos (PQ),¹ Vitor F. Ferreira (PQ),² Fernando de C. da Silva (PQ)¹

fernandapauli@id.uff.br; fcsilva@id.uff.br

¹Instituto de Química, Departamento de Química Orgânica – UFF; ²Departamento de Tecnologia Farmacêutica, Faculdade de Farmácia – UFF.

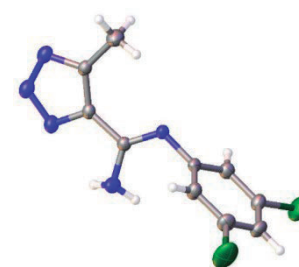
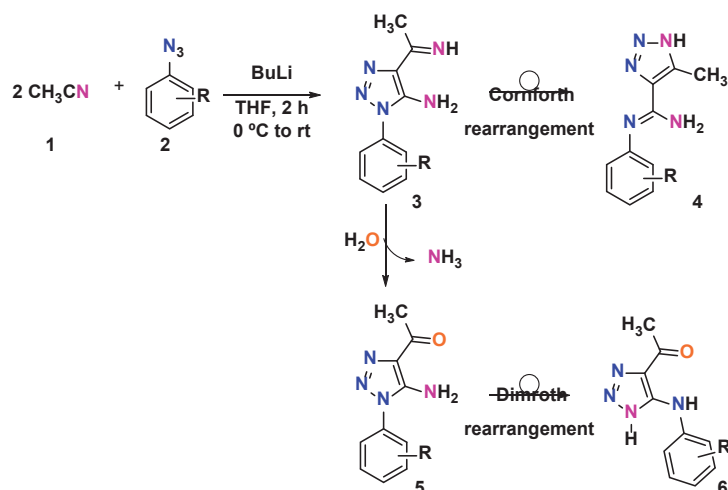
Key words: *triazole rearrangement, carboximidamide-triazole, amino-triazole.*

Highlights

A multicomponent approach via Dimroth and Cornforth rearrangements were used as strategy to access novel triazole derivatives.

Resumo/Abstract

The 1,2,3-triazoles are classified as an important class of heterocyclic compounds and have attracted considerable attention due to the wide diversity of biological activities they exhibit. Although many synthetic methodologies have been developed in recent years, the most widespread reaction to synthesize the 1,2,3-triazole nucleus is click chemistry.¹ However, the potential toxicity associated with these catalysts promote the study of metal-free methodologies.¹ In this work, the multicomponent synthesis via Cornforth and Dimroth rearrangement (Scheme 1) was used as an approach to access 21 new 1,2,3-triazole-4-carboximidamide **4** (Scheme 2), 5-amino-triazole **5** and 5-phenylamino-1,2,3-triazole **6** in 13-42% yields.²



Scheme 2. Ortep representation of **4** (Orthorhombic crystalline system; Pbc_a space group)

Scheme 1. Synthesis of 1,2,3-triazole compounds **4**, **5** and **6**

References

- Opsomer, T.; Dehaen, W. Metal-free syntheses of N-functionalized and NH-1,2,3-triazoles: an update on recent developments. *Chemical Communications* **2021**, 57(13), 1568–1590.
- Gomes, A. T. P. C.; M, Priscila R. C.; Rocha, D. R.; Neves, M. G. P. M. S.; Ferreira, V. F.; Silva A. M. S.; Cavaleiro, J. A. S.; da Silva, F. C. Consecutive Tandem Cycloaddition between Nitriles and Azides; Synthesis of 5-Amino-1H-[1,2,3]-triazoles. *Synlett*, **2013**, 24, 41-44.

Agradecimentos/Acknowledgments

CAPES, CNPq, FAPERJ, LDRX-UFF and FIOCRUZ.

46ª Reunião Anual da Sociedade Brasileira de Química: "Química: Ligando ciências e neutralizando desigualdades"

Multicomponent Synthesis of SAHA-DHPMs hybrids

Elise A. M. Rios (PG)^{1*}, Guilherme A. Justen (PG)², Camila M. Dea (IC)¹, Eron R. Bueno (IC)¹, Marcelo G. M. D'Oca (PQ)², Caroline R. M. D'Oca (PQ)¹ *elise.maluf@gmail.com; carolinedoca@ufpr.br

¹Medicinal and Agrochemical Organic Synthesis Group (SOMA), Chemistry Department, Federal University of Paraná, UFPR, 81530-000; ²Kolbe Organic Synthesis Group (KOLBE), Chemistry Department, Federal University of Paraná, UFPR.

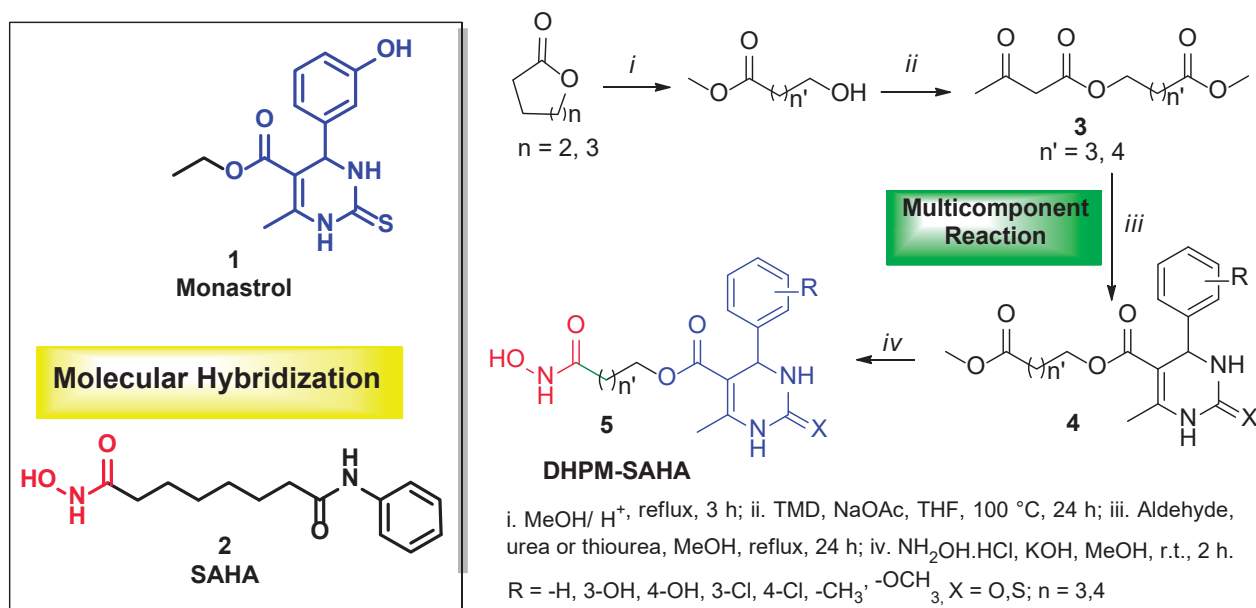
Palavras Chave: Monastrol, SAHA, Multicomponent Reaction. Dihydropyrimidinones (DHPMs)

Highlights

Molecular Hybridization as tool for new drug design.
DHPM and SAHA analogues as template to synthesis of new molecular hybrids.
Synthesis of 1,3-dicarbonyl compounds from ring opening reactions.

Abstract

Molecular hybridization is a powerful tool in design of new compounds with biological activity.^{1,2} Considering the antitumor activities present in Monastrol (**1**), a dihydropyrimidinone (DHPM) that acts by inhibition of kinesin,³ and suberoyl hydroxamic acid, SAHA (**2**), active substance present in Vorinostat, that act as histone deacetylases inhibitor,⁴ the aim of this work was the multicomponent synthesis of new molecular hybrids SAHA-DHPM's (**5**, Scheme 1). Initially, the 1,3-dicarbonyl compounds **3** were synthesized from 6- and 7-membered lactones, via ring opening reaction.⁵ Next, the Biginelli's reaction was explored to obtain the DHPMs analogues **4**, from several aldehydes, urea or thiourea, and the 1,3-dicarbonyl compounds **3** (70% yield). Finally, the DHPM-SAHA hybrid's synthesis occurred via aminolysis reaction of **4**, in the presence of NH₂OH.HCl.



Scheme 1. New SAHA-DHPM hybrids (**5**) through Biginelli MCR.

References:

- ¹Nepali, K. et. al. *Eur. J. Med. Chem.* **2014**, 77, 422;
- ²Cabrera, D. C. et.al. *Med. Chem. Commun.*, **2016**,7, 2167;
- ³Tron, G. C. et. al. *Eur. J. Org. Chem.* **2011**, 2011, 5541;
- ⁴Grant, S. et. al. *Nat. Rev. Drug Discov.* **2007**, 6, 21;
- ⁵Cerniauskaite, *Eur. J. Org. Chem.* **2011**, 12, 2293.

Agradecimentos/Acknowledgments

Gratefully acknowledge to Federal University of Paraná (UFPR), CAPES, CNPq and LabRMN.

New mechanistic insights of flavanone-enabled reduction of copper species in the stereoselective synthesis of 1,2,3-triazole-naringenin

Eloah P. Ávila (PD),¹ Gabriela L. P. Suhett (IC),¹ Hélio F. Dos Santos (PQ)¹, Brenno A. D. Neto (PQ)², Mauro V. de Almeida (PQ)¹

eloahavila@ice.ufjf.br

¹Departament of Chemistry, Federal University of Juiz de Fora, 36036-900, Juiz de Fora – MG, Brazil

²Laboratory of Medicinal and Technological Chemistry, University of Brasília, Chemistry Institute (IQ-UnB), Campus Universitário Darcy Ribeiro, Brasília, 70910-900, DF, Brazil

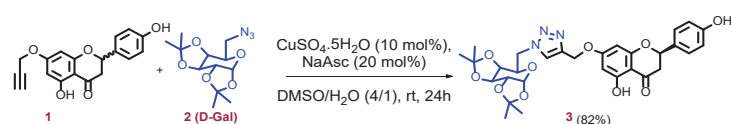
Key words: Naringenin, Click chemistry, DFT studies, HRMS

Highlights

Naringenin (NAR) is a bioactive flavanone and its skeleton bridged to pharmacophoric 1,2,3-triazole moieties emerges as a source of new candidates for drug prototypes.¹ Herein we reported mechanistic insights of both flavanone-enabled reduction process and stereoselective *click* reaction of NAR-alkyne guided by density functional theory (DFT) and high-resolution mass spectrometry (HRMS).

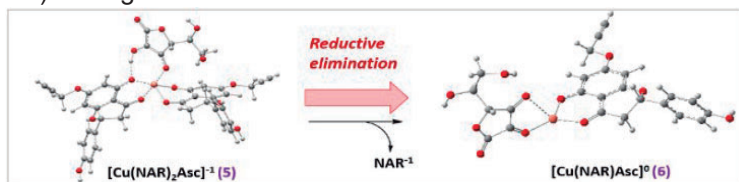
Abstract

The *click* reaction between *rac*-NAR-alkyne **1** and enantiopure galactopyrano-azide **2** led to the 1,2,3-triazole **3** as the only diastereomer (82% yield, Scheme 1). Also, the complete conversion of the racemate into (*R*)-NAR skeleton indicates a possible dynamic kinetic resolution. Thus, our mechanistic studies started investigating **1** as a possible chiral-inducing agent in the catalytic cycle. The control experiments of **1** with CuSO₄/ascorbate (Asc) system, as well as the click reactions, were performed by real-time HRMS monitoring and guided by DFT studies.



Scheme 1. Preparation of 1,2,3-triazole **3** by *click* reaction

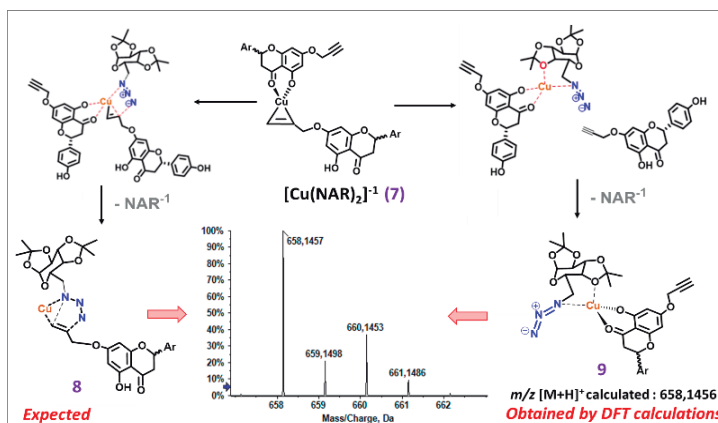
First, it is suggested a NAR-enabled reduction process from [Cu^{II}-(NAR)₂] **4** (*m/z* of 704.07 ([M + H + Na]⁺). The reducing agent **5** is proposed when it was observed Asc fully oxidized as ligand of [Cu^I] **6** (*m/z* of 545.02 ([M – H]⁻). Two possible pathways are being studied: a reductive elimination (Scheme 2) or single electron transfer from **5** to **4**.



Scheme 2. Proposed reductive elimination step of **5** guided by DFT calculations of species.

After, [CuNAR]⁰ (*m/z* 370.99, [M]⁻), could form the activated alkyne-copper species **7** (*m/z* 681.08, [M]⁻) as a precursor of

After, [CuNAR]⁰ (*m/z* 370.99, [M]⁻), could form the activated alkyne-copper species **7** (*m/z* 681.08, [M]⁻) as a precursor of click reaction. However, DFT calculations converged to structure related to its isomer **9** (Scheme 3), with a secondary interactions of galactose portion to copper.



Scheme 3. Mechanistic proposal of click reaction based on DFT calculations

Finally, our preliminary results suggests the monocopper molecular complex species are enough reactive to form triazole-derivatives. It is worth mentioning that his approach is different from the classical pathways already reported in the literature.^{2,3} Mechanistic studies by DFT are in progress to elucidate the origin of stereoselectivity of kinetically favored step (*k_{fast}*).

¹ Mendes, L. A. O. et al. *Chem. Biol. Interact.* **2020**, 331, 109218; ² Worrell, B. T.; Malik, J. A.; Fokin, V. V. *Science* (80), **2013**, 340 (6131), 457; ³ Iacobucci, C.; Reale, S.; Gal, J.-F.; De Angelis, F. *Angew. Chemie Int. Ed.* **2015**, 54 (10), 3065.

Acknowledgments

CAPES, CNPq e FAPEMIG

New Ugi-Smiles-multicomponent strategy toward the diastereoselective synthesis of 1,2,3,4-tetrahydroquinolines

Karina de Souza Quaglio* (PG),¹ Vitor A. F. da Silva (PG),¹ Márcio W. Paixão (PQ).¹

karinaquaglio@estudante.ufscar.br

¹ Laboratory for Sustainable Organic Synthesis and Catalysis - Department of Chemistry, Federal University of São Carlos – UFSCar, São Carlos, São Paulo, Brazil

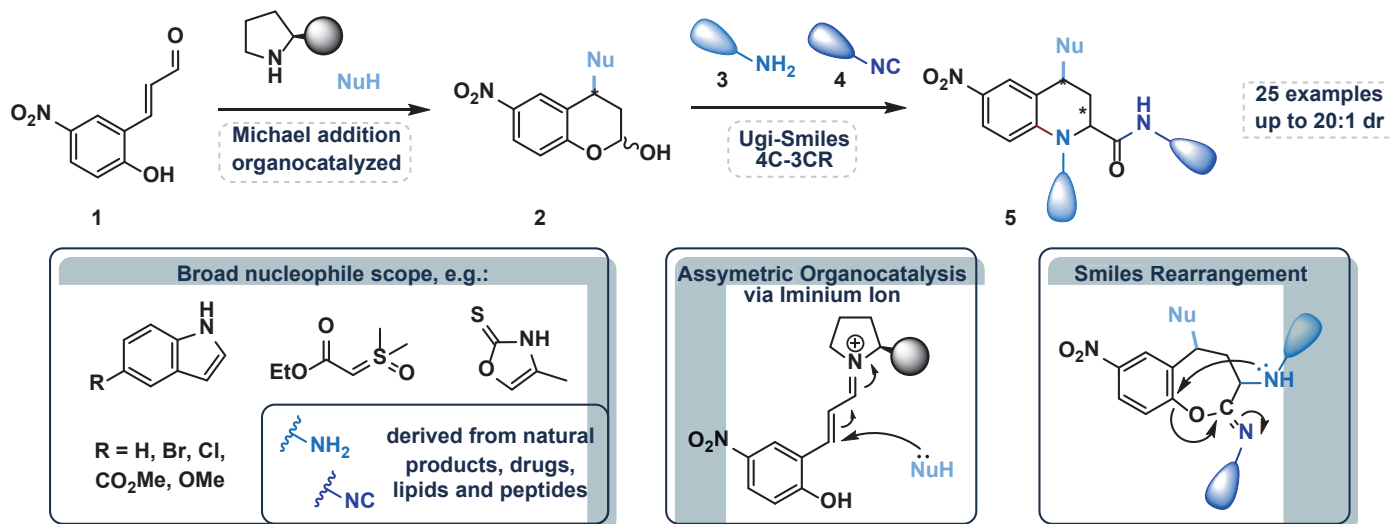
Keywords: Organocatalysis, Multicomponent reactions, Diastereoselective synthesis.

Highlights

A diastereoselective synthesis of highly functionalized tetrahydroquinolines – important chemical motif present in biologically active natural products and pharmacologically relevant therapeutic agents¹ – is achieved in a short reaction sequence. The combination of easy to handle reactions, namely organocatalytic and multicomponent protocols, allows the preparation of peptide-type structure with a wide functional group diversity.

Resumo/Abstract

The widespread presence of tetrahydroquinolines in compounds of interest to the chemical industries places the synthesis of this scaffold's derivative as an interesting field of research.² In this context and in an effort to develop efficient and greener synthetic routes for the synthesis of highly substituted tetrahydroquinolines derivatives, we herein describe an organocatalytic Michael Addition followed by an Ugi-Smiles reaction to precisely assembly this architecture, strategy that has been successful in our research group. This association allows the diastereoselective achievement of a small set of 1,2,3,4-tetrahydroquinolines under sustainable and mild reaction conditions.



¹ Jampilek, J. Heterocycles in Medicinal Chemistry. *Molecules*. MDPI AG, 2019. <https://doi.org/10.3390/molecules24213839>.

² Muthukrishnan, I.; Sridharan, V.; Menéndez, J. C. *Chem. Rev.* **2019**, 5057.

³ Echemenda, R.; de La Torre, A. F.; Monteiro, J. L.; Pila, M.; Corrêa, A. G.; Westermann, B.; Rivera, D. G.; Paixão, M. W. *Angew. Chem. Int. Ed.* **2015**, 54, 1. b) Echemendía, R.; da Silva, G. P.; Kawamura, M. Y.; de la Torre, A. F.; Corrêa, A. G.; Ferreira, M. A. B.; Rivera, D. G.; Paixão, M. W. *Chem. Commun.*, **2019**, 55, 286. c) Fernandes, V. A.; Lima, R. N.; Broterson, Y. B.; Kawamura, M. Y.; Echemendia, R.; de la Torre, A. F.; Rivera, D. G.; Paixão, M. W. *Chem. Sci.*, **2021**, 12, 15862.

Agradecimentos/Acknowledgments

We are grateful to CNPq (INCT Catálise Grants No 444061/ 2018-5 and Universal Project 405052/2021-9) and FAPESP (21/06099-5 for MWP). This study was financed in part by the Coordenação de Aperfeiçoamento de Pessoal de Nível Superior – Brasil (CAPES) – Finance Code 001.

Novel Arylsulfonamide-chalcones Hybrids: Synthesis, Leishmanicidal Activity and Molecular Modeling Studies

Nathália S. Oliveira (PG),¹ Edgar Schaeffer (PG),¹ Ariely R. R. Barreto (PG),² Luana G. de Souza (PQ),¹ Bartira R. Bergmann (PQ),² Alcides J. M. Silva (PQ).^{1*}

nathalia.oliveira@ufrj.br; alcides@ippn.ufrj.br

¹Instituto de Pesquisas de Produtos Naturais Walter Mors, UFRJ. ²Instituto de Biofísica Carlos Chagas Filho, UFRJ

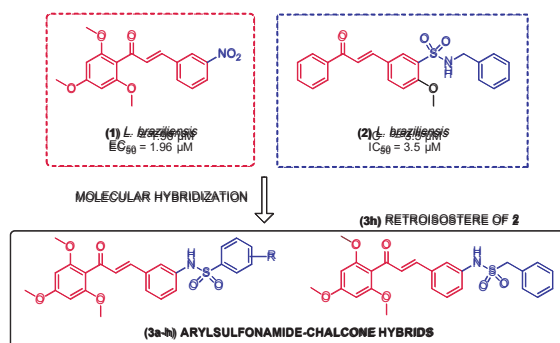
Keywords: Synthesis, Chalcone, Sulfonamide, Hybridization, Leishmaniasis, Docking molecular.

Highlights

A new series of arylsulfonamides-chalcones was synthesized and evaluated against *L. amazonensis*. Docking Molecular assays with the *Leishmania* cTXNPx target enzyme have been in progress.

Resumo/Abstract

Leishmaniasis is a set of diseases caused by a variety of protozoan species of the genus *Leishmania*. In this work, the molecular hybridization, between the trimethoxylated chalcone (**1**) and the sulfonamide group (**2**), is used as a central purpose for the construction of novel arylsulfonamide-chalcones (Scheme 1).^{1,2} The chalcones were synthesized using as starting material 2',4',6'-trimethoxyacetophenone, and 3-nitro-benzaldehyde through the Claisen-Schmidt condensation, followed by the chemoselective reduction of the NO₂ group. A series containing 8 unpublished arylsulfonamide-chalcone hybrids were prepared using the classical methodology with commercial arylsulfonyl chlorides, pyridine, and dichloromethane, providing chemical yields ranging from 65-95%. Arylsulfonamides-chalcones were tested in promastigotes of the *L. amazonensis* specie, evaluating the anti-promastigotes and cytotoxic activity. In general, all substances were active with IC₅₀ between 1.72 and 3.19 µM. However, only three substances were selected to continue the tests because they presented a SI ~ 10, indicating that it was more selective to the parasite. In addition, the cytosolic trypanodioxin peroxidase (cTXNPx) is considered a molecular target for chalcones in a variety of *Leishmania* species.¹ The Molecular Docking assays of hybrids arylsulfonamide-chalcone were performed with the theoretical model cTXNPx of *L. amazonensis* obtaining satisfactory results.



Scheme 1: Structural design of arylsulfonamide-chalcone.

1. Escrivani D. O. *et al.* PLoS Negl Trop Dis. 2021, 15(11).

2. Andrighetti-Fröhner, C. R. *et al.* Europ. J. Med. Chem. 2009, 44, 755.

Agradecimentos/Acknowledgments

CAPES, CNPQ, IBCCF, IPPN, UFRJ.

Optimization of One-pot Telescoped Synthesis of Thiazole Derivatives from β -Diketones and Thioamides Promoted by Trihaloisocyanuric Acids

Tatiana Medeiros Boaventura (IC), Paula Fernandes de Aguiar (PQ), Marcio C. S. de Mattos* (PQ)

tatimb.ufri@gmail.com; mmattos@iq.ufri.br

Instituto de Química, UFRJ

Palavras Chave: Trihaloisocyanuric acids, One-pot telescoped synthesis, Thiazole, Plackett-Burman design.

Highlights

- New methodology for preparation of thiazoles derivatives from β -diketones and thioamides
- Easily available reagents
- Safer and greener reaction conditions

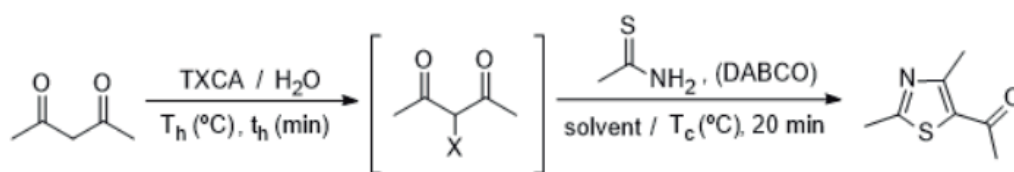
Resumo/Abstract

Thiazoles and their derivatives have long inspired researchers due to their associations with compounds of biological and pharmacological activity. Traditionally, the chosen method for the preparation of these compounds is via the Hantzsch thiazole synthesis, which presents as an inconvenient the preparation or manipulation of toxic α -haloketones.¹ In this regard, the telescoping of multi-step reaction is an interesting and safer pot-economical approach that avoids exposure to hazardous or toxic compounds, besides reducing operational costs.²

Recently, we have been exploring the chemistry of trihaloisocyanuric acids (TXCA, X = Cl, Br) as green reagents for electrophilic bromination of diverse reactions.² One of these approaches involves the generation in situ of a highly watery halogenated intermediate in the preparation of thiazoles.

Herein, we present the study of one-pot telescoped synthesis of thiazoles derivatives from β -diketones and thioamides promoted by trihaloisocyanuric acid.

Initially the study consisted in an optimization of the reaction with acetylacetone and TBCA/TCCA, followed by condensation with thioacetamide to produce the thiazole. Since we aimed to study several parameters, the Plackett-Burman design was chosen to reduce the number of experiments and determine the main variables that will be modeled. The variables optimized were: the molar ratio of acetylacetone:TXCA:thioacetamide, halogenation temperature (T_h), halogenation time (t_h), halogenation agent (TXCA, X=Cl, Br), condensation temperature (T_c), condensation time (t_c), solvent and the use of DABCO in the condensation reaction. The condensation time was fixed in 20 minutes, since preliminary results indicated that by this time all intermediate produced in the first reaction had been consumed.



The response of the experiments were evaluated by Hydrogen Nuclear Magnetic Resonance (^1H NMR), using acetophenone as internal standard. So far, we obtained 5-acetyl-2,4-dimethylthiazole in 15-29% yield after a simple extraction with CH_2Cl_2 .

1. de Andrade, V.S.C.; de Mattos, M.C.S., *Synthesis*, **2018**, *50*, 4867.
2. de Andrade, V.S.C.; de Mattos, M.C.S., *Quim. Nova*, **2021**, *44*, 912.

Agradecimentos/Acknowledgments

CNPq / PIBIC

Palladium-catalyzed heterocyclization/carbonylation/arylation reaction to access pyrazoline-ketone scaffold

Mateus Oliveira Costa (PG),¹ Juliana A. Dantas (PG),^{1*} Camila P. de Oliveira (IC),² Amanda Lemos Quintela (PG),² Tadeu Luiz Gomes Cabral (PG),² Claudio Francisco Tormena (PQ),² Marco Antonio B. Ferreira (PQ).¹

mateuscosta0595@gmail.com; juarantesdantas@gmail.com

¹Departamento de Química, UFSCar; ²Instituto de Química, Unicamp

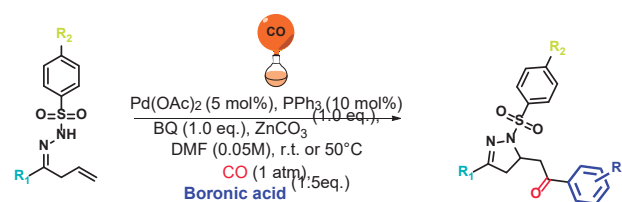
Palavras Chave: Palladium, Catalysis, Carbonylation, Heterocycle, Prediction, Boronic Acid.

Highlights

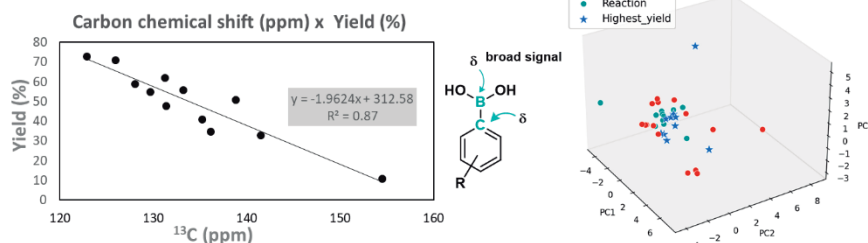
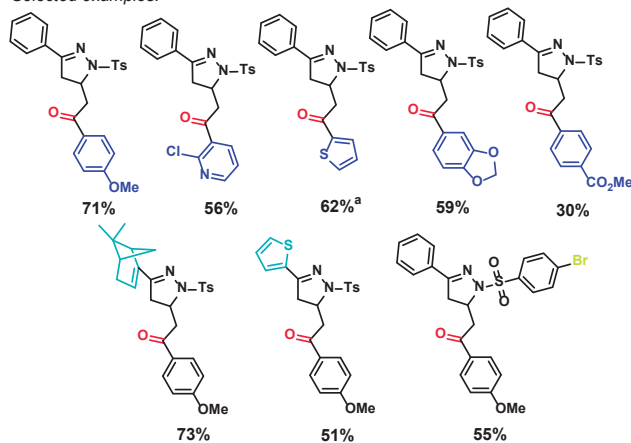
Aza-Wacker reaction with widely available reagents to functionalization. Statistical analysis with experimental and calculated parameters providing insights about the robustness of the methodology.

Resumo/Abstract

The great variety of heterocycle compounds have led organic chemists in pursuit of efficient methods to synthesize molecules containing this type of core which are present in many natural products with important biological activity like pyrazoline, where studies indicate activity against cancer, diabetes and inflammations¹. The pyrazoline nucleus can be obtained through aza-Wacker reactions, by the intramolecular 5-*exo-trig* cyclization leading to the heterocycle, which can undergo to further functionalization. In our work, we were able to achieve those transformations sequentially after the heterocyclization using widely available and cheap reagents, as the carbonylation by CO atmosphere and subsequent arylation with arylboronic acids, with mediation of Pd catalysis. We obtained products in moderate yields using electron-rich arylboronic acids, electron-withdrawing groups led to low yields and alkylboronic acids were unreactive. We also explore the nature of hydrazones, which presented excellent robustness admitting many electronic and steric variations with no big influence on yield. Exploring the range of boronic acid derivatives, we were able to find a strong dependence on the ¹³C NMR chemical shifting with the yield. The correlation found led us to explore the vast chemical space of different boronic acids that could be used in our reaction, applying statistical tools such as PCA analysis and linear regressions we were able to predict the range and efficiency of our methodology.



Selected examples:



[1] (a) P.-F. Wang, H.-Y. et al, *Chem. Biol. Drug Des.* **2015**, 86, 1405. (b) J. Shi, Z. et al. *J. Med. Chem.*, **2018**, 61, 681 [2] (a) M.-N. Yang, et al, *Org. Lett.*, **2017**, 19, 5208–5211 (b) J. Chen, M.-N. Yang. et al, *Org. Lett.*, **2018**, 20, 3314.

Agradecimentos/Acknowledgments



Process Number (2020/10246-0;
2020/01255-6;2022/11314-5)



Process Number (88882.332787/2019-01)



Process Number (140710/2022-1)

Paramagnetic Relaxation Agents for Time Saving in Quantitative NMR

João P. Brussolo (PG),^{1*} Cláudio F. Tormena (PQ).¹

joaopedrobrussolo@gmail.com; tormena@unicamp.br

¹Instituto de Química, UNICAMP - Campinas - Brazil.

Palavras Chave: NMR, Relaxation, Paramagnetic, qNMR, NMR-PRE.

Highlights

Long experimental times required for some NMR experiments can be reduced by addition of a relaxation agent. Allowing to acquire quantitative ¹³C NMR (qNMR) spectra in a reasonable time.

Abstract

Currently, one of the biggest challenges encountered in the use of nuclear magnetic resonance is the long experiment times associated with quantitative measurement [1] necessary for mechanistic studies [2] in the organic chemistry. These long experimental times, ranging from hours to days, are due to the longitudinal relaxation time (T_1) of the nuclear spins. To improve the accuracy in qNMR measurements it is mandatory to wait at least 5 times the longest T_1 of the nuclei present in the molecule, for the magnetization returns to equilibrium between each scan. In the case of ¹³C NMR, T_1 is much longer when compared with ¹H and considering the low natural abundance of ¹³C, several scans are necessary for achieving good signal-to-noise ratio (SNR), imposing long experimental times.

It's known that paramagnetic compounds [3], such as Cr(acac)₃ reduce T_1 of the nuclei. Recently Cr(acac)₃ (fig. 1) was used to acquire quantitative ¹³C NMR spectra applied to Kinetic Isotope Effect (KIE) determination[4]. However, there is no information in the literature about how and in which extension relaxation agents affect all nuclei present in a molecule. Thus, the aim of this work is to evaluate the effect of Cr(acac)₃ as relaxation agent in a series of organic molecules containing different functional groups to determine the best proportion between analyte and Cr(acac)₃, to acquire a ¹³C qNMR spectrum in a short time as possible. The T_1 values for all carbon atoms were measured using two different pulse sequences, namely Inversion Recovery (IR) [5] and Saturation Recovery (SR) to evaluate the performance (accuracy and time of experiment) for both sequences.

Figure 1

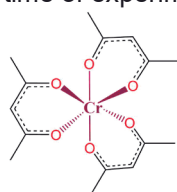


Figure 2

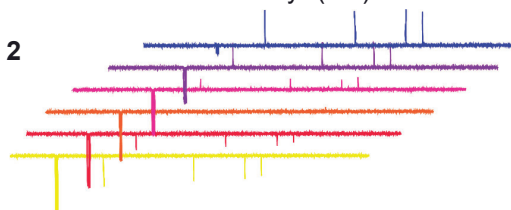


Figure 1: structure of paramagnetic relaxation agent Cr(acac)₃ ; Figure 2: Schematic ¹³C NMR Inversion-Recovery experiment of 1-butanol.

The results show that the effect of the relaxation agent is different for each atom, depending on its position in the molecular structure in relation to the complexing site of the agent. This result suggests that it is very important to establish the proportion of relaxation agent depending on each carbon atom (sp, sp², sp³) that interests us and also the functional group(s) present in the molecule.

References:

1. Henderson, Terry J. J. Amer. Chem. Soc., 126, 3682-3683 (2004).
2. Kwan, Eugene E. et al. Nat. Chem.10, 917-923 (2018).
3. Mulder, Frans AA; Tenori, Leonardo; Luchinat, Claudio. Angew. Chem. Int. Ed. 131, 15427-15430 (2019).
4. Kawamura, Meire Y. et al. Chem. Eur. J. 28, e202202294 (2022).
5. Frye, J. S. Conc. Magn. Reson. 1, 27-33 (1989).

Agradecimentos/Acknowledgments

We thank CAPES and FAPESP for financial support (grants #2020/10246-0) and the IQ-UNICAMP for the infrastructure and NMR facilities.

Predicting the selectivity of organocatalyzed aldol reactions: a multivariate approach

Giovanna Scalli Tâmega (IC),¹ Attilio Chiavegatti Neto (PG),¹ Marco Antonio Barbosa Ferreira (PQ),¹

giovanna.tamega@estudante.ufscar.br; attilio@estudante.ufscar.br; marco.ferreira@ufscar.br

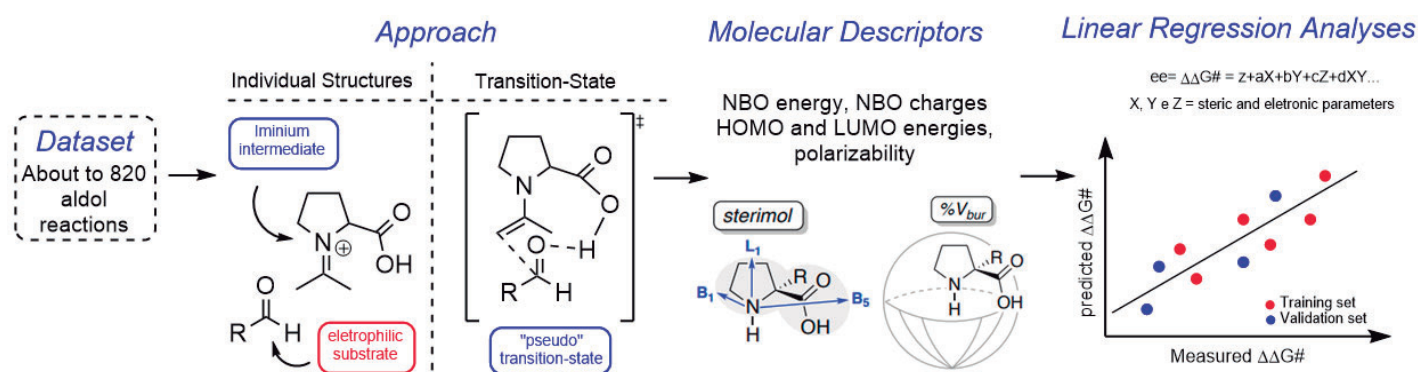
¹Departamento de Química, UFSCar

Palavras Chave: Catalysis, Aldol Reaction, Computational Chemistry, Organic Chemistry

Highlights

Exploration of the enantioselectivity of aldol reaction through the enamine intermediate and its transition states. Application of computational chemistry tools to build linear regression models aiming to predict the enantioselectivity of literature cataloged aldol reactions.

Resumo/Abstract



Persuading organic molecules to react in a controlled manner is a constant challenge in organic synthesis. In this context, reactions promoted using catalysts are ubiquitous. Over the years, several studies of catalytic organic reactions have been published, either describing new processes or rationalizing the existing ones. Here we explore the aldol reaction, a classical reaction for carbon-carbon bond formation. For the stereoselective variants of the aldol reaction, the multifactorial nature of selectivity makes the consolidation of a predictive model an arduous task, when considering only the chemist's intuition. On the other hand, advances in computational chemistry made it possible to evaluate the selectivity *in silico*. Thus, this work aims to explore multivariate linear models capable of predicting the enantioselectivity of aldol reactions catalyzed by chiral enamines. Using a library of 820 reactions carefully curated from the literature, we calculated chemical descriptors describing sterical and electronic features of the catalysts, nucleophiles, and electrophiles employed in these reactions. These descriptors were then related to the enantiomeric excess of these reactions employing a statistical analysis. Preliminary studies demonstrated that although relevant predictive models could be obtained using this protocol, they cannot be simplified enough for practical use. Consequently, we sought to include a new set of parameters. Using a prototypical transition state for the aldol reaction and modern low-cost protocols of computational chemistry we could obtain structures that retain the main interactions of the real transition states, with emphasis on the hydrogen-bond donors present in the organocatalysts employed in the aldol reactions. Then, we compare the predictive power of each type of selectivity model and the effect of introducing mechanistic-derived parameters relative to more general descriptors.

Agradecimentos/Acknowledgments



Process Number (2020/10246-0; 2020/13563-7;
2021/08236-0; 2022/11314-5)



Process Number
(88887.597433/2021-
00)



Secretaria Geral
de Informática



Núcleo de Atendimento em Computação de Alto Desempenho

Process Development for the Synthesis of Cannabidiol under Continuous Flow

Érica A. Araujo (IC),¹ João G. H. Rosa (IC),¹ Felipe L. N. Da Silva (PG),¹ Raquel A. C. Leão (PQ),¹ Nelson F. C. Junior (PQ),² Edison P. Wendler (PQ),² Bruna R. A. Cavizioli (PQ),² Rodrigo O. M. A. De Souza (PQ).^{1*}

erica.araujo@ufri.br, souzarod21@gmail.com*

¹Laboratório de Biocatálise e Síntese Orgânica, Instituto de Química da Universidade Federal do Rio de Janeiro – IQ – UFRJ.

²Prati-Donaduzzi - Rua Mitsugoro Tanaka, 145, Centro Ind. Nilton Arruda, Toledo/PR, CEP 85903-630; CNPq – Conselho Nacional de Desenvolvimento Científico e Tecnológica.

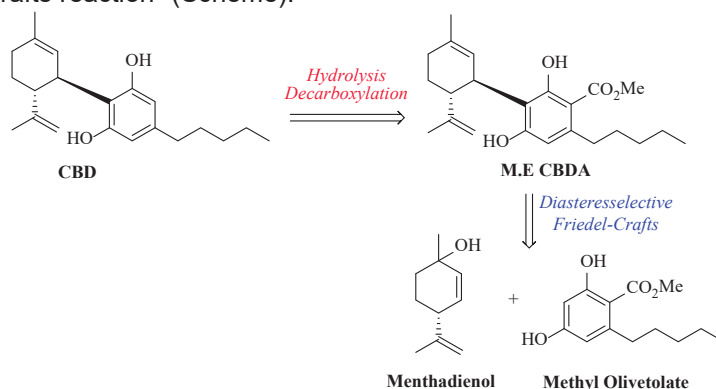
Keywords: Cannabidiol, Continuous Flow, Organic Synthesis.

Highlights

Study of the reaction to obtaining cannabidiol (CBD), an important drug used for treatment of several disease under continuous flow conditions and several catalysts.

Abstract

Throughout millennia, Cannabis sativa has been used by different cultures for its therapeutic properties. These properties originate from cannabinoids, natural terpene-phenolic compounds of which Δ^9 -tetrahydrocannabinol (THC) and cannabidiol (CBD) are the main ones.^{1,2} Among the cannabinoids, CBD has stood out for its pharmacological and non-psychoactive properties, which has been awakening interest in several countries around the world. In this work, we seek a new route of synthesis of CBD from menthadienol. CBD is synthesized from M.E CBDA by basic hydrolysis followed by thermal decarboxylation.³ E.M CBDA is synthesized from menthadienol and methyl olivetolate via a diastereoselective Friedel-Crafts reaction⁴ (Scheme).



Scheme. Retrosynthesis of CBD in the two Steps.

The big challenge in this step is the rapid degradation of menthadienol upon heating. This degradation generates products of elimination, rearrangement and by reacting with the nucleophile of the reaction, with coupling byproducts. Our best result was obtained under the fed-batch condition of menthadienol under reaction. Under these conditions we achieved partial conversion of methyl olivetolate and selectivity between 50 - 60% of M.E CBDA. In face of the results found, we observe that the boronic acid explored so far did not perform well. We now plan to explore Other boronic acids and Lewis acid catalysts, in order to achieve full conversion of methyl olivetolate and selectivity in the formation of M.E CBDA.

Acknowledgments

CNPq, CAPES and FAPERJ

1. Bonini, S. A. et al. *J. Ethnopharm.* **2018**, 227, 300-315.
2. Mechoulam, R.; Hanus, L. *Chem. Physic Lipids*, **2002**, 121, 35-40.
3. Steup, et al. US2010298579A1. **2010**.
4. Hall, D. G. et al. *Euro. J. Org. Chem.*, **2015**, 21, 4218-4223.

Process Intensification for Synthesis of (S)- γ -Hydroxymethyl- γ -butyrolactone from Cyrene™

Isabela G. da Silva (IC), Caio M. Pacheco (PG), Wesley Lima (PG), Marcelo A. Nascimento (PG), Raquel A. C. Leão (PQ), Rodrigo O.M.A. de Souza (PQ).*

isabelagds15@gmail.com; souzarod21@gmail.com*

Laboratório de Biocatálise e Síntese Orgânica, Instituto de Química da Universidade Federal do Rio de Janeiro – IQ – UFRJ.

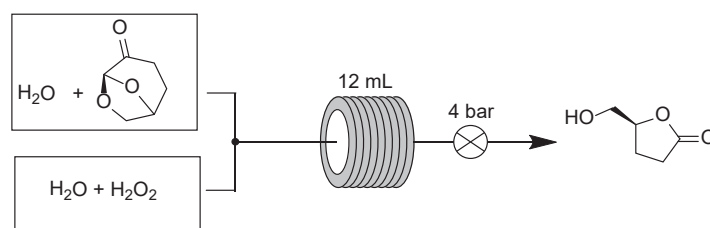
Keywords: Continuous Flow, Cyrene, Lactone.

Highlights

The present work describes the flow synthesis of (S)- γ -Hydroxymethyl- γ -butyrolactone from Cyrene, which is a commercial green solvent derivative from paper industry.

Abstract

With the advancement of methods used in organic chemistry, continuous flow synthesis is one of the techniques that is currently being explored. Flow synthesis reactors are capable of controlling several reaction variables, such as temperature, pressure and residence time.¹ These equipment can scale up production due to the capacity of the system to constantly maintain ideal conditions for the reaction. Therefore, it is possible to use them in order to increase the product space-time yield, that is, product mass per reactor volume and time. In this work, we aim to use a coil-type reactor to intensify the synthesis process of (S)- γ -hydroxymethyl- γ -butyrolactone (2H-HBO) from Cyrene™.² Allais and his collaborators reported the green synthesis of 2H-HBO, through a Baeyer-Villiger type reaction using only water and hydrogen peroxide. Therefore, the reaction can be adapted for flow synthesis system (Scheme).³



Scheme: 2H-HBO Flow Synthesis.

The first studies showed promising results for the reaction using this method (Table), where the product is formed with conversion and selectivity above 99 % through gas chromatography analysis coupled to a flame ionization detector with a residence time of only 3.75 min at 150 °C and space-time yield of 3.9 g.mL¹.h⁻¹. As perspectives, we will be performing a study of hydrogen peroxide equivalents, a more detailed study of temperature and residence time followed by alcohol oxidation and cyclic ester hydrolysis.

Table. Conversion and selectivity values in the studied parameters.

T (°C)	R.T. (min)	Conv. (%)	Select. (%)
100	15	>99	99
	7.5	>99	94
	3.75	>99	99
150	15	>99	99
	7.5	>99	96
	3.75	>99	99

Acknowledgments

CNPq, CAPES and FAPERJ

1. De Oliveira, K.T.; De Souza, R. O. M. A.; Pastre, J. C. et al. *Anais Acad. Bras. Cien.* **2018**, *90*, 1131 – 1169.

2. Clark, J. H.; Hunt, A. J.; Farmer, T. J. et al. *Chem. Comm.* **2014**, *50*, 9650 – 9652.

3. Allais, F.; Flourat, A. L.; Bonneau, G. et al. *Green Chemistry.* **2018**, *20*, 2455 – 2458.

Área: **ORG**
 (Inserir a sigla da seção científica para qual o resumo será submetido. Ex: ORG, BEA, CAT)

Rational design and synthesis of menadione-triazole-selenoester hybrids with potential activity against *Mycobacterium tuberculosis*

Ruan Carlos B. Ribeiro (PQ),^{1,*} **Acácio S. de Souza** (PQ),^{2,*} Sandy P. Valle (IC),¹ Lais M. Marins (IC),¹ Cláudio José C. Carvalho (PG),¹ Vanessa Nascimento (PQ),¹ Luana S. M. Forezi (PQ),¹ Fernando de C. da Silva (PQ),¹ Vitor F. Ferreira (PQ)²

acacio.farma@gmail.com; ruancarlos@id.uff.br

¹Departamento de Química Orgânica, Instituto de Química, UFF; ²Departamento de Tecnologia Farmacêutica, Faculdade de Farmácia UFF.

Palavras Chave: Tuberculosis, Naphthoquinone, Organoselenium, Triazoles.

Highlights

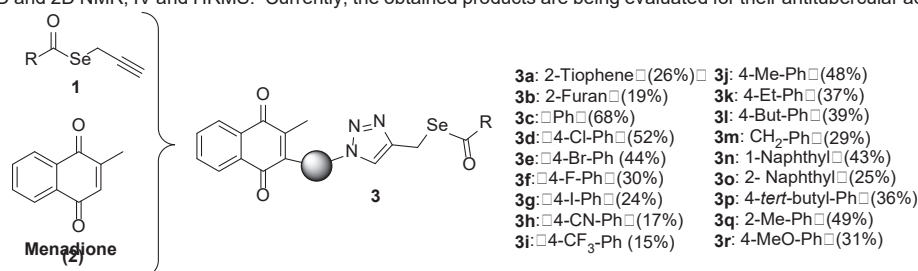
It is a search for hybrid menadione-triazole-selenoesters acting as antitubercular agents. Thus, it is intended to investigate how the hybridization of such systems may influence the activity against different *M. tuberculosis* strains.

Resumo/Abstract

Caused by the bacillus *Mycobacterium tuberculosis*, Tuberculosis (TB) is a communicable respiratory disease that is a major cause of ill health and one of the leading causes of death worldwide. About a quarter of the global population is estimated to have been infected with *M. tuberculosis*, with a total of 1.6 million people died in 2021 by TB disease, making it the second leading cause of death from a single infectious agent, ranking below COVID-19.¹ TB medicines have been used for decades and strains that are resistant to one or more of the medicines have been documented in every country surveyed, with emphasis on multidrug-resistant tuberculosis (MDR-TB).¹ In this context, the literature has presented naphthoquinone, organoselenium compounds and triazole derivatives, independently, and as well as menadione-organoselenium conjugates as promising scaffolds for new antitubercular drugs.²

The objective of this work is to search for new naphthoquinone-organoselenium hybrids connected by a 1,2,3-triazole spacer, looking for a good relation between the structure and the activity, and possibly even acting as antitubercular agent. Thus, we intend to investigate how the combination of such systems - naphthoquinone, selenoesters and 1,2,3-triazole - may have an influence on the activity of these new molecules.

For the synthesis of the new hybrids **3**, elemental selenium was reduced by NaBH₄, in ethanol, and then treated with the respective acyl chlorides and propargyl bromide to provide the selenoesters **1**, which were promptly reacted with the menadione derivatives in the presence of a catalytic amount of copper sulfate pentahydrate and excess sodium ascorbate under ultrasonic irradiation. The new compounds **3a-r** were obtained in the form of yellow solids, with yields ranging from 15 to 68% (Scheme 1). Their structures were confirmed using different physical methods of analysis such as 1D and 2D NMR, IR and HRMS. Currently, the obtained products are being evaluated for their antitubercular activity.



¹ Tuberculosis; World Health Organization: Geneva, 2022. <https://www.who.int/news-room/fact-sheets/detail/tuberculosis>. Accessed in 28/01/2023.

² Busquet, R.C.B.; Marins, D.B.; Di Leo, I.; *et al. Eur. J. Med. Chem.* 2021, 209, 112859.

Formatado: Inglês (Estados Unidos)

Agradecimentos/Acknowledgments

FAPERJ, CAPES, FIOCRUZ and CNPq.

46ª Reunião Anual da Sociedade Brasileira de Química: "Química: Ligando ciências e neutralizando desigualdades"

Regioselective and directing-group free photochemical C(2)-arylation of indoles

Bruno M. da S. Santos (PG),¹ Gabriel V. de Lucena (IC),¹ Fernanda G. Finelli (PQ).^{1*}

brunomaiasantos@gmail.com; finelli@ippn.ufrj.br

¹Instituto de Pesquisas de Produtos Naturais (IPPN/UFRJ)

Keywords: Arylation, EDA complex, Indole, Photochemistry, Regioselective.

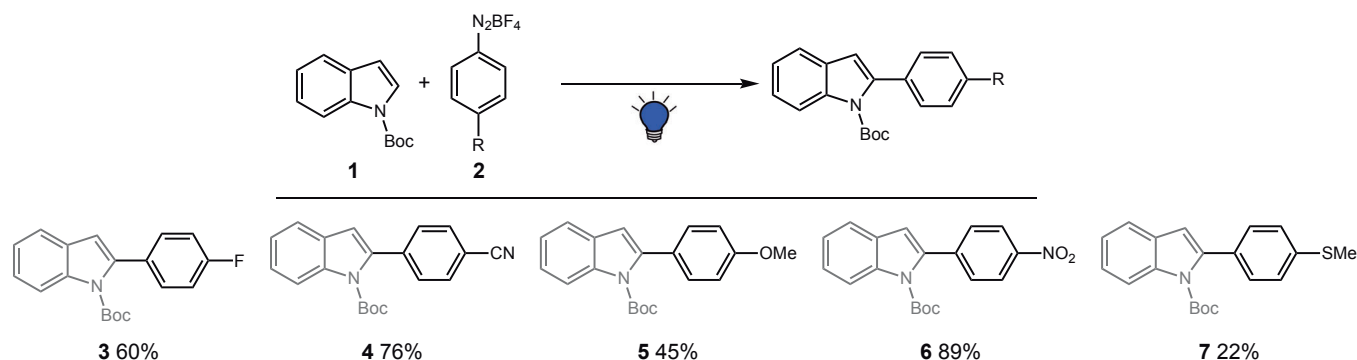
Highlights

An extremely simple and mild protocol for transition metal and photocatalyst-free selective C(2)-arylation of indoles is reported. Aryl diazonium salts are used as arylating agents.

Abstract

Indole motif is an important pharmacophore found in many natural products and biologically active substances. 2-Aryl indoles have been investigated for its promising activities against some cancer cell lines,¹ and selective protocols for indole arylation usually rely on precious metal catalysis, harsh conditions, and the use of directing groups.² This work presents our efforts in developing a mild, regioselective and directing-group free photochemical protocol for indole arylation using diazonium salts as arylating agents.

A model reaction between *N*-Boc-indole and 4-fluorobenzenediazonium was used to optimize the reaction conditions, which provided the C(2)-arylated product in 60% yield (Scheme 1, Structure 3). We could detect the formation of a photoactive electron donor-acceptor complex between the indole and the diazonium salt as responsible for triggering the reaction without the use of photocatalysts. To check the generality of the reaction, a scope is proposed using different starting materials. To date, we have two other examples, indicating both electron-poor and electron-rich diazonium salts are suitable for the reaction, although with different yields (Scheme 1, Structures 4 and 5).



Scheme 1. Initial scope investigation.

In conclusion, we propose an extremely simple, transition metal and photocatalyst-free protocol for selective indole arylation. We are moving forward to an evaluation of starting material's electronics effect in regioselectivity and kinetics, as well as a more detailed mechanistic investigation.

¹Bakherad, Z. *et al. Research on Chemical Intermediates* **2019**, 45 (5), 2827-2854; ²Pandey, D. K. *et al. Journal of Organic Chemistry* **2019**, 84 (20), 12800-12808.

Acknowledgments

The authors thanks CAPES, FAPERJ and CNPq for financial support.

Regioselectivity nitration of eugenol: a joint theoretical and experimental reinvestigation

Jaqueline R. C. Barbosa (PG),^{1*} Murillo H. Queiroz (PG)¹, Silvio Cunha (PQ)¹, Roberto Rivelino (PQ)²; Luciano Morais Lião (PQ)³ Gerlon de Almeida Ribeiro Oliveira (PQ)³
 1) Instituto de Química, Universidade Federal da Bahia, 40170-115
 2) Instituto de Física, Universidade Federal da Bahia, 40170-115
 3) Instituto de Química, Universidade Federal de Goiás, 40170-115
 *e-mail: jaquelinerosa.cb@gmail.com

Palavras Chave: (nitration, eugenol, bismuth nitrate, regioselectivity).

Highlights

The elusive straightforward synthesis of 5-nitro-eugenol from eugenol affords isomeric 6-nitro-eugenol.

Resumo/Abstract

Eugenol **1** is a versatile starting material for organic synthesis.¹ In an ongoing synthesis of guanidine from eugenol, we needed to prepare 6-nitro-eugenol **2** and 5-nitro-eugenol **3**, already described in the literature.²⁻⁴ To the synthesis of these isomers the main strategies use nitrate salts as a nitrating agent. To prepare **2** was applied the method in that nitronium ion comes from sodium nitrate in silica gel.² To obtain the regioisomer **3** was used the method developed by Banik and extensively applied by Barbosa, and both suggested a direct synthesis of **3** using bismuth nitrate.^{3,4} However, **3** never was formed using bismuth nitrate, and both salts afforded the same product, that is, both conditions afforded **2**, as presented in Figure 1, confirmed by NMR studies (including 2D NMR, H-C and H-N heterocorrelations). 5-Nitro-eugenol **3** could be prepared from eugenol acetate, in a three steps route and confirmed by NMR studies (including 2D NMR, H-C and H-N heterocorrelations). Currently, theoretical calculation within density functional theory [M06-2X/6-311++G(d,p)] is under investigation to understand the reaction mechanism of this nitration and explain the regioselectivity nitration of eugenol and eugenol acetate. In conclusion, our results suggests that all data relating the synthesis and biological activity of derivatives obtained from the elusive straightforward synthesis of 5-nitro-eugenol from eugenol and bismuth nitration should be revised.

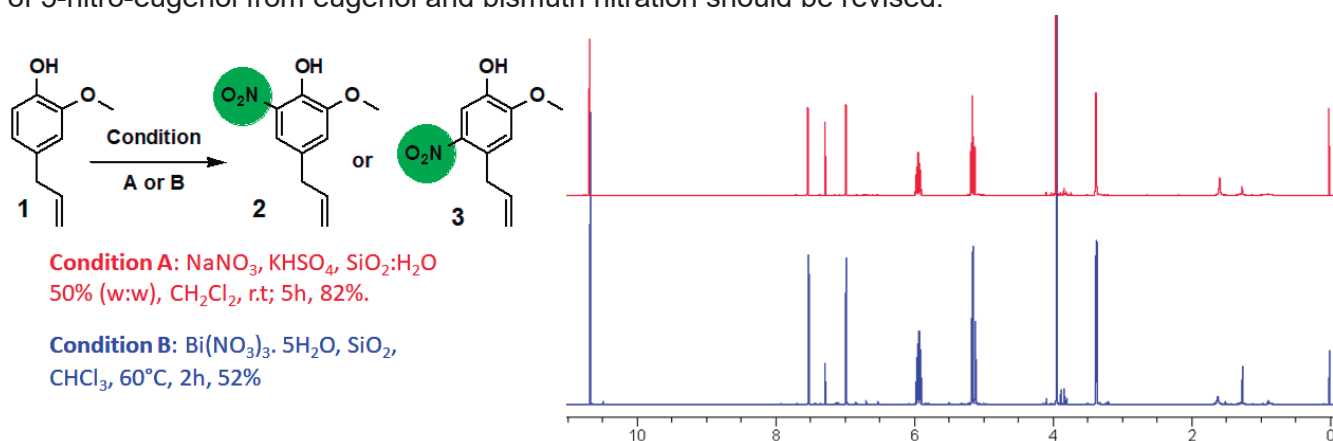


Figure 1. Nitration of eugenol in different conditions and their respective ¹H NMR.

Agradecimentos/Acknowledgments



- KAUFMAN, T. S. J. Braz. Chem. Soc., 26, 1055–1085, 2015.
- CARRASCO A., H. et al. J. Braz. Chem. Soc., 19, 543–548, 2008.
- CANALES, L.; BANDYOPADHYAY, D.; BANIK, B. K. Organic and Medicinal Chemistry Letters, 1, 9–11, 2011.
- BARBOSA, H. A., et al. Chemistry & Biodiversity, 18(5), e2100066, 2021.

Síntese de derivados 3-(1,3,4-oxadiazolil)-4-hidroxiquinolínicos como potenciais candidatos ao tratamento da doença de Alzheimer

Alan I. Ribeiro (IC),¹ Guilherme C. Valles (IC),¹ Mariana de P. Batista (IC),¹ Amanda R. P. Costa (PG),¹ Fernanda da C. S. Boechat (PQ),¹ Maria C. B. V. de Souza (PQ),¹ Pedro N. Batalha (PQ).^{1*}

alanimperatori@id.uff.br; pedrobatalha@id.uff.br

¹ Departamento de Química Orgânica, Universidade Federal Fluminense

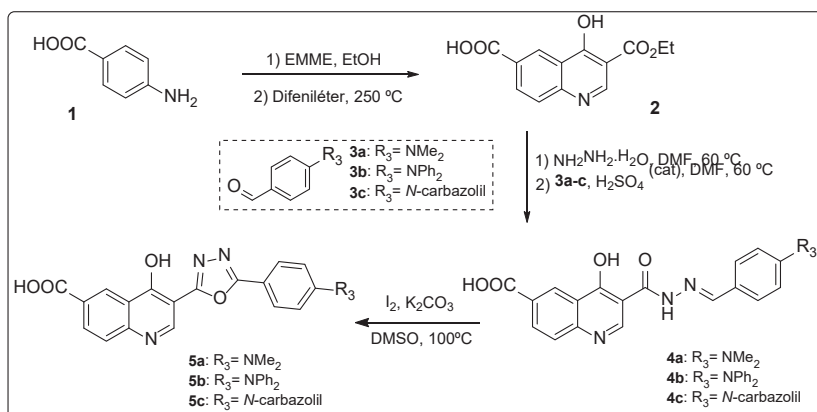
Palavras Chave: 1,3,4-Oxadiazoles, 4-Quinolines, Heterocycles, Alzheimer, Acetylcholinesterase

Highlights

Synthesis of 3-(1,3,4-oxadiazolyl)-4-hydroxyquinoline derivatives as potential candidates for the treatment of Alzheimer's disease. Oxadiazoles and quinolines are heterocyclic compounds with biological activity widely described in the literature. In this work, 3-(1,3,4-oxadiazolyl)-4-hydroxyquinoline derivatives were synthesized.

Resumo/Abstract

A doença de Alzheimer (DA) é uma doença neurodegenerativa e sem cura que causa a deterioração progressiva das funções cerebrais. Nesse contexto, um dos alvos farmacológicos visados no tratamento da doença é a enzima Acetilcolinesterase (AChE), pela promoção de efeitos neuroprotetores ocasionados por sua inibição.¹ Sendo assim, a busca por novos agentes inibidores da AChE se revela uma alternativa promissora para o manejo farmacológico da DA, por retardarem a progressão dos sintomas da doença. Os derivados de 1,3,4-oxadiazóis e de quinolinas são uma importante classe de compostos heterocíclicos com atividade biológica amplamente descrita na literatura, tais como antitumoral, antibacteriana, antiviral, anti-Alzheimer e outras.^{1,2} Devido a isso, já é relatada a existência de híbridos de quinolinas, 1,3,4-oxadiazóis e outros compostos como potenciais agentes anti-Alzheimer.^{1,3} Neste trabalho, portanto, uma nova série de derivados 3-(1,3,4-oxadiazolil)-4-hidroxiquinolínicos (**5a-c**) foi racionalmente planejada. Inicialmente, o ácido p-aminobenzóico (**1**) foi submetido a uma reação de condensação com etoximetilenomalonato de dietila (EMME), seguida de ciclização térmica, para formação do intermediário ácido 4-hidroxiquinolino-carboxílico (**2**). Após, esta substância foi reagida com monidrato de hidrazina, seguido de acidificação do meio reacional e adição de diferentes aldeídos aromáticos (**3a-c**), em uma estratégia *one-pot*. As acilidrazonas (**4a-c**) foram, por fim, convertidas nos compostos **5a-c** em uma etapa de ciclização oxidativa (Esquema 1). Assim, espera-se que o grupo carboxilato, ligado ao núcleo 4-hidroxiquinolínico, forneça um sítio capaz de formar ligações de hidrogênio com os alvos enzimáticos e, da mesma forma, pretende-se avaliar os diferentes efeitos eletrônicos dos grupamentos ligados à porção oxadiazólica no perfil farmacodinâmico destas substâncias no futuro.



Esquema 1. Rota sintética para obtenção dos compostos **5a-c**.

Agradecimentos/Acknowledgments

CNPq, FAPERJ, PPGQ-UFF, PROAP-UFF, CNPq - PIBIC, CAPES (Finance Code 001).

¹ KHAN, B. A.; et al., *Pharmaceuticals*, **2023**, 16 (1), 11.

² REHMAN, A.; et al., *Cogent Chemistry*, **2018**, 4: 1472197.

³ ZAIB, S.; et al., *Molecules*, **2021**, 26 (21), 6573.

Síntese de derivados 4-oxoquinolino-3-carboxamídicos com potencial atividade antitumoral

Jordana de Paula Alves (IC),¹ Leticia M. dos Santos (IC),¹ Thiago M. Do Vale (PG),¹ Aislan Cristina Rheder Fagundes Pascoal (PQ),² Vinícius Dávila Bitencourt Pascoal (PQ),² Pedro Netto Batalha (PQ),¹ Maria Cecília B. V. de Souza (PQ),¹ Fernanda S. Boechat (PQ).¹

alvesjordana@id.uff.br; fernandacostasantos@id.uff.br;

¹Laboratório de Nucleosídeos, Heterociclos e Carboidratos, Departamento de Química Orgânica, UFF;

²Grupo de Pesquisa de produtos naturais e moléculas bioativas- Laboratório Multiusuário de Pesquisa Biomédica- ISNF-UFF

Palavras Chave: quinolonas. 4-oxoquinolinas, atividade antitumoral

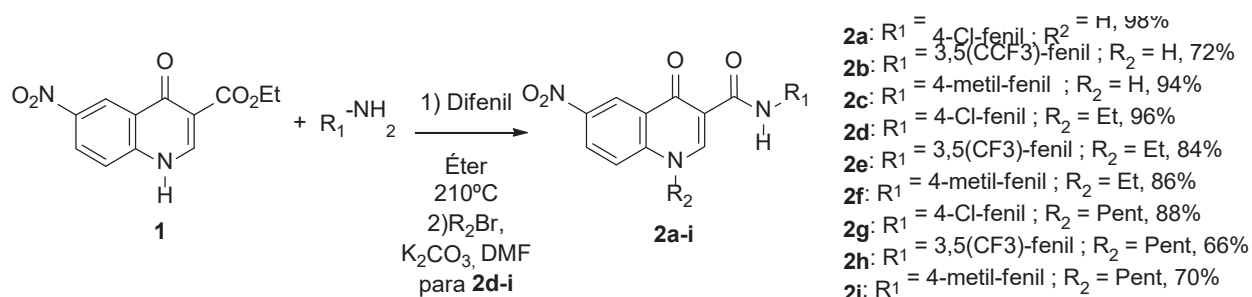
Highlights

Synthesis of 4-oxoquinoline-3-carboxamide derivatives with potential antitumor activity

Design, synthesis and antitumoral evaluation of 4-oxoquinoline derivatives in the search of new anticancer agents

Resumo/Abstract

A busca por agentes antitumorais com melhor potência terapêutica e menos efeitos colaterais motiva pesquisas pelo mundo inteiro, a fim de uma melhor eficácia no tratamento contra o câncer e melhora na qualidade de vida dos pacientes. As 4-oxoquinolinas são substâncias muito conhecidas por sua versatilidade sintética, e consequentemente, biológica, das quais podemos destacar sua atividade antitumoral. Da mesma forma, carboxamidas são amplamente estudadas na busca de novos agentes quimioterápicos. Nosso grupo de pesquisas tem sintetizado ao longo dos anos séries de derivados 4-oxoquinolino-carboxamídicos com relevante atividade antiproliferativa, frente a diversas linhagens celulares. Neste contexto, continuando com nossos estudos na busca de potenciais agentes antitumorais, a síntese de uma série de compostos 4-oxoquinolino-3-carboxamídicos é observada no Esquema 1, a seguir:



A 6-nitro-4-oxoquinolina (1) foi obtida previamente a partir da metodologia clássica de Gould Jacobs, amplamente utilizada pelo nosso grupo de pesquisas. Para obtenção das carboxamidas correspondentes, esta 4-oxoquinolina foi submetida à reação de substituição nucleofílica à carbonila utilizando-se diferentes anilinas como nucleófilos. Uma vez obtidas e devidamente caracterizadas, a série de quinolonocarboxamidas sofreu uma reação de *N*-alquilação, utilizando-se como agentes alquilantes brometo de etila ou de pentila. Os derivados **2a-i** foram obtidos com rendimentos que variaram entre 66 e 98%. Estes compostos sintéticos foram encaminhados para avaliação de sua atividade antitumoral. Estudos iniciais indicam que o derivado **2b** foi capaz de inibir o crescimento de células escamosas de câncer de boca, em 80% a 25 µM.

Agradecimentos/Acknowledgments

O presente trabalho foi realizado com apoio da Coordenação de Aperfeiçoamento de Pessoal de Nível Superior - Brasil (CAPES) - Código de Financiamento 001; CNPq; FAPERJ; PPGQ-UFF; PROAP-UFF.

Síntese de Derivados Cumarínicos via Funcionalização da 4-Hidroxycumarina com Organoselênio

Cristal V. T. Martins (IC),¹ **Acácio S. de Souza** (PQ),² **Ruan C. B. Ribeiro** (PQ),¹ **Pâmela S. Cordeiro** (PG),¹ **Vanessa Nascimento** (PQ),¹ **Luana S. M. Forezi** (PQ),^{1*}

luanaforezi@id.uff.br

¹Departamento de Química Orgânica, Instituto de Química, UFF; ²Departamento de Tecnologia Farmacêutica, Faculdade de Farmácia UFF.

Palavras Chave: 4-Hidroxycumarina, Organoselênio, Calcogênio, Bioatividade.

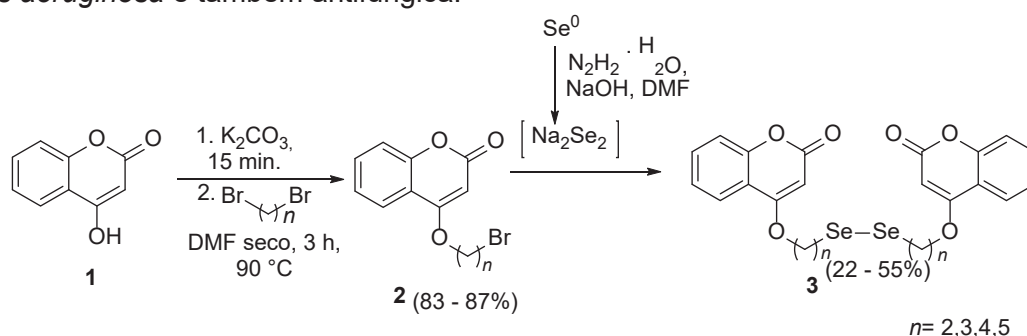
Highlights

Obtaining new coumarin derivatives via functionalization of 4-hydroxycoumarin with organoselenium. Coumarins and organoselenium compounds exhibit numerous individual biological properties.

Resumo/Abstract

A busca por novas moléculas bioativas inicia-se pela sua relevância na literatura, como é o caso das 4-hidroxycumarinas (**1**) e de compostos organoselênio, cujos estudos farmacológicos relatados mostram variadas propriedades biológicas quando avaliados individualmente. Assim, o objetivo deste trabalho consiste na síntese de novos derivados cumarínicos obtidos via funcionalização da 4-hidroxycumarina (**1**) com derivados organoselênio (Esquema 1).

Para preparação das cumarinas *O*-alquiladas **2**, a 4-hidroxycumarina (**1**) foi reagida com os dibromoalcanos correspondentes, em presença de carbonato de potássio, DMF seco, a 90 °C durante 3 horas (Esquema 1). Em seguida, os derivados alquilados **2** foram reagidos com o disseleneto de sódio, gerado in situ pela redução do selênio elementar com hidrazina, formando os disselenetos **3** em rendimentos moderados. Todos os disselenetos foram obtidos como sólidos amarelos e conforme aumenta-se a cadeia alquílica o disseleneto vai ganhando uma coloração amarela mais forte. Tais disselenetos serão empregados como nucleófilos em reações com diferentes eletrófilos. Após a obtenção das cumarinas funcionalizadas com organoselênio de interesse, estas serão enviadas para avaliação biológica anti-virulência contra *Pseudomonas aeruginosa* e também antifúngica.



Esquema 1. Síntese dos disselenetos cumarínicos.

1. Krief A.; Derock M. *Synlett* **2005**, 6, 1012–1014.
2. Forezi, L. S. M.; Froes, T. Q.; Cardoso, M. F. C.; Maciel, C. A. O.; Nicastro, G. G.; Baldini, R. L.; Costa, D. C. S.; Ferreira, V. F.; Castilho, M. S.; Silva, F. C. *Current Topics in Medicinal Chemistry* **2018**, 18, 149-156.

Agradecimentos/Acknowledgments

FAPERJ, CAPES, FIOCRUZ and CNPq.

Síntese de novas diarilssulfonimididas derivadas de 4-quinolonas com perfil de atividade antitumoral.

Mayra S. Coutinho (PG)¹; **Bruno A. Pereira** (IC)¹; Maria Cecília B. V. de Souza (PQ)¹; Pedro Netto Batalha (PQ)^{1*}.
alvesbruno@id.uff.br; pedrobatalha@id.uff.br

¹Instituto de Química, Departamento de Química Orgânica, UFF.

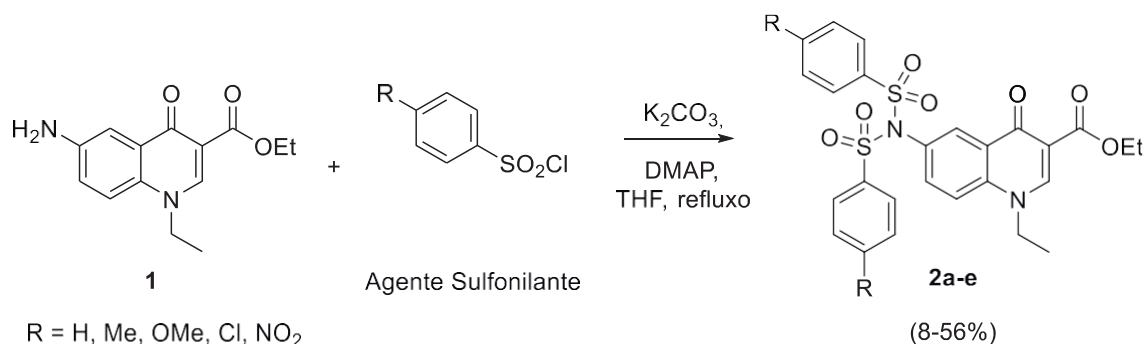
Palavras Chave: Quinolona, Sulfonimida, Intermediário sintético, Heterociclos.

Highlights

“Synthesis of novel diarylsulfonimides derived from 4-quinolones with antitumor activity profile.” Mild conditions were applied for the synthesis of the products and their intermediates. New 4-quinolone derivatives as intermediates for the synthesis of bioactive substances.

Resumo/Abstract

O aumento significativo no número de casos de câncer no Brasil, nos últimos anos, faz com que o desenvolvimento de novas estratégias mais eficientes para o combate a esta doença seja desenvolvido. Considerando a baixa seletividade do arsenal quimioterapêutico disponível na clínica, diferentes grupos de pesquisa têm despendido esforços no planejamento e síntese de novas substâncias com atividade antitumoral potencializada e maior seletividade. Derivados quinolônicos são substâncias de grande interesse medicinal, cujas características químicas possibilitam sua aplicação em diferentes áreas, incluindo no desenvolvimento de novos fármacos frente às mais diversas patologias. Desse modo, a busca por métodos sintéticos que levem a modificação em diferentes posições desse núcleo é uma estratégia da Química-Medicinal para obtenção de substâncias de amplo espectro biológico, em especial antitumoral. Estudos indicam que o núcleo 4-quinolônico e o grupo funcional sulfonamida estão presentes em diferentes substâncias capazes de atuar seletivamente contra à diferentes linhagens celulares. Contudo, o grupamento sulfonimida, ou *N*-sulfonilsulfonamida, é pouco explorado tornando-se um grupamento interessante para ser investigado. Dessa forma, neste trabalho é descrita a síntese de uma série de derivados 6-sulfonimido-4-quinolono (**2**) com potencial atividade anticâncer. A síntese das substâncias **2** se deu a partir da reação de sulfonilação empregando-se 6-amino-4-quinolono **1** e o agente sulfonilante adequado, na presença de *N,N*-dimetilaminopiridina (DMAP) e K₂CO₃. Estas substâncias tiveram suas estruturas confirmadas por métodos espectroscópicos de análise (IV, RMN de ¹H e de ¹³C), e tiveram seus pontos de fusão determinados.



Esquema 1 - Rota sintética para obtenção dos derivados **2**.

Agradecimentos/Acknowledgments

PPGQ-UFF, CAPES (Código de Financiamento 001), FAPERJ e CNPq

Síntese de novas tiossemicarbazonas contendo o núcleo 1*H*-1,2,3-triazol com potencial atividade antitumoral

Thais B. Santos (PG),¹ Rafaela M. de A. C. Ribeiro (IC),¹ Leonardo G. C. de Moraes (PG),¹ Vítor F. Ferreira (PQ),² David R. da Rocha (PQ),¹

thaisbarreto@id.uff.br

¹Departamento de Química, Universidade Federal Fluminense; ²Faculdade de Farmácia, Universidade Federal Fluminense

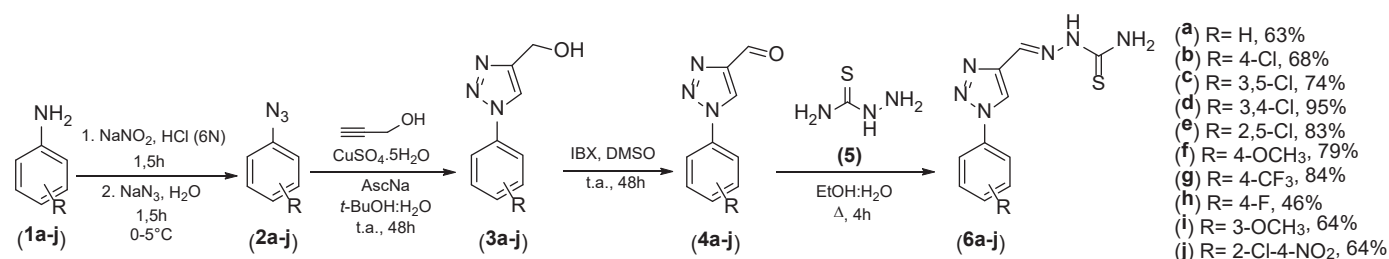
Palavras Chave: bases de Schiff, tiossemicarbazida, núcleo triazólico, câncer

Highlights

Synthesis of new thiosemicarbazone-linked 1*H*-1,2,3-triazoles with potential antitumor activity. Chemoselective condensation of thiosemicarbazide with triazolic aldehydes. Ten new Schiff bases containing triazole moiety.

Resumo/Abstract

O câncer é a segunda maior causa de morte no mundo e ainda um desafio no que diz respeito ao seu tratamento de forma bem-sucedida, tornando fundamental o desenvolvimento de novas substâncias, principalmente mais seletivas.¹ O núcleo 1*H*-1,2,3-triazol, heterociclo aromático de cinco membros contendo três átomos de nitrogênio vizinhos, vem sendo amplamente estudado, dadas as suas diferentes atividades biológicas, tais como antibacteriana, antifúngica, antiviral, analgésica e anticâncer.^{2,3,4,5} Recentemente, foi descrita uma série de tiossemicarbazonas contendo o núcleo 1,2,3-triazol que demonstrou atividade inibitória frente a diferentes linhagens de células tumorais, com destaque para a atividade em células leucêmicas.⁶ Nesse sentido, o objetivo deste trabalho é a síntese de tiossemicarbazonas inéditas contendo o núcleo 1*H*-1,2,3-triazol, com posterior avaliação de seus efeitos frente a diferentes linhagens tumorais. Para isso, a estratégia sintética inicia-se através da reação de diazotação seguida de substituição nucleofílica aromática de diferentes anilinas (**1a-j**), formando as azidas (**2a-j**). Estas são transformadas nos álcoois triazólicos (**3a-j**), através de uma cicloadição 1,3-dipolar catalisada por cobre.⁷ Uma reação subsequente de oxidação branda dos álcoois levou a formação dos aldeídos triazólicos (**4a-j**). Por fim, uma condensação quimiosseletiva da tiossemicarbazida (**5**) com os respectivos aldeídos permitiu a síntese das tiossemicarbazonas triazólicas inéditas (**6a-j**) com rendimentos variando de 46% a 95%, conforme descrito no Esquema 1.⁸ Assim, neste trabalho foram sintetizadas quarenta moléculas, das quais dez são as bases de Schiff inéditas, que atualmente se encontram em avaliação biológica frente a diferentes linhagens tumorais.



Esquema 1. Síntese das tiossemicarbazonas triazólicas (**6a-j**)

Agradecimentos/Acknowledgments

CAPES, CNPq e FAPERJ

¹Gregoric, T. *et al. Eur. J. Med. Chem.* **2017**, *125*, 1247-1267.

²Silva, T. B. *et al. Bioorg. Chem.* **2021**, *116*, 105250.

³Costa, D. C. S. *et al. Chemistry Select.* **2022**, *7*, e202201334.

⁴Wu, X. *et al. Bentham Science Pub.* **2022**, *22*, 1406-1425.

⁵Slavova, K. I. *et al. Bentham Science Pub.* **2020**, *15*, 92-112.

⁶Othman, E. M. *et al. Bioorg. Chem.* **2022**, *127*, 105968

⁷Jordão, A. *et al. Bioorg. Med. Chem.* **2011**, *19*, 1860.

⁸Wang, D. *et al. Molecules* **2019**, *24*, 4003.

Síntese de novos derivados ácidos 4-quinolono-3-hidroxiâmicos com potencial antiviral.

Joice Cristina de O. Andrade (PG),^{1*} Pedro N. Batalha (PQ),¹ Maria Cecília B. V. de Souza (PQ),¹ Fernanda da C. S. Boechat (PQ).¹

joicecristina@id.uff.br

¹Universidade Federal Fluminense, Instituto de Química, Departamento de Química Orgânica – Outeiro de São João Batista s/nº, Niterói / RJ, 24020-141

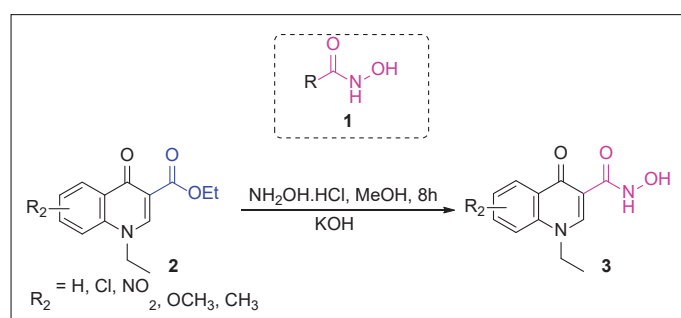
Palavras Chave: Ácido hidroxiâmico, 4-quinolona, Síntese, Otimização reacional

Highlights

Synthesis of new 4-quinolone-3-hydroxamic acids with potential antiviral activity. Reaction conditions toward the synthesis of new hydroxamic acids derived from 4-quinolone ester precursors.

Resumo/Abstract

As 4-quinolonas constituem uma classe de substâncias orgânicas amplamente estudadas, em razão do seu amplo espectro de atividades biológicas.¹ Seus derivados são conhecidos classicamente por apresentarem atividade antibacteriana, no entanto, também são utilizados no tratamento de doenças relacionadas a diferentes patógenos, como: vírus, fungos, parasitas e outros. O Elvitegravir,² por exemplo, é um derivado 4-quinolônico com perfil antiviral, atualmente utilizado como medicamento na clínica para o tratamento da *AIDS*, através da inibição da enzima integrase associada a replicação do HIV. Diante do exposto, é importante investir em novas modificações estruturais a partir deste núcleo estrutural na busca por novos derivados bioativos. Os ácidos hidroxiâmicos são substâncias que compõem o grupo funcional (R-NHOH). Estes derivados são agentes quelantes de diversos íons catiônicos e, apresentam grupos doadores e aceptores de ligação hidrogênio conferindo ao grupo um perfil bioativo diversificado.³ Dessa forma, o objetivo do trabalho é a combinação do grupo funcional ácido hidroxiâmico **1** ao arcabouço estrutural 4-quinolônico **2**, para a obtenção de novos derivados do tipo **3** através do estudo e otimização das condições reacionais.



Esquema 1. Síntese dos derivados ácidos-4-quinolono-3-hidroxiâmicos.

Os derivados **3** foram obtidos através de uma reação de substituição nucleofílica ao carbono carbonílico do grupamento éster utilizando-se um nucleófilo (NH₂OH) obtido *in situ* através da reação prévia entre NH₂OH.HCl e KOH em meio metanólico (**Esquema 1**). No geral, os rendimentos obtidos para os derivados ácidos 4-quinolono-3-hidroxiâmicos foram em torno de 79% e, após o isolamento, estes derivados foram estruturalmente caracterizados por métodos físicos de análise (p.f., IV, MS e RMN de ¹H), tendo suas estruturas confirmadas. A metodologia utilizada será aplicada a outros precursores, para que uma nova série congênere de derivados do tipo **3** seja preparada e posteriormente avaliada quanto ao seu perfil antiviral.

Referências

- 1-MESITI, F. et al. 4-Oxoquinolines and monoamine oxidase: When tautomerism matters. *European Journal of Medicinal Chemistry*, v. 213, 2021.
- 2-HAUSER, W. B.; RENFROW, Jr. **BENZOYDROXAMIC ACID**. *Org. Synth*, Vol.19, p.15, 1939.
- 3-OSIPOV, V. N. et al. Biologically active quinazoline-based hydroxamic acids. *Medicinal Chemistry Research*, v. 29, n. 5, p. 831–845, 2020.

Agradecimentos/Acknowledgments

CNPq, FAPERJ, CAPES (Finance Code 0001)

46ª Reunião Anual da Sociedade Brasileira de Química: "Química: Ligando ciências e neutralizando desigualdades"

Síntese e avaliação anti-SARS-CoV-2 de novos análogos de aciclonucleosídeos fosfonatos derivados de ácidos 4-quinolono-3-carboxílicos (ANPs).

Alan G. de Souza (PG),^{1*} Guilherme C. Valles (IC),¹ Leticia V. Faro (PQ),¹ Fernanda C. S. Boechat (PQ),¹ Thiago Moreno L. de Souza,² Maria Cecília B. V. de Souza (PQ).¹

alangoncalves@id.uff.br; mceciliabvs@gmail.com

¹Instituto de Química, Departamento de Química Orgânica, UFF; ²Fundação Oswaldo Cruz – FIOCRUZ.

Palavras-Chave: Aciclonucleosídeo, Quinolona, Fosfonato, COVID-19, Antiviral.

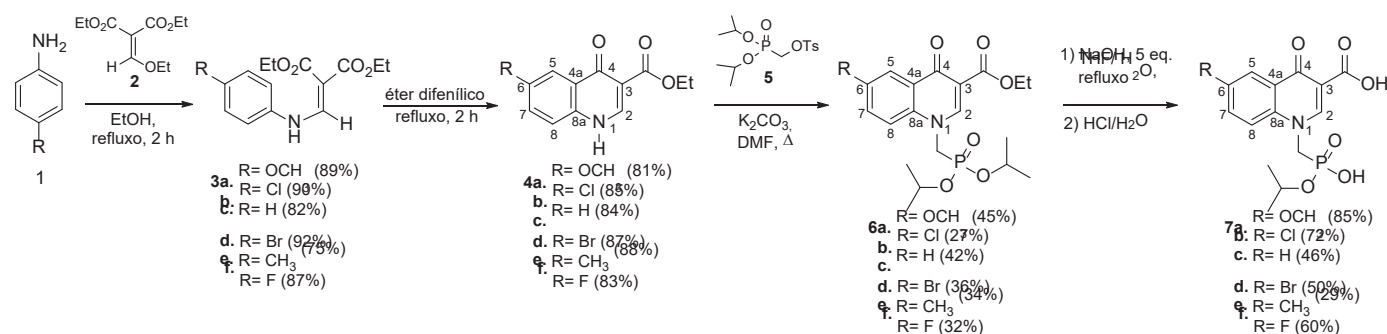
Highlights

Synthesis and anti-SARS-CoV-2 evaluation of novel acyclonucleosides phosphonates 4-quinolone-3-carboxylic acids analogues.

The lack of specific drugs for the treatment of viruses makes the synthesis of new antiviral substances urgent and necessary.

Resumo/Abstract

Com o cenário alarmante da pandemia causada pelo SARS-CoV-2, evidencia-se que o desenvolvimento de novas substâncias que possam atuar como fármacos de potencial ação antiviral frente a este vírus se faz urgente e necessário. O coronavírus (COVID-19) causou milhões de óbitos em todo o mundo e continua gerando novas vítimas com as suas subvariantes. A inexistência de fármacos específicos para tratamento dessa infecção viral corrobora com a importância da busca por novas substâncias antivirais com foco no vírus citado. Nesse sentido, foi preparada uma série de aciclonucleosídeos fosfonatos (ANPs) do tipo ácidos 4-quinolono-3-carboxílicos **7**, através da sequência reacional que envolveu a reação entre as anilinas **1** e o etoximetilnomalonato de dietila (**2**), gerando os anilinoacrilatos de etila **3**, que por ciclização térmica produziram as 4-quinolonas **4**. Estas, submetidas à reação de *N*-alquilação com diisopropil-*p*-toluenosulfoniloximetanofosfonato (**5**), levaram aos intermediários ANPs 4-quinolonônicos **6**, que foram convertidos aos ANPs **7** por hidrólise básica, seguida de neutralização do meio reacional. Estes novos ANPs **7**, assim como os precursores **6**, tiveram suas estruturas confirmadas por RMN de ¹H e de ¹³C, por espectroscopia na região do IV e por espectrometria de massas de alta resolução, e foram submetidos a avaliação biológica frente ao vírus SARS-CoV-2 em células Calu-3 infectadas. Os resultados obtidos indicaram percentuais de inibição entre 12 e 40% e, de modo geral, os derivados ácidos **7** se mostraram mais ativos do que seus precursores **6**. Buscando-se o desenvolvimento da estratégia de se obter pró-fármacos ativos contra este vírus, estes ANPs **7** constituem-se em protótipos para o planejamento de futuras pró-drogas com potencial ação anti-SARS-CoV-2.



Esquema 1. Esquema reacional para obtenção dos derivados ANPs de ácidos 4-quinolono-3-carboxílicos **7**

Agradecimentos/Acknowledgments

O presente trabalho foi realizado com apoio da Fundação de Amparo à Pesquisa do Estado do Rio de Janeiro (FAPERJ), do Conselho Nacional de Desenvolvimento Científico e Tecnológico (CNPq) e da Coordenação de Aperfeiçoamento de Pessoal de Nível Superior - Brasil (CAPES) - Código de Financiamento 001.

Síntese e Prospecção Biológica de uma Nova Série de Ariloxi-1,2-naftoquinonas como Agentes Antiparasitários

Camille C. Cruz* (IC), Searitha C. Rodrigues (PG), Maria Tereza M. Martins (PG),
Raphael Silva M. de Moraes (PG), Gabriel Tavares de A. Pinto (IC), Anna Claudia Cunha* (PQ).

Departamento de Química Orgânica, Programa de Pós-Graduação em Química, Universidade Federal Fluminense, Niterói, RJ, Brasil.

*e-mail: camillecruz@id.uff.br; annacunha@id.uff.br

Palavras Chave: *Trypanosoma cruzi*, 1,2-Naftoquinonas, Fenóis.

Highlights

Synthesis and characterization of a series of aryloxy-1,2-naphthoquinones as candidate antiparasitic agents.

Resumo/Abstract

A doença de Chagas (DC), também conhecida como Tripanossomíase Americana, é uma enfermidade infecciosa parasitária negligenciada com endemia em 21 países do continente americano.¹ Esta patologia desencadeia em infecções com alto índice de morbidez e mortalidade, constituindo um relevante problema de saúde pública.²

Atualmente, a terapêutica da DC é muito limitada, restringindo-se apenas a dois fármacos nitro-heterocíclicos: benznidazol e o nifurtimox (descontinuado no Brasil). Ambos os fármacos são ineficazes na fase crônica da doença, além de provocarem graves efeitos colaterais.³ Neste contexto, a busca por novas substâncias com atividade tripanomicida se faz necessária face à gravidade da DC.

Relatos na literatura⁴ mostram que ariloxi-1,4-naftoquinonas **1a-b** (Figura) são capazes de inibir a atividade do protozoário *Trypanosoma cruzi*, apresentando valores de CI_{50} expressivos na faixa de 0,7 a 1,7 μ M. Diante deste contexto, este trabalho descreve a síntese de uma série de ariloxi-1,2-naftoquinonas **4a-g** (Esquema) via reação de substituição nucleofílica do sal 4-sulfonato de sódio 1,2-naftoquinona **2** com fenol **3a** e seus derivados **3b-g**. As substâncias alvo **4a-g** foram obtidas com rendimentos que variam de 27 a 62%. As estruturas químicas de **4a-g** foram elucidadas por métodos espectroscópicos tais como, espectroscopia na região do Infravermelho (IV) e Ressonância Magnética Nuclear de Hidrogênio (¹H) e Carbono (¹³C). Estas substâncias serão encaminhadas para avaliação de seus efeitos contra as formas morfológicas do *T. cruzi*.

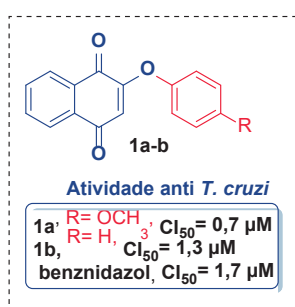
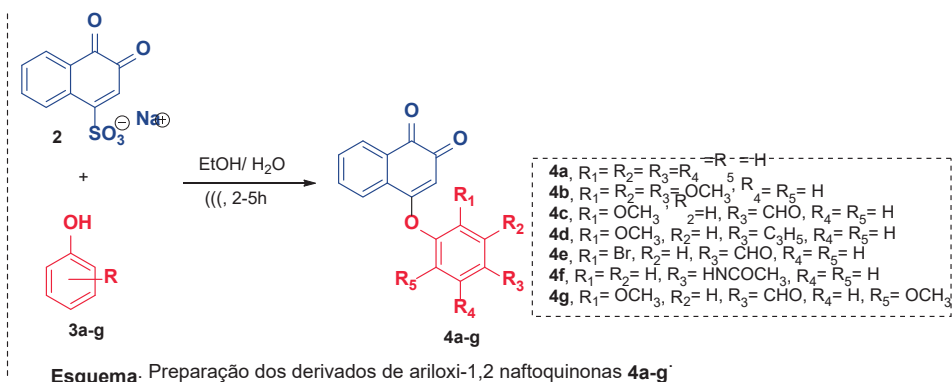


Figura: Fármaco de referência e derivados de 1,4-naftoquinonas com atividade tripanomicida.



Agradecimentos/Acknowledgments

CAPES, UFF, PPGQ-UFF, FAPERJ, PIBITI/CNPq.

Referências Bibliográficas:

- ¹Kann, S.; Dib, J. C.; Aristizabal, A.; Mendoza, G. C.; Lacouture, H. D. S.; Hartmann, M.; Frickmann, H.; Kreienbrock, L. *Microorganism.*, **2022**, 10, 1427.
- ²Lara, L. D.; Lechuga, G. C.; Orlando, L. M. R.; Ferreira, B. S.; Souto, B. A.; Santos, M. S.; Pereira, M. C. S. *Pharm.*, **2022**, 14, 995.
- ³Duchowicz, P. R.; Fiorelli, S. E.; Bacelo, D. E. *Results Chem.*, **2022**, 4, 10256.
- ⁴Bolognesi, L. M.; Lizzi, F.; Perozzo, R.; Reto, B.; Cavalli, A. *Bioorganic Med. Chem. Lett.*, **2008**, 18, 2272.

Síntese mecanoquímica de derivados α -carbetoxy- β -(anilino)acrilatos de etila

Mayra S. Coutinho (PG)¹; **Rodrigo Luís M. Gomes** (PG)¹; Alan I. Ribeiro (IC)¹; Maria Cecília B. V. de Souza (PQ)¹; Fernanda C. S. Boechat (PQ),¹ Pedro Netto Batalha (PQ)^{1*}.

gomesrodrigo@id.uff.br; pedrobatalha@id.uff.br

¹Instituto de Química, Departamento de Química Orgânica, UFF.

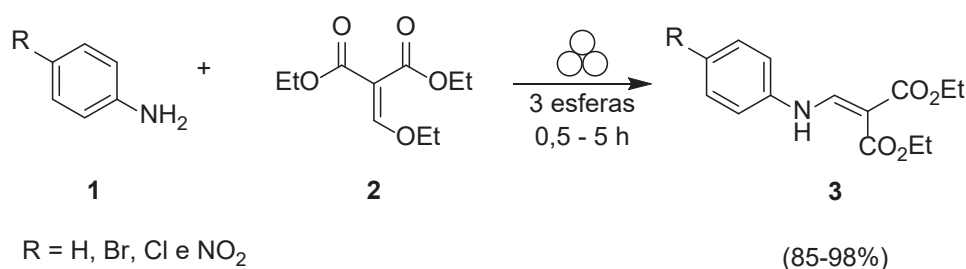
Palavras Chave: Acrilato, Mecanoquímica, Intermediário sintético, Livre de solvente, Química Verde.

Highlights

"Mechanochemical synthesis of ethyl α -carbetoxy- β -(anilino)acrylate derivatives". In this work we use a ball mill to synthesize α -carbetoxy- β -(anilino)acrylate derivatives under mild, solvent free conditions.

Resumo/Abstract

A síntese de substâncias via processos mecanoquímicos tem atraído considerável atenção nos últimos anos, em razão de ser um método eficaz e limpo, que dispensa o uso de solventes e proporciona maior eficiência energética e menores tempos de reação. Desse modo, a mecanoquímica é uma alternativa sustentável para obtenção de numerosos compostos orgânicos. α -Carbetoxy- β -(anilino)acrilatos de etila são intermediários sintéticos versáteis para a construção de diferentes tipos de *N*-heterociclos bioativos com diferentes perfis de atividade biológica, como por exemplo, no caso de derivados quinolônicos. Ademais, estes intermediários são utilizados no preparo industrial de polímeros para a geração de plásticos, revestimentos, adesivos, elastômeros, tintas e polidores. Em metodologias clássicas, a síntese dessas substâncias requer o uso de solvente, usualmente em condições de refluxo. Neste trabalho propõe-se uma metodologia verde, com foco na síntese de uma série de derivados α -carbetoxy- β -(anilino)acrilatos de etila (**3**) em condições livres de solvente e sem aquecimento. A síntese das substâncias do tipo **3** se deu a partir de uma reação de condensação, reagindo-se anilinas devidamente substituídas (**1**) com etoximetilenomalonato de dietila (**2**), utilizando-se um moinho de bolas do modelo Ultra Turrax Tube Drive UTDD IKA Workstation. Estas substâncias foram obtidas em excelentes rendimentos e sem a necessidade de etapas de purificação posteriores. Tiveram suas estruturas confirmadas por métodos espectroscópicos de análise (IV, RMN de ¹H e de ¹³C), assim como tiveram seus pontos de fusão determinados, estando de acordo com os relatados na literatura científica. Os resultados obtidos até o momento foram promissores e indicam que é possível otimizar a metodologia de síntese de α -carbetoxy- β -(anilino)acrilatos de etila sem aquecimento, na ausência de solventes, e com menor tempo reacional, quando comparada com a metodologia tradicional.



Esquema 1 - Rota sintética para obtenção dos derivados **3**.

Agradecimentos/Acknowledgments

PPGQ-UFF, CAPES (Código de Financiamento 001), FAPERJ e CNPq

Referências

- MATETI, S. *et al.* **Chemical Communications**, v. 57, n. 9, p. 1080-1092, 2021.
- LIU, X. *et al.* **Advanced Materials**, v. 34, n. 46, p. 2108327, 20 mar. 2022.

Sequential Multicomponent Reactions Applied to the Synthesis of Furoxan Nitrogen-Heterocycles as Potential Nitric Oxide Donors

Nicolas S. Anjos (PG),^{1*} Luiz S. Longo Jr. (PQ)¹

nicolas.anjos@unifesp.br; luiz.longo@unifesp.br

¹Departamento de Ciências Farmacêuticas, Instituto de Ciências Ambientais, Químicas e Farmacêuticas
Universidade Federal de São Paulo – campus Diadema

Keywords: Multicomponent Reactions; Nitrogen-based Heterocycles; Furoxans; Nitric Oxide Donors

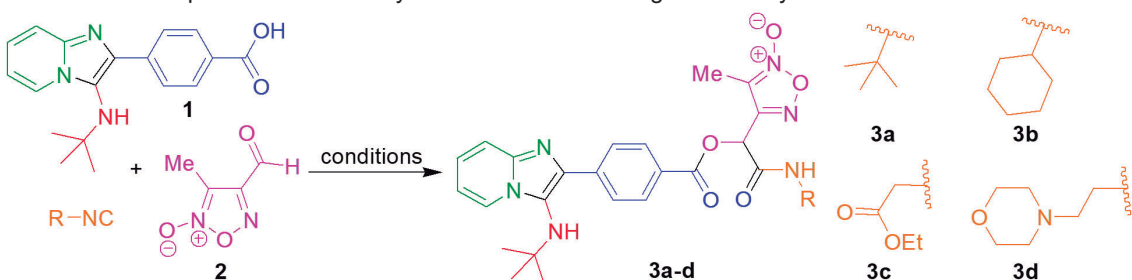
Highlights

Imidazo[1,2-a]pyridines containing the furoxan moiety as potential nitric oxide donors can be synthesized in moderate to good yields via sequential Groebke-Blackburn-Bienaymé/Passerini reactions.

Resumo/Abstract

In a tumor microenvironment, high concentrations of nitric oxide (NO) lead to cytotoxic effect against tumor cells (antitumor activity).^[1] In this context, organic compounds containing the 1,2,5-oxadiazole-2-oxide scaffold (furoxan), can play an important role as exogenous NO donors under physiological conditions and, therefore, act as potential antitumor compounds. Sequential multicomponent reactions are useful synthetic tools for the rapid and efficient construction of structurally diverse nitrogen-fused heterocycles containing the furoxan scaffold. Previously, we reported the Groebke-Blackburn-Bienaymé (GBB) reaction catalyzed by reusable Brønsted-acidic ionic liquids, affording a series of imidazo-fused heterocycles in moderate to excellent yields.^[2] In this study, we investigated the sequential GBB/Passerini reactions to synthesize imidazo[1,2-a]pyridines containing the furoxan moiety. Firstly, the Passerini reaction between carboxylic acid **1** (obtained via GBB reaction),^[2] 3-methyl-4-furoxancarbaldehyde **2** and *tert*-butyl isocyanide was evaluated under different conditions to afford **3a** in 59-75% yield (Table 1, entries 1-4). Next, the best reaction condition to obtain **3a** (entry 4) was applied to prepare a series of new furoxan nitrogen-heterocycles **3b-d** in moderate to good yields (54-73%; entries 5-7). Further studies on the expansion of the furoxan nitrogen-heterocycles library as well as its NO release quantification are under investigation by our group.

Table 1. Passerini reaction optimization for the synthesis of furoxan nitrogen-heterocycles **3a-d**.



Entry	Catalyst	Conditions	Time (h)	Product/Yield
1	-	CH ₂ Cl ₂ , rt.	24	3a (59%)
2	-	CH ₂ Cl ₂ , rt.	48	3a (74%)
3	-	CH ₂ Cl ₂ , MW, 80°C	2	3a (70%)
4	-	CH₂Cl₂, MW, 80°C	4	3a (75%)
5	-	CH ₂ Cl ₂ , MW, 80°C	4	3b (73%)
6	-	CH ₂ Cl ₂ , MW, 80°C	4	3c (54%)
7	-	CH ₂ Cl ₂ , MW, 80°C	4	3d (61%)

Reagents and conditions: isocyanide (1,0 mmol), **1** (1,0 mmol), **2** (1,0 mmol), dichloromethane (3,0 mL), closed vial, MONOWAVE 300 (Anton Paar).

References:

- [1] H. P. Monteiro, E. G. Rodrigues, A. K. C. Amorim Reis, L. S. Longo, F. T. Ogata, A. I. S. Moretti, P. E. da Costa, A. C. S. Teodoro, M. S. Toledo, A. Stern, *Nitric Oxide - Biol. Chem.* **2019**, *89*, 1–13.
[2] N. S. Anjos, A. I. Chapina, A. R. Santos, P. Licence, L. S. Longo, *Eur. J. Med. Chem.* **2022**, e202200615.

Agradecimentos/Acknowledgments

CAPES, FAPESP, PPG Q-CTS, UNIFESP.

Statistical Models for Selectivity Prediction in Phosphoric Acid-Catalyzed Ugi-Type reactions

Vitor A. Fernandes (PG), Marco A. B. Ferreira (PQ), Márcio W. Paixão (PQ)*

vitorafs.alcantara@gmail.com; mwpaixao@ufscar.br

Laboratory for Sustainable Organic Synthesis and Catalysis - Department of Chemistry, Federal University of São Carlos – UFSCar, São Carlos, São Paulo, Brazil

Keywords: Ugi reaction, Brønsted acid, organocatalysis, stereoselectivity, statistical model

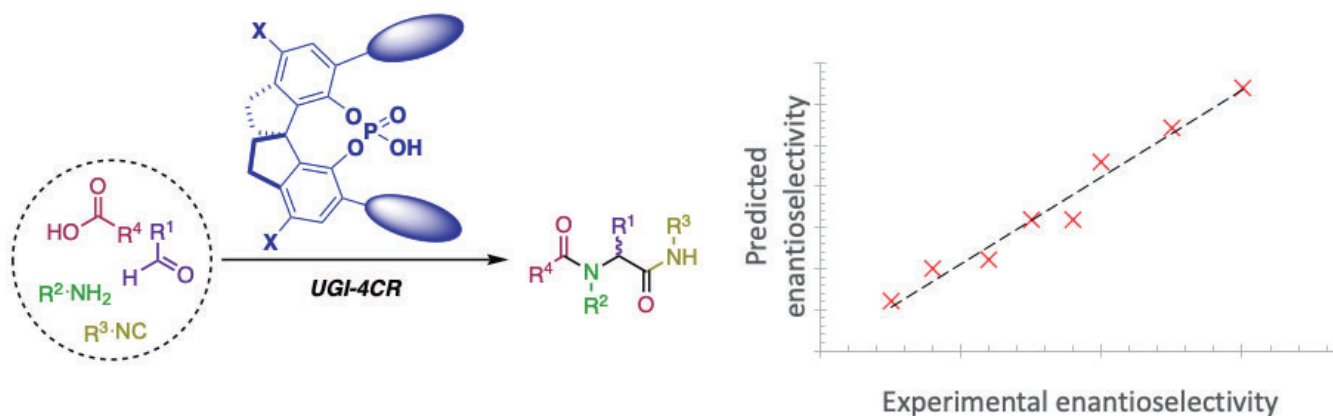
Highlights

Statistical modeling meets the Ugi reaction! Statistical models assist on the understanding of asymmetric phosphoric acid-catalyzed Ugi four-component reaction.

Resumo/Abstract

The four-component Ugi reaction (Ugi-4CR) is a useful synthetic tool for the one-pot construction of peptide-like structures through the combination of a carbonyl compound, an amine, an acid, and an isocyanide.¹ Even though its huge potential to be applied in drug discovery, stereochemical challenges narrow the application of this reaction and it is a long-term problem for the synthetic community. Just a few years ago, Zhang *et al.* reported the first enantioselective Ugi reaction by using chiral phosphoric acids as catalysts.² Despite the great contribution given by this work, there are still some limitations to be addressed, for example, the restriction in the substrate scope.

Foretelling the suitable asymmetric catalyst for a particular reaction might be challenging, because the optimal molecular features for one reaction do not always translate to another. For that reason, researchers have been using statistical models to predict the outcome of organic transformations. In order to better understand the features that govern the enantioselectivity and to design new optimal catalysts, we have developed statistical models for the prediction of enantioselectivity of the phosphoric acid-catalyzed Ugi reaction.



1. I. Ugi, R. Meyr, U. Fetzer, C. Steinbrückner, *Angew. Chem.* **1959**, *71*, 386.
2. J. Zhang, P. Yu, S.-Y. Li, H. Sun, S.-H. Xiang, J. Wang, K. N. Houk, B. Tan, *Science* **2018**, *361*, 1087.

Agradecimentos/Acknowledgments

We are grateful to CNPq (INCT Catalise), FAPESP (15/17141-1, 19/01973-9, 20/01255-6, 21/10246-3 and 22/11314-5) and GSK for financial support. This study was financed in part by the Coordenação de Aperfeiçoamento de Pessoal de Nível Superior – Brasil (CAPES) – Finance Code 001.

Stereoselective synthesis of bioactive β -amino alcohols derived from (-)- β -pinene through biocatalysis

Gustavo dos Santos Martins (PG)¹, Bruno Maia da Silva dos Santos (PG)², Fernanda Gadini Finelli (PQ)², Ivana Côrrea Ramos Leal (PQ).^{1*}

martinsufri.farma@gmail.com; ivanafarma@yahoo.com.br

¹Faculdade de Farmácia - UFRJ; ²Instituto de Pesquisa de Produtos Naturais - UFRJ

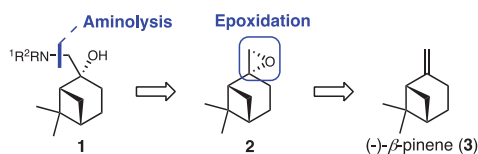
Keywords: Epoxidation, Beta-Pinene, Monoterpene.

Highlights

Herein we present our efforts toward the stereoselective synthesis of valuable β -amino alcohols derived from (-)- β -pinene through two reaction steps involving a biocatalytic epoxidation and aminolysis.

Abstract

Monoterpenes, such as β -pinene, are secondary metabolites widely used in food and fragrance industries. The β -amino alcohols **1** derived from β -pinene (**3**) are valuable intermediates for pharmaceuticals, such as β -blockers, antifungals and antibiotics¹. The synthetic strategy to obtain the target molecules consists of the aminolysis reaction with the appropriated epoxides obtained from (-)- β -pinene (**3**) (Scheme 1).



Scheme 1. Synthetic strategy for the synthesis of β -amino alcohols

We started our studies comparing different protocols for (-)- β -pinene epoxidation, employing immobilized lipases, *N,N'*-dicyclohexylcarbodiimide (DCC) and Oxone® as oxidant, evaluating the efficiency and the diastereoselectivity of the reactions (Table 1).

Table 1. Epoxidation of (-)- β -pinene (**3**) to substance **2**

Entry	Conditions ^{a,2,3,4}	Yield ^b	dr
1	0.1 equiv. of Novozyme 435®, 2.25 equiv. of UHP, EtOAc, 45 °C, 225 rpm, 3 h	58%	4.8:1
2	2 equiv. of DCC, 2 equiv. of KHCO ₃ , MeOH, r.t., 24 h	58%	>98:2
3	10 equiv. of acetone, 1 equiv. of Oxone®, pH 10, H ₂ O/EtOAc (1:1), r.t., 5 h	5%	>99

^aAll the reactions performed with 1 mmol of **3** as limitant reactant; ^bDetermined through ¹H qNMR analysis using 1,3-benzodioxole as internal standard and based on the ratio of signals with δ 2.6 ppm and δ 2.4 ppm in ¹H qNMR.

The biocatalytic pathway exhibited promising results, leading to product in 58% yield in only 3 h (Entry 1). The use of DCC (Entry 2) leads to similar yields and better selectivities, but produces several byproducts, making the purification process difficult. Based on this preliminary investigation, we demonstrated that the enzymatic procedure is suitable for the epoxidation of β -pinene, with short reaction times and good yields. We are currently moving forward to the optimization of this process to improve its efficiency and the aminolysis of **2** to produce the desired β -amino alcohols **1**.

¹ Bhaskar et al. *Journal of the Brazilian chemical society*, v. 29, p. 639-648, 2018. ² MARTINS et al. *Biotechnology Letters*, v. 44, n. 7, p. 867-878, 2022. ³ MAJETICH et al. *The Journal of Organic Chemistry*, v. 63, n. 8, p. 2564-2573, 1998. ⁴ HASHIMOTO and KANDA, *Organic process research & development*, v. 6, n. 4, p. 405-406, 2002.

Acknowledgments

46ª Reunião Anual da Sociedade Brasileira de Química: "Química: Ligando ciências e neutralizando desigualdades"

Sociedade Brasileira de Química (SBQ)

The authors would like to thank FAPERJ, CNPQ and CAPES.

Structural modifications in microbial naphthoquinone

Vitor T. Moraes (IC),¹ Franco J. Caires (PG),¹ Luiz A. B. Moraes (PQ),^{2*} Giuliano C. Clososki (PQ)^{1*}

vtmx00@usp.br; gclososki@usp.br

¹Departamento de Ciências Biomoleculares/Clososki Research Group, FCFRP/USP RP; ²Departamento de Química/Laboratório de Massas, FFCLRP/USP RP.

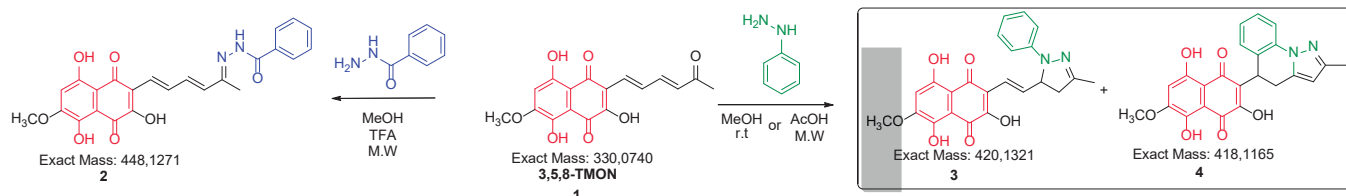
Palavras Chave: Naphthoquinones, Phenylhydrazine, Isoniazid, Heterocycles, Dihydropyrazole.

Highlights

The microbial naphthoquinone isolated from the fungus *Cordyceps* sp. was reacted with phenylhydrazine and isoniazid. The products were characterized by EI/MS⁺ and NMR and sent to biological evaluation.

Abstract

Naphthoquinones are part of an important group of natural products. This class includes some well-known compounds, such as lapachol and shikonin. These molecules are largely explored as starting materials for structural modification reactions, aiming at biological activity. Thus, this work aimed to perform structural modification reactions with the microbial naphthoquinone 3,5,8-TMON. *Cordyceps* sp. was fermented and the culture broth was extracted using ethyl acetate at pH 2 and the organic phase was analyzed in LC-MS. A dehydration reaction was used to transform Erythrostominone into 3,5,8-TMON (**1**), increasing the yield of the process and the final product was centrifuged.¹ Structural modification reactions of 3,5,8-TMON were performed using isoniazid² and phenylhydrazine³ based on modified methodologies. The reactions with both reagents were carried out with variations in both the solvents, AcOH or MeOH (acid-catalyzed), and the heating methods, micro-wave, oil bath or room temperature. The bests conditions for each reaction are showed on the scheme bellow. The reaction with isoniazid generated a low solubility product (**2**) that couldn't be characterize by NMR being possible to observe only the fragmentation patterns, that indicate the occurrence of the reaction in the side chain. The reaction with phenylhidrazine generated four products, two isomers (420u) and their respective oxidation products (418u). It was observed that different solvents and heating methods affects directly the proportion between those products. The reaction was purified by preparative HPLC and the products were characterized (**3** and **4**). All the products were submitted to antiinflammatory bioassay. In conclusion, the method of production and extraction were appropriated since we could get a high purity starting material 3,5,8-TMON without any additional purification step. It is also possible to infer that the reaction occurs majorly in the side chain, since the final products had the naphthoquinone ring intact, a fact confirmed by the MS/MS fragments, which presented losses related to the side chain and ions with the mass corresponding to fragments with the naphthoquinone moiety. It was still possible to propose the structure for two molecules, which are new structures in the literature and with great potential from the biological point of view due to the presence of the heterocycle.⁴



1- Mendonça, J. N.; Tese de doutorado na Faculdade de Filosofia, Ciências e Letras de Ribeirão Preto da Universidade de São Paulo, Ribeirão Preto, **2016**.; **2**- Dandawate et. al. *Bioorg. Med. Chem. Lett.* **22** (2012) 3104–3108; **3**- Carvalho et. al. *Dyes and Pigments*, **52** (2002) 209-214.; **4**- George et. al. *Bioorganic Chemistry* **99** (2020) 103780

Acknowledgments

Conselho Nacional de Desenvolvimento Científico e Tecnológico (CNPq); Fundação de Amparo à Pesquisa do Estado de São Paulo (FAPESP)

Studies on C1'-Quaternized C-Nucleosides: Novel Isoxazolyl Nucleoside Synthesis and Perspectives

Julia de Paula Santos (IC),^a Sarah M. R. do Nascimento (PG),^a Leandro Soter de Mariz e Miranda (PQ)*^a

julia.psantos1864@gmail.com; sarahrodrigues17.ufrj@gmail.com; leandrosoter@iq.ufrj.br

^a *Biocatalysis and Organic Synthesis Group, IQ-UFRJ Universidade Federal do Rio de Janeiro, Av Athos da Silveira Ramos 149, Centro de Tecnologia, Bl A, 21941909 Ilha do Fundão, Rio de Janeiro, Brazil.*

Palavras Chave: *nucleosides, 1,3-dipolar cycloaddition, quaternization*

Highlight

Studies on C1'-Quaternized C-Nucleosides: novel Isoxazolyl Nucleoside Synthesis and Perspectives

- C-alkynyl-Ribosides of the type **2** are versatile intermediate on the synthesis of different nucleosides.
- The reaction of riboside **2** with nitrile oxides furnishes isoxazolyl-nucleosides that can be further quaternized.

Abstract

5'-Phosphorylated nucleosides, termed nucleotides, are a class of molecules present in all living organisms and viruses. These molecules and their polymers are responsible for many vital processes such as storing, transcription, and translation of genetic information. Over the last century, these vital roles have fueled the interest of researchers to develop structural analogues that could interfere with these processes. Special attention was given to analogues that could interfere with the transcription and translation of genetic information and disrupt the cell division process.

As part of our continuous efforts in the study of C1'-quaternized C-ribonucleosides, we decided to explore the versatility of the ribosylpropiolate **2** in the reaction with nitrile oxides for the synthesis of C1'-quaternized C-isoxazolyl-ribonucleosides.

For such, the alkylation of the ribonolactone **1** with the lithium propiolate followed by the quenching of the intermediate hemiketal with acetic anhydride furnished the ribosyl-propiolate **2**. The reaction of **2** with a model nitrile oxide derived from the oxidation of **3** yielded the isoxazoles **4a, b**. These intermediates will be used as substrates for the study of the quaternization reaction as depicted in Scheme 1.

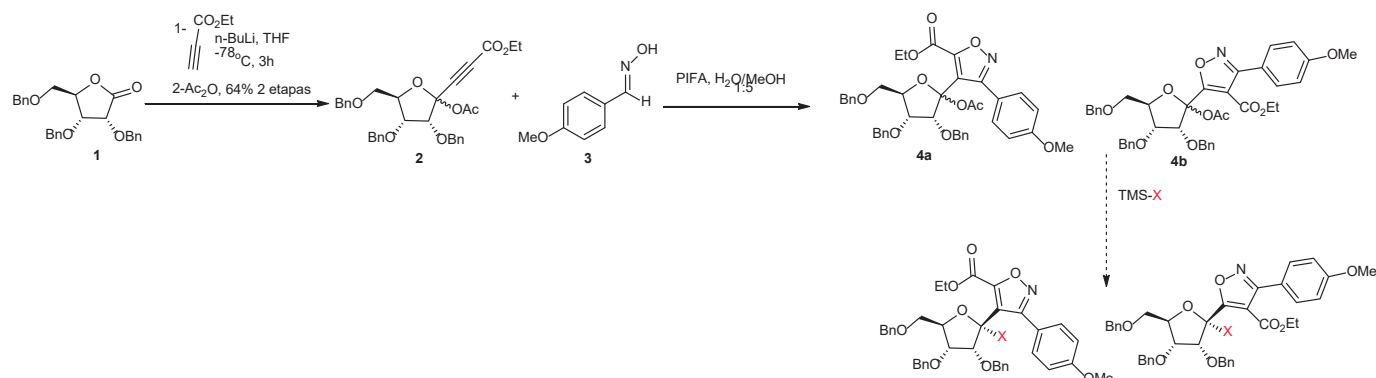


Figure 1. The synthesis of quaternized and spirocyclic nucleosides **3** and **4**

Acknowledgments



Studies on the Synthesis of C1'-Quaternized-Triazolyl-C-Ribosides

Sarah M. R. do Nascimento (PG),^b Nina Bozinovic (PQ),^a Viviane Marques de Aguiar (PG),^b Angélique Ferry (PQ),^a Florian Gallier (PQ),^a Nadège Lubin-Germain (PQ),^a Jacques Uziel (PQ)^a Leandro Soter de Mariz e Miranda (PQ)*^b

sarahrodrigues17.ufri@gmail.com; leandrosoter@iq.ufri.br;

^a CY Cergy Paris Université, CNRS, BioCIS, 95000, Cergy-Pontoise, France

^b Biocatalysis and Organic Synthesis Group, Universidade Federal do Rio de Janeiro, Av Athos da Silveira Ramos 149, Centro de Tecnologia, Bl A, 21941909 Ilha do Fundão, Rio de Janeiro, Brazil.

Palavras Chave: Nucleosides, 1,3 dipolar cycloaddition, spirocyclic nucleosides

Highlight

Studies on the Synthesis of 1'-CN-Triazolyl-C-Ribosides

- The synthesis of the 1'-CN-Triazolyl-C-Ribosides is achieved by the cyanation reaction of 1'-OAc ribosyl propiolate followed by the [3+2] cycloaddition with benzylazide.

Resumo/Abstract

5'-Phosphorylated nucleosides, termed nucleotides, are a class of molecules present in all living organisms and viruses. These molecules and their polymers are responsible for many vital processes such as storing, transcription, and translation of genetic information. Over the last century, these vital roles have fueled the interest of researchers to develop structural analogues that could interfere with these processes. Special attention was given to analogues that could interfere with the transcription and translation of genetic information and disrupt the cell division process.

As part of our continuous efforts in the study of 1,2,3-triazolyl-C-ribonucleosides, we decided to explore the possibility of a C1' quaternization with a nitrile function. The introduction of the C1' nitrile group, as present in Remdesivir, a C-nucleoside recently approved against SARS-CoV-2, would allow us to address the importance of this structural modification on the known biological activity of these triazolyl-C-ribonucleosides. For such, cyanation reaction on ribosylpropiolate **2**, with TMS-CN and TMSOTf at 0°C and the subsequent 1,3 dipolar cycloaddition, furnished the desired 1'-CN-ribosides in 68% yield from **2** in an anomeric ratio of 87:13 favoring the anomer where the -CN group occupies the alpha position.

Interestingly when regioisomers **3a,b** were heated overnight in a saturated methanolic ammonia solution, for amidation of the ester present in **3a,b**, a mixture of products was observed from which guanosine analogue **4** which could be isolated in 38% yield as a single regioisomer. This reaction sequence allows the synthesis of two new class of nucleosides, the C1-quaternized 1,2,3-triazolyl-C-ribonucleosides **3** and the new spirocyclic nucleoside **4**.

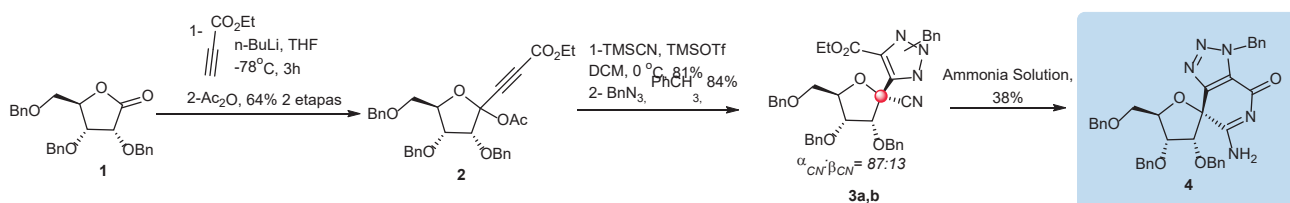


Figure 1. The synthesis of C1-quaternized 1,2,3-triazolyl-C-ribonucleosides **3** and the new spirocyclic nucleoside **4**.

Agradecimentos/Acknowledgments



Study of new maleic and succinic acid derivatives as corrosion inhibitors for mild steel 1020 in 1 mol L⁻¹ HCl solution

Brenno D.V. Evangelista (PG),^{1*} Beatriz H. da Rocha (IC),¹ Jéssica N. da Cunha (PG),¹ Eliane D'Elia (PQ),¹ Amanda V. Xavier (IC),¹ Michelle J.C. Rezende (PQ).¹

brennodanho@gmail.com

¹Universidade Federal do Rio de Janeiro, Instituto de Química, Cidade Universitária, Rio de Janeiro, Brazil.

Keywords: *Inhibitors corrosion, organic synthesis, maleic acid, succinic acid.*

Highlights

Synthesis of new organics molecules from maleic acid (MA) and succinic acid (SA). Acid maleic derivative reached inhibition efficiency of 93.5% for 24 h of immersion. Biomass derivatives products.

Resumo/Abstract

Corrosion is a common issue in industry due to the use of acidic solutions in boiler cleaning, acid pickling of metals, acid descaling, acidification of oil wells and chemical cleaning. Corrosion can be controlled using corrosion inhibitors – natural or synthetic substances capable of preventing the reaction of the metal with the corrosive environment.¹⁻³ Studies of environmentally friendly organic compounds as corrosion inhibitors have grown.⁴ The objective of this work is the synthesis of candidate products for corrosion inhibitor from maleic acid or succinic acid and the study of the anticorrosive activity of these derivatives in highly corrosive environment (1 mol L⁻¹ HCl solution), through weight loss tests. The products were synthesized in two steps. The first consisted of the esterification of maleic acid or succinic acid with methanol using sulfuric acid as a catalyst. In the second step, the dimethyl maleate or dimethyl succinate was submitted to amidation condition with 1,3-diaminopropane without solvent, concomitantly promoting the Michael addition in the case of dimethyl maleate. The products were obtained with a yield of 80% for maleic derivative (**3**) and 71% for succinic derivative (**5**), characterized by Hydrogen and Carbon Nuclear Magnetic Resonance, Infrared Spectroscopy and High-Resolution Mass Spectrometry. For the evaluation of the anticorrosive activity of the products **3** and **5** against corrosion of mild steel in 1 mol L⁻¹ HCl solution, mass loss tests were performed varying the inhibitor concentration (5x10⁻⁵, 1x10⁻⁴, 5x10⁻⁴ and 1x10⁻³ mol L⁻¹) in 24 h of immersion. The results are shown in **Tables 1** and **2**. The mass loss tests showed a high inhibition efficiency of the products, reaching 93.5% and 92.6% for maleic and succinic acid derivatives, respectively, in 1x10⁻³ mol L⁻¹ and 24 h of immersion. The results indicate that the synthesized products are strong candidates for mild steel corrosion inhibitors in 1 mol L⁻¹ HCl solution. References: ¹ SANTANA, C. A. Orientadora: Eliane D'Elia. 2018. 114 f. Dissertação (Mestrado). Curso de Química, Universidade Federal do Rio de Janeiro, Rio de Janeiro, 2018. ² Rocha JC, Gomes JACP, D'Elia E. Corrosion Science, v. 52, n. 7, p. 2341-2348, 2010. ³ DA SILVA, A. B. et al. International Journal of Electrochemical Science, v. 8, n. 7, p. 9317-9331, 2013. ⁴ DE ASSIS, B.V.R. et al. Revista Virtual de Química, v. 7, n. 5, p. 1830-1840, 2015.

Table 1: Preparation of maleic derivative **3** and results of weight loss.

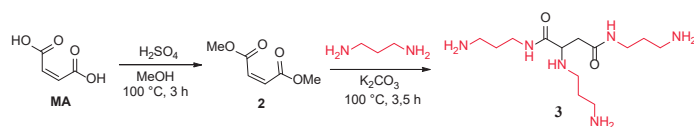
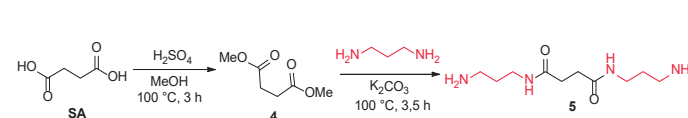


Table 2: Preparation of succinic derivative **5** and results of weight loss.



Conc. (mol L ⁻¹)	W _{corr} (g cm ⁻² h ⁻¹)	I.E. (%)	Error (%)
0	0.01990	-	-
5E-05	0.00179	91.0	0.5
1E-04	0.00178	91.0	0.6
5E-04	0.00117	94.1	0.7
1E-03	0.00130	93.5	0.8
MA	0.00138	13.0	3.0

Conc. (mol L ⁻¹)	W _{corr} (g cm ⁻² h ⁻¹)	I.E. (%)	Error (%)
0	0.021990	-	-
5E-05	0.005281	76.0	1.2
1E-04	0.003763	82.9	1.0
5E-04	0.002314	89.5	0.2
1E-03	0.001617	92.6	0.5
AS	0.00159	69.9	3.2

Agradecimentos/Acknowledgments

ANP, PRH20.1, FINEP, Petrobras, Instituto de Química – UFRJ e PGQu.

Synthesis and application of new tellurium-pillar[5]arene as catalysts in aqueous media

Ingrid C. Chipoline,¹ Beatrice F. A. B. Brasil,¹ Alix Y. Bastidas Ángel,² Eduardo E. Alberto,²
Vanessa Nascimento *¹

chipoline.ingrid@gmail.com; nascimentovanessa@id.uff.br*

¹ Department of Chemistry, Universidade Federal Fluminense, UFF, 24210-20; ² Department of Chemistry, Universidade Federal de Minas Gerais, UFMG, 31270-901

Keywords: Catalysis, macrocycle, nitrile, selenium, tellurium.

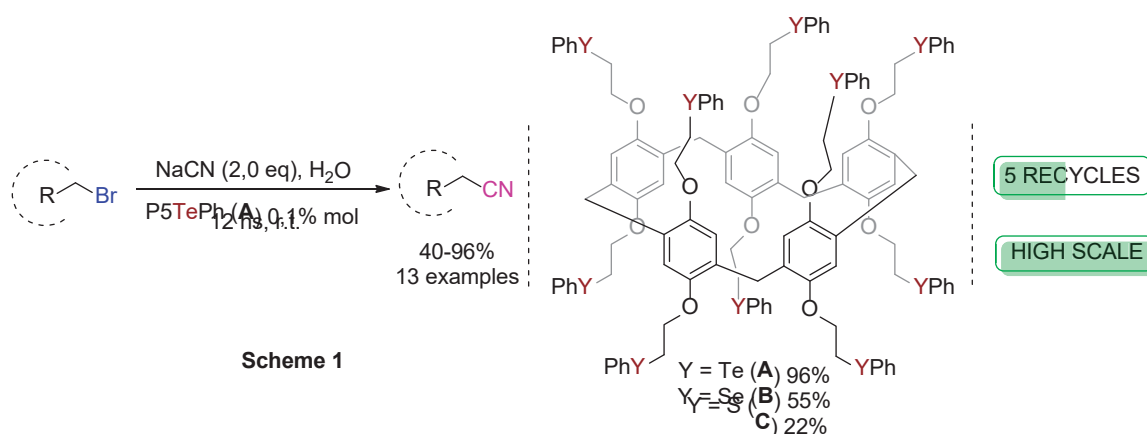
Highlights

In this work, a new pillar[5]arene functionalized with organotellurium compound was developed. This macrocycle showed promising results as a phase transfer catalyst for nucleophilic substitution in water.

Abstract

Pillar[n]arenes are macrocycles that have different applications, one of which is as a catalyst in organic reactions.¹ In this sense, chalcogens are also a class of substances that have aroused interest in this area.² The objective of this work was to synthesize chalcogen-pillar[n]arene hybrids and evaluate their catalytic potentials. Thus, pillar[5]arenes functionalized with sulphide, selenide and phenyl telluride were successfully synthesized.

As can be seen in scheme 1, pillar[5]arene containing tellurium (**A**) was the best catalyst. After optimizing the reaction conditions (12 hours, 0,1% mol **A**, r.t.) from catalyst **A** was possible the synthesis of 13 different nitriles, starting from the corresponding bromides, with yields ranging from moderate to excellent. In addition, it was observed that the new tellurium-pillar[5]arene was efficient for large-scale reaction (5 mmol – 92%) and did not lose its efficiency even after five recycles. In addition, some ¹H-NMR experiments were conducted to confirm the involvement of the macrocycle cavity in the role of the reaction and the results showed good prospects for its application in supramolecular catalysis. Furthermore, it was determined that mechanism is not radical, corroborating with the literature.²



All the data from this research will soon be available in the form of a scientific article.

Acknowledgments

FAPERJ, CNPq, CAPES, PPGQ-UFF

- Xiao X, Bai Y., Liu J., Wang J.; *J Incl Phenom Macrocycl Chem*, **2017**, 87, 29.
- Martins N.S., Angel A. Y. B., Anghinoni J. M., Lenardão E. J., Barcellos T., Alberto E. E.; *Adv Synth*, **2021**, 363, 1.

Synthesis and biological evaluation of new menadione-organosulfur hybrids against *Plasmodium falciparum*

Ruan Carlos B. Ribeiro (PQ),^{1,*} Carolina B. G. Teles (PQ),² Alcione S. de Carvalho (PQ),³ Fernando de C. da Silva (PQ),¹ Vitor F. Ferreira (PQ)³

ruancarlos@id.uff.br*

¹Instituto de Química, Departamento de Química Orgânica – UFF; ²Fundação Oswaldo Cruz - Unidade de Rondônia, FIOCRUZ – RO; ³Departamento de Tecnologia Farmacêutica, Faculdade de Farmácia – UFF.

Palavras Chave: Malaria, Naphthoquinones, Organosulfur compounds.

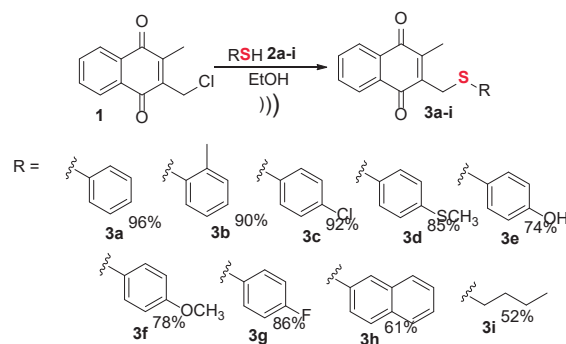
Highlights

Considering the biological activity of naphthoquinones and organosulfur compounds, in this work we report the synthesis of new menadione-organosulfur hybrids and the evaluation of their in vitro anti-*P. falciparum* activity.

Abstract

According to the World Health Organization (WHO), neglected diseases affect about one billion people in the world.¹ Among those, malaria stands out as an acute, febrile, infectious disease transmitted to humans through the bite of female *Anopheles* mosquitoes infected with *Plasmodium*. There are five species of *plasmodia* responsible for transmission in humans: *P. falciparum*, *P. vivax*, *P. ovale*, *P. malariae* and *P. knowlesi*. However, *P. falciparum* is the most aggressive one, being responsible for 90% of deaths in the world.² In that way, the search for new therapeutical options to treat such condition is of the utmost importance. In this context, naphthoquinones are a characteristic group of quinones widely distributed in nature with importance in different areas of chemistry and biochemistry.³ Broadly, the design of the scaffold was based on two fragments: one being menadione (naphthoquinone) and the other, the sulfur functionalized moiety. The desired products were obtained in good to excellent yields (52-96%).

The biological evaluation was carried out at the Department of Malaria and Leishmaniasis Bioassays, at Fundação Oswaldo Cruz, Rondônia. The compounds were evaluated against the W2 strain, using fluorescence detectors technique at initial concentrations of 200 to 1.56 μM , and the medium was incubated for 48 hours. Among the nine tested compounds, four were active, presenting IC_{50} values between 1.94 – 10.84 μM . Compounds with $\text{IC}_{50} > 15 \mu\text{M}$ were considered inactive. It worth to highlight that compound 3f was the most potent against the parasite.



Scheme 1. Synthesis of menadione-organosulfur hybrids 3a-i.

Compound	IC_{50} (μM)
3f	1.94
3a	3.72
3i	6.22
3h	10.84

Table 1. IC_{50} values for the most active hybrids against the W2 strain of *P. falciparum*.

The preliminary results of the biological evaluation have shown that the new menadione-organosulfur hybrids displayed promising activity against *P. falciparum*. Next, we intent to study the activity of such molecules against other strains, as well as their toxicity profile.

1.WHO, World Health Organization. Neglected tropical diseases. https://www.who.int/neglected_diseases. access in January, 2023.

2.WHO, World Health Organization. <https://www.who.int/newsroom/factsheets/detail/malaria>. access in January, 2023.

3.da Silva, F. de C.; Ferreira, V. F. Curr. Synth. 2016, 13, 334

Acknowledgments

FAPERJ, CAPES, CNPq, and FIOCRUZ-RO.

Synthesis and biological evaluation of chalcogenonaphthoquinones with potential application against tuberculosis

Nathália L. B. Santos (PG),¹ Luana S. Gomes (PG),¹ Ingrid C. Chipoline (PG),¹ Ruan C. B. Ribeiro (PG),² Alcione S. de Carvalho (PQ),² Maria Cristina S. Lourenço (PQ),³ Vitor F. Ferreira (PQ),² Fernando C. da Silva (PQ),² Vanessa Nascimento (PQ).^{1*}

nl_botelho@id.uff.br; nascimentoivanessa@id.uff.br

¹SupraSelen Laboratory – Department of Organic Chemistry – UFF; ²LabSOA Laboratory – Department of Organic Chemistry – UFF; ³Laboratory of Bacteriology and Bioassays – Campus Manguinhos – FIOCRUZ

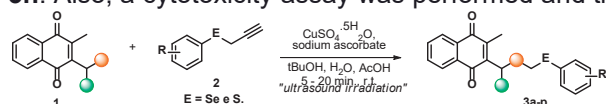
Keywords: selenium; naphthoquinones; organochalcogens.

Highlights

Due to the biological importance of chalcogenic nuclei and 1,4-naphthoquinones, this work consists of the design, synthesis and biological assays of promising structures against tuberculosis.

Resumo/Abstract

Tuberculosis treatment remains a worldwide public health challenge. According to the World Health Organization (WHO), the COVID-19 pandemic has set back years of progress in the fight against TB, due to reduced access to diagnosis and treatment of the disease. In 2021, 68,271 new cases of TB were registered in Brazil, which corresponds to an incidence rate of 32.0 cases per 100,000 inhabitants.¹ Thus, the need to search for new, more effective treatments is evident.² In this sense, the combination of organochalcogens with naphthoquinones to combat tuberculosis has been shown to be efficient.³ Thus, following our research group's interest in combating neglected diseases,⁴ the objective of this work is to obtain new chalcogenonaphthoquinones and their application against tuberculosis. The target compounds were obtained through the reaction between menadione derivatives and alkynes containing chalcogen atoms (Se and S). The formation of chalcogenonaphthoquinones with an important linker was provided by the Cu(I) catalyzed 1,3-dipolar cycloaddition reaction (**Scheme 1**). With this methodology it was possible to obtain 16 new molecules with good to excellent yields. The synthesized compounds were tested against *Mycobacterium tuberculosis* H37Rv ATCC 27294. The best results were found for compounds **3a**, **3d**, **3f**, **3g** and **3h** (**Figure 1**). A complementary microbiological assay was also performed in order to detect susceptibility/resistance against the strain of *M. tuberculosis* T113 (resistant to rifampicin and isoniazid). Optimum results were obtained with MIC values $\leq 3.12 \mu\text{g/ml}$ for compounds **3a**, **3d**, **3g** and **3h**. Also, a cytotoxicity assay was performed and the results are shown in **Table 1**.



● = alkyl and aryl.
○ = linker.
R = H, 3-CF₃-C₆H₄, 2,4,5-Me-C₆H₂, 4-Cl-C₆H₄, 2-Me-C₆H₄, naphthyl, furan.

Scheme 1. Synthetic route to obtain products 3a-p

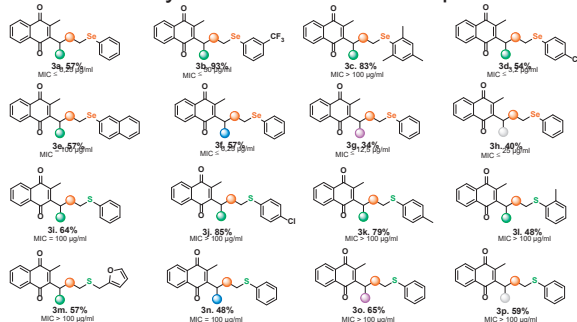


Figure 1. Structure of the products obtained 3a-p.

Compound	MIC <i>Mtb</i> T 113 (µg/ml)	CC50 (µg/ml)
3a	$\leq 3,12$	Não se aplica
3b	> 100	-
3d	$\leq 3,12$	Não se aplica
3f	50	-
3g	$\leq 3,12$	> 100
3h	$\leq 3,12$	67,54
<i>Mtb</i> T 113	1,0	

Table 1. Results of screening

Agradecimentos/Acknowledgments

UFF, CAPES, FAPERJ, CNPq, PPGQ-UFF, SBQ-RJ

¹Carvalho, A. C. C. *et al. J. Bras. Pneumol.* **2022**, 44, 134. ²Branco, F. S. C.; Pinto, A. C.; Boechat, N. *Ver. Virtual Quim.* **2012**, 4, 287. ³Nascimento, V. *et al. Eur. J. Med. Chem.* **2021**, 209, 112859. ⁴Nascimento, V. *et al. Eur. J. Med. Chem.* **2022**, 243, 114687.
46^o Reunião Anual da Sociedade Brasileira de Química: "Química: Ligando ciências e neutralizando desigualdades"

Synthesis and molluscicidal activity of 3-aryl-2-hydroxy-1,4-naphthoquinones

Nayane A. A. e Silva (PG),¹ Leonardo S. Rangel (PG),² Jose A. A. dos Santos (PG),² Robson X. Faria (PQ),² Vitor F. Ferreira (PQ),³ Daniela de L. Martins (PQ)^{1*}

nayaneabreu@id.uff.br; dlmartins@id.uff.br

¹ Universidade Federal Fluminense, Grupo de Pesquisa em Catálise e Síntese (CSI), Laboratório 413, Niterói, RJ, Brasil, www.danielamartinsgroup.com.br; ² Fiocruz, Laboratório de Avaliação e Promoção de Saúde Ambiental, Rio de Janeiro, RJ, Brasil; ³ Universidade Federal Fluminense, Departamento de Tecnologia Farmacêutica, Niterói, RJ, Brasil

Keywords: *Biomphalaria glabrata*, Suzuki, Esquistossomose

Highlights

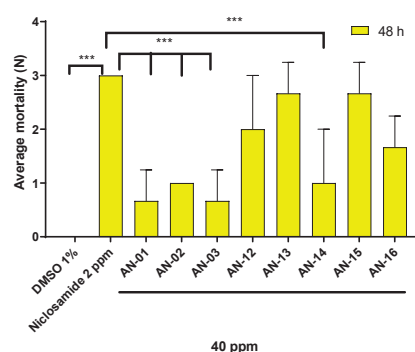
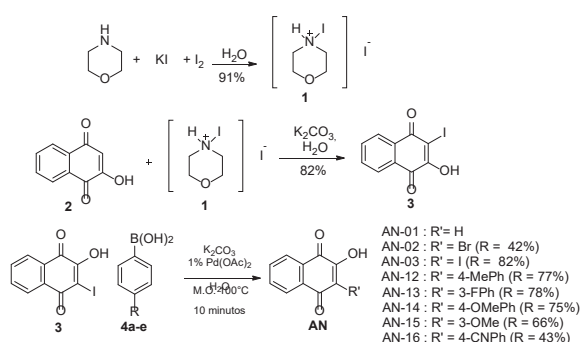
Synthesis of 3-aryl-2-hydroxy-1,4-naphthoquinones using the Suzuki reaction.

3-aryl-2-hydroxy-1,4-naphthoquinones with molluscicidal activity.

The synthetic molecule **AN-15** showed molluscicidal activity against *B. glabrata* with potency superior to niclosamide, the molluscicide approved by the WHO (LC₉₀ 0,98 ± 6 ppm in 48 h).

Abstract

Schistosomiasis is the second parasitic disease that most affects individuals worldwide, second only to malária.¹ This disease is caused by helminths of the genus *Schistosoma*.² This parasite uses snails of the genus *Biomphalaria* as an intermediate host; in Brazil, *Biomphalaria glabrata* is the main species associated with the transmission of schistosomiasis.³ Only niclosamide (1) is used on a large scale as a pesticide against *B. glabrata*,⁴ therefore, it is of great importance to research and develop new substances with molluscicidal activity that are safe, inexpensive and selective. In this work, 3-aryl-2-hydroxy-1,4-naphthoquinones were synthesized using the Suzuki reaction. The substances obtained were evaluated against *B. glabrata*, generating promising results regarding molluscicidal activity. Initially morpholino-iodine complex **1** was prepared with 91% yield, then it was used in the iodination of 1,4-naphthoquinone **2**. 2-iodo-3-hydroxy-1,4-naphthoquinone **3**, obtained in 82% yield, was used in Suzuki reactions with different arylboronic acids (**4a-e**), employing microwave irradiation for 10 minutes at 100 °C (Scheme 1).⁵



Scheme 1. Synthesis of 3-aryl-2-hydroxy-1,4-naphthoquinones

Figure 1- Molluscicidal activity of naphthoquinones

The lethal concentration of naphthoquinones was determined by exposing *B. glabrata* to the compounds for 48 hours. AN-15 showed the highest mortality (CL₉₀ 0.98 ± 6 ppm) (Figure 1), in addition, *in silico* studies demonstrated less potential for environmental toxicity for this compound, when compared to niclosamide.⁵

Acknowledgments

The authors thank CNPq, CAPES, FAPERJ, PPGQ-UFF.

¹ Chitsulo, L.; Engels, D.; Montresor, A.; Savioli, L. *Acta Tropica* **2000**, *77*, 41. ²Nelwan, M. *Curr. Ther. Res. Clin. Exp.* **2019**, *91*, 5. ³Zanardi, V. S.; et al. *Rev. Soc. Bras. Med. Trop.* **2019**, *52*, e20190171. ⁴Coelho, P. M. Z.; Caldeira, R. L. *Infect. Dis. Poverty*, **2016**, *5*, 57. ⁵ Martins, D. L., Silva, N. A. A., Ferreira, V. F., Rangel, L. S., Santos, J. A. A., Farias, R. X. *Acta Tropica* **2022**, *231*, 106414.

46^o Reunião Anual da Sociedade Brasileira de Química: "Química: Ligando ciências e neutralizando desigualdades"

Synthesis and Photophysical and Electrochemical Characterization of Thiocompounds from 4-Hydroxycoumarin.

Yuri P. V. Carvalho (IC),¹ Amanda A. Borges (PG),¹ Vitor F. Ferreira (PQ),² Fernando de C. da Silva (PQ),¹ Bernardo A. Iglesias (PQ),³ Luana da S. M. Forezi (PQ)^{1*}

luanaforezi@id.uff.br

¹Chemistry Institute, Department of Organic Chemistry, UFF; ²University of Pharmacy, Department of Pharmacy Technology, UFF; ³Laboratory of Bioinorganic and Porphyrins Materials – LBMP, Chemistry Department, UFSM.

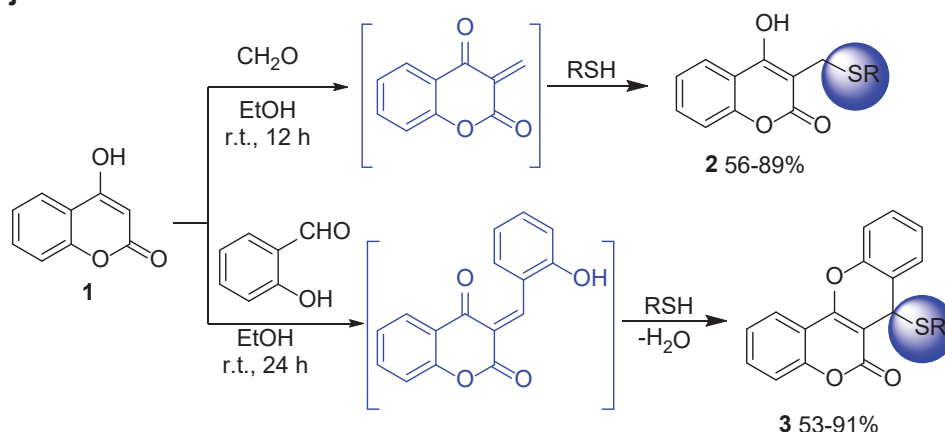
keywords: Coumarin, Multicomponent reaction, Thiocompounds, Photophysics, Electrochemistry.

Highlights

Thiocoumarins were obtained with satisfactory yields. Photophysical properties, solvatochromic effects, photobiological properties and electrochemical behavior were evaluated.

Abstract

Coumarins are a class of heterocycles compounds that exhibit interesting biological and redox properties. Thus, the present work reports the synthesis of thiocompounds from coumarin and their photophysical analyses, solvatochromic effects, photobiological properties and electrochemical behavior (Scheme 1). The syntheses of the thiocoumarins **2** and **3** were performed via three-component reaction by reacting 4-hydroxycoumarin (**1**) with an aldehyde (salicylaldehyde or formalin) and an appropriate thiol. In general, these reactions involve Knoevenagel condensation of compound **1** with aldehydes, *in situ*, forming a double Michael acceptor that undergo 1,4-thiol addition. Compounds **2a-i** are result of the Knoevenagel condensation between **1** and formalin followed by thiol 1,4-addition. It should be noted that the reaction with salicylaldehyde follow the same route but undergo to a cyclocondensation in the coumarin framework leading the tetracyclic derivatives **3a-j**.



Scheme 1. Synthetic routes to obtain coumarin derivatives **2a-i** and **3a-j**.

- Forezi, L. S. M.; Froes, T. Q.; Cardoso, M. F. C.; Maciel, C. A. O.; Nicastro, G. G.; Baldini, R. L.; Costa, D. C. S.; Ferreira, V. F.; Castilho, M. S.; Silva, F. C. *Current Topics in Medicinal Chemistry* **2018**, *18*, 149-156.
- Kotali, A.; Nasiopoulou, D. A.; Tsoleridis, C. A.; Harris, P. A.; Kontogiorgis, C. A.; Hadjipavlou-Litina, D. J. *Molecules* **2016**, *21*, 138.

Acknowledgments

CAPES, CNPq, FAPERJ and FAPERGS.

Synthesis of activated carbon from eucalyptus coal residue, an industrial waste, and its application in the retention of copper ions.

Sávio E.O. Miranda (PG),¹ **Sandro L. Barbosa** (PQ),² **David Lee Nelson** (PQ),² **Abraão J.S. Viana** (TM),³ **Yuno Raphael Ferreira Araújo** (IC),² **Líncon Oliveira Guimarães** (IC).²

savio.eduardo@ufvjm.edu.br

¹Instituto de Engenharia, Ciência e Tecnologia, UFVJM; ²Departamento de Farmácia, UFVJM, ³Laboratório Multiusuário-LIPEMVALE, UFVJM

Keywords: Adsorption; Activated charcoal; Quality control; Green Chemistry; Biofuels

Highlights

Synthesis of activated charcoal from eucalyptus charcoal residue, an industrial waste, and its application in the retention of copper ions.

Reuse of waste from the charcoal industry.

The most demanding quality standards of European legislation is one of the main barriers for exportation of Brazilian sugar cane spirits.

Cooper retention by adsorption.

Resumo/Abstract

Brazil produced 10 million tons of charcoal in 2020. This number represents 11% of the total charcoal produced globally, which makes Brazil the largest producer on the planet. Due to its high friability, however, charcoal generates a large amount of particulates during handling, usually called “moinha”, which can reach 25% of the total produced. This material, because of its low granulometry, is now considered to be an industrial waste that cannot be used directly in the blast furnace and, consequently, is accumulated in the industrial sites. A carbonaceous matrix, ground charcoal, was used because it is an important residue from the biofuel production chain with a strategic position in the national energy matrix. A 10-g portion of ground charcoal, provided by Aperam BioEnergia, was initially washed with two 250-mL portions of distilled water and then dried in an oven at 100 °C for 12 hours. The particle size of the charcoal was standardized with a 100 mesh sieve. This sample was heated at 600 °C in a muffle furnace for 4 hours. After cooling in a desiccator, the sample was again washed twice with 250-mL portions of distilled water to remove any combustion products such as nitrogen oxides, sulfur oxides, ash and other contaminants that might have formed during thermal activation. The sample was finally dried in an oven at 100 °C for 12 hours to furnish a 41% yield..



The production of cachaça in Brazil is approximately 1.3 billion liters per year, and about 25% is produced in copper stills. Only 1% to 2% of the cachaça produced is exported. One of the main technical barriers for exporting the product to commercial centers, such as countries belonging to the European Union, is the presence of copper ions in concentrations greater than 1 mg.L⁻¹. A recent publication by this research group¹, which atested to the effectiveness of an activated charcoal for the purification of crude glycerol, encouraged the development of a technique for the removal of copper ions from cachaça samples. A 20-mL aliquot of cachaça was passed through 2.0 g of the charcoal product. Copper analysis was performed by atomic absorption spectrometry, as recommended by the ABPM. The technique proved to be satisfactory, retaining 100% of the copper ions present in the sample (2.54 ppm). On the basis of these results, studies for the physical-chemical characterization of the charcoal are planned because the work has shown potential for application in stills for quality control in relation to the copper contaminant. This control would facilitate the eligibility for exportation and increase the potential of this appetizing beverage.

1. BARBOSA, Sandro L. et al. Preparation of activated charcoal from *Acrocomia aculeata* for purification of pretreated crude glycerol. Biomass Conversion and Biorefinery. Available in: <<http://hdl.handle.net/11449/200517>>.

Agradecimentos/Acknowledgments

PRPPG -UFVJM

46ª Reunião Anual da Sociedade Brasileira de Química: "Química: Ligando ciências e neutralizando desigualdades"

Synthesis of an Ibuprofen Intermediate by a Selective Electrochemical Iodination of Isobutylbenzene

Maria F.A. Magalhães (PG),¹ Guilherme M. Martins (PQ),¹ Timothy J. Brocksom (PQ),¹ Kleber T. de Oliveira (PQ),^{1*}

mmagalhaes@estudante.ufscar.br; kleber.oliveira@ufscar.br

¹Departament of Chemistry, Federal University of Sao Carlos (UFSCar);

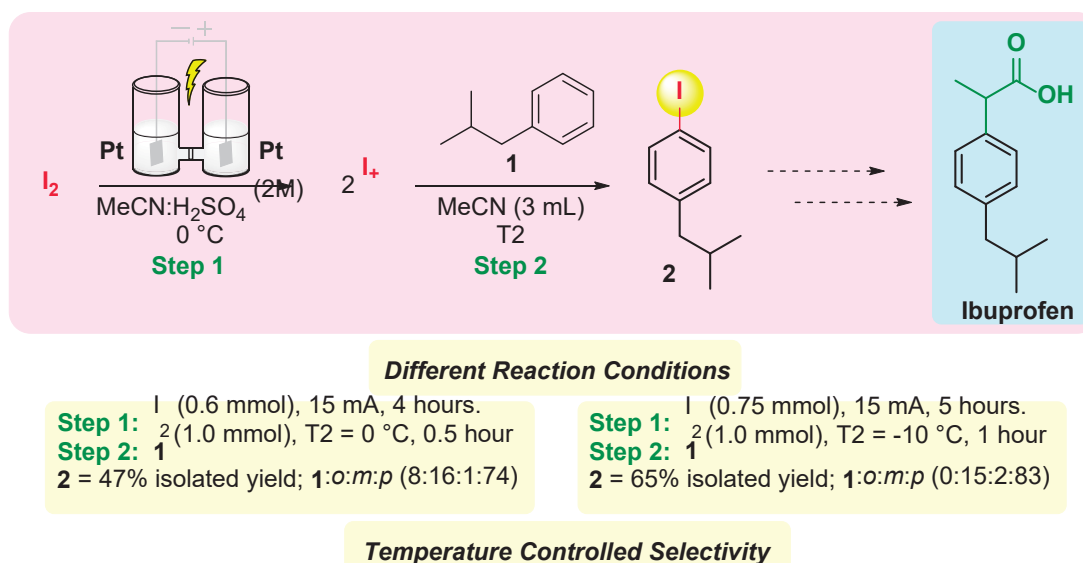
Keywords: Selective Iodination, Electrosynthesis, Ibuprofen.

Highlights

The electrochemical generation of the iodonium ion (I^+) at the anode of a divided electrochemical cell allows the electrophilic iodination of isobutylbenzene with greater regioselectivity and efficiency when compared to the iodination with $(Py)_2IBF_4$, thus providing an important intermediate for Ibuprofen synthesis.

Resumo/Abstract

Ibuprofen is an anti-inflammatory drug widely used to treat pain and fever, being considered one of the most useful analgesics in the World, with a demand of thousands of tons/year and revenues of almost \$300 million per year. A new synthetic route has been developed, using enabling technologies such as electrosynthesis and continuous flow chemistry. The regioselective iodination of isobutylbenzene, through the generation of I^+ in a divided electrochemical cell was performed, thus generating the *para*- isomer preferentially.



Scheme 1. Electrochemical generation of I^+ and iodination of isobutylbenzene.

Initially, we carried out the synthesis of **2** in batch, using $(Py)_2IBF_4$ in the presence of triflic acid. Compound **2** was obtained in 51% yield and *o:m:p* = 22:3:75 regioselectivity. Thus, a temperature controlled electrochemical reaction was performed mixing the anodic solution containing I^+ with the isobutylbenzene solution allowing us to obtain a better selectivity (*o:m:p* = 15:2:83) of the desired product **2**. This reaction has been now evaluated under different reaction conditions, and a scale up will be studied in order to transpose this protocol to continuous flow. Then the synthesis of Ibuprofen will be studied.

Agradecimentos/Acknowledgments

The authors would like to thank the São Paulo Research Foundation FAPESP (grant numbers: 2020/06874-6 (K.T.O.), 2022/00074-3 (G.M.M.) and 2022/10687-2 (M.F.A.M.)) as well as the Conselho Nacional de Pesquisa - CNPq (K.T.O. research fellowship 303890/2019-3) and CAPES - Financial Code 001.

¹ Davies, N. M. *Clinical Pharmacokinetics* 1998, 34, 101.

² Kataoka, K. et al. *OPR&D*, v. 12, n. 6, p. 1130-1136, 2008.

³ Bando, T.; Namba, Y.; Shishido, K. *Tetrahedron: Asymmetry*, v. 8, n. 13, p. 2159-2165, 1997.

⁴ De Souza, A. A. N. et al. *The Journal of Organic Chemistry*, v. 83, n. 24, p. 15077-15086, 2018.

Synthesis of (-)-Cannabidiol via Silver Triflate-Catalyzed Friedel-Crafts Reaction

Marcos Accioly Jr (PG) and Cristiano Raminelli (PQ)*

marcos.accioly@unifesp.br; raminelli@unifesp.br

Instituto de Ciências Ambientais, Químicas e Farmacêuticas, Universidade Federal de São Paulo

Keywords: cannabinoids, semi-synthesis, asymmetric synthesis, silver triflate catalysis, bioactive compound.

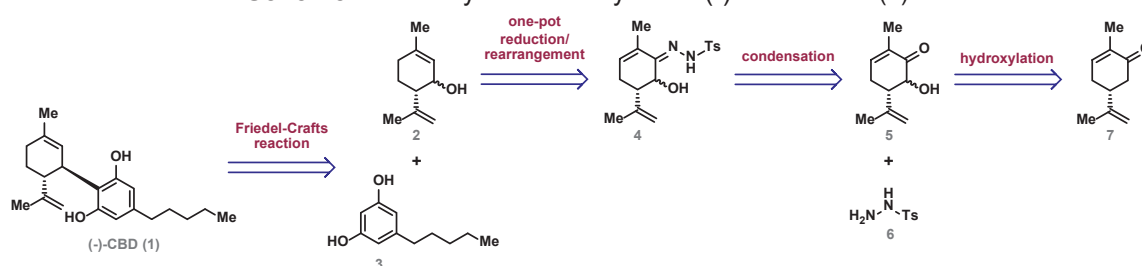
Highlights

(-)-CBD was synthesized from (*R*)-(-)-carvone in 6 steps with an overall yield of 4.5% for pharmacological studies. The key Friedel-Crafts reaction has been achieved by catalysis with silver triflate.

Abstract

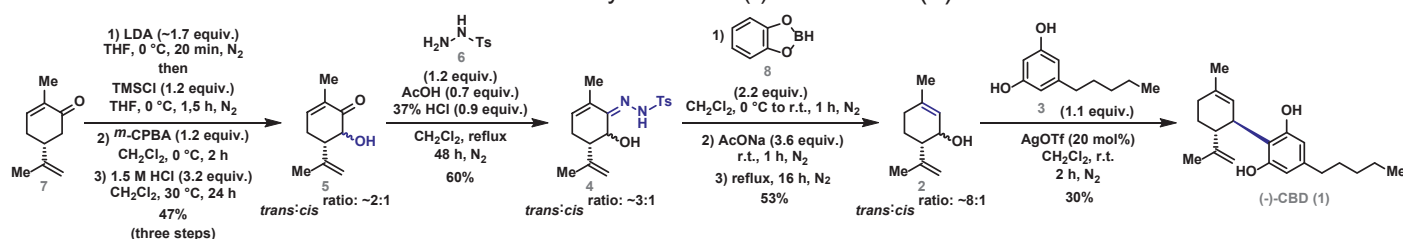
(-)-Cannabidiol ((-)-CBD) (**1**) is a non-psychoactive phytocannabinoid present in *Cannabis* species, with pharmaceutical applications, including the treatment of epileptic convulsions related to Lennox-Gastaut and Dravet syndromes.¹ However, the current drug control policies prohibit hemp cultivation, due to its recreational drug use.² Hence, scalable semi-synthetic approaches to provide natural cannabinoids are of considerable interest to produce these compounds.³ Herein, we report a straightforward route to obtain (-)-CBD (**1**),³ which involves an unprecedented silver triflate-catalyzed Friedel-Crafts key reaction, according to the retrosynthetic analysis outlined in **Scheme 1**.

Scheme 1. Retrosynthetic analysis for (-)-cannabidiol (**1**).



The synthesis of (-)-CBD (**1**) was initiated by converting (*R*)-(-)-carvone (**7**) into the intermediate **5** after 3 steps in 47% yield as a *trans:cis* mixture with a ~2:1 ratio. Diastereoisomeric mixture **5** was subjected to a condensation with *p*-tosyl hydrazide (**6**) in the presence of AcOH and 37% HCl, allowing the formation of compound **4** in 60% yield as a *trans:cis* mixture with a ~3:1 ratio. One-pot reduction/rearrangement of mixture **4** was carried out using catecholborane (**8**) and AcONa to provide isopiperitenol (**2**) in 53% yield as a *trans:cis* mixture with a ~8:1 ratio. The coupling between the diastereoisomeric mixture **2** and olivetol (**3**) was performed by a Friedel-Crafts reaction catalyzed by AgOTf,⁴ affording (-)-CBD (**1**) in 30% isolated yield (**Scheme 2**).

Scheme 2. Synthesis of (-)-cannabidiol (**1**).



(-)-Cannabidiol (**1**) was synthesized in 6 steps with an overall yield of 4.5%, employing in the key step a silver triflate-catalyzed Friedel-Crafts reaction. (-)-CBD (**1**) is currently under pharmacological studies in models that evaluate conditioned fear memory.

¹ Morales, P.; Reggio, P. H.; Jagerovic, N. *Front. Pharmacol.* **2017**, *8*, 422.

² Citti, C.; Linciano, P.; Cannazza, G. *Drug. Discov.* **2020**, *25*, 628.

³ Gollither, A. E.; Tenorio, A. J.; Dimauro, N. O.; Mairata, N. R.; Holguin, F. O.; Maio, W. *Tetrahedron Lett.*, **2021**, *67*, 152891.

⁴ Anand, R.; Cham, P. S.; Gannedi, V.; Sharma, S.; Kumar, M.; Singh, R.; Vishwakarma, R. A.; Singh, P. P. *J. Org. Chem.* **2022**, *87*, 4489.

Acknowledgments

We are grateful to FAPESP and CNPq for the financial support. M.A. Jr thanks CAPES for the scholarship.

Synthesis of enantioenriched helical complexes

Lucas S. Cunha (PG),¹ Caio C. Oliveira (PQ)*¹

I262829@dac.unicamp.br; caio.oliveira@unicamp.br

¹State University of Campinas. Institute of Chemistry. Rua Monteiro Lobato 270, 13083-862, Campinas, SP, Brazil

Keywords: Chiral-at-metal complexes, Helical, Cross-coupling, Asymmetric catalysis

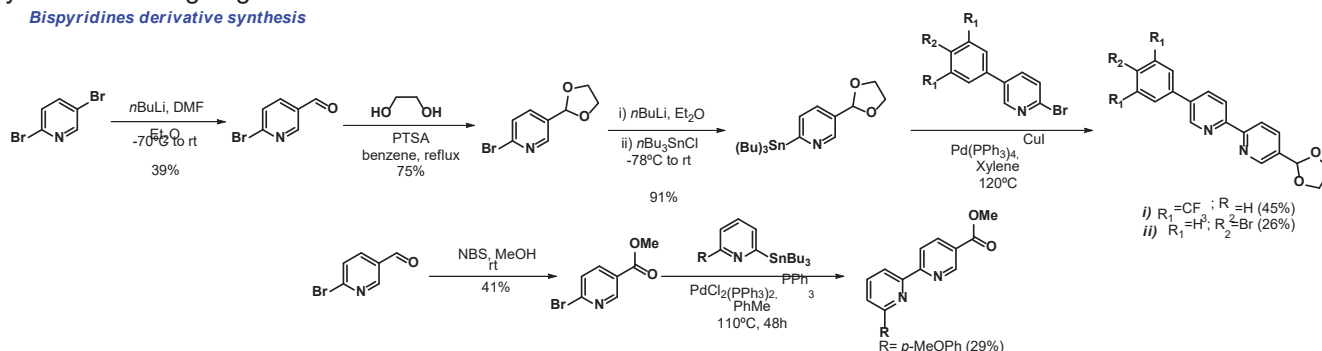
Highlights

- Synthesis of helical metal complexes;
- Distal chirality induction.

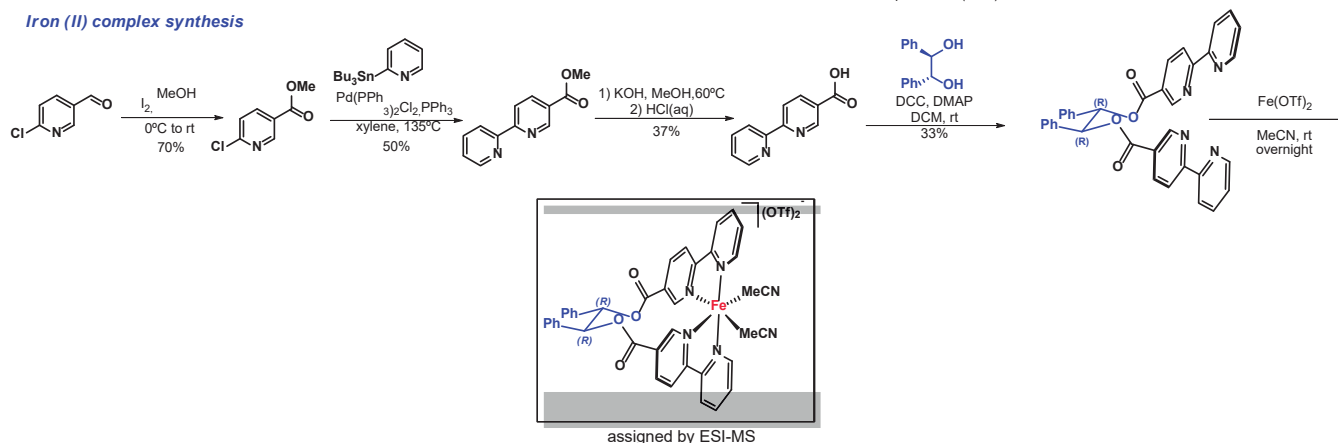
Resumo/Abstract

Bipyridines and their derivatives are commonly used in catalysis and metal complexes synthesis.^[1] In this way, this work focus in the synthesis of bisbipyridines, by introducing chiral backbone to yield helical enantioenriched complexes. The synthetic of the bipyridines was achieved by cross-coupling reactions and the chiral diol backbone was attached by Steglich reaction. A new iron(II) complex was obtained using this strategy and catalytic studies and novel complexes synthesis are ongoing.

Bispyridines derivative synthesis



Iron (II) complex synthesis



[1] E. C. Constable, C. E. Housecroft, *Molecules* **2019**, *24*, 3951

Agradecimentos/Acknowledgments



Processo: (2019/15883-1)

Synthesis of fluorescent squaramides using ultrasonic irradiation

Alexandre Barros-Barbosa (PG)^{1,*}, Marina Ávila-Costa (PQ)¹, Luiz F. Cappa de Oliveira (PQ)², Claudio L. Donnici (PQ)^{1,*}

cdonnici@terra.com.br; alexandrebb96@gmail.com

¹Departamento de Química, UFMG; ²Departamento de Química, UFJF

Palavras Chave: híbridos moleculares doador-aceptor, esquamidas, fluorescência, irradiação de ultrassom.

Highlights

Squaramides are aza-squaric acid derivatives with many applications. The present work reports the conventional and the ultrasonic irradiated syntheses of highly fluorescent mono- and bis-squaramides.

Resumo/Abstract

NIR ("Near-InfraRed") emitting materials have attracted great attention for potential applications, such as organic light emitting diodes (OLEDs) and biomarkers. The squaric acid (3,4-dihydroxycyclobut-3-ene-1,2-dione (**1**)) - is a versatile organic building block that can be used in a variety of fields ranging from dyes, optoelectronic materials to bioconjugates. Among some useful squaric derivatives, fluorescent squaramides with donor-acceptor molecular hybridization (**D-A**) can be synthesized connecting the squaric electron-acceptor unit (**A**) and electron-donating substituents (**D**) through the chemical reaction between high reactive electrophilic squaric derivatives (**A**) and fluorescent aromatic amines (**D**). In the present work, we report the synthesis of eleven mono- (**SQ-1NAr**, **3.1**) and eleven bis-squaramides (**SQ-2NAr**, **3.2**) in a two-step straight forward route, as reported in Figure 1. The intermediate dimethylsquarate (**2**) was obtained in good yield (95%) by direct condensation of squaric acid (**1**) with equimolar amount of trimethyl orthoformate in methanol under reflux. The synthesis of these novel mono-squaramides (**3.1**), in high yields, were carried out from the condensation reactions between **2** and the corresponding eleven different aromatic amines in ethanol at room temperature under magnetic stirring for 1h. On

the other hand, all bis-squaramides (**3.2**) were obtained, also in high yields, in toluene/DMF (19:1 vol/vol) under magnetic stirring and reflux during 12 h. It is noteworthy that both the mono-1-naphthyl- and the di-1-naphthyl-squaramides could not be obtained by conventional heating due to the great steric hindrance in this amine and, actually, only the ultrasound irradiation method was effective to prepare these 1-naphthyl derivatives. Indeed, the ultrasonic irradiation made the reactions much faster, easier and efficient and the preparation of all mono-squaramides (**3.1**) occurred in 15 minutes (ethanol, r.t.) and all bis-squaramides (**3.2**) could be obtained in only 1 hour of reaction and even at room temperature. All squaramides could be easily purified with ethanol to remove the residues of starting materials and drying. All the precursors, intermediates and final products were fully characterized by the usual spectrometric techniques (¹H-NMR, ¹³C-NMR, IR, etc...). Finally, these new donor-acceptor (**D-A**) molecular hybrid mono- and bis-squaramides showed quite intense fluorescence and their applications as NIR agents are still under investigation.

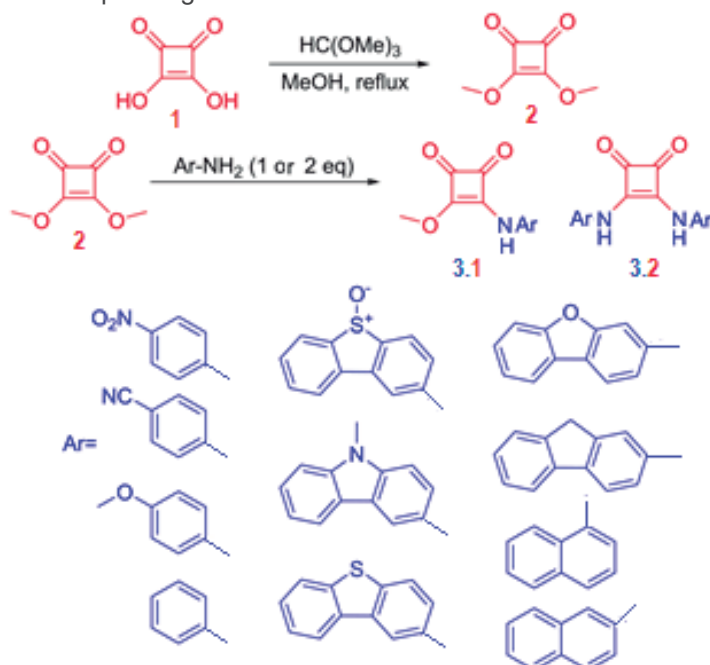


Figure 1. Synthetic route for mono- (**3.1**) and bis-squaramides (**3.2**)

Agradecimentos/Acknowledgments

UFMG, CAPES, CNPq, FAPEMIG (PPM-00281-17) and INCT-MIDAS (MCT/CNPQ/CAPES/FAPS,16/2014)

Synthesis of N-aryl-azacoumestans with potential antileishmanial activity.

Rachel de C. V. Novas (PG),¹ **Felipe H. Ribas** (IC),² **Leonardo S. A. Carneiro** (PQ),³ **Camilla D. Buarque** (PQ),⁴
chemistrykel@gmail.com

¹Departamento de Química, PUC-Rio; ²Departamento de Química Orgânica, Instituto de Química, UFRRJ

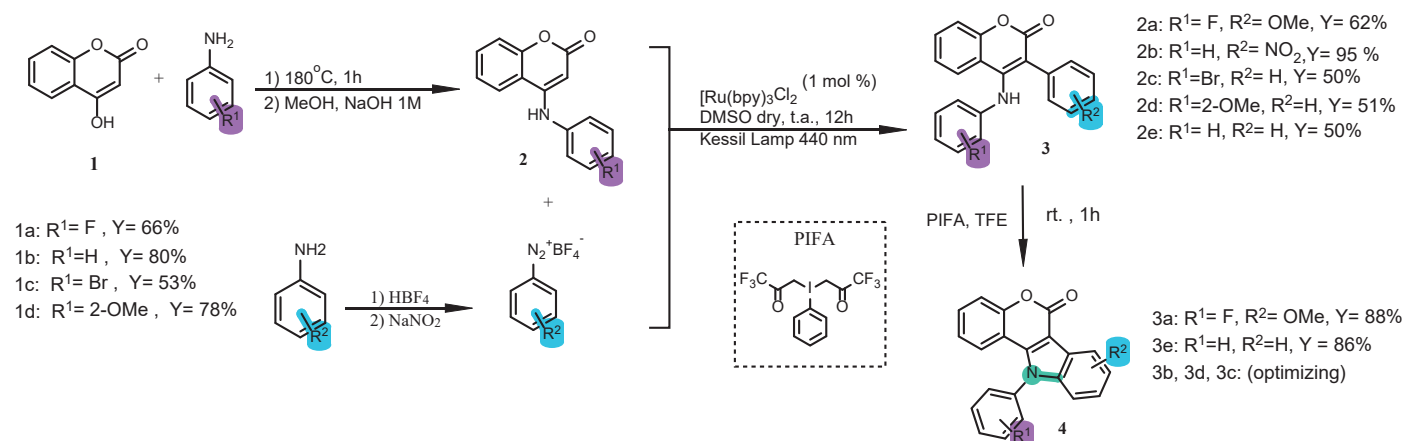
Palavras Chave: Azacoumestan, Coumarin, Photoredox Catalysis, Hypervalent Iodine.

Highlights

A coumarin (**2a**) with excellent action against leishmaniasis was discovered by our group. Therefore, is being synthesized your respective azacoumestan to evaluate the influence of molecular rigidity on antileishmaniasis activity.

Resumo/Abstract

Coumarins are an important class of benzopyrones found mostly in plants with notable biological activities.¹ The functionalization at positions C-3 and C-4 is prone to transform this natural product in azacoumestans (**4**). The compound **4** could be synthesized from the oxidative amination of **3**, which is obtained from the amination of **1** followed by the radical arylation of **2** (Scheme 1). Previously, we showed that **2a** exhibited $IC_{50} = 9.64 \mu M$ against the amastigote form of *Leishmania amazonensis* and a selective index higher than 62.2.² The obtention of the azacoumestans derivatives would add rigidity in the structure that could affect its biological activity. The aim of this work is to propose the synthesis of **4** from **3** based on the oxidative amination using hypervalent iodines. To do so, we are optimizing the reaction conditions, so that until now, yields of 86 and 88% have been obtained. The scope of this reaction is now being expanded to evaluate the influence of substituents at the antileishmanial activity and also in the reaction mechanism.

**Agradecimentos/Acknowledgments**

CAPES, CNPq, Faperj and Central Analítica Pe. Leopoldo Heinberger (DQ/PUC-Rio)

¹ Patra, P. et al. *Bentham Science*. **2022**

² Carneiro, L.S.A. et al. *Bioorganic Chemistry*. **2021**, 114, 105141.

Synthesis of new bis-1,2,3-triazole glycoconjugates with potential antifungal application

João Pedro de Paiva S. Duarte (IC), Ingrid C. Chipoline (PQ), Sabrina B. Ferreira* (PQ).

joaop.duarte@gradu.iq.ufrj.br; *sabinab@iq.ufrj.br

Universidade Federal do Rio de Janeiro, Instituto de Química Laboratório de Síntese e Prospecção Biológica, Rio de Janeiro, RJ, Brasil

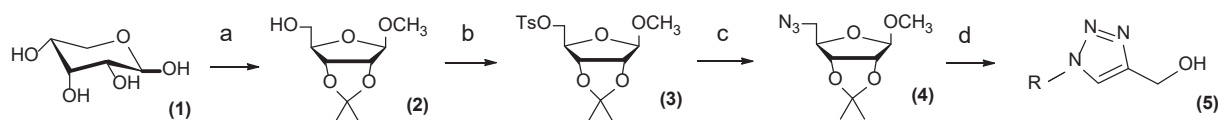
Keywords: Carbohydrate, Fungus, Galactose, Heterocycles, Mannose, Ribose.

Highlights

The combination of carbohydrates, through the triazole rings present in each one of them, originates molecules that will be of great importance in the fight against fungi.

Abstract

Triazole rings are aromatic heterocycles, of synthetic origin and their derivatives have proven biodynamicity, demonstrating activities such as antiviral, antibacterial, antitumor and antifungal, the latter being the activity of interest for the work in question. These molecules can be used to unite two nuclei of interest. In this sense, compounds that have also shown notorious antifungal potential, among other biological activities, are carbohydrates. Thus, the objective of this work is to efficiently synthesize, through carbohydrates and triazoles, new glycoconjugated bis-1,2,3-triazoles, varying the portion of the carbohydrates which are D-ribose (**1**), D-galactose and D-mannose. To obtain these derivatives, the synthesis begins with the carbohydrate to form the protected carbohydrate (**2**). Then, tosyl group was added to synthesize compound (**3**). In sequence, the azido group was added through a nucleophilic substitution, forming compound (**4**). And, to form the first triazole ring (**5**) from product (**4**), a 1,3-dipolar cycloaddition was performed. The hydroxyl moiety in the next step will be reacted in the presence of propargyl bromide in a SN2 reaction to obtain the terminal alkyne. Finally, from the terminal alkynes and with the initial azido-carbohydrates, the second cycloaddition reaction will be carried out to form the triazole ring and coupling the two carbohydrate units. The scheme below shows the sequence of reactions already done with D-ribose.



a. Acetone, MeOH, H_2SO_4 , 25 minutes, 75% yield; **b.** TsCl, Pyridine, DMAP, 16h, r.t., 60% yield; **c.** NaN_3 , DMF, reflux, 24h, 90% yield; **d.** H_2O , CH_2Cl_2 , $CuSO_4 \cdot 5H_2O$, Sodium Ascorbate, 3h.
R = Carbohydrate

It is worth noting that the three types of carbohydrates will be combined with each other, generating six symmetric molecules that can have their solubility modulated by their deprotection to have free hydroxyls, thus obtaining six other compounds. The biological part will be carried out with a partner research group.

Acknowledgments

The authors gratefully acknowledge the financial support from FAPERJ, Fiocruz and UFRJ.

¹Evangelista, T. C. S. *et al. Journal of Carbohydrate Chemistry* (2021), 40, 243-268.

²Reddy, B. J. *et al. Russ J Gen Chem* (2016), 86, 1424–1429.

³Abdel-Wahab, B. F. *et al. European Journal of Medicinal Chemistry*, (2012), 52, 263-268.

Synthesis of new indirubins containing 1,2,3-triazole ring

Ana Flávia S. Fuzaro* (PG),¹ Gabriela L. P. Suhett (IC),² Richard M. Grazul (PQ)¹, Mauro V. de Almeida (PQ), Eloah P. Ávila (PQ).

aninhafufuquimica@hotmail.com

1. Departamento de Química, Instituto de Ciências Exatas, Universidade Federal de Juiz de Fora, 36036-900, Juiz de Fora – MG, Brasil.

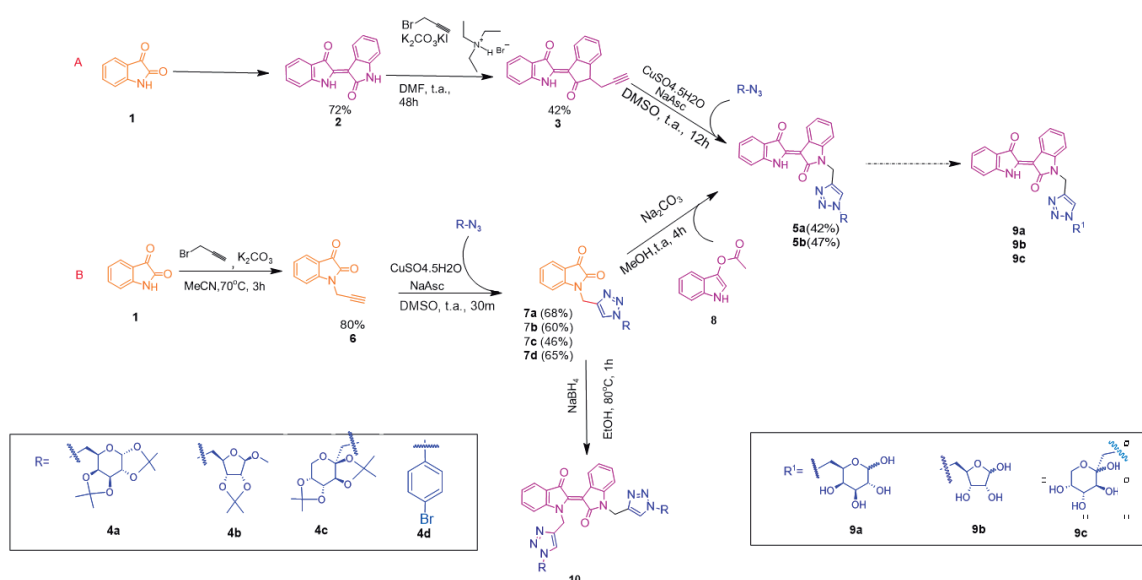
Key words: Indirubin, Click Chemistry, Reductive coupling reaction.

Highlights

Indirubin is a bioactive molecule and a promising prototype of new drugs, however it has limited bioavailability, requiring its functionalization to improve its biological properties.¹

Abstract

Functionalization of indirubin skeleton with lipophilic and hydrophilic groups bridged to 1,2,3-triazole portion may delineate a new approach to improve the biological properties. Herein, we proposed the development of methodologies for the preparation of new 1,2,3-triazole-indirubin compounds¹. The triazole ring insertion was performed by copper(I)-catalyzed alkyne-azide cycloaddition (CuAAC) with different azides **4a-4d**. The system 20mol% CuSO₄·5H₂O and 20mol% sodium ascorbate (NaAsc) was used as precatalyst species². The excess of NaAsc amounts prevented the re-oxidation catalytic of Cu^I species and ensured complete reduction of Cu^{II}. For monofunctionalized adducts **5a-5b** (Scheme 1a), the viability of route **A** was first evaluated. The starting material *N*-propargyl-indirubin **3** was obtained in two steps: reductive coupling of isatin **1**, followed by propargylation of **2** in basic medium. However, this strategy is limited for synthesis of the monofunctionalized ones. The second strategy, Pathway **B** (Scheme 1b), started from an aldol condensation reaction between 1,2,3-triazol-isatin **7a-7d** derivatives and acetoxy-indole **8** leading to compounds **5**. Moreover, this route allows to access of disubstituted indirubin scaffolds **10** by reductive coupling. In this condition, the formation of a mixture of diastereoisomers was observed, justified by the partial reduction process carried out from NaBH₄. Finally, the hydrolysis step is being optimized to obtain the hydrophilic carbohydrate indirubin compounds **9a-9c**.



Scheme 1: Proposed synthesis of indirubins containing 1,2,3-triazole ring

[1] Hoessel, R. et al. *Nature Cell Biology*, v. 1, n. 1, p. 60–67, 1999; [2] *Quim. Nova*, Vol. 34, No. 10, 1791-1804, 2011.

Acknowledgments

FAPEMIG, CAPES and CNPQ for the financial support.;

Synthesis of new pyrido-indoles as potential inhibitors of SARS-CoV-2 Mpro

Anna Paula P.M. da Silva (PG)¹, Pedro Henrique O. Borges (PG)¹, Floriano P. S. Junior (PQ)², Ingrid C. Chipoline (PQ)^{1,2}, Sabrina B. Ferreira* (PQ)¹

appmsilva@ufrj.br; sabrinab@iq.ufrj.br

¹Universidade Federal do Rio de Janeiro, Instituto de Química Laboratório de Síntese e Prospecção Biológica, Rio de Janeiro, RJ, Brasil; ²Fundação Oswaldo Cruz, Instituto Oswaldo Cruz, Laboratório de Bioquímica Experimental e Computacional de Fármacos, Rio de Janeiro, RJ, Brasil

Keywords: COVID-19, Drugs, Hydrazine, Machine learning, Pyrido-indole

Highlights

Based on active fragment-like compounds previously identified by machine learning approaches a new series of pyrido indole derivatives were synthesized to obtain potential Mpro SARS-CoV-2 inhibitors.

Abstract

COVID-19 is a pandemic disease caused by a severe acute respiratory syndrome (SARS-CoV-2) that has already killed more than six million people worldwide according to the World Health Organization (WHO) since 2019¹. To contain the pandemic, the scientific community has been looking for alternatives such as safe medicines by repositioning drugs and vaccines against the virus. However, there is still a limited number of effective treatments against COVID-19². In this scenario, computational technologies have been useful to boost and assist in the discovery and optimization of new drugs such as inhibitors of the SARS-CoV-2 Mpro enzyme. Previously, our group has explored a deep learning approach known as generative modeling³ to identify fragment-like compounds active on this target⁴. One of the most active fragments contains a pyrido indole scaffold, which is present in other compounds with known anti-infective (antimalarial) activity⁵. Therefore, the objective of this work was to synthesize a series of compounds analog to the prototype pyrido indole fragment (**5**) selected by machine learning. In the figure **1** it was proposed a synthetic route for the synthesis of pyrido indole derivatives.

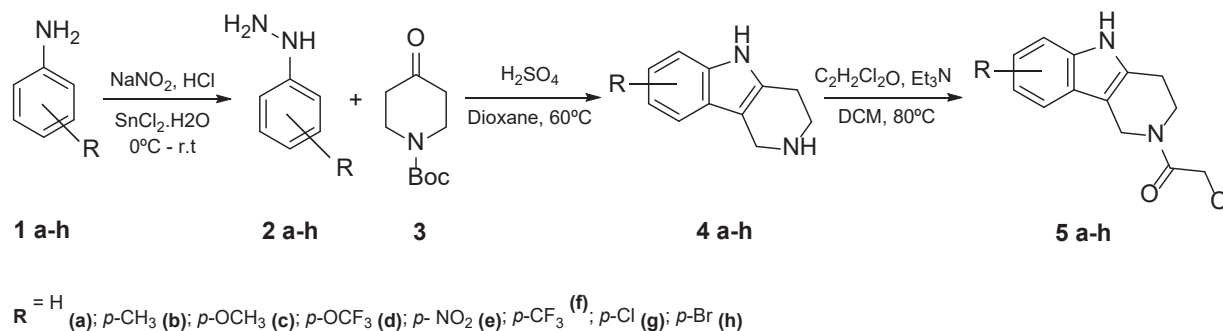


Figure 1. Synthetic route to pyrido indole derivatives.

The synthesis begins with commercial anilines (**1**) to obtain hydrazines (**2**) with yields varying between 30% - 85%. The formation of the indole nucleus, obtained by a Fischer-indole reaction between (**2**) and (**3**), was accomplished for compounds **4a** and **4b** until the present moment. The structures of the synthesized substances were analyzed by ¹H and ¹³C NMR spectra, and infrared spectroscopy. Methodologies of the first two steps are being optimized in parallel with the synthesis of end products. The pyrido-indol subsequently tested for inhibition of SARS-CoV-2 Mpro.

Acknowledgments

CAPES, FAPERJ, CNPq and PGQu - UFRJ.

¹ WHO Coronavirus (COVID-19) Dashboard., n.d. Web. 30 Jan.2023.

² Saul, S.; Einav, S. ACS Infectious Diseases **2020**, 6 (9), 2304–2318.

³ Santana, M. V. S.; Silva-Jr, F. P. BMC Chemistry **2021**, 15 (1), 1-20.

⁴ Mathada, B. S.; Somappa, S. B. Journal of Molecular Structure **2022**, 1261, 1-19.

⁵ Saramago, L.; Santana, M., Silva-Jr, F.P et al.2023. AI-Driven Discovery of SARS-CoV-2 Main Protease fragment-like Inhibitors with antiviral activity in vitro. Manuscript submitted for publication. Fundação Oswaldo Cruz, Instituto Oswaldo Cruz.

46^o Reunião Anual da Sociedade Brasileira de Química: "Química: Ligando ciências e neutralizando desigualdades"

Synthesis of Non-anomeric C-Glycosyl Pyrazolidinones Derivatives via Photoredox Catalysis

Renan O. Gonçalves (PG),^{1*} Pedro H. R. Oliveira (PQ),¹ Iva S. de Jesus (PQ),¹ Natalí P. Debia (PG),² Diogo S. Lüttke (PQ),² Marcio W. Paixão (PQ).¹

renangoncalves@estudante.ufscar.br

¹Laboratory for Sustainable Organic Synthesis and Catalysis - Chemistry Department – Federal University of São Carlos – UFSCar;
²Institute of Chemistry, Federal University of Rio Grande do Sul, Porto Alegre, RS, Brazil.

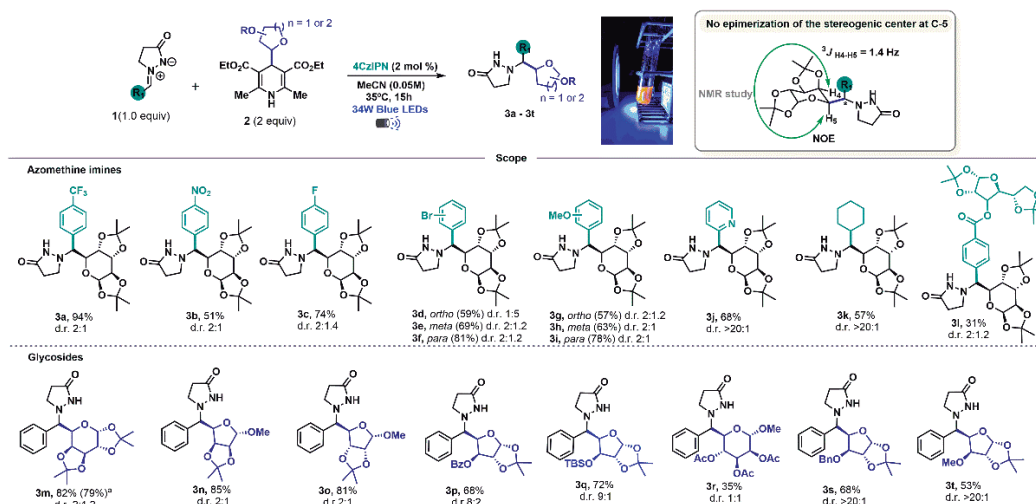
Keywords: Photoredox catalysis, Azomethine imines, Radical C-glycosyl.

Highlights

Herein we report an operationally simple visible-light photocatalytic approach for the glycosylation of azomethine imines using DHPs 4-glycosyl-1,4-dihydropyridines as a radical source.

Abstract

C-glycosides have gained considerable attention in recent decades. This class of structurally complex C-linked glycoconjugates has greater chemical stability concerning hydrolytic cleavage under both acidic and basic conditions as well as in the presence of several proteases.¹ The "non-anomeric" or "C-reversed" class of glycosides has been less investigated - with fewer methods reported in the literature for their synthesis - despite their promising applicability in medicinal chemistry. Among them, nitrogen-containing C-glycosides stand out as privileged structural motif in drug development.² In this regard, we developed an operationally simple, photocatalytic strategy for the glycosylation of azomethine imines, using 4-substituted 1,4-dihydropyridines (DHPs) as a glycosyl radical source. We selected azomethine imines as coupling partners due to their reactivity and applicability as a biologically relevant building block.³ With the optimal reaction condition in hands, we investigated the scope of the azomethine imines (**3a-3l**). The developed methodology accommodates a variety of substrates containing both electron-withdrawing and, electron-donating groups, heterocycles, and cycloaliphatic moieties. Subsequently, the generality concerning the glycosyl radicals was evaluated, and different types of functionalized glycosidic scaffolds were successfully employed (**3m-3t**), providing the desired products in good yields and moderate diastereoselectivity. Furthermore, a 1D NOE study showed that the formed glycosyl radical retains its initial configuration once we have observed a similar coupling-constant (1.4 Hz) of the starting materials (0.8 Hz).



Scheme 1: Scope of azomethine imines and glycosides.

¹Dumoulin, A.; Matsui, J. K.; Gutiérrez-Bonet, Á.; Molander, G. A. *Angew. Chem. Int. Ed.* **2018**, *2*, 228. ²Koester, D. C.; Holkenbrink, A.; Werz, D. B. *Synthesis* **2010**, *19*, 3217. ³Schantl, J. G. *Science of Synthesis*, **2004**, *27*, 731-738.

Acknowledgments

The authors are grateful to FAPESP (grant 2021/06099-5) and CAPES – Finance code 001 for the financial support during this research.

46^o Reunião Anual da Sociedade Brasileira de Química: "Química: Ligando ciências e neutralizando desigualdades"

Synthesis of Novel Chiral Ruthenium Complexes and Evaluation in Asymmetric Catalysis

Erick M. C. Pinheiro (PG),¹ Caio C. Oliveira (PQ).¹

e265994@dac.unicamp.br; caio.oliveira@unicamp.br

¹Institute of Chemistry, University of Campinas (UNICAMP)

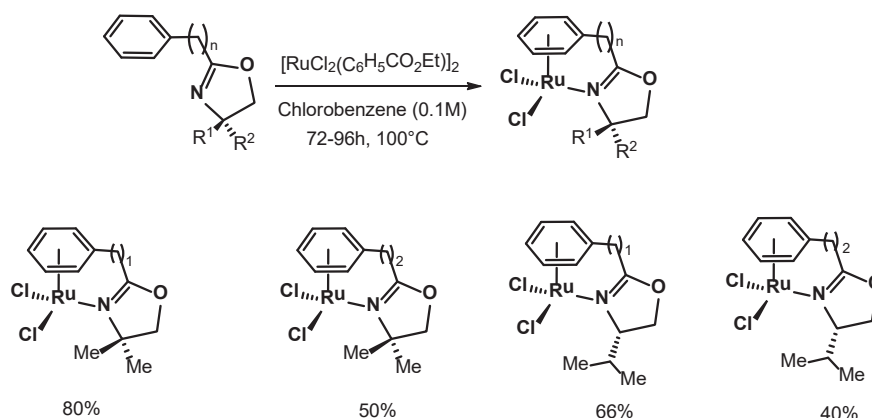
Keywords: Asymmetric catalysis, Chiral complexes, Ruthenium.

Highlights

Development of novel Ruthenium (II) complexes bearing chiral η^6 -arene ligands is a challenging task in asymmetric catalysis.¹ Herein, the synthesis of novel chiral Ruthenium complexes is presented, alongside with some perspectives in catalysis.

Abstract

An overview of literature indicates that p-cymene ruthenium catalyst is the more widely employed ruthenium source in C-H functionalization.¹ In this context, an adaptation of the protocol reported by Wills group, using $[\text{RuCl}_2(\text{C}_6\text{H}_5\text{CO}_2\text{Et})_2]$ successfully allowed the synthesis of novel arene-ruthenium (II) complexes bearing an oxazoline ligand.² Furthermore, these complexes are air-stable and easily purified. Next steps involve the evaluation of these complexes as catalysts in C-H functionalization.



Scheme 1. Novel arene-Ruthenium (II) complexes

References:

- Liang, H.; Guo, W.; Li, J.; Jiang J.; Wang J. *Angew, Chem Int. Ed.* 2022, 61, e202204926.
- Soni, R.; Jolley, K.E.; Clarkson, G.J.; Wills, M. *Org. Lett.* 2013, 15, 19, 5110–5113.

Acknowledgments



Synthesis of oxadiazole and hydantoin derivatives as potential zika virus NS3 helicase inhibitors

Ana C. B. Bernardes (IC),^{1*} Herika D. A. Vidal (PG),¹ Luana G. Morao (PQ),² Nathalya C. M. R. Mesquita (PQ),² Rafael V. C. Guido (PQ),² Glaucius Oliva (PQ)² and Arlene G. Corrêa (PQ)¹¹ Centre of Excellence for Research in Sustainable Chemistry, Department of Chemistry, Federal University of São Carlos. ² Centre for Research and Innovation in Biodiversity and Pharmaceuticals, Institute of Physics of São Carlos, University of São Paulo, SP, Brazil. *anabergler@estudante.ufscar.br

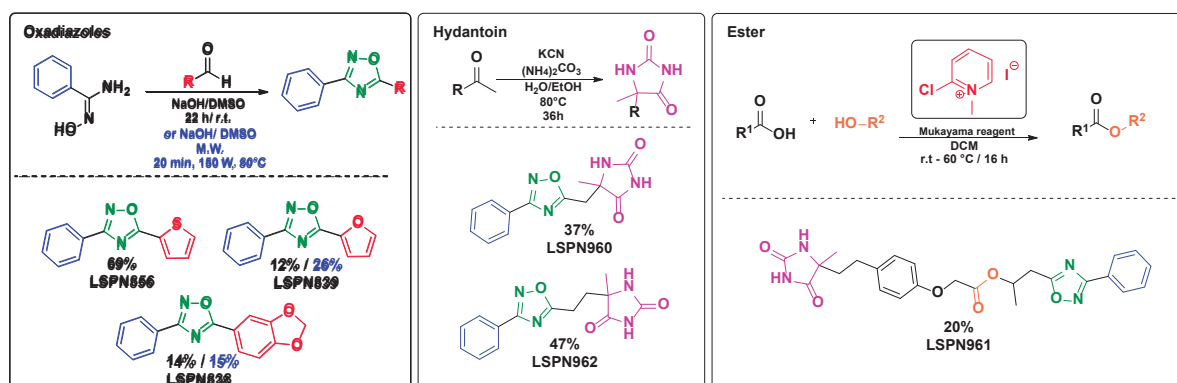
Keywords: zika virus, oxadiazole, hydantoin, NS3 helicase, enzymatic inhibitors.

Highlights

Synthesis of possible Zika virus inhibitors containing fragments of oxadiazole and hydantoin.

Abstract

Zika virus infections are associated with triggering severe neurological problems, however, so far, there are no efficient and specific antivirals to treat the disease. In this sense, a high-throughput screening (HTS) study identified hydantoin and oxadiazole scaffolds as promising fragments to compose NS3 helicase (non-structural protein that has vital enzymatic activity for the virus life cycle) ligands.¹ Herein, the synthesis of possible inhibitors containing the cited fragments is described. For the synthesis of hydantoins, the Bucherer-Bergs² reaction has been used showing good yields and simple purifications. The formation of oxadiazole involves an amidoxime in the presence of esters³ and aldehydes,⁴ and despite the low yields obtained from aldehydes under traditional conditions (r.t. for 22 h), the use of microwave (M.W.) irradiation improved the yield in only 20 minutes. Furthermore, the Steglich esterification reaction, using the Mukaiyama coupling reagent, allowed the synthesis of compound **LSPN961**.⁵



Based on these synthetic routes, greener conditions are being explored, including alternative solvents, reduced reaction time and less waste production. Furthermore, the biological activity of compounds **LSPN856**, **LSPN838**, **LSPN839**, **LSPN960**, **LSPN961** against NS3-helicase was evaluated, obtaining promising results for **LSPN839**, **LSPN960** and **LSPN961**.

References:

- Mesquita, N. C. M. R.; Guido, R. V. C., Oliva, G., unpublished results.
- Bucherer, H. T.; Lieb, V. A. Über die Bildung substituierter Hydantoine aus Aldehyden und Ketonen. Synthese von Hydantoinen, *J. Prakt. Chem.*, **1934**, *141*, 5.
- Du, W.; Qi, Q.T.H.; Guo, Y.; Chobanian, H. R.; Hagmann, W. K.; Hale, J. J. A one-pot synthesis of 3-substituted-5-carbonylmethyl-1,2,4-oxadiazoles from β -keto esters and amidoximes under solvent-free conditions. *Tetrahedron Lett.* **2007**, *48*, 2231.
- Shetneva, A. A.; Pankratiev, V. E.; Kunichkin, A. S.; Vlasova, A. S.; Proskurin, I. K.; Kotov, A. D.; Korsakova, M. K. Synthesis of 3,5-Disubstituted 1,2,4-Oxadiazoles from Amidoximes and Aldehydes in the Superbasic System NaOH/DMSO. *Russ. J. Org. Chem.* **2020**, *56*, 1064.
- Jordan, A.; Whymark, K. D.; Sydenham, J.; Sneddon, H. F. A solvent-reagent selection guide for Steglich-type esterification of carboxylic acids. *Green Chem.* **2021**, *23*, 6405.

Acknowledgments

We thank FAPESP (2013/07600-3, 2014/50249-8 and 2022/07493-1), GlaxoSmithKline, CAPES (Financial Code 001) and CNPq (grants 429748/2018-3 and 302140/2019-0) for funding and grants.

Área: ORG

Synthesis of piperine linked with 1,2,3-triazole for application as efflux pumps inhibitors

Quelli Larissa O. de Santana (PG),¹ Floriano P. Silva-Jr (PQ)²; Sabrina Baptista Ferreira (PQ)*¹.

quellilarissa@pos.iq.ufrj.br; sabrinab@iq.ufrj.br

¹Universidade Federal do Rio de Janeiro, Instituto de Química Laboratório de Síntese e Prospecção Biológica, Rio de Janeiro, RJ, Brasil; ²Fundação Oswaldo Cruz, Instituto Oswaldo Cruz, Laboratório de Bioquímica Experimental e Computacional de Fármacos, Rio de Janeiro, RJ, Brasil

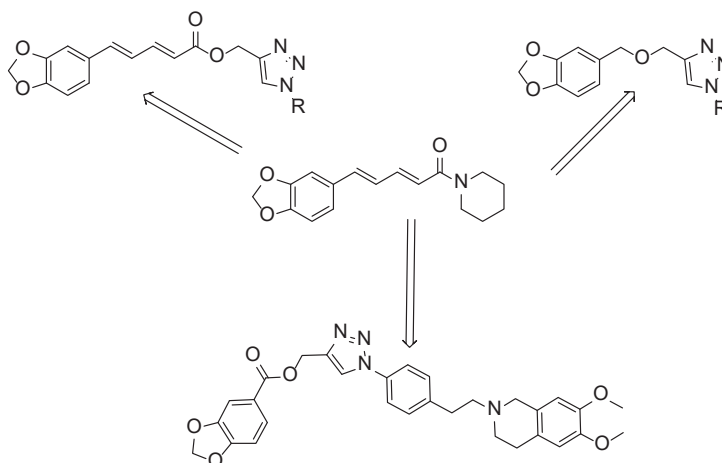
Palavras Chave: Piperine, 1,2,3-Triazole, Multidrug resistance, Efflux pumps.

Highlights

Synthesis of piperine derivatives linked with 1,2,3-triazole as new efflux pumps inhibitors with potential application as drugs targeting multidrug resistant cancer types and infectious agents.

Resumo/Abstract

Efflux mechanisms are widely recognized as major components of resistance to many classes of chemotherapeutic as well as anti-infective agents. Multidrug resistance (MDR) has expanded dramatically across a wide range of organisms from bacteria to humans, resulting in a global increase in life-threatening infections and deaths¹. That makes it a serious threat to public health around the world and needs action in all government sectors. An example of a natural product described in the literature with efflux pump inhibitory activity is piperine² This work aims to synthesize piperine hybrids containing the 1,2,3-triazole moiety, starting from the terminal alkynes of piperine with carbohydrates, 6,7-dimethoxy-tetrahydroisoquinoline and aromatic azides. To obtain the piperine coupled to triazole, the click chemistry concept was used, the Cu (I) -catalyzed 1,3-dipolar cycloaddition reaction using terminal alkynes with organic azides³. It was obtained three families of compounds with yields from 35-80%.



1. <https://www.who.int/health-topics/antimicrobial-resistance>.

2. Szumowski JD, Adams KN, Edelstein PH, Ramakrishnan L. *Curr Top Microbiol Immunol*. 2013, 374, 200-230.

3. Kolb, Hartmuth C.; Finn, M.G.; Sharpless, K. B. *Click chemistry: diverse chemical function from a few good reactions*. *Angewandte Chemie International Edition*, 2001, 40.11: 2004-2021.

Agradecimentos/Acknowledgments

The authors gratefully acknowledge the financial support from CAPES, FAPERJ, Fiocruz and UFRJ

Synthesis of pyrazole-imidazoline and pyridine-pyrazole-imidazoline hybrids

Leonardo C. Lemos (PG), Maurício S. dos Santos¹ (PQ)*

leocensi@unifei.edu.br; mauriciosantos@unifei.edu.br

Laboratório de Síntese de Sistemas Heterocíclicos (LaSSH), Universidade Federal de Itajubá (UNIFEI), Itajubá, MG, Brasil.

Keywords: Synthesis, heterocycles, imidazoline, pyrazole, pyridine.

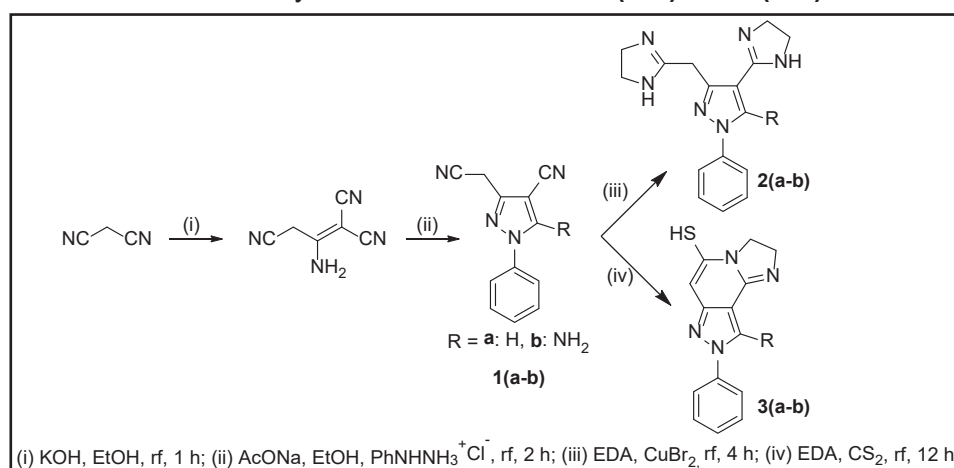
Highlights

The use of heterocycles in the pharmaceutical industry is well established, once approximately 85% of the drugs have in their molecular structure at least one of these rings.¹ Our research group have published synthetic methodologies to obtain a variety of heterocyclic systems.^{2,3} In this work, we investigated the synthesis of heterocycles using the key intermediates 1-aryl-4-cyano-3-(cyanomethyl)-1H-pyrazoles.

Abstract

The intermediates **1(a-b)** were obtained from malononitrile after 2 steps as showed in the scheme 1. The synthesis of the final compounds **2(a-b)** were carried out from copper(II) bromide (CuBr₂) and ethylenediamine (EDA), under reflux for 4 h. On the other hand, **3(a-b)** were synthesized using carbon disulfide (CS₂) and EDA, at 100°C for 12 h. All compounds are being characterized using Fourier transform infrared spectroscopy (FT-IR), high resolution mass spectrometry (HRMS) and nuclear magnetic resonance (NMR) for the nucleus ¹H and ¹³C.

Scheme 1. Synthetic route to obtain **2(a-b)** and **3(a-b)**.



¹ Qadir, T.; et al. The Open Med. Chem. J. 2021, 16, 197.

² Rosa, G. S.; et al. J. of Heterocyclic Chem. 2019, 56, 1825.

³ Lara, L. S.; et al. Pharmaceutics. 2022, 14, 195.

Acknowledgments



Synthesis of quercetin derivatives as potential modulators of cellular signalling processes

Rodrigo S. de Almeida (PG)¹, Leonardo Natal M. da Silva (PG)¹, Jaqueline D. Senra (PQ)², Alessandro B. C. Simas (PQ)^{1*}

rodrigoipn19@gmail.com; abcsimas@ippn.ufrj

¹ Universidade Federal do Rio de Janeiro, Instituto de Pesquisas de Produtos Naturais Walter Mors, CCS, Cidade Universitária, Rio de Janeiro, RJ. ² Universidade do Estado do Rio de Janeiro, Instituto de Química, Maracanã, Rio de Janeiro, RJ.

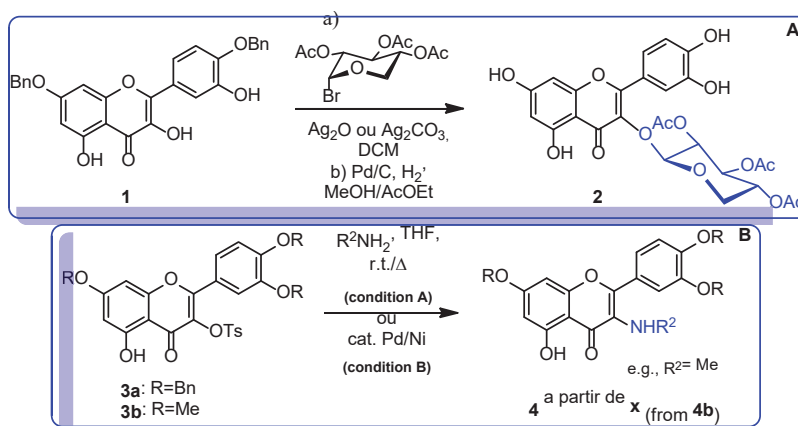
Keywords: Flavonoid, Quercetin, Glycoside, Signal Transduction.

Highlights

The practical preparation of partially-derivatized 3-O-glycosides and 3-deoxy-3-amino derivatives of quercetin as prospective modulators signal transduction pathways will be presented.

Abstract

Flavonoids are known to display diverse biological activities. Herein, we present part of the results on the synthesis of quercetin derivatives to be assayed towards signal transduction pathways. Thus, di-O-benzylated^[1] quercetin **1** was reacted, among other examples, with *D*-xylose acetobromide. Hydrogenolysis of the product led to β -O-*D*-xyloside^[2] **2** (**Scheme 1a**). As for the 3-deoxy-3-nitrogenated derivatives, 3-O-tosylates were reacted with different nitrogen nucleophiles in a uncatalyzed manner (Condition A), thereby broadening the scope of the literature protocol^[3]. A catalyzed version (Condition B) has also been studied (**Scheme 1b**).



Scheme 1. Synthetic approach to the synthesis of quercetin derivatives.

Parallel to these efforts, synthetic innovation at the benzopyranone moiety construction is sought.

[1] REN, Xuhong *et al.* Synthesis of Quercetin 3-O-[6''-O-(trans-p-Coumaroyl)]- β -D-Glucopyranoside. *Journal of Carbohydrate Chemistry*, (2011), v. 30, n. 3, p. 119-131.

[2] KAJJOUT, M.; ROLANDO, C. Regiospecific synthesis of quercetin O-b-D-glucosylated and O-b-D-glucoranidated isomers. *Tetrahedron*, (2011), 67, 4731.

[3] TAKECHI, A; TAKIKAWA, H; MIYAKE, H.; SASAKI, M. Synthesis of 3-aminoflavones from 3-Hydroxyflavones via 3-Tosyloxy or 3-Mesyloxyflavones. *Chemistry Letters*, 1,35, (2006)

Acknowledgments

FAPERJ and CNPq for financial support. Central Analítica/IPPNUFRJ, IQ-UFRJ and CEMBIO/IBCCF-UFRJ for analytical data.

Synthesis of substances for the phytosanitary control of *Xylella fastidiosa*

Leticia N.S. Tavares (PG),¹ Caio C. Oliveira (PQ).^{1*}

l219480@dac.unicamp.br; caio.oliveira@unicamp.br

¹Institute of Chemistry, University of Campinas (UNICAMP)

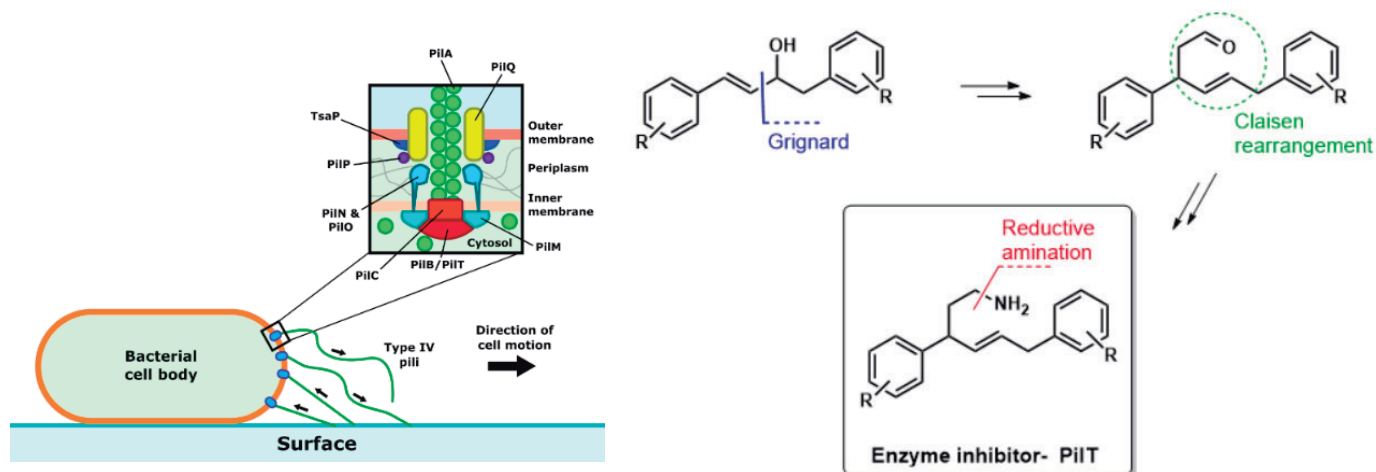
Keywords: Organic synthesis; Enzyme inhibitor; *Xylella fastidiosa*.

Highlights

The PilT enzyme is responsible for the proliferation of the bacterium *Xylella fastidiosa* in the xylem of plants. This work aims to synthesize enzymatic inhibitors for PilT.

Abstract

Xylella fastidiosa is a pathogen that causes disease in several agricultural crops. This bacterium attacks the xylem of plants, spreading and obstructing the passage of water and nutrients throughout the entire plant length, thus causing it to suffocate. The twitching motility mechanism, responsible for the proliferation of bacteria in the xylem, is totally dependent on the action of the PilT enzyme. Based on previous biochemical and computational studies, this work aims at the organic synthesis of potential inhibitors for the PilT enzyme to prevent the proliferation of the pathogen. Two target molecules have already been reached.



Acknowledgments



SYNTHESIS OF SUBSTITUTED COUMARINS VIA FORMAL OXA-[4+2] CYCLOADDITION OF 2-HYDROXI-ALDEHYDES AND MALEIMIDES

Fernando Barretto (PG)^{1,2*} and Silvio Cunha (PQ)^{1,2}

1) Instituto de Química, Universidade Federal da Bahia, UFBA, 40170-115

2) INCT-Instituto Nacional de Ciência e Tecnologia em Energia e Ambiente, Universidade Federal da Bahia, UFBA, 40170-230

*e-mail: fernando.barretto@hotmail.com

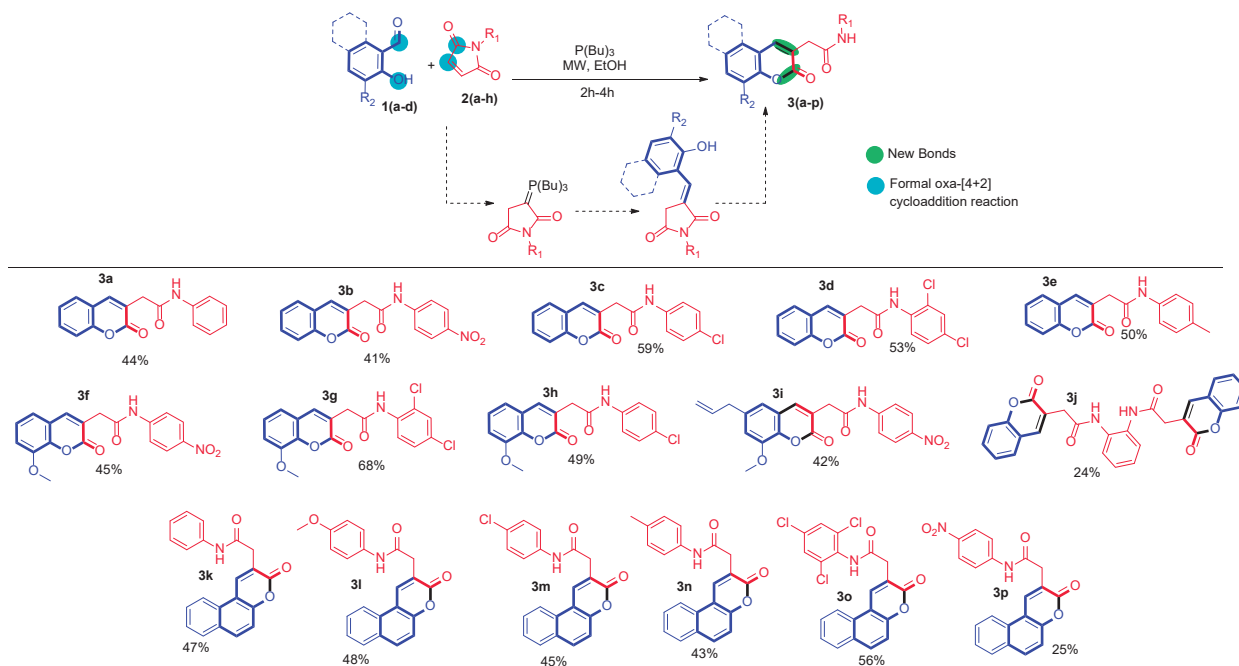
Palavras Chave: (Coumarins, maleimides, aldehydes e tributylphosphine).

Highlights

Substituted coumarins were obtained by formal oxa-[4+2] cycloaddition reaction of 2-hydroxi-aldehydes, maleimides and tributylphosphine under microwave heating.

Resumo/Abstract

The coumarins have an aromatic nucleus condensed to a piran-2-one and shown biological activity. These compounds have a high interest due to their use as starting materials for synthesis of complex heterocyclic compounds.¹ In general, coumarins are obtained by classical methodologies such as Pechmann/Knoevenagel/Wittig/Perkin reactions.² Wittig reaction is the most of important reaction that promotes olefination.³ Herein, we developed a new route to access a set of coumarins **3(a-p)** by Wittig reaction *in situ* of **1(a-d)** with **2(a-h)** and tributylphosphine under microwave heating in EtOH. The products were obtained by simple purification process because all coumarins precipitated. Therefore, we developed a cascade route to substituted coumarins obtained by formal oxa-[4+2] cycloaddition reaction of 2-hydroxi-aldehydes, maleimides and tributylphosphine as promotor, which involves *in situ* ylide formation/Wittig reaction/intramolecular ester formation.



¹(a) YUE, JIAN-MIN, et al. *Eur. J. Med. Chem.*, 45, 5258-5264, **2010**; (b) CHEN, C. H. et al., *Tetrahedron*, 68, 2598-2606, **2012**; (c) SARDARI, S. et al. *Bioorg. Med. Chem.*, 7, 1933-1940, **1999**; (d) RAZAVI, S. M. *Int. J. Biol. Chem.*, 5, 86-90, **2011**; (e) GRIMES, P. E. *Clinics in Dermatology* 15, 921-926, **1997**; (f) BORDIN, F., *Int. J. of Photoenergy*, 1, 1-6, **1999**; (g) GUIOTTO, A. et al., *J. Med. Chem.* 27, 959-967, **1984**; (h) Mokale S.N. et al. *Biomed. & Pharmacother.* 89, 966-972, **2017**; (i) CHILIN, A. et al. *J. Med. Chem.* 56, 1830-1842, **2013**.

²(a) CUNHA, S. et al. *Quim. Nova*, 38, 1125-1131, **2015**; (b) GALLEYS, R. G.; ZINMER, H. *Tetrahedron Lett.*, 32, 2839-2844, **1970**.

³TSOLOMITI, G. et al. *Heterocycl. Comun.* 12, 3-4, **2006**.

Agradecimentos/Acknowledgments

CAPES, FAPESB, INCT and CNPq.

Synthesis of triazolic thionaphthoquinones with antineoplastic potential

Leonardo G. C. de Moraes (PG),¹ Samara G. Silva (IC),¹ Vitor F. Ferreira (PQ),² David R. da Rocha (PQ).¹

leonardocavaliere@id.uff.br

¹Departamento de Química, UFF; ²Departamento de Tecnologia Farmacêutica, UFF

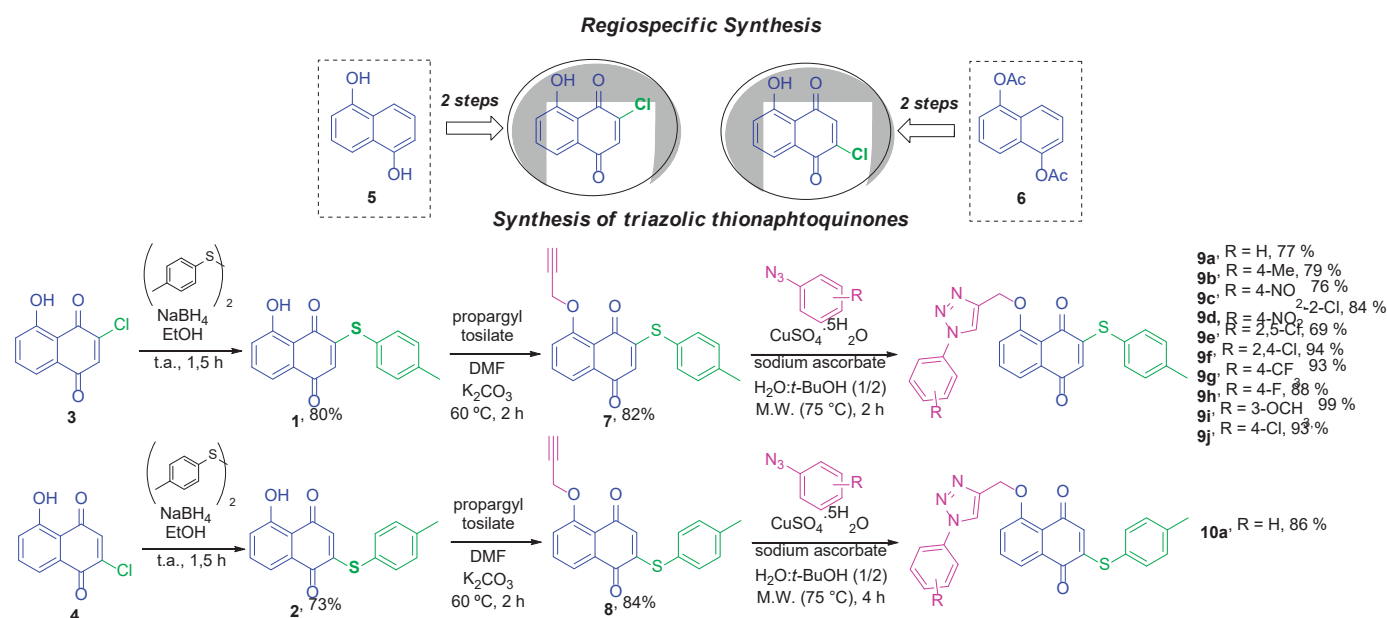
Palavras Chave: Regiospecific, Naphthoquinone, Cancer, Triazole, Microwave

Highlights

In this work, unpublished thionaphthoquinones modified in the aromatic ring with triazole moiety and with great antineoplastic potential were synthesized in a regiospecific way with excellent yields.

Resumo/Abstract

Naphthoquinones are a class of substances widely studied in the literature due to their wide variety of biological activities. Thionaphthoquinones have recently demonstrated excellent antineoplastic activity and selectivity against leukemia cell lines, especially thionaphthoquinone **1** and **2**. Likewise, the 1*H*-1,2,3-triazole is of great importance due to its plurality of biological activities and there is a lack of studies in the literature that promote the modification of naphthoquinones with this triazole moiety on the aromatic ring. In this context, this work aims at the synthesis of hybrids of thionaphthoquinones and 1*H*-1,2,3-triazole rings. The synthetic route starts with the regiospecific synthesis of the chlorinated intermediates **3** and **4** starting from **5** and **6**, respectively. The chlorine atom is then replaced by the *p*-thiocresol group producing thionaphthoquinones **1** and **2**. The thionaphthoquinones were then propargylated on the aromatic ring providing **7** and **8**. Finally, **5** and **6** reacted with aromatic azides through a cycloaddition catalyzed by copper I producing hybrids **9** and **10**, respectively. The developed synthetic route proved to be efficient and other analogues of **10**, varying the substitution pattern, are still being synthesized.



Agradecimentos/Acknowledgments

FAPERJ, CAPES and CNPQ

Synthetic Studies Towards Wedelienone

Lucas D.P. Gonçalves (IC),^{1*} Victor C.S. Santana (PG),¹ Julian C.S. Pavan (PG),² Vladimir C.G. Heleno (PQ),² Emilio C. de Lucca Jr. (PQ).¹

l239920@dac.unicamp.br

¹ Institute of Chemistry, University of Campinas; ² Research Center in Exact and Technological Sciences, University of Franca.

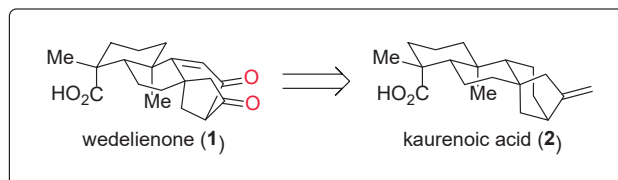
Keywords: Catalysis, Natural products, Diterpenes, C—H oxidation.

Highlights

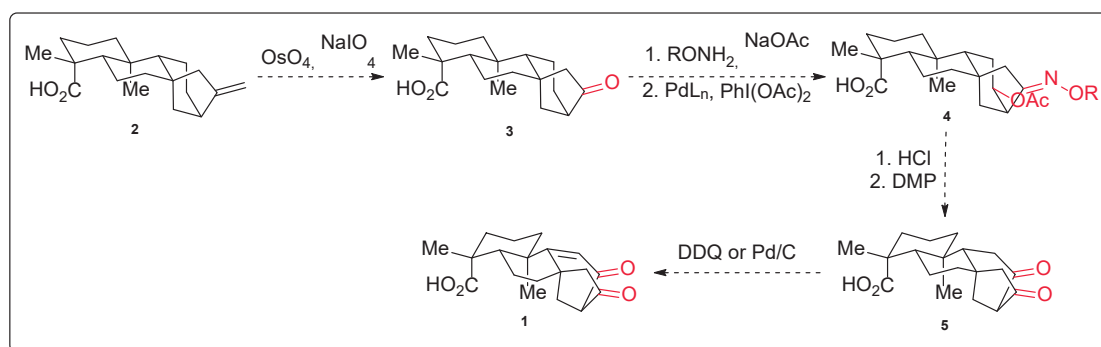
Studies towards the synthesis of complex natural *ent*-kaurane diterpenoid wedelienone. Our approach utilizes a selective palladium-mediated Sanford acetoxylation of a kaurenoic acid derivative as the key step.

Abstract

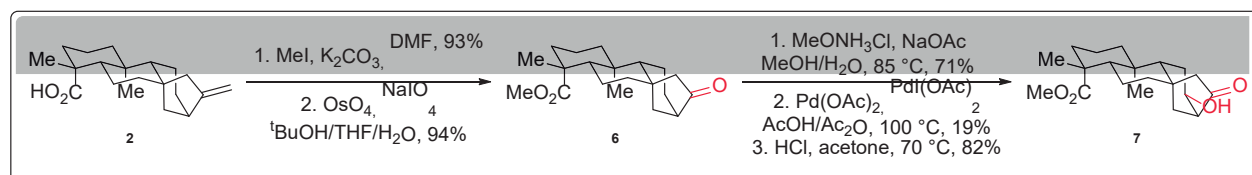
The study aims to investigate a synthetic route to obtain the natural product wedelienone (**1**),¹ through oxidation of C—H bonds. This product is found in the plant *Wedelia chinensis* and, since it is an *ent*-kaurene type, we propose synthesizing **1** from kaurenoic acid (**2**).



In view of our recent report for the acetoxylation of the C17 position of *ent*-beyerane isosteviol derivatives² and previous works³ using Pd(OAc)₂ as catalyst, we envisioned to use this strategy in the synthesis of natural product **1**.



Using these reactions, we have progressed in our efforts to synthesize wedelienone. Given the 19% yield in the acetoxylation reaction, optimizing this step is a priority to enhance the overall yield. The stereochemistry of product **7** was confirmed by 1D and 2D NMR.



References:

- (1) Rany Das, K.; Iwasaki, A.; Suenaga, K.; Kato-Noguchi, H. *Tetrahedron Lett.* **2020**, *61*, 151600.
- (2) Santana, V. C. S.; Rocha, E. C. S.; Pavan, J. C. S.; Heleno, V. C. G.; de Lucca, E. C., Jr. *J. Org. Chem.* **2022**, *87*, 10462–10466.
- (3) Zhou, S.; Guo, R.; Yang, P.; Li, A. *J. Am. Chem. Soc.* **2018**, *140*, 9025–9029.

Acknowledgments

IQ/Unicamp, FAPESP, FAEPEX, CNPq and CAPES.

Targeting Nitrogenated Aromatics: Tandem Diels-Alder/Aromatization Reaction of Chitin-Derived Furans

Camila Souza Santos (PD),¹ Renan Rodini Mattioli (PG),¹ Julia Soares Baptista (IC),¹ Vitor H. Menezes da Silva (PD),¹ Julio Cezar Pastre (PQ)^{1,*}
 cssantos12@gmail.com; jpastre@unicamp.br.

¹Institute of Chemistry, University of Campinas - UNICAMP, 13083-970, Campinas, SP, Brazil.

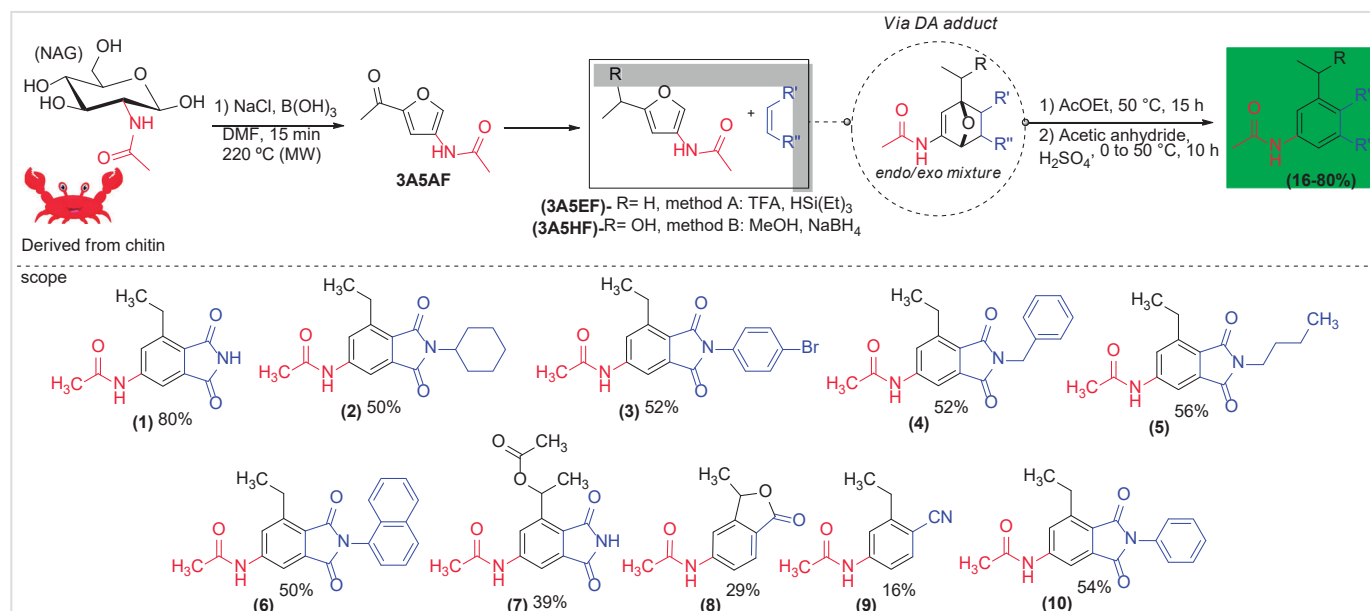
Palavras Chave: Diels-Alder, chitin-derived, aromatic compounds

Highlights

The application of biomass-derived furans in sequential Diels-Alder (DA)/aromatization reactions is a promising approach for the preparation of aromatic compounds. We addressed the formation of *N*-containing aromatic compounds from chitin-derived furans.

Resumo/Abstract

Chitin is the second most abundant biopolymer in nature and the main constituent of the exoskeleton of insects and crustaceans. Chitin has a unique potential for obtaining nitrogen-containing derivatives, such as *N*-acetyl-*D*-glucosamine (NAG), *D*-glucosamine, *N*-acetylglycine, *N*-acetyl sorbitol, *N*-acetyl isosorbide, and 3-acetamido-5-acetylfuran (3A5AF).^{1,2} 3A5AF is particularly valuable as it contains a substitution pattern that is difficult to install synthetically, thus representing a real opportunity for chemical valorization.³ We addressed the challenge of using chitin-derived furans, 3-acetamido-5-ethylfuran (3A5EF) and 3-acetamido-5-(1-hydroxyethyl)furan (3A5HF), for the formation of 4-acetylaminophthalimides and other *N*-containing aromatic compounds. The transformation is carried out sequentially and involves the formation of the DA adduct, 7-oxa-norbornene, which in an acidic/acylating medium undergoes a dehydration/aromatization reaction providing the compounds in yields ranging from 16–80%. To the best of our knowledge, this is the first report involving a chitin derivative for the formation of 4-acetylaminophthalimides, which is the first step towards expanding the toolbox of chitin-derived furans in the synthesis of nitrogenated aromatic compounds *with the nitrogen atom directly attached to the benzene ring*. The 4-aminophthalimide, combined with *N*-linked electron-donating groups in the phthalimide scaffold, is well known to exhibit high fluorescence. Thus, its derivatives continually attract great attention for biological applications, especially as fluorescent markers, and environment-sensitive probes.⁴



References: [1] *ACS Sustain. Chem. Eng.*, **2018**, 6, 12411-12418; [2] *Green Chem.*, **2017**, 19, 3350-3356; [3] *Green Chem.*, **2021**, 23, 9800-9814; [4] *J. Pharm. Biomed. Anal.*, **2014**, 92, 63-68.

Agradecimentos/Acknowledgments

The authors gratefully acknowledge financial support from the São Paulo Research Foundation - FAPESP (Awards N.: JCP, 2021/06661-5; CSS, 2022/00774-5; RRM, 2019/26450-9), the Brazilian National Council for Scientific and Technological Development - CNPq (JCP), and the Coordination for the Improvement of Higher Education Personnel - CAPES (RRM).

The Second Generation of the In-tandem Enantioselective Heck-Matsuda Arylations of Unactivated Olefins Directly from Anilines

Luiz P. M. O. Leão (PG),^{1*} Valdeir C. Oliveira (PG),¹ Carlos R. D. Correia (PQ).^{1*}

l264637@dac.unicamp.br; roque@iqm.unicamp.br

¹Instituto de Química, Unicamp, 13083-970

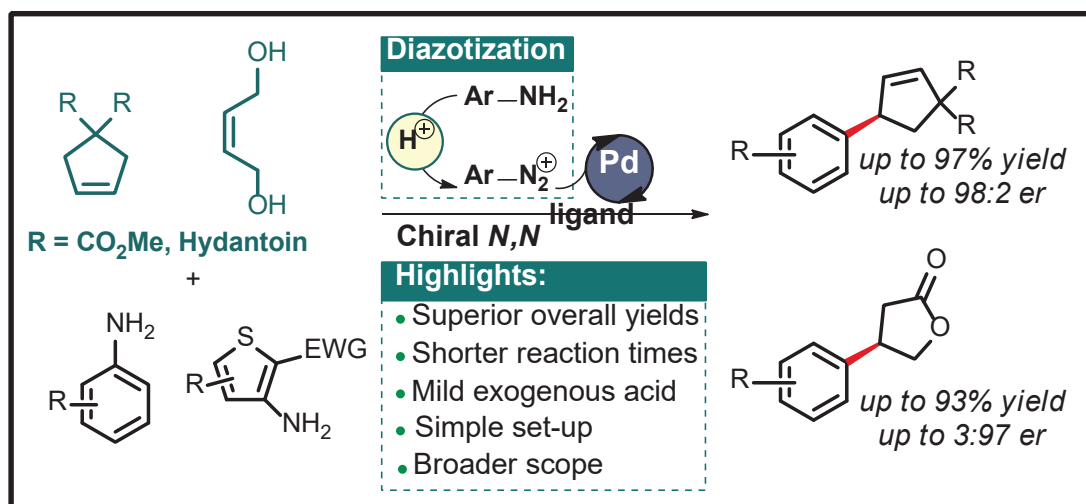
Palavras Chave: (Enantioselective Catalysis, In Tandem Reaction, Palladium Catalysis, Olefin Desymmetrization, In Situ Diazotization)

Highlights

In tandem enantioselective Heck-Matsuda reactions directly from anilines under mild exogenous acidic conditions; Improved yields and shorter reaction times; Broader scope and simple reaction set-up.

Resumo/Abstract

A much improved second generation of the sequential one-pot enantioselective Heck-Matsuda reaction directly from aniline derivatives has been developed.¹ This new, simple, and effective arylation method relies on the *in situ* diazotization of the electronically diverse anilines and, aminothiophenes, followed by the enantioselective Heck-Matsuda reaction under mildly acidic conditions, skipping the need for the preparation of unstable arenediazonium salts. This effective and very practical protocol was used to perform, among other processes, the desymmetrization of unactivated olefins leading to the synthesis of enantioenriched cyclopentenes and β -aryl- γ -lactones in high yields (up to 99%) and er (up to 99:1). Importantly, the protocol was also applied in the formal total synthesis of the biologically active compound VPC01091, a drug candidate for multiple sclerosis with excellent yield (94%), in 97:3 er and >20:1 dr. The method is amenable to multigram-scale reactions.



Agradecimentos/Acknowledgments

We acknowledge the financial support of FAPESP (2014/25770-6), the Coordination for the Improvement of Higher Education Personnel (CAPES) for the fellowship to L.P.M.O.L. (88887.486174/2020-00), and CNPq for the fellowship to V.C.O. (140326/2019-7)

Reference: For the first generation of these reactions, see: Herrera, C. L., Santiago, J. V., Pastre, J. C., Correia, C. R. D. *Adv. Synth. Catal.* **2022**, 364, 1863–1872.

Ultrafast Transition Metal-Free Synthesis of Functionalized Oxindoles and Dihydroquinoline-2-ones Under Microwave Irradiation

Júlia L. Couto (PG),¹ Milene M. Hornink (PG),¹ Vinicius R. do Nascimento (PG),¹ Leandro H. Andrade (PQ).¹

jlcouto@usp.br

¹ Laboratory of Fine Chemistry and Biocatalysis, Institute of Chemistry, USP

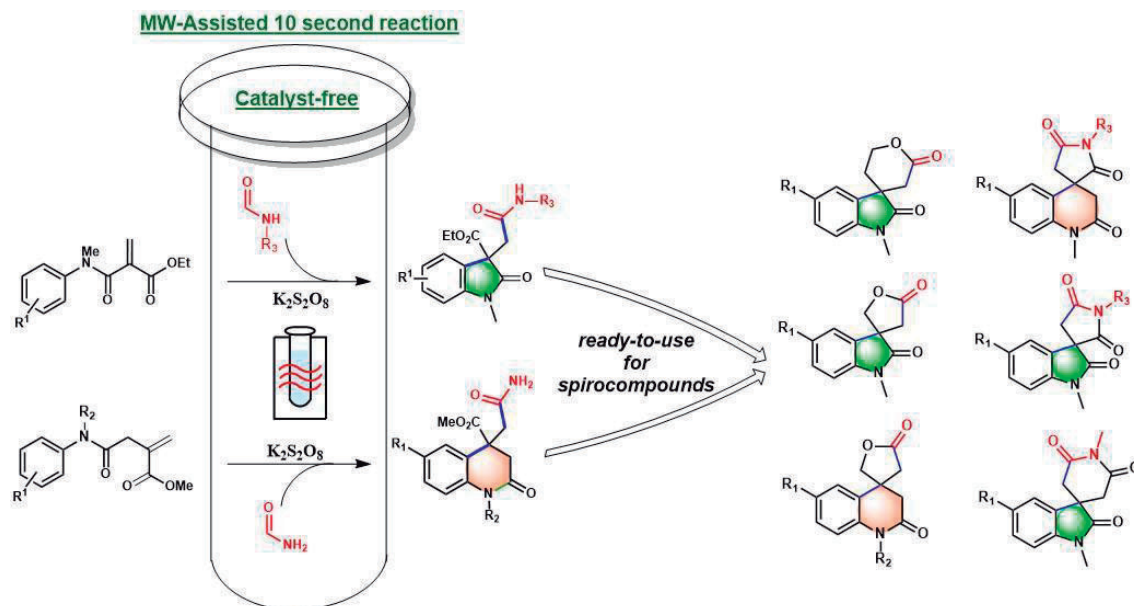
Microwave, catalyst-free, metal-free, ultrafast synthesis, formamide, oxindoles; dihydroquinolin-2-ones.

Highlights

A ultrafast transition metal-free methodology for the synthesis of highly functionalized heterocycles was developed. The exploitation of formamide or *N*-methylformamide and potassium persulfate under microwave irradiation resulted in a reaction of 10 s. The functionalized oxindoles and dihydroquinoline-2-ones allowed us to access several spiro lactones and spiroimides.

Resumo/Abstract

A ultrafast transition metal-free and synthetic methodology for generating a broad scope of highly functionalized oxindoles and dihydroquinolin-2-ones was developed. The exploitation of formamide or *N*-methylformamide (reagent/solvent) and potassium persulfate (radical initiator) under microwave irradiation resulted in a ultrafast radical reaction of 10 s. The functionalized oxindoles and dihydroquinoline-2-ones allowed us to readily access several spiro compounds such as spiro[oxindole- γ -lactones], spiro[oxindole- δ -lactones], spiro[dihydroquinoline-2-one- γ -lactones], spiro[oxindole-imides] and spiro[dihydroquinoline-2-one-imides].



Acknowledgments: Conselho Nacional de Desenvolvimento Científico e Tecnológico (National Council for Scientific and Technological Development, CNPq, grant no. 312751/2018-4 and 132280/2018-3), Coordenação de Aperfeiçoamento de Pessoal de Nível Superior (Coordination for the Improvement of Higher Education Personnel, CAPES), and Fundação de Amparo à Pesquisa do Estado de São Paulo (The São Paulo Research Foundation, FAPESP, grant nos. 2017/02854-8, 2018/07152-4, 2019/10762-1 and 2021/12555-3) for financial support.

Visible-Light Mediated Carbamylation of Nitrones via Continuous Flow

Pedro H. R. Oliveira*(PQ), Everton A. Tordato (PG), Jeimy A.C Velez (PG), Pablo S. Carneiro (IC) and Márcio W. Paixão (PQ)

*e-mail: peddrms@gmail.com

Laboratory for Sustainable Organic Synthesis and Catalysis - Chemistry Department – Federal University of São Carlos – UFSCar, 13565-905

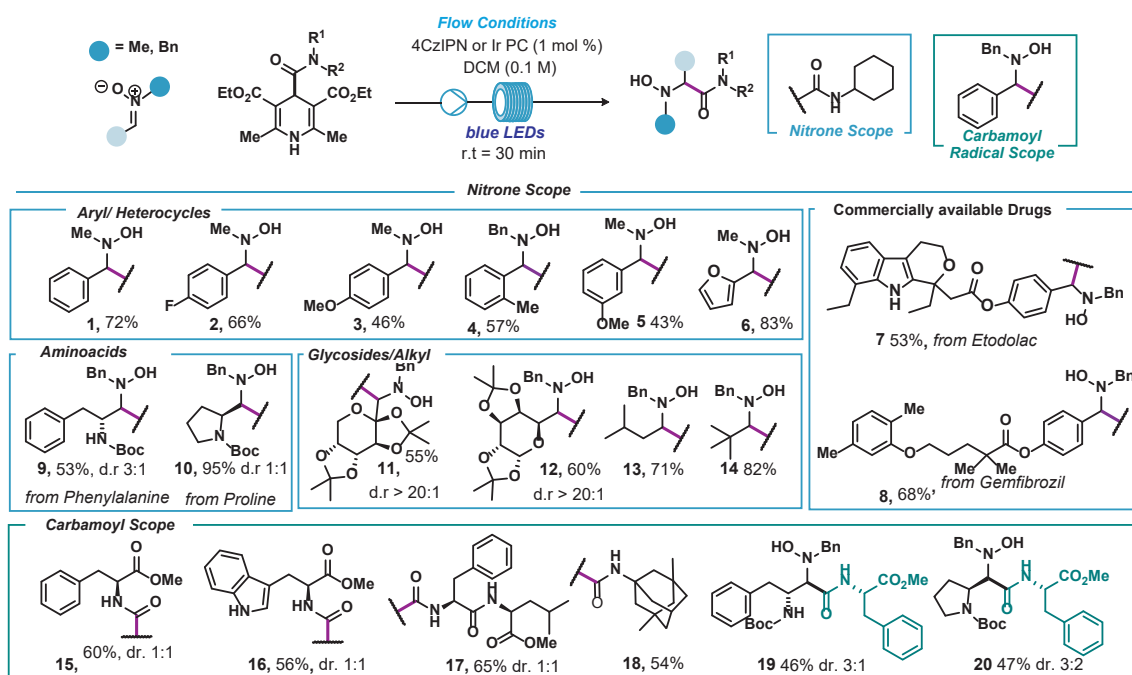
Keywords: Photoredox Catalysis, Continuous Flow, Nitrones

Highlights

A fast and efficient photocatalytic protocol for the carbamylation of Nitrones under continuous flow conditions was developed.

Resumo/Abstract

Nitrones are important starting materials for the synthesis of biologically relevant nitrogen-containing scaffolds. Among established synthetic protocols, the selective addition of nucleophilic species to nitrones stands as a straightforward route for accessing *N,N*-disubstituted hydroxylamines. Although appealing, some of these strategies require harsh conditions that significantly hedge its applicability and functional group tolerance.¹ More recently, photoredox catalysis has emerged as an important trend in the context of amide preparation, given its milder reaction conditions and compatibility with a wide range of substrates.^{2,3} Considering these aspects, we developed an efficient time-economical and easy-to-scale photocatalytic strategy for the amidation of nitrones using 1,4-dihydropyridines (DHPs) as carbamoyl radical sources under a continuous flow regime. The optimized protocol showed better yields compared to batch conditions and allowed the preparation of a wide library of compounds comprising pharmaceutical active ingredients, amino acids, peptides, and glycosides, requiring only 30 minutes of residence time.



Agradecimentos/Acknowledgments

We are grateful to the Brazilian funding agencies CNPq (INCT Catálise, Grants No 444061/ 2018-5 and Universal Project 405052/2021-9) and FAPESP (2021/06099-5 for MWP). This study was financed in part by the Coordenação de Aperfeiçoamento de Pessoal de Nível Superior - Brasil CAPES 23038.003012/2020-16- Financial code 001;

References

- Murahashi, S.-I.; Imada, Y. *Chem. Rev.* **2019**, *119* (7), 4684–4716.
- Matsuo, B. T.; Oliveira, P. H. R.; Pissinati, E. F.; Vega, K. B.; de Jesus, I. S.; Correia, J. T. M.; Paixão, M. *Chem. Commun.* **2022**, *58* (60), 8322–8339.
- Matsuo, B. T.; Oliveira, P. H. R.; Correia, J. T. M.; Paixão, M. W. *Org. Lett.* **2021**, *23* (17), 6775–6779.

Visible light-mediated diastereoselective synthesis of novel C-Glycoamino acids and Glycopeptides under sustainable conditions.

Antonio Orestes de Souza Neto (PG)^{1*}, Pedro H. R. Oliveira (PQ),² Kimberly Benedetti Vega (PG),² Jeimy A. C. Velez (PG)², Iva S. de Jesus(PQ)² Marcio W. Paixão. (PQ).²

antoniosouza@estudante.ufscar.br

Laboratory for Sustainable Organic Synthesis and Catalysis - Chemistry Department – Federal University of São Carlos – UFSCar.

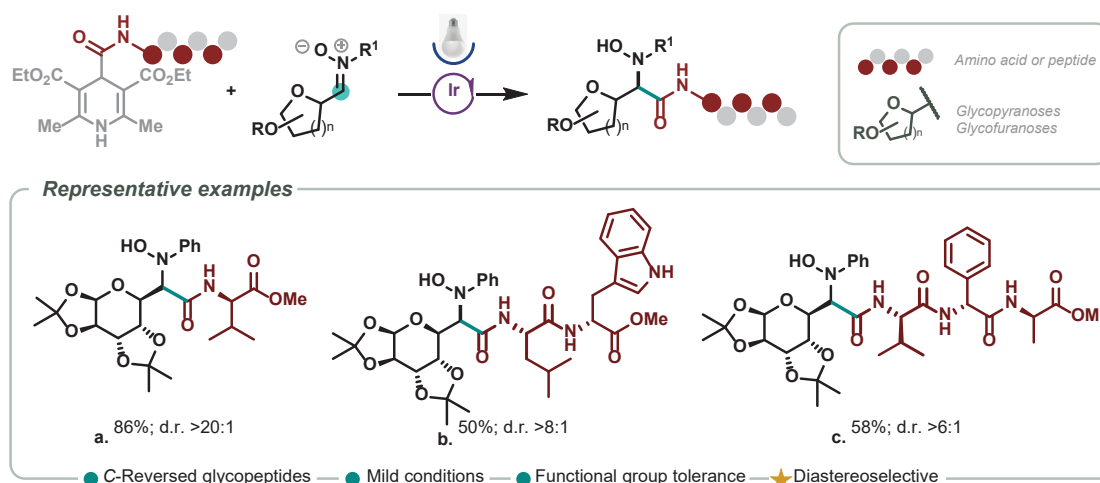
Key words: Glycoamino Acids, Glycopeptides, diastereoselectivity, photocatalysis.

Highlights

Herein we report an operationally simple photocatalytic approach for the synthesis of C-glycopeptides using derived 1,4-dihydropyridines (DHP) as carbamoyl radical source.

Abstract

Glycoamino acids are commonly found among natural products and living organisms. This class of compounds consists of a pyranose or furanose directly linked to an amino acid moiety. Moreover, the glycosylation of drug molecules and lead compounds stands as a valuable tool in drug discovery as they can improve metabolic stability, biodistribution and target-binding interactions. The glycosylation process can be achieved through different types of linkages (C-, O- and N-glycosylations). Among those, the C-glycosyl linkage is the most stable under both acid and basic conditions, as well in the presence of different types of proteases.^{1, 2} Recognizing the importance of such strategy in the drug design scenario, herein we report the developed a new photocatalytic strategy for the preparation of C-glycopeptides using amino acids and peptides derived 1,4-dihydropyridines (DHP) as carbamoyl radical sources, and glycosyl nitrones as acceptors.³ Having the optimized reaction condition in hands, the scope and limitation towards a set of carbamoyl radicals were further evaluated. In this regard, polar, non-polar, aromatics amino acids, and different types of peptides were successfully employed providing therefore the desired products in moderate/good yields and excellent diastereoselectivities. As a perspective, we will challenge new glycosyl nitrones and peptides to our optimized reaction condition.



¹ Qi, R.; Wang, C.; Ma, Z.; Wang, H.; Chen, Q.; Liu, L.; Pan, D. A. *Angew. Chem.Int. Ed* **2022**, 61, 134. ² .. Liu, Y.; Xia, Y.; Gulzar, T.; Wei, B.; Li, H.; Zhu, D.; Hu, Z.; Xu, P.; Yu, B. *Nat Commun* **2021**, 12, 4924. ³ Matsuo, B. T.; Oliveira, P. H. R.; Correia, J. T. M.; Paixão, M. W. *Org. Lett.* **2021**, 23, 6775-6779.

Acknowledgments

We are grateful to the Brazilian funding agencies CNPq (INCT Catálise, Grants No 444061/ 2018-5 and Universal Project 405052/2021-9) and FAPESP (2021/06099-5 for MWP).

46^o Reunião Anual da Sociedade Brasileira de Química: "Química: Ligando ciências e neutralizando desigualdades"

Visible Light Promoted C-H Functionalization of 4-Aminoquinazoline

Jhonathan Renner N. dos Santos (PG),^{1*} Alice Karoline de Almeida Martinez (IC),¹ Arlene G. Corrêa (PQ)¹¹Centre of Excellence for Research in Sustainable Chemistry, Department of Chemistry, Federal University of São Carlos, São Carlos, SP, Brazil. *jhonathanquimica@gmail.com

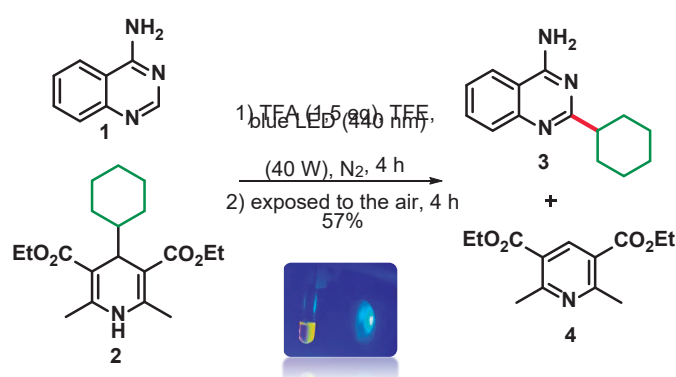
keywords: Quinazoline, Dihydropyridine, C-H functionalization

Highlights

The construction of a C-C bond at C-2 position of 4-amino-quinazoline via C-H functionalization mediated by blue LED irradiation with dihydropyridine as radical precursor was evaluated.

Abstract

N-Heterocyclic compounds are targets of interest due to their wide range of pharmacological interest,^[1] and among this class are the quinazolines that have their biological potential already reported.^[2] Studies based on the functionalization of *N*-heterocycles have received great attention, however, still face some challenges such as the use of drastic conditions with the adoption of metal catalysts, toxic solvents, and lack of selectiveness, among others. In this regard, Chen *et al.* reported the use of 1,4-dihydropyridines (DHPs) as an alternative for the functionalization of azaarenes.^[3] Based on this work, we are investigating the reaction of 4-amino-quinazoline (**1**) with cyclohexyl-1,4-dihydropyridine (DHP) (**2**) under blue LED (40 W) irradiation in the presence of trifluoroacetic acid (TFA) and 2,2,2-trifluoroethanol (TFE). In our first attempt, product **3** was obtained in 57% yield (Entry 1).



Entry	Modifications to standard conditions	Yield (%)
1	-	57
2	Two LEDs	13
3	Dark	-
4	Air exposure	-
5	Absence of acid	-
6	CHF ₃ O ₃ S	traces
7	BF ₃ .OEt ₂	8
8	AcOH	traces

In this context, studies were carried out using two blue LEDs, but there was a decrease in yield (Entry 2), and in the absence of light, it was noted that the product of interest was not obtained (Entry 3). Moreover, the need of an inert atmosphere (Entry 4) and acid (Entry 5) were also verified, and we observed that there was no progress of the reaction. Optimization of the process aiming at greener conditions are undergoing, as well as the evaluation of the scope and limitations and understanding the reaction mechanism.

References: [1] Obaid, R. J.; Mughal, E. U.; Naeem, N.; Al-Rooqi, M. M.; Sadic, A.; Jassas, R. S.; Moussa, Z.; Ahmed, S. A. Pharmacological significance of nitrogen-containing five and six-membered heterocyclic scaffolds as potent cholinesterase inhibitors for drug discovery. *Process Biochem.*, **2022**, *120*, 250-259. [2] Gomaa, H. A. M. A comprehensive review of recent advances in the biological activities of quinazolines. *Chem. Biol. Drug Design* **2022**, *100* (5), 639-655. [3] Chen, X.; Luo, X.; Wang, K.; Liang, F.; Wang, P. Late-Stage Alkylation of *N*-Containing Heteroarenes Enabled by Homolysis of Alkyl-1, 4-dihydropyridines under Blue LED Irradiation. *Synlett* **2021**, *32* (7), 180-197.

Acknowledgments

FAPESP (14/50249-8 and 21/050012-3), GSK, CNPq and CAPES (Finance Code 001)

QPN

Produtos Naturais

46^a Reunião
Anual da **SBQ**

28 a 31 de Maio de 2023

Águas de Lindóia · SP
Hotel Monte Real

Analysis of carotenoids and antioxidant activity of coffee beans using smartphone

Daiane E. Blank (PG),¹ Antonio J. Demuner (PQ),^{1*} Maria J.M. Firmino (IC),¹ Cristiane I. Cerceau (PQ),¹ Iara F. Demuner (PQ),² Marcela R. Coura (PG),² Marcelo H. Santos (PQ).¹

ademuner@ufv.br

¹Departamento de Química, UFV; ²Laboratório de celulose e Papel, UFV

Keywords: Coffee, Lycopene, β -carotene, Phenolic, Antioxidant, PhotoMetrix®.

Highlights

Coffee has antioxidant potential due to its chemical composition. Chemical determination of coffee extract using PhotoMetrix® application. Low-cost chemical determination analytical methods.

Abstract

Coffee is one of the most important agricultural products in world, and its pulp is one of the main by-products during its processing. The chemical composition of coffee is a fundamental parameter in distinguishing the different varieties of this product, since in it phenolic compounds and a variety of other bioactive compounds are found. Several approaches for the determination of phenolic compounds and antioxidants use sophisticated and high-cost equipment. To overcome these disadvantages the Photometrix® app associated with a smartphone was used as a simple, inexpensive, and alternative method, that use minimal quantities of reagents employing spectrophotometric techniques associated with image analysis. PhotoMetrix® is an app installed for free from the Google Play Store in which digital images captured are decomposed in primary colors (red, green and blue) using RGB model. The intensity of the color developed in the chemical reaction is measured as a function of the primary colors that compose it, being directly proportional to the concentration of the analyte. In the present study, phenolic compounds, carotenoids, and antioxidant activity were investigated in different coffee samples grown in Minas Gerais. The pulp and seed of each coffee sample were segregated for extraction by maceration technique. Subsequently, the determination of phenolic and antioxidant capacity using DPPH methodology¹, and β -carotene and lycopene¹ content were quantified by PhotoMetrix® using analytical standard. The results were compared with traditional UV-Vis spectrophotometer. The results in both methods of analysis were similar. The samples showed high content of phenolic compounds (425.08-812.91 mg/100 g) in coffee samples identified using PhotoMetrix®. The antioxidant activities were from 24.44-33.90 mg/g, according to the maturation stage. The lycopene concentration was from 3.05-9.03 mg/100 g and β -carotene 2.17-4.88 mg/100 g. The method of analysis using PhotoMetrix® can be an alternative for the investigation of carotenoid, especially in Institutions without financial resources for chemical analysis.

¹ Bazani, E. J. O.; Barreto, M. S.; Demuner, A. J.; Santos, M. H.; Cerceau, C. I.; Blank, D. E.; Firmino, M. J. M.; Souza, G. S. F.; Franco, M. O.; Suarez, W. T.; Stringheta, P. C. *Food Analytical Methods*, v. 14, p. 631-640, 2021. Doi: <https://doi.org/10.1007/s12161-020-01907-z>

Acknowledgments

The authors thank FAPEMIG, CNPq, CAPES for financial support and scholarship.

Analysis of chemodiversity related to stingless bees by MS-based Molecular Networking and larvicidal activity of their propolis against *Aedes aegypti*.

Luís G. P. Feitosa (PG),*¹ Juliana M. Feres (PQ),² Thais Guaratini (PQ),² Lorena C. Albernaz (PQ),³ Laila S. Espindola (PQ),³ Norberto P. Lopes (PQ)¹

***luis.feitosa@usp.br**

¹Núcleo de Pesquisa em Produtos Naturais e Sintéticos, School of Pharmaceutical Sciences of Ribeirão Preto - University of São Paulo; ²Heborá Ltda; ³Pharmacognosy Laboratory, School of Health Sciences/Medicine - University of Brasília

Palavras Chave: *Stingless bees, Honey, Propolis, Aedes aegypti, Mass spectrometry, Molecular Networking*

Highlights

Micromolecular composition of stingless bees honey and propolis may be influenced by floral substrates. The geopropolis from *M. quadrifasciata* may contain bioactive diterpenes against *Aedes aegypti*.

Resumo/Abstract

Stingless bees (SB) play an important ecological role in the pollination of plants in Neotropical region, including Brazilian ecosystems. More than 240 species of SB are found in Brazil, 87 of which are endemics. The honey and (geo)propolis produced by SB present several biological activities, highlighting the antibacterial effects. However, environmental factors are related to variations in the chemical composition of these products. Thus, metabolomics of stingless bees honey (SBH) and propolis (SBP) based in *tandem* mass spectrometry and Molecular Networking may increase the knowledge about potentially bioactive metabolites, and molecules involved in interactions between SB and their environments. We analyzed SBH samples of different species collected in meliponaries located in São Carlos city (SP) and SBP from Bandeirantes city (PR), including genera *Melipona*, *Tetragonisca*, *Tetragona*, *Nannotrigona*, *Scaptotrigona*, and others. The samples were submitted to cleanup by SPE in C18 cartridge and then analyzed by HPLC-HRESI-MS/MS (QTOF, positive mode), using a C18 column and elution with gradient of formic acid 0.1%: ACN. MS/MS data were preprocessed in the MZmine 2 software and uploaded to the web-based platform GNPS (Global Natural Products Social Molecular Networking) to processing with FBMN tool. Annotations were based in public spectral libraries of GNPS, *in silico* predictions of NAP, MS2LDA computational tool, chemical data from literature, as well manual dereplication of analogues. It was observed that chemical diversity of SBH and SBP mainly includes flavonoids (glycosides and free aglycones), as well amino acids and derivatives, and terpenes. Literature data associate the presence of flavonoids with the antioxidant, anti-inflammatory and antimicrobial properties of SBH. The molecular networks showed differences in the occurrence of some molecular families between both SBH and SBP samples. These data suggest that different species of SB in the same environment may present different behaviors in their floral visits and collection of substrates with distinct chemical compositions to produce honey and propolis. Furthermore, this work increases the micromolecular inventory related to SB found in Brazil. We also evaluated the larvicidal activities of SBP against mosquito *Aedes aegypti*, which is the vector of dengue, zika and chikungunya arboviruses. It was verified that three of four propolis with highest mortality of larvae were produced by genus *Melipona*. Unlike the other products evaluated in the test, *Melipona* produces the geopropolis from the mixture of floral resins with clay/soil. Nevertheless, the SBP molecular network did not showed clusters of metabolites with exclusive occurrence in the genus *Melipona*. It was observed that some nodes were more restricted to the most active geopropolis from *M. quadrifasciata*. These metabolites were annotated as congeners of diterpenes with abiatatriene skeleton, such as dehydroabietic acid derivatives, which were previously described in this species. At the present, these data suggest that terpenes may be related to the larvicidal activity observed for *M. quadrifasciata* geopropolis. In addition, these results may contribute with the strategies for the control of *Aedes aegypti* based in natural products.

Agradecimentos/Acknowledgments

Coordenação de Aperfeiçoamento de Pessoal de Nível Superior (CAPES).
Fundação de Amparo à Pesquisa do Estado de São Paulo (FAPESP).

Anthelmintic effect of *Pterogyne nitens* and its phenolic compounds against *Haemonchus contortus*

Gabriela M. Payão (PG),¹ Caroline S. Lima (PG),¹ Ana C. S. Chagas (PQ),² Hervé Hoste (PQ),³ Luis O. Regasini (PQ).^{1*}

gabriela.payao@unesp.br; luis.regasini@unesp.br

¹Laboratório de Antibióticos e Quimioterápicos, Unesp São José do Rio Preto- SP, Brasil; ²Embrapa Pecuária Sudeste, São Carlos-SP, Brasil; ³INRA –Interactions Hôte Agents Pathogènes, Toulouse-França

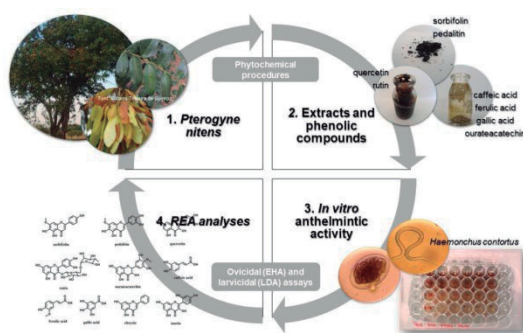
Palavras Chave: *Pterogyne nitens*, anthelmintic, *Haemonchus contortus*, antiparasitic, flavonoid, phenylpropanoid

Highlights

Extracts and phenolic compounds showed anthelmintic activity. Phenolic acids were more active than flavonoids. This the first investigation on the anthelmintic activity of sorbifolin, pedaltin and chrysin.

Abstract

Due to high prevalence and large pathogenicity, *Haemonchus contortus* is the main gastrointestinal nematode in tropical and subtropical regions. This species is responsible for severe economic losses to sheep and goat breeders in Brazil. The control of this parasite is currently compromised, mainly, due to anthelmintic resistance. In the search for natural anthelmintic alternatives, *Pterogyne nitens*, a native Brazilian tree with potential medicinal effect, was evaluated. The aim of this study was to evaluate the anthelmintic activity of ethanolic extracts and phenolic compounds from *P. nitens*, as well as two commercial flavonoids (chrysin and morin), to derive structure-activity relationship. The ovicidal and larvicidal activity of ethanolic extracts from leaves (EEL) and fruits (EEFR), as well as natural compounds from *P. nitens* on *H. contortus* were evaluated through egg hatch assay (EHA) and larval development assay (LDA). The results showed that all extracts, especially the phenolic compounds were active in the EHA and LDA. The egg hatch inhibitory effects of EEL ($EC_{50} = 316 \mu\text{g/mL}$) were more potent than EEFR ($EC_{50} = 512 \mu\text{g/mL}$). However, larval development inhibitory effects of EEL ($EC_{50} = 47 \mu\text{g/mL}$) and EEFR ($EC_{50} = 35 \mu\text{g/mL}$) were similar. Among the compounds, the flavones (sorbifolin, pedaltin, and chrysin) did not have inhibitory effects on egg hatching but presented some activity against larval development of *H. contortus*. In contrast, the flavonols (quercetin, rutin, and morin) showed high activity in the EHA but were inactive in the LDA. The addition of a hydroxyl group and a rutinosyl group to the flavonoid structure increased the ovicidal and larvicidal activity, respectively. The phenolic acids showed potent anthelmintic activity: caffeic acid, ferulic acid, and gallic acid had the highest anthelmintic effects, presenting EC_{50} values of 1.48, 0.56, and $4.93 \mu\text{g/mL}$ in the EHA; and 31, 22, and $33 \mu\text{g/mL}$ in the LDA, respectively. These results suggest that *P. nitens* might be a source of effective alternative compounds to control *H. contortus*.



Acknowledgments

The authors gratefully acknowledge financial support from (CAPES, finance code 001), (CNPq) (Grants 471129/2013-5, 306251/2016-7 and 429322/2018-6), (FAPESP) (Grants 2014/18330-0 and 2018/15083-2) and (FAPESP 2009/53989-4). GMP thanks CAPES for her scholarship.

ANTIFUNGAL ACTIVITY AND ANALYSIS BY MOLECULAR NETWORKS OF ETHANOLIC AND AQUEOUS EXTRACTS OF CURCUMA LONGA L.

Felipe A. C. Pinto (IC) ^{1*}, Joyce Nogueira Gonçalves (IC) ¹, Renata Nátili Schimiloski (IC) ¹, Rafaela Echlin Schimiloski (IC) ¹, Conceição de Fátima Alves Olguin (PQ) ¹, Lucília Kato ².

felipe_chimenez99@hotmail.com

¹Departamento de Química, UNIOESTE ²Departamento de Química, UFG.

Palavras Chave: Fitopatógenos, GNPS, Redes Moleculares, Antioxidante, Curcuminóides.

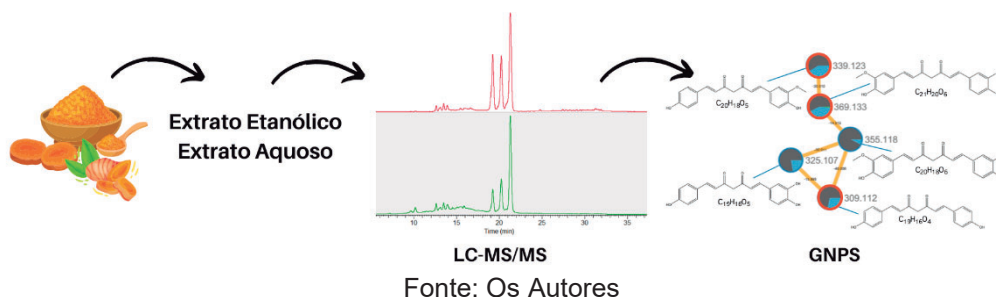
Highlights

Antifungal activity and analysis by molecular networks of ethanolic and aqueous extracts of curcuma longa l. Natural products are widely used in treatment of phytopathogens. Turmeric has compounds with antifungal and antioxidant activity capacity. The GNPS assisted in the determination of the compounds.

Resumo/Abstract

A alta demanda da produção de alimentos no território brasileiro, como por exemplo de frutas, gera preocupação em relação as perdas causadas por doenças pós-colheita causadas por fitopatógenos.¹ Dessa forma, métodos convencionais como a utilização de fungicidas sintéticos tem aumentado e com isso a preocupação com o meio ambiente e a saúde do homem, devido a toxicidade e a resistência fúngica a longo prazo. Métodos alternativos como extratos e óleos essenciais de plantas, como a *Curcuma longa* L. por exemplo, são importantes, uma vez que são menos prejudiciais ao ser humano e ao meio ambiente.² Portanto, o objetivo deste trabalho foi avaliar o potencial antifúngico dos extratos etanólico e aquoso da *C. longa* L. frente aos fungos *Colletotrichum musae*, *Alternaria sp*, *Fusarium sp*, *Fusarium paridorosium* e *Aspergillus flavus*, assim como sugerir por meio de redes moleculares da plataforma GNPS os principais compostos presentes nos extratos. A atividade antifúngica foi realizada pelo método de difusão em meio BDA, a atividade antioxidante foi realizada pelo método de DPPH, e posteriormente foi criado pelo método clássico as redes moleculares na plataforma GNPS. O teste antifúngico apresentou resultados positivos do extrato etanólico frente a *A. flavus*, *A. sp* e *F. sp* e este extrato também foi o que apresentou maior atividade antioxidante, com IC₅₀ = 48,44. Foi possível anotar os compostos curcumina, demetoxicurcumina e bisdemetoxicurcumina, assim como possíveis derivados (Figura 1). Pode-se concluir que o extrato etanólico possui potencial inibitório frente aos fungos testados, e podemos sugerir que os responsáveis pela atividade sejam os compostos anotados.

Figura 1: Fluxograma do trabalho realizado



Referências

- ABDULLAHI, A. et al. Phytochemical profiling and antimicrobial activity of ginger (*Zingiber officinale*) essential oils against important phytopathogens. *Arabian Journal of Chemistry*, v. 13, n. 11, p. 8012-8025, 2020.
- ARASU, M. V. et al. Bioactive potential of *Albizia lebbek* extract against phytopathogens and protective properties on tomato plant against speck disease in greenhouse. *Physiological and Molecular Plant Pathology*, v. 117, p. 101750, 2022.

Agradecimentos/Acknowledgments

UNIOESTE – Centro de Engenharias e Ciências Exatas, Toledo-PR e Programa de Educação Tutorial - PET

Antifungal activity of volatile compounds produced by rhizobacteria against yellow wilt in black pepper (*Piper nigrum* L.)

Lais S. Almeida (PG),¹ Suzana Kaory G. Inoue (PG),¹ Beatriz G. H. Silva (IC),² Pablo Luís B. Figueiredo (PQ),³ Eloisa Helena A. Andrade (PQ),⁴ Massuo Kato (PQ),⁵ Joyce Kelly R. da Silva (PQ).^{1,2*}

lais.almeida@icb.ufpa.br; joycekellys@ufpa.br

¹Programa de Pós-graduação em Biotecnologia, UFPA; ²Programa de Bolsas de Iniciação Científica, CNPq. ³Departamento de Ciências Naturais, UEPA; ⁴Programa de Pós-graduação em Química; ⁵Laboratório de Química de Produtos Naturais, USP.

Key words: bacterial VOCs, 2-ethyl hexanol, Biocontrol, *Fusarium oxysporum* f. sp. *piperis*.

Highlights

The isolated rhizobacteria presented *in vitro* antifungal activity against *Fusarium oxysporum*.

2-Ethyl hexanol was identified by GC-MS as the major bacterial volatile compound.

Resumo/Abstract

Black pepper (*Piper nigrum*) is the most important spice, and Brazil is the second largest producer in the world¹. However, the species is susceptible to diseases caused by fungi of the genus *Fusarium*, such as yellow wilt caused by *F. oxysporum* f. sp. *piperis*. In this context, microorganisms, especially rhizobacteria, can be an eco-friendly alternative for the biocontrol of plant diseases replacing synthetic fungicides. Thus, this work aimed to isolate rhizobacteria with antagonistic activity against the fungus *F. oxysporum* and identify its volatiles organic compounds (VOCs).

Bacterial strains were isolated from soil samples from the *P. nigrum* rhizosphere, and the antagonistic effect was evaluated against *F. oxysporum* on TSA medium by dual culture technique. Each bacterial strain (overnight cultures) was drop-inoculated (10 µl), and, in parallel was placed a mycelial plug (1 cm diameter) from actively growing *F. oxysporum*. Plates were incubated at 28°C, and inhibition of fungal growth was noted after seven days. Petri-plate without bacterial inoculation served as a control. VOCs from bacterial biomass (4.0 g) were extracted by the Likens-Nickerson apparatus and identified by Gas Chromatography-Mass spectrometer (GC-MS). The selected strain PN1-32 showed a mycelial inhibition of 53,1±1,1% (Fig 1).

Figure 1. *In vitro* antagonism effect of rhizobacteria against *F. oxysporum* (A) Dual culture, (B) control plate.

The Gram test showed that the strain has a bacillus morphology and is Gram-positive. The aspect colonies were white, opaque, big, and filamentous. The major and only compound identified was the alcohol 2-Ethyl hexanol (95.03%). This compound has been described in bacteria, yeast, and endophytic fungi.

Table 1. Bacterial volatile composition.

Compound	RI _c	RI _L	%
2-Ethyl hexanol	1023	1030	95.03
RT:29.792	1503		3.46
RT:62.817	2425		0.4

RI_c=calculated retention index, RI_L=Literature Retention Index, RT=Retention time.

In the literature 2-Ethyl hexanol was reported as a potent antifungal chemical against various phytopathogens. 2-ethyl hexanol was the best volatile compound for inhibiting *Fusarium incarnatum*, with a percentage inhibition of 74.28%².

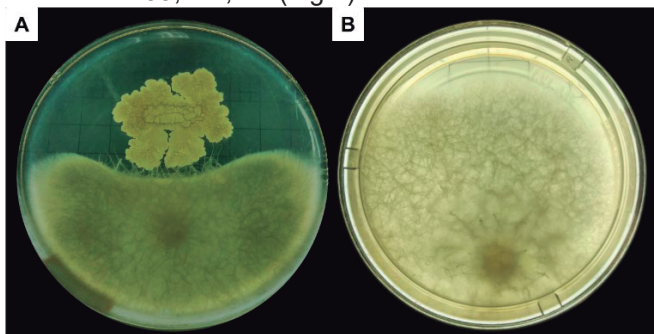
In addition, the culture method in milk agar showed that the strain could produce protease enzymes. Proteases are important hydrolytic enzyme that targets the peptide bonds in the glycosaminopeptide in the fungal cell wall³.

More tests are necessary to identify the bacterial specie. Nevertheless, the results show a significant ecological potential of the rhizobacteria PN1-32 as a biocontrol agent against *Fusarium oxysporum* f. sp. *piperis*.

¹International Pepper Community, 2020.

²Itana, W. et al. Journal of Fungi, 7(1), 46. 2021.

³Ensign, J.C., Wolfe, R.S., 1966. Journal of Bacteriology 91, 524–534.



Agradecimentos/Acknowledgments

We are grateful for Fundação Amazônia de Amparo a Estudos e Pesquisas (FAPESPA), Conselho Nacional de Desenvolvimento Científico e Tecnológico (CNPq), and Coordenação de Aperfeiçoamento de Pessoal de Nível Superior (CAPES) for their financial support.

Anti-*Trypanosoma cruzi* activity of phenylpropanoids from *Baccharis ligustrina*

Matheus L. Silva* (PG),¹ Leila Gimenes (PQ),² Paulete Romoff (PQ),³ Marisi G. Soares (PQ),⁴ Fernanda F. Camilo (PQ),⁵ Erica Valadares de C. Levatti (PQ),⁶ André G. Tempone (PQ),⁶ João Henrique G. Lago (PQ).^{1*}

matheus.lopes@ufabc.edu.br; joao.lago@ufabc.edu.br*

¹Centro de Ciências Naturais e Humanas, UFABC; ²Centro de Pesquisa e Desenvolvimento de Recursos Genéticos Vegetais, IAC; ³Centro de Ciências e Humanidades, UPM; ⁴Instituto de Química, UNIFAL; ⁵Instituto de Ciências Ambientais, Químicas e Farmacêuticas, UNIFESP; ⁶Centro de Parasitologia e Micologia, IAL

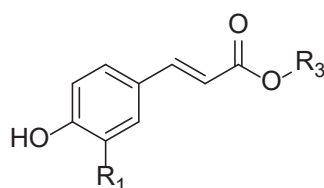
Palavras Chave: *Phenylpropanoids*, *Trypanosoma cruzi*, *Baccharis*, *amastigotes forms*

Highlights

Phenylpropanoids obtained from *Baccharis ligustrina* were evaluated against amastigote forms of parasite *Trypanosoma cruzi*. The results points that the presence of a long-chain alkyl side chain is a crucial chemical moiety for the activity to be observed.

Abstract

In the present work, dried aerial parts of *Baccharis ligustrina* (Asteraceae) were subjected to extraction using an aqueous solution with 1-butyl-3-methylimidazolium bromide (BMImBr) in the microwave assisted extraction (MAE). The obtained extract was successively partitioned using hexane and EtOAc. Using reduced amounts of extracts and efficient chromatographic steps, four acyl C₆C₃ derivatives (*n*-hexacosyl ferulate (3), *n*-hexacosyl (4), *n*-octacosyl (5), and *n*-triacontyl (6) *p*-coumarates) were obtained from hexane phase whereas two C₆C₃ ferulic (1) and *p*-coumaric (2) acids were obtained from EtOAc phase. Isolated phenylpropanoids were evaluated against amastigote forms of parasite *Trypanosoma cruzi*. As result, it was observed that *p*-coumaric and ferulic acids were inactives whereas alkyl derivatives displayed effective concentration at 50% (EC₅₀) values of 6.5 μM (*n*-octacosyl *p*-coumarate), 9.3 μM (*n*-triacontyl *p*-coumarate), 15.7 μM (*n*-hexacosyl *p*-coumarate), and 32.2 μM (*n*-hexacosyl ferulate). All tested compounds displayed reduced toxicity against NCTC cells, with cytotoxic concentration at 50% (CC₅₀) larger than 200 μM. These results suggest that the presence of the alkyl group is crucial for the activity against amastigotes, being potentially intensified with the increase of the side chain. Such an observation would possibly be associated with an increase of these esters lipophilicity in terms of log P_{ow} values when in comparison with free *p*-coumaric and ferulic acids. This characteristic may cause such compounds to acquire an amphiphilic character, thus allowing them to cross the cell membrane and reach the parasites inside the cells. These results allow us to suggest, in the future, the performance of studies on the structure/activity relationship with *p*-coumaric acid esters containing different alkyl groups followed by the evaluation of activity against amastigotes of *T. cruzi*.



- 1 R₁ = OMe, R₂ = H
 2 R₁ = OMe, R₂ = n-C
 3 R₁ = H, R₂ = n-C₂₆H₅₃
 4 R₁ = H, R₂ = n-C₂₆H₅₃
 5 R₁ = H, R₂ = n-C₂₈H₅₇
 6 R₁ = H, R₂ = n-C₃₀H₆₁

Acknowledgments

This work was funded by grants and fellowships provided by Fundação de Amparo a Pesquisa do Estado de São Paulo (FAPESP – project 2021/02789-7). We also thank CNPq scientific research award to J. H. G. L. and A. G. T. and CAPES to fellow M. L. S..

Antitrypanosomal effect of enyne acetogenins from *Porcelia macrocarpa* involves increase in ATP and ROS levels

Fernanda Thevenard (PG),¹ Dalete Christine S. Souza (PG),¹ Thais A. Costa-Silva (PQ),² André G. Tempone (PQ),² João Henrique G. Lago (PQ).¹

joao.lago@ufabc.edu.br;

¹Centro de Ciências Humanas e Naturais, UFABC; ²Centro de Parasitologia e Micologia, Instituto Adolfo Lutz

Keywords: *Porcelia macrocarpa*, *Trypanosoma cruzi*, Acetogenins, ATP, ROS

Highlights

Four new enyne acetogenins (**1** – **4**) have been identified in a bioactive fraction obtained from the MeOH extract of *Porcelia macrocarpa* fruit peels. Antitrypanosomal activity of these compounds is related to increase in ATP and ROS levels and reduction of intracellular calcium.

Abstract

Natural products, including those from plants, offer a wide range of chemical structures that may be used for drug development.¹ Chagas disease, resulting from *Trypanosoma cruzi* infection, may lead to a fatal chronic phase which affects thousands worldwide. Current treatment is limited to two pharmaceuticals, benznidazole and nifurtimox^{2,3}, which further exemplifies the urgency for new drugs. Bioassay guided fractionation of the MeOH extract of *P. macrocarpa* fruit peels led to a bioactive fraction I with EC₅₀ values of 4.9 and 2.4 µg/mL against trypomastigotes and amastigotes, respectively, and CC₅₀ > 200 µg/mL against NCTC cells. ¹H and ¹³C NMR analysis, as well as LC/ESI-HRMS demonstrated that fraction I consists of mixture of four new enyne acetogenins **1** – **4** (Figure 1) where the main differences are presence or lack of a terminal double bond as well as a shorter or longer side chain (C₁₈ or C₂₀). Selectivity indexed for both forms of the parasite were higher than those determined for the standard drug benznidazole. The mechanism of action assays for trypomastigote forms showed that fraction I did not affect the parasite cell membrane but caused decrease in intracellular calcium levels. Further investigation showed no acidocalcisome alkalization, which corroborates with the Ca²⁺ levels observed, as well as no effect of the mitochondrial membrane potential, both organelles important for maintaining calcium homeostasis.^{4,5} A great increase in ATP and ROS levels (Figures 2A and 2B, respectively) may indicate death due to oxidative stress.

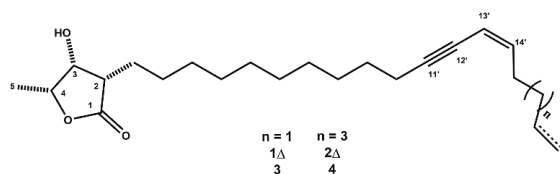


Figure 1 - Structures of compounds **1** – **4**, characterized in fraction I by NMR and ESI-HRMS

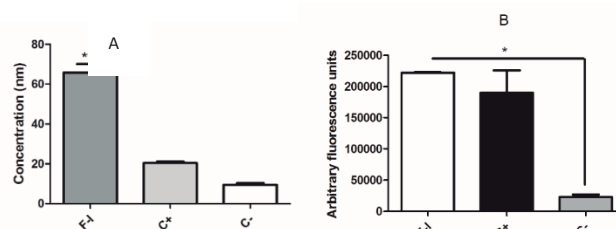


Figure 2 – A) ATP levels after treatment with fraction I, positive control (c+); parasites treated with CCCP; B) ROS levels after treatment for 2 h (H2DCFA dye), parasites treated with azide as positive control (c+). Untreated parasites were used as negative control (c-).

References: ¹Thomford, N. E. *et al. Int. J. Mol. Sci.* **2022**, 19, 1578.;²World Health Organization, **2022**; ³Drugs for neglected diseases *initiative*, **2023**; ⁴RefDocampo, R. Huang, G. *Cell Calcium.* **2015**, 57, 194-202; ⁵Kaczanowski, S, *et al. Parasit. Vectors.* **2011**, 4, 44.

Acknowledgments

FAPESP, CAPES and CNPq

46^o Reunião Anual da Sociedade Brasileira de Química: "Química: Ligando ciências e neutralizando desigualdades"

Application of metabolomics tools to investigation of benzodiazepine alkaloids derivatives from ferruginous cave-dwelling bacteria.

Natália Naomi Kato (PG),¹ Aline Figueredo Cardoso (PQ),² José Augusto Pires Bitencourt (PQ),² Norberto Peporine Lopes (PQ)^{1*}.

nataliakato@usp.br; npelopes@fcrp.usp.br

¹Núcleo de Pesquisa de Produtos Naturais e Sintéticos, Faculdade de Ciências Farmacêuticas de Ribeirão Preto, USP; ²Instituto Tecnológico da Vale de Desenvolvimento Sustentável, ITVDS.

Palavras Chave: *Mass spectrometry; Metabolomics; Caves; Chemical ecology; Metagenomics*

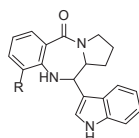
Highlights

Bacterial strains were isolated from ferruginous cave and aphotic zone.

Benzodiazepine alkaloids and cyclopeptides derivatives were the main classes annotated by tools in the GNPS platform.

Abstract

Caves are underground ecosystems hosting the heterogeneous microbial community, surviving even in low organic matter substrates and aphotic environments. Molecular analysis and Next-Generation Sequencing advances allowed better taxonomic classification in an ecosystem and promoted studies in cave microbiomes, revealing magnificent microbial diversity and their ecological functions. Despite the microbial richness and abundance already described in the literature, there are limited chemical studies and their biological effects. Some cave-dwelling bacteria are producers of antibiotic and cytotoxic compounds and may be the key to new drug discovery. In this way, this research aimed to determine the chemical profile of bacterial strains isolated from a ferruginous cave localized in the Carajás National Forest (PA) through mass spectrometry analysis and metabolomics tools. Sediment samples were collected from the aphotic zone with a high concentration of iron ore and low organic content. The thirteen bacterial strains were cultivated and isolated in the TSA (Tryptic Soy Agar) solid medium, also used for fermentation in a liquid medium incubated for a week at 28°C, under agitation in the shaker. The metabolites from the liquid medium were obtained by liquid-liquid partition using ethyl acetate as a solvent. The data acquisition was realized by High-Performance Liquid Chromatography coupled with Mass Spectrometry (HPLC-MS/MS) for untargeted analysis aiming at the chemical diversity associated with bacterial strains isolated from ferruginous caves. All spectral data were processed using the Global Natural Products Social Molecular Network (GNPS) platform for molecular network analysis. The ionized metabolites from crude extracts were organized into clusters according to their spectral similarity and compared to the GNPS library. Among the metabolites annotated, the high-intensity peaks correspond to the benzodiazepine alkaloids derivatives, which are produced from eight isolated bacteria. Others chemical classes were detected in the samples, such as alkaloids and cyclopeptide derivatives, corresponding to low-intensity peaks. This set of bacteria presented different chemical profiles inside the same chemical groups and a potential source of new active compounds.



Lukoseviciute, L., Lebedeva, J., & Kuisiene, N. (2021). Diversity of Polyketide Synthases and Nonribosomal Peptide Synthetases Revealed Through Metagenomic Analysis of a Deep Oligotrophic Cave. *Microbial Ecology*, 81(1), 110–121. <https://doi.org/10.1007/s00248-020-01554-1>

Ghosh, S., Kuisiene, N., & Cheeptham, N. (2017). The cave microbiome as a source for drug discovery: Reality or pipe dream? *Biochemical Pharmacology*, 134, 18–34. <https://doi.org/10.1016/j.bcp.2016.11.018>

Acknowledgments

The authors would like to thank the financial agencies: FAPESP (2022/05378-0), CAPES, CNPq for the project grant and fellowship support.

As metilas da resistência: um arsenal perdido?

Maria Clara S. Aguiar (PG)¹, Marcelo M. Freitas (PG)², Carlos A. Freitas (PG)², João B. Fernandes (PQ)¹, Renato L. Carneiro (PQ)¹, Maria Fátima G.F. da Silva (PQ)¹, Arlindo L. Boiça-Junior (PQ)², Moacir R. Forim (PQ)¹

mforim@ufscar.br; clarasantanaaguiar@gmail.com

¹Departamento de Química, UFSCar; ²Departamento de Ciência da Produção Agrícola, UNESP.

Palavras Chave: (*Glycine max*, Mecanismos de resistência; *Spodoptera cosmioides*, Análises metabolômica, Supressão rotas biossintéticas).

Highlights

The wild genotype from *Glycine max* presented a resistance mechanism against *Spodoptera cosmioides* (Lepidoptera) using methylated flavonoids. We did not identify this mechanism in commercial cultivars of soybean.

Resumo/Abstract

As plantas desenvolveram mecanismos de adaptação aos estresses biótico e abiótico para superar a sua imobilidade. Estas respostas evolutivas, que podem ser pré-existentes ou induzidas, vão desde a formação de estruturas morfológicas a produção de novas moléculas. Dentre as moléculas de defesa sintetizadas, os flavonoides compõem uma classe química que auxilia as plantas a se adaptarem ao ambiente e responderem a estímulos externos. Contudo, o empenho em produzir cultivares com maior rendimento e melhoria nas características agrônômicas pode interferir na capacidade de alguns genótipos em produzir substâncias de defesa. Afinal, a produção dessas substâncias é controlada pela carga genética, variável que pode ser alterada pelas técnicas de melhoramento das plantas.

Neste contexto, um estudo de caso que merece destaque é o da soja, uma leguminosa de importância mundial como fonte de proteínas, óleo e micronutrientes. Na década de 1990, a Embrapa Soja já havia observado que mais de 60% dos cultivares de soja estudados não apresentavam a rutina, molécula associada à resistência a insetos desfolhadores. Assim, cabe o questionamento: o desenvolvimento de cultivares de soja com características comerciais favoráveis interferiria na capacidade de defesa das plantas, aumentando a necessidade do uso de agroquímicos?

Com base neste questionamento, avaliamos como as técnicas de transgenia e melhoramento genético podem interferir na resposta da soja à ação de insetos herbívoros. Para isto, utilizamos dez cultivares de soja classificados em transgênicos, com melhoramento genético e não comercial. Avaliamos a resposta das plantas a herbivoria por lagartas de *Spodoptera cosmioides* por meio de análises metabolômicas não direcionadas.

Os resultados destacam que em condições de cultivo normais, o cultivar não comercial apresentou uma maior indução de flavonoides metilados e maior diversidade de metabólitos. Além disso, sob estresse biótico, este cultivar foi considerado resistente à *S. cosmioides*, pelo menor consumo foliar. As análises multivariadas demonstraram que após o estresse ocorreu um aumento na biossíntese das mesmas moléculas metiladas, com a ativação da rota dos fenilpropanoides. Por outro lado, os cultivares transgênicos e com melhoramento genético apresentaram maior acúmulo de flavonoides glicosilados não metilados como uma das respostas à herbivoria. Estas moléculas auxiliam no crescimento das folhas, na formação e na morfologia das vagens, além de promoverem a proteção dos tecidos - características desejadas pelos melhoristas para o desenvolvimento de novos cultivares. Entretanto, o acúmulo destas substâncias nas folhas pode ser atrativo para a alimentação dos insetos, fato observado nos ensaios de preferência alimentar e que sugerem uma maior suscetibilidade destes cultivares à *S. cosmioides*. Cabe destacar que, dentre os cultivares transgênicos e submetidos ao melhoramento genético, após a ação da herbivoria, dois cultivares mobilizaram seu arsenal químico para a biossíntese de flavonoides aglicônicos, dentre eles alguns flavonoides metilados, e apresentaram menor consumo foliar pelas lagartas de *S. cosmioides*. Assim, estes dados sugerem que as alterações promovidas pelos melhoristas podem ocasionar em cultivares mais susceptíveis à *S. cosmioides* pela redução na biossíntese de flavonoides metilados associados à mecanismos de resistência.

Agradecimentos/Acknowledgments

Os autores agradecem ao CNPq, CAPES e FAPESP pelo suporte financeiro concedido.

Área: **QPN**

AVALIAÇÃO DA ATIVIDADE ANTI-HELMÍNTICA *IN VITRO* E *IN VIVO* DO DEIDRODIEUGENOL B ISOLADO DE *Nectandra leucantha* (LAURACEAE)

Vinicius C. Rocha (PG),¹ Ana C. Mengarda (PG)², Josué de Moraes (PQ),² João Henrique G. Lago (PQ).³
vc.rocha@unifesp.br

¹Departamento de Química, Universidade Federal de São Paulo – UNIFESP; ²Núcleo de Pesquisa em Doenças Negligenciadas (NPDN), Universidade de Guarulhos – UnG; ³Centro de Ciências Naturais e Humanas, Universidade Federal do ABC – UFABC

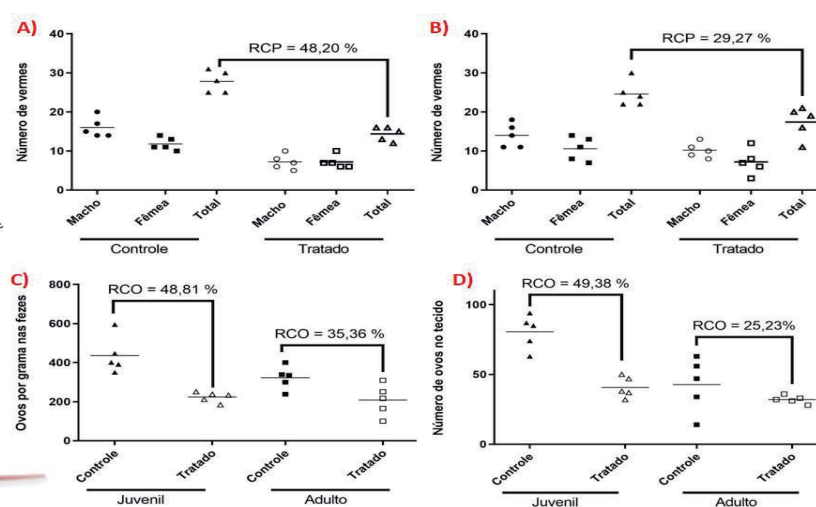
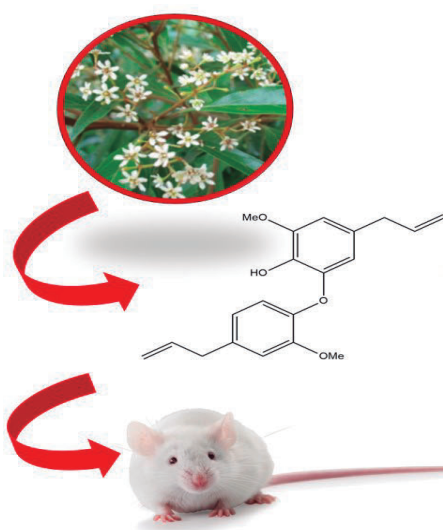
Key-Words: Schistosomiasis, *Schistosoma mansoni*, *Nectandra leucantha*, dehydrodieugenol B.

Highlights

EVALUATION OF *IN VITRO* AND *IN VIVO* ANTIHELMTIC ACTIVITY OF DEHYDRODIEUGENOL B ISOLATED FROM *Nectandra leucantha* (LAURACEAE). Dehydrodieugenol B, a neolignan isolated from *Nectandra leucantha* (Lauraceae), displayed *in vitro* and *in vivo* activity against *Schistosoma mansoni*.

Resumo

Esquistossomose é uma doença negligenciada que afeta mais 200 milhões de pessoas em todo o mundo. Sendo o praziquantel o único fármaco disponível para tratamento desta doença, faz-se necessária a busca por novas entidades bioativas. Considerando a ampla biodiversidade brasileira, o presente estudo teve como objetivo inicial avaliar a atividade anti-helmíntica do extrato hexânico das folhas de *Nectandra leucantha*, o qual apresentou 100% de morte do parasito a 300 µg/mL. Frente a esse resultado, foi realizado um estudo químico totalmente biomonitorado o que permitiu o isolamento da neolignana deidrodieugenol B, cuja identificação estrutural foi realizada via análise dos espectros de RMN e de massas. Posteriormente, foi avaliada a atividade anti-*S. mansoni in vitro* do deidrodieugenol B cujo valor de CE₅₀ foi determinado como 31,9 µM, com reduzida toxicidade para *Vero cells* (CC₅₀ > 100 µM). Como controle positivo, foi utilizado o fármaco praziquantel (CE₅₀ = 0,7 µM e CC₅₀ > 100 µM). Sequencialmente, foi avaliada a eficácia da substância em modelo murino (*in vivo*) sendo a análise de eficácia terapêutica baseada na carga parasitária e produção de ovos nas fezes e no tecido do intestino do animal tratado. Como resultado, nos animais albergando vermes adultos foi detectada redução de vermes de 29,27%, redução de ovos nas fezes de 35,36% (método Kato Katz) enquanto que a redução de ovos imaturos de 25,23%, por meio da avaliação por oograma (análise morfológica por microscopia). Animais albergando vermes na fase juvenil, a redução da carga parasitária (RCP), da carga de ovos (RCO) nas fezes e nos tecidos foram mais significativas, apresentando valores de 48,20%, 48,81% e 49,38%, respectivamente. Assim os resultados obtidos podem ser considerados promissores no que tange a ação anti-helmíntica do deidrodieugenol B, em especial pela destacada ação *in vivo*, e podem contribuir para o desenvolvimento de novos protótipos moleculares para o avanço na produção de drogas para o tratamento dessa enfermidade.



Legenda: A) Vermes juvenil; B) Vermes adultos; C) Ovos nas fezes; D) Ovos no tecido do intestino.

Agradecimentos

FAPESP, CNPq, CAPES, UFABC, UNIFESP, NPDN

46ª Reunião Anual da Sociedade Brasileira de Química: "Química: Ligando ciências e neutralizando desigualdades"

Avaliação da atividade anti-*Trypanosoma cruzi* de lignanas dibenzilbutirolactólicas dos galhos de *Piper truncatum*

Marina de M. Gonçalves (PG),^{1*} Erica Valadares de C. Levatti (PQ),² Maiara A. de Oliveira (PG),² Guilherme M. Antar (PQ),³ André G. Tempone (PQ),² João Henrique G. Lago (PQ).¹
marina.monroe@ufabc.edu.br

¹Centro de Ciências Naturais e Humanas, Universidade Federal do ABC (UFABC); ²Centro de Parasitologia e Micologia, Instituto Adolfo Lutz (IAL); ³Departamento do Ciências Agrárias e Biológicas da Universidade Federal do Espírito Santo (UFES)

Palavras Chave: Lignanas dibenzilbutirolactólicas, *Piper truncatum*, doença de Chagas

Highlights

Evaluation of the anti-*T. cruzi* activity of dibenzylbutyrolactolic lignans from twigs of *P. truncatum*. This work reports the isolation and chemical characterization of lignans **1 – 6** and their activities against the parasite *T. cruzi*.

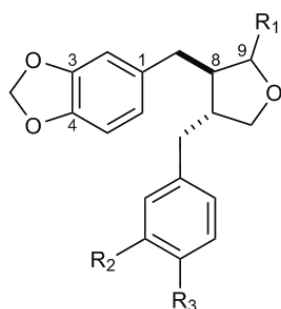
Resumo

A doença de Chagas possui elevada taxa de mortalidade e o arsenal terapêutico voltado para o tratamento desta moléstia é escasso, estando limitado ao benznidazol que apresenta baixa eficácia e diversos efeitos colaterais. Como parte do nosso trabalho contínuo visando a busca de protótipos naturais bioativos, foi observado que o extrato hexânico dos galhos de *P. truncatum* mostrou atividade frente as formas tripomastigotas de *T. cruzi*. Frente a esse resultado, o mesmo foi submetido a fracionamento cromatográfico fornecendo oito grupos (A – H). Após a avaliação da atividade anti-*T. cruzi* destes, foi possível constatar que todos os grupos, com exceção do H, se mostraram bioativos. Os grupos E e F foram submetidos a diferentes processos fracionamentos (sílica gel 60, Sephadex LH-20 e CLAE) permitindo o isolamento de seis compostos (**1 – 6**). Após as análises de espectros RMN uni e bidimensionais, espectros de massas de alta resolução e rotação óptica específica, foi possível caracterizar seis lignanas dibenzilbutirolactólicas: cubebina (**1**), (-)-9 α -O-metilcubebina (**2**), (+)-9 β -O-metilcubebina (**3**), 3',4'-dimetoxi-3,4-desmetilenodioxicubebina (**4**), truncatina A (**5**) e truncatina B (**6**), sendo as duas últimas inéditas na literatura. Os compostos isolados foram submetidos a avaliação da atividade anti-*T. cruzi* para formas tripomastigotas (CI₅₀), além da citotoxicidade frente a células NCTC (CC₅₀), cujos resultados estão apresentados na tabela 1.

Tabela 1 - CI₅₀ e CC₅₀ dos compostos **1 – 6**

compostos	CI ₅₀ (μM)	CC ₅₀ (μM)
1	41,6 ± 23,8	88,4 ± 0,2
2	NA	>200
3	21,0 ± 13,3	>200
4	NA	>200
5	NA	26,0 ± 4,2
6	39,6 ± 14,0	115,4 ± 7,6
BNZ	11,6 ± 1,0	>200

NA: Não ativo; BNZ: Benznidazol



- | | |
|--|--|
| 1. R ₁ : ~ OH
R ₂ = R ₃ : OCH ₂ O | 4. R ₁ : ~ OH
R ₂ = R ₃ : OCH ₃ |
| 2. R ₁ : α-OCH ₃
R ₂ = R ₃ : OCH ₂ O | 5. R ₁ : α-OCH ₃
R ₂ = R ₃ : OCH ₃ |
| 3. R ₁ : β-OCH ₃
R ₂ = R ₃ : OCH ₂ O | 6. R ₁ : β-OCH ₃
R ₂ = R ₃ : OCH ₃ |

Dentre os compostos testados, **1**, **3** e **6** foram ativos para as formas tripomastigotas do parasita e, com exceção de **1**, apresentaram reduzida toxicidade frente a células NCTC. Considerando-se as estruturas moleculares de **1 – 6** foi possível inferir que a presença do sistema metilenodioxílico em R₂ e R₃ (compostos **1 – 3**) desempenha um papel importante para a atividade anti-*T. cruzi*, visto que os compostos contendo grupos metoxílicos em R₂ e R₃ (**4 – 6**) se mostraram menos ativos. Além disso, a configuração do grupo metoxílico em C-9 também se mostrou crucial para a atividade, uma vez que somente os compostos **3** e **6** (C-8/C-9 – *cis*) apresentaram potencial frente a *T. cruzi*, enquanto os compostos **2** e **5** (C-8/C-9- *trans*) foram inativos. Finalmente, a possibilidade dos compostos **2** e **3/5** e **6** serem artefatos foi excluída, uma vez que foi detectada a presença destes metabólitos no extrato hexânico bruto via EM de alta resolução.

Agradecimentos

UFABC, CAPES, CNPq e FAPESP.

Avaliação da capacidade antioxidante e potencial fotoprotetor do extrato etanólico da casca da Jabuticaba (*Plinia cauliflora*)

Rafael Luis Barros de Oliveira (PG),¹ Messias de Oliveira Silva (PG),¹ Monika B. S. Oliveira (PQ)¹, Iara B. Valentim (PQ)², Marília Oliveira Fonseca Goulart (PQ),¹ Jadriane de Almeida Xavier (PQ)^{1*}

rafael.oliveira@iqb.ufal.br; jadrianexavier@iqb.ufal.br

¹ Instituto de Química e Biotecnologia, UFAL; ² Instituto Federal de Alagoas, IFAL – Maceió AL

Palavras Chave: Antioxidante, Fotoproteção, Jabuticaba, Espécies reativas

Highlights

The ethanolic extract of jabuticaba (EECJ) bark showed activity scavenging of HOCl and O₂^{•-}. EECJ showed SPF ≥6, which is the minimum limit established by ANVISA for a material to be considered photoprotective.

Resumo

A exposição crônica à radiação UV tem efeitos pronunciados sobre a pele, induzindo o envelhecimento prematuro e o desenvolvimento de câncer. O uso de protetores solares é a alternativa mais eficaz contra os efeitos nocivos causados pelos raios UV, no entanto um dos filtros UV mais utilizados em produtos para a pele, a benzofenona, tem sido associada à toxicidade humana e ao ambiente aquático. Desse modo, o extrato de jabuticaba foi avaliado frente ao seu potencial antioxidante e fotoprotetor, visando o desenvolvimento de um produto multifuncional para a pele. Os resultados da capacidade antioxidante estão expressos na Tabela 1, diferentes ensaios foram utilizados a fim de obter o perfil antioxidante do extrato. O Fator de Proteção Solar (FPS) do extrato foi determinado a partir de soluções diluídas nas concentrações de 0,25 a 8,0 mg mL⁻¹, utilizando o método espectrofotométrico *in vitro* desenvolvido por Mansur e colaboradores, 1986.² Os resultados se encontram na Tabela 2.

Tabela 1. Conteúdo Total de Compostos Fenólicos (CTF), Capacidade antioxidante sequestradora de radicais (DPPH^{*}), redutora de ferro (FRAP) e captura do ânion radical superóxido (O₂^{•-}) e do ácido hipocloroso (HOCl).

Extrato	CTF (mg de EAG/g de extrato seco)	DPPH [*] (IC ₅₀)	FRAP (μmol de ET/g de extrato seco)	O ₂ ^{•-} (%Inibição)	HOCl (%Inibição)
EECJ	104,4 ± 0,8	30,1 ± 0,9	210,2 ± 1,2	17,9 ± 3,9	65,9 ± 1,5

CTF: Conteúdo de fenóis totais; EAG: Equivalentes de ácido gálico; ET: Equivalentes de Trolox, EECJ: Extrato Etanólico da Casca da Jabuticaba.

Tabela 2. FPS das diluições do extrato etanólico da casca da Jabuticaba.

Amostra	Diluições (mg mL ⁻¹)					
	0,25	0,5	1,0	2,0	4,0	8,0
EECJ	5,8 ± 0,1	10,8 ± 0,1	21,3 ± 0,5	35,0 ± 0,9	36,4 ± 1,6	35,9 ± 2,1

EECJ: Extrato Etanólico da Casca da Jabuticaba

Os resultados mostram que o EECJ apresentou propriedades antioxidantes, sendo capaz de sequestrar espécies reativas de importância biológica como o O₂^{•-} e o HOCl. Além de apresentar FPS ≥ 6 nas concentrações de 0,5 a 8,0 mg mL⁻¹, que é o valor mínimo estabelecido pela ANVISA. As formulações contendo o extrato estão sendo elaboradas e o FPS das formulações também serão calculados. A utilização de princípios ativos em produtos de cuidado com a pele que sejam seguros e atribuam propriedades multifuncionais tem sido requisitada cada vez mais e o extrato da casca da jabuticaba tem se mostrado bastante promissor.

¹David Fivenson, MD. Sunscreens: UV filters to protect us: Part 2-Increasing awareness of UV filters and their potential toxicities to us and our environment, v. 7, n. 1, p. 45-69, 2021.

²Mansur, J. D. S. et al., An. Bras. Dermatol, 61, (1986), 121 – 124.

Agradecimentos/Acknowledgments

UFAL, CAPES, CNPQ and FAPCAL.

Área: QPN

Avaliação do potencial antiparasitário de alcaloides isolados de *Porcelia ponderosa* (Annonaceae)

Carlos H. Totini (PG)¹; Beatriz A. de Andrade (PG)²; Emerson A. Oliveira (PQ)³; Érica V. C. Levatti (PQ)²; André G. Tempone (PQ)²; João Henrique G. Lago (PQ)^{1*}

carlos.totini@ufabc.edu.br

¹Centro de Ciências Naturais e Humanas (CCNH), Universidade Federal do ABC, Santo André – SP; ²Centro de Parasitologia e Micologia, Instituto Adolfo Lutz (IAL); ³Instituto de Ciências Ambientais, Químicas e Farmacêuticas, Universidade Federal de São Paulo, SP.

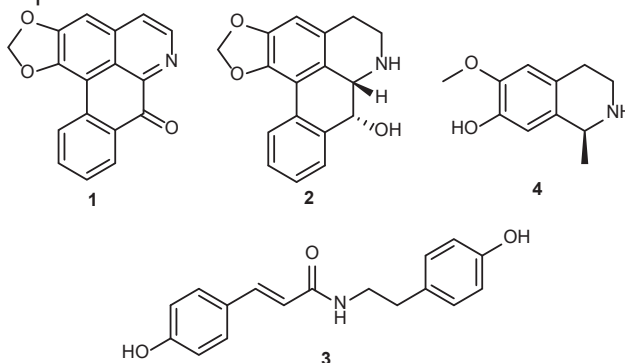
Palavras Chave: Atividade Anti-*T. cruzi*; Propriedades farmacocinéticas *in silico*; Alcaloides aporfínicos; *Porcelia ponderosa*.

Highlights

Antiparasitic potential of isolated alkaloids from *Porcelia ponderosa*. Alkaloidal extract of roots from *Porcelia ponderosa* displayed activity against *T. cruzi* and afforded three alkaloids, liriodenine (**1**), norushinsunine (**2**), *N-trans-p-coumaroyl* tiramine (**3**) and (-)-6-methoxy-salsolinol (**4**).

Resumo

A doença de Chagas, causada pelo parasita *Trypanosoma cruzi*, é uma enfermidade considerada endêmica no território nacional e, atualmente, possui escassas fontes terapêuticas para o seu tratamento¹. Dentro de produtos naturais, a busca por novos compostos com ação anti-*T. cruzi* tem evidenciado os resultados obtidos pela classe dos alcaloides². Nesse contexto, o presente trabalho descreve a investigação do potencial antiparasitário de alcaloides obtidos das raízes de *Porcelia ponderosa*. Para esse estudo, foi realizada a extração com MeOH seguida da extração ácido-base para obtenção da fase alcaloídica. Essa fase foi purificada empregando os processos de separação por cromatografia em coluna (SiO₂) e UHPLC (C18), resultando em três alcaloide: liriodenina (**1**), norushinsunina (**2**) e (-)-6-metóxi-salsolinol (**4**), e uma amida fenólica: *N-trans-p-coumaroil* tiramina (**3**), que tiveram suas estruturas definidas por espectros de RMN uni- e bidimensionais e espectros de massas.



Os alcaloides **1** e **2** foram descritas previamente para a espécie *P. macrocarpa*³ bem como em outros gêneros de Annonaceae, sendo essa a primeira ocorrência em *P. ponderosa*. Por outro lado, essa é a primeira descrição das substâncias **3** e **4** no gênero *Porcelia*. Do ponto de vista quimiotaxonômico a ocorrência desses compostos se encontrava, até então, restrita em gêneros taxonomicamente distantes⁶ do gênero *Porcelia* tais como *Polyalthia suberosa*⁵ e *Bocaeopsis canescens*⁴, respectivamente. Visto que a fase alcaloídica resultou na morte de 100% de tripomastigotas de *T. cruzi* a 300 µg/mL, os alcaloides **1** – **4** foram avaliados individualmente quanto a esse potencial. Assim, o composto **1** mostrou CE₅₀ de 41,4 ± 16,7 µM contra as formas tripomastigotas do parasita ao passo que os demais se mostraram inativos. Do ponto de vista de *drug-likeness*, os dados *in silico* obtidos por meio da plataforma SwissADME mostraram que o composto **1** apresenta excelente aderência quanto as propriedades físico-químicas previstas inclusive quanto aos filtros de Lipinski, Ghose e Veber, apresentam uma boa absorção no TGI e não demonstram nenhum alerta de PAINS, indicando que o composto **1** pode ser considerado um bom candidato para o desenvolvimento de futuros protótipos para o desenvolvimento de fármacos para o tratamento da Doença de Chagas.

Referências: ¹Jurberg, J. *et al.*, FIOCRUZ, 2014; ²Fernández, L.R. *et al.*, *Curr Clin Microbiol Rep.* 2021, 8(2), 68-86; ³Chaves, M.H. *et al.*, *J Nat Prod.* 2001, 64(2), 240-242; ⁴Soares E.R. *et al.*, *Biochem Syst Ecol.* 2019, 85, 76-78; ⁵Tuchinda P. *et al.*, *Phytochemistry.* 2000, 53, 1079-1082; ⁶Guo, X. *et al.*, *Scientific Reports* 2017, 7(7323), 1-11.

Agradecimentos

UFABC, IAL, CAPES, CNPq e FAPESP.

46ª Reunião Anual da Sociedade Brasileira de Química: "Química: Ligando ciências e neutralizando desigualdades"

Bioprospecting diketopiperazines produced by the endophytic fungus *Penicillium setosum* CMLD 18

Cláudia M. da S. C. de Oliveira (PG),^{1*} Milena P. S. Rivero (PG),¹ Milena C. Bassicheto (IC),² Ana C. de Carvalho (PQ),³ Gilvan F. da Silva (PQ),⁴ Thiago A. M. Veiga (PQ),¹ Lívia S. de Medeiros (PQ)¹.

coliveira08@unifesp.br; livia.soman@unifesp.br

¹Instituto de Ciências Ambientais, Químicas e Farmacêuticas, UNIFESP; ²Laboratório de Química Bio-Orgânica Otto Richard Gottlieb (LaBiORG); ³The Novo Nordisk Foundation Center for Biosustainability; ⁴Embrapa Amazônia Ocidental.

Keywords: *Penicillium setosum*, diketopiperazines, dereplication, antimicrobials, leukemia.

Highlights

Diketopiperazines are produced by the fungus *P. setosum* and antileukemia activity has been reported for Fellutanine C. Considering the biological potential of this metabolite sub-class, this work focuses on the discovery of other diketopiperazines biosynthesized by the strain (known or still unknown) with anticancer activity.

Abstract

The genus *Penicillium* represents one of the largest sources of all known fungal chemodiversity. Therefore represents a promising source for the discovery of new therapeutic agents through the chemical and biological prospecting of its secondary metabolome. Interestingly, the occurrence of cryptic biosynthetic gene clusters in fungi suggests that a large part of the natural products, likely to be produced by the genus, has not yet been accessed. Fortunately, many of these clusters responsible for the production of secondary metabolites are susceptible to biotic and abiotic environmental modifications to which microorganisms are exposed and may promote the production of compounds with pharmacological activities, as a chemical and biological response. In a previous work performed in our research group (LaBiORG) we identified the species *Penicillium setosum* CMLD 18, an endophytic fungus isolated from the Atlantic Forest region plant, *Swinglea glutinosa*. This microorganism was described only in 2019, and its metabolism is still poorly understood in the chemical, genomic and biological scope. Diketopiperazines (DKPs) represents a class of bioactive substances commonly produced by fungi, with diverse biological activities, including antibiotic, cytotoxic, and antitumor. Recently, the identification of a diketopiperazine produced by the endophytic fungus *P. setosum*, CMLD18, Fellutanine C, was reported. It has been confirmed its cytotoxic effects, being the first report of antileukemic activity of this diketopiperazine so far¹. Therefore, this work aims to explore the metabolic pathways for the production of other cytotoxic DKPs compounds produced by *P. setosum*. The growth of the strain applying the variation of nutritional media culture was performed, by means of the OSMAC (One Strain Many Compounds) technique². The micro extracts were analyzed by high-performance liquid chromatography coupled to high-performance mass spectrometry (HPLC-HRMS). The molecular dereplication is being performed through manual inspection, the use of in silico metabolomic tools, as well as data analysis in GNPS platform³. According to the obtained annotations, it was possible to identify and widely explore potentially known and new diketopiperazines, as well as still unknown secondary metabolites produced by *P. setosum*. Isolation of the target compounds will be performed by chromatographic techniques, with sequential structural determination via nuclear resonance spectroscopic data (NMR1 and 2D) as well as HRMS/MS data. To investigate the biological potential of the target compounds, they will be submitted to antibiosis tests against multi-resistant bacteria and cytotoxicity tests on human leukemia cells.

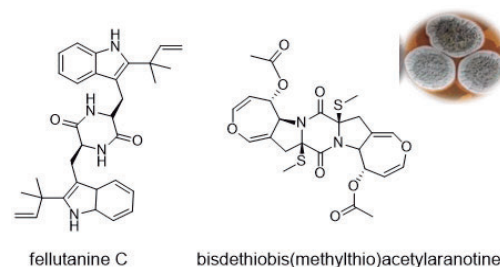


Figure 1: Diketopiperazine compounds isolated from *Penicillium setosum*¹.

References: 1. de Carvalho, A. C.; and Veiga, T. A. M.; *Metabolites*, 13., 1-19 (2022). 2. Björn, B. H. and Zeeck, A.; *ChemBioChem*, 3., 619-627 (2002). 3. Wang, M., Carver, J., Phelan, V. et al. *Nat. Biotechnol.*, 34., 828–837 (2016).

Acknowledgments

Capes 88887.671409/2022-00; FAPESP Project 2020/08270-0

Biosynthetic potential of the mushroom *Gymnopilus imperialis* - A metabolomic and genomic approach

Lhais Caldas^{*1,4} (PG), Douglas Soares² (PG), Nelson Menoli³ (PQ), Cassius Stevani² (PQ), Jorge Navarro⁴ (PQ), Jérôme Collemare⁴ (PQ), Patrícia Sartorelli¹ (PQ).

lhais.caldas@unifesp.br*; psartorelli@unifesp.br

¹Instituto de Ciências Ambientais, Químicas e Farmacêuticas, Universidade Federal de São Paulo, 09972-270, Diadema, SP, Brazil; ²Departamento de Química Fundamental, Instituto de Química, Universidade de São Paulo, São Paulo, Brazil; ³Instituto Federal de Educação, Ciência e Tecnologia de São Paulo, Campus São Paulo (SPO), Departamento de Ciências da Natureza e Matemática (DCM), Subarea de Biologia (SAB), São Paulo, SP, Brazil; ⁴Westerdijk Fungal Biodiversity Institute, Uppsalalaan 8, 3584 CT Utrecht, The Netherlands.

Keywords: Mushroom, metabolomics, genomics, molecular networking, biosynthesis.

Highlights

Retro-biosynthetic approach on *Gymnopilus imperialis* extracts based on metabolomics and genomics techniques to assign biosynthetic gene clusters of styrylpyrones and terpenoids.

Resumo/Abstract

Gymnopilus consists of a widely distributed genus of mushroom-forming fungi, especially in tropical regions of the world. Literature on *Gymnopilus* representatives reports the presence of oligoisoprenoids, and styrylpyrones. Considering the large number of secondary metabolites that basidiomycetes might contain, dereplication tools such as GNPS (Global Natural Products Social Molecular Networking), have become important in prospecting metabolites, saving time and work on isolation and characterization of natural products. Thus, this work aims to dereplicate the extracts of *G. imperialis* with the aid of GNPS to annotate metabolites, and based on the annotated molecules, to use genomics, metabolomics, and molecular biology to identify gene clusters related to the biosynthesis of the annotated molecules through a “retro-biosynthetic” approach. So, the basidiomycetes (50g) were freeze-dried, grinded and extracted with methanol. After evaporation of the solvent under reduced pressure, the obtained crude extract (7 g) was resuspended in MeOH/H₂O (2:1) and then partitioned with dichloromethane (2.36 g) and ethyl acetate (0.83 g). The UHPLC-ESI-HRMS/MS data was obtained in a MicroTOF-QII (Bruker Daltonics, USA) equipped with an electrospray ion source (ESI). The precursor ion mass tolerance for GNPS was set to 0.02 Da and a MS/MS fragment ion tolerance of 0.02 Da. A network was then created where edges were filtered to have a cosine score above 0.65 and more than 6 matched peaks. Additionally, the biosynthetic gene clusters of *G. imperialis* were predicted in addition to three correlated species *Galerina marginata*, *Gymnopilus chrysopilus* and *Gymnopilus junonius* using fungiSMASH (doi: 10.1093/nar/gkz310). These predictions were further analyzed using the BGCtoolkit software (unpublished) that is being developed in the Fungal Natural Products group. Phylogenetic and comparative genomics analyses were performed on the major biosynthetic classes, sesquiterpene synthases and polyketide synthases, to identify candidate pathways for already reported or novel metabolites. As results it was possible to annotate 24 oligoisoprenoids from methanol, dichloromethane, and ethyl acetate extracts of *G. imperialis*, 4 of them from GNPS spectral library match, and 20 from the prediction based on molecular network; and 6 terpenoids, being 3 of them sesquiterpenes. Moreover, HRMS-ESI-(+) dereplication of the acetate extract annotated bisnoryangonin and hispidin, hybrid NRPS-PKS molecules. According to the genome mining analyses, it was possible to access the full biosynthetic potential of the species, assign biosynthetic gene clusters to the dereplicated molecules and select 10 biosynthetic clusters candidates for heterologous expression, being of them 7 sesquiterpene synthases, and 3 PKSs. Future perspectives of this project involve the heterologous expression in *Aspergillus oryzae* of the clusters and screening for the production of secondary metabolites.

Agradecimentos/Acknowledgments

Hatfield, G.M.; Brady, L.R. 1969. J Pharm Sci. 58(10):1298-9.

Mosunova, O.; Navarro-Muñoz, J.C.; Collemare, J. 2020.

Encyclopedia of Mycology. doi:10.1016/B978-0-12-809633-8.21072-8

Zhang, J.J.; Tang, X.; Moore, B.S. 2019. Nat. Prod. Rep., 36, 1313-1332.

Área: QPN*(Inserir a sigla da seção científica para qual o resumo será submetido. Ex: ORG, BEA, CAT)***Caffeine content and antioxidant potential in different forms of guarana powder from Maués – AM****Karollyna B. B. Martins**² (PG), **Marcos Batista Machado**² (PQ), **Kidney Neves**² (TC), **Ingrity S. Costa Sá**⁴ (PG) **Sergio M. Nunomura**³ (PQ), **Rita C.S. Nunomura**⁴ (PQ)karollbia17b@gmail.com; ritasn@ufam.edu.br¹Graduate Program in Chemical Engineering, UFAM; ²Federal University of Amazonas and Magnetic Resonance Laboratory; ³National Institute for Amazonian Research. Coordination of Technology and Innovation; ⁴Federal University of Amazonas. Chemistry Department.Keywords: *Paullinia cupana*; qNMR; DPPH.**Highlights**

The antioxidant potential and caffeine content in organic guarana powder produced by different processing methods by a cooperative in Maués - AM were investigated. The antioxidant activity and caffeine content were more significant in samples of whole guarana seeds than seeds with the tegument removed.

Resumo/Abstract

Guarana fruit (*Paullinia cupana* Kunth), native to the Amazon region, is highly appreciated for its stimulating and antioxidant properties. Its commercialization began in the municipality of Maués - AM and nowadays covers the state of Bahia and small plantations in Venezuela (SMITH & ATROCH, 2010). However, the different forms of production of the powder raise the question regarding the variation in the chemical composition, caffeine content, and antioxidant activity of the several forms of commercialization. This work aimed to quantify caffeine and analyze the antioxidant potential of powdered guarana extracts obtained by different processing: R1 – seeds roasted with the tegument and subsequently ground; R2 - seeds with seed coat automatically removed and toasted; R3 - seeds with tegument removed and selected manually and then toasted; R4 - handmade sticks. For the quantitative analysis of caffeine, the qNMR (PULCON) technique was performed in a Bruker Avance III HD, 500.13 MHz for ¹H and 125.8 MHz for ¹³C, BBFO Plus SmartProbe™ (OLIVEIRA, 2021). The antioxidant potential was performed by the DPPH method in BioTek equipment, Elx800, at 515 nm. As a reference standard, gallic acid (IC₅₀ = 11.53 µg/mL) was used (BRAND-WILLIAMS, 1995). The highest levels of caffeine were observed in unselected seed samples.

Table 1 – Average caffeine content (%) in guarana samples R1, R2, R3 and R4.

Sample	qNMR (mg)	PULCON/Sample ratio	% Content of extractives	% caffeine content in dry seeds
R1	2,74	55%	3,695	2,02
R2	3,43	69%	5,066	3,48
R3	1,87	37%	4,072	1,51
R4	2,08	42%	2,598	1,08

*R1 – seeds roasted with the shell and then ground; R2 - seeds with the tegument removed automatically, which were not selected; R3 - seeds with tegument removed and manually selected; R4 – guarana handmade stick.

The antioxidant activity of samples of guarana powder with tegument showed a higher antioxidant potential, with R1 with IC₅₀ = 35 µg/mL and R4 with IC₅₀ = 14.72 µg/mL. The samples from which the tegument was removed showed an IC₅₀ of 44.01 µg/mL (R2) and 43 µg/mL (R3). Given the observed results, we suggest that the presence of the tegument in the seeds contributes to the more higher caffeine content. Usually, guarana products are produced from guarana seeds with tegument, and it is suggested that this is the best way of production.

SMITH, N.; ATROCH, A. L. *eCAN*, 7 (3) 279-282, 2010.OLIVEIRA, E. S. C. et al. *Journal of Pharmaceutical and Biomedical Analysis*, v. 201, p. 1 – 8, 2021.BRAND-WILLIAMS, et al. *Lebensm-Wiss. u.-Technol.*, 28.25-30, 1995.**Agradecimentos/Acknowledgments**

The authors are grateful to Central Analítica (UFAM) for analysis, UFAM, FAPEAM for financial support and COPERMAUES for providing samples.

Área: QPN

CARACTERIZAÇÃO MOLECULAR E AVALIAÇÃO DO POTENCIAL ANTILEISHMANIA DE ACETOGENINAS ACETILÊNICAS DAS SEMENTES DE *Porcelia macrocarpa* (WARM.) R. E. FRIES (ANNONACEAE)

Ivanildo A. Brito (PG)¹, Erica V. Castro Levatti (PG)², Andre G. Tempone (PQ)², João Henrique G. Lago (PQ)¹.

ivanildo.brito@ufabc.edu.br

¹Centro de Ciências Naturais e Humanas, Universidade Federal do ABC, Santo André, SP; ²Instituto Adolfo Lutz, São Paulo, SP.Palavras Chave: *Porcelia macrocarpa*, Annonaceae, acetogeninas acetilênicas.

Highlights

This work reports the isolation and evaluation of the antileishmanial activity of eight chemically related acetylenic acetogenins (**1 – 8**), obtained from *Porcelia macrocarpa* seed extracts.

Resumo

As plantas vêm se destacando como importantes fontes de moléculas a serem exploradas para o desenvolvimento de protótipos e potenciais fármacos frente ao tratamento das mais diversas doenças, principalmente aquelas consideradas negligenciadas. Uma dessas é a leishmaniose, que atinge mais de 12 milhões de indivíduos e cujo arsenal efetivo terapêutico disponível para o tratamento ainda é bastante reduzido e insatisfatório.^{1,2} Em continuação aos nossos estudos visando a descoberta de protótipos com ação anti-*Leishmania infantum*, o presente trabalho descreve o isolamento de oito acetogeninas acetilênicas (**1 – 8**) biossinteticamente relacionadas (**Figura 1**) do extrato diclorometano das sementes de *Porcelia macrocarpa* R.E. Fries (Annonaceae). As estruturas destes compostos foram definidas por diferentes métodos espectroscópicos/espectrométricos, incluindo RMN e EM, o que permitiu concluir que os compostos **1**, **3-5**, **7 e 8** são inéditos na literatura.

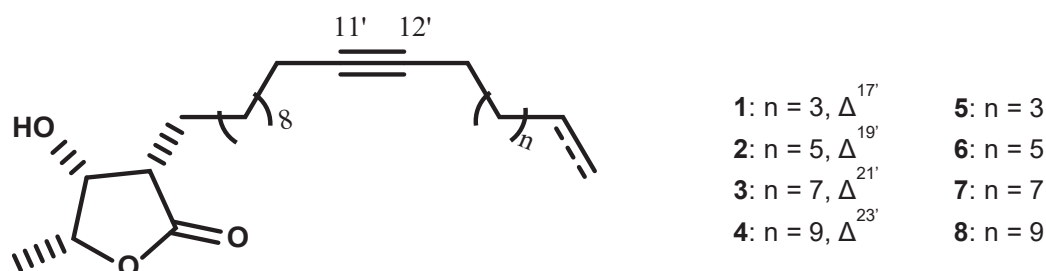


Figura 1. Estruturas química das acetogeninas acetilênicas **1 - 8** isoladas das sementes de *P. macrocarpa*

O potencial dos compostos **1 - 8** foi avaliado *in vitro* frente às formas amastigotas (intracelulares) de *L. infantum* enquanto que a toxicidade foi determinada para células NCTC. Tais resultados permitiram inferir que as acetogeninas acetilênicas **1**, **2**, **7 e 8** apresentaram CE_{50} de 11,3; 23,5; 44,8 e 37,0 μ M, respectivamente ao passo que **3 - 6** foram inativos ($CE_{50} > 200 \mu$ M). Com relação à citotoxicidade em células de mamífero (NCTC), os resultados obtidos demonstraram que os compostos **1 – 8** apresentaram $CC_{50} > 200 \mu$ M. Após o cálculo do índice de seletividade ($IS = CC_{50}/EC_{50}$) foi possível inferir que os compostos **1 e 2** forneceram IS maior que 17,7 e 8,5 respectivamente, mostrando potencial superior que o fármaco padrão, miltefosina ($IS > 6,5$). No que tange os aspectos estrutura e atividade das acetogeninas acetilênicas **1 - 8**, foi observado que o aumento da extensão da cadeia lateral associado com a presença da ligação dupla terminal causa redução do potencial, como observado para os compostos inativos **3 e 4**. Por outro lado, a ausência dessa insaturação e o aumento da extensão da cadeia lateral favoreceu o incremento da atividade, como observado para as substâncias **7 e 8**. Diante dos resultados obtidos, este estudo contribui para o conhecimento da atividade antileishmania de metabolitos de *P. macrocarpa*, o que pode contribuir para o desenvolvimento de novos protótipos moleculares para obtenção de novos fármacos frente ao tratamento da leishmaniose.

Agradecimentos

Agradecimentos: FAPESP, CNPq e CAPES.

Referências: [1] World Health Organization, **2021**. Disponível em <<http://www.who.int/leishmaniasis/en/>>(2021). [2] SUNDAR, S.; CHAKRAVARTY, J. Expert Opin. Pharmacother. **2015**, 16, 237.

Cell Membrane Chromatography (CMC) experiments guided the identification of antileukemia metabolites from *Myrsine guianensis* (Primulaceae)

Fernando Cassas (PG)¹, Cauê Santos Lima (PG)², Heron F. V. Torquato (PQ)², Edgar J. Paredes-Gamero (PQ)³, Luciano Caseli (PQ)⁴, Livia Soman de Medeiros (PQ)⁴ and Thiago A. M. Veiga* (PQ)⁴

fernando.machado@unifesp.br

¹Programa de Pós-Graduação em Biologia Química, Federal University of São Paulo - UNIFESP, Diadema, Brazil; ²Department of Biochemistry, Federal University of São Paulo – UNIFESP, São Paulo, Brazil; ³Faculty of Pharmaceutical Sciences, Food and Nutrition - Federal University of Mato Grosso do Sul – UFMS, Brazil; ⁴Department of Chemistry, Federal University of São Paulo - UNIFESP, Diadema, Brazil

Key words: Cell membrane chromatography, CMC, Dereplication, Leukemia assays, *Myrsine guianensis*, HRMS.

Highlights

CMC experiments showed that myrsinoic acid A (**MA**) interacted with Jurkat cells receptors or ligands. To prove this hypothesis, **MA** was purified and submitted to the cytotoxic assays. Additionally, we are also investigating its behavior on cell membrane models through Langmuir monolayers.

Abstract

Natural Products (NPs) are known as promising sources of specialized metabolites with cytotoxic effects¹. The combination of hyphenated analytical techniques, bio-monitored fractionation and molecular dereplication are modern approaches increasingly used to access these metabolites². In addition, Cell Membrane Chromatography (CMC) experiments allow us to determine the characteristics of interaction between membrane ligands and receptors, which led to a rapid and efficient identification of target metabolites³. Based on these contexts, nine extracts obtained from *Myrsine guianensis* (Aubl.) Kuntze (Primulaceae) (called here as **MGs**) were submitted to cell viability assays against two human leukemia cell lines, **Kasumi-1** and **Jurkat**. After 24 hours, three of them (**MG 4**, **6** and **7**) were cytotoxic once they inhibited cell proliferation by 80% at 100 µg/mL. The active extracts were submitted to **CMC** experiments against Jurkat cells.

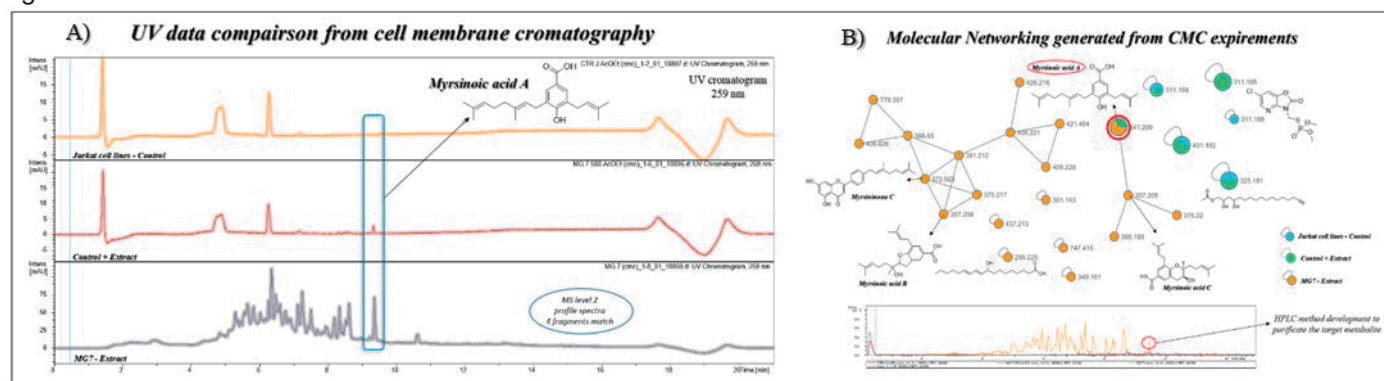


Figure 1 – (A) UV and MS/MS data comparison from CMC experiments; (B) Molecular networking obtained from CMC experiments.

Data showed that Myrsinoic acid A (**MA**) interacted with the cell membrane (Figure 1 A). According to these results, the active extracts were purified through preparative HPLC to provide 32.3 mg of **MA**, which is being evaluated against Jurkat cells. Additionally, we are investigating **MA** behavior on cell membrane models through Langmuir monolayers by employing the lipids DPPC and DPPS to verify if structural changes on the scaffold of **MA** modulated the interaction with the phospholipids at the air-water interface. Finally, through MS/MS data, the extracts were dereplicated resulting in the creation of Molecular Networking for the annotation of unrelated metabolites for *M. guianensis* (Figure 1B).

¹ Ashis K. Mukherjee, Sourav Basu, Nabanita Sarkar, Anil C. Ghosh "Advances in Cancer Therapy with Plant Based Natural Products" *Current Medicinal Chemistry*, Volume 8, Issue 12, 2001.

² SMYTH, W. F. et al "Dereplication of phytochemicals in plants by LC-ESI-MS and ESI-MSn". *TrAC Trends in Analytical Chemistry*, v.33, n. 46, 2012.

³ MA, W. et al "Advances in cell membrane chromatography" *Journal of Chromatography A*, 1639 (2021) 46191

Acknowledgments

FAPESP (2018/04095-0; 2020/08270-0), CNPq and CAPES.

CHEMICAL COMPOSITION AND ANTIBACTERIAL ACTIVITY OF THE ESSENTIAL OIL FROM THE LEAVES OF *Callistemon viminalis* (MYRTACEAE)

Ana Clara L.N. Silva (PG),^{1*} Marisi G. Soares (PQ),² Daniel de Oliveira Miranda (PG),² Jackson Monteiro (PG)¹, Marcelo Afonso Vallim (PQ)¹, Renata Castiglioni Pascon (PQ)¹, Patricia Sartorelli (PQ).¹

clara.nunes17@unifesp.br

¹Programa de Pós-Graduação em Biologia Química, Instituto de Ciências Ambientais Químicas e Farmacêuticas, Universidade Federal de São Paulo – UNIFESP;

² Institute of Chemistry, Federal University of Alfenas, Minas Gerais, Brazil.

Keywords: *Callistemon viminalis*, bioactive metabolites, essential oil, antibacterial activity.

Highlights

The essential oil of *Callistemon viminalis* is mainly composed of monoterpenes that have an antibacterial activity.

Abstract

Since the dawn of mankind, there are reports of the use of plants for medicinal purposes, due to some species presenting low toxicity and efficiency in fighting certain diseases. There is *in vitro* evidence showing that volatile oils can be antibacterial agents against several pathogenic bacterial strains¹. Essential oils of Myrtaceae have demonstrated antibacterial, anti-inflammatory, fungicidal, antioxidant and antiviral properties². Chemical studies conducted from the essential oil (EO) obtained from the leaves of *Callistemon viminalis* (Myrtaceae) showed the majority presence of 1,8-cineole, in addition to other significant monoterpenes, these being α -pinene, α -terpineol, and p-cymene that have high antibacterial activity. The present work aims to carry out an investigation of the chemical components of the essential oil from the leaves of *C. viminalis*, in view of the evaluation of the antimicrobial activity. The EO was obtained by Clevenger distillation and the constituents determined by gas chromatography associated with mass spectrometry (GC/MS) and was evaluated for antimicrobial potential against strains of *Staphylococcus aureus* and *Escherichia coli* using the disk diffusion method to evaluate the antimicrobial susceptibility of microorganisms performing following the CLSI protocol (M2-A8). As results, the EO of the leaves showed a yield of 0.58%, with the data obtained by GC/MS and comparing the mass spectrum present in the literature it was possible to identify eucalyptol (1,8 cineole) (51.80%) as the major compound, confirming what has already been reported in the literature where there is a percentage variation from 39.4 to 83.2%^{3,4}, the second peak with the highest intensity was α -pinene (10,57%), , in addition to compounds such as and p-cymene (4,70%) and phellandrene (3.18%). The difference of the constituents and their concentrations in the oil from the data of literature can end up interfering in the biological characteristics, this is due to factors such as geographical position, climate, light, latitude, among others that have a direct influence. In order to evaluate the antimicrobial activity of the essential oil, disco-diffusion assay against the *S. aureus* strain was performed according to literature⁵. The oil showed an inhibition halo of 0.7 cm, under the 400 μ g concentration, while, no halo of inhibition was observed against *E. coli*, possibly due to the difference in concentration of the monoterpenes present in the oil composition. From these data the next step will be to perform disc-diffusion with other gram-positive bacteria and yeasts, and to evaluate the minimum inhibitory concentration (MIC). However, the essential oil from the leaves of *Callistemon viminalis* can be exploited as a potential antibacterial source of a natural product.

References

- 1 LARAYETAN, R. A., OKOH, O. O., SADIMENKO, A., *et al.* "Terpene constituents of the aerial parts, phenolic content, antibacterial potential, free radical scavenging and antioxidant activity of *Callistemon citrinus* (Curtis) Skeels (Myrtaceae) from Eastern Cape Province of South Africa", BMC Complementary and Alternative Medicine, v. 17, n. 1, p. 1–9, 2017.
- 2 GAD, H. A., AYOUB, I. M., WINK, M. "Phytochemical profiling and seasonal variation of essential oils of three *Callistemon* species cultivated in Egypt", PLoS ONE, v. 14, n. 7, p. 1–15, 2019.
- 3 AWEKE, N., YESHANEW, S. "Chemical composition and antibacterial activity of essential oil of *Callistemon citrinus* from Ethiopia", European Journal of Medicinal Plants, v. 21:1-7, 2016.
- 4 AHMAD, K., ATHAR, F. "Phytochemistry and pharmacology of *Callistemon viminalis* (Myrtaceae): A review". The Natural Products Journal, v. 7(3): 166-175, 2017.
- 5 SILVA, F.B.D., SANTOS, N.O.D., PASCON, R.C., VALLIM, M.A., FIGUEIREDO, C.R., MARTINS, R.C.C., SARTORELLI, P. "Chemical Composition and *In Vitro* Cytotoxic and Antimicrobial Activities of the Essential Oil from Leaves of *Zanthoxylum monogynum* St. Hill (Rutaceae)", Medicines (Basel). v. 19;4(2):31, 2017.

Acknowledgments

FAPESP, CAPES and CNPq.

Chemical composition, antioxidant and antimicrobial activities of extracts from the bark and branches of *Lafoensia replicata* Pohl

Débora M. Lima (PG),¹ Anna L. Oliveira (PG),² Carlos H. G. Martins (PQ),² Raquel M. F. Sousa (PQ)¹

deboramalima@gmail.com

¹Instituto de Química, ²Instituto de Ciências Biomédicas, Universidade Federal de Uberlândia

Keywords: phenolic compounds, mass spectrometry, antioxidant, antibiologic activities

Highlights

Valorization of the Cerrado species. Chemical composition of organic extracts of *Lafoensia replicata* Pohl. Comparison of the biological and antioxidant activities between bark and branches extracts.

Abstract

Lafoensia replicata Pohl (mangabeira) is an endemic tree from Brazil that occurs in the Cerrado of Goiás and Minas Gerais. An ethnopharmacological study¹ showed the popular use of the bark of this species to treat diseases related to the liver and kidneys, inflammations in general, wound healing, gastritis, high blood pressure, headache and stomach pain. The bark and branches of *L. replicata* were collected on BR 497 (Uberlândia/Prata, MG, 18°59'20.3"S 48°25'14.5"W). After the vegetable material was dried and crushed, they were submitted to extraction by maceration at room temperature with hexane for 48 hours (5x) (HE), followed by ethanol extraction for 48 hours (5x) (EE). The antimicrobial activity (Table 1) was performed by the broth microdilution technique and expressed as minimum inhibitory concentration (MIC). The antioxidant activity (Table 2) was analyzed by the DPPH radical scavenging techniques, expressed as EC₅₀ (µg mL⁻¹), and by the iron reducing capacity (FRAP) method, expressed as Trolox Equivalent (µmol g⁻¹).

Table 1: Minimum inhibitory concentration (MIC) of plant extracts *L. replicata*.

Microorganisms	Minimum inhibitory concentration (MIC) – µg mL ⁻¹			
	HE barks	HE branches	EE barks	EE branches
<i>Staphylococcus aureus</i>	> 800	> 800	100	50
<i>Escherichia coli</i>	> 800	> 800	> 800	> 800
<i>Pseudomonas aeruginosas</i>	800	> 800	100	200
<i>Candida albicans</i>	800	100	1.56	3.12

Table 2: Antioxidant activities of plant extracts *L. replicata*

Sample	FRAP – Trolox	DPPH
	Equivalent µmol g ⁻¹	(EC ₅₀ µg mL ⁻¹)
HE barks	46.42 ± 2.78	> 200
HE branches	156.25 ± 3.25	> 200
EE barks	389.23 ± 8.61	4.5 ± 0.37
EE branches	548.17 ± 7.31	3.52 ± 0.1

According to Kuete², the antimicrobial activity of plant extracts can be classified as significant when the MIC value is lower than 100 µg mL⁻¹; moderate for MICs between 100 and 625 µg mL⁻¹, and weak when MIC is higher than 625 µg mL⁻¹. It was found that EE showed significant results for all microorganisms evaluated, except *E. coli* and *P. aeruginosas* for the branch extract. HE presented weaker activities compared to EE. According to Reynertson et. Al³, for EC₅₀<50 µg mL⁻¹, the antioxidant activity intensity is considered high and for EC₅₀>200 µg mL⁻¹, it is considered inactive. For the FRAP method, the more Fe²⁺ at the end of the reaction (the higher the amount of equivalent in Trolox/g of the sample), the higher the antioxidant activity will be. Thus, it can be seen from Table 2 that EE presented antioxidant activities better than HE. The annotation of the compounds present in EE was performed through liquid chromatography coupled to mass spectrometry with an electrospray ionization system (LC/ESI-MS/MS-negative mode). Compounds of the tannin class, flavonoids, phenolic acids, and derivatives were annotated, including ellagic acid, gallic acid, sorbitol, HHDP-glucose, HHDP-galoyl glucose, digaloyl-HHDP-glucose, trisgaloyl-HHDP-glucose, galoyl glucose, punicalagin, galoyl punicalin, sorbitol, tetragaloyl hexose, galoyl quercetrin, canferol hexoside, and quercetin.

¹ SOBRINHO et al., *Desenvolv. Meio Ambiente*, **2016**, 39, 207; ² KUETE *Planta Med.* **2010**, 76, 1479 ³ REYNERTSON et. al. *Ethnobot. Res. Appl.*, **2005**, 3, 25.

Acknowledgments

FAPEMIG, IQUFU, CAPES, CNPq

Área: QPN

Chemical constituents and evaluation of antioxidant, antimicrobial and antiproliferative activities of *Moquiniastrium sordidum* (Asteraceae)

Tamires Cordeiro (PG)^{1*}, Isabella C. dos Santos (PG)¹, Bianca D. B. Sahm (PG)², Elizabeth Figueiredo Pires (PG)³, Aline Pivetta (PG)³, Letícia Costa Lotufo (PQ)², Tatiana Shioji Tiunan (PQ)³, Marta Regina Barroto do Carmo (PQ)⁴, Maria Helena Sarragiotto (PQ)¹, Debora Cristina Baldoqui (PQ)¹

iscdsan@gmail.com; tamih.cordeiro@gmail.com

¹Departamento de Química, UEM, Maringá-PR, Brazil; ²Instituto de Ciências Biomédicas, USP, São Paulo, SP, Brazil; ³Universidade Tecnológica Federal do Paraná, Toledo-PR, Brazil; ⁴Departamento de Biologia Geral, UEPG, Ponta Grossa-PR, Brazil.

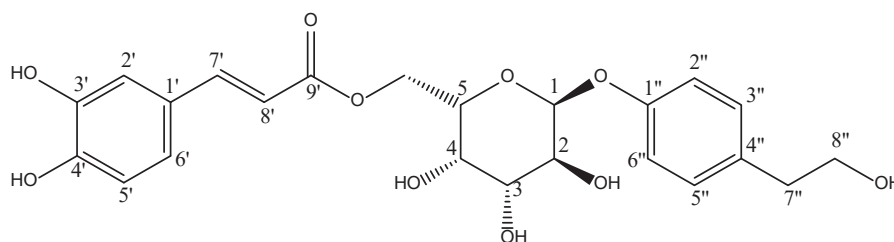
Palavras Chave: *Moquiniastrium sordidum*, *Gochnatia sordida*, Phenolic derivatives, Biological activity.

Highlights

This is the first phytochemical study of *Moquiniastrium sordidum*. A new glycosylated phenolic derivative was isolated and exhibited potent antioxidant activity.

Resumo/Abstract

Moquiniastrium genus, which was previously described by Cabrera as a section of *Gochnatia*, belongs to the Asteraceae family. This genus comprises twenty-one species, and seven have already been studied. The main classes of specialized metabolites described of this genus are sesquiterpene lactones, diterpenes, triterpenes and flavonoids. In this work, we proposed the first phytochemical and biological investigation of *Moquiniastrium sordidum*. Dried aerial parts of *M. sordidum* (668 g), collected in April 2019, in Ponta Grossa-PR, were powered and exhaustively extracted with ethanol at room temperature. Vacuum concentration yielded the crude extract (118 g), which was suspended in MeOH:H₂O (1:1) and partitioned into hexane, dichloromethane and EtOAc. The crude extract, fractions and pure compounds were submitted the evaluation of antioxidant (ABTS and FRAP), antimicrobial and antiproliferative activity. Hexane, dichloromethane and ethyl acetate fractions were subjected to successive chromatographic columns on silica gel, silica flash and sephadex LH-20, resulting in the isolation of seven compounds, that were characterized by comparing their uni and bidimensional NMR spectroscopic data, with literature data, as simiarenol, oleanolic acid, tyrosol, hispidulin, genkwanin, apigenin and a new glycosylated phenolic derivative (1). Another six compounds were identified by UHPLC-HRMS/MS-based dereplication from the dichloromethane and ethyl acetate fractions, being two triterpenes, ursolic acid and betulinic acid, and four flavonoids, quercetin, rutin, dihydrokaempferol and isoliquiritin. It is important to note that of the thirteen specialized metabolites identified in this species, five are being reported for the first time in the genus *Moquiniastrium*, the triterpene simiarenol, the flavonoids quercetin, dihydrokaempferol and isoquiritin, in addition to tyrosol and the new phenolic derivative. Regarding the results of antioxidant activity, it was observed that the ethyl acetate fraction presented a high potential in the two methodologies applied, ABTS (2763.0 μmol of Trolox g^{-1}) and FRAP (9652.6 μmol of Fe(II) g^{-1}), and the new phenolic derivative (1), isolated from this fraction, also showed potent antioxidant activity (1111.1 μmol of Trolox g^{-1} and 4293.0 μmol of Fe(II) g^{-1}). Oleanolic acid and apigenin were active against the Gram-positive bacterium *Bacillus cereus*, with MIC of 130 and 30 $\mu\text{g mL}^{-1}$, respectively. To evaluate the antiproliferative potential, the extract and fractions were tested in tumor cell cultures of colon carcinoma (HCT-116), and only the dichloromethane fraction showed activity, inhibiting cell growth by 92.11% at the maximum concentration tested, however, it did not show growth inhibition greater than 50% at the lowest concentration tested.



1

Agradecimentos/Acknowledgments

UEM, CAPES, CNPq, INCT-BioNat.

Chemical constituents of volatile oil from leaves of *Ludwigia elegans* (Onagraceae)

Ana Beatriz M. Salero (IC),¹ Lorena S. Meirelles (IC),¹ Edgard A. Ferreira (PQ).^{1*}

ana.salero@mackenzista.com.br; edgard.ferreira@mackenzie.br*

¹School of Engineering, Mackenzie Presbyterian University.

Keywords: Essential Oils, Aquatic Macrophytes, Onagraceae, Dereplication.

Highlights

Hidrodistillation of leaves of *Ludwigia elegans*, an aquatic macrophyte, followed by dereplication of volatile oil by means of GC-MS analysis, comparison with spectral library NIST17 and retention index indicated presence of 34 compounds, in which majority of compounds tentatively identified are alcohols and aliphatic hydrocarbons.

Resumo/Abstract

Aquatic macrophytes, popularly known as aquatic plants are representative species of flora, due to its importance to ecosystem in which they belong. In Brazil, they are found in all biomes and in all forms of adaption to the environment in which they live in. In general, these species can be described as herbaceous species that grow in water, soils covered by water or even soils saturated by water.¹ However, studies involving chemical composition and biological properties of compounds are reduced to a few reports in literature when compared with number of all species. As part of the Brazilian aquatic flora, genus *Ludwigia*, that belongs to Onagraceae family and presents a considerable number of 48 species in Brazil.² However, like most aquatic macrophytes, studies concerning these species are insufficient, which reflects in poor information about the potential of these species as source of bioactive molecules and chemotaxonomic aspects, even more about composition and biological effects of volatile oils. As part of our research group studies focusing on molecular diversity and biological effects of compounds from aquatic macrophytes, *Ludwigia elegans* was collected in Nazaré Paulista, São Paulo State and their leaves were submitted to extraction of volatile oils by hydrodistillation using Cleavenger apparatus for a period of four hours, affording volatile oil with yield of 0.01%. As next stage, the content of extraction was submitted to molecular dereplication by GC-MS in which resulted spectral data was submitted to comparison with NIST 17 library, besides obtention of each retention index and comparison with data available on literature.³ Dereplication revealed 34 compounds, in which mostly composed by alcohol and aliphatic compounds, in which *cis*-phytol was major compound (**1**, 87.6%), followed by heptacosane (**2**, 1.7%), 1-octen-3-ol (**3**, 1.6%) (*E*)-nerolidol (**4**, 0.6%), heptadecane (**5**, 0.5%), *n*-hexadecanoic acid (**6**, 0.5), (*Z*)-3-hexenyl benzoate (**7**, 0.5%), (*Z*)-3-hexen-1-ol (**8**, 0.4%), *n*-tricosane (**9**, 0.2%), respectively (**Figure 1**). These results may contribute with this genus in terms of chemotaxonomic aspects, whereas the same class of compounds have already been described in *Ludwigia stolonifera*.⁴

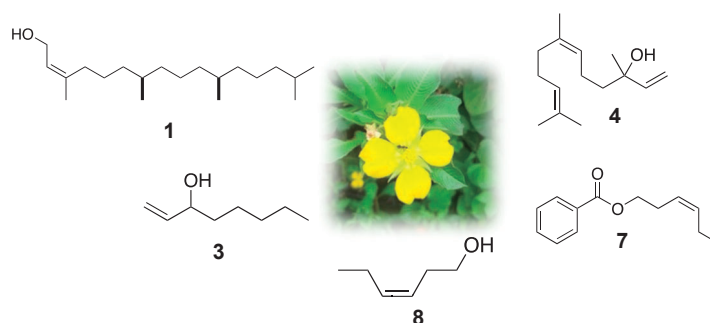


Figure 1: Compounds from volatile oil of *Ludwigia sericea*.

References: ¹Irgang, *et al.*, **1994**, *Roessléria*, 395-404; Souza *et al.*, **2019**, *Rodriguésia*, e01392018; ³Adams, R. P., Identification of Essential Components by Gas Chromatography/Mass Spectroscopy, **2009**. ⁴Baky, *et al.*, **2021**, *ACS Omega*, 24788.

Agradecimentos/Acknowledgments

Mackpesquisa and CNPq for fellowship to Lorena S. Meirelles and Ana Beatriz M. Saleiro, respectively. Sumiko Honda of Municipal Herbarium of São Paulo (PMSP) for identification of plant species.

Área: QPN

Chemical dereplication, genome mining of *Penicillium limosum* CMLD 19 for discovery Brefeldin analogs/Fatty acids biosynthetic precursors cytotoxics.

Milena C. Bassicheto (IC), ^{1*}, Cláudia M. da S. C. de Oliveira (PG), ¹, Milena P. S. Rivero (PG), ¹, Ana C. de Carvalho (PQ), ², Héron F. V. Torquato (PQ), ³, Gilvan F. da Silva (PQ), ⁴, Thiago A. M. Veiga (PQ), ¹, Livia S. de Medeiros (PQ), ¹.

bassicheto.milena@unifesp.br

¹Chemistry Department, UNIFESP; ²DTU Biosustain, Denmark; ³Biochemistry Department, UNIFESP; ⁴EMBRAPA CCAA

Key words: *P. limosum*, Leukemia, Cytotoxicity, Fatty acids, Brefeldin's precursors, Genome mining

Highlights

HPLC-HRMS/MS data of *P. limosum* rice extract showed production brefeldin A, likely analogs/biosynthetic precursors. Cytotoxic activity from the rice extract was detected against leukemia cell lines.

Abstract

P. limosum CMLD 19 was isolated as an endophytic fungus from *Swinglea glutinosa* (Biodiversity - Atlantic Forest). The strain was cultivated in different culture media and the methanolic extracts were obtained aiming to unveil their metabolic profiling and to verify the cytotoxicity potential of the produced metabolites against leukemia cells (Jurkat and Kasumi-1). The performed bioassays indicated a cellular inhibition of more than 80 e 95% for the rice extract. Moreover, the microorganism whole genome sequencing was performed which provided further genome mining studies through the use of FungiSmash platform. Preliminary results showed the detection of a biosynthetic gene cluster with 50% of similarity to the biosynthetic cluster corresponding to the production of 4-epi-15-epi-brefeldin A. Brefeldin A is known as a commercial anti-cancer compound. Indeed, the production of brefeldin by the fungus was confirmed by HPLC-HRMS/MS based dereplication data analysis and manual inspection of the fragmentation spectrum from the target compound. The use of GNPS platform was applied, pointing toward some likely analogues of Brefeldin A, as well as major fatty acids present into the rice extract, which may represent biosynthetic precursors of these compounds. Therefore, the ongoing work seeks the discovery of new brefeldin A analogues as well as its biosynthetic precursors in order to find new cytotoxic agents against leukemia cells.

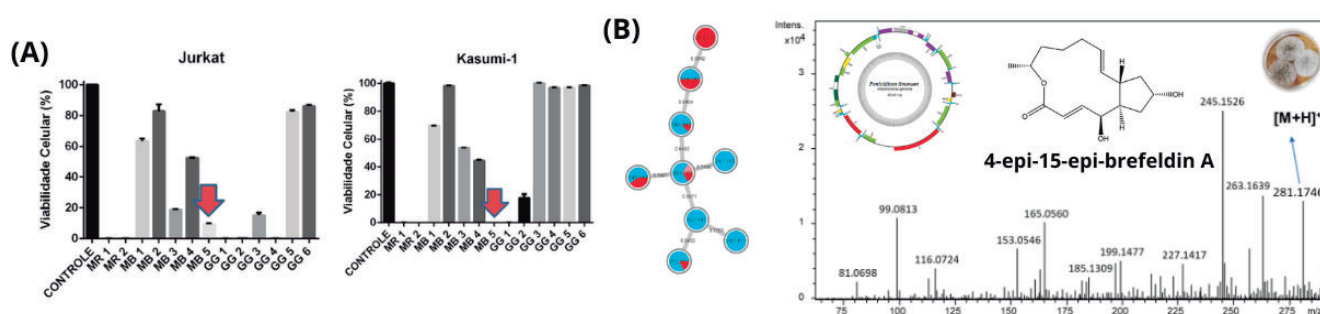


Figure 1a) Cell viability of rice extract; 1b) Mass spectrum/Molecular networking results of rice extract

Acknowledgments



FAPESP: 2020/08270-0 e 2018/04095-0 PIBIC: 143487/2022-1

Chemical study and antifungal activity of the marine fungus *Penicillium citrinum*-4A14 extract

Wanderson Z. Cosme (PG)^{1*}, Carla A. S. Lopes (PG)¹, Rodrigo Sorrechia (PG)², Rosemeire C. L. R. Pietro (PQ)², Gustavo M. Dias (PQ)³, Marcos A. Soares (PQ)⁴, Marcio L. A. Silva (PQ)¹, Wilson R. Cunha (PQ)¹, Patrícia M. Pauletti (PQ)¹, Ana H. Januario (PQ)¹.

wanderson_cosme@outlook.com

¹Universidade de Franca, UNIFRAN; ²Universidade Estadual Paulista, Araraquara, UNESP; ³Universidade Federal do ABC, UFABC. ⁴Universidade Federal de Mato Grosso, UFMT.

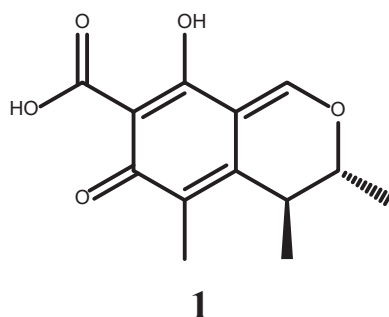
Keywords: Citrinin, Dermatophyte fungi, *Didemnum perlucidum*.

Highlights

This work reports the isolation of citrinin and antifungal activity of the EtOAc extract of marine fungus *Penicillium citrinum*-4A14 against dermatophyte fungi *Trichophyton rubrum* e *Microsporum canis*

Abstract

Microorganisms are found in virtually all habitats on Earth including the marine ecosystem. Marine fungi have aroused enthusiasm in several topics as a prosperous source in the bioprospecting of new molecules, with high potential for applicability in the pharmacological field¹. The purpose of this work was to carry out a chemical study of marine fungus *Penicillium citrinum*-4A14 associated with the ascidian *Didemnum perlucidum* cultivated in malt and to evaluate its antimicrobial potential against dermatophyte fungi. The fungus was cultivated in malt medium for 15 days and extracted with EtOAc. The extract was subjected to reverse phase chromatographic purifications using a flash chromatography system, Buchi Pure 850®, operating in a binary gradient system, supplied with a DAD detector, equipped with a cartridge filled with C-18, allowing the isolation of compound **1**. The antimicrobial evaluation was carried out by the microdilution method, against the *Trichophyton rubrum* and *Microsporum canis* strains. Samples were diluted in concentrations of 2.500-2.44 µg/mL and amphotericin B was used as a positive control, in concentrations of 16.00 - 0.007 µg/mL. Fractionation in the mentioned medium pressure system led to the isolation of the mycotoxin, citrinin (**1**). Additionally, **1** was analyzed on HPLC-DAD in reversed phase, in analytical mode, showing RT of 24.49 min and λ_{max} 240 and 324nm. The chemical structure of **1** was established by ¹H NMR and by comparison with data described in the literature². The 4A14 extract showed antifungal activity against *T. rubrum* (clinical isolate) with MIC and CFM of 625 µg/mL, and against *M. canis* with MIC of 1250 µg/mL and CFM of 625 µg/mL. These results confirm the antifungal potential of *P. citrinum*-4A14 and the importance in studying marine endophytic fungi as an attractive and alternative source in the search for specialized metabolites, which may help in the knowledge of the applicability of this strain.



References

- ¹ Ayuningrum, D, *et al.* PLoS One, 14(3), e0213797, 2019.
- ² Valente, A. M. M. P, *et al.* Applied Magnetic Resonance, 45(3), 207-215, 2014.

Acknowledgments

This research was supported by CAPES, CNPq and FAPESP.

Chemodiversity and cytotoxic activity of *Fusarium solani* isolated from red marine seaweed *Dichotomania marginata*.

Edelson J. S. Dias (PG),^{1*} Augusto L. Santos (PQ),¹ Givaldo S. Silva (PG),¹ Ana C. Zanatta (PQ),² Dulce H. S. Silva (PQ)¹

edelson.dias@unesp.br; dulce.silva@unesp.br

¹Nucleus of Bioassays, Biosynthesis and Ecophysiology of Natural Products (NuBBE), Department of Biochemistry and Organic Chemistry, Institute of Chemistry, Universidade Estadual Paulista - UNESP, Araraquara - SP, Brazil.; ²Faculty of Pharmaceutical Science, University of São Paulo, USP, Ribeirão Preto, SP, Brazil

Keywords: *Fusarium solani*, *Dichotomania marginata*, endophytic fungi, chemodiversity.

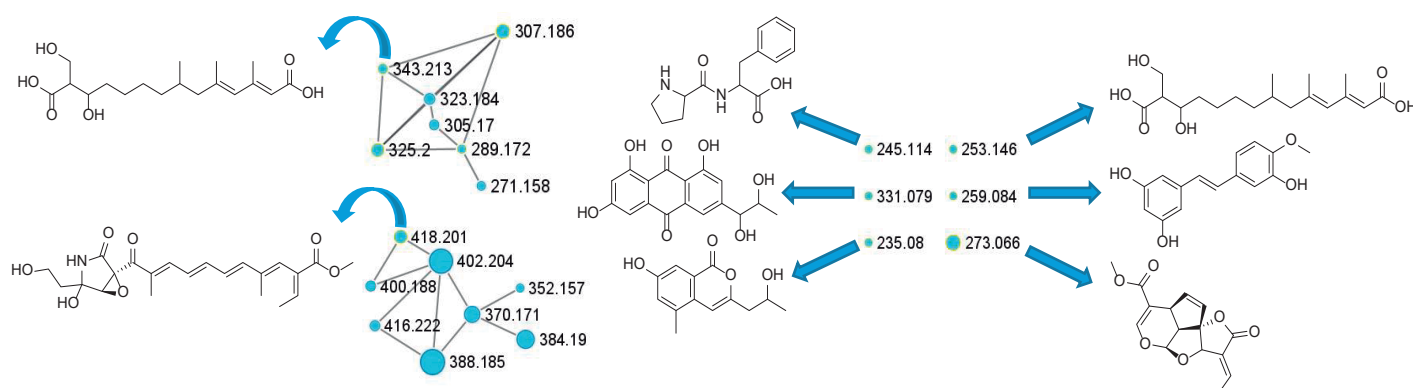
Highlights

- *F. solani* extract at 25 days showed cytotoxic activity with maximum inhibition of 81%.
- Molecular network approach allowed the annotation of phenolic compounds, terpenoids and polyketides in *F. solani*.

Abstract

Endophytic fungi are present in different organisms, they are endosymbionts that inhabit the interior of plant or other organisms tissues and do not trigger any apparent damage to their host during their endophytic phase (1). *Fusarium* is one of the most abundant fungal genera in nature, and in many cases it is considered as a phytopathogen, causing root and fruit rot. On the other hand it is also reported as an endophytic fungus presenting a rich chemodiversity, producing secondary metabolites that may present several bioactivities (2). In this work, *F. solani* was grown in 300 mL of malt extract in static mode at several time intervals of 5, 10, 15, 20, 25, 30, 35 and 40 days. After filtration each sample was partitioned with EtOAc to yield solutions which were dried under reduced pressure to afford crude extracts. The extracts were subjected to cytotoxicity test against HTC-116 cells (rectal colon carcinoma) and the extract obtained at 25 days showed the highest percentage of inhibition (81%) and was subjected to analysis by high resolution mass spectrometry (ESI-QTOF-MS) in positive and negative mode. The LC-HRMS data were submitted to the GNPS platform and a molecular network was generated which enabled the annotation of terpenoids and phenolic substances, including polyketides.

Annotated compounds from GNPS analyses of *Fusarium solanii* extract obtained at 25 days of fermentation



1. FARHAT, H. *et al.* **Biocatalysis and Agricultural Biotechnology**, v. 18, n. 101043, 2019.
2. KHAN, N. *et al.* **Toxicology Reports**, v. 05, 2018.

Acknowledgments

CAPES, CNPq (INCT/BioNat), FINEP and FAPESP (Cepid/CibFar and INCT/BioNat) for research financial support and fellowships.

Área: QPN

(Inserir a sigla da seção científica para qual o resumo será submetido. Ex: ORG, BEA, CAT)

Comparison of different processing of guarana seed by UHPLC-ESI-MS/MS and molecular networking dereplication

Sergio Massayoshi Nunomura (PQ),¹ Josiel do Nascimento Amazonas (IC),^{2*} Rita Cynara de Oliveira Salles (PQ),¹ Magno Perea Muniz (TC),¹ Rita de Cássia Saraiva Nunomura (PQ).²

smnunomu@inpa.gov.br; siel.nasc16@gmail.com

¹ National Institute for Amazon Research – INPA, Coordination of Technology and Innovation-COTEI; ² Federal University of Amazonas- UFAM, Chemistry Department- DQ

Key-words: *Paullinia cupana*, dereplication, GNPS, flavonoids, UHPLC-ESI-qQ-TOF-MS

Highlights

- GNPS platform in the dereplication of guarana samples of different types of seed processing by UHPLC-ESI-MS/MS.
- Metabolites from guarana seeds identified by GNPS are similar to other procedures.
- Flavonoids identified, including dimers and trimers of procyanidins and catechins

Abstract

Paullinia cupana H. B. K var. *sorbilis* (Mart.) Duke (Sapindaceae) is worldwide known and is considered to be native to the Amazon region of Maués (AM). Guarana seeds generate different products (syrup, powdered seeds, and others) that are very much appreciated and well-traded. Many studies described the seed's chemical composition. Methylxanthines, especially caffeine, along with phenolic compounds, are the main constituents. In this work, we have analyzed samples of guarana seeds processed differently, hot-dried (traditional) and cold-dried (lyophilization). Previously we have successfully developed an LC-MS method to discriminate the seeds according to their geographic origin (Salles *et al*, 2022) and also processed them in different conditions. Here, we used the molecular networking created by GNPS (Global Natural Products Social Molecular Networking) to identify the compounds that discriminated samples submitted to these two different seed processing. The sample extracts were prepared from the ground seeds and with a mixture of ACN and TFA (pH=2.0) in a sonic bath for 1 hour, centrifuged, and dried. A solution of 1 mg/mL was prepared from each sample and submitted to UHPLC-ESI-qQ-TOF-MS/MS from Bruker using a Phenomenex Luna PFP2 column (5 µm, 15 cm, 2.0 mm), eluted in a linear gradient of ACN (0.1% formic acid) and an aqueous solution of formic acid at 0,1%. An electrospray ionization (ESI) interface in negative mode was used and the MS range was set to m/z 120-1200. After the acquisition, the converted data were submitted to GNPS tools for molecular annotation and molecular networking. We were able to find a coherent molecular network, as compared to our previous studies, setting tolerance to 0.02 Da and ion-fragmentation tolerance (MS/MS) of 0.02 Da. In order to enhance the ion identity, we have used some other *in silico* tools such as Library Search, Network Annotation Propagation (NAP), Dereplicator+ as described by GNPS MolNetEnhancer. We have achieved some molecular families containing flavonoids, phenylpropanoids and catechins. The most frequent ion identities were typical procyanidins of guarana seeds, including dimers and trimers, that are responsible for the seed's process discrimination (hot vs. cold drying). GNPS have successfully helped identify the key-guarana seed compounds and speed the compound identification process.

SALLES, R.C.O. *et al*. *Food Chemistry*, v. 371, p. 131068, 2022.

Acknowledgments

The authors thank INPA (MCTI /CNPq) and FAPEAM for the scholarships and financial support.

Confirmation Through Structural Modification of Tri-Acyl-Glyceride (TAG) Isolated from the Seed of *Joannesia princeps*, (Cutieira a *Euphorbiaceae*).

Eduarda Freitas da Silva dos S. Oliveira IC),¹ Jhones T. Hubner (IC),¹ Milena R. Oliveira (IC),¹ Miguel Francisco da S. Filho (IC),¹ Francisco de Assis Da Silva (PQ).^{1*}

dufreitas2000@gmail.com; fasilva@ufrj.br

¹Departamento de Química Fundamental – IQ – UFRJ.

Palavras Chave: Cutieira; Euphorbiaceae; Oleico; Linoleico; *Joannesia princeps* Velloso

Highlights

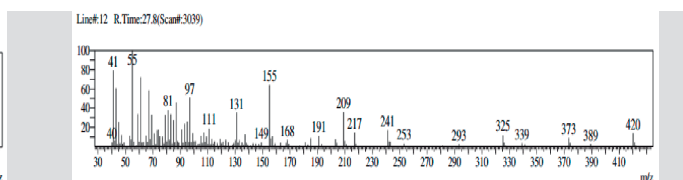
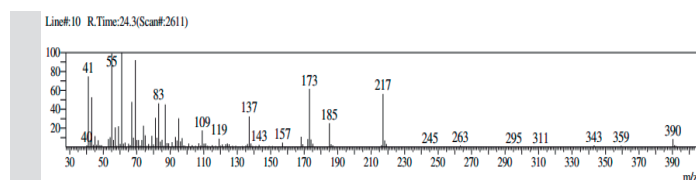
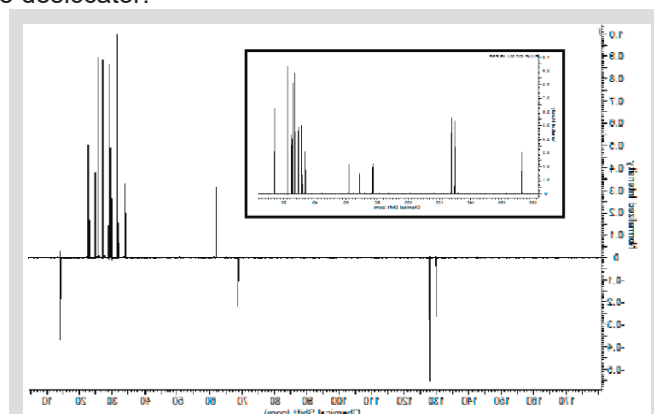
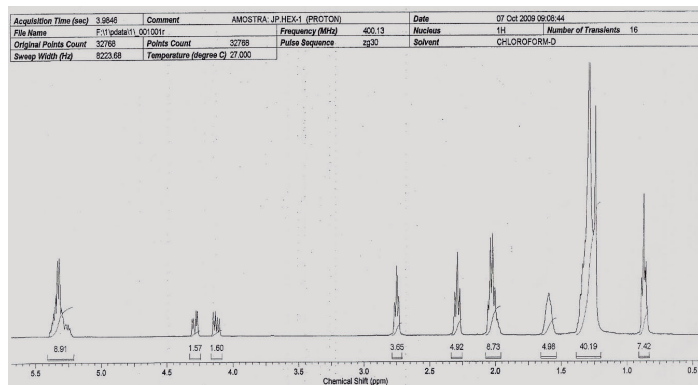
From seed of cutieira one **oil was isolated**. The structure was determined by spectrometric analysis. Data are indicating that the observed signals are of the compound with two linoleic and oleic units.

Resumo/Abstract

Through institutional interaction with researchers of the Pharmacology and Physiology, it was demonstrated that:

- Cutieira seed oil accelerates the closure of skin wounds, increases angiogenesis, keratinocyte migration and fibroblast activity, while reducing the inflammatory process and oxidative damage [1];
- Investigations on the cytotoxic and genotoxic potential and using *Allium cepa* and micronucleus assays demonstrated no mutagenic effects [2];
- New studies have shown that this oil has an antinociceptive and anti-inflammatory action through its topical and systemic administration, promoted by the inhibition of leukocyte recruitment and cytokine production [3].

In this present work, by hexane extraction with soxhlet apparatus a **triglyceride-oil was isolated, from seed of *Joannesia princeps* Vell, a *Euphorbiaceae***. The proposed structure to TAG was determined by spectrometric analysis (alt resolution GC/MS; Infra-red; ¹³C and ¹H NMR). Also, analysis by: H x H COSY and HMQC spectroscopy are indicating that all observed signals in the NMR spectra are of only one compound, a TAG formed by two linoleic unities and oleic unity. The proposed structure is confirmed by acid and basic hydrolysis (CH₃OH/ CH₃ONa) as well as confirmed by literature data. Reaction with dimethyl- disulfide after hydrolysis define double bond position by mass spectroscopy and revealed a probable product from thermic rearrangement (390 and 420g.mol⁻¹). The final structure is a triglyceride with molecular mass of 880g.mol⁻¹ and total formula C₅₇H₁₀₀O₆. Another TAG, with molecular mass of 878g.mol⁻¹, was detected after the seed's storage period on the desiccator.



1. Da Silva, F. A.; Marinho, B. G.; et al; *Journal of Ethnopharmacology*; **2021**; vol. 268; 113554
2. De Lima, V.M.; Da Silva, F.A.; Borba, H.R.; et al; *Journal of Life Sciences*. 2013. Vol 7, N° 12. PP. 1249-1254.
3. Donato-Trancoso, A.; Gonçalves, L.; Monte-Alto-Costa, A.; Da Silva, F.A.; Romana-Souza, B.; *Acta Histochemica*. 2014; Vol 116. pp 1169-1177.

Agradecimentos/Acknowledgments

Our Thanks: Raimundo Braz Filho (PQ); Luciano Suzart (PQ) and Eline Pena Berty (FM) for collaborations.

Constituents of volatile oils from leaves, stems and roots of *Cosmos sulphureus* Cav. (Asteraceae)

João Pedro V. Moriconi (IC),¹ Lorena S. Meirelles (IC),¹ Ana Beatriz M. Salero (IC),¹ Edgard A. Ferreira (PQ).^{1*}

jp.valdomoriconi@gmail.com; edgard.ferreira@mackenzie.br*

¹School of Engineering, Mackenzie Presbyterian University

Keywords: Essential Oil, Dereplication, Sesquiterpene

Highlights

Hydrodistillation of leaves, stems and roots of *Cosmos sulphureus*;
The dereplication of volatile oils revealed 40 compounds;
Sesquiterpene is the main class of compounds identified.

Resumo/Abstract

Asteraceae family is represented by approximately 25000 species distributed in more than 1000 genera. Predominantly, these species are found in temperate and semi-arid regions of the tropics and subtropics.¹ In Brazil, the Asteraceae family has 1900 species among 196 genera.² The species *Cosmos sulphureus*, has wide occurrence and easy dissemination. Due to its beauty, it has been widely used for ornamental purposes. In previous studies, the allelopathic potential of the chemical constituents of *C. sulphureus* was reported³, besides *in vitro* schistosomicidal properties of essential oil of flowers.⁴ Herewith, to expand knowledge about molecular diversity, the present study reports molecular dereplication of volatile oils from the leaves, stems and roots of the constituents of *C. sulphureus*. Thus, the plant was collected in the city of Atibaia, São Paulo State. Then, fresh leaves, stems and roots were submitted to the extraction of volatile oils separately by means of hydrodistillation using Cleavenger apparatus for a period of four hours with yields of 0.03, 0.01 and 0.01%, respectively. Then, dereplication was performed on the bases of GC-MS analysis of oils. The spectral data of all compounds were compared with NIST 11 Library, besides obtention of each retention index and comparison with data available in literature.⁵ As a result, 40 compounds were identified in different parts of the plant, and major compounds in leaves and stems were quite similar, β -elemene (**1**, 12.9%, 3.2%), β -copaene (**2**, 3.2%, 6.8%), D-germacrene (**3**, 17.23%, 34.57%), β -ylangene (**4**, 16.30%, 14.03%) and bicyclogermacrene (**5**, 27.09%, 5.09%), respectively (**figure 1**). The major compounds identified in roots were β -elemene (**1**, 12.4%), D-germacrene (**2**, 11.2%) and Longifolene (**6**, 7.0%) (**figure 1**). As next stage of the study, volatile oils will be subjected to evaluation of potential anti-*Trypanosoma cruzi* and anti-*Schistosoma mansoni*.

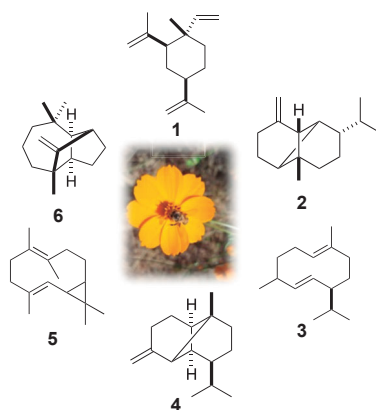


Figure 1: Major compounds of volatile oils from *Cosmos sulphureus* Cav.

References: ¹Bessada, *et al.*, **2015**, *Ind. Crops. Prod.* 76:604-615; ²Hattori and Nakajima, **2008**, *Rodriguésia* 59 (4):687-749; ³Respatie *et al.*, **2019**, *AIP Conference Proceedings* 2202, 020077; ⁴Aguiar, *et al.*, **2013**, *Nat. Prod. Res.*, 27(10), 920–924; ⁵Adams, R. P., Identification of Essential Components by Gas Chromatography/Mass Spectroscopy, **2009**.

Agradecimentos/Acknowledgments

Mackpesquisa and CNPq for fellowship to Lorena S. Meireles and Ana Beatriz M. Saleiro, respectively. Sumiko Honda of São Paulo Municipal Herbarium (PMSP) for identification of plant species.

Cytotoxic Activity and Chemical Profile of the Ethanol Extract Obtained from the Leaves of the Plant Species *Allophylus edulis* (SAPINDACEAE)

Beatriz I. M. do Carmo (IC),¹ Ivana B. Suffredini (PQ),² Patricia Sartorelli (PQ),³ Waldemar A. Ribeiro Filho (PQ),¹ Daniela C. Russo (PG).^{3*}

beatriz.carmo@fatec.sp.gov.br; daniela.russo@unifesp.br

¹ Laboratório de Química Instrumental, FATEC-PG; ² Núcleo de Pesquisas Biodiversidade, NPBio-UNIP; ³ Laboratório de Química Bio-Orgânica – Otto Richard Gottlieb, UNIFESP.

Keywords: *Allophylus edulis*. Chemical Profile. Anticarcinogenic potential.

Highlights

The phytochemical study carried out with the ethanolic extract of *Allophylus edulis* allowed the identification of the presence of different classes of secondary metabolites. Hydrogen-1 and Carbon-13 NMR spectra, obtained by the Nuclear Magnetic Resonance Spectrometry technique, suggest the presence of Terpenes. Cytotoxic potential assays showed that the ethanolic extract is active against tumor cell lines of non-metastatic breast adenocarcinoma (MCF-7), prostate adenocarcinoma (PC-3), and metastatic breast adenocarcinoma (MDA-MB-231).

Abstract

Natural products have become increasingly relevant for the treatment of diseases, due to the biodiversity of plant species and the structural chemodiversity of molecules, in addition to the wide acceptance of the use of plants in natural drugs.¹ Nowadays, it is recorded that about 7.6 million people on the planet die from cancer annually, while here in Brazil about 280,000 people die due to this disease.² The specie *Allophylus edulis* (A.St.-Hil., A. Juss. & Campess. Radlk.), the plant selected for this study, has been commonly used based on popular tradition.³ However, there is not a significant amount of studies of the chemical composition and biological activity of its metabolites. Thus, this study aimed to carry out a chemical and biological study with the leaves of the plant species *Allophylus edulis*, to verify the chemical profile and anticarcinogenic potential. For this, the collected plant material was extracted with ethanol, and later analyses were carried out through chromatographic and spectrometric techniques. The fractionation of the ethanolic extract was carried out through column chromatography with solvents of increasing polarity. At the end of this process, 16 fractions were obtained. The phytochemical study allowed the identification of the presence of different classes of secondary metabolites, such as flavonoids and terpenes. Cytotoxic activity assays showed that the metabolites present in the ethanolic extract and the selected fractions (AeF7 and AeF8) showed activity against tumor cell lines MCF-7, MDA-MB-231, and PC-3.

¹ VALLI, Marília; RUSSO, Helena M.; BOLZANI, Vanderlan S. The potential contribution of the natural products from Brazilian biodiversity to bioeconomy. *Anais da Academia Brasileira de Ciências* [online]. **2018**, v. 90, n. 1 Suppl 1.

² INCA – INSTITUTO NACIONAL DO CÂNCER. CÂNCER: o que é câncer? **2021**. Disponível em: inca.gov.br/o-que-e-cancer. Acesso em: 26 fev. 2022.

³ TREVIZAN, Lucas Noboru Fatori *et al.* Anti-inflammatory, antioxidant and anti-Mycobacterium tuberculosis activity of viridiflorol: the major constituent of *Allophylus edulis*. *Journal Of Ethnopharmacology*, Grande Dourados, p. 510-515, 06 set. **2016**.

Acknowledgments



Dehydroabietic acid from *Pinus elliottii* as precursor for new derivatives prepared by amidation reactions

Julian C.S. Pavan^{1*} (PG), Taís A.M. Figueredo¹ (PG), Mário F. C. Santos² (PQ), Vladimir C.G. Heleno¹ (PQ).

*julian.c.s.pavan@hotmail.com

¹Research Nucleus in Exact and Technological Sciences - University of Franca, Franca, SP.

²Exact Sciences Center - Federal University of Espírito Santo, Alegre, ES.

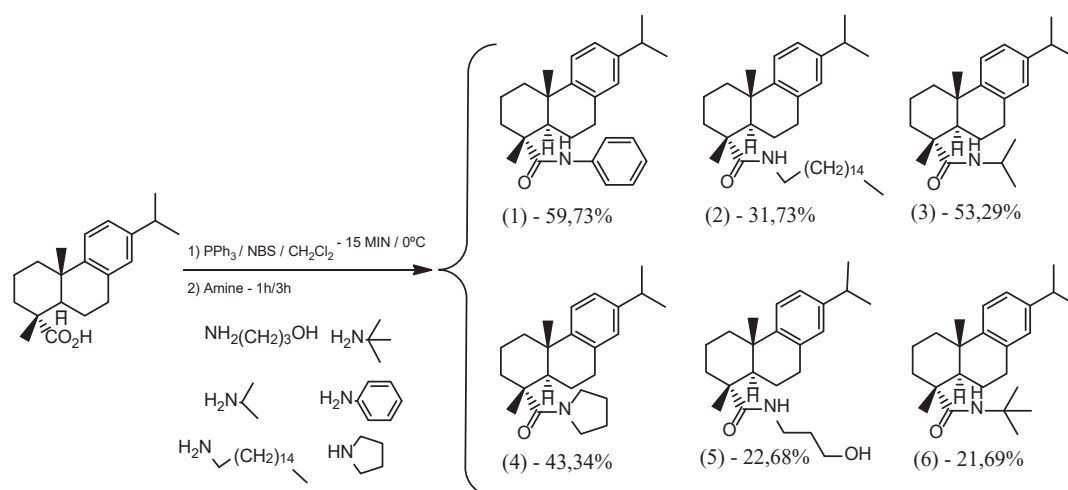
Keywords: Diterpenes, abietanes, structural modification, semi synthesis.

Highlights

The dehydroabietic acid was isolated from *Pinus elliottii* resin and was subjected to amidation reactions, yielding six derivatives, including four new compounds; all six identified by ¹H and ¹³C NMR.

Abstract

Pinus elliottii resin is composed of a non-volatile fraction, made up of bicyclic and tricyclic acid diterpenes, and a volatile fraction, which contains compounds from the monoterpene and sesquiterpene class that evaporate, facilitating the concentration of diterpenes^{1,2}. DA is one of the main compounds reported from coniferous plants belonging to *Pinus elliottii*³, and it presents a broad spectrum of bioactivity against several pathologies^{4,5}, what makes it an interesting starting material for the development of new semi-synthetic active compounds. The isolation of DA was performed in Reduced Pressure Chromatography and HPLC in reversed phase. With the objective to reach substances with improved interesting activities, DA was submitted to reactions through well-known methodologies described in the literature⁶. Six amide derivatives were obtained, as shown in the scheme below, four of which (3, 4, 5 and 6) are unpublished. All substances were properly identified by ¹H and ¹³C Nuclear Magnetic Resonance techniques. Derivatives and DA were submitted to biological assays to assess cytotoxicity.



References

¹NEIS, F. A. *et al.* Industrial Crops & Products. Vol. 132, p. 76-83, 2019. ²KEELING, C. I. Phytochemistry. Vol. 67, p. 2415-2423, 2006. ³GONÇALVES, M. D. *et al.* Fitoterapia, v. 128, p. 224-232, 2018. ⁴PERTINO, M. W. *et al.* Molecules, v. 22, n. 3, p. 369, 2017. ⁵VAHERMO, M. *et al.* Medicinal Chemistry Communication, v. 7, n. 3, p. 457-463, 2015. ⁶BANDGAR, R. P.; BETTIGERI, S. V. Communications. Vol. 34, p. 2917-2924, 2004.

Acknowledgments

This research was financial by CAPES, CNPq, and FAPESP.

Dehydrodieugenol B, a neolignan obtained from *Nectandra leucantha* aerial parts, is suitable for olefin cross-metathesis aiming preparation of antichagasic new derivatives

Anderson K. Ueno (PG),^{1*} Thalita S. Galhardo (PQ),² Thaís A. C. Silva (PQ),^{3,4} André G. Tempone (PQ),³ Dalmo Mandelli (PQ),² Cédric Fischmeister⁵, Christian Bruneau⁵ João Henrique G. Lago (PQ),² ueno@unifesp.com

¹Instituto de Ciências Ambientais, Químicas e Farmacêuticas, Universidade Federal de São Paulo (UNIFESP); ²Centro de Ciências Naturais e Humanas, Universidade Federal do ABC (UFABC); ³Centro de Parasitologia e Micologia, Instituto Federal Adolfo Lutz, (IFAL); ⁴Instituto SENAI de Inovação em Biotecnologia SENAI; ⁵Institut des Sciences Chimiques de Rennes, Université de Rennes

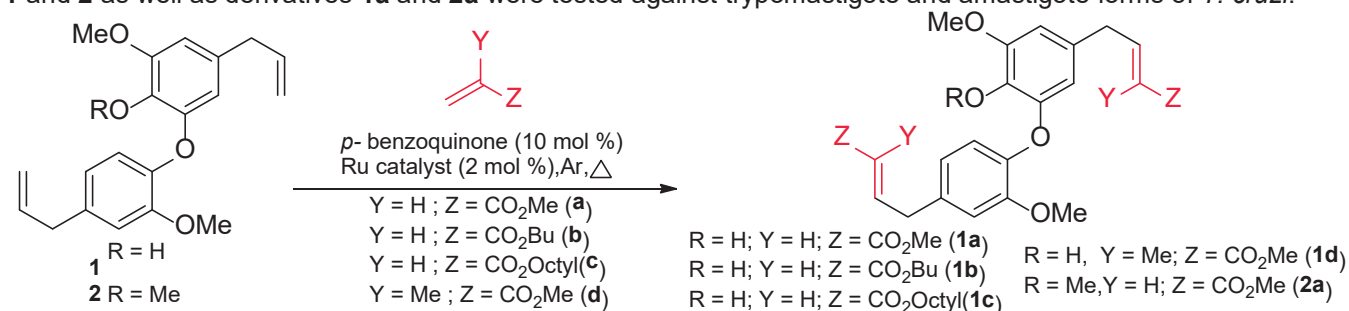
Key words: olefin cross metathesis, *Trypanosoma cruzi*, dehydrodieugenol B.

Highlights

This work presents the preparation and anti-*Trypanosoma cruzi* activity of five alkylformyl derivatives from dehydrodieugenol B and methyl dehydrodieugenol B isolated from *Nectandra leucantha*, via olefin cross-metathesis reaction. Additionally, mechanism of action of the most bioactive derivatives on parasite were investigated.

Abstract

Chagas disease is a tropical disease caused by *T. cruzi*.¹ It was estimated that at least one million people are infected in Brazil. Therapy is restricted to two drugs: benznidazole and nifurtimox, with severe side effects.¹ In this work, it was described the preparation of methyl, n-butyl, octyl and methylmetaformyldehydrodieugenol B (**1a-d**), and methylformyl-methyldehydrodieugenol B (**2a**) using dehydrodieugenol B (**1**) and methyldehydrodieugenol B (**2**), isolated from *Nectandra leucantha* twigs², by cross-metathesis reaction using methyl acrylate catalyzed by the second generation Hoveyda Grubbs catalyst (2 mol%) at 80°C in the environmentally friendly dimethyl carbonate solvent. Natural products **1** and **2** as well as derivatives **1a** and **2a** were tested against trypomastigote and amastigote forms of *T. cruzi*.



	trypomastigote (μM)			amastigote (μM)		
	IC ₅₀	CC ₅₀	NCTC	IC ₅₀	CC ₅₀	NCTC
1	38.6 ± 13.6	86.5 ± 10.4	>200	13.5 ± 11.0	10.2 ± 2.8	139.8
2	NA	NA	>200	23.0 ± 2.1	6.1 ± 0.7	>200
BNZ	5.5 ± 0.9	18.7 ± 4.1	>200	5.5 ± 0.9	18.7 ± 4.1	>200

Fig.1. Preparation of compounds **1a** and **2a** via olefin cross metathesis reaction from **1** and **2** and respective IC₅₀ and CC₅₀ values against trypomastigote and amastigote forms of *T. cruzi* (positive control: benznidazole – BNZ)

As observed, the addition of methylformyl group at allyl side chain in starting material caused enhancement of antiparasitic activity, mainly against amastigote forms since compounds **1a** and **2a** displayed IC₅₀ values of 10.2 ± 2.8 and 6.1 ± 0.7 μM, respectively, superior than natural products **1** and **2** and standard drug benznidazole (IC₅₀ 18.7 ± 4.1 μM). However, **1a** showed slightly toxicity (CC₅₀ = 139.8 μM) while **2a** was non-toxic (CC₅₀ > 200 μM) against NCTC cells. Based on these results, possible phenotypical mechanisms of action of **1a** and **2a** were evaluated. Initially, a depolarization of the plasma membrane electric potential of the parasite was observed for both derivatives as they were capable to depolarize the mitochondria membrane until two hours of incubation. Considering the effect on bioactivity through enhancement of the length of alkyl chain, derivatives **1b** – **1d** will be evaluated against *T. cruzi* on *in vitro* essays. Those future data will clear the role of alkyl chain for structure-activity relationship studies for a DHDB core prototype for possible Chagas disease treatment.

¹Secretaria de Vigilância em Saúde, Ministério da Saúde, Boletim – Territorialização e vulnerabilidade para doença de Chagas crônica. 2022

²Grecco, S.S. et al. *J. Venom. Anim. Toxins Incl. Trop. Dis.* 2018, 24 (5), 122.

Acknowledgments

FAPESP, CNPq, CAPES, UFABC, Université de Rennes.

Área: QPN

(Inserir a sigla da seção científica para qual o resumo será submetido. Ex: ORG, BEA, CAT)

Dereplication by GC-MS/Molecular Networking and Antimicrobial Activity of Essential Oil of *Duguetia lanceolata* (Annonaceae).

Jackson Monteiro (PG)¹, Geovanna N. Antonelli (IC)¹, Erick Dantas (PG)¹, Marisi G. Soares (PQ)², João H. G. Lago (PQ)³, Renata Pascon (PQ)¹, Marcelo Vallim (PQ)¹, Patricia Sartorelli (PQ)^{1*}

jackson.monteiro@unifesp.br; psartorelli@unifesp.br

¹Universidade Federal de São Paulo – UNIFESP; ²Instituto de Química, Universidade Federal de Alfenas – UNIFAL; ³Centro de Ciências Naturais e Humanas, Universidade Federal do ABC – UFABC;

Key-words: *Duguetia lanceolata*, Terpenes, Antifungal activity, Essential oil.

Highlights

The essential oil of *Duguetia lanceolata* leaves was analyzed for chemical composition by GC-FID and GC-MS, identified corresponding to 83.73% of the total composition of the oil. A molecular network was constructed via the *Global Natural Products Social Molecular Networking* (GNPS) for the visual exploration of the volatile constituents among *Duguetia* species.

Resumo/Abstract

The use of antibiotics currently has several side effects, such as the risk of bacterial resistance and adverse reactions.¹ Antimicrobial activity investigations using natural product-based, such as essential oils are increasingly important against pathogenic microorganisms. However, essential oils are highly complex and require modern analytical and computational approaches to streamline the identification of bioactive substances. This study combined a GC-MS analysis and molecular network approach with specific antimicrobial assays as a novel strategy for the discovery of potential bioactive substances in complex biologicals. The essential oil of *Duguetia lanceolata* leaves was analyzed for chemical composition by GC-FID and GC-MS, and 13 compounds were identified corresponding to 83.73% of the total composition of the oil with bisabolene (24.87%), germacrene-D (18.60%) and α -gurjurenene (12.08%) as main compounds using the NIST 08 mass spectra library for identification, as well as by comparison with mass spectra available in the literature. A consecutive molecular network was constructed through the *Global Natural Products Social Molecular Networking* (GNPS) for the visual exploration of volatile constituents among *Duguetia* species allowing the identification of another 11 compounds that had not been previously identified in NIST 08. The essential oil, fractions and subfractions were evaluated for antimicrobial potential against *Candida albicans*, *Cryptococcus neoformans* and *Saccharomyces cerevisiae* strains. The crude oil showed antimycotic activity against *C. neoformans* and *S. cerevisiae*. The fraction III showed antifungal activity against *C. albicans* and *C. neoformans*. Although (β -bisabolene) did not show separate antifungal activity, in association these compounds showed antifungal activity against *C. albicans* strains, *C. neoformans*, thus suggesting potential synergism between the compounds the essential oil.

¹Morrison, Lindsay, and Teresa R. Zembower. *Antimicrobial resistance; Gastrointestinal Endoscopy Clinics* (2020): 619-635.

²Hobson, Christian, Andrew N. Chan, and Gerard D. Wright. *The antibiotic resistome: a guide for the discovery of natural products as antimicrobial agents; Chemical Reviews* (2021): 3464-3494.

Agradecimentos/Acknowledgments

FAPESP, CAPES and CNPq.

Dereplication of extracts of endophytic fungi obtained from *Calea pinnatifida* (Asteraceae)

Bianca B. Fernandes (PG)^{1*}, Marcelo J. P. Ferreira (PQ)², Suzan P. Vasconcellos (PQ)¹, Patricia Sartorelli (PQ)¹.
bianca.barna@unifesp.br; psartorelli@unifesp.br

¹ Instituto de Ciências Ambientais, Química e Farmacêutica, UNIFESP; ² Instituto de Biociências, USP

Palavras Chave: *Calea pinnatifida*, endophytic fungi, dereplication, GNPS, molecular network.

Highlights

Seventeen endophytic fungi were obtained from *Calea pinnatifida* leaves; Were cultivated in two culture media to increase and diversify metabolic production; Terpenes and alkaloids were annotated through the GNPS platform from the crude extracts of two strains.

Resumo/Abstract

The search for new drugs, through bioactive substances from plants and microorganisms, is becoming increasingly interesting. Endophytic microorganisms gain prominence due to the production of a great diversity of classes and metabolites. *Calea pinnatifida* is a native Brazilian plant belonging to the Asteraceae family and is widely used in folk medicine to treat stomach pain, giardiasis and amoebiasis. However, this species was not investigated in relation to their endophytic microbiota and, here, it was the object of study. Seventeen endophytic fungi were isolated from leaves and stem of the plant, in order to cultivate them in different culture media such as potato dextrose and rice. Aiming a better fungal growth and development, the One Strain Many Compounds (OSMAC) cultivation technique was applied to obtain better yield and metabolic diversity produced by the endophytic fungi. The analysis of the extracts was performed by liquid chromatography coupled to mass spectrometer (HPLC-MS/MS) and in association with the Global Natural Product Social Molecular Networking (GNPS) platform, it was possible to perform the organization and dereplication of the extracts to increase the efficiency of the search for bioactive compounds. MS/MS spectra were obtained in maXis QToF ESI (+) mode. All MS/MS data were then converted to mzXML format to perform dereplication in GNPS for database matching. Structural annotations of compounds fusaproliferin (terpene) and caffeic acid (polyphenol) were detected in the fungal metabolome of CPFF12A and CPFF13A strains cultured in rice. In this way, it was possible to observe the variety of classes of compounds produced by endophytic fungi, highlighting the potential of these microorganisms for prospecting new drugs.

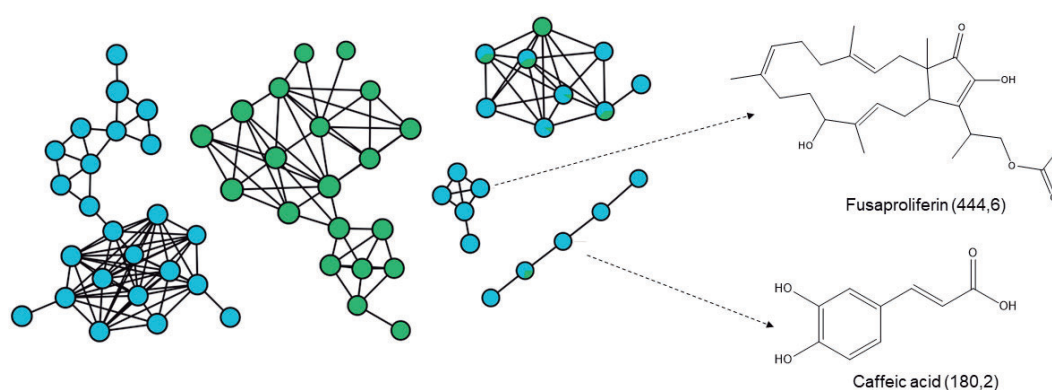


Figure 1 – GNPS-generated molecular network with annotation of fusaproliferin and acid caffeic. National Center for Biotechnology Information (2023).

Agradecimentos/Acknowledgments

To the collaborators and funding agencies: Capes, CNPq and FAPESP.

Dereplication of secondary metabolites associated with the phytopathogenic fungus *Austropuccinia psidii*, a major threat to the *Myrtaceae* family

Stephanie N. Silva (PG),¹ Carolina A. A. Hayashibara (PQ),² Maria C. Quecine (PQ),² Taicia P. Fill (PQ).^{1*}

s230061@dac.unicamp.br; taicia@unicamp.br

¹Departamento de Química orgânica, Unicamp, Campinas-SP, Brazil; ²Departamento de Genética, ESALQ, Piracicaba-SP, Brazil.

Palavras Chave: *Austropuccinia psidii*, Secondary metabolites, UHPLC-MS/MS, Molecular Networking.

Highlights

This study evaluated the secondary metabolism of *Austropuccinia psidii*, isolated from *Eucalyptus grandis*, using UHPLC-MS/MS combined with bioinformatics tools such as *Molecular Networking*.

Abstract

Austropuccinia psidii is a biotrophic fungus capable of infecting about 460 species and 73 genera of the *Myrtaceae* family, including plants with significant commercial importance, such as species of the genus *Eucalyptus* spp., which can be used as raw material for the cellulose and paper industry in Brazil.¹ Nowadays, the pathogen control strategies involve genomic tools for selection of new rust-resistance genotypes or application of fungicides. However, these strategies involve many problems, such as the high costs and health risk concerns. Studies related to the understanding of the pathogen-host interaction have been focused on the physiological adaptation and response of the plant.² On the other hand, pathogenic mechanisms of the fungus are little investigated, especially the secondary metabolites produced that may contribute to the establishment of the infection. So, understanding the metabolism of *A. psidii* can guide efficient, economical and environmentally friendly biological control strategies.

The aim of this study was to evaluate the secondary metabolism of *A. psidii*, detecting and investigating the biological role of these compounds in the phatosystem. For this, metabolites were extracted from the spores, isolated from a *Eucalyptus grandis* plant infected with the pathogen, using two different methods and analyzed using UHPLC-MS/MS. Data dereplication was performed using tools of Global Natural Products Social Molecular Networking (GNPS) platform.

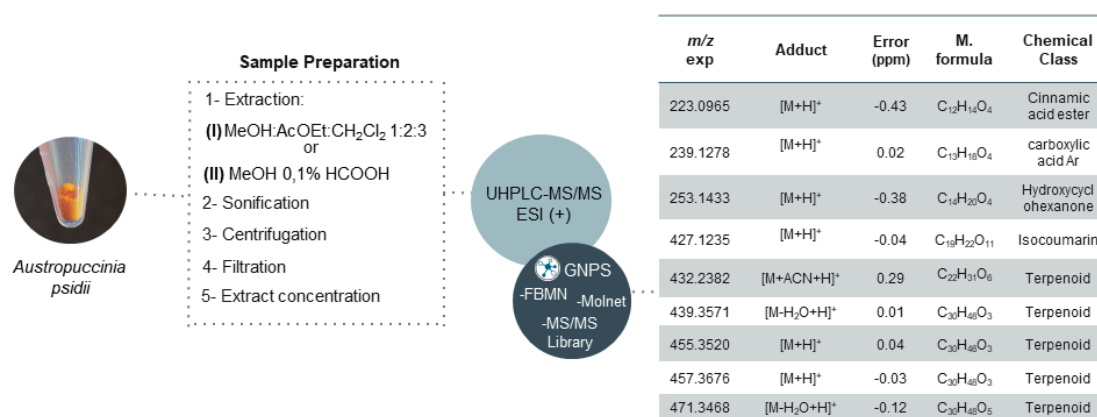


Figure 1. Applied extraction methods, analysis and annotated metabolite in the study.

Analysis of *A. psidii* metabolism using UHPLC-MS/MS allowed annotation of 9 metabolites of different chemical classes (**Figure 1**), mainly terpenoids, based on the exact mass of the ion, RT and MS/MS fragmentation pattern. The results indicate possible metabolic pathways related to plant-pathogen interaction, a first step towards the development of new fungus control strategies.

1. Sekiya, A. et al. *Front. Plant Sci.*, 2021, 11, 604849. 2. Moffitt, M. C. et al. *Microorganisms*, 2022, 10, 383.

Acknowledgments

The authors are grateful to the institutions Fundação de Amparo à pesquisa do Estado de São Paulo (FAPESP) and Coordenação de Aperfeiçoamento de Pessoal de Nível Superior – Brasil (CAPES) for the financial support.

46ª Reunião Anual da Sociedade Brasileira de Química: "Química: Ligando ciências e neutralizando desigualdades"

Desreplicação molecular e avaliação da atividade anti-*Trypanosoma cruzi* in vitro do óleo essencial das partes aéreas de *Vernonanthura polyanthes* (Asteraceae)

Felipe S. Sales (PG),¹ Beatriz A. de Andrade (PG),² Dayana A. S. Ferreira (PG),² Gustavo F. Bitencourt (PG),¹ Dalmo Mandelli (PQ),¹ André G. Tempone (PQ),² João Henrique G. Lago (PQ),^{1*}

felipe.sales@ufabc.edu.br; joao.lago@ufabc.edu.br

¹Centro de Ciências Naturais e Humanas (CCNH), Universidade Federal do ABC (UFABC), Santo André – SP; ²Centro de Parasitologia e Micologia, Instituto Adolfo Lutz (IAL).

Palavras Chave: óleo essencial, assa-peixe, *Vernonanthura polyanthes*, sesquiterpenos, *T. cruzi*.

Highlights

Molecular dereplication and in vitro evaluation of anti-*Trypanosoma cruzi* of the essential oil from *Vernonanthura polyanthes* (Asteraceae). The E.O. of *V. polyanthes* was dereplicated and indicated to be composed by sesquiterpenes. The crude oil showed anti-*T. cruzi* activity against trypomastigotes with higher potency than benznidazole

Resumo

A Doença de Chagas, causada pelo protozoário *Trypanosoma cruzi*, afeta milhões de indivíduos ao redor do mundo, sendo países do continente americano os mais acometidos¹. No Brasil, entre 2010 e 2019, a quantidade de óbitos causados por esta enfermidade chegou a um patamar superior a 45 mil registros². O principal fármaco utilizado para o tratamento da infecção por *T. cruzi* é o benznidazol, o qual apresenta diversos efeitos adversos aos usuários por conta da sua toxicidade³. Frente a essa problemática, a busca de novos agentes quimioterápicos faz-se necessária sendo os produtos naturais uma fonte importante de novos compostos bioativos. Nesse contexto, a espécie vegetal *Vernonanthura polyanthes*, conhecida popularmente como “assa-peixe”, é usada, na medicina popular, como antipirético, diurético e no tratamento de reumatismos, disfunções do sistema respiratório e também para tratamento da malária⁴. Estudos anteriores realizados por nosso grupo de pesquisa descreveu a ocorrência de triterpenos livres e acetilados, especialmente α - e β -amirina além de ψ -taraxasterol e lupeol. Devido a uso popular dessa espécie como antiparasitário, no presente trabalho foi investigada a composição química do óleo essencial das partes aéreas de *V. polyanthes* seguido da avaliação in vitro da atividade anti-*T. cruzi*. Assim, do material vegetal coletado na região de Pindamonhangaba/SP em julho/2021, os compostos voláteis foram extraídos via hidrodestilação em aparelho do tipo Clevenger. Posteriormente, o óleo bruto foi submetido à desreplicação molecular por meio de cromatografia a gás acoplada a espectrometria de massas (CG/EM) bem como pelo cálculo do índice de Kovats o que permitiu a identificação de 32 compostos (95,4% do total). Dentre as substâncias identificadas, destacam-se os sesquiterpenos 9-*epi*-(*E*)-cariofileno (3,8%), biclogermacreno (9,8%), β -cariofileno (11,8%), α -humuleno (12,8%) e germacreno D (16,4%) como os majoritários. Estudos anteriores com essa espécie vegetal indicaram que o óleo essencial das folhas é composto principalmente por monoterpenos, em especial não oxigenados, além de apresentar atividade in vitro frente a *L. infantum*⁵, demonstrando que o óleo analisado apresenta um perfil químico diferenciado. Após avaliação do potencial frente a formas tripomastigotas do parasita *T. cruzi*, foi obtido um valor de CE₅₀ de 11,5 μ g/mL, indicativo de potencial superior ao observado para o controle positivo benznidazol com CE₅₀ de 18,7 μ g/mL⁶. No que tange a toxicidade, o óleo essencial das partes aéreas de *V. polyanthes* mostrou CC₅₀ > 200 μ g/mL frente a células NCTC, fornecendo, portanto, um índice de seletividade superior a 17,4. Frente aos resultados obtidos é possível inferir que este estudo indica aplicação de plantas medicinais brasileiras bastante comuns no território nacional, como a *V. polyanthes*, para o desenvolvimento de novos protótipos no tratamento da Doença de Chagas.

Referências: ¹WHO, **Chagas disease**, 2021; ²Brasil, **Ministério da Saúde**, 2022; ³Ferreira, A. M. et al., **Cad. Saúde Colet.** 2019, 27 (3), 354-362; ⁴Brasil, **Vernonia polyanthes**, 2014; ⁵Moreira R. R. D., et al., **Nat. Prod. Res.** 2017, 31(24), 2905-2908; ⁶Conserva, G. A. A. et al., **PLoS ONE** 2021, 16(2), 1-18.

Agradecimentos

CAPES, CNPq, FAPESP, IAL e UFABC.

Área: QPN

DESREPLICATION OF EXTRACTS FROM *Agaricus subrufescens* BY UHPLC-ESI-HRMS/MS COMBINED WITH MOLECULAR NETWORK

Andreisa C. Monteiro (PG),^{1*} Lhais Araujo Caldas (PG),¹ Diego Cunha Zied (PQ),² Patrícia Sartorelli (PQ).¹

andreisa.monteiro@unifesp.br; lhais.caldas@unifesp.br; dczied@gmail.com; psartorelli@unifesp.br

¹Institute of Environmental, Chemical and Pharmaceutical Sciences, UNIFESP, Brazil;

²College of Agricultural and Technological Sciences, UNESP, Brazil.

Keyword: *Agaricus subrufescens*, Natural Products, Metabolomics, GNPS.

Highlights

Chemical profiling of *A. subrufescens* extracts by LC-ESI-MS/MS through molecular network approach using GNPS. Analyzed by molecular network associated with the GNPS platform.

Abstract

Although we currently have an arsenal of bioactive substances from natural sources, such as plants and fungi, we still have much to advance in order to prospect novel bioactive metabolites. In this sense, in recent years there has been an increasing search for substances with bioactive properties for the production of new drugs and the treatment of diseases, such as cancer. The macrofungus *Agaricus subrufescens* is a basidiomycete belonging to the Agaricaceae popularly known as "cogumelo-do-sol", the species is native to Brazil and is distributed worldwide, mostly due to its nutritional, environmental, economic, and medicinal potential¹. Thus, the present study aims to access the chemical profile of *A. subrufescens*, as well as obtaining molecular network from different extracts of the basidiomycete with the aid of GNPS (Global Natural Products Social Molecular Networking). Samples were analyzed in UHPLC-ESI-MS/MS (qTOF) in positive mode electrospray ionization on three strains of *A. subrufescens*. The resulting MS/MS data were organized in the form of a molecular network highlighting the structural families using the GNPS platform². Through the resulting molecular network it was possible to obtain 282 clusters, grouped into 26 spectral families, 20 molecules of the following classes of metabolites were annotated: fatty acids, amides, amines, amino acids and phospholipids in smaller quantities. Using the molecular network, for example, the molecules pantothenic acid (m/z 220.12), 13-Docosenamide (m/z 338.34) and palmitamide (m/z 256.26) were annotated. Of which, the pyroglutaminylytyrosine (m/z 293.11) and octadecanamide (m/z 284.29) molecules showed correlation between the IAP and ABZC lineages, while the C-18:2 alpha-linolenic acid (m/z 352.29) and Glutamine-C18:2 (m/z 409.29) molecules showed correlation between the IAP and 0403P lineages. In addition, no correlation was identified for the molecule L-Tryptophan (m/z 205.09), since it is only found in IAP. However, the present analysis showed spectral correlations in most of the annotated compounds, as well as, showed indications of production and divergence of production of certain metabolites among the different strains. It is also concluded that the performance of the analysis through the use of the GNPS platform is an important tool for obtaining the mapping of the chemical profile in the studied species, thus facilitating the investigation in an objective, fast and reliable way.

[1] FIRENZUOLI, F, GORI L, Lombardo G. The medicinal mushroom *Agaricus blazei murrill*: review of literature and pharmaco-toxicological problems. **Evidence-Based Complementary and Alternative Medicine** 5:3–15.2008.

[2] WANG, MINGXUN, et al. "Sharing and community curation of mass spectrometry data with Global Natural Products Social Molecular Networking." **Nature Biotechnology** 34.8 (2016): 828-837. PMID: 27504778, <https://www.nature.com/articles/nbt.3597>

Acknowledgments

This study was funded by CAPES, CNPQ and FAPESP.

Determination of phenolic and xanthinic markers in specialty coffee beans for sensory quality, post-harvest processing and geographical origin correlation

Heloísa Tieghi (IC),¹ Luana de Almeida Pereira (PG),¹ Derielsen Brandão Santana (PG),² Ronaldo Luiz Mincato (PQ),² Daniela Aparecida Chagas de Paula (PQ),¹ Danielle Ferreira Dias (PQ),¹ Marisi Gomes Soares (PQ),¹ Willem Guilherme de Araújo,³ Paula Carolina Pires Bueno (PQ)^{1*}.

heloisa.tieghi@sou.unifal-mg.edu.br; paula.bueno@unifal-mg.edu.br

¹Institute of Chemistry, UNIFAL-MG; ²Institute of Natural Sciences, UNIFAL-MG; ³Empresa de Assistência Técnica e Extensão Rural do Estado de Minas Gerais, EMATER-MG

Palavras Chave: Coffea arabica, Metabolomics, specialty coffee

Highlights

- Phenolic and xanthinic compounds in specialty coffee samples were analyzed by HPLC-UV-DAD
- The multivariate data analysis included the sensorial score, the region of origin, the post-harvesting protocol and the chemical profile
- Changes were observed in the quantitative chemical profile of samples from regions of higher altitude
- The post-harvesting processing may influence the chemical profile and the sensorial analysis.

Abstract

Coffee is an important commodity, grown in more than 80 countries¹ and traded in all continents. Brazil is the main producer and exporter. The state of Minas Gerais accounts for half of the national production, with large cultivation areas distributed in the regions 'Sul de Minas', 'Cerrado', 'Chapada de Minas', and 'Matas de Minas'². The species *Coffea arabica* is the most sold and consumed in the world due to its sensory characteristics, such as sweetness, acidity and aroma. These attributes are a consequence of the chemical composition of the coffee bean, which can be influenced by external factors, soil and climate conditions, or by processes carried out between its harvesting and consumption. One of the most valuable niches in the market is the specialty coffee, for which both production and analysis are certified by specialized evaluators (Q-graders) and internationally carried out according to the protocols described by the Specialty Coffee Association (SCA). For such coffees, 10 sensory attributes are evaluated: fragrance/aroma, uniformity, clean cup, sweetness, flavor, acidity, body, aftertaste, balance, overall, and defects³, which allows the sensory characterization of different coffee samples/cultivars and influences their pricing. However, despite being standardized, it is a subjective analysis in which it is not possible to distinguish the presence or content of different classes of chemical substances commonly present. Therefore, the present study aims at the chemical analysis of specialty coffees produced in different regions of the state of Minas Gerais, in order to determine the relative composition of chemical markers that complement the sensorial classification, as well as to provide chemical parameters for the evaluation of their quality, authentication of origin and national and international valuation. In order to achieve this goal, a targeted metabolomics approach was used. The quantitative analyses were performed by HPLC-UV-DAD and the optimized method employed reversed-phase gradient elution (C18, 150 x 4.6 mm x 5 µm), using water acidified with 0.2% formic acid (A) and methanol containing 10% ACN and 0.2% formic acid (B). Analytical curves were prepared using authentic standards of trigonelline, theobromine, theophylline, chlorogenic acid, caffeine, caffeic acid, ferulic acid, and *p*-coumaric acid. Samples of green coffee beans (traditional and pulped) were extracted at the ratio of 100 mg of powder to 1 mL of 80% MeOH containing naringenin as internal standard, with the aid of an ultrasound bath for 15 min. The extracts were centrifuged, filtered through a 0.22 µm PTFE membrane, diluted with the extracting solvent and analyzed (n=3). The uni and multivariate statistical analyses included the quantitative chemical profile of the analyzed samples, the geographical origin, the score obtained in the sensorial analysis and the processing protocol. The results show that the content of the analyzed markers varies among the Matas de Minas, Sul de Minas and Cerrado regions. The sensory analysis also reflected the processing type and the profile of xanthines and phenolic compounds

¹Semedo, J. N. et al., 2018. *Climate Change Management*, p. 465

²ABIC, 2021

³Malta, M. R. et al., 2021. *Frontiers in Sustainable Food Systems*, v. 5, p. 715385

Acknowledgments

Authors are grateful to FAPEMIG (011/2022), Emater-MG and Unifal-MG.

Determination of the relative configuration of a new labdane from *Austro eupatorium inulaefolium* using pip-HSQMBC-IPAP technique

Francielli Alana Pereira* (PG),¹ Maria Eduarda V. de Souza (IC),¹ Cleverton S. Fernandes (PQ),¹ Beatriz P. Moreno (PQ),¹ Bianca D. B. Sahm (PG),² Andressa L. Ieque (PG),³ Marta R. B. do Carmo (PQ),⁴ Regiane B. de L. Scodro (PQ),³ Leticia V. Costa-Lotufu (PQ),² Ernani A. Basso (PQ),¹ Maria H. Sarragiotto (PQ),¹ Debora C. Baldoqui (PQ).¹

dcbaldoqui@uem.br; alanafranhp@gmail.com

¹Departamento de Química, UEM; ²Instituto de Ciências Biomédicas, USP; ³Laboratório de Bacteriologia Médica, UEM; ⁴Departamento de Biologia Geral, UEPG.

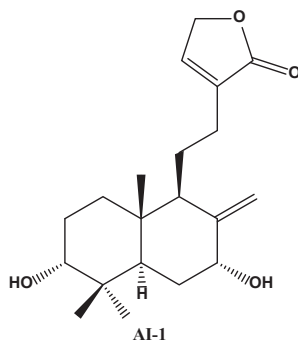
Palavras Chave: *Austro eupatorium inulaefolium*; Labdane; Dereplication; antiproliferative activity; anti-*Mycobacterium tuberculosis* activity;

Highlights

Although *Austro eupatorium inulaefolium* has been extensively studied, a new labdane derivative was isolated. Others twenty compounds were putatively identified from using dereplication techniques.

Resumo/Abstract

Austro eupatorium inulaefolium, popularly known as "Salvia amarga" and "erva de Santa Maria", is among of the plants most empirically used as medicine in Colombian Andes. In Paraguay it is used as a contraceptive, and in Colombia it is employed to treat snake bites. For this reason, *A. inulaefolium* is the most studied species from *Austro eupatorium* genus, and labdane-type diterpenes are the main specialized metabolites found in this species. Dried aerials parts of *A. inulaefolium* (540 g), collected in Ponta Grossa, Paraná, were ground and exhaustively extracted with ethanol at room temperature. Vacuum concentration yielded the crude extract (117 g, AI-CM), a part of the extract (2 g) was resuspended in MeOH:H₂O (1:1) and partitioned into hexane (230 mg, AI-FHEX), dichloromethane (160 mg, AI-FDC), ethyl acetate (290 mg, AI-FEA) and hydromethanolic (150 mg, AI-FHM) fractions. A dereplication study of AI-FDC and AI-FEA fractions were carried out using ultra-high performance liquid chromatography coupled with high performance mass spectrometry (UHPLC-HRMS) for data acquisition, and molecular networking for data analysis study, which led to the putative identification of twenty compounds, and nine of them are labdanes. Another part of the AI-CM (10 g) was resuspended in MeOH:H₂O (1:1) and partitioned using dichloromethane. Dichloromethane fraction (5,75 g) was submitted to chromatographic column over silica gel and afforded a new diterpene of labdane type (1,92 g, **AI-1**). It is important to note that **AI-1** is the major compound present in this species, and although this plant has been extensively studied, this is the first report of this compound. The relative configuration of **AI-1** was determined using the J³CH coupling constants obtained by the pip-HSQMBC-IPAP technique. Through this technique, considering the values of the coupling constants, the sin and anti-relationships between the methyl groups and the other stereogenic centers were identified, allowing to determine the relative stereochemistry. The analysis was performed on a Bruker Avance III HD operating at 500MHz for the ¹H core employing a 1.7 mm probe. The crude extract, fractions and the new labdane derivative (**AI-1**) of *A. inulaefolium* were inactive when evaluated for their antiproliferative and anti-*Mycobacterium tuberculosis* potential.



Agradecimentos/Acknowledgments

UEM, CAPES, CnPq, INCT-BioNat.

Development and Application of a 2D-LC-MS on-flow methodology to assess cholinesterases inhibition activity of complex natural extracts.

João V.P.O. Elói (PG),^{1*} Carmen L. Cardoso (PQ).¹

joaovitorpoe@usp.br; ccardoso@ffclrp.usp.br

¹Faculdade de Filosofia, Ciências e Letra de Ribeirão Preto, USP.

Keywords: Natural products, Alzheimer's disease, Immobilized enzyme reactors, Cholinesterases, 2D-LC-MS

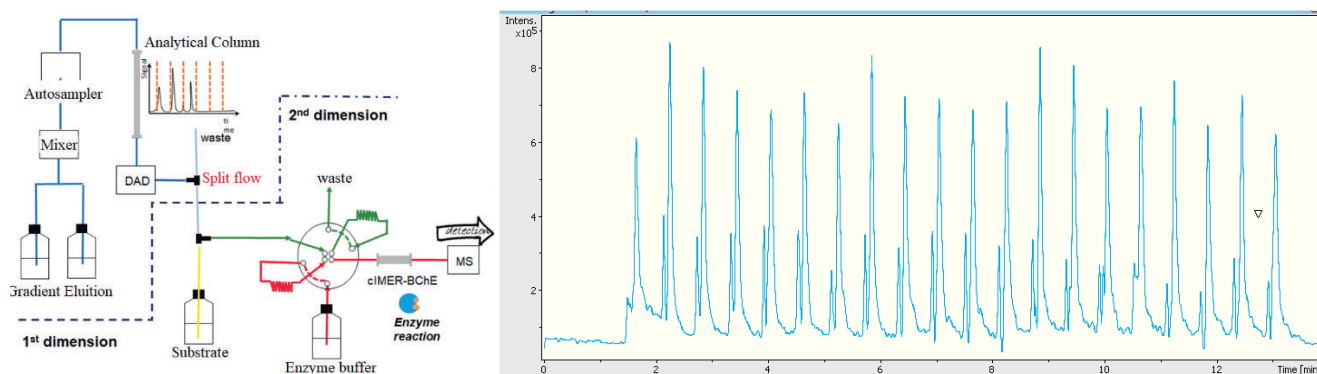
Highlights

Search for inhibitors of Acetylcholinesterase and Butyrylcholinesterase, enzymes associated to Alzheimer's disease, with a new efficient methodology that avoids traditional method's drawbacks.

Resumo/Abstract

Alzheimer's disease (AD) is a neurodegenerative disorder originated by multifactorial causes, which affect the central nervous system, causing, among other effects, brain atrophy, memory loss and cognition decrease¹. The cognition decrease has been associated with high acetylcholinesterase (AChE) activity and, for more advanced stages of the disease, Butyrylcholinesterase (BChE)¹. As a potential source of bioactive compounds, Natural products show characteristic complexity that makes the identification of bioactive compounds time-consuming. Two-dimension liquid chromatography with mass spectrometry detection is an innovative technique applied for crude extract analysis: In one run, it is possible to separate the parts of an extract in one chromatography dimension and transfer each fraction from the analytical column (LCxLC), or just the fractions of interest (LC-LC) to the other dimension². Herein, in the second dimension we used a capillary Immobilized enzyme reactor (cIMER) to directly identify each fraction's inhibitory enzyme's activity when it is passing through the IMER, to accelerate the identification of actives compounds. Using the previously developed methodology³, the enzyme BChE was covalently immobilized on capillary fused silica producing an cIMER-BChE. After the immobilization, its catalytic activity was monitored by detection of the product of the enzymatic reaction, choline (104 m/z) post second dimension (Figure 1). In conclusion, the immobilization was successful, and the enzyme was active in the analysis conditions. For the method's validation, a mixture of standard inhibitors, containing galanthamine, tacrine and donepezil was used.

Figure 1: Schematic representation of 2D-LC system. Peaks produced by the detection of the ion choline (104 m/z), in different modulation times, which indicates the successful immobilization of active BChE:



¹ Carreiras, M. C.; Marco, J. L. *Current Pharmaceutical design*, v. 10, n. 25, p. 3167, 2004. doi: 10.2174/1381612043383421

² Stoll, D. R.; Carr, P. W. *Analytical Chemistry*, v.89, 1, 519–531, 2017. doi.org/10.3389/fmolb.2022.868597

³ Seidl, C. et al. *Front. Mol. Biosci.* 9: n 868597, 2022. doi: 10.3389/fmolb.2022.868597

Agradecimentos/Acknowledgments

The authors thank São Paulo State Foundation FAPESP (grants 2022/00432-7; and 2014/50249-8 and GSK), National Council for Scientific and Technological Development CNPq and Coordenação de Aperfeiçoamento de Pessoal de Nível Superior, Brazil (CAPES), Finance Code 001, for financial support and scholarship.

46ª Reunião Anual da Sociedade Brasileira de Química: "Química: Ligando ciências e neutralizando desigualdades"

Diversity of bile salts in anuran gallbladders from the Atlantic Forest using a molecular networking approach

Ana C. Zanatta (PQ),¹ Andrés E. Brunetti (PQ),² Norberto Peporine Lopes (PQ).^{1*}

anczanatta@usp.com; npelopes@fcrp.usp.br

¹Faculty of Pharmaceutical Science, University of São Paulo, USP, Ribeirão Preto, SP, Brazil; ²Instituto de Biología Subtropical (IBS) – CONICET, Universidad Nacional de Misiones – UnaM, Posadas, Misiones, Argentina

Palavras Chave: Bile salts, Anuran, Gallbladders, Diet, Mass spectrometry, Molecular networking.

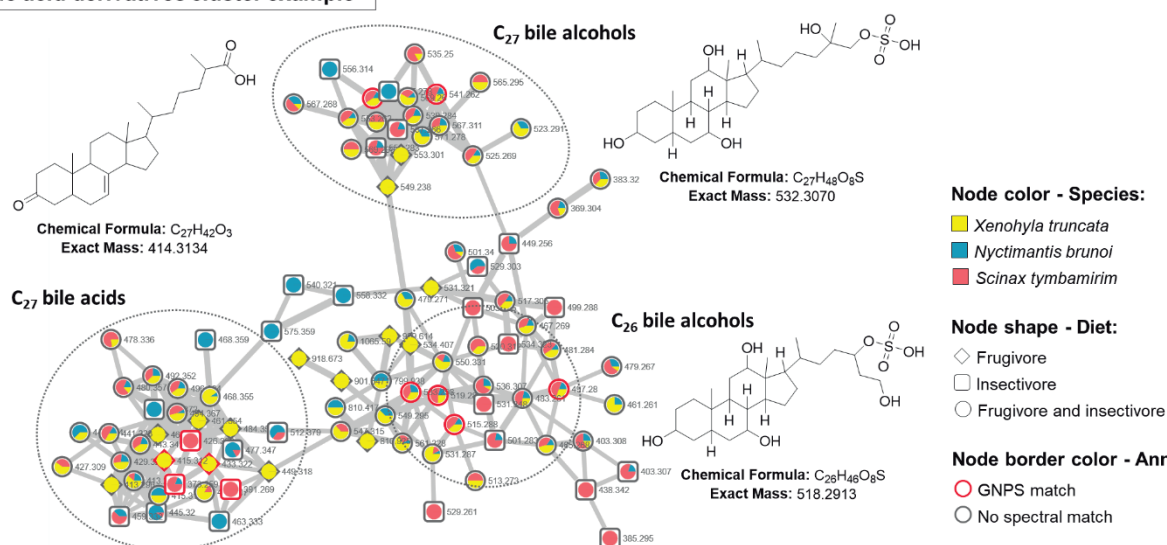
Highlights

- LC-MS-based molecular networking approach allowed the annotation of 15 bile salts derivatives.
- Anurans with different diets showed variations in the composition of bile salts.

Resumo/Abstract

Bile acids and bile-acid-like molecules are produced by vertebrates with important physiological functions in the absorption, transport and storage of dietary substances.¹ Anuran species have some of the most complex bile salt profiles.^{2,3} In this regard, to better understand the chemical composition of the gallbladder of anuran species from the Atlantic Forest on a dietary basis, we conducted a thorough study using LC-MS data analysis technique. The study helped obtain a profile of bile acids and derivatives of three anuran species of the Hylidae family with different diet types - frugivore, *Xenohyla truncata* and insectivore, *Nyctimantis brunoi* and *Scinax tymbamirim*. The chemical profile of the gallbladder methanol/water 8:2 (v/v) extracts was obtained by HPLC-ESI-HRMS/MS analysis in positive ionization mode. The data were uploaded onto the GNPS platform following the workflow⁴ to generate the molecular networking. Visual inspection of these data showed variation in bile salt composition according to individual species and diet. The use of molecular networking contributed toward in the annotation of 15 bile salts derivatives including C₂₇ bile alcohols, C₂₆ bile alcohols, C₂₇ bile acids, and C₂₄ bile acids. In addition, biliverdin derivatives, a green bile pigment in many amphibians, was also found. These results support the complexity of bile salts in anurans. The variation in bile salt structures observed may be related to evolutionary relationships for each species or by diet-induced processes.

Bile acid derivatives cluster example



¹Kuipers, F.; et al. *Nat. Rev. Endocrinol.* **2014**, *10*, 488–498.; ²Hagey, L.R.; et al. *Physiol. Biochem. Zool.* **2010**, *83*, 308–321.; ³Hofmann, A.F.; et al. *J. Lipid Res.* **2010**, *51*, 226–246.; ⁴Wang, M.; et al., *Nat. Biotechnol.* **2016**, *34*, 828–837.

Agradecimentos/Acknowledgments

The authors would like to acknowledge the Brazilian research funding agencies CNPq, CAPES and FAPESP. 46^o Reunião Anual da Sociedade Brasileira de Química: "Química: Ligando ciências e neutralizando desigualdades"

Docking, Larvicidal and Oviposition Deterrence activities of Beta-Germacrene-4-ol against *Aedes aegypti*

Daniela Maria do Amaral Ferraz Navarro (PQ),^{1*} Bheatriz Nunes de Lima Albuquerque (PG),¹ Marcelo Felipe Rodrigues da Silva (PG),¹ Patrícia Cristina Bezerra da Silva (PG),¹ Camila Soledade de Lira Pimentel (PG),¹ Suyana Karolyne Lino da Rocha (PG),¹ Júlio César Ribeiro de Oliveira Farias de Aguiar (PG),¹ Afonso Cordeiro Agra Neto(PQ),² Matheus Gabriel Moura Gomes(PG),³ Edeildo Ferreira da Silva-Júnior (PQ).³

daniela.navarro@ufpe.br

¹Departamento de Química Fundamental, UFPE; ²Jardim Botânico de Recife, Pernambuco, Brasil; ³Instituto de Química e Biotecnologia, UFAL.

Palavras Chave: *β*-germacrene-D-4-ol, atividade larvicida, atividade deterrente de oviposição.

Highlights

Larvicidal activity of *A. aegypti* (LC₅₀) were 18.23 ppm for *β*-germacrene-D-4-ol. *β*-germacrene-D-4-ol exhibited oviposition deterrence activity in 5, 10 and 50 ppm. *β*-germacrene-D-4-ol achieves deterrence by interacting with OBP1

Resumo/Abstract

The chromatographic profile of *Piper corcovadensis* leaves was compared oils obtained from hydrodistillation, maceration, supercritical fluid, headspace, steam distillation and ultrasound techniques. This procedure was used to determine the best extraction method for the obtaining of *β*-germacrene-D-4-ol. 1-butyl-3,4-methylenedioxybenzene, *β*-germacrene-D-4-ol and trans-caryophyllene, which were identified as major compounds in these oils. The maceration method extracted *β*-germacrene-D-4-ol with the highest yield, isolated from ethanolic extract of *Piper corcovadensis* leaves. Larvicidal bioassay showed a LC₅₀ of 18.23 ± 1.19 ppm for *β*-germacrene-D-4-ol and 6.71 ± 0.16 ppm for the oil. The maceration oil and the *β*-germacrene-D-4-ol were submitted to the oviposition bioassay showing an oviposition deterrence against the mosquito *Aedes aegypti* at concentrations of 5, 10 and 50 ppm. Docking study showed that oviposition deterrence may occurs by interacting with *β*-germacrene-D-4-ol with odorant-binding protein 1 (OBP1) in *Aedes aegypti*. The maceration oil and *β*-germacrene-D-4-ol demonstrate a considerable potential of use for the *A. aegypti* control.

Agradecimentos/Acknowledgments

Thanks to FACEPE, APQ-0443-1.06/15) and National Council of Scientific and Technological Development (CNPq: 303404/2019-1 and 422233/2018-8) for the financial support. Thanks to Prof. Dr. Raydonal Ospina Martinez (Statistics Department at UFPE) for helping to calculate the CL50.

Enediyne γ -lactones and fatty acids from *Porcelia ponderosa* (Annonaceae)

Dalete Christine S. Souza* (PG),¹ Carlos H. Totini (PG),¹ Andreas Russo (IC),¹ Patricia Sartorelli (PQ)¹, Emerson A. Oliveira (PQ),² João Henrique G. Lago (PQ)¹

christine.silva@ufabc.edu.br

¹Center of Natural and Human Sciences, Federal University of ABC, SP; ²Institute of Environmental, Chemical and Pharmaceutical Sciences, Federal University of Sao Paulo, SP.

Palavras-chave: *Porcelia ponderosa*, enediyne system, fatty acids.

Highlights

Molecular dereplication processes using NMR and UPLC/MS² made it possible to identify two new enediyne γ -lactones (**1** and **2**) and fatty acids (**3** and **4**) from seeds of *Porcelia ponderosa*.

Abstract

As part of our continuous studies with Annonaceae species, in the present work the CH₂Cl₂ extract from seeds of *Porcelia ponderosa* was chromatographed over Sephadex LH-20 to afford five groups (A – E). HPLC analysis indicated that group C was composed by two enediyne γ -lactones due to the observation, in the ¹³C NMR spectrum, of signals at δ 172.3 (C-1), 162.3 (C-3), 149.8 (C-4), 146.5 (C-16'), 108.6 (C-17'), 105.3 (C-2), 92.5 (C-5), 85.1 (C-12'), 78.5 (C-14'), 71.8 (C-13'), and 65.1 (C-15'). Furthermore, were detected two signals at δ 137.5 (C-23') and 115.1 (C-24'), referring to the terminal double bond carbons, as well as one signal of methyl group at δ 14.0 (C-24'), suggested the presence of a mixture of unsaturated (**1**) and saturated (**2**) terminal side chain.² UPLC/ESI-HRMS² analysis was performed and displayed [M – H]⁻ ion peaks at *m/z* 435.2921 and 437.3072, compatible for the molecular formulas C₂₉H₄₀O₃ (**1**) and C₂₉H₄₂O₃ (**2**). Finally, positioning of enediyne system in the side chain at C-12' was proposed by observation of fragmentation peaks at *m/z* 263.1665 and 263.1639 for compounds **1** and **2**, respectively. Similarly, HPLC analysis of group E indicated a mixture of two enediyne derivatives, due to the absorption bands at λ 212.30, 267.64, 283.62 and 211.94, 267.01, 283.10 nm. Analysis of its ¹³C NMR spectrum confirmed the presence of the enediyne system due to the signals at δ 146.5 (C-18), 108.6 (C-19), 85.2 (C-14), 78.4 (C-16), 71.9 (C-15), and 65.0 (C-17).³ Signals attributed to aliphatic carbons from side chain were observed at δ 27 – 32 whereas those assigned to terminal double bond and methyl group were detected, respectively, at δ 137.6/115.1 and 13.9, suggesting, as observed to compounds **1** and **2**, the presence of a mixture of two compounds containing sp² (**3**) and sp³ (**4**) carbons at C-25/C-26. Considering the absence of signals attributed to γ -lactone unity⁴ but the observance of one peak at δ 177.7, it was suggested that compounds **3** and **4** correspond to fatty acids. UPLC/ESI-HRMS analysis displayed [M – H]⁻ ion peaks at *m/z* 383.2946 and 385.3103, compatible for the molecular formulas C₂₆H₄₀O₂ (**3**) and C₂₆H₄₂O₂ (**4**). This information allowed the identification of fatty acids **3** and **4**, the biosynthetic precursors of γ -lactones **1** and **2**, all of those being reported at first time in the literature.

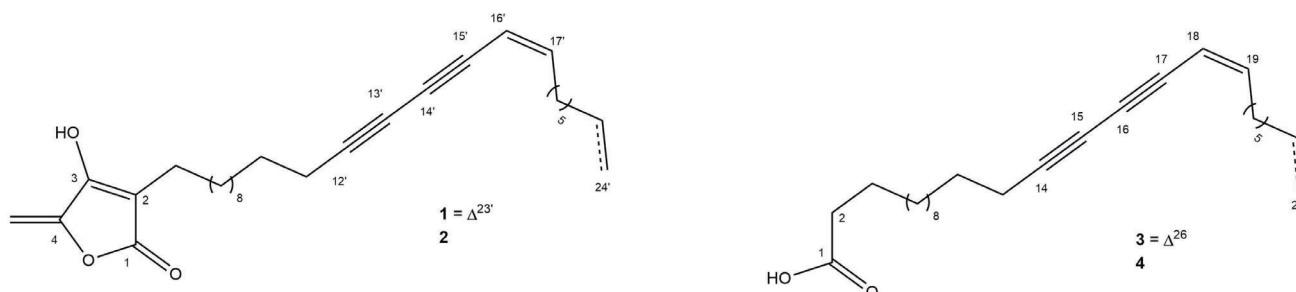


Figure 1 – Enediyne γ -lactones (**1** and **2**) and fatty acids (**3** and **4**) from seeds of *Porcelia ponderosa*.

References ¹Cardellina II, J. H. *J. Nat. Prod.* **1983**, 46 (2) 196-199. ²Brito, I. A. et al. *J. Braz. Chem. Soc.* **2021**, 32, 447-453. ³Bousseroue, H. et al. *Phytochem. Lett.* **2012**, 5, 29–32. ⁴Oliveira, E. A. et al. *J. Nat. Prod.* **2019**, 82, 1177-1182.

Acknowledgments

CAPES, CNPq and FAPESP.

Enhanced biosynthesis of key secondary metabolites in soybean during water stress

Luana de Almeida Pereira (PG),¹ **Vinicius Fortes da Silva (IC)**¹, **Marisi Gomes Soares (PQ)**,¹ **Daniela Aparecida Chagas de Paula (PQ)**¹, **Danielle Ferreira Dias (PQ)**¹, **Liliane Marcia Mertz-Henning (PQ)**³, **Alexandre Lima Nepomuceno (PQ)**³, **Noberto Peporine Lopes (PQ)**², **Paula Carolina Pires Bueno (PQ)**¹

luana.almeidaunifal@gmail.com

¹Institute of Chemistry Federal University of Alfenas, UNIFAL; ²University of São Paulo, Faculty of Pharmaceutical Sciences of Ribeirão Preto, FCFRP; ³Embrapa Soja.

Palavras Chave: *Glycine max*, Metabolomics, Water stress

Highlights

- Glyceollins are biosynthesized phytoalexins from the isoflavonoid pathway and are known for their role in plant defense against biotic stressors.
- Plants were grown under flooded and controlled conditions and analyzed UHPLC-DAD-MS/MS.
- Untargeted metabolomics followed by statistical and multivariate data analysis showed glyceollins along with other isoflavone derivatives were targeted as key compounds in soybean subjected to water stress.
- Knowing how plants of food interest adapt to abiotic stresses is essential to ensure food security in the future, given the unpredictability of climate change and population growth.

Resumo/Abstract

Soybean (*Glycine max*) is a noble representative of the legume family and is one of the main food plant species cultivated, marketed and used worldwide. However, for soybean as well as for other species that form the basis of the food system, environmental factors such as water stresses cause major concerns in crop production since these cannot be controlled¹. Therefore, this work presents the analysis and interpretation of metabolomic data focused on secondary metabolism, for the evaluation and selection of molecular indicators of resistance and/or susceptibility to water stress in soybean, aiming to contribute to the mechanistic elucidation of the adaptation processes of plant species to abiotic stresses. For this purpose, samples were grown under control and hypoxia-induced waterlogging conditions. Leaves and roots were analyzed following a non-target metabolomic analysis protocol, whose data were obtained by UHPLC-DAD-MS/MS. The multidimensional data were subjected to multivariate analysis and validated by permutation and cross-validation tests. The results pointed out substances such as pterocarpanes (glyceollidin I/II), isoflavone derivatives (glycosylated and prenylated) and flavones as significantly altered and determinant markers in signaling response or adaptation to hypoxia, mainly in roots. The results provide new data for the functional understanding of these secondary metabolites in the face of abiotic stresses, since we demonstrate that such compounds are induced in soybean not only by pathogens or by herbivory, as previously demonstrated, but also by water stress².

¹MOUSAVI-DERAZMAHALLEH, M. et al. Adapting legume crops to climate change using genomic approaches. **Plant Cell Environment**, v. 42, p. 6-19, 2019.

²KALLI, Sylvia et al. Induction of promising antibacterial prenylated isoflavonoids from different subclasses by sequential elicitation of soybean. **Phytochemistry**, v. 179, p. 112496, 2020.

Agradecimentos/Acknowledgments

Authors are grateful to IQ-UNIFAL, CAPES, CNPq and Embrapa Soja and JIRCAS (Japan International Research Center for Agricultural Sciences).

Área: QPN

Essential oil chemical profile, DNA barcoding and genetic variability of Lauraceae species from Amazon

Júlia Karla A. M. Xavier (PG)¹, Oscar Victor C. Alegria (PG)², Adriana R. Carneiro (PQ)², Pablo Luis B. Figueiredo (PQ)³, Joyce Kelly R. da Silva (PQ)^{1,*}

joycekellys@ufpa.br; julia.xavier@icen.ufpa.br.

¹Programa de Pós-Graduação em Química, UFPA; ²Centro de Genômica e Biologia de Sistemas, UFPA, 66075-900, Belém, Brazil;

³Departamento de Ciências Naturais, UEPA, 66087-662, Belém, Brazil.

Keywords: Terpenoids, Benzenoids, Statistical multivariate analysis, DNA Barcode, *psbA-trnH*.

Highlights

Lauraceae essential oils were classified into two main groups rich in terpenoids and benzenoids. DNA barcodes were developed and *psbA-trnH* provided greater discrimination among the samples.

Resumo/Abstract

Lauraceae species are widely represented in the Amazon, presenting a significant essential oil yield content with various biological applications and economic potentials¹. Taxonomically, the family represents a challenging group due to the accentuated morphological uniformity, even among taxa from a different genus². In this work, the essential oils (EOs) and genetic material (DNA) were extracted from the leaves of twenty-four Lauraceae specimens occurring in the metropolitan region of Belém (PA, Brazil). The analysis of EO by Gas Chromatography coupled with mass spectrometry (GC-MS) annotated 417 compounds in the samples, where only those with amounts above 3% were submitted to Hierarchical Cluster Analysis (HCA) for comparison of chemical profiles, which formed two main groups. Group I was composed of a more significant number of samples (17 spp.) grouping EO rich in sesquiterpene hydrocarbons, oxygenated sesquiterpenes, and benzenoids from the species *Endlicheria* sp. (ENDsp), *E. verticellata* (EVE), *Mezilaurus mahuba* (MMA1, MMA2), *M. itauba* (MIT), *Ocotea* sp. (OCOsp), *O. cernua* (OCE1 e OCE2), *O. guianensis* (OGU), *Nectandra cuspidata* (NCU1, NCU2, NCU3, NCU4), *N. japurensis* (NJA) and Lauraceae sp. (LAU1, LAU2). The compounds with contents above 10% were α -copaene, β -caryophyllene, viridiflorene, δ -cadinene, spathulenol, caryophyllene oxide, benzyl benzoate, and benzyl salicylate. Group II grouped the EO rich in monoterpene hydrocarbons, sesquiterpene hydrocarbons, oxygenated sesquiterpenes, benzenoids, and fatty acid derivatives including *Licaria* sp. (LICsp), *L. armeniaca* (LAR), *Ocotea* sp. (OCOsp2), *O. floribunda* (OFL) and Lauraceae sp. These samples were characterized by α -pinene, β -pinene, β -caryophyllene, caryophyllene oxide, benzaldehyde, benzyl benzoate, benzyl salicylate, and 2-tridecanone (LAU3, LAU4). DNA Barcodes (DNA Barcode) were developed for phylogenetic analysis using chloroplastic regions of the *matK*, *psbA-trnH*, and *rbcl* genes. Maximum Likelihood (ML) and Bayesian Inference (IB) were used with the markers separately and combined. The trees constructed with the individual markers *matK* and *psbA-trnH* formed the *Ocotea* complex and the *Mezilaurus* group. The *psbA-trnH* sequences provided greater discrimination for the species and statistical support for the internal clades. The association of the three regions (*matK+psbA-trnH+rbcl*) formed clades strongly supported by IB (PP: 1.0) and ML (BS: 100 %). The chemical profile showed a significant correspondence with the molecular data of the Lauraceae species. Thus, the DNA barcode tool helped in the identification, classification, and evolutionary study, as well as in the delimitation of chemical groups of Lauraceae species.

¹MAIA, J. G. S. et al. **Plantas aromáticas na Amazônia e seus óleos essenciais**. Museu Paraense Emílio Goeldi, 2001.

²VAN DER WERFF, H., RICHTER, V.D H. G. *Annals of the Missouri Botanical Garden*, 83, 409-418. 1996.

Agradecimentos/Acknowledgments

Coordenação de Aperfeiçoamento de Pessoal de Nível Superior (CAPES-Coordination for the Improvement of Higher Education Personnel) for granting the scholarship and Aromatic Plant Research Center (APRC, UT, EUA) for their financial support for the execution of this project.

Estudo químico da doença bolor azul causada pelo fungo *Penicillium italicum* em *Citrus sinensis* utilizando técnicas de espectrometria de massas

Aline Midori Kanashiro (PG),^{1*} Alana Kelyene Pereira (PQ),² Taicia Pacheco Fill (PQ).¹

A263427@dac.unicamp.br

¹Instituto de Química da Unicamp; ²Biology Institute, Leiden University, Leiden, Netherlands.

Palavras-Chave: Citros, fitopatógeno, virulência, *Penicillium italicum*.

Chemical study of blue mold disease caused by *Penicillium italicum* in *Citrus sinensis* using mass spectrometry techniques

In this work, we conducted a metabolomic study combining IMS (imaging mass spectrometry) and HPLC-MS/MS analyses to understand the pathogen-host interaction in the blue mold disease.

Resumo

No setor agrícola, a citricultura é uma das mais importantes atividades no mundo¹, sendo o Brasil o maior produtor e exportador de suco de laranja². Todavia, quedas consideráveis na produção de laranja são observadas anualmente devido a ocorrência de doenças fúngicas durante o período pós-colheita, como a doença bolor azul causada pelo fungo *Penicillium italicum*. Métodos alternativos de controle destas doenças têm sido explorados com o intuito de substituir os defensivos agrícolas químicos utilizados atualmente, que apresentam alta toxicidade para a saúde humana e para o meio ambiente. Neste sentido, o primeiro passo para o desenvolvimento de estratégias seguras e eficientes de controle é o estudo da interação patógeno-hospedeiro e dos mecanismos de infecção e virulência do fungo. Nesse estudo, o metabolismo do patógeno *P. italicum* durante o processo de interação com o hospedeiro cítrico (*Citrus sinensis*) foi investigado por meio de análises de cromatografia líquida acoplada a espectrometria de massas (HPLC-MS/MS) e imageamento químico via espectrometria de massas (IMS – Imaging Mass Spectrometry) de amostras de laranja infectadas com o fungo *P. italicum* e amostras de *Citrus sinensis* sadias (controle). Ferramentas de bioinformática foram utilizadas para monitorar as alterações metabólicas do hospedeiro na presença do patógeno, além de realizar o estudo estatístico por meio de análises multivariadas dos dados. Como principais resultados, foram anotados metabólitos presentes apenas durante a infecção, sendo que alguns já foram relatados como Produtos Naturais de *P. italicum*, como a deoxiisoaustamida³ e a dehidrodeoxibrevianamida E⁴, ambos compostos observados também nas amostras infectadas e analisadas via IMS. Ainda, foram anotados outros metabólitos nunca descritos para o fungo, apesar de já ser relatados em outras espécies do gênero, como é o caso da Brevianamida F, que já foi relatada sendo produzido por *P. vinaceum*⁵ e com atividade antimicrobiana⁶. Todavia não há estudos relacionados a funcionalidade destes metabólitos secundários na infecção de *P. italicum* em frutas cítricas, sendo desconhecidos os seus papéis durante a doença, o que reforça a importância de desenvolver maiores estudos nessa inter-relação entre *P. italicum* e *C. sinensis*. Em suma, esse estudo apresentou resultados promissores para compreender os PNs produzidos na interação patógeno-hospedeiro, servindo como base para futuras investigações sobre os mecanismos de virulência do fungo responsável pela doença bolor azul em citros.

Referências

¹ Papoutsis, et al. *Trends in Food Science and Technology*. 86, p. 479-491, (2019), ² Araújo, et al. *Food Chemistry*, 301, 1-6 (2019), ³ Brase, et al. *Marine Drugs*. 19. 32 (2021), ⁴ Scott, et. al. *Applied Microbiology*. 25, p. 892-894, (1974). ⁵ Asiri, et. al. *Phytochemistry Letters*. 13, p. 53-58, (2021), ⁶ Zhang, et. al., *Natural Product Sciences*, 13, p. 257-264, (2007).

Agradecimentos

Os autores agradecem à Sociedade Brasileira de Química pela oportunidade, ao Coordenação de Aperfeiçoamento de Pessoal de Nível Superior (CAPES) e a Fundação de Amparo à Pesquisa no Estado de São Paulo (FAPESP) pelo incentivo e apoio financeiro.

Estudo químico e avaliação da virulência de um novo fitopatógeno de citros no Brasil

Mayra Pinheiro (PG),^{1*} Evandro Silva (PQ),² Taicia Fill (PQ).²

m234915@dac.unicamp.br

¹Pós-graduação em Química – Unicamp; ²Instituto de Química – Unicamp.

Palavras-Chave: Citros, fitopatógeno, virulência, micotoxina.

Chemical study and virulence evaluation of a new citrus phytopathogen in Brazil

In this work we carried out chemical and biological investigations of a new phytopathogen isolated from a citrus host.

Resumo

Fungos dos gêneros *Penicillium*, *Colletotrichum* e *Fusarium* são frequentemente relatados como agentes causadores de doenças em hospedeiros citros, incluindo bolor verde, antracnose e podridão seca, respectivamente.^{1,2,3} Algumas dessas doenças provocam danos substanciais nas frutas no período pós-colheita, outras são diagnosticadas ainda no estágio de desenvolvimento da planta, e conseqüentemente, o fruto perde seu valor agregado, evitando seu consumo e sua exportação.¹ Deste modo, os fitopatógenos representam uma grande ameaça para a segurança alimentar global, devido a redução da produtividade na citricultura.⁴ Pesquisas envolvendo fitopatógenos concentram-se principalmente no tratamento contra os sintomas da doença, entretanto, pouco se sabe sobre o metabolismo secundário destes micro-organismos e os fatores de virulência produzidos durante a interação com hospedeiros citros.⁵ Neste sentido, esse estudo visa realizar uma investigação química e biológica de um novo fitopatógeno de hospedeiro citros, pois caso ocorra a propagação de uma nova doença na citricultura brasileira é de suma importância que estratégias sejam desenvolvidas para combatê-la. Neste estudo, o fitopatógeno LaBioQuiMi 01 foi isolado de uma variedade de citros na região do nordeste brasileiro, inoculado em ágar batata dextrose (BDA) e armazenados em BOD à 25 °C. Inicialmente foi realizado a otimização das condições de crescimento do fungo em diferentes meios de cultura (BDA, Czapek, YES) para avaliar a diversidade de metabólitos produzidos pelo micro-organismo. Após o período de 7 dias as culturas foram submetidas a extração usando uma mistura de solventes MeOH:AcEOT:CHCl₃ (1:2:3 v. v. v). Testes de patogenicidade foram realizados em diferentes partes da planta para confirmar a virulência do fungo, e posteriormente análise de identificação por PCR. Técnicas cromatográficas em escala analítica e preparativa em HPLC foram utilizadas para análise do perfil cromatográfico e isolamento de compostos, bem como cromatografia líquida acoplada a espectrometria de massas (LC-MS/MS) para identificação de metabólitos produzidos *in vitro* e *in vivo* durante a infecção. Os resultados obtidos confirmaram a patogenicidade do fungo LaBioQuiMi 01 em hospedeiro citros. A produção de metabólitos biossintetizados pelo fungo *in vitro* abrange diferentes classes de compostos, os quais foram identificados putativamente pela plataforma GNPS. Dentre eles, um composto majoritário foi isolado e caracterizado como uma micotoxina. Portanto, os resultados alcançados até o presente momento contribuem na compreensão do metabolismo do fungo LaBioQuiMi 01 e na identificação de compostos tóxicos que possam estar envolvidos na patogenicidade de LaBioQuiMi 01 e que podem atuar como fatores de virulência. Por fim, este trabalho tem resultados promissores que servem de base para desenvolver estratégias de controle da doença.

Referências

¹ Kanashiro, et al. *Frontiers in Microbiology*. 11, 606852, (2020), ² Huang, et al. *Fungal Diversity*., 61, 61-74 (2013), ³ Kurt, et al. *J Gen Plant Pathol.*, 86, 326–332 (2020), ⁴ Costa, et al. *Scientific Reports*., 9, 18647 (2019). ⁵ Chen, et al. *Metabolites*. 9, 169, (2019).

Agradecimentos

Os autores agradecem à Sociedade Brasileira de Química pela oportunidade, ao Conselho Nacional de Desenvolvimento Científico e Tecnológico (CNPq, Brasil) 142600/2021-0 e a Fundação de Amparo à Pesquisa no Estado de São Paulo (FAPESP) pelo incentivo e apoio financeiro.

Evaluation of anti-*Trypanosoma cruzi* activity of patagonic acid, isolated from leaves of *Echinodorus grandiflorus* (Alismataceae), and its methyl ester

Mariana M. Borges (IC),¹ Vinicius S. Londero (PG),² Andre G. Tempone (PQ)³, João Henrique G. Lago (PQ),² Edgard A. Ferreira (PQ).^{1*}

mari_borges@terra.com.br; edgard.ferreira@mackenzie.br*

¹School of Engineering, Mackenzie Presbyterian University; ²Center of Natural Sciences and Humanities, Federal University of ABC; ³Adolfo Lutz Institute, São Paulo.

Keywords: Neglected Tropical Diseases, Chagas disease, clerodane

Highlights

Fractionation of *n*-hexane extract of *E. grandiflorus* afforded patagonic acid, with moderate activity against trypomastigote forms of *T. cruzi* (EC₅₀ of 41.7 μM) and reduced toxicity against NCTC cells.

Resumo

Popularly known as aquatic plants, aquatic macrophytes, throughout their evolutionary process have been adapted to the aquatic environment efficiently and are spread across different biomes and growing conditions. They are represented approximately by 2600 species among proximately 450 genera. The aquatic macrophyte *Echinodorus grandiflorus*, popularly known as "leather hat" in Brazil is a traditional plant with applications in folk medicine as anti-inflammatory, anti-hypertensive, anti-arthritis, throat inflammation, among others.¹ According to reports, isolated compounds from *Echinodorus* genus belong mainly to three chemical classes, phenolic compounds, cembranes and especially diterpenes. However, studies to investigate biological effects of these isolated compounds in this genus are scarce.²⁻⁴ As part of a continuous study aiming to explore chemical diversity and biological effects of compounds from aquatic macrophytes, the *n*-hexane extract from leaves of Brazilian native species *E. grandiflorus* displayed activity against trypomastigote forms of *T. cruzi* (100% of death at 300 μg/mL). Based on this result, the crude extract was subjected to an activity-guided chromatographic separation over silica gel (eluted with increasing amounts of EtOAc in *n*-hexane) to afford a bioactive fraction. This material was purified by semi-preparative HPLC to afford patagonic acid. Its structure was defined by analysis of ¹H and ¹³C NMR and HR-MS spectral data and comparison with those reported in the literature.⁵ Anti-*T. cruzi* activity of patagonic acid was evaluated against trypomastigote forms of the parasite and exhibited EC₅₀ value of 41.7 ± 2.9 μM with reduced toxicity against NCTC cells (CC₅₀ > 200 μM). Comparatively, the positive control benznidazole exhibited EC₅₀ of 17.7 ± 2.1 μM to trypomastigotes, indicating that patagonic acid displayed moderate activity. Evaluation of ADME proprieties *in silico* suggested that the esterification of carboxylic acid to afford methyl ester cause important alterations in different parameters such as lipophilicity, pharmacokinetic and other physicochemical properties, suggesting a higher effect to this semi-synthetic derivative against trypomastigotes. Therefore, after preparation and evaluation of activity *in vitro*, the EC₅₀ was determined as 17.3 ± 5.1 μM with no toxicity against NCTC cells (CC₅₀ > 200 μM), similar to positive control. In view of these results, this work contributes to obtaining new bioactive compounds with antiparasitic potential through simple chemical modification using *in silico* analysis.

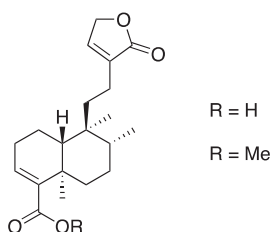


Table 1. Effects of patagonic acid and its methyl ester derivative against extracellular forms of *T. cruzi* and NCTC cells.

Compounds	<i>T. cruzi</i>	NCTC
	EC ₅₀ / μM trypomastigote	CC ₅₀ / μM
Patagonic acid	41.7 ± 2.9	> 200
Patagonic acid methyl ester	17.3 ± 5.1	> 200
Benznidazole*	17.7 ± 2.1	> 200

EC₅₀: 50% Effective concentration; CC₅₀: 50% Cytotoxic concentration.
*Standard drug.

References: ¹Marques, *et al.*, **2017**, *Food Chem. Toxicol.* 109:1032-1047; ²Kobayashi *et al.*, **2000**, *Tetrahedron Lett.* 41(16):2939-2943; ³Kobaiashi *et al.*, **2000**, *J. Nat. Prod.* 63(3):375-377; ⁴Shigemori, *et al.*, **2002**, *J. Nat. Prod.* 65(1):82-84; ⁵Pinto, *et al.* **2010**, *J. Braz. Chem. Soc.* 21(10):1819-1824.

Acknowledgments

Authors thanks FAPESP, CNPq, CAPES, and Mackpesquisa for financial support and fellowships, Sumiko Honda of São Paulo Municipal Herbarium (PMSP) for identification of plant species.

Evaluation of the antagonist potential and *in vitro* control of phytopathogenic fungi by *Bacillus* bacteria

Joyce N. Gonçalves (IC),^{1*} Renata N. Schimiloski (IC)¹, Conceição de F. A. Olguin, (PQ)¹.

joyce.nog.gon@gmail.com;

¹Centro de Engenharias e Ciências Exatas, UNIOESTE – Campus Toledo, PR;

Palavras-Chave: Biofungicidas, agentes antagonistas, *Bacillus*, fungos fitopatógenos.

Highlights

The *Bacillus* genus is potential antagonistic agents on the growth of some species of phytopathogenic fungi. *Colletotrichum musae*, *Alternaria* sp., *Fusarium* sp. and *Fusarium pallidoroseum* was inhibited by some *Bacillus* genus.

Resumo/Abstract

Various diseases can affect Brazilian crops, the most harmful are those caused by phytopathogenic fungi, affecting all parts of plants, from the beginning to the end of cultivation¹. To combat these diseases, pesticides are generally used. However, biological control using bacteria of the genus *Bacillus* is presented as an alternative methodology in addition to preserving the environment and human health. We can define biological control as a relationship between pathogenic microorganisms and antagonists, involving several interactions in a biological pathogen/host/antagonist system². The use of bacteria of the genus *Bacillus* is alternative method, because they have the ability to produce secondary metabolites, that have antifungal activity, with potential use as biofungicidas³. Therefore, the objective of this study was to evaluate the effect caused by potential antagonistic agents on the growth of some species of phytopathogenic fungi. The colony pairing method was used for evaluation of potential antagonists and the methodology of pairing/striation in circle¹, observing the growth diameter of pathogens (mm) and calculating the Percentage of Inhibition of Mycelial Growth (ICP) (%). The tests were done in duplicates, with readings performed every 24 hours for 7 days. The antagonistic agents used for the experiments were: *B. subtilis*, *B. licheniformis*, *B. megaterium*, *B. amyloliquefaciens*, *B. pumilus* and *B. thuringiensis* in front of phytopathogenic fungi: *Colletotrichum musae*, *Fusarium* sp., *F. paridorosium*, *Alternaria* sp. and *Aspergillus flavus*. It was possible to notice that *B. subtilis*, *B. licheniformis* (Figure 1) and *B. amyloliquefaciens* obtained the best results of inhibition of growth *C. musae* and *A. sp.* from the 3rd and 4th day of analysis, respectively. On the other hand, to *Fusarium* sp. and *F. pallidoroseum*, *B. licheniformis* was more efficient compared to *B. subtilis* and *B. amyloliquefaciens*, from the 2nd and 3rd day of analysis. It was observed that none of the *Bacillus* used in the tests was able to inhibit *A. flavus*. We can conclude that bacteria *B. subtilis*, *B. licheniformis* and *B. amyloliquefaciens* have potential for biofungicidas, because they were able to inhibit the growth of four of the five fungi analyzed.

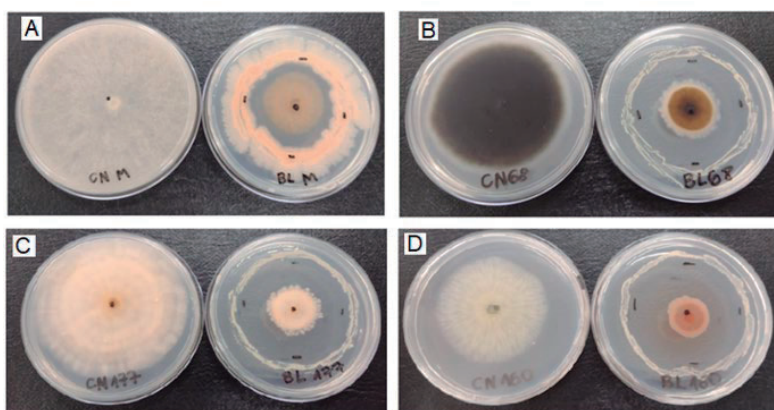


Figure 1: Antifungal activity by bacteria (BL) *Bacillus licheniformis*, against phytopathogenic fungi: (A) *Colletotrichum musae*, (B) *Fusarium* sp., (C) *F. paridorosium* and (D) *Alternaria* sp.

¹ JUNIOR *et al.*, Biota Amazônia, p. 45-51, v. 7, n. 3, 2017.

² BETTIOL *et al.*, EMBRAPA, v. 1, 1991.

³ MELO *et al.*, Research, Society and Development, p. 1-22, v. 10, n. 9, 2021.

Agradecimentos/Acknowledgments

To the Programa de Educação Tutorial (PET) Química and UNIOESTE - Campus Toledo, PR.

Evaluation of the antibacterial activity of prenylated compounds from propolis and their semisynthetic derivatives against cariogenic bacteria

Tatiana M. Vieira (PG),^{1*} Julia G. Barco (IC),¹ Sara L. Souza (IC),² Anna L. O. Santos (IC),² Carlos H. G. Martins (PQ),² Antônio E. M. Crotti (PQ).¹

*tati.manzini@gmail.com; millercrotti@ffclrp.usp.br

¹Faculdade de Filosofia, Ciências e Letras de Ribeirão Preto (FFCLRP-USP), Ribeirão Preto – SP, Brasil; ²Universidade Federal de Uberlândia (UFU), Uberlândia – MG, Brasil

Key Words: antimicrobial activity, cariogenic bacteria, phenylpropanoids, prenylation, própolis

Highlights

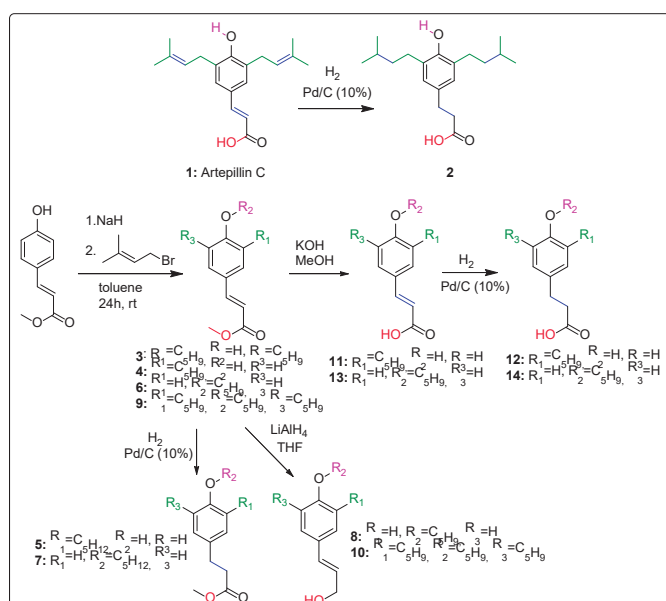
Due to the highlighted antimicrobial potential of artepillin C, this work aims to evaluate the antibacterial activity of synthetic artepillin C derivatives and analogs against a representative panel of cariogenic bacteria.

Resumo/Abstract

Artepillin C (**1**, **Scheme 1**) is one of the major prenylated phenolic acids found in green propolis (*Baccharis dracunculifolia*).^[1] Several biological activities are attributed to artepillin C, including antimicrobial activity.^[1] However, data on the antimicrobial potential against oral bacteria of artepillin C and its derivatives are still scarce in the literature, which makes this class of compounds very attractive to be explored.

Compound **1** (Artepillin C) investigated in this study was isolated by Arruda and coworkers^[1]. Other prenylated phenolic derivatives were obtained by prenylation with prenyl bromide,^[2] followed by reduction with LiAlH₄, hydrolysis,^[3] and/or catalytic hydrogenation (**Scheme 1**). The antimicrobial activity of compounds **1-14** against cariogenic bacteria was evaluated using the microplate microdilution method, according to the CLSI protocol. The minimum inhibitory concentrations (MIC) were performed against *Streptococcus mutans*, *S. mitis*, *S. sanguinis*, *S. sobrinus*, *S. salivarius*, *Enterococcus faecalis*, and *Lactobacillus casei*. Chlorhexidin (Positive Control) and compounds **1-14** were tested at concentrations of 2000 and 0.98 µg/mL, respectively. The most promising results were observed for compounds **4** and **5** (*S. mitis* and *S. mutans*, MIC=31.25 µg/mL), **11** (*S. mutans*, MIC=125 µg/mL; *S. sobrinus*, MIC=125 µg/mL), and **2** (*S. mitis* MIC=62.5 µg/mL). Furthermore, compound **4** was more

active^[4] than artepillin C (**1**). Comparison between the MIC values of artepillin C (**1**) with those of compounds **2-13** indicated that compound **4**, which contains only one prenyl in the *orto* position to the phenolic hydroxyl, was more active than artepillin C and its methyl ester **3** (di-C-prenylated).



Scheme 1. Synthesis of compounds **1-14** from methyl coumarate.

References

- [1] Arruda, C., et al. *J. Pharm. Biomed. Anal.*, **2020**, 178, 112922.
- [2] Patra, T., et al. *Angew. Chem. Int. Ed.* **2016**, 55, 7751–7755.
- [3] Uto, Y., et al. *J. Org. Chem.* **2002**, 67, 2355-2357.
- [4] Oliveira, T. A. S. *Chem. Biodiversity*. **2022**, 19, e202200097.

Agradecimentos/Acknowledgments

The authors acknowledge São Paulo Research Foundation (FAPESP) for research financial support (proc. 2019/11700-0 and 2017/04138-8).

Área: QPN

Evaluation of the antifungal activity of geopropolis extracts produced by *Melipona quadrifasciata anthidioides*

Gabriel F. dos Santos (PG),^{1*} Rafael F. dos Santos (PG),¹ Wesley S. Freitas (IC),¹ Gabriel T. S. Ribeiro (IC),¹ Aguida A. de Oliveira (PQ),² Rosane N. Castro (PQ).¹

gabriel.fulgencio21@gmail.com

¹Departamento de Química Orgânica-IQ – UFRRJ; ²Departamento de microbiologia e imunologia veterinária-IV - UFRRJ.

Keywords: Mandaçaia, antifungal activity, *Sporothrix schenckii*, *Sporothrix brasiliensis*.

Highlights

In this work, the ethanol extract of mandaçaia geopropolis was evaluated for its antioxidant potential, total phenolic and flavonoid and against strains of *Sporothrix schenckii* and *Sporothrix brasiliensis*.

Resumo/Abstract

In Brazil there are several types of stingless bees (Tribo Meliponini), among them, *Melipona quadrifasciata* (mandaçaia) stands out, object of this work and which produces geopropolis. It is a resinous substance of complex chemical composition, collected by bees from different parts of the plant tissue, plus soil and/or clay (1). Several biological activities of geopropolis have been evaluated, such as antibacterial, antifungal, antiviral and antioxidant. Sporotrichosis is a severe mycosis caused by fungi of the genus *Sporothrix*, and this disease affects both humans and animals. Brazil has a high prevalence of sporotrichosis caused by fungi, and in particular, cats are the most infected by *S. brasiliensis*, and play an important role in zoonotic transmission (2). Treatment options for sporotrichosis include itraconazole and amphotericin B, drugs generally associated with adverse and deleterious reactions. In addition, the use of these drugs has been hampered by the emergence of new fungal isolates with resistance to the drugs already used. Thus, due to the need to search for new antifungal compounds in the treatment of sporotrichosis this work aimed to evaluate the profile of phenolic compounds and antioxidant capacity of different geopropolis extracts of mandaçaia and to investigate the *in vitro* antifungal activity against *S. schenckii* and *S. brasiliensis*, the major causative agents of sporotrichosis. Geopropolis was collected from an apiary located in Bosque da Barra, Rio de Janeiro. The pulverized sample of geopropolis (4 g) was extracted for six hours with 150 mL of ethanol. The extracts were then combined and concentrated by rotary evaporation to provide geopropolis ethanolic extract (EEGP-M). The EEGP-M (350,8 mg) was solubilized in methanol:water (7:3 v/v) and partitioned with n-hexane, dichloromethane and ethyl acetate, respectively, providing the following fractions: Fr-Hex (206.9 mg), Fr-DCM (116.9 mg) and Fr-Ac (5.2 mg). The qualitative chemical profile was evaluated by analytical thin layer chromatography, revealed in an ultraviolet lamp at a length of 254 nm and in a sulfuric vanillin solution, and high-performance liquid chromatography coupled to a diode array detector. It was possible to observe that different polarity solvents helped to simplify the constituents of the complex geopropolis matrix. The total phenolic and flavonoid content were evaluated compared to gallic acid (GA) and quercetin (QE) standards, respectively. The Fr-DCM fraction showed the highest results for phenolic (18.9 mg EGA g⁻¹) and flavonoid (4.2 mg EQE g⁻¹), while the EEGP-M showed 6.3 mg EGA g⁻¹ and 1.5 mg EQE g⁻¹ and Fr-Ac 11.9 mg EGA g⁻¹ and 3.0 mg EQE g⁻¹. The Fr-Hex fraction did not show detectable levels. The DPPH (2,2-Diphenyl-1-picrylhydrazyl) assay was used to determine the antioxidant capacity of the extract and its fractions, again the Fr-DCM presented the highest results (EC₅₀ = 0.200 mg mL⁻¹) being consistent with the results of total phenolic and flavonoid content, since the literature relates antioxidant activity to the presence of phenolic substances and flavonoids, and Fr-Hex did not show antioxidant activity. The EEGP-M showed EC₅₀ = 0.203 mg mL⁻¹ and Fr-Ac EC₅₀ = 0.404 mg mL⁻¹. The antifungal activity was investigated against strains of *S. schenckii* and *S. brasiliensis*. The best result with *S. schenckii* was observed in Fr-Ac (MIC = 0.75 mg mL⁻¹) indicating that the more polar extract was important for the antifungal activity. EEGP-M, Fr-Hex and Fr-DCM showed MIC above 6 mg mL⁻¹ compared to the positive control Itraconazole (MIC = 5 x 10⁴ mg mL⁻¹). Tests with *S. brasiliensis* again indicated that Fr-Ac (MIC = 0.75 mg mL⁻¹) had the best inhibition, although EEGP-M also showed promising results (MIC = 1.5 mg mL⁻¹). For *S. brasiliensis* again the best result was for Fr-Ac (MIC = 0.75 mg mL⁻¹), EEGP-M also obtained promising result (MIC = 1.5 mg mL⁻¹). Fr-Hex and Fr-DCM presented MIC greater than 6 mg mL⁻¹ and the positive control was Itraconazole (MIC = 8 x 10³ mg mL⁻¹). The antifungal activity test showed the inhibition potential of the ethanol extract and the acetate fraction against *S. schenckii* and *S. brasiliensis*, demonstrating that this natural product is promising for the treatment of sporotrichosis.

Bibliography: (1) CARDOSO, et al. Revista Virtual de Química. v. 7 (6), p. 2457-2474, 2015.

(2) WALLER et al. Science and animal health. V.5 N.2. P. 151-165. 2017.

Agradecimentos/Acknowledgments

CAPES, FAPERJ, CNPq, UFRRJ.

Evaluation of the antioxidant capacity and photoprotective formulations of ethanolic extracts of *Genipa americana* L.

Messias de O. Silva (PG)¹, Estela Vitória A. Miranda (IC)¹, Luiz Artur L. Melo (IC)¹, Monika B. S. Oliveira (PQ)¹, Iara B. Valentim (PQ)², Marília O. F. Goulart (PQ)¹, Jadriane de A. Xavier (PQ)^{1*}

messias.silva@iqb.ufal.br; jadrianexavier@iq.ufal.br

¹Instituto de Química e Biotecnologia, Universidade Federal de Alagoas; ²Instituto Federal de Alagoas, IFAL – Maceió/AL

Key Words: *Genipap*, *Photoprotection*, *Formulations*, *Antioxidant Capacity*, *Reactive Species*.

Highlights

The jenipap bark extract was the most promising in the antioxidant assays employed. The photoprotective formulations containing the extracts presented SPF values > 6, according to the RDC No. 30/2012 of ANVISA.

Abstract

Exposure to the sun can be beneficial, such as for the production of vitamin D in the body, but it can also have negative effects through overexposure, which can cause premature aging or even skin cancer. Benzophenones (BFs) are widely used as UV filters, but have aroused concern due to their human and ecological toxicity^{1,2}. Given the above, the present work aims to evaluate the antioxidant and photoprotective capacity of ethanolic extracts of *Genipap* for use in multifunctional photoprotective formulations to replace BFs.

Table 1. Yield, total phenolic compound content (CTF) and antioxidant capacity of the extracts.

Extract	Yield (%)	CTF (mg de EAG/g of dry extract)	DPPH• (RSA%)	FRAP (µmol de ET/g of dry extract)	O ₂ ^{•-} IC ₅₀ (µg mL ⁻¹)	HOCI IC ₅₀ (µg mL ⁻¹)
EEPJ	30,5	114,7 ± 1,4	13,8 ± 0,1	141,6 ± 19,8	186,8 ± 3,7	>600 µg mL ⁻¹
EESEJ	41,5	46,8 ± 1,0	25,7 ± 0,0	81,7 ± 4,4	NA*	193,38 ± 13,1
EECJ	7,3	486,1 ± 7,9	23,1 ± 1,0	30,7 ± 0,0	NA*	5,6 ± 2,17
Quercetin	-	-	-	-	28,6 ± 2,8	8,2 ± 2,7

EEPJ (Ethanolic extract *genipap* of pulp); EESEJ (Ethanolic extract *genipap* of seed + endocarp); EECJ (Ethanolic extract *genipap* of bark); *Not active up to a concentration of 800 µg mL⁻¹; CTF= Total Content of Phenolic Compounds; EAG= Gallic Acid Equivalent; RSA= Radical Scavenging Ability; ET=Trollox Equivalent.

In general, the extracts showed antioxidant potential, being EECJ the most promising, especially in the elimination of HOCl being more active than quercetin, used as a positive standard. Regarding the formulations containing the extracts at a concentration of 5% (m/m), SPF values ranging from 6 to 32 were obtained. Formulations containing the standard benzophenone-3 (5%, m/m) and the extracts (5%, m/m) in the proportions of 1:1 and 1:5 (m/m) were also produced, in order to decrease the concentration of BF-3 without decreasing the SPF. It was observed that in all formulations, from the concentration of 5 mg mL⁻¹ on, there was no significant difference between the SPF of the formulations that were prepared with the addition of only BF-3, and those in which BF-3 was used in association with the extracts. All formulations evaluated obtained SPF values higher than 6, being all in accordance with the RDC No. 30/2012 of ANVISA. Thus, EEPJ, EESEJ and EECJ extracts can be considered active ingredients in the preparation of sunscreens and multifunctionals, since they are also able to stabilize reactive species that contribute to premature skin aging.

¹GE, Jiali. et al., *Water Research*, 2019.

²DO, N. S. et al., *International Journal of Women's Dermatology*, 2021.

Acknowledgments

UFAL, CAPES, CNPQ and FAPAL.

Área: QPN

Extraction efficiency of bioactive compounds of *Morus nigra* leaves using Natural Deep Eutectic Solvents.

Nicole F N Golia (PG)^{1*} and Daniel Rinaldo (PQ)².

nicole.golia@unesp.br; daniel.rinaldo@unesp.br

¹Institute of Chemistry, UNESP, Araraquara; ²School of Science, UNESP, Bauru.

Palavras Chave: NADES, Green Chemistry, *Morus nigra*, Extraction, Medicinal plants, HPLC.

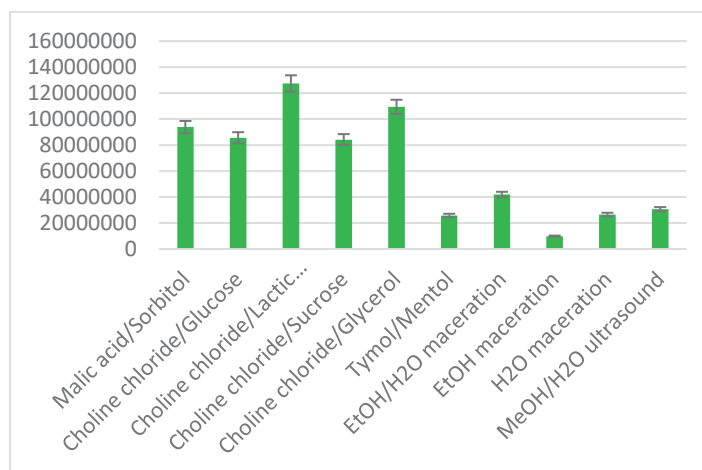
Highlights

Extractions based on green chemistry. Using NADES as solvents. More efficient than usually used methods. Applied to the worldly famous medicinal plant: *Morus nigra*.

Resumo/Abstract

Morus nigra, popularly known as blackberry, is a plant well known for its fruits and it's explored as a medicinal plant. It presents bioactive compounds and several studies show their very important action in the human body. The industry is increasingly interested in such products, but the analysis and extractions are still ineffective and the use of low-toxic solvents are few. Therefore, this work sought to use natural deep eutectic solvents (NADES), which are green solvent methods that do not harm the environment, to perform extractions and propose a more efficient method. The microwave-assisted extraction (MAE), considered very efficient, was used as extraction technique and NADES were used as solvents. To assess the efficiency of these green solvents, popular extraction methods of the literature¹⁻² were used. The best NADES was based on choline chloride and lactic acid. And it was 68% better than the most efficient solvent reproduced here.

Fig.1 – Quantitative extraction comparison



¹QBAL, S., *et al.* Proximate Composition and Antioxidant Potential of Leaves from Three Varieties of Mulberry (*Morus sp.*): A Comparative Study. *International Journal of Molecular Sciences*, 2012.

²PADILHA, M.M. *et al.* Antiinflammatory properties of *Morus nigra* leaves. *Phytother*, 2010.

Agradecimentos/Acknowledgments

This work was financed in part by the CAPES – Finance Code 001 and INCTBioNat (CNPq grant # 465637/2014-0 and FAPESP grant # 2014/50926-0), Brazil.

Furanditerpenes and tocotrienols association promote antagonistic antiproliferative activity on MCF-7 breast cancer cell line

Kaio E. Buglio (PG)^{1*}, Daniele D. Affonso (PG)², Rogério J. M. Júnior (PG)¹, Mayra G. Biccigo (PG)², Ana L. T. G. Ruiz (PQ)², João E. Carvalho (PQ)², Mary A. Foglio (PQ).^{1,2}.

foglioma@unicamp.br; kaiobuglio@gmail.com

¹Faculty of Medical Sciences (FCM), University of Campinas (UNICAMP), 13083-887 Campinas, SP, Brazil; ²Faculty of Pharmaceutical Sciences (FCF), University of Campinas (UNICAMP), 13083-871 Campinas, SP, Brazil.

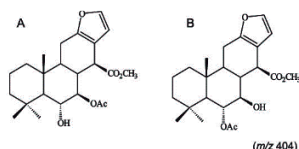
Key words: Voucapan; tocotrienol; MCF-7; 3D cell culture; isobolographic analysis

Highlights

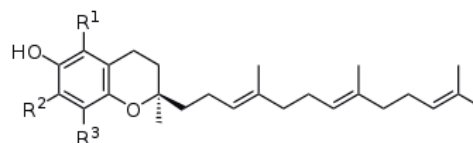
Association of isomers voucapan with 70% tocotrienol fraction produce antagonistic outcome when tested on MCF-7 cell line highlighting the need of safety and efficacy evaluation in drug development.

Resumo/Abstract

The interest in studying synergistic or antagonistic effects through experiments with associations has increased immensely over the years. Scientific reports show how often the pharmacological action of one isolated compound differs from the action found in crude extracts, suggesting that the advantage of herbal medicines results from synergistic interactions that potentiate their pharmacological effects with reduced side effects. Previously our group investigated *in vitro* antiproliferative activities of *Bixa orellana*'s unsaponifiable extract and resulting fractions, among others, a 70% enriched tocotrienol fraction, on human tumoral cells. The fraction is a by-product of an industrial process to produce bixin carotenoid dye [1]. Another research, undertaken by our group, also reported the activity of *Pterodon pubescens* Benth. crude dichloromethane extract and isomers voucapan 6 α -hydroxy-7 β -acetoxy-voucapan-17 β -oate methyl ester and 6 α -acetoxy-7 β -hydroxyvoucapan-17 β -oate methyl ester (m/z 404) isolated from the species. These results prompted the study on the effect of the association of the voucapan isomers with the 70% enriched tocotrienol fraction tested on *in vitro* 2D and 3D antiproliferative activity models on MCF-7 (breast cancer cell line). The isomers voucapan 6 α -hydroxy-7 β -acetoxy-voucapan-17 β -oate methyl ester and 6 α -acetoxy-7 β -hydroxyvoucapan-17 β -oate methyl ester (m/z 404) were isolated from crude *Pterodon pubescens* Benth. fruit extract by column chromatography (25 \times 500 mm), using solvent gradient of hexane and ethyl acetate. Nuclear Magnetic Resonance (NMR) and Mass Spectrometry (MS) compared the purified compounds data to previously identified compounds [2]. The association interaction characterized by isobolographic analysis assume that the combinations were constituted by equally effective doses of the individual drugs. After determination of the effective concentration for each compound/fraction, specific combinations of the associations were tested on *in vitro* antiproliferative activity with MCF-7 cell line for the construction of the isobologram. Both isomers 404 and 70% enriched tocotrienol fraction, with the same TGI (total growth inhibition) of 34 μ g/mL, showed a moderate cytostatic effect. The association of both samples produced antagonism outcome, suggesting that Tocotrienols antioxidant activity interferes with cancer cell inhibition of isomers 404.



Isomers 404



Tocotrienol

References: [1] Basting et.al.; Natural Product Research v. 1, p. 1-6, 2020; [2] Biomedicine & Pharmacotherapy 112 (2019) 108693;

Acknowledgments: CAPES, CNPq, and FAPESP grant numbers 2021/01280-3 & 2017/21801-2

Green extraction of compounds from *Prunus dulcis* residues

Gabriela Cremasco (PG)¹, Adam Sutton (PQ)², Cristiano S. Funari (PQ)³, Dario Arrua (PQ)², Emily F. Hilder (PQ)², Kelly Johana Dussán Medina (PQ)¹, Vanderlan S. Bolzani¹ and Daniel Rinaldo (PQ)^{1,4}.

gabriela.cremasco@unesp.br.

¹Institute of Chemistry University (UNESP - Araraquara); ²University of South Australia (UniSA); ³School of Agricultural Sciences (UNESP - Botucatu); ⁴School of Sciences (UNESP - Bauru).

Keywords: Almond hull, Design of experiment. Green Chemistry, NADES.

Highlights

Extraction of tannins and flavonoids in almond hull using NADES, via microwave. Chemometrics for optimization of the developed method.

Abstract

The great concern with sustainability, together with the UN goals for the 2030 Agenda, has led researchers to study practices to reduce the production of toxic waste in order to protect from the environment to human health [1]. As well as the advancement of techniques for environmental preservation, plant residues have also been studied, as they have compounds of economic and practical interest, as is the case of agricultural residues of *Prunus dulcis* (almonds). In this context, 10 Natural Deep Eutectic Solvents (NADES) were prepared and used as extracting solvent subjected to Microwave assisted extraction (MAE) miniaturized technique. Then analyzed by HPLC-DAD, using as a parameter, the total area of integration of the chromatographic bands corresponding to compounds of interest (phenolic compounds); larger area, greater extraction efficiency. The best extractor NADES was optimized through a central composite design (CCD) in which 3 parameters were analyzed: plant/solvent ratio [X1 (mass/mass)]; Temperature [X2 (°C)] and Time [X3 (min)]. Using the Analytical AGREEness (AGREE) metric [5], it was possible to quantify the environmental impact of the developed method and compare it with the methods reproduced in the literature.

It is possible to observe in the graph of Figure 1 that the method developed was more efficient than the methods reproduced in the literature that use methanol in an acid medium, acetone and ethanol as solvents, through dynamic maceration. The method in the literature that showed the highest efficiency was the Meshikini method (2016), but the method developed in this work was approximately 2.4 times more efficient. From the input data entered for the extractions, the method developed in this work was the one that presented the greatest green character (Figure 2), that is, these results obtained by the AGREE metric indicate that the method developed for the extraction of metabolites in the residues of *P. dulcis* by NADES-MAE is the one that presents the greatest coverage of the principles of Green Analytical Chemistry, and can be classified as a green method.

This work resulted in an optimized, efficient and low environmental impact alternative for extracting the high value-added compounds present in almond hulls. The NADES lactic acid:glycerol 1:1 (containing 20% water) is easy to prepare, has low viscosity and can be a suitable substitute for frequently used reference solvents.

¹ONU. Organização das Nações Unidas. Disponível em: <<https://www.un.org/en/>>. Access: Mar 2022; ²Pinelo, M. et al. Extraction of antioxidant phenolics from almond hulls (*Prunus amygdalus*) and pine sawdust (*Pinus pinaster*). *Food Chemistry*, v. 85, n. 2, p. 267-273, 2004; ³Rubiular, M. et al.. Separation and HPLC-MS Identification of Phenolic Antioxidants from Agricultural Residues: almond hulls and grape pomace. *Journal Of Agricultural And Food Chemistry*, [s.l.], v. 55, n. 25, p. 10101-10109, dez. 2007. ⁴Meshikini, A. Acetone extract of almond hulls provides protection against oxidative damage and membrane protein degradation. *Journal of acupuncture and meridian studies*, v. 9, n. 3, p. 134- 142, 2016. ⁵Pena-Pereira, F.; et al. AGREE-Analytical GREEnness Metric Approach and Software. *Analytical Chemistry*, v. 92, n. 14, p. 10076-10082, 2020.

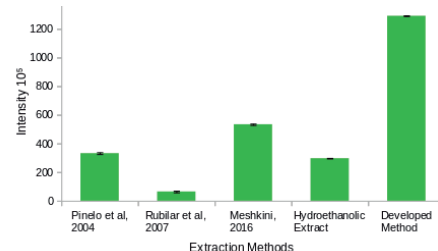


Figure 1: Comparison between extraction methods

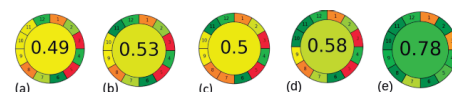


Figure 2: Pictograms AGREE metric (a) [2]; (b) [3]; (c) [4]; (d) hydroethanolic extract and (e) developed method.

Acknowledgments

National Council for Scientific and Technological Development (CNPq, Conselho Nacional de Desenvolvimento Científico e Tecnológico), National Institute of Science and Technology (INCT BioNat – Brazil) [grant # 465637/2014-0]. and the State of São Paulo Research Foundation (FAPESP, Fundação de Amparo à Pesquisa do Estado de São Paulo (grants # 2016/08179-8, 2014/50926-0 and 2020/15024-6)).

Green synthesis of silver nanoparticles of eugenol and its antimicrobial activity against multidrug-resistant *Pseudomonas aeruginosa*

Larissa V.F. Oliveira (PQ),^{1*} Fernanda F. Camilo (PQ),² André G. Tempone (PQ),³ João Henrique G. Lago (PQ).¹

larissa.verena@ufabc.edu.br

¹Center of Natural Sciences and Humanities, Federal University of ABC (UFABC); ²Chemistry Department, Institute of Environmental, Chemical and Pharmaceutical Sciences, Federal University of São Paulo (UNIFESP); ³Centre for Parasitology and Mycology, Adolfo Lutz Institute (IAL)

Keywords: Silver Nanoparticles, Green synthesis, Eugenol, Multidrug-resistant bacteria, *Pseudomonas aeruginosa*.

Highlights

Green synthesis of AgNP of eugenol. Evaluation of antimicrobial activity of the mixtures AgNP-eugenol against multidrug resistant bacteria *Pseudomonas aeruginosa*.

Abstract

There has been a considerable increase in infections by multidrug-resistant microorganisms in the last few years¹ so, new alternative treatments to diseases caused by these microorganisms are urgent and necessary. One alternative is to use nanomaterials, particularly, silver nanoparticles (AgNP). The plant-based method to synthesize AgNP has received great attention in recent years due to the advantages of this method like simplicity, cost, use of eco-friendly reagents and biocompatibility.² Thus, in this work a one-step biosynthetic method for the synthesis of AgNP with natural phenylpropanoid eugenol is presented. AgNP formation was confirmed by UV-Vis spectroscopy and TEM images. Differently of the majority of the studies from the literature that uses plant extracts as reducing agent in the biosynthesis of metallic nanoparticles, in this work it was used an isolated natural compound, so it was possible to analyze the products of the redox reaction. After NMR and ESI-HRMS analyzes it was suggested that an oxidation coupling reaction occurred and dehydrodieugenol was obtained. This is the first time that such mechanism is observed in green synthesis of AgNP by isolated phytochemicals. The antimicrobial activity of these samples was evaluated against multi-resistant bacteria *Pseudomonas aeruginosa* and displayed expressive potential (Table 1).

Table 1: Minimum inhibitory concentration ($\mu\text{g/mL}$) of the compounds tested against multidrug-resistant *Pseudomonas aeruginosa*.

Sample	<i>Pseudomonas aeruginosa</i>	
	MIC concentration ($\mu\text{g/mL}$)	
Eugenol_AgNP_1 mM	31.3	
Eugenol_AgNP_2 mM	15.6	
Eugenol_AgNP_5 mM	15.6	
Eugenol	250	
Dehydrodieugenol	250	
AgNP	125	

As could be seen, pure eugenol and dehydrodieugenol displayed reduced activity against multidrug-resistant *Pseudomonas aeruginosa*. Otherwise, AgNP exhibited activity against this bacterium (MIC 125 mg/mL) indicating the effect of this nanoparticle. However, when eugenol was incorporated to AgNP in different concentrations, the effect against this multidrug-resistant bacteria was intensified since MIC values were calculated as 31.3 mg/mL (1 mM) and 15.6 mg/mL (2 and 5 mM), indicating the synergic effect of this phenylpropanoid in association with AgNP.

References: ¹C. Reygaert et al. *AIMS Microbiol.* **2018**, 4, 482-501. ²Anand U, et al. *Sci Total Environ.* **2022**, 821,153472.

Acknowledgments

FAPESP (2021/07971-8, 2021/07297-5 and 2021/02789-7).

46ª Reunião Anual da Sociedade Brasileira de Química: "Química: Ligando ciências e neutralizando desigualdades"

Área: QPN

Halogenated azaphilones produced by *Penicillium* sp. isolated from stingless bee colonies

Jullio Kennedy C. Soares (PG) ^{1,2*}, **Michelle M. Morais (PQ)** ¹, **Livia S. de Medeiros (PQ)** ^{1,2}.

jullio.kennedy@unifesp.br; livia.soman@unifesp.br

¹ Instituto de Ciências Ambientais, Químicas e Farmacêuticas, UNIFESP; ² Laboratório de Química Bio-Orgânica Otto Richard Gottlieb (LaBiORG)

Keywords: Antimicrobials, Chemical Ecology, Fungi, Halogenated Azaphilones, *Penicillium*, Stingless Bees.

Highlights

Chemical dereplication based on HPLC-HRMS/MS data from *Penicillium* spp. isolated from stingless bees (*Melipona marginata* and *Melipona quadrifasciata*) is being executed to find azaphilones.

Abstract

The eusociality of stingless bees (Hymenoptera: Meliponini) makes their dense populations more willing to be infected by entomopathogenic agents. The ecological association of these insects with microorganisms is a defensive strategy to avoid compromising the health of the colony through the natural exploration of antimicrobial compounds by the bees. Thus, the aim of this study is to explore the chemical diversity of secondary metabolites of fungi of the genus *Penicillium* isolated from colonies of stingless bees called manduri (*Melipona marginata*) and mandaçaia (*Melipona quadrifasciata*), focusing on the search for antifungal agents that may act in symbiont-mediated protection. Eleven *Penicillium* spp. with different pigmentations have already been obtained from the UNIFESP meliponary, stored at the CMLD (Coleção Micológica LaBiORG Diadema) under the codes 32, 39, 40, 44, 45, 53, 64, 72, 83, 85, and 86. Dereplication strategies are being applied for the analysis of microextracts obtained from solid and liquid cultures. Until the moment, the analysis of the microextracts by HPLC-HRMS/MS has indicated the presence of halogenated azaphilones by the strain *Penicillium* sp. CMLD 72 (Figure 1). Azaphilones represent a polyketide subclass recognized for their structural diversity and mainly their biological activities, like antibiotic and antifungal properties, which may play an important role in the interaction between bees and their associated fungi. Then, the most promising fungi will be selected for the production of azaphilones and other substances with biological properties against ecologically relevant fungi. For this, large-scale cultivations will be carried out aiming the isolation and structural characterization of these compounds, preferably of new structures, by spectroscopic and spectrometric techniques. That way, this work aims to contribute to the elucidation of potential defensive symbioses little understood in stingless bees, in addition to enriching the chemical knowledge of the genus *Penicillium* obtained from underexplored niches.

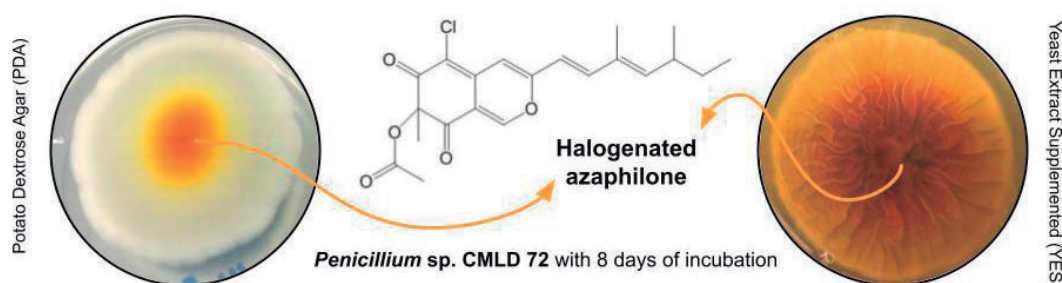


Figure 1. Strain *Penicillium* sp. CMLD 72 and literature example of structure of chlorinated azaphylone by Hebra *et al.* (2021).

HEBRA, T.; *et al.* **Metabolites**, v. 11, n. 7, p. 1-18, 2021.

Acknowledgments

The authors thank the CAPES (88887.798945/2022-00) and the FAPESP (2020/08270-0) for financial support.

Área: PN

(Inserir a sigla da seção científica para qual o resumo será submetido. Ex: ORG, BEA, CAT)

Herbivory alters the volatile profile of *Piper lindbergii* (Piperaceae) and increases the emission of compounds recognized by a specialist herbivore

Massuo J. Kato (PQ),¹ Mariana A. Stanton (PQ).

majokato@iq.usp.br; mariana.a.stanton@gmail.com

¹Departamento de Química Fundamental, IQ-USP

Palavras Chave: *Volatile Organic Compounds*; *GC-EAD*; *herbivore-induced plant volatiles*; *Lepidoptera*; *host plant selection*

Highlights

Volatile organic compounds (VOCs) are released by *Piper lindbergii* plants after herbivory by larvae of the specialist herbivore *Eois nr multistrigaria* (Lepidoptera: Geometridae). Gas chromatography coupled with electroantennographic detection (GC-EAD) assays show that female *E. nr multistrigaria* moths can perceive more of these VOCs than male moths of the same species.

Resumo/Abstract

Plants of the genus *Piper* (Piperaceae) make up a large proportion of the understory of tropical forests, and despite previous studies characterizing the diverse chemistry of many of these plants and studies suggesting that this phytochemical diversity is linked to a higher degree of insect herbivore specialization and parasitoids diversity, little is known of the role of volatile organic compounds (VOCs) in mediating ecological interactions with these higher trophic levels. VOCs can lead to changes in ecological communities by mediating changes in animal distribution, diversity and abundance. Specifically, VOCs can change insect behavior, such as influencing host plant selection through attraction or repellence, or acting as signals of the presence of caterpillars to foraging predators and parasitoids, which in turn control herbivore populations. Therefore, improving our understanding of the effects of natural products produced by plants on their ecological interactions can help to understand mechanisms that structure and maintain biodiversity in natural communities. While there is extensive literature on essential oil characterizations of *Piper* plants, essential oils do not always accurately represent the volatile blends that are released into the air by the plant and their composition is subjected to changes caused by harsh conditions during distillation and residual leaf enzymatic activity. Here we used a static headspace VOC sampling method with polydimethyl-siloxane (PDMS) tubes under field conditions with native plants and herbivores in a fragment of Atlantic Forest at the Reserva Biológica da Serra do Japi in Jundiá (São Paulo state). We show that the VOC profile of *Piper lindbergii* consists of a blend of mono- and sesquiterpenes and increases in complexity and abundance after herbivory by larvae of the specialist herbivore *Eois nr multistrigaria* (Lepidoptera: Geometridae), a previously undescribed species of neotropical moth. Laboratory gas chromatography coupled with electroantennographic detection (GC-EAD) assays show that female *E. nr multistrigaria* moths can perceive more of these VOCs than male moths of the same species, suggesting they may be used as cues for host plant choice for oviposition in this specialist herbivore. Field assays to test the potential role of VOCs as cues for parasitoids were inconclusive and require further studies.

Agradecimentos/Acknowledgments

The authors acknowledge funding from FAPESP (2014/50316-7, 2015/26823-9) and CNPq (166551/2020-1) Dr. Simeão M. Moraes for molecular and morphological identification of *Eois* specimens, and Dr Lydia F. Yamaguchi, Dr Variluska Fragoso, Welber S. Neves and Joaquim L. Matheus for assistance in the field.

Induction of secondary metabolites through Coculture of endophytic fungi strains isolated from marine red algae

Iatã do C. Mendonça^{1*} (PG), Givaldo S. da Silva¹ (PG); Victor H. L. Rufino¹ (PG), Edelson de J. S. Dias¹ (PG), Lucas H. S. Moura¹ (PG), Dulce H. S. Silva¹ (PQ)

iata.mendonca@hotmail.com

¹NuBBE - Núcleo de Bioensaios, Biossíntese e Ecofisiologia de Produtos Naturais Instituto de Química-UNESP, Araraquara, SP.
Keywords: Marine algae, Endophytic fungi, Chemical prospection, *Asparagopsis taxiformis*, *Humicola fuscoatra*, *Nemania bipapillata*.

Highlights

Coculture impacts on the metabolic dynamics of endophytic fungi; UPLC-MS/MS and GNPS molecular networking tools allowed the annotation of the fungal extracts chemical constituents.

Resumo/Abstract

The chemodiversity of natural products may inspire studies on biodiversity due to both scientific and economic interests. Plants, insects and microorganisms are important sources of bioactive compounds, and organisms belonging to marine ecosystems may be highlighted owing to their huge biodiversity, comparable to tropical forests. Due to environmental pressure, marine organisms, as well as their associated microorganisms, exhibit specific biochemical characteristics, representing great potential for bioprospecting. However, most genes related to the biosynthesis of microorganisms remain silenced under standard laboratory growth conditions. Some approaches have been used to solve this problem, such as coculture. This methodology consists of inoculating two or more microorganism strains together, allowing them to induce physiological and chemical stimuli, and trigger activation of silenced biosynthetic pathways. The fungal strains used in this work, encoded as At02 and At05, were isolated from red seaweed *Asparagopsis taxiformis*, and identified as *Humicola fuscoatra* (At02) and *Nemania bipapillata* (At05). They were grown in Petri dishes containing PDA culture medium and incubated for 10 days at 25° C. Then the two strains were inoculated both separately and together in Erlenmeyer flasks containing ultrapure water and malt growth medium, and held at 25° C in static mode, for 21 days. After that, the mycelium was separated from the fermented broths by vacuum filtration and the aqueous filtrate was subjected to liquid/liquid partition with ethyl acetate followed by solvent evaporation to yield the extracts. The control extracts (monoculture) and the coculture extract were analyzed by UPLC-MS/MS and the data submitted to the Global Natural Product Social (GNPS) molecular networking platform, which provided annotation of possible chemical constituents produced only in coculture. As the alkaloid isoeresespin (1), the monoterpene gentiopicroside (2), and a cluster (figure 1) with two diterpenes, Kaurenoic acid (3) and 17-Hydroxy-15,16-epoxykauran-18-oic acid (4) and a sesquiterpenoid, Verrucarol (5), in addition to four other possible terpenes that did not match the platform library and might be isolated and identified in the next steps.

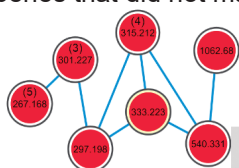
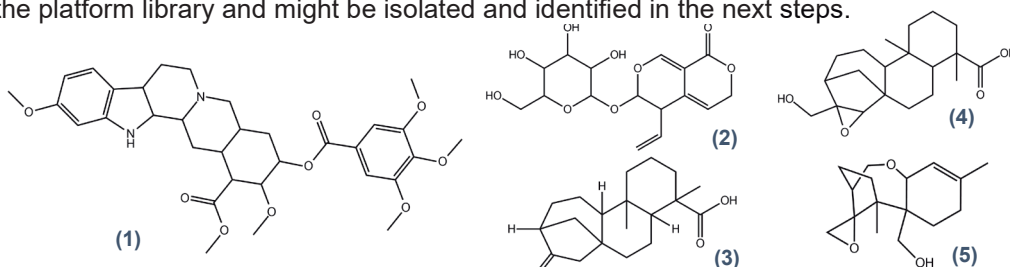


Figure 1: Terpene cluster found only in coculture extract.



References:

- Newman, D. J. Predominately uncultured microbes as sources of bioactive agents. *Front Microbiol.*, v. 7, n. 1832, p. 1-15, 2016
- RAJAMANIKYAM, M. et al. Endophytic Fungi as Novel Resources of natural Therapeutics. *Braz. Arch. Biol. and Technol.*, v. 60, p. 1–26, 2017.
- Scherlach, K., Hertweck, C. Triggering cryptic natural product biosynthesis in microorganisms. *Org Biomol Chem.*, v. 7, p. 1753–1760, 2009.
- WANG, M. et al. Sharing and community curation of mass spectrometry data with Global Natural Products Social Molecular Networking. *Nature Biotechnol.*, v. 34, n. 8, p. 828–837, 2016.

Agradecimentos/Acknowledgments



Integration of HPLC-DAD-ESI-MS/MS and NMR for profiling in mixture the monoterpene indole alkaloids of *Psychotria rhytidocarpa* (Rubiaceae)

Erick F. V. Gagliano (PG),¹ Virginia G. Correa (PG),^{1,2} Victor F. de Jesus (PG),¹ Jéssica O. Costa,¹ Mário Gomes (PQ),³ Alvicler Magalhães (PQ),¹ Marcelo R. R. Tappin (PQ),² Rodolfo S. Barboza (PQ),^{1*} Ligia M. M. Valente (PQ).^{1*}

erickgaglianos@gmail.com; rodolfosb@iq.ufrj.br; valente@iq.ufrj.br

¹Universidade Federal do Rio de Janeiro, Instituto de Química, Av. Athos da Silveira Ramos 149, C.T. Bl. A; ²Fundação Oswaldo Cruz, Instituto de Tecnologia em Fármacos, R. Sizenando Nabuco 100; ³Instituto de Pesquisas Jardim Botânico do Rio de Janeiro, R. Pacheco Leão 195.

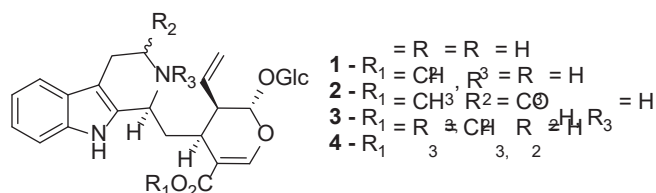
Palavras Chave: *Psychotria rhytidocarpa*, Rubiaceae, alkaloids, HPLC-DAD-ESI-MS/MS, solid-phase extraction, NMR.

Highlights

Use of SPE to obtain alkaloid-rich fractions from the crude extract. Use of MS molecular network to expand knowledge of alkaloids present in the species.

Abstract

Psychotria L. is the largest genus in the Rubiaceae family with near to 2000 species worldwide, mostly distributed in tropical regions. The species *P. rhytidocarpa* Müll.Arg. occurs in the Brazilian Southeastern region, and so far, to the best of our knowledge, there are no publications of phytochemical study on it. In this work, by using online HPLC-DAD-ESI-MS/MS and NMR techniques, without isolation, we were able to profile the major monoterpene indole alkaloids (MIA) present in the leaves of the species. The species was collected in 2019 at the municipality of Araras, RJ state. A species voucher is deposited at the Herbarium of the Botanic Garden of Rio de Janeiro, RJ state, under number RB 799025. SisGen/MMA/Brazil as A9C4B8A. Dried and milled leaves (4.7 g) were sonically extracted with MeOH and the solvent was evaporated under low pressure yielding 0.5 g of crude extract. The extract was submitted to SPE in semi-preparative scale performed in homemade cartridges filled with silica gel C18 (40 - 63 µm) yielding six alkaloid-rich fractions (A = 6.9 mg, B = 13.1 mg, C = 18.5 mg, D = 19.5 mg, E = 6.5 mg, and F = 8.4 mg). These fractions were analyzed by HPLC-DAD-ESI-MS/MS in a Nexera Prominence liquid chromatograph (Shimadzu) coupled to a QTOF mass spectrometer (Bruker) equipped with an electrospray ionization (ESI) source. Separation was performed on a C18 XBridge (3.5 µm, 150 x 4.6 mm i.d.) column and a gradient elution with H₂O-0.1% HCOOH (A) and MeOH (B) as mobile phase as previously described.¹ The compounds monitoring was performed at 254 nm. Fraction D was submitted to 1D and 2D NMR techniques (¹H, DEPT, HSQC and HMBC) recorded on a Bruker Avance III HD 400 spectrometer in CD₃OD. Three MIA were identified in the alkaloid-rich fractions: strictosidinic acid (**1**), strictosidine (**2**), and 5-carboxystrictosidine (**3**). Identification was possible by comparing the R_t, UV-vis spectra, MS recorded in full scan and MS/MS product ion scan mode with standards analyzed under the same conditions for compounds **1** and **2**, and by UV-vis spectrum, MS spectra and comparison with similar literature data for compound **3**.²⁻⁴ NMR data and key signals, and their 2D correlations, analyzed in mixture, allowed to confirm the presence of these MIA.^{2,3,5} The MS data when compiled and treated using Global Natural Product Social Molecular Networking (GNPS) platform, led to suggest, in addition to compounds **1-3**, the presence of the alkaloid 4-*N*-strictosidine (dolichantoside) (**4**).



Cpd nº	Rt (min)	[M+H] ⁺ (m/z)	MS ² main fragments (m/z)
1	26.49	517.2129	500.1896; 352.1544; 144.0811
2	31.22	531.2286	514.2059; 352.1544; 144.0816
3	29.47	575.2174	396.1442; 238.0856; 188.0706
4	31.49	545.2450	

References

1. Klein-Júnior et al. *J. Chromatogr. A* 1463, 71–80, 2016; 2. Jesus et al. XVII ERSBQ-RJ, 2019; 3. Costa et al. *J. Braz. Chem. Soc.* 30, 2104-2113, 2020; 4. Santos et al. *Rapid Commun Mass Spectrom.* 34(S3):e8683.4, 2020; 5. Carvalho Junior et al. *Molecules* 22, 2-22, 2017.

Acknowledgments

FAPERJ, CNPQ

Isolation and identification of Dinaphthalenone Derived from a alga Endophytic fungus *Annulohypoxyton stygium*

Givaldo S. da Silva (PG),^{1,2*} Rafael Vieira (PG),^{1,3} Ana Caroline Zanatta Silva (PQ),¹ Camila Luiza Cunha (PQ),¹ Dulce H. S. Silva (PQ).¹

givaldo.silva@unesp.br;

¹Nucleus of Bioassays, Biosynthesis and Ecophysiology of Natural Products (NuBBE), Institute of Chemistry, São Paulo State University - UNESP, Araraquara, SP, Brazil; ²Federal Institute of Education, Science and Technology of Acre – IFAC, AC, Brazil; ³Federal Institute of Education, Science and Technology of Rondônia – IFRO, RO, Brazil.

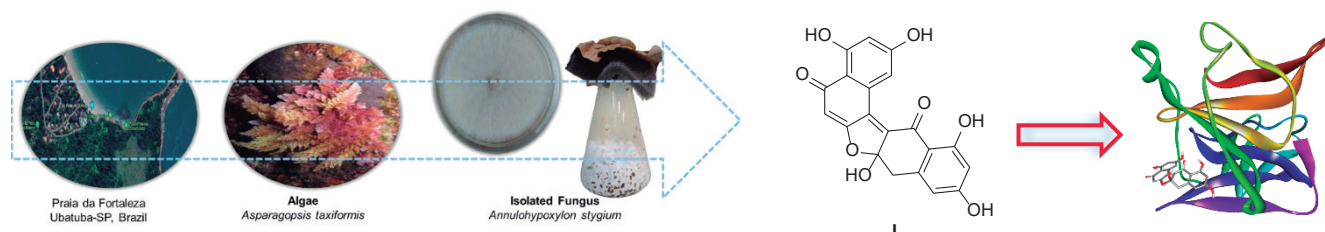
Palavras Chave: Marine fungi; Asperlones; Endophytic fungus; *Annulohypoxyton*. molecular docking

Highlights

MPLC and Sephadex LH-20 applied to the isolation and purification of dinaphthalenone derivative The structure was established by employing ESI-QqTOF-MS and spectroscopic method as 1D and 2D NMR spectra.

Resumo/Abstract

Different types of naphthalene derivatives are widely found in *Annulohypoxyton* species. Naphthalene derivatives such as truncatone A and B were isolated from *A. leptascum*, truncatone C was obtained from *Annulohypoxyton* sp, while truncatone D was isolated from *A. cf. truncatum*. Truncatone A, B and D showed cytotoxic activity against mouse fibroblast cell (2). The fungus used in this study was isolated from red alga *Asparagopsis taxiformis* and identified as *Annulohypoxyton stygium*. The fungal strain *A. stygium* was grown on red rice solid medium (50 g red rice and 150 mL water) at 25 °C static for 20 days. After incubation it was extracted twice with 300 mL of CH₃OH within a 24 hours interval. The solvent was removed under reduced pressure at ≤40 °C. The CH₃OH extract was dissolved in 100 mL of CH₃OH:H₂O solution (4:1) and defatted with n-hexane by liquid partitioning (3 x 50 mL). The hydromethanolic fraction was evaporated to yield 1.2 g of organic extract, which was subjected to silica column MPLC (C18) in gradient elution (CH₃OH:H₂O from 05:95 to 95:05 (v/v)) to generate 16 fractions (Fr. 1-16). Fr.11 was further purified by Sephadex LH-20 eluted with MeOH to yield 15 fractions (Fr. 1-15), with Fr. 11-12 identified as a dynaphthalenone derivative, Asperlone B (1.7 mg), isolated as an amorphous red powder, of molecular formula C₂₀H₁₂O₈ determined by ESI-QqTOF-MS, in positive mode, with peak *m/z* 381.0616 [M+H]⁺ (calculated mass for C₂₀H₁₂O₈ 380.0537). The structure of the isolated compound was established by extensive analysis of 1D- and 2D-NMR spectra, ESI-QqTOF-MS data and comparison with literature data. This work describes the first occurrence of asperlone B as a fungal metabolite of the genus *Annulohypoxyton*. Based on the results from molecular docking, the structure of Asperlone B shows effectiveness in modulating the biomacromolecular target of Mayaro virus, confirmed by the release of -7.0 kcal/mol. This is mainly due to the resonance effect inherent to its aromatic rings, which allows PI-type interactions with amino acids lysine-138 and alanine-256, as well as Van der Waals interactions with 10 other amino acids in the reaction site. Thus, once this ligand is complexed in the hydrophobic site of the molecule, the virus capsid bonds are not effective, thus interrupting its cycle.



1. SUDARMAN, E. *et al.* *Tetrahedron*, v. 72, n. 41, p. 6450-6454, 2016.

Agradecimentos/Acknowledgments

CAPES, CNPq (INCT/BioNat), FINEP and FAPESP (Cepid/CibFar and INCT/BioNat) for research financial support and fellowships.

Isolation of bioactive compounds from *Banisteriopsis caapi* by Dry Column Chromatography

Sinésio Boaventura Júnior (PQ), Adriana da Silva Santos de Oliveira (PG), Emily Freitas Oliveira (TM), Marili Villa Nova Rodrigues (PQ)*

sinesio@unicamp.br; marili@unicamp.br

Pluridisciplinary Research Center for Chemistry, Biology and Agriculture (CPQBA), State University of Campinas (UNICAMP)

Keywords: *Banisteriopsis caapi*, Dry column chromatography

Highlights

Dry column chromatography as a pre-purification methodology. Study of the therapeutic potential of drugs containing alkaloids.

Resumo/Abstract

Banisteriopsis caapi is a woody, robust climbing plant with thick and crooked stems, native to the Amazon region in upland forests. Popularly known as mariri, yage or ayahuasca, it has hallucinogenic and medicinal effects and is widely used by indigenous communities¹. In its chemical composition, the alkaloids harmine, harmaline and tetrahydroarmine stand out. The objective of this work was to isolate the bioactive compounds present in the leaves of *Banisteriopsis caapi* cultivated in the CPQBA by means of Dry Column Chromatography. This type of chromatography is a “non-elution” method of column chromatography, meaning, the separated substances remain in the column at the end of the chromatographic process². Dry column fractionation was carried out from 1.22 g of hexane extract obtained by cold mechanical extraction of dry leaves of *Banisteriopsis caapi*, which was placed on top of the cellulose acetate column (support), containing about 87 g of silica gel 60 (0.063 to 0.2 mm) as stationary phase. A solution of hexane / ethyl acetate 80:20 was used as the mobile phase. After elution, the column was divided into 10 fractions of 5 cm and numbered from 1 to 10 (Fr 1 to Fr 10). After filtration and concentration, the fractions were analyzed by Thin Layer Chromatography (TLC) and Gas Chromatography coupled with a Spectrometer Mass Detector (GCMS). The chemical composition of the main fractions obtained in Dry Column Chromatography are described below (table 1).

Table 1. Relative percentages of compounds identified by GCMS

Compound	MM (g.mol ⁻¹)	Hexane Extract	Fr 1	Fr 3	Fr 4	Fr 5	Fr 6
Nonacosane	408	24.8	37.0	1.1	ND	ND	ND
Vitamin E	430	9.2	8.1	1.5	ND	ND	ND
γ-sitosterol	414	14.3	ND	1.1	15.4	65.6	66.1
Lupeol	426	5.7	ND	56.7	31.6	3.0	ND
Campesterol	400	2.0	15.1	ND	1.9	10.4	12.2

Subtitle: Name of compound; MM- Molecular mass; Fr 1,3,4,5,6- main fractions obtained with the mobile phase hexane and ethyl acetate (80:20); ND- Not detected

Thus, we conclude that under the conditions employed, the dry column chromatography technique showed medium resolution and can be indicated for the pre-purification of compounds, proving to be a simple, fast, low-cost tool with great potential when applied in the phytochemical study of *Banisteriopsis caapi*.

Agradecimentos/Acknowledgments

Pro-Rectorate of Research at UNICAMP for funding through the CAF 2023 project (FAEPEX 519292).

¹ Lorenzi, H.; “Plantas Medicinais no Brasil. Nativas e Exóticas”, 2^a ed.

² Kovac-Besovic, E.E; Duric, K.; Kalodera, Z.; Sofic, E.; “Identification and isolation of pharmacologically active triterpenes in *Betulae cortex*, *Betula pendula* Roth., Betulaceae”, *Bosnian Journal of Basic Medical Sciences*, v. 9 (1), p. 31-38, 2009.

Isolation Of C-Methylated Flavanones From Geopropolis *Melipona rufiventris* With Potential Trypanocidal Activity.

Rafael F. dos Santos (PG),^{1*} Afonso S. M. M. Velez (PG),¹ Débora D. R. de Lima (PQ),² Marco Edilson F. de Lima (PQ),¹ Paulo P. dos Santos (PG),¹ Rosane N. Castro (PQ).¹

rafael.ssantos097@hotmail.com

¹Instituto de Química– UFRRJ; ² Instituto de Veterinária - UFRRJ.

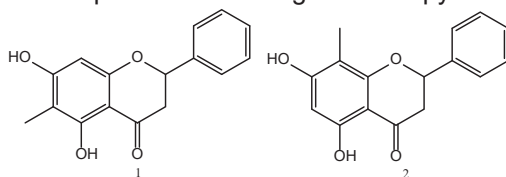
Keywords: *Brazilian stingless bee*, Biological activity, *Trypanosoma cruzi*, Chagas Disease, methylflavanones.

Highlights

Geopropolis Ethanol Extract was evaluated against mutant strains of *T. cruzi*, which causes Chagas disease. Using the VLC (vacuum liquid chromatography) separation technique, it was possible to isolate two new methylflavanones (Strobopinin and Cryptostrobin) with potential antiparasitic activity.

Resumo/Abstract

Geopropolis consists of a mixture of resinous and balsamic material, collected by stingless bees, with the addition of earth and/or clay. There is a lack of consistent data on the chemical profile and biological properties presented by this resin. This fact supports the development of studies related to this natural product, which appears as a viable natural alternative, still little explored for the treatment of several diseases, with a special focus on neglected tropical diseases (NTD's). Among the NTD's, Chagas' disease stands out, with around 6 to 7 million infected people worldwide. In Brazil, the only drug available for the treatment of this zoonosis is Benznidazole, which has low efficacy in chronic patients, in addition to having numerous deleterious effects. Therefore, in view of the need to investigate the chemical constituents of geopropolis, and the current scenario related to the unsatisfactory availability of chemotherapy for chronic chagasic patients, this work aimed to evaluate the antiparasitic potential of the ethanolic extract of geopropolis from the stingless bee *Melipona rufiventris* (EEGP), and isolate key bioactive chemicals responsible for the biological activity of interest. The pulverized sample of geopropolis (20 g), acquired in Bosque da Barra da Tijuca - RJ, was subjected three times to ultrasonic extraction for two hours with 150 mL of grain alcohol. The extracts were then combined and concentrated by rotary evaporation to provide geopropolis ethanolic extract (EEGP, 3.4441 g). About 950 mg of EEGP was solubilized in methanol:water (7:3 v/v) and partitioned with n-hexane and dichloromethane, respectively, to give the following fractions: Fr-Hex (580.4 mg), Fr-DCM (333.6 mg) and Fr-MeOH:H₂O (17.5 mg). The crude extract and the fractions obtained from the EEGP were tested against the amastigotes form of the mutant strain of *Trypanosoma cruzi* (Tulahuen C2C4 LacZ). In the bioassay carried out, the EEGP presented IC₅₀ = 4.79 µg/mL, the most active fraction was Fr-HEX (IC₅₀ = 3.88 µg/mL), Fr-DCM presented IC₅₀ = 9.54 µg/mL and Fr-MeOH:H₂O was the least active fraction with an IC₅₀ = 48.07 µg/mL, which can be explained by the fact that this fraction contains compounds of greater polarity, such substances being more difficult to cross cell membranes. Furthermore, the FR-DCM fraction showed a less complex chemical profile by reverse-phase DAD-HPLC when compared to the chemical profile of Fr-Hex. The FR-DCM fraction also showed peaks with ultraviolet curves in its chromatogram that suggested flavanone skeletons (UV_{max} = 290 nm). Then, the FR-DCM fraction was subjected to vacuum liquid chromatography (VLC), using silica gel 60 for TLC and CHCl₃:Acetone 1% as mobile phase, and two new methylflavanones (**1**-Strobopinin and **2**-Cryptostrobin) were isolated in Brazilian geopropolis, the which were characterized by spectrometric techniques (NMR, UV, EM). Both substances had their antiparasitic potential evaluated, showing IC₅₀ = 5.69 µg/mL (21.08 µM) and 2.83 µg/mL (10.48 µM), respectively, with the positive control Benznidazole (IC₅₀ = 0.45 µg/mL; 1.74 µM). The extracts and isolated substances showed considerable activity, suggesting antiparasitic potential. Although the preliminary results of geopropolis from stingless bees are encouraging, further studies are essential to validate the safety and efficacy of products from these bee species in antichagasic therapy.



Agradecimentos/Acknowledgments

CAPES, FAPERJ, CNPq, UFRRJ.

Isolation of neolignans from *Licaria aritu* Ducke wood residues using LC/DAD-SPE/NMR

Jennifer Araújo de Oliveira Lima (PG),¹ Noam Gadelha da Silva (PQ),² Claudete Catanhede do Nascimento (PQ),¹ Lyege Magalhães Oliveira (PQ),³ Sergio Scherrer Thomasi (PQ),⁴ Antonio Gilberto Ferreira (PQ),⁵ Maria da Paz Lima (PQ)^{1*}

mdapaz@inpa.gov.br; jaol2108@gmail.com

¹Coordenação de Tecnologia e Inovação, INPA; ²IFAM, Campus Itacoatiara; ³IFAM, Campus Manaus; ⁴Departamento de Química, Departamento de Química, UFLA; ⁵Departamento de Química, UFSCar

Palavras Chave: Louro-aritu, Lauraceae, Lignoids, Phenylpropanoids

Highlights

Using LC-DAD-SPE/NMR, analyses of fractions 2 of the methanolic extract from wood residues of *Licaria aritu* was performed, and nine compounds were identified including five new neolignans

Resumo/Abstract

Licaria aritu Ducke, is an arboreous Lauraceae species of the Amazon region which occurs in regular abundance in the vicinity of Manaus. The wood of this species is known as louro-aritu in which the presence of neolignans licarin A 1 and B has been reported.¹ Samples of louro-aritu were identified by macroscopic analysis and comparison with samples in the Xylotheque Laboratory of Wood Technology at the Instituto Nacional de Pesquisas da Amazonia. Using LC-DAD-SPE/NMR, analyses of fractions 2 of the methanolic extract from wood residues was performed, and we identified neolignans of types 8.1', uncommon with allyl group transposed to C-4' (1, 2 and 4), 8.O.4' (3 and 5) and 8.1' (6 and 7), in addition to phenylpropanoids 8 and 9 (Fig 1). The hexane extract also provided compound 1 (266 mg), obtained by recrystallization. Compounds 1 and 3 are neolignans known as aurein A¹ and virolongin B², respectively. The phenylpropanoids 8 and 9 are also known in the literature as isoelemycin and elemycin. The neolignans 2 and 4-7 were identified here for the first time based on the ¹H and ¹³C NMR spectra, HSQC and HMBC. The use of LC-DAD-SPE/NMR hyphenation technique allowed us to perform a faster study of the most promising fraction of the extracts of *Licaria aritu*.

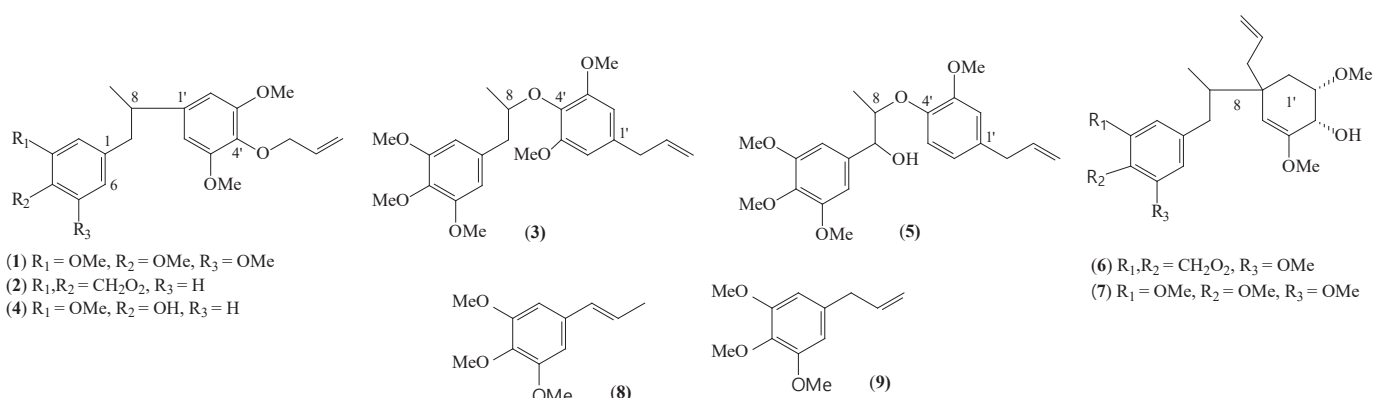


Fig 1. Compounds identified from *Licaria aritu*

¹Marmara Pharmaceutical Journal 20: 390-400, 2016.

²Phytochemistry 31, 360-361, 1992

Agradecimentos/Acknowledgments

The authors are grateful for the support from the Fundação de Amparo à Pesquisa Estado do Amazonas (FAPEAM), Grant No 01.02.016301.03412/2021-78.

LC-MS- and GC-MS-based metabolomics unravels metabolites involved in the development of a Heliantheae-specialist insect

Marília E. Gallon (PG),^{1*} Leonardo Gobbo-Neto (PQ).¹

mariliagallon@hotmail.com.br

¹ Núcleo de Pesquisa em Produtos Naturais e Sintéticos, School of Pharmaceutical Sciences of Ribeirão Preto, University of São Paulo (USP), Av. do Café s/n°, Ribeirão Preto, SP 14040-903, Brazil

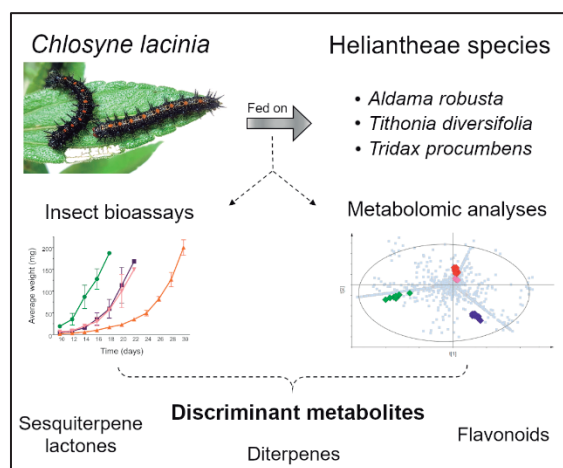
Palavras Chave: *Chlosyne lacinia*, *Tithonia diversifolia*, *Tridax procumbens*, *Aldama robusta*, Asteraceae, Chemical ecology

Highlights

Chlosyne lacinia caterpillars fed on Heliantheae species exhibited differential development. We putatively identified 51 metabolites. Diterpenes may be involved in insect development and diapause rate.

Resumo/Abstract

Plant-insect interactions are greatly mediated by secondary metabolites, playing fundamental roles in ecosystem evolution. For insect herbivores (i.e., plant-feeding insects), a balanced nutritional intake is required to ensure an adequate larval development and metamorphosis. Herein, we explored the metabolites involved in the development of *Chlosyne lacinia*, an insect that feeds preferably on plants of the Heliantheae tribe (Asteraceae family). To this end, *C. lacinia* caterpillars were fed on leaves of three different Heliantheae species (*Tithonia diversifolia*, *Tridax procumbens* and *Aldama robusta*) and we performed insect development assays along with liquid chromatography coupled to mass spectrometry (LC-MS)- and gas chromatography coupled to mass spectrometry (GC-MS)-based metabolomics of plant and insect samples. *C. lacinia* caterpillars fed on all Heliantheae species showed an appropriated development and completed metamorphosis to adulthood. However, according to the plant species provided as diet, we observed a distinctive larval development in terms of mean weight of the caterpillars, development time until the pupal stage, larval and pupal viabilities, and diapause rate. *C. lacinia* caterpillars fed on *T. diversifolia* leaves completed their development to pupae within 18 days and exhibited larval and pupal viability of 100%. Caterpillars that were fed on *T. procumbens* leaves took approximately 20 days to complete their development to pupae. For *C. lacinia* caterpillars fed on *A. robusta* leaves, the development period was longer and lasted approximately 30 days. Additionally, caterpillars fed on *A. robusta* leaves showed a diapause rate much greater (70%) than caterpillars fed on *T. procumbens* (10%) or *T. diversifolia* leaves (2%). To assess the discriminant metabolites, we combined the LC-MS and GC-MS data to perform principal component analysis (PCA) and partial least squares discriminant analysis (PLS-DA) for each set of samples (plant species, *C. lacinia* frass and *C. lacinia* caterpillars). Fifty-one metabolites were putatively identified, and included flavonoids, sesquiterpene lactones, monoterpene derivatives, sesquiterpenoids, diterpenes, triterpenes, oxygenated terpene derivatives, steroids and lipid derivatives. Diterpenes were appointed as discriminant metabolites and were detected only in *A. robusta* leaves and insects that were fed on this diet. Considering that the caterpillars fed on *A. robusta* leaves took longer to complete their development to adults and exhibited greater diapause rate, we hypothesized that diterpenes may be involved in the differential larval development. Therefore, for this Heliantheae-specialist insect, the sesquiterpene lactones typically present in its host plants were not related to detrimental effects across insect development. However, diterpenes may be associated with longer development periods and modulation of feeding behavior in *C. lacinia* caterpillars. Also, triterpenes, steroids and lipid derivatives may be involved in larval and pupal viabilities. Taken together, our findings provided insights into metabolites that play a role in insect development and behavior, pointing out relevant directions for integrative studies in insect physiology, behavior and nutritional ecology.



Agradecimentos/Acknowledgments

Authors are grateful to the São Paulo Research Foundation—FAPESP (grant #2017/17023-4) and Coordination for the Improvement of Higher Education Personnel—CAPES.

***In vitro* anticandidal activity of *Microlicia parviflora* flower extracts.**

Diego G. Prado (PG)^{1*}, Tiara da C. Silva (PG)¹, Mariana B. Santiago (PG)³, Alessandra G. Medeiros (IC)¹, Rafael A. C. Souza (PG)¹, Júlia M. G. D. Reis (IC)¹, Mário M. Martins (PG)⁵, Raquel M. F. de Sousa (PQ)¹, Luís C. S. Cunha (PQ)², Carlos H. G. Martins (PQ)³, Rosana Romero (PQ)⁴, Alberto de Oliveira (PQ)¹.

diego_godina@yahoo.com.br

¹Instituto de Química, UFU; ²Departamento de Química, IFTM; ³Instituto de Ciências Biomédicas, UFU; ⁴Instituto de Biologia, UFU; ⁵Instituto de Biotecnologia, UFU.

Microlicia parviflora, *Candida*, Cerrado, HPLC-ESI-MS/MS, flavonoids, Hydrolyzable tannins

Highlights

Promising anticandidal activity. Chemical study by HPLC-ESI-MS/MS of *Microlicia parviflora* flower extracts.

Resumo/Abstract

Fungal infections are responsible for approximately 1.5 million deaths per year. These infections occur more commonly in people with low immunity, making them particularly worrisome. Another problem with fungal infections is their treatment. Because they are eukaryotic organisms, it is more difficult to find effective substances against them. The few available drugs also have certain toxicities to patients, such as the class of azoles, which is the most commonly used to treat these infections^{1,2}. Thus, there is a need to search for new substances that can help in the treatment of these type of infections, especially considering that microorganisms can developed resistance to the substances used. In this aspect, the use of plants as a source of new active substances, or substances that serve as inspiration for the discovery of new drugs, has played a relevant role throughout history³. Therefore, this work aims to study that ability of extracts of the flowers of an endemic species from the Cerrado⁴, *Microlicia parviflora*, to inhibit the growth of *Candida* species, which are the species that most commonly cause fungal infections in humans, and to chemically evaluate the extracts that show good inhibition values for the evaluated species. For this, the extracts were prepared sequentially by maceration with hexane (HE) and 95% ethanol (EE) and were evaluated *in vitro* using the broth microdilution method. Promising MIC values obtained for EE against three species studied as shown in table 1.

Table 1: MIC values for the *Candida* species studied

	Espécies de <i>Candida</i>		
Amostra	<i>C. albicans</i>	<i>C. tropicalis</i>	<i>C. glabrata</i>
EH	1500	3000	187.50
EE	11.72	46.875	2.93

CP: amphotericin

As the EE was the more active, its chemical composition was evaluated by mass spectrometry, in its composition were found benzoic acids such as gallic acid and derivatives, flavonoids such as quercetin and some flavonoid derivatives such as quercetin galloyl-hexoside, rutin, myricitrin, kaempferol galloyl-hexoside, among others. Hydrolyzable tannins such as ellagic acid have also been identified.

¹BONGOMIN, F. et al., *Journal of fungi (Basel, Switzerland)*. 2017. ²HOKKEN, M. W. J. et al., *Fungal Genetics and Biology* 2019. ³NEWMAN, CRAGG., *Journal of Natural Products*. 2020. ⁴PACIFICO, R. F., Jardim Botânico do Rio de Janeiro, disponível em: <https://floradobrasil.jbrj.gov.br/reflora/floradobrasil/FB9983>, acesso em 03/01/2022

Agradecimentos/Acknowledgments

FAPEMIG, IQUFU, CAPES, CNPq, ProPP, UFU

In vitro leishmanicidal activity of essential oils

Adriana da Silva Santos de Oliveira (PG),^{1,2*} Nathalia Grazzia (PG),³ Gabrielly Galdino Conrado (PQ),⁴ Danilo Ciccone Miguel (PQ),³ Vera Lúcia Garcia (PQ),^{1,2}

***adriana@cpqba.unicamp.br**

¹Divisão de Química Orgânica e Farmacêutica, CPQBA-UNICAMP; ²Programa de Pós-Graduação FCF-UNICAMP; ³Departamento de Biologia Animal, IB-UNICAMP; ⁴Aluna de pós-doutorado Aché.

Palavras Chave: *Leishmanicidal activity, Essential oil, Baccharis dracunculifolia, Baccharis trimera, Varronea verbenacea, Aldama arenaria.*

Highlights

Four essential oils (*Baccharis dracunculifolia*, *Baccharis trimera*, *Varronea verbenacea*, and *Aldama arenaria*) were evaluated *in vitro* regarding their action against the promastigote parasite *Leishmania amazonensis*.

Abstract

Leishmaniasis is a neglected tropical disease that affects more than 12 million people around the world. It is transmitted by different species of infected sandflies (genus *Phlebotomus*). In Brazil, it is very common to find two species, *Leishmania* (Vianna) *braziliensis*, and *Leishmania amazonensis*. Four essential oils (*Baccharis dracunculifolia*, *Baccharis trimera*, *Varronea verbenacea*, and *Aldama arenaria*) were evaluated *in vitro* regarding their action against the promastigote parasite *Leishmania amazonensis*. The oils were obtained by hydrodistillation in Clevenger and analyzed by GC-MS. Activity evaluation was performed in promastigote forms cultured in 25 mL flasks. Samples were diluted in dimethyl sulfoxide (maximum final concentration of 0.07%) and, then, submitted to the biological activity test according to the MTT method (3-[4,5-dimethyl-triazol-2-yl]-2,5-diphenyltetrazolium bromide) in 96-well plates.¹ Results were expressed as percentages of cell viability compared to the group of untreated parasites (control group, equivalent to 100%). Using the cell viability curves drawn with at least 8 different concentrations and at least two independent assays was possible to calculate EC₅₀ (effective concentration for a 50% reduction in cell viability). The viability curves demonstrated that more than 25 µg.mL⁻¹ was needed to begin the reduction of cellular growth in parasites. Regarding the chemical composition of essential oils, we can highlight mono, sesqui, and diterpenes compounds. The essential oils showed the following EC₅₀ values (Table 1):

Table 1. EC₅₀ values (µg.mL⁻¹) obtained from tests in duplicate and majority compounds of essential oils evaluated for *L. amazonensis* promastigote parasites.

Essential Oil	EC ₅₀ (µg.mL ⁻¹)		Majority compounds identified by GC-MS (Relative percentage)
<i>V. verbenacea</i>	19,6	30,8	α-Pinene, trans-Caryophyllene, α-Humulene and Alloaromadendrene
<i>B. trimera</i>	112,7	75,8	trans-Caryophyllene, Germacrene D, Bicyclogermacrene and δ-Cadinene
<i>B. dracunculifolia</i>	33,3	51,9	β-Pinene, Limonene, Nerolidol and Spathulenol
<i>A. arenaria</i>	16,8	19,7	α-Pinene, Carotol, Pimaradiene and ent-8(14),15-pimaradien-3β-ol

With these data, we can understand that *V. verbenacea* and *A. arenaria* oils were more active than oils from the *Baccharis* genus species.

Reference:

¹Oliveira ADSS, Conrado GG, Grazzia N, Miguel DC, Franchi Júnior GC, Garcia VL. In Vitro Cytotoxic and Leishmanicidal Activity of Isolated and Semisynthetic ent-Pimaranes from *Aldama arenaria*. *Planta Med.* 2022 Oct; 88(13):1163-1174.

Acknowledgments

CNPq, CAPES, FAPEAM, FAPESP, and EDUCORP-UNICAMP by the financial support.

Marine fungi *Cunninghamella echinulata*-9A5 as a biosurfactant in tannery leather treatment waste

Mariana B. Nascimento (PG)^{1*}, Heber E. Andrada (PG)¹, Kátia R. Prieto (PQ)¹, Eduardo F. Molina (PQ)¹, Gustavo M. Dias (PQ)², Marcos A. Soares (PQ)³, Marcio L. A. Silva (PQ)¹, Wilson R. Cunha (PQ)¹, Patrícia M. Pauletti (PQ)¹, Ana H. Januário (PQ)¹.

marianab158@gmail.com

¹ Universidade de Franca-UNIFRAN; ² Universidade Federal do ABC-UFABC; ³ Universidade Federal de Mato Grosso-UFMT.

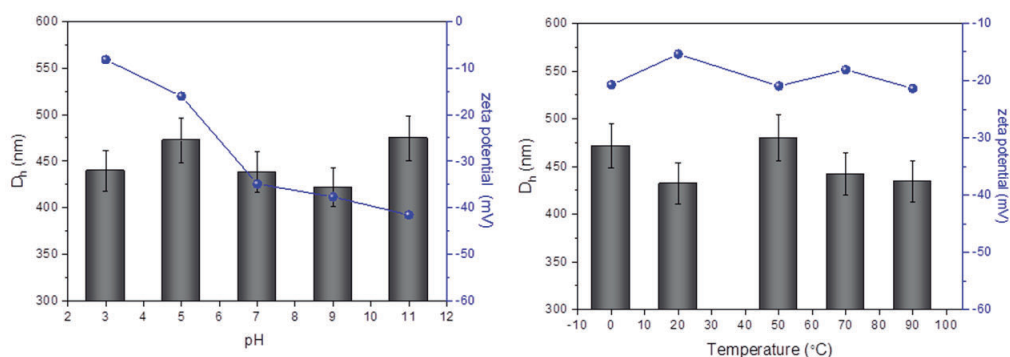
Keywords: Emulsification index, Filamentous fungi, *Trididemnum orbiculatum*, Zeta potential.

Highlights

Malt broth extract of the marine fungi *Cunninghamella echinulata*-9A5 showed biosurfactant action against vegetable oils, used engine oil and tannery sample, as well as the capacity for emulsification, dispersion, and stability with the variation of pH and temperature.

Abstract

Microorganisms as bacteria, yeasts and fungi are major producers of biosurfactant agents with diverse biotechnological applications in replacing synthetic surfactants, as well as in reducing environmental pollution through remediation¹⁻³. The present work aimed to evaluate the biosurfactant potential of malt broth extract of the marine fungi *Cunninghamella echinulata*-9A5. After 5 days of cultivation in sterile medium, the E24 emulsification index and oil displacement were evaluated using vegetable oils (soybean, sunflower, corn) used motor oil and residue from the leather treatment process. The chemical profile of the extract was delineated by GC/MS, NMR and HPLC-DAD and stability were determined by the zeta potential and hydrodynamic diameter (D_h). Concerning the emulsification index E24(%) the best results were found for maltextract along with burnt engine oil and leather industrial waste 78.10± 0.05 and 77.10± 0.00, respectively. Regarding the zeta potential, the maltextract showed an anionic profile with good stability against temperature variations (0° to 90°C) and pH (3 to 11) represented in the following graphics. The presence of triglycerides and free and esterified fatty acids was confirmed by GC/MS and ¹H NMR. Our results indicate marine fungi *Cunninghamella echinulata*-9A5 as a sustainable alternative for removing crude oils from the environment, which collaborate existing literature on biosurfactants from different strains of *Cunninghamella echinulata*, highlighting the scarcity of studies focused on the fungal strain of marine origin.



References:

- Andrade, Rosileide FS *et al.* Advances in Materials Science and Engineering, v. 2018, 2018.
- Silva, Artemisia Carla Santos da *et al.* Archives of Institute Biological, v. 85, 2018.
- Srivastava, Rajesh Kumar *et al.* Archives of Microbiology, v. 204, 2022.

Acknowledgments

This research was supported by CAPES, CNPQ and FAPESP.

46ª Reunião Anual da Sociedade Brasileira de Química: "Química: Ligando ciências e neutralizando desigualdades"

Metabolic profile of extracts from flowers of the genus *Aristolochia* by HPLC-ESI-IT-MS/MS and GC-MS

Camila Luiza Cunha (PQ),^{1*} Isabele Rodrigues Nascimento (PQ),¹ Ana C. Zanatta Silva (PQ).²

camila.cunha@unesp.br; isabele.nascimento@unesp.br

¹Institute of Chemistry, São Paulo State University, UNESP, Araraquara, SP, Brazil;

²Faculty of Pharmaceutical Science, University of São Paulo, USP, Ribeirão Preto, SP, Brazil;

Palavras Chave: *Aristolochiaceae*. *Aristolochia*. Flowers. Dereplication.

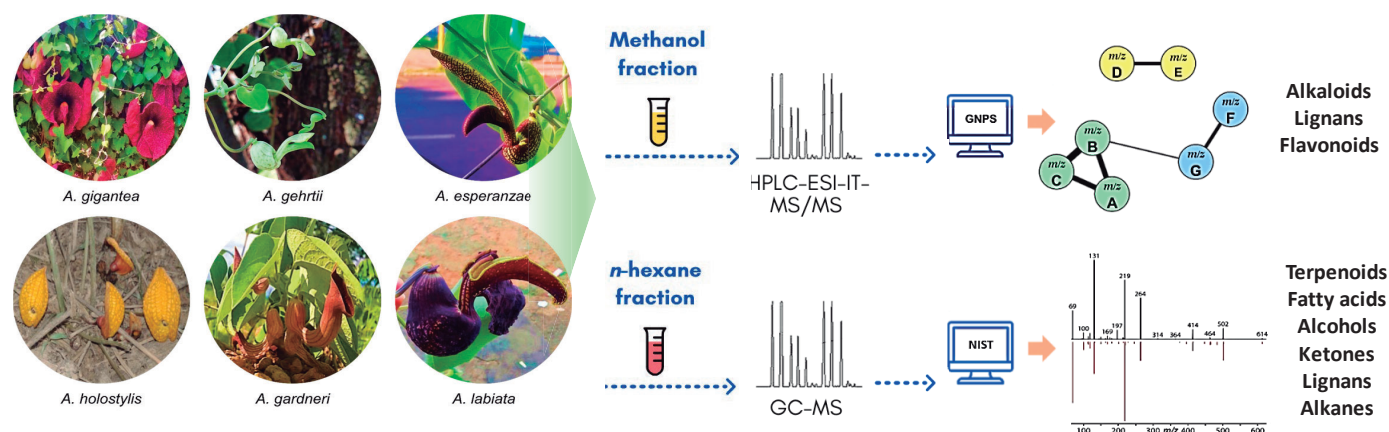
Highlights

- HPLC-ESI-IT-MS/MS and GC-MS analysis of the flowers of six *Aristolochia* species.
- Molecular networking and mass spectral libraries as metabolite annotation strategies.

Abstract

Plants of the genus *Aristolochia* (Aristolochiaceae) have flowers with very peculiar morphological characteristics and pollination mechanism.^{1,2} The aim of this work was to analyze and compare the organic extracts of six species of *Aristolochia* using HPLC-ESI-IT-MS/MS and GC-MS (Figure 1). The analysis of the methanol fractions of the species *A. esperanzae*, *A. gardneri*, *A. gehrtii*, *A. gigantea*, *A. holostylis*, and *A. labiata* by HPLC-ESI-IT-MS/MS, using the molecular network approach, allowed to note 17 compounds belonging to the classes of alkaloids, lignans and flavonoids. Regarding the GC-MS analysis of the hexane fractions of these species, it was possible to suggest the presence of 37 compounds belonging to the classes of terpenoid, fatty acids, alcohols, ketones, lignans, in addition to alkanes homologues. This is the first dereplication study involving flowers of *Aristolochia*.

Figure 1. Fractionation methodology and instrumental analysis of *Aristolochia* flowers.



1. HIPÓLITO, J. et al. *Botany*, v. 90, n. 9, p. 815-829, 2012.

2. MARTIN, K. R. et al. *Flora*, v. 232, p. 153-168, 2017.

Acknowledgments

The authors thank CAPES, CNPq, FINEP, and FAPESP for the financial support and research grants.

Metabolomics approach to study pathogen-host interaction in Huanglongbing disease in *Citrus sinensis* roots

Hellen B. Barbieri (PG),¹ João Guilherme de M. Pontes (PQ),¹ Beatriz P. Sanchez,² Josiane Darolt,² Nelson A. Wulff,² Taícia P. Fill (PQ).^{1*}

hellen.hbb@gmail.com; taicia@gmail.com

¹Departamento de Química Orgânica, Universidade Estadual de Campinas.

²Fundo de Defesa da Citricultura, FUNDECITRUS.

Palavras Chave: Metabolômica, Huanglongbing, Raízes, Interação patógeno-hospedeiro, Cromatografia líquida acoplada a espectrometria de massas, *Citrus sinensis*.

Highlights

Metabolomics approach to study host-pathogen interaction in *Huanglongbing* disease in *Citrus sinensis* roots

The results indicate that infection by CLAs causes significant differences in the roots secondary metabolism.

Resumo/Abstract

Huanglongbing disease (HLB) is a devastating disease that affects citrus species and has been reported in several regions of the world. The bacteria *Candidatus* Liberibacter asiaticus (CLAs), *Candidatus* Liberibacter americanus, and *Candidatus* Liberibacter africanus are the causative agents of HLB in citrus. In Florida, there was a 75% reduction in citrus production due to the presence of HLB in 100% of the orchards [1]. Studies have already described the presence of CLAs in the roots of infected citrus [2] and one of the symptoms is the loss of fibrous roots, which begins before the appearance of foliar symptoms [3]. Furthermore, symptomatic trees infected by HLB are more affected by temperature and humidity extremes than healthy trees, a characteristic associated with the loss of fibrous roots in the infected citrus [2]. Therefore, the metabolomics approach is an important tool to study the plants' response through metabolites involved in processes that play an important role in this host-pathogen interaction [1]. This work, therefore, aims to understand the CLAs-citrus interaction in citrus roots through a metabolomics approach via LC-MS combined with platforms for metabolite annotation and statistical analysis. Through principal component analysis (PCA), a separation was noted between the group of roots infected by CLAs and healthy roots (Figure 1A) with an explained variance more significant than 80%, which indicates a metabolic differentiation between the two groups studied. Some secondary metabolites classes were observed up-regulated and statistically significant in the distinction between roots affected by CLAs and the control group (Figure 1B), such as coumarins, fatty acyls, prenol lipids, phenylpropanoids, and organic acids. These metabolic classes play essential roles in the plant's defense system against stress and pathogen attacks. For example, the exudation of organic acids by the roots, for example, can improve the absorption of soil minerals such as zinc, iron, and phosphorus [4]. The foliar symptoms of HLB-diseased citrus are similar to those generated by deficiencies of nutrients [5] such as zinc and iron [6]. Infection by CLAs, therefore, would impact nutrient uptake and root growth and, consequently, alter the plant ionome [5].

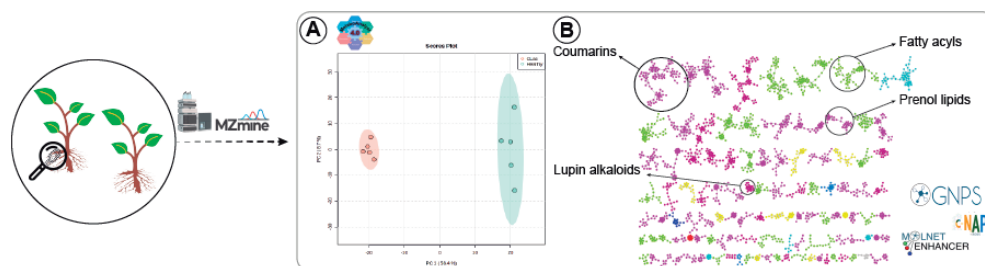


Figure 1. Metabolomic analysis of CLAs-citrus interaction in roots. (A) Principal component analysis. (B) Classes of up-regulated metabolites in roots affected by the disease compared to the control group.

[1]: 10.1094/PHYTO-08-21-0354-FI. [2] Doi: 10.1094/PDIS-01130021-RE. [3] Doi: 10.1016/j.scienta.2021.110511. [4] Doi: 10.1093/jxb/erab019; [5] Doi: 10.1007/s40858-020-00389-y; [6] 10.3389/fntpr.2023.1045364.

Agradecimentos/Acknowledgments

We thank FAPESP (2021/00728-0; 201/08947-3), CNPq, CAPES, and UNICAMP for financial support.
46ª Reunião Anual da Sociedade Brasileira de Química: "Química: Ligando ciências e neutralizando desigualdades"

Microencapsulation of *Schinus terebinthifolius* essential oil: Application in Integrated Pest Management

Regina S. Acácio (PG),¹ Miguel Angel M. Gutierrez (PG),¹ Henrique F. Goulart (PG),¹ Antônio Euzébio G. Santana (PQ).^{1*}

regina.acacio@iqb.ufal.br; aegs@ceca.ufal.br

¹Centro de Ciências Agrárias, UFAL

Keywords: Spray-drying, Repellent Activity, *Alphitobius diaperinus*.

Highlights

The essential oil was microencapsulated by spray drying; Repellent activity against *Alphitobius diaperinus* in four arm bioassays; Daily weight loss in different places of microparticles.

Resumo/Abstract

Schinus terebinthifolius é conhecida popularmente como aroeira, é utilizada na medicina popular devido à sua ação antialérgica, anti-inflamatória e antimicrobiano, e tem sido citada na literatura por sua atividade inseticida e antifúngica. A técnica de microencapsulação por spray-drying é um processo físico que realiza uma secagem por atomização, e tem sido utilizada para otimizar a estabilidade e o uso de agentes bioativos como fármacos, aromas, probióticos e mais recentemente, óleos essenciais. *Alphitobius diaperinus* é um inseto praga em aviários de difícil controle e causa prejuízos por transmitir patógenos para os aviários. O presente trabalho teve como objetivo microencapsular o óleo essencial de aroeira por spray-drying, realizar a caracterização das micropartículas, observar sua perda de massa diária em função do tempo, e testar a atividade repelente do óleo essencial puro e microencapsulado frente ao inseto praga de grãos armazenados *A. diaperinus*. O óleo essencial foi obtido pela técnica de hidrodestilação e a obtenção dos produtos microencapsulados foi realizada no equipamento spray-dryer utilizando como agentes encapsulantes a maltodextrina, goma arábica e como agente dispersante o dióxido de silício. A caracterização morfológica das micropartículas foi realizada por Microscopia Eletrônica de Varredura (MEV), a presença do óleo nas micropartículas foi comprovada pela técnica de cromatografia gasosa acoplada ao detector de ionização em chamas (GC-FID), e a atividade repelente foi testada em quadruplicata em olfátometro de 4 braços com 200 insetos. As micrografias obtidas por Microscopia Eletrônica de Varredura (MEV) indicam que as micropartículas formadas são esféricas e uniformes com tamanho médio de 5 µm. Os resultados expressos no gráfico 1 indicam que há estabilidade das microcápsulas formadas em ambiente fechado e aumento no rendimento obtido quanto maior for o volume utilizado durante a secagem. Os resultados obtidos foram analisados por regressão linear. Notou-se que as amostras em laboratório não tiveram alterações significativas na perda de massa no período analisado. O perfil cromatográfico apresenta variação na porcentagem dos voláteis. As amostras em casa de vegetação adquiriram umidade do ambiente alterando suas características físico-químicas e apresentando alterações em sua massa.

Figura 1: Bioensaios em olfátometro 4-arm

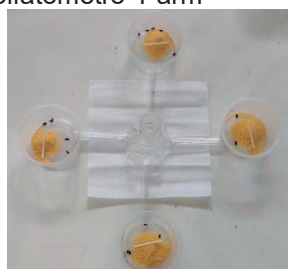


Figura 2: Cromatogramas de 1 e 5 dias e micropartículas

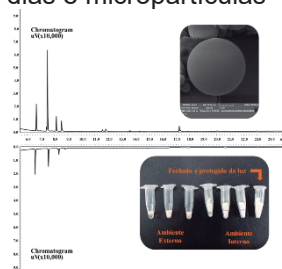
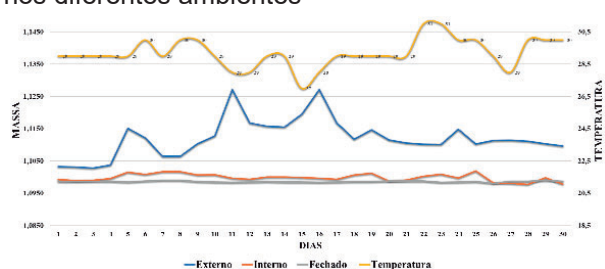


Gráfico 1: Variação de massa das micropartículas nos diferentes ambientes



Agradecimentos/Acknowledgments

Agradecemos aos órgãos de fomento FAPEAL, CAPES e CNPq. À Universidade Federal de Alagoas e ao Instituto Federal de Alagoas pela estrutura para o desenvolvimento do trabalho.

Molecular Dereplication and Cytotoxic Evaluation of Isoflavonoids from *Vicia faba* (FABACEAE)

Victor M. Sipoloni (PG),^{1*} Cauê S. Lima (PG),² Heron F. V. Torquato (PQ),² Edgard J. Paredes-Gamero (PQ),³ Livia Soman de Medeiros (PQ),⁴ Thiago A. M. Veiga (PQ)⁴.

victor.sipoloni@unifesp.br

¹Programa de Pós-Graduação em Biologia Química, Universidade Federal de São Paulo – UNIFESP; ²Departamento de Bioquímica, Universidade Federal de São Paulo – UNIFESP; ³Faculdade de Ciências Farmacêuticas, Alimentos e Nutrição, Universidade Federal do Mato Grosso do Sul – UFMS; ⁴Departamento de Química, Universidade Federal de São Paulo – UNIFESP.

Palavras Chave: Natural Products, Isoflavones, *Vicia faba*, dereplication, leukemia.

Highlights

Our approaches are exploring compounds from *Vicia faba* with cytotoxic activity by molecular networking that allowed us to the isolation of isoflavonoids, which was not reported for *Vicia* genus yet.

Resumo/Abstract

The search for Natural Products (NPs) with a biological activity has grown in the last decades and many researchers have highlighted their potential for clinical trials against several diseases, including cancer.¹ In recent years, the use of hyphenated analytical techniques has boosted the discovery of new bioactive compounds, promoting more effective strategies for the investigation of known or completely unknown metabolites.^{2, 3} Based on this, our proposal aims to use molecular dereplication of anti-leukemia compounds from *Vicia faba* (Fabaceae). Therefore, we submitted our MS/MS data to the GNPS database to construct a Molecular Network (Figure 1), which allowed us to annotate isoflavonoids in the fractions assayed (at 100 µg/mL; 24 and 48 hours) against different human leukemia cell lines: Jurkat, KG-1, Kasumi-1, Raji and K562 (Figure 2). Interestingly, there is no previous reports for this class of NPs in *Vicia* species. Based on these data, to prove the presence of isoflavonoids in *V. faba*, the most active fractions were submitted to different purification steps. So far, two isoflavones were purified and identified by NMR and HRMS: alfarone (**1**) and 8-O-methylretusin (**2**) (Figure 3). Thus, our dereplication approaches were powerful tools to increase the chemodiversity of *Vicia* genus. Additionally, other four substances were isolated, and their structures are under identification. Finally, all compounds will be submitted to anti-leukemia assays to determine their cytotoxic activities and their possible mechanisms of action will be elucidated.

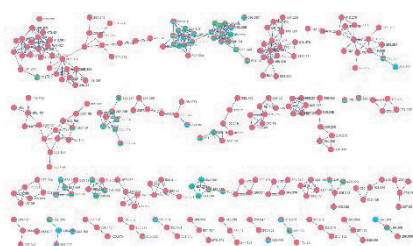


Figure 1: Molecular Network

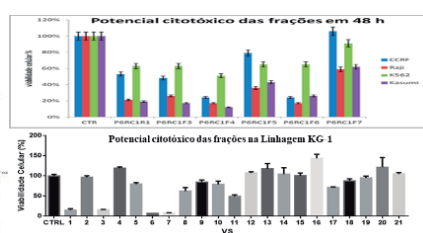


Figure 2: Preliminary cytotoxic assays

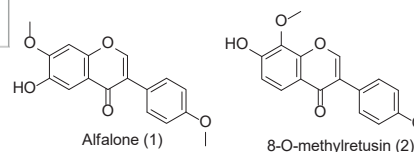


Figure 3: Isolated compounds

¹ NEWMAN, David J. Journal Of Natural Products, 83, 770-803 (2020). <http://dx.doi.org/10.1021/acs.jnatprod.9b01285>;

² KATZ, Leonard; et al. Journal Of Industrial Microbiology And Biotechnology, 43, 155-176 (2016).

<http://dx.doi.org/10.1007/s10295-015-1723-5>; ³ OLIVEIRA, Gibson de et al. Planta Medica, 83, 636-646 (2016).

<http://dx.doi.org/10.1055/s-0042-118712>.

Agradecimentos/Acknowledgments



Molecular dereplication of volatile oil from leaves of *Ludwigia sericea* (Cambess) H.Hara (Onagraceae)

Lorena S. Meirelles (IC),¹ Ana Beatriz M. Salero (IC),¹ Edgard A. Ferreira (PQ).^{1*}

lorena.meirelles@mackenzista.com.br; edgard.ferreira@mackenzie.br*

¹School of Engineering, Mackenzie Presbyterian University

Keywords: Essential Oil, Aquatic Macrophyte, Onagraceae, Dereplication.

Highlights

Hidrodistillation of leaves of aquatic macrophyte *Ludwigia sericeae* followed by dereplication of volatile oil based on GC-MS analysis, comparison with spectral libraries and retention index revealed presence of 70 compounds, in which alcohols and aliphatic hydrocarbons are the most representative classes.

Resumo/Abstract

Among groups of vegetal species that cover all biomes in Brazil, there are aquatic macrophytes, popularly known as aquatic plants. They are herbaceous species that grow in water, soils covered by water or even soils saturated by water.¹ Despite the geographic range of these species, that are found throughout the Brazilian territory due to the versatility of adaptation to different biomes, few studies are related to chemical composition and biological properties of their compounds. As part of the Brazilian aquatic flora, genus *Ludwigia* belongs to Onagraceae family and has 48 species.² However, studies involving species of this genus are scarce, which reflects in poor information about chemotaxonomic aspects and bioactive compounds. Studies concerning chemical composition and biological effects of essential oils are even more restricted. Then, as part of our research group studies focusing on molecular diversity and biological effects of compounds obtained from aquatic macrophytes, the present study reports molecular dereplication of volatile oils from leaves of *L. sericea*, collected in Nazaré Paulista, São Paulo State. Thus, leaves were submitted to extraction of volatile oils by hydrodistillation using Cleavenger apparatus for a period of four hours with yield of 0.01%. Then, the obtained product of hydrodistillation was analyzed by GC-MS. The obtained data from CG-MS analysis was subjected to dereplication by means of comparison with mass spectra library of compounds NIST 17 Library jointly with retention index of each compound and comparison with data available on literature.³ This procedure revealed a substantial number of 70 compounds distributed in different classes as alcohols, carboxylic acids, aldehydes and aliphatic hydrocarbons, in which major compounds were *n*-tricosane (**1**, 13.96 %), *cis*-phytol (**2**, 7.63%), *n*-hexacosane (**3**, 7.1%), *n*-pentacosane (**4**, 6.46%), *n*-hexadecanoic acid (**5**, 5.81%), *n*-tetracosane (**6**, 3.49%), (9Z, 12Z, 15Z)-octadecatrienoic acid (**7**, 2.89%), linalool (**9**, 2.9%), (*E*)-nerolidol (**8**, 2.8%), 6,10,14-trimethylpentadecanone (**10**, 2.17%), pentadecanal (**11**, 1.28%) and fokienol (**12**, 1.25%) (**Figure 1**). These results may contribute with chemotaxonomic aspects of this genus, whereas compounds of the same classes have already described for *L. stolonifera*.⁴

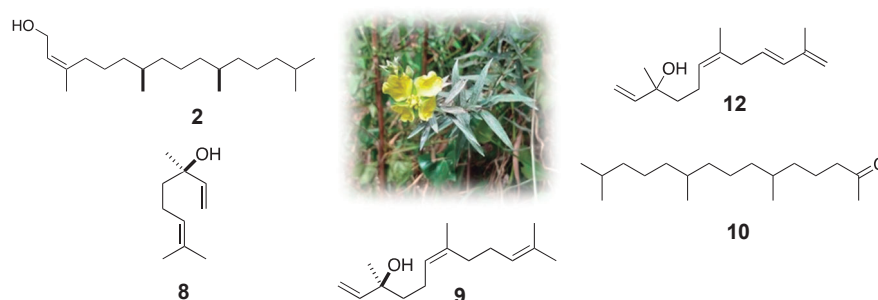


Figure 1: Compounds from volatile oil of *Ludwigia sericea*.

References: ¹Irgang, *et al.*, **1994**, *Roessléria*, 395-404; ²Souza *et al.*, **2019**, *Rodriguésia*, e01392018; ³Adams, R. P., Identification of Essential Components by Gas Chromatography/Mass Spectroscopy, **2009**. ⁴Baky, *et al.*, **2021**, *ACS Omega*, 24788.

Agradecimentos/Acknowledgments

Mackpesquisa and CNPq for fellowship to Lorena S. Meireles and Ana Beatriz M. Salero, respectively. Sumiko Honda and São Paulo Municipal Herbarium (PMSP) for identification of plant species.

Natural product diversity of two ecologically distinct *Penicillium brasilianum* strains: are meroterpenes involved in fungal environmental adaptation?

Daniel Yuri Akiyama (PG),^{1*} Marina Ferreira Maximo (IC),¹ Taicia Pacheco Fill (PQ).¹

d195888@dac.unicamp.br; taicia@unicamp.br

¹Departamento de Química Orgânica, Instituto de Química, UNICAMP.

Keywords: chemical ecology, chemical biology, natural products, metabolomics, meroterpenes.

Highlights

Metabolomics of two ecologically distinct *P. brasilianum* were performed through LC-MS/MS. Meroterpenes were differentially produced. Could these molecules be involved in fungal environment adaptation?

Abstract

Penicillium brasilianum is a filamentous fungi isolated from many ecologically distinct niches such as soil, in association with marine sponges, as an endophyte of *Melia azedarach* and as a phytopathogen of *Allium cepa* L.. Although its metabolism has been extensively studied, bioinformatic analyses indicate that many biosynthetic gene clusters remain cryptic. To expand our knowledge of the natural product diversity in *P. brasilianum* and correlate such molecules to its adaptation to different lifestyles, we investigated the metabolome of two different *P. brasilianum* strains: LaBioMMi 136, isolated as an endophyte from the root bark of *M. azedarach*, and MG11, isolated from soil. Both fungi were inoculated in four different culture media. Secondary metabolites were extracted with methanol and analyzed through LC-MS/MS. Data analysis comprised feature finding through mzMine3 and Feature-Based-Molecular Networking in the GNPS platform. Our results indicate that meroterpenes are differentiated in both strains. Meanwhile LaBioMMi 136 produces austinol-related meroterpenes (not shown in this abstract), MG11 biosynthesizes austalides and mycophenolic acid (Fig 1).

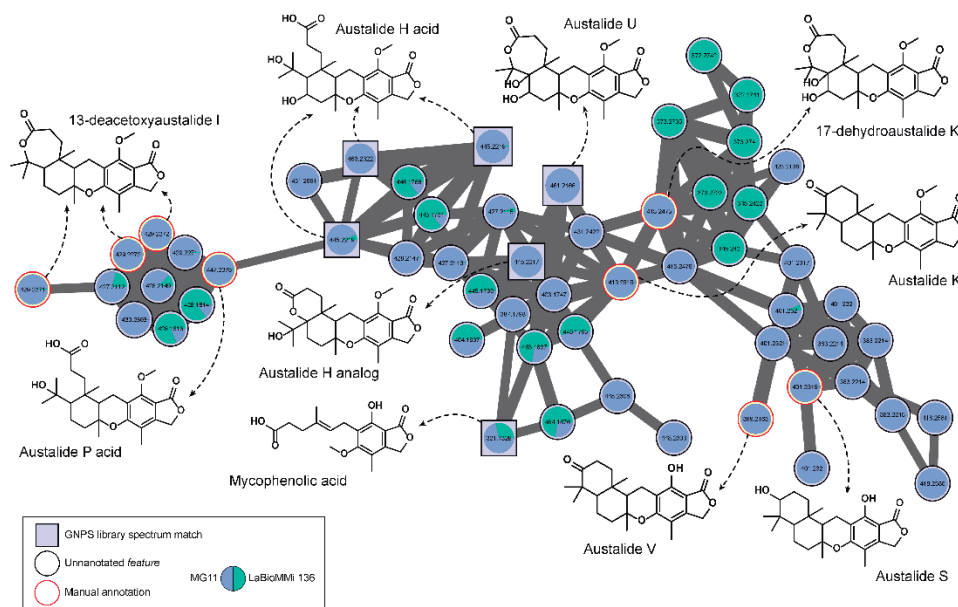


Figure 1. Spectral family relate to austalides, being produced only by *P. brasilianum* MG11.

Due to the common biosynthetic origin of austalides, mycophenolic acid and austinol, we believe a divergence in the biosynthetic gene cluster of these meroterpenes may have occurred in the studied strains. Molecular biology experiments will be carried out to elucidate the biosynthetic pathway and correlate this divergence with fungal adaptation to different lifestyles.

Acknowledgments



New methodologies and natural products control of leaf cutting ants, and their fungus.

João B. Fernandes (PQ)^{1*}, Artur S. Cruz (PG)¹, Yara P. F. Pio (PG)¹, Lulliana T. Franco (IC)¹, Gabriele F. Silva (IC)¹, Sean S. Araújo (PG)¹, Dorai P. Zandonai (PG)¹, Ronaldo C. Faria (PQ)¹, Moacir R. Forim (PQ)¹, M. Fátima G. F. da Silva (PQ)¹, Rose M. Carlos (PQ)¹, Marisa N. Fernandes (PQ)², Odair C. Bueno (PQ)³.

djbf@ufscar.br

¹Chemistry Department, CCET - UFSCar; ²Physiologic Science Department, CCBS – UFSCar, ³CEIS, UNESP-Rio Claro

Key-words: Leaf cutting ants, Bioinsecticides, Natural products, Fungus, Biosensors

Highlights

The control of leaf-cutting and fire ants, which causes severe damage to agriculture, must be done without influencing the environment. Natural products from *Toona ciliata*, *Vismia guianensis* and *Hymatatus articulatus* are under study and tests as insecticides and fungicides, as well as action of acetylcholinesterase (using a disposable electrochemical device (DED) show good results.

Abstract

Leaf-cutter and fire ants are agricultural pests and research on their controls is under development using new technologies applied to natural products, such as micro and nanoencapsulation, disposable electrochemical device (DES) using acetylcholinesterase enzyme (AChE), co-cultivation technique of nests members, mass spectrometry associated with statistical tools, including PCA (Principal Component Analysis), PLS (Partial Least Squares), HCA (hierarchical cluster analysis), HeatMap method (heat map) and GNPS Platform (Global Natural Products Social).

In the world supply of agricultural products, Brazil is very important and pest ants are the main problems for Brazilian agriculture, causing enormous damage to agribusiness. New natural products and techniques are being developed by the Natural Products Group, specially to reduce costs and the amount of insecticides applied. Ants of the genus *Atta* (saúvas) and *Acromyrmex* (quenquéns), are characterized by cultivating a single species of fungus, *Leucoagaricus gongylophorus*, a mutualistic fungus essential for their survival.

This communication presents the chemical studies of the plants *Toona ciliata*, *Vismia guianensis* and *Hymatatus articulatus* and tests as insecticides and fungicides, as well as the action of acetylcholinesterase. These plants are characterized respectively by the presence of limonoids (1), benzophenones (2) and lactonic iridoids (3).

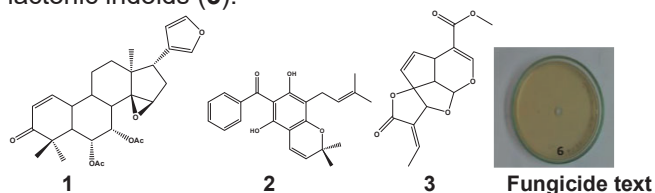


Figure 1. Structure of type of compounds isolated and *Leucoagaricus gongylophorus* fungicide text.

The alcoholic extract of the bark of *Hymatatus articulatus* present 100% of inhibition of the culture of

Leucoagaricus gongylophorus. Its fractionation led to the isolation of 6 lactonic iridoids and all were active, inhibiting the fungus 100%.

The ethanolic extract of leaves of *V. guianensis* showed 100% of inhibition of the enzyme acetylcholinesterase and was fractionated yielding benzophenones as the main compounds. The result indicates the insecticidal potential of this plant and the isolated compound. Benzophenones in the extracts, and the literature (KUMAR, S et al. 2013, OLIVEIRA, A.H. et al. 2017) presents the inhibition power of this class of compounds. Isolated compounds were identified by analysis of the ¹H and ¹³C NMR of 1D, 2D and HRMS.

Application of DEDs with the following reagents: Poly(diallyldimethylammonium chloride) (PDDA) solution; glutathione-decorated gold nanoparticles (AUNPs-GSH); 1-ethyl-3-(3-dimethylaminopropyl) carbodiimide (EDC) and Hydroxybenzotriazole (HOBT); the AChE and ethanolamine solution to block non-specific bonds is a viable alternative for faster tests in bioassays. AChE (DED-AChE) modified DED was applied in inhibition studies using the Square Wave Voltammetry (SWV) technique (Scheme 1).



Scheme 1. Schematic representation of DES-AChE construction.

KUMAR, S. et al. *Fitoterapia*, 89, 86–125, 2013.
OLIVEIRA, A.H. et al. *J. Ethnoph.* 195, 266–274, 2017.

Acknowledgments

FAPESP, 2012/25299-6, CAPES, CNPq, 312366/2018-3

Novos compostos de *Trichilia pseudostipularis* (Meliaceae)

Renata R. da S. Robaina (PG),^{1*} Michel de Souza Passos (PG),¹ Raimundo Braz-Filho (PQ),² Ivo José Curcino Vieira (PQ)¹

renatarobainadasilva@gmail.com

¹Laboratório de Ciências Químicas, Universidade Estadual do Norte Fluminense Darcy Ribeiro, Campos dos Goytacazes-RJ;

²Departamento de Química, Universidade Federal Rural do Rio de Janeiro, Seropédica-RJ.

Palavras Chave: Meliaceae, *Trichilia*, RMN

Highlights

New compounds from *Trichilia pseudostipularis* (Meliaceae). The phytochemical study of the wood and roots of *Trichilia pseudostipularis* resulted in the isolation and identification of four compounds, two of which are new in the literature.

Resumo/Abstract

Trichilia P. Browne é um dos gêneros mais numerosos da família Meliaceae¹. Segundo dados da WFO Plant List (2022), existem cerca de 102 espécies aceitas nesse gênero². Trabalhos envolvendo, tanto extratos quanto substâncias isoladas, de diferentes espécies de *Trichilia* apresentaram uma variedade de atividades biológicas, tais como, citotóxica¹, antifeedante² e antimicrobiana³. *Trichilia pseudostipularis* é uma espécie nativa e endêmica, podendo ser encontrada ao longo de toda a costa Brasileira, do sul do estado de Santa Catarina até a Bahia⁴. Nenhum artigo descrevendo estudos fitoquímicos desta espécie foi encontrado na literatura. Devido à importância das espécies do gênero *Trichilia* e da inexistência de quaisquer pesquisas sobre sua constituição química, o caule e as raízes de *T. pseudostipularis* foram submetidas a um estudo fitoquímico, que resultou no isolamento e identificação de 3 compostos do caule, 10-isopropil-3-metil-8,9-dihidronaftaleno-7(2H)ona (1), 2-hidroxi-10-isopropil-3-metil-8,9-dihidronaftaleno-7(2H)ona (2), e pseudostipulariol (3). Das raízes de *T. pseudostipularis*, foi obtida a γ -lactona, (2S,3S,4R)-3-Hidroxi-4-metil-2-(13"-fenil-1"-n-tridecil)-butanolideo (4). Os compostos foram identificados utilizando RMN e espectrometria de massas de alta resolução, sendo que os compostos 3 e 4 estão sendo relatados pela primeira vez na literatura.

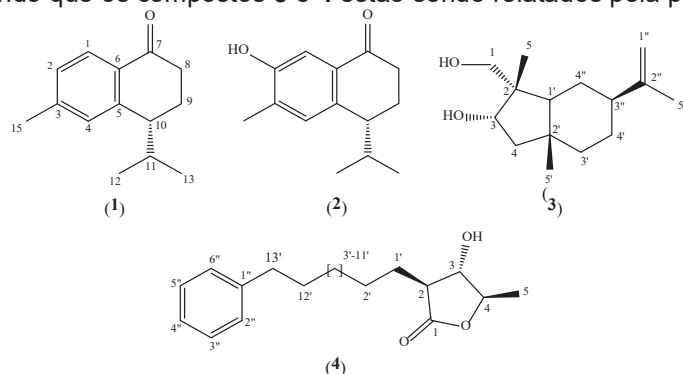


Figura 1. Substâncias isoladas de *Trichilia pseudostipularis*.

1. Pennington, T. D., Clarkson, J. J. A revision of *American Trichilia* (Meliaceae). *Phytotaxa* 256, 6-17, 2016.
2. WFO Plant List. 2011-2020. Acesso Jan 2023. <https://wfo.plantlist.org/plant-list/taxon/wfo-4000038940-2022-12>
3. Ji, K. L. et al. Cytotoxic limonoids from *Trichilia americana* leaves. *Phytochemistry* 118, 61-67, 2015.
4. Wheeler, D. A., Isman, M. B. Antifeedant and toxic activity of *Trichilia americana* extract against the larvae of *Spodoptera litura*. *Entomol Exp Appl* 98, 9-16, 2001.
5. Aladesanmi, A. J. & Odeiran, S. A. Antimicrobial activity of *Trichilia heudelotti* leaves. *Fitoterapia* 71, 179-182, 2000.
6. Pennington, T. D., Styles, B. T., Taylor, D. A. H. A monograph of neotropical Meliaceae. The. New York Botanical Garden Press, 1981.

Agradecimentos/Acknowledgments



POTENCIAL ALELOPÁTICO DE ALGUMAS PLANTAS AQUÁTICAS FRENTE AS PLANTAS INVASORAS *BIDENS PILOSA L.* E *DIGITARIA INSULARIS*

Michelly Maira Caovilla* (PG),¹ Conceição de Fátima Alves Olguin (PQ)

cfolguin@gmail.com; michy_caovilla@hotmail.com

¹Centro de Engenharias e Ciências Exatas, UNIOESTE – Campus Toledo, PR;

Palavras Chave: Plantas aquáticas, Atividade alelopática, Picão-preto, Capim-amargoso

Highlights

Allelopathic potential of some aquatic plants against invasive plants *Bidens pilosa* L. and *Digitaria insularis*. The use of synthetic herbicides can cause damage to the environment and to humans. Plants extracts can be used as natural herbicides. Aquatic plants can be an alternative for weed control.

Resumo/Abstract

A utilização de plantas com efeito alelopático tem se intensificado na agricultura, com o intuito de diminuir a utilização de herbicidas sintéticos para o controle de plantas invasoras, preservando assim o meio ambiente e contribuindo para a agricultura sustentável¹. Este trabalho avaliou o potencial alelopático do extrato hidroalcoólico de oito espécies de plantas aquáticas da região do Oeste do Paraná: *Azolla caroliniana*, *Eichornia crassipes* (parte aérea e raiz), *Egeria densa*, *Ludwigia peploides* (parte aérea e raiz), *Hydrocotyle ranunculoides* (parte aérea e raiz), *Oxycaryum cubens* (parte aérea e raiz), *Pistia stratiotes* (parte aérea e raiz) e *Salvinia sprucei* (parte aérea e raiz). Os extratos foram avaliados em bioensaios de germinação, crescimento e biomassa utilizando como alvo as sementes de picão-preto (*Bidens pilosa* L.) e capim-amargoso (*Digitaria insularis*). O teste foi realizado segundo a metodologia de Cunico e col² utilizando solução de ácido 2-morfolino-etanosulfônico (MES), com soluções dos extratos nas concentrações de 0,1; 0,2; 0,4; 0,8 mg/mL. O teste foi realizado em quadruplicata. Foram utilizados também os herbicidas sintéticos glifosato e atrazina, que foram testados nas mesmas concentrações que os extratos. Foi realizado o tratamento estatístico para o teste de germinação, crescimento e biomassa seca no programa STATISTICA. Também foi avaliado o teor de fenóis totais e os resultados expressos em miligramas de EAT (equivalentes de ácido tânico) por grama (g) de extrato.³ No bioensaio de germinação, os extratos da *L. peploides* (raiz), *E. densa* e *A. caroliniana* causaram uma inibição de 28%, 35% e 35% respectivamente, sendo observado para o glifosato e atrazina, uma inibição de 28%. No bioensaio de crescimento, os extratos mais ativos frente ao picão-preto foram a *L. peploides* aérea e *E. crassipes* aérea que provocaram uma inibição no crescimento de 66,33% e 67,15%, respectivamente. No teste de biomassa seca, podemos destacar os extratos *E. crassipes* (parte aérea e raiz) e *P. stratiotes* (raiz) que em suas maiores concentrações (0,8 mg/mL) apresentaram redução na massa das radículas de 90,65%, 89,49% e 93,03%, respectivamente. Com relação ao capim amargoso, os extratos das macrófitas não foram eficientes, entretanto, os herbicidas sintéticos conseguiram inibir em torno de 80% a germinação desta invasora. Na determinação dos fenóis totais destacam-se os extratos da *L. peploides* aérea (78,4 mg EAT g⁻¹) e raiz (75,82 mg EAT g⁻¹), sugerindo que o efeito alelopático observado para esta planta frente ao picão-preto pode estar correlacionado com o teor fenólico obtido. Os resultados observados neste trabalho, estimulam a continuidade de estudos nesta área de pesquisa uma vez que, ainda é pouco explorado o potencial biológico das plantas aquáticas, principalmente como bioherbicidas.

Referências

¹ Ferreira, A.G & Aquila, M.E.A. Revista Brasileira De Fisiologia Vegetal 12: 175-204, 2000.

² Cunico et al. Química Nova, v. 29, n.4, 746-749, 2006.

³ Roesler et al. Ciência e Tecnologia de Alimentos, v. 27, n.1, 53-60, 2007.

Agradecimentos/Acknowledgments

UNIOESTE - Campus Toledo, PR.

Raman and surface-enhanced Raman scattering spectroscopy characterization of the metabolic profile of *Coffea arabica* green beans

Lenize F. Maia (PQ),^{1*} Rafael de Oliveira (PG),² Mariana T. C. Campos (PG),² Raquel C. Ribeiro (PG),¹ Antonio Carlos Sant'Ana (PQ),² Luiz Fernando C. de Oliveira (PQ),² Cláudia M. Rezende (PQ)¹

rafael5@ice.uuff.br ; lenmaia@uol.com.br

¹ Instituto de Química, UFRJ; ² Instituto de Ciências Exatas, UFJF

Keywords: Green Coffee, *C. arabica*, SERS Spectroscopy, Raman Imaging, Adenine, Trigonelline

Highlights

- Raman and SERS spectroscopies were used to characterize coffee compounds directly on the green coffee bean
- Normal Raman spectral analysis highlighted the presence of phenolic acids, while SERS evidenced the alkaloid trigonelline and the purine base adenine
- Both techniques were suitable to identify different classes of metabolites present in the green coffee bean without pre-treatment of the sample

Abstract

The main chemical components of coffee beans are alkaloids, terpenes, phenolic acids, and volatile compounds that contribute to the aroma, and taste of the beverage. This work first demonstrates the combination of Raman and surface-enhanced Raman scattering (SERS) spectroscopy to characterize some of the *C. arabica* metabolites. The aim is to prove that *in situ* Raman spectroscopy can be used to identify compounds directly on the surface of beans without the need for extraction and purification. Figure 1A presents a normal Raman spectrum showing strong bands at 1630 and 1606 cm^{-1} assigned to $\nu(\text{C}=\text{C})$, attributed mainly to phenolic acids (caffeic acid), and chlorogenic acids (CGAs), while the broad band around 1692 cm^{-1} assigned to $\nu(\text{C}=\text{O})$ was addressed to xanthines and CGAs. The most intense bands observed in the SERS spectrum (Fig. 1A) were attributed to trigonelline (1032 cm^{-1}) and adenine (732 cm^{-1}), when compared with the standard compounds (Fig. 1 B and C, respectively). The latter is known to be the biosynthetic precursor of xanthines such as caffeine, theobromine, and theophylline. The presence of such xanthines could be confirmed due to the observation of low-intensity SERS bands in the region from 700 to 500 cm^{-1} , as well the superposition with adenine bands at 1376 and 1330 cm^{-1} . The spectral integration of SERS signals at 1032 and 732 cm^{-1} (Fig. 1 D, and E, respectively), represented as chemical maps suggest homogeneous distributions of trigonelline and adenine on the endosperm. These results show that both Raman and SERS techniques are suitable for selectively identifying compounds in coffee beans non-invasively and without complex sample preparations.

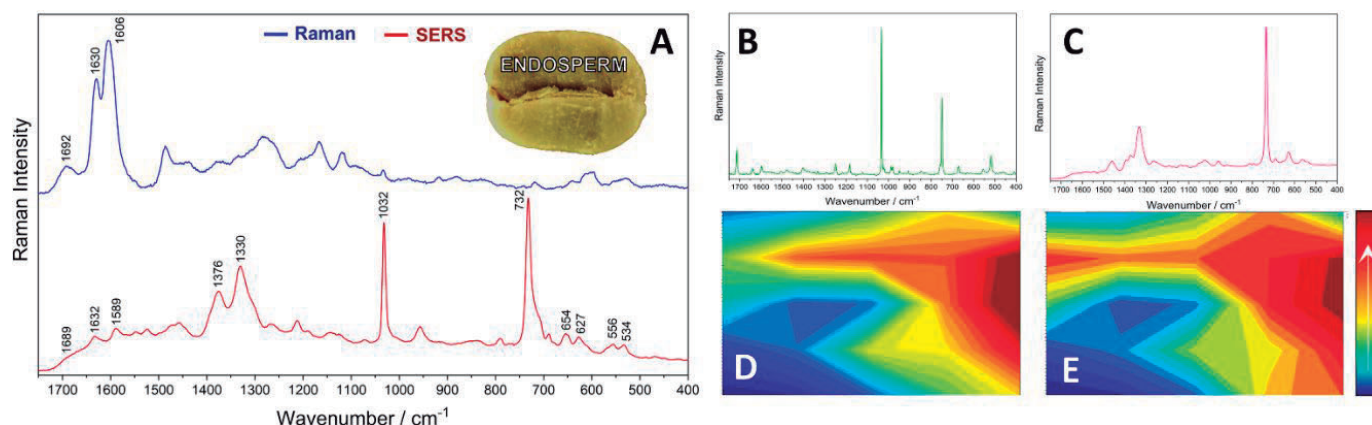


Figure 1. (A) Raman and SERS spectra ($\lambda_0 = 632.8 \text{ nm}$) collected from the endosperm of *C. arabica* bean (Ouro Fino, MG), shown in the inset. SERS spectra of (B) trigonelline and (C) adenine. SERS intensity mapping of bands at (D) 1032 cm^{-1} (trigonelline) and (E) 732 cm^{-1} (adenine). The color gradient in the chemical map is correlated with the integrated area of the band.

Agradecimentos/Acknowledgments

The authors thank UFRJ, UFJF, and the funding agencies CNPq, CAPES, FAPERJ, and FAPEMIG.

Secondary metabolites in the interaction between *Penicillium digitatum* and a new isolate fungus LBQM02 - A “Fleming” case against citrus green mold

Rodolfo Dantas Lima Junior (PG),^{1*} Éder de Vilhena Araújo (PG),¹ Pedro Luís Theodoro dos Santos Júnior (IC)¹, Taicia Pacheco Fill (PQ).¹

r197412@dac.unicamp.br; taicia@unicamp.br.

¹Institute of Chemistry, University of Campinas (UNICAMP)

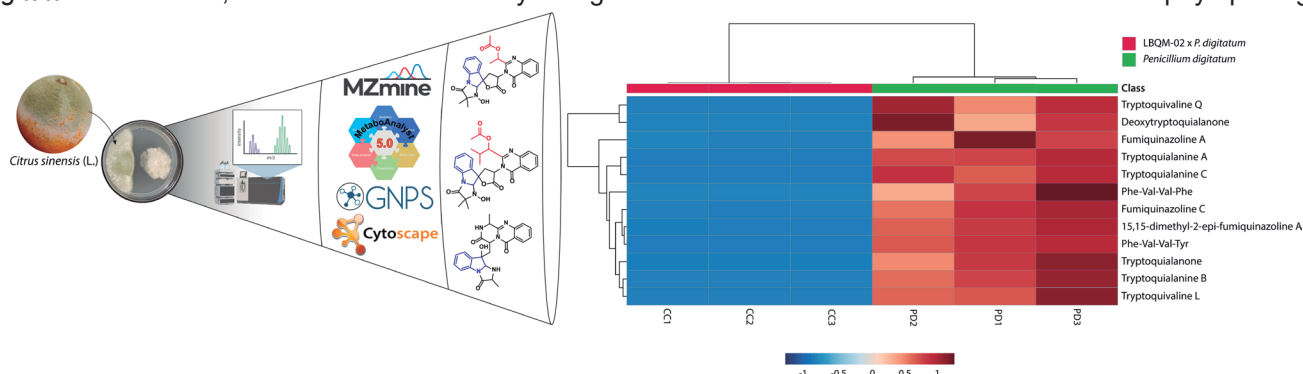
Keywords: Microbial metabolomics, Liquid co-culture, Antagonistic fungi.

Highlights

A fungal isolate obtained from a Petri dish contamination showed potent growth inhibition of *P. digitatum* and reduced the levels of secondary metabolites involved in the competition for the host.

Abstract

Green mold, caused by *Penicillium digitatum*, is the main post-harvest disease affecting the citrus market worldwide.[1] This disease can result in losses of up to 90% to the citrus industry.[1] Therefore, control strategies involving antagonistic fungi prospection as a source of new secondary metabolites with antifungal potential have emerged as an alternative to synthetic fungicides.[2] One of the ways to promote the prospection of fungi with unexplored antimicrobial metabolic potential is by carrying out paired cultivation in the same environment, a co-culture strategy.[3] Within this perspective, the purpose of this work fits into the study of the secondary metabolites involved in the interaction between the pathogen *P. digitatum* with a fungus (LBQM02) isolated as a contamination of a Petri dish containing *P. digitatum*. Analogous to the unexpected event that occurred with Alexander Fleming in the discovery of penicillin, the presence of the LBQM02 isolate showed potent inhibition of the phytopathogenic fungus, which led us to question the chemical control mechanisms involved in this interaction and how this interaction would help in the search by metabolites with antifungal character. Thus, analyses by liquid chromatography coupled to high-resolution mass spectrometry (LC-HRMS) associated with chemometric analyses, molecular network, and manual and database annotation of compounds indicated that the liquid co-culture between *P. digitatum* and LBQM02 induced the biosynthesis of the thiodiketopiperazine class analogs, the same molecules class observed in LBQM02 axenic culture. These molecules may be associated with mycelial growth inhibition, and cell wall deformation observed in-vitro. Furthermore, quinazoline-containing indole alkaloids such as tryptoquialanines and tryptoquivalines family, as well as fumiquinazolines analogs, have been significantly reduced in the co-culture. Understanding that the alkaloids produced can participate in the host colonization once they showed to be highly phytotoxic against the host seeds process as an attack mechanism against other pathogens, it is valid to infer that the decrease in the levels of these metabolites in co-culture indicates that the compounds produced by LBQM02 are a prolific source of secondary metabolites capable of disarming *P. digitatum*. Our hypothesis that the metabolites produced by LBQM02 may be involved in this decrease in alkaloid production levels opens up new hope for finding key structures capable of acting efficiently against *P. digitatum*. Therefore, more efforts are already being made to evaluate the in-vitro and in-vivo anti-phytopathogenic



action of the molecules found.

[1] doi:10.1002/jsfa.8865; [2] doi:10.3390/antibiotics11111604; [3] doi: 10.3390/md12021043

Acknowledgments

Sociedade Brasileira de Química (SBQ)

We thank FAPESP (proc. 21/00728-0), CNPq, CAPES, and UNICAMP for financial support.

Selective anti-*Trypanosoma cruzi* activity of natural dicentrine and its diastereomeric *N*-oxide derivatives

Daniela C. Tristão (PG),¹ Erica V. de Castro Levatti (PQ),² Beatriz A. Andrade (PG),² André G. Tempone (PQ),² João Henrique G. Lago (PQ)*¹

daniela.tristao@ufabc.edu.br

¹Center for Natural and Human Sciences, Federal University of ABC (UFABC), Sao Paulo, SP; ²Department of Parasitology, Adolfo Lutz Institute, Sao Paulo, SP.

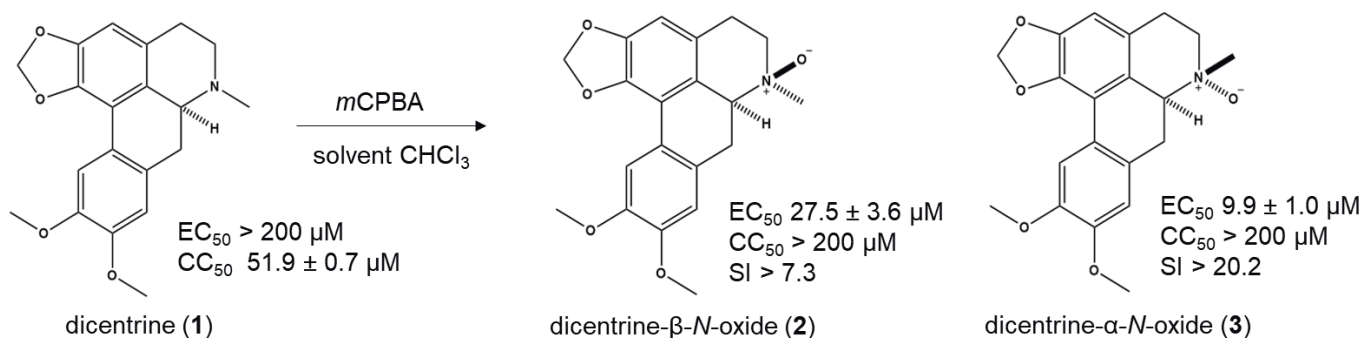
Palavras Chave: *aporphine alkaloids*, *N*-oxide, *Chagas Disease*.

Highlights

Dicentrine (**1**) was used as starting material for preparation of two diastereomeric *N*-oxide derivatives (**2** and **3**) which displayed selective activity against amastigote forms of *T. cruzi*.

Resumo/Abstract

The World Health Organization estimates that Neglected Tropical Diseases (NTDs) affect more than 1 billion people worldwide¹. Chagas Disease (CD) is a life-threatening NTD transmitted by the protozoan *Trypanosoma cruzi* that affects 6-7 million people and leads about 10 thousand to death every year¹. In Brazil, CD is endemic, and despite its discovery more than 100 years ago, the therapeutic available is limited, since the two approved drugs - benznidazole and nifurtimox – show effectiveness only during the acute phase of CD and present several side effects². It is therefore urgent the search for new potential substances, especially effective on the chronic stage of the disease, characterized by the presence of amastigote form of *T. cruzi*. As part of our continuous study aiming the identification of new prototypes, the alkaloid dicentrine (**1**) was isolated as the main compound of *Ocotea puberula* (Lauraceae) and used as starting material for preparation of *N*-oxide derivatives – dicentrine- β -*N*-oxide (**2**) and dicentrine- α -*N*-oxide (**3**)³.



After isolation by HPLC and characterization by NMR and MS, these compounds **1** – **3** were evaluated against amastigotes forms of *T. cruzi*. As result, it was observed that natural dicentrine (**1**) was inactive ($EC_{50} > 200 \mu M$) whereas the *N*-oxide derivative **3** exhibited similar potential ($EC_{50} 9.9 \pm 1.0 \mu M$) than positive control benznidazole ($EC_{50} 6.5 \pm 3.0 \mu M$). However, diastereomeric derivative **2** displayed reduced activity against amastigotes ($EC_{50} 27.5 \pm 3.6 \mu M$). Concerning the toxicity against NCTC, natural dicentrine showed $CC_{50} 51.9 \pm 0.7 \mu M$ whereas *N*-oxides **2** and **3** exhibited $CC_{50} > 200 \mu M$ and SI values of > 7.3 and > 20.2 . These results indicated that the presence of *N*-oxide moiety plays an important role in the antitrypanosomal activity, which is intensified by the *S* configuration of nitrogen atom (**3**). Additionally, the *N*-oxidation of (**1**) caused the alkaloids to become more selective. The presented study contributes to the understanding of the potential use of aporphines as drug candidates for CD treatment, bringing to light possible structural modifications to optimize selectivity of such compounds.

References: ¹<https://www.who.int/health-topics/neglected-tropical-diseases>. ²Martín-Escolano et al. *ACS Infect. Dis.* **2020**, 6, 2830-2843. ³Shafiee, A. et al. *J. Nat. Prod.* **1998**, 61, 1564 – 1565.

Agradecimentos/Acknowledgments

FAPESP, CAPES and CNPq.

Semi-Synthesis of (-)-Palitantin Derivatives for Bioassay Testing

Pedro M. Santucci (PG),^{1*} Gabriel H. S. Rosa (IC),² Kleber T. de Oliveira (PQ),² Roberto G. S. Berlinck (PQ).¹pedro.santucci@usp.br¹Instituto de Química de São Carlos, Universidade de São Paulo, CP 780, CEP 13560-970, São Carlos, SP, Brazil; ²Departamento de Química, Universidade Federal de São Carlos, São Carlos 13565-905, Brazil.

Palavras Chave: Palitantin, semi-synthesis, derivatization, marine fungus.

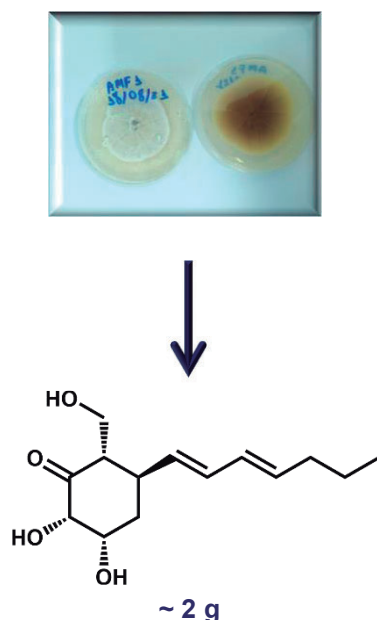
Highlights

A fungal strain *Geomyces* sp. produces large amounts of (-)-palitantin, a multi-functionalized bioactive natural product. To explore its biological activities, new nitrogenated derivatives were prepared.

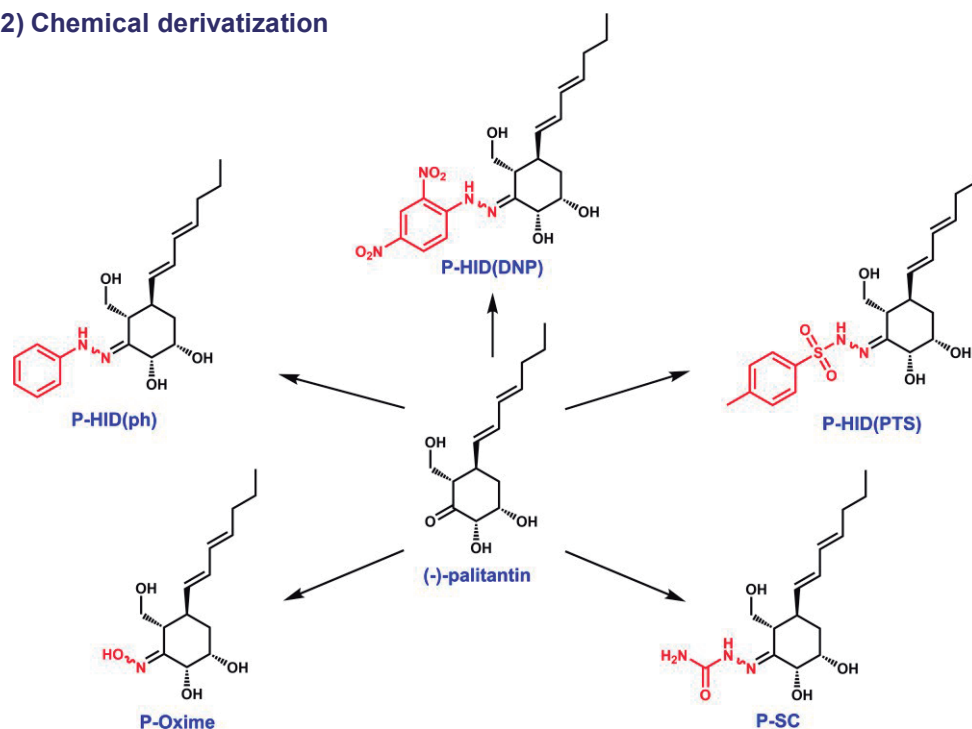
Resumo/Abstract

The derivatization of bioactive natural products aiming to explore and/or to improve their biological activities is currently a subject of much interest. This work reports the isolation and characterization of (-)-palitantin from culture media produced by *Geomyces* sp., in a yield of 200 mg/L. Subsequently, we have been able to prepare three hydrazones, an oxime and a semicarbazone derivatives. The compounds were completely identified by HPLC-PDA-MS and NMR spectroscopy and will be sent to biological assays.

1) NP isolation



2) Chemical derivatization



Agradecimentos/Acknowledgments

Organic Chemistry of
Biological SystemsLaboratório de Química Bio-Orgânica
LQBO

FAPESP

CNPq

CAPES

Sesquiterpenos com ação anti-helmíntica de *Drimys brasiliensis* Miers.

Eric Umehara¹ (PG), Stephani L. Pereira¹ (IC), Ana C. Mengarda² (PG), Josué de Moraes² (PQ) e João Henrique G. Lago¹ (PQ)

ericumehara@hotmail.com

¹Centro de Ciências Naturais e Humanas, Universidade Federal do ABC, Santo André – SP

²Centro de pesquisas de doenças negligenciadas, Universidade de Guarulhos, Guarulhos - SP

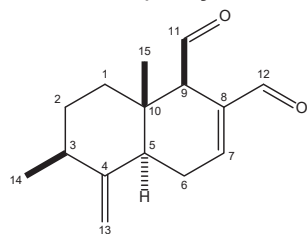
Palavras Chave: *Drimys brasiliensis*, sesquiterpenos, atividade antihelmíntica, *Schistosoma mansoni*

Highlights

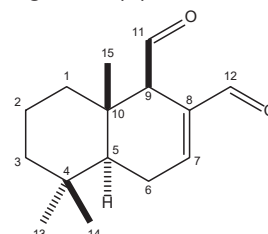
Sesquiterpenes with antihelmintic action from *Drimys brasiliensis* Miers. In the present work two sesquiterpenes 9-deoximuzigadial (**1**) and polygodial (**2**) were isolated from twigs of *D. brasiliensis* and *in vitro* anthelmintic effect against *Schistosoma mansoni* was evaluated.

Resumo

Como parte do nosso trabalho envolvendo a busca de metabolitos especiais bioativos, no presente trabalho, o extrato hexânico dos galhos de *Drimys brasiliensis* mostrou potencial frente à *Schistosoma mansoni*. Desta forma, o fracionamento cromatográfico permitiu, até o momento, o isolamento de dois sesquiterpenos (**1** e **2**). No espectro de RMN de ¹H de **1** foram observados aqueles em δ 0,72 (s, H-15), 9,51 (d, $J = 4,4$ Hz, H-11), 9,49 (s, H-12) e em δ 7,12 (t, $J = 2,5$ Hz, H-7) sugerindo a presença de dois grupos aldeído e um sistema carbonílico α,β -insaturado. Nesse espectro foi observado também um tripleto em δ 4,91 ($J = 1,5$ Hz, H-13), além de multipletos em δ 1,60 (H-1), 1,70 (H-2), 2,00 (H-3), 2,10 (H-5) e em 2,44 (H-6) além de um duplete em 1,09 ($J = 6,5$ Hz, H-14). Os espectros de RMN de ¹³C mostraram 15 sinais, sendo dois metílicos, quatro metilênicos, seis metínicos e três carbonos não hidrogenados, sendo aqueles em δ 106,0 e 151,3 atribuídos aos carbonos de ligação dupla exocíclica C-13 e C-4, respectivamente. Além desses, os sinais em δ 201,1 (C-11) e δ 193,2 (C-12) são referentes aos carbonos de grupo aldeído enquanto que aqueles em δ 152,9 (C-7) e δ 137,9 (C-8) foram atribuídos aos carbonos de ligação dupla endocíclica conjugada. A análise desses dados seguido da comparação àqueles descritos na literatura, permitiram identificar o composto **1** como sendo o 9-deoximuzigadial¹. O espectro de RMN de ¹H do composto **2** se mostrou similar ao de **1**, sendo a única diferença referente a ausência dos sinais atribuídos a C-13 e C-14 enquanto que foram observados dois simples, integrando para três hidrogênios cada, em δ 0,96 (H-13) e 0,93 (H-14). Assim, foi sugerida que a diferença entre **1** e **2** consiste, no caso desse último, na presença de duas metilas geminadas ligadas a C-4, o que foi confirmada pela análise do espectro de RMN de ¹³C e comparação dos dados espectrais para o poligodial² (**2**).



9-Deoximuzigadial (**1**)



Poligodial (**2**)

Concentração / μM	Morte / %		Redução da atividade motora / %		Morte / %		Redução da atividade motora / %	
	M	F	M	F	M	F	M	F
50,0	60	60	60	60	100	100	100	100
25,0	NA	NA	NA	NA	100	100	100	100
12,5	NA	NA	NA	NA	30	30	30	30
DMSO (0,5 %)	0	0	0	0	0	0	0	0
Praziquantel (2,0 μM)	100	100	100	100	100	100	100	100

M/F = indivíduo macho/fêmea;

Como observado, o composto **2** se mostrou promissor em diferentes concentrações causando 100% de morte e de redução da atividade motora do parasita (machos e fêmeas) a 50,0 e a 25,0 μM ao passo que o composto **1** se mostrou totalmente inativo para concentrações de 25,0 e 12,5 μM , mostrando potencial moderado apenas para 50,0 μM . Do ponto de vista estrutural, a única diferença entre os dois compostos consiste na ausência da ligação dupla exocíclica entre C-4/C-13 e na posição da metila C-14 no anel A, sugerindo que o arranjo adequado desses substituintes é de grande importância para a atividade anti-helmíntica.

Referências: ¹Al-Said, et al., *Phytochemistry*, 29, 975-977, 1990. ²Corrêa, et al., *Parasitology Research*, 109, 231-236, 2011

Agradecimentos

FAPESP, CAPES, CNPq e UFABC

Área: QPN
(Inserir a sigla da seção científica para qual o resumo será submetido. Ex: ORG, BEA, CAT)

Extraction sStandardization protocol for the analysis of foam nests' metabolites of the foam nest from *Physalaemus nattereri* frog (Anura: Family Leptodactylidae) by MALDI-TOF by MALDI-TOF

Jamicelly R. G. da Silva (PG),^{1*} Andrés E. Brunetti (PQ),² Norberto P. Lopes (PQ),^{2,1}

Jamicelly.ravanna@gmail.com

¹ Departamento de Ciências Biomoleculares, Universidade de São Paulo, Faculdade de Ciências Farmacêuticas de Ribeirão Preto;

² Instituto de Biología Subtropical, UNAM-CONICET, Misiones Argentina

Palavras Chave: AnurosAnfibiosAnurans, Foam nests, Peptides, Alkaloids, *Physalaemus nattereri*.

Highlights

We propose one extraction and analysis the metabolites present in the foam nests from *P. nattereri* by MALDI-TOF was standard. In the MALDI-TOF analOur analyses revealed the presence the aqueous extract presented a peak corresponding to 1360 Da, suggesting of defense peptides and, and the methanolic extract showed a peak of 496 Da, suggestive of alkaloid-like compounds.

Formatado: Inglês (Estados Unidos)

Resumo/Abstract

Introduction: *Physalaemus nattereri* is a frog measuring approximately 4cm long, widely distributed th occurrence in Brazil, occurring in the Cerrado hotspot, the, in central Brazil to the transition areas between Caatinga and in the western part of the states of Bahia and Piauí (FREITAS; SILVA, 2007). During the reproductive period, females of *P. nattereri* lay their eggs in a structure called the foam nest. This nest is formed by proteins released from the oviduct that are vigorously shaken by the hindlimbs of both he the male and the female, frogs release their skin secretions and clean their hind limbs on the back to form stable foams nest last for months. Recently, few studies have investigated extractions at different polarities to identify a diversity of metabolites in anurans substrates. The research about frog skin, at the moment, focuses on the comprehension of the protein and carbohydrate composition present in their structure, but the information on the nest chemical composition, pharmacological potentials, and ecological relationships relevance has been neglected. **Objective:** To standardize the extraction protocol for the analysis with MALDI-TOF that maximizes the chemical profile of metabolites occurring in foam nests of *P. nattereri* using MALDI-TOF. **Methodology:** Seven lyophilized samples of *P. nattereri* foam nests were extracted sequentially in solvents with different polarities (hexane, ethyl acetate, methanol, and water), centrifuged for 15 minutes at 3000 rpm and dried in gaseous nitrogen. For Matrix Assisted Laser Ionization/Desorption Time-of-Flight (MALDI-TOF) analysis, the samples were resuspended in water and acetonitrile (1:1) and added a saturated solution of HCCA (α -hydroxycinnamic acid) and DHB (2,5-dihydroxybenzoic acid). The parameters used to obtain the spectra were: 1000 laser shots per spectra, PIE (Pulsed Ion Extraction) 120 ns, positive mode, and 1000 Hz laser frequency, setting the detection range to 0-2500 m/z. A mixture of synthetic peptides and synthetic quercetin was used for the calibration of to calibrate the equipment. The laser energy was set above the threshold for ion production. A range of 0-2500 m/z was used for the digital identification of metabolites from *P. nattereri*. Spectra were measured generated in triplicate using the AutoExecute tool of the Flexcontrol acquisition software (version 2.4; Bruker-Daltonik GmbH). The raw spectra were preprocessed by FlexAnalysis software (BrukerDaltonik). **Results and discussion:** Qualitative analysis of the chemical constitution of the extracts showed the presence of more metabolites in the that extracts prepared with methanol and water (1:1; v/v) and water only had more metabolites compared to the other than the other solvents used. The aqueous extract showed a high intensity high-intensity signal of mass 1360 Da and an MS/MS fragmentation pattern, suggestive of compatible with a peptide T, while in the extraction with methanol and water showed, a signal of mass 496 Da suggests compatible with an the alkaloid-like compound. **Conclusion:** At moment, This study represents the alkaloids are not documented in foam nests, but this research described the first report of this secondary metabolite class in this biological matrix. Regarding peptides, only one study (SHAH RUDIN et al., 2017) found in the foam nest of the species *Polypedates leucomystax*, a peptide of the brevenin class; however, our results suggest the first description of peptides in these metabolite classes in foam nests in the species of *P. nattereri*. In addition, The they results contribute with information about the importance of considering the solvent polarity for the extraction of different chemical substances in anurans metabolites also, new metabolites were detected in *P. nattereri* nests. It also demonstrating stress the capacity of this biological matrix for the discovery of new molecules with the potential to the development of drugs while, improve our the understanding of the ecological relationships of anurans, as well as the reproduction of species, which that produce this biofoam.

Formatado: Inglês (Estados Unidos)

Sociedade Brasileira de Química (SBQ)

Referências:

Shahrudin, S., Ismail, M. N., Kwan, S. H., & Najimudin, N. (2017). Ecology and protein composition of Polypedates leucomystax (Gravenhorst, 1829)(Anura: Rhacophoridae) foam nests from Peninsular Malaysia. *Annual Research & Review in Biology*, 14(6):1-10.

Freitas, M. A.; Silva, T. F. S. (2007) Guia ilustrado - A herpetofauna das caatingas e áreas de altitudes do nordeste brasileiro. Editora USEB, 388p.

Agradecimentos/Acknowledgments

Agradecemos ao Conselho Nacional de Desenvolvimento Científico e Tecnológico (CNPQ), a Coordenação de Aperfeiçoamento de Pessoal de Nível Superior (CAPES) e a Fundação de Amparo à Pesquisa do Estado de São Paulo (FAPESP) pelo financiamento, bem como a Faculdade de Ciências Farmacêuticas de Ribeirão Preto da Universidade de São Paulo (FCFRP-USP) e ao Núcleo de Pesquisa em Produtos Naturais e Sintéticos pela estrutura física e ao Consejo Nacional de Investigaciones Científicas y Técnicas- Conicet – Argentina, PIP 2021-2023 por todo o suporte (Agencia – CONICET, Argentina – PICT-2020-SERIEA-02939).

STRUCTURAL AND BIOLOGICAL EVALUATION OF THE PEPTIDES FROM *Tityus stigmurus* SCORPION

Adriana M.S. Parente (PG),¹ Suedson C.S. Rodrigues (PG),² Allanny A Furtado (PG),¹ Jarbas M Resende (PQ),³ Matheus F.F. Pedrosa (PQ),¹ Renata M. Araújo (PQ),²

renata.mendonca@ufrn.br

¹Departamento de Bioquímica, UFRN; ²Instituto de Química, UFRN; ³Departamento de química, UFMG.

Keywords: Antimicrobial Activity, Antimicrobial peptides, 3D peptide structure

Highlights

Antimicrobial peptides designed from a native peptide of a scorpion venom, showed higher biological activity and presented α -helix structure when analyzed by Nuclear Magnetic Resonance and Circular Dichroism.

Resumo/Abstract

Antibiotic resistance is a worldwide problem that has grown and alerted researchers [1], becoming interested in the search for new molecules with antimicrobial activity. Recent studies show that some peptides from scorpion venom have great potential. Analogous peptides from Stigmurin (FFSLIPSLVGGGLISAFK-NH₂) present in the venom of the scorpion *Tityus stigmurus* have demonstrated that changes in its amino acid sequence can increase its antimicrobial activity [2]. This work proposes the structural and biological characterization of the bioactive peptides StigA8 (FFSLIPKLVGKLISAFK-NH₂) and StigA18 (FFSLIPKLVGKLKAFK-NH₂), both designed from Stigmurin and obtained commercially. For both peptides, it was observed that the change of amino acid residues for lysine in positions 7 and 11 and in positions 7, 11 and 14, respectively, resulted in increased *in vitro* antimicrobial activity against Gram-positive and Gram-negative multidrug-resistant bacteria when compared to the native peptide, peptides StigA8 presented higher activity than StigA18. In addition, these substitutions resulted in a greater α -helix structure, high amphipathic character, as well as structural stability when compared to Stigmurin. For the structural evaluation, the two peptides were analyzed by circular dichroism (CD) in different solvents and by nuclear magnetic resonance (NMR). Through CD analyses we could observe a shift in structure when these peptides are in different mediums, random structure in aqueous medium and α -helix when in hydrophobic mediums (TFE and SDS). And from NMR evaluation in TFE, a higher number of NOE correlations for the StigA8 peptide could be observed and that resulted in a longer helix for this peptide, indicating that the addition of lysine at position 14 favored the folding of this peptide, this is corroborated with CD results in hydrophobic mediums. A high amphipathic feature of StigA8 and StigA18 was demonstrated by NMR, which, together with their positive net charge (+4 and +5, respectively), are very important properties in peptides with significant antimicrobial activity, and this may explain the higher activity observed for the analog peptides compared to the native peptide. The longer helix structure presented by the peptide StigA8, when compared to the peptide StigA18 and the native peptide Stigmurin, may explain the higher antimicrobial activity observed for this peptide. Therefore, in this study we present the structural elucidation of the peptides StigA8 and StigA18 together with their high antimicrobial activity.

[1] Kwon, J. H.; Powderly, W. G. *Science*, 2021, v. 373, n. 6554, p. 471–471.

[2] Furtado, A. A., *et al. Pharmacological Research*, 2022, v. 181, n. 7, p. 106245.

Agradecimentos/Acknowledgments

UFRN, CAPES, FAPERN, INCTBioNat.

Structural elucidation of a lactam isolated from *Bunchosia glandulifera* and antioxidant activity

Daiane E. Blank¹ (PG), Antonio J. Demuner¹ (PQ), Vitor C. Baía¹ (PG), Elson S. Alvarenga¹ (PQ), Cristiane I. Cerceau¹ (PQ), Neusa F. Moura² (PQ)

daiane.blank@ufv.br

¹Departamento de Química, UFV

²Grupo de Pesquisas em Produtos Naturais-FURG

Keywords: *Bunchosia glandulifera*, Lactam, DP4, Theoretical calculation, Antioxidant

Highlights

Novel lactam isolated from *Bunchosia glandulifera*. Structural identification by high field NMR spectroscopy. Theoretical calculations to assist in the structure identification.

Abstract

Bunchosia glandulifera is a red-colored fruit, belonging to the family *Malpighiaceae*, an exotic species, source of bioactive compounds with antioxidant potential. The fruit was collected in the city of Santo Antonio Patulha-Brazil. 3,6-Dihydropyridin-2(1H)-one was isolated from *B. glandulifera* seed extract and D-mannitol was isolated from the pulp. The structural elucidation of 3,6-dihydropyridin-2(1H)-one was carried out using spectrometric methods. Theoretical calculations of ¹H and ¹³C NMR chemical shifts for three candidate structures were performed. Calculated chemical shifts were compared with experimental values using the DP4 statistical method. DP4 probability for carbon and hydrogen was 100% for the candidate structure R1 (3,6-dihydropyridin-2(1H)-one), confirming the structure proposed by the interpretation of the spectrometric data. Antioxidant activities of the isolated compounds were evaluated using the method of 2,2-azino-bis(3-ethylbenzothiazoline-6-sulfonic acid) (ABTS), 2,2-diphenyl-1-picrylhydrazyl (DPPH) method, iron reduction (FRAP), and reducing power. 3,6-Dihydropyridin-2(1H)-one was isolated for the first time from the extract of *B. glandulifera*. 3,6-Dihydropyridin-2(1H)-one was characterized by the spectrometric methods and the structure was confirmed with the assistance of theoretical calculations. Antioxidant activities were measured, and the δ -lactam (3,6-dihydropyridin-2(1H)-one) presented a greater antioxidant capacity than D-mannitol.

Acknowledgments

Conselho Nacional de Desenvolvimento Científico e Tecnológico (CNPq)

Fundação de Amparo à Pesquisa de Minas Gerais (FAPEMIG)

Coordenação de Aperfeiçoamento de Pessoal de Nível Superior (CAPES)

Área: QPN

Studies of biosynthetic induction from the microbial co-culture between *Penicillium* sp. CML-3020 and *Penicillium setosum*.

Milena P.S. Rivero (PG),^{1,2} **Claudia M. S. Costa** (PG),^{1,2} **Milena C. Bassicheto** (IC),^{1,2} **Thiago A. M. Veiga** (PQ),^{1,2} **Lívia S. de Medeiros** (PQ).^{1,2*}

milena.rivero@unifesp.br; livia.soman@unifesp.br

¹Institute of Environmental, Chemical and Pharmaceutical Sciences, UNIFESP; ²Otto Richard Gottlieb Bio-Organic Chemistry Laboratory (LaBiORG).

Palavras Chave: Metabólitos secundários, Co-cultura, *Penicillium*, Antimicrobials, Anti leukemia agents.

Highlights

This work investigates the production of bioactive fungal metabolites by means of crosstalk approach, testing the co-culture of *Penicillium* sp. CML-3020 with *Penicillium setosum*. The production of some compounds by *Penicillium* sp. CML-3020 only during the co-culture was observed. The application of this strategy suggested the possible activation of biosynthetic genes clusters for this specie.

Resumo/Abstract

Given the continuous search for therapeutic agents of natural origin, the exploration of the secondary metabolism of *Penicillium* species today represents a promising potential for new discoveries². One of the forms of microbial metabolic expression is the use of biotic inducers in the growth condition of the species under study. Within this context, the use of microbial co-cultures has been a successful strategy for the discovery of new fungal natural products¹. In this work the potential production of new bioactive fungal metabolites is investigated, through the co-culture of *Penicillium* sp. CML-3020 and *Penicillium setosum*. The experiments were performed in solid culture medium BDA and YES. The investigation of the obtained micro-extracts was performed by the analysis of data obtained in high-performance liquid chromatography coupled to high resolution mass spectrometry (HPLC-DAD-HRMS). Through inspection of accurate masses and queries submitted to Natural Products databases, such as Antibase, Dictionary of Natural Products and GNPS platform³, chemical dereplication of the compounds biosynthesized by *Penicillium* sp. CML-3020 in response to microbial interactions was performed. Metabolic induction and a significant increase of some compounds produced by *Penicillium* sp. CML-3020 were observed when it was subjected to joint growth with *Penicillium setosum*. The isolation of the target metabolites will be performed by various chromatographic techniques, with sequential structural determination via nuclear magnetic resonance (NMR 1/2D) spectroscopic data, as well as HRMS/MS data. Subsequently, the compounds will be submitted to cytotoxicity tests against leukemia cells and antimicrobial assays against pathogenic bacteria and fungi in humans. Therefore, this strategy of mimicking microbial interactions evidenced the possible activation of genes responsible for coding and synthesis of secondary metabolites before not produced by *Penicillium* sp. CML-3020.

Referências:

1. Kildgaard, Sara, et al. "Cyclopiamines C and D: epoxide spiroindolinone alkaloids from *Penicillium* sp. CML 3020." *Journal of natural products* 81.4 (2018): 785-790.
2. Nielsen, Jens Christian, et al. "Global analysis of biosynthetic gene clusters reveals vast potential of secondary metabolite production in *Penicillium* species." *Nature microbiology* 2.6 (2017): 1-9.
3. Wang, Mingxun, et al. "Sharing and community curation of mass spectrometry data with Global Natural Products Social Molecular Networking." *Nature biotechnology* 34.8 (2016): 828-837.

Agradecimentos/Acknowledgments

CAPES-88887.663155/2022-00, Projeto FAPESP 2020/08270-0.

Targeted metabolomics and transcriptomics revealing the influence of abiotic stresses on the specialized metabolism biosynthesis in transgenic soybean

Paula C. P. Bueno (PQ),^{1,2,3*} Helena Mannocho-Russo (PQ),⁴ Amira S. V. Nieva (PQ),² Mayla Molinari,⁵ Alexander Erban (PQ),² Joachim Kopka (PQ),² Liliame M. Mertz-Henning (PQ)⁵, Alexandre L. Nepomuceno (PQ)⁵, Norberto P. Lopes (PQ)¹

paulabueno@yahoo.com

¹Faculty of Pharmaceutical Sciences of Ribeirão Preto, FCFRP-USP; ²Max Planck Institute of Plant Molecular Physiology, MPI-MP; ³Institute of Chemistry, UNIFAL-MG; ⁴Skaggs School of Pharmacy and Pharmaceutical Sciences, UC; ⁵Embrapa Soybean

Key words: *Glycine max*, Metabolomics, Abiotic stress, Transcriptomics

Highlights

- Secondary metabolites have relevant biological properties related to human health and in plant performance
- The isoflavones biosynthesis in conventional and transgenic soybean subjected to water stresses was studied
- Twelve isoflavones from roots and shoots were analyzed, along with their biosynthetic pathway transcripts
- The integration of metabolomics and transcriptomics brings new information about the mechanisms plants use to keep their performance in challenging environments

Abstract

The high worldwide soybean productivity, which is one of the pillars of our food system, is only possible due to the constant development of cultivars with a greater capacity to adapt to biotic and abiotic events. The significance of secondary metabolism in the modulation of abiotic stresses in plant species, and the association between crops metabolome and agronomic traits have been frequently emphasized in the investigations about the molecular mechanisms lying behind soybean stress tolerance¹. In soybean, the biosynthesis of secondary metabolites derived from phenylalanine, along with a complete understanding about of their accumulation, has been impeded because they are highly influenced by genotypic and environmental effects, as well as by their interactions, which are not well understood². Therefore, the present study aimed to compare the levels of 12 isoflavones and their corresponded transcripts in a conventional soybean cultivar (drought susceptible) and two transgenic events modified with an ATGolS2 gene (GolS) coding the expression of galactinol synthase (drought resistant)³. Both events and the original genotype were cultivated under controlled and water stress conditions. The extraction parameters and chromatographic method were defined by experimental planning and certified by quality evaluation. Shoots and roots were harvested, lyophilized, grounded, extracted, and measured by HPLC-DAD-ESI-MS/MS. The targeted isoflavones daidzin, glycitin, genistin 6-O-malonyldaidzin, 6"-O-malonylglycitin 6"-O-acetyldaidzin, 6"-O-acetylglycitin, 6"-O-acetylgenistin, 6"-O-malonylgenistin, daidzein, glycitein, and genistein, were detected, measured and quantified in the different genotypes and treatments. Leaf transcriptomics allowed to integrate the information through the isoflavones biosynthetic pathway. Results suggest that under flooding, eight of the twelve isoflavones were significantly reduced in the roots of the moderately resistant mutant, while five of them were reduced under drought. Under both water stresses, two acetylated and not methoxylated isoflavones were significantly decreased in this mutant. Additionally, the methoxylated aglycone glycitein tended to decrease under flooding and to rise under drought in all genotypes. The moderately drought-resistant mutant showed a more vigorous response under controlled conditions, suggesting that the genetic change produced by the GolS insertion may influence the production of isoflavones in soybean.

¹ Zhao B. et al., 2021. *Plant, Cell & Environment*, v. 44, p. 1379

² Gutierrez-Gonzalez, J. J. et al, 2010. *Plant & Cell Physiology*, v. 51, p. 936

³ Honna, P. T. et al., 2016. *Molecular Breeding*, v. 36, p. 157

Acknowledgments

The authors acknowledge the support of the São Paulo Research Foundation (FAPESP grants #2017/19702-6 and # 2019/08477-7 (PCPB) and #2014/50265-3 (NPL).

The impact of strawberry by-products' freeze-drying process on the stability parameters of phenolic & flavonoids content and antioxidant activity

Mayra G. Biccigo (PG),^{1*} Camila S. Soares (PG),¹ Luan S. D. Rabelo (PG),¹ Ailane S. Freitas (PG),¹ Ilza M. O. Sousa (PQ),¹ Kaio E. Buglio (PG),² Rogério J. Machado Jr. (PG),² Daniele D. Affonso (PG),¹ Ana L. G. T. Ruiz (PQ),¹ João E. de Carvalho (PQ),¹ Mary Ann Foglio (PQ).¹

mayrabiccigo@gmail.com

¹Faculdade de Ciências Farmacêuticas, FCF-Unicamp; ²Faculdade de Ciências Médicas, FCM-Unicamp

Palavras Chave: *Strawberry, Freeze-drying process, Antioxidant, Phenolic compounds, Stability.*

Highlights

Herein the stability of phenolic & flavonoids content and antioxidant activity of freeze-dried strawberry agricultural by-products is reported. These data highlight benefit to this culture production waste.

Resumo/Abstract

Fragaria ananassa Duch, popularly known as strawberry, is a pseudo fruit highly appreciated both processed and *in natura*, rich in various bioactive compounds, such as vitamins and phenolic compounds. Anthocyanins are the most abundant class among the plant's phenolic content. This chemical class is responsible for strawberries' intense red color with antioxidant & anti-inflammatory activity, and neuroprotective potential. In the production chain, a large volume of waste is generated, which can reach more than 50% of by-products, due to the pseudo fruit's highly perishable characteristic (IBRAF, 2008). This prompted the evaluation of the pharmacological potential of the resulting by-product of the agricultural production.

Drying processes in foods are essential for their stabilization. Among the many strategies, freeze-drying allow for the elimination of water at low pressure, nevertheless the drawback is process time and high cost. Herein the stability of phenolic & flavonoids content and antioxidant activity of freeze-dried strawberry agricultural by-products compared to *in natura* samples is reported. *Fragaria* is exempt of registration with SisGen, according to Normative Instruction nº 23 of 2017.

Both by products of *in natura* strawberry (10g) and freeze-dried strawberry (1g) were extracted at 5°C with 70% acidified ethanol using mechanical stirring. Solvent was removed using vacuum, providing 20% yield. Folin-Ciocalteu method analyzed the total phenolic content, using gallic acid (GA) as standard. Colorimetric method using catechin (C) as standard measured flavonoid content by. The pH differential method determined total anthocyanin content (Giusti & Wrolstad, 2001), and the antioxidant activity was quantified by the DPPH method (2,2-Diphenyl-1-picrylhydrazyl), expressed in Trolox® equivalents (Aryal et al, 2019) (Table 1).

Table 1: Data of *Fragaria* agriculture waste product evaluated for phenolic & flavonoid content and antioxidant activity.

Analyzes	<i>In natura</i> Strawberry	Freeze-dried Strawberry
Total phenolic content	14 µg GAE/mg of sample	43,3 µg GAE/mg of sample
Total flavonoid content	4 µg CE/mg of sample	9,9 µg CE/mg of sample
Total anthocyanin content	142,44 mg/100g of sample	166 mg/100g of sample
DPPH	2,5 mg/mL	1,5 mg/mL

Data demonstrates that the freeze-dried material reproduces the contents of *in natura* samples, considering *Fragaria*'s approximately 88% water content providing a product with less damage from external effects, such as light, humidity and microorganisms' attack. Freeze-dried *Fragaria* samples had higher anthocyanin contents compared to fresh or frozen samples. This is due to the capacity of the freeze-drying process to release higher phenolic compound content by extracellular matrix disintegration, corroborated by Taghavi (2022). Therefore, freeze-dried waste samples become an interesting plant input, maintaining anthocyanin content for applications in health benefit products. Moreover, the technique has the advantage of stabilizing the product, increasing shelf life, reducing high yield waste.

Acknowledgments

Faculdade de Ciências Farmacêuticas – Unicamp, LAFTEEx, STAW Agricultura, CAPES, FAPESP, CNPq.

Total syntheses and antibacterial mode of action of rare retrochalcones

Patrick R. Ozanique (PG),¹ Alvaro L. Helena (PG),¹ Janaina C. Orlandi (PQ),² Carlos H. G. Martins (PQ),³ Henrique Ferreira (PQ),⁴ Luis O. Regasini (PQ).^{1,*}

patrick.ozanique@unesp.br; luis.regasini@unesp.br

¹Laboratório de Antibióticos e Quimioterápicos, IBILCE, Unesp São José do Rio Preto – SP, Brasil; ²Departamento de Ciências Fisiológicas, UNICAMP Piracicaba -SP, Brasil; ³Instituto de Ciências Biomédicas, UFU Uberlândia – MG, Brasil; ⁴ Departamento de Bioquímica e Microbiologia, Unesp Rio Claro – SP, Brasil.

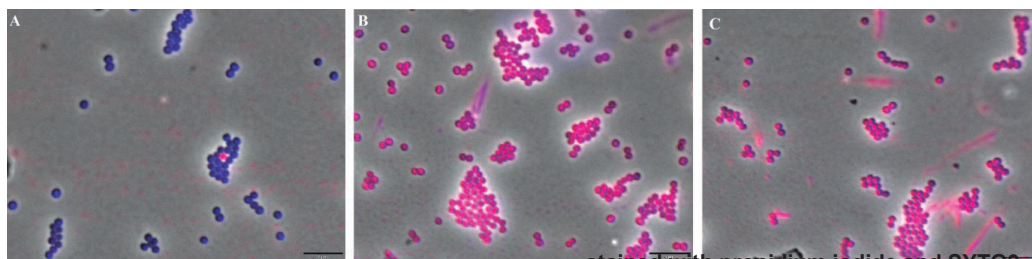
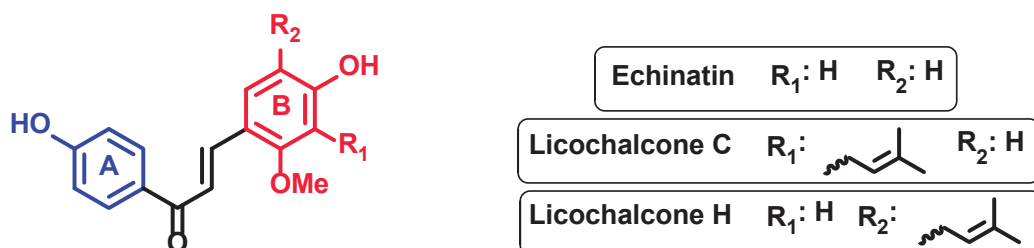
Palavras-Chave: Retrochalcone, Antibacterial, Biofilm, *Staphylococcus aureus*; *Galleria mellonella*, Membranes.

Highlights

Retrochalcones are rare secondary metabolites and restricted to *Glycyrrhiza* genus. A new regioselective syntheses of echinatin and licochalcones C and H were carried out. The mode of action of retrochalcones were firstly elucidated, indicating membrane disruption of MSSA and MRSA cells.

Abstract

The resurgence of drug-resistant bacteria is a challenge to the discovery of new antibacterial agents. Thus, efforts are urgent to discover and develop drugs with innovative structural and mechanistic patterns. The present work aimed the synthesis and evaluation of three rare retrochalcones; echinatin and licochalcones C and H, which are restricted to *Glycyrrhiza* genus. The total syntheses included iodination and Suzuki coupling reactions, which allowed regioselective C-prenylations. The overall yields ranged from 18 to 33 % using five-seven steps. The antibacterial and antimycobacterial activities of retrochalcones were evaluated against Gram-positive, Gram-negative and mycobacteria species, displaying an activity against Gram-positive (MIC = 6.25 – 50.0 µg/mL), *Mycobacterium* species (MIC = 36.25 – 125 µg/mL) and *Helicobacter pylori* (MIC = 3.9 -12.5 µg/mL). Retrochalcones showed no synergic effect when combined with tetracycline or vancomycin, but retrochalcones inhibited biofilm formation of *Staphylococcus aureus* (MSSA and MRSA) with MBIC₅₀ values of 6.25 µg/mL. The mode of action of retrochalcones were elucidated, and the *S. aureus* membrane disruption was confirmed by fluorescence microscopy. Retrochalcones proved to have no systemic toxicity according to assays with *Galleria mellonella* larvae. In brief, this is the first study on the regioselective syntheses and antibacterial mode of action of rare retrochalcones, indicating their potential as antibacterial hits.



Fluorescence microscopy of *Staphylococcus aureus* stained with propidium iodide and SYTO9.
(A) negative control (cells treated with 1% DMSO); (B) positive control (cells treated with nisin); (C) cells treated with LCC solution in DMSO for 15 minutes. Magnification 100×; Scale bar 5 µm.

Acknowledgments

The authors gratefully acknowledge financial support from the Coordination for the Improvement of Higher Education Personnel (CAPES, finance code 001), Brazilian Council for Scientific and Technological Development (CNPq) (Grants 471129/2013-5, 306251/2016-7 and 429322/2018-6), the São Paulo Research Foundation (FAPESP) (Grants 2014/18330-0 and 2018/15083-2) and Multiuser Centre for Biomolecular Innovation (FAPESP 2009/53989-4). PRO thanks CAPES for his scholarship.

Triterpenes and flavonoids from *Vernonanthura discolor* (Asteraceae)

Anderson Valdiney Gomes Ramos (PG)^{1*}, Yasmin Irineu dos Santos (PG)¹, Julia Martino Caldato (IC)², Francielli Alana Pereira (PG)¹, Marta Regina Barroto do Carmo (PQ)², Maria Helena Sarragiotto (PQ)¹, Debora Cristina Baldoqui (PQ)¹

dcbaldoqui@uem.br; yasminirineu@yahoo.com.br

¹Departamento de Química, UEM, Maringá-PR, Brazil; ²Departamento de Biologia Geral, UEPG, Ponta Grossa-PR, Brazil

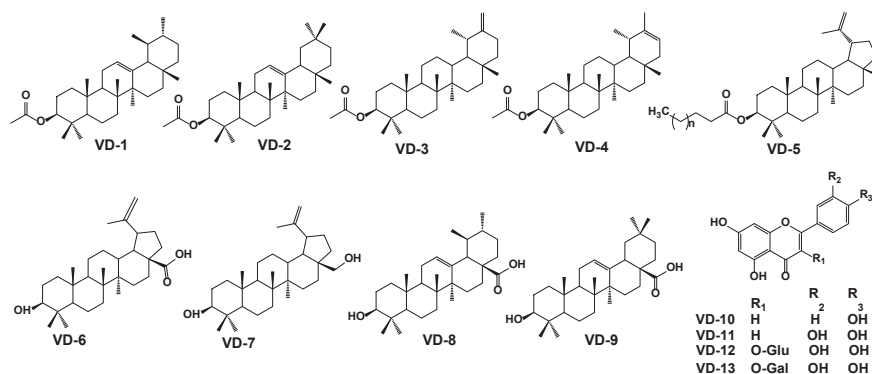
Keywords: Asteraceae, Phytochemistry, Chemophenetic study, metabolites

Highlights

Thirteen compounds were isolated from *Vernonanthura discolor*. Ten of these compounds are being reported for the first time in the species.

Abstract

Vernonanthura discolor (Spreng.) is a species popularly known as a “vassourão de folha larga” or “cambará-guaçú”, it is a medium-sized tree (10 to 20 m high), native to Brazil, occurring in the Northeast, Midwest, Southeast and South¹. The triterpenes friedelin and friedelanol were previously reported in this species², in addition to flavonoids and phenolic acids by LC-MS/MS dereplication strategy³. This work aimed to carry out a phytochemical study of the *Vernonanthura discolor*, as well as to contribute to chemophenetic studies of the genus *Vernonanthura* H. Rob. The aerial parts of *V. discolor* were collected in the Campos Gerais region, in Ponta Grossa, Paraná State. The crude ethanolic extract was produced by exhaustive maceration (32.5 g) which was suspended in MeOH:H₂O (1:1), and then partitioned into hexane, CH₂Cl₂, and EtOAc. Part of the hexane fraction (4.7 g) was subjected to successive chromatographic columns over silica gel 60 to afford a mixture of five compounds (VD-1 to VD-5). The dichloromethane fraction (3.0) was subjected to a silica gel 60 column chromatography providing the isolation of four compounds (VD-6 to VD-9). Part of the polar fraction (EtOAc) (2.5 g) was subjected to filtration on a Sephadex LH-20 column resulting in four compounds (VD-10 to VD-13). The known isolated compounds were identified by comparison of their spectroscopic data (1D and 2D NMR) with those reported in the literature^{4,5,6}. The mixture composition was the triterpenes α -amyrin acetate (VD-1), β -amyrin acetate (VD-2), taraxasterol acetate (VD-3), pseudotaraxasterol acetate (VD-4), lupeol derivative esterified with fatty acid (VD-5). Betulinic acid (VD-6), betulin (VD-7), ursolic acid (VD-8) and oleanolic acid (VD-9), in addition to the flavonoids apigenin (VD-10), luteolin (VD-11), quercetin-3-O- β -D-glucopyranoside (VD-12) and quercetin-3-O- β -D-galactopyranoside (VD-13) were identified and ten of these compounds are being reported for the first time in this species, only the flavonoids apigenin (VD-10), luteolin (VD-11), quercetin-3-O- β -D-glucopyranoside (VD-12) were previously described.



[1] Marquardt, R.T. et al. *Acta Biológica Catarinense*. 5, 14-21, 2018.

[2] Bazon, J. N. et al. *Phytochemistry*. 44, 1535, 1997.

[3] Gallon, M. E. et al. *Phytochemistry*. 150, 93-105, 2018.

[4] Ebajo V.D. J. R. et al. *J Appl Pharm Sci*. 5, 69-72, 2015.

[5] Silva, L. A. L. et al. *Revista Brasileira de Farmacognosia*, 25, 375-381, 2015.

[6] Mahato e Kundu. *Phytochemistry*. 37, 1517-1575, 1994.

Acknowledgments

Sociedade Brasileira de Química (SBQ)

UEM, CAPES, CnPq, INCT-BioNat.

Triterpenes, steroids and xanthone isolated from *Macrolobium acaciifolium* leaves and branches hexane extracts

David Ribeiro da Silva (PG),^{1,2} Cecilia Veronica Nunez (PQ).^{1*}

david.ribeiro07@gmail.com; cecilia@inpa.gov.br

¹Instituto Nacional de Pesquisas da Amazônia, INPA; ²Doutorando PPGQ-UFAM

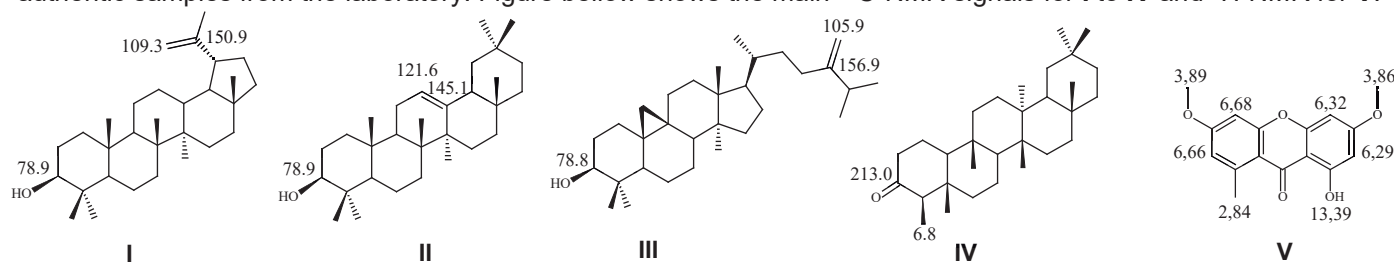
Key-words: Triterpenes, Xanthone, Steroids, β -Amyrin, Friedelin, Lupeol.

Highlights

Four triterpenes: lupeol (I), β -amyrin (II), 24-methylenecycloartenol (III), friedelin (IV), two steroids: β -sitosterol and stigmasterol and a xanthone: lichexanthone (V) were isolated from *Macrolobium acaciifolium* leaves and branches hexane extracts and identified by ¹H and ¹³C NMR analysis.

Resumo/Abstract

Leaves and branches of *M. acaciifolium* were collected nearby Catalão lake, Amazonas, Brazil. The plant parts were dried in a force ventilation oven and then, ground in a knife mill (leaves, 468 g) and crushed in a hammer mill (branches, 1,1 Kg). Then extracted with hexane, followed by methanol and distilled water, using an ultrasound bath. Comparative thin layer chromatography (TLC) analyzes of the hexane extracts obtained (leaves, 2,5 g; branches 1,6 g) were performed and observed the presence of terpenoids compounds when revealed with sulfuric anisaldehyde. The hexane extracts were then fractionated by open column chromatography with silica eluted with hexane/ethyl acetate mixtures: 95:5, 9:1, 8:2, 7:3 and 1:1. Fractions 3-4 (472 mg) from hexane extract of leaves were pooled and subjected to fractionation on an open silica column with hexane/chloroform mixtures 7:3, 6:4, 1:1 and chloroform 100%. Fraction 1 (35 mg) showed to be a terpenoid mixture, being purified by CLAE in isocratic mode ACN 67% in aqueous solution, where the triterpenes lupeol (36.56 min, I, 5 mg), β -amyrin (38.42 min, II, 3 mg) and 24-methylenecycloartenol (47.28 min, III, 2 mg) were collected. Fractions 5-7 from hexane extract of leaves showed to be the mixture of β -sitosterol and stigmasterol steroids. Fraction 3 from hexane extract of branches presented white amorphous solid, which was identified as the triterpene friedelin (IV, 9 mg) and the xanthone lichexanthone (V, 3 mg) as a mixture in 3:1 proportion and fraction 5 was the mixture of β -sitosterol and stigmasterol steroids. Lupeol showed ¹³C NMR signals in δ 150.9 and 109.3 (C20 and C29) as well as ¹H multiplets in δ 4.69 and 4.57 (H-20_a and H-20_b), β -amyrin showed δ 145.1 and 121.6 (C13 and C12) in addition to ¹H multiplet in δ 5.19 (H-12) while 24-methylenecycloartenol, δ 156.9 and 105.9 (C24 and C31) including ¹H multiplet in δ 4.71 and 4.66 (H-31_a and H-31_b). Lupeol, β -amyrin and 24-methylenecycloartenol showed 3β -OH group presence by ¹H multiplets in δ 3.20 ppm with δ 78.9, δ 3.23 ppm with δ 78.9 and δ 3.28 ppm linked to ¹³C δ 78.8 ppm. The 3β -OH group was absent in the friedelin in addition to ¹³C δ 213 ketone group and 6.8 methyl. Lichexanthone showed duplet in δ 6.68 ($J = 2,3$ Hz, 1H) and multiplet in δ 6.66, duplets δ 6.32 and 6.29 ($J = 2,3$ Hz, 1H, each), two methoxyl groups in δ 3.89 and 3.86, one methyl in δ 2.84, besides hydroxyl in δ 13.89 linked by hydrogen bond with carbonyl group (δ 182.3). All data were compared with literature¹ and/or authentic samples from the laboratory. Figure below shows the main ¹³C-NMR signals for I to IV and ¹H-NMR for V.



Agradecimentos/Acknowledgments

To CAPES, CNPq and FAPEAM for the financial support and fellowships. To the technicians Magno Perea Muniz and Sabrina Kelly Reis de Moraes from the Analytical Center of the Thematic Laboratory of Chemistry of Natural Products (CA-LTQPN) of the INPA for the NMR and mass analyses.

Reference: ¹Olea, R.S.G. & Roque, N.F. (1990) Análise de misturas de triterpenos por RMN de ¹³C. *Química Nova*, 13(4), 278-281.

Triterpenoids from the fruits of *Trichilia hirta* (Meliaceae)

Milena Gonçalves Curcino Vieira (FM),^{1*} Raimundo Braz Filho (PQ),² Ivo J. Curcino Vieira (PQ).²

milena.uff@gmail.com

¹Instituto Federal Fluminense, Campos dos Goytacazes, RJ - Brasil; ²Laboratório de Ciências Químicas, Universidade Estadual do Norte Fluminense Darcy Ribeiro, Campos dos Goytacazes, RJ – Brasil.

Key words: limonoids, protolimonoids, *Trichilia hirta*, Meliaceae.

Highlights

The phytochemical study of the fruits of *Trichilia hirta* resulted in the isolation and identification of three limonoids and three protolimonoids compounds.

Abstract

The Meliaceae family, belonging to the Order Rutales, is economically important as a source of wood. The *Trichilia* genus belonging to this family consists of approximately 102 species, distributed mainly in Tropical America¹. Species of this genus have been studied for some years by the research Natural Product Chemistry laboratory group of the UENF, showing promising chemical results and great biological potential². The present work involved the phytochemical study of the *Trichilia hirta* species, leading to the identification and characterization of three limonoids: methyl 6-hydroxy-11 β -acetoxoy-12 α -(2-methylpropanoyloxy)-3,7-dioxo-14 β ,15 β -epoxy-1,5-meliacadien-29-oate (I) and methyl 6-hydroxy-11 β -propanoyloxy-12 α -(2-methylpropanoyloxy)-3,7-dioxo-14 β ,15 β -epoxy-1,5-meliacadien-29-oate (II), obtained as a mixture and other called curcinomarcoide (III); and three protolimonoids: nilocitin (IV), (21*R*)-21,25-dimethoxymeliandiol (V) and (21*S*)-21,25-dimethoxymeliandiol (VI), obtained as a mixture³. The compounds were identified using spectroscopic and spectrometric methods and comparison with literature data.

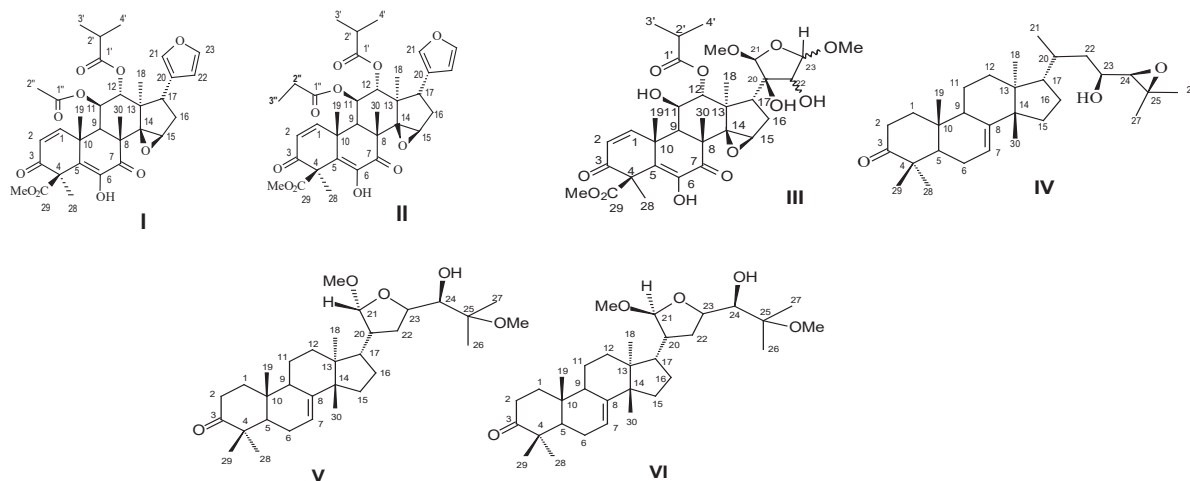


Figure 1 Compounds of *T. hirta*.

1. WFO Plant List. 2011-2020. Acesso Jan 2023. <https://wfoplantlist.org/plant-list/taxon/wfo-4000038940-2022-12>
2. Terra, W.; Vieira, I. J.C.; Braz-Filho, R.; Freitas, W.; Kanashiro, M.; Torres, M. Lepidotrichilins A and B, New Protolimonoids with Cytotoxic Activity from *Trichilia lepidota* (Meliaceae). *Molecules*, 18, 12180-12191, 2013.
3. Vieira, M.G.C.; Braz-Filho, R.; Vieira, I. J.C. Curcinomarcoide, a Novel Limonoid From *Trichilia hirta* (Meliaceae)-Complete ¹H and ¹³C Chemical Shift Assignments. *Natural Product Communications*, 14, p. 1934578X1984361, 2019

Acknowledgments



TRYPANOCIDAL POTENTIAL OF *Schinus molle* L. ESSENTIAL OILS

Nelsa P. I. Uombe (PG)¹, Bruna C. Borges (PG)¹, Frank S. da Silva (PG)², Rafael A. C. Souza (PG)², Sérgio A. L. Morais (PQ)², Luís C. S. Cunha (PQ)³, Jesús J. P. Segovia (PQ)⁴, Marco R. Arones (PQ)⁴, Cláudio V. da Silva (PQ)¹, Francisco J. T. de Aquino (PQ)^{2*}

aquino@ufu.br, nelsauombe@gmail.com

¹ Instituto de Ciências Biomédicas, Universidade Federal de Uberlândia; ² Instituto de Química, Universidade Federal de Uberlândia, 38000-902, Uberlândia-MG, Brasi; ³ Instituto Federal de Educação, Ciência e Tecnologia do Triângulo Mineiro/Uberaba-MG; ⁴ Departamento de Medicina Humana, Universidad Nacional de San Cristóbal de Huamanga, 05001, Huamanga, Ayacucho, Perú.

Palavras-Chave: *Schinus molle* L., *T. cruzi*, Toxicity, Cell viability.

Highlights

Schinus molle L. essential oils, Chagas disease, Trypanocidal effect on Tissue Culture derived Trypomastigote (TCT), Vero-cells presented IC₅₀ lower than those observed in TCT.

Resumo/Abstract

Chagas disease (CD) is a neglected disease, endemic in Latin America, and affects about 8 million people. The treatment for CD currently has only two drugs, whose side effects can worsen the patient's clinical condition. Therefore, the search for new therapies is necessary. Essential oils have several biological activities: antiviral, anti-diabetic, cancer suppressor, acaricide, among others. Leaves and fruits from *Schinus molle* L. (aroeira-mansa) contain essential oils rich in mono and sesquiterpenes with known microbicidal, insecticidal and antitumor action. In this context, the present study aims to investigate the trypanocidal effects of different fractions of *S. molle* L. essential oil from Peru, province of Huamanga (altitude of 2620 m) on the Vero cell and Tissue Culture derived Trypomastigote (TCT) forms of *Trypanosoma cruzi* strain G. The essential oils extracted from the fruit of the plant, collected in 2022 Mars, were fractionated by steam distillation, at 90-91 °C (548 mmHg) and 80-81 °C (150 mmHg under vacuum), generating fractions of the AE and AF series, respectively. GC-MS analysis of these oils identified the presence of several hydrocarbon terpenes and oxygenated terpenes with recognized biological activities (Spathulenol, 2.9%; Schyobunol, 3.6%; β-Copaene, 3.9%; Caryophyllene oxide, 5.4%; Beta-Caryophyllene, 8.1%; Bicyclogermacrene, 14.7%; γ-Cadinene, 14.2%, for example), including trypanocidal activity. Subsequently, Vero-cell cultures and TCT were treated with different concentrations (1024, 512, 256, 128, 64, 32, 16 and 8 μg/mL) of essential oil fractions, for 48 h, and their viability was determined 24 h after application of resazurin. The fractions tested demonstrated, in fact, to have toxicity in the Vero-cells and a trypanocidal effect on TCT. IC₅₀ (TCT) values for series AF (0, 1 and 5) and AE (0, 1, 2 and 5) were observed among the highest concentrations (1024 to 512 μg/mL). In the case of the Vero-cells, all fractions presented IC₅₀ lower than those observed in TCT. The AF6 fraction (aliquot collected in the period of 330 a 360 min) showed the highest toxicity when compared to the other fractions for Vero-cells and TCT-cells, (IC₅₀=16.25 and 81.94 μg/mL respectively). Otherwise, the AE2 fraction showed the lowest toxicity (IC₅₀ > 512 μg/mL) for Vero-cells and TCT. The results obtained indicate that the essential oils of *S. molle* L. have trypanocidal effects on TCT. Further tests are in progress using different concentrations to elucidate the therapeutic potential of these essential oils.

Agradecimentos/Acknowledgments

FAPEMIG, CAPES, CNPq, and Universidad Nacional de San Cristóbal de Huamanga (the project financier in Peru).

Uma abordagem metabolômica e de Imageamento por Espectrometria de Massas para a investigação da doença Vassoura-de-Bruxa em cacau

Marina Ferreira Maximo (PG),^{1*} **Daniel Yuri Akiyama** (PG),¹ **Jonas Henrique Costa** (PQ),² **Renata Moro Baroni** (PQ),³ **Alana Kelyene Pereira** (PQ),⁴ **Mario Ramos de Oliveira Barsottini** (PQ)³, **Jorge Maurício Costa Mondego** (PQ),⁵ **Gonçalo Amarante G. Pereira** (PQ),³ **Taicia Pacheco Fill** (PQ)¹

m203139@dac.unicamp.br; taicia@unicamp.br

¹Departamento de Química Orgânica, Instituto de Química, UNICAMP; ²Baylor College of Medicine; ³Instituto de Biologia, UNICAMP; ⁴Leiden University, LEIDEN, Holanda; ⁵Instituto Agrônomo de Campinas.

Palavras Chave: Vassoura de Bruxa, *Moniliophthora perniciosa*, Metabolômica, Imageamento por Espectrometria de Massas

Highlights

A metabolomics and Mass Spectrometry Imaging (MSI) approach to investigate the Witches' broom disease (WBD) in cacao fruits. The WBD is the most threatening disease in cacao. Metabolomics and MSI show metabolic differences between healthy and infected cacao. Would those be promising biomarkers for this disease diagnosis?

Resumo

Moniliophthora perniciosa é um fungo hemibiotrófico patógeno causador da doença devastadora Vassoura-de-Bruxa em cacau (*Theobroma cacao*), a qual é responsável por grandes perdas econômicas e ainda não possui uma estratégia eficiente de controle. Este estudo teve o objetivo de comparar o metabolismo de frutos de cacaueiros saudáveis e infectados na fase necrotrófica da doença através de análises de LC-HRMS/MS e de Imageamento por Espectrometria de Massas (MSI), visando estudar o efeito provocado pelo fungo no metabolismo dos frutos infectados. Análises de PCA dos perfis metabólicos de frutos infectados e saudáveis, coletados em campo no estado da Bahia, mostram uma evidente separação entre os grupos, sugerindo alteração do metabolismo após a infecção (Figura 1). Observou-se redução significativa de flavonas, flavonoides e alguns açúcares típicos da planta, sugerindo biodegradação destes metabólitos pelo fungo na fase necrotrófica, e um aumento de lipídeos em frutos infectados, sugerindo envolvimento destes metabólitos na defesa da planta. Essas moléculas são potenciais biomarcadores da doença, já que possuem sua concentração alterada após a infecção, confirmadas por MSI (Figura 1). Este estudo apresenta o MSI como uma ferramenta promissora para diagnóstico da doença Vassoura-de-bruxa em cacau.

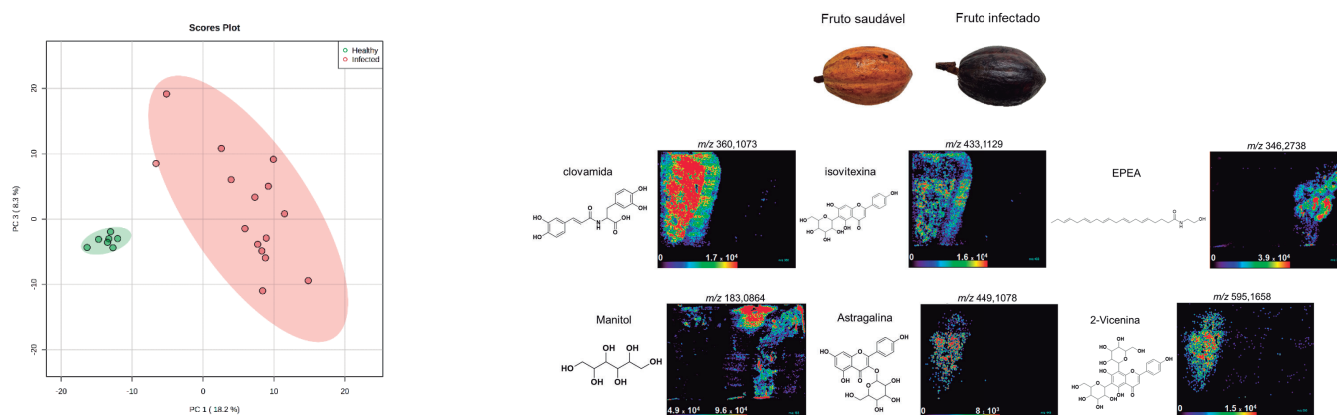


Figura 1. PCA dos grupos de frutos saudáveis e infectados (esquerda) e DESI-MSI de frutos saudáveis e infectados (direita), mostrando a distribuição espacial de m/z de alguns possíveis biomarcadores (preto indica baixa concentração e vermelho, alta concentração).

Agradecimentos



Volatile Organic Compounds from rhizobacteria control fusariosis (*F. solani* f. sp. *piperis*) in black pepper.

Suzana Kaory G. Inoue (PG),¹ Laís S. Almeida (PG),¹ Beatriz G. Holanda Silva (IC)², Pablo Luis B. Figueiredo (PQ)³, Joana M. Marques (PQ)¹, Oriel F. de Lemos (PQ),⁵ Massuo Jorge Kato (PQ)⁶, Joyce Kelly R. da Silva (PQ).^{1*}

suzana.inoue@icb.ufpa.br; joycekellys@ufpa.br

¹Programa de Pós-Graduação em Biotecnologia, UFPA; ²Programa Institucional de Bolsas de Iniciação Científica-CNPq; ⁴Departamento de Ciências Naturais, UEPA; ⁵Embrapa Amazônia Oriental; ⁶Laboratório de Química de Produtos Naturais, USP.

Palavras-Chave: *Piper nigrum*, antagonistic effects, Dual-culture assay, Dodecanal, Undecanal, 2-ethyl-Hexanol.

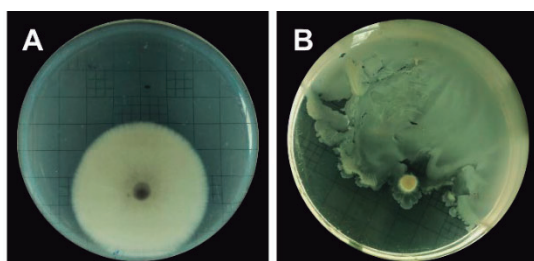
Highlights

The isolate PN3-73 from the rhizosphere of *P. nigrum* exhibited potent antibiosis against *F. solani* f. sp. *piperis*, possibly due to its capacity to produce antifungal volatile organic compounds.

Abstract

The incidence of fusariosis disease (*Fusarium solani* f. sp. *piperis*) (FS) in black pepper (*Piper nigrum* L.) (PN) has been causing a reduction in the production rates of the spice in Brazil since there are no forms of satisfactory control. Plant growth-promoting rhizobacteria (PGPR) as a biocontrol strategy has become a non-polluting alternative to chemical fungicides. The present study evaluated several bacterial isolates' potential to control fusariosis and their Volatile Organic Compound (VOC) production. Rhizobacteria were isolated from soil near the roots of healthy *Piper nigrum* plants in a commercial field in Castanhal city (Pará State). The phytopathogen FS was obtained from the collection of fungi of EMBRAPA Amazônia Oriental (Belém, PA). The antagonistic effect of the rhizobacteria was evaluated by dual culture with FS in Tryptic Soy Agar (TSA). The inhibition percentual was calculated compared to the control TSA plate with FS only. Bacterial volatile compounds were extracted from a 5-day-old culture by the Likens-Nickerson apparatus, and the analysis was performed by Gas Chromatography-Mass spectrometry (GC-MS). The rhizobacterial isolate PN3-72 exhibited potent antifungal activity against FS in vitro: the percentual inhibition was 62.6±0.8% (Figure 1). The chemical profile of the volatile concentrate showed the presence of 6 compounds with relative abundances above 1% (Table 1). The major compounds were dodecanal (77.81%), undecanal (6.95%), and 2-ethyl-hexanol (4.05%). The aldehydes dodecanal and undecanal have been reported as antibiotic substances against *F. oxysporum* (1) and *Rhizoctonia solani* (2). The antifungal activity of alcohol 2-ethyl-Hexanol against *Monilina frutigena* has also been reported (3). Other studies will be carried out to understand the antibiosis of PN3-72 against FS, such as evaluating the extracts and plant inoculation, aiming to develop a product to be applied under field conditions.

Figure 1: Antagonistic effect of PN3-72 against *F. solani* f. sp. *piperis*. **A:** Control plate with only FS. **B:** Dual culture of PN3-72 and FS.



(1) RAZA et al. Biological Control, v. 80, p. 89-95, 2015.

(2) CHANPRAPAI; KUBO; CHAVASIRI. Science & Technology Asia, p. 32-41, 2018.

(3) GUO et al. Chinese Journal of Biological Control, v. 36, n. 4, p. 575, 2020.

Table 1: Chemical profile of volatile organic compounds produced by PN3-72

Compound	RIC	RA (%)
2-ethyl-hexanol	1023	4.05
n-decanal	1205	3.28
undecanal	1306	6.95
dodecanal	1409	77.81
trans-Dodec-2-en-1-ol	1480	3.85
NI	1855	2.77

RIC: Calculated Retention Index; RA: Relative Abundance.

Acknowledgments

Fundação Amazônia de Amparo a Estudos e Pesquisas-FAPESPA and Conselho Nacional de Desenvolvimento Científico e Tecnológico-CNPq for their financial support for the execution of this project.

QVE

Química Verde

46^a Reunião
Anual da **SBQ**

28 a 31 de Maio de 2023

Águas de Lindóia · SP
Hotel Monte Real

Blue light-mediated synthesis of α -carbonyl selenocyanates and 2-arylimidazo[1,2-a]pyridines

João M. Anghinoni (PG),¹ Sabrina S. Ferreira (IC),¹ Filipe Penteado (PQ),^{2,*} and Eder J. Lenardão (PQ)^{1,*}

lenardao@ufpel.edu.br; filipe.penteado@ufsm.br

¹ Centro de Ciências Químicas, Farmacêuticas e de Alimentos – CCQFA, Universidade Federal de Pelotas – UFPel, P.O. box 354, CEP 96010-900, Pelotas – RS, Brazil.

² Departamento de Química, Centro de Ciências Naturais e Exatas – CCNE, Universidade Federal de Santa Maria – UFSM, Avenida Roraima, CEP 97105-340, Santa Maria – RS, Brazil.

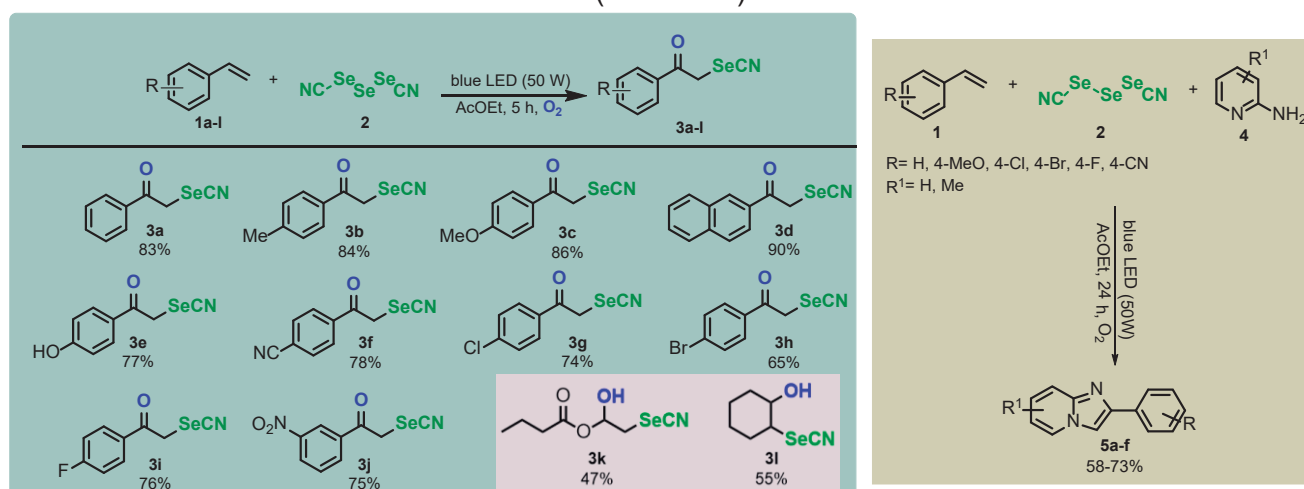
Palavras Chave: Organoselenium, Visible light, Imidazopyridines, Selenocyanate, Green chemistry.

Highlights

α -Carbonyl selenocyanates and 2-substituted imidazo[1,2-a]pyridines were efficiently obtained through a novel visible light-driven oxidative coupling of alkenes with triselenodicyanide (TSD).

Resumo/Abstract

Selenium-containing molecules have found widespread applications in organic synthesis and drug discovery.¹ Continuous efforts have been devoted to the development of new and efficient methods for the incorporation of selenium groups into organic molecules.² In this context, α -carbonyl selenocyanates is an interesting class of compounds, which can be further manipulated, including cyclization to prepare heterocyclic compounds.³ Imidazo[1,2-a]pyridines, in turn, are very studied due to their pharmacological activities.⁴ Most of the current used methods to prepare organoselenium derivatives and imidazopyridines use harsh conditions, like high temperatures, use of strong bases or acids, or heavy metals. To circumvent these drawbacks, we developed a visible light-driven oxidative coupling of alkenes **1** with triselenodicyanide (TSD, **2**). α -Carbonyl selenocyanates **3a-j** were obtained from styrene derivatives **1a-j** (5 h; 65-90% yield), while α -hydroxy selenocyanates **3k** and **3l** (47% and 55% yield) were obtained respectively from vinyl ester **1k** and cyclohexene **1l**. No reaction was observed in the absence of light. The new procedure was used in the *in situ* synthesis of 2-arylimidazo[1,2-a]pyridines **5a-f** (24 h; 58-73% yield), as an alternative to the use of α -bromo ketones (Scheme 1).



Scheme 1. Synthesis of α -carbonyl selenocyanates and 2-arylimidazo[1,2-a]pyridines.

References: 1) Z. Chen, H. Lai, L. Hou and T. Chen, *Chem. Commun.*, 2020, **56**, 179. 2) A. D. Sonawane and M. Koketsu, *Curr. Org. Chem.*, 2019, **23**, 3206. 3) M. Besev and L. Engman, *Org. Lett.*, 2000, **2**, 1589. 4) B. M. Vieira, N. B. Padilha, N. M. Nascimento, G. Perin, D. Alves, R. F. Schumacher and E. J. Lenardão, *Arquivoc.* 2019, **2019**, 6.

Agradecimentos/Acknowledgments

CNPq, CAPES, FAPERGS, and FINEP.

Development of hydrophobic deep eutectic solvents (hDES) for removal of inorganic contaminants in sewage

Rafaela S. Lamarca (PQ)^{1*}, Éder R. Paganini (PG)¹, Natália S. Ferreira (PG)¹, Sabrina S. Ferreira (PG)¹, Clarice B. D. Amaral (PQ)², Paulo C. F. de Lima Gomes (PQ)³, Mario H. Gonzalez (PQ)¹

*Rafaela.lamarca@unesp.br

¹Department of Chemistry and Environmental Science, National Institute for Alternative Technologies of Detection, Toxicological Evaluation and Removal of Micropollutants and Radioactives (INCT-DATREM), São Paulo State University (UNESP), São José do Rio Preto, São Paulo, Brazil; ²Federal University of Paraná, Department of Chemistry, Curitiba, Paraná, Brazil; ³Department of Analytical Chemistry, Physical Chemistry and Inorganic Chemistry, National Institute for Alternative Technologies of Detection, Toxicological Evaluation and Removal of Micropollutants and Radioactives (INCT-DATREM), Institute of Chemistry, São Paulo State University (UNESP), Araraquara, São Paulo, Brazil.

Keywords: Green solvents, Elemental determination, ICP-MS

Highlights

- Syntheses of two new hydrophobic deep eutectic solvents (hDES).
- Analytical Eco-Scale was used to evaluate the greenness of the hDES preparation.
- Extraction of inorganic contaminants from sewage.

Resumo/Abstract

In the last decades in the analytical chemistry, area a current of study called Green Analytical Chemistry, started priorities to reduce or eliminate the use of products, by-products, and toxic solvents for humans and the environment.^{1,2} In this context, the development of green sustainable solvents, such as hydrophobic deep eutectic solvents (hDES) has been highlighted. The hDES have particularities such as simple and fast preparation, biodegradability, high extraction efficiency and low cost.³ The aim of this study was to prepare two different hDES and apply it in the extraction of inorganic contaminants present in sewage samples. The prepared solvents were: 1) acetic acid with DL-menthol at molar ration of 1:1 (hDES1); 2) DL-menthol, pyruvic acid and acetic acid at molar ration 1:1:1 (hDES2). All hDES were prepared in triplicate using simple procedure such as, under stirring and heating at 200 rpm for 15 min at 60 °C. The solvents were characterized by density, viscosity, infrared spectroscopy (ATR- FTIR mode, wavenumber 4000 - 400 cm⁻¹) and DSC at low temperature (-70 to 350 °C) to obtain the melting point (T_m). Table 1 presents the density and viscosity obtained for these assays. By DSC the values of T_m were 27.8 °C and 7.80 °C for hDES1, and hDES2, respectively. As observed, the T_m of both solvents were lower than those of the starting materials. The vibrational characterization of the precursor and hDES via FTIR allowed the identification of vibration frequencies of the main functional groups, as well as the vibrational shifts when compared with the precursors. From the FTIR spectra, it was possible to verify a shift of the vibrational mode assigned to the symmetric stretching of carbonyl (C=O) group from 1704 to 1713 cm⁻¹, which indicates the formation of solvents. The preliminary results were performed in triplicate with 100 mg of sample certified containing 1.3 mg kg⁻¹ Hg and 57 mg kg⁻¹ Pb, respectively. 100 mg of this sample was inserted in 5.0 mL of each hDES, followed by 60 seconds of stirring and vortex. Afterwards, the solution was filtered and analyzed by ICP-MS in the standard mode, with calibration curves (0.50 - 50.0 µg L⁻¹), LOD 0.20 µg L⁻¹ and LOQ 0.50 µg L⁻¹ to both analytes. The hDES developed were efficient to remove 78% of Hg and 85% of Pb present in the certified sewage samples. Moreover, Analytical Eco-Scale method was used to evaluate the hDES prepare. This metric assigns penalty points for methods that do not comply with green chemistry. The hDES prepared only scored 98 of a total of 100 points possible, featuring an excellent greenness.⁴

Table 1: Physicochemical properties of the solvents prepared

Solvent	Density (g mL ⁻¹)	Viscosity (mPa s)
DL-menthol and acetic acid (hDES1)	0.930	6.54
DL-menthol, pyruvic acid and acetic acid (hDES2)	0.988	4.27

References

¹Armenta S, Garrigues S, de la Guardia M, *TrAC Trends in Analytical Chemistry*, 27, 2008, 497-511; ²Sajid M, Plotka-Wasylyka J, *Talanta*, 238, 2022, 123046; ³Florindo C, et al, *Journal of Molecular Liquids*, 297, 2020, 111841; ⁴Galuszka A, et al, *TrAC Trends in Analytical Chemistry*, 37, 2012, 61-72.

Acknowledgments

São Paulo Research Foundation (FAPESP grants #2014/50945-4, #2018/2500-2, #2021/14581-1 and #2021/14759-5), CAPES (grant #88887.485183/2020-00), CNPQ (grant ##465571/2014-0), IBILCE-UNESP-São José do Rio Preto, and INCT-DATREM.

Extraction and Physicochemical Analysis of Favela oil (*Cnidoscopus quercifolius pohl*) to obtain fatty acid alkyl esters

Erika P.L. da Costa (IC),¹ Paloma B. Coelho (TC),¹ Guilherme Antonio Finazzi,² Yariadner C.B. Spinelli (PQ).^{3*}

erika.paes@discente.univasf.edu.br; yariadner.brito@univasf.edu.br

¹Colegiado de Ciências da Natureza, UNIVASF; ²Laboratório de química Geral, UNIVASF; ³Colegiado de Ecologia, UNIVASF

Palavras Chave: Favela, *Cnidoscopus quercifolius*, Extração de óleo, Transesterificação, Biodiesel.

Highlights

Favela oil has shown an outstanding potential to compose the biodiesel production chain in the semi-arid region of Brazil. Favela oil has a percentage of fatty acids similar to soybean oil.

Resumo/Abstract

Biodiesel has stood out as an alternative source of energy obtained from oils and plant or animal fat. In this scenario, the Favela plant (*Cnidoscopus quercifolius Pohl*) is considered endemic in Brazil, occurring in parts of the Northeast region and showing significant drought resistance. The advantage of using favela oil in transesterification reactions to obtain biodiesel becomes attractive when alternative raw materials can be used to replace soybean oil, in addition to the possibility of strengthening the local agriculture in the semi-arid region and widening the Brazilian energy matrix of biofuels. From this perspective, the main objective of this study was to extract favela seed oil and evaluate its physicochemical properties for later use in transesterification reactions. The favela oil was extracted using a Soxhlet extractor at various times (2, 4, and 6 hours) and using different solvents (ethanol and hexane). The concentration (%) of fatty acids present in the favela oil was determined by gas chromatography coupled to mass spectroscopy, and the acidity index (mg of KOH/g sample) followed the methodology of the Adolfo Lutz Institute [1]. The approximate percentage of oil obtained from favela seeds was 35 % during 4 h, at 80 °C, in ethanol and 39 %, 6 h, 80 °C in hexane. (Figure 1). The acidity index was approximately 0.059, and the highest concentration percentage of fatty acids corresponded to linoleic acid (52,8 %) followed by palmitic and oleic acid, with 21.5 % and 17.5 %, respectively (Table 1). The results corroborate the data obtained in the literature [2], showing properties similar to soybean oil [3], constituting a strong indicator of the potential of this species as a raw material for biodiesel production. The transesterification reactions are still ongoing and conversions into fatty acid alkyl esters (FAAEs) have shown promising results. However, more analyses are required for a better result effectuation.

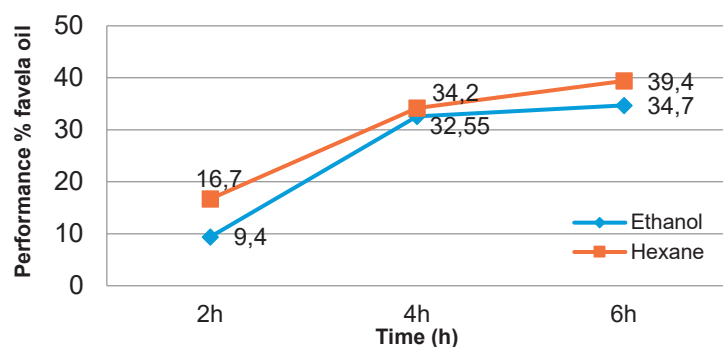


Figure 1: Performance of Favela oil as a function of the time and type of solvent.

Table 1: Concentration of (%) fatty acids in favela oil.

	AG	Concentration (%)
Myristic	C14	0,3
Palmitic	C16	21,5
Stearic	C18	7,7
Oleic	C18:1	17,5
Linoleic	C18:2	52,2
Linolenic	C18:3	0,9
Arachidonic	C:20	0,3

Source: the authors

- [1] Instituto Adolfo Lutz. Métodos físico-químicos para análise de alimentos ZENEBAON, O.; PASCUET, S. N. e TIGLEA, P., p. 1020, 2008;
 [2] SANTOS, K.A., FILHO, O.P.A., AGUIAR, C.M., MILINSK, M.C., SAMPAIO, S.C., PALÚ, F., DA SILVA, E.A. Chemical composition, antioxidant activity and thermal analysis of oil extracted from favela (*Cnidoscopus quercifolius*) seeds. *Industrial Crops and Products*, v. 97, p.368-373, 2017;
 [3] CARVALHO, G. C.; Composição de ácidos graxos em óleos vegetais obtida por cromatografia gasosa e sua correlação com propriedades térmicas, reológicas, espectroscópicas e outras propriedades físico-químicas. tese Doutorado, UFRN, 2019.

Agradecimentos/Acknowledgments

To the Nucleus of Ecology and Environmental Monitoring - NEMA/UNIVASF, the *Projeto de Integração do Rio São Francisco com as Bacias Hidrográficas do Nordeste Setentrional* – PISF, and the Regional Development Ministry - MDR for providing the seeds. To the Catalysis and Chemical Reactivity Group (*Grupo de Catálise e Reatividade Química*) – GCAR/UFAL for the analysis of favela oil samples.

Functionalized biochars obtained from water hyacinth biomass as sustainable catalysts for multicomponent reactions

Bruno Salarini Peixoto (PQ),¹ Nívea L. Aguiar (IC),¹ Cristina M. Hüther (PQ),² Marcela C. Moraes (PQ),¹ Gilberto A. Romeiro (PQ),¹ Vitor F. Ferreira (PQ),^{1,3} Fernando C. Silva,¹ Carolina G. S. Lima (PQ)^{1*}

brunosalarini@id.uff.br; *cgslima@id.uff.br

¹Departamento de Química Orgânica, Instituto de Química, Universidade Federal Fluminense

²Departamento de Engenharia Agrícola e Meio Ambiente, Escola de Engenharia, Universidade Federal Fluminense

³Departamento de Tecnologia Farmacêutica e Cosmético, Faculdade de Farmácia, Universidade Federal Fluminense

Keywords: biochar, biomass upgrading, heterogeneous catalysis, Biginelli reaction, pyrimidinones

Highlights

Biochars from *Eichhornia crassipes* were prepared and had their catalytic activity evaluated in the Biginelli reaction. Preliminary tests demonstrated the potential of the newly obtained biochars.

Resumo/Abstract

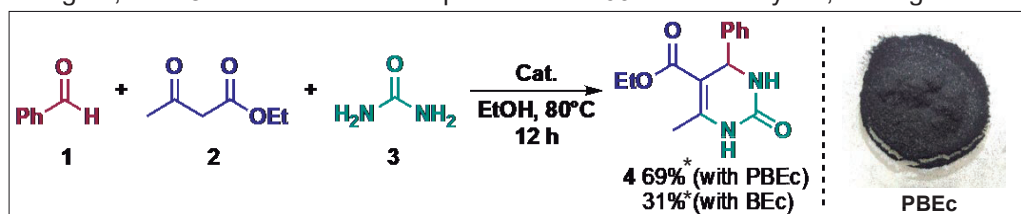
Water hyacinth (*Eichhornia crassipes*) is as an aquatic plant indigenous to South America that has spread worldwide in the few past decades (Figure 1).¹ Its rapid growth and ability to thrive in adverse conditions make this species an



Figure 1. *Eichhornia crassipes* specimen

environmental concern, and the main solution to remediate this problem is the mechanical collection of the plants, which end up in landfills.² On the other hand, in the past few years, several strategies have been devised for the upgrading of plant biomass waste into value-added chemicals and materials such as biochars.³ Biochars are carbonaceous materials produced via the transformation of lignocellulosic biomass through heating in a low O₂ environment (pyrolysis), and such materials have attracted considerable interest within the last decades as a consequence of their physicochemical features. Indeed, biochars have been finding applications within several areas in recent years, for instance in soil enrichment, water treatment, and as catalyst's supports. Considering these facts, in this work we aimed to produce biochars from *E. crassipes* biomass and evaluate the catalytic activity of the resulting materials in multicomponent reactions. In order accomplish that, the collected plant specimens were collected, washed, and dried, and subsequently, submitted to slow pyrolysis processes under N₂ atmosphere in the presence or absence of phosphoric acid (the obtained biochars were named **BEc** and **PBEc**, respectively). Both materials were evaluated in the Biginelli reaction between benzaldehyde (**1**), ethyl acetoacetate (**2**) and urea (**3**) to produce 1,4-dihydropyrimidinones (**4**), biologically important molecules, using ethanol as a green solvent (Scheme 1). To our delight, under preliminary experimental conditions, using 20 mg of catalyst to each 1 mmol of reagent, **PBEc** led to the desired product with 69% isolated yield, having showed

considerably superior activity than the **BEc** biochar (31%). Further studies on the optimization of the reaction conditions are currently ongoing, as well as the evaluation of the scope and applications of this protocol.



Scheme 1. Biginelli reaction promoted by hyacinth biomass-derived biochars * Isolated yield

- References: [1]. T. Dalu, R. J. Wasserman, *Ecology to Conservation Management*, Elsevier, 2022.
[2]. A. Sharma. et al. *J. Environ. Sci. Technol.* 2016, 9, 26.
[3]. Y. X. Seow et al. *J. Environ. Chem. Eng.* 2022, 10, 107017.

Agradecimentos/Acknowledgments

The authors gratefully acknowledge FAPERJ for funding (E-26/210.377/2022) and scholarships. (E-26/203.964/2022 and E-26/205.535/2022).

NEW GREEN PREPARATION AND CHARACTERIZATION OF AMINO ACID-BASED DEEP EUTECTIC SOLVENTS

Mario Henrique Gonzalez (PQ)^{1*}, Sabrina S. Ferreira (PG)¹, Éder R. Paganini (PG)¹, Rafaela S. Lamarca (PQ)¹, Clarice B.D. Amaral (PQ)², Paulo C.F. de Lima Gomes (PQ)³.

mario.gonzalez@unesp.br

¹Department of Chemistry and Environmental Science, National Institute for Alternative Technologies of Detection, Toxicological Evaluation and Removal of Micropollutants and Radioactives (INCT-DATREM), São Paulo State University (UNESP), São José do Rio Preto, São Paulo, Brazil;

²Federal University of Paraná, Department of Chemistry, Curitiba, Paraná, 81531-980, Brazil; ³Department of Analytical Chemistry, Physical Chemistry and Inorganic Chemistry, National Institute for Alternative Technologies of Detection, Toxicological Evaluation and Removal of Micropollutants and Radioactives (INCT-DATREM), Institute of Chemistry, São Paulo State University (UNESP), Araraquara, São Paulo, Brazil

Keywords: Green analytical chemistry, Green solvent, NADES, Physicochemical properties.

Highlights

Development of new green methods to prepare AADES.

AADES can be prepared without heating the precursor mixture.

Different preparation methods can modulate the viscosity of water-based AADES.

Abstract

Reducing the production and use of harmful chemicals, and minimizing exposure to them, are crucial for ensuring compliance with sustainability objectives¹. The development of new sustainable solvents, as substitutes for toxic solvents, is one of the significant efforts being made to reduce the environmental impact of chemical analyses, which often generate hazardous waste during the analytical process². Natural deep eutectic solvents (NADES) are considered green solvents, consisting of natural precursors that undergo interaction involving a hydrogen bond donor (HBD) compound and a hydrogen bond acceptor (HBA) compound³. These solvents have been widely used in green methods of sample preparation, aiming to obtain reliable and accurate results, while prioritizing the sustainability of the analytical process. When at least one of the precursors is an amino acid, the solvent is classified as an amino acid-based deep eutectic solvent (AADES). In this work, AADES were prepared using two simple and cheap methods. Also, the physicochemical properties of these solvents were characterized and compared. AADES based on citric acid/ β -alanine/water at a ratio⁴ of 42.75:12.50:43.75 (% m m⁻¹), were prepared by stirring (ST) and rotaevaporation (RT) methods. Following, this solvent was characterized by Fourier transform infrared spectroscopy (FTIR) in attenuated total reflectance (ATR) mode, as well as by density and viscosity measurements. These new methods were compared with the reference prepare method involving stirring with heating (SH)⁵. The ATR-FTIR spectrum for the solvents prepared by the three methods showed an intense absorption band between 3573 and 3095 cm⁻¹, characteristic of the stretching vibrations of OH groups, due to the presence of water⁵. In addition, the presence of a downward shift of ν OH was observed at lower wavelengths between 2550 and 2000 cm⁻¹ which indicated the formation of hydrogen bonds between the precursors. In comparison with the initial reagents, the C=O stretching was shifted to a higher wavenumber, from 1696 to 1710 cm⁻¹, which also supported the interactions between the used HBD and HBA. The density values obtained (ST: 1.26 \pm 0.0009 g mL⁻¹; SH: 1.27 \pm 0.0003 g mL⁻¹; RT: 1.30 \pm 0.001 g mL⁻¹) indicated that there was significant variation (t-test with 95% confidence) of this property among the solvents prepared by the different preparation methods. The viscosity values increased in the following order: ST (10.96 mPa s) < SH (11.22 mPa s) < RT (26.24 mPa s) which could be explained by the different amount of water which volatilize depending on the method of preparation. The results showed that the proposed methods are effective for the AADES preparation and offer the potential to modulate the physical properties, such as viscosity, of water-based solvents.

References:

¹ United Nations, A/70/1, 2015; ² Pacheco-Fernández, I., Pino, V., *Curr. Opin. Green Sustain. Chem.*, v. 18, 2019; ³ Dai, Y. et al., *Anal. Chim. Acta*, v. 766, 61-68, 2013; ⁴ Guimarães, T.G.S. et al., *J. Mol. Liq.*, v. 345, 117887, 2022. ⁵ Santana, A.P.R. et al., *Talanta*, v. 216, 2020.

Acknowledgments

The authors are grateful for scholarships provided by the Coordination for the Improvement of Higher Education Personnel (CAPES). Financial assistance was provided by FAPESP (#2021/14759-5 and #2021/14581-1) and the National Institute of Alternative Technologies for The Detection, Toxicological Evaluation and Removal of Micropollutants and Radioactive Drugs - INCT-DATREM (FAPESP, #14/50945-4; CNPq, #465571/2014-0).

SBQ for a sustainable Brazil: The tackling of five significant challenges to impact sustainable development in Brazil through chemistry

Izadora R. S. Menezes (PG)^{1*}, Maryna M. Barros (PG)¹, Ingrid F. Silva (PQ)², Larissa L. Maia (PG)³, Carolina Maria M. de C. Andrade (PQ)¹, Romeu C. Rocha Filho (PQ)⁴, Shirley Nakagaki (PQ)⁵, Rochel M. Lago (PQ)¹, Ana Paula de C. Teixeira (PQ)^{1*}.

menezes.irs@gmail.com; anapct@ufmg.br

¹Departamento de Química, ICEx, UFMG; ²Department of Colloid Chemistry, MPIKG; ³Instituto de Ciências Exatas e Tecnológicas, UFV; ⁴Instituto de estudos avançados, UFSCAR; ⁵Departamento de Química, UFPR.

Keywords: chemistry post 2022 movement, action plan, sustainability.

Highlights

The SBQ wants to promote Brazil's sustainable development. The five significant challenges involve important topics related to Chemistry that need to be continuously tackled for the advancement of sustainable development in Brazil.

Abstract

The action plan "Chemistry and its Players for a Sustainable and Sovereign Brazil", one of the fronts of the "Chemistry Post 2022 Movement – Sustainability and Sovereignty" launched by the Brazilian Chemical Society (SBQ) in mid-2021, expresses ways to impact the sustainable development of Brazil through chemistry. Within this plan, after three stages of intense discussion, two Chemistry Objectives for Sustainable Development (OQDS) and five Chemistry Challenges for a Sustainable Brazil were established. OQDS 1 aims to promote sustainability through basic education in chemistry, while OQDS 2 intends to advance Science, Technology, Innovation & Education in industry and academia, promoting their connection for fast and effective technological transfer. With this abstract, we aim to divulge the five challenges. Starting in 2023, actions/projects related to these challenges will be implemented in accordance with each OQDS, considering past and current efforts from other players, and thus joining forces whenever possible.

Challenge 1 – FIGHTING CLIMATE CHANGE: There is an urgent need for initiatives that mitigate impacts and for solutions/alternatives that reduce the influence of human activity on the environment due to the various problems faced by society today arising from climate change. Some of the biggest tasks in this regard are decarbonization (defossilization), which refers to the reduction of the emission into the atmosphere of greenhouse gases (especially CO₂) derived from fossil fuels, and the development of new renewable energy sources. The subtopics to be prioritized are **CO₂ capture and use, biofuels and green hydrogen**.

Challenge 2 – TREATING WASTE: Some type of waste is generated in almost all industrial or domestic activities, from production to disposal of products. However, billions of tons of residues can somehow be treated and reintroduced into the economy, with added value. Thus, arises the Circular Economy, which favours the preservation of feedstocks and contributes to pollution reduction. The subtopics of this challenge were selected according to their basic composition, namely: **plastic, mineral, and biomass waste**.

Challenge 3 – USING WATER SUSTAINABLY: Water is one of the fundamental resources for biological survival. However, most of the time it is not used in a sustainable way, resulting in its pollution and increased scarcity. The pollution of rivers, lakes and groundwater caused by the inadequate disposal of residential, industrial, and agricultural wastes is a major problem that is being faced by society today. Therefore, some subtopics of this challenge are **treatment of industrial and domestic effluents, reuse of water and monitoring of water quality**.

Challenge 4 – DEVELOPING MATERIALS FOR SUSTAINABILITY: The development of new materials that bring positive impacts in the context of sustainability and allow replacing materials that are harmful to the environment is extremely relevant for our society. The subtopics to be explored within this challenge are **obtention of new renewable/sustainable materials** (developed from renewable sources or using sustainable processes), **materials for clean energy generation and storage, and materials based on bioresources**.

Challenge 5 – PRODUCING FOOD SUSTAINABLY: Agribusiness is of great economic importance for Brazil; thus, initiatives that increase the sustainability of food production are crucial in the transition to a sustainable country. Chemistry can contribute to the implementation of a sustainable agriculture, focused on preserving the fauna, flora and natural resources throughout the production and distribution chain. Some subtopics to be explored within this challenge are **use of natural resources in plant and animal nutrition, pest control and post-harvest processes**. From 2023 on, the SBQ ought to promote the tackling of these challenges to impact sustainable development in Brazil as guidelines to the whole society for the next 30 years, besides assisting the action projects related to them in each OQDS. The movement intends to have a national impact, integrating all regions and sectors of Brazil. **Please join us!**

Acknowledgments

Capes, CNPq, FAPEMIG, INCT Midas, SBQ, Abiquim, CFQ, Escalab and our interviewed collaborators.

46^o Reunião Anual da Sociedade Brasileira de Química: "Química: Ligando ciências e neutralizando desigualdades"

Using a cyanobacteria *Synechocystis* sp. to produce the biopolymer polyhydroxyalkanoate (PHA) by mixotroph cultivation

Pedro B. Miragaia (PG),^{1*} Arthur B. D. Pereira (PG),¹ Dielle P. Procópio (PQ),¹ Renato S. Freire (PQ),¹ Cassius V. Stevani (PQ).¹

pedro.miragaia@usp.br

¹Department of Fundamental Chemistry, Institute of Chemistry, USP, São Paulo, Brazil

Keywords: Polyhydroxyalkanoates, Biopolymer, Cyanobacteria, Mixotrophic Cultivation.

Highlights

A cyanobacterium uses mixotrophic pathway to capture CO₂ & biosynthesis PHA. PHA prod. peaked (26% w/v) at 8 days, [Ac] = 0.3% w/v & [P] = 10 mg L⁻¹. More acetate & shorter times enhance PHA yield.

Abstract

Polymers, a widely used material in modern society, continue to heavily rely on petroleum and its derivatives, which are highly polluting and challenging to decompose. To address this issue, the world needs to adopt greener alternatives, such as polyhydroxyalkanoates (PHA). These polymers degrade in a matter of months in soil and can be used as standalone materials or blended with other environmentally-friendly polymers.¹ The widespread adoption of PHA could reduce the accumulation of waste from disposable plastics and packaging, thus promoting a cleaner environment. The present work focuses on a newly isolated cyanobacteria, *Synechocystis* sp. B12, which was obtained from a contaminated mangrove in Santos, SP.² Using a cyanobacteria are particularly attractive for its ability to produce PHA through mixotrophic pathways, making it a promising option for capturing CO₂ (via photo-autotrophic) and converting it into a biopolymer. Additionally, this cyanobacterium could be cultivated using agro-industrial waste as a nutrient medium. To optimize PHA production, the study utilized two strategies combined: *feast and famine* and experimental planning. The *feast and famine* approach involved growing the cyanobacteria in two phases: an abundance of nutrients (*feast*) and nitrogen-free medium with limited phosphate availability (*famine*), both under atmospheric aeration and artificial light (fig 1). The experimental planning (table 1 and 2) involved manipulating three factors: incubation period (2, 8, and 14 days), sodium acetate (Ac) concentration (0.2%, 0.3%, and 0.4% w/v), and potassium phosphate (P) concentration (0, 10, and 20 mg L⁻¹). The best conditions for PHA production were determined based on the yield relative to total dry mass. The optimal results were found to be at the center of the experimental design (8 days, sodium acetate concentration of 0.3%, and potassium phosphate concentration of 10 mg L⁻¹), with a yield of 26.0 ± 3.6%. The study also noted two trends: increased acetate concentration and shorter incubation periods resulted in higher PHA production. Further investigation is underway to consider other factors, such as light intensity and alternative substrates.

Table 1. Experimental Design

#	Acetate	Potassium phosphate	Incubation	Yield
1	-1	-1	-1	9%
2	1	-1	-1	15%
3	-1	1	-1	5%
4	1	1	-1	18%
5	-1	-1	1	4%
6	1	-1	1	6%
7	-1	1	1	3%
8	1	1	1	3%
9	0	0	0	23%
10	0	0	0	30%
11	0	0	0	25%

Table 2. Experimental Factors

Variable	Level		
	-1	0	1
Acetate (% w/v)	0,2	0,3	0,4
K ₃ PO ₄ (mg L ⁻¹)	0	10	20
Incubation (days)	2	8	14



Fig. 1 – Incubation system

¹Carpine R, Olivieri G, Hellingwerf K, et al; *Processes*. 2020, 8, 1-23.

²Gracioso L, Bellan A, Karolski B, Cardoso L, et al; *Bioresource Technol.* 2021, 320, 124379.

Acknowledgments

The authors thank Capes (88887.675818/2022-00) and Fapesp/RCG2I (20/15230-5) for the financial support.

TEC

Química Tecnológica

46^a Reunião
Anual da **SBQ**

28 a 31 de Maio de 2023

Águas de Lindóia · SP
Hotel Monte Real

Application of natural extracts with antioxidant properties in biodiesel.

Nathan F. Silva (IC),¹ Eduardo G. de Souza (IC),¹ Heloisa H. P. Silva (IC),¹ Julia W. Campos (IC),¹ Maria C. Brandão,¹ Marco A. J. Clemente (PG),¹ Letícia T. Chendynski (PQ),² Dionisio Borsato (PQ).^{1*}

nathan.ferreira@uel.br; dborsato@uel.br

¹Departamento de Química, UEL; ²Instituto Federal do Paraná, Campus Ivaiporã - PR

Keywords: *Induction period, Rate constant, Simplex-centroid, Phenolic compounds*

Highlights

Antioxidant activity was observed in all extracts. Extracts of jabuticaba peel, gabirola leaves and hibiscus flowers reduced biodiesel oxidation. The natural extracts are a good alternative to synthetic substances.

Resumo/Abstract

The use of biofuels has been presented as a viable alternative in the search for clean and renewable energy sources. Among biofuels, biodiesel is highlighted with an increasingly important role in the energy matrix of several countries and its demand grows every year. However, due to the nature of the raw material used in biodiesel production, it degrades more quickly than fossil fuels, which are relatively inert and maintain their essential characteristics during storage. The oxidation resulting from exposure to atmospheric air is one of the main degradation problems. In order to inhibit or delay the biodiesel oxidation, chemical compounds with antioxidant properties are used. An alternative to replace synthetic antioxidants are natural extracts with antioxidant properties, such as those produced from fruit peels, condiments, leaves and flowers. To evaluate the efficiency of antioxidants in biodiesel, individually or in mixtures, experimental design coupled with multiresponse optimization algorithms are used. The objective of this research was to present an efficiency analysis of natural extracts with antioxidant properties when added to biodiesel, using the mixture experimental design, as well as to study the biodiesel oxidation kinetics by monitoring the oxidation reaction at 110 °C. The biodiesel used was obtained from the transesterification reaction of a mixture of refined palm oil with refined soybean oil, in the proportion of 50% w/w, with potassium hydroxide as a catalyst at a concentration of 0.8% w/w. Jabuticaba peels, gabirola leaves and hibiscus flowers were dried in an oven at 60 °C, separately. Each extract was prepared by mixing 10 g of the dry sample in 250 mL of absolute ethanol and kept in the dark for 48 hours. Then, the mixture was filtered. The volume of each sample was reduced with the aid of a heating plate at 60 °C, to approximately 50 mL, transferred to volumetric flasks and completed with absolute ethanol. Biodiesel samples were individually prepared by adding 7.5 mL of each extract in 100 g of biodiesel and kept at rest for 24 hours. Then, the binary and ternary mixtures were prepared according to the simplex-centroid design. The oxidative stability of the control biodiesel and of each sample containing only one type of natural extract and in binary and ternary mixtures were analyzed in a Rancimat at 110 °C and the rate constants (k) were determined for each assay considering the first order reaction. With the application of the simplex-centroid experimental design, special cubic models were obtained for the induction period and rate constant. The jabuticaba peels, gabirola leaves and hibiscus flowers extracts increased the biodiesel induction period and decrease the rate constant compared to the control sample, showing that they can act as an antioxidant additive to delay the biodiesel oxidation reaction. The simplex-centroid designs proved to be an adequate tool to evaluate the inhibition of the oxidative process and the efficiency of natural extracts, with antioxidant properties, added to biodiesel obtained from a mixture of soybean and palm oil. The mathematical models obtained showed determination coefficients greater than 94% and non-significant lack of fit at the 5% level, indicating that they can be used for predictive purposes. The proportions optimization of the natural extracts, considering the maximization of the induction period and minimization of the rate constant, showed that a mixture containing 0.2868% of jabuticaba peels, 0.6227% of gabirola leaves and 0.0905% of hibiscus flowers results in an induction period of 10.43 h and 0.2365 h⁻¹. The gabirola leaves extract and its mixture with the jabuticaba peels extract provided the highest increase in the induction period and the lowest rate constant. The use of inedible products, such as peels, leaves and flowers, with antioxidant properties in the industrial biofuel's production, in addition to meeting the recommendation and legislation of many countries, has proved to be a good alternative to synthetic substances to delay the reaction of biodiesel oxidation.

Agradecimentos/Acknowledgments

To UEL, CNPq, CAPES and Araucaria Foundation.

Construction of an Arduino-based calorimeter for undergraduate-level experiments

Renato P. Gomes (IC),^{1*} Regina M. Takeuchi (PQ),¹ André L. Santos (PQ),¹

renato.gomes@ufu.br

¹Instituto de Ciências Exatas e Naturais do Pontal, UFU.

Keywords: Enthalpy of neutralization, Waste minimization, Calorimetry.

Highlights

A simple calorimeter built with Arduino UNO and DS18B20 sensor. Enthalpy of neutralization was determined with 1 mL of each solution. A promising way to combine technology and didactic experiments.

Resumo/Abstract

Calorimetry is an important topic discussed in general chemistry courses which not only provides initial insights about the interconnections between chemical reactions and energy but also introduces important thermodynamics concepts such as enthalpy. The simple “coffee-cup” calorimeter is the classical device used to estimate the enthalpy of chemical reactions mainly for neutralization reactions. The combination of this simple calorimeter and technological tools such as miniaturized temperature sensors and microcontrollers is a promising approach to improve the accuracy of heat transfer measures, minimize the consumption and waste of chemicals, and make the calorimetric experiment more attractive. Therefore, in this study, we have used an Arduino UNO as the main hardware coupled to a DS18B20 temperature sensor to build an accurate and eco-friendly calorimeter (Fig. 1) Different types of recipients with different volumes of solutions (Table 1) were used as the reaction vessel to study the neutralization of NaOH by HCl. The acidic and alkaline solutions were prepared at a nominal concentration of 1.0 mol L⁻¹ and further standardized by volumetry of neutralization. The concentration of NaOH was kept slightly lower than HCl so that NaOH was the limiting reagent in the neutralization reaction.

Fig1. Calorimeter with the glass vial

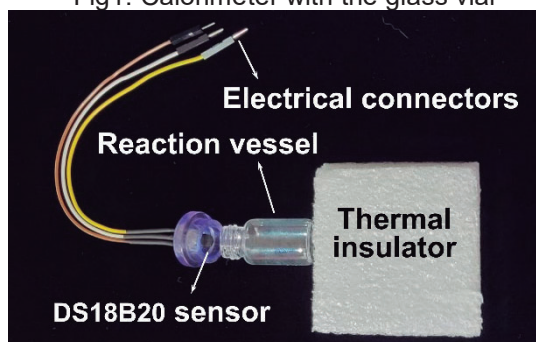


Table 1 – Enthalpies of neutralization for HCl and NaOH solutions, both 1 mol L⁻¹.

Reaction vessel	Volume / mL	Temperature sensor	$-\Delta H_{\text{neut.}} / \text{kJ mol}^{-1}$ *	R % [#]
Aluminum can	25	pH-meter	56 ± 4	+11
		Arduino	62 ± 4	+1.6
Eppendorf tube	1	Arduino	64 ± 9	+14
Glass-vial		Arduino	57.9 ± 0.6	+3.6

*Average value ± standard deviation (n = 3). [#]R% = relative error versus the theoretical value -55,9 kJ mol⁻¹ [1]

We have observed that the results obtained with the Arduino-based calorimeter were statistically equivalent to those from a pH-meter temperature sensor (at a 95 % confidence level). The best results were achieved using a glass vial as the reaction vessel and 1 mL of each solution. At this low volume, the NaOH and HCl solutions could be added to the reaction vessel with a micropipette and no solution stirring was necessary since the turbulence generated by the addition of the HCl solution to the NaOH provided efficient solution mixing. This remarkably simplifies the calorimeter assembly and temperature reading. Therefore, it can be concluded that the Arduino-based calorimeter developed in this study combines satisfactory accuracy and simplicity. Also, it is environmentally friendly since enables calorimetric measurements in solution volumes as low as 2 mL. Finally, the approach described here could be a promising ally to provide a first contact between undergraduate students and technological tools.

Agradecimentos/Acknowledgments

FAPEMIG (APQ-01316-22)

[1] RUSSEL, J.B. *Química Geral*, 2ª Ed, 1994. Makron Books: Rio de Janeiro. V. 1. Cap. 12. P. 564.

Evaluation of the impact of fuel mixtures containing charcoal on injector nozzles of a diesel engine

Ana Luíza Freitas Ferreira (PQ),^{1*} Andrey Teixeira Portela (PQ),¹ Egídio Teixeira de Almeida Guerreiro (PQ),¹ Pedro Bacillon Ventin Muniz (PQ),¹ Julio César Câmara Chaves (PQ),¹ Lilian Lefol Nani Guarieiro (PQ)¹, Maurício Lerina Bonifatti (PQ),¹ Thomaz Barros de Carvalho Prado (PQ).¹

lilian.guarieiro@fieb.org.br; ana.freitas@fbter.org.br;

¹SENAI CIMATEC

Keywords: bunker, HVO, MGO, charcoal, injector nozzles, deposits, diesel engine.

Highlights

- Fuels containing charcoal combust in diesel engines;
- The increase in the concentration of charcoal in fuel mixtures generates its deposition in the nozzle orifice.

Resumo/Abstract

The search for alternative marine biofuels to the use of bunkers led to the development of two fuel concepts based on charcoal. Fuel Blends 1 (Bunker, MGO – marine diesel, and coal) with 1, 5, 10, 15 and 20% coal, and Fuel Blends 2 (HVO and coal) with 1, 5, 12, 18 and 30% of coal. This work aimed to analyze the combustion capacity of these fuels and evaluate the impacts of their different compositions on the injector nozzle. For this, the fuels were submitted to a test of 15 min of operation in a single-cylinder diesel engine (White BDA 18.0TE). In the intervals between the tests, the engine was maintained and the injector nozzles were replaced.

All tested fuel Blends combusted. The tests with higher percentages of coal (Blend 1 – 20% and Blends 2 – 18% and 30%) were interrupted between 3 and 5 min of operation, due to the deposition of materials in the nozzle orifices, which made it difficult to inject fuel into the combustion chamber [1].

Fig. 1 shows that fuels with bunker (Blends 1) resulted in a greater formation of deposits in the injector nozzles. The nozzles used in the tests with pure HVO and HVO with 1% of charcoal, and HVO with 5% and 12% of charcoal, the deposition of solid particles was observed (Fig. 2 – H, I, J). While in the test nozzles with HVO with 18% and 30% of charcoal there was also a slight deformation in the contour of the nozzle orifice (Fig. 2 – L and M).

Due to the high fuel deposition on the outer surface, there was no clear visualization of the test hole at 30% (Fig. 2 – L and M). In tests with Fuel Blends 1, bunker accumulation in the holes was observed. Tests of this concept with 1% and 5% charcoal showed a high deposition rate (Fig. 2 – C, D), making it difficult to visualize the hole. In the test with 10% it is possible to observe the beginning of deformation of the contour of the orifice (Fig. 2 – E). Behavior that intensifies in the tests with 15% and 20% of charcoal (Fig. 2 – F and G). In the case of the test with 20% charcoal, there was also obstruction of the orifice (Fig. 2 – G). Videoscopy of the engine was also carried out, which showed the

deposition of fuel on the cylinder walls and on the piston after the tests with the bunker.

Fig. 1 - Images of the injectors used in the tests.

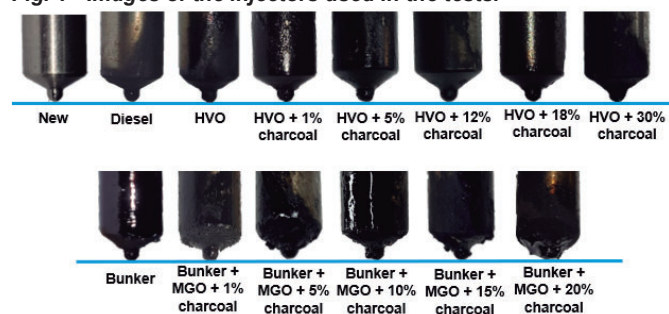
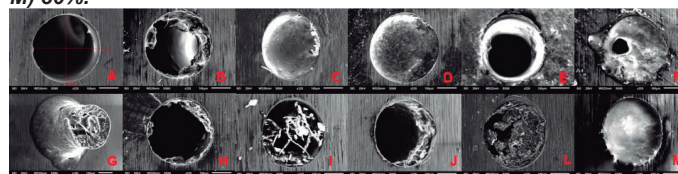


Fig. 1 – MEV of the nozzle orifices. A) New; B) Bunker; Concept 1 (Bunker, MGO and charcoal): C) 1%, D) 5%, E) 10%, F) 15%, G) 20%; Concept 2 (HVO and charcoal): H) 1%, I) 5%, J) 12%, L) 18%, M) 30%.



Fuel Blends 1 fuels were more aggressive to the injector nozzles and internal engine components, a fact associated with their high viscosity related to the presence of bunker oil [2]. Fuel blends with lower percentages of charcoal allowed operation for a longer period due to the non-clogging of the nozzle holes.

[1] ACHEBE, C. H. et al. Analysis of diesel engine injector nozzle spray characteristics fueled with residual fuel oil. *Heliyon*, v. 6, n. 8, p. e04637, 2020.

[2] PETROBRÁS. Combustíveis marítimos – Informações técnicas. 2021. Disponível em: <https://petrobras.com.br/data/files/02/83/FA/2C/5A39C710E2EF93B7B8E99EA8/Manual_Combustiveis_Maritimicos_2021.pdf>. Acesso em: 30 jan. 2023.

Agradecimentos/Acknowledgments

Ao CNPq, EMBRAPPII e TECNORED.

Hybrid Systems Used for Behavior Detection in a Plug Flow Reactor (PFR)

William Tonello S. Borges (IC)*, Fabio R. Chavarette (PQ).

william.tonello@unesp.br; fabio.chavarette@unesp.br

Instituto de Química, UNESP Araraquara

Palavras Chave: *Sistemas Híbridos, Algoritmos Inteligentes, Indústria 4.0, Reatores*

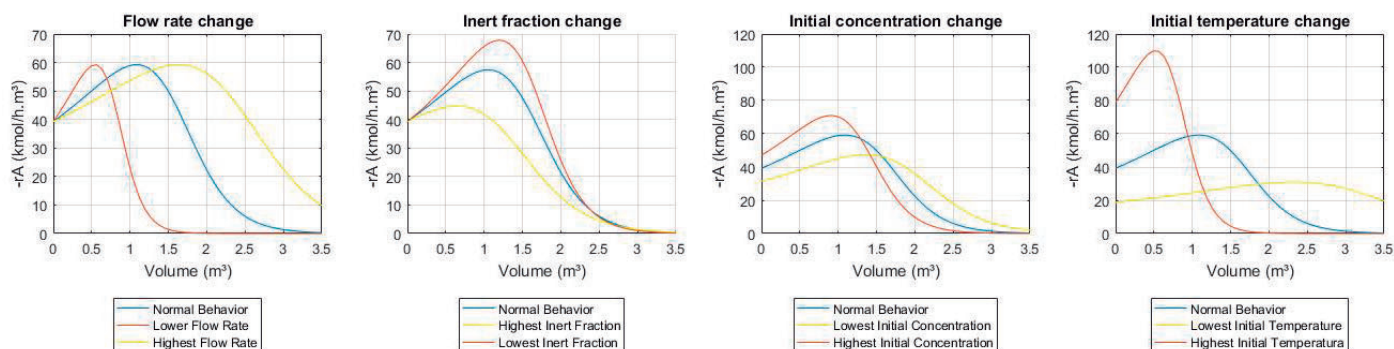
Highlights

The PFR model showed the expected physical-chemical and kinetic behavior.

The immuno-wavelet hybrid system was able to detect changes in reactor behavior with high efficiency.

Resumo/Abstract

The use of modeling and intelligent computing are some of the various techniques and approaches that industry 4.0 has been using to generate higher quality products and services. In the chemical industry, modeling is of great importance because its use does not interfere with the operating system. This work proposes a hybrid immuno-wavelet system for monitoring behaviors in a PFR reactor model. The reactor is modeled using ordinary differential equations obtained using the laws of conservation of mass and energy and molar, mass and energy balance. Then these equations were applied to an interactive software and the fourth order RungeKutta method is used for resolution. For the model was used a case study of a reversible isomerization reaction of n-butane into isobutane. The hybrid system is composed of a negative selection algorithm with a wavelet transform to enhance the dynamic properties of the signal. Below is a visualization of the change in behavior in extreme cases of highest and lower change in parameters:



The table below shows the success rate of the algorithm in detecting changes in behavior in each case:

	Normal signals	Fault signals	Normal signals detect	Fault signals detect	Success rate (%)
Flow rate change	164	147	164	147	100
Inert fraction change	101	25	101	25	100
Initial concentration change	96	140	96	139	100
Initial temperature change	111	54	111	54	100

The immuno-wavelet hybrid system proved to be extremely efficient in identifying changes in the behavior of the reactor, reaching 100% accuracy in all cases analyzed.

Agradecimentos/Acknowledgments

The author thanks the advisor and the SISPLEXOS laboratory for the academic support. The author also thanks FAPESP for financial support to the Project (Proc. FAPESP No. 2022/06342-0).

Permeability modification of ceramic membranes for aromatics recovery system and photocatalytic reactor applications.

Marcelo H. Armoa* (PQ)¹; **Miguel Jafelicci Jr.**²

marcelo.armoa@fatec.sp.gov.br

¹Faculdade de Tecnologia Nilo De Stéfani de Jaboticabal.

²Instituto de Química de Araraquara – UNESP.

Palavras Chave: *Ceramic membranes, Silica, Polydimethylsiloxane, Anatase, Membrane Aromatic Recovery System, Photocatalytic Membrane Reactor.*

Highlights

Ceramic membranes for Membrane Aromatic Recovery Systems (MARS) and Photocatalytic Membrane Reactor (PMR). Membrane surface properties of the modification with polydimethylsiloxane and titanium dioxide (Anatase).

Resumo/Abstract

Ceramic membranes have a wide range of industrial and environmental applications, showing superiority over polymeric membranes in terms of thermal, mechanical and chemical inertia. Among the various technologies that use membranes for environmental purposes, we can mention the membrane aromatic recovery system (MARS) and the photocatalytic membrane reactor (PMR). MARS uses highly hydrophobic membranes to remove undesirable organic compounds in an aqueous medium. PMR uses photocatalysts, usually TiO₂, supported in various ways to provide photocatalytic activity to the membrane. However, for both technologies we found several works that use polymeric membranes as substrate and almost total absence of works with ceramic membranes. This work presents the differences in behavior in terms of water permeability of SiO₂ membranes modified with polydimethylsiloxane (PDMS – 5000 cS) and TiO₂ (anatase), characterized in a tangential filtration pilot. SiO₂ macroporous membranes (SIL-HT) were obtained by hydrothermal treatment of borosilicate glasses. Chemical modification of the silica surface was carried out with PDMS – 5000 cS, by acid catalysis, obtaining hydrophobic inorganic membranes (SIL-HT-HFB). It has also been deposited by capillarity TiO₂ (anatase) on the inner longitudinal surface of SiO₂ membranes (SIL-HT-Ti) to provide photocatalytic activity. Furthermore, the TiO₂-coated membranes were subjected to UV radiation during the permeation tests. It was obtained for the variants of the membrane, the variation of the transmembrane flux (J) in relation to the pressure and the coefficient of permeability (Q_w), showing the evident difference in the physical-chemical behavior of the same ones. It is verified for the unmodified SiO₂ membrane Q_w=12038 L h⁻¹ m⁻², compared to the hydrophobized membrane, with Q_w=3187 L h⁻¹ m⁻². For the TiO₂ membrane, the phenomenon of photoinduced hydrophilicity was verified, when activated by a source of UV radiation, with a reversible and expressive increase in membrane permeability, attributed to the dissociative adsorption of water molecules. SiO₂ membranes modified by PDMS show prospects for application in aromatic recovery membrane systems (MARS). Membranes modified with TiO₂ show application in photocatalytic membrane reactors (PMR) and also as chemical valves.

Long-Fei, R.; Mister, A.; Jun, L.; Cong, X.; Zheng, X.; Xiaofan, Z.; Jiahui, S.; Yiliang, H. Phenol separation from phenol-laden saline wastewater by membrane aromatic recovery system-like membrane contactor using superhydrophobic/organophilic electrospun PDMS/PMMA membrane, **Water Research** 135 (2018) 31- 43

Inamuddin, Boddula, R. Asiri, A. M. Self-standing Substrates Materials and Applications, Engineering Materials, p. 119-145, Springer Nature Switzerland 2020.

Zakria, H. S.; Othman, M. H. D.; Kamaludin, R.; Kadir, S. H. S. A.; Kurniawan, T. A.; Jilani, A. Immobilization techniques of a photocatalyst into and onto a polymer membrane for photocatalytic activity. **RSC Adv.**, 2021, 11, 6985.

Ainali, N.M.; Kalaronis, D.; Evgenidou, E.; Bikiaris, D.N.; Lambropoulou, D.A. Insights into Biodegradable Polymer-Supported Titanium Dioxide Photocatalysts for Environmental Remediation. **Macromol** 2021, 1, 201–233. <https://doi.org/10.3390/macromol1030015>

Agradecimentos/Acknowledgments

À CAPES

Ao IQ/UNESP – Araraquara

Ao CEETEPS

Plano de Ação SBQ para impactar a sustentabilidade no Brasil: OQDS 2 - promovendo interação entre indústrias e universidades

Maryna M. Barros (PG)¹, Ingrid F. Silva (PQ)², Izadora R. S. Menezes (PG)¹, Larissa L. Maia (PG)³, Carolina Maria M. de C. Andrade¹, Shirley Nakagaki (PQ)⁴, Rochel M. Lago (PQ)¹, Ana Paula de C. Teixeira (PQ)^{1*}.

maryna.moreira@hotmail.com; anapct@ufmg.br

¹Departamento de Química, ICEx, UFMG; ²Department of Colloid Chemistry, MPIKG; ³Instituto de Ciências Exatas e Tecnológicas, UFV; ⁴Departamento de Química, UFPR

Palavras-Chave: Sustentabilidade, Plano de ação, Interação Indústria-Universidade, Brasil.

Highlights

SBQ Action Plan to impact sustainability in Brazil: OQDS 2 - promoting interaction between industries and universities

- Objetivos da Química para o Desenvolvimento Sustentável
- OQDS 2: Promover a sustentabilidade através de CTI&E em química na indústria e na universidade

Resumo/Abstract

A SBQ está elaborando, desde meados de 2021, o Plano de Ação “Química e Seus Atores para um Brasil Sustentável e Soberano”, o qual tem o intuito de impactar a sustentabilidade e soberania no país por meio da Química.¹ Este Plano é formado por dois Objetivos de Química para o Desenvolvimento Sustentável (OQDS), seis eixos de ação e cinco desafios direcionadores (Fig. 1)² e, a partir deles, estão sendo realizadas ações e projetos. Assim, este trabalho tem como objetivo apresentar os diferentes projetos e ações que estão sendo desenvolvidos dentro do OQDS 2 em 2023.

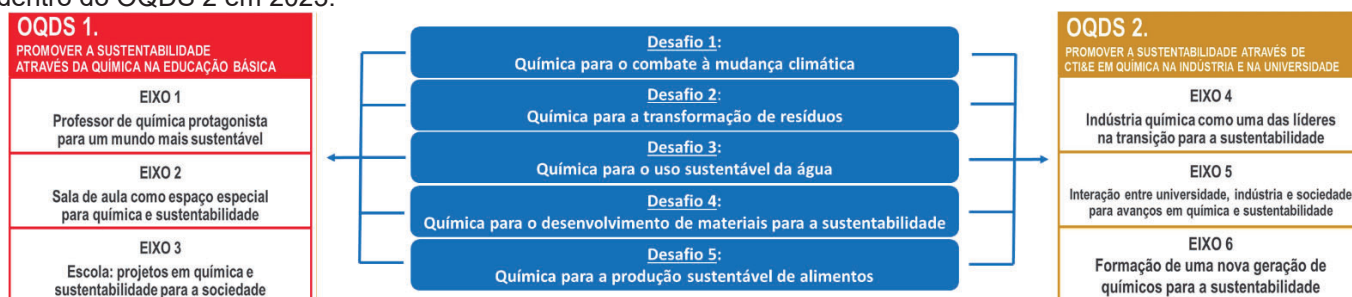


Figura 1 –OQDS, eixos de ação e desafios direcionadores do Plano de Ação SBQ

O OQDS 2 foi estruturado para promover sustentabilidade em indústrias e universidades por meio de Ciência, Tecnologia, Inovação e Educação (CTI&E) em química. Para isso, atualmente três projetos/ações estão em execução:

- Mapeamento de tecnologias maduras relacionadas aos 5 desafios em sustentabilidade em Universidades por meio do programa Escalase Summit, desenvolvido em parceria com a FAPEMIG, empresas parceiras e o Escalab, um Centro de escalonamento de tecnologias e modelagem de negócios do INCT MIDAS- UFMG. Neste programa, as tecnologias selecionadas passarão pelos processos de aceleração e escalonamento e as finalistas receberão um aporte de até R\$ 100.000,00.

- Criação de um programa de levantamento de demandas das indústrias na área dos cinco desafios e indução de P&D nas Universidades. A partir dele, pretende-se articular mecanismos de financiamento desses projetos com indústrias e governo.

- Criação de uma série de webinários com temas dentro dos 5 desafios para promover conexão entre indústrias e universidades, resultando em um evento final presencial.

Algumas dessas iniciativas já estão ou serão executadas na forma de projetos pilotos em 2023 em alguns polos específicos do Brasil, para que então em 2024 seja possível a sua replicação e expansão para as cinco regiões do país. Além disso, a partir de 2024 tem-se como objetivo incorporar aos projetos outras áreas das ciências.

Referências:

- 1- SBQ. Movimento química pós 2022. Disponível em: <http://www.s bq.org.br/mqp2022/>
- 2- Silva, I. F.; et al. Movimento Química pós 2022: construção de um Plano de Ação para que a química e seus atores impactem a sustentabilidade e soberania no Brasil. Química Nova, Vol. 45, No. 4, 497-505, 2022

Agradecimentos/Acknowledgments

Capes, CNPq, FAPEMIG, INCT Midas, SBQ, Abiquim, CFQ, Escalab e aos participantes do Grupo de Inteligência.

Re-refining of aeroturbine industrial lubricating oils: reaction routes and prospects for a sustainable environmental

¹Simone O. Ribeiro (TM),²Lucas G. L. L da Silva (IC),³ Arthur F. S. Lima (TC),⁴ Ana C. M. da Silva (PQ),⁵ Leocádia T. C. Beltrame (PQ),⁶ Michelle S. G. Dantas (PQ).

Simoneoliveira0704@gmail.com; lucasgabrielrn2@gmail.com; arthur.felipe@ifrn.edu.br;
acristinasilva@ufba.br; leocadia.beltrame@ufrpe.br; michelle.dantas@ifrn.edu.br

^{1,3,6} Diretoria Acadêmica de Indústria (DIACIN/ CNAT) - IFRN; ² Diretoria Acadêmica de Recursos Naturais (DIAREN/ CNAT) - IFRN;
⁴ Engenharia de Minas – UFBA; ⁵ Engenharia Ambiental – UFRPE,

Key words: Re-refinig; Lubrificants; Aeroturbines; Enviroment.

Highlights

Lubricants are of great importance for the functioning of the mechanical elements presente in the wind tower. Wind energy has been gaining notoriely for the generation of clean energy. Re-refinig is an economic alternative for reuse the lubricants.

Abstract

Lubricants are of the great importance for the functioning of the mechanical elements present in the wind tower, as they guarantee maximum reliability in operation and increase the useful life of equipment parts. In this sense, wind energy has been gaining notoriety for the generation of clean energy, but it is important to highlight that lubricating base oils, after fulfilling their role, lose their optimal properties and are contaminated with various toxic compounds, becoming a hazardous waste that can cause immeasurable environmental damage. This study aims to evaluate the recovery process of oils obtained from aeroturbines of an offshore wind farm, located on the white coast of Rio Grande do Norte, through chemical treatments for reuse of these oils. The material was subjected to solvent extraction [isopropanol (IPPOL) and ethanol (EtOH)], followed by centrifugation at 3000rpm/ 20 minutes, which showed clear separation and clarification in both samples, and was characterized physicochemically along with lubricant samples new and used. The results allowed concluding that tests with IPPOL resulted in a higher extraction yield (85%) compared to EtOH (57%). IR tests made is possible to monitor oxidation products, additives and some impurities in the samples, as well as flash point tests. Considering that the wind farm in the state has been growing by an average of 50% each year, the need to implement actions of this nature is notorious, integrating companies and the population on the negative impacts that this waste generates on the environment and human health.

Acknowledgments

UFRN for IV analysis

Costa Branca Wind farm in RN for the samples provided

Storage time estimation of biodiesel in mixture with jabuticaba peel extract

Eduardo G. de Sousa (IC),¹ **Heloisa H.P. Silva** (IC),¹ **Nathan F. Silva** (IC),¹ **Júlia W. Campos** (IC),¹ **Marco A.J. Clemente** (PG),¹ **Dionisio Borsato** (PQ).¹

Sousa.eduardo047@uel.br; dborsato@uel.br

¹Departamento de Química, UEL

Keywords: Oxidative stability, Kinetic parameters, Natural antioxidant.

Highlights

The biodiesel oxidation reaction was studied. The Jabuticaba peels extract was evaluated as a natural antioxidant. The extract inhibited the biodiesel oxidation reaction and increasing storage time.

Abstract

Biofuels are considered renewable energy sources, making it possible to reduce the use of fossil fuels and the emissions of gasses derived from sulfur oxides. It is one of the alternatives to petroleum-derived diesel due to its similar physicochemical properties¹. According to the type of raw material used, biodiesel may present a greater number of unsaturated esters such as oleate, linoleate, and methyl linolenate, which is favor the oxidation reaction, reducing its oxidative stability². Natural extracts with antioxidant properties, even at low concentrations, act to prevent the oxidation reaction of biodiesel through the inactivation of free radicals³. This research evaluated the antioxidant potential of jabuticaba peels extract in the oxidative stability, the kinetic oxidation reaction, and the biodiesel storage period at 25 °C in the absence of light. The oxidative stability of the biodiesel samples, with and without the extract of jabuticaba peels, were analyzed in Rancimat model 743 equipment (Metrohm®), at temperatures of 110, 115, 120 and 125 °C according to the EN14112 standard⁴. The values of the induction periods can be found in table 1. As expected, for all samples, the induction period decreased with increasing temperature, and biodiesel sample containing the jabuticaba peel extract presented, at a temperature of 110 °C, induction period of 14.31 h, value above that found in the control sample, 8.54 h, and above the minimum required by Brazilian legislation, which is 12 h. Considering the first order reaction, the rate and energy constants of activation of the oxidation reaction in the presence and absence of extract were determined. The addition of the extract decreased the rate constants at all test temperatures and the activation energy of the control sample was lower than that verified with the addition of the extract. To evaluate the storage time of biodiesel, in the presence and absence of the natural extract, oxidative stability data, at temperatures of 110, 115, 120, 125 °C were converted to the natural logarithm and the graphs obtained, as a function of temperatures, were adjusted linearly and extrapolated to the temperature of 25 °C. The biodiesel sample containing only extract of jabuticaba peels presented an estimated 10218 days at 25 °C, being approximately 15 times higher than the value found by the control at 673 days. This shows that the antioxidant properties of jabuticaba peels have acted in reducing the oxidative process of biodiesel by increasing its storage time. The use of natural antioxidant proved to be effective in delaying the oxidation reaction of biodiesel, proven by the higher values of induction period of these samples when compared to the control. Data extrapolation is a useful technique for estimating the oxidative stability of biodiesel under more realistic storage conditions.

Table 1. Induction period values of assays conducted at 110, 115, 120, and 125 °C.

Sample	Induction period (h)			
	110°C	115°C	120°C	125°C
Control	8.54	6.24	3.64	2.54
Biodiesel + jabuticaba peel	14.31	9.39	4.09	2.97

Source: Author

¹HOANG, A. T., et al. **Renewable and Sustainable Energy Reviews**, v. 135, p. 110204, 2021.

²CORREIA, I. A. S., et al. **Renewable Energy**, v. 160, p. 288-296, 2020.

³ROMOLA, C. J., et al. **Renewable and Sustainable Energy Reviews**, v. 145, p. 111109, 2021.

⁴EN 14112. European Committee for Standardization: 2020.

Agradecimentos/Acknowledgments

To UEL, CNPq, CAPES and Araucaria Foundation.

TEO

Química Teórica

46^a Reunião
Anual da **SBQ**

28 a 31 de Maio de 2023

Águas de Lindóia · SP
Hotel Monte Real

Área:

TEO

(Inserir a sigla da seção científica para qual o resumo será submetido. Ex: ORG, BEA, CAT)

A DFT Investigation of CH₄ Activation and Dehydrogenation on Ceria Clusters

Carina S. T. Peraca (PG)¹, Karla F. Andriani (PQ)¹, Mauricio J. Piotrowski (PQ)², Juarez L. F. Da Silva (PQ)¹

carinaperaca@usp.br, juarez_dasilva@iqsc.usp.br.

¹São Carlos Institute of Chemistry, University of São Paulo, PO Box 780, 13560-970, São Carlos, SP, Brazil; Department of Physics, Federal University of Pelotas, PO Box 354, 96010-900, Pelotas, RS, Brazil.

Key words: Methane conversion, DFT, UBI-QEP, CeO₂ cluster.

Highlights

Methane has a high propensity to be converted into syngas and other important compounds for the production of energy inputs.

Resumo/Abstract

Methane is a greenhouse gas that has a high potential to trap radiation in the atmosphere. It also a major constituent of natural gas and offers the possibility of being converted into other chemicals, making it a valuable resource for the production of energy during the transition from non-renewable to renewable sources. Due to the high stability of this molecule, one of the great problems of this process relates to the CH₄ activation, which allows the first C-H bond break. In recent decades, finding catalytic materials that can transform methane into high-value chemicals like CH₃OH and H₂ has been suggested as a potential solution. In this sense Ceria based materials can be a great catalyst candidate since the interaction between the H atom from molecule and O⁻ centered from the cerium oxide can lead to the activation of methane and the subsequent dehydrogenation. Then, in this work we report a computational investigation about the CH₄ activation and dehydrogenation considering (CeO₂)₁₀ cluster as a catalyst. Our calculations are based on Density Functional Theory (DFT), employing the Perdew-Burke-Ernzerhof (PBE) formalism, combined with the Unity Bond Index-Quadratic Exponential Potential approach (UBI-QEP). To improved the correct description of the coulomb interaction for localized *f*-states from Ce atoms and the long-range interactions, we employed the Hubbard term (U) and the van der Waals corrections (D3), respectively. Our results showed that the adsorption of this species generates a polaron leading the presence of Ce³⁺ and a consequent geometric distortions which affects the reactivity of the material. In this sense, the H co-adsorption site can influence the energetic barrier value of the first C-H bond break that varies from 0.54 eV to 0.81 eV and are considered a destabilizing factor, once compete for the same adsorption site of the molecule. As the dehydrogenation becomes, a strong tendency towards complete dehydrogenation was observed leading to the formation of other compounds, e.g. CH₃OH and syngas, two essential chemicals for the generation of energy inputs.

1 – Peraça, C. S. T.; Andriani K. F.; Piotrowski, J. M.; Da Silva, J. L. F. *J. Phys. Chem C*, **2022**, *126*, 11937–11948.

2 - Da Silva, J. L. F.; Ganduglia-Pirovano, M. V.; Sauer, J.; Bayer, V.; Kresse, G. *Phys. Rev. B*, **2007**, *75*, 045121.

3 - Zibbordi-Besse, L.; Seminovski, Y.; Rosalino, I.; Guedes-Sobrinho, D.; Da Silva, J. L. F. *J. Phys. Chem C*, **2018**, *122*, 27702-27712.

Agradecimentos/Acknowledgments

The authors gratefully acknowledge the support from FAPESP (São Paulo Research Foundation, Grant Numbers 2017/11631-2, 2018/21401-7, 2018/11152-0, 2019/05561-7, and 2021/03357-3), Shell and the strategic importance of the support given by ANP (Brazil's National Oil, Natural Gas and Biofuels Agency) through the R&D levy regulation.

A joint experimental and theoretical investigation on the $\text{La}_2(\text{WO}_4)_3$ nanoparticles: Synthesis and characterization

Amanda F. Gouveia (PQ),^{1*} Eliezer C. Silva (PQ),² Içamira C. Nogueira (PQ),² Edson R. Leite (PQ),^{3,4} Elson Longo (PQ),³ Juan Andrés (PQ).^{1,3,4}

gouveiad@uji.es

¹Departament of Physical and Analytical Chemistry, UJI, Spain; ²Federal University of Amazonas, UFAM, Brazil; ³CDMF, UFSCar, Brazil; ⁴Brazilian Nanotechnology National Laboratory, CNPEM, Brazil;

Keywords: $\text{La}_2(\text{WO}_4)_3$, Synthesis and Characterization, First-principles calculations, Structure, Electronic and Optical properties.

Highlights

Experimental and theoretical investigation on the $\text{La}_2(\text{WO}_4)_3$ based-materials. Structure and electronic properties of the $\text{La}_2(\text{WO}_4)_3$ have been elucidated.

Abstract

Complex metal tungstates are important materials with tailorable optical and electronic properties with a wide range of applications such as luminescence, photocatalysis, and scintillators. Among them, lanthanum tungstate, $\text{La}_2(\text{WO}_4)_3$, exhibits outstanding physical and chemical stabilities owing to their compact crystal structure. Here, $\text{La}_2(\text{WO}_4)_3$ nanoparticles were synthesized via the direct chemical precipitation method and further heat treatment at 550 and 600 °C by 2h. The crystal structures were characterized by XRD with Rietveld refinement, Raman, and FE-SEM spectroscopy techniques.

Density functional theory calculations at the B3LYP level were performed to study the structure and electronic properties of the $\text{La}_2(\text{WO}_4)_3$ structure. The lattice parameters (a , b , c , α , β , γ) were optimized and the electronic properties and Infrared and Raman frequencies were computed. A detailed comparison between experimental and theoretical results were performed.

Acknowledgments

We acknowledge *Fundação de Amparo à Pesquisa do Estado de São Paulo* (FAPESP), grant number 2013/07296 and 2022/08048-1. A.F.G. acknowledges the Generalitat Valenciana (Conselleria de Innovación, Universidades, Ciencia y Sociedad Digital) for the postdoctoral contract (CIAPOS/2021/106). J.A. acknowledges Universitat Jaume I (project UJI-B2019-30), and Generalitat Valenciana (Conselleria de Innovación, Universidades, Ciencia y Sociedad Digital – project CIAICO/2021/122) for financially supporting this research.

Akamptisomeric porphyrins as molecular photo-switches: computational evaluation of chromophore groups as substituents

Natalia M. Raffaelli (IC),¹ Karine N. de Andrade (PG),¹ Fernando M. dos Santos Junior (PG),¹ Rodolfo G. Fiorot (PQ)¹

nataliamarques@id.uff.br

¹Programa de Pós Graduação em Química, Universidade Federal Fluminense, Niterói, RJ, Brasil

Keywords: Bond angle inversion, DFT, Isomerism, Molecular machine, TD-DFT

Highlights

We computationally explored the akamptisomerism through the bond angle inversion in chromophore-substituted porphyrins (naphthoquinone and BODIPY), seeking to design molecular photoswitches.

Resumo/Abstract

Molecular photoswitches are substances that are transformed into stable states with distinct properties in the presence of light.[1] A new fundamental type of isomerism (akamptisomerism) based on the bond angle inversion (BAI) of a strained bridge anchored in porphyrin macrocycles, such as (F)B–O–B(F), was discovered.[2] To have isolatable isomers, the BAI barrier must be higher than 22 kcal mol⁻¹. In this process, the planarity of the conjugated bonds is affected (**Figure 1a**), influencing their electronic properties, thus allowing the design of photoswitches. Herein, we evaluate how structural modifications affect the process of akamptisomerisation and their optical properties. The BAI of -(N)₂FB–O–BF(N)₂- with the fluorides in *transoid* configuration (conversion *t*₁ → *t*₂) was explored by means of DFT (B3LYP-D3/6-31+G(d,p)) and TD-DFT (CAM-B3LYP/6-31+G(d,p)) calculations. The substituent effect was evaluated by inserting boron dipyrromethene (BODIPY) in the *meso* position of the porphyrin using three different π spacers: none **1**, benzene **2**, and ethyne **3**. The addition of β,β-dinaphthoquinones was also explored **4** (**Figure 1b**).

Each system demonstrated to yield isolatable akamptisomers, with energy barriers higher than 25 kcal mol⁻¹. The smaller the torsion between the BODIPY-porphyrin, the greater the electronic delocalization between the macrocycles. [3] This becomes evident in the average shift of the bands (**Figure 1c**) to regions of longer wavelength (red shift) for the different π spacers: Δλ=37 nm for **2** (biggest torsion), and 61 nm for **3** (minor torsion), in comparison with the unsubstituted porphyrin (**Po**). The simulated mean red shift of the β,β-dinaphthoquinone was 79 nm. Regarding the difference in the absorption between akamptisomers *t*₁/*t*₂, we noticed a maximum displacement of λ(*t*₁/*t*₂)=15 nm and 4 nm for the system with naphthoquinone and meso-ethyne-BODIPY, respectively. Thus, the insertion of the two naphthoquinones in the β,β-pyrrole positions promotes a more significant separation in the absorption of the akamptisomeric isomers. Although this value is not sufficient to work as photoswitches, the phenomenon of BAI allows obtaining isolatable species with different photochemical properties. New structural modifications will be carried out seeking to increase the difference between the absorption profiles of the akamptisomer pairs.

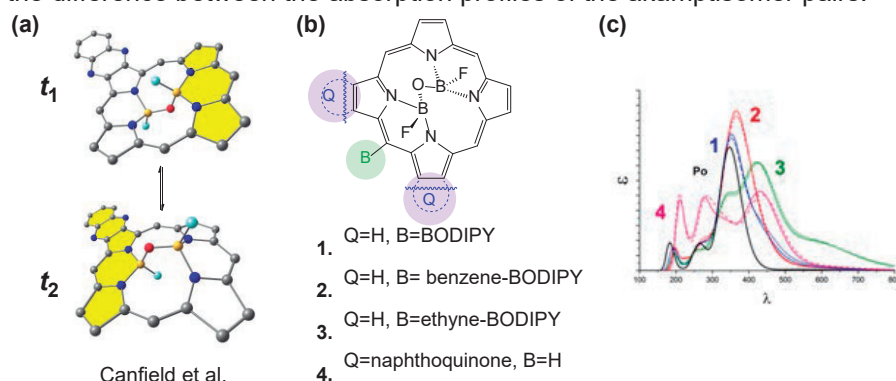


Figure 1. a) Process of BAI *t*₁→*t*₂ b) General porphyrins structure evaluated, and c) theoretical UV/Vis spectra for all the systems.

References

[1] WANG, G.; ZHANG, J. Journal of Photochemistry and Photobiology. C: Photochemistry Reviews. 2012 v. 43, n. 4, p. 299-309; [2] CANFIELD, P. J et al. Nature Chemistry. 2018 v. 10, p. 615-624; [3] NAMUANGRUK, S. et al. Dalton Trans. 2014, v. 43, p 9166–9176

Agradecimentos/Acknowledgments

Ao órgão de fomento FAPERJ e super computador NACAD (a22006).

46ª Reunião Anual da Sociedade Brasileira de Química: "Química: Ligando ciências e neutralizando desigualdades"

Antibody structure modeling and simulation for demyelinating disease study

Jéssica Cristiane Magalhães Ierich (PQ),^{1*} Doralina Guimarães Brum Souza (PQ),² Pamela Soto Garcia (PQ),^{3,4} Luiz Carlos Gomide Freitas (PQ),¹ Fabio de Lima Leite (PQ),⁵ André Farias de Moura (PQ)¹

jessica.ierich@gmail.com; jcmierich@alumni.usp.br

¹Department of Chemistry, Federal University of São Carlos (UFSCar); ²Department of Neurology, Psychology and Psychiatry, São Paulo State University (UNESP); ³Biomaterials Laboratory, Pontifical Catholic University of São Paulo (PUC-SP) Sorocaba-SP; ⁴Pure and Applied Biochemistry Laboratory, Lund University; ⁵Department of Physics, Chemistry and Mathematics, Federal University of São Carlos (UFSCar Sorocaba).

Palavras Chave: Myelin Basic Protein, Anti-Myelin Basic Protein, Multiple Sclerosis, Molecular Modeling, Molecular Docking, Molecular Dynamics.

Highlights

An autoantibody was modeled by *in silico* protocols. Complementarity-determining region of a well-known antibody was mutated. The designed model recognized a putative multiple sclerosis target.

Resumo/Abstract

Demyelinating diseases, such as multiple sclerosis (MS), present a critical and complex involvement of autoimmune processes. Targets of the immune system and their interaction with important immunological components, like self-reactive antibodies, are still unknown. Myelin Basic Protein (MBP) is a protein involved in the structural maintenance of the myelin layer on neurons, which highly increases the speed of electrical impulses. MBP is strongly highlighted as an MS immune target. Here, we described the structure of an antibody against MBP peptides combining Molecular Modeling, Docking, and Molecular Dynamics (MD). A well-known structure of an anti-myelin antibody (PDB code 1PKQ) was used as a template for the mutating protocol, described as follows: (1) identification of complementarity-determining region residues in the template antibody that anchors the antigen using abYsis¹ and PDBSum² servers; (2) target residues were replaced by randomly selected residues in the template structure using Swiss-PDB viewer³ and Visual Molecular Dynamics⁴ tools; (3) Twenty models were designed and ranked according to their affinity to MBP 85-99 peptide by AutoDock Vina⁵; (4) the top-ranked model based on affinity values to MBP were simulated by MD in a TIP3P water box for structure validation and MBP binding description. The modeled antibody and MBP peptide system in water was minimized using the steepest descent algorithm and a 1000 ns MD simulation system equilibration step, followed by the NPT ensemble (T=309.65 K and P=1 bar) simulation using CHARMM 36 force field⁶ within GROMACS 2021.1 package⁷. The designed antibody-MBP 85-99 complex showed to be stable in water, with a large contribution of the heavy chain of the antibody in the complex formation, as also described for similar antibody-antigen simulation^{8,9}. Residues ARG99, LYS93, ASN94, HIS90, PHE92, ASN86, and VAL96 of MBP peptide contributed more to the complex formation and maintenance, as also pointed out by experimental studies of MBP 85-99¹⁰.

References: **1.** Swindells, M. B. *et al. J. Mol. Biol.* 429, 356–364 (2016); **2.** Laskowski, R. A. *et al. Protein Sci.* 27, 129–134 (2018); **3.** Guex, N. *et al. Electrophoresis* 30 Suppl 1, S162-73 (2009); **4.** Humphrey, W. *et al. J. Mol. Graph.* 14, 33–38 (1996); **5.** Trott, O. & Olson, A. J. *J. Comput. Chem.* 31, 455–461 (2010); **6.** Huang, J. & MacKerell, A. D. *J. Comput. Chem.* 34, 2135–2145 (2013); **7.** Van Der Spoel, D. *et al. J. Comput. Chem.* 26, 1701–1718 (2005); **8.** Osajima, T. *et al. J. Mol. Graph. Model.* 53, 128–139 (2014); **9.** Osajima, T. & Hoshino, T. *Comput. Biol. Chem.* 64, 368–383 (2016). **10.** Wucherpfennig, K. W. *et al. J. Clin. Invest.* 100, 1114–1122 (1997).

Agradecimentos/Acknowledgments

São Paulo Research Foundation (FAPESP 2014/12082–4, 2014/21530-0, 2019/25972-1, 2022/05157-4, 2013/07296-2), Coordination for the Improvement of Higher Education Personnel (CAPES), and Brazilian National Council for Scientific and Technological Development (CNPq). We also acknowledge SDumont supercomputer (National Laboratory for Scientific Computing, LNCC/MCTI, Brazil) for computational resources.

Applying normal modes to understand complex systems: a case study.

Weverson Rodrigues Gomes (PQ)^{1*}, André Farias de Moura (PQ)¹.

gomeswr@gmail.com;

¹Departamento de Química, UFSCAR;

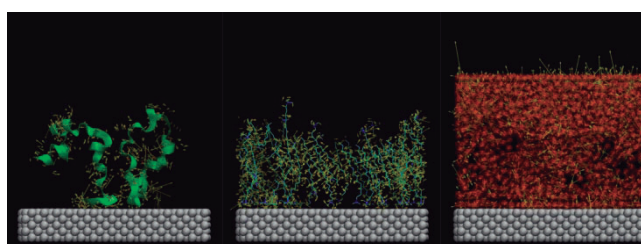
keywords: *Normal modes, Nanomaterials, gold, peptide, hIAPP.*

Highlights

The normal mode represents an important insight into complex systems. We analysed individual modes to understand the assembling of hIAPP into fibrils on gold surfaces covered with surfactant.

Abstract

Normal modes are ubiquitous in interacting systems, from molecular scale to astronomical object. The normal mode represents an important insight about those systems and describes the complex movement of a system in terms of collective coordinates taking into account many-body effects, showing the relationship between structure and dynamical behavior. In this work, we studied the effects of the gold surface and the surfactant on the assembling of hIAPP into fibrils. The model system consisted of a periodic planar gold slab with adsorbed CTAB and hIAPP (human islet amyloid polypeptides) using gromacs and ProDy programs, we had to handle over 37,000 individual normal modes. Although informative, we must recognize that high-frequency/low-amplitude modes from bond stretching and angle bending inside the molecules should be regarded as being unlike to contribute to the large scale reorganization of hIAPP monomers into fibers. This occurrence is expected to occur due to the intermolecular coupling between neighboring hIAPP molecules, possibly with the mediation of both the gold surface and the peptides (in the figure below). It is noteworthy that atoms lying closer to the gold surface have displacement vectors with components parallel to the planar surface larger than the projection in the perpendicular direction. Even though the gold surface is vibrationally decoupled from the adsorbed molecules, it still exerts an appreciable entropic interaction, arising from the excluded volume that breaks the symmetry and limits which degrees of freedom are accessible and which are not.



¹ M.J. Abraham, T. Murtola, R. Schulz, S. Páll, J.C. Smith, B. Hess, and E. Lindahl, "GROMACS: High performance molecular simulations through multi-level parallelism from laptops to supercomputers," *SoftwareX* (2015).

² Zhang S, Krieger JM, Zhang Y, Kaya C, Kaynak B, Mikulska-Ruminska K, Doruker P, Li H, Bahar I ProDy 2.0: Increased scale and scope after 10 years of protein dynamics modelling with Python 2021 *Bioinformatics*, btab187.

Acknowledgments

The authors acknowledge FINEP (01.22.181.00), CNPq, CAPES, FAPESP (2013/07296-2) and the access to the HPC resources of the SDumont supercomputer.

Assessment of a computational protocol for calculating the first hyperpolarizability of ruthenium complexes

Júlio P. C. Oliveira (IC),^{1*} Hélio F. dos Santos (PQ),² Diego F. S. Paschoal (PQ).^{1*}

julio.pco@hotmail.com; diegofspaschoal@macae.ufrj.br

¹Núcleo de Química Teórica e Computacional de Macaé, Polo Ajuda, Campus UFRJ Macaé, Universidade Federal do Rio de Janeiro, Macaé-RJ, Brazil.

²Núcleo de Estudos em Química Computacional, Departamento de Química – ICE, Universidade Federal de Juiz de Fora, Campus Universitário, 36.036-900, Juiz de Fora, Mg, Brazil.

Keywords: First hyperpolarizability, Ruthenium complexes, Basis set, DFT, Computational protocol.

Highlights

Computational protocol (DFT-functional/Ruthenium-basis-set/Ligands/basis-sets/IEF-PCM(UFF) for predicting β .

Calculated β with B3LYP/jorge-TZP(Ru)/def2-TZVP(ligands)/IEF-PCM protocol presenting a deviation of 1.21%.

Abstract

Nonlinear optical properties are important descriptors to be evaluated to correlate with the biological activity of ruthenium complexes, due to the intrinsic characteristics of the electronic structure.^{1,2} The computational prediction of these properties is strongly dependent on the theoretical approach. The present study assess the role of the ruthenium (RUBS) and ligands (LBS) basis sets in predicting the first hyperpolarizability (β) of ruthenium complexes.

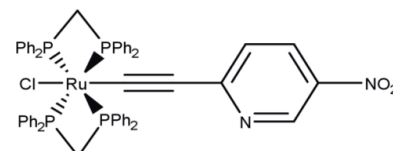


Figure 1: 2D structure of complex 1.

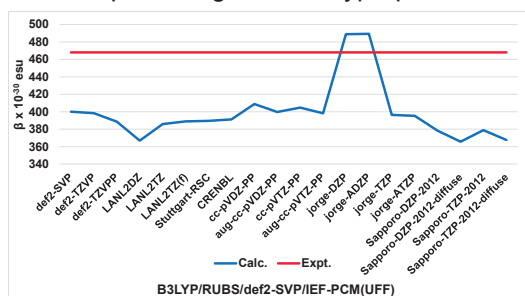


Figure 2: Calculated β_{tot} ($\times 10^{-30}$ esu) at B3LYP/RUBS/def2-SVP/IEF-PCM(UFF).

procedures (B3LYP/RUBS/LBS/IEF-PCM) were evaluated.

In general, the analysis of RUBS (Figure 2) showed no significant differences between the distinct effective core potentials (ECP) and with the increase of the valence basis set from double- ζ to triple- ζ . The analysis of the LBS (Figure 3) showed an improvement in calculated β values when the basis sets is increased from double- ζ to triple- ζ . The protocols B3LYP/def2-SVP(Ru)/def2-TZVP(ligands)/IEF-PCM, B3LYP/jorge-TZP(Ru)/def2-TZVP(ligands)/IEF-PCM, and B3LYP/jorge-DZP(Ru)/def2-SVP(ligands)/IEF-PCM presenting the smallest relative deviations (RD = 2.64%, 1.21% and 4.47 respectively).

Subsequently, the role of the DFT functional was also assessed and a new basis set was developed for the Ru atom. Furthermore, the best obtained protocols are being applied in the study of other Ru complexes.

¹Yankova, R. et al., J Mol Struct, v. 1268, p. 133712, 2022; ²De, S. et al., J Organomet Chem, v. 785, p. 72-76, 2015;

³Naulty, R. H. et al. J Organomet Chem, v. 563, p. 137-146, 1998.

Acknowledgments

The authors would like to thank the Brazilian agencies FAPERJ (E-26/201.336/2022 – BOLSA) and CAPES (Finance Code 001), and Prefeitura Municipal de Macaé for the financial support.

46ª Reunião Anual da Sociedade Brasileira de Química: "Química: Ligando ciências e neutralizando desigualdades"

Assessment of a computational protocol for predicting standard reduction potential of Fe(III) complexes.

Rayane M. Cavalcante (IC),^{1*} Diego F. S. Paschoal (PQ).^{1*}

rayanemeloc@gmail.com; diegofspaschoal@macae.ufrj.br

¹Núcleo de Química Teórica e Computacional de Macaé, Polo Ajuda, Campus UFRJ Macaé, Universidade Federal do Rio de Janeiro, Macaé-RJ, Brazil.

Keywords: Cancer, Fe(III) complexes, Reduction potential, Computational protocol, DFT, Basis sets.

Highlights

Computational protocols (DFT-Functional/Basis-sets/Solvent-effects/Relativistic-effects) will be presented.

Variations of 817 mV are observed according to the considered DFT functional, with BLYP, revTPSS, and PWP1 being selected.

Abstract

Some iron (Fe) complexes have shown activity against resistant cancer cells, selective cytotoxicity and mechanisms of action different from conventional drugs.¹ In this context, the computational study of Fe complexes is an important tool to aid the development of new complexes with antineoplastic potential. Therefore, the present work presents the construction of a computational protocol for predicting the reduction potential (ϵ^0) in Fe(III) complexes.

Initially, the $[\text{Fe}(\text{H}_2\text{O})_6]^{3+}/[\text{Fe}(\text{H}_2\text{O})_6]^{2+}$ redox process, which has experimental data ($\epsilon^0 = 0.77 \text{ V}$) available,² was selected as a reference. The geometry of the complexes was optimized and characterized as a local minimum on the potential energy surface at the DFT-functional/Basis-sets, where a set of 32 distinct DFT functionals were tested. The ϵ^0 was obtained according to equation: $\epsilon^0 \text{ (V)} = 27.2114 \times (G_{\text{ox}} - G_{\text{red}}) - \epsilon_{\text{abs}}^0(\text{SHE})$,^{2,3} using the ΔG values obtained from the construction of a thermodynamic cycle, with the optimized structures and thermal corrections obtained in the gas phase. For the inclusion of solvent effects, the implicit SMD model was used, with the dielectric constant set for water. All calculations were performed with ORCA 5.0.3 program.

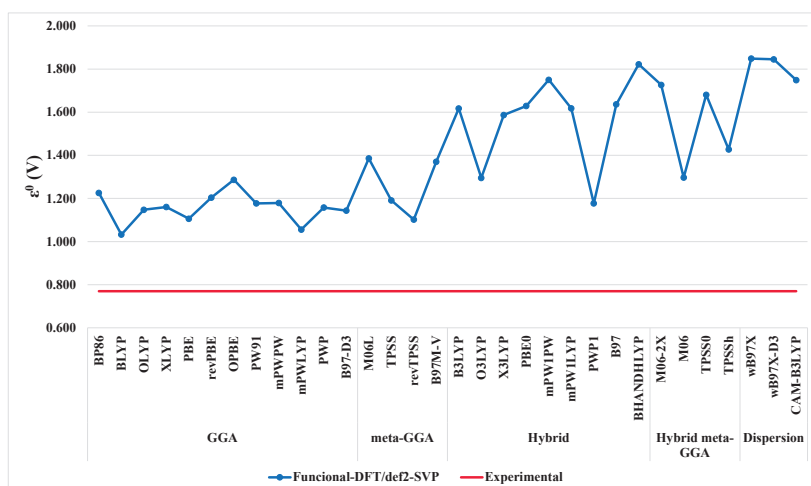


Figure 1. Calculated reduction potential for $[\text{Fe}(\text{H}_2\text{O})_6]^{3+}/[\text{Fe}(\text{H}_2\text{O})_6]^{2+}$ redox process at DFT-functional/def2-SVP level with SMD solvation model.

The calculated results showed AD of 489 mV, 377 mV, and 276 mV, respectively, showing that for this process the hybrid functional presents a better description of ϵ^0 . In general, the revTPSS functional presents similar errors between the studied complexes (326 mV and 377 mV), and the PWP1 functional presented a smaller mean absolute deviation (MAD = 339 mV). In the next steps, the role of the basis sets, considering both three DFT functionals, and relativistic effects are also being evaluated.

¹Basu, U. et al., *Coord. Chem. Rev.*, v. 417, p. 21339, 2020; ²Rulisek, L. J. *Phys. Chem. C.*, v. 117, p. 16871-16877, 2013; ³Srnc, M. et al., *J. Am. Chem. Soc.*, v. 130, p. 10947-10954, 2008.

Acknowledgments

The authors would like to thank the Brazilian agency FAPERJ (E-26/201.336/2022 – BOLSA).

Assessment of DFT functional in predicting the nonlinear optical properties of Pt(II) complexes

Milena de A. Pereira (IC),^{1*} Diego F. S. Paschoal (PQ).^{1*}

Milenaaguiairj18@gmail.com; diegofspaschoal@macae.ufrj.br

¹Núcleo de Química Teórica e Computacional de Macaé, Polo Ajuda, Campus UFRJ Macaé, Universidade Federal do Rio de Janeiro, Macaé-RJ, Brazil.

Keywords: First hyperpolarizability, Platinum complexes, DFT, Basis set, Computational protocol.

Highlights

Computational protocol (DFT-functional/LANL2TZ(f)/def2-SVP/IEF-PCM(UFF) for predicting first hyperpolarizability.

Calculated $\mu\beta_{\text{vec}}$ with B3LYP/LANL2TZ(f)/def2-SVP/IEF-PCM(UFF) protocol presenting a deviation of 1.8%.

Abstract

In the field of second-order nonlinear optics, coordination metal complexes are attractive, since they present characteristics such as low energy and high intensity charge transfer electronic transitions, and they can be regulated by the choice of the ligands.¹ Platinum (Pt) complexes have shown particularly large quadratic hyperpolarizabilities with a variety of ligands.¹ The theoretical prediction of NLO properties is very dependent on the computational protocol, which includes the DFT-functional, basis sets and solvent effects. Thus, in the present study an assessment of the DFT functional for predicting the first hyperpolarizability of Pt(II) complexes is presented.

Initially, the N^{^C^N}-1,3-bis[5-(trifluoromethyl)pyridin-2-yl]-4,6-difluorobenzene platinum(II) p-dimethylaminophenylacetylide complex (Figure 1), which presents an experimental value of $\mu\beta_{\text{EFISH}}(1907 \text{ nm}) = -2020 \times 10^{-48} \text{ esu}$ in DMF, was selected.² The complex was optimized and characterized as a minimum point on the potential energy surface (PES) at B3LYP/LANL2TZ(f)/def2-SVP/IEF-PCM(UFF) level. Then, the β was calculated according to equation: $\beta_{\text{vec}}(-2\omega; \omega, \omega) = \sum_{i=1}^3 \frac{\mu_i \beta_i}{|\mu|}$, where the β_{ijk} tensors were obtained considering the **B** convention with the Coupled-Perturbed Kohn-Sham (CPKS) method.³ Computational protocols at DFT-Functional/LANL2TZ(f)/def2-SVP/IEF-PCM(UFF) level, considering a set of 25 functionals, were constructed DMF solvent with a wavelength of 1907 nm, in the Gaussian 16 Rev. C.01 program.

The calculated results (Table 1) show an extremely strong dependence of the calculated $\mu\beta_{\text{vec}}$ values with the DFT functional. When a GGA functional is considered, relative deviation (RD) above 1000% are found, decreasing to ~250% with meta-GGA functionals. For the other functionals, RD below 100% are found, with the smallest RD being found with the hybrid functionals. The DFT functionals B3LYP, B3PW91, and mPW3PBE, which showed the smallest RD, 1.8%, 2.3%, and 2.4%, respectively, were selected for further application in other Pt(II) complexes.

Table 1. Calculated $\mu\beta_{\text{vec}}(1907 \text{ nm}) \times 10^{-48} \text{ esu}$ values at DFT-functional/LANL2TZ(f)/def2-SVP/IEF-PCM(UFF) protocols.

Functional	$\mu\beta_{\text{vec}}$	Functional	$\mu\beta_{\text{vec}}$	Functional	$\mu\beta_{\text{vec}}$	Functional	$\mu\beta_{\text{vec}}$	Functional	$\mu\beta_{\text{vec}}$
BLYP	-21250	M06L	-7228	B3PW91	-2067	BHandH	-544	SOGGA11X	-692
BP86	-24970	M11L	-7826	mPW1LYP	-1500	BHandHLYP	-483	B1B95	-1396
PBE	-23918	B3LYP	-2057	mPW1PW91	-1502	M06	-1402	LC-BLYP	-211
B97D3	-24061	X3LYP	-1836	mPW3PBE	-2069	M06-2X	-487	CAM-B3LYP	-456
SOGGA11	-36843	B3P86	-2125	PBE0	-1498	M11	-260	wB97xD	-359

Experimental value of $\mu\beta_{\text{EFISH}}(1907 \text{ nm}) = -2020 \times 10^{-48} \text{ esu}$.²

¹Colombo, A. et al., *Coord. Chem. Rev.*, v. 446, p. 214-113, 2021; ²Rossi, E. et al., *Chem. – Eur. J.*, v. 19, p. 9875-9883, 2013; ³Paschoal, D. et al., *Org. Electron.*, v. 28, p. 111-117, 2016.

Acknowledgments

The authors would like to thank the Brazilian agencies FAPERJ (E-26/201.336/2022 – BOLSA) and PIBIC-UFRJ for the financial support.

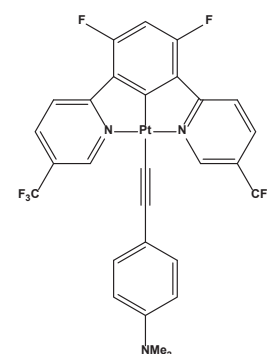


Figure 1. Pt(II) complex studied

Computational-Experimental Study of Variants of Concern of SARS-CoV-2

Layla Uliana Pinheiro (PG),^{1,*} Jessica Cristiane Magalhães Ierich (PQ),¹ Paulo Ricardo Leitão do Carmo (PG),¹ Weverton Rodrigues Gomes (PQ),¹ André Farias de Moura (PQ),¹.

layla.uliana@estudante.ufscar.br;

¹Departamento de Química, UFSCAR.

Keywords: Molecular Dynamics, SARS-CoV-2, Omicron Variant, Spike Protein, Receptor-Binding Domain, Angiotensin-Converting Enzyme 2.

Highlights

Omicron RBD bound to a human ACE2 cellular receptor were investigated by MD simulations. Complex anchoring patterns were identified and may allow the mapping of different virus infection mechanisms.

Abstract

About three years after the first report of COVID-19 cases in Wuhan, China,¹ the scientific community faces the challenge of rising new variants of SARS-CoV-2 with a higher infective ability, which can potentially re-infect people by escaping the natural immune system or antibodies derived from the vaccine. In this context, the spike (S) protein plays a crucial role in the virus binding to the cell receptor,² the human angiotensin-converting enzyme (ACE2), which can be related to this immunological evasion process of SARS-CoV-2. We modeled the complex between omicron spike receptor-binding domain (RBD) and ACE2 receptor based on an experimental structure available at the Protein Data Bank repository (PDB code 7WK6).³ The protocol used for the omicron RBD protein system with ACE2 molecular dynamics (MD) simulation in water is described as follows: (1) system minimization using the steepest descent algorithm; (2) system equilibration using a 1 μ s MD simulation system; and (3) NPT ensemble (T=309.65 K and P=1 bar) simulation using CHARMM 36 force field⁴ within GROMACS 2021.3 package⁵. The conformational changes in the protein measured by the RMSD and the radius of gyration during MD demonstrate complex stability in water. Figure 1 shows energy values obtained for the interaction between water molecules and each protein, with oscillating profiles with opposite trends (negative peaks of one interaction correlate with positive peaks of the other). This finding suggests that a conformational change occurring in the ACE2 structure receptor causes a response in the RBD structure, reflecting the dynamics of this interaction. Observed system fluctuation during interaction indicated an ACE2 higher RMSD (0.23 ± 0.017 nm) than the spike binding domain (0.16 ± 0.013 nm), which reflects ACE2 function as a cellular receptor and, thus, requires more flexibility.⁶ The average number of hydrogen bond interactions between the two proteins was (9 ± 2), consistent with the literature data for the complex under study.

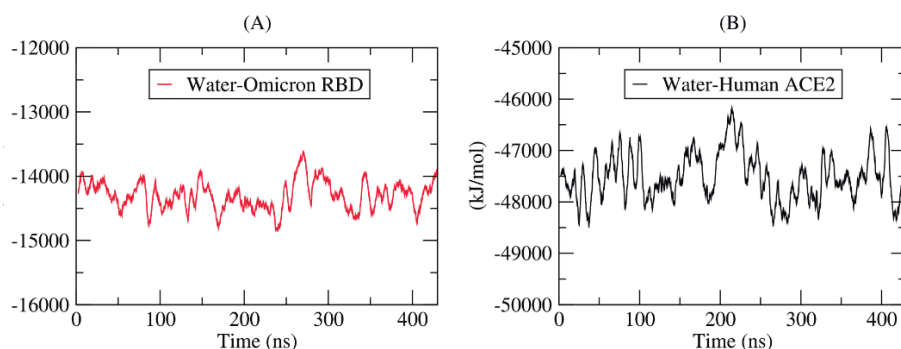


Figure 01: Water interaction energy for selections: (A) - Omicron RBD, (B) - Human ACE2.

References: **1.** Hu, B. *et al.* *Nat. Rev. Microbiol.* 19, 141–154 (2021); **2.** Tai, W. *et al.* *Cell Mol. Immunol.* 17, 613–620 (2020); **3.** Hong, Q., *et al.* *Nature* 604: 546–552 (2022); **4.** Huang, J. & MacKerell, A. D. *J. Comput. Chem.* 34, 2135–2145 (2013); **5.** van der Spoel, D. *et al.* *J. Comput. Chem.* 26, 1701–1718 (2005); **6.** Zhu L., Frenkel D, Bolhuis P. G. *Phys Rev Lett.* 106, 168103 (2011).

Acknowledgments

Coordenação de Aperfeiçoamento de Pessoal de Nível Superior – Brasil (CAPES) – Finance Code 001. São Paulo Research Foundation (FAPESP 2013/07296-2). We also acknowledge the National Laboratory for Scientific Computing (LNCC/MCTI, Brazil) for providing HPC resources of the SDumont supercomputer.

Computational study of the electrocatalytic CO₂ reduction reaction using a non-noble metal complex

Gabriela Garcia (PG),^{1*} Atualpa A. C. Braga (PQ)¹.

ggarcia@iq.usp.br; atualpa@iq.usp.br

¹Departamento de Química Fundamental, Instituto de Química da USP (IQ-USP).

Keywords: Computational Chemistry, Electrochemistry, Homogeneous Catalysis, Electrocatalysis, CO₂, Carbon-carbon bond.

Highlights

Theoretical calculations of CO₂ electroreduction's reaction path to form acetic acid, using a manganese complex with corrole ligand. A carbon-carbon bond is formed between two CO₂ molecules from the saturated atmosphere.

Abstract

The manganese complex with corrole ligand was used as the catalyst (Figure 1) for the CO₂ reduction reaction (CO₂RR). Based on this, a reaction mechanism was proposed, through computational methods, as a proof of concept to this type of reaction (Figure 2). The calculations were carried out with unrestricted B3LYP functional and Def2-SVP basis set. Since this is an open shell system, all structures were optimized with different multiplicities, resulting that they all are more stable as triplets or quartets, depending on how much electrons they gain. No spin contamination was found in any structure.

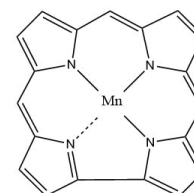


Figure 1: Mn-Corr Catalyst

It was verified that the species which activate the CO₂ comes from the electroreduction of the initial Mn (III) (R1) to Mn (II) (I1). As it follows, the intermediate I2 receives a proton from water (20% in acetonitrile solution). After receiving another electron, I3 becomes able to activate a second CO₂ molecule, forming the carbon-carbon bond, which is the most interesting step for this work, since its goal is to form C₂₊ products. On the following ones, the reaction undergoes successive proton coupled electron transfers, that in the end will release acetic acid and restore the initial catalyst.

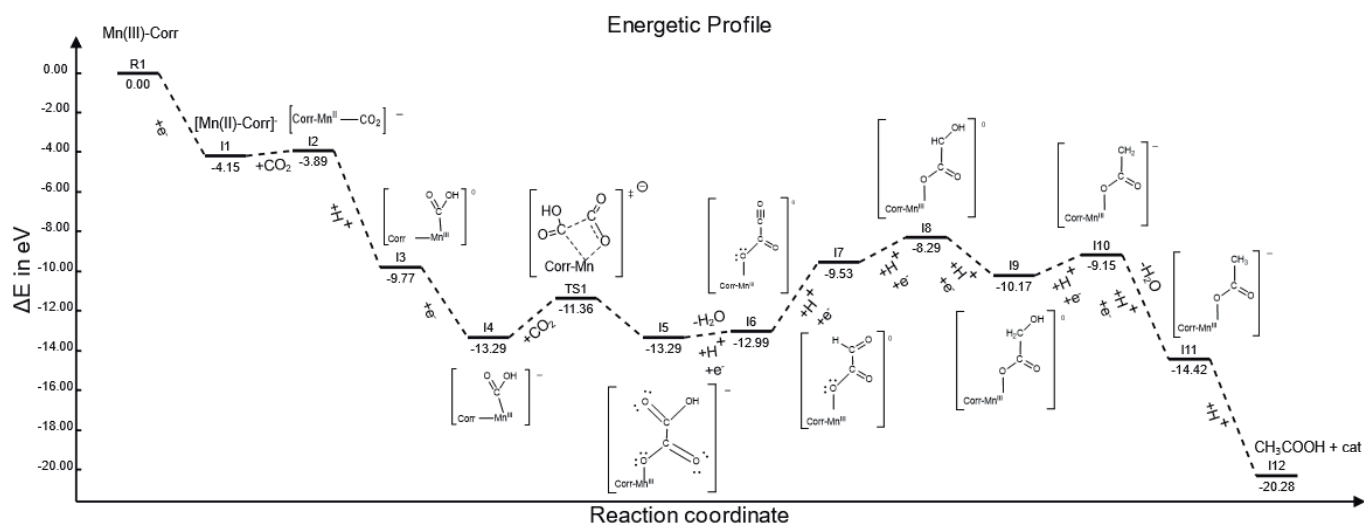


Figure 2: Energetic Profile

Acknowledgments



Computational study of the relative stability of lactic acid enantiomers in a chiral dipeptide system.

Davi A. Mattoso (IC),^{1*} Dr. André F. de Moura (PQ).¹

dmattoso@estudante.ufscar.br; davi.augusto.mattoso@gmail.com

¹Departamento de Química, Universidade Federal de São Carlos.

Palavras Chave: Chirality, Enantioselectivity, Biomolecules, Chiral Catalysis, Statistical Mechanics.

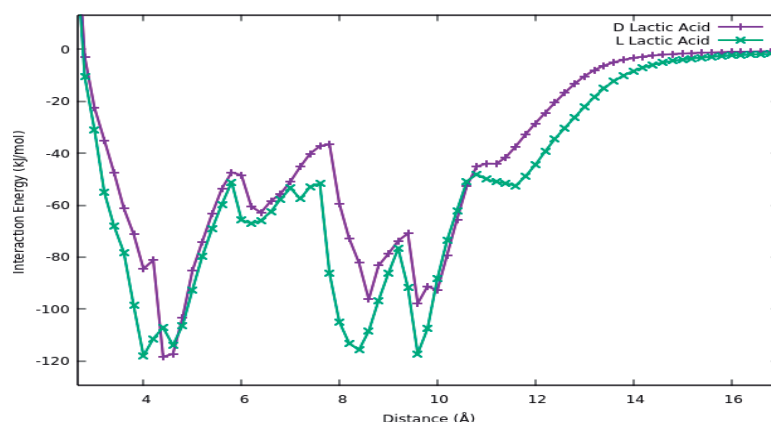
Highlights

Interaction of lactic acid enantiomers with cysteine-threonine dipeptide. Chiral catalysis of pyruvic to lactic acid (D,L). Free energy reaction coordinate.

Abstract

The ability to efficiently obtain chiral compounds in an efficient manner and with a high selectivity towards one specific enantiomer is a huge challenge for synthetic chemistry. Among the many obstacles encountered, the choice of catalyst holds a central place. The present investigation aims at providing a microscopic view on the relative stability of the D and L enantiomers of lactic acid when a heterogeneous catalyst is employed, based on gold nanoparticles with a surface coating of surfactant molecules and a chiral peptide. Preliminary experimental screening indicates that this catalyst has a high degree of photo-asymmetric transfer hydrogenation of pyruvic acid to lactic acid (D,L). We first conducted thorough molecular dynamics simulations of the catalytic systems with either D or L lactic acid and after 5 μ s of simulation the systems were still not fully relaxed, which demonstrated that the direct simulation of the process could not achieve the chiral discrimination of the products formed, since the differences in the interaction energy of each enantiomer was smaller than the observed fluctuations, as might be expected for a complex and sizable structure.

Although these simulation could not assess the chiral discrimination mechanism on their own, they are nonetheless a very thorough sampling of the conformational space of the molecules of interest in a realistic chemical environment, with a composition consistent with the actual catalytic system experimental setup. Bearing this in mind, we sampled the configurations of lactic acid (D and L) and the cystein-threonine (CT) peptide along the simulations and computed their Helmholtz free energy of interaction. Free energies were computed using the statistical mechanics software *Themis*¹ to compute the partition function along the reaction coordinate between lactic acid and the CT peptide, sampling the distance and the relative orientation between the molecules by means of predefined grids. The typical free energy profile along the reaction coordinate has multiple minima due to large number of polar and charged groups in both molecules (Figure 1). A large sample of molecular conformations for both lactic acid and CT peptide is under investigation now to obtain an average free energy profile, in order to remove the arbitrariness of the geometry choice and to take into account the internal energy penalties of each molecular conformation.



1 - Colombari, Felipe, et al. "Themis: a software to assess association free energies via direct estimative of partition functions." (2020).

Acknowledgments

São Paulo Research Foundation (FAPESP), Processes 2013/07296-2 and 2021/03516-4.

46ª Reunião Anual da Sociedade Brasileira de Química: "Química: Ligando ciências e neutralizando desigualdades"

Development of a computational protocol to study the aquation reaction of Pt(II) complexes with nitrogenous ligands with antineoplastic potential

Leticia S. Amorim (PG),^{1*} Willian T. G. Novato (PQ),¹ Diego F. S. Paschoal (PQ).^{1*}

leticia.amorim05@gmail.com; diegofspaschoal@macae.ufrj.br

¹Núcleo de Química Teórica e Computacional de Macaé, Polo Ajuda, Campus UFRJ Macaé, Universidade Federal do Rio de Janeiro, Macaé-RJ, Brazil.

Keywords: Cancer, Pt(II) complexes, Kinetics, Aquation, Computational Protocol.

Highlights

Computational protocols (DFT-Functional/Platinum-basis-set/Ligands-basis-sets/solvent-effects/relativistic-effects).

Mean absolute deviation less than 0.50 kcal mol⁻¹ for the aquation reaction of Pt(II) complexes.

Abstract

Considering that the aquation reaction of Pt(II) complexes is an important descriptor to be considered in the search for new Pt(II) complexes with antineoplastic potential,¹ Paschoal et al.² assessed the influence of the platinum basis set (PTBS) and relativistic effects (REL) on the prediction of the reactivity of cisplatin. However, a gap still remained regarding the role of the DFT functional and the ligands basis set (LBS).² Thus, the present study aims to extend these analyzes evaluating the influence of the DFT functional and the LBS, and applying in the study of the aquation reaction of the other Pt(II) complexes with N-ligands (Figure 1).

First, the cisplatin aquation reaction was studied through the supermolecule approximation, considering an associative mechanism, where the transition state (TS) was proposed as a distorted trigonal bipyramidal and the intermediate 1 (I1) was found through intrinsic reaction coordinate (IRC) calculation. The Gibbs free energy of activation (ΔG_a) was calculated using the equation: $\Delta G_a = G(\text{TS}) - G(\text{I1})$. Computational protocols considering 5 PTBS, 6 LBS and 17 DFT functionals were constructed. Solvent effects were considered using the CPCM continuous solvation model and scalar relativistic effects were considered in some protocols using the 2nd-Order Douglas-Kroll-Hess (DKH2) approach. The calculations were performed in ORCA 4.2.1 program.

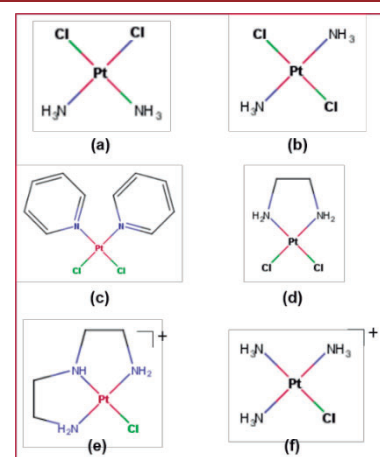


Figure 1. Pt(II) complexes with N-ligands: (a) cisplatin, (b) transplatin, (c) *cis*-[PtCl₂(py)₂], (d) [PtCl₂(en)], (e) [PtCl(dien)]⁺, (f) [PtCl(NH₃)₃]⁺.

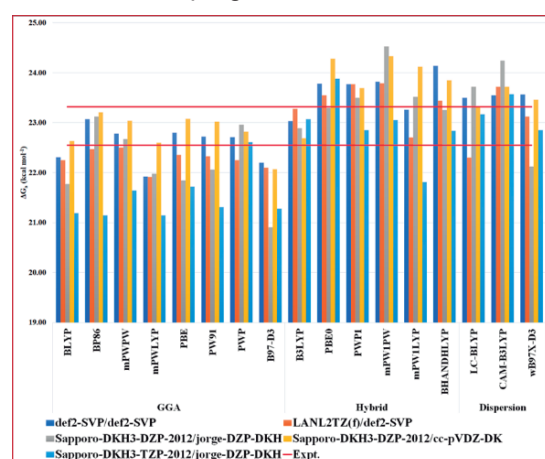


Figure 2. Calculated ΔG_a for the first aquation reaction of cisplatin at DFT-functional/PTBS/LBS computational protocols.

The calculated results suggest that the ligands basis sets def2-SVP, jorge-DZP-DKH and cc-pVDZ-DK present the best description of the kinetic parameters. Regarding the DFT functional, the GGA PWP and Hybrid B3LYP functionals showed the smallest relative deviations (RD) in relation to the mean experimental value ($\Delta G_a = 22.94$ kcal mol⁻¹). A total of 32 computational protocols presented ΔG_a values within the experimental range available in the literature ($\Delta G_a = 22.55 - 23.32$ kcal mol⁻¹), as Figure 2, with a maximum RD of only 1.66%, being considered suitable for application in the study of the aquation reaction of other Pt(II) complexes with nitrogenous ligands.

In the next step, the other Pt(II) complexes (Figure 1) will be studied. So far, considering the cisplatin, transplatin, *cis*-[PtCl₂(py)₂], and [PtCl₂(en)] complexes, the protocol B3LYP/LANL2TZ(f)/def2-SVP/CPCM presents a mean absolute deviation (MAD) and a mean relative deviation (MRD) only of 0.37 kcal mol⁻¹ and 1.66%, respectively.

¹Kozelka, J. et al.; Coord. Chem. Rev. 1999, 190-192, 61-82. ²Paschoal, D.F.S.; Gomes, M.S.; Machado, L.P.N.; Santos, H.F.; Basis Sets for Heavy Atoms. In: E. Perlt (eds). Lecture Notes in Chemistry: Basis Sets in Computational Chemistry. Springer, 2021, 107, 183-214.

Acknowledgments

The authors would like to thank the Brazilian agency FAPERJ (E-26/201.336/2022 – BOLSA) and CAPES (Finance Code 001) for the financial support.

Docking Studies of Endocrine Disruptors at Estrogen Receptor α and Metabolite Prediction

Rafaela M. de Angelo¹ (PG), Kathia M. Honório^{1,2} (PQ)

rafaela.molina.angelo@usp.br;

¹University of São Paulo – EACH USP, São Paulo, Brazil; ²University Federal of ABC – UFABC, Santo André, Brasil

Keywords: Endocrine Disruptors; Estrogen Receptor Alpha; Docking.

Highlights

- The present exploratory study showed that three endocrine disruptors (ethinyl-estradiol, acetochlor, and glyphosate) may have significant interactions with the hormone receptor (in particular, estrogen receptor alpha) and interactions that have not yet been described in the literature.
- In this work, metabolite prediction tools were used to better understand whether the products generated via the degradation of these endocrine disruptors could be even more toxic than the compounds themselves.
- Based on the analyses of physicochemical and toxicity properties, it was possible to verify that some predicted metabolites, such as glyphosate derivatives, presented a more toxic potential than the initial molecule.

Resumo/Abstract

Endocrine disruptors (EDs) are chemicals that can interfere with hormone systems and produce adverse effects on the developmental, reproductive, neurological, and immune systems. The hormone receptor chosen for this study is the alpha estrogen receptor (ER α). ERs, in particular, are not very specific and this feature makes them susceptible to activation by a variety of compounds present in many products that often bear little resemblance to the high-affinity ligand (estradiol). Therefore, from chemical structures already recognized as endocrine disruptors (acetochlor, ethinyl estradiol, and glyphosate) we investigated their ligand-receptor interactions, as well as evaluated their physicochemical properties and their possible metabolites. So, this work aims to study and understand the properties and possible mechanisms of action of three endocrine disruptors on the α estrogen receptor and its possible metabolites, searching to analyze and verify the possible relationships between toxicological and physicochemical properties. The docking simulations were carried out considering the score values of each conformation and the number of polar and non-polar interactions since due to the high hydrophobicity of the binding site and the hydrophobic regions of the endocrine disruptors, the small contacts were analyzed. For this, the structures of the three endocrine disruptors were prepared in the Sybyl package, with the calculation of the MOPAC charges, and after these structures were submitted to docking simulations at RE α . To validate the chosen parameters, the redocking step was performed, in which the GoldScore function had better results, with the site delimited at 7Å and rigid residues. Metabolite prediction and toxicity analysis were performed using the GLORYx and eMolTox servers, respectively. From the obtained results, the endocrine disruptor ethinyl estradiol showed hydrogen interactions with His524 and Ala350 via two hydroxyl groups, which are found in opposite positions of the molecule. It is worth mentioning that the center of the ligand with four rings and the ethinyl region showed non-polar interactions, classified as “small contacts” with two residues that the literature cites as conserved (Leu384 and Met421). Regarding the endocrine disruptor glyphosate, due to its low molecular volume, the compound does not fill the binding site, leaving a lot of space. However, it has a phosphonated moiety that can interact more easily with residues that are close to the active site. This would explain why most of the results obtained from docking simulations show interactions with residues that are not actually in the cavity of the binding site. Even so, the compound showed significant hydrogen interactions with Leu346, Glu353, Arg394, Leu391, and Leu387. Finally, the interactions of acetochlor at the endocrine receptor were also analyzed, which did not show polar bonds, only non-polar ones. We observed that the side chains of the leucine residues are all oriented towards the non-polar portions of the compound and among the cited residues; Leu384 also appears very close, interacting with the side chain of acetochlor. In the *in silico* prediction of metabolites, simulating the process of metabolizing substances from different metabolic pathways and systems and using a set of rules for each route, it was possible to identify that the glyphosate metabolite has the potential to interrupt or cause damage in some metabolic pathways. Therefore, from the results obtained in this study, it was possible to understand the possible molecular behaviors of some endocrine disruptors at ER α , as well as predict the toxicity of possible metabolites from these substances.

Agradecimentos/Acknowledgments



(2017/10118-0)

Experimental and theoretical elucidation of graphitic carbon nitride structure

Caio V. Caetano (PG),^{1,*} Ivo F. Teixeira (PQ),² Nadezda V. Tarakina,³ André F. Moura (PQ)²

caiovinciuscaetano@hotmail.com

¹Programa de Pós-Graduação em Química, UFSCar; ²Departamento de Química, UFSCar; ³Max-Planck-Institut für Kolloid- und Grenzflächenforschung

Keywords: Graphitic carbon nitride, Molecular dynamics, Electronic microscopy, Radial distribution function.

Highlights

Na⁺ and Mg²⁺ were stable inside the PHI pores. Na⁺ stay closer to the nitrogen atoms as compared to Mg²⁺ due to the higher stability of water molecules in the first hydration layer of the latter.

Abstract

Molecular dynamics (DM) simulations using the GROMACS package [1], with the CHARMM36 force field [2], were carried out in order to elucidate how the Na⁺ and Mg²⁺ are organized inside the graphitic carbon nitride structure (Na-PHI and Mg-PHI, respectively). The simulation protocol consisted of 3 steps: (1) energy minimization; (2) 500 ps NVT simulation; and (3) 1 μ s NPT simulation. The last structure of each DM was used to build a more realistic set of model systems in an ethanol box, selecting the nanosheets along with the cations and the water molecules which were inside the pores, which amounted to 181 and 262 water molecules for Na-PHI and Mg-PHI, reaching the experimental compositions of 16.1% m/m and 23.3% m/m water, respectively. The same simulation protocol described for the aqueous systems were employed to equilibrate the ethanol model systems and the 1 μ s production runs were used to perform the radial distribution function (PDF) analyses.

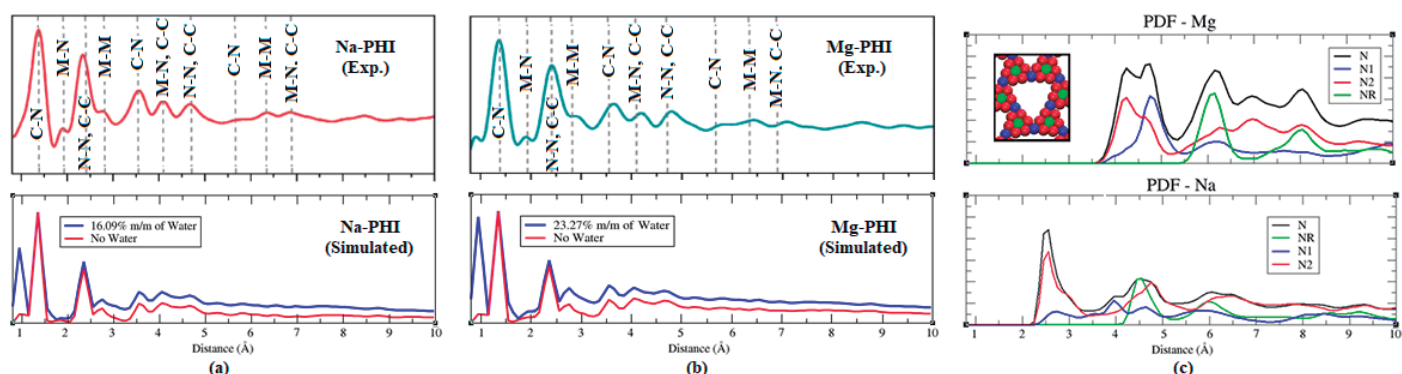


Figure 1: Total radial distribution function (PDF) for the (a) Na-PHI, (b) Mg-PHI and (c) Mg²⁺ and Na⁺ in relation to each pore nitrogen.

The total theoretical PDFs are consistent with the experimental ones (Figure 1a and 1b), except for the N-H (due to the presence of NH₂ groups at the vertices of the model PHI sheets) and water O-H correlation peaks close to 1 Å, which indicate that water molecules have been probably eliminated during samples preparation for the electronic microscopy analyses and that synthesized PHI systems have only small contributions of NH₂ groups, if any. Na⁺ cations presented the same distribution profiles for both systems (Figure 1c), remaining closer to N₂ type nitrogen atoms, with a maximum correlation peak at 2.6 Å (Figure 1c, bottom). On the other hand, the Mg²⁺ cations stay farther from any nitrogen atom, with correlation peaks at 4.2 Å with respect to N₂ type (Figure 1c, top). An explanation for this is due to the ionic radius of Mg²⁺ is smaller as compared to Na⁺ and its charge is twofold larger, yielding a much larger charge density for Mg²⁺, leading to a stable hydration layer that prevents direct interactions between magnesium and PHI. It is also important to point out that both ions and their hydration layers were located preferentially inside the large pores or along the lateral grooves in PHI, but not free in the ethanol solution.

[1] M. J. Abraham, T. Murtola, R. Schulz, S. Páll, J. C. Smith, B. Hess, E. Lindahl, *SoftwareX*, 2015, 1–2, 19.

[2] R. B. Best, X. Zhu, J. Shim, P. E. M. Lopes, et al. *J. Chem. Theory Comput.*, 2012, 8, 3257.

Acknowledgments

We thank FAPESP (2013/07296-2) and CAPES (Project 001) for financial support, and LNCC for access to the SDumont supercomputer.

Improved pKa from the Hellmann–Feynman Theorem at the DFT Level

Felipe R. Dutra (PG),¹ Rogério Custodio (PQ).^{1*}

feliperd6@hotmail.com; rogerct@unicamp.br

¹Departamento de Físico-Química, Instituto de Química, UNICAMP

Keywords: Direct method, pKa, Hellmann-Feynman theorem, Basis set, Density functional theory

The direct method is used for pKa calculations from density functional theory for a series of carboxylic acids. An accuracy lower than 0.5 units of pKa is achieved by modifying the basis set to satisfy the Hellmann-Feynman theorem.

Abstract

• Introduction

The pKa constant have stimulated the development of computational protocols for its determination from electronic structure calculations. The most recent and simple approach have been developed considering the direct reaction and a proton-adjustable parameter¹. The objective of the present work is to evaluate the performance of the direct method for pKa prediction with newly modified basis functions to satisfy the Hellmann–Feynman theorem.

• Methodology

The proton-adjustable method determines the Gibbs energy of the solvated proton based on the reaction: $AH_{aq} \rightleftharpoons A_{aq}^- + H_{aq}^+$. Thus, the mean proton energy ($\overline{G}_{aq}(H^+)$) can be estimated from a set of N training molecules with well-defined pKa experimental values and theoretical Gibbs energies in solution of the acid and the respective conjugate base at each level of theory. Different training sets were tested and referred to as: Set I (global average), Set II (six straight-chain acids) and Set III (six distinct acids). The calculations were performed using the Gaussian16 program at a temperature of 298.15 K, for 44 monocarboxylic acids. All calculations were carried out considering 7 functionals. The inclusion of the solvent was done using the SMD solvation model and explicit water molecules at the carboxylic group. The basis set were obtained from the aug-cc-pVDZ basis. Preserving only the s contracted basis sets from the aug-cc-pVDZ and adding p and d functions with the same exponents then the s primitives to reduce the electric field at each nucleus at the equilibrium geometry, the resulting basis set satisfies the Hellmann-Feynman theorem.

• Results and Discussion

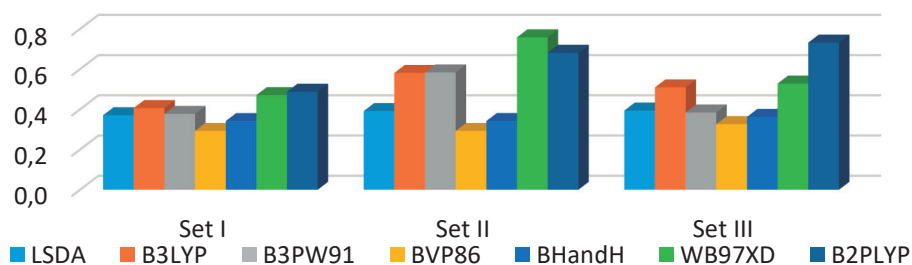


Figure 1: Mean absolute errors in units of pKa for 44 carboxylic acids

Figure 1 shows that the mean absolute errors are below 1.0 unit of pKa regardless of the functional used. Excellent results for all carboxylic acids were obtained, especially for hybrid functionals.

• Reference

1. Dutra, F. R.; Silva, C. D. S.; Custodio, R. J. *Phys. Chem. A* 2021, 125 (1), 65–73.

Acknowledgments

The authors are grateful for the support of process n° 2021/03201-3 – FAPESP, Center for Computational Engineering and Sciences, grants 2013/08293-7 and 2017/11485-6 - FAPESP and FAEPEX-UNICAMP.

46ª Reunião Anual da Sociedade Brasileira de Química: "Química: Ligando ciências e neutralizando desigualdades"

In silico investigation of the spectroscopic properties of molecular knots**Walber G. Guimarães (PQ),¹ André F. de Moura (PQ)¹****walber@ufscar.br; moura@ufscar.br**¹Departamento de Química, UFSCar, São Carlos – SP.

Keywords: Molecular Knot, Electronic Circular dichroism, Density Functional Theory, Spectroscopy.

Highlights

Molecular knot self-assembly leads to an intrinsic chirality. The Density Theory Functional calculations can decipher the structural and electronic properties, employing spectroscopies simulations.

Abstract

In chemistry, a molecular knot (MK) is a topologically interlocked molecular architecture that is analogous to a macroscopic knot.¹ Tying MK with different topologies, on larger length scales, remains challenging, not to mention the difficulties with harnessing their topological characteristics to elucidate their properties.² Furthermore, the MK is one of the bearers for the future of material chemistry allowing unlimited possibilities for its application. In the core of this outlook, Wu and co-workers,³ synthesized an iron(II)-templated contra-helical trefoil knot series (**Figure 1a**), which we are now investigating in collaboration with the experimental group.

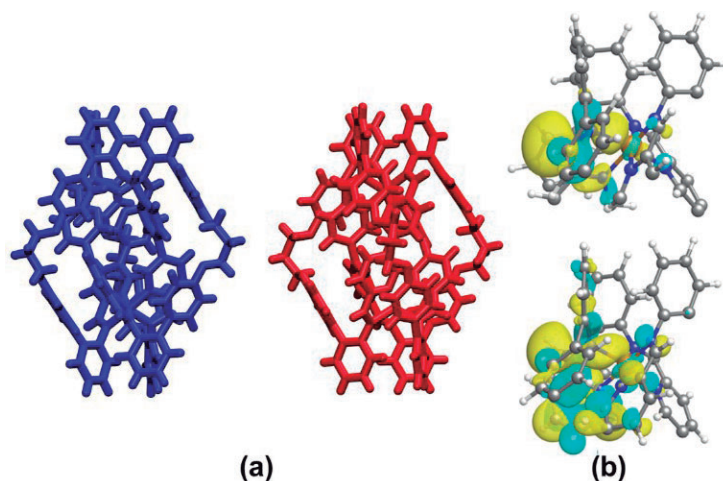


Figure 1 – (a) Λ -(+)-MK-Fe (**Blue**) and Δ -(-)-MK-Fe (**Red**)³ and (b) Frontier orbitals HOMO (**Top**) and LUMO (**Bottom**). Color code: Fe (ochre), O (red), N (blue), C (silver), H (white).

We perform in the all-geometry optimization calculations using the hybrid exchange–correlation PBE0 functional with Grimme’s D3 dispersion correction. The balanced full electron polarized triple- ζ def2-TZVP(-f) basis set was used for all atoms. Solvent effects were included in calculations by using the continuum model, in which the solvent was the THF. The calculations were performed using the ORCA package. The preliminary results are in good agreement with the experimental data. The Fe – Fe, O – O, and Fe – N average bond length errors, are lower than 5%. The frontier orbitals are localized in the Fe – N bond. The HOMO and LUMO are localized preferentially over N-atoms and Fe-atoms with degenerate aromatic orbitals, respectively. The simulation process of the absorption spectra, and also the vibrational frequencies calculation is being carried out on the optimized geometry, employing exchange–correlation CAM-B3LYP functional. Moreover, the correlations between ECD spectra, mechanical strain, and critical points are in progress at this step.

References

- (1) Fielden, S. D. P.; Leigh, D. A. *Angew. Chemie* **2017**, *129* (37), 11318–11347.
- (2) Lukin, O.; Vögtle, F. *Angew. Chemie Int. Ed.* **2005**, *44* (10), 1456–1477.
- (3) Wu, L., et. al. *Nat. Synth.* **2022**, *2* (1), 17–25.

Acknowledgments

CNPQ, CAPES, FAPESP (2013/07296-2) and FINEP (01.22.181.00).

Ab initio Study of Catalytic Properties of 2D CuS_x Nanolayer, with x = 0.5, 1.0, and 1.5, in CO₂ Reduction

Henrique A. B. Fonseca (PG),¹ Lucas G. Verga,¹ Juarez L. F. Da Silva.¹

henrique.alves.fonseca@usp.br; juarez_dasilva@iqsc.usp.br

¹ São Carlos Institute of Chemistry, University of São Paulo. P.O. Box 780, 13560-970 São Carlos, SP, Brazil

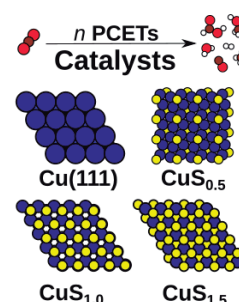
Palavras Chave: Two-dimensional, CuS, Chalcogenide, CO₂RR, CHE model.

Highlights

We explored the adsorption of several CO₂RR-related intermediates on 2D CuS_x using the CHE model. CuS₁ and CuS_{1.5} were favorable to the CO and HCOOH formation. For CuS_{1.5} we investigated beyond CO.

Resumo/Abstract

Global warming problems are becoming increasingly alarming nowadays and are mainly caused by anthropogenic activities such as the burning fossil fuels that increase greenhouse gas emissions, for example, the CO₂. This atmospheric CO₂ is an inexpensive C1 resource that we can use to transform into products with aggregate values, such as CO, HCOOH, and CH₄, which are very useful chemicals. So, one of the potential solutions that have received a lot of interest is CO₂ reduction reaction (CO₂RR) via an electrochemical pathway, owing to the possibility of being carried out under normal temperature and pressure conditions, as well as being associated with a source of clean energy like solar energy or wind energy.^[1] But for this, we need catalysts. Copper has gained a lot of attention because it reduces CO₂ to several products, despite its low selectivity. Copper sulfide, for example, is an environment-friendly and abundant material and has also attracted extensive attention for the production of formate in CO₂ electroreduction.^[2] In the same way, the 2D transition-metal dichalcogenides materials have many implications, mainly because of their different structures, active sites, defects, and so on. So, in this work, we performed DFT calculations using the Vienna Ab initio Simulation Package (VASP), with the Perdew-Burke-Ernzerhof (PBE) exchange-correlation functional and van der Waals correction D3, to study the effect of Cu/S ratio of the CuS_x layers on the CO₂RR reaction pathways toward C1 products. We used the Computational Hydrogen Electrode model^[3] and observed that the reaction step CO₂ → *COOH was the potential determinant step (PDS) for CO formation on all materials. Meanwhile, for HCOOH formation the PDS depends on the considered substrate. As compared to the results for Cu(111), the CuS_{0.5} system has a high onset potential, while the CuS and CuS_{1.5} systems have small onset potential values for CO and HCOOH. Additionally, we also investigate the possibility of CH₄ formation for CuS_{1.5}.



[1] Sonali Das, Javier Pérez-Ramírez, Jinlong Gong, Nikita Dewangan, Kus Hidajat, Bruce C. Gates, and Sibudjing Kawi. Coreshell structured catalysts for thermocatalytic, photocatalytic, and electrocatalytic conversion of CO₂. *Chem. Soc. Rev.*, 49:2937–3004, 2020.

[2] Yun Huang, Yilin Deng, Albertus D. Handoko, Gregory K. L. Goh, and Boon Siang Yeo. Rational design of sulfur-doped copper catalysts for the selective electroreduction of carbon dioxide to formate. *ChemSusChem*, 11(1):320–326, 2018.

[3] J. K. Nørskov, J. Rossmeisl, A. Logadottir, L. Lindqvist, J. R. Kitchin, T. Bligaard, and H. Jónsson. Origin of the overpotential for oxygen reduction at a fuel-cell cathode. *J. Phys. Chem. B*, 108:17886–17892, 2004.

Agradecimentos/Acknowledgments

Grant nº 2021/05728-9, São Paulo Research Foundation (FAPESP). The opinions, hypotheses and conclusions or recommendations expressed in this material are the responsibility of the author(s) and do not necessarily reflect the views of FAPESP.

In silico investigation of MOF SIFSIX-3-Cu for natural gas separationSabrina Grigoletto* (PG)¹, Guilherme Ferreira de Lima (PQ)¹, Heitor Avelino de Abreu (PQ)¹

sgrigoletto@ufmg.br

¹Chemistry Department, Federal University of Minas Gerais (UFMG), Belo Horizonte, MG - Brazil;

Key words: Metal-organic Frameworks, adsorption, natural gas, Monte Carlo, Molecular Dynamics.

Highlights

The MOF SIFSIX-3-Cu presented the potential to separate natural gas mixtures.

The calculations were performed through Monte Carlo and molecular dynamics methods.

Abstract

Natural gas is often referred as the energy transition fuel. This is due to the large reserves distributed worldwide, which can supply part of the rising power demand, and for being the most environmentally friendly among the fossil fuels[1]. Natural gas is mainly composed of CH₄, H₂O, N₂, and light hydrocarbon fractions (C_{2s} and C_{3s}). In this sense, to avoid pipeline corrosion and enhance energetic efficiency, all those fractions must be separated. Currently, the separation is made through cryogenic distillation with high pressures and temperatures below the boiling point of the molecules, resulting in a high-cost process. To face this problem, microporous materials for selective adsorption have received considerable attention, highlighting the emerging metal-organic frameworks (MOFs). These crystalline and highly porous materials stand out due to their pore size tunability and chemical properties. The anion-pillared framework SIFSIX-3-Cu, constituted by SiF₆²⁻, pyrazine and Cu²⁺ cations, showed great potential to capture CO₂[2]. The combination of the metal node, the anionic complex and the organic ligand results in functionalized cavities with promisor selectivity. With this in mind, this work aims to investigate the MOF SIFSIX-3-Cu to separate mixtures of methane, ethane, ethene, propane, propene and N₂. We performed computational simulations using Monte Carlo and molecular dynamics methods in RASPA software. The Lennard-Jones parameters for the gas molecules are from the TraPPE force field, UFF force field for Cu atom and DREIDING force field for C, H, Si and F atoms. The Lennard-Jones cross-interactions were described using Lorentz-Berthelot mixing rules and the framework was simulated as rigid. The atomic charges of MOFs were calculated with the charge equilibration method[3].

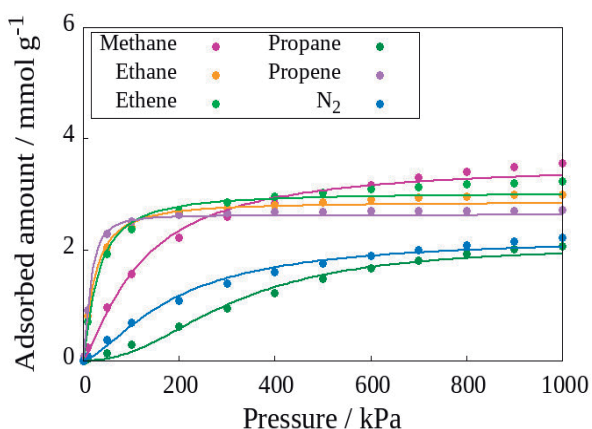


Figure 1: Fitted adsorption isotherms for gases molecules at SIFSIX-3-Cu.

reaching $S_{\text{ads}} = 3$ in binary mixtures with molar fractions of 0.5 and 0.75 of CH₄ at 100 kPa. The calculated adsorption enthalpy (ΔH_{ads}) is $-27.2 \text{ kJ mol}^{-1}$ and $-26.6 \text{ kJ mol}^{-1}$, for CH₄ and N₂, respectively. In this sense, it is expected that the separation of CH₄ against the other hydrocarbons happens in lower pressures as a size-sieving effect, while the separation between CH₄ and N₂ may happen due to different kinds of interactions established between SIFSIX-3-Cu and the adsorbed molecules, since they have similar diameters.

References:

- [1] R. Sahoo and M. C. Das, *Coord Chem Rev*, vol. 442, p. 213998, 2021.
- [2] O. Shekhah *et al.*, "*Nat Commun*", vol. 5, pp. 1–7, 2014.
- [3] C. E. Wilmer *et al.*, *Journal of Physical Chemistry Letters*, vol. 3, no. 17, pp. 2506–2511, 2012.

Acknowledgments

The following institutions: CNPq, FAPEMIG, CAPES, and INCT Acqua for financial support.
46^o Reunião Anual da Sociedade Brasileira de Química: "Química: Ligando ciências e neutralizando desigualdades"

Área: TEO

Mechanistic Study of Palladium(II) Catalyzed Annulation Reaction of *N*-Methoxy Amides and Arynes via C–H Bond Activation and C–N Cleavage.

Erick H. de S. Alves (IC),¹ Daniel A. S. Oliveira (PG),¹ Atualpa A. C. Braga (PQ),¹

erick_004@iq.usp.br

¹Department of Fundamental Chemistry, Institute of Chemistry, University of São Paulo, São Paulo - SP, Brazil

Keywords: C–H activation, annulation, DFT, catalysis

Highlights

Computational study of Pd(II)-catalyzed annulation of hydroxamates with arynes supported by C–H activation and *N*-methoxy amide as a directing group.

Abstract

In recent years, C–H functionalization reactions have received much attention from specialized authors. Countless products can be conceived with the propitious conditions and catalysts, usually with a higher atom economy compared with other techniques.

Based on the experimental work of Xiu-Feng Cheng and Ting Yu *et al.*,¹ we aim to develop a reliable computational model for the *N*-Methoxy amide directed C–H activation reaction catalyzed by the palladium(II) complex. The model to be developed attempts to clarify all steps, and its nuances, required to obtain the desirable products and recover the catalyst, helping to enhance process efficiency with better understanding of its kinetics and stereoselectivity. The calculations were performed using M06L density functional,² with the basis set Def2-SVP³ for geometry optimizations and frequency calculations.

A probable mechanism was proposed to the reaction (**Figure 1**).¹ So far, the intermediates and N–H/C–H activation transition states were determined in the gaseous phase, shown in **Figure 2**. The C–H activation represents the highest free-energy activation barrier up to now and it takes place through a concerted metalation-deprotonation (CMD) mechanism. The latter was facilitated by the *N*-methoxy amide group, functioning as a directing group for *ortho* C–H activation, demonstrated by N–H activation.

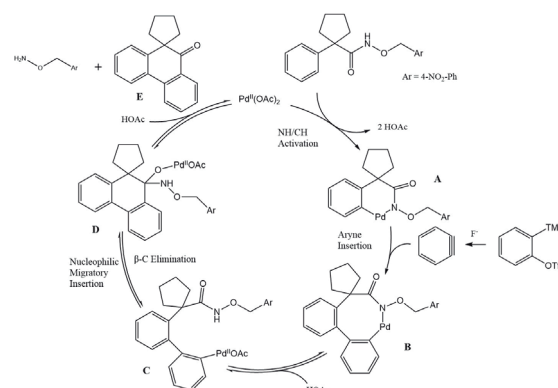


Figure 1. Proposed mechanism for the reaction

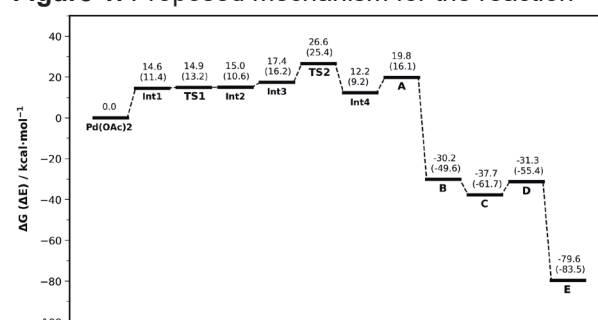


Figure 2. Energy reaction profile

- [1] X. Cheng, T. Yu, Y. Liu, N. Wang, Z. Chen, G. Zhang, L. Tong, B. Tang, *Organic Letters* **2022**, 24, 11, 2087-2092.
 [2] Y. Zhao, D. G. Truhlar, *J. Chem. Phys.* **2006**, 125, 194101.
 [3] F. Weigend, R. Ahlrichs, *Phys. Chem. Chem. Phys.*, **2005**, 7, 3297. *Phys. Chem. Chem. Phys.*, **2006**, 8, 1057.

Acknowledgments

We acknowledge the Institute of Chemistry of University of São Paulo and the financial support from FAPESP.

Área: TEO

(Inserir a sigla da seção científica para qual o resumo será submetido. Ex: ORG, BEA, CAT)

Nucleophilic Addition of Methyl Amine to Quinoline-5,8-dione

Paulo C. M. L. Miranda^{1a}; Nelson H. Morgon (PQ)^{1b,*}

nhmorgon@unicamp.br

¹Departamentos de Química Orgânica^a e de Físico Química^b, Instituto de Química (UNICAMP)

Palavras Chave: Nucleophilic Addition, Methyl Amine, Quinoline ring, B3LYP, SMD.

Highlights

- * Nucleophilic addition of Methyl Amine to Quinoline-5,8-dione.
- * B3LYP-D3(BJ)/(6-311++G(3df,2p) or ECP)/SMD (1,4-Dioxane).
- * A second Methyl Amine molecule catalyzes the reactions.
- * The obtained product at position **7** is energetically favored.

Resumo/Abstract

Alkaloids bearing nitrogen or oxygen atoms at position **7** of an isoquinoline nucleus are a common scaffold in several natural products such as caulibugulone, mansouramycin, and saframycin. Nevertheless, an ample number of alkaloids also have nitrogen or oxygen atoms at position **6** instead, as can be and both alkaloid subgroups stand out as privileged structures in biologically active alkaloids [*J. Org. Chem.* **2022**, *87*, 12, 7610–7617]. An analysis of the free energy reaction profile of the nucleophilic addition of Methyl Amine to the Quinoline-5,8-dione was carried out at DFT level of theory. The quantum chemical approach employed to determine the electronic and molecular structures was the Becke three-parameter hybrid method using the Lee-Yang-Parr correlation functional. The basis sets used for calculations were 6-311++G(3df,2p). Solvent effects (1,4-dioxane) were described by SMD model and D3 version of Grimmes's dispersion with Becke-Johnson damping. All calculations were performed using the Gaussian 16 program. Our results reveal minor differences in electronic densities and frontier orbitals at carbons **6** and **7**, which could justify to some extent the observed regioselectivity of the reaction. The reaction profile (potential energy surface – PES) is only obtained with the presence of a second Methyl Amine molecule. And the obtained product at position **7** was energetically favored in analogy to the experimental results.

Agradecimentos/Acknowledgments

This work was supported by the Foundation of the State of São Paulo (FAPESP, grants 2013/08293-7 and 2015/22338-9), and the National Council for Scientific and Technological Development (CNPq, grant 303581/2018-2).

Pharmacophore modeling of pleurotin with target on human Thioredoxin Reductase

Daniel B. Quintanilha (IC)¹ and Hélio F. Dos Santos (PQ)^{1*}.

dbquintanilha@ice.ufjf.br; helio.santos@ufjf.edu.br

¹ Núcleo de Estudos em Química Computacional, Departamento de Química, UFJF

Palavras Chave: Pleurotin, Molecular modeling, TrxR, Pharmacophore

Highlights

Proposed a pharmacophore model to improve the interaction of pleurotin with TrxR. Predicted a new derivative better than the pleurotin. The important residues in the TrxR catalytic site was defined.

Resumo/Abstract

The TrxR is an enzyme over expressed in tumor cells and a promising target to small inhibitors. In this study, we performed an analysis of the binding modes for pleurotin and its analogues to TrxR catalytic site. The goal was evaluate the contribution of each active pharmacophore moieties (Fig. 1) for the enzyme inhibition. Furthermore, the results allow to improve the knowledge of the catalytic site of TrxR.

Pleurotin was taken as template to establish the pharmacophore based on the analysis of the binding mode on TrxR. In the first step, 13 analogues were divided into four groups based on the moiety which was evaluated for interactions with TrxR. Figure 1 shows the regions on pleurotin backbone which had the principal modification in each group.

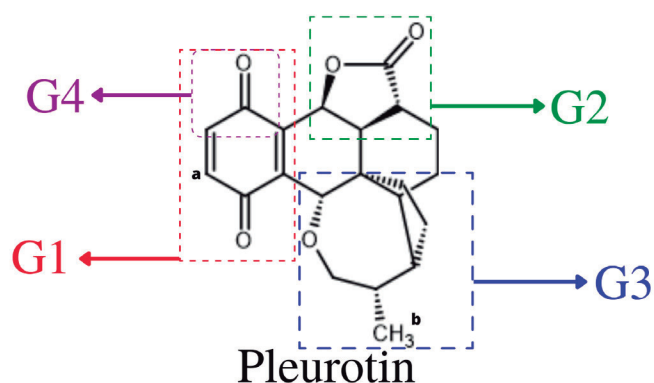


Figure 1. Structure of pleurotin with emphases on the four moieties that were evaluated as pharmacophore.

The ligands and receptor were optimized with the softwares Gaussian 03 and Visual Molecular Dynamics program, respectively. To improve the model, molecular docking and molecular dynamics were performed for all

compounds with Autodock4 and Amber16 softwares, respectively. The complex stability was estimated from Molecular Dynamics trajectory using the MM/GBSA method.

The results indicated that the inhibitor fitted in TrxR catalytic site in one favorable conformation, in which the hydrophilic moiety (G1 and G2) is exposed to solvent, and the other portion (G3) direct toward the inner part of the binding site. Moreover, it was observed that the better structure for the inhibitor is the pleurotin backbone with a non-polar group at position “a” (e.g. CH₃), and a polar H-bond donor group at position “b” (e.g. NH₂). However, the group at position “b” cannot be an OH, which decreases the affinity by the TrxR.

Thus, to test the proposed pharmacophore model, 17 derivatives were proposed with modifications at the positions “a” and “b”. These analogues were submitted to docking simulations. The results indicated that the model was accurate and could predict an inhibitor that the complex with TrxR was ~10% more stable than with pleurotin. This new derivative has a CH₃ at “a” and a NH₂ at “b”. Therefore, the results may motivate the synthesis of this new pleurotin analogue.

References

- Quintanilha et al. *J. Biomol. Struct. Dyn.* 2022, 00, 1-14; <https://doi.org/10.1080/07391102.2022.2092553>
- Sandargo et al. Molecules* 2018, 23(10), 2697; <https://doi.org/10.3390/molecules23102697>
- Hoskin et al. J. Am. Chem. Soc.* 2022, 144, 31, 14042–14046. <https://doi.org/10.1021/jacs.2c06504>

Agradecimentos/Acknowledgments

The authors would like to express gratitude to the financial support from CNPq (307018/2021-0), FAPEMIG, CAPES and UFJF that provided continuous support to our laboratory.

Predicting the Xe-129 NMR chemical Shift using the new NMR-ZORA basis sets for XeF₂, XeF₄ and XeF₆

Simone F. T. Marques (IC),^{1*} Diego F. S. Paschoal (PQ).^{1*}

simonefloreny@gmail.com; diegofspaschoal@macae.ufrj.br

¹Núcleo de Química Teórica e Computacional de Macaé, Polo Ajuda, Instituto Multidisciplinar de Química, Centro Multidisciplinar UFRJ-Macaé, Universidade Federal do Rio de Janeiro, 27.971-525, Macaé, RJ, Brasil.

Keywords: Xenon, NMR, Xe-129 chemical shift, Computational protocol, Relativistic effects, DFT.

Highlights

New NMR-ZORA basis sets for predicting NMR properties.

Computational protocol (NMR//Geometry) for predicting the structures and the Xe-129 NMR chemical shift.

Resumo/Abstract

The development of Noble Gas chemistry has shown a variety of applications, as those observed for xenon (Xe) in ultraviolet lamps, propellant for space travel, and anesthetic power [1]. Thus, there is great interest in studying and obtaining new Xe compounds, where NMR spectroscopy can be a powerful tool given the suitability of ¹²⁹Xe nucleus due to its favorable magnetic properties [1]. Therefore, computational chemistry resources are advantageous for the prediction of NMR properties. The present study aims to develop a computational protocol for predicting Xe-129 NMR chemical shift ($\delta^{129}\text{Xe}$) using the new NMR-ZORA basis set.

The xenon fluorides XeF₂, XeF₄, XeF₆, which present experimental data in gas phase for $\delta^{129}\text{Xe}$, were selected. Initially, a computational protocol for predicting the structures of compounds was proposed at DFT-Functional/def2-SVP, with a set of 32 DFT functionals being tested. Furthermore, the Xe-129 shielding constant ($\sigma^{129}\text{Xe}$) was calculated at GIAO-SSB-D-SC-ZORA/NMR-ZORA protocol, where the NMR-ZORA basis set for Xe atom was developed in the present study. Then, the chemical shift was obtained according to equation: $\delta^{129}\text{Xe} = \sigma^{129}\text{Xe}_{\text{ref}} - \sigma^{129}\text{Xe}_{\text{calc}}$, where atomic Xe was used as internal reference. All calculations were carried out in NWChem 7.0.2 program.

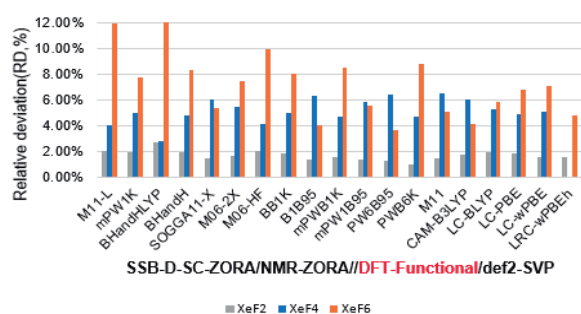


Figure 1. Relative deviation (RD, %) for the calculated $\delta^{129}\text{Xe}$ in XeF₂, XeF₄ e XeF₆ (C_{3v}).

It was observed that only DFT functionals with at least 28% of HF exchange adequately described the experimentally observed C_{3v} symmetry for the XeF₆ molecule [2], except for the M11-L. Concerning the $\delta^{129}\text{Xe}$, only the geometries obtained with 19 functionals were considered. The $\delta^{129}\text{Xe}$ of XeF₂ was not sensitive to the functional considered in the geometry, with relative deviations (DR) ranging from 0.03% to 2.67%. On the other hand, XeF₄ and XeF₆ showed a greater dependence on the considered geometry, with DR ranging from 2.77% to 8.13% and 1.97% to 12.05%, respectively. Considering all molecules, the lowest mean relative deviation (MRD) was only of 3.79% with PW6B95 functional.

The results show that the NMR-ZORA basis sets present a good description of the $\delta^{129}\text{Xe}$ in the studied xenon fluorides, with the protocol GIAO-SSB-D-SC-ZORA/NMR-ZORA//PW6B95/def2-SVP presenting a MRD of only 3.79%. Furthermore, the basis sets effect in geometries and NMR functionals in NMR will be analyzed to improve the consistency of the protocol.

[1] Chhandak, A. K. et al. *Int. J. Curr. Microbiol. App. Sci.* **2017**, 6, 2063.

[2] Paschoal, D. F. S.; Dos Santos, H. F. *Phys. Chem. Chem. Phys.* **2021**, 23, 7240.

Agradecimentos/Acknowledgments

The authors would like to thank the Brazilian agency FAPERJ (E-26/201.336/2022 – BOLSA) and PIBIC-UFRJ for the financial support.

RELATIONSHIPS BETWEEN CHEMICAL PROPERTIES AND THE BIOLOGICAL ACTIVITY OF THE ENDOCRINE DISRUPTOR CHLORHEXIDINE

Thiago C. B. Guimarães¹ (IC), Rafaela M. de Angelo¹ (PG), Michell O. Almeida² (PQ), Renata Colombo¹ (PQ), Kathia M. Honório^{1,3} (PQ)

kmhonorio@usp.br; thiago_borem@usp.br

¹EACH USP, São Paulo, ²IQSC-USP, São Carlos, ³UFABC, Santo André

Keywords: Chlorhexidine, Endocrine disruptors, Molecular docking, Molecular dynamics.

Highlights

- Chlorhexidine has high toxicity rates for aquatic organisms.
- Chlorhexidine has a profile with potential harm to human health, mainly related to the endocrine system since the results obtained indicate that this substance has affinity for the binding site of the alpha estrogen receptor, and may alter or even inhibit this hormonal pathway.
- Possible metabolites may be formed from the metabolism of chlorhexidine in the human body and most of these metabolites may be harmful to the aquatic environment.
- In this work, we verified that chlorhexidine and metabolite 6 have a high potential to be classified as endocrine disruptors.
- It is suggested to look for ways of metabolizing chlorhexidine that prioritize the formation of metabolites similar to metabolite 3, which could be a possible solution to avoid contamination in water treatment plants.

Resumo/Abstract

Most of the existing biocides end up acting mainly as endocrine disruptors, that is, substances capable of acting as hormone mimetics or inhibitors. Thus, an endocrine disruptor can bind to a specific hormone receptor, usually estradiol, generating a response that differs from normal hormonal action, in the case of mimicking substances, or no response in the case of inhibition. These substances can cause serious hormonal regulation problems and even problems such as sexual dystrophies and diseases linked to the endocrine system. In this study, molecular modeling techniques were employed to evaluate the possible endocrine action of chlorhexidine using docking tools, in particular, the GOLD program. In addition, *in silico* tools were used to generate possible metabolites of chlorhexidine and, consequently, their fitting in 3D structures of endocrine receptors (in this case, estrogen receptor alpha). Finally, the complexes formed by chlorhexidine/metabolites and the hormone receptor were submitted to molecular dynamics simulations using the AMBER program¹⁸. From the results obtained, we verified that chlorhexidine can present high levels of toxicity for aquatic organisms. In addition, it presented a profile with potential harm to human health, mainly related to the endocrine system, since the docking results indicate that this substance has affinity for the alpha estrogen receptor's binding site, which may alter or even inhibit this hormonal pathway. Added to this, this work can serve as a basis for future experimental analyses, since it contemplated possible metabolites that may be formed from the metabolism of chlorhexidine in the human body. The results also suggested that most of these metabolites may be harmful to the aquatic ecosystem, and one metabolite (6) showed a high level of toxicity, similar to chlorhexidine. On the other hand, metabolite 3 was the only one that presented a non-harmful profile for the aquatic environment. Finally, from molecular dynamics simulations, we can conclude that chlorhexidine and metabolite 6 have a high potential to be classified as endocrine disruptors, reinforcing the relevance of experimental analyses. In turn, metabolite 3 showed a low interaction potential, presenting a profile that does not suggest significant risks for both the aquatic ecosystem and the human organism. Based on these results, it is relevant to look for ways to metabolize chlorhexidine that prioritize the formation of metabolites similar to metabolite 3, which could be a possible solution to avoid contamination of water stations containing chlorhexidine or some metabolite with toxic potential for the aquatic environment and the human being.

Agradecimentos/Acknowledgments



(2017/10118-0)



S_NAr Trifluoromethylation of Activated Aryl Bromide by Crown Ether CatalysisGabryelle C. Marçal Salgado (PG),^{1*} Josefredo R. Pliego Jr. (PQ).¹

gabryellecarvalhomarçalsalgado@gmail.com; pliego@ufsj.edu.br.

¹Departamento de Ciências Naturais (DCNat), Universidade Federal de São João del-Rei – UFSJ

Keywords: Phase-transfer Catalysis, Nucleophilic Trifluoromethylation, Crown Ether, Free energy profile.

Highlights“S_NAr trifluoromethylation catalyzed by crown ether is kinetically viable with activated aryl bromide”**Abstract**

Nucleophilic substitutions reactions (S_NAr) are among the most useful processes in organic chemistry, with important recent advances.¹ Thus, the approach of aromatic trifluoromethylation reaction via S_NAr becomes interesting, because the insertion of the trifluoromethyl nucleophile (CF₃⁻) in organic molecules enhances its effectiveness in agrochemicals and pharmaceuticals.² In view of this, the development of trifluoromethylation methods is worthwhile. In this work, we have hypothesized that trifluoromethylation of aryl bromides could be achieved through phase transfers catalysis with the crown ether 18-crown-6 (18C6). The mechanistic proposal is the solubilization of the solid KOH (or CH₃OK) with 18C6, forming a complex. This complex would react with the source of CF₃⁻ ((C₂H₅)₃SiCF₃) generating KCF₃(18C6). Such a complex would react with the aryl bromide substrates (PhBr and *para*-BrAr(CN)). Therefore, we intend to evaluate the difference in the kinetics of this S_NAr reaction between the two substrates. The theoretical calculations were performed with the ORCA 5 program, using the ωB97X-D3/def2-SVP level of theory for geometry optimization calculations, harmonic frequencies and solvent effect (SMD), and the ωB97M-V/def2-TZVPP level for single point energy calculation. The calculations has indicated an easy solubilization of the KOH, and subsequent formation of the KCF₃(18C6) complex (with ΔG_{sol} = -20,8 kcal/mol and low barrier of ΔG[‡]). Thus, the rate-determining step is the next step, the S_NAr reaction. The free energy profile of the S_NAr reactions are described in Figs 1 and 2, being noticeable that when KCF₃(18C6) reacts with the aryl bromides, the ΔG[‡] of the reaction with BrAr(CN) (22.7 kcal/mol) is 7 lower kcal/mol than the reaction with PhBr (29.7 kcal/mol). This is the effect of the activating CN group on the aromatic ring. As the cyanide ion is an electron-withdrawing group in the ortho/para position in relation to the leaving group (Br), there is a stabilization of the aromatic ring.¹ Thus, based on our findings, we can predict that while the trifluoromethylation reaction with PhBr is kinetically very slow even at reflux of acetonitrile, the reaction with BrAr(CN) is fast and easy to carry out. In summary, our results point out for the feasibility of the trifluoromethylation reaction via S_NAr process and crown ether catalysis using (C₂H₅)₃SiCF₃ as CF₃ source for activated aryl bromides.

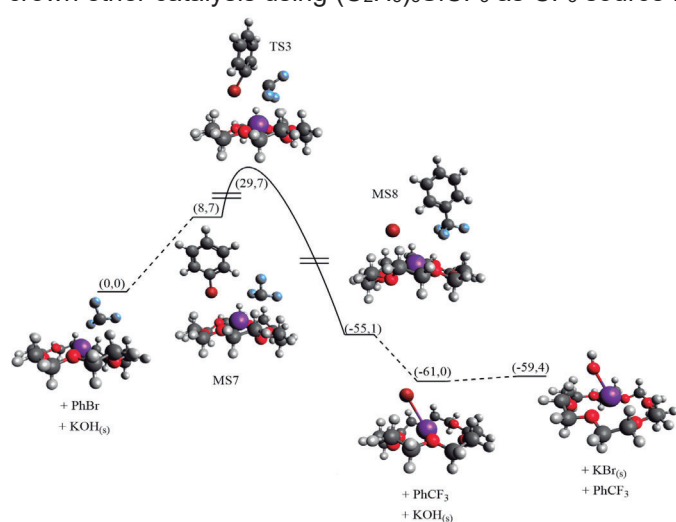


Fig. 1. Free energy profile with PhBr as substrate

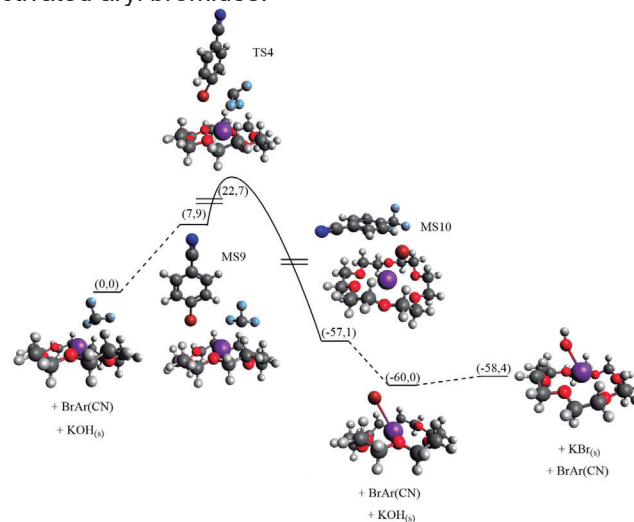


Fig. 2. Free energy profile with BrAr(CN) as substrate

¹ROHRBACH, S. et al. Concerted Nucleophilic Aromatic Substitution Reactions. *Angewandte Chemie - International Edition*, v. 58, n. 46, p. 16368–16388, 2019. ²CHO, E. J. et al. The palladium-catalyzed trifluoromethylation of aryl chlorides. *Science*, v. 328, n. 5986, p. 1679–1681, 2010.

Acknowledgments

CNPq, CAPES and FAPEMIG.

46ª Reunião Anual da Sociedade Brasileira de Química: “Química: Ligando ciências e neutralizando desigualdades”

Study of perovskite surfaces aiming electrocatalytic applications

Laura Menezes (PG),¹ Luis Henrique Lacerda (PQ),² Miguel A. San-Miguel (PQ)^{1*}

lauramenezes337@gmail.com; smiguel@unicamp.br

¹Instituto de Química, Unicamp; ²Departamento de Química UFSC

Palavras Chave: *Perovskite, DFT, Electrocatalysis*

Highlights

Perovskites are promising materials for catalysts in the glycerol oxidation reaction.

We use DFT calculations to analyze the electronic properties and attain trends in the catalytic activity of these materials.

We specifically focus on LaMnO₃, LaNiO₃, LaCoO₃, and LaFeO₃.

Abstract

The increased concern of nations about sustainability policies and the strong advent impact of Green Chemistry in recent years motivates and increasingly pressures the search for alternatives that minimize the effects generated by the emission of polluting gases into the atmosphere and promote new alternatives to energy obtainment. In this scenario, the electrocatalytic valorization of biomass, ideally powered by renewable electricity, rises as a sustainable path to produce transportable fuels and value-added chemicals.[1] In particular, the electrooxidation of glycerol is an attractive path since it is the main product of biodiesel obtainment allied to the capability of generating high-purity H₂ at the cathode. Nowadays, many electrocatalysts are based on noble metals, whose practical application is complex due to their high cost and scarcity. Thus, it is urgent to develop novel catalysts based on non-noble metals with high catalytic activity. In this scenario, perovskite-type oxides are prominent candidates.[2] Cooperative experimental results show that the oxides LaNiO₃ and LaCoO₃ present good catalytic activity for glycerol oxidation, while the LaMnO₃ and LaFeO₃ have poor activity. In this work, we investigate different surfaces of LaNiO₃, LaCoO₃, LaMnO₃, and LaFeO₃ perovskites from density functional theory calculations using the CRYSTAL17 code to understand the catalytic activity for the glycerol oxidation reaction. The four investigated perovskites are discussed in terms of band structure, charge carriers calculations, and density of states projections.

[1] H. Zhou et al. Chem. J. Chinese Universities, 41, 1449-1460, 2020.

[2] O.J. Bockris, J. Electrochem. Soc., 131, 290, 1984.

Acknowledgments

This work is supported by Coordenação de Aperfeiçoamento de Pessoal de Nível Superior - Brasil (CAPES) - Finance Code 001 and FAPESP (grants 2013/07296-2, 2016/23891-6, 2017/26105-4, and 2020/03780-0).

Study of reverse docking of acetogenins and synthetic analogues with leishmanicidal activity

João P.P. Encide (PG),¹ Ivanildo A. Brito (PG).^{1*} João H.G. Lago (PQ),¹ Kathia M. Honorio (PQ),^{1; 2}
joao.portilho@ufabc.edu.br; ivanildo.brito@ufabc.edu.br*

¹ Centro de Ciências Naturais e Humanas, UFABC; ² Escola de Artes, Ciências e Humanidades, USP

Keywords: (*L. infantum*, Natural products, neglected diseases, Reverse Docking).

Highlights

This work aims to propose possible mechanisms of action of natural products and analogues with activity against *L. infantum* through reverse docking studies.

Resumo/Abstract

Leishmaniasis is a tropical disease considered neglected by the World Health Organization, affecting several continents and is present in all Brazilian states. The species *Leishmania infantum* is the etiological agent of visceral leishmaniasis, a non-contagious infectious disease capable of causing splenomegaly and hepatomegaly and can be lethal when untreated. Its therapy involves aggressive antimonials to the body with harmful side effects, requiring the development of less toxic drugs¹. A natural product (**1**) obtained from *Porcelia Macrocarpa* seed extract and two analogous compounds (**1a** and **1b**) were recently reported with activity against *L. infantum* in in vitro tests. Such activity depends on the unsaturation of carbons C19'-C20', as their absence renders the inactive compounds (**2**, **2a** and **2b**)² shown in Fig. 1. To investigate such dependence, the reverse docking methodology was used in order to assess which enzyme(s) previously validated as molecular targets may be acting as a receptor. Nine enzymes described in the literature as essential for the survival of the parasite were selected. Their three-dimensional structures

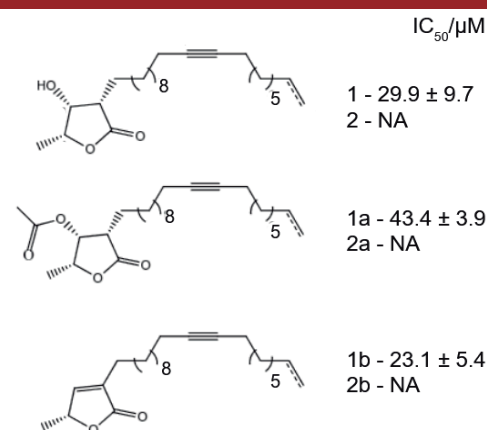


Figure 1 - Structure of acetogenins (1 and 2) and synthetic analogues (1a, 2a, 1b and 2b). NA = Not Active.

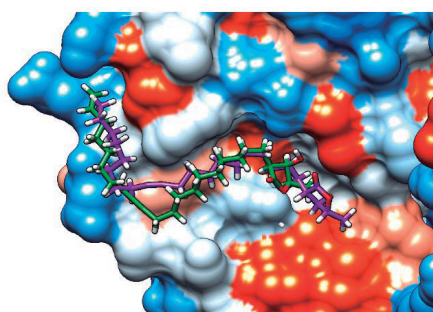


Figure 2 - Results of dockings with Trypanothione Reductase for compounds 1 (green) and 2 (purple).

were obtained from the PDB³ database. To perform the docking calculations, the GOLD⁴ program was used with the Python API extension to automate the protocols. The docking approach for trypanothione reductase (one of the most important targets against infection) with active and inactive compounds obtained scores slightly below that presented by the crystallographic ligand. Non-polar residues such as tryptophan, methionine and some leucines close to the catalytic site of the enzyme contributed to the accommodation of the ligands. Compound 2 obtained the highest score among the molecules, followed by 1 and 1a, similarly arranged in the cleft, shown in Fig. 2. The high scores attributed to the inactive compounds in relation to the active ones indicate the possibility of inhibiting another target. There is also the possibility that they are pro-drugs, therefore computationally idealized metabolites will also be tested on *L. infantum* enzymes.

¹ NEVES, D. P. *et al.* **Parasitologia Humana**. 11 ed. Atheneu; ² BRITO, I. A. *et al.* **Molecules**, 27(3):893; ³ Burley, S. K. *et al.* **Nucleic Acids Research** 49:D437–D451; ⁴ Jones, G. *et al.* **Journal of Molecular Biology**. 267(3);

Agradecimentos/Acknowledgments

CNPq, CAPES, FAPESP

Sulfonic Acid contaminant as hidden catalyst in the formation of α,β -unsaturated imines in aprotic solvents

Virginia C. Rufino (PG),¹ Josefredo R. Pliego Jr. (PQ),¹

virginiacamila12@gmail.com; pliego@ufs.br

¹Departamento de Ciências Naturais (DCNat), Universidade Federal de São João del-Rei – UFSJ

Keywords: Simple addition, Conjugate 1,4-addition, Acid catalysis, DFT, Selectivity.

Highlights

Methanesulfonic acid is a powerful catalyst for the α,β -unsaturated imine formation reaction, effective even in trace amounts.

Abstract

In recent years, theoretical calculations have pointed out that carboxylic acid impurity in the reaction medium could act as catalysts and explain the kinetics viability of imine formation in aprotic solvents.¹ In this work, we have investigated another class of acid impurity: sulfonic acids. The substrate is α,β -unsaturated aldehyde (crotonaldehyde) reacting with benzylamine (BnNH₂) and catalyzed by methanesulfonic acid (CH₃SO₂OH) in a toluene solution. The reaction can take place via 1,2-addition (imine formation, path in green, Figure 1) or 1,4-addition (aza-Michael product, path in blue). In both mechanisms, there is the formation of an ion pair between the amine and the acid (MS1PI, $\Delta G_{\text{sol}} = -4.8$ kcal mol⁻¹). Then, the crotonaldehyde can react along two different paths, as shown in Figure 1. In the first pathway (blue), in the counterclockwise catalytic cycle, the rate-determining step is the formation of the enol MS1cc, whose transition state (TS) does not have the participation of the methanesulfonic acid, presents $\Delta G^{\ddagger} = 30.8$ kcal mol⁻¹ in relation to MS1PI, kinetically unfeasible. After the formation of MS1cc, CH₃SO₂OH catalyzes the formation of a highly stable ion pair between 1,4-addition product and CH₃SO₃⁻ (MS6sc, $\Delta G_{\text{sol}} = -8.0$ kcal mol⁻¹), whose respective TS has $\Delta G^{\ddagger} = 13.6$ kcal mol⁻¹. This intermediate MS6sc is more stable than the product MS2ct ($\Delta G_{\text{sol}} = 1.4$ kcal mol⁻¹). On the other hand, in the clockwise catalytic cycle (green), there is the formation of an ion pair MS4ac ($\Delta G_{\text{sol}} = -4.8$ kcal mol⁻¹) through a catalyzed TS with $\Delta G^{\ddagger} = 14.1$ kcal mol⁻¹ in relation to MS1PI. In the sequence, there is the formation of MS4bt ($\Delta G_{\text{sol}} = -3.2$ kcal mol⁻¹), the rate-determining step, whose step also catalyzed by CH₃SO₂OH has $\Delta G^{\ddagger} = 14.3$ kcal mol⁻¹ in relation to MS1PI. In this case, the free species, MS2bt (imine), H₂O and CH₃SO₂OH have a free energy in solution of -2.1 kcal mol⁻¹. If we consider the kinetic law and a concentration of only 0.01 mol% of CH₃SO₂OH, the observed ΔG^{\ddagger} rises from 14.3 to 20.6 kcal mol⁻¹. Thus, even the presence of CH₃SO₂OH in the reaction medium in trace amounts is able to catalyze the formation of the imine as presented by the microkinetic modeling in Figure 1.

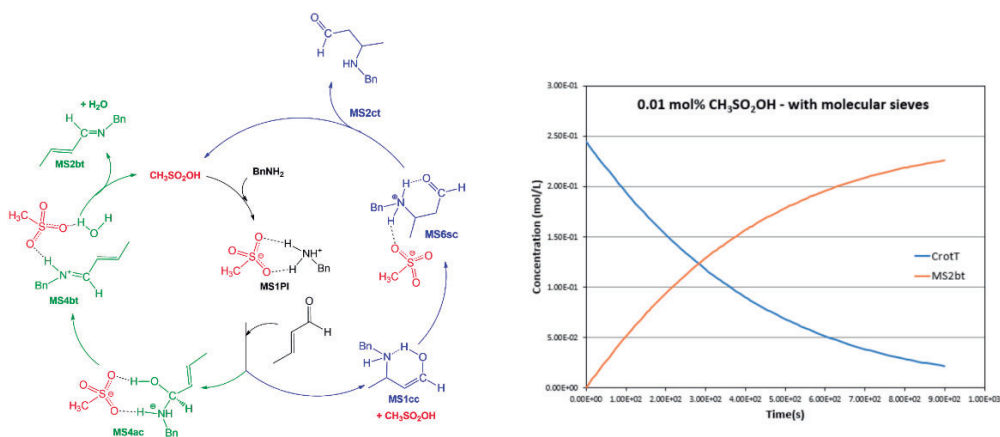


Figure 1: Catalytic cycle for the reaction between crotonaldehyde and benzylamine catalyzed by CH₃SO₂OH and the microkinetic modeling with a reaction time of 15 minutes.

¹ V. C. Rufino, J. R. Pliego, *Comput. Theor. Chem.* **2020**, 1191, 113053

Acknowledgments

CNPq, CAPES and FAPEMIG

46ª Reunião Anual da Sociedade Brasileira de Química: "Química: Ligando ciências e neutralizando desigualdades"

Área: TEO

(Inserir a sigla da seção científica para qual o resumo será submetido. Ex: ORG, BEA, CAT)

Theoretical Screening of Two Dimensional MQ_x Chalcogenides ($M = \text{Cu, Ag}$; $Q = \text{S, Se, Te}$, and $x = 0.5, 1.0, 1.5, 2.0$) via Density Functional Theory

Guilherme K. Inui (PG),¹ Rafael Besse (PQ),¹ Juarez L. F. Da Silva (PQ)¹

guiinui@gmail.com; juarez_dasilva@iqsc.usp.br

¹São Carlos Institute of Chemistry, University of São Paulo, São Carlos, SP, Brazil

Palavras Chave: DFT, Chalcogenides, Ab initio, Two-dimensional, Monolayer, Photovoltaics.

Highlights

Theoretical screening of 258 two-dimensional chalcogenides revealed 22 potentially stable. Nine show semiconductor properties with diverse bandgaps for solar energy harvesting.

Resumo/Abstract

Two-dimensional (2D) chalcogenides have attracted great interest for the development of photovoltaic devices due to its semiconductor properties with tunable band gaps within the optimal range for solar energy harvesting. Since most studies focused on particular compounds and composition of transition metal dichalcogenides (TMDs), e.g., MoS_2 , MoSe_2 , WS_2 , and WSe_2 , extending our knowledge on novel 2D chalcogenides structures is a promising route. Therefore, we used two crystal structure databases, the Inorganic Crystal Structure Database (ICSD) and Computational 2D Materials Database (C2DB), to select 2D structure prototypes that were then employed for MQ_x , where $M = \text{Cu, Ag}$, $Q = \text{S, Se, Te}$, $x = 0.5, 1.0, 1.5, 2.0$, leading to 258 systems. To improve the atomistic understanding of the physical-chemical properties of 2D copper and silver chalcogenides, Density Functional Theory (DFT) calculations with Perdew-Burke-Ernzerhof Generalized Gradient Approximation (PBE-GGA) with van der Waals D3 correction were performed to obtain structural, energetic, and electronic characterization of these materials. We found a logarithmic correlation between the average bond distance and effective coordination number (ECN) of cations and anions. Based on phonons dispersion analyses, we selected a set of 22 potentially stable MQ_x monolayers, classified as stable or semi-stable according to a criterion of maximum tolerance for negative frequencies. Among these monolayers, we identified 9 semiconductors (2 CuQ_x and 7 AgQ_x), with band gaps from 0.07 eV up to 1.67 eV (5 direct and 4 indirect), while the remaining 13 systems have a metallic character. The comparison of similar systems shows that an increase in anion size decreases the band gap, which can be explained by the increase in energy of anion Q p -levels that originates band edge states. Furthermore, an increase in the atomic radius of the Q species (i.e. from S to Te) increases the monolayer cohesive energies (E_{coh}) (ranging from -3.63 eV to -2.55 eV) and due to enhanced delocalization of the Ag d -states compared with Cu, the absolute value of E_{coh} is smaller for Ag compounds. Moreover, with the anion size increase, the work function it decreases for nearly all MQ_x monolayers (ranging from 3.00 eV to 6.24 eV) due to easier electron removal from outer layers. The potentially stable MQ_x monolayers investigated in this study will be explored further as a CO_2 reduction catalyst.

Agradecimentos/Acknowledgments

The authors gratefully acknowledge support from FAPESP (São Paulo Research Foundation, Grant Numbers 2017/11631-2, 2018/21401-7, 2018/17460-8, and 2022/06925-5), Shell and the strategic importance of the support given by ANP (Brazil's National Oil, Natural Gas and Biofuels Agency) through the R&D levy regulation.

Theoretical study of merocyanine isomers in methanol by Monte Carlo simulations

Débora A. Cunha (PG),¹ Ana Beatriz Oliveira (IC), Juliana Fedoce Lopes (PQ)².

¹Laboratório de Química Computacional (LaQC), Instituto de Física e Química, Universidade Federal de Itajubá, Itajubá, 37500-903, Minas Gerais, Brazil.

Keywords: Merocyanine, Explicit solvation, Monte Carlo simulation.

Highlights

Definition of the first and second solvation shells. Indication of the strong hydrogen bonds between methanol and a merocyanine isomer.

Abstract

The chromism phenomena occur when some substance is exposed to an external factor such as radiation, high or low temperatures, solvents with different polarity, and changed their structure which is observed by the change of color¹. Depending upon solvent, Merocyanines show different colours², and to study them, the interactions between the MC-TTC isomers in methanol were analyzed. For that, the software DICE was used in ensemble NPT, with 400000 Monte Carlo steps to determine the radial function distribution (RDF) between the atoms and the center of mass of the solute-solvent system. The RDF analysis between the centers of mass provides information on the distance at which the first shell of solvent molecules is located around the solute and their amounts, as shown in figure-X, also the groups contributing to the electronic transition of MC-TTC² were observed, highlighting the benzopyrene of the nitro group interacting with the hydrogen of the hydroxyl of the solvent.

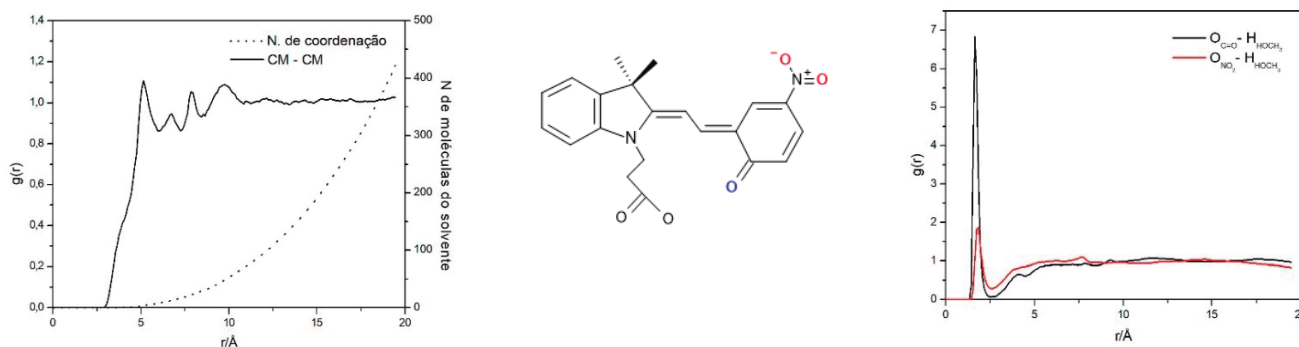


Figure 1. Left to right: RDF of solute and solvent centers of mass, with the number of molecules and their distances; Structure of MC-TTC with emphasis on groups containing oxygen; RDF of interactions between methanol hydroxyl hydrogen and the oxygens of benzopyran and nitro group.

Defining the first and second solvation shells, it is possible to analyze the maximum point of the first two peaks, that is the average maximum distance of 5.15 Å and 6.75 Å. When the number of solvent molecules is crossed between these points, there are approximately 4 and 13 molecules, respectively. The first peak has a greater intensity than the second, indicating stronger interactions. The $\text{-C=O}\cdots\text{HOCH}_3$ interaction was considerably more intense. The electronic density of the carbonyl group is more concentrated, with oxygen being more electronegative than carbon. According to theoretical calculations, the carbonyl group has a charge of -0.6339 while the nitrogen group has a charge of -0.4553, explaining why the hydrogens in methanol are more attracted to the more negative charge. These results are of great importance for the aqueous study of MC-TTC, because its orbitals contribute to the electronic transition in the molecule. The relevance of these interactions can be verified by comparing a study in different solvents with the same solute.

Acknowledgments

UNIFEI, CNPq, CAPES, FAPEMIG e PPGMQ-MG.

¹BAMFIELD, P., HUTCHINGS, M. *Chromic Phenomena Technological Applications of Colour Chemistry*. 2010, 3rd ed., p. 3-10,160-167.

²MENZONATTO, T. G., LOPES, J.F. *The role of intramolecular interactions on the stability of the conformers of a spiropyran derivative*. 2022. Chemical Physics.

Thermodynamic and Kinetic Aspects of Proton Reduction Involving Tridentate N3 based Nickel Complexes - A Quantum Mechanical Investigation

Murugesan Panneerselvam,¹ Madhavan Jaccob^{2*} and Luciano T Costa^{1*}

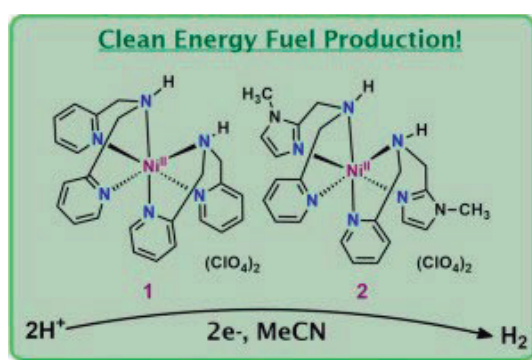
¹Universidade Federal Fluminense, Department of Physical Chemistry, Niterói – RJ, Brazil.

²Department of Chemistry, Loyola College, Chennai, India.

E-mail: panneerchem130491@gmail.com

Abstract

Detailed theoretical calculations were performed to understand the thermodynamic and kinetic aspects of proton reduction involving tridentate N3 based nickel $[\text{Ni}(\text{L}1)_2]^{2+}$ and $[\text{Ni}(\text{L}2)_2]^{2+}$ complexes have been investigated with the help of quantum chemical calculations, where L is (pyridin-2-ylmethyl)amine (L1) and 1-(1-methyl-1H-imidazol-2-yl)-N-(pyridin-2-ylmethyl)methanamine (L2) complexes for hydrogen production. Reaction free energies for mechanistic roots were computed along with their respective reduction potential and $\text{p}K_a$ values. Based on the computed formation free energies, the involvement of TsOH is less significant in altering the key intermediate formation (Ni(III)–Hydride) for proton reduction. The calculated $\text{p}K_a$ values clearly indicate that Ni(III)–hydride species is more acidic. This leads to electrochemical hydrogen generation at acidic pH condition instead of neutral pH medium. Also, proton coupled electron transfer (PCET) pathway is investigated for proton reduction involving similar catalysts and PCET is seems to be more favourable for Ni. Higher catalytic stability of tridentate N3 based ligand is clearly witnessed from the computed protonation free energy of the pyridine nitrogen. The acidic/basic nature of transient $\text{Ni}^{\text{III/II}}\text{-H}$ intermediate and choosing an appropriate reaction conditions based on the electronic nature of Ni catalysts are the main factors in improving the catalytic efficiency of Ni based molecular electrocatalysts involving tridentate N3 based ligand backbone. The calculated results and geometrical properties are in good agreement with the experimental observations. Based on our theoretical remarks, both ligands showed similar kind of electrocatalytic activity and more reactivity was observed for distorted octahedral coordination geometry than octahedral geometries of tridentate N3 based nickel catalysts.



Keywords: A DFT study, Nickel catalysts, Tridentate N3, PCET Mechanism and Proton Reduction.

References:

1. *Catalysis Today*, **2022**, XX, XX-XX. ([10.1016/j.cattod.2022.12.003](https://doi.org/10.1016/j.cattod.2022.12.003)).
2. *Inorg. Chem.* **2018**, 57, 14, 8116–8127.

What's behind their various activities? Towards a relationship between the morphology and forbidden energy gap of semiconductors from experiments to DFT calculations

Juan Andrés (PQ),^{1*} Amanda F. Gouveia (PQ),¹ Edson R. Leite (PQ),^{2,3} Fabricio R. Sensato (PQ),⁴ Elson Longo (PQ)²

andres@gfa.uji.es

¹Department of Analytical and Physical Chemistry, UJI, Spain; ²CDMF, UFSCar, ³Brazilian Nanotechnology National Laboratory, CNPEM, Brazil; ⁴Departament of Chemistry, Institute of Environmental, Chemical and Pharmaceutical Sciences, Unifesp, Brazil

Keywords: *Inorganic Semiconductor Oxides*, Surface Energy, Morphology, Band Gap, Wulff Construction, DFT Calculations.

Highlights

A relationship between morphology and band gap. Available morphologies of SnO₂, TiO₂, ZnO, Fe₂O₃, Co₃O₄, and Ag₃PO₄. Surface energy and band gap.

Abstract

The functional properties of inorganic semiconductor oxides as well as other materials not only are strongly dependent on its morphology and band gap, but also determine its relevance and merit for the applications. Adjusting morphologies, surface structures, and band gap is an effective way for understanding the underlying mechanisms to explore novel functions or controlling and optimizing specific properties. However, control and design of reaction conditions along synthesis of inorganic semiconductor oxides to acquire desirable band gap and morphology is a complex and difficult process.

Here, we combined density functional theory calculations and a Wulff construction to develop a simple computational model predicting the available morphologies for SnO₂, TiO₂, ZnO, Fe₂O₃, Co₃O₄, and Ag₃PO₄. The morphological transformations driven by the energy values of the exposed surface at a given morphology are capable to tune the band gap, and by analyzing the reported experimental morphologies, based on electron microscopy images, we disclose a detailed relationship between morphology and forbidden energy gap.

Importantly, our explicitly dynamic approach elucidates the atomic arrangements and stability of the exposed surfaces to provide a close match between experimental field emission scanning electron microscopy images and computational simulation. These findings highlight the role of the energetics, structural and electronic properties of the exposed surfaces at the morphology. Also, it can potentially set a foundation for establishing methods of synthesis to drive the morphology evolution through the control of temperature/pressure, and/or based on surface interactions of the selective adsorption of solvents/surfactants.

Acknowledgments

We acknowledge *Fundação de Amparo à Pesquisa do Estado de São Paulo (FAPESP)*, grant number 2013/07296 and 2022/08048-1. A.F.G. acknowledges the Generalitat Valenciana (Conselleria de Innovación, Universidades, Ciencia y Sociedad Digital) for the postdoctoral contract (CIAPOS/2021/106). J.A. acknowledges Universitat Jaume I (project UJI-B2019-30), and Generalitat Valenciana (Conselleria de Innovación, Universidades, Ciencia y Sociedad Digital – project CIAICO/2021/122) for financially supporting this research.